

spatiotemporal cats  
or, try herding 11 cats

*spatiotemp*, rev. 9051:

last edit Predrag Cvitanović, 2025-01-17

Predrag Cvitanović, Han Liang, Matthew N. Gudorf,  
Sidney V. Williams, Xuanqi Wang, Ibrahim Abu-hijeh,  
Rana Jafari, Li Han, Adrien K. Saremi and Boris Gutkin

January 17, 2025

# Contents

<b>1</b>	<b>Bernoulli map</b>	<b>13</b>
1.1	Temporal Bernoulli system . . . . .	13
1.2	Bernoulli map, beta transformation . . . . .	14
1.3	Any piecewise linear map has “linear code” . . . . .	29
	References . . . . .	30
<b>2</b>	<b>Cat map</b>	<b>37</b>
2.1	Adler-Weiss partition of the Thom-Arnol’d cat map . . . . .	37
2.2	Adler-Weiss partition of the Percival-Vivaldi cat map . . . . .	39
2.3	Cat map: Hamiltonian formulation . . . . .	45
2.3.1	Adler-Weiss partition of the cat map state space . . . . .	45
2.3.2	Counting Hamiltonian cat map periodic orbits . . . . .	46
2.3.3	An example: Fundamental parallelogram for period-2 cycle points . . . . .	49
2.3.4	An example: period-4 orbits . . . . .	51
2.3.5	Adler / Adler98 . . . . .	52
2.3.6	Percival and Vivaldi / PerViv . . . . .	52
2.3.7	Isola / Isola90 . . . . .	53
2.3.8	Creagh / Creagh94 . . . . .	54
2.3.9	Keating / Keating91 . . . . .	55
2.4	Green’s function for 1-dimensional lattice . . . . .	56
2.5	Green’s blog . . . . .	59
2.6	Chebyshev series . . . . .	64
2.6.1	Spectral methods . . . . .	64
2.6.2	Discretizing with Chebyshev polynomials . . . . .	65
2.7	Cat map blog . . . . .	67
	References . . . . .	80
2.8	Examples . . . . .	86
	exercises 91	
<b>3</b>	<b>Temporal Hénon</b>	<b>101</b>
3.1	Hénon blog . . . . .	101
3.2	Anti-integrable limit . . . . .	101
3.2.1	The meaning of source terms $m_t$ . . . . .	106

## CONTENTS

---

3.2.2	Anti-integrable blog	107
3.3	Hénon map symmetries	111
3.4	“Center of mass” puzzle	112
3.5	Symmetries of the symbol square	125
3.5.1	Symmetry lines	125
	References	126
3.6	*	134
	exercises	134
<b>4</b>	<b>Field theory</b>	<b>141</b>
4.1	Lattice discretization of a field theory	142
4.1.1	Transfer matrix	144
4.2	Laplacians	146
4.2.1	Laplacian notes 2012-2018	147
4.2.2	Laplacian notes	150
4.3	Deterministic lattice field theory	160
4.4	A partition function in terms of prime periodic states	161
4.4.1	Retiling the tiles, ver. 2023-02-28	163
4.4.2	Retiling the tiles, ver. 2023-01-19	164
4.4.3	Repeats of prime periodic states (failed attempt)	169
4.4.4	Resolvent of $W$	169
4.5	Orbit stability	170
4.5.1	Primitive cell stability of a periodic state	171
4.6	Orbit Jacobian matrices as block matrices	172
4.7	Observables	173
4.7.1	Birkhoff sums	174
4.7.2	Reject rate	175
4.7.3	Expectation values, à la Josh & Sam	175
4.8	Nonlinear lattice field theory	180
4.9	Internal symmetries	181
4.10	Deterministic $\phi^3$ lattice field theory	182
4.10.1	Spatiotemporal lattice Hénon theory	184
4.10.2	Biham-Wenzel potential	185
4.11	Deterministic $\phi^4$ lattice field theory	185
4.12	Historical context	188
4.12.1	1-dimensional lattice field theories	188
4.12.2	Nonlinear field theories	188
4.12.3	Deterministic lattice field theory	188
4.12.4	A $\phi^3$ field theory	189
4.12.5	A $\phi^4$ field theory	191
4.12.6	$\phi^4$ : Discrete Nonlinear Klein-Gordon	192
4.12.7	Anastassiou <i>et al.</i> AnBoBa17 $\phi^4$ notes	194
4.13	$\phi^k$ field theory blog	196
4.13.1	Letter from Ping Ao	206
4.14	Correlations	207
4.15	Semiclassical quantization	214

4.16	Noise is your friend . . . . .	215
4.16.1	Noisy Gábor . . . . .	220
4.17	Complex Ginzburg-Landau equation . . . . .	222
4.18	Kuramoto–Sivashinsky equation . . . . .	222
4.19	Elastodynamic equilibria of 2D solids . . . . .	223
4.20	Field theory blog . . . . .	223
	References . . . . .	241
<b>5</b>	<b>Computing periodic states</b>	<b>251</b>
5.1	Inverse iteration method . . . . .	251
5.2	Shadow state, temporal Hénon . . . . .	253
5.3	Shadow state, $\phi^3$ . . . . .	256
5.3.1	Primitive cell stability of a shadow periodic state . . . . .	258
5.4	Schneider papers . . . . .	259
5.4.1	Farano <i>et al.</i> FCRDS18 . . . . .	259
5.4.2	Azimi and Schneider Azimi2020 . . . . .	260
5.4.3	Parker and Schneider ParSch22a . . . . .	260
5.4.4	Parker, Ashtari and Schneider PaAsSc23 . . . . .	261
5.4.5	Ashtari and Schneider AshSch23 . . . . .	261
5.4.6	Page, Norgaard, Brenner and Kerswel PNBK22 . . . . .	261
5.5	Variational method, Dong 2020 paper DoLiLi20 . . . . .	261
5.6	Dong 2021 paper LDJL21 . . . . .	264
5.7	Wang and Lan 2022 paper WanLan22 . . . . .	264
5.8	Computing periodic states blog . . . . .	266
	exercises 270	
	References . . . . .	271
<b>6</b>	<b>Group theory</b>	<b>275</b>
6.1	A dancer, a parquet floor . . . . .	275
6.2	Group theory snippets . . . . .	276
6.3	Temporal lattice systems . . . . .	278
6.3.1	Temporal cat . . . . .	278
6.3.2	Periodic states . . . . .	279
6.3.3	Reflection-symmetric periodic states . . . . .	280
6.4	Time reversal symmetry reduction . . . . .	288
6.4.1	Laplacians (and time reversal?) . . . . .	288
6.4.2	Primitive cell Hill determinant for a 1-order system . . . . .	292
6.4.3	Time reversal blog . . . . .	295
6.4.4	Poles of dynamical zeta functions . . . . .	303
6.5	Time reversal literature . . . . .	305
6.5.1	Grava <i>et al.</i> 2021 paper GKMM21 . . . . .	305
6.5.2	Baake <i>et al.</i> 2008 paper BaRoWe08 . . . . .	310
6.5.3	Baake <i>et al.</i> 1997 paper BaHePI97 . . . . .	315
6.5.4	Baake 2018 paper Baake18 . . . . .	316
6.5.5	Lamb and Roberts 1998 paper lamb98 . . . . .	316
6.5.6	Calogero 2007 paper BrCaDr07 . . . . .	317

## CONTENTS

---

6.6	A Lind zeta function for flip systems . . . . .	319
6.6.1	Counting periodic states . . . . .	322
6.6.2	Counting square and rectangle states . . . . .	324
6.7	Permutation representations . . . . .	325
6.8	Internal symmetry factorization . . . . .	331
6.8.1	Internal symmetry blog . . . . .	332
6.9	Symmetry factorization blog . . . . .	336
6.10	Group theory and symmetries: a review . . . . .	341
6.10.1	Regular representation . . . . .	341
6.10.2	Irreducible representations . . . . .	342
6.10.3	Projection operator . . . . .	344
6.11	Examples . . . . .	345
6.12	Discrete factorization of the dynamical zeta function . . . . .	368
6.12.1	Factorization of $C_3$ and $D_3$ . . . . .	369
6.12.2	Factorization of $C_n$ and $D_n$ . . . . .	371
	References . . . . .	376
<b>7</b>	<b>Bloch, Brilluoin, ...</b> . . . . .	<b>382</b>
7.1	Reduction to the reciprocal lattice . . . . .	383
7.1.1	Hill determinant: Reciprocal lattice evaluation . . . . .	386
7.1.2	Integration over Brillouin zone . . . . .	393
	References . . . . .	396
<b>8</b>	<b>Spatiotemporal cat</b> . . . . .	<b>399</b>
8.1	Coupled map lattices . . . . .	400
8.1.1	Coupled map lattices . . . . .	400
8.1.2	Hamiltonian coupled map lattices . . . . .	401
8.2	Helmoltz type equations . . . . .	405
8.2.1	Poisson and Laplace's equations . . . . .	406
8.2.2	Screened Poisson equation . . . . .	406
8.2.3	Klein–Gordon equation . . . . .	407
8.2.4	Spatiotemporal cat equation . . . . .	408
8.2.5	Helmholtz blog . . . . .	408
8.3	Green's function for 2-dimensional square lattice . . . . .	410
8.4	Toeplitz tensors . . . . .	412
8.5	Green's blog . . . . .	413
8.6	Generating functions; temporal cat . . . . .	424
8.6.1	Lagrangian formulation . . . . .	427
8.6.2	Temporary: Cat map in the Lagrangian formulation . . . . .	429
8.7	Lattice points enumeration . . . . .	432
8.7.1	Integer lattice in $d$ dimensions . . . . .	432
8.7.2	A cryptographic perspective . . . . .	436
8.7.3	Primitive parallelogram . . . . .	445
8.7.4	Tensor eigenvalues . . . . .	449
8.8	Difference equations . . . . .	450
8.8.1	Time quasilattices . . . . .	453

8.9	Generating functions	456
8.10	Resistor networks	463
8.11	Counting periodic states	481
8.12	Integer lattices literature	482
	References	483
<b>9</b>	<b>Counting</b>	<b>499</b>
9.1	Enumeration of prime periodic states	499
9.1.1	Covering alphabet	499
9.1.2	Admissible prime periodic states	502
9.2	Counting prime periodic states	509
9.2.1	Enumeration of one-dimensional necklaces	512
9.2.2	Enumeration of two-dimensional necklaces	514
	References	516
<b>10</b>	<b>Zeta functions in 2D</b>	<b>517</b>
	References	530
<b>11</b>	<b>Spatiotemporal stability</b>	<b>534</b>
11.1	Temporal lattice	534
11.1.1	Second-order difference equation	536
11.1.2	Third-order difference equation	536
11.1.3	Bountis and Helleman 1981 paper Bount81	537
11.2	Repeats of a prime primitive cell	540
11.2.1	Primitive cell repeats symmetrized	541
11.2.2	Repeats blog	543
11.3	Spatiotemporal lattice	546
11.4	Noether's theorem	546
11.5	Stability blog	547
11.6	Generating function literature	553
	References	554
<b>12</b>	<b>Hill's formula</b>	<b>558</b>
12.1	An overview over "Hill's formulas"	558
12.2	Generating functions; action	559
12.3	Homoclinic and periodic orbit actions in chaotic systems	560
12.4	Hill's formula, Lagrangian setting	562
12.5	Spatiotemporal cat Hill's formula	563
12.6	Hill's formula for relative periodic orbits	568
12.7	Han's 1st order difference eq. Hill's formula	570
12.7.1	Hill's formula for a first-order system	572
12.8	Han's temporal cat Hill's formula	576
12.9	Han's 2nd order difference eq. Hill's formula	577
12.9.1	Hill's formula for a second-order system	578
12.10	Han's spatiotemporal cat Hill's formula	580
12.10.1	Han's relative-periodic Hill's formula	581

## CONTENTS

---

12.11 Han's Hénon map Hill's formula . . . . .	583
12.12 Hill's formula blog . . . . .	585
References . . . . .	601
<b>13 Chronotopic musings</b>	<b>607</b>
13.1 Chronotopic literature . . . . .	607
13.2 PolTor92b Towards a statistical mechanics of spatiotemporal chaos	611
13.3 PolTor92 Periodic orbits in coupled Hénon maps . . . . .	615
13.4 PoToLe98 Lyapunov exponents from node-counting . . . . .	616
13.5 PolPuc92 Invariant measure in coupled maps . . . . .	617
13.6 PolTor09 Stable chaos . . . . .	617
13.7 Spatiotemporal Floquet-Bloch theory . . . . .	619
References . . . . .	623
<b>14 Symbolic dynamics: a glossary</b>	<b>626</b>
14.1 Symbolic dynamics, inserts . . . . .	630
References . . . . .	631
<b>15 Statistical mechanics applications</b>	<b>632</b>
15.1 Cat map . . . . .	632
15.2 New example: Arnol'd cat map . . . . .	632
References . . . . .	636
<b>16 Ising model in 2D</b>	<b>637</b>
16.1 Ihara zeta functions . . . . .	647
16.1.1 Clair / Clair14 . . . . .	648
16.1.2 Ihara blog . . . . .	651
16.1.3 Maillard . . . . .	663
16.2 Gaussian model . . . . .	668
16.3 Tight-binding Hamiltonians . . . . .	672
16.4 Discrete Schrödinger equation . . . . .	675
16.5 Harper's model . . . . .	679
16.6 The sine-Gordon equation . . . . .	682
16.7 Frenkel-Kontorova model . . . . .	683
16.8 Mean field theory for the Ising model . . . . .	688
16.9 Clock model . . . . .	689
16.10 XY model . . . . .	691
16.11 Rigid rotors model, dimer model . . . . .	693
16.12 Many-body quantum chaos . . . . .	696
16.13 Lattice QED . . . . .	698
16.14 Seiberg lattice papers . . . . .	701
References . . . . .	705

<b>17 Normalizing flows, machine learning, information</b>	<b>715</b>
17.1 Normalizing flows	715
17.2 Information	724
17.2.1 Information blog	728
References	736
<b>18 Heat kernel</b>	<b>738</b>
18.1 Heat kernel, continuous space, fictitious time	738
18.2 Wanderings of a drunken snail	739
18.2.1 Newton flows	749
18.2.2 Heat equation	751
References	752
<b>19 Conformal field theory</b>	<b>754</b>
19.1 Complex plane	754
19.1.1 Integer lattice	754
19.2 Elliptic functions	755
19.3 Zeta function regularization	774
19.4 Computing log det of Hill determinant	781
19.5 Maloney-Witten partition functions, MalWit07	782
References	787
<b>20 Metamaterials</b>	<b>791</b>
20.1 Checkerboard model	791
20.1.1 Checkerboard literature	792
20.2 Zero bulk modulus model	792
References	796
<b>21 Article edits</b>	<b>797</b>
21.1 Cats' GHJSC16blog	797
21.1.1 Cats/nonlin-v2/ GHJSC16 revisions	813
21.2 Kittens' CL18blog	817
21.2.1 Prime Bravais lattices	841
21.3 Reversal' LC21blog	880
21.3.1 Counting periodic states	888
21.3.2 Hill determinant: fundamental parallelepiped evaluation	890
21.4 Hill determinant: stability of an orbit vs. its time-evolution stability	900
21.4.1 Hill determinant: time-evolution evaluation	901
21.4.2 Hill's formula: stability of an orbit vs. its time-evolution stability	903
21.4.3 Hill's formula	904
21.5 Hill's formula LC22blog	907
21.6 Nonlinear deterministic field theory WWL AFC22blog	910
References	911



## CONTENTS

---

<b>22 Sidney's blog</b>	<b>917</b>
22.1 2020 blog	917
22.2 2021 blog	947
22.3 2022 blog	988
22.4 2024 blog	1036
References	1067
<b>23 Xuanqi's blog</b>	<b>1071</b>
23.1 2022 blog	1072
23.2 Notes on zeta function	1113
23.3 2024 blog, continued	1117
References	1134
<b>24 Han's blog</b>	<b>1136</b>
24.1 Rhomboid corner partition	1137
24.2 Rhomboid center partition	1154
24.2.1 Reduction to the reciprocal lattice	1164
24.3 Time reversal	1166
24.4 Reduction to the fundamental domain	1171
24.5 Spatiotemporal cat partition	1173
24.6 Running blog	1183
24.6.1 Stability of a periodic point vs. stability of the orbit	1231
24.6.2 Temporal cat counting by determinant recursion	1232
24.7 Cycle expansion	1341
24.7.1 Temporal Bernoulli escape rate and field expectation value	1341
24.7.2 Correlation function of temporal Bernoulli	1343
24.7.3 Correlation function of the 'golden mean' map	1344
24.7.4 Temporal cat escape rate and field expectation value	1345
24.7.5 Correlation function of temporal cat	1345
References	1370
<b>25 Spatiotemporal cat, blogged</b>	<b>1375</b>
References	1398
<b>26 Pow Wows</b>	<b>1402</b>
26.1 Pow wow 2020-12-08	1402
26.2 Pow wow 2020-12-28	1403
26.3 Pow wow 2021-01-08	1403
26.4 Pow wow 2021-03-22	1404
26.5 Pow wow 2021-04-02	1404
26.6 Pow wow 2021-04-09	1405
26.7 Pow wow 2021-04-27	1406
26.8 Pow wow 2021-05-04	1406
26.9 Pow wow 2021-05-07	1407
26.10 Pow wow 2021-05-14	1408
26.11 Pow wow 2024-10-21	1408

*CONTENTS*

---

26.12Pow wow 2024-10-24 . . . . . 1412  
26.13Pow wow 2024-11-08 . . . . . 1415  
26.14Pow wow 2025-01-07 . . . . . 1416  
26.15Pow wow 2025-01-09 . . . . . 1419  
26.16Pow wow 2025-01-14 . . . . . 1423  
26.17Pow wow 2025-01-16 . . . . . 1425  
References . . . . . 1429

## CONTENTS

---

This cat has been skinned in more ways than any other cat in the history of cats.

— Professore Gatto Nero

This is a project of many movable parts, so here is a guide where to blog specific topics (or where to find them)

- sect. ?? 1-dimensional / cat map lattice Green's functions
- sect. ?? cat map blog
- sect. 2.8 Examples: Cat map
- chapter 8  $d$ -dimensional spatiotemporal cat
- sect. ??  $d$ -dimensional / spatiotemporal cat Green's function
- sect. ?? Reduction to the reciprocal lattice
- chapter 12 Hill's formula
- chapter 18 Heat kernel
- sect. 12.2 1-dimensional action
- sect. ?? Herding five cats [1] edits
- chapter 14 Symbolic dynamics: a glossary
- chapter 16 2D Ising model; Ihara and multi-dimensional zetas
- chapter 20 Metamaterials
- chapter 22 Sidney's blog
- chapter 23 Xuanqi's blog
- chapter 24 Han's blog - the most important blog
- chapter ?? Rana's blog (uncomment in blogCats.tex)
- chapter ?? Adrien's blog (uncomment in blogCats.tex)
- chapter 25 Spatiotemporal cat blog

Blog fearlessly: this is your own lab-book, a chronology of your learning and research that you might find invaluable years hence.



# Chapter 1

## Bernoulli map

2021-01-04 Predrag discussed here:

[ChaosBook example 14.5](#) *Bernoulli shift map state space partition*

[ChaosBook exercise 27.3](#) *Lyapunov exponents for 1-dimensional maps.*

2022-06-17 Looks misplaced, fix [ChaosBook here!](#)

[ChaosBook eq. \(28.11\)](#), the end of [ChaosBook section 28.4](#) *Analyticity of spectral determinants.*

[ChaosBook example 28.2](#) *Bernoulli shift eigenfunctions.*

[ChaosBook exercise 28.5](#) *Bernoulli shift on  $L$  spaces.*

2022-06-17 Looks misplaced, fix [ChaosBook here!](#)

[ChaosBook example 29.1](#) *Return times for the Bernoulli map.*

[ChaosBook appendix 28.5](#) *Pruned Bernoulli shift.*

example [4.1](#) *Bernoulli map correlations.*

Han's sect. [24.7.1](#) *Temporal Bernoulli escape rate and field expectation value.*

Remark [1.1](#) *Bernoulli map.* remark [1.2](#) *Bernoulli shift.*

See discussion around [\(1.18\)](#).

See [\(8.144\)](#).

[wiki: Dyadic transformation](#) also known as the dyadic map, bit shift map,  $2x \bmod 1$  map, Bernoulli map, doubling map, sawtooth map.

### 1.1 Temporal Bernoulli system

To motivate our formulation of a spatiotemporal deterministic field theory to be developed in the sequel [\[7\]](#), we recast the local initial value, time-evolution Bernoulli map problem as a *temporal lattice* fixed point condition, the problem of enumerating and determining all global solutions.

‘Temporal’ here refers to the state (field)  $\phi_t$ , and the winding number (source)  $m_t$  taking their values on the lattice sites of a 1-dimensional *temporal* integer lattice  $t \in \mathbb{Z}$ . Over a finite lattice segment, these can be written compactly as a *periodic state* and the corresponding *symbol block*

$$\Phi^\top = (\phi_{t+1}, \dots, \phi_{t+n}), \quad \mathbf{M}^\top = (m_{t+1}, \dots, m_{t+n}), \quad (1.1)$$

where  $(\dots)^\top$  denotes a transpose. The Bernoulli equation, rewritten as a first-order difference equation

$$\phi_t - s\phi_{t-1} = -m_t, \quad \phi_t \in [0, 1), \quad (1.2)$$

takes the matrix form

$$\mathcal{J}\Phi = -\mathbf{M}, \quad \mathcal{J} = \mathbf{1} - sr^{-1}, \quad (1.3)$$

where the  $[n \times n]$  matrix

$$r_{jk} = \delta_{j+1,k}, \quad r = \begin{pmatrix} 0 & 1 & & & \\ & 0 & 1 & & \\ & & & \ddots & \\ & & & & 0 & 1 \\ 1 & & & & & 0 \end{pmatrix}, \quad (1.4)$$

implements the shift operation, a cyclic permutation that translates forward in time the periodic state  $\Phi$  by one site,  $(r\Phi)^\top = (\phi_2, \phi_3, \dots, \phi_n, \phi_1)$ . The time evolution law must be of the same form for all times, so the shift operator  $r$  has to be time-translation invariant, with  $r_{n+1,n} = r_{1n} = 1$  matrix element enforcing the periodicity. After  $n$  shifts, a periodic state returns to the initial state,

$$r^n = \mathbf{1}. \quad (1.5)$$

## 1.2 Bernoulli map, beta transformation

**2020-01-27 Predrag** Much of ergodic theory can be illustrated by a Bernoulli map [3, 8]. One can explicitly construct a Perron-Frobenius operator, and compute its eigenvalues and its eigenvectors; construct the dynamical zeta function, and count periodic states and orbits [6].

As a gentle introduction for a reader too busy [4] to study the book [6], we disguise a brief course on chaos theory as something everyone understands, a Bernoulli coin toss.

one determines the total number of periodic states by computing the Hill determinant of the *orbit Jacobian matrix*

The observation that a Bernoulli system can be viewed as a discretization of a first-order in time ODE, with solutions whose temporal global linear stability is described by the orbit Jacobian matrix  $\mathcal{J}_{tt'} = \delta F[\Phi]_t / \delta \phi_{t'}$ ,

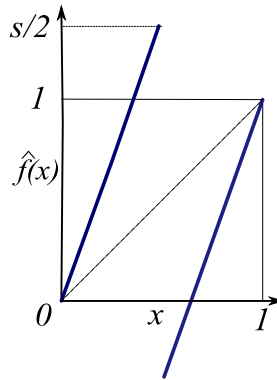


Figure 1.1:  $\hat{f}(\phi)$ , the full space sawtooth map (1.7),  $s > 2$ .

has profound implications for dissipative spatiotemporal systems such as Navier–Stokes and Kuramoto–Sivashinsky [11].

As we shall here have to traverse territory unfamiliar to many, we follow Mephistopheles pedagogical dictum “You have to say it three times” [10], and sing our song thrice.

(for  $r$  written out as a matrix, see (1.25))

**2019-07-30 Predrag** Since all coefficients in (2.80) are integers, the periodic states  $\phi_t$  are always rational. This allows for their exact evaluation by integer arithmetic.

**2019-12-18 Predrag** (dropped from CL18.tex)

Restrict the admissible field values  $\phi_t$  at time-lattice site  $t$  to the symmetric unit interval  $\phi \in [-1/2, 1/2)$ , with ??-letter alphabet

$$\mathcal{A} = \{\underline{4}, \underline{3}, \underline{2}, \underline{1}, 0, 1, 2, 3, 4\}. \quad (1.6)$$

It maps the unit interval onto itself, with fixed points  $\phi_0 = 0, \phi_1 = 1$ .

reduction  $\hat{f}(\phi_t) \mapsto f(\phi_t)$

Recall how the subpartitions of figure 1.2 were used to obtain the total number of periodic points (??), as every subpartition contained one and only one periodic point.

The closely related *sawtooth map*, sketched in figure 1.1, with ‘stretching’ parameter  $s > 2$ ,

$$\hat{x}_{t+1} = \hat{f}(\hat{x}_t) = \begin{cases} s\hat{x}_t, & \hat{x}_t \in [0, 1/2) \\ s\hat{x}_t + 1 - s, & \hat{x}_t \in (1/2, 1] \end{cases} \quad (1.7)$$

Since the relation between  $m_t$  symbol sequences and  $\phi_t$  states is linear, it is straightforward to go back and forth between a periodic state and its symbolic representation.

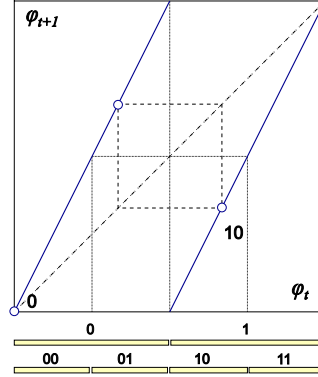


Figure 1.2: The Bernoulli map (1.7) for  $s = 2$ , together with the  $\bar{0}$  fixed point, and the  $\bar{01}$  2-cycle. Preimages of the critical point  $\phi_c = 1/2$  partition the unit interval into  $\{\mathcal{M}_0, \mathcal{M}_1\}, \{\mathcal{M}_{00}, \mathcal{M}_{01}, \mathcal{M}_{10}, \mathcal{M}_{11}\}, \dots$ , subintervals. As the map is a circle map,  $\phi_5 = 1 = 0 = \phi_0 \pmod{1}$ .

The  $n$ th preimages  $b^{-(n-1)}(\phi)$  of the critical point  $\phi_c = 1/2$  partition the state space into  $2^n$  subintervals, each labeled by the first  $n$  binary digits of points  $\phi = .m_1m_2m_3\dots$  within the subinterval: figure 1.2 illustrates such 4-intervals state space partition  $\{\mathcal{M}_{00}, \mathcal{M}_{01}, \mathcal{M}_{11}, \mathcal{M}_{10}\}$  for  $n = 2$ . known as the *doubling* map if  $s = 2$ ,

$$\phi_{t+1} = 2\phi_t \pmod{1}, \tag{1.8}$$

and  $s$ -*tupling* map, figure 1.6 (b), for integer stretching parameter  $s \geq 3$ . The relation is linear, and a given block  $M$ , or ‘code’ in terms of alphabet (??), corresponds to a unique temporal periodic state  $\Phi$  given by the lattice Green’s function

$$\Phi = g M, \quad g = -\frac{r}{r - s \mathbf{1}}, \tag{1.9}$$

provided we specify the boundary conditions (bc’s) for the shift operator  $r$ .

The power of the linear encoding of the temporal Bernoulli condition (1.18) is that the *integer-valued* symbols  $m_t$  from the finite alphabet (??) encode the *real-valued* lattice site states  $\phi_t$ .

For the piecewise linear map of figure 1.2 we can evaluate the dynamical zeta function in closed form. Each branch has the same value of the slope, and the map can be parameterized by the single parameter  $s$ . The larger  $s$  is, the stronger is the stretching action of the map.

The power of the code

$$M^\top = (m_t, m_{t+1}, \dots, m_{t+k}) \tag{1.10}$$



for the temporal cat (2.80) is that one can use *integers*  $m_t$  to encode the *real-valued* periodic states  $\phi_t$ .

$$(\partial - (s - 1)r^{-1})\Phi = -M. \quad (1.11)$$

For the  $s = 3$  cat map example at hand, they are

$$\{M_j\} = (M_1, M_2, M_3, M_4, M_5, \dots) = (1, 2, 5, 10, 24, \dots), \quad (1.12)$$

Visualizing the volume relation (8.122) for a general  $n$ -dimensional fundamental parallelepiped is not easy, but

As the temporal Bernoulli (1.19) and (1.3) is linear, eigenmodes of  $\mathcal{J}$ , shifted by  $M$  as in (1.19) for each distinct periodic state, are also periodic states of temporal Bernoulli.

**2020-01-17 Han** The determinant of  $\mathcal{J}$  from (1.19) is negative, so we cannot use the determinant trace formula directly. A correct way: first rewrite the  $\mathcal{J}$  as in (1.9)

$$\mathcal{J} = \mathbf{1} - sr^{-1} = -\frac{s}{r} \left( \mathbf{1} - \frac{r}{s} \right).$$

Note that  $\text{Det}(r) = (-1)^{n-1}$ . The Hill determinant of  $\mathcal{J}$  is:

$$\text{Det } \mathcal{J} = \det \left( \frac{r}{s} - \mathbf{1} \right) s^n (-1)^{n-1} = -s^n \text{Det} \left( \mathbf{1} - \frac{r}{s} \right).$$

Then use the determinant-trace formula:

$$\ln \text{Det} \left( \mathbf{1} - \frac{r}{s} \right) = \text{Tr} \ln \left( \mathbf{1} - r/s \right) = - \sum_{k=1}^{\infty} \frac{1}{k} \frac{\text{Tr}(r^k)}{s^k},$$

and use  $\text{Tr } r^k = n\delta_{k, nr}$  if  $k$  is a multiple of  $n$ , 0 otherwise (follows from  $r^n = \mathbf{1}$ ),

$$\ln \text{Det} \left( \mathbf{1} - \frac{r}{s} \right) = - \sum_{r=1}^{\infty} \frac{1}{r} \frac{1}{s^{nr}} = \ln(1 - s^{-n}),$$

and the Hill determinant of  $\mathcal{J}$  is:

$$\text{Det } \mathcal{J} = -s^n \text{Det} \left( \mathbf{1} - \frac{r}{s} \right) = 1 - s^n, \quad (1.13)$$

which is negative. So for the temporal Bernoulli the count is:

$$N_n = |\text{Det } \mathcal{J}| = s^n - 1,$$

in agreement with the time-evolution count.

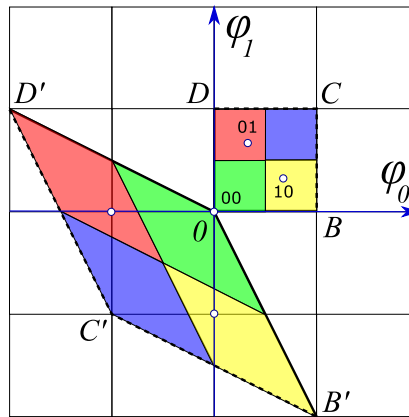


Figure 1.3: (2020-02-14 Predrag: his is “wrong”, now superseded with the updated figure in ref. [7]; 2020-09-11 the whole example seems misplaced here, move it to wherever it belongs) The base-2 Bernoulli map (1.14) period-2 periodic points  $\Phi_p = (\phi_0, \phi_1)$  are  $\bar{0} = (0, 0)$ ,  $\bar{1} = (1, 1)$  fixed point repeats, and the 2-cycle  $\Phi_{01} = (1/3, 2/3)$ , see figure 1.2. They all lie within the unit square  $[0BCD]$ , one within each  $\mathcal{M}_{m_0 m_1}$  subregion, and are mapped by the  $[2 \times 2]$  orbit Jacobian matrix  $\mathcal{J}$  into the parallelogram  $[0B'C'D']$ , whose area is 4 times the unit area. The images of periodic points  $\Phi_p$  land on the integer lattice, and are sent back into the origin by integer translations  $M_p$ , in order to satisfy the fixed point condition  $\mathcal{J}\Phi_p + M_p = 0$ .

**2020-01-25 Predrag: A Bernoulli map example.** The action of orbit Jacobian matrix  $\mathcal{J}$  for the period-2 periodic points of the base-2 Bernoulli map, figure 1.2, which partitions the unit interval into 2 subintervals  $\{\mathcal{M}_m\}$ , is

$$\phi_{t+1} = 2\phi_t - m_{t+1}, \quad \phi_t \in \mathcal{M}_{m_t}, \quad (1.14)$$

where  $m_t$  takes values in the 2-letter alphabet

$$m \in \mathcal{A} = \{0, 1\}. \quad (1.15)$$

should suffice to convey the idea. In this case, the  $[2 \times 2]$  orbit Jacobian matrix, the unit square basis vectors, and their images are

$$\begin{aligned} \mathcal{J} &= \begin{pmatrix} 1 & -2 \\ -2 & 1 \end{pmatrix}; \quad \Phi_B = \begin{pmatrix} 1 \\ 0 \end{pmatrix}, \quad \Phi_D = \begin{pmatrix} 0 \\ 1 \end{pmatrix} \\ \Phi_{B'} &= \mathcal{J}\Phi_B = \begin{pmatrix} 1 \\ -2 \end{pmatrix}, \quad \Phi_{D'} = \begin{pmatrix} -2 \\ 1 \end{pmatrix}, \end{aligned} \quad (1.16)$$

with the resulting fundamental parallelogram of area 4 shown in figure 1.3. The volume of the fundamental parallelogram lattice  $\mathcal{L}$  (8.97) is

$$\text{Det}(\mathcal{L}) = \text{Det}(\Phi_{B'}|\Phi_{D'}) = \text{Det}(\mathcal{J})\text{Det}(\Phi_B|\Phi_D) = -3, \quad (1.17)$$

where in this case the unit cell matrix  $(\Phi_B|\Phi_D) = \mathbf{1}$ .

The  $[3 \times 3]$  orbit Jacobian matrix and the unit cube basis vectors are

$$-\mathcal{J} = \begin{pmatrix} -1 & 0 & 2 \\ 2 & -1 & 0 \\ 0 & 2 & -1 \end{pmatrix}, \quad (\Phi_B|\Phi_C|\Phi_D) = \begin{pmatrix} 1 & 0 & 0 \\ 0 & 1 & 0 \\ 0 & 0 & 1 \end{pmatrix}.$$

Clearly  $\text{Det}(-\mathcal{J}) = s^3 - 1$ , and so on, reproducing the periodic states count for Bernoulli. No point of looking at  $\text{Det}(-\mathcal{J})$ , as that changes sign at every order - always evaluate  $|\text{Det}(\mathcal{J})|$ .

**2020-02-18 Predrag** Clipped here from *Ising.tex*, might be relevant to generalizing Bernoulli to 2-dimensional lattice, as a warm-up to spatiotemporal cat zeta functions:

Roettger [18], *Periodic points classify a family of Markov shifts*, writes:

Ledrappier introduced the following type of space of doubly indexed sequences over a finite abelian group  $G$ ,

$$X_G = \{(x_{s,t}) \in G^{\mathbb{Z}^2} | x_{s,t+1} = x_{s,t} + x_{s+1,t} \text{ for all } s, t \in \mathbb{Z}\}.$$

The group  $\mathbb{Z}^2$  acts naturally on the space  $X_G$  via left and upward shifts.

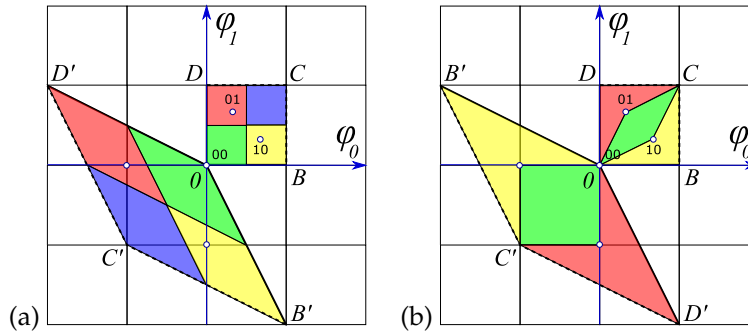


Figure 1.4: [OLD VERSION] The Bernoulli map (??) period-2 periodic states  $\Phi_M = (\phi_0, \phi_1)$  are the  $\bar{0} = (0, 0)$  fixed point, and the 2-cycle  $\Phi_{01} = (1/3, 2/3)$ , see figure 1.2. They all lie within the unit square  $[0BCD]$ , one within each  $\mathcal{M}_{m_0 m_1}$  subregion, and are mapped by the  $[2 \times 2]$  orbit Jacobian matrix  $\mathcal{J}$  (??) into the fundamental parallelepiped  $[0B'C'D']$ . The images of periodic points  $\Phi_M$  land on the integer lattice, and are sent back into the origin by integer translations  $M$ , in order to satisfy the fixed point condition  $\text{refeq}\{\text{tempFixPoint}\}, \mathcal{J}\Phi_M + M = 0$ . Figure 1.2 suggests subdividing the fundamental parallelepiped into (a) 4 areas, but they are not unit areas. The theory of integer lattices dictates instead (b) covering the fundamental parallelepiped by 3 unit area rectangles, with all vertices on the integer lattice.

2020-02-19 Predrag Suarez [21] *Difference equations and a principle of double induction*, ([click here](#)) studies this as a “partial difference equations,” that is, difference equations in two or more variables. He refers to many books on the subject. His example is a first order hyperbolic equation, with initial conditions on space and time axes, which describes some thermal properties,

$$f(r, m) = f(r, m - 1) + f(r - 1, m).$$

The goal is to calculate, step by step, all the values of the temperature  $T(m, n)$ , starting with the initial and boundary conditions. But then I do not get the rest of the papers. Perhaps best not to use much time on ‘spatiotemporal’ Bernoulli.

2020-03-28 Predrag The Bernoulli first-order difference equation

$$\phi_t - s\phi_{t-1} = -m_t, \quad \phi_t \in [0, 1), \quad (1.18)$$

characteristic equation (for  $m_t=0$ )

$$\Lambda - s = 0, \quad (1.19)$$

has one characteristic root  $\{s\}$ .

Comparing with (8.146) we see that we need to solve a first-order inhomogeneous difference equation with a constant forcing term  $(s - 1)$ .

Weijie Chen does this pedagogically in his 2011 lecture notes ([click here](#)), sect. 1.2.1 *One Example*, where he considers

$$\phi_t - s\phi_{t-1} = M, \quad (1.20)$$

and finds the particular solution by taking  $\phi_{p,n} = \phi_p$  for all  $n$ ,

$$\phi_p - s\phi_p = M \quad \rightarrow \quad \phi_p = -M/(s-1).$$

Hence the solution is

$$\phi_n = \phi_{c,n} + \phi_{p,n} = c s^n - \frac{M}{s-1}, \quad (1.21)$$

with  $c$  determined by the initial value  $\phi_0 = c s^0 - M/(s-1)$ . Bernoulli starts with  $\phi_0 = 0$ , and according to (8.146),  $M = (s-1)$ , so  $c = 1$ .

Weijie Chen also works out the particular solution when  $s = 1$ . He also 2CB remarks that in econometrics the shift operator  $r$  is called the *lag operator*.

Questions

- Why is it OK to take site-independent particular solution?
- $M/(s-1)$  looks awkward, can one reformulate? so instead of  $M$ , have  $M/(s-1) \rightarrow 1$
- I am guessing that  $M = (s-1)$  in (1.20) something like the total number of 'letters' I can add to the count  $N_n$  at time  $n$ . Something like that.
- Similarly for  $M = 2\mu^2$  forcing term in temporal cat second-order difference equation (8.158).
- This is still just a verification of my guess recurrence (8.146). Make this argument into a derivation.

**2020-02-23 Predrag** Just curious - what does the Bernoulli fundamental parallelepiped defined by the columns of  $[3 \times 3]$  orbit Jacobian matrix

$$\mathcal{J} = \begin{pmatrix} 1 & -2 & 0 \\ 0 & 1 & -2 \\ -2 & 0 & 1 \end{pmatrix}, \quad N_3 = |\text{Det } \mathcal{J}| = 2^3 - 1, \quad (1.22)$$

look like in a 3-dimensional rendition? Hopefully it is not symmetric, like figure ?? (b).

**2020-03-01 Predrag** Wilf [26] *Generatingfunctionology* starts out in his sect. 1.1 *An easy 2-term recurrence*, with our Bernoulli periodic points count (8.144) and (8.155) as a trivial example of a two-term recurrence (first-order difference equation).

2020-12-21 Predrag Counting temporal Bernoulli periodic states removed from CL18.tex → Bernoulli.tex, replaced by refsects:Hill1stOrd

To evaluate the Hill determinant (8.122), observe that from (1.19) it follows that

$$\text{Det}(-\mathcal{J}) = \text{Det}(s/r) \text{Det}(\mathbf{1} - r/s),$$

where  $|\text{Det}(s/r)| = s^n$ . Expand  $\ln \text{Det}(\mathbf{1} - r/s) = \text{Tr} \ln(\mathbf{1} - r/s)$  as a series in  $1/s$ ,

$$\text{Tr} \ln\left(\mathbf{1} - \frac{r}{s}\right) = -\sum_{k=1}^{\infty} \frac{1}{k} \frac{\text{Tr}(r^k)}{s^k}. \quad (1.23)$$

It follows from  $r^n = \mathbf{1}$  that  $\text{Tr} r^k = n\delta_{k, rn}$  is non-vanishing if  $k$  is a multiple of  $n$ , 0 otherwise:

$$\ln \text{Det}(\mathbf{1} - r/s) = -\sum_{r=1}^{\infty} \frac{1}{r} \frac{1}{s^{nr}} = \ln(1 - s^{-n}).$$

### 2020-12-09 Predrag Temporal Bernoulli

After  $n$  shifts, the periodic state  $\Phi$  returns to the initial state,  $r^n = \mathbf{1}$ . This relation leads to the explicit expression for the orbit Jacobian matrix (1.9),

$$\mathbf{g} = \frac{r}{s \mathbf{1} - r} = \frac{1}{\mathbf{1} - \frac{r}{s}} \frac{r}{s} = \sum_{k=1}^{\infty} \frac{r^k}{s^k} = \frac{s^n}{s^n - 1} \sum_{k=1}^n \frac{r^k}{s^k}. \quad (1.24)$$

From (1.9) it then follows that the last field in  $\Phi$  is the field at lattice site  $n$

$$\phi_n = \frac{s^n}{s^n - 1} \cdot m_1 m_2 m_3 \cdots m_n = \frac{1}{s - 1} \frac{s^{n-1} m_1 + \cdots + s m_{n-1} + m_n}{s^{n-1} + \cdots + s + 1}, \quad (1.25)$$

and the rest are obtained by cyclic permutations of  $M$ .

For example, for  $s = 2$ , the lattice fields are (they are always rational-valued),

$$\begin{aligned} \phi_{m_1 m_2 \cdots m_n} &= \sum_{k=1}^n \frac{m_k}{2^k} \sum_{m=0}^{\infty} \frac{1}{2^{nm}} = \frac{2^n}{2^n - 1} \cdot m_1 m_2 \cdots m_n \\ &= \frac{1}{2^n - 1} \sum_{k=1}^n m_k 2^{n-k}, \end{aligned} \quad (1.26)$$

where  $p = \overline{m_1 m_2 \cdots m_n}$  is an orbit of period  $n$ , with stability multiplier  $\Lambda_p = 2^n$ .

For a Bernoulli map, the rational  $\phi_0$  are either periodic or land eventually on a periodic orbit (the base- $s$  version of the familiar fact that the decimal expansion of a rational number is eventually periodic), while the orbit of a normal irrational  $\phi_0$  is ergodic.

2020-12-09, 2020-12-11 Predrag Quotienting the temporal Bernoulli system

$$\phi_t - s\phi_{t-1} = -m_t, \quad \phi_t \in [0, 1), \quad (1.27)$$

by its dynamical  $D_1 = \{e, \sigma\}$  symmetry

$$\sigma\phi_t = 1 - \phi_t, \quad \sigma m_t = (s - 1) - m_t, \quad \text{for all } t \in \mathbb{Z}, \quad (1.28)$$

where  $m_t$  takes values in the  $s$ -letter alphabet

$$m \in \mathcal{A} = \{0, 1, 2, \dots, s - 1\}. \quad (1.29)$$

Define the fundamental domain to be  $\hat{\phi}_t \in [0, 1/2]$ . We construct the Bernoulli fundamental domain lattice system, with '1/2' unit hypercube  $\hat{\Phi} \in [0, 1/2]^n$ , as in [ChaosBook Group  \$D\_1\$  and reduction to the fundamental domain](#), see figure 1.5 (b), and the fundamental domain symbolic dynamics  $\hat{\mathcal{A}}$ . The temporal lattice Bernoulli condition (1.27) is now two conditions (Bernoulli)/ $D_1$ . They are different for  $s$  even or odd:

$$\begin{aligned} \hat{\phi}_{t+1} - s\hat{\phi}_t &= -m_{t+1}, & \hat{\phi}_t \in \mathcal{M}_{m_t}, & \quad s \text{ even} \\ \hat{\phi}_{t+1} + s\hat{\phi}_t &= 1 + m_{t+1}, & \hat{\phi}_t \in \mathcal{M}_{\sigma m_t} & \\ \hat{\mathcal{A}} &= \{\{m\}, \{\sigma m\}\}, & \{m\} = \{0, 1, 2, \dots, s/2\}, & \end{aligned} \quad (1.30)$$

$$\begin{aligned} \hat{\phi}_{t+1} - s\hat{\phi}_t &= \quad, & s \text{ odd} & \\ \hat{\mathcal{A}} &= \{\{m\}, (s - 1)/2, \{\sigma m\}\}, & m \in \{0, 1, 2, \dots, (s - 3)/2\}. & \end{aligned} \quad (1.31)$$

As an example, case  $s = 6$ ,  $m_t \in \{0, 1, 2\}$  is worked out in figure 1.5 (c). (Plot also the fundamental domain map for odd values of  $s$ .)

In the matrix form (1.27), the orbit Jacobian matrix

$$\mathcal{J} \Phi = -M, \quad \mathcal{J} = \mathbf{1} - sr^{-1}, \quad (1.32)$$

is independent of  $M$ . Not so for the symmetry reduced orbit Jacobian matrix  $\hat{A}_M$  in (1.30): it depends on  $M$ , as its diagonal takes values  $\pm s$ . We need to prove that the Hill determinant  $\text{Det } \hat{A}$  does not.

I had not noticed before that this parametrization converts Bernoulli into tent map, with full state space 2-cycles turned into negative slope fixed points.

By the inclusion-exclusion principle (24.251)

$$N_n = \hat{N}_n + \sigma\hat{N}_n - \hat{N}_n \cap (\sigma\hat{N}_n) = 2\hat{N}_n - \hat{N}_n \cap (\sigma\hat{N}_n). \quad (1.33)$$

Let's call the number of points in the shared boundary  $I$ . The  $\phi = 0$  is in  $I$  for any  $n$ , if I am allowed to identify  $\phi = 1 \rightarrow 0$ , and that is the

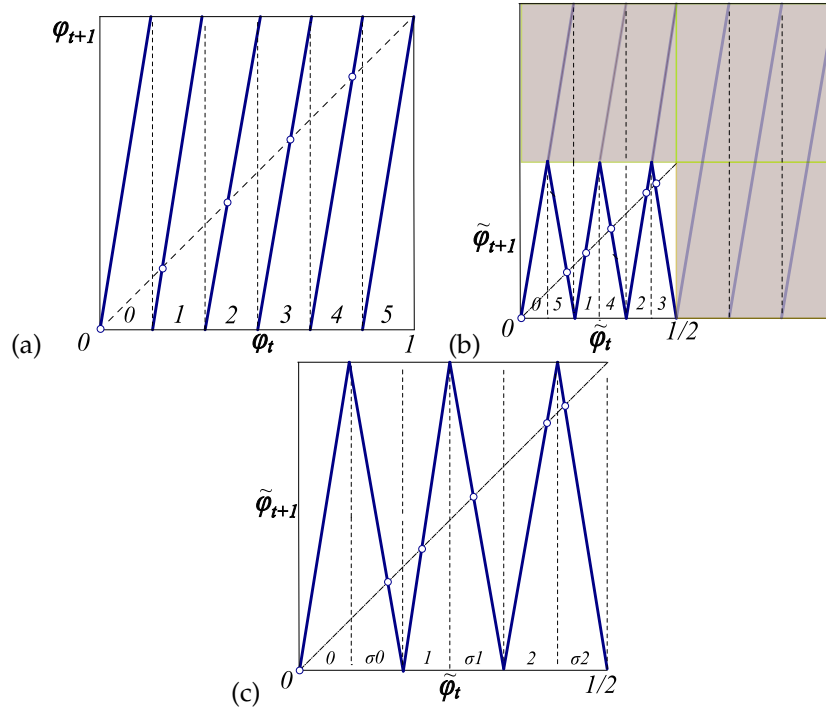


Figure 1.5: (a) The Bernoulli map  $f$  with the stretching parameter  $s = 6$  partitions the unit interval into 6 subintervals  $\{\mathcal{M}_m\}$ , labeled by the 6-letter alphabet (1.29). As the map is a circle map,  $\phi_5 = 1 = 0 = \phi_0 \pmod{1}$ . (b) The Bernoulli map is quotiented by the dynamical  $G = D_1 = \{e, \sigma\}$  symmetry to (c) the fundamental domain  $\hat{\phi}_t \in [0, 1/2]$  map  $\hat{f} = f/G$  partitions the half interval into the three  $1/12$  subintervals  $\{\mathcal{M}_0, \mathcal{M}_1, \mathcal{M}_2\}$ , and their reflections, the three 3 subintervals  $\{\mathcal{M}_{\sigma_0}, \mathcal{M}_{\sigma_1}, \mathcal{M}_{\sigma_2}\}$ , labeled by a 6-letter reduced system's alphabet. Reduced space fixed points  $\{\bar{\sigma}_0, \bar{\sigma}_1, \bar{\sigma}_2\}$  correspond to self-dual 2-cycles  $\{0\bar{5}, \bar{1}4, \bar{2}3\}$  in the full space. Fixed point  $\bar{0}$  is in the border, and thus over-counted;  $\bar{1}$  corresponds to  $\{\bar{1}, \bar{4}\}$ , and  $\bar{2}$  corresponds to  $\{\bar{2}, \bar{3}\}$ .



only point in the boundary. Presumably this leads to the denominator  $(1 - z)$  in (1.34). I guess that the symmetric irrep of  $D_1 = \{e, \sigma\}$  leads to  $N_+ = s^n$  and the numerator  $(1 - sz)$ , while the antisymmetric irrep leads to  $N_- = 0$ , and a trivial factor 1 contribution to the numerator (1.34).

$$1/\zeta_{\text{AM}}(z) = \frac{1 - sz}{1 - z}. \quad (1.34)$$

Temporal cat should be more interesting. Also any nonlinear  $s$ -branch map ‘Bernoulli-like’ lattice with a *dynamical*  $D_1$  symmetry; then the weights  $t_p$  do not necessarily cancel for the antisymmetric irrep.

**2021-08-23 Predrag** We have omitted “Quotienting the temporal Bernoulli system” (1.27) from LC21.

**2020-09-30 Predrag** The Bernoulli equation rewritten as a first-order difference equation:

$$\phi_t - s\phi_{t-1} = -m_t, \quad \phi_t \in [0, 1). \quad (1.35)$$

For a Bernoulli system

$$\begin{aligned} 1/\zeta_{\text{AM}}(z) &= \exp[\ln(1 - sz) - \ln(1 - z)] \\ &= \frac{1 - sz}{1 - z}. \end{aligned} \quad (1.36)$$

Define

$$d(s) = z^{-1} - s \quad (1.37)$$

then (compare with (16.39))

$$1/\zeta_{\text{AM}}(z) = \frac{d(s)}{d(2)} = 1 + \frac{d(s) - d(2)}{d(2)} = 1 + (s - 1) \frac{1}{d(2)} \quad (1.38)$$

The numerator  $(1 - sz)$  says that a Bernoulli system is a full shift [5]: there are  $s$  fundamental periodic states and every other periodic state is built from their concatenations and repeats.

**2018-12-27 Linas Vepstas** *On the Beta Transformation* [arXiv:1812.10593](https://arxiv.org/abs/1812.10593): The beta transformation is the iterated map (1.39). The  $\beta = 2$  is known as the Bernoulli map, and is exactly solvable. The Bernoulli map provides a model for pure, unrestrained chaotic (ergodic) behavior: it is the full invariant shift on the Cantor space. The beta transformation defines a sub-shift: iterated on the unit interval, it singles out a subspace of the Cantor space, in such a way that it is invariant under the action of the left-shift operator. That is, lopping off one bit at a time gives back the same subspace. The beta transform seems to capture something basic about the multiplication of two real numbers:  $\beta$  and  $x$ . It offers a window into understanding the nature of multiplication. Iterating on multiplication, one would get exponentiation; although the mod 1 of the beta transform conorts this in interesting ways. The work presented here is a research diary:

a pastiche of observations and some shallow insights. The eigenvalues of the transfer operator seem to lie on a circle of radius  $1/\beta$  in the complex plane. Given that the transfer operator is purely real, the appearance of such a quasi-unitary spectrum seems surprising. The spectrum appears to be the limit of a dense set of quasi-cyclotomic polynomials, the positive real roots of which include the Golden and silver ratios, the Pisot numbers, the n-bonacci (tribonacci, tetranacci, etc.) numbers.

Beta transformation

$$T_\beta(x) = \beta x \pmod{1}, \quad 1 < \beta \leq 2 \quad (1.39)$$

was introduced by Alfréd Rényi [17] in 1957, and an invariant measure for it was given by Alexander Gelfond in 1959 and independently by Bill Parry [16] in 1960.

[Beta transformation literature review and references.](#)

[A concise intro to beta-transformations?](#) has references.

**2020-09-08 Predrag Bing Li** *Some fractal problems in beta-expansions* (video) (slides)

For greedy beta-expansions, we study some fractal sets of real numbers whose orbits under beta-transformation share some common properties. For example, the partial sum of the greedy beta-expansion converges with the same order, the orbit is not dense, the orbit is always far from that of another point etc. The usual tool is to approximate the beta-transformation dynamical system by Markov subsystems. We also discuss the similar problems for intermediate beta-expansions.

**2021-01-05 Predrag Hofbauer and Keller [13]** *Zeta-functions and transfer-operators for piecewise linear transformations* (1984) has no Bernoulli zeta. Not useful to us at this time.

**2021-01-05 Predrag Takahashi [22]** *Fredholm determinant of unimodal linear maps* has lots of detail and examples. I might have missed something, but Bernoulli zeta is not there, or anything we care about.

**2021-01-04 Predrag Flatto, Lagarias and Poonen [9]** *The zeta function of the beta transformation* (1994)

which should have the  $\beta = 2$  Bernoulli zeta function as the trivial case.

Sakaguchi [20] *Breakdown of the phase dynamics* was the first to study a coupled Bernoulli maps lattice (in  $D = 2$ ).

Kawasaki and Sasa [14] *Statistics of unstable periodic orbits of a chaotic dynamical system with a large number of degrees of freedom*, study a coupled Bernoulli maps lattice (in spatial  $D = 1$ ); Bernoulli forward in time, but tanh-coupled to the nearest spatial neighbors, so that the natural invariant measure for spin configurations coincides with the canonical distribution for an Ising spin Hamiltonian. The most significant feature of

the Bernoulli CML is that it respects a detailed balance and the resulting measure coincides with the canonical distribution of the 1D Ising model. There is a one-to-one correspondence between symbol sequences and periodic orbits, as proven by Yutaka Ishii, *Note on a paper by Kawasaki and Sasa on Bernoulli coupled map lattices*. Then they commit the Japanese heresy: “In summary, we have demonstrated that the macroscopic properties of the Bernoulli CML can be calculated with high accuracy using only one periodic orbit sampled from the special periodic orbit ensemble.”

Takeuchi and Sano [24] *Role of unstable periodic orbits in phase transitions of coupled map lattices* also study the spatially periodic Bernoulli CML (in spatial  $D = 1$ ).

**2021-01-05 Han** Notes from Flatto, Lagarias and Poonen [9] paper:

$\beta$ -transformation map is:

$$f_\beta(x) = \beta x \pmod{1},$$

where  $\beta > 1$ ,  $x \in [0, 1]$ . The symbolic dynamics of  $f_\beta$  is based on the fact that the graph of  $f_\beta$  consists of  $\lfloor \beta \rfloor + 1$  monotone pieces which they call laps, which are assigned by the symbols  $0, 1, \dots, \lfloor \beta \rfloor$ . When  $\beta \in \mathbb{Z}^+$ , the piece  $\lfloor \beta \rfloor$  consists of a single point, and the symbol  $\lfloor \beta \rfloor$  only appears in the itinerary of 1. To each  $x \in [1, 0]$  its itinerary is  $I_\beta(x) = A_0 A_1 A_2 \dots$ , where the symbol

$$A_n := A_n(x) = \lfloor \beta f_\beta^n(x) \rfloor.$$

In particular the itinerary of 1,  $I_\beta(1) = A_0^* A_1^* A_2^* \dots$  encodes complete information about the behavior of  $f_\beta$ .

They introduced a power series with integer coefficients:

$$\phi_\beta(z) = A_0^* z + A_1^* z^2 + A_2^* z^3 + \dots = \sum_{n=0}^{\infty} A_n^* z^{n+1}.$$

This function is related to the iterates of 1 by:

$$\phi_\beta(z) = 1 + (\beta z - 1) \left( \sum_{n=0}^{\infty} f_\beta^n(1) z^n \right).$$

Then the zeta function is:

$$\zeta_\beta(z) = \frac{1}{1 - \phi_\beta(z)},$$

if  $\beta$  is not a simple  $\beta$ -number, and

$$\zeta_\beta(z) = \frac{1 - z^N}{1 - \phi_\beta(z)},$$

if  $\beta$  is a simple  $\beta$ -number, and  $N$  is minimal with  $f_\beta^N(1) = 0$ . Simple  $\beta$ -numbers are the  $\beta$ -numbers such that for some  $n$ ,  $f_\beta^n(1) = 0$ . This formula gives the correct topological zeta function of temporal Bernoulli.

Associated with the  $\beta$ -transformation is the set  $X_\beta$  of all  $I_\beta(x)$  for  $0 \leq x < 1$ . The  $\beta$ -shift  $S_\beta$  is a symbolic dynamical system obtained as the smallest closed (two-sided) subshift of  $\{1, 2, \dots, \lfloor \beta \rfloor\}^{\mathbb{Z}}$  generated by all finite substrings of  $X_\beta$ . For simple  $\beta$ -numbers  $S_\beta$  is a subshift of finite type.

There is a zeta function associated to the  $\beta$ -shift  $S_\beta$ , which is studied by Takahashi [23], who showed that

$$\hat{\zeta}_\beta(z) = \frac{1}{1 - \phi_\beta(z)}.$$

This formula is closely related to  $\zeta_\beta(z)$  but differs from it for simple  $\beta$ -numbers, in which case the closure operation defining  $S_\beta$  adds some extra periodic points.

**2021-01-11 Predrag** Seth Lloyd *et al.*. *Quantum algorithm for nonlinear differential equations* [arXiv:2011.06571](https://arxiv.org/abs/2011.06571):

[1] showed how to map the problem of solving a general linear differential equation to that of matrix inversion, which can then be performed using the quantum linear systems algorithm [12-13]. Consider a linear differential equation of the form,

$$\frac{dx}{dt} + Ax = b(t), \tag{6}$$

where as above  $x, b \in \mathbb{C}^d$  and  $A$  is a  $[d \times d]$  matrix.

Discretize the equation in time at intervals  $\delta\tau$ , and take  $k$  to be the index for the discretized time, so that  $x_k$  and  $b_k$  are the values of  $x$  and  $b$  at time label  $k$ .

We wish to integrate equation (6) numerically starting from the initial state  $x_0 \equiv b_0$ . We obtain a series of equations of the form:

$$x_0 = b_0 \quad x_1 = x_0 - \delta\tau Ax_0 + \delta\tau b_1 \quad \dots \quad x_{k+1} = x_k - \delta\tau Ax_k + \delta\tau b_k \quad \dots \tag{7}$$

Here, we have used the Euler forward method for numerical integration, but it is straightforward to implement implicit methods such as Euler backward, Crank-Nicholson, Runge-Kutta, etc. [3]. Written in matrix form, these equations become

$$-\begin{pmatrix} -I & 0 & 0 & \dots & 0 & 0 \\ I - \delta\tau A & -I & 0 & \dots & 0 & 0 \\ 0 & I - \delta\tau A & -I & \dots & 0 & 0 \\ & & \dots & & & \\ 0 & 0 & 0 & \dots & -I & 0 \\ 0 & 0 & 0 & \dots & I - \delta\tau A & -I \end{pmatrix} \begin{pmatrix} x_0 \\ x_1 \\ x_2 \\ \dots \\ x_{T-1} \\ x_T \end{pmatrix} = \begin{pmatrix} b_0 \\ \delta\tau b_1 \\ \delta\tau b_2 \\ \dots \\ \delta\tau b_{T-1} \\ \delta\tau b_T \end{pmatrix},$$

### 1.3 Any piecewise linear map has “linear code”

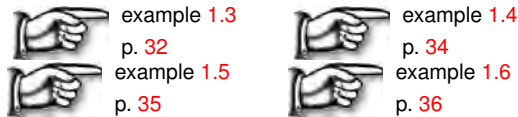
2CB

For reasons unbeknownst to me, it is below the dignity of any cat to work out any problem in ChaosBook, or in the online course, no matter how often I point out that it is easier to understand what we do for cat maps if you first work it out for 1-dimensional maps.

So I have to do these exercises myself - I’m forced to it, so Li Han can be motivated to re-derive his polynomials (as described in Bird and Vivaldi [2], see my notes of 2016-05-21, -12-12 below), rather than to fit them to Mathematica grammar rule counts for integer  $s$ .

Basically, I am baffled by why should “linear code” be such a big deal that it has to go into the title of our paper [12]. *Every* example of symbolic dynamics worked out in ChaosBook is a “linear code.” The strategy is always the same - find a topological conjugacy from your map to a piecewise linear map, and then use the fact that any piecewise linear map has “linear code.” The pruning theory is always the same - kneading orbit separates admissible from the inadmissible, also in the infinite 1-dimensional discrete lattice case worked out in the *Diffusion* chapter in the ChaosBook, and the appendix (chapter 15 reproduced here) that no one wants to read either.

A tent map is a 1-dimensional example (a simpler one is Bernoulli, and its sawtooth generalizations). The 2-dimensional examples are the Belykh map, example 1.5, and the Lozi map, example 1.6. Belykh map is of particular interest to us, as it is in form very close to the cat map. Both maps have the pruning front conjecture is proven for them, for some sets of parameters.



### Commentary

**Remark 1.1.** Bernoulli map. The Bernoulli shift map (??) and the doubling map (1.8) are also known as the dyadic transformation, dyadic map, bit shift map, angle doubling map or sawtooth map (??). There are many fine books that discuss it in depth, for example Driebe [8]. See also remark 1.2.

**Remark 1.2.** Bernoulli shift. For a more in-depth discussion, consult chapter 3 of ref. [8]. The extension of Fredholm theory to the case of Bernoulli shift on  $\mathbb{C}^{k+\alpha}$  (in which the Perron-Frobenius operator is *not* compact – technically it is only *quasi-compact*. That is, the essential spectral radius is strictly smaller than the spectral radius) has been given by Ruelle [19]: a concise and readable statement of the results is contained in ref. [1]. We see from (??) that for the Bernoulli shift the exponential decay rate of correlations coincides with the Lyapunov exponent: while such an identity holds for a number of systems, it is by no means a general result, and there exist explicit counterexamples. See also remark 1.1.

2CB



example 1.1  
p. 32

## References

- [1] V. Baladi, Dynamical zeta functions, in *Real and Complex Dynamical Systems: Proceedings of the NATO ASI*, edited by B. Branner and P. Hjorth (1995), pp. 1–26.
- [2] N. Bird and F. Vivaldi, “Periodic orbits of the sawtooth maps”, *Physica D* **30**, 164–176 (1988).
- [3] A. Boyarsky and P. Góra, *Laws of Chaos: Invariant Measures and Dynamical Systems in One Dimension* (Birkhäuser, Boston, 1997).
- [4] P. Cvitanović, “Recurrent flows: The clockwork behind turbulence”, *J. Fluid Mech. Focus Fluids* **726**, 1–4 (2013).
- [5] P. Cvitanović, “Counting”, in *Chaos: Classical and Quantum* (Niels Bohr Inst., Copenhagen, 2023).
- [6] P. Cvitanović, R. Artuso, R. Mainieri, G. Tanner, and G. Vattay, *Chaos: Classical and Quantum* (Niels Bohr Inst., Copenhagen, 2024).
- [7] P. Cvitanović and H. Liang, *A chaotic lattice field theory in two dimensions*, In preparation, 2024.
- [8] D. J. Driebe, *Fully Chaotic Maps and Broken Time Symmetry* (Springer, New York, 1999).
- [9] L. Flatto, J. C. Lagarias, and B. Poonen, “The zeta function of the beta transformation”, *Ergodic Theory Dynam. Systems* **14**, 237–266 (1994).
- [10] J. W. von Goethe, *Faust I, Studierzimmer 2*. M. Greenberg, transl. (Yale Univ. Press, 1806).
- [11] M. N. Gurdorf, N. B. Budanur, and P. Cvitanović, *Spatiotemporal tiling of the Kuramoto-Sivashinsky flow*, In preparation, 2022.
- [12] B. Gutkin, L. Han, R. Jafari, A. K. Saremi, and P. Cvitanović, “Linear encoding of the spatiotemporal cat map”, *Nonlinearity* **34**, 2800–2836 (2021).
- [13] F. Hofbauer and G. Keller, “Zeta-functions and transfer-operators for piecewise linear transformations”, *J. Reine Angew. Math. (Crelle)* **1984**, 100–113 (1984).
- [14] M. Kawasaki and S. Sasa, “Statistics of unstable periodic orbits of a chaotic dynamical system with a large number of degrees of freedom”, *Phys. Rev. E* **72**, 037202 (2005).
- [15] D. Li and J. Xie, “Symbolic dynamics of Belykh-type maps”, *Appl. Math. Mech.* **37**, 671–682 (2016).
- [16] W. Parry, “On the  $\beta$ -expansions of real numbers”, *Acta Math. Acad. Sci. Hung.* **11**, 401–416 (1960).

- [17] A. Rényi, “Representations for real numbers and their ergodic properties”, *Acta Math. Acad. Sci. Hung.* **8**, 477–493 (1957).
- [18] C. G. J. Roettger, “Periodic points classify a family of markov shifts”, *J. Number Theory* **113**, 69–83 (2005).
- [19] D. Ruelle, “An extension of the theory of Fredholm determinants”, *Inst. Hautes Études Sci. Publ. Math.* **72**, 175–193 (1990).
- [20] H. Sakaguchi, “Breakdown of the phase dynamics”, *Progr. Theor. Phys.* **84**, 792–800 (1990).
- [21] R. Suarez, “Difference equations and a principle of double induction”, *Math. Mag.* **62**, 334–339 (1989).
- [22] Y. Takahashi, “Fredholm determinant of unimodal linear maps”, *Scientific Papers Coll. Gen. Ed. Univ. Tokyo* **31**, 61–87 (1981).
- [23] Y. Takahashi, “Shift with orbit basis and realization of one-dimensional maps”, *Osaka J. Math.* **20**, 599–629 (1983).
- [24] K. Takeuchi and M. Sano, “Role of unstable periodic orbits in phase transitions of coupled map lattices”, *Phys. Rev. E* **75**, 036201 (2007).
- [25] T. Tél, “Fractal dimension of the strange attractor in a piecewise linear two-dimensional map”, *Phys. Lett. A* **97**, 219–223 (1983).
- [26] H. S. Wilf, *Generatingfunctionology* (Academic Press, New York, 1994).

**Example 1.1. Temporal Bernoulli shadowing.**

<sup>1</sup> As the temporal Bernoulli condition (1.19) is a linear relation, a given block  $M$ , or 'code' in terms of alphabet (??), corresponds to a unique temporal periodic state  $\Phi$  given by the temporal lattice Green's function

$$\Phi_M = g M, \quad g = \frac{r/s}{\mathbb{1} - r/s}. \quad (1.40)$$

For an infinite lattice  $t \in \mathbb{Z}$ , this Green's function can be expanded as a series in  $\Lambda^{-k}$ ,

$$g = \frac{r/\Lambda}{\mathbb{1} - r/\Lambda} = \sum_{k=1}^{\infty} \frac{r^k}{\Lambda^k}, \quad (1.41)$$

where  $\Lambda = s$  is the 1-time step stability multiplier for the Bernoulli system. From (1.40) it follows that the influence of a source  $m_{t'}$  back in the past, at site  $t'$ , falls off exponentially with the temporal lattice distance  $t - t'$ ,

$$\phi_t = \sum_{t'=-\infty}^{t-1} g_{tt'} m_{t'}, \quad g_{tt'} = \frac{1}{\Lambda^{t-t'}}, \quad t > t', \quad 0 \text{ otherwise}. \quad (1.42)$$

That means that an ergodic periodic state segment of length  $n$  (or a periodic periodic state of a longer period) is shadowed by the periodic periodic state (??) with the same  $n$ -sites symbol block  $M$ ,<sup>2</sup>

$$\phi_t = \frac{1}{1 - 1/\Lambda^n} \left( \frac{m_1}{\Lambda} + \frac{m_2}{\Lambda^2} + \dots + \frac{m_{n-1}}{\Lambda^{n-1}} + \frac{m_n}{\Lambda^n} \right), \quad (1.43)$$

with exponentially decreasing shadowing error of order  $O(1/\Lambda^{n+1})$ . The error is controlled by the (4.126) prefactor  $1/|\text{Det } \mathcal{J}| = 1/|\det(\mathbb{1} - \mathbb{J}_M)|$ , with the determinant arising from inverting the orbit Jacobian matrix  $\mathcal{J}$  to obtain the Green's function (1.19).

This error estimate is deeper than what it might seem at the first glance. In fluid dynamics, pattern recognition, neuroscience and other high or  $\infty$ -dimensional settings distances between 'close solutions' (let's say pixel images of two faces in a face recognition code) are almost always measured using some arbitrary yardstick, let's say a Euclidean  $L_2$  norm, even though the state space has no Euclidean symmetry. Not so in the periodic orbit theory: here  $1/|\text{Det } \mathcal{J}|$  is the intrinsic, coordinatization and norm independent measure of the distance between similar spatiotemporal states.

[click to return: p. 30](#)

**Example 1.2. Linear code for a piecewise linear map.** the piecewise linear map of figure 1.6

[click to return: p. ??](#)

**Example 1.3. Tent map linear code.** The simplest example of a piece-wise linear unimodal map with a binary (in general, pruned) symbolic dynamics is the tent map,

$$f(x) = \begin{cases} f_0(x) = \Lambda x & \text{if } x < 1/2 \\ f_1(x) = \Lambda(1 - x) & \text{if } x > 1/2 \end{cases}, \quad (1.44)$$

with  $1 < \Lambda < \infty$  and  $x \in \mathcal{M} = [0, 1]$ . (Everything would go through for a skew tent map with  $\Lambda_0 \neq -\Lambda_1$ , but there is no need here for that complication.) For this family of

<sup>1</sup>Predrag 2024-03-03: Moved to dasbuch/book/Examples/. Then made it a section in dasbuch/QMlectures/lectQM.tex chaoticFT.tex, so edit only there!

<sup>2</sup>Predrag 2020-02-16: Do I need to derive this?



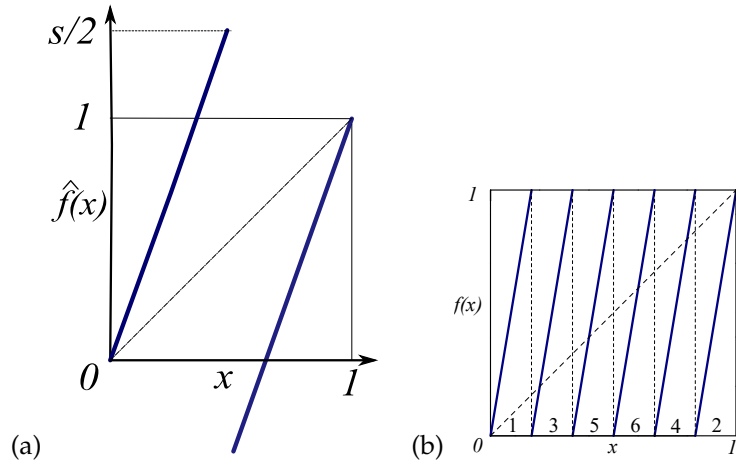


Figure 1.6: (a)  $\hat{f}(\hat{x})$ , the full space sawtooth map (??),  $\Lambda > 2$ . (b)  $f(x)$ , the sawtooth map restricted to the unit circle (??),  $\Lambda = 6$ .

unimodal maps the coarse (covering) partition of the unit interval  $\mathcal{M} = \mathcal{M}_0 \cap C \cap \mathcal{M}_1$  is given by intervals  $\mathcal{M}_0 = [0, 1/2)$ ,  $\mathcal{M}_1 = (1/2, 1]$ , and the critical point  $C = 1/2$ . Let's rewrite this as a linear first-order difference equation, in the manner of cat lovers enamoured of matters feline:

$$\frac{1}{\Lambda} x_{t+1} + (2m_t - 1)x_t = m_t, \quad \begin{cases} m_t = 0 & \text{if } x_t < 1/2 \\ m_t = 1 & \text{if } x_t > 1/2 \end{cases} \quad (1.45)$$

That every such code is a 'linear code' is best understood by computing a periodic orbit for a specified itinerary.

The fixed point condition  $f^n(x) = x$  for  $n$ -cycle  $\overline{m_1 m_2 m_3 \dots m_{n-1} m_n}$  is a linear relation between the finite alphabet  $m_t \in \{0, 1\}$  code, and the  $x_t \in \mathbb{R}$  orbit

$$\Delta(m)q(m) = m(m) \quad (1.46)$$

with orbit-dependent inverse propagator  $\Delta(m) =$

$$\begin{pmatrix} 2m_n - 1 & 0 & 0 & \dots & 0 & \Lambda^{-1} \\ \Lambda^{-1} & 2m_{n-1} - 1 & 0 & \dots & 0 & 0 \\ 0 & \Lambda^{-1} & 2m_{n-2} - 1 & \dots & 0 & 0 \\ \vdots & \vdots & \vdots & \ddots & \vdots & \vdots \\ 0 & 0 & 0 & \dots & 2m_2 - 1 & 0 \\ 0 & 0 & 0 & \dots & \Lambda^{-1} & 2m_1 - 1 \end{pmatrix},$$

$$q(m) = \begin{pmatrix} x_n \\ x_{n-1} \\ x_{n-2} \\ \vdots \\ x_2 \\ x_1 \end{pmatrix}, \quad m(m) = \begin{pmatrix} m_n \\ m_{n-1} \\ m_{n-2} \\ \vdots \\ m_2 \\ m_1 \end{pmatrix},$$

and  $m(m)$  is needed to fold the stretched orbit back into the unit interval. While the off-diagonal “1”s do generate cyclic shifts, the diagonal  $\pm\Lambda$  terms are not shift invariant, so I do not believe this can be diagonalized by a discrete Fourier transform. I had worked it out for  $\Lambda = 2$  in *ChaosBook*, but not sure if there are elegant tricks for arbitrary  $\Lambda \neq 2$ . For an orbit

$$q(m) = \Delta(m)^{-1}m(m) \tag{1.47}$$

to be admissible, no point should be to the right of the kneading value  $x_\kappa = f(C)$ . It follows from the kneading theory for unimodal maps (dike map with slope  $\Lambda = 2$  being the canonical example) that if a periodic orbit exists for a given  $\Lambda$ , it exists for all larger  $\Lambda$ , and that all orbits exist for  $\Lambda \geq 2$ .

In other words,  $\Lambda$  is the “stretching parameter” for this problem, and the rational polynomial expressions in  $\Lambda$  for  $x_i$  correspond to Li Han’s polynomials for cat maps.

[click to return: p. 29](#)

**Example 1.4. Periodic points of a tent map.**

**Exercise** Check (1.47) for fixed point(s).

**Exercise** Check (1.47) for the 2-cycle  $\overline{01}$ .

$$\Delta(m) = \begin{pmatrix} -\Lambda & 1 \\ 1 & \Lambda \end{pmatrix}, \quad m(m) = \Lambda \begin{pmatrix} 0 \\ 1 \end{pmatrix}.$$

$$\Delta^{-1} = \frac{1}{\Lambda^2 + 1} \begin{pmatrix} -\Lambda & 1 \\ 1 & \Lambda \end{pmatrix}, \quad \det \Delta(m) = -(\Lambda^2 + 1)$$

$$\begin{pmatrix} x_{01} \\ x_{10} \end{pmatrix} = \frac{\Lambda}{\Lambda^2 + 1} \begin{pmatrix} -\Lambda & 1 \\ 1 & \Lambda \end{pmatrix} \begin{pmatrix} 0 \\ 1 \end{pmatrix} = \frac{\Lambda}{\Lambda^2 + 1} \begin{pmatrix} 1 \\ \Lambda \end{pmatrix}.$$

For the Ulam tent map this yields the correct periodic points  $\{x_{01}, x_{10}\} = \{2/5, 4/5\}$ . In the  $\Lambda \rightarrow 1$  limit, this 2-cycle collapses into the critical point  $C = 1/2$ .

**Exercise** Check (1.47) for the two 3-cycles. For the Ulam tent map case, the periodic points are

$$\{\gamma_{001}, \gamma_{010}, \gamma_{100}\} = \{2/9, 4/9, 8/9\}$$

$$\{\gamma_{011}, \gamma_{110}, \gamma_{101}\} = \{2/7, 4/7, 6/7\}.$$

**Exercise** Check (1.47) for  $\Lambda =$  golden mean. The  $\overline{001} \rightarrow \overline{0C1}$  as  $\Lambda \rightarrow$  golden mean from above. Do you get all admissible cycles? That is worked out in *ChaosBook*, but not in this formulation.

**Exercise** Is there a systematic solution to (1.47) for arbitrary  $n$ -cycle? The  $\Lambda = 2$  case has the elegant solution described in *ChaosBook*; whatever polynomials you find, they should agree with that particular factorization. In other words, think of the sums (1.48) and (1.49) as the expansion of a real number in terms of the digits  $w_i$  in the nonintegral base  $\Lambda$ . As the symbolic dynamics of a cycle is independent of  $\Lambda$ , the Ulam tent map calculation, in the familiar base 2 clinches the arbitrary tent map case.

The rest of the section might even be right - has to factorize in agreement with my Ulam tent map computations. Please fix at your leisure, if I am wrong.

If the repeating string  $m_1 m_2 \dots m_n$  contains an even number of '1's, the repeating string of well ordered symbols  $w_1 w_2 \dots w_n$  is of the same length. The cycle-point  $x$  is a geometrical sum which we can rewrite as the odd-denominator fraction

$$\begin{aligned} x(\overline{m_1 m_2 \dots m_n}) &= \sum_{t=1}^n \frac{w_t}{\Lambda^t} + \frac{1}{\Lambda^{-n}} \sum_{t=1}^n \frac{w_t}{\Lambda^t} + \dots \\ &= \frac{1}{\Lambda^n - 1} \sum_{t=1}^n w_t \Lambda^{n-t} \end{aligned} \quad (1.48)$$

If the repeating string  $m_1 m_2 \dots m_n$  contains an odd number of '1's, the string of well ordered symbols  $w_1 w_2 \dots w_{2n}$  has to be of the double length before it repeats itself. The cycle-point  $x$  is a geometrical sum which we can rewrite as the odd-denominator fraction

$$\begin{aligned} x(\overline{m_1 m_2 \dots m_n}) &= \sum_{t=1}^{2n} \frac{w_t}{\Lambda^t} + \frac{1}{\Lambda^{-2n}} \sum_{t=1}^{2n} \frac{w_t}{\Lambda^t} + \dots \\ &= \frac{1}{(\Lambda^n - 1)(\Lambda^n + 1)} \sum_{t=1}^{2n} w_t \Lambda^{2n-t} \end{aligned} \quad (1.49)$$

[click to return: p. 29](#)

**Example 1.5. Belykh map linear code.** Li and Xie [15] Symbolic dynamics of Belykh-type maps: " The symbolic dynamics of a Belykh-type map (a two-dimensional discontinuous piecewise linear map) is investigated. The pruning front conjecture (the admissibility condition for symbol sequences) is proved under a hyperbolicity condition. Using this result, a symbolic dynamics model of the map is constructed according to its pruning front and primary pruned region. "

The Belykh map is a piecewise linear map given by

$$\begin{pmatrix} x_{n+1} \\ y_{n+1} \end{pmatrix} = \begin{pmatrix} \sigma_n - ax_n + by_n \\ x_n \end{pmatrix} = \begin{pmatrix} \sigma_n \\ 0 \end{pmatrix} + \begin{pmatrix} -a & b \\ 1 & 0 \end{pmatrix} \begin{pmatrix} x_n \\ y_n \end{pmatrix} .$$

where

$$\sigma_n = \begin{cases} 1 & \text{if } x_n \geq 0 \\ -1 & \text{if } x_n < 0 \end{cases} .$$

The two branches of the map are

$$f_{\pm} = \begin{cases} \pm 1 - ax + by \\ x \end{cases} .$$

In the 3-term recurrence formulation (the linear code), the map is an asymmetric tridiagonal Toeplitz matrix

$$x_{n+1} + ax_n - bx_{n-1} = \sigma_n ,$$

or

$$\square x_n + (2 + a)x_n - (1 + b)x_{n-1} = \sigma_n . \quad (1.50)$$

For  $b = -1$  (the Hamiltonian, time-reversible case) this is almost the cat map, with  $a = -s$ , except that the single sawtooth discontinuity is across  $x = 0$ , there is no mod 1 condition.

Li and Xie consider the  $a, b > 0$  case. The strange attractor (for example, for  $a = 1.5$  and  $b = 0.3$ ) looks like a fractal set of parallel lines. They define the pruning front, the primary pruned region, plot them in the symbol plane, and prove the pruning front conjecture for this map. In the symbol plane there is a symmetry under rotation by  $\pi$ , but they do not seem to exploit that.

They call the past and the future itineraries of the tail and the head, and start the head with  $s_0$ .

Tél [25] Fractal dimension of the strange attractor in a piecewise linear two-dimensional map computes the box-counting dimension of this map (which he does not call Belykh map).

**Example 1.6. Lozi map linear code.** The Lozi map

$$x_{n+1} = 1 - \sigma_n a x_n + b x_{n-1}.$$

written as a 3-term recurrence relation

$$x_{n+1} - 2x_n + x_{n-1} + (2 + \sigma_n a)x_n - (b + 1)x_{n-1} = 1. \quad (1.51)$$

That has the same nonlinear term  $\sigma_n x_n$  as (1.45), so maybe we can figure out the pruning front as well, in this formulation.

[click to return: p. 29](#)

# Chapter 2

## Cat map

If space is infinite, we are in no particular point in space.  
If time is infinite, we are in no particular point in time.

— [The Book of Sand](#), by Jorge Luis Borges

What is a natural way to cover the torus, in such a way that the dynamics and the partition borders are correctly aligned? You are allowed to coordinatize the unit torus by any set of coordinates that covers the torus by a unit area. The origin is fixed under the action of  $\mathbf{A}$ , and straight lines map into the straight lines, so Adler and Weiss did the natural thing, and used parallelograms (following Bowen [20] we shall refer to such parallelograms as ‘rectangles’) with edges parallel to the two eigenvectors of  $\mathbf{A}$ . Adler and Weiss observed that the torus in the new eigen-coordinates is covered by two rectangles, labelled  $A$  and  $B$  in figure 2.1.<sup>1</sup>

### 2.1 Adler-Weiss partition of the Thom-Arnol’d cat map

Figure 2.1 for the canonical Thom-Arnol’d cat map

remark ??

$$A = \begin{bmatrix} 2 & 1 \\ 1 & 1 \end{bmatrix}. \tag{2.1}$$

String people, [arXiv:1608.07845](#), find the identity

$$\begin{bmatrix} 2 & 1 \\ 1 & 1 \end{bmatrix} = \begin{bmatrix} 1 & 1 \\ 0 & 1 \end{bmatrix} \begin{bmatrix} 1 & 0 \\ 1 & 1 \end{bmatrix} = LL^T \tag{2.2}$$

significant: “The map corresponds to successive kicks, forwards and backwards along the light cone [...]”

<sup>1</sup>Predrag 2018-02-09: (1) motivate Manning multiples by doing the 1D circle map first. Maybe Robinson [75] does that.

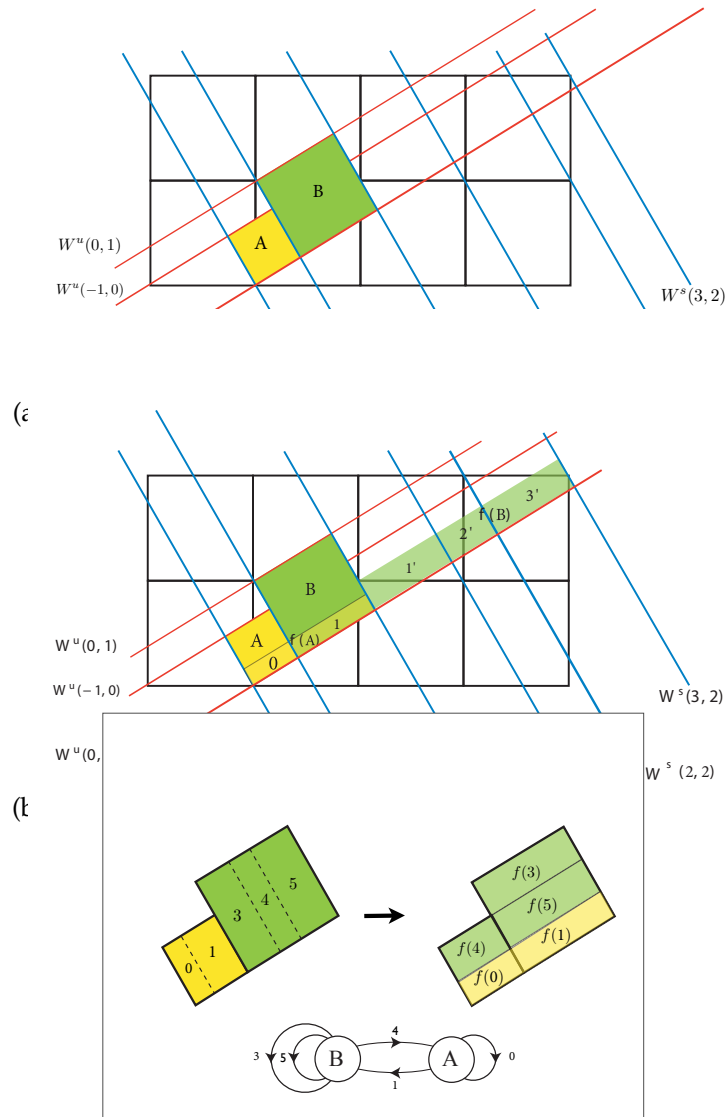


Figure 2.1: (a) Two-rectangles Adler-Weiss generating partition for the canonical Arnold's cat map (2.1), with borders given by stable-unstable manifolds of the unfolded cat map lattice points near to the origin. (b) The first iterate of the partition. (c) The iterate pulled back into the generating partition, and the corresponding 5-letter transition graph. In (b) and (c) I have not bothered to re-label Crutchfield partition labels with our shift code. This is a "linear code," in the sense that for each square one can count how many side-lengths are needed to pull the overhanging part of  $f(x)$  back into the two defining squares. (Figure by Crutchfield [25])

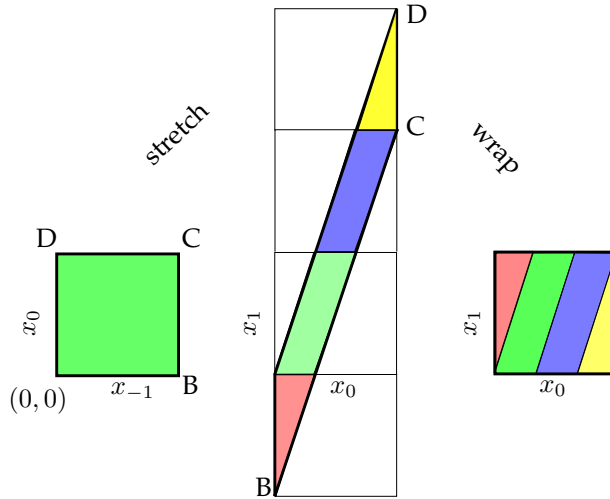


Figure 2.2: (Color online) The  $s = 3$  Percival-Vivaldi cat map matrix (2.5) stretches the unit square into a parallelogram. Translations by  $m_0$  from alphabet  $\mathcal{A} = \{-1, 0, 1, 2\} = \{\text{red, green, blue, yellow}\}$  bring stray regions back onto the torus.

As another example, with  $s = 4$ , Manning [64] discusses a Markov partition for the cat map (also discussed by Anosov, Klimenko and Kolutsky [5])

$$A = \begin{bmatrix} 3 & 1 \\ 2 & 1 \end{bmatrix}. \quad (2.3)$$

In order to count all admissible walks, one associates with the transition graph such as the one in figure 2.1 (c) the *connectivity matrix*

$$C = \begin{bmatrix} 1 & 1 \\ 1 & 2 \end{bmatrix}, \quad (2.4)$$

where  $C_{ij}$  is the number of ways (number of links) of getting to  $i$  from  $j$ .

## 2.2 Adler-Weiss partition of the Percival-Vivaldi cat map

As illustrated in figure 2.2, the action of the cat map in the Percival-Vivaldi [70] “two-configuration representation” is given by the antisymmetric area preserving  $[2 \times 2]$  matrix

$$\mathbf{A} = \begin{bmatrix} 0 & 1 \\ -1 & s \end{bmatrix} \quad (2.5)$$

For the Arnol'd value  $s = 3$ , in one time step the map stretches the unit square into a parallelogram, and then wraps it around the torus 3 times, as in figure 2.2. Visualise the phase space as a bagel, with  $x_0$  axis a circle on the outside of the bagel. This circle is divided into three color segments, which map onto each other as you go in the  $x_1$  axis direction. Now apply the inverse map - you get 3 strips intersecting the the above strips, for 9 rectangles in all: a full shift, i.e., a ternary Smale horseshoe. So on the torus there are only 3 strips - there is no distinction between the two outer letters  $\mathcal{A}_1 = \{-1, 2\} = \{\text{red, yellow}\}$ , it is the same third strip. The division into 2 triangles is an artifact of plotting the torus as a unit square. All complicated pruning of (the current draft of) Gutkin *et al.* [45] is a red herring, due to over-partitioning of the torus with a 4-letter alphabet.

*This is stupid.*

How do Adler-Weiss coordinates work out for the Arnol'd cat map in the Percival-Vivaldi representation (2.5) used here? First one needs to construct the eigen-coordinates.



example 2.1  
p. 86

For  $s > 2$  the stability multipliers  $(\Lambda^+, \Lambda^-) = (\Lambda, \Lambda^{-1})$  are real,

$$\Lambda^\pm = \frac{1}{2}(s \pm \sqrt{D}), \quad \Lambda = e^\lambda, \quad (2.6)$$

where

$$\begin{aligned} s &= \Lambda + \Lambda^{-1} = 2 \cosh(\lambda), \\ \sqrt{D} &= \Lambda - \Lambda^{-1} = 2 \sinh(\lambda) \end{aligned} \quad (2.7)$$

discriminant  $D = s^2 - 4$ , with a positive Lyapunov exponent  $\lambda > 0$ , and the right, left eigenvectors:

$$\begin{aligned} \{\mathbf{e}^{(+)}, \mathbf{e}^{(-)}\} &= \left\{ \begin{bmatrix} \Lambda^{-1} \\ 1 \end{bmatrix}, \begin{bmatrix} \Lambda \\ 1 \end{bmatrix} \right\} \\ \begin{bmatrix} \mathbf{e}_{(+)} \\ \mathbf{e}_{(-)} \end{bmatrix} &= \begin{bmatrix} [-\Lambda^{-1}, 1] \\ [\Lambda, -1] \end{bmatrix}, \end{aligned} \quad (2.8)$$

(where the overall scale is arbitrary). As the matrix is not symmetric, the  $\{\mathbf{e}^{(j)}\}$  do not form an orthogonal basis.

What does this do to the partition of figure 2.2? The origin is still the fixed point. For a state space point in the new, dynamically intrinsic right eigenvector Adler-Weiss coordinate basis  $x'$

$$\begin{pmatrix} x'_{t-1} \\ x'_t \end{pmatrix} = \begin{pmatrix} -\Lambda x_t + x_{t-1} \\ -\Lambda^{-1} x_t + x_{t-1} \end{pmatrix}.$$

the abscissa ( $x_{t-1}$  direction) is not affected, but the ordinate ( $x_t$  direction) is flipped and stretched/shrunk by factor  $-\Lambda, -\Lambda^{-1}$  respectively,

$$\begin{pmatrix} x'_t \\ x'_{t+1} \end{pmatrix} = \begin{bmatrix} \Lambda^{-1} & 0 \\ 0 & \Lambda \end{bmatrix} \begin{pmatrix} x'_{t-1} \\ x'_t \end{pmatrix} - \begin{pmatrix} 0 \\ m_t \end{pmatrix},$$



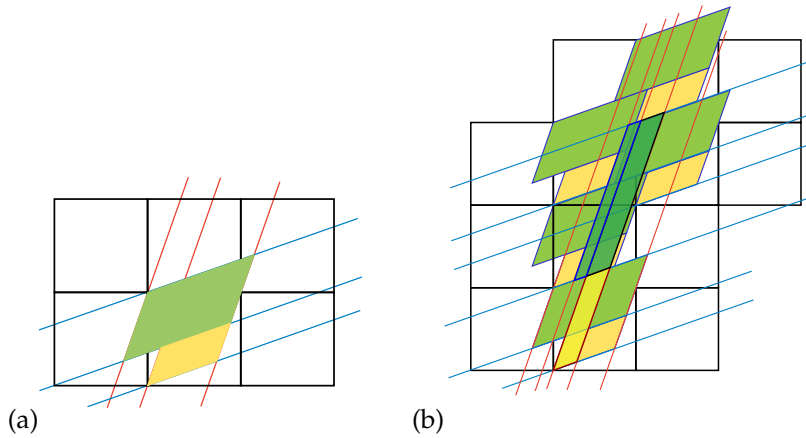


Figure 2.3: (a) An abandoned two-rectangle Adler-Weiss generating partition for the Percival-Vivaldi cat map (2.5), with borders given by cat map stable-unstable manifolds. (b) An abandoned attempt to identify the finite partition, since superseded by the partition of figure 2.6 (b) and figure 2.9.

preserving the vertical strip nature of the partition of figure 2.2. In the Adler-Weiss right eigenbasis,  $A$  acts by stretching the  $e^{(+)}$  direction by  $\Lambda$ , and shrinking the  $e^{(-)}$  direction by  $\Lambda^{-1}$ , without any rotation of either direction.

Thus the Adler-Weiss coordinates preserve the convenient feature of the Percival-Vivaldi cat map, figure 2.2: the torus ‘rewrapping’ translations remain all vertical, specified by a single integer.

The angles of stable / unstable manifolds are irrational respective to the lattice, and they never hit another vertex (and so they do not close onto themselves under quotienting of translations).

Note that from figure 2.4(a) to figure 2.4(b) we have used the continuous translation invariance to center the large tile  $A$  within the unit square. That makes the time reversal invariance more explicit. It might not be obvious that the two parallelograms of figure 2.3(a) tile the square lattice, but they do, as illustrated in figure 2.4 (a). Such tilings are known as ‘Pythagorean’.

Given the stable/unstable eigenvectors, the natural eigen-coordinates are given. I had first constructed a 2-rectangle generating partition for the Percival-Vivaldi [70] two-configuration representation (2.5) - it is a squashed and rotated version of figure 2.1 (a) drawn in figure 2.3 (a). The point is, after a linear change of coordinates one has finite grammar Adler-Weiss symbolic dynamics, and the symbolic dynamics is a linear code in sense of Boris, but this time with all admissible sequences generated as walks on a transition graph isomorphic to the one in figure 2.1 (c).

remark 2.2

I actually like better the three-rectangle, time reversal symmetric generating partition of figure 2.5 and figure 2.6.

Thus we have constructed Percival-Vivaldi cat map coordinate transforma-

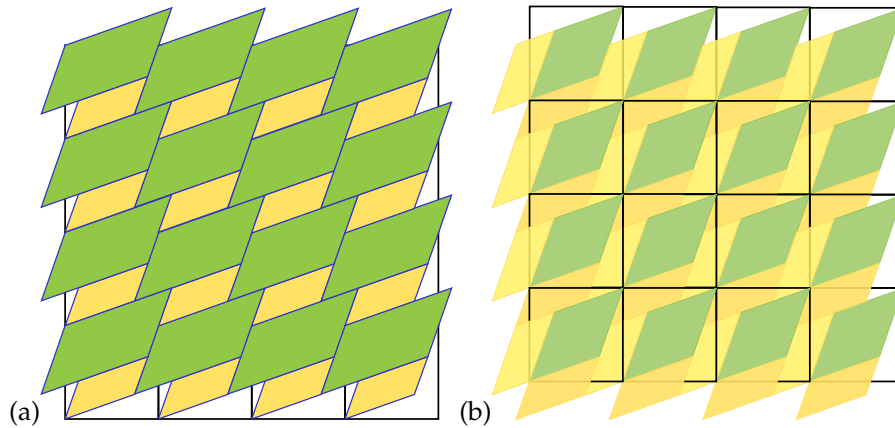


Figure 2.4: (a) [Abandoned] Tiling of the square lattice by the two-rectangle Adler-Weiss generating partition of figure 2.3(a) for the Percival-Vivaldi cat map (2.5). (b) Tiling of the square lattice by the three-rectangle, time reversal symmetric generating partition. Note that we have used the continuous translation invariance to center the large tile  $A$  within the unit square (continued in figure 2.5(a)).

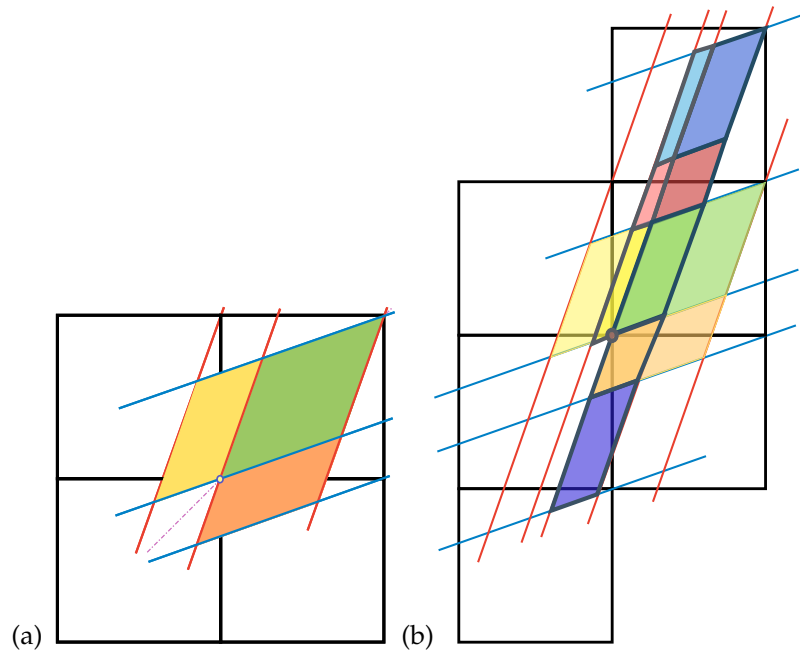


Figure 2.5: (a) The three-rectangle, time reversal symmetric generating partition for the Percival-Vivaldi cat map (2.5), with borders given by cat map stable-unstable manifolds. (b) The three-rectangle mapped one step forward in time.

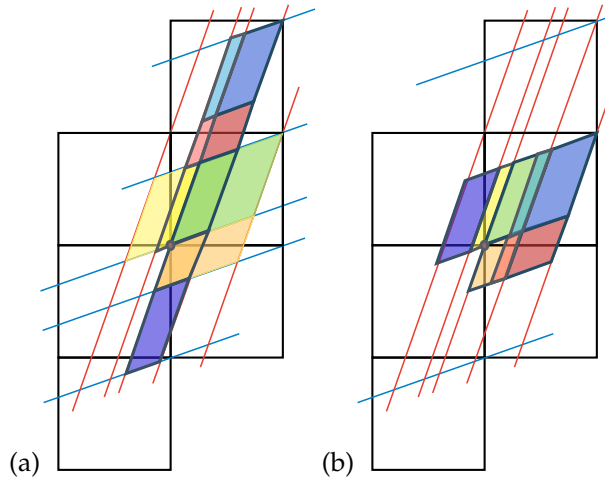


Figure 2.6: (a) The three-rectangle mapped one step forward in time. (b) The three-rectangle wrapped back onto the torus, along the unstable direction, yields 8-letter alphabet generating partition, with three-nodes transition graph. One could have kept the two-rectangle Adler-Weiss generating partition of figure 2.3 (a), in which case the alphabet is the standard 5 letters.

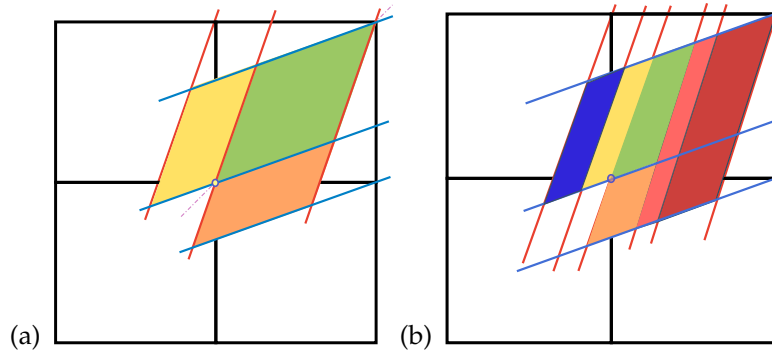


Figure 2.7: Figure 2.6 continued. (a) The three-rectangle, time reversal symmetric generating partition for the Percival-Vivaldi cat map (2.5), with borders given by cat map stable-unstable manifolds. (b) The three-rectangle subpartition, one step forward in time.  $A$  into three strips,  $B$  into three strips,  $B'$  into two strips, for a total of 8 forward links in the graph (continue with a sensible coloring of these regions). Label the graph links by translations that bring these pieces back into the unit square. Under time reversal, interchange  $B$  and  $B'$ , get the same partition going backwards in time. Then make it Lagrangian, meaning the combined graph should have undirected links (?).

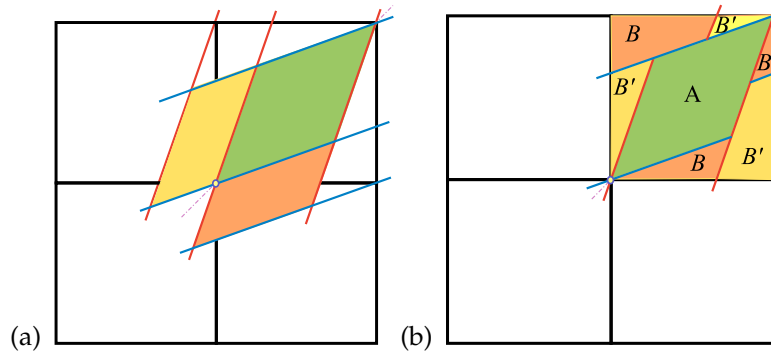


Figure 2.8: (a) The three-rectangle, time reversal symmetric generating partition for the Percival-Vivaldi cat map (2.5), with borders given by cat map stable-unstable manifolds. (b) The three-rectangle partition of the unit square (torus laid out). In this partition  $A$  already lies entirely within the unit square, while  $B$  and  $B'$  are wrapped around the torus, and only seem to consist of three pieces each, an artifact of the wrapping. The unit square borders have no physical meaning.

tion from the square to the intrinsic Adler-Weiss eigencoordinate basis. This is a LINEAR transformation. As this has been falling on deaf ears for last few years, let me say it again:

This is a **LINEAR** code,

as is every code in ChaosBook, as illustrated by the examples of sect. 1.3 that I worked out for feline pleasure some years back. Got that?

As Adler-Weiss partition is generating, there is nothing for Dirichlet boundary conditions Green's functions to accomplish - all admissible symbol blocks are known. The problem is now *trivial*, in the Soviet sense (i.e., after a few years of work, I understand it).

What is wrong with the argument so far? I used Newtonian, evolution-in-time thinking to generate the  $d = 1$  partition. That will not work in higher dimensions, so the above argument has to be recast in the Lagrangian form.

Be my guest - I'm going to bed:)

A few side, symmetry related remarks: we *must* quotient translation symmetries, do calculations in the elementary cell or, better still, the fundamental domain.

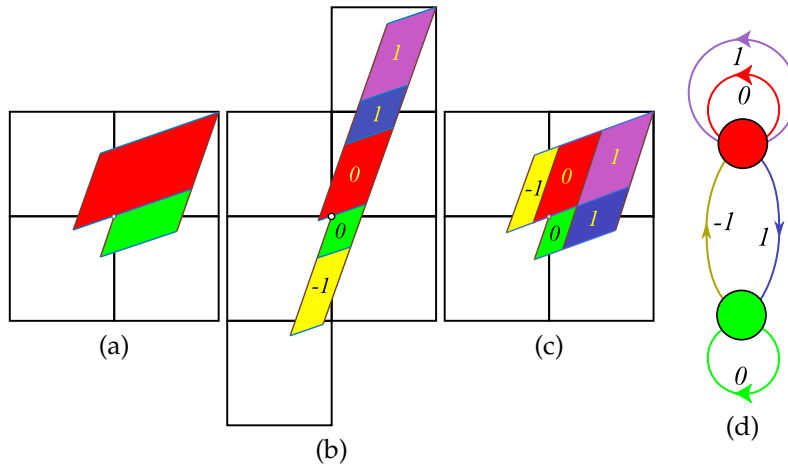


Figure 2.9: (Color online) (a) An Adler-Weiss generating partition of the unit torus for the  $s = 3$  Percival-Vivaldi cat map (2.75), with rectangle  $\mathcal{M}_A$  (red) and  $\mathcal{M}_B$  (green) borders given by the cat map stable (blue) and unstable (dark red) manifolds, i.e., along the two eigenvectors corresponding to the eigenvalues (??). (b) Mapped one step forward in time, the rectangles are stretched along the unstable direction and shrunk along the stable direction. Sub-rectangles  $\mathcal{M}_j$  that have to be translated back into the partition are indicated by color and labeled by their lattice translation  $m_j \in \mathcal{A} = \{1, 0, 1\}$ , which also doubles as the 3-letter alphabet  $\mathcal{A}$ . (c) The sub-rectangles  $\mathcal{M}_j$  translated back into the initial partition yield a generating partition, with the finite grammar given by the transition graph (d). The nodes refer to the rectangles  $A$  and  $B$ , and the five links correspond to the five sub-rectangles induced by one step forward-time dynamics. For details, see appendix 2.3 and ChaosBook [27].

## 2.3 Cat map: Hamiltonian formulation

2

### 2.3.1 Adler-Weiss partition of the cat map state space

Cat maps, also known as Thom-Anosov diffeomorphisms, or Thom-Anosov-Arnol'd-Sinai cat maps [6, 30, 90], have been extensively studied as the simplest examples of chaotic Hamiltonian systems.

Percival-Vivaldi cat map (2.75) is a discrete time non-autonomous Hamiltonian system, time-forced by 'pulses'  $m_t$ . The  $m_t$  translations reshuffle the state space, as in figure 2.9, thus partitioning it into regions  $\mathcal{M}_m$ , labeled with letters  $m$  of the  $|\mathcal{A}|$ -letter alphabet  $\mathcal{A}$ , and associating a symbol sequence  $\{m_t\}$  to the

<sup>2</sup>Predrag 2019-12-12: Make sure no clip & paste from ref. [45]

dynamical trajectory  $\{x_t\}$ . As the relation (2.75) between the trajectory  $x_t$  and its symbolic dynamics encoding  $m_t$  is linear, Percival and Vivaldi refer to  $m_t$  as a ‘linear code’.

As explained in the companion paper [45], the deep problem with the Percival-Vivaldi code prescription is that it does not yield a generating partition; the borders (i.e.,  $x_0, x_1$  axes) of their unit-square partition  $(x_{t-1}, x_t) \in (0, 1] \times (0, 1]$  do not map onto themselves, resulting in the infinity of, to us unknown, grammar rules for inadmissible symbol sequences.

This problem was resolved in 1967 by Adler and Weiss [2, 3, 6] who utilized the stable/unstable manifolds of the fixed point at the origin to cover a unit area torus by a two-rectangles generating partition; for the Percival-Vivaldi cat map (2.75), such partition [27] is drawn in figure 2.9. Following Bowen [20], one refers to parallelograms in figure 2.9 as ‘rectangles’; for details see Devaney [30], Robinson [75], or ChaosBook [27]. Siemaszko and Wojtkowski [79] refer to such partitions as the ‘Berg partitions’, and Creagh [24] studies their generalization to weakly nonlinear mappings. Symbolic dynamics on this partition is a subshift of finite type, with the 3-letter alphabet

$$\mathcal{A} = \{\underline{1}, 0, 1\} \tag{2.9}$$

that indicates the translation needed to return the given sub-rectangle  $\mathcal{M}_j$  back into the two-rectangle partition  $\mathcal{M} = \mathcal{M}_A \cup \mathcal{M}_B$ .

While Percival and Vivaldi were well aware of Adler-Weiss partitions, they felt that their “coding is less efficient in requiring more symbols, but it has the advantage of linearity.” Our construction demonstrates that one can have both: an Adler-Weiss generating cat map partition, and a linear code. The only difference from the Percival-Vivaldi formulation [70] is that one trades the single unit-square cover of the torus of (2.75) for the dynamically intrinsic, two-rectangles cover of figure 2.9, but the effect is magic - now every infinite walk on the transition graph of figure 2.9(d) corresponds to a unique admissible orbit  $\{x_t\}$ , and the transition graph generates all admissible itineraries  $\{m_t\}$ .

To summarize: an explicit Adler-Weiss generating partition, such as figure 2.9, completely solves the Hamiltonian cat map problem, in the sense that it generates all admissible orbits. Rational and irrational initial states generate periodic and ergodic orbits, respectively [56, 71], with every state space orbit uniquely labeled by an admissible bi-infinite itinerary of symbols from alphabet  $\mathcal{A}$ .

### 2.3.2 Counting Hamiltonian cat map periodic orbits

The five sub-rectangles  $\mathcal{M}_j$  of the two-rectangle Adler-Weiss partition of figure 2.9(c) motivate introduction of a 5-letter alphabet

$$\bar{\mathcal{A}} = \{1, 2, 3, 4, 5\} = \{A^0A, B^1A, A^1A, B^0B, A^1B\}, \tag{2.10}$$

see figure 2.10(b), which encodes the links of the transition graph of figure 2.9(d). The loop expansion of the determinant [26] of the transition graph  $T$  of fig-

ure 2.10 (b) is given by all non-intersecting walks on the graph

$$\det(1 - zT) = 1 - z(t_1 + t_3 + t_4) - z^2(t_{25} - (t_1 + t_3)t_4), \quad (2.11)$$

where  $t_p$  are traces over fundamental cycles, the three fixed points  $t_1 = T_{A^0A}$ ,  $t_3 = T_{A^1A}$ ,  $t_4 = T_{B^0B}$ , and the 2-cycle  $t_{25} = T_{B^1A}T_{A^1B}$ .

As the simplest application, consider counting all admissible cat map periodic orbits. This is accomplished by setting the non-vanishing links of the transition graph to  $T_{ji} = 1$ , resulting in the cat map topological zeta function [27, 52] (6.199), (16.43),

$$1/\zeta_{\text{AM}}(z) = \frac{1 - 3z + z^2}{(1 - z)^2}, \quad (2.12)$$

where the numerator  $(1 - z)^2$  corrects the overcounting of the fixed point at the origin due to assigning it to both  $\mathcal{M}_A$  (twice) and  $\mathcal{M}_B$  rectangles [63] (see figure 2.12 (a) for an example of such over-counting). 2CB

According to ChaosBook count [26],  $N_n$ , the number of *periodic points* of period  $n$  is given by the logarithmic derivative of the topological zeta function

$$\sum_{n=1} N_n z^n = -\frac{z}{1/\zeta_{\text{AM}}} \frac{d}{dz} (1/\zeta_{\text{AM}}). \quad (2.13)$$

Substituting the cat map topological zeta function (2.12) we obtain

$$\begin{aligned} \sum_{n=1} N_n z^n &= z + 5z^2 + 16z^3 + 45z^4 + 121z^5 + 320z^6 + 841z^7 \\ &\quad + 2205z^8 + 5776z^9 + 15125z^{10} + O(z^{11}) \end{aligned} \quad (2.14)$$

The number of *prime* cycles can be computed recursively as in (9.20) or by the Möbius inversion formula (9.21). Hence

$$\begin{aligned} \sum_{n=1} M_n z^n &= z + 2z^2 + 5z^3 + 10z^4 + 24z^5 + 50z^6 + 120z^7 \\ &\quad + 270z^8 + 640z^9 + 1500z^{10} \dots, \end{aligned} \quad (2.15)$$

in agreement with the Bird and Vivaldi [15] census. These counts are tabulated in table 21.1.

This derivation was based on the Adler-Weiss generating partition, a clever explicit visualization of the cat map dynamics, whose generalization to several coupled maps (let alone spatially infinite coupled cat maps lattice) is far from obvious: one would have to construct covers of high-dimensional parallelepipeds by sets of sub-volumes. However, as Keating [56] explains, no such explicit generating partition is needed to count cat map periodic orbits. Cat map (2.75) periodic points are the fixed points of

$$\begin{bmatrix} q_t \\ p_t \end{bmatrix} = \begin{bmatrix} q_{t+n} \\ p_{t+n} \end{bmatrix} = A^n \begin{bmatrix} q_t \\ p_t \end{bmatrix} \pmod{1},$$

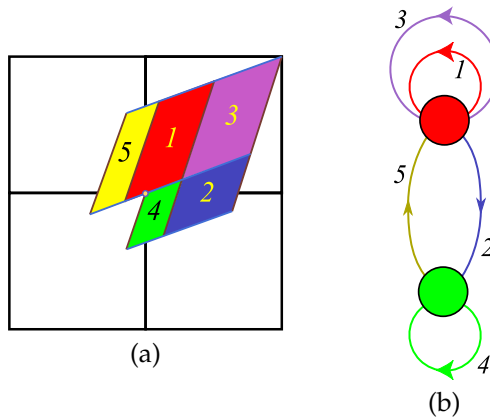


Figure 2.10: (Color online) (a) The sub-rectangles  $\mathcal{M}_j$  of figure 2.9 (c). (b) Admissible orbits correspond to walks on the transition graph of figure 2.9 (d), with rectangles  $\mathcal{M}_A$  (red) and  $\mathcal{M}_B$  (green) as nodes, and the links labeled by 5-letter alphabet (2.10), see the loop expansion (2.11).

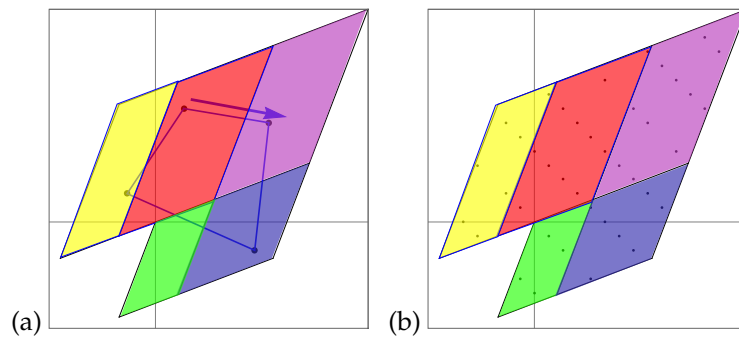


Figure 2.11: (a) An example of a 4-cycle:  $X_{0111}$ . (b) All period 4 orbits periodic points land in the partition of figure 2.10 (a).



so on the unwrapped phase space lattice, tiled by repeats of the unit square of the cat map torus,

$$(A^n - \mathbf{1}) \begin{bmatrix} q_t \\ p_t \end{bmatrix} = \begin{bmatrix} m_t^q \\ m_t^p \end{bmatrix}, \quad (m_t^q, m_t^p) \in \mathbb{Z}^2, \quad (2.16)$$

matrix  $(A^n - \mathbf{1})$  stretches the unit square into what Keating calls the ‘fundamental parallelogram’ (an example is drawn in figure 2.12). The number of periodic points of period  $n$  is given by the area of this parallelogram

$$N_n = |\det(A^n - \mathbf{1})| = \Lambda^n + \Lambda^{-n} - 2, \quad (2.17)$$

where the  $\Lambda$  is the stability multiplier (??) of the Hamiltonian time evolution matrix  $A$  in (??).

Jaidee, Moss and Ward [53], *Time-changes preserving zeta functions*, say that a Lehmer–Pierce sequence [60, 72], with  $n$ th term  $|\det(A^n - I)|$  for some integer matrix  $A$ , counts periodic points for an ergodic toral endomorphism if it is non-zero for all  $n \geq 1$ .

Substituting the numbers of periodic points  $N_n$  into the *topological* or *Artin-Mazur zeta function* [7, 26] we obtain (2.28), (6.199), (16.43)

$$\begin{aligned} 1/\zeta_{\text{AM}}(z) &= \exp\left(-\sum_{n=1}^{\infty} \frac{z^n}{n} N_n\right) = \exp\left(-\sum_{n=1}^{\infty} \frac{z^n}{n} (\Lambda^n + \Lambda^{-n} - 2)\right) \\ &= \exp[\ln(1 - z\Lambda) + \ln(1 - z\Lambda^{-1}) - 2\ln(1 - z)] \\ &= \frac{(1 - z\Lambda)(1 - z\Lambda^{-1})}{(1 - z)^2} \\ &= \frac{1 - sz + z^2}{(1 - z)^2}, \end{aligned} \quad (2.18)$$

in agreement with Isola [52], as well as the Adler-Weiss generating partition topological zeta function (2.12). As explained in ChaosBook [26], topological zeta functions count *prime* orbits (1.12), i.e., the time invariant sets of periodic points, rather than the individual periodic points.

### 2.3.3 An example: Fundamental parallelogram for period-2 cycle points

To visualize the fundamental parallelogram (2.16) counting of periodic solutions, consider Percival-Vivaldi  $s = 3$  cat map (2.75) acting on states  $x_t$  within the unit square  $(x_{t-1}, x_t) \in (0, 1] \times (0, 1]$ , as in figure 2.12 (a). In 2 time steps matrix  $(A^2 - \mathbf{1})$  stretches the unit square into the fundamental parallelogram, with integer points within the parallelogram corresponding to periodic points of period 2. Note however that the integer points on the vertices of the fundamental parallelogram over-count the number distinct solutions, as was already noted in the construction of the topological zeta function (2.12).

The  $(x_{t-1}, x_t) = (0, 0)$  solution is a repeat of the fixed point solution for  $n = 1$ , so the total number of period-2 orbits is 2, as given in (1.12).

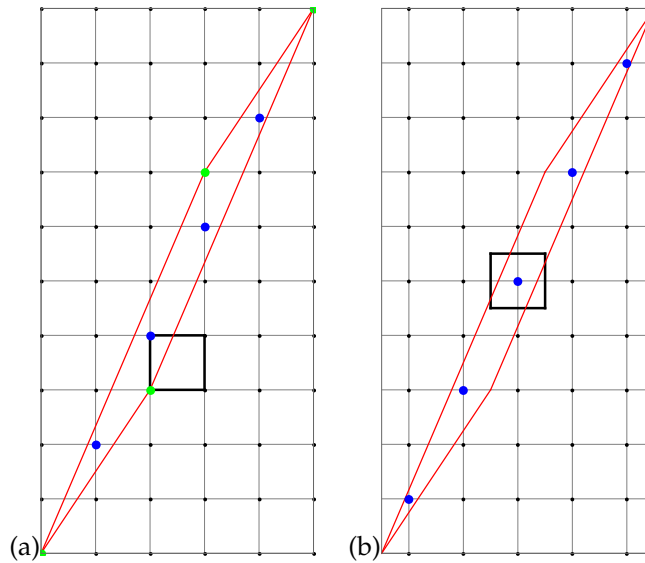


Figure 2.12: (Color online) (a) The corner-centered [black] unit square  $(0, 1] \times (0, 1]$  is stretched by  $(A^2 - 1)$  into the [red] fundamental parallelogram. By (2.16), each integer point within the fundamental parallelogram corresponds to a periodic point solution of period 2. The 4 internal integer points are marked by the blue dots. Note however that the 4 vertex integer points [green] are the same point  $\pmod 1$ , and thus have to be counted as 1 fixed point solution. (b) The face-centered [black] (Wigner-Seitz cell?) unit square  $(-1/2, 1/2] \times (-1/2, 1/2]$  is stretched by  $(A^2 - 1)$  into the [red] fundamental parallelogram. Now all 5 integer points [blue] are within the fundamental parallelogram, yielding again 5 periodic point solutions of period 2, but without any over-counting. Percival-Vivaldi cat map (2.75),  $s = 3$ .

### 2.3.4 An example: period-4 orbits

As a hands-on example, let us count the  $M_4 = 10$  admissible period 4 orbits, as stated in (1.12). The admissible blocks  $M_p$  can be read off as walks on either the 5-letter alphabet (2.10) graph, see figure 2.10 (b), or the 3-letter alphabet (2.9) graph, see figure 2.9 (d). They are, in 5-letter (top), and 3-letter (bottom) alphabets<sup>3</sup>

$$\begin{array}{ccccc} \overline{1113} & \overline{1125} & \overline{1245} & \overline{1253} & \overline{1325} \\ 0001 & 001\bar{1} & 010\bar{1} & 01\bar{1}\bar{1} & 01\bar{1}\bar{1} \\ \overline{1133} & \overline{3325} & \overline{3331} & \overline{3245} & \overline{4452} \\ 0011 & 111\bar{1} & 1110 & 110\bar{1} & 00\bar{1}\bar{1} \end{array} \cdot \quad (2.19)$$

The corresponding periodic orbits  $X_p$  are computed using Green's function (??) (the inverse of the - of the  $[4 \times 4]$  orbit Jacobian matrix (??), easiest to evaluate by discrete Fourier transforms, see appendix ??):

$$M_{0001} \Rightarrow X_{0001} = g \begin{bmatrix} 0 \\ 0 \\ 0 \\ 1 \end{bmatrix} = \frac{1}{15} \begin{bmatrix} 3 \\ 2 \\ 3 \\ 7 \end{bmatrix}.$$

Likewise,<sup>4</sup>

$$\begin{aligned} X_{001\bar{1}}^\top &= \frac{1}{15} \begin{bmatrix} -1 & 1 & 4 & -4 \end{bmatrix}, & X_{010\bar{1}}^\top &= \frac{1}{15} \begin{bmatrix} 0 & 5 & 0 & -5 \end{bmatrix} \\ X_{01\bar{1}\bar{1}}^\top &= \frac{1}{15} \begin{bmatrix} 4 & 6 & -1 & 6 \end{bmatrix}, & X_{01\bar{1}\bar{1}}^\top &= \frac{1}{15} \begin{bmatrix} 2 & 8 & 7 & -2 \end{bmatrix} \\ X_{0011}^\top &= \frac{1}{15} \begin{bmatrix} 5 & 5 & 10 & 10 \end{bmatrix}, & X_{111\bar{1}}^\top &= \frac{1}{15} \begin{bmatrix} 9 & 11 & 9 & 1 \end{bmatrix} \\ X_{1110}^\top &= \frac{1}{15} \begin{bmatrix} 12 & 13 & 12 & 8 \end{bmatrix}, & X_{110\bar{1}}^\top &= \frac{1}{15} \begin{bmatrix} 7 & 8 & 2 & -2 \end{bmatrix} \\ X_{00\bar{1}\bar{1}}^\top &= \frac{1}{15} \begin{bmatrix} 1 & -1 & -4 & 4 \end{bmatrix}. \end{aligned} \quad (2.20)$$

One can verify that for each of these 10 period 4 orbits the periodic points  $(x_t, x_{t+1})$  visit the rectangles  $\mathcal{M}_A$  or  $\mathcal{M}_B$  of figure 2.9 (b) in the temporal order dictated by the transition graph, and thus they are all admissible cycles.<sup>5</sup>



example 2.6  
p. 90

<sup>3</sup>Predrag 2019-12-20: For covering symbolic dynamics, use/refer to ChaosBook. Order (24.12) lexically.

<sup>4</sup>Predrag 2019-12-20: To Han: order lexically.

<sup>5</sup>Predrag 2019-09-11: Add here the blog figure that has all points in the partition.

### 2.3.5 Adler / Adler98

Predrag 2017-10-02 excerpts from or notes on Adler [1] *Symbolic dynamics and Markov partitions*, ([click here](#)) an excellent overview of symbolic dynamics techniques.

$$A = \begin{pmatrix} a & b \\ c & d \end{pmatrix}, \tag{2.21}$$

where  $a, b, c, d$  and  $\det A = 1$ . The row vectors

$$\{\mathbf{e}_{(+)}, \mathbf{e}_{(-)}\} = \{[c, \Lambda - a], [c, \Lambda^{-1} - a]\} \tag{2.22}$$

are the left expanding / contracting eigenvectors. The matrix (2.21) is in general not symmetric, so  $\{\mathbf{e}_{(j)}\}$  do not form an orthogonal basis. For matrix (2.5) the left eigenvectors are

$$\{\mathbf{e}_{(+)}, \mathbf{e}_{(-)}\} = \{[-1, \Lambda], [-1, \Lambda^{-1}]\}, \tag{2.23}$$

in agreement with (2.8). I prefer the right eigenvectors basis  $\{\mathbf{e}^{(j)}\}$ , as it lies in the first quadrant.

### 2.3.6 Percival and Vivaldi / PerViv

Predrag 2016-05-29 excerpts from or notes on

Percival and Vivaldi [70] *A linear code for the sawtooth and cat maps* ([click here](#))

“Completely chaotic systems are comparatively well understood, but they have been neglected as a starting point for the study of systems with divided phase space. It is the purpose of this and related papers to remedy this.”

“When one starts with an integrable system, and perturbs it to introduce some chaos, new orbits and new classes of orbits keep on appearing by bifurcation processes, and they are very difficult to follow or to classify. It is better to start with a purely chaotic system and then reduce the chaos by *removing* orbits.”<sup>6</sup>

“In this paper we present the symbolic dynamics of the sawtooth maps, and in the companion paper [71] *Arithmetical properties of strongly chaotic motions* the number theory for the periodic orbits of the automorphisms of the torus, including the cat maps.”

“we start with the simplest systems that show the phenomena of interest-area preserving maps. The sawtooth maps are piecewise linear systems. They depend on a parameter  $K$  and for positive  $K$  they are completely chaotic. For positive *integer*  $K$  they are automorphisms of the torus, of which the simplest is the Arnol’d-Sinai cat map, with  $K = 1$ . We shall refer to all such toral automorphisms, with positive integer  $K$ , as cat maps. They are Anosov systems, continuous on the torus. On the other hand, when  $K$  is not an integer, the sawtooth map is discontinuous.”

<sup>6</sup>Predrag 2016-05-29: totally agree - they say it well

2CB

2CB

“Most of this paper is concerned with a ‘linear code’ for the symbolic dynamics of the sawtooth maps, including the cat maps. This code is chosen for its convenience in practice, and differs from the usual codes for the Arnol’d-Sinai cat.”

“In section 3 a practical problem of stabilisation is considered, that provides a concrete model for the sawtooth and cat maps, and a natural introduction to the linear codes. An explicit linear transformation from the itinerary to the orbit is given.”

<sup>7</sup> Every Anosov diffeomorphism of the torus is topologically conjugate to a hyperbolic automorphism. These are represented by  $[2 \times 2]$  matrices with integer entries (for continuity), unit determinant (for area preservation) and real eigenvalues (for hyperbolicity), and are known as cat maps.

In order to describe certain collective properties of cat map orbits Hannay and Berry [46] introduced a function closely related to the least common multiple of their periods.

### 2.3.7 Isola / Isola90

Predrag 2016-06-02 excerpts from or notes on  
S. Isola [52]  *$\zeta$ -functions and distribution of periodic orbits of toral automorphisms*

Bellissard’s friend Isola gives counting formulas of the usual type - could easily be turned into examples/exercises for ChaosBook. But I am looking for symbolic dynamics - not even mentioned here.

We consider canonical automorphisms of the torus  $T^2$ , i.e. maps of the form

$$T(x, y) = (ax + by, cx + dy) \pmod{1},$$

which are implemented by the group of  $[2 \times 2]$  matrices with integer entries, determinant 1, and eigenvalues (15.12).

To study the properties of this dense set of unstable periodic orbits, observe that the periodic orbits of  $T$  consist precisely of those points having rational coordinates  $(p_l/q_l, p_z/q_z)$ . If  $p_1, q_1$  are coprime and  $g$  is the least common multiple of  $q_1$  and  $q_z$ , then the square lattice of size  $l/g$  is invariant under  $T$ .

In this direction, Percival and Vivaldi [15, 70, 71] have constructed a nice translation of the dynamical problem into the language of modular arithmetic, allowing a profound understanding of the structure of periodic orbits. Here, however, we follow another approach where a general expression for the  $N$ ’s is derived through a simple iterative scheme. Consider the numbers

$$u_n = \frac{\Lambda^n - \Lambda^{-n}}{\sqrt{D}}. \tag{2.24}$$

The first two terms of the series are  $u_0 = 0, u_1 = 1$  and each term after is given by

$$u_n = su_{n-1} - u_{n-2}. \tag{2.25}$$

---

<sup>7</sup>Predrag 2016-06-02: verbatim from Keating [55]

[stuff to work out: Isola has nice figures that illustrate the partitions of the 2-torus]

For the number of periodic points he finds, for any integer  $s > 2$

$$N_n = \Lambda^n + \Lambda^{-n} - 2, \tag{2.26}$$

in agreement with the numerics of ref. [69]. Walters [94] defines the topological entropy as

$$h = \lim_{n \rightarrow \infty} \frac{1}{n} \ln N_n, \tag{2.27}$$

This yields  $h = \log \Lambda$ , i.e., the Sinai theorem for the entropy of an automorphism [6, 82].

The topological zeta function for cat-map class of models is

$$1/\zeta_{\text{AM}}(z) = \frac{(1 - \Lambda z)(1 - \Lambda^{-1}z)}{(1 - z)^2} = \frac{1 - sz + z^2}{(1 - z)^2}. \tag{2.28}$$

The denominator  $(1 - z)^2$  takes care of the over-counting of the fixed point at the origin due to the 2-periodicity on the torus.<sup>8</sup>

He also gives the number of orbits of period  $n$ , which is as usual given in terms of the Moebius function  $\mu(m)$ ,

$$P_n = \frac{1}{n} \sum_{m|n} \mu(m) N_{n/m}. \tag{2.29}$$

### 2.3.8 Creagh / Creagh94

Predrag 2016-06-02 excerpts from or notes on

Creagh [24], *Quantum zeta function for perturbed cat maps* (click here), who says: “ The behavior of semiclassical approximations to the spectra of perturbed quantum cat maps is examined as the perturbation parameter brings the corresponding deterministic system into the nonhyperbolic regime. The approximations are initially accurate but large errors are found to appear in the traces and in the coefficients of the characteristic polynomial after nonhyperbolic structures appear. Nevertheless, the eigenvalues obtained from them remain accurate up to large perturbations. ”

Thom-Arnol’d cat map

$$A = \begin{pmatrix} 1 & 1 \\ 1 & 2 \end{pmatrix}, \quad \det A = 1. \tag{2.30}$$

This system can be written as:

$$\begin{pmatrix} q_{t+1} \\ p_{t+1} \end{pmatrix} = A \begin{pmatrix} q_t \\ p_t \end{pmatrix} \pmod{1} \tag{2.31}$$

<sup>8</sup>Predrag 2016-06-02: I wonder whether the fact that this is quadratic in  $z$  has something to do with the time-reversibility, and the unsigned graph’s Ihara zeta functions, see sect. 16.1 and (6.189).

It is possible to construct a symbolic coding with finite grammar, as described in Devaney [30]. Robinson [75] goes through the construction clearly, step by step. The coding is constructed for an antisymplectic map whose double iteration is (2.31) - orbits of the cat map are then coded by sequences whose length is even. A brief summary of the construction follows (see Devaney [30] for figures and details). The stable and unstable manifolds coming from the fixed point at  $(q, p) = (0, 0)$  are used to divide the phase space into 3 rectangles  $R_1$ ,  $R_2$  and  $R_3$ . Under iteration of the antisymplectic map,  $R_1$  is mapped into  $R_2 \cup R_3$ ,  $R_2$  into  $R_1 \cup R_3$  and  $R_3$  is mapped completely into  $R_2$ . Therefore orbits of the antisymplectic map are coded by sequences of 3 symbols (1,2,3), where 1 must be followed by 2 or 3, 2 is followed by 1 or 3, and 3 must be followed by 2. The full cat map is coded by even sequences of symbols following the same grammar. We can alternatively code orbits of the full map with 5 symbols denoting the admissible pairs of the symbols above:  $(a, b, c, d, e) = (12, 13, 21, 23, 32)$ .

The integers that must be subtracted from the phase space coordinates following application of the linear map in (2.31) in order to take the point back into the unit torus are fixed for each pair of symbols. The equation defining a periodic orbit can be written out as an explicit affine equation and solved for each itinerary. In this way a complete list of primitive periodic orbits is obtained for the unperturbed map.

### 2.3.9 Keating / Keating91

Keating [56] *The cat maps: quantum mechanics and classical motion.*

the action of map on the vector  $(p, q)$  can be described as the motion in the phase space specified by the Hamiltonian [56]

$$H(p, q) = (k^2 - 4)^{-1/2} \sinh^{-1}[(k^2 - 4)^{-1/2}/2][m_{12}p^2 - m_{21}q^2 + (m_{11} - m_{22})pq]. \quad (2.32)$$

Here,  $(p, q)$  are taken modulo 1 at each observation (the integer part is ignored), and observations occur at integer points of time.

The paper has a nice discussion of (possible discrete symmetries of cat maps.

Keating and F. Mezzadri [57] *Pseudo-symmetries of Anosov maps and spectral statistics.*<sup>9</sup>

Earlier work: Rykken [77] constructed new types of Markov partitions. Snively [86] studied the connectivity matrices of Markov partitions for hyperbolic automorphisms of  $T^2$ . He found that for Berg partitions the connectivity matrices are conjugated to the dynamics. He also found a way to list all such matrices and hence to classify the shapes of Berg partitions. He relied on the result of Adler [1] that such partitions are indeed present for any toral automorphism. Manning [64] gave a powerful generalization of this to  $T^n$ .

2CB

---

<sup>9</sup>Predrag 2016-08-29: not useful for the deterministic case

Anosov, Klimenko and Kolutsky [5] give an introduction to Anosov diffeomorphisms, ways to represent their chaotic properties and some historical remarks on this subject: “As far as we know, the first example of such kind was pointed out by J. Hadamard about 1900. A couple of decades earlier H. Poincaré discovered the “homoclinic points” which now serve as the main “source” of “chaoticity”; however, Poincaré himself spoke only that the “phase portrait” (i.e., the qualitative picture of trajectories’ behaviour in the phase space) near such points is extremely complicated. A couple of decades after Hadamard, E. Borel encountered a much simpler example of the “chaoticity” where it is easy to understand the “moving strings” of this phenomenon. We shall begin with a description of his example. About 100 years later it remains the simplest manifestation of the fact that a dynamical system (which, by definition, is deterministic) can somehow resemble a stochastic process.”

## 2.4 Green’s function for 1-dimensional lattice

Cat map is a second order difference equation

$$-x_{t+1} + (s x_t - m_t) - x_{t-1} = 0, \quad (2.33)$$

with the unique integer “winding number”  $m_t$  at every time step  $t$  ensuring that  $s x_t$  lands in the unit interval. This is a 1-dimensional discrete screened Poisson equation of form

$$\mathcal{D}x = m, \quad (2.34)$$

where  $x_t$  are periodic states, and  $m_t$  are the ‘sources’. Since  $\mathcal{D}_{tt'}$  is of a tridiagonal form, its inverse, or its Green’s discrete matrix  $g$  on infinite lattice satisfies

$$(\mathcal{D}g)_{t0} = \delta_{t0}, \quad t \in \mathbb{Z} \quad (2.35)$$

with a point source at  $t = 0$ . By time-translation invariance  $g_{tt'} = g_{t-t',0}$ , and by time-reversal invariance  $g_{t',t} = g_{t,t'}$ . In this simple, tridiagonal case,  $g$  can be evaluated explicitly [65, 70],

$$g_{tt'} = \frac{1}{\Lambda^{|t'-t|}} \frac{1}{\Lambda - \Lambda^{-1}}, \quad (2.36)$$

where, in the hyperbolic  $s > 2$  case, the cat map “stretching” parameter  $s$  is related to the 1-time step cat map eigenvalues  $\{\Lambda, \Lambda^{-1}\}$  by

$$s = \Lambda + \Lambda^{-1} = e^\lambda + e^{-\lambda} = 2 \cosh \lambda, \quad \lambda > 0. \quad (2.37)$$

While the “Laplacian” matrix  $\mathcal{D}$  is sparse, it is non-local (i.e., not diagonal), and its inverse is the full matrix  $g$ , whose key feature, however, is the prefactor  $\Lambda^{-|t'-t|}$  which says that the magnitude of the matrix elements falls off exponentially with their distance from the diagonal. For this it is crucial that the  $\mathcal{D}$  eigenvalues (2.37) are hyperbolic. In the elliptic,  $-2 < s < 2$  case, the  $\sinh$ ’s



and cosh's are replaced by sines and cosines,  $s = 2 \cos \theta = \exp(i\theta) + \exp(-i\theta)$ , and there is no such decay of the off-diagonal matrix elements.

For a finite-time lattice with  $n$  sites we can represent  $\mathcal{D}$  by a symmetric tridiagonal  $[n \times n]$  Toeplitz matrix. The matrix

$$\mathcal{D}_n = \begin{pmatrix} s & -1 & 0 & 0 & \dots & 0 & 0 \\ -1 & s & -1 & 0 & \dots & 0 & 0 \\ 0 & -1 & s & -1 & \dots & 0 & 0 \\ \vdots & \vdots & \vdots & \vdots & \ddots & \vdots & \vdots \\ 0 & 0 & \dots & \dots & \dots & s & -1 \\ 0 & 0 & \dots & \dots & \dots & -1 & s \end{pmatrix} \quad (2.38)$$

satisfies *Dirchlet boundary conditions*, in the sense that the first and the last site do not have a left (right) neighbor to couple to. We distinguish it from the circulant matrix (2.45) by emphasising that  $(\mathcal{D}_n)_{0,n-1} = (\mathcal{D}_n)_{n-1,0} = 0$ . As the time-translation invariance is lost, the matrix elements of its inverse, the Green's  $[n \times n]$  matrix  $\mathbf{g}_{tt'}$ , with a delta-function source term and the Dirichlet boundary conditions

$$\begin{aligned} (\mathcal{D}\mathbf{g})_{tt'} &= \delta_{tt'} & t, t' \in 0, 1, 2, \dots, n-1 \\ 0 &= \mathbf{g}_{-1,t'} = \mathbf{g}_{t,-1} = \mathbf{g}_{nt'} = \mathbf{g}_{tn} \end{aligned} \quad (2.39)$$

depend on the point source location  $t$ , and no formula for its matrix elements as simple as (2.36) is to be expected. In general, a finite matrix inverse is of the form

$$\mathcal{D}^{-1} = \frac{1}{\det \mathcal{D}} (\text{cofactor matrix of } \mathcal{D})^\top.$$

While the cofactor matrix might be complicated, the key here is, as in formula (2.36), that the prefactor  $1/\det \mathcal{D}$  falls off exponentially, and for Toeplitz matrices can be computed recursively.

Associated with this simple tridiagonal matrix are the Chebyshev polynomials of the first and the second kind

$$T_n(s/2) = \cosh(n\lambda), \quad U_n(s/2) = \sinh(n+1)\lambda / \sinh(n\lambda),$$

generated by a three-term recursion relation (second-order difference equation [34]).

The identity

$$2T_n(s/2) = \Lambda^n + \Lambda^{-n} \quad (2.40)$$

follows from  $s = \Lambda + \Lambda^{-1}$ , see (21.151).

The inverse of the Dirichlet boundary conditions matrix  $\mathcal{D}_n$  (2.38) can be determined explicitly, in a number of different ways [50, 80, 85, 89]. Here we find it convenient to write the inverse of  $\mathcal{D}_n$  in the Chebyshev polynomial form [97]. The determinant of  $\mathcal{D}_n$ , i.e., the Jacobian of the linear transformation (2.34) is well known [40]

$$\det \mathcal{D}_n = U_n(s/2), \quad (2.41)$$

and the matrix elements of the Green's function in the Chebyshev polynomial form [50, 97] are explicitly

$$\mathbf{g}_{ij} = \frac{1}{\det \mathcal{D}_n} \times \begin{cases} U_{i-1}(s/2) U_{n-j}(s/2) & \text{for } i \leq j \\ U_{j-1}(s/2) U_{n-i}(s/2) & \text{for } i > j. \end{cases} \quad (2.42)$$

$\det \mathcal{D}_n$  is also known as the determinant of the *Dirichlet kernel* (see [wiki](#))

$$D_n(x) = \sum_{k=-n}^n e^{ikx} = 1 + 2 \sum_{k=1}^n \cos(kx) = \frac{\sin((n+1/2)x)}{\sin(x/2)}. \quad (2.43)$$

It follows from the recurrence relation  $x_{i+1} = sx_i - x_{i-1}$ , mod 1, that  $U_n(s/2)$  Chebyshev polynomials have the generating function

$$\begin{aligned} \sum_{n=0}^{\infty} U_n(s/2) z^n &= \frac{1}{1 - sz + z^2} \\ &= 1 + sz + (s^2 - 1)z^2 + (s^3 - 2s)z^3 + \dots, \end{aligned} \quad (2.44)$$

with  $U_n(s/2) \approx s^n \approx \Lambda^n$ , and for a hyperbolic system the off-diagonal matrix elements  $\mathbf{g}_{tt'}$  are again falling off exponentially with their separation  $|t' - t|$ , as in (2.36), but this time only in an approximate sense.

<sup>10</sup> Alternatively, for finite time  $n$  we can represent  $\mathcal{D}$  by a symmetric tridiagonal  $[n \times n]$  circulant matrix with *periodic boundary conditions*

$$\mathcal{D}_n = \begin{pmatrix} s & -1 & 0 & 0 & \dots & 0 & -1 \\ -1 & s & -1 & 0 & \dots & 0 & 0 \\ 0 & -1 & s & -1 & \dots & 0 & 0 \\ \vdots & \vdots & \vdots & \vdots & \ddots & \vdots & \vdots \\ 0 & 0 & \dots & \dots & \dots & s & -1 \\ -1 & 0 & \dots & \dots & \dots & -1 & s \end{pmatrix}. \quad (2.45)$$

In the periodic boundary conditions case the determinant (in contrast to the Dirichlet case (2.41)) is obtained by Fourier-transform diagonalization

$$\det \mathcal{D}_n = \prod_{j=0}^{n-1} \left[ s - 2 \cos\left(\frac{2\pi j}{n}\right) \right] = 2 T_n(s/2) - 2, \quad (2.46)$$

see (2.40). <sup>11</sup>

Now the discrete matrix Green's function  $\mathbf{g}_{tt'}$  satisfies periodic boundary conditions

$$\begin{aligned} (\mathcal{D}\mathbf{g})_{t1} &= \delta_{t1}, & t &= 1, 2, \dots, n \\ \mathbf{g}_{n+1,t'} &= \mathbf{g}_{1t'}, & \mathbf{g}_{t,n+1} &= \mathbf{g}_{t1}. \end{aligned} \quad (2.47)$$

<sup>10</sup>Predrag 2017-09-20: Probably should do circulants first, then the complicated Dirichlet case next, or drop it altogether, in the spirit of starting out with the infinite lattice case (2.36).

<sup>11</sup>Han 2018-12-01: I still have to derive and recheck this formula!

Note that the Green's matrix is strictly negative for both the periodic and Dirichlet boundary conditions.

**Boris version:** An alternative way to evaluate  $g_{i,j}$  is to use Green's function  $g$  and take antiperiodic sum (similar method can be used for periodic and Neumann boundary conditions)

$$g_{i,j} = \sum_{n=-\infty}^{\infty} g_{i,j+2n(n+1)} - g_{i,-j+2n(n+1)}. \quad (2.48)$$

This approach has an advantage of being extendable to the  $\mathbb{Z}^2$  case. After substituting  $g$  and taking the sum one obtains (2.42).

See also sect. 2.6 *Chebyshev series*.

## 2.5 Green's blog

**2017-08-24,2017-09-09 Predrag** This to all curious cats, but mostly likely only Boris might care: OK now I see why Chebyshevs...

Chebyshev expansions are used here because of the recurrence relations that they satisfy.

2CB

A *Toeplitz matrix*,  $T$ , is a matrix that is constant along each diagonal, i.e.,  $T_{jk} = t_{j-k}$ . A *Hankel matrix*,  $H$ , is a matrix that is constant along each anti-diagonal, i.e.,  $H_{jk} = h_{j+k}$ . There is also the *Laurent matrix* or *doubly infinite Toeplitz matrix*.

R. M. Gray (2009) [Toeplitz and Circulant Matrices: A Review](#) focuses on bounds of sums of eigenvalues - I see nothing here that is of immediate use to us, with maybe the exception of the discussion of the diagonalization of circulant matrices (discrete Fourier series).

2CB

A look at a Toeplitz matrix evokes time evolution of a periodic orbit symbolic block: it looks like successive time shifts stacked upon each other, every entry is doubly periodic on a torus of size  $[n_p \times n_p]$ . Does that have to do something with Chebyshev polynomials (rather than with the usual discrete Fourier series)? One uses Chebyshev polynomials of the first, second, third, and fourth kind, denoted by  $T_n, U_n, V_n, W_n$ , if, as an example, one looks at a pentadiagonal symmetric Toeplitz matrix, a generalization of the 3rd order spatial derivative.

Circulant matrices are discussed in Aitkenref. [4] (1939).

Maybe some of the literature cited here illuminates this:

**2022-01-23 Predrag** This "assignment" by Chen Jing seems like a [good overview](#) of available methods for Toeplitz matrices. Our orbit Jacobian matrices are circulant and banded, should be easier.

**2017-09-09 Predrag** The eigenvalues and eigenvectors for the finite symmetric tridiagonal Toeplitz matrix might have been obtained by Streater [89] *A bound for the difference Laplacian*, but I do not see where in the article they are. They seem to also be given in Smith [85] *Numerical Solution of Partial Differential Equations: Finite Difference Methods*.

Hu and O'Connell [50] *Analytical inversion of symmetric tridiagonal matrices* " present an analytical formula for the inversion of symmetrical tridiagonal matrices. As an example, the formula is used to derive an exact analytical solution for the one-dimensional discrete screened Poisson equation (DPE) with Dirichlet boundary conditions. " The  $n$  eigenvalues and orthonormal  $n$ -dimensional eigenvectors of  $\mathcal{D}$  are <sup>12</sup>

$$\begin{aligned}\gamma_k &= s + 2 \cosh \frac{k\pi}{n+1}, \quad k = 1, 2, \dots, n \\ e_n^{(k)} &= \sqrt{\frac{2}{n+1}} \sinh \frac{kn\pi}{n+1}\end{aligned}\tag{2.49}$$

(see, for example, refs. [50, 97]). This is a typical inverse propagator, see ChaosBook [9]

$$(\varphi_k^\dagger \cdot \Delta \cdot \varphi_{k'}) = \left( -2 \cos \left( \frac{2\pi}{N} k \right) + 2 \right) \delta_{kk'}\tag{2.50}$$

The inverse (the Green's function)  $g\mathcal{D} = 1$  is [50] <sup>13</sup>

$$g_{jk} = \frac{\cosh(n+1-|k-j|)\lambda - \cosh(n+1-j-k)\lambda}{2 \sinh \lambda \sinh(n+1)\lambda}\tag{2.51}$$

The above paper is applied to physical problems in Hu and O'Connell [48] *Exact solution for the charge soliton in a one-dimensional array of small tunnel junctions*, and in Hu and O'Connell [49] *Exact solution of the electrostatic problem for a single electron multijunction trap*. The **erratum** is of no importance for us, unless the - sign errors affect us.

A cute fact is that they also state the solution for  $s = 2$ , which, unlike (2.51) has no exponentials - it's a power law.

Eigenvalues, eigenvectors and inverse for  $[n \times n]$  matrix  $\mathcal{D}$  (2.38),  $-2 < s < 2$ ,

$$\begin{aligned}\lambda_k &= -s + 2 \cos \frac{k\pi}{n+1} \\ e_k &= \sqrt{\frac{2}{n+1}} \left( \sin \frac{k\pi}{n+1}, \sin \frac{2k\pi}{n+1}, \dots, \sin \frac{nk\pi}{n+1} \right) \\ (\mathcal{D}^{-1})_{kn} &= \frac{2}{n+1} \sum_{m=1}^n \frac{\sin \frac{km\pi}{n+1} \sin \frac{nm\pi}{n+1}}{-s + 2 \cos \frac{k\pi}{n+1}}\end{aligned}\tag{2.52}$$

<sup>12</sup>Predrag 2017-09-09: recheck!

<sup>13</sup>Predrag 2017-09-09: It is shown in ref. [97] that is the same as the formula (2.42) Boris uses (without a source citation).

are computed in Meyer [66] *Matrix Analysis and Applied Linear Algebra*.

Yamani and Abdelmonem [97] *The analytic inversion of any finite symmetric tridiagonal matrix* rederive Hu and O'Connell [50], using the theory of orthogonal polynomials in order to write down explicit expressions for the polynomials of the first and second kind associated with a given infinite symmetric tridiagonal matrix  $H$ .

The matrix representation of many physical operators are tridiagonal, and some computational methods, are based on creating a basis that renders a given system Hamiltonian operator tridiagonal. The advantage lies in the connections between tridiagonal matrices and the orthogonal polynomials, continued fractions, and the quadrature approximation which can be used to invert the tridiagonal matrix by finding the matrix representation of the Green's functions.

The Green's function  $G(z)$  associated with the matrix  $H$  is defined by the relation

$$(H - zI)G = I. \quad (2.53)$$

It is more convenient to calculate the inverse of the matrix  $(H - zI)$  instead of the inverse of the matrix  $H$ . Note that in this formulation  $G$  is the *resolvent* of  $H$ .

Simons [80] *Analytical inversion of a particular type of banded matrix* rederives Hu and O'Connell [50] by a "a simpler and more direct approach". The structure of (2.53) is that of a homogeneous difference equation with constant coefficients and therefore one looks for a solution of the form

$$G_{pq} = A_q e^{p\lambda} + A_q e^{-p\lambda}, \quad (2.54)$$

with appropriate boundary conditions. This leads to the Hu and O'Connell formulas for the inverses of  $G$ .

**How to invert** a very regular banded Toeplitz matrix.

Yueh [98] *Explicit inverses of several tridiagonal matrices* has a bunch of fun tri-diagonal Toeplitz matrix inverses, full of integers - of no interest to us.

Dow [31] *Explicit inverses of Toeplitz and associated matrices*: " We discuss Toeplitz and associated matrices which have simple explicit expressions for their inverses. We first review existing results and generalize these where possible, including matrices with hyperbolic and trigonometric elements. In Section 4 we invert a tridiagonal Toeplitz matrix with modified corner elements. A bunch of fun tri-diagonal Toeplitz matrix inverses, full of integers - of no interest to us.

Noschese, Pasquini and Reichel [68] *Tridiagonal Toeplitz matrices: properties and novel applications* use the eigenvalues and eigenvectors of tridiagonal Toeplitz matrices to investigate the sensitivity of the spectrum. Of no interest to us.

Berlin and Kac [14] *The spherical model of a ferromagnet* use bloc-circulant matrices; see also

Davis [29] *Circulant Matrices*.

**2017-09-09 Predrag Gover [38]** *The Eigenproblem of a Tridiagonal 2-Toeplitz Matrix* seems less useful: “ The characteristic polynomial of a tridiagonal 2-Toeplitz matrix is shown to be closely connected to polynomials which satisfy the three point Chebyshev recurrence relationship. This is an extension of the well-known result for a tridiagonal Toeplitz matrix. When the order of the matrix is odd, the eigenvalues are found explicitly in terms of the Chebyshev zeros. The eigenvectors are found in terms of the polynomials satisfying the three point recurrence relationship. ”

Gover [38] motivates his paper by reviewing a tridiagonal 1-Toeplitz, or Toeplitz matrix, referring to the original literature. Consider a tridiagonal  $[\ell \times \ell]$  Toeplitz matrix with Dirchlet boundary conditions (2.38), with eigenvalues (2.49).

Kübra Duru and Bozkurt [58] *Integer powers of certain complex pentadiagonal 2-Toeplitz matrices*

Elouafi [35] *On a relationship between Chebyshev polynomials and Toeplitz determinants*: “Explicit formulas are given for the determinants of a band symmetric Toeplitz matrix  $T_n$  with bandwidth  $2r + 1$ . The formulas involve  $r \times r$  determinants whose entries are the values of Chebyshev polynomials on the zeros of a certain  $r$ th degree  $q$  which is independent of  $n$ . ”

**2017-09-09 Predrag Felsner and Heldt** *Lattice paths* seem to be all on graphs - I see no 2-dimensional lattice here.

*Spectral asymptotics in one-dimensional periodic lattices with geometric interaction*

**2022-04-17 Predrag Feynman trick (click here)** might be the way to do such integrals. See also

[Wolfram Mathworld \(click here\)](#),

[many different derivations \(click here\)](#),

[Differentiation under the integral sign \(click here\)](#).

[Another derivation \(click here\)](#):

$$\int_0^\pi \ln(b \cos x + c) dx = \pi \ln \left( \frac{c + \sqrt{c^2 - b^2}}{2} \right). \quad (2.55)$$

Using (21.151) one verifies (24.351):

$$\int_0^\pi \ln(-2 \cos x + s) dx = \pi \ln \left( \frac{s + \sqrt{s^2 - 4}}{2} \right) = \pi \ln \Lambda. \quad (2.56)$$

2024-07-08 Predrag Used in CL18, verified here:

$$\begin{aligned}\lambda &= \frac{1}{2\pi} \int_{-\pi}^{\pi} dk \ln \left[ 4 \sin^2 \frac{k}{2} + \mu^2 \right] = \ln \left[ \frac{2 + \mu^2 + \sqrt{\mu^2(\mu^2 + 4)}}{2} \right] \\ &= \ln \mu^2 + \ln \left[ \frac{1}{2} + \frac{1}{\mu^2} + \frac{1}{2} \sqrt{1 + \frac{4}{\mu^2}} \right],\end{aligned}\quad (2.57)$$

where the stability exponent  $\lambda$  is the cat map Lyapunov exponent [45, 61], written in a form that makes the anti-integrable limit explicit.

2024-07-08 Predrag Gradshteyn and Ryzhik [40] Eq. 4.226 2. (click here)

$$\frac{1}{2\pi} \int_0^{\pi} \ln(1 + a \sin^2 x) dx = \ln \frac{1 + \sqrt{1+a}}{2}, \quad a \geq -1. \quad (2.58)$$

Set  $a = 4/\mu^2$ ,  $x = k/2$

$$\frac{1}{2\pi} \int_0^{2\pi} \ln \left( 1 + \frac{4}{\mu^2} \sin^2 \frac{k}{2} \right) \frac{dk}{2} = \ln \frac{1 + \sqrt{1 + \frac{4}{\mu^2}}}{2}. \quad (2.59)$$

$$\frac{1}{2\pi} \int_0^{2\pi} \left[ \ln \left( \mu^2 + 4 \sin^2 \frac{k}{2} \right) - \ln \mu^2 \right] dk = 2 \ln \frac{\mu + \sqrt{\mu^2 + 4}}{2\mu}. \quad (2.60)$$

$$\begin{aligned}\frac{1}{2\pi} \int_0^{2\pi} \ln \left[ 4 \sin^2 \frac{k}{2} + \mu^2 \right] dk &= 2 \ln \mu + 2 \ln \frac{\mu + \sqrt{\mu^2 + 4}}{2\mu}. \quad (2.61) \\ &= 2 \ln \frac{\mu + \sqrt{\mu^2 + 4}}{2} = \ln \mu^2 + 2 \ln \frac{1 + \sqrt{1 + 4/\mu^2}}{2} \\ &= \ln \frac{\mu^2 + 2\mu\sqrt{\mu^2 + 4} + \mu^2 + 4}{4} \\ &= \ln \frac{\mu^2 + 2 + \sqrt{\mu^2(\mu^2 + 4)}}{2}\end{aligned}$$

This verifies Han's (2.57), as used in in CL18.

2023-04-03 Predrag Gradshteyn and Ryzhik [40] Eq. 1.317.1 (click here)

$$2 \sin^2 (\theta/2) = 1 - \cos (\theta) \quad (2.62)$$

For time period  $n$  primitive cell:

$$\begin{aligned}\Lambda_m &= \mu^2 + 2 - 2 \cos k_m = \mu^2 + 4 \sin^2 (k_m/2) \\ &= \left( \mu - i 2 \sin \left( \frac{k_m}{2} \right) \right) \left( \mu + i 2 \sin \left( \frac{k_m}{2} \right) \right) \\ &= \left( \mu + e^{ik_m/2} - e^{-ik_m/2} \right) \left( \mu + e^{ik_m/2} - e^{-ik_m/2} \right)^* \\ &\quad \text{where } k_m = 2\pi m/n\end{aligned}\quad (2.63)$$

Note also relations (2.64) convenient for Hill determinant evaluations:

$$\ln(2 - 2 \cos(2\pi x)) = 2 \ln |2 \sin(\pi x)| = 2 \ln |1 - e^{2\pi i x}|. \quad (2.64)$$

2024-02-16 Predrag

$$I(\Lambda) = \int_0^\pi d\theta \ln(1 - 2\Lambda \cos \theta + \Lambda^2) = 2\pi \ln \Lambda, \quad \Lambda \geq 1, \quad (2.65)$$

or

$$I(\Lambda) = \int_0^\pi d\theta \ln(\Lambda + \Lambda^{-1} - 2 \cos \theta) - \pi \ln \Lambda, \quad \Lambda \geq 1.$$

There are lots of derivations:

[Dedalus post](#) is mostly clumsy, but has a drawing that explains where the integrand comes from. I like robjohn's contour integral solution best, see also robjohn in [Julien post](#).

[Moor Xu blog](#) has 5 ways of solving this, including Chebyshev polynomials (not pretty). A physics answer is a point mass falling towards a unit circle mass centered around the origin. He also has contour integral version.

[Gradshteyn and Ryzhik](#) lists the answer as Eq. 4.225 15.

## 2.6 Chebyshev series

Chebyshev series are Fourier (cosine) series in disguise.

— Jason Mireles-James

The canonical reference is Boyd [21] *Chebyshev and Fourier Spectral Methods* ([click here](#)). Perhaps check also:

[Keaton J. Burns](#) *Chebyshev Spectral Methods with applications to Astrophysical Fluid Dynamics*.

Philippe Grandclement [41] *Introduction to spectral methods* [arXiv:gr-qc/0609020](#).

### 2.6.1 Spectral methods

The basic idea of all numerical techniques is to approximate any function  $u(x)$  by polynomials,  $\hat{u} = \sum_{n=0}^N \hat{u}_n p_n(x)$  where the  $p_n(x)$  are polynomial *trial functions*. Depending on the choice of trial functions, one has various classes of numerical techniques. For example, the *finite difference* schemes are obtained by choosing local polynomials of low degree. In *spectral methods* the  $p_n(x)$  are global polynomials, typically Legendre or Chebyshev. Spectral methods can reach very good accuracy with only moderate computational resources; for  $C^\infty$  functions, the error decays exponentially, as one increases the degree of the approximation.

A function  $u$  can be described either by its value  $u(x_i)$  at each collocation point  $x_i$  or by the coefficients  $\tilde{u}_i$  of the *interpolant* of  $u$

$$[I_N u](x) = \sum_{n=0}^N \tilde{u}_n p_n(x). \quad (2.66)$$



The computation of  $\tilde{u}$  only requires evaluation of  $u$  at the  $N + 1$  collocation points. The interpolant of  $u$  is the spectral approximate of  $u$  in terms of polynomials of degree  $N$  that coincide with  $u$  at each collocation point:

$$[I_N u](x_i) = u(x_i) \quad \forall i \leq N.$$

If the values at collocation points are known one is working in the *configuration space*, and in the *coefficient space* if  $u$  is given in terms of its coefficients.

Depending on the operation one has to perform, one choice of space is usually more suited than the other. The derivative of  $u$  can be evaluated in the coefficient space by approximating  $u'$  by the derivative of the interpolant,

$$u'(x) \approx [I_N u]'(x) = \sum_{n=0}^N \tilde{u}_n p_n'(x).$$

This requires only the knowledge of the coefficients of  $u$  and the derivatives of the basis polynomials. This approximate derivative is not the interpolant of  $u'$ , as the polynomials that represent  $(I_N u)'$  do not coincide with  $u'$  at the collocation points.

## 2.6.2 Discretizing with Chebyshev polynomials

To use Chebyshev series as a basis, one shifts the problem to functions defined over  $x \in [-1, 1]$ , and expands them in Chebyshev polynomial of the first kind  $T_k(x)$

$$\phi(x) = \phi_0 + 2 \sum_{n=1}^{\infty} \phi_n T_n(x), \quad (2.67)$$

where  $T_k(z)$  are defined by 3-term recurrence (16.30).

Expanded as Chebyshev series, the product of functions

$$a(x) = a_0 + 2 \sum_{n=1}^{\infty} a_n T_n(x), \quad b(x) = b_0 + 2 \sum_{n=1}^{\infty} b_n T_n(x),$$

satisfies the Fourier-like convolution formula <sup>14</sup>

$$(a \cdot b)(x) = (a * b)_0 + 2 \sum_{n=1}^{\infty} (a * b)_n T_n(x)$$

where

$$(a * b)_n = \sum_{k_1+k_2=n} a_{|k_1|} b_{|k_2|}, \quad k_1, k_2 \in \mathbb{Z}$$

---

<sup>14</sup>Predrag 2020-06-07: I think of Fourier convolution formula as a statement of the translation invariance condition on matrices, not sure how to think about this.

Chebyshev polynomials are an analogue of the Fourier expansion for non periodic functions on an interval and, as the Chebyshev polynomials of the first kind [21] satisfy

$$T_n(\cos(x)) = \cos(nx), \tag{2.68}$$

they are Fourier series in disguise. Mapping (2.68) geometric interpretation: the  $n$ th Chebyshev polynomial is the projection onto a plane of the function  $y = \cos(nx)$  drawn on a cylinder.

For  $x = 0$ ,  $T_n(1) = 1$ . For  $x = 2\pi k/n$ ,  $k = 0, 1, \dots, n - 1$ ,  $\cos(2\pi k/n)$  is the  $k$ th root of equation

$$T_n(x) - 1 = 0.$$

This equation can be written as a product over the eigenvalues

$$T_n(x) - 1 = 2^{n-1} \prod_{k=0}^{n-1} [x - \cos(2\pi k/n)]. \tag{2.69}$$

Here the coefficient  $2^{n-1}$  comes from matching the coefficient of  $x^n$  term in the definition of  $T_n(x) = \dots + 2^{n-1}x^n$ . For  $x = s/2$ , this is the orbit Jacobian matrix determinant formula

$$N_n = \prod_{k=0}^{n-1} [s - 2 \cos(2\pi k/n)] = 2T_n(s/2) - 2. \tag{2.70}$$

Three different types of partial differential equation solvers [41] are the *Tau-method*, the *collocation method* and the *Galerkin method*.

The basic idea of the Galerkin method is to expand the solution as a linear combinations of polynomials -the *Galerkin basis*- that fulfill the boundary conditions.

The Chebyshev polynomials  $T_n$  are an orthogonal set on  $[-1, 1]$  for the measure  $w = \frac{1}{\sqrt{1-x^2}}$ ,

$$\int_{-1}^1 \frac{T_n T_m}{\sqrt{1-x^2}} dx = \frac{\pi}{2} (1 + \delta_{0n}) \delta_{mn}. \tag{2.71}$$

**2020-06-03 Jason Mireles-James talk**, *Parameterization of unstable manifolds for delay differential equations*: Delay differential equations (DDEs) are important in physical applications where there is a time lag in communication between subsystems. They provide natural examples of infinite dimensional dynamical systems. He discusses Chebyshev spectral numerical methods for computing invariant manifolds for DDEs.

**2020-06-03 Jean-Phillipe Lessard talk**, *Rigorous integration of infinite dimensional dynamical systems via Chebyshev series*: In this talk we introduce recent general methods to rigorously compute solutions of infinite dimensional Cauchy problems. The idea is to expand the solutions in time using

Chebyshev series and use the contraction mapping theorem to construct a neighbourhood about an approximate solution which contains the exact solution of the Cauchy problem. We apply the methods to some semi-linear parabolic partial differential equations (PDEs) and delay differential equations (DDEs).

For my screen grabs from the 2 talks, ([click here](#)).

**2023-09-16 Predrag** Yan and Beck *Distinguished correlation properties of Chebyshev dynamical systems and their generalisations*, [arXiv:2006.06786](#), has lots of cute facts about Chebyshev mappings in dynamical systems and in coupled map lattices.

**2020-06-03 Predrag** We (John Gibson [channelflow.org](#), etc.) use Chebyshev in the wall-normal directions in Navier-Stokes channel flow high-accuracy integrators, as the Laplacian is a banded matrix in the Chebyshev basis. But I do not like them, as they put all wiggles close to the walls, and lots of interesting turbulence is going on in the middle of the channel, around the middle of the  $[-1, 1]$  interval.

Dear Abby, am I just being prejudiced for no good reason?

## 2.7 Cat map blog

2CB

**2016-05-18 Predrag** I start with our 2011 *Notes for cat map* (former *appendStatMnotes.doc* in *dasbuch/book/notes*), to be eventually merged with *chapter/appendStatM.tex*.

**2011-05-14 Jean-Luc Thiffeault** I figured out that the grouping of periodic orbits is crucial, and moreover that there is something delicate with the fixed point of the cat map, which lies on the boundary of Markov boxes.

**2011-05-14 Predrag** For Anosov (linear Anosov?) - Arnol'd cat map - it should work like ton of rocks, but you have to note that because of the periodicity there is one fixed point, not two. If you screw up an early term in the series, then it converges very slowly. I think the Stephen Creagh [24] tested it on weakly nonlinearly perturbed cat map (weakly, so golden-mean grammar is working) and it converged super-exponentially (you know the grammar, flow has bounded hyperbolicity, so weight-truncated cycle expansions are not needed - they perform less well).

**2011-05-14 Jean-Luc Thiffeault** I know how to do it with the Markov partition now, and it works much better. Keep in mind this is a warmup problem: what I really have in mind (with my collaborator Erwan Lanneau [59]) is to compute periodic orbits for Teichmuller flow, where the periodic orbits themselves are actually now pseudo-Anosovs!

**2011-05-16 Hans-Henrik Rugh** The situation as I recall it is roughly as follows:

When you construct the symbolic dynamics you may start by picking one periodic orbit, typically the fixed point  $p = f(p)$  (but the following depends on the choice). You then cut the torus into pieces following  $s/u$ -manifolds until you get a small collection of  $N$  rectangles.

$$R_1, \dots, R_N$$

Associated to this collection you have a transition matrix (for SINGLE rectangles). Now, you also need to construct a transition matrix for PAIRS of rectangles, e.g.  $(R_1, R_2) \rightarrow (R_2, R_1)$  and then TRIPLES of rectangles ...  $(R_1, R_2, R_3) \rightarrow (R_2, R_1, R_3)$ , etc.... These  $k$ 'th - order transitions comes from the fact that there is a fixed point/periodic cycle on the boundary of the Markov partition elements.

You get determinants  $d_k(z)$  for each of these  $k$ 'th-order transition matrices. NB :  $(R_1, R_2) \rightarrow (R_2, R_1)$  is a periodic orbit of prime length 2 even if it represents a fixed point of  $f$ . I think (but is not sure?) that the weights in the determinant are calculated in the same way...

The final determinant is  $d(z) = d_1(z)d_3(z).../(d_2(z)d_4(z)...) if I am not mistaken. This is related to the so-called Manning trick [63] for counting real orbits related to$

$$\det(1 - s) = 1 - \text{tr } s + \text{tr } s \wedge s - \dots$$

where  $s$  is a permutation. What is not obvious is that  $d(z)$  is entire, but it is!

It's a kind of model problem anyway. In more realistic systems I suppose that one may run into the problem of having several orbits on boundaries.

One of the tricky points is to see how such an orbit in the 'higher' order zeta-functions/Fredholm-det.

As mentioned in e.g.  $d_1(z)$  a 'physical' fixed point may appear zero times, or twice, or,...? In  $d_2(z)$  a fixed point may actually appear as a period two orbit, so should be treated as such when looking for cancelling terms.

Great, if you have managed to make it work in practice. I don't think that one can call it a standard trick but one may perhaps get it implicitly from the paper of Ruelle [76]. But it is difficult to digest and even more difficult to convert into computable formulae.

**2018-02-10 Predrag** Manning [63] writes: " According to Bowen [20], a Markov partition is a finite cover of state space by closed subsets called *rectangles*. The rectangles are pairwise disjoint except possibly for the intersection of their boundaries. [...] At the boundaries of the rectangles, that is where they intersect, several periodic points individual rectangles may be mapped to the same periodic point in the full state space. "

" Counting the periodic points involves also certain auxiliary subshifts of finite type to remedy overcounting of points in the boundaries of the rectangles. "

**2011-05-18 Jean-Luc Thiffeault** emailed to Predrag pdf file *Notes on periodic orbit expansions for Teichmüller flow* (saved as *POexp.pdf* in *dasbuch/book/notes/*), which maybe figures out cat map symbolic dynamics. He writes:

“ Updated notes: on page 4-5 I used the Markov boxes to compute the PO expansion. I used a trick to deal with the orbit on the boundary: include several copies of the orbit, but divide by the correct factor. It makes the series very nicely convergent. I don’t know if this is a standard trick but it seems to work well. ”

**2011-05-17 Predrag** It is standard, it is in ChaosBook.org Chapter *Counting*, Sect *Counting cycles*. I introduced it in Roberto Artuso, Erik Aurell and Predrag Cvitanović [8], *Recycling of strange sets: II. applications*, see eq. (4) and Fig. 6, but Manning [63] did it in 1971 (if that’s what he did), and Ruelle [76] at the same time, according to Hans Henrik. ChaosBook says: “Smale [84] conjectured rationality of the zeta functions for Axiom A diffeomorphisms, later proved by Guckenheimer [44] and Manning [63],” and ChaosBook cannot be wrong.

The rule of thumb is that all credit should go to old white male mathematicians whose names one knows how to spell.

The argument is something like this: the correct object, the Fredholm determinant, can be written as ratios of products of skew products (AKA determinants of different dimensions), each one being the not correct object, but historically the first thing written down (dynamical or Ruelle zeta function).

The ones on partition boundaries (what I currently call ‘ridges’) are of lower dimensions, either downstairs or upstairs in these ratios. They account for overcounting of the boundary fixed and periodic points.

ChaosBook does something of that when explaining the relation between Fredholm determinants and dynamical zeta functions, but is so far silent on explicit examples of the Manning multiples. That is why I would really like us to write up the cat map symbolic dynamics simply and elegantly. Jean-Luc is not the only person who has gotten lost here, anybody mathematician who thinks that Arnol’d is the simplest exercise to try sinks precisely at this spot (physicists train on unimodal maps and the 3-disk system, remaining blissfully ignorant of the Manning multiples)

Hans Henrik might have more elegant way of saying this. Vivianne still more elegant.

**2012-03-01 Predrag** I’ve been dreaming about this forever, see for example my post of [2012-03-01], *pipes repository, A letter to our experimental friends*:

“ For large aspect systems I imagine we fit local templates whose 2-dimensional or 3-dimensional volume is concentrated on a region big enough to capture interaction of close-by structures, but small enough not to track weakly interacting ones.

In other words, cover 3-dimensional volume with a finite-size template that tracks a neighborhood for a finite time. It's OK to make it spatially periodic, as long as distance is measured in finite size spatiotemporal windows. That is what we already do when we use unstable periodic orbits - we use temporally-infinite periodic solution (that cannot be seen in experiment) to identify a finite-time neighboring segment of a chaotic trajectory.

It has not been tried, so I might be wrong (again). "

**2016-05-04 Predrag** I am not suggesting that we should study this, but it's something to maybe keep in mind: Slipantschuk, Bandtlow and Just [83], *Complete spectral data for analytic Anosov maps of the torus*, construct a family of analytic hyperbolic diffeomorphisms of the torus (of which Arnol'd cat map is a special case) for which the spectral properties of the associated transfer operator acting on a suitable Hilbert space can be computed explicitly. They introduce an example of an analytic hyperbolic diffeomorphism on the complex unit torus, of which the cat map is a special, linear case. The real representation of the map, Eq. (2) is area-preserving and thus provides an example of a chaotic Hamiltonian system. Unlike the situation for one-dimensional non-invertible maps, here is no distinction between Perron-Frobenius operators and Koopman operators as diffeomorphism is area-preserving.

Note that the eigenvalues of the evolution (transfer) operators come in doublets or quadruplets, presumably because of the discrete symmetries of the unit square.

Just looking at their Figs. 1 is inspirational.

The cat map can always be written as a composition of area preserving orientation reversing linear automorphisms. They define a two-parameter area-preserving family, Eq. (85), and show that measures for such maps, where the determinant of the Jacobian varies, may have fractal properties, see Fig. 2.

**2016-05-16 PC** Weirdly, Wolfram's Weisstein [95] is wrong: what he calls "Lyapunov characteristic exponents" for Arnol'd cat map are certainly not "exponents" but multipliers. Maybe you guys could alert him, ask him to fix it.

The eigenvectors are correct. They are the same for all periodic points and thus parallel: cat map is uniformly hyperbolic (the same stability exponents for all orbits), a nice example of the Anosov Axim A system, with the stable and unstable manifolds transverse everywhere, at the same intersection angle.

**2016-05-16 PC** The boyscout version of ChaosBook Appendix N *Statistical mechanics applications*, Artuso's Sect. N.1 *Diffusion in sawtooth and cat maps* sure merits a read. The pruning rules are given there. Exercise e-Per-P-Cats gives the exact number of  $T$ -periodic points of the cat map.

**2016-05-17 Predrag** I have added for the time being chapter [15](#) *Statistical mechanics applications* from ChaosBook to this blog. Note that there are yet more references to read in the Commentary to the chapter [15](#).

**2016-05-21 Predrag** I had included Percival and Vivaldi [[15](#), [70](#), [71](#)] among the papers to read (search for **2016-05-16 PC**; see remark [15.1](#)). Percival and Vivaldi [[71](#)] *Arithmetical properties of strongly chaotic motions* is about cat maps. ChaosBook material included in sect. ?? might be based on that, but I do not remember now, I had last worked on that section in 1996 :)

Maybe working out exercise ?? to exercise ?? is the fastest way to make sure one understands this symbolic dynamics...

**2016-05-17 Li Han** Uploaded to `siminos/mathematica` two Mathematica notebooks. *CatMap - single cat map symbolic dynamics and statistics* counts the single cat map symbols and determines their statistics. It is interactive and one can modify the parameters and play with it. *CatMap - single cat map periodic orbits and topological zeta functions* verifies the number of periodic orbits and the topological zeta functions for a single cat map.

**2016-05-21 Predrag** Adrien and Rana wondered why are (??) and (??) the same equation. Have a look at the two forms of the [Hénon equation](#) in the ChaosBook Example 3.6. Or see (??) (eq. (2.2) in Percival and Vivaldi [[70](#)]). Does that help in understanding the relation? Once you do, write it up in your reports.

**2016-06-01 Predrag** As no one has written anything down, I am not sure what happened in the rest of the WebEx session, but my impression is that perhaps we should step a step back back and first work through some more introductory material for cat-map dynamics to start making sense. Do not be discouraged - it is all very different in flavor from what one learns in most traditional physics courses (though once you learn the stuff, deep connections to statistical mechanics emerge). My recommendation is that Rana and Adrien work through [week 9](#), [week 10](#), and at least parts of [week 12](#) (skip Chap. 23. Cycle expansions).

Could one of you focus on understanding the cat-map ‘the linear code’ part of Percival and Vivaldi [[70](#)] - perhaps just complete sect. [2.3.6](#) started by me.

The other one could describe the ‘standard’ generating partition code allegedly given in Arnol’d and Avez [[6](#)] and in most of the references in remark [15.1](#), so we all understand what Boris means when he says that code is not good for a study of spatiotemporal chaos.

**2016-07-01 Li Han :**

code: `mathematica/Catmap - single cat map symbol diagram and symbol frequencies.nb`

Single cat map symbol diagram and symbol frequencies. Analytical results of 2-symbol frequencies, up to a gap of 5. Great thanks to the new geometry package in Mathematica 10.

**2016-07-06 Li Han :**

code: *mathematica/Catmap - single cat map symbol diagram and symbol frequencies v2.nb*

Modified the form of matrix  $A$  so that area calculation is easier;  
Added sections for 3-7 symbol frequencies (joint probability).

Total pruning rules for consecutive  $n$  symbols of single Arnol'd cat map,  $s = \text{tr}[A] = 3$ , see table 2.1. Compare with Rana's table ??: the number of inadmissible sequences that she found for  $n_a = 7$  differs.

It would take 12 core\*hours to run all (up to 6 symbols: 1 core\*hour)

**2016-07-10 Rana** I agree with Li Han table 2.1 on the numbers of pruned blocks.

**2016-07-20 Li Han :**

code: *mathematica/Catmap - single cat map symbol diagram and symbol frequencies v3.nb*

Total pruning rules for consecutive  $n$  symbols of single Arnol'd cat map,  $s = \text{tr}[A] = 3$  up to length 12, see table 2.1. Compare with Rana's table ??: the number of inadmissible sequences that she found for  $n_a = 7$  differs.

For  $s = 3$  up to ...:

length 7:  $\approx 1$  Core\*hour

length 10:  $\approx 3$  Core\*days

length 12:  $\approx 15 - 20$  Core\*days

**2016-08-01 Predrag :** According to table 2.1, there is a single new pruning rule for each prime-number period. Li Han lists it as 2, but by the reflection symmetry there is only one. One should really quotient the symmetry, and it is not just by removing overall factor 2 in the table: there are pruning blocks that map into each other by the reflection symmetry, and there are pruning blocks that are self-dual under reflection, giving one pruning rule rather than two in the not-desymmetrized listing of this table.

- Is this surmise something proved by Dyson [33]? Or does Behrends [12, 13] explain it?
- Does this new rule have a simple geometric interpretation, in terms of the inequalities? What is the code of the pruned block?

None of

0, 2, 22, 132, 684, 3164, 13894, 58912, 244678, 1002558, 4073528, 16460290  
= 2(1, 11, 66, 342, 1582, 6947, 29456, 122339, 501279, 2036764, 8230145)



$$0, 2, 8, 2, 30, 2, 70, 16, 198, 2, 528, 2, \dots$$

$$= 2(1, 4, 1, 15, 1, 35, 8, 99, 1, 264, 1, \dots)$$

sequences is in the [On-Line Encyclopedia](#) of Integer Sequences, which is bad news. It means that not only this is a number-theoretic problem that has to do with prime factorization (bad news) but in addition it is not one of the standard number-theoretic problems. Means this is an undecidable problem, unlikely to have any simple explanation. Do not waste any more time on it.

**2018-07-26 Li Han** [lhan629@gmail.com](mailto:lhan629@gmail.com)

Added to the repo my notes [han/catMapItiners.pdf](#) on the cat map symbolic sequence, mostly about the empirical (polynomial) fit of the total and new pruning rules  $\tilde{N}_n$ , table II, which displays the “anomalous” behavior with periodicity of 6, i.e. at

$$n = 2 + 6m = 2, 8, 14, 20, \dots \quad m = 0, 1, 2, 3, \dots$$

At even lengths  $n = 2\ell$  there are always 2 new pruning rules  $\{-1, 0, 0, 0, -1\}$  and (reflection symmetry related sequence)  $\{s - 1, s - 2, s - 2, s - 2, s - 1\}$ .

At  $n = 2$  the anomalous new pruning rules are vanishing.

Still a mystery: why anomalies at 2, 8, 14, ...? and what will be further occurrences? Explicit formula?

Learning some new math theory in progress, mirror symmetry (here of elliptic curve?), topological recursion from random matrix theory, which might give clue to these numbers.

**2018-07-29 Predrag** My interpretation of table 2.1 is that the “anomalous” behavior happens when  $n - 1$  is prime, is now confirmed by  $n - 1 = 3, 5, 7, 11, \dots$  Li Han’s *catMapItiners.pdf* table II, also for  $n - 1 = 13, 17, 19$ . Perhaps even higher, as the table is cut off at the right edge. I do not see what Li Han’s  $n = 2 + 6m$  anomalies are...

**2016-08-15 Predrag** : I need Arnol’d cat map in [ChaosBook.org](#), because an example of a tractable Hamiltonian system is useful, and because so many people refer to it.

I say “stupid” because it is very seductive (as much of number theory is), and totally useless as physics. The moment one goes away from the piece-wise linear (and integer!) cat map to any physical nonlinear flow, all this symbol counting falls apart, and one needs cycle expansions ([ChaosBook.org/course1](#), the 2nd course) to describe the physics. I had **wasted too much time** on number theory in my life to be ever dragged into that again, as sooner or later you discover you are assuming the Riemann Hypothesis holds true :)

**2016-11-11 Predrag** For fun and games with the cat map, check out Hunt and Todd [51, 91] *On the Arnol'd cat map and periodic boundary conditions for planar elongational flow*

**2016-08-11 Predrag** Read Gozzi [39] *Counting periodic trajectories via topological classical mechanics* (click here): " We prove that the number of periodic trajectories of arbitrary period  $T$  on the flow tangent to periodic trajectories in phase space of the same period  $T$ , is equal to the Euler number of the underlying phase-space. This result holds for systems with compact phase-space and isolated periodic orbits. "

Giulietti, Liverani and Pollicott [36] *Anosov flows and dynamical zeta functions* (click here): " We study the Ruelle and Selberg zeta functions for an Anosov flow on a compact smooth manifold. We prove several results, the most remarkable being (a) for  $C^\infty$  flows the zeta function is meromorphic on the entire complex plane; (b) for contact flows satisfying a bunching condition, the zeta function has a pole at the topological entropy and is analytic in a strip to its left; (c) under the same hypotheses as in (b) we obtain sharp results on the number of periodic orbits. " A good paper, deserving a deeper study.

A discussion of determinants of graphs - says that Levins [73] illuminated a connection between the characteristic polynomial and the feedback loops of a sparse matrix: D. Cates Wylie [96] *Linked by loops: Network structure and switch integration in complex dynamical systems*, arXiv:0704.3640 (2007).

Wylie [96]: for the stability of control systems ref. [87] (click here).

**2016-12-12 Predrag** Percival and Vivaldi [70] write: "The linear code described here may be considered as a development of the code used by Bullett [22] for the piecewise linear tent map." But Bullett mentions no tent map, I see nothing there... :) His piecewise linear standard map is the simplest possible area preserving piecewise linear twist homeomorphism of zero flux.

**2016-12-12 Predrag** Beardon, Bullett and Rippon [11] *Periodic orbits of difference equations* (click here) might be of interest.

**2022-05-06 Predrag** Crampin [23] *Piecewise linear recurrence relations* (1992): " A standard method for investigating a second order system, be it recurrence relation or a differential equation, is to reduce it to a first order system in twice as many variables. "

Lyness [62] 2731. *Linear recurrence relations* (1957); cute, probably best ignored...

**2016-12-12 Predrag** Pondering Li Han's undisputable polynomial fits in  $s$  to the (new) pruned blocks  $\tilde{N}_n$ . Li Han now has a set of polynomials that counts the number of pruning rules  $\tilde{N}_n(s)$  for small finite  $n$ , but any  $s$ .

$n$	$N_n$	$\tilde{N}_{n-1}$
2	2	0
3	22	2
4	132	$8 = 2 \cdot 2 \cdot 2$
5	684	2
6	3164	$30 = 2 \cdot 3 \cdot 5$
7	13894	2
8	58912	$70 = 2 \cdot 5 \cdot 7$
9	244678	$16 = 2 \cdot 2 \cdot 2 \cdot 2$
10	1002558	$198 = 2 \cdot 3 \cdot 3 \cdot 11$
11	4073528	2
12	16460290	$528 = 2 \cdot 2 \cdot 2 \cdot 2 \cdot 3 \cdot 11$
13	??	2
14	??	1326
15	??	124
16	??	3410
17	??	2
18	??	9264
19	??	2

Table 2.1:  $N_n$  is the total number of pruned blocks of length  $n = n_a$  for the  $s = 3$  Arnol'd cat map.  $\tilde{N}_n$  is the number of *new* pruned blocks of length  $n_a$ , with all length  $n_a$  blocks that contain shorter pruned blocks already eliminated. Note that (empirically) there is a single new pruning rule for each prime-number period (it is listed as 2 rules, but by the reflection symmetry there is only one).  $n = 14$  to  $n = 19$  added 2018-07-28.

(table 2.1 lists them only for  $s = 3$ , but Li Han has new tables, not included in the blog as yet).

What’s so unique about primes? I think that if cycle period  $n - 1 = p$  is a prime, there is always one “most monotone  $(p + 1)$ -cycle” such that cycle points order themselves monotonically along the spatial coordinate  $q$ ,

$$q_{1/(p+1)} < q_{2/(p+1)} < \dots < q_{p/(p+1)},$$

and one would have to show that this forces  $1 < q_{p/(p+1)}$ , so that one  $(p + 1)$ -cycle is pruned, but all the rest are somehow protected and fall within the unit interval. Keating [55] is all about orbits, so maybe this is explained there - or if not there, maybe in Percival-Vivaldi [71]? Percival and Vivaldi [70] and Boris’ Green’s functions are polynomial functions of  $s$ , so maybe the answer is there already.

What about non-prime periods  $n = p_1 p_2 \dots p_m$ ? Perhaps one has to replace the cat map  $f$  by the commuting set of maps  $f_{p_\ell} = f^{p_\ell}$ , one for each prime, and argue about pruning rules for  $f^n = f_{p_1} \circ f_{p_2} \circ \dots \circ f_{p_m}$ . Will be messy. But while cat map  $f$  is linear in  $s$ ,  $f_p$  are polynomial in  $s$ , and that might lead to Li Han’s polynomials for  $\tilde{N}_n(s)$ .

**2016-05-21, -12-12 Predrag** I had included Bird and Vivaldi [15] *Periodic orbits of the sawtooth maps* among the papers to read, but the paper remained woefully unread. Now Li Han has no choice but to read it :)

They assert that for the Arnol’d cat map there are 11 440 548 orbits of period 20.

Percival and Vivaldi [70] refer to the discrete Laplacian as the “central difference operator.”

The special case  $s = 2$  corresponds to an unperturbed twist map, for which orbits represent uniform motions of a free rotor.

The one-parameter  $s$  family of sawtooth maps (of the 2-torus), within which reside infinitely many Anosov diffeomorphisms. Sawtooth maps are piecewise linear, and for this reason we are able to construct the parameter dependence of the sawtooth orbits explicitly in terms of rational functions with integer coefficients.

(i) for integral  $s$  the sawtooth map reduces to a toral automorphism, and the structure of periodic orbits of such maps is known [71]. They are found to coincide with points having rational coordinates, and can be dealt with using arithmetical techniques, one can locate and count all periodic orbits.

(ii) if an orbit is known for one value of  $s$ , it can be computed for any other value.

We represent orbits as doubly infinite sequences of integers (words), where the integers are drawn from a finite set (alphabet). An orbit is written in terms of the configuration coordinate  $x_t$  alone and is denoted by  $(x_t)$ .

The word we denote by  $(m_t)$ . For  $s > 2$  the code is an isomorphism. For a given  $s$ , the possible values of the  $m_t$  are bounded in magnitude by  $|m_t| \leq \text{Int}(1 + s/2)$ . The itinerary of a given orbit is independent of the parameter. The orbit is recovered by Green's function (2.36):

$$q_t = \frac{1}{\sqrt{D}} \sum_{s \in \mathbb{N}} \frac{1}{\Lambda^{|t-s|}} b_s \quad , \quad (2.72)$$

The leading eigenvalue of the cat map Jacobian matrix  $M$  is given by (2.151). For an  $n$ -cycle  $x_t$  are rational functions of  $\Lambda$ , given by the quotient of two reflexive polynomials (for example,  $P_t(\Lambda) = \Lambda^n P_t(1/\Lambda)$ ),

$$\begin{aligned} x_t &= \Lambda P_t(\Lambda)/Q(\Lambda) \\ P_t(\Lambda) &= \sum_{\tau=1}^{n-1} \Lambda^{n-\tau} (\Lambda m_{t+\tau-1} + m_{t-\tau}) \\ Q(\Lambda) &= (\Lambda^2 - 1) (\Lambda^n - 1) \end{aligned} \quad (2.73)$$

Bird and Vivaldi [15] then discuss pruning, give formulas for the numbers of orbits for integer  $s$ , etc.. Most likely Li Han's polynomials are implicit in these formulas.

**2016-12-15 Predrag to Roberto, Going catty:** What is the main question? **My Question of the Day** is:

In ChaosBook Diffusion chapter we show that whenever the critical point of the 1D sawtooth map (the rightmost highest point) is pre-periodic, we have finite grammar and an analytic cycle expansion formula (essentially the topological zeta function, with the uniform expansion rate stuck into  $z^n$ ) for the diffusion constant.

As far as I can tell, both you and Boris ignore the issues of the grammar, get some long-time limit estimate of the diffusion constant.

Usually in 2D there is a fractal set of critical points (AKA pruning front) - we had worked it out for the Lozi map and the Hénon map. If the strange set is a strange repeller, there we have infinitely many examples of finite grammars. But it never happens for non-repelling sets, like the cat map for integer trace  $s$ . There there is a new (only one!) pruning rule for each prime period set of cycles (ie, are we on the way to prove Riemann conjecture?) and a messy set of rules for non-prime periods (which can be described by a polynomial in  $s$ ).

**The Question:** Is the cat map pruning front a fractal set? Is there a systematic set of formulas for the diffusion constant, one for each set of grammar rules? Is this implicit in papers of Vivaldi and/or Keating?

I'm attaching the list of table 2.1, generated by Li Han. He (and not only he) operates on a different astral plane, so getting him to commit his results to our blog or draft of the paper is harder than pulling teeth . He

has the grammar rules count to length 17 and the polynomials in  $s$ , but that I have only seen on his laptop screen.

PS - I am throwing in for a good measure a tent map, sect. 1.3, to illustrate what these polynomials in the stretching rate ( $s$  for cat,  $\Lambda$  for tent) are.

Now, what was YOUR main question that is still blowing in the wind?

**2016-12-12 Roberto Artuso** The main question, as I thought of it in my work of many years ago [10] (see ChaosBook.org Appendix *Statistical mechanics applications*, included in this blog as chapter 15), was to understand the behavior of  $D$  as  $K \rightarrow 0$ , since it seems to get an extra factor  $D \sim K^{2.5}$ , while  $D \sim K^2$  is the usual quasilinear result. The Percival-Vivaldi linear code seemed to me appealing since it selects allowed itineraries within a sort of rhombus in many dimensions, and the symbols are directly linked to transport, while usual Markov partitions for integer  $K$  are not. My thought was that non-integer  $K$  behavior could be linked to the number of lattice points within the "rhombus", and that the  $K$  correction (as well as oscillations with respect to quasilinear estimate), could be related to estimates of errors in volumes *vs.* number of lattice points (something like Dyson-Bleher [16–19] work for ellipses).

**2017-09-29 Predrag Vienti** [92] *Ergodic properties of the discontinuous sawtooth map* might be worthy of a read.

**2017-09-27 Predrag Vallejos and Saraceno** [93] *The construction of a quantum Markov partition* (1999), present in Figure 6 the 5-rectangles Markov partition of the Arnol'd cat map of Adler-Weiss [3] *Similarity of automorphisms of the torus*. Work it out for our  $A'$ .

The three regions partition of the cat map is explained at length in [Tabrizian's](#) notes.

[Chernov](#) (see his Fig. 1) writes: "If the matrix  $A'$  is not symmetric, the stable and unstable lines for on the torus may not be orthogonal. Then, the atoms of Markov partitions are, geometrically, parallelograms rather than rectangles. In early works on Markov partitions [81], the term 'parallelogram' was used instead of 'rectangle'.

Check also [Nonnenmacher](#) notes, and the Sect. 5 of [Huntsman's](#) paper.

From [math stockexchange](#): A reference would be the Handbook of dynamical systems by Hasselblatt and Katok [47], Volume 1, starting on page 324. The cat map example is on pages 327-328. Another good source is the original paper by Adler-Weiss [2] from 1967 and R. Bowen's paper on Axiom A from 1970. Constructing Markov partitions for higher dimensional tori is much more complicated, as the borders of their atoms are fractal and not differentiable, hence the nice rectangles only happen to exist in 2 dimensions.

The two and  $M$  regions partition of the cat map are drawn in [Vorobets'](#) lecture.

Here is a beautifully laid out [problem set](#).

For a cat map, the SRB measure is just the Lebesgue measure, which also serves as a probability measure.

[Bruin](#), in his Sect. 12 discussion of *Toral automorphisms*, asserts that Arnol'd didn't seem to like cats. So, never ever forget to blame the [cat](#). Whatever you do, the cat will be [back](#).

**2018-02-11 Predrag** Ignore the following cryptic remark about symbolic dynamics intrinsic to being in the stable / unstable manifolds coordinates: The symbolic dynamics is 2-dimensional: a partition can be  $\{\text{left, right}\} = \{L, R\}$  with respect to the unstable eigendirection through the origin, and  $\{\text{up, down}\} = \{U, D\}$  with respect to the stable eigendirection, so partitions are labeled by pairs of symbols (the canonical Arn 3-letter alphabet)

$$\{h_j, v_j\} \in \{RU, LU, RD\},$$

with  $\{LD\}$  forbidden.

**2012-01-15 Predrag** Read Jézéquel [54] *Global trace formula for ultra-differentiable Anosov flows*: “[...] we prove that a trace formula that holds for Anosov flows in a certain class of regularity. The main ingredient of the proof is the construction of a family of anisotropic Hilbert spaces of generalized distributions on which the generator of the flow has discrete spectrum.

**2020-03-28 Predrag** Weijie Chen solves the temporal cat pedagogically in his lecture notes ([click here](#)), sect. 2 *Second-Order Difference Equation*.

## Commentary

**Remark 2.1.** Phase space. The cylinder phase is  $[-1/2, 1/2) \times \mathbb{R}$ : the map is originally defined in  $[-1/2, 1/2)^2$ , and is generalized over the cylinder by symmetry requirements. <sup>15</sup>

**Remark 2.2.** Pythagorean tiling or *two squares tessellation* is a tiling of a Euclidean plane by squares of two different sizes, in which each square touches four squares of the other size on its four sides (see [wikipedia.org/wiki/Pythagorean\\_tiling](http://wikipedia.org/wiki/Pythagorean_tiling)). This tiling has four-way rotational symmetry around each of its squares. When the ratio of the side lengths of the two squares is an irrational number such as the golden ratio, its cross-sections form aperiodic sequences with a Fibonacci-type recursive structure. It has a cyclic set of symmetries around the corresponding points, giving it **p4** symmetry: square lattice, point group  $C_4$ , two rotation centres of order four ( $90^\circ$ ), and one rotation centre of order two ( $180^\circ$ ). It has no reflections or glide reflections. It is a chiral pattern, meaning that it is impossible to superpose it on top of its mirror image using only translations and rotations; a Pythagorean tiling is not symmetric under mirror reflections. Although a Pythagorean tiling is itself periodic (it has a square lattice of

<sup>15</sup>Predrag 2016-08-03: missing eq. refeqtra-sym reference.

translational symmetries) its cross sections can be used to generate one-dimensional aperiodic sequences.

**Remark 2.3.** Symmetries of the symbol square. For a discussion of symmetry lines of [example 3.6](#) see refs. [[42](#), [43](#), [67](#), [74](#), [78](#)]. It is an open question (see remark ??) as to how time reversal symmetry can be exploited for reduction of cycle expansions of chapter ?. For example, the fundamental domain symbolic dynamics for reflection symmetric systems is discussed in some detail in [sect. 6.11](#), but how does one recode from time-reversal symmetric symbol sequences to desymmetrized  $1/2$  state space symbols? In discussion of [example 3.5](#), we have followed refs. [[32](#), [37](#), [88](#)].<sup>16</sup>

**Remark 2.4.** XXX.

## References

- [1] R. L. Adler, “Symbolic dynamics and Markov partitions”, *Bull. Amer. Math. Soc.* **35**, 1–56 (1998).
- [2] R. L. Adler and B. Weiss, “Entropy, a complete metric invariant for automorphisms of the torus”, *Proc. Natl. Acad. Sci. USA* **57**, 1573–1576 (1967).
- [3] R. L. Adler and B. Weiss, *Similarity of Automorphisms of the Torus* (Amer. Math. Soc., Providence RI, 1970).
- [4] A. Aitken, *Determinants & Matrices* (Oliver & Boyd, Edinburgh, 1939).
- [5] D. V. Anosov, A. V. Klimenko, and G. Kolutsky, *On the hyperbolic automorphisms of the 2-torus and their Markov partitions*, 2008.
- [6] V. I. Arnol’d and A. Avez, *Ergodic Problems of Classical Mechanics* (Addison-Wesley, Redwood City, 1989).
- [7] M. Artin and B. Mazur, “On periodic points”, *Ann. Math.* **81**, 82–99 (1965).
- [8] R. Artuso, E. Aurell, and P. Cvitanović, “Recycling of strange sets: II. Applications”, *Nonlinearity* **3**, 361–386 (1990).
- [9] R. Artuso and P. Cvitanović, “Deterministic diffusion”, in *Chaos: Classical and Quantum*, edited by P. Cvitanović, R. Artuso, R. Mainieri, G. Tanner, and G. Vattay (Niels Bohr Inst., Copenhagen, 2023).
- [10] R. Artuso and R. Strepparava, “Recycling diffusion in sawtooth and cat maps”, *Phys. Lett. A* **236**, 469–475 (1997).
- [11] A. F. Beardon, S. R. Bullett, and P. J. Rippon, “Periodic orbits of difference equations”, *Proc. Roy. Soc. Edinburgh Sect. A* **125**, 657–674 (1995).
- [12] E. Behrends, “The ghosts of the cat”, *Ergod. Theor. Dynam. Syst.* **18**, 321–330 (1998).

<sup>16</sup>Predrag 2021-04-03: Improve references; eventually return to ChaosBook *cycles.tex*.



- [13] E. Behrends and B. Fielder, “Periods of discretized linear Anosov maps”, *Ergod. Theor. Dynam. Syst.* **18**, 331–341 (1998).
- [14] T. H. Berlin and M. Kac, “The spherical model of a ferromagnet”, *Phys. Rev.* **86**, 821–835 (1952).
- [15] N. Bird and F. Vivaldi, “Periodic orbits of the sawtooth maps”, *Physica D* **30**, 164–176 (1988).
- [16] P. Bleher, “Trace formula for quantum integrable systems, lattice-point problem, and small divisors”, in *Emerging Applications of Number Theory*, edited by D. A. Hejhal, J. Friedman, M. C. Gutzwiller, and A. M. Odlyzko (Springer, 1999), pp. 1–38.
- [17] P. M. Bleher and F. J. Dyson, “Mean square limit for lattice points in a sphere”, *Acta Arith.* **68**, 383–393 (1994).
- [18] P. M. Bleher and F. J. Dyson, “Mean square value of exponential sums related to representation of integers as sum of two squares”, *Acta Arith.* **68**, 71–84 (1994).
- [19] P. M. Bleher and F. J. Dyson, “The variance of the error function in the shifted circle problem is a wild function of the shift”, *Commun. Math. Phys.* **160**, 493–505 (1994).
- [20] R. Bowen, “Markov partitions for Axiom A diffeomorphisms”, *Amer. J. Math.* **92**, 725–747 (1970).
- [21] J. P. Boyd, *Chebyshev and Fourier Spectral Methods*, 2nd ed. (Dover, New York, 2000).
- [22] S. Bullett, “Invariant circles for the piecewise linear standard map”, *Commun. Math. Phys.* **107**, 241–262 (1986).
- [23] M. Crampin, “Piecewise linear recurrence relations”, *Math. Gaz.* **76**, 355–359 (1992).
- [24] S. C. Creagh, “Quantum zeta function for perturbed cat maps”, *Chaos* **5**, 477–493 (1995).
- [25] J. Crutchfield, *Roadmap for Natural Computation and Self-Organization*, tech. rep., Physics 256A course (U. California, Davis, 2017).
- [26] P. Cvitanović, “Counting”, in *Chaos: Classical and Quantum* (Niels Bohr Inst., Copenhagen, 2023).
- [27] P. Cvitanović, R. Artuso, R. Mainieri, G. Tanner, and G. Vattay, *Chaos: Classical and Quantum* (Niels Bohr Inst., Copenhagen, 2024).
- [28] P. Cvitanović, R. Artuso, L. Rondoni, and E. A. Spiegel, “Transporting densities”, in *Chaos: Classical and Quantum*, edited by P. Cvitanović, R. Artuso, R. Mainieri, G. Tanner, and G. Vattay (Niels Bohr Inst., Copenhagen, 2023).
- [29] P. J. Davis, *Circulant Matrices*, 2nd ed. (Amer. Math. Soc., Providence RI, 1979).

- [30] R. L. Devaney, *An Introduction to Chaotic Dynamical systems*, 2nd ed. (Westview Press, Cambridge, Mass, 2008).
- [31] M. Dow, “Explicit inverses of Toeplitz and associated matrices”, *ANZIAM J.* **44**, E185–E215 (2003).
- [32] H. R. Dullin, J. D. Meiss, and D. G. Sterling, “Symbolic codes for rotational orbits”, *SIAM J. Appl. Dyn. Sys.* **4**, 515–562 (2005).
- [33] F. J. Dyson and H. Falk, “Period of a discrete cat mapping”, *Amer. Math. Monthly* **99**, 603–614 (1992).
- [34] S. Elaydi, *An Introduction to Difference Equations*, 3rd ed. (Springer, Berlin, 2005).
- [35] M. Elouafi, “On a relationship between Chebyshev polynomials and Toeplitz determinants”, *Appl. Math. Comput.* **229**, 27–33 (2014).
- [36] P. Giulietti, C. Liverani, and M. Pollicott, “Anosov flows and dynamical zeta functions”, *Ann. Math.* **178**, 687–773 (2013).
- [37] A. Gómez and J. D. Meiss, “Reversible polynomial automorphisms of the plane: The involutory case”, *Phys. Lett. A* **312**, 49–58 (2003).
- [38] M. J. C. Gover, “The eigenproblem of a tridiagonal 2-Toeplitz matrix”, *Linear Algebra Appl.* **197**, 63–78 (1994).
- [39] E. Gozzi, “Counting periodic trajectories via topological classical mechanics”, *Chaos Solit. Fract.* **4**, 653–660 (1994).
- [40] I. S. Gradshteyn and I. M. Ryzhik, *Tables of Integrals, Series and Products*, 8th ed. (Elsevier LTD, Oxford, New York, 2014).
- [41] P. Grandclément, “Introduction to spectral methods”, *EAS Publications Series* **21**, 153–180 (2006).
- [42] J. M. Greene, “A method for determining a stochastic transition”, *J. Math. Phys.* **20**, 1183–1201 (1979).
- [43] J. M. Greene, R. S. MacKay, F. Vivaldi, and M. J. Feigenbaum, “Universal behaviour in families of area-preserving maps”, *Physica D* **3**, 468–486 (1981).
- [44] J. Guckenheimer, “On the bifurcation of maps of the interval”, *Inv. Math.* **39**, 165–178 (1977).
- [45] B. Gutkin, L. Han, R. Jafari, A. K. Saremi, and P. Cvitanović, “Linear encoding of the spatiotemporal cat map”, *Nonlinearity* **34**, 2800–2836 (2021).
- [46] J. H. Hannay and M. V. Berry, “Quantization of linear maps on a torus – Fresnel diffraction by a periodic grating”, *Physica D* **1**, 267–290 (1980).
- [47] B. Hasselblatt and A. Katok, *Handbook of Dynamical Systems* (Elsevier, New York, 2002).
- [48] G. Y. Hu and R. F. O’Connell, “Exact solution for the charge soliton in a one-dimensional array of small tunnel junctions”, *Phys. Rev. B* **49**, 16773–16776 (1994).

- [49] G. Y. Hu and R. F. O’Connell, “Exact solution of the electrostatic problem for a single electron multijunction trap”, *Phys. Rev. Lett.* **74**, 1839–1842 (1995).
- [50] G. Y. Hu and R. F. O’Connell, “Analytical inversion of symmetric tridiagonal matrices”, *J. Phys. A* **29**, 1511 (1996).
- [51] T. A. Hunt and B. D. Todd, “On the Arnold cat map and periodic boundary conditions for planar elongational flow”, *Molec. Phys* **101**, 3445–3454 (2003).
- [52] S. Isola, “ $\zeta$ -functions and distribution of periodic orbits of toral automorphisms”, *Europhys. Lett.* **11**, 517–522 (1990).
- [53] S. Jaidee, P. Moss, and T. Ward, “Time-changes preserving zeta functions”, *Proc. Amer. Math. Soc.* **147**, 4425–4438 (2019).
- [54] M. Jézéquel, “Global trace formula for ultra-differentiable Anosov flows”, *Commun. Math. Phys.* **385**, 1771–1834 (2021).
- [55] J. P. Keating, “Asymptotic properties of the periodic orbits of the cat maps”, *Nonlinearity* **4**, 277 (1991).
- [56] J. P. Keating, “The cat maps: quantum mechanics and classical motion”, *Nonlinearity* **4**, 309–341 (1991).
- [57] J. P. Keating and F. Mezzadri, “Pseudo-symmetries of Anosov maps and spectral statistics”, *Nonlinearity* **13**, 747–775 (2000).
- [58] H. Kübra Duru and D. Bozkurt, *Integer powers of certain complex pentadiagonal 2-Toeplitz matrices*, 2017.
- [59] E. Lanneau and J.-L. Thiffeault, “On the minimum dilatation of pseudo-Anosov homeomorphisms on surfaces of small genus”, *Ann. Inst. Fourier* **61**, 105–144 (2011).
- [60] D. H. Lehmer, “Factorization of certain cyclotomic functions”, *Ann. of Math. (2)* **34**, 461–479 (1933).
- [61] H. Liang and P. Cvitanović, “A chaotic lattice field theory in one dimension”, *J. Phys. A* **55**, 304002 (2022).
- [62] R. C. Lyness, “2731. linear recurrence relations”, *Math. Gaz.* **41**, 285–287 (1957).
- [63] A. Manning, “Axiom A diffeomorphisms have rational zeta function”, *Bull. London Math. Soc.* **3**, 215–220 (1971).
- [64] A. Manning, “A Markov partition that reflects the geometry of a hyperbolic toral automorphism”, *Trans. Amer. Math. Soc.* **354**, 2849–2864 (2002).
- [65] B. D. Mestel and I. Percival, “Newton method for highly unstable orbits”, *Physica D* **24**, 172 (1987).
- [66] C. Meyer, *Matrix Analysis and Applied Linear Algebra* (SIAM, Philadelphia, 2000).

- [67] C. Mira, *Chaotic dynamics – From one dimensional endomorphism to two dimensional diffeomorphism* (World Scientific, Singapore, 1987).
- [68] S. Noschese, L. Pasquini, and L. Reichel, “Tridiagonal Toeplitz matrices: properties and novel applications”, *Numer. Linear Algebra Appl.* **20**, 302–326 (2013).
- [69] A. M. Ozorio de Almeida and J. H. Hannay, “Periodic orbits and a correlation function for the semiclassical density of states”, *J. Phys. A* **17**, 3429 (1984).
- [70] I. Percival and F. Vivaldi, “A linear code for the sawtooth and cat maps”, *Physica D* **27**, 373–386 (1987).
- [71] I. Percival and F. Vivaldi, “Arithmetical properties of strongly chaotic motions”, *Physica D* **25**, 105–130 (1987).
- [72] T. A. Pierce, “The numerical factors of the arithmetic forms  $\prod(1 \pm \alpha_i^m)$ ”, *Ann. of Math. (2)* **18**, 53–64 (1916).
- [73] C. Puccia and R. Levins, *Qualitative Modeling of Complex Systems: An Introduction to Loop Analysis and Time Averaging* (Harvard Univ. Press, 1985).
- [74] P. H. Richter, H.-J. Scholz, and A. Wittek, “A breathing chaos”, *Nonlinearity* **3**, 45–67 (1990).
- [75] R. C. Robinson, *An Introduction to Dynamical Systems: Continuous and Discrete* (Amer. Math. Soc., New York, 2012).
- [76] D. Ruelle, “An extension of the theory of Fredholm determinants”, *Inst. Hautes Études Sci. Publ. Math.* **72**, 175–193 (1990).
- [77] E. Rykken, “Markov partitions for hyperbolic toral automorphisms of  $T^2$ ”, *Rocky Mountain J. Math.* **28**, 1103–1124 (1998).
- [78] S. J. Shenker and L. P. Kadanoff, “Critical behavior of a KAM surface: i. Empirical results”, *J. Stat. Phys.* **27**, 631–656 (1982).
- [79] A. Siemaszko and M. P. Wojtkowski, “Counting Berg partitions”, *Nonlinearity* **24**, 2383–2403 (2011).
- [80] S. Simons, “Analytical inversion of a particular type of banded matrix”, *J. Phys. A* **30**, 755 (1997).
- [81] Y. G. Sinai, “Construction of Markov partitions”, *Funct. Anal. Appl.* **2**, 245–253 (1968).
- [82] Y. G. Sinai, *Introduction to Ergodic Theory* (Princeton Univ. Press, Princeton NJ, 1976).
- [83] J. Slipantschuk, O. F. Bandtlow, and W. Just, “Complete spectral data for analytic Anosov maps of the torus”, *Nonlinearity* **30**, 2667 (2017).
- [84] S. Smale, “Generalized Poincaré’s conjecture in dimensions greater than four”, *Ann. Math.* **74**, 199 (1961).

- [85] G. D. Smith, *Numerical Solution of Partial Differential Equations: Finite Difference Methods* (Clarendon Press, Oxford UK, 1985).
- [86] M. R. Snavely, "Markov partitions for the two-dimensional torus", *Proc. Amer. Math. Soc.* **113**, 517–517 (1991).
- [87] E. D. Sontag, *Mathematical Control Theory: Deterministic Finite Dimensional Systems* (Springer, New York, 1998).
- [88] D. G. Sterling, H. R. Dullin, and J. D. Meiss, "Homoclinic bifurcations for the Hénon map", *Physica D* **134**, 153–184 (1999).
- [89] R. F. Streater, "A bound for the difference Laplacian", *Bull. London Math. Soc.* **11**, 354–357 (1979).
- [90] R. Sturman, J. M. Ottino, and S. Wiggins, *The Mathematical Foundations of Mixing* (Cambridge Univ. Press, 2006).
- [91] B. D. Todd, "Cats, maps and nanoflows: some recent developments in nonequilibrium nanofluidics", *Molec. Simul.* **31**, 411–428 (2005).
- [92] S. Vaienti, "Ergodic properties of the discontinuous sawtooth map", *J. Stat. Phys.* **67**, 251–269 (1992).
- [93] R. O. Vallejos and M. Saraceno, "The construction of a quantum Markov partition", *J. Phys. A* **32**, 7273 (1999).
- [94] P. Walters, *An Introduction to Ergodic Theory* (Springer, New York, 1982).
- [95] E. W. Weisstein, *Arnold's Cat Map*, MathWorld—A Wolfram Web Resource.
- [96] D. C. Wylie, "Linked by loops: Network structure and switch integration in complex dynamical systems", *Physica A* **388**, 1946–1958 (2009).
- [97] H. A. Yamani and M. S. Abdelmonem, "The analytic inversion of any finite symmetric tridiagonal matrix", *J. Phys. A* **30**, 2889 (1997).
- [98] W.-C. Yueh, "Explicit inverses of several tridiagonal matrices", *Appl. Math. E-Notes* **6**, 74–83 (2006).

## 2.8 Examples

**Example 2.1. Projection operator decomposition of the cat map:** Let's illustrate how the decomposition works for the Percival-Vivaldi [70] "two-configuration representation" of the Arnol'd cat map by the  $[2 \times 2]$  matrix

$$\mathbf{A} = \begin{bmatrix} 0 & 1 \\ -1 & s \end{bmatrix}. \quad (2.74)$$

To interpret  $m_n$ 's, consider the action of the this map (2.80) on a 2-dimensional state space point  $(x_{n-1}, x_n)$ ,

$$\begin{pmatrix} x_n \\ x_{n+1} \end{pmatrix} = \mathbf{A} \begin{pmatrix} x_{n-1} \\ x_n \end{pmatrix} - \begin{pmatrix} 0 \\ m_n \end{pmatrix}. \quad (2.75)$$

In Percival and Vivaldi [70] this representation of cat map is referred to as "the two-configuration representation". As illustrated in figure 2.2, in one time step the area preserving map  $A'$  stretches the unit square into a parallelogram, and a point  $(x_0, x_1)$  within the initial unit square in general lands outside it, in another unit square  $m_n$  steps away. As they shepherd such stray points back into the unit torus, the integers  $m_n$  can be interpreted as "winding numbers" [56], or "stabilising impulses" [70]. The  $m_n$  translations reshuffle the state space, thus partitioning it into  $|\mathcal{A}|$  regions  $\mathcal{M}_m, m \in \mathcal{A}$ .

Associated with each root  $\Lambda^i$  in (??) is the projection operator  $P^i = \prod (\mathbf{A} - \Lambda^j \mathbf{1}) / (\Lambda^i - \Lambda^j), j \neq i$ ,

$$P^+ = \frac{1}{\sqrt{D}} (\mathbf{A} - \Lambda^{-1} \mathbf{1}) = \frac{1}{\sqrt{D}} \begin{bmatrix} -\Lambda^{-1} & 1 \\ -1 & \Lambda \end{bmatrix} \quad (2.76)$$

$$P^- = -\frac{1}{\sqrt{D}} (\mathbf{A} - \Lambda \mathbf{1}) = \frac{1}{\sqrt{D}} \begin{bmatrix} \Lambda & -1 \\ 1 & -\Lambda^{-1} \end{bmatrix}. \quad (2.77)$$

Matrices  $P^\pm$  are orthonormal and complete. The dimension of the  $i$ th subspace is given by  $d_i = \text{tr } P_i$ ; in case at hand both subspaces are 1-dimensional. From the characteristic equation it follows that  $P^\pm$  satisfy the eigenvalue equation  $\mathbf{A} P^\pm = \Lambda^\pm P^\pm$ , with every column a right eigenvector, and every row a left eigenvector. Picking –for example– the first row/column we get the right and the left eigenvectors:

$$\begin{aligned} \{\mathbf{e}^{(+)}, \mathbf{e}^{(-)}\} &= \left\{ \frac{1}{\sqrt{D}} \begin{bmatrix} -\Lambda^{-1} \\ -1 \end{bmatrix}, \frac{1}{\sqrt{D}} \begin{bmatrix} \Lambda \\ 1 \end{bmatrix} \right\} \\ \{\mathbf{e}_{(+)}, \mathbf{e}_{(-)}\} &= \left\{ \frac{1}{\sqrt{D}} [-\Lambda^{-1}, 1], \frac{1}{\sqrt{D}} [\Lambda, -1] \right\}, \end{aligned} \quad (2.78)$$

with overall scale arbitrary.<sup>17</sup> The matrix is not symmetric, so  $\{\mathbf{e}^{(j)}\}$  do not form an orthogonal basis. The left-right eigenvector dot products  $\mathbf{e}_{(j)} \cdot \mathbf{e}^{(k)}$ , however, are orthogonal,

$$\mathbf{e}_{(i)} \cdot \mathbf{e}^{(j)} = c_j \delta_{ij}.$$

What does this do to the partition figure 2.2? The origin is still the fixed point. A state space point in the new, dynamically intrinsic right eigenvector Adler-Weiss [3] coordinate basis is

$$\begin{pmatrix} x_{n-1} \\ x_n \end{pmatrix} = (P^+ + P^-) \begin{pmatrix} x_{n-1} \\ x_n \end{pmatrix}$$

<sup>17</sup>Predrag 2017-10-02: compare with (2.22)

$$\begin{aligned}
 &= \frac{1}{\sqrt{D}} \begin{bmatrix} -\Lambda^{-1} & 1 \\ -1 & \Lambda \end{bmatrix} \begin{pmatrix} x_{n-1} \\ x_n \end{pmatrix} + \frac{1}{\sqrt{D}} \begin{bmatrix} \Lambda & -1 \\ 1 & -\Lambda^{-1} \end{bmatrix} \begin{pmatrix} x_{n-1} \\ x_n \end{pmatrix} \\
 &= \frac{1}{\sqrt{D}} \begin{pmatrix} x_n - \Lambda^{-1}x_{n-1} \\ \Lambda x_n - x_{n-1} \end{pmatrix} + \frac{1}{\sqrt{D}} \begin{pmatrix} -x_n + \Lambda x_{n-1} \\ -\Lambda^{-1}x_n + x_{n-1} \end{pmatrix} \\
 &= -(\Lambda x_n - x_{n-1}) \frac{1}{\sqrt{D}} \begin{bmatrix} -\Lambda^{-1} \\ -1 \end{bmatrix} + (-\Lambda^{-1}x_n + x_{n-1}) \frac{1}{\sqrt{D}} \begin{bmatrix} \Lambda \\ 1 \end{bmatrix} \\
 &= (-\Lambda x_n + x_{n-1}) P^+ + (-\Lambda^{-1}x_n + x_{n-1}) P^-.
 \end{aligned}$$

The abscissa ( $x_{n-1}$  direction) is not affected, but the ordinate ( $x_n$  direction) is flipped and stretched/shrunk by factor  $-\Lambda$ ,  $-\Lambda^{-1}$  respectively, preserving the vertical strip nature of the partition figure 2.2. In the Adler-Weiss right eigenbasis,  $\mathbf{A}$  acts by stretching the  $e^{(+)}$  direction by  $\Lambda$ , and shrinking the  $e^{(-)}$  direction by  $\Lambda^{-1}$ , without any rotation of either direction.

**Example 2.2. A linear cat map code.** Eqs. (12.100,12.101) are the discrete-time Hamilton's equations, which induce temporal evolution on the 2-torus  $(x_n, p_n)$  phase space. For the problem at hand, it pays to go from the Hamiltonian  $(x_n, p_n)$  phase space formulation to the Newtonian (or Lagrangian)  $(x_{n-1}, x_n)$  state space formulation [70], with  $p_n$  replaced by  $p_n = (x_n - x_{n-1})/\Delta t$ . Eq. (??) then takes the 3-term recurrence form (the discrete time Laplacian  $\square$  formula for the second order time derivative  $d^2/dt^2$ , with the time step set to  $\Delta t = 1$ ),

$$\square x_n \equiv x_{n+1} - 2x_n + x_{n-1} = P(x_n) \pmod{1}, \quad (2.79)$$

i.e., Newton's Second Law: "acceleration equals force." For a cat map, with force  $P(x)$  linear in the displacement  $x$ , the Newton's equation of motion (2.79) takes form

$$(\square + 2 - s)x_n = -m_n, \quad (2.80)$$

with  $\pmod{1}$  enforced by  $m_n$ 's, integers from the alphabet

$$\mathcal{A} = \{1, 0, \dots, s-1\}, \quad (2.81)$$

necessary to keep  $x_n$  for all times  $t$  within the unit interval  $[0, 1)$ . The genesis of this alphabet is illustrated by figure 2.2. We have introduced here the symbol  $\underline{|m_n|}$  to denote  $m_n$  with the negative sign, i.e.,  $\underline{1}$  stands for symbol  $-1$ '.

**Example 2.3. Perron-Frobenius operator for the Arnol'd cat map.** The two-rectangle partition  $[2 \times 2]$  Markov matrix, where one sums over all admissible transitions, should suffice (for notation, see (24.10) and ref. [28]):

$$\begin{bmatrix} \phi'_A \\ \phi'_B \end{bmatrix} = L\phi = \begin{bmatrix} L_{A^0A} + L_{A^1A} & L_{A^1B} \\ L_{B^1A} & L_{B^0B} \end{bmatrix} \begin{bmatrix} \phi_A \\ \phi_B \end{bmatrix} \quad (2.82)$$

$$\begin{aligned}
 L &= \begin{bmatrix} L_{A^0A} + L_{A^1A} & L_{A^1B} \\ L_{B^1A} & L_{B^0B} \end{bmatrix} = \begin{bmatrix} \frac{|\mathcal{M}_1| + |\mathcal{M}_3|}{|\mathcal{M}_A|} & \frac{|\mathcal{M}_5|}{|\mathcal{M}_A|} \\ \frac{|\mathcal{M}_2|}{|\mathcal{M}_B|} & \frac{|\mathcal{M}_4|}{|\mathcal{M}_B|} \end{bmatrix} \\
 &= \frac{1}{\Lambda} \begin{bmatrix} 2 & \Lambda - 2 \\ \Lambda - 1 & 1 \end{bmatrix}.
 \end{aligned} \quad (2.83)$$

in compact notation  $\{A^0A, B^1A, A^1A, B^0B, A^1B\} = \{1, 2, 3, 4, 5\}$ . Then

$$\begin{aligned} \text{Det}(1 - zL) &= \begin{vmatrix} 1 - 2z/\Lambda & -z(\Lambda - 2)/\Lambda \\ -z(\Lambda - 1)/\Lambda & 1 - z/\Lambda \end{vmatrix} \\ &= 1 - 3\frac{z}{\Lambda} + 2\frac{z^2}{\Lambda^2} - \frac{z^2}{\Lambda^2}(\Lambda - 1)(\Lambda - 2) \\ &= 1 - 3\frac{z}{\Lambda} - \frac{z^2}{\Lambda}(\Lambda - 3), \end{aligned} \quad (2.84)$$

in agreement with the loop expansion (2.89).

**Example 2.4. Perron-Frobenius operator for the Arnol'd cat map.** For a piecewise linear maps acting on a finite generating partition the Perron-Frobenius operator takes the finite, transfer matrix form (see ref. [28]).

$$\mathbf{L}_{ij} = \frac{|\mathcal{M}_i \cap f^{-1}(\mathcal{M}_j)|}{|\mathcal{M}_i|}, \quad \rho' = \rho\mathbf{L} \quad (2.85)$$

The two rectangles and five sub-rectangle areas  $|\mathcal{M}_j|$  are given by inspection of figure 2.10 (a):<sup>18</sup>

$$\begin{aligned} |\mathcal{M}_A| &= \Lambda/(\Lambda + 1), & |\mathcal{M}_B| &= 1/(\Lambda + 1), \\ |\mathcal{M}_1| &= |\mathcal{M}_A|/\Lambda, & |\mathcal{M}_2| &= (\Lambda - 1)|\mathcal{M}_B|/\Lambda, & |\mathcal{M}_3| &= |\mathcal{M}_A|/\Lambda, \\ |\mathcal{M}_4| &= |\mathcal{M}_B|/\Lambda, & |\mathcal{M}_5| &= (\Lambda - 2)|\mathcal{M}_A|/\Lambda, \end{aligned} \quad (2.86)$$

where  $\Lambda$  and  $D$  are given in (??), and we are considering the  $s = 3$  Arnol'd cat map case (the generalization to  $s > 3$ . is immediate) The areas are symplectic invariants, and thus the same in any choice of cat-map coordinates. As in the ChaosBook example exam:FP\_eigs\_Ulam (currently 19.1), the Adler-Weiss partitioned Percival-Vivaldi cat map is an expanding piecewise-linear map, so we can construct the associated transfer matrix explicitly, by weighing the links of transition graph figure 2.10 (a) by the ratios of out-, in-rectangle areas  $T_{kj} = |\mathcal{M}_{m_k}|/|\mathcal{M}_{m_j}|$ :<sup>19</sup>

$$\begin{bmatrix} \phi'_1 \\ \phi'_2 \\ \phi'_3 \\ \phi'_4 \\ \phi'_5 \end{bmatrix} = \mathbf{T}\phi = \frac{1}{\Lambda} \begin{bmatrix} 1 & \Lambda - 2 & 1 & 0 & 0 \\ 0 & 0 & 0 & \Lambda - 1 & 1 \\ 1 & \Lambda - 2 & 1 & 0 & 0 \\ 0 & 0 & 0 & 1 & \Lambda - 1 \\ 1 & \Lambda - 1 & \frac{\Lambda - 2}{\Lambda - 1} & 0 & 0 \end{bmatrix} \begin{bmatrix} \phi_1 \\ \phi_2 \\ \phi_3 \\ \phi_4 \\ \phi_5 \end{bmatrix} \quad (2.87)$$

The probability for starting in initial state  $j$  is conserved,  $\sum_k L_{kj} = 1$ , as it should be. Such non-negative matrix whose columns conserve probability is called Markov, probability or stochastic matrix. Thanks to the same expansion everywhere, and a finite transition graph, the Fredholm determinant is the characteristic polynomial of the transfer matrix (currently ChaosBook Eq. (18.13)) defined by the transition graph of figure 2.1 (c), expanded in non-intersecting loops  $t_A = T_{A^0A}, t'_A = T_{A^1A}, t_B = T_{B^0B}, t_{AB} = T_{A^1B}T_{B^1A}$  :

$$\det(1 - z\mathbf{T}) = 1 - z(t_A + t'_A + t_B) - z^2 t_{AB} + z^2(t_A + t'_A)t_B = 1 - 3\frac{z}{\Lambda} - (\Lambda - 3)\frac{z^2}{\Lambda}, \quad (2.88)$$

<sup>18</sup>Predrag 2018-02-16: to Han: PLEASE RECHECK

<sup>19</sup>Predrag 2018-02-11: the matrix is NOT CORRECT yet, FIX!



$$\det(1 - z\mathbf{T}) = 1 - 3\frac{z}{\Lambda} - (\Lambda - 3)\frac{z^2}{\Lambda}, \quad (2.89)$$

in agreement with (2.11). This counts the fixed point at the origin thrice (it lives in the invariant subspace spanned by stable and unstable manifolds, the border) so that has to be divided out.

Due to probability (unit area) conservation,  $\mathbf{T}$  has a unit eigenvalue  $z = 1 = e^{s_0}$ , with constant density eigenvector  $\rho_0 = \rho_1$ .

In the orbit-counting case one retrieves Isola's  $\zeta$ -function [52] (??).

This simple explicit matrix representation of the Perron-Frobenius operator is a consequence of the piecewise linearity of the time-forward map, and the restriction of the densities  $\rho$  to the space of piecewise constant functions.

**Example 2.5. Counting temporal cat periodic states.**

The temporal cat equation (??) is a linear 2nd-order inhomogeneous difference equation (3-term recurrence relation) with constant coefficients that can be solved by standard methods [34] that parallel the theory of linear differential equations.<sup>20</sup> Inserting a solution of form  $x_t = \Lambda^t$  into the associated ( $m_t=0$ ) homogenous 2nd-order difference equation

$$x_{t+1} - s x_t + x_{t-1} = 0 \quad (2.90)$$

yields the characteristic equation

$$\Lambda^2 - s\Lambda + 1 = 0, \quad (2.91)$$

which, for  $|s| > 2$ , has two real roots  $\{\Lambda, \Lambda^{-1}\}$ ,

$$\Lambda = \frac{1}{2}(s + \sqrt{(s-2)(s+2)}), \quad (2.92)$$

and the so-called complementary solution of form

$$x_{c,t} = a_1 \Lambda^t + a_{-1} \Lambda^{-t}. \quad (2.93)$$

A difference of any pair of solutions to the temporal cat inhomogenous equation (??) is a solution of the homogenous difference equation (2.90), so the general solution is a sum of the complementary solution (2.93) and a particular solution  $x_p$ ,

$$x_t = x_{c,t} + x_{p,t}. \quad (2.94)$$

Eq. (2.90) is time-reversal invariant,  $x_t = x_{-t}$ , so  $a_1 = a_{-1} = a$ . To determine the particular solution, assume that both the source  $m_t = m$  and  $x_{p,t} = x_p$  in (??) are site-independent,

$$x_p - s x_p + x_p = -m, \quad (2.95)$$

so  $x_p = m/(s-2)$ . Hence the solution is

$$x_t = x_{c,t} + x_{p,t} = a(\Lambda^t + \Lambda^{-t}) + m/(s-2), \quad (2.96)$$

with  $a_i$  determined by fields at two lattice sites,

$$x_0 = 2a + m/(s-2), \quad x_1 = a(\Lambda + \Lambda^{-1}) + m/(s-2), \quad .$$

Temporal cat starts with  $N_0 = 0$ , and according to (??),  $N_1 = s-2$ , so  $a = 1$ ,  $m = -2(s-2)$ , and the number of temporal periodic states of period  $n$  is

$$N_n = \Lambda^n + \Lambda^{-n} - 2. \quad (2.97)$$

<sup>20</sup>Predrag 2020-06-10: Comparing with (8.158) we see that we need to solve a second-order inhomogeneous difference equation with a constant forcing term  $2(s-2)$ .

**Example 2.6. Temporal cat shadowing.**

As the relation between the symbol blocks  $M$  and the corresponding periodic states  $X_M$  is linear, for  $M$  an admissible symbol block, the corresponding periodic state  $X_M$  is given by the Green's function

$$X_M = g M, \quad g = \frac{1}{-d + s \mathbf{1} - d^{-1}}, \quad (2.98)$$

as in the Bernoulli case (??).

As in sect. ??, the Green's function (2.98) decays exponentially with the distance from the origin, a fact that is essential in establishing the 'shadowing' between periodic states sharing a common sub-block  $M$ . For an infinite temporal lattice  $t \in \mathbb{Z}$ , the lattice field at site  $t$  is determined by the sources  $m_{t'}$  at all sites  $t'$ , by the Green's function  $g_{tt'}$  for one-dimensional discretized heat equation [65, 70],

$$x_t = \sum_{t'=-\infty}^{\infty} g_{tt'} m_{t'}, \quad g_{tt'} = \frac{1}{\Lambda - \Lambda^{-1}} \frac{1}{\Lambda^{|t-t'|}}, \quad (2.99)$$

with  $\Lambda$  is the expanding stability multiplier defined in (??).

Suppose there is a non-vanishing point source  $m_0 \neq 0$  only at the present,  $t' = 0$  temporal lattice site. Its contribution to  $x_t \sim \Lambda^{-|t|}$  decays exponentially with the distance from the origin. More generally, as in the Bernoulli case (1.43), if two periodic states  $X, X'$  share a common sub-block  $M$  of length  $n$ , they shadow each other with accuracy of order of  $O(1/\Lambda^n)$ .

[click to return: p. 51](#)

**Example 2.7. Two-degrees of freedom Hamiltonian flows:** <sup>21</sup> For a 2-degrees of freedom Hamiltonian flow the energy conservation eliminates one phase-space variable, and restriction to a Poincaré section eliminates the marginal longitudinal eigenvalue  $\Lambda = 1$ , so a periodic orbit of 2-degrees of freedom hyperbolic Hamiltonian flow (or of a 1-degree of freedom hyperbolic Hamiltonian map) has one expanding transverse eigenvalue  $\Lambda, |\Lambda| > 1$ , and one contracting transverse eigenvalue  $1/\Lambda$ . The weight in (??) is expanded as follows:

$$\frac{1}{|\det(\mathbf{1} - M_p^r)|} = \frac{1}{|\Lambda|^r (1 - 1/\Lambda_p^r)^2} = \frac{1}{|\Lambda|^r} \sum_{k=0}^{\infty} \frac{k+1}{\Lambda_p^{kr}}. \quad (2.100)$$

The spectral determinant exponent can be resummed,

$$-\sum_{r=1}^{\infty} \frac{1}{r} \frac{e^{(\beta A_p - s T_p)r}}{|\det(\mathbf{1} - M_p^r)|} = \sum_{k=0}^{\infty} (k+1) \log \left( 1 - \frac{e^{\beta A_p - s T_p}}{|\Lambda_p| \Lambda_p^k} \right),$$

and the spectral determinant for a 2-dimensional hyperbolic Hamiltonian flow rewritten as an infinite product over orbits

$$\det(s - \mathcal{A}) = \prod_p \prod_{k=0}^{\infty} \left( 1 - t_p / \Lambda_p^k \right)^{k+1}. \quad (2.101)$$

<sup>22</sup>

exercise ??

[click to return: p. ??](#)

<sup>21</sup>Predrag 2018-12-13: if edited, return to ChaosBook

<sup>22</sup>Predrag 2015-03-09: state here also the  $d$ -dimensional result ala Gaspard

**Example 2.8. Dynamical zeta function in terms of determinants, 2-dimensional Hamiltonian maps:** <sup>23</sup> For 2-dimensional Hamiltonian flows the above identity yields <sup>24</sup>

$$\frac{1}{|\Lambda|} = \frac{1}{|\Lambda|(1-1/\Lambda)^2} (1 - 2/\Lambda + 1/\Lambda^2),$$

so

$$1/\zeta = \frac{\det(1 - z\mathcal{L}) \det(1 - z\mathcal{L}_{(2)})}{\det(1 - z\mathcal{L}_{(1)})^2}. \quad (2.102)$$

<sup>25</sup> This establishes that for nice 2-dimensional hyperbolic flows the dynamical zeta function is meromorphic. <sup>26</sup>

[click to return: p. ??](#)

**Example 2.9. Dynamical zeta functions for 2-dimensional Hamiltonian flows:** <sup>27</sup> The relation (2.102) is not particularly useful for our purposes. Instead we insert the identity

$$1 = \frac{1}{(1-1/\Lambda)^2} - \frac{2}{\Lambda} \frac{1}{(1-1/\Lambda)^2} + \frac{1}{\Lambda^2} \frac{1}{(1-1/\Lambda)^2}$$

<sup>28</sup> into the exponential representation (??) of  $1/\zeta_k$ , and obtain <sup>29</sup>

$$1/\zeta_k = \frac{\det(1 - z\mathcal{L}_{(k)}) \det(1 - z\mathcal{L}_{(k+2)})}{\det(1 - z\mathcal{L}_{(k+1)})^2}. \quad (2.103)$$

Even though we have no guarantee that  $\det(1 - z\mathcal{L}_{(k)})$  are entire, we do know (by arguments explained in sect. ?!) <sup>30</sup> that the upper bound on the leading zeros of  $\det(1 - z\mathcal{L}_{(k+1)})$  lies strictly below the leading zeros of  $\det(1 - z\mathcal{L}_{(k)})$ , and therefore we expect that for 2-dimensional Hamiltonian flows the dynamical zeta function  $1/\zeta_k$  generically has a double leading pole coinciding with the leading zero of the  $\det(1 - z\mathcal{L}_{(k+1)})$  spectral determinant. This might fail if the poles and leading eigenvalues come in wrong order, but we have not encountered such situations in our numerical investigations. This result can also be stated as follows: the theorem establishes that the spectral determinant (2.101) is entire, and also implies that the poles in  $1/\zeta_k$  must have the right multiplicities to cancel in the  $\det(1 - z\mathcal{L}) = \prod 1/\zeta_k^{k+1}$  product.

↓PRIVATE

↑PRIVATE

[click to return: p. ??](#)

## Exercises boyscout

### 2.1. Cat map Green's function, infinite lattice.

<sup>23</sup>Predrag 2018-12-13: if edited, return to ChaosBook

<sup>24</sup>Predrag 2015-03-09: define  $\det(1 - z\mathcal{L}_{(2)})$

<sup>25</sup>Predrag 2015-03-09: compare with  $1/\zeta = \frac{F^2}{F_1 F_{-1}}$  of the preceding section

<sup>26</sup>Predrag 2015-03-09: write out Ruelle's alternating product for any dimensions

<sup>27</sup>Predrag 2018-12-13: if edited, return to ChaosBook

<sup>28</sup>Predrag 2015-03-09: seems the same as (2.102)?

<sup>29</sup>Predrag 2015-03-09: recheck, looks wrong

<sup>30</sup>Predrag 2015-03-09: find the sect. referred to

(a) Show that the eigenvalues of the cat map  $M$  are given by

$$\Lambda^\pm = \frac{1}{2}(s \pm \sqrt{D}), \quad \Lambda = e^\lambda, \quad (2.104)$$

where  $\Lambda \equiv \Lambda^+$ ,  $s = \Lambda + \Lambda^{-1}$ ,  $\sqrt{D} = \Lambda - \Lambda^{-1}$ , and the discriminant is  $D = s^2 - 4$ .

(b) Verify by substitution that the Green's function is given by

$$\mathfrak{g}_{nn'} = \frac{1}{\sqrt{D}} \frac{1}{\Lambda^{|n'-n|}}. \quad (2.105)$$

(c) Show that the orbit is then recovered by

$$x_n = \frac{1}{\sqrt{D}} \sum_{n' \in \mathbb{Z}} \Lambda^{-|n-n'|} m_{n'}. \quad (2.106)$$

2.2. **Cat map Green's function for a periodic orbit.** Show that the Green's function for a periodic orbit of period  $n_p$  is obtained by summing (2.105) over period  $n_p$ :

$$g_{nn'}^p = \sum_{j=-\infty}^{\infty} g_{n-n', j n_p} = \frac{1}{\sqrt{D}} \frac{\Lambda^{-|n-n'|} + \Lambda^{-n_p + |n-n'|}}{1 - \Lambda^{-n_p}}. \quad (2.107)$$

Verify this formula by explicit matrix inversion for a few periodic points of cycles  $p$  of periods  $n_p = 1, 2, 3, 4, \dots$ .

2.3.  **$d = 2$  cat map guess Green's function, infinite lattice.** Show by substitution that a  $d = 2$  "Green's function" guess given by

$$\mathfrak{g}_{zz'} = \frac{1}{2} \frac{1}{\sqrt{D}} \frac{1}{\Lambda^{|\ell' - \ell| + |t' - t|}}, \quad (2.108)$$

(and similarly, in arbitrary dimension  $d > 1$ ) does not satisfy the Green's function conditions

$$(\mathcal{D}\mathfrak{g})_{zz'} = \delta_{zz'} = \delta_{U'V'} \delta_{t't'}, \quad (2.109)$$

Here the eigenvalues of the cat map  $M$  are

$$\Lambda^\pm = \frac{1}{2}(s/2 \pm \sqrt{D}), \quad \Lambda = e^\lambda, \quad (2.110)$$

where  $\Lambda \equiv \Lambda^+$ ,  $s/2 = \Lambda + \Lambda^{-1}$ ,  $\sqrt{D} = \Lambda - \Lambda^{-1}$ , and the discriminant is  $D = (s/2)^2 - 4$ .

Hint: the check works just like for exercise 2.1.

2.4. **Periodic orbits of Arnol'd cat map.**

- (a) Describe precisely how you actually pick "random  $q_1$  and  $q_2$ "
- (b) Explain what happens if  $q_1$  and  $q_2$  are rational
- (c) Can you get a periodic orbit if  $q_1$  and  $q_2$  are irrational?

- (d) What do you mean by period 0?
- (e) Does the Arnol'd cat map have periodic orbits of any period?
- (f) Derive analytically that  $m_j \in \{-1, 0, 1, 2\}$  (you can continue the exposition that I started in sect. ??, if that helps). Does your result agree with Percival and Vivaldi [70]?

2.5. **The second iterate generating partition.** Figure 2.10 is very helpful in giving us a visual understanding of what a Hamiltonian cat map does, and how the generating partition comes about. Draw the corresponding Adler-Weiss generating partition for  $s = 3$ , the second,  $n = 2$  iterate, to verify that the  $n = 1$  determines a generating partition for all subsequent times.

2.6. **One-dimensional Hill determinant integral, ver. 1.** Show that

$$I(\Lambda) = \int_0^\pi d\theta \ln(1 - 2\Lambda \cos \theta + \Lambda^2) = 2\pi \ln \Lambda, \quad \Lambda \geq 1, \quad (2.111)$$

## Chapter 2. Cat map

**Solution 2.1 - Cat map Green's function, infinite lattice.**

- (a) It's just the roots of a quadratic equation, with  $s = \Lambda + \Lambda^{-1}$ , and  $\sqrt{D} = \Lambda - \Lambda^{-1}$ .
- (b) The Green's function (2.105)

$$\mathbf{g}_{tt'} = \frac{1}{\sqrt{D}} \frac{1}{\Lambda^{|t'-t|}} \quad (2.112)$$

for the discrete damped Poisson equation (2.34) was first computed explicitly by Percival and Vivaldi [70], using the methods introduced in Mestel and Percival [65]. It should satisfy

$$(\mathcal{D}\mathbf{g})_{ij} = \sum_k \mathcal{D}_{ik} \mathbf{g}_{kj} = \delta_{ij}. \quad (2.113)$$

Since we are considering infinite 1D lattice, we do not need to specify the boundary conditions.  $\mathcal{D}$  is a Toeplitz matrix

$$\mathcal{D}_{ik} = s\delta_{ik} - \delta_{i-1,k} - \delta_{i+1,k} \quad (2.114)$$

Substituting (2.114) into (2.113)

$$\sum_k \mathcal{D}_{ik} \mathbf{g}_{kj} = s\mathbf{g}_{ij} - \mathbf{g}_{i-1,j} - \mathbf{g}_{i+1,j} = \delta_{ij}, \quad (2.115)$$

and substituting (2.105)

$$\mathbf{g}_{ij} = \frac{1}{\sqrt{D}} \frac{1}{\Lambda^{|j-i|}} = \begin{cases} \frac{1}{\sqrt{D}} \frac{1}{\Lambda^{i-j}} & \text{if } j < i \\ \frac{1}{\sqrt{D}} & \text{if } j = i \\ \frac{1}{\sqrt{D}} \frac{1}{\Lambda^{j-i}} & \text{if } j > i \end{cases}. \quad (2.116)$$

into (2.115), one verifies that (2.105) is indeed the Green's function for the infinite lattice. By translational invariance, for  $i = j$  consider

$$s\mathfrak{g}_{00} - \mathfrak{g}_{-1,0} - \mathfrak{g}_{10} = \frac{1}{\sqrt{D}} \left( s - \frac{2}{\Lambda} \right) = \frac{1}{\sqrt{D}} \left( \Lambda - \frac{1}{\Lambda} \right) = 1. \quad (2.117)$$

For  $i > j$  consider

$$s\mathfrak{g}_{10} - \mathfrak{g}_{00} - \mathfrak{g}_{20} = \frac{1}{\sqrt{D}} \left( \frac{s}{\Lambda} - 1 - \frac{1}{\Lambda^2} \right) = \frac{1}{\sqrt{D}} \frac{1}{\Lambda} \left( s - \Lambda - \frac{1}{\Lambda} \right) = 0. \quad (2.118)$$

(c) The orbit is recovered by:

$$x_n = \sum_{n' \in \mathbb{Z}} \mathfrak{g}_{nn'} m_{n'} = \frac{1}{\sqrt{D}} \sum_{n' \in \mathbb{Z}} \Lambda^{-|n-n'|} m_{n'}. \quad (2.119)$$

(Han Liang)

**Solution 2.2 - Cat map Green's function for a periodic orbit.** Express the periodic orbit Green's function in terms of the infinite lattice by using a periodic source  $m_{n'} = m_{n'} + n_p$ ,

$$\begin{aligned} \sum_{n'=-\infty}^{\infty} \mathfrak{g}_{nn'} m_{n'} &= \sum_{r=-\infty}^{\infty} \sum_{n'=rn_p}^{rn_p+n_p-1} \mathfrak{g}_{nn'} m_{n'} = \sum_{r=-\infty}^{\infty} \sum_{n'=0}^{n_p-1} \mathfrak{g}_{n,n'+rn_p} m_{n'+rn_p} \\ &= \sum_{r=-\infty}^{\infty} \sum_{n'=0}^{n_p-1} \mathfrak{g}_{n-n',rn_p} m_{n'} \end{aligned} \quad (2.120)$$

Comparing with the expression for the Green's function of a periodic orbit:

$$\sum_{n'=0}^{n_p-1} \mathfrak{g}_{nn'}^{n_p} m_{n'} \quad (2.121)$$

we see that

$$\mathfrak{g}_{nn'}^{n_p} = \sum_{r=-\infty}^{\infty} \mathfrak{g}_{n-n',rn_p} \quad (2.122)$$

Substituting (2.105) into (2.122) we have:

$$\begin{aligned} \mathfrak{g}_{nn'}^{n_p} &= \frac{1}{\sqrt{D}} \sum_{r=-\infty}^{\infty} \frac{1}{\Lambda^{|n-n'-rn_p|}} \\ &= \frac{1}{\sqrt{D}} \left( \frac{1}{\Lambda^{|n-n'|}} + \sum_{r=1}^{\infty} \frac{1}{\Lambda^{rn_p-(n-n')}} + \sum_{r=-1}^{-\infty} \frac{1}{\Lambda^{(n-n')-rn_p}} \right) \\ &= \frac{1}{\sqrt{D}} \left( \frac{1}{\Lambda^{|n-n'|}} + \frac{1}{\Lambda^{-|n-n'|}} \frac{1}{\Lambda^{n_p-1}} + \frac{1}{\Lambda^{|n-n'|}} \frac{1}{\Lambda^{n_p-1}} \right) \\ &= \frac{1}{\sqrt{D}} \frac{1}{1-\Lambda^{-n_p}} (\Lambda^{-|n-n'|} + \Lambda^{-n_p+|n-n'|}) \end{aligned} \quad (2.123)$$

This verifies (2.107).

Bird and Vivaldi [15] show that for an  $n$ -cycle  $x_n$  are rational functions of  $\Lambda$ , given by the quotient of two reflexive polynomials (for example,  $P_t(\Lambda) = \Lambda^n P_t(1/\Lambda)$ ),

$$\begin{aligned} x_t &= \Lambda P_t(\Lambda)/Q(\Lambda) \\ P_t(\Lambda) &= \sum_{\tau=1}^{n-1} \Lambda^{n-\tau} (\Lambda m_{t+\tau-1} + m_{t-\tau}) \\ Q(\Lambda) &= (\Lambda^2 - 1)(\Lambda^n - 1) \end{aligned} \quad (2.124)$$

Bird and Vivaldi [15] then discuss pruning, give formulas for the numbers of orbits for integer  $s$ , etc..

(Han Liang)

**Solution 2.3** -  $d = 2$  cat map guess Green's function, infinite lattice. The Green's function  $g$  for the Toeplitz matrix (tensor) in 2 dimensions

$$\begin{aligned} \mathcal{D}_{lt,l't'} &= [-\square + 2(s/2 - 2)]_{lt,l't'} \\ &= \left( \frac{s}{2} \delta_{ll'} - \delta_{l-1,l'} - \delta_{l+1,l'} \right) \delta_{tt'} \\ &\quad + \delta_{ll'} \left( \frac{s}{2} \delta_{tt'} - \delta_{t-1,t'} - \delta_{t+1,t'} \right). \end{aligned} \quad (2.125)$$

should satisfy (2.109), or, substituting (2.125) into (2.109),

$$\begin{aligned} 2 \delta_{ll'} \delta_{tt'} &= \frac{s}{2} \mathfrak{g}_{ll',tt'} - \mathfrak{g}_{l-1,l',tt'} - \mathfrak{g}_{l+1,l',tt'} \\ &\quad + \frac{s}{2} \mathfrak{g}_{ll',tt'} - \mathfrak{g}_{ll',t-1,t'} - \mathfrak{g}_{ll',t+1,t'}. \end{aligned} \quad (2.126)$$

Let's check this. By translational invariance, need to look only at different values of  $l - l'$  and  $t - t' = 0$ . For  $l = l'$  and  $t = t'$  it suffices that we consider the  $l = l' = t = t' = 0$  case. Using (2.110) we have

$$\begin{aligned} &\frac{s}{2} \mathfrak{g}_{00,00} - \mathfrak{g}_{-1,0,00} - \mathfrak{g}_{10,00} \\ &+ \frac{s}{2} \mathfrak{g}_{00,00} - \mathfrak{g}_{00,-1,0} - \mathfrak{g}_{00,10} \\ &= \frac{2}{\sqrt{D}} \left( \frac{s}{2} - \frac{2}{\Lambda} \right) = \frac{2}{\sqrt{D}} \left( \Lambda - \frac{1}{\Lambda} \right) = 2, \end{aligned} \quad (2.127)$$

verifies (2.125).

For  $l > l'$  and  $t = t'$  it suffices to consider  $l = 1, l' = 0, t = t' = 0$  case.

$$\begin{aligned} &\frac{s}{2} \mathfrak{g}_{10,00} - \mathfrak{g}_{00,00} - \mathfrak{g}_{20,00} \\ &+ \frac{s}{2} \mathfrak{g}_{10,00} - \mathfrak{g}_{10,-1,0} - \mathfrak{g}_{10,10} \\ &= \frac{1}{2\sqrt{D}} \left( \frac{s/2}{\Lambda} - 1 - \frac{1}{\Lambda^2} \right) + \frac{1}{2\sqrt{D}} \left( \frac{s/2}{\Lambda} - \frac{2}{\Lambda^2} \right) \\ &= \frac{1}{2\Lambda\sqrt{D}} \left( \frac{s}{2} - \frac{2}{\Lambda} \right) = \frac{1}{2\Lambda\sqrt{D}} \left( \Lambda - \frac{1}{\Lambda} \right) = \frac{1}{2\Lambda}. \end{aligned} \quad (2.128)$$

So, the guess (2.108) already does not work.

Substitute (2.108) into (2.126) we get:

$$\sum_{z''} \mathcal{D}_{zz''} \mathfrak{g}_{z''z'} = \begin{cases} \frac{1}{\sqrt{D}} \frac{1}{\Lambda^{|\ell' - \ell| + |t' - t|}} (s - 2\Lambda - 2\Lambda^{-1}) & \text{if } l \neq l' \text{ and } t \neq t' \\ \frac{1}{\sqrt{D}} (s - 4\Lambda^{-1}) & \text{if } l = l' \text{ and } t = t' \end{cases} \quad (2.129)$$

To satisfy (2.109),  $s$ ,  $\sqrt{D}$  and  $\Lambda$  must satisfy:

$$\begin{cases} s = 2\Lambda + 2\Lambda^{-1} \\ \sqrt{D} = 2\Lambda - 2\Lambda^{-1} \end{cases} \quad (2.130)$$

So we will have:

$$\begin{cases} \Lambda = \frac{1}{4}(s + \sqrt{s^2 - 16}) \\ \Lambda^{-1} = \frac{1}{4}(s - \sqrt{s^2 - 16}) \end{cases} \quad (2.131)$$

Now the problem is, if  $l \neq l'$  but  $t = t'$ , (2.129) become:

$$\sum_{z''} \mathcal{D}_{zz''} \mathfrak{g}_{z''z'} = \frac{1}{\sqrt{D}} \frac{1}{\Lambda^{|\ell' - \ell| + |t' - t|}} (s - \Lambda - 3\Lambda^{-1}) \quad (2.132)$$

and this is not satisfied by (2.131). So (2.108) does not work for the 2-dimensional case. I haven't figured out the correct Green's function for the 2 dimensions.

(Han Liang)

**Solution 2.3** -  $d = 2$  cat map guess Green's function, infinite lattice. The guess Green's function (2.108) doesn't work. For  $l = 2$ ,  $l' = 0$  and  $t = t' = 0$ , the correct form of (2.128) is:

$$\begin{aligned} & \frac{s}{2} \mathfrak{g}_{10,00} - \mathfrak{g}_{00,00} - \mathfrak{g}_{20,00} \\ & + \frac{s}{2} \mathfrak{g}_{10,00} - \mathfrak{g}_{10,10} - \mathfrak{g}_{10,-10} \end{aligned} \quad (2.133)$$

$$= \frac{1}{2\sqrt{D}} \left( \frac{s}{2\Lambda} - 1 - \frac{1}{\Lambda^2} \right) + \frac{1}{2\sqrt{D}} \left( \frac{s}{2\Lambda} - \frac{1}{\Lambda^2} - \frac{1}{\Lambda^2} \right) \quad (2.134)$$

$$= \frac{1}{2\sqrt{D}} \frac{1}{\Lambda} \left( \frac{s}{2} - \Lambda - \frac{1}{\Lambda} \right) + \frac{1}{2\sqrt{D}} \frac{1}{\Lambda} \left( \frac{s}{2} - \frac{1}{\Lambda} - \frac{1}{\Lambda} \right) \quad (2.135)$$

$$= 0 + \frac{1}{2\Lambda} \quad (2.136)$$

As in (2.128), this does not work .

(Han Liang)

**Solution 2.4** - Periodic orbits of Arnol'd cat map. No solution available.

**Solution 2.5** - The second iterate generating partition. Figure 2.13 is the generating partition with  $s = 3$  evolved after 2 steps. In the Markov diagram figure 2.13 (d) there are 7 self cycles, two of which are the over-counted fixed points at the origin. So there are actually 5 periodic points with period 2, including 1 fixed point and 2 length-2 orbits, as given by (1.12).

Figure 2.13 is a very nice illustration of a generating partition subrectangles being further subdivided.

**Solution 2.6** - One-dimensional Hill determinant integral, ver. 1. Gradshteyn and Ryzhik lists this integral as Eq. 4.225 15.



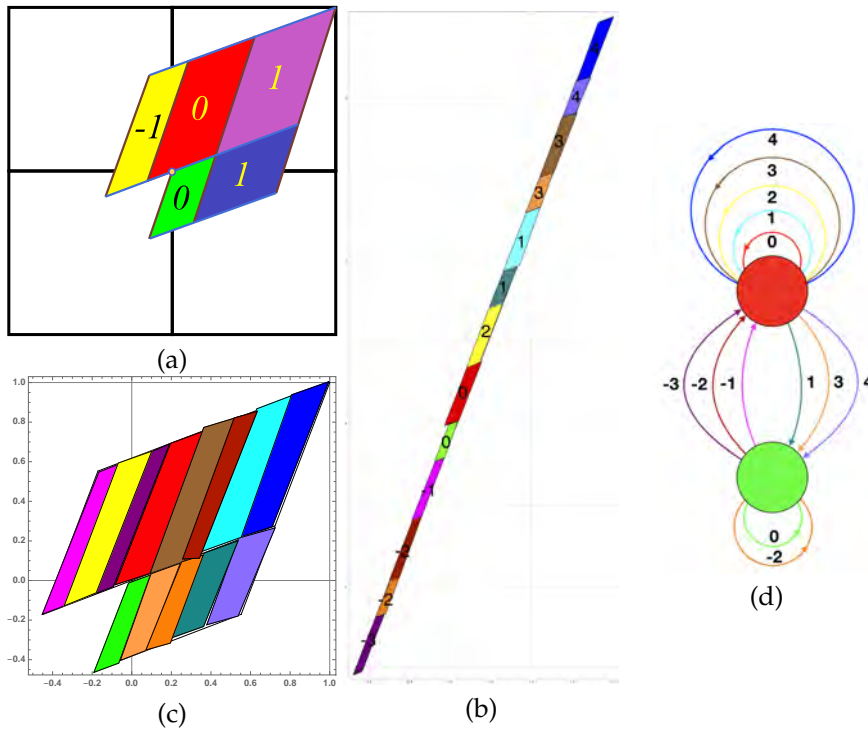


Figure 2.13: (a) An Adler-Weiss one step forward in time partition of the unit torus for the  $s = 3$  Percival-Vivaldi cat map figure 2.9 (c). (b) Mapped two steps forward in time, the rectangles are stretched along the unstable direction and shrunk along the stable direction. Sub-rectangles  $\mathcal{M}_j$  that have to be translated back into the partition are indicated by color and labeled by their lattice translation  $m_j$ . (c) The sub-rectangles  $\mathcal{M}_j$  translated back into the unit square yield a two steps forward in time generating partition (a subpartition of rectangles in (a)), with (d) the finite grammar given by the transition graph for this partition. The nodes refer to the rectangles  $A$  and  $B$ , and the 13 links correspond to the 13 sub-rectangles induced by two step forward-in-time dynamics.

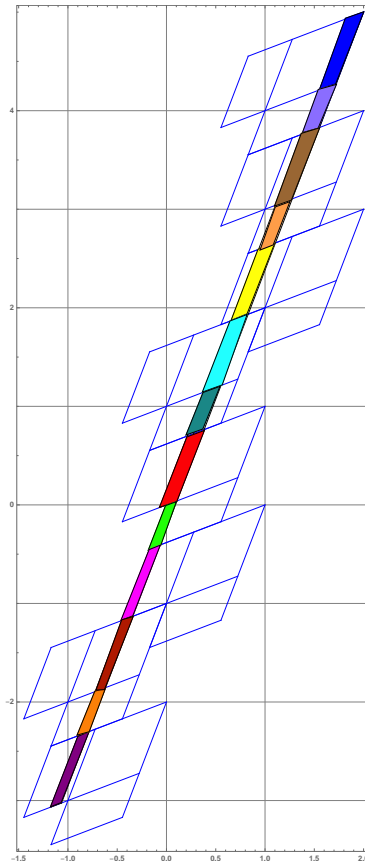


Figure 2.14: This figure is used to track where each sub-rectangles in figure 2.13 goes. Note that two step forward-in-time requires both vertical and horizontal shifts, unlike the one step forward-in-time Percival-Vivaldi cat map (2.75).

## Exercises boyscout

---

There are many derivations of the integral. [Dedalus post](#) is mostly clumsy, but has a drawing that explains where the integrand comes from. I like robjohn's contour integral solution best, see also robjohn in [Julien post](#).

[Moor Xu blog](#) has 5 ways of solving this, including also the contour integral version.

r

## Chapter 3

# Temporal Hénon

### 3.1 Hénon blog

2020-03-17 **Predrag** Moving some of the text into the tigers' paper, the shared sect. 4.10 *Deterministic  $\phi^3$  lattice field theory*.

2021-02-15 **Predrag** Added Hénon map examples (to be edited and returned to ChaosBook):

example 3.1 *Hénon map*

example 3.2 *Temporal Hénon*

example 3.4 *Temporal Hénon stability*

example 3.5 *Hamiltonian Hénon map, reversibility*

example 3.6 *Symmetry lines of the standard map*

example 3.7 *Symmetry lines of the cat map*

Study also chronotopic literature:

sect. 13.2 *PolTor92b Towards a statistical mechanics of spatiotemporal chaos*

sect. 13.3 *PolTor92 Periodic orbits in coupled Hénon maps*

sect. 13.4 *PoToLe98 Lyapunov exponents from node-counting*

sect. 13.6 *PolTor09 Stable chaos*

2021-02-17 **Predrag** My key 2005 contribution was presumably the time-reversal symmetry induced, temporal lattice cycle by cycle full square (3.34) and (3.33).

### 3.2 Anti-integrable limit

2021-12-23 **Predrag** See also sect. 4.12.5 *Deterministic  $\phi^4$  lattice field theory*

**2021-12-22 Jim Meiss:** "The concept of anti-integrability was introduced by Aubry and Abramovici [7] in 1983 for the standard map (PC: 1983? maybe he means Aubry and Le Daeron [8]?), viewed as a linear chain of particles connected by springs in a periodic potential. They reasoned that the integrable limit corresponded to vanishing potential energy, so that the springs dominated giving equal spacing at equilibrium. By contrast, anti-integrability corresponds to vanishing kinetic energy, so that particles sit at critical points of the potential. What is most interesting about this limit is that it is relatively easy, using a contraction mapping style argument, to show that AI states persist, and this gives conjugacy to a shift on a symbolic dynamics."

**2024-10-06 Predrag David Campbell,** Flach and Kivshar [21] *Localizing energy through nonlinearity and discreteness* (2004):

" the late 1980s by the discovery that intrinsic localized modes(ILMs), AKA discrete breathers (DBs), are, in fact, typical excitations in perfectly periodic but strongly nonlinear systems.

A DB is a localized, oscillatory excitation that is stabilized against decay by the discrete nature of the periodic lattice.

An ILM is an excitation that is localized in space by the intrinsic nonlinearity of the medium, rather than by a defect or impurity.

By the early 1990s, researchers following these two paths had converged on the insight that stable localized periodic modes, whether called ILMs or DBs, were generic excitations in discrete nonlinear systems, and that to study them systematically, one should start with a system of uncoupled nonlinear oscillators -the "anti-continuum limit"- and treat the coupling as a weak perturbation.

Now consider exciting one oscillator strongly but the second one only weakly so that most of the energy is initially localized at the first oscillator. Because the frequencies depend on the amplitudes, we can, in principle, choose amplitudes such that the frequencies of each oscillator are irrationally related. For strictly incommensurate frequencies, no possible resonances exist between any of the oscillators' harmonics. If we now turn on the coupling between the oscillators, intuition suggests that the transfer of energy from one to the other must be very difficult, if even possible.

That heuristic result can be formalized by the powerful Kolmogorov-Arnold-Moser (KAM) theorem of nonlinear dynamical systems, which establishes that the incommensurate motions do remain rigorously stable for sufficiently weak coupling and ensures that the excitation energy remains localized on the first oscillator.

(Predrag: This is the essence of our argument that Sinai-Bunimovich CML is the weak coupling theory, sect. 8.1.1 *Coupled map lattices*.)

The Euler–Lagrange equation (4.137) for the  $d = 1$  scalar lattice  $\phi^4$  field theory (see (23.22)),

$$\frac{d^2\phi_n}{dt^2} - \frac{1}{(\Delta x)^2}(\phi_{n+1} + \phi_{n-1} - 2\phi_n) - \phi_n + \phi_n^3 = 0, \quad (3.1)$$

nearest spatial neighbors coupling strength  $1/(\Delta x)^2 = -1/\mu^2$ , here  $\mu^2$  is the Klein-Gordon mass.

They plot frequency versus wave-number for linear oscillations (green) for  $\Delta x = 10$

$$\omega(k)^2 = 2 + (2/\Delta x)^2 \sin^2 k/2 = \frac{1}{\mu^2}(2\mu^2 + p(k)^2) \quad p = 2 \sin \frac{k}{2}. \quad (3.2)$$

and two isolated frequencies  $\omega_b$  from the range of possible frequencies corresponding to the types of ILMs

Fermi-Pasta-Ulam-Tsingou (FPUT) models with cubic and quartic potentials are referred to as the  $\alpha$ -FPUT and  $\beta$ -FPUT models, respectively. The Toda model approximates the dynamics of the  $\alpha$ -FPUT system at short times.

Their references to continuous time, 1-dimensional discrete space Hamiltonians:

R. T. Birge , H. Spooner ,Phys. Rev. 28 , 259 (1926 )

J. W. Ellis, Phys. Rev. 33 , 27 (1929 )

B. R. Henry , W. Siebrand , J. Chem. Phys. 49 , 5369 (1968 )

A. A. Ovchinnikov , Sov. Phys. JETP 30 , 147 (1970 )

R. Bruinsma et al, Phys. Rev. Lett. 57 , 1773 (1986 )

A. S. Davydov , Solitons in Molecular Systems , E. S. Kryachko , trans., Kluwer, Hingham , Mass . (1985 ).

"

**2024-10-06 Predrag** Discretize time in (3.1) with temporal lattice constant  $\Delta t = 1$ :

$$\phi_{t+1} + \phi_{t-1} - 2\phi_t - \frac{1}{(\Delta x)^2}(\phi_{n+1} + \phi_{n-1} - 2\phi_n) - \phi_n + \phi_n^3 = 0. \quad (3.3)$$

Chose lattice constants in space and time to be equal,  $(\Delta t)^2 = (\Delta x)^2 = -\mu^2$ . Go to imaginary time, so  $\mu^2 > 0$ . That theory is the  $d$ -dimensional Euclidean  $\phi^4$  theory, with Euclidean Laplacian  $\square$ ,

$$-\square\phi_z + \mu^2(\phi_z - \phi_z^3) = 0. \quad (3.4)$$

Curiously, this version of  $\phi^4$  theory seems to not be even mentioned in Kevrekidis and Cuevas-Maraver [20, 49] *A Dynamical Perspective on the  $\phi^4$  Model: Past, Present and Future* (2019).

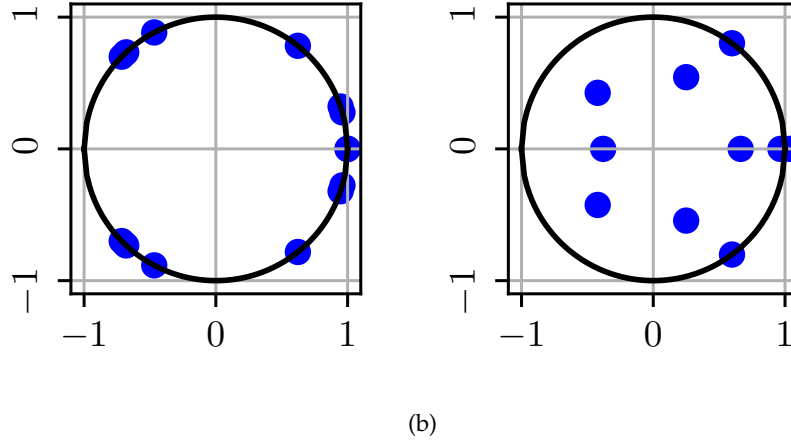


Figure 3.1: Floquet multipliers of a stable seed mode  $k_0 = 1$   $q$ -breather (a) and an unstable composite periodic orbit (b) in an 8-particle  $\alpha$ -FPUT system. From ref. [48].

**2024-10-06 Predrag** Karve, Rose and Campbell [48] *Periodic orbits in Fermi-Pasta-Ulam-Tsingou systems* (2024); [arXiv:2406.10790](https://arxiv.org/abs/2406.10790).

Figure 3.1 illustrates stability multiplies of a purely oscillator breather orbit, and a hyperbolic spatiotemporal doubly-periodic unstable orbit of two FPUT systems.

**2024-10-06 Predrag** Campbell [20] *Historical overview of the  $\phi^4$  model* (2019)

**2021-12-07 Ibrahim** I do not understand sources  $m_t$  in (4.181) and (4.182). In temporal cat (4.180) they are a finite integer-valued alphabet that translates the field to the right fixed point, but for the nonlinear field theories they are simply a constant? A constant that can be changed by shifting fields?

**2021-12-08, 2021-12-10 Predrag** You are right - we should think of  $m_t$  is a (in general, a real number) shift that centers the map on a given nonlinear segment. Read sect. 4.16.1, see whether you have a good formulation that cover all cases.

Hénon map

$$\begin{aligned} x_{n+1} &= 1 - ax_n^2 + by_n \\ y_{n+1} &= x_n \end{aligned} \quad (3.5)$$

Written as a 2nd-order inhomogeneous difference equation (3-term recurrence relation), the temporal Hénon Euler–Lagrange equation is

$$F[\mathbf{X}]_t = -\phi_{t+1} + b\phi_{t-1} - a\phi_t^2 + 1 = 0. \quad (3.6)$$



Where  $F[X]_t$  is the local deviation of an approximate periodic state from the exact 2-step recurrence form of the Hénon map  $F[X]_t = 0$ .

For fixed  $\phi_{t-1}, \phi_{t+1}$  there are two values of  $\phi_t$  satisfying  $F[X]_t = 0$ . These solutions are the two extremal points of a local cubic Biham-Wenzel [12] “potential” function (no sum on  $t$ )<sup>1</sup>

$$F[X]_t = \frac{\partial}{\partial \phi_t} S[X], \quad S[X] = \sum_t^{\mathcal{L}} \left\{ \phi_t(\phi_{t+1} - b\phi_{t-1}) + \frac{a}{3}\phi_t^3 - \phi_t \right\}. \quad (3.7)$$

Assuming that the two extremal points are real, one is a local minimum of  $V_t(\phi)$  and the other is a local maximum.

(3.5)

Garden variety scalar field theory actions  $S[X]$  are smooth, often of polynomial type. In the examples below we add a potential [2–4, 28, 35, 50]

$$V(\phi_t, \varphi_t^{(m)}) = -\frac{g}{k}\phi_t^k + \phi_t^2 + \varphi_t^{(m)}\phi_t \quad (3.8)$$

at each lattice site  $t$  to the Laplacian, where  $\varphi_t^{(m)}$  is a translation of field  $\phi_t$  adjusted so that for the  $m$ th fixed point solution the potential is centered so that fixed point is at  $\phi = 0$ .

The discrete Euler–Lagrange equations now take form of 3-term recurrence, second-order difference equations

$$-\square \phi_t - V'(\phi_t, \varphi_t^{(m)}) = 0. \quad (3.9)$$

For a constant (fixed point) periodic state the Laplacian  $\square \phi_t$  in (3.9) does not contribute, so fixed points  $\phi_t = \phi$  are the  $(k - 1)$  solutions of (3.8)

$$V'(\phi, m) = -g\phi^{k-1} + 2\phi + \varphi_t^{(m)} = 0. \quad (3.10)$$

second-order difference Euler–Lagrange equations (3.9) that we call, in the cases considered here, the ‘temporal cat’, ‘temporal Hénon’, and ‘temporal  $\phi^4$  theory’, respectively:

$$-\phi_{t+1} + s\phi_t - \phi_{t-1} = m_t \quad (3.11)$$

$$-\phi_{t+1} + a\phi_t^2 - \phi_{t-1} = m_t \quad (3.12)$$

$$-\phi_{t+1} + g\phi_t^3 - \phi_{t-1} = m_t \quad (3.13)$$

Written as a 2nd-order inhomogeneous difference equation [28], (4.186) takes the *temporal Hénon* 3-term recurrence form (4.187), explicitly time-translation and time-reversal invariant Euler–Lagrange equation,

$$-\phi_{t+1} + a\phi_t^2 - \phi_{t-1} = 1.$$

---

<sup>1</sup>Predrag 2022-04-07: **WRONG** cannot write a global action  $S[X] = \sum_t V_t(\phi)$ !

Just as the kicked rotor (12.100,12.101), the map can be interpreted as a kicked driven anaharmonic oscillator [44], with the nonlinear, cubic Biham-Wenzel [12] lattice site potential (3.8)

$$V(\phi_t, m_t) = -\frac{a}{3}\phi_t^3 + \phi_t^2 + m_t \phi_t, \quad m_t = -1, \quad (3.14)$$

giving rise to kicking pulse (12.101), so we refer to this field theory as  $\phi^3$  theory.

For a sufficiently large stretching parameter  $a$ , lattice site field values of this  $\phi^3$  theory are in one-to-one correspondence to the unimodal Hénon map Smale horseshoe repeller, cleanly split into the ‘left’, positive stretching and ‘right’, negative stretching lattice site field values.

fix (arbitrarily) the stretching parameter value to  $a = 6$ , in order to guarantee that all  $2^n$  periodic points  $\phi = f^n(\phi)$  of the Hénon map (4.186) exist, see table 3.1. The symbolic dynamics is binary, as simple as the temporal Bernoulli (1.15),

### 3.2.1 The meaning of source terms $m_t$

Make sure that the coupling constant  $g$  in (3.8) is sufficiently strong so you are in the anti-integrable regime, meaning that for constant field  $\phi_t = \phi$  periodic state  $V'(\phi_t, m_t)$  in has (3.9) has  $k$  distinct real roots

$$\phi_m^* = m\varphi_m, \quad (3.15)$$

i.e., there are  $k$  fixed-point, constant  $X_m$  periodic states (this might require further nonleading terms in (3.8), perhaps see the history review in [arXiv:1512.08645](https://arxiv.org/abs/1512.08645), “problems close to *hyperbolicity*, concerning number of (may be, positive or negative) real roots of a polynomial”).

The alphabet  $m_t \in \mathcal{A}$  will have  $(k - 1)$  letters, all  $n^{k-1}$  periodic states  $M$  should be be admissible.

$$-\phi_{t+1} + (g\phi_t^{k-1} - m_t\varphi_m) - \phi_{t-1} = 0. \quad (3.16)$$

Here  $m_t\varphi_m$  should be a translation that places  $m$ th root at the origin.

Let’s engineer potentials that give symmetrically disposed fixed points:

Odd  $k, \ell = (k - 1)/2$ :

$$\prod_{\alpha=1}^{\alpha=\ell} (\phi^2 - m_\alpha^2 \varphi_\alpha^2) = 0, \quad \mathcal{A} = \{-\ell, \dots, -1, 1, \dots, \ell\}.$$

Even  $k, \ell = k/2$ :

$$\phi \prod_{\alpha=1}^{\alpha=\ell} (\phi^2 - m_\alpha^2 \varphi_\alpha^2) = 0, \quad \mathcal{A} = \{-\ell, \dots, -1, 0, 1, \dots, \ell\}$$

$\phi^3$ /Hénon field theory

$$(\phi - \varphi)(\phi + \varphi) = \phi^2 - \varphi^2 = 0, \quad \mathcal{A} = \{-1, 1\}$$

compare with fixed points (22.17).

$\phi^4$  field theory

$$\phi(\phi - \varphi)(\phi + \varphi) = \phi^3 - \varphi^2\phi = 0, \quad \mathcal{A} = \{-1, 0, 1\},$$

compare with the calculation following (23.1).

### 3.2.2 Anti-integrable blog

**2021-09-12 to 2021-12-22 Predrag** I have added my guess (4.228) for the infinite coupling  $g$  anti-integrable limit of  $\phi^4$  theory. That gives a 3-letter alphabet  $\mathcal{A} = \{-1, 0, 1\}$ . One can use it to find by continuation any periodic state, at  $g$  as low as possible. ‘Generalized Hénon maps’ AKA  $\phi^4$  field theory posts are in sect. 4.12.5 *Deterministic  $\phi^4$  lattice field theory*.

**2021-06-04 Predrag** David Meiss’ student David G. Sterling [65] much (undeservedly) un-cited [PhD thesis](#), Univ. of Colorado, *Anti-Integrable Continuation and the Destruction of Chaos* has much to teach us. He studies *coupled Hénon map lattices* in both Hamiltonian and Lagrangian formulations; his definition seems pretty much consistent with our (22.12), though he has a coupling parameter  $c$  used to make spatial couplings weak. The “anti-integrable” refers to our choice  $a \geq 6$ , I believe - parameter regimes in which all of the horseshoe orbits exists.

“Specifying the anti-integrable state for an orbit of a coupled map lattice requires a multidimensional symbolic object which we call a symbol tensor.”

His Figures 6.7, 6.18 are reminiscent of my pruning front.

Thesis abstract: [...] Recurrent phenomena, the simplest of which is periodic motion, are particularly interesting and practical objects of study. Scientists have long been captivated by the near periodic motions of the planets. Among them, Poincaré was the first to truly recognize the importance of periodic solutions in understanding more complex dynamical behavior. [...] This research has two complementary aspects. Not only do we develop a technique for locating periodic orbits in discrete dynamical systems, but we then use these orbits to study bifurcations, most significantly the global bifurcation that signals the destruction of chaos. Our technique embodies the following basic principles:

- (1) periodic orbits are conveniently described by a variational principle,
- (2) in a special case, the variation principle simplifies, and
- (3) continuation from this limiting case is an effective method for studying periodic orbits. We illustrate this approach on the Hénon map.

**2021-09-12 Sidney, Predrag** In the  $a \rightarrow \infty$ , *anti-integrable* limit [64] the Hénon's original map (3.21) goes to  $a(\phi^*)^2 = 1$ , so

$$\phi_t = m_t \phi^*, \quad \phi^* = a^{-1/2}, \quad m_t \in \{-, +\}. \quad (3.17)$$

The small perturbation parameter for the problem is  $\phi^* = a^{-1/2}$ , so replace

$$\phi_t = m_t \phi^* + \hat{\phi}_t, \quad (3.18)$$

study the temporal Hénon equations for  $\hat{\phi}_t$ .

**2021-09-12 Sidney** The process for perturbations that you're describing sounds very reminiscent of what is in chapter 11 of Townsend, would that be worth trying to copy here?

**2021-12-22 Predrag** Moved 'generalized Hénon maps' AKA  $\phi^4$  field theory posts to sect. 4.12.5 *Deterministic  $\phi^4$  lattice field theory*.

**2021-06-04 Predrag** Read also

Aubry and Le Daeron [8] *The discrete Frenkel-Kontorova model and its extensions. I. Exact results for the ground-states* (1983)

Sterling and Meiss [64] *Computing periodic orbits using the anti-integrable limit* (1988)

Aubry and Abramovici [7], *Chaotic trajectories in the standard map. The concept of anti-integrability*, (1990)

Aubry [6] *Anti-integrability in dynamical and variational problems* (1995)

Chen [24]

Yi-Chuan Chen *A Proof of Devaney–Nitecki region for the Hénon mapping using the anti-integrable limit*, *Adv. Dyn. Systems Appl.* **13**, 33–43 (2018).

He seems to not have been active the past 3 years.

Treschev, D. and Zubelevich [67] *The anti-integrable limit* (2009)

**2021-12-21 Predrag** Hagiwara and Shudo [43] *An algorithm to prune the area-preserving Hénon map* (2004) describes Sterling's anti-integrable method.

Starting with the temporal Hénon second-order difference equation (3.23), changing variables to  $z = \epsilon x$ ,  $\epsilon = a^{-1/2}$  gives

$$-\epsilon(z_{t-1} + z_{t+1}) + z_t^2 - 1 = 0. \quad (3.19)$$

At the anti-integrable limit  $\epsilon \rightarrow 0$ , the map reduces to  $z_t^2 = 1$ , with every orbit an arbitrary sequence of  $\pm 1$ .

**2021-06-04 Predrag** They are probably deep and good, but I find

Bolotin and MacKay [14] *Multibump orbits near the anti-integrable limit for Lagrangian systems*, (1997)

Bolotin and Treschev [15] *The anti-integrable limit* (2015)

hard to read. Gave up.

**2021-06-04 Predrag** We all might find the Sect. III of Wen's 2014 project [Chaos-Book.org/projects/Wen14.pdf](https://Chaos-Book.org/projects/Wen14.pdf) interesting.

Wen says that the original Hénon's [45] Hamiltonian Hénon map is equivalent to the harmonic oscillator system. By that he means it can be interpreted as a kicked driven harmonic oscillator with a nonlinear, cubic potential kicking term [44]. When we write about temporal Hénon, include this as a physical motivation.

2023-11-03 Predrag] Included the above in `FTlatt.tex`.

**2021-06-04 Predrag** Check out also Zalmond C. Barney [Master's Thesis](#) *Derivation of planar diffeomorphisms from Hamiltonians with a kick*.

Butusov *et al.* [19] *Discrete chaotic maps obtained by symmetric integration* might be of interest for adding a reflection symmetry to the Hénon map.

**2021-09-07 Predrag 2 Sidney** .

1. Plot lattice field values for  $a \gg 1$ , then try to look at a perturbation theory treatment of this.
2. Learn about the perturbative treatments of field theories.

**2021-09-09 Predrag** Re. 1. above: I quickly tried to sketch how  $a \gg 1$ , did not get anything sensible. Might be yet another crazy idea that met instant death, do not worry about it for now.

**2021-09-12 Sidney** I did some preliminary calculations of  $a \gg 1$  using the Gallas scaling (so not quite field theory, but I good test) and as  $a$  got larger, the less variation in lattice site values occurred. There were still negative, and positive values, but in the large  $a$  limit the lattice site values all approached an equal absolute value. I am not sure if that is useful, perhaps if we looked at the asymptotic behavior of both large and small  $a$  we could come up with some interesting "asymptotic temporal Hénon" theory.

**2021-09-12 Predrag** That sounds very good: in this limit the fields are apparently  $\phi_t = m_t \phi^*$ ,  $m_t \in \{-, +\}$ , where  $- \rightarrow 0$ ,  $+ \rightarrow 1$  is the binary label corresponding to lattice site  $t$ .

Basically you get a theory even simpler than the temporal cat.

Perturbation theory for large but finite  $a$  would come from replacement  $\phi_t \rightarrow \phi^* + \epsilon \hat{\phi}_t$  in the equations, and ordering terms by powers  $\epsilon^k$  and  $a^{-\ell}$ . Probably  $a^{-\ell}$  only.

**2021-09-12 Predrag** Do you have the analytic value of  $\phi^*$ ?

**2021-09-13 Sidney** I have changed my code so that it can be easily switched between the Hénon [45] (3.21), and Endler and Gallas [32] rescaled (3.38),

I have added this updated code *Relaxation Method Henon with Orbit Jacobian.py* to *siminos/williams/python/relax*.

So, let's see if I understand, if we plug (3.17) into the Hénon form (3.21), expand and keep only linear terms of  $\hat{\phi}_t$ , we get a new temporal Hénon of form:

$$\hat{\phi}_{t+1} + 2m_t a^{1/2} \hat{\phi}_t + \hat{\phi}_{t-1} = -(m_{t+1} + m_{t-1}) \phi^*, \quad (3.20)$$

where  $m_t$  is determined by the cycle itinerary. Is that the form you were thinking of? If this is the correct procedure, I can't see a way of extending this to a second-order perturbation theory, as that is just reproducing temporal Hénon.

**2021-09-13 Predrag** I have not thought through your (3.20) yet. Maybe  $\hat{\phi}_t \rightarrow \phi^* \hat{\phi}_t$  helps a bit.

You have analytic formulas for fixed points (??), period-2 periodic states (??). You might find useful approximate large  $a$  formulas for all period- $n$  periodic states. They might already be in David Sterling's [PhD thesis](#).

Maybe Hill determinants have interesting expansions in powers of  $a^{-\ell/2}$ ...

**2022-01-23 Predrag** Beck [11] *Spontaneous symmetry breaking in a coupled map lattice simulation of quantized Higgs fields* abstract:

We study a class of coupled map lattices with a  $Z(2)$ ,  $U(1)$ , and  $SU(2)$  symmetry, respectively. We point out that these types of coupled maps have applications in particle physics, since they arise from the field equations of stochastically quantized Higgs fields in the anti-integrable limit. For  $d$ -dimensional lattices we investigate the dependence of the vacuum expectation of the field on the coupling constant. Spontaneous symmetry breaking is observed at various critical coupling strengths.

He uses the stochastic quantization method with a Langevin equation, so I will ignore the paper for now, perhaps unfairly. The  $Z(2)$  symmetry is what I tend to call 'dynamical'  $\phi \rightarrow -\phi$  symmetry of the  $\phi^4$  potential.

For the contraction parameter value  $b = -1$  the Hénon map [45] is orientation and area preserving, and can be written as a 3-term recurrence relation

$$x_{t-1} = 1 - ax_t^2 - x_{t+1}. \quad (3.21)$$

Multiply both sides by  $-2a$  and define the Hénon 'field' at lattice site  $t$  to be  $\phi_t = -2ax_t$ . We shall refer to this form of Hénon as the *temporal Hénon*:

$$\phi_{t+1} - \frac{1}{2}\phi_t^2 + \phi_{t-1} = -2a. \quad (3.22)$$

or we can multiply both sides by  $-2$  and define the Hénon 'field' at lattice site  $t$  to be  $\phi_t = -2x_t$ , yielding temporal Hénon of form:

$$\phi_{t+1} - \frac{a}{2}\phi_t^2 + \phi_{t-1} = -m_t, \quad m_t = 2, \quad (3.23)$$

with the ‘coupling constant’  $a$  the analogue of the stretching factor  $s$  in temporal cat (6.8), and a constant source  $m_t$ .

The fixed points  $\phi_j = \phi$  satisfy

$$\phi^2 - \frac{4}{a}\phi - \frac{4}{a} = 0, \quad \phi_{\pm} = \frac{2}{a} \pm \sqrt{\frac{4}{a^2} + \frac{16}{a}} \quad (3.24)$$

Temporal Hénon is  $\phi^3$  lattice field theory. Biham-Wenzel [12] find Hénon periodic states by constructing a cubic action density (4.148),

$$S[\phi]_t - m_t \phi_t = \phi_{t+1}\phi_t + \phi_t\phi_{t-1} - \frac{a}{3!}\phi_t^3 - m_t \phi_t, \quad m_t = 2. \quad (3.25)$$

Still to check: is  $m_t = \pm 2$  the Biham-Wenzel method? Looks like it, as that amounts to flipping the sign of the cubic term while keeping the variation across there sits of the same magnitude.

I took  $+2\phi_n$  out of  $S[\phi]$  to treat it as a source density term  $m_t\phi_t$ .

Now the orbit Jacobian matrix (3.26) is of the same form as the temporal cat orbit Jacobian matrix (6.11),

$$\mathcal{J}[X] = \begin{pmatrix} d_0 & -1 & 0 & 0 & \cdots & 0 & 0 & -1 \\ -1 & d_1 & -1 & 0 & \cdots & 0 & 0 & 0 \\ 0 & -1 & d_2 & -1 & \cdots & 0 & 0 & 0 \\ \vdots & \vdots & \vdots & \vdots & \ddots & \vdots & \vdots & \vdots \\ 0 & 0 & 0 & 0 & \cdots & -1 & d_{n-2} & -1 \\ -1 & 0 & 0 & 0 & \cdots & 0 & -1 & d_{n-1} \end{pmatrix}, \quad (3.26)$$

but with the stretching factor at site  $t$  depending on the particular periodic state,  $d_t = \phi_t$ , and once you have an expression for Hill determinant  $\|\mathcal{J}[X]\|$  in terms of traces  $\text{Tr } \mathcal{J}^k$ , i.e., the  $D_n$  invariant orbital sums for products of fields on consecutive lattice sites, they will be the same for the temporal cat and the temporal Hénon.

### 3.3 Hénon map symmetries

We note here the symmetries of the Hénon map (3.5). For  $b \neq 0$  the Hénon map is reversible: the backward iteration of (3.6) is given by

$$x_{n-1} = -\frac{1}{b}(1 - ax_n^2 - x_{n+1}). \quad (3.27)$$

Hence the time reversal amounts to  $b \rightarrow 1/b$ ,  $a \rightarrow a/b^2$  symmetry in the parameter plane, together with  $x \rightarrow -x/b$  in the coordinate plane, and there is no need to explore the  $(a, b)$  parameter plane outside the strip  $b \in \{-1, 1\}$ . For  $b = -1$  the map is orientation and area preserving Hamiltonian Hénon map

$$x_{n-1} = 1 - ax_n^2 - x_{n+1}, \quad (3.28)$$

the backward and the forward iteration are the same, and the non-wandering set is symmetric across the  $x_{n+1} = x_n$  diagonal. We can write this as a nonlinear field equation with a Laplacian (4.6) and a “cubic” potential (4.148)

$$\square x_n + (a x_n + 2) x_n = 1. \quad (3.29)$$

Endler and Gallas [32] prefer the equivalent, rescaled form (3.38).

This is one of the simplest models of a return map for a Hamiltonian flow.

For the orientation reversing  $b = 1$  case we have ‘golden Hénon’ (in analogy with (6.194))

$$x_{n-1} = 1 - a x_n^2 + x_{n+1}, \quad (3.30)$$

and the non-wandering set is symmetric across the  $x_{n+1} = -x_n$  diagonal.

2023-04-19 Removed from CL18 the obsolete form (3.28) period-2 calculation:

$$-x_{t+1} + (a x_t^2 - 1) - x_{t-1} = 0. \quad (3.31)$$

$$X_p = \frac{1}{a} \begin{pmatrix} -1 - \sqrt{a-3} \\ -1 + \sqrt{a-3} \end{pmatrix}.$$

$$E(k)^\pm = -2(1 \pm \sqrt{a-3 + \cos^2 k}),$$

### 3.4 “Center of mass” puzzle

Some of Predrag’s unpublished 2004 drafts and calculations are in

```
% dasbuch/book/FigSrc/gnu/Gallas % just a link
dасbuch/WWW/library/Gallas-chiral.pdf
dасbuch/WWW/projects/revHenon/Gallas0101305.txt etc
dасbuch/book/Fig/COM0001011.eps COM0001101.eps COM0001111.eps
COM0011.eps COM011.eps
dасbuch/book/OldProblems/soluCOM011005.tex
```

*predrag/reports/referee/Gallas.txt* on the unpublished

*Periodic orbits are not necessarily independent from each other*

Some of Predrag’s unpublished 2004 drafts and calculations of Jan 26, 1999 suggests many references where similar work was published. The revised paper appeared as Gallas [36] *Nonlinear dependencies between sets of periodic orbits*, I believe.

*Gallas-chiral.pdf* ([click here](#)) has the Endler-Gallas Hénon map polynomials up to period 8, and nothing else.

[ChaosBook.org/projects/revHenon](http://ChaosBook.org/projects/revHenon) has lots of stuff:



1. *chiral.pdf* is an unfinished draft of Endler, Gallas and Cvitanović paper, based on *Gallas-chiral.pdf*. Much of the introduction is utterly delirious. Notation for ‘orbits’, eq. (10) is redundant and the indices of  $x_j$  are useless, they label roots of different polynomials, ordered by increasing  $x_j$ . Figures illustrate ‘chiral’ orbit pairs,  $A_n = 0$ ;  $B_n = 0$  and  $C_n = 0$  self-dual orbits. Fig. 4 might be  $C_n = 0$  for value of  $a$  other than 6.
2. From: Jason Alfredo Carlson Gallas (14 Jan 2005) fortran *plot\_orbit.f*, generates \*.eps files, see *Fig-7cycles.txt*, *Gallas0101305.txt*.
3. *per7.pdf* 18 period-7 orbits.
4. *chiral\_p8.pdf* 3 period-8 time-asymmetric pairs.
5. *per8.pdf*: 18 self-dual period-8 orbits (not sure that is a complete list).
6. *FourClasses.pdf*: defines four classes of orbits under time reversal; perhaps useful, still need to find the LaTeX file.
7. *tres.pdf*: period-6, symmetries with respect to the main diagonal of 3 6-cycles “corresponding to a  $\sigma^3$  factor,” plotted for  $a = 7$ . No idea what that is...
8. *Gallas0101305.txt* says he does not understand me.
9. *Predrag011304.txt* my last attempt to explain symbolic dynamics and why is this a time-reversal symmetry. “Please use ‘time reversal’ rather than ‘chiral’. It is a standard part of the lore of Hamiltonian dynamics, and especially Hamiltonian/symplectic mappings.” Hopeless.
10. *puzzle.pdf*, *puzzle.tex* is January 25, 2005 version of Endler and Gallas [32] (submitted December 25, 2005?) that uses ChaosBook notation - Table 1 can be used as a check on Sidney’s periodic orbits. Other versions: *puzzle011305.tex* of 13 Jan 2005; *puzzle.tex* and *puzzle2dasbuch.tex* of 27 Jan 2005;
 

They published in *Reductions and simplifications of orbital sums in a Hamiltonian repeller* [33] without me as a coauthor. Algebraic number expressions for periodic points show interesting patterns, their eqs. (22), (23) and (28), that would not be noticed from their numerical values.

They use binary labelling also in Endler and Gallas [31] *Conjugacy classes and chiral doublets in the Hénon Hamiltonian repeller*, without mentioning me or ChaosBook at all.
11. *citation.txt* and *puzzle.end* is the footnote which Gallas would not accept: *endnote27 This exact equation was discovered by P. Cvitanović during discussion and in collaboration with the authors.*
12. *old/puzzle011805.pdf* has my comments

13. *solRevHen.pdf* is extracted from [ChaosBook.org/projects](https://ChaosBook.org/projects), version 11.2.2, Mar 10 2005. I believe all that is in ChaosBook, ignore.
14. *revHenon.pdf*, *revHenon.zip* is a template for a [ChaosBook.org/projects](https://ChaosBook.org/projects) extracted from Jason Gallas, Predrag edited *puzzle.tex*, Gallas text removed 18 Feb 2006. I believe no one took up the project.

To summarize, this 2005 work agrees with current Han’s work, but does not clarify the problems we are dealing with now. The figures might be useful as crosschecks for Sidney’s Hénon orbits.

**2021-02-16 Predrag**<sup>2</sup> Here are my notes on the work of Gallas and collaborators; they have written many papers on polynomial maps [29–33, 38–40]. What I had contributed (unpublished, I believe) is to show Gallas how to use time-reversal, (??), (3.33) and (3.56), wrote a draft of a paper (click on [chiral.pdf](#)), and –when he was not interested in it– requested my traditional citation,

This exact equation was discovered by P. Cvitanović during discussion and in collaboration with the authors.

but he refused to credit me for that, so I - what’s the point - I stopped following their papers. I remember him being stubborn in a male kind of way. Absolutely refuses to understand binary symbolic dynamics, that what he understands [37] to be ‘spatial  $x \leftrightarrow y$  symmetry’

“[...] three algebraic conjugacy classes with respect to a spatial reflection  $R(x, y) = (y, x)$  about the  $y = x$  symmetry diagonal in phase-space.”

is time reversal, and he would not try to understand ChaosBook symmetry factorizations. But it is quite possible that they (or younger me?) did the right thing and quotiented the time reversal... Check the papers and the papers they refer to.

As he has worked on this for at least 20 years, there are many details specific to quadratic mappings that I think we can ignore here. Here is an overview from my point of view: Gallas *et al.* observe that

1. for polynomial mapping (3.41) the *orbital sum*

$$\sigma_p = \sum_{i \in p} x_{p,i} \tag{3.32}$$

is a *prime cycle p invariant* that satisfies a (factorized!) polynomial equation  $\mathbb{S}_n(\sigma) = 0$  of the order  $n_p$ , the period of the cycle, see for example (??).

---

<sup>2</sup>Predrag 27dec2004: Extracted from the ChaosBook.org boyscout, version of 2018-08-02 tex files. Edited here, so eventually return to ChaosBook.

**Predrag addendum:** Hill determinants are *symmetric polynomials* in lattice fields  $\{\phi_1, \phi_2, \dots, \phi_n\}$ , which are, by construction, all *prime cycle  $p$  invariants*. The orbital sum (3.32) is one example. Another one is the bilinear (22.21).

2. the cycle-points  $x_{p,i}$  of a given cycle are roots of a polynomial (3.41) of order  $n_p$ , see for example (?). This is remarkable, as higher iterates of a polynomial mapping are polynomials of a horrendous order.
3. time-reversal invariance (my interpretation, not theirs) induces the

$$\mathbb{S}_n = C_n^2 D_n N_n . \quad (3.33)$$

factorization of such polynomials, where D='diagonal' class, N='non-diagonal' class, and 'C='chiral' class, see below.

For me this is the key result.

This  $\mathbb{S}_n$  is very smart, as it has a zero for every *prime* orbit. Perhaps we can bring this to a full square, by including the boundary into the definition of the temporal lattice fundamental domain, with  $(CDN)$  orbits (perhaps in the Fourier space - they talk about 'cyclotomic polynomials')

$$\mathbb{S} = \frac{(CDN)^2}{DN} \quad (3.34)$$

by taking care of the temporal fundamental domain boundary by the inclusion-exclusion principle (24.251), and proceed to zeta-function factorization in the spirit of (6.47), (6.57), for each Hamiltonian Hénon cycle separately.

I believe factorization (3.34) should apply to periodic orbits of *any time-reversible* mapping, not just Hénon and temporal cat, but the 'N class' worries me.

(6.47)

$$\begin{aligned} (d - \mathbf{1}) &= \tilde{d}\tilde{\partial} \\ (d^{-1} - \mathbf{1})(d - \mathbf{1}) &= -\tilde{\partial}^2 = \square \\ \mathcal{J} &= \square - \mu^2 \mathbf{1} = (\tilde{\partial} + \mu \mathbf{1})(\tilde{\partial} - \mu \mathbf{1}) \\ \tilde{\mathcal{J}} &= \tilde{\partial} - \mu \mathbf{1} = \tilde{d} - \mu \mathbf{1} - \tilde{d}^{-1} \end{aligned} \quad (3.35)$$

**2021-02-19 Predrag** Gallas [37] *Counting orbits in conjugacy classes of the Hénon Hamiltonian repeller* counts the numbers  $C_n, D_n, N_n$  of (3.34) orbits (switched to calling 'prime cycles' orbits, like Gallas does) in each class, for any arbitrary period  $n$ .

$n$	1	2	3	4	5	6	7	8	9	10	11
$N_n$	2	4	8	16	32	64	128	256	512	1024	.
$M_n$	2	1	2	3	6	9	18	30	56	99	186

Table 3.1: Periodic states and orbit counts for the  $a = 6$  Hénon map. Compare with the golden (Fibonacci [9]) cat map table 6.2 and (6.198).

$n$	1	2	3	4	5	6	7	8	9	10	11	12	13	14	15
$\tilde{N}_n$	2	2	4	4	8	8	16	16	32	32	.	.	.	.	.
$\tilde{M}_n$	3	.	.	.	.	.	.	.	.	.	.	.	.	.	.

Table 3.2: Temporal periodic states and  $\mu = 1$  golden cat map. See (6.198) and the counting of walks on the “half time-step” Markov graph figure 6.5.

$D_n$  is sensible, relatively simply related to the number of points on the time-reversal diagonal; one expects something like that for any system.

$N_n$  is funky, has to do with the parabola symmetry line, might be what we call "dynamical".

$C_n$  is just the remainder  $M_n - D_n - N_n$ :  $C_1 = \dots = C_5 = 0$ , and then (Gallas Table 1), starting with  $C_6/2 = 1$ :

$$1, 2, 6, 14, 30, 62, 127, 252, 500, 968, 25446, \dots \quad (3.36)$$

This is not in *On-Line Encyclopedia of Integer Sequences OEIS*, (It is close to [OEIS:A000918](#) A000918  $a(n) = 2^n - 2$  and  $a(n + 1) = 2 + 2a(n)$ ) so it has to be reverse engineered to find the  $\tilde{N}_n$ , the numbers of periodic points of the yet to be written down  $\sqrt{\text{Hénon map}}$ .

The number of  $C_n/2$  periodic points:

$$\tilde{N}_6 = 1 * 6 = 6, \tilde{N}_7 = 2 * 7 = 14, \tilde{N}_8 = 6 * 8 = 48, \tilde{N}_9 = 14 * 9 = 126,$$

Actually,  $\tilde{N}_n = n C_n/2 + n(D_{2n} + N_{2n})$  looks more sensible

$$\tilde{N}_6 = **, \tilde{N}_7 = 2*7+1 = 5, \tilde{N}_8 = 6*8+1 = 19, \tilde{N}_9 = 14*9+2*2+1 = 61,$$

MacKay had these numbers already listed in Table 1.2.3.5.1 of his 1982 PhD thesis [53] ([click here](#)).

Assuming that (6.57) applies, we can compute  $\tilde{N}(\mu)_n$  from  $N(s)_n$

$$\begin{aligned} 2^n &= \tilde{N}(\mu)_n^2, & n \text{ odd} \\ 2^n &= \tilde{N}(\mu)_{2n}, & n \text{ even.} \end{aligned} \quad (3.37)$$

**2022-02-21 Predrag** In **2021-05-05 Predrag** I requested that Sidney use the Gallas form (22.11), but in **2021-08-29 Predrag** I recognized the error of my ways - *mea culpa*, and ever since (4.187) has been our convention for all scalar field theories.

The Hénon map, as introduced by Hénon [45], is (4.186). Written as a 2nd-order inhomogeneous difference equation [28], (4.186) takes the *temporal Hénon* 3-term recurrence form (4.187). Its Smale horseshoe is generated by iterates of the region plotted in figure 5.1.

**2004-12-27 Predrag** These extracts from ChaosBook.org are meant to complement and perhaps add to the Endler and Gallas explanation [32] of the “center of mass” puzzle for the cycles listed in table 5.3, first observed numerically by G. Vattay in ref. [10].

**2016-09-19 Predrag** <sup>3</sup>

We present exact formulas solving the problem of partitioning the total number  $M_k$  of period- $k$  orbits of the area-preserving Hénon map into the number of orbits building its three possible conjugacy classes. The formulas are valid for any arbitrary period  $n$ . They are derived with combinatorial methods, by an application of the number-theoretic Moebius inversion formula to a key problem in physics and dynamical systems. A handy MAPLE implementation of the formulas is also provided.

A number of orbital symmetries and asymmetries computed analytically and systematically for the Hamiltonian (area-preserving)  $b = -1$  limit of the Hénon map have been studied in refs. [31, 33].

Endler and Gallas [32] prefer the equivalent, rescaled form  $x \rightarrow x/a$  of the Hamiltonian Hénon map (3.29):

$$x_{n-1} - 2x_n + x_{n+1} + (x_n + 2)x_n = a, \quad (3.38)$$

They write: “ The advantage of this equation is that it generates *monic* minimal polynomials, i.e. polynomials having 1 as the leading coefficient. ”

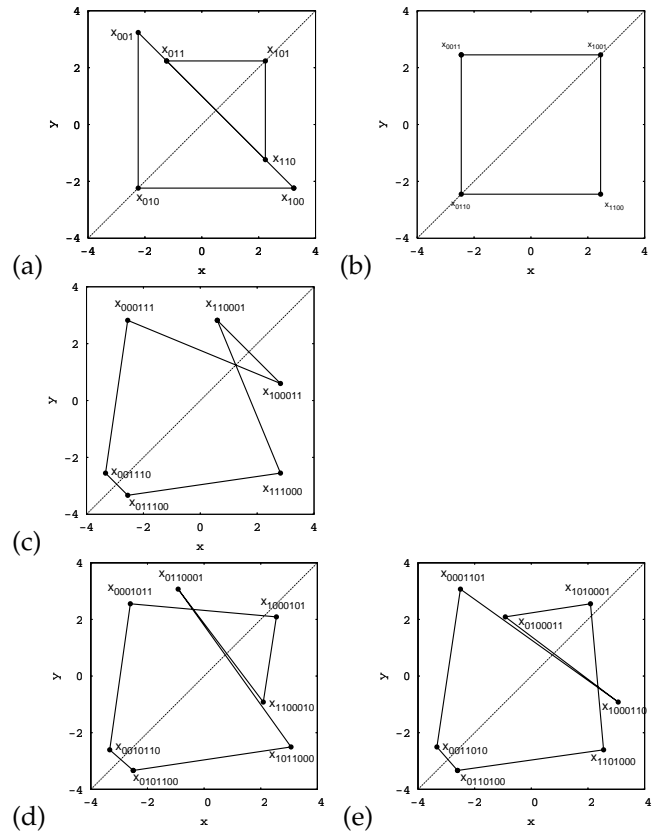
The key result reported was the existence of a natural segregation of all orbits into three algebraic conjugacy classes with respect to a spatial reflection  $R(x,y)=(y,x)$  about the  $y=x$  symmetry diagonal in state space. Under reflection, every periodic orbit was found to fall into one of three classes:

- D diagonal class, formed by symmetric orbits with points on the time-reversal symmetry diagonal. An odd period symmetric cycle has an odd number of points on the boundary, see figure 3.2 (a). An even period symmetric cycle has an even number of points on the boundary, see figure 3.2 (b).

---

<sup>3</sup>Predrag 2021-02-15: Copied from *DBblog.tex* - return eventually, as there are edits here. Not sure where the next few paragraphs came from.

Figure 3.2: Periodic orbits of the Hamiltonian Hénon map (3.28): (a) An odd-period orbit can have a point on the boundary, and thus belong to the diagonal class D. Example: the 3-cycles  $\overline{001}$ ,  $\overline{011}$ . (b) An even-period orbit can have two points on the boundary, and thus belong to the diagonal class D. Example: the 4-cycle  $\overline{0011}$ . (c) An even-period orbit can belong to the non-diagonal class N. Example: the 6-cycle  $\overline{000111}$ , with no points on the boundary. (d) Almost all longer orbits are asymmetric, ‘chiral’ class C. Example: the 7-cycle  $\overline{0001011}$ , and (e) its partner  $\overline{0001101}$  under flip across the diagonal and time-reversal. Under the time reversal periodic points symbol sequences are mirrored into their symmetry partners point by point. For spatiotemporal cat examples, see figure 24.5, figure 24.6, figure 24.18, figure 24.20, figure 24.22.



N non-diagonal class, formed by self-symmetric orbits without points on the symmetry diagonal, see figure 3.2 (c).

C chiral class, formed by pairs of asymmetric cycles that map into each other, see figure 3.2 (d,e).

Each class contains a characteristic algebraic signature embodied by a specific orbital decompositions (factorizations) [31]. The orbital segregation is independent of the control parameters and is specially interesting for  $a_h > 5.69931 \dots$ , the value beyond which there is a complete Smale horseshoe and all orbits are real. This Letter reports exact analytical expressions that count the numbers  $C_n$ ,  $D_n$ ,  $N_n$  of orbits in each class, for any arbitrary period  $n$ .

4

The problem of counting periodic orbits and its partitions is among the first problems that one needs to address [13, 16, 18, 22, 23, 51, 52, 68]. For

<sup>4</sup>Predrag 2022-02-25: Re figure ??: If anybody ever gives some thought to orbit Jacobian matrix eigenvalues of figure 22.2 (right), the corresponding eigenvectors might illuminate this point.

Table 3.3: The temporal Hénon period-5 and -6 symmetric periodic states of type figure 6.1 (b), with symmetry indicated in the  $\sigma$ -reflection format (??). For odd  $n = 2m + 1$ , symmetric orbits reduce to blocks of length  $m + 1$ . For even  $n = 2m$ , their lengths are either  $m + 1$  or  $m$ . The period-5 periodic states are plotted in figure ?? (to supersede figure 22.2 (left)). There is no asymmetric period-5, the first  $C_n$  asymmetric pair is period-6. Indicated: the binary code  $s_j$  of the field  $x_j$  at the lattice site  $j = 0, 1, 2, 3, 4$ .

$C_5$	$x_{-2}x_{-1} x_0 x_1x_2 $	$D_5$
11110	11 0 11	0 11
00011	10 0 01	0 01
00101	01 0 10	0 10
00001	00 1 00	1 00
11010	10 1 01	1 01
11100	01 1 10	1 10

$C_6$	$x_0x_1x_2x_3x_4x_5$	$D_6$
001011	001011	001011
110100	110100	
	$x_0 x_1x_2 x_3 x_2x_1$	
010001	0 10 0 01	0 10 0
011111	0 11 1 11	0 11 1
001110	0 01 1 10	0 01 1
100000	1 00 0 00	1 00 0
101110	1 01 1 10	1 01 1
	$x_0x_1x_2 x_2x_1x_0 $	
001100	001 100	001
011110	011 110	011

the paradigmatic quadratic map it was addressed very early by [Myrberg](#), in what appears to be one of the first applications of computers to dynamics [56–60]. Apart from counting orbits, he knew well how to exploit symbolic dynamics and what was later named “itineraries” and “kneading sequences” [54] to efficiently tabulate parameters with no less than 11 digits of accuracy. The problem of counting orbits for the Hénon map was also addressed very early, in a pioneering work by Simó [62] using an approach centered in the strange attractor creation/destruction.

The direct combinatorial problem of determining the partitions  $C_n, D_n, N_n$  individually seems to be very hard. However there is an efficient way of getting indirectly to them by counting the orbital points lying on symmetry axis of the problem. This is what we do. The approach is a nice application of enumerative combinatorics and the number-theoretic Moebius inversion formula to a key problem in physics and dynamical systems. Several complementary aspects of combinatorial dynamics are discussed in ref. [1].

**2021-02-18 Predrag** [Predrag: as the logistic map \(??\) is not invertible map, I expect no information about the time reversal factorization from this group of papers:](#)

Gallas [38] *Equivalence among orbital equations of polynomial maps* [arXiv:1809.05399](#)

Gallas [39] *Orbital carriers and inheritance in discrete-time quadratic dynamics* [arXiv:2008.01073](#):

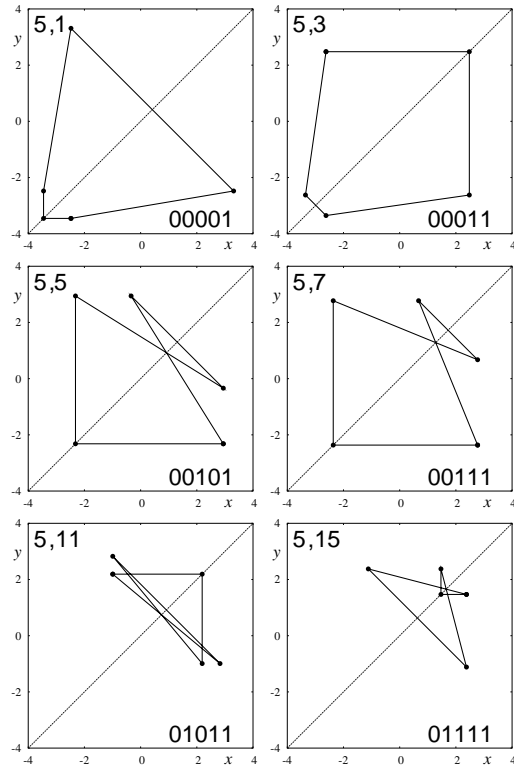


Figure 3.3: The 6 period-5 orbits are of Endler-Gallas class D (here called odd period symmetric cycles ( $o$ ), see (??)): they are symmetric under reflection across the diagonal, have a single point on it, corresponding to 2 successive field values of an even-reflection pair. Compare with the periodic state plots of figure ?? . The pairs 5,1 & 5,3 and 5,1 & 5,3 have an additional symmetry under reflection and stretch (Predrag: what is that? I do not see it) across the other diagonal.

[...] may be all conveniently extracted from just a single mathematical object, a polynomial called an *orbital carrier*, see for example (??). All orbits may be encoded simultaneously by a single carrier, with  $p$  orbit parameterized by the orbital sum  $\sigma_p$ .

recurrence

from Pincherle's relation

Simó [62] *On the Hénon-Pomeau attractor* is a very fine early paper. Cite it in Hénon remark. No mention of symmetry lines, though.

MacKay [53] 1982 PhD thesis, published as *Renormalisation in Area-preserving Maps* has a chapter on reversible maps. Do cite in our paper(s).

The theory comes from deVogelaere [27] *On the structure of symmetric periodic solutions of conservative systems, with applications* (1958)

**Orbits and periodic points** A periodic point is a solution  $(x, n)$ ,  $x \in \mathbb{R}^d$ ,  $n \in \mathbb{Z}$  of the periodic orbit condition

$$x = f^n(x) \tag{3.39}$$



for a given mapping  $f$ . Each periodic point  $x = x_{p,i} \in p$  belongs to a *time orbit*, a *orbit*  $p$  of period  $n_p$ , and its  $n_p$  distinct images

$$f^k(x_{p,i}) = x_{p,i+k}, \quad i+k \bmod n_p$$

are the successive periodic points along the cycle.

A *orbit*  $p$  of period  $n_p$  is a single traversal of the orbit.

We list the number of orbits up to length 10 for the 2-letter complete symbolic dynamics in tables ?? and ??.

<sup>5 6</sup> Consider the  $n$ -periodic point condition  $0 = f^n(x) - x$ . This polynomial of order  $2^n$  has zeros at all shorter, period  $d$  orbits if  $d$  is a divisor of  $n$ . Dividing those out, we arrive at the polynomial [55]

$$Q_n(x) = \prod_{d|n} (f^d(x) - x)^{\mu(n/d)}, \quad (3.40)$$

with  $nM_n$  zeros corresponding to the  $n$  periodic points for each orbit  $p$  of period  $n_p = n$ ,  $Q_n(x) = \prod_p P_p(x)$ , where the  $n$ th order polynomial

$$P_p(x) = \prod_{i \in p} (x - x_{p,i}) = 0, \quad n_p = n \quad (3.41)$$

has zeros at all periodic points in orbit  $p$ . Except for some values of  $a$ , at which bifurcations occur, these are simple zeros.

The coefficients in the expansion of (3.44) are symmetric polynomials in  $x_i$ , all reducible to powers of the orbital sum  $\sigma_p$  (3.32), a orbit  $p$  invariant, For example, the  $x^{n-2}$  coefficient

$$2 \sum_{i < j} x_i x_j = \sigma^2 - \sum_i x_i^2 = \sigma^2 + 2\sigma - n_p a$$

can be expressed in terms of  $\sigma^2$ ,  $\sigma$  and  $a$

$$P_p(x) = x^{n_p} - \sigma_p x^{n_p-1} + (\sigma^2 + 2\sigma - n_p a) x^{n_p-2} + \dots \pm (\sigma^{n_p} \dots). \quad (3.42)$$

We refer to  $\sigma$  as the “center of mass” of cycle  $p$  (up to an overall prefactor of  $1/n_p$ ). It was introduced by Friedland and Milnor [35], who refer to it as ‘the center of gravity’.

By cyclic invariance of periodic points in  $p$ ,  $\sigma_p$  is invariant under  $x \rightarrow f(x)$ , so it is an intrinsic property of the orbit  $p$ , hence it can take at most  $M_n$  distinct values corresponding to the  $M_n$  orbits  $p$  of period  $n_p = n$ .

Endler and Gallas [32] succeeded - after considerable algebra - in computing explicitly the  $M_n$ -th order polynomials

$$S_n(\sigma) = 0, \quad (3.43)$$

<sup>5</sup>Predrag 27dec2004: table ?? derived from knead.tex

<sup>6</sup>Predrag 27dec2004: extracted from smale.tex

<sup>7</sup> for  $n_p \leq n$ . The  $M_n$  root  $\sigma = \sigma_p$  substituted into the  $n$ th order polynomial

$$P_n(x, \sigma_p, a) = \prod_{i \in p} (x - x_i) = 0, \quad (3.44)$$

yields the  $n$  periodic points  $x = x_{p,i}$  belonging to the orbit  $p$  as the roots of  $P_n(x, \sigma_p, a) = 0$ . As the reduction of symmetric polynomial coefficients does not rely on the shape of a given orbit  $p$ ,  $P_n$  has the same form for all  $n_p = n$ .

**Smale horseshoe** Smale horseshoes and symbolic dynamics labeling of the dynamics - it's really great, once you get it, because the label tells you everything about the periodic point and the cycle it belongs too. From table ?? you can read off the shape and symmetry of individual cycles, and the factorization of  $S$  - at least the highest power of  $\sigma$  in each of the monic polynomials it factors into.

The Jacobian matrix for the  $n$ th iterate of the Hamiltonian Hénon map is

$$M^n(x_0) = \prod_{m=n}^1 \begin{bmatrix} -2x_m & -1 \\ 1 & 0 \end{bmatrix}, \quad x_m = f_1^m(x_0, y_0). \quad (3.45)$$

<sup>8</sup> The determinant of the Hénon one time-step Jacobian matrix (3.45) is constant,

$$\det M = \Lambda_1 \Lambda_2 = 1 \quad (3.46)$$

so only one eigenvalue  $\Lambda_1 = 1/\Lambda_2$  needs to be determined.

Iterating  $x_{n+1} = f(x_n)$  and checking the sign of  $x_k$  associates a temporally ordered topological itinerary  $s_{-m} \cdots s_{-1} s_0$  with a given trajectory,

$$s_k = \begin{cases} 1 & \text{if } x_k > 0 \\ 0 & \text{if } x_k < 0 \end{cases}. \quad (3.47)$$

**Time reversal symmetry** Under the time reversal (3.58) the points in the symbol square for an orientation preserving map are symmetric across the diagonal  $\gamma = \delta$ . Consequently the periodic orbits appear either in dual pairs  $p = s_1 s_2 s_3 \cdots s_n$ ,  $\bar{p} = s_n s_{n-1} s_{n-2} \cdots s_1$ , or are self-dual under time reversal,  $S_p = S_{\bar{p}}$ .

<sup>9</sup> For the orientation preserving case a self-dual cycle of odd period has at least one point (or odd number of points) on the symmetry diagonal. In particular, all fixed points lie on the symmetry diagonal.

A self-dual cycle of even period has no, or even number of points on the symmetry diagonal.

One distinguishes three kinds of cycles: asymmetric cycles  $a$ , symmetric cycles  $s$  built by repeats of irreducible segments  $\tilde{s}$ , and boundary cycles  $b$ .

<sup>7</sup>Predrag 27dec2004: fill in the explanation

<sup>8</sup>Predrag 27dec2004: main text - explain the order of multiplication

<sup>9</sup>Predrag 27dec2004: insert this into the book

**Asymmetric cycles C** ('chiral' class): A periodic orbits is not symmetric if  $\{x_a\} \cap \{\mathbf{R}x_a\} = \emptyset$ , where  $\{x_a\}$  is the set of periodic points belonging to the cycle  $a$ . Thus  $\mathbf{R}$  generates a second orbit with the same number of points and the same stability properties.

For this class of cycles for any  $n$ ,

$$P_a(x, \sigma, a) = \prod_{i=1}^p (x - x_{a,i}) \quad (3.48)$$

has  $n$  distinct roots  $\{x_{a,i}\}$ . The associated equation for is  $C(\sigma)^2 = 0$ .

**Example** : Follow the successive periodic points in the orbit  $\overline{0001011}$ , figure 3.2(d); then flip across the diagonal, reverse the direction along the cycle, and you are now on the orbit  $\overline{0001101}$ , the time reversed partner of  $\overline{0001011}$ .

**Symmetric cycles, no boundary point N** ('non-diagonal' class): A cycle  $s$  is reflection symmetric if operating with  $\mathbf{R}$  on the set of periodic points reproduces the set. The period of a symmetric cycle is always even ( $n_s = 2m$ ) and the mirror image of the  $x_s$  periodic point is reached by traversing the irreducible segment  $\bar{s}$  of length  $m$ ,  $f^m(x_s) = \mathbf{R}x_s$ .

$$P_N(x, \sigma, a) = (x - x_1)(x - x_2)^2 \cdots (x - x_m)^2(x - x_{m+1}) \quad (3.49)$$

has  $m + 1$  distinct roots.

$$\sigma_p = x_1 + 2x_2 + \cdots + 2x_m + x_{m+1} \quad (3.50)$$

**Example** : Symmetric (or self-dual orbit):

Draw 4-cycles  $\overline{0001}$  and  $\overline{0111}$ . They map into themselves under flip and time reversal. That means that if you know 2 periodic points, the other 2 are given by symmetry.

**Even symmetric cycles, 2 boundary points D** ('diagonal' class):

$$P_D(x, \sigma, a) = \prod_{i=1}^p (x - x_{s,i})^2 \quad (3.51)$$

has  $n_{\bar{s}}$  distinct roots.

$$\sigma_p = 2 \sum_i^{n_{\bar{s}}} x_{p,i} \quad (3.52)$$

3 or more boundary points are not possible for orbits.

Cycle  $\overline{0011}$  is an example of even-period boundary orbit . Two periodic points  $x_{1001}$ ,  $x_{0110}$  are on the symmetry diagonal, and reflection symmetry of

the remaining  $x_{0011}, x_{1100}$  pair forces a square-shaped trajectory in the  $[x, y]$  plane, see figure 3.2:<sup>10</sup>

$$\left[ \begin{array}{c} x_{1001} \\ x_{1001} \end{array} \right], \left[ \begin{array}{c} -x_{1001} \\ x_{1001} \end{array} \right], \left[ \begin{array}{c} -x_{1001} \\ -x_{1001} \end{array} \right], \left[ \begin{array}{c} x_{1001} \\ -x_{1001} \end{array} \right]$$

Hence  $\sigma_{0011} = 0$ , and

$$P_{0011} = (x^2 - x_{0011}^2)^2. \quad (3.53)$$

with  $x_{0011} = \sqrt{a}$ . Note that this 4-cycle is more robust than the 2-cycle given in (??) - it exists for  $a > 0$ , and is not the period-doubling relative of the 2-cycle.

**Odd symmetric cycles  $n = 2m + 1$ , 1 boundary point D** ('diagonal' class):

$$P_B(x, \sigma, a) = (x - x_1)^2 \cdots (x - x_m)^2 (x - x_{m+1}) \quad (3.54)$$

has  $m + 1$  distinct roots.

$$\sigma_p = 2x_1 + 2x_2 + \cdots + 2x_m + x_{m+1} \quad (3.55)$$

**Example** Boundary cycles:

Draw 3-cycles  $00\bar{1}$  and  $0\bar{1}\bar{1}$ . They have a point on the diagonal, indicated in the table S.1.

The time reversal symmetry of the state space (this is true for *all* Hamiltonian time-reversible flows whose Poincaré section is symmetric under  $[q, p] \rightarrow [p, q]$  diagonal flip, not just polynomial mappings) implies - but we need to cleanly explain it for this case that  $S_n(\sigma)$  *always* factorizes into form (3.33). Endler and Gallas [32] indeed observe that the polynomials  $S = S_n(\sigma)$  factorize into product of polynomials over the above three kinds of cycles.

For each  $n$ , the  $P_n(x, \sigma, a)$  polynomial should be written explicitly for each of the 3 symmetry classes  $[a, s, b]$ . In particular, for  $P_s(x, \sigma, a)$  the factorization over  $1/2$  of the state space

$$P_s(x, \sigma, a) = \left( \prod (x - x_{\bar{s},i}) \right)^2 \quad (3.56)$$

is expected, as exemplified by the 6-cycle figure 3.2 (c).

**Remark 3.1.** "Center of mass" puzzle. The "center of mass" notions play important role in a number of physical problems, such as: (1) the periodic-orbit formulation of the deterministic drift and diffusion (2) the kinematic dynamo problem [10, 41], and (3) Sullivan's formulation [5, 25, 47, 61] of the Feigenbaum  $\delta$  eigenvalue problem in the period-doubling renormalization theory.

The "center of mass" puzzle for the cycles listed in table 5.3 was first observed numerically by G. Vattay in ref. [10], and was resolved by Endler and Gallas [32]. Their method of solution resembles the methods earlier employed for quadratic polynomials

<sup>10</sup>Predrag 27dec2004: make into an exercise

(and their Julia sets) by Brown [17]<sup>11</sup> and Stephenson [63]. Brown gives cycles up to length 6 for the logistic map, employing symmetric functions of periodic points. Hitzl and Zele [46] study the Hénon map for cycle lengths up to period 6.

All explicit values of periodic points for the Hamiltonian Hénon map displayed here are taken from ref. [32]. Method of ref. [32] applies to cycles of polynomial maps only, in this case the quadratic map.

**Remark 3.2.** Complete Smale horseshoe, Hamiltonian Hénon map. It was proved by Devaney and Nitecki [26, 64] that there is indeed a hyperbolic horseshoe when  $a > 5 + 2\sqrt{5}$ . Numerical studies indicate that [64, 66]

$$a > 5.699310786700 \dots \quad (3.57)$$

### 3.5 Symmetries of the symbol square

<sup>12</sup> Depending on the type of dynamical system, the symbol square might have a variety of symmetries. Under the time reversal

$$\dots s_{-2}s_{-1}s_0.s_1s_2s_3 \dots \rightarrow \dots s_3s_2s_1.s_0s_{-1}s_{-2} \dots \quad (3.58)$$

the points in the symbol square for an orientation preserving map are symmetric across the diagonal  $\gamma = \delta$ , and for the orientation reversing case they are symmetric with respect to the  $\gamma = 1 - \delta$  diagonal. Consequently the periodic orbits appear either in dual pairs  $p = s_1s_2s_3 \dots s_n, \bar{p} = s_ns_{n-1}s_{n-2} \dots s_1$ , or are self-dual under time reversal,  $S_p = S_{\bar{p}}$ . For the orientation preserving case a self-dual cycle of odd period has at least one point on the symmetry diagonal. In particular, all fixed points lie on the symmetry diagonal. Determination of such symmetry lines can be of considerable practical utility, as it reduces some of the periodic orbit searches to 1-dimensional searches.<sup>13</sup>

#### 3.5.1 Symmetry lines

discuss symmetry lines



example 3.6

p. 133

example 3.7

p. 133

<sup>11</sup>Predrag : Brown [17] did all the right algebra for the logistic case. but computed approximate numbers rather than algebraic ones.

<sup>12</sup>Predrag 2021-04-03: Moved to here from ChaosBook *appendFiniteGr*. Return once updated here.

<sup>13</sup>Predrag 2021-03-24: create appendix chapter/appendCont.tex, include add JH Jan 18, 2008 *Desymmetrization of large spaces, thinking is extra price version* from halcrow/blog/TEX/symm.tex; create Problems/exerAppCont.tex, Problems/soluAppCont.tex, include halcrow/blog/TEX/zeglache.tex; create chapter/refsAppCont.tex.

## References

- [1] L. Alsedà, J. Llibre, and M. Misiurewicz, *Combinatorial Dynamics and Entropy in Dimension One* (World Scientific, Singapore, 2000).
- [2] S. Anastassiou, “Complicated behavior in cubic Hénon maps”, *Theoret. Math. Phys.* **207**, 572–578 (2021).
- [3] S. Anastassiou, A. Bountis, and A. Bäcker, “Homoclinic points of 2D and 4D maps via the parametrization method”, *Nonlinearity* **30**, 3799–3820 (2017).
- [4] S. Anastassiou, A. Bountis, and A. Bäcker, “Recent results on the dynamics of higher-dimensional Hénon maps”, *Regul. Chaotic Dyn.* **23**, 161–177 (2018).
- [5] R. Artuso, E. Aurell, and P. Cvitanović, “Recycling of strange sets: II. Applications”, *Nonlinearity* **3**, 361–386 (1990).
- [6] S. Aubry, “Anti-integrability in dynamical and variational problems”, *Physica D* **86**, 284–296 (1995).
- [7] S. Aubry and G. Abramovici, “Chaotic trajectories in the standard map. The concept of anti-integrability”, *Physica D* **43**, 199–219 (1990).
- [8] S. Aubry and P. Y. Le Daeron, “The discrete Frenkel-Kontorova model and its extensions. I. Exact results for the ground-states”, *Physica D* **8**, 381–422 (1983).
- [9] M. Baake, N. Neumärker, and J. A. G. Roberts, “Orbit structure and (reversing) symmetries of toral endomorphisms on rational lattices”, *Discrete Continuous Dyn. Syst.* **33**, 527–553 (2013).
- [10] N. J. Balmforth, P. Cvitanović, G. R. Ierley, E. A. Spiegel, and G. Vattay, “Advection of vector fields by chaotic flows”, *Ann. New York Acad. Sci.* **706**, 148–160 (1993).
- [11] C. Beck, “Spontaneous symmetry breaking in a coupled map lattice simulation of quantized Higgs fields”, *Phys. Lett. A* **248**, 386–392 (1998).
- [12] O. Biham and W. Wenzel, “Characterization of unstable periodic orbits in chaotic attractors and repellers”, *Phys. Rev. Lett.* **63**, 819 (1989).
- [13] R. L. Bivins, J. D. Louck, N. Metropolis, and M. L. Stein, “Classification of all cycles of the parabolic map”, *Physica D* **51**, 3–27 (1991).
- [14] S. Bolotin and R. MacKay, “Multibump orbits near the anti-integrable limit for Lagrangian systems”, *Nonlinearity* **10**, 1015–1029 (1997).
- [15] S. V. Bolotin and D. V. Treschev, “The anti-integrable limit”, *Russ. Math. Surv.* **70**, 975–1030 (2015).
- [16] A. Bridy and R. A. Pérez, “A count of maximal small copies in Multibrot sets”, *Nonlinearity* **18**, 1945–1953 (2005).
- [17] A. Brown, “Equations for periodic solutions of a logistic difference equation”, *J. Austral. Math. Soc. Ser. B* **23**, 78–94 (1981).

- [18] K. M. Brucks, “MSS sequences, colorings of necklaces, and periodic points of  $f(z) = z^2 - 2$ ”, *Adv. Appl. Math.* **8**, 434–445 (1987).
- [19] D. N. Butusov, A. I. Karimov, N. S. Pyko, S. A. Pyko, and M. I. Bogachev, “Discrete chaotic maps obtained by symmetric integration”, *Physica A* **509**, 955–970 (2018).
- [20] D. K. Campbell, Historical overview of the  $\phi^4$  model, in *A Dynamical Perspective on the  $\phi^4$  Model* (Springer, 2019) Chap. 1, pp. 1–22.
- [21] D. K. Campbell, S. Flach, and Y. S. Kivshar, “Localizing energy through nonlinearity and discreteness”, *Phys. Today* **57**, 43–49 (2004).
- [22] O. Chavoya-Aceves, F. Angulo-Brown, and E. Piña, “Symbolic dynamics of the cubic map”, *Physica D* **14**, 374–386 (1985).
- [23] W. Y. C. Chen and J. D. Louck, “Necklaces, MSS sequences, and DNA sequences”, *Adv. Appl. Math.* **18**, 18–32 (1997).
- [24] Y.-C. Chen, “Bernoulli shift for second order recurrence relations near the anti-integrable limit”, *Discrete & Continuous Dynamical Systems - B* **5**, 587–598 (2005).
- [25] F. Christiansen, P. Cvitanović, and H. H. Rugh, “The spectrum of the period-doubling operator in terms of cycles”, *J. Phys. A* **23**, 713–717 (1999).
- [26] R. L. Devaney and Z. Nitecki, “Shift automorphisms in the Hénon mapping”, *Commun. Math. Phys.* **67**, 137–146 (1979).
- [27] R. DeVogelaere, “IV. On the structure of symmetric periodic solutions of conservative systems, with applications”, in *Contributions to the Theory of Nonlinear Oscillations (AM-41), Volume IV* (Princeton Univ. Press, Princeton NJ, 1958), pp. 53–84.
- [28] H. R. Dullin and J. D. Meiss, “Generalized Hénon maps: the cubic diffeomorphisms of the plane”, *Physica D* **143**, 262–289 (2000).
- [29] A. Endler and J. A. C. Gallas, “Period four stability and multistability domains for the Hénon map”, *Physica A* **295**, 285–290 (2001).
- [30] A. Endler and J. A. C. Gallas, “Arithmetical signatures of the dynamics of the Hénon map”, *Phys. Rev. E* **65**, 036231 (2002).
- [31] A. Endler and J. A. C. Gallas, “Conjugacy classes and chiral doublets in the Hénon Hamiltonian repeller”, *Phys. Lett. A* **356**, 1–7 (2006).
- [32] A. Endler and J. A. C. Gallas, “Reductions and simplifications of orbital sums in a Hamiltonian repeller”, *Phys. Lett. A* **352**, 124–128 (2006).
- [33] A. Endler and J. A. C. Gallas, “Reductions and simplifications of orbital sums in a Hamiltonian repeller”, *Phys. Lett. A* **352**, 124–128 (2006).
- [34] M. J. Engel, *Short Course on Symmetry and Crystallography*, 2011.
- [35] S. Friedland and J. Milnor, “Dynamical properties of plane polynomial automorphisms”, *Ergodic Theory Dynam. Systems* **9**, 67–99 (1989).

- [36] J. A. C. Gallas, “Nonlinear dependencies between sets of periodic orbits”, *Europhysics Lett.* **47**, 649–655 (1999).
- [37] J. A. C. Gallas, “Counting orbits in conjugacy classes of the Hénon Hamiltonian repeller”, *Phys. Lett. A* **360**, 512–514 (2007).
- [38] J. A. C. Gallas, “Equivalence among orbital equations of polynomial maps”, *Int. J. Modern Phys. C* **29**, 1850082 (2018).
- [39] J. A. C. Gallas, “Orbital carriers and inheritance in discrete-time quadratic dynamics”, *Int. J. Modern Phys. C* **31**, 2050100 (2020).
- [40] J. A. C. Gallas, “Preperiodicity and systematic extraction of periodic orbits of the quadratic map”, *Int. J. Modern Phys. C* **31**, 2050174 (2020).
- [41] A. D. Gilbert and S. Childress, *Stretch, Twist, Fold: the Fast Dynamo* (Springer, Berlin, 1995).
- [42] M. N. Gudorf, *Orbithunter: Framework for Nonlinear Dynamics and Chaos*, tech. rep. (School of Physics, Georgia Inst. of Technology, 2021).
- [43] R. Hagiwara and A. Shudo, “An algorithm to prune the area-preserving Hénon map”, *J. Phys. A* **37**, 10521 (2004).
- [44] J. F. Heagy, “A physical interpretation of the Hénon map”, *Physica D* **57**, 436–446 (1992).
- [45] M. Hénon, “A two-dimensional mapping with a strange attractor”, *Commun. Math. Phys.* **50**, 94–102 (1976).
- [46] D. L. Hitzl and F. Zele, “An exploration of the Hénon quadratic map”, *Physica D* **14**, 305–326 (1985).
- [47] Y. Jiang, T. Morita, and D. Sullivan, “Expanding direction of the period doubling operator”, *Commun. Math. Phys.* **144**, 509–520 (1992).
- [48] N. Karve, N. Rose, and D. Campbell, “Periodic orbits in Fermi-Pasta-Ulam-Tsingou systems”, *Chaos: An Interdisciplinary Journal of Nonlinear Science* **34**, 093117 (2024).
- [49] P. G. Kevrekidis and J. Cuevas-Maraver, eds., *A Dynamical Perspective on the  $\phi^4$  Model: Past, Present and Future* (Springer, Berlin, 2019).
- [50] M.-C. Li and M. Malkin, “Bounded nonwandering sets for polynomial mappings”, *J. Dynam. Control Systems* **10**, 377–389 (2004).
- [51] M. Lutzky, “Counting stable cycles in unimodal iterations”, *Phys. Lett. A* **131**, 248–250 (1988).
- [52] M. Lutzky, “Counting hyperbolic components of the Mandelbrot set”, *Phys. Lett. A* **177**, 338–340 (1993).
- [53] R. S. MacKay, *Renormalisation in Area-preserving Maps* (World Scientific, Singapore, 1993).
- [54] J. Milnor and W. Thurston, “On iterated maps of the interval”, in *Dynamical Systems*, edited by J. C. Alexander (Springer, New York, 1988), pp. 465–563.



- [55] J. W. Milnor, *Orbits, external rays and the Mandelbrot set: An expository account*, 1999.
- [56] P. J. Myrberg, “Iteration der reellen Polynome zweiten Grades I”, *Ann. Acad. Sc. Fenn. A* **256**, 1–10 (1958).
- [57] P. J. Myrberg, “Iteration von quadratwurzeloperationen”, *Ann. Acad. Sc. Fenn. A* **259**, 1–10 (1958).
- [58] P. J. Myrberg, “Iteration der reellen Polynome zweiten Grades II”, *Ann. Acad. Sc. Fenn. A* **268**, 1–13 (1959).
- [59] P. J. Myrberg, “Sur l’itération des polynômes réels quadratiques”, *J. Math. Pures Appl.* **41**, 339–351 (1962).
- [60] P. J. Myrberg, “Iteration der reellen Polynome zweiten Grades III”, *Ann. Acad. Sc. Fenn. A* **336**, 1–13 (1963).
- [61] M. Pollicott, “A note on the Artuso-Aurell-Cvitanovic approach to the Feigenbaum tangent operator”, *J. Stat. Phys.* **62**, 257–267 (1991).
- [62] C. Simó, “On the Hénon-Pomeau attractor”, *J. Stat. Phys.* **21**, 465–494 (1979).
- [63] J. Stephenson and D. T. Ridgway, “Formulae for cycles in the Mandelbrot set II”, *Physica A* **190**, 104–116 (1992).
- [64] D. Sterling and J. D. Meiss, “Computing periodic orbits using the anti-integrable limit”, *Phys. Lett. A* **241**, 46–52 (1998).
- [65] D. G. Sterling, *Anti-integrable Continuation and the Destruction of Chaos*, PhD thesis (Univ. Colorado, Boulder, CO, 1999).
- [66] D. G. Sterling, H. R. Dullin, and J. D. Meiss, “Homoclinic bifurcations for the Hénon map”, *Physica D* **134**, 153–184 (1999).
- [67] D. Treschev and O. Zubelevich, “The anti-integrable limit”, in *Introduction to the Perturbation Theory of Hamiltonian Systems* (Springer, Berlin, 2009), pp. 131–142.
- [68] F.-G. Xie and B. L. Hao, “Counting the number of periods in one-dimensional maps with multiple critical points”, *Physica A* **202**, 237–263 (1994).

2CB

**Example 3.1. Hénon map.** The map

$$\begin{aligned} x_{n+1} &= 1 - ax_n^2 + by_n \\ y_{n+1} &= x_n \end{aligned} \tag{3.59}$$

is a nonlinear 2-dimensional map frequently employed in testing various hunches about chaotic dynamics. Written as a 2nd-order inhomogeneous difference equation (3-term recurrence relation), the temporal Hénon is

$$x_{n+1} = 1 - ax_n^2 + bx_{n-1}. \tag{3.60}$$

An  $(n + 1)$ -term recurrence relation is the discrete-time analogue of an  $n$ th order differential equation, and it can always be replaced by a set of  $n$  1-step relations.

Always plot the dynamics of such maps in the  $(x_n, x_{n+1})$  plane, rather than in the  $(x_n, y_n)$  plane, and make sure that the ordinate and abscissa scales are the same, so  $x_n = x_{n+1}$  is the  $45^\circ$  diagonal. There are several reasons why one should plot this way: (a) we think of the Hénon map as a model return map  $x_n \rightarrow x_{n+1}$ , and (b) as parameter  $b$  varies, the attractor will change its  $y$ -axis scale, while in the  $(x_n, x_{n+1})$  plane it goes to a parabola as  $b \rightarrow 0$ , as it should.

2CB

**Example 3.2. Temporal Hénon.** For  $b = -1$  parameter value the Hénon map (3.5) is the simplest example of a nonlinear Hamiltonian map, a 2-dimensional orientation preserving, area preserving map, often studied to better understand topology and symmetries of Poincaré sections of 2-degrees of freedom Hamiltonian flows.

We find it convenient [32] to multiply (3.60) by  $a$  and absorb the  $a$  factor into the definition the lattice field  $\phi = ax$ . This brings the Hamiltonian Hénon map to the form

$$\begin{aligned} \phi_{n+1} &= a - \phi_n^2 - p_n \\ p_{n+1} &= \phi_n, \end{aligned} \tag{3.61}$$

or, equivalently, the temporal Hénon (3.38) 3-term recurrence relation of form

$$\phi_{i+1} + \phi_i^2 + \phi_{i-1} = a, \quad i = 1, \dots, n_p. \tag{3.62}$$

We can write this as a lattice field equation with lattice Laplacian (4.6)

$$\square \phi_n + (\phi_n + 2) \phi_n = a. \tag{3.63}$$

The field equation is nonlinear, with the cubic potential (4.148).

For definitiveness, in numerical calculations in examples to follow we shall fix (arbitrarily) the stretching parameter value to  $a = 6$ , a value large enough to guarantee that all roots of  $0 = f^n(x) - x$  (periodic points) are real.

exercise ??  
click to return: p. ??

**Example 3.3. Temporal Hénon fixed points.** Since we are looking for fixed points  $p_q$  of (3.61), each successive step is the same as the previous,

$$\begin{pmatrix} \phi_q \\ p_q \end{pmatrix} = \begin{pmatrix} a - \phi_q^2 - p_q \\ \phi_q \end{pmatrix}.$$

Thus there two fixed points, given by the roots of the quadratic equation  $\phi^2 - 2\phi - a = 0$ ,  
<sup>14</sup>

$$\begin{aligned} \phi_0 &= -1 - \sqrt{1 + a} \\ \phi_1 &= -1 + \sqrt{1 + a}. \end{aligned} \tag{3.64}$$

<sup>14</sup>Predrag 2021-04-28: agrees with Endler and Gallas [32]  $a = 6$  values

<sup>15</sup>  $\overline{01}$  periodic points are (??)

$$\phi_{10} = 1 + \sqrt{a-3}, \quad \phi_{01} = 1 - \sqrt{a-3}. \quad (3.65)$$

[click to return: p. ??](#)

**Example 3.4. Temporal Hénon stability.** For the Hénon map (3.61) the temporal evolution Jacobian matrix for the  $n$ th iterate of the map is the product of consecutive one time-step Jacobian matrices

$$J^n(\phi_0) = \prod_{m=n}^1 \begin{bmatrix} -2\phi_m & -1 \\ 1 & 0 \end{bmatrix}, \quad \phi_m = f_1^m(\phi_0, p_0). \quad (3.66)$$

The decreasing order in the indices of the products in above formulas is a reminder that the successive time steps correspond to multiplication from the left,  $J_p(\phi_1) = J(\phi_{n_p}) \cdots J(\phi_1)$ .

The determinant of the Hénon one time-step Jacobian matrix in (3.66) is a constant,

$$\det J = 1, \quad (3.67)$$

so the map is Hamiltonian (symplectic) in the sense that it preserves areas in the  $[\phi, p]$  plane.

The Floquet matrix  $J_p$  for a orbit  $p$  of length  $n_p$  of the Hénon map (3.61) is evaluated by picking any periodic point as a starting point, running once around a orbit, and multiplying the individual periodic point Jacobian matrices (3.66),

$$J_p(x_0) = \prod_{k=n_p}^1 \begin{bmatrix} -2\phi_k & -1 \\ 1 & 0 \end{bmatrix}, \quad \phi_k \in \mathcal{M}_p, \quad (3.68)$$

Once we have a periodic orbit of Hénon map, we also have its Floquet matrix. Only the expanding eigenvalue  $\Lambda_1 = 1/\Lambda_2$  needs to be determined, as  $\det J = \Lambda_1 \Lambda_2 = 1$ .

The orbit Jacobian matrix is the  $\delta/\delta\phi_k$  derivative of the temporal Hénon (3.62) 3-term recurrence relation

$$\begin{aligned} \mathcal{J}_p &= \sigma + 2\mathbb{X}_p + \sigma^{-1} \\ &= \begin{bmatrix} 2\phi_0 & 1 & 0 & 0 & \dots & 0 & 1 \\ 1 & 2\phi_1 & 1 & 0 & \dots & 0 & 0 \\ 0 & 1 & 2\phi_2 & 1 & \dots & 0 & 0 \\ \vdots & \vdots & \vdots & \vdots & \ddots & \vdots & \vdots \\ 0 & 0 & \dots & \dots & \dots & 2\phi_{n-2} & 1 \\ 1 & 0 & \dots & \dots & \dots & 1 & 2\phi_{n-1} \end{bmatrix}, \end{aligned} \quad (3.69)$$

where  $\mathbb{X}_p$  is a diagonal matrix with  $p$ -periodic state  $\phi_k$  in the  $k$ th row/column, and the 1's in the upper right and lower left corners enforce the periodic boundary conditions.

The trace of the orbit Jacobian matrix is twice the orbital sum [40]

$$\sigma_p = \sum_{i \in p} \phi_{p,i} \quad (3.70)$$

a prime cycle  $p$  invariant that satisfies a polynomial equation  $\mathbb{S}_n(\sigma) = 0$  of the order  $n_p$ , the period of the cycle. <sup>16</sup>

<sup>15</sup>Predrag 2021-04-28: make into na exercise: Show that (3.64)...

<sup>16</sup>Predrag 2021-05-04: Perhaps include the example (??)?

The two fixed points (3.65) are hyperbolic for  $a > 3$ , with expanding eigenvalues

$$\begin{aligned}\Lambda_0 &= 1 + \sqrt{1+a} + (1+a)^{1/4} \sqrt{\sqrt{1+a} + 2} \\ \Lambda_1 &= 1 - \sqrt{1+a} - (1+a)^{1/4} \sqrt{\sqrt{1+a} - 2},\end{aligned}\tag{3.71}$$

The action of the temporal Hénon orbit Jacobian matrix can be hard to visualize, as a period-2 periodic state is a 2-torus, period-3 periodic state a 3-torus, etc.. Still, the fundamental parallelepiped for the period-2 and period-3 periodic states, should suffice to convey the idea. The fundamental parallelepiped basis vectors (??) are the columns of  $\mathcal{J}$ . The  $[2 \times 2]$  orbit Jacobian matrix and its Hill determinant follow from (3.64)

$$\mathcal{J} = \begin{pmatrix} 2\phi_0 & 2 \\ 2 & 2\phi_1 \end{pmatrix}, \quad \text{Det } \mathcal{J} = 4(\phi_0\phi_1 - 1) = -4(a - 3).\tag{3.72}$$

The resulting fundamental parallelepiped shown in figure ?? (a). Period-3 periodic states for  $s = 3$  are contained in the half-open fundamental parallelepiped of figure ?? (b), defined by the columns of  $[3 \times 3]$  orbit Jacobian matrix

$$\mathcal{J} = \begin{pmatrix} 2\phi_0 & 1 & 1 \\ 1 & 2\phi_1 & 1 \\ 1 & 1 & 2\phi_2 \end{pmatrix}, \quad \text{Det } \mathcal{J} = 8\phi_0\phi_1\phi_2 - 2(\phi_0 + \phi_2 + \phi_3) + 2,\tag{3.73}$$

and for an period- $n$  periodic state,<sup>17</sup>

$$\text{Det } \mathcal{J} = 2^n \phi_0\phi_1\phi_2 \cdots \phi_{n-1}, \quad n > 3.\tag{3.74}$$

**Example 3.5. Hamiltonian Hénon map, reversibility.** The Hénon map (??) is reversible, with its inverse interchanging the roles of  $x$  and  $y$ :

$$\begin{aligned}x_{n-1} &= y_n \\ y_{n-1} &= a - y_n^2 - x_n,\end{aligned}\tag{3.75}$$

hence the dynamics is symmetric in the  $[x, y]$  plane: a trajectory maps into a trajectory under the flip across the  $x = y$  diagonal

$$\begin{bmatrix} y \\ x \end{bmatrix} = R \begin{bmatrix} x \\ y \end{bmatrix} = \begin{bmatrix} 0 & 1 \\ 1 & 0 \end{bmatrix} \begin{bmatrix} x \\ y \end{bmatrix}\tag{3.76}$$

and the time reversal. The reversor  $R$  is orientation reversing,  $\det[\partial R] = -1$ , and is an involution,  $R^2 = \mathbf{1}$ . In other words, the Hamiltonian Hénon map is conjugate to its inverse  $f \circ R = R \circ f^{-1}$ , and can be factored into a pair of orientation reversing involutions,  $f = (fR) \circ R = T \circ R$ , with

$$T \begin{bmatrix} x \\ y \end{bmatrix} = \begin{bmatrix} x \\ a - x^2 - y \end{bmatrix}.\tag{3.77}$$

Equivalently, writing  $f = S \circ (Sf) = S \circ U$ , the reversor

$$U \begin{bmatrix} x \\ y \end{bmatrix} = \begin{bmatrix} a - y^2 - x \\ y \end{bmatrix}\tag{3.78}$$

factorizes the Hénon map as  $f = ST$ .

[click to return: p. ??](#)

<sup>17</sup>Predrag 2021-05-04: A guess, **absolutely wrong - Fix!**

**Example 3.6. Symmetry lines of the standard map.** *In practice the search for important classes of periodic orbits for the standard map takes advantage of its remarkable symmetry:  $A$  can be written as the product of two involutions,  $A = T_2 \cdot T_1$ , (involution means that the square of the map is the identity):*

remark 2.3

$$\begin{aligned} T_1(x, y) &= (-x, y - k \sin x) \\ T_2(x, y) &= (-x + y, y). \end{aligned} \quad (3.79)$$

Now define symmetry lines  $\mathcal{L}_1$  and  $\mathcal{L}_2$  as the sets of fixed points of the corresponding involution:  $\mathcal{L}_1$  consists of the lines  $x = 0, \pi$ ,  $\mathcal{L}_2$  of  $x = y/2 \pmod{2\pi}$ . There are deep connections between symmetry lines and periodic orbits: we just give an example with the following statement: if  $(x_0, y_0) \in \mathcal{L}_1$  and  $A^M(x_0, y_0) \in \mathcal{L}_1$  (i.e. they are both fixed points of  $T_1$ ), then  $(x_0, y_0)$  is a periodic point of period  $2M$ .<sup>18</sup> As a matter of fact

$$\begin{aligned} A^{2M}(x_0, y_0) &= A^{M-1}T_2T_1A^{M-1}T_2T_1(x_0, y_0) \\ &= A^{M-1}T_2A^{M-1}T_2(x_0, y_0) \end{aligned} \quad (3.80)$$

by the fixed point property. Now the involution property implies

$$T_2A = T_1 \quad AT_1 = T_2 \quad (3.81)$$

and thus

$$AT_2AT_2 = AT_1T_2 = \mathbf{1} \quad (3.82)$$

and

$$A^P T_2 A^P T_2 = A^{P-1} T_2 A^{P-1} T_2 \quad (3.83)$$

from which it easily follows that  $(x_0, y_0)$  belongs to a  $2M$  cycle.

(Continued in example 3.7.)

[click to return: p. 125](#)

**Example 3.7. Symmetry lines of the cat map.** (Continued from example 3.6.) Instead of standard map, consider its linear relative, the cat map, obtained by substituting  $k \sin x \rightarrow Kx$  in (3.79).  $A$  can now be written as the matrix product of two involutions,  $A = T_2 T_1$ ,

$$\begin{aligned} T_1(x, p) = (-x, p - Kx) &\Rightarrow T_1 = \begin{bmatrix} -1 & 0 \\ s-2 & 1 \end{bmatrix} \\ T_2(x, p) = (-x + p, p) &\Rightarrow T_2 = \begin{bmatrix} -1 & 1 \\ 0 & 1 \end{bmatrix} \\ &\Rightarrow A = \begin{bmatrix} s-1 & 1 \\ s-2 & 1 \end{bmatrix}. \end{aligned} \quad (3.84)$$

$T_1$  and  $T_2$  are involutions as their squares are the identity. We have substituted  $K = -s + 2$ , where  $s = \text{tr } A$ .

<sup>19</sup> Now define symmetry lines  $\mathcal{L}_1$  and  $\mathcal{L}_2$  as the sets of fixed points of the corresponding involution:  $\mathcal{L}_1$  consists of the lines  $x = 0 \pmod 1$ ,  $\mathcal{L}_2$  of  $p = 2x$ . There are deep connections between symmetry lines and periodic orbits: we just give an example

<sup>18</sup>Predrag 2021-04-03: Bad notation -  $M$  is monodromy matrix

<sup>19</sup>Predrag 2021-04-10: complete the rewrite here.

with the following statement: if  $(x_0, p_0) \in \mathcal{L}_1$  and  $A^M(x_0, p_0) \in \mathcal{L}_1$  (i.e. they are both fixed points of  $T_1$ ), then  $(x_0, p_0)$  is a periodic point of period  $2M$ . As a matter of fact

$$\begin{aligned} A^{2M}(x_0, p_0) &= A^{M-1}T_2T_1A^{M-1}T_2T_1(x_0, p_0) \\ &= A^{M-1}T_2A^{M-1}T_2(x_0, p_0) \end{aligned} \quad (3.85)$$

by the fixed point property. Now the involution property implies

$$T_2A = T_1 \quad AT_1 = T_2 \quad (3.86)$$

and thus

$$AT_2AT_2 = AT_1T_2 = \mathbf{1} \quad (3.87)$$

and

$$A^P T_2 A^P T_2 = A^{P-1} T_2 A^{P-1} T_2 \quad (3.88)$$

from which it easily follows that  $(x_0, p_0)$  belongs to a  $2M$  cycle.

I see no  $\mathcal{J} = \tilde{\mathcal{J}}^\top \tilde{\mathcal{J}}$  factorization in style of (6.49)

[click to return: p. 125](#)

## 3.6 \*

### Exercises boyscout

3.1. **“Center of mass” puzzle.** Why is the “center of mass,” tabulated in exercise 5.1, often a rational number?

3.2. **Hénon temporal lattice.**

1-dimensional temporal Hénon lattice (see [ChaosBook Example 3.5](#)) is given by a 3-term recurrence

$$x_{n+1} + ax_n^2 - bx_{n-1} = 1.$$

The parameter  $a$  quantifies the “stretching” and  $b$  quantifies the “contraction”.

The single Hénon map is nice because the system is a nonlinear generalization of temporal cat 3-term recurrence CL18 eq. `catMapNewt`, with no restriction to the unit hypercube XXX, but has binary dynamics.

There is still a tri-diagonal orbit Jacobian matrix  $\mathcal{J}$  CL18 eq. `tempCatFixPoint`, but CL18 eq. (Hessian) is now periodic state dependent. Also, I believe Han told me that CL18 sect. s:Hill *Hill determinant: stability of an orbit vs. its time-evolution stability* block matrices derivation of Hill’s formula does not work any more. Neither does the ‘fundamental fact’, as each periodic state’s orbit Jacobian matrix is different, and presumably does not count periodic states, as there is no integer lattice within the Hill determinant volume.

Does the [ChaosBook flow conservation](#) sum rule [ChaosBook ed. \(27.15\)](#) (or CL18.tex eq. Det(jMorb)eights) still work?

The assignment: Implement the variational searches for periodic states in Matt's OrbitHunter [42], find all periodic states up to  $n = 6$ .

(a)  $a = 1.4$   $b = 0.3$ , compare with [ChaosBook Table 34.2](#).

(b) For  $b = -1$  the system is time-reversible or 'Hamiltonian', see [ChaosBook Example 8.5](#). For definitiveness, in numerical calculations in examples to follow we fix (arbitrarily) the stretching parameter value to  $a = 6$ , a value large enough to guarantee that all roots of the periodic point condition  $0 = f^n(x) - x$  are real.

Note also [ChaosBook sect A10.3 Hénon map symmetries](#) and [ChaosBook Exer. 7.2 Inverse iteration method](#).

The deviation of an approximate trajectory from the 3-term recurrence is

$$v_n = x_{n+1} - (1 - ax_n^2 + bx_{n-1})$$

In classical mechanics force is the gradient of a potential, which Biham-Wenzel [12] construct as a cubic potential

$$V_n = x_{n+1}x_n - bx_nx_{n-1} + (ax_n^3 - x_n). \quad (3.89)$$

With the cubic potential at lattice site  $n$  we can start to look for orbits variationally. Note that the potential is time-reversal invariant for  $b = 1$ .

Compare with XXX

- 3.3. **Engel Point Groups 1.** (Engel's [34] [Point Groups](#) Exercise 1): The molecule on the left has  $C_{1s}$  which signifies that it has reflection symmetry over one axis. The molecule on the right has  $C_3$  symmetry, signifying that it is symmetric by rotations of  $\frac{2\pi}{3}$  or one third of a full circle.

M. Engel

- 3.4. **Engel Point Groups 3.** (Engel's [34] [Point Groups](#) Exercise 3): Three point groups for  $C_2H_6$ : a.  $C_{3v}$  because rotating it by  $1/3$  of a circle leaves it invariant, and one can cut the molecules into three identical pieces. b.  $C_s$  because the top and bottom have the same orientation, it is like looking in a mirror, so can apply reflection symmetry. c. Unsure, perhaps inversion symmetry  $C_i$ .

M. Engel

- 3.5. **The matrix square root.** Consider matrix

$$A = \begin{bmatrix} 4 & 10 \\ 0 & 9 \end{bmatrix}.$$

Generalize the square root function  $f(x) = x^{1/2}$  to a square root  $f(A) = A^{1/2}$  of a matrix  $A$ .

a) Which one(s) of these is/are the square root of  $A$

$$\begin{bmatrix} 2 & 2 \\ 0 & 3 \end{bmatrix}, \begin{bmatrix} -2 & 10 \\ 0 & 3 \end{bmatrix}, \begin{bmatrix} -2 & -2 \\ 0 & -3 \end{bmatrix}, \begin{bmatrix} 2 & -10 \\ 0 & -3 \end{bmatrix} ?$$

b) Assume that the eigenvalues of a  $[d \times d]$  matrix are all distinct. How many square root matrices does such matrix have?

c) Given a  $[2 \times 2]$  matrix  $A$  with a distinct pair of eigenvalues  $\{\lambda_1, \lambda_2\}$ , write down a formula that generates all square root matrices  $A^{1/2}$ . Hint: one can do this using the 2 projection operators associated with the matrix  $A$ .  
2 points

### Chapter 3. Hénon map

#### Solution 3.2 - Hénon temporal lattice.

(a) Here's my initial attempt, I'm trying to see if the flow conservation law CL18 eq. Det(jMorb)eights still works for the Hénon map:

$$\phi_{n+1} + a\phi_n^2 - b\phi_{n-1} = 1$$

The first step seems to be to construct the orbit Jacobian matrix  $\mathcal{J}$ :

$$F[\Phi] = \mathcal{J}\Phi - I \tag{3.90}$$

Where  $I$  is the identity matrix, and  $F$  is the function where we want to find the zeros for (the orbits). We can rewrite this as:

$$(\sigma + aI\Phi - b\sigma^{-1})\Phi = I \tag{3.91}$$

Therefore,  $\mathcal{J}$  is

$$\mathcal{J} = \sigma + aI\Phi - b\sigma^{-1} = \begin{bmatrix} a\phi_1 & 1 & 0 & \dots & -b \\ -b & a\phi_2 & 1 & \dots & 0 \\ 0 & \ddots & \ddots & \ddots & \vdots \\ \vdots & \dots & -b & a\phi_{n-1} & 1 \\ 1 & 0 & \dots & -b & a\phi_n \end{bmatrix} \tag{3.92}$$

Before I take a crack at seeing if this flow conservation still holds, I do have some questions:

Q1 Sidney It appears that the derivation from chapter 23 (eqn 23.17, I don't know how to cite that specifically) the denominator of the sum rule is a product of the eigenvalues  $\Lambda_{pi}$ , which (if I remember correctly) are just the eigenvalues of the orbit Jacobian matrix of the flow or map, which from basic linear algebra I know to be just the determinant of the orbit Jacobian matrix. It cannot be that straightforward, where is the flaw in my logic?



Q2 Sidney How do I go from the periodic orbit formulation of the sum rule from Ch 23 to the lattice formulation? My initial thought is that since periodic states are akin to a periodic orbit (right?) that the sum can just be immediately changed from a sum over all periodic orbits, to a sum over all periodic states. Is this reasoning correct?

Comment Sidney I now realize that the flow sum rule involving the orbit Jacobian matrix (NOT the Hill matrix) is a fundamental property that applies to all systems (at least all closed systems), what I now know is that I need to work out if I can convert between the determinant of the orbit Jacobian matrix and the determinant of the Hill matrix.

Plan Sidney I am going to try to see what I can do with the block matrix proof, and I will get back to everyone on Friday

Update Sidney I tried working out the proof with the block matrices for just the regular Bernoulli map, I understand everything except the sentence "For a period- $n$  periodic state  $\Phi_M$ , the orbit Jacobian matrix (15) is now a  $[nd \times nd]$  matrix function of the  $[d \times d]$  block matrix  $J$ ." It sort of seemed like it was much like "poof! And then a miracle happens!" I will keep exploring.

I shall now correct my mistake with the derivation of the orbit Jacobian matrix/Hill matrix  $\mathcal{J}$  I shall use the differential definition:

$$\mathcal{J}_{ij} = \frac{\delta F[\Phi]_j}{\delta \phi_i}$$

Which gives us that  $\mathcal{J} = \sigma + 2aI\Phi_n - b\sigma^{-1}$ . Now I will use the differential definition of the local Jacobian, where  $f$  is a functions such that  $f(\phi_n) = \phi_{n+1}$

$$J_{ij} = \frac{\partial f(\phi_n)_i}{\partial \phi_{n,j}}$$

Which gives us that  $J(\phi_n) = -2a\phi_n$ . So we can rewrite  $\mathcal{J} = \sigma - J(\phi_n)I - b\sigma^{-1}$ , with the understanding that  $J$  changes along the diagonal. I am not quite sure how to bring this to the sum rule, but I will soon (hopefully), how do I math things like  $\phi$  and  $\Phi$  bold?

Update Sidney I need to do a proper mathematical look at the flow conservation, but the Hénon map is not flow conserving (some trajectories are inadmissible) so the sum rule does not equal 1, I will try later to look at what it does equal analytically, but until then I will tackle the computation. I have made great progress with that, with help from Matt I was able to create a working code that gave me the correct orbits up to length 10 (I could not check past that). The code is in my blog. Once Matt has completed the current round of OrbitHunter [42] updates I shall try to use that to reproduce my results.

Solution Sidney (a) The flow conservation sum rule does not sum to 1 so it does not work as before, I still need to try to relate the global Hill matrix to the local Jacobian matrix, I think I may be close to reworking the block matrix proof. Anyway, here are the periodic points I found (please note that the code cannot be used to find fixed points ( $n=1$ ) so I just did it analytically, I will try to add that to the code later):

$$\begin{aligned} n = 1 & \quad - 1.13135447 \\ n = 1 & \quad 0.63135447 \\ n = 2 & \quad [0.97580005, -0.47580005] \end{aligned}$$

$$n = 4 \quad [1.12506994, -0.70676678, 0.63819399, 0.21776177]$$

$$n = 6 \quad [1.03805954, -0.41515894, 1.07011813, -0.72776163, 0.57954366, 0.31145232]$$

$$n = 6 \quad [1.1579582, -0.8042199, 0.44190995, 0.48533586, 0.80280173, 0.2433139]$$

When I tried to find  $n = 3$  and  $n = 5$  the code returned nothing, this matches with what is tabulated in table 34.2. I will try using some of the analytical pruning techniques to prove that  $n = 3$  and  $n = 5$  are not allowed.

(Sidney Williams 2021-01-20)

**Solution 3.3 - Engel Point Groups 1.** The molecule on the left has  $C_i$  symmetry which is inversion symmetry NOT reflection symmetry because the top and bottom arrangements are not like they would be if placed in front of a mirror. The molecule on the right has  $C_{3v}$  symmetry, which is pyramidal symmetry which corresponds to the fact that one could take three slices of the molecule and they would each be identical, not just the configuration would be preserved by a rotation.

(Sidney Williams 2021-03-07)

**Solution 3.4 - Engel Point Groups 3.** Apparently, it depends based on whether we are dealing with staggered Ethane or not. If it is staggered, then it has inversion symmetry, if it is not, it has reflection symmetry, it should have  $C_3$  symmetry instead of  $C_{3v}$  which confuses me a great deal. If I remember correctly it should correspond to a reflection vertical plane, which it should have, so I do not understand. The third one is  $C_2$  which I do not understand how it is different from the inversion symmetry. Although, looking at simulations from [here](#), it looks like the  $C_2$  group can be used to rotate about axes that are different in orientation from just right through the middle. (Sidney Williams) 2021-03-07

**Solution 3.5 - The matrix square root.**

a) It is easy to check that

$$A = \begin{bmatrix} 4 & 10 \\ 0 & 9 \end{bmatrix} = \left(A_{ij}^{1/2}\right)^2$$

for the matrices

$$\begin{aligned} A_{++}^{1/2} &= \begin{bmatrix} 2 & 2 \\ 0 & 3 \end{bmatrix}, & A_{+-}^{1/2} &= \begin{bmatrix} -2 & 10 \\ 0 & 3 \end{bmatrix} \\ A_{--}^{1/2} &= \begin{bmatrix} -2 & -2 \\ 0 & -3 \end{bmatrix}, & A_{-+}^{1/2} &= \begin{bmatrix} 2 & -10 \\ 0 & -3 \end{bmatrix} \end{aligned} \quad (3.93)$$

Being upper-triangular, the eigenvalues of the four matrices can be read off their diagonals: there are four square root  $\pm$  eigenvalue combinations  $\{3,2\}$ ,  $\{-3,2\}$ ,  $\{3,-2\}$ , and  $\{-3,-2\}$ .

Associated with each set  $\lambda_i \in \{\lambda_1, \lambda_2\}$  is the projection operator

$$P_{ij}^{(1)} = \frac{1}{\lambda_1 - \lambda_2} (A_{ij}^{1/2} - \lambda_2 \mathbf{1}) = \begin{bmatrix} 0 & 2 \\ 0 & 1 \end{bmatrix} \quad (3.94)$$

$$P_{ij}^{(2)} = \frac{1}{\lambda_2 - \lambda_1} (A_{ij}^{1/2} - \lambda_1 \mathbf{1}) = \begin{bmatrix} 1 & -2 \\ 0 & 0 \end{bmatrix}. \quad (3.95)$$

Note that all 'square root' matrices have the same projection operators / eigenvectors as the matrix  $A$  itself, so one can drop the  $ij$  subscripts on  $P^{(1)}, P^{(2)}$ .

## Exercises boyscout

---

b) If the eigenvalues of a  $[d \times d]$  matrix are all distinct, the matrix is diagonalizable, so the number of square root  $\pm$  combinations is  $2^d$ . However, for general matrices things can get crazy - there can be *no, or some, or  $\infty$*  of 'square root' matrices.

c) We know  $\{\lambda_1, \lambda_2\}$  and  $P^{(\alpha)}$  for  $A$ , and the four 'square root' eigenvalues are clearly  $\{\pm\lambda_1^{1/2}, \pm\lambda_2^{1/2}\}$ . That suggest finding the 'square root' matrices (3.93) by reverse-engineering (3.94), (3.95):

$$A_{ij}^{1/2} = (\lambda_1 - \lambda_2)P^{(1)} + \lambda_2 \mathbf{1},$$

which is, of course, how the problem was cooked up. For example,

$$A_{+-}^{1/2} = (+3 - (-2)) \begin{bmatrix} 0 & 2 \\ 0 & 1 \end{bmatrix} + (-2) \begin{bmatrix} 1 & 0 \\ 0 & 1 \end{bmatrix}.$$



# Chapter 4

## Field theory

Be wise, discretize.

— Mark Kac

**2022-01-31 Predrag** My [quantum field theory](#) notes take one semester to go through, not something we have time for right now. There is a part you already know much about: [Lattice field theory](#). Our [partition function](#) is as in the notes, but while in QED and in the notes one focuses on the weak coupling perturbation expansion [Feynman diagrams](#), our current project is to *start* from the anti-integrable, strong coupling side of the theory, and the method is the WKB or [saddle point](#) or [stationary phase](#) approximation (Laplace method every theorist needs to know), in which - good luck for us - deterministic solutions (our periodic states) dominate, with the [deterministic partition function eq. \(9\)](#), or the [ChaosBook deterministic trace formula eq. \(21.9\)](#) as our starting point. That's in no textbook that I know of, other than the ChaosBook.org, that cover this from our global perspective.

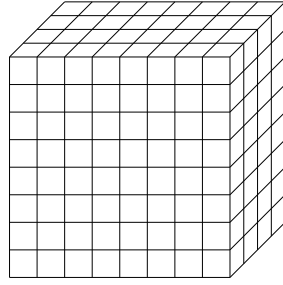
**2021-09-24 Predrag to everybody** A deep but important question for reformulating all of "dynamics" as (lattice) field theory:

How does pruning work in the global, lattice formulation? Can we see it on the reciprocal lattice? In the fundamental domain, where we only see orbits, not the range of lattice states of which perhaps only one strays into the inadmissible territory?

Fundamental (to me) is the pruning theory, the criteria for inadmissible orbits, see [ChaosBook sect. 14.5 Kneading theory](#) and [ChaosBook sect. 15.4 Prune Danish](#).

Is there a pruning criterion on the reciprocal lattice?

I would start by the reciprocal kneading value lattice state for a tent map or Bernoulli map (maybe that one first?), color all pruned orbits a differ-



$$\begin{aligned}
 x &= (x_1, x_2, \dots, x_d) \rightarrow \\
 z &= (z_1, z_2, \dots, z_d) \\
 x &= a z = \text{lattice site}
 \end{aligned}$$

Figure 4.1: In lattice field theory the  $d$  continuous coordinates  $x \in \mathbb{R}^d$  are replaced by a set of lattice sites  $z \in \mathcal{L}$  (from ref. [107]).

ent color, and see whether there is a ‘pruning front’ in the fundamental domain?

Now, none of the above has “Burnside” in their index.

## 4.1 Lattice discretization of a field theory

In Euclidean field theory the fields  $\phi(x)$  depend on the  $d$  Euclidean coordinates, so introduce a discretized spacetime in form of a  $d$ -periodic hypercubic *integer lattice*  $\mathbb{Z}^d/L^d$  (see figure 4.1), with lattice spacing  $a_i = \Delta x_i$  and lattice period  $L_i = 1/\Delta x_i$  along the unit vector

$$\hat{n}_i \in \{\hat{n}_1, \hat{n}_2, \dots, \hat{n}_d\}$$

pointing in the  $i$ th positive direction. The (scalar) *field*  $\phi(x)$  is evaluated only on the lattice points

$$\phi_z = \phi(x), \quad x = a z = \text{lattice point}, \quad z \in \mathbb{Z}^d/L^d. \quad (4.1)$$

It is periodic

$$\phi_z = \phi_{z+L_i \hat{n}_i}.$$

in all directions. We refer to the set of values of  $\Phi = \{\phi_z\}$  as a *periodic state*.

In order to discretize field-theoretic partial differential equations, we need to define lattice derivatives. The *forward partial lattice derivative*

$$(\partial_i \phi)_z = \frac{\phi(x + \Delta x_i \hat{n}_i) - \phi(x)}{\Delta x_i} = \frac{\phi_{z+\hat{n}_i} - \phi_z}{\Delta x_i} \quad (4.2)$$

depends explicitly on the lattice spacing. For our purposes it is convenient to reformulate the problem as a discretization on an integer lattice. This is attained by converting all continuum partial *derivatives* into discrete partial *differences* by  $\partial_i \rightarrow L_i \partial_i$  rescaling of the partial derivatives. After this rescaling  $\partial_i$  is an integer lattice forward partial *difference operator*

$$\partial_i = r_i - 1. \quad (4.3)$$

Higher lattice partial difference operators can be defined as [55]

$$\partial_i^k = \sum_{j=0}^k (-1)^j \binom{k}{j} r_i^{k-j}, \quad (4.4)$$

with support on  $k + 1$  forward points. For example

$$\begin{aligned} \partial_i^2 &= r_i^2 - 2r_i + \mathbf{1} \\ \partial_i^3 &= r_i^3 - 3r_i^2 + 3r_i - \mathbf{1}. \end{aligned} \quad (4.5)$$

The even ones can be centered to be reflection symmetric (symmetric under transposition) by translation by  $k$  sites,

$$\begin{aligned} \square_i &= -\partial_i^\top \partial_i = r_i - 2\mathbf{1} + r_i^{-1} \\ \square_i^2 &= r_i^2 - 4r_i + 6\mathbf{1} - 4r_i^{-1} + 6r_i^{-2}, \end{aligned} \quad (4.6)$$

where  $\square = \sum \square_i$  stands for the lattice Laplacian (or d'Alambertian).

Spacetime integrals are now replaced by spacetime sums,

$$\int d^d x \quad \longrightarrow \quad \sum_x a^d,$$

and the lattice free field action is

$$\begin{aligned} S &= \sum_z a^d \left\{ \frac{1}{2} \sum_{\mu=1}^d (\partial_\mu \phi)_z^2 + \frac{\mu^2}{2} \phi_z^2 \right\} \\ &= \sum_z a^d \left\{ \frac{1}{2} \sum_{i=1}^d \phi_z (-\square_i + \mu^2)_{zz'} \phi_{z'} \right\}. \end{aligned} \quad (4.7)$$

In the functional integrals the measure

$$\mathcal{D}\phi = \prod_x d\phi(x)$$

involves the lattice points  $x$  only, so for a finite lattice this is a finite dimensional integral.

involves the lattice points  $x$  only, so we have a discrete set of variables to integrate. If the lattice is taken to be finite, we just have finite dimensional integrals.

The momenta are also discretized,

$$p_\mu = \frac{2\pi}{a} \frac{l_\mu}{L_\mu} \quad \text{with } l_\mu = 0, 1, 2, \dots, L_\mu - 1,$$

and the momentum-space integration is replaced by finite sums

$$\int \frac{d^d p}{(2\pi)^d} \quad \longrightarrow \quad \frac{1}{a^d L^{d-1} T} \sum_{l_\mu}.$$

All “functional integrals” are now regularized, finite expressions.

The best-developed numeric tool for QFT at strong coupling is lattice field theory. The first step in constructing a lattice field theory is to choose a lattice that respects as well as possible the isometries of the target manifold and to understand the UV and IR cut-off effects, which are referred to as lattice spacing and finite volume errors, respectively. A lattice field theory calculation replaces the continuum manifold with a finite lattice spacing (a UV cut-off) and a finite volume  $V$  (IR cut-off).

To recover physics in a continuous and infinite spacetime, one needs to take the infinite volume limit,

$$L, T \longrightarrow \infty,$$

and the continuum limit,

$$a \longrightarrow 0.$$

We shall not discuss the continuum limit of a lattice field theory here.

### 4.1.1 Transfer matrix

Picking out a ‘time direction’ and evolving in time slices (what we call Hamiltonian formulation) is here called ‘transfer matrix’, presumably in reference to the similar formulation for the Ising model.

Split the 4D hypercubic lattice  $z = (z_1, z_2, z_3, z_4)$  into 3-dimensional ‘spatial’ directions  $\mathbf{z} = (z_1, z_2, z_3)$  and the ‘temporal’ direction  $z_4 = t$ . Let

$$\Phi_t = \{\phi_{\mathbf{z}} | z_4 = t\} \tag{4.8}$$

be a field configuration on a Euclidean time slice  $z_4 = t$ . Decompose the lattice action as

$$S[\phi] = \sum_t L[\Phi_{t+1}, \Phi_t] \tag{4.9}$$

This sum looks like the usual 1D temporal lattice action (12.3). Here

$$L[\Phi_{t+1}, \Phi_t] = \sum_{\mathbf{z}} \frac{1}{2} (\phi_{\mathbf{z}, t+1} - \phi_{\mathbf{z}t})^2 + \frac{1}{2} (L_1[\Phi_t] + L_1[\Phi_{t+1}]) \tag{4.10}$$

with (here I drop a non-harmonic potential terms)

$$L_1[\Phi_t] = \sum_{\mathbf{z}} \frac{1}{2} \left\{ \sum_{k=1}^3 (\phi_{\mathbf{z}+\hat{k}, t} - \phi_{\mathbf{z}t})^2 + \frac{m^2}{2} \phi_{\mathbf{z}t}^2 \right\} \tag{4.11}$$

Eq. (4.10) looks like a sensible generalization of the temporal lattice generating function (8.80).

The transfer matrix is defined as

$$T[\Phi_{t+1}, \Phi_t] = e^{-L[\Phi_{t+1}, \Phi_t]} \tag{4.12}$$



As the matrices are presumably not commuting, it is not obvious to me that repeated application of the transfer operator adds up to the lattice action  $S[\phi]$  (4.9) in the exponent. Take a field  $\Psi_t$  defined on  $t$  time-slice. Then the transfer operator evolves the initial time-slice by matrix multiplication,

$$T^n \Psi_t = \Psi_{t+n} \quad (4.13)$$

As it stands, it is not obvious how this is supposed to work, but Montvay and Münster [105] do give the standard differential formulation, explain correlations, etc., so it's probably OK. For a time-periodic lattice of time period  $T$  they say that

$$Z = \text{Tr } T^n \quad (4.14)$$

is the *partition function*.

**2020-07-04 Predrag** Would be happier if (4.14) were a  $\text{Det}$ , i.e., if there were a  $T = 1 - zJ$  kind of expression. But ... I do not see a quick way from here to the Hill's formula, so I abandon this path for now.

**2023-08-05 Predrag** **Jorge L. deLya** *The Gaussian Model: An Exploration into the Foundations of Quantum Field Theory* is a pedagogical introduction into discrete scalar field theory, covering much the same ground as CL18. Big shortcoming from our point of view is that there is not as much as a mention of a Bravais lattice.

He has opinions: "Although using the classical theory as an intuitive guide for the construction of the quantum theory may be a very good idea, the conceptual derivation must be from the quantum theory to the classical one, and *not* the other way around. In other words, while the 'quantization' of a classical theory belongs to the realm of imaginative guesswork, the derivation of the classical limit of a quantum theory should be precise deductive work. [...] our approach to the subject, unlike the traditional one, in both the classical and quantum cases, will not be based on equations of motion but rather on the action functional as the object defining the physical models."

His notion of a 'classical solution' has no relation to our 'deterministic field theory': "[...] classical solution of the model is a configuration which minimizes the action locally, that is, at which the action has a local *minimum*. [...] For the action of the free theory the classical solution is the identically null configuration. [...] in principle, the action may have more than one local minimum and when this happens, we will have more than one classical solution."

I like this: "[...] the finite-difference operator ends up associated in a natural way to links [...] a fact that leads us to think that the association of finite differences to links has a certain character of inevitability."

"[...] the operator  $\square$  has a null eigenvector, or a zero mode, on the torus."

He defines the forward and backward difference operators (4.6) that satisfy

$$\square = \Delta^{(+)}\Delta^{(-)} = \Delta^{(-)}\Delta^{(+)} \quad (4.15)$$

“[...] the concept of *momentum* space will be of great importance both for the solution of the mathematical problems of the theory and in relation to its physical interpretation. [...] The fields are written as functions of the sites integer coordinates. [...] the space of all possible fields as the space of field configurations.in the *position* space. [...] momentum space is obtained by means of a linear transformation that effects a change of basis in the space of configurations. The integer coordinates of the position sites will be mapped on a new set of integer coordinates that index the *modes* of the lattice. The name originates from the classical concept of normal modes of oscillation. ”

“[...] the zero-momentum ( $k = 0$ ) transform of the field is its average value inside the box. This average is also called the *zero mode* of the field and it will play a special role in the subsequent development of the theory.”

He introduces the *linear momentum*

$$p_j = 2 \sin \frac{k_j}{2} (\times \text{a phase factor}) \quad (4.16)$$

as eigenvalues of  $\Delta^{(+)}$ ,  $\Delta^{(-)}$ .

“[...] The relation  $p^2 + \mu^2 = 0$  is referred to as the *on-shell condition* and is a characteristic of the plane waves that constitute the relativistically invariant classical solutions of the theory in non-Euclidean space. ”

Figure 2.10.1 shows a period-25,  $d = 1$  Green’s function. Looks sharper for  $d = 2$ .

Beyond that, nothing that we need right now. As a curiosity, there are maybe 2 or three citations for the whole book.

**2024-02-19 Predrag** Kevin Costello *Integrable lattice models from four-dimensional field theories*, [arXiv:1308.0370](https://arxiv.org/abs/1308.0370), defines transfer matrix on rectangular primitive cells on p. 4, as a mathematician would.

## 4.2 Laplacians

There seems to be whole body of literature on our unexplored project on Dirac equation on lattice (4.33).

See also:

sect. 6.4.1 *Laplacians (and time reversal?)*

sect. 16.1.1 *Clair / Clair14*

sect. 16.1.2 *Ihara blog*

Discussion around (8.205).

Momentum (4.16), (4.31), (6.99)  
 Laplacian (4.15)

### 4.2.1 Laplacian notes 2012-2018

See also sect. 17.2 *Information*.

**Graph Laplacians** Predrag’s notes on graph Laplacians and explain the Laplacian introduced at the beginning of page 472 of Schlueter-Kuck and Dabiri [125] *Coherent structure colouring: identification of coherent structures from sparse data using graph theory*, arXiv:1610.00197. They also have a similar paper in Chaos: Schlueter-Kuck and Dabiri [126] *Identification of individual coherent sets associated with flow trajectories using coherent structure coloring*, arXiv:1708.05757.

Another such article of potential interest is Candelaresi, Pontin and Hornig [33] *Quantifying the tangling of trajectories using the topological entropy*

This topic appears closely related to sect. 16.1 *Ihara zeta functions*. It started with pipes blog 2017-12-15 **Ashley - An alternative norm’?**. He saw a talk on *Coherent Structure Colouring* at APS-DFD Denver. Could the method be used to colour’ regions in the state space with similar (short time) symbolic dynamics? It could be rather expensive to calculate, however, comparing figures 4 and 5 in the JFM [125], they are able to get decent results with much grainier data than finite-time Lyapunov exponents.

Schlueter-Kuck and Dabiri define coherence’ as the kinematic similarity of Lagrangian fluid trajectories, regardless of their spatial proximity.” They measure this similarity by computing the coherent structure colouring (CSC) field.”

The approach is data driven, and it could be in the Matt-Predrag’s spatiotemporal project spirit. Except I disapprove of time-averaging definition of weight link (4.19). Given the trajectories of a set of Lagrangian fluid particles strobed at a set of time steps, one can think of the data set as a spatiotemporal graph, wherein each node represents the position of a fluid particle at a given instant. Traditionally one weighs the edges of such a graph based on the proximity of the fluid trajectories (e.g. using Euclidian distance), but they use a weight based on *kinematic dissimilarity*.

They claim that coherent structures can be identified more robustly by quantifying the extent to which fluid trajectory kinematics are different, rather than the extent to which fluid particle trajectories remain in proximity over time.

If one distinguishes between two or more paths connecting the same two regions, that is encoded by the *adjacency* matrix with non-negative integer entries [41],

$$A_{ij} = \begin{cases} k & \text{if a transition } \mathcal{M}_j \rightarrow \mathcal{M}_i \text{ is possible in } k \text{ ways} \\ 0 & \text{otherwise.} \end{cases} \quad (4.17)$$

More generally, we shall encounter  $[m \times m]$  matrices which assign different real or complex weights to different transitions,

$$A_{ij} = \begin{cases} A_{ij} \in \mathbb{R} \text{ or } \mathbb{C} & \text{if } \mathcal{M}_j \rightarrow \mathcal{M}_i \text{ is allowed} \\ 0 & \text{otherwise.} \end{cases} \quad (4.18)$$

In statistical physics one refer to these as *transfer* matrices, but here (see Gallier below) such matrix is called a weighted adjacency" matrix  $A$ , where  $a_{ij}$  is the weight of the edge connecting particle  $i$  and particle  $j$ .

To this end, each edge, representing the connection between a pair of particles, is weighted by the standard deviation of the distance between the two fluid trajectories over their duration, normalized by the average distance between the fluid particle trajectories during the same period:

$$a_{ij} = \frac{1}{\bar{r}_{ij} T^{1/2}} \sum_{k=0}^{T-1} [(\bar{r}_{ij} - r_{ij}(t_k))^2]^{1/2} \quad (4.19)$$

where  $r_{ij}(t_k)$  is the distance between two particles  $i$  and  $j$  at time  $t_k$ , and  $\bar{r}_{ij}$  is the average distance between the two fluid particle trajectories. In other words,  $a_{ij}$  is the standard deviation (square root of the diffusion constant?) for the pairwise distance  $r_{ij}(t)$ , except that the prefactor  $1/\bar{r}_{ij}$  makes it dimensionless, and  $1/2d$  prefactor (for the number of dimensions) is also missing. Why are weights dimensionless? Mhm...

I am similarly confused in ChaosBook.org, boyscout sect. 16.3.1 *How good is my orbit?*. There I think of the numerical round-off errors along a trajectory as uncorrelated and acting as noise, so the errors  $(\phi(t + \delta\tau) - f^{\delta\tau}(\phi(t)))^2$  are expected to accumulate as the sum of squares of uncorrelated steps, linearly with time. Hence the accumulated numerical noise along an orbit of period  $T_p$  sliced by  $N$  intermediate sections separated by  $\delta\tau_k = t_{k+1} - t_k \sim T_p/N$  can be characterized by an effective diffusion tensor (covariance matrix) <sup>1</sup>

$$\Delta_{ij}^p = \left\langle \sum_{k=0}^{n_p-1} \frac{1}{\delta\tau_k} (\phi_{k+1} - f^{\delta\tau_k}(\phi_k))_i (\phi_{k+1} - f^{\delta\tau_k}(\phi_k))_j^T \right\rangle, \quad (4.20)$$

where  $\langle \dots \rangle$  denotes an average over a number of different attempt to determine the cycle  $p$ . In contrast to (4.19), this at least makes sense dimensionally, even though a  $1/2d$  prefactor is still missing.

They go on to show that colours can be assigned via solution of an eigenvalue problem. They maximize

$$z = \frac{1}{2} \sum_{i=1}^N \sum_{j=1}^N (x_i - x_j)^2 a_{ij}$$

where  $N$  is the number of rows and columns in the weighted adjacency matrix  $A$  (i.e. the number of particles) and  $X$  is a row vector containing the value of coherent structure coloring (CSC) associated with each particle. By maximizing  $z$  they determine CSC values such that fluid particle trajectories that are kinematically dissimilar (i.e. where the weight of the edge between them  $a_{ij}$  is large) and the CSC values that are as different as possible. They define

<sup>1</sup>Predrag 2018-03-21: should define  $\langle \dots \rangle$ ?

the (weighted) degree matrix  $D$ , which contains the row sums of the adjacency matrix along the diagonal, as

$$d_{ij} = \begin{cases} 0, & i \neq j \\ \sum_{k=1}^N a_{ik}, & i = j. \end{cases}$$

and the associated graph Laplacian,  $L = D - A$ , with which

$$z = X^\top LX$$

(that is an exercise, worked out in the paper), and the generalized eigenvalue for the graph Laplacian is

$$LX = \lambda DX. \quad (4.21)$$

The eigenvector  $X$  that maximizes  $z$  is the eigenvector corresponding to the maximum eigenvalue of (4.21). Each element of  $X$  assigns that value of CSC to the corresponding fluid particle. The CSC vector can be used to color the original flow, in whatever spatial representation of the particles. Then the regions in the flow with a similar coherent structure coloring indicate coherence.

[mathworld.wolfram.com](http://mathworld.wolfram.com): The Laplacian matrix is a discrete analog of the Laplacian operator and serves a similar purpose by measuring to what extent a graph differs at one vertex from its values at nearby vertices."

$$(Lf)_i = D_{ii}f_i - \sum_{j \neq i} w_{ij}f_j$$

where  $w_{ij}$  is the weight of the  $j \rightarrow i$  edge (link), and  $D_{ii} = \sum_{j \neq i} w_{ij}$ .

[wikipedia.org](http://wikipedia.org): It can also be used to construct low dimensional embeddings, which can be useful for a variety of machine learning applications."

A current research example: For a discrete  $d$ -dimensional Euclidean space-time the Laplacian is given by

$$\square \phi_n \equiv \phi_{n+1} - 2\phi_n + \phi_{n-1} \quad (4.22)$$

$$\square \phi_{n_1 n_2} \equiv (\square_1 + \square_2) \phi_{n_1 n_2} \quad (4.23)$$

$$\square_1 \phi_{n_1 n_2} = \phi_{n_1+1, n_2} - 2\phi_{n_1 n_2} + \phi_{n_1-1, n_2}$$

$$\square_2 \phi_{n_1 n_2} = \phi_{n_1, n_2+1} - 2\phi_{n_1 n_2} + \phi_{n_1, n_2-1}$$

in  $d = 1, 2, \dots$  dimensions. For 1-dimensional periodic chain with  $N$  sites, the  $[N \times N]$  matrix representation of the lattice Laplacian is:

$$\square = \begin{bmatrix} -2 & 1 & & & & & & & & & 1 \\ 1 & -2 & 1 & & & & & & & & \\ & & 1 & -2 & 1 & & & & & & \\ & & & & & 1 & -2 & 1 & & & \\ & & & & & & & \ddots & & & \\ & & & & & & & & 1 & -2 & 1 \\ 1 & & & & & & & & & 1 & -2 \end{bmatrix}. \quad (4.24)$$

The lattice Laplacian measures the second variation of a field  $\phi_\ell$  across three neighboring sites. On the diagonal you have the *degree* of the vertex (the degree of a graph vertex is the number of graph edges (links) which touch it). Off diagonal you have a '1' for every vertex connected to it. Each vertex (or node) has a field (some scalar value) associated with it - the Laplacian matrix measures the variation of the field across the neighboring nodes. If the field is the same, it returns zero.

Jean Gallier course notes CIS 515 are quite nice: [Graphs and Graph Laplacians](#):

The terminology *walk* is often used instead of *path*, the word path being reserved to the case where the nodes  $v_i$  are all distinct, except that  $v_0 = v_k$  when the path is closed.

*Incidence matrix*  $B$  entries are  $b_{ij} = \pm 1$ , depending on whether  $v_i$  is a *target* or a *source*. If the graph is undirected, all entries in the incidence matrix are nonnegative.

Graph Laplacians are fundamentally associated with undirected graph.

**Proposition 17.2.** [Godsil and Royle [65]] Given any directed graph  $G$  if  $B$  is the incidence matrix of  $G$ ,  $A$  is the adjacency matrix of  $G$ , and  $D$  is the degree matrix such that  $D_{ii} = d(v_i)$ , then

$$BB^T = D - A. \tag{4.25}$$

The matrix  $L = D - A$  is called the (unnormalized) graph Laplacian of the graph  $G$ .  $BB^T$  is independent of the orientation of  $G$  and  $D-A$  is symmetric, positive, semidefinite; that is, the eigenvalues of  $D$ .

Each row of  $L$  sums to zero (because  $B^T \mathbf{1} = 0$ ). Consequently, the vector  $\mathbf{1}$  is in the nullspace of  $L$ .

The eigenvalues  $0 = \lambda_0 < \lambda_1 \leq \lambda_2 \leq \dots \leq \lambda_m$  of  $L$  are real and non-negative, and there is an orthonormal basis of eigenvectors of  $L$ . (A way to prove that  $L$  is positive semidefinite is to evaluate the quadratic form  $x^T Lx$ .) If the graph  $G$  is connected, then the second eigenvalue  $\lambda_1$  is strictly positive. The eigenvalue  $\lambda_1$  (the Fiedler number) contains a lot of information about the graph  $G$  (assuming that  $G$  is an undirected graph).

All this generalizes to weighted graphs, and is in some deep way related to sect. 16.1 *Ihara zeta functions*. For example, the *deformed Laplacian*

$$\Delta(s) = I - sA + s^2(D - I)$$

where  $I$  is the unit matrix,  $A$  is the adjacency matrix,  $D$  is the degree matrix, and  $s$  is a (complex-valued) number. The standard Laplacian is  $\Delta(1)$ .

## 4.2.2 Laplacian notes

2016-10-05 Predrag Loebland and Somberg [96] *Discrete Dirac operators, critical embeddings and Ihara-Selberg functions*.

The main theme: a formulation of a discrete analogue of the claim made by Alvarez-Gaume *et al.* that the partition function of free fermion on a

closed Riemann surface of genus  $g$  is a linear combination of Pfaffians of Dirac operators. [...] we overcome the limitations and obstacles for the determinant-type reasoning, and replace the determinants by the Ihara-Selberg functions of the graph  $G$ .

They define the discrete Dirac operator  $D(s)$  of a bipartite graph  $G = (V, E)$  as the weighted adjacency matrix, but I get lost very quickly.

**2018-04-05 Predrag** All this is very instructive about how Laplacian'' graphs implement time-reversal invariance. My hunch is that the correct formulation is a Laplacian'' representation such as (16.22). Briefly,  $B$  is the (directed) incidence matrix of our directed graph  $G$  transition graph, giving us our 7-rectangles partition, and  $A$  is the adjacency matrix of (undirected)  $G$ .

That gives us a reformulation of directed graphs as undirected graphs, and maybe we will know how to do it directly, rather than via (to me unappealing) Ihara zeta functions route.

We still have to take care of space-reversal invariance. I think we need to go to the fundamental domain figure 24.26 (a).

**2020-11-22 Uzy** To dig out the Levit-Smilansky theorem'' you had to be a real archaeologist. A more profound representation is in the subsequent paper, about the phase space representation of the path integral, Levit and Smilansky [91] *The Hamiltonian path integrals and the uniform semiclassical approximations for the propagator*, (1977); cited over 50 times. The stability operator turns out to be a Dirac like (and not Schrödinger like) operator, with spectrum which covers the entire line. Yet, we wrote a similar expression for its regularized determinant and the Maslov index turns out to be the excess of negative eigenvalues. The phase space representation is of dimension  $(1+1)$  (not in your sense) but still it might be related by some miracle/good reason???

**2021-04-14 Predrag to Stephen** In spirit of our square root' philosophy, [Wolfram Physics Project](#) writes:

Another promising possibility relates to the distinction between fermions and bosons. We're not sure yet, but it seems as if Fermi-Dirac statistics may be associated with multiway graphs where we see only non-merging branches, while Bose-Einstein statistics may be associated with ones where we see all branches merging. Spinors may then turn out to be as straightforward as being associated with directed rather than undirected spatial hypergraphs.

The problem is that I cannot find a technical paper on that, if it exists. I do not find any hint of this in his Wolfram [143] *A Project to Find the Fundamental Theory of Physics*.

That jives with our spatiotemporal cat work. There the graph is just a  $d$ -dimensional undirected hypercubic lattice, but reflection symmetry reduces the graph to a pair of directed graphs, much like reducing the Klein-Gordon Laplacian to two Dirac operators, perhaps see sect. 16.13 *Lattice QED*.

**2021-04-15 Stephen** There's nothing yet on our home pages.

Very interesting! Now I just went searching in your material ... and couldn't find this either. Can you point me to this?

I'm wondering if it's at all related to the (disappointingly vague) [notes-9-16-discrete-quantum-mechanics](#). (2021-04-16 **Predrag**: Read this, do not see any connection to our work.)

I saw various Klein-Gordan-like equations in your works ... but nothing Dirac like (did I miss it?)

The  $d$ -dimensional hypercubic lattice obviously has certain discrete symmetry. Does the "square root lattice" have some other identifiable, and perhaps spinorial, symmetry?

By the way ... if you're up for it sometime, I'd love to try to talk through the "geodesic-balls-in-hypergraphs-have-limiting-symmetries-that-are-Lie-groups story. Your hypercubic lattice is too special" ... but imagine a random  $d$ -dimensional lattice (for integer  $d$ ). Then presumably the invariances of the geodesic ball limit to  $SO(d)$ . But what happens with one-way vs two-way connections? How does it affect representations? What about fractional  $d$ ? Etc. etc. I have a suspicion that with your help this might be able to be cracked...

**2021-09-23 Martin Richter** <martin.richter@nottingham.ac.uk>

A question: Is there an intuitive reason why the Klein-Gordon equation shows up? Why not something first order, for example? Either like the eikonal equation or better something linear like Dirac? There is probably a very simple answer to this but I was just wondering. Is there a geometrical reason, for example? Nothing of urgency, otherwise I would have shouted earlier.

**2021-10-11 Predrag** That will precisely be the technical part: Klein-Gordon shows up because of the nearest neighbor coupling, and it has to be second order because of the reflection symmetry, so Laplacian. So far, we have only looked at the Euclidean version, to keep things as simple as possible. Yes, we can take the "square root" of Laplacian and get two 1st order, time-asymmetric equations and a factorized Hill determinant, but I am not sure what to make of it. So far the field theory is only a scalar, single field component per site. I'm very reluctant to get into Dirac spin-1/2 fields at this time, because of lattice no-go-theorems, and the usual fermion nonsense in lattice formulations. But have a look at sect. 16.13 *Lattice QED*.



**2020-11-22 Uzy** To dig out the Levit-Smilansky theorem" you had to be a real archaeologist. A more profound representation is in the subsequent paper, about the phase space representation of the path integral, Levit and Smilansky [91] *The Hamiltonian path integrals and the uniform semiclassical approximations for the propagator*, (1977); cited over 50 times. The stability operator turns out to be a Dirac like (and not Schrödinger like) operator, with spectrum which covers the entire line. Yet, we wrote a similar expression for its regularized determinant and the Maslov index turns out to be the excess of negative eigenvalues. The phase space representation is of dimension (1+1) (not in your sense) but still it might be related by some miracle/good reason???

**2023-02-15 Predrag** Shouvik Datta Choudhury, *Root Laplacian Eigenmaps with their application in spectral embedding* [arXiv:2302.02731](https://arxiv.org/abs/2302.02731) is too verbose for my taste, and probably not helpful to us, but anyway:

"[...] the square root of Laplacian which can be obtained in complete Riemannian manifolds in the Gromov sense has an analog in graph theory as a square root of graph-Laplacian."

" **Kato's square root conjecture** is a mathematical conjecture that states that, for a large class of differential operators, the square root of the operator is a well-defined and bounded operator. [...] The existence, as well as the uniqueness of the square root, enables us to the possible implementation of the square root in the spectral embedding context of machine learning as well as the geometric deep learning. "

Kato's square root conjecture is too abstract for our needs, I believe.

**2023-02-20 Predrag** If we want to get into fermions: Christos, [...] and Subir Sachdev, *A model of d-wave superconductivity, antiferromagnetism, and charge order on the square lattice*, [arXiv:2302.07885](https://arxiv.org/abs/2302.07885), formulates a standard version of massless fundamental Dirac fermions on a square lattice.

**2023-09-09 Predrag** For a one-dimensional lattice

$$p^2 + \mu^2 \mathbf{1} = (p + i\mu \mathbf{1})(p - i\mu \mathbf{1})$$

so the steady state Hill determinant is square of a Hill determinant of a propagator linear in momentum and Klein-Gordon mass  $\mu$

$$|\text{Det}(p^2 + \mu^2 \mathbf{1})| = |\text{Det}(p + i\mu \mathbf{1})|^2. \quad (4.26)$$

This can be diagonalized with the discrete Fourier transform (??)

$$\text{Det}(p + i\mu \mathbf{1}) = \prod_{m=0}^{n-1} (p_m + i\mu), \quad p_m = \lambda^m - 1 = \lambda^{m/2} 2i \sin(\pi m/n).$$

$$|\text{Det}(p + i\mu \mathbf{1})| = \prod_{m=0}^{n-1} |(1 - i\mu) - \lambda^m|, \quad \lambda = e^{i 2\pi/n}.$$

That we can evaluate by substituting  $x = 1 - i\mu$  into the characteristic polynomial

$$x^n - 1 = (x - 1)(x - \lambda)(x - \lambda^2) \cdots (x - \lambda^{n-1})$$

associated with the shift matrix characteristic equation `refeq shift1n`.

$$|\text{Det}(p + i\mu \mathbf{1})|^2 = ((1 - i\mu)^n - 1)^* ((1 - i\mu)^n - 1) = (1 + \mu^2)^n + \cdots + 1.$$

**2023-08-05 Predrag** My last attempt to attract Tiger's eye to how beautiful the Ivashkevich *et al.* [80] formulation of the above is (discussed in the blog). We really want to write the Hill determinant as a square of (19.30)!: Partition function with twisted boundary conditions (tilts in both time and space directions)

$$Z_{\alpha,\beta}^2(\mu) = \prod_{n=0}^{N-1} \prod_{m=0}^{M-1} 4 \left[ \sin^2 \left( \frac{\pi(n+\alpha)}{N} \right) + \sin^2 \left( \frac{\pi(m+\beta)}{M} \right) + 2 \text{sh}^2 \mu \right] \quad (4.27)$$

$\alpha = 0$  corresponds to the periodic boundary conditions in the  $N$ -direction while  $\beta$  controls boundary conditions in  $M$ -direction. The partition function with twisted boundary conditions  $Z_{\alpha,\beta}$  can be transformed into simpler form

$$Z_{\alpha,\beta}(\mu) = \prod_{n=0}^{N-1} 2 \left| \text{sh} \left[ M\omega_\mu \left( \frac{\pi(n+\alpha)}{N} \right) + i\pi\beta \right] \right| \quad (4.28)$$

where lattice dispersion relation

$$\omega_\mu(k) = \text{arcsinh} \sqrt{\sin^2 k + 2 \text{sh}^2 \mu} \quad (4.29)$$

is the relation between energy  $\omega_\mu$  and momentum  $k$  of a free quasi-particle on the square lattice.

In this section, we use 2-dimensional steady state as an example of computation of the Hill determinants over a finite volume primitive cell  $\mathbb{A}$ . For a given  $\mathcal{L}_{\mathbb{A}}$ -periodic state, the Hill determinant of the finite volume primitive cell  $\mathbb{A}$  orbit Jacobian matrix is given by the product of its eigenvalues (??).

The steady state orbit Jacobian matrix (4.103), with no periodic state dependence,  $d_z = s$ , is diagonalized by going to the reciprocal lattice.

As wave-numbers  $k_j$  are not integers, but proportional to integers  $m_j$ , it is convenient to index reciprocal lattice sites (discrete wave-numbers  $k_1, k_2$ ) by integer pairs  $m_1 m_2$ .

For the square-lattice spatiotemporal cat the explicit formula for Hill determinant of the primitive cell  $\mathbb{A}$  orbit Jacobian matrix in terms of lattice

momenta:

$$\begin{aligned}
 |\text{Det } \mathcal{J}_A| &= \prod_{m_1=0}^{L-1} \prod_{m_2=0}^{T-1} [p(k_1)^2 + p(k_2)^2 + \mu^2] \\
 k_1 &= \frac{2\pi}{L} m_1, \quad k_2 = \frac{2\pi}{T} \left(-\frac{S}{L} m_1 + m_2\right). \quad (4.30)
 \end{aligned}$$

**2023-09-22 Predrag** For two-dimensional square lattice, factorization (4.26) has been noted in refs. [80, 102], as holomorphic factorization', valid for each geometry separately, but not for the partition sum over geometries.

For one-dimensional temporal lattice, factorization (4.26) leads to the factorization of the partition sum over geometries, and the factorization of Isola topological zeta function [79, 93] (??).

For what follows, it is convenient to define a lattice momentum' operator in  $j$ th lattice direction as the forward lattice difference operator,

$$p_j = r_j - \mathbf{1}, \quad (4.31)$$

where  $r$  is the shift operator, lattice spacing is set to 1, and the  $d$ -dimensional lattice Laplacian is the lattice momentum operator squared,

$$\square = -\sum_{j=1}^d p_j^\top p_j = \sum_{j=1}^d (r_j - 2\mathbf{1} + r_j^{-1}). \quad (4.32)$$

**2023-09-09 Predrag** Presumably one can insert Pauli matrices, and in general Dirac spinors into (6.48) to square-root' the Klein-Gordon propagator, and the  $d$ -dimensional Hill determinant,

$$-\square + \mu^2 = \left( \sum_{\nu=1}^d p_\nu \gamma^\nu + \mu \right)^2. \quad (4.33)$$

**2024-05-20 Predrag** .

Ginestra Bianconi *The topological Dirac equation of networks and simplicial complexes* (2021), [arXiv:2106.02929](https://arxiv.org/abs/2106.02929).

Consider a network  $G = (V, E)$  formed by a set  $V$  of  $N$  nodes (or vertices)  $\{1, 2, \dots, N\}$  and a set  $E$  of  $M$  links (or edges)  $\{\ell_1, \ell_2, \dots, \ell_M\}$  connecting the nodes by pairwise interactions. The network  $G$  has an arbitrary topology, including chains and square lattices.

The topology of the network is given by the incidence matrix  $\mathbf{B}_{[1]}$  representing the boundary operator of the network mapping each link  $\ell$  of the network to a linear combination of its two endnodes. In particular

the incidence matrix  $\mathbf{B}_{[1]}$  of a network (indicated here simply by  $\mathbf{B}$ ) is a rectangular matrix of size  $N \times M$ ,

$$\mathbf{B}_{i\ell} = \begin{cases} 1 & \text{if } \ell = [j, i], \\ -1 & \text{if } \ell = [i, j], \\ 0 & \text{otherwise.} \end{cases} \quad (4.34)$$

The incidence matrix  $\mathbf{B}$  defines the graph Laplacian  $\mathbf{L}_{[0]}$  describing diffusion from node to node through links, and the 1-down-Laplacian  $\mathbf{L}_{[1]}^{down}$  describing diffusion from link to link through nodes:

$$\mathbf{L}_{[0]} = \mathbf{B}\mathbf{B}^\dagger, \quad (4.35)$$

$$\mathbf{L}_{[1]}^{down} = \mathbf{B}^\dagger\mathbf{B}. \quad (4.36)$$

The Dirac operator (also called the chiral operator), see Lloyd *et al.* below, of a network is defined by the square  $(N + M) \times (N + M)$  matrix

$$\mathcal{D} = \begin{pmatrix} 0 & b\mathbf{B} \\ b^*\mathbf{B}^\dagger & 0 \end{pmatrix},$$

where  $b \in \mathbb{C}$  has absolute value  $|b| = 1$  and where  $b^*$  is its complex conjugate. Typically we can choose  $b$  equal to the real unit ( $b = b^* = 1$ ) or  $b$  equal to the imaginary unit ( $b = -b^* = i$ ).

The square of the Dirac operator is a topological Laplacian represented by a block diagonal matrix formed by two blocks: one acting on the nodes degree of freedom and reducing to the graph Laplacian and one acting on the link degree of freedom and reducing to the 1-up-Laplacian, i.e.

$$\mathcal{L} = (\mathcal{D})^2 = \begin{pmatrix} \mathbf{L}_{[0]} & 0 \\ 0 & \mathbf{L}_{[1]}^{down} \end{pmatrix}.$$

This Dirac operator defines a topological Dirac equation over a network. When the Dirac and the Schrödinger equations are put on a lattice, typically it is assumed that the wave function is defined on the nodes of the lattice (network). Here we assume that the wave function of a network is not only defined by a set of variables  $\phi$  defined on the nodes of the network but includes also a set of variable  $\chi$  defined on the links of the network. Therefore we relax a bit the notion of point-like definition of the wave function and consider also degree of freedoms associated to links. We consider the wave function described by the topological spinor

$$\psi = \begin{pmatrix} \phi \\ \chi \end{pmatrix}, \quad (4.37)$$

with  $\phi$  indicating a 0-cochain and  $\chi$  indicating a 1-cochain associated to the network, i.e.

$$\phi = \begin{pmatrix} \phi_1 \\ \phi_2 \\ \vdots \\ \phi_N \end{pmatrix}, \quad \chi = \begin{pmatrix} \chi_{\ell_1} \\ \chi_{\ell_2} \\ \vdots \\ \chi_{\ell_M} \end{pmatrix},$$

where a 0-cochain and a 1-cochain indicate functions defined on nodes  $\{1, 2, \dots, N\}$  and links  $\{\ell_1, \ell_2, \dots, \ell_M\}$  respectively. While in Sec. 5 we will touch on the problem of modelling a discrete Lorentzian spacetime, to start with we consider that the network, although of arbitrary topology only captures the discrete space, while we keep time as a continuous variable.

Consider a directional topological Dirac equation in which also time is discretized on a  $1 + d$  dimensional lattice with  $d \in \{1, 2\}$  space dimensions, with space the isotropic portion of the lattice in  $\mathbb{R}^{d+1}$ , with sides of length  $N^{1/(d+1)}$ , and periodic boundary conditions. For  $1 + 1$  lattice incidence matrix  $\mathbf{B}$  can be decomposed as

$$\mathbf{B} = \mathbf{B}_{(x)} + \mathbf{B}_{(t)} \quad (4.38)$$

for  $1 + 2$  lattice the incidence matrix can be decomposed as

$$\mathbf{B} = \mathbf{B}_{(x)} + \mathbf{B}_{(y)} + \mathbf{B}_{(t)} \quad (4.39)$$

where  $\mathbf{B}_{(w)}$  with  $w \in \{x, y, t\}$  indicates the directional incidence matrix defined by refeq Bdir.

The *directional* Dirac operator is

$$\bar{\mathcal{D}} = \sum_w \mathcal{D}_{(w)} \quad (4.40)$$

where for  $1 + 1$  lattices the sum extends to  $w \in \{x, y\}$  and for  $1 + 2$  lattices it extends to  $w \in \{x, y, t\}$ . Here the  $w$ -directional Dirac operators  $\mathcal{D}_{(w)}$  corresponding to the spatial directions  $w \in \{x, y\}$  have the same definition as for  $d$  dimensional spatial lattices, with the directional Dirac operator  $\mathcal{D}_{(t)}$  corresponding to the temporal direction is defined as

$$\mathcal{D}_{(t)} = \begin{pmatrix} 0 & i\mathbf{B}_{(t)} \\ i[\mathbf{B}_{(t)}]^\dagger & 0 \end{pmatrix}.$$

While  $\mathcal{D}_{(x)}$  and  $\mathcal{D}_{(y)}$  are Hermitian, we have chosen  $\mathcal{D}_{(t)}$  to be anti-Hermitian. With this choice of the  $t$ -directional Dirac operator  $\mathcal{D}_{(t)}$ , the anti-commutator between  $\beta$  and  $\mathcal{D}_{(w)}$  vanishes,

$$\{\mathcal{D}_{(w)}, \beta\} = 0,$$

for  $w \in \{x, y, t\}$ . However the anti-commutator between  $\mathcal{D}_{(w)}$  with  $w \in \{x, y\}$  and  $\mathcal{D}_{(t)}$  is given by

$$\{\mathcal{D}_{(w)}, \mathcal{D}_{(t)}\} = \begin{pmatrix} \mathbf{0} & \mathbf{0} \\ \mathbf{0} & i([\mathbf{B}_{(w)}]^\dagger \mathbf{B}_{(t)} + [\mathbf{B}_{(t)}]^\dagger \mathbf{B}_{(w)}) \end{pmatrix}.$$

The directional topological Dirac equation on this  $1 + d$  space-time is given by the eigenvalue problem

$$(\bar{\mathcal{D}} + m_0\beta) \psi = 0$$

with the topological spinor  $\psi = (\phi, \chi)^\top$  defined in (4.37). By writing this eigenvalue problem for the component  $\phi$  and the component  $\chi$  separately, where the component  $\chi$  is decomposed according to the type of link in which the 1-cochain is defined,  $\chi = (\chi_{(x)}, \chi_{(t)})^\top$  we obtain

$$\begin{aligned} \mathbf{B}_{(x)}\chi_{(x)} + i\mathbf{B}_{(t)}\chi_{(t)} + m_0\phi &= \mathbf{0}, \\ \mathbf{B}_{(x)}^\dagger\phi - m_0\chi_{(x)} &= \mathbf{0}, \\ i\mathbf{B}_{(t)}^\dagger\phi - m_0\chi_{(t)} &= \mathbf{0}. \end{aligned} \quad (4.41)$$

From this system of equations it is possible to observe that  $\phi$  must be an eigenvector of the discrete D'Alembert operator

$$\square = \mathbf{L}_{(t)} - \mathbf{L}_{(x)} = \mathbf{B}_{(t)}\mathbf{B}_{(t)}^\dagger - \mathbf{B}_{(x)}\mathbf{B}_{(x)}^\dagger$$

with eigenvalue  $m_0^2$ . Therefore the component  $\phi$  of the topological spinor calculated on a node  $i$  of coordinates  $(t_i, x_i)$  is given by

$$\phi_i = \mathcal{N} e^{-i(\omega t_i - k_x x_i)}$$

where  $\mathcal{N}$  is a normalization constant. Here  $\omega = 2\pi\bar{n}_\omega/N^{1/2}$ ,  $k_x = 2\pi\bar{n}_x/\sqrt{N}$  with  $0 \leq \bar{n}_w \leq N^{1/2} - 1$ . Let us indicate with  $\lambda_x$  and  $E_t$  the eigenvalues of the directional incidence matrices  $\mathbf{B}_{(x)}$  and  $\mathbf{B}_{(t)}$  with with

$$|\lambda_w| = 2 \sin(k_w/2), \quad (4.42)$$

for  $w \in \{x, y\}$ . In order to satisfy the directional topological Dirac equation on  $1 + 1$  space-time  $E_t$  and  $\lambda_x$  must satisfy the dispersion relation

$$|E_t|^2 = |\lambda_x|^2 + m_0^2, \quad (4.43)$$

which, given the discrete nature of the spectrum can impose constraints on the possible value of the mass  $m_0$  and eigenvalues of  $\mathbf{B}_t$  and  $\mathbf{B}_x$  that might be considered. If this relation can be satisfied the eigenstate exists, and the topological Dirac equation on discrete space time has a solution with the components  $\chi_{(x)}$  and  $\chi_{(y)}$  given by

$$\begin{aligned} \chi_{(x)} &= \frac{1}{m_0} \mathbf{B}_{(x)}^\dagger \phi, \\ \chi_{(t)} &= i \frac{1}{m_0} \mathbf{B}_{(t)}^\dagger \phi. \end{aligned} \quad (4.44)$$

By following similar steps it is possible to show that for the  $1 + 2$  topological Dirac equation, the component  $\phi$  is an eigenvector of the operator

$$\square = \mathbf{L}_{(t)} - \mathbf{L}_{(x)} - \mathbf{L}_{(y)} = \mathbf{B}_{(t)}\mathbf{B}_{(t)}^\dagger - \mathbf{B}_{(x)}\mathbf{B}_{(x)}^\dagger - \mathbf{B}_{(y)}\mathbf{B}_{(y)}^\dagger \quad (4.45)$$

with eigenvalue  $m_0^2$  and its element  $\phi_i$  calculated on a node  $i$  of coordinates  $(t_i, x_i, y_i)$  is given by


$$\phi_i = \mathcal{N} e^{-i(\omega t_i - k_x x_i - k_y y_i)}$$


where  $\mathcal{N}$  is a normalization constant and  $k_w = 2\pi\bar{n}_w/N^{1/3}$  with  $0 \leq \bar{n}_w \leq N^{1/3} - 1$ . Indicating with  $\lambda_x, \lambda_y$  and  $E_t$  the eigenvalues of the directional incidence matrices  $\mathbf{B}_{(x)}, \mathbf{B}_{(y)}$  and  $\mathbf{B}_{(t)}$  respectively we see that for 1 + 2 dimensional space-time this eigenvalues must satisfy the dispersion relation

$$|E_t|^2 = |\lambda_x|^2 + |\lambda_y|^2 + m_0^2.$$

Therefore, due to the discrete nature of the spectrum, solving for the spectrum of the directional topological Dirac equation reduces to a problem connected to number theory.

**2024-05-21 Ginestra Bianconi** [Homepage](#) [ICTP seminar](#)

 *Lecture 3: The Dirac operator in Topological Machine Learning*

I was in the [3rd lecture](#). Here are a few [slides](#) from it. All four lectures  have been recorded.

An interesting overview. Introduces higher order topological Kuramoto models. Dirac operator. Dirac patterns are different from Turing patterns. Dirac operator outperforms Hodge Laplacian. I find the whole development fascinating...

I told her that I teach field theory starting with lattice scalar field theory, but then have to introduce Dirac spinors as continuum  $SO(n)$  spin representations voodoo, and asked her whether their discrete network Dirac operators go into usual spinors in a hypercubic lattice continuum limit. Turns out she absolutely avoids continuum, and hopes her discrete spinors do not have such connections to continuum.

Wierdly enough, she's cool with time being continuous, so all equations are differential equations in time, discrete on network (including lattices).

**2024-05-20 Predrag** Seth Lloyd, Silvano Garnerone, Paolo Zanardi *Quantum algorithms for topological and geometric analysis of big data* (2014), [arXiv:1408.3106](#), [DOI](#).

Because  $\mathbf{B}^2$  is the sum of the combinatorial Laplacians,  $\mathbf{B}$ , their eq. (3) is sometimes called the Dirac operator', since the original Dirac operator was the square root of the Laplacian.

### 4.3 Deterministic lattice field theory

A scalar field  $\phi(x)$  over  $d$  Euclidean coordinates can be discretized by replacing the continuous space by a  $d$ -dimensional hypercubic integer lattice  $\mathbb{Z}^d$ , with lattice spacing  $a$ , and evaluating the field only on the lattice points [105, 107]

$$\phi_z = \phi(x), \quad x = az = \text{lattice point}, \quad z \in \mathbb{Z}^d. \quad (4.46)$$

A *field configuration* (here in one spatiotemporal dimension)

$$\Phi = \cdots \phi_{-3} \phi_{-2} \phi_{-1} \phi_0 \phi_1 \phi_2 \phi_3 \phi_4 \cdots, \quad (4.47)$$

takes any set of values in system's  $\infty$ -dimensional *state space*  $\phi_z \in \mathbb{R}$ . A periodic field configuration satisfies

$$\Phi_{z+R} = \Phi_z \quad (4.48)$$

for any discrete translation  $R \in \mathcal{L}_a$  in the *Bravais lattice*

$$\mathcal{L}_a = \left\{ \sum_{i=1}^d n_i \mathbf{a}_i \mid n_i \in \mathbb{Z} \right\} = \{ \mathbf{n} \mathbf{A} \mid \mathbf{n} \in \mathbb{Z}^d \} \quad (4.49)$$

(2023-02-11 Predrag Wrong: if  $\mathbf{n}$  is a row vector,  $\mathbf{a}_j$  should also be row vectors.)

where the matrix  $\mathbf{A}$  whose columns are  $d$  independent integer lattice vectors  $\mathbf{a}_j$

$$\mathbf{A} = [\mathbf{a}_1, \cdots, \mathbf{a}_d] \in \mathbb{R}^{d \times d} \quad (4.50)$$

defines a *primitive cell* basis.

The determinant of lattice  $\mathcal{L}_a$  is the volume of (i.e., the number of lattice sites within) the parallelepiped spanned by the primitive cell basis

$$N_a = |\det \mathbf{A}|. \quad (4.51)$$

The action in (??) is given as primitive cell sum over the Lagrangian density

$$S_a[\Phi] = \sum_z^a \left\{ \frac{1}{2} \sum_{\mu=1}^d (\partial_\mu \phi)_z^2 + V(\phi_z) \right\}, \quad (4.52)$$

The variational extremum condition (4.53)

$$F[\Phi_c]_z = \frac{\delta S[\Phi_c]}{\delta \phi_z} = 0, \quad (4.53)$$

yields the Euler–Lagrange equations of  $\phi^k$  theory (4.137) on a  $d$ -dimensional hypercubic lattice, with *periodic state*  $\Phi_c$  a global deterministic (or ‘classical’) solution satisfying this local extremal condition on every lattice site  $z$ .

Each periodic state is a distinct deterministic solution  $\Phi_c$  to the discretized Euler–Lagrange equations (4.53), so its probability density is a  $N_L$ -dimensional Dirac delta function (that’s what we mean by the system being *deterministic*), a



delta function per site ensuring that Euler–Lagrange equation (4.53) is satisfied everywhere, with probability

$$P_c = \frac{1}{Z} \int_{\mathcal{M}_c} d\Phi \delta(F[\Phi]), \quad \Phi_c \in \mathcal{M}_c, \quad (4.54)$$

where  $\mathcal{M}_c$  is an open neighborhood, sufficiently small that it contains only the single periodic state  $\Phi_c$ .

In ref. [93] we verify that this definition agrees with the forward-in-time Perron-Frobenius probability density evolution [44]. However, we find field-theoretical formulation vastly preferable to the forward-in-time formulation, especially when it comes to higher spatiotemporal dimensions [47].

$n$ -point correlation functions or ‘Green functions’ [121]

$$\langle \phi_i \phi_j \cdots \phi_\ell \rangle = \frac{1}{Z[0]} \int D\phi e^{-S[\phi]} \phi_i \phi_j \cdots \phi_\ell. \quad (4.55)$$

The deterministic field theory partition sum has support only on lattice field values that are solutions to the Euler–Lagrange equations (4.53), and the partition function (4.95) is now a sum over configuration state space (4.47) *points*, what in theory of dynamical systems is called the ‘deterministic trace formula’ [42],

$$Z[0] = \sum_c P_c = \sum_p \sum_{r=1}^{\infty} P_{p^r}, \quad P_c = \frac{1}{|\text{Det } \mathcal{J}_c|}, \quad (4.56)$$

and we refer to the  $[N_{\mathcal{L}} \times N_{\mathcal{L}}]$  matrix of second derivatives

$$(\mathcal{J}_c)_{z'z} = \frac{\delta F_{z'}[\Phi_c]}{\delta \phi_z} = S[\Phi_c]_{z'z} \quad (4.57)$$

as the *orbit Jacobian matrix*, and to its determinant  $\text{Det } \mathcal{J}_c$  as the *Hill determinant*. Support being on state space *points* means that we do not need to worry about potentials being even or odd (thus unbounded), or the system being energy conserving or dissipative, as long as its nonwandering periodic states  $\Phi_c$  set is bounded in state space. In what follows, we shall deal only with deterministic field theory and mostly omit the subscript ‘ $c$ ’ in  $\Phi_c$ .

## 4.4 A partition function in terms of prime periodic states

2

---

<sup>2</sup>Predrag 2023-02-12: I think sect. 4.4.1 should go to Han’s thesis,

This section is an old version of summing over all *finite volume* primitive cell  $\mathbb{A}$  repeats on *compact* 2-tori. Superseded in CL18 by all calculations done on the *infinite* Bravais lattice. Go directly for Bloch theorem and compute the band, without constructing the set of all finite 2-tori first.

Do fix the normalization  $Z$ .

See also sect. 11.2 *Repeats of a prime primitive cell.*

A single *prime* periodic state  $\Phi_p$  over primitive cell  $\mathbb{A}$  has the same Hill determinant and Birkhoff sum  $A_{\mathbb{A}}[\Phi_p]$  for the  $V_{\mathbb{A}}$  periodic states in its group orbit, so its contribution to the partition function (??) is

$$e^{V_p W_{\mathbb{A}}[\beta]_p} = \frac{V_p}{|\text{Det}_{\mathbb{A}} \mathcal{J}_p|} e^{\beta V_p a_p}, \quad V_p = V_{\mathbb{A}} = L_{\mathbb{A}} T_{\mathbb{A}}, \quad (4.58)$$

For the prime periodic state  $\Phi_p$  over a *repeated* primitive cell tile  $\mathbb{A}\mathbb{R}$  (21.131), the contribution to the partition function is

$$e^{V_{\mathbb{A}\mathbb{R}} W_{\mathbb{A}\mathbb{R}}[\beta]_p} = \frac{V_p}{|\text{Det}_{\mathbb{A}\mathbb{R}} \mathcal{J}_p|} e^{\beta V_{\mathbb{A}\mathbb{R}} a_p}, \quad V_{\mathbb{A}\mathbb{R}} = r_1 r_2 V_p. \quad (4.59)$$

The nuisance here is that the Hill determinant  $\text{Det}_{\mathbb{A}\mathbb{R}} \mathcal{J}_p$  has no simple multiplicative relation to  $\text{Det}_{\mathbb{A}} \mathcal{J}_p$ ; has to be computed for each repeat separately, though in the infinite lattice limit they all might get replaced by a band in the first Brillouin zone.

Summing over all prime orbit  $p$  repeats (all  $\mathbb{A}\mathbb{R}$  primitive cells), we have the  $p$  contribution to the partition sum

$$Z[\beta]_p = e^{V_p W[\beta]_p} = \sum_{r_1=1}^{\infty} \sum_{r_2=1}^{\infty} \frac{V_p}{|\text{Det}_{\mathbb{A}\mathbb{R}} \mathcal{J}_p|} e^{\beta r_1 r_2 V_p a_p}, \quad (4.60)$$

and to the expectation value of observable  $a_z = a(\phi_z)$

$$\langle a \rangle_p = \frac{1}{V_p} \frac{\partial}{\partial \beta} W[\beta]_p \Big|_{\beta=0} = a_p w'_p, \quad w'_p = \frac{1}{Z_p} \sum_{r_1=1}^{\infty} \sum_{r_2=1}^{\infty} \frac{r_1 r_2}{|\text{Det}_{\mathbb{A}\mathbb{R}} \mathcal{J}_p|}. \quad (4.61)$$

Finally, summing over all prime orbits we have the mother of spatiotemporal partition functions and expectation values

$$Z[\beta] = e^{W[\beta]} = \sum_p e^{V_p W[\beta]_p}, \quad \langle a \rangle = \sum_p a_p w_p. \quad (4.62)$$

Prime orbits  $p$  are themselves searched for and ordered by the hierarchy of primitive cells

$$\sum_p \cdots = \sum_{r_1=1}^{\infty} \sum_{r_2=1}^{\infty} \sum_{r_3=0}^{r_1-1} \cdots, \quad (4.63)$$

Now, all this is what ChaosBook calls a ‘trace formula’, everything contributes to orbit weights  $w_p$  with positive signs, there are *no shadowing cancellations*. For that one needs a cumulant expansion of the Helmholtz ‘free energy’  $W[\beta] = \ln Z[\beta]$ .

And all stability calculations have to be done in the first Brillouin zone.

I’ll be grateful if you do it, but if not, I’ll try.

### 4.4.1 Retiling the tiles, ver. 2023-02-28

**2023-02-12 Predrag** This section or similar goes into Han's thesis, we have replaced it in CL18 by sect. *Tile multiples*.

A Bravais lattice  $\mathcal{L}_\mathbb{A}$  is a sublattice of a Bravais lattice  $\mathcal{L}_\mathbb{B}$  if its primitive vectors are integer multiples of the  $\mathcal{L}_\mathbb{B}$  primitive vectors [52],

$$\mathbb{A} = \mathbb{B}\mathbb{M}, \quad |\det \mathbb{B}| > 1, |\det \mathbb{M}| > 1. \quad (4.64)$$

We now reformulate this as a condition on which primitive cells  $\mathbb{B}$  can tile a primitive cell  $\mathbb{A}$ , see figure 24.82.

Bravais lattices  $\mathcal{L}_\mathbb{A} = [L_a \times T_a]_{S_a}$ ,  $\mathcal{L}_\mathbb{B} = [L_b \times T_b]_{S_b}$ , and the integer multipliers of lattice  $\mathcal{L}_\mathbb{B}$  are given by Hermite normal form primitive vectors (7.4)

$$\mathbb{A} = \begin{bmatrix} L_a & S_a \\ 0 & T_a \end{bmatrix}, \quad \mathbb{B} = \begin{bmatrix} L_b & S_b \\ 0 & T_b \end{bmatrix}, \quad \mathbb{M} = \begin{bmatrix} r_1 & m_{12} \\ 0 & r_2 \end{bmatrix}. \quad (4.65)$$

<sup>3</sup> It follows from (4.64) that the primitive cell  $\mathbb{B}$  tiles the primitive cell  $\mathbb{A}$  if and only if

$$\mathbb{M} = \mathbb{B}^{-1}\mathbb{A} = \begin{bmatrix} L_a/L_b & (S_a T_b - S_b T_a)/L_b T_b \\ 0 & T_a/T_b \end{bmatrix} \quad (4.67)$$

is a matrix with integer elements, i.e., only if  $L_a$  is a multiple of  $L_b$ ,  $T_a$  is a multiple of  $T_b$ , and the area spanned by the two 'tilted' primitive vectors (see figure 24.82 (a))

$$S_a T_b - T_a S_b = \det [\mathbf{a}_2, \mathbf{b}_2] \quad (4.68)$$

is an integer multiple of the  $\mathcal{L}_\mathbb{B}$  primitive cell area  $L_b T_b$ .

As a simple but perhaps surprising example, consider  $\mathcal{L} = [2 \times 2]_0$ ,  $\mathcal{L}_\mathbf{p} = [2 \times 1]_1$ . The Bravais lattice  $[2 \times 2]_0$  is a sublattice of  $[2 \times 1]_1$ , since

$$\begin{bmatrix} L/L_p & S/L_p - S_p T/L_p T_p \\ 0 & T/T_p \end{bmatrix} = \begin{bmatrix} 1 & -1 \\ 0 & 2 \end{bmatrix} \quad (4.69)$$

is an integer matrix (see also sect. ??). <sup>4</sup>

Figure 24.82 is another example of such tiling of a Bravais sublattice primitive cell by a finer Bravais lattice primitive cell. Bravais lattice  $[3 \times 2]_1$  (red dots) is a subset of Bravais lattice  $[3 \times 1]_2$  (blue and red dots). Figure 24.82 (b) shows that one can choose primitive cells for these two lattices such that the primitive cell of  $[3 \times 2]_1$  is tiled by the primitive cell of  $[3 \times 1]_2$ , using a translation of  $[3 \times 1]_2$ .

<sup>3</sup>Predrag 2023-02-13:

$$\mathbb{A} = \mathbb{B}\mathbb{M} = \begin{bmatrix} r_1 L_b & m_{12} L_b + r_2 S_b \\ 0 & r_2 T_b \end{bmatrix}, \quad m_{12} L_b + r_2 S_b \pmod{(r_1 L_b)} \quad (4.66)$$

Compare with (21.131). Is  $(m_{12} - r_1)L_b \pmod{(r_1 L_b)} \neq 0$ ?

<sup>4</sup>Predrag 2023-02-13:

$$\begin{bmatrix} 1 & -1 \\ 0 & 2 \end{bmatrix} = \begin{bmatrix} 1 & 1 \\ 0 & 2 \end{bmatrix}, \quad m_{12} L_p + r_2 S_p \pmod{(r_1 L_p)} \quad (4.70)$$

Compare with (21.131).

$\mathbb{B}$  is not necessarily the smallest tile that tiles the primitive cell  $\mathbb{A}$ . If  $|\det \mathbb{B}|$  is not a prime number, the above procedure can be repeated, tiling the primitive cell  $\mathbb{B}$  by repeats of a smaller tile. And the smallest possible tile, the integer lattice  $\mathbb{Z}^2$  unit square tiles any larger tile.

#### 4.4.2 Retiling the tiles, ver. 2023-01-19

For the temporal cat and spatiotemporal cat, the 1-dimensional fields is defined on the sites of the  $d$ -dimensional (hyper-cubic) integer lattice  $\mathbb{Z}^d$ . So the periodicities can only be given by lattices with integer components, i.e., a sublattice of  $\mathbb{Z}^d$ . To make  $\mathcal{L}_a$  a sublattice of  $\mathbb{Z}^d$  the basis must only consist of integers,

$$\mathbf{A} = [\mathbf{a}_1, \dots, \mathbf{a}_d] \in \mathbb{Z}^{d \times d}. \quad (4.71)$$

For a 2-dimensional lattice, the choice of lattice basis  $\mathbf{A} \in \mathbb{Z}^{2 \times 2}$  is not unique. The infinity of equivalent bases are related by unimodular transformations [128]:  $\mathcal{L}_a = \mathcal{L}_b$  if and only if  $\mathbf{A} = \mathbf{B}\mathbf{U}$ , where  $\mathbf{U} \in \mathbb{Z}^{2 \times 2}$  and  $\det \mathbf{U} = \pm 1$ . Nevertheless, each 2-dimensional lattice has a unique *Hermite normal form* [37] basis,

$$\mathbf{A} = \begin{bmatrix} L & S \\ 0 & T \end{bmatrix}, \quad (4.72)$$

where  $L, T$  are respectively the spatial, temporal lattice periods, and the ‘tilt’ [109]  $0 \leq S < L$  imposes the relative-periodic ‘shift’bc’s). We label the lattice  $\mathcal{L}_a$  with  $\mathbf{A}$  in Hermite normal form (7.4) by  $[L \times T]_S$ . An example of the  $[3 \times 2]_1$  lattice is shown in figure ??.

A lattice  $\mathcal{L}_a$  is a sublattice of lattice  $\mathcal{L}_b$  if and only if the basis of  $\mathcal{L}_a$  is in the lattice  $\mathcal{L}_b$ , i.e.,

$$\mathbf{A} = \mathbf{B}\mathbf{Q}, \quad \mathbf{Q} \in \mathbb{Z}^{2 \times 2}. \quad (4.73)$$

If  $\mathcal{L}_a$  is a sublattice of  $\mathcal{L}_b$ , we can choose the fundamental domain of  $\mathcal{L}_b$  that can tile the fundamental domain of  $\mathcal{L}_a$ .

If  $|\det \mathbf{A}|$  is not a prime number or 1, it can be decomposed into the product of two integer matrices:  $\mathbf{A} = \mathbf{B}\mathbf{Q}$ , where neither  $\mathbf{B}$  nor  $\mathbf{Q}$  is unimodular [52].<sup>5</sup> So if  $|\det \mathbf{A}|$  is not a prime number or 1,  $\mathcal{L}_a$  is a sublattice of a lattices other than the integer lattice  $\mathbb{Z}^2$ . If  $|\det \mathbf{A}|$  is a prime number,  $\mathcal{L}_a$  is not a sublattice of other lattices except for the integer lattice  $\mathbb{Z}^2$  and we call  $\mathcal{L}_a$  prime lattice. If  $|\det \mathbf{A}|$  is 1,  $\mathcal{L}_a$  is  $\mathbb{Z}^2$ .

Write the basis of  $\mathcal{L}_a$  and  $\mathcal{L}_b$  in the Hermite normal form:

$$\mathbf{A} = [\mathbf{a}_1 \quad \mathbf{a}_2] = \begin{bmatrix} L_a & S_a \\ 0 & T_a \end{bmatrix}, \quad \mathbf{B} = [\mathbf{b}_1 \quad \mathbf{b}_2] = \begin{bmatrix} L_b & S_b \\ 0 & T_b \end{bmatrix}. \quad (4.74)$$

<sup>5</sup>Predrag 2020-09-08: In *siminos/spatiotemp/chapter/integLatt.tex* Dudgeon and Mersereau [52] explain clearly that if  $\det \mathcal{L}$  is a prime number, then  $\mathcal{L}$  is a *prime matrix*. If  $\mathcal{L}$  is neither prime nor unimodular, it is *composite*, and can be decomposed, nonuniquely - up to a unimodular transformation - into a product of two non-unimodular matrices  $\mathcal{L} = P\mathbf{Q}$ . Then one can “quotient”  $\mathbf{Q}$  by “dividing” by  $P$ .

Use definitions preceding (8.116)?

By (4.73),  $\mathbf{Q} = \mathbf{B}^{-1}\mathbf{A}$  is an integer matrix if  $\mathcal{L}_a$  is a sublattice of  $\mathcal{L}_b$ , and this is satisfied only if  $L_a$  is a multiple of  $L_b$ ,  $T_a$  is a multiple of  $T_b$ , and the two tile ‘tilts’ satisfy that the area spanned by the two ‘tilted’ primitive vectors

$$\det \begin{bmatrix} \mathbf{a}_2 & \mathbf{b}_2 \end{bmatrix} = S_a T_b - T_a S_b \quad (4.75)$$

is a multiple of the  $\mathcal{L}_b$  tile area  $L_b T_b$ .

A given Bravais lattice  $\mathcal{L}$  can be defined by any of the infinity of primitive cells, each defined by a different pair of primitive vectors  $(\mathbf{a}_1, \mathbf{a}_2)$ , but equivalent under unimodular,  $\text{SL}(2, \mathbb{Z})$  transformation [89].<sup>6</sup> Each such family contains a unique primitive cell of the *Hermite normal form* [37], which, for a 2-dimensional square lattice, can be chosen to have the first primitive vector pointing in the spatial direction [95]

$$\mathbf{a}_1 = \begin{pmatrix} L \\ 0 \end{pmatrix}, \quad \mathbf{a}_2 = \begin{pmatrix} S \\ T \end{pmatrix}, \quad (4.76)$$

where  $L, T$  are respectively the spatial, temporal lattice periods, and the ‘tilt’ [109]  $0 \leq S < L$  imposes the relative-periodic ‘shift’ bc’s [42] (in the integer lattices literature these are also referred to as ‘helical’ [94] vs. ‘toroidal’ [81]; ‘twisted’ and ‘twisting factor’ [94]; ‘screw’ bc’s). We label primitive cell (4.76) and the corresponding Bravais lattice  $\mathcal{L}$  by  $[L \times T]_S$ . An example is the  $[3 \times 2]_1$  Bravais lattice is shown in reffig f:BravaisLatt.

For brevity, we shall refer to periodic state  $\Phi$  as a *invariant 2-torus* if it satisfies

$$\Phi(z + R) = \Phi(z) \quad (4.77)$$

for any discrete translation  $R = n_1 \mathbf{a}_1 + n_2 \mathbf{a}_2 \in \mathcal{L}$ , where  $\{n_1, n_2\}$  are any integers, and  $(\mathbf{a}_1, \mathbf{a}_2)$  is a pair of  $\mathbb{Z}^2$  integer lattice vectors that define a *primitive cell*. We shall always refer to a Bravais sublattice (sublattice of  $\mathbb{Z}^2$ ) by its unique Hermite normal form primitive cell (4.76) (basis?), and denote it  $\mathcal{L} = [L \times T]_S$ , a 2-dimensional doubly-periodic (relative) *invariant 2-torus*

$$\phi_{nt} = \phi_{n+L, t} = \phi_{n+S, t+T}, \quad (n, t) \in \mathbb{Z}^2 \quad (4.78)$$

with periods  $(L, T)$  and tilt  $S$ .

**2020-03-17 Han** In order to determine all prime tiles

$$\mathbf{b}_1 = \begin{pmatrix} L_p \\ 0 \end{pmatrix}, \quad \mathbf{b}_2 = \begin{pmatrix} S_p \\ T_p \end{pmatrix}, \quad (4.79)$$

that tile a larger tile

$$\mathbf{a}_1 = \begin{pmatrix} L \\ 0 \end{pmatrix}, \quad \mathbf{a}_2 = \begin{pmatrix} S \\ T \end{pmatrix}, \quad (4.80)$$

<sup>6</sup>Predrag 2020-09-05: recheck Lang [89] *Linear Algebra*, or replace! It is possible that it does not reference modular group at all...

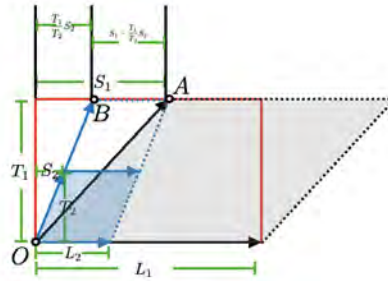


Figure 4.2: The gray parallelogram is the primitive cell of the large tile and the blue parallelogram is the primitive cell of the prime tile  $p$ ,  $T = 2T_p$  and  $L = 3L_p$ . The repeat the prime tile in the temporal direction reaches the upper boundary of the large tile at point  $B$ . If the prime tile can tile the large tile then the periodic boundary of the prime tile should satisfy the periodic boundary of the large tile. So the field value at point  $B$  should be same as the field value at point  $A$ . The distance between point  $B$  and point  $A$  should be equal to  $L_p$  multiplied by an integer.

observe that a prime tile tiles the larger tile only if its width  $L$  is a multiple of  $L_p$ , its height  $T$  is a multiple of  $T_p$ , and the tile ‘tilts’ are related by

$$\mathbf{a}_2 = n\mathbf{b}_1 + \frac{T}{T_p}\mathbf{b}_2 \quad \rightarrow \quad S = nL_p + \frac{T}{T_p}S_p \quad (4.81)$$

i.e., the area spanned by the two ‘tilted’ primitive vectors  $\mathbf{a}_2 \times \mathbf{b}_2 = ST_p - TS_p$  must be a multiple of the prime tile area  $L_pT_p$ .

Another way to understand the prime tile condition is illustrated in figure 4.2. The gray parallelogram is the primitive cell of the larger tile and the blue parallelogram is the primitive cell of the prime tile. In this figure we assume that the first two relations,  $L_p$  divides  $L$  and  $T_p$  divides  $T$  are already satisfied. In the periodic field over the larger tile, the field value at the tip of  $\mathbf{a}_2$  (marked  $A$ ) is the same as the field value at the origin  $O$ . And for the periodic field of the prime tile, the field value at the tip of  $(T/T_p)\mathbf{b}_2$  (marked  $B$ ) is same as the field value on the origin, hence the field values at points  $A$  and  $B$  are the same,  $\mathbf{a}_2 = (T/T_p)\mathbf{b}_2$  which requires that  $A - B$  can be divided by  $L_p$ . So  $S - (T/T_p)S_p$  must be divisible by  $L_p$ .

2020-06-05 Han Suppose a Bravais lattice  $\mathcal{L}$  with basis

$$\mathbf{\Lambda} = [ \mathbf{a}_1 \mid \mathbf{a}_2 ] = \begin{bmatrix} a_{11} & a_{12} \\ a_{21} & a_{22} \end{bmatrix}$$

$$\det \mathcal{L} = a_{11}a_{22} - a_{12}a_{21} . \quad (4.82)$$

is tiled by a finer lattice  $\mathcal{L}_p$  with a basis

$$\begin{aligned}\mathbf{\Lambda}_p &= [\mathbf{a}_1^p \mid \mathbf{a}_2^p] = \begin{bmatrix} a_{11}^p & a_{12}^p \\ a_{21}^p & a_{22}^p \end{bmatrix} \\ \det \mathcal{L}_p &= a_{11}^p a_{22}^p - a_{12}^p a_{21}^p.\end{aligned}\quad (4.83)$$

As  $\mathcal{L}$  is a sublattice of  $\mathcal{L}_p$ , the basis must satisfy

$$\mathbf{\Lambda} = [k\mathbf{a}_1^p + l\mathbf{a}_2^p \mid m\mathbf{a}_1^p + n\mathbf{a}_2^p] = \mathbf{\Lambda}_p \begin{bmatrix} k & m \\ l & n \end{bmatrix}, \quad (4.84)$$

where  $k, l, m$  and  $n$  are integers. Solving this equation we have

$$\begin{aligned}k &= \frac{a_{11}a_{22}^p - a_{21}a_{12}^p}{\det \mathcal{L}_p}, & l &= \frac{a_{21}a_{11}^p - a_{11}a_{21}^p}{\det \mathcal{L}_p} \\ m &= \frac{a_{12}a_{22}^p - a_{22}a_{12}^p}{\det \mathcal{L}_p}, & n &= \frac{a_{22}a_{11}^p - a_{12}a_{21}^p}{\det \mathcal{L}_p},\end{aligned}\quad (4.85)$$

and

$$\frac{\det \mathcal{L}}{\det \mathcal{L}_p} = \det \begin{bmatrix} k & m \\ l & n \end{bmatrix} = kn - lm. \quad (4.86)$$

To satisfy these relations,  $|\mathbf{a}_1 \times \mathbf{a}_1^p|$ ,  $|\mathbf{a}_1 \times \mathbf{a}_2^p|$ ,  $|\mathbf{a}_2 \times \mathbf{a}_1^p|$  and  $|\mathbf{a}_2 \times \mathbf{a}_2^p|$  need to be multiples of the prime tile area  $\det \mathcal{L}_p$ , with one relation on these integers imposed by the volume ratio (4.86) also being an integer.

**2020-08-15 Predrag** Is

$$\text{tr} \begin{bmatrix} k & m \\ l & n \end{bmatrix} = \text{tr} (\mathbf{\Lambda}_p^{-1} \mathbf{\Lambda}) \quad (4.87)$$

an important invariant?

**2020-08-15 Predrag** Any integer  $[2 \times 2]$  matrix with nonvanishing determinant defines a primitive cell, so we can turn the above argument around. The form of (4.84) suggests that if we have two prime lattices, we can construct a 'non-prime' (?) Bravais lattice by multiplication

$$\mathbf{\Lambda}_{pp'} = \mathbf{\Lambda}_p \mathbf{\Lambda}_{p'}. \quad (4.88)$$

Can we construct all Bravais lattices this way? Not clear, as the two primitive cells do not commute,  $\mathbf{\Lambda}_p \mathbf{\Lambda}_{p'} \neq \mathbf{\Lambda}_{p'} \mathbf{\Lambda}_p$ . Their volumes do multiply  $\det \mathbf{\Lambda}_{pp'} = \det \mathbf{\Lambda}_p \det \mathbf{\Lambda}_{p'}$ , so it is still possible they generate the same Bravais lattice, or two within an relative periodic orbit family of the same volume, but different tilt.

The ordered concatenations of primes, [ChaosBook Appendix A18.2 Prime factorization for dynamical itineraries](#) might do the trick.

See also the factorization algorithm (8.116).

**2020-08-15 Predrag** This checks with the Hermite normal form basis (4.79), where  $a_{21} = a_{21}^p = 0$ :

$$k = \frac{LT_p}{\det \mathcal{L}_p} = \frac{L}{L_p}, \quad l = 0,$$

$$m \det \mathcal{L}_p = ST_p - TS_p, \quad n = \frac{TL_p}{\det \mathcal{L}_p} = \frac{T}{T_p},$$

The volume relation

$$\frac{\det \mathcal{L}}{\det \mathcal{L}_p} = \det \begin{bmatrix} k & m \\ 0 & n \end{bmatrix} = kn \quad (4.89)$$

is trivially true. The trace (4.90)

$$\text{tr} \begin{bmatrix} k & m \\ l & n \end{bmatrix} = \frac{L}{L_p} + \frac{T}{T_p} \quad (4.90)$$

does not depend on  $S$ , so it is not an invariant that we are looking for.

**2020-08-15 Predrag** Consider now the prime primitive cell whose volume is a prime number,

$$\det \mathcal{L}_p = p.$$

Its only divisor is the unit cell of  $\mathbb{Z}^2$ , so (4.85) becomes

$$\begin{bmatrix} k & m \\ l & n \end{bmatrix} = \begin{bmatrix} a_{11} & a_{12} \\ a_{21} & a_{22} \end{bmatrix}. \quad (4.91)$$

In the Hermite normal form basis (4.79) we chose  $L = p, T = 1$ , so

$$\begin{bmatrix} k & m \\ l & n \end{bmatrix} = \begin{bmatrix} L & S \\ 0 & T \end{bmatrix}, \quad S = 0, 1, \dots, p-1. \quad (4.92)$$

According to (4.85) the unimodular-transformation invariant formula (is it?) for  $S$  is

$$S = \mathbf{a}_2 \times \mathbf{a}_2^p = a_{12}a_{22}^p - a_{22}a_{12}^p, \quad (4.93)$$

where  $\Lambda_p$  is an unit area primitive cell (not necessarily the unit square) that tiles  $\mathcal{L}$ .

Some of discussion in the **2020-07-11 Predrag** post, around eq. (8.116), might be relevant.

**2020-08-15 Predrag** As an example of an arbitrary primitive cell  $\Lambda$ , consider the prime Bravais lattice figure 8.1, with the 'integral basis' vectors (8.96) and  $\det \mathcal{L} = 7$

$$\begin{bmatrix} a_{11} & a_{12} \\ a_{21} & a_{22} \end{bmatrix} = \begin{bmatrix} 3 & 2 \\ 1 & 3 \end{bmatrix}. \quad (4.94)$$



### 4.4.3 Repeats of prime periodic states (failed attempt)

2023-06-08 Predrag Not sure this is the right file retiling.tex

2022-10-05 Predrag This section is WRONG IF probability of a repeat assumed in (4.97) is not multiplicative, as is the case for orbit Jacobian matrices, see (4.111). But (4.99) is a subsum, only the rectangles, no slants.

A field configuration  $\Phi_{\mathbf{a}}$  occurs with probability density

$$P[\Phi_{\mathbf{a}}] = \frac{1}{Z_{\mathbf{a}}} e^{-S_{\mathbf{a}}[\Phi_{\mathbf{a}}]}, \quad Z_{\mathbf{a}} = Z_{\mathbf{a}}[0]. \quad (4.95)$$

Here  $Z_{\mathbf{a}}$  is a normalization factor, given by the *partition sum*, the sum (in continuum, the integral) over probabilities of all configurations,

$$Z_{\mathbf{a}}[J_{\mathbf{a}}] = e^{N_{\mathbf{a}}W_{\mathbf{a}}} = \int d\Phi_{\mathbf{a}} P[\Phi_{\mathbf{a}}] e^{\Phi_{\mathbf{a}} \cdot J_{\mathbf{a}}}, \quad d\Phi_{\mathbf{a}} = \prod_z d\phi_z, \quad (4.96)$$

where  $J = \{j_z\}$  is an external source  $j_z$  that one can vary site by site, and  $S_{\mathbf{a}}[\Phi]$  is the action that defines the theory (discussed in more detail in sect. 4.12.2). The dimension of the partition function integral equals the number of lattice sites  $N_{\mathbf{a}}$ , i.e., the lattice volume (8.97).

A repeat of a *prime* primitive cell  $\mathcal{L}_{\mathbf{a}}$  along direction  $a_1$  is given by

$$Z_{\mathbf{a}}^2 = \int d\Phi_{\mathbf{a}} P[\Phi_{\mathbf{a}}] P[\Phi_{\mathbf{a}}] e^{2\Phi_{\mathbf{a}} \cdot J_{\mathbf{a}}}. \quad (4.97)$$

Summing over all repeats we get

$$Z_{\mathbf{a}}[J_{\mathbf{a}}; z_1] = \int d\Phi_{\mathbf{a}} \frac{P[\Phi_{\mathbf{a}}]z_1}{1 - P[\Phi_{\mathbf{a}}]z_1} = \int d\Phi_{\mathbf{a}} \frac{e^{N_{\mathbf{a}}W_{\mathbf{a}}z_1}}{1 - e^{N_{\mathbf{a}}W_{\mathbf{a}}z_1}}. \quad (4.98)$$

(fix up the notation!)

In the case of an Euclidean theory symmetric under all spacetime axes  $a_j$  interchanges, we need only one generating function variable,  $z_j = z$ . Carrying out the summation for a 2-dimensional spatiotemporal square lattice, we re-sum by summing first over the equal area (anti) diagonals  $N_{\mathbf{a}} = L_{\mathbf{a}} + T_{\mathbf{a}}$ , then over  $N_{\mathbf{a}}$ , obtaining

$$Z_{\mathbf{a}}[J_{\mathbf{a}}; z] = \int d\Phi_{\mathbf{a}} \frac{P[\Phi_{\mathbf{a}}]z}{(1 - P[\Phi_{\mathbf{a}}]z)^2} = \int d\Phi_{\mathbf{a}} \frac{e^{N_{\mathbf{a}}W_{\mathbf{a}}z}}{(1 - e^{N_{\mathbf{a}}W_{\mathbf{a}}z})^2}. \quad (4.99)$$

(Now sum over all primes, do cumulant expansion (??), get cycle expansions for observables.)

### 4.4.4 Resolvent of $W$

<sup>7</sup> We assume that the deterministic system under consideration is *uniformly hyperbolic*, i.e., that the stability eigen-exponents  $\lambda_{c,\alpha} = \ln |\Lambda_{c,\alpha}|/V_c$  of every

<sup>7</sup>Predrag 2024-09-10: What follows is edits of text initially copied from ChaosBook average.tex

periodic state are finite and strictly bounded from above and below,

$$-\infty < \lambda_{min} \leq \lambda_{c,\alpha} \leq \lambda_{max}.$$

Hence every primitive cell partition sum is exponentially bounded,

$$\lambda_{min} \leq W_{\mathbb{A}}[0] \leq \lambda_{max}.$$

It is reasonable to suppose that there exist constants  $M > 0$ ,  $s_0 \geq 0$  such that

$$Z_{\mathbb{A}} = e^{tW_{\mathbb{A}}} \leq M e^{ts_0} \text{ for all } t \geq 0, \quad t = V_{\mathbb{A}}$$

What does that mean? We are assuming that no value of  $e^{tW_{\mathbb{A}}}\rho(\phi)$  grows faster than exponentially for any choice of function  $\rho(\phi)$ , so that the fastest possible growth can be bounded by  $e^{ts_0}$ , a reasonable expectation in the light of the simplest example studied so far, the escape rate. If that is so, multiplying  $e^{tW_{\mathbb{A}}}$  by  $e^{-ts_0}$  we construct a new operator  $e^{-ts_0}e^{tW_{\mathbb{A}}} = e^{t(W-s_0I)}$  which decays exponentially for large  $t$ ,  $\|e^{t(W-s_0I)}\| \leq M$ . We say that  $e^{-ts_0}e^{tW_{\mathbb{A}}}$  is an element of a *bounded* semigroup with generator  $W - s_0I$ . Given this bound, it follows by the Laplace transform

$$\int_0^\infty dt e^{-st} e^{tW_{\mathbb{A}}} = \frac{1}{s - W}, \quad \text{Re } s > s_0, \quad (4.100)$$

<sup>8</sup> that the *resolvent* operator  $(s - W)^{-1}$  is bounded

$$\left\| \frac{1}{s - W} \right\| \leq \int_0^\infty dt e^{-st} M e^{ts_0} = \frac{M}{s - s_0}. \quad (4.101)$$

If one is interested in the spectrum of  $\mathcal{L}$ , as we will be, the resolvent operator is a natural object to study; it has no Bravais lattice volume dependence, and it is bounded. It is clear that the leading eigenvalue  $s_0(\beta)$  corresponds to the pole in (4.101).

The main lesson of this brief aside is that for continuous time flows, the Laplace transform is the tool that brings down the XXX in refeq3.16a into the resolvent form (4.100) and enables us to study its spectrum.

## 4.5 Orbit stability

The central insight of spatiotemporal field theory is the notion of *global* orbit stability. What we lack is the associated flow (analogue of the temporal Perron-Frobenius operator).

It might be the *Laplacian as a generator of diffusion* (18.21).

It might be the stability of *Newton descent*, page 548.

It might be *Gel'fand-Yaglom theorem's 'Fredholm' operator*, page 599.

<sup>8</sup>Predrag 2024-05-27:  $W$  might have the sign wrong here. More importantly, I'm mixing up the operator (a 'matrix' kernel) here, and the Laplace integral over its trace.

For field theories considered here, the orbit Jacobian operators are of form

$$\mathcal{J}_{zz'} = -\square_{zz'} + V''(\phi_z) \delta_{zz'}, \quad (4.102)$$

with the free field  $\phi^3, \phi^4$  orbit Jacobian operators

$$\mathcal{J}_{zz'} = -\square_{zz'} + \mu^2 \delta_{zz'}, \quad (4.103)$$

$$\mathcal{J}_{zz'} = -\square_{zz'} - 2\mu^2 \phi_z \delta_{zz'}, \quad (4.104)$$

$$\mathcal{J}_{zz'} = -\square_{zz'} + \mu^2(1 - 3\phi_z^2) \delta_{zz'}. \quad (4.105)$$

Sometimes it is convenient to lump the diagonal terms of the discrete Laplace operator together with the site potential  $V''(\phi_z)$ . In that case, the orbit Jacobian operator takes the  $2d + 1$  banded form

$$\mathcal{J} = \sum_{j=1}^d (-r_j + \mathcal{D} - r_j^{-1}), \quad \mathcal{D}_{zz'} = d_z \delta_{zz'}, \quad d_z = V''(\phi_z)/d + 2 \quad (4.106)$$

where  $r_j$  shift operators translate the field configuration by one lattice spacing in the  $j$ th hypercubic lattice direction, and we refer to  $d_z$  as the *stretching factor* at lattice site  $z$ . For the free field and spatiotemporal cat (4.103),  $\phi^3$  (4.159),  $\phi^4$  (4.105) theories the stretching factor  $d_z$  is, respectively,

$$s = \mu^2/d + 2, \quad (4.107)$$

$$d_z = -2\mu^2 \phi_z/d + 2, \quad (4.108)$$

$$d_z = \mu^2(1 - 3\phi_z^2)/d + 2. \quad (4.109)$$

In solid state physics operator (4.106) is known as the discrete Schrödinger operator [26, 129].

In what follows, it is crucial to distinguish the  $[V_{\mathbb{A}} \times V_{\mathbb{A}}]$  orbit Jacobian matrix, evaluated over a finite volume primitive cell  $\mathbb{A}$ , from the orbit Jacobian operator (4.106) that acts on the infinite Bravais lattice  $\mathcal{L}_{\mathbb{A}}$ .

#### 4.5.1 Primitive cell stability of a periodic state

Solutions of a nonlinear field theory are in general not translation invariant, so the orbit Jacobian matrix (4.57) (or the ‘discrete Schrödinger operator’ [26, 129])

$$\mathcal{J}_c = \begin{pmatrix} d_0 & -1 & 0 & 0 & \cdots & 0 & -1 \\ -1 & d_1 & -1 & 0 & \cdots & 0 & 0 \\ 0 & -1 & d_2 & -1 & \cdots & 0 & 0 \\ \vdots & \vdots & \vdots & \vdots & \ddots & \vdots & \vdots \\ 0 & 0 & 0 & 0 & \cdots & d_{n-2} & -1 \\ -1 & 0 & 0 & 0 & \cdots & -1 & d_{n-1} \end{pmatrix} \quad (4.110)$$

is not a circulant matrix: each periodic state  $\Phi_c$  has its own orbit Jacobian matrix  $\mathcal{J}_c = \mathcal{J}[\Phi_c]$ , with the ‘stretching factor’  $d_t = V''(\phi_t) + 2$  at the lattice site  $t$  a function of the site field  $\phi_t$ .

The orbit Jacobian matrix of a period- $(mn)$  periodic state  $\Phi$ , which is a  $m$ -th repeat of a period- $n$  prime periodic state  $\Phi_p$ , has a tri-diagonal block circulant matrix form that follows by inspection from (4.110):

$$\mathcal{J}_{pr} = \begin{pmatrix} \mathbf{s}_p & -\mathbf{r} & & -\mathbf{r}^\top \\ -\mathbf{r}^\top & \mathbf{s}_p & -\mathbf{r} & \\ & \ddots & \ddots & \ddots \\ & & -\mathbf{r}^\top & \mathbf{s}_p & -\mathbf{r} \\ -\mathbf{r} & & & -\mathbf{r}^\top & \mathbf{s}_p \end{pmatrix}, \quad (4.111)$$

where block matrix  $\mathbf{s}_p$  is a  $[n \times n]$  symmetric Toeplitz matrix

$$\mathbf{s}_p = \begin{pmatrix} d_0 & -1 & & & 0 \\ -1 & d_1 & -1 & & \\ & \ddots & \ddots & \ddots & \\ & & -1 & d_{n-2} & -1 \\ 0 & & & -1 & d_{n-1} \end{pmatrix}, \quad \mathbf{r} = \begin{pmatrix} 0 & \cdots & 0 \\ & \ddots & \vdots \\ 1 & & 0 \end{pmatrix} \quad (4.112)$$

and  $\mathbf{r}$  and its transpose enforce the periodic bc's. This period- $(mn)$  periodic state  $\Phi$  orbit Jacobian matrix is as translation-invariant as the temporal cat, but now under Bravais lattice translations by multiples of  $n$ . One can visualize this periodic state as a tiling of the integer lattice  $\mathbb{Z}$  by a generic periodic state field decorating a tile of length  $n$ . The orbit Jacobian matrix  $\mathcal{J}$  is now a block circulant matrix which can be brought into a block diagonal form by a unitary transformation, with a repeating  $[n \times n]$  block along the diagonal.

## 4.6 Orbit Jacobian matrices as block matrices

By reshaping the  $d$ -dimensional periodic states as vectors the tensors, the multi-index orbit Jacobian matrices  $\mathcal{J}$  can be rewritten as block matrices. For example consider a  $[L \times T]_0$  periodic state  $\Phi_c$  of a two-dimensional spatiotemporal  $\phi^4$  theory (??). Reshape the spatiotemporal periodic state as a temporal periodic state with the spatial dependence treated as a multicomponent field at each temporal lattice site. Then the orbit Jacobian matrix is a  $[T \times T]$  block matrix,

$$\mathcal{J}_A = \begin{pmatrix} \mathbf{s}_0 & -\mathbf{1} & & -\mathbf{1} \\ -\mathbf{1} & \mathbf{s}_1 & -\mathbf{1} & \\ & \ddots & \ddots & \ddots \\ & & -\mathbf{1} & \mathbf{s}_{T-2} & -\mathbf{1} \\ -\mathbf{1} & & & -\mathbf{1} & \mathbf{s}_{T-1} \end{pmatrix}, \quad (4.113)$$

with  $[L \times L]$  matrix block  $\mathbf{s}_t$

$$\mathbf{s}_t = \begin{pmatrix} d_{0,t} & -1 & & & -1 \\ -1 & d_{1,t} & -1 & & \\ & \ddots & \ddots & \ddots & \\ & & -1 & d_{L-2,t} & -1 \\ -1 & & & -1 & d_{L-1,t} \end{pmatrix}, \quad (4.114)$$

and  $\mathbf{1}$  a  $[L \times L]$  identity matrix. For a periodic state with periodicity  $[L \times T]_S$  the orbit Jacobian matrix is still a tri-diagonal block matrix, but with relative periodic boundary conditions, imposed by the non-zero shift  $S$ :

$$\mathcal{J} = \begin{pmatrix} \mathbf{s}_0 & -\mathbf{1} & & & -r_1^S \\ -\mathbf{1} & \mathbf{s}_1 & -\mathbf{1} & & \\ & \ddots & \ddots & \ddots & \\ & & -\mathbf{1} & \mathbf{s}_{T-2} & -\mathbf{1} \\ -r_1^S & & & -\mathbf{1} & \mathbf{s}_{T-1} \end{pmatrix}, \quad (4.115)$$

where  $r_1$  is a  $[L \times L]$  cyclic shift matrix  $(r_1)_{n,n'} = \delta_{n+1,n'}$ .

A spatiotemporal lattice field theory which couples adjacent field values by discrete Laplace operator (4.139) has orbit Jacobian matrices with tri-diagonal form similar to (4.113). For example, a  $[L \times T]_0$  periodic state of a uniform stretching systems such as the two-dimensional spatiotemporal cat (??) has orbit Jacobian matrix (4.113)–(4.114) but  $s_{i,t}$  is a constant  $2s$  that does not depend on the field values at each lattice site. The spatiotemporal-translation invariance allows one to compute the eigenvalues of the orbit Jacobian matrix using the discrete Fourier transform.

## 4.7 Observables

**2022-01-19, 2023-02-11 Predrag** Because of the dependence of the orbit Jacobian matrix (4.111) on the primitive cell  $\mathbf{A}$  repeat number  $r$ , we have to distinguish the partition function  $Z_{\mathbf{A}}$  defined over the finite lattice volume  $N_{\mathcal{L}} = N_{\mathbf{A}}$  primitive cell from the (infinite) lattice partition function  $Z_{\mathcal{L}}$ , which is the sum over all distinct primitive cells.

A field configuration  $\Phi$  over a primitive cell  $\mathbf{A}$  of lattice  $\mathcal{L}$  occurs with probability density

$$P_{\mathbf{A}}[\Phi] = \frac{1}{Z} e^{-S_{\mathbf{A}}[\Phi]}, \quad Z = Z_{\mathcal{L}}[0]. \quad (4.116)$$

Here  $Z_{\mathcal{L}}$  is a normalization factor, given by the *partition sum*, the sum (in continuum, the integral) over probabilities of all configurations,

$$Z_{\mathcal{L}}[J] = e^{N_{\mathcal{L}}W_{\mathcal{L}}} = \int_{\mathcal{L}} d\Phi P[\Phi] e^{\Phi \cdot J}, \quad d\Phi = \prod_z^{\mathcal{L}} d\phi_z, \quad (4.117)$$

where  $J = \{j_z\}$  is an external source  $j_z$  that one can vary site by site, and  $S[\Phi]$  is the action that defines the theory (discussed in more detail in sect. 4.12.2). The dimension of the partition function integral equals the number of lattice sites  $N_{\mathcal{L}}$ , i.e., the lattice volume (8.97).

Birkhoff sum [88] over primitive cell  $c$

$$A_c = \sum_{z \in c} a_z. \quad (4.118)$$

Birkhoff average over primitive cell  $c$

$$\langle a \rangle_c = \frac{A_c}{N_c}. \quad (4.119)$$

The free energy (the large-deviation potential?)

$$\begin{aligned} Z_{\mathbf{A}}[0] &= \sum_c e^{N_{\mathcal{L}} W_c[0]} \\ e^{N_{\mathcal{L}} W_c[0]} &= \int_{\mathcal{M}_c} d\Phi \delta(F[\Phi]) = \frac{1}{|\text{Det } \mathcal{J}_c|} \end{aligned} \quad (4.120)$$

was originally snuck into (??) (see (4.226), (4.306), (16.99)) See also partition function (4.14), (4.179), (4.291); partition sum (4.179); Gaussian (16.55); Ising (19.26).

### 4.7.1 Birkhoff sums

**2022-04-17 Predrag** In number theory, probability theory and dynamical systems literature the integrated observable is sometimes called a ‘Birkhoff sum’, and the time average along an orbit is sometimes called a ‘Birkhoff average’.

What I (used to) call in ChaosBook the ‘integrated observable’ mathematicians (sometimes?) call the ‘Birkhoff sum’,

$$A_k = \sum_{j=1}^k a_j \quad (4.121)$$

and the time average along an orbit is sometimes called a ‘Birkhoff average’. See Oliver Knill *Birkhoff sum*.

see [ChaosBook Appendix: Averaging](#)  
 see [ChaosBook Remark A20.1. Cumulants](#)

### 4.7.2 Reject rate

ChaosBook: “Local quantities, such as the eigenvalues of equilibria and periodic orbits and global quantities, such as Lyapunov exponents, metric entropy, and fractal dimensions, are examples of dynamical system properties that are independent of coordinate choice.”

**2024-07-02 Predrag and Han** In dynamical systems theory, for open systems the rate at which trajectories leave the system per unit time is called *escape rate*, see [ChaosBook eq. \(1.3\)](#),

**2024-07-02 Predrag** For the relation between stability exponent  $\lambda$ , metric entropy  $h$  and escape rate  $\gamma$ , see [ChaosBook eq. \(22.11\)](#).

### 4.7.3 Expectation values, à la Josh & Sam

From CL18:

For a given  $\mathcal{L}_p$ -periodic prime periodic state  $\Phi_p$ , the *Birkhoff average* of observable  $a[\Phi]_z$  is given by the Birkhoff sum  $A_p$ ,

$$\langle a \rangle_p = \frac{1}{V_p} A_p, \quad A_p = \sum_{z \in \mathbb{A}_p} a[\Phi_p]_z. \quad (4.122)$$

$$Z_{\mathbb{A}}[\beta] = \sum_c \int_{\mathcal{M}_c} d\Phi_{\mathbb{A}} \delta(F[\Phi]) e^{V_{\mathbb{A}}\beta \cdot a_{\mathbb{A}}[\Phi]} = \sum_c \frac{1}{|\text{Det} \mathcal{J}_c|} e^{V_{\mathbb{A}}\beta \cdot \langle a \rangle_c}, \quad (4.123)$$

$$Z_{\mathbb{A}}[\beta] = \sum_c Z_c, \quad Z_c = e^{V_{\mathbb{A}}(\beta \cdot \langle a \rangle_c - \lambda_c)}, \quad (4.124)$$

The orbit Jacobian operator of a periodic state  $\Phi_c$ :

$$(\mathcal{J}_c)_{zz'} = \frac{\delta F[\Phi_c]_z}{\delta \phi_{z'}}, \quad z \in \mathbb{Z}^d, \quad (4.125)$$

and its determinant, the *Hill determinant*  $\text{Det} \mathcal{J}_c$ .

The stabilities of periodic states can be evaluated using either the orbit Jacobian matrix [\(21.135\)](#), a high-dimensional matrix computed globally over the periodic state, or the forward-in-time Floquet matrix  $\mathbb{J}_c$ , a low-dimensional matrix computed at a given periodic state time instant. The two ways of computing stability are related by the *Hill's formula*:

$$|\text{Det} \mathcal{J}_c| = |\det(\mathbf{1} - \mathbb{J}_c)|. \quad (4.126)$$

In the companion paper I [\[93\]](#) we derive the Hill's formula for temporal systems. The derivation of Hill's formula for spatiotemporal systems is similar.

For a one-dimensional, temporal Bravais lattice, the generating function of the deterministic partition function (21.98) is known as the deterministic trace formula (see ChaosBook eq. (21.24)), see (21.160) As here every periodic state weight contributes with a positive sign, there are no cancelations, and the key property of hyperbolic flow trajectories, that they are shadowed by shorter trajectories, is here not taken into account. That is accomplished by reorganizing the periodic state contributions into the dynamical zeta function [124] (4.128).

Our spatiotemporal zeta function - a two-dimensional generalization of the dynamical zeta function (4.128) - is related to the deterministic generating partition function (two-dimensional generalization of the deterministic trace formula (21.160)) by the usual logarithmic derivative relation between the partition sum and the zeta function

$$Z[\beta, z] = z \frac{d}{dz} \ln \zeta[\beta, z] = \sum_p V_p \sum_{n=1}^{\infty} \frac{nt_p^n}{1 - t_p^n}, \quad (4.127)$$

see, for example, ChaosBook eq. (18.24).

From (4.122):

$$V_p \langle a \rangle_p = \sum_{z \in \mathbb{A}_p} a_z.$$

From (4.123), (21.98):

$$W[\beta] = \ln \sum_p V_p Z_p[\beta], \quad Z_p[\beta] = e^{W_p[\beta]}$$

$$\left. \frac{\partial}{\partial \beta} W[\beta] \right|_{\beta=0} = \frac{1}{Z[0]} \sum_p V_p Z_p[0] \left. \frac{\partial W_p[\beta]}{\partial \beta} \right|_{\beta=0}. \quad Z_p[0] = \frac{V_p}{|\text{Det} \mathcal{J}_p|}$$

For a 1-dimensional, temporal lattice (21.160), this agrees with Josh & Sam (maybe I did not get all  $V_p$  right).

[... the above is TO BE REWRITTEN]

**2023-02-10, 2024-03-31, 2024-04-13 Han and Predrag's** derivation of Josh & Sam's prime orbits expectation value formula (4.132), as given in the current draft of Joshua L. Pughe-Sanford, Sam Quinn, Teodor Balabanski, and Roman O. Grigoriev *Computing chaotic time-averages from a small number of periodic orbits* (2024).

Start with the Euler product form of the dynamical zeta function [124],

$$1/\zeta = \prod_p (1 - t_p) \quad (4.128)$$

$$t_p = \frac{1}{|\Lambda_p|} e^{T_p \langle a \rangle_p - s}, \quad z = e^{-s}. \quad (4.129)$$



In [ChaosBook eq. \(23.25\)](#), the cycle averaging formula

$$\langle a \rangle = \langle A \rangle_\zeta / \langle T \rangle_\zeta = - \frac{\partial}{\partial \beta} \frac{1}{\zeta} \bigg/ \frac{\partial}{\partial s} \frac{1}{\zeta} \bigg|_{\beta=0, s=s_0}$$

is evaluated ordered by increasing pseudocycle periods,

$$\langle A \rangle_\zeta = \sum' A_\pi t_\pi \langle T \rangle_\zeta = \sum' T_\pi t_\pi, \quad (4.130)$$

with the 'escape rate'  $= -s_0$  in the weight  $t_p$  determined by the leading zero of the dynamical zeta function [\(4.128\)](#).

Josh & Sam take instead the derivative of each term  $(1 - t_p)$  in the formal product [\(4.128\)](#), for a confined, probability conserving  $s_0 = 0$  escape rate, resulting in the cute but troubled

$$\frac{\partial}{\partial \beta} \ln(1/\zeta) \bigg|_{\beta=0} = -1/\zeta \sum_p \frac{1}{1 - t_p} \frac{\partial t_p}{\partial \beta} \bigg|_{\beta=0}, \quad \frac{\partial t_p}{\partial \beta} = A_p t_p. \quad (4.131)$$

Prior to 0/0 setting  $s = 0$ , the overall  $-1/\zeta$ 's factors cancel, resulting in Josh & Sam's über-simple probability  $P_p$  of prime orbit  $p$  weighted formula

$$\langle a \rangle = \sum_p P_p \langle a \rangle_p, \quad P_p = \frac{T_p / (|\Lambda_p| - 1)}{\sum_{p'} T_{p'} / (|\Lambda_{p'}| - 1)}. \quad (4.132)$$

What's not nice about it, is that it is not ordered by increasing  $z^N$ .

**Proposal:** cut off the  $z$  power series at the period  $T = T_{p'}$  of the longest prime  $p'$  included, keep the  $p$  repeat terms in the geometric series expansion of  $1/(1 - t_p)$  only up to  $rT_p \leq T$ . Exponential convergence. No pseudocycles, so no shadowing. Plot  $\langle a \rangle_T$ . It might be OK.

Various way of seeing [\(4.132\)](#) is not nice. The simplest, I think, is [ChaosBook sect 22.4 False zeros](#). Or, as Han explains below, due to [ChaosBook sect 23.4 Flow conservation sum rules](#), both the expectation value and mean period series are divergent at  $s = s_0$  escape rate, where we are using them.

**2024-03-31 Han** The numerator, denominator of [\(4.130\)](#) are

$$- \frac{\partial}{\partial \beta} \ln(1/\zeta) \bigg|_{\beta=0, s=s_0} = \sum_p \frac{T_p \langle a \rangle t_p}{1 - t_p} \bigg|_{\beta=0, s=s_0} = \sum_p \frac{T_p \langle a \rangle}{|\Lambda_p| - 1},$$

$$\frac{\partial}{\partial s} \ln(1/\zeta) \bigg|_{\beta=0, s=s_0} = \sum_p \frac{T_p t_p}{1 - t_p} \bigg|_{\beta=0, s=s_0} = \sum_p \frac{T_p}{|\Lambda_p| - 1},$$

specializing to bound systems'  $s_0 = 0$  in the third terms.

In Josh & Sam's formula (4.132), the denominator increases linearly as more prime orbits are included, since for prime orbits with period  $T$ :

$$\lim_{T \rightarrow \infty} \sum_{p: T_p=T} \frac{T_p}{|\Lambda_p| - 1} = \lim_{T \rightarrow \infty} \sum_{p: T_p=T} \frac{T_p}{|\Lambda_p|} = 1 \quad (4.133)$$

for a bound system. If a system is not bound, add a  $e^{\gamma T_p}$  factor to every  $T_p$  so the exponential increase of number of prime orbits and exponential decrease of weight sum balance out, and the relation (4.133) still holds.

Our generating function (ChaosBook deterministic trace formula)

$$\begin{aligned} Z[\beta, z] &= \sum_p Z_p[\beta, z] \\ Z_p[\beta, z] &= V_p \sum_{r=1}^{\infty} t_p^r = \frac{V_p t_p}{1 - t_p}, \end{aligned} \quad (4.134)$$

with the primitive cell volume  $V_p = T_p$  equal to the time period of a prime orbit of temporal evolution equation  $\phi_{t+1} - f(\phi_t) = 0$  is similar to the numerator of (4.132), but I have not yet used its relation to the zeta function in order to actually compute this numerator. The derivative of the trace formula with respect to  $\beta$  is:

$$\left. \frac{\partial}{\partial \beta} Z[\beta, z] \right|_{z=1, \beta=0} = \sum_p \frac{T_p^2 \langle a \rangle_p}{|\Lambda_p| - 1} + ?$$

There is an extra  $T_p$  because the numerator of (4.132) is proportional to  $\frac{\partial}{\partial \beta} \zeta$ , while using (4.127) our computation of the partition function is:

$$\frac{\partial}{\partial \beta} Z[\beta, z] = z \frac{\partial^2}{\partial \beta \partial z} \ln \zeta.$$

The extra  $\partial/\partial z$  brings out one more  $T_p$ .

2022-02-13 Josh & Sam Questions about how to best (and practically) evaluate cycle averaging formulas:

1. The numbers of terms in the expansion grows so quickly with respect to the minimal symbol length orbit excluded that we are not quite sure how and where to truncate the sum, even moderately sized collections of orbits.
2. Has anyone attempted to compute periodic orbits averages by numerically computing the zero and derivative of  $F = \prod_p(1 - t_p)$  directly?

2022-02-11 Predrag .

1. Nobody so far has had enough understanding of Navier–Stokes periodic orbits to evaluate truncation errors. For low-dimensional systems:
  - (a) If grammar is known, exponentially decreasing errors kick in only after ‘fundamental’ cycles are accounted for, read the end of [ChaosBook sect. 18.3 Determinant of a graph](#)
  - (b) If symbolic dynamics is not understood, [ChaosBook sect. 23.7 Stability ordering of cycle expansions](#)
2. None has attempted it - an idea worth exploring.
  - (a) Watch out for [ChaosBook sect. 22.4 False zeros](#): the unexpanded product  $\prod_p(1 - t_p)$  is only a shorthand, just like for the original Riemann zeta function.
  - (b) If you expand the terms as a (pseudo)cycle expansion, numerically “computing the zero and derivative” seems to be what we already do?
3. But your question does lead to something that Matt Gudorf never explored in his thesis: Perhaps the most important insight of the spatiotemporal reformulation of ‘chaos’ is that the weight of periodic orbits ( $N$ -torus, if theory has  $N$  continuous symmetries) is given by its Hill determinant, see [LC21 sect 8.2 Periodic orbit theory for the retarded](#).
  - (a) Can you think of new/better ways to evaluate  $\text{Det } \mathcal{J}$ ? Orbit Jacobian matrix  $\mathcal{J}$  is big, but very sparse, and  $\text{Det } \mathcal{J}$  has a nice geometrical interpretation as a [LC21 fundamental parallelepiped](#)? The edges of the parallelepiped are the columns of the orbit Jacobian matrix, which are sparse, so maybe it is computable?
  - (b) In the continuum limit (more appropriate to Navier–Stokes?), maybe the best was is to follow [LC21 Hill and Poincaré](#), and truncate Fourier series?
  - (c) For viscous flows, like Navier–Stokes, the infinity of transient, strongly dissipative modes immediately damp put, so the Hill determinant should only have the dimension of the [inertial manifold](#). Does it?

## 4.8 Nonlinear lattice field theory

Consider a continuum scalar, one-component field,  $d$ -dimensional Euclidean  $\phi^k$  theory defined by action [85, 115, 142]

$$S[\Phi] = \int d^d x \left\{ \frac{1}{2} [\partial_\mu \phi(x)]^2 + \frac{\mu^2}{2} \phi^2(x) - \frac{g}{k!} \phi^k(x) \right\}, \quad (4.135)$$

with the Klein-Gordon mass  $\mu \geq 0$ , and the strength of the self-coupling  $g \geq 0$ . Note the inverted potential - we are interested in unstable periodic states.

The discretized  $\phi^k$  theory [106] is defined as the lattice sum over the Euclidean Lagrangian density

$$S[\Phi] = \sum_z \left\{ \frac{1}{2} \sum_{\mu=1}^d (\partial_\mu \phi)_z^2 + \frac{\mu^2}{2} \phi_z^2 - \frac{g}{k!} \phi_z^k \right\}, \quad (4.136)$$

where we set lattice constant  $a = 1$  throughout. In the spirit of anti-integrability [11], we split the action into 'kinetic' and the local 'potential' parts  $S[\Phi] = -\frac{1}{2} \Phi^\top \square \Phi + V[\Phi]$ , where the nonlinear self-interaction part is

$$V[\Phi] = \sum_z V(\phi_z), \quad V(\phi) = \frac{1}{2} \mu^2 \phi^2 - \frac{g}{k!} \phi^k, \quad k \geq 3 \quad (4.137)$$

with  $V(\phi_z)$  a nonlinear potential, intrinsic to the lattice site  $z$ . The part bilinear in fields is the free field theory action

$$S_0[\Phi] = \frac{1}{2} \Phi^\top (-\square + \mu^2 \mathbf{1}) \Phi, \quad (4.138)$$

Here the lattice Laplacian

$$\square \phi_z = \sum_{\|z'-z\|=1} (\phi_{z'} - \phi_z) = \sum_{\|z'-z\|=1} \phi_{z'} - 2d \phi_z \quad \text{for all } z, z' \in \mathcal{L} \quad (4.139)$$

is the average of the lattice field variation  $\phi_{z'} - \phi_z$  over the sites nearest to the site  $z$ . For a hypercubic lattice in one and two dimensions this discretized Laplacian is given by

$$\square \phi_t = \phi_{t+1} - 2\phi_t + \phi_{t-1} \quad (4.140)$$

$$\square \phi_{jt} = \phi_{j,t+1} + \phi_{j+1,t} - 4\phi_{jt} + \phi_{j,t-1} + \phi_{j-1,t}. \quad (4.141)$$

Discretizing  $\partial/\partial t$  as the backward partial difference operator,

$$\frac{\partial \phi(t)}{\partial t} = \frac{\phi_t - \phi_{t-1}}{\Delta t}, \quad (4.142)$$

setting  $\Delta t = 1$ , the discretized Hamilton's equations take form

$$\begin{aligned} \phi_{t+1} - \phi_t &= p_{t+1}, \\ p_{t+1} - p_t &= -V'(\phi_t), \end{aligned} \quad (4.143)$$

To go to the Lagrangian formulation, replace the momentum by the discretized velocity  $p_t = \phi_t - \phi_{t-1}$ ,

$$\phi_{t+1} - \phi_t = \phi_t - \phi_{t-1} - V'(\phi_t).$$

For the discrete scalar field theory (4.136) the Euler–Lagrange equations take form of a 3-term recurrence (second-order difference equation)

$$\square \phi_z + V'(\phi)_z = 0. \quad (4.144)$$

9

Seen from the perspective of conventional scalar field theory, we are interested in the “lattice formulation, broken-symmetry phase” or the “Goldstone phase” setting. By “spontaneous breaking of the symmetry” in  $\phi^4$  theory one means that a solution does not satisfy  $\phi \rightarrow -\phi$ . That is obvious for our spatiotemporal chaotic, “turbulent” solutions. We work “beyond perturbation theory”, as we start out in the anti-integrable, strong coupling regime, in contrast to much of the literature that often studies weak coupling expansions around one of the minima.

## 4.9 Internal symmetries

In addition to spacetime ‘geometrical’ symmetries: invariance of the shape of a periodic state under coordinate translations, rotations, and reflections, a field theory might have *internal* symmetries, groups of transformations that leave the Euler–Lagrange equations invariant, but act only on a lattice site *field*, not on site’s location in the spacetime lattice.

Consider a general transformation of lattice field,  $\phi_z \rightarrow g(\phi_z)$ . The new Euler–Lagrange equation  $F_z[g(\phi_z)]$  will be equivalent, but different in form. In that case, we need a convention to pick a particular form of the equation.

For example, under field inversion,  $\phi \rightarrow -\phi$ , the orbit (the set of all actions  $g$ ) of temporal Hénon (or  $\phi^3$  theory) consists of two distinct but equivalent Euler–Lagrange equations, differing in the sign of the stretching coefficient  $a$  in (3.6). In contrast, the potential of the  $\phi^4$  theory is invariant under field inversion. In such case, where potential is invariant under all transformations  $g \in G$ , all Euler–Lagrange equations in the group orbit of  $G$  are of the same form.

A theory has an internal symmetry, if the defining equation of the system is invariant under some transformations of the fields, without reference to their spacetime location. It maps solutions to equivalent solutions.

For example, the temporal Bernoulli (1.19) and the temporal cat (4.180) (but not the temporal Hénon) have an internal  $D_1$  symmetry. The Euler–Lagrange equations of the temporal Bernoulli and the temporal cat are invariant under order-2 dihedral group  $D_1$  inversion of the fields though the center of the  $0 \leq \phi_z < 1$  unit interval,

$$\bar{\phi}_z = 1 - \phi_z \pmod{1}, \quad \text{for all } j \in \mathcal{L}, \quad (4.145)$$

---

<sup>9</sup>Predrag 2022-04-22: **probably WRONG again**, recheck references to (4.144)!

and the corresponding inversion of lattice site symbol  $m_z$ .

For the temporal cat with a given integer stretching parameter  $s$  the alphabet ranges over  $|\mathcal{A}| = s+1$  possible values for  $m_t$ ,

$$\mathcal{A} = \{\underline{1}, 0, \dots, s-1\}, \quad (4.146)$$

necessary to keep  $\phi_t$  for all times  $t$  within the unit interval  $[0, 1)$ .

Inspection of the temporal cat figure ?? suggests that there is an internal symmetry under inversion though the center of the  $0 \leq \phi_z < 1$  unit interval. Indeed, if  $M = \{m_{nt}\}$ , composed of symbols from a given alphabet, corresponds to a 2-dimensional lattice state  $\Phi_M = \{\phi_{nt}\}$ , its internal symmetry partner

$$\bar{M} = \{\bar{m}_{nt}\}, \quad \bar{m}_{nt} = 2(s-2) - m_{nt}, \quad (4.147)$$

corresponds to lattice state  $\bar{\Phi}_{\bar{M}} = \{1 - \phi_{nt}\}$ .

If  $\Phi = \{\phi_z\}$  is a periodic state of the system, the inversion  $\bar{\Phi} = \{\bar{\phi}_z\}$  is also an admissible periodic state. So, every periodic state of the temporal Bernoulli and the temporal cat either belongs to a pair of asymmetric periodic states  $\{\Phi, \bar{\Phi}\}$ , or is symmetric (self-dual) under the inversion.

See also sect. 6.8 *Internal symmetry factorization* and sect. 6.8.1 *Internal symmetry blog*.

**2024-11-09 Predrag** Quotient the internal  $D_1$  symmetry for  $\phi^4$ , as in [Chaos-Book fig. 11.5](#).

**2021-07-17 Predrag to Han, Xaunqi and Sidney** Looking at figure ??: The temporal cat (but not the temporal Hénon) has a *internal symmetry* under the simultaneous inversion  $S$  through the center of the  $0 \leq \phi_j < 1$  unit interval, see (4.145). Can you check whether the (6.199), (6.192) Isola zeta function factorization is a consequence of this dynamical inversion symmetry?  $S^2 = 1$  should give you the projection operators.

## 4.10 Deterministic $\phi^3$ lattice field theory

Consider the non-Laplacian part of the action (4.136), with cubic Biham-Wenzel [21] lattice site potential (4.137)

$$V(\phi) = \frac{\mu^2}{2} \phi^2 - \frac{g}{3!} \phi^3 = -\frac{g}{3!} (\phi^3 - 3\lambda \phi^2), \quad \lambda = \mu^2/g, \quad (4.148)$$

parametrized by the Klein-Gordon mass  $\mu > 0$  and the self-coupling constant  $g \geq 0$ . We will scale away one of the two parameters, in two ways. In sect. 4.10.1 we shall bring the theory to the normal, Hénon form. Here we bring it to the anti-integrable [10, 11, 136] form, suitable for the analysis of theory's strong coupling limit.

We start by a field translation  $\phi \rightarrow \phi + \epsilon$ :

$$-\frac{g}{3!} \left( (\phi + \epsilon)^3 - 3\lambda(\phi + \epsilon)^2 \right) = -\frac{g}{3!} \left( \phi^3 + 3(\epsilon - \lambda)\phi^2 + 3\epsilon(\epsilon - 2\lambda)\phi \right) + (\text{const}).$$

Choose the field translation  $\epsilon = \lambda$ , such that the  $\phi^2$  term vanishes,

$$-\frac{g}{3!} (\phi^3 - 3\lambda^2\phi) + (\text{const}).$$

Drop the (const) term, and rescale the field  $\phi \rightarrow 2\lambda\phi$ :

$$-4\lambda^2\mu^2 \left( \frac{\phi^3}{3} - \frac{\phi}{4} \right).$$

The  $\phi^3$  scalar field theory action (4.136) takes form

$$S[\Phi] = \sum_z \left\{ -\frac{1}{2} \phi_z \square \phi_z - \mu^2 \left( \frac{\phi_z^3}{3} - \frac{\phi_z}{4} \right) \right\}. \quad (4.149)$$

The Euler–Lagrange equation (4.53) for the scalar lattice  $\phi^3$  field theory is now, in the  $d = 1$  temporal lattice case

$$-\phi_{t+1} + 2\phi_t - \phi_{t-1} + \mu^2(-\phi_t^2 + 1/4) = 0, \quad (4.150)$$

and in the  $d$ -dimensional spatiotemporal lattice case,<sup>10</sup>

$$\sum_{||z'-z||=1} (\phi_{z'} - \phi_z) - \mu^2(\phi_z^2 - 1/4) = 0, \quad (4.151)$$

parametrized by a *single* parameter, the Klein-Gordon mass  $\mu^2$ , with the “coupling constant”  $g$  in (4.136) scaled away.

Next, we compute the period-1 and period-2 periodic states.

**Period-1 periodic states.** From the Euler–Lagrange equation (4.150) it follows that the period-1, constant periodic states,  $\phi_t = \bar{\phi}$ , for the  $d = 1$  lattice are the zeros of function

$$F[\bar{\phi}] = \frac{4\mu^6}{g^2} \left( \bar{\phi}^2 - \frac{1}{4} \right), \quad (4.152)$$

with two real roots  $\bar{\phi}_m$

$$(\bar{\phi}_L, \bar{\phi}_R) = \left( -\frac{1}{2}, \frac{1}{2} \right). \quad (4.153)$$

---

<sup>10</sup>Predrag 2024-03-07: Removed prefactor  $1/d$  from the Laplacian here.

**Period-2 periodic states.** To determine the four period-2 periodic states  $\bar{\Phi}_m = \bar{\phi}_0 \bar{\phi}_1$ , set  $x = \phi_{2k}$ ,  $y = \phi_{2k+1}$  in the Euler–Lagrange equation (4.150), and seek the zeros of

$$F[x, y] = \begin{pmatrix} 2(x - y) - \mu^2(x^2 - 1/4) \\ 2(y - x) - \mu^2(y^2 - 1/4) \end{pmatrix}. \quad (4.154)$$

That is best done using the Friedland and Milnor [62] ‘the center of gravity’ and Endler and Gallas [57, 58] ‘center of mass’ or ‘orbit’ polynomials, but for the period-2 periodic states it suffices to eliminate  $y$  using  $F_1 = 0 \Rightarrow y(x) = x - \frac{\mu^2}{2}(x^2 - 1/4)$ , and seek zeros of the second component,

$$F_2[x, y(x)] = -\mu^2 \left( x - \frac{1}{2} \right) \left( x + \frac{1}{2} \right) \left( \frac{\mu^4}{4} x^2 - \mu^2 x + \left( 2 - \frac{\mu^4}{16} \right) \right) \quad (4.155)$$

The first 2 roots are the  $x = y$  period-1 periodic states (4.249). There is one period-2 periodic state  $\underline{12}$

$$x, y = \frac{2 \pm 2\sqrt{\frac{\mu^4}{16} - 1}}{\mu^2}, \quad (4.156)$$

so the prime period-2 periodic state exists for  $\mu^2 > 4$ . For  $\mu^2 = 4$  the period-2 periodic states pairs coalesce with the positive period-1 periodic states

$$F_2[x, y(x)] = -4 \left( x^2 - \frac{1}{4} \right) \left( x^2 - \frac{1}{2} \right)^2. \quad (4.157)$$

In the anti-integrable limit [10, 11]  $\mu \rightarrow \infty$ , the site field values

$$F_2[x, y(x)] \rightarrow -\frac{\mu^6}{4} \left( x - \frac{1}{2} \right)^2 \left( x + \frac{1}{2} \right)^2 \quad (4.158)$$

tend to the two steady states (4.249).  
the orbit Jacobian matrix

$$\mathcal{J}_{zz'} = -\square_{zz'} - 2\mu^2 \phi_z \delta_{zz'}, \quad (4.159)$$

#### 4.10.1 Spatiotemporal lattice Hénon theory

The primary advantage of studying  $\phi^3$  is that it can readily be connected to the well studied temporal Hénon map **needs citations**. We can see this connection through a straightforward linear transformation. As temporal Hénon is most commonly studied in one-dimension, for the following analysis  $d$  in (4.151) will be set to 1. To transform between  $\phi^3$  and temporal Hénon we can apply the transformation  $\phi_t = c\varphi_t + \varepsilon$  to (4.151), setting  $\varepsilon = \frac{1}{\mu^2}$  yields

$$-\varphi_{t+1} - \mu^2 c \varphi_t^2 - \varphi_{t-1} = \frac{4 - \mu^4}{4\mu^2 c} = 1$$



Where the last equality is a condition enforced to maintain the form of temporal Hénon with inverted lattice values ( $\varphi \rightarrow -\varphi$ ). Finally, we set  $-\mu^2 c = a$  to recover the classical temporal Hénon parameter. Solving our two conditions and enforcing that all binary symbolic dynamics are admissible with  $a = 6$ , we find  $c = -\frac{2}{\sqrt{3}}$  and  $\mu^2 = 3\sqrt{3}$ . So, the transformation which brings  $\phi^3$  into temporal Hénon is

$$\phi = -\frac{2}{\sqrt{3}}\varphi + \frac{1}{3\sqrt{3}} \quad (4.160)$$

#### 4.10.2 Biham-Wenzel potential

Biham and Wenzel [21] (see [ChaosBook sect. 34.1 Fictitious time relaxation](#)) construct a time-asymmetric cubic action

$$S[\Phi] = \sum_{t \in \mathbb{Z}} \left( \phi_{t+1} \phi_t - b \phi_t \phi_{t-1} + \frac{a}{3} \phi_t^3 - \phi_t \right), \quad (4.161)$$

whose Euler–Lagrange equation is the temporal Hénon 3-term recurrence equation (3.6), with dissipation,

$$F_t[\Phi] = -\phi_{t+1} + b \phi_{t-1} - a \phi_t^2 + 1, \quad (4.162)$$

and the orbit Jacobian operator

$$\mathcal{J}_{zz'} = -r + b r^{-1} - 2a \phi_t. \quad (4.163)$$

With the cubic potential at lattice site  $n$  we can start to look for orbits variationally. Note that the potential is time-reversal invariant for  $b = 1$ .

### 4.11 Deterministic $\phi^4$ lattice field theory

Consider the discrete scalar one-component field,  $d$ -dimensional  $\phi^4$  theory [121] defined by the Euclidean action (4.136)

$$S[\Phi] = \sum_z \left\{ \frac{1}{2} \sum_{\mu=1}^d (\Delta_\mu \phi_z)^2 + \frac{\mu^2}{2} \phi_z^2 - \frac{g}{4!} \phi_z^4 \right\}, \quad (4.164)$$

with the Klein-Gordon mass  $\mu \geq 0$ , quartic lattice site potential (4.137),

$$V(\phi) = \frac{1}{2} \mu^2 \phi^2 - \frac{g}{4!} \phi^4, \quad (4.165)$$

the strength of the self-coupling  $g \geq 0$ , and we set lattice constant  $a = 1$  throughout.

A popular way [98] to rewrite the quartic action (4.164) is to complete the square

$$V(\phi) = -\frac{g}{4!} \left( \phi_z^2 - 3! \frac{\mu^2}{g} \right)^2 + (\text{const}),$$

drop the (const) term, and rescale the field  $\phi_z^2 \rightarrow 3! \frac{\mu^2}{g} \phi_z^2$  :

$$S[\Phi] = 3! \frac{\mu^2}{g} \sum_z \left\{ -\frac{1}{2} \phi_z \square \phi_z - \frac{1}{4} \mu^2 (\phi_z^2 - 1)^2 \right\}. \quad (4.166)$$

The Euler–Lagrange equation (4.137) for the  $d = 1$  scalar lattice  $\phi^4$  field theory,

$$-\phi_{t+1} + [-\mu^2 \phi_t^3 + (\mu^2 + 2) \phi_t] - \phi_{t-1} = 0, \quad (4.167)$$

is thus parametrized by a *single* parameter, the Klein-Gordon mass  $\mu^2 = s - 2$ , with the “coupling constant”  $g$  in (4.164) scaled away. Next, we compute the period-1 and period-2 periodic states.

**Period-1 periodic states.** From the Euler–Lagrange equation (23.22) it follows that the period-1 periodic states,  $\phi_t = \bar{\phi}$ , for the  $d = 1$  lattice are the zeros of function

$$F[\bar{\phi}] = \mu^2 (1 + \bar{\phi}) \bar{\phi} (1 - \bar{\phi}). \quad (4.168)$$

As long as the Klein-Gordon mass is positive, there are 3 real roots  $\bar{\phi}_m$

$$(\bar{\phi}_L, \bar{\phi}_C, \bar{\phi}_R) = (-1, 0, 1). \quad (4.169)$$

The period-1 primitive cell orbit Jacobian matrix  $\mathcal{J}$  is a  $[1 \times 1]$  matrix

$$\mathcal{J} = d_m = \frac{dF[\bar{\phi}]}{d\bar{\phi}} = \mu^2 (1 - 3\bar{\phi}_m^2) = \mu^2 \text{ or } -2\mu^2, \quad (4.170)$$

so the “stretching” factor for the 3 steady periodic states is

$$(d_L, d_C, d_R) = (-2\mu^2, \mu^2, -2\mu^2). \quad (4.171)$$

**Period-2 periodic states.** To determine the nine period-2 periodic states  $\bar{\Phi}_m = \bar{\phi}_0 \bar{\phi}_1$ , set  $x = \phi_{2k}$ ,  $y = \phi_{2k+1}$  in the Euler–Lagrange equation (23.22), and seek the zeros of

$$F[x, y] = \begin{pmatrix} -(s-2)x^3 + sx - 2y \\ -(s-2)y^3 + sy - 2x \end{pmatrix}. \quad (4.172)$$

That is best done using the Friedland and Milnor [62] ‘the center of gravity’ and Endler and Gallas [57, 58] ‘center of mass’ or ‘orbit’ polynomials, but for the period-2 periodic states it suffices to eliminate  $y$  using  $F_1 = 0 \Rightarrow 2y(x) = -x^3 + sx$ , and seek zeros of the second component,

$$F_2[x, y(x)] = \frac{\mu^8}{8} (x-1) x (x+1) \left( x^2 - 1 - \frac{4}{\mu^2} \right) \left( x^4 - \left( 1 + \frac{2}{\mu^2} \right) x^2 + \frac{4}{\mu^4} \right) \quad (4.173)$$

The first 3 roots are the  $x = y$  period-1 periodic states (4.169). There is one symmetric period-2 periodic state  $\bar{LR}$

$$x = -y = \pm \sqrt{1 + 4/\mu^2}, \quad (4.174)$$

and a pair of period-2 asymmetric periodic states  $\overline{LC}, \overline{CR}$  related by reflection symmetry (time reversal).

For  $\mu^2 = 2$  the period-2 asymmetric periodic states pairs coalesce with the two period-1 asymmetric periodic states

$$2x(x^2 - 3)(x^2 - 1)^3. \quad (4.175)$$

To get a complete horseshoe (all  $3^n$  3-symbol bimodal map itineraries are realized), you know what to do next (see figure 2. in ref. [62]). Numerical work indicates [141] that for  $\mu^2 > 2.95$  the horseshoe is complete.

In the anti-integrable limit [10, 11]  $\mu \rightarrow \infty$ , the site field values

$$F_2[x, y(x)] \rightarrow \frac{\mu^8}{8} (x+1)^3 x^3 (x-1)^3 \quad (4.176)$$

tend to the three steady states (4.169).

## 4.12 Historical context

### 4.12.1 1-dimensional lattice field theories

**Spatiotemporal cat** the temporal lattice Laplacian

$$\square \phi_t \equiv \phi_{t+1} - 2\phi_t + \phi_{t-1} = (s - 2)\phi_t - m_t, \quad (4.177)$$

with the time step set to  $\Delta t = 1$ .

the cat map forcing pulse (12.101) is linear in the angular displacement  $\phi$ ,  
 $P(\phi_t) = -V'(\phi_t) = (s - 2)\phi$

the temporal cat Euler–Lagrange equation takes form (see free action (4.138))

$$(-\square + \mu^2 \mathbf{1}) \Phi = M, \quad (4.178)$$

where the Klein-Gordon mass  $\mu$  is related to the cat-map stretching parameter  $s$  by  $\mu^2 = d(s - 2)$ .

### 4.12.2 Nonlinear field theories

partition function, the integral over probabilities of all configurations,

$$Z[j] = e^{W[j]} = \int d\Phi e^{-S[\Phi] + \Phi \cdot J}, \quad d\Phi = \prod_z d\phi_z, \quad (4.179)$$

where  $J = \{j_z\}$  is an external ‘source’

Field theorists do not like odd potentials, such as the temporal Hénon (3.25), for symmetry reasons, as well as that they are not bounded from below.

### 4.12.3 Deterministic lattice field theory

second-order difference Euler–Lagrange equations (4.144) that we call, in the cases considered here, the ‘temporal cat’, ‘temporal Hénon’, and ‘temporal  $\phi^4$  theory’, respectively:

$$-\phi_{t+1} + s\phi_t - \phi_{t-1} = m_t \quad (4.180)$$

$$-\phi_{t+1} + a\phi_t^2 - \phi_{t-1} = m_t \quad (4.181)$$

$$-\phi_{t+1} + g\phi_t^3 - \phi_{t-1} = m_t \quad (4.182)$$

for the Hamiltonian,  $b = -1$  Hénon map (4.186), the 1-time step Jacobian matrix (4.185) is

$$\mathbb{J}_t = \begin{pmatrix} -2a\phi_t & -1 \\ 1 & 0 \end{pmatrix}, \quad (\phi_t, \varphi_t) = f^t(\phi_0, \varphi_0). \quad (4.183)$$

So, once we have a determined a temporal Hénon periodic state  $\Phi_p$ , we have its Floquet matrix  $\mathbb{J}_p$ . When  $\mathbb{J}_p$  is hyperbolic, only the expanding eigenvalue

$\Lambda_1 = 1/\Lambda_2$  needs to be determined, as the determinant of the Hénon 1-time step Jacobian matrix (4.183) is unity,

$$\det \mathbb{J}_p = \Lambda_1 \Lambda_2 = 1. \quad (4.184)$$

The map is Hamiltonian  
the linearized equation

$$\Delta \phi_t - \mathbb{J}_{t-1} \Delta \phi_{t-1} = 0, \quad (\mathbb{J}_t)_{ij} = \frac{\partial f(\phi_t)_i}{\partial \phi_{t,j}}, \quad (4.185)$$

where  $\mathbb{J}_t = \mathbb{J}(\phi_t)$  is the 1-time step  $[d \times d]$  Jacobian matrix, evaluated on lattice site  $t$ .

#### 4.12.4 A $\phi^3$ field theory


The simplest such nonlinear action turns out to correspond to the paradigmatic dynamicist's model of a 2-dimensional nonlinear dynamical system, the Hénon map [75]

$$\begin{aligned} x_{t+1} &= 1 - a x_t^2 + b y_t \\ y_{t+1} &= x_t. \end{aligned} \quad (4.186)$$

For the contraction parameter value  $b = -1$  this is a Hamiltonian map (see (4.184) below).

The Hénon map is the simplest map that captures chaos that arises from the smooth stretch & fold dynamics of nonlinear return maps of flows such as Rössler [120]. Written as a 2nd-order inhomogeneous difference equation [53], (4.186) takes the *temporal Hénon* 3-term recurrence form, explicitly time-translation and time-reversal invariant Euler–Lagrange equation (4.181),

$$-\phi_{t+1} + a \phi_t^2 - \phi_{t-1} = 1. \quad (4.187)$$

Just as the kicked rotor (12.100,12.101), the map can be interpreted as a kicked driven anaharmonic oscillator [74], with the nonlinear, cubic Biham-Wenzel [21] lattice site potential (4.137) 

$$V(\phi_t, m_t) = -\frac{a}{3} \phi_t^3 + \phi_t^2 - \phi_t, \quad (4.188)$$

giving rise to kicking pulse (12.101), so we refer to this field theory as  $\phi^3$  theory.

For a sufficiently large stretching parameter  $a$ , lattice site field values of this  $\phi^3$  theory are in one-to-one correspondence to the unimodal Hénon map Smale horseshoe repeller, cleanly split into the 'left', positive stretching and 'right', negative stretching lattice site field values. A plot of this horseshoe, given in, for example, [ChaosBook Example 15.4](#) is helpfull in understanding that state space of deterministic solutions of strongly nonlinear field theories has fractal support. Devaney, Nitecki, Sterling and Meiss [51, 136, 137] have shown that

the Hamiltonian Hénon map has a complete Smale horseshoe for ‘stretching parameter’  $a$  values above

$$a > 5.699310786700 \dots \quad (4.189)$$

In numerical [42] and analytic [58] calculations we fix (arbitrarily) the stretching parameter value to  $a = 6$ , in order to guarantee that all  $2^n$  periodic points  $\phi = f^n(\phi)$  of the Hénon map (4.186) exist, see table 3.1. The symbolic dynamics is binary, as simple as the temporal Bernoulli (1.15), in contrast to the temporal cat which has nontrivial pruning, see table ??.

The simplest such nonlinear action turns out to correspond to the paradigmatic dynamicist’s model of a 2-dimensional nonlinear dynamical system, the Hénon map [75]

$$\begin{aligned} x_{t+1} &= 1 - a x_t^2 + b y_t \\ y_{t+1} &= x_t. \end{aligned} \quad (4.190)$$

For the contraction parameter value  $b = -1$  this is a Hamiltonian map.



example 4.2  
p. 209



example 4.3  
p. 209

The Hénon map is the simplest map that captures chaos that arises from the smooth stretch & fold dynamics of nonlinear return maps of flows such as Rössler [120]. Written as a 2nd-order inhomogeneous difference equation [53], (4.190) takes the *temporal Hénon* 3-term recurrence form, explicitly time-translation and time-reversal invariant Euler–Lagrange equation (4.181),

$$-\phi_{t+1} + a \phi_t^2 - 1 - \phi_{t-1} = 0. \quad (4.191)$$

**Period-1** (replaces Gallas (22.17))

$$\phi_{0,1} = \frac{1 \pm \sqrt{1+a}}{a} \rightarrow \frac{1 \pm \sqrt{7}}{6} \quad (4.192)$$

**Period-2** (replaces Gallas (22.19)) The periodic points in the 10 orbit are

$$\phi_{1,2} = \frac{1 \pm \sqrt{a-3}}{a} \rightarrow \frac{1 \pm \sqrt{3}}{6} \quad (4.193)$$

(PLEASE Crosscheck THIS misCALCULATION) A cubic function can be brought to the canonical, single parameter  $p$  form [140]

$$f(x) = x^3 + p x, \quad (4.194)$$

by a field translation  $\phi \rightarrow \phi + \epsilon$ :

$$-\phi_{t+1} - \phi_{t-1} - \frac{\mu^2}{2} \left( \phi_t^2 + \frac{4}{\mu^2} \phi_t + \frac{2}{\mu^4} - \frac{2}{\mu^4} + 1 \right) = 0, \quad (4.195)$$

$$-\phi_{t+1} - \phi_{t-1} - \frac{\mu^2}{2} \left( \phi_t + \frac{2}{\mu^2} \right)^2 + \frac{1}{\mu^2} + \frac{\mu^2}{2} = 0, \quad (4.196)$$

$$-\phi_{t+1} - \phi_{t-1} + \frac{4}{\mu^2} - \frac{\mu^2}{2} \phi_t^2 + \frac{1}{\mu^2} + \frac{\mu^2}{2} = 0, \quad (4.197)$$

Another choice: a field translation  $\phi \rightarrow \phi + \epsilon$ :

$$-\frac{g}{3!} \left( (\phi + \epsilon)^3 - 3\lambda(\phi + \epsilon)^2 \right) = -\frac{g}{3!} \left( \phi^3 + 3(\epsilon - \lambda)\phi^2 + 3\epsilon(\epsilon - 2\lambda)\phi \right) + (\text{const}).$$

Choose the field translation  $\epsilon = 2\lambda$ , such that the  $\phi$  term vanishes,

$$V(\phi) = -\frac{g}{3!} (\phi^3 + 3\lambda\phi^2) + (\text{const}).$$

Rescale the field  $\phi \rightarrow \lambda\phi$ , and drop the (const) term:

$$V(\phi) = -\frac{g}{3!} \phi^3 - \frac{\mu^2}{2} \phi^2 \rightarrow -\lambda^2 \frac{\mu^2}{3!} (\phi^3 + 3\phi^2).$$

The  $\phi^3$  scalar field theory action (4.136) takes form

$$S[\Phi] = \frac{\mu^4}{g^2} \sum_z \left\{ -\frac{1}{2} \phi_z \square \phi_z - \frac{\mu^2}{3!} (\phi_z^3 + 3\phi_z^2) \right\}. \quad (4.198)$$

The Euler–Lagrange equation (4.53) for the scalar lattice  $\phi^3$  field theory (in the  $d = 1$  temporal lattice example),

$$-\phi_{t+1} + \frac{4 - \mu^2}{2} \phi_t - \phi_{t-1} - \frac{\mu^2}{2} \phi_t^2 = 0, \quad (4.199)$$

is thus again parametrized by a *single* parameter, the Klein-Gordon mass  $\mu^2$ , the “coupling constant”  $g$  in (4.136) was but a Fata Morgana.

#### 4.12.5 A $\phi^4$ field theory

If a symmetry forbids the odd-power potentials such as (4.148), one starts instead with the Klein-Gordon [8, 18, 19, 25, 27] quartic potential (4.137)

$$V(\phi_t, m_t) = -\frac{g}{4} \phi_t^4 + \phi_t^2, \quad (4.200)$$

leading to our example of the lattice ‘scalar  $\phi^4$  field theory’ [85, 115] (4.182),

$$-\phi_{t+1} + g \phi_t^3 - \phi_{t-1} = 0. \quad (4.201)$$

Topology of the state space of  $\phi^4$  theory is very much like what we had learned for the unimodal Hénon map  $\phi^3$  theory, except that the repeller set is now bimodal. As long as coupling  $g$  is sufficiently large, the repeller is a full 3-letter

shift. Indeed, while Smale’s first horseshoe [132], his fig. 1, was unimodal, he also sketched the  $\phi^4$  bimodal repeller, his fig. 5.

===== Ignore the rest for now: =====  
 quartic potential (3.8)

$$V(\phi_t, m_t) = -\frac{g}{4}\phi_t^4 + \phi_t^2 + m_t \phi_t, \tag{4.202}$$

leading to our example of the ‘ $\phi^4$  lattice field theory’ [85, 115],

$$-\phi_{t+1} + (g \phi_t^3 - m_t) - \phi_{t-1} = 0. \tag{4.203}$$

Topology of the state space of  $\phi^4$  theory is very much like what we had learned for the unimodal Hénon map  $\phi^3$  theory, except that the repeller set is now bimodal. As long as coupling  $g$  is sufficiently large, the repeller is a full 3-letter shift.

Orbit Jacobian matrix:

$$\mathcal{J} = \begin{vmatrix} \mu^2 + 2 - 3x^2 & -2 \\ -2 & \mu^2 + 2 - 3y^2 \end{vmatrix} \tag{4.204}$$

$$\begin{aligned} \text{Det}(\mathcal{J}) &= (\mu^2 + 2 - 3x^2)(\mu^2 + 2 - 3y^2) - 4 \\ &= 9(xy)^4 + 4\mu^2 + \mu^4. \end{aligned} \tag{4.205}$$

Now you have 3 values  $m_t \in \{L, C, R\}$ , but you want to quotient the reflection symmetry. See example 6.6 *A reflection–symmetric 1d map.*

The Hill determinant  $\|\mathcal{J}[\Phi]\|$  is again of the same form (3.26), with the stretching factor at site  $t$  depending on the coupling constant  $g$ , the lattice site field for the given periodic state.

For example, the Hill determinant of the  $[4 \times 4]$  orbit Jacobian matrix  $\mathcal{J}$  is (correct this!):

$$\begin{aligned} \text{Det}(\mathcal{J}) &= \begin{vmatrix} d_1 & -1 & 0 & -1 \\ -1 & d_2 & -1 & 0 \\ 0 & -1 & d_3 & -1 \\ -1 & 0 & -1 & d_4 \end{vmatrix} \\ &= d_1 d_2 d_3 d_4 + d_1 d_2 d_3 + d_2 d_3 d_4 \\ &\quad + d_1 d_2 + d_2 d_3 + d_1 d_4 + d_3 d_4 + d_1 + d_2 + d_3 + d_4. \end{aligned} \tag{4.206}$$

### 4.12.6 $\phi^4$ : Discrete Nonlinear Klein-Gordon

2024-03-14 Predrag Frantzeskakis, Karachalios, Kevrekidis, Koukouloyannis, and Vetas *Dynamical transitions between equilibria in a dissipative Klein–Gordon lattice* Journal of Mathematical Analysis and Applications, 472, 546-576 (2019). [...] the energy landscape of a dissipative Klein–Gordon lattice



(DKG model) with a  $\phi^4$  on-site potential. Continuous in time  $\ddot{\phi}$  together with a linear dissipation of strength  $\delta > 0$  term  $\delta \dot{\phi}$ . [...] The goal is to reveal and discuss the structure of the set of the possible equilibria of (1.1), which serve as potential attractors.

The system belongs in the class of a finite dimensional second-order gradient system, for which the Hamiltonian energy serves as a Lyapunov function. They prove that all bounded solutions converge to a single *global* equilibrium, i.e., a solution of the stationary problem. While in terms of the topology of the phase space, the structure of the global attractor is trivial (since it consists of the single equilibrium), they show that the structure of the set of equilibrium (steady-state) solutions is quite non-trivial. [...] They characterizing the bifurcating equilibrium branches by the number of sign-changes of the associated equilibrium solutions. [...] the evolution of the Hamiltonian energy is an effective diagnostic for the potential metastable dynamics. [...] On each lattice site there is a quartic oscillator governed by a linearly damped Duffing equation, see their Fig. 1, with 2 equilibria that we call  $\pm 1$ , and the unstable saddle at  $\phi_z = 0$ .

The Duffing oscillator is described by Duffing's equation: a second-order differential equation of the form

$$\mu \ddot{\phi}_z + c \dot{\phi}_z + k \phi_z + h \phi_z^3 = f(t). \quad (4.207)$$

So idea seems to be the same as Biham-Wentzel - use dissipation and a potential to slide into equilibria.

[...] [...] [...] [...] [...]

The unknown  $\phi_z(t)$  stands for the displacement of the atom  $n$ , while the lattice may be infinite ( $n \in \mathbb{Z}$ ) or finite ( $|n| \leq N$ ). The parameters  $m > 0, \delta \geq 0$  are related to the mass of the atoms and some possible linear damping effects respectively. The system (?1) is known as the

*Discrete Nonlinear Klein-Gordon equation* (DKG).

[...] Discretization of the (Hamiltonian variant of ???) the model, conservative DKG equation, is studied in

V. Achilleos, A. Álvarez, J. Cuevas, D.J. Frantzeskakis, N.I. Karachalios, P.G. Kevrekidis, B. Sánchez-Rey *Escape dynamics in the discrete repulsive model* Phys. D, 244 (2013), pp. 1-24

Anninos, Oliveira and Matzner *Fractal structure in the scalar  $\lambda(\phi^2 - 1)^2$  theory*, Phys. Rev. D, 44 (1991), pp. 1147-1160

Karachalios, Kyriazopoulos and Vetas, *The Lefever–Lejeune nonlinear lattice: Convergence dynamics and the structure of equilibrium states*, Physica D: Nonlinear Phenomena 409, 132487 (2020)

The dissipative variant of the model, the linearly damped DKG equation:

Comte, Marquié and Remoissenet *Dissipative lattice model with exact traveling discrete kink-soliton solutions: discrete breather generation and reaction diffusion regime* Phys. Rev. E, 60, 7484–7489 (1999).

Filatrella and Malomed *The alternating-current-driven motion of dislocations in a weakly damped Frenkel–Kontorova lattice* J. Phys., Condens. Matter, 11, 7103–7114 (1999)

#### 4.12.7 Anastassiou *et al.* AnBoBa17 $\phi^4$ notes

Notes on, excerpts from Anastassiou, Bountis and Bäcker [8] *Homoclinic points of 2D and 4D maps via the parametrization method* (2017).

Breathers and multibreathers in 1-dimensional Hamiltonian lattices [18, 19, 25, 27] (4.211) are homoclinic orbits at the intersections of stable and unstable manifolds of the origin, which, if hyperbolic, is a saddle point of the map (4.217). It suffices to locate the primary homoclinic point at which the manifolds first meet, since it generates under repeated application of  $f$  and  $f^{-1}$  all other points of the associated homoclinic orbit. The paper gives a parametrization method to locate such homoclinic orbits, compute their points of intersection. They also give the critical value of the dissipation parameter for which homoclinic intersections no longer exist.

Hénon map [75]

$$h(x, y) = (1 + y - ax^2, bx), \quad (4.208)$$

More convenient: its conjugate

$$h(x, y) = (y, -bx + a - y^2). \quad (4.209)$$

Generalized Hénon maps [66, 97]

$$H(x, y) = (y, -\delta x + p(y)), \quad (4.210)$$

where  $p(y)$  is a univariate polynomial. Dullin and Meiss [53, 54] and this paper take a third degree  $p(y)$ . Zhang [145] gives sufficient conditions for hyperbolicity for arbitrary polynomials  $p(y)$ . Bifurcations of homoclinic tangencies involving intersections of invariant manifolds [67] for (4.210).

The dynamics of discrete breather solutions on 1-dimensional lattices (or chains) of nonlinearly interacting particles is described by the discrete nonlinear Klein-Gordon system of ordinary differential equations

$$\ddot{u}_n = -V'(u_n) + \alpha(u_{n+1} - 2u_n + u_{n-1}), \quad V(x) = \frac{1}{2}Kx^2 + \frac{1}{4}x^4, \quad (4.211)$$

where  $u_n$  for  $-\infty < n < \infty$  is the amplitude of the  $n$ -th particle,  $\alpha > 0$  is a parameter indicating the strength of coupling between nearest neighbors, and  $V(x)$  is the on-site potential with primes denoting differentiation with respect to the argument of  $V(x)$ . Discrete nonlinear Schrödinger equation is similar.

A discrete breather: insert a Fourier series

$$u_n(t) = \sum_{k=-\infty}^{\infty} A_{n,k} \exp(ik\omega_b t) \quad (4.212)$$

where  $\omega_b$  the frequency of the breather, obtain

$$-k^2 \omega_b^2 A_{n,k} = \alpha (A_{n+1,k} - 2A_{n,k} + A_{n-1,k}) - K A_{n,k} - \sum_{k_1+k_2+k_3=k} A_{n,k_1} A_{n,k_2} A_{n,k_3}, \quad (4.213)$$

A breather solution to the lowest order approximation: substitute  $u_n(t) = 2A_{n,1} \cos(\omega_b t)$  in (4.213),  $A_{n,1} = A_{n,-1} = A_n$ , obtain a 3-term recurrence

$$A_{n+1} - \frac{2+K-\omega_b^2}{\alpha} A_n - \frac{3}{\alpha} A_n^3 + A_{n-1} = 0. \quad (4.214)$$

They set  $c = (2+K-\omega_b^2)/\alpha$ , rescale the Fourier coefficients  $A_n \rightarrow \alpha^{1/2} A_n$ :

$$A_{n+1} - (c+3A_n^2)A_n + A_{n-1} = 0. \quad (4.215)$$

2022-03-10 Predrag Compare with (23.22), (23.15)

$$\phi_t = -A_t, \quad g = -3, \quad s = c. \quad (4.216)$$

To get a 2-dimensional area-preserving map, set  $A_{n-1} = x$ ,  $A_n = y$ :

$$f(x, y) = (y, -x + cy + 3y^3), \quad (4.217)$$

This is the generalized Hénon map (4.210) for  $p(y) = cy + 3y^3$ . Its inverse is given by

$$f^{-1}(x, y) = (cx - y + 3x^3, x). \quad (4.218)$$

The mapping is Hamilton, reflection symmetric  $\sigma(x, y) = (-x, -y)$  with three fixed points on the diagonal, the origin and

$$\pm \sqrt{(2-c)/3}. \quad (4.219)$$

The (0, 0) fixed point stability multipliers are

$$\Lambda_s = \frac{1}{2} (c - \sqrt{c^2 - 4}), \quad \Lambda_u = \frac{1}{2} (c + \sqrt{c^2 - 4}), \quad (4.220)$$

Their choice  $c = -5/2$  yields a saddle point at the origin, and theorem of Zhang [145] ensures existence of a complete horseshoe repeller. The eigenvalues of the saddle at the origin are <sup>11</sup>

$\Lambda_u = -2$  and  $\Lambda_s = -1/2$   
 eigenvectors  
 $(-1, 2)$  and  $(-2, 1)$ .

---

<sup>11</sup>Predrag 2022-02-18: Signs opposite of (4.220)?

### 4.13 $\phi^k$ field theory blog

**2021-12-23 Predrag** The simplest field theory is a self-interacting scalar field, described by its action. All  $\phi^k$  lattice field theories fit under the “generalized Hénon map” umbrella. Hence  $\phi^3$  is covered in sect. 3.2 *Temporal Hénon; anti-integrable limit*.

**2022-03-26 Predrag** This  $\phi^4$  has a  $D_1$  symmetry under the transformation  $\phi \rightarrow -\phi$ . This is an example of an *internal* symmetry, in contrast to a *spacetime* symmetry.

**2024-01-10 Predrag** Recheck: What we call an *internal* symmetry, field-theorists call a *global* symmetry, in contradistinction to the local gauge symmetry.

**2020-03-15 Predrag** Some of the formulas in sect. 4.1 were initially extracted from G. Münster and M. Walzl [107] *Lattice Gauge Theory - A Short Primer*, arXiv:hep-lat/0012005. Used in CL18 [47].

Scholarpedia [Lattice quantum field theory](#) [106].

Maybe already used for CL18 [47]:

$\phi_\ell = \phi(a\ell)$ , where  $\phi(a\ell)$  is defined by the value of the continuum field  $\phi(\phi)$  at the lattice point  $\phi_\ell = a\ell$

(Here we work in Euclidean space.)

**2020-03-15 Predrag**

$$\partial_\mu \phi(x) = \frac{1}{a} (\phi(x + a\hat{\mu}) - \phi(x)),$$

**2020-03-15 Predrag** Let us assume a hypercubic lattice with length  $L_1 = L_2 = L_3 = L$  in every spatial direction and length  $L_4 = T$  in Euclidean time,

$$x_\mu = an_\mu, \quad n_\mu = 0, 1, 2, \dots, L_\mu - 1,$$

with finite volume  $V = L^3T$ , and periodic boundary conditions

$$\phi(x) = \phi(x + aL_\mu \hat{\mu}),$$

where  $\hat{\mu}$  is the unit vector in the  $\mu$ -direction.

**2022-03-26 Predrag** For the  $s < 2$ , a discrete free field theory is a harmonic spring mattress. All field theory courses are basically the same. They start with a spring mattress, add weak anaharmonicities, go to Feynman diagrams. None address our strong coupling, strong stretching chaotic field theory.

See, for example

Smit [133] *Introduction to Quantum Fields on a Lattice* (2002) has a nice discussion of discretization, his sect. 2.5 *Latticization of the scalar field*. But otherwise gauge field theory, fermions, etc.

Jared Kaplan [sect. 2.3 Balls and Springs](#)

John McGreevy [sect. 1 QFT from springs](#). Note that on p. 14 the potential -sum of  $\phi^k$  terms, all with positive signs- in the action enters with the overall '-' sign.

We might find the [sect. 5.2  \$\mathbb{Z}^2\$  lattice gauge theory](#) a good starting point for getting into the lattice gauge theory, if we get that far.

Niklas Beisert [sect. 2.1 Spring Lattice](#) is nice. Note that the time is continuous. He writes down the dispersion relation, his eq. (2.8).

Ashvin Vishwanath [Demystifying quantum field theory](#).

**2016-08-20 Predrag** Might be worth a look - several papers on coupled map lattices, see also ref. [77] on order and chaos in a continuous time, 1-dimensional latticel  $\phi^4$  model - if you read that literature, please share what you have learned by writing it up there.

**2021-08-11 Predrag** Karimipour and Zarei [86] *Completeness of classical  $\phi^4$  theory on two-dimensional lattices* [arXiv:1201.4558](#):

The 2-dimensional  $\phi^4$  Hamiltonian for all discrete scalar field theories on a two dimensional square lattice with periodic boundary conditions

$$H_c = \sum_{\langle r,s \rangle} K_{r,s} (\phi_r - \phi_s)^2 + \sum_r h_r \phi_r + m_r \phi_r^2 + q_r \phi_r^4, \quad (4.221)$$

where  $K_{r,s} \in \{i, -i\}$ ,  $i = \sqrt{-1}$  and the real parameters  $h_r$ ,  $m_r$  and  $q_r$  denote respectively the inhomogeneous external field, the quadratic (mass term) and quartic coupling strengths. The linear terms  $\{h_r\}$  are also necessary for completeness.

**2021-12-07 Predrag** Vierhaus's masters thesis [138] *Simulation of  $\phi^4$  theory in the strong coupling expansion beyond the Ising Limit* (DOI) has a clear discussion of the [Ising limit of  \$\phi^4\$](#) . Note the reformulation (4.224) of the action, his eq. (2.15). Compare with the Scholarpedia [Triviality of the 4D lattice  \$\phi^4\$](#)  [142] action (4.224).

the discrete  $\phi^4$  theory Euclidean action [106] defined in terms of the Euclidean Lagrangian [138]

$$S[\Phi] = \sum_z \left\{ \frac{1}{2} \sum_{\mu=1}^d (\Delta_\mu \phi_z)^2 + \frac{\mu^2}{2} \phi_z^2 + \frac{g}{4!} \phi_z^4 \right\} \quad (4.222)$$

with the scalar one component field  $\phi$ , the Klein-Gordon mass  $\mu$ , the strength of the self-coupling  $g$  and the dimension  $d$ , and we set lattice constant  $a = 1$  throughout.

Wolff [142] sets  $\mu^2 < 0$  and presumably  $g > 0$  in (4.222), but in order to agree with spatiotemporal cat I think we need to set  $\mu^2 > 0$  and  $g < 0$  in

(4.222), as currently written, in order to have double-well shaped density with *maxima* at

$$\phi_z \equiv \pm \bar{\phi} \text{ with } \bar{\phi}^2 = -6\mu_0^2/g_0$$

Note - for this formulation, one can discuss  $\mu = 0, g = -1$  case. The period-1 periodic states coalesce, and so does the period-2 asymmetric periodic states pair:

$$F_2[x, y(x)] = \frac{1}{8}x^3(x-2)(x+2)(x^2-2)^2 \quad (4.223)$$

However, cannot do this for the Ising action, as (4.173) has an explicit overall factor of  $\mu^2$ .

**2022-03-09 Predrag** Aizenman [5] *Proof of the triviality of  $\phi^4$  field theory and some mean-field features of Ising models for  $D > 4$*  (1981)

refers to Simon-Griffiths' method, Simon and Griffiths [130] *The  $\phi^4$  field theory as a classical Ising model* (1973), but I do not see the action (4.224) in this paper.

Aizenman [6] *Geometric analysis of  $\phi^4$  fields and Ising models. Parts I and II* (1982)

**2022-03-10 Predrag** The next 3 Lüscher and Weisz papers are all about weak coupling expansion and renormalization. We do not want to get into that, I believe. I hope :)

Lüscher and Weisz [98] *Scaling laws and triviality bounds in the lattice  $\phi^4$  theory (I). One-component model in the symmetric phase* (1987)

A complete solution obtained in the sense that all low energy amplitudes can be computed with reasonable estimated accuracy for arbitrarily chosen bare coupling and mass in the symmetric phase region.

For notational convenience, we choose lattice units throughout this paper, which means that all length scales are measured in numbers of lattice spacings.

correlation functions (4.256)

A popular way to write the action of the lattice  $\phi^4$  theory is (4.224). So I still do not know who to refer to as doing it first.

$$S = \sum_x \left[ \varphi_z^2 + \lambda (\varphi_z^2 - 1)^2 \right] - \beta \sum_{\langle zz' \rangle} \varphi_z \varphi_{z'}. \quad (4.224)$$

and the parameters are restricted to the range  $\beta \geq 0, \lambda \geq 0$ .

$$\phi = \sqrt{\beta} \varphi, \quad \mu^2 = (1 - 2\lambda) \frac{2}{\beta} - 2d, \quad g = 4! \frac{\lambda}{\beta^2}. \quad (4.225)$$

For  $d = 4 \lambda = 0, \kappa = 1/8$  and the point at  $\lambda = \infty$

Lüscher and Weisz [99] *Scaling laws and triviality bounds in the lattice  $\phi^4$  theory (II). One-component model in the phase with spontaneous symmetry breaking* (1988)

They consider the one component  $\phi^4$  theory in the phase, where the reflection symmetry  $\phi \rightarrow -\phi$  is spontaneously broken.

At strong coupling, the low energy properties of the model are therefore likely to be more complicated in the broken symmetry phase than in the symmetric phase, in particular, it is conceivable that bound state particles form. In the Ising model limit of the theory such bound states do in fact occur.

The broken symmetry phase is more difficult to treat than the symmetric phase, because for general bare coupling  $\lambda$ , there is no known (practical) expansion for  $\beta \rightarrow \infty$ .

Lüscher and Weisz [100] *Scaling laws and triviality bounds in the lattice  $\phi^4$  theory (III). n-component model* (1989)

**2021-12-05 Predrag**  $\phi^4$  theory also shows up in Brézin & Zinn-Justin (see sect. 16.8) *Mean field theory for the Ising model*. Their formulation suggests that the partition function (4.179) should be written as (16.99) where  $f[\Phi]$  is free energy (the large-deviation potential)

$$Z[j] = e^{-N_{\mathcal{L}} f[j]} . \tag{4.226}$$

and  $N_{\mathcal{L}}$  is the number of lattice sites.

Scalar  $\phi^4$  field theory textbook references: G. Kane [85], *Modern Elementary Particle Physics* and P. Ramond [115], *Field Theory: A Modern Primer*.

**2021-12-22 Predrag** An unchecked reverse engineering guess: Starting with the second-order difference equation for  $\phi^4$  theory:

$$-\epsilon(z_{t-1} + z_{t+1}) + z_t(z_t - 1)(z_t + 1) = 0 . \tag{4.227}$$

At the anti-integrable limit  $\epsilon \rightarrow 0$ , the map reduces to  $z_t(z_t - 1)(z_t + 1) = 0$ , with every orbit an arbitrary sequence of  $\{-1, 0, 1\}$ . Then go back to (23.22), using  $\phi = z/\epsilon$ ,  $\epsilon = g^{-1/3}$ .

$$-\phi_{j-1} + g\phi_j^3 - \phi_{j+1} = g^{2/3}\phi_j . \tag{4.228}$$

Probably not the right thing; note that (4.233) scales the linear term differently, by  $\epsilon$ .

**2021-12-22 Predrag** Must study Anastassiou [7] *Complicated behavior in cubic Hénon maps*, (2021). He defines the generalized Hénon map of the plane onto itself as

$$H: \mathbb{R}^2 \rightarrow \mathbb{R}^2, \quad H(x, y) = (y, bx + p(y)), \tag{4.229}$$

The determinant of the Jacobian matrix connected to the dissipation of the system is equal to  $-b$ . If the polynomial  $p(y)$  is odd, then the map  $H(x, y)$  is symmetric under the transformation

$$\sigma(x, y) = (-x, -y). \quad (4.230)$$

For  $-b = 1$ , the map is a symplectomorphism (or symplectic map) because it preserves the natural symplectic form of the plane,  $dx \wedge dy$ .

Anastassiou studies cubic polynomial  $p(y)$  Hénon maps,

$$H: \mathbb{R}^2 \rightarrow \mathbb{R}^2, \quad H(x, y) = (y, -bx + g(y^3 - y)), \quad (4.231)$$

studied from a different perspective in his earlier articles [8, 9]. He locates the region of the state space

$$\mathcal{A} = \left\{ (x, y) \in \mathbb{R}^2 : |x|, |y| \leq \sqrt{1 + \frac{2}{g}} \right\}, \quad (4.232)$$

where the bounded non-wandering set exists, and finds parameter values  $g > 4$  for which this non-wandering set is hyperbolic. Read his proof - it is instructive. Remember that these are just very crude bounds - the stable/unstable manifolds will give tight bounds. He shows that his map is conjugate to the Bernoulli three-shift, using the anti-integrability technique [10, 12, 23, 34].

$$\phi_{n+1} - g(\phi_n - \phi_n^3) + \phi_{n-1} = 0,$$

Define  $\epsilon = 1/g$

$$-\epsilon(\phi_{n+2} + \phi_{n+1}) + \phi_{n+1}^3 = \epsilon \phi_n, \quad (4.233)$$

It is customary to say that such a complex behavior is ‘chaotic’ because of Devaney’s definition [14].

**2021-06-04 Predrag** See also Anastassiou, Bountis and Bäcker [9] (2018) *Recent results on the dynamics of higher-dimensional Hénon maps*, their fig. 1. They take

$$p(y) = cy + 3y^3 \quad (4.234)$$

They chose  $c = -\frac{5}{2}$  throughout their publication (we should too, to compare results). “This choice is pictorially convenient, since  $c$  values in that range produce large scale manifolds that are clearly visible in the figures.”

The cubic mapping possesses three fixed points: saddle point at the origin, for all parameter values, a symmetric pair at

$$\left( \pm \sqrt{(2-c)/3}, \pm \sqrt{(2-c)/3} \right).$$



The  $(0, 0)$  fixed point Floquet multipliers are

$$\frac{1}{2} \left( c - \sqrt{c^2 - 4} \right), \frac{1}{2} \left( c + \sqrt{c^2 - 4} \right). \quad (4.235)$$

Since  $c = -5/2$  and  $\delta = 1$ , the Floquet multipliers of the origin are  $\Lambda_u = -2$  and  $\Lambda_s = -1/2$  with normalized eigenvectors  $(-1/\sqrt{5}, 2/\sqrt{5})$  and  $(-2/\sqrt{5}, 1/\sqrt{5})$ . The origin is thus a saddle, with a 1-dimensional stable and a 1-dimensional unstable manifold, whose parametric computation they explain.

**2021-06-04 Predrag** Friedland and Milnor [62] *Dynamical properties of plane polynomial automorphisms* (1989) introduced the generalized Hénon map. Their theorem 2.6 on the normal form of such maps is nice. In their fig. 2 they do the 0th order version of the plot that Xuanqi has plotted in figure 23.4: the three-fold horseshoe associated with a real cubic polynomial.

Dullin and Meiss [53] do that, their fig. 13 (right). They also give a not-very-tight bound on the parameter region in which the horseshoe is complete, their fig. 12. I do not know how to relate that to our parameters.

**2021-06-04 Predrag** Dullin and Meiss [53] *Generalized Hénon maps: the cubic diffeomorphisms of the plane* (2000):

The Euler–Lagrange equation associated with this action is

$$m(\phi_{t-1} + \phi_{t+1}) = U'(\phi_t) \quad (4.236)$$

which is the Lagrangian form of the Hénon map. They concentrate on the area-preserving cubic maps. [...] These are reversible and have an additional symmetry on a codimension-one line in parameter space. Such symmetry is usually referred to as ‘internal’.

**2021-06-04 Predrag** The Arneodo–Coullet–Tresser maps (referred to in [92]) are 5-term recurrence equations with  $\phi_t^k$  nonlinear term, ignore for now.

Li and Malkin [92] *Bounded non-wandering sets for polynomial mappings* (2004)

**2022-02-17 Predrag** For sufficiently strong coupling, periodic state have support on horseshoe repellers. That does not square with our intuition that QFT should be unitary (probability conserving). Our experience with semiclassical quantization of helium is perhaps the clue, **Chaos-Book sect. 42.2 Chaos, symbolic dynamics and periodic orbits**: “As soon as we switch on electron-electron interaction these states are no longer bound states; they turn into resonant states which decay into a bound state of the helium ion and a free outer electron. This might not come as a big surprise if we have the classical analysis of the previous section in mind: we already found that one of the classical electrons will almost always escape after some finite time. More remarkable is the fact that the first,  $N = 1$  series consists of true bound states for all  $n$ , an effect which can only be understood by quantum arguments.”

2022-02-28, 020-03-02 Predrag Parenthetically, wiki [Cubic function](#) [140] answers my question: the canonical form of a cubic map is

$$f(x) = x^3 + px$$

there is only one parameter  $p$ , and qualitatively only its sign or being 0 determines the number of its real roots, which is 3 if  $p < 0$ :

$$(\bar{\phi}_L, \bar{\phi}_C, \bar{\phi}_R) = (-\sqrt{-p}, 0, \sqrt{-p}). \quad (4.237)$$

Multiply by  $g$ , set  $gp = -\mu^2$ ,  $g > 0$ , get (4.169) with 3 real roots:

$$g(x) = gx^3 - \mu^2 x \quad (4.238)$$

2023-01-14 Predrag I have a paper copy of particle physicist Soper [135] monograph *Classical Field Theory* (1976). It covers various classical field theory topics (EM, Eulerian fluids) but is not of much help to us when it comes to understanding dissipative field theories, such as  $\phi^3$  / Hénon for  $b \neq -1$ .

We have also a PDF of Franklin [61] *Classical Field Theory* (2017) ([click here](#)). The same problem.

2023-04-18 Predrag A  $\phi^4$  paper for Tigers to check:

Bazzani, Giovannozzi, Montanari and Turchetti *Performance analysis of indicators of chaos for nonlinear dynamical systems*, [arXiv:2304.08340](#): The efficient detection of chaotic behavior in orbits [...] The challenge is to predict chaotic behavior based on the analysis of orbits of limited length. In this paper, the performance analysis of past and recent indicators of chaos, in terms of predictive power, is carried out in detail using the dynamical system characterized by a symplectic Hénon-like cubic polynomial map.

2023-10-28 Predrag A  $\phi^3$  paper for Tigers to check. Knill writes in [Quantum-Calculus.org](#): "looked at coupled standard maps which emerged when looking at extremization problems of Wilson type. The paper was called "Nonlinear dynamics from the Wilson Lagrangian". It is quite a neat variational problem to maximize the functional  $\text{tr}((D + i\mu)^4)$  on some space of operators, where  $\mu$  is a mass parameter. This naturally leads in the simplest case to Hénon type cubic symplectic maps and in higher dimensions to coupled map lattices where one can prove the existence of bounded solutions using the anti-integrable limit of Aubry. "

2023-05-20 Predrag A reputable series of papers, some on what we call  $\phi^4$ , from Georgia Tech, 20+ years ago.

Chow, Mallet-Paret and Van Vleck [36] *Dynamics of lattice differential equations* (1996), fetch from [Shui-Nee Chow et al.](#). Should refer to it in our paper III [141].

They survey work (there is much of it, check the references) on the dynamics of lattice differential equations, and discuss spatial chaos in the

equilibrium states (what we call periodic states) of spatially discrete reaction-diffusion systems.

They start with  $\phi^4$  theory, their eq. (4)

$$V(\phi)' = (\phi^2 - 1)(\phi - a)/\alpha. \quad (4.239)$$

The parameter  $-1 < a < 1$  is known as the *detuning parameter*: only for  $a = 1$  one has the internal symmetry  $\phi \rightarrow -\phi$  (see sect. 4.9). They seem (?) to work at  $\alpha$  value such that the equilibria  $\phi = \pm 1$  are stable, while  $\phi = a$  is an unstable equilibrium. When they get 'mosaics' they switch to the 'double-obstacle' function eq. (28). To have alphabet  $\{-1, 0, 1\}$  they require some 'double-obstacle', or Cahn-Hilliard equation (27) conditions I have not tried to understand. An  $d$ -mosaic, or simply a mosaic, is a mapping  $\Phi : \mathbb{Z}^d \rightarrow \{-1, 0, 1\}$ , that is, an assignment of -1, 0, or 1, to each point of the lattice  $\mathbb{Z}^d$ . Let  $M_d$  denote the set of all  $d$ -mosaics.

After eq. (35) they even define  $[2 \times 1]_0$  'bricks' :)

Everything is done with equations continuous in time, so their equilibrium solutions are our periodic states. They focus on stable equilibria, we focus on the unstable ones. Their Fig. 5 shows  $[2 \times 1]_1$  and  $[3 \times 1]_1$  periodic states. Their Fig. 6. "Striped type mosaic solutions" (a) is a weird  $[8 \times 2]_1$ , and (b) has a  $[4 \times 4]_0$  prime primitive cell that tiles  $[8 \times 8]_0$  by 2 space reflections and one  $\phi^4$  internal  $D_1$  symmetry (!).

[...] the  $a$ -corkscrew boundary condition  $\phi(i + a, j) = \phi(i, j + 1)$  for all  $(i, j) \in \mathbb{Z}^2$  is presumably our relative/slant primitive cell.

[...] There are some old numerical mosaics that were obtained for a spatially discrete Cahn-Hilliard equation (27) on a finite square lattice with the discrete analogue of periodic and Neumann boundary conditions.

[...] spatially discrete Cahn-Hilliard eq. (27) seems to involve next-nearest neighbors.

[...] In eq. (35) they define the spatial entropy, for arbitrary finite alphabets.

**2024-10-01 Francesco Fedele See**

Vittorio Erba, Freya Behrens, Florent Krzakala, Lenka Zdeborová *Quenches in the Sherrington-Kirkpatrick model*; [arXiv:2405.04267](https://arxiv.org/abs/2405.04267).

"The Sherrington-Kirkpatrick (SK) model is a prototype of a complex non-convex energy landscape. Dynamical processes evolving on such landscapes and locally aiming to reach minima are generally poorly understood. Here, we study quenches, i.e. dynamics that locally aim to decrease energy. We analyse the energy at convergence for two distinct algorithmic classes, single-spin flip and synchronous dynamics, focusing on greedy and reluctant strategies. We provide precise numerical analysis of the finite size effects and conclude that, perhaps counter-intuitively, the reluctant algorithm is compatible with converging to the ground state

energy density, while the greedy strategy is not. These synchronous processes can be analysed using dynamical mean field theory (DMFT), and a new backtracking version of DMFT. Notably, this is the first time the backtracking DMFT is applied to study dynamical convergence properties in fully connected disordered models."

See their sect. 3.1 *Dynamical mean field theory* (DMFT)

**2024-10-01 Predrag to Francesco** EBKZ24 DMFT partition sum eq. (3.10) indeed starts out deterministic (Dirac deltas!), and does look like a bit like our deterministic partition sum (Dirac deltas!), CL18 eq. (36). The argument of delta function in our case is the local spacetime Euler-Lagrange equation, in their case the forward time map, they can be related by Hill's formulas, I expect.

There are many differences, but maybe not fatal.

Our deterministic theory has no randomness whatsoever. Our "counting" comes from the spacetime lattice discretization of multi-periodic solutions (Bravais lattices), resulting in the very pretty exact spatiotemporal partition sum, CL18 eq. (116). The Bravais lattices solutions counting carries over to continuous spacetime, I believe (that we have not verified yet).

EBKZ24 "discretize", in order to be able to count, by introducing random initial conditions, for a set of temporal, finite time deterministic trajectories. Why would one do that? They start with a statistical SK model, so it seems natural to them. But their "zero temperature quenches" are the deterministic backbone of the non-zero temperature model. Their time evolution is the deterministic dynamical rule

$$x_i(t + 1) = \sigma(x_i(t), h_i(t)),$$

so they could use that to construct our partition sum.

"This is a classic dynamics for the SK model, a synchronous Glauber dynamics ("sync-Glauber", to stress its synchronous nature)."

While we have the exact, spatiotemporal deterministic partition sum, they are stuck in 2nd millennium, evolving random initial points forward in time, because what else can they do, if they do not even know that spatiotemporally invariant solutions exist, let alone how to use them? In my opinion, there is no sense in introducing randomness and then trying to mitigate it by DMFT averaging, when one has the exact 3rd millennium theory.

As I have not studied their work in any depth, everything I say might be wrong.

**2024-12-26 Predrag** For *Dynamical mean field theory* EBKZ24 refer to

[8] Antoine Georges, Gabriel Kotliar, Werner Krauth, and Marcelo J Rozenberg. Dynamical mean-field theory of strongly correlated fermion systems and the limit of infinite dimensions. *Reviews of Modern Physics*, 68(1):13, 1996.

[9] H. Eissfeller and M. Opper *Mean-field Monte Carlo approach to the Sherrington-Kirkpatrick model with asymmetric couplings*. *Phys. Rev. E*, 50:709–720, 1994; DOI

"We use the technique of dynamical generating functions, which are a type of path integral that are very convenient for the description of stochastic dynamical systems [24–26]."

[10] Hwang, Folli, Lanza, Parisi, Ruocco, and Zamponi *On the number of limit cycles in asymmetric neural networks*, *Journal of Statistical Mechanics: Theory and Experiment*, 2019(5):053402, 2019; DOI; arXiv:1810.09325.

"The shape of the recurrent connectivity matrix plays a crucial role [...] Tanaka and Edwards [...] evaluate the mean number of fixed points in a fully connected model at thermodynamic limit. [...] Our study [...] evaluates the mean number of attractors of any given length  $L$  for different degrees of symmetry in the connectivity matrices."

**2024-12-26 Predrag Check**

L. F. Cugliandolo, *Recent applications of dynamical mean-field methods* (2023); arXiv:2305.01229.

### 4.13.1 Letter from Ping Ao

2020-12-16 from **Ping Ao**, aoping@sjtu.edu.cn

*Distinguished Professor Shanghai Center for Quantitative Life Sciences and Physics Department Shanghai University; and Shanghai Center for Systems Biomedicine Shanghai Jiao Tong University Shanghai, China*

Dear Prof. Predrag Cvitanovic, Many thanks for your inspiring pandemic seminar on "Spatiotemporal Cat: A Chaotic Field Theory". It is very interesting to use "chaotic attractors" as building blocks for field theories. Here I have one remark and one question which may be of an interest to you.

In dynamical systems it is known that there are three generic classes of systems: fixed points or linear; limit cycles; chaotic attractors. The last two must be nonlinear, as well explained during your talk. For dissipative dynamical systems we have explicitly constructions for all three:

1. *Structure of stochastic dynamics near fixed points*, C Kwon, P Ao, DJ Thouless. PNAS 102 (2005) 13029 ([click here](#))
2. *Limit cycle and conserved dynamics*, XM Zhu, L Yin, P Ao. Intl J Modern Physics B20 (2006) 817 ([click here](#))
3. *Exploring a noisy van der Pol type oscillator with a stochastic approach*, Yuan, R.-S.; Wang, X.-A.; Ma, Y.-A.; Yuan, B. & Ao, P. . Phys Rev E87 (2013) 062109 ([click here](#))
4. *Potential function in a continuous dissipative chaotic system: Decomposition scheme and role of strange attractor*, Yian Ma, Qijun Tan, Ruoshi Yuan, Bo Yuan and Ping Ao. Intl J Bifur Chaos 24 (2014) 1450015 ([click here](#))
5. A summary of our method is here: *SDE decomposition and A-type stochastic interpretation in nonequilibrium processes*, Ruoshi Yuan, Ying Tang, Ping Ao Frontiers of Physics 12 (2017) 120201 ([click here](#))

To my knowledge, we were the first group to explicitly construct the "Hamiltonian" for limit cycles and chaotic attractors, thought not possible before our work. I would be happy to be updated on this, due to our limited knowledge.

My remark is that, our explicit construction for chaotic attractors revealed a hidden structure which may be useful for your construction, too.

My question is, is there a field theory constructed upon limit cycles?

Will be happy to receive your feedback.

2022-01-31 - Predrag still has no answered Ping Ao, but it must be done, if you get inspired, please do it :)

## 4.14 Correlations

Spacetime is a text in which correlations between words are given by some gauge theory. But note that I'm not saying that if you know the correlations of War and Peace, you can understand what War and Peace is all about.

—Sasha Polyakov, via Ronnie Mainieri

2022-05-02 excerpts from Vladimir & Xu-Yao notes on [arXiv:2204.13655](https://arxiv.org/abs/2204.13655)  
*Correlation functions in linear chaotic maps* [78] are the initial draft of this section, for eventual inclusion in ChaosBook.org examples:



example 4.1  
p. 208

**Example 4.1. Bernoulli map correlations.**

Bernoulli map invariant measure is constant over  $(0, 1)$ .  
 functions  $f(x)$  and  $g(x)$  two-point correlation function

$$\langle f(x_t)g(x_0) \rangle = \int_0^1 dx_0 f(x_t)g(x_0). \quad (4.240)$$

break up the integral in (4.240) into regions, with integer  $n$  to implement the mod 1,

$$\langle f(x_t)g(x_0) \rangle = \sum_{n=0}^{2^t-1} \int_{n2^{-t}}^{(n+1)2^{-t}} dx_0 f(2^t x_0 - n)g(x_0).$$

Isolate the highest power in the correlation function  $\langle x_t^k x_0^k \rangle$  by looking at correlation functions of the Bernoulli polynomials  $B_k(x)$ :

$$\langle B_k(x_t)B_k(x_0) \rangle = \frac{(k!)^2 \zeta(2k)}{2^{2k-1} \pi^{2k}} \frac{1}{2^{kt}}, \quad (4.241)$$

where  $\zeta(x)$  is the Riemann zeta function, and  $B_k(x)$  is a  $k$ 'th order Bernoulli polynomial.  
 can compute the correlation of any pair of functions by expanding them in Bernoulli polynomials

**Fourier series expansion.**

$x_t$  is periodic  $f(x_t + 1) = f(x_t)$ , so expand

$$f(x_t) = \sum_{n=-\infty}^{\infty} f_n e^{2\pi i n x_t}, \quad g(x_0) = \sum_{m=-\infty}^{\infty} g_m e^{2\pi i m x_0}.$$

this replaces  $x_t$  with  $x_0 2^t$ , mod 1 is automatic.

time-translation invariant correlation function  $\langle f(x_{t+\tau})g(x_\tau) \rangle = \langle f(x_t)g(x_0) \rangle$ ,  $\tau \in \mathbb{Z}$

Bernoulli has no time reversal symmetry  $t \rightarrow -t$

correlation function (4.240):

$$\langle f(x_t)g(x_0) \rangle = \sum_{n,m=-\infty}^{\infty} f_n g_m \int_0^1 dx_0 e^{2\pi i (2^t n + m) x_0} = \sum_{n=-\infty}^{\infty} f_n g_{-2^t n}. \quad (4.242)$$

initial mode of wavenumber  $n$  becomes a mode of effective wavenumber  $2^t n$ ,

$$e^{2\pi i n x_t} = e^{2\pi i (2^t n) x_0}.$$

chaos stretches in state space  $2^t x_0$ . For the correlator  $\langle f(x_t)g(x_0) \rangle$  to be nonzero at large  $t$ ,  $g(x)$  needs support in high wavenumber modes.

Geometric intuition: correlation functions of reasonably smooth functions rapidly decay with time because, a reasonably smooth function has exponentially small high wavenumber modes.

Bernoulli polynomials Fourier series,

$$B_k(x) = \frac{-k!}{(2\pi i)^k} \sum_{n \neq 0} \frac{e^{2\pi i n x}}{n^k}. \quad (4.243)$$



inserting into (4.242) reproduces the correlator of two Bernoulli polynomials (4.241):

$$\langle B_k(x_t)B_k(x_0) \rangle = \left( \frac{k!}{(2\pi i)^k} \right)^2 \sum_{n \neq 0} \frac{1}{n^k} \frac{1}{(-2^t n)^k} = \frac{(k!)^2}{2^{2k-1} \pi^{2k}} \frac{\zeta(2k)}{2^{kt}},$$

X.-Y. Hu and V. Rosenhaus [78]

[click to return: p. 207](#)

**Example 4.2. From Hénon map to spatiotemporal  $\phi^3$ .** The Hénon map, as introduced by Hénon [75], is (4.186). Written as a 2nd-order inhomogeneous difference equation [53], it takes the temporal Hénon 3-term recurrence form (4.187). Its Smale horseshoe is generated by iterates of the region plotted in figure 5.1.

For  $b = -1$  parameter value the Hénon map is the simplest example of a nonlinear Hamiltonian map, a 2-dimensional orientation preserving, area preserving map, often studied to better understand topology and symmetries of Poincaré sections of 2-degrees of freedom Hamiltonian flows.

With the  $d$ -dimensional Laplacian (4.6) separated out, the  $d$ -dimensional spatiotemporal Hénon Euler–Lagrange equation (4.187) takes form

$$-\square \varphi_z - (a\varphi_z^2 + 2d\varphi_z - 1) = 0, \quad z \in \mathbb{Z}^d. \quad (4.244)$$

The field equation is nonlinear, with the cubic potential (4.148). To bring it to our  $d$ -dimensional ‘anti-integrable’ form (4.245), we translate the field  $\varphi = \varphi'^2 - d/a$ , complete the square, and rescale the field  $\varphi' = 2\sqrt{a+d^2}\phi/a$ ,<sup>12</sup>

$$\begin{aligned} -\square \varphi'_z - a \left( \varphi'_z{}^2 - \frac{a+d^2}{a^2} \right) &= 0 \\ -\square \phi_z + \mu^2 (1/4 - \phi_z^2) &= 0 \\ \mu^2 &= 2\sqrt{a+d^2} = 2d\sqrt{1+a/d^2}. \end{aligned} \quad (4.245)$$

Devaney, Nitecki, Sterling and Meiss [51, 136, 137] have shown that the Hamiltonian Hénon map has the complete Smale horseshoe for ‘stretching’ parameter  $a$  and temporal Hénon /  $\phi^3$  Klein-Gordon mass  $\mu^2$  values above

$$\begin{aligned} a &> 5.699310786700\dots \\ \mu^2 &= 5.176605369043\dots \end{aligned} \quad (4.246)$$

In numerical [42] and analytic [58] calculations we fix (arbitrarily) the Hénon stretching parameter value to

$$\begin{aligned} a &= 6 \\ \mu^2 &= 2\sqrt{7} = 5.291502622\dots, \end{aligned} \quad (4.247)$$

in order to guarantee that all  $2^n$  periodic states of the Hénon map (4.186), i.e., the 1-dimensional temporal  $\phi^3$  exist.

[click to return: p. 190](#)

**Example 4.3. Spatiotemporal  $\phi^3$  periodic states.**

**Period-1 periodic states.** For period-1, constant periodic states  $\phi_z = \phi$ , the Laplacian in the Euler–Lagrange equation (4.150) does not contribute, so it follows that in any spatiotemporal dimension  $d$  constant periodic states are the zeros of

$$F[\phi] = -\mu^2 \left( \phi^2 - \frac{1}{4} \right), \quad (4.248)$$

with two real roots

$$(\phi_L, \phi_R) = \left( -\frac{1}{2}, \frac{1}{2} \right). \quad (4.249)$$

**Period-2  $[2 \times 1]_0$  periodic states.** For the spatial period-2 periodic states  $\Phi_m = \overline{\phi_0 \phi_1}$ , set even sites fields to  $\phi_{2k,z} = \phi_0$ , odd sites fields to  $\phi_{2k+1,z} = \phi_1$ , where  $z \in \mathbb{Z}^{d-1}$  refers to all other lattice directions along which the field is constant valued. In  $d = 2$  dimensions, we refer to this periodic states as  $[2 \times 1]_0$ . Figure 9.2 is the color coding of such periodic states with periodicity  $[2 \times 1]_1$ ,  $[3 \times 2]_1$  and  $[3 \times 2]_0$ .

The Laplacian in the Euler–Lagrange equation (4.150) acts only on the first, ‘spatial’ direction, so for any spatiotemporal dimension  $d$ , the spatial period-2 periodic states are the zeros of

$$F[\Phi] = \begin{pmatrix} 2(\phi_0 - \phi_1) - \mu^2(\phi_0^2 - 1/4) \\ 2(\phi_1 - \phi_0) - \mu^2(\phi_1^2 - 1/4) \end{pmatrix}, \quad (4.250)$$

redefine the fields  $x = \mu^2(\phi_0 + \phi_1)$ ,  $y = \mu^2(\phi_0 - \phi_1)$ :

$$\begin{aligned} 2y + \mu^4/4 - \mu^4\phi_0^2 &= 0 \\ -2y + \mu^4/4 - \mu^4\phi_1^2 &= 0, \end{aligned}$$

add, subtract the two equations to obtain

$$x = 4, \quad y^2 = \mu^4 - 16,$$

eliminate  $y$ . The period-2 periodic state  $\Phi_m = \overline{\phi_0 \phi_1}$  is

$$\begin{aligned} \phi_0 &= \frac{2}{\mu^2} + \frac{1}{2} \sqrt{1 - \frac{16}{\mu^4}} \\ \phi_1 &= \frac{2}{\mu^2} - \frac{1}{2} \sqrt{1 - \frac{16}{\mu^4}}. \end{aligned} \quad (4.251)$$

The Klein-Gordon mass has to be larger than  $\mu^2 > 4$  for period-2 periodic state to exist. Numerical work indicates [141] that for  $\mu^2 \geq 5$  all periods periodic state solutions are real, so in our numerical calculations we set  $\mu^2 = 5$ . In the anti-integrable limit [10, 11]  $\mu^2 \rightarrow \infty$ , the site field values tend to the two steady lattice states (4.249).

<sup>12</sup>Predrag 2023-04-21: This differs from the earlier (??), which is presumably wrong. It agrees with the critical values for the existence of period-2 periodic states, from (3.65)  $a = 3$ , and from (4.251)  $\mu^2 = 4$ . I believe it to be right. Han seems to agree.

**Period- $L$   $[L \times 1]_0$  periodic states.** For the spatial period- $L$  periodic states set sites fields to  $\phi_{lz} = \phi_\ell$ ,  $\ell = l \bmod L$ , where  $z \in \mathbb{Z}^{d-1}$  refers to all other lattice directions along which the field is constant valued. In  $d = 2$  dimensions, we refer to this periodic states as  $[2 \times 1]_0$ . The spatial period- $L$  periodic states  $[L \times 1]_0$  are the zeros of the 1-dimensional lattice Euler–Lagrange equations

$$F[\Phi] = \begin{bmatrix} -\phi_{L-1} + 2\phi_0 - \phi_1 - \mu^2(\phi_0^2 - 1/4) \\ -\phi_0 + 2\phi_1 - \phi_2 - \mu^2(\phi_1^2 - 1/4) \\ -\phi_1 + 2\phi_2 - \phi_3 - \mu^2(\phi_2^2 - 1/4) \\ \dots \\ -\phi_{L-2} + 2\phi_{L-1} - \phi_0 - \mu^2(\phi_{L-1}^2 - 1/4) \end{bmatrix}. \quad (4.252)$$

Translational invariance organizes the solutions into orbits, so a smart organization of this calculation should rely on translational invariant quantities. Add all equations: we see that the solutions depend on Birkhoff sums  $\sum \phi_z$ ,  $\sum \phi_z^2$  (what Friedland and Milnor [62] call ‘the center of gravity’ and Endler and Gallas [57, 58] call ‘center of mass’ or ‘orbit’ polynomials. Such observation lead to analytical evaluation of many of the low-period orbits: we will not pursue these methods here, as anyway most of the solutions that we need can only be evaluated numerically.

**$[2 \times 1]_1$  periodic states.** For spatiotemporal period- $[2 \times 1]_1$  periodic state  $\Phi = \phi_0 \phi_1$  (figure 9.2 (a)), each lattice field value  $\phi_0$  has 4  $\phi_1$  neighbors. The Euler–Lagrange equations are:

$$F[\Phi] = \begin{bmatrix} 4(\phi_0 - \phi_1) - \mu^2(\phi_0^2 - 1/4) \\ 4(\phi_1 - \phi_0) - \mu^2(\phi_1^2 - 1/4) \end{bmatrix} = \begin{bmatrix} 0 \\ 0 \end{bmatrix}, \quad (4.253)$$

with periodic states solutions

$$\begin{aligned} \phi_0 &= \frac{4}{\mu^2} - \frac{1}{2} \sqrt{1 - \frac{64}{\mu^4}} \\ \phi_1 &= \frac{4}{\mu^2} + \frac{1}{2} \sqrt{1 - \frac{64}{\mu^4}}, \end{aligned} \quad (4.254)$$

so must have  $\mu^2 > 8$  for  $[2 \times 1]_1$  periodic state to exist.

**$[3 \times 1]_1$  periodic states.** Consider  $[3 \times 1]_1$ . The pairs of neighbors in figure 9.1 (c) yield Euler–Lagrange equations:

$$F[\Phi] = \begin{bmatrix} -2\phi_2 + 4\phi_0 - 2\phi_1 - \mu^2(\phi_0^2 - 1/4) \\ -2\phi_0 + 4\phi_1 - 2\phi_2 - \mu^2(\phi_1^2 - 1/4) \\ -2\phi_1 + 4\phi_2 - 2\phi_0 - \mu^2(\phi_2^2 - 1/4) \end{bmatrix} = \begin{bmatrix} 0 \\ 0 \\ 0 \end{bmatrix}, \quad (4.255)$$

[click to return: p. 190](#)

**2022-05-12 Predrag** From Keller [87]: I discuss methods of calculating the Ruelle-Pollicott resonances of the perturbed cat map. The Ruelle-Pollicott (RP) resonances are the stable eigenvalues of the coarse-grained Frobenius-Perron (FP) operator (which governs the classical dynamics of chaotic systems) in the semiclassical limit. The RP resonances describe the decay of correlation functions and are important in the link between classical and quantum chaotic systems. [...] I describe two different methods of calculating the classical RP resonances using the perturbed cat map with a linear perturbation as a toy model to test them. The first method makes use of a trace formula to connect the spectral determinant of the FP operator to the periodic orbits of the map. The second method involves truncating the infinite-dimensional FP operator to a finite dimension. The matrix elements of this truncated FP operator are constructed using trigonometric basis states, and the eigenvalues of the reduced matrix are calculated. [...] I discuss the quantization of the perturbed cat map and the quantum RP resonances. Several methods for calculating the quantum resonances were attempted, none of which yielded accurate results.

It has been demonstrated [112, 113, 122, 123] that the RP resonances describe the exponential decay of correlation functions.

**2022-03-10, 2022-05-02 Predrag** Let's take

Rothe [121] *Lattice Gauge Theories - An Introduction* (2005), ([click here](#)) as a standard to check our definitions.

His definition of the free scalar field action eq. (3.10) agrees 100% with our (4.138).

$n$ -point correlation functions [121]

$$\langle \phi_i \phi_j \cdots \phi_\ell \rangle = \frac{1}{Z[0]} \int D\phi e^{-S[\phi]} \phi_i \phi_j \cdots \phi_\ell. \quad (4.256)$$

he calls 'Green functions' eq. (3.9a).

the circular Dirac delta eq. (3.15)

$$\delta_{t't} = \int_{-\pi}^{\pi} \frac{dk}{2\pi} e^{ik(t'-t)} \quad (4.257)$$

The "momentum" integration is restricted to the Brillouin zone (BZ)  $[-\pi, \pi]$ .

Eq. (3.19b), with lattice spacing explicit (see (6.52)), together with the inverse propagator on the reciprocal lattice:

$$\tilde{k}_m = \frac{2}{a} \sin \frac{k_m a}{2}, \quad \sum_{\mu} \tilde{k}_m^2 + \mu^2, \quad (4.258)$$

where  $\tilde{k}$  denotes the “momentum measured in lattice units”.

His Example 2, eq. (4.11) might be of interest to us: he discusses what we call Bernoulli first-order in time operator (1.11), as the simplest example of how the discretization of an equation can lead to a *doubling* of solutions, see his fermion doubling fig. 4-1.

Eq. (13-6a)

The  $\phi^3$ -theory, Rothe sect. 13.2

$$S[\Phi] = \sum_z \left\{ -\frac{1}{2}\phi_z \square \phi_z + \frac{\mu^2}{2}\phi_z^2 + \frac{g}{3!}\phi_z^3 \right\}. \quad (4.259)$$

is the simplest non-trivial example of a scalar field theory. Note that the sign of the cubic term differs from our (4.135). This is the convention used by other authors - for  $\phi^4$ , see for example eq. (2.51) in Sommer [134]; eq. (2.50) in Smit [133].

Beyond this, Rothe is no of use to us, his focus is on lattice gauge theories, and for scalar case, weak coupling expansions.

**2016-10-15 Predrag** Boris is thinking about temporal and spatial correlations in spatiotemporal cats. Here is some literature on the topic, just for cat maps:

Brini *et al.* [29] *Decay of correlations for the automorphism of the torus  $T^2$*

García-Mata and Saraceno [63] *Spectral properties and classical decays in quantum open systems* (who study the Arnol'd cat map with a small sinusoidal perturbation write that Blank, Keller and Liverani [22] and Nonnenmacher [108] provide a rigorous theoretical underpinning to their calculations for quantum and deterministic maps on the torus.

Blank, Keller and Liverani [22] *Ruelle-Perron-Frobenius spectrum for Anosov maps* extend a number of results from one-dimensional dynamics based on spectral properties of the Ruelle–Perron–Frobenius transfer operator to Anosov diffeomorphisms on compact manifolds.

Nonnenmacher [108] studies deterministic and quantum maps on the torus phase space, in the presence of noise. We focus on the spectral properties of the noisy evolution operator, and prove that for any amount of noise, the quantum spectrum converges to the deterministic one in the semiclassical limit.

**2021-01-04 Predrag** See remark 1.2 *Bernoulli shift*

**2022-06-10 Predrag 2 Han** Thanks to my very smart colleague Arkady, Cvitanović and Pikovsky [48] *Cycle expansion for power spectrum* (1993), [click here](#), is a good paper on recycling correlations, I should have included it in ChaosBook. Check it out.

I have more explicit calculations in LaTeX source files for earlier drafts of that paper.

Aside: Not sure it is wise to do Birkhoff sums over  $a_{j,m}$ :

$$A_m = \sum_{j \in p} a_{j,m}, \quad a_{j,m} = \phi_j \phi_{j+m}. \quad (4.260)$$

You might also want to have a look at the calculations of

Grossmann and Thomaes [69] *Invariant distributions and stationary correlation functions of one-dimensional discrete processes* (1977).

Beck [15] *Higher correlation functions of chaotic dynamical systems - a graph theoretical approach* (1991).

## 4.15 Semiclassical quantization

2022-12-07 Predrag Excerpts (mashed together in random order) from P. Cvitanović, R. Artuso, R. Mainieri, G. Tanner and G. Vattayet *al.* [43] *Chaos: Classical and Quantum*, (2022)

ChaosBook Chap. 36 *Quantum mechanics - the short short version*

In what is excerpted here we omit all correction terms, as we are interested only into the leading behavior.

A given wave function can be expanded in the energy eigenbasis

$$\psi(q, t) = \sum_n c_n e^{-iE_n t/\hbar} \phi_n(q), \quad (4.261)$$

where the expansion coefficient  $c_n$  is given by the projection of the initial wave function  $\psi(q, 0)$  onto the  $n$ th eigenstate

$$c_n = \int dq' \psi(q', 0) \phi_n^*(q'). \quad (4.262)$$

By substituting (4.262) into (4.261), we can cast the evolution of a wave function into a multiplicative form

$$\psi(q, t) = \int dq' K(q, q', t) \psi(q', 0),$$

with the kernel

$$K(q, q', t) = \sum_n \phi_n(q) e^{-iE_n t/\hbar} \phi_n^*(q') \quad (4.263)$$

called the *quantum evolution operator*, or the *propagator*.

For time-independent Hamiltonians, the time dependence of the wave functions is known as soon as the eigenenergies  $E_n$  and eigenfunctions  $\phi_n$  have been determined. With time dependence taken care of, it makes sense to focus on the *Green's function*, which is the Laplace transform of the propagator

$$G(q, q', E) = \frac{1}{i\hbar} \int_0^\infty dt e^{\frac{i}{\hbar} E t} K(q, q', t) = \sum_n \frac{\phi_n(q) \phi_n^*(q')}{E - E_n}. \quad (4.264)$$

The eigenenergies show up as poles in the Green's function with residues corresponding to the wave function amplitudes. If one is only interested in spectra, one may restrict oneself to the (formal) trace of the Green's function,

$$\text{Tr } G(E) = \int dq G(q, q, E) = \sum_n \frac{1}{E - E_n}, \quad (4.265)$$

where  $E$  is complex, with a positive imaginary part, and we have used the eigenfunction orthonormality (??).

## 4.16 Noise is your friend

**2021-11-27 Predrag** Excerpts (mashed together in random order) from Cvitanović, Dettmann, Mainieri and Vattay *Trace formulae for stochastic evolution operators*:

*Weak noise perturbation theory* [45] (1998), [arXiv:chao-dyn/9807034](https://arxiv.org/abs/1907.034), and *Smooth conjugation method* [46] (1998) [arXiv:chao-dyn/9811003](https://arxiv.org/abs/1907.1003).

These are the first two papers to treat time evolution as a 1-dimensional temporal lattice field theory. They start out by expressing the weak noise expansions in terms of Dirac  $\delta$  and its derivatives. In what is excerpted here we omit all correction terms, as we are interested only into the leading behavior.

The central object in the theory, the trace of the evolution operator, is a discrete path integral, similar to those found in field theory and statistical mechanics.

The theory is cast in the standard field theoretic formalism, and weak noise perturbation theory written in terms of Feynman diagrams.

The noise tends to regularize the theory, replacing the deterministic delta function evolution operators by smooth distributions. While in this paper we are interested in effects of weak but *finite* noise, the  $\sigma \rightarrow 0$  limit is also important as a tool for identifying the natural measure [28, 124, 131] for deterministic flows.

We have cast the theory in the standard field theoretic language [39], in the spirit of approaches such as the Martin-Siggia-Rose [103] formalism, the Parisi-Wu [111] stochastic quantization, and the Feigenbaum and Hasslacher [59] study of noise renormalization in period doubling.

The form of the perturbative expansions is reminiscent of perturbative calculations of field theory, but in some aspects the calculations undertaken here are relatively more difficult. The main difference is that there is no translational invariance along the chain, so unlike the case of usual field theory, the propagator is not diagonalized by a Fourier transform. We do our computations in configuration coordinates. Unlike the most field-theoretic literature, we are neither “quantizing” around a trivial vacuum, nor a countable infinity of stable soliton saddles, but around an infinity of nontrivial unstable hyperbolic saddles.

[...] our results are *a priori* far from obvious: [...] a more subtle and surprising result, repeats of prime cycles can be resummed and theory reduced to the dynamical zeta functions and spectral determinants of the same form as the for the deterministic systems.

[...] a discrete time 1-dimensional discrete Langevin equation [84, 90],

$$x_{n+1} = f(x_n) + \sigma \xi_n, \quad (4.266)$$

with  $\xi_n$  independent normalized random variables, suffices to reveal the structure of the perturbative corrections.

We shall treat a chaotic system with such Gaussian weak external noise by replacing the the deterministic evolution  $\delta$ -function kernel by  $\mathcal{L}_{FP}$ , the Fokker-Planck kernel corresponding to (4.266), a sharply peaked noise distribution function

$$\mathcal{L}_{FP} = \delta_\sigma(y - f(x)), \quad (4.267)$$

where  $\delta_\sigma$  is the Gaussian kernel

$$\delta_\sigma(z) = \frac{1}{\sqrt{2\pi\sigma^2}} e^{-z^2/2\sigma^2}. \quad (4.268)$$

In the weak noise limit the kernel is sharply peaked, so it makes sense to expand it in terms of the Dirac delta function and its derivatives:

$$\delta_\sigma(y) = \sum_{m=0}^{\infty} \frac{a_m \sigma^m}{m!} \delta^{(m)}(y) = \delta(y) + a_2 \frac{\sigma^2}{2} \delta^{(2)}(y) + \dots \quad (4.269)$$

where

$$\delta^{(k)}(y) = \frac{\partial^k}{\partial y^k} \delta(y),$$

and the coefficients  $a_m$  depend on the choice of the kernel. We have omitted the  $\delta^{(1)}(y)$  term in the above because in our applications we shall impose the saddle-point condition, that is, we shift  $f$  by a constant to ensure that the noise peak corresponds to  $y = 0$ , so  $\delta'_\sigma(0) = 0$ . For example, if  $\delta_\sigma(y)$  is a Gaussian kernel, it can be expanded as

$$\delta_\sigma(y) = \frac{1}{\sqrt{2\pi\sigma^2}} e^{-y^2/2\sigma^2} = \delta(y) + \frac{\sigma^2}{2} \delta^{(2)}(y) + \dots \quad (4.270)$$

We start our computation of the weak noise corrections to the spectrum of  $\mathcal{L}_{FP}$  by calculating the trace of the  $n$ th iterate of the stochastic evolution operator  $\mathcal{L}_{FP}$  for a one-dimensional analytic map  $f(x)$  with additive noise  $\sigma$ . This trace is an  $n$ -dimensional integral on  $n$  points along a discrete periodic chain, so  $x$  becomes an  $n$ -vector  $x_a$  with indices  $a, b, \dots$  ranging from 0 to  $n-1$  in a cyclic fashion

$$\begin{aligned} \text{tr } \mathcal{L}_{FP}^n &= \int \prod_{a=0}^{n-1} dx_a \delta_\sigma(y_a) \\ y_a(x) &= f(x_a) - x_{a+1}, \quad x_n = x_0. \end{aligned} \quad (4.271)$$



If the map is smooth, the periodic points of given finite period  $n$  are isolated and the noise broadening  $\sigma$  sufficiently small so that they remain separated, the dominant contributions come from neighborhoods of periodic points; in the *saddlepoint approximation* the trace (4.271) is given by

$$\mathrm{tr} \mathcal{L}_{FP}^n \longrightarrow \sum_{x_c \in \mathrm{Fix} f^n} e^{W_c}, \quad (4.272)$$

As traces are cyclic,  $e^{W_c}$  is the same for all periodic points in a given cycle, independent of the choice of the starting point  $x_c$ . Hence it is customary to rewrite this sum in terms of prime cycles and their repeats,

$$\mathrm{tr} \mathcal{L}_{FP}^n |_{\text{saddles}} = \sum_p n_p \sum_{r=1}^{\infty} e^{W_{p^r}}, \quad (4.273)$$

where  $p^r$  labels the  $r$ th repeat of prime cycle  $p$ .

A fixed point and its repeats are of particular interest having the same interaction at every site, as does the usual field theory. What we do here is to formulate [...] the field theory on finite periodic 1-dimensional discrete chains.

Defining  $y = f(x) - x$ , we can write the fixed point trace as

$$\mathrm{tr} \mathcal{L}_{FP} = \int dx \delta_\sigma(f(x) - x) = \int dy \frac{1}{|y'(x)|} \delta_\sigma(y). \quad (4.274)$$

We start by calculating the trace of the  $n$ th iterate of the stochastic evolution operator  $\mathcal{L}_{FP}$  for a one-dimensional analytic map  $f(x)$  with additive Gaussian noise  $\sigma$ . This trace is an  $n$ -dimensional integral on  $n$  points along a discrete periodic chain, so  $x$  becomes an  $n$ -vector  $x_a$  with indices  $a, b, \dots$  ranging from 0 to  $n-1$  in a cyclic fashion

$$\begin{aligned} \mathrm{tr} \mathcal{L}_{FP}^n &= \int [dx] \exp \left\{ -\frac{1}{2\sigma^2} \sum_a [x_{a+1} - f(x_a)]^2 \right\} \\ x_n &= x_0, \quad [dx] = \prod_{a=0}^{n-1} \frac{dx_a}{\sqrt{2\pi\sigma^2}}. \end{aligned} \quad (4.275)$$

As we are dealing with a path integral on a finite discrete chain, we find it convenient to rewrite the exponent in matrix notation

$$\mathrm{tr} \mathcal{L}_{FP}^n = \int [dx] e^{-[r^{-1}x - f(x)]^2 / 2\sigma^2}, \quad r_{ab} = \delta_{a,b+1}, \quad (4.276)$$

where  $x$  and  $f(x)$  are column vectors with components  $x_a$  and  $f(x_a)$  respectively, and  $r$  is the left cyclic shift or hopping matrix satisfying  $r^n = 1$ ,  $r^{-1} = r^T$ . Unless stated otherwise, we shall assume the repeated index summation convention throughout, and that the Kronecker  $\delta$  function is the periodic one, defined by

$$\delta_{ab} = \frac{1}{n} \sum_{k=0}^{n-1} e^{i2\pi(a-b)k/n}. \quad (4.277)$$

[...] if the noise is weak, the path integral (4.275) is dominated by periodic deterministic trajectories. Assuming that the periodic points of given finite period  $n$  are isolated and the trajectory broadening  $\sigma$  sufficiently small so that they remain clearly separated, the dominant contributions come from neighborhoods of periodic points; in the *saddlepoint approximation* the trace (4.275) is given by

$$\mathrm{tr} \mathcal{L}_{FP}^n \longrightarrow \sum_{x_c \in \mathrm{Fix} f^n} e^{W_c}, \quad (4.278)$$

where the sum goes over all periodic points  $x_c = x_{c+n}$  of period  $n$ ,  $f^n(x_c) = x_c$ . The contribution of the  $x_c$  neighborhood is obtained by shifting the origin of integration to

$$x_a \rightarrow x_a + \phi_a,$$

where from now on  $x_a$  refers to the position of the  $a$ -th periodic point, and expanding  $f$  in Taylor series around each of the periodic points in the orbit of  $x_c$ .

The contribution of the neighborhood of the periodic point  $x_c$  is given by

$$\begin{aligned} e^{W_c} &= \int [d\phi] e^{-(M^{-1}\phi - V'(\phi))^2 / 2\sigma^2} \\ &= |\det M| \int [d\phi] e^{\sum \frac{1}{k} \mathrm{tr} (MV''(\phi))^k} e^{-\varphi^2 / 2\sigma^2} \end{aligned} \quad (4.279)$$

where the propagator and interaction terms are collected in

$$M^{-1}{}_{ab}\phi_b = -f'(x_a)\phi_a + \phi_{a+1}, \quad V(\phi) = \sum_a \sum_{m=2}^{\infty} f^{(m)}(x_a) \frac{\phi_a^{m+1}}{(m+1)!}. \quad (4.280)$$

We find it convenient to also introduce a bidirectional propagator  $C = MM^T$  for reasons that will become apparent below. In the second line of (4.279) we have changed coordinates,

$$\varphi = M^{-1}\phi - V'(\phi), \quad (4.281)$$

and used the matrix identity  $\ln \det M = \mathrm{tr} \ln M$  on the Jacobian

$$\frac{1}{\det (M^{-1} - V'')} = \frac{\det M}{\det (1 - MV'')} = \det M e^{-\mathrm{tr} \ln (1 - MV'')}. \quad (4.282)$$

The functional dependence of  $\phi = \phi(\varphi)$  is recovered by iterating (4.281)

$$\phi_a = M_{ab}\varphi_b + M_{ab}V'_b(\phi). \quad (4.283)$$

The above manipulations are standard [103] and often used in the stochastic quantization literature [49, 111].

As the sum is cyclic,  $e^{W_c}$  is the same for all periodic points in a given cycle, independent of the choice of the starting point  $x_c$ . In the saddlepoint approximation we assume that the map is analytic and the extrema  $f^n$  are isolated.

From the second path integral representation in (4.279) it follows that  $M$  can be interpreted as the “free” propagator. As  $M$  will play a central role in what follows, we write its inverse in its full  $[n \times n]$  matrix form:

$$M^{-1} = r^{-1} - \mathbf{f}' = \begin{pmatrix} -f'_0 & 1 & & & \\ & -f'_1 & 1 & & \\ & & -f'_2 & 1 & \\ & & & \ddots & \\ 1 & & & & -f'_{n-1} \end{pmatrix} \quad (4.284)$$

where  $\mathbf{f}'$  is a diagonal matrix with elements  $f'_a = f'(x_a)$  a shorthand notation for stability of the map at the periodic point  $x_a$ . The determinant of  $M$  is

$$\det M = \frac{(-1)^n}{\Lambda_c - 1}, \quad \Lambda_c = \prod_{a=0}^{n-1} f'(x_a), \quad (4.285)$$

with  $\Lambda_c$  the *stability* of the  $n$  cycle going through the periodic point  $x_c$ . We shall assume that we are dealing with a chaotic dynamical system, and that all cycles are unstable,  $|\Lambda_c| > 1$ .

The formula for propagator itself is obtained by inverting (4.284) and using relation  $(r\mathbf{f}')^n = \Lambda_c$ , (due to the periodicity of the chain):

$$\begin{aligned} M &= -\frac{1}{1 - \mathbf{f}'^{-1}r^{-1}} \mathbf{f}'^{-1} = -\sum_{k=0}^{\infty} (\mathbf{f}'^{-1}r^{-1})^k \mathbf{f}'^{-1} \\ &= -\frac{1}{\Lambda_c - 1} \sum_{k=0}^{n-1} r(\mathbf{f}'r)^k \end{aligned} \quad (4.286)$$

In the full matrix form, the propagator is given by

$$M = \frac{-1}{\Lambda_c - 1} \begin{pmatrix} f'_1 \cdots f'_{n-1} & f'_2 \cdots f'_{n-1} & f'_3 \cdots f'_{n-1} & \cdots & 1 \\ 1 & f'_2 \cdots f'_0 & f'_3 f'_4 \cdots f'_0 & \cdots & f'_0 \\ f'_1 & 1 & f'_3 \cdots f'_0 f'_1 & \cdots & f'_0 f'_1 \\ f'_1 f'_2 & f'_2 & 1 & \ddots & f'_0 f'_1 f'_2 \\ f'_1 f'_2 f'_3 & f'_2 f'_3 & f'_3 & \ddots & \vdots \\ \vdots & \vdots & \vdots & \vdots & \vdots \\ f'_1 \cdots f'_{n-2} & f'_2 \cdots f'_{n-2} & \cdots & \cdots & 1 & f'_0 \cdots f'_{n-2} \end{pmatrix} \quad (4.287)$$

or, more compactly,

$$M_{ab} = \frac{-1}{\Lambda_c - 1} \prod_{d=b+1}^{a-1} f'(x_d), \quad M_{a,a-1} = \frac{-1}{\Lambda_c - 1}, \quad (4.288)$$

where  $d$  increases cyclically through the range  $b + 1$  to  $a - 1$ ; for example, if  $a = 0$ ,  $a - 1 = n - 1$ . We note that  $M$  is invertible only for cycles which are not marginal,  $|\Lambda_c| \neq 1$ .

The saddlepoint approximation (4.279) is a discrete path integral on periodic chain of  $n$  points which we shall evaluate by standard field-theoretic methods. Separating the quadratic terms we obtain

$$e^{W_c} = \frac{1}{|\Lambda_c - 1|} \int [d\varphi] e^{-S_0(\varphi) - S_I(\varphi)}, \quad (4.289)$$

where

$$S_0(\varphi) = \varphi^2 / 2\sigma^2, \quad S_I(\varphi) = - \sum_{k=1}^{\infty} \frac{1}{k} \text{tr} [MV''(\phi(\varphi))]^k \quad (4.290)$$

The terms collected in  $S_I(\varphi)$ , linear or higher in  $\varphi$ , are the interaction vertices.

Next introduce a source term  $J_a$  and define a partition function

$$\begin{aligned} e^{W_c(J)} &= \frac{1}{|\Lambda_c - 1|} \int [d\varphi] e^{-S_0(\varphi) - S_I(\varphi) + J_a \varphi_a} \\ &= \frac{1}{|\Lambda_c - 1|} e^{-S_I(\frac{d}{dJ})} \int [d\varphi] e^{-S_0(\varphi) + J_a \varphi_a} \\ &= \frac{1}{|\Lambda_c - 1|} e^{-S_I(\frac{d}{dJ})} e^{\frac{\sigma^2}{2} J^2}. \end{aligned} \quad (4.291)$$

Here we have used standard formulas for Gaussian integrals together with the normalization (4.275).

[...] yields the perturbation expansion

$$W_c = -\ln |\Lambda_c - 1| + \sum_{k=1}^{\infty} W_{c,2k} \sigma^{2k}. \quad (4.292)$$

In field-theoretic calculations the  $W_{c,0}$  term is usually an overall volume term that drops out in the expectation value computations. In contrast, here the  $W_{c,0} = -\ln |\Lambda_c - 1|$  term is the deterministic weight of the cycle which plays the key role both in the classical and stochastic trace formulas.

If efficient methods are found for computing numerical periodic solutions of spatially extended systems, the method might apply to the field theory as well.

### 4.16.1 Noisy Gábor

1998-03-04 Gábor Vattay The initial version.

2021-12-08 Predrag Tweaked Gábor's note a bit. The approach is safe for multimodal maps, and it should work for finite-grammar Smale horseshoe

repellers (Smale's original horseshoe [132], his fig. 1 was unimodal, but he also explicitly gives our  $\phi^4$  bimodal map, his fig. 5.

For generic, no finite grammar case, who knows... Will be messier, pruning front style. Perhaps.

Suppose we have a 'bimodal' system with three distinct, monotone segments such as (6.225), with map  $f_i(\phi_t)$  for  $i$ th segment. Associate with each monotone segment one of three Perron-Frobenius operators (24.362),

$$\mathcal{L}_i(x, y) = \delta(x - f_i(y)), \quad i = \{0, 1, 2\}. \quad (4.293)$$

To compute the spectral determinant

$$F(z) = \det(1 - z(\mathcal{L}_0 + \mathcal{L}_1 + \mathcal{L}_2)), \quad (4.294)$$

write

$$F(z) = \exp(\text{tr} \log(1 - z(\mathcal{L}_0 + \mathcal{L}_1 + \mathcal{L}_2))) = \exp\left(-\sum_n \frac{z^n}{n} \text{tr}(\mathcal{L}_0 + \mathcal{L}_1 + \mathcal{L}_2)^n\right), \quad (4.295)$$

expand the  $n$ th power,

$$\text{tr}(\mathcal{L}_0 + \mathcal{L}_1 + \mathcal{L}_2)^n = \sum_p \sum_{r|n=n_p \cdot r} n_p \text{tr} \mathcal{L}_p^r, \quad (4.296)$$

where  $p$  denotes a period  $n_p$  prime symbol sequence composed of 0, 1, 2, and  $r$  is its repetition number. Say  $p = 011$ , then  $\mathcal{L}_{011} = \mathcal{L}_0 \mathcal{L}_1 \mathcal{L}_1 = \mathcal{L}_0 \mathcal{L}_1^2$ , up to a cyclic permutation. For a given  $n$  we get contributions only from primitive orbits for which  $n_n = r n_p$ . Then, as usual one can write

$$F(z) = \exp\left(-\sum_{p,r} \frac{z^{n_p r}}{r} \text{tr} \mathcal{L}_p^r\right), \quad (4.297)$$

and after  $r$  summation we get

$$F(z) = \prod_p \det(1 - z^{n_p} \mathcal{L}_p). \quad (4.298)$$

In case of the noisy maps we can introduce -let's say- the three branches of the map  $f_i(x)$  corresponding to the symbols  $f(x) = f_i(x)$  if  $x$  is in the state space region  $\mathcal{M}_i$ , and define operators

$$\mathcal{L}_i(x', x) = \frac{1}{\sqrt{2\pi\sigma}} e^{-\frac{1}{2\sigma^2}(x' - f_i(x))^2}. \quad (4.299)$$

Map  $f_i$  acts only on the state space region  $\mathcal{M}_i$ , but it maps to all regions  $\mathcal{M}_j$  allowed by system's transition graph. If you visualize this operator as a matrix,  $\mathcal{L}$  is an  $[n \times n]$  matrix, while  $\mathcal{L}_i$  is -say-  $[n \times n/3]$  matrix, the matrix elements

where the initial  $x$  is in the state space region  $\mathcal{M}_j \neq \mathcal{M}_i$  are all zero. For these operators we can apply (4.298) and get the spectral determinant as a product of spectral determinants of primitive orbits. The operators are defined on piecewise monotonic maps, so there is only one periodic point on each.

So, this way can get rid of repeats in an early stage, and concentrate only on computing prime orbits. Tomorrow (March 4, 1998 - tomorrow never came) on the train I will try to give the matrix representation elements [45] of  $L_p$  in the unperturbed basis (eg. on  $x^k$ ) and hope to end up with simpler formulas.

### 4.17 Complex Ginzburg-Landau equation

2016-08-04 PC Afraimovich and Pesin [2] *Hyperbolicity of infinite-dimensional drift systems* study the discrete versions of the complex Ginzburg-Landau equation.

$$u_{n,t+1} = u_{n,t} + \tau(u_{n,t}, \sigma) + \gamma(u_{n,t} - u_{n,t-1}) + \frac{\epsilon}{2}[u_{n-1,t} - 2u_{n,t} + u_{n+1,t}], \quad (4.300)$$

where  $\tau(u_{n,t}, \sigma)$  is local time dynamics,  $\gamma$  is a parameter of “connection”, a memory of the previous step, so this has a time evolution component that could be written as a time Laplacian, with remainder presumably playing role of a friction. Not sure why this would be a good idea, as complex Ginzburg-Landau is the first order in time. Literature worries about the stability of the space-homogeneous state in chains of maps. They consider a special ‘drift’ type of perturbation, at which point they lost me.

### 4.18 Kuramoto–Sivashinsky equation

Assume a 2-dimensional square lattice with period  $L$  in the spatial direction and period  $T$  in the temporal direction, finite volume  $LT$ , and periodic boundary conditions. We use  $L = 1/\Delta x, T = 1/\Delta t$  discretization.

Given the Kuramoto–Sivashinsky equation of form

$$u_t + u u_x + u_{xx} + u_{xxxx} = 0, \quad x \in [0, L]. \quad (4.301)$$

the corresponding discretized Kuramoto–Sivashinsky equation is

$$T\partial_t U + \frac{L}{2}\partial_x U^2 + L^2 \square_x U + L^4 \square_x^2 U = 0. \quad (4.302)$$

In continuum the Kuramoto–Sivashinsky equation is Galilean invariant: if  $u(x, t)$  is a solution, then  $v + u(x - vt, t)$ , with  $v$  an arbitrary constant velocity, is also a solution. On a spacetime torus, the velocity have to be ‘quantized’, satisfy something like  $n\Delta x - vt\Delta t = \frac{n}{L} - v\frac{t}{T} \in \mathbb{Z}$ , i.e., if you have relative

periodic orbit  $[L \times T]_S$ , allowed velocities are

$$v = k \frac{n T}{t L}, \quad k \in \mathbb{Z}.$$

FIX  $S$  dependence in THIS! But would like to check that one gets a sensible spatiotemporal orbit Jacobian matrix  $\mathcal{J}$  and  $\text{Det } \mathcal{J}$ , at least for the  $U = 0$  fixed point...

**2016-01-12, 2016-08-04 PC** Chen, Chen, and Yuan [35] *Topological horseshoes in travelling waves of discretized nonlinear wave equations* is a mathematical paper. They concentrate on describing relative equilibria of a discretized version of a PDE that has Kuramoto–Sivashinsky, KdV and Burgers as special cases. They define discretized derivatives up to the 5th, if we ever need them. They write “Applying the concept of anti-integrable limit to coupled map lattices originated from space-time discretized nonlinear wave equations, we show that there exist topological horseshoes in the phase space formed by the initial states of travelling wave solutions. In particular, the coupled map lattices display spatiotemporal chaos on the horseshoes.” 2CB

**2016-08-04 Predrag** Elder *et al.* [56] *Spatiotemporal chaos in the damped Kuramoto–Sivashinsky equation*: “A discretized version of the damped Kuramoto–Sivashinsky (DKS) equation is constructed to provide a simple computational model of spatiotemporal chaos in one dimension. The discrete map is used to study the transition from periodic solutions to disordered solutions (i.e., spatiotemporal chaos). The numerical evidence indicates a jump discontinuity at this transition.”

## 4.19 Elastodynamic equilibria of 2D solids

**Predrag 2018-08-23** this section is now in *book/chapters/mattress.tex*, removed from here.

## 4.20 Field theory blog

**2021-07-20 Chris Crowley** I am looking for a good citation to use that suggests that periodic orbit theory like thinking could be useful for quantum field theories. I have a few references at the very end of a paper, see that try to establish that this framework could extend to other systems and want to add quantum field theory to the list because it sounds sexy in the current zeitgeist.

**2021-08-04 Predrag** For the Quantum Field Theory I think I am still the main proponent, I tend to cite [40]

```
@Article{CFTsketch,
  author = {P. Cvitanovi{\ 'c}},
  journal = {Physica A},
  title = {Chaotic field theory: {A} sketch},
  year = {2000},
  pages = {61},
  volume = {288},
  doi = {10.1016/s0378-4371(00)00415-5},
}
```

**2022-03-31 Predrag** *partition function*, the integral over probabilities of all configurations (4.179).

the ‘deterministic trace formula’ [42],

$$Z[0] = \sum_c \int_{\mathcal{M}_c} d\Phi \delta(F[\Phi]) = \sum_c \frac{1}{|\text{Det } \mathcal{J}_c|} \quad (4.303)$$

The orbit Jacobian matrix of a period- $(mn)$  periodic state  $\Phi$ , which is a  $m$ -th repeat of a period- $n$  prime periodic state  $\Phi_p$ , has a tri-diagonal block circulant matrix form that follows by inspection from (3.26):

$$\mathcal{J} = \begin{pmatrix} \mathbf{s}_p & -\mathbf{r} & & & -\mathbf{r}^\top \\ -\mathbf{r}^\top & \mathbf{s}_p & -\mathbf{r} & & \\ & \ddots & \ddots & \ddots & \\ & & & -\mathbf{r}^\top & \mathbf{s}_p & -\mathbf{r} \\ -\mathbf{r} & & & -\mathbf{r}^\top & \mathbf{s}_p \end{pmatrix}, \quad (4.304)$$

where block matrix  $\mathbf{s}_p$  is a  $[n \times n]$  symmetric Toeplitz matrix

$$\mathbf{s}_p = \begin{pmatrix} d_0 & -1 & & & 0 \\ -1 & d_1 & -1 & & \\ & \ddots & \ddots & \ddots & \\ & & -1 & d_{n-2} & -1 \\ 0 & & & -1 & d_{n-1} \end{pmatrix}, \quad \mathbf{r} = \begin{pmatrix} 0 & \dots & 0 \\ & \ddots & \\ 1 & & 0 \end{pmatrix} \quad (4.305)$$

and  $\mathbf{r}$  and its transpose enforce the periodic bc’s. This period- $(mn)$  periodic state  $\Phi$  orbit Jacobian matrix is as translation-invariant as the temporal cat (??), but now under Bravais lattice translations by multiples of  $n$ . One can visualize this periodic state as a tiling of the integer lattice  $\mathbb{Z}$  by a generic periodic state field decorating a tile of length  $n$ . The orbit Jacobian matrix  $\mathcal{J}$  is now a block circulant matrix which can be brought into a block diagonal form by a unitary transformation, with a repeating  $[n \times n]$  block along the diagonal.



**2020-10-31 Predrag** Relation to field theory is discussed in sect. 4.1 *Lattice discretization of a field theory.*

**2018-09-26 Predrag** The Lagrangian formulation (8.4) suggests that the action (integral over the Lagrangian density, one-step generating function (8.69)) is given by

$$Z[M] = e^{W[M]} = \int [d\Phi] e^{S[\Phi] + \Phi \cdot M}, \quad (4.306)$$

$$W[M] = \Gamma[\Phi] + \Phi \cdot M. \quad (4.307)$$

with “source” symbol block  $M$ .

Were  $\Phi$  not confined to a unit hypercube, the Gaussian integral for quadratic action

$$S[\Phi] = -\frac{1}{2} \Phi^\top (-\square + \mu^2 \mathbf{1}) \Phi \quad (4.308)$$

could be integrated out in the usual way,

$$Z[M] = |\det(-\square + \mu^2 \mathbf{1})|^{-1/2} e^{\frac{1}{2} M^\top (-\square + \mu^2 \mathbf{1})^{-1} M}, \quad (4.309)$$

leading to determinants and traces

$$W[0] = \ln Z[0] = -\frac{1}{2} \ln \det(-\square + \mu^2 \mathbf{1}) = -\frac{1}{2} \text{tr} \ln(-\square + \mu^2 \mathbf{1}). \quad (4.310)$$

**2020-09-24 Predrag** The trace formula is logarithmic derivative of the determinant,

$$\text{tr} \frac{1}{-\square + \mu^2} = \frac{d}{d\mu^2} \ln \det(-\square + \mu^2). \quad (4.311)$$

To recover  $\det(-\square + \mu^2)$  integrate both sides with respect to  $\mu^2$ ,

$$\int_{\mu_0^2}^{\mu^2} du \text{tr} \frac{1}{-\square + u} = \ln \frac{\det(-\square + \mu^2)}{\det(-\square + \mu_0^2)},$$

and exponentiate. In this form, the determinant is regularized, as the divergent, large wave-numbers  $k$  contribution cancels out

$$\begin{aligned} \frac{\det(-\square + \mu^2)}{\det(-\square + \mu_0^2)} &= \exp \left( \int_{\mu_0^2}^{\mu^2} du \text{tr} \frac{1}{-\square + u} \right) \\ &= \exp \left( \int_0^\infty dt \int_{\mu_0^2}^{\mu^2} du \text{tr} e^{-t(-\square + u)} \right) \\ &= \exp \left( - \int_0^\infty dt \frac{1}{t} \text{tr} \left( e^{-t(-\square + \mu^2)} - e^{-t(-\square + \mu_0^2)} \right) \right). \end{aligned}$$

This appears to be the natural form of topological zeta functions, see (16.42), with the Laplacian value  $\mu_0 = 0$ .

(Another variant, following worldline formalism:) The free scalar propagator for the Euclidean Klein-Gordon equation [4, 127] is

$$g_{zz'} = \left( \frac{1}{-\square + \mu^2} \right)_{zz'}. \quad (4.312)$$

Exponentiate the denominator following Schwinger,

$$g_{zz'} = \int_0^\infty dt e^{-\mu^2 t} \left( e^{-t(-\square)} \right)_{zz'}, \quad (4.313)$$

Replace the operator in the exponent by a path integral, i.e., the sum over random walks (see [Wanderings of a drunken snail](#))

$$g_{zz'} = \int_0^\infty dt e^{-\mu^2 t} \int_{x(0)=x'}^{x(t)=x} \mathcal{D}x(\tau) e^{-\int_0^t d\tau \frac{1}{4} \dot{x}^2}, \quad (4.314)$$

where  $\tau$  is a proper-time parameter (the fifth parameter [60]), and the dot denotes a derivative with respect to the proper time. This is the *worldline path integral* representation of the relativistic propagator of a scalar particle in Euclidean space-time. In the vacuum (no background field), it is easily evaluated by standard methods and leads to the usual space and momentum space free propagators,<sup>13</sup>

$$\int_{x(0)=x'}^{x(t)=x} \mathcal{D}x(\tau) e^{-\int_0^t d\tau \frac{1}{4} \dot{x}^2} = \frac{1}{(4\pi t)^{d/2}}, \quad (4.315)$$

should be one derivation of (8.17).

**2018-10-09 Predrag** I have been trying to write up a standard Euclidean lattice field theory formulation of generating functions  $Z[J]$  and  $W[J]$ , mostly following Montvay and Münster [105] *Quantum Fields on a Lattice*, though there are many references, and some others might be smarter.

What I have done so far is in section *Lattice action* of the course [QFT notes](#).

Like Han, they single out one “time” direction, and reformulate the theory as a “transfer matrix” calculation, which is essentially the Hamiltonian formulation, I believe. I have not written that part up yet.

**2021-11-29 Predrag** Might need to introduce the inverse temperature  $\beta = 1/T$  and the free energy  $F$ , as in (4.226), multiplied by ‘volume’  $N$  the number of lattice sites;

$$Z[J] = e^{W[J]}, \quad W[J] = \beta N F[\Phi]$$

So,  $W[J]$  is not the ‘free energy’.

Hill’s formula here is the discrete Hill’s formula [24, 101] (12.17).

<sup>13</sup>Predrag 2017-06-17: Here a study of Sect. 6. *Worldline formalism* of Gelis and Tanji [64] might be helpful - it reexpresses the integral as an average over Wilson loops.

**2021-11-29 Predrag** The temporal Bernoulli orbit Jacobian matrix  $\mathcal{J} = \partial/\partial t - (s-1)r^{-1}$  is a differential operator whose determinant one usually computes by a Fourier transform diagonalization. The Fourier discretization approach goes all the way back to Hill's 1886 paper [76];

**2020-02-19 Predrag** In Berenstein and García-García15 [17] *A universal quantum constraints on the butterfly effect*, [arXiv:1510.08870](#), cat maps were generalized to products of such vector spaces that can be put on a lattice, with a variables at each site and variables at different sites commuting with each other, for nearest neighbors on a lattice in any dimension. As they write, "This generates a system with nearest neighbor hopping and local scrambling." They write down a periodic (circulant) banded matrix, so the eigenvalues have a band structure similar to a periodic potential with nearest neighbor hopping. The evolve forward in time, i.e., their is a quantized Hamiltonian formulation.

Berenstein [16] *A toy model for time evolving QFT on a lattice with controllable chaos*, [arXiv:1803.02396](#) from UC Santa Barbara. is perhaps a precursor to Gutkin and our spatiotemporal cat.

He discusses two points of view on how the Lyapunov exponents appear in real time correlation functions in quantum field theory and will them compute them in the case of the cat map dynamics. The Kubo's formula point if view is in semiclassical physics, and the second point of view is statistical. They both amount to different ways of making a quantity with an indefinite sign positive.

He considers 1-dimensional spatial lattice, and carries out computations on a spatial lattice with only two sites. He composes a local cat map at each site with a nearest neighbor entangler and after the system is constructed one iterates the automorphism. The system will also be determined by a  $[2m \times 2m]$  matrix. Each  $[2 \times 2]$  block on the diagonal represents  $(P_i; Q_i)$ . The local cat map acts on each of these as a  $[2 \times 2]$  matrix, and the nearest neighbor entangler is a matrix that, at least for a lattice on a line, is near the diagonal giving rise to a banded matrix. The eigenvalues of this bigger matrix are the Lyapunov exponent of the system.

Iterating over a general M produces a cat map dynamics on the Q, and the 'inverse' cat dynamics on the P. The dynamics on P is actually built from the inverse transpose, but that has the same eigenvalues as the inverse of M.

As noted in ref. [17], models with nearest neighbor properties also mimic the Lieb-Robinson bound [18] for propagation of information and thus can in principle serve as toy models for relativistic field theories (they have the equivalent of a speed of light).

He sets up a one dimensional spatial lattice, with nearest neighbor entanglers whose dynamics can be encoded by an 'Dirichlet' upper triangular matrix, his eq. (64) and sketch (65), with eigenvalues 1, and thus

not chaotic. However, with periodic bc's it is chaotic. The paper here falls short of Gutkin and Osipov [72].

Berenstein and Teixeira [16] *Maximally entangling states and dynamics in one dimensional nearest neighbor Floquet systems*, [arXiv:1901.02944](https://arxiv.org/abs/1901.02944), describe conditions for generating entanglement between two regions at the optimal rate in a class of one-dimensional quantum circuits with Floquet dynamics. I do not get it, but it does cite Prosen [20] see 2019-11-18 Boris below.

I do not think we need to cite him, but should send him links to our papers: [David Berenstein](#)

**2021-02-04 Predrag** van der Kamp [83] *Initial value problems for lattice equations studies periodic solutions of partial difference equations (PΔEs):*

consider  $(s_1, s_2)$  relative periodic initial value problem. [...] In the Cauchy directions, assuming the equation to be multi-linear, the periodic solution can be obtained uniquely by iteration of a simple mapping, whose dimension is a piecewise linear function of  $(s_1, s_2)$ .

van der Kamp [83] paper offers geometric understanding, and shows how to pose initial value problems for general lattice equations. He provides explicit reductions of an integrable 5-point equation.

If well-posed, the periodic solutions are uniquely determined by iteration of single-valued mappings. Here,  $s$ -periodicity on the band of initial values implies  $s$  periodicity of the solution on  $\mathbb{Z} \times \mathbb{Z}$ .

His mappings can be obtained by using the equation only  $r = \gcd(s_1, s_2)$  times.

He performs different reductions for the integrable 5-point equation of Bruschi, Calogero and Droghei [30] *Tridiagonal matrices, orthogonal polynomials and Diophantine relations: I*. Also, read sect. 6.5.6, add your notes to the subsection there.

**Do have a look at:**

Papageorgiou, Nijhoff and Capel [110] *Integrable mappings and nonlinear integrable lattice equations*: Periodic reductions for lattice equations defined on a square.

Quispel, Capel, Papageorgiou and Nijhoff [114] *Integrable mappings derived from soliton equations*: They realized that such reductions provide traveling wave solutions.

A general description of  $s$ -reduction, with  $s \in \mathbb{Z} \times \mathbb{Z}$ , is given in Rojas, van der Kamp and Quispel [116] *Lax representations for integrable maps OΔEs*.

Adler and Veselov [1] *Cauchy problem for integrable discrete equations on quad-graphs* give a criterion for the well-posedness of Cauchy problems for integrable equations defined on the square, on a so-called quad-graph (a planar graph with quadrilateral faces).

**2021-11-27 Predrag** The Cvitanović and Vattay unpublished draft *Variational principle for noisy dynamics* explains how the leading noisy  $\sqrt{\text{Det } \mathcal{J}}$  becomes the classical  $\text{Det } \mathcal{J}$  (I believe that is included into ChaosBook, but I have not checked). So that would be one way to go from noisy dynamics to the deterministic limit, but I hope we can avoid this in the current paper.

Cvitanović, Dettmann, Mainieri and Vattay *Trace formulae for stochastic evolution operators: Weak noise perturbation theory* [45] and *Smooth conjugation method* [46] starts out by expressing the weak noise expansions in terms of Dirac  $\delta$  and its derivatives. (For now) you are interested in keeping only the leading term, i.e., the Dirac  $\delta$  that yields  $1/\text{Det } \mathcal{J}$ . Exponentiated action appears naturally. See sect. 4.16 *Noise is your friend*.

None of the above have orbit Jacobian matrix, they are all formulated as time-stepping. I think we want to emphasize the primacy of the orbit Jacobian matrix, consider time-evolution as one (awkward) way of formally evaluating  $\text{Det } \mathcal{J}$ , I say “formally” as time evolution stability cannot be implemented in practice due to exponential overflows / underflows in any numerical evaluation.

Field theorists think of euclidean field theory as sum over probabilities  $p(\phi) = \exp(-S[\phi])/Z$ , see (17.3). The papers cited there might have a reference to a simple derivation of that formula. I derive it in Cvitanović [39] *Field Theory*, but I hope you do not have to go through that, that takes 1/3 of a semester-long course.

The  $\epsilon$  trick I talked about is the ‘Gaussian damping factor’, see mu *Field Theory* [39] sect. 3B *Gaussian integrals*, eq. (3.8).

**2020-12-16 Predrag** My 2000 *Chaotic Field Theory: A sketch* [40] gets cited every so often. Most citations seems useless, with the exception of these two:

Stam Nicolis *Supersymmetry and Deterministic Chaos* (2020): We show that the fluctuations of the periodic orbits of deterministically chaotic systems can be captured by supersymmetry, in the sense that they are repackaged in the contribution of the absolute value of the determinant of the noise fields, defined by the equations of motion.

[...] In a chaotic phase there are infinitely many periodic orbits and there have been attempts to use them to construct the measure they define, using perturbative field theoretic techniques [40] (that’s me). [...] He] discusses another way to address this issue, that does not rely on perturbation theory, following the approach of his earlier papers, he writes a *lattice action* and computes the identities that the correlation functions that the noise fields would be expected to satisfy, were the system consistently closed.

Bernd Mümken *A Dynamical Zeta Function for Pseudo Riemannian Foliations* (2006): “We investigate a generalization of geodesic random walks to pseudo Riemannian foliations. The main application we have in mind

is to consider the logarithm of the associated zeta function as grand canonical partition function in a theory unifying aspects of general relativity, quantum mechanics and dynamical systems.”

It looks familiar in glimpses, but the math is killing me...

**2023-09-16 Predrag Campos, López and Sierra [32]** *Integrability and scattering of the boson field theory on a lattice* (2021), [arXiv:2009.03338](#) construct factorized scattering models using the Boltzmann weights of the free boson on a lattice. The former models describe the elastic scattering of particles, typically solitons, in a relativistic quantum field theory with an infinite number of conserved quantities. The scattering of these particles can be factorized into the product of two-particle scattering amplitudes that, for consistency, satisfy the Yang-Baxter equation. It turns out that some solutions of the Yang-Baxter equation can be used as Boltzmann weights of a Statistical Mechanical model or, alternatively, as scattering  $S$  matrices in a relativistic quantum field theory with the appropriate identifications of variables. They show that the Boltzmann weights of the boson model can be promoted to scattering  $S$  matrices with the special feature that the particles carry a continuous degree of freedom, unlike the more common models where it is discrete. They construct two  $S$  matrix models, one using the trigonometric functions, and another using Jacobi elliptic functions. They are similar to those proposed by Mussardo and Penati for the elliptic version of the sinh-Gordon model.

**2020-06-30 Moshe Rozali** *Effective Field Theory for Chaotic CFTs* “ Relations between chaos and hydrodynamics are one of the unique feature of holographic CFTs. The early time Lyapunov regime can be described by an effective field theory of a single mode, which for maximally chaotic systems is an hydrodynamic mode. We describe that effective field theory for conformal field theories, both in two dimensions and in higher dimensions, and show how it captures maximal chaos and pole skipping. We discuss the relation of the theory to other formulations of CFTs and show how it captures interesting objects such as conformal blocks and partial waves. We speculate on what is needed to extend the discussion to non maximal chaos. ”

[arXiv:1712.04963](#); [arXiv:1808.02898](#); [arXiv:1909.05847](#)

[arXiv:1612.06330](#); [arXiv:1811.09641](#); [arXiv:1812.10073](#);

G.J. Turiaci [arXiv:1901.04360](#); [arXiv:1912.02810](#)

**2020-07-02 Ruairí Brett** *From two to three-body systems in lattice QCD*

Problem: finite box has no continuous spectrum, scattering.

[arXiv:1911.09047](#) 2-body scattering: quantization condition is given by the Lüscher formula, stated as a determinant.

[arXiv:1707.05817](#) implements is with group theory, octahedral  $O_h$  crystallographic irreps for a cubic box which mix some the continuous limit

O(4). They also compute on elongated boxes, with different discrete symmetry. These are elongated in the  $z$ , not the temporal  $t$  direction) yields many more states.

[arXiv:1901.00483](#)

relation to relativistic formulation [arXiv:1905.12007](#)

[arXiv:1709.08222](#) 2-body scattering is a sub-calculation in the 3-body scattering.

“Wrap-around effects” arise from finite temporal size of the lattice.

The cleanest example is  $\pi^+\pi^+\pi^+$  elastic scattering. Lattice simulation data are surprisingly sharp. They are close to 3 non-interacting pions. The agreement with the determinant zeros (infinite volume limit) using only 2-body scattering data, no fit are very sharp. So the 3-body contact term will be small (they are working on that now)

The latest 3-pion formalism: [arXiv:2003.10974](#)

**2022-02-24 Predrag .**

Zied Ammari, Marco Falconi and Marco Olivieri *Semiclassical analysis of quantum asymptotic fields in the Yukawa theory* [arXiv:2111.03352](#):

we then show that  $\mu_0$  concentrates on a set of classical asymptotic radiationless states, from which no radiation is coming out or in. The later notion is similar to that of trapped trajectories in finite dimensional semiclassical analysis.

As for the quantum theory and asymptotic vacuum states (20), at the classical level there is a notion of asymptotic radiationless states. These are the phase space points in the kernel of the classical wave operator.

**Predrag** Their Schrödinger-Klein-Gordon equation eq. (45) has an extra ‘ $z$ ’ field to it. I have Googled “radiationless” solutions; they start with Sommerfeld and Schott in electromagnetism, as ways of avoiding QM, and in study of solitons on discrete lattices. Might explain why our lattice fields theories live on Cantor sets, but I gave up on searching further.

**2022-03-13 Predrag (move to Hill determinants?)**

Yuhang Hou and Santosh Kandel *Asymptotic analysis of determinant of discrete Laplacian* [arXiv:1910.02887](#). Lots of good stuff in it, but on a very sophisticated level:

[...] study the relation between the partition function of the free scalar field theory on hypercubes with boundary conditions and asymptotics of discrete partition functions on a sequence of “lattices” which approximate the hypercube as the mesh approaches to zero. More precisely, we show that the logarithm of the zeta regularized determinant of Laplacian on the hypercube with Dirichlet boundary condition appears as the constant term in the asymptotic expansion of the log-determinant of the discrete Laplacian up to an explicitly computable constant.

They are mostly interested in the restriction to the functions which vanish on the boundary, call it the discrete Laplacian with Dirichlet boundary condition. They also investigate similar problems for the massive Laplacian on tori.

They refer to our free field theory action (4.138) as ‘massive Laplacian’, and to discrete hypercube as ‘ $d$ -dimensional orthotope’.


For  $d = 2$ , there is a very special relationship between determinants of the massive discrete Laplacian on the torus and on the hypercube, which they state. They use formulas like the ones we use, for example

$$\prod_{k=1}^{n-1} \left( 2x - 2 \cos \left( \frac{k\pi}{n} \right) \right) = (x + \sqrt{x^2 - 1})^n + (x - \sqrt{x^2 - 1})^n - 2. \quad (4.316)$$

Kenyon [7] derived a partial asymptotic expansion for the determinant of the corresponding discrete Laplacian on rectilinear polygonal domains. [...] log determinant of discrete Laplacians with free boundary condition, is studied by Louis [12].

**2022-01-25 Michele Schiavina** (ETH Zürich)

Hadfield, Kandel and Schiavina [73] *Ruelle zeta function from field theory* [arXiv:2002.03952](https://arxiv.org/abs/2002.03952) has lots of good stuff in it, but on a very sophisticated level.

 *Ruelle Zeta Function from Field Theory* I will discuss a field-theoretic interpretation of Ruelle’s zeta function, which “counts” prime geodesics on hyperbolic manifolds, as the partition function for a topological field theory (BF) with an unusual gauge fixing condition available on contact manifolds. This suggests a rephrasing of a conjecture due to Fried, on the equivalence between Ruelle’s zeta function (at zero) and the analytic torsion, as gauge-fixing independence in the Batalin–Vilkovisky formalism.

**2022-03-26 Predrag** Campellone, Parisi and Virasoro [31] *Replica method and finite volume corrections* (2009) evaluate a set of extremal points of action (saddle points) but I do not see relevance to our field theories.

**2022-03-26 Predrag** Reading [physics.stackexchange.com](https://physics.stackexchange.com) is interesting:

Saddle points in QFT, or the [stationary phase approximation](#)

$$\int_{\mathbb{R}^n} dx g(x) e^{iS(x)/\hbar} \simeq (2\pi\hbar)^{n/2} \int_{\text{Crit}(S)} \frac{e^{i\frac{\pi}{4} \text{sgn}(\text{Hess}(S))}}{\sqrt{|\det(\text{Hess}(S))|}} g(x_0) e^{iS(x_0)/\hbar} \quad (4.317)$$

The integral on the left over  $\mathbb{Z}^n$  is approximated by the integral on the right over the set  $\text{Crit}(S)$  of critical points of  $S$ .

**2020-04-16 ‘adithya’** writes in [physics.stackexchange.com](https://physics.stackexchange.com): “In Coleman’s *Aspects of Symmetry*, chapter 7, section 3.2, he makes a claim that configurations of finite action form a set of zero measure and are therefore unimportant. Further, he goes on to prove the claim in Appendix 3 of the same



chapter and says that the finite action contribution to the path integral must be zero."

**2023-11-01 Predrag** Chap. 7 *The uses of instantons*, sect. 3.2 *The winding number* does not seem to contain a sum over saddles? Appendix 3 maybe does it, but I do not get it anyway :( .

**2023-11-01 Predrag** It might be that WHAT we call *periodic states*, other people call **instantons**

...becomes formally a sum over **instantons**, i.e. classical field configurations.

I think not, as " An instanton is a classical solution to equations of motion with a *finite*, non-zero action, either in quantum mechanics or in quantum field theory. More precisely, it is a solution to the equations of motion of the classical field theory on a Euclidean spacetime [...]. solutions to the equations of motion may be thought of as critical points of the action. The critical points of the action may be local maxima of the action, local minima, or saddle points [...]. In the context of soliton theory the corresponding solution is known as a kink. In view of their analogy with the behaviour of classical particles such configurations or solutions, as well as others, are collectively known as pseudoparticles or pseudoclassical configurations [...]. "Periodic instantons" are a generalization of instantons, expressible in terms of Jacobian elliptic functions which are periodic functions. "

Our periodic state is not localized in spacetime, it is repeated over an infinite Bravais lattice, so no finite action.

**2020-04-16 'Chiral Anomaly'** answers: " Consider the path integral for a lattice QFT. On a finite lattice, all configurations have finite action. What happens in the continuum limit?

If we apply the saddle-point approximation first and then take the continuum limit, no problems arise. Coleman's comments apply to the continuum limit of the original path integral and so do not contradict the legitimacy of the saddle point approximation. Actually, Coleman's comments also apply to the result of the saddle-point approximation: after applying

the saddle-point approximation to the lattice QFT, the only path integral remaining is a gaussian path integral,

and Coleman's comments apply to the continuum limit of that gaussian path integral. [...] The guiding principle is: taking the continuum limit should be the last thing we do, if we ever do it at all. "

John Dougherty writes: Consider **stationary phase approximation** says that (4.317).  $\text{Crit}(S)$  is a finite subset of  $\mathbb{R}^n$ .  $\text{Crit}(S)$  has measure zero

in  $\mathbb{R}^n$ , and Coleman's claim is that the set of critical points is "unimportant" to the integral on the left. However,  $\text{Crit}(S)$  is the entire domain of integration on the right hand side, not unimportant there.

Might be helpful: Notes from [Sidney Coleman's Physics 253a](#). [Swanson](#) is good on historical sources of QFT.

**2022-01-26 Andrey Bagrov** andrey.bagrov@ru.nl (assistant professor, Radboud University, Nijmegen, the Netherlands) writes:

" Your ref. [93] [arXiv:2201.11325](#) establishing the connections between quantum field theory and chaos in dynamical systems has attracted our attention [...] we think you might find our paper

Ageev, Bagrov and Iliaso [3] *Deterministic chaos and fractal entropy scaling in Floquet conformal field theories* (2021)

useful. From the technical point of view, the setting considered by us is somewhat different from yours, - we study continuous field theory, and the dynamical system is implemented on the level of conformal transformations of the CFT, - it is still pretty similar ideologically. We also show that a certain, quite atypical type of chaos can be induced in a one-dimensional quantum system as a result of the composition of field theory operators.

It would be interesting to search for more specific relations between the two approaches. For example, did you try to study the asymptotics of low-order correlation functions and/or scaling of the von Neumann entropy in your setting? Is there a chance to have some fractal structures in your model? "

**2022-01-30 Predrag** So far, I do not understand Ageev, Bagrov and Iliaso [3] paper.

I think our field theory is as 'continuous field theory' as theirs, except that so far we had no motivation to venture into the complex plane to represent the dynamics.

They are able to continue the Ulam map and the Ulam tent map analytically into complex plane - hence 'conformal field theories' and there might be something interesting there for us to learn.

**2022-01-30 Predrag** Starting to draft the email response:

" Our article has too many unfamiliar things to say as is, so in [figure 12\(b\)](#) we only *hint* at the fractal spectrum of nonlinear theories. One of our priorities has been to explore the fractal nature of this spectrum for  $\phi^3$  and  $\phi^4$  scalar field theories, providing our group is able to carry out the calculations. The students have started the calculation more than a year ago. So far we have no results to report.

However, we do know that in the anti-integrable, strong coupling limit the eigenvalues are

$$\lambda_j = g \phi_j + O\left(\frac{1}{\langle \phi \rangle}\right), \quad (4.318)$$

where  $g$  is the coupling constant, and lattice site fields  $\phi_j$ 's are embedded into Smale horseshoes, a unimodal (two branches) horseshoe for  $\phi^3$ , and bimodal (three branches) for  $\phi^4$  strongly coupled scalar field theories, so there is no doubt that the spectrum is fractal. But, you would be more easily persuaded were our group to show you a plot of such fractal.

We have not gotten yet to low-order correlation functions, their asymptotics, and to metric (Kolmogorov) entropy, but we eventually can and should. We do have the partition function, our article [eq. \(9\)](#), but we are still struggling with details of Hill determinant weights for symmetric orbits, such as our article [eq. \(151\)](#). "

**2022-05-09 Predrag 2 Carlos Martínez López** (the best [ChaosBook.org/course1](#) student, who is starting his PhD with Javier Jiménez): Now you have a job to do. Javier misunderstood my last conference talk, and got an impression that our global, field-theoretic formulation of spatiotemporal turbulence / chaos [ChaosBook.org/overheads/spatiotemporal](#) works only for Hamiltonian systems, ie, for Euler and not Navier-Stokes. But our simplest example, the Bernoulli map, is a non-Hamiltonian dynamical system with infinite contraction ("dissipation") in one time step, and we have explored the '1d Navier-Stokes', ie., Kuramoto–Sivashinsky, in a great detail.

**2016-11-13 Predrag** A thing to rethink: Green's functions for periodic lattices are in ChaosBook sections D.3 Lattice derivatives and on, for the Hermitian Laplacian and  $s = 2$ . For real  $s > 2$  cat map, the potential is inverted harmonic oscillator, the frequency is imaginary (Schrödinger in imaginary time), eigenvectors real - should be a straightforward generalization. Have done this already while studying Ornstein-Uhlenbeck with Lippolis and Heninger - the eigenfunctions are Hermite polynomials times Gaussians.

Predrag's formula, removed by Boris 2017-01-15:

As the 3-point discretization of the second time derivative  $d^2/dt^2$  (central difference operator) is  $\square \phi_t \equiv \phi_{t+1} - 2\phi_t + \phi_{t-1}$  (with the time step set to  $\Delta t = 1$ ), the *temporal* cat map [\(8.58\)](#) can be rewritten as the discrete time Newton equation for inverted harmonic potential,

$$(\square + 2 - s) \phi_t = m_t. \quad (4.319)$$

**2021-12-14 Predrag** I now avoid the pesky overall "--" sign; it arises from  $m_{t+1} = \lfloor s\phi_t \rfloor$ , being the integer part of  $s\phi_t$  by having redefined the temporal Bernoulli. Han's [\(8.82\)](#) is the way to go.

By noting that the temporal lattice Laplacian can be written as  $\square = \partial^\top \partial = r^\top r - 2\mathbf{1}$ , where the  $[n \times n]$  matrix  $\partial = (\mathbf{1} - r)/\Delta t$  is the discrete time derivative [refeq{1stepVecEq}](#), the temporal cat Lagrangian density [\(8.80\)](#) and the action [\(24.189\)](#) can be written in the more familiar, field-theoretic form

$$S[\Phi] = \sum_{t=1}^n \left\{ \frac{1}{2} (\partial \phi_t)^2 + \frac{1}{2} \mu^2 \phi_t^2 \right\} + \sum_{t=1}^n m_t \phi_t. \quad (4.320)$$

For  $0 \leq s < 2$  this is the action for a 1-dimensional chain of nearest-neighbor coupled harmonic oscillators. Here we are, however, interested in the everywhere hyperbolic, unstable, anti-integrable or inverted parabolic potential,  $s \geq 2$  case.

**2022-01-19 Predrag** “If a potential that is bounded from below is needed to make sense of the probabilistic interpretation of the configuration weight [\(4.95\)](#)” from “one starts with a quartic potential [\(4.137\)](#) i.e., [\(23.14\)](#)” because our potential is inverted.

Note the inverted potential in [\(4.135\)](#) - we are interested in unstable periodic states.


**2025-01-10 Predrag** Nonlinear Schrödinger equation (NLS) [\(wiki\)](#) in one dimension:

$$i\partial_t \psi = -\frac{1}{2} \partial_x^2 \psi + \kappa |\psi|^2 \psi. \quad (4.321)$$

The case with negative  $\kappa$  is called focusing and allows for bright soliton solutions (localized in space, and having spatial attenuation towards infinity) as well as breather solutions. The  $\kappa$  positive case is the defocusing NLS which has dark soliton solutions (having constant amplitude at infinity, and a local spatial dip in amplitude).

The Discrete Nonlinear Schrodinger (DNLS) equation is likely to be not integrable.

Spatially 2-dimensional DNLS lattices admit localized ‘vortex-breathers’. They become unstable as the coupling is increased.

 [Monica Visan \*Determinants, commuting flows, and recent progress on completely integrable systems\* \(2021\)](#), explains how to define regularized determinants, Hilbert-renormalized, in the continuum  $\phi^4$ , theory when nonlinear term is weak, with sufficiently small Hilbert-Schmidt norm (I think), using the  $\sqrt{R}$  of the resolvent  $R$  of the free Klein-Gordon (for her, ‘Lax’, as she is interested in integrability). This takes care of high frequencies in the unregularized ‘Hill’ determinant.

**2022-08-05 Predrag** .

Minos Axenides, Emmanuel Floratos and Stam Nicolis *Arnol’d cat map lattices* [arXiv:2208.03267](#) is temporal cat with our scalar field  $\phi_t$  on lattice site  $t \in \mathbb{Z}$  replaced by a  $n$ -dimensional vector field of  $n$  coupled cat maps

$q_t$  on lattice site  $t \in \mathbb{Z}$ , with Euler–Lagrange equations (the call them ‘Newton’s discrete time equations’)

$$q_{t+1} - 2q_t + q_{t-1} = q_t C^2 \quad (4.322)$$

Left hand side is  $\square q$ , the 1-dimensional (temporal) discretized lattice Laplacian (4.140). The invertible symmetric mass matrix  $C$  generalizes the scalar theory (4.178) Klein-Gordon mass  $\mu$ .

They define the  $[2 \times 2]$  integer matrix

$$C \equiv \begin{pmatrix} k_1 & c \\ c & k_2 \end{pmatrix} \quad (4.323)$$

However, I do not see the winding numbers  $m_t$  in their (4.322)?

As the matrix  $C^2$  is positive definite, the coupling is repulsive, so (4.322) describes coupled *inverted* harmonic oscillators. The phase space of each of these particles is a two-dimensional torus, so the motion is strongly chaotic and mixing (cf. also [50]).

They decouple the modes of Newton’s equations and diagonalize  $C$  by (finite) Fourier transform,  $F^\dagger C F \equiv D$  where  $F_{IJ} = e^{2\pi i I J / n} / \sqrt{n} \equiv \omega_n^{IJ} / \sqrt{n}$ . We define the mode variable  $r_m$  by  $q_m \equiv r_m F$ . The mode variable  $r_m$  satisfies Newton’s equation of motion in the form:

$$r_{m+1} - 2r_m + r_{m-1} = r_m D^2 \quad (4.324)$$

where  $D_{IJ} = \delta_{IJ} D_J$ , with

$$D_J = K + 2G \cos \frac{2\pi J}{n} \quad (4.325)$$

for the case of nearest-neighbor interactions. We note here that, if  $n$  is even, then the mode  $J_0 = n/2$  has zero eigenvalue, when  $K = 2G$ . If  $n$  is odd, a zero mode cannot exist, because  $K$  and  $G$  are positive integers.

It is possible to include the case of couplings beyond nearest-neighbors, i.e.  $G_l$ , with  $1 < l \leq (n-1)/2$ , as follows:

$$D_J = K + 2 \sum_{l=1}^{\frac{n-1}{2}} \left( G_l \cos \frac{2\pi l J}{n} \right) \quad (4.326)$$

2022-04-14 Predrag 2 Vladimir Rosenhaus vrosenhaus@gc.cuny.edu.

Your 2022-04-13 talk on Rosenhaus and Smolkin [119] *Feynman rules for wave turbulence*, [arXiv:2203.08168](https://arxiv.org/abs/2203.08168), was great and very helpful to me, thanks!

Your Dirac delta eq. (2.14) which ensures that the equations of motion are satisfied, see e.g. ref. [13, 70, 103, 144, 146] is (almost) equivalent to our [93] ‘deterministic trace formula’ eq. (9).

Then we get a divorce. While you, and the mostly already dead friends, work with weak coupling  $\phi^4$ , we work with the strong coupling, nonperturbative  $\phi^4$ , our [eq. \(56\)](#). For us the chaos comes from the deterministic dynamics, and we absolutely *do not* stick in any Gaussian forcing terms.

Gurarie and Migdal [\[70\]](#) *Instantons in the Burgers equation* (1996) is just the usual gymnastics (I have it in ChaosBook noisy chapters) of starting with Gaussian forcing  $f$ , and sticking in an integral over  $\delta(F[\Phi] - f)$  to replace  $f$  in the Gaussian exponent by Euler-Lagrange equation in terms of state space fields  $\Phi$ . No deterministic condition  $\delta(F[\Phi])$  there, as far as I can see.

Wyld [\[144\]](#) *Formulation of the theory of turbulence in an incompressible fluid* (1961) is close to us (see p. 31 of [this talk](#)): “For the *stationary* problem it is convenient, to Fourier analyze the velocity field with respect to both space and time” - his eqs. (4), (7) - “a large four-dimensional box of volume  $V$  and temporal extent  $T$ , and we suppose that there are periodic boundary conditions on the sides of the box,” except that we do not take the  $V, T \rightarrow \infty$  limit. However, by his eq (12) Wyld gets into perturbation theory, so nothing for us to cite there.

I do not see your Dirac delta eq. (2.14) in the Martin-Siggia-Rose [\[103\]](#) (1973) paper, or Balkovsky, Falkovich, Kolokolov and Lebedev [\[13\]](#) *Intermittency of Burgers’ turbulence* (1997).

I’m impressed that you do QFT without  $\hbar$  or  $iS$  anywhere; so we simple southern gents have been [Quefithing](#) all along, without knowing we were doing it?

**2022-07-19 Predrag** Vladimir Rosenhaus [\[117\]](#) *Chaos in the quantum field theory S-matrix* (2021)

David Gross and Vladimir Rosenhaus [\[68\]](#) *Chaotic scattering of highly excited strings* (received 31 March 2021)

**2022-07-19 Predrag** Vladimir Rosenhaus [\[118\]](#) *Chaos in a many-string scattering amplitude* (received 24 March 2022) is a continuation of the above refs. [\[68, 117\]](#).

Abstract: “String theory provides a compact integral expression for the tree-level scattering amplitude of an arbitrary number of light strings. [...] We pick out a particular pole in the amplitude of weakly coupled bosonic, one corresponding to successive photon scatterings, which lead to an intermediate state with a highly excited string in a definite state. [...] erratic behavior of the amplitude suggests that this may serve as a simple and explicit illustration of chaos in many-particle scattering.”

The 3 papers are too hard to read for me, but the gist is “the physical process of starting with a tachyon and successively scattering photons off of it, and after each scattering event picking out the intermediate string state that is on shell.”

“There is no generally accepted notion of what chaos in quantum field theory or string theory means. In ref. [117] I proposed that chaos be diagnosed by erratic behavior of a many-particle amplitude under a change in the momentum of one of the particles.”

He finds by inspecting the amplitude that “For some generic excited string, the distribution looks erratic.”

I should read his refs [1-15] :(

2022-05-02 Predrag & Han 2 Vladimir & Xu-Yao notes on

[arXiv:2204.13655](https://arxiv.org/abs/2204.13655) *Correlation functions in linear chaotic maps* [78]

1. Can you emphasize that these systems are **not** linear: they are *piece-wise* linear, which makes them extremely nonlinear: ([click here](#)). For example, Bernoulli map is a limit of the ‘cubic’ potential map [ChaosBook fig. 11.4](#) with the slope of middle interval going to infinity.
2. It is not a ‘the recently introduced “spatiotemporal” cat map’; it’s not a ‘map’ at all, it is the Euler–Lagrange equation condition applied to every lattice site. There is no evolution (a map) forward in time - hence *spatiotemporal cat*.
3. Not **area-preserving**. Temporal Bernoulli is not volume preserving - it is infinitely contracting in one time-step, and it is noninvertible. It is crucial that the lattice field theory covers both Hamiltonian /symplectic and dissipative systems. See the text after [eq. \(71\)](#), [eq. \(88\)](#), 2nd paragraph on p. 58, search for ‘dissipative’ throughout the manuscript.
4. ‘they should be viewed as discrete-time dynamical systems’. Actually, our message in Gutkin *et al.* [71] is ‘The cat map is generalized to the spatiotemporal cat map by considering a 1- dimensional spatial lattice’, not a ‘discrete-time dynamical system’.
5. ‘Ruelle resonances’ → Ruelle-Pollicott resonances’
6. For the Bernoulli map discrete time is unnecessary. We may consider the continuous time map,  $\delta_t x(t) = \log 2 x(t)$ , where again  $x(t)$  is confined to live on a circle. The solution is  $x(t) = x_0 2^t$ , so the map is just viewing the system at discrete time intervals.  
**2022-05-02 Predrag** Correct. True of any 1st order ODE, solutions are exponentials, real (AKA hyperbolic) or complex (AKA oscillatory). However, the mod operation is essential, not ‘just’, it makes the map piece-wise linear, i.e. strongly nonlinear.
7. “chaos, which involves stretching and folding” - for temporal Bernoulli and temporal cat it is “stretching and winding”, there is no folding.

## Commentary

**Remark 4.1.** Lattice field theory. In his 1983 *Six Lectures on Lattice Field Theory* Michael Stone explains that the free, non-interacting partition function (??) is the sum over all loop (returning walks), i.e., related to the trace of the propagator (??).<sup>14</sup> This goes back to Symanzik, and is probably explained at length in Federico Camia *Brownian Loops and Conformal Fields*, [arXiv:1501.04861](https://arxiv.org/abs/1501.04861).

Check Rosenfelder *Path Integrals in Quantum Physics*, [arXiv:1209.1315](https://arxiv.org/abs/1209.1315).


<sup>14</sup>Predrag 2018-10-07: Incorporate Stone explanation, with hops weighted by fugacity  $h = \exp(-\mu)$ .



Meyer [104] *Lattice QCD: A brief introduction*.

Check out also online Simons, Lecture I: Simons courses *Collective Excitations: From Particles to Fields* *Free Scalar Field Theory: Phonons*; and *Quantum Condensed Matter Field Theory*; as well as Piers Coleman [38] *Introduction to Many-Body Physics* ([click here](#)) + ([click here](#)).

Further reading on lattice field theories: Sommer [134] *Introduction to Lattice Gauge Theories*; Wiese [139] *An Introduction to Lattice Field Theory*; Rothe [121] *Lattice Gauge Theories*; Jansen [82] *Lattice field theory* focuses on the lattice QCD; Smit [133] *Introduction to Quantum Fields on a Lattice*; Münster and M. Walzl [107] *Lattice gauge theory - A short primer*, [arXiv:hep-lat/0012005](#); Montvay and G. Münster [105] *Quantum Fields on a Lattice*.

Perhaps watch  *Shadow state for everyone* (1:21 min). Not required :)

## References

- [1] V. E. Adler and A. P. Veselov, “Cauchy problem for integrable discrete equations on quad-graphs”, *Acta Appl. Math.* **84**, 237–262 (2004).
- [2] V. S. Afraimovich and Y. B. Pesin, “Hyperbolicity of infinite-dimensional drift systems”, *Nonlinearity* **3**, 1–19 (1990).
- [3] D. S. Ageev, A. A. Bagrov, and A. A. Iliashov, “Deterministic chaos and fractal entropy scaling in Floquet conformal field theories”, *Phys. Rev. B* **103**, 1100302 (2021).
- [4] N. Ahmadinia, A. Bashir, and C. Schubert, “Multiphoton amplitudes and generalized Landau-Khalatnikov-Fradkin transformation in scalar QED”, *Phys. Rev. D* **93**, 045023 (2016).
- [5] M. Aizenman, “Proof of the triviality of  $\phi^4$  field theory and some mean-field features of Ising models for  $D > 4$ ”, *Phys. Rev. Lett.* **47**, 1–4 (1981).
- [6] M. Aizenman, “Geometric analysis of  $\phi^4$  fields and Ising models. Parts I and II”, *Commun. Math. Phys.* **86**, 1–48 (1982).
- [7] S. Anastassiou, “Complicated behavior in cubic Hénon maps”, *Theoret. Math. Phys.* **207**, 572–578 (2021).
- [8] S. Anastassiou, A. Bountis, and A. Bäcker, “Homoclinic points of 2D and 4D maps via the parametrization method”, *Nonlinearity* **30**, 3799–3820 (2017).
- [9] S. Anastassiou, A. Bountis, and A. Bäcker, “Recent results on the dynamics of higher-dimensional Hénon maps”, *Regul. Chaotic Dyn.* **23**, 161–177 (2018).
- [10] S. Aubry, “Anti-integrability in dynamical and variational problems”, *Physica D* **86**, 284–296 (1995).
- [11] S. Aubry and G. Abramovici, “Chaotic trajectories in the standard map. The concept of anti-integrability”, *Physica D* **43**, 199–219 (1990).

- [12] C. Baesens, Y.-C. Chen, and R. S. MacKay, “Abrupt bifurcations in chaotic scattering: view from the anti-integrable limit”, *Nonlinearity* **26**, 2703–2730 (2013).
- [13] E. Balkovsky, G. Falkovich, I. Kolokolov, and V. Lebedev, “Intermittency of Burgers’ turbulence”, *Phys. Rev. Lett.* **78**, 1452–1455 (1997).
- [14] J. Banks, J. Brooks, G. Cairns, G. Davis, and P. Stacey, “On Devaney’s definition of chaos”, *Amer. Math. Monthly* **99**, 332–334 (1992).
- [15] C. Beck, “Higher correlation functions of chaotic dynamical systems - a graph theoretical approach”, *Nonlinearity* **4**, 1131 (1991).
- [16] D. Berenstein, *A toy model for time evolving QFT on a lattice with controllable chaos*, 2018.
- [17] D. Berenstein and A. M. García-García, *A universal quantum constraints on the butterfly effect*, 2015.
- [18] J. M. Bergamin, T. Bountis, and C. Jung, “A method for locating symmetric homoclinic orbits using symbolic dynamics”, *J. Phys. A* **33**, 8059–8070 (2000).
- [19] J. M. Bergamin, T. Bountis, and M. N. Vrahatis, “Homoclinic orbits of invertible maps”, *Nonlinearity* **15**, 1603–1619 (2002).
- [20] B. Bertini, P. Kos, and T. Prosen, “Entanglement spreading in a minimal model of maximal many-body quantum chaos”, *Phys. Rev. X* **9**, 021033 (2019).
- [21] O. Biham and W. Wenzel, “Characterization of unstable periodic orbits in chaotic attractors and repellers”, *Phys. Rev. Lett.* **63**, 819 (1989).
- [22] M. Blank, G. Keller, and C. Liverani, “Ruelle-Perron-Frobenius spectrum for Anosov maps”, *Nonlinearity* **15**, 1905–1973 (2002).
- [23] S. Bolotin and R. MacKay, “Multibump orbits near the anti-integrable limit for Lagrangian systems”, *Nonlinearity* **10**, 1015–1029 (1997).
- [24] S. V. Bolotin and D. V. Treschev, “Hill’s formula”, *Russ. Math. Surv.* **65**, 191 (2010).
- [25] T. Bountis, H. W. Capel, M. Kollmann, J. C. Ross, J. M. Bergamin, and J. P. van der Weele, “Multibreathers and homoclinic orbits in 1-dimensional nonlinear lattices”, *Physics Letters A* **268**, 50–60 (2000).
- [26] T. Bountis and R. H. G. Helleman, “On the stability of periodic orbits of two-dimensional mappings”, *J. Math. Phys* **22**, 1867–1877 (1981).
- [27] T. Bountis and H. Skokos, *Complex Hamiltonian Dynamics* (Springer, Berlin, 2012).
- [28] R. Bowen, *Equilibrium States and the Ergodic Theory of Anosov Diffeomorphisms* (Springer, Berlin, 1975).
- [29] F. Brini, S. Siboni, G. Turchetti, and S. Vaienti, “Decay of correlations for the automorphism of the torus  $T^2$ ”, *Nonlinearity* **10**, 1257–1268 (1997).

- [30] M. Bruschi, F. Calogero, and R. Droghei, “Tridiagonal matrices, orthogonal polynomials and Diophantine relations: I”, *J. Phys. A* **40**, 9793–9817 (2007).
- [31] M. Campellone, G. Parisi, and M. A. Virasoro, “Replica method and finite volume corrections”, *J. Stat. Phys.* **138**, 29–39 (2009).
- [32] M. Campos, E. López, and G. Sierra, “Integrability and scattering of the boson field theory on a lattice”, *J. Phys. A* **54**, 055001 (2021).
- [33] S. Candelaresi, D. I. Pontin, and G. Hornig, “Quantifying the tangling of trajectories using the topological entropy”, *Chaos* **27**, 093102 (2017).
- [34] Y.-C. Chen, “Anti-integrability in scattering billiards”, *Dyn. Sys.* **19**, 145–159 (2004).
- [35] Y.-C. Chen, S.-S. Chen, and J.-M. Yuan, “Topological horseshoes in travelling waves of discretized nonlinear wave equations”, *J. Math. Phys.* **55**, 042701 (2014).
- [36] S.-N. Chow, J. Mallet-Paret, and E. S. Van Vleck, “Dynamics of lattice differential equations”, *Int. J. Bifurcation Chaos* **06** (1996) 10 . 1142 / s0218127496000977.
- [37] H. Cohen, *A Course in Computational Algebraic Number Theory* (Springer, Berlin, 1993).
- [38] P. Coleman, *Introduction to Many-Body Physics* (Cambridge Univ. Press, Cambridge UK, 2015).
- [39] P. Cvitanović, *Field Theory*, Notes prepared by E. Gyldenkerne (Nordita, Copenhagen, 1983).
- [40] P. Cvitanović, “Chaotic Field Theory: A sketch”, *Physica A* **288**, 61–80 (2000).
- [41] P. Cvitanović, “Walkabout: Transition graphs”, in *Chaos: Classical and Quantum*, edited by P. Cvitanović, R. Artuso, R. Mainieri, G. Tanner, and G. Vattay (Niels Bohr Inst., Copenhagen, 2023).
- [42] P. Cvitanović, R. Artuso, R. Mainieri, G. Tanner, and G. Vattay, *Chaos: Classical and Quantum* (Niels Bohr Inst., Copenhagen, 2024).
- [43] P. Cvitanović, R. Artuso, R. Mainieri, G. Tanner, and G. Vattay, *Chaos: Classical and Quantum* (Niels Bohr Inst., Copenhagen, 2024).
- [44] P. Cvitanović, R. Artuso, L. Rondoni, and E. A. Spiegel, “Transporting densities”, in *Chaos: Classical and Quantum*, edited by P. Cvitanović, R. Artuso, R. Mainieri, G. Tanner, and G. Vattay (Niels Bohr Inst., Copenhagen, 2023).
- [45] P. Cvitanović, C. P. Dettmann, R. Mainieri, and G. Vattay, “Trace formulas for stochastic evolution operators: Weak noise perturbation theory”, *J. Stat. Phys.* **93**, 981–999 (1998).

- [46] P. Cvitanović, C. P. Dettmann, R. Mainieri, and G. Vattay, “Trace formulae for stochastic evolution operators: Smooth conjugation method”, *Nonlinearity* **12**, 939 (1999).
- [47] P. Cvitanović and H. Liang, *A chaotic lattice field theory in two dimensions*, In preparation, 2024.
- [48] P. Cvitanović and A. Pikovsky, “Cycle expansion for power spectrum”, *Proc. SPIE* **2038**, 290–298 (1993).
- [49] P. H. Damgaard, H. Hüffel, and A. Rosenblum, eds., *Probabilistic Methods in Quantum Field Theory and Quantum Gravity* (Springer, New York, 1990).
- [50] G. De Palma and L. Hackl, “Linear growth of the entanglement entropy for quadratic Hamiltonians and arbitrary initial states”, *SciPost Physics* **12**, 021 (2022).
- [51] R. L. Devaney and Z. Nitecki, “Shift automorphisms in the Hénon mapping”, *Commun. Math. Phys.* **67**, 137–146 (1979).
- [52] D. Dudgeon and R. M. Mersereau, *Multidimensional Digital Signal Processing* (Prentice-Hall, Englewood Cliffs, NJ, 1984).
- [53] H. R. Dullin and J. D. Meiss, “Generalized Hénon maps: the cubic diffeomorphisms of the plane”, *Physica D* **143**, 262–289 (2000).
- [54] H. R. Dullin and J. D. Meiss, “Quadratic volume-preserving maps: Invariant circles and bifurcations”, *SIAM J. Appl. Dyn. Sys.* **8**, 76–128 (2008).
- [55] S. Elaydi, *An Introduction to Difference Equations*, 3rd ed. (Springer, Berlin, 2005).
- [56] K. R. Elder, H. Xi, M. Deans, and J. D. Gunton, “Spatiotemporal chaos in the damped Kuramoto-Sivashinsky equation”, *AIP Conf. Proc.* **342**, 702–708 (1995).
- [57] A. Endler and J. A. C. Gallas, “Conjugacy classes and chiral doublets in the Hénon Hamiltonian repeller”, *Phys. Lett. A* **356**, 1–7 (2006).
- [58] A. Endler and J. A. C. Gallas, “Reductions and simplifications of orbital sums in a Hamiltonian repeller”, *Phys. Lett. A* **352**, 124–128 (2006).
- [59] M. J. Feigenbaum and B. Hasslacher, “Irrational decimations and path-integrals for external noise”, *Phys. Rev. Lett.* **49**, 605–609 (1982).
- [60] V. Fock, “Die Eigenzeit in der klassischen und in der Quantenmechanik”, *Physik. Z* **12**, Transl. Proper time in classical and quantum mechanics, 404–425 (1937).
- [61] J. Franklin, *Classical Field Theory* (Cambridge Univ. Press, 2017).
- [62] S. Friedland and J. Milnor, “Dynamical properties of plane polynomial automorphisms”, *Ergodic Theory Dynam. Systems* **9**, 67–99 (1989).
- [63] I. García-Mata and M. Saraceno, “Spectral properties and classical decays in quantum open systems”, *Phys. Rev. E* **69**, 056211 (2004).

- [64] F. Gelis and N. Tanji, “Schwinger mechanism revisited”, *Prog. Part. Nucl. Phys.* **87**, 1–49 (2016).
- [65] C. Godsil and G. F. Royle, *Algebraic Graph Theory* (Springer, New York, 2013).
- [66] S. V. Gonchenko, J. D. Meiss, and I. I. Ovsyannikov, *Regul. Chaotic Dyn.* **11**, 191–212 (2006).
- [67] V. S. Gonchenko, Y. A. Kuznetsov, and H. G. E. Meijer, “Generalized Hénon map and bifurcations of homoclinic tangencies”, *SIAM J. Appl. Dyn. Syst.* **4**, 407–436 (2005).
- [68] D. J. Gross and V. Rosenhaus, “Chaotic scattering of highly excited strings”, *J. High Energy Phys.* **2021**, 048 (2021).
- [69] S. Grossmann and S. Thomae, “Invariant distributions and stationary correlation functions of one-dimensional discrete processes”, *Z. Naturf. A* **32**, 1353–1363 (1977).
- [70] V. Gurarie and A. Migdal, “Instantons in the Burgers equation”, *Phys. Rev. E* **54**, 4908–4914 (1996).
- [71] B. Gutkin, L. Han, R. Jafari, A. K. Saremi, and P. Cvitanović, “Linear encoding of the spatiotemporal cat map”, *Nonlinearity* **34**, 2800–2836 (2021).
- [72] B. Gutkin and V. Osipov, “Classical foundations of many-particle quantum chaos”, *Nonlinearity* **29**, 325–356 (2016).
- [73] C. Hadfield, S. Kandel, and M. Schiavina, “Ruelle zeta function from field theory”, *Ann. Inst. H. Poincaré* **21**, 3835–3867 (2020).
- [74] J. F. Heagy, “A physical interpretation of the Hénon map”, *Physica D* **57**, 436–446 (1992).
- [75] M. Hénon, “A two-dimensional mapping with a strange attractor”, *Commun. Math. Phys.* **50**, 94–102 (1976).
- [76] G. W. Hill, “On the part of the motion of the lunar perigee which is a function of the mean motions of the sun and moon”, *Acta Math.* **8**, 1–36 (1886).
- [77] W. G. Hoover and K. Aoki, “Order and chaos in the one-dimensional  $\phi^4$  model : N-dependence and the Second Law of Thermodynamics”, *Commun. Nonlinear Sci. Numer. Simul.* **49**, 192–201 (2017).
- [78] X.-Y. Hu and V. Rosenhaus, Correlation functions in linear chaotic maps, 2022.
- [79] S. Isola, “ $\zeta$ -functions and distribution of periodic orbits of toral automorphisms”, *Europhys. Lett.* **11**, 517–522 (1990).
- [80] E. V. Ivashkevich, N. S. Izmailian, and C.-K. Hu, “Kronecker’s double series and exact asymptotic expansions for free models of statistical mechanics on torus”, *J. Phys. A* **35**, 5543–5561 (2002).

- [81] N. S. Izmailian, K. B. Oganesyan, and C.-K. Hu, “Exact finite-size corrections for the square-lattice Ising model with Brascamp-Kunz boundary conditions”, *Phys. Rev. E* **65**, 056132 (2002).
- [82] K. Jansen, “Lattice field theory”, *Int. J. Mod. Phys. E* **16**, 2638–2679 (2007).
- [83] P. H. van der Kamp, “Initial value problems for lattice equations”, *J. Phys. A* **42**, 404019 (2009).
- [84] N. G. van Kampen, *Stochastic Processes in Physics and Chemistry*, 3rd ed. (Elsevier, Amsterdam, 2007).
- [85] G. Kane, *Modern Elementary Particle Physics* (Addison-Wesley, Redwood City, 1987).
- [86] V. Karimipour and M. H. Zarei, “Completeness of classical  $\phi^4$  theory on two-dimensional lattices”, *Phys. Rev. A* **85**, 032316 (2012).
- [87] E. D. Keller, *Ruelle-Pollicott Resonances of the Perturbed Cat Map*, PhD thesis (2007).
- [88] O. Knill and F. Tangerman, “Self-similarity and growth in Birkhoff sums for the golden rotation”, *Nonlinearity* **24**, 3115–3127 (2011).
- [89] S. Lang, *Linear Algebra* (Addison-Wesley, Reading, MA, 1987).
- [90] A. Lasota and M. MacKey, *Chaos, Fractals, and Noise; Stochastic Aspects of Dynamics* (Springer, New York, 1994).
- [91] S. Levit and U. Smilansky, “The Hamiltonian path integrals and the uniform semiclassical approximations for the propagator”, *Ann. Phys.* **108**, 165–197 (1977).
- [92] M.-C. Li and M. Malkin, “Bounded nonwandering sets for polynomial mappings”, *J. Dynam. Control Systems* **10**, 377–389 (2004).
- [93] H. Liang and P. Cvitanović, “A chaotic lattice field theory in one dimension”, *J. Phys. A* **55**, 304002 (2022).
- [94] T. M. Liaw, M. C. Huang, Y. L. Chou, S. C. Lin, and F. Y. Li, “Partition functions and finite-size scalings of Ising model on helical tori”, *Phys. Rev. E* **73**, 041118 (2006).
- [95] D. A. Lind, “A zeta function for  $Z^d$ -actions”, in *Ergodic Theory of  $Z^d$  Actions*, edited by M. Pollicott and K. Schmidt (Cambridge Univ. Press, 1996), pp. 433–450.
- [96] M. Loebl and P. Somberg, “Discrete Dirac operators, critical embeddings and Ihara-Selberg functions”, *Electron. J. Combin.* **22**, P1–10 (2015).
- [97] H. E. Lomelí and J. D. Meiss, “Quadratic volume-preserving maps”, *Nonlinearity* **11**, 557–574 (1998).
- [98] M. Lüscher and P. Weisz, “Scaling laws and triviality bounds in the lattice  $\phi^4$  theory (I). One-component model in the symmetric phase”, *Nucl. Phys. B* **290**, 25–60 (1987).

- [99] M. Lüscher and P. Weisz, “Scaling laws and triviality bounds in the lattice  $\phi^4$  theory (II). One-component model in the phase with spontaneous symmetry breaking”, *Nucl. Phys. B* **295**, 65–92 (1988).
- [100] M. Lüscher and P. Weisz, “Scaling laws and triviality bounds in the lattice  $\phi^4$  theory (III). n-component model”, *Nucl. Phys. B* **318**, 705–741 (1989).
- [101] R. S. MacKay and J. D. Meiss, “Linear stability of periodic orbits in Lagrangian systems”, *Phys. Lett. A* **98**, 92–94 (1983).
- [102] A. Maloney and E. Witten, “Quantum gravity partition functions in three dimensions”, *J. High Energy Phys.* **2010**, 029 (2010).
- [103] P. C. Martin, E. D. Siggia, and H. A. Rose, “Statistical dynamics of classical systems”, *Phys. Rev. A* **8**, 423–437 (1973).
- [104] H. B. Meyer, “Lattice QCD: A brief introduction”, in *Lattice QCD for Nuclear Physics*, edited by H.-W. Lin and H. B. Meyer (Springer, York New, 2015), pp. 1–34.
- [105] I. Montvay and G. Münster, *Quantum Fields on a Lattice* (Cambridge Univ. Press, Cambridge, 1994).
- [106] G. Münster, “Lattice quantum field theory”, *Scholarpedia* **5**, 8613 (2010).
- [107] G. Münster and M. Walzl, *Lattice gauge theory - A short primer*, 2000.
- [108] S. Nonnenmacher, “Spectral properties of noisy classical and quantum propagators”, *Nonlinearity* **16**, 1685–1713 (2003).
- [109] Y. Okabe, K. Kaneda, M. Kikuchi, and C.-K. Hu, “Universal finite-size scaling functions for critical systems with tilted boundary conditions”, *Phys. Rev. E* **59**, 1585–1588 (1999).
- [110] V. G. Papageorgiou, F. W. Nijhoff, and H. W. Capel, “Integrable mappings and nonlinear integrable lattice equations”, *Phys. Lett. A* **147**, 106–114 (1990).
- [111] G. Parisi and Y. S. Wu, “Perturbation-theory without gauge fixing”, *Scientia Sinica* **24**, 483–496 (1981).
- [112] M. Pollicott, “On the rate of mixing of Axiom A flows”, *Inv. Math.* **81**, 413–426 (1985).
- [113] M. Pollicott, “Meromorphic extensions of generalised zeta functions”, *Inv. Math.* **85**, 147–164 (1986).
- [114] G. R. W. Quispel, H. W. Capel, V. G. Papageorgiou, and F. W. Nijhoff, “Integrable mappings derived from soliton equations”, *Physica A* **173**, 243–266 (1991).
- [115] P. Ramond, *Field Theory* (Routledge, 1981).
- [116] P. H. Rojas O. van der Kamp and G. R. W. Quispel, *Lax representations for integrable maps  $O\Delta E$ s*, 2007.

- [117] V. Rosenhaus, “Chaos in the quantum field theory S-matrix”, *Phys. Rev. Lett.* **127**, 021601 (2021).
- [118] V. Rosenhaus, “Chaos in a many-string scattering amplitude”, *Phys. Rev. Lett.* **129**, 031601 (2022).
- [119] V. Rosenhaus and M. Smolkin, *Feynman rules for wave turbulence*, 2022.
- [120] O. E. Rössler, “An equation for continuous chaos”, *Phys. Lett. A* **57**, 397–398 (1976).
- [121] H. J. Rothe, *Lattice Gauge Theories - An Introduction* (World Scientific, Singapore, 2005).
- [122] D. Ruelle, “Locating resonances for Axiom A dynamical systems”, *J. Stat. Phys.* **44**, 281–292 (1986).
- [123] D. Ruelle, “Resonances of chaotic dynamical systems”, *Phys. Rev. Lett.* **56**, 405–407 (1986).
- [124] D. Ruelle, *Thermodynamic Formalism: The Mathematical Structure of Equilibrium Statistical Mechanics*, 2nd ed. (Cambridge Univ. Press, Cambridge, 2004).
- [125] K. L. Schlueter-Kuck and J. O. Dabiri, “Coherent structure colouring: identification of coherent structures from sparse data using graph theory”, *J. Fluid Mech.* **811**, 468–486 (2016).
- [126] K. L. Schlueter-Kuck and J. O. Dabiri, “Identification of individual coherent sets associated with flow trajectories using coherent structure coloring”, *Chaos* **27**, 091101 (2017).
- [127] C. Schubert, “Lectures on the Worldline Formalism”, in *School of Spinning Particles in Quantum Field Theory: Worldline Formalism, Higher Spins and Conformal Geometry*, edited by C. Schubert (Universidad Michoacana San Nicholas de Hidalgo, 2012).
- [128] C. L. Siegel and K. Chandrasekharan, *Lectures on the Geometry of Numbers* (Springer Berlin Heidelberg, Berlin, Heidelberg, 1989).
- [129] B. Simon, “Almost periodic Schrödinger operators: A review”, *Adv. Appl. Math.* **3**, 463–490 (1982).
- [130] B. Simon and R. B. Griffiths, “The  $\phi^4$  field theory as a classical Ising model”, *Commun. Math. Phys.* **33**, 145–164 (1973).
- [131] Y. G. Sinai, “Gibbs measures in ergodic theory”, *Russian Math. Surveys* **27**, 21 (1972).
- [132] S. Smale, “Differentiable dynamical systems”, *Bull. Amer. Math. Soc.* **73**, 747–817 (1967).
- [133] J. Smit, *Introduction to Quantum Fields on a Lattice* (Cambridge Univ. Press, Cambridge, 2002).
- [134] R. Sommer, *Introduction to Lattice Gauge Theories*, tech. rep. (Humboldt Univ., 2015).



- [135] D. E. Soper, *Classical Field Theory* (Dover, 1976).
- [136] D. Sterling and J. D. Meiss, “Computing periodic orbits using the anti-integrable limit”, *Phys. Lett. A* **241**, 46–52 (1998).
- [137] D. G. Sterling, H. R. Dullin, and J. D. Meiss, “Homoclinic bifurcations for the Hénon map”, *Physica D* **134**, 153–184 (1999).
- [138] I. Vierhaus, Simulation of  $\phi^4$  Theory in the Strong Coupling Expansion beyond the Ising Limit, MA thesis (Humboldt-Univ. Berlin, Math.-Naturwissen. Fakultät I, 2010).
- [139] U.-J. Wiese, *An Introduction to Lattice Field Theory*, tech. rep. (Univ. Bern, 2009).
- [140] Wikipedia contributors, *Cubic function — Wikipedia, The Free Encyclopedia*, 2022.
- [141] S. V. Williams, X. Wang, H. Liang, and P. Cvitanović, *Nonlinear chaotic lattice field theory*, In preparation, 2024.
- [142] U. Wolff, “Triviality of four dimensional  $\phi^4$  theory on the lattice”, *Scholarpedia* **9**, 7367 (2014).
- [143] S. Wolfram, *A Project to Find the Fundamental Theory of Physics* (Wolfram Media Inc., 2020).
- [144] H. W. Wyld, “Formulation of the theory of turbulence in an incompressible fluid”, *Ann. Phys.* **14**, 143–165 (1961).
- [145] X. Zhang, “Hyperbolic invariant sets of the real generalized Hénon maps”, *Chaos Solit. Fract.* **43**, 31–41 (2010).
- [146] J. Zinn-Justin, *Quantum Field Theory and Critical Phenomena* (Oxford Univ. Press, Oxford, 1989).



# Chapter 5

## Computing periodic states

The latest blog post at the bottom for this chapter, page 271

Unlike the temporal Bernoulli and the temporal cat, for which the periodic state fixed point condition is linear and easily solved, for nonlinear lattice field theories the periodic states are roots of polynomials of arbitrarily high order. While Gallas and collaborators [3, 16–20, 24–26, 47] have developed a powerful theory that yields Hénon map periodic orbits in analytic form, it would be unrealistic to demand such explicit solutions for general field theories on multi-dimensional lattices. We take a pragmatic, numerical route, and search for the fixed-point solutions starting with the deviation of an approximate trajectory from the 3-term recurrence (4.144) -in  $d$  spatiotemporal dimensions  $(2d + 1)$ -term recurrence- given by the lattice deviation vector

$$v_t = -\square \phi_t + V'(\phi_t) - j_t, \quad (5.1)$$

and minimizing this error term by any convenient variational or optimization method, perhaps in conjunction with a high-dimensional variant of the Newton method [10, 31, 36].

### 5.1 Inverse iteration method

(Gábor Vattay, Sidney V. Williams and P. Cvitanović)

The ‘inverse iteration method’ for determining the periodic orbits of 2-dimensional repeller was introduced by G. Vattay as a ChaosBook.org exercise 5.1 *Inverse iteration method for a Hénon repeller*. (See also the solution on page 271.) The idea of the method is to


- (1) Guess a lattice configuration  $\phi_t^{(0)}$  that qualitatively looks like the desired periodic state. For that, you need a qualitative, symbolic dynamics description of system’s admissible periodic states. You can get started by a peak at ChaosBook Table 18.1.

↓PRIVATE

↑PRIVATE

- (2) Compare the ‘stretched’ field  $\phi_t^{(0)}$  to its neighbors, using system’s defining equation. For example,  $\phi^3$  (or temporal Hénon) Euler–Lagrange equation (4.150) is

$$-\phi_{t+1} - \left( \mu^2 \phi_t^2 - 2\phi_t + \frac{\mu^2}{4} \right) - \phi_{t-1} = 0.$$


Perhaps watch  *What’s “The Law”?* (4 min).

- (3) Use the amount by which  $\phi_t$  ‘sticks out’ in violation of the defining equations to obtain a better value  $\phi_t^{(1)}$ , for every lattice site  $t$ . Vattay does that by inverting the equation, determining  $\phi_t^{(1)}$  from its neighbors

$$\phi_t^{(m+1)} = \sigma_t \frac{1}{\sqrt{a}} \left( 1 + \phi_{t+1}^{(m)} + \phi_{t-1}^{(m)} \right)^{1/2} \quad (5.2)$$

where  $\sigma_t$  is the sign of the target site field  $\sigma_t = \phi_t/|\phi_t|$ , prescribed in advance by specifying the desired Hénon symbol block

$$\sigma_t = 1 - 2m_t, \quad m_t \in \{0, 1\}. \quad (5.3)$$

Perhaps watch  *Inverse iteration method* (14:28 min).

- (4) Wash and repeat,  $\phi_t^{(m)} \rightarrow \phi_t^{(m+1)}$ . Sidney starts the iteration by setting the initial guess lattice site fields to

$$\phi_t^{(0)} = \sigma_t / \sqrt{a},$$

and then loops (5.2) through all lattice site fields to obtain  $\phi_t^{(1)}$ . When  $|\phi_t^{(m+1)} - \phi_t^{(1)}|$  for all periodic states is smaller than a desired tolerance, the loop terminates, and the periodic state is found. An example of the resulting periodic states is given in figure ??.

The meat of the method is contained in these two loops:

```
for i in range(0, len(symbols)):
    cycle[i]=signs[i]*np.sqrt(abs(1-np.roll(cycle,1)[i]-np.roll(cycle,-1)[i])/a)
for i in range(0, len(symbols)):
    deviation[i]=np.roll(cycle,-1)[i]-(1-a*(cycle[i])**2-np.roll(cycle,1)[i])
```

The method applies to strongly coupled  $\phi^3$  field theory in any spatiotemporal dimension. For example, in 2 spacetime dimensions, the  $m$ th inverse iterate (5.2) compares the ‘stretched’ field  $\phi_{nt}^{(0)}$  to its 4 neighbors,

$$\phi_{nt}^{(m+1)} = \sigma_{nt} \frac{1}{\sqrt{2a}} \left( 2 + \phi_{n,t+1}^{(m)} + \phi_{n,t-1}^{(m)} + \phi_{n+1,t}^{(m)} + \phi_{n-1,t}^{(m)} \right)^{1/2}. \quad (5.4)$$

It is applied to each of the  $LT$  lattice site fields  $\{\phi_{nt}^{(m)}\}$  of a doubly periodic primitive cell  $[L \times T]_S$ . Here  $\sigma_{nt}$  is the sign of the target site field  $\sigma_{nt} = \phi_{nt}/|\phi_{nt}|$ , prescribed in advance by specifying the desired Hénon symbol block  $M$ ,

$$\sigma_{nt} = 1 - 2m_{nt}, \quad m_{nt} \in \{0, 1\}. \quad (5.5)$$

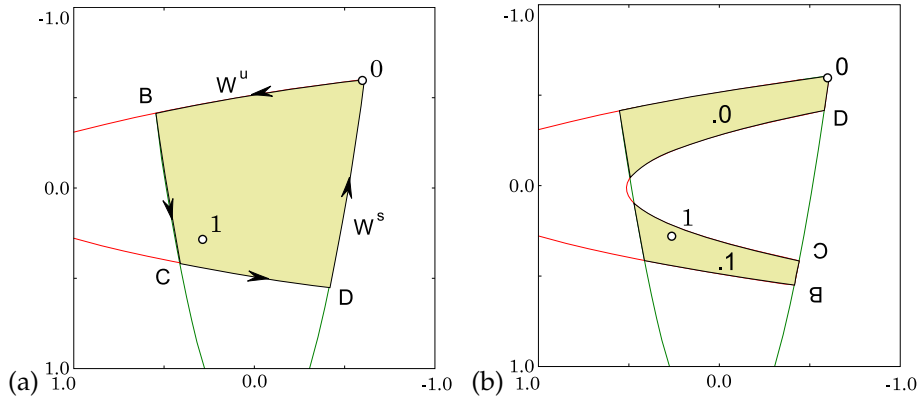


Figure 5.1: Temporal Hénon (4.186), (4.187) stable-unstable manifolds Smale horseshoe partition in the  $(\phi_t, \phi_{t+1})$  plane for  $a = 6, b = -1$ : fixed point  $\bar{0}$  with segments of its stable, unstable manifolds  $W^s, W^u$ , and fixed point  $\bar{1}$ . The most positive field value is the fixed point  $\phi_0$ . The other fixed point  $\phi_1$  has negative stability multipliers, and is thus buried inside the horseshoe. (a) Their intersection bounds the region  $\mathcal{M} = OBCD$  which contains the non-wandering set  $\Omega$ . (b) The intersection of the forward image  $f(\mathcal{M})$  with  $\mathcal{M}$  consists of two (future) strips  $\mathcal{M}_0, \mathcal{M}_1$ , with points  $BCD$  brought closer to fixed point  $\bar{0}$  by the stable manifold contraction. (The same as [ChaosBook fig. 15.5](#), with  $\phi_t = -x_t$ .)

For the *temporal Hénon* 3-term recurrence (4.187), the system's state space Smale horseshoe is again generated by iterates of the region plotted in figure 5.1. So, positive field  $\phi_{nt}$  value has  $m_{nt} = 0$ , negative field  $\phi_{nt}$  value has  $m_{nt} = 1$ .

## 5.2 Shadow state, temporal Hénon

1

*Have:* a partition of state space  $\mathcal{M} = \mathcal{M}_A \cup \mathcal{M}_B \cup \dots \cup \mathcal{M}_Z$ , with regions  $\mathcal{M}_m$  labelled by an  $|\mathcal{A}|$ -letter finite alphabet  $\mathcal{A} = \{m\}$ . The simplest example is temporal Hénon partition into two regions, labelled '0' and '1',

$$m_t \in \mathcal{A} = \{0, 1\}, \quad (5.6)$$

plotted in figure 5.1 (b). Prescribe a symbol block  $M$  over a finite primitive cell of a  $d$ -dimensional lattice. A 1-dimensional example:

$$M = (m_0, \dots, m_{n-1}). \quad (5.7)$$

*Want:* the periodic state  $\Phi_M$  whose lattice site fields  $\phi_t$  lie in state space domains  $\phi_t \in \mathcal{M}_m$ , as prescribed by the given symbol block  $M$ . A 1-dimensional

<sup>1</sup>Predrag 2022-02-24: The initial version, parametrized by Hénon map parameter  $a$ . Superseded by sect. 5.3. To be made into an appendix.

example:

$$\Phi_M = (\phi_0, \dots, \phi_{n-1}), \quad \phi_t \in \mathcal{M}_m, \quad (5.8)$$

By *periodic state*  $\Phi$  we mean a point in the  $n$ -dimensional state space that is a solution of the defining Euler–Lagrange equation. For the temporal Hénon example, that equation is the 3-term recurrence (4.187),

$$-\phi_{t+1} + a\phi_t^2 - \phi_{t-1} = j_t, \quad j_t = 1, \quad (5.9)$$

with all  $a = 6$  period-5 periodic states plotted in figure ??.

**Shadow state method.** Periodic states are the skeleton for dynamics in the uniformly invariant subset, thus it is necessary that we have a systematic algorithm to find periodic states numerically. One of the most powerful method among such is shadow state method, which involves constructing a shadow state based on symbolic dynamics as the initial guess and the minimize the deviation function.

Construct a *shadow state*  $\bar{\Phi}_M$  and the *forcing*  $j(M)_t$  such that the site-by-site deviation

$$\varphi_t = \phi_t - \bar{\phi}_t \quad (5.10)$$

is small. Determine the desired periodic state  $\Phi_M$  as the neighboring  $|\Phi_M - \bar{\Phi}_M|$  fixed point of the  $M$ -forced Euler–Lagrange equation.

*Desideratum:* Plot the first,  $n = 6$  temporal Hénon asymmetric periodic state  $\Phi_M$  and shadow state  $\bar{\Phi}_M$ , to illustrated the idea.

First, determine the fixed points (solutions with a constant field on all lattice sites)  $\phi_t = \bar{\phi}_m$ . For temporal Hénon there are two,  $\bar{\phi}_0$  and  $\bar{\phi}_1$  (see figure 5.1), labeled by the alphabet (5.6).

Next, construct the simplest configuration from  $|\mathcal{A}|$  fields  $\bar{\phi}_m$ , each field in the domain of state space prescribed by the symbol block  $M$ . In the shadow state method, we pick a fixed point  $\bar{\phi}_m$  in each domain as domain's representative  $\bar{\phi}_m \in \mathcal{M}_m$ . For the temporal Hénon example, the fixed-points *shadow state* is:

$$\bar{\Phi}_M = (\bar{\phi}_0, \dots, \bar{\phi}_{n-1}), \quad \text{where } \bar{\phi}_t = \begin{cases} \bar{\phi}_0 & \text{if } m_t = 0 \\ \bar{\phi}_1 & \text{if } m_t = 1 \end{cases}. \quad (5.11)$$

In general, the shadow state  $\bar{\Phi}_M$  does not satisfy the Euler–Lagrange equation (5.9), violating it by amount  $\bar{j}(M)_t$

$$-\bar{\phi}_{t+1} + a\bar{\phi}_t^2 - \bar{\phi}_{t-1} = 1 - \bar{j}(M)_t, \quad (5.12)$$

where the forcing  $\bar{j}(M)_t$  depends on  $\bar{\phi}_t$  and its neighbors. For the temporal Hénon example, it takes the values tabulated in table 5.2.

Subtract (5.21) from (5.9) to obtain the 3-term recurrence for  $\varphi_t = \phi_t - \bar{\phi}_t$ , the deviations (5.19) from the shadow state,

$$-\varphi_{t+1} + a(\phi_t^2 - \bar{\phi}_t^2) - \varphi_{t-1} = \bar{j}(M)_t.$$

Substituting  $\phi_t^2 = (\varphi_t + \bar{\phi}_t)^2$  and  $j(M)_t = \bar{j}(M)_t - a\bar{\phi}_t^2$ , we obtain

$m_{t-1}m_t m_{t+1}$	$\bar{j}(M)_t$
0 0 0	0
0 0 1 = 1 0 0	-A = $\bar{\phi}_1 - \bar{\phi}_0$
0 1 0	-B = $a(\bar{\phi}_1^2 - \bar{\phi}_0^2)$
1 0 1	B = $a(\bar{\phi}_0^2 - \bar{\phi}_1^2)$
1 1 0 = 0 1 1	A = $\bar{\phi}_0 - \bar{\phi}_1$
1 1 1	0

Table 5.1: Temporal Hénon fixed-points shadow state  $\bar{\Phi}_M$  forcing  $\bar{j}(M)_t$  depends on the  $t$  lattice site and its two neighbors  $m_{t-1}m_t m_{t+1}$ . It takes values  $(0, \pm A, \pm B)$ . If period-2 or longer periodic states are utilized as shadows, more neighbors contribute.

### M-forced Euler–Lagrange equation

for the deviation  $\varphi_M$  from the shadow lattice state configuration  $\bar{\Phi}_M$ :


$$-\varphi_{t+1} + a(\varphi_t + \bar{\phi}_t)^2 - \varphi_{t-1} = j(M)_t. \quad (5.13)$$

<sup>2</sup> This is to be solved by whatever code you find optimal. For example:

**Vattay inverse iteration** (5.2) is now

$$\varphi_t^{(m+1)} = -\bar{\phi}_t + \sigma_t \frac{1}{\sqrt{a}} \left( j(M)_t + \varphi_{t+1}^{(m)} + \varphi_{t-1}^{(m)} \right)^{1/2}, \quad (5.14)$$

and that should converge like a ton of rocks.

Perhaps watch  *Shadow state conspiracy* (35:26 min)

### Overview

1. The M-forced Euler–Lagrange equation is *exact*, the only difference from the starting Euler–Lagrange equation (5.9) is that lattice fields  $\phi_t$  have been translated by constant amounts (5.19) in order to center it on the M-th saddlepoint ‘landscape’. There is one such M-forced Euler–Lagrange equation for each admissible symbol block M.
2. M-forced 3-term recurrence (5.22) is *exact*. It is superior to the original recurrence as it has built-in symbolic dynamics. The deviations  $\varphi_t = \phi_t - \bar{\phi}_t$  should be small, and the topological guess based on M-forcing should be robust. The recurrence can be solved by any method you like.

<sup>2</sup>Predrag 2022-02-22: Clearly I have to recompute the violation table table 5.2, but that’s for another day.

3.  $\phi^4$  field theory works the same, with the M-forced 3-term recurrence for the deviations  $\varphi_t$  now built from approximate 3-field values  $(\bar{\phi}_L, \bar{\phi}_C = 0, \bar{\phi}_R)$ . If using Vattay (5.23), the Hénon sign  $\sigma_t$  needs to be rethought.
4. Implement M-forced 3-term recurrence for symmetric states boundary conditions.
5. Generalization to higher spatiotemporal dimensions is immediate (see, for example, the 2-dimensional Vattay iteration (5.4)).
6. As one determines larger and larger primitive cell periodic states, one can use the already computed ones instead of the initial  $(\bar{\phi}_0, \bar{\phi}_1)$  to get increasingly better M-forced shadowing.
7. The boring forcing term  $j_t = 1$  on RHS of the temporal Hénon recurrence (5.9) has been replaced by a non-trivial forcing  $j(M)_t$  in (5.22), as hoped for.
8. This is not the Biham-Wentzel method: it's based on exact Euler–Lagrange equations, there are no artificially inverted potentials, as we are not constructing an attractor; all our solutions are and should be unstable.
9. The Newton method requires evaluation of the orbit Jacobian matrix  $\mathcal{J}$ . As we have only *translated* field values  $\phi_t \rightarrow \varphi_t$ ,  $\mathcal{J}$  is the same as for the original 3-term recurrence. For large periodic states variational methods discussed below should be far superior to simple Newton.
10. Have a look at Fourier transform of (5.22). Anything gained in Fourier space? Remember, we have not quotiented translation symmetry, we are still computing  $n$  periodic states on the spatiotemporal lattice.
11. Shadowing method was first formulated by Kai Hansen [33] in *Alternative method to find orbits in chaotic systems* (1995).

### 5.3 Shadow state, $\phi^3$

3 4

*Have:* a partition of state space  $\mathcal{M} = \mathcal{M}_A \cup \mathcal{M}_B \cup \dots \cup \mathcal{M}_Z$ , with regions  $\mathcal{M}_m$  labelled by an  $|\mathcal{A}|$ -letter finite alphabet  $\mathcal{A} = \{m\}$ . The simplest example is temporal  $\phi^3$  theory (which can be easily mapped into temporal Hénon via [put equation here](#)) which partitions its domain into two regions, labelled '0' and '1',

$$m_t \in \mathcal{A} = \{0, 1\}, \tag{5.15}$$

<sup>3</sup>Predrag 2022-02-24: The rewrite of sect. 5.2, now parametrized by  $\phi^3$  parameter  $\mu^2$ .

<sup>4</sup>Sidney 2024-02-15: Sidney rewrite for the current definition of  $\phi^3$ , to replace siminos/tigers/state.tex when finalized here.



plotted in figure 5.1 (b). We can prescribe a symbol block  $M$  over a finite primitive cell of a  $d$ -dimensional lattice. A 1-dimensional example is:

$$M = (m_0, \dots, m_{n-1}). \quad (5.16)$$

*Want:* the periodic state  $\Phi_M$  whose lattice site fields  $\phi_t$  lie in state space domains  $\phi_t \in \mathcal{M}_m$ , as prescribed by the given symbol block  $M$ . The one-dimensional temporal lattice case:

$$\Phi_M = (\phi_0, \dots, \phi_{n-1}), \quad \phi_t \in \mathcal{M}_m, \quad (5.17)$$

By *periodic state*  $\Phi$  we mean a point in the  $n$ -dimensional state space that is a solution of the defining Euler–Lagrange equation. For the  $\phi^3$  example example, that equation is the 3-term recurrence (4.187),

$$-\phi_{t+1} + 2\phi_t - \phi_{t-1} + \mu^2 \left( -\phi_t^2 + \frac{1}{4} \right) = j_t, \quad j_t = 0, \quad (5.18)$$

with all  $a = 6$  period-5 periodic states plotted in figure ?? (needs to be changed to  $\phi^3$ ).

**Shadow state method.** Construct a *shadow state*  $\bar{\Phi}_M$  and the *forcing*  $j(M)_t$  such that the site-by-site deviation

$$\varphi_t = \phi_t - \bar{\phi}_t \quad (5.19)$$

is small. Determine the desired periodic state  $\Phi_M$  as the neighboring  $|\Phi_M - \bar{\Phi}_M|$  fixed point of the  $M$ -forced Euler–Lagrange equation.

*Desideratum:* Plot the first,  $n = 6$  temporal Hénon asymmetric periodic state  $\Phi_M$  and shadow state  $\bar{\Phi}_M$ , to illustrated the idea.

First, determine the fixed points (solutions with a constant field on all lattice sites)  $\phi_t = \bar{\phi}_m$ . For temporal  $\phi^3$  there are two,  $\bar{\phi}_0$  and  $\bar{\phi}_1$  (see figure 5.1), labeled by the alphabet (5.6).

Next, construct the simplest configuration from  $|\mathcal{A}|$  fields  $\bar{\phi}_m$ , each field in the domain of state space prescribed by the symbol block  $M$ . In the shadow state method, we pick a fixed point  $\bar{\phi}_m$  in each domain as domain's representative  $\bar{\phi}_m \in \mathcal{M}_m$ . For the temporal  $\phi^3$  example, the fixed-points *shadow state* is:

$$\bar{\Phi}_M = (\bar{\phi}_0, \dots, \bar{\phi}_{n-1}), \quad \text{where } \bar{\phi}_t = \begin{cases} \bar{\phi}_0 & \text{if } m_t = 0 \\ \bar{\phi}_1 & \text{if } m_t = 1 \end{cases}. \quad (5.20)$$

In general, the shadow state  $\bar{\Phi}_M$  does not satisfy the Euler–Lagrange equation (5.9), violating it by amount  $\bar{j}(M)_t$

$$-\phi_{t+1} + 2\phi_t - \phi_{t-1} + \mu^2 \left( -\phi_t^2 + \frac{1}{4} \right) = -\bar{j}(M)_t, \quad (5.21)$$

$m_{t-1}m_t m_{t+1}$	$\bar{j}(M)_t$
0 0 0	0
0 0 1 = 1 0 0	-A = $\bar{\phi}_1 - \bar{\phi}_0$
0 1 0	-B = $2(\bar{\phi}_0 - \bar{\phi}_1) + \mu^2(\bar{\phi}_1^2 - \bar{\phi}_0^2)$
1 0 1	B = $2(\bar{\phi}_1 - \bar{\phi}_0) + \mu^2(\bar{\phi}_0^2 - \bar{\phi}_1^2)$
1 1 0 = 0 1 1	A = $\bar{\phi}_0 - \bar{\phi}_1$
1 1 1	0

Table 5.2: Temporal  $\phi^3$  fixed-points shadow state  $\bar{\Phi}_M$  forcing  $\bar{j}(M)_t$  depends on the  $t$  lattice site and its two neighbors  $m_{t-1}m_t m_{t+1}$ . It takes values  $(0, \pm A, \pm B)$ . If period-2 or longer periodic states are utilized as shadows, more neighbors contribute.

where the forcing  $\bar{j}(M)_t$  depends on  $\bar{\phi}_t$  and its neighbors. For the temporal  $\phi^3$  example, it takes the values tabulated in table 5.2.

Subtract (5.21) from (5.9) to obtain the 3-term recurrence for  $\varphi_t = \phi_t - \bar{\phi}_t$ , the deviations (5.19) from the shadow state,

$$-\varphi_{t+1} + 2\varphi_t - \varphi_{t-1} + \mu^2(-\phi_t^2 + \bar{\phi}_t^2) = \bar{j}(M)_t.$$

Substituting  $\phi_t^2 = (\varphi_t + \bar{\phi}_t)^2$  and  $j(M)_t = \bar{j}(M)_t + a\bar{\phi}_t^2$ , we obtain

### M-forced Euler–Lagrange equation

for the deviation  $\varphi_M$  from the shadow lattice state configuration  $\bar{\Phi}_M$ :


$$-\varphi_{t+1} + 2\varphi_t - \varphi_{t-1} - \mu^2(\varphi_t + \bar{\phi}_t)^2 = j(M)_t. \quad (5.22)$$

<sup>5</sup> This is to be solved by whatever code you find optimal. For example:

**Vattay inverse iteration** (5.2) is now

$$\varphi_t^{(m+1)} = -\bar{\phi}_t + \sigma_t \frac{1}{\sqrt{a}} \left( j(M)_t + \varphi_{t+1}^{(m)} + \varphi_{t-1}^{(m)} \right)^{1/2}, \quad (5.23)$$

and that should converge like a ton of rocks.

Perhaps watch  *Shadow state conspiracy* (35:26 min)

### 5.3.1 Primitive cell stability of a shadow periodic state

Comparing with the free field (4.103) orbit Jacobian matrix,

$$\mathcal{J}_{zz'} = -\square_{zz'} + \mu^2 \delta_{zz'},$$

<sup>5</sup>Sidney 2024-02-15: I still have to recompute the violation table table 5.2.

the effective shadow state, site dependent Klein-Gordon masses in orbit Jacobian operators for  $\phi^3$  (4.159) are  $\pm\mu^2$  (see (4.159), seems to conflict: check!), and for  $\phi^4$  (4.105) either  $\mu^2$  or  $-2\mu^2$  (see (4.170)),

$$\overline{\mathcal{J}}_{zz'} = -\square_{zz'} + \overline{\mu}_z^2 \delta_{zz'}, \quad \overline{\mu}_z^2 = m_z \mu^2, \quad m_z \in \{-1, 1\}, \quad (5.24)$$

$$\overline{\mathcal{J}}_{zz'} = -\square_{zz'} + \overline{\mu}_z^2 \delta_{zz'}, \quad \overline{\mu}_z^2 = (1 - 3|m_z|)\mu^2, \quad m_z \in \{-1, 0, 1\} \quad (5.25)$$

In the anti-integrable, strong coupling regime, one can drop the Laplacian in  $\text{Det } \overline{\mathcal{J}}_p$ , so the shadow Hill determinant is approximately the product of the above lattice-site dependent masses, and the shadow stability exponent is

$$\text{Det } \overline{\mathcal{J}}_p = \prod_z^{\mathbb{A}} \overline{\mu}_z^2, \quad \overline{\lambda}_p = \frac{2}{V_{\mathbb{A}}} \sum_z^{\mathbb{A}} \ln |\overline{\mu}_z|, \quad (5.26)$$

so for  $\phi^3$  and spatiotemporal cat the anti-integrable limit of shadow stability exponent is periodic state-independent, simply  $\overline{\lambda}_p = \ln \mu^2$ , while for  $\phi^4$  theory  $\overline{\lambda}_p$  depends on the number of '0's in periodic state's mosaic.

## 5.4 Schneider papers

### 5.4.1 Farano *et al.* FCRDS18

Farano, Cherubini, Robinet, De Palma and Schneider [21] *Computing heteroclinic orbits using adjoint-based methods* (2019):

Transitional turbulence in shear flows is supported by a network of unstable exact invariant solutions of the Navier–Stokes equations. The network is interconnected by heteroclinic connections along which the turbulent trajectories evolve between invariant solutions. While many invariant solutions in the form of equilibria, travelling waves and periodic orbits have been identified, computing heteroclinic connections remains a challenge. We propose a variational method for computing orbits dynamically connecting small neighbourhoods around equilibrium solutions. Using local information on the dynamics linearized around these equilibria, we demonstrate that we can choose neighbourhoods such that the connecting orbits shadow heteroclinic connections. The proposed method allows one to approximate heteroclinic connections originating from states with multi-dimensional unstable manifold and thereby provides access to heteroclinic connections that cannot easily be identified using alternative shooting methods. For plane Couette flow, we demonstrate the method by recomputing three known connections and identifying six additional previously unknown orbits.

They compute nine heteroclinic connections nine heteroclinic connections linking seven unstable equilibria originally found by Halcrow, Gibson, Cvitanović and Viswanath [32] *Heteroclinic connections in plane Couette flow*. They also find six previously unknown heteroclinic connections, and also offer a movie.

They fix energy shells  $E_{0,ut}$  and  $E_{0,in}$ , around the initial and final equilibria. Their Figure 4. is cute, it shows two distinct connections for  $EQ5 \rightarrow EQ1$ , one for departing  $EQ5$  along the unstable eigenvector, the other for departing along the opposite direction. That does not lead to a heteroclinic cycle (which would suggest nearby periodic orbits) - they did not find any.

The claim that “the algorithm finds the only existing connection,” but Predrag doubts that - if the starting equilibrium is embedded into chaotic sea, there must be an infinity of connections. Only for isolated, boring unstable equilibrium  $\rightarrow$  stable equilibrium connection one expects a single connection.

Reetz, Kreilos and Schneider [44] *Exact invariant solution reveals the origin of self-organized oblique turbulent-laminar stripes* (2019)

demonstrate the dynamical-systems origin for such patterns, for plane Couette flow via two pitchfork and one saddle-node bifurcation. These patterns exist between angles of approximately  $17^\circ$  and  $30^\circ$  degrees.

#### 5.4.2 Azimi and Schneider Azimi2020

Azimi and Schneider [2] *Self-similar invariant solution in the near-wall region of a turbulent boundary layer at asymptotically high Reynolds numbers*, [arXiv:1912.04850](#) (2020)

Patterns of well-ordered, long-wavelength oblique turbulent-laminar bands are phenomena observed in large domain DNS and experimental wall-bounded shear flows. Similarly, Kuramoto–Sivashinsky large domain DNS simulations seem to indicate existence of preferential angles in observed patterns.

Azimi, Ashtari and Schneider [1] *Constructing periodic orbits of high-dimensional chaotic systems by an adjoint-based variational method*, [arXiv:2007.06427](#) (2022)

Parker and Schneider [42] *Variational methods for finding periodic orbits in the incompressible Navier-Stokes equations*, [arXiv:2108.12219](#) (2022)

#### 5.4.3 Parker and Schneider ParSch22a

Parker and Schneider [41] *Invariant tori in dissipative hyperchaos*, [arXiv:2207.05163](#) (2022)

[...] study of **non-chaotic** yet dynamically unstable invariant solutions embedded in the system’s chaotic attractor.

[...] higher-dimensional invariant tori representing quasi-periodic dynamics have **rarely** been considered. [...] higher dimensional unstable invariant tori have never been considered as generic invariant structures embedded in a chaotic attractor and instead have only been studied as isolated exotic objects. Here we show that unstable tori are generically embedded in the chaotic attractor of a dissipative system and can be identified numerically [...] their stability properties be computed. Consequently, including tori in a dynamical systems description of chaos now based on the complete set of invariant solution types appears feasible.

Predrag: maybe, but 1) relative periodic orbits live on tori [9], see also ref. [5–7];

2) papers with Lan

... we assume that only one iteration of the Poincaré return map is necessary [...] We follow the method of Lan *et al.* [35] (they refer to it as [24])

They credit Chian *et al.* [8] *Amplitude-phase synchronization at the onset of permanent spatiotemporal chaos* (2010) for spatiotemporal chaos being associated with a large number of positive Lyapunov exponents (so-called ‘hyperchaos’) and a high dimensional attractor, with invariant tori thus presumed to be generic, and conjectured to be as important as the periodic orbits.

For  $M \geq 3$ , in the absence of symmetries  $M$ -tori are structurally unstable (they cite Newhouse [39] (1978), Kaneko book (1986), investigate!) and so we do not expect them to play an important role in chaotic dynamics, even for higher dimensional systems. In cases with a continuous symmetry, 2-tori become ‘relative’ 2-tori, a special case of 3-tori which are structurally stable due to the symmetry, so become relevant, but these can be handled by careful modifications of the algorithms for 2-tori, analogously to the study of relative periodic orbits. Therefore, the equilibria, periodic orbits and 2-tori represent a complete collection of non-chaotic solutions which form the skeleton of chaos.

Stable tori have nevertheless been studied in dissipative systems as the breakdown of a 2-torus is one of the possible routes to chaos

#### 5.4.4 Parker, Ashtari and Schneider PaAsSc23

Parker, Ashtari and Schneider *Predicting chaotic statistics with unstable invariant tori*, [arXiv:2301.10626](#) (2023)

#### 5.4.5 Ashtari and Schneider AshSch23

Ashtari and Schneider *Jacobian-free variational method for constructing connecting orbits in nonlinear dynamical systems*, [arXiv:2301.11704](#) (2023)

#### 5.4.6 Page, Norgaard, Brenner and Kerswel PNBK22

Page, Norgaard, Brenner and Kerswel [40] *Recurrent flow patterns as a basis for turbulence: predicting statistics from structures*, [arXiv:2212.1188](#) (2022)

### 5.5 Variational method, Dong 2020 paper DoLiLi20

Some of the text that follows is copy & paste from Dong, Liu and Li [15] *Unstable periodic orbits analysis in the generalized Lorenz-type system* (2020). That is probably copy & paste from earlier Dong papers, have not checked that.

Their description of our variational method [10, 36] looks better than our own, or the ChaosBook text (which is not in the public edition yet).

2CB

[...] a local, time-dependent scaling factor is used to adjust the period

$$\lambda(s_n) \equiv \Delta t_n / \Delta s_n, \quad (5.27)$$

where  $\Delta s_n = s_{n+1} - s_n, n = 1, \dots, N - 1, \Delta s_N = 2\pi - (s_N - s_1)$  and  $\Delta t_n$  follows the same pattern. The scaling factor guarantees the loop increment  $\Delta s_n$  is proportional to its counterpart  $\Delta t_n + \delta t_n$  on the periodic orbit when the loop approaches the cycle, with  $\delta t_n \rightarrow 0$  as  $L \rightarrow p$ .

The Jacobian matrix  $\mathbf{J}(x, t) = dx(t) / dx(0)$  is obtained by integrating

$$\frac{d\mathbf{J}}{dt} = \mathbf{A}\mathbf{J}, \mathbf{A}_{ij} = \frac{\partial v_i}{\partial x_j}, \quad \text{with } \mathbf{J}(x, 0) = \mathbf{1}. \quad (5.28)$$

[Predrag is getting tired of copying LaTeX from Dong, Liu and Li [15]. Whoever continues this, remember to turn on *MathJax*, upper right corner of paper's homepage.]

The variational evolution equation containing the crux of the method of finding periodic orbits

$$\frac{\partial^2 \tilde{x}}{\partial s \partial \tau} - \lambda \mathbf{A} \frac{\partial \tilde{x}}{\partial \tau} - \mathbf{v} \frac{\partial \lambda}{\partial \tau} = \lambda \mathbf{v} - \tilde{\mathbf{v}}. \quad (5.29)$$

Rewriting as

$$\frac{\partial \tilde{\mathbf{v}}}{\partial \tau} - \lambda \frac{\partial \mathbf{v}}{\partial \tau} = -(\tilde{\mathbf{v}} - \lambda \mathbf{v}), \quad (5.30)$$

yields

$$(\tilde{\mathbf{v}} - \lambda \mathbf{v}) = e^{-\tau} (\tilde{\mathbf{v}} - \lambda \mathbf{v})|_{\tau=0}, \quad (5.31)$$

a minimizing cost function:

$$F^2[\tilde{x}] = \frac{1}{2\pi} \oint_{L(\tau)} d\tilde{x} [\tilde{v}(\tilde{x}) - \lambda v(\tilde{x})]^2. \quad (5.32)$$

As the loop descends toward a periodic orbit, the cost function decreases monotonically the differences between  $\tilde{v}(\tilde{x})$  and  $v(\tilde{x})$ , converging in the  $\tau \rightarrow \infty$  limit to the periodic orbit. On the periodic orbit, by (5.27),  $\lambda(s, \infty) = (dt/ds)(\tilde{x}(s, \infty))$ , and the period is given by

$$T_P = \int_0^{2\pi} \lambda(\tilde{x}(s, \infty)) ds. \quad (5.33)$$

The finite difference scheme is employed in a discretization of a loop

$$\tilde{\mathbf{v}}_n \equiv \left. \frac{\partial \tilde{\mathbf{x}}}{\partial s} \right|_{\tilde{x}=\tilde{x}(s_n)} \approx (\hat{\mathbf{D}}\tilde{\mathbf{x}})_n \quad (5.34)$$

and the five-point approximation is adopted

$$\hat{D} = \frac{1}{12h} \begin{pmatrix} 0 & 8 & -1 & & & & & & & & 1 & -8 \\ -8 & 0 & 8 & -1 & & & & & & & & 1 \\ 1 & -8 & 0 & 8 & -1 & & & & & & & \\ & & & & & \dots & & & & & & \\ & & & & & & 1 & -8 & 0 & 8 & -1 & \\ -1 & & & & & & & 1 & -8 & 0 & 8 & \\ 8 & -1 & & & & & & & 1 & -8 & 0 & \end{pmatrix}, \quad (5.35)$$

where  $h = 2\pi/N$ , and each entry represents a  $[d \times d]$  matrix in (5.35),  $8 \rightarrow 8 \mathbf{1}$ , etc; the blanks in the matrix represent zeros. The two  $[2d \times 2d]$  matrices, found in the upper right-corner and the lower-left corner of (5.35), respectively, can be written as

$$M_1 = \begin{pmatrix} \mathbf{1} & -8\mathbf{1} \\ 0 & \mathbf{1} \end{pmatrix}, \quad M_2 = \begin{pmatrix} -\mathbf{1} & 0 \\ 8\mathbf{1} & -\mathbf{1} \end{pmatrix},$$

and are related to the periodic boundary conditions.

After discretization, (5.29) can be written as

$$\begin{pmatrix} \hat{A} & -\hat{v} \\ \hat{a} & 0 \end{pmatrix} \begin{pmatrix} \delta\tilde{x} \\ \delta\lambda \end{pmatrix} = \delta\tau \begin{pmatrix} \lambda\hat{v} - \hat{v} \\ 0 \end{pmatrix}, \quad (5.36)$$

where  $\hat{A} = \hat{D} - \lambda \text{diag}[A_1, A_2, \dots, A_N]$  and  $A_n = \mathbf{A}(\tilde{x}(s_n))$  is defined in (5.28).

$$\hat{v} = (v_1, v_2, \dots, v_N)^T \quad \text{with} \quad v_n = \mathbf{v}(\tilde{x}(s_n)),$$

are the two column vectors that we match everywhere during the evolution of the loop.  $\hat{a}$  is an  $Nd$ -dimensional row vector that restricts the coordinate variations. The deformation of the loop coordinates  $\delta\tilde{x}$  and period  $\delta\lambda$  can be calculated by inverting the  $[(Nd + 1) \times (Nd + 1)]$  matrix on the left-hand side of (5.36).

We use the banded lower-upper (LU) decomposition scheme. Due to the structure of the matrix in (5.36), the Woodbury formula is adopted on the cyclic and boundary terms in the calculations [43], thus enabling an efficient search for periodic orbits.

The variational approach is a good choice to search cycles in a low-dimensional dissipative system. This method is not only suitable for the determination of periodic orbits but also for the homoclinic and heteroclinic orbits [13]. In the previous work, the periodic orbits in various chaotic systems were calculated efficiently using the variational method [11, 12, 14], which illustrates the practicability of this method in the GLTS.

The variational method can also be used to analyze bifurcation phenomena. When the parameters of a dynamical system change continuously, we can observe the conditions under which the periodic orbit is created or disappears through deformations of the periodic orbit.

## 5.6 Dong 2021 paper LDJL21

Liu, Dong, Jie, and Li [38] *Topological classification of periodic orbits in the generalized Lorenz-type system with diverse symbolic dynamics* (2021) ([click here](#)).

I like their explanation of the variational method for finding periodic orbits, and their use of it to study bifurcations by homotopy evolution, which I believe to be authors' original contribution to the subject.

I wish they would consider quotienting symmetries of a given dynamical system prior to their symbolic dynamics analysis. For the 3-disk system quotienting the  $D_3$  symmetry vastly improves the convergence of cycle expansions, see [ChaosBook Table 23.2](#), with symmetry reduction illustrated by [ChaosBook Figure 11.1](#), and explained at length in ChaosBook, also for the Lorenz flow, see [ChaosBook Example 14.4](#), and the text leading up to it.

Reduction of the Lorenz  $D_1$  symmetry might not seem like much, but even that is pretty impressive - the period of a prime or pre-periodic orbit is  $|G|/|G_p|$ -th root of the full state space orbit period, and that leads to a significant simplification of the given problem. For example, in ref. [37], [Figure 8 \(e\)](#) that led to the 3-letter, bi-modal return map instead of a numerically unmanageable 9-letter return map in the symmetry-unreduced, original state space.

In authors' example, symmetry reduction would reduce their Table 1 cycles 0,1; 001, 011; 0001,0111 etc to a single cycle, and 01 to repeat 1-cycle, 0011 to a repeat of a prime 2-cycle, and in general of  $1/2$  period. Table 2 is another illustration, with 2,3; barred 2,3 to a single letter, 23 a repeat of 1-cycle, ..., etc, and the co-existing attractors of Figure 9 reduced to a single attractor. Would be nice to visualize self-linking in the symmetry-reduced state space.

How the reduced symbolic dynamics is related to unreduced one (the kind used by the authors) is explained in ref. [34] [ChaosBook Sect. 25.5  \$D\_1\$  factorization](#).

## 5.7 Wang and Lan 2022 paper WanLan22

Wang and Yueheng Lan have a new paper [49]: *A reduced variational approach for searching cycles in high-dimensional systems*:

They accelerate the variational approach for finding periodic orbits in systems with chaotic dynamics on inertial manifold [...]. An effective loop evolution equation greatly reduces the storage and computing time, with repeated modification of local coordinates and evolution of the guess loop being carried out alternately. The dimension of local coordinate subspaces is generally larger than the number of nonnegative Lyapunov exponents to ensure the exponential convergence.

Ref. [36] scheme describes a periodic orbit with a loop of discrete points, with the topological constraint built into the loop representation. The method requires the storage and inversion of an  $(Nd + 1) \times (Nd + 1)$  matrix ( $d$  is the dimension of system and  $N$  is the number of lattice points on the guess loop).



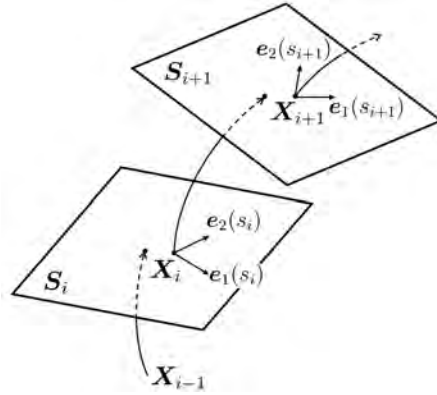


Figure 5.2: The local coordinate frames  $\{e_k(s_i)\}$  ( $k = 1, 2, \dots, n$ ;  $i = 1, 2, \dots, N$  and  $n \leq d$ ), along the orbit parametrized by  $s_i$ , where  $S_i$  represents the hyperplane spanned by the vectors  $e_k(s_i)$  ( $k \leq d$ ).

In search of connecting orbits [13] an automatic mesh allocation scheme [51] alleviates the problem to some extent.

In ref. [50], an automatic allocation scheme of lattice points is adopted to minimize  $N$ . Here we consider systems where the dimension  $d$  of the system is much greater than  $N$ , and try to accelerate the variational method by reducing the effective dimension of the local coordinate system.

Most computation load originates from the  $(Nd + 1) \times (Nd + 1)$  matrix

$$\begin{pmatrix} \hat{A} & -\hat{v} \\ \hat{a} & 0 \end{pmatrix} \quad (5.37)$$

Not all directions are equally important for orbit adjustment when approaching a periodic orbit from a guess loop. On a hyperplane perpendicular to the periodic orbit, the vicinity of an orbit point is stretched in a few directions and compressed in others. The convergence along the compressed directions is automatic, but the deviation in the stretching or neutral directions has to be corrected by the variational scheme.

We find a family of local coordinate frames  $\{e_k(s_i)\}$  ( $k = 1, 2, \dots, n$ ;  $i = 1, 2, \dots, N$  and  $n \leq d$ ) along these important directions, giving the projection sketched in figure 5.2, and rewrite the original variational equation in reduced coordinate frames.

[...] The size of the velocity gradient matrix  $\partial v_k / \partial x_j$  obtained by numerical differentiation, is much smaller than that of the original velocity gradient  $A = \partial v / \partial x$  if  $n \ll d$ . The matrix (5.37) is reduced to  $(Nn + 1) \times (Nn + 1)$ , with  $Nn + 1$  much smaller than the original one  $Nd + 1$ , and the storage and computing time are greatly cut down. The larger the dimension  $d$ , the more prominent the benefits of this reduction.

(Predrag: have not gotten into the nitty-gritty, but it looks like something we might want to use).

## 5.8 Computing periodic states blog

**2022-02-26 Predrag** Variational methods are central to the spatiotemporal chaos program, so they are involved in any line of attack. Here is an attempt at a list (incomplete) of variational links:

They were central to Yuehang Lan's PhD work:

Y. Lan [34] *Dynamical Systems Approach to 1 – d Spatiotemporal Chaos – A Cyclist's View* (2004)

Cvitanović and Lan [10] *Turbulent fields and their recurrences* (2003)

Lan and Cvitanović [36] *Variational method for finding periodic orbits in a general flow* (2004)

Lan, Chandre and Cvitanović [35] *Variational method for locating invariant tori* (2006)

They are a recurring theme throughout DasBuch:

[ChaosBook Chapter Relaxation for cyclists](#)

[ChaosBook Section Least action method](#)

[ChaosBook Appendix Dynamicist's vision of turbulence](#)

[ChaosBook Section Cost function](#)

[ChaosBook eq. \(7.5\) Newton setup for flows.](#)

[ChaosBook Q. 8.1 Dynamics equals a Hamiltonian plus a bracket](#)

Variational methods were central to Matt Gudorf's PhD work:

Matt Gudorf [30] *Spatiotemporal Tiling of the Kuramoto–Sivashinsky Equation* (2020), click [here](#)

[Orbithunter: Framework for Nonlinear Dynamics and Chaos](#)

Then there are several *siminos*/ repo blogs (you have to go there first, and compile them before these links can work):

[is space time?](#) - mostly continuous PDEs, Matt Gudorf, the main parallel variational methods blog, full of important posts

[Navier-Stokes Zipped!](#) - fluid dynamics, many variational methods posts

[Desymmetrization and its discontents](#) - mostly slicing, many variational methods posts

Gao, Gao, Li, Tong and Lee [28] *Detecting unstable periodic orbits of nonlinear mappings by a novel quantum-behaved particle swarm optimization non-Lyapunov way* (2009)

Gao, Xie and Lan [27] *Accelerating cycle expansions by dynamical conjugacy* (2012)

Dong and Lan [13] *A variational approach to connecting orbits in nonlinear dynamical systems* (2014)

Dong and Lan [14] *Organization of spatially periodic solutions of the steady Kuramoto–Sivashinsky equation* (2014)

Wang and Lan [49] *A reduced variational approach for searching cycles in high-dimensional systems* (2022)


**2022-02-25 Burak** Your shadow state method looks very much like the **predictor–corrector method**.



**2022-02-28 Predrag** I do not quite see it. Both methods are implicit, but predictor–corrector is forward in time, while shadow state is global. We should check whether there is a Hill’s formula relation between the two - might help us transfer some of the predictor–corrector techniques into the global setting.


**2022-04-14 Predrag** Looking at *Examples of Hidden Convexity in Nonlinear PDEs* ([click here](#)).



**2022-02-11 Predrag** We have the extraordinarily gifted **Molei Tao** on campus, and we should try to get his advice as we move forward, especially if we make enough progress to be able to move into fluid dynamics.

I enjoyed his latest talk (really, two talks packed into 80 minutes, which summarize earlier ones) very much:

 [ML meets dynamics](#) (2022). What I find interesting that - while we get rid of (position, momentum) as fast as possible, he introduces artificial momentum, shows that it accelerates his forward-in-time integration.

 Data-driven prediction of general Hamiltonian dynamics via learning exactly-symplectic maps (2021);  5 min version; [arXiv:2103.14166](#), [arXiv:2103.05632](#). Their algorithm’s convergence compared to anything else is incredible.

 Stochasticity of deterministic gradient descent: Large learning rate for multiscale objective function (2020)

 Variational optimization on Lie groups with examples of leading (generalized) eigenvalue problems (2020);  17 min version; [pdf](#); [arXiv:2103.14166](#)

See also *Hessian-free high-resolution Nesterov acceleration for sampling* [arXiv:2006.09230](#)

This goes on, Molei is crazy productive...

**2022-02-23 Predrag 2 all Tigers** Molei will join our Zoom Tigers meeting

**4:15-5:15pm on Friday March 18.**

Please be ready to explain your calculations to someone who has never been a part of our discussions.

2020-03-18, 2020-03-23 Molei Tao Here are some references / thoughts:

- ▶ *Lattice field theory* (15:53)
- ▶ *Vattay inverse iteration* (7:14 min)
- ▶ *Use L-BFGS quasi Newton method* (19:17 min. Predrag: internal to GaTech, this video can be seen by a club so exclusive that I doubt Molei is its member)

I don't have a GitHub code for the action minimization, but if students would like to try my suggestions, I will be happy to help.

Regarding my thoughts on the research, which I agree is indeed very interesting, here is a list of possible things to try after more thinking:

- (1) preconditioning >
- (2) implicit-explicit scheme (what we did) >
- (3) L-BFGS

1. The quasi-Newton method is the famous BFGS, the initials of Broyden [4], Fletcher [22], Goldfarb [29] and Shanno [45]. There is also a version for large-scale problems called L-BFGS (limited memory BFGS), see the [wiki](#).
2. Meanwhile, gradient-flow for solving the Euler–Lagrange equation is still a great idea, at least in our opinion, as that is what we used for finding maximal likelihood transition between metastable states in SDEs and SPDEs (e.g., my ref. [48] ([click here](#)) and our ref. [46] ([click here](#))) The setup is in fact sharing some similarities because path integral and Freidlin–Wentzell [23] action are structurally analogous. The only difference is we first do the first variation of the action and then discretize the Euler–Lagrange equation, and you first discretize the action (for impeccable reasons) and then do the variation. Gradient descent still works. In terms of numerics, however, we sometimes do preconditioning which could be helpful in your case too –
3. Your action is

$$-\langle \Phi, \square \Phi \rangle / 2 - \sum_z V(\phi_z) \tag{5.38}$$

where  $\Phi$  is a vector and  $\square$  is a symmetric matrix. The corresponding Euler–Lagrange equation you want to solve is

$$-(\square \Phi)_z - \nabla V(\phi_z) = 0, \quad \text{for all } z \tag{5.39}$$

One could use a fictitious time  $\tau$  gradient flow to solve it,

$$\partial_\tau \Phi = -(\square \Phi + dV), \quad \text{where } dV_i = \nabla V(\phi_i)$$

which discretizes to

$$\Phi^{(k+1)} = \Phi^{(k)} - h(\square \Phi^{(k)} - dV^{(k)}) \tag{5.40}$$

4. What we [46, 48] did in the 2010s is

$$\phi^{(k+1)} = \phi^{(k)} - h(L(\phi^{(k)} + \phi^{(k+1)}) - dV^{(k)}) \quad (5.41)$$

which allows  $h$  to be much larger than that needed for (5.40), and the need for small  $h$  is why (5.40) doesn't work for high-spatial dimension (i.e. your problem)

5. I feel it will give faster convergence if (5.40) gets preconditioned like

$$\phi^{(k+1)} = \phi^{(k)} - h(\phi^{(k)} - \square^{-1}dV^{(k)})$$

where  $\square^{-1}dV^{(k)}$  is computed by spectrally (i.e. Fourier) solving the Poisson equation.

6. If  $\Phi$  is really too high dimensional, one can try 'Random coordinate descent' (see wiki) which was supposed to help large-scale optimization problems like those in machine learning, but contemporary machine learning uses gradient descent to optimize with  $\Phi$  being  $\sim 10^{10}$  dimensional (in fact, GPT3 has 1.75E+11 parameters). So, yes, gradient descent can be slow (preconditioning could help), but its scalability is fantastic.

**2022-02-25 Predrag** Matt commits a breakthrough: using an L-BFGS solver, in the course of the Tigers' Friday meeting he codes in Python an L-BFGS solver for  $\phi^4$  (23.22), and computes all periodic states up to  $n = 6$  or whatever period- $n$  you desire, for Xuanqi's  $\mu^2 = 3.5$  or larger. I have no time to edit this recording -3 hours and 14 minutes- so you will have to skate through it. Highlights:

 Matt does  $\phi^4$ .

4:25 Xuanqi has the  $\phi^4$  horseshoe, its diamond's boundary are the  $LR$  period-2 periodic state stable/unstable manifolds.

1:55:00 using a 'shadow of the shadow state' (4.169) as the initial condition for each combination of  $\mathcal{A} = \{L, C, R\}$  letters,

2:21:00 Matt finds period- $n$  periodic states. They look like they will fit snugly into Xuanqi's diamond.

2:45:00 Matt: could someone explain what orbit Jacobian matrix *means*?

3:00:02 the end.

Links discussed

- Verlet integration
- A version of FIRE
- J. Burkardt molecular dynamics simulation.

None of them are needed for Matt's implementation.

Table 5.3: All periodic orbits up to  $n = 6$  for the Hamiltonian Hénon map repeller (5.42) with  $a = 6$ . Listed are the cycle itinerary, its expanding eigenvalue  $\Lambda_p$ , and its “center of mass.” The “center of mass” is listed because it turns out that it is often a simple rational or a quadratic irrational. All orbits up to topological length  $n = 20$  have been computed.

$p$	$\Lambda_p$	$\sum \phi_{p,i}$
0	$0.715168 \times 10^1$	-0.607625
1	$-0.295285 \times 10^1$	0.274292
10	$-0.989898 \times 10^1$	0.333333
100	$-0.131907 \times 10^3$	-0.206011
110	$0.558970 \times 10^2$	0.539345
1000	$-0.104430 \times 10^4$	-0.816497
1100	$0.577998 \times 10^4$	0.000000
1110	$-0.103688 \times 10^3$	0.816497
10000	$-0.760653 \times 10^4$	-1.426032
11000	$0.444552 \times 10^4$	-0.606654
10100	$0.770202 \times 10^3$	0.151375
11100	$-0.710688 \times 10^3$	0.248463
11010	$-0.589499 \times 10^3$	0.870695
11110	$0.390994 \times 10^3$	1.095485
100000	$-0.545745 \times 10^5$	-2.034134
110000	$0.322221 \times 10^5$	-1.215250
101000	$0.513762 \times 10^4$	-0.450662
111000	$-0.478461 \times 10^4$	-0.366025
110100	$-0.639400 \times 10^4$	0.333333
101100	$-0.639400 \times 10^4$	0.333333
111100	$0.390194 \times 10^4$	0.548583
111010	$0.109491 \times 10^4$	1.151463
111110	$-0.104338 \times 10^4$	1.366025

## Exercises boyscout

### 5.1. Inverse iteration method for a Hénon repeller.

<sup>6,7</sup> Consider the Hénon map (3.5) for the area-preserving (“Hamiltonian”) parameter value  $b = -1$ . The coordinates of a periodic orbit of length  $n_p$  satisfy the equation

$$\phi_{p,i+1} + \phi_{p,i-1} = 1 - a\phi_{p,i}^2, \quad i = 1, \dots, n_p, \quad (5.42)$$

with the periodic boundary condition  $\phi_{p,0} = \phi_{p,n_p}$ . Verify that the itineraries and the stabilities of the short periodic orbits for the Hénon repeller (5.42) at  $a = 6$  are as listed in table 5.3.

**Hint:** you can use any cycle-searching routine you wish, but for the complete repeller case (all binary sequences are realized), the cycles can be evaluated by inverse iteration  $\phi_{p,i}^{(m+1)} \rightarrow \phi_{p,i}^\infty = \phi_{p,i}$ , estimating the midpoint by

<sup>6</sup>Predrag 14oct2021: Return to ChaosBook eventually

<sup>7</sup>Predrag 27dec2004: give the center of mass paper reference somewhere

square-root of (5.42)

$$\phi_{p,i}^{(m+1)} = \sigma_{p,i} \sqrt{\frac{1 - \phi_{p,i+1}^{(m)} - \phi_{p,i-1}^{(m)}}{a}}. \quad (5.43)$$

Here  $\sigma_{p,i}$  are the signs of the corresponding periodic point coordinates,  $\sigma_{p,i} = \phi_{p,i}/|\phi_{p,i}|$ , related in the obvious way to desired periodic orbit's binary itinerary,

$$\sigma_i + 1 = 2m_i, \quad m_i \in \{0, 1\}. \quad (5.44)$$

see figure ??.

G. Vattay

## Chapter 3. Hénon map

**Solution 5.1 - Inverse iteration method for a Hamiltonian repeller.** For the complete repeller case (all binary sequences are realized), the cycles can be evaluated variationally, as follows. According to (3.5), the coordinates of a periodic orbit of length  $n_p$  satisfy the equation

$$\phi_{p,i+1} + \phi_{p,i-1} = 1 - a\phi_{p,i}^2, \quad i = 1, \dots, n_p, \quad (5.45)$$

2CB

with the periodic boundary condition  $\phi_{p,0} = \phi_{p,n_p}$ .

In the complete repeller case, the Hénon map is a realization of the Smale horseshoe, and the symbolic dynamics has a very simple description in terms of the binary alphabet  $\epsilon \in \{0, 1\}$ ,  $\epsilon_{p,i} = (1 + S_{p,i})/2$ , where  $S_{p,i}$  are the signs of the corresponding periodic point coordinates,  $S_{p,i} = \phi_{p,i}/|\phi_{p,i}|$ . We start with a preassigned sign sequence  $S_{p,1}, S_{p,2}, \dots, S_{p,n_p}$ , and a good initial guess for the coordinates  $\phi_{p,i}$ . Using the inverse of the equation (5.42)

$$\phi_{p,i}'' = S_{p,i} \sqrt{\frac{1 - \phi_{p,i+1}' - \phi_{p,i-1}'}{a}} \quad i = 1, \dots, n_p$$

we converge iteratively, at exponential rate, to the desired periodic points  $\phi_{p,i}$ . Given the periodic points, the cycle stabilities and periods are easily computed using (3.66). The itineraries and the stabilities of the short periodic orbits for the Hénon repeller (5.45) for  $a = 6$  are listed in table 5.3; in actual calculations all orbits up to topological length  $n = 20$  have been computed.

G. Vattay

## References

- [1] S. Azimi, O. Ashtari, and T. M. Schneider, "Constructing periodic orbits of high-dimensional chaotic systems by an adjoint-based variational method", *Phys. Rev. E* **105**, 014217 (2022).
- [2] S. Azimi and T. M. Schneider, "Self-similar invariant solution in the near-wall region of a turbulent boundary layer at asymptotically high Reynolds numbers", *J. Fluid Mech.* **888**, 014217 (2020).
- [3] A. Brown, "Equations for periodic solutions of a logistic difference equation", *J. Austral. Math. Soc. Ser. B* **23**, 78–94 (1981).

- 
- [4] C. G. Broyden, "The convergence of a class of double-rank minimization algorithms 1. General considerations", *IMA J. Appl. Math.* **6**, 76–90 (1970).
  - [5] N. B. Budanur, D. Borrero-Echeverry, and P. Cvitanović, "Periodic orbit analysis of a system with continuous symmetry - A tutorial", *Chaos* **25**, 073112 (2015).
  - [6] N. B. Budanur and P. Cvitanović, "Unstable manifolds of relative periodic orbits in the symmetry-reduced state space of the Kuramoto-Sivashinsky system", *J. Stat. Phys.* **167**, 636–655 (2015).
  - [7] N. B. Budanur, P. Cvitanović, R. L. Davidchack, and E. Siminos, "Reduction of the SO(2) symmetry for spatially extended dynamical systems", *Phys. Rev. Lett.* **114**, 084102 (2015).
  - [8] A. C.-L. Chian, W. M. Santana, E. L. Rempel, F. A. Borotto, T. Hada, and Y. Kamide, "Chaos in driven Alfvén systems: Unstable periodic orbits and chaotic saddles", *Nonlin. Proc. Geophys.* **14**, 17–29 (2007).
  - [9] P. Cvitanović, D. Borrero-Echeverry, K. Carroll, B. Robbins, and E. Siminos, "Cartography of high-dimensional flows: A visual guide to sections and slices", *Chaos* **22**, 047506 (2012).
  - [10] P. Cvitanović and Y. Lan, Turbulent fields and their recurrences, in *Correlations and Fluctuations in QCD : Proceedings of 10. International Workshop on Multiparticle Production*, edited by N. Antoniou (2003), pp. 313–325.
  - [11] C. Dong, "Topological classification of periodic orbits in Lorenz system", *Chin. Phys. B* **27**, 080501 (2018).
  - [12] C. Dong, "Topological classification of periodic orbits in the Yang-Chen system", *Europhys. Lett.* **123**, 20005 (2018).
  - [13] C. Dong and Y. Lan, "A variational approach to connecting orbits in nonlinear dynamical systems", *Phys. Lett. A* **378**, 705–712 (2014).
  - [14] C. Dong and Y. Lan, "Organization of spatially periodic solutions of the steady Kuramoto-Sivashinsky equation", *Commun. Nonlinear Sci. Numer. Simul.* **19**, 2140–2153 (2014).
  - [15] C. Dong, H. Liu, and H. Li, "Unstable periodic orbits analysis in the generalized Lorenz-type system", *J. Stat. Mech.* **2020**, 073211 (2020).
  - [16] A. Endler and J. A. C. Gallas, "Period four stability and multistability domains for the Hénon map", *Physica A* **295**, 285–290 (2001).
  - [17] A. Endler and J. A. C. Gallas, "Arithmetical signatures of the dynamics of the Hénon map", *Phys. Rev. E* **65**, 036231 (2002).
  - [18] A. Endler and J. A. C. Gallas, "Conjugacy classes and chiral doublets in the Hénon Hamiltonian repeller", *Phys. Lett. A* **356**, 1–7 (2006).
  - [19] A. Endler and J. A. C. Gallas, "Reductions and simplifications of orbital sums in a Hamiltonian repeller", *Phys. Lett. A* **352**, 124–128 (2006).



- [20] A. Endler and J. A. C. Gallas, “Reductions and simplifications of orbital sums in a Hamiltonian repeller”, *Phys. Lett. A* **352**, 124–128 (2006).
- [21] M. Farano, S. Cherubini, J.-C. Robinet, P. De Palma, and T. M. Schneider, “Computing heteroclinic orbits using adjoint-based methods”, *J. Fluid Mech.* **858**, R3 (2019).
- [22] R. Fletcher, “A new approach to variable metric algorithms”, *Comput. J.* **13**, 317–322 (1970).
- [23] M. I. Freidlin and A. D. Wentzel, *Random Perturbations of Dynamical Systems* (Springer, Berlin, 1998).
- [24] J. A. C. Gallas, “Equivalence among orbital equations of polynomial maps”, *Int. J. Modern Phys. C* **29**, 1850082 (2018).
- [25] J. A. C. Gallas, “Orbital carriers and inheritance in discrete-time quadratic dynamics”, *Int. J. Modern Phys. C* **31**, 2050100 (2020).
- [26] J. A. C. Gallas, “Preperiodicity and systematic extraction of periodic orbits of the quadratic map”, *Int. J. Modern Phys. C* **31**, 2050174 (2020).
- [27] A. Gao, J. Xie, and Y. Lan, “Accelerating cycle expansions by dynamical conjugacy”, *J. Stat. Phys.* **146**, 56–66 (2012).
- [28] F. Gao, H. Gao, Z. Li, H. Tong, and J.-J. Lee, “Detecting unstable periodic orbits of nonlinear mappings by a novel quantum-behaved particle swarm optimization non-Lyapunov way”, *Chaos Solit. Fract.* **42**, 2450–2463 (2009).
- [29] D. Goldfarb, “A family of variable-metric methods derived by variational means”, *Math. Comput.* **24**, 23–26 (1970).
- [30] M. N. Gudorf, *Spatiotemporal Tiling of the Kuramoto-Sivashinsky Equation*, PhD thesis (School of Physics, Georgia Inst. of Technology, Atlanta, 2020).
- [31] M. N. Gudorf, *Orbithunter: Framework for Nonlinear Dynamics and Chaos*, tech. rep. (School of Physics, Georgia Inst. of Technology, 2021).
- [32] J. Halcrow, J. F. Gibson, P. Cvitanović, and D. Viswanath, “Heteroclinic connections in plane Couette flow”, *J. Fluid Mech.* **621**, 365–376 (2009).
- [33] K. T. Hansen, “Alternative method to find orbits in chaotic systems”, *Phys. Rev. E* **52**, 2388–2391 (1995).
- [34] Y. Lan, *Dynamical Systems Approach to 1 – d Spatiotemporal Chaos – A Cyclist’s View*, PhD thesis (School of Physics, Georgia Inst. of Technology, Atlanta, 2004).
- [35] Y. Lan, C. Chandre, and P. Cvitanović, “Variational method for locating invariant tori”, *Phys. Rev. E* **74**, 046206 (2006).
- [36] Y. Lan and P. Cvitanović, “Variational method for finding periodic orbits in a general flow”, *Phys. Rev. E* **69**, 016217 (2004).
- [37] Y. Lan and P. Cvitanović, “Unstable recurrent patterns in Kuramoto-Sivashinsky dynamics”, *Phys. Rev. E* **78**, 026208 (2008).

- 
- [38] H. Liu, C. Dong, Q. Jie, and H. Li, “Topological classification of periodic orbits in the generalized Lorenz-type system with diverse symbolic dynamics”, *Chaos, Solitons & Fractals* **154**, 111686 (2022).
- [39] S. Newhouse, D. Ruelle, and F. Takens, “Occurrence of strange Axiom A attractors near quasi periodic flows on  $T^m$ ,  $m \leq 3$ ”, *Comm. Math. Phys.* **64**, 35–40 (1978).
- [40] J. Page, P. Norgaard, M. P. Brenner, and R. R. Kerswell, “Recurrent flow patterns as a basis for two-dimensional turbulence: Predicting statistics from structures”, *Proc. Natl. Acad. Sci.* **121**, 23 (2024).
- [41] J. P. Parker and T. M. Schneider, “Invariant tori in dissipative hyperchaos”, *Chaos* **32**, 113102 (2022).
- [42] J. P. Parker and T. M. Schneider, “Variational methods for finding periodic orbits in the incompressible Navier-Stokes equations”, *J. Fluid. Mech.* **941**, A17 (2022).
- [43] W. H. Press, B. P. Flannery, S. A. Teukolsky, and W. T. Vetterling, *Numerical Recipes*, 3rd ed. (Cambridge Univ. Press, Cambridge UK, 2007).
- [44] F. Reetz, T. Kreilos, and T. M. Schneider, “Exact invariant solution reveals the origin of self-organized oblique turbulent-laminar stripes”, *Nat. Commun.* **10**, 2277 (2019).
- [45] D. F. Shanno, “Conditioning of quasi-Newton methods for function minimization”, *Math. Comput.* **24**, 647–656 (1970).
- [46] A. N. Souza and M. Tao, “Metastable transitions in inertial Langevin systems: What can be different from the overdamped case?”, *Eur. J. Appl. Math.* **30**, 830–852 (2018).
- [47] J. Stephenson and D. T. Ridgway, “Formulae for cycles in the Mandelbrot set II”, *Physica A* **190**, 104–116 (1992).
- [48] M. Tao, “Hyperbolic periodic orbits in nongradient systems and small-noise-induced metastable transitions”, *Phys. D* **363**, 1–17 (2018).
- [49] D. Wang and Y. Lan, *A reduced variational approach for searching cycles in high-dimensional systems*, 2022.
- [50] D. Wang, P. Wang, and Y. Lan, “Accelerated variational approach for searching cycles”, *Phys. Rev. E* **98**, 042204 (2018).
- [51] X. Zhou, W. Ren, and E. W., “Adaptive minimum action method for the study of rare events”, *J. Chem. Phys.* **128**, 104111 (2008).

## Chapter 6

# Group theory

### 6.1 A dancer, a parquet floor

Think of a dancer on a parquet floor. Or a skater skating over the skating ring's ice. Or a cat over spacetime.

A parquet board  $t$  is a site of our lattice  $\mathcal{L}$ , the *coordinate* system over which the dancer dances.

The disposition of the dancer on a parquet board  $t$  is given by the *field*  $\phi_t$ .

A *periodic state* is a set of field values  $\Phi = \{\phi_z\}$  over the  $d$ -dimensional lattice  $z \in \mathbb{Z}^d$  that satisfies a given Euler–Lagrange equation.

**Space group.** ‘State space’  $\mathcal{M}$  is the totality of ‘states’  $\Phi$ : all possible arrangements of cats, dancers, ... - ‘fields’  $\phi_t$  and their names  $M$ .

‘Coordinates’ refer to markings on the floor that they stand on.

If you mark every inch on a blank linoleum floor, that is a ‘discretization’.

If you compare dancers on adjoining parquet boards, this is a *lattice derivative*. The floor is still a floor; lattice derivative is property of the floor, what parquet boards are adjoining boards in  $d$  dimensions.

If dancer strikes the same pose on a different parquet board, we call that translational or  $(C_\infty)^d$  symmetry.

If the dancer strikes the same pose on a parquet board of a different orientation, we refer to such coordinate system symmetry as a *space group*  $G$ . An example is a dancer that cannot tell left from right on a 1-dimensional lattice. Then the coordinate system symmetry is the dihedral group  $D_\infty$ .

If the theory has a Lagrangian formulation, the Lagrangian is -by construction- *invariant* under all symmetries.

Its first variation, the Euler–Lagrange equation is *equivariant* under these symmetries. For example, for a 2-dimensional square integer lattice, a possible symmetry of the theory can be the *space group*  $p4mm$  symmetry operations (23.83).

The individual lattice states either have no symmetry at all (they are, after all, ‘turbulent’), or are invariant under subgroups of space group  $p4mm$ .

In what follows we quotient only the translational symmetries, and postpone dazzling the captive reader with the full  $D_4$  point group reduction to a later, more ponderous publication.

## 6.2 Group theory snippets

We used to be stuck on reflection-symmetry reduction needed to factorize the zeta functions. But no more - see sect. 6.6 *A Lind zeta function for flip systems*.  
deterministic field theory on  $d$ -dimensional lattice

$$(\square - \mu^2) \Phi + F[\Phi] = -M, \tag{6.1}$$

Definitions:

The matrix *symmetry group*  $G$  of a matrix  $M$ :

$$\mathcal{S}(M) = \{g \in G \mid gMg^{-1} = M\}. \tag{6.2}$$

The *reversing matrix symmetry group*  $R$  of a matrix  $M$ :

$$\mathcal{R}(M) = \{s \in R \mid sMs^{-1} = M^{-1}\}. \tag{6.3}$$

A matrix  $M$  is *reversible* if it is conjugate to its inverse within matrix group  $R$ .

Park [62] refers to (??) as ‘skew-commuting’:

“The ‘covering space’ has two actions,  $f$  and  $s$ , where  $f$  is a  $\mathbb{Z}$ -action,  $s$  is a map of order two, and  $s$  and  $T$  skew-commute; that is,  $sfs = f^{-1}$ .”

Let  $(\mathcal{M}, f)$  be an invertible dynamical system. A homeomorphism  $s : \mathcal{M} \rightarrow \mathcal{M}$  is a *flip* if

$$s \circ f \circ s = f^{-1}, \quad s^2 = 1. \tag{6.4}$$

The triple  $(\mathcal{M}, f, s)$  is called a *flip system* [49].

For a shift space a flip is a non-abelian group action, see (6.7). A flip system  $(\mathcal{M}, f, s)$  is *shift-flip system of finite type* if  $(\mathcal{M}, f)$  is a shift of finite type.

Notation follows **Dihedral group** and **Regular polygons** wikis.

$T$  is a normal subgroup of  $G$ .

For space groups, the cosets by translation subgroup  $T$  (the set all translations) form the *factor* (also known as *quotient*) group  $G/T$ , isomorphic to the point group  $g$ . The normal subgroup of a line group  $G$  is its translational subgroup  $T$ , with its factor group  $G/T$  isomorphic to the *isogonal point group*  $P$  of discrete symmetries of its 1-dimensional unit cell  $x \in [0, 1)$ .

$$r_i r_j = r_{i+j}, \quad r_i s_j = s_{i+j}, \quad s_i r_j = s_{i-j}, \quad s_i s_j = r_{i-j}, \tag{6.5}$$

As the order in which a translation and a reflection are applied is not commutative, dihedral groups are nonabelian.

1

To omit from the paper:

As any two flips result in a rotation, alternative presentation for  $D_n$ ,  $n$  even, is generated by a horizontal (short axis) reflection, and a diagonal (long axis) reflection, rather than the usual  $(r, s)$  set. (I have not checked this for the odd  $n$ .)

an even index  $2k$  reflection  $s_{2k}$  reflects the lattice across the  $k$ th lattice site, while an odd index reflection  $s_{2k+1}$  reflects the lattice across the midpoint between sites  $k$  and  $k+$ .

**Definition: Coset.** Let  $H = \{e, b_2, b_3, b_4, \dots\} \subseteq G$  be a subgroup of  $G$ . The set of  $h$  elements  $\{c, cb_2, cb_3, cb_4, \dots\}$ ,  $c \in G$  but not in  $H$ , is called left coset  $cH$ . For a given subgroup  $H$  the group elements are partitioned into  $H$  and  $m - 1$  cosets, where  $m = |G|/|H|$ .

There are a  $2n$  left cosets of subgroup  $H(n)$  in  $D_\infty$  (6.245), with the quotient group  $D_\infty/H(n)$  isomorphic to the dihedral group  $D_n$ .

There are  $n$  infinite dihedral  $H(n, k)$  subgroups of  $D_\infty$ , with  $n$  left cosets (6.246) and the quotient group  $D_\infty/H(n, k)$  isomorphic to the cyclic group  $C_n$ .

A typical turbulent trajectory of fluid flow has no symmetry beyond the identity, so its symmetry group is the trivial subgroup  $\{e\}$ .

In summary: You can visualize an periodic states invariant under a translation subgroup  $H(a)$ , figure 6.1 (a), as a tiling of the lattice  $\mathbb{Z}$  by a periodic state tiles with a fish painted on it, swimming upstream, and no reflection symmetry.

Note that as  $H(10, 9)$  and  $H(10, 0)$  are not conjugate subgroups, there is no translation or reflection that maps periodic state of the first type into periodic state of the second.

An orbit is by construction a *symmetry invariant* notion: as the set of all periodic states that can be reached  $\Phi$  by symmetries, it is an invariant set, as any group action merely permutes it. The full state space  $\mathcal{M}$  is a union of such orbits.

If  $G$  is a symmetry, intrinsic properties of an orbit  $p$  (period, Floquet multipliers) evaluated anywhere along its  $G$ -orbit are the same.

A symmetry thus reduces the number of inequivalent periodic states  $\mathcal{M}_p$ . So we also need to describe the symmetry of a *solution*, as opposed to the symmetry of the *system*.

A generic orbit might be ergodic, unstable and essentially uncontrollable. The ChaosBook strategy is to populate the state space by a hierarchy of orbits which are *compact invariant sets* (equilibria, periodic orbits, invariant tori, . . .), each computable in a finite time. They are to a generic orbit what fractions are to normal numbers on the unit interval.

While for the infinite lattice case there are no 'long axes', 'short axes', an even index  $2k$  reflection  $s_{2k}$  still reflects the lattice across the  $k$ th lattice site (a 'vertex' of a triangle or a square in the finite example), while an odd index

---

<sup>1</sup>Predrag 2021-07-17: Fig. 2.1 in [Damjanović and Milošević](#) is cute:) So is [this illustration](#) of the group elements  $D_8$ .

$2k - 1$  reflection  $s_{2k-1}$  reflects the lattice across the midpoint between sites  $k - 1$  and  $k$  (an 'edge' of a square in the finite example).<sup>2</sup>

Not sure we need this, so I dropped it for now: " For odd  $n$ , there are  $(n - 1)/2$  such classes. For even  $n$ , there are  $(n - 2)/2$  such pairs, with the rotation by half a circle a class  $\{r_{n/2}\}$  by itself. "

Dihedral groups are *ambivalent* groups – every element is conjugate to its inverse. Thus, all the irreducible representations of a dihedral group over the complex numbers can be realized over the real numbers. Etc.

As  $D_n$  elements are combinations of one-step translations and reflections, its group presentation is

$$D_n = \langle r, s \mid r^n = s^2 = 1, rs = sr^{n-1} \rangle . \quad (6.6)$$

A presentation of the *infinite dihedral group* [49] is

$$D_\infty = \langle r, s \mid srs = r^{-1}, s^2 = 1 \rangle . \quad (6.7)$$

$D_1, D_2, D_3, D_4, \dots$

Examples are the  $D_3$  Cayley table 6.11 and the  $D_6$  Cayley table 6.12.

So far, ChaosBook works out zeta function factorizations for  $D_1$  (example 6.11),  $D_2$  (known as **Klein four-group**),  $D_3$  (symmetric group  $S_3$ ), and  $D_4$ .



example 6.15  
p. 353



example 6.17  
p. 353



example 6.18  
p. 354

## 6.3 Temporal lattice systems

For temporal Bernoulli, see sect. 1.1.

### 6.3.1 Temporal cat

Written out as a second-order difference equation, the Percival-Vivaldi map takes a particularly elegant, *temporal cat* form

$$\phi_{t+1} - s\phi_t + \phi_{t-1} = -m_t , \quad (6.8)$$

or, in terms of a periodic state  $\Phi$ , the corresponding symbol block  $M$  (1.1), and the  $[n \times n]$  shift operator  $r$  (1.4),

$$(r - s\mathbf{1} + r^{-1})\Phi = -M , \quad (6.9)$$

very much like the temporal Bernoulli condition (1.3). 'Temporal' again refers to the global periodic state (field)  $\Phi$ , and the winding numbers (sources)  $M$  taking their values on the lattice sites of a 1-dimensional *temporal* lattice  $t \in \mathbb{Z}$ .

<sup>2</sup>Han 2021-08-13: This is correct only when we define that  $s$  is the reflection across the 0th lattice site.

where the  $[n \times n]$  orbit Jacobian matrix  $\mathcal{J}$  is now given by

$$\mathcal{J} = r - s \mathbf{1} + r^{-1} \quad (6.10)$$

a tri-diagonal Toeplitz matrix (constant along each diagonal,  $\mathcal{J}_{kl} = j_{k-l}$ ) of circulant form,

$$\mathcal{J} = \begin{pmatrix} -s & 1 & \cdot & \cdot & \dots & \cdot & 1 \\ 1 & -s & 1 & \cdot & \dots & \cdot & \cdot \\ \cdot & 1 & -s & 1 & \dots & \cdot & \cdot \\ \vdots & \vdots & \vdots & \vdots & \ddots & \vdots & \vdots \\ \cdot & \cdot & \dots & \dots & \dots & -s & 1 \\ 1 & \cdot & \dots & \dots & \dots & 1 & -s \end{pmatrix}. \quad (6.11)$$

### 6.3.2 Periodic states

A periodic state  $\Phi$  is *periodic* if it satisfies

$$\Phi(x + R) = \Phi(x) \quad (6.12)$$

for any discrete translation  $R = n\mathbf{a} \in \mathcal{L}$ , where  $n$  is any integer, and  $\mathbf{a}$  is the integer lattice vector that defines the *primitive cell* (or, the Bravais sublattice of  $\mathbb{Z}$ ).

The basic ‘atom’ of a reflection-symmetric period  $n$  periodic state is a ‘half’ of it, the length  $m$  orbit, and its reflection

$$\tilde{\Phi} = \phi_1 \phi_2 \phi_3 \cdots \phi_m, \quad s\tilde{\Phi} = \phi_m \cdots \phi_3 \phi_2 \phi_1, \quad (6.13)$$

in terms of which a periodic state  $\Phi$  has one of the four symmetries:

$$(a) \quad \tilde{\Phi} \quad m = n \quad (6.14)$$

$$(o) \quad \boxed{\phi_0} \tilde{\Phi} | s\tilde{\Phi} \quad m = (n-1)/2, \quad n \text{ odd} \quad (6.15)$$

$$(ee) \quad \boxed{\phi_0} \tilde{\Phi} \boxed{\phi_{m+1}} | s\tilde{\Phi} \quad m = (n-2)/2, \quad n \text{ even} \quad (6.16)$$

$$(eo) \quad \tilde{\Phi} | s\tilde{\Phi} \quad m = n/2, \quad n \text{ even} \quad (6.17)$$

While the defining equation for temporal cat or temporal Hénon is equivariant under the integer lattice *space group*  $p1m$  symmetry operations, the individual periodic states either have no symmetry at all (they are, after all, ‘turbulent’), or are invariant under subgroups of space group  $p1m$ .

In addition, the temporal cat (but not the temporal Hénon) has an *internal*  $D_1$  symmetry (see sect. 4.9) under the inversion  $S$  through the center of the  $0 \leq \phi_j < 1$  unit interval,

$$\bar{\phi}_j = S\phi_j = 1 - \phi_j, \quad \text{for all } j \in \mathcal{L}. \quad (6.18)$$

Indeed, if  $\Phi_M = \{\phi_i\}$  is a periodic state, its internal symmetry partner  $\bar{\Phi} = \{1 - \phi_i\}$  is also a periodic state (see sect. 4.9). So, every periodic state either belongs to a conjugate pair  $\{\Phi, \bar{\Phi}\}$ , or is self-dual under conjugation.

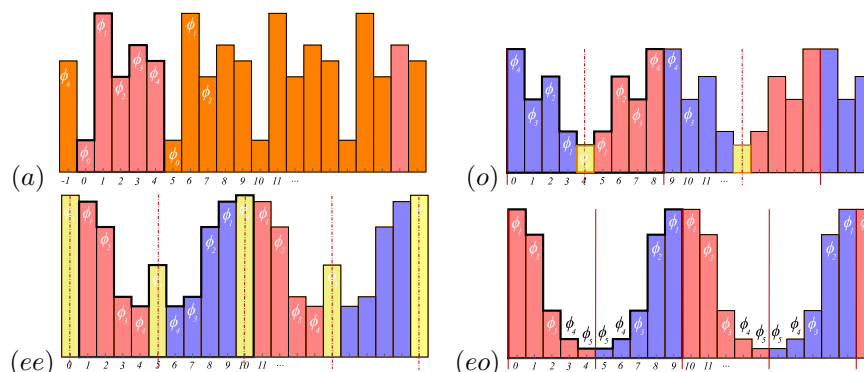


Figure 6.1: (Color online) A periodic state  $\Phi$  has one of the 4 possible symmetries, illustrated by: (a) *No reflection symmetry*: an  $H_5$  invariant period-5 periodic state (12.123). For its  $G$ -orbit, see figure ?? . (o) *Odd period, reflection-symmetric*: an  $H_{9,8}$  invariant period-9 periodic state (??), reflection symmetric over the lattice sites interval [8-9] midpoint and over the lattice site 4. (ee) *Even period, even reflection-symmetric*: an  $H_{10,0}$  invariant period-10 periodic state (12.124), reflection symmetric over lattice sites 0 and 5. (eo) *Even period, odd reflection-symmetric*: an  $H_{10,9}$  invariant period-10 periodic state (12.125), reflection symmetric over the [4-5] and [9-10] interval midpoints. Horizontal: lattice sites labelled by  $t \in \mathbb{Z}$ . Vertical: value of field  $\phi_t$ , plotted as a bar centred at lattice site  $t$ . Time reversed blocks indicated in blue, boundary sites in yellow. Even reflection axes dashed, odd reflections full line.

### 6.3.3 Reflection-symmetric periodic states

2021-08-14 Predrag Much of this section is misguided or wrong. Thread carefully, delete eventually...

Consider a periodic state

$$\cdots \phi_{-3} \phi_{-2} \phi_{-1} \phi_0 \phi_1 \phi_2 \phi_3 \phi_4 \cdots \tag{6.19}$$

over an infinite 1-dimensional integer lattice  $\mathbb{Z}$ . Assume for the moment that the system is linear so a sum of periodic states is also a periodic state.

If the periodic state is antisymmetric under an even reflection, the antisymmetric subspace is 2-dimensional. The periodic state tiles the infinite lattice as:

$$\overline{\boxed{0} \phi_1 \phi_2 \boxed{0} \phi_2 \phi_1}, \tag{6.20}$$

Go to any lattice site  $k$ , reflect the periodic state and average the two, using the translate-reflect operator <sup>3</sup>

$$P_k = \frac{1}{2}(\mathbf{1} + s_k). \tag{6.21}$$

<sup>3</sup>Predrag 2021-10-08: Was 'shift-reflect', but Burak says in fluid dynamics translation is one direction, but 'reflect' is in a transverse direction; changed to avoid confusion.



The result is a periodic state reflection-symmetric across lattice site  $k$ . From (??) it follows that for odd  $k$ , all  $P_k$  operators are in the same conjugacy class as  $P_1$ , and for even  $k$ , all  $P_k$  are in the same conjugacy class as  $P_0$ . It suffices to do the computation only once for each class.

$$P_{\pm} = (1 \pm s)/2$$

$$P_+ = \frac{1}{2} \begin{pmatrix} 2 & 0 & 0 & 0 & 0 \\ 0 & 1 & 0 & 0 & 1 \\ 0 & 0 & 1 & 1 & 0 \\ 0 & 0 & 1 & 1 & 0 \\ 0 & 1 & 0 & 0 & 1 \end{pmatrix}, \quad \text{tr } P_+ = 3 \quad (6.22)$$

with two orthogonal nul eigenvectors

$$e_4 = 2^{-1/2}(0, 0, 1, -1, 0), e_5 = 2^{-1/2}(0, 1, 0, 0, -1),$$

suggesting an orthogonal basis

$$e_1 = (1, 0, 0, 0, 0), e_2 = 2^{-1/2}(0, 0, 1, 1, 0) e_3 = 2^{-1/2}(0, 1, 0, 0, 1)$$

Stack them up into a diagonalization matrix

$$V = \begin{pmatrix} 1 & 0 & 0 & 0 & 0 \\ 0 & 0 & 1 & 0 & 1 \\ 0 & 1 & 0 & 1 & 0 \\ 0 & 1 & 0 & -1 & 0 \\ 0 & 0 & 1 & 0 & -1 \end{pmatrix}, \quad V^{-1} = \frac{1}{2} \begin{pmatrix} 2 & 0 & 0 & 0 & 0 \\ 0 & 0 & 1 & 1 & 0 \\ 0 & 1 & 0 & 0 & 1 \\ 0 & 0 & 1 & -1 & 0 \\ 0 & 1 & 0 & 0 & -1 \end{pmatrix} \quad (6.23)$$

(I gave up on this - too manual)

$$P_- = \frac{1}{2} \begin{pmatrix} 0 & 0 & 0 & 0 & 0 \\ 0 & 1 & 0 & 0 & -1 \\ 0 & 0 & 1 & -1 & 0 \\ 0 & 0 & -1 & 1 & 0 \\ 0 & -1 & 0 & 0 & 1 \end{pmatrix}, \quad \text{tr } P_- = 2. \quad (6.24)$$

The determinant of a  $[3 \times 3]$  matrix can be written as the antisymmetrized trace of the matrix [23]:

$$\begin{aligned} \text{Det } M &= \text{tr}_3 AM = \frac{1}{3} \sum_{k=1}^3 (-1)^{k-1} (\text{tr}_{3-k} AM) \text{tr } M^k \\ &= \frac{1}{3} ((\text{tr}_2 AM) \text{tr } M - (\text{tr } M) \text{tr } M^2 + \text{tr } M^3) \\ \text{tr}_2 AM &= \frac{1}{2} ((\text{tr } M)^2 - \text{tr } M^2), \end{aligned} \quad (6.25)$$

where  $A$  is the antisymmetrization projection operator, and 3 is the dimension of the matrix  $M$ .

Apply the (6.21) operator  $P_0 = (1 + s)/2$  to periodic state (6.19). We obtain a periodic state

$$\cdots \tilde{\phi}_4 \tilde{\phi}_3 \tilde{\phi}_2 \tilde{\phi}_1 \boxed{\phi_0} \tilde{\phi}_1 \tilde{\phi}_2 \tilde{\phi}_3 \tilde{\phi}_4 \cdots, \quad (6.26)$$

symmetric under reflection, where  $\tilde{\phi}_j = (\phi_{-j} + \phi_j)/2$ , are pairwise symmetric under the reflection  $s$ , with  $\overline{\phi_0} = (\phi_0 + \phi_0)/2$  indicating that the field at the lattice site 0 is unchanged by reflection.

Next apply the projection operator  $P_1 = (1 + sr)/2$  from (6.21) to a periodic state (6.19). We obtain a periodic state

$$\cdots \tilde{\phi}_4 \tilde{\phi}_3 \tilde{\phi}_2 \tilde{\phi}_1 | \tilde{\phi}_1 \tilde{\phi}_2 \tilde{\phi}_3 \tilde{\phi}_4 \cdots, \quad (6.27)$$

where  $|$  indicates that the state is symmetric under reflection across midpoint between lattice sites 0 and 1, and the successive lattice pair averages  $\tilde{\phi}_j = (\phi_j + \phi_{1-j})/2$ ,  $j = 1, 2, 3, \dots$ , are pairwise symmetric under the reflection  $s_1$ .

In summary, as reflection operators  $s_0 = s$  and  $s_1 = sr$  belong to the two dihedral group  $D_\infty$  classes, all other periodic states symmetric with respect to reflection  $s_k$ , for any integer  $k$ , are conjugate to the above two types of symmetric periodic states.

The orbit Jacobian matrix (3.26), 3 symmetry cases:

*Odd period primitive cell* (??), is  $[(m+1) \times (m+1)]$ -dimensional (compare with (24.307)): <sup>4</sup>

$$\mathcal{J}[\Phi] = \begin{pmatrix} d_0 & -2 & 0 & 0 & \cdots & 0 & 0 & 0 \\ -1 & d_1 & -1 & 0 & \cdots & 0 & 0 & 0 \\ 0 & -1 & d_2 & -1 & \cdots & 0 & 0 & 0 \\ \vdots & \vdots & \vdots & \vdots & \ddots & \vdots & \vdots & \vdots \\ 0 & 0 & 0 & 0 & \cdots & -1 & d_{m-1} & -1 \\ 0 & 0 & 0 & 0 & \cdots & 0 & -1 & d_m - 1 \end{pmatrix}. \quad (6.28)$$

*Even period  $n = 2m + 2$ , even reflection  $k$*  (12.124) (compare with (24.309)):

$$\mathcal{J}[\Phi] = \begin{pmatrix} d_0 & -2 & 0 & 0 & \cdots & 0 & 0 & 0 \\ -1 & d_1 & -1 & 0 & \cdots & 0 & 0 & 0 \\ 0 & -1 & d_2 & -1 & \cdots & 0 & 0 & 0 \\ \vdots & \vdots & \vdots & \vdots & \ddots & \vdots & \vdots & \vdots \\ 0 & 0 & 0 & 0 & \cdots & -1 & d_m & -1 \\ 0 & 0 & 0 & 0 & \cdots & 0 & -2 & d_{m+1} \end{pmatrix}. \quad (6.29)$$

*Even period  $n = 2m$ , odd reflection  $k$*  (12.125) (compare with (24.308)):

$$\mathcal{J}[\Phi] = \begin{pmatrix} d_1 - 1 & -1 & 0 & \cdots & 0 & 0 & 0 \\ -1 & d_2 & -1 & \cdots & 0 & 0 & 0 \\ \vdots & \vdots & \vdots & \ddots & \vdots & \vdots & \vdots \\ 0 & 0 & 0 & \cdots & -1 & d_{m-1} & -1 \\ 0 & 0 & 0 & \cdots & 0 & -1 & d_m - 1 \end{pmatrix}. \quad (6.30)$$

<sup>4</sup>Predrag 2021-09-01: The bottom, odd, looks like Neumann boundary condition, see Pozrikidis [63] (click here) eq. (1.5.4). The top, time-direction symmetry breaking b.c. I do not recognize.

orbit Jacobian matrix  $\mathcal{J}$  evaluated on the periodic state commutes with  $s$ ,

$$\mathcal{J}s = \begin{pmatrix} d_0 & -1 & 0 & 0 & -1 \\ -1 & d_1 & -1 & 0 & 0 \\ 0 & -1 & d_2 & -1 & 0 \\ 0 & 0 & -1 & d_2 & -1 \\ -1 & 0 & 0 & -1 & d_1 \end{pmatrix} \begin{pmatrix} 1 & 0 & 0 & 0 & 0 \\ 0 & 0 & 0 & 0 & 1 \\ 0 & 0 & 0 & 1 & 0 \\ 0 & 0 & 1 & 0 & 0 \\ 0 & 1 & 0 & 0 & 0 \end{pmatrix} = s\mathcal{J}. \quad (6.31)$$

*Even period examples:* For even dimensions, there are two classes of reflections, the even ones, figure 6.1 (*ee*), that leave two ‘yellow’ site fields fixed, swap the rest, and the odd ones, figure 6.1 (*eo*), that swap the ‘reds’ and ‘blues’. This is illustrated by the  $D_4$  permutation representation of the even  $s$ , odd  $s_3$  reflection symmetries of a square, figure 6.2 (*b*):

2CB

$$s = \begin{pmatrix} 1 & 0 & 0 & 0 \\ 0 & 0 & 0 & 1 \\ 0 & 0 & 1 & 0 \\ 0 & 1 & 0 & 0 \end{pmatrix}, \quad s_3 = \begin{pmatrix} 0 & 0 & 0 & 1 \\ 0 & 0 & 1 & 0 \\ 0 & 1 & 0 & 0 \\ 1 & 0 & 0 & 0 \end{pmatrix}. \quad (6.32)$$

The even reflection keeps two site fields fixed,

$$(s\Phi)^\top = (\phi_0, \phi_3, \phi_2, \phi_1),$$

in agreement with (12.124). while the odd reflection reverses the order of site fields

$$(s_3\Phi)^\top = (\phi_3, \phi_2, \phi_1, \phi_0),$$

in agreement with (12.125),

(24.324) is invariant under the 1/2 lattice spacing reflection:

$$s = \begin{pmatrix} 0 & 0 & 0 & 0 & 0 & 0 & 0 & 1 \\ 0 & 0 & 0 & 0 & 0 & 0 & 1 & 0 \\ 0 & 0 & 0 & 0 & 0 & 1 & 0 & 0 \\ 0 & 0 & 0 & 0 & 1 & 0 & 0 & 0 \\ 0 & 0 & 0 & 1 & 0 & 0 & 0 & 0 \\ 0 & 0 & 1 & 0 & 0 & 0 & 0 & 0 \\ 0 & 1 & 0 & 0 & 0 & 0 & 0 & 0 \\ 1 & 0 & 0 & 0 & 0 & 0 & 0 & 0 \end{pmatrix}. \quad (6.33)$$

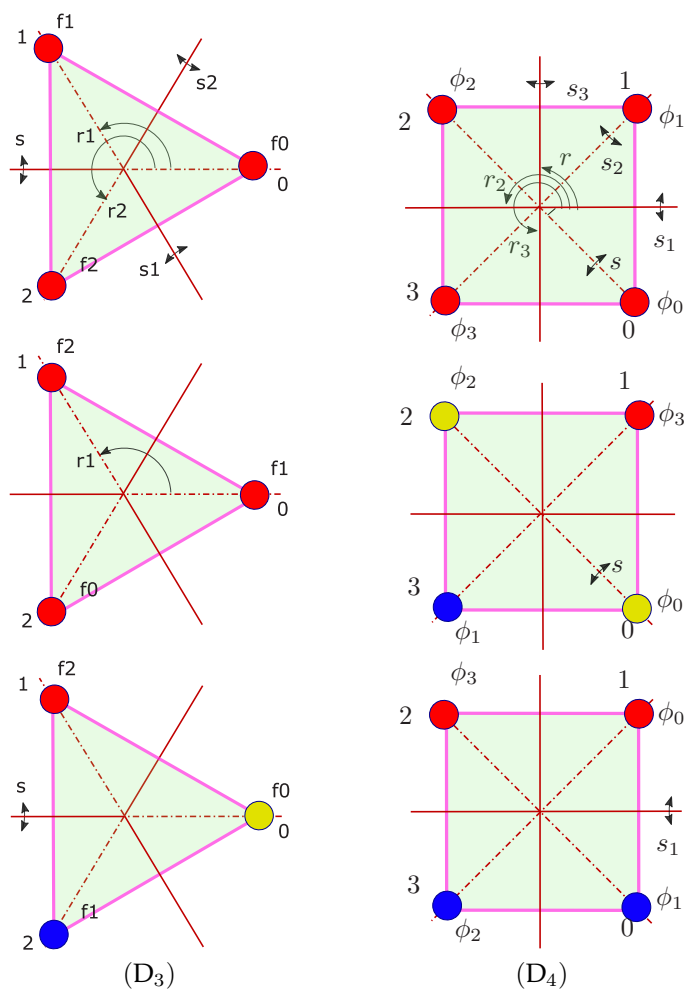


Figure 6.2: (Color online)  $(D_3)$  Question to Han, and everybody else: Is this figure easier to understand than the LC21 figure 8(a)?  $(D_4)$  Dihedral group  $D_4$ , the group of all symmetries that overlie a square onto itself, consists of 3 rotations  $r_j$  that permute the sites cyclically and 4 rotate-reflect  $s_k$  elements that reflect the sites across reflection axes, exchanging the red and the blue sites. An even reflection (long diagonal, dashed line reflection axis), here  $s$ , leaves a pair of opposite sites fixed (marked yellow), while an odd reflection axis (short diagonal, full line), here  $s_1$ , bisects the opposite edges, and flips all sites. Compare with figure 6.4.

(24.327) the corresponding reflection operator leaves sites 1 and 4 invariant:

$$s_1 = \begin{pmatrix} 1 & 0 & 0 & 0 & 0 & 0 & 0 & 0 & 0 \\ 0 & 0 & 0 & 0 & 0 & 0 & 0 & 0 & 1 \\ 0 & 0 & 0 & 0 & 0 & 0 & 0 & 1 & 0 \\ 0 & 0 & 0 & 0 & 0 & 1 & 0 & 0 & 0 \\ 0 & 0 & 0 & 0 & 1 & 0 & 0 & 0 & 0 \\ 0 & 0 & 0 & 1 & 0 & 0 & 0 & 0 & 0 \\ 0 & 0 & 1 & 0 & 0 & 0 & 0 & 0 & 0 \\ 0 & 1 & 0 & 0 & 0 & 0 & 0 & 0 & 0 \end{pmatrix}. \quad (6.34)$$

Combination  $r + r^{-1}$  commutes with  $s_k$ , and  $s_k$  conjugacy reverses  $\mathbb{S}$

$$\begin{aligned} s_k \mathcal{J} s_k &= -r + s_k \mathbb{S} s_k - r^{-1} \\ &= \begin{pmatrix} d_{n-1} & -1 & 0 & 0 & \dots & 0 & -1 \\ -1 & d_{n-2} & -1 & 0 & \dots & 0 & 0 \\ 0 & -1 & d_2 & -1 & \dots & 0 & 0 \\ \vdots & \vdots & \vdots & \vdots & \ddots & \vdots & \vdots \\ 0 & 0 & \dots & \dots & \dots & d_2 & -1 \\ -1 & 0 & \dots & \dots & \dots & -1 & d_1 \end{pmatrix} \end{aligned} \quad (6.35)$$

where  $\mathbb{S}$  is a diagonal matrix with the lattice site  $k$  'stretching' factor  $d_k$  in the  $k$ th row/column.

If a period-9 orbit is invariant under the reflection operator (see (24.328))

$$s = \begin{pmatrix} 0 & 0 & 0 & 0 & 0 & 0 & 0 & 0 & 1 \\ 0 & 0 & 0 & 0 & 0 & 0 & 0 & 1 & 0 \\ 0 & 0 & 0 & 0 & 0 & 0 & 1 & 0 & 0 \\ 0 & 0 & 0 & 0 & 0 & 1 & 0 & 0 & 0 \\ 0 & 0 & 0 & 0 & 1 & 0 & 0 & 0 & 0 \\ 0 & 0 & 0 & 1 & 0 & 0 & 0 & 0 & 0 \\ 0 & 0 & 1 & 0 & 0 & 0 & 0 & 0 & 0 \\ 0 & 1 & 0 & 0 & 0 & 0 & 0 & 0 & 0 \\ 1 & 0 & 0 & 0 & 0 & 0 & 0 & 0 & 0 \end{pmatrix}. \quad (6.36)$$

If a period-8 orbit is of form (see (12.124))

$$\overline{\phi_0 \phi_1 \phi_2 \phi_3 \phi_4 \phi_3 \phi_2 \phi_1}, \quad (6.37)$$

the corresponding reflection operator leaves sites 0 and 4 invariant (see (24.328)):

$$s = \begin{pmatrix} 1 & 0 & 0 & 0 & 0 & 0 & 0 & 0 \\ 0 & 0 & 0 & 0 & 0 & 0 & 0 & 1 \\ 0 & 0 & 0 & 0 & 0 & 0 & 1 & 0 \\ 0 & 0 & 0 & 0 & 0 & 1 & 0 & 0 \\ 0 & 0 & 0 & 0 & 1 & 0 & 0 & 0 \\ 0 & 0 & 0 & 1 & 0 & 0 & 0 & 0 \\ 0 & 0 & 1 & 0 & 0 & 0 & 0 & 0 \\ 0 & 1 & 0 & 0 & 0 & 0 & 0 & 0 \end{pmatrix}. \quad (6.38)$$

**2021-08-23 Predrag** I still worry about the antisymmetric states (24.311), (24.312); here (6.39) and (6.39) look wrong as they force the fixed lattice site fields to be zero. Cannot be true for nonlinear field theories, such as temporal Hénon. Presumably, individual symmetric periodic states are either symmetric or antisymmetric under the swap, not just the reflection-reduced orbit Jacobian matrix  $\mathcal{J}$ . I wish someone would actually show me how this works for individual temporal cat or temporal Hénon periodic states? I'll plod on...

**2021-08-28 Predrag** For example, if the period of the periodic states is 6, we have two kinds of reflections. If the periodic state is antisymmetric under an odd reflection, the antisymmetric subspace is 3-dimensional, and the periodic state tiles  $\mathcal{L}$  as:

$$\overline{\phi_1 \phi_2 \phi_3 | \underline{\phi_3} \underline{\phi_2} \underline{\phi_1} |}, \quad (6.39)$$

where the underline is a shorthand for  $\phi_j = -\phi_j$ .

**2021-08-29 Predrag** A period-5 reflection *antisymmetric periodic state* tiles the infinite lattice as:

$$\cdots \underline{\phi_2} \underline{\phi_1} \overline{\phi_0} \phi_1 \phi_2 | \underline{\phi_2} \underline{\phi_1} \overline{\phi_0} \phi_1 \phi_2 | \cdots, \quad (6.40)$$

The thing to get used to is that a reflection of the primitive cell leads to

$$s \overline{\phi_0} \phi_1 \phi_2 | \underline{\phi_2} \underline{\phi_1} = \overline{\phi_0} \underline{\phi_1} \underline{\phi_2} | \phi_2 \phi_1,$$

which is not a translation; length-2 block  $(\phi_1, \phi_2)$  lattice fields have changed signs. I assume that is OK because the overall number of '-'s does not change.

$$\begin{aligned} -d_0 \phi_0 &= -m_0 \\ \phi_0 - d_2 \phi_1 + \phi_2 &= -m_1. \\ \phi_1 - (d_3 + 1) \phi_2 &= -m_2 \end{aligned}$$

Note, this differs from (24.312), where it is assumed that the antisymmetry forces  $\phi_0 = 0$  (which is indeed the case for a multiplicative symmetrization operator with eigenvalue -1, but we are not doing that here, I think).

orbit Jacobian matrix

$$\begin{aligned} \mathcal{J}_- &= \begin{pmatrix} -d_0 & 0 & 0 \\ 1 & -d_1 & 1 \\ 0 & 1 & -d_2 - 1 \end{pmatrix} \text{ or } \begin{pmatrix} -d_1 & 1 \\ 1 & -d_2 - 1 \end{pmatrix} \\ \text{Det } \mathcal{J}_- &= -d_0(d_1 d_2 + d_2 - 1) \end{aligned} \quad (6.41)$$


where the  $[2 \times 2]$  matrix comes from assuming that separately fixed.

As temporal cat fields are always presented mod 1, there the asymmetric states do not look asymmetric. That would be much easier to see in plots of temporal Hénon periodic states of table 3.3 and figure 3.3.

For  $d_j = 3$  the determinant of this orbit Jacobian matrix is  $3 \cdot 11$  or 11. Are there 11 antisymmetric periodic states, i.e., the corresponding 2 antisymmetric 5-orbits? I assume  $\phi_j = 0$  fixed point counts as 'antisymmetric'. Seems to agree with table 24.3.

Starting with the block  $(\phi_2, \phi_1)$ , followed by  $\boxed{\phi_0}$  presumably results in a time-reversed orbit Jacobian matrix  $s\mathcal{J}s$ . From this construction it is not clear how to connect this to the 5-dimensional primitive cell; so, see also (??), and the continuation in (24.307).

**2021-10-18 Predrag to Han** You might enjoy the discussion of "fundamental domains" in

 [Knots in hyperbolic space](#).

now in CB

**2021-10-31 Predrag to Han** Does not mention 'Burnside', but seems like [Matt Macauley](#) ([homepage](#)) on visualizing group actions is a possible path to understanding Burnside marks...

The course is [here](#), and it, as well as Dana Ernst's online [An inquiry-based approach to abstract algebra](#) are inspired by

Nathan Carter's [Visual Group Theory](#), (read it online through [GaTech-Library](#)) seems very good.

**2021-10-31 Predrag** Matt Macauley has a nice discussion of [dihedral  \$D\_\infty\$](#)  in his [Chapter 1: Groups, intuitively](#).

## 6.4 Time reversal symmetry reduction

### 6.4.1 Laplacians (and time reversal?)

The symmetric (self-adjoint) Laplacian  $\square = -\partial^\top \partial$  suggests that time-reversal desymmetrized dynamics is given by a first order derivative  $\partial = r - 1$  (also known as the integer lattice forward difference operator, see (4.3), (4.4)). The symmetric (self-adjoint) combination  $\square = -\partial^\top \partial$  is the Laplacian

$$\mathcal{J} = -\square + \mu^2 \mathbf{1} = (r^{-1} - 1)(r - 1) + \mu^2 \mathbf{1}, \quad (6.42)$$

where

$$\mu = \sqrt{s - 2}. \quad (6.43)$$

is the Yukawa mass parameter (8.27) in  $d = 1$  dimension.

Note that  $\partial^\top \partial = -\square$  is a symmetric operator, with nonnegative eigenvalues (?recheck the conditions?), so it is a good practice to always prepend a minus sign to the Laplacian, write it as  $-\square$ . With that choice, the Green's function (8.36), (8.42) is strictly nonnegative (?recheck the conditions?).

Define lattice momentum as forward lattice difference operator, and the Laplacian as the hermitian operator

$$\begin{aligned} p &= i(r - 1) \\ \square &= -p^\dagger p = (r^{-1} - 1)(r - 1) = -r + 2\mathbf{1} - r^{-1} \end{aligned} \quad (6.44)$$

For a one-dimensional lattice

$$\begin{aligned} \mathcal{J} &= p^\dagger p + \mu^2 \mathbf{1} = \hat{\mathcal{J}}^\dagger \hat{\mathcal{J}}, \quad \hat{\mathcal{J}} = p + \mu \mathbf{1} = ir + (\mu - i) \mathbf{1} \\ \text{Det } \mathcal{J} &= |\text{Det } \hat{\mathcal{J}}|^2. \end{aligned}$$

In  $d$  dimensions, the free-field orbit Jacobian operator takes the  $2d+1$  banded form

$$\begin{aligned} \mathcal{J} &= \sum_{j=1}^d (-r_j + 2\mathbf{1} - r_j^{-1}) + \mu^2 \mathbf{1} \\ &= \sum_{j=1}^d p^\dagger p + \mu^2 \mathbf{1}, \end{aligned} \quad (6.45)$$

For purposes of the time-reversal desymmetrization it might be more convenient to work with the centered, reflection antisymmetric difference operators (4.6),

$$\begin{aligned} \tilde{\partial} &= \tilde{r} - \tilde{r}^{-1}, \quad \tilde{r} = r^{1/2} \\ &= -\tilde{\partial}^\top, \end{aligned} \quad (6.46)$$



constructed by interpolating 1/2-unit spacing lattice  $\tilde{\mathcal{L}}$  points between the integer lattice  $\mathcal{L}$  points, with the derivatives written as

$$\begin{aligned} (r - \mathbf{1}) &= \tilde{r}\tilde{\partial} \\ (r^{-1} - \mathbf{1})(r - \mathbf{1}) &= -\tilde{\partial}^2 = \square \end{aligned} \quad (6.47)$$

Alternative version: Define lattice momentum as 1/2-lattice centered lattice derivative  $ip_j = r_j^{\frac{1}{2}} - r_j^{-\frac{1}{2}}$ . In  $d$  dimensions, the free-field orbit Jacobian operator takes the  $2d + 1$  banded form

$$\begin{aligned} \mathcal{J} &= \sum_{j=1}^d (-r_j + 2\mathbf{1} - r_j^{-1}) + \mu^2 \mathbf{1} \\ &= \sum_{j=1}^d -(\tilde{r}_j - \tilde{r}_j^{-1})(\tilde{r}_j - \tilde{r}_j^{-1}) + \mu^2 \mathbf{1} \\ &= \sum_{j=1}^d p_j^2 + \mu^2 \mathbf{1}, \end{aligned} \quad (6.48)$$

where  $r_j$  shift operators translate the field configuration by one lattice spacing in the  $j$ th hypercubic lattice direction.

$$\begin{aligned} \mathcal{J} &= \square - \mu^2 \mathbf{1} = \tilde{\mathcal{J}}^\top \tilde{\mathcal{J}} \\ \tilde{\mathcal{J}} &= \tilde{\partial} - \mu \mathbf{1} = \tilde{r} - \mu \mathbf{1} - \tilde{r}^{-1} \\ \tilde{\mathcal{J}}^\top &= \tilde{\partial} + \mu \mathbf{1} = \tilde{r} + \mu \mathbf{1} - \tilde{r}^{-1} \end{aligned}$$

Written out in the matrix form, the  $\mathcal{J} = \tilde{\mathcal{J}}^\top \tilde{\mathcal{J}}$  factorization can be checked by matrix multiplication<sup>5</sup>

$$\begin{aligned} \mathcal{J}[\Phi] &= \begin{pmatrix} -d_0 & 0 & 1 & 0 & \dots & 1 & 0 \\ 0 & -d_1 & 0 & 1 & \dots & 0 & 1 \\ 1 & 0 & -d_2 & 0 & \dots & 0 & 0 \\ \vdots & \vdots & \vdots & \ddots & \vdots & \vdots & \vdots \\ 0 & 0 & \dots & 0 & -d_{n-3} & 0 & 1 \\ 1 & 0 & \dots & 1 & 0 & -d_{n-2} & 0 \\ 0 & 1 & \dots & 0 & 1 & 0 & -d_{n-1} \end{pmatrix} \\ \tilde{\mathcal{J}} &= \begin{pmatrix} -\mu_0 & -1 & 0 & 0 & \dots & 0 & 1 \\ 1 & -\mu_1 & -1 & 0 & \dots & 0 & 0 \\ 0 & 1 & -\mu_2 & -1 & \dots & 0 & 0 \\ \vdots & \vdots & \vdots & \vdots & \ddots & \vdots & \vdots \\ 0 & 0 & \dots & \dots & \dots & -\mu_{n-2} & -1 \\ -1 & 0 & \dots & \dots & \dots & 1 & -\mu_{n-1} \end{pmatrix}, \end{aligned} \quad (6.49)$$

<sup>5</sup>Predrag 2021-09-14: Checked that factorization (6.49), metal temporal lattice condition (6.50) works also for the orbit  $\Phi$  dependent case (3.26).

where  $\mu_t^2 = d_t - 2$  is the lattice site "Klein-Gordon mass", "stretching factor", respectively, and  $\mathcal{J}, \tilde{\mathcal{J}}^\top, \tilde{\mathcal{J}}$  act on the 1/2-unit spacing lattice  $\tilde{\mathcal{L}}$ , i.e., remember (perhaps reintroduce  $\Delta t$  lattice spacing explicitly?) that  $\tilde{r} = r^{1/2}$  in (6.47) is the shift operator on the 1/2 lattice spacing. So two applications of 1/2 lattice shift operator give you one full lattice spacing.

Written out as a second-order difference equation, the metal map takes a temporal lattice form

$$\tilde{\phi}_{t+1} - \mu_t \tilde{\phi}_t - \tilde{\phi}_{t-1} = -\tilde{m}_t, \quad (6.50)$$

or, in terms of a periodic state  $\Phi$ , the corresponding symbol block'  $M$ , and the  $[n \times n]$  shift operator  $r$ ,

$$(\tilde{r} - \mu[\Phi] \mathbf{1} - \tilde{r}^{-1}) \tilde{\Phi} = -\tilde{M}, \quad (6.51)$$

where  $\mu[\Phi] \mathbf{1}$  stands for site-dependent diagonal Klein-Gordon mass matrix.

$\tilde{\mathcal{J}}$  discrete Fourier diagonalization

$$\begin{aligned} \lambda_m &= \mu^2 + 2 - 2 \cos(k_m) = \mu^2 + 4 \sin^2(k_m/2) \\ &= \left( \mu - i 2 \sin\left(\frac{k_m}{2}\right) \right) \left( \mu + i 2 \sin\left(\frac{k_m}{2}\right) \right) \\ &= \left( \mu + e^{ik_m/2} - e^{-ik_m/2} \right) \left( \mu + e^{ik_m/2} - e^{-ik_m/2} \right)^* \\ &\text{where } k_m = 2\pi m/n \end{aligned} \quad (6.52)$$

i.e., the  $\sin^2(k_m/2)$  version of the eigenvalues is there for a reason, a consequence of the time-reversal symmetry, with  $\tilde{\mathcal{J}}$  eigenvalues being

$$-2i \sin(k_m/2) = e^{ik_m/2} - e^{-ik_m/2}.$$

Phase is  $k_m/2$  because the fundamental domain is 1/2 of the full line. The square root is natural because the Yukawa mass  $\mu^2 = d(s-2)$  parameter (8.27).

Note also relations (16.96) convenient for Hill determinant evaluations:

$$\ln(2 - 2 \cos(2\pi x)) = 2 \ln |2 \sin(\pi x)| = 2 \ln |1 - e^{2\pi i x}|. \quad (6.53)$$

Discrete Fourier diagonalization  $\mathcal{J} = \mathcal{J}_- \mathcal{J}_+$ , turns  $\tilde{r}$  into its eigenvalues  $\exp(ik_m/2)$ , and the temporal cat Hill determinant (24.241) factorizes as

$$\begin{aligned} \text{Det } \mathcal{J} &= \text{Det } \mathcal{J}_- \text{Det } \mathcal{J}_+ \\ \text{Det } \mathcal{J}_+ &= \mu \prod_{m=1}^{\ell-1} (\mu + p_m), \quad p_m = 2i \sin \frac{k_m}{2}, \quad k_m = \frac{2\pi m}{\ell} \\ \text{Det } \mathcal{J}_- &= \mu \prod_{m=1}^{\ell-1} (\mu - p_m). \end{aligned} \quad (6.54)$$

$n$	1	2	3	4	5	6	7	8	9	10	11
$N_n$	1	5	16	45	121	320	841	2205	5776	15125	39601
$M_n$	1	2	5	10	24	50	120	270	640	1500	3600

Table 6.1: Periodic states and orbit counts for the  $s = 3$  cat map. Compare with the golden (Fibonacci [8]) cat map table 6.2 and (6.198).

$n$	1	2	3	4	5	6	7	8	9	10	11	12	13	14	15
$\tilde{N}_n$	1	1	4	5	11	16	29	45	76	121	199	320	521	841	1364
$\tilde{M}_n$	1	0	1	1	2	2	4	5	8	11	18	25	40	58	90

Table 6.2: Temporal periodic states and orbit counts for the  $\mu = 1$  golden cat map. See (6.198) and the counting of walks on the “half time-step” Markov graph figure 6.5.

By derivation (do it!) analogous to the Isola’s cat map  $\zeta(Z)$  (2.28), the topological zeta function for metal cat maps is

$$\frac{1}{\tilde{\zeta}(t)} = \frac{1 - \mu t - t^2}{(1 - t)^2}, \quad (6.55)$$

where  $z = t^2$ , in agreement with (6.197) for  $\mu = 1$ . See also (8.152).

Denote the  $[\tilde{n} \times \tilde{n}]$  orbit Jacobian matrix  $\tilde{\mathcal{J}}(\mu)$  of the  $1/2$  time-step lattice  $\tilde{\mathcal{L}}$  as  $\tilde{\mathcal{J}}_{\tilde{n}}$ , where  $\tilde{n}$  is the period of the periodic state  $\tilde{\Phi}$  on the half interval lattice  $\tilde{\mathcal{L}}$ . Denote the orbit Jacobian matrix  $\mathcal{J}(s)$  of the temporal cat lattice  $\mathcal{L}$  as  $\mathcal{J}_n$ , where  $n$  is the period of the periodic state  $\Phi$  on the integer lattice  $\mathcal{L}$ . For odd, respectively even periods, the determinants of  $\tilde{\mathcal{J}}$  and  $\mathcal{J}$  are related as:

$$\begin{aligned} \det(\tilde{\mathcal{J}}_{2m+1}^\top \tilde{\mathcal{J}}_{2m+1}) &= \det(\mathcal{J}_{2m+1}) \\ \det(\tilde{\mathcal{J}}_{2n}^\top \tilde{\mathcal{J}}_{2n}) &= \det(\mathcal{J}_n)^2, \end{aligned} \quad (6.56)$$

hence <sup>6</sup>

$$\begin{aligned} N(s)_n &= \det \mathcal{J}_n = (\det \tilde{\mathcal{J}}_n)^2 = \tilde{N}(\mu)_n^2, \quad n \text{ odd} \\ N(s)_n &= |\det \mathcal{J}_n| = |\det \tilde{\mathcal{J}}_{2n}| = \tilde{N}(\mu)_{2n}, \quad n \text{ even}. \end{aligned} \quad (6.57)$$

For odd  $n$ , see (6.88) and compare odd entries in table 21.1 and table 6.2.

For even  $n$ , compare the  $n$  entries in table 21.1 with the  $\tilde{n} = 2n$  entries in table 6.2.

$\hat{\mathcal{J}} = \tilde{\mathcal{J}}^\top \tilde{\mathcal{J}}$  is the orbit Jacobian matrix of the temporal cat on the half interval lattice  $\tilde{\mathcal{L}}$  (denoted  $\mathcal{J}$  in (6.49)).  $\hat{\mathcal{J}}_{2n} = \tilde{\mathcal{J}}_{2n}^\top \tilde{\mathcal{J}}_{2n}$  is the orbit Jacobian matrix of

<sup>6</sup>Predrag 2021-02-13: Have not checked whether absolute values  $|\dots|$  are needed for the even case.

the temporal cat on the half lattice with period  $2n$ , which is period  $n$  in the unit lattice. But  $\hat{\mathcal{J}}_{2n}$  is different from  $\mathcal{J}_n$ , the orbit Jacobian matrix of the temporal cat on the unit lattice, because it has more lattice sites. Note that:

$$\hat{\mathcal{J}}_{2n} = \mathcal{J}_n \otimes \mathbf{1}_{[2 \times 2]}.$$

Using the second identity in (12.20) we can get the second relation in (6.56).

$\hat{\mathcal{J}}_{2n+1} = \hat{\mathcal{J}}_{2n+1}^\top \hat{\mathcal{J}}_{2n+1}$  is the orbit Jacobian matrix of the temporal cat on the half lattice with period  $2n + 1$ , which has period  $n + 1/2$  on the unit lattice.  $\hat{\mathcal{J}}_{2n+1}$  is same as the  $\mathcal{J}_{2n+1}$  after a permutation, which leads to the first relation in (6.56).

The “functional equation” [2]

$$\hat{\zeta}(z) = \zeta(1/z) \quad (6.58)$$

is for us the obvious statement of time-reversal invariance. Note also under the time reversal  $t \rightarrow 1/t$

$$\frac{1}{\tilde{\zeta}(1/t)} = -\frac{1}{\tilde{\zeta}(-t)}. \quad (6.59)$$

## 6.4.2 Primitive cell Hill determinant for a 1-order system

7

Consider a one-dimensional, temporal lattice period- $n$  periodic state  $\Phi_p = \{\phi_1, \phi_2, \dots, \phi_n\}$ , with the orbit Jacobian matrix

$$\tilde{\mathcal{J}}_p = \begin{pmatrix} \sigma_1 & -1 & 0 & \cdots & 0 & 0 \\ 0 & \sigma_2 & -1 & \cdots & 0 & 0 \\ 0 & 0 & \sigma_3 & \cdots & 0 & 0 \\ \vdots & \vdots & \vdots & \ddots & \vdots & \vdots \\ 0 & 0 & 0 & \cdots & \sigma_{n-1} & -1 \\ -1 & 0 & 0 & \cdots & 0 & \sigma_n \end{pmatrix} = -r(\mathbf{1} - r^{-1}\tilde{\mathcal{S}}_p), \quad (6.60)$$

It suffices to work out a temporal period  $n = 3$  example to understand the calculation for any period. In terms of the  $[3 \times 3]$  matrix shift matrix  $r$ , the orbit Jacobian matrix can be written as

$$\begin{aligned} -r^{-1}\tilde{\mathcal{J}}_p &= \mathbf{1} - r^{-1}\tilde{\mathcal{S}}_p \\ r^{-1} &= \begin{bmatrix} 0 & 0 & 1 \\ 1 & 0 & 0 \\ 0 & 1 & 0 \end{bmatrix}, \quad \tilde{\mathcal{S}}_p = \begin{bmatrix} \sigma_1 & 0 & 0 \\ 0 & \sigma_2 & 0 \\ 0 & 0 & \sigma_3 \end{bmatrix}. \end{aligned} \quad (6.61)$$

<sup>7</sup>Predrag 2024-10-19: An attempt to streamline Xuanqi’s separation of stability into primitive cell Hill determinant and  $p(k)^2$  parts. Transfer to WWLAF22 [76]. Once incorporated, remove from here.

Next, note that is  $r\tilde{\mathcal{S}}_p$  comutator permutes cyclicly the diagonal elements of  $\tilde{\mathcal{S}}_p$ ,

$$\begin{aligned} (r^{-1}\tilde{\mathcal{S}}_p)^2 &= r^{-2} \begin{bmatrix} \sigma_2\sigma_1 & 0 & 0 \\ 0 & \sigma_3\sigma_2 & 0 \\ 0 & 0 & \sigma_1\sigma_3 \end{bmatrix} \\ (r^{-1}\tilde{\mathcal{S}}_p)^3 &= \begin{bmatrix} \sigma_2\sigma_1\sigma_3 & 0 & 0 \\ 0 & \sigma_3\sigma_2\sigma_1 & 0 \\ 0 & 0 & \sigma_1\sigma_3\sigma_2 \end{bmatrix}. \end{aligned}$$

As  $r^{\pm n} = \mathbf{1}$  for any periodic state of period  $n$ , the trace of  $[n \times n]$  matrix

$$\text{tr} (r^{-1}\tilde{\mathcal{S}}_p)^\ell = \delta_{\ell, rn} n \sigma_p^r, \quad \sigma_p = \sigma_n\sigma_{n-1} \cdots \sigma_2\sigma_1$$

is non-vanishing only if  $\ell$  is a multiple of  $n$ .

Now we can evaluate the Hill determinant by expanding

$$\begin{aligned} \ln \text{Det} (\tilde{\mathcal{J}}_p) &= \text{tr} \ln(\mathbf{1} - r^{-1}\tilde{\mathcal{S}}_p) = - \sum_{\ell=1}^{\infty} \frac{1}{\ell} \text{tr} (r^{-1}\tilde{\mathcal{S}}_p)^\ell \\ &= - \sum_{r=1}^{\infty} \frac{1}{r} \sigma_p^r = \ln(1 - \sigma_p), \end{aligned} \quad (6.62)$$

where we have used the unitarity of finite group representations,  $\text{Det} r = 1$ . The Hill determinant for a 2-term difference equation (6.60) on a temporal lattice

$$\text{Det} (\tilde{\mathcal{J}}_p) = 1 - \sigma_p, \quad \sigma_p = \sigma_n\sigma_{n-1} \cdots \sigma_2\sigma_1. \quad (6.63)$$

In the temporal Bernoulli case, the field  $\phi_t$  is a constant, a period  $n_c$  repeat periodic state  $\Phi_c$  Hill determinant is

$$\text{Det} \tilde{\mathcal{J}}_c = 1 - s^{n_c}, \quad (6.64)$$

in agreement with the Bernoulli Hill determinant (1.13).

Remarks:

- This generalizes the Bernoulli map, chapter 1, with steady state (1.3) stretching factor  $s$ , to prime periodic state of any temporal evolution system.
- See Han's sect. 11.1.3 summary of Bountis and Helleman paper.
- This is almost (except for '1' term) the orbit Jacobian matrix of the anti-integrable theory, with couplings to spatiotemporal neighbors dropped. So maybe we know the answer in any dimension, something like (not quite right, might need Lind  $2d$  formula):

$$\text{Det} \tilde{\mathcal{J}}_p = 1 - \sigma_p \quad (???), \quad \sigma_p = \prod_z^{\mathbb{A}} \sigma_z. \quad (6.65)$$

- Predrag’s derivation is formal (AKA wrong) because of sign issues. It should be fixed, as Han does on page 17, and Predrag on page 22.
- The derivation applies to both scalar and multi-component field theories, if rewritten as in sect. 12.7.1. Can treat  $\ell_p$  rows as a  $\ell_p$ -component fields, perhaps. Hope we can avoid that.
- From (6.289), we also know the anti-integrable primitive cell zeta function in one (and perhaps) any dimension,

$$\begin{aligned} 1/\zeta_p &= \exp [\ln(1 - \sigma_p z^n) - \ln(1 - z)] \\ &= \frac{1 - \sigma_p z^n}{1 - z}. \end{aligned} \tag{6.66}$$

- Hopefully this is a ‘square root’ of an one-dimensional temporal lattice, time reversal invariant, Laplacian theory, see sect. ?? . We are using notation  $\sigma_j$  for stretching factors in (6.60), in anticipation that they are square roots of the second-order system’s stretching factors,  $d_j = \sigma_j^2$ .
- Predrag would prefer a lattice momentum formulation, as in (6.47).
- Rewrite the above finite matrix (6.60) in terms of the infinite Bravais lattice orbit Jacobian operator.
- To go to continuous  $k$  stability exponents, need to include primitive cells for all repeats of period- $n$  periodic state  $\Phi_p$ . With ‘1’ in (6.62) replaced by something like  $r^{-n}$  (???) .

Or, maybe, replace unit lattice shift  $r$  by arbitrary spacing shift (equal or larger than 1), which does not satisfy  $r^{\pm n} = \mathbf{1}$  for any integer  $n$ , but is diagonalized by a continuous Fourier transform to the Brillouin zone  $k \in (-\pi/n, \pi/n]$ .

- Generalization to one-dimensional Laplacian, time-reversal invariant field theories hopefully follows from Hill determinant factorization (6.54), and Laplacian factorization (6.73), perhaps (6.77).  
 $\text{Det } \mathcal{J} = \text{Det } \tilde{\mathcal{J}}_1 \text{Det } \tilde{\mathcal{J}}$ .
- Generalization to two-dimensional square and rectangular Bravais lattice Laplacians might require Pauli matrices (???) , see (4.33).
- Have given no thought to Bravais lattices with tilts.
- The orbit Jacobian matrix of a period- $(mn)$  periodic state  $\Phi$ , which is a  $m$ th repeat of a period- $n$  prime periodic state  $\Phi_p$ , has a bi-diagonal block circulant matrix form that follows by inspection from (6.60):

$$\mathcal{J} = \begin{pmatrix} \mathbf{s}_p & -\mathbf{r} & & & \mathbf{0} \\ \mathbf{0} & \mathbf{s}_p & -\mathbf{r} & & \\ & \ddots & \ddots & \ddots & \\ & & & \mathbf{0} & \mathbf{s}_p & -\mathbf{r} \\ -\mathbf{r} & & & & \mathbf{0} & \mathbf{s}_p \end{pmatrix}, \tag{6.67}$$

where block matrix  $s_p$  is a  $[n \times n]$  symmetric Toeplitz matrix

$$s_p = \begin{pmatrix} d_0 & -1 & & & 0 \\ 0 & d_1 & -1 & & \\ & \ddots & \ddots & \ddots & \\ & & 0 & d_{n-2} & -1 \\ 0 & & & 0 & d_{n-1} \end{pmatrix}, \quad \mathbf{r} = \begin{pmatrix} 0 & \cdots & 0 \\ & \ddots & \vdots \\ 1 & & 0 \end{pmatrix},$$

and  $\mathbf{r}$  enforces the periodic bc's. This period- $(mn)$  periodic state  $\Phi$  orbit Jacobian matrix is translation-invariant under Bravais lattice translations by multiples of  $n$ . One can visualize this periodic state as a tiling of the integer lattice  $\mathbb{Z}$  by a prime periodic state  $\Phi_p$  decorating a tile of length  $n$ .

### 6.4.3 Time reversal blog

**2007-11-20 Keating, Marklof and Williams** The cat map  $A$  acting on  $(q_t, p_t)$  must be symplectic, and time-reversal symmetric,

$$TAT = A^{-1} \tag{6.68}$$

where  $T$  is the time-reversal operator

$$T = \begin{bmatrix} 1 & 0 \\ 0 & -1 \end{bmatrix} \tag{6.69}$$

An example is

$$A = \begin{bmatrix} 2 & 1 \\ 3 & 2 \end{bmatrix} \tag{6.70}$$

The Percival-Vivaldi 2-configuration map (2.5) acts on a 2-dimensional state space point  $(\phi_{n-1}, \phi_n)$ , so time reversal permutes the two entries,

$$A = \begin{bmatrix} 0 & 1 \\ -1 & s \end{bmatrix}, \quad T = \begin{bmatrix} 0 & 1 \\ 1 & 0 \end{bmatrix}. \tag{6.71}$$

Not sure what  $T$  is for cat map of form (8.58).

**2004-11-01 Predrag and Lan** We implemented the “half-step” figure 6.5 reduction for the Kuramoto–Sivashinsky spatial reflection symmetry in *Unstable recurrent patterns in Kuramoto–Sivashinsky dynamics* [52], see figure 6.3. It happens in sect. B *Curvilinear coordinates, center repeller* of the paper, and the result is the 3-letter bimodal return map of figure 6.3 (c). Without quotienting the  $D_1$  symmetry, the return map would have up to 11 letters, and be an unmanageable holly mess.

**2018-04-12 Predrag** For our many (failed) attempts to find an Adler-Weiss forward and backward in time symmetric partition, see sect. 24.3 *Time reversal*.

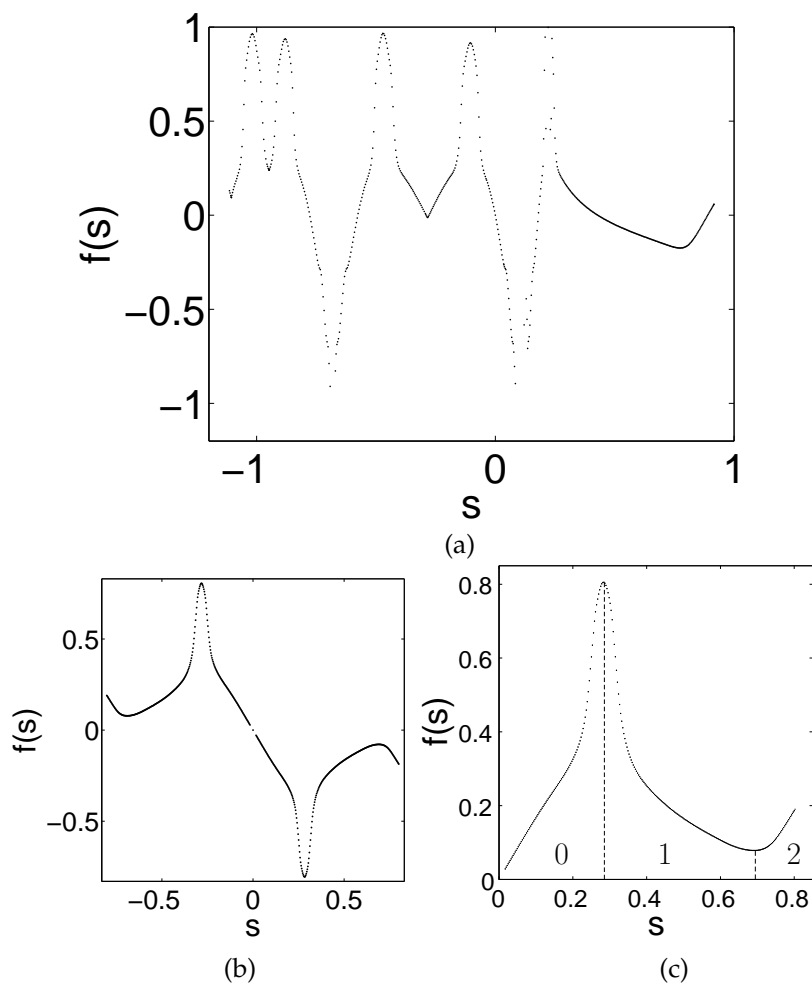


Figure 6.3: The return map on the Poincaré section  $\mathcal{P}_C$  of the unstable manifold of equilibrium  $C$ , antisymmetric subspace of Kuramoto–Sivashinsky, the intrinsic coordinate: (a) There are 11 monotone segments, requiring an 11-letter alphabet. However, in the (Kuramoto–Sivashinsky)/ $D_1$ -spatial reflection symmetry reduced state space, (b) the return map simplifies to an antisymmetric return map, which becomes (c) a 3-letter bimodal return map in the fundamental domain, with the symbolic dynamics given by three symbols  $\{0, 1, 2\}$ . It's a **wild**  $\sqrt{\text{time}}$  simplification of the dynamics! enabling us to populate the neighboring strange attractor with many periodic orbits. (Taken from fig. 8 (e) of Lan and Cvitanović [52]).



**2018-04-12 Predrag** [Birdtracks.eu](https://birdtracks.eu) Sect. 8.2.3 *Time reversal symmetry* might be relevant to spatiotemporal cat: when the Hamiltonian is invariant under time reversal, the symmetry group is enlarged.

**2016-11-16 Predrag** Maillard group, Anglès d’Auriac, Boukraa and Maillard [2] *Functional relations in lattice statistical mechanics, enumerative combinatorics, and discrete dynamical systems* state the “functional equation”

$$\zeta(z) = \zeta(1/z) \tag{6.72}$$

which for us is the obvious statement of time-reversal invariance.

**2016-11-16 Predrag** Note also (6.59) under the presumed time reversal  $t \rightarrow 1/t$  This all has to do with time reversibility - we should exploit time and space reversal symmetries in this way, and - who knows - understand Ihara zeta functions better.

**2020-12-24 Predrag** Note that in the discussion of time-reversal invariant recurrence relations (8.167) (see (2.38), etc.) the characteristic equation factors as  $a(\phi) = \ell(\phi)\ell(1/\phi)$  where the factors  $\ell(\phi)$  and  $\ell(1/\phi)$  of  $a(\phi)$  are known as the *Hurwitz factors*.

**2023-08-05 Predrag** This time following deLyra factorization (4.15)  $\square = \Delta^{(+)}\Delta^{(-)}$ , with

$$\Delta^{(+)} = -\mathbf{1} + r, \quad \Delta^{(-)} = r^T \Delta^{(+)} = \mathbf{1} - r^T. \tag{6.73}$$

The forward difference operator (see (4.3), (4.4)),

$$\Delta^{(+)} = \begin{pmatrix} -1 & 1 & 0 & 0 & \dots & 0 & 0 \\ 0 & -1 & 1 & 0 & \dots & 0 & 0 \\ 0 & 0 & -1 & 1 & \dots & 0 & 0 \\ \vdots & \vdots & \vdots & \vdots & \ddots & \vdots & \vdots \\ 0 & 0 & \dots & \dots & \dots & \mu & 1 \\ 1 & 0 & \dots & \dots & \dots & 0 & -1 \end{pmatrix}, \tag{6.74}$$

the backward difference operator (see (4.142), (24.435)),

$$\Delta^{(-)} = \begin{pmatrix} 1 & 0 & 0 & 0 & \dots & 0 & -1 \\ -1 & 1 & 0 & 0 & \dots & 0 & 0 \\ 0 & -1 & 1 & 0 & \dots & 0 & 0 \\ \vdots & \vdots & \vdots & \vdots & \ddots & \vdots & \vdots \\ 0 & 0 & \dots & \dots & \dots & 1 & 0 \\ 0 & 0 & \dots & \dots & \dots & -1 & 1 \end{pmatrix}. \tag{6.75}$$

The *linear momentum*  $p_m = 2 \sin \frac{k_m}{2}$  ( $\times$  a phase factor) as eigenvalue of  $\Delta^{(+)}, \Delta^{(-)}$ :

$$\begin{aligned} \Delta^{(+)}\varphi_m &= (-1 + e^{ik_m})\varphi_m = ie^{ik_m/2} 2 \sin \frac{k_m}{2} \\ \Delta^{(-)}\varphi_m &= (1 - e^{-ik_m})\varphi_m = ie^{-ik_m/2} 2 \sin \frac{k_m}{2}, \end{aligned} \tag{6.76}$$

**2020-01-10 Predrag** The “square root”  $C$  (6.188) might be related to resistor networks’s Laplace-like operator factorization  $L = RR^\top$ , see (8.205), with no transpose needed in this example, as  $C$  is symmetric.

**2020-02-06 Predrag**  $\mathcal{J} = \tilde{\mathcal{J}}^\top \tilde{\mathcal{J}}$  factorization [63], as in (24.270):

$$\tilde{\mathcal{J}} = \begin{pmatrix} \mu & -1 & 0 & 0 & \dots & 0 & 1 \\ 1 & \mu & -1 & 0 & \dots & 0 & 0 \\ 0 & 1 & \mu & -1 & \dots & 0 & 0 \\ \vdots & \vdots & \vdots & \vdots & \ddots & \vdots & \vdots \\ 0 & 0 & \dots & \dots & \dots & \mu & -1 \\ -1 & 0 & \dots & \dots & \dots & 1 & \mu \end{pmatrix}. \quad (6.77)$$

$$\tilde{\mathcal{J}}^\top = \begin{pmatrix} \mu & 1 & 0 & 0 & \dots & 0 & -1 \\ -1 & \mu & 1 & 0 & \dots & 0 & 0 \\ 0 & -1 & \mu & 1 & \dots & 0 & 0 \\ \vdots & \vdots & \vdots & \vdots & \ddots & \vdots & \vdots \\ 0 & 0 & \dots & \dots & \dots & \mu & 1 \\ 1 & 0 & \dots & \dots & \dots & -1 & \mu \end{pmatrix}. \quad (6.78)$$

Note that Pozrikidis [63]  $L = RR^\top$  factorization (8.205) the factors  $R$  are bi-diagonal, as in the forward difference operator (6.42). He does not seem to introduce  $1/2$  lattice spacing central difference operator (6.46), and considers only the Helmholtz equation  $\mu = 0$  case, not our tri-diagonal map. I do not see our symmetry reduction there...

$\mathcal{J}$  is time reversal (6.82) invariant (self-adjoint; Hermitian),  $R\mathcal{J}R^\top = \mathcal{J}$ , but  $\tilde{\mathcal{J}}^\top = \tilde{R}\tilde{\mathcal{J}}\tilde{R}^\top$  is time reversed, as a first order derivative should.

**2020-09-30 Predrag** Note that in (6.199) Maillard *et al.* [2] quotient the time reversal (reflection) symmetry for  $s = 3$  temporal cat.

The reflection-symmetric operator

$$T_{ij} = \sum_{\mu=1}^d [(r^\mu)_{ij} + (r^\mu)_{ji}], \quad (6.79)$$

generates all steps of length 1. The symmetric (self-adjoint) combination  $\Delta = -\partial^\top \partial = \partial^2$  (note this notation for  $\square$ )

$$\begin{aligned} \Delta - \mu^2 \mathbf{1} &= - \sum_{\mu=1}^d \{ (r_\mu^{-1} - \mathbf{1}) (r_\mu - \mathbf{1}) + \mu^2 \mathbf{1} \} \\ &= \mathcal{J} = \sum_{\mu=1}^d (r_\mu^{-1} + r_\mu - s \mathbf{1}) \\ &= (T - ds \mathbf{1}) \end{aligned} \quad (6.80)$$

relates the walker  $T$  to the lattice Laplacian and the orbit Jacobian matrix  $\mathcal{J}$ .

**2020-10-31 Predrag** Han, what does Gradshteyn and Ryzhik [39] have to say about formulas (6.54)? Sine is a cosine rotated by  $\pi/2$ .

Still have to factorize the zeta function, as in (6.199). Clearly  $\det \mathcal{J}_+(\mu) = (-1)^\ell \det \mathcal{J}_-(-\mu)$ , so, up to a complex phase,  $\det \mathcal{J}_+$  is a square root of  $\mathcal{J}$ . Not sure anything is attained by computing one rather than the other...

A guess for factorization in  $d$  dimensions (still wrong) is something like

$$\begin{aligned} \Delta - d(s-2)\mathbf{1} &= -\sum_{\mu=1}^d \{(r_\mu^{-1} - 1)(r_\mu - 1) + (s-2)\mathbf{1}\} \\ &= -\sum_{\mu=1}^d \{-i(r_\mu^{-1} - 1) + \sqrt{s-2}\mathbf{1}\} \\ &\quad \{i(r_\mu - 1) + \sqrt{s-2}\mathbf{1}\} \end{aligned} \quad (6.81)$$

**2020-09-30 Predrag** Failed attempt, can safely ignore. In  $d = 1$  temporal cat case the time reflection operator  $R, R^2 = \mathbf{1}$ , is

$$R = \begin{pmatrix} 0 & 0 & 0 & 0 & \dots & 0 & 1 \\ 0 & 0 & 0 & 0 & \dots & 1 & 0 \\ 0 & 0 & 0 & \dots & 1 & 0 & 0 \\ \vdots & \vdots & \vdots & \vdots & \ddots & \vdots & \vdots \\ 0 & 1 & \dots & \dots & \dots & 0 & 0 \\ 1 & 0 & \dots & \dots & \dots & 0 & 0 \end{pmatrix}. \quad (6.82)$$

with projection operators (for  $n = 3$ )

$$P_{A_1} = \frac{1}{2} \begin{pmatrix} 1 & 0 & 1 \\ 0 & 2 & 0 \\ 1 & 0 & 1 \end{pmatrix}, \quad P_{A_2} = \frac{1}{2} \begin{pmatrix} 1 & 0 & -1 \\ 0 & 0 & 0 \\ -1 & 0 & 1 \end{pmatrix} \quad (6.83)$$

$$d_{A_1} = \text{tr } P_{A_1} = 2, \quad d_{A_2} = \text{tr } P_{A_2} = 1 \quad (6.84)$$

For any  $n$

$$d_{A_1} = \text{tr } P_{A_1} = \frac{1}{2}(\text{tr } \mathbf{1} + \text{tr } R) = \frac{1}{2}(n+1), \quad d_{A_2} = \frac{1}{2}(n-1) \quad (6.85)$$

This can only work for  $n$  odd. For even ones there must be another irrep?

$$\mathcal{J}_{A_1} = \frac{1}{2} \begin{pmatrix} 1-s & 2 & 1-s \\ 2 & -2s & 2 \\ 1-s & 2 & 1-s \end{pmatrix}, \quad \mathcal{J}_{A_2} = \frac{1}{2} \begin{pmatrix} -1-s & 0 & 1+s \\ 0 & 0 & 0 \\ 1+s & 0 & -1-s \end{pmatrix} \quad (6.86)$$

$$\mathcal{J}_{A_1} = \mathbf{1} + \begin{pmatrix} -\frac{1+s}{2} & 1 & \frac{1-s}{2} \\ 1 & -(1+s) & 1 \\ \frac{1-s}{2} & 1 & -\frac{1+s}{2} \end{pmatrix} \quad (6.87)$$

We know that for  $[3 \times 3]$  orbit Jacobian matrix

$$\mathcal{J} = \begin{pmatrix} -s & 1 & 1 \\ 1 & -s & 1 \\ 1 & 1 & -s \end{pmatrix}$$

$$N_3 = |\text{Det } \mathcal{J}| = (s-2)(s+1)^2 = [\mu(\mu^2 + 3)]^2, \quad (6.88)$$

but clearly

$$\text{Det } \mathcal{J}_{A_1} = 0, \quad \text{Det } \mathcal{J}_{A_2} = \frac{1}{4} (0(1+s)^2 - 0(1+s)^2) = 0. \quad (6.89)$$

As det of sum is not sum of det's,  $\mathcal{J}_{A_1}$ ,  $\mathcal{J}_{A_2}$  are not fundamental parallelepipeds, and have no geometrical meaning, both have vanishing determinants. Actually,  $\mathcal{J}_{A_1}$  should be invariant under time reversal, so what did I screw up? **Failed attempt, done.**

**2021-03-22 Predrag** Grava *et al.* [40] eq. (6.131) suggests what went wrong with the above failed  $D_1$  factorization attempt: we should have started from the Hamiltonian formulation, decompose the one-time step temporal evolution  $[2 \times 2]$  Jacobian matrix  $\hat{\mathbf{J}}_1$  that generates a time orbit by acting on the 2-dimensional 'phase space' of successive temporal lattice points (21.241) with time reversal  $\mathbf{T}$  (6.71) decomposing the 2nd order Percival-Vivaldi time-evolution equation into two 1st order invariant subspace evolution equations:

$$\mathbf{T} = \begin{bmatrix} 0 & 1 \\ 1 & 0 \end{bmatrix}, \quad \mathbf{P}^+ = \frac{1}{2} \begin{bmatrix} 1 & 1 \\ 1 & 1 \end{bmatrix}, \quad \mathbf{P}^- = \frac{1}{2} \begin{bmatrix} 1 & -1 \\ -1 & 1 \end{bmatrix}. \quad (6.90)$$

so

$$\hat{\mathbf{J}}_1 = \begin{bmatrix} 0 & 1 \\ -1 & s \end{bmatrix}; \quad \hat{\mathbf{J}}_1^+ = \frac{1}{2} \begin{bmatrix} 1 & 1 \\ s-1 & s-1 \end{bmatrix}, \quad \hat{\mathbf{J}}_1^- = \frac{1}{2} \begin{bmatrix} -1 & 1 \\ -s-1 & s+1 \end{bmatrix}. \quad (6.91)$$

Next: verify the Hill's formula, sect. 12.9.1, and/or sect. 5. *Hill determinant: stability of an orbit vs. its time-evolution stability of siminos/kittens/CL18.tex* for period- $n$  periodic states;

$$\text{Det } \mathcal{J}_{\pm} = \det \left[ \mathbf{1} - (\hat{\mathbf{J}}_1^{\pm})^n \right]. \quad (6.92)$$

This establishes, following Fejér [37, 64] (1916) Fejér and Riesz lemma sect. 6.5.1, -doubting Thomases notwithstanding- that the time reversal

invariance leads to factorization of zeta functions for -hopefully- any temporal lattice systems with time-inversion  $t \rightarrow -t$  invariance.

As far as I can tell, we are the first to make this claim for time evolution, not for spatially discrete or  $N$ -body systems.

Sidney and Han, please go to sect. 26.4 *Pow wow 2021-03-22* and do the homework. Call me any time for any clarifications you need. As always, everything prof says might be wrong, so remain vigilant. And stay safe.

**2021-03-22 Predrag** The above might be a failed attempt again..., as Percival-Vivaldi form is not right:  $[\mathbf{T}, \mathbf{J}_1] \neq 0$ :

$$\mathbf{T} = \begin{bmatrix} 0 & 1 \\ 1 & 0 \end{bmatrix}, \quad \mathbf{P}^+ = \frac{1}{2} \begin{bmatrix} 1 & 1 \\ 1 & 1 \end{bmatrix}, \quad \mathbf{P}^- = \frac{1}{2} \begin{bmatrix} 1 & -1 \\ -1 & 1 \end{bmatrix}. \quad (6.93)$$

so

$$\hat{\mathbf{J}}_1 = \begin{bmatrix} 0 & 1 \\ -1 & s \end{bmatrix}; \quad \hat{\mathbf{J}}_1^+ = \frac{1}{2} \begin{bmatrix} 1 & 1 \\ s-1 & s-1 \end{bmatrix}, \quad \hat{\mathbf{J}}_1^- = \frac{1}{2} \begin{bmatrix} -1 & 1 \\ -s-1 & s+1 \end{bmatrix}. \quad (6.94)$$

**2020-11-18 Predrag** Factorization (2.2)

$$A = \begin{bmatrix} 2 & 1 \\ 1 & 1 \end{bmatrix} = \begin{bmatrix} 1 & 1 \\ 0 & 1 \end{bmatrix} \begin{bmatrix} 1 & 0 \\ 1 & 1 \end{bmatrix} = LL^\top \quad (6.95)$$

leads to

$$\det(1 - tL^\top) \det(1 + tL) = \det(1 - zA) \quad (6.96)$$

which also verifies (6.199). Both (6.185), (2.2) are symmetric under transposition. What about the asymmetric Percival-Vivaldi (2.5)? The similarity transformation (8.110) that maps (2.1) into (2.5),

$$\mathbf{A} = \begin{bmatrix} 2 & 1 \\ 1 & 1 \end{bmatrix}, \quad \mathbf{B} = \begin{bmatrix} 0 & 1 \\ -1 & 3 \end{bmatrix}, \quad (6.97)$$

is

$$\mathbf{B} = \mathbf{S}^{-1} \mathbf{A} \mathbf{S}, \quad (6.98)$$

where

$$\mathbf{S} = \mathbf{S}^{-1} = \begin{bmatrix} -1 & 2 \\ 0 & 1 \end{bmatrix}.$$

See also discussion around (8.111) and (24.40).

**2021-02-10 Predrag** I looked cursorily at it and did not spot anything, but it is of possible interest:

Terry Loring and Fredy Vides *Computing Floquet Hamiltonians with Symmetries* [arXiv:2007.06112](https://arxiv.org/abs/2007.06112)

**2021-04-10 Predrag** For specializing example 3.6 *Symmetry lines of the standard map* to cat map, see example 3.7 *Symmetry lines of the cat map*.

**2021-04-10 Predrag** For a scholarly discussion of many facets of “time-reversal”, see the essay *Time Reversal* by Bryan W. Roberts (2019).

**2021-04-17 Predrag to Tony Kennedy** <Tony.Kennedy@ed.ac.uk>

You might be The Man for the job:

We are stuck on reflection-symmetry reduction needed to factorize the zeta functions. Here is a simple way to explain what the problem is:

Think of a discrete time dynamical system (iterations of a map) as a 1-dimensional lattice with the field on each site labeled by integer time. An period- $n$  periodic state lives on a discrete 1-torus (a ring or necklace) of period  $n$ , and if the law is time-independent, sets of solutions are invariant under cyclic perturbations. The symmetry is  $C_n$ , and one needs to distinguish  $C_n$  orbits (“prime cycles” in ChaosBook; one per each orbit). The right way to do this is by going to  $C_n$  irreps, ie, by the discrete Fourier transform, with all reciprocal lattice Brillouin zone solutions orbits in an  $1/n$  sliver of a  $n$ -gon. If  $n$  is prime, this is irreducible; if it is a multiple of a prime, one should remove those solutions, as they have already been accounted for.

If, in addition, the law is time-reversal (or time-inversion) invariant, the symmetry includes time-reflection, ie, it is dihedral group  $D_n$  with  $2n$  elements, so the reciprocal lattice should be a half of the above  $1/n$  sliver of a  $n$ -gon, and irreps are now either 1 or 2 dimensional. Even  $n$  is different from odd  $n$ , and solutions either appear in pairs, or are self dual under reflection in 3 different ways.

ChaosBook works out zeta function factorizations for  $D_1$ ,  $D_2$  (known as **Klein four-group**),  $D_3$  (symmetric group  $S_3$ ), and  $D_4$ , but somehow I get confused by all the invariant subspaces of solutions for  $D_n$ , so we are stuck... Not to mention counting orbits for a Bravais lattices (doubly periodic periodic states) for spatiotemporal cat. There we do not know how to write down the zeta function, let alone factorize it into irreps of the discrete symmetry group of a given Bravais lattice.

For more detail, see refsect s:latt1d *Dihedral groups*.

**2017-09-11 Predrag** Define ‘lattice momentum’ operator in  $j$ th lattice direction as a centered lattice derivative,

$$ip_j = r_j^{1/2} - r_j^{-1/2}. \quad (6.99)$$

In terms of momenta, second lattice derivatives in, for example, Laplace operator, are

$$r_j - 2\mathbf{1} + r_j^{-1} = \left( r_j^{1/2} - r_j^{-1/2} \right)^2,$$

and the  $d$ -dimensional lattice Laplace operator is the lattice momentum

operator squared

$$\square = \sum_{j=1}^d (r_j - 2\mathbf{1} + r_j^{-1}) = -\sum_{j=1}^d p_j^2. \quad (6.100)$$

**2023-12-10 Predrag** Should we be using Pfaffians (16.5)? Still have to add mass  $\mu^2$  as  $\text{Det}(p) = 0$ , so probably I'm wrong, but with the antisymmetric  $ip$  (6.99), sketchily

$$\text{Det}(p^2) = (\text{Det}(p))^2 = (\text{Pf}(p))^4? \quad (6.101)$$

On primitive cell finite matrices one might have a problem for odd periods, and in the factors in (6.49), the  $\mu$  on the diagonal breaks antisymmetry, so probably no Pfaffians for us... Not sure why they are so prominent for 2D Ising model (16.5), but do not appear here.

#### 6.4.4 Poles of dynamical zeta functions

**1993-03-11 Predrag** A clip from (boyscouts only) ChaosBook Chapter *Quantum pinball*, taken from Predrag's `c.tex` [33], Casati and Shilnikov [18].

**2020-11-07 Predrag** In 1993 I have not thought of (6.104) as clue to time-reversal factorization, but the Hamiltonian weight, one per each degree of freedom,

$$\det(\mathbf{1} - \mathbf{J}_p) = (1 - \Lambda_p)(1 - 1/\Lambda_p) = -\Lambda_p + 2 - 1/\Lambda_p \quad (6.102)$$

sure looks suggestive, in the spirit of (24.242). It leads to factorization (6.111),

$$1/\zeta_j = \frac{F_j}{F_{j+1}} \frac{F_{j+2}}{F_{j+1}}, \quad (6.103)$$

compare with (6.199).

For a Hamiltonian two degree of freedom system,  $\mathbf{J}_p$  is a  $[2 \times 2]$  matrix with unit determinant. If the cycle is unstable, the eigenvalues  $\Lambda_p$  and  $1/\Lambda_p$  are real, and we denote the expanding eigenvalue by  $\Lambda_p$ . The denominator can then be expanded in a geometric series

$$1/|\det(\mathbf{J}_p - \mathbf{1})| = |\Lambda_p|^{-1} (1 - 1/\Lambda_p)^{-2} = |\Lambda_p|^{-1} \sum_{j=0}^{\infty} (j+1) \Lambda_p^{-j}. \quad (6.104)$$

Performing the  $r$  summation and interchanging sums and logarithms one ends up with  $\Omega(s) = \frac{\partial}{\partial s} \ln F(s)$ , where  $F(s)$  is the *deterministic Fredholm determinant*

$$F(s) = \prod_p \prod_{j=0}^{\infty} (1 - |\Lambda_p|^{-1} \Lambda_p^{-j} e^{sT_p})^{j+1}. \quad (6.105)$$

As  $\Omega(s)$  is a logarithmic derivative, its poles are given by the zeros and poles of  $F(s)$ . Denoting the deterministic weight of the cycle  $p$  by

$$t_p = z^{n_p} e^{sT_p} / |\Lambda_p| \quad (6.106)$$

and defining *dynamical zeta function* [68]

$$1/\zeta_j = \exp \left( - \sum_p \sum_{r=1}^{\infty} \frac{1}{r} (t_p / \Lambda_p^j)^r \right) = \prod_p (1 - t_p / \Lambda_p^j) , \quad (6.107)$$

the Fredholm determinant (6.105) can be written as an infinite product over  $1/\zeta_j$ :

$$F(s) = \prod_p \prod_{j=0}^{\infty} (1 - t_p / \Lambda_p^j)^{j+1} = \prod_{j=0}^{\infty} 1/\zeta_j^{j+1} . \quad (6.108)$$

We have introduced a bookkeeping variable  $z$  raised to the power of the topological length (number of disk collisions in a cycle) in order to be able to systematically expand the infinite products in terms of increasing topological cycle length.

The double pole is not as surprising as it might seem at the first glance; indeed, the theorem that establishes that the deterministic Fredholm determinant (6.108) is entire implies that the poles in  $1/\zeta_j$  must have right multiplicities in order that they be cancelled in the  $F = \prod 1/\zeta_j$  product. More explicitly,  $1/\zeta_j$  can be expressed in terms of weighted Fredholm determinants

$$F_j = \exp \left( - \sum_p \sum_{r=1}^{\infty} \frac{1}{r} \frac{(t_p / \Lambda_p^j)^r}{(1 - 1/\Lambda_p^r)^2} \right) \quad (6.109)$$

by inserting the identity

$$1 = \frac{1}{(1 - 1/\Lambda)^2} - \frac{2}{\Lambda} \frac{1}{(1 - 1/\Lambda)^2} + \frac{1}{\Lambda^2} \frac{1}{(1 - 1/\Lambda)^2} \quad (6.110)$$

into the exponential representation (6.107) of  $1/\zeta_j$ . This yields

$$1/\zeta_j = \frac{F_j F_{j+2}}{F_{j+1}^2} , \quad (6.111)$$

and we conclude that for 2-dimensional Hamiltonian flows the dynamical zeta function  $1/\zeta_j$  has a *double* leading pole coinciding with the leading zero of the  $F_{j+1}$  Fredholm determinant.



## 6.5 Time reversal literature

### 6.5.1 Grava *et al.* 2021 paper GKMM21

Notes on Grava, Kriecherbauer, Mazzuca and McLaughlin [40] *Correlation functions for a chain of short range oscillators*, [arXiv:2010.09612](https://arxiv.org/abs/2010.09612):

[C]onsider a system of  $N = 2M + 1$  particles interacting with a short range harmonic potential with Hamiltonian of the form

$$H = \sum_{j=0}^{N-1} \frac{p_j^2}{2} + \sum_{s=1}^m \frac{\kappa_s}{2} \sum_{j=0}^{N-1} (q_j - q_{j+s})^2, \quad (6.112)$$

and Hamiltonian density

$$e_j = \frac{p_j^2}{2} + \frac{1}{2} \left( \sum_{s=1}^m \tau_s (q_{j+s} - q_j) \right)^2,$$

local in the variables  $(\mathbf{p}, \mathbf{q})$  for fixed  $m$ . If we let  $N \rightarrow \infty$ , the quantity  $e_j$  involves a finite number of physical variables  $(\mathbf{p}, \mathbf{q})$ . We always take periodic boundary conditions, the indices  $j$  are taken from  $\mathbb{Z}/N\mathbb{Z}$  and therefore

$$q_{N+j} = q_j, \quad p_{N+j} = p_j$$

holds for all  $j$ .

The relative shift  $S$  boundary condition  $q_{N+1} = q_1 + S$  can be also be considered (see e.g. ref. [72]). The periodic boundary condition is recovered by change of coordinates  $q_j \rightarrow q_j - \frac{S}{N}(j-1)$ .

The coefficients  $\tau_s$  are the entries of the circulant localized square root  $T$  of the matrix  $A$  by which we mean a solution of the equation (6.117) of the form (6.118).

The Hamiltonian (6.112) can be rewritten in the form

$$H(\mathbf{p}, \mathbf{q}) := \frac{1}{2} \langle \mathbf{p}, \mathbf{p} \rangle + \frac{1}{2} \langle \mathbf{q}, A\mathbf{q} \rangle, \quad (6.113)$$

where  $\mathbf{p} = (p_0, \dots, p_{N-1})$ ,  $\mathbf{q} = (q_0, \dots, q_{N-1})$ ,  $\langle \cdot, \cdot \rangle$  denotes the standard scalar product in  $\mathcal{R}^N$  and where  $A \in \text{Mat}(N, \mathcal{R})$  is a positive semidefinite symmetric circulant matrix generated by the vector  $\mathbf{a} = (a_0, \dots, a_{N-1})$  namely  $A_{kj} = a_{(j-k) \bmod N}$  or

$$A = \begin{bmatrix} a_0 & a_1 & \dots & a_{N-2} & a_{N-1} \\ a_{N-1} & a_0 & a_1 & & \\ \vdots & a_{N-1} & a_0 & \ddots & \vdots \\ a_2 & & \ddots & \ddots & a_1 \\ a_1 & a_2 & \dots & a_{N-1} & a_0 \end{bmatrix}, \quad (6.114)$$

The harmonic oscillator with only nearest neighbour interactions is recovered by choosing

$$a_0 = 2\kappa_1, \quad a_1 = a_{N-1} = -\kappa_1,$$

and the remaining coefficients are set to zero.

The equations of motion for the Hamiltonian  $H$  take the form

$$\frac{d^2}{dt^2} q_j = \sum_{s=1}^m \kappa_s (q_{j+s} - 2q_j + q_{j-s}), \quad j \in \mathbb{Z}/N\mathbb{Z}. \quad (6.115)$$

The integration is obtained by studying the dynamics in Fourier space. [...] Following the standard procedure in the case of nearest neighbour interactions we replace the vector of position  $\mathbf{q}$  by a new variable  $\mathbf{r}$  so that the Hamiltonian takes the form

$$H = \frac{1}{2} \langle \mathbf{p}, \mathbf{p} \rangle + \frac{1}{2} \langle \mathbf{r}, \mathbf{r} \rangle.$$

Such a change of variables may be achieved by any linear transformation

$$\mathbf{r} = T\mathbf{q}, \quad (6.116)$$

with an  $N \times N$  matrix  $T$  that satisfies

$$A = T^T T, \quad (6.117)$$

where  $T^T$  denotes the transpose of  $T$ .

In the case of nearest neighbour interactions one may choose

$$r_j = \sqrt{\kappa_1} (q_{j+1} - q_j)$$

corresponding to a circulant matrix  $T$  generated by the vector

$$\boldsymbol{\tau} = \sqrt{\kappa_1} (-1, 1, 0, \dots, 0).$$

We show that short range interactions given by matrices  $A$  of the form (6.114) also admit such a *localized square root*. More precisely, there exists a circulant  $N \times N$  matrix  $T$  of the form

$$T = \begin{bmatrix} \tau_0 & \tau_1 & \dots & \tau_m & 0 & \dots & 0 \\ 0 & \tau_0 & \tau_1 & \dots & \tau_m & 0 & \\ & & \ddots & \ddots & \ddots & & \\ \tau_m & 0 & \ddots & \ddots & \ddots & \ddots & \\ & \ddots & \ddots & \ddots & \ddots & \ddots & \ddots \\ \tau_2 & \dots & \tau_m & 0 & \dots & \tau_0 & \tau_1 \\ \tau_1 & \tau_2 & \dots & \tau_m & 0 & 0 & \tau_0 \end{bmatrix}. \quad (6.118)$$

that satisfies (6.117). The crucial point here is that  $T$  is not the standard (symmetric) square root of the positive semidefinite matrix  $A$  but a localized version

generated by some vector  $\tau$  with zero entries everywhere, except possibly in the first  $m + 1$  components. [...] Note that  $\mathbf{1} = (1, \dots, 1)^\top$  satisfies  $T\mathbf{1} = 0$  since  $\langle \mathbf{1}, A\mathbf{1} \rangle = 0$ . This implies

$$\sum_{s=0}^m \tau_s = 0, \quad r_j = \sum_{s=1}^m \tau_s (q_{j+s} - q_j) \quad \text{and} \quad \sum_{j=0}^{N-1} r_j = (1, \dots, 1)^\top T\mathbf{q} = 0.$$

The local energy  $e_j$  takes the form

$$e_j = \frac{1}{2}p_j^2 + \frac{1}{2}r_j^2.$$

Due to the spatial translation invariance of the Hamiltonian

$$H(\mathbf{p}, \mathbf{q}) = H(\mathbf{p}, \mathbf{q} + \lambda\mathbf{1}),$$

$\lambda \in \mathcal{R}$ , that corresponds to the conservation of total momentum, we reduce the Hamiltonian system by one degree of freedom, with the reduced phase space

$$\mathcal{M} := \left\{ (\mathbf{p}, \mathbf{q}) \in \mathcal{R}^N \times \mathcal{R}^N : \sum_{k=0}^{N-1} p_k = 0; \sum_{k=0}^{N-1} q_k = 0 \right\}. \quad (6.119)$$

[...] the dispersion relation  $|\omega(k)|$  for the harmonic oscillator with short range interaction in the limit  $N \rightarrow \infty$  obtaining

$$f(k) = |\omega(k)| = \sqrt{2 \sum_{\ell=1}^m \kappa_\ell (1 - \cos(2\pi k\ell))}, \quad (6.120)$$

[...] we show that the evolution equations for the generalized position, momentum can be written in the form of conservation laws which have a potential function. For the case of the harmonic oscillator with nearest neighbour interaction, we show that this function is a Gaussian random variable and determine the leading order behaviour of its variance as  $t \rightarrow \infty$ .

[...] some notation. First of all, a matrix  $A$  of the form (6.114) with  $\mathbf{a} \in \mathcal{R}^N$  is called a circulant matrix generated by the vector  $\mathbf{a}$ .

**$m$ -physical vector and half- $m$ -physical vector** Fix  $m \in \mathbb{N}$ . For any odd  $N > 2m$ , a vector  $\tilde{\mathbf{x}} \in \mathcal{R}^N$  is said to be  $m$ -physical generated by  $\mathbf{x} = (x_0, x_1, \dots, x_m) \in \mathcal{R}^{m+1}$  if  $x_0 = -2 \sum_{s=1}^m x_s$  and

$$\tilde{x}_0 = x_0, \quad (6.121)$$

$$\tilde{x}_1 = \tilde{x}_{N-1} = x_1 < 0, \quad \tilde{x}_m = \tilde{x}_{N-m} = x_m < 0, \quad (6.122)$$

$$\tilde{x}_k = \tilde{x}_{N-k} = x_k \leq 0, \quad \text{for } 1 < k < m, \quad (6.123)$$

$$\tilde{x}_k = 0, \quad \text{otherwise,} \quad (6.124)$$

while the vector  $\tilde{\mathbf{x}} \in \mathcal{R}^N$  is called *half- $m$ -physical* generated by  $\mathbf{y} \in \mathcal{R}^{m+1}$  if  $y_0 = -\sum_{s=1}^m y_s$  and

$$\begin{aligned} \tilde{x}_k &= y_k, \text{ for } 0 \leq k \leq m \\ \tilde{x}_k &= 0, \text{ for } m < k \leq N - 1. \end{aligned}$$

Following the proof of a lemma by Fejér and Riesz, one can show that a circulant symmetric matrix  $A$  of the form (6.113) generated by a  $m$ -physical vector  $\mathbf{a}$  always has a circulant localized square root  $T$  that is generated by a half- $m$ -physical vector  $\boldsymbol{\tau}$ .

**Fejér and Riesz [64, pg. 117 f] lemma** asserts that every positive trigonometric polynomial can be represented by the square of the absolute value of another trigonometric polynomial whose coefficients are, in general, complex.

Fix  $m \in \mathbb{N}$ . Let the circulant matrix  $A$  be generated by an  $m$ -physical vector  $\mathbf{a}$ , then there exist a circulant matrix  $T$  generated by an half- $m$ -physical vector  $\boldsymbol{\tau}$  such that:

$$A = T^\top T. \tag{6.125}$$

Moreover, we can choose  $\boldsymbol{\tau}$  such that  $\sum_{s=1}^m s\tau_s > 0$ . Then one has  $\sum_{s=1}^m s\tau_s = \sqrt{\sum_{s=1}^m s^2 \kappa_s}$ .

For example, if we consider  $m = 1$ , and  $a_0 = 2\kappa_1$  and  $a_1 = a_{N-1} = -\kappa_1$ . The matrix  $T$  is generated by the vector  $\boldsymbol{\tau} = (\tau_0, \tau_1)$  with  $\tau_0 = -\sqrt{\kappa_1}$  and  $\tau_1 = \sqrt{\kappa_1}$ . When  $m = 2$  and  $a_0 = 2\kappa_1 + 2\kappa_2$ ,  $a_1 = a_{N-1} = -\kappa_1$ ,  $a_2 = a_{N-2} = -\kappa_2$ . The matrix  $T$  is generated by the vector  $\boldsymbol{\tau} = (\tau_0, \tau_1, \tau_2)$  with

$$\begin{aligned} \tau_0 &= -\frac{\sqrt{\kappa_1}}{2} - \frac{1}{2}\sqrt{\kappa_1 + 4\kappa_2}, \quad \tau_1 = \sqrt{\kappa_1}, \\ \tau_2 &= -\frac{\sqrt{\kappa_1}}{2} + \frac{1}{2}\sqrt{\kappa_1 + 4\kappa_2}, \end{aligned}$$

so that the quantities  $r_j$  are defined as

$$r_j = \tau_1(q_{j+1} - q_j) + \tau_2(q_{j+2} - q_j), \quad j \in \mathbb{Z}/N\mathbb{Z}.$$

[...] The Hamiltonian  $H(\mathbf{p}, \mathbf{q})$  represents clearly an integrable system that can be integrated passing through Fourier transform. Let  $\mathcal{F}$  be the discrete Fourier transform with entries  $\mathcal{F}_{j,k} := \frac{1}{\sqrt{N}}e^{-2\text{Im}\pi jk/N}$  with  $j, k = 0, \dots, N - 1$ . It is immediate to verify that

$$\mathcal{F}^{-1} = \bar{\mathcal{F}} \quad \mathcal{F}^\top = \mathcal{F}. \tag{6.126}$$

Thanks to the above properties, the transformation defined by

$$(\hat{\mathbf{p}}, \hat{\mathbf{q}}) = (\bar{\mathcal{F}}\mathbf{p}, \mathcal{F}\mathbf{q}) \tag{6.127}$$

is canonical. Furthermore  $\bar{\hat{\mathbf{p}}}_j = \hat{\mathbf{p}}_{N-j}$  and  $\bar{\hat{\mathbf{q}}}_j = \hat{\mathbf{q}}_{N-j}$ , for  $j = 1, \dots, N-1$ , while  $\hat{\mathbf{p}}_0$  and  $\hat{\mathbf{q}}_0$  are real variables. The matrices  $T$  and  $A$  are circulant matrices and so they are reduced to diagonal form by  $\mathcal{F}$ :

$$\mathcal{F}A\mathcal{F}^{-1} = \mathcal{F}T^\top T\mathcal{F}^{-1} = \overline{(\mathcal{F}T\mathcal{F}^{-1})}^\top (\mathcal{F}T\mathcal{F}^{-1}).$$

Let  $\omega_j$  denote the eigenvalues of the matrix  $T$  ordered so that  $\mathcal{F}T\mathcal{F}^{-1} = \text{diag}(\omega_j)$ . Then  $|\omega_j|^2$  are the (non negative) eigenvalues of the matrix  $A$  and

$$|\omega_j|^2 = \sqrt{N}(\overline{\mathcal{F}\tilde{\mathbf{a}}})_j, \quad \omega_j = \sqrt{N}(\overline{\mathcal{F}\tilde{\boldsymbol{\tau}}})_j, \quad j = 0, \dots, N-1, \quad (6.128)$$

where  $\tilde{\mathbf{a}}$  is the  $m$ -physical vector generated by  $\mathbf{a}$  and  $\tilde{\boldsymbol{\tau}}$  is the half  $m$ -physical vector generated by  $\boldsymbol{\tau}$ . It follows that

$$\omega_0 = 0, \quad \omega_j = \bar{\omega}_{N-j}, \quad j = 1, \dots, N-1, \quad (6.129)$$

which implies  $|\omega_j|^2 = |\omega_{N-j}|^2$ ,  $j = 1, \dots, N-1$ .

### Circulant hierarchy of integrals

In this section we construct a complete set of conserved quantities that have local densities. The harmonic oscillator with short range interaction is clearly an integrable system. A set of integrals of motion is given by the harmonic oscillators in each of the Fourier variables:  $\hat{H}_j = \frac{1}{2}(|\hat{\mathbf{p}}_j|^2 + |\omega_j|^2|\hat{\mathbf{q}}_j|^2)$ ,  $j = 0, \dots, \frac{N-1}{2}$ . However, when written in the physical variables  $\mathbf{p}$  and  $\mathbf{q}$ , the quantities

$$\hat{H}_j = \frac{1}{2} \sum_{k,l=0}^{N-1} \mathcal{F}_{j,k} \overline{\mathcal{F}_{j,l}} (p_k p_l + |\omega_j|^2 q_k q_l)$$

depend on all components of the physical variables. We now construct integrals of motion each having a density that involves only a limited number of components of the physical variables and this number only depends on the range  $m$  of interaction.

For this purpose we denote by  $\{\mathbf{e}_k\}_{k=0}^{N-1}$  the canonical basis in  $\mathcal{R}^N$ .

**Local conserved quantities** Let us consider the Hamiltonian

$$H(\mathbf{p}, \mathbf{q}) = \frac{1}{2} \mathbf{p}^\top \mathbf{p} + \frac{1}{2} \mathbf{q}^\top A \mathbf{q}, \quad (6.130)$$

with the symmetric circulant matrix  $A$  as in (6.113), (6.114). Define the matrices  $\{G_k\}_{k=1}^M$  to be the symmetric circulant matrix generated by the vector  $\frac{1}{2}(\mathbf{e}_k + \mathbf{e}_{N-k})$  and  $\{S_k\}_{k=1}^M$  to be the antisymmetric circulant matrix generated by the

vector  $\frac{1}{2}(\mathbf{e}_k - \mathbf{e}_{N-k})$ . Then the family of Hamiltonians defined as

$$H_k(\mathbf{p}, \mathbf{q}) = \frac{1}{2} \mathbf{p}^\top G_k \mathbf{p} + \frac{1}{2} \mathbf{q}^\top T^\top G_k T \mathbf{q} = \frac{1}{2} \sum_{j=0}^{N-1} [p_j p_{j+k} + r_j r_{j+k}], \quad (6.131)$$

$$H_{k+\frac{N-1}{2}}(\mathbf{p}, \mathbf{q}) = \mathbf{p}^\top T^\top S_k T \mathbf{q} = \frac{1}{2} \sum_{j=0}^{N-1} \left[ \left( \sum_{\ell=0}^m \tau_\ell p_{j+\ell} \right) (r_{j+k} - r_{j-k}) \right], \quad k = 1, \dots, \frac{N-1}{2} \quad (6.132)$$

together with  $H_0 := H$  forms a complete family  $(H_j)_{0 \leq j \leq N-1}$  of integrals of motion that, moreover, is in involution. [...] Now we introduce the local densities corresponding to the just defined integrals of motion

$$e_j^{(k)} = \begin{cases} \frac{1}{2} (p_j p_{j+k} + r_j r_{j+k}), & \text{for } k = 1, \dots, \frac{N-1}{2} \\ \left( \sum_{l=0}^m \tau_l p_{j+l} \right) (r_{j+k} - r_{j-k}), & \text{for } k = \frac{N+1}{2}, \dots, N. \end{cases} \quad (6.133)$$

[...]

### Nonlinear regime

In this section we consider a nonlinear perturbation of the harmonic oscillators with short range interactions of the form

$$H(\mathbf{p}, \mathbf{q}) = \sum_{j=0}^{N-1} \frac{p_j^2}{2} + \sum_{s=1}^m \kappa_s \left( \frac{1}{2} \sum_{j=0}^{N-1} (q_j - q_{j+s})^2 + \frac{\chi}{3} \sum_{j=0}^{N-1} (q_j - q_{j+s})^3 + \frac{\gamma}{4} \sum_{j=0}^{N-1} (q_j - q_{j+s})^4 \right). \quad (6.134)$$

We consider examples with different strengths of nonlinearity namely

$$m = 2, \kappa_1 = 1, \kappa_2 = \frac{1}{4}, \begin{cases} \chi = 0.01 \text{ and } \gamma = 0.001 \\ \chi = 0.1 \text{ and } \gamma = 0.01 \end{cases}$$

$$m = 3, \kappa_1 = 1, \kappa_2 = \frac{1}{8}, \kappa_3 = \frac{7}{72}, \begin{cases} \chi = 0.01 \text{ and } \gamma = 0.001 \\ \chi = 0.1 \text{ and } \gamma = 0.01 \end{cases}.$$

### 6.5.2 Baake *et al.* 2008 paper BaRoWe08

2017-09-27, 2021-02-03 Predrag reading Baake, Roberts and Weiss [10] *Periodic orbits of linear endomorphisms on the 2-torus and its lattices* [arXiv:0808.3489](https://arxiv.org/abs/0808.3489).

2021-02-03 Predrag Summary

1. The main result is the third matrix invariant: the ‘gmc’ that fixes the conjugacy class of a given lattice in an invariant way, unlike the Hermite normal form (8.123) that breaks the ‘spatiotemporal’ symmetry; mention and cite in CL18 [26], even if we do not use it.

2. They do counting for the golden (Fibonacci [8]) cat map (6.194), see table 6.2 and (6.198), as the simplest example; we do not need to cite their counting in CL18 [26], cite 1997 sect. 6.5.3 Baake, Hermisson and Pleasants [7] instead. (I'm somewhat sure that name 'golden cat' is not already in 1967 Smale [71], or 1995 Katok and Hasselblatt [47]. Perhaps better to call it "Fibonacci" [8]?) There is no mention that this is a time-reversal reduction of the  $s = 3$  cat map in Baake *et al.* [10]. Perhaps Katok and Hasselblatt [47] mention that?
3. They do not mention any time-reversal symmetry reduction connection to the periodic states and orbit counts for the  $s = 3$  cat map table 21.1; do not cite them for that.

Their focus on the relation between global and local aspects and between the dynamical zeta function on the torus and its analogue on finite lattices. The situation on the lattices, up to local conjugacy, is completely determined by the determinant, the trace and a third invariant of the matrix defining the toral endomorphism.

In introduction they refer to much literature on cat maps on lattices, and I've not read much of it.

[...] the system  $(\Omega, T)$  is called *chaotic* when the periodic orbits of  $T$  are dense in  $\Omega$  and when also a dense orbit exists, see Banks *et al.* [12] *On Devaney's definition of chaos* for details. Knowledge of the periodic orbits can be used to detect characteristic properties of  $T$ . For example, if  $T'$  represents another continuous mapping of  $\Omega$ , then a necessary condition for  $T$  and  $T'$  to be topologically conjugate is that they share the same number of periodic points of each period. 2CB

[...] endomorphisms of the 2-torus, represented by the action (mod 1) of an integer matrix  $M \in Mat(2, \mathbb{Z})$  on  $\mathbb{T}^2 \simeq \mathbb{R}^2/\mathbb{Z}^2$ . A well-studied subclass consists of the toral automorphisms, represented by elements of the group  $GL(2, \mathbb{Z})$ , being the subgroup of matrices with determinant  $\pm 1$  within the ring  $Mat(2, \mathbb{Z})$ . Particularly important are the hyperbolic ones (meaning that no eigenvalue is on the unit circle), which are often called *cat maps*. Since these are expansive, all periodic point counts are finite. Hyperbolic toral automorphisms are also topologically mixing and intrinsically ergodic, see refs. [47, 74]. By the Bowen-Sinai theorem, this has the consequence that the integral of a continuous function over  $\mathbb{T}^2$  equals its average value over the points fixed by  $M^m$  in the limit as  $m \rightarrow \infty$ .

The topological entropy of a hyperbolic toral automorphism  $M \in GL(2, \mathbb{Z})$  is given by  $\log |\lambda_{\max}|$ , where  $\lambda_{\max}$  is the eigenvalue of  $M$  with modulus  $> 1$ . This is also the metric (or Kolmogorov-Sinai) entropy of  $M$ , and completely determines the dynamics up to metric isomorphism, compare ref. [1]. This does not imply topological conjugacy though, and one important difference emerges from the periodic orbits, which live on a set of measure 0. Indeed, on  $\mathbb{T}^2$ , it is well-known that the periodic orbits of hyperbolic linear endomorphisms lie on the invariant lattices given by the sets of rational points with a given denominator  $n$ , also known as  $n$ -division points. One of our main themes in this paper

is the interplay between the periodic orbit statistics on a certain lattice (which we call *local statistics*) versus periodic orbit statistics on the union of all lattices (which we call *global statistics*). What determines when two cat maps have the same global statistics? What determines when two cat maps have the same local statistics on a certain lattice or on all lattices?

The time of recurrence of a hyperbolic  $M \in GL(2, \mathbb{Z})$  on the toral rational lattice with denominator  $n$  is denoted by  $per(M, n)$ , where this is the least common multiple of the periods present on the  $n$ -division points.

[...] for symmetries or (time) reversing symmetries of a cat map, these being automorphisms of the torus that commute with the cat map, respectively conjugate it into its inverse.

[...] there has been quite some interest in dealing with this challenge of so-called pseudo-symmetries of quantum maps that are not quantisations of symmetries of the cat map on the torus, but instead are manifestations of local symmetries of the cat map restricted to some lattice [48, 50].

Conjugacy of  $GL(2, \mathbb{Z})$  matrices is another topic that has arisen in a broad variety of contexts and has been considered by many. Conjugacy is determined by a triple of invariants, namely the determinant, the trace and one other invariant which can be related to ideal classes, representation by binary quadratic forms or topological properties. Conjugacy in  $GL(2, \mathbb{Z})$  can also be completely decided by using the amalgamated free product structure of  $PGL(2, \mathbb{Z})$ , which attaches a finite sequence of integers to each element which corresponds to its normal form as a word in the generators of the amalgamated free product [9].

There are various ways of deciding  $GL(2, \mathbb{Z})$ -conjugacy, amounting to exploiting a third and final conjugacy invariant.

**Result of this paper:** The *matrix gcd* is a key quantity. It is preserved by  $GL(2, \mathbb{Z})$  conjugacy, so it provides a quick tool to see that two  $GL(2, \mathbb{Z})$  matrices with different matrix gcd are not conjugate on the torus. If two integer matrices share the same determinant, trace and matrix gcd they are linearly conjugate on all rational lattices of the torus. As an illustration of this result, consider cat maps and time-reversal symmetry. The fact that any  $M \in SL(2, \mathbb{Z})$  shares determinant, trace and matrix gcd with  $M^{-1}$  means that the two matrices are conjugate on *all* rational lattices, though not necessarily by matrices that derive from one and the same matrix on the torus.

Consider a compact space  $\Omega$  and some (continuous) mapping  $T$  of  $\Omega$  into itself. Let  $Fix_m(T) := \{x \in \Omega \mid T^m x = x\}$  be the set of fixed points of  $T^m$ . Of particular interest are the *fixed point counts*, defined as

$$a_m := \text{card}\{x \in \Omega \mid T^m x = x\} = \text{card}(Fix_m(T)). \quad (6.135)$$

The quantity  $a_m$  has the disadvantage that one keeps recounting the contributions  $a_\ell$  for all  $\ell \mid m$ . Clearly, the fixed points of *genuine* order  $m$  permit a partition into disjoint cycles, each of length  $m$ . If  $c_m$  is the number of such cycles, one thus has the relation

$$a_m = \sum_{d \mid m} d c_d. \quad (6.136)$$



An application of a standard inclusion-exclusion argument, here by means of the Möbius inversion formula from elementary number theory, results in the converse identity,

$$c_m = \frac{1}{m} \sum_{d|m} \mu\left(\frac{m}{d}\right) a_d, \quad (6.137)$$

where  $\mu(k)$  is the Möbius function.

[...] a toral endomorphism  $M \in \text{Mat}(2, \mathbb{Z})$  is *hyperbolic* if it has no eigenvalue on the unit circle  $\mathbb{S}^1$ . The standard 2-torus is  $\mathbb{T}^2 \simeq \mathbb{R}^2 / \mathbb{Z}^2$ , where  $\mathbb{Z}^2$  is the square lattice in the plane. It is a compact Abelian group, which can be written as  $\mathbb{T}^2 := [0, 1)^2$ , with addition defined mod 1.

[...] the abbreviation  $\mathbb{Z}_n = \mathbb{Z}/n\mathbb{Z}$  for the finite integer ring mod  $n$ , and  $\mathbb{Z}_n^\times = \{1 \leq k \leq n \mid \gcd(k, n) = 1\}$  for its unit group.

Some 'obvious' number theory defines gcd, but I have not put in the effort needed to understand it.

For counting orbits, this might be useful:

Let  $M \in \text{Mat}(2, \mathbb{C})$  be a non-singular matrix, with  $D := \det(M) \neq 0$  and  $T := \text{tr}(M)$ . Define a two-sided sequence of (possibly complex) numbers  $p_m$  by the initial conditions  $p_{-1} = -1/D$  and  $p_0 = 0$  together with the recursion

$$\begin{aligned} p_{m+1} &= Tp_m - Dp_{m-1}, \quad \text{for } m \geq 0, \\ p_{m-1} &= \frac{1}{D}(Tp_m - p_{m+1}), \quad \text{for } m \leq -1. \end{aligned} \quad (6.138)$$

This way, as  $D \neq 0$ ,  $p_m$  is uniquely defined for all  $m \in \mathbb{Z}$ . Note that the sequence  $(p_m)_{m \in \mathbb{Z}}$  depends only on the determinant and the trace of  $M$ . When  $M \in \text{Mat}(2, \mathbb{Z})$ , one has  $p_m \in \mathbb{Q}$ , and  $p_m \in \mathbb{Z}$  for  $m \geq 0$ . When  $M \in \text{GL}(2, \mathbb{Z})$ , all  $p_m$  are integers.

Note an interesting property, which follows from a straight-forward induction argument (in two directions):

The two-sided sequence of rational numbers defined by the recursion (6.138) satisfies the relation

$$p_m^2 - p_{m+1}p_{m-1} = D^{m-1}, \quad (6.139)$$

for all  $m \in \mathbb{Z}$ .

To deal with combinatorial quantities such as the fixed point counts  $a_m$ , it is advantageous to employ generating functions. Here, the concept of a *dynamical zeta function* is usually most appropriate. Consequently, given a matrix  $M \in \text{Mat}(2, \mathbb{Z})$ , we set

$$\zeta_M(t) := \exp\left(\sum_{m=1}^{\infty} \frac{a_m}{m} t^m\right), \quad (6.140)$$

where, from now on,  $a_m := \text{card}\{x \in \text{Fix}_m(M) \mid x \text{ is isolated}\}$  is the number of *isolated* fixed points of  $M^m$ .

The ordinary power series generating function for the counts  $a_m$  can be calculated from  $\zeta_M(t)$  as  $\sum_{m \geq 1} a_m t^m = t \frac{d}{dt} \log(\zeta_M(t))$ . The significance of the

formulation used in Eq. (6.140) follows from the fact that it has a unique Euler product decomposition as

$$\frac{1}{\zeta_M(t)} = \prod_{\text{cycles } \mathcal{C}} (1 - t^{|\mathcal{C}|}) = \prod_{m \geq 1} (1 - t^m)^{c_m}, \quad (6.141)$$

where  $|\mathcal{C}|$  stands for the length of the cycle  $\mathcal{C}$  and  $c_m$  is now the number of *isolated* cycles of  $M$  on  $\mathbb{T}^2$  of length  $m$ , as determined from Formula (6.137). Consequently, the role of cycles in dynamics is similar to that of primes in elementary number theory.

The dynamical zeta function, a special case of which was also given in ref. [35].

Let  $M \in GL(2, \mathbb{Z})$  be hyperbolic, and define  $\sigma = \text{sgn}(\text{tr}(M))$ . Then, with the coefficients  $a_m = \text{card}\{x \in \mathbb{T}^2 \mid M^m x = x \pmod{1}\}$ , the dynamical zeta function (6.140) of  $M$  on  $\mathbb{T}^2$  is given by

$$\zeta_M(t) = \frac{(1 - \sigma t)(1 - \sigma t \det(M))}{\det(\mathbf{1} - \sigma t M)} = \frac{(1 - \sigma t)(1 - \sigma \det(M) t)}{1 - |\text{tr}(M)| t + \det(M) t^2}.$$

In particular,  $\zeta_M(t)$  is a rational function, with numerator and denominator in  $\mathbb{Z}[t]$ . The denominator is a quadratic polynomial that is irreducible over  $\mathbb{Z}$ . Its zero  $t_{\min}$  closest to 0 gives the radius of convergence of  $\zeta_M(t)$ , as a power series around 0, via  $r_c = |t_{\min}|$ .

If  $M$  is hyperbolic, the general formula for the  $a_m$

$$a_m = \sigma^m (\text{tr}(M^m) - (1 + \det(M)^m))$$

can be derived by observing that the two eigenvalues of  $A$  can be written as  $\lambda$  and  $\det(A)/\lambda$ . For the detailed argument, one may assume  $|\lambda| > 1$  and check the different cases. Note that a hyperbolic toral automorphism is never of trace 0.

The formula for the zeta function now follows from (6.140) by inserting the expression for  $a_m$ . The statement on the nature of the rational function is then clear. With  $M \in GL(2, \mathbb{Z})$ , the denominator only factorises for  $\text{tr}(M) = 0$ ,  $\det(M) = -1$  or for  $\text{tr}(M) = \pm 2$ ,  $\det(M) = 1$ , both cases being impossible for hyperbolic matrices.

Two hyperbolic  $GL(2, \mathbb{Z})$ -matrices with the same trace and determinant possess the same dynamical zeta function, hence the same fixed point counts. The converse is slightly more subtle.

3.3. *Generating functions on lattices: I tried reading this before, I tried on 2017-09-27 again, and on 2021-02-03 again, and I still do not get it.*

Consider a  $2 \times 2$ -matrix

$$M = \begin{pmatrix} a & b \\ c & d \end{pmatrix} \quad (6.142)$$

If  $M \in Mat(2, \mathbb{Z})$ , the quantity

$$\text{mgcd}(M) := \text{gcd}(b, c, d - a),$$

is called the *matrix gcd* of  $M$ , or *mgcd* for short. Here, we take the gcd to be a non-negative integer, and set  $mgcd(M) = 0$  when  $b = c = d - a = 0$ . The last convention matches that of the ordinary gcd, and is compatible with modular arithmetic.

For  $M \in Mat(2, \mathbb{Z})$ , the following statements are equivalent:

- (a) The matrix gcd satisfies  $mgcd(M) = 0$ .
- (b)  $M = k\mathbf{1}$  for some  $k \in \mathbb{Z}$ .
- (c) The minimal polynomial of  $M$  is of degree 1.

Consequently, whenever  $mgcd(M) = r \in \mathcal{N}$ ,  $M$  cannot be a multiple of the identity, and its characteristic and minimal polynomials coincide.

Most significantly, the matrix gcd satisfies the following invariance property:

If  $M, M' \in Mat(2, \mathbb{Z})$  are two integer matrices that are conjugate via a  $GL(2, \mathbb{Z})$ -matrix, one has  $mgcd(M') = mgcd(M)$ . In particular, the matrix gcd is constant on the conjugacy classes of  $GL(2, \mathbb{Z})$ .

consider the integer matrices

$$M = \begin{pmatrix} a & b \\ c & d \end{pmatrix} \quad \text{and} \quad C = \begin{pmatrix} 0 & -D \\ 1 & T \end{pmatrix} \quad (6.143)$$

with  $D = \det(M)$  and  $T = \text{tr}(M)$ . Here,  $C$  is the standard companion matrix for the characteristic polynomial

$$x^2 - Tx + D \quad (6.144)$$

of the matrix  $M$ . [...]

2017-09-27, 2021-02-03 **Predrag** read superficially Llibre and Neumärker [56] *Period sets of linear toral endomorphisms on  $T^2$* ; did not understand much.

### 6.5.3 Baake *et al.* 1997 paper BaHePl97

In 1997 Baake, Hermisson and Pleasants [7] *The torus parametrization of quasiperiodic LI-classes* (click here) refer to time-reversal as ‘inversion’ symmetry, and discuss the golden (Fibonacci [8]) cat map. Before giving up on them, do have a look at their eq. (18) zeta function and Table 2. *Inflation orbit counts for 1D cut-and-project patterns with inflation*, compare with table 6.2; compare their Table 4. with table 21.1. Their eq. (18) zeta function is not our Kim *et al.* [49] (6.162). Do cite in CL18 [26]!

**Sect. 2.3 Symmetry** The only kind of point symmetry possible for 1D chains is mirror symmetry, which we shall usually refer to as *inversion symmetry* in order to have the same terminology for all dimensions (‘inversion’ meaning

the isometry  $x \rightarrow -x$ ). Inversion symmetric chains correspond to points  $\mathbf{t}$  on the torus with  $\mathbf{t} = -\mathbf{t}$ , i.e.  $2\mathbf{t} = \mathbf{0}$ . There are four such points

$$(0, 0) \left(\frac{1}{2}, 0\right) \left(0, \frac{1}{2}\right) \left(\frac{1}{2}, \frac{1}{2}\right), \quad (6.145)$$

that form the discrete subgroup of ‘two-division points’ of  $T^2$ , isomorphic to  $C_2 \times C_2$ .

They count many inversion-symmetric patterns in various dimensions, but I do not think any of that applies to temporal cat or spatiotemporal cat.

### 6.5.4 Baake 2018 paper Baake18

Read this:

Michael Baake [6] *A brief guide to reversing and extended symmetries of dynamical systems* [arXiv:1803.06263](https://arxiv.org/abs/1803.06263).

### 6.5.5 Lamb and Roberts 1998 paper lamb98

Lamb and Roberts [51] *Time reversal symmetry in dynamical systems: A survey* (1998) is a very extensive compendium of references on reversibility. Even though they touch upon discrete lattice settings (the Frenkel-Kontorova model [5]) I see no place a reference to group-theoretic description of  $D_\infty$  lattices that we undertake in LC21 [53].

section 16.7 Example 3.4. Symmetric difference equations of the form

$$\phi_{n+l} - f(\phi_n) + \phi_{n-1} = 0 \quad (6.146)$$

the Frenkel-Kontorova model which is equivalent to the area-preserving Chirikov-Taylor standard mapping.

Remarkably, (6.146) is not only reversible, but the associate ‘time’ mapping is also area-preserving. Many area-preserving (symplectic) mappings studied in the literature are reversible (e.g. the well-studied area-preserving Hénon map, cf. Roberts and Quispel [66] (1992) and references therein).

**2021-03-25 Predrag** See example 3.5; shouldn’t “time-reversal operator” just reverse momentum/velocity (6.69)? The definitive review of the nomenclature is Roberts and Quispel [66] *Chaos and time-reversal symmetry. Order and chaos in reversible dynamical systems*.

It turns out that symmetry naturally arises in the study of return maps of flows of time-periodic vector fields with mixed space-time symmetries. In a natural way these space-time symmetries form a group under composition.

#### 4.1. Symmetric periodic orbits

a result on periodic orbits is by far the most well known and used result in reversible dynamical systems. In 1915, Birkhoff [Birkhoff, 1915] described the use of reversibility to find periodic orbits of the restricted three-body problem. In 1958 DeVogelaere [27] described the method again, but now as a tool for searching for symmetric periodic orbits of reversible systems (by computer).

Definition 4.1 (Symmetric orbits). An orbit of a dynamical system is  $s$ -symmetric or symmetric with respect to  $s$  when the orbit is setwise invariant under  $s$ .

Theorem 4.2 (Symmetric orbits for maps) is the same as LC21 [53] classification of 3 kinds of symmetric orbits (Predrag believes).

Theorem 4.1 or 4.2 is used in almost every paper discussing reversible dynamical systems. In particular, these theorems imply efficient techniques for tracking down  $s$ -symmetric periodic orbits, as it justifies searching for them in only a subset of the full phase space.

A well-known property of linear reversible systems is that their eigenvalue structure is similar to that of Hamiltonian systems.

Theorem 4.4 (Eigenvalues of linear reversible systems)...

### 6.5.6 Calogero 2007 paper BrCaDr07

Bruschi, Calogero and Droghei [15] *Tridiagonal matrices, orthogonal polynomials and Diophantine relations: I*.

If the equations of motion and the solution of their initial-value problems involve only algebraic operations: finding the zeros of explicitly known polynomials of degree  $N$ , finding the eigenvectors and eigenvalues of explicitly known  $N \times N$  matrices, the dynamical system is called *solvable*.

It is well known that the eigenvalues of tridiagonal matrices can be identified with the zeros of polynomials satisfying three-term recursion relations and being therefore members of an orthogonal set. They consider the class of monic polynomials  $p_n(s)$ , of degree  $n$  in the variable  $s$ , defined by the three-term recursion relation

$$p_{n+1}(s) - (s + a_n)p_n(s) - b_n p_{n-1}(s) = 0, \quad (6.147)$$

They associate a tridiagonal  $[n \times n]$  matrix  $M$  with it, related to  $p_n(s)$  via the “well-known” formula

$$p_n(s) = \det(s - M). \quad (6.148)$$

The  $n$  zeros of the polynomial  $p_n(s)$  coincide with the  $n$  eigenvalues of the tridiagonal matrix  $M$ .

**Favard’s theorem:** a sequence of polynomials satisfying a suitable 3-term recurrence relation of the form  $p(s)_{n+1} = (s - c_n)p(s)_n - d_n p(s)_{n-1}$  for some numbers  $c_n$  and  $d_n$ , then the polynomials  $p(s)_n$  form a sequence of orthogonal polynomials. **We are interested in this, because we would like to understand Hill determinants polynomials factorization, such as in (21.125).**

See also **Jacobi operator**. The self-adjoint *Jacobi operators* act on the Hilbert space of square summable sequences over the  $\ell^2(\mathbb{N})$ :

$$Jf_0 = a_0 f_1 + b_0 f_0, \quad Jf_n = a_n f_{n+1} + b_n f_n + a_{n-1} f_{n-1}, \quad n > 0,$$

where the coefficients are assumed to satisfy

$$a_n > 0, \quad b_n \in \mathbb{R}.$$

The solution  $p_n(s)$  of the recurrence relation

$$J p_n(s) = s p_n(s), \quad p_0(s) = 1 \text{ and } p_{-1}(s) = 0,$$

is a polynomial of degree  $n$  and these polynomials are orthonormal. Here  $J$  can be interpreted as a lattice right-shift operator, i.e., for a temporal lattice this is related to the evolution in time. This recurrence relation can also be written as

$$a_{n+1} p_{n+1}(s) - (s - b_n) p_n(s) + a_n p_{n-1}(s) = 0, \quad (6.149)$$

(Compare with (8.158).)

or (if one replaces  $s \rightarrow \mu^2$ )

$$(-J + \mu^2) p_n(\mu^2) = 0,$$

reminiscent of the Klein–Gordon equation (8.26). The operator will be bounded if and only if the coefficients are bounded. The case  $a(n) = 1$  is known as the discrete one-dimensional Schrödinger operator. It also arises in:

- The Lax pair of the Toda lattice (see **2020-08-02 Predrag** Toda post)
- The three-term recurrence relationship of orthogonal polynomials.
- Algorithms devised to calculate Gaussian quadrature rules, derived from systems of orthogonal polynomials.

## 6.6 A Lind zeta function for flip systems

Let  $G$  be a group,  $\mathcal{M}$  a set and  $f : G \times \mathcal{M} \rightarrow \mathcal{M}$  a  $G$ -action on  $\mathcal{M}$ . The Lind zeta function [54] is defined by

$$\zeta_{Lind}(t) = \exp \left( \sum_H \frac{N_H}{|G/H|} t^{|G/H|} \right), \quad (6.150)$$

where the sum is over all finite-index subgroups  $H$  of  $G$ , such that  $|G/H| < \infty$ , and  $N_H$  is defined by (see (6.156)):

$$N_H = |\{x \in \mathcal{M} : \text{all } h \in H \quad f(h, x) = x\}|. \quad (6.151)$$



example 6.16  
p. 353

A flip system  $(\mathcal{M}, f, s)$  is a dynamical system, where  $\mathcal{M}$  is a topological space and  $f : \mathcal{M} \rightarrow \mathcal{M}$  is a homeomorphism.  $s : \mathcal{M} \rightarrow \mathcal{M}$  is flip for  $(\mathcal{M}, f)$  that satisfy:

$$s \circ f \circ s = f^{-1} \quad \text{and} \quad s^2 = 1. \quad (6.152)$$

Kim *et al.* [49] showed that the zeta function  $\zeta_s$  of a flip system  $(\mathcal{M}, f, s)$  can be defined as a Lind zeta function  $\zeta_{Lind}$  of the  $D_\infty$ -action  $f : D_\infty \times \mathcal{M} \rightarrow \mathcal{M}$  that is given by:

$$f(r, x) = f(x) \quad \text{and} \quad f(s, x) = s(x). \quad (6.153)$$

Every finite index subgroup of the infinite dihedral group  $D_\infty$  is either

$$H(n) = \langle r^n \rangle \quad \text{or} \quad H(n, k) = \langle r^n, r^k s \rangle, \quad (6.154)$$

with indices

$$|D_\infty/H(n)| = 2|n| \quad \text{or} \quad |D_\infty/H(n, k)| = |n|. \quad (6.155)$$

8

If  $n$  is a positive integer and  $k$  is an integer, then  $N_{n,k}^s$  will denote the number of points in  $\mathcal{M}$  fixed by  $f^n$  and  $f^k \circ s$ :<sup>9</sup>

$$N_{n,k}^s = |\{x \in \mathcal{M} : f^n(x) = f^k \circ s(x) = x\}|. \quad (6.156)$$

They obtain<sup>10</sup>

$$\zeta_s(t) = \exp \left( \sum_{n=1}^{\infty} \frac{N_n}{2n} t^{2n} + \sum_{n=1}^{\infty} \sum_{k=0}^{n-1} \frac{N_{n,k}^s}{n} t^n \right). \quad (6.157)$$

<sup>8</sup>Han 2021-07-16: The infinite dihedral group  $D_\infty$  is the point group of a 1-dimensional Bravais lattice.

The subgroup  $H(n)$  is a translation group of a sublattice of the 1-dimensional Bravais lattice. The subgroup  $H(n, k)$  is the symmetry group of a 1-dimensional lattice with a picture in the unit cell that is invariant under  $s_k = sr^k$ .

<sup>9</sup>Predrag 2021-07-04, 2021-08-25: our notation, replaced subscript  $f, s$  by noting.

<sup>10</sup>Predrag 2021-07-04: my own notation, replaced subscript  $f, s$  by superscript  $s$ .

The first sum factors as an Artin-Mazur zeta function (6.242):

$$\exp\left(\sum_{n=1}^{\infty} \frac{t^{2n}}{2n} N_n\right) = \sqrt{\zeta_{top}(t^2)} \quad (6.158)$$

The definition of a flip (6.156) tells us that

$$N_{n,k}^s = N_{n,k+n}^s = N_{n,k+2}^s \quad (6.159)$$

and this implies

$$N_{n,k}^s = \begin{cases} N_{n,0}^s & \text{if } n \text{ is odd,} \\ N_{n,0}^s & \text{if } n \text{ and } k \text{ are even,} \\ N_{n,1}^s & \text{if } n \text{ is even and } k \text{ is odd.} \end{cases} \quad (6.160)$$

Hence <sup>11</sup>

$$\sum_{k=0}^{n-1} \frac{N_{n,k}^s}{n} = \begin{cases} N_{n,0}^s & \text{if } n \text{ is odd,} \\ \frac{N_{n,0}^s + N_{n,1}^s}{2} & \text{if } n \text{ is even.} \end{cases} \quad (6.161)$$

so the Lind zeta function of the flip triple system  $(\mathcal{M}, f, s)$  is

$$\zeta_s(t) = \sqrt{\zeta_{top}(t^2)} e^{h(t)}, \quad (6.162)$$

where  $\zeta_{top}$  is the Artin-Mazur zeta function (6.242), and the counts of symmetric orbits

$$h(t) = \sum_{m=1}^{\infty} \left\{ N_{2m-1,0}^s t^{2m-1} + (N_{2m,0}^s + N_{2m,1}^s) \frac{t^{2m}}{2} \right\}. \quad (6.163)$$

they call the “generating function.”

The  $\exp(h(t))$  in (6.162) can be factored into terms that presumably correspond – in the particular, Hénon case – to the  $D_n N_n$  factors in (3.33), but this is now totally general, in the spirit of table 24.3, for any time-reversal discrete time dynamical system. Should be generalizable also to systems with continuous time.

The zeta function  $\zeta_s$  can be written as a product over orbits. Let  $O_1$  be the collection of finite orbits with time reversal (flip) symmetry, and  $O_2$  be the

<sup>11</sup>Han 2021-07-07: To understand  $N_{n,k} = N_{n,k+2}$ : Note that  $rH_{n,k}r^{-1} = H_{n,k+2}$ . Let  $x$  be a periodic point that is fixed by group  $H_{n,k}$ :

$$h \cdot x = x, \forall h \in H_{n,k}.$$

For simplicity here I denote  $f(h, x)$  as  $h \cdot x$ . There is a periodic point  $r \cdot x$  that is fixed by group  $H_{n,k+2} = rH_{n,k}r^{-1}$ :

$$rhr^{-1}r \cdot x = rh \cdot x = r \cdot x, \forall h \in H_{n,k}.$$

So the numbers of periodic points fixed by group  $H_{n,k}$  and  $H_{n,k+2}$  are equal.



collection of the pairs of orbits without time reversal symmetry, each an orbit and the flipped orbit. A finite orbit  $p$  is a periodic points set

$$p = \{x, f(x), \dots, f^{n_p-1}(x)\}$$

if  $p \in O_1$ , and

$$p = \{x, f(x), \dots, f^{k-1}(x)\} \cup \{s(x), f \circ s(x), \dots, f^{k-1} \circ s(x)\}$$

if  $p \in O_2$ , where  $k = n_p/2$ .

If  $p \in O_1$ ,

$$\zeta_p(t) = \sqrt{\frac{1}{1-t^{2n_p}}} \exp\left(\frac{t^{n_p}}{1-t^{n_p}}\right), \quad (6.164)$$

and if  $p \in O_2$ ,

$$\zeta_p(t) = \frac{1}{1-t^{n_p}}. \quad (6.165)$$

The product form of the zeta function is:

$$1/\zeta_s(t) = \sqrt{\prod_{p_1 \in O_1} (1-t^{2n_{p_1}})} \exp\left(-\frac{t^{n_{p_1}}}{1-t^{n_{p_1}}}\right) \prod_{p_2 \in O_2} (1-t^{n_{p_2}}). \quad (6.166)$$

**2021-07-28 Predrag** Checked: [Douglas Lind](#) does have a Lind zeta function (6.150) in Lind [54]. His Theorem 5.4 presumably is the product formula for his zeta.

More important for us, going forward to spatiotemporal cat, he knows how to count prime tiles in any  $\mathbb{Z}^d$  lattice, see his Table 1.

**2024-03-17 Predrag** The Lind zeta function [54] (6.150) possibly follows from the *Cauchy–Frobenius Lemma*. From [arXiv:2007.15106](#):

If the group  $G$  acts on the set  $\mathcal{M}$ , the *orbit* of the element  $X \in \mathcal{M}$  is

$$\text{orb}(X) = \{gX : g \in G\}, \quad (6.167)$$

and let

$$\text{fix}(g) = \{X \in \mathcal{M} : gX = X\} \quad (6.168)$$


be the set of element invariant under the action of a given group element  $g$ . The orbits partition  $\mathcal{M}$ , and the *orbit-counting lemma* shows how to compute the number of orbits.

**The Orbit-Counting Lemma.** Suppose a finite group  $G$  acts on the finite set  $\mathcal{M}$ . Then the number of orbits of  $\mathcal{M}$  is

$$\frac{1}{|G|} \sum_{g \in G} |\text{fix}(g)|. \quad (6.169)$$

**TheoremOfTheDay** illustrates it for the tetrahedral group.

The Hidden Library of Mathematics

 *Group Theory Lecture 6.5 Cauchy-Frobenius Theorem (AKA Burnside's Lemma)* proves the lemma.

**Mathworld:** (Unintelligible definition. Commentary:) The lemma was known by Cauchy (1845) and Frobenius (1887) prior to Burnside's (1900) rediscovery, as Burnside's lemma, the orbit-counting theorem, the Pólya-Burnside lemma, or even "the lemma that is not Burnside's!" It was extended and refined by Pólya (1937) for applications in combinatorial counting problems. In this form, it is known as **Pólya enumeration theorem**.

**2021-07-28 Predrag** Rather than Lind's nebulous 'index' [54], for  $|G/H|$  in (6.150) I would like to use **ChaosBook p. 166**:

**Definition: Multiplicity.** For a finite discrete group, the multiplicity of orbit  $p$  is  $m_p = |G|/|G_p|$ .

**Predrag** Caved in eventually, now we use 'index' as does everyone else.

**2022-02-01 Predrag to Yanxin Feng** Can you give me a good reference for "index". I call it multiplicity, because "index" says nothing to me, but I always have to refer to the "official" nomenclature as well.

We use 'multiplicity' in the current LC21 **eq. (175)**, but Lind called it an "index".

**2022-02-01 Yanxin Feng** "Index" is popular in math books. One reference [75] could be our omniscient **wiki**.

Parenthetically, Cima [19] *On the relation between index and multiplicity* has nothing to do with finite groups, ignore.

**2022-02-01 Chris DuPre** p.90 of Dummit and Foote [31] *Abstract Algebra* has it, **(click here)**. The book is a massive resource for groups.

**2022-02-01 Predrag to Yanxin Feng** Reading the wiki you gave me I do not really understand this:

When  $G$  is infinite,  $|G : H|$  is a nonzero cardinal number that may be finite or infinite. For example,  $|\mathbb{Z} : 2\mathbb{Z}| = 2$ , but  $|\mathbb{R} : \mathbb{Z}|$  is infinite.

Maybe the way to understand is to first establish it for  $D_n$  subgroups of  $D_\infty$  and then take  $n \rightarrow \infty$ , show it applies to  $D_\infty$  as well?

### 6.6.1 Counting periodic states

Given the topological zeta function (6.157) we can count the number of fixed points from the generating function:

$$\frac{-t \frac{d}{dt}(1/\zeta_s(t))}{1/\zeta_s(t)} = \sum_{n=1}^{\infty} N_n t^{2n} + \sum_{n=1}^{\infty} \sum_{k=0}^{n-1} N_{n,k}^s t^n = \sum_{m=1}^{\infty} a_m t^m, \quad (6.170)$$

where the coefficients are:

$$a_m = \begin{cases} \sum_{k=0}^{m-1} N_{m,k}^s = mN_{m,0}^s, & m \text{ is odd,} \\ N_{m/2} + \sum_{k=0}^{m-1} N_{m,k}^s = N_{m/2} + \frac{m}{2} (N_{m,0}^s + N_{m,1}^s), & m \text{ is even.} \end{cases} \quad (6.171)$$

Using the product formula of topological zeta function (6.166) and the numbers of orbits with length up to 5 from the table 24.3, we can write the topological zeta function:

$$\begin{aligned} 1/\zeta_s(t) &= \sqrt{1-t^2} \exp\left(-\frac{t}{1-t}\right) (1-t^4) \exp\left(-\frac{2t^2}{1-t^2}\right) (\sqrt{1-t^6})^3 \\ &\quad \exp\left(-\frac{3t^3}{1-t^3}\right) (1-t^6)(1-t^8)^3 \exp\left(-\frac{6t^4}{1-t^4}\right) \\ &\quad (1-t^8)^2(1-t^{10})^5 \exp\left(-\frac{10t^5}{1-t^5}\right) (1-t^{10})^6 \dots \end{aligned} \quad (6.172)$$

The generating function is:

$$\frac{-t \frac{d}{dt}(1/\zeta_s)}{1/\zeta_s} = t + 7t^2 + 12t^3 + 41t^4 + 55t^5 + \dots, \quad (6.173)$$

which is in agreement with (6.171), where the  $N_n$  and  $N_n^s$  are the  $C_n$  and  $SF_n$  in the table 24.3.

We are not able to retrieve the numbers of fixed points by their symmetry groups using this topological zeta function (6.157), unless we rewrite the topological zeta function with two variables:

$$\zeta_s(t, u) = \exp\left(\sum_{n=1}^{\infty} \frac{N_n}{2n} t^{2n} + \sum_{n=1}^{\infty} \sum_{k=0}^{n-1} \frac{N_{n,k}^s}{n} u^n\right). \quad (6.174)$$

Using this topological zeta function  $\zeta_s(t, u)$  we can write two generating functions:

$$\frac{-t \frac{\partial}{\partial t}(1/\zeta_s(t, u))}{1/\zeta_s(t, u)} = \sum_{n=1}^{\infty} N_n t^{2n}, \quad (6.175)$$

and

$$\frac{-u \frac{\partial}{\partial u}(1/\zeta_s(t, u))}{1/\zeta_s(t, u)} = \sum_{n=1}^{\infty} \sum_{k=0}^{n-1} N_{n,k}^s u^n. \quad (6.176)$$

Using the product formula of this topological zeta function and the numbers of orbits with length up to 5 from the table 24.3, the topological zeta function

is:

$$\begin{aligned}
 1/\zeta_s(t, u) &= \sqrt{1-t^2} \exp\left(-\frac{u}{1-u}\right) (1-t^4) \exp\left(-\frac{2u^2}{1-u^2}\right) \left(\sqrt{1-t^6}\right)^3 \\
 &\quad \exp\left(-\frac{3u^3}{1-u^3}\right) (1-t^6)(1-t^8)^3 \exp\left(-\frac{6u^4}{1-u^4}\right) \\
 &\quad (1-t^8)^2(1-t^{10})^5 \exp\left(-\frac{10u^5}{1-u^5}\right) (1-t^{10})^6 \dots \quad (6.177)
 \end{aligned}$$

And the generating function from this topological zeta function is:

$$\frac{-u \frac{\partial}{\partial u}(1/\zeta_s(t, u))}{1/\zeta_s(t, u)} = u + 6u^2 + 12u^3 + 36u^4 + 55u^5 + \dots, \quad (6.178)$$

which is in agreement with (6.176), where the  $N_n^s$  is the  $SF_n$  in the table 24.3.

### 6.6.2 Counting square and rectangle states

2024-06-23 Predrag By doing PDEs I learned what love is.

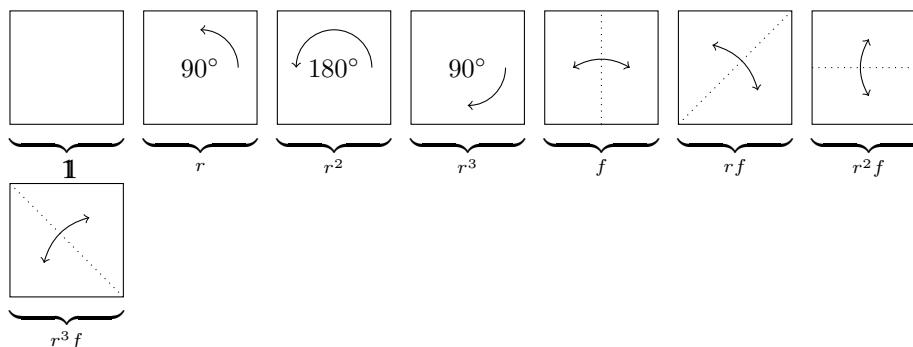


Figure 6.4: Illustrations of the eight group actions of the dihedral group of the square  $D_8$ : “identity”, “90° rotation”, “180° rotation”, “−90° rotation”, “horizontal reflection”, “diagonal reflection”, “vertical reflection”, and “antidiagonal reflection” respectively [46]. Compare with figure 6.2.

2024-06-23 Predrag S. N. Ethier and J. Lee [36] *Parrondo games with two-dimensional spatial dependence* (2015), [arXiv:1510.06947](https://arxiv.org/abs/1510.06947).

Mihailović and Rajković [59] *Cooperative Parrondo’s games on a two-dimensional lattice* (2006).

In Parrondo’s game lattice sites values are ‘0’ (loser) and ‘1’ (winner), and recoding a 2-dimensional lattice state in terms of binary number might be of interest to us.

**2024-06-23 Predrag** Banda, Caughman, Cenek and Teuscher [11] *Shift-symmetric configurations in two-dimensional cellular automata: Irreversibility, insolubility, and enumeration* (2019).

“understand symmetry of configurations in decentralized toroidal architectures” “The concept of ‘configuration shift-symmetry’ is applied to two-dimensional cellular automata.” “using compact enumeration formulas and bounding the number of shift-symmetric configurations for a given lattice size, we efficiently calculate the probability of a configuration being shift-symmetric.” “we devise an algorithm detecting the presence of shift-symmetry in a configuration.”

## 6.7 Permutation representations

Burnside’s *Table of marks*, whose rows are the orbit types, and the columns are the subgroups seems related to ChaosBook determinant factorizations.

**Marks wiki:** Much as character theory simplifies working with group representations, ‘marks’ simplify working with permutation representations and the Burnside ring (for the  $D_3$  example, see (24.314)).

See also **ncatlab Table of marks**. Possibly **DOI** contains the tables we might want to use.

**GAP** is an amazing system for computational discrete algebra. In particular, it computes *tables of marks*.

**Permutation representations wiki:**

Associated to a periodic state  $X$  is a vector space with the  $X$  lattice sites as the basis. An action of a finite group  $G$  on  $X$  induces a linear action on this vector space, called a *permutation representation*.

$H \subseteq G$  is a subgroup of  $G$ .

The table of marks of the group  $G$  is computed from the *lattice of subgroups* of  $G$ .

The *mark* of  $H$  on  $X$  is the number of elements of  $X$  that are fixed by every element of  $H$ :  $m_X(H) = |X^H|$ , where

$$X^H = \{x \in X \mid h \cdot x = x, \forall h \in H\}.$$

If  $H$  and  $K$  are conjugate subgroups, then  $m_X(H) = m_X(K)$  for any finite  $G$ -set  $X$ ; indeed, if  $K = gHg^{-1}$  then  $X^K = gX^H$ .

Let  $G_1 = \mathbf{1}, G_2, \dots, G_N = G$  be representatives of the  $N$  conjugacy classes of subgroups of  $G$ , ordered in such a way that whenever  $G_i$  is conjugate to a subgroup of  $G_j$ , then  $i \leq j$ . Now define the  $[N \times N]$  table (square matrix) whose  $(i, j)$ th entry is  $m(G_i, G_j)$ . This matrix is lower triangular, and the elements on the diagonal are non-zero so it is invertible.

The table of marks (Burnside matrix) entries are the number of elements in the orbit  $G/K$  fixed by the subgroup  $H$ .

The first column is the degree of the representation. The bottom row is 1’s because  $G/G$  is a single point. The diagonal terms are (CONTINUE)

Table 6.3:  $D_3$  table of marks, from [Montaldi](#). For  $D_6$  see table [24.4](#).

$D_3$	$\mathbf{1}$	$D_2$	$C_3$	$D_3$
$D_3/\mathbf{1}$	6			
$D_3/D_2$	3	1		
$D_3/C_3$	2	0	2	
$D_3/D_3$	1	1	1	1

$D_3$  table of marks is given in table [6.3](#), and  $D_6$  table of marks in table [24.4](#). Corresponding sets of periodic states are given by Burnside rings ([24.314](#)) and ([24.318](#))

**Theorem (Burnside 1897):** If  $X$  is a  $G$ -set, and  $u_i = m_X(G_i)$  its row vector of marks, then  $X$  decomposes as a disjoint union of  $a_i$  copies of the orbit of type  $G_i$ , where the vector  $a$  satisfies ([24.316](#))

$$\mathbf{a}M = \mathbf{u}, \tag{6.179}$$

and  $M$  is the matrix of the table of marks.

**2021-06-27 Predrag** Study example [6.30](#) discussion of the  $D_3$  symmetry: compact and elegant.

**2021-06-21 Predrag** Montaldi discussion of  $D_3$  is instructive.

In agreement with our results, his  $D_3$  permutation representation is

$$D_3 : A_0 + E, \tag{6.180}$$

see for example figure ??.

His “orientation permutation” representation on the set of 3 edges of the triangle, is  $A_1 + E$ . I do not think we use that representation.

Montaldi *Product structure in Burnside Ring* seems to be a variant of the class operators multiplication tables.

**2021-06-21 Predrag** [James Montaldi](#) has a cute overview of the  $D_2$  to  $D_6$  irreps. Our fields  $\phi_i$  are defined on  $n$  lattice sites, not on links

*Dihedral irrep:*

**2021-06-21 Predrag** Character tables in physics and chemistry use the *Mulliken symbols* as the representations names, such as  $A_1$  or  $T_{2g}$ . Montaldi adheres to that notation, except that he denotes the trivial representation by  $A_0$  rather than  $A_1$ .

$D_3$  permutation representation on the

- 3 vertices of an equilateral triangle is  $A_0 + E$

$D_4$  permutation representation on the

- 4 vertices of the square is  $A_0 + B_1 + E$
- not used: 4 edges of the square is  $A_0 + B_2 + E$
- not used: 2 diagonals of the square is  $A_0 + A_1$

$D_5$  permutation representation on the

- 5 vertices of the pentagon is  $A_0 + E_1 + E_2$

$D_6$  permutation representation on the

- 6 vertices of the hexagon is  $A_0 + B_1 + E_1 + E_2$
- not used: 3 diagonals joining opposite vertices of the hexagon is  $A_0 + E_2$

Table 6.4:  $D_n$  permutation representation irreps (from [J. Montaldi](#)).

Montaldi [Notes on circulant matrices](#) (2012) are very pedagogical. He discusses (as we do, calling this the permutation rep) the representation theory of the cyclic group (or dihedral group in the symmetric case) acting on  $\mathbb{R}^n$ .

For each  $\ell = 1, \dots, [(n-1)/2]$  let  $A_\ell$  be the irreducible 1-dimensional real representation of  $D_n$ : let the rotation  $r$  act by rotation through  $2\pi\ell/n$  and let  $s$  act by a reflection (this is independent of the choice of reflection as any two reflections are conjugate, and the resulting irreps equivalent).

Here  $[q]$  denotes the greatest integer less than or equal to  $q$ .

$A_0$  is the trivial rep and if  $n$  is even,  $A_{n/2}$  is the 1-dimensional rep where  $r$  and  $s$  act by multiplication by  $-1$ . These irreducible representations are also irreps for the cyclic group  $C_n$  (ignoring  $s$ ). The real 1-dimensional reps  $E_r$  are irreducible but not absolutely irreducible, and their complexification splits as a sum of two 1-d reps.

**Proposition 1** The above (permutation) representation decomposes as a sum of irreps:

$$A_0 \oplus A_1 \cdots \oplus A_{n/2} \tag{6.181}$$

This is called the *isotypic decomposition* of  $\mathbb{R}^n$  for this action (or representation).

The eigenvectors of  $M$  are the same for any circulant matrix  $M$ . Define the vectors  $u^{(\ell)}, v^{(\ell)} \in \mathbb{R}^n$ , with components

$$u_j^{(\ell)} = \cos(2\pi j\ell/n), \quad v_j^{(\ell)} = \sin(2\pi j\ell/n). \tag{6.182}$$

Note that  $u^{(n-\ell)} = u^{(\ell)}$  and  $v^{(n-\ell)} = -v^{(\ell)}$ . In particular,  $v^{(0)} = 0$  and if  $n$  is even then  $v^{(n/2)} = 0$ . There is therefore a total of  $n$  linearly independent vectors

$$u^{(\ell)} \quad (\ell = 0, \dots, \lfloor \frac{n}{2} \rfloor) \text{ and } v^{(\ell)} \quad (\ell = 1, \dots, \lfloor \frac{n-1}{2} \rfloor). \quad (6.183)$$

They form a basis for  $\mathbb{R}^n$  (there is more complex components detail in Montaldi notes).

In particular,  $u^{(0)} = (1, 1 \dots, 1)^\top$  and  $u^{(n/2)} = (1, -1, 1, \dots, -1)^\top$  (the latter if  $n$  is even) are real eigenvectors.

**Proposition 2** The component  $A_\ell$  is spanned by the vectors  $u_\ell, v_\ell$ .

**Proposition 3** A matrix  $M$  is circulant iff it commutes with the action of  $C_n$ , and it is symmetric and circulant iff it commutes with  $D_n$ .  $\lambda_0$  and (if  $n$  is even)  $\lambda_{n/2}$  are simple, while the other  $\lambda_\ell$  are double eigenvalues.

**2021-06-27 Predrag** The *markaracter table* of a finite group was introduced by Shinsaku Fujita.

**2021-07-04 Predrag** For a bit of history, see J. E. Humphreys review of [Pioneers of representation theory](#).

**2021-07-07 Predrag** Dirac characters (Harter's central operators, see [Harter's Sect. 3.2 First stage of non-Abelian symmetry analysis](#)) were introduced by Dirac [28] in *The Principles of Quantum Mechanics* (1930) ([click here](#)): "[...] what is called in group theory a character of the group of permutations."

Corson [22] *Note on the Dirac character operators* (1948) writes:

[...] the evaluation of Dirac and similar character operators is all that is required for the solution of the standard molecular problems in the spirit of Dirac's original program which avoids appeal to formal group theory.

Dirac characters (??) use not only the abstract group information, but also account for the symmetry information contained in the basis set used. The diagonalization of Dirac characters has three main advantages:

1. It can be realized by means of a quite simple and general algorithm.
2. The projective irreps obtained are just the ones that are needed to reduce the starting basis set into irreducible sets.
3. No tabulated quantities are required to construct the projective irreps.



The scheme is completely general, in the sense that it applies to all space groups.

Cini and Stefanucci [21] *Antiferromagnetism of the two-dimensional Hubbard model at half-filling: The analytic ground state for weak coupling*, [arXiv:cond-mat/0009058](#), uses Dirac characters to diagonalize a square integer  $[N \times N]$  lattice with  $D_4$  symmetry. Might help us with the temporal cat desymmetrization.

Cini [20] *Topics and Methods in Condensed Matter Theory* (2007) ([click here](#))


Jacobs [44] *Group Theory with Applications in Chemical Physics*, ([click here](#)) (2005)


El-Batanouny and Wooten [13] *Symmetry and Condensed Matter Physics: A Computational Approach* (2008) ([click here](#)). In sect. 4.3 they describe the Burnside's method. They give an example of Mathematica code that constructs the character table. If needed, one might use Dixon's method, which is more clever for numerical computations.

Big Chemical Encyclopedia, [Dirac character](#)


The [CRYSTAL](#) package performs ab initio calculations of the ground state energy, energy gradient, electronic wave function and properties of periodic systems. Uses Dirac characters.

**2021-07-08 Predrag** Ananda Dasgupta had 1.68K followers on YouTube, now he has one more.


 playlist for his *Symmetries in Physics* course:

 *Lecture 15* (start at about 35 min into the lecture) has a nice discussion of Dirac characters, their relation to characters, and motivates the algorithmic Burnside's method for computing characters via class multiplication tables  $(H_i)_{jk}$ .

example 6.22

 *PH4213 Discussion Class 8* applies Burnside's method to  $D_4$ .

Less interesting, but anyway, you might learn something:

 *PH4213 Discussion Class 9* gets projection operators out of characters.

 *Lecture 16* Projection operators, the Wigner-Eckart theorem.

A discussion from the Group Theory course:

[Sect. 2.10 What are cosets good for?](#)

**Henriette Roux** asks: What are cosets good for? Apologies for glossing over their meaning in the lecture. I try to minimize group-theory jargon, but cosets cannot be ignored.

Dresselhaus *et al.* [29] ([click here](#)) Chapter 1 *Basic Mathematical Background: Introduction* needs them to show that the dimension of a subgroup is a divisor of the dimension of the group. For example,  $C_3$  of dimension 3 is a subgroup of  $D_3$  of dimension 6.

In [ChaosBook Chapter 10. Flips, slides and turns](#) cosets are absolutely essential. The significance of the coset is that if a periodic state has a symmetry, then the elements in a coset act on the periodic state the same way, and generate all equivalent copies of this periodic state. Example 10.7. *Subgroups, cosets of  $D_3$*  should help you understand that.

**Henriette Roux** writes: When talking about the cosets of a subgroup we demonstrated multiplication between cosets with a specific example, but this wasn't leading to something along the lines of that the set of all left cosets of a subgroup (or the set of all the right cosets of a subgroup) form a group, correct? It didn't appear so in the example since the "unit"  $\{E, A\}$  we looked appears to only have the properties of an identity with multiplication from one direction (the direction depending on if it is the set of left cosets or the set of right cosets). In the context of the lecture I think this point was related to Lagrange's theorem (although we didn't call it that) and I vaguely remember cosets being used in the proof of Lagrange's theorem but I wasn't connecting it today. Are we going to cover that in a future lecture?

**Predrag** You are right - Lagrange's theorem (see the [wiki](#)) simply says the order of a subgroup has to be a divisor of the order of the group. We used cosets to partition elements of  $G$  to prove that. But what we really need cosets for is to define (see Dresselhaus *et al.* [29] Sect. 1.7) *Factor Groups* whose elements are cosets of a self-conjugate subgroup ([click here](#)). I will not cover that in a subsequent lecture, so please read up on it yourself.


**Henriette Roux** You talked about the period of an element  $X$ , and said that that *period* is the set

$$\{E, X, \dots, X^{n-1}\}, \quad (6.184)$$

where  $n$  is the *order* of the element  $X$ . I had thought that set was the subgroup generated by the element  $X$  and that the period of the element  $X$  was a synonym for the order of the element  $X$ ? Is that incorrect?

**Predrag** To keep things as simple as possible, in Thursday's lecture I followed Sect. 1.3 *Basic Definitions* of Dresselhaus *et al.* textbook [29], to the letter. In Def. 3 the *order* of an element  $X$  is the smallest  $n$  such that  $X^n = E$ , and they call the set (6.184) the *period* of  $X$ . I do not like that usage (and do not remember seeing it anywhere else). As you would do, in ChaosBook.org Chap. [Flips, slides and turns](#) I also define the smallest  $n$  to be the *period* of  $X$  and refer to the set (6.184) as the *orbit* generated by  $X$ . When we get to compact continuous groups, the orbit will be a (great) circle generated by a given Lie algebra element, and look more like what we usually think of as an orbit.

I am not using my own [ChaosBook.org](#) here, not to confuse things further by discussing both time evolution and its discrete symmetries. Here we focus on the discrete group only (typically spatial reflections and finite angle rotations).

- Sect. 7.1 *Reduction to the reciprocal lattice*
  - See (8.116) for Dudgeon and Mersereau [30] explaining clearly how to get the “quotient”  $Q$  when “dividing” by  $P$ .  $|\det \Lambda|/|\det Q| = |\det P|$  is then the number of cosets.
-  Canals and Schober [16] *Introduction to group theory*. It is very concise and precise, a bastard child of Bourbaki and Hamermesh [42]. Space groups show up only once, on p. 24: “By working with the cosets we have effectively factored out the translational part of the problem.”

## 6.8 Internal symmetry factorization

Here we shall distinguish “geometrical symmetry” invariance of a shape of an object under coordinate translations, reflections, and rotations from (what???) (see also sect. 4.9).

Physical Symmetry *vs.* Symmetry

A dynamical symmetry is often a *hidden* symmetry. The classic example would be the Hydrogen atom. Naively, we would only expect an  $SO(3)$  symmetry associated with rotational symmetry. This would be the geometrical symmetry, which leads to the conserved angular momentum vector. In fact, the full symmetry of the system is  $SO(4)$ ; this is exhibited by there being another conserved vector, the Laplace-Runge-Lenz (LRL) vector. Since the LRL vector is peculiar to the particular potential of the hydrogen atom and does not emerge as the result of some general geometrical feature shared by a whole class of systems (like rotational symmetry), it is referred to as a *dynamical symmetry*.

Noether?

the symmetry of a particular figure or lattice in a two- or three-dimensional Euclidean space is defined by a subgroup of the group of all translations, rotations, reflections and inversions — the subgroup that converts the object into itself.

Associated with each geometric object is the set of symmetry operations that leave invariant the relation between the object and a coordinate system. These conceptions of symmetry and operations of symmetry have their basis in Euclidean geometry.

Symmetry in physics means invariance under any kind of transformation, for example arbitrary coordinate transformations.

The invariance group of an equation is an intrinsic property of the equation.

To avoid this problem, we will henceforth use the words *intrinsic symmetry* and *intrinsic symmetry groups* when speaking of invariance properties of equations and functions. If functions or equations are left invariant by the operations of a group of transformations, the group will be said to be an *intrinsic symmetry group* of the functions or equations.

The hyperspherical symmetry of Kepler Hamiltonians is a truly dynamical symmetry — a symmetry present when there is motion. It is a symmetry that exists only when motion is allowed.

The phrase hidden symmetry is sometimes used to signify the presence of dynamical symmetry greater than ordinary geometrical symmetry.

Note; we do not know yet how this section relates to sect. 6.4.1 *Laplacians and (time) reversal*.

### 6.8.1 Internal symmetry blog

**2016-11-16 Predrag** Note that [3] the canonical Thom-Arnol'd cat map (2.1) can be written as

$$\begin{bmatrix} 2 & 1 \\ 1 & 1 \end{bmatrix} = \begin{bmatrix} 1 & 1 \\ 1 & 0 \end{bmatrix}^2, \quad (6.185)$$

so each of equivalence classes with respect to centralizer is split into two equivalence classes with respect to the group  $\{\pm A^n \mid n \in \mathbb{Z}\}$ . (See also (6.189).)

Jaidee, Moss and Ward [45] *Time-changes preserving zeta functions* say that

$$N_n = \text{tr} \begin{bmatrix} 1 & 1 \\ 1 & 0 \end{bmatrix}^n, \quad (6.186)$$

is a 'golden mean' system, and  $N_n$  is the  $n$ th Lucas number  $(1, 3, 4, 7, 11, \dots)$ , with zeta function

$$\frac{1}{\zeta(t)} = 1 - t - t^2, \quad (6.187)$$

(compare with (6.197)).

**2016-11-16 Predrag** Maillard group, Anglès d'Auriac, Boukraa and Maillard [2] *Functional relations in lattice statistical mechanics, enumerative combinatorics, and discrete dynamical systems* note that (see (6.185), (2.2))

$$A = \begin{pmatrix} 2 & 1 \\ 1 & 1 \end{pmatrix} = \begin{pmatrix} 1 & 1 \\ 1 & 0 \end{pmatrix}^2 = C^2. \quad (6.188)$$

Anosov, Klimenko and Kolutsky [3] say: "so each of equivalence classes with respect to centralizer is split into two equivalence classes with respect to the group  $\{\pm A^n \mid n \in \mathbb{Z}\}$ ." (whatever that means)

Factorization

$$\det(1 - tC) \det(1 + tC) = \det(1 - zC^2) \quad (6.189)$$

leads then to (6.199) (see (2.28), (2.18), (16.43); here corrected by Han (6.199))

**2020-09-30 Predrag** (I have no generalization guess of (6.189) yet.)

The Yukawa massive field mass parameter is related to the spatiotemporal cat stretching parameter  $s$  by (8.27)

$$\mu^2 = d(s - 2). \quad (6.190)$$

Observe that

$$\begin{aligned} \left(1 - \frac{t^2}{\mu^2}\right)^2 - t^2 &= 1 - sz + z^2, & t^2 &= \mu^2 z \\ &= \left(1 - t - \frac{t^2}{\mu^2}\right) \left(1 + t - \frac{t^2}{\mu^2}\right) \\ (\mu^2 - t^2)^2 - \mu^4 t^2 &= \mu^4(1 - sz + z^2) \\ &= (\mu^2(1 - t) - t^2) (\mu^2(1 + t) - t^2) \\ \frac{(\mu^2 - t^2)^2}{\mu^4} &= (1 - z)^2, \end{aligned} \quad (6.191)$$

so Predrag gets (see (6.199)) time-reflection factorized  $1/\tilde{\zeta}(t)$ .

$$\begin{aligned} \frac{1}{\zeta(z)} &= \frac{1 - sz + z^2}{(1 - z)^2} = \frac{1}{\zeta_{A_1}(t)} \frac{1}{\zeta_{A_1}(-t)} \\ \frac{1}{\zeta_{A_1}(t)} &= \frac{\mu^2(1 - t) - t^2}{\mu^2 - t^2} = 1 - \frac{\mu^2 t}{\mu^2 - t^2}. \end{aligned} \quad (6.192)$$

The antisymmetric  $A_2$  subspace dynamical zeta function  $\zeta_{A_2}$  differs from  $\zeta_{A_1}$  only by a minus sign for cycles with an odd number of 0's, see (6.286).

This is presumably the same as metal cat map zeta (6.55) except here I chose to count the symmetry-reduced cycles by the  $t = \sqrt{\mu^2} z$  expansion.

I suspect that the factorization (8.171) is another example of such factorization, but for a cubic lattice.

**2020-10-31 Predrag** Note that time-reversal factorization of zeta functions naturally leads to formulas in terms of the mass  $\mu = \sqrt{s - 2}$ , see (6.52) and (6.81).

**2020-11-06 Han**

$$\frac{1}{\zeta(z)} = \frac{\det(1 - zA)}{\det(1 - zB)}, \quad B = \begin{pmatrix} 1 & 0 \\ 0 & 1 \end{pmatrix}.$$

Using the factorization:

$$\det(1 - tB) \det(1 + tB) = \det(1 - zB)$$

we have (6.199).

**2020-12-09, 2020-12-11 Predrag** Reread the “quotienting the temporal Bernoulli system” (1.27) by its dynamical  $D_1 = \{e, s\}$  symmetry (1.28); figure 1.5.

**2020-12-29 Predrag** Temporal cat dynamical  $D_1 = \{e, s\}$  symmetry is (24.259)

$$sx_t = 1 - x_t, \quad ss_t = \mu^2 - s_t, \quad \text{for all } t \in \mathbb{Z}, \quad (6.193)$$

where  $s_t$  takes values in the  $s$ -letter alphabet (24.258).

**2021-01-13 Han** The factorization of (6.199) can be interpreted as the product of the topological zeta function of a half time step cat map, see (24.263) and what follows.

**2017-09-27, 2021-02-03 Predrag** reading Baake, Roberts and Weiss [10] *Periodic orbits of linear endomorphisms on the 2-torus and its lattices* arXiv:0808.3489, see sect. 6.5.2:

They discuss zeta functions of toral automorphisms, see their Table 1. Fixed point and orbit counts for the golden cat map. Example 2 is amusing:

The best known hyperbolic toral automorphism is the ‘classic’ or golden (Fibonacci [8]) cat map (see also (8.152))

$$M = \begin{pmatrix} 0 & 1 \\ 1 & 1 \end{pmatrix}. \quad (6.194)$$

It has  $\det(M) = -1$  and is thus orientation reversing (sometimes, as in ref. [47], its square is used instead). One obtains

$$\zeta_M(t) = \frac{1 - t^2}{1 - t - t^2} = \prod_{m \geq 1} (1 - t^m)^{-c_m} \quad (6.195)$$

with  $a_m = f_{m+1} + f_{m-1} - (1 + (-1)^m)$  and  $c_m$  according to Eq. (6.137), see also entries A001350 and A060280. Here,  $f_m$  are the Fibonacci numbers, defined by the recursion  $f_{m+1} = f_m + f_{m-1}$ , for  $m \geq 0$ , together with the initial condition  $f_0 = 0$  and  $f_{-1} = 1$ . The first few terms of the counts are given in table 6.2. Note that  $\zeta_M(t) = 1 + \sum_{m=0}^{\infty} f_m t^m$ , and one has  $M^m = f_m M + f_{m-1} \mathbf{1}$ , the latter being valid for all  $m \in \mathbb{Z}$ .

**2021-02-12 Han** By derivation (do it!) analogous to the Isola’s cat map  $\zeta(Z)$  (2.28), the topological zeta function for metal cat maps is (6.55) where  $z = t^2$ , in agreement with (6.197) for  $\mu = 1$ . See also (8.152).

**2021-02-12 Predrag** What is this square root of  $z$ ? This is expected, see Chaos-Book sect. 25.5  $Z_2 = D_1$  factorization: [...] if a cycle  $p$  is invariant under the symmetry subgroup  $\mathcal{H}_p \subseteq G$  of order  $h_p$ , its weight can be written as a repetition of a fundamental domain cycle

$$t_p = t_p^{h_p} \quad (6.196)$$

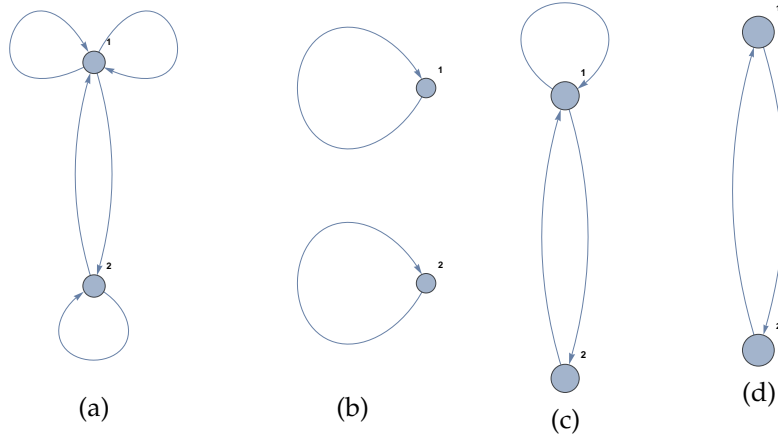


Figure 6.5: (a), (b), (c) and (d) are the Markov diagrams corresponding to the transition matrices  $A$ ,  $B$ ,  $A'$  and  $B'$ . We can get (a) and (b) by mapping (c) and (d) two time steps forward.  $1/\zeta(z)$  is the topological zeta function of the Markov diagram (a) with periodic orbits in (b) eliminated.  $1/\tilde{\zeta}(t)$  is the topological zeta function of the Markov diagram (c) with periodic orbits in (d) eliminated.

computed on the irreducible segment that corresponds to a fundamental domain cycle. [...] In the  $D_1$  case,  $t_p$  is a orbit, or a double repeat of a orbit,  $t_p = t_p^2$ , hence the square root.

For the  $\mu = 1$  golden (Fibonacci [8]) cat zeta function (24.264) or (6.199) or [45] (6.187):

$$\frac{1}{\tilde{\zeta}(t)} = \frac{1 - t - t^2}{(1 - t)^2}, \quad (6.197)$$

$\tilde{N}_n$ , the number of *periodic states* of period  $n$  is given by the logarithmic derivative of the golden cat zeta function (2.13),

$$\begin{aligned} \sum_{n=1} \tilde{N}_n t^n &= -\tilde{\zeta} t \frac{d}{dt} \frac{1}{\tilde{\zeta}} \\ &= t + t^2 + 4t^3 + 5t^4 + 11t^5 + 16t^6 + 29t^7 \\ &\quad + 45t^8 + 76t^9 + 121t^{10} + 199t^{11} + \dots \end{aligned} \quad (6.198)$$

So this is the golden (Fibonacci [8]) cat map count, table 6.2 of Baake *et al.* [10] *Periodic orbits of linear endomorphisms on the 2-torus and its lattices*. It is also the number of walks on Han's reduced Markov diagram, figure 6.5.

$$\frac{1}{\zeta(z)} = \frac{1}{\tilde{\zeta}(t)\tilde{\zeta}(-t)} = \frac{1-t-t^2}{(1-t)^2} \cdot \frac{1+t-t^2}{(1+t)^2} = \frac{1-3z+z^2}{(1-z)^2}, \quad (6.199)$$

where  $z = t^2$ .

**2021-04-03 Predrag** The temporal Hénon (3.38) is a 3-term recurrence relation of form (3.62)

$$\phi_{i+1} + \phi_i^2 + \phi_{i-1} = a, \quad i = 1, \dots, n_p. \quad (6.200)$$

## 6.9 Symmetry factorization blog

For the latest entry, go to the bottom of this section

**2018-09-02 Predrag** Miles [60] *A dynamical zeta function for group actions*, [arXiv:1506.08555](https://arxiv.org/abs/1506.08555): “introduces and investigates the basic features of a dynamical zeta function for group actions, motivated by the deterministic dynamical zeta function of a single transformation. A product formula for the dynamical zeta function is established that highlights a crucial link between this function and the zeta function of the acting group.

The zeta function of a dynamical system is a fundamental invariant that has warranted considerable attention since the definitive work of Artin and Mazur [4]. Ruelle [67] provides an introduction to various guises of this function, and Sharp [69] (seems to be lacking from [here](#)) provides a comprehensive survey by in the context of periodic orbits of hyperbolic flows.”

“The relevance of the dynamical zeta function in questions of orbit growth is also considered.”

**2020-09-24, 2020-12-16 Predrag to Robert S. MacKay** (see discussion around (24.501))

My thoughts in that directions (that is in my temporal cat talk, and in this blog, see (8.167), (16.39), (16.42), (16.49)) are that for the 1-dimensional temporal cat [26, 41]

$$x_{n,t+1} + x_{n,t-1} - 2s x_t + x_{n+1,t} + x_{n-1,t} = -s_t, \quad s_t \in \mathcal{A}, \quad (6.201)$$

with alphabet

$$\mathcal{A} = \{-3, -2, -1, 0, \dots, \mu^2 + 1, \mu^2 + 2, \mu^2 + 3\}, \quad (6.202)$$

and the Yukawa mass squared of the scalar field  $x$

$$\mu^2 = 2(s - 2). \quad (6.203)$$



The  $\zeta$  function has to satisfy all spatiotemporal symmetries of the square lattice

$$D_4 = \{1, r, r^2, r^3, s, s_1, s_2, s_3, \}. \quad (6.204)$$

See [ChaosBook sect. A25.1](#).

In the international crystallographic notation, this square lattice space point group is referred to as  $p4mm$  [29].

2CB

**2019-01-28 Predrag** Useful wikis:

[Dihedral group  \$D\_4\$](#)

Wolfram Demonstrations:

[Dihedral Group n of Order 2n](#)

[Cosine and Sine Identities with Dihedral Transformations](#)

[The symmetry group of a square](#): I find their “different Cayley graph” interesting: here  $D_4$  is generated by a horizontal (short axis) reflection, and a diagonal (long axis) reflection, rather than the usual  $(r, s)$  set.

[Linear representation theory of dihedral groups](#) summarizes everything worth knowing:

**2021-01-08 Predrag** taken from [ChaosBook remark 11.2](#): *Examples of systems with discrete symmetries.*

$D_2 = C_{2v} = V_4 = Z_2 \times Z_2$  symmetry in the stadium billiard [65]. Cvitanović, Davidchack and Siminos [25] eq. (2.13)

See [ChaosBook sect. A25.2](#).

$D_4 = C_{4v}$  symmetry: in quartic oscillators [32, 57], in the pure  $x^2y^2$  potential [17, 58] and in hydrogen in a magnetic field [34].

$D_n$  symmetry: see [Ding thesis example 2.9](#).

Pdflatex *siminos/lyapunov/blog.tex*, read sect. 7.11.2 *Factorization of  $C_n$  and  $D_n$* .

**2020-12-20 Predrag** This square lattice symmetry group is the space group  $p4mm$ , with point group  $D_4$  (6.204), so all calculations should be carried out on the reciprocal lattice, with a  $1/8$ th of a square Brilluion zone, figure 6.6.

Furthermore, one should quotient the temporal cat (24.501) by its  $D_1 = \{e, \sigma\}$  dynamical symmetry

$$\sigma x_t = 1 - x_t, \quad \sigma s_t = \mu^2 - s_t, \quad \text{for all } t \in \mathbb{Z}, \quad (6.205)$$

where  $s_t$  takes values in the  $s$ -letter alphabet (10.6). Define the fundamental domain to be  $\hat{x}_t \in [0, 1/2]$ . We construct the temporal cat fundamental domain lattice system, with ‘ $1/2$ ’ unit hypercube  $\hat{X} \in [0, 1/2]^n$ , as in [ChaosBook Group  \$D\_1\$  and reduction to the fundamental domain](#), see figure 1.5(b), and the fundamental domain symbolic dynamics  $\hat{A}$ . That leads to [ChaosBook chapter 25 Discrete symmetry factorization](#) of zeta functions.

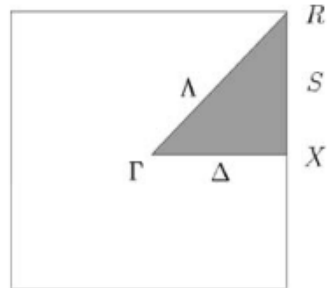


Figure 6.6: The shaded (or yellow) area indicates a *fundamental domain*, i.e., the smallest part of the pattern whose repeats tile the entire plane. For the most symmetric 2D square lattice, with point group  $p4mm$ , the fundamental domain is indicated by the shaded triangle  $\Gamma\Lambda R S X \Delta \Gamma$  which constitutes  $1/8$  of the Brillouin zone, and contains the basic wave vectors and the high symmetry points (Fig. 10.2 of Dresselhaus *et al.* [29]).

**2021-06-08 Predrag** 🗣️ *Lecture 7* (Unedited as of 2021-06-18)

- We work out the symmetry reduction and a breaking of the  $D_3$  symmetry in the  $[3 \times 3]$  permutation matrices representation

**2021-06-20 Predrag** I'll have to rerecord the above video from scratch, example 6.30 discussion of the  $D_3$  symmetry is much more compact and elegant.

**2021-06-20 Predrag** This analysis of  $D_n$  irreps does not apply to symmetric orbits. For that one has to look at the subgroup structure of dihedral groups, see [groupprops wiki](#), the subgroup called there  $\langle x \rangle$ . Han's discussion of (6.265), (6.266) and (4.304) counts the broken rotational invariance solutions.

**2021-06-21 Predrag** Paul Garrett (2014) course notes *Harmonic analysis of dihedral group* contain a nice discussion of use of discrete Fourier basis for representation of fields (i.e., scalar functions) on  $D_n$  lattices. His *Representation theory* course contains many interesting nuggets.

**2018-07-04 Predrag** Siemaszko and Wojtkowski [70] *Counting Berg partitions* describe symmetries of Adler-Weiss partitions. They are present for reversible toral automorphisms.

**2021-07-04 Predrag** The full symmetry group of a toral automorphism was studied by Baake and Roberts [9].

**2021-07-04 Predrag** The *infinite dihedral group*  $D_\infty$  (6.7) was introduced by Kim, Lee and Park [49] *A zeta function for flip systems* (2003).

Kim, Lee and Park [49] give the explicit formula (6.162) for the Lind zeta function [54]  $\zeta_s$  (search for “Lind96” to find more about it) of a flip system  $(\mathcal{M}, f, s)$  (6.4).

[...] investigate dynamical systems with flip maps (6.4), regarded as infinite dihedral group actions. We introduce a zeta function for flip systems, and find its basic properties including a product formula. When the underlying  $C_n$ -action is conjugate to a topological Markov shift, the flip system is represented by a pair of matrices, and its zeta function is expressed explicitly in terms of the representation matrices.

[...] Any topological Markov shift whose transition matrix is symmetric has a natural flip.

[...] establish a zeta function for flip systems which is a conjugacy invariant, and give a finite description of the function when the underlying  $\mathbb{Z}$ -action is conjugate to a topological Markov shift.

**2021-07-04 Predrag** The much desired -see (3.34)- square root and dependence on  $t^2$  finally makes an appearance in the Lind zeta function (6.162)!

**2021-07-04 Predrag** S. Ryu *The Lind Zeta functions of reversal systems of finite order* [arXiv:1712.03519](https://arxiv.org/abs/1712.03519) (2017) deals with a more general case of reversing operators, but the LaTeX file was useful for clip & paste.

If  $(\mathcal{M}, f)$  is a shift of finite type, then there exists a square matrix  $A$  with non-negative integer entries such that the number of fixed points  $N_n$  can be expressed in terms of matrices [55]

$$N_n = \text{tr } A^n \quad (m = 1, 2, \dots) \quad (6.206)$$

Similarly, when  $(\mathcal{M}, f, s)$  is a shift-flip system of finite type, the number of fixed points  $N_n^s$  can be expressed in terms of matrices [49].

They write: “ Since there is a dynamical system  $(X, T)$  which is not conjugate to its time reversal  $(X, T^{-1})$ , not every dynamical system has a flip. See p. 104 of Boyle, Marcus and Trow [14].

**Note:** Predrag does not understand that page. Worse still, Predrag does not understand any page in the entire monograph :(

In Park [62] it is shown that if the underlying  $\mathbb{Z}$ -actions are Kolmogorov and isomorphic, there are examples of non-isomorphic  $D_\infty$ -actions. ”

**2021-08-11 Predrag** Park [62] *On ergodic foliations* (1988).

The ‘covering space’ has two actions,  $f$  and  $s$ , where  $f$  is a  $\mathbb{Z}$ -action,  $s$  is a map of order two, and  $s$  and  $T$  skew-commute; that is,  $sfs = f^{-1}$ .

**Note:** Predrag does not understand this paper, not at all.

**2021-07-04 Predrag** Still to read:

Boyle, Marcus and Trow [14] *Resolving maps and the dimension group for shifts of finite type* (1987).

Nordin and Noorani [61] *Counting finite orbits for the flip systems of shifts of finite type* (2021).

Yumiko Hironaka *Zeta functions of finite groups by enumerating subgroups*, [arXiv:1410.4326](https://arxiv.org/abs/1410.4326) (2014) is potentially interesting: Hironaka forms zeta function like Riemann, rather than Artin-Mazur.

Richard Miles *Orbit growth for algebraic flip systems* [DOI](#) (2014)

Sieye Ryu [PhD thesis](#) *The Lind Zeta Function and Williams' Decomposition Theorem for Sofic Shift-Reversal Systems of Finite Order* (2014)

Golubitsky and Stewart [38] *The Symmetry Perspective*, chapters *Time Periodicity and Spatio-Temporal Symmetry and Periodic Solutions of Symmetric Hamiltonian Systems* (2002)



example 6.11  
p. 349  
example 6.30  
p. 362



example 6.35  
p. 366  
example 6.31  
p. 362



example 6.32  
p. 364

## 6.10 Group theory and symmetries: a review

<sup>12</sup> <sup>13</sup> In quantum mechanics, whenever a system exhibits some symmetry, the corresponding symmetry group commutes with the Hamiltonian of this system, namely,  $[U(g), H] = U(g)H - HU(g) = 0$ . Here  $U(g)$  denotes the operation corresponding to symmetry  $g$  whose meaning will be explained soon. The set of eigenstates with degeneracy  $\ell$ ,  $\{\phi_1, \phi_2, \dots, \phi_\ell\}$ , corresponding to the same system energy  $H\psi_i = E_n\psi_i$ , is invariant under the symmetry since  $U(g)\psi_i$  are also eigenvectors for the same energy. This information helps us understand the spectrum of a Hamiltonian and the quantum mechanical selection rules. We now apply the same idea to the deterministic evolution operator  $\mathcal{L}^t(x_e, x_s)$  for a system  $f^t(x)$  equivariant under a discrete symmetry group  $G = \{e, g_2, g_3, \dots, g_{|G|}\}$  of order  $|G|$ :

$$f^t(D(g)x) = D(g)f^t(x) \quad \text{for } \forall g \in G. \quad (6.207)$$

We start with a review of some basic facts of the group representation theory. Some examples of good references on this topic are ref. [43, 73].

Suppose group  $G$  acts on a linear space  $V$  and function  $\rho(x)$  is defined on this space  $x \in V$ . Each element  $g \in G$  will transform point  $x$  to  $D(g)x$ . At the same time,  $\rho(x)$  is transformed to  $\rho'(x)$ . The value  $\rho(x)$  is unchanged after state point  $x$  is transformed to  $D(g)x$ , so  $\rho'(D(g)x) = \rho(x)$ . Denote  $U(g)\rho(x) = \rho'(x)$ , so we have

$$U(g)\rho(x) = \rho(D(g)^{-1}x). \quad (6.208)$$

This is how functions are transformed by group operations. Note,  $D(g)$  is the representation of  $G$  in the form of space transformation matrices. The operator  $U(g)$ , which acts on the function space, is not the same as group operation  $D(g)$ , so (6.208) does not mean that  $\rho(x)$  is invariant under  $G$ . Example 6.12 gives the space transformation matrices of  $C_3$ .



example 6.12  
p. 351

### 6.10.1 Regular representation

An operator  $U(g)$  which acts on an infinite-dimensional function space is too abstract to analyze. We would like to represent it in a more familiar way. Suppose there is a function  $\rho(x)$  with symmetry  $G$  defined in full state space  $\mathcal{M}$ , then full state space can be decomposed as a union of  $|G|$  tiles each of which is obtained by transforming the fundamental domain,

$$\mathcal{M} = \bigcup_{g \in G} g\hat{\mathcal{M}}, \quad (6.209)$$

<sup>12</sup>Predrag 2021-06-19: A copy of the 2017-03-09 section from Xiong Ding's thesis `siminos/xiong/thesis/chapters/symGroup.tex`.

<sup>13</sup>Predrag 2021-06-19: Update/replace the ChaosBook version, as now  $Z_2 \rightarrow D_1, Z_3 \rightarrow C_3$ .

where  $\hat{\mathcal{M}}$  is the chosen fundamental domain. So  $\rho(x)$  takes  $|G|$  different forms by (6.208) in each sub-domain in (6.209). Now, we obtained a natural choice of a set of bases in this function space called the *regular basis*,

$$\{\rho_1^{reg}(\hat{x}), \rho_2^{reg}(\hat{x}), \dots, \rho_{|G|}^{reg}(\hat{x})\} = \{\rho(\hat{x}), \rho(g_2\hat{x}), \dots, \rho(g_{|G|}\hat{x})\}. \quad (6.210)$$

Here, for notation simplicity we use  $\rho(g_i\hat{x})$  to represent  $\rho(D(g_i\hat{x}))$  without ambiguity. These bases are constructed by applying  $U(g^{-1})$  to  $\rho(\hat{x})$  for each  $g \in G$ , with  $\hat{x}$  a point in the fundamental domain. The  $[|G| \times |G|]$  matrix representation of the action of  $U(g)$  in basis (6.210) is called the (*left*) *regular representation*  $D^{reg}(g)$ . Relation (6.208) says that  $D^{reg}(g)$  is a permutation matrix, so each row or column has only one nonzero element.

We have a simple trick to obtain the regular representation quickly. Suppose the element at the  $i$ th row and the  $j$ th column of  $D^{reg}(g)$  is 1. It means  $\rho(g_i\hat{x}) = U(g)\rho(g_j\hat{x})$ , which is  $g_i = g^{-1}g_j \implies g^{-1} = g_i g_j^{-1}$ . Namely,

$$D^{reg}(g)_{ij} = \delta_{g^{-1}, g_i g_j^{-1}}. \quad (6.211)$$

So if we arrange the columns of the multiplication table by the inverse of the group elements, then setting positions with  $g^{-1}$  to 1 defines the regular representation  $D^{reg}(g)$ . Note, the above relation can be further simplified to  $g = g_j g_i^{-1}$ , but it exchanges the rows and columns of the multiplication table, so  $g = g_j g_i^{-1}$  should not be used to get  $D^{reg}(g)$ . On the other hand, it is easy to see that the regular representation of group element  $e$  is always the identity matrix.



example 6.13  
p. 351

### 6.10.2 Irreducible representations

$U(g)$  is a linear operator under the regular basis. Any linearly independent combination of the regular bases can be used as new basis, and then the representation of  $U(g)$  changes respectively. So we ask a question: can we find a new set of bases

$$\rho_i^{irr} = \sum_j S_{ij} \rho_j^{reg} \quad (6.212)$$

such that the new representation  $D^{irr}(g) = S D^{reg}(g) S^{-1}$  is block-diagonal for any  $g \in G$ ?

$$D^{irr}(g) = \begin{bmatrix} D^{(1)}(g) & & \\ & D^{(2)}(g) & \\ & & \ddots \end{bmatrix} = \bigoplus_{\mu=1}^r d_\mu D^{(\mu)}(g). \quad (6.213)$$

In such a block-diagonal representation, the subspace corresponding to each diagonal block is invariant under  $G$  and the action of  $U(g)$  can be analyzed subspace by subspace. It can be easily checked that for each  $\mu$ ,  $D^{(\mu)}(g)$  for all

$g \in G$  form another representation (*irreducible representation*, or *irrep*) of group  $G$ . Here,  $r$  denotes the total number of irreps of  $G$ . The same irrep may show up more than once in the decomposition (6.213), so the coefficient  $d_\mu$  denotes the number of its copies. Moreover, it is proved [43] that  $d_\mu$  is also equal to the dimension of  $D^{(\mu)}(g)$  in (6.213). Therefore, we have a relation

$$\sum_{\mu=1}^r d_\mu^2 = |G|.$$



example 6.14  
p. 352

**Character tables.** Finding a transformation  $S$  which simultaneously block-diagonalizes the regular representation of each group element sounds difficult. However, suppose it can be achieved and we obtain a set of irreps  $D^{(\mu)}(g)$ , then according to Schur's lemmas [43],  $D^{(\mu)}(g)$  must satisfy a set of orthogonality relations:

$$\frac{d_\mu}{|G|} \sum_g D_{il}^{(\mu)}(g) D_{mj}^{(\nu)}(g^{-1}) = \delta_{\mu\nu} \delta_{ij} \delta_{lm}. \quad (6.214)$$

Denote the trace of irrep  $D^{(\mu)}$  as  $\chi^{(\mu)}$ , which is referred to as the *character* of  $D^{(\mu)}$ . Properties of irreps can be derived from (6.214), and we list them as follows:

1. The number of irreps is the same as the number of classes.
2. Dimensions of irreps satisfy  $\sum_{\mu=1}^r d_\mu^2 = |G|$
3. Orthonormal relation I:  $\sum_{i=1}^r |K_i| \chi_i^{(\mu)} \chi_i^{(\nu)*} = |G| \delta_{\mu\nu}$ .  
Here, the summation goes through all classes of this group, and  $|K_i|$  is the number of elements in class  $i$ . This weight comes from the fact that elements in the same class have the same character. Symbol  $*$  means the complex conjugate.
4. Orthonormal relation II:  $\sum_{\mu=1}^r \chi_i^{(\mu)} \chi_j^{(\mu)*} = \frac{|G|}{|K_i|} \delta_{ij}$ .

The characters for all classes and irreps of a finite group are conventionally arranged into a *character table*, a square matrix whose rows represent different classes and columns represent different irreps. Rules 1 and 2 help determine the number of irreps and their dimensions. As the matrix representation of class  $\{e\}$  is always the identity matrix, the first row is always the dimension of the corresponding representation. All entries of the first column are always 1, because the symmetric irrep is always one-dimensional. To compute the remaining entries, we should use properties 3, 4 and the class multiplication tables. Spectroscopists conventions use labels  $A$  and  $B$  for symmetric, respectively antisymmetric nondegenerate irreps, and  $E, T, G, H$  for doubly, triply, quadruply, quintuply degenerate irreps.



example 6.20  
p. 356

### 6.10.3 Projection operator

We have listed the properties of irreps and the techniques of constructing a character table, but we still do not know how to construct the similarity transformation  $S$  which takes a regular representation into a block-diagonal form. Think of it in another way, each irrep is associated with an invariant subspace, so by projecting an arbitrary function  $\rho(x)$  into its invariant subspaces, we find the transformation (6.212). One of these invariant subspaces is  $\sum_g \rho(g\hat{x})$ , which is the basis of the one-dimensional symmetric irrep  $A$ . For  $C_3$ , it is (6.230). But how to get the others? We resort to the projection operator:

$$P_i^{(\mu)} = \frac{d_\mu}{|G|} \sum_g \left( D_{ii}^{(\mu)}(g) \right)^* U(g). \tag{6.215}$$

It projects an arbitrary function into the  $i$ th basis of irrep  $D^{(\mu)}$  provided the diagonal elements of this representation  $D_{ii}^{(\mu)}$  are known.  $P_i^{(\mu)} \rho(x) = \rho_i^{(\mu)}$ . Here, symbol  $*$  means the complex conjugate. For unitary groups  $\left( D_{ii}^{(\mu)}(g) \right)^* = D_{ii}^{(\mu)}(g^{-1})$ . Summing  $i$  in (6.215) gives

$$P^{(\mu)} = \frac{d_\mu}{|G|} \sum_g \left( \chi^{(\mu)}(g) \right)^* U(g). \tag{6.216}$$

This is also a projection operator which projects an arbitrary function onto the sum of the bases of irrep  $D^{(\mu)}$ .

Note, for one-dimensional representations, (6.216) is equivalent to (6.215). The projection operator is known after we obtain the character table, since the character of an one-dimensional matrix is the matrix itself. However, for two-dimensional or higher-dimensional representations, we need to know the diagonal elements  $D_{ii}^{(\mu)}$  in order to get the basis of invariant subspaces. That is to say, (6.215) should be used instead of (6.216) in this case. Example 6.21 illustrates this point. The two one-dimensional irreps are obtained by (6.216), but the other four two-dimensional irreps are obtained by (6.215).



example 6.21  
p. 357

The  $C_3$  and  $D_3$  examples used in this section can be generalized to any  $C_n$  and  $D_n$ . For references, Example 6.26, example 6.33 and example 6.34 give the character tables of  $C_n$  and  $D_n$ .



example 6.26  
p. 359



example 6.33  
p. 365



example 6.34  
p. 366



## Commentary

**Remark 6.1. Time reversal.** (2021-01-27 Predrag harmonize this remark with the same in ChaosBook discrete.tex)

Some background on  $D_\infty$  symmetry of the temporal cat and  $\phi^4$  1d lattice field theory, refsect s:latt1d *Translations and reflections*. Time-reversed periodic states (if not self-dual under reflection) are counted as pairs, see for example ChaosBook fig. 11.6, ChaosBook example 11.11, ChaosBook Example 15.6  $C_2$  recoded, ChaosBook fig. 15.15, ChaosBook table 18.1 *The 4-disk orbits up to period 8*, ChaosBook table 34.1, the time-reversal discussion in ChaosBook section 42.2.3, and ChaosBook fig. 42.5.

This is a many-years outstanding frustration, see ChaosBook Remark 16.3 *Symmetries of the symbol square* and ChaosBook Remark 25.2 *Other symmetries*.

42.2.3 Periodic orbits

The zeta functions are still to be factorized in the  $z \rightarrow t^2$  sense, perhaps as in (6.197). Then the corresponding ChaosBook chapters have to be rewritten.

## 6.11 Examples

**Example 6.1. Discrete groups of order 2 on  $\mathbb{R}^3$ .** Three types of discrete group of order 2 can arise by linear action on our 3-dimensional Euclidean space  $\mathbb{R}^3$ :



$$\begin{aligned} \text{reflections: } s(x, y, z) &= (x, y, -z) \\ \text{rotations: } r(x, y, z) &= (-x, -y, z) \\ \text{inversions: } P(x, y, z) &= (-x, -y, -z). \end{aligned} \tag{6.217}$$

$s$  is a reflection (or an inversion) through the  $[x, y]$  plane.  $r$  is  $[x, y]$ -plane, constant  $z$  rotation by  $\pi$  about the  $z$ -axis (or an inversion thorough the  $z$ -axis).  $P = rs$  is an inversion (or parity operation) through the point  $(0, 0, 0)$ . Singly, each operation generates a group of order 2:  $D_1 = \{e, s\}$ ,  $C_2 = \{e, r\}$ , and  $D_1 = \{e, P\}$ . Together, they form the dihedral group  $D_2 = \{e, s, r, sr\}$  of order 4. (continued in example 6.2)

[click to return: p. ??](#)

**Example 6.2. Discrete operations on  $\mathbb{R}^3$ .** (Continued from example 6.1.) The matrix representation of reflections, rotations and inversions defined by (6.217) is

2CB

$$D(s) = \begin{pmatrix} 1 & 0 & 0 \\ 0 & 1 & 0 \\ 0 & 0 & -1 \end{pmatrix}, \quad D(r) = \begin{pmatrix} -1 & 0 & 0 \\ 0 & -1 & 0 \\ 0 & 0 & 1 \end{pmatrix}, \quad D(P) = \begin{pmatrix} -1 & 0 & 0 \\ 0 & -1 & 0 \\ 0 & 0 & -1 \end{pmatrix}, \tag{6.218}$$

with  $\det D(r) = 1$ ,  $\det D(s) = \det D(P) = -1$ ; that is why we refer to  $r$  as a rotation, and  $s, P$  as inversions. As  $g^2 = e$  in all three cases, these are groups of order 2. (continued in example 6.3)

[click to return: p. ??](#)

**Example 6.3. Equivariance of the Lorenz flow.** (Continued from example 6.2) The velocity field in Lorenz equations (??)

exercise ??

$$\begin{bmatrix} \dot{x} \\ \dot{y} \\ \dot{z} \end{bmatrix} = \begin{bmatrix} \sigma(y - x) \\ \rho x - y - xz \\ xy - bz \end{bmatrix} \tag{6.219}$$

is equivariant under the action of cyclic group  $C_2 = \{e, r\}$  acting on  $\mathbb{R}^3$  by a  $\pi$  rotation about the  $z$  axis,

$$r(x, y, z) = (-x, -y, z). \tag{6.220}$$

(continued in example 6.4)

[click to return: p. ??](#)

**Example 6.4. Desymmetrization of Lorenz flow.** (Continuation of example 6.3) Lorenz equation (6.219) is equivariant under (6.220), the action of order-2 group  $C_2 = \{e, r\}$ , where  $r$  is  $[x, y]$ -plane, half-cycle rotation by  $\pi$  about the  $z$ -axis:

$$(x, y, z) \rightarrow r(x, y, z) = (-x, -y, z). \tag{6.221}$$

$r^2 = 1$  condition decomposes the state space into two linearly irreducible subspaces  $\mathcal{M} = \mathcal{M}^+ \oplus \mathcal{M}^-$ , the  $z$ -axis  $\mathcal{M}^+$  and the  $[x, y]$  plane  $\mathcal{M}^-$ , with projection operators onto the two subspaces given by (see sect. ??)

$$P^+ = \frac{1}{2}(1 + r) = \begin{pmatrix} 0 & 0 & 0 \\ 0 & 0 & 0 \\ 0 & 0 & 1 \end{pmatrix}, \quad P^- = \frac{1}{2}(1 - r) = \begin{pmatrix} 1 & 0 & 0 \\ 0 & 1 & 0 \\ 0 & 0 & 0 \end{pmatrix}. \tag{6.222}$$

As the flow is  $C_2$ -invariant, so is its linearization  $\dot{x} = Ax$ . Evaluated at  $E_0$ ,  $A$  commutes with  $r$ , and, as we have already seen in example ??, the  $E_0$  stability matrix decomposes into  $[x, y]$  and  $z$  blocks.<sup>14</sup>

The 1-dimensional  $\mathcal{M}^+$  subspace is the fixed-point subspace, with the  $z$ -axis point-wise invariant under the group action

$$\mathcal{M}^+ = \text{Fix}(C_2) = \{x \in \mathcal{M} \mid gx = x \text{ for } g \in \{e, r\}\} \tag{6.223}$$

(here  $x = (x, y, z)$  is a 3-dimensional vector, not the coordinate  $x$ ). A  $C_2$ -fixed point  $x(t)$  in  $\text{Fix}(C_2)$  moves with time, but according to (??) remains within  $x(t) \in \text{Fix}(C_2)$  for all times; the subspace  $\mathcal{M}^+ = \text{Fix}(C_2)$  is flow invariant. In case at hand this jargon is a bit of an overkill: clearly for  $(x, y, z) = (0, 0, z)$  the full state space Lorenz equation (6.219) is reduced to the exponential contraction to the  $E_0$  equilibrium,<sup>15</sup>

$$\dot{z} = -bz. \tag{6.224}$$

However, for higher-dimensional flows the flow-invariant subspaces can be high-dimensional, with interesting dynamics of their own. Even in this simple case this subspace plays an important role as a topological obstruction: the orbits can neither enter it nor exit it, so the number of windings of a trajectory around it provides a natural, topological symbolic dynamics.

The  $\mathcal{M}^-$  subspace is, however, not flow-invariant, as the nonlinear terms  $\dot{z} = xy - bz$  in the Lorenz equation (6.219) send all initial conditions within  $\mathcal{M}^- = (x(0), y(0), 0)$  into the full,  $z(t) \neq 0$  state space  $\mathcal{M}/\mathcal{M}^+$ . (continued in example ??)

[click to return: p. 972](#)

(E. Siminos and J. Halcrow)

**Example 6.5. Discrete symmetries of the plane Couette flow.** The plane Couette flow is a fluid flow bounded by two countermoving planes, in a cell periodic in streamwise and spanwise directions. The Navier-Stokes equations for the plane Couette flow have two discrete symmetries: reflection through the (streamwise, wall-normal) plane, and rotation by  $\pi$  in the (streamwise, wall-normal) plane. That is why the system has equilibrium and periodic orbit solutions, as well as relative equilibrium and relative periodic

2CB

↓PRIVATE

↑PRIVATE

2CB

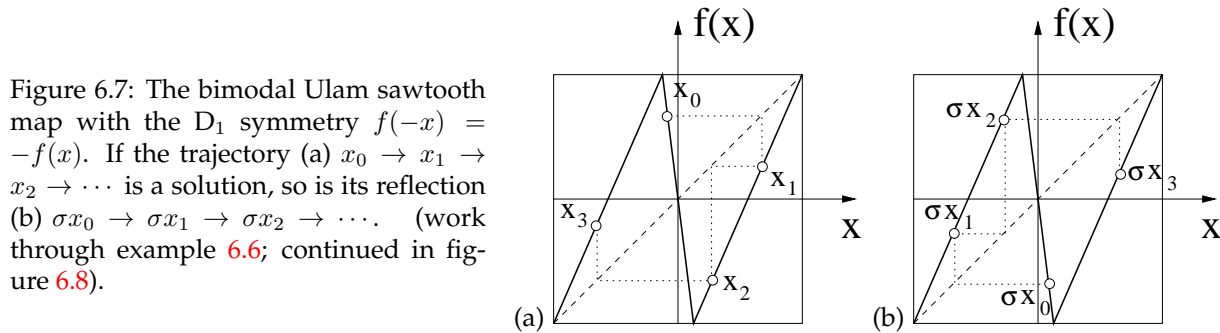


Figure 6.7: The bimodal Ulam sawtooth map with the  $D_1$  symmetry  $f(-x) = -f(x)$ . If the trajectory (a)  $x_0 \rightarrow x_1 \rightarrow x_2 \rightarrow \dots$  is a solution, so is its reflection (b)  $\sigma x_0 \rightarrow \sigma x_1 \rightarrow \sigma x_2 \rightarrow \dots$ . (work through example 6.6; continued in figure 6.8).

orbit solutions discussed in chapter ??). They belong to discrete symmetry subspaces. (continued in example ??)

[click to return: p. ??](#)

**Example 6.6. A reflection-symmetric 1d map.** Consider a 1-dimensional bimodal 'sawtooth' map  $f$  shown in figure 6.7.

$$x_{t+1} = \begin{cases} f_L(x_t) = \Lambda(x_t + 1) - 1, & x_t \in \mathcal{M}_0 = [-1, -\ell/2] \\ f_C(x_t) = \Lambda_C x_t, & x_t \in \mathcal{M}_C = [-\ell/2, \ell/2] \\ f_R(x_t) = \Lambda(x_t - 1) + 1, & x_t \in \mathcal{M}_1 = (\ell/2, 1], \end{cases} \quad (6.225)$$

with  $\ell = 2/|\Lambda_C|$ , and  $2/|\Lambda| + 1/|\Lambda_C| = 1$ . The map is piecewise-linear on the state space  $\mathcal{M} = [-1, 1]$ , a compact 1-dimensional line interval, split into three regions  $\mathcal{M} = \mathcal{M}_L \cup \mathcal{M}_C \cup \mathcal{M}_R$ . The map is reflection-symmetric,  $f(-x) = -f(x)$ .

Denote the reflection operation by  $\sigma x = -x$ . The 2-element group  $G = \{e, \sigma\}$  goes by many names, such as  $Z_2$  or  $C_2$ . Here we shall refer to it as  $D_1$ , dihedral group generated by a single reflection. The  $G$ -equivariance of the map implies that if  $\{x_n\}$  is a trajectory, then also  $\{\sigma x_n\}$  is a symmetry-equivalent trajectory because  $\sigma x_{n+1} = \sigma f(x_n) = f(\sigma x_n)$ .

In the temporal lattice formulation, there is a triplet of fields  $\phi_t = (\phi_t^L, \phi_t^C, \phi_t^R)$  at each lattice site  $t$ . Just like the temporal Bernoulli (?), temporal periodic states satisfy a linear first-order difference equation

$$\phi_t - f \circ \phi_{t-1} = 0, \quad (6.226)$$

but now for a triplet of fields satisfying the local condition (6.225) at each lattice site. As the local slope can be either  $\Lambda$  or  $\Lambda_C$ , the  $[3n \times 3n]$  orbit Jacobian matrix  $\mathcal{J}$  takes a block-diagonal form, and depends on the symbol block of a particular periodic state.

**Challenge:** write down the Hill determinant for a given symbol block, not only using Hill's formula, but also directly, without time evolution.

(continued in example 6.7)<sup>16</sup>

[click to return: p. ??](#)

**Example 6.7.  $D_1$ -asymmetric cycles.** (Continued from example 6.6)<sup>17</sup> The  $D_1$ -

<sup>14</sup>Predrag 20171-07-24: create example in sect. ?? from the last sentence

<sup>15</sup>Predrag 2017-07-24: pointer to turbulence chapter here

<sup>16</sup>Predrag 2021-06-12: write up exercise exer:ReflectA: write down the formula for the map of figure 6.7, verify its  $D_1$ -equivariance.

<sup>17</sup>Predrag 2019-02-18: REPLACE discreteD1.mp4, eventually.

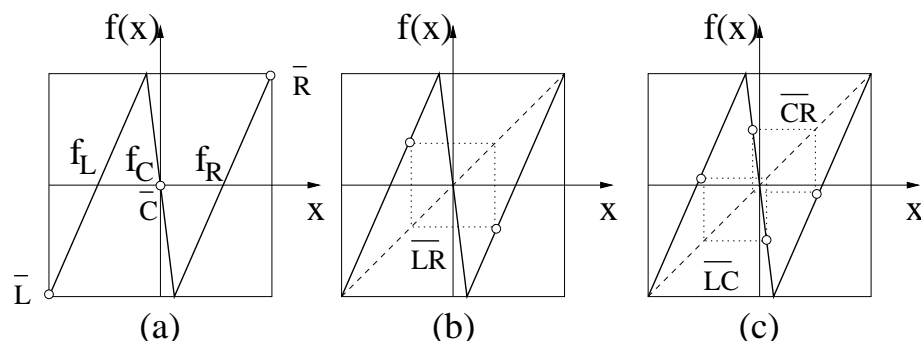


Figure 6.8: The  $D_1$ -equivariant bimodal sawtooth map of figure 6.7 has three types of periodic orbits: (a)  $D_1$ -fixed fixed point  $\bar{C}$ , asymmetric fixed points pair  $\{\bar{L}, \bar{R}\}$ . (b)  $D_1$ -symmetric (setwise invariant) 2-cycle  $\bar{L}\bar{R}$ , composed of the relative cycle segment from  $L$  to  $R$  and its repeat from  $R$  to  $L$ . (c) Asymmetric 2-cycles pair  $\{\bar{L}\bar{C}, \bar{C}\bar{R}\}$ . (study example 6.7; continued in figure 6.9) (Y. Lan,)

equivariance of a map,  $D_1 = \{e, \sigma\}$ , implies that, in particular, if a finite set of states  $\mathcal{M}_p = \{x_n\}$  constitutes a periodic orbit  $p$ , so does its reflection  $\mathcal{M}_{\sigma p} = \{\sigma x_n\}$ , with the same period and the same stability properties.

Label the three regions  $\mathcal{M} = \{\mathcal{M}_L, \mathcal{M}_C, \mathcal{M}_R\}$  of the bimodal ‘sawtooth’ map of figure 6.8, with a 3-letter alphabet  $L$ (eft),  $C$ (enter), and  $R$ (ight). This symbolic dynamics is complete ternary dynamics, with any sequence of letters  $\mathcal{A} = \{L, C, R\}$  corresponding to an admissible trajectory (‘complete’ means no additional grammar rules required, see example ?? below).

If  $a$  is an asymmetric cycle  $\tilde{\mathcal{M}}_a$ ,  $\sigma$  maps it into the reflected cycle  $\sigma\tilde{\mathcal{M}}_a$ , with no points in common,  $\tilde{\mathcal{M}}_a \cap \sigma\tilde{\mathcal{M}}_a = \emptyset$ . Examples are the fixed points pair  $\{\bar{L}, \bar{R}\}$  and the 2-cycles pair  $\{\bar{L}\bar{C}, \bar{C}\bar{R}\}$  in figure 6.8 (c).

click to return: p. ??

2CB

**Example 6.8.  $D_1$ -symmetric cycles.** (Continued from example 6.7) For  $D_1$  the period of a set-wise symmetric cycle is even ( $n_s = 2n_{\bar{s}}$ ), and the mirror image of the  $x_s$  periodic point is reached by traversing the relative periodic orbit segment  $\bar{s}$  of length  $n_{\bar{s}}$ ,  $f^{n_{\bar{s}}}(x_s) = \sigma x_s$ , see figure 6.8 (b).

click to return: p. ??

2CB

**Example 6.9.  $D_1$ -invariant cycles.**

$\text{Fix}(G)$ , the set of points invariant under group action of  $D_1$ ,  $\tilde{\mathcal{M}} \cap \sigma\tilde{\mathcal{M}}$ , is just this fixed point  $x = 0$ , the reflection symmetry point.

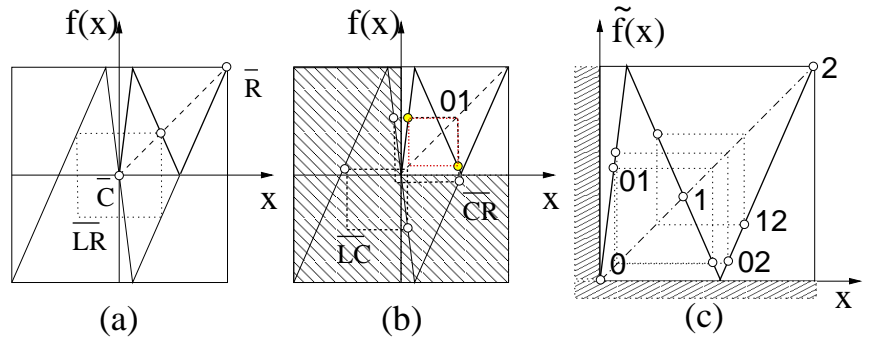
In the example at hand there is only one  $G$ -invariant (point-wise invariant) orbit, the fixed point  $\bar{C}$  at the origin, see figure 6.8 (a). As reflection symmetry is the only discrete symmetry that a map of the interval can have, this example completes the group-theoretic analysis of 1-dimensional maps. We shall continue analysis of this system in example 6.10, and work out the symbolic dynamics of such reflection symmetric systems in example 6.11).

click to return: p. ??

2CB

**Example 6.10.  $D_1$  reduction to the fundamental domain.** Consider again the reflection-symmetric bimodal Ulam sawtooth map  $f(-x) = -f(x)$  of example 6.7, with

Figure 6.9: The bimodal Ulam sawtooth map of figure 6.8 with the  $D_1$  symmetry  $f(-x) = -f(x)$ , restricted to the fundamental domain.  $f(x)$  is indicated by the thin line, and fundamental domain map  $\tilde{f}(\tilde{x})$  by the thick line. (a) Boundary fixed point  $\bar{C}$  is the fixed point  $\bar{0}$ . The asymmetric fixed point pair  $\{\bar{L}, \bar{R}\}$  is reduced to the fixed point  $\bar{2}$ , and the full state space symmetric 2-cycle  $\overline{LR}$  is reduced to the fixed point  $\bar{1}$ . (b) The asymmetric 2-cycle pair  $\{\overline{LC}, \overline{CR}\}$  is reduced to 2-cycle  $\overline{01}$ . (c) All fundamental domain fixed points and 2-cycles. (work through example 6.10) (Y. Lan,)



symmetry group  $D_1 = \{e, \sigma\}$ . The state space  $\mathcal{M} = [-1, 1]$  can be tiled by half-line  $\tilde{\mathcal{M}} = [0, 1]$ , and  $\sigma\tilde{\mathcal{M}} = [-1, 0]$ , its image under a reflection across  $x = 0$  point. The dynamics can then be restricted to the fundamental domain  $\tilde{x}_k \in \tilde{\mathcal{M}} = [0, 1]$ ; every time a trajectory leaves this interval, it is mapped back using  $\sigma$ .

In figure 6.9 the fundamental domain map  $\tilde{f}(\tilde{x})$  is obtained by reflecting  $x < 0$  segments of the global map  $f(x)$  into the upper right quadrant.  $\tilde{f}$  is also bimodal and piecewise-linear, with  $\tilde{\mathcal{M}} = [0, 1]$  split into three regions  $\tilde{\mathcal{M}} = \{\tilde{\mathcal{M}}_0, \tilde{\mathcal{M}}_1, \tilde{\mathcal{M}}_2\}$  which we label with a 3-letter alphabet  $\tilde{\mathcal{A}} = \{0, 1, 2\}$ . The symbolic dynamics is again complete ternary dynamics, with any sequence of letters  $\{0, 1, 2\}$  admissible.

However, the interpretation of the ‘desymmetrized’ dynamics is quite different - the multiplicity of every periodic orbit is now 1, and relative periodic segments of the full state space dynamics are all periodic orbits in the fundamental domain. Consider figure 6.9:

In (a) the boundary fixed point  $\bar{C}$  is also the fixed point  $\bar{0}$ . The asymmetric fixed point pair  $\{\bar{L}, \bar{R}\}$  is reduced to the fixed point  $\bar{2}$ , and the full state space symmetric 2-cycle  $\overline{LR}$  is reduced to the fixed point  $\bar{1}$ . (b) The asymmetric 2-cycle pair  $\{\overline{LC}, \overline{CR}\}$  is reduced to the 2-cycle  $\overline{01}$ . Finally, the symmetric 4-cycle  $\overline{LCRC}$  is reduced to the 2-cycle  $\overline{02}$ . This completes the conversion from the full state space for all fundamental domain fixed points and 2-cycles, frame (c).<sup>18</sup>

[click to return: p. ??](#)

**Example 6.11.  $D_1$ -reduced binary symbolic dynamics.**

2CB

<sup>19</sup> Consider a nonlinear,  $D_1$ -symmetric ‘bent Bernoulli’ map of figure 6.10; like the bimodal map figure 6.8, but with the middle interval squeezed to a point, so the symbolic dynamics is simpler, complete binary with a 2-letter alphabet  $L$ (eft),  $R$ (ight).

In figure 6.11 the fundamental domain map  $\tilde{f}(\tilde{\phi})$  is obtained by reflecting  $\phi < 0$  segments of the global map  $f(\phi)$  into the upper right quadrant.  $\tilde{f}$  also has two branches, with  $\tilde{\mathcal{M}} = [0, 1]$  split into two regions  $\tilde{\mathcal{M}} = \{\tilde{\mathcal{M}}_0, \tilde{\mathcal{M}}_1\}$  which we label with a 2-letter

<sup>18</sup>Predrag 2019-02-18: draw this cycle both in the full and in the fundamental domain. in figure 6.9 (a) double label, with  $\bar{0}$ ,  $\bar{1}$  and  $\bar{2}$ .

<sup>19</sup>Predrag 2017-09-20: Extracted this from ChaosBook `symm.tex` *Discrete symmetry factorization*, ChaosBook sect. 25.5  $Z_2 = D_1$  factorization (version of 2015-04-07).

Figure 6.10: The  $D_1$ -equivariant ‘bent Bernoulli’ map has two types of periodic orbits: (a) asymmetric pairs, such as the fixed points pair  $\{\bar{L}, \bar{R}\}$ . (b)  $D_1$ -symmetric (setwise invariant) periodic orbits, such as the 2-cycle  $\bar{LR}$ , composed of the relative cycle segment from  $L$  to  $R$  and its repeat from  $R$  to  $L$ . (study example 6.11; continued in figure 6.11)

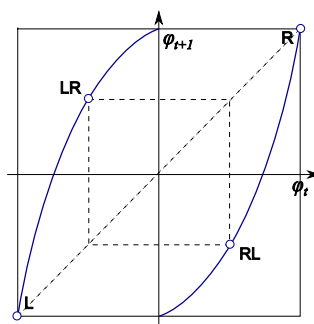
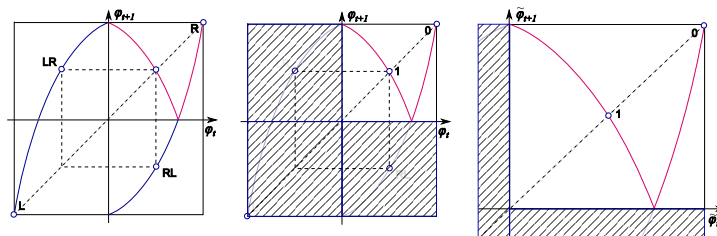


Figure 6.11: The ‘bent Bernoulli’ map of figure 6.10 with the  $D_1$  symmetry  $f(-\phi) = -f(\phi)$ , restricted to the fundamental domain.  $f(\phi)$  is indicated by a blue line, and fundamental domain map  $\tilde{f}(\tilde{\phi})$  by the purple line. The asymmetric fixed point pair  $\{\bar{L}, \bar{R}\}$  is reduced to the fixed point  $\bar{0}$ , and the full state space symmetric 2-cycle  $\bar{LR}$  is reduced to the fixed point  $\bar{1}$ . (work through example 6.11)



alphabet  $\tilde{A} = \{0, 1\}$ . While the full state space map has two monotone branches with positive slopes, the symmetry reduced map is a unimodal map, with negative slope branch  $\tilde{f}_1$ .

The negative slope branch is the consequence of relative periodicity: the mirror image of the  $x_s$  periodic point is reached by traversing the relative periodic orbit segment  $\tilde{s}$  of length  $n_{\tilde{s}}$ ,  $f^{n_{\tilde{s}}}(x_s) = \sigma x_s$ , see the  $LR$  2-cycle in figure 6.10, so the relative periodic orbit temporal Jacobian matrix carries a minus sign.

We could have illustrated this with the Bernoulli piecewise linear map, figure 1.2, whose symmetry-reduced map is the Ulam tent map, but there the  $D_1$  symmetry is so obvious that it is hidden in the plain sight.<sup>20</sup>

The symbolic dynamics is again complete binary dynamics, with any sequence of letters  $\{0, 1\}$  admissible. Assume that all periodic orbits are strictly unstable,  $|\Lambda_p| > 0$ , so that each orbit or orbit is uniquely labeled by an infinite string  $\{s_i\}$ ,  $s_i \in \{R, L\}$ , and that the dynamics is invariant under the  $R \leftrightarrow L$  interchange, i.e., it is  $D_1$  symmetric. The periodic orbits separate into the symmetric orbits  $s \in \{RL, RRLL, RRLLLL, RLLRLRRL, \dots\}$ , with multiplicity  $m_s = 1$ , and the asymmetric orbit pairs  $a \in \{R, L, RRL, LLR, \dots\}$ , with multiplicity  $m_a = 2$ . For example, as there is no distinction between the ‘left’ or the ‘right’ branch of the map, the weights  $t_R = t_L$ ,  $t_{RRL} = t_{RLL}$ , are equal, and so on.

exercise ??

The symmetry reduced labeling  $\tilde{s}_i \in \{0, 1\}$  is related to the full state space labels

<sup>20</sup>Predrag 2021-08-03: Make up the Bernoulli  $D_1$ -symmetry example, setting up example 6.36, will need it for LC21.

Table 6.5: Correspondence between the  $D_1$  symmetry reduced cycles  $\tilde{p}$  and the full state space periodic orbits  $p$ , together with their multiplicities  $m_p$ . Also listed are the two shortest cycles (length 6) related by time reversal, but distinct under  $D_1$ .

$\tilde{p}$	$p$	$m_p$
0	R	2
1	LR	1
01	LLRR	1
011	LLR	2
001	LLLRRR	1
0111	LRLRLRR	1
0001	LRRR	2
0011	LLLLRRR	1
01111	LRLRL	2
00111	LRLRLRRR	1
11010	LRLLRLLR	1
00011	LRLRLRRR	1
10100	LLRR	2
00001	LLLLRRRR	1
110100	LRLLRLLRRR	1
110010	LRRLRLLLR	1

$s_i \in \{L, R\}$  by

$$\begin{aligned} \text{If } s_i &= s_{i-1} \text{ then } \tilde{s}_i = 0 \\ \text{If } s_i &\neq s_{i-1} \text{ then } \tilde{s}_i = 1 \end{aligned} \tag{6.227}$$

For example, both  $\bar{L} = \dots LLLL \dots$  and  $\bar{R} = \dots RRRR \dots$  map into  $\dots 000 \dots = \bar{0}$ ,  $\bar{LR} = \dots LRLR \dots$  maps into  $\dots 111 \dots = \bar{1}$ ,  $\bar{LRRL} = \dots LLRLLRR \dots$  maps into  $\dots 0101 \dots = \bar{01}$ , and so forth. A list of such reductions is given in table 6.5.<sup>21</sup> (continued in example 6.35, illustrated by the Bernoulli example 6.36)

[click to return: p. 340](#)

**Example 6.12. A matrix representation of cyclic group  $C_3$ .** A 3-dimensional 2CB matrix representation of the 3-element cyclic group  $C_3 = \{e, r, r^2\}$  is given by the three rotations by  $2\pi/3$  around the  $z$ -axis in a 3-dimensional state space,

$$\begin{aligned} D(e) &= \begin{bmatrix} 1 & & \\ & 1 & \\ & & 1 \end{bmatrix}, \quad D(r) = \begin{bmatrix} \cos \frac{2\pi}{3} & -\sin \frac{2\pi}{3} & \\ \sin \frac{2\pi}{3} & \cos \frac{2\pi}{3} & \\ & & 1 \end{bmatrix}, \\ D(r^2) &= \begin{bmatrix} \cos \frac{4\pi}{3} & -\sin \frac{4\pi}{3} & \\ \sin \frac{4\pi}{3} & \cos \frac{4\pi}{3} & \\ & & 1 \end{bmatrix}. \end{aligned}$$

(continued in example 6.13)

(X. Ding, )

[click to return: p. 341](#)

**Example 6.13. The regular representation of cyclic group  $C_3$ .** (continued from 2CB example 6.12) Take an arbitrary function  $\rho(x)$  over the state space  $x \in \mathcal{M}$ , and define

<sup>21</sup>Predrag 2021-08-02: please recheck table 6.5: I have interchanged '0' and '1' compared to ChaosBook, might have introduced errors.

Table 6.6: The multiplication tables of the dihedral group  $D_1$ , and cyclic group  $C_3$ .

$D_1$	$e$	$s$
$e$	$e$	$s$
$s$	$s$	$e$

$C_3$	$e$	$r^{-1}$	$r^{-2}$
$e$	$e$	$r^2$	$r$
$r$	$r$	$e$	$r^2$
$r^2$	$r^2$	$r$	$e$

a fundamental domain  $\hat{\mathcal{M}}$  as a  $1/3$  wedge, with axis  $z$  as its (symmetry invariant) edge. The state space is tiled with three copies of the wedge,

$$\mathcal{M} = \hat{\mathcal{M}}_1 \cup \hat{\mathcal{M}}_2 \cup \hat{\mathcal{M}}_3 = \hat{\mathcal{M}} \cup r\hat{\mathcal{M}} \cup r^2\hat{\mathcal{M}}.$$

Function  $\rho(x)$  can be written as the 3-dimensional vector of functions over the fundamental domain  $\hat{x} \in \hat{\mathcal{M}}$ ,

$$(\rho_1^{reg}(\hat{x}), \rho_2^{reg}(\hat{x}), \rho_3^{reg}(\hat{x})) = (\rho(\hat{x}), \rho(r\hat{x}), \rho(r^2\hat{x})). \tag{6.228}$$

The multiplication table of  $C_3$  is given in table 6.6. By (6.211), the regular representation matrices  $D^{reg}(g)$  have ‘1’ at the location of  $g^{-1}$  in the multiplication table, ‘0’ elsewhere. The actions of the operator  $U(g)$  are now represented by permutations matrices (blank entries are zeros):

$$D^{reg}(e) = \begin{bmatrix} 1 & & \\ & 1 & \\ & & 1 \end{bmatrix}, \quad D^{reg}(r) = \begin{bmatrix} & 1 & \\ & & 1 \\ 1 & & \end{bmatrix}, \quad D^{reg}(r^2) = \begin{bmatrix} & & 1 \\ 1 & & \\ & 1 & \end{bmatrix}. \tag{6.229}$$

(X. Ding,)

[click to return: p. 342](#)

2CB

**Example 6.14. Irreps of cyclic group  $C_3$ .** (continued from example 6.13) For  $D_1$ , whose multiplication table is in table 6.6, we can form the symmetric base  $\rho(\hat{x}) + \rho(s\hat{x})$  and the antisymmetric base  $\rho(\hat{x}) - \rho(s\hat{x})$ . You can verify that in this new basis,  $D_1$  is block-diagonalized. We would like to generalize this symmetric-antisymmetric decomposition to the order 3 group  $C_3$ . Symmetrization can be carried out on any number of functions, but there is no obvious anti-symmetrization. We draw instead inspiration from the Fourier transformation for a finite periodic lattice, and construct from the regular basis (6.228) a new set of bases

$$\rho_0^{irr}(\hat{x}) = \frac{1}{3} [\rho(\hat{x}) + \rho(r\hat{x}) + \rho(r^2\hat{x})] \tag{6.230}$$

$$\rho_1^{irr}(\hat{x}) = \frac{1}{3} [\rho(\hat{x}) + \omega \rho(r\hat{x}) + \omega^2 \rho(r^2\hat{x})] \tag{6.231}$$

$$\rho_2^{irr}(\hat{x}) = \frac{1}{3} [\rho(\hat{x}) + \omega^2 \rho(r\hat{x}) + \omega \rho(r^2\hat{x})]. \tag{6.232}$$

Here  $\omega = e^{2i\pi/3}$ . The representation of group  $C_3$  in this new basis is block-diagonal by inspection:

$$D^{irr}(e) = \begin{bmatrix} 1 & & \\ & 1 & \\ & & 1 \end{bmatrix}, \quad D^{irr}(r) = \begin{bmatrix} 1 & 0 & 0 \\ 0 & \omega & 0 \\ 0 & 0 & \omega^2 \end{bmatrix}, \quad D^{irr}(r^2) = \begin{bmatrix} 1 & 0 & 0 \\ 0 & \omega^2 & 0 \\ 0 & 0 & \omega \end{bmatrix}. \tag{6.233}$$



So  $C_3$  has three 1-dimensional irreps. Generalization to any  $C_n$  is immediate: this is just a finite lattice, discrete Fourier transform. (X. Ding, )

[click to return: p. 343](#)

**Example 6.15.  $C_\infty$  group.** Consider the integer lattice  $\mathbb{Z}$ . The infinite cyclic group  $C_\infty$  is generated by  $r$ , the right shift by one lattice spacing 2CB

$$C_\infty = \langle r \mid r^\ell, \ell \in \mathbb{Z} \rangle. \quad (6.234)$$

Every finite index subgroup of the infinite cyclic group  $C_\infty$  is also cyclic, isomorphic to  $C_n$

$$H(n) = \langle r^n \rangle, \quad (6.235)$$

with index

$$|C_\infty/H(n)| = |n|. \quad (6.236)$$

The infinite cyclic group elements are all shifts

$$\begin{aligned} C_\infty &= \langle r_j \mid r_j = r^j; j \in \mathbb{Z} \rangle \\ &= \{ \dots, r_{-2}, r_{-1}, 1, r_1, r_2, r_3, \dots \}, \end{aligned} \quad (6.237)$$

where  $r_j = r^j$  denotes translation by  $j$  lattice sites.  $r_0 = 1$  denotes the identity. Cyclic group multiplication adds translations.

[click to return: p. 278](#)

**Example 6.16. Marching forward in time: Artin-Mazur zeta function.** Consider the integer lattice  $\mathbb{Z}$ , invariant under infinite cyclic group shifts by one or integer number of lattice spacings (see example 6.15):

$$C_\infty = \langle r \mid r^\ell, \ell \in \mathbb{Z} \rangle. \quad (6.238)$$

Every period  $n$  sublattice is  $n$ -steps infinite cyclic group,

$$H(n) = \langle r^n \rangle, \quad (6.239)$$

with the quotient  $C_\infty/H(n)$  isomorphic to  $C_n$ , with multiplicity

$$|C_\infty/H(n)| = |n|. \quad (6.240)$$

Let  $N_n$  denote the number of points in  $\mathcal{M}$  fixed by  $f^n$ :

$$N_n = |\{x \in \mathcal{M} : f^n(x) = x\}|. \quad (6.241)$$

The corresponding Lind zeta function (6.150) is known as the Artin-Mazur zeta function [4, 24]

$$1/\zeta_{AM}(t) = \exp\left(-\sum_{n=1}^{\infty} \frac{t^n}{n} N_n\right) \quad (6.242)$$

[click to return: p. 319](#)

**Example 6.17.  $D_\infty$  group multiplication table.** The infinite dihedral group [49] 2CB elements are all shifts and translate-reflections

$$\begin{aligned} D_\infty &= \langle r_i, s_j \mid r_i s_j = s_j r_{-i}; s_j^2 = 1; i, j \in \mathbb{Z} \rangle \\ &= \{ \dots, r_{-2}, s_{-2}, r_{-1}, s_{-1}, 1, s, r_1, s_1, r_2, s_2, \dots \}. \end{aligned} \quad (6.243)$$

where  $r_j = r^j$  denotes translation by  $j$  lattice sites, and  $s_j = sr^j$  denotes reflection across the  $j$ th lattice site.  $r_0 = 1$  denotes the identity, and by definition  $s_0 = s$ . Dihedral group multiplication table 6.7 adds up translations, or translates and then reverses their direction.

[click to return: p. 278](#)

Table 6.7:  $C_\infty$  cyclic group multiplication adds up translations.  $D_\infty$  dihedral group multiplication adds up translations, or translates and then reverses their direction.

$C_\infty$	$r_j$
$r_i$	$r_{i+j}$

$D_\infty$	$r_j$	$s_j$
$r_i$	$r_{i+j}$	$s_{j-i}$
$s_i$	$s_{i+j}$	$r_{j-i}$

**Example 6.18.  $D_\infty$  subgroups and cosets.**  $H(n)$ , any  $n$ , is a translation subgroup of  $D_\infty$  (a 1-dimensional Bravais sublattice  $\mathcal{L}$  (??), with a basis vector  $\mathbf{a}$  that defines the primitive cell of length  $n$ ) with group elements  $\langle r^n \rangle$ , or, more explicitly:

$$H(n) = \{ \dots, r_{-2n}, r_{-n}, 1, r_n, r_{2n}, \dots \}. \quad (6.244)$$

There are a  $2n$  left cosets of subgroup  $H(n)$  in  $D_\infty$ :

$$\begin{aligned} H(n) &= \{ \dots, r_{-2n}, r_{-n}, 1, r_n, r_{2n}, \dots \} \\ sH(n) &= \{ \dots, s_{-2n}, s_{-n}, s, s_n, s_{2n}, \dots \} \\ rH(n) &= \{ \dots, r_{-2n+1}, r_{-n+1}, r, r_{n+1}, r_{2n+1}, \dots \} \\ s_1H(n) &= \{ \dots, s_{-2n+1}, s_{-n+1}, s_1, s_{n+1}, s_{2n+1}, \dots \} \\ &\vdots \\ r_{n-1}H(n) &= \{ \dots, r_{-n-1}, r_{-1}, r_{n-1}, r_{2n-1}, r_{3n-1}, \dots \} \\ s_{n-1}H(n) &= \{ \dots, s_{-n-1}, s_{-1}, s_{n-1}, s_{2n-1}, s_{3n-1}, \dots \}. \end{aligned} \quad (6.245)$$

Using elements  $\{1, s, r, s_1, \dots, r_{n-1}, s_{n-1}\}$  as representatives of these cosets we see that the quotient group  $D_\infty/H(n)$  is isomorphic to the dihedral group  $D_n$ .

There are  $n$  infinite dihedral  $H(n, k)$  subgroups of  $D_\infty$ , for any  $n$ ,  $0 \leq k < n$  (primitive cell of length  $n$ , with reflection point shifted  $k$  steps):

$$H(n, k) = \{ \dots, r_{-2n}, s_{-2n+k}, r_{-n}, s_{-n+k}, 1, s_k, r_n, s_{n+k}, r_{2n}, s_{2n+k}, \dots \}.$$

The left cosets of the subgroup  $H(n, k)$  in  $D_\infty$  are:<sup>22</sup>

$$\begin{aligned} H(n, k) &= \{ \dots, r_{-2n}, s_{-2n+k}, r_{-n}, s_{-n+k}, 1, \\ &\quad s_k, r_n, s_{n+k}, r_{2n}, s_{2n+k}, \dots \} \\ rH(n, k) &= \{ \dots, r_{-2n+1}, s_{-2n+k+1}, r_{-n+1}, s_{-n+k+1}, r \\ &\quad s_{k+1}, r_{n+1}, s_{n+k+1}, r_{2n+1}, s_{2n+k+1}, \dots \} \\ &\vdots \\ r_{n-1}H(n, k) &= \{ \dots, r_{-n-1}, s_{-n+k-1}, r_{-1}, s_{k-1}, r_{n-1}, \\ &\quad s_{n+k-1}, r_{2n-1}, s_{2n+k-1}, r_{3n-1}, s_{3n+k-1}, \dots \}. \end{aligned} \quad (6.246)$$

Using  $\{1, r, \dots, r_{n-1}\}$  as representatives of these cosets we see that the quotient group  $D_\infty/H(n, k)$  is isomorphic to the cyclic group  $C_n$ .

<sup>22</sup>Predrag 2021-07-24: Explain that  $s_j H(n, k)$  is a rearrangement.

Table 6.8:  $D_3$  group and class operator multiplication tables.

$D_3$	1	$r$	$r_2$	$s_1$	$s_2$	$s_3$
1	1	$r$	$r_2$	$s_1$	$s_2$	$s_3$
$r$	$r$	$r_2$	1	$s_3$	$s_1$	$s_2$
$r_2$	$r_2$	1	$r$	$s_2$	$s_3$	$s_1$
$s_1$	$s_1$	$s_2$	$s_3$	1	$r$	$r_2$
$s_2$	$s_2$	$s_3$	$s_1$	$r_2$	1	$r$
$s_3$	$s_3$	$s_1$	$s_2$	$r$	$r_2$	1

$D_3$	$C_1$	$C_2$	$C_3$
$C_1$	$C_1$	$C_2$	$C_3$
$C_2$	$C_2$	$2C_1+C_2$	$2C_3$
$C_3$	$C_3$	$2C_3$	$3C_1+3C_2$

To show that  $H(n, k)$  is not a normal subgroup: using (??) we have:  $r_i s_k r_i^{-1} = s_{k-2i}$ . For  $i \neq n$ , generally  $s_{k-2i} = r_{2i} s_k$  is not an element of  $H(n, k)$ .

Let  $\phi(n)$  be a periodic state that is invariant under the action of subgroup  $H(n)$ :

$$H(n)\phi(n) = \phi(n), \tag{6.247}$$

and  $\phi(n, k)$  be a periodic state that is invariant under the action of subgroup  $H(n, k)$ :

$$H(n, k)\phi(n, k) = \phi(n, k). \tag{6.248}$$

Since  $H(n)$  is a normal subgroup of  $D_\infty$ , we have:

$$\begin{aligned} H(n)g\phi(n) &= gH(n)g^{-1}g\phi(n) \\ &= gH(n)\phi(n) \\ &= g\phi(n), \quad g \in D_\infty. \end{aligned} \tag{6.249}$$

So  $g\phi(n)$  with  $g \in D_\infty$  is also a periodic state that is invariant under  $H(n)$ . For the periodic state  $\phi(n, k)$  we have:

$$\begin{aligned} gH(n, k)g^{-1}g\phi(n, k) &= gH(n, k)\phi(n, k) \\ &= g\phi(n, k), \quad g \in D_\infty. \end{aligned} \tag{6.250}$$

Since  $H(n, k)$  is not a normal subgroup,  $gH(n, k)g^{-1}$  is a conjugate subgroup of  $H(n, k)$ . So  $g\phi(n, k)$  with  $g \in D_\infty$  is not invariant under  $H(n, k)$ , but invariant under a conjugate subgroup of  $H(n, k)$ .

(H. Liang, 2021-07-28) [click to return: p. 278](#)



example 6.19  
p. 355

**Example 6.19. The regular representation of dihedral group  $D_3$ .**

2CB

$D_3 = \{e, r, r_2, s, s_1, s_2\}$  represents the symmetries of a triangle with equal sides.  $r$  and  $r_2$  are rotations by  $2\pi/3$  and  $4\pi/3$  respectively.  $s, s_1$  and  $s_2$  are the 3 reflections, see figure 6.2(a). The regular basis in this case are

$$(\rho(\hat{x}), \rho(s\hat{x}), \rho(s_1\hat{x}), \rho(s_2\hat{x}), \rho(r\hat{x}), \rho(r_2\hat{x})).$$

It helps us obtain the multiplication table quickly by the following relations

$$s_2 = s_1 r, \quad s_1 = r_2 s, \quad r s = s r_2, \quad r_2 s = s r. \tag{6.251}$$

Table 6.9: The multiplication table of  $D_3$ , the group of symmetries of an equilateral triangle.

$D_3$	$e$	$s$	$s_{-1}$	$s_{-2}$	$r_{-1}$	$r_{-2}$
$e$	$e$	$s$	$s_1$	$s_2$	$r_2$	$r$
$s$	$s$	$e$	$r$	$r_2$	$s_2$	$s_1$
$s_1$	$s_1$	$r_2$	$e$	$r$	$s$	$s_2$
$s_2$	$s_2$	$r$	$r_2$	$e$	$s_1$	$s$
$r$	$r$	$s_2$	$s$	$s_1$	$e$	$r_2$
$r_2$	$r_2$	$s_1$	$s_2$	$s$	$r$	$e$

The multiplication table of  $D_3$  is given in table 6.9. By (6.211), the 6 regular representation matrices  $D^{reg}(g)$  have '1' at the location of  $g^{-1}$  in the multiplication table, '0' elsewhere. For example, the regular representation of the action of operators  $U(s_1)$  and  $U(r_2)$  are, respectively:

$$D^{reg}(s_1) = \begin{bmatrix} 0 & 0 & 1 & 0 & 0 & 0 \\ 0 & 0 & 0 & 0 & 0 & 1 \\ 1 & 0 & 0 & 0 & 0 & 0 \\ 0 & 0 & 0 & 0 & 1 & 0 \\ 0 & 0 & 0 & 1 & 0 & 0 \\ 0 & 1 & 0 & 0 & 0 & 0 \end{bmatrix}, \quad D^{reg}(r) = \begin{bmatrix} 0 & 0 & 0 & 0 & 1 & 0 \\ 0 & 0 & 0 & 1 & 0 & 0 \\ 0 & 1 & 0 & 0 & 0 & 0 \\ 0 & 0 & 1 & 0 & 0 & 0 \\ 0 & 0 & 0 & 0 & 0 & 1 \\ 1 & 0 & 0 & 0 & 0 & 0 \end{bmatrix}.$$

(X. Ding, )

[click to return: p. 355](#)

Table 6.10: Character tables of  $D_3$ ,  $C_3$  and  $D_3$ . The classes  $\{s_{12}, s_{13}, s_{14}\}$ ,  $\{r, r^2\}$  are denoted  $3s$ ,  $2C$ , respectively.

$D_1$	$A$	$B$	$C_3$	$A$	$E$	$D_3$	$A$	$B$	$E$
$e$	1	1	$e$	1	1	$e$	1	1	2
$s$	1	-1	$r$	1	$\omega$	$3s$	1	-1	0
			$r^2$	1	$\omega^2$	$2C$	1	1	-1

**Example 6.20. Character table of  $D_3$ .** (continued from example ??) Let us construct table 6.10. one-dimensional representations are denoted by  $A$  and  $B$ , depending on whether the basis function is symmetric or antisymmetric with respect to transpositions  $s_{ij}$ .  $E$  denotes the two-dimensional representation. As  $D_3$  has 3 classes, the dimension sum rule  $d_1^2 + d_2^2 + d_3^2 = 6$  has only one solution  $d_1 = d_2 = 1, d_3 = 2$ . Hence there are two one-dimensional irreps and one two-dimensional irrep. The first row is 1, 1, 2, and the first column is 1, 1, 1 corresponding to the one-dimensional symmetric representation. We take two approaches to figure out the remaining 4 entries. First, since  $B$  is an antisymmetric one-dimensional representation, so the characters should be  $\pm 1$ . We anticipate  $\chi^B(s) = -1$  and can quickly figure out the remaining 3 positions. Then we check that the obtained table satisfies the orthonormal relations. Second, denote  $\chi^B(s) = x$  and  $\chi^E(s) = y$ , then from the orthonormal relation of the second column

with the first column and itself, we obtain  $1 + x + 2y = 0$  and  $1 + x^2 + y^2 = 6/3$ . Then we get two sets of solutions, one of which is incompatible with other orthonormal relations, so we are left with  $x = -1, y = 0$ . Similarly, we can get the other two characters. (X. Ding, )

[click to return: p. 344](#)

**Example 6.21. Bases for irreps of  $D_3$ .** (continued from example ??) We use 2CB projection operator (6.216) to obtain a basis of irreps of  $D_3$ . From table 6.10, we have

$$P^A \rho(\hat{x}) = \frac{1}{6} [\rho(\hat{x}) + \rho(s\hat{x}) + \rho(s_2\hat{x}) + \rho(s_1\hat{x}) + \rho(r\hat{x}) + \rho(r^2\hat{x})] \quad (6.252)$$

$$P^B \rho(\hat{x}) = \frac{1}{6} [\rho(\hat{x}) - \rho(s\hat{x}) - \rho(s_2\hat{x}) - \rho(s_1\hat{x}) + \rho(r\hat{x}) + \rho(r^2\hat{x})]. \quad (6.253)$$

For projection into irrep  $E$ , we need to figure out the explicit matrix representation first. Obviously, the following 2 by 2 matrices are  $E$  irreps.

$$D^E(e) = \begin{bmatrix} 1 & 0 \\ 0 & 1 \end{bmatrix}, \quad D^E(r) = \begin{bmatrix} \omega & 0 \\ 0 & \omega^2 \end{bmatrix}, \quad D^E(r^2) = \begin{bmatrix} \omega^2 & 0 \\ 0 & \omega \end{bmatrix} \quad (6.254)$$

$$D^E(s) = \begin{bmatrix} 0 & 1 \\ 1 & 0 \end{bmatrix}, \quad D^E(s_2) = \begin{bmatrix} 0 & \omega^2 \\ \omega & 0 \end{bmatrix}, \quad D^E(s_1) = \begin{bmatrix} 0 & \omega \\ \omega^2 & 0 \end{bmatrix}. \quad (6.255)$$

So apply projection operator (6.215) on  $\rho(\hat{x})$  and  $\rho(s\hat{x})$ , we get

$$P_1^E \rho(\hat{x}) = \frac{1}{6} [\rho(\hat{x}) + \omega\rho(r\hat{x}) + \omega^2\rho(r^2\hat{x})] \quad (6.256)$$

$$P_2^E \rho(\hat{x}) = \frac{1}{6} [\rho(\hat{x}) + \omega^2\rho(r\hat{x}) + \omega\rho(r^2\hat{x})] \quad (6.257)$$

$$P_1^E \rho(s\hat{x}) = \frac{1}{6} [\rho(s\hat{x}) + \omega\rho(s_1\hat{x}) + \omega^2\rho(s_2\hat{x})] \quad (6.258)$$

$$P_2^E \rho(s\hat{x}) = \frac{1}{6} [\rho(s\hat{x}) + \omega^2\rho(s_1\hat{x}) + \omega\rho(s_2\hat{x})]. \quad (6.259)$$

The above derivation has used formulas (6.251). In the invariant basis

$$\left\{ P^A \rho(\hat{x}), P^B \rho(\hat{x}), P_1^E \rho(\hat{x}), P_2^E \rho(\hat{x}), P_1^E \rho(s\hat{x}), P_2^E \rho(s\hat{x}) \right\},$$

we have

$$D^{irr}(s_2) = \begin{bmatrix} 1 & 0 & 0 & 0 & 0 & 0 \\ 0 & -1 & 0 & 0 & 0 & 0 \\ 0 & 0 & 0 & \omega^2 & 0 & 0 \\ 0 & 0 & \omega & 0 & 0 & 0 \\ 0 & 0 & 0 & 0 & 0 & \omega^2 \\ 0 & 0 & 0 & 0 & \omega & 0 \end{bmatrix} \quad D^{irr}(r) = \begin{bmatrix} 1 & 0 & 0 & 0 & 0 & 0 \\ 0 & 1 & 0 & 0 & 0 & 0 \\ 0 & 0 & \omega & 0 & 0 & 0 \\ 0 & 0 & 0 & \omega^2 & 0 & 0 \\ 0 & 0 & 0 & 0 & \omega & 0 \\ 0 & 0 & 0 & 0 & 0 & \omega^2 \end{bmatrix}.$$

(X. Ding, )

[click to return: p. 344](#)

**Example 6.22. The class multiplication table for  $D_3$ .**

2CB

See table 6.11.

Table 6.11:  $D_3$  group and class operator multiplication tables.

$D_3$	1	$r$	$r_2$	$s$	$s_1$	$s_2$
1	1	$r$	$r_2$	$s$	$s_1$	$s_2$
$r$	$r$	$r_2$	1	$s_2$	$s$	$s_1$
$r_2$	$r_2$	1	$r$	$s_1$	$s_2$	$s$
$s$	$s$	$s_1$	$s_2$	1	$r$	$r_2$
$s_1$	$s_1$	$s_2$	$s$	$r_2$	1	$r$
$s_2$	$s_2$	$s$	$s_1$	$r$	$r_2$	1

$D_3$	$\mathbf{1}$	$\mathcal{R}$	$\mathcal{S}$
$\mathbf{1}$	$\mathbf{1}$	$\mathcal{R}$	$\mathcal{S}$
$\mathcal{R}$	$\mathcal{R}$	$2\mathbf{1} + \mathcal{R}$	$2\mathcal{S}$
$\mathcal{S}$	$\mathcal{S}$	$2\mathcal{S}$	$3(\mathbf{1} + \mathcal{R})$

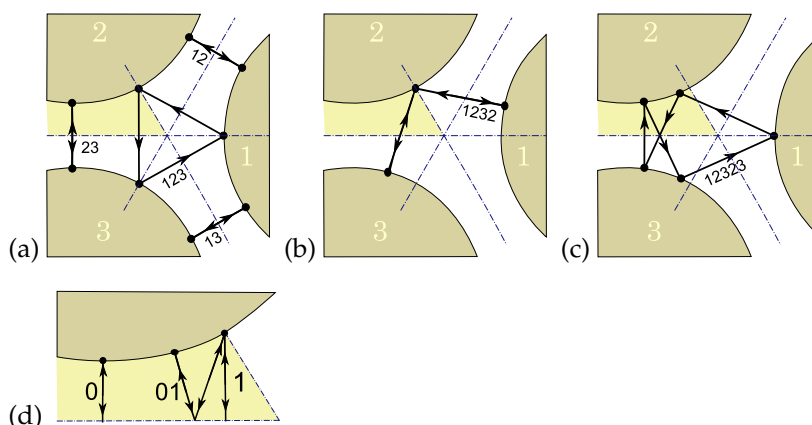


Figure 6.12: The 3-disk pinball orbits: (a)  $\overline{12}$ ,  $\overline{13}$ ,  $\overline{23}$ ,  $\overline{123}$ ; the clockwise  $\overline{132}$  not drawn. (b) Orbit  $\overline{1232}$ ; the symmetry related  $\overline{1213}$  and  $\overline{1323}$  not drawn. (c) Orbit  $\overline{12323}$ ; orbits  $\overline{12123}$ ,  $\overline{12132}$ ,  $\overline{12313}$ ,  $\overline{13131}$  and  $\overline{13232}$  not drawn. (d) The fundamental domain, i.e., the light-shaded  $1/6$ th wedge in (a), consisting of a section of a disk, two segments of symmetry axes acting as straight mirror walls, and the escape gap to the left. The above 14 full-space orbits restricted to the fundamental domain and recoded in binary reduce to the two fixed points  $\overline{0}$ ,  $\overline{1}$ , period-2 orbit  $\overline{10}$ , and period-5 orbit  $\overline{00111}$  (not drawn).

**Example 6.23. Subgroups, cosets of  $D_3$ .** (Continued from example ??) 2CB  
 The 3-disks symmetry group, the  $D_3$  dihedral group (??) has six subgroups

$$\{e\}, \{e, s\}, \{e, s_1\}, \{e, s_2\}, \{e, r, r_2\}, D_3. \quad (6.260)$$

The left cosets of subgroup  $D_1 = \{e, s\}$  are  $\{r, s_1\}, \{r_2, s_2\}$ . The coset of subgroup  $C_3 = \{e, r, r_2\}$  is  $\{s, s_1, s_2\}$ . The significance of the coset is that if a solution has a symmetry  $H$ , for example the symmetry of a 3-cycle  $\overline{123}$  is  $C_3$ , then all elements in a coset act on it the same way, for example  $\{s, s_1, s_2\}\overline{123} = \overline{132}$ .

The nontrivial subgroups of  $D_3$  are  $D_1 = \{e, \sigma\}$ , consisting of the identity and any one of the reflections, of order 2, and  $C_3 = \{e, r, r_2\}$ , of order 3, so possible cycle multiplicities are  $|G|/|G_p| = 1, 2, 3$  or 6. Only the fixed point at the origin has full symmetry  $G_p = G$ . Such equilibria exist for smooth potentials, but not for the 3-disk billiard. Examples of other multiplicities are given in figure 6.12 and figure ?? (continued in example 6.24)

[click to return: p. ??](#)

**Example 6.24. Classes of  $D_3$ .** (Continued from example 6.23) 2CB  
 The three classes of the 3-disk symmetry group  $D_3 = \{e, r, r_2, s, s_1, s_2\}$ , are the identity, any one of the reflections, and the two rotations,

$$\{e\}, \left\{ \begin{matrix} s \\ s_1 \\ s_2 \end{matrix} \right\}, \left\{ \begin{matrix} r \\ r_2 \end{matrix} \right\}. \quad (6.261)$$

In other words, the group actions either flip or rotate. (continued in example ??)

[click to return: p. ??](#)

**Example 6.25. Cyclic groups.** The cyclic group  $C_n \subset SO(2)$  (sometimes called 2CB  
 $Z_n$ ) of order  $n$  is generated by one element a shift  $r$ , the  $1/n$  circle rotation by  $2\pi/n$ .

[click to return: p. ??](#)

**Example 6.26. Character table of cyclic group  $C_n$ .** The symmetry under a discrete 2CB  
 rotation by angle  $2\pi/n$  gives birth to a cyclic group  $C_n = \{e, r, r^2, \dots, r^{n-1}\}$ . Since  $C_n$  is Abelian, each element forms a separate class, and thus  $C_n$  has  $n$  one-dimensional irreducible representations. The characters multiply as group elements:  $\chi_\alpha(r^i)\chi_\alpha(r^j) = \chi_\alpha(r^{i+j}) \pmod n$ . Therefore, we get table 6.14. (X. Ding,)

[click to return: p. 344](#)

**Example 6.27. Dihedral groups.** The dihedral group  $D_n \subset O(2)$ ,  $n = 1, 2, 3, \dots$  2CB  
 (sometimes called  $C_{nv}$ ), can be generated by two elements one at least of which must orientation reversing. For example, take  $s$  corresponding to reflection across the  $x$ -axis.  $s^2 = e$ ; such operation is called an involution.  $r$  to rotation through  $2\pi/n$ , then  $D_n = \langle s, r \rangle$ , and the defining relations are  $s^2 = r^n = e, (rs)^2 = e$ .

[click to return: p. ??](#)

**Example 6.28.  $D_4$  reflection symmetric, antisymmetric permutation representation subspaces.** The characteristic equation  $s^2 = 1$ , with eigenvalues  $\{+1, -1\}$ , enables us to start the symmetry reduction of the  $n$ -dimensional permutation representation of  $D_n$  by splitting it into the reflection symmetric or antisymmetric subspaces by means of projection operators.

When the period  $n$  of the periodic states is even, there are two classes of reflections. For example, when the period of the periodic states is 4, reflection operators  $s$  and  $s_1 = sr$  (see example 6.17) belong to distinct dihedral group  $D_4$  classes:

$$s = \begin{bmatrix} 0 & 0 & 0 & 1 \\ 0 & 0 & 1 & 0 \\ 0 & 1 & 0 & 0 \\ 1 & 0 & 0 & 0 \end{bmatrix}, \quad s_1 = \begin{bmatrix} 0 & 0 & 1 & 0 \\ 0 & 1 & 0 & 0 \\ 1 & 0 & 0 & 0 \\ 0 & 0 & 0 & 1 \end{bmatrix}, \quad (6.262)$$

where  $r$  is the shift matrix. Either one splits the  $n$ -dimensional permutation representation of  $D_n$  into the reflection symmetric and antisymmetric subspaces. For  $s$  the two projection operators are

$$\begin{aligned}
 P_{0+} &= \frac{s - (-1)\mathbf{1}}{1 - (-1)} = \frac{1}{2} \begin{bmatrix} 1 & 0 & 0 & 1 \\ 0 & 1 & 1 & 0 \\ 0 & 1 & 1 & 0 \\ 1 & 0 & 0 & 1 \end{bmatrix} \\
 P_{0-} &= \frac{s - \mathbf{1}}{-1 - 1} = \frac{1}{2} \begin{bmatrix} 1 & 0 & 0 & -1 \\ 0 & 1 & -1 & 0 \\ 0 & -1 & 1 & 0 \\ -1 & 0 & 0 & 1 \end{bmatrix}, \quad (6.263)
 \end{aligned}$$

and for  $s_1$  they are

$$\begin{aligned}
 P_{1+} &= \frac{\mathbf{1} - (-1)s_1}{1 + 1} = \frac{1}{2} \begin{bmatrix} 1 & 0 & 1 & 0 \\ 0 & 2 & 0 & 1 \\ 1 & 0 & 1 & 0 \\ 0 & 0 & 0 & 2 \end{bmatrix} \\
 P_{1-} &= \frac{\mathbf{1} + (-1)s_1}{1 + 1} = \frac{1}{2} \begin{bmatrix} 1 & 0 & -1 & 0 \\ 0 & 0 & 0 & 0 \\ -1 & 0 & 1 & 0 \\ 0 & 0 & 0 & 0 \end{bmatrix}. \quad (6.264)
 \end{aligned}$$

Either splits the  $n$ -dimensional permutation representation, but in a different way. The dimensions  $d_\alpha = \text{tr } P_\alpha$  of the pairs of subspaces are  $d_{s+} = 2$ ,  $d_{s-} = 2$ , and  $d_{s_1+} = 3$ ,  $d_{s_1-} = 1$ . They are reducible further by each other, and by the translation operator characteristic equation  $r^4 = 1$ . Of course, there is no reason to single out reflection operators  $s$  and  $s_1$ . For a systematic, all commuting operator approach, see example 6.31 for the Burnside, class operator full reduction.

[click to return: p. 972](#)

**Example 6.29.  $D_6$  reflection symmetric, antisymmetric permutation representation subspaces.** The characteristic equation  $s^2 = 1$ , with eigenvalues  $\{+1, -1\}$ , enables us to start the symmetry reduction of the  $n$ -dimensional permutation representation of  $D_n$  by splitting it into the reflection symmetric or antisymmetric subspaces by means of projection operators.

When the period  $n$  of the periodic states is even, there are two classes of reflections. For example, when the period of the periodic states is 6, reflection operators  $s$  and  $rs$  belong to distinct dihedral group  $D_6$  classes:

$$s = \begin{bmatrix} 0 & 0 & 0 & 0 & 0 & 1 \\ 0 & 0 & 0 & 0 & 1 & 0 \\ 0 & 0 & 0 & 1 & 0 & 0 \\ 0 & 0 & 1 & 0 & 0 & 0 \\ 0 & 1 & 0 & 0 & 0 & 0 \\ 1 & 0 & 0 & 0 & 0 & 0 \end{bmatrix}, \quad (6.265)$$



and<sup>23</sup>

$$rs = \begin{bmatrix} 1 & 0 & 0 & 0 & 0 & 0 \\ 0 & 0 & 0 & 0 & 0 & 1 \\ 0 & 0 & 0 & 0 & 1 & 0 \\ 0 & 0 & 0 & 1 & 0 & 0 \\ 0 & 0 & 1 & 0 & 0 & 0 \\ 0 & 1 & 0 & 0 & 0 & 0 \end{bmatrix}, \quad (6.266)$$

where  $r$  is the shift matrix. Either one splits the  $n$ -dimensional permutation representation of  $D_n$  into the reflection symmetric and antisymmetric subspaces. For  $s$  the two projection operators are

$$P_{0+} = \frac{s - (-1)\mathbf{1}}{1 - (-1)} = \frac{1}{2} \begin{bmatrix} 1 & 0 & 0 & 0 & 0 & 1 \\ 0 & 1 & 0 & 0 & 1 & 0 \\ 0 & 0 & 1 & 1 & 0 & 0 \\ 0 & 0 & 1 & 1 & 0 & 0 \\ 0 & 1 & 0 & 0 & 1 & 0 \\ 1 & 0 & 0 & 0 & 0 & 1 \end{bmatrix}$$

$$P_{1-} = \frac{rs - \mathbf{1}}{-1 - 1} = \frac{1}{2} \begin{bmatrix} 0 & 0 & 0 & 0 & 0 & 0 \\ 0 & 1 & 0 & 0 & 0 & -1 \\ 0 & 0 & 1 & 0 & -1 & 0 \\ 0 & 0 & 0 & 0 & 0 & 0 \\ 0 & 0 & -1 & 0 & 1 & 0 \\ 0 & -1 & 0 & 0 & 0 & 1 \end{bmatrix}, \quad (6.267)$$

and for  $rs$  they are

$$P_{0-} = \frac{s - \mathbf{1}}{-1 - 1} = \frac{1}{2} \begin{bmatrix} 1 & 0 & 0 & 0 & 0 & -1 \\ 0 & 1 & 0 & 0 & -1 & 0 \\ 0 & 0 & 1 & -1 & 0 & 0 \\ 0 & 0 & -1 & 1 & 0 & 0 \\ 0 & -1 & 0 & 0 & 1 & 0 \\ -1 & 0 & 0 & 0 & 0 & 1 \end{bmatrix}$$

$$P_{1+} = \frac{rs - (-1)\mathbf{1}}{1 - (-1)} = \frac{1}{2} \begin{bmatrix} 2 & 0 & 0 & 0 & 0 & 0 \\ 0 & 1 & 0 & 0 & 0 & 1 \\ 0 & 0 & 1 & 0 & 1 & 0 \\ 0 & 0 & 0 & 2 & 0 & 0 \\ 0 & 0 & 1 & 0 & 1 & 0 \\ 0 & 1 & 0 & 0 & 0 & 1 \end{bmatrix}. \quad (6.268)$$

Either splits the  $n$ -dimensional permutation representation, but in a different way. The dimensions  $d_\alpha = \text{tr } P_\alpha$  of the pairs of subspaces are  $d_{0+} = 3$ ,  $d_{0-} = 3$ , and  $d_{1+} = 4$ ,  $d_{1-} = 2$ . They are reducible further by each other, and by the translation operator characteristic equation  $r^6 = 1$ . Of course, there is no reason to single out reflection operators  $s$  and  $rs$ . For a systematic, all commuting operator approach, see example 6.31 for the Burnside, class operator full reduction. (H. Liang, 2021-05-11)

[click to return: p. 1292](#)

<sup>23</sup>Predrag 2021-07-25: I would prefer  $s_1 = sr$ , to be consistent with the wiki convention of example 6.17.

**Example 6.30.**  $D_3$  **multiplication tables and the permutation rep.** For period-3 periodic states, the class operators are the identity  $\mathbf{1}$  and

$$\mathcal{R} = \begin{bmatrix} 0 & 1 & 1 \\ 1 & 0 & 1 \\ 1 & 1 & 0 \end{bmatrix}, \quad \mathcal{S} = \begin{bmatrix} 1 & 1 & 1 \\ 1 & 1 & 1 \\ 1 & 1 & 1 \end{bmatrix} = \mathbf{1} + \mathcal{R}, \quad (6.269)$$

so either  $\mathcal{R}$  or  $\mathcal{S}$  can be eliminated from the class multiplication table 6.11. In the spirit of the presentation of a dihedral group in terms of two flips, let's eliminate  $\mathcal{R} = \mathcal{S} - \mathbf{1}$ :

$D_3$	$\mathbf{1}$	$\mathcal{S}$	
$\mathbf{1}$	$\mathbf{1}$	$\mathcal{S}$	
$\mathcal{S}$	$\mathcal{S}$	$3\mathcal{S}$	

(6.270)

From this  $D_3$  class operator multiplication table follows the Hamilton-Cayley equation for its 3-dimensional permutation rep, with two eigenvalues,

$$\mathcal{S}(\mathcal{S} - 3\mathbf{1}) = 0, \quad (6.271)$$

with projection operators

$\lambda$		projection op.	$d$
$3$	$P_3 =$	$\mathcal{S}/3$	$1$
$0$	$P_0 =$	$(3\mathbf{1} - \mathcal{S})/3$	$2$

(6.272)

Note that the zero-eigenvalue  $P_0$  is the Laplacian operator.

Take orbit Jacobian matrix of form common to both the temporal cat (8.79) and the temporal Hénon (21.219), and use the spectral resolution  $\mathbf{1} = P_0 + P_3$ :

$$d = 3 \quad \mathcal{J} = \begin{bmatrix} -\mathcal{J}_{00} & 1 & 1 \\ 1 & -\mathcal{J}_{11} & 1 \\ 1 & 1 & -\mathcal{J}_{22} \end{bmatrix} = P_0 - (\mathcal{J} - \mathbf{1}), \quad (6.273)$$

Study also [wiki: Character of the permutation representation](#).

Dixon, J. D. and Mortimer, Permutation Groups, Springer

[click to return: p. 340](#)

**Example 6.31.**  $D_6$  **multiplication tables.** From the  $D_6$  class operator multiplication table follow the Hamilton-Cayley equations (for any matrix representation; in our application (??) that is the 6-dimensional matrix representation of permutations), with 16 eigenvalues as listed,<sup>24</sup>

$$\begin{aligned} (\mathcal{R}_3 - \mathbf{1})(\mathcal{R}_3 + \mathbf{1}) &= 0 \\ (\mathcal{R}_1 - \mathbf{1})(\mathcal{R}_1 + \mathbf{1})(\mathcal{R}_1 - 2\mathbf{1})(\mathcal{R}_1 + 2\mathbf{1}) &= 0 \\ (\mathcal{R}_2 - \mathbf{1})(\mathcal{R}_2 + \mathbf{1})(\mathcal{R}_2 - 2\mathbf{1})(\mathcal{R}_2 + 2\mathbf{1}) &= 0 \\ \mathcal{S}_0(\mathcal{S}_0 - 3\mathbf{1})(\mathcal{S}_0 + 3\mathbf{1}) &= 0 \\ \mathcal{S}_1(\mathcal{S}_1 - 3\mathbf{1})(\mathcal{S}_1 + 3\mathbf{1}) &= 0, \end{aligned} \quad (6.274)$$

<sup>24</sup>Predrag 2021-06-16:  $\mathcal{R}_2$  is a guess, I have not derived it.

Table 6.12: The  $D_6$  Cayley table (group multiplication (??) table), and the class operator multiplication table. The class operator multiplication table is symmetric under transposition, so it suffices to fill up the upper half-triangular region. The 6 classes correspond to 4 1-dimensional irreps, and the 2 1-dimensional irreps.

$D_6$	1	$r^3$	$r$	$r^5$	$r^2$	$r^4$	$s$	$s_2$	$s_4$	$s_1$	$s_3$	$s_5$
1	1	$r^3$	$r$	$r^5$	$r^2$	$r^4$	$s$	$s_2$	$s_4$	$s_1$	$s_3$	$s_5$
$r^3$	$r^3$	1	$r^4$	$r^2$	$r^5$	$r$	$s_3$	$s_5$	$s_1$	$s$	$s_1$	$s_2$
$r$	$r$	$r^4$	$r^2$	1	$r^3$	$r^5$	$s_1$	$s_3$	$s_5$	$s_2$	$s_4$	$s$
$r^5$	$r^5$	$r^2$	1	$r^4$	$r$	$r^3$	$s_5$	$s_1$	$s_3$	$s$	$s_2$	$s_4$
$r^2$	$r^2$	$r^5$	$r^3$	$r$	$r^4$	1	$s_2$	$s_4$	$s$	$s_3$	$s_5$	$s_1$
$r^4$	$r^4$	$r$	$r^5$	$r^3$	1	$r^2$	$s_4$	$s$	$s_2$	$s_5$	$s_1$	$s_3$
$s$	$s$	$s_3$	$s_1$	$s_5$	$s_2$	$s_4$	1	$r^4$	$r^2$	$r^5$	$r^3$	$r$
$s_2$	$s_2$	$s_5$	$s_3$	$s_1$	$s_4$	$s$	$r^2$	1	$r^4$	$r$	$r^5$	$r^3$
$s_4$	$s_4$	$s_2$	$s_5$	$s_3$	$s$	$s_2$	$r^4$	$r^2$	1	$r^3$	$r$	$r^5$
$s_1$	$s_1$	$s_4$	$s_2$	$s$	$s_3$	$s_5$	$r$	$r^5$	$r^3$	1	$r^4$	$r^2$
$s_3$	$s_3$	$s$	$s_4$	$s_2$	$s_5$	$s_1$	$r^3$	$r$	$r^5$	$r^2$	1	$r^4$
$s_5$	$s_5$	$s_3$	$s$	$s_4$	$s_1$	$s_3$	$r^5$	$r^3$	$r$	$r^4$	$r^2$	1

$D_6$	$\mathbf{1}$	$\mathcal{R}_3$	$\mathcal{R}_1$	$\mathcal{R}_2$	$\mathcal{S}_0$	$\mathcal{S}_1$
$\mathbf{1}$	$\mathbf{1}$	$\mathcal{R}_3$	$\mathcal{R}_1$	$\mathcal{R}_2$	$\mathcal{S}_0$	$\mathcal{S}_1$
$\mathcal{R}_3$	.	$\mathbf{1}$	$\mathcal{R}_2$	$\mathcal{R}_1$	$\mathcal{S}_1$	$\mathcal{S}_0$
$\mathcal{R}_1$	.	.	$2\mathbf{1}+\mathcal{R}_2$	$2\mathcal{R}_3+\mathcal{R}_1$	$2\mathcal{S}_1$	$2\mathcal{S}_0$
$\mathcal{R}_2$	.	.	.	$2\mathbf{1}+\mathcal{R}_2$	$2\mathcal{S}_0$	$2\mathcal{S}_1$
$\mathcal{S}_0$	.	.	.	.	$3(\mathbf{1}+\mathcal{R}_2)$	$3(\mathcal{R}_3+\mathcal{R}_1)$
$\mathcal{S}_1$	.	.	.	.	.	$3(\mathbf{1}+\mathcal{R}_2)$

so there is lots of redundancy - there are only 6 irreps.

$$\begin{aligned}
 \mathcal{R}_3 : \lambda = 1 &\rightarrow P_1 = (\mathbf{1} + \mathcal{R}_3)/2 \\
 \mathcal{R}_3 : \lambda = -1 &\rightarrow P_{-1} = (\mathbf{1} - \mathcal{R}_3)/2 \\
 \mathcal{S}_0 : \lambda = 0 &\rightarrow P_{0,0} = (2\mathbf{1} - \mathcal{R}_2)/3 \\
 \mathcal{S}_0 : \lambda = 3 &\rightarrow P_{0,3} = (\mathbf{1} + \mathcal{R}_2 + \mathcal{S}_0)/6 \\
 \mathcal{S}_0 : \lambda = -3 &\rightarrow P_{0,-3} = (\mathbf{1} + \mathcal{R}_2 - \mathcal{S}_0)/6 \\
 \mathcal{S}_1 : \lambda = 0 &\rightarrow P_{1,0} = P_{0,0} \\
 \mathcal{S}_1 : \lambda = 3 &\rightarrow P_{1,3} = (\mathbf{1} + \mathcal{R}_2 + \mathcal{S}_1)/6 \\
 \mathcal{S}_1 : \lambda = -3 &\rightarrow P_{1,-3} = (\mathbf{1} + \mathcal{R}_2 - \mathcal{S}_1)/3.
 \end{aligned} \tag{6.275}$$

Split  $P_{0,-3}$  using  $P_1$ :

$$P_1 P_{0,-3} = (\mathbf{1} + \mathcal{R}_3 + \mathcal{R}_1 + \mathcal{R}_2 - \mathcal{S}_0 - \mathcal{S}_1)/12. \tag{6.276}$$

$\mathcal{S}_j$  equations are the same form as for  $D_3$  1-dimensional irrep, so the number of such equations presumably equals the number of 1-dimensional irrep, and the same for  $\mathcal{R}_j, j \neq n/2$  equations.

$\mathcal{S}_j$  equations presumably contain symmetric/antisymmetric solutions, in the spirit of (6.265) and (6.266).

For even dimensions  $\mathcal{R}_{n/2}$  presumably leads to 4 1-dimensional irreps, of which I assume the two antisymmetric ones do not contribute to the  $n$ -dimensional matrix representation of permutations, while all 1-dimensional irrep do.

That is probably easier to count using the character formulas.

[click to return: p. 340](#)

**Example 6.32.  $D_6$  permutation rep.** For period-6 periodic states, the class operators are the identity, and:

$$\mathcal{R}_3 = \begin{bmatrix} 0 & 0 & 0 & 1 & 0 & 0 \\ 0 & 0 & 0 & 0 & 1 & 0 \\ 0 & 0 & 0 & 0 & 0 & 1 \\ 1 & 0 & 0 & 0 & 0 & 0 \\ 0 & 1 & 0 & 0 & 0 & 0 \\ 0 & 0 & 1 & 0 & 0 & 0 \end{bmatrix}, \tag{6.277}$$

$$\mathcal{R}_1 = \left[ \begin{array}{ccc|ccc} 0 & 1 & 0 & 0 & 0 & 1 \\ 1 & 0 & 1 & 0 & 0 & 0 \\ 0 & 1 & 0 & 1 & 0 & 0 \\ \hline 0 & 0 & 1 & 0 & 1 & 0 \\ 0 & 0 & 0 & 1 & 0 & 1 \\ 1 & 0 & 0 & 0 & 1 & 0 \end{array} \right], \quad \mathcal{R}_2 = \left[ \begin{array}{ccc|ccc} 0 & 0 & 1 & 0 & 1 & 0 \\ 0 & 0 & 0 & 1 & 0 & 1 \\ 1 & 0 & 0 & 0 & 1 & 0 \\ \hline 0 & 1 & 0 & 0 & 0 & 1 \\ 1 & 0 & 1 & 0 & 0 & 0 \\ 0 & 1 & 0 & 1 & 0 & 0 \end{array} \right]. \tag{6.278}$$

$$\mathcal{S}_0 = \left[ \begin{array}{ccc|ccc} 0 & 1 & 0 & 1 & 0 & 1 \\ 1 & 0 & 1 & 0 & 1 & 0 \\ 0 & 1 & 0 & 1 & 0 & 1 \\ \hline 1 & 0 & 1 & 0 & 1 & 0 \\ 0 & 1 & 0 & 1 & 0 & 1 \\ 1 & 0 & 1 & 0 & 1 & 0 \end{array} \right], \quad \mathcal{S}_1 = \left[ \begin{array}{ccc|ccc} 1 & 0 & 1 & 0 & 1 & 0 \\ 0 & 1 & 0 & 1 & 0 & 1 \\ 1 & 0 & 1 & 0 & 1 & 0 \\ \hline 0 & 1 & 0 & 1 & 0 & 1 \\ 1 & 0 & 1 & 0 & 1 & 0 \\ 0 & 1 & 0 & 1 & 0 & 1 \end{array} \right]. \tag{6.279}$$

The reflection operators eigenvalues are +1 and -1, corresponding to the reflection symmetric and antisymmetric subspaces.

To compute the dimensions of irreps obtained from (6.274), we need the characters of the permutation representation class operators:

$$\text{tr } \mathbf{1} = 6, \text{tr } \mathcal{R}_3 = 0, \text{tr } \mathcal{R}_1 = 0, \text{tr } \mathcal{R}_2 = 0, \text{tr } \mathcal{S}_0 = 0, \text{tr } \mathcal{S}_1 = 6. \quad (6.280)$$

(Predrag: I do not see why  $\mathcal{S}_1$  is special...) In particular, we have a vanishing dimension  $\lambda = -3$  representation, so

$$\mathcal{S}_1, \lambda = -3 \rightarrow P_{1,-3} = (\mathbf{1} + \mathcal{R}_2 - \mathcal{S}_1)/2 = 0, \quad (6.281)$$

Taking trace of (6.276) we find that also  $P_1 P_{0,-3}$  is 0-dimensional, so, 6-dimensional permutation representation is not faithful, and the classes are not independent (you can check this by inspecting eqs. (6.279) to (6.278)):

$$\begin{aligned} \mathcal{S}_0 &= \mathcal{R}_3 + \mathcal{R}_1 \\ \mathcal{S}_1 &= \mathbf{1} + \mathcal{R}_2, \end{aligned} \quad (6.282)$$

so forget the last two equations in (6.274) for the  $n$ -dimensional permutation representations of  $D_n$ . I think it is clear from (6.276) that this means no antisymmetric 1-dimensional reps.

Lecturing about the "projector analysis" of  $D_3$  I was such a fool - I forgot to follow [birdtracks.eu](http://birdtracks.eu), which explains very clearly that whenever there is a matrix equation =0, that means a relationship between matrices, they are not independent.

Now one can eliminate  $\mathcal{S}_j$  from projection operators (6.275):

$$\begin{aligned} \mathcal{S}_0 : \lambda = 3 &\rightarrow P_{0,3} = (\mathbf{1} + \mathcal{R}_3 + \mathcal{R}_1 + \mathcal{R}_2)/6 \\ \mathcal{S}_1 : \lambda = 3 &\rightarrow P_{1,3} = (\mathbf{1} + \mathcal{R}_2)/3, \end{aligned} \quad (6.283)$$

To summarize - this is rather inelegant, but the main result is that the flip classes  $\mathcal{S}_0, \mathcal{S}_1, \mathcal{S}_2, \dots$  do not contribute to the reduction of the permutation representation; it can be done purely in terms of the rotation classes  $\mathcal{R}_1, \mathcal{R}_2, \mathcal{R}_3, \dots$ . This strikes me as a big deal, as this is isomorphic - I believe - to the cyclic group  $C_{n/2}$  (for the even period  $n$ ). I tentatively submit table 6.13 being sufficient to construct all irreducible projection operators. Of course,  $C_6$  is the only normal subgroup of  $D_6$ , but we do not use that - we use only 4 classes rather than the 6 of  $C_6$ . Looks pretty illegal.)

Can you check that you get 2 symmetric 1-dimensional irreps, and the two 1-dimensional ones?

[click to return: p. 340](#)

**Example 6.33. Character table of dihedral group  $D_n$ ,  $n$  odd.** The  $D_n$  group

2CB

$$D_n = \{e, r, r^2, \dots, r^{n-1}, s, rs, \dots, r^{n-1}s\}$$

has  $n$  rotation elements and  $n$  reflections. Group elements satisfies  $r^i \cdot r^j s = r^j s \cdot r^{n-i}$ , so  $r^i$  and  $r^{n-i}$  form a class. Also,  $r^{n-i} \cdot r^{2i+j} s = r^j s \cdot r^{n-i}$  implies that  $r^j s$  and  $r^{2i+j} s$  are in the same class. Therefore, there are only three different types of classes:  $\{e\}$ ,  $\{r^k, r^{n-k}\}$  and  $\{s, rs, \dots, r^{n-1}s\}$ . The total number of classes is  $(n+3)/2$ . In this case, there are 2 one-dimensional irreducible representations (symmetric  $A_1$  and antisymmetric  $A_2$ ) and  $(n-1)/2$  two-dimensional irreducible representations. In the  $j$ th two-dimensional irreducible representation, class  $\{e\}$  has form  $\begin{pmatrix} 1 & 0 \\ 0 & 1 \end{pmatrix}$ , class  $\{r^k, r^{n-k}\}$  has form  $\begin{pmatrix} \exp(\frac{i2\pi k j}{n}) & 0 \\ 0 & \exp(-\frac{i2\pi k j}{n}) \end{pmatrix}$ , and class  $\{s, rs, \dots, r^{n-1}s\}$  has form  $\begin{pmatrix} 0 & 1 \\ 1 & 0 \end{pmatrix}$ . We get table 6.15. (X. Ding.)

[click to return: p. 344](#)

Table 6.13: A tentative  $D_6$  class operator multiplication table restricted to the permutations matrix representation, with flip classes eliminated using (6.282).

$D_6$	$\mathbf{1}$	$\mathcal{R}_3$	$\mathcal{R}_1$	$\mathcal{R}_2$
$\mathbf{1}$	$\mathbf{1}$	$\mathcal{R}_3$	$\mathcal{R}_1$	$\mathcal{R}_2$
$\mathcal{R}_3$	.	$\mathbf{1}$	$\mathcal{R}_2$	$\mathcal{R}_1$
$\mathcal{R}_1$	.	.	$2\mathbf{1}+\mathcal{R}_2$	$2\mathcal{R}_3+\mathcal{R}_1$
$\mathcal{R}_2$	.	.	.	$2\mathbf{1}+\mathcal{R}_2$

Table 6.14: Character table of cyclic group  $C_n$ . Here  $k, j = 1, 2, \dots, n - 1$ .

$C_n$	$A$	$\Gamma_j$
$e$	$1$	$1$
$r^k$	$1$	$\exp(\frac{i2\pi kj}{n})$

**Example 6.34. Character table of dihedral group  $D_n, n$  even.** In this case, there are  $(n+6)/2$  classes:  $\{e\}, \{r_{n/2}\}, \{r_k, r_{n-k}\}, \{s, sr_2, \dots, sr_{n-2}\}$  and  $\{sr_1, sr_3, \dots, sr_{n-1}\}$ . There are four different one-dimensional irreducible representations, whose characters are  $\pm 1$  under reflection  $s$  and translate-reflect operation  $sr_1$ . We get table 6.16. (X. Ding, )

[click to return: p. 344](#)

**Example 6.35.  $D_1$  factorization.** (Continued from example 6.11)

Depending on the maximal symmetry group  $\mathcal{H}_p$  that leaves an orbit  $p$  invariant (see [refsects degene Dynami as well as example 6.7](#)), the contributions to the full state space dynamical zeta function factor as

$$\begin{aligned} \mathcal{H}_p = \{e\} : (1 - t_{\hat{p}})^2 &= (1 - t_{\hat{p}})(1 - t_{\hat{p}}) \\ \mathcal{H}_p = \{e, s\} : (1 - t_{\hat{p}})^2 &= (1 - t_{\hat{p}})(1 + t_{\hat{p}}), \end{aligned} \tag{6.284}$$

For example:

$$\begin{aligned} \mathcal{H}_{RRL} = \{e\} : (1 - t_{RRL})^2 &= (1 - t_{001})(1 - t_{001}) \\ \mathcal{H}_{RL} = \{e, s\} : (1 - t_{RL}) &= (1 - t_0)(1 + t_0), \quad \text{where } t_{RL} = t_0^2. \end{aligned}$$

The  $A_1$  subspace dynamical zeta function has the same form as the full state space  $\mathcal{M}$  binary expansion refeq curvbin:

$$\begin{aligned} 1/\zeta_{A_1} &= 1 - t_0 - t_1 - (t_{01} - t_1 t_0) - (t_{001} - t_0 t_{10}) - (t_{011} - t_1 t_{10}) \\ &\quad - (t_{0001} - t_0 t_{001}) - (t_{0111} - t_1 t_{011}) \\ &\quad - (t_{0011} - t_{001} t_1 - t_0 t_{011} + t_0 t_0 t_1) - \dots \end{aligned} \tag{6.285}$$

The form is the same, however, the weights  $t_{\hat{p}}$  are different - a symmetric orbit weight is a square root of the corresponding full state space orbit weight. The asymmetric orbits retain the same weight, but contribute only once.

Table 6.15: Character table of dihedral group  $D_n$ ,  $n$  odd.

$D_n$ ( $n$ odd)	$A_1$	$A_2$	$E_j$
$e$	1	1	2
$r^k, r^{n-k}$	1	1	$2 \cos(\frac{2\pi kj}{n})$
$s, sr^1, \dots, sr^{n-1}$	1	-1	0

Table 6.16: Character table of dihedral group  $D_n$ ,  $n$  even. Here  $k, j = 1, 2, \dots, n - 1$ .

$D_n$ ( $n$ even)	$A_1$	$A_2$	$B_1$	$B_2$	$E_j$
$e$	1	1	1	1	2
$r_{1/2}$	1	1	$(-1)^{n/2}$	$(-1)^{n/2}$	$2(-1)^j$
$r_k, r_{n-k}$ ( $k$ odd)	1	1	-1	-1	$2 \cos(\frac{2\pi kj}{n})$
$r_k, r_{n-k}$ ( $k$ even)	1	1	1	1	$2 \cos(\frac{2\pi kj}{n})$
$s, sr_2, \dots, sr_{n-2}$	1	-1	1	-1	0
$sr_1, sr_3, \dots, sr_{n-1}$	1	-1	-1	1	0

The antisymmetric  $A_2$  subspace dynamical zeta function  $\zeta_{A_2}$  differs from  $\zeta_{A_1}$  by a minus sign for cycles with an odd number of 0's:

$$\begin{aligned}
 1/\zeta_{A_2} &= (1+t_0)(1-t_1)(1+t_{10})(1-t_{100})(1+t_{101})(1+t_{1000}) \\
 &\quad (1-t_{1001})(1+t_{1011})(1-t_{10000})(1+t_{10001}) \\
 &\quad (1+t_{10010})(1-t_{10011})(1-t_{10101})(1+t_{10111}) \dots \\
 &= 1+t_0-t_1+(t_{10}-t_1t_0)-(t_{100}-t_{10}t_0)+(t_{101}-t_{10}t_1) \\
 &\quad -(t_{1001}-t_1t_{001}-t_{101}t_0+t_{10}t_0t_1)-\dots \dots \dots \quad (6.286)
 \end{aligned}$$

Note that the group theory factors do not destroy the curvature corrections (the cycles and pseudo cycles are still arranged into shadowing combinations).

If the system under consideration has a boundary orbit (cf. *refsect bound-o*) with group-theoretic factor  $h_p = (e + \sigma)/2$ , the boundary orbit does not contribute to the antisymmetric subspace

$$\begin{matrix} A_1 & A_2 \\ \text{boundary: } (1-t_p) &= (1-t_{\hat{p}})(1-0t_{\hat{p}}) \end{matrix} \quad (6.287)$$

This is the  $1/\zeta$  part of the boundary orbit factorization discussed in example 6.7, where the factorization of the corresponding spectral determinants for the 1-dimensional reflection symmetric maps is worked out in detail.

[click to return: p. 340](#)

**Example 6.36.  $D_1$ -symmetry factorization of the temporal Bernoulli zeta function.**

<sup>25</sup> For the particularly simple, linear Bernoulli case at hand, the field  $x_t$  is a scalar, the

<sup>25</sup>Predrag 2021-08-03: Making up the Bernoulli  $D_1$ -symmetry example, will need it for LC21.

1-time step  $[1 \times 1]$  time-evolution Jacobian matrix (12.57) at every lattice point  $t$  is simply  $\mathbb{J}_t = s$ , and the orbit Jacobian matrix (1.19) is the same for all, in general distinct periodic states of period  $n$ , so

$$N_n = |\text{Det } \mathcal{J}| = s^n - 1; \tag{6.288}$$

all itineraries are allowed, except that the periodicity of  $r^n = \mathbf{1}$  accounts for  $\bar{0}$  and  $\overline{s-1}$  fixed points (see figure 1.2) being a single periodic point.

For a Bernoulli system (6.288),

$$\begin{aligned} 1/\zeta_{AM}(z) &= \exp\left(-\sum_{n=1}^{\infty} \frac{z^n}{n}(s^n - 1)\right) = \exp[\ln(1 - sz) - \ln(1 - z)] \\ &= \frac{1 - sz}{1 - z}. \end{aligned} \tag{6.289}$$

The numerator  $(1 - sz)$  says that a Bernoulli system is a full shift [24]: there are  $s$  fundamental periodic states, in this case fixed points  $\{x_0, x_1, \dots, x_{s-1}\}$ , and every other periodic state is built from their concatenations and repeats. The denominator  $(1 - z)$  compensates for the single overcounted periodic state, the fixed point  $x_{s-1} = x_0 \pmod{1}$  of figure 1.2 and its repeats.

The dynamical  $D_1$ -symmetry factorized zeta function, analogous to (6.199), follows from (6.284):

$$\begin{aligned} \frac{1}{\zeta(z)} &= \frac{1}{\zeta_{A_1}(t)} \frac{1}{\zeta_{A_1}(-t)}, \quad z = t^2, \quad s = \mu^2 \\ \frac{1}{\zeta_{A_1}(t)} &= \frac{1 - \mu t}{1 - t}. \end{aligned} \tag{6.290}$$

The antisymmetric  $A_2$  subspace dynamical zeta function  $\zeta_{A_2}$  differs from  $\zeta_{A_1}$  only by a minus sign for cycles with an odd number of 1's, see (6.286). At the level of the linear Bernoulli map, this seems a triviality, but for a nonlinear example 6.11, it is not; all cycles are computed numerically in the  $D_1$ -symmetry-reduced fundamental domain figure 6.11.

[click to return: p. ??](#)

**Example 6.37. XXX.**

## 6.12 Discrete factorization of the dynamical zeta function

<sup>26</sup> When a dynamical system has a discrete symmetry, the cycle averaging formula can be simplified substantially, and the expansion needs much fewer orbits to achieve the desired accuracy. In this section, we discuss how the dynamical zeta function can be factorized by a product of contributions from each irreps of this discrete symmetry.



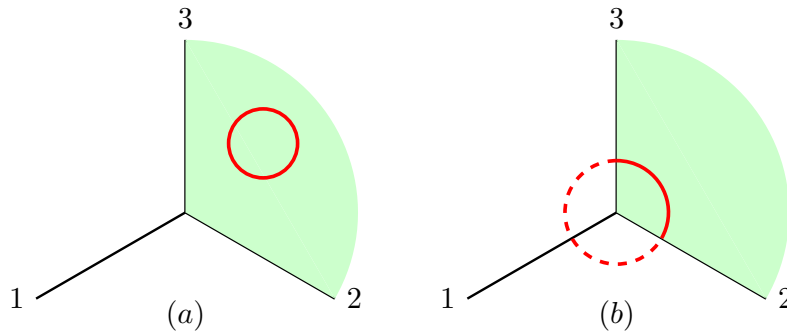


Figure 6.13: The two different kinds of periodic orbits in a system with  $C_3$  symmetry. The green region is the chosen fundamental domain. The red cycles are periodic orbits.

### 6.12.1 Factorization of $C_3$ and $D_3$

$C_3$  has two subgroups  $\{e\}$  and  $\{e, r, r_2\}$ , so there are two types of periodic orbits as shown in figure 6.13. A type-(a) orbit has symmetry  $\{e\}$ , i.e., no symmetry, and it has two replicas by rotation  $r$  and  $r_2$  respectively, which are not shown in this figure. So the contribution from a type-(a) orbit to the dynamical zeta function is  $(1 - t_p)^3$ . The cubic order refers to the fact that there are three sibling orbits together. Also, since the entire orbit is in the fundamental domain, we have

$$1/\zeta_a = (1 - t_{\hat{p}})^3.$$

The hat on  $p$  means that  $t_{\hat{p}}$  is evaluated only on the part of the orbit that is in the fundamental domain. A type-(b) orbit is invariant under  $e, r$  and  $r_2$ . This orbit has no siblings and only one third of this orbit is in the fundamental domain. The other two thirds are replicas by rotation  $r$  and  $r_2$  of the part in the fundamental domain. So, its contribution to dynamical zeta function is

$$1/\zeta_b = 1 - t_p = 1 - t_{\hat{p}}^3.$$

Here, relation  $t_p = t_{\hat{p}}^3$  is easily obtained by its definition in (??). On the other hand, by example 6.13, we know that the regular representations of  $e, r,$  and  $r_2$  are respectively

$$D^{reg}(e) = \begin{bmatrix} 1 & & \\ & 1 & \\ & & 1 \end{bmatrix}, \quad D^{reg}(r) = \begin{bmatrix} & 1 & \\ & & 1 \\ 1 & & \end{bmatrix}, \quad D^{reg}(r_2) = \begin{bmatrix} & & 1 \\ 1 & & \\ & 1 & \end{bmatrix}.$$

You can easily verify that

$$(1 - t_{\hat{p}})^3 = \det(1 - D^{reg}(e)t_{\hat{p}}), \quad 1 - t_p^3 = \det(1 - D^{reg}(r)t_{\hat{p}}) = \det(1 - D^{reg}(r_2)t_{\hat{p}}).$$

<sup>26</sup>Predrag 2021-06-19: A copy of the 2017-03-09 Xiong Ding's section, not included in his thesis siminos/xiong/thesis/chapters/symFactor.tex.

Therefore, you see that the contribution from periodic orbits to the dynamical zeta function in a system with  $C_3$  symmetry are related to the regular representation of  $C_3$ .

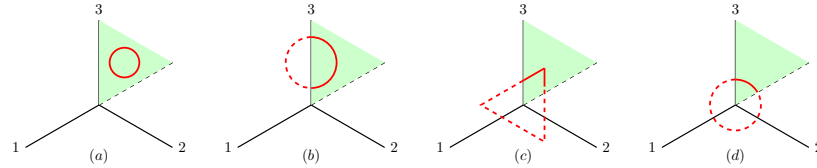


Figure 6.14: The four different kinds of periodic orbits in a system with  $D_3$  symmetry. The green region is the chosen fundamental domain. The red cycles are periodic orbits.

Let us check out another example - a system with  $D_3$  symmetry.  $D_3$  has four different kinds of subgroups  $\{e\}$ ,  $\{e, s\}$ ,  $\{e, r, r_2\}$ , and  $D_3$  itself. Here  $s$  can be any one of  $s_{12}$ ,  $s_{23}$  or  $s_{31}$ . Accordingly, there are four types of periodic orbits as shown in figure 6.14. The fundamental domain is one sixth of the full state space. Similar to the analysis of the two orbits in the  $C_3$  case, we have

$$1/\zeta_a = (1 - t_{\hat{p}})^6, \quad 1/\zeta_b = (1 - t_{\hat{p}}^2)^3, \quad 1/\zeta_c = (1 - t_{\hat{p}}^3)^2, \quad 1/\zeta_d = 1 - t_{\hat{p}}^6.$$

Example ?? gives the regular representation of  $D_3$ . You can also verify that

$$\begin{aligned} (1 - t_{\hat{p}})^6 &= \det(1 - D^{reg}(e)t_{\hat{p}}), & (1 - t_{\hat{p}}^2)^3 &= \det(1 - D^{reg}(s)t_{\hat{p}}) \\ (1 - t_{\hat{p}}^3)^2 &= \det(1 - D^{reg}(r)t_{\hat{p}}), & 1 - t_{\hat{p}}^6 &=? . \end{aligned}$$

I leave a question mark above since no analogous expression exists for it. We will come back to it after proving the identity (6.291).

We can generalize the above observation for a system invariant under a general discrete group  $G = \{e, g_2, g_3, \dots, g_{|G|}\}$ . Let  $h$  be an element of  $G$  with order (period)  $m$ , i.e.,  $m$  is the smallest positive integer such that  $h^m = e$ . Then we have

$$(1 - t^m)^{\frac{|G|}{m}} = \det(1 - D^{reg}(h)t). \tag{6.291}$$

The proof starts from the matrix identity  $\ln \det = \text{tr} \ln$ , by which we have

$$\ln \det(1 - D^{reg}(h)t) = \text{tr} \ln(1 - D^{reg}(h)t) = - \sum_{k=1}^{\infty} \frac{\text{tr} D^{reg}(h^k)t^k}{k}.$$

The last identity above comes from the Taylor expansion  $\ln(1-x) = - \sum_{k=1}^{\infty} \frac{x^k}{k}$ . As we know, the regular representation of a group element has nonzero trace if and only if this group element is  $e$ . So we have,

$$\ln \det(1 - D^{reg}(h)t) = - \sum_{k=1}^{\infty} \frac{|G|t^{mk}}{mk} = - \frac{|G|}{m} \sum_{k=1}^{\infty} \frac{t^{mk}}{k} = \frac{|G|}{m} \ln(1 - t^m).$$

Therefore, we obtain (6.291). This is why we have the observation in the  $C_3$  and  $D_3$  example. However, for the type-(d) orbit in figure 6.14, the symmetry group of this orbit is  $\{e, s_{12}, s_{32}, s_{13}, r, r_2\}$ . The order of  $s$  is 2 while the order of  $r$  is 3. The least common multiple is 6. Therefore, the contribution to the dynamical zeta function is  $(1 - t_{\tilde{p}}^6)^{-1}$  and it cannot be written as form  $\det(1 - D^{reg}(h)t_{\tilde{p}})$  with some  $h \in G$ .

Actually, we can write

$$1 - t_{\tilde{p}}^6 = \det(1 - D^{reg}(r)t_{\tilde{p}}^2), \quad \text{or} \quad 1 - t_{\tilde{p}}^6 = \det(1 - D^{reg}(s)t_{\tilde{p}}^3)$$

With  $D^{reg}(r)$  the  $[3 \times 3]$  representation of  $r$  in group  $C_3$  and  $D^{reg}(s)$  the  $[2 \times 2]$  representation of  $s$  in reflection group  $\{e, s\}$ . Anyway, for the type-(d) orbit we have no choice but to give up the regular representation of  $D_3$ .

### 6.12.2 Factorization of $C_n$ and $D_n$

for a discrete symmetry group  $G = \{e, g_2, \dots, g_{|G|}\}$ . The orthogonality and completeness of projection operator can be easily verified by the orthogonality relation among characters of irreducible representation. Define  $\mathcal{L}_\alpha = \mathcal{P}_\alpha \mathcal{L}$ , then the trace of evolution operator  $\mathcal{L}$  can be decomposed into a sum of  $\sum_\alpha \text{tr} \mathcal{L}_\alpha$  because of the completeness of projection operators.<sup>27</sup> So we only need to investigate the projected trace formula:

$$\begin{aligned} \text{tr} \mathcal{L}_\alpha &= \frac{d_\alpha}{|G|} \sum_{hg \in G} \chi_\alpha(h) \mathbf{h}^{-1} \int_{\mathcal{M}} dx \mathcal{L}(x, x) \\ &= \frac{d_\alpha}{|G|} \sum_{hg \in G} \chi_\alpha(h) \mathbf{h}^{-1} \sum_{ag \in G} \int_{\tilde{\mathcal{M}}} d(a\tilde{x}) \mathcal{L}(a\tilde{x}, a\tilde{x}) \\ &= \frac{d_\alpha}{|G|} \sum_{hg \in G} \chi_\alpha(h) \mathbf{h}^{-1} \cdot |G| \int_{\tilde{\mathcal{M}}} d(\tilde{x}) \mathcal{L}(\tilde{x}, \tilde{x}) \\ &= d_\alpha \sum_{hg \in G} \chi_\alpha(h) \int_{\tilde{\mathcal{M}}} d\tilde{x} \mathcal{L}(\mathbf{h}^{-1}\tilde{x}, \tilde{x}) \end{aligned}$$

In the above derivation, we have used the invariance of evolution operator under group transform. For a periodic orbit in the fundamental domain  $\tilde{p}$ , we follow the standard argument in Chaosbook and get

$$\int_{\tilde{\mathcal{M}}} d\tilde{x} \mathcal{L}(\mathbf{h}^{-1}\tilde{x}, \tilde{x}) = n_{\tilde{p}} \sum_{r=1}^{\infty} \frac{e^{r\beta \cdot A_{\tilde{p}}}}{|\det(\mathbf{1} - \tilde{M}_{\tilde{p}}^r)|} \delta_{n, n_{\tilde{p}}r} \delta_{h, h_{\tilde{p}}^r};$$

<sup>27</sup>XD 2014-05-03: Here the decomposition of trace just relies on the completeness of projection operators, we haven't used the commuting relation between evolution operator and group transform. Am I right?

so, the spectral determinant is

$$\begin{aligned}
 F(z) &= \prod_{\alpha} F_{\alpha}(z)^{d_{\alpha}} \\
 F_{\alpha}(z) &= \exp \left( - \sum_{\bar{p}} \sum_{r=1}^{\infty} \frac{1}{r} \frac{\chi_{\alpha}(h_{\bar{p}}^r) z^{n_{\bar{p}} r} e^{r\beta \cdot A_{\bar{p}}}}{|\det(\mathbf{1} - \tilde{M}_{\bar{p}}^r)|} \right), \quad (6.292)
 \end{aligned}$$

which is discrete factorization for maps. The same method can be applied to flows with discrete symmetry:

$$F_{\alpha}(z) = \exp \left( - \sum_{\bar{p}} \sum_{r=1}^{\infty} \frac{1}{r} \frac{\chi_{\alpha}(h_{\bar{p}}^r) e^{r(\beta \cdot A_{\bar{p}} - s T_{\bar{p}})}}{|\det(\mathbf{1} - \tilde{M}_{\bar{p}}^r)|} \right)$$

Making an approximation  $|\det(\mathbf{1} - \tilde{M}_{\bar{p}}^r)| \approx |\Lambda_{\bar{p}}|$  where  $\Lambda_{\bar{p}}$  is the product of all expanding multipliers, we get the factorized zeta function:

$$F_{\alpha}(z) = \exp \left( - \sum_{\bar{p}} \sum_{r=1}^{\infty} \frac{1}{r} \chi_{\alpha}(h_{\bar{p}}^r) t_{\bar{p}}^r \right) \quad (6.293)$$

Formula (6.293) is the ultimate goal of Discrete Factorization, which basically tells us that, equipped with character table of the group in question, we can write down all the factorized zeta function for all classes of this group. On the other hand, in order to verify our result, let's calculate the zeta function in the full state space.

$$\begin{aligned}
 F(z) &= \prod_{\alpha} F_{\alpha}(z)^{d_{\alpha}} \\
 &= \exp \left( - \sum_{\bar{p}} \sum_{r=1}^{\infty} \frac{1}{r} \sum_{\alpha} (d_{\alpha} \chi_{\alpha}(h_{\bar{p}}^r)) t_{\bar{p}}^r \right) \\
 &= \exp \left( - \sum_{\bar{p}} \sum_{r=1}^{\infty} \frac{1}{r} |G| \delta_{h_{\bar{p}}^r} t_{\bar{p}}^r \right) \\
 &= \exp \left( - \sum_{\bar{p}} \sum_{k=1}^{\infty} \frac{|G|}{mk} t_{\bar{p}}^{mk} \right),
 \end{aligned}$$

that is

$$F(z) = \left( 1 - t_{\bar{p}}^{\frac{|G|}{m}} \right)^m, \quad (6.294)$$

where  $m$  is the smallest positive number such that  $h_{\bar{p}}^m = e$ , namely the multiplicity of the periodic orbit in the full state space. Formula (6.294) is just the

left side of

$$(1 - t_{\bar{p}}^{h_p})^{g/h_p} = \det(1 - D(h_{\bar{p}})t_{\bar{p}}) = \prod_{\alpha} \det(1 - D_{\alpha}(h_{\bar{p}})t_{\bar{p}})^{d_{\alpha}} \quad (6.295)$$

in Chaosbook and actually formula (6.293) is the right side of it. For completeness, I derive their equivalence here. By the definition of character and representation of a group,  $\chi_{\alpha}(h_{\bar{p}}^r) = \text{tr } D_{\alpha}(h_{\bar{p}}^r) = \text{tr } (D_{\alpha}(h_{\bar{p}}))^r$  where  $D$  is the regular representation of this group, so (6.293) can be rewritten as follows,

$$\begin{aligned} F_{\alpha}(z) &= \exp\left(-\text{tr} \sum_{\bar{p}} \sum_{r=1}^{\infty} \frac{1}{r} (D_{\alpha}(h_{\bar{p}}))^r t_{\bar{p}}^r\right) \\ &= \exp\left(\text{tr} \sum_{\bar{p}} \ln(1 - D_{\alpha}(h_{\bar{p}}))\right) \\ &= \prod_{\bar{p}} \det(1 - D_{\alpha}(h_{\bar{p}})) \end{aligned}$$

Here, we have used relation  $\text{tr } \ln = \ln \det$ . All calculation of factorized zeta function in Chaosbook is conducted by  $\det(1 - D_{\alpha}(h_{\bar{p}}))$ , but I tend to use (6.293) because it doesn't contain information about any specific representation.<sup>28</sup> All the following examples are analyzed by (6.293).

$C_n$  case

When  $h_{\bar{p}} = e$ ,

$$F_A = F_{\Gamma_j} = \exp\left(-\sum_{r=1}^{\infty} \frac{1}{r} t_{\bar{p}}^r\right) = 1 - t_{\bar{p}},$$

Where we only investigate the contribution from one specific periodic orbit and ignore the summation  $\sum_{\bar{p}}$ .

When  $h_{\bar{p}} = C_n^k$ , Similarly,

$$\begin{aligned} F_A &= 1 - t_{\bar{p}} \\ F_{\Gamma_j} &= \exp\left(-\sum_{r=1}^{\infty} \frac{1}{r} e^{\frac{i2\pi kjr}{n}} t_{\bar{p}}^r\right) = 1 - e^{\frac{i2\pi kj}{n}} t_{\bar{p}}, \end{aligned}$$

In sum,

$$\begin{array}{lcl} h_{\bar{p}} & & A \quad \Gamma_j \\ e: & (1 - t_{\bar{p}})^n & = (1 - t_{\bar{p}}) \quad (1 - t_{\bar{p}}) \\ C_n^k: & (1 - t_{\bar{p}}^n)^{\frac{n}{n}} & = (1 - t_{\bar{p}}) \quad (1 - \exp(\frac{i2\pi kj}{n})t_{\bar{p}}) \end{array}$$

---

<sup>28</sup>XD 2014-05-05: I am not sure whether I understand it correctly here.

$D_n$  ( $n$  odd) case: When  $h_{\bar{p}} = e$ ,

$$F_{A_1} = F_{A_2} = \exp\left(-\sum_{r=1}^{\infty} \frac{1}{r} t_{\bar{p}}^r\right) = 1 - t_{\bar{p}}$$

$$F_{E_j} = \exp\left(-\sum_{r=1}^{\infty} \frac{2}{r} t_{\bar{p}}^r\right) = (1 - t_{\bar{p}})^2$$

When  $h_{\bar{p}} = C_n^k$ , the same goes for  $A_1$  and  $A_2$ :  $F_{A_1} = F_{A_2} = 1 - t_{\bar{p}}$ , but for  $E_j$ , it requires a little special treatment.

$$\begin{aligned} F_{E_j} &= \exp\left(-\sum_{r=1}^{\infty} \frac{1}{r} 2 \cos \frac{2\pi k j r}{n} t_{\bar{p}}^r\right) \\ &= \exp\left(-\sum_{r=1}^{\infty} \frac{1}{r} \left(\exp\left(\frac{i2\pi k j r}{n}\right) + \exp\left(-\frac{i2\pi k j r}{n}\right)\right) t_{\bar{p}}^r\right) \\ &= \left(1 - \exp\left(\frac{i2\pi k j}{n}\right) t_{\bar{p}}\right) \left(1 - \exp\left(-\frac{i2\pi k j}{n}\right) t_{\bar{p}}\right) \\ &= 1 - 2 \cos \frac{2\pi k j}{n} t_{\bar{p}} + t_{\bar{p}}^2 \end{aligned}$$

When  $h_{\bar{p}} \in \{s, s_1, \dots, s_{n-1}\}$ ,  $h_{\bar{p}}^2 = e$ .

$$F_{A_1} = 1 - t_{\bar{p}}$$

$$F_{A_2} = \exp\left(-\sum_{r=even}^{\infty} \frac{1}{r} t_{\bar{p}}^r + \sum_{r=odd}^{\infty} \frac{1}{r} t_{\bar{p}}^r\right) = (1 + t_{\bar{p}})$$

$$F_{E_j} = \exp\left(-\sum_{r=even}^{\infty} \frac{1}{r} 2 t_{\bar{p}}^r\right) = (1 - t_{\bar{p}}^2)$$

In sum,

$h_{\bar{p}}$	$A_1$	$A_2$	$E_j$
$e$ :	$(1 - t_{\bar{p}})^{2n}$	$(1 - t_{\bar{p}}) (1 - t_{\bar{p}})$	$(1 - t_{\bar{p}})^4$
$C_n^k, C_n^{n-k}$ :	$(1 - t_{\bar{p}}^{\frac{2n}{m}})^{\frac{2n}{m}}$	$(1 - t_{\bar{p}}) (1 - t_{\bar{p}})$	$(1 - 2 \cos(\frac{2\pi k j}{n}) t_{\bar{p}} + t_{\bar{p}}^2)^2$
$s, s_1, \dots, s_{n-1}$ :	$(1 - t_{\bar{p}}^2)^n$	$(1 - t_{\bar{p}}) (1 + t_{\bar{p}})$	$(1 - t_{\bar{p}}^2)^2$

$D_n$  ( $n$  even) case:

Similar calculation gives us the following factorized zeta function table.

$$\begin{array}{l}
 h_{\bar{p}} \\
 e: \\
 r_{n/2}: \\
 r_k \\
 \text{(odd):} \\
 r_k \\
 \text{(even):} \\
 s: \\
 rs:
 \end{array}
 \begin{array}{l}
 (1-t_{\bar{p}})^{2n} \\
 (1-t_{\bar{p}}^2)^n \\
 (1-t_{\bar{p}}^m)^{\frac{2n}{m}} \\
 (1-t_{\bar{p}}^n)^{\frac{2n}{m}} \\
 (1-t_{\bar{p}}^2)^n \\
 (1-t_{\bar{p}}^2)^n
 \end{array}
 =
 \begin{array}{l}
 A_1 \\
 A_2 \\
 A_1 \\
 A_2 \\
 A_1 \\
 A_2 \\
 A_1 \\
 A_2 \\
 A_1 \\
 A_2
 \end{array}
 \begin{array}{l}
 (1-t_{\bar{p}}) \\
 (1-t_{\bar{p}}) \\
 (1-t_{\bar{p}}) \\
 (1-t_{\bar{p}}) \\
 (1-t_{\bar{p}}) \\
 (1-t_{\bar{p}}) \\
 (1-t_{\bar{p}}) \\
 (1-t_{\bar{p}}) \\
 (1-t_{\bar{p}}) \\
 (1-t_{\bar{p}})
 \end{array}
 \begin{array}{l}
 B_1 \\
 B_2 \\
 B_1 \\
 B_2 \\
 B_1 \\
 B_2 \\
 B_1 \\
 B_2 \\
 B_1 \\
 B_2
 \end{array}
 \begin{array}{l}
 (1-t_{\bar{p}}) \\
 (1-t_{\bar{p}}) \\
 (1-t_{\bar{p}}) \\
 (1-t_{\bar{p}}) \\
 (1-t_{\bar{p}}) \\
 (1-t_{\bar{p}}) \\
 (1-t_{\bar{p}}) \\
 (1-t_{\bar{p}}) \\
 (1-t_{\bar{p}}) \\
 (1-t_{\bar{p}})
 \end{array}
 \begin{array}{l}
 B_1 \\
 B_2 \\
 B_1 \\
 B_2 \\
 B_1 \\
 B_2 \\
 B_1 \\
 B_2 \\
 B_1 \\
 B_2
 \end{array}
 \begin{array}{l}
 E_j \\
 (1-t_{\bar{p}})^4 \\
 (1-t_{\bar{p}})^4 \\
 (1-2\cos(\frac{2\pi k j}{n})t_{\bar{p}}+t_{\bar{p}}^2)^2 \\
 (1-2\cos(\frac{2\pi k j}{n})t_{\bar{p}}+t_{\bar{p}}^2)^2 \\
 (1-t_{\bar{p}}^2)^2 \\
 (1-t_{\bar{p}}^2)^2
 \end{array}$$

When it comes to continuous symmetry, projection operator is

$$P_m = d_m \int_G dg \chi_m(g^{-1}) O_g. \quad (6.296)$$

The corresponding trace formula in the irreducible subspace is

$$\sum_{\beta=0}^{\infty} \frac{1}{s - s_{m,\beta}} = d_m \sum_p \ell_p \sum_{r=1}^{\infty} \chi_m(g_p^r) \frac{e^{r(\beta A_p - s \ell_p)}}{|\det(\mathbf{1} - \tilde{M}_{m,p}^r)|}. \quad (6.297)$$

Therefore the spectral determinant is factorized as

$$\begin{aligned}
 \det(s - \mathcal{A}) &= \prod_{\alpha} F_{\alpha}(z)^{d_{\alpha}} \\
 F_{\alpha}(z) &= \exp \left( - \sum_{\bar{p}} \sum_{r=1}^{\infty} \frac{1}{r} \chi_{\alpha}(g_{\bar{p}}^r) z^{n_{\bar{p}} r} e^{r \beta \cdot A_{\bar{p}}} \right)
 \end{aligned} \quad (6.298)$$

It differs from the discrete case on that now the group operator  $g_{\bar{p}}$  is continuous and the factorization may have infinite terms.

**Used formulas** Here I list several formulas used in the above post.

$$\frac{1}{2\pi} \sum_{n=-\infty}^{\infty} e^{inx} = \delta(x) \quad (6.299)$$

This identity comes from one definition of delta function  $\delta(x) = \lim_{N \rightarrow \infty} \frac{1}{2\pi} \frac{\sin(N+1/2)x}{\sin(\frac{1}{2}x)}$  and simple calculation gives  $\sum_{n=-N}^N e^{inx} = \frac{\sin(N+1/2)x}{\sin(\frac{1}{2}x)}$ .

$$\sum_R \chi_{\alpha}(R) \chi_{\beta}(SR^{-1}) = \frac{|G|}{d_{\alpha}} \delta_{\alpha,\beta} \chi_{\alpha}(S) \quad (6.300)$$

This is the orthogonality between characters of irreducible representations. If we set  $S = e$ , then it reduces to  $\sum_R \chi_\alpha(R)\chi_\beta(R^{-1}) = |G|\delta_{\alpha,\beta}$ . The orthogonality of projection operators can be checked:

$$\begin{aligned} P_\alpha P_\beta &= \frac{d_\alpha}{|G|} \frac{d_\beta}{|G|} \sum_{h,sg \in G} \chi_\alpha(h)\chi_\alpha(s)\mathbf{h}^{-1}\mathbf{s}^{-1} \\ &= \frac{d_\alpha}{|G|} \frac{d_\beta}{|G|} \sum_{sg \in G} \frac{|G|}{d_\alpha} \delta_{\alpha,\beta} \chi_\alpha(sh)(\mathbf{s}\mathbf{h})^{-1} \\ &= \delta_{\alpha,\beta} \frac{d_\alpha}{|G|} \sum_{sg \in G} \chi_\alpha(s)\mathbf{s}^{-1} \\ &= \delta_{\alpha,\beta} P_\alpha \end{aligned}$$

The last formula is

$$\sum_\alpha d_\alpha \chi_\alpha(R) = |G| \delta_{e,R} \tag{6.301}$$

which comes from orthogonality relation above. For regular representation, the trace of  $R$  in terms of irreducible representations is  $\chi(R) = \sum_\alpha a_\alpha \chi_\alpha(R)$ , so the summation of all group elements gives

$$\sum_R \chi(R)\chi_\alpha(R^{-1}) = \sum_\alpha a_\alpha \sum_R \chi_\alpha(R)\chi_\alpha(R^{-1}) = |G| a_\alpha$$

On the other hand,  $\chi(R) = |G| \delta_{e,R}$  for regular representation, then the left side of the above expression is just  $|G| \chi_\alpha(e)$ , so  $a_\alpha = \chi_\alpha(e) = d_\alpha$  the dimension of  $\alpha_{th}$  irreducible representation. In this way, we obtain (6.301). Now the completeness of projection operator can be checked:

$$\sum_\alpha P_\alpha = \sum_\alpha \frac{d_\alpha}{|G|} \sum_{hg \in G} \chi_\alpha(h)\mathbf{h}^{-1} = \frac{1}{|G|} \sum_{hg \in G} \left( \sum_\alpha d_\alpha \chi_\alpha(h) \right) \mathbf{h}^{-1} = e$$

## References

- [1] R. L. Adler and B. Weiss, "Entropy, a complete metric invariant for automorphisms of the torus", *Proc. Natl. Acad. Sci. USA* **57**, 1573–1576 (1967).
- [2] J.-C. Anglès d'Auriac, S. Boukraa, and J.-M. Maillard, "Functional relations in lattice statistical mechanics, enumerative combinatorics, and discrete dynamical systems", *Ann. Comb.* **3**, 131–158 (1999).
- [3] D. V. Anosov, A. V. Klimenko, and G. Kolutsky, *On the hyperbolic automorphisms of the 2-torus and their Markov partitions*, 2008.
- [4] M. Artin and B. Mazur, "On periodic points", *Ann. Math.* **81**, 82–99 (1965).



- [5] S. Aubry and G. Abramovici, “Chaotic trajectories in the standard map. The concept of anti-integrability”, *Physica D* **43**, 199–219 (1990).
- [6] M. Baake, “A brief guide to reversing and extended symmetries of dynamical systems”, in *Ergodic Theory and Dynamical Systems in their Interactions with Arithmetics and Combinatorics*, edited by S. Ferenczi, J. Kułaga-Przymus, and M. Lemańczyk (Springer, New York NY, 2018), pp. 117–135.
- [7] M. Baake, J. Hermisson, and A. B. Pleasants, “The torus parametrization of quasiperiodic LI-classes”, *J. Phys. A* **30**, 3029–3056 (1997).
- [8] M. Baake, N. Neumärker, and J. A. G. Roberts, “Orbit structure and (reversing) symmetries of toral endomorphisms on rational lattices”, *Discrete Continuous Dyn. Syst.* **33**, 527–553 (2013).
- [9] M. Baake and J. A. G. Roberts, “Reversing symmetry group of  $GL(2, \mathbb{Z})$  and  $PGL(2, \mathbb{Z})$  matrices with connections to cat maps and trace maps”, *J. Phys. A* **30**, 1549 (1997).
- [10] M. Baake, J. A. G. Roberts, and A. Weiss, “Periodic orbits of linear endomorphisms on the 2-torus and its lattices”, *Nonlinearity* **21**, 2427 (2008).
- [11] P. Banda, J. Caughman, M. Cenek, and C. Teuscher, “Shift-symmetric configurations in two-dimensional cellular automata: Irreversibility, insolvability, and enumeration”, *Chaos* **29**, 063120 (2019).
- [12] J. Banks, J. Brooks, G. Cairns, G. Davis, and P. Stacey, “On Devaney’s definition of chaos”, *Amer. Math. Monthly* **99**, 332–334 (1992).
- [13] M. El-Batanouny and F. Wooten, *Symmetry and Condensed Matter Physics: A Computational Approach* (Cambridge Univ. Press, Cambridge UK, 2008).
- [14] M. Boyle, B. Marcus, and P. Trow, *Resolving Maps and the Dimension Group for Shifts of Finite Type* (Amer. Math. Soc., 1987).
- [15] M. Bruschi, F. Calogero, and R. Droghei, “Tridiagonal matrices, orthogonal polynomials and Diophantine relations: I”, *J. Phys. A* **40**, 9793–9817 (2007).
- [16] B. Canals and H. Schober, “Introduction to group theory”, *EPJ Web Conf.* **22**, 00004 (2012).
- [17] A. Carnegie and I. C. Percival, “Regular and chaotic motion in some quartic potentials”, *J. Phys. A* **17**, 801 (1984).
- [18] G. Casati and B. V. Chirikov, *Quantum Chaos: Between Order and Disorder* (Cambridge Univ. Press, Cambridge UK, 1995).
- [19] A. Cima, “On the relation between index and multiplicity”, *J. London Math. Soc.* **57**, 757–768 (1998).
- [20] M. Cini, *Topics and Methods in Condensed Matter Theory - From Basic Quantum Mechanics to the Frontiers of Research* (Springer, Berlin, 2007).

- [21] M. Cini and G. Stefanucci, “Antiferromagnetism of the two-dimensional Hubbard model at half-filling: The analytic ground state for weak coupling”, *J. Phys.: Condens. Matter* **13**, 1279–1294 (2001).
- [22] E. M. Corson, “Note on the Dirac character operators”, *Phys. Rev.* **73**, 57–60 (1948).
- [23] P. Cvitanović, *Group Theory: Birdtracks, Lie’s and Exceptional Groups* (Princeton Univ. Press, Princeton NJ, 2008).
- [24] P. Cvitanović, “Counting”, in *Chaos: Classical and Quantum* (Niels Bohr Inst., Copenhagen, 2023).
- [25] P. Cvitanović, R. L. Davidchack, and E. Siminos, “On the state space geometry of the Kuramoto-Sivashinsky flow in a periodic domain”, *SIAM J. Appl. Dyn. Syst.* **9**, 1–33 (2010).
- [26] P. Cvitanović and H. Liang, *A chaotic lattice field theory in two dimensions*, In preparation, 2024.
- [27] R. DeVogelaere, “IV. On the structure of symmetric periodic solutions of conservative systems, with applications”, in *Contributions to the Theory of Nonlinear Oscillations (AM-41), Volume IV* (Princeton Univ. Press, Princeton NJ, 1958), pp. 53–84.
- [28] P. A. M. Dirac, *The Principles of Quantum Mechanics* (Oxford Univ. Press, 1930).
- [29] M. S. Dresselhaus, G. Dresselhaus, and A. Jorio, *Group Theory: Application to the Physics of Condensed Matter* (Springer, New York, 2007).
- [30] D. Dudgeon and R. M. Mersereau, *Multidimensional Digital Signal Processing* (Prentice-Hall, Englewood Cliffs, NJ, 1984).
- [31] D. S. Dummit and R. M. Foote, *Abstract Algebra* (Wiley, 2003).
- [32] B. Eckhardt, G. Hose, and E. Pollak, “Quantum mechanics of a classically chaotic system: Observations on scars, periodic orbits, and vibrational adiabaticity”, *Phys. Rev. A* **39**, 3776–3793 (1989).
- [33] B. Eckhardt, G. Russberg, P. Cvitanović, P. E. Rosenqvist, and P. Scherer, “Pinball scattering”, in *Quantum Chaos: Between Order and Disorder*, edited by G. Casati and B. Chirikov (Cambridge Univ. Press, Cambridge UK, 1995).
- [34] B. Eckhardt and D. Wintgen, “Symbolic description of periodic orbits for the quadratic Zeeman effect”, *J. Phys. B* **23**, 355–363 (1990).
- [35] M. D. Esposti and S. Isola, “Distribution of closed orbits for linear automorphisms of tori”, *Nonlinearity* **8**, 827–842 (1995).
- [36] S. N. Ethier and J. Lee, “Counting toroidal binary arrays II”, *J. Integer Seq.* **18**, 15.8.3 (2015).
- [37] L. Fejér, “Über trigonometrische Polynome”, *J. Reine Angew. Math. (Crelle)* **1916**, 53–82 (1916).

- [38] M. Golubitsky and I. Stewart, *The Symmetry Perspective* (Birkhäuser, Boston, 2002).
- [39] I. S. Gradshteyn and I. M. Ryzhik, *Tables of Integrals, Series and Products*, 8th ed. (Elsevier LTD, Oxford, New York, 2014).
- [40] T. Grava, T. Kriecherbauer, G. Mazzuca, and K. D. T.-R. McLaughlin, “Correlation functions for a chain of short range oscillators”, *J. Stat. Phys.* **183**, 1 (2021).
- [41] B. Gutkin, L. Han, R. Jafari, A. K. Saremi, and P. Cvitanović, “Linear encoding of the spatiotemporal cat map”, *Nonlinearity* **34**, 2800–2836 (2021).
- [42] M. Hamermesh, *Group Theory and Its Application to Physical Problems* (Dover, New York, 1962).
- [43] M. Hamermesh, *Group Theory and Its Application to Physical Problems* (Dover, New York, 1962).
- [44] P. Jacobs, *Group Theory with Applications in Chemical Physics* (Cambridge Univ. Press, 2005).
- [45] S. Jaidee, P. Moss, and T. Ward, “Time-changes preserving zeta functions”, *Proc. Amer. Math. Soc.* **147**, 4425–4438 (2019).
- [46] P. Kagey and W. Keehn, “Counting tilings of the  $n \times m$  grid, cylinder, and torus”, *J. Integer Seq.* **27**, 24.6.1 (2024).
- [47] A. Katok and B. Hasselblatt, *Introduction to the Modern Theory of Dynamical Systems* (Cambridge Univ. Press, Cambridge, 1995).
- [48] J. P. Keating and F. Mezzadri, “Pseudo-symmetries of Anosov maps and spectral statistics”, *Nonlinearity* **13**, 747–775 (2000).
- [49] Y.-O. Kim, J. Lee, and K. K. Park, “A zeta function for flip systems”, *Pacific J. Math.* **209**, 289–301 (2003).
- [50] P. Kurlberg and Z. Rudnick, “Hecke theory and equidistribution for the quantization of linear maps of the torus”, *Duke Math. J.* **103**, 47–77 (2000).
- [51] J. S. W. Lamb and J. A. G. Roberts, “Time reversal symmetry in dynamical systems: A survey”, *Physica D* **112**, 1–39 (1998).
- [52] Y. Lan and P. Cvitanović, “Unstable recurrent patterns in Kuramoto-Sivashinsky dynamics”, *Phys. Rev. E* **78**, 026208 (2008).
- [53] H. Liang and P. Cvitanović, “A chaotic lattice field theory in one dimension”, *J. Phys. A* **55**, 304002 (2022).
- [54] D. A. Lind, “A zeta function for  $Z^d$ -actions”, in *Ergodic Theory of  $Z^d$  Actions*, edited by M. Pollicott and K. Schmidt (Cambridge Univ. Press, 1996), pp. 433–450.
- [55] D. A. Lind and B. Marcus, *An Introduction to Symbolic Dynamics and Coding* (Cambridge Univ. Press, Cambridge, 1995).

- [56] J. Llibre and N. Neumärker, “Period sets of linear toral endomorphisms on  $T^2$ ”, *Topology Appl.* **185-186**, 41–49 (2015).
- [57] C. C. Martens, R. L. Waterland, and W. P. Reinhardt, “Classical, semi-classical, and quantum mechanics of a globally chaotic system: integrability in the adiabatic approximation”, *J. Chem. Phys.* **90**, 2328 (1989).
- [58] S. G. Matanyan, G. K. Savvidy, and N. G. Ter-Arutyunyan-Savvidy, “Classical Yang-Mills mechanics. Nonlinear color oscillations”, *Sov. Phys. JETP* **53**, 830–838 (1981).
- [59] Z. Mihailović and M. Rajković, “Cooperative Parrondo’s games on a two-dimensional lattice”, *Physica A* **365**, 244–251 (2006).
- [60] R. Miles, “A dynamical zeta function for group actions”, *Monatsh. Math.* **182**, 683–708 (2016).
- [61] A. Nordin and M. S. M. Noorani, “Counting finite orbits for the flip systems of shifts of finite type”, *Discrete Continuous Dyn. Syst.* **41**, 4515–4529 (2021).
- [62] K. Park, “On ergodic foliations”, *Ergod. Theor. Dyn. Syst.* **8**, 437–457 (1988).
- [63] C. Pozrikidis, *An Introduction to Grids, Graphs, and Networks* (Oxford Univ. Press, Oxford, UK, 2014).
- [64] F. Riesz and B. Sz.-Nagy, *Functional Analysis* (Dover Publ., Mineola, NY, 1955).
- [65] J. M. Robbins, “Discrete symmetries in periodic-orbit theory”, *Phys. Rev. A* **40**, 2128–2136 (1989).
- [66] J. A. G. Roberts and G. R. W. Quispel, “Chaos and time-reversal symmetry. Order and chaos in reversible dynamical systems”, *Phys. Rep.* **216**, 63–177 (1992).
- [67] D. Ruelle, “Dynamical zeta functions and transfer operators”, *Notices Amer. Math. Soc.* **95**, 887–895 (2002).
- [68] D. Ruelle, *Thermodynamic Formalism: The Mathematical Structure of Equilibrium Statistical Mechanics*, 2nd ed. (Cambridge Univ. Press, Cambridge, 2004).
- [69] R. Sharp, “Periodic orbits of hyperbolic flows”, in *On Some Aspects of the Theory of Anosov Systems*, edited by G. A. Margulis (Springer, Berlin, 2004), pp. 73–138.
- [70] A. Siemaszko and M. P. Wojtkowski, “Counting Berg partitions”, *Nonlinearity* **24**, 2383–2403 (2011).
- [71] S. Smale, “Differentiable dynamical systems”, *Bull. Amer. Math. Soc.* **73**, 747–817 (1967).
- [72] H. Spohn, “Nonlinear fluctuating hydrodynamics for anharmonic chains”, *J. Stat. Phys.* **154**, 1191–1227 (2014).

- [73] M. Tinkham, *Group theory and quantum mechanics* (Dover, New York, 2003).
- [74] P. Walters, *An Introduction to Ergodic Theory* (Springer, New York, 1982).
- [75] Wikipedia contributors, [Index of a subgroup — Wikipedia, The Free Encyclopedia](#), 2022.
- [76] S. V. Williams, X. Wang, H. Liang, and P. Cvitanović, [Nonlinear chaotic lattice field theory](#), In preparation, 2024.

## Chapter 7

# Bloch, Brilluoin, ...

An invariant 2-torus on a 2-dimensional spatiotemporally infinite  $\mathbb{Z}^2$  lattice has more complicated pattern than a cat map periodic orbit. An invariant 2-torus can tile the infinitely large 2-dimensional space not only by repeating in the time or space direction, but also by moving in both of the spatiotemporal directions. The repeating pattern can generally be described by a Bravais lattice:

$$\mathcal{L} = \{n_1 \mathbf{a}_1 + n_2 \mathbf{a}_2 | n_i \in \mathbb{Z}\}. \quad (7.1)$$

And the invariant 2-tori tile the infinitely large 2-dimensional space by:

$$x_{\mathbf{z}} = x_{\mathbf{z}+\mathbf{R}}, \quad \mathbf{R} \in \mathcal{L}. \quad (7.2)$$

The  $\mathbf{z}$  here is a two-dimensional vector which labels the position and time of the field. The screened Poisson equation can be written as:

$$(-2s + \sigma_1 + \sigma_1^\top + \sigma_2 + \sigma_2^\top)x_{\mathbf{z}} = -m_{\mathbf{z}}, \quad (7.3)$$

where the  $\sigma_i$  is a translation operator which can translate the field in the positive  $i$ th direction by length one and  $\sigma_i^\top$  is the inverse of the operator  $\sigma_i$  which translates the field in the negative  $i$ th direction. Here we can assume that  $\sigma_1$  is a translation in the time and  $\sigma_2$  is a translation in space. But since the system is invariant under the exchange of space and time, we don't need to distinguish these two directions.

Note that in (7.3) the operators, field and source are defined on infinitely large 2-dimensional space (lattice). For an invariant 2-torus, which is a periodic tile, the screened Poisson equation (7.3) is also satisfied on this finite tile. But in this case, the translation operators need to satisfy the periodic bc's specified by this invariant 2-torus. And the  $-2s + \sigma_1 + \sigma_1^\top + \sigma_2 + \sigma_2^\top$  on the finite region is the orbit Jacobian matrix of this specific periodic pattern.

Following the same procedure as counting the periodic points of a cat map, we know that the number of periodic points is given by the determinant of the orbit Jacobian matrix. To find the determinant and the inverse of the orbit Jacobian matrix, we need to first find the eigenvectors and eigenvalues.

The eigenvectors here are fields defined in this finite tile. The elements of these eigenvectors are generally complex numbers. If we tile the whole 2-dimensional space with one of these finite fields using the periodic condition, we will get an eigenvector of the operator in (7.3) defined in the infinite 2-dimensional space. And the eigenvalue remains unchanged. So we can find the eigenvectors and eigenvalues in the infinite 2-dimensional space then reduce the field into the finite tiles.

## 7.1 Reduction to the reciprocal lattice

My *Phys 7143 zipped! World Wide Quest to Tame Group Theory* course notes are [here](#). See in particular [birdtracks.eu Sect. 8.2.2, One-dimensional line groups](#), and Gutkin [lecture notes](#) *Lecture 7 Applications III. Energy Band Structure*, Sects. 1. *Lattice symmetries* and 2. *Band structure*.

Other good reads: Dresselhaus *et al.* [11] ([click here](#)) chapter 9. *Space Groups in Real Space*, and Cornwell [9] ([click here](#)) chapter 7. *Crystallographic Space Groups*. Walt De Heer learned this stuff from Herzberg [15] *Molecular Spectra and Molecular Structure*. Condensed matter people like Kittel [18] *Introduction to Solid State Physics*, but I am not a fan, because simple group theoretical facts are there presented as solid state phenomena. Quinn and Yi [22] *Solid State Physics: Principles and Modern Applications* introduction to space groups looks compact and sensible.

Martin Mourigal found the Presqu'île Giens, May 2009 *Contribution of Symmetries in Condensed Matter Summer School* very useful. Villain [27] *Symmetry and group theory throughout physics* gives a readable overview. The overheads are [here](#), many of them are of potential interest. Mourigal recommends Ballou [3] *An introduction to the linear representations of finite groups* appears rather formal (and very erudite).

Grenier, B. and Ballou [13] *Crystallography: Symmetry groups and group representations*.

Schober [24] *Symmetry characterization of electrons and lattice excitations* gives an eminently readable discussion of space groups.

Rodríguez-Carvajal and Bourée [23] *Symmetry and magnetic structures*

Schweizer [25] *Conjugation and co-representation analysis of magnetic structures* deals with black, white and gray groups that Martin tries not to deal with, so all Mourigal groups are gray.

If you are curious about graphene, work out Gutkin [lecture notes](#) *Lecture 7 Applications III. Energy Band Structure*, Sect. 7.3 *Band structure of graphene*. Villain [27] discusses graphene in the Appendix A of *Symmetry and group theory*

The symmetry is  $C_n$ , and one needs to distinguish  $C_n$  orbits ("prime cycles" in ChaosBook; one per each orbit). The right way to do this is by going to  $C_n$  irreps, ie, by the discrete Fourier transform, with all reciprocal lattice Brillouin zone solutions orbits in an  $1/n$  sliver of a  $n$ -gon. If  $n$  is prime, this is irreducible;

if it is a multiple of a prime, one should remove those solutions, as they have already been accounted for.

The translation group  $T$ , the set of translations  $\vec{t}$  that put the crystallographic structure in coincidence with itself, constitutes the *lattice*.  $T$  is a normal subgroup of  $G$ . It defines the *Bravais lattice*. In 1 dimension translations are of the form

$$\vec{t} = \vec{t}_{\vec{n}} = n\vec{a}, \quad n \in \mathbb{Z}.$$

The basis vector  $\vec{a}$  spans the *unit cell*. The lattice unit cell is always a *generating region* (a tile that tiles the entire space), but the smallest generating region –*the fundamental domain*– may be smaller than the lattice unit. At each lattice point the identical group of “atoms” constitutes the *motif*. A *primitive cell* is a minimal region repeated by lattice translations. The lattice and the motif completely characterize the crystal.

There is also the *conventional cell*, see [unit cell wiki](#): A conventional cell (which may or may not be primitive) is a unit cell with the full symmetry of the lattice and may include more than one lattice point. The conventional unit cells are parallelotopes in  $n$  dimensions.

In the *Wigner–Seitz cell*, the lattice point is at the center of the cell, and for most Bravais lattices, the shape is not a parallelogram or parallelepiped. This is a type of Voronoi cell.

The Wigner–Seitz cell of the reciprocal lattice in momentum space is called the Brillouin zone.

The cosets by translation subgroup  $T$  (the set all translations) form the *factor* (AKA *quotient*) group  $G/T$ , isomorphic to the point group  $g$  (rotations). All irreducible representations of a space group  $G$  can be constructed from irreducible representations of  $g$  and  $T$ . This step, however, is tricky, as, due to the non-commutativity of translations and rotations, the quotient group  $G/T$  is not a normal subgroup of the space group  $G$ .

The quantum-mechanical calculations are executed by approximating the infinite crystal by a periodic one, and going to the *reciprocal* space by deploying  $C_N$  discrete Fourier transform. This implements the  $G/T$  quotienting by translations and reduces the calculation to a finite *Brillouin zone*. That is the content of the ‘*Bloch theorem*’ of solid state physics. Further work is then required to reduce the calculations to the point group irreps.

One would think that the one-dimensional *line groups*, which describe systems exhibiting translational periodicity along a line, such as carbon nanotubes, would be simpler still. But even they are not trivial – there are 13 of them.

The normal subgroup of a line group  $L$  is its translational subgroup  $T$ , with its factor group  $L/T$  isomorphic to the *isogonal point group*  $P$  of discrete symmetries of its 1-dimensional unit cell  $x \in (-a/2, a/2]$ . In the reciprocal lattice  $k$  takes on the values in the first Brillouin zone interval  $(-\pi/a, \pi/a]$ . In *Irreducible representations of the symmetry groups of polymer molecules. I*, Božović, Vujičić and Herbut [6] construct all the reps of the line groups whose isogonal point groups are  $C_n, C_{nv}, C_{nh}, S_{2n}$ , and  $D_n$ . For some of these line groups the irreps are obtained as products of the reps of the translational subgroup and the irreps of



the isogonal point group.

According to W. De Heer, the Mintmire, Dunlap and White [20] paper *Are Fullerene tubules metallic?* which took care of chiral rotations for nanotubes by a tight-binding calculation, played a key role in physicists' understanding of line groups.

Consequences of time-reversal symmetry on line groups are discussed by Božović [5]; In the case when the Hamiltonian is invariant under time reversal [14], the symmetry group is enlarged:  $L + \theta L$ . It is interesting to learn if the degeneracy of the levels is doubled or not.

Johnston [17] *Group theory in solid state physics* is one of the many reviews that discusses Wigner's time-reversal theorems for a many-electron system, including the character tests for time-reversal degeneracy, the double space groups, and the time-reversal theorems (first discussed by Herring [14] in *Effect of time-reversal symmetry on energy bands of crystals*).

Consider

$$\rho_{\vec{G}}(\vec{x}) = e^{i\vec{G} \cdot \vec{r}(\vec{x})},$$

where  $\vec{G}$  is a reciprocal lattice vector. By definition,  $\vec{G} \cdot \vec{a}$  is an integer multiple of  $2\pi$ ,  $\rho_{\vec{G}} = 1$  for lattice vectors. For any other state, reciprocal periodic state is given by

$$e^{i\vec{G} \cdot \vec{u}(\vec{x})} \neq 1.$$

When a cube is a building block that tiles a 3D cubic lattice, it is referred to as the 'elementary' or 'Wigner-Seitz' cell, and its Fourier transform is called 'the first Brillouin zone' in 'the reciprocal space'.

**Han:** *Hermite normal form* primitive cell, with upper-triangular basis,

$$\mathbb{A} = \begin{bmatrix} \ell & S \\ 0 & \ell \end{bmatrix}, \quad V_{\mathbb{A}} = \ell\ell, \quad (7.4)$$

reciprocal primitive cell is also of Hermite normal form, but with lower-triangular basis,

$$\tilde{\mathbb{A}} = \frac{(2\pi)^2}{V_{\mathbb{A}}} \begin{bmatrix} \ell & 0 \\ S & \ell \end{bmatrix}, \quad (7.5)$$

**wiki Reciprocal lattice:**

Some lattices may be skew, which means that their primary lines may not necessarily be at right angles.

The Brillouin zone is a Wigner-Seitz cell of the reciprocal lattice.

The spatial periodicity of this wave is defined by its wavelength  $\lambda$ , where  $k\lambda = 2\pi$ ; hence the corresponding wavenumber in reciprocal space will be  $k = 2\pi/\lambda$ .

The magnitude of a wavevector is called wavenumber.

Let  $\mathcal{L}_{\mathbb{A}} \subseteq \mathbb{R}^n$  be a lattice. That is,  $\mathcal{L}_{\mathbb{A}} = \mathbb{A}\mathbb{Z}^n$  for some matrix  $\mathbb{A}$ .

If matrix  $\mathbb{A}$  has primitive vectors as columns, then the matrix

$$\tilde{\mathbb{A}} = \mathbb{A} \frac{1}{\mathbb{A}^T \mathbb{A}} \quad (7.6)$$

columns are primitive wavevectors of the reciprocal lattice.

But this looks wrong:  $2\pi$ 's are missing (this is a dual lattice, not the reciprocal one), and:

$$\tilde{\mathbb{A}} = \mathbb{A} (\mathbb{A}^\top \mathbb{A})^{-1} = \mathbb{A} \mathbb{A}^{-1} (\mathbb{A}^\top)^{-1} = (\mathbb{A}^\top)^{-1} \quad (7.7)$$

Checking

$$\mathbb{A}^\top \mathbb{A} = \begin{bmatrix} \ell & 0 \\ S & \ell \end{bmatrix} \begin{bmatrix} \ell & S \\ 0 & \ell \end{bmatrix} = \begin{bmatrix} \ell^2 & S\ell \\ S\ell & S^2 + \ell^2 \end{bmatrix}$$

### 7.1.1 Hill determinant: Reciprocal lattice evaluation

$$\omega = e^{2i\pi/n}$$

$$\tilde{\phi}_k = x_k + i y_k = |\tilde{\phi}_k| e^{i\theta_k}$$

$$q_k = 2\pi k/n,$$

$n$  is the primitive cell period

The temporal Bernoulli orbit Jacobian matrix  $\mathcal{J} = \partial/\partial t - (s - 1)r^{-1}$  is a differential operator whose determinant one usually computes by a Fourier transform diagonalization (see sect. ??). The Fourier discretization approach goes all the way back to Hill's 1886 paper [16].

The first advantage of using the reciprocal lattice is that it provides a way to compute the Hill determinant. If the orbit Jacobian matrix (4.57) commutes with the translation operator, the plane waves are eigenvectors of the orbit Jacobian matrix. Using these eigenvectors one can find the eigenvalues and the determinant of the orbit Jacobian matrix. In the  $n$ -dimensional space of periodic states with period- $n$ , the one-lattice spacing translation operator is a shift matrix (??), whose eigenvectors are plane waves  $\tilde{e}_k$ :

$$r \tilde{e}_k = \omega^k \tilde{e}_k. \quad (7.8)$$

For example, the eigenvalues of the temporal Bernoulli orbit Jacobian matrix (1.19) are

$$(s \mathbf{1} - r) \tilde{e}_k = (s - \omega^k) \tilde{e}_k, \quad (7.9)$$

and the Hill determinant is simply a polynomial whose roots are the  $n$ th roots of unity,

$$\text{Det}(s \mathbf{1} - r) = \prod_{k=0}^{n-1} (s - \omega^k) = s^n - 1. \quad (7.10)$$

see (21.111). The eigenvalues of the temporal cat orbit Jacobian matrix (??) are:

$$(-r + s \mathbf{1} - r^{-1}) \tilde{e}_k = (s - 2 \cos(2\pi k/n)) \tilde{e}_k, \quad (7.11)$$

and the Hill determinant is:

$$\begin{aligned} \text{temporal cat: } \text{Det}(-r + s \mathbf{1} - r^{-1}) &= \prod_{k=0}^{n-1} [s - 2 \cos(2\pi k/n)] \\ &= 2T_n(s/2) - 2, \end{aligned} \quad (7.12)$$

where  $T_n$  is the Chebyshev polynomial of the first kind.

Explain figure ??.

**2019-10-10, 2023-09-04 Predrag Brillouin [7]** *Les électrons libres dans les métaux et le rôle des réflexions de Bragg* (1930), Appendix seems to be the reference to Bloch theorem.

Grayson Smith and Wilhelm [12] *Superconductivity*, (1935)? They plot the "energy momentum curve".

Seitz and Johnson [26] *Modern theory of solids I* (1937) review "The zone theory of solids", that accounts for the periodic potential distribution in the solid lattice; they refer to earlier textbooks on this.

"If we have a crystal block containing  $N$  unit cells, the energy spectrum of the electrons has to be divided into sets of  $N$  levels. Within each such set, the  $N$  levels are always so closely spaced that, for all practical purposes, they form a continuous band. We shall refer to such a band of  $N$  levels as a zone. In the one-dimensional case, each continuous range of energy between the discontinuities in the  $E(u)$  function contains the  $N$  energy levels comprised in one zone."

Bohm [4] *Note on a theorem of Bloch concerning possible causes of superconductivity* (1949) has no mention of periodic potentials, so this is not 'our' Bloch theorem.

There is no reason to refer to Watanabe [28] *A proof of the Bloch theorem for lattice models* (2019), [arXiv:1904.02700](https://arxiv.org/abs/1904.02700):

"The Bloch theorem states that the expectation value of the  $U(1)$  current operator averaged over the entire space vanishes for large quantum systems. The theorem applies as long as all terms in the Hamiltonian are finite ranged. Finite systems are sensitive to the boundary conditions. Under the periodic boundary condition, one can only prove that the current expectation value is inversely proportional to the linear dimension of the system, while the current expectation value completely vanishes before taking the thermodynamic limit when the open boundary condition is imposed. We also provide simple tight-binding models that clarify the limitation of the theorem in dimensions higher than one."

"the result is applicable not only to periodic lattice with arbitrary number of sub-lattices but also, for example, to quasi-crystals or disordered systems."

His Fig. 2 (a) shows the band structure of the tight-binding model for  $L = 12$ , much like ours, so ours is a "tight-binding model with the nearest neighbor hopping".

**2020-01-10 Predrag** A very pedagogical, down to earth textbook: Pozrikidis [21] *An introduction to grids, graphs, and networks*, ([click here](#)).

He discusses Sect 2.6.1 *Bravais Lattices*, the reciprocal lattice, the discrete Brillouin zone or Wigner-Seitz cell.

**2018-03-18 Predrag** Check sect. [24.2.1](#) *Reduction to the reciprocal lattice* for possibly useful material.

**2018-03-30, 2023-03-10 Predrag** Read [ChaosBook Chapter 24](#) *Deterministic diffusion*. You also might find my online lectures, [Week 13](#) helpful. Maybe also have a glance at [ChaosBook Appendix A24](#) *Deterministic diffusion*. As Dan has already covered everything, you can pick and chose: maybe redo the 1-dimensional example sect. [24.2](#) *Diffusion induced by chains of 1-dimensional maps* using the discrete Fourier that you are using for cat maps? Doing some nontrivial partitions, as in figure [24.4](#) of example [24.4](#)?

My Group Theory course [birdtracks.eu/course3](#) might be of interest. Cyclic group  $C_n$  shows up in [week 2](#) Examples 2.3 and 2.4.

Because of the reflection symmetries, the cat map and spatiotemporal cat symmetry is actually not  $C_n$ , but the dihedral group  $D_n$ , whose irreducible representations are not the complex 1-dimensional  $\exp(2\pi i k j / \ell)$ , but the real 2-dimensional  $(\cos(2\pi i k j / \ell), \sin(2\pi i k j / \ell))$ , see [week 4](#) Exercises 4.3 and 4.4.

The most important for you is [week 8](#) *Space groups*. The symmetries of our spatiotemporal cat are summarized by figure [8.1](#) and in the exercise [8.1](#). *Band structure of a square lattice*. The elastic (not chaotic) cousin of spatiotemporal cat is described in sect. [8.2](#) *Elastodynamic equilibria of 2D solids*.

The whole course is a subversion repository that I can give you access to, if you want to reuse any of the LaTeX, or see the solution sets.

**2018-03-18 Predrag** to Han - can you have a look at the Group Theory course [week 8](#) exercises, [solution 8.3](#)? I should know this, but I do not, and you have thought about it:

is spatiotemporal cat in any illuminating sense related to a tight-binding model? (see sect. [16.3](#)) We are not doing QM, but if we formulate the problem in the continuous space  $x \in \mathbb{R}^d$ , rather than the integer lattice  $x \in \mathbb{Z}^d$ , our Hamiltonian is  $\delta$  function on each site, and its neighbors.

If there is a relation, we definitely have to explain that in our paper, as many colleagues care about couple spin chains and lattices.

**2018-05-22 Han** For the Fourier transform of all the admissible period-5 see figure [24.35](#). For a 1-dimensional lattice with lattice spacing 1, the reciprocal lattice has spacing  $2\pi/1 = 2\pi$ , with the (first) Brillouin zone from  $k = -\pi$  to  $k = \pi$ . Due to the time reversal, all  $k = 2\pi/5$  irrep states are the same as the  $k = 4\pi/5$  irrep states.

**2018-04-18 Predrag** I would expect the time-reversal pairs to be the complex-conjugate pairs in Fourier space, as  $C_4$  shift moves them in opposite directions.

**2019-09-11 Predrag** Perhaps - if that helps: copy to here the nomenclature used in [week 8 Space groups](#).

**2020-01-23 Predrag** Barvinok [arXiv:/math/0504444](https://arxiv.org/abs/math/0504444):

Let  $V$  be a  $d$ -dimensional real vector space with the scalar product  $\langle \cdot, \cdot \rangle$  and the corresponding Euclidean norm  $\| \cdot \|$ . Let  $\mathcal{L} \subset V$  be a lattice and let  $\mathcal{L}^* \subset V$  be the *dual* or the *reciprocal* lattice

$$\mathcal{L}^* = \left\{ x \in V : \langle x, y \rangle \in \mathbb{Z} \text{ for all } y \in \mathcal{L} \right\}.$$

For  $\tau > 0$ , we introduce the *theta function*

$$\begin{aligned} \theta_{\mathcal{L}}(x, \tau) &= \tau^{d/2} \sum_{m \in \mathcal{L}} \exp \{ -\pi\tau \|x - m\|^2 \} \\ &(\det \mathcal{L})^{-1} \sum_{l \in \mathcal{L}^*} \exp \{ -\pi \|l\|^2 / \tau + 2\pi i \langle l, x \rangle \}, \end{aligned} \quad (7.13)$$

where  $x \in V$ . The last equality is the reciprocity relation for theta series (essentially, the Poisson summation formula).

**2021-02-27 Sidney** Figure [22.1](#) shows all Hamiltonian Hénon [\(3.28\)](#),  $a = 6$  periodic states of period  $n = 6$ , in the  $C_6$  reciprocal lattice.

Compare with Han's figure [24.59](#).

**2021-08-10 Han Reciprocal periodic state**

An infinite periodic state is periodic if the state is invariant under the action of a translation group. A translation group can be described by a Bravais lattice, the vector in which determines the direction and distance of the translation. When the dynamical system has time translation symmetry, the defining equation of the system is invariant under translations. So it is natural to use the eigenvectors of the translation operator to study the periodic states of the system.

The eigenvectors of translation operators are plane waves defined on the lattice. But to study the periodic states, we need to require that the plane wave also satisfies the periodic condition. Generally, a  $d$ -dimensional Bravais lattice can be described by:

$$\mathcal{L} = \left\{ \sum_{i=1}^d n_i \mathbf{b}_i \mid n_i \in \mathbb{Z} \right\}, \quad (7.14)$$

where  $\mathbf{b}_i$  is the  $i$ th primitive vector of the Bravais lattice. And a plane wave on the  $d$ -dimensional lattice is:

$$f_{\mathbf{k}}(\mathbf{z}) = e^{i\mathbf{k} \cdot \mathbf{z}}, \quad (7.15)$$

where  $\mathbf{z}$  is the position of a lattice site, and  $\mathbf{k}$  is the wave vector. The periodicity given by the Bravais lattice  $\mathcal{L}$  requires that:

$$f_{\mathbf{k}}(\mathbf{z} + \mathbf{R}) = f_{\mathbf{k}}(\mathbf{z}), \quad \mathbf{R} \in \mathcal{L}. \quad (7.16)$$

This condition can only be satisfied if the wave vector  $\mathbf{k}$  exists on the reciprocal lattice of the lattice  $\mathcal{L}$ :

$$\bar{\mathcal{L}} = \left\{ \sum_{j=1}^d n_j \mathbf{b}_j \mid n_j \in \mathbb{Z} \right\}, \quad (7.17)$$

the basis vectors of which satisfy:

$$\mathbf{b}_i \cdot \mathbf{a}_j = 2\pi\delta_{ij}. \quad (7.18)$$

Using these eigenvectors we can transform periodic states into reciprocal periodic states by discrete Fourier transform. Any periodic state with the periodicity given by the Bravais lattice  $\mathcal{L}$  can be spanned by the plane waves with wave vectors in the reciprocal lattice  $\bar{\mathcal{L}}$ . And since a periodic state only has values on lattice sites, we only need a finite number of plane waves to span the periodic state.

**2021-09-06 Han** See my post on page [1311](#), and sect. [24.2.1](#) *Reduction to the reciprocal lattice*.

**2020-06-08 Predrag** dropped from LC21: The periodicity of a periodic states is described by the  $d$ -dimensional Bravais lattice:

$$\Lambda = \left\{ \sum_{i=1}^d n_i \mathbf{a}_i \mid n_i \in \mathbb{Z} \right\}. \quad (7.19)$$

The orbit Jacobian matrix (??) is constructed from  $d$  commuting translation operators  $\sigma_i$  with  $i = 1, \dots, d$ . The eigenvectors of these translation operators are plane waves:

$$f_{\mathbf{k}}(z) = e^{i\mathbf{k} \cdot z}, \quad (7.20)$$

where  $\mathbf{k}$  is a  $d$ -dimensional wave vector. A general plane wave does not satisfy the periodicity (??), unless

$$e^{i\mathbf{k} \cdot R} = 1. \quad (7.21)$$

Since  $R$  is a vector from the Bravais lattice  $\mathcal{L}$ , the wave vector  $\mathbf{k}$  must lie in the reciprocal lattice of  $\Lambda$ :

$$\mathbf{k} \in \Lambda^*, \quad \Lambda^* = \left\{ \sum_{i=1}^d m_i \mathbf{b}_i \mid m_i \in \mathbb{Z} \right\}, \quad (7.22)$$

where the primitive reciprocal lattice vectors  $\mathbf{b}_i$  satisfy:

$$\mathbf{b}_i \cdot \mathbf{a}_j = 2\pi\delta_{ij} . \quad (7.23)$$

To get the eigenvectors and the corresponding eigenvalues of the orbit Jacobian matrix, note that

$$(\sigma_j + \sigma_j^{-1})e^{ik \cdot z} = e^{i(k \cdot z - k_j)} + e^{i(k \cdot z + k_j)} = (2 \cos k_j)e^{ik \cdot z} , \quad (7.24)$$

where the  $\mathbf{k} = (k_1, k_2, \dots, k_d)$ . Hence the eigenvalue of the orbit Jacobian matrix (??) corresponding to the eigenvector with the wave vector  $\mathbf{k}$  (7.20) is

$$\lambda_{\mathbf{k}} = \sum_{j=1}^d (2 \cos k_j - s) . \quad (7.25)$$

and compute its inverse, the Green's function.

The generalization to  $d$  spatiotemporal dimensions is immediate. A periodic state  $\mathbf{X} = \{x_z\}$ ,  $z \in \mathbb{Z}^d$  is a point within the  $(\ell_1 \ell_2 \dots \ell_d)$ -dimensional unit hyper-cube  $[0, 1]^{\ell_1 \ell_2 \dots \ell_d}$ , where  $\ell_j$  is the lattice period in direction  $j$ , and the  $(\ell_1 \ell_2 \dots \ell_d)^2$ -dimensional orbit Jacobian matrix  $\mathcal{J}_{zz'}$  is given by

$$\mathcal{J} = \sum_{j=1}^d (\sigma_j - s \mathbf{1} + \sigma_j^{-1}) . \quad (7.26)$$

Here  $\sigma_i$  is a shift operator (??) which translates the field in the  $i$ th direction by one lattice spacing. Its inverse  $\sigma_i^{-1}$  translates the field in the negative  $i$ th direction.

From now on we specialize to the 2-dimensional,  $z = (n, t) \in \mathbb{Z}^2$  spatiotemporal lattice, and replace the  $(\ell_1, \ell_2)$  notation for lattice periods by  $(\ell, \ell)$ , where  $\ell$  is the 'spatial', and  $\ell$  the 'temporal' lattice period. The field  $x_i$  takes values in the  $\ell\ell$ -dimensional unit hyper-cube  $\mathbf{X} \in [0, 1]^{\ell\ell}$ .

Throw away all blocks which are repeats of shorter blocks in the temporal direction. What remains in  $N_k$  prime periodic blocks  $p$  of the same size  $[\ell_p \times \ell_p] = [\ell_k \times \ell_k]$ .

This is essential to all that follows, as the Lagrangian formulation will apply to spatiotemporal cat in any number of spatial dimensions as well.

**2023-04-04 Predrag Kuchment [19] Analytic and algebraic properties of dispersion relations (Bloch varieties) and Fermi surfaces. What is known and unknown, (2023), arXiv:2304.01478;** very interesting high level mathematical bird's eye view of reciprocal lattices.

Let  $\mathcal{L} = \mathbb{Z}^d$  act on  $\mathbb{R}^d$  by shifts. Irreps of  $\mathcal{L}$  are  $e^{ik \cdot \gamma}$ , with *quasimomentum*

$$k \in \mathbb{R}^d \text{ mod } \mathcal{L}^* , \quad (7.27)$$

<sup>1</sup>Predrag 2023-04-05: What is  $\gamma$ ?

where  $\mathcal{L}^* = 2\pi\mathbb{Z}^d$  is the dual lattice to  $\mathcal{L} = \mathbb{Z}^d$ . The corresponding eigenspace  $\mathcal{H}_k$  for  $\mathcal{L}$  consists of Bloch functions of form

$$v(x) = e^{ik \cdot x} p(x), \quad (7.28)$$

where  $p$  is  $\mathcal{L}$ -periodic.

We fix choices of a fundamental domain  $W$  (Wigner-Seitz cell)<sup>2</sup> for action of  $\mathcal{L}$  on  $\mathbb{R}^d$  and of a fundamental domain  $B$  (Brillouin zone) for action of  $\mathcal{L}^*$ . Functions that are  $\mathcal{L}$ -periodic can be considered as functions on the torus  $\mathbb{T} := \mathbb{R}^d/\mathcal{L}$ . Analogously,  $\mathcal{L}^*$ -periodic functions can be identified with functions on the ‘‘Brillouin torus’’  $\mathbb{T}^* := \mathbb{R}^d/\mathcal{L}^*$ . We will denote the corresponding normalized to the volume 1 measures by  $dx$  and  $dk$  correspondingly.

All  $\mathcal{L}$ -invariant linear partial differential operators are of the form

$$L = L(x, D) = \sum a_\alpha(x) D^\alpha \quad (7.29)$$

with  $\mathcal{L}$ -periodic functions  $a_\alpha$ .

If we denote by  $L(k)$  the operator  $L$  acting on the functions from  $\mathcal{H}_k$ , then we have the following direct integral expansion

$$L = \int_{k \in \mathbb{T}^*}^{\oplus} L(k) dk \quad (7.30)$$

A convenient representation of  $L(k)$  for a periodic operator  $L = L(x, D)$  is the following:

**Lemma:**  $L(k) = L(x, D + k)$  acting on function on the torus  $T := \mathbb{R}^d/\mathcal{L}$ .

In particular, if  $L = -\Delta + V(x) = (D)^2 + V(x)$ , then<sup>3</sup>

$$L(k) = \left(\frac{1}{i}\nabla + k\right)^2 + V(x) = -\Delta + \frac{2}{i}k \cdot \nabla + k^2 + V(x),$$

acting on  $\mathcal{L}$ -periodic functions (i.e., functions on  $\mathbb{T}$ ).

The Bloch variety (dispersion relation) of operator  $L$ :<sup>4</sup>

$$\mathbb{B}_L := \{(k, \lambda) \mid \lambda \in \sigma(L(k))\}.$$

- The advantage of the operators  $L(k)$  in comparison with  $L$  is that they act on a compact manifold (torus) and if they are elliptic, their spectra are discrete.

<sup>2</sup>Predrag 2023-04-05: We call this ‘primitive cell’.

<sup>3</sup>Predrag 2023-04-05: Note that he refers to what for us is a partial difference equation Euler–Lagrange equation as a partial differential ‘operator’, and goes to the analogue of ‘QM time-independent Schrödinger eq.’, in  $k$ th subspace.

<sup>4</sup>Predrag 2023-04-05: Note that  $L(k)$  is our Euler–Lagrange equation (a state space vector), not our orbit Jacobian matrix. So how is that an operator?



- Since the correspondence between quasimomenta  $k$  and irreps of  $\mathcal{L}$  is not one-to-one, it is often convenient to introduce the *Floquet multiplier*

$$z := e^{ik} := (e^{ik_1}, \dots, e^{ik_d}) \in (\mathbb{C} \setminus \{0\})^d. \quad (7.31)$$

If  $k$  is real,  $z$  is in “Brillouin torus”  $\mathbb{T}^* := \mathbb{R}^d / \mathcal{L}^*$ .

One can observe that in the discrete case, in the Floquet multipliers rather than quasimomenta representation, the Bloch and Fermi varieties become algebraic.

**2023-06-21 Predrag** If you want to know what 2nd, 4rd, etc Brillouin zones look like, check out [this](#). We do not need them.

**2023-01-13 Predrag** As Han points out, Predrag’s term ‘Bravais cell’ is not used in the standard crystallographic and solid state literature. For now, I have replaced the term by a macro ‘*pcell*’ for ‘primitive cell’ in CL18 [10], where ‘primitive cell’ is defined by  $d$  independent vectors such that the primitive cell contains exactly one Bravais lattice point.

We should eventually do this through out this blog and the related papers.

Arfken, Weber and Harris [1] supplementary chapter [31 Periodic Systems](#) uses ‘Bravais cell’ for a multiple of the ‘primitive cell’, i.e., not in the sense we have been using it here.

**2024-11-27 Predrag** [Viebahn](#) lecture notes [Introduction to Floquet theory, Boulder School 2021](#), is pedagogical, and covers also Bloch theory - the difference is that the Floquet is applied to periodically forced *time* evolution while Bloch theory is applied to *space*. He has an example, we with two Bloch bands (e.g. a two-site tight-binding model) in with a resonant driving at the frequency of the band separation, resulting in the Floquet-Bloch dispersion. But none of this feels related to our spatiotemporal Hill determinants.

**2024-11-27 Predrag** Giuseppe E. Santoro [Introduction to Floquet](#)

## 7.1.2 Integration over Brillouin zone

**2024-05-05 Predrag to Martin Mourigal** We have a Hessian  $J_{z'z}$  (second derivative of action) over a hyper-cubic lattice, have to evaluate the integral over a *single* band

$$\int dk^d \ln \det J(k)$$

over the 1st Brillouin zone for arbitrary Bravais lattice (we do this for hundreds and thousands of Bravais lattices) - do you do that someplace in the course?

PS We know  $\ln \det = \text{tr} \ln$ , so if one diagonalizes  $J$ , we can integrate over the band for each eigenvalue separately, but as the determinant is simpler than individual eigenvalues, looks like I should do it directly.

PPS We don't expect anything analytical, except in the simplest case of Bravais lattice states of period 2. You might have open source software pointers about that?

**2024-05-05 Martin** I am curious: how many Bravais lattices exist in dimensions  $D > 3$ ?

**2024-05-05 Predrag** [Gabriele.Nebe](#) goes up to  $D = 40$  and higher.

**2024-05-05 Predrag** I see - for a professional there are 5 Bravais lattices over a  $D = 2$ , two-dimensional space.

Our turbulent/chaotic field is described by all  $D=2$  doubly periodic lattices whose (primitive cell's) primitive vectors are on a square (integer hypercubic) lattice  $\mathbb{Z}^2$ . Not anyplace in the  $\mathbb{R}^2$  continuum.

There is an infinity of them, and we know how to correctly count them. Do you have a name for them, if 'Bravais' is too confusing?

**2024-05-06 Predrag** I changed CL18 [10] text in Bravais lattice section to:

[...] For systems characterized by several translational symmetries, one has to take care of multiple periodicities, or, in parlance of crystallography, organize the periodic orbit sums by corresponding *Bravais lattices* [2].

In crystallography there are 5 Bravais lattices over a two-dimensional space. The square lattice is one of them. For brevity, at risk of annoying crystallographers: whenever we refer here to a 'Bravais lattice', we mean a 'full rank sublattice of the square lattice' [8].

**2024-05-06 Predrag** Looking at computer science literature, sect. 8.7.2, for example Daniele Micciancio's [course notes](#): we are supposed to call these lattices 'full rank sublattices'? That's soooo boring...

**2024-05-07 Martin** Sublattices here are what we would call "conventional" or "non-primitive" unit-cell choices. Primitive unit cells cover only one lattice point, while conventional and non-primitive cells do not.

**2024-05-06 Predrag** Yech - 'gauge' is a sexy, descriptive word by these standards.

As we say, hear me out.

You have a primitive cell that contains 17 atoms. Your fundamental discovery is that to make the 2nd quantum revolution, you flip the 5th cobalt to shmobalt in every 3rd repeat of the starting primitive cell. Your new Bravais sublattice primitive cell fits perfectly over Zweistein's original Bravais lattice (which had 1 point per primitive cell), but contains

51 atoms, has 1 point per the new 51-atom primitive cell, and that one shmobalt is your ticket to Stockholm.

Then a drone like me has to compute the conductance. I have to correctly weigh relative contributions of Zweistein's cobalt and Mourigal's shmobalt, ie, compute  $\ln \det J(k)$  for each.

In *our* 1st revolution of 3rd millennium, we do not engineer with tweezers Mourigal's 51 atom shmobalt: we include all possible Lego-block mutations of Zweistein's 20th century naive guess, consistent with Schrödinger, and compute conductance of each. As you had intuited,  $\ln \det J(k)$  approaching a singularity is a big deal, the secret of revolutionary Mourigistor.

Also: a typical sublattice primitive cell is a 'turbulent' in the sense that it looks like a pointillist jumble of colored atoms. And it's legal, Schrödinger allows it. That is, the problem of turbulence is solved.

The 1st revolution of the 3rd millennium, and I'm supposed to call it "conventional"? Goes where no human eye has set foot before, and its "conventional" !??? Or worse still, refer to "Mourigal revolution" by prefix "non-Zweistein same-old"?

Give me something better :)

**2024-05-07 Martin** For computations, we prefer to work with primitive cells when we can. All the rest is redundant for us. We even have a way to construct THE primitive cell — a.k.a the Wigner-Seitz cell — that has visibly the point symmetry of the Bravais lattice itself. For the square lattice, all of this is trivial.

**2024-05-07 Predrag** Yes, origin, diagonals, diagonal planes correspond to point group's symmetry subgroups, That's standard, nein?

You mean, to evaluate Bloch states, you use the original lattice to include all contributions to the Bravais sublattice primitive cell? That gives a good, nearly three 17-dimensional blocks diagonalization of the 51-dimensional Bloch state. How else could one do it?

**2024-05-05 Martin** Numerical integrals over the BZ in spatial dimensions smaller than 3 or 4 are typically done with the cubature technique:

[github.com/stevengj/cubature](https://github.com/stevengj/cubature)

a C package for adaptive multidimensional integration (cubature) of vector-valued integrands over hypercubes, written by **Steven G. Johnson**. The code implements two algorithms for adaptive integration.

The first, h-adaptive integration, recursively partitions the integration domain into smaller subdomains, applying the same integration rule to each, until convergence is achieved.

The second, p-adaptive integration, repeatedly doubles the degree of the quadrature rules until convergence is achieved, is based on a tensor product of Clenshaw–Curtis quadrature rules. This algorithm is often superior to h-adaptive integration for smooth integrands in a few ( $\leq 3$ ) dimensions.

**2024-05-05 Predrag** Undergraduate John D. Joannopoulos, Steven G. Johnson, Joshua N. Winn, and Robert D. Meade textbook *Photonic Crystals: Molding the Flow of Light*, Chap. 5 *Two-Dimensional Photonic Crystals*, p. 66, might be a good reading for us.

“In fact, the essentials of this theorem were discovered independently at least four different times (in four languages), by Hill (1877), Floquet (1883), Lyapunov (1892), and Bloch (1928).”

**2024-05-05 Martin** For higher-dimensional integrals, what about a simple Monte-Carlo integration? I used this in some 6D vertex calculations, where 2 momenta must be summed in a 3D BZ.

**2024-05-05 Martin** Do you expect singularities in the  $\ln(\det J(k))$  function?

**2024-05-05 Predrag** We work in the parameter regimes where all eigenvalues of  $\ln \det J(k)$  are real, but we are very interested in singularity, ‘bifurcation’ parameter value regions, where at least one eigenvalue goes through 0. What does that mean for a crystallographer?

## References

- [1] G. B. Arfken, H. J. Weber, and F. E. Harris, *Mathematical Methods for Physicists: A Comprehensive Guide*, 7th ed. (Academic, New York, 2013).
- [2] N. W. Ashcroft and N. D. Mermin, *Solid State Physics* (Holt, Rinehart and Winston, 1976).
- [3] R. Ballou, “An introduction to the linear representations of finite groups”, *EPJ Web Conf.* **22**, 00005 (2012).
- [4] D. Bohm, “Note on a theorem of Bloch concerning possible causes of superconductivity”, *Phys. Rev.* **75**, 502–504 (1949).
- [5] I. B. Božović, “Irreducible representations of the symmetry groups of polymer molecules. III. Consequences of time-reversal symmetry”, *J. Phys. A* **14**, 1825 (1981).
- [6] I. B. Božović, M. Vujičić, and F. Herbut, “Irreducible representations of the symmetry groups of polymer molecules. I”, *J. Phys. A* **11**, 2133 (1978).
- [7] L. Brillouin, “Les électrons libres dans les métaux et le rôle des réflexions de Bragg”, *J. Phys. Radium* **1**, 377–400 (1930).

- [8] J. W. S. Cassels, *An Introduction to the Geometry of Numbers* (Springer, Berlin, 1959).
- [9] J. F. Cornwell, *Group theory in physics: an introduction* (Academic, New York, 1997).
- [10] P. Cvitanović and H. Liang, *A chaotic lattice field theory in two dimensions*, In preparation, 2024.
- [11] M. S. Dresselhaus, G. Dresselhaus, and A. Jorio, *Group Theory: Application to the Physics of Condensed Matter* (Springer, New York, 2007).
- [12] H. Grayson Smith and J. O. Wilhelm, "Superconductivity", *Rev. Mod. Phys.* **7**, 237–271 (1935).
- [13] B. Grenier and R. Ballou, "Crystallography: Symmetry groups and group representations", *EPJ Web Conf.* **22**, 00006 (2012).
- [14] C. Herring, "Effect of time-reversal symmetry on energy bands of crystals", *Phys. Rev.* **52**, 361–365 (1937).
- [15] G. Herzberg, *Molecular Spectra and Molecular Structure* (Van Nostrand, Princeton NJ, 1950).
- [16] G. W. Hill, "On the part of the motion of the lunar perigee which is a function of the mean motions of the sun and moon", *Acta Math.* **8**, 1–36 (1886).
- [17] D. F. Johnston, "Group theory in solid state physics", *Rep. Prog. Phys.* **23**, 66 (1960).
- [18] C. Kittel, *Introduction to Solid State Physics*, 8th ed. (Wiley, 2004).
- [19] P. Kuchment, Analytic and algebraic properties of dispersion relations (Bloch varieties) and Fermi surfaces. What is known and unknown, 2023.
- [20] J. W. Mintmire, B. I. Dunlap, and C. T. White, "Are Fullerene tubules metallic?", *Phys. Rev. Lett.* **68**, 631–634 (1992).
- [21] C. Pozrikidis, *An Introduction to Grids, Graphs, and Networks* (Oxford Univ. Press, Oxford, UK, 2014).
- [22] J. J. Quinn and K. S. Yi, *Solid State Physics: Principles and Modern Applications* (Springer, Berlin, 2009).
- [23] J. Rodríguez-Carvajal and F. Bourée, "Symmetry and magnetic structures", *EPJ Web Conf.* **22**, 00010 (2012).
- [24] H. Schober, "Symmetry characterization of electrons and lattice excitations", *EPJ Web Conf.* **22**, 00012 (2012).
- [25] J. Schweizer, "Conjugation and co-representation analysis of magnetic structures", *EPJ Web Conf.* **22**, 00011 (2012).
- [26] F. Seitz and R. P. Johnson, "Modern theory of solids I", *J. Appl. Phys.* **8**, 84–97 (1937).


- [27] J. Villain, “Symmetry and group theory throughout physics”, EPJ Web Conf. **22**, 00002 (2012).
- [28] H. Watanabe, “A proof of the Bloch theorem for lattice models”, J. Stat. Phys. **177**, 717–726 (2019).

## Chapter 8

# Spatiotemporal cat

**2016-09-09 Predrag** I have added this chapter with intention to include it as several examples in ChaosBook.org.

**2020-12-16 Predrag** The abstract of my online Mathematical Physics Webinar, Rutgers University - the most attended of the series :)

 *Spatiotemporal cat - a chaotic field theory* (55 min seminar)

1

When I refer to a physical phenomenon -such as motions of a Navier-Stokes fluid- as ‘chaotic’, or ‘turbulent’, I am often told: We understand ‘chaos’ for a system such as Lorenz attractor, but what is a ‘chaotic’ field, a field with infinitely many degrees of freedom?

The goal of the seminar is to answer this question pedagogically, as a sequence of pencil and paper calculations. First I will explain what is ‘deterministic chaos’ by walking you through its simplest example, the coin toss or Bernoulli map, but reformulated as problem of enumerating admissible global solutions on an integer-time lattice. Then I will do the same with the ‘kicked rotor’, the simplest mechanical system that is chaotic. Finally, I will take an infinity of ‘rotors’ coupled together on a spatial lattice to explain what ‘chaos’ or ‘turbulence’ looks like in the spacetime.

What emerges is a spacetime which is very much like a big spring mattress that obeys the familiar harmonic oscillator field theory equations, the discrete Helmholtz equation (or the tight-binding model), but instead of being ‘springy’, this metamaterial is a discretization of the Euclidean Klein-Gordon equation, with an unstable rotor at every lattice site, that gives, rather than pushes back, a theory formulated in terms of Hill determinants and zeta functions. We call this mother of all chaotic field theories the ‘spatiotemporal cat’.

---

<sup>1</sup>Predrag 2024-03-03: This text included in dasbuch/QMlectures/lectQM.tex chaoticFT.tex .

This is the simplest example of reformulating a space and time translationally invariant, exponentially unstable ‘turbulent’ field theory as a (D+1)-dimensional spatiotemporal system which treats space and time on equal footing. Here there is no ‘evolution in time’: there is only the enumeration of the repertoire of admissible tilings of spacetime by invariant (D+1)-dimensional tori, or ‘periodic orbits’, very much as the partition function of the Ising model is a weighted sum formed by enumerating its lattice states. But that is a story for another seminar.

And if you don’t know, [now you know](#)

## 8.1 Coupled map lattices

Diffusive coupled map lattices (CML) were introduced by Kaneko [145, 146]:

$$x_{n,t+1} = g(x_{n,t}) + \frac{\epsilon}{2}[g(x_{n-1,t}) - 2g(x_{n,t}) + g(x_{n+1,t})] = (1 + \epsilon \square)g(x_{n,t}) \quad (8.1)$$

where the individual site dynamical system  $g(x)$  is a 1D map such as the logistic map.

[QuantumCalculus.org](#): “Coupled map lattice is a quite general frame work, where one considers a graph  $G$  and at each node runs a dynamical system, which can be a map or a differential equation.”

### 8.1.1 Coupled map lattices

In order to solve a partial differential equation (PDE) on a computer, one represents it by a finite number of computational elements. The simplest discretization of a scalar spacetime field  $x(\vec{q}, \tau)$  is by specifying its values  $x_{n_1 n_2 \dots n_d t} = x(q_n, \tau_t)$  on lattice points  $(\vec{n}, t) \in \mathbb{Z}^d$ . Once spatial and temporal derivatives are replaced by their discretizations, the PDE is reduced to dynamics of a coupled map lattice, a spatially extended system with discrete time, discrete space, and a set of continuous fields on each site. For many PDEs, CML conceptual advantage is not only numerical, but also that the technical problems such as existence and uniqueness of the field theory are regularized away, and the essence of spatiotemporal chaos is revealed in a transparent form.

Often one starts out by coupling neighbors harmonically, and thinks of this starting, free field theory formulation as a spring mattress [258] to which weakly coupled nonlinear terms are then added. Similarly, the conventional CML models, mostly motivated by discretizations of dissipative PDEs, start out with chaotic on-site dynamics weakly coupled to neighboring sites, with a strong space-time asymmetry. An example are the diffusive coupled map lattices introduced by Kaneko [145, 146], with time evolution given by

$$\begin{aligned} x_{n,t+1} &= (1 + \epsilon \square)g(x_{nt}) \\ &= g(x_{nt}) + \epsilon[g(x_{n-1,t}) - 2g(x_{nt}) + g(x_{n+1,t})], \end{aligned} \quad (8.2)$$



where the individual spatial site's dynamical system  $g(x)$  is a 1-dimensional map, such as the logistic map, coupled to its nearest neighbors by  $\square$ , the spatial version of the Laplacian for the discretized second order *spatial* derivative  $d^2/dx^2$  (we always set the lattice spacing constant equal to unity).

The form of time-step map  $g(x_{nt})$  is the same for all times, i.e., the law of temporal evolution is invariant under the group of discrete *time translations*. Spatially homogenous lattice models also invariant under discrete *space translations* were studied by Bunimovich and Sinai [41] in the case when  $g(x_{nt})$  is a one-dimensional expanding map.

The observation that for spatiotemporally chaotic systems space and time should be considered on the same footing goes back to the 'chronotopic' program of Politi and collaborators [96, 162, 163, 212] who, in their studies of propagation of spatiotemporal disturbances in extended systems, discovered that the spatial stability analysis can be combined with the temporal stability analysis, with orbit weights depending exponentially both on the space and the time variables,  $t_p \propto e^{-\ell_1 \ell_2 \lambda_p}$ . Politi and Torcini [211] study of periodic states of *spatiotemporal Hénon*, a (1+1)-spacetime lattice of Hénon maps with solutions periodic both in space and time is the closest to the present investigation. They explain why the dependence of the lattice field at time  $x_{t+1}$  on the two previous time steps prevents an interpretation of dynamics as the composition of a local chaotic evolution with a diffusion process (8.2). In the CML tradition, they study the weak coupling regime  $\epsilon \approx 0$ , but note that the  $b = -1$  case could be an interesting example of a nonlinear Hamiltonian lattice field theory.

### 8.1.2 Hamiltonian coupled map lattices

For quantum mechanics and statistical mechanics applications, one needs the dynamics to be Hamiltonian, motivating models such as coupled standard map lattice [147] and  $\phi^4$  lattice [119]. Lattice recurrence relations [192] of the type studied below arise in the Frenkel-Kontorova lattice, Hamiltonian lattice models for ferromagnetism, many-body quantum chaos [107–109, 193, 225], and in discretizations of elliptic PDEs.

Pesin and Sinai [207] were the first to study such lattices, with chains of coupled Anosov maps. In order to establish rigorously the desired statistical properties of coupled map lattices, such as the continuity of their SRB measures, they, and most of the subsequent statistical mechanics literature, relied on the structural stability of Anosov automorphisms under small perturbations. For such lattices the neighboring sites have to be coupled sufficiently weakly (small  $\epsilon$  in (8.2)) so that the site cat maps could be conjugated to a lattice of uncoupled Anosov automorphisms, with a finite Markov partition, the key ingredient required for the proofs.

This exploration, as well as the companion paper [106] for Dirichlet bc's, starts with the study of a coupled  $\ell$ -body Hamiltonian system undertaken by Gutkin and Osipov [109]. If the reader wants to quantize an  $\ell$ -body Hamiltonian system, Gutkin and Osipov article covers the formalism in depth, so we do not review the Hamiltonian formulation here.

**2018-12-15 Predrag** In the discretization of a spacetime field  $q(x, t)$  on lattice points  $(x_n, t_j)$ , the field is replaced by its lattice point value  $q_{n,j} = q(x_n, t_j)$ . For a Hamiltonian set of fields we also have  $p_{n,j} = p(x_n, t_j)$ . In the spatiotemporal cat, a cat map at each periodic lattice site is coupled diffusively to its nearest neighbors:

$$\begin{aligned} q_{n,j+1} &= p_{n,j} + (s - 3)q_{n,j} - (q_{n+1,j} - 2q_{n,j} + q_{n-1,j}) - m_{n,j+1}^q \\ p_{n,j+1} &= p_{n,j} + (s - 4)q_{n,j} - (q_{n+1,j} - 2q_{n,j} + q_{n-1,j}) - m_{n,j+1}^p \end{aligned} \quad (8.3)$$

The spatiotemporal symbols follow from the Newtonian equations in  $d$  spatiotemporal dimensions

$$\begin{aligned} (q_{n,j+1} - 2q_{n,j} + q_{n,j-1}) + (q_{n+1,j} - 2q_{n,j} + q_{n-1,j}) - (s - 4)q_{n,j} &= m_{n,j} \\ (-\square + \mu^2 \mathbf{1}) \mathbf{q} &= -\mathbf{m}. \end{aligned} \quad (8.4)$$

The  $\square + 2d\mathbf{1}$  part is the standard statistical mechanics diffusive inverse propagator that counts paths on a  $d$ -dimensional lattice [61],  $\mu^2 = d(s - 2)$  is the Yukawa mass parameter (8.27), and  $-s\mathbf{1}$  is the on-site cat map dynamics, described by the stretching parameter  $s$ . For  $d = 1$  lattice,  $s = 3$  is the usual Arnold's cat map.

**2018-12-15 Predrag** Frahm and Shepelyansky [92] *Small world of Ulam networks for chaotic Hamiltonian dynamics*, and the related Shepelyansky work is of potential interest.

“Ulam method” replaces discrete dynamics by an Ulam approximate [91] of the Perron-Frobenius operator (UPFO). The Ulam method produces directed “Ulam networks” with weighted probability transitions between nodes corresponding to phase-space cells. From a physical point of view the finite cell size of UPFO corresponds to the introduction of a finite noise with amplitude given by a discretization cell size. Ulam networks have small-world properties, meaning that almost any two nodes are indirectly connected by a small number of links.

They show that the Ulam method applied to symplectic maps generates Ulam networks which belong to the class of small-world networks. They analyze the small-world examples of the Chirikov standard map and the Arnold cat map, showing that the number of degrees of separation grows logarithmically with the network size for the regime of strong chaos, due to the instability of chaotic dynamics. The presence of stability islands leads to an algebraic growth with the network size.

The usual case of the cat map corresponds to  $L = 1$ . The map on a torus of longer integer size  $L > 1$  generates a diffusive dynamics [80]. For  $L \gg 1$  the diffusive process for the probability density is described by the Fokker-Planck equation.

The time scales related with the degrees of separation and the relaxation times of the Perron-Frobenius operator have different behaviors. The

largest relaxation times remain size independent in the case of a diffusive process, like for the Arnold cat map on a long torus.

In the Appendix they show that the exact linear form of the cat map allows for very efficient and direct *exact Ulam network* network size  $10^8$  computation of the transition probabilities needed for the UPFO. Shepelyansky tends to omit boring formulas, so I see no stability multipliers which are so important in our computations.

In UPFO discretizations of the standard map they use the Arnoldi method. The main idea of the Arnoldi method is to construct a subspace of “modest”, but not too small, dimension (the Arnoldi-dimension) generated by the vectors that span a Krylov space; the Arnoldi method in ref. [91] is quite interesting.

The construction of the Ulam networks is (verbally?) described in ref. [91], but I have not understood it. As graphs are directed (?), there is probably no Laplacian. There might be a related undirected network model, with a graph Laplacian (16.22). In that case a Lagrangian formulation (in terms of graph Laplacians) might be a more powerful formulation than their Hamiltonian one. “Arrow of time” is perhaps encoded by the orientations of the links in a directed complex network.

2CB

**2018-12-15 Predrag** Ermann and Shepelyansky [80] *The Arnold cat map, the Ulam method and time reversal* show that the “Ulam method” coarse-graining leads to irreversibility.

**2020-05-31 Predrag** Houlik [123] *Periodic orbits in a two-variable coupled map* computes periodic orbits in  $1 + 1$  spacetime CML for a linear map composed of two coupled Chaté-Manneville maps [45] [tent map + linear branch] (see (8.2))

$$x_{n,t+1} = f(x_{n,t}) + \frac{\epsilon}{2}[f(x_{n-1,t}) - 2f(x_{n,t}) + f(x_{n+1,t})] \quad (8.5)$$

what we call the  $[2 \times n]_0$  family periodic orbits, using symbol blocks blocks  $M$  defined as the direct product of the single-map symbols  $\mathcal{A} = \{0, 1, 2\}$ . He credits Bunimovich and Sinai [41] with introducing the  $(D+1)$ -dimensional spatiotemporal symbolic dynamics.

The  $[2 \times 2]$  matrix

$$A = \begin{pmatrix} 1 - \epsilon & \epsilon \\ \epsilon & 1 - \epsilon \end{pmatrix} = (1 - \epsilon)\mathbf{1} + \epsilon(r + r^{-1}) \quad (8.6)$$

and sources

$$B(M) = \sum_{n-1}^{k=0} J(s_{n-1}) \cdots J(s_{k+1}) A \mathbf{b} \quad (8.7)$$

He finds the  $[2 \times n]_0$  periodic orbits by solving

$$(1 - J(M))X = B(M) \quad (8.8)$$

The fixed point condition (8.8) has a periodic orbit solution

$$X = \frac{1}{1 - J(M)} B(M) \quad (8.9)$$

for each admissible brick  $M$ , where this needs still to be rewritten in the  $n$ -dimensional temporal periodic state formulation, hence the partial products of  $[2 \times 2]$  stability matrices in (8.7). The admissible periodic states and the pruning criterion are easily visualized in the  $(\phi_{1,0}, \phi_{2,0})$  plane.

**2016-01-12, 2016-08-04 PC** Literature related to Gutkin and Osipov [109] *Classical foundations of many-particle quantum chaos*:

The existence of 2D symbolic dynamics was demonstrated in ref. [209], for a particular model of coupled lattice map.

“In general, calculating periodic orbits of a non-integrable system is a non-trivial task. To this end a number of methods have been developed,” and then, for some reason, they refer to ref. [21].

Pethel *et al.* [208] *Symbolic dynamics of coupled map lattices*

Pethel *et al.* [209] *Deconstructing spatiotemporal chaos using local symbolic dynamics*

Amigó, Zambrano and Sanjuán [8] *Permutation complexity of spatiotemporal dynamics* study diffusive logistic coupled map lattices (CML) (8.2).

Sun *et al.* [236] *A method of recovering the initial vectors of globally coupled map lattices based on symbolic dynamics* study CMLs with logistic, Bernoulli, and tent chaotic maps. They cite refs. [208, 209]. Gundlach and Rand [105] study coupled circle maps (the results of subsequent papers in this series are wrong, see Jiang [138]), which is too mathematical for me to understand. Sad.

Coutinho and Fernandez [56] *Extended symbolic dynamics in bistable CML: Existence and stability of fronts*, (1997) has a discrete model of reaction diffusion dynamics, with a *linear spatiotemporal code*.

W. Just [140]

Just [141] *Equilibrium phase transitions in coupled map lattices: A pedestrian approach*. A class of piecewise linear coupled map lattices with simple symbolic dynamics is constructed. It can be solved analytically in terms of the statistical mechanics of spin lattices. The corresponding Hamiltonian is written down explicitly in terms of the parameters of the map. The method works only for map lattices with repelling invariant sets. Not of interest to us, I think.

Just [142] *On symbolic dynamics of space-time chaotic models*

Atay, Jalan and Jost [14] study coupled map networks with multiple time delays; of no current interest for us.

**2016-11-13 Predrag Potential inserts, varied temptations**

B. Fernandez and P. Guiraud [82]

B. Fernandez and M. Jiang [83]: “two diffusively coupled identical unimodal maps [...] the eventual periodicity of the position of orbits with respect to the diagonal of the square phase space and the asymptotic periodicity for orbits whose coordinates have the same sign. [...] a global condition for the existence of symmetric orbits.

**2022-02-19 Predrag** W. Just and F. Schmüser [143] *On phase transitions in coupled map lattices*: “ In order to tackle such a problem one assigns *symbol lattice* to each spatio-temporal pattern. One dimension of the symbol lattice corresponds to the temporal evolution in the dynamical system whereas the other dimensions of the symbol lattice take the spatial extension of the dynamical system into account.

Thus we end up with a nearest neighbour coupled two-dimensional Ising model.

Summarising, by adopting a symbolic description and translating the time into a lattice dimension dynamical properties may be reformulated within the concepts of canonical equilibrium statistical mechanics. For expansive dynamical systems we obtain Hamiltonians with short range interaction.”

R. S. MacKay, Dynamics of networks: features that persist from the uncoupled limit, in “Stochastic and spatial structures of dynamical systems”, eds. S. J. van Strien, S. M. Verduyn Lunel (North Holland, 1996), 81–104.

Ya. B. Pesin, Ya. G. Sinai [207] (1988).

## 8.2 Helmholtz type equations

The inhomogeneous *Helmholtz equation* is an elliptical equation of form

$$(\square + k^2) \phi(x) = -4\pi\rho(x), \quad x \in \mathbb{R}^d, \quad (8.10)$$

where the field  $\phi(x)$  is a  $C^2$  function of coordinates, and  $\rho(x)$  is a density function with compact support. Its Green’s function satisfies

$$(\square + k^2) g(x, x') = \delta(x - x'). \quad (8.11)$$

For example, in  $d = 3$  dimensions the stationary wave, the outgoing wave and the incoming wave Green’s functions are:

$$\begin{aligned} g_0(x, x') &= -\frac{\cos(k|x - x'|)}{4\pi|x - x'|} \\ g_+(x, x') &= -\frac{e^{ik|x - x'|}}{4\pi|x - x'|} \\ g_-(x, x') &= -\frac{e^{-ik|x - x'|}}{4\pi|x - x'|}. \end{aligned} \quad (8.12)$$

Furthermore, to these any solution to the homogeneous Helmholtz equation

$$(\square + k^2) f_0(x, x') = 0$$

can be added. On infinite space, the solution of (8.10) is of the form

$$\phi(x) = \phi_0(x) - \int_V d^d x' \rho(x') g(x, x'), \quad (8.13)$$

where  $(\square + k^2) \phi_0(x) = 0$ .

### 8.2.1 Poisson and Laplace's equations

The *Poisson equation* is the  $k \rightarrow 0$  limit of the Helmholtz equation;

$$\square \phi(x) = -4\pi\rho(x), \quad x \in \mathbb{R}^d, \quad (8.14)$$

with Green's function

$$g(x, x') = -\frac{1}{4\pi|x - x'|}. \quad (8.15)$$

For  $\rho = 0$ , the equation is known as *Laplace's equation*.

### 8.2.2 Screened Poisson equation

For the  $\mu^2 = -k^2 > 0$  (imaginary  $k$ ), the equation

$$(-\square + \mu^2) \phi(x) = 4\pi\rho(x), \quad x \in \mathbb{R}^d, \quad (8.16)$$

is known as the *screened Poisson equation* [84], Klein–Gordon or *Yukawa equation*.

The name arises from its applications to electric field screening in plasmas. In chemistry the equation governs steady-state diffusion in presence of the solute  $\rho(x)$  piped in or generated by a chemical reaction, or of heat diffusion in presence of heat sources.

The solutions of the screened Poisson equation (8.16) are of the same form as for the Helmholtz equation, but with the oscillatory  $\sin$ ,  $\cos$ , and  $\exp(i \cdot \cdot \cdot)$  solutions replaced by the hyperbolic  $\sinh$ ,  $\cosh$ , and  $\exp(- \cdot \cdot \cdot)$ .

The outgoing Green's function (8.12) is here known as the *Yukawa potential*, the static, spherically symmetric solution

$$g(x, x') = -\frac{e^{-\mu|x-x'|}}{4\pi|x-x'|}. \quad (8.17)$$

to the Klein–Gordon equation. The Fourier transform relates the Yukawa potential to the massive scalar particle propagator, i.e., Green's function of the static Klein–Gordon equation (8.25),

$$V(\mathbf{r}) = \frac{-g^2}{(2\pi)^3} \int e^{i\mathbf{k}\cdot\mathbf{r}} \frac{4\pi}{k^2 + \mu^2} d^3k.$$

In  $d = 2$  this integral can be explicitly evaluated as a Bessel function,<sup>2</sup>

$$g(\mathbf{r}, 0) = \frac{1}{2\pi} \int_0^{+\infty} dk_r \frac{k_r J_0(k_r r)}{k_r^2 + \mu^2} = \frac{1}{2\pi} K_0(r\mu). \quad (8.18)$$

### 8.2.3 Klein–Gordon equation

**wiki says:** The Klein–Gordon equation for a scalar particle of mass  $m$  and complex-valued function  $\psi(t, \mathbf{x})$  of the time variable  $t$  and space variables  $\mathbf{x}$ ,

$$\frac{1}{c^2} \frac{\partial^2}{\partial t^2} \psi - \nabla^2 \psi + \frac{m^2 c^2}{\hbar^2} \psi = 0, \quad (8.19)$$

is derived by requiring that its plane-wave solutions

$$\psi = e^{-i\omega t + i\mathbf{k} \cdot \mathbf{x}} = e^{ik_\mu x^\mu} \quad (8.20)$$

obey the energy–momentum relation of special relativity,

$$-p_\mu p^\mu = E^2 - \mathbf{p}^2 = \omega^2 - \mathbf{k}^2 = -k_\mu k^\mu = \mu^2, \quad (8.21)$$

with  $(-, +, +, +)$  metric. It is written compactly in *natural units*,

$$(\square + \mu^2)\psi = 0, \quad (8.22)$$

where  $\mu = mc/\hbar$ , and

$$\square = -\partial_\nu \partial^\nu = \frac{1}{c^2} \frac{\partial^2}{\partial t^2} - \nabla^2 \quad (8.23)$$

is the *d'Alembert operator*, while the scalar operator

$$\Delta = \nabla^2 = \frac{\partial^2}{\partial x^2} + \frac{\partial^2}{\partial y^2} + \frac{\partial^2}{\partial z^2}, \quad (8.24)$$

is called the *Laplacian* or the *Laplace operator*.

Writing the equation as

$$-\partial_t^2 \psi + \nabla^2 \psi = \mu^2 \psi, \quad (8.25)$$

we note that for the time-independent solutions, the Klein–Gordon equation becomes the homogeneous *screened Poisson equation*

$$(\nabla^2 - \mu^2) \psi(\mathbf{r}) = 0. \quad (8.26)$$

---

<sup>2</sup>Predrag 2020-10-31: Recheck the  $2\pi$  factors

### 8.2.4 Spatiotemporal cat equation

The Yukawa massive field mass parameter is related to the spatiotemporal cat stretching parameter  $s$  by

$$\mu^2 = d(s - 2). \quad (8.27)$$

The  $d$ -dimensional, purely hyperbolic  $\mu^2 > 0$  spatiotemporal cat

$$(-\square + \mu^2 \mathbf{1})_{zz'} \phi_{z'} - m_z = 0, \quad \phi_z \in \mathbb{T}^1, \quad m_z \in \mathcal{A}^1, \quad z \in \mathbb{Z}^d, \quad (8.28)$$

that we study is a discretization of the inhomogeneous *screened Poisson equation* (8.26), while the discretization of the Helmholtz equation corresponds to  $s < 2$ .

We denote the differential operator by the d'Alembert  $\square$  rather than the Laplacian  $\Delta$  (8.24) to emphasize that we are studying the spatiotemporal spatiotemporal cat rather than the temporally static solutions (8.26).

### 8.2.5 Helmholtz blog

**wiki:** In the inhomogeneous case, the only difference between the inhomogeneous screened Poisson equation and the inhomogeneous Helmholtz equation is the the sign of the  $\mu^2$  parameter.

**2017-09-11 Predrag** Katsura [151] *Lattice Green's function. Introduction:* The Helmholtz equation for the wavefunction  $\psi(r)$  in the continuous space is given by

$$\left( \frac{1}{2} \Delta + E \right) \psi = 0 \quad (8.29)$$

The Green's function  $g(E, r)$  is the solution of

$$\left( \frac{1}{2} \Delta + E \right) g = \delta(r) \quad (8.30)$$

**2020-10-31 Predrag** In sect. 1.30 *Introduction*, Gradshteyn and Ryzhik write:

The trigonometric and hyperbolic sines are related by the identities

$$\sinh x = \frac{1}{i} \sin(ix), \quad \sin x = \frac{1}{i} \sinh(ix). \quad (8.31)$$

The trigonometric and hyperbolic cosines are related by the identities

$$\cosh x = \cos(ix), \quad \cos x = \cosh(ix). \quad (8.32)$$

Because of this duality, every relation involving trigonometric functions has its formal counterpart involving the corresponding hyperbolic functions, and vice versa. In many cases, both pairs of relationships are meaningful.



In sect. 6.94 *Relationships between eigenfunctions of the Helmholtz equation in different coordinate systems* they define the scalar Helmholtz equation as

$$(\nabla^2 + k^2)\Psi = 0, \quad (8.33)$$

with a 3-dimensional Laplacian (8.24), and a Cartesian particular solution of form

$$\Psi_{k_x k_y k_z}(x, y, z) \propto e^{i(k_x x + k_y y + k_z z)} \text{ with } k^2 = k_x^2 + k_y^2 + k_z^2. \quad (8.34)$$

**2017-09-09 Predrag** Hu and O’Connell [124] also state the discretized version of the solution (8.15) for  $s = 2$ , which, unlike (2.51) has no exponentials - it’s a power law.

I find **Robert E. Hunt notes** quite good, both for the continuum case, and for solving the lattice discretization.

**2020-10-31 Predrag** In publications, it would be nice if we could refer to Gradshteyn and Ryzhik [101] whenever we mention continuum limits of our discretized equations. It’s the best known, classical reference.

Unfortunately, Gradshteyn and Ryzhik [101] do not define the Laplace equation and (damped?) screened Poisson equation, see [wiki](#). For that, we should combine our definitions (8.11), (8.29), (8.201), (8.202), see also **2017-09-09 Predrag**, **2020-01-13 Predrag**, and discretizations of Helmholtz [67, 168] and screened Poisson [42, 68, 100, 124, 125] (also known as Klein–Gordon or Yukawa) equations.

**2023-07-15 Predrag** In the case of fully periodic BC, the most natural (and efficient) approach to the problem is the reciprocal space treatment.

[physics.stackexchange](#) has a clean derivation:

The Fourier transform

$$G(x, y) = \int \frac{d^d k}{(2\pi)^d} \frac{e^{ik \cdot (x-y)}}{k^2 + \mu^2}. \quad (8.35)$$

In  $d$  dimensions:

$$(-\square^2 + \mu^2)G(\mathbf{x}, \mathbf{x}') = A\delta(\mathbf{x} - \mathbf{x}'), \text{ b.c. } \lim_{|\mathbf{x} - \mathbf{x}'| \rightarrow \infty} G(\mathbf{x}, \mathbf{x}') = 0 \quad (8.36)$$

The solution is radially symmetric

$$G(r) = \frac{A}{(2\pi)^{d/2}} \left(\frac{\mu}{r}\right)^{d/2-1} K_{d/2-1}(\mu r), \quad r = |\mathbf{x} - \mathbf{x}'|, \quad (8.37)$$

where  $K_{d/2-1}(r)$  is the modified Bessel function of the second kind.

$d = 1$  (fix normalization?)

$$G(r) = \frac{1}{2\mu} e^{-\mu r}, \quad (8.38)$$

$d = 2$  is given by (??).

$d = 3$

$$G(r) = \frac{1}{4\pi r} e^{-\mu r}, \quad (8.39)$$

Asymptotics for  $r$  large

$$K_\nu(\mu r) \sim \sqrt{\frac{\pi}{2\mu r}} e^{-\mu r} \quad (8.40)$$

seems to contradict (8.38)?

Let  $g(x, x')$ , with  $x, x' \in \mathcal{R}$  be the corresponding Green's function on a bounded, simply connected domain  $\mathcal{R} \subset \mathbb{R}^d$ , satisfying some boundary condition (e.g., periodic, Dirichlet or Neumann) at  $\partial\mathcal{R}$ . The Green's function identity allows us to connect the values of  $x_z$  inside of  $\mathcal{R}$  with the ones attained at the boundary (an arbitrary Soviet citation):

$$\begin{aligned} x(z) &= \int_{\mathcal{R}} g(z, z') m(z') dz' \\ &- \int_{\partial\mathcal{R}} \nabla_n g(z, z'') x(z'') dz'' + \int_{\partial\mathcal{R}} \nabla_n x(z'') g(z, z'') dz''. \end{aligned} \quad (8.41)$$

The Neumann boundary condition can be imposed by extending the original field symmetrically across its sides, so that the extended field, which is four times bigger, is symmetric and periodic.

At the risk of sounding repetitive: it's crazy to formulate this problem in terms of the symmetry-breaking domains with Dirichlet boundary conditions, when all that is needed are the trivial periodic solutions on 2-dimensional tori. To appreciate how difficult the Dirichlet problem is, you can at your leisure study the paper *On the solution of the Helmholtz equation on regions with corners* by Soviet mathematicians Serkh and Rokhlin [222] (one of them a Member of The National Academy of Sciences of The USA), who solve several boundary value problems for the Helmholtz equation on polygonal domains. In terms of the boundary integral equations of potential theory, the solutions are representable by series of appropriately chosen Bessel functions. Making the space discrete does not make these calculations any easier.

### 8.3 Green's function for 2-dimensional square lattice

Copied to here from *siminos/cats/GHJSC16.tex*

2019-10-31

The free Green's function  $\mathbf{g}(z, z') \equiv \mathbf{g}(z - z', 0) \equiv \mathbf{g}_{zz'}$  solves the equation

$$(-\square + \mu^2)\mathbf{g}_{zz'} = \delta_{zz'}, \quad z = (n, t) \in \mathbb{Z}^2. \quad (8.42)$$

The solution is given by the double integral [181]

$$\mathfrak{g}_{z0} = \frac{1}{\pi^2} \int_0^\pi \int_0^\pi \frac{\cos(nx) \cos(ty)}{s - 2 \cos x - 2 \cos y} dx dy, \quad (8.43)$$

an expression which can, in turn, be recast into single integral form,

$$\begin{aligned} \mathfrak{g}_{z0} &= \frac{1}{2\pi^3} \int_{-\infty}^{+\infty} d\eta \int_0^\pi \int_0^\pi \frac{\cos(nx) \cos(ty)}{(s/2 - 2 \cos x - i\eta)(s/2 - 2 \cos y + i\eta)} dx dy \\ &= \frac{1}{2\pi} \int_{-\infty}^{+\infty} d\eta \frac{\mathcal{L}(\eta)^{-n} \mathcal{L}^*(\eta)^{-t}}{|\mathcal{L}(\eta) - \mathcal{L}(\eta)^{-1}|^2}, \end{aligned} \quad (8.44)$$

where

$$\mathcal{L}(\eta) + \mathcal{L}(\eta)^{-1} = s/2 + i\eta, \quad |\mathcal{L}(\eta)| > 1. \quad (8.45)$$

The above equation can be thought as the integral over a product of two  $\mathbb{Z}^1$  functions:

$$\mathfrak{g}_{z0} = \frac{1}{2\pi} \int_{-\infty}^{+\infty} d\eta \mathfrak{g}_{n0}(s/2 + i\eta) \mathfrak{g}_{t0}(s/2 - i\eta). \quad (8.46)$$

An alternative representation is given by modified Bessel functions  $I_n(x)$  of the first kind [181]:

$$\mathfrak{g}_{z0} = \int_0^{+\infty} d\eta e^{-s\eta} I_n(\eta) I_t(\eta), \quad (8.47)$$

which demonstrates that  $\mathfrak{g}_{zz'}$  is positive for all  $z = (n, t)$ . The representation (8.47) enables explicit evaluation of the  $n = t$  diagonal elements in terms of a Legendre function,

$$\mathfrak{g}_{z0} = \frac{1}{2\pi i} Q_{n-1/2}(s^2/8 - 1), \quad s^2/8 - 1 > 1, \quad z = (n, n).$$

**Dirichlet boundary conditions.** Consider next the Green's function  $\mathfrak{g}_{zz'}$  which satisfies (8.42) within the rectangular domain  $\mathcal{R} = \{(n, t) \in \mathbb{Z}^2 | 1 \leq n \leq \ell_1, 1 \leq t \leq \ell_2\}$  and vanishes at its boundary  $\partial\mathcal{R}$ . By applying the same method as in the case of 1-dimensional lattices we get

$$\begin{aligned} \mathfrak{g}_{zz'} &= \sum_{j_1, j_2 = -\infty}^{+\infty} \mathfrak{g}_{n-n'+2j_1(\ell_1+1), t-t'+2j_2(\ell_2+1)} + \mathfrak{g}_{n+n'+2j_1(\ell_1+1), t+t'+2j_2(\ell_2+1)} \\ &\quad - \mathfrak{g}_{n-n'+2j_1(\ell_1+1), t+t'+2j_2(\ell_2+1)} - \mathfrak{g}_{n+n'+2j_1(\ell_1+1), t-t'+2j_2(\ell_2+1)}, \end{aligned}$$

where  $\mathfrak{g}_{zz'}$  is the free Green's function (8.43). Substituting (8.46) yields the spatiotemporal Green's function as a convolution of the two 1-dimensional Green's functions (??)

$$\mathfrak{g}_{zz'} = \frac{1}{2\pi} \int_{-\infty}^{+\infty} d\eta \mathfrak{g}_{nn'}(s/2 + i\eta) \mathfrak{g}_{tt'}(s/2 - i\eta). \quad (8.48)$$

## 8.4 Toeplitz tensors

In sect. 18.2 we worked out the propagator in the only in  $d = 1$  configuration space, and stated the result for  $d > 1$  after the Fourier transform diagonalization. What are the generalizations of Toeplitz matrices to  $d > 1$ ? They are called *Toeplitz tensors*.

**2018-02-24 Predrag** This one I think is not relevant to us: Lim [170] *Singular values and eigenvalues of tensors: A variational approach* - " A theory of eigenvalues, eigenvectors, singular values, and singular vectors for tensors based on a constrained variational approach much like the Rayleigh quotient for symmetric matrix eigenvalues. An illustration: a multilinear generalization of the Perron-Frobenius theorem. "

**2018-02-24 Predrag** Khoromskaia and Khoromskij [156] *Block circulant and Toeplitz structures in the linearized Hartree-Fock equation on finite lattices: Tensor approach* seems quite relevant to our project - they work out the  $D = 3$  lattice case: " grid-based tensor approach to solution of the elliptic eigenvalue problem for the 3D lattice-structured systems. We consider the linearized Hartree-Fock equation over a spatial  $L_1 \times L_2 \times L_3$  lattice for both periodic and non-periodic case. In the periodic case the low-rank tensor structure in the diagonal blocks of the Fock matrix in the Fourier space reduces the conventional 3D FFT to the product of 1D FFTs. "

Xie, Jin and Wei [255] *A fast algorithm for solving circulant tensor systems*: " Circulant tensors is a generalization of the circulant matrix. We define the generalized circulant tensors which can be diagonalized by a Fourier matrix, and solve the circulant tensor system by a fast FFT algorithm. "

Cui *et al.* [60] *An eigenvalue problem for even order tensors with its applications*: " Using the matrix unfolding of even order tensors, we can establish the relationship between a tensor eigenvalue problem and a multi-level matrix eigenvalue problem. We show that higher order singular values are the square root of the eigenvalues of the product of the tensor and its conjugate transpose, as in the matrix case. Also we study an eigenvalue problem for Toeplitz/circulant tensors, and give the lower and upper bounds of eigenvalues of Toeplitz tensors. "

Rezghi and Eldén [218] *Diagonalization of tensors with circulant structure*: " A tensor of arbitrary order, which is circulant with respect to two modes, can be diagonalized in those modes by discrete Fourier transforms. This property can be used in the efficient solution of linear systems involving contractive products of tensors with circulant structure. Tensors with circulant structure occur in models with periodic boundary conditions. "

**2018-02-24 Predrag** In 2007 the N-way Toolbox, Tensor Toolbox, and Multilinear Engine were software packages for working with tensors.

block-Toeplitz matrix

A tensor can be regarded as a multidimensional array of data. The order of a tensor is the number of dimensions. The dimensions of a tensor also are known as *ways* or *modes*.

Multilevel matrices arise in multidimensional applications.

## 8.5 Green's blog

**2016-07-13 Predrag** Cat map Green's functions are standard 'lattice propagators' for discrete lattices, obtained by discrete Fourier transform diagonalization of discrete Laplacian. Working through ChaosBook sections *D.3 Lattice derivatives* to *D.5.2 Lattice Laplacian diagonalized* might help you understand this material.

Note: All eq. numbers refer to svn ver. 5020 of [160521Gutkin.pdf](#) and ChaosBook.org [ver. 15.7](#). You can also use [current ver.](#), but the chapter numbering is different.

**2017-02-17 Predrag** For diffusion, a linear (symmetric, Vivaldi) code is needed. For spatiotemporal cat

1. linear code seems needed. Have not proven that.
  2. its partition volumes have no relation to 2-tori weights
  3. linear code pruning rules undercount 2-tori pruning rules
  4. 2-tori are intrinsic to the flow, there might exist Markov partitions
- Boris 2017-02-17** Markov partitions for spatiotemporal cats exist, but their complexity grows exponentially with number of cats.
- Predrag 2017-03-04** That is what you keep saying, but if you mean *finite* Markov partitions for *the* spatiotemporal cat, even on a finite spatially periodic domain, I have never seen it. It would require high-dimensional unstable/stable manifolds of the fixed point at the origin to map onto each other, in order to get a generating partition consisting of a finite number of volumes. Pretty amazing.

**2017-08-25 Predrag** I have not understood this before, but the  $\mathcal{R} = [2 \times 1]$  block

$$M = \begin{bmatrix} s_{11} & s_{21} \end{bmatrix}$$

is not just a 1D temporal cat - the Dirichlet boundary conditions make this nasty as well,

$$M \cup \partial\mathcal{R} = \begin{bmatrix} x_{12}x_{22} \\ x_{01}s_{11}s_{21}x_{31} \\ x_{10}x_{20} \end{bmatrix}.$$

**2017-08-25 Predrag**  $\partial\mathcal{R} = \{x_1, x_2, \dots, x_8\}$  is not consistent with our notation: they live on sites, and should be labelled by index pairs  $\partial\mathcal{R} = \{x_z\}_r$  in

$\mathcal{R} = [2 \times 1]$  example as  $\partial\mathcal{R} = \{x_{01}, x_{02}, x_{13}, \dots, x_{10}\}$ . That is consistent with the cat map, where the corresponding block + boundary points is correctly labelled as  $x_0 s_1 s_2 x_3$ . The crazy thing is that even with the correct notation, there is no rhyme nor reason in the above 8 inequalities.

$$\begin{aligned} 0 &\leq (x_{01} + x_{10} - s_{12})(s^2 - 2) + (x_{13} + x_{02} + x_{31} + x_{20} - s_{22} - s_{11})s + (x_{23} + x_{32} - s_{21})2 \leq \nu_s \\ 0 &\leq (x_{02} + x_{13} - s_{22})(s^2 - 2) + (x_{01} + x_{10} + x_{23} + x_{32} - s_{12} - s_{21})s + (x_{20} + x_{31} - s_{11})2 \leq \nu_s \\ 0 &\leq (x_{20} + x_{31} - s_{11})(s^2 - 2) + (x_{01} + x_{10} + x_{23} + x_{32} - s_{12} - s_{21})s + (x_{02} + x_{13} - s_{22})2 \leq \nu_s \\ 0 &\leq (x_{23} + x_{32} - s_{21})(s^2 - 2) + (x_{13} + x_{02} + x_{31} + x_{20} - s_{22} - s_{11})s + (x_{01} + x_{10} - s_{12})2 \leq \nu_s \end{aligned}$$

**2017-08-30 Boris** In principle you are right, but keeping 2 indices would only make things look terribly “heavy” (without a good justification, as anyway “there is no rhyme nor reason”). The single index notation for the boundary points seems to me the least evil. **2017-09-09 Predrag** not convinced, but this is really a minor point. We follow Boris’ convention.

**2017-09-09 Predrag** Dorr [68] *The direct solution of the discrete Poisson equation on a rectangle*

Hu, Ryu and O’Connell [125] *Analytical solution of the generalized discrete Poisson equation* “ present an analytical solution to the generalized discrete Poisson equation (DPE), a matrix equation which has a tridiagonal matrix with fringes having an arbitrary value for the diagonal elements.”

Many physical problems require the numerical solution of the Poisson equation on a rectangle. In general, one uses the finite-difference method [68], where the rectangle is replaced by an  $N \times k$  grid, and the Poisson equation is solved in the finite-difference representation. In this way, the problem is reduced to the discrete Poisson equation (DPE) on an  $[N \times k]$  grid, a matrix equation  $\mathcal{D}x = s$  having a tridiagonal matrix  $[k \times k]$  with fringes, of form

$$\mathcal{D} = \begin{pmatrix} M & 1 & 0 & 0 & \dots & 0 & 0 \\ 1 & M & 1 & 0 & \dots & 0 & 0 \\ 0 & 1 & M & 1 & \dots & 0 & 0 \\ \vdots & \vdots & \vdots & \vdots & \ddots & \vdots & \vdots \\ 0 & 0 & \dots & \dots & \dots & M & 1 \\ 0 & 0 & \dots & \dots & \dots & 1 & M \end{pmatrix}, \quad (8.49)$$

where  $M$  is a  $[N \times N]$  symmetric tridiagonal matrix (2.38), with constant  $-s$  along the diagonal, and the  $[N \times N]$  identity matrix  $1$  as the off-diagonal elements. Thus, the matrix  $\mathcal{D}$  consists of  $[k \times k]$  submatrices of  $[N \times N]$  elements. An important special case is  $s = 4$ , which is the matrix form for the Poisson equation on a rectangle arising from the difference method.

They invert  $\mathcal{D}$  in three steps:

1. By applying the results of ref. [124], invert  $\mathcal{D}$  into  $\mathcal{D}^{-1}$ . This generalizes (2.51) to a (sub)matrix formula, with  $g_{jk}$  replaced by submatrix  $\Theta_{jk}$ , where  $\Theta$  is an  $[N \times N]$  matrix defined by

$$-2 \cosh \Theta = M$$

2. The eigenvalues and eigenfunctions for the submatrices of the block matrix  $g = \mathcal{D}^{-1}$  are given by (2.49).
3. Evaluate analytically each of the individual elements in the inverted matrix  $\mathcal{D}^{-1}$  by the Schur decomposition scheme [100].

I find the procedure inelegant and cumbersome, as the two dimensions are treated in different ways. The result is, however, a bit more symmetric (but not written fully symmetric), written in terms of coefficients such as:

$$\alpha_{lm}(n) = \sqrt{\frac{2}{N+1}} \sinh \frac{ln\pi}{N+1} \sinh \frac{mn\pi}{N+1}.$$

In contrast, Boris formulation (8.43) is symmetric.

My intuition is explained in sect. 18.2 - the  $d$  translations commute, so should compute eigenvalues for each direction separately. Works out for periodic boundary conditions.

As a wild guess, in  $d$ -dimensional the Jacobian (2.41) for Dirchlet b.c. would generalize to the product of  $d$  Jacobians, one for each direction

$$\det(\mathcal{D}_{\ell_1 \times \ell_2 \times \dots \times \ell_d}) = U_{\ell_1}(s/2)U_{\ell_2}(s/2) \cdots U_{\ell_d}(s/2). \quad (8.50)$$

For example,

$$\det(\mathcal{D}_{1 \times 1}) = U_1(s/2)U_1(s/2) = s^2, \quad (8.51)$$

and

$$\det(\mathcal{D}_{2 \times 2}) = U_2(s/2)U_2(s/2) = (s^2 - 1)^2. \quad (8.52)$$

This naive guess is almost certainly wrong...

How does one get cosh's and sinh's in the circulant matrix case?

**2017-09-09 Predrag** A few more links to digest:

*Eigenvalues of periodic lattice Laplacian?* uses the Kronecker product, and Harshaw gives sensible, symmetric eigenvalues for a doubly-periodic torus, something like

$$\lambda_{jk}^{[\ell_1 \times \ell_2]} = -\mu^2 - 2 \cos \frac{j\pi}{\ell_1} - 2 \cos \frac{k\pi}{\ell_2}, \quad (8.53)$$

where,  $0 \leq j \leq \ell_1 - 1$ ,  $0 \leq k \leq \ell_2 - 1$ , and  $d = 2$ . Their problem is the usual diffusive Laplacian on a square lattice, has no  $s$  term, so this is still only a guess.

Andreas Wipf [250] *Statistical Approach to Quantum Field Theory: An Introduction* ([click here](#)).

[arXiv:math/0010135](#) *Integrable Lattices: Random Matrices and Random Permutations*

[arXiv:1702.00339](#) *Block circulant and Toeplitz structures in the linearized Hartree-Fock equation on finite lattices: tensor approach*

**2017-09-08 Predrag** Giles and Thorn [97] *Lattice approach to string theory*. The Giles-Thorn (GT) discretization of the worldsheet begins with a representation of the free closed or open string propagator as a lightcone worldsheet path integral defined on a lattice.

The sequel Papathanasiou and Thorn [201] *Worldsheet propagator on the lightcone worldsheet lattice* give in Appendix B 2D lattice Neumann open string, Dirichlet open string, and closed string propagators.

*Discrete Green's functions* are explained, for example, by Chung and Yau [49] who give explicitly, in their Theorem 6, a 2-dimensional lattice Green's function for a rectangular  $R^{[\ell_1 \times \ell_2]}$ . I do not understand the paper - in any case, I see no determinants in it. This paper is cited over 100 times, maybe there is a better answer in that list.

**2017-09-11 Boris** Some caution on Green's functions: In 1D everything is explicit and simple. The real problem is  $2D$ . For the paper we need two facts – positivity of its elements, and exponential decay (both for Dirichlet boundary conditions). I was unable to extract them from the literature (which is bizarre), but checked numerically. Proofs are still lacking, but should be within reach.

**2017-09-20 Predrag** Continued feline misery. From the periodic orbit theory point of view, it is insane to work with finite lattice blocks with Dirichlet boundary conditions. The theory demands periodic boundary conditions. They preserve translational invariance which makes Green's matrices trivially diagonalizable by discrete Fourier transforms. Now that Boris is such a mensch that he can do it, I am writing up a pedagogical Dirichlet/periodic b.c.'s Green's matrices appendix to ref. [106] (or per chance even a section of the paper proper, as this is no afterthought - this is the central point of the paper), an appendix whose ultimate goal is to show that the matrix elements are decaying exponentially as

$$\mathcal{D}_{zz'} \approx e^{-\lambda|z-z'|^d}, \quad (8.54)$$

i.e., in our humble  $d = 2$  example as  $\exp(-\lambda|z - z'|^2)$ . If the coauthors were to understand or (gasp!) contribute to the write up, we would be in cat heaven.

So far, still writing up the  $d = 1$  temporal cat example of sect. 2.4, but the determinant of the Helmholtz operator for any finite  $d = 2$  rectangular lattice region of sect. 8.4 should play out the same way.



To Matt and Andy: This goes lock, stock and barrel into the continuum field theories, such as Kuramoto–Sivashinsky, with the Euclidian metric in (8.54) replaced by the (still to be thought through) correct Kuramoto–Sivashinsky spacetime metric.

**2017-10-18 Predrag** Glaser [98] *Numerical solution of waveguide scattering problems by finite-difference Green's functions* computes a 2-dimensional Green's function with boundary conditions on arbitrary shape approximated by a discrete boundary: "A finite-difference Green's function method for solving time-harmonic wave guide scattering problems involving metallic obstacles of finite size is applied to the two-dimensional problem of a TE<sub>10</sub> mode impinging on cylindrical metallic posts of arbitrary shape in a rectangular waveguide."

**2017-10-19 Predrag** de la Llave [174] *Variational methods for quasiperiodic solutions of partial differential equations* has a pedagogical discussion of the discrete lattices gradient flows.

**2019-11-04 Predrag** Doyle and Snell [69] [arXiv:math/0001057](https://arxiv.org/abs/math/0001057) present the connection between random walks and electric networks.

**2020-05-09 Predrag** Sunada [238] *Topological Crystallography* ([click here](#)) Chap. 9 is all about random walks on lattices.

2CB

**2020-05-10 Predrag** Some general graph-theory definitions, from different sources, will eventually be all in ChaosBook *appendMarkov.tex* :

Many follow the definitions in Serre [223] and Stark and Terras [233].

Let  $G = (V, E)$  be a connected *non-directed* graph, with  $V$  the set of  $|V|$  vertices or nodes (assume that there are no 1-degree vertices),  $E$  the set of  $|E|$  unoriented edges (possibly multiple edges and 1-loops) labeled  $e_1, \dots, e_{|E|}$ .

The *adjacency matrix* for an undirected graph with  $n$  nodes is an  $[n \times n]$  matrix (16.11) with  $(i,j)$ -th entry specifying the number of non-directed edges from node  $i$  to  $j$  with  $i$ -th diagonal entry being twice the number of self-adjointing loops on  $i$ -th node.

A graph is *finite* if it has a finite number of and edges. It is *connected* if every node can be reached by traversing a path.

A *rooted graph* is a pair  $(G, v)$ , where  $G$  is a graph and  $v \in V$  is a vertex of  $G$ , called the root.

A graph is *simple* if it has no loops, i.e., no edges of the form  $(u, u)$   $u \in V$  and there is at most a single edge between any two vertices.

A graph is *bi-partite* if its vertices can be partitioned into two disjoint sets  $U$  and  $W$  such that no vertex in  $U$  is adjacent to any other vertex in  $U$  and likewise for  $W$ ; the graph has edges only between "U" and "W" vertices.

In order to define a closed path in a non-directed graph orient the edges in an arbitrary but fixed way. Oriented edge  $e = (u, v) \in E(G)$  joins two vertices, the origin  $u = o(e)$  to the tip  $v = t(e)$ .

The vertices  $o(e)$  and  $t(e)$  are the *extremities* of the edge  $E$ . Two vertices are *adjacent* if they are extremities of an edge.

The *degree* of a vertex  $v$  is  $\text{deg}v = \text{Card}\{e \in E_v : o(e) = v\}$ . A graph is *d-regular* if each vertex has degree  $d$ .

The in-degree (respectively out-degree) of any vertex of a directed graph is the number of in-coming (respectively out-going) edges. For a *directed regular* graph all vertices have equal in-degrees and out-degrees.

A graph is *vertex transitive* if there is a group of automorphisms which is transitive on the vertices. Such a graph is *regular*.

In the physics literature regular trees are called Bethe lattices.

Denote by  $e^{-1} = (v, u)$  the inverse of  $e = (u, v)$ , with the origin  $v$  and the tip  $u$ .

Let  $G'$  be the graph with  $2|E|$  oriented edges built from such oriented graph  $G$  by adding the opposing oriented edges  $e_{|E|+1} = (e_1)^{-1}, \dots, e_{2|E|} = (e_{|E|})^{-1}$ .

If  $e_i$  belongs to an oriented loop,  $e_{i+|E|} = (e_i)^{-1}$  belongs to oriented loop going through the same pair of vertices.

A path  $P = (e_1, \dots, e_n)$  has a backtracking if  $e_{i+1}^{-1} = e_i$ . The path has a *tail* if  $e_0 = e_{n-1}^{-1}$ .

The *inverse cycle* of a cycle  $C = (e_1, \dots, e_n)$  is the cycle  $C^{-1} = (e_n^{-1}, \dots, e_1^{-1})$ .

The cycle  $C$  is called *reduced* if  $C^2$  has no backtrack, and *prime* if it can not be expressed as  $C = D^f$  for any cycle  $D$  and  $f \geq 2$ .

A cycle  $C$  is *prime* if it is not a repeat of a strictly smaller cycle.

Cycles  $C_1 = (e_1, \dots, e_n)$  and  $C_2 = (f_1, \dots, f_n)$  are called *equivalent* if there exists  $k$  such that  $f_j = e_j + k$  for all  $j$ . Let  $[C]$  be the equivalence class which contains a cycle  $C$ .

For a cycle  $C$ , the equivalence class  $[C]$  is the set of cyclic permutations of  $C$ , i.e., cycles are equivalent up to choice of the initial/terminal vertex.

A 'prime cycle' ('orbit') is non-backtracking, tailless and not a  $r$ -multiple cycle.

A geodesic in a graph is a path without back-tracking, consistent with Riemannian geometry where a geodesic is a path which is locally distance minimizing. A closed geodesic is a closed path without back-tracking or tails.

A *tree* is a connected nonempty graph without geodesic loops.

In Riemannian geometry geodesics are locally distance minimizing paths and the difference between a *geodesic loop* and a *closed geodesic* is that the latter is required to be differentiable also at the starting/ending point.

A path is closed if  $e_0 = e_n$ . A geodesic is a path without backtracking. A geodesic loop (or circuit in Serre's terminology) is a closed path that is a geodesic. A closed geodesic is a closed path with no tail and without backtracking.

The path of length zero counts as a closed geodesic and, therefore, is a geodesic loop. Additionally, every closed path with one edge counts as a closed geodesic. Any length two geodesic loop is also a closed geodesic, but the closed path  $e e^{-1}$  is neither.

A *prime* geodesic is an equivalence class of closed geodesics  $[C]$  (where the equivalence class is forgetting the starting point) which is primitive in the sense that it is not a power of another closed geodesic. The latter means by definition that there is no closed geodesic  $d$  and integer  $n > 1$  such that  $[C] = [d^n]$ , which says in words that  $c$  is not just a geodesic that traverses another one  $n$  number of times.

In graph theory the names for "closed geodesics" or "geodesic loops", range from circuits, loops etc, to closed paths without backtracking and no tails.

In terms of a graph  $G = (V, E)$ , a random walk is a stochastic process associated with a positive-valued function  $p$  on  $E$  satisfying

$$\sum_{e \in E_v} p(e) = 1.$$

$p(e)$  is the transition probability that a random walker at  $o(e)$  moves to  $t(e)$  along the edge  $e$ . The transition operator  $P : C(V) \rightarrow C(V)$ ,  $C(V)$  the space of functions on  $V$ , is defined by

$$Pf(x) = \sum_{e \in E_v} p(e)f(t(e)).$$

The  $n$ -step transition probability  $p(n, x, y)$  is the probability that after the  $n$ -steps a random walker at the initial site  $x$  is found at  $y$ ,

$$(P^n) f(x) = \sum_{y \in V} p(n, x, y)f(y).$$

The *simple random walk* on  $G = (V, E)$  is the walk such that the probabilities moving along out-going edges from a vertex are the same, with the transition probability  $p(e) = 1/\deg o(e)$ .

The operator  $P - I$  is the discrete Laplacian associated with the weight functions  $m_V(v) = \deg v$ ,  $m_E = 1$ ,

$$((P^n - I)f)(v) = \frac{1}{\deg v} \sum_{e \in E_v} [f(t(e)) - f(o(e))]. \quad (8.55)$$

$P_v - I$  is the discrete analogue of the *twisted Laplacian* [237]<sup>4 5</sup>

Let  $\Lambda$  be a Bravais lattice. Then  $P$  is  $\Lambda$ -equivariant, and is related to the transition operator  $P_0$  associated with the simple random walk on over a finite graph  $G_0 = (V_0, E_0)$  as

$$P(f \circ \omega) = (P_0(f)) \circ \omega,$$

where  $f$  is an arbitrary function on  $V_0$ , and  $\omega : G \rightarrow G_0$  is the covering map.

**2020-05-11 Predrag** Bharatram Rangarajan *A combinatorial proof of Bass's determinant formula for the zeta function of regular graphs*, [arXiv:1706.00851](https://arxiv.org/abs/1706.00851):

For an integer  $d \geq 2$ , let  $G = (V, E)$  be a finite  $d$ -regular undirected graph with adjacency matrix  $A$ . A *walk* on the graph  $G$  is a sequence  $v_0 v_1 \dots v_k$  where  $v_0, v_1, \dots, v_k$  are (not necessarily distinct) vertices in  $V$ , and for every  $0 \leq i \leq k-1$ ,  $(v_i, v_{i+1}) \in E$ . The vertex  $v_0$  is referred to as the *root* (or *origin*) of the above walk,  $v_k$  is the *terminus* of the walk, and the walk is said to have length  $k$ .

It is often useful to equivalently define a walk as a sequence of directed or oriented edges. Associate each edge  $e = (v, w) \in E$  with two directed edges (or rays) denoted

$$\vec{e} = (v \rightarrow w)$$

$$\vec{e}^{-1} = (w \rightarrow v)$$

Note that the origin  $org(\vec{e})$  is the vertex  $v$  and its terminus  $ter(\vec{e})$  is the vertex  $w$ . Similarly, the origin  $org(\vec{e}^{-1})$  is the vertex  $w$  and its terminus  $ter(\vec{e}^{-1})$  is the vertex  $v$ . Let  $\vec{E}$  denote the set of  $m = nd$  directed edges of  $G$ . So a walk of length  $k$  can equivalently be described as a sequence  $\vec{e}_1 \vec{e}_2 \dots \vec{e}_k$  of  $k$  (not necessarily distinct) oriented edges in  $\vec{E}$  such that for every  $1 \leq i \leq k-1$ ,

$$ter(\vec{e}_i) = org(\vec{e}_{i+1})$$

This is a walk that starts at  $org(\vec{e}_1)$  and ends at  $ter(\vec{e}_k)$ .

It is easy to show that for any  $k \in \mathbb{Z}$ , the number of walks of length  $k$  between vertices  $u, v \in V$  is exactly  $(A^k)_{u,v}$ . In particular, the total number of rooted cycles of length  $k$  in  $G$  is exactly

$$\text{tr}(A^k)$$

A *non-backtracking walk* of length  $k$  from  $v_0 \in V$  to  $v_k \in V$  is a walk  $v_0 v_1 \dots v_k$  such that for every  $1 \leq i \leq k-1$ ,

$$v_{i-1} \neq v_{i+1}$$

<sup>4</sup>Predrag 2020-05-05: Looked at Sunada [237], but still not sure what is a 'twisted' Laplacian.

<sup>5</sup>Predrag 2020-05-13: Why  $1/\deg v$  in (8.55)?

Equivalently, a non-backtracking walk of length  $k$  from  $v \in V$  to  $w \in V$  is a walk  $\vec{e}_1 \vec{e}_2 \dots \vec{e}_k$  such that  $org(\vec{e}_1) = v$ ,  $ter(\vec{e}_k) = w$  and for every  $1 \leq i \leq k-1$ ,

$$\vec{e}_{k+1} \neq \vec{e}_k^{-1}$$

Non-backtracking random walks on graphs have been studied in the context of mixing time [cite alon], cut-offs [cite peres], and exhibit more useful statistical properties than ordinary random walks. In [cite peres], the authors obtain further interesting results on the eigendecomposition of the Hashimoto matrix  $H$ .

A rooted, non-backtracking cycle of length  $k$  with root  $v$  is a non-backtracking walk  $v, v_1, v_2, \dots, v_{k-1}, v$  with the additional boundary constraint that

$$v_1 \neq v_{k-1}$$

Let  $\mathcal{C}$  denote the set of all rooted, non-backtracking, closed walks in  $G$ , and for  $C \in \mathcal{C}$ , let  $|C|$  denote the length of the walk  $C$ . There are two elementary constructions we can carry out to generate more elements of  $\mathcal{C}$  from a given cycle  $C$ :

- *Powering*: Given a rooted, non-backtracking closed walk  $C \in \mathcal{C}$  of length  $k$  of the form

$$C = \vec{e}_1 \vec{e}_2 \dots \vec{e}_k$$

then for  $m \geq 1$  define a power

$$C^m = \underbrace{\vec{e}_1 \dots \vec{e}_k \vec{e}_1 \dots \vec{e}_k \dots \vec{e}_1 \dots \vec{e}_k}_{m \text{ times}}$$

which is a concatenation of the string of edges corresponding to the walk  $C$  with itself  $m$  times. Note that  $C^m$  is also a rooted, non-backtracking closed walk in  $G$  of length  $mk$ . Essentially,  $C^m$  represents the walk obtained by repeating or winding the walk  $C$   $m$  times. Also note that  $C$  and  $C^m$  are both rooted at the same vertex.

- *Cycle class*: Given a rooted, non-backtracking closed walk  $C \in \mathcal{C}$  of length  $k$  of the form

$$C = \vec{e}_1 \vec{e}_2 \dots \vec{e}_k$$

we can form another walk

$$C^{(2)} = \vec{e}_2 \vec{e}_3 \dots \vec{e}_k \vec{e}_1$$

which is also a rooted, non-backtracking closed walk in  $G$  of length  $k$ , but now rooted at the origin of the directed edge  $\vec{e}_2$  (or the terminus of  $\vec{e}_1$ ). More generally, for  $1 \leq j \leq k$ , define

$$C^{(j)} = \vec{e}_j \vec{e}_{j+1} \dots \vec{e}_k \vec{e}_1 \vec{e}_2 \dots \vec{e}_{j-1}$$

which is a cyclic permutation of the walk  $C$  obtained by choosing a different root. So given a walk  $C \in \mathcal{C}$  of length  $k$ , we get  $k - 1$  additional walks in  $\mathcal{C}$  of length  $k$  for free this way. In fact, this defines an equivalence class  $\sim$  on  $\mathcal{C}$ , and the set

$$[C] = \{C^{(1)}, C^{(2)}, \dots, C^{(k)}\}$$

is called the equivalence class of  $C$ . An element  $[C] \in \mathcal{C} / \sim$  represents a non-backtracking closed walk modulo a choice of root.

**2019-10-31 Predrag Guttman [110]** *Lattice Green's functions in all dimensions* starts the way I understand, with random walks on lattices ( **Wanderings of a drunken snail**), apparently discussed eruditely by Hughes [127] and also used in the calculation of the effective resistance of resistor networks [58], but then quickly leads to an amazing range of deep mathematics which we can safely ignore (though not some of the references).

“ for a translationally invariant walk on a  $d$ -dimensional periodic Bravais lattice, a natural question to ask is the probability that a walker starting at the origin of a lattice will be at position  $z$  after  $n$  steps. The probability-generating function is known as the lattice Green's function  $g_{z,0}$ . [...] the *structure function* of the lattice and is given by the discrete Fourier transform of the individual step probabilities. For example, for the  $d$ -dimensional hypercubic lattice, the structure function is

$$\lambda(k) = \frac{1}{d}(\cos k_1 + \cos k_2 + \dots + \cos k_d).$$

Harshaw (8.53) seem to be in the same spirit.

[...] The probability of returning to the origin is

$$1 - 1/g_{0,0}.$$

Since  $g_{0,0}$  diverges for two-dimensional lattices, the probability of returning to the origin by a random walker in two dimensions is certain. [...] For the infinite square lattice, the result is remarkably simple:

$$g_{z,0}(u) = \frac{2}{\pi} K(u)$$

where  $K(u)$  is the complete elliptic integral of the first kind (8.170), with hypergeometric representation

$$K(u) = \frac{\pi}{2} {}_2F_1\left(\frac{1}{2}, \frac{1}{2}; 1; u\right) \tag{8.56}$$

For the square lattice, we can also use the equivalent structure function

$$\lambda(k) = \cos k_1 \cos k_2,$$

demonstrating that structure functions for a given lattice are not unique. [...] In  $d = 3$  the result for the simple cubic case is a saga in itself. [...] ”

**2020-02-09 Predrag** Chen [46] *On the solution of circulant linear systems*: In the case where multidimensional problems are concerned, the matrices of coefficients of the resulting linear systems are block circulant matrices. After some transformations and permutations we are led to a block diagonal matrix with circulant blocks on the diagonal. This reduces the problem to the solution of  $n$  circulant linear systems, which may be performed in parallel. An important example is the finite difference approximate solution of elliptic equations over a rectangle with periodic boundary conditions [42, 251].

Sect. 4: A block matrix is a matrix defined by smaller matrices, called blocks. A block matrix  $M$ , where each of the blocks  $M_i$  is itself a circulant, is called block circulant with circulant blocks. He first extracts eigenvalues of circulant blocks, then inserts them into the large matrix.

It is well known [42] that the approximation of Poisson's equation on a rectangle subject to periodic boundary conditions in both directions by the standard five-term difference scheme on a uniform mesh results in the block circulant linear system.

He also solves biharmonic (Laplacian squared) equation with the standard 13-term difference approximation.

**2020-02-16 Predrag** An example computed for *CL18.tex*, using *siminos/mathematica/Tensors.nb*

Block circulant with circulant blocks [42, 46]  $\mathcal{J}_{[4 \times 2]} =$

$$\left( \begin{array}{cccc} \begin{pmatrix} -2s & 2 \\ 2 & -2s \end{pmatrix} & \begin{pmatrix} 1 & 0 \\ 0 & 1 \end{pmatrix} & \begin{pmatrix} 0 & 0 \\ 0 & 0 \end{pmatrix} & \begin{pmatrix} 1 & 0 \\ 0 & 1 \end{pmatrix} \\ \begin{pmatrix} 1 & 0 \\ 0 & 1 \end{pmatrix} & \begin{pmatrix} -2s & 2 \\ 2 & -2s \end{pmatrix} & \begin{pmatrix} 1 & 0 \\ 0 & 1 \end{pmatrix} & \begin{pmatrix} 0 & 0 \\ 0 & 0 \end{pmatrix} \\ \begin{pmatrix} 0 & 0 \\ 0 & 0 \end{pmatrix} & \begin{pmatrix} 1 & 0 \\ 0 & 1 \end{pmatrix} & \begin{pmatrix} -2s & 2 \\ 2 & -2s \end{pmatrix} & \begin{pmatrix} 1 & 0 \\ 0 & 1 \end{pmatrix} \\ \begin{pmatrix} 1 & 0 \\ 0 & 1 \end{pmatrix} & \begin{pmatrix} 0 & 0 \\ 0 & 0 \end{pmatrix} & \begin{pmatrix} 1 & 0 \\ 0 & 1 \end{pmatrix} & \begin{pmatrix} -2s & 2 \\ 2 & -2s \end{pmatrix} \end{array} \right) \quad (8.57)$$

is of  $[L \times L]$  block form,  $L = 4$ , with  $[T \times T]$  blocks,  $T = 2$ .

**2023-10-05 Predrag** M. Bak *Two-particle lattice Green functions on a two-dimensional rectangular lattice with next-nearest neighbor hopping* is an extension of Katsura and Inawashiro [149] *Lattice Green's functions for the rectangular and the square lattices at arbitrary points*, and its reformulation in the language of elliptic integrals. It has an extensive lattice Green's functions reference list, if needed.

**2023-10-05 Predrag** Kogan and Gumbs *Green's functions and DOS for some 2D Lattices* (2021), [arXiv:2008.05544](https://arxiv.org/abs/2008.05544), looks clean, pedagogical and maybe right for us: should study!

## 8.6 Generating functions; temporal cat

Lagrangian systems are conservative dynamical systems which have a variational formulation. To understand the relation between the discrete time Hamiltonian and Lagrangian formulations, one needs to understand the discrete mapping generating function, such as (11.37).<sup>6</sup>

Consider a cat map [11] of form

$$\begin{pmatrix} q_{t+1} \\ p_{t+1} \end{pmatrix} = A \begin{pmatrix} q_t \\ p_t \end{pmatrix} \pmod 1, \quad A = \begin{pmatrix} s-1 & 1 \\ s-2 & 1 \end{pmatrix}, \quad (8.58)$$

with both  $q_t$  and  $p_t$  in the unit interval,  $A$  a linear, state space (area) preserving map of a 2-torus onto itself, and  $s = \text{tr } A > 2$  an integer. Implement explicitly, as in (2.75), the  $\pmod 1$  operation by introducing  $m^q$  and  $m^p$  winding numbers,

$$\begin{pmatrix} q_{t+1} \\ p_{t+1} \end{pmatrix} = A \begin{pmatrix} q_t \\ p_t \end{pmatrix} - \begin{pmatrix} m_{t+1}^q \\ m_{t+1}^p \end{pmatrix}. \quad (8.59)$$

This is a non-autonomous, time-forced Hamiltonian equation of motion of form (12.100,12.101):

$$q_{t+1} = q_t + p_{t+1} + (s_{t+1}^p - s_{t+1}^q) \quad (8.60)$$

$$p_{t+1} = p_t + \mu^2 q_t - s_{t+1}^p, \quad (8.61)$$

with the force and the corresponding potential energy given by

$$P(q_t) = -\frac{dV(q_t)}{dq_t} = \mu^2 q_t - s_{t+1}^p, \quad (8.62)$$

$$V(q_t) = -\frac{1}{2}\mu^2 q_t^2 + s_{t+1}^p q_t. \quad (8.63)$$

As always, the Lagrangian, or, in the parlance of discrete time dynamics, the *generating function*  $L(q_i, q_{i+1})$ , is given by the difference of the kinetic and potential energies, where in the literature [34, 176, 177, 183] there are different choices of the instant in time at which  $V(q)$  is be evaluated. We define the generating function as

$$L(q_t, q_{t+1}) = \frac{1}{2}p_{t+1}^2 - V(q_t).$$

Next one eliminates momenta in favor of velocities, using (8.60)

$$\begin{aligned} L(q_t, q_{t+1}) &= \frac{1}{2}(q_{t+1} - q_t - s_{t+1}^p + s_{t+1}^q)^2 + \frac{1}{2}\mu^2 q_t^2 - s_{t+1}^p q_t \\ &= \frac{1}{2}q_{t+1}^2 + \frac{s-1}{2}q_t^2 - q_t q_{t+1} \\ &\quad - q_{t+1} s_{t+1}^p + q_{t+1} s_{t+1}^q - q_t s_{t+1}^q + \text{constant}. \end{aligned} \quad (8.64)$$

<sup>6</sup>Predrag 2019-08-05: In preparing this summary we have found expositions of Lagrangian dynamics for discrete time systems by MacKay, Meiss and Percival [177, 183], and Li and Tomsovic [166] particularly helpful.



And this generating function satisfies (8.74).

Consider a symplectic (“area preserving”) map acting on phase space

$$x_{t+1} = M(x_t), \quad x_t = (q_t, p_t)$$

that maps  $x_t$  to  $x_{t+1}$  while preserving the symplectic area.

A *path* is any set of successive *configuration space* points

$$\{q_i\} = \{q_t, q_{t+1}, \dots, q_{t+k}\}. \quad (8.65)$$

In a Lagrangian system each path of finite length in the configuration space is assigned an *action*.<sup>7</sup>

To get the action of an orbit from time  $t_0$  to  $t_n$ , we only need to sum (8.64) over intermediate time steps:

$$S(q_{t_0}, q_{t_0+1}, \dots, q_{t_n-1}, q_{t_n}) = \sum_{t=t_0}^{t_n-1} L(q_t, q_{t+1}). \quad (8.66)$$

For example, in a discrete-time one-degree-of-freedom Lagrangian system with the configuration coordinate  $q_i$  at the discrete time  $i$ , and *generating function* (“Lagrangian density”)  $L(q_i, q_{i+1})$ , the action of path  $\{q_i\}$  is

$$S_{t,t+k} \equiv \sum_{i=t}^{t+k-1} L(q_i, q_{i+1}), \quad (8.67)$$

For 1-dof systems, the geometrical interpretation of the action  $S_{t,t+k}$  is that  $L(q_t, q_{t+1})$  is, up to an overall constant, the phase-space area below the  $p_t$  to  $p_{t+k}$  graph for the  $(q_t, q_{t+k})$  path in the  $(q, p)$  phase plane.<sup>8</sup>

Denoting the derivatives of the generating function  $L(q, q')$  as

$$\begin{aligned} L_1(q, q') &= \frac{\partial}{\partial q} L(q, q'), & L_2(q, q') &= \frac{\partial}{\partial q'} L(q, q') \\ L_{12}(q, q') &= L_{21}(q, q') = \frac{\partial^2}{\partial q \partial q'} L(q, q'), \end{aligned} \quad (8.68)$$

the *momenta* are given by [177, 183]

$$p_n = -L_1(q_n, q_{n+1}), \quad p_{n+1} = L_2(q_n, q_{n+1}). \quad (8.69)$$

The twist condition

$$\partial p_{n+1} / \partial q_n \neq 0 \text{ for all } p_{n+1}, q_n, \quad (8.70)$$

---

<sup>7</sup>Predrag 2019-08-04: repeat of text in catLagrang.tex; 2020-07-04 no recollection of where that is?

<sup>8</sup>Predrag 2016-11-11, 2018-09-26: What follows is (initially) copied from Li and Tomsovic [166], *Exact relations between homoclinic and periodic orbit actions in chaotic systems* arXiv source file, then merged with the MacKay-Meiss-Percival action principle refs. [177, 183].

ensures that

$$L_{12}(q_n, q_{n+1}) \neq 0. \quad (8.71)$$

We distinguish a *path* (8.65), which is any set of successive points  $\{q_n\}$  in the configuration space, from the *orbit segment*  $M^k(x_n)$  from  $x_n$  to  $x_{n+k}$ , a set of successive *phase space* points

$$\{x_i\} = \{x_n, x_{n+1}, \dots, x_{n+k}\}. \quad (8.72)$$

that extremizes the *action* (8.67), with momenta given by (8.69). In other words, not only  $q_n$ , but also  $p_n$  have to align from phase space point to phase space point [205],

$$\frac{\partial}{\partial q_n} (L(q_{n-1}, q_n) + L(q_n, q_{n+1})) = 0. \quad (8.73)$$

Any finite path for which the action is stationary with respect to variations of the segment keeping the endpoints fixed, is called an orbit segment or *trajectory* [61]. Infinite paths for which each finite segment is an orbit segment are called *orbits*.

Given by Keating [154], for the 1-dimensional cat map (2.75), the action of a one-step orbit (which is the generating function) from  $(x_t, p_t)$  to  $(x_{t+1}, p_{t+1})$  can be written as (8.83). And the map (8.59) can be generated using [177, 183]:

$$p_t = -\partial L(x_t, x_{t-1})/\partial x_t, \quad p_{t+1} = \partial L(x_t, x_{t-1})/\partial x_{t+1} \quad (8.74)$$

9

Setting the first variation of the action  $\delta S$  to 0 we get:

$$\frac{\partial S}{\partial x_t} = \frac{\partial L(x_t, x_{t+1})}{\partial x_t} + \frac{\partial L(x_{t-1}, x_t)}{\partial x_t} = 0 \quad (8.75)$$

$$\Rightarrow -x_{t-1} + s_t x_t - x_{t+1} = s_{t+1} x_t - s_t x_t + s_t p_t. \quad (8.76)$$

This is the Percival-Vivaldi second-order difference equation of the cat map with  $s_t = s_{t+1} x_t - s_t x_t + s_t p_t$ .

Using (8.64–8.66) we can compute the action of any finite trajectory. For a trajectory  $\dots x_{t-1} x_t x_{t+1} x_{t+2} \dots$ , the action can be written as:

$$S(\mathbf{x}) = -\frac{1}{2} \mathbf{x}^\top \mathcal{J} \mathbf{x} - \mathbf{s}^\top \mathbf{x}, \quad (8.77)$$

where  $\mathbf{x}$  and  $\mathbf{s}$  are column vectors,

$$\mathbf{x} = \begin{bmatrix} \vdots \\ x_{t-1} \\ x_t \\ x_{t+1} \\ x_{t+2} \\ \vdots \end{bmatrix}, \quad \mathbf{s} = \begin{bmatrix} \vdots \\ s_{t-1} \\ s_t \\ s_{t+1} \\ s_{t+2} \\ \vdots \end{bmatrix}, \quad (8.78)$$

<sup>9</sup>Han 2019-08-01: (8.83) is given by Keating [154] but I cannot find the derivation of this generating function in that paper and the papers referred [153, 206]. The following derivation of generating function is from our blog.

and the orbit Jacobian matrix  $\mathcal{J}$  is a Toeplitz matrix

$$-\mathcal{J} = \begin{bmatrix} \ddots & \ddots & \ddots & \ddots & \ddots & \ddots & \ddots & \ddots & \ddots \\ \ddots & s & -1 & 0 & 0 & \dots & 0 & 0 & \ddots \\ \ddots & -1 & s & -1 & 0 & \dots & 0 & 0 & \ddots \\ \ddots & 0 & -1 & s & -1 & \dots & 0 & 0 & \ddots \\ \ddots & \vdots & \vdots & \ddots & \ddots & \ddots & \vdots & \vdots & \ddots \\ \ddots & 0 & 0 & \dots & \dots & \dots & s & -1 & \ddots \\ \ddots & 0 & 0 & \dots & \dots & \dots & -1 & s & \ddots \\ \ddots & \ddots & \ddots & \ddots & \ddots & \ddots & \ddots & \ddots & \ddots \end{bmatrix}. \quad (8.79)$$

For an orbit with finite length, we need to know the bc's to find the action at boundaries. Note that the action computed in this way will not have the constant terms in (8.64). The matrix  $\mathcal{J}$  has same effect as  $(s - \square - 2)$  where the  $\square$  is the discrete one-dimensional Laplacian defined in (4.177).

### 8.6.1 Lagrangian formulation

<sup>10</sup> While introduction of ‘temporal Bernoulli’ might have seem unmotivated (as we had already shown, there are many way to skin a cat), in mechanics the ‘temporal’ formulation is as old as the modern mechanics itself, and known as the Lagrangian, or variational formulation, the additional twist being phase space volume conservation. In the simplest, 1-degree of freedom kicked rotor example, that means area preservation.

An area-preserving map (12.100,12.101) that describes a kicked rotor subject to a discrete time sequence of angle-dependent impulses  $P(x_t)$  has a Lagrangian (*generating function*) for a particle moving in potential  $V(x)$  at the *lattice site* (time instant)  $t$ ,

$$L(x_t, x_{t+1}) = \frac{1}{2}(x_t - x_{t+1})^2 - V(x_t), \quad P(x) = -\frac{dV(x)}{dx}. \quad (8.80)$$

In the Lagrangian formulation a global periodic state  $\mathbf{X}$  is assigned an *action* functional  $S[\mathbf{X}] = \sum_t L(x_t, x_{t+1}) + \mathbf{X}^\top \mathbf{M}$ , for a prescribed symbol block  $\mathbf{M}$  of sources  $s_t$ . The action can be written down by inspection,

$$S[\mathbf{X}] = \frac{1}{2} \mathbf{X}^\top \mathcal{J} \mathbf{X} + \mathbf{X}^\top \mathbf{M} = \frac{1}{2} \sum_{t,t'=1}^{\ell} x_{t'} \mathcal{J}_{t't} x_t + \sum_{t=1}^{\ell} s_t x_t, \quad (8.81)$$

as its first variation  $\delta S / \delta \mathbf{X}^\top = 0$  has to yield  $\mathcal{J} \mathbf{X}_M + \mathbf{M} = 0$ , the temporal cat fixed point condition (4.178). The solutions  $\mathbf{X}_M$  of the variational condition of

<sup>10</sup>Predrag 2020-07-24: This is a former subsection *Lagrangian formulation of cat.tex*, called by *CL18.tex*.

$\delta S/\delta X^\top = 0$  are stationary points of the action, so they are sometimes called *stationary* configurations; here we refer to them as ‘periodic states’. The form is the same as the Bernoulli fixed point condition `refeq{tempFixPoint}`, but with the temporal cat orbit Jacobian matrix  $\mathcal{J}$  given by the symmetric  $[n \times n]$  matrix of second variations `refeq{Hessian}`  $\mathcal{J}_{tt'} = \partial^2 S/\partial x_t \partial x_{t'}$ , in mechanics often referred to as the *Hessian* matrix. Here, due to the fact that the temporal stability multipliers `refeq{StabMtlpr}` are the same for all temporal periodic states of the same period  $\ell$ , this orbit Jacobian matrix depends only on the period of the periodic state. That does not hold for general nonlinear cat maps [57], where each periodic temporal periodic state  $X_M$  has its own stability.

**2023-11-01 Predrag** The determinant of the **Hessian matrix**, when evaluated at a critical point of a function, is equal to the Gaussian curvature of the function considered as a manifold. The eigenvalues of the Hessian at that point are the principal curvatures of the function, and the eigenvectors are the principal directions of curvature.

**2020-01-17 Han** In my previous computation, the orbit Jacobian matrix is  $\mathcal{J} = -r + s\mathbf{1} - r^{-1}$ . And I think my  $\mathcal{J}$  is correct. One way to show this is:  $S[X] = \sum_t L(x_t, x_{t+1}) + X^\top M$ , and in the Lagrangian (8.80) if you expand the first term there will be a  $-x_t x_{t+1}$  term. So the subdiagonal elements of  $\mathcal{J}$  should be  $-1$ .

And  $\square = \partial^\top \partial = r^\top r - 2\mathbf{1}$  is not right. In the first chapter of your Quantum Field Theory notes, section of Lattice Laplacian, you have  $\square = -\partial^\top \partial$ .

$\partial^\top \partial = 2\mathbf{1} - r^\top - r$ . So using my orbit Jacobian matrix  $\mathcal{J} = -r + s\mathbf{1} - r^{-1}$  the action has form:

$$S[X] = \sum_{t=1}^n \left\{ \frac{1}{2} (\partial x_t)^2 - \frac{1}{2} \mu^2 x_t^2 \right\} + \sum_{t=1}^n s_t x_t. \quad (8.82)$$

**2020-01-31 Predrag** I would love to have your convention  $\mathcal{J} = -r + s\mathbf{1} - r^{-1}$ . But there is no avoiding the pesky overall “-” sign; it arises from  $s_{t+1} = \lfloor s x_t \rfloor$ , being the integer part of  $s x_t$ . This leads to (??), and there is no logically clean rational for changing the sign of  $s_t$ . But I do have to ponder again the meaning of  $\partial^\top \partial = 2\mathbf{1} - r^\top - r$  for the Lagrangian formulation

**2023-09-16 Predrag** Read this paper: Li and Tomsovic *Homoclinic orbit expansion of arbitrary trajectories in chaotic systems: classical action function and its memory*, [arXiv:2009.12224](https://arxiv.org/abs/2009.12224): [...] as demonstrated in previous publications [Phys. Rev. E 95, 062224 (2017), Phys. Rev. E 97, 022216 (2018) [166]], the determination of homoclinic orbits is sufficient for the exact calculation of classical action functions of unstable periodic orbits. [...] partitions the trajectories into short segments of transient visits to the neighborhoods of successive periodic orbits, giving rise to a periodic orbit expansion

scheme which is equivalent to the homoclinic orbit expansion. [...] homoclinic and periodic orbits are equally valid skeletal structures for the tessellation of phase-space dynamics.

### 8.6.2 Temporary: Cat map in the Lagrangian formulation

===== the rest: TEMPORARY TEXT =====

Rewrite (2.75) back to (8.58)'s form, and let  $m^q$  and  $m^p$  be the winding numbers, we can get (8.59).

<sup>11</sup> The action of the system in this one-step motion is [154] <sup>12</sup>

$$L(q_t, q_{t-1}) = \frac{1}{2}[(s-1)q_{t-1}^2 - 2q_{t-1}(q_t + m_t^q) + (q_t + m_t^q)^2 - 2m_t^p q_t]. \quad (8.83)$$

The action of a longer orbit is the sum of the one-step actions at each time step. The Lagrangian equations of motion are obtained by demanding that the first variation of the action vanishes:

$$\frac{\partial L(q_{t+1}, q_t)}{\partial q_t} + \frac{\partial L(q_t, q_{t-1})}{\partial q_t} = 0 \quad (8.84)$$

$$-q_{t-1} + sq_t - q_{t+1} = m_{t+1}^q - m_t^q + m_t^p = m_t, \quad (8.85)$$

which gives us the screened Poisson equation (2.95) with  $m_t = m_{t+1}^q - m_t^q + m_t^p$ . If the orbit has periodic bc's with period  $n$ ,  $q_t = q_{t+n}$ , the action of the periodic orbit can be written as (24.189), where the  $n \times n$  matrix  $\mathcal{J}$  is given by `refeq{Hessian}`, and

$$\mathbf{x} = \begin{bmatrix} x_1 \\ x_2 \\ x_3 \\ \vdots \\ x_n \end{bmatrix}, \quad \mathbf{m} = \begin{bmatrix} m_1 \\ m_2 \\ m_3 \\ \vdots \\ m_n \end{bmatrix}. \quad (8.86)$$

$\mathcal{J}_n$  is called the orbit Jacobian matrix (or the Hessian matrix) of period  $n$ . The element of matrix  $-\mathcal{J}_n$  is  $-(\mathcal{J}_n)_{ij} = \partial^2 L(\mathbf{x}) / \partial x_i \partial x_j$ . Letting the first derivative of action (24.189) be 0, we can see that a periodic point of cat map with

<sup>11</sup>Predrag 2019-08-04: Percival-Vivaldi [205] (3.1) uses only  $m^p$ , no need for this confusing additional  $m^q$ , for their Hamiltonian (2.1), with no specialization to the Percival-Vivaldi cat map.

<sup>12</sup>Predrag 2019-08-04: By MacKay, Meiss and Percival [177, 183] convention (3.2), and Li and Tomsovic [166] convention (9) we should always have  $L(q_t, q_{t+1})$ . Unfortunately Keating [154] definition (3) corresponds to  $L(q_t, q_{t-1})$ , but we do not take that one.

period  $n$  satisfies:

$$\begin{bmatrix} s & -1 & 0 & \dots & -1 \\ -1 & s & -1 & \dots & 0 \\ 0 & -1 & s & \dots & 0 \\ \vdots & \vdots & \vdots & \ddots & \vdots \\ -1 & 0 & 0 & \dots & s \end{bmatrix} \begin{bmatrix} x_1 \\ x_2 \\ x_3 \\ \vdots \\ x_n \end{bmatrix} = \begin{bmatrix} m_1 \\ m_2 \\ m_3 \\ \vdots \\ m_n \end{bmatrix}, \quad \begin{bmatrix} m_1 \\ m_2 \\ m_3 \\ \vdots \\ m_n \end{bmatrix} \in \mathbb{Z}^n, \quad (8.87)$$

13

$$L(x_{t+1}, x_t) = \frac{1}{2}[(s-1)x_t^2 - 2x_t(x_{t+1} + m_{t+1}^x) + (x_{t+1} + m_{t+1}^x)^2 - 2m_{t+1}^p x_{t+1}]. \quad (8.88)$$

14 15

Consider cat map of form (8.58).

$$L(q_t, q_{t+1}) = \frac{1}{2}(q_{t+1} - q_t)^2 - V(q_t), \quad P(q) = -\frac{dV(q)}{dq}, \quad (8.89)$$

The problem with formulation (8.63) is that the potential energy contribution is defined asymmetrically in (8.89). We should really follow Bolotin and Treschev [34] eq. (2.5), and define a symmetric generating function

$$L(q_t, q_{t+1}) = \frac{1}{2}(q_{t+1} - q_t)^2 - \frac{1}{2}[V(q_t) + V(q_{t+1})], \quad (8.90)$$

The first variation (12.13) of the action vanishes,

$$\begin{aligned} 0 &= L_2(q_{t+1}, q_t) + L_1(q_t, q_{t-1}) \\ &= q_t - q_{t+1} + \mu^2 q_t - s_{t+1}^p + q_t - q_{t-1} \\ &= -q_{t+1} + s q_t - q_{t-1} - s_{t+1}^p, \end{aligned} \quad (8.91)$$

hence

$$q_{t+1} - s q_t + q_{t-1} = -s_{t+1}^p. \quad (8.92)$$

Defining  $s_t = -s_{t+1}^p$ , we recover the screened Poisson equation (2.95).

Alternatively, Han's generating function (1-step Lagrangian density) is:

$$\begin{aligned} L(q_{n+1}, q_n) &= \frac{1}{2}[p_{n+1}(q_{n+1}, q_n)]^2 - V(q_n) \\ &= \frac{1}{2}(q_{n+1} - q_n + m_{n+1}^q - m_{n+1}^p)^2 + \frac{1}{2}\mu^2 q_n^2 - m_{n+1}^p q_n. \end{aligned} \quad (8.93)$$

<sup>13</sup>Predrag 2019-05-27: For a more detailed discussion, see for example (12.104) in *spatiotemp/chapter/Hill.tex*; *spatiotemp/chapter/examCatMap.tex* text: *generating function* (8.89) This generating function is the discrete time Lagrangian for a particle moving in potential  $V(x)$ .

<sup>14</sup>Han 2019-06-10: (8.83) is already given by Keating [154]. Do we want to add our procedure here? I got the Lagrangian (12.108) which is different from (8.88) only by a constant.

<sup>15</sup>Han 2019-06-12: The generating function of a 2-dimensional spatiotemporal cat (11.37) in given by Gutkin and Osipov [109].

The action is the sum over the Lagrangian density over the orbit. The first variation (12.13) of the action vanishes,

$$\begin{aligned}
 0 &= L_2(q_{n+1}, q_n) + L_1(q_n, q_{n-1}) \\
 &= q_n - q_{n+1} + m_{n+1}^p - m_{n+1}^q \\
 &\quad + \mu^2 q_n - m_{n+1}^p + q_n - q_{n-1} + m_n^q - m_n^p \\
 &= -q_{n+1} + sq_n - q_{n-1} - (m_{n+1}^q - m_n^q + m_n^p),
 \end{aligned} \tag{8.94}$$

hence

$$-q_{n+1} + sq_n - q_{n-1} = m_{n+1}^q - m_n^q + m_n^p. \tag{8.95}$$

Letting  $m_n = m_{n+1}^q - m_n^q + m_n^p$ , we recover the Lagrangian formulation `refeq{eq:CatMapNewt}`, **except for the wrong sign for  $m_n$** . Now we see why  $m_n$ 's are called 'sources'.

## 8.7 Lattice points enumeration

God made the integers, all else is the work of man.  
— Leopold Kronecker

### 8.7.1 Integer lattice in $d$ dimensions

Since we are interested in combinatorial rather than metric properties, it suffices to consider the case of the standard integer lattice  $\mathbb{Z}^d \subset \mathbb{R}^d$ . The case of a general lattice  $\mathcal{L}$  in  $\mathbb{R}^d$  reduces to that of  $\mathbb{Z}^d$  by a change of the coordinates.

2020-01-23 Predrag .

**wiki:** *Lattice (group)*: A lattice  $\mathcal{L}$  in  $\mathbb{R}^d$  has the form

$$\mathcal{L} = \left\{ \sum_{i=1}^d a_i v_i \mid a_i \in \mathbb{Z} \right\}$$

where

$$\{v_1, v_2, \dots, v_d\} \tag{8.96}$$

is a basis (or ‘integral basis’) that defines the primitive cell. One convention is that an integral basis is ordered according to the length of its elements; i.e.  $|v_1| \leq |v_2| \leq \dots \leq |v_d|$ .

**wiki:** *A lattice graph*, mesh graph, or grid graph, is a graph whose drawing, embedded in  $\mathbb{R}^d$ , forms a regular tiling. In  $d = 2$  a lattice graph (or a square grid graph) is the graph whose vertices correspond to the points in the plane with integer coordinates.

The determinant (‘discriminant’ or ‘volume’) of lattice  $\mathcal{L}$  is

$$d(\mathcal{L}) = |\det(v_1|v_2|\dots|v_d)|. \tag{8.97}$$

The determinant is the reciprocal of the average density of points in the lattice. Different bases can generate the same lattice, but the absolute value of the determinant is uniquely determined by  $\mathcal{L}$ . If one thinks of a lattice as dividing the whole of  $\mathbb{R}^d$  into equal polyhedra (copies of an  $d$ -dimensional parallelepiped, the ‘fundamental region’ of the lattice), then  $d(\mathcal{L})$  is equal to the  $d$ -dimensional volume of this polyhedron. This is why  $d(\mathcal{L})$  is sometimes called the *covolume* of the lattice. If it equals 1, the lattice is called unimodular.

The master of counting integer lattice points in various domains (and all dimensions) is Alexander **Barvinok**. Barvinok **lectures** are very clear and simple. On p. 20 he defines the fundamental parallelepiped, and then shows that

**Theorem 2.** The number of integer points in the fundamental parallelepiped is equal to the volume of the parallelepiped.



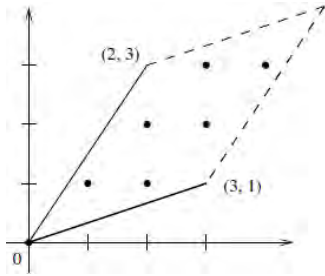


Figure 8.1: A parallelepiped spanned by  $(3,1)$  and  $(2,3)$  contains  $\text{Det} \begin{pmatrix} 3 & 2 \\ 1 & 3 \end{pmatrix} = 7$  points. Note that  $(3,1)$ ,  $(2,3)$  and the far vertex  $(5,4)$  are not counted. Barvinok [22] Fig. 81.

Note that the fundamental parallelepiped is half-open, as indicated by dashed lines in figure 8.1 so that its translates form a partition of the whole space.

Barvinok [22] *A Course in Convexity*, ([click here](#))

Barvinok [23] *Integer Points in Polyhedra*, ([click here](#)) seems to be a harder read, and not helpful for our integer lattice points counting.

1831 pages [Handbook of Discrete and Computational Geometry](#) might be of some use.

Hadamard's inequality. Let  $v_1, v_2, \dots, v_d$  be any basis for  $\mathcal{L}$ . Then

$$d(\mathcal{L}) \leq |v_1| |v_2| \cdots |v_d|, \quad (8.98)$$

as the volume of a parallelepiped is never greater than the product of the lengths of its sides. Hadamard's inequality is an equality if and only if the basis vectors are orthogonal. A theorem of Hermite says that every lattice has a basis that is reasonably orthogonal (see (8.123)), where the amount of nonorthogonality is bounded solely in terms of the dimension. A *reduced basis* is an integral basis that minimizes the product of lengths (8.98) over all bases of the lattice. Lattice  $\mathcal{L}$  is *bounded* by  $T$ , if it has a reduced basis consisting of vectors of length at most  $T$ .

**LattE** is an "Lattice point Enumeration" program that count lattice points contained in convex polyhedra defined by linear equations and inequalities with integer coefficients [65]. In 1994 Barvinok [24] gave an algorithm that counts lattice points in convex rational polyhedra in polynomial time when the dimension of the polytope is fixed. LattE counts the lattice points using multivariate generating functions  $P(a)$ ,  $z^a = z^{a_1} z^{a_2} \dots z^{a_d}$ , implementing Barvinok algorithm. At the end,  $f(P)$  is written as a sum of "short" rational functions.

LattE [home page](#).

Maple code.

Simplicial cone: Let (8.96) be a set of  $k$  linearly independent integral vectors in  $\mathbb{R}^d$ , where  $k \leq d$ . Consider simplicial cone  $K$  and parallelepiped  $S$  generated by (8.96),

$$K = \{\lambda_1 v_1 + \lambda_2 v_2 + \dots + \lambda_k v_k\}, \quad 0 \leq \lambda_i \quad (8.99)$$

$$S = \{\lambda_1 v_1 + \lambda_2 v_2 + \dots + \lambda_k v_k\}, \quad 0 \leq \lambda_i < 1 \quad (8.100)$$

The generating function for the lattice points in  $K$  equals [232]<sup>16</sup>

$$\sum_{\beta \in K \cap \mathbb{Z}^d} z^\beta = \left( \sum_{\tau \in S \cap \mathbb{Z}^d} z^\tau \right) \prod_{i=1}^k \frac{1}{1 - z^{v_i}} \quad (8.101)$$

A unimodular cone is a simplicial cone with all  $\lambda = 1$  which forms an integral basis for the lattice  $\mathbb{R}\{v_1, v_2, \dots, v_k\} \cap \mathbb{Z}^d$ . In this case the numerator of the formula has a single monomial; in other words, the parallelepiped has only one lattice point. The number of points in the parallelepiped is obtained by setting  $z_i = 1$  in the generating function

$$f(S; z) = \left( \sum_{\tau \in S \cap \mathbb{Z}^d} z^\tau \right) \quad (8.102)$$

However, the generating function is not constructed by enumerating all the integer points in  $S$ , but rather as a signed sum of rational functions that can be derived from the description of  $S$ . They all count points in a general polyhedron; counting them in a parallelepiped should be a simple special case, but I have not seen that discussed separately.

Note that this count does not identify opposing sides of the parallelepiped. If we need to enumerate periodic points one-by-one, John Voight [mathoverflow](#) question might be a start.

[Stumbling Robot](#) derives the area of a polygon whose vertices are lattice points.

The study of integer points in convex polyhedra is motivated by questions such as "how many nonnegative integer-valued solutions does a system of linear equations with nonnegative coefficients have" or "how many solutions does an integer linear program have".

[wiki](#): *Minkowski's theorem* relates the number  $d(\mathcal{L})$  and the volume of a symmetric convex set  $S$  to the number of lattice points contained in  $S$ . The number of lattice points contained in a polytope all of whose vertices are elements of the lattice is described by the polytope's Ehrhart polynomial. Formulas for some of the coefficients of this polynomial involve  $d(\mathcal{L})$  as well.

<sup>16</sup>Predrag 2020-01-25: I cannot find this formula in Stanley [232], ([click here](#)).

**wiki:** An integral polytope has an associated *Ehrhart polynomial* that encodes the relationship between the volume of a polytope and the number of integer points the polytope contains. A generating function for the Ehrhart polynomials, or the Ehrhart series is a rational function - this suggest that we should be able to convert this series into a zeta function. This wiki has some intriguing explicit examples.

**2020-09-18 Predrag** Subramaniam and Balani have an **E-book** with a cute chapter on **lattices**, but it standard Bravais lattice crystallography, of no use to us. Ignore.

**2020-07-31 Predrag** The spatiotemporal cat orbit Jacobian matrix (21.239) in the Hill determinant  $\det \mathcal{J}$  computation for a  $[L \times T]_0$  rectangular primitive cell is expressed naturally and spacetime symmetrically in terms of 'horizontal', 'vertical' translation generators  $r_1, r_2$ .

I expect that for an arbitrary primitive cell, such as figure 8.1, the corresponding translation generators should act along the 'integral basis' vectors (8.96) that define the primitive cell  $\mathcal{L}$ , i.e., the spatiotemporal cat Hill determinant should be given by

$$\det \mathcal{J} = \det (\mathcal{J}\mathcal{L}) / \det \mathcal{L}, \quad (8.103)$$

where spatiotemporal cat orbit Jacobian matrix  $\mathcal{J}$  should be expressed in terms of translations along the primitive cell primitive vectors, and the Hill determinant should be expressed terms of invariant quantities that can be constructed from them. The simplest is the volume (8.97), the others are presumably related to traces  $\text{tr } \mathcal{L}^k$  and the corresponding subvolumes. Not sure what they are, but someone has surely thought about that. My understanding is summarized in [birdtracks.eu](http://birdtracks.eu).

Han and I have an answer of asymmetric form for the orbit Jacobian matrix (21.239) for a tilted primitive cell (relative periodic orbit) (12.46), with the relative periodicity all in the 'comoving frame' translation generator  $r_1^{-S/T} \otimes r_2$ .

This space-time asymmetry is a consequence of choosing the Hermite normal form (8.123) to define the primitive cell. So - even though we are computing the representation-independent determinants, we do not have an invariant statement of cell's 'tilt'. There must be a more elegant answer to this. Some of this discussion is in the **2020-07-11 Predrag** post, around eq. (8.116).

But that might lead us too deep into the role that prime numbers play in characterizing equivalent primitive cells  $\mathcal{L}$  and their volumes. Whenever your result depends on factorization in primes, it is time to sound a potentially deep number theory **red alert** :)

**2023-02-12 Predrag** This is the case of a single finite, doubly periodic lattice. For the infinite lattice deterministic field theory partition function, refor-

ulated in terms of prime periodic states, see sect. 4.4 *A partition function in terms of prime periodic states.*

### 8.7.2 A cryptographic perspective

2020-01-23 Predrag Oded Regev is good on this - will post more links. He uses Micciancio and Goldwasser [186] *Complexity of Lattice Problems - A Cryptographic Perspective* (click here) as his course textbook.

Oded Regev: Definition 5 defines  $d(\mathcal{L})$ , the determinant of a lattice in terms of the basis matrix that might be useful to us.

Lattices, Convexity and Algorithms lecture notes from 2013 might be better. Check out "Gram Schmidt Orthogonalization," which I think is his construction of the Hermite normal basis, and "Equivalence of Lattice Definitions." Also check out his *Fundamental Parallelepiped and the Determinant* lecture.

2020-12-12 Predrag Haviv and Regev arXiv:1311.0366 address the Lattice Isomorphism Problem (LIP). I like their definitions.

Two lattices  $\mathcal{L}_1$  and  $\mathcal{L}_2$  are isomorphic if there exists an orthogonal linear transformation mapping  $\mathcal{L}_1$  to  $\mathcal{L}_2$ .

An orthogonal linear transformation (or isometry)  $O : V_1 \rightarrow V_2$  is a linear transformation that preserves inner products, that is,  $\langle x, y \rangle = \langle O(x), O(y) \rangle$  for every  $x, y \in V_1$ . For a set  $A \subseteq V_1$  we use the notation  $O(A) = \{O(x) \mid x \in A\}$ .

For a matrix  $B$  we denote its  $i$ th column by  $b_i$ , and  $O(B)$  stands for the matrix whose  $i$ th column is  $O(b_i)$ .  $\text{span}(B)$  stands for the subspace spanned by the columns of  $B$ .

Let  $B$  and  $D$  be two matrices satisfying  $B^T \cdot B = D^T \cdot D$ . Then there exists an orthogonal linear transformation  $O : \text{span}(B) \rightarrow \text{span}(D)$  for which  $D = O(B)$ .

An  $m$ -dimensional lattice  $\mathcal{L} \subseteq \mathcal{R}^m$  is the set of all integer combinations of a set of linearly independent vectors  $\{b_1, \dots, b_n\} \subseteq \mathcal{R}^m$ , i.e.,  $\mathcal{L} = \{\sum_{i=1}^n a_i b_i \mid \forall i. a_i \in \mathbb{Z}\}$ . The set  $\{b_1, \dots, b_n\}$  is called a *basis* of  $\mathcal{L}$  and  $n$ , the number of vectors in it, is the *rank* of  $\mathcal{L}$ . Let  $B$  be the  $m$  by  $n$  matrix whose  $i$ th column is  $b_i$ . We identify the matrix and the basis that it represents and denote by  $\mathcal{L}(B)$  the lattice that  $B$  generates.

A basis of a lattice is not unique: two bases  $B_1$  and  $B_2$  generate the same lattice of rank  $n$  if and only if  $B_1 = B_2 \cdot U$  for a unimodular matrix  $U \in \mathbb{Z}^{n \times n}$ , i.e., an integer matrix satisfying  $|\det(U)| = 1$ .

The determinant of a lattice  $\mathcal{L}$  is defined by

$$\det(\mathcal{L}) = \sqrt{|\det(B^T B)|}, \tag{8.104}$$

where  $B$  is a basis that generates  $\mathcal{L}$ .  $\det(\mathcal{L})$  is independent of the choice of the basis. A set of (not necessarily linearly independent) vectors that generate a lattice is called a *generating set* of the lattice.

A lattice  $\mathcal{M}$  is a *sublattice* of a lattice  $\mathcal{L}$  if  $\mathcal{M} \subseteq \mathcal{L}$ , and it is a *strict sublattice* if  $\mathcal{M} \subsetneq \mathcal{L}$ . If a lattice  $\mathcal{L}$  and its sublattice  $\mathcal{M}$  span the same subspace, then the *index* of  $\mathcal{M}$  in  $\mathcal{L}$  is defined by  $|\mathcal{L} : \mathcal{M}| = \det(\mathcal{M})/\det(\mathcal{L})$ . If  $\mathcal{M}$  is a sublattice of  $\mathcal{L}$  such that  $|\mathcal{L} : \mathcal{M}| = 1$  then  $\mathcal{M} = \mathcal{L}$ .

They define lattices by their *Gram matrices*. The *Gram matrix* of a matrix  $B$  is defined to be the matrix

$$G = B^T \cdot B, \quad (8.105)$$

or equivalently,

$$G_{ij} = \langle b_i, b_j \rangle, \quad \text{for every } i \text{ and } j. \quad (8.106)$$

A Gram matrix specifies a basis only up to rotation.

In the Lattice Isomorphism Problem the input consists of two Gram matrices  $G_1$  and  $G_2$ , and the goal is to decide if there exists a unimodular matrix  $U$  for which  $G_1 = U^T \cdot G_2 \cdot U$ .

The *dual lattice* of a lattice  $\mathcal{L}$ , denoted by  $\mathcal{L}^*$ , is defined as the set of all vectors in  $\text{span}(\mathcal{L})$  that have integer inner product with all the lattice vectors of  $\mathcal{L}$ , that is,

$$\mathcal{L}^* = \{u \in \text{span}(\mathcal{L}) \mid \forall v \in \mathcal{L}. \langle u, v \rangle \in \mathbb{Z}\}.$$

The *dual basis* of a lattice basis  $B$  is denoted by  $B^*$  and is defined as the one which satisfies  $B^T \cdot B^* = I$  and  $\text{span}(B) = \text{span}(B^*)$ , that is,  $B^* = B(B^T B)^{-1}$ . It is well known that the dual basis generates the dual lattice, i.e.,  $\mathcal{L}(B)^* = \mathcal{L}(B^*)$ .

The relations between parameters of lattices and parameters of their dual are known as *transference theorems*.

**2020-02-14 Predrag** Given a nondegenerate lattice  $\mathcal{L}$ , we can construct an invariant by choosing a basis, and taking the determinant of the matrix whose  $(i,j)$  entry is the inner product of the  $i$ -th primitive vector with the  $j$ -th primitive vector. The matrix is called the Gram matrix of the basis, and the determinant is a rough measure of how loosely packed the lattice vectors are in  $\mathcal{L} \otimes \mathbb{R}$ .

**2020-02-14 Predrag** I have run (once) into ‘fundamental parallelepiped’ being called ‘fundamental parallelotope’.

**2020-12-12 Predrag** For our choice of Hermite normal form (8.124), (4.80), the Gram matrix (8.105) is

$$G = \begin{bmatrix} L^2 & LS \\ LS & L^2 + T^2 \end{bmatrix}, \quad (8.107)$$

so the lattice  $\mathcal{L}$  determinant (8.104) of is

$$\det(\mathcal{L}) = L\sqrt{T^2 + L^2 - S^2}, \quad (8.108)$$

which looks wrong.

**2020-09-08 Predrag Daniele Micciancio** is very economical. I propose we follow his exposition, and use Micciancio and Goldwasser [186] *Complexity of Lattice Problems - A Cryptographic Perspective* (click here). They say (I have not looked at any of these, so they might be even better than Micciancio and Goldwasser, for our purposes):

“Classical references about lattices are Cassels [44] (or 1971) (click here) and Gruber and Lekerkerker [103] (click here). Another very good reference is Siegel [226] (click here). For a brief introduction to the applications of lattices in various areas of mathematics and science the reader is referred to (Lagarias 1995) and (Gritzmman and Wills 1993), which also touch some complexity and algorithmic issues. A very good survey of algorithmic application of lattices is (Kannan 1987a).”

Lattices are regular arrangements of points in Euclidean space. The simplest example of lattice in  $n$ -dimensional space is  $\mathbb{Z}^d$ , the set of all  $d$ -dimensional vectors with integer entries. More generally, a lattice is the result of applying a nonsingular linear transformation  $B \in \mathbb{R}^{m \times d}$  to the integer lattice  $\mathbb{Z}^d$ , to obtain the set  $B(\mathbb{Z}^m) = \{Bx : x \in \mathbb{Z}^d\}$ . etc. - you fill it in.

To Han: can you replace our ‘Bravais’ by Micciancio and Goldwasser [186] lattice definitions?

Is the ‘Hermite normal form’ the same as the ‘Gram-Schmidt orthogonalization method’?

**2020-09-11 Han** Gram Schmidt orthogonalization constructs orthogonal with primitive vectors whose tips are not on  $\mathbb{Z}^d$  lattice; not Hermite normal form, forget it.

**2018-01-31 Han** The similarity transformation  $\mathbf{S}$  that maps (2.1) into (2.5),

$$\mathbf{A} = \begin{bmatrix} 2 & 1 \\ 1 & 1 \end{bmatrix}, \quad \mathbf{B} = \begin{bmatrix} 0 & 1 \\ -1 & 3 \end{bmatrix}, \quad (8.109)$$

is

$$\mathbf{B} = \mathbf{S}^{-1}\mathbf{A}\mathbf{S}, \quad (8.110)$$

where

$$\mathbf{S} = \mathbf{S}^{-1} = \begin{bmatrix} -1 & 2 \\ 0 & 1 \end{bmatrix}.$$

**2018-04-27 Predrag** Note that  $\det \mathbf{S} = -1$ . Why? That can be fixed by multiplying it by  $i$ , but why? It is also not unique, one could, for example, use

$$\mathbf{S}' = \mathbf{S}'^{-1} = \begin{bmatrix} 0 & -1 \\ 1 & 0 \end{bmatrix} \begin{bmatrix} -1 & 2 \\ 0 & 1 \end{bmatrix} \begin{bmatrix} 0 & 1 \\ -1 & 0 \end{bmatrix} = \begin{bmatrix} 1 & 0 \\ -2 & -1 \end{bmatrix}.$$

For a systematic discussion, see sect. 4. *Global versus local conjugacy and orbit statistics* of Baake *et al.* [18], and sect. 2.5. *Results for  $d = 2$*  of Baake *et al.* [17] *Orbit structure and (reversing) symmetries of toral endomorphisms on rational lattices*. The main point (for us) is that maps that are in the same conjugacy class need to have 3 invariants in common; the trace, the determinant, and the mgcd (the matrix greatest common denominator). For the Thom-Arnol'd cat map (2.1),  $\text{mgcd}(A) = 1$

Baake *et al.* [17] discuss “pretails” to periodic orbits at length.

**2018-04-27 Predrag** Next, one can transform Arnold cat map “square root”  $\mathbf{C}$  (or, according to Baake *et al.* [18], the ‘classic’ or golden orientation reversing cat map, or the Fibonacci cat map [17], with  $\det(\mathbf{C}) = -1$ )

$$\mathbf{A} = \mathbf{C}^2, \quad \mathbf{C} = \begin{bmatrix} 1 & 1 \\ 1 & 0 \end{bmatrix} \quad (8.111)$$

to the Percival-Vivaldi version

$$\mathbf{B} = \tilde{\mathbf{C}}^2, \quad \tilde{\mathbf{C}} = \mathbf{S}^{-1}\mathbf{C}\mathbf{S} = \begin{bmatrix} -2 & 1 \\ -1 & 1 \end{bmatrix}. \quad (8.112)$$

As noted in (6.199), taking this “square root” expresses the zeta function as a product of a time-reversal pair of zeta’s.  $\mathbf{B}$  and  $\tilde{\mathbf{C}}$  have the same eigenvectors, but as  $\det \tilde{\mathbf{C}} = -1$ , one of the stability multipliers is a negative square root of the  $\mathbf{B}$  multipliers (21.151),

$$\tilde{\Lambda} = \tilde{\Lambda}_1 = \frac{1 + \sqrt{5}}{2}, \quad \tilde{\Lambda}_2 = \frac{1 - \sqrt{5}}{2}. \quad (8.113)$$

The issue of reversibility seems complicated [17]. When  $M \in \text{SL}(2, \mathbb{Z})$ , also its inverse is in  $M^{-1} \in \text{SL}(2, \mathbb{Z})$ , and  $M$  and  $M^{-1}$  share the same determinant, trace and mgcd:

$$\mathbf{M} = \begin{bmatrix} a & b \\ c & d \end{bmatrix}, \quad \mathbf{M}^{-1} = \begin{bmatrix} d & -b \\ -c & a \end{bmatrix}.$$

The the golden (Fibonacci [17]) cat map (8.111) is not reversible in  $\text{GL}(2, \mathbb{Z})$  (while its square  $A$  is [17]).

**2020-02-19 Predrag** *Linear recurrences with constant coefficients: the multivariate case* by Mireille Bousquet-Mélou1a and Marko Petkovšek, (DOI) has the right feel and a few 2-dimensional integer lattice recurrences and the corresponding functional equations, but I do not see how to apply it to the 2-dimensional spatiotemporal cat.

**2020-07-11 Predrag** Woods [252] (2012) (click here) is very clear, what follows is excerpted from it. As Woods says, his starting chapters are taken from Lim [169] *Two-dimensional Signal and Image Processing* (click here) (click

here), who copies from Dudgeon and Mersereau [72] (1984) *Multidimensional Digital Signal Processing* (click here) which cover the same ground.

A 2-dimensional field  $\phi_{nt}$  is periodic with period  $[L \times T]_0$ , if the following equalities hold for all integers  $n, t$ :

$$\phi_{nt} = \phi_{n+L, t} = \phi_{n, t+T}, \quad (8.114)$$

where  $L$  and  $T$  are positive integers. This type of periodicity occurs often for 2-dimensional signals and is referred to as *rectangular periodicity*. We call the resulting period the *rectangular period*.

Given a periodic function, the period effectively defines a basic cell in the plane, which can be repeated to form the function over all integers  $n, t$ . As such, we often want the minimum size unit cell for efficiency of both specification and storage. In the case of the rectangular period, we seek the smallest nonzero integers that will suffice for  $[L \times T]_0$  to form this basic cell.

**Horizontal Wave.** Consider the sine wave  $\phi_{nt} = \sin(2\pi n/4)$ . The horizontal period is  $L = 4$ . In the vertical direction, the signal is constant, so we can use any positive integer  $T$ . The smallest such value is  $T = 1$ . Thus the rectangular period is  $[L \times T]_0 = [4 \times 1]_0$ , and the basic cell consists of the set of points  $\{(nt) = [(0, 0), (1, 0), (2, 0), (3, 0)]\}$  or any translate of this set.

In general, ‘periodicity’ refers to a repetition of blocks, not necessarily rectangular blocks or blocks occurring on a rectangular repeat grid, with the periodicity represented with two integer vectors,

$$v_1 = \begin{pmatrix} L \\ c_{21} \end{pmatrix}, \quad v_2 = \begin{pmatrix} S \\ T \end{pmatrix}.$$

While they note the nonuniqueness of primitive cells with respect to unimodular transformations, image processing textbooks seem not to use the Hermite normal form (8.123) to eliminate  $c_{21}$ .

The 2-dimensional field  $\phi_{nt}$  is periodic with period  $(v_1, v_2) = \Lambda$  if the following hold for all integers  $n, t$ :

$$\phi_{nt} = \phi_{n+L, t+c_{21}} = \phi_{n+S, t+T}, \quad (8.115)$$

To avoid degenerate cases, restrict the integers in  $v_j$  with the condition

$$\det(v_1, v_2) \neq 0.$$

“We leave it to the reader to show that” the number of samples in this region is  $\det \Lambda$ , i.e., the absolute value of the determinant of the periodicity matrix gives the number of samples of  $\phi_n$  contained in one period.



The matrix  $\Lambda$  is called the *periodicity matrix*. In matrix notation, the periodic field satisfies

$$\phi_{\mathbf{n}} = \phi_{\mathbf{n} + \Lambda \mathbf{r}}, \quad \mathbf{r} = \begin{pmatrix} r_1 \\ r_2 \end{pmatrix}.$$

Two integer vectors  $\mathbf{m}$  and  $\mathbf{n}$  are *congruent* with respect to the matrix modulus  $\Lambda$  if  $\mathbf{m} = \mathbf{n} + \Lambda \mathbf{r}$  for some integer vector  $\mathbf{r}$ .

In the case that  $\Lambda$  is a diagonal matrix,  $\phi_{\mathbf{n}}$  is *rectangularly periodic*.

If  $P$  is any integer matrix, then  $P\Lambda$  is also be a periodicity matrix for  $\phi_{\mathbf{n}}$ . Thus the periodicity matrix is not unique for any periodic sequence.

A matrix  $E$  for which  $\det E = 1$  is called a *unimodular matrix*.  $E^{-1}$  is then also a unimodular matrix. Unimodular matrices are the only integer matrices whose inverses are also integer matrices. If  $\det \Lambda$  is a prime number, we will say that  $\Lambda$  is a *prime matrix*. If  $\Lambda$  is neither prime nor unimodular, we say that it is *composite*, and can be decomposed, nonuniquely - up to a unimodular transformation - into a product of two non-unimodular matrices

$$\Lambda = PQ. \tag{8.116}$$

If either  $P$  or  $Q$  is composite, one continues the process, until  $\det \Lambda$  is the product of its prime factors.

Dudgeon and Mersereau [72] then explain clearly how to get the “quotient”  $Q$  when “dividing” by  $P$ .  $|\det \Lambda|/|\det Q| = |\det P|$  is then the number of cosets. In the image-processing, Fourier transforms trade this non-prime factorization is known as “decimation-in-time Cooley-Tukey FFT algorithm,” “twiddle factors,” and “butterflies.”<sup>17</sup>

**Example** Relative equilibrium field  $\sin[2\pi(n/8 + t/16)]$  is constant along the line  $2n + t = 16$ . The basis vectors are

$$v_1 = \begin{pmatrix} 4 \\ 8 \end{pmatrix}, \quad v_2 = \begin{pmatrix} 1 \\ -2 \end{pmatrix}, \quad \text{with } \det \Lambda = 16.$$

**Definition 1.1-1: Linear System** [⋯]

**Definition 1.1-2: Shift Invariance** [⋯]

“Linear shift-invariant discrete systems are generally implemented using difference equations. Although multidimensional difference equations represent a generalization of 1-dimensional difference equations, they are considerably more complex and are, in fact, quite different. A number of important issues associated with multidimensional difference equations, such as the direction of recursion and the ordering relation, are really not issues in the 1-dimensional case.

---

<sup>17</sup>Predrag 2020-07-15: Use this to define prime factorization in ref. [63]?

[...] they define multidimensional recursive systems and consider the issues associated with multidimensional difference equations; [...] define the multidimensional Z-transform. ”

**2-dimensional Convolution** If a system is *linear shift-invariant* (LSI), then [...] the field  $h$  is called the LSI system’s *impulse response*. [...] He defines the 2-dimensional convolution operator [...]

**Properties of 2-dimensional Convolution or Convolution Algebra** [...] All 5 properties of convolution hold for any 2-dimensional fields  $x, y$ , and  $z$ , for which convolution is defined (i.e., for which the infinite sums exist). His Figure 1.1-9 illustrates a convolution.

**Stability in 2-dimensional Systems**<sup>18</sup> Stable systems are those for which a small change in the input gives a small change in the output. We define bounded-input bounded-output (BIBO) stability for 2-dimensional systems analogously to that in 1-dimensional system theory. A spatial or 2-dimensional system will be stable if the response to every uniformly bounded input is itself uniformly bounded. For an LSI system the condition is equivalent to the impulse response being absolutely summable,

$$\sum_{k_1, k_2} |h_{k_1, k_2}| < \infty. \tag{8.117}$$

**Sect. 1.2 2-dimensional discrete-space Fourier transform** The Fourier transform is important in 1-dimensional signal processing because it effectively explains the operation of linear time-invariant (LTI) systems via the concept of frequency response, i.e., the Fourier transform of the system impulse response. While convolution provides a complicated description of the LTI system operation, with the input at all locations  $n$  affects the output at all locations, the frequency response provides a simple interpretation as a scalar weighting in the Fourier domain, where the output at each frequency  $\omega$  depends only on the input at that same frequency. A similar result holds for 2-dimensional systems that are LSI.

**2020-07-15 Predrag** Note that the discrete Fourier transform of a Bravais lattice always carries the prefactor  $1/\det \Lambda$ . Going back involves a volume  $(2\pi)^d$ .

**Definition 1.2-1: 2-dimensional Fourier Transform** [...] In the 2-dimensional Fourier transform the frequency variable  $\omega_1$  is called *horizontal frequency*, and the variable  $\omega_2$  is called *vertical frequency*. [...] As  $n, t$  are integers, the 2-dimensional Fourier transform is periodic with rectangular period  $2\pi \times 2\pi$ , and only needs be calculated for one period, usually taken to be  $[-\pi, \pi] \times [-\pi, \pi]$ .

<sup>18</sup>Predrag 2020-07-11: I do not understand BIBO, but maybe we should?

[...] the 2-dimensional Fourier transform is a *separable operator*, because it can be performed as the concatenation of 1-dimensional operations on the rows followed by 2-dimensional operations on the columns.

**Inverse 2-dimensional Fourier Transform** [...]

**Fourier Transform of 2-dimensional or Spatial Convolution**

**Theorem 1.211: Fourier Convolution Theorem** [...]

[...] As a 2-dimensional or spatial LSI system is characterized by its impulse response  $h_{n,t}$ , its frequency response  $H_{\omega_1, \omega_2}$  suffices to characterize such a system. And the Fourier transform  $Y$  of the output equals the product of the frequency response  $H$  and the Fourier transform  $X$  of the input. When the frequency response  $H$  takes on only values 1 and 0, the system is an *ideal filter*, filtering out some frequencies and passing others unmodified. More generally, the term filter include all such LSI systems, and has been extended to shift-variant and even nonlinear systems through the concept of the Volterra series of operators.<sup>19</sup>

**Some Important Properties of the FT Operator** [...]

**Some Useful Fourier Transform Pairs** [...]

**Example 1.2-4: Fourier Transform of Separable Signal** [...]

**Symmetry Properties of the Fourier Transform** [...]

Generally, we think of the Fourier transform as the evaluation of the Z-transform on the unit polycircle  $\{|z_1| = |z_2| = 1\}$ ; however, this assumes the polycircle is in the region of convergence of  $X(z_1, z_2)$ , which is not always true.

[...] linear shift-invariant systems with sinusoidal excitations are naturally described by the Fourier transform. The Z-transform is a generalization of the Fourier transform which allows us to treat exponential inputs.

[...] Exponentials of the form  $x_{n_1 n_2} = z_1^{n_1} z_2^{n_2}$  are eigenfunctions of 2-dimensional linear shift invariant systems.

The 2-dimensional Z-transform of a discrete field  $X$  is defined as

$$X_{z_1 z_2}^Z = \sum_{n_1=-\infty}^{\infty} \sum_{n_2=-\infty}^{\infty} x_{n_1 n_2} z_1^{-n_1} z_2^{-n_2}. \quad (8.118)$$

---

<sup>19</sup>Predrag 2020-07-11: ‘Volterra series of operators’? Defined in S. Thurnhofer and S. K. Mitra, *A General Framework for Quadratic Volterra Filters for Edge Enhancement*, IEEE Trans. Image Process., vol. 5, June, pp. 950-963, 1996.

**Example 3.4-5: Comparison of Fourier Transform and Z-Transform** [· · ·]

The Fourier transform is not strictly a subset of the Z-transform, because it can use impulses and other singularity functions, which are not permitted to Z-transforms.

[· · ·] The Fourier transform is used primarily to describe signals and to describe the actions that systems will have on them. The Z-transform is used to describe systems and to provide an additional tool for manipulating difference equations. While the 2-dimensional Z-transform is related to its 1-dimensional counterpart, the two transforms are actually quite different.

For  $z_1 = e^{i\omega_1}, z_2 = e^{i\omega_2}$  the Z-transform reduces to the Fourier transform. The corresponding surface in the Z-domain is the called 2-dimensional unit *bicircle*. 2-dimensional Z-transform converges on the *Reinhardt domain*, the 2-dimensional analog of the annulus for 1-dimensional case.

**2020-02-23 Predrag** Continuing on the multivariate generating functions, the *integer-point transform* introduced in this textbook in integer lattices counting: Beck and Robins [27] *Computing the Continuous Discretely*, ([click here](#)), might be helpful:

Let  $\mathbf{a} = (a_1, \dots, a_d) \in \mathbb{Z}^d$  be an integer point. The Laurent monomial  $\mathbf{z}^{\mathbf{a}}$  is defined as

$$\mathbf{z}^{\mathbf{a}} := z_1^{a_1} z_2^{a_2} \dots z_d^{a_d}, \quad \mathbf{z}^{\mathbf{0}} := 1 \tag{8.119}$$

where  $\mathbf{0} := (0, 0, \dots, 0)$ . For a given rational cone or rational polytope  $S \subset \mathbb{R}^d$ ,

$$\sigma_S(\mathbf{z}) = \sigma_S(z_1, z_2, \dots, z_d) := \sum_{\mathbf{a} \in S \cap \mathbb{Z}^d} \mathbf{z}^{\mathbf{a}} \tag{8.120}$$

is called the *integer-point transform* of  $S$ . The function  $\sigma_S$  lists all integer points in  $S$  not as a list of vectors, but as a sum of monomials. This  $\sigma_S$  also goes by the name *moment generating function* or simply *generating function* of  $S$ .

They start with the usual trivial example of a geometric series in Example 3.3, and work out a 2-dimensional  $\{(1, 1), (-2, 3)\}$  Bravais lattice in example Example 3.4, see figure 8.2. They call the  $\mathbb{R}^2$  interior of the half-open primitive cell ‘fundamental parallelogram  $\Pi$ ’, and tile the two-dimensional cone  $\mathcal{K}$  with its non-negative translations. That results in the rational polynomial formula for the integer-point transform of the cone  $\mathcal{K}$

$$\sigma_{\mathcal{K}}(\mathbf{z}) = \frac{1 + z_2 + z_2^2 + z_1^{-1} z_2^2 + z_1^{-1} z_2^3}{(1 - z_1 z_2)(1 - z_1^{-2} z_2^3)} \tag{8.121}$$

of the form that I had suggested to Han for the spatiotemporal cat.

Check also:

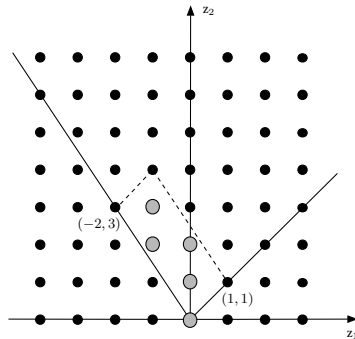


Figure 8.2: The cone  $\mathcal{K}$  and its fundamental parallelogram, fig 3.3 from ref. [27].

- **2020-03-02 Predrag** notes below, on Wilf [249] sect. 1.5 *Two independent variables*.
- *Characteristic function* or “five-point stencil” (8.168)

**2020-03-03 Predrag** OK, the fundamental parallelepiped determinant (8.97) counts integer points

$$N_n = |\text{Det } \mathcal{J}| = |\text{Det}(v_1|v_2|\cdots|v_n)|. \quad (8.122)$$

What does  $\text{tr } \mathcal{J}$  do? That is also an invariant under  $SLG(n)$  lattice transformations.

### 8.7.3 Primitive parallelogram

**2020-01-25 Predrag** A lattice vector is called *primitive*, if there is no other lattice points on the segment between 0 and the tip.

or:

An integer vector  $v \in \mathbb{Z}^d$  is *primitive* if it cannot be written as an integer multiple  $m \neq 1$  of some other integer vector  $w \in \mathbb{Z}^d$ .

or:

A lattice point is a primitive lattice point if it is not a multiple of any other lattice point, that is, the greatest common divisor of its coordinates is one.

or:

A primitive lattice point is a lattice point visible from the origin.

Let  $A$  be an integer  $[d \times d]$ -matrix with nonzero determinant  $k$  and primitive row vectors. The common divisors of the entries of each row of  $A$  are preserved under multiplication on the right by any matrix  $X \in SL(d, \mathbb{Z})$ .

A lower triangular integer matrix

$$C = \begin{pmatrix} c_{11} & 0 & \cdots & 0 \\ c_{21} & c_{22} & \ddots & 0 \\ \vdots & & \ddots & 0 \\ c_{d1} & \cdots & c_{d(d-1)} & c_{dd} \end{pmatrix} \quad (8.123)$$

is said to be in (lower) *Hermite normal form* if  $0 < c_{11}$  and  $0 \leq c_{ij} < c_{ii}$  for all  $j < i$ .

I would prefer the vectors to be column vectors, as in Lind (24.163). In particular, in the case of 2-dimensional square lattice,

$$C = \begin{pmatrix} L & S \\ 0 & T \end{pmatrix} \quad (8.124)$$

The primitive cell basis column vectors are

$$v_1 = \begin{pmatrix} L \\ 0 \end{pmatrix}, \quad v_2 = \begin{pmatrix} S \\ T \end{pmatrix},$$

where  $0 \leq S < L$  is the relative-periodic ‘shift,’ or ‘screw’ for a screw-boundary condition, and our convention is  $L \geq T$ , the rest obtained by discrete symmetries.

Orbit of  $\Lambda$ , a matrix in Hermite normal form with primitive row vectors, is denoted  $\{A\Lambda \mid A \in \text{SL}(2, \mathbb{Z})\}$ .

**Lemma**[Cohen [54], Theorem 2.4.3] Assume  $k > 0$ . Given an arbitrary matrix  $A \in M_{n,k}$ , the orbit  $ASL(n, \mathbb{Z})$  contains a unique matrix  $\Lambda$  in Hermite normal form.

**Samuel Holmin** PhD thesis [118] is a user-friendly overview of his papers, such as *Counting nonsingular matrices with primitive row vectors* [117] [arXiv:1211.2716](https://arxiv.org/abs/1211.2716). Holmin defines a *primitive* parallelogram: “Consider a parallelogram with integer coordinates which cannot be decomposed into smaller parallelograms with integer coordinates. We will call such an object a primitive parallelogram; see figure 8.3 for an illustration. How many primitive parallelograms are there with an area of 10? There are infinitely many such primitive parallelograms: in fact, starting with a single primitive parallelogram, we can produce another one with the same area by for example shifting it an integer distance up or to the right, or by shearing it, and by repeating either of these operations we can produce arbitrarily many different parallelograms, all of which are primitive and have the same area.”

Curiously, even though in his 2nd papers he mentions that different primitive cells correspond to the same *lattice*, his claim of figure 8.3 is wrong.

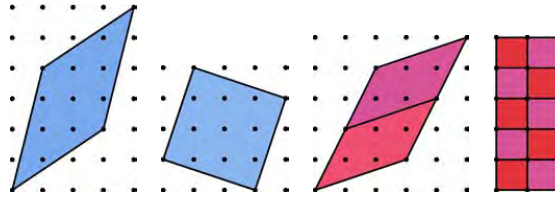


Figure 8.3: Four primitive cells of area 10, a figure from Holmin’s PhD thesis [118]. The two blue primitive cells are not ‘primitive’ (i.e., prime), as they are clearly tiled by smaller prime primitive cells. Homlin claims that the two blue primitive cells are primitive, but that is wrong, see (24.216).

Wigman [248] *Counting singular matrices with primitive row vectors*: “ Let us consider the set of singular  $[n \times n]$  matrices with integer entries. We are interested in the question how many among these matrices have primitive row vectors, that is each row is not a nontrivial multiple of an integer vector. We count the matrices according to the maximal allowed Euclidean length of the rows. Without the constraint of primitivity the problem of counting such matrices was solved by Katznelson [??].”

Wigman [248] and Katznelson focus on asymptotic counting, which we probably do not need.

**2020-02-19 Predrag** Alexander Gorodnik [lecture notes](#) discuss cat map  $(A^n - 1)$  and says “The number of such solutions is exactly the area  $\det(A^n - 1)$  of fundamental parallelepiped in virtue of the

**Pick’s theorem** (Gorodnik’s Theorem 1.5.3, and A.4.1). Let  $i$  be the number of points with integer coordinates in the interior of parallelogram  $P$  and  $b$  be the number of points with integer coordinates on the perimeter of  $P$ . Then,  $\text{Area}(P) = i + (b/2) + 1$ , with points on the edges are counted as half and all vertices count as a single point.

He proves the theorem. As usual, Pick’s theorem is for  $\mathbb{R}^2$ , not general enough for us.

**2020-02-19 Predrag** Baake, Hermisson and Pleasants [16] *The torus parametrization of quasiperiodic LI-classes* call this theorem a “Fundamental fact” (their eq. (10)), and prove it, in Appendix for  $d$ -dimensional tori maps, i.e., in the case that we need. They use it to count all manner of tilings. What they emphasize, and what we might have to pay attention to, is the structure of the symmetry solutions on  $\mathbb{T}^d$ .

**2020-02-21 Predrag** Jezierski and Marzantowicz [137] [\(click here\)](#) write:

let  $f : X \rightarrow X$  be a self-map of a set  $X$ .

(1.0.4) Definition. If  $x \in X$  is a periodic point of  $f$  then any  $m \in \mathbb{N}$  such that  $f^m(x) = x$  is called a period of  $x$ . The smallest period of  $x$  is called the

minimal period of  $x$  with respect to  $f$ . The set of all minimal periods of  $x \in X$  is called the set of minimal periods of  $f$  and denoted by  $\text{Per}(f)$ .

We will define the fundamental algebraic invariants of a map  $f$  which allow us to study the following notions:

- Lefschetz number  $L(f)$  (cf. (2.3.12)), correspondingly Lefschetz numbers  $L(fm)$  of all iterations and their algebraic combinations, informing about the existence of fixed, respectively periodic points.
- Nielsen number  $N(f)$  (cf. (4.1.2)), correspondingly Nielsen periodic numbers  $NFm(f)$  (cf. (5.1.16)),  $NPm(f)$  (cf. (5.1.14)) estimating from below the number of fixed, respectively points of period  $m$  and  $m$ -periodic points.

[...] This theory was initiated by Jakob Nielsen [195] in 1920 by the observation that every self-map of the two-dimensional torus  $f : \mathbb{T}^2 \rightarrow \mathbb{T}^2$  has at least  $|\det(I-A)|$  fixed points (here  $I, A \in M_{2 \times 2}(\mathbb{Z})$  are respectively the identity matrix and the matrix representing the induced homotopy homomorphism  $f_{\#}$  of  $\pi_1(\mathbb{T}^2) = \mathbb{Z}^2$ ).

In 1975 R. Brooks, B. Brown J. Pak, and D. Taylor [39] derived a nice formula for the Nielsen number  $N(f)$  for the torus map: the Nielsen number equals the absolute value of the Lefschetz number. [...] The following theorem has been proved in ref. [39].

(4.3.14) Theorem. For every self-map of the torus  $f : \mathbb{T}^d \rightarrow \mathbb{T}^d$ ,  $L(f) = \det(I-A)$  and  $N(f) = |L(f)|$ .

Proof. Since the Lefschetz and Nielsen numbers are homotopy invariants we may assume that  $f = f_A$ , i.e.  $f$  is induced by the linear map  $A$ .

1.  $f_A$  has exactly  $|\det(I-A)|$  fixed points,
2. no two fixed points of  $f_A$  are Nielsen related,
3. the index of each fixed point equals  $\text{sgn}(\det(I-A))$ .

[...] the fundamental theorem which allows us to extend the Nielsen fixed point theory from tori into nilmanifolds. This theorem was proved simultaneously by Anosov [An], and also Fadell and Husseini [FaHu2].

(6.3.13) Theorem. Let  $f : X \rightarrow X$  be a self-map of a compact nilmanifold. Then  $N(f) = |L(f)|$  and  $L(f) = \det(I-A)$ , where  $A$  denotes the linearization matrix of  $f$  (cf. Definition (6.3.4), Proposition (6.3.6)).

**2020-02-22 Predrag** Brooks *et al.* [39] *Nielsen numbers of maps of tori:*

If  $f : X \rightarrow X$  is any map on a  $k$ -dimensional torus  $X$ , then the Nielsen number and Lefschetz number of  $f$  are related by the formula  $N(f) = |L(f)|$ . Thus, on the torus, the Lefschetz number gives information, not just on the existence of fixed points, but on the number of fixed points as well. No other compact Lie group has this property.



**1995-09-08, 2020-12-08 Predrag** Fel'shtyn and Hill [81] *Trace formulae, Zeta functions, congruences and Reidemeister torsion in Nielsen theory* [arXiv:chaodyn/9509009](https://arxiv.org/abs/chaodyn/9509009) paper is rich in examples of trace formulas and zeta functions, but it's probably safe to ignore all this...

"The Artin-Mazur zeta function and its modification count periodic points of a map geometrically, the Lefschetz's type zeta functions do this algebraically (with weight given by index theory). Another way to count the periodic points is given by Nielsen theory.

The Lefschetz zeta function is always rational function of  $z$  and is given by a determinant formula. Manning [178] proved the rationality of the Artin-Mazur zeta function for diffeomorphisms of a compact smooth manifold satisfying Smale's Axiom A.

In Nielsen theory the 'fixed point class' is determined by the 'lifting class'. A fixed point class is called *essential* if its index is nonzero. The number of lifting classes (and hence the number of fixed point classes, empty or not) is called the *Reidemeister Number*. Generating functions for these numbers are called the Reidemeister zeta and Nielsen zeta functions. They are homotopy invariants. "

#### 8.7.4 Tensor eigenvalues

In principle Han has solved the periodic states counting problem for  $d$ -dimensional hypercubic lattices by the discrete Fourier transform diagonalization formula (24.176). A conceptual problem is that the answer is stated in terms of  $\cos$ 's of rational angles, and it is not obvious how those combine to yield an integer as the final result, the number of periodic states.

For that reason it might be nice to perform the inverse Fourier transform to the configuration space, to see what the basis vectors and the fundamental parallelogram of the 2-dimensional integer lattice look like, and unify the treatment of the 1-dimensional and higher-dimensional lattice points counting. We have looked at the relationship between the periodic states and their Fourier representation in (24.29), figure 24.24, (24.53), etc..

Also we have some suggestive lattice solutions, such as (24.62), figure 24.29 (unit cube have been preferable - this is in the cube center coordinates).

There is much literature on eigenvectors of tensors - probably we can figure it out on our own, but I'm recording possible references just for record here:

**2018-02-06 Predrag** A job candidate Glen Evenbly talked about "Tensor Networks", (also known as "birdtracks", but getting a citation out of computer nerds who do it is harder than pulling teeth - at best I can pass under "Penrose diagrams"). If you want to see a lot of non-birdtracky pictures, Román Orús [has them](#). Basically, if you are solving a 1D lattice problem, the transfer operator is a matrix. However, if you are acting on a 2-dimensional or higher lattice, the transfer operator has pairs of more indices replacing each index of the 1D matrix, hence "tensor." We

need to understand that as we go from cat map Toeplitz matrices to their  $d$ -dimensional generalizations.

**2020-02-14 Predrag** Mateusz Michałek and Bernd Sturmfels [187] *Invitation to Nonlinear Algebra*, ([click here](#)) discuss symmetric  $[n \times n]$  matrices tensor eigenvectors in Sect. 9.1.

The main monograph in this subject is Qi, Chen and Chen [215] *Tensor Eigenvalues and Their Applications*, ([click here](#)).

They find convenient to replace the  $n$ -dimensional affine space with the  $(n-1)$ -dimensional projective space, where two nonzero vectors are identified if they are parallel.

Papers not looked at yet:

*All Real Eigenvalues of Symmetric Tensors* DOI:

*Generalized Tensor Eigenvalue Problems* DOI:

*On determinants and eigenvalue theory of tensors* DOI:

## 8.8 Difference equations

sect. 2.3 Linear homogenous equations with constant coefficients, Elaydi [74]

Consider  $k$ th-order difference equation

$$\phi_{n+k} + p_1 \phi_{n+k-1} + p_2 \phi_{n+k-2} + \cdots + p_k \phi_n = 0, \quad (8.125)$$

where  $p_i$  are constants and  $p_k \neq 0$ . A  $k$ th-order difference equation with constant coefficients is often referred to as  $(k + 1)$ -term recurrence relation, see sect. 8.9. Assuming a solution of form  $\phi_n = \Lambda^n$  leads to the *characteristic equation* (see also ‘characteristic function’ (8.167))

$$\Lambda^k + p_1 \Lambda^{k-1} + p_2 \Lambda^{k-2} + \cdots + p_k = 0, \quad (8.126)$$

with characteristic roots  $\{\Lambda_1, \Lambda_2, \dots, \Lambda_k\}$ . If the roots are distinct,

$$\{\Lambda_1^n, \Lambda_2^n, \dots, \Lambda_k^n\}$$

is a set of fundamental solutions, and the general solution is of form

$$\phi_n = \sum_{i=1}^k a_i \Lambda_i^n, \quad (8.127)$$

where constants  $a_i$  are determined by the initial conditions  $\{\phi_0, \phi_1, \dots, \phi_{k-1}\}$ .

If the roots are not distinct, one also has fundamental solutions of form  $n^m \Lambda_i^n$ .

**sect. 2.4 Linear inhomogenous equations, Elaydi [74]**

$$\phi_{n+k} + p_1 \phi_{n+k-1} + p_2 \phi_{n+k-2} + \cdots + p_k \phi_n = g_n \quad (8.128)$$

represents a physical system in which the *forcing term* (or *external force*, or *control*, or *input*)  $g_n$  is the input, and  $\phi_n$  the output,

$$g_n \rightarrow \text{system} \rightarrow \phi_n .$$

The solutions of (8.128) do not form a vector space, i.e., their linear combinations are not also solutions. However, a difference of any pair of solutions is a solution of the homogenous difference equation (8.125), and a general solution of the linear inhomogenous system (8.128) is a sum of the *complementary* solution (a homogenous solution  $\phi_c$  of (8.125), and a *particular* solution  $\phi_p$

$$\phi_n = \phi_{c,n} + \phi_{p,n} \quad (8.129)$$

A simple example of a particular solution: if  $g_n = a^n$ , then  $\phi_{p,n} = c_1 a^n$ .

**2020-03-28 Predrag** There are many books on difference equations.

I like Elaydi [74] ([click here](#)), but I have also downloaded

Kelley and Peterson [155] ([click here](#))

Agarwal [1] ([click here](#))

Agarwal [2] ([click here](#))

Allen, Aulbach, Elaydi and Sacker [7] ([click here](#))

Galor [95] ([click here](#))

Ozisk, Orlande, Colaco and Cotta [200] ([click here](#))

Micciancio and Goldwasser [186]

**2022-05-06 Predrag** Mariconda and Tonolo [179] *Linear recurrence relations* (2016), ([click here](#)) seems like a good textbook on many counting and linear things.

they call  $j_t$  "a sequence of non-homogeneous terms of the recurrence. The recurrence is called homogeneous if the sequence of non-homogeneous terms is the null sequence."

Fibonacci recurrence:  $f_m$  are the Fibonacci numbers, defined by the recursion  $f_{m+1} = f_m + f_{m-1}$ , for  $m \geq 0$ , together with the initial condition  $f_0 = 0$  and  $f_{-1} = 1$  see (6.195).

**2020-04-13 Predrag** Dannan, Elaydi and Liu [64] *Periodic solutions of difference equations* is a treasure trove of results on periodic solutions of difference equations: marginal eigenvalues, Floquet exponents and multipliers, Fredholm alternative.

**2020-08-10 Predrag** Lick [168] *Difference Equations from Differential Equations* ([click here](#)) we probably do not need.

The most general, quasi-linear, second-order PDE in two independent variables is his eq. (2.0.2). Depending on coefficients, the equation can be *hyperbolic*, such as the  $d = 2$  spacetime wave equation (2.0.3). He focuses on *parabolic* ( $s = 2$  for us), such as the time dependent diffusion equation given by (2.0.4).

Elliptic equations usually describe the steady-state limit of problems where the time-dependent problem is described by parabolic or hyperbolic partial differential equations. The most common elliptic equation is  $d = 2$  space'time' symmetric Laplace's equation (2.0.5).

He defines Helmholtz equation (4.0.5), Laplace's equation (4.0.6), and Poisson's equation (4.0.7). His emphasis is on the discretized Helmholtz equation (4.1.3).

Sect. 2.4 *Algorithms for Two-Dimensional Problems* has the 5-term recurrence, his eq. (2.4.3) and (4.1.3).

Difference equations arising from elliptic equations generally necessitate the solution of a large set of linear algebraic equations. The matrix corresponding to this set of equations is generally sparse and good solution methods take advantage of this fact. [...] the direct solution of these difference equations is quite time consuming. When the number of equations is large, iterative methods of solution are usually more efficient.

(4.2.8) defines *Jacobi iteration*, a method of improving initial guess solution. (4.2.9) method is known as Gauss-Seidel iteration or the method of successive relaxation.

**2016-07-11 Predrag** Boris cites P. A. Martin [181] *Discrete scattering theory: Green's function for a square lattice*

The *lattice Green's function* is the main subject of the paper.

We consider the simplest problem, with a two-dimensional, square lattice. Each lattice point can move out of the plane of the lattice, and that each point is connected to its neighbours by springs; only nearest-neighbour interactions are included. This leads to a system of partial difference equations. The same equations are obtained if the two-dimensional Helmholtz equation is discretized using the central-difference approximation (lattice d'Alembert operator) for the Laplacian.

**2017-09-11 Predrag** Morita [190] *Useful procedure for computing the lattice Green's function - square, tetragonal, and bcc lattices:* " A recurrence relation, which gives the values of the lattice Green's function along the diagonal direction from a couple of the elliptic integrals of the first (8.170) and second kind, is derived for the square lattice by an elementary partial integration. The values of the square lattice Green's function at an arbitrary site are then calculated in a successive way with the aid of the difference equation defining the function. " The method yields a recursion formula for a peculiar lattice Green's function on a 2d lattice, but not the LGF itself.

2017-09-09, 2024-01-07 **Predrag** Simons [228] uses (8.127) in his (2.54) to invert a particular banded matrix.

Berry Simon refers to what we call orbit Jacobian operator  $\mathcal{J}$ , as a ‘Jacobi matrix’ [228], or discrete Schrödinger operator, see [arXiv:2011.12335](#).

[Encycl. of Math](#) defines a square tridiagonal matrix a Jacobi matrix, does not do anything more with it.

[wiki tridiagonal Jacobi operator](#) uses to specify systems of orthonormal polynomials, does not elaborate much.

The usual [wiki Jacobian matrix and determinant](#) is not a banded matrix.

### 8.8.1 Time quasilattices

2018-10-10, 2020-03-12 **Predrag** Felix Flicker writes: “My student Leon Zaporski and I have been investigating the topological entropy of substitution sequences in the symbolic dynamics of periodic orbits in discrete-time dynamical systems. We were hoping you might be willing to take a look at our draft, Zaporski and Flicker [257] *Superconvergence of topological entropy in the symbolic dynamics of substitution sequences*, [arXiv:1811.00331](#), and to send any thoughts you might have, both in terms of whether you think the results would be of interest to the community, and if there is a journal you might recommend for us to submit to.”

2CB

I failed to read it. But it needs to be included in ChaosBook, as well as many of the references.

Their Fig. 1 is the topological entropy as a function of a control parameter of the logistic map [204]. [...] In the cases that accumulation points correspond to generalised time quasilattices, the Boyle-Steinhardt class [38] is indicated above the curve.

Predrag: I made several attempts to get some kind of renormalization theory for the Sharkovsky sequence, with no interesting results to report. Dahlquist wrote up his attempt [ChaosBook \(click here\)](#).

[...] Period doubling continues to be of importance to cutting edge research: recent experiments established the existence of (discrete) time crystals, which spontaneously break the symmetry of a periodic driving by returning a robust period-doubled response, made rigid to perturbations and finite temperature by the local interactions of many degrees of freedom. [...] periodically-driven nonlinear systems can feature not just period-doubled responses, but robust responses with the symmetries of one-dimensional (generalised) *time quasilattices* [88]. [...] Quasilattice substitution rules fall within the set we consider, and, by considering a simple generalisation of the basic quasilattice concept, we find that we are able to identify aperiodic orbits corresponding to all physically relevant quasilattices, extending previous results identifying two cases. Generalizing further we consider a set of substitutions additionally covering,

for example, the period-doubling cascade. [...] Whereas the topological entropy is zero for all sequences in the period-doubling cascade, for other substitution sequences it increases monotonically. [...] We find that the topological entropy of the wide class of substitution sequences we consider converges as a double exponential onto its accumulation point. [...] We demonstrate that all one-dimensional quasilattices can appear as stable orbits in nonlinear dynamical systems.

Here is something we might find useful for spatiotemporal cat:

[...] we focus on the *generalised composition rules*, which systematically generate admissible words by a substitution process [40].

[...] The universal order of periodic windows coincides with the *parity-lexicographic order* of words, defined through the relation ' $\prec$ ' in the following way:

$$L \prec C \prec R$$

and for two admissible words they state it in a way that is perhaps superior to [ChaosBook](#) [ChaosBook](#). Cite it there.

[...] **Word operations**

- $\bar{A}\bar{B}$  indicates the concatenation of words  $\bar{A}$  and  $\bar{B}$
- $|\bar{A}|$  returns the number of letters in  $\bar{A}$
- $|\bar{A}|_{R,L}$  returns the number of letters  $R, L$  in  $\bar{A}$
- $\bar{A}|_C$  substitutes the final letter of  $\bar{A}$  with the letter  $C$ .

Inverse words are defined as follows (Predrag - I do not understand this):

$$\begin{aligned} \bar{A}^{-1}(\bar{A}\bar{B}) &= \bar{B} \\ (\bar{A}\bar{B})\bar{B}^{-1} &= \bar{A}. \end{aligned} \tag{8.130}$$

**Theorem 8.1.** *Substitution rules generating a cascade with initial word  $\bar{W}_1 = R$  and  $\bar{W}_2 = \bar{R}$  can be restated as a second order linear recursive relation  $\bar{W}_{n+2} = g(\bar{W}_n, \bar{W}_{n+1})$  under concatenation if  $\bar{W}_3 = g(\bar{W}_1, \bar{W}_2)$ .*

[...] Consider a  $[2 \times 2]$  growth matrix

$$A = \begin{pmatrix} a & b \\ c & d \end{pmatrix} \tag{8.131}$$

which quantifies the growth in the numbers of each letter type:

$$\begin{pmatrix} |\bar{W}_n|_R \\ |\bar{W}_n|_L \end{pmatrix} \rightarrow \begin{pmatrix} a & b \\ c & d \end{pmatrix} \begin{pmatrix} |\bar{W}_{n-1}|_R \\ |\bar{W}_{n-1}|_L \end{pmatrix} = \begin{pmatrix} |\bar{W}_{n+1}|_R \\ |\bar{W}_{n+1}|_L \end{pmatrix} \tag{8.132}$$

The class of substitutions we consider can then be written as

$$\bar{W}_n = \bar{W}_{n-1} \mathcal{P} \left( \bar{W}_{n-1}^{\text{tr}(A)-1} \bar{W}_{n-2}^{-\det(A)} \right) \tag{8.133}$$

for  $n > 2$ , with  $\bar{W}_1 = R$ , and  $\bar{W}_2$  a specified word. The symbol  $\mathcal{P}$  indicates an unspecified permutation. The characteristic equation of the growth matrix  $A$  is

$$\lambda^2 - \text{tr}(A)\lambda + \det(A) = 0. \quad (8.134)$$

The eigenvalues of  $A$  must be real, either integer or quadratic irrational (when we consider quasilattices). The ratio of the components of the eigenvector associated to the largest eigenvalue gives the relative frequencies of the two cell types [38]. Eq. (8.134) can be seen as the  $n \rightarrow \infty$  limit of the defining equation of some integer sequence  $W_n$  given by

$$W_n = \text{tr}(A)W_{n-1} - \det(A)W_{n-2} \quad (8.135)$$

for  $n > 2$ ,  $W_1 = |\bar{W}_1| = 1$ , and  $W_2 = |\bar{W}_2|$ . The ratio  $W_n/W_{n-1}$  gives the best possible rational approximation, for denominators not larger than  $W_{n-1}$ , to the largest eigenvalue of the growth matrix, *i.e.* the larger of the solutions to Eq. (8.134).

[...] As an example, the period-doubling substitutions lead to the integer sequence

$$W_n = W_{n-1} + 2W_{n-2} \quad (8.136)$$

for  $n > 2$ , with  $W_1 = |\bar{W}_1| = |R| = 1$  and  $W_2 = |\bar{W}_2| = |RL| = 2$ . Explicitly, the first few terms are

$$1, 2, 4, 8, 16, 32, 64, \dots \quad (8.137)$$

*i.e.*  $W_n = 2^{n-1}$ .

Predrag: This is perhaps related to  $s = 2$  version of (2.96).

Then they do Fibonacci. [...] The eigenvalues of a  $[2 \times 2]$  growth matrix  $A$  are real and given by

$$\lambda_{\pm} = \frac{1}{2} \left( s \pm \sqrt{s^2 - 4\det A} \right), \quad s = \text{tr} A. \quad (8.138)$$

If  $s^2 = 4\det A$  they are integers. Otherwise, the larger eigenvalue is a quadratic irrational ‘Pisot-Vijayaraghavan’ (PV) number: the largest root of an irreducible monic polynomial, all of whose Galois conjugates have modulus strictly less than one. [...] The three conditions are necessary and sufficient for the substitutions to correspond to quasilattice inflation rules [38]:

1. the growth matrix must be unimodular,  $|\det A| = 1$
2. there must be two spacings between each symbol
3. the largest eigenvalue of the growth matrix must be a PV number.

The condition  $|\det A| = 1$ , implies the inverse of the growth matrix is also an integer matrix. The inflation (substitution) of any quasilattice sequence can therefore be undone with a well-defined deflation. This endows quasilattices with a discrete scale invariance [37]. The third, PV numbers condition is necessary for the interpretation of the quasilattice sequence in terms of a cut through a higher-dimensional regular lattice.

The concept of quasilattices relating to higher-dimensional lattices is discussed at length in refs. [38, 88].

Predrag: So our  $s = 3$  temporal cat  $\lambda^2 - 3\lambda + 1 = 0$  eigenvalue  $\frac{3+\sqrt{5}}{2}$  turns out to be a PV number. So is  $s = 4$  temporal cat  $\lambda^2 - 4\lambda + 1 = 0$  eigenvalue  $2 + \sqrt{3}$ . Both are the Boyle-Steinhardt [38] quasilattices, of class 1, respectively 3.

[...] Starting from an orbit described by the word  $R$ , repeated application of the inflation rules will lead to a cascade of stable periodic orbits of increasing length. After an infinite number of substitutions, *i.e.* at the accumulation point of the sequence, lies a stable orbit described by an aperiodic word: a *time quasilattice*. [...] Characteristic equation

$$\lambda^2 = 4\lambda - 1. \tag{8.139}$$

leads to the (modulus of the) Clapeyron numbers  $C_n$  (A125905 in the [On-Line Encyclopedia of Integer Sequences](#))

$$C_n = 4C_{n-1} - C_{n-2} \tag{8.140}$$

for  $n > 2$  with  $C_1 = 1, C_2 = 4$ .

Predrag: In conclusion, temporal cat is related to counting of quasilattice words. Not sure it is of any use to us.

**2020-04-12 Predrag** Have a look at Flicker, Simon and Parameswaran [89] *Classical dimers on Penrose tilings*. [...] [...] [...] [...] [...] [...] [...] [...] [...]

## 8.9 Generating functions

(Note, there is also a totally unrelated Lagrangian ‘generating function’, sect. 11.6, nothing to do with this section of the blog.)

**Definition [27].** Let  $f(x)$  be a series in powers of  $x$ . Then by the symbol  $[x^n]f(x)$  we will mean the coefficient of  $x^n$  in the series  $f(x)$ .

**2020-03-20 Predrag** The theory generating function (AKA Z-transforms) is pedagogically explained by Elaydi [74], including a table of common Z-transform pairs, in analogy with the familiar Laplace transform tables.



**2020-09-30 Predrag** Online [Signals and Systems](#) has pedagogical chapters on Z-transforms.

**2020-07-11 Predrag** Woods [252] *Multidimensional signal, image, and video processing and coding*, Chap. 3 *Two-Dimensional Systems and Z-Transforms* (2012) ([click here](#)).

**2020-01-23 Predrag** For multivariate generating functions

$$N(z), \quad z^n = z^{n_1} z^{n_2} \dots z^{n_d}, \quad (8.141)$$

see (8.101), (8.119), (8.120), (8.121) .

Other examples of generating functions: (2.44), (8.190), (16.5) .

**2020-04-07 Han** Perhaps we need three generating function variables

$$N(z_1, z_2, z_3) = \sum_{L=1} N_{[L \times T]_S} z_1^L z_2^T z_3^S, \quad (8.142)$$

Here  $z_3^S$  sum is finite,  $-L < S < L$ , and that feels not sufficiently invariant, as it depends on Hermite normal form convention. Need something invariant...

**2020-03-01 Predrag** Cute but true; Wilf [249] *Generatingfunctionology* defines the periodic points counting generating function as

$$N(z) = \sum_{n \geq 0} N_n z^n, \quad (8.143)$$

and starts out in his sect. 1.1 *An easy 2-term recurrence*, with our Bernoulli periodic points count (for the  $s = 2$  case only)

$$N_n = s^n - 1, \quad (8.144)$$

as a trivial example of a two-term recurrence (first-order difference equation [74])

$$N_{n+1} = 2N_n + 1, \quad (s = 2; n \geq 0, N_0 = 0), \quad (8.145)$$

and (Predrag's insert) for  $s \neq 2$ ,

$$N_{n+1} - sN_n = (s - 1), \quad (n \geq 0, N_0 = 0), \quad (8.146)$$

and its conversion to the periodic points count generating function (8.143). For (8.145) he derives and expands in partial fractions

$$N(z; 2) = \frac{z}{(1-z)(1-2z)} = \frac{2z}{1-2z} - \frac{z}{1-z}, \quad (8.147)$$

and (Predrag's addition) for  $s \neq 1$ ,

$$N(z; s) = (s-1)z + (s-1)(s+1)z^2 + (s-1)(s^2+s+1)z^3 + \dots, \quad (8.148)$$

verifying the Bernoulli periodic points count (8.144). Take  $N_n = (s-1)\hat{N}_n$ , then (8.146) leads to

$$\hat{N}_{n+1} - s\hat{N}_n = 1, \quad (n \geq 0, \hat{N}_0 = 0, \hat{N}_1 = 1). \quad (8.149)$$

$$\hat{N}(z; s) = z + (s+1)z^2 + (s^2+s+1)z^3 + \dots, \quad (8.150)$$

For  $s = 1$  this is a complicated way to generate integers.

Then he does, as an example of a 3-term recurrence (second-order difference equation [74]), the Fibonacci recurrence

$$F_{n+1} = F_n + F_{n-1} \quad ; \quad (n \geq 1, F_0 = 0, F_1 = 1), \quad (8.151)$$

and derives

$$N(z) = \frac{z}{1-z-z^2} = \frac{1}{z^{-1}-1-z}. \quad (8.152)$$

Here the expansion in partial fractions is in terms of roots of the ('golden mean') polynomial  $1-z-z^2$ .

He notes that the Stirling numbers of the first kind satisfy a 3-term recurrence relation.

**2020-06-20 Predrag** Oscar Levin *Discrete Mathematics: An Open Introduction* Sect. 5.1 **Generating Functions** works out a 3-term recurrence  $a_n = 3a_{n-1} - 2a_{n-2}$ , with  $a_0 = 1, a_1 = 3$  in Example 5.1.6. Surprisingly, one gets again (!)

$$a_n = 2^{n+1} - 1.$$

**2020-06-20 Predrag** Check out also Al Doerr and Ken Levasseur *Applied Discrete Structures*:

*Sect. 8.3 Recurrence relations.*

*Sect. 8.5.2 Solution of a Recurrence Relation Using Generating Functions.*

**2020-03-04 Predrag** Ron Knott writes:

The series of natural numbers 1, 2, 3, 4, ... has the generating function

$$\frac{1}{(1-z)^2} = \frac{1}{1-2z+z^2} \quad (8.153)$$

and the 3-term recurrence (second-order difference equation [74])

$$\phi_n - 2\phi_{n-1} + \phi_{n-2} = 0$$

and compare that with the denominator of the generating function, namely:

$$1 - 2z + z^2$$

which might be a way to understand why  $s = 2$  is special.

A variant of Fibonacci: 0,1,3,8,21,... is generated by

$$\frac{z}{z^2 - 3z + 1} = \frac{1}{z - 3 + z^{-1}}$$

which looks temporal cat-like.

**2020-03-02 Predrag** In sect. 1.4 *A three term boundary value problem* Wilf [249] considers a 3-term recurrence with Dirichlet bc's

$$au_{n+1} + bu_n + cu_{n-1} = d_n, \quad (n = 1, 2, \dots, N-1; u_0 = u_N = 0) \quad (8.154)$$

where the positive integer  $N$ , the constants  $a, b, c$  and the sequence  $\{d_n\}_{n=1}^{N-1}$  are given in advance. The eqs (8.154) determine the sequence  $\{u_i\}_0^N$  uniquely. Such boundary value problems arise in applications such as the interpolation by spline functions.

**2020-03-01 Predrag** Compare (8.146) to our [63] Bernoulli 1-step difference condition

$$\phi_t - s\phi_{t-1} = -s_t, \quad \phi_t \in [0, 1]. \quad (8.155)$$

This suggests that the periodic points count is obtained by

$$\phi_t \rightarrow N_n, s_t \rightarrow 1 - s. \quad (8.156)$$

The temporal cat second-order difference equation is

$$\phi_{t+1} - s\phi_t + \phi_{t-1} = -s_t, \quad (8.157)$$

Mimicking (8.156), my guess for the recurrence for periodic points count is

$$N_{n+1} - sN_n + N_{n-1} = 2(s-2), \quad (n \geq 1, N_0 = 0, N_1 = s-2). \quad (8.158)$$

$$N_{n+1} - (\mu^2 + 2)N_n + N_{n-1} = 2\mu^2, \quad (n \geq 1, N_0 = 0, N_1 = \mu^2). \quad (8.159)$$

Indeed, this generates the correct series for arbitrary  $s$  (compare with (2.97), (6.149).)

$$N(z; s) = (s-2)z + (s-2)(s+2)z^2 + (s-2)(s+1)^2z^3 + (s-2)(s+2)s^2z^4 + \dots \quad (8.160)$$

$$N(z; \mu^2) = \mu^2z + \mu^2(\mu^2 + 4)z^2 + \mu^2(\mu^2 + 3)^2z^3 + \mu^2(\mu^2 + 4)(\mu^2 + 2)^2z^4 + \dots \quad (8.161)$$

Take  $N_n = \mu^2 \hat{N}_n$ , then (8.158) leads to

$$\hat{N}_{n+1} - s\hat{N}_n + \hat{N}_{n-1} = 2, \quad (n \geq 1, \hat{N}_0 = 0, \hat{N}_1 = 1). \quad (8.162)$$

$$\hat{N}(z; s) = z + (s + 2)z^2 + (s + 1)^2 z^3 + (s + 2) s^2 z^4 + (s^2 + s - 1)^2 z^5 + (s^2 - 1)^2 (s + 2) z^6 + \dots \quad (8.163)$$

$$\hat{N}(z; s) = z + (\mu^2 + 4)z^2 + (\mu^2 + 3)^2 z^3 + (\mu^2 + 4)(\mu^2 + 2)^2 z^4 + (\mu^4 + 3\mu^2 + 5)^2 z^5 + (\mu^2 + 1)^2 (\mu^2 + 3)^2 (\mu^2 + 4) z^6 + \dots \quad (8.164)$$

For  $\mu = 0$  this is a complicated way to generate integers squared (see also (8.153))

$$\hat{N}(z; 2) = z + 4z^2 + 9z^3 + 16z^4 + 25z^5 + 36z^6 + \dots \quad (8.165)$$

Recurrence (8.160) appears correct for the  $s = 3$  count (have not rechecked)

$$N(z; 3) = z + 5z^2 + 16z^3 + 45z^4 + 121z^5 + 320z^6 + 841z^7 + 2205z^8 + 5776z^9 + 15125z^{10} + 39601z^{11} + \dots \quad (8.166)$$

**2020-03-02 Predrag** In sect. 1.5 *Two independent variables* and 1.6 *Another 2-variable case* Wilf [249] considers problems that involve functions of two discrete variables. His example is combinatorial, probably not what we need.

A generating function with the  $1/n!$ 's thrown into the coefficients, is called an *exponential generating function*. After his eq. (1.6.12), he explains the

$$x(d/dx) \log$$

operation. He works it out for the “Bell numbers”, and derives that the Bell numbers satisfy the recurrence depending on all previous Bell numbers, much like the ChaosBook formulas for cumulants.

He says, comfortingly: “[...] there’s no need for the guilt, because the various manipulations can be carried out in the ring of formal power series, where questions of convergence are nonexistent.”

**2012-06-19 Predrag** In **ChaosBook example** 18.12 (edition 16.4.5), I show that for alphabet  $\mathcal{A} = \{a, cb^k; \bar{b}\}$ , the cycle counting  $\zeta$ -function is

$$1/\zeta_{\mathcal{AM}} = 1 - 3z + z^2,$$

i.e., the Isola [130]  $\zeta$ -function (2.28) for  $s = 3$ , without the  $(1 - z)^2$  factor (see (??), (2.18), (6.199), (16.43)). That might be a simple statement of the cat map symbolic dynamics.

**2020-02-09 Predrag** Fischer, Golub, Hald, Leiva and Widlund [86] *On Fourier-Toeplitz methods for separable elliptic problems* solve linear equations, where  $M$  arises from a finite difference approximation to an elliptic partial differential equation.

Such a situation arises for those problems that can be handled by the classical separation-of-variables technique. Their methods are a computer

implementation of the separation of variables carried out on a discretized model of the elliptic differential equation.

In one-dimensional lattice, the *characteristic function*  $a(x)$  of a symmetric  $2k$ -banded Toeplitz matrix  $A$  is defined as

$$a(x) = a_k x^k + \cdots + a_0 + \cdots + a_k x^{-k} \quad (8.167)$$

(see (2.38), for example). Such matrices occur in fourth, or higher, order accurate finite difference approximation to second order elliptic problems, when solving the bi-harmonic problem by a Fourier method, in higher order spline interpolation, etc.

For a 1-dimensional lattice one assumes that the characteristic function  $a(x)$  has no roots on the unit circle. Then they factor  $a(x) = l(x) \ell(l/x)$ , where  $l(x) = b_0 + \cdots + b_k x^k$ ,  $b_0 > 0$ , is a real polynomial with no roots inside the unit circle, their Lemma 1. The factors  $l(x)$  and  $\ell(l/x)$  of  $a(x)$  are known as the *Hurwitz factors*. Predrag has not found any useful literature on these.

Their algorithm applied to the temporal cat tri-diagonal case (2.45) with  $a_1 = -1$  and  $a_0 > 2$ , has linear convergence; see obscure references

[3] F. L. Bauer, "Ein direktes Iterationsverfahren zur Hurwitz-Zerlegung eines Polynoms," Arch. Elec. Ubertr., v. 9, 1955, pp. 285-290.

[4] F. L. Bauer, "Beiträge zur Entwicklung numerischer Verfahren für programmgesteuerte Rechenanlagen. II. Direkte Faktorisierung eines Polynoms," Bayer. Akad. Wiss. Math.-Nat. Kl. S.-B., v. 1956, pp. 163-203.

[18] M. Malcolm & J. Palmer, A Fast Method for Solving a Class of Tri-Diagonal Linear Systems, Computer Science Report 323, Stanford University, 1972,

[24] V. Thomée, "Elliptic difference operators and Dirichlet's problem," Contributions to Differential Equations, v. 3, 1964, pp. 301-324.

[25] O. B. Widlund, "On the use of fast methods for separable finite difference equations for the solution of general elliptic problems," Sparse Matrices and Their Applications, edited by D. J. Rose and R. A. Willoughby, Plenum Press, New York, 1972.

which we hopefully can ignore.

In the *semidefinite* case,  $a_0 = 2$ , one still has convergence, but the error decreases only as  $l/n$ .

2-dimensional lattice: When the characteristic function depends on several variables, a factorization like the one of their Lemma 1 is possible only in exceptional cases. They seek an appropriate factorization of the *characteristic function* for 2-dimensional lattice Laplacian

$$a(x_1, x_2) = -x_1 - x_2 + 4 - x_1^{-1} - x_2^{-1} \quad (8.168)$$

which cannot be factored in a useful way. They turn to the separation of variables technique.

“Characteristic function” (8.167) does not seem to be a commonly used name; compare with (8.167).

our preference is to call this *characteristic equation*, as in (8.126).

Lothar Reichel refers to (8.168) as the standard “five-point stencil” for discretization of the Poisson equation on a rectangle by finite differences.

**2020-06-15 Predrag** Insert into (8.168)  $x_i^{n_i} \rightarrow \Lambda_i^{n_i}$  to get characteristic equation for the 2-dimensional homogenous linear 2nd-order difference equation

$$\frac{1}{x_1}(x_1^2 - sx_1 + 1) + c\frac{1}{x_2}(x_2^2 - sx_2 + 1) = 0,$$

where  $[c] = [\ell_1]/[\ell_2]$  is dimensionally the ‘velocity’ parameter.

We can write

$$x_2(\Lambda - x_1)(\Lambda^{-1} - x_1) + cx_1(\Lambda - x_2)(\Lambda^{-1} - x_2) = 0,$$

with each term separately zero for  $x_1 = x_2 = 0$  and 4 combinations  $x_i \in \{\Lambda, 1/\Lambda\}$ . Though there there is no reason to set terms separately to zero, so there are 1-dimensional families of roots,

$$\begin{aligned} x_2(\Lambda - x_1)(\Lambda^{-1} - x_1) &= b \\ cx_1(\Lambda - x_2)(\Lambda^{-1} - x_2) &= -b, \end{aligned} \quad (8.169)$$

parametrized by  $b$ . So I too am lost as to how to use characteristic equations in higher dimensions...

## 8.10 Resistor networks

**2017-09-11 Predrag** A textbook: Blanchard and Volchenkov [33] *Random Walks and Diffusions on Graphs and Databases*, ([click here](#)); Chapter 6 *Random walks and electric resistance networks*. They cite Doyle and Snell 1984; Tetali 1991; Chandra et al. 1996; Bollobas 1998 (have not looked at any of these).

They define the discrete representation of the Laplace operator on a lattice in their eq. (4.22). The matrix (4.38) corresponds to the normalized Laplace operator.

“ It was established in Tetali (1991) and Chandra et al. (1996) that the effective resistance might be interpreted as the expected number of times a random walker visits all nodes of the network in a random round trip from  $i$  to  $j$  and back. ”

**2020-01-10 Predrag** A textbook: A very pedagogical, down to earth textbook: Pozrikidis [214] *An introduction to grids, graphs, and networks*, ([click here](#)) discusses this in Chap. 6 *Network performance*. In part based on Wu [253], cited below. My notes are below, search for **2020-01-10 Predrag**.

**2020-01-13 Predrag** A textbook: Grimmett [102] *Probability on Graphs: Random Processes on Graphs and Lattices*, ([click here](#)). Not sure we need this now, but it is a modern stat mech book on percolation, Schramm–Löwner evolution, Gibbs states and Markov fields, the Ising and Potts models.

Chapter 1 is devoted to the relationship between random walks (on graphs) and electrical networks. This leads to the Thomson and Rayleigh principles, and thence to a proof of Pólya’s theorem.

Early papers are

Venezian [243] *On the resistance between two points on a grid*

Atkinson and van Steenwijk [15] *Infinite resistive lattices*

leading to much cited:

**2020-01-13 Predrag** Cserti [58] *Application of the lattice Green’s function for calculating the resistance of an infinite network of resistors*:

In the network of resistors it is assumed here that the resistances of all the edges of the hypercube are the same, say  $R$ . The goal is to find the resistance between the origin and a given lattice point of the infinite hypercube. Ohm’s and Kirchhoff’s laws for potential at a lattice site are expressed in terms of the lattice Laplacian. To find the resistance one solves a Poisson-type equation by using the lattice Green’s function.

The 1-dimensional case, his eq. (23) is very simple.

The energy-dependent lattice Green’s function of the tight-binding Hamiltonian for a square lattice, his eq. (30), has energy  $E$  playing the role of our stretching parameter  $s$ .

He does the actual derivations on finite  $d$ -tori, but only as a step preliminary to taking the infinite-lattice limit; no actual calculations for finite  $d$ -tori.

[...] The value of  $G(0,0,0)$  was evaluated for the first time by Watson [21] and subsequently by Joyce [22] in a closed form in terms of the complete elliptic integral of the first kind

$$K(k) = \int_0^{\pi/2} d\theta \frac{1}{\sqrt{1 - k^2 \sin^2 \theta}} \quad (8.170)$$

It is worth mentioning that a simpler result was obtained by Glasser and Zucker [23] (see also Doyle and Snell's book [69]), [arXiv:math/0001057](https://arxiv.org/abs/math/0001057), who calculated the integrals in terms of gamma functions:

$$2G(0,0,0) = \frac{\sqrt{3} - 1}{96\pi^3} \Gamma^2(1/24) \Gamma^2(11/24). \quad (8.171)$$

Predrag finds this form intriguing, as he expects symmetry factorizations in the spirit of (6.197).

Glasser and Montaldi [27] gave other useful integral representations of the lattice Green's function for the hypercubic lattice for arbitrary dimension  $d$ . It was shown by Joyce [22] that the function  $G(E;0,0,0)$  can be expressed in the form of a product of two complete elliptic integrals of the first kind. (Predrag: presumably a symmetry factorization.)

This work is continued in ref. [59]:

**2019-11-04 Predrag** Cserti, Széchenyi and Dávid [59] *Uniform tiling with electrical resistors*: " The resistance between two arbitrary nodes of a network of resistors is studied when the network is perturbed by connecting an extra resistor between two arbitrary nodes in the perfect lattice. The lattice Green's function and the resistance of the perturbed network are expressed in terms of those of the perfect lattice by solving Dyson's equation. A comparison is carried out between numerical and experimental results for a square lattice. "

The electric resistance between two arbitrary nodes on any infinite lattice structure of resistors that is a periodic tiling of space is obtained, using the lattice Green's function of the Laplacian matrix associated with the network. The method can be extended to the random walk problem or to electron dynamics in solid state physics. The results may be used to calculate the wavefunctions at the lattice points for complicated lattice structures.

I do not think we need this paper at the present stage - understanding 'undecorated' square lattice is all we need...

**2019-11-01 Predrag** Introduction of Owaidat, Asad and Tan [199] *Resistance computation of generalized decorated square and simple cubic network lattices*



has a very exhaustive lattice Green functions literature discussion, starting with

Kirchhoff [157] *Üeber die Auflösung der Gleichungen, auf welche man bei der Untersuchung der linearen Vertheilung galvanischer Ströme geführt wird*, which, weirdly enough, reminds me that I've computed for my PhD [62] the determinants for QED that we here seek to compute for a much simpler lattice problem.

Their work follows the Green's function theory presented by Cserti [58]. They say that the lattice Green's functions are usually evaluated as the elliptic integrals (8.170) or by recurrence relations methods.

They do display a determinant of a Laplacian, eq. (B.11) in their Appendix B. *The matrix elements of the Green's function for the generalized decorated simple cubic lattice*, but it is a determinant of a single Fourier mode (in each of the three directions of a cubic lattice). Han has the analogue for the square lattice - what we do not have is the product formula, in which all eigenvalues (cosines, etc) average out, and all that is left is a polynomial in  $s$

**2019-11-04 Predrag** Jafarizadeh, Sufiani and Jafarizadeh [135] *Calculating two-point resistances in distance-regular resistor networks* provide an algorithm for the calculation of the resistance between two arbitrary nodes in an arbitrary distance-regular resistor network.

Past efforts have been focused mainly on infinite lattices, with little attention paid to finite networks. They present a general formulation for computing two-point resistances in finite networks.

Their starting point is the Laplacian matrix associated with a network. The Laplacian is a matrix whose off-diagonal entries are the conductances connecting pairs of nodes. Just as in graph theory where everything about a graph is described by its adjacency matrix (whose element is 1 if two vertices are connected and 0 otherwise), everything about an electric network is described by its Laplacian.

The two-point resistances on a network depend only on the Stieltjes function  $G_\mu(x)$  corresponding to the network. The Stieltjes function corresponding to an infinite network possesses a unique representation as an infinite continued fraction. In the cases for which the parameters iterate themselves after some finite steps, one can find a closed form for the infinite continued fraction. This situation takes place, for instance, in the infinite line network. But in most cases, this situation does not occur and one cannot obtain a closed form for the Stieltjes function of the network.

**2019-11-04 Predrag** Wu [253] *Theory of resistor networks: the two-point resistance* is a foundational paper, where a theory to calculate the resistance between arbitrary nodes for a finite lattice of resistors is given in terms of the eigenvalues and eigenvectors of the graph Laplacian matrix.

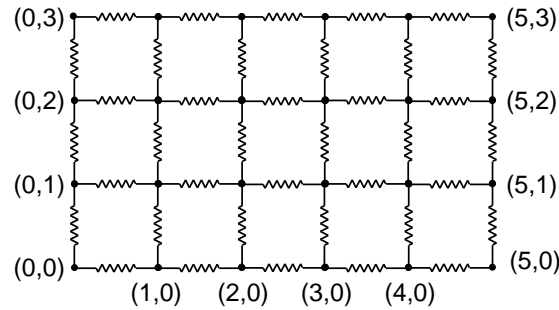


Figure 8.4: A  $[5 \times 4]$  rectangular resistor network: resistors with resistances  $r$  and  $s$  on edges of the network in, respectively, horizontal and vertical directions.

Wu gives a closed-form expression, his eq. (43), for the resistance  $R_{z_1 z_2}^{[L \times T]}$  of a finite square lattice between nodes  $z_1 = (x_1, y_1)$  and  $z_2 = (x_2, y_2)$  for free, periodic and cylindrical boundary conditions.

The paper is very clear and explicit, with many examples, including the 1-dimensional periodic chain (sect. 3.2. *Periodic boundary conditions*) and the doubly periodic  $[L \times T]$  square lattice, his sect. 5. *Two-dimensional network* and figure 8.4. His eq. (43) gives the resistance between nodes  $z_1 = (x_1, y_1)$  and  $z_2 = (x_2, y_2)$

$$\begin{aligned}
 R_{z_1 z_2}^{[L \times T]} &= \sum_{m=0}^{M-1} \sum_{\substack{n=0 \\ (m,n) \neq (0,0)}}^{N-1} \frac{|\psi_{(m,n);(x_1,y_1)} - \psi_{(m,n);(x_2,y_2)}|^2}{\lambda(m,n)} \\
 &= \frac{r}{N} \left[ |x_1 - x_2| - \frac{(x_1 - x_2)^2}{M} \right] + \frac{s}{M} \left[ |y_1 - y_2| - \frac{(y_1 - y_2)^2}{N} \right] \\
 &+ \frac{1}{MN} \sum_{m=1}^M \sum_{n=1}^N \frac{1 - \cos [2(x_1 - x_2)\theta_m + 2(y_1 - y_2)\phi_n]}{r^{-1}(1 - \cos 2\theta_m) + s^{-1}(1 - \cos 2\phi_n)},
 \end{aligned} \tag{8.172}$$

The result depends only on the differences  $|x_1 - x_2|$  and  $|y_1 - y_2|$ , as it should by translational invariance. This is a double sum over Fourier modes, and I see no determinant calculation where these are summed over and what remains is some sensible polynomial.

However, his sect. 10. *Summation and product identities* might be just what we need:

He shows that

$$\begin{aligned} F_N(\ell) &= \frac{1}{N} \sum_{n=1}^{N-1} \frac{1 - \cos(\ell\phi_n)}{1 - \cos\phi_n} \\ &= |\ell| - \frac{1}{N} \left( \frac{\ell^2 + |\ell|}{2} - \left\lfloor \frac{|\ell|}{2} \right\rfloor \right) \end{aligned} \quad (8.173)$$

where  $[x]$  denotes the integral part of  $x$ . Similarly

$$G_N(\ell) = \frac{1}{N} \sum_{n=1}^{N-1} \frac{1 - \cos(2\ell\phi_n)}{1 - \cos 2\phi_n}.$$

is evaluated as a special case of the identity (8.176), using the recursion relation

$$G_N(\ell) - G_N(\ell - 1) = 1 - \frac{1}{N}(2\ell - 1)$$

which yields

$$G_N(\ell) = |\ell| - \ell^2/N. \quad (8.174)$$

*Proposition: Define*

$$I_\alpha(\ell) = \frac{1}{N} \sum_{n=0}^{N-1} \frac{\cos(\alpha \ell \frac{n\pi}{N})}{\cosh \lambda - \cos(\alpha \frac{n\pi}{N})}, \quad \alpha = 1, 2.$$

Then the following identities hold for  $\lambda \geq 0$ ,  $N = 1, 2, \dots$ ,

$$I_1(\ell) = \frac{\cosh(N - \ell)\lambda}{(\sinh \lambda) \sinh(N\lambda)} + \frac{1}{N} \left[ \frac{1}{\sinh^2 \lambda} + \frac{1 - (-1)^\ell}{4 \cosh^2(\lambda/2)} \right], \quad 0 \leq \ell < 2N, \quad (8.175)$$

$$I_2(\ell) = \frac{\cosh(\frac{N}{2} - \ell)\lambda}{(\sinh \lambda) \sinh(N\lambda/2)}, \quad 0 \leq \ell < N. \quad (8.176)$$

Remarks:

3. In the  $N \rightarrow \infty$  limit both (8.175) and (8.176) become the integral

$$\frac{1}{\pi} \int_0^\pi \frac{\cos(\ell\theta)}{\cosh \lambda - \cos \theta} d\theta = \frac{e^{-\ell\lambda}}{\sinh \lambda} \quad \ell \geq 0.$$

4. Set  $\ell = 0$  in (8.175), multiply by  $\sinh \lambda$  and integrate over  $\lambda$ , we obtain the product identity

$$\prod_{n=0}^{N-1} \left( \cosh \lambda - \cos \frac{n\pi}{N} \right) = (\sinh N\lambda) \tanh(\lambda/2). \quad (8.177)$$

5. Set  $\ell = 0$  in (8.176), multiply by  $\sinh \lambda$  and integrate over  $\lambda$ . We obtain the product identity

$$\prod_{n=0}^{N-1} \left( \cosh \lambda - \cos \frac{2n\pi}{N} \right) = \sinh^2(N\lambda/2). \quad (8.178)$$

Proof:

Introduce

$$S_\alpha(\ell) = \frac{1}{N} \sum_{n=0}^{N-1} \frac{\cos(\ell \theta_n)}{1 + a^2 - 2a \cos \theta_n}, \quad a < 1, \quad \alpha = 1, 2 \quad (8.179)$$

so that

$$I_\alpha(\ell) = 2a S_\alpha(\ell), \quad a = e^{-\lambda}. \quad (8.180)$$

It is readily seen that we have the identity

$$S_\alpha(1) = \frac{1}{2a} \left[ (1 + a^2) S_\alpha(0) - 1 \right]. \quad (8.181)$$

1. Proof of (8.175):

First we evaluate  $S_1(0)$  by carrying out the following summation, where  $\mathcal{R}e$  denotes the real part, in two different ways. First we have

$$\begin{aligned} \mathcal{R}e \frac{1}{N} \sum_{n=0}^{N-1} \frac{1}{1 - a e^{i\theta_n}} &= \mathcal{R}e \frac{1}{N} \sum_{n=0}^{N-1} \frac{1 - a e^{-i\theta_n}}{|1 - a e^{i\theta_n}|^2} \\ &= \frac{1}{N} \sum_{n=0}^{N-1} \frac{1 - a \cos \theta_n}{1 + a^2 - 2a \cos \theta_n} \\ &= S_1(0) - a S_1(1) \\ &= \frac{1}{2} \left[ 1 + (1 - a^2) S_1(0) \right]. \end{aligned} \quad (8.182)$$

Secondly by expanding the summand we have

$$\mathcal{R}e \frac{1}{N} \sum_{n=0}^{N-1} \frac{1}{1 - a e^{i\theta_n}} = \mathcal{R}e \frac{1}{N} \sum_{n=0}^{N-1} \sum_{\ell=0}^{\infty} a^\ell e^{i\ell n\pi/N}$$

and carry out the summation over  $n$  for fixed  $\ell$ . It is clear that all  $\ell =$  even terms vanish except those with  $\ell = 2mN, m = 0, 1, 2, \dots$  which yield  $\sum_{m=0}^{\infty} a^{2mN} = 1/(1 - a^{2N})$ . For  $\ell =$  odd  $= 2m + 1, m = 0, 1, 2, \dots$  we have

$$\mathcal{R}e \sum_{n=0}^{N-1} e^{i(2m+1)n\pi/N} = \mathcal{R}e \frac{1 - (-1)^{2m+1}}{1 - e^{i(2m+1)\pi/N}} = 1$$

after making use of

$$\mathcal{R}e \left( \frac{1}{1 - e^{i\theta}} \right) = \frac{1}{2}, \quad 0 < \theta < 2\pi. \quad (8.183)$$

So the summation over  $\ell = \text{odd}$  terms yields  $N^{-1} \sum_{m=0}^{\infty} a^{2m+1} = a/N(1 - a^2)$ , and we have

$$\mathcal{R}e \sum_{n=0}^{N-1} \frac{1}{1 - a e^{i\theta_n}} = \frac{1}{1 - a^{2N}} + \frac{a}{N(1 - a^2)} \quad (8.184)$$

Equating (8.182) with (8.184) we obtain

$$S_1(0) = \frac{1}{1 - a^2} \left[ \left( \frac{1 + a^{2N}}{1 - a^{2N}} \right) + \frac{2a}{N(1 - a^2)} \right]. \quad (8.185)$$

To evaluate  $S_1(\ell)$  for general  $\ell$ , we consider the summation

$$\begin{aligned} \mathcal{R}e \frac{1}{N} \sum_{n=0}^{N-1} \frac{1 - (a e^{i\theta_n})^\ell}{1 - a e^{i\theta_n}} &= \mathcal{R}e \frac{1}{N} \sum_{n=0}^{N-1} \frac{(1 - a^\ell e^{i\ell\theta_n})(1 - a e^{-i\theta_n})}{|1 - a e^{i\theta_n}|^2} \\ &= S_1(0) - a S_1(1) - a^\ell S_1(\ell) + a^{\ell+1} S_1(\ell - 1), \end{aligned} \quad (8.186)$$

where the second line is obtained by writing out the real part of the summand as in (8.182). On the other hand, by expanding the summand we have

$$\begin{aligned} \mathcal{R}e \frac{1}{N} \sum_{n=0}^{N-1} \frac{1 - (a e^{i\theta_n})^\ell}{1 - a e^{i\theta_n}} &= \mathcal{R}e \frac{1}{N} \sum_{n=0}^{N-1} \sum_{m=0}^{\ell-1} a^m e^{i\pi m n / N} \\ &= 1 + \mathcal{R}e \frac{1}{N} \sum_{m=1}^{\ell-1} a^m \left( \frac{1 - (-1)^m}{1 - e^{i\pi m / N}} \right) \\ &= 1 + \frac{a(1 - a^\ell)}{N(1 - a^2)}, \quad \ell = \text{even} < 2N \\ &= 1 + \frac{a(1 - a^{\ell-1})}{N(1 - a^2)}, \quad \ell = \text{odd} < 2N \end{aligned} \quad (8.187)$$

where again we have used (8.183).

Equating (8.187) with (8.186) and using (8.181) and (8.185), we obtain the recursion relation

$$S_N(\ell) - a S_N(\ell - 1) = A a^{-\ell} + B_\ell \quad (8.188)$$

where

$$A = \frac{a^{2N}}{1 - a^{2N}}, \quad B_\ell = \frac{a^{(1+(-1)^\ell)/2}}{N(1 - a^2)}. \quad (8.189)$$

The recursion relation (8.188) can be solved by standard means. Define the generating function

$$G_\alpha(t) = \sum_{\ell=0}^{\infty} S_\alpha(\ell) t^\ell, \quad \alpha = 1, 2. \quad (8.190)$$

Multiply (8.188) by  $t^\ell$  and sum over  $\ell$ . We obtain

$$(1 - at)G_1(t) - S_1(0) = \frac{A a^{-1}t}{1 - a^{-1}t} + \frac{t + at^2}{N(1 - a^2)(1 - t^2)}. \quad (8.191)$$

This leads to

$$\begin{aligned} G_1(t) &= \frac{1}{1 - at} \left[ S_1(0) + \frac{A a^{-1}t}{1 - a^{-1}t} + \frac{t + at^2}{N(1 - a^2)(1 - t^2)} \right] \\ &= \frac{1}{(1 - a^2)(1 - a^{2N})} \left[ \frac{1}{1 - at} + \frac{a^{2N}}{1 - a^{-1}t} \right] \\ &\quad + \frac{1}{2N(1 - a)^2(1 - t)} - \frac{1}{2N(1 + a)^2(1 + t)}, \end{aligned}$$

from which one obtains

$$\begin{aligned} S_1(\ell) &= \frac{a^\ell + a^{2N-\ell}}{(1 - a^2)(1 - a^{2N})} + \frac{1}{2N(1 - a)^2} - \frac{(-1)^\ell}{2N(1 + a)^2} \\ &= \frac{a^\ell + a^{2N-\ell}}{(1 - a^2)(1 - a^{2N})} + \frac{1}{2N} \left[ \frac{4a}{(1 - a^2)^2} + \frac{1 - (-1)^\ell}{(1 + a^2)^2} \right] \end{aligned} \quad (8.192)$$

It follows that using  $I_1(\ell) = 2a S_1(\ell)$  we obtain (8.175) after setting  $a = e^{-\lambda}$ .

2. Proof of (8.176):

Again, we first evaluate  $S_2(0)$  by carrying out the summation

$$\mathcal{R}e \frac{1}{N} \sum_{n=0}^{N-1} \frac{1}{1 - a e^{i2\theta_n}}, \quad a < 1$$

in two different ways. First as in (8.182) we have

$$\mathcal{R}e \frac{1}{N} \sum_{n=0}^{N-1} \frac{1}{1 - a e^{i2\theta_n}} = \frac{1}{2} \left[ 1 + (1 - a^2)S_2(0) \right], \quad (8.193)$$

where  $S_2(\ell)$  is defined in (8.179). Secondly by expanding the summand we have

$$\frac{1}{N} \sum_{n=0}^{N-1} \frac{1}{1 - a e^{i2\theta_n}} = \frac{1}{N} \sum_{n=0}^{N-1} \sum_{\ell=0}^{\infty} a^\ell e^{i2\ell n\pi/N} = \frac{1}{1 - a^N} \quad (8.194)$$

where by carrying out the summation over  $n$  for fixed  $\ell$  all terms in (8.184) vanish except those with  $\ell = mN, m = 0, 1, 2, \dots$ . Equating (8.194) with (8.193) we obtain

$$S_2(0) = \frac{1}{1-a^2} \left( \frac{1+a^N}{1-a^N} \right) \quad (8.195)$$

and from (8.181)

$$S_2(1) = \frac{1}{1-a^N}.$$

We consider next the summation

$$\mathcal{R}e \frac{1}{N} \sum_{n=0}^{N-1} \frac{1 - (a e^{i2\theta_n})^\ell}{1 - a e^{i2\theta_n}} \quad a < 1. \quad (8.196)$$

Evaluating the real part of the summand directly as in (8.186), we obtain

$$\mathcal{R}e \frac{1}{N} \sum_{n=0}^{N-1} \frac{1 - (a e^{i2\theta_n})^\ell}{1 - a e^{i2\theta_n}} = S_2(0) - a S_2(1) - a^\ell S_2(\ell) + a^{\ell+1} S_2(\ell - 1) \quad (8.197)$$

Secondly, expanding the summand in (8.196) we obtain

$$\begin{aligned} \frac{1}{N} \sum_{n=0}^{N-1} \frac{1 - (a e^{i2\theta_n})^\ell}{1 - a e^{i2\theta_n}} &= \frac{1}{N} \sum_{n=0}^{N-1} \sum_{m=0}^{\ell-1} a^m e^{i2\pi mn/N} \\ &= \frac{1}{N} \left[ N + \sum_{m=1}^{\ell-1} \frac{1 - e^{i2m\pi}}{1 - e^{i2m\pi/N}} \right] \\ &= 1 \quad m < \ell \leq N. \end{aligned} \quad (8.198)$$

Equating (8.198) and (8.197) and making use of (8.195) for  $S_2(0)$ , we obtain

$$S_2(\ell) - a S_2(\ell - 1) = \frac{a^{N-\ell}}{1-a^N} \quad (8.199)$$

The recursion relation (8.199) can be solved as in the above. Define the generating function  $G_2(t)$  by (8.190). We find

$$\begin{aligned} G_2(t) &= \frac{1}{1-at} \left[ S_2(0) + \frac{a^{N-1}t}{(1-a^N)(1-a^{-1}t)} \right] \\ &= \frac{1}{(1-a^2)(1-a^{2N})} \left[ \frac{1}{1-at} + \frac{a^N}{1-a^{-1}t} \right], \end{aligned} \quad (8.200)$$

from which one reads off

$$S_2(\ell) = \frac{a^\ell + a^{N-\ell}}{(1-a^2)(1-a^{2N})}.$$

Using the relation  $I_2(\ell) = 2a S_2(\ell)$  with  $a = e^{-\lambda}$ , we obtain (8.176).

**2019-11-04 Predrag** Tzeng and Wu have extended this impedance networks, where the Laplacian matrix has complex matrix elements; I think we do not care about this at this time.

**2019-11-04 Predrag** The corner-to-corner resistance and its asymptotic expansion for various boundary conditions were calculated by Izmailian and Huang [134] *Asymptotic expansion for the resistance between two maximally separated nodes on an  $M$  by  $N$  resistor network*: “ The computation of the asymptotic expansion of the corner to-corner resistance, in other word the resistance between two maximally separated nodes of a rectangular resistor network is of interest as its value provides a lower bound to the resistance of compact percolation clusters in the Domany-Kinzel model of a directed percolation [15]. ”

They take a  $[L \times T]$  array, use a ton of funky identities, and manage to reduce Wu’s double sum (8.172) to a single, highly non-obvious sum, their eq. (33). Then there are Kronecker’s double series expressed in terms of the complete elliptic integrals  $K(s)$  and  $E(s)$ .

**2020-01-11 Predrag** Dienstfrey, Hang and Huang [67] *Lattice sums and the two-dimensional, periodic Green’s function for the Helmholtz equation*. They compute the Green’s function for the Helmholtz equation in two dimensions with doubly periodic boundary conditions, on a fundamental cell  $[-1/2, 1/2]^2$ . I believe this is not relevant to us, it solves a continuous problem over the unit cell, rather than a problem on discrete lattice.

Due to the translation invariance, the Green’s function has a convolution structure,  $G(x, x_0) = G(y)$ ,  $y = x - x_0 \in [-1, 1]^2$ . A periodic Helmholtz equation can be computed via the method of images over the zeroth-order Hankel function of the first-kind. The sums can also be evaluated by recognizing an identity between the so-called ‘spectral’ and ‘spatial’ representations of  $G$ . For a square array, there are symmetries which allow for further simplification.

**2020-01-10 Predrag** Stewart and Gökyaydin [234] *Symmetries of quotient networks for doubly periodic patterns on the square lattice*, ([click here](#)). Read for sect. 24.4 *Reduction to the fundamental domain* that has still to be completed.

**2020-01-10 Predrag** A very pedagogical, down to earth textbook: Pozrikidis [214] *An introduction to grids, graphs, and networks*, ([click here](#)):

*Graphs* are finite or infinite sets of vertices connected by edges in structured or unstructured configurations.

Infinite *lattices* and tiled surfaces are described by highly ordered graphs parametrized by an appropriate number of indices.

*Networks* consist of nodes connected by physical or abstract links with an assigned conductance in spontaneous or engineered configurations. In



physical and engineering applications, networks are venues for conducting or convecting a transported entity, such as heat, mass, or digitized information according to a prevailing transport law.

*Finite difference* and finite element *grids* can be regarded as networks whose link conductance is determined by the differential equation, as well as by the chosen finite difference or finite element approximation.

A finite difference grid for solving ordinary or partial differential equations consists of rectilinear grid lines that can be regarded as conveying links intersecting at nodes.

Topics: The node adjacency, Laplacian, and Kirchhoff matrices; The computation of the regular and generalized lattice Green's function describing the response to a nodal source; The pairwise resistance of any two nodes.

Consider the Poisson equation in one dimension for an unknown function of one variable,  $f(x)$ ,

$$\frac{d^2 f}{dx^2} + g(x) = 0, \quad (8.201)$$

to be solved in a finite domain,  $[a, b]$ , where  $g(x)$  is a given source function. When  $g(x) = 0$ , the Poisson equation reduces to Laplace's equation. When  $g(x) = \alpha f(x)$ , the Poisson equation reduces to the Helmholtz's equation,

$$\left( \frac{d^2}{dx^2} + \alpha \right) f(x) = 0, \quad (8.202)$$

where  $\alpha$  is a real or complex constant. (See also sect. 8.2 *Helmholtz and screened Poisson equations*.)

Applying the Poisson equation at the  $i$ th node, approximating the second derivative with a central difference

$$f_{i+1} - 2f_i + f_{i-1} = -g_i \quad (8.203)$$

where  $f_i = f(x_i)$ ,  $g_i = g(x_i)$ . He says: "The signs on the left- and right-hand sides of (8.203) were chosen intentionally to conform with standard notation in graph theory regarding the Laplacian, as discussed in Section 1.7."

The discretized Helmholtz's equation:

$$f_{i+1} - 2f_i + f_{i-1} + \alpha f_i = 0, \quad (8.204)$$

so for us  $\alpha = 2 - s$ .

For any boundary conditions -Neumann, Dirichlet, or periodic- the coefficient matrix of the linear system admits the factorization

$$L = RR^\top \quad (8.205)$$

where  $R$  is a square or rectangular matrix. This factorization is the discrete counterpart of the second derivative constructed as the sequential application of the first derivative. Note that the commutative property  $RR^T = R^T R$  is not always satisfied.

When the Dirichlet boundary condition is specified at both ends of the solution domain, the first and last values,  $f_1$  and  $f_{n+1}$ , are known. Collecting the difference equations (8.203) for the interior nodes,  $i = 2, \dots, n$ , we obtain a system of linear equations where  $L$  is  $(n - 1) \times (n - 1)$  symmetric tridiagonal Toeplitz matrix, a matrix with constant diagonal lines. The  $m = 1, 2, \dots, n - 1$  eigenvalues of  $L$  are

$$\lambda_m = 2 - 2 \cos \alpha_m = 4 \sin^2 \left( \frac{1}{2} \alpha_m \right), \quad \alpha_m = \pi \frac{m}{n} \quad (8.206)$$

He also lists eigenvectors and factorizes as in (8.205), and discusses the Neumann boundary condition, in which case  $L$  is a “nearly Toeplitz matrix.” as well. In factorization (8.205),  $R$  is now a rectangular matrix.

For periodic boundary conditions,  $L$  is a “nearly tridiagonal matrix.” Because of the zero eigenvalue of the Laplacian,  $\lambda_0 = 0$ , corresponding to a constant eigenvector, the matrix  $L$  is singular. The rest of the eigenvectors are pure harmonic waves. The identity

$$f^T \cdot L \cdot f = \sum_{i=1}^n (f_{i+1} - f_i)^2 \geq 0 \quad (8.207)$$

for arbitrary periodic field  $f$  demonstrates that the matrix  $L$  is positive semidefinite.

The periodic Laplacian is a circulant matrix.

He defines the graph Laplacian.

The adjacency matrix  $A$ , defined as  $A_{ij} = 1$  if nodes  $i$  and  $j$  are connected by a grid line or link, 0 otherwise, with the convention that  $A_{ii} = 0$ . Thus, by convention, the diagonal line of the adjacency matrix is zero. .

The number of paths that return to an arbitrary node after  $s$  steps have been made, summed over all starting nodes, is

$$n_s = \sum_{j=1}^n \mu_j^s \quad (8.208)$$

where  $\mu_j$  are eigenvalues of  $A$ .

The degree of the  $i$ th node, denoted by  $d_i$ , is defined as the number of links attached to the node, which is equal to the sum of the elements in the corresponding row or column of the adjacency matrix. The Laplacian equals  $L = D - A$ , where  $D$  is a diagonal matrix whose  $i$ th diagonal element is equal to the corresponding node degree  $d_i$ .

He introduces the oriented incidence matrix  $R$ , by labeling nodes and links sequentially, and shows it leads to the factorization (8.205). All of these notions generalize to graphs.

A uniform two-dimensional Cartesian (square) lattice.

An Archimedean lattice consists of an infinite doubly periodic array regular polygons. In particular, each node is surrounded by the same sequence of polygons. There are 11 Archimedean lattices.

The Archimedean  $4^4$  lattice, also known as the square lattice, is a Bravais lattice consisting of a doubly periodic array of empty squares.

Laves lattices are the duals of the Archimedean lattices. A Laves lattice arises by introducing vertices in the middle of the tiles (faces) of an Archimedean lattice and then connecting the vertices to cross the edges of the Archimedean lattice. The dual of the square lattice is the same square lattice.

The nodes of a two- or three-dimensional regular lattice, regarded as a structured network, can be identified by two or three indices assigned to the individual lattice directions. The spectra of lattice networks Laplacians are used in computing of lattice Green's functions.

His figure 8.5 is interesting: I think it is a plot of the lowest eigenstates ("spectral partitioning") of a  $[17 \times 17]$  square lattice ("Cartesian network") consisting of a complete set of horizontal and vertical links. As an example, the spectral partitioning of a square network is shown in Figure 2.2.1.

In spectral partitioning (a weighed sum of eigenvectors of the Laplacian matrix) roughly an equal number of eigenvector components with positive and negative sign appear. Eigenvector corresponding to the zero eigenvalue of the Laplacian matrix is uniform over the nodes of a network; the eigenvector corresponding to the zero eigenvalue is filled with ones. Orthogonality of the set of eigenvectors requires that all other eigenvectors have mean zero, his Eq. (2.2.8). Higher eigenvectors partition the network into two or a higher number of pieces (spectral partitioning). To partition a network, we may group together nodes whose eigenvector components corresponding to a specified eigenvalue have the same sign. The eigenvalue with the second smallest magnitude, is chosen for division into two fragments, while higher eigenvalues are chosen for division into a higher number of fragments.

A network whose structure is isomorphic to that of a square lattice consists of two intersecting one-dimensional arrays of links. A theorem due to Fiedler [10, 85] states that the eigenvectors of the Laplacian matrix for certain types of boundary conditions are tensor products of those of the constituent one-dimensional graphs, and the eigenvalues are the sums of the eigenvalues of the Laplacian of the constituent one-dimensional graphs. This property reflects the separability of the discrete Laplace operator in Cartesian coordinates.

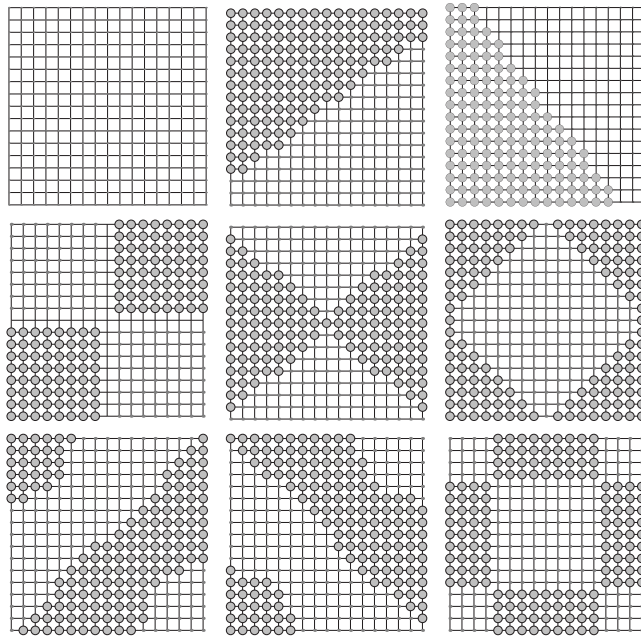


Figure 8.5: A  $[17 \times 17]$  rectangular Helmholtz (8.204) network. Positive components of an eigenvector are marked as filled circles, negative components are marked as dots, and zero components are unmarked. The network shown consists of  $N = 17^2 = 289$  nodes connected by  $L = 544$  links. The degree of the 4 corner nodes is 2, the 60 edge nodes is 3, and 225 interior nodes is 4. Exact expressions for the eigenvalues and eigenvectors of the Laplacian of the square network are discussed in Pozrikidis Chapter 3. The first nine eigenvalues corresponding to the eigenvectors shown here are  $\lambda_i = 0, 0.0341$  (double),  $0.0681, 0.1351$  (double),  $0.1691$  (double), and  $0.2701$ . Pozrikidis [214] Fig 2.2.1.

We need to understand spatiotemporal cat eigenmodes. If  $s < 2$  lattice is a spring mattress, with spring constant  $2 - s$ , what are the normal modes of the  $s > 2$  spatiotemporal cat? In the above he discusses the Helmholtz,  $s = 2$  Laplacian eigenmodes case (8.204).

**2020-01-21 Predrag** Fruchart, Zhou and Vitelli [93] *Dualities and non-Abelian mechanics* seems interesting. The abstract: “ Dualities are mathematical mappings that reveal links between apparently unrelated systems in virtually every branch of physics. Systems mapped onto themselves by a duality transformation are called self-dual and exhibit remarkable properties, as exemplified by the scale invariance of an Ising magnet at the critical point. Here we show how dualities can enhance the symmetries of a dynamical matrix (or Hamiltonian), enabling the design of metamaterials with emergent properties that escape a standard group theory analysis. As an illustration, we consider twisted kagome lattices, reconfigurable mechanical structures that change shape by means of a collapse mechanism. We observe that pairs of distinct configurations along the mechanism exhibit the same vibrational spectrum and related elastic moduli. We show that these puzzling properties arise from a duality between pairs of configurations on either side of a mechanical critical point. The critical point corresponds to a self-dual structure with isotropic elasticity even in the absence of spatial symmetries and a twofold-degenerate spectrum over the entire Brillouin zone. The spectral degeneracy originates from a version of Kramers’ theorem in which fermionic time-reversal invariance is replaced by a hidden symmetry emerging at the self-dual point. The normal modes of the self-dual systems exhibit non-Abelian geometric phases that affect the semiclassical propagation of wavepackets, leading to non-commuting mechanical responses. ”

Mechanical structures are described at the linear level by normal modes of vibration and their oscillation frequencies. Both are determined by the dynamical matrix  $\hat{D}$ , which summarizes the Newton equations of motion in the harmonic approximation [...] our analysis also applies when  $\hat{D}$  is replaced by other linear operators, such as the Maxwell operator of a photonic crystal[ref28], the mean-field Hamiltonian of a quantum system (in which case the eigenvalues are energies) or the dynamical matrix of an electrical circuit [6, 160, 196].

A *symmetry* is a transformation that maps a system onto itself. A *duality* relates distinct models or structures. In self-dual systems, the distinction between dualities and symmetries is blurred: additional symmetries can emerge at a self-dual point even if the spatial symmetries are unchanged. Such dualities can be harnessed to engineer material properties from wave propagation to static responses that are not predicted by a standard symmetry analysis based on space groups.

This one as well: Souslov and Vitelli [231] *Geometry for mechanics*: “ The mechanics of many materials can be modelled by a network of balls con-

nected by springs. A bottom-up approach based on differential geometry now captures changes in mechanics upon network growth or merger, going beyond the linear deformation regime. ”

**2021-01-09 Predrag** Fruchart, Zhou and Vitelli [93] cite

Ningyuan *et al.* [196] *Time- and site-resolved dynamics in a topological circuit*: I think we can ignore this paper. Though supplemental material explains: (1) The Harper-Hofstadter model, and its extension to spinful systems. (2) Photonic lattices, in both massive and massless limits. (3) Adding topology to photonic lattice models. (4) Mathematical tools for the calculation of band-structure, corresponding band Chern numbers, and two-point response of photonic lattice models. (5) Mathematical tools for calculating band- and edge- structure of finite strips.

Albert, Glazman and Jiang [6] *Topological properties of linear circuit lattices* have a 3-site lattice example, where the Lagrangian contribution of the link between neighboring sites is built from a (kinetic) capacitive part with what we call orbit Jacobian matrix  $\mathcal{J}$ , and a (potential) inductive part with what we call shift matrix  $r$ .

**2021-01-09 Predrag** Fruchart, Zhou and Vitelli [93] cite Lee *et al.* [160] *Topological circuits*. The normal mode frequency matrix of our circuit is unitarily equivalent to the hopping matrix of a quantum spin Hall insulator.

Circuits consisting of resistor, inductor and capacitor (RLC) components are governed by its circuit Laplacian, which is analogous to the Hamiltonian describing the energetics of a physical system. Here we show that topological insulating and semimetallic states can be realized in a periodic RLC circuit.

Any electrical circuit network can be represented by a graph whose nodes and edges correspond to the circuit junctions and connecting wires/elements. The circuit behavior is fundamentally described by Kirchhoff’s law. As an initial step towards identifying circuits with tight-binding lattice models, they rewrite Kirchhoff’s law in a matrix form, and consider circuits made up of periodic sublattices, with periodic boundary conditions (i.e. without grounded terminations).

What we call orbit Jacobian matrix  $\mathcal{J}$  they call ‘the grounded Laplacian’  $\mathcal{J}$ .

The regularized inverse of  $\mathcal{J}$  known as the circuit Green’s function (regularization in this context means that 0 modes are omitted). The Laplacian is defined in terms of the conductances by  $L = D - C$ , where  $C$  is the (adjacency) matrix of conductances and  $D$  lists the total conductances out of each node. They call the set of eigenvalues the band structure of the circuit, and also refer to the nodes as sites.

RLC circuits obey a linear 2nd order ordinary differential equation (ODE), just like a mechanical system with springs, dampers and masses.

**2023-09-27 Predrag** Inspiring [Andrea Liu](#) *Learning about learning with physical networks* [Rutgers seminar](#) on modeling 'physical' learning by heterogeneous, finite, not translation invariant resistor networks. One of the lessons, I believe, is that going analog makes learning computations much faster than running it on a digital machine(?). The paper, including a video presentation: [\(click here\)](#).

What I find inspirational is the eigenfunction of the leading eigenvalue of the learning Hessian (orbit Jacobian matrix  $\mathcal{J}$  for us, I believe): it clearly separates the resistor network in different regions.

It is not our, chaotic field theory situation, where the square lattice is the same everywhere - it is a 'neuronal' network that has "learned", ie, a highly heterogeneous network, with very different link strengths.

**2023-09-27 Greg Huber To Predrag Cvitanović** I've been working through Pierre Nolin *et al.* *Backbone exponent for two-dimensional percolation*, [arXiv:2309.05050](#).

Abstract: "We derive an exact expression for the celebrated backbone exponent for Bernoulli percolation in dimension two at criticality. It turns out to be a root of an elementary function. Contrary to previously known arm exponents for this model, which are all rational, it has a transcendental value. Our derivation relies on the connection to the SLE  $\kappa$  bubble measure, the coupling between SLE and Liouville quantum gravity, and the integrability of Liouville conformal field theory. Along the way, we derive a formula not only for  $\kappa = 6$  (corresponding to percolation), but for all  $\kappa \in (4, 8)$ ."

Claims a theory of the percolation backbone. If correct, it is a breakthrough. Also gets all the  $q=0$  to  $q=4$  backbones in the Potts models. It looks correct, but did they work backwards to get the right numbers and hide the jumps in reasoning somewhere? It is related to conductivity and trees too of course. The odd thing is that they claim the scaling dimensions are transcendental numbers, not rational numbers. This is a bit strange for 2D percolation exponents. But the hull of the backbone should be rational?! For instance, I know the hull dimension of the percolation backbone is exactly  $4/3$ . Or they would say the co-dimension is  $2-4/3=2/3$ . I think they try to scare children with it. The basic argument at the core is very simple, but they invoke Liouvillean 2D quantum gravity.

Typical francophonic move...

**2023-09-27 Predrag** I scanned through the paper, and wow! I could not possibly digest it in the years still allotted to me in the Book of Life. Curiously, Nolin has not published anything on this since 2007 or 2011 or so, though he does publish a paper every few years. If other papers are like this one, no wonder.

Amusing: the first figure in Nolin *et al.* looks identical to Liu's figure of the leading learning Hessian eigenfunction:)

The coauthors are impossible to track on arXiv. It has to start using Orcid numbers.

**2023-09-27 Greg** The thing about Nolin *et al.* - they combine deep results with absolutely trivial proofs/observations — why do that?? Why the rigor god ridiculously simple statements mixed with the truly deep things?

I think a lot of the terms are there to scare away children - the crux of the argument is obscured by 'Liouville quantum gravity' talk. SLE though is essential. See the review by Gruzberg and Kadanoff for that I would say.

You can easily master this stuff - they just want you to think that it's hard.

**2024-11-13 Predrag Eleni Katifori** and her student G. Gounaris, *Geometry Matters: Spatial Considerations in the Design of Physical Networks* [Rutgers seminar](#)

"Networks optimized for one or several cost functions are commonplace in nature and engineering. Their topology is usually at least partially determined by the functions the networks need to satisfy. However, when there is a notion of distance between the nodes and the graph is embedded in physical space, geometry also influences the optimal architecture. We explore two instances where spatial embedding determines the optimal form, sometimes in counterintuitive ways.

(1) we consider a spatially embedded graph traversed by random walkers and investigate the structure of the graph that minimizes the average mean first passage time for the walkers.

(2) We generalize our findings to energy landscapes, modeling them as networks with nodes representing energy minima and edges denoting transition pathways with Arrhenius-dependent rates. We find that reducing infinite barriers isolating metastable states can paradoxically increase search time. Additionally, we establish a lower bound for the mean first passage time, showing that search efficiency depends primarily on the ground state's energy and connectivity. "

The papers, including a video presentation: (TO BE found) ([click here](#)).



## 8.11 Counting periodic states

20 21

For a 2-dimensional spatiotemporal cat map, we want to find eigenvectors with periodicity given by the Bravais lattice (7.1), where  $\mathbf{a}_1$  and  $\mathbf{a}_2$  are two 2-dimensional primitive vectors. The general form of these primitive vectors are  $\mathbf{a}_1 = \{l_1, l_2\}$  and  $\mathbf{a}_2 = \{l_3, l_4\}$ . For a given Bravais lattice, the choice of primitive vectors is not unique. It is shown by Lind [172], (click here) that we can choose primitive vectors with form  $\mathbf{a}_1 = \{l_1, 0\}$  and  $\mathbf{a}_2 = \{l_3, l_4\}$  without loss of generality.<sup>22</sup> Then the reciprocal lattice is:

$$\bar{\mathcal{L}} = \{n_1 \mathbf{b}_1 + n_2 \mathbf{b}_2 | n_i \in \mathbb{Z}\}, \quad (8.209)$$

where the vectors  $\mathbf{b}_1$  and  $\mathbf{b}_2$  satisfy:

$$\mathbf{b}_i \cdot \mathbf{a}_j = 2\pi \delta_{ij}. \quad (8.210)$$

The eigenvectors of the translation operator which satisfy the periodicity of the Bravais lattice (7.1) are plane waves of form:

$$f_{\mathbf{k}}(\mathbf{z}) = e^{i\mathbf{k} \cdot \mathbf{z}}, \quad \mathbf{k} \in \bar{\mathcal{L}}, \quad (8.211)$$

where the wave vector  $\mathbf{k}$  is on the reciprocal lattice  $\bar{\mathcal{L}}$ . For the primitive vectors  $\mathbf{a}_1 = \{l_1, 0\}$  and  $\mathbf{a}_2 = \{l_3, l_4\}$ , the primitive vectors of the corresponding reciprocal lattice are  $\mathbf{b}_1 = 2\pi/l_1 l_4 \{l_4, -l_3\}$  and  $\mathbf{b}_2 = 2\pi/l_1 l_4 \{0, l_1\}$ . The expression of eigenvector with wave vector  $\mathbf{k} = n_1 \mathbf{b}_1 + n_2 \mathbf{b}_2$  is:

$$f_{\mathbf{k}}(\mathbf{z}) = e^{i\mathbf{k} \cdot \mathbf{z}} = \exp\left[i \frac{2\pi}{l_1 l_4} (n_1 l_4 z_1 - n_1 l_3 z_2 + n_2 l_1 z_2)\right], \quad (8.212)$$

where the  $\mathbf{z} = (z_1, z_2)$ . The eigenvalue of the operator  $s - \sigma_1 - \sigma_1^\top - \sigma_2 - \sigma_2^\top$  corresponding to this eigenvector is:

$$\lambda_{\mathbf{k}} = s - 2 \cos\left(\frac{2\pi n_1}{l_1}\right) - 2 \cos\left(-\frac{2\pi n_1 l_3}{l_1 l_4} + \frac{2\pi n_2}{l_4}\right). \quad (8.213)$$

It is sufficient to use the wave vectors  $\mathbf{k}$  with  $n_1$  from 0 to  $l_1 - 1$  and  $n_2$  from 0 to  $l_4 - 1$  to get all of the eigenvectors. Any wave vector on the reciprocal lattice outside of this range will give an eigenvector which is equivalent to an eigenvector with the wave vector in the range. So the number of eigenmodes we can get is  $l_1 l_4$ , which is the number of lattice sites in a smallest repeating tile.

<sup>20</sup>Han 2019-06-25: This section is a version of kittens refsect s:dDcatMap that starts from 2D cat map without giving the formula of general  $d$ -dimensional spatiotemporal cat. I feel this is less clear than start with the  $d$ -dimensional spatiotemporal cat, but it directly follows the section of spatiotemporal cat map. Eventually this text was not used not used in kittens [63].

<sup>21</sup>Han 2019-06-17: I will need to rewrite this paragraph to make it clearer.

<sup>22</sup>Predrag 2020-02-15: This is called 'Hermite normal form', see (8.123).

Using the counting formula (??), we can find the number of the periodic points by computing the determinant of the orbit Jacobian matrix, which is the operator  $-2s + \sigma_1 + \sigma_1^\top + \sigma_2 + \sigma_2^\top$  defined on the finite tile with periodic bc's:

$$N = \prod_{\mathbf{k}} \lambda_{\mathbf{k}} = \prod_{n_1=0}^{l_1-1} \prod_{n_2=0}^{l_4-1} \left[ 2s - 2 \cos\left(\frac{2\pi n_1}{l_1}\right) - 2 \cos\left(-\frac{2\pi n_1 l_3}{l_1 l_4} + \frac{2\pi n_2}{l_4}\right) \right]. \quad (8.214)$$

This is the number of periodic points with the periodicity given by Bravais lattice (7.1) with the primitive vectors  $\mathbf{a}_1 = \{l_1, 0\}$  and  $\mathbf{a}_2 = \{l_3, l_4\}$ .

Using the eigenvectors we can do a Fourier transform to the orbit Jacobian matrix and get the inverse which is the Green's function.

## 8.12 Integer lattices literature

There are many reasons why one needs to compute an “orbit Jacobian matrix” Hill determinant  $|\text{Det } \mathcal{J}|$ , in fields ranging from number theory to engineering, and many methods to accomplish that:

- discretizations of Helmholtz [67, 84, 168] and screened Poisson or Klein–Gordon or Yukawa [68, 100, 124, 125] equations

- Green's functions on integer lattices [10, 13, 32, 42, 46, 49, 85, 98, 120, 121, 149–151, 174, 181, 184, 190, 191, 205, 234, 251]

- linearized Hartree-Fock equation on finite lattices [156]

- random walks, resistor networks, electrical circuits [6, 15, 33, 58, 59, 69, 102, 110, 127, 157, 160, 196, 214, 238, 243, 253]

- Gaussian model [90, 144, 180, 224]

- tight-binding Hamiltonians [58, 59, 73]

- discrete Schrödinger equation [203], Harper or Hofstadter model [111, 116] or almost Mathieu operator [227]

- quasilattices [38, 88]

- circulant tensor systems [42, 46, 187, 215, 218, 255]

- Ising model [26, 113, 114, 126, 128, 131–133, 152, 167, 175, 182, 197, 210, 254],

- Ising model transfer matrices [198, 254]

- lattice field theory [136, 185, 189, 194, 220, 229, 230, 247]

- many-body quantum chaos [3–5, 28–31, 75–79, 219]

- modular transformations [43, 159, 261]

- lattice string theory [97, 201]

- spatiotemporal stability in coupled map lattices [9, 94, 259]

- Van Vleck determinant, Laplace operator spectrum, semiclassical Gaussian path integrals [55, 164, 165, 242]

- Jacobi operator

- time reversal

- Hill determinant [34, 55, 176]; discrete Hill's formula and the Hill discriminant, Toda lattice [241]

- Lindstedt-Poincaré technique [244–246]

heat kernel [47, 71, 74, 139, 148, 184, 205, 256]  
chronotopic models [212]  
lattice points enumeration [22, 23, 27, 65]  
cryptography [186]  
primitive parallelogram [16, 39, 195, 248]  
difference equations [64, 86, 235]  
Bernoulli map [36, 70, 115], beta transformation [87, 202, 217]  
digital signal processing [72, 169, 252]  
generating functions, Z-transforms [74, 249]  
integer-point transform [27]  
graph Laplacians [50, 99, 173, 213]  
graph zeta functions [12, 20, 25, 35, 51–53, 66, 71, 104, 112, 122, 129, 158, 161, 213, 216, 221, 223, 233, 239, 240, 260]  
zeta functions for multi-dimensional shifts [19, 171, 172, 188]  
zeta functions on discrete tori [47, 48, 256]

## References

- [1] R. P. Agarwal, *Difference Equations and Inequalities* (Taylor & Francis, 2000).
- [2] R. P. Agarwal and K. Perera, *Proc. Conf. Differential & Difference Eqs. and Appl.* (Hindavi, New York, 2006).
- [3] M. Akila, B. Gutkin, P. Braun, D. Waltner, and T. Guhr, “Semiclassical prediction of large spectral fluctuations in interacting kicked spin chains”, *Ann. Phys.* **389**, 250–282 (2018).
- [4] M. Akila, D. Waltner, B. Gutkin, P. Braun, and T. Guhr, “Semiclassical identification of periodic orbits in a quantum many-body system”, *Phys. Rev. Lett.* **118**, 164101 (2017).
- [5] M. Akila, D. Waltner, B. Gutkin, and T. Guhr, “Particle-time duality in the kicked Ising spin chain”, *J. Phys. A* **49**, 375101 (2016).
- [6] V. V. Albert, L. I. Glazman, and L. Jiang, “Topological properties of linear circuit lattices”, *Phys. Rev. Lett.* **114**, 173902 (2015).
- [7] L. Allen, B. Aulbach, S. Elaydi, and R. Sacker, eds., *Difference Equations and Discrete Dynamical Systems : Proc. 9th Intern. Conf.* (World Sci., Singapore, 2005).
- [8] J. M. Amigó, S. Zambrano, and M. A. F. Sanjuán, “Permutation complexity of spatiotemporal dynamics”, *Europhys. Lett.* **90**, 10007 (2010).
- [9] R. E. Amritkar, P. M. Gade, A. D. Gangal, and V. M. Nandkumaran, “Stability of periodic orbits of coupled-map lattices”, *Phys. Rev. A* **44**, R3407–R3410 (1991).
- [10] W. N. Anderson and T. D. Morley, “Eigenvalues of the Laplacian of a graph”, *Lin. Multilin. Algebra* **18**, 141–145 (1985).

- [11] V. I. Arnol'd and A. Avez, *Ergodic Problems of Classical Mechanics* (Addison-Wesley, Redwood City, 1989).
- [12] F. Arrigo, P. Grindrod, D. J. Higham, and V. Noferini, "On the exponential generating function for non-backtracking walks", *Linear Algebra Appl.* **556**, 381–399 (2018).
- [13] J. H. Asad, "Differential equation approach for one- and two-dimensional lattice green's function", *Mod. Phys. Lett. B* **21**, 139–154 (2007).
- [14] F. M. Atay, S. Jalan, and J. Jost, "Symbolic dynamics and synchronization of coupled map networks with multiple delays", *Phys. Lett. A* **375**, 130–135 (2010).
- [15] D. Atkinson and F. J. van Steenwijk, "Infinite resistive lattices", *Am. J. Phys* **67**, 486–492 (1999).
- [16] M. Baake, J. Hermisson, and A. B. Pleasants, "The torus parametrization of quasiperiodic LI-classes", *J. Phys. A* **30**, 3029–3056 (1997).
- [17] M. Baake, N. Neumärker, and J. A. G. Roberts, "Orbit structure and (reversing) symmetries of toral endomorphisms on rational lattices", *Discrete Continuous Dyn. Syst.* **33**, 527–553 (2013).
- [18] M. Baake, J. A. G. Roberts, and A. Weiss, "Periodic orbits of linear endomorphisms on the 2-torus and its lattices", *Nonlinearity* **21**, 2427 (2008).
- [19] J.-C. Ban, W.-G. Hu, S.-S. Lin, and Y.-H. Lin, *Zeta Functions for Two-dimensional Shifts of Finite Type*, Vol. 221, *Memoirs Amer. Math. Soc.* (Amer. Math. Soc., Providence RI, 2013).
- [20] R. Band, J. M. Harrison, and C. H. Joyner, "Finite pseudo orbit expansions for spectral quantities of quantum graphs", *J. Phys. A* **45**, 325204 (2012).
- [21] M. Baranger, K. T. R. Davies, and J. H. Mahoney, "The calculation of periodic trajectories", *Ann. Phys.* **186**, 95–110 (1988).
- [22] A. Barvinok, *A Course in Convexity* (Amer. Math. Soc., New York, 2002).
- [23] A. Barvinok, *Integer Points in Polyhedra* (European Math. Soc. Pub., Berlin, 2008).
- [24] A. I. Barvinok, "A polynomial time algorithm for counting integral points in polyhedra when the dimension is fixed", *Math. Oper. Res.* **19**, 769–779 (1994).
- [25] H. Bass, "The Ihara-Selberg zeta function of a tree lattice", *Int. J. Math.* **3**, 717–797 (1992).
- [26] R. J. Baxter, "The bulk, surface and corner free energies of the square lattice Ising model", *J. Phys. A* **50**, 014001 (2016).
- [27] M. Beck and S. Robins, *Computing the Continuous Discretely* (Springer, New York, 2007).

- [28] B. Bertini, P. Kos, and T. Prosen, “Exact spectral form factor in a minimal model of many-body quantum chaos”, *Phys. Rev. Lett.* **121**, 264101 (2018).
- [29] B. Bertini, P. Kos, and T. Prosen, “Entanglement spreading in a minimal model of maximal many-body quantum chaos”, *Phys. Rev. X* **9**, 021033 (2019).
- [30] B. Bertini, P. Kos, and T. Prosen, “Exact correlation functions for dual-unitary lattice models in 1+1 dimensions”, *Phys. Rev. Lett.* **123**, 210601 (2019).
- [31] B. Bertini, P. Kos, and T. Prosen, “Operator entanglement in local quantum circuits i: Chaotic dual-unitary circuits”, *SciPost Physics* **8**, 067 (2020).
- [32] H. S. Bhat and B. Osting, “Diffraction on the two-dimensional square lattice”, *SIAM J. Appl. Math.* **70**, 1389–1406 (2010).
- [33] P. Blanchard and D. Volchenkov, *Random Walks and Diffusions on Graphs and Databases* (Springer, Berlin, 2011).
- [34] S. V. Bolotin and D. V. Treschev, “Hill’s formula”, *Russ. Math. Surv.* **65**, 191 (2010).
- [35] R. Bowen and O. Lanford, Zeta functions of restrictions of the shift transformation, in *Global Analysis (Proc. Sympos. Pure Math., Berkeley, CA, 1968)*, Vol. 1, edited by S.-S. Chern and S. Smale (1970), pp. 43–50.
- [36] A. Boyarsky and P. Góra, *Laws of Chaos: Invariant Measures and Dynamical Systems in One Dimension* (Birkhäuser, Boston, 1997).
- [37] L. Boyle, M. Dickens, and F. Flicker, “Conformal quasicrystals and holography”, *Phys. Rev. X* **10**, 011009 (2020).
- [38] L. Boyle and P. J. Steinhardt, *Self-similar one-dimensional quasilattices*, 2016.
- [39] R. B. S. Brooks, R. F. Brown, J. Pak, and D. H. Taylor, “Nielsen numbers of maps of tori”, *Proc. Amer. Math. Soc.* **52**, 398–398 (1975).
- [40] N. G. de Bruijn, “Sequences of zeros and ones generated by special production rules”, *Indag. Math. Proc.* **84**, 27–37 (1981).
- [41] L. A. Bunimovich and Y. G. Sinai, “Spacetime chaos in coupled map lattices”, *Nonlinearity* **1**, 491 (1988).
- [42] B. L. Buzbee, G. H. Golub, and C. W. Nielson, “On direct methods for solving Poisson’s equations”, *SIAM J. Numer. Anal.* **7**, 627–656 (1970).
- [43] J. L. Cardy, “Operator content of two-dimensional conformally invariant theories”, *Nucl. Phys. B* **270**, 186–204 (1986).
- [44] J. W. S. Cassels, *An Introduction to the Geometry of Numbers* (Springer, Berlin, 1959).
- [45] H. Chaté and P. Manneville, “Transition to turbulence via spatiotemporal intermittency”, *Phys. Rev. Lett.* **58**, 112 (1987).

- [46] M. Chen, “On the solution of circulant linear systems”, *SIAM J. Numer. Anal.* **24**, 668–683 (1987).
- [47] G. Chinta, J. Jorgenson, and A. Karlsson, “Zeta functions, heat kernels, and spectral asymptotics on degenerating families of discrete tori”, *Nagoya Math. J.* **198**, 121–172 (2010).
- [48] G. Chinta, J. Jorgenson, and A. Karlsson, “Heat kernels on regular graphs and generalized Ihara zeta function formulas”, *Monatsh. Math.* **178**, 171–190 (2014).
- [49] F. Chung and S.-T. Yau, “Discrete Green’s functions”, *J. Combin. Theory A* **91**, 19–214 (2000).
- [50] D. Cimasoni, “The critical Ising model via Kac-Ward matrices”, *Commun. Math. Phys.* **316**, 99–126 (2012).
- [51] B. Clair, “The Ihara zeta function of the infinite grid”, *Electron. J. Combin.* **21**, P2–16 (2014).
- [52] B. Clair and S. Mokhtari-Sharghi, “Zeta functions of discrete groups acting on trees”, *J. Algebra* **237**, 591–620 (2001).
- [53] B. Clair and S. Mokhtari-Sharghi, “Convergence of zeta functions of graphs”, *Proc. Amer. Math. Soc.* **130**, 1881–1887 (2002).
- [54] H. Cohen, *A Course in Computational Algebraic Number Theory* (Springer, Berlin, 1993).
- [55] Y. Colin de Verdière, “Spectrum of the Laplace operator and periodic geodesics: thirty years after”, *Ann. Inst. Fourier* **57**, 2429–2463 (2007).
- [56] R. Coutinho and B. Fernandez, “Extended symbolic dynamics in bistable CML: Existence and stability of fronts”, *Physica D* **108**, 60–80 (1997).
- [57] S. C. Creagh, “Quantum zeta function for perturbed cat maps”, *Chaos* **5**, 477–493 (1995).
- [58] J. Cserti, “Application of the lattice Green’s function for calculating the resistance of an infinite network of resistors”, *Amer. J. Physics* **68**, 896–906 (2000).
- [59] J. Cserti, G. Széchenyi, and G. Dávid, “Uniform tiling with electrical resistors”, *J. Phys. A* **44**, 215201 (2011).
- [60] L.-B. Cui, C. Chen, W. Li, and M. K. Ng, “An eigenvalue problem for even order tensors with its applications”, *Lin. Multilin. Algebra* **64**, 602–621 (2015).
- [61] P. Cvitanović, R. Artuso, R. Mainieri, G. Tanner, and G. Vattay, *Chaos: Classical and Quantum* (Niels Bohr Inst., Copenhagen, 2024).
- [62] P. Cvitanović and T. Kinoshita, “Feynman-Dyson rules in parametric space”, *Phys. Rev. D* **10**, 3978–3991 (1974).
- [63] P. Cvitanović and H. Liang, *A chaotic lattice field theory in two dimensions*, In preparation, 2024.

- [64] F. Dannan, S. Elaydi, and P. Liu, "Periodic solutions of difference equations", *J. Difference Equations and Applications* **6**, 203–232 (2000).
- [65] J. A. De Loera, R. Hemmecke, J. Tauzer, and R. Yoshida, "Effective lattice point counting in rational convex polytopes", *J. Symbolic Comp.* **38**, 1273–1302 (2004).
- [66] A. Deitmar, "Ihara zeta functions of infinite weighted graphs", *SIAM J. Discrete Math.* **29**, 2100–2116 (2015).
- [67] A. Dienstfrey, F. Hang, and J. Huang, "Lattice sums and the two-dimensional, periodic Green's function for the Helmholtz equation", *Proc. Roy. Soc. Ser A* **457**, 67–85 (2001).
- [68] F. W. Dorr, "The direct solution of the discrete Poisson equation on a rectangle", *SIAM Rev.* **12**, 248–263 (1970).
- [69] P. G. Doyle and J. L. Snell, "Random walks and electric networks", in *Intelligent Systems, Control and Automation: Science and Engineering* (Springer, 2012), pp. 259–265.
- [70] D. J. Driebe, *Fully Chaotic Maps and Broken Time Symmetry* (Springer, New York, 1999).
- [71] J. Dubout, *Zeta functions of graphs, their symmetries and extended Catalan numbers*.
- [72] D. Dudgeon and R. M. Mersereau, *Multidimensional Digital Signal Processing* (Prentice-Hall, Englewood Cliffs, NJ, 1984).
- [73] E. N. Economou, *Green's Functions in Quantum Physics* (Springer, Berlin, 2006).
- [74] S. Elaydi, *An Introduction to Difference Equations*, 3rd ed. (Springer, Berlin, 2005).
- [75] T. Engl, J. Dujardin, A. Argüelles, P. Schlagheck, K. Richter, and J. D. Urbina, "Coherent backscattering in Fock space: A signature of quantum many-body interference in interacting bosonic systems", *Phys. Rev. Lett.* **112**, 140403 (2014).
- [76] T. Engl, P. Plöss, J. D. Urbina, and K. Richter, "The semiclassical propagator in fermionic Fock space", *Theor. Chem. Acc.* **133**, 1563 (2014).
- [77] T. Engl, J. D. Urbina, Q. Hummel, and K. Richter, "Complex scattering as canonical transformation: A semiclassical approach in Fock space", *Ann. Phys.* **527**, 737–747 (2015).
- [78] T. Engl, J. D. Urbina, and K. Richter, "Periodic mean-field solutions and the spectra of discrete bosonic fields: Trace formula for Bose-Hubbard models", *Phys. Rev. E* **92**, 062907 (2015).
- [79] T. Engl, J. D. Urbina, and K. Richter, "The semiclassical propagator in Fock space: dynamical echo and many-body interference", *Philos. Trans. Royal Soc. A* **374**, 20150159 (2016).

- [80] L. Ermann and D. L. Shepelyansky, “The Arnold cat map, the Ulam method and time reversal”, *Physica D* **241**, 514–518 (2012).
- [81] A. Fel’shtyn and R. Hill, “Trace formulae, Zeta functions, congruences and Reidemeister torsion in Nielsen theory”, *Forum Mathematicum* **10**, 641–664 (1998).
- [82] B. Fernandez and P. Guiraud, “Route to chaotic synchronisation in coupled map lattices: Rigorous results”, *Discrete Continuous Dyn. Syst. Ser. B* **4**, 435–456 (2004).
- [83] B. Fernandez and M. Jiang, “Coupling two unimodal maps with simple kneading sequences”, *Ergod. Theor. Dynam. Syst.* **24**, 107–125 (2004).
- [84] A. L. Fetter and J. D. Walecka, *Theoretical Mechanics of Particles and Continua* (Dover, New York, 2003).
- [85] M. Fiedler, “Algebraic connectivity of graphs”, *Czech. Math. J* **23**, 298–305 (1973).
- [86] D. Fischer, G. Golub, O. Hald, C. Leiva, and O. Widlund, “On Fourier-Toeplitz methods for separable elliptic problems”, *Math. Comput.* **28**, 349–349 (1974).
- [87] L. Flatto, J. C. Lagarias, and B. Poonen, “The zeta function of the beta transformation”, *Ergodic Theory Dynam. Systems* **14**, 237–266 (1994).
- [88] F. Flicker, “Time quasilattices in dissipative dynamical systems”, *SciPost Phys.* **5**, 001 (2018).
- [89] F. Flicker, S. H. Simon, and S.-A. Parameswaran, “Classical dimers on Penrose tilings”, *Phys. Rev. X* **10**, 011005 (2020).
- [90] E. Fradkin, *Field Theories of Condensed Matter Physics* (Cambridge Univ. Press, Cambridge UK, 2013).
- [91] K. M. Frahm and D. L. Shepelyansky, “Ulam method for the Chirikov standard map”, *Eur. Phys. J. B* **76**, 57–68 (2010).
- [92] K. M. Frahm and D. L. Shepelyansky, “Small world of Ulam networks for chaotic Hamiltonian dynamics”, *Phys. Rev. E* **98**, 032205 (2018).
- [93] M. Fruchart, Y. Zhou, and V. Vitelli, “Dualities and non-Abelian mechanics”, *Nature* **577**, 636–640 (2020).
- [94] P. M. Gade and R. E. Amritkar, “Spatially periodic orbits in coupled-map lattices”, *Phys. Rev. E* **47**, 143–154 (1993).
- [95] O. Galor, *Discrete Dynamical Systems* (Springer, Berlin, 2007).
- [96] G. Giacomelli, S. Lepri, and A. Politi, “Statistical properties of bidimensional patterns generated from delayed and extended maps”, *Phys. Rev. E* **51**, 3939–3944 (1995).
- [97] R. Giles and C. B. Thorn, “Lattice approach to string theory”, *Phys. Rev. D* **16**, 366–386 (1977).



- [98] J. I. Glaser, “Numerical solution of waveguide scattering problems by finite-difference Green’s functions”, *IEEE Trans. Microwave Theory Tech.* **18**, 436–443 (1970).
- [99] C. Godsil and G. F. Royle, *Algebraic Graph Theory* (Springer, New York, 2013).
- [100] G. H. Golub and C. F. Van Loan, *Matrix Computations*, 4th ed. (J. Hopkins Univ. Press, Baltimore, MD, 2013).
- [101] I. S. Gradshteyn and I. M. Ryzhik, *Tables of Integrals, Series and Products*, 8th ed. (Elsevier LTD, Oxford, New York, 2014).
- [102] G. Grimmett, *Probability on Graphs: : Random Processes on Graphs and Lattices* (Cambridge Univ. Press, 2009).
- [103] P. Gruber and C. G. Lekkerkerker, *Geometry of numbers* (North-Holland, Amsterdam, 1987).
- [104] D. Guido, T. Isola, and M. L. Lapidus, “A trace on fractal graphs and the Ihara zeta function”, *Trans. Amer. Math. Soc.* **361**, 3041–3041 (2009).
- [105] V. M. Gundlach and D. A. Rand, “Spatio-temporal chaos. I. Hyperbolicity, structural stability, spatio-temporal shadowing and symbolic dynamics”, *Nonlinearity* **6**, 165 (1993).
- [106] B. Gutkin, L. Han, R. Jafari, A. K. Saremi, and P. Cvitanović, “Linear encoding of the spatiotemporal cat map”, *Nonlinearity* **34**, 2800–2836 (2021).
- [107] B. Gutkin and V. Osipov, “Clustering of periodic orbits and ensembles of truncated unitary matrices”, *J. Stat. Phys.* **153**, 1049–1064 (2013).
- [108] B. Gutkin and V. Osipov, “Clustering of periodic orbits in chaotic systems”, *Nonlinearity* **26**, 177 (2013).
- [109] B. Gutkin and V. Osipov, “Classical foundations of many-particle quantum chaos”, *Nonlinearity* **29**, 325–356 (2016).
- [110] A. J. Guttmann, “Lattice Green’s functions in all dimensions”, *J. Phys. A* **43**, 305205 (2010).
- [111] P. G. Harper, “Single band motion of conduction electrons in a uniform magnetic field”, *Proc. Phys. Soc. London, Sect. A* **68**, 874–878 (1955).
- [112] K. Hashimoto, “Zeta functions of finite graphs and representations of p-adic groups”, *Adv. Stud. Pure Math.* **15**, 211–280 (1989).
- [113] H. Hobrecht and F. Hucht, “Anisotropic scaling of the two-dimensional Ising model I: the torus”, *SciPost Phys.* **7**, 026 (2019).
- [114] H. Hobrecht and F. Hucht, “Anisotropic scaling of the two-dimensional Ising model II: surfaces and boundary fields”, *SciPost Phys.* **8**, 032 (2020).
- [115] F. Hofbauer and G. Keller, “Zeta-functions and transfer-operators for piecewise linear transformations”, *J. Reine Angew. Math. (Crelle)* **1984**, 100–113 (1984).

- [116] D. R. Hofstadter, "Energy levels and wave functions of Bloch electrons in rational and irrational magnetic fields", *Phys. Rev. B* **14**, 2239–2249 (1976).
- [117] S. Holmin, "Counting nonsingular matrices with primitive row vectors", *Monatsh. Math.* **173**, 209–230 (2013).
- [118] S. Holmin, *Geometry of Numbers, Class Group Statistics and Free Path Lengths*, PhD thesis (KTH Royal Inst. Technology, Stockholm, 2015).
- [119] W. G. Hoover and K. Aoki, "Order and chaos in the one-dimensional  $\phi^4$  model : N-dependence and the Second Law of Thermodynamics", *Commun. Nonlinear Sci. Numer. Simul.* **49**, 192–201 (2017).
- [120] T. Horiguchi, "Lattice Green's function for the simple cubic lattice", *J. Phys. Soc. Jpn.* **30**, 1261–1272 (1971).
- [121] T. Horiguchi and T. Morita, "Note on the lattice Green's function for the simple cubic lattice", *J. Phys. C* **8**, L232 (1975).
- [122] M. D. Horton, "Ihara zeta functions of digraphs", *Linear Algebra Appl.* **425**, 130–142 (2007).
- [123] J. M. Houlrik, "Periodic orbits in a two-variable coupled map", *Chaos* **2**, 323–327 (1992).
- [124] G. Y. Hu and R. F. O'Connell, "Analytical inversion of symmetric tridiagonal matrices", *J. Phys. A* **29**, 1511 (1996).
- [125] G. Y. Hu, J. Y. Ryu, and R. F. O'Connell, "Analytical solution of the generalized discrete Poisson equation", *J. Phys. A* **31**, 9279 (1998).
- [126] A. Hucht, "The square lattice Ising model on the rectangle I: finite systems", *J. Phys. A* **50**, 065201 (2017).
- [127] B. D. Hughes, *Random Walks and Random Environments: Vol. I, Random Walks* (Clarendon Press, Oxford, 1995).
- [128] C. A. Hurst and H. S. Green, "New solution of the Ising problem for a rectangular lattice", *J. Chem. Phys.* **33**, 1059–1062 (1960).
- [129] Y. Ihara, "On discrete subgroups of the two by two projective linear group over p-adic fields", *J. Math. Soc. Japan* **18**, 219–235 (1966).
- [130] S. Isola, " $\zeta$ -functions and distribution of periodic orbits of toral automorphisms", *Europhys. Lett.* **11**, 517–522 (1990).
- [131] E. V. Ivashkevich, N. S. Izmailian, and C.-K. Hu, "Kronecker's double series and exact asymptotic expansions for free models of statistical mechanics on torus", *J. Phys. A* **35**, 5543–5561 (2002).
- [132] N. S. Izmailian, "Finite-size effects for anisotropic 2D Ising model with various boundary conditions", *J. Phys. A* **45**, 494009 (2012).
- [133] N. S. Izmailian and C.-K. Hu, "Finite-size effects for the Ising model on helical tori", *Phys. Rev. E* **76**, 041118 (2007).

- [134] N. S. Izmailian and M.-C. Huang, “Asymptotic expansion for the resistance between two maximally separated nodes on an  $M$  by  $N$  resistor network”, *Phys. Rev. E* **82**, 011125 (2010).
- [135] M. A. Jafarizadeh, R. Sufiani, and S. Jafarizadeh, “Calculating two-point resistances in distance-regular resistor networks”, *J. Phys. A* **40**, 4949–4972 (2007).
- [136] K. Jansen, “Lattice field theory”, *Int. J. Mod. Phys. E* **16**, 2638–2679 (2007).
- [137] J. Jezierski and W. Marzantowicz, *Homotopy Methods in Topological Fixed and Periodic Points Theory* (Springer, Berlin, 2006).
- [138] M. Jiang, “Equilibrium states for lattice models of hyperbolic type”, *Nonlinearity* **8**, 631–659 (1995).
- [139] J. Jorgenson and S. Lang, “The ubiquitous heat kernel”, in *Mathematics Unlimited - 2001 and Beyond* (Springer, Berlin, 2001), pp. 655–683.
- [140] W. Just, “Analytical approach for piecewise linear coupled map lattices”, *J. Stat. Phys.* **90**, 727–748 (1998).
- [141] W. Just, “Equilibrium phase transitions in coupled map lattices: A pedestrian approach”, *J. Stat. Phys.* **105**, 133–142 (2001).
- [142] W. Just, “On symbolic dynamics of space-time chaotic models”, in *Collective Dynamics of Nonlinear and Disordered Systems* (Springer, 2005), pp. 339–357.
- [143] W. Just and F. Schmüser, “On phase transitions in coupled map lattices”, in *Dynamics of Coupled Map Lattices and of Related Spatially Extended Systems*, edited by J.-R. Chazottes and B. Fernandez (Springer, 2005), pp. 33–64.
- [144] L. P. Kadanoff, *Statistical Physics: Statics, Dynamics and Renormalization* (World Scientific, Singapore, 2000).
- [145] K. Kaneko, “Transition from torus to chaos accompanied by frequency lockings with symmetry breaking: In connection with the coupled-logistic map”, *Prog. Theor. Phys.* **69**, 1427–1442 (1983).
- [146] K. Kaneko, “Period-doubling of kink-antikink patterns, quasiperiodicity in antiferro-like structures and spatial intermittency in coupled logistic lattice: Towards a prelude of a “field theory of chaos””, *Prog. Theor. Phys.* **72**, 480–486 (1984).
- [147] H. Kantz and P. Grassberger, “Chaos in low-dimensional Hamiltonian maps”, *Phys. Let. A* **123**, 437–443 (1987).
- [148] A. Karlsson and M. Neuhauser, “Heat kernels, theta identities, and zeta functions on cyclic groups”, *Contemp. Math.* **394**, 177–190 (2006).
- [149] S. Katsura and S. Inawashiro, “Lattice Green’s functions for the rectangular and the square lattices at arbitrary points”, *J. Math. Phys.* **12**, 1622–1630 (1971).

- [150] S. Katsura, S. Inawashiro, and Y. Abe, “Lattice Green’s function for the simple cubic lattice in terms of a Mellin-Barnes type integral”, *J. Math. Phys.* **12**, 895–899 (1971).
- [151] S. Katsura, T. Morita, S. Inawashiro, T. Horiguchi, and Y. Abe, “Lattice Green’s function. Introduction”, *J. Math. Phys.* **12**, 892–895 (1971).
- [152] B. Kaufman, “Crystal statistics. II. Partition function evaluated by spinor analysis”, *Phys. Rev.* **76**, 1232–1243 (1949).
- [153] J. P. Keating, “Asymptotic properties of the periodic orbits of the cat maps”, *Nonlinearity* **4**, 277 (1991).
- [154] J. P. Keating, “The cat maps: quantum mechanics and classical motion”, *Nonlinearity* **4**, 309–341 (1991).
- [155] W. G. Kelley and A. C. Peterson, *Difference Equations : An Introduction with Applications* (Academic, San Diego, 2001).
- [156] V. Khoromskaia and B. N. Khoromskij, “Block circulant and Toeplitz structures in the linearized Hartree-Fock equation on finite lattices: Tensor approach”, *Comput. Methods Appl. Math.* **17**, 43–455 (2017).
- [157] G. Kirchhoff, “Über die Auflösung der Gleichungen, auf welche man bei der Untersuchung der linearen Vertheilung galvanischer Ströme geführt wird”, *Ann. Phys. Chem.* **148**, 497–508 (1847).
- [158] M. Kotani and T. Sunada, “Zeta functions of finite graphs”, *J. Math. Sci. Univ. Tokyo* **7**, 7–25 (2000).
- [159] S. Lang, *Linear Algebra* (Addison-Wesley, Reading, MA, 1987).
- [160] C. H. Lee, S. Imhof, C. Berger, F. Bayer, J. Brehm, L. W. Molenkamp, T. Kiessling, and R. Thomale, “Topoelectrical circuits”, *Commun. Phys.* **1**, 39 (2018).
- [161] D. Lenz, F. Pogorzelski, and M. Schmidt, “The Ihara zeta function for infinite graphs”, *Trans. Amer. Math. Soc.* **371**, 5687–5729 (2018).
- [162] S. Lepri, A. Politi, and A. Torcini, “Chronotopic Lyapunov analysis. I. A detailed characterization of 1D systems”, *J. Stat. Phys.* **82**, 1429–1452 (1996).
- [163] S. Lepri, A. Politi, and A. Torcini, “Chronotopic Lyapunov analysis. II. Towards a unified approach”, *J. Stat. Phys.* **88**, 31–45 (1997).
- [164] S. Levit and U. Smilansky, “A new approach to Gaussian path integrals and the evaluation of the semiclassical propagator”, *Ann. Phys.* **103**, 198–207 (1977).
- [165] S. Levit and U. Smilansky, “A theorem on infinite products of eigenvalues of Sturm-Liouville type operators”, *Proc. Amer. Math. Soc.* **65**, 299–299 (1977).
- [166] J. Li and S. Tomsovic, “Exact relations between homoclinic and periodic orbit actions in chaotic systems”, *Phys. Rev. E* **97**, 022216 (2017).

- [167] T. M. Liaw, M. C. Huang, Y. L. Chou, S. C. Lin, and F. Y. Li, “Partition functions and finite-size scalings of Ising model on helical tori”, *Phys. Rev. E* **73**, 041118 (2006).
- [168] W. J. Lick, *Difference Equations from Differential Equations* (Springer, Berlin, 1989).
- [169] J. S. Lim, *Two-dimensional Signal and Image Processing* (Prentice Hall, Englewood Cliffs, N.J, 1990).
- [170] L.-H. Lim, Singular values and eigenvalues of tensors: A variational approach, in *1st IEEE International Workshop on Computational Advances in Multi-Sensor Adaptive Processing* (2005).
- [171] D. Lind and K. Schmidt, “Symbolic and algebraic dynamical systems”, in *Handbook of Dynamical Systems*, Vol. 1, edited by B. Hasselblatt and A. Katok (Elsevier, New York, 2002), pp. 765–812.
- [172] D. A. Lind, “A zeta function for  $Z^d$ -actions”, in *Ergodic Theory of  $Z^d$  Actions*, edited by M. Pollicott and K. Schmidt (Cambridge Univ. Press, 1996), pp. 433–450.
- [173] D. A. Lind and B. Marcus, *An Introduction to Symbolic Dynamics and Coding* (Cambridge Univ. Press, Cambridge, 1995).
- [174] R. de la Llave, Variational methods for quasiperiodic solutions of partial differential equations, in *Hamiltonian Systems and Celestial Mechanics (HAMSYS-98)*, edited by J. Delgado, E. A. Lacomba, E. Pérez-Chavela, and J. Llibre (2000).
- [175] I. Lyberg, “Free energy of the anisotropic Ising lattice with Brascamp-Kunz boundary conditions”, *Phys. Rev. E* **87**, 062141 (2013).
- [176] R. S. MacKay and J. D. Meiss, “Linear stability of periodic orbits in Lagrangian systems”, *Phys. Lett. A* **98**, 92–94 (1983).
- [177] R. S. MacKay, J. D. Meiss, and I. C. Percival, “Transport in Hamiltonian systems”, *Physica D* **13**, 55–81 (1984).
- [178] A. Manning, “Axiom A diffeomorphisms have rational zeta function”, *Bull. London Math. Soc.* **3**, 215–220 (1971).
- [179] C. Mariconda and A. Tonolo, *Discrete Calculus - Methods for Counting* (Springer, 2016).
- [180] E. C. Marino, *Quantum Field Theory Approach to Condensed Matter Physics* (Cambridge Univ. Press, Cambridge UK, 2017).
- [181] P. A. Martin, “Discrete scattering theory: Green’s function for a square lattice”, *Wave Motion* **43**, 619–629 (2006).
- [182] B. M. McCoy and T. T. Wu, *The Two-Dimensional Ising Model*, 2nd ed. (Dover, 1973).
- [183] J. D. Meiss, “Symplectic maps, variational principles, and transport”, *Rev. Mod. Phys.* **64**, 795–848 (1992).

- [184] B. D. Mestel and I. Percival, “Newton method for highly unstable orbits”, *Physica D* **24**, 172 (1987).
- [185] H. B. Meyer, “Lattice QCD: A brief introduction”, in *Lattice QCD for Nuclear Physics*, edited by H.-W. Lin and H. B. Meyer (Springer, York New, 2015), pp. 1–34.
- [186] D. Micciancio and S. Goldwasser, *Complexity of Lattice Problems - A Cryptographic Perspective* (Springer, New York, 2002).
- [187] M. Michałek and B. Sturmfels, *Invitation to Nonlinear Algebra* (MPI Leipzig, 2020).
- [188] R. Miles, “A dynamical zeta function for group actions”, *Monatsh. Math.* **182**, 683–708 (2016).
- [189] I. Montvay and G. Münster, *Quantum Fields on a Lattice* (Cambridge Univ. Press, Cambridge, 1994).
- [190] T. Morita, “Useful procedure for computing the lattice Green’s function - square, tetragonal, and bcc lattices”, *J. Math. Phys.* **12**, 1744–1747 (1971).
- [191] T. Morita and T. Horiguchi, “Calculation of the lattice Green’s function for the bcc, fcc, and rectangular lattices”, *J. Math. Phys.* **12**, 986–992 (1971).
- [192] B. Mramor and B. Rink, “Ghost circles in lattice Aubry-Mather theory”, *J. Diff. Equ.* **252**, 3163–3208 (2012).
- [193] S. Müller, S. Heusler, P. Braun, F. Haake, and A. Altland, “Semiclassical foundation of universality in quantum chaos”, *Phys. Rev. Lett.* **93**, 014103 (2004).
- [194] G. Münster and M. Walzl, *Lattice gauge theory - A short primer*, 2000.
- [195] J. Nielsen, “Über die Minimalzahl der Fixpunkte bei den Abbildungstypen der Ringflächen”, *Math. Ann.* **82**, 83–93 (1920).
- [196] J. Ningyuan, C. Owens, A. Sommer, D. Schuster, and J. Simon, “Time- and site-resolved dynamics in a topological circuit”, *Phys. Rev. X* **5**, 021031 (2015).
- [197] Y. Okabe, K. Kaneda, M. Kikuchi, and C.-K. Hu, “Universal finite-size scaling functions for critical systems with tilted boundary conditions”, *Phys. Rev. E* **59**, 1585–1588 (1999).
- [198] L. Onsager, “Crystal statistics. I. A Two-dimensional model with an order-disorder transition”, *Phys. Rev.* **65**, 117–149 (1944).
- [199] M. Q. Owaidat, J. H. Asad, and Z.-Z. Tan, “Resistance computation of generalized decorated square and simple cubic network lattices”, *Results Phys.* **12**, 1621–1627 (2019).
- [200] N. Ozisik, H. R. B. Orlande, M. J. Colaco, and R. M. Cotta, *Finite Difference Methods in Heat Transfer* (Apple Academic Press, 2017).

- [201] G. Papathanasiou and C. B. Thorn, “Worldsheet propagator on the light-cone worldsheet lattice”, *Phys. Rev. D* **87**, 066005 (2013).
- [202] W. Parry, “On the  $\beta$ -expansions of real numbers”, *Acta Math. Acad. Sci. Hung.* **11**, 401–416 (1960).
- [203] R. Peierls, “Zur Theorie des Diamagnetismus von Leitungselektronen”, *Z. Phys.* **80**, 763–791 (1933).
- [204] S.-L. Peng, K.-F. Cao, and Z.-X. Chen, “Devil’s staircase of topological entropy and global metric regularity”, *Phys. Lett. A* **193**, 437–443 (1994).
- [205] I. Percival and F. Vivaldi, “A linear code for the sawtooth and cat maps”, *Physica D* **27**, 373–386 (1987).
- [206] I. Percival and F. Vivaldi, “Arithmetical properties of strongly chaotic motions”, *Physica D* **25**, 105–130 (1987).
- [207] Y. B. Pesin and Y. G. Sinai, “Space-time chaos in the system of weakly interacting hyperbolic systems”, *J. Geom. Phys.* **5**, 483–492 (1988).
- [208] S. D. Pethel, N. J. Corrion, and E. Bollt, “Symbolic dynamics of coupled map lattices”, *Phys. Rev. Lett.* **96**, 034105 (2006).
- [209] S. D. Pethel, N. J. Corrion, and E. Bollt, “Deconstructing spatiotemporal chaos using local symbolic dynamics”, *Phys. Rev. Lett.* **99**, 214101 (2007).
- [210] A. Poghosyan, N. Izmailian, and R. Kenna, “Exact solution of the critical Ising model with special toroidal boundary conditions”, *Phys. Rev. E* **96**, 062127 (2017).
- [211] A. Politi and A. Torcini, “Periodic orbits in coupled Hénon maps: Lyapunov and multifractal analysis”, *Chaos* **2**, 293–300 (1992).
- [212] A. Politi, A. Torcini, and S. Lepri, “Lyapunov exponents from node-counting arguments”, *J. Phys. IV* **8**, 263 (1998).
- [213] M. Pollicott, *Dynamical zeta functions*, in *Smooth Ergodic Theory and Its Applications*, Vol. 69, edited by A. Katok, R. de la Llave, Y. Pesin, and H. Weiss (2001), pp. 409–428.
- [214] C. Pozrikidis, *An Introduction to Grids, Graphs, and Networks* (Oxford Univ. Press, Oxford, UK, 2014).
- [215] L. Qi, H. Chen, and Y. Chen, *Tensor Eigenvalues and Their Applications* (Springer, Singapore, 2018).
- [216] P. Ren, T. Aleksić, D. Emms, R. C. Wilson, and E. R. Hancock, “Quantum walks, Ihara zeta functions and cospectrality in regular graphs”, *Quantum Inf. Process.* **10**, 405–417 (2010).
- [217] A. Rényi, “Representations for real numbers and their ergodic properties”, *Acta Math. Acad. Sci. Hung.* **8**, 477–493 (1957).
- [218] M. Rezghi and L. Eldén, “Diagonalization of tensors with circulant structure”, *Linear Algebra Appl.* **435**, 422–447 (2011).

- [219] K. Richter, J. D. Urbina, and S. Tomsovic, “Semiclassical roots of universality in many-body quantum chaos”, *J. Phys. A* **55**, 453001 (2022).
- [220] H. J. Rothe, *Lattice Gauge Theories - An Introduction* (World Scientific, Singapore, 2005).
- [221] I. Sato, “Bartholdi zeta functions of group coverings of digraphs”, *Far East J. Math. Sci.* **18**, 321–339 (2005).
- [222] K. Serkh and V. Rokhlin, “On the solution of the Helmholtz equation on regions with corners”, *Proc. Natl. Acad. Sci. USA* **113**, 9171–9176 (2016).
- [223] J.-P. Serre, *Trees* (Springer, Berlin, 1980).
- [224] R. Shankar, *Quantum Field Theory and Condensed Matter* (Cambridge Univ. Press, Cambridge UK, 2017).
- [225] M. Sieber and K. Richter, “Correlations between periodic orbits and their role in spectral statistics”, *Phys. Scr.* **2001**, 128 (2001).
- [226] C. L. Siegel and K. Chandrasekharan, *Lectures on the Geometry of Numbers* (Springer Berlin Heidelberg, Berlin, Heidelberg, 1989).
- [227] B. Simon, “Almost periodic Schrödinger operators: A review”, *Adv. Appl. Math.* **3**, 463–490 (1982).
- [228] S. Simons, “Analytical inversion of a particular type of banded matrix”, *J. Phys. A* **30**, 755 (1997).
- [229] J. Smit, *Introduction to Quantum Fields on a Lattice* (Cambridge Univ. Press, Cambridge, 2002).
- [230] R. Sommer, *Introduction to Lattice Gauge Theories*, tech. rep. (Humboldt Univ., 2015).
- [231] A. Souslov and V. Vitelli, “Geometry for mechanics”, *Nature Physics* **15**, 623–624 (2019).
- [232] R. P. Stanley, *Enumerative Combinatorics*, Vol. 1 (Cambridge Univ. Press, 2009).
- [233] H. M. Stark and A. A. Terras, “Zeta functions of finite graphs and coverings”, *Adv. Math.* **121**, 124–165 (1996).
- [234] I. Stewart and D. Gökyaydin, “Symmetries of quotient networks for doubly periodic patterns on the square lattice”, *Int. J. Bifur. Chaos* **29**, 1930026 (2019).
- [235] R. Suarez, “Difference equations and a principle of double induction”, *Math. Mag.* **62**, 334–339 (1989).
- [236] L.-S. Sun, X.-Y. Kang, Q. Zhang, and L.-X. Lin, “A method of recovering the initial vectors of globally coupled map lattices based on symbolic dynamics”, *Chin. Phys. B* **20**, 120507 (2011).
- [237] T. Sunada, “Unitary representations of fundamental groups and the spectrum of twisted Laplacians”, *Topology* **28**, 125–132 (1989).
- [238] T. Sunada, *Topological Crystallography* (Springer, Tokyo, 2013).



- [239] A. Tarfulea and R. Perlis, “An Ihara formula for partially directed graphs”, *Linear Algebra Appl.* **431**, 73–85 (2009).
- [240] A. Terras, *Zeta Functions of Graphs: A Stroll through the Garden* (Cambridge Univ. Press, 2010).
- [241] M. Toda, *Theory of Nonlinear Lattices* (Springer, Berlin, 1989).
- [242] J. H. Van Vleck, “The correspondence principle in the statistical interpretation of quantum mechanics”, *Proc. Natl. Acad. Sci.* **14**, 178–188 (1928).
- [243] G. Venezian, “On the resistance between two points on a grid”, *Am. J. Phys* **62**, 1000–1004 (1994).
- [244] D. Viswanath, “The Lindstedt-Poincaré technique as an algorithm for finding periodic orbits”, *SIAM Rev.* **43**, 478–496 (2001).
- [245] D. Viswanath, “Symbolic dynamics and periodic orbits of the Lorenz attractor”, *Nonlinearity* **16**, 1035–1056 (2003).
- [246] D. Viswanath, “The fractal property of the Lorenz attractor”, *Physica D* **190**, 115–128 (2004).
- [247] U.-J. Wiese, *An Introduction to Lattice Field Theory*, tech. rep. (Univ. Bern, 2009).
- [248] I. Wigman, “Counting singular matrices with primitive row vectors”, *Monatsh. Math.* **144**, 71–84 (2005).
- [249] H. S. Wilf, *Generatingfunctionology* (Academic Press, New York, 1994).
- [250] A. Wipf, *Statistical Approach to Quantum Field Theory: An Introduction* (Springer, Berlin, 2013).
- [251] W. L. Wood, “Periodicity effects on the iterative solution of elliptic difference equations”, *SIAM J. Numer. Anal.* **8**, 439–464 (1971).
- [252] J. Woods, *Multidimensional Signal, Image, and Video Processing and Coding* (Academic Press, Amsterdam, 2012).
- [253] F. Y. Wu, “Theory of resistor networks: the two-point resistance”, *J. Phys. A* **37**, 6653–6673 (2004).
- [254] M.-C. Wu and C.-K. Hu, “Exact partition functions of the Ising model on  $M \times N$  planar lattices with periodic-aperiodic boundary conditions”, *J. Phys. A* **35**, 5189–5206 (2002).
- [255] Z.-J. Xie, X.-Q. Jin, and Y.-M. Wei, “A fast algorithm for solving circulant tensor systems”, *Lin. Multilin. Algebra* **65**, 1894–1904 (2016).
- [256] Y. Yamasaki, “An explicit prime geodesic theorem for discrete tori and the hypergeometric functions”, *Math. Z.* **289**, 361–376 (2017).
- [257] L. Zaporski and F. Flicker, “Superconvergence of topological entropy in the symbolic dynamics of substitution sequences”, *SciPost Phys.* **7**, 018 (2019).

- [258] A. Zee, *Quantum Field Theory in a Nutshell*, 2nd ed. (Princeton Univ. Press, Princeton NJ, 2010).
- [259] Q. Zhilin, A. Gangal, M. Benkun, and T. Gang, “Spatiotemporally periodic patterns in symmetrically coupled map lattices”, *Phys. Rev. E* **50**, 163–170 (1994).
- [260] D. Zhou, Y. Xiao, and Y.-H. He, “Seiberg duality, quiver gauge theories, and Ihara’s zeta function”, *Int. J. Mod. Phys. A* **30**, 1550118 (2015).
- [261] R. M. Ziff, C. D. Lorenz, and P. Kleban, “Shape-dependent universality in percolation”, *Physica A* **266**, 17–26 (1999).

# Chapter 9

## Counting

The latest entry at the bottom for this chapter, page 515

This chapter comprises our notes paralleling  
[ChaosBook chap. 18 Counting](#)  
[ChaosBook appendix A18 Counting](#)  
but now focusing on prime Bravais lattices.

Should be studied in tandem with the more sophisticated chapter [10 Zeta functions in 2D](#).

See also:

Much counting in chapter [1](#), examples:  
example [1.1 Temporal Bernoulli shadowing](#).  
example [1.3 Tent map linear code](#).

Compare characteristic equation [\(8.126\)](#) to the characteristic function  $a(z)$  [\(8.167\)](#).

Much counting in cat map chapter [2](#).

### 9.1 Enumeration of prime periodic states

#### 9.1.1 Covering alphabet

Our algorithm for generating all prime  $[L \times T]_S$  Bravais lattices consists in picking the lexically lowest block for every set of blocks related by spatial and temporal translations:

1. Fill the first row  $[s_{11} s_{21} \cdots s_{L1}]$  by lexically ordered symbols,  $s_{j1} \leq s_{j+1,1}$ , keep one block for each set of spatially cyclically related permutations.
2. Picking the lexically ordered first row representatives uses up the cyclic invariance under spatial translations, so for the second  $[s_{12} s_{22} \cdots s_{L2}]$  and higher rows fill in all  $|\mathcal{A}|^T$  combinations of symbols.
3. The count is the same for all  $[L \times T]_S$  relative-periodic blocks.

4. Group blocks into sets related by cyclic permutations in the time direction. For each such set, pick a representative that has lexically lowest first row, throw away the rest.
5. Throw away all blocks which are repeats of shorter blocks in the spatial direction.
6. Throw away all blocks which are repeats of shorter blocks in the temporal direction. What remains in  $N_k$  prime periodic blocks  $p$  of the same size  $[L_p \times T_p] = [L_k \times T_k]$ .
7. The total number of (doubly) periodic blocks is the sum of all cyclic permutations of prime blocks,

$$|\mathcal{A}|^{LT} = \sum_p N_p [L_p \times T_p]_{S_p}$$

where the sum goes over prime tilings of the  $[L \times T]_S$  block.

This completes the list of prime periodic states, with the alphabet  $\mathcal{A}$  taken as a *covering* alphabet, i.e., we have generated all possible prime blocks, under assumption of no grammar rules.

The number of prime periodic states is given recursively by (see (9.20)),

$$M_p = \frac{1}{LT} \left( N_p - \sum_{p'} L_{p'} T_{p'} M_{p'} \right), \quad (9.1)$$

where the sum is over  $p'$ , the prime 'divisors' of  $p$  that satisfy tiling conditions (21.74).

*Example:*  $[2 \times 2]_0$  Bravais lattices prime blocks.

Consider  $[2 \times 2]_0$  Bravais lattices prime block

$$M_p = \begin{bmatrix} s_{01} & s_{11} \\ s_{00} & s_{10} \end{bmatrix}, \quad (9.2)$$

and the relative-periodic  $[2 \times 1]_1$  block with 1 site-shift periodic boundary, which is periodic after the second repeat in the time direction,

$$M_p = \begin{bmatrix} [s_{00} & s_{10}] & s_{10} \\ [s_{00} & s_{10}] & \end{bmatrix}. \quad (9.3)$$

According to (9.1), the number of prime  $[2 \times 2]_0$  periodic states is

$$M_{[2 \times 2]_0} = \frac{1}{2 \cdot 2} (N_{[2 \times 2]_0} - 2M_{[2 \times 1]_0} - 2M_{[1 \times 2]_0} - 2M_{[2 \times 1]_1} - M_{[1 \times 1]_0}), \quad (9.4)$$

We can work this out explicitly as follows:

(1) Fill the first row  $[s_{11} \ s_{21}]$  by lexically ordered symbols, one for each set of

spatially cyclically related permutations. For the alphabet (??) there are 36 such length 2 strings.

(2) As we have already ‘used up’ the cyclic invariance under spatial translations by picking the lexically ordered first row representatives, for the second  $[s_{12} s_{22}]$  and higher rows all 81 combinations of 9 symbols are allowed. We now have  $36 \times 81 = 2916$  blocks in all.

(3) The  $[2 \times 1]_1$  relative-periodic block (9.3) is counted as the  $[2 \times 2]_0$  periodic state; as in (1), after spatial cyclic rotations, there are 36 such prime blocks.

(4) Group blocks into sets related by cyclic permutations in the time direction. For each such set, pick a representative that is lexically lowest in the first row, throw away the rest.

(5) Throw away all blocks which are repeats of shorter blocks. There are three kinds of repeating small blocks:

$$[2 \times 1]_0 = \begin{bmatrix} a & b \\ a & b \end{bmatrix}, \quad [1 \times 2]_0 = \begin{bmatrix} b & b \\ a & a \end{bmatrix}, \quad [2 \times 1]_1 = \begin{bmatrix} & a & b \\ a & b & \end{bmatrix}.$$

(6) The result is 1584  $[2 \times 2]_0$  prime blocks.

There are also 36 prime  $[2 \times 1]_0$  blocks repeating in time, 36 prime  $[1 \times 2]_0$  blocks repeating in space, 36 prime  $[2 \times 1]_1$  blocks repeating in time with 1/2-shift periodic boundary, and 9 blocks which are repeats of one-symbol prime  $[1 \times 1]_0$  block. The total number of  $[2 \times 2]_0$  blocks is recovered by all cyclic permutations of prime blocks (21.128):

$$\begin{aligned} N_{[2 \times 2]_0} &= 9^{2 \times 2} = 6561 & (9.5) \\ &= 1584 [2 \times 2]_0 + 36 [2 \times 1]_0 + 36 [1 \times 2]_0 + 36 [2 \times 1]_1 + 9 [1 \times 1]_0, \end{aligned}$$

where  $\overline{\dots}$  stands for the number of prime blocks of a given shape. This completes the count with the alphabet (??) taken as a *covering* alphabet, i.e., we have generated all possible prime blocks, were there no further grammar rules.

*Example:*  $[3 \times 2]_0$  Bravais lattices prime blocks.

Consider the Bravais lattice

$$M = \begin{bmatrix} s_{12} & s_{22} & s_{32} \\ s_{11} & s_{21} & s_{31} \end{bmatrix}. \quad (9.6)$$

According to (9.1), the number of prime  $[3 \times 2]_0$  periodic states is

$$M_{[3 \times 2]_0} = \frac{1}{3 \cdot 2} (N_{[3 \times 2]_0} - 3M_{[3 \times 1]_0} - 2M_{[1 \times 2]_0} - M_{[1 \times 1]_0}), \quad (9.7)$$

Unlike the  $[2 \times 2]_0$  case (9.3), there no sub-blocks with relative-periodic boundary contributing to the  $[3 \times 2]_0$  blocks count, since  $[3 \times 1]_0$  and  $[1 \times 2]_0$  sub-blocks cannot fit into the  $[3 \times 2]_0$  doubly-periodic Bravais lattice without a shift.

Following the same algorithm as for  $[2 \times 2]_0$  blocks, we get 88440  $[3 \times 2]_0$  prime blocks, 240 prime  $[3 \times 1]_0$  blocks repeating in time, 36 prime  $[1 \times 2]_0$  blocks repeating in space, and 9 blocks which are repeats of one symbol prime  $[1 \times 1]_0$

Table 9.1: The numbers of the  $\mu^2 = 1$  spatiotemporal cat  $[L \times T]_S$  periodic states:  $N_{[L \times T]_S}$  is the number of periodic states,  $M_{[L \times T]_S}$  is the number of prime orbits, and  $R_{[L \times T]_S}$  is the number of prime orbits in the  $D_4$  symmetries orbit.

$[L \times T]_S$	$M$	$N$	$R$
$[1 \times 1]_0$	1	1	1
$[2 \times 1]_0$	2	$5 = 2 [2 \times 1]_0 + 1 [1 \times 1]_0$	2
$[2 \times 1]_1$	4	$9 = 4 [2 \times 1]_1 + 1 [1 \times 1]_0$	
$[3 \times 1]_0$	5	$16 = 5 [3 \times 1]_0 + 1 [1 \times 1]_0$	
$[3 \times 1]_1$	16	$49 = 16 [3 \times 1]_1 + 1 [1 \times 1]_0$	
$[4 \times 1]_0$	10	$45 = 10 [4 \times 1]_0 + 2 [2 \times 1]_0 + 1 [1 \times 1]_0$	
$[4 \times 1]_1$	54	$225 = 54 [4 \times 1]_1 + 4 [2 \times 1]_1 + 1 [1 \times 1]_0$	
$[4 \times 1]_2$	60	$245 = 60 [4 \times 1]_2 + 2 [2 \times 1]_0 + 1 [1 \times 1]_0$	
$[2 \times 2]_0$	52	$225 = 52 [2 \times 2]_0 + 2 [2 \times 1]_0 + 2 [1 \times 2]_0$ $+ 4 [2 \times 1]_1 + 1 [1 \times 1]_0$	1
$[2 \times 2]_1$	60	$245 = 60 [2 \times 2]_1 + 2 [1 \times 2]_0 + 1 [1 \times 1]_0$	
$[3 \times 2]_0$	850	$5120 = 850 [3 \times 2]_0 + 5 [3 \times 1]_0$ $+ 2 [1 \times 2]_0 + 1 [1 \times 1]_0$	
$[3 \times 2]_1$	1012	$6125 = 1012 [3 \times 2]_1 + 16 [3 \times 1]_2$ $+ 2 [1 \times 2]_0 + 1 [1 \times 1]_0$	
$[3 \times 3]_0$	68281	$614656 = 68281 [3 \times 3]_0 + 5 [3 \times 1]_0$ $+ 16 [3 \times 1]_1 + 16 [3 \times 1]_2 + 5 [1 \times 3]_0 + 1 [1 \times 1]_0$	1
$[3 \times 3]_1$	70400	$633616 = 70400 [3 \times 3]_1 + 5 [1 \times 3]_0 + 1 [1 \times 1]_0$	

block. The total number of  $[3 \times 2]_0$  blocks is recovered by all cyclic permutations of prime blocks:

$$\begin{aligned}
 N_{[3 \times 2]_0} &= 9^{3 \times 2} = 531441 \\
 &= 88440 [3 \times 2]_0 + 240 [3 \times 1]_0 + 36 [1 \times 2]_0 + 9 [1 \times 1]_0. \quad (9.8)
 \end{aligned}$$

### 9.1.2 Admissible prime periodic states

To determine the *admissible* blocks, compute  $X_p$  for each prime block  $M_p$ , and eliminate every  $X_p$  which contains a lattice site or sites on which the value of the field violates the admissibility condition  $x_z \in [0, 1]^2$ .

**2019-11-22 Han** For  $s = 5/2, \mu^2 = 1$  spatiotemporal cat the pruning is very severe. Of 1584 covering alphabet prime blocks in (9.5), only 52 prime  $[2 \times 2]_0$  blocks are admissible. As for the repeats of smaller blocks, there are 2 admissible  $[1 \times 2]_0$  blocks repeating in time and 2  $[2 \times 1]_0$  blocks repeating in space. There are 4 admissible 1/2-shift periodic boundary  $[1 \times 2]_0$  blocks. And there is 1 admissible block  $[1 \times 1]_0$  which is a repeat of letter 0. The total number of  $[2 \times 2]_0$  of periodic states is obtained by all cyclic permutations of admissible prime blocks (a significant pruning,

Table 9.2: The numbers of spatiotemporal cat periodic states for Bravais lattices  $\Lambda = [L \times T]_S$  up to  $[3 \times 3]_2$ . Here  $N_\Lambda(s)$  is the number of doubly periodic periodic states,  $M_\Lambda(s)$  is the number of prime invariant 2-tori, and  $R_\Lambda$  is the number of prime invariant 2-tori in the  $D_4$  symmetries orbit. The stretching parameter  $s$  can take half-integer or integer values.

$\Lambda$	$N_\Lambda(s)$	$M_\Lambda(s)$	$R$
$[1 \times 1]_0$	$2(s-2)$	$2(s-2)$	1
$[2 \times 1]_0$	$2(s-2)2s$	$2(s-2)\frac{1}{2}(2s-1)$	2
$[2 \times 1]_1$	$2(s-2)2(s+2)$	$2(s-2)\frac{1}{2}(2s+3)$	
$[3 \times 1]_0$	$2(s-2)(2s-1)^2$	$2(s-2)\frac{1}{3}(s-1)s$	
$[3 \times 1]_1$	$2(s-2)4(s+1)^2$	$2(s-2)\frac{1}{3}(2s+1)(2s+3)$	
$[4 \times 1]_0$	$2(s-2)8(s-1)^2s$	$2(s-2)\frac{1}{5}(2s-3)(2s-1)s$	
$[4 \times 1]_1$	$2(s-2)8s^2(s+2)$	$2(s-2)\frac{1}{5}(s+2)(2s-1)(2s+1)$	
$[4 \times 1]_2$	$2(s-2)8(s+1)^2s$	$2(s-2)\frac{1}{5}(2s+3)(2s+1)s$	
$[4 \times 1]_3$	$2(s-2)8s^2(s+2)$	$2(s-2)\frac{1}{5}(s+2)(2s-1)(2s+1)$	
$[5 \times 1]_0$	$2(s-2)(4s^2-6s+1)^2$	$2(s-2)\frac{4}{3}(s-1)(2s-3)(2s-1)s$	
$[5 \times 1]_1$	$2(s-2)16(s^2+s-1)^2$	$2(s-2)\frac{1}{3}(2s-1)(2s+3)(4s^2+4s-5)$	
$[2 \times 2]_0$	$2(s-2)8s^2(s+2)$	$2(s-2)\frac{1}{2}(2s-1)(2s^2+5s+1)$	1
$[2 \times 2]_1$	$2(s-2)8s(s+1)^2$	$2(s-2)\frac{1}{2}(2s+1)(2s+3)s$	
$[3 \times 2]_0$	$2(s-2)2s(2s-1)^2(2s+3)^2$	$2(s-2)\frac{2}{3}(2s-1)(4s^3+10s^2+3s-5)s$	
$[3 \times 2]_1$	$2(s-2)32s^3(s+1)^2$	$2(s-2)\frac{2}{6}(2s-1)(2s+1)(8s^3+16s^2+10s+3)$	
$[3 \times 3]_0$	$2(s-2)16(s+1)^4(2s-1)^4$		
$[3 \times 3]_1$	$2(s-2)(2s-1)^2(8s^3+12s^2-1)^2$		

compared to the full shift count (9.5)),

$$\begin{aligned} N_{[2 \times 2]_0} &= 225 & (9.9) \\ &= 52 [2 \times 2]_0 + 2 [2 \times 1]_0 + 2 [1 \times 2]_0 + 4 [2 \times 1]_1 + 1 [1 \times 1]_0. \end{aligned}$$

**2019-11-23 Han** For  $s = 5/2, \mu^2 = 1$  spatiotemporal cat only 850 prime  $[3 \times 2]_0$  blocks are admissible. There are 5 admissible repeating prime  $[3 \times 1]_0$  blocks, 2 admissible repeating prime  $[1 \times 2]_0$  blocks, and 1 admissible block which is a repeat of 0. The total number of admissible solutions obtained by all cyclic permutations of admissible prime blocks is:

$$N_{[3 \times 2]_0} = 5120 = 850 [3 \times 2]_0 + 5 [3 \times 1]_0 + 2 [1 \times 2]_0 + 1 [1 \times 1]_0, \quad (9.10)$$

in agreement with the counting formula (??) for the  $[3 \times 2]_0$  periodic states.

**2020-06-09 Han** The admissible prime periodic states counts for any half-integer or integer  $s$  are listed in table 9.2. Note that  $N_{[3 \times T]_1}(s) = N_{[3 \times T]_2}(s)$ , by reflection symmetry, as  $N_{[3 \times T]_2}(s) = N_{[3 \times T]_{-1}}(s)$ .

Table 9.3: The numbers of spatiotemporal cat periodic states for primitive cells  $\mathbb{A} = [L \times T]_S$  up to  $[3 \times 3]_2$ . Here  $N_{\mathbb{A}}(\mu^2)$  is the number of periodic states,  $M_{\mathbb{A}}(\mu^2)$  is the number of prime orbits, and  $R_{\mathbb{A}}$  is the number of prime orbits in the  $D_4$  point-group orbit. The Klein-Gordon mass  $\mu^2$  can take only integer values.

$\mathbb{A}$	$V_{\mathbb{A}}(\mu^2)$	$M_{\mathbb{A}}(\mu^2)$	$R$
$[1 \times 1]_0$	$\mu^2$	$\mu^2$	1
$[2 \times 1]_0$	$\mu^2(\mu^2 + 4)$	$\mu^2(\mu^2 + 3)/2$	2
$[2 \times 1]_1$	$\mu^2(\mu^2 + 8)$	$\mu^2(\mu^2 + 7)/2$	
$[3 \times 1]_0$	$\mu^2(\mu^2 + 3)^2$	$\mu^2(\mu^2 + 2)(\mu^2 + 4)/3$	2
$[3 \times 1]_1$	$\mu^2(\mu^2 + 6)^2$	$\mu^2(\mu^2 + 5)(\mu^2 + 7)/3$	
$[4 \times 1]_0$	$\mu^2(\mu^2 + 2)^2(\mu^2 + 4)$	$\mu^2(\mu^2 + 1)(\mu^2 + 3)(\mu^2 + 4)/4$	2
$[4 \times 1]_1$	$\mu^2(\mu^2 + 4)^2(\mu^2 + 8)$	$\mu^2(\mu^2 + 3)(\mu^2 + 4)(\mu^2 + 5)/4$	
$[4 \times 1]_2$	$\mu^2(\mu^2 + 4)(\mu^2 + 6)^2$	$\mu^2(\mu^2 + 4)(\mu^2 + 5)(\mu^2 + 7)/4$	
$[4 \times 1]_3$	$\mu^2(\mu^2 + 4)^2(\mu^2 + 8)$	$\mu^2(\mu^2 + 3)(\mu^2 + 5)(\mu^2 + 8)/4$	
$[5 \times 1]_0$	$\mu^2(\mu^4 + 5\mu^2 + 5)^2$	$\mu^2(\mu^2 + 1)(\mu^2 + 2)(\mu^2 + 3)(\mu^2 + 4)/5$	2
$[5 \times 1]_1$	$\mu^2(\mu^4 + 10\mu^2 + 23)^2$	$\mu^2(\mu^2 + 3)(\mu^2 + 7)(\mu^4 + 10\mu^2 + 19)/5$	
$[2 \times 2]_0$	$\mu^2(\mu^2 + 4)^2(\mu^2 + 8)$	$\mu^2(\mu^2 + 3)/2 \times (\mu^4 + 13\mu^2 + 38)/2$	1
$[2 \times 2]_1$	$\mu^2(\mu^2 + 4)(\mu^2 + 6)^2$	$\mu^2(\mu^2 + 7)/2 \times (\mu^2 + 4)(\mu^2 + 5)/2$	
$[3 \times 2]_0$	$\mu^2(\mu^2 + 3)^2(\mu^2 + 4)(\mu^2 + 7)^2$	$\mu^2(\mu^2 + 3)(\mu^2 + 4)(\mu^6 + 17\mu^4 + 91\mu^2 + 146)/6$	2
$[3 \times 2]_1$	$\mu^2(\mu^2 + 4)^3(\mu^2 + 6)^2$	$\mu^2(\mu^2 + 3)(\mu^2 + 5)(\mu^6 + 16\mu^4 + 85\mu^2 + 151)/6$	
$[3 \times 3]_0$	$\mu^2(\mu^2 + 3)^4(\mu^2 + 6)^4$		1
$[3 \times 3]_1$	$\mu^2(\mu^2 + 3)^2(\mu^6 + 15\mu^4 + 72\mu^2 + 111)^2$		
$[3 \times 3]_2$	$\mu^2(\mu^2 + 3)^2(8s^3 + 3(\mu^2 + 4)^2 - 1)^2$		



These two expressions do not fit into the table format:

$$M_{[3 \times 3]_0} = 2(s-2) \frac{1}{9} (256s^8 + 512s^7 - 128s^6 - 640s^5 + 16s^4 + 320s^3 - 48s^2 - 72s + 9). \quad (9.11)$$

**2020-06-09 Han** The last, currently unreduced formula exemplifies what is non-intuitive about the Fourier space results; it is not at all obvious that this

$$M_{[3 \times 3]_1} = M_{[3 \times 3]_2} = 2(s-2) \frac{1}{9} (1-2s)^2 \times \left\{ \left[ 2s+1 - 2 \sin\left(\frac{\pi}{18}\right) \right]^2 \left[ 2s+1 + 2 \cos\left(\frac{\pi}{9}\right) \right]^2 \left[ \left( 2s+1 - 2 \cos\left(\frac{2\pi}{9}\right) \right)^2 - 1 \right] \right\} \quad (9.12)$$

is an integer for any half-integer or integer  $s$  (i.e., integer  $\mu^2$ ).

**2023-09-01 Predrag** Rewriting (9.12) the Klein-Gordon way, in terms of lattice momentum:

$$M_{[3 \times 3]_1} = M_{[3 \times 3]_2} = \mu^2 (\mu^2 + 3)^2 \times \frac{1}{9} \left\{ \left[ \mu^2 + 3 - p\left(\frac{\pi}{9}\right) \right]^2 \left[ \mu^2 + 3 + p\left(\frac{2\pi}{9}\right) \right]^2 \left[ \left( \mu^2 + 3 - p\left(\frac{4\pi}{9}\right) \right)^2 - 1 \right] \right\} \quad (9.13)$$

Here divisors  $m = 0, 3, 6$  simplify –the first three factors– and  $1/9 = 8/9, 2/9 = 7/9, 4/9 = 5/9$  don't, the remaining 6 factors.

Please recheck - I surely have introduced errors. The '-1' at the end sure looks strange...

**2023-08-10 Predrag** Instead of (??), we can write

$$(\tilde{\mathcal{J}}_{\mathbb{A}})_{m_1 m_2} = [p^2(k_{m_1}) + p^2(k_{m_2} - k_{m_1} S/T) + \mu^2]. \quad (9.14)$$

I find the angle  $\theta = k_{m_2} - k_{m_1} S/T$  hard to understand.

**2023-08-10 Predrag** The (momentum)<sup>2</sup> along  $\mathbf{a}_2$  is by Pythagoras a sum of time-direction (momentum)<sup>2</sup>, and the tilt in space direction (momentum)<sup>2</sup>

$$p_{\mathbf{a}_2}^2 = p(k_{m_2})^2 + p(k_{m_1} S/T)^2, \quad \text{Hipparchus } p(\theta) = 2 \sin \frac{\theta}{2},$$

so the Laplacian in (??) becomes

$$p^2 = p(k_{m_1})^2 + p(k_{m_1} S/T)^2 + p(k_{m_2})^2. \quad (9.15)$$

This would explain why Hill determinants increase monotonically with  $S$ : the length of the wave-vector  $\mathbf{p}_{\mathbf{a}_2}$  increases monotonically as it is stretched out by  $S$ . If true, this formula is prettier than (??), but I haven't *derived* it from (??). I checked it manually only for (??). You can check it with Mathematica for a few more examples: if it works, then we derive it.

2023-08-31 Han so  $(\tilde{\mathcal{J}}_{\mathbb{A}})_{11}$  eigenvalue is

$$\Lambda_{11} = 6 + \mu^2$$

while using (9.15) gives

$$\Lambda_{11} = p(\pi)^2 + p(\pi/2)^2 + p(\pi)^2 + \mu^2 = 10 + \mu^2 .$$

2023-09-01 Predrag However, with a minus sign,

$$\Lambda_{11} = p(\pi)^2 - p(\pi/2)^2 + p(\pi)^2 + \mu^2 = \mu^2 + 6 .$$

But then for  $V_{[2 \times 1]_1} = \mu^2(\mu^2 + 8)$  Hill determinant, table 9.3, with Laplacian  $\mathbf{p}^2$  eigenvalues laid out on a square Brillouin zone, (9.14) fails :)

$$\begin{array}{|c|c|} \hline \Lambda_{00} & \Lambda_{10} \\ \hline \hline \hline \end{array} = \begin{array}{|c|c|} \hline 0 & 0 \\ \hline \hline \hline \end{array} \quad (9.16)$$

In this case (9.15) works, but the minus sign modification fails! So the cheap guess (9.15) is wrong.

<sup>1</sup>

2023-08-31 Predrag Example:  $[2 \times 2]_1$  Orbit Jacobian matrix eigenvalues.

We have  $S/T = 1/2$ , so lattice momentum  $p(k) = 2 \sin(k/2)$  can take values

$$p(0) = 0, \quad p(\pm\pi) = \pm 2, \quad p(\pm\pi/2) = \pm\sqrt{2},$$

and the eigenvalues of the Laplacian  $\mathbf{p}^2$  evaluated on the  $V_{\mathbb{A}} = 4$  lattice sites of the square reciprocal primitive cell, are

$$\begin{array}{|c|c|} \hline \mathbf{p}_{01}^2 & \mathbf{p}_{11}^2 \\ \hline \mathbf{p}_{00}^2 & \mathbf{p}_{10}^2 \\ \hline \hline \hline \end{array} = \begin{array}{|c|c|} \hline 6 & 6 \\ \hline 0 & 4 \\ \hline \hline \hline \end{array} . \quad (9.17)$$

2023-08-31 Han Correct,  $[2 \times 2]_1$  eigenvalues give the Hill determinant

$$\text{Det}_{[2 \times 2]_1} = \mu^2(\mu^2 + 4)(\mu^2 + 6)^2 \text{ in table 9.3.}$$

2023-09-04 Predrag For the  $[3 \times 2]_1$ , we have  $S/T = 1/2$ ,

$$k_1 = 0, 2\pi/3, 4\pi/3, \quad k_2 = 0, \pi$$

$$\mathbf{p}^2 = p(k_1)^2 + p(k_2 - k_1/2)^2 .$$

<sup>1</sup>Predrag 2023-09-01: See the discussion about (no possible) simplification into  $\mu^2$  polynomials of  $[3 \times 3]_1$  individual eigenvalues in Hill determinant (9.12).

and lattice momentum  $p(k) = 2 \sin(k/2)$ , of periodicity  $4\pi$ , takes values

$$p(\pm 2\pi/3) = \pm\sqrt{3}, \quad p(\pm\pi/3) = \pm 1, \quad ,$$

$$p(0) = 0, \quad p(\pm\pi) = \pm 2, \quad ,$$

$4\pi$  periodicity:  $p(4\pi/3) = -p(2\pi/3)$ .

$$\begin{aligned} p_{00}^2 &= p(0)^2 &&= 0 \\ p_{10}^2 &= p\left(\frac{2\pi}{3}\right)^2 + p\left(\frac{\pi}{3}\right)^2 &&= 3 + 1 \\ p_{20}^2 &= p\left(\frac{4\pi}{3}\right)^2 + p\left(\frac{2\pi}{3}\right)^2 &&= 3 + 3 \\ p_{01}^2 &= p(0)^2 + p(\pi)^2 &&= 0 + 4 \\ p_{11}^2 &= p\left(\frac{2\pi}{3}\right)^2 + p\left(\frac{2\pi}{3}\right)^2 &&= 3 + 3 \\ p_{21}^2 &= p\left(\frac{4\pi}{3}\right)^2 + p\left(\frac{\pi}{3}\right)^2 &&= 3 + 1 \end{aligned}$$

$$\begin{array}{|c|c|c|} \hline p_{01}^2 & p_{11}^2 & p_{21}^2 \\ \hline p_{00}^2 & p_{10}^2 & p_{20}^2 \\ \hline \end{array} = \begin{array}{|c|c|c|} \hline 4 & 6 & 4 \\ \hline 0 & 4 & 6 \\ \hline \end{array} \quad (9.18)$$

so  $(\tilde{\mathcal{J}}_{\mathbb{A}})_{11}$  eigenvalue is

$$\Lambda_{11} = 6 + \mu^2,$$

and so on.

Compare with  $\text{Det} = \mu^2(\mu^2 + 4)^3(\mu^2 + 6)^2$

**2023-09-01 Predrag** For the  $[3 \times 3]_S$  family, we still have not simplified  $[3 \times 3]_1$  (9.12) into a  $\mu^2$  polynomial.

We have  $S/T = 1/3$  and lattice momentum  $p(k) = 2 \sin(k/2)$ , of periodicity  $4\pi$ , takes values

$$p(\pm 2\pi/3) = \pm\sqrt{3}, \quad ,$$

$$\begin{array}{|c|c|c|} \hline p_{02}^2 & p_{12}^2 & p_{22}^2 \\ \hline p_{01}^2 & p_{11}^2 & p_{21}^2 \\ \hline p_{00}^2 & p_{10}^2 & p_{20}^2 \\ \hline \end{array} = \begin{array}{|c|c|c|} \hline 3 & * & * \\ \hline 3 & * & * \\ \hline 0 & * & * \\ \hline \end{array} \quad (9.19)$$

$$\begin{aligned} p_{00}^2 &= p(0)^2 &&= 0 \\ p_{01}^2 &= p\left(\frac{2\pi}{3}\right)^2 &&= 3 \\ p_{02}^2 &= p\left(\frac{2\pi}{3} \cdot 2\right)^2 = p_{01}^2 &&= 3 \\ p_{10}^2 &= p\left(\frac{2\pi}{3}\right)^2 + p\left(\frac{2\pi}{3} \cdot \frac{1}{3}\right)^2 &&= 3 + p\left(\frac{2\pi}{9}\right)^2 \\ p_{20}^2 &= p\left(\frac{2\pi}{3} \cdot 2\right)^2 + p\left(\frac{2\pi}{3} \cdot 2 \cdot \frac{1}{3}\right)^2 &&= 3 + p\left(\frac{4\pi}{9}\right)^2 \\ p_{11}^2 &= p\left(\frac{2\pi}{3}\right)^2 + p\left(\frac{2\pi}{3} - \frac{2\pi}{3} \cdot \frac{1}{3}\right)^2 &&= 3 + p\left(\frac{4\pi}{9}\right)^2 \\ p_{12}^2 &= p\left(\frac{2\pi}{3}\right)^2 + p\left(\frac{2\pi}{3} \cdot 2 - \frac{2\pi}{3} \cdot \frac{1}{3}\right)^2 &&= 3 + p\left(\frac{5\pi}{9}\right)^2 \\ p_{21}^2 &= p\left(\frac{2\pi}{3} \cdot 2\right)^2 + p\left(\frac{2\pi}{3} - \frac{2\pi}{3} \cdot 2 \cdot \frac{1}{3}\right)^2 &&= 3 + p\left(\frac{2\pi}{9}\right)^2 \\ p_{22}^2 &= p\left(\frac{2\pi}{3} \cdot 2\right)^2 + p\left(\frac{2\pi}{3} \cdot 2 - \frac{2\pi}{3} \cdot 2 \cdot \frac{1}{3}\right)^2 &&= 3 + p\left(\frac{8\pi}{9}\right)^2 \end{aligned}$$

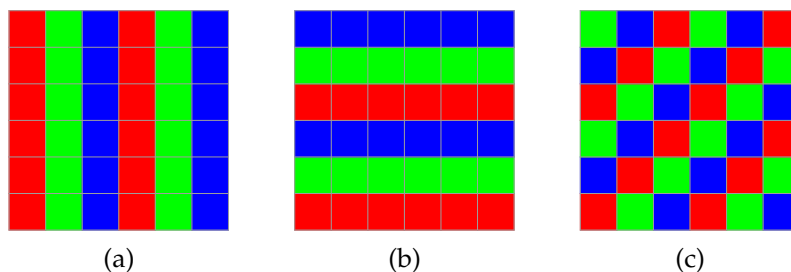


Figure 9.1: Examples of  $[L \times T]_s$  periodic blocks together with their spatiotemporal Bravais lattice tilings (??). (a)  $[3 \times 1]_0$ , primitive vectors  $\mathbf{a}_1 = \{3, 0\}$  and  $\mathbf{a}_2 = \{0, 1\}$ ; (b)  $[1 \times 3]_0$ , primitive vectors  $\mathbf{a}_1 = \{1, 0\}$  and  $\mathbf{a}_2 = \{0, 3\}$ ; (c)  $[3 \times 1]_1$ , primitive vectors  $\mathbf{a}_1 = \{3, 0\}$  and  $\mathbf{a}_2 = \{1, 1\}$ ;

where we have used the  $4\pi$  periodicity:

$$p(4\pi/3) = -p(2\pi/3),$$

$$p(8\pi/9) = -p(2\pi/9).$$

This does not look pretty eigenvalue by eigenvalue, because of period 9 (or 18?) brought in by the tilt term  $p(2\pi/9)$ .

**2020-06-09 Han** The admissible prime periodic states counts are listed in table 9.1. This list verifies the counting formula (??).

**2019-11-24 Han** The interior alphabet depends on the value of  $s$  and the admissible range of  $x_z$ . For  $s = 5/2, \mu^2 = 1, x_z \in [0, 1)$ , the interior alphabet is  $\mathcal{A}_0 = \{0, 1\}$  (see eq. (38) in ref. [7]). For  $s = 7/2, x_z \in [0, 1)$ , the interior alphabet is  $\mathcal{A}_0 = \{0, 1, 2, 3\}$  (eq. (46) in ref. [7]).

**2020-06-09 Han** Figures 9.1 and 9.2 are the plots of the periodic blocks by color. The three figures in figure 9.1 are the blocks with periodicity  $[1 \times 3]_0, [3 \times 1]_0$  and  $[3 \times 1]_1$ , which can show the periodicity of the space-equilibria, time-equilibria and time-relative equilibria. Figure 9.2 is the color coding of the periodic blocks with periodicity  $[2 \times 1]_1, [3 \times 2]_1$  and  $[3 \times 2]_0$ .

**2019-11-23 Predrag** We always reduce relative-shift symmetries, so I am not happy about the  $[2 \times 1]_1$  relative-periodic block (9.3) being counted as the  $[2 \times 2]_0$  periodic state. We'll have to revisit symmetry reduction...

**2019-11-23 Predrag** For uses of the lexical ordering, ChaosBook table **ChaosBook 18.1: Orbits for the binary symbolic dynamics up to length 9**, and appendix **ChaosBook A18.2 Prime factorization for dynamical itineraries** might be of interest.

In the paper, we will probably first review the temporal cat counting, something along the lines of the above tables.

suggestion of constructing covering prime blocks wildly overcounts the candidates for admissible prime periodic states, so we should give up

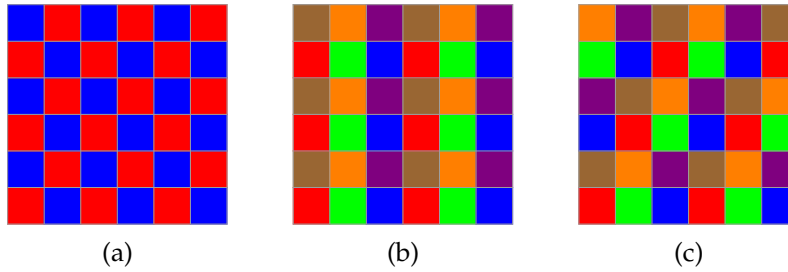


Figure 9.2: Examples of  $[L \times T]_S$  periodic blocks together with their spatiotemporal Bravais lattice tilings (??). (a)  $[2 \times 1]_1$ , primitive vectors  $\mathbf{a}_1 = \{2, 0\}$  and  $\mathbf{a}_2 = \{1, 1\}$ ; (b)  $[3 \times 2]_0$ , primitive vectors  $\mathbf{a}_1 = \{3, 0\}$  and  $\mathbf{a}_2 = \{0, 2\}$ ; (c)  $[3 \times 2]_1$ , primitive vectors  $\mathbf{a}_1 = \{3, 0\}$  and  $\mathbf{a}_2 = \{1, 2\}$ ;

this avenue of constructing them - no need to count any larger Bravais lattices.

**2020-03-17 Han** *PrimeTiles.nb* generates all prime tiles that can tile a larger tile. It gives some not obvious results. For example, let the large tile be  $[3 \times 2]_1$ , and consider the full-shift 9-symbol  $[3 \times 2]_1$  blocks. The number  $[3 \times 2]_0$  blocks is given by (9.8). The program shows that the  $[3 \times 2]_0$  tile can only be tiled by  $[1 \times 1]_0$ ,  $[1 \times 2]_0$  and  $[3 \times 1]_0$  tiles. So we get the result in (9.8):

$$N_{[3 \times 2]_0} = 9^{3 \times 2} = 88440 [3 \times 2]_0 + 240 [3 \times 1]_0 + 36 [1 \times 2]_0 + 9 [1 \times 1]_0.$$

For the full-shift the number of periodic blocks is given by the area of the larger tile, and number of  $[3 \times 2]_S$  blocks is the same for all  $S$ . But now  $[3 \times 1]_0$  tile cannot tile the  $[3 \times 2]_1$  tile. Instead, the  $[3 \times 2]_1$  can be tiled by  $[1 \times 1]_0$ ,  $[3 \times 1]_2$  and  $[1 \times 2]_0$  tiles,

$$N_{[3 \times 2]_1} = 9^{3 \times 2} = 88440 [3 \times 2]_1 + 240 [3 \times 1]_2 + 36 [1 \times 2]_0 + 9 [1 \times 1]_0.$$

*A priori* is not obvious that  $[3 \times 1]_2$  tile can tile a  $[3 \times 2]_1$  tile. But if you stack  $[3 \times 1]_2$  tile in the shifted temporal direction by 2 then the left edge of the tile is shifted by 4 in the spatial direction. With the spatial period being 3, shifted by 4 in the spatial direction is same as shifted by 1. So the bc's of  $[3 \times 2]_1$  tile are satisfied by the  $[3 \times 1]_2$  tiles.

## 9.2 Counting prime periodic states

**2004-01-13 Predrag** Note that Endler and Gallas  $\mathbb{S}_n$  polynomial (3.33) is very smart, as it has a zero for every *prime* orbit.

**2016-10-05 Predrag** For the (Ihara) graph-theoretic notion of prime, reduced cycles see (16.26).

now in CL

**2020-07-11 Predrag** For *prime matrices* and *composite matrices*, see (8.116).

**2019-11-22 Han** The algorithm for generating all  $[2 \times 2]$  and  $[3 \times 2]$  Bravais lattices prime blocks moved to 2022-04-29 CL18 draft [3], [sect. 3.7 Prime Bravais lattices](#).

**2020-01-18 Predrag** The number of *prime cycles* can be computed recursively

$$M_n = \frac{1}{n} \left( N_n - \sum_{d|n, d < n} dM_d \right), \quad (9.20)$$

(see *siminos/mathematica/CatMaptopZeta.nb*) or by the Möbius inversion formula

$$M_n = n^{-1} \sum_{d|n} \mu\left(\frac{n}{d}\right) N_d. \quad (9.21)$$

where the Möbius function  $\mu(1) = 1$ ,  $\mu(n) = 0$  if  $n$  has a squared factor, and  $\mu(p_1 p_2 \dots p_k) = (-1)^k$  if all prime factors are different.

**2020-01-18 Predrag** did not know how to use `MoebiusMu[]`.

**2022-01-02 Predrag** There are exactly (9.23) binary necklaces of length  $\ell$ . The set  $W_p$  of prime necklaces consists of ones that cannot be written as a periodic concatenation of substrings. There exists an exact periodic orbit expansion for the spectral density in terms of prime binary necklaces.

See [Wolfram Necklace](#), [Lyndon word](#), [irreducible polynomial](#), [counting necklaces](#), [Combinatorica ListNecklaces](#),

**2022-04-13 Predrag to Sidney** If you do the [homework](#), doing the needed calculations will be a bit easier.

My Mathematica codes *PrimCyc.m* and *zeta.m* are in *siminos/mathematica/*.

[Adam Prügel-Bennett](#) codes

[P. Andréßen](#) code

There are other codes for zetas on [ChaosBook.org/extras](#), as well as on the [ChaosBook.org/projects](#), if you have patience to fish them out.

Evangelos (ask him for help if stuck: [evangelos.siminos@gmail.com](mailto:evangelos.siminos@gmail.com)) has Mathematica code that generates cycle expansions for full binary code in his code repo

```
svn checkout svn://zero.physics.gatech.edu/vaggelis
```

*vaggelis/mathematica/trunk/* contains *zeta.nb* and *zeta.m*.

Burak has his own codes somewhere, you can ask him what he has.

2CB

**2022-04-29 Han to Sidney and Ibrahim** To generate prime symbolic strings, first generate all of them in a list. Then for each one of strings  $a$ , use cyclic permutation to generate a set of strings,  $a_i = \sigma_i a$ , where  $\sigma_i$  is the cyclic shift operator, which shifts the string by  $i$  steps. Then go to the list and search for the string  $a_i$ , and delete it. Then move to the next symbolic string and repeat. If you move to a string that is deleted, just skip it.

To avoid slowing down your program, when "deleting" a string, you should not actually delete it from the list, which is very time consuming. The program will remove one element from the list, and move every element after it one position forward. So instead, you should change the target string to something that obviously does not belong to the list, for example, -100 or an irrational number (I used  $\pi$ ). Another advantage of doing this is that it doesn't change the rank of each element. For example, if you generate the list by running a for loop, to find the string (0, 1, 0), you will go to the element with rank  $0 \times 2^2 + 1 \times 2^1 + 0 \times 2^0 = 2$  (assuming 2-letter symbolic dynamics). Otherwise you will need to search for the string in the list, which is also time consuming.

The pseudocode is:

```
new empty list M;
//For example, finding lattice states with length 3.
//Assuming 2-letter symbolic dynamics.
for(i=0; i<=1; i++)
    for(j=0; j<=1; j++)
        for(k=0; k<=1; k++)
            appendto(M, [i, j, k]);
for(i=0; i<length(M), i++)
    a=M[i];
    if(a==[-100,-100,-100]) continue; //skip one iteration
    for(j=1; j<3; i++)
        k = (sigma_j a)[0];
        l = (sigma_j a)[1];
        m = (sigma_j a)[2];
        M[k*2^2 + l*2^1 + m*2^0] = [-100,-100,-100];
delete [-100,-100,-100] from M;
```

By doing this you will delete not only periodic states from cyclic permutation, but also repeats of shorter prime orbits. For example, if I have an orbit 010101, which is a repeat of 01, using the shift operator will delete 5 periodic states generated by  $\sigma_i$  with  $i$  from 1 to 5. The periodic state generated by  $\sigma_2$  and  $\sigma_4$  is itself, so this periodic state itself will be deleted. However, if you want to quotient the time reversal symmetry, orbits with time reversal symmetry will delete themselves. But this can be easily fixed by adding a line of code like

```
if(a==reflection of a) don't delete itself;
```

I'm sure this is not the most efficient algorithm of finding prime orbits, and it is not elegant at all. But considering that you will delete most of strings in the list so you will not run over the entire list, the complexity of this algorithm is not too bad.

**2022-04-29 Han** To significantly reduce the complexity of the algorithm, I think you need to generate prime orbits directly, i.e., not generate the list of all strings. I don't have a good idea of how to do that...

**2022-04-29 Predrag** Now that you are thinking about this, it's a good time to learn about the Möbius function (9.21), invented for this purpose. You might enjoy [ChaosBook appendix A18 Counting](#). Here is a post about generate prime orbits directly, moved to here from Han's blog:

**2019-11-23 Predrag** For uses of the lexical ordering, table [ChaosBook 18.1: Orbits for the binary symbolic dynamics up to length 9](#), and appendix [ChaosBook A18.2 Prime factorization for dynamical itineraries](#) might be of interest.

**2022-11-10 Predrag** [Tobias Rossmann \[11\] Computing local zeta functions of groups, algebras, and modules arXiv:1602.00919 \(2017\)](#). Lecture notes [here](#).

By considering associated Dirichlet series, various algebraic counting problems give rise to a *global zeta function*  $Z(s)$  which admits a natural Euler product factorisation

$$Z(s) = \prod_p Z_p(s) \quad (9.22)$$

into *local zeta functions*  $Z_p(s)$  indexed by rational primes  $p$ . For example,  $Z(s)$  could be the Dirichlet series enumerating subgroups of finite index within a finitely generated nilpotent group and  $Z_p(s)$  might enumerate those subgroups of  $p$ -power index only.

In the special case of the infinite cyclic group, one recovers the classical Euler factorisation  $\zeta(s) = \prod_p 1/(1 - p^{-s})$  of the Riemann zeta function.

I do not understand what these zeta functions are, so I give up for now...

### 9.2.1 Enumeration of one-dimensional necklaces

**2024-08-01 Predrag** There is a huge number of papers on necklaces, i.e., one-dimensional periodic primitive cells.

Definition: A circular word or a necklace is an equivalence class of a word under cyclic shift.

[ChaosBook sect. 18.7.2 Counting prime cycles](#).

[ChaosBook remark 18.8 Counting prime cycles](#) has a few references.

[Necklaces wiki](#).

[Necklaces Wolfram Mathworld](#) considers not only the cyclic, but also the dihedral (time-reversal), 'bracelet' (?) case.

[Online necklace generator](#).

[Necklaces Code Golf](#)



Fredricksen and Maiorana *Necklaces of beads in  $k$  colors and  $k$ -ary de Bruijn sequences* Discrete Math. DOI (1978)

H Fredricksen and Kessler *An algorithm for generating necklaces of beads in two colors* Discrete Math. DOI (1986)

Frank Ruskey, Carla Savage and Terry Min Yih Wang *Generating necklaces*, DOI (1991), analyze an algorithm due to Fredricksen, Kessler, and Maiorana

**2021-05-10 Predrag** To all Tigers - always number sites of length- $n$  periodic chains (necklaces) as

$$\{0, 1, 2, \dots, n - 1\},$$

otherwise discrete Fourier transforms will go awkward on you.

2CB

**2022-01-02 Predrag** Not sure this is good for anything, so just for the record: Blümel and Dabaghian [1] *Combinatorial identities for binary necklaces from exact ray-splitting trace formulae* (2001) [arXiv:math-ph/0107026](https://arxiv.org/abs/math-ph/0107026):

two words  $w$  and  $w'$  are equivalent in our context, and code for the same periodic orbit, if they are of the same length (i.e. they consist of the same number of symbols) and their respective symbol sequences are identical up to cyclic permutations. Sequences of objects that are identical up to cyclic permutations are called (Pólya) necklaces [10] (see also **necklace**). If the number of objects they consist of is two, they are called binary necklaces. The periodic orbits can be coded with the help of binary necklaces over the symbols  $\mathcal{L}$  and  $\mathcal{R}$ . It is remarkable that every Newtonian or non-Newtonian periodic orbit can be mapped one-to-one onto a binary necklace. In other words, “pruning” is not necessary for the binary necklaces relevant to us.

Given two letters, for instance  $\mathcal{L}$  and  $\mathcal{R}$ , we can form  $2^\ell$  words of length  $\ell$ . But, in general, many of these words will be cyclically equivalent, and correspond to the same necklace. So, how many necklaces of length  $\ell$  are there? This question is answered by the following formula. There are exactly [10]

$$N(\ell) = \frac{1}{\ell} \sum_{n|\ell} \phi(n) 2^{\ell/n} \tag{9.23}$$

binary necklaces of length  $\ell$ , where the symbol “ $n|\ell$ ” denotes “ $n$  is a divisor of  $\ell$ ”, and  $\phi(n)$  is Euler’s totient function defined as the number of positive integers smaller than  $n$  and relatively prime to  $n$  with  $\phi(1) = 1$  as a useful convention. Thus the first four totients are given by  $\phi(1) = 1$ ,  $\phi(2) = 1$ ,  $\phi(3) = 2$  and  $\phi(4) = 2$ .

Next we define the set  $W_p$  of prime necklaces as the ones that cannot be written as a periodic concatenation of substrings. There exists an exact periodic orbit expansion for the spectral density in terms of prime binary necklaces (see also ref. [4]).

**necklace** J. H. van Lint and R. M. Wilson, *A Course in Combinatorics* (Cambridge University Press, Cambridge, 1992).

**intro** J. Riordan [10], *An Introduction to Combinatorial Analysis* (1958)

## 9.2.2 Enumeration of two-dimensional necklaces

2024-08-14 **Predrag to Carlos Márcio De Oliveira E Silva Filho:**

You could be a match for what our group is currently working on, [Chaos-Book.org/overheads/spatiotemporal](https://Chaos-Book.org/overheads/spatiotemporal), with possible publishable work on if you join us for the whole academic year. But it is very different problem - combinatorics - from what you have worked on so far, learning curve is steep, you would be on your own, leading this effort, and, as we have not worked on it, I do not know whether it is hard or impossible. So have a look, and do not do it, unless you really enjoy combinatorial problems like, let's say, Rubik's cube. I don't, but nature seems to want us to do it:

I believe that in order to understand turbulence, one has to be able to enumerate and name all patterns allowed by laws governing it.

We [3, 9] describe how we believe this should be accomplished in

**LC21** *A chaotic lattice field theory in one dimensions*

**CL18** *A chaotic lattice field theory in two dimensions*

Your project would be to enumerate and name all distinct *prime* mosaics (see **CL18** Sect. 3.1. *Periodic states, mosaics*) for  $\phi^3$ , possibly also  $\phi^4$  theory. It might be already accomplished in some of the papers listed below. Or papers we have not found yet. In any case, we do not understand these papers.

Have look, and if this appeals to you, let me know.

2024-08-01 **Predrag** Moving on to two-dimensional necklaces (discrete tori):

Duncan Adamson, Argyrios Deligkas, Vladimir V. Gusev and Igor Potapov talk: *Multidimensional necklaces: Enumeration, generation, ranking and un-ranking* (2020).

Duncan Adamson, Argyrios Deligkas, Vladimir V. Gusev and Igor Potapov *Combinatorial algorithms for multidimensional necklaces*, [arXiv:2108.01990](https://arxiv.org/abs/2108.01990).

**Duncan Adamson:** "I am interested in capturing symmetry on words, such as reflective and, in the multidimensional setting, translational symmetries."

*Harmonious colourings of temporal matchings.*

They do not do slants.

"Given a unit cell in  $d$  dimensions of size  $N_1 \times N_2 \times \dots \times N_d$ , and  $k - 1$  types of ions, how many ways of arrainging ions in the cell are there up to translational equivalence?"

Definition: A necklace is the lexicographically smallest representation of a cyclic string.

A multidimensional necklace is the lexicographically smallest rotation of a cyclic string.

**2024-06-23, 2024-08-01 Predrag .**

Peter Kagey and William Keehn [8] *Counting tilings of the  $n \times m$  grid, cylinder, and torus* (2024), [arXiv:2311.13072](#) from [Prison Mathematics Project](#).

[William Henry Keehn II](#), Inmate ID: #62041-018, age 60, is due for release 2047-02-02. All his appeals so far had been rejected.

His sentence seems steep, considering what he actually did. Beginning 2005, Keehn [hid video cameras](#) in the bathrooms of his residence in order to obtain naked images of several minors in his custody. Along the way, Keehn amassed a hoard of child pornography. In 2014, Keehn, a 52-year-old former software developer, covertly taped himself molesting a 17-year-old girl in his home (here journalists go overboard: “6,500-square-foot, five-bedroom, six-bathroom spacious 11 acres estate, owned by his wife, a health-care professional”). You can shoot any number of people here, and get a lighter, or no sentence.

But we are not here to judge that.

They have a ton of nice figures, such as figure [6.4](#).

**2024-06-23 Predrag** Toroidal binary arrays., or what we call  $\phi^3$ :

S. N. Ethier [5] *Counting toroidal binary arrays* (2013), [arXiv:1301.2352](#).

S. N. Ethier and J. Lee [6] *Counting toroidal binary arrays II* (2015), [arXiv:1502.03792](#).

What is strange about this is that they seem only to do square and rectangle primitive cells, no slanted  $S > 0$  primitive cells.

**OEIS:** *Number of distinct  $N_1 \times N_2$  toroidal binary arrays.*

Veronika Irvine, *Lace Tessellations: A mathematical model for bobbin lace and an exhaustive combinatorial search for patterns*, PhD Dissertation, University of Victoria (2016).

T. A. Gulliver, *New optimal ternary linear codes*, IEEE Trans. Inform. Theory 41, pp. 1182-1185, (1995).

**2022-01-03 Predrag 2 Predrag** Check what this ChaosBook reference:

Cattell *et al.* [2] *Fast algorithms to generate necklaces, unlabeled necklaces, and irreducible polynomials over  $GF(2)$*  is about?

Tomasz Kociumaka, Jakub Radoszewski and Wojciech Rytter *Computing  $k$ -th Lyndon Word and Decoding Lexicographically Minimal de Bruijn Sequence* (2014), [DOI](#).

## References

- [1] R. Blümel and Y. Dabaghian, “Combinatorial identities for binary necklaces from exact ray-splitting trace formulas”, *J. Math. Phys.* **42**, 5832–5839 (2001).
- [2] K. Cattell, F. Ruskey, J. Sawada, M. Serra, and C. R. Miers, “Fast algorithms to generate necklaces, unlabeled necklaces, and irreducible polynomials over  $\text{GF}(2)$ ”, *J. Algorithms* **37**, 267–282 (2000).
- [3] P. Cvitanović and H. Liang, “A chaotic lattice field theory in two dimensions”, In preparation, 2024.
- [4] Y. Dabaghian, R. V. Jensen, and R. Blümel, “Exact trace formulas for a class of one-dimensional ray-splitting systems”, *Phys. Rev. E* **63**, 066201 (2001).
- [5] S. N. Ethier, “Counting toroidal binary arrays”, *J. Integer Seq.* **16**, 13.4.7 (2013).
- [6] S. N. Ethier and J. Lee, “Counting toroidal binary arrays II”, *J. Integer Seq.* **18**, 15.8.3 (2015).
- [7] B. Gutkin, L. Han, R. Jafari, A. K. Saremi, and P. Cvitanović, “Linear encoding of the spatiotemporal cat map”, *Nonlinearity* **34**, 2800–2836 (2021).
- [8] P. Kagey and W. Keehn, “Counting tilings of the  $n \times m$  grid, cylinder, and torus”, *J. Integer Seq.* **27**, 24.6.1 (2024).
- [9] H. Liang and P. Cvitanović, “A chaotic lattice field theory in one dimension”, *J. Phys. A* **55**, 304002 (2022).
- [10] J. Riordan, *An Introduction to Combinatorial Analysis* (Wiley, New York, 1958).
- [11] T. Rossmann, “Computing local zeta functions of groups, algebras, and modules”, *Trans. Amer. Math. Soc.* **370**, 4841–4879 (2017).

# Chapter 10

## Zeta functions in 2D

This chapter is a sophisticated cousin of chapter 9 *Counting*.

“symbols” are sometimes called “colors”.

2CB

<sup>1</sup> Let  $\mathbb{Z}^2$  be a two-dimensional planar lattice. For any  $m, n \geq 1$  and  $(i, j) \in \mathbb{Z}^2$ , the  $m \times n$  rectangular lattice with the left-bottom vertex  $(i, j)$  is denoted by

$$\mathbb{Z}_{m \times n}((i, j)) = \{(i + m', j + n') \mid 0 \leq m' \leq m - 1, 0 \leq n' \leq n - 1\} .$$

and  $\mathbb{Z}_{m \times n} = \mathbb{Z}_{m \times n}((0, 0))$ . Let  $\mathcal{S}_p$  be an alphabet of  $p (\geq 2)$  symbols. For  $m, n \geq 1$ ,  $\Sigma_{m \times n}(p) = \mathcal{S}_p^{\mathbb{Z}_{m \times n}}$  is the set of all  $m \times n$  local patterns or rectangular blocks, and  $\Sigma_{m \times n}(\mathcal{B})$  is the set of admissible  $m \times n$  patterns.  $\Sigma(\mathcal{B})$  is the set of all admissible patterns in  $\mathcal{B}$ .

**2016-11-07 Predrag** There is much literature on multi-dimensional shifts [2–6, 8, 9, 17, 21, 23, 24, 33, 34, 43, 45]. It does not seem to directly relevant to the 2-dimensional spatiotemporal symbolic dynamics studied by us.

**2016-05-04 Predrag** There is much literature on multi-dimensional shifts that we have to understand (or at least understand whether it is relevant to our 2-dimensional symbolic dynamics):

Ward [48] *An algebraic obstruction to isomorphism of Markov shifts with group alphabets* introduced  $\mathbb{Z}^2$ -subshift, or the space of doubly indexed sequences over a finite abelian compact group  $G$ .

Ward [45] *Automorphisms of  $\mathbb{Z}^d$ -subshifts of finite type*

Ward and Miles [46] *A directional uniformity of periodic point distribution and mixing*: “ For mixing actions generated by commuting automorphisms of a compact abelian group, we investigate the directional uniformity of the rate of periodic point distribution and mixing. When each of these automorphisms has finite entropy, it is shown that directional mixing and

---

<sup>1</sup>Predrag 2016-10-11: From Ban *et al.* [3], on two-dimensional  $\mathbb{Z}^2$ -shifts of finite type

directional convergence of the uniform measure supported on periodic points to Haar measure occurs at a uniform rate independent of the direction. ”

Miles and Ward [36] *The dynamical zeta function for commuting automorphisms of zero-dimensional groups*: “ For a  $\mathbb{Z}^d$ -action  $\alpha$  by commuting homeomorphisms of a compact metric space, Lind [27], (click here) introduced a dynamical zeta function that generalizes the dynamical zeta function of a single transformation. We investigate this function when  $\alpha$  is generated by continuous automorphisms of a compact abelian zero-dimensional group. We address Lind’s conjecture concerning the existence of a natural boundary for the zeta function and prove this for two significant classes of actions, including both zero entropy and positive entropy examples. The finer structure of the periodic point counting function is also examined and, in the zero entropy case, we show how this may be severely restricted for subgroups of prime index in  $\mathbb{Z}^d$ . ”

Ward and Miles [47] *Directional uniformities, periodic points, and entropy*: “ For dynamical systems generated by  $d \geq 2$  commuting homeomorphisms, dynamical invariants like entropy and periodic point data, become more complex and permit multiple definitions. A powerful theory of directional entropy and periodic points can be built. An underlying theme is uniformity in dynamical invariants as the direction changes, and the connection between this theory and problems in number theory; we explore this for several invariants and highlight Fried’s notion of average entropy and its connection to uniformities in growth properties. ”

Al Refaei 2011 “The group  $\mathbb{Z}^2$  acts natural on the space ?? via left and upward shifts” is gibberish, ignore it.

Roettger [44], *Periodic points classify a family of Markov shifts*, writes:

Ledrappier introduced the following type of space of doubly indexed sequences over a finite abelian group  $G$ ,

$$X_G = \{(x_{s,t}) \in G^{\mathbb{Z}^2} \mid x_{s,t+1} = x_{s,t} + x_{s+1,t} \text{ for all } s, t \in \mathbb{Z}\}.$$

The group  $\mathbb{Z}^2$  acts naturally on the space  $X_G$  via left and upward shifts.

Chow, Mallet-Paret and Van Vleck [8, 9, 33, 34] *Pattern formation and spatial chaos in spatially discrete evolution equations*

(Actually, Bunimovich might have worked on this)

Friedland [17] *On the entropy of  $\mathbb{Z}^d$  subshifts of finite type*

Quas and Trow [43] *Subshifts of multi-dimensional shifts of finite type*

Desai [12] *Subsystem entropy for  $\mathbb{Z}^d$  sofic shifts*

Ban and Lin [4, 5] *Patterns generation and transition matrices in multi-dimensional lattice models*

Boyle, Pavlov and Schraudner [6] *Multidimensional sofic shifts without separation and their factors*

Hochman and Meyerovitch [21] *A characterization of the entropies of multi-dimensional shifts of finite type*

Ban, Hu, Lin, and Lin [3], *Verification of mixing properties in two-dimensional shifts of finite type*

Hu and Lin [23] *Nonemptiness problems of plane square tiling with two colors*

Hu and Lin [24], *On spatial entropy of multi-dimensional symbolic dynamical systems*, discuss multi-dimensional shift space for a rectangular spatial entropy which is the limit of growth rate of admissible local patterns on finite rectangular sublattices.

**2016-05-04 Predrag** Ban, Hu, Lin, and Lin [2], *Zeta functions for two-dimensional shifts of finite type* seems to be a **must read**, with exhaustive references. The zeta functions of two-dimensional shifts of finite type which generalizes the Artin-Mazur [1] zeta function was given by Lind [27], ([click here](#)) for  $\mathbb{Z}^2$ -action. The rotationally symmetric trace operator is the transition matrix for  $x$ -periodic patterns with period  $n$  and height 2. The rotational symmetry induces the reduced trace operator, and the zeta function in the  $x$ -direction is now a reciprocal of an infinite product of polynomials. The zeta function can be presented in the  $y$ -direction and in the coordinates of any unimodular transformation in  $GL_2(\mathbb{Z})$ . Therefore, there exists a family of zeta functions that are meromorphic extensions of the same analytic function. The Taylor series for these zeta functions at the origin are equal with integer coefficients, yielding a family of identities, which are of interest in number theory.

Their **Example 7.2**

Let  $F_2 = \{0, 1\}$  and

$$\mathbb{Z} = \{ \phi_{nt} = \phi_{n,t+1} + \phi_{n,t-1} + \phi_{n+1,t} + \phi_{n-1,t} \text{ for all } nt \in \mathbb{Z}^2 \} \quad (10.1)$$

is about the harmonic patterns on square-cross lattice  $\mathcal{L}$  studied by F. Ledrappier, *Un champ markovien peut être d'entropie nulle et mélangeant*, C. R. Acad. Sc. Paris Ser. A 287 (1978), 561-562. For us, this is a bit strange - our 'harmonic' value would be  $4\phi_{nt}$ , not  $\phi_{nt}$ .

**2016-10-11 Predrag Boris Gutkin** has explained the strategy of Ban *et al.* [2], approach that he himself has used: one constructs  $\zeta$  functions for finite periodic domain in one direction, i.e., infinite strip  $\mathbb{Z}_{\infty \times L}$  or  $\mathbb{Z}_{T \times \infty}$ . with a transfer operator generating the other, infinite direction, as in figure 10.1 (b). Those zeta functions are multiplied. The infinite products, a different formula for each direction, describe the same set of admissible patterns, resulting in some unexpected identities.

I find this very unnatural - intelligent zeta should account for all commuting directions democratically.

**2020-03-05 Predrag** Douglas Lind's [website](#).

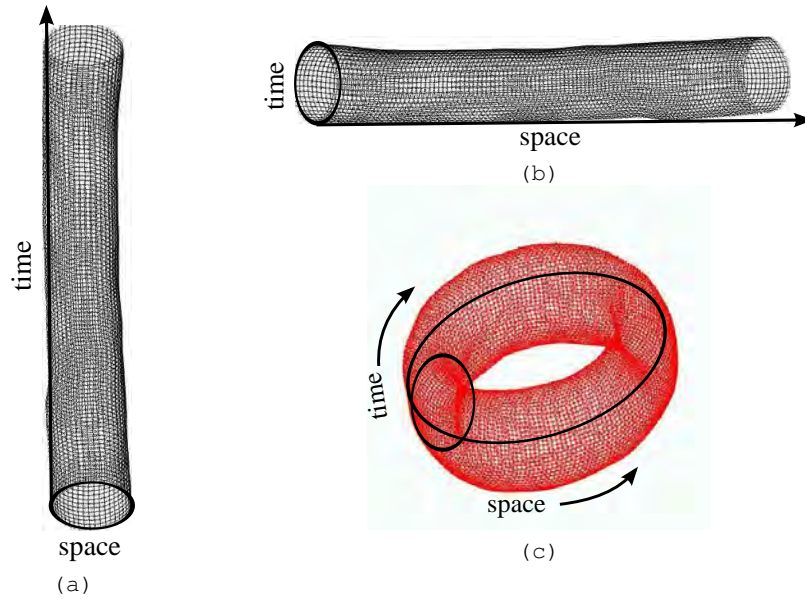


Figure 10.1: (a) A fixed  $L$  periodic spatial domain, all  $t$ . (b) A fixed  $T$  periodic temporal domain, all  $x$ . (c) A fixed  $LT$ , doubly periodic spatiotemporally invariant 2-torus.

Lind [27]: Let  $f : X \rightarrow X$  be a homeomorphism of a compact space and  $N_n(f)$  denote the number of points in  $X$  fixed by  $f^n$ . We assume that  $N_n(f)$  is finite for all  $n \geq 1$ . [⋯] The zeta function has the product formula

$$1/\zeta_{AM}(z) = \prod_p (1 - z^{n_p}) \tag{10.2}$$

where the product is over all finite orbits  $p$  of  $f$  and  $n_p$  denotes the number of points in  $p$ .

To compute  $e_d(n)$  we use the Hermite normal form of an integer matrix (see ref. [29], Thm. 22.1).

[10] Mac Duffee [29] *The Theory of Matrices*, (Chelsea, New York, 1956) (click here); Y. Katznelson, Ergodic automorphisms of  $T^n$  are Bernoulli, Israel J. Math. 10 (1971), 186-195.

The following question was suggested to us by David Ruelle:

**Problem 7.5.** Compute explicitly the thermodynamic zeta function for the 2-dimensional Ising model, where  $\alpha$  is the  $\mathbb{Z}^2$  shift action on the space of configurations.

2021-07-28 Predrag Here is a cute “interesting zeta function” over  $\mathbb{Z}$  with the



product formula, apparently known to Gauss:

$$\prod_n \frac{1}{1 - z^n} = \sum_\ell p_\ell z^\ell \quad (10.3)$$

where  $p_\ell$  of is the number of partitions of  $\ell$ .

**2018-10-09 Predrag** Lind and Schmidt [26] *Symbolic and algebraic dynamical systems*, ([click here](#)) studies zeta functions for  $\mathbb{Z}^d$  actions.

**2018-09-02, 2018-10-09 Predrag** Einsiedler, Lindenstrauss, Michel and Venkatesh [14] *Distribution of periodic torus orbits and Duke's theorem for cubic fields*: " We study periodic torus orbits on spaces of lattices. Using the action of the group of adelic points of the underlying tori, we define a natural equivalence relation on these orbits, and show that the equivalence classes become uniformly distributed. This is a cubic analogue of Duke's theorem about the distribution of closed geodesics on the modular surface: suitably interpreted, the ideal classes of a cubic totally real field are equidistributed [...]"

*Homogeneous toral sets* do not seem to be defined. They generalize the groupings of compact orbits (I believe these compact orbits are what we call -at this moment- prime tori).

They define two invariants for homogeneous toral sets, *volume* (defined in their eq. (13), measuring how "large" it is) and *discriminant* (measuring its arithmetic complexity). I have no intuition about what this discriminant is in our applications.

The periodic orbits are grouped into equivalence classes, equivalent orbits having the same volume and discriminant. An equivalence class of compact orbits is a *packet*. Compact orbits in the same packet have the same stabilizer and the same discriminant.

**2020-12-18 Predrag** Esposti and Isola [15] *Distribution of closed orbits for linear automorphisms of tori* (1995) develop zeta functions for  $d$ -dimensional tori; then they specialized to  $D$  dof symplectic matrices acting on  $2D$ -dimensional tori, of which Isola's  $d = 2$  is a special case. But I'm confused. I do not think that has to do with lattice zeta functions we seek...

**2020-11-22 RSM** The November 20, 2020 Matthew Gudorf *Spatiotemporal tiling of the Kuramoto-Sivashinsky system* thesis dissertation defense interests me. At the conceptual level it was already in Pesin & Sinai [39] 1988 *Space-time chaos in the system of weakly interacting hyperbolic systems*, for CML, and in my MacKay [31] *Space-time phases* 2012 lecture notes, but claiming it applies to Kuramoto-Sivashinsky is bold. I suppose it does not fit perfectly, but interesting if it fits approximately.

Is there a paper I can read?

**2022-021-19 Predrag** I see no ‘symbol table’ in Pesin & Sinai [39] (1988). Bunimovich and Sinai [7] (1988) has two-dimensional ‘symbolic representation’.

R.S. MacKay [30] *Indecomposable coupled map lattices with non-unique phase* (2005) refers to ‘symbol tables’.

Coutinho and Fernandez [10] (1997) call this ‘spatiotemporal code’.

**2020-11-22 Predrag** to Han: please read MacKay [31] *Space-time phases: Statistical properties of dynamics on large networks* ([click here](#)), Sect. 2.2 *Statistical Phases for Uniformly Hyperbolic Attractors of Finite-Dimensional Deterministic Dynamical Systems* and related, and please take notes here on anything that is related to our project.

**2020-12-16 RSM** Cf. section 7.2.3 *Uniformly hyperbolic dynamics on networks* in our 2013 LMS lecture notes [31] “Masters of Complexity Science” ([click here](#)).

**2020-12-16 Predrag** Han Liang and I have been studying your *Space-time phases: Statistical properties of dynamics on large networks* [31], and I was supposed to report back to you. I like the proof of hyperbolicity for the spatiotemporal CML. Other than sect. 13.1 *Chronotopic literature*, this is the closest to our spatiotemporal work.

**2020-12-16 RSM** Perhaps the analogue of the MM formula that is relevant is the formula on line 4 of p. 436, of which I am proud but it was also found by Bricmont and Kupiainen, and they published before I did.

**2020-12-23 Predrag** Bricmont and Kupiainen, *High temperature expansions and dynamical systems* [arXiv:chao-dyn/9504015](#): “ We develop a resummed high-temperature expansion for lattice spin systems with long range interactions, in models where the free energy is not, in general, analytic. We establish uniqueness of the Gibbs state and exponential decay of the correlation functions. Then, we apply this expansion to the Perron-Frobenius operator of weakly coupled map lattices.”

They credit D. L. Volevich, *Kinetics of coupled map lattices*, *Nonlinearity* 4, 37-45 (1991); *The Sinai -Bowen-Ruelle measure for a multidimensional lattice of interacting hyperbolic mappings*, *Russ. Acad. Dokl. Math.* 47, 117-121 (1993); and *Construction of an analogue of Bowen-Ruelle-Sinai measure for a multidimensional lattice of interacting hyperbolic mappings*, *Russ. Acad. Math. Sbornik* 79, 347-363 (1994).

**2020-12-16 Predrag** Spatially homogenous lattice models also invariant under discrete *space translations* were studied by Bunimovich and Sinai [7] in the case when  $g(\phi_{nt})$  is a one-dimensional expanding map.

Regarding your “symbol tables” (what we call symbol blocks): the previous examples of  $(D+1)$ -dimensional spatiotemporal symbolic dynamics: Pesin and Sinai [39], Bunimovich and Sinai [7], Pethel, Corron and

Boltt [40, 41]. In other literature, I noticed that Houlrik [22] gives Bunimovich and Sinai [7] the credit.

The key insight [7, 20]—an insight that applies to coupled-map lattices [40–42], and field theories modeled by them, not only the system considered here— is that a field  $X = \{\phi_z\}$  over a  $d$ -dimensional spacetime lattice  $z \in \mathbb{Z}^d$  has to be described by a corresponding symbol block  $M = \{m_z\}$ , over the same  $d$ -dimensional spacetime lattice  $z \in \mathbb{Z}^d$ , rather than a 1-dimensional temporal symbol sequence (1.10), as one does when describing a finite coupled “ $N$ -particle” system in the Hamiltonian formalism.

Other than the “symbol tables”, Bunimovich and Sinai [7] (1988) and Pesin and Sinai [39] are profoundly different, nothing to do with the spatiotemporal cat. Bunimovich has heard me talk about it, Sinai not.

As spatiotemporal cat equations are symmetric under interchange of the ‘space’ and the ‘time’ directions, their temporal and spatial dynamics are strongly coupled, corresponding to  $\epsilon \approx O(1)$  in (8.2), in contrast to the traditional spatially weakly coupled CML [7].

The conventional CML models start out with chaotic on-site dynamics weakly coupled to neighboring sites, with strong spacetime asymmetry. In order to establish the desired statistical properties of CML, such as the continuity of their SRB measures, refs. [7, 39] and most of the subsequent mathematical literature rely on the structural stability of Anosov automorphisms under small perturbations. Contrast this with the non-perturbative 2-dimensional Gutkin-Osipov [20] *spatiotemporal cat* (24.43).

Unlike the systems studied in ref. [7], spatiotemporal cat cannot be conjugated to a product of non-interacting cat maps; a way to see that is to compare the numbers of invariant 2-tori in the two cases – they differ.

In all other coupled maps literature I am aware of, the starting point is time evolution of a non-interacting particle at each site, with its 1-dimensional temporal symbolic dynamics, with spatial coupling to  $D$  spatial neighbors subsequently tacked on. While the spacetime *coordinate* of site is  $(D+1)$ -dimensional, its symbolic dynamics is 1-dimensional.

Your paper I found most eye-opening was the Hill’s formula of [32] *Linear stability of periodic orbits in Lagrangian systems*.

We do not derive the formula the way you did it (ours also works for dissipative systems), but the paper made the light bulb turn on...

Is there something else?

The thing we’ve been struggling with the most, that has kept the paper from a publication is unimodular invariance of the defining (primitive cell) of a lattice (tiling of spacetime) so I have not been able to write down a rational spatiotemporal topological zeta function in terms of prime (non-repeating) 2-tori (spatiotemporal periodic orbits). Should be doable (the Green’s function is elliptic K function), but I just do not get it.)

**2020-12-16 RSM** Yes, neat to consider cat map as a second order recurrence on one variable rather than a first order one on two variables (I hadn't appreciated the advantage when Vivaldi was talking about it way back then) and then it indeed looks like a discrete field theory and extends naturally to space-time and you can code all solutions by lattices of integers, one for each point in space-time.

In the general "uniformly hyperbolic" situation (in quotes because it is the way to connect with dyn sys, but the point is to escape from time-evolution view, as you do, and consider solutions as being zeroes of some function from states on spatiotemporal lattice to the spatiotemporal lattice and then u hyp just means the derivative of the function has bounded inverse), expect to be able to code all solutions by some set of allowed symbol tables, via spatiotemporal shadowing (which is just shadowing in the more general context, again having nothing to do with time-evolution). Not sure to what extent I mentioned this in my lecture notes, but perhaps it appears in the article I wrote for Chazottes & Fernandez earlier. I have certainly waved spatiotemporal shadowing around as providing an answer, but never really done it for any particular system. Will think about it.

Will also think about your question of zeta fn for the Gutkin-Osipov CML. It will be a straightforward answer once we have thought of it, but a question of keeping everything straight in one's mind. I'm not clear where your obstacle is. We can count all spatiotemporal periodic solutions and so make a zeta fn; you want to reduce it to an expression in terms of prime ones? or to one in terms of collections of disjoint elementary cycles? (I put elementary in there because graph theorists use closed walk for what you might call a cycle and cycle for what I'm calling an elementary one) "Just" need to work out the spatiotemporal analogue. Maybe I need to wake up fresh tomorrow morning to do it. Or have a whisky now to do it (except I don't have any in the house right now!).

**2020-12-17 RSM** I found the Percival-Vivaldi [37] paper (having first found their other one [38] from 1987 on the periodic orbits). As I remembered, they do not appear to derive finite-type conditions on their coding. I suspect it is not of finite type. Thus I'd say it is pretty useless, compared to the Adler-Weiss partition.

I wasn't convinced by Percival-Vivaldi [37] as it is not obvious (to me) what are the constraints on the sequence of integers  $m_t$ . Do you know? Say we take  $\phi_{t+1} - 3\phi_t + \phi_{t-1} = 0 \pmod{1}$ ,  $\phi \in [-1/2, 1/2)$  then we can get  $\{-2, -1, 0, 1, 2\}$ , but not all sequences of such integers are possible because that would give entropy  $\log 5$  whereas it is supposed to be  $\log(3 + \sqrt{5})/2$ , or  $\log(s + \sqrt{(s-2)(s+2)})/2$  in general. There should be a simple finite-type condition. Do you know it?

**2020-12-18 Predrag** I agree. It's ridiculous, arbitrary frame on the unit torus, contra natura, ignoring stable/unstable manifolds, painful to implement

– Dirichlet conditions destroy the time-translational invariance of the lattice. That is why I included [figure 2](#) and [table 2](#) – an impossible number-theoretic problem created by ignoring the well-known generating partition construction. There Vivaldi and Percival got it wrong.

Aside: Nobody listens to me, and in particular Russians, so I had to watch and assist Gutkin and 3 grad students push this pointless torture of a paper. The problem is that quantum chaos crowd profoundly lacks understanding of periodic orbit theory – I wrote a whole book to explain that periodic orbit calculations are general nonlinear coordinate transformation invariant, that one does not need nowhere differentiable probability measures, to no avail. Russians make it worse by idolizing Sinai and believing that one has to construct explicit, coordinate-dependent generating partitions – that never works except in 3 or so examples which are the only ones they are always taught.

**2020-12-17 RSM** Do you have a way around it?

**2020-12-18 Predrag** Yes, we construct the Adler-Weiss generating partition for Percival-Vivaldi 2-configuration map in ChaosBook.org (not polished yet, but for you I’ve promoted it from internal to publicly readable text): [ChaosBook Example 14.12](#) *Adler-Weiss partition of the cat map state space*.

While Percival and Vivaldi were well aware of Adler-Weiss partitions, they felt that their “coding is less efficient in requiring more symbols, but it has the advantage of linearity.” Our construction demonstrates that one can have both: an Adler-Weiss generating cat map partition, and a linear code. The only difference from the Percival-Vivaldi formulation [\[37\]](#) is that one trades the single unit-square cover of the torus of [\(2.75\)](#) for the dynamically intrinsic, two-rectangles cover, but the effect is magic – now every infinite walk on the transition graph corresponds to a unique admissible orbit  $\{\phi_t\}$ , and the transition graph generates all admissible itineraries  $\{m_t\}$ .

But the Hamiltonian formulation is stupid. The great advantage of the Lagrangian, temporal lattice formulation is that the fundamental fact yields the number of periodic solutions and the zeta function without any explicit time-evolution generating partition. I believe that explicit time-evolution generating partitions are impossible to generalize to spatial lattices evolving in time.

**2020-12-17 RSM** You cited Isola [\[25\]](#) for the  $\zeta$ -function for the cat map but I thought people like Manning had calculated it earlier. I looked up his 1971 paper on rationality of zeta for Axiom A and see he cites Smale’s 1967 review for toral automorphisms.

**2020-12-18 Predrag** I doubt it. In his 1971 *Axiom A diffeomorphisms have rational zeta function* [\[35\]](#) he explains rationality of topological (orbit counting) of Smale’s school zeta functions in terms of ‘Manning multiples’, what I

understand as inclusion-exclusion principle (when sets share boundaries, boundary has to be –recursively- subtracted not to be overcounted).

It is easy enough to construct, but I have not seen cat map zeta function earlier than the one written down by Isola. Will change the citation if we find an earlier one.

**2020-12-18 RSM** OK, you map the Adler-Weiss partition into  $(x, x')$  coordinates and then reduce by translation into that fundamental domain instead of the standard one. Got it. I thought you had some magic for the standard fundamental domain. I agree the tedious thing about counting periodic orbits of toral automorphisms is the ambiguity of coding for orbits on the partition boundaries. A cute thing is that if you consider the map on a sphere (with 4 conical points) induced by quotienting by reflection through 0,0 then you get exactly  $\text{tr } A^n$  fixed points of  $A^n$ , see Libre and MacKay [28] *Pseudo-Anosov homeomorphisms on a sphere with four punctures have all periods* (1992).

**2020-12-18 Predrag** A very cute paper, but it will not help me here, will it?

**2020-12-18 RSM** OK, I might look up Pollicott on zeta fns for toral autos because I think he has some lecture notes in which he gives history.

On your big question, can I phrase it as how many orbits under  $\text{SL}(2, \mathbb{Z})$  are there for its action on integer parallelograms of given area (based at 0)? Equivalently, how many sublattices of given area are there in  $\mathbb{Z}^2$ ?

**2020-12-18 Predrag** It's the first step, a warm-up exercise - we all can do it. But then you have to count the number of invariant 2-tori that live on each parallelogram. The paper explains that we know how to do it, but if we had the zeta functions, it would generate all these numbers.

It could be that the sensible zeta function is a double series in  $(z_1^L, z_2^T)$ , in which case we want to count integer parallelograms of periods  $(L, T)$ , not lump them into areas  $A = LT$ , and have a zeta function which is a series in single  $z^A$ .

**2020-12-18 RSM** It is the sort of thing Marklof probably knows. But we can think about it too. For area 1 I get 1 because I can map any unit parallelogram to the unit square by the inverse of the matrix representing its sides, which is in  $\text{SL}(2, \mathbb{Z})$ . For area 2, I think I get two, by observing that to have area 2, the matrix has one row or column divisible by 2 and then dividing that out and using its inverse to map to one of the two standard rectangles. For area 3 I didn't get an answer yet. But I wonder if it is something trivial like the area. This would fit with your fundamental fact.

**2020-12-18 RSM** I see I was wrong in getting only two orbits of parallelograms for area 2. There's also the diamond. I must have missed something with the rows and columns calculation (which admittedly I did while in bed)!

Ah yes, I remember I did see one more solution and then forgot it by the time I go up. Here it is done properly:

**Number of sublattices of  $\mathbb{Z}^2$ .** "I would like to count the number of sublattices  $\mathcal{L}$  of  $\mathbb{Z}^2$  of index  $n = |\det \mathcal{L}|$ ."

**2020-12-19 Predrag** This example lists  $\det \mathcal{L} = 2$  parallelograms as (columns are their primitive vectors)

$$\begin{bmatrix} 2 & 0 \\ 0 & 1 \end{bmatrix}, \begin{bmatrix} 0 & 1 \\ 2 & 0 \end{bmatrix}, \begin{bmatrix} 1 & -1 \\ 1 & 1 \end{bmatrix}. \quad (10.4)$$

The third one is not in the Hermite normal form, but presumably a unimodular transformation (have not checked it) brings it to the upper diagonal form  $[2 \times 1]_1$  invariant 2-torus that we use.

This example counts parallelograms under distinct translations (must make sure that each unimodular orbit is counted only once). Guido, Isola and Lapidus [18] (or **ChaosBook chapter 25 Discrete symmetry factorization**) count parallelograms distinct under reflections.

I think counting  $\det \mathcal{L} = A$  parallelograms is easy. What we need is a generating function that counts numbers of invariant 2-tori, and the related zeta that counts the numbers of *prime* invariant 2-tori.

**2020-12-18 Predrag** If it is any help, for small areas answers are listed in **table 2**.

**2020-12-18 RSM** The question is how to make a zeta fn from these counts. Take simplest case of Bernoulli on  $s$  symbols. For each area  $n$ , we have  $T_n = \sum d$  over divisors of  $n$ , sublattices. Each can be populated by  $s^n$  patterns (not worrying about patterns with a smaller lattice), so there are  $s^n T_n$  patterns with an area  $n$ . I suppose it is natural to divide by  $n$  because we could move the origin to any of the  $n$  points. So propose  $\zeta(z) = \exp \sum_n s^n z^n T_n / n$  for this example. Need to look up some number theory to simplify this but I think it is some standard formula.

**2020-12-18 RSM** Ah, I see from (86) of your draft paper that I have made a mistake. Yes, have identified my error now. Here is **a useful page**. So, OK, number of Bravais lattices has zeta fn (with respect to area)  $= \prod_L (1 - z^L)$ . But you already knew this. Your question at the bottom of p. 21 is to count prime lattices or perhaps the more subtle one of counting prime periodic patterns taking the finite-type conditions of spatiotemporal cat into account.

**2020-12-19 RSM** If define  $\zeta(z) = \exp \sum_n z^n / n N_n$  where  $N_n$  is the number of periodic states that have a period parallelogram of area  $n$ , and we let prime patterns be ones that are not repetitions of ones with a smaller area, and regarded as equivalent if differ by a translation, then I get  $\zeta(z) = \prod_\gamma F(z^{|\gamma|})$  over orbits  $\gamma$ , where  $F(x) = \prod_m (1 - x^m)^{-1/m}$ . Not sure if  $F$  can be simplified.

**2020-12-16 Predrag** We have not been able to make that one work. Square lattice is separable, so one hopes for something like that. The problem is that in the addition to double periodicity, there is a third integer – parallelogram come with different tilts (screw bc's). Some details are towards the end of the current draft [11], Predrag Cvitanović and Han Liang *Spatiotemporal cat: A chaotic field theory* rough draft, (November 2020) on [spatiotemporal homemade](#).

**2020-12-20 RSM** I have some thoughts about the 2D  $\zeta$  function, in particular the question of how to generalise  $\det(I - zW)$  from finite type conditions (or more generally weights  $W$ ) for nearest nbr chains to finite type conditions (or more generally weights from cliques) for 2D lattices. I think it proceeds in same way as I did for Gibbs measures for CML.

**2020-09-24, 2020-12-16 Predrag** My thoughts in that directions (that is in my spatiotemporal cat talk, and in this blog, see (8.167), (16.39), (16.42), (16.49)) are that for the 2-dimensional spatiotemporal cat [11, 19]

$$\phi_{n,t+1} + \phi_{n,t-1} - 2s\phi_{nt} + \phi_{n+1,t} + \phi_{n-1,t} = -m_{nt}, \quad m_{nt} \in \mathcal{A}, \quad (10.5)$$

with alphabet

$$\mathcal{A} = \{-3, -2, -1, 0, \dots, \mu^2 + 1, \mu^2 + 2, \mu^2 + 3\}, \quad (10.6)$$

and the Yukawa mass squared of the scalar field  $\phi$

$$\mu^2 = 2(s - 2). \quad (10.7)$$

The  $\zeta$  function has to satisfy all spatiotemporal symmetries of the square lattice (6.204)

$$C_{4v} = D_4 = \{E, C_{4z}^+, C_{4z}^-, C_{2z}, \sigma_y, \sigma_x, \sigma_a, \sigma_b\}. \quad (10.8)$$

See [ChaosBook sect. A25.1](#).

In the international crystallographic notation, this square lattice space point group is referred to as  $p4mm$  [13].

**2020-12-16 Predrag** The simplest rational  $\zeta$  function that satisfies these symmetries is of form

$$1/\zeta_{AM}(z_1, z_2) = d(s)/d(2) = 1 - \mu^2/d(2), \quad (10.9)$$

where

$$d(s) = z_1 + z_2 - 2s + z_1^{-1} + z_2^{-1} \quad (10.10)$$

$d(s)$  is the Z-transform (discrete Laplace transform) of (24.501). Fischer *et al.* [16] call this the *characteristic function*, a somewhat over-abused nothing-saying appellation.

Anything more complicated would be a disappointment :)



**2020-12-20 Predrag** Its massless  $\mu^2 = 0$ , Poisson equation value  $d(2)$  is the Z-transform of the  $d = 2$  lattice Laplacian.  $d(s)$  can be written in a  $D_4$ -symmetric form

$$\begin{aligned} d(s) &= (1 - \Lambda z_1)(1/z_1 - 1/\Lambda) + (1 - \Lambda z_2)(1/z_2 - 1/\Lambda) \\ d(2) &= (1 - z_1)(1/z_1 - 1) + (1 - z_2)(1/z_2 - 1). \end{aligned} \quad (10.11)$$

Here  $(\Lambda, 1/\Lambda)$  are the roots of the  $d = 1$  characteristic equation

$$\Lambda^2 - s\Lambda + 1 = 0, \quad (10.12)$$

which, for  $|s| > 2$ , has two real roots  $\{\Lambda, \Lambda^{-1}\}$ ,

$$\Lambda = \frac{1}{2}(s + \sqrt{(s-2)(s+2)}), \quad (10.13)$$

$$\Lambda = \frac{1}{2}(\mu^2 + 2 + \mu^2 \sqrt{1 + \left(\frac{2}{\mu}\right)^2}), \quad (10.14)$$

$$s = \Lambda + \Lambda^{-1} = e^\lambda + e^{-\lambda} = 2 \cosh \lambda, \quad \lambda > 0. \quad (10.15)$$

Derivatives, integrations with respect to the parameter  $(z_1, z_2)$ , should relate this to the numbers of periodic states generating function, but Han tells me that does not work. Perhaps, in the spirit of Schwinger and Feynman 'tricks' derivatives, integrations with respect to the stretching parameter  $s$  or squared mass  $\mu^2$  do the job.

Decomposition (10.11) is dodgy - in higher dimesnions there are other eigenvalues than (10.13).

**2020-12-17 RSM** I found [...] Percival-Vivaldi [37] [... see above ...] There should be a simple finite-type condition. Do you know it?

2CB

**2020-12-20 Predrag** As for the cat map, we split the  $\mu^2 + 7$  letter alphabet  $\mathcal{A} = \mathcal{A}_0 \cup \mathcal{A}_1$  into the interior  $\mathcal{A}_0$  and exterior  $\mathcal{A}_1$  alphabets [19]

$$\mathcal{A}_0 = \{0, \dots, \mu^2\}, \quad \mathcal{A}_1 = \{-3, -2, -1\} \cup \{\mu^2 + 1, \mu^2 + 2, \mu^2 + 3\}. \quad (10.16)$$

For example, for  $\mu^2 = 1$  (ie,  $s = 5/2$ ) the interior, respectively exterior alphabets are

$$\mathcal{A}_0 = \{0, 1\}, \quad \mathcal{A}_1 = \{-3, -2, -1\} \cup \{2, 3, 4\}. \quad (10.17)$$

If all  $m_z \in M$  belong to  $\mathcal{A}_0$ ,  $M$  is admissible, i.e.,  $\mathcal{A}_0^{\mathbb{Z}^2}$  is a full shift [19]. All grammar rules involve exterior alphabet  $\mathcal{A}_1$ . I do not know whether there is a finite grammar, or the grammar is the infinite one investigated by Gutkin *et al.* [19]. My claim is that it does not matter, as we know how to count all  $[L \times T]_S$ , and for each we can read off all admissible  $M$  by listing all integer points within the  $\mathcal{J}_M$  fundamentele parallelepiped.

Curiously, even the Poisson  $\mu = 0$  case looks chaotic, numerically (though how would our graduate students notice logarithmic corrections due to the 0-mode?), see [figure 5 \(c\)](#) of Gutkin *et al.* [19]. That presumably arises from the intersection set (the boundary) of the (6.205) fundamental domain and its reflection.

## References

- [1] M. Artin and B. Mazur, “On periodic points”, *Ann. Math.* **81**, 82–99 (1965).
- [2] J.-C. Ban, W.-G. Hu, S.-S. Lin, and Y.-H. Lin, *Zeta Functions for Two-dimensional Shifts of Finite Type*, Vol. 221, *Memoirs Amer. Math. Soc.* (Amer. Math. Soc., Providence RI, 2013).
- [3] J.-C. Ban, W.-G. Hu, S.-S. Lin, and Y.-H. Lin, *Verification of mixing properties in two-dimensional shifts of finite type*, 2015.
- [4] J.-C. Ban and S.-S. Lin, “Patterns generation and transition matrices in multi-dimensional lattice models”, *Discrete Continuous Dyn. Syst. Ser. A* **13**, 637–658 (2005).
- [5] J.-C. Ban, S.-S. Lin, and Y.-H. Lin, “Patterns generation and spatial entropy in two-dimensional lattice models”, *Asian J. Math.* **11**, 497–534 (2007).
- [6] M. Boyle, R. Pavlov, and M. Schraudner, “Multidimensional sofic shifts without separation and their factors”, *Trans. Amer. Math. Soc.* **362**, 4617–4653 (2010).
- [7] L. A. Bunimovich and Y. G. Sinai, “Spacetime chaos in coupled map lattices”, *Nonlinearity* **1**, 491 (1988).
- [8] S.-N. Chow, J. Mallet-Paret, and W. Shen, “Traveling waves in lattice dynamical systems”, *J. Diff. Equ.* **149**, 248–291 (1998).
- [9] S.-N. Chow, J. Mallet-Paret, and E. S. Van Vleck, “Pattern formation and spatial chaos in spatially discrete evolution equations”, *Random Comput. Dynam.* **4**, 109–178 (1996).
- [10] R. Coutinho and B. Fernandez, “Extended symbolic dynamics in bistable CML: Existence and stability of fronts”, *Physica D* **108**, 60–80 (1997).
- [11] P. Cvitanović and H. Liang, *A chaotic lattice field theory in two dimensions*, In preparation, 2024.
- [12] A. Desai, “Subsystem entropy for  $Z^d$  sofic shifts”, *Indag. Math.* **17**, 353–359 (2006).
- [13] M. S. Dresselhaus, G. Dresselhaus, and A. Jorio, *Group Theory: Application to the Physics of Condensed Matter* (Springer, New York, 2007).

- [14] M. Einsiedler, E. Lindenstrauss, P. Michel, and A. Venkatesh, “Distribution of periodic torus orbits and Duke’s theorem for cubic fields”, *Ann. Math.* **173**, 815–885 (2011).
- [15] M. D. Esposti and S. Isola, “Distribution of closed orbits for linear automorphisms of tori”, *Nonlinearity* **8**, 827–842 (1995).
- [16] D. Fischer, G. Golub, O. Hald, C. Leiva, and O. Widlund, “On Fourier-Toeplitz methods for separable elliptic problems”, *Math. Comput.* **28**, 349–349 (1974).
- [17] S. Friedland, “On the entropy of  $Z^d$  subshifts of finite type”, *Linear Algebra Appl.* **252**, 199–220 (1997).
- [18] D. Guido, T. Isola, and M. L. Lapidus, “Ihara zeta functions for periodic simple graphs”, in *C\*-algebras and Elliptic Theory II*, edited by D. Burghelea, R. Melrose, A. S. Mishchenko, and E. V. Troitsky (Birkhäuser, Basel, 2008), pp. 103–121.
- [19] B. Gutkin, L. Han, R. Jafari, A. K. Saremi, and P. Cvitanović, “Linear encoding of the spatiotemporal cat map”, *Nonlinearity* **34**, 2800–2836 (2021).
- [20] B. Gutkin and V. Osipov, “Classical foundations of many-particle quantum chaos”, *Nonlinearity* **29**, 325–356 (2016).
- [21] M. Hochman and T. Meyerovitch, “A characterization of the entropies of multidimensional shifts of finite type”, *Ann. Math.* **171**, 2011–2038 (2010).
- [22] J. M. Houlrik, “Periodic orbits in a two-variable coupled map”, *Chaos* **2**, 323–327 (1992).
- [23] W.-G. Hu and S.-S. Lin, “Nonemptiness problems of plane square tiling with two colors”, *Proc. Amer. Math. Soc.* **139**, 1045–1059 (2011).
- [24] W.-G. Hu and S.-S. Lin, “On spatial entropy of multi-dimensional symbolic dynamical systems”, *Discrete Continuous Dyn. Syst. Ser. A* **36**, 3705–3717 (2016).
- [25] S. Isola, “ $\zeta$ -functions and distribution of periodic orbits of toral automorphisms”, *Europhys. Lett.* **11**, 517–522 (1990).
- [26] D. Lind and K. Schmidt, “Symbolic and algebraic dynamical systems”, in *Handbook of Dynamical Systems*, Vol. 1, edited by B. Hasselblatt and A. Katok (Elsevier, New York, 2002), pp. 765–812.
- [27] D. A. Lind, “A zeta function for  $Z^d$ -actions”, in *Ergodic Theory of  $Z^d$  Actions*, edited by M. Pollicott and K. Schmidt (Cambridge Univ. Press, 1996), pp. 433–450.
- [28] J. Llibre and R. S. MacKay, “Pseudo-Anosov homeomorphisms on a sphere with four punctures have all periods”, *Math. Proc. Cambridge Philos. Soc.* **112**, 539–549 (1992).
- [29] C. C. Mac Duffee, *The Theory of Matrices* (Springer, Berlin, 1933).

- [30] R. S. MacKay, “Indecomposable coupled map lattices with non-unique phase”, in *Dynamics of Coupled Map Lattices and of Related Spatially Extended Systems*, edited by J.-R. Chazottes and B. Fernandez (Springer, 2005), pp. 65–94.
- [31] R. S. MacKay, “Space-time phases: Statistical properties of dynamics on large networks, The Warwick Master’s Course”, in *Complexity Science*, edited by R. Ball, V. Kolokoltsov, and R. S. MacKay (Cambridge Univ. Press, Cambridge UK, 2013).
- [32] R. S. MacKay and J. D. Meiss, “Linear stability of periodic orbits in Lagrangian systems”, *Phys. Lett. A* **98**, 92–94 (1983).
- [33] J. Mallet-Paret and S.-N. Chow, “Pattern formation and spatial chaos in lattice dynamical systems. I”, *IEEE Trans. Circuits Systems I Fund. Theory Appl.* **42**, 746–751 (1995).
- [34] J. Mallet-Paret and S.-N. Chow, “Pattern formation and spatial chaos in lattice dynamical systems. II”, *IEEE Trans. Circuits Systems I Fund. Theory Appl.* **42**, 752–756 (1995).
- [35] A. Manning, “Axiom A diffeomorphisms have rational zeta function”, *Bull. London Math. Soc.* **3**, 215–220 (1971).
- [36] R. Miles and T. Ward, “The dynamical zeta function for commuting automorphisms of zero-dimensional groups”, *Ergod. Th. & Dynam. Sys.* **38**, 1564–1587 (2016).
- [37] I. Percival and F. Vivaldi, “A linear code for the sawtooth and cat maps”, *Physica D* **27**, 373–386 (1987).
- [38] I. Percival and F. Vivaldi, “Arithmetical properties of strongly chaotic motions”, *Physica D* **25**, 105–130 (1987).
- [39] Y. B. Pesin and Y. G. Sinai, “Space-time chaos in the system of weakly interacting hyperbolic systems”, *J. Geom. Phys.* **5**, 483–492 (1988).
- [40] S. D. Pethel, N. J. Corrion, and E. Bollt, “Symbolic dynamics of coupled map lattices”, *Phys. Rev. Lett.* **96**, 034105 (2006).
- [41] S. D. Pethel, N. J. Corrion, and E. Bollt, “Deconstructing spatiotemporal chaos using local symbolic dynamics”, *Phys. Rev. Lett.* **99**, 214101 (2007).
- [42] A. Politi and A. Torcini, “Towards a statistical mechanics of spatiotemporal chaos”, *Phys. Rev. Lett.* **69**, 3421–3424 (1992).
- [43] A. N. Quas and P. B. Trow, “Subshifts of multi-dimensional shifts of finite type”, *Ergod. Theor. Dynam. Syst.* **20**, 859–874 (2000).
- [44] C. G. J. Roettger, “Periodic points classify a family of markov shifts”, *J. Number Theory* **113**, 69–83 (2005).
- [45] T. Ward, “Automorphisms of  $Z^d$ -subshifts of finite type”, *Indag. Math.* **5**, 495–504 (1994).

- [46] T. Ward and R. Miles, “A directional uniformity of periodic point distribution and mixing”, *Discrete Continuous Dyn. Syst.* **30**, 1181–1189 (2011).
- [47] T. Ward and R. Miles, “Directional uniformities, periodic points, and entropy”, *Discrete Continuous Dyn. Syst. Ser. B* **20**, 3525–3545 (2015).
- [48] T. B. Ward, “An algebraic obstruction to isomorphism of Markov shifts with group alphabets”, *Bull. London Math. Soc.* **25**, 240–246 (1993).

# Chapter 11

## Spatiotemporal stability

### 11.1 Temporal lattice

Assume that a periodic orbit  $x(T_p + t) = x(t)$  of a continuous time flow  $\dot{x} = v(x)$  is known ‘numerically exactly’, that is to say, to arbitrary (but not infinite) precision. One way to present the solution is to give a single point  $x(0)$  in the orbit, and let the reader reconstruct the orbit  $p$  by integrating forward in time,  $x(t) = f^t(x(0))$ ,  $t \in [0, T_p]$ .

However, for a linearly unstable periodic orbit a single point does not suffice to present the orbit, because there is always a finite ‘Lyapunov time’  $t_{Lyap}$  beyond which  $f^t(x(0))$  has lost all memory of the periodic orbit  $p$ . This problem is particularly severe in searches for ‘exact coherent structures’ embedded in turbulence, where even the shortest period solutions have to be computed to the (for everyday fluid dynamics excessive) machine precision [20, 21, 37] in order to complete the first return to the initial state.

Instead of relying on forward-in-time numerical integration, *global methods* for finding periodic orbits [8] view them as equations for the vector fields  $\dot{x}$  on spaces of closed curves. In numerical implementations one discretizes the periodic orbit  $p$  into sufficiently many short segments [8, 12, 13, 15, 24], and lists a point for each segment

$$p = (x_1, x_2, \dots, x_{n_p}). \quad (11.1)$$

For a  $d$ -dimensional discrete time map  $f$  obtained by cutting the flow by a set of Poincaré sections, with the periodic orbit  $p$  of discrete period  $n_p$ , every segment can be reconstructed by a short time integration, and satisfies

$$x_{k+1} = f(x_k), \quad (11.2)$$

to high accuracy, as for sufficiently short times the exponential instabilities are numerically controllable.

So, how accurate is such an orbit, i.e., how fast do errors grow for such globally specified orbit? In numerical work we know the cycle points only to a

finite precision

$$\hat{p} = (\hat{x}_1, \hat{x}_2, \dots, \hat{x}_{n_p}), \quad \hat{x}_k = x_k + \Delta x_k, \quad (11.3)$$

where  $x_k$  are the exact periodic orbit points. Define the error field by  $F(\hat{p}) = f(\hat{p}) - \sigma\hat{p}$ , an operator which compares the forward map of every point in  $\hat{p}$  with the next point  $\sigma\hat{p}$ , a  $(n_p \times d)$ -dimensional vector field obtained by stacking  $n_p$  state space points  $\hat{x}_k$

$$F(\hat{x}) = F \begin{pmatrix} \hat{x}_1 \\ \hat{x}_2 \\ \dots \\ \hat{x}_{n_p} \end{pmatrix} = \begin{pmatrix} \hat{x}_1 - \hat{f}_{n_p} \\ \hat{x}_2 - \hat{f}_1 \\ \dots \\ \hat{x}_{n_p} - \hat{f}_{n_p-1} \end{pmatrix}, \quad \hat{f}_k = f(\hat{x}_k), \quad (11.4)$$

which measures the misalignment of every finite forward-in-time segment  $f(\hat{x})_k$  with the next listed point  $\hat{x}_{k+1}$  on the periodic orbit.

By (11.2), the exact discretized cycle (11.1) is a zero of this vector field,  $F(x) = 0$ . Assuming that the  $d$ -dimensional vectors  $\Delta x_k$  are small in magnitude, and Taylor expanding the one discrete time-step map  $f$  to linear order around the exact solution,

$$f(x_t + \Delta x_t) = x_{t+1} + \mathbb{J}_t \Delta x + (\dots),$$

where

$$[\mathbb{J}_t]_{ij} = \frac{\partial f_i(x_t)}{\partial x_j}, \quad t = (1, 2, \dots, n_p), \quad i, j = (1, 2, \dots, d) \quad (11.5)$$

one finds that the neighborhood of entire cycle  $p$  is linearly deformed by the  $[n_p d \times n_p d]$  orbit Jacobian matrix

$$\Delta x' = \mathcal{J}(x) \Delta x, \quad \mathcal{J}_{ij}(x) = \frac{\partial F(x)_i}{\partial x_j}, \quad (11.6)$$

with

$$\mathcal{J} = 1 - \sigma \mathbb{J},$$

the one discrete time-step temporal  $[d \times d]$  diagonal Jacobian matrix  $\mathbb{J}$  evaluated on the entire cycle  $p$ , and  $\sigma$  the shift matrix

$$\sigma = \begin{pmatrix} 0 & & & & \mathbf{1} \\ \mathbf{1} & 0 & & & \\ & \mathbf{1} & 0 & & \\ & & \mathbf{1} & & \\ & & & \ddots & 0 \\ & & & & \mathbf{1} & 0 \end{pmatrix}, \quad \mathbb{J} = \begin{pmatrix} \mathbb{J}_1 & & & & \\ & \mathbb{J}_2 & & & \\ & & \mathbb{J}_3 & & \\ & & & \ddots & \\ & & & & \mathbb{J}_{n_p-1} \\ & & & & & \mathbb{J}_{n_p} \end{pmatrix}, \quad (11.7)$$

with  $\mathbf{1}$  in the upper right corner assuring periodicity,  $\sigma^{n_p} = \mathbf{1}$ .<sup>1</sup>

Next, we address two questions: (i) how is the high-dimensional orbit Jacobian matrix  $\mathcal{J}$  related to the temporal  $[d \times d]$  Jacobian matrix  $\mathbb{J}$ ? and (ii) how does one evaluate the orbit Jacobian matrix  $\mathcal{J}$ ?

<sup>1</sup>Predrag 2019-10-10: this is  $\sigma^{-1}$  shift operator as defined in ChaosBook.

### 11.1.1 Second-order difference equation

2

A second-order difference equation with constant coefficients has the form

$$x_{t+2} + p_1 x_{t+1} + p_2 x_t = 0 \quad (11.8)$$

Let  $x_{0,t} = x_t$ ,  $x_{1,t} = x_{t+1}$ , and rewrite this as a pair of coupled first-order difference equations

$$\begin{aligned} \mathbf{X}_{t+1} &= A \mathbf{X}_t, & \mathbf{X}_t &= (x_{0,t}, x_{1,t})^\top \\ A &= \begin{pmatrix} 0 & 1 \\ -p_2 & -p_1 \end{pmatrix}. \end{aligned} \quad (11.9)$$

The characteristic equation

$$\lambda^2 + p_1 \lambda + p_2 = 0 \quad (11.10)$$

can be obtained by substitution  $x_t = \lambda^n$  into the two-term recursion (11.8).

If  $\lambda_1 \neq \lambda_2$ ,  $\lambda_j$  real, then the solution of (11.8) is

$$x_t = c_1 \lambda_1^t + c_2 \lambda_2^t. \quad (11.11)$$

If  $\lambda_1 = \lambda_2 = \lambda$ , then the solution is

$$x_t = c_1 \lambda^t + c_2 t \lambda^t. \quad (11.12)$$

If  $\lambda_1 = \alpha + i\beta$ ,  $\lambda_2 = \alpha - i\beta$ , then the solution is

$$x_t = |\lambda|^t (c_1 \cos t\omega + c_2 \sin t\omega), \quad (11.13)$$

where  $\omega = \arctan(\beta/\alpha)$ . To solve such second-order difference equation, one has to specify initial conditions, for example  $x_0 = 1, x_1 = 0$ .

(Based on Elaydi [18])

### 11.1.2 Third-order difference equation

One can always reformulate an  $k$ -term recursion relation (8.125) as a set of  $k$  coupled first-order difference equations (delay equations). For example, one can rewrite the three-term recursion relation (third-order difference equation)

$$x_{t+3} + p_1 x_{t+2} + p_2 x_{t+1} + p_3 x_t = 0 \quad (11.14)$$

as three coupled first-order difference equations

$$\begin{aligned} x_{0,t+1} &= x_{1,t}, \\ x_{1,t+1} &= x_{2,t}, \\ x_{2,t+1} &= -p_3 x_{0,t} - p_2 x_{1,t} - p_1 x_{2,t}. \end{aligned} \quad (11.15)$$

---

<sup>2</sup>Predrag 2020-12-15: Transfer to ChaosBook.org. Once incorporated, remove from here)



where  $x_{0,t} = x_t, x_{1,t} = x_{t+1}, x_{2,t} = x_{t+2}$ . Compactly

$$\begin{aligned} X_{t+1} &= AX_t, & X_t &= (x_{0,t}, x_{1,t}, x_{2,t})^\top \\ A &= \begin{pmatrix} 0 & 1 & 0 \\ 0 & 0 & 1 \\ -p_3 & -p_2 & -p_1 \end{pmatrix}. \end{aligned} \quad (11.16)$$

The eigenvalues of  $A$  are the characteristic roots of (11.14), see (8.126) and (8.167).

The discrete time derivative of a periodic state  $X$  evaluated at the lattice site  $t$  is given by the *difference operator*

$$\dot{X}_t = \left[ \frac{\partial X}{\partial t} \right]_t = \frac{x_t - x_{t-1}}{\Delta t} \quad (11.17)$$

Eq. (11.16) can be viewed as a time-discretized, first-order ODE dynamical system

$$\dot{X} = v(X), \quad (11.18)$$

with the time increment set to  $\Delta t = 1$

(Based on Elaydi [17])

### 11.1.3 Bountis and Helleman 1981 paper Bount81

**2024-11-22 Predrag** We should add Bountis and Helleman [5] to the collection 2CL of our "bibles". Has so much stuff in it that it is probably Bountis PhD thesis.

**2016-11-11 Predrag** Bountis and Helleman On the stability of periodic orbits of two-dimensional mappings: " We apply our criterion and derive a sufficient stability condition for a large class of periodic orbits of the widely studied "standard mapping" describing a periodically 'kicked' free rotor. "

I find this paper quite interesting, because the computation of Floquet multipliers, i.e., linearization of periodically 'kicked' free rotor, is full of matrices that look like Laplacians + a diagonal term which varies along the periodic orbit. For cat maps this term is constant, essentially the stretching factor  $s$ . This might help with interpreting coupled 'kicked' rotor lattices.

This is presumably related to the block circulant stability matrices [1, 19] for spatially and temporally periodic orbits in coupled map lattices.

**2024-11-20 Han** Bountis and Helleman [5] studied the stability of two-dimensional mappings. They applied the Floquet-Bloch theorem to Hill's equation:

$$-\Delta x_{t+1} - \Delta x_{t-1} + d_t \Delta x_t = 0, \quad (11.19) \quad 2CL$$

which is exactly what we are doing. To study the stability they compute the determinant of the matrix:

$$H(k) = \begin{pmatrix} d_1 & -e^{ik} & 0 & \cdots & 0 & -e^{-ik} \\ -e^{-ik} & d_2 & -e^{ik} & \cdots & 0 & 0 \\ 0 & -e^{-ik} & d_3 & \cdots & 0 & 0 \\ \vdots & \vdots & \vdots & \ddots & \vdots & \vdots \\ 0 & 0 & 0 & \cdots & d_{n-1} & -e^{ik} \\ -e^{ik} & 0 & 0 & \cdots & -e^{-ik} & d_n \end{pmatrix} \quad (11.20)$$

which is the  $k$ -dependent submatrix of our block-diagonalized orbit Jacobian operator, and  $H(0)$  is the primitive cell orbit Jacobian matrix. They set  $\text{Det } H(k) = 0$  to see if the periodic solution is stable. The stability criterion they got is:

$$|2 + \text{Det } H(0)| \begin{cases} < 2 & \text{stable or "elliptic",} \\ > 2 & \text{unstable or "hyperbolic",} \\ = 2 & \text{marginally (un)stable, "parabolic".} \end{cases} \quad (11.21)$$

This is perhaps the hyperbolicity assumption from the orbit Jacobian matrix that we are looking for?

If  $k$  in  $\text{Det } H(k)$  is not set to 0, their equation (2.18a) is Xuanqi's one-dimensional equation (23.75),

$$\text{Det } H(k) = \text{Det } H(0) + 2 - 2 \cos(nk). \quad (11.22)$$

**2024-11-22 Predrag** They study the Hamiltonian second difference eq. (2.2), with  $\phi^3$  orbit Jacobian operator eq. (2.3). They first do stability analysis using forward in time  $[2 \times 2]$  Jacobian, eq. (2.4). Then they look at the global orbit Jacobian operator eq. (2.10), with stretching factor  $d_t$ . Then the Floquet's theorem [24,25] establishes that Hill's equation eq. (2.10-2.11) possesses two linearly independent solutions.

Hill determinant eq. (2.18).

The Floquet characteristic exponent  $\beta$  value (see [26] for difference equations, real versus complex determines whether the solutions of eq. (2.10) are bounded or not. They have a simple derivation of Xuanqi's Bloch theorem equation. We should use their stability criterion eq. (2.18). They say their  $\text{Det } H(0)$  is particularly simple, do not write it out explicitly, except [7,9] as a tr of the time-stepping Jacobian, in eq. (2.19). [...] the trace of such a product for 2-D Ising model in the presence of magnetic field was given as the integral eq. (2.20) in [27].

**2024-11-22 Predrag** Their Sect. III is an interesting investigation of the "border of order" for the standard map, starting with low "stretching" parameter  $K$  stable orbits. The longer the period of the orbit the sooner it may turn

unstable, as  $K$  increases. [...] The estimates obtained from eq. (3.23) are significantly lower than the actual values at which the corresponding orbit turns unstable. For instance, for the period 3 orbit, eq. (3.23) yields  $K_3 \approx 0.355$  while the actual orbit turns unstable at  $K_3 \approx 1.52$ .

**2024-11-22 Predrag** We might follow them, and replace the ‘stretching’ term by the humble ‘diagonal term’ notation,  $s_t \rightarrow d_t$ . We are not using  $d_z$  for anything, are we? 2CL

**2024-11-22 Predrag** Bountis and Helleman [5] Sec. IV *Stability criterion for dissipative mappings* considers area-contracting mappings, which model dissipative systems. Be careful about the sign of  $b$ ! For the temporal Hénon eqs. (4.2), (4.3). In their formulation, Hill’s difference equation eq. (4.6) leads to rescaled stretching terms  $b^{-1/2}d_t$  on the diagonal, eq. (4.10), with attendant definition of hyperbolicity eqs. (4.11).

Near a stable periodic orbit of the dissipative equation eq. (4.3) solutions are attracted to it, whereas in the conservative case nearby solutions forever "circle" around it. Eq. (A6) describes our temporal cat’s well-behaved harmonic sister, if anybody ever asks. The cacluation is cast into a recursion of ‘Dirichlet’ orbit Jacobian matrices (no ‘1’s in the corners).

In eq. (4.12) they redistribute the contraction factor symmetrically among the two shifts  $b^{1/2}r^{\pm 1}$ . That’s the form more natural for us - we should use it in the Tigers paper.

Then the ‘large dissipation limit  $|b| \rightarrow 0$ ’ is what we call the anti-integrable limit. Makes sense - it’s a repeller in the sense that the non-wondering set pushes the rest of states space away. Precedes Aubry [2, 3] by 9 years. (Wow !:)

Bountis and Helleman credit May (1976) [31]. But I cannot see why - his paper is all about 1-dimensional maps, nothing but words about ‘higher dimensions’.

For  $b$  small (are you listening, comrade X?), the orbit Jacobian matrix becomes diagonally dominant. This is convenient for calculating its eigenvalues (and hence its determinant) using iterative algorithms [32]. One may also approximate Hill determinant by expanding it in powers of  $b$ , eq. (13),

$$\det H_b + p^2(m\pi/2) = \sigma_p + b\sigma_1 + b^2\sigma_2 + \dots, \quad (11.23)$$

where  $\sigma_p$  is Predrag’s (6.63), (12.94), (24.333) and  $\sigma_j =$  [all terms obtained by deleting any pair of consecutive  $d_t, \dots$ ] cf. eq. (2.19) and footnote [33]. Compare this with (4.206).

**2019-01-28 Predrag** A whole book on the subject that we might have to have a look at: Magnus and Winkler [30] *Hill’s Equation*; (click here). There is also a more compact MagWin66.djvu version.

2024-11-22 Predrag Barouch [4] *On the Ising model in the presence of magnetic field* (1980), or related 2D Ising papers might be of interest.

Considers a square doubly-periodic  $N \times N$  nearest-neighbour interaction Ising lattice.

**References .**

[7] Hénon [26] (1969); see also R. H. G. Helleman, "Iterative Solution of a Stochastic Mapping," in *Statistical Mechanics and Statistical Methods*, edited by U. Landman (Plenum, New York, 1978).  
The expansion eq. (2.10) there is meant to be the standard expansion of a determinant.

[9] Greene [22, 23] (1979), (1968).

[24] Magnus and Winkler [30] *Hill's Equation* (1966).

[25] L. A. Pars, *Analytical Dynamics* (Wiley, New York, 1965), esp. See sects. 23.5, 23.6, and 26.3.

[26] T. Fort, *Finite Differences and Difference Equations in the Real Domain* (Oxford U. P., Oxford, 1948); also H. Levy and F. Lessamn, *Finite Difference Equations* (MacMillan, New York, 1961).

[27] Barouch [4] *On the Ising Model in the Presence of Magnetic Field* (1980).

[31] May [31] (1976); [\(click here\)](#)

[32] J. Wilkinson, *The Algebraic Eigenvalue Problem* (1965).

## 11.2 Repeats of a prime primitive cell

2021-06-11 Han

A periodic state  $X_p$  is *prime* if it is not a repeat of a smaller periodic state. The orbit Jacobian matrix of a period- $(rn)$  periodic state  $X$  which is a  $r$ -th repeat of a period- $n$  prime periodic state  $X_p$  has a tri-diagonal block circulant matrix form

$$\mathcal{J} = \begin{bmatrix} s_p & -\mathbf{r} & & & -\mathbf{r}^\top \\ -\mathbf{r}^\top & s_p & -\mathbf{r} & & \\ & & \ddots & \ddots & \ddots \\ & & & -\mathbf{r}^\top & s_p & -\mathbf{r} \\ -\mathbf{r} & & & & -\mathbf{r}^\top & s_p \end{bmatrix}, \tag{11.24}$$

where  $\mathbf{s}_p$ ,  $\mathbf{r}$  and  $\mathbf{r}^\top$  are  $[n \times n]$  block matrices

$$\mathbf{s}_p = \begin{bmatrix} d_0 & -1 & & & 0 \\ -1 & d_1 & -1 & & \\ & \ddots & \ddots & \ddots & \\ & & -1 & d_{n-2} & -1 \\ 0 & & & -1 & d_{n-1} \end{bmatrix},$$

$$\mathbf{r} = \begin{bmatrix} 0 & \cdots & 0 \\ & \ddots & \vdots \\ 1 & & 0 \end{bmatrix}, \quad \mathbf{r}^\top = \begin{bmatrix} 0 & & 1 \\ \vdots & \ddots & \\ 0 & \cdots & 0 \end{bmatrix}, \quad (11.25)$$

and  $\mathbf{r}$  and its transpose enforce the periodic bc's.

As  $\mathcal{J}$  is a block circulant matrix, it brought into a block diagonal form by a unitary transformation, with a repeating block along the diagonal.

Note that matrices  $\mathbf{s}_p$ ,  $\mathbf{r}$  and  $\mathbf{r}^\top$  are not circulant, the matrix  $\mathcal{J}$  is *not* a block circulant with circulant blocks [6, 7, 38].

### 11.2.1 Primitive cell repeats symmetrized

2021-06-11 Han

The tri-diagonal block matrix can be projected into the symmetric subspace of the shorter periodic state. As an example, take the shorter periodic state of period  $n = 4$ , and the long periodic state given by the shorter periodic state repeated 4 times. Then the reflection operator can also be written into the 16-



the orbit Jacobian matrix is projected into the symmetric subspace and it still has the tri-diagonal form:

$$\mathcal{J}P_{\hat{R}^+} = \begin{bmatrix} \frac{\mathbf{s}_p P_{\hat{R}^+}}{-\mathbf{r}^\top P_{\hat{R}^+}} & \frac{-\mathbf{r} P_{\hat{R}^+}}{\mathbf{s}_p P_{\hat{R}^+}} & 0 & \frac{-\mathbf{r}^\top P_{\hat{R}^+}}{0} \\ \frac{-\mathbf{r}^\top P_{\hat{R}^+}}{0} & \frac{\mathbf{s}_p P_{\hat{R}^+}}{-\mathbf{r}^\top P_{\hat{R}^+}} & \frac{-\mathbf{r} P_{\hat{R}^+}}{\mathbf{s}_p P_{\hat{R}^+}} & \frac{-\mathbf{r}^\top P_{\hat{R}^+}}{-\mathbf{r} P_{\hat{R}^+}} \\ 0 & \frac{-\mathbf{r}^\top P_{\hat{R}^+}}{0} & \frac{\mathbf{s}_p P_{\hat{R}^+}}{-\mathbf{r}^\top P_{\hat{R}^+}} & \frac{-\mathbf{r} P_{\hat{R}^+}}{\mathbf{s}_p P_{\hat{R}^+}} \\ \frac{-\mathbf{r} P_{\hat{R}^+}}{0} & 0 & \frac{-\mathbf{r}^\top P_{\hat{R}^+}}{\mathbf{s}_p P_{\hat{R}^+}} & \frac{\mathbf{s}_p P_{\hat{R}^+}}{-\mathbf{r} P_{\hat{R}^+}} \end{bmatrix}. \quad (11.28)$$

### 11.2.2 Repeats blog

**2016-09-28 Predrag** Amritkar *et al.* [1, 19] have investigated the stability of spatiotemporally periodic orbits in one- and two-dimensional coupled map lattices, i.e., 1 + 1 and 1 + 2 spatiotemporal dimensions. They derive conditions for the stability of periodic solutions in terms of the criteria for smaller orbits.

**2020-06-01 Predrag** Gade and Amritkar [19] *Spatially periodic orbits in coupled-map lattices* (a preliminary version of a part of this work was published as Amritkar, Gade, Gangal and Nandkumaran [1] *Stability of periodic orbits of coupled-map lattices*):

They are interested in stability, rather than our focus on instability.

They take CMLs with periodic orbits over  $[L \times T]_0$  and study the stability of their periodic orbit ‘replicas’  $[kL \times T]_0$  obtained by repeating  $[L \times T]_0$   $k$  times in the spatial direction, and show that orbit Jacobian matrix eigenvalues of the replica follow from the small periodic orbit. Not obvious, as the replica periodic orbit has more directions to be stable/unstable in. The trick is observing that the replica orbit Jacobian matrix is a block circulant with circulant blocks. The stability matrices for such periodic states are block circulant and hence can be brought onto a block diagonal form through a unitary transformation, their eq. (19).

The textbook they use is Davis [11] *Circulant Matrices*.

They write:

We call  $X_{n,r}$  the  $r$  replica solution of  $X_{n,1}$ . We address the problem of what can be stated about the stability properties of such spatially and temporally periodic solutions  $X_{n,r}$ , from the analysis of the stability matrices for  $X_{n,1}$  of the building blocks [1]. In other words the question is, What is the effect of enlargement of phase space and the couplings on the stability of the replica solutions?

(Their eq. (16) is our (4.304). Note their block-circulant matrix eq. (18))

The trick is observing that the replica orbit Jacobian matrix is a block circulant with circulant blocks. The stability matrices for such periodic states are block circulant and hence can be brought onto a block diagonal form through a unitary transformation, their eq. (19). The unitary matrix which affects the block diagonalization is a direct product of Fourier matrices of sizes  $[r \times r]$  and  $[n \times n]$ .

(2022-01-12 Predrag: but block matrix  $s_p$  in (4.304) is not circulant?)

The effects on the stability due to the enlargement of the state space and couplings manifest themselves through the eigenvalues of the additional blocks.

Our analysis leads to the following important conclusion about unstable periodic orbits. The matrix  $s_p$  appears as a block of the matrix  $\mathcal{J}$ . Hence, a solution built out of the replicas of unstable periodic orbits will also be unstable. Enlargement of state space and the effect of couplings cannot stabilize an unstable replica solution. The unstable periodic orbits are dense on the chaotic attractor. They are supposed to form the backbone of the dynamics on the attractor.

Our formalism will be useful if one tries to use unstable periodic orbits to analyze the spatially extended systems. It is clear that the replica solutions can be used to construct a hierarchy of unstable periodic orbits based on the orbits for building blocks. This may help in the organization of spatio-temporal chaos on the lines of arguments in ref. [9].

We have also discussed the two-dimensional extension of our formalism. From the convenient form in which the equations can be set, it is obvious that the generalization to higher dimensions is also possible. If one tries to analyze the problems similar to the ones analyzed here, in oscillator arrays this procedure can be easily used to simplify the computation.

Cited Gade and Amritkar [19] in LC21 as an early investigation of a lattice orbit Jacobian matrix. They did not know about 'Hill's formula.

**2016-09-28 Predrag** Zhilinet *al.* [39] *Spatiotemporally periodic patterns in symmetrically coupled map lattices* write: " The stability of the deduced orbits is investigated and we can reduce the problem to analyze much smaller matrices corresponding to the building block of their spatial periodicity or to the building block of the spatial periodicity of the original orbits from which we construct the new orbits. In the two-dimensional case the problem is considerably simplified. "

**2019-02-04 Predrag** A relative periodic block  $\hat{p}$  is always preperiodic to a periodic block whose period  $T_p = rT_{\hat{p}}$ , so you can always Fourier-transform this larger torus. But the right way of doing is acting relative periodic block  $\hat{p}$  with the translation  $r^r$  that makes it periodic, and then Fourier-transforming the minimal  $d$ -torus.

In this case we are still solving (24.155) except the rank  $2d$  tensor is no longer a circulant tensor.

**2019-02-04 Predrag** The orbit Jacobian matrix times the translation  $r^r$  is circulant, I believe. That is how we compute the Jacobian matrices of relative periodic orbits in ChaosBook. But we can still solve for the eigenvectors. I have shown how to compute the eigenvectors and eigenvalues in



(24.119–24.129) and verified this is correct for small blocks. In (24.130–24.136) I proved this is correct in any dimension. Using these eigenvectors we can diagonalize the orbit Jacobian matrix and get the inverse (Green’s function). The only problem is even though the counting formula is very compact, it seems to me that now it is hard to simplify the topological zeta function.

**2019-02-04 Predrag** I doubt it. In ChaosBook we show that after symmetry reduction, counting relative periodic orbits is not any harder than counting periodic orbits.

**2021-05-04 Predrag** Can one write the orbit Jacobian matrix of a repeat of a  $p$ -cycle as a product of  $p$ -cycle orbit Jacobian matrices?

**(2021-06-14 Predrag** This is now accomplished by the block matrix formulation (11.28).)

$$\begin{aligned} \mathcal{J}_p^{(2)} \mathcal{J}_p^{(1)} &= \begin{bmatrix} 1 & 0 & 0 & 0 & 0 & 0 \\ 0 & 1 & 0 & 0 & 0 & 0 \\ 0 & 0 & 1 & 0 & 0 & 0 \\ 0 & 0 & 0 & \phi_0 & 1 & 1 \\ 0 & 0 & 0 & 1 & \phi_1 & 1 \\ 0 & 0 & 0 & 1 & 1 & \phi_2 \end{bmatrix} \begin{bmatrix} \phi_0 & 1 & 1 & 0 & 0 & 0 \\ 1 & \phi_1 & 1 & 0 & 0 & 0 \\ 1 & 1 & \phi_2 & 0 & 0 & 0 \\ 0 & 0 & 0 & 1 & 0 & 0 \\ 0 & 0 & 0 & 0 & 1 & 0 \\ 0 & 0 & 0 & 0 & 0 & 1 \end{bmatrix} \\ &\neq \begin{bmatrix} \phi_0 & 1 & 0 & 0 & 0 & 1 \\ 1 & \phi_1 & 1 & 0 & 0 & 0 \\ 0 & 1 & \phi_2 & 1 & 0 & 0 \\ 0 & 0 & 1 & \phi_0 & 1 & 0 \\ 0 & 0 & 0 & 1 & \phi_1 & 1 \\ 1 & 0 & 0 & 0 & 1 & \phi_2 \end{bmatrix}, \end{aligned} \quad (11.29)$$

Another try:

$$\begin{aligned} \mathcal{J}_p^{(2)} \mathcal{J}_p^{(1)} &= \begin{bmatrix} 1 & 0 & 0 & 0 & 0 & 1 \\ 0 & 1 & 0 & 0 & 0 & 0 \\ 0 & 0 & 1 & 1 & 0 & 0 \\ 0 & 0 & 1 & \phi_0 & 1 & 0 \\ 0 & 0 & 0 & 1 & \phi_1 & 1 \\ 1 & 0 & 0 & 0 & 1 & \phi_2 \end{bmatrix} \begin{bmatrix} \phi_0 & 1 & 0 & 0 & 0 & 1 \\ 1 & \phi_1 & 1 & 0 & 0 & 0 \\ 0 & 1 & \phi_2 & 1 & 0 & 0 \\ 0 & 0 & 1 & 1 & 0 & 0 \\ 0 & 0 & 0 & 0 & 1 & 0 \\ 1 & 0 & 0 & 0 & 0 & 1 \end{bmatrix} \\ &\neq \begin{bmatrix} \phi_0 + 1 & 1 & 0 & 0 & 0 & 2 \\ 1 & \phi_1 & 1 & 0 & 0 & 0 \\ 0 & 1 & \phi_2 + 1 & 2 & 0 & 0 \\ 0 & 0 & 1 & \phi_0 + 1 & 1 & 0 \\ 0 & 0 & 0 & 1 & \phi_1 & 1 \\ \phi_0 + \phi_2 & 0 & 0 & 0 & 1 & \phi_2 + 1 \end{bmatrix}, \end{aligned} \quad (11.30)$$

(partly wrong, but does not matter), so orbit Jacobian matrices do not multiply.

But they do not add up, either, cannot reconcile the small block periodic bc’s with the repeated block bc’s. Defeated again.

**2021-08-22 Predrag** I believe was wrong in asking that we look at the stability of repeats of a shorter period block, eq. (4.304) above. That does not arise in the new formulation of periodic orbit theory; the Hill determinant is computed on any periodic state  $X$  in the orbit  $\mathcal{M}_c$  of a periodic state  $X_c$ . There are only orbits, nothing is computed on repeats. There should be no repeats summation in the derivation of zeta functions.

**2022-01-22 Predrag** believes today that he was very wrong on **2021-08-22** :)

The projection operator on the  $k$ th Fourier mode is

$$P_k = \prod_{j \neq k} \frac{r - \omega_j \mathbf{1}}{\omega_k - \omega_j}. \quad (11.31)$$

The set of the projection operators is complete,

$$\sum_k P_k = \mathbf{1}, \quad (11.32)$$

and orthonormal

$$P_k P_j = \delta_{kj} P_k \quad (\text{no sum on } k). \quad (11.33)$$

[TO BE CONTINUED]

### 11.3 Spatiotemporal lattice

In spatiotemporal settings,  $\mathbb{J}_p$  can be defined only for finite numbers of spatial sites, and it gets funkier and funkier as the spatial direction increases (that is why we are able to work only with very small spatial domain Kuramoto–Sivashinsky discretizations). But, as shown for the spatiotemporal cat in ref. [10],  $\text{Det } \mathcal{J}_p$  works just fine on any spatiotemporal torus. In particular, for any invariant 2-torus Kuramoto–Sivashinsky discretization.

### 11.4 Noether's theorem

**2018-05-04 Predrag** Moved this section to spacetime continuous systems  
spatiotemp/blog.tex

## 11.5 Stability blog

**2023-06-07 Predrag** *ChaosBook 4.7 Neighborhood volume* computes the determinant of the forward-in-time jacobian  $J^t(x_0)$  (not the Hill determinant) by the continuity equation (evolution of density in time) which relates it to the time average of the divergence of the state space velocity.

1. Rewrite this continuous time formula as a discrete temporal lattice formula.
2. Is there a Hill's formula relating it to  $\text{Det } \mathcal{J}$ ?
3. Can one use Euler-Lagrange equation to get an equation for Hill determinant  $\text{Det } \mathcal{J}$  in the infinite spacetime, Bravais-lattice limit?

**2019-10-10 Predrag** Reread Lindstedt-Poincaré [34] Fourier method papers by Viswanath [35, 36]; his most accurate resolution of fractal structure of the Lorenz attractor. It is a very thin fractal, stable manifold thickness is of the order  $10^{-4}$ . He has computed all 111011 periodic orbits corresponding to symbol sequences of length 20 or less, all with 14 digits accuracy.

**2019-10-13 Predrag** Viswanath [34] writes: "The Lindstedt-Poincaré technique uses a nearby periodic orbit of the unperturbed differential equation as the first approximation to a perturbed differential equation. One of the examples presents what is possibly the most accurate computation of Hill's orbit of lunation since its justly celebrated discovery in 1878.

The eigenvalues excluding 1 are called characteristic multipliers.

AUTO [14, 15] collocation method, Guckenheimer and Meloon [24], Choe and Guckenheimer [8] all set up their periodic orbits as in (11.4). Since the linear systems that they form are sparse, the cost of solution is only linear in the number of mesh points.

There are other variants of this forward multiple shooting algorithm: one is a symmetric multiple shooting algorithm and another is based on Hermite interpolation.

He dismisses harmonic balance methods for computing periodic orbits (Lau, Cheung and Wu [?15], and Ling and Wu [?16]) as being too expensive, of order  $O(n^3)$ , where the Fourier series are of width  $n$ , whereas his method is of order  $O(n \ln n)$ .

Wiswanath algorithm for computing periodic orbits is a "polyphony of three themes:" the Lindstedt-Poincaré technique from perturbation theory, Newton's method for solving nonlinear systems, and Fourier interpolation.

To compute  $n$  Fourier coefficients of  $x(t)$ , the fast Fourier transform (FFT) is applied to the function evaluated at  $n$  equispaced points in  $[0, 2\pi)$ . The width  $n$  of the Fourier series must be sufficiently large to pick up all the coefficients above a desired accuracy threshold.

If  $(x_1, x_2, \dots, x_m)$  are  $2\pi$  periodic, so is  $f(x_1, x_2, \dots, x_m)$ . To obtain its Fourier series from those of the  $x_i$ , interpolate  $x_i$  at equispaced points, evaluate  $f$  at those points, and apply the FFT. The inverse FFT can be used to interpolate a Fourier series at equispaced points [33]. In  $d$  state space dimensions, one needs  $d$  Fourier series, one for each coordinate in  $\mathbb{R}^d$ .

His 4 coupled Josephson junctions (10-dimensional state space) uses 64 Fourier modes.

”

The implementation of the algorithm must pay attention to the possibility of aliasing.

**2019-10-13 Predrag** Viswanath [35] writes: “ The representation of periodic orbits by Fourier series is both accurate and efficient because, when a periodic orbit is analytic, the Fourier coefficients decrease exponentially fast, making its Fourier representation compact.

”

**2019-10-13 Predrag** Guckenheimer and Meloon [24] set up their periodic orbits as in (11.4), and have the same  $d$ -dimensional orbit Jacobian matrix variant of (12.61), but with extra, time-direction fixing diagonals, as they are looking at continuous time flows. Instead of the cyclic group, they use LU factorization. They get  $1 - J_p$  matrix.

**2019-10-14 Predrag** Notes on Choe and Guckenheimer [8], a clear and enjoyable read:

Instead of relying on forward-in-time numerical integration, *global methods* for finding periodic orbits view the vector field as an equation on a function space of closed curves. Here  $f$  is a Lipschitz continuous vector field on a smooth manifold  $\mathcal{M}$ , and  $p : S^1 \rightarrow \mathcal{M}$  is a  $C^1$  closed curve in  $\mathcal{M}$ .

Computer implementation of global methods for computing periodic orbits requires discretization of closed curves and approximation of the periodic orbit equations. One defines finite-dimensional submanifolds of the space of closed curves and approximates the periodic orbit equations as a map defined on this space.

They keep the number of discretization points fixed and increase the accuracy by *automatic differentiation*, constructing the Taylor series of trajectories at discretization points. They also compute stability matrix derivatives of the Taylor series coefficients with respect to the state space variables for use in the Newton iteration. As the degree of the computed Taylor series increases, their curves converge since the trajectories are analytic.

The Taylor series is obtained by repeated differentiation of the differential equation  $\dot{x} = v(x)$  and recursive substitution of the values of derivatives

$x^{(k)}(t)$  of increasing degree. To make the approximate curve smooth and continuous, they use a somewhat funky interpolation function they call  $\beta(t)$ .

[Predrag’s aside: hopefully our strategy of using Fourier transforms has much faster convergence than Taylor series. Even if one wants polynomials, I suspect Chebyshev or Hermite or some other orthogonal sets would be better.]

Indeed, the Hermite splines, interpolating functions that arc polynomials of degree  $2d + 1$ , gave the best results in their computations.

They eliminate the time translation marginal eigenvalue by using sets of Poincaré section hyperplanes transverse to the vector field, and solving for points that lie on the intersection of Poincaré section with the periodic orbit. They use the orthogonal complements to the vector field  $v(x_i)$  at the mesh points  $x_i$ . The normal subspace to the vector field at  $x_i$ , is determined by computing the QR factorization of the  $[d \times (d + 1)]$  matrix. There is a whole PhD thesis worth of detail here.

The structure of the Jacobian matrices that are used in the root finding has a simple sparsity pattern that can be exploited in its inversion. Explicit inversion of this block matrix in terms of the inverses of the individual blocks yields a relationship between the regularity of the root finding problem and the hyperbolicity of the periodic orbit. They relate the regularity of orbit Jacobian matrix  $\mathcal{J}$  to the periodic orbit’s monodromy matrix, their sect. 3. *Analysis*, using LU factorization. They show that  $\mathcal{J}$  is invertible (needed for Newton schemes) if and only if the monodromy matrix  $M$  of the Poincaré section does not have 1 as an eigenvalue.

Since their methods produce smooth approximations to periodic orbits, they can evaluate the distance between the tangent vectors to a computed curve and the vector field along that curve. These error estimates enable them to develop strategies for mesh refinement that balance the error in different mesh intervals. Since the approximating solution in a mesh interval is determined entirely by its endpoints, mesh refinement is a simple process and does not change the structure of the discretized periodic orbit equations.

They define the error field (11.4) as operator  $F(p) = f(p) - \sigma p$ , with periodic orbits solutions satisfying  $F = 0$ .  $p$  are analytic curves, but Choe-Guckenheimer approximations are not analytic.

The starting data is an  $N$ -point *discrete closed curve* (11.3), a cyclically ordered collection of  $N$  points. Given a map  $S$ , on seeks seek systems of  $(n_p \times d)$ -dimensional vector field equations  $F_S = 0$  whose solutions yield good approximations to periodic orbits of  $f$ . The convergence is takes place on a fixed mesh, but with increasing degree  $d$  of map  $S_d$ . They compute the orbit Jacobian matrix  $\mathcal{J}$  and invert it to use in the Newton routine, but do not mention or discuss computing  $\det \mathcal{J}$ .

They test their algorithm with the Hodgkin-Huxley equations, a moderately stiff 4-dimensional vector field with strongly stable directions. They do not boast, but their residual errors are of order  $10^{-11}$ .

**2022-05-06 Predrag** Check out Wolfram Demonstrations Project [Learning Newton's Method](#).

**2022-05-06 Predrag** Check out Kevin Zeng, Alec J. Linot and Michael D. Graham *Data-driven control of spatiotemporal chaos with reduced-order neural ODE-based models and reinforcement learning* [arXiv:2205.00579](#): We combine data-driven nonlinear manifold dynamics with deep RL to control spatiotemporal chaos in the Kuramoto–Sivashinsky equation. The approach discovers and stabilizes a low-dissipation steady state!

Linot and Graham [29] *Data-driven reduced-order modeling of spatiotemporal chaos with neural ordinary differential equations*, (2022)

Also: M. A. Bucci, O. Semeraro, A. Allauzen, G. Wisniewski, L. Cordier, and L. Mathelin. *Control of chaotic systems by deep reinforcement learning*, Proceedings of the Royal Society A, 475(2231):20190351, 2019 [DOI](#).

**2022-07-11 Predrag** Study these 2 papers which compute and discuss Hessian spectra:

Le Cun, Kanter and Solla [27] *Second order properties of error surfaces: Learning time and generalization* (1990), ([click here](#)).

Le Cun, Kanter and Solla [28] *Eigenvalues of covariance matrices: Application to neural-network learning* (1991), ([click here](#)).

The dynamical behavior of learning algorithms based on the minimization of the learning error function  $E(W)$  through gradient descent is controlled by the second-order properties of  $E(W)$ , as represented by its Hessian matrix  $H$ . The cost function is quadratic in  $W$ , and can be rewritten in terms of a symmetric non-negative covariance matrix (or Hessian) of the inputs.

The diagonalization of  $R$  provides a diagonal matrix  $A$  formed by its eigenvalues and a matrix  $Q$  formed by its eigenvectors.

The spectral density follows from a standard Fresnel representation for the determinant of a symmetric matrix.

**2023-01-18 Predrag** It's not clear why we should care about the eigen-values, -vectors of an orbit Jacobian matrix  $\mathcal{J}$ . Perhaps they are natural because of the translation invariance, which lead to the diagonalization of  $\mathcal{J}$  on the reciprocal lattice. Eigenvectors are the natural basis if one repeats the same map od state space onto itself time after time, but orbit Jacobian matrices do not have such multiplicative structure. So far we had only used them to derive and evaluate their Hill determinants, but there are many ways of computing determinants. In particular, QR (used much by

Xiong Ding), SVD, and other factorizations might offer efficient numerical evaluations methods.

One such widely used method is *singular value decomposition* (here in part paraphrased from the [wiki](#), restricted to our case of real square matrices)

Singular value decomposition (SVD) factorizes *any* real square  $[m \times m]$  matrix as  $\mathbf{M} = \mathbf{U}\mathbf{\Sigma}\mathbf{V}^\top$ , where matrices  $\mathbf{U}$  and  $\mathbf{V}^\top$  are rotations and/or reflections,  $\mathbf{V}^\top$  is the transpose of  $\mathbf{V}$ , and  $\mathbf{\Sigma}$  is a diagonal matrix with positive real numbers on the diagonal. If  $\mathbf{M}$  has a positive determinant, then  $\mathbf{U}$  and  $\mathbf{V}^\top$  can be chosen to be pure rotations. If the determinant is negative, one of them has to include a reflection.

The diagonal entries  $\sigma_j = \Sigma_{jj}$  are the *singular values* of  $\mathbf{M}$ . The columns of  $\mathbf{U}$  and the columns of  $\mathbf{V}$  are left-singular vectors and right-singular vectors of  $\mathbf{M}$ , respectively. They form two sets of orthonormal bases  $u_1, \dots, u_m$  and  $v_1, \dots, v_m$ , typically sorted so that  $\sigma_j \geq \sigma_{j+1} > 0$  (we assume  $\det \mathbf{M} \neq 0$ ). The singular value decomposition can be written as

$$\mathbf{M} = \sum_{j=1}^m \mathbf{u}_j \sigma_j \mathbf{v}_j^\top. \quad (11.34)$$

The singular values can be interpreted as the lengths of the semiaxes of an hyper-ellipse in  $m$  dimensions. Singular value is the length of a semiaxis, while singular vector is its direction.

The eigenvalue decomposition and SVD of  $\mathbf{M}$  differ: (a) the eigenvalue decomposition is  $\mathbf{M} = \mathbf{U}\mathbf{D}\mathbf{U}^{-1}$ , where  $\mathbf{U}$  is not necessarily unitary and  $\mathbf{D}$  is not necessarily positive semi-definite, while (b) the SVD is  $\mathbf{M} = \mathbf{U}\mathbf{\Sigma}\mathbf{V}^\top$ , where  $\mathbf{\Sigma}$  is diagonal and positive semi-definite, and  $\mathbf{U}$  and  $\mathbf{V}$  are rotation matrices that are not necessarily related except through the matrix  $\mathbf{M}$ . Thus the SVD decomposition represents any linear transformation of  $\mathbb{R}^m$  as three successive transformations: a rotation / reflection  $\mathbf{V}^\top$ , followed by a coordinate-by-coordinate scaling  $\mathbf{\Sigma}$ , followed by another rotation / reflection  $\mathbf{U}$ .

While only non-defective square matrices have an eigenvalue decomposition, *any*  $[m \times m]$  matrix has a SVD.

**2023-01-18 Predrag** Pondering a possible temporally asymmetric ‘directed’, ‘dissipative’ propagator, quantum partition function (modeled after QFT charged particle and fermion propagators):

$$Z[\mathbf{J}, \bar{\mathbf{J}}] = \int d\mathbf{X} e^{i(S[\mathbf{X}, \bar{\mathbf{X}}] + \mathbf{X} \cdot \bar{\mathbf{J}} + \bar{\mathbf{X}} \cdot \mathbf{J})}, \quad d\mathbf{X} = \prod_z \frac{dx_z}{\sqrt{2\pi}}, \quad d\bar{\mathbf{X}} = \prod_z d\bar{x}_z, \quad (11.35)$$

‘semiclassical’ approximation

$$S[\mathbf{X}, \bar{\mathbf{X}}] = S[\mathbf{X}_c, \bar{\mathbf{X}}_c] + (\bar{\mathbf{X}} - \bar{\mathbf{X}}_c)^\top \mathcal{J}_c (\mathbf{X} - \mathbf{X}_c) + \dots$$

orbit Jacobian matrix is asymmetric

$$(\mathcal{J}_c)_{z'z} = \left. \frac{\delta^2 S[\mathbf{X}]}{\delta \bar{x}_{z'} \delta x_z} \right|_{\mathbf{X}=\mathbf{X}_c}$$

Fourier integral over  $n$  lattice sites, neighborhood of deterministic solution  $\mathbf{X}_c$  gives a Fourier series Dirac delta, (FIX THIS!)

$$\int_c [d\mathbf{X}] e^{\frac{i}{\hbar} \frac{1}{2} \mathbf{X}^\top \mathcal{J}_c \mathbf{X}} = \frac{1}{|\text{Det } \mathcal{J}_c|} \quad (11.36)$$

But forget semiclassics for now. Probably start with the (two?) Euler–Lagrange equation(s), enforce by deterministic delta functions; use SVD to diagonalize  $\mathcal{J}_c$ , get the correct Hill determinant.

Test on

1. temporal Bernoulli
2. dissipative  $b \neq -1$  temporal Hénon, see (3.6), (3.7), (3.60), (3.89), (3.92)



## 11.6 Generating function literature

For the latest entry, go to the bottom of this section

**2016-11-11 Predrag** I still cannot get over how elegant the Gutkin-Osipov [25] spatiotemporal cat is. It is *linear!* ( mod 1, that is - the map is continuous for integer  $s$ ). A 1-dimensional cat map has a Hamiltonian (2.32), and they have written down the 2-dimensional Lagrangian, their Eq. (3.1) (or the “generating function”, as this is a mapping). Their spatiotemporal cat generating function is defined on a spatiotemporal cylinder, infinite in time direction,

$$S(q_t, q_{t+1}) = - \sum_{n=1}^N q_{nt} q_{1+n,t} - \sum_{n=1}^N q_{nt} (q_{n,t+1} + m_{n,t+1}^q) + \frac{a}{2} \sum_{n=1}^N q_{nt}^2 + \frac{b}{2} \sum_{n=1}^N (q_{n,t+1} + m_{n,t+1}^q)^2 - m_{n,t+1}^p q_{n,t+1}, \quad (11.37)$$

where  $q_t = \{q_{nt}\}_{n=1}^N$  is a spatially periodic state at time  $t$ , with  $q_{nt}$  being the coordinate of  $n$ th “particle”  $n = 1 \dots N$  at the moment of time  $t \in \mathbb{Z}$ , and  $m_{n,t+1}^q, m_{n,t+1}^p$  are integer numbers which stand for winding numbers along the  $q$  and  $p$  directions of the  $2N$ -torus. Note that  $x_{1+n,t} = x_{1+(n \bmod N),t}$ . The coefficients  $a, b, s = a + b$  are integers which they specify. Gutkin and Osipov refer to the map generated by the action (11.37) as non-perturbed *coupled cat map*, and to an invariant 2-torus  $p$  as a “many-particle periodic orbit” (MPO) if  $q_{nt}$  is doubly-periodic, or “closed,” i.e.,

$$q_{nt} = q_{n+L,t+T}, \quad n = 1, 2, \dots, L, \quad t = 1, 2, \dots, T.$$

**2D symbolic representation** Encode each invariant 2-torus (many-particle periodic orbit)  $p$  by a two dimensional (periodic) lattice of symbols  $a_{nt}, (nt) \in \mathbb{Z}^2$ , where symbols  $a_{nt}$  belong to some alphabet  $\mathcal{A}$  of a small size. Each invariant 2-torus  $p$  is represented by  $L \times T$  toroidal array of symbols:

$$\bar{\mathcal{A}}_p = \{a_{nt} | (nt) \in \mathbb{Z}_{LT}^2\}.$$

The Hamiltonian equations of motion can be generated using (8.69) but who needs them? Remember, a field theorist would formulate a space-time symmetric field theory in a Lagrangian way, with the invariant action.

**2016-11-11 Predrag** Percival and Vivaldi [32] state the Lagrangian variational principle in Sect. 6. *Codes, variational principle and the static model:*<sup>3</sup>

<sup>3</sup>Predrag 2016-11-12: eventually move to remark 15.1

The Lagrangian variational principle for the sawtooth map on the real line states that the action sum (8.89) is stationary with respect to variations of any finite set of configurations  $x_t$ . Their discussion of how “elasticity” works against the “potential” is worth reading. For large values of stretching parameter  $s$ , the potential wins out, and the state  $x_t$  falls into the  $m_t$ th well: “the code may be considered as a labelling of the local minima of the Lagrangian variational principle.”

Dullin and Meiss [16] *Stability of minimal periodic orbits* does the calculations in great detail.

**2016-11-11 Predrag** “mean action” = the action divided by the period

**2018-12-07 Predrag** as shown in (copied here from ChaosBook) example 2.7, example 2.8, and example 2.9 Hamiltonian spectral determinant and dynamical zeta function have a special form. Recheck against our cat map  $1/\zeta_{AM}$ .

**2019-10-14 Predrag** The Jacobi operator acts on a discrete periodic lattice as

$$Lu(t) = a(t+1)u(t+1) + b(t)u(t) + a(t-1)u(t-1),$$

where  $a(t)$  and  $b(t)$  are real valued for each  $t \in \mathbb{Z}$ , and  $M$ -periodic in  $t$ . Jacobi operators are the discrete analogue of Sturm–Liouville operators, with many similarities to Sturm–Liouville theory.

**2022-12-23 Predrag** Lego blocks for Matt to play with

1. which pairs fit spacewise, timewise by coordinate translations?
2. which pairs fit spacewise by coordinate reflections?
3. which pairs fit by Galilean field translations
4. what are their orbit Jacobian matrices?
5. what are their Hill determinants?
6. what are their orbit Jacobian matrices on reciprocal lattice?

**2023-04-18 Predrag** Check this out: Kartik Krishna, Steven L. Brunton and Zhuoyuan Song *Finite Time Lyapunov Exponent Analysis of Model Predictive Control and Reinforcement Learning*, [arXiv:2304.03326](https://arxiv.org/abs/2304.03326)

**2022-02-19 Predrag** JAX is said to make evaluation of Jacobians trivial.

## References

- [1] R. E. Amritkar, P. M. Gade, A. D. Gangal, and V. M. Nandkumar, “Stability of periodic orbits of coupled-map lattices”, *Phys. Rev. A* **44**, R3407–R3410 (1991).

- [2] S. Aubry, “Anti-integrability in dynamical and variational problems”, *Physica D* **86**, 284–296 (1995).
- [3] S. Aubry and G. Abramovici, “Chaotic trajectories in the standard map. The concept of anti-integrability”, *Physica D* **43**, 199–219 (1990).
- [4] E. Barouch, “On the Ising model in the presence of magnetic field”, *Physica D* **1**, 333–337 (1980).
- [5] T. Bountis and R. H. G. Helleman, “On the stability of periodic orbits of two-dimensional mappings”, *J. Math. Phys* **22**, 1867–1877 (1981).
- [6] B. L. Buzbee, G. H. Golub, and C. W. Nielson, “On direct methods for solving Poisson’s equations”, *SIAM J. Numer. Anal.* **7**, 627–656 (1970).
- [7] M. Chen, “On the solution of circulant linear systems”, *SIAM J. Numer. Anal.* **24**, 668–683 (1987).
- [8] W. G. Choe and J. Guckenheimer, “Computing periodic orbits with high accuracy”, *Computer Meth. Appl. Mech. and Engin.* **170**, 331–341 (1999).
- [9] P. Cvitanović, R. Artuso, R. Mainieri, G. Tanner, and G. Vattay, *Chaos: Classical and Quantum* (Niels Bohr Inst., Copenhagen, 2024).
- [10] P. Cvitanović and H. Liang, *A chaotic lattice field theory in two dimensions*, In preparation, 2024.
- [11] P. J. Davis, *Circulant Matrices*, 2nd ed. (Amer. Math. Soc., Providence RI, 1979).
- [12] X. Ding, H. Chaté, P. Cvitanović, E. Siminos, and K. A. Takeuchi, “Estimating the dimension of the inertial manifold from unstable periodic orbits”, *Phys. Rev. Lett.* **117**, 024101 (2016).
- [13] X. Ding and P. Cvitanović, “Periodic eigendecomposition and its application in Kuramoto-Sivashinsky system”, *SIAM J. Appl. Dyn. Syst.* **15**, 1434–1454 (2016).
- [14] E. J. Doedel, “Nonlinear numerics”, *J. Franklin Inst.* **334**, 1049–1073 (1997).
- [15] E. J. Doedel, A. R. Champneys, T. F. Fairgrieve, Y. A. Kuznetsov, B. Sandstede, and X. Wang, *AUTO: Continuation and Bifurcation Software for Ordinary Differential Equations* (2007).
- [16] H. R. Dullin and J. D. Meiss, “Stability of minimal periodic orbits”, *Phys. Lett. A* **247**, 227–234 (1998).
- [17] S. Elaydi, *An Introduction to Difference Equations*, 3rd ed. (Springer, Berlin, 2005).
- [18] S. N. Elaydi, *Discrete Chaos* (Chapman and Hall/CRC, 2007).
- [19] P. M. Gade and R. E. Amritkar, “Spatially periodic orbits in coupled-map lattices”, *Phys. Rev. E* **47**, 143–154 (1993).
- [20] J. F. Gibson, *Channelflow: A spectral Navier-Stokes simulator in C++*, tech. rep., [Channelflow.org](http://Channelflow.org) (U. New Hampshire, 2019).

- [21] J. F. Gibson, J. Halcrow, and P. Cvitanović, “Visualizing the geometry of state-space in plane Couette flow”, *J. Fluid Mech.* **611**, 107–130 (2008).
- [22] J. M. Greene, “Two-dimensional measure-preserving mappings”, *J. Math. Phys.* **9**, 760 (1968).
- [23] J. M. Greene, “A method for determining a stochastic transition”, *J. Math. Phys.* **20**, 1183–1201 (1979).
- [24] J. Guckenheimer and B. Meloon, “Computing periodic orbits and their bifurcations with automatic differentiation”, *SIAM J. Sci. Comput.* **22**, 951–985 (2000).
- [25] B. Gutkin and V. Osipov, “Classical foundations of many-particle quantum chaos”, *Nonlinearity* **29**, 325–356 (2016).
- [26] M. Hénon, “Numerical study of quadratic area-preserving mappings”, *Quart. Appl. Math.* **27**, 291–312 (1969).
- [27] Y. Le Cun, I. Kanter, and S. A. Solla, Second order properties of error surfaces: Learning time and generalization, in *Adv. neural information processing systems*, Vol. 3, edited by R. P. Lippmann, J. Moody, and D. Touretzky (1990).
- [28] Y. Le Cun, I. Kanter, and S. A. Solla, “Eigenvalues of covariance matrices: Application to neural-network learning”, *Phys. Rev. Lett.* **66**, 2396–2399 (1991).
- [29] A. J. Linot and M. D. Graham, “Data-driven reduced-order modeling of spatiotemporal chaos with neural ordinary differential equations”, *Chaos* **32**, 073110 (2022).
- [30] W. Magnus and S. Winkler, *Hill’s Equation* (Dover, 1966).
- [31] R. M. May, “Simple mathematical models with very complicated dynamics”, *Nature* **261**, 459–467 (1976).
- [32] I. Percival and F. Vivaldi, “A linear code for the sawtooth and cat maps”, *Physica D* **27**, 373–386 (1987).
- [33] L. N. Trefethen, *Spectral Methods in MATLAB* (SIAM, Philadelphia, 2000).
- [34] D. Viswanath, “The Lindstedt-Poincaré technique as an algorithm for finding periodic orbits”, *SIAM Rev.* **43**, 478–496 (2001).
- [35] D. Viswanath, “Symbolic dynamics and periodic orbits of the Lorenz attractor”, *Nonlinearity* **16**, 1035–1056 (2003).
- [36] D. Viswanath, “The fractal property of the Lorenz attractor”, *Physica D* **190**, 115–128 (2004).
- [37] A. P. Willis, *Openpipeflow: Pipe flow code for incompressible flow*, tech. rep., [openpipeflow.org](http://openpipeflow.org) (U. Sheffield, 2014).
- [38] W. L. Wood, “Periodicity effects on the iterative solution of elliptic difference equations”, *SIAM J. Numer. Anal.* **8**, 439–464 (1971).

- [39] Q. Zhilin, A. Gangal, M. Benkun, and T. Gang, “Spatiotemporally periodic patterns in symmetrically coupled map lattices”, *Phys. Rev. E* **50**, 163–170 (1994).

# Chapter 12

## Hill's formula

### 12.1 An overview over “Hill's formulas”

To be written up as Liang and Cvitanović LC22 [44] *A derivation of Hill's formulas* (2024), [siminos/hill/](https://siminos.github.io/hill/).

A succinct explanation of the Hill's formula:

If you evaluate stability of the 3-term recurrence (16.81) on a periodic lattice you get the orbit Jacobian matrix  $\mathcal{J}$ ; if you evaluate it by multiplying the ‘two-configuration representation’ matrix  $J$ , you get the ‘time evolution’ side of the Hill's formula.

We should emphasize that, while discovered first in Lagrangian setting, Hill's formulas are much more general, they apply also to dissipative dynamical systems as well, see

CL18 [sect. 1.5](#) *Stability of an orbit vs. its time-evolution stability*

CL18 [appendix C](#) *Spatiotemporal stability*

[sect. 12.2](#) *Generating functions; action*

[sect. 12.4](#) *Hill's formula, Lagrangian setting*

[sect. 12.5](#) *Spatiotemporal cat Hill's formula*

[sect. 12.6](#) *Hill's formula for relative periodic orbits*

[sect. 12.8](#) *Han's temporal cat Hill's formula*

[sect. 12.10](#) *Han's spatiotemporal cat Hill's formula*

[sect. 12.10.1](#) *Han's relative-periodic Hill's formula*

[sect. 12.11](#) *Han's Hénon map Hill's formula*

All work in this chapter is done for finite-dimensional matrices.

‘Hill's formula’ for infinite-dimensional linear operators is called the ‘Gel'fand-Yaglom’ formula, which relates the zeta-regularized determinant of a differential operator to the solution of an initial value problem, a relation between a Fredholm determinant and a zeta-regularized determinants, see Ludwig and Shea in

[sect. 19.3](#) *Zeta function regularization*

Proposal for possible inclusion into Hill's formula paper ref. [44] (but only after the current material is written up in publication-ready form!):

After deriving the primitive cell formulas, take the continuous time limit of the temporal 1-dimensional lattice, derive the continuous time Hill-Gel'fand-Yaglom formula for ODEs.

Apply that to what most  $N$ -body literature [45, 63] computes, continuous time evolution of systems with discrete periodic  $N$ -body chains forward-in time stability.

Hopefully, that gets us half way to the continuous time, continuous space Gel'fand-Yaglom formula.

sect. 19.4 *Computing log det of Hill determinant*

## 12.2 Generating functions; action

<sup>1</sup> For discrete-time one-degree-of-freedom Lagrangian systems satisfying a periodicity condition (i.e., cat map):

$$L(q + 1, q' + 1) = L(q, q') + C, \quad (12.1)$$

one can consider relative periodic paths (or pre-periodic paths, also called periodic paths of type  $(r, n)$  by Mackay and Meiss [47]), with <sup>2</sup>

$$q_{i+n} = q_i + r. \quad (12.2)$$

Every  $q_i$  returns to its value after time period  $n$ , but shifted by  $r$ . Orbits satisfying (12.2) are given by stationary points of the action

$$S = \sum_{i=0}^{q-1} L(q_i, q_{i+1}) \quad (12.3)$$

in the space of periodic paths of type  $(r, n)$ . For periodic paths, it suffices to consider one period, because an orbit is periodic if and only if it is a stationary point of the action of one period in the space of periodic paths.

If the constant  $C$  (the **Calabi invariant** [8]) in the periodicity condition (12.1) is zero, and the Lagrangian satisfies a convexity condition

$$L_{12}(q, q') < 0, \quad (12.4)$$

where subscript  $k$  refers to the derivative with respect to the  $k$ th argument, then the action of periodic paths of type  $(r, n)$  is bounded below, so there is a minimising path. Since its action is stationary, it gives a periodic orbit of type  $(r, n)$ .

---

<sup>1</sup>Predrag 2016-11-11, 2018-09-26: What follows is (initially) copied from Li and Tomsovic [42], *Exact relations between homoclinic and periodic orbit actions in chaotic systems* arXiv source file, then merged with the MacKay-Meiss-Percival action principle refs. [48, 51].

<sup>2</sup>Predrag 2018-09-29: presumably they are relative periodic orbits, or pre-periodic orbits, with a rational winding number  $p/q$ .

<sup>3</sup> For orbit  $p$  of period  $n_p$ , the action of the orbit is:

$$S_p \equiv \sum_{n=0}^{n_p-1} L(q_n, q_{n+1}). \quad (12.5)$$

$S_p$  is the generating function that maps a point along the orbit for one (prime) period. For the case of a fixed point  $p$  of period  $n_p = 1$ , the action is

$$S_p = L(q_p, q_p), \quad (12.6)$$

where the generating function  $L(q_p, q_p)$  maps  $x_p$  into itself in one iteration.

### 12.3 Homoclinic and periodic orbit actions in chaotic systems

<sup>4</sup> For an aperiodic orbit  $\{x_0\}$  going through the point  $x_0$ , the action, evaluated as the sum over an infinity of successive mappings,

$$S_{\{x_0\}} \equiv \lim_{N \rightarrow \infty} \sum_{n=-N}^{N-1} L(q_n, q_{n+1}) = \lim_{N \rightarrow \infty} S_{-N, N}, \quad (12.7)$$

is not necessarily convergent. However, the MacKay-Meiss-Percival action principle [48, 51] can be applied to obtain well defined action differences between pairs of orbits. For example, the *relative action*  $\Delta S_{\{h_0\}\{x\}}$  between a fixed point  $x_p$  and its homoclinic orbit  $\{h_0\}$ , where  $h_{\pm\infty} \rightarrow x_p$ :

$$\begin{aligned} \Delta S_{\{h_0\}\{x_p\}} &\equiv \lim_{N \rightarrow \infty} \sum_{i=-N}^{N-1} [L(h_i, h_{i+1}) - L(x_p, x_p)] \\ &= \int_{U[x_p, h_0]} pdq + \int_{S[h_0, x_p]} pdq = \oint_{US[x_p, h_0]} pdq \\ &= \mathcal{A}_{US[x_p, h_0]}^\circ \end{aligned} \quad (12.8)$$

where  $U[x_p, h_0]$  is the segment of the unstable manifold from  $x_p$  to  $h_0$ , and  $S[h_0, x_p]$  the segment of the stable manifold from  $h_0$  to  $x_p$ . The  $\circ$  superscript on the last line indicates that the area is interior to a path that forms a closed loop, and the subscript indicates the path:  $US[x_p, h_0] = U[x_p, h_0] + S[h_0, x_p]$ . The clockwise enclosure of an area is positive, counterclockwise negative.  $\Delta S_{\{h_0\}\{x_p\}}$  gives the action difference between the homoclinic orbit segment  $[h_{-N}, \dots, h_N]$  and the length- $(2N + 1)$  fixed point orbit segment  $[x_p, \dots, x_p]$  in the limit

<sup>3</sup>Predrag 2018-01-21: Is this true? To go from the Hamiltonian  $(x_t, p_t)$  phase space formulation to the Newtonian (or Lagrangian)  $(x_{t-1}, x_t)$  state space formulation, replace  $p_t$  by  $p_t = (x_t - x_{t-1})/\Delta t$ , where  $\Delta t = 1$ .

<sup>4</sup>Predrag 2018-09-29: What follows is copied from Li and Tomsovic [42].



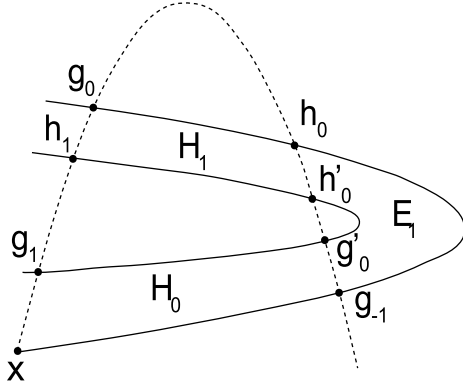


Figure 12.1: A sketch of a partial homoclinic tangle which forms a complete horseshoe structure. The unstable (stable) manifold of  $x$  is the solid (dashed) curve. There are two primary homoclinic orbits  $\{h_0\}$  and  $\{g_0\}$ .  $\mathcal{R}$  is the closed region bounded by loop  $\mathcal{L}_{USUS[x, g_{-1}, h_0, g_0]}$ . (From ref. [42])

$N \rightarrow \infty$ . In later sections, upon specifying the symbolic code of the homoclinic orbit  $\{h_0\} \Rightarrow \bar{0}\gamma\bar{0}$ , we also denote  $\Delta S_{\{h_0\}\{x_p\}}$  alternatively as

$$\Delta S_{\{h_0\}\{x_p\}} = \Delta S_{\bar{0}\gamma\bar{0}, \bar{0}} \quad (12.9)$$

by replacing the orbits in the subscript with their symbolic codes.

Likewise, a second important case is for the relative action between a pair of homoclinic orbits  $\{h'_0\} \Rightarrow \bar{0}\gamma'\bar{0}$  and  $\{h_0\} \Rightarrow \bar{0}\gamma\bar{0}$ , which results in

$$\begin{aligned} \Delta S_{\{h'_0\}\{h_0\}} &\equiv \lim_{N \rightarrow \infty} \sum_{i=-N}^{N-1} [L(h'_i, h'_{i+1}) - L(h_i, h_{i+1})] \\ &= \lim_{N \rightarrow \infty} [L(h'_{-N}, h'_N) - L(h_{-N}, h_N)] \\ &= \int_{U[h_0, h'_0]} p dq + \int_{S[h'_0, h_0]} p dq = \mathcal{A}_{US[h_0, h'_0]}^\circ \\ &= \Delta S_{\bar{0}\gamma'\bar{0}, \bar{0}\gamma\bar{0}} \end{aligned} \quad (12.10)$$

where  $U[h_0, h'_0]$  is the segment of the unstable manifold from  $h_0$  to  $h'_0$ , and  $S[h'_0, h_0]$  the segment of the stable manifold from  $h'_0$  to  $h_0$ . Due to the fact that the endpoints approach  $x_p$  forward and backward in time, one can also write

$$\Delta S_{\{h'_0\}\{h_0\}} = \lim_{N \rightarrow \infty} [L(h'_{-(N+n)}, h'_{N+m}) - L(h_{-N}, h_N)] - (n+m)\mathcal{F}_0. \quad (12.11)$$

## 12.4 Hill's formula, Lagrangian setting

<sup>5</sup> There can be more than one minimising path. In particular, translating one minimising path by an integer in time or space or both gives another. This implies existence of saddle points of the action in between the minima, with one downward direction [1-3]. They are called minimax points, and give rise to minimax periodic orbits of type  $(r, n)$ . The statement of the existence of at least two periodic orbits of each type  $(r, n)$  is known as the Poincaré-Birkhoff theorem.

As a corollary, Mackay and Meiss [47] rederive the old result that when the convexity condition is satisfied, the multipliers of a minimising orbit are a reciprocal pair of positive reals, and those of a minimax orbit are either a complex conjugate pair on the unit circle, or a reciprocal pair of negative reals. The result for minimising orbits was shown by Poincaré [58] for two-degree-of-freedom continuous-time systems, and Birkhoff [1] discusses the minimax case.

The linear stability of a periodic orbit is determined by its multipliers, the eigenvalues of the derivative of the return map round the orbit. While the first variation of the action is by definition zero for an orbit, the multipliers of a periodic orbit can be related to the second variations of the action in the space of periodic paths. This has been shown in various cases. Hill [23] and Poincaré [58] derived a formula for the multipliers in the case of one-degree-of-freedom systems of the form kinetic minus potential [23], using a Fourier representation for periodic paths. In his study of periodic orbits of the three-body problem, Hill obtained a formula connecting the characteristic polynomial of the monodromy matrix of a periodic orbit with the infinite determinant of the Hessian of the action functional. Mackay and Meiss [47] derived a formula (12.17) for the multipliers of a periodic orbit for general discrete-time one-degree-of-freedom systems. Bolotin and Treschev [6] give two multidimensional generalizations of Hill's formula: for discrete Lagrangian systems (symplectic twist maps) and for continuous Lagrangian systems, and discuss implications of symmetries and reversibility. Bountis and Helleman [7] and Greene [19] treated the case of discrete-time one-degree-of-freedom systems with

$$L_{12}(q, q') = -1. \quad (12.12)$$

Schmidt [60] determined  $n$ -tupling bifurcations by the criterion that the matrix of second variations of the action with respect to periodic paths of  $n$  times the period have a zero eigenvalue.

Mackay and Meiss [47] relate the multipliers of a periodic orbit to the second variations of the action about the orbit, and compute the Hill determinant of the matrix of second variations of the action in the space of periodic paths of period  $T$ .

---

<sup>5</sup>Predrag 2016-11-11, 2018-09-26: The current draft of this section starts out with excerpts from Mackay and Meiss [47] *Linear stability of periodic orbits in Lagrangian systems*, and Bolotin and Treschev [6] *Hill's formula*.

Stationarity (8.73) of the action for an orbit of a discrete-time one-degree-of-freedom system implies that

$$L_2(q_{i-1}, q_i) + L_1(q_i, q_{i+1}) = 0. \quad (12.13)$$

Thus the tangent orbits  $\delta x_i$  satisfy [...]. The multipliers  $\Lambda$  of a periodic orbit of period  $q$  are defined by existence of a tangent orbit satisfying [...] residue of a periodic orbit one can easily solve for multipliers. [... losing steam]

Mackay and Meiss [47] formulas for the multipliers of minimising and minimax orbits follow. Under the convexity condition (12.4), the denominator is positive. At a minimum of action (whether local or global):

$$D(1) \leq 0, \quad (12.14)$$

so the multipliers are real and positive. At a minimax with one downward direction:

$$D(1) \geq 0, \quad (12.15)$$

so the multipliers are on the unit circle or the negative real axis.

Residue [19]  $R$  of a periodic orbit  $p$  of period  $n_p$

$$4R = \det(\mathbf{1} - J_p) = \text{tr}(\mathbf{1} - J_p) = 2 - \Lambda_p - 1/\Lambda_p \quad (12.16)$$

is related to the Hill determinant  $D(\Lambda)$  by what the discrete Hill's formula [6]:  
6

$$\det(\mathbf{1} - J_p) = -D(1) \left( \prod_{i=0}^{n_p-1} (-L_{12}[i, i+1]) \right)^{-1}. \quad (12.17)$$

This formula was derived by Mackay and Meiss [47] and Allroth [2] (Allroth eq. (12)). It applies to general "one-degree-of-freedom" systems, i.e., 1D lattices with only the nearest neighbor interactions. For a finite set of neighbors, i.e., higher-dimensional discrete-time systems, Allroth [2] has some partial results in the context of Frenkel-Kontorova models.

$D(1)$  is the Hill determinant of the matrix of second variations of the action in the space of periodic paths of period  $q$ . So we have related the multipliers of a periodic orbit to the second variations of the action about the orbit.

## 12.5 Spatiotemporal cat Hill's formula

2020-07-23 Predrag I have everything in place for deriving spatiotemporal cat (and temporal cat as a special case) Hill's formula from the elementary Kronecker product (12.18) block matrix rules

1. multiplication (21.237) leads to shift (21.251) accruing correctly.
2. Hill determinant (12.20), (21.252); yields correct  $\ln \det = \text{tr} \ln$  reduction to periodic  $J_p$

---

<sup>6</sup>Predrag 2018-09-30: See Bolotin and Treschev [6] eqs. (2.8) and (2.13)

3.  $\mathbf{A} \otimes \mathbf{B}$  being similar to  $\mathbf{B} \otimes \mathbf{A}$  by (21.238) explains why  $[2L \times 2L]$  phase space is equivalent to the  $[L \times L]$  orbit stability.

2020-07-23 Predrag Next: streamline, move to CL18.tex

2020-07-27 Predrag Essential parts copied to CL18.tex, *siminos/kittens/Hill.tex*

The  $d = 2$  lattice spatiotemporal cat equations can be recast in a matrix form, by rewriting the defining equations as block matrices [11, 17, 27], constructed by the Kronecker product  $\mathbf{A} \otimes \mathbf{B}$ ,<sup>7</sup> an operation that replaces elements of the  $[n \times n]$  matrix  $\mathbf{A}$  by  $[m \times m]$  matrix 'blocks'  $\mathbf{B}$ , resulting in an  $[mn \times mn]$  block matrix [4, 73]

$$\mathbf{A} \otimes \mathbf{B} = \begin{bmatrix} a_{11}\mathbf{B} & \cdots & a_{1n}\mathbf{B} \\ \vdots & \ddots & \vdots \\ a_{n1}\mathbf{B} & \cdots & a_{nn}\mathbf{B} \end{bmatrix}. \quad (12.18)$$

Consider  $\mathbf{A}, \mathbf{C}$  square matrices of size  $[n \times n]$ , and  $\mathbf{B}, \mathbf{D}$  square matrices of size  $[m \times m]$ . The matrix product of two block matrices is a block matrix [4, 72],

$$(\mathbf{A} \otimes \mathbf{B})(\mathbf{C} \otimes \mathbf{D}) = (\mathbf{AC}) \otimes (\mathbf{BD}). \quad (12.19)$$

The trace and the determinant of a block matrix are given by

$$\begin{aligned} \text{tr}(\mathbf{A} \otimes \mathbf{B}) &= \text{tr} \mathbf{A} \text{tr} \mathbf{B} \\ \det(\mathbf{A} \otimes \mathbf{B}) &= \det(\mathbf{A}^m) \det(\mathbf{B}^n). \end{aligned} \quad (12.20)$$

The two  $[mn \times mn]$  block matrices  $\mathbf{A} \otimes \mathbf{B}$  and  $\mathbf{B} \otimes \mathbf{A}$  are equivalent by a similarity transformation

$$\mathbf{B} \otimes \mathbf{A} = \mathbf{P}^\top (\mathbf{A} \otimes \mathbf{B}) \mathbf{P}, \quad (12.21)$$

where  $\mathbf{P}$  is permutation matrix. As  $\det \mathbf{P} = 1$ , the block matrix determinant  $\det(\mathbf{A} \otimes \mathbf{B}) = \det(\mathbf{B} \otimes \mathbf{A})$  is independent of the order in which blocks are constructed.

Now, apply this formalism to a  $[L \times T]_0$  rectangular primitive cell. In the Kronecker product block matrix notation (12.18), the orbit Jacobian matrix `refeq{eq:BxAtemp}` can be written as a  $[LT \times LT]$  block matrix

$$\mathcal{J} = \mathbf{1}_1 \otimes (r_2 + r_2^{-1}) - 2s \mathbf{1}_1 \otimes \mathbf{1}_2 + (r_1 + r_1^{-1}) \otimes \mathbf{1}_2, \quad (12.22)$$

where the (12.18) matrix  $\mathbf{A}$  and identity  $\mathbf{1}_1$  matrix are 'spatial'  $[L \times L]$  matrices, with blocks  $\mathbf{B}$  and identity  $\mathbf{1}_2$  'temporal'  $[T \times T]$  matrices, with indices '1', '2' referring to 'spatial', 'temporal' lattice directions, respectively.

<sup>7</sup>Predrag 2020-08-01: The Zehfuss product (1858), really. The Hill determinant is from 1886, though it does not look recognizably anything like out the Hill determinants... These things are everywhere!

Our goal is to compute the Hill determinant  $|\det \mathcal{J}|$ . As we have shown in the example `refsect{s:catLattRel3x2}`, this is best done directly, by computing the volume of the fundamental parallelepiped. <sup>8</sup>

However, in classical and statistical mechanics, one often computes the Hill determinant using a Hamiltonian, or 'transfer matrix' formulation. An example is the temporal cat 3-term recurrence (8.157) in the Percival-Vivaldi [55] 'two-configuration' cat map representation (2.75)

$$\hat{\mathbf{x}}_{t+1} = \hat{\mathbf{J}}_1 \hat{\mathbf{x}}_t - \hat{\mathbf{s}}_t, \quad (12.23)$$

with the one-time step temporal evolution  $[2 \times 2]$  Jacobian matrix  $\hat{\mathbf{J}}_1$  generating a time orbit by acting on the 2-dimensional 'phase space' of successive configuration points

$$\hat{\mathbf{J}}_1 = \begin{bmatrix} 0 & 1 \\ -1 & s \end{bmatrix}, \quad \hat{\mathbf{x}}_t = \begin{pmatrix} x_{t-1} \\ x_t \end{pmatrix}, \quad \hat{\mathbf{s}}_t = \begin{pmatrix} 0 \\ s_t \end{pmatrix}, \quad (12.24)$$

Similarly, for the  $d = 2$  spatiotemporal cat lattice at hand, one can recast the 5-term recurrence (XX) (compare with the (8.167))

$$\begin{aligned} x_{nt} &= x_{nt} \\ x_{n,t+1} &= -x_{n,t-1} + (-x_{n-1,t} + 2s x_{nt} - x_{n+1,t}) - s_{nt} \end{aligned} \quad (12.25)$$

in the 'two-configuration' matrix form (21.240) by picking the vertical direction (indexed '2') as the 'time', with temporal 1-time step Jacobian  $[2L \times 2L]$  block matrix

$$\hat{\mathbf{J}}_1 = \left[ \begin{array}{c|c} \mathbf{0} & \mathbf{1}_1 \\ \hline -\mathbf{1}_1 & -\mathcal{J}_1 \end{array} \right], \quad (12.26)$$

(known as a transfer matrix in statistical mechanics [52, 53]) generating a time orbit by acting on a  $2L$ -dimensional 'phase space' lattice strip  $\hat{\mathbf{x}}_t$  along the 'spatial' direction (indexed '1'),

$$\hat{\mathbf{x}}_t = \begin{bmatrix} \mathbf{x}_{t-1} \\ \mathbf{x}_t \end{bmatrix}, \quad \hat{\mathbf{s}}_t = \begin{bmatrix} \mathbf{0} \\ \mathbf{s}_{1t} \end{bmatrix}, \quad \mathbf{x}_t = \begin{bmatrix} x_{1t} \\ \vdots \\ x_{Lt} \end{bmatrix}, \quad \mathbf{s}_t = \begin{bmatrix} s_{1t} \\ \vdots \\ s_{Lt} \end{bmatrix}, \quad (12.27)$$

where the hat  $\hat{\phantom{x}}$  indicates a  $2L$ -dimensional 'two-configuration' state, and  $\mathcal{J}_1$  is the spatial  $[L \times L]$  orbit Jacobian matrix of form (XX),

$$\mathcal{J}_1 = r_1^{-1} - 2s\mathbf{1}_1 + r_1 \quad (12.28)$$

The 'two-configuration' coupled cat maps system (21.240) is a generalization of the Bernoulli map time evolution formulation (XX) to a higher-dimensional spatially-coupled lattice. Just as in the temporal Bernoulli condition `refeq {temp-FixPoint}`, the first order in time difference equation (21.240) can be viewed as

<sup>8</sup>Predrag 2020-07-27: Insert `refsect{s:catLattRel3x2}` example here?

a periodic state fixed point condition  $\text{refeq}\{\text{tempFixPoint}\}$ , a zeros of the function  $F[\hat{X}] = \hat{\mathcal{J}}\hat{X} + \hat{M} = 0$ , with the entire periodic *periodic state*  $\hat{X}_M$  treated as a single fixed *point* in the  $2LT$ -dimensional unit hyper-cube, and the  $[2LT \times 2LT]$  block matrix orbit Jacobian matrix given either by

$$\hat{\mathcal{J}} = \hat{\mathbf{1}} - \hat{\mathbf{J}}_1 \otimes r_2^{-1}, \quad (12.29)$$

or by

$$\hat{\mathcal{J}}' = \hat{\mathbf{1}} - r_2^{-1} \otimes \hat{\mathbf{J}}_1. \quad (12.30)$$

Here the unity  $\hat{\mathbf{1}} = \hat{\mathbf{1}}_1 \otimes \mathbf{1}_2$  is a  $[2LT \times 2LT]$  block matrix, and the time-evolution Jacobian matrix  $\hat{\mathbf{J}}_1$  (21.243) is a  $[2L \times 2L]$  matrix.

The order in which the block matrix blocks are composed does not matter, yielding the same the Hill determinant  $\det \hat{\mathcal{J}} = \det \hat{\mathcal{J}}'$  by (21.238). However, written out explicitly, the two orbit Jacobian matrices (21.247) and (21.250) are of a very different form.

For example, for the  $[L \times T]_0$  rectangular primitive cell, the spatiotemporal cat orbit Jacobian matrix (XX) involves the  $[T \times T]$  time shift operator block matrix  $r_2$  (XX) with the one-time-step  $[2L \times 2L]$  time-evolution Jacobian matrix  $\hat{\mathbf{J}}_1$  (21.243)

$$\hat{\mathcal{J}} = \left[ \begin{array}{c|c} \mathbf{1}_1 \otimes \mathbf{1}_2 & -\mathbf{1}_1 \otimes r_2^{-1} \\ \hline \mathbf{1}_1 \otimes r_2^{-1} & \mathbf{1}_1 \otimes \mathbf{1}_2 + \mathcal{J}_1 \otimes r_2^{-1} \end{array} \right], \quad (12.31)$$

and for spatiotemporal cat (21.242) this is a time-periodic  $[T \times T]$  shift operator block matrix  $r_2$  (XX), each block now a space-periodic  $[2L \times 2L]$  matrix  $\hat{\mathbf{J}}_1$  (21.243).

If a block matrix is composed of four blocks, **its determinant** can be factorized by Schur's (1917) formula [61, 72]

$$\det \left[ \begin{array}{c|c} \mathbf{A} & \mathbf{B} \\ \hline \mathbf{C} & \mathbf{D} \end{array} \right] = \det(\mathbf{A}) \det(\mathbf{D} - \mathbf{C}\mathbf{A}^{-1}\mathbf{B}). \quad (12.32)$$

so, noting (21.237), (21.239) and (21.244), we find that the  $[2LT \times 2LT]$  'phase space'  $\det \hat{\mathcal{J}}$  defined by (21.247) is actually the desired Hill determinant of  $[LT \times LT]$  orbit Jacobian matrix  $\mathcal{J}$ ,

$$\begin{aligned} \det \hat{\mathcal{J}} &= \det \left[ \begin{array}{c|c} \mathbf{1}_1 \otimes \mathbf{1}_2 & -\mathbf{1}_1 \otimes r_2^{-1} \\ \hline \mathbf{1}_1 \otimes r_2^{-1} & \mathbf{1}_1 \otimes \mathbf{1}_2 + \mathcal{J}_1 \otimes r_2^{-1} \end{array} \right] \\ &= \det [\mathbf{1}_1 \otimes \mathbf{1}_2 + \mathcal{J}_1 \otimes r_2^{-1} + (\mathbf{1}_1 \otimes r_2^{-1})(\mathbf{1}_1 \otimes \mathbf{1}_2)(\mathbf{1}_1 \otimes r_2^{-1})] \\ &= \det [\mathbf{1}_1 \otimes \mathbf{1}_2 + \mathcal{J}_1 \otimes r_2^{-1} + \mathbf{1}_1 \otimes r_2^{-2}] \\ &= \det(r_2^{-1}) \det [\mathbf{1}_1 \otimes r_2^{-1} + (r_1^{-1} - 2s\mathbf{1}_1 + r_1) \otimes \mathbf{1}_2 + \mathbf{1}_1 \otimes r_2] \\ &= \det \mathcal{J}, \end{aligned} \quad (12.33)$$

where we have used  $\det \mathbf{1}_1 = \det \mathbf{1}_2 = \det r_1 = \det r_2 = 1$ .

Consider next (21.246), the equivalent way of forming of the block matrix for the  $[L \times T]_0$  rectangular primitive cell, with temporal period taken for definitiveness  $T = 4$ . The spatiotemporal cat orbit Jacobian matrix (21.246) is now constructed as the  $[4 \times 4]$  time shift operator block matrix  $r_2$  (XX), with the one-time-step  $[2L \times 2L]$  time-evolution Jacobian matrix  $\hat{\mathbf{J}}_1$  (21.243) and unit matrix  $\hat{\mathbf{1}}_1$  as blocks

$$\hat{\mathcal{J}}' = \mathbf{1}_2 \otimes \hat{\mathbf{1}}_1 - r_2^{-1} \otimes \hat{\mathbf{J}}_1 = \begin{bmatrix} \hat{\mathbf{1}}_1 & \mathbf{0} & \mathbf{0} & -\hat{\mathbf{J}}_1 \\ -\hat{\mathbf{J}}_1 & \hat{\mathbf{1}}_1 & \mathbf{0} & \mathbf{0} \\ \mathbf{0} & -\hat{\mathbf{J}}_1 & \hat{\mathbf{1}}_1 & \mathbf{0} \\ \mathbf{0} & \mathbf{0} & -\hat{\mathbf{J}}_1 & \hat{\mathbf{1}}_1 \end{bmatrix}. \quad (12.34)$$

To evaluate the Hill determinant  $\det \hat{\mathcal{J}}'$ , note that from the block-matrix multiplication rule (21.237) and the determinant rule (12.20) it follows that

$$(r_2^{-1} \otimes \hat{\mathbf{J}}_1)(r_2^{-1} \otimes \hat{\mathbf{J}}_1) = r_2^{-2} \otimes \hat{\mathbf{J}}_1^2, \quad (r_2^{-1} \otimes \hat{\mathbf{J}}_1)^k = r_2^{-k} \otimes \hat{\mathbf{J}}_1^k, \quad (12.35)$$

and

$$\det (r_2^{-1} \otimes \hat{\mathbf{J}}_1) = (\det r_2)^{-L} (\det \hat{\mathbf{J}}_1)^T = \det \hat{\mathbf{J}}_p, \quad \hat{\mathbf{J}}_p = \hat{\mathbf{J}}_1^T, \quad (12.36)$$

where  $\hat{\mathbf{J}}_p$  is the Jacobian matrix of a temporal periodic orbit  $p$ . Expand  $\ln \det \hat{\mathcal{J}}' = \text{tr} \ln \hat{\mathcal{J}}'$  as a series using (12.20) and (21.251),

$$\text{tr} \ln \hat{\mathcal{J}}' = \text{tr} \ln (\mathbf{1} - r_2^{-1} \otimes \hat{\mathbf{J}}_1) = - \sum_{k=1}^{\infty} \frac{1}{k} \text{tr} (r_2^{-k}) \text{tr} \hat{\mathbf{J}}_1^k, \quad (12.37)$$

and use  $\text{tr} r_2^k = T$  if  $k$  is a multiple of  $T$ , 0 otherwise (follows from  $r_2^T = \mathbf{1}$ ):

$$\ln \det (\mathbf{1} - r_2^{-1} \otimes \hat{\mathbf{J}}_1) = - \sum_{r=1}^{\infty} \frac{1}{r} \text{tr} \hat{\mathbf{J}}_p^r = \ln \det (\hat{\mathbf{1}}_1 - \hat{\mathbf{J}}_p).$$

So for the spatiotemporal cat the orbit Jacobian matrix and the temporal evolution (21.240) stability  $\hat{\mathbf{J}}_p$  are related by the remarkable Hill's formula

$$|\det \mathcal{J}| = |\det (\hat{\mathbf{1}}_1 - \hat{\mathbf{J}}_p)|. \quad (12.38)$$

which expresses the Hill determinant of the arbitrarily large orbit Jacobian matrix  $\hat{\mathcal{J}}'$  in terms of a determinant of a small  $[2L \times 2L]$  time-evolution Jacobian matrix  $\hat{\mathbf{J}}_1$ .

**Remark** From (21.257) we have

2CB

$$\det \hat{\mathbf{J}}_1 = \det \begin{bmatrix} \mathbf{0} & \mathbf{1}_1 \\ -\mathbf{1}_1 & -\mathcal{J}_1 \end{bmatrix} = \det (\mathcal{J}_1) \det (\mathcal{J}_1^{-1}) = 1, \quad (12.39)$$

so  $\hat{\mathbf{J}}_1$  is a canonical, or phase-space volume preserving transformation, as one expects of Hamiltonian systems.

**Remark** The reformulation of the spatiotemporal cat 5-term recurrence (21.242) as the ‘two-configuration’ form (21.240) is really just the usual passage from Lagrangian to the Hamiltonian formulation, but we chose to short-circuit it, as all that heavy general formalism is not needed for the problem at hand.<sup>9</sup>

**Remark** I am not a big fan of the Kronecker product (12.18) as it treats the time and the space differently. Nicer notion would be a tensor product that treats all directions in  $d$ -dimensional on equal, symmetric footing. Perhaps the ‘outer product’ does that (see the [wiki](#)) explains the outer product of tensors, and its relation to the Kronecker product. Arfken, Weber & Harris [4] *Mathematical Methods for Physicists: A Comprehensive Guide* ([click here](#)) call it the *direct tensor* or *Kronecker product*, see [AWH eq. \(2.55\)](#).

Perhaps Steeb and Hardy [65] *Matrix Calculus, Kronecker Product and Tensor Product* (I have not downloaded the book) deals with that. Not sure if that is different from Steeb and Hardy [64] *Matrix Calculus and Kronecker Product - A Practical Approach to Linear and Multilinear Algebra*.

Kowalski and Steeb [36] *Nonlinear Dynamical Systems and Carleman Linearization* ([click here](#)) already goes beyond the other Kronecker product references I had looked at, as it emphasizes commutators of Kronecker products.

Horn and Johnson [25] *Matrix Analysis* ([click here](#)) promises to do Kronecker product in the companion volume Horn and Johnson [26] *Topics in Matrix Analysis* that I have not looked yet.

Schur’s (1917) formula (21.248) is derived in exercise A.12 of Stone and Goldbart [66] *Mathematics for Physics* ([click here](#)).

## 12.6 Hill’s formula for relative periodic orbits

As a first try, let’s reverse-engineer relative periodicity for the more familiar ‘two-configuration’ spatiotemporal cat (21.240). The stability matrix of a temporally periodic orbit

$$\delta \hat{\mathbf{x}}_T = \hat{\mathbf{J}}_1^T \delta \hat{\mathbf{x}}_0, \quad (12.40)$$

corresponds spatiotemporally to a  $[L \times T]_0$  rectangular primitive cell, while the stability matrix of a relative periodic orbit includes the relative shift  $S$ ,

$$\delta \hat{\mathbf{x}}_T = r_1^S \hat{\mathbf{J}}_1^T \delta \hat{\mathbf{x}}_0, \quad (12.41)$$

and corresponds spatiotemporally to a  $[L \times T]_S$  parallelepipedal primitive cell, which can be convert into a rectangular cell by going into a co-moving frame, with the temporal 1-time step Jacobian  $[2L \times 2L]$  block matrix (21.243) replaced by

$$\tilde{\mathbf{J}}_1 \Rightarrow r_1^{S/T} \hat{\mathbf{J}}_1 = \left[ \begin{array}{c|c} \mathbf{0} & r_1^{S/T} \\ \hline -r_1^{S/T} & -r_1^{S/T} \mathcal{J}_1 \end{array} \right], \quad (12.42)$$

<sup>9</sup>Predrag 2020-07-15: Perhaps refer to [ChaosBook 8.1 Hamiltonian flows](#). Mention transfer matrix formulation of lattice field theories?



and  $\hat{\mathcal{J}}'_{[L \times T]_s}$  is of the rectangular cell form, with replacement  $\hat{\mathbf{J}}_1 \rightarrow \tilde{\mathbf{J}}_1$  in (21.250). In evaluating the corresponding determinants we can use (21.252),

$$\det(r_2^{-1} \otimes \tilde{\mathbf{J}}_1) = (\det r_2)^{-L} (\det \tilde{\mathbf{J}}_1)^T = \det \tilde{\mathbf{J}}_p, \quad \tilde{\mathbf{J}}_p = r_1^S \hat{\mathbf{J}}_1^T, \quad (12.43)$$

where  $\tilde{\mathbf{J}}_p$  is the Jacobian matrix of the temporal prime relative periodic orbit  $p$ .

Now we can reverse-engineer relative periodicity for the  $d = 2$  lattice. We have just worked out  $\hat{\mathcal{J}}'$  defined by (21.246). Consider next  $\hat{\mathcal{J}}$  (21.245), with 'time' and 'space' blocked in the other order, defined by (21.245), (21.247) and (12.42),

$$\hat{\mathcal{J}} = \left[ \begin{array}{c|c} \mathbf{1}_1 \otimes \mathbf{1}_2 & -r_1^{S/T} \otimes r_2^{-1} \\ \hline r_1^{S/T} \otimes r_2^{-1} & \mathbf{1}_1 \otimes \mathbf{1}_2 + \mathcal{J}_1 r_1^{S/T} \otimes r_2^{-1} \end{array} \right], \quad (12.44)$$

We next evaluate the  $[2LT \times 2LT]$  'phase space'  $\det \hat{\mathcal{J}}$  defined by (21.247), and show again that it equals the Hill determinant of  $[LT \times LT]$  orbit Jacobian matrix  $\mathcal{J}$ ,

$$\begin{aligned} \det \hat{\mathcal{J}} &= \det \left[ \mathbf{1}_1 \otimes \mathbf{1}_2 + \mathcal{J}_1 r_1^{S/T} \otimes r_2^{-1} + r_1^{2S/T} \otimes r_2^{-2} \right] \\ &= \det \left[ r_1^{S/T} \otimes r_2^{-1} + (r_1^{-1} - 2s\mathbf{1}_1 + r_1) \otimes \mathbf{1}_2 + r_1^{-S/T} \otimes r_2 \right] \\ &= \det \mathcal{J}, \end{aligned} \quad (12.45)$$

The orbit Jacobian matrix (21.239) for a tilted primitive cell (relative periodic orbit) is thus a  $[LT \times LT]$  block matrix

$$\mathcal{J}_{[L \times T]_s} = \left( r_1^{S/T} \otimes r_2^{-1} + r_1^{-S/T} \otimes r_2 \right) - 2s \mathbf{1}_1 \otimes \mathbf{1}_2 + (r_1 + r_1^{-1}) \otimes \mathbf{1}_2. \quad (12.46)$$

All the relative periodicity is in the  $r_1^{-S/T} \otimes r_2$ . This space-time asymmetry is a consequence of choosing the Hermite normal form (8.123) to define the primitive cell, so we are not home yet - even though we are computing the representation-independent determinants, we do not have an invariant statement of cell's 'tilt'.

What do I mean? An example of an invariant condition is the statement that a prime lattice  $\mathcal{L}_p$  tiles the given lattice  $\mathcal{L}$  only if the area spanned by the two 'tilted' primitive vectors

$$\mathbf{a}_2 \times \mathbf{a}_2^p = ST_p - TS_p \quad (12.47)$$

is a multiple of the prime tile area  $L_p T_p$ .

**Remark** Perhaps we can use Floquet theory analogue of a comoving frame (12.42) to put the generally time-varying  $(\hat{\mathbf{J}}_1)_t$  into an average, constant per time step form  $\tilde{\mathbf{J}}_1$ , in order to use the block-matrix formalism.

## 12.7 Han's 1st order difference eq. Hill's formula

2019-10-04 Han I haven't found the proof of (12.73), so I will prove it here.

Assuming we have a  $d$ -dimensional map. The state of the system at time  $t$  is give by a  $d$ -dimensional vector  $\mathbf{X}(t) = \{x_1(t), x_2(t), \dots, x_d(t)\}$ . The forward-time Jacobian matrix is:

$$J(t)_{ij} = \frac{\partial x_i(t+1)}{\partial x_j(t)}. \quad (12.48)$$

A block matrix is a matrix defined by smaller matrices, called blocks. The matrix  $H$  (12.61) is now an  $[n_p d \times n_p d]$  block matrix:

$$H(\mathbf{x}_p) = \begin{pmatrix} \mathbf{1} & & & & -\mathbf{J}(n_p) \\ -\mathbf{J}(1) & \mathbf{1} & & & \\ & \cdots & \mathbf{1} & & \\ & & \cdots & \mathbf{1} & \\ & & & -\mathbf{J}(n_p - 1) & \mathbf{1} \end{pmatrix}, \quad (12.49)$$

where  $\mathbf{1}$  is a  $d$ -dimensional identity matrix and  $\mathbf{J}(t)$  is the  $[d \times d]$  forward-time Jacobian matrix. To evaluate the determinant of the matrix  $H$ , we will eliminate the off diagonal elements in the lower triangular region start from the second row. Eventually the matrix  $H$  becomes:

$$\tilde{H}(\mathbf{x}_p) = \begin{pmatrix} \mathbf{1} & & & & -\mathbf{J}(n_p) \\ 0 & \mathbf{1} & & & -\mathbf{J}(1)\mathbf{J}(n_p) \\ & 0 & \mathbf{1} & & -\mathbf{J}(2)\mathbf{J}(1)\mathbf{J}(n_p) \\ & & 0 & \mathbf{1} & \cdots \\ & & & 0 & \mathbf{1} - \mathbf{J} \end{pmatrix}, \quad (12.50)$$

where  $\mathbf{J} = \mathbf{J}(n_p - 1)\mathbf{J}(n_p - 2) \dots \mathbf{J}(2)\mathbf{J}(1)\mathbf{J}(n_p)$ . The determinant of the block matrix  $\tilde{H}$  is equal to the product of the determinant of the matrices on the diagonal, which is the determinant of  $\mathbf{1} - \mathbf{J}$ .

The cat map is a 2-dimensional map that can be written as 1-dimensional time delay map. A general form of this map is <sup>10</sup>

$$x_{t+1} = f(x_t, x_{t-1}). \quad (12.51)$$

The forward-time Jacobian matrix can be written as:

$$\mathbf{J}(t) = \frac{\partial(x_t, x_{t+1})}{\partial(x_{t-1}, x_t)} = \begin{pmatrix} 0 & 1 \\ f_2(x_t, x_{t-1}) & f_1(x_t, x_{t-1}) \end{pmatrix}, \quad (12.52)$$

where the subscript of  $f_k$  refers to the derivative with respect to the  $k$ th argu-

<sup>10</sup>Predrag 2019-10-11: Note to myself: Reference the cat map equation in the text. Explain how imposing "direction" of time is in this case arbitrary, but related to Hamiltonian formulation (which this is not)

ment of  $f$ . For a periodic orbit  $p$ , the matrix  $H$  is:

$$H(\mathbf{x}_p) = \begin{pmatrix} 1 & & & -f_2(x_{n_p}, x_{n_p-1}) & -f_1(x_{n_p}, x_{n_p-1}) \\ -f_1(x_1, x_{n_p}) & 1 & & & -f_2(x_1, x_{n_p}) \\ -f_2(x_2, x_1) & -f_1(x_2, x_1) & & & \\ & & 1 & & \\ & & \dots & & \\ & & & 1 & \\ -f_2(x_{n_p-1}, x_{n_p-2}) & -f_1(x_{n_p-1}, x_{n_p-2}) & & & 1 \end{pmatrix}. \quad (12.53)$$

To change this matrix to upper triangular form,<sup>11</sup> first add  $f_1(x_1, x_{n_p})$  times the first row to the second row:

$$\begin{pmatrix} 1 & & & -f_2(x_{n_p}, x_{n_p-1}) & -f_1(x_{n_p}, x_{n_p-1}) \\ 0 & 1 & & -f_2(x_{n_p}, x_{n_p-1})f_1(x_1, x_{n_p}) & -f_2(x_1, x_{n_p}) - f_1(x_{n_p}, x_{n_p-1})f_1(x_1, \\ -f_2(x_2, x_1) & -f_1(x_2, x_1) & & & \\ & & 1 & & \\ & & \dots & & \\ & & & 1 & \\ -f_2(x_{n_p-1}, x_{n_p-2}) & -f_1(x_{n_p-1}, x_{n_p-2}) & & & 1 \end{pmatrix}$$

Note that the  $[2 \times 2]$  block on the upper-right corner is  $-\mathbf{J}(1)\mathbf{J}(n_p)$ . After we finish the first two rows, when we eliminate the elements on the  $t$ th row in the lower triangular region, we will add  $f_2(x_{t-1}, x_{t-2})$  times the  $(t-2)$ th row plus  $f_1(x_{t-1}, x_{t-2})$  times the  $(t-1)$ th row to the  $t$ th row. If the  $[2 \times 2]$  block on the right end of the  $(t-2)$ th and  $(t-1)$ th row is  $-\mathbf{J}_{t-1}$ , after we eliminate the sub-diagonal elements on the  $t$ th row the  $[2 \times 2]$  block on the right end of the  $(t-1)$ th and  $t$ th row is  $-\mathbf{J}(t-1)\mathbf{J}_{t-1}$ .

Repeat this procedure until we reach the  $(n_p - 1)$  row. The  $[2 \times 2]$  block on the right end of the  $(n_p - 2)$ th and  $(n_p - 1)$ th row is:

$$\begin{pmatrix} 0 & 0 \\ 1 & 0 \end{pmatrix} - \mathbf{J}_{n_p-1},$$

where  $\mathbf{J}_{n_p-1} = \mathbf{J}(n_p - 2) \dots \mathbf{J}(1)\mathbf{J}(n_p)$ . The next step is eliminating the off-diagonal elements in the last row. We will only eliminate the element on the  $(n_p - 2)$ th column by adding  $f_2(n_p - 1, n_p - 2)$  times the  $(n_p - 2)$ th row plus  $f_1(n_p - 1, n_p - 2)$  times the  $(n_p - 1)$ th row to the last row. The  $[2 \times 2]$  block on the lower-right corner is now:

$$\mathbf{1} - \mathbf{J}(n_p - 1)\mathbf{J}_{n_p-1}.$$

---

<sup>11</sup>Predrag 2019-10-11: to Han - can you derive this more elegantly using the  $C_N$  formulation of (11.7)?

Now the matrix  $H$  becomes an upper-triangular block matrix:

$$\tilde{H}(\mathbf{x}_p) = \begin{pmatrix} \mathbf{1} & & & -\mathbf{J}(1)\mathbf{J}(n_p) \\ & \mathbf{1} & & \cdots \\ & & \mathbf{1} & \cdots \\ & & & \mathbf{1} \\ & & & & \mathbf{1} - \mathbf{J} \end{pmatrix}, \quad (12.55)$$

where  $\mathbf{1}$  is a 2-dimensional identity matrix and  $\mathbf{J} = \mathbf{J}(n_p-1)\mathbf{J}(n_p-2) \dots \mathbf{J}(1)\mathbf{J}(n_p)$ . The determinant of matrix  $H$  is equal to the product of the determinant of the matrices on the diagonal, which is equal to the determinant of  $\mathbf{1} - \mathbf{J}$ .

**2019-10-13 Predrag** to Han - can you have a look at my Guckenheimer and Meloon [20] "symmetric multiple shooting algorithm" notes, sect. 12.12? First verify and understand that their argument that the orbit Jacobian matrix for their (12.120) is equivalent to the orbit Jacobian matrix for the 'forward shooting' case.

Then do the same for the time-reversible 'error' field (12.120) with self-adjoint (symmetric orbit Jacobian matrix) orbit Jacobian matrix (12.122). We have to show that its determinant is the Hill's formula.

### 12.7.1 Hill's formula for a first-order system

12

Consider an period- $n$  periodic state  $X_p$ , with  $d$  fields  $\{x_{t,1}, x_{t,2}, \dots, x_{t,d}\}$  on each temporal lattice site  $t$  satisfying the condition

$$x_t - f(x_{t-1}) = 0, \quad t = 1, 2, \dots, n, \quad (12.56)$$

where  $f(x)$  is a  $d$ -dimensional function. A deviation  $\Delta X$  from  $X_p$  then satisfies the linearized condition

$$\Delta x_t - \mathbb{J}_{t-1} \Delta x_{t-1} = 0, \quad (\mathbb{J}_t)_{ij} = \left. \frac{\partial f(x)_i}{\partial x_j} \right|_{x_j = x_{t,j}}, \quad (12.57)$$

where  $\mathbb{J}_t$  is the 1-time step  $[d \times d]$  Jacobian matrix.

It suffices to work out a temporal period  $n = 3$  example to understand the calculation for any period. In terms of the  $[3d \times 3d]$  matrix shift matrix  $r$ , the orbit Jacobian matrix can be written as

$$\mathcal{J}_p = \mathbf{1} - r^{-1}\mathbb{J}, \quad r^{-1} = \begin{bmatrix} 0 & 0 & \mathbf{1}_d \\ \mathbf{1}_d & 0 & 0 \\ 0 & \mathbf{1}_d & 0 \end{bmatrix}, \quad \mathbb{J} = \begin{bmatrix} \mathbb{J}_1 & 0 & 0 \\ 0 & \mathbb{J}_2 & 0 \\ 0 & 0 & \mathbb{J}_3 \end{bmatrix}, \quad (12.58)$$

<sup>12</sup>Predrag 2020-12-15, 2024-10-18: Transfer to LC22 [44]. Once incorporated, remove from here - too much duplication, as is;

where  $\mathbf{1}_d$  is the  $d$ -dimensional identity matrix. Next, note that

$$(r^{-1}\mathbb{J})^2 = r^{-2} \begin{bmatrix} \mathbb{J}_2\mathbb{J}_1 & 0 & 0 \\ 0 & \mathbb{J}_3\mathbb{J}_2 & 0 \\ 0 & 0 & \mathbb{J}_1\mathbb{J}_3 \end{bmatrix}, \quad (r^{-1}\mathbb{J})^3 = \begin{bmatrix} \mathbb{J}_2\mathbb{J}_1\mathbb{J}_3 & 0 & 0 \\ 0 & \mathbb{J}_3\mathbb{J}_2\mathbb{J}_1 & 0 \\ 0 & 0 & \mathbb{J}_1\mathbb{J}_3\mathbb{J}_2 \end{bmatrix},$$

as  $r^{-3} = \mathbf{1}$ . Likewise, as  $r^n = \mathbf{1}$  for any period  $n$ , the trace of  $[nd \times nd]$  matrix

$$\text{tr} (r^{-1}\mathbb{J})^k = \delta_{k, rn} n \text{tr} \mathbb{J}_p^r, \quad \mathbb{J}_p = \mathbb{J}_n\mathbb{J}_{n-1} \cdots \mathbb{J}_2\mathbb{J}_1$$

is non-vanishing only if  $k$  is a multiple of  $n$ , with  $\mathbb{J}_p$  the forward-in-time  $[d \times d]$  Jacobian matrix of the periodic orbit  $p$ .

Now we can evaluate the Hill determinant (8.122) by expanding

$$\begin{aligned} \ln \text{Det} (\mathcal{J}_p) &= \text{tr} \ln(\mathbf{1} - r^{-1}\mathbb{J}) = - \sum_{k=1}^{\infty} \frac{1}{k} \text{tr} (r^{-1}\mathbb{J})^k \\ &= -\text{tr} \sum_{r=1}^{\infty} \frac{1}{r} \mathbb{J}_p^r = \ln \det (\mathbf{1}_d - \mathbb{J}_p). \end{aligned} \quad (12.59)$$

The Hill determinant for a 2-term difference equation (??) on a temporal lattice

$$\text{Det} (\mathcal{J}_p) = \det (\mathbf{1}_d - \mathbb{J}_p)$$

thus relates the global orbit stability to the Floquet, temporal evolution stability. In the temporal Bernoulli case, the field  $x_t$  is a scalar, and the 1-time step  $[1 \times 1]$  time-evolution Jacobian matrix (12.57) at every lattice point  $t$  is simply  $\mathbb{J}_t = s$ , so

$$N_n = |\text{Det} \mathcal{J}| = s^n - 1, \quad (12.60)$$

in agreement with the time-evolution count.

**Example 12.1. Temporal lattice stability of a 3-cycle.** For a 1-dimensional map  $f$ , orbit Jacobian matrix is an  $[n_p \times n_p]$  matrix:

$$\mathcal{J}(x) = \begin{pmatrix} 1 & & & & -f'_{n_p} \\ -f'_1 & 1 & & & \\ & \cdots & 1 & & \\ & & \cdots & 1 & \\ & & & -f'_{n_p-1} & 1 \end{pmatrix}. \quad (12.61)$$

Let us invert a 3-cycle orbit Jacobian matrix  $\mathcal{J}(x)$  for such 1-dimensional map by hand, step by step. According to (11.6), the initial small  $\delta x$  deviations from the periodic orbit (11.3) are mapped into deviations  $\delta x'$  a time step later by

$$\begin{pmatrix} \delta x'_1 \\ \delta x'_2 \\ \delta x'_3 \end{pmatrix} = \begin{pmatrix} 1 & 0 & -f'_3 \\ -f'_1 & 1 & 0 \\ 0 & -f'_2 & 1 \end{pmatrix} \begin{pmatrix} \delta x_1 \\ \delta x_2 \\ \delta x_3 \end{pmatrix},$$

where the  $d$ -dimensional vector  $\Delta x_i = \hat{x}_i - x_i$  is the error at  $i$ th periodic point. In terms of the shift matrix  $\sigma$ , the one-time step cycle Jacobian matrix (12.61) can be written as

$$\mathcal{J} = \mathbf{1} - \sigma f', \quad \sigma = \begin{pmatrix} 0 & 0 & 1 \\ 1 & 0 & 0 \\ 0 & 1 & 0 \end{pmatrix}, \quad f' = \begin{pmatrix} f'_1 & 0 & 0 \\ 0 & f'_2 & 0 \\ 0 & 0 & f'_3 \end{pmatrix}. \quad (12.62)$$

Suppose all  $|f'_k| > 1$ , so forward in time the errors are growing. We can make errors contract by going backwards in time, i.e., evaluating the inverse matrix  $\mathcal{J}$ , and noting that every 3rd power  $(\sigma f')^3 = J_p \mathbf{1}$  is diagonal,

$$\begin{aligned} \frac{1}{\mathbf{1} - \sigma f'} &= \sum_{j=0}^{\infty} (\sigma f')^j = \sum_{k=0}^{\infty} J_p^k \sum_{\ell=0}^2 (\sigma f')^\ell = \frac{1}{1 - J_p} [\mathbf{1} + \sigma f' + (\sigma f')^2] \quad (12.63) \\ &= \frac{1}{1 - J} \left[ \mathbf{1} + \sigma \begin{pmatrix} f'_1 & 0 & 0 \\ 0 & f'_2 & 0 \\ 0 & 0 & f'_3 \end{pmatrix} + \sigma^2 \begin{pmatrix} f'_2 f'_1 & 0 & 0 \\ 0 & f'_3 f'_2 & 0 \\ 0 & 0 & f'_1 f'_3 \end{pmatrix} \right], \end{aligned}$$

where  $J_p = f'_3 f'_2 f'_1$  is the forward-in-time stability of the cycle  $p$ , so

$$\begin{pmatrix} \Delta x_1 \\ \Delta x_2 \\ \Delta x_3 \end{pmatrix} = \frac{1}{1 - J_p} \begin{pmatrix} \delta x'_1 + f'_3 \delta x'_3 + f'_3 f'_2 \delta x'_2 \\ \delta x'_2 + f'_1 \delta x'_1 + f'_1 f'_3 \delta x'_3 \\ \delta x'_3 + f'_2 \delta x'_2 + f'_2 f'_1 \delta x'_1 \end{pmatrix}.$$

For an unstable cycle, the error gets contracted by overall factor  $1/(1 - J)$ , with the earlier errors amplified by the orbit instability; for example,  $\Delta x_3$  receives a contribution from two time steps in the past of form  $f'_2 f'_1 \delta x'_1$ .

By explicit evaluation, for 1-dimensional maps<sup>13</sup>  $\mathcal{J}(x)^3 = (1 - J_p)\mathbf{1} + (\dots)$  and

$$\text{Det } \mathcal{J}_p = \det(1 - J_p) \quad (12.64)$$

for the  $d$ -dimensional case.  $\mathcal{J}(x)$  is a cycle rotation by one time step; for a 3-cycle we are back, times a constant, uniform factor multiplying all errors by the rotation invariant scalar quantity  $\det(1 - J_p)$ , whose inverse happens to be the cycle-expansions' size of the neighborhood of cycle  $p$ .

### Example 12.2. Temporal lattice stability of a 3-cycle.

Consider an period- $n$  periodic state  $X_p$ , with  $d$  fields  $\{x_{t,1}, x_{t,2}, \dots, x_{t,d}\}$  on each lattice site  $t$  satisfying the condition

$$x_t - f(x_{t-1}) = 0, \quad t = 1, 2, \dots, n, \quad (12.65)$$

where  $d$ -dimensional time evolution function. A deviation  $\Delta X$  from  $X_p$  must satisfy the linearized condition

$$\Delta x_t - \mathbb{J}_{t-1} \Delta x_{t-1} = 0, \quad (\mathbb{J}_t)_{ij} = \left. \frac{\partial f(x)_i}{\partial x_j} \right|_{x_i = x_{t,i}}, \quad (12.66)$$

where  $\mathbb{J}_t$  is the 1-time step  $[d \times d]$  time-evolution Jacobian matrix. Let  $\mathbf{1}_d$  be a  $d$ -dimensional identity matrix. For an period- $n$  periodic state  $X_p$ , the orbit Jacobian matrix

<sup>13</sup>Predrag 2019-10-10: Still have to derive this formula, probably by  $\ln \det = \text{tr } \ln$  relation

$\mathcal{J}_p \Delta X = 0$  is an  $[nd \times nd]$  matrix

$$\mathcal{J}_p = \mathbf{1} - r^{-1}\mathbb{J} = \begin{pmatrix} \mathbf{1}_d & & & -\mathbb{J}_n \\ -\mathbb{J}_1 & \mathbf{1}_d & & \\ & -\mathbb{J}_2 & \ddots & \\ & & & \mathbf{1}_d \\ & & & -\mathbb{J}_{n-1} & \mathbf{1}_d \end{pmatrix}, \quad (12.67)$$

where the  $[nd \times nd]$  matrix

$$r = \begin{pmatrix} 0 & \mathbf{1}_d & & \\ & 0 & \mathbf{1}_d & \\ & & & \ddots \\ & & & 0 & \mathbf{1}_d \\ \mathbf{1}_d & & & & 0 \end{pmatrix}, \quad (12.68)$$

implements the shift operation, a cyclic permutation that translates forward in time the periodic state  $X_p$  by one site,  $(rX)^T = (x_2, x_3, \dots, x_n, x_1)$ .

To evaluate the Hill determinant (??), note that  $r^n = \mathbf{1}$ , that  $\text{tr}((r^{-1}\mathbb{J})^k) = n\delta_{k, rn} \text{tr} \mathbb{J}_p^r$  is non-vanishing only if  $k$  is a multiple of  $n$ , and expand

$$\begin{aligned} \ln \text{Det}(\mathcal{J}_p) &= \text{tr} \ln(\mathbf{1} - r^{-1}\mathbb{J}) = - \sum_{k=1}^{\infty} \frac{1}{k} \text{tr}((r^{-1}\mathbb{J})^k) \\ &= - \text{tr} \sum_{r=1}^{\infty} \frac{1}{r} \mathbb{J}_p^r = \ln \det(\mathbf{1}_d - \mathbb{J}_p). \end{aligned} \quad (12.69)$$

So, the Hill determinant for any hyperbolic 2-term difference equation on a temporal lattice is

$$\text{Det}(\mathcal{J}_p) = \det(\mathbf{1}_d - \mathbb{J}_p).$$

In the temporal Bernoulli case, the field  $x_t$  is a scalar, and the 1-time step  $[d \times d]$  time-evolution Jacobian matrix (12.66) at any time is simply  $\mathbb{J}_t = s$ , so

$$N_n = |\text{Det} \mathcal{J}| = s^n - 1, \quad (12.70)$$

in agreement with the time-evolution count.

In terms of the shift matrix  $r$ , the one-time step cycle Jacobian matrix (12.61) can be written as

$$\mathcal{J}_p = \mathbf{1} - r^{-1}\mathbb{J}, \quad r = \begin{pmatrix} 0 & 0 & \mathbf{1}_d \\ \mathbf{1}_d & 0 & 0 \\ 0 & \mathbf{1}_d & 0 \end{pmatrix}, \quad \mathbb{J} = \begin{pmatrix} \mathbb{J}_1 & 0 & 0 \\ 0 & \mathbb{J}_2 & 0 \\ 0 & 0 & \mathbb{J}_3 \end{pmatrix}. \quad (12.71)$$

Suppose all  $\mathbb{J}_p \neq 1$ . Note that every  $n$ th power  $(r\mathbb{J})^3 = \mathbb{J}_p\mathbb{J}$  is diagonal,

$$\begin{aligned} \frac{1}{\mathbf{1} - r\mathbb{J}} &= \sum_{j=0}^{\infty} (r\mathbb{J})^j = \sum_{k=0}^{\infty} \mathbb{J}_p^k \sum_{\ell=0}^2 (r\mathbb{J})^\ell = \frac{1}{\mathbf{1} - \mathbb{J}_p} [\mathbb{J} + r\mathbb{J} + (r\mathbb{J})^2] \\ &= \frac{\mathbf{1}}{\mathbf{1} - \mathbb{J}} \left[ \mathbb{J} + r \begin{pmatrix} \mathbb{J}_1 & 0 & 0 \\ 0 & \mathbb{J}_2 & 0 \\ 0 & 0 & \mathbb{J}_3 \end{pmatrix} + r^2 \begin{pmatrix} \mathbb{J}_2\mathbb{J}_1 & 0 & 0 \\ 0 & \mathbb{J}_3\mathbb{J}_2 & 0 \\ 0 & 0 & \mathbb{J}_1\mathbb{J}_3 \end{pmatrix} \right], \end{aligned} \quad (12.72)$$

where  $\mathbb{J}_p = \mathbb{J}_3\mathbb{J}_2\mathbb{J}_1$  is the forward-in-time stability of the cycle  $p$ .

To summarize, a discretized, temporal lattice periodic orbit linear stability can be computed in two ways - either by computing the  $[n_p d \times n_p d]$  Jacobian matrix  $\mathcal{J}(x)$ , or by computing  $\mathbb{J}_p$

$$|\text{Det } \mathcal{J}_p| = |\det(1 - \mathbb{J}_p)|, \quad (12.73)$$

where  $\mathbb{J}_p$  is the  $n_p$  time-steps  $[d \times d]$  forward-time Jacobian matrix. In the limit of discretization  $n_p \rightarrow \infty$  the left hand side is a *functional* determinant of an  $\infty$ -dimensional *operator*. Nevertheless, thanks to the discrete Fourier diagonalization of  $\mathcal{J}(x)$ , appendix ??, the determinant  $\text{Det } \mathcal{J}_p$  is easier to compute than the ill-posed  $\mathbb{J}_p$ .<sup>14 15</sup>

## 12.8 Han's temporal cat Hill's formula

The orbit Jacobian matrix of the  $T = 4$  temporal cat has form:

$$\mathcal{J} = \begin{pmatrix} -s & 1 & 0 & 1 \\ 1 & -s & 1 & 0 \\ 0 & 1 & -s & 1 \\ 1 & 0 & 1 & -s \end{pmatrix}.$$

For example, the  $T = 4$  the orbit Jacobian matrix expressed in the terms of the one-step  $[2 \times 2]$  temporal Jacobian matrix (21.240) is:

$$\hat{\mathbf{J}}_1 = \mathbf{1} - r^{-1} \otimes J \quad (12.74)$$

$$= \begin{pmatrix} 1 & 0 & 0 & 0 & 0 & 0 & 0 & -1 \\ 0 & 1 & 0 & 0 & 0 & 0 & 1 & -s \\ \hline 0 & -1 & 1 & 0 & 0 & 0 & 0 & 0 \\ 1 & -s & 0 & 1 & 0 & 0 & 0 & 0 \\ \hline 0 & 0 & 0 & -1 & 1 & 0 & 0 & 0 \\ 0 & 0 & 1 & -s & 0 & 1 & 0 & 0 \\ \hline 0 & 0 & 0 & 0 & 0 & -1 & 1 & 0 \\ 0 & 0 & 0 & 0 & 1 & -s & 0 & 1 \end{pmatrix}.$$

$$\det(\mathbf{1} - r^{-1} \otimes J) = \det(\mathbf{1} - J \otimes r^{-1}) = \det[(\mathbf{1} - J \otimes r^{-1})(\mathbf{1}_{[2 \times 2]} \otimes r)],$$

<sup>14</sup>Predrag 2019-10-10:  $\mathcal{J}(x)$  is block-diagonalized by the discrete Fourier transform on a periodic lattice of three sites. Write up next the discrete Fourier evaluation of  $\text{Det } \mathcal{J}_p$ .

<sup>15</sup>Predrag 2019-10-10: Rewrite the derivation of the Hill-Poincaré-Van Vleck stability matrix (12.55) for symplectic / Lagrangian Hessians (orbit Jacobian matrix) using the shift matrix (12.62).



where:

$$\mathbf{1} - J \otimes r^{-1} = \left( \begin{array}{cccc|cccc} 1 & 0 & 0 & 0 & 0 & 0 & 0 & -1 \\ 0 & 1 & 0 & 0 & -1 & 0 & 0 & 0 \\ 0 & 0 & 1 & 0 & 0 & -1 & 0 & 0 \\ 0 & 0 & 0 & 1 & 0 & 0 & -1 & 0 \\ \hline 0 & 0 & 0 & 1 & 1 & 0 & 0 & -s \\ 1 & 0 & 0 & 0 & -s & 1 & 0 & 0 \\ 0 & 1 & 0 & 0 & 0 & -s & 1 & 0 \\ 0 & 0 & 1 & 0 & 0 & 0 & -s & 1 \end{array} \right),$$

and

$$(\mathbf{1} - J \otimes r^{-1}) (\mathbf{1}_{[2 \times 2]} \otimes r) = \left( \begin{array}{cccc|cccc} 0 & 1 & 0 & 0 & -1 & 0 & 0 & 0 \\ 0 & 0 & 1 & 0 & 0 & -1 & 0 & 0 \\ 0 & 0 & 0 & 1 & 0 & 0 & -1 & 0 \\ \hline 1 & 0 & 0 & 0 & 0 & 0 & 0 & -1 \\ 1 & 0 & 0 & 0 & -s & 1 & 0 & 0 \\ 0 & 1 & 0 & 0 & 0 & -s & 1 & 0 \\ 0 & 0 & 1 & 0 & 0 & 0 & -s & 1 \\ 0 & 0 & 0 & 1 & 1 & 0 & 0 & -s \end{array} \right).$$

A block matrix is a matrix defined by smaller matrices, called blocks. The determinant of a block matrix is [72] (see [wiki](#)):

$$\det \begin{pmatrix} A & B \\ C & D \end{pmatrix} = \det(A) \det(D - CA^{-1}B). \quad (12.75)$$

or

$$\det \begin{pmatrix} A & B \\ C & D \end{pmatrix} = \det(D) \det(A - BD^{-1}C). \quad (12.76)$$

## 12.9 Han's 2nd order difference eq. Hill's formula

**2022-01-16 Han** A map of form  $x_{t+1} = f(x_{t-1}, x_t)$  can be replaced by a pair of 1st order difference equation for the 2-component field  $\hat{x}_t = (x_{t-1}, x_t)$ :

$$\hat{x}_{t+1} = \hat{f}(\hat{x}_t) = \begin{pmatrix} \hat{x}_{t,2} \\ f(\hat{x}_{t,1}, \hat{x}_{t,2}) \end{pmatrix} = \begin{pmatrix} x_t \\ f(x_{t-1}, x_t) \end{pmatrix}. \quad (12.77)$$

The trace of the Perron-Frobenius operator is:

$$\begin{aligned} \text{tr } \mathcal{L}^n &= \int d\hat{x}_0 \delta(\hat{x}_0 - \hat{f}^n(\hat{x}_0)) \\ &= \int \prod_{t=0}^{n-1} (d\hat{x}_t \delta(\hat{x}_{t+1} - \hat{f}(\hat{x}_t))), \quad \hat{x}_{t+n} = \hat{x}_t. \\ &= \int \prod_{t=0}^{n-1} (d\hat{x}_{t,1} d\hat{x}_{t,2} \delta(\hat{x}_{t+1,1} - \hat{x}_{t,2}) \delta(\hat{x}_{t+1,2} - f(\hat{x}_{t,1}, \hat{x}_{t,2}))). \end{aligned} \quad (12.78)$$

Integrating over the first components  $d\hat{x}_{t,1}$  and using the trivial Dirac delta  $\delta(\hat{x}_{t+1,1} - \hat{x}_{t,2})$ , we can drop the  $d\hat{x}_{t,1}$  and rewrite  $\hat{x}_{t,1}$  as  $\hat{x}_{t-1,2}$ . So the trace becomes:

$$\begin{aligned} \text{tr } \mathcal{L}^n &= \int d\hat{x}_0 \delta(\hat{x}_0 - \hat{f}^n(\hat{x}_0)) \\ &= \int \prod_{t=0}^{n-1} (d\hat{x}_{t,2} \delta(\hat{x}_{t+1,2} - f(\hat{x}_{t-1,2}, \hat{x}_{t,2}))) . \end{aligned} \quad (12.79)$$

Now write  $\hat{x}_{t,2}$  as  $x_t$ , we have:

$$\begin{aligned} \text{tr } \mathcal{L}^n &= \int \prod_{t=0}^{n-1} (dx_t \delta(x_{t+1} - f(x_{t-1}, x_t))) \\ &= \int [d\mathbf{X}] \prod_{t=0}^{n-1} \delta(x_{t+1} - f(x_{t-1}, x_t)), \quad d\mathbf{X} = \prod_{t=0}^{n-1} dx_t . \end{aligned} \quad (12.80)$$

Note that before we integrate the Dirac delta function, we should write the map  $\hat{f}_t$  as a map from  $\hat{x}_t$  to  $\hat{x}_{t+1}$ .

**2022-01-16 Predrag** That looks about right - I have a small notational suggestion in *LC21.tex*. Can you try to polish that section, while I move on with editing to other sections? I think this derivation is the simpler than any I have seen for Hamiltonian systems. Doin it as delta-function deterministic kernels really helps.

### 12.9.1 Hill's formula for a second-order system

16

Consider an period- $n$  periodic state  $X_p$ , with  $d$  fields  $\{x_{t,1}, x_{t,2}, \dots, x_{t,d}\}$  on each temporal lattice site  $t$  satisfying the condition

$$x_{t+1} - f(x_{t-1}) + x_{t-1} = 0, \quad t = 1, 2, \dots, n, \quad (12.81)$$

where  $f(x)$  is a  $d$ -dimensional function.

Consider one-dimensional Schrödinger equation [22, 24, 54, 62],  $H = -d^2/dx^2 + V(x)$  with  $V(x)$  almost periodic and the discrete (= tight binding) analog, i.e., the doubly infinite Jacobi matrix

$$h_{ij} = \delta_{i,j+1} + V_i \delta_{ij} + \delta_{i,j-1} \quad (12.82)$$

with  $V_n$  almost periodic on the integers.

A deviation  $\Delta X$  from  $X_p$  then satisfies the linearized condition

$$\Delta x_t - \mathbb{J}_{t-1} \Delta x_{t-1} = 0, \quad (\mathbb{J}_t)_{ij} = \left. \frac{\partial f(x)_i}{\partial x_j} \right|_{x_j = x_{t,j}}, \quad (12.83)$$

<sup>16</sup>Predrag 2020-12-15: Merge sect. ?? *Spatiotemporal cat Hill's formula* into his, to transfer to CL18.tex. Once incorporated, remove from here (too much duplication, as is)

where  $\mathbb{J}_t$  is the two-configuration  $[d \times d]$  Jacobian matrix.

In our notation (16.81) is written as (2.95)

$$x_{\ell+1} - d_\ell x_\ell + x_{\ell-1} = -s_\ell, \quad (12.84)$$

He, as everybody else, sooner or later, rewrites (16.84) in the ‘Percival-Vivaldi’ ‘two-configuration representation’ [24, 55] matrix  $J$  (2.5),

$$\begin{bmatrix} \Delta\phi_t \\ \Delta\phi_{t+1} \end{bmatrix} = \begin{bmatrix} 0 & \mathbf{1}_d \\ -\mathbf{1}_d & \mathbb{J}_t \end{bmatrix} \begin{bmatrix} \Delta\phi_{t-1} \\ \Delta\phi_t \end{bmatrix}. \quad (12.85)$$

(note ‘upside-down’ 2D vector), and concerns himself with the rational, energy  $\text{tr } J^m < 2$ , oscillatory case.

Note, it’s only about the order of recurrence, nobody says the systems should be Hamiltonian / Lagrangian, works for dissipative systems as well.

A deviation  $\Delta X$  from  $X_p$  then satisfies the linearized condition

$$\Delta x_t - \mathbb{J}_{t-1} \Delta x_{t-1} = 0, \quad (\mathbb{J}_t)_{ij} = \left. \frac{\partial f(x)_i}{\partial x_j} \right|_{x_j = x_{t,j}}, \quad (12.86)$$

where  $\mathbb{J}_t$  is the two-configuration  $[d \times d]$  Jacobian matrix.

It suffices to work out a temporal period  $n = 3$  example to understand the calculation for any period. In terms of the  $[3d \times 3d]$  matrix shift matrix  $r$ , the orbit Jacobian matrix can be written as

$$\mathcal{J}_p = \mathbf{1} - r^{-1}\mathbb{J}, \quad r^{-1} = \begin{bmatrix} 0 & 0 & \mathbf{1}_d \\ \mathbf{1}_d & 0 & 0 \\ 0 & \mathbf{1}_d & 0 \end{bmatrix}, \quad \mathbb{J} = \begin{bmatrix} \mathbb{J}_1 & 0 & 0 \\ 0 & \mathbb{J}_2 & 0 \\ 0 & 0 & \mathbb{J}_3 \end{bmatrix}, \quad (12.87)$$

where  $\mathbf{1}_d$  is the  $d$ -dimensional identity matrix. Next, note that

$$(r^{-1}\mathbb{J})^2 = r^{-2} \begin{bmatrix} \mathbb{J}_2\mathbb{J}_1 & 0 & 0 \\ 0 & \mathbb{J}_3\mathbb{J}_2 & 0 \\ 0 & 0 & \mathbb{J}_1\mathbb{J}_3 \end{bmatrix}, \quad (r^{-1}\mathbb{J})^3 = \begin{bmatrix} \mathbb{J}_2\mathbb{J}_1\mathbb{J}_3 & 0 & 0 \\ 0 & \mathbb{J}_3\mathbb{J}_2\mathbb{J}_1 & 0 \\ 0 & 0 & \mathbb{J}_1\mathbb{J}_3\mathbb{J}_2 \end{bmatrix},$$

as  $r^{-3} = \mathbf{1}$ . Likewise, as  $r^n = \mathbf{1}$  for any period  $n$ , the trace of  $[nd \times nd]$  matrix

$$\text{tr} (r^{-1}\mathbb{J})^k = \delta_{k, rn} n \text{tr } \mathbb{J}_p^r, \quad \mathbb{J}_p = \mathbb{J}_n \mathbb{J}_{n-1} \cdots \mathbb{J}_2 \mathbb{J}_1$$

is non-vanishing only if  $k$  is a multiple of  $n$ , with  $\mathbb{J}_p$  the forward-in-time  $[d \times d]$  Jacobian matrix of the periodic orbit  $p$ .

Now we can evaluate the Hill determinant (8.122) by expanding

$$\begin{aligned} \ln \text{Det} (\mathcal{J}_p) &= \text{tr} \ln (\mathbf{1} - r^{-1}\mathbb{J}) = - \sum_{k=1}^{\infty} \frac{1}{k} \text{tr} (r^{-1}\mathbb{J})^k \\ &= - \text{tr} \sum_{r=1}^{\infty} \frac{1}{r} \mathbb{J}_p^r = \ln \det (\mathbf{1}_d - \mathbb{J}_p). \end{aligned} \quad (12.88)$$

The Hill determinant for a 2-term difference equation (??) on a temporal lattice

$$\text{Det}(\mathcal{J}_p) = \det(\mathbf{1}_d - \mathbb{J}_p)$$

thus relates the global orbit stability to the Floquet, temporal evolution stability. In the temporal Bernoulli case, the field  $x_t$  is a scalar, and the 1-time step  $[1 \times 1]$  time-evolution Jacobian matrix (12.57) at every lattice point  $t$  is simply  $\mathbb{J}_t = s$ , so

$$N_n = |\text{Det } \mathcal{J}| = s^n - 1, \quad (12.89)$$

in agreement with the time-evolution count.

## 12.10 Han's spatiotemporal cat Hill's formula

Consider a  $[L \times T]_0$  rectangular primitive cell. In the Kronecker product block matrix notation (12.18), the orbit Jacobian matrix  $\text{refeq}\{\text{eq:BxAtemp}\}$  is the  $[LT \times LT]$  block matrix (21.239):

$$\mathcal{J} = \mathbf{1}_1 \otimes (r_2 + r_2^{-1}) - 2s\mathbf{1} + (r_1 + r_1^{-1}) \otimes \mathbf{1}_2.$$

The temporal Jacobian matrix  $\mathbf{J}$  is:

$$\mathbf{J} = \begin{pmatrix} \mathbf{0}_1 & \mathbf{1}_1 \\ -\mathbf{1}_1 & -\hat{\mathcal{J}}_1 \end{pmatrix},$$

where  $\hat{\mathcal{J}}_1$  is a  $[L \times L]$  matrix (21.244):

$$\hat{\mathcal{J}}_1 = r_1^{-1} - 2s\mathbf{1}_1 + r_1.$$

There is another  $[2LT \times 2LT]$  orbit Jacobian matrix:

$$\mathcal{J}' = \mathbf{1} - r_2^{-1} \otimes \mathcal{J}_1.$$

Here we will show that:

$$\det \mathcal{J} = \det \mathcal{J}'.$$

$$\begin{aligned} \det \mathcal{J}' &= \det(\mathbf{1} - r_2^{-1} \otimes \mathcal{J}_1) = \det(\mathbf{1} - \mathcal{J}_1 \otimes r_2^{-1}) \\ &= \det[(\mathbf{1} \otimes r_2)(\mathbf{1} - \mathcal{J}_1 \otimes r_2^{-1})] \\ &= \det(\mathbf{1} \otimes r_2 - \mathcal{J}_1 \otimes \mathbf{1}_2) \\ &= \det \left\{ \begin{pmatrix} \mathbf{1}_1 \otimes r_2 & 0 \\ 0 & \mathbf{1}_1 \otimes r_2 \end{pmatrix} - \begin{pmatrix} 0 & \mathbf{1}_1 \otimes \mathbf{1}_2 \\ -\mathbf{1}_1 \otimes \mathbf{1}_2 & -\hat{\mathcal{J}}_1 \otimes \mathbf{1}_2 \end{pmatrix} \right\} \\ &= \det \begin{pmatrix} \mathbf{1}_1 \otimes r_2 & -\mathbf{1}_1 \otimes \mathbf{1}_2 \\ \mathbf{1}_1 \otimes \mathbf{1}_2 & \mathbf{1}_1 \otimes r_2 + \hat{\mathcal{J}}_1 \otimes \mathbf{1}_2 \end{pmatrix} \\ &= \det(\mathbf{1}_1 \otimes r_2 + \hat{\mathcal{J}}_1 \otimes \mathbf{1}_2 + \mathbf{1}_1 \otimes r_2^{-1}) \\ &= \det \mathcal{J}. \end{aligned} \quad (12.90)$$

### 12.10.1 Han's relative-periodic Hill's formula

Consider a 'tilted' or 'relative periodic'  $[L \times T]_S$  primitive cell for which we have after one time period:

$$\hat{\mathbf{J}}_p \hat{\mathbf{u}}_t = \hat{\mathbf{u}}_{t+T} = \mathbf{g}_S^{-1} \hat{\mathbf{u}}_t,$$

so

$$\left( \hat{\mathbf{1}}_1 - \mathbf{g}_S \hat{\mathbf{J}}_p \right) \hat{\mathbf{u}}_t = 0.$$

First we will show that:

$$\det \hat{\mathcal{J}}' = \det \left( \hat{\mathbf{1}}_1 - \mathbf{g}_S \hat{\mathbf{J}}_p \right), \quad (12.91)$$

where

$$\mathbf{g}_S = \left[ \begin{array}{c|c} r_1^S & 0 \\ \hline 0 & r_1^S \end{array} \right], \quad (12.92)$$

The right hand side of (12.91) is different from (12.38), because ...

Note that  $\mathbf{g}_S$  and  $\hat{\mathbf{J}}_1$  commute. Let  $u_{nt}$  be a variation on the field  $x_{nt}$ .

$$\hat{\mathbf{u}}_t = \left[ \begin{array}{c} \mathbf{u}_{t-1} \\ \mathbf{u}_t \end{array} \right], \quad \mathbf{u}_t = \left[ \begin{array}{c} u_{1t} \\ \vdots \\ u_{Lt} \end{array} \right].$$

Now we need to know the form of  $\hat{\mathcal{J}}'$  in (12.91). Let:

$$\hat{\mathbf{u}} = \left[ \begin{array}{c} \hat{\mathbf{u}}_1 \\ \hat{\mathbf{u}}_2 \\ \vdots \\ \hat{\mathbf{u}}_{T-1} \\ \hat{\mathbf{u}}_T \end{array} \right].$$

Then

$$\hat{\mathcal{J}}' = \left[ \begin{array}{cc|cc} \hat{\mathbf{1}}_1 & & & -\hat{\mathbf{J}}_1 \mathbf{g}_S \\ -\hat{\mathbf{J}}_1 & \hat{\mathbf{1}}_1 & & \\ & & \ddots & \\ & & -\hat{\mathbf{J}}_1 & \hat{\mathbf{1}}_1 \end{array} \right],$$

where  $\mathbf{g}_S$  is the 'tilt' (12.92), and  $\hat{\mathcal{J}}' \hat{\mathbf{u}} = 0$  for a periodic perturbation field. In an analogy with the usual construction of Floquet matrices, let  $\mathbf{g}_S^{1/T}$  be a  $T$ 'th root of the total relative shift  $\mathbf{g}_S$ . Change the field to a co-moving frame  $\hat{\mathbf{u}}_t \rightarrow \hat{\mathbf{w}}_t$ , where  $\hat{\mathbf{u}}_t = \mathbf{g}_S^{-t/T} \hat{\mathbf{w}}_t$ . Now  $\hat{\mathcal{J}}'$  is replaced by  $\hat{\mathcal{J}}'_S$ :

$$\hat{\mathcal{J}}'_S = \hat{\mathbf{1}} - r_2^{-1} \otimes \left( \hat{\mathbf{J}}_1 \mathbf{g}_S^{1/T} \right).$$

Then we have  $\hat{\mathcal{J}}'_S \hat{\mathbf{w}} = 0$  when  $\hat{\mathcal{J}}' \hat{\mathbf{u}} = 0$ . Using the method from (21.253),

$$\det \hat{\mathcal{J}}'_S = \det \left[ \hat{\mathbf{1}}_1 - \left( \hat{\mathbf{J}}_1 \mathbf{g}_S^{1/T} \right)^T \right] = \det \left( \hat{\mathbf{1}}_1 - \hat{\mathbf{J}}_1^T \mathbf{g}_S \right) = \det \left( \hat{\mathbf{1}}_1 - \mathbf{g}_S \hat{\mathbf{J}}_1^T \right).$$

When we change to the co-moving frame  $\hat{\mathbf{u}}_t \rightarrow \hat{\mathbf{w}}_t$ , all of the operators are changed by a similarity transformation:

$$\hat{\mathcal{J}}'_S = \hat{\mathbf{P}} \hat{\mathcal{J}}' \hat{\mathbf{P}}^{-1},$$

where

$$\hat{\mathbf{P}} = \text{diag} \left( \mathbf{g}_S^{1/T}, \mathbf{g}_S^{2/T}, \dots, \mathbf{g}_S^{(T-1)/T}, \mathbf{g}_S \right)$$

is a  $[2LT \times 2LT]$  block diagonal matrix. In the co-moving frame, we have  $\hat{\mathbf{w}}_t = \mathbf{g}_S^{t/T} \hat{\mathbf{u}}_t$ ,  $\hat{\mathbf{w}} = \hat{\mathbf{P}} \hat{\mathbf{u}}$  and  $\mathbf{w} = \mathbf{P} \mathbf{u}$ , where

$$\mathbf{u} = \begin{bmatrix} \mathbf{u}_1 \\ \mathbf{u}_2 \\ \vdots \\ \mathbf{u}_{T-1} \\ \mathbf{u}_T \end{bmatrix},$$

and

$$\mathbf{P} = \text{diag} \left( r_1^{S/T}, r_1^{2S/T}, \dots, r_1^{(T-1)S/T}, r_1^S \right).$$

Now we can prove that (12.46) is the orbit Jacobian matrix for the tilted primitive cell in the co-moving frame. The orbit Jacobian matrix for the tilted primitive cell in the original frame is:

$$\mathcal{J}_{[L \times T]_S} = \begin{pmatrix} \mathcal{J}_1 & \mathbf{1}_1 & & r_1^S \\ \mathbf{1}_1 & \mathcal{J}_1 & \mathbf{1}_1 & \\ & \ddots & \ddots & \ddots \\ & & \mathbf{1}_1 & \mathcal{J}_1 & \mathbf{1}_1 \\ r_1^{-S} & & & \mathbf{1}_1 & \mathcal{J}_1 \end{pmatrix},$$

which can also be written as:

$$\mathcal{J}_{[L \times T]_S} = 2s \mathbf{1}_2 \otimes \mathbf{1}_1 + \mathbf{1}_2 \otimes (r_1 + r_1^{-1}) + \mathbf{B},$$

where

$$\mathbf{B} = \begin{pmatrix} 0 & \mathbf{1}_1 & & r_1^S \\ \mathbf{1}_1 & 0 & \mathbf{1}_1 & \\ & \ddots & \ddots & \ddots \\ & & \mathbf{1}_1 & 0 & \mathbf{1}_1 \\ r_1^{-S} & & & \mathbf{1}_1 & 0 \end{pmatrix}$$

and the rest of  $\mathcal{J}_{[L \times T]_S}$  is the diagonal part. The diagonal part commutes with  $\mathbf{P}$  since  $\mathcal{J}_1$  and  $r_1^{-S/T}$  commute. So the diagonal part is unchanged after the similarity transformation. The block matrix  $\mathbf{B}$  becomes:

$$\mathbf{PBP}^{-1} = \begin{pmatrix} 0 & r_1^{-S/T} & & & r_1^{S/T} \\ r_1^{S/T} & 0 & r_1^{-S/T} & & \\ & \ddots & \ddots & \ddots & \\ & & r_1^{S/T} & 0 & r_1^{-S/T} \\ r_1^{-S/T} & & r_1^{S/T} & 0 & 0 \end{pmatrix} = r_2 \otimes r_1^{-S/T} + r_2^{-1} \otimes r_1^{S/T}.$$

So the orbit Jacobian matrix in the co-moving frame is:

$$\mathbf{P}\mathcal{J}_{[L \times T]_S}\mathbf{P}^{-1} = r_2 \otimes r_1^{-S/T} + r_2^{-1} \otimes r_1^{S/T} + \mathbf{1}_2 \otimes (r_1 + r_1^{-1}) + 2s \mathbf{1}_2 \otimes \mathbf{1}_1.$$

## 12.11 Han's Hénon map Hill's formula

The temporal evolution Jacobian matrix of the Hénon map (3.61) is:

$$J(\phi_n) = \frac{\partial(\phi_n, \phi_{n+1})}{\partial(\phi_{n-1}, \phi_n)} = \begin{bmatrix} 0 & 1 \\ -1 & -2a\phi_n \end{bmatrix}.$$

For the periodic orbit  $X_p$  with period  $n$ , we have two orbit Jacobian matrices: The  $[n \times n]$  orbit Jacobian matrix from the 3-term recurrence relation (3.62),

$$\mathcal{J}_p = \begin{bmatrix} 2\phi_0 & 1 & 0 & 0 & \dots & 0 & 1 \\ 1 & 2\phi_1 & 1 & 0 & \dots & 0 & 0 \\ 0 & 1 & 2\phi_2 & 1 & \dots & 0 & 0 \\ \vdots & \vdots & \vdots & \vdots & \ddots & \vdots & \vdots \\ 0 & 0 & \dots & \dots & \dots & 2\phi_{n-2} & 1 \\ 1 & 0 & \dots & \dots & \dots & 1 & 2\phi_{n-1} \end{bmatrix},$$

and the  $[2n \times 2n]$  orbit Jacobian matrix from the first-order difference equation,

$$\hat{\mathcal{J}}_p = \begin{bmatrix} \mathbf{1} & & & & -J(\phi_0) \\ -J(\phi_1) & \mathbf{1} & & & \\ & \ddots & \ddots & & \\ & & -J(\phi_{n-2}) & \mathbf{1} & \\ & & & -J(\phi_{n-1}) & \mathbf{1} \end{bmatrix},$$

where  $\mathbf{1}$  is the  $[2 \times 2]$  identity matrix.

To show

$$|\text{Det } \mathcal{J}_p| = |\text{Det } \hat{\mathcal{J}}_p|,$$

we need to use the  $[2n \times 2n]$  permutation matrix  $P$  to change the form of  $\hat{\mathcal{J}}_p$ . The matrix elements of  $P$  is the Kronecker (circular) delta function:

$$P_{kj} = \delta_{2k-2+\lceil k/n \rceil, j} = \frac{1}{2n} \sum_{l=0}^{2n-1} e^{i \frac{2\pi}{2n} (2k-2+\lceil k/n \rceil - j)l}, \quad (12.93)$$

where the  $\lceil x \rceil$  is the ceiling function. Using the permutation matrix  $P$ , the orbit Jacobian matrix  $\hat{\mathcal{J}}_p$  can be transformed into a block matrix:

$$P \hat{\mathcal{J}}_p P^\top = \left[ \begin{array}{ccccc|ccccc} 1 & 0 & \cdots & 0 & 0 & 0 & 0 & \cdots & 0 & -1 \\ 0 & 1 & \cdots & 0 & 0 & -1 & 0 & \cdots & 0 & 0 \\ \vdots & \vdots & \ddots & \vdots & \vdots & \vdots & \ddots & \ddots & \vdots & \vdots \\ 0 & 0 & \cdots & 1 & 0 & 0 & \cdots & -1 & 0 & 0 \\ 0 & 0 & \cdots & 0 & 1 & 0 & \cdots & 0 & -1 & 0 \\ \hline 0 & 0 & \cdots & 0 & 1 & 1 & 0 & \cdots & 0 & 2a\phi_0 \\ 1 & 0 & \cdots & 0 & 0 & 2a\phi_1 & 1 & \cdots & 0 & 0 \\ \vdots & \ddots & \ddots & \vdots & \vdots & \vdots & \ddots & \ddots & \vdots & \vdots \\ 0 & \cdots & 1 & 0 & 0 & 0 & \cdots & 2a\phi_{n-2} & 1 & 0 \\ 0 & \cdots & 0 & 1 & 0 & 0 & \cdots & 0 & 2a\phi_{n-1} & 1 \end{array} \right].$$

Then use (21.248) we have  $|\text{Det } \mathcal{J}_p| = |\text{Det } \hat{\mathcal{J}}_p|$ .

Now we will evaluate the Hill determinant  $|\det(\hat{\mathcal{J}}_p)|$  and prove the Hill's formula:

$$|\det(\hat{\mathcal{J}}_p)| = |\det(\mathbf{1} - J_p)|,$$

Where  $J_p = J(\phi_{n-1})J(\phi_{n-2}) \cdots J(\phi_1)J(\phi_0)$ .

Write the orbit Jacobian matrix  $\hat{\mathcal{J}}_p$  as:

$$\hat{\mathcal{J}}_p = \hat{\mathbf{1}} - \tilde{\mathcal{J}}_p,$$

where  $\hat{\mathbf{1}}$  is the  $[2n \times 2n]$  identity matrix and  $\tilde{\mathcal{J}}_p$  is a block matrix:

$$\tilde{\mathcal{J}}_p = \left[ \begin{array}{cccccc} 0 & & & & & J(\phi_0) \\ J(\phi_1) & 0 & & & & \\ & \ddots & \ddots & & & \\ & & J(\phi_{n-2}) & 0 & & \\ & & & J(\phi_{n-1}) & 0 & \end{array} \right].$$

Expand  $\ln \det \hat{\mathcal{J}}_p = \text{tr} \ln \hat{\mathcal{J}}_p$  as a series:

$$\text{tr} \ln \hat{\mathcal{J}}_p = \text{tr} \ln (\hat{\mathbf{1}} - \tilde{\mathcal{J}}_p) = - \sum_{k=1}^{\infty} \frac{1}{k} \text{tr} \tilde{\mathcal{J}}_p^k.$$



Note that  $\text{tr } \tilde{\mathcal{J}}_p^k$  is non-zero only when  $k$  is a multiple of  $n$ , and

$$\tilde{\mathcal{J}}_p^n = \begin{bmatrix} J(\phi_0)J(\phi_{n-1}) \dots J(\phi_1) & & & & & & \\ & J(\phi_1) \dots J(\phi_2) & & & & & \\ & & \ddots & & & & \\ & & & & & & \\ & & & & J(\phi_{n-2}) \dots J(\phi_{n-1}) & & \\ & & & & & & \\ & & & & & & J(\phi_{n-1}) \dots J(\phi_0) \end{bmatrix},$$

is a block diagonal matrix, with the  $j$ th block on the diagonal:

$$\begin{bmatrix} (\tilde{\mathcal{J}}_p^n)_{2j-1,2j-1} & (\tilde{\mathcal{J}}_p^n)_{2j-1,2j} \\ (\tilde{\mathcal{J}}_p^n)_{2j,2j-1} & (\tilde{\mathcal{J}}_p^n)_{2j,2j} \end{bmatrix} = J(\phi_{j-1})J(\phi_{j-2}) \dots J(\phi_1)J(\phi_0)J(\phi_{n-1})J(\phi_{n-2}) \dots J(\phi_{j+1})J(\phi_j).$$

So we have:

$$\ln \det \hat{\mathcal{J}}_p = - \sum_{k=1}^{\infty} \frac{1}{k} \text{tr } \tilde{\mathcal{J}}_p^k = - \sum_{r=1}^{\infty} \frac{1}{r} \text{tr } J_p^r = \text{tr } \ln (\mathbf{1} - J_p) = \ln \det (\mathbf{1} - J_p).$$

And we have proved the Hill's formula:

$$|\det (\hat{\mathcal{J}}_p)| = |\det (\mathbf{1} - J_p)|.$$

## 12.12 Hill's formula blog

For the latest entry, go to the bottom of this section

**2024-10-06 Predrag** Alternative titles for what is currently Liang and Cvitanović [44]

*A derivation of Hill's formulas* (2024), [siminos/hill/](https://siminos.github.io/hill/).

*Chaotic lattice field theory Hill's formulas*

**2022-01-30 Predrag** We have omitted (or forgotten? from exhaustion...) to mention in LC21 [43] four more ways of evaluating Hill determinants:

1. Symmetric polynomials (3.32), (22.21), (3.42), (3.44), (24.337). Please correct (4.206).
2. Hill determinant time-reversal factorization (6.54).
3. Kim-Lee-Park zeta function (6.162) gives a hint, but we still do not know how to use Endler and Gallas  $D_n$  factorization (3.34).
4. In the anti-integrable limit all stretching parameters  $d_j$  on  $\mathcal{J}$  diagonal are arbitrarily large, the 'kinetic energy' (off-diagonal '-1's) is swamped by the potential energy (4.318), so

$$\text{Det } (\mathcal{J}) \rightarrow \prod_{j=0}^{n-1} d_j. \quad (12.94)$$

Gershgorin circle theorem (22.54) is a refinement of the anti-integrable limit for  $d_j$  moderately large.

**2019-10-13 Predrag** Viswanath [71] describes, and numerically solves Hill's problem: " In 1878, Hill [23] derived the equations that describe the planar motion of the moon around the earth:

$$\begin{aligned} \ddot{x} - 2\dot{y} &= \frac{\partial \Omega}{\partial x} \\ \ddot{y} + 2\dot{x} &= \frac{\partial \Omega}{\partial y}, \quad \Omega = \frac{3}{2}x^2 + (x^2 + y^2)^{-1/2}. \end{aligned} \quad (12.95)$$

The Jacobi integral  $2\Omega - \dot{x}^2 - \dot{y}^2$  is constant along the solutions of Hill's equation, so each orbit is characterized by a "Jacobi constant." The orbits Viswanath (and Hill) computes are symmetric with respect to both the  $x$  and the  $y$  axes -  $C_2 \times C_2$ -symmetric, so it suffices to compute them to quarter-period  $T/4$ . He uses a Fourier series of width 64 and filters out 20% of the frequencies at the high end after each iteration.

I do not see Hill's formula in this paper. "

**2018-10-27 Predrag** Petrisor [56] *Twist number and order properties of periodic orbits* works mostly with the standard-like maps, but we might find her article useful both as a review of the standard literature, as well as an aid in understanding the  $\mathcal{J}$  of the cat map, and perhaps the twisted bc's (relative) invariant 2-tori of spatiotemporal cat as well.

Petrisor [57] *Monotone gradient dynamics and the location of stationary  $(p, q)$ -configurations* might also be of interest.

A standard-like map is a twist map  $F_\epsilon$ , defined by a Lagrangian generating function of the form

$$h(x, x') = \frac{1}{2}(x - x')^2 - \epsilon V(x),$$

where  $V$  is a fixed 1-periodic even function. Classical standard map corresponds to the potential  $V(x) = -\frac{1}{(2\pi)^2} \cos(2\pi x)$ . The twist map  $F_\epsilon$  is reversible, i.e. it factorizes as  $F_\epsilon = I \circ R$ , where  $R$  and  $I$  are the involutions. [...] The  $R$ -invariant orbits are called symmetric orbits.

A numerical characteristic associated with a periodic orbit is the rotation number, which measures the average rotation of the orbit around the annulus. Mather [50] defined also the amount of rotation, which is called twist number or torsion number. [...] Angenent [3] proved that in the space of  $(p, q)$ -sequences a critical point of the  $W_{pq}$  action [...] is connected by the negative gradient flow of the action.

The 1-cone function is defined on the phase space of a twist map and takes negative values within the region where the map exhibits strong folding property. We prove that the restriction of this function to a periodic orbit gives information on the eigenvalues of the orbit Jacobian matrix  $\mathcal{J}_q$  associated with that orbit.

[...] we revisit the definition and properties of the twist number of a periodic orbit based on the structure of the universal covering group of the group  $SL(2, \mathbb{R})$ . The twist number is defined as the translation number of a circle map induced by the monodromy matrix associated with the periodic orbit. [...] we give the relationship between the twist number value of a  $(p, q)$ -periodic orbit, and the position of the real number 0 with respect to the sequence of interlaced eigenvalues of the orbit Jacobian matrix  $\mathcal{J}_q$ , associated with the corresponding  $(p, q)$ -sequence, and of a symmetric matrix derived from  $H_q$ .

Petrisor eq. (11) expresses the Hessian in terms of the 1-step forward Jacobian matrix, and gives references to the related literature. In particular, the discrete Hill's formula, the characteristic polynomial of a periodic Jacobi matrix (16.79), and the Hill discriminant are presented in Toda [68].

The orbit Jacobian matrix  $\mathcal{J}_q$  of the  $W_{pq}$  action associated with a  $(p, q)$ -periodic orbit,  $q \leq 3$ , is a Jacobi periodic matrix (i.e. a symmetric tridiagonal matrix with non-null entries in the upper right, and left lower corners, and the next-to-diagonal entries have the same sign), see Petrisor eq. (19). For  $q = 2$ ,  $H_q$  is simply a symmetric matrix.

Let  $\mathcal{J}_q$  be the orbit Jacobian matrix of the action  $W_{pq}$  at a critical point  $x = (x_n)$ . The signature (the number of negative and positive eigenvalues) of the Hessian  $\mathcal{J}_q$ , at a non-degenerate minimizing sequence is  $(0, q)$ , while at the corresponding mini-maximizing sequence it is  $(1, q-1)$ . The number of negative eigenvalues is called the Morse index of the critical sequence.

**2020-08-02 Predrag** Toda [68] *Theory of Nonlinear Lattices* ([click here](#)).

Chapt. 4. *Periodic Systems* has way more wisdom than what I am capable of learning this Sunday.

Toda studies the classical mechanics of one-dimensional lattices (chains) of particles with nearest neighbor interaction; they are discrete and infinite in space, continuous in time.

When the force is proportional to displacement, that is, when Hooke's law is obeyed, the spring is said to be linear, the potential is quadratic. While for us that leads to site stretching rate  $s$ , for Toda it leads to the Laplacian ( $s = 2$ ), not sure why...

The *inverse scattering method* for an infinite lattice makes use of the discrete Schrodinger equation. For periodic systems this gives a discrete Hill's equation, and in place of the scattering data, it is convenient to use the spectrum of the discrete Hill's equation and the auxiliary spectrum for fixed boundary conditions of the same equation. In this case the fundamental solutions and the discriminant of the discrete Hill's equation play important roles. The discriminant is a polynomial of the spectrum, and the integral of motion is given in terms of elliptic integrals. Thus the initial value problem reduces to the inverse problem (Jacobi's inverse problem), or inverse spectral theory.

His discrete Hill's equation is continuous in time, so presumably most work is for stationary states; I have probably misunderstood the formulation...

He works with a 3-term recurrence (4.1.3a), and defines a 2-configuration monodromy matrix (4.1.11).

For special values of  $A$ , the solution of (4.1.4) can be periodic, but more generally it is relative periodic (4.1.16), or the Bloch function (its existence given by the Floquet theorem) which he relates to the trace of the monodromy matrix (4.1.19). The simplest example is his (4.1.23). His orbit Jacobian matrix (4.1.28) has variable diagonal and off diagonal elements, corresponding to nontrivial nonlinear solutions for  $d = 1$  lattice.

He says that the  $L = 3$  three-particle system [4.8] is important because, though the simplest, it shows nearly all the characteristic features which  $L$ -particle systems exhibit.

#### 2023-11-22 Percy Deift with

Luen-Chau Li, Herbert Spohn, Carlos Tomei, Thomas Trogdon, *On the open Toda chain with external forcing*, [arXiv:2012.02244](https://arxiv.org/abs/2012.02244), [Rutgers seminar](#): We consider the open Toda chain with external forcing, and in the case when the forcing stretches the system, we derive the longtime behavior of solutions of the chain. Using an observation of Jürgen Moser, we then show that the system is completely integrable, in the sense that the  $2N$ -dimensional system has  $N$  functionally independent Poisson commuting integrals, and also has a Lax-Pair formulation. In addition, we construct action-angle variables for the flow. In the case when the forcing compresses the system, the analysis of the flow remains open.

Predrag's comments:

1. There seems to be an equilibrium  $q_i = 0$  solution for  $c = -1$ . They should compute the spectrum of its Hessian. If it has complex pair eigenvalues, it would explain why the dynamics is oscillatory (they see something like that numerically). The weak perturbation probably makes it nearly chaotic.
2. Michael Berry: "I suffer from cognitive dissonance here. Isn't this chaotic scattering? Shouldn't there be a measure zero non-escaping set here?"
3. They should redo it in Lagrangian formalism, as we do.
4. Their space is discrete and finite ( $N$ -body). Fixed, not periodic bc's. Their time is continuous, the formulation is Hamiltonian. Possibly discrete time would make things nicer.
5. We could do all of that, if we had manpower:(

2020-07-24 Predrag Bolotin and Treschev [6] *Hill's formula*: give two multidimensional generalizations of Hill's formula:

1. to discrete Lagrangian systems (symplectic twist maps)
2. to continuous Lagrangian systems

They discuss additional aspects which appear in the presence of symmetries or reversibility.

1. study the change of the Morse index of a periodic trajectory after the reduction of order in a system with symmetries
2. applications to stability of periodic orbits

"In his study of periodic orbits of the 3 body problem, Hill obtained a formula relating the characteristic polynomial of the monodromy matrix of a periodic orbit and an infinite determinant of the Hessian of the action functional. A mathematically correct definition of the Hill determinant and a proof of Hill's formula were obtained later by Poincaré."

Hill computed  $\det H$  approximately replacing  $H$  by a  $3 \times 3$  matrix, which gave quite a good approximation. Hill did not prove convergence for the infinite determinant  $\det H$ . Poincaré [59] (Vol. I: Solutions périodiques. Non-existence des intégrales uniformes. Solutions asymptotiques) explained the meaning of the Hill determinant and presented a rigorous proof of Hill's formula. The equation appeared in 1983 for discrete Lagrangian systems in ref. [47] and independently in ref{4}. Here  $H$  is the finite Hessian matrix associated with the action functional at the critical point generated by the periodic solution. In ref{5} (see also ref{6}) a general form of Hill's formula was obtained for a periodic solution of an arbitrary Lagrangian system on a manifold. In this case  $H$  is a properly regularized Hessian operator of the action functional at the critical point determined by a periodic solution.

Hill's relates  $P$ , the monodromy matrix of the periodic trajectory, to the second variation of the action functional at the periodic trajectory, with  $H$  the corresponding Hessian operator.

2CB

The first dynamical application of Hill's formula is the well known statement that the Poincaré degeneracy of a periodic trajectory (that is, the condition that 1 is an eigenvalue of  $P$ ) is equivalent to the variational degeneracy (the condition  $\det H = 0$ ).

**2019-01-30 Predrag** Downloaded the monograph by Treschev and Zubelevich [69] *Introduction to the Perturbation Theory of Hamiltonian Systems* ([click here](#)) which contains a chapter *Hill's formula*. Here are some clippings:

"In 1886, in his study of stability of the lunar orbit, Hill [23] published a formula which expresses the characteristic polynomial of the monodromy matrix for a second order time periodic equation in terms of the determinant of a certain infinite matrix."

**2018-09-29 Predrag** Some papers that follow up on Bolotin and Treschev [6]:

Xu and Weng [74] *The calculation for characteristic multiplier of Hill's equation in case with positive mean*

Hu and Wang [30] *Conditional Fredholm determinant for the  $S$ -periodic orbits in Hamiltonian systems*

Hu and Wang [31] *Conditional Fredholm determinant and trace formula for Hamiltonian systems: a survey*

Hu, Ou and Wang [28] *Trace formula for linear Hamiltonian systems with its applications to elliptic Lagrangian solutions*. Their eq. (1.17) Krein formula for eigenvalues of a linear Hamiltonian systems with  $D$  degree of freedoms is intriguing.

Krein [38] *The basic propositions of the theory of  $\lambda$ -zones of stability of a canonical system of linear differential equations with periodic coefficients* (have not found a free version on line)

Davletshin [15] *Hill's formula for  $g$ -periodic trajectories of Lagrangian systems*

Hu and Wang [32] *Eigenvalue problem of Sturm-Liouville systems with separated bc's*

Hu and Wang [33] *Hill-type formula and Krein-type trace formula for  $S$ -periodic solutions in ODEs*, [arXiv:1504.01815](https://arxiv.org/abs/1504.01815)

Hu, Ou and Wang [29] *Hill-type formula for Hamiltonian system with Lagrangian bc's*, [arXiv:1711.09182](https://arxiv.org/abs/1711.09182): "The Hill-type formula connects the infinite determinant of the Hessian of the action functional with the determinant of matrices which depend on the monodromy matrix and bc's. Consequently, we derive the Krein-type trace formula and give nontrivial estimation for the eigenvalue problem. "

Hu, Wu and Yang [34] *Morse index theorem of Lagrangian systems and stability of brake orbit*

Sunada [67] *Trace formula for Hill's operators*

Carlson [10] *Eigenvalue estimates and trace formulas for the matrix Hill's equation*

**2019-01-28 Predrag** Downloaded monographs (have not started studying them as yet):

Maybe [encyclopediaofmath.org](https://encyclopediaofmath.org) *Hill equation* is a starting point for this literature.

Added a Bolotin conference abstract ([click here](#)) and a Hu conference abstract ([click here](#)).

**2019-04-21 Predrag** Kozlov [37] *Problem of stability of two-link trajectories in a multidimensional Birkhoff billiard* has a simple derivation of Hill's formula for billiards, where the Hessian is the second derivative of the length function.

**2018-09-29 Predrag** Agrachev [1] *Spectrum of the second variation*, [arXiv:1807.10527](#)

writes: Second variation of a smooth optimal control problem at a regular extremal is a symmetric Fredholm operator. We study the spectrum of this operator and give an explicit expression for its determinant in terms of solutions of the Jacobi equation.

We study the spectrum of the second variation  $D_u^2\varphi$  that is a symmetric Fredholm operator of the form  $I + K$ , where  $K$  is a compact Hilbert-Schmidt operator.  $K$  is NOT a trace class operator so that the trace of  $K$  and the determinant of  $I + K$  are not well-defined in the standard sense.

[...] A simple example: for the 1-dimensional linear control system  $\dot{x} = ax + u$  with the quadratic cost  $\varphi(u) = \int_0^1 u^2(t) - (a^2 + b^2)x^2(t) dt$  our determinantal identity reads:

$$\prod_{n=1}^{\infty} \left( 1 - \frac{a^2 + b^2}{a^2 + (\pi n)^2} \right) = \frac{a \sin b}{b \operatorname{sh} a}; \quad (12.96)$$

the case  $a = 0$  corresponds to the famous Euler identity

$$\prod_{n=1}^{\infty} \left( 1 - \frac{b^2}{(\pi n)^2} \right) = \frac{\sin b}{b}. \quad (12.97)$$

The example is simple, but, unfortunately, the paper itself is a hell to read...

**2018-12-07 Predrag** Reread Kook and Meiss [35] *Application of Newton's method to Lagrangian mappings*. They describe an Newton's method algorithm for finding periodic orbits of Lagrangian mappings. The method is based on block-diagonalization of the orbit Jacobian matrix of the action function. The explicit form of the Hessian displayed by Kook and Meiss reminds me of Bolotin discrete Hill's formula (sect. 12.2, Predrag post **2018-09-29** above, eq. (12.105)), maybe that's the way to derive it.

**2018-09-26 Han** I worked through the cat map example. The equation of motion is:

$$\begin{bmatrix} q_{n+1} \\ p_{n+1} \end{bmatrix} = \begin{bmatrix} s-1 & 1 \\ s-2 & 1 \end{bmatrix} \begin{bmatrix} q_n \\ p_n \end{bmatrix} \pmod{1}. \quad (12.98)$$

Rewrite this equation as:

$$\begin{aligned} q_{n+1} &= q_n + p_n + (s-2)q_n - s_{n+1}^q \\ p_{n+1} &= p_n + (s-2)q_n - s_{n+1}^q - (s_{n+1}^p - s_{n+1}^q). \end{aligned} \quad (12.99)$$

and compare with (12.101),

$$q_{n+1} = q_n + p_{n+1} \pmod{1}, \quad (12.100)$$

$$p_{n+1} = p_n + P(q_n), \quad (12.101)$$

so

$$\begin{aligned} q_{n+1} &= q_n + p_{n+1} \\ p_{n+1} &= p_n + (s-2)q_n - s_{n+1}^p. \end{aligned} \quad (12.102)$$

where the  $s_{n+1}^q$  seems happily absorbed into  $p_{n+1}$ . The generating function (1-step Lagrangian density) is

$$L(q_n, q_{n+1}) = \frac{1}{2}(q_{n+1} - q_n)^2 - V(q_n), \quad P(q) = -\frac{dV(q)}{dq}, \quad (12.103)$$

and the potential energy is:

$$V(q_n) = -\frac{s-2}{2}q_n^2 + s_{n+1}^p q_n. \quad (12.104)$$

The problem with this formulation is that the potential energy contribution is defined asymmetrically in (8.89). We should really follow Bolotin and Treschev [6] eq. (2.5), and define a symmetric generating function

$$L(q_n, q_{n+1}) = \frac{1}{2}(q_{n+1} - q_n)^2 - \frac{1}{2}[V(q_n) + V(q_{n+1})], \quad (12.105)$$

The first variation (12.13) of the action vanishes,

$$\begin{aligned} 0 &= L_2(q_{n+1}, q_n) + L_1(q_n, q_{n-1}) \\ &= q_n - q_{n+1} + (s-2)q_n - s_{n+1}^p + q_n - q_{n-1} \\ &= -q_{n+1} + sq_n - q_{n-1} - s_{n+1}^p, \end{aligned} \quad (12.106)$$

hence

$$q_{n+1} - sq_n + q_{n-1} = -s_{n+1}^p. \quad (12.107)$$

Letting  $s_n = -s_{n+1}^p$ , we recover the Lagrangian formulation (2.95).

Alternatively, Han's generating function (1-step Lagrangian density) is:

$$\begin{aligned} L(q_{n+1}, q_n) &= \frac{1}{2}[p_{n+1}(q_{n+1}, q_n)]^2 - V(q_n) \\ &= \frac{1}{2}(q_{n+1} - q_n + m_{n+1}^q - m_{n+1}^p)^2 + \frac{s-2}{2}q_n^2 - m_{n+1}^p q_n. \end{aligned} \quad (12.108)$$

The action is the sum over the Lagrangian density over the orbit. The first variation (12.13) of the action vanishes,

$$\begin{aligned} 0 &= L_2(q_{n+1}, q_n) + L_1(q_n, q_{n-1}) \\ &= q_n - q_{n+1} + m_{n+1}^p - m_{n+1}^q \\ &\quad + (s-2)q_n - m_{n+1}^p + q_n - q_{n-1} + m_n^q - m_n^p \\ &= -q_{n+1} + sq_n - q_{n-1} - (m_{n+1}^q - m_n^q + m_n^p), \end{aligned} \quad (12.109)$$



hence

$$-q_{n+1} + sq_n - q_{n-1} = m_{n+1}^q - m_n^q + m_n^p. \quad (12.110)$$

Letting  $m_n = m_{n+1}^q - m_n^q + m_n^p$ , we recover the Lagrangian formulation (2.95), **except for the wrong sign for  $m_n$** . Now I see why  $m_n$ 's are called 'sources'.

But I think I missed something. I believe (4.308) is correct. Because  $\square - \mu^2 \mathbf{1}$  has negative determinant, so we can do the Gaussian integral. But it seems like the action  $S[X]$  is the negative of the sum of Lagrangian along the orbit? Because if we sum (12.108) along the orbit, the sign before  $s$  should be positive but in (4.308) it is negative...

**2020-07-14 Han** To prove the Hill's formula (??) for the cat map, first note that both the left hand side and right hand side are polynomials with the same leading terms  $s^n$ . The left hand side is the determinant of the tri-diagonal Toeplitz matrix (??). From the (??) and (2.17), the right hand side can be written in the form

$$\begin{aligned} |\det(\mathbb{J}^n - \mathbf{1})| &= \Lambda^n + \Lambda^{-n} - 2 \\ &= 2 \cosh(n\lambda) - 2 \\ &= 2 \cosh \left[ n \operatorname{arc} \cosh \left( \frac{s}{2} \right) \right] - 2, \end{aligned} \quad (12.111)$$

where we used  $s = 2 \cosh(\lambda)$ . As the Chebyshev polynomial of the first kind can be written as  $T_n(x) = \cosh[n \operatorname{arc} \cosh(x)]$ , the right hand side of (??) is

$$|\det(\mathbb{J}^n - \mathbf{1})| = 2T_n \left( \frac{s}{2} \right) - 2,$$

which has the leading term  $s^n$ .

Let  $u = (u_j)_{j=1,2,\dots,n}$  be the variation to the periodic orbit  $X$  with length  $n$ .  $\mathcal{J}u = 0$  only if  $\mathbb{J}^n w = w$  where  $w = (u_1, u_2)$ . Then  $|\det(\mathbb{J}^n - \mathbf{1})| = 0$  is equivalent to  $|\operatorname{Det} \mathcal{J}| = 0$ . Then the polynomials  $|\operatorname{Det} \mathcal{J}|$  and  $|\det(\mathbb{J}^n - \mathbf{1})|$  have the same roots and the same leading terms so they are equal.

**2020-07-17 Han** Let  $s$  go to infinity. Then the stability multipliers becomes:

$$\begin{aligned} \lim_{s \rightarrow \infty} \Lambda &= \lim_{s \rightarrow \infty} \frac{s + \sqrt{s^2 - 4}}{2} = s, \\ \lim_{s \rightarrow \infty} \Lambda^{-1} &= \lim_{s \rightarrow \infty} \frac{2}{s + \sqrt{s^2 - 4}} = \lim_{s \rightarrow \infty} \frac{1}{s} = 0. \end{aligned} \quad (12.112)$$

Then in the limit:

$$\lim_{s \rightarrow \infty} |\det(\mathbb{J}^n - \mathbf{1})| = \lim_{s \rightarrow \infty} \Lambda^n + \Lambda^{-n} - 2 = s^n, \quad (12.113)$$

So the leading term of the right hand side of (??) is  $s^n$ .

$$\begin{aligned}
 |\det(\mathbb{J}^n - \mathbf{1})| &= \Lambda^n + \Lambda^{-n} - 2 \\
 &= \left(\frac{s + \sqrt{s^2 - 4}}{2}\right)^n + \left(\frac{s - \sqrt{s^2 - 4}}{2}\right)^n - 2 \\
 &= \frac{1}{2^n} \sum_{k=0}^{\frac{n}{2}} \binom{2k}{n} s^{n-2k} (s^2 - 4)^k - 2, \quad (12.114)
 \end{aligned}$$

**2019-09-25 PC** Levit and Smilansky [41] *A theorem on infinite products of eigenvalues of Sturm-Liouville type operators* computes a Gaussian path integral with a Laplacian kernel. Looks simple, but I do not understand it.

Levit and Smilansky [40] *A new approach to Gaussian path integrals and the evaluation of the semiclassical propagator*.

**2019-09-25 PC** Han, can you clean up the rest, make it (12.116) and beyond into a derivation of the Hill's formula for our paper - what follows is just a sketch in (close to) our notations:

Colin de Verdière [12] *Spectrum of the Laplace operator and periodic geodesics: thirty years after* discusses the mathematical history of "Semi-classical trace formula," a formula expressing the smoothed density of states of the Laplace operator on a compact Riemannian manifold in terms of the periodic geodesics. This seems to be an elaboration of these lectures from which one can clip & paste.

Colin de Verdière [12] and Levit and Smilansky [40] are deriving "semi-classical" or "Gaussian path integral" evolution trace formulas, which lead to  $|\det(\mathbf{1} - M_p)|^{\frac{1}{2}}$  rather than the classical  $|\det(\mathbf{1} - M_p)|$ . That does not matter for our purposes, which is the derivation of the Hill's formula, sketched in (12.116), and on.

What we call periodic orbit's monodromy matrix  $M$  he seems to call (linear) Poincaré map  $\Pi$  a closed orbit computed on a hypersurface transverse to the orbit, an "invertible (symplectic) endomorphism of the tangent space". The periodic orbit weight  $|\det(\mathbf{1} - M_p)|$  shows up in his eq. (5.5).

In his Theorem 11, Sect. 11, Colin de Verdière evaluates the integral over  $\exp(iS(x)/\hbar)$  in the stationary phase approximation, with  $S(W)$  having support on a critical manifold  $W$  has a measure  $d\mu_W$  given by the quotient of the measure  $|dx|$  by the "Riemannian measure" on the normal bundle to  $W$  associated to the Hessian of  $S$

$$d\mu_W = \frac{|dx|}{|\det(\partial_{\alpha\beta}^2 S)|^{\frac{1}{2}} |dz|}, \quad (12.115)$$

where  $z = (z_\alpha)$  are the coordinates on the normal bundle.

The Hessian is associated to a periodic Sturm-Liouville operator for which many regularizations have been proposed.

Elsewhere [40, 70]  $\det(\partial_{\alpha\beta}^2 S)$  is known as the Van Vleck determinant. Irrelevant to the problem at hand, but a fun history read [Nicholas Wheeler is here](#). In Sect. 11.6 *Regularized Determinants of continuous Sturm-Liouville operators* he discretizes the  $n$ -cycle Hessian just as we do (except he allows  $s$  to vary along the path), with Dirichlet, or periodic boundary conditions,

$$\mathcal{H}_n = \begin{pmatrix} A & B & 0 & \dots & 0 & B^\top \\ B^\top & A & B & \dots & 0 & 0 \\ 0 & B^\top & A & \dots & 0 & 0 \\ \vdots & \vdots & \vdots & \ddots & \vdots & \vdots \\ 0 & 0 & 0 & \dots & A & B \\ B & 0 & 0 & \dots & B^\top & A \end{pmatrix} \quad (12.116)$$

In general the  $[2 \times 2]$  matrices

$$A = \frac{1}{*} \begin{pmatrix} a_{11} & a_{12} \\ a_{21} & a_{22} \end{pmatrix}, \quad B = -\frac{1}{*} \begin{pmatrix} * & * \\ * & * \end{pmatrix} \quad (12.117)$$

are time dependent,  $(A_t, B_t)$ , but for our simple temporal cat they are constant,  $(A_t, B_t) = (A, B)$ . For some choices, see sect. ?? *Adrien's blog*. Denote  $b = -\det B$ , and by

$$\begin{pmatrix} x_1 \\ x_2 - x_1 \end{pmatrix} = J \begin{pmatrix} x_0 \\ x_1 - x_0 \end{pmatrix} \quad (12.118)$$

the 1-time step symplectic (canonical) transformation

$$J = \begin{pmatrix} \alpha & \beta \\ \gamma & \delta \end{pmatrix}. \quad (12.119)$$

From his theorem 13 he gets Hill's formula  $\det H = \det(1 - J_p)$  for the periodic case.

**2025-01-12 PC** An interesting discussion [The invariance of the Hessian and its eigenvalues, determinant, and trace](#) of why the eigenvalues, determinant and trace of the Hessian invariant under reparametrization.

**2019-09-28 PC** It is clearer and clearer that the smart way of doing the multi-shooting Newton and various related "noisy" dynamics problems is by discrete Fourier ( $C_n$  cyclic group) irreps diagonalization. So I might have to rework several earlier papers:

I had inverted Newton Jacobian matrix often, see for example eq. (16) and onward in Cvitanović, Dettmann, Mainieri and Vattay [13], [click here](#). I have also introduced the notation for finite-time (shorter than the period) Jacobian matrices, see for example eq. (69) in Cvitanović and

Lippolis [14], [click here](#). But I have never done it the way I should have, by a discrete Fourier transform, into sum of irreps of  $C_n$  (AKA Fourier modes). Probably best to use characters?

**2019-09-28 PC** I think I have finally committed the long awaited conceptual breakthrough. To remind everyone - one unsolved problem in Matt and my work [21] is "Hill's formula" for the first-order time derivative dissipative dynamics, which relates linear stability of a spatiotemporal pattern to  $(1 - J)$  temporal evolution stability.

**2019-10-01 PC** Cao and Voth [9] *Semiclassical approximations to quantum dynamical time correlation functions* ([click here](#)): " find an alternative to evaluate the Jacobi matrices (16.79) and have thereby found it necessary to derive the initial-value expression from a new perspective. Straight-forward and self-contained, this derivation leads to a discretized expression for the Jacobi matrices and a simple interpretation of the Maslov-like index. "

They derive the Jacobi equations from a discretization, their Appendix B. These equations evolve subblocks of the Jacobian that maintain the symplectic invariance.

Langouche, Roekaerts and Tirapegui [39] *WKB Expansion for arbitrary Hamiltonians* might be of interest, but I have not studied it.

**2019-10-13 Predrag** Guckenheimer and Meloon [20] define a "symmetric multiple shooting algorithm" as is a small modification of the forward multiple shooting method that makes the method time reversible. Let  $p = (x_1, x_2, \dots, x_{n_p})$ , as in (11.1). They evaluate some "Taylor polynomials" at time-interval midpoints, I admit not to see how their formulas are time reversible. I believe they replace (11.4) by segments that traverse a time interval in both direction

$$F_{GM}(\hat{x}) = \begin{pmatrix} \hat{f}_{n_p} - \hat{f}_1^{-1} \\ \hat{f}_1 - \hat{f}_2^{-1} \\ \dots \\ \hat{f}_{n_p-1} - \hat{f}_{n_p}^{-1} \end{pmatrix}, \quad \hat{f}_k = f(\hat{x}_k), \quad (12.120)$$

Now the orbit Jacobian matrix (12.61) picks up the derivatives of inverse map along the diagonal (instead of the identity matrices). They manipulate it and show it is the same Jacobian as the forward shooting one.

For my taste having a diagonal and sub-diagonal is not time-symmetric enough. Inspired by the formula for the discrete Laplacian (4.177), I suggest trying the tri-diagonal vector field

$$H(\hat{x}) = \begin{pmatrix} \hat{f}_2^{-1} - 2\hat{x}_1 + \hat{f}_{n_p} \\ \hat{f}_3^{-1} - 2\hat{x}_2 + \hat{f}_1 \\ \dots \\ \hat{f}_{n_p-1}^{-1} - 2\hat{x}_{n_p} + \hat{f}_{n_p-1} \end{pmatrix}, \quad \hat{f}_k = f(\hat{x}_k), \quad (12.121)$$

that reverses its direction under time reversal. The orbit Jacobian matrix

$$\mathcal{H} = (\sigma J)^{-1} - 2J + \sigma J, \quad (12.122)$$

is of self-adjoint form. We have to show that its determinant is the Hill's formula.

Is it what we need for the Hessian / Lagrangian case? I suspect that the temporal cat case - uniform stretching, is easily brought to the temporal cat orbit stability form, by rescaling (12.122) so that off-diagonal  $J'$ s are absorbed into the diagonal  $\mu^2$  factors.

Read Doedel *et al.* [16] (click here). They show how two-point boundary value problem continuation software like AUTO [Doedel *et al.*, 1997; Doedel *et al.*, 2000] can be used to compute families of periodic solutions of conservative systems, i.e. systems having a first integral. Seems the same as chaos book as far as adding and additional constraint is concerned. See no word "determinant" anywhere...

**2020-08-01 Predrag** I guess I should have looked more closely. The original the Hill determinant (see [mathworld.wolfram](#)) is, with various terms absorbed into our stretching parameter  $s$ , a 3-term recurrence which is *exactly* our  $d = 1$  temporal cat, with our Hill determinant, except Hill did it for the oscillatory parameter value  $\mu^2 < 0$ .

Check Morse, P. M. and Feshbach, H. *Methods of Theoretical Physics*, Part I. New York: McGraw-Hill, pp. 555-562, (1953).

Magnus and Winkler [49] *Hill's Equation* (click here).

Dan Rothman told me to look at J. J. Stoker (but it is not in *Differential geometry*), so it's in the wave mechanics book... Have not found it yet.

**2022-06-06 Predrag** Playing with symmetry-reduced Hill determinants again. Copied (12.126), (12.123–12.125) from ref. [43]:

A periodic state  $X$  has one of the four symmetries:

$$(a) \quad \begin{array}{l} \text{asymmetric, no reflection symmetry} \\ \overline{x_0 x_1 x_2 x_3 \cdots x_{n-1}} \\ \text{index } m_X = 2n \end{array} \quad (12.123)$$

periodic state invariant under the translation group  $H_n$ . Its  $G$ -orbit, generated by all actions of  $D_\infty$ , results in  $2n$  distinct,  $D_n$  related periodic states.

$$(ee) \quad \begin{array}{l} \text{even period } n = 2m + 2, \text{ even reflection } k \\ \overline{x_0} x_1 x_2 \cdots x_m \overline{x_{m+1}} x_m \cdots x_2 x_1 \\ \text{index } m_X = n \end{array} \quad (12.124)$$

periodic state invariant under the dihedral group  $H_{n,k}$ ,  $k$  even.

$$(eo) \quad \frac{\text{even period } n = 2m, \text{ odd reflection } k}{x_1 x_2 x_3 \cdots x_m | x_m \cdots x_2 x_1 |} \quad (12.125)$$

index  $m_X = n$

periodic state invariant under the dihedral group  $H_{n,k}$ ,  $k$  odd.

The determinants of the symmetry reduced orbit Jacobian matrices for temporal cat are:

$$\begin{aligned} \text{Det } \mathcal{J}_o &= \sqrt{(s-2)} \text{Det } \mathcal{J}, \\ \text{Det } \mathcal{J}_{ee} &= \sqrt{(s-2)(s+2)} \text{Det } \mathcal{J}, \\ \text{Det } \mathcal{J}_{eo} &= \sqrt{\frac{(s-2)}{(s+2)}} \text{Det } \mathcal{J}, \end{aligned} \quad (12.126)$$

where  $\text{Det } \mathcal{J}$  is computed on the full primitive cell.  $\text{Det } \mathcal{J}$ ,  $\text{Det } \mathcal{J}_o$ ,  $\text{Det } \mathcal{J}_{ee}$  and  $\text{Det } \mathcal{J}_{eo}$  count numbers of periodic periodic states that satisfy the symmetries defined by (12.123–12.125) respectively.

Rewriting (12.126) as the three symmetry factorizations:

$$\begin{aligned} o: \quad \text{Det } \mathcal{J} &= \frac{1}{\mu^2} (\text{Det } \mathcal{J}_p)^2 \\ \mathcal{J} &= \begin{bmatrix} s_0 & -\sigma \mathbf{r} & -\mathbf{r}^\top \\ -\mathbf{r} & \mathcal{J}_p & -\sigma \vec{r} \\ -\sigma \mathbf{r}^\top & -\mathbf{r} & \sigma \mathcal{J}_p \sigma^{-1} \end{bmatrix} \\ ee: \quad \text{Det } \mathcal{J} &= \frac{1}{\mu^2(\mu^2+4)} (\text{Det } \mathcal{J}_p)^2 \\ \mathcal{J} &= \begin{bmatrix} s_0 & -\sigma \vec{r}^\top & 0 & -\vec{r}^\top \\ -\vec{r} & \mathcal{J}_p & -\sigma \vec{r} & \mathbf{0} \\ 0 & -\vec{r}^\top & s_{n/2} & -\sigma \vec{r}^\top \\ -\sigma \vec{r} & \mathbf{0} & -\vec{r} & \sigma \mathcal{J}_p \sigma^{-1} \end{bmatrix} \\ eo: \quad \text{Det } \mathcal{J} &= \frac{\mu^2+4}{\mu^2} (\text{Det } \mathcal{J}_p)^2 \\ \mathcal{J} &= \begin{bmatrix} \mathcal{J}_p & -\mathbf{r} - \mathbf{r}^\top \\ -\mathbf{r} - \mathbf{r}^\top & \sigma \mathcal{J}_p \sigma^{-1} \end{bmatrix}, \end{aligned} \quad (12.127)$$

The orbit Jacobian matrix of a period- $(n)$  periodic state  $X$  which is a 1-st repeat of a period- $n$  prime periodic state  $X_p$  has a tri-diagonal block circulant matrix form (11.24), where Dirichlet  $\mathcal{J}_p$ , block shifts  $\mathbf{r}$  and  $\mathbf{r}^\top =$

$\sigma\sigma^{-1}$  are  $[m \times m]$  block matrices

$$\mathcal{J}_p = \begin{bmatrix} d_1 & -1 & & & 0 \\ -1 & d_2 & -1 & & \\ & \ddots & \ddots & \ddots & \\ & & -1 & d_{m-1} & -1 \\ 0 & & & -1 & d_m \end{bmatrix},$$

$$\mathbf{r} = \begin{bmatrix} 0 & \cdots & 0 \\ & \ddots & \vdots \\ 1 & & 0 \end{bmatrix}, \quad \vec{r} = \begin{bmatrix} 0 \\ \vdots \\ 0 \\ 1 \end{bmatrix}, \quad (12.128)$$

and  $\mathbf{r}$  and its transpose enforce the periodic bc's.

**2023-11-24 Predrag** This might go into Liang and Cvitanović [44] *A derivation of Hill's formulas* (2024): The setting is much more general, but the formulas seem to be Hill's formulas, relating zeta-regularized determinants of Jacobian operators with positive spectrum to Fredholm determinants of Hessians (forward in time determinants?).

**Matthias Ludewig** *Path Integrals on Manifolds with Boundary and their Asymptotic Expansions* **PhD thesis** (2016).

Ludewig [46] *Heat kernel asymptotics, path integrals and infinite-dimensional determinants*, [arXiv:1607.05891](#). A hard read...

Let us now discuss the determinant of the Hessian of the action. If  $T$  is a bounded linear operator on a separable Hilbert space  $\mathcal{H}$ , then its determinant can be defined if it has the form  $T = \mathbf{1} + W$  with a trace-class operator  $W$ . We will call such operators *determinant-class* and their *Fredholm determinant* can be defined by

$$\det(T) := \prod_{j=1}^{\infty} (1 + \lambda_j),$$

where  $\lambda_j$  are the eigenvalues of  $W$ , repeated with algebraic multiplicity. [...] the trace-class condition means that  $\sum_{j=1}^{\infty} |\lambda_j| < \infty$  [...]

[...] another possible choice for the determinant of an operator on an infinite-dimensional space is the zeta determinant [...] replace the Fredholm determinant by the zeta determinant of the Jacobi-operator  $-\nabla_s^2 + \mathcal{R}_\gamma$ .

This determinant [...] depends on the Jacobi-operator eigenvalues, [...] the *zeta function* (21.137) [...] the *zeta-regularized determinant* (21.139).

**Multiplicativity.** Let  $\mathcal{H}$  be a Hilbert space, let  $P$  be a closed and invertible operator on  $\mathcal{H}$  with positive spectrum and let  $T := \mathbf{1} + W$  with  $W$  trace-

class on  $\mathcal{H}$ . If  $P$  is zeta-admissible, then so are  $PT$  and  $TP$  and we have

$$\det_{\zeta}(PT) = \det_{\zeta}(TP) = \det_{\zeta}(P)\det(T),$$

where  $\det(T)$  denotes the usual Fredholm determinant.

Generally  $\det_{\zeta}(AB) \neq \det_{\zeta}(A)\det_{\zeta}(B)$ . The above is the correct replacement for this product rule.

**Zeta Relativity.** Let  $P_1, P_2$  be positive self-adjoint Laplace type operators with Dirichlet boundary conditions on the interval  $[0, t]$ , acting on the bundle  $\gamma^*TM$ , where  $\gamma$  is a smooth path in some Riemannian manifold  $M$ . Suppose that the difference  $P_1 - P_2$  is of order zero and that  $P_1$  and  $P_2$  have trivial kernels. Then [...] we have

$$\det(P_1^{-1}P_2) = \frac{\det_{\zeta}(P_2)}{\det_{\zeta}(P_1)},$$

where the left hand side is the usual Fredholm determinant.

**Gel'fand-Yaglom theorem.** [18] Let  $V_i, i = 1, 2$  [...] be functions with values in symmetric matrices and consider the differential operators

$$P_i := -\frac{d^2}{ds^2} + V_i.$$

Assume that all eigenvalues of  $P_1$  and  $P_2$  are positive. Then we have

$$\frac{\det_{\zeta}(P_2)}{\det_{\zeta}(P_1)} = \frac{\det(J_2(t))}{\det(J_1(t))},$$

where the  $J_i(s)$  are the unique matrix-valued solutions of

$$J_i''(s) = V_i(s)J_i(s), \quad J_i(0) = 0, \quad J_i'(0) = \mathbf{1}.$$

**2023-11-24 Predrag** Han, you need to study Gel'fand and Yaglom [18] *Integration in functional spaces and its applications in quantum physics* (1960).

It starts out by our, discrete Hill's theorem, then takes their continuous limit.

**2023-11-24 Predrag** This also might go into Liang and Cvitanović [44]:

Meredith Shea *Discrete Systems in Quantum and Statistical Mechanics* [PhD thesis](#) (2022).

Shea *Generalized Gel'fand-Yaglom formula for a discretized quantum mechanic system* [arXiv:2011.02996](#)

We consider operators in the physics literature and explore their discretized counterparts for a better understanding of their behavior. In chapter 2, we discretize a standard Hamiltonian model from quantum mechanics and, in this setting, develop a discretized Gel'fand- Yaglom



formula. From this discrete set up we are able to develop an alternative regularization for the determinant of a class of operators. We refer to this as the lattice-regularization.

The Gel'fand-Yaglom formula relates the regularized determinant of a differential operator to the solution of an initial value problem. Here we develop a generalized Gel'fand-Yaglom formula for a Hamiltonian system with Lagrangian boundary conditions in the discrete and continuous settings. Later we analyze the convergence of the discretized Hamilton-Jacobi operator and propose a lattice regularization for the determinant.

There is the usual ChaosBook.org mess of the forward-in-time Jacobian for a Hamiltonian flow. Shea then discretizes time. The orbit Jacobian matrix is the usual elegant thing (set  $\epsilon = 1$  in Shea eq. (37)  $A_4$  example). Then he takes continuum limit - we do not need to do that.

Only the Neumann and Dirichlet boundary conditions, no periodic case. For his Gel'fand-Yaglom theorem, he credits Burghlelea, Friedlander, and Kappeler. He has a total of 7 references:)

**2024-09-11 Predrag** from Xiaodong "Will" An:

Solé and Bascompte [63] *Measuring chaos from spatial information* (1995).

[...] Define and evaluate numerically a new class of Lyapunov exponents when very short time series are obtained from a spatially distributed dynamical system instead of a long macroscopic time series. The underlying hypothesis in our approach deals with the existence of a common deterministic mechanism operating at each point. Our proposal is that we can compare different points in order to know how two dynamically close local states will separate.

I'm vaguely unhappy about Solé and Bascompte method, but do not remember why:)

**2024-10-06 Predrag** Livi, Politi, Ruffo and Vulpiani [45] *Liapunov exponents in high-dimensional symplectic dynamics* (1987).

Should understand why temporal Lyapunov exponents tend to order themselves decaying linearly, while orbit Jacobian matrix stability exponents are fluctuating around  $\mu^2$ ...

The continuous time, discrete periodic  $N$ -body chain forward-in time stability is sketched in the Appendix eq. (A.2). We might want to check the corresponding Hill's formula.

The above two papers compute temporal evolution stability. I believe the right way to do this is our spatiotemporal approach.

## References

- [1] A. Agrachev, *Spectrum of the second variation*, 2018.

- [2] E. Allroth, "Ground state of one-dimensional systems and fixed points of  $2n$ -dimensional map", *J. Phys. A* **16**, L497 (1983).
- [3] S. B. Angenent, "The periodic orbits of an area preserving twist-map", *Commun. Math. Phys.* **115**, 353–374 (1988).
- [4] G. B. Arfken, H. J. Weber, and F. E. Harris, *Mathematical Methods for Physicists: A Comprehensive Guide*, 7th ed. (Academic, New York, 2013).
- [5] J. Barrow-Green, *Poincaré and the Three Body Problem* (Amer. Math. Soc., Providence RI, 1997).
- [6] S. V. Bolotin and D. V. Treschev, "Hill's formula", *Russ. Math. Surv.* **65**, 191 (2010).
- [7] T. Bountis and R. H. G. Helleman, "On the stability of periodic orbits of two-dimensional mappings", *J. Math. Phys.* **22**, 1867–1877 (1981).
- [8] E. Calabi, "On the group of automorphisms of a symplectic manifold", in *Problems in Analysis: A Symposium in Honor of Salomon Bochner* (Princeton Univ. Press, Princeton NJ, 1970), pp. 1–26.
- [9] J. Cao and G. A. Voth, "Semiclassical approximations to quantum dynamical time correlation functions", *J. Chem. Phys.* **104**, 273–285 (1996).
- [10] R. Carlson, "Eigenvalue estimates and trace formulas for the matrix Hill's equation", *J. Diff. Eqn.* **167**, 211–244 (2000).
- [11] M. Chen, "On the solution of circulant linear systems", *SIAM J. Numer. Anal.* **24**, 668–683 (1987).
- [12] Y. Colin de Verdière, "Spectrum of the Laplace operator and periodic geodesics: thirty years after", *Ann. Inst. Fourier* **57**, 2429–2463 (2007).
- [13] P. Cvitanović, C. P. Dettmann, R. Mainieri, and G. Vattay, "Trace formulas for stochastic evolution operators: Weak noise perturbation theory", *J. Stat. Phys.* **93**, 981–999 (1998).
- [14] P. Cvitanović and D. Lippolis, Knowing when to stop: How noise frees us from determinism, in *Let's Face Chaos through Nonlinear Dynamics*, edited by M. Robnik and V. G. Romanovski (2012), pp. 82–126.
- [15] M. N. Davletshin, "Hill's formula for  $g$ -periodic trajectories of Lagrangian systems", *Trans. Moscow Math. Soc.* **74**, 65–96 (2014).
- [16] E. J. Doedel, R. C. Paffenroth, H. B. Keller, D. J. Dichmann, J. Galan, and A. Vanderbauwhede, "Computation of periodic solutions of conservative systems with application to the 3-body problem", *Int. J. Bifur. Chaos* **13**, 1353–1381 (2003).
- [17] F. W. Dorr, "The direct solution of the discrete Poisson equation on a rectangle", *SIAM Rev.* **12**, 248–263 (1970).
- [18] I. M. Gel'fand and A. M. Yaglom, "Integration in functional spaces and its applications in quantum physics", *J. Math. Phys.* **1**, 48–69 (1960).
- [19] J. M. Greene, "A method for determining a stochastic transition", *J. Math. Phys.* **20**, 1183–1201 (1979).

- [20] J. Guckenheimer and B. Meloon, "Computing periodic orbits and their bifurcations with automatic differentiation", *SIAM J. Sci. Comput.* **22**, 951–985 (2000).
- [21] M. N. Gudorf, N. B. Budanur, and P. Cvitanović, *Spatiotemporal tiling of the Kuramoto-Sivashinsky flow*, In preparation, 2022.
- [22] P. G. Harper, "Single band motion of conduction electrons in a uniform magnetic field", *Proc. Phys. Soc. London, Sect. A* **68**, 874–878 (1955).
- [23] G. W. Hill, "On the part of the motion of the lunar perigee which is a function of the mean motions of the sun and moon", *Acta Math.* **8**, 1–36 (1886).
- [24] D. R. Hofstadter, "Energy levels and wave functions of Bloch electrons in rational and irrational magnetic fields", *Phys. Rev. B* **14**, 2239–2249 (1976).
- [25] R. A. Horn and C. R. Johnson, *Matrix Analysis* (Cambridge Univ. Press, Cambridge, 1990).
- [26] R. A. Horn and C. R. Johnson, *Topics in Matrix Analysis* (Cambridge Univ. Press, Cambridge UK, 1994).
- [27] G. Y. Hu, J. Y. Ryu, and R. F. O'Connell, "Analytical solution of the generalized discrete Poisson equation", *J. Phys. A* **31**, 9279 (1998).
- [28] X. Hu, Y. Ou, and P. Wang, "Trace formula for linear Hamiltonian systems with its applications to elliptic Lagrangian solutions", *Arch. Ration. Mech. Anal.* **216**, 313–357 (2014).
- [29] X. Hu, Y. Ou, and P. Wang, "Hill-type formula for Hamiltonian system with Lagrangian boundary conditions", *J. Diff. Equ.* **267**, 2416–2447 (2019).
- [30] X. Hu and P. Wang, "Conditional Fredholm determinant for the  $S$ -periodic orbits in Hamiltonian systems", *J. Funct. Analysis* **261**, 3247–3278 (2011).
- [31] X. Hu and P. Wang, "Conditional Fredholm determinant and trace formula for Hamiltonian systems: a survey", in *Emerging Topics on Differential Equations and Their Applications* (World Scientific, Singapore, 2013), pp. 12–23.
- [32] X. Hu and P. Wang, "Eigenvalue problem of Sturm-Liouville systems with separated boundary conditions", *Math. Z.* **283**, 339–348 (2015).
- [33] X. Hu and P. Wang, "Hill-type formula and Krein-type trace formula for  $S$ -periodic solutions in ODEs", *Discrete Continuous Dyn. Syst. Ser. A* **36**, 763–784 (2016).
- [34] X. Hu, L. Wu, and R. Yang, *Morse index theorem of Lagrangian systems and stability of brake orbit*, 2018.
- [35] H.-T. Kook and J. D. Meiss, "Application of Newton's method to Lagrangian mappings", *Physica D* **36**, 317–326 (1989).

- [36] K. Kowalski and W.-H. Steeb, *Nonlinear Dynamical Systems and Carleman Linearization* (World Scientific, Singapore, 1991).
- [37] V. V. Kozlov, "Problem of stability of two-link trajectories in a multidimensional Birkhoff billiard", *Proc. Steklov Inst. of Math.* **273**, 196–213 (2011).
- [38] M. G. Krein, "The basic propositions of the theory of  $\lambda$ -zones of stability of a canonical system of linear differential equations with periodic coefficients", in *Operator Theory: Advances and Applications* (Birkhäuser, Basel, 1983), pp. 1–105.
- [39] F. Langouche, D. Roekaerts, and E. Tirapegui, "WKB expansion for arbitrary Hamiltonians", *Il Nuovo Cimento A* **64**, 357–377 (1981).
- [40] S. Levit and U. Smilansky, "A new approach to Gaussian path integrals and the evaluation of the semiclassical propagator", *Ann. Phys.* **103**, 198–207 (1977).
- [41] S. Levit and U. Smilansky, "A theorem on infinite products of eigenvalues of Sturm-Liouville type operators", *Proc. Amer. Math. Soc.* **65**, 299–299 (1977).
- [42] J. Li and S. Tomsovic, "Exact relations between homoclinic and periodic orbit actions in chaotic systems", *Phys. Rev. E* **97**, 022216 (2017).
- [43] H. Liang and P. Cvitanović, "A chaotic lattice field theory in one dimension", *J. Phys. A* **55**, 304002 (2022).
- [44] H. Liang and P. Cvitanović, *A derivation of Hill's formulas*, In preparation, 2024.
- [45] R. Livi, A. Politi, S. Ruffo, and A. Vulpiani, "Liapunov exponents in high-dimensional symplectic dynamics", *J. Stat. Phys.* **46**, 147–160 (1987).
- [46] M. Ludewig, "Heat kernel asymptotics, path integrals and infinite-dimensional determinants", *J. Geom. Phys.* **131**, 66–88 (2018).
- [47] R. S. MacKay and J. D. Meiss, "Linear stability of periodic orbits in Lagrangian systems", *Phys. Lett. A* **98**, 92–94 (1983).
- [48] R. S. MacKay, J. D. Meiss, and I. C. Percival, "Transport in Hamiltonian systems", *Physica D* **13**, 55–81 (1984).
- [49] W. Magnus and S. Winkler, *Hill's Equation* (Dover, 1966).
- [50] J. N. Mather, "Amount of rotation about a point and the Morse index", *Commun. Math. Phys.* **94**, 141–153 (1984).
- [51] J. D. Meiss, "Symplectic maps, variational principles, and transport", *Rev. Mod. Phys.* **64**, 795–848 (1992).
- [52] I. Montvay and G. Münster, *Quantum Fields on a Lattice* (Cambridge Univ. Press, Cambridge, 1994).
- [53] L. Onsager, "Crystal statistics. I. A Two-dimensional model with an order-disorder transition", *Phys. Rev.* **65**, 117–149 (1944).

- [54] R. Peierls, "Zur Theorie des Diamagnetismus von Leitungselektronen", *Z. Phys.* **80**, 763–791 (1933).
- [55] I. Percival and F. Vivaldi, "A linear code for the sawtooth and cat maps", *Physica D* **27**, 373–386 (1987).
- [56] E. Petrisor, "Twist number and order properties of periodic orbits", *Physica D* **263**, 57–73 (2013).
- [57] E. Petrisor, "Monotone gradient dynamics and the location of stationary (p,q)-configurations", *J. Phys. A* **47**, 045102 (2014).
- [58] H. Poincaré, "Sur les déterminants d'ordre infini", *Bull. Soc. Math. France* **14**, 77–90 (1886).
- [59] H. Poincaré, *Les méthodes nouvelles de la mécanique céleste*, For a very readable exposition of Poincaré's work and the development of the dynamical systems theory up to 1920's see ref. [5]. (Guthier-Villars, Paris, 1899).
- [60] G. Schmidt, "Hamilton's principle and the splitting of periodic orbits", in *Statistical Physics and Chaos in Fusion Plasmas*, edited by C. W. Horton Jr. and L. E. Reichl (John Wiley and Sons, 1984), p. 57.
- [61] I. Schur, "Über Potenzreihen, die im Innern des Einheitskreises beschränkt sind", *J. reine angewandte Math.* **147**, 205–232 (1917).
- [62] B. Simon, "Almost periodic Schrödinger operators: A review", *Adv. Appl. Math.* **3**, 463–490 (1982).
- [63] R. V. Solé and J. Bascompte, "Measuring chaos from spatial information", *J. Theor. Biol.* **175**, 139–147 (1995).
- [64] W.-H. Steeb and Y. Hardy, *Matrix Calculus and Kronecker Product - A Practical Approach to Linear and Multilinear Algebra*, 2nd ed. (World Scientific, Singapore, 2011).
- [65] W.-H. Steeb and Y. Hardy, *Matrix Calculus, Kronecker Product and Tensor Product* (World Scientific, Singapore, 2011).
- [66] M. Stone and P. Goldbart, *Mathematics for Physics: A Guided Tour for Graduate Students* (Cambridge Univ. Press, Cambridge, 2009).
- [67] T. Sunada, "Trace formula for Hill's operators", *Duke Math. J.* **47**, 529–546 (1980).
- [68] M. Toda, *Theory of Nonlinear Lattices* (Springer, Berlin, 1989).
- [69] D. Treschev and O. Zubelevich, "Hill's formula", in *Introduction to the Perturbation Theory of Hamiltonian Systems* (Springer, Berlin, 2009), pp. 143–162.
- [70] J. H. Van Vleck, "The correspondence principle in the statistical interpretation of quantum mechanics", *Proc. Natl. Acad. Sci.* **14**, 178–188 (1928).
- [71] D. Viswanath, "The Lindstedt-Poincaré technique as an algorithm for finding periodic orbits", *SIAM Rev.* **43**, 478–496 (2001).

- [72] Wikipedia contributors, [Block matrix](#) — Wikipedia, The Free Encyclopedia, 2020.
- [73] Wikipedia contributors, [Kronecker product](#) — Wikipedia, The Free Encyclopedia, 2020.
- [74] R. Xu and A. Weng, "The calculation for characteristic multiplier of Hill's equation in case with positive mean", *Nonlinear Anal. Real World Appl.* **9**, 949–962 (2008).

## Chapter 13

# Chronotopic musings

The chronotope is how a configuration of time and space is represented in language and discourse.

— [Wikipedia : Chronotope](#)

- Mikhail Mikhailovich Bakhtin (1937)
- Politi, Giacomelli, Lepri, Torcini [13] (1996)
- Gutkin and Osipov (2016)
- ChaosBook.org [spatiotemporal homepage](#) (2020)

### 13.1 Chronotopic literature

The latest entry at the bottom for this blog

**2016-03-02 Boris** Just stumbled upon Lepri, Politi and Torcini [13] *Chronotopic Lyapunov analysis. I. A detailed characterization of 1D systems*.

Are you familiar with this? Somewhere in the direction I thought about.

**2016-03-02, 2016-09-03 Predrag** Politi and collaborators work is very close to our way of spatiotemporal thinking. See [refsects:GiLePo95](#), [refsects:LePoTo96](#), [refsects:LePoTo97](#) and sect. [13.4](#).

Alessandro Torcini writes: Potete trovare tutto nella mia web page e scariare tutto

[perso.u-cergy.fr/~atorcini/prepri.html](http://perso.u-cergy.fr/~atorcini/prepri.html)

Boris, if you read that literature, please share what you have learned by writing it up there.

**2016-03-02 Predrag** Also Pazó *et al.* [20] *Structure of characteristic Lyapunov vectors in spatiotemporal chaos*. Actually (I hesitated to bring it up) this line of inquiry goes smoothly into Xiong Ding's inertial manifold dimension project.

Not sure Li *et al.* [16] *Lyapunov spectra of coupled chaotic maps* is of any interest, but we'll know only if we read it.

**2016-09-06 Matt Chronotopic Approach** I've been reading refs. [7, 13, 14, 30] on chronotopic approach to spatiotemporal chaos.

**Rafael 2016-09-29** I spent a lot of time in the coupled cat maps, but in the regime of small coupling. One thing I did explore numerically is when the conjugacy given by the structural stability breaks down as one turns up the coupling.

**Rafael 2016-10-10** The main paper about the coupled maps is the paper with Miaohua Jiang. We show that the local chains of Anosov remain Anosov under local couplings. The partitions remain the same if you make changes of coordinates that are essentially local.

Of course, the fact that there is a regime of large perturbations in which this does not happen begs the question of studying the transition. Some of this has been studied also by Bastien Fernandez [5].

I have done some preliminary numerics (too crude to show). One possibility is that some of the Lyapunov exponents go to zero. Another is that the Lyapunov exponents remain away from zero but that the angle between the splittings goes to zero. There are heuristic arguments that the second possibility should occur. (Almost a proof when there is a system small coupling to another more massive one).

There were other points of the discussion. The space dynamics for PDE's. This contains references to older papers notably Kirchgassner and Mielke as well as applications to some papers.

I think Weinstein [32] is related.

**2011-02-17 PC** *A large-deviation approach to space-time chaos* by Pavel V. Kuptsov and Antonio Politi [12], [arXiv:1102.3141](https://arxiv.org/abs/1102.3141). They say:

" We show that the analysis of Lyapunov-exponents fluctuations contributes to deepen our understanding of high-dimensional chaos. This is achieved by introducing a Gaussian approximation for the entropy function that quantifies the fluctuation probability. More precisely, a diffusion matrix  $D$  (a dynamical invariant itself) is measured and analyzed in terms of its principal components. The application of this method to four (conservative, as well as dissipative) models, allows: (i) quantifying the strength of the effective interactions among the different degrees of freedom; (ii) unveiling microscopic constraints such as those associated to a symplectic structure; (iii) checking the hyperbolicity of the dynamics. "



**2016-09-28 Predrag** Isola, Politi, Ruffo and Torcini [10] *Lyapunov spectra of coupled map lattices*.

Fontich, de la Llave and Martín [6] *Dynamical systems on lattices with decaying interaction I: A functional analysis framework*. [...] consider weakly coupled map lattices with a decaying interaction. [...] applications of the framework are the study of the structural stability of maps with decay close to uncoupled possessing hyperbolic sets and the decay properties of the invariant manifolds of their hyperbolic sets, in the companion paper by Fontich et al. (2011).

**2016-11-18 Matt** : There is a storm in the distance however, as this general procedure is ruined for the spatial problem. According to the chronotopic literature [7, 13, 14, 30], iteration in space typically does not converge to the same attractor as iteration in time, and generally corresponds to a strange repeller. Therefore I cannot hope to form an initial guess loop from using a Poincaré section in the spatial direction, as typically all of my Fourier coefficients go off to infinity before a recurrence is found.

**2016-09-06 Matt** Branching out to get a better grasp of what's out there, I read Pikovsky and Politi [21] *Dynamic localization of Lyapunov vectors in space-time chaos*. It discusses the complex Ginzburg-Landau equation, two types of coupled maps, as well as Kuramoto-Sivashinsky equation, so I thought it might be useful somehow.

**2016-09-06 Predrag** Pikovsky and Politi [21] is a stat mech paper about using KPZ equations in pattern formation, no need to study it right now.

**2024-06-01 Predrag** They write:

The main difference connected to distributed systems is the existence of the so-called thermodynamic limit, corresponding to the system size  $L$  tending to infinity, that must be taken together with the usual limit  $T \rightarrow \infty$ , where  $T$  is the observation time.

The key element for understanding this universality is the interpretation of the logarithm of the local amplitude of the perturbation as a rough drifting surface.

**2017-03-02 Predrag** I asked GaTech library to order Pikovsky and Politi [22] *Lyapunov Exponents: A Tool to Explore Complex Dynamics*. I have since stolen it, [\(click here\)](#).

**2017-11-07 Matt** My *spatiotemp/blog* comments of 2017-11-02 were mainly predicated by the fact that once we find these roots, I don't think we can apply the same type of reasoning as Politi and Torcini [28] as they aren't truly fixed points of a fictitious dynamical system, like so,  $F(\hat{a}_{k,j}, T, L) = \hat{a}_{k,j}, T, L$ . But rather, like I have already described, they are the roots of a system of nonlinear algebraic equations,  $F(\hat{a}_{k,j}, T, L) = 0$ .

**2019-05-11 Predrag** My extensive notes on extensivity in Carlu, Ginelli, Lucarini and Politi [3] *Lyapunov analysis of multiscale dynamics: the slow bundle of the two-scale Lorenz 96 model* are in `lyapunov/dailyBlog.tex`.

**2020-12-16 Alessandro Torcini** `alessandro.torcini@u-cergy.fr`  
to Domenico:

si avevo visto l'annuncio della tesi di Gudorf ma alla fine non avevo partecipato, se ho capito bene lui e' riuscito a fare nello spazio-tempo continuo una cosa che io e Politi avevamo tentato nel 1990 in tempo discreto e spazio discreto (mappe accoppiate), cioe' riscrivere come un modello Markoviano la evoluzione spazio-temporale di un sistema con caos spazio temporale in termini di unita' spazio temporali, tipo i mattoncini del Tetris.

(I had seen the announcement of the thesis of Gudorf but in the end I had not participated, if I understood well he was able to do in continuous space-time something that Politi and I had tried in 1990 in discrete time and discrete space (coupled maps), that is to rewrite as a Markovian model the spatio-temporal evolution space-time evolution of a system with space-time chaos in terms of space-time units time-space units, like Tetris bricks.)

Io ci ho speso 6 mesi sopra e credo di avere ancora quaderni su quaderni, ma alla fine non pubblicammo mai nulla con Politi. A parte un PRL del 1992 molto poco citato ed un Chaos.

(I spent 6 months on it and I think I still have notebooks upon notebooks, but in the end we never published anything with Politi. Except for a 1992 PRL very little cited and a Chaos.)

Poi scrivemmo 3 lavori con Lepri su chronotopic approach al caos spazio temporale, questa roba e' finita in 2 o 3 libri, ma di fatto la linea di ricerca e' stata molto poco seguita, infine nel 2013 siamo riusciti a calcolare tutto lo spettro dei i comoving Lyapunov exponents (lavoro ignoto ai piu),

(Then we wrote 3 papers with Lepri on chronotopic approach to space-time chaos. time chaos, this stuff ended up in 2 or 3 books, but in fact the research line of research was very little followed, finally in 2013 we managed to calculate the whole spectrum of the the whole spectrum of comoving Lyapunov exponents, work unknown to most,)

A. K. Jiotsa, A. Politi, and A. Torcini [11], *Convective Lyapunov Spectra* J. Phys. A 46 (2013) 254013.

Spero di riuscire a studiare la tesi di Gudorf prima o poi.

(I hope to be able to study Gudorf's thesis sooner or later.)

A presto

## 13.2 PolTor92b Towards a statistical mechanics of spatiotemporal chaos

**2017-10-31 Burak** I looked everywhere but could not find Politi and Torcini [28] *Towards a statistical mechanics of spatiotemporal chaos* (1992) in this blog. The abstract:

Coupled Hénon maps are introduced to model in a more appropriate way chaos in extended systems. An effective technique allows the extraction of spatiotemporal periodic orbits, which are then used to approximate the invariant measure. A further implementation of the  $\zeta$ -function formalism reveals the extensive character of entropies and dimensions, and allows the computation of the associated multifractal spectra. Finally, the analysis of short chains indicates the existence of distinct phases in the invariant measure, characterized by a different number of positive Lyapunov exponents.

We should all read it very carefully. They use Biham-Wenzel [1] to infer spatiotemporal periodic orbits and their symbolic dynamics by introducing a continuous fictitious time.

I'm not sure if they are using periodic orbits of different chain spatial period  $L$  in order to estimate the statistics of the system at thermodynamic limit  $L \rightarrow \infty$ . If that's the case and the dynamical  $\zeta$  function is designed for this purpose, then this paper is very similar to what we have in mind.

**2017-10-31 Matt** I find it interesting that they use a continuous fictitious Biham-Wenzel [1] dynamics for a spatiotemporal system of mappings, while I have a discrete fictitious time (in the form of my spatiotemporal mapping) introduced for continuous (albeit discretized) spatiotemporal equations.

Currently the paper has **13** APS and **22** Google Scholar citations.

To motivate the Politi and Torcini [28] coupled Hénon map lattice, we start by a review a single Hénon map, written using the conventions of [Chaos-Book.org](#).

**Note:** Politi and Torcini say that in the case of  $\epsilon = 0$  that the original Hénon map is retrieved, but if you actually do this then indices don't match the original equation.

$$\begin{aligned}x_{n+1} &= 1 - ay_{n+1}^2 + bx_{n-1} \\y_{n+1} &= x_n,\end{aligned}\tag{13.1}$$

or, as a 3-term recurrence

$$\phi_{n+1} + a\phi_n^2 - b\phi_{n-1} = 1.$$

The parameter  $a$  quantifies the “stretching” and  $b$  quantifies the “contraction”.

The single Hénon map is nice because the system is not linear, but has binary dynamics.

The deviation of an approximate trajectory from the 3-term recurrence is

$$v_n = \phi_{n+1} - (1 - a\phi_n^2 + b\phi_{n-1})$$

In classical mechanics force is the gradient of potential, which Biham-Wenzel [1] construct as a cubic potential

$$V_n = \phi_n(\phi_{n+1} - b\phi_{n-1} - 1) + a\phi_n^3 \quad (13.2)$$

With the cubic potential of a single Hénon map we can start to look for orbits with initial conditions of two points (two point recurrence relation requires this) and make the guess as we iterate in time. A particular guess is to choose a sequence of maxima/minima of the potential.

In order to accurately enumerate the orbit with symbolic dynamics, in order to choose which way you “roll” the potential needs to be modified by  $\pm 1$ , as when viewed from the perspective of the cubic potential, trajectories roll downhill, so in order to flip the direction one must apply a flip. The symbolic dynamics is therefore binary and determined by these flips. One can just list the binary sequences and see if the orbit is realized by the system. [Chaosbook](#) does this up to sequences of length 13, while it has been done by Grassberger, Kantz and Moenig [8] to symbol length 32. This means that there could be as many as  $2^{32}/32$  distinct periodic orbits.

In the Politi-Torcini [28] coupled Hénon map equations  $t$  is the index associated to time, while  $n$  is the index associated with space: <sup>1</sup>

$$\begin{aligned} \phi_{n,t+1} + y_{nt}^2 - b\phi_{n,t-1} &= a \\ y_{nt} &= \phi_{nt} + \frac{\epsilon}{2}(\phi_{n+1,t} - 2\phi_{nt} + \phi_{n-1,t}) \end{aligned} \quad (13.4)$$

In the Hamiltonian  $b = -1$  case the only parameter is the stretching  $a$ ; when it is small some orbits become stable, not everyone is unstable and admissible. If there’s not strong stretching then there is a mixture as the hyperbolicity isn’t dominating. All of these coupled maps, say something wild happens at each site (alternating between 1 and -1 is far in this case), and THEN you couple it weakly to its neighbors.

But when the coupling with neighbors is very strong, its a very different phenomena. The cats have written a Helmholtz in Euclidean space and time

<sup>1</sup>Matt 2017-11-08: Politi-Torcini Hénon map form differs from the ChaosBook convention (13.1). If we take their claim that in the  $\epsilon = 0$  case we should retrieve the classical Hénon equations very strictly, this is how they should appear I believe. The difference lies in the time index  $t + 1$  versus  $t$  of the  $y$  terms.

$$\begin{aligned} \phi_{n,t+1} &= 1 - a(y_{n,t+1})^2 + b\phi_{n,t-1} \\ y_{n,t+1} &= (1 + \epsilon)\phi_{nt} + \frac{\epsilon}{2}(\phi_{n+1,t} + \phi_{n-1,t}). \end{aligned} \quad (13.3)$$

where the Laplacian is weighted by  $+1$  as opposed to  $1, -1$  in the Minkowski case. Second order operator that has different weights (as determined by some metric) its called the Beltrami operator. Predrag also thinks the sign is different. This is 1992 though, and there's not much there because its Phys. Rev. Lett. so there must be real work somewhere.

They cite the fact that most people don't use it for invertible dynamics. Then they say the spatially and temporally periodic orbits are extracted using the Newton method. What they actually do, they take  $L = 1, 2, 3, 4$  only. They don't elucidate on interesting tricks, like how to use the method for coupled maps. The density of periodic orbits in the invariant measure is stated, but this is only really known for single maps, Predrag doubts this.

Politi and Torcini [28] is one of the first papers that uses spatiotemporal symbolic dynamics, as seen by Predrag in the literature. Symbol of a torus is really just a lattice label. Politi and Torcini use doubly periodic boundary conditions, with canonical values from Hénon for the parameters.

When you write the equations in diagonal form you'll likely take a square root of it. Then, they say some orbits are pruned, some exist only with uncoupled case. That helps them because if you can prove you only lose orbits and never gain orbits you can see if certain orbits are realized or not.

It is important to realize that not all periodic states belong to the inertial manifold. There are isolated orbits, corresponding to fixed points.

The orbits are found with Newton method.

They discarded all of the cycles that had a sequence, specifically  $0\bar{0}0$  in symbolic dynamics, is not allowed. The application of the zeta function, "they don't know what they are doing, so ignore it".

Their intuition is that the inertial manifold is extensive: if you double the spatial length, you should double the number of physical Lyapunov exponents as you go in time. They compute some Jacobian, they are just the standard forward-in-time Jacobians. Using these they compute  $2J \times 2J$  sized matrices for the spatiotemporal domain, (thinks Bloch theorem doesn't apply, maybe). They also say to take the logarithm and divide it by the size of the domain. Their entropy is a sum of temporal Lyapunov exponents divided by  $L$ . They have an intuition but its hard to check because of the small  $L$ . One possible solution is to use the fixed point, as its a representative of the stretching rate in the neighborhood. "Let's just say the typical stretching rate is roughly the same no matter the domain size." I.e. they assume its a frozen state so it doesn't matter how big the domain gets. Grand canonical formalism for the Zeta function, but it can be "safely ignored". Multifractal stuff seems useless, look at this  $h$ , instead of plotting everything from infinity to infinity, but can subtract something and it works out and they get a plot. But there seems to be an envelope which may be connected to the quantity they try to claim, maybe.

Different phases, but they notice that different periodic orbits have different number of positive Lyapunov exponents. They interpret periodic orbits with the same number belong to the same 'phase'.

The problem only uses Biham in time; Not clear why they did it because they say its invertible, which makes sense because Hamiltonian.

For a particular solution, the potential is just a set of numbers, even though it depends on  $x$ . It will have to be evaluated at the linearization of the nonlinear equations and evaluated along the orbit. e.g. stability of orbits do not look like constant anything. PC Thinks the Jacobian will work out somehow.

**2017-10-31 Matt Part Two: Discussions from the Invariant Solns Meeting**

Ignore the last third of the paper. The one thing PC doesn't understand, is that they are studying coupled Hénon maps because they're invertible, but he doesn't understand why they care.

They use the standard parameter values of Hénon.

Fictitious time isn't important, the method is the method of Biam where they derive a cubic potential such that its derivative is the Hénon map.

The coupling is what determines the type of behavior here, in the weak coupling limit, everything looks unstable on its own, but when the coupling is strong, the model is ergodic, because it is fully developed due to the length scale imposed but no laminar patches (No point where there are a different number of unstable directions).

If we write it carefully, take a Hamiltonian map, rewrite in terms of Beltrami operator (Laplacian with metric). Looking at this operator, its bilinear in derivative, but the derivatives have different weights and can have opposite signs.

Elliptic structure in PC's case, but thinks the Hénon there should be a negative sign.

If you have a spatially periodic chain, (they still think of a chain in space evolved in time, but they change this in the future). They say if you have periodic lattice, you should use Bloch theorem, which is what is done in condensed matter. They write the Bloch theorem, but we don't know why. PC believes it may be because the coupling is weak, so deformations are long wavelength deformations.

Explicitly the stretching parameter, changed from small to large, the problem becomes hyperbolic and sines and cosines change to hyperbolic sines and cosines.

In order to rewrite the equations in one scalar field that has a spatiotemporal Beltrami operator, we need to modify (13.3). First we write the set of equations as two step recurrence in one field,

$$\phi_{n,t+1} + b\phi_{n,t-1} = 1 - a((1 + \epsilon)\phi_{n,t} + \frac{\epsilon}{2}(\phi_{n,t+1} + \phi_{n-1,t}))^2, \quad (13.5)$$

Then we can add and subtract  $2\phi_n^j$  to the LHS of the equation (Predrag 2024-12-30 this looks wrong),

$$(\square_t - 2)\phi_{n,t} = 1 - a((1 + \epsilon)\phi_{n,t} + \frac{\epsilon}{2}(\phi_{n+1,t} + \phi_{n-1,t}))^2, \quad (13.6)$$

Because the quadratic nonlinearity is where the spatial part of the Beltrami or Laplacian is, I don't know how to get around this and combine space and time currently. I recall Predrag mentioning something about a square root but it doesn't seem very well motivated because the spatial coupling is completely separated from time coupling unless I'm missing some type of approximation.

**2020-06-25 Predrag** Perhaps the easiest thing would be to replace the Hénon in (13.4) by the Lozi map?

### 13.3 PolTor92 Periodic orbits in coupled Hénon maps

**2020-05-31 Predrag** Politi and Torcini [27] *Periodic orbits in coupled Hénon maps: Lyapunov and multifractal analysis* is quite close to our spatiotemporal cat. The problem is harder, as the Hénon map is nonlinear; MUST CITE in ref. [4].

They study *spatiotemporal Hénon*, a (1+1)-spacetime lattice of Hénon maps orbits which are periodic both in space and time, and note that the dependence of the lattice field at time  $\phi_{t+1}$  on the two previous time steps prevents an interpretation of dynamics as the composition of a local chaotic evolution with a diffusion process, and that the  $|b| = 1$  case(s) could be important as examples of Hamiltonian lattice field theories. (**Predrag:** they do not comment on the role of the spacetime asymmetry of spatiotemporal Hénon.)

Their numerical method is an extension of Biham and Wenzel [1] for the single Hénon map, with symbols  $s_{nt}$  in  $\mathcal{A} = \{0, 1\}$ . Any fixed point in fictitious time corresponds to a spatio-temporal cycle  $[L \times T]_S$ .

The search of periodic orbits is further simplified by the fact that a small coupling prunes some of cycles which are present for  $\epsilon = 0$ . Therefore, the knowledge of the topological structure of the single Hénon map yields a symbolic encoding of the dynamics and allows for restricting the set of candidate admissible symbol blocks to be investigated. For  $a = 1.4$ ,  $b = 0.3$  this works well for  $\epsilon = 0.1$ .

They comment on existence both time-equilibria  $[L \times 1]_0$  and time-relative equilibria  $[L \times 1]_S$ ,  $S \neq 0$  (seen as stationary patterns in a reference frame moving with a constant velocity).

A problem in reconstructing the statistical properties of an attractor from periodic orbits is ensuring that all orbits used belong to the natural invariant measure. For instance, in the single Hénon map, one of the two fixed points is isolated and it does not belong to the strange attractor. Something similar should occur in the CML.

A family of specific Lyapunov exponents is defined, which estimate the growth rate of spatially inhomogeneous perturbations, related to the co-moving Lyapunov exponents.

The  $\zeta$ -function formalism is used to analyze the scaling structure of the invariant measure both in space and time.

**(Predrag:** here things fall apart. They do numerics for various small fixed  $L$  or  $T$ , but have no path to constructing a spacetime  $\zeta$ -function.)

In the case of a CML, the periodic orbit weights depend exponentially both on space and time variables,  $t_j = r_j^{LT}$ . This suggests that the  $\zeta$ -function formalism could be effectively extended, by performing an additional sum over all spatial periods. Unfortunately, a straight implementation of this scheme is not so effective as in the low-dimensional case. Therefore, we limit ourselves to apply the standard formalism, checking afterwards the dependence on the length chain  $L$ .

### 13.4 PoToLe98 Lyapunov exponents from node-counting

Politi, Torcini and Lepri [30] *Lyapunov exponents from node-counting arguments* is a promising start, but there does not seem to have been any followup since 1998..

The *chronotopic approach* aims to extending the concept of Lyapunov spectrum to spatially inhomogeneous perturbations.

The main result of the chronotopic approach is the existence of a dynamical invariant, the entropy potential, the knowledge of which allows to determine all properties of the evolution of localized as well as extended perturbations.

One can describe the spatial structure of a generic Lyapunov vector with a single complex number  $\tilde{\mu} = \mu + ik$ , the real part of which is the exponential growth rate, while the imaginary part is the wavenumber. The frequency  $\omega$  can be read as the imaginary part of the complex number  $\tilde{\lambda} = \lambda + i\omega$ , where  $\lambda$  is the temporal growth rate (i.e. the Lyapunov exponent) of the given perturbation. The analyticity properties of the "dispersion relation" connecting  $\tilde{\mu}$  with  $\tilde{\lambda}$  furnish the last ingredient to "prove" the existence of an entropy potential [14].

This paper introduces a wavenumber by define "rotation numbers" as the imaginary counterpart of the Lyapunov exponents. They compute the Lyapunov spectrum by using the transfer matrix approach. The approach is limited to a class of coupled map lattices (CMLs) with everywhere expanding multipliers.

(First) they assume a time-stationary spatiotemporal solution and compute the 1 spatial dimension orbit Jacobian matrix. That resembles the tight-binding approximation of the 1D Schrödinger equation (with imaginary time) in the presence of a random potential, i.e., the Anderson model. They note the close analogy with the computation of the vibrational spectrum of a chain with random masses. The spectrum of the Schrödinger problem can be determined without diagonalizing the operator (which is the sum of the discretized spatial Laplacian and a diagonal operator). Its symmetry ensures the applicability of the node theorem which states that the eigenfunctions are ordered according to the number of their zeros [19].



For a time-stationary spatiotemporal solution, one can always redefine site fields  $\phi_{nt}$  to make them all a constant field  $\phi_{oo}$ . Then the spatial structure of the corresponding Lyapunov vector counts the nodes. Furthermore, all eigenvalues are real, i.e., no rotations in tangent space.

(Second), they consider orbits of temporal period  $T > 2$ . The operator is a banded matrix (of width  $2T + 1$ ) so that we are dealing with a sort of Schrodinger problem with long-range hopping. The fundamental difference is that no similarity transformation can turn the operator into a symmetric matrix, hence generic existence of complex eigenvalues. That's a problem for them, as the node theorem is proved only for operators with a strictly real and positive spectrum. They waffle.

Still, they do a numerical calculation for  $[L_{11} \times T_7]_{S_0}$  and  $[L_7 \times T_5]_{S_0}$  primitive cells and get the correct counting, their figs. 2 and 3. They finish with

“More important, in our opinion, is the question whether the same approach can be extended to continuous-time and -space systems. We believe that instead of checking numerically whether this is true or not, it is more important to look for the possibly deep reasons that lie behind the apparent validity of the conjectures presented in this paper.”

**2020-04-18 Predrag** A long shot, but maybe Pastur and Figotin [19] *Spectra of Random and Almost-Periodic Operators* Chap. III offers some estimate of the Kuramoto–Sivashinsky spectra, and provides mean node-count for Kuramoto–Sivashinsky?

## 13.5 PolPuc92 Invariant measure in coupled maps

**2016-11-06 Predrag** Politi and Puccioni [26] *Invariant measure in coupled maps* write: “ The state of affairs is much less clear when we pass from closed chains (as above) to sub-chains of an-in principle-infinite lattice. This corresponds to the canonical-ensemble picture of statistical mechanics: the system of interest (sub-chain of length  $E$ ) is coupled with a thermal bath given by the rest of the chain. From the previous considerations, the attractor corresponding to an isolated system would fill, for  $E$  sufficiently large, a  $\rho E$ -dimensional manifold. The main effect of the coupling with the heat bath is to add a sort of “external noise” dressing the manifold along all directions, and thus making the resulting invariant measure to become  $E$ -dimensional. ”

This paper is lots of hand-waving, so I gave up on reading it.

## 13.6 PolTor09 Stable chaos

Politi and Torcini [29] *Stable chaos* (2009), [arXiv:0902.2545](https://arxiv.org/abs/0902.2545)

They consider a chain of chain of Duffing oscillators.

Chaos is associated with an exponential sensitivity to tiny perturbations in the initial conditions, so that the presence of at least one positive Lyapunov exponent is considered as a necessary and sufficient condition for the occurrence of irregular dynamics in deterministic dynamical systems. In fact, the first observation in coupled-map models of stochastic-like behaviour accompanied by a negative maximum Lyapunov exponent came as a big surprise. The unexpected coexistence of local stability and chaotic behaviour, due to the phenomenon was called stable chaos (SC). The irregular behaviour is a transient phenomenon that is restricted to finite-time scales.

We might want to study the 'chronotopic approach' of eqs. (10) to (17).

## 13.7 Spatiotemporal Floquet-Bloch theory

2024-12-28 Predrag .

Dear Arkady,

For (many) years now we have been preparing a series of papers on the spatiotemporal theory of turbulence. For us, one of the essential innovations of our approach has been the computation of spatiotemporal stability exponents over infinite Bravais lattices, rather than temporal Floquet/Lyapunov stability of compact, finite time solutions see [CL18 figure 9](#). As far as I can tell, this is never done in the ‘standard’ Gutzwiller-Ruelle periodic orbit theory (as developed in our [ChaosBook.org](#)).

We would like to give credit where the credit is due. Current list:

1. Is there an earlier paper? Is this already in Hill [9] and Poincaré [25]?
2. Bountis and Helleman (1981) [2]
3. Also mention (?) Mackay and Meiss (1983) [18] *Linear stability of periodic orbits in Lagrangian systems*
4. Pikovsky (1989) [24] *Spatial development of chaos in nonlinear media*
5. Also mention (?) Lepri, Politi and Torcini (1996) [13] *Chronotopic Lyapunov analysis: (I) A comprehensive characterization of 1D systems,*

though I don’t see what would be the point of giving credit to people who did it second, third, etc.?

Is it fair to say that the Bloch/Floquet approach to stability was first utilized by Bountis (1981) for temporal evolution, and Pikovsky (1989) for spatiotemporal systems? Should we cite any other papers for essential contributions to this notion of stability of deterministic solutions of spatiotemporal systems?

2024-12-30 Arkady .

Suppose one has a finite-dimensional dynamical system and a periodic orbit  $\vec{X}(t) = \vec{X}(t + T)$  there. Then the stability of this orbit reduces to finding solutions of a linear system with  $T$ -periodic in time coefficients. Floquet theory says that the solutions of this linear system define characteristic multipliers, which can be complex, their absolute values define stability of the periodic orbit. Practically the same holds for finite-dimensional maps (in fact, Bountis and Helleman give a reference [26] to some old books).

If one wants to calculate stability of non-periodic orbit, one has to find solutions of a linear system with chaotic/random coefficients. Instead of multipliers, one has according to the Oseledets multiplicative ergodic theorem real-valued Lyapunov exponents that determine stability of the orbit.

Suppose one has a partial differential equation, where a state  $\vec{X}(x, t)$  depends on the spatial coordinate  $x$  in a domain  $0 \leq x \leq L$ . Again, if a solution is a periodic function of time, multipliers can be defined (in fact an infinite set of multipliers) that determine stability. In the case of a chaotic solution, stability is determined by the Lyapunov exponents.

Suppose now that the domain is infinite  $-\infty < x < \infty$ , but the basic solution  $\vec{X}(x, t) = \vec{X}(x + L, t)$  is periodic in space. First, one can as above determine multipliers/Lyapunov exponents assuming that the linear solution is also  $L$ -periodic in space. But, if one wants to explore stability with respect to non-periodic in space perturbation, one has to look for generic space dependent solutions of a linear problem with space-periodic coefficients. In my opinion, fundamental solutions here have the form  $\vec{U}(x, t) \exp[ik_1 x]$  where  $\vec{U}(x, t) = \vec{U}(x + L, t)$  is space-periodic, and  $k_1$  is “quasi-momentum”. The linear equation for  $\vec{U}(x, t)$  will contain  $k_1$  as a parameter. In the case of a periodic in time basic trajectory  $\vec{X}(x, t) = \vec{X}(x + L, t + T)$  one obtains multipliers that depend on  $k_1$  as on a parameter. In the case of a chaotic in time trajectory, one obtains Lyapunov exponents depending on  $k_1$  as on a parameter. These Lyapunov exponents, dubbed that time as Lyapunov-Bloch exponents, is the essence of what I did in 80-ies. I am not 100% sure, but maybe I was the first to introduce them. On the other hand I am pretty sure there is a long history of defining multipliers depending on  $k_1$  in the realm of secondary stability of time-periodic patterns and waves.

Lepri and Politi in their chronotopic Lyapunov analysis considered also complex or purely imaginary quasimomentum  $k_1$ .

I think, all above is directly applicable also to discrete in space systems (coupled ODEs) or discrete in space and time systems (coupled map lattices). It appears also reasonable that in case of two- or three-dimensional in space patterns, the quasi-momentum becomes also two- or three-dimensional.

There is a symmetric reformulation of the above approach if one exchanges space and time variables, and considers evolution in space of a time-dependent field. For example, in nonlinear optics one uses spatial coordinate  $z$  in the direction of a beam propagation as an equivalent of time variable; the field  $E(z = 0, t)$  plays a role of an “initial condition”.

In general, however, in PDEs one can consider evolution along some directions in space and time, but I am not sure how to formulate the approaches above for such “skewed” cases.

Interestingly, in some cases it is not easy to recognize, what is “time” and what is “space”. Consider, e.g., a simple set of ODEs

$$\frac{dx_n}{dt} = -x_n + f(x_{n-1}), \quad n = 1, 2, \dots$$

where  $f(x) = 1 - 2x^2$  is a chaotic map. One here has to define the boundary field  $x_0(t)$  and to look at its evolution along space  $n$ . It appears, that

it is suitable to treat  $n$  as a new discrete time and  $t$  as a space. Then the field  $x_n(t)$  will be chaotic in space direction  $n$ . On the other hand, all Lyapunov exponents in time-direction are  $-1$ .

**2024-12-30 Predrag** The main advance in our work, we believe, is that we work in infinite spacetime, not with infinite space, compact periodic time solutions. The orbit Jacobian operator, our [eq. \(70\)](#) and [eq. \(56\)](#), the orbit stability exponent [eq. \(111\)](#), and the amazingly pretty exact (in this example one-space, one-time dimension) deterministic zeta function [eq. \(129\)](#) are defined democratically over what you might call Bloch quasi-momenta, and Floquet quasi-energies: what we call spacetime lattice momenta. The "thermodynamic parameter" is not the time  $T$  or spatial extent  $L$ , but the **spacetime** primitive cell volume  $V$  ( $V = LT$  in the 2-dimensional example).

Its Euclidean spacetime "sum over Bravais lattices" form should be correct not only for discretized spacetime, but turbulent PDEs as well. We believe, but have not explored that as yet.

**2024-05-18 Predrag** to Antonio Politi: "Who did first the spacetime coupled maps stability ("entropy per unit spacetime volume"? in spatial "thermodynamic" limit number of spatial lattice sites  $\rightarrow \infty$ ) as an integral over Brillouin zone? And where? "

(your chronopic gruppie)

**2024-05-20 Antonio** There are three papers of mine where I addressed the point you mention.

S. Lepri, A. Politi, A. Torcini [\[13\]](#) *Chronotopic Lyapunov analysis: (I) A comprehensive characterization of 1D systems*, J. Stat. Phys. 82, 1429 (1996); ([click here](#)); see sect. [13.2](#)

S. Lepri, A. Politi, A. Torcini [\[15\]](#) *Entropy potential and Lyapunov exponents*, Chaos 7, 701 (1997); ([click here](#))

S. Lepri, A. Politi, A. Torcini [\[14\]](#) *Chronotopic Lyapunov analysis: (II) Towards a unified approach*, J. Stat. Phys. 88, 31 (1997); ([click here](#))

The same issue is addressed also in my book with Arkady on Lyapunov exponents [\[22\]](#).

**2024-12-30 Predrag** We would preced the above three papers with Politi and Torcini [\[28\]](#) *Towards a statistical mechanics of spatiotemporal chaos* (1992), see sect. [13.2](#). The use spatial Bloch wavenumber  $k$ , both for equilibria and temporally periodic solutions, but no temporal Floquet "quasi-energy".

**2024-05-22 Predrag** The interesting thing is that chronotopians use Bloch only for spatial infinity, but not the temporal infinity. So our paper I [\[17\]](#) would be the first to do that, were it not for Pikovsky (1989) [\[24\]](#), who computes Bloch bands for solutions periodic in time :).

Reading Pikovsky and Politi [22] *Lyapunov Exponents: A Tool to Explore Complex Dynamics*, (2016), ([click here](#)).

Section *Bloch-Lyapunov exponents*

In spatially uniform systems (either unbounded or in the presence of periodic boundary conditions), the spatially homogeneous state is invariant as well as all the states with arbitrary periodicity in space. Indeed, if the initial field configuration is  $L$ -periodic on an infinite lattice, then this property holds at all times. On the other hand, a linear perturbation must not have the same periodicity. As in the standard theory of linear waves in a periodic potential, here the Bloch ansatz allows one to reduce the dynamics of the perturbation to the original domain.

The corresponding Lyapunov exponent depends on the quasi-momentum  $k$ , which attains values in the interval  $[-\pi/L, \pi/L]$ . The value  $k = 0$  corresponds to the internal exponent (i.e. to perturbations that do not violate the original periodicity), while the other  $k \neq 0$  values correspond to the transverse exponents.

It seems Pikovsky did it first, but only for the spatial dimension: “For applications of these Bloch-Lyapunov exponents, see Pikovsky [24] (1989) and Straube and Pikovsky [31] (2011).

**2024-05-22 Predrag** Pikovsky [23] *On the interaction of strange attractors* (1984); Pikovsky [24] *Spatial development of chaos in nonlinear media* (1989); ([click here](#))

calls Bloch bands ‘quasi-Lyapunov exponents’.

Sect. 6. *Spatial-temporal analogy and temporal development of spatial chaos*

Using a spatial-temporal analogy, the problem of the temporal development of spatial chaos may be transformed to the problem described above of the spatial development of temporal chaos. Indeed, unstable waves in an infinite medium may be governed by the complex Ginzburg-Landau equation in the “dual” form [...]

which Pikovsky gives credit for to

[3] H.T. Moon, P. Huerre and L.G. Redekopp, *Physica D* 7 (1983) 135.

(Predrag: I do not see anything we need to cite in the above paper)

He also considers a continuous (but periodic) time, discrete space  $\phi^4$  model.

And now, music to [Lyapunov | Bloch](#).

**2024-05-22 Predrag** Arthur V. Straube, Markus Abel, Arkady Pikovsky *Temporal chaos versus spatial mixing in reaction-advection-diffusion systems* (2004); [arXiv:nlin/0404057](#).

The transverse Lyapunov exponent governing the stability of the homogeneous state can be represented as a combination of Lyapunov exponents for spatial mixing and temporal chaos.

**2024-05-22 Predrag** Straube and Pikovsky *Pattern formation induced by time-dependent advection* [31] (2011); ([click here](#))

[...] study pattern-forming instabilities in periodic-in-space mixing flows, based on the calculation of Lyapunov-Bloch exponents [24]. [...] using a discrete-in-time model, where reaction, advection, and diffusion act as successive operators. This enormously simplifies the calculations, while yielding a qualitatively correct picture.

**2024-05-22 Predrag** Pikovsky slides *Lyapunov exponents and all that* ([click here](#)):

[...] Lyapunov-Bloch exponent: Take a system of size  $L$  and calculate the Lyapunov exponent  $\lambda(k)$  of the perturbation  $v = \exp(ikx)$ . It determines stability of space-periodic states.

**2024-09-29 Predrag** Working on illustrating the difference between periodic and aperiodic perturbations of a periodic state, see [CL18 figure 9](#). The value  $k = 0$  corresponds to the ‘internal’ exponent (i.e. to perturbations that do not violate the original periodicity), while the  $k \neq 0$  values correspond to the ‘transverse’ exponents.

**2024-11-22 Predrag** We should add Bountis and Helleman [2], see sect. [11.1.3 Bountis and Helleman 1981 paper](#), to the collection of our “bibles”. Has so much stuff in it that it is probably Bountis PhD thesis.

**2024-12-11 Han** Reread Mackay and Meiss (1983) [18], see post on page [1369](#). They apply Floquet theorem to iterated map temporal stability, without explicitly calling it that. Their Floquet multiplier  $\lambda$  is the Floquet-Bloch theorem phase factor  $e^{iqk}$ .

## References

- [1] O. Biham and W. Wenzel, “Characterization of unstable periodic orbits in chaotic attractors and repellers”, *Phys. Rev. Lett.* **63**, 819 (1989).
- [2] T. Bountis and R. H. G. Helleman, “On the stability of periodic orbits of two-dimensional mappings”, *J. Math. Phys.* **22**, 1867–1877 (1981).
- [3] M. Carlu, F. Ginelli, V. Lucarini, and A. Politi, “Lyapunov analysis of multiscale dynamics: the slow bundle of the two-scale Lorenz 96 model”, *Nonlinear Processes Geophys.* **26**, 73–89 (2019).
- [4] P. Cvitanović and H. Liang, *A chaotic lattice field theory in two dimensions*, In preparation, 2024.
- [5] B. Fernandez, “Breaking of ergodicity in expanding systems of globally coupled piecewise affine circle maps”, *J. Stat. Phys.* **154**, 999–1029 (2014).
- [6] E. Fontich, R. de la Llave, and P. Martín, “Dynamical systems on lattices with decaying interaction I: A functional analysis framework”, *J. Diff. Equ.* **250**, 2838–2886 (2011).

- [7] G. Giacomelli, S. Lepri, and A. Politi, "Statistical properties of bidimensional patterns generated from delayed and extended maps", *Phys. Rev. E* **51**, 3939–3944 (1995).
- [8] P. Grassberger, H. Kantz, and U. Moenig, "On the symbolic dynamics of Hénon map", *J. Phys. A* **22**, 5217–5230 (1989).
- [9] G. W. Hill, "On the part of the motion of the lunar perigee which is a function of the mean motions of the sun and moon", *Acta Math.* **8**, 1–36 (1886).
- [10] S. Isola, A. Politi, S. Ruffo, and A. Torcini, "Lyapunov spectra of coupled map lattices", *Phys. Lett. A* **143**, 365–368 (1990).
- [11] A. K. Jiotsa, A. Politi, and A. Torcini, "Convective Lyapunov spectra", *J. Phys. A* **46**, 254013 (2013).
- [12] P. V. Kuptsov and A. Politi, "Large-deviation approach to space-time chaos", *Phys. Rev. Lett.* **107**, 114101 (2011).
- [13] S. Lepri, A. Politi, and A. Torcini, "Chronotopic Lyapunov analysis. I. A detailed characterization of 1D systems", *J. Stat. Phys.* **82**, 1429–1452 (1996).
- [14] S. Lepri, A. Politi, and A. Torcini, "Chronotopic Lyapunov analysis. II. Towards a unified approach", *J. Stat. Phys.* **88**, 31–45 (1997).
- [15] S. Lepri, A. Politi, and A. Torcini, "Entropy potential and Lyapunov exponents", *Chaos* **7**, 701–709 (1997).
- [16] X. Li, Y. Xue, P. Shi, and G. Hu, "Lyapunov spectra of coupled chaotic maps", *Int. J. Bifur. Chaos* **18**, 3759–3770 (2008).
- [17] H. Liang and P. Cvitanović, "A chaotic lattice field theory in one dimension", *J. Phys. A* **55**, 304002 (2022).
- [18] R. S. MacKay and J. D. Meiss, "Linear stability of periodic orbits in Lagrangian systems", *Phys. Lett. A* **98**, 92–94 (1983).
- [19] L. Pastur and A. Figotin, *Spectra of Random and Almost-Periodic Operators* (Springer, Berlin, 1992).
- [20] D. Pazó, I. G. Szendro, J. M. López, and M. A. Rodríguez, "Structure of characteristic Lyapunov vectors in spatiotemporal chaos", *Phys. Rev. E* **78**, 016209 (2008).
- [21] A. Pikovsky and A. Politi, "Dynamic localization of Lyapunov vectors in spacetime chaos", *Nonlinearity* **11**, 1049–1062 (1998).
- [22] A. Pikovsky and A. Politi, *Lyapunov Exponents: A Tool to Explore Complex Dynamics* (Cambridge Univ. Press, Cambridge, 2016).
- [23] A. S. Pikovsky, "On the interaction of strange attractors", *Z. Phys. B* **55**, 149–154 (1984).
- [24] A. S. Pikovsky, "Spatial development of chaos in nonlinear media", *Phys. Lett. A* **137**, 121–127 (1989).



- [25] H. Poincaré, “Sur les déterminants d’ordre infini”, *Bull. Soc. Math. France* **14**, 77–90 (1886).
- [26] A. Politi and G. P. Puccioni, “Invariant measure in coupled maps”, *Physica D* **58**, 384–391 (1992).
- [27] A. Politi and A. Torcini, “Periodic orbits in coupled Hénon maps: Lyapunov and multifractal analysis”, *Chaos* **2**, 293–300 (1992).
- [28] A. Politi and A. Torcini, “Towards a statistical mechanics of spatiotemporal chaos”, *Phys. Rev. Lett.* **69**, 3421–3424 (1992).
- [29] A. Politi and A. Torcini, “Stable chaos”, in *Understanding Complex Systems* (Springer, Berlin, 2009), pp. 103–129.
- [30] A. Politi, A. Torcini, and S. Lepri, “Lyapunov exponents from node-counting arguments”, *J. Phys. IV* **8**, 263 (1998).
- [31] A. V. Straube and A. Pikovsky, “Pattern formation induced by time-dependent advection”, *Math. Model. Nat. Pheno.* **6**, 138–148 (2011).
- [32] A. Weinstein, “Periodic nonlinear waves on a half-line”, *Commun. Math. Phys.* **99**, 385–388 (1985).

## Chapter 14

# Symbolic dynamics: a glossary

Analysis of a low-dimensional chaotic dynamical system typically starts [4] with establishing that a flow is locally stretching, globally folding. The flow is then reduced to a discrete time return map by appropriate Poincaré sections. Its state space is partitioned, the partitions labeled by an alphabet, and the qualitatively distinct solutions classified by their temporal symbol sequences. Thus our analysis of the cat map and the spatiotemporal cat requires recalling and generalising a few standard symbolic dynamics notions.

**Partitions, alphabets.** A division of state space  $\mathcal{M}$  into a disjoint union of distinct regions  $\mathcal{M}_A, \mathcal{M}_B, \dots, \mathcal{M}_Z$  constitutes a *partition*. Label each region by a symbol  $m$  from an  $N$ -letter *alphabet*  $\mathcal{A} = \{A, B, C, \dots, Z\}$ , where  $N = n_{\mathcal{A}}$  is the number of such regions. Alternatively, one can distinguish different regions by coloring them, with colors serving as the “letters” of the alphabet. For notational convenience, in alphabets we sometimes denote negative integer  $m$  by underlining it, as in  $\mathcal{A} = \{-2, -1, 0, 1\} = \{\underline{2}, \underline{1}, 0, 1\}$ .

**Itineraries.** For a dynamical system evolving in time, every state space point  $x_0 \in \mathcal{M}$  has the *future itinerary*, an infinite sequence of symbols  $S^+(x_0) = m_1 m_2 m_3 \dots$  which indicates the temporal order in which the regions shall be visited. Given a trajectory  $x_1, x_2, x_3, \dots$  of the initial point  $x_0$  generated by a time-evolution law  $x_{n+1} = f(x_n)$ , the itinerary is given by the symbol sequence

$$m_n = m \quad \text{if} \quad x_n \in \mathcal{M}_m. \quad (14.1)$$

The *past itinerary*  $S^-(x_0) = \dots m_{-2} m_{-1} m_0$  describes the order in which the regions were visited up to arriving to the point  $x_0$ . Each point  $x_0$  thus has associated with it the bi-infinite itinerary

$$S(x_0) = S^- . S^+ = \dots m_{-2} m_{-1} m_0 . m_1 m_2 m_3 \dots, \quad (14.2)$$

or simply ‘itinerary’, if we chose not to use the decimal point to indicate the present,

$$\{m_i\} = \cdots m_{-2}m_{-1}m_0m_1m_2m_3\cdots \quad (14.3)$$

**Shifts.** A forward iteration of temporal dynamics  $x \rightarrow x' = f(x)$  shifts the entire itinerary to the left through the ‘decimal point’. This operation, denoted by the shift operator  $r$ ,

$$r(\cdots m_{-2}m_{-1}m_0.m_1m_2m_3\cdots) = \cdots m_{-2}m_{-1}m_0m_1.m_2m_3\cdots, \quad (14.4)$$

denotes the current partition label  $m_1$  from the future  $S^+$  to the past  $S^-$ . The inverse shift  $r^{-1}$  shifts the entire itinerary one step to the right.

The set of all itineraries that can be formed from the letters of the alphabet  $\mathcal{A}$  is called the *full shift*

$$\hat{\Sigma} = \{(m_k) : m_k \in \mathcal{A} \text{ for all } k \in \mathbb{Z}\}. \quad (14.5)$$

The itinerary is infinite for any trapped (non-escaping or non-wandering set orbit) orbit (such as an orbit that stays on a chaotic repeller), and infinitely repeating for a periodic orbit  $p$  of period  $n_p$ . A map  $f$  is said to be a *horse-shoe* if its restriction to the non-wandering set is hyperbolic and topologically conjugate to the full  $\mathcal{A}$ -shift.

**Lattices.** Consider a  $d$ -dimensional hypercubic lattice infinite in extent, with each site labeled by  $d$  integers  $z \in \mathbb{Z}^d$ . Assign to each site  $z$  a letter  $m_z$  from a finite alphabet  $\mathcal{A}$ . A particular fixed set of letters  $m_z$  corresponds to a particular periodic state  $M = \{m_z\}$ . In other words, a  $d$ -dimensional lattice requires a  $d$ -dimensional code  $M = \{m_{n_1n_2\cdots n_d}\}$  for a complete specification of the corresponding state  $X$ . In the lattice case, the *full shift* is the set of all  $d$ -dimensional symbol blocks that can be formed from the letters of the alphabet  $\mathcal{A}$

$$\hat{\Sigma} = \{\{m_z\} : m_z \in \mathcal{A} \text{ for all } z \in \mathbb{Z}^d\}. \quad (14.6)$$

**Commuting discrete translations.** For an autonomous dynamical system, the evolution law  $f$  is of the same form for all times. If  $f$  is also of the same form at every lattice site, the group of lattice translations (sometimes called multi-dimensional shifts), acting along  $j$ th lattice direction by shift  $r_j$ , is a spatial symmetry that commutes with the temporal evolution. A temporal mapping  $f$  that satisfies  $f \circ r_j = r_j \circ f$  along the  $d-1$  spatial lattice directions is said to be *shift invariant*, with the associated symmetry of dynamics given by the  $d$ -dimensional group of discrete spatiotemporal translations.

Assign to each site  $z$  a letter  $m_z$  from the alphabet  $\mathcal{A}$ . A particular fixed set of letters  $m_z$  corresponds to a particular lattice symbol array  $M = \{m_z\} = \{m_{n_1n_2\cdots n_d}\}$ , which yields a complete specification of the corresponding state  $X$ . In the lattice case, the *full shift* is the set of all  $d$ -dimensional symbol arrays that can be formed from the letters of the alphabet  $\mathcal{A}$

as in (14.6)

A  $d$ -dimensional spatiotemporal field  $X = \{x_z\}$  is determined by the corresponding  $d$ -dimensional spatiotemporal symbol array  $M = \{m_z\}$ . Consider next a finite block of symbols  $M_{\mathcal{R}} \subset M$ , over a finite rectangular  $[\ell_1 \times \ell_2 \times \cdots \times \ell_d]$  lattice region  $\mathcal{R} \subset \mathbb{Z}^d$ . In particular, let  $M_p$  over a finite rectangular  $[\ell_1 \times \ell_2 \times \cdots \times \ell_d]$  lattice region be the  $[\ell_1 \times \ell_2 \times \cdots \times \ell_d]$   $d$ -periodic block of  $M$  whose repeats tile  $\mathbb{Z}^d$ .

**Blocks.** In the case of temporal dynamics, a finite itinerary  $M_{\mathcal{R}} = m_{k+1}m_{k+2} \cdots m_{k+\ell}$  of symbols from  $\mathcal{A}$  is called a *block* of length  $\ell = n_{\mathcal{R}}$ . More generally, let  $\mathcal{R} \subset \mathbb{Z}^d$  be a  $[\ell_1 \times \ell_2 \times \cdots \times \ell_d]$  rectangular lattice region,  $\ell_k \geq 1$ , whose lower left corner is the  $n = (n_1 n_2 \cdots n_d)$  lattice site

$$\mathcal{R} = \mathcal{R}_n^{[\ell_1 \times \ell_2 \times \cdots \times \ell_d]} = \{(n_1 + j_1, \cdots, n_d + j_d) \mid 0 \leq j_k \leq \ell_k - 1\}. \quad (14.7)$$

The associated finite block of symbols  $m_z \in \mathcal{A}$  restricted to  $\mathcal{R}$ ,  $M_{\mathcal{R}} = \{m_z \mid z \in \mathcal{R}\} \subset M$  is called the block  $M_{\mathcal{R}}$  of volume  $n_{\mathcal{R}} = \ell_1 \ell_2 \cdots \ell_d$ . For example, for a 2-dimensional lattice a  $\mathcal{R} = [3 \times 2]$  block is of form

$$M_{\mathcal{R}} = \begin{bmatrix} m_{12} & m_{22} & m_{32} \\ m_{11} & m_{21} & m_{31} \end{bmatrix} \quad (14.8)$$

and volume (in this case, an area) equals  $3 \times 2 = 6$ . In our convention, the first index is ‘space’, increasing from left to right, and the second index is ‘time’, increasing from bottom up.

**Cylinder sets.** While a particular admissible infinite symbol array  $M = \{m_z\}$  defines a point  $X$  (a unique periodic state) in the state space, the *cylinder set*  $\mathcal{M}_{M_{\mathcal{R}}}$ , corresponds to the totality of state space points  $X$  that share the same given finite block  $M_{\mathcal{R}}$  symbolic representation over the region  $\mathcal{R}$ . For example, in  $d = 1$  case

$$\mathcal{M}_{M_{\mathcal{R}}} = \{\cdots a_{-2} a_{-1} \cdot m_1 m_2 \cdots m_{\ell} a_{\ell+1} a_{\ell+2} \cdots\}, \quad (14.9)$$

with the symbols  $a_j$  outside of the block  $M_{\mathcal{R}} = [m_1 m_2 \cdots m_{\ell}]$  unspecified.

**Periodic orbits, invariant  $d$ -tori.** A state space point  $x_z \in X$  is spatiotemporally *periodic*,  $x_z = x_{z+\ell}$ , if its spacetime orbit returns to it after a finite lattice shift  $\ell = (\ell_1, \ell_2, \cdots, \ell_d)$  over region  $\mathcal{R}$  defined in (14.7). The infinity of repeats of the corresponding block  $M_{\mathcal{R}}$  then tiles the lattice. For a spatiotemporally periodic state  $X$ , a *prime* block  $M_p$  (or  $p$ ) is a smallest such block  $\ell_p = (\ell_1, \ell_2, \cdots, \ell_d)$  that cannot itself be tiled by repeats of a shorter block.

The periodic tiling of the lattice by the infinitely many repeats of a prime block is denoted by a bar:  $\overline{M}_p$ . We shall omit the bar whenever it is clear from the context that the state is periodic. <sup>1 2</sup>

In  $d = 1$  dimensions, a prime block is called an *orbit*  $p$ , a single traversal of the orbit; its label is a block of  $n_p$  symbols that cannot be written as a repeat of a shorter block. Each *periodic point*  $x_{m_1 m_2 \cdots m_{n_p}}$  is then labeled by the starting

<sup>1</sup>Predrag 2019-01-19: eliminate  $\_m_{-m+1} \cdots m_0$  and  $[m_{-m+1} \cdots m_0]$  notation in favor a single convention

<sup>2</sup>Predrag 2018-11-07: Generalize to invariant  $d$ -tori.

symbol  $m_1$ , followed by the next  $(n_p - 1)$  steps of its future itinerary. The set of periodic points  $\mathcal{M}_p$  that belong to a given periodic orbit form a *cycle*

$$p = \overline{m_1 m_2 \cdots m_{n_p}} = \{x_{m_1 m_2 \cdots m_{n_p}}, x_{m_2 \cdots m_{n_p} m_1}, \cdots, x_{m_{n_p} m_1 \cdots m_{n_p-1}}\}. \quad (14.10)$$

More generally, a state space point is *spatiotemporally periodic* if it belongs to an invariant  $d$ -torus, i.e., its symbolic representation is a block over region  $\mathcal{R}$  defined by (14.7),

$$\mathcal{M}_p = \mathcal{M}_{\mathcal{R}}, \quad \mathcal{R} = \mathcal{R}_0^{[\ell_1 \times \ell_2 \times \cdots \times \ell_d]}, \quad (14.11)$$

that tiles the periodic state  $\mathcal{M}$  periodically, with period  $\ell_j$  in the  $j$ th lattice direction.

**Generating partitions.** A temporal partition is called *generating* if every bi-infinite itinerary corresponds to a distinct point in state space. In practice almost any generating partition of interest is infinite. Even when the dynamics assigns a unique infinite itinerary  $\cdots m_{-2} m_{-1} m_0 . m_1 m_2 m_3 \cdots$  to each distinct orbit, there generically exist full shift itineraries (14.5) which are not realized as orbits; such sequences are called *inadmissible*, and we say that the symbolic dynamics is *pruned*.

**Dynamical partitions.** If the symbols outside of given temporal block  $b$  remain unspecified, the set of all admissible blocks of length  $n_b$  yield a dynamically generated partition of the state space,  $\mathcal{M} = \cup_b \mathcal{M}_b$ .

**Subshifts.** A dynamical system  $(\mathcal{M}, f)$  given by a mapping  $f : \mathcal{M} \rightarrow \mathcal{M}$  together with a partition  $\mathcal{A}$  induces *topological dynamics*  $(\Sigma, r)$ , where the *subshift*

$$\Sigma = \{(m_k)_{k \in \mathbb{Z}}\}, \quad (14.12)$$

is the set of all *admissible* itineraries, and  $r : \Sigma \rightarrow \Sigma$  is the shift operator (14.4). The designation ‘subshift’ comes from the fact that  $\Sigma$  is a subset of the full shift.

Let  $\hat{\Sigma}$  be the full lattice shift (14.5), i.e., the set of all possible periodic state  $\mathcal{M}$  labelings by the alphabet  $\mathcal{A}$ , and  $\hat{\Sigma}(\mathcal{M}_{\mathcal{R}})$  is the set of such blocks over a region  $\mathcal{R}$ . The principal task in developing the symbolic dynamics of a dynamical system is to determine  $\Sigma$ , the set of all *admissible* itineraries/periodic states, i.e., all states that can be realized by the given system.

**Pruning, grammars, recoding.** If certain states are inadmissible, the alphabet must be supplemented by a *grammar*, a set of pruning rules. Suppose that the grammar can be stated as a finite number of pruning rules, each forbidding a block of finite size,

$$\mathcal{G} = \{b_1, b_2, \cdots b_k\}, \quad (14.13)$$

where a *pruned block*  $b$  is an array of symbols defined over a finite  $\mathcal{R}$  lattice region of size  $[\ell_1 \times \ell_2 \times \cdots \times \ell_d]$ . In this case we can construct a finite Markov partition by replacing finite size blocks of the original partition by letters of a new alphabet. In the case of a 1-dimensional, the temporal lattice, if the longest forbidden block is of length  $L+1$ , we say that the symbolic dynamics is Markov, a shift of finite type with  $L$ -step memory.

**Subshifts of finite type.** A topological dynamical system  $(\Sigma, r)$  for which all admissible states  $M$  are generated by recursive application of the finite set of pruning rules (14.13) is called a subshift of *finite type*.

2CB

If a map can be topologically conjugated to a linear map, the symbolic dynamics of the linear map offers a dramatically simplified description of all admissible solutions of the original flow, with the temporal symbolic dynamics and the state space dynamics related by linear recoding formulas. For example, if a map of an interval, such as a parabola, can be conjugated to a piecewise linear map, the kneading theory [5] classifies *all* of its admissible orbits.

## 14.1 Symbolic dynamics, inserts

**2019-01-19 Predrag** Merge everything here to chapter 14 *Symbolic dynamics: a glossary* then `svn rm` this file.

**2017-08-05 Predrag** Consult / harmonize with ChaosBook.org Chapter *Charting the state space* (source file knead.tex).

to Predrag: check that all this is in ChaosBook, then erase:

The set of all bi-infinite itineraries that can be formed from the letters of the alphabet  $\mathcal{A}$  is called the *full shift* (or *topological Markov chain*)

Here we refer to this set of all conceivable itineraries as the *covering* symbolic dynamics.

Orbit that starts out as a finite block followed by infinite number of repeats of another block  $p = (m_1 m_2 m_3 \cdots m_\ell)$  is said to be *heteroclinic* to the cycle  $p$ . An orbit that starts out as  $p^\infty$  followed by a different finite block followed by  $(p')^\infty$  of another block  $p'$  is said to be a *heteroclinic connection* from cycle  $p$  to cycle  $p'$ .

Suppose that the grammar can be stated as a finite number of pruning rules, each forbidding a block of finite length,

$$\mathcal{G} = \{b_1, b_2, \cdots b_k\}, \quad (14.14)$$

where a *pruned block*  $b$  is a sequence of symbols  $b = m_1 m_2 \cdots m_{n_b}$ ,  $m \in \mathcal{A}$ , of finite length  $n_b$ .

**Subshifts of finite type.** A topological dynamical system  $(\Sigma, \sigma)$  for which all admissible itineraries are generated by a finite transition matrix

$$\Sigma = \{(m_k)_{k \in \mathbb{Z}} : T_{s_k s_{k+1}} = 1 \text{ for all } k\} \quad (14.15)$$

is called a subshift of *finite type*.

**Reflection symmetries.** Symmetries of the cat map induce invariance with respect to corresponding symbol exchanges. Define  $\bar{m} = s - m - 2$  to be the conjugate of symbol  $m \in \mathcal{A}$ . For example, the two exterior alphabet  $\mathcal{A}_1$  symbols are conjugate to each other, as illustrated by (2.75).<sup>3</sup> If  $b = m_1 m_2 \dots m_\ell$  is

<sup>3</sup>Predrag 2019-05-27: fix this eq. reference; edit it away

a block, and  $\bar{b} = \bar{m}_1 \bar{m}_2 \dots \bar{m}_\ell$  its conjugate, then by reflection symmetry of the cat map we have  $|\mathcal{P}_b| = |\mathcal{P}_{\bar{b}}|$ . Similarly, if  $b^* = m_\ell m_{\ell-1} \dots m_1$ , the time reversal invariance implies  $|\mathcal{P}_b| = |\mathcal{P}_{b^*}|$ .

There are many ways to skin a cat. For example, due to the space reflection symmetry about  $x = 1/2$  of the Percival-Vivaldi cat map (2.75), it is natural (especially in studies of deterministic diffusion on periodic lattices [1–3]) to center the phase space unit interval [6] as  $x \in [-1/2, 1/2)$ . In this formulation the Percival-Vivaldi cat map has a 5-letter alphabet  $\mathcal{A} = \{\underline{2}, \underline{1}, 0, 1, 2\}$ , in which the spatial reflection symmetry is explicit (the “conjugate” of a symbol  $m \in \mathcal{A}$  is  $\bar{m} = -m$ ).

## References

- [1] R. Artuso and P. Cvitanović, “Deterministic diffusion”, in *Chaos: Classical and Quantum*, edited by P. Cvitanović, R. Artuso, R. Mainieri, G. Tanner, and G. Vattay (Niels Bohr Inst., Copenhagen, 2023).
- [2] R. Artuso and P. Cvitanović, “Deterministic diffusion”, in *Chaos: Classical and Quantum*, edited by P. Cvitanović, R. Artuso, R. Mainieri, G. Tanner, and G. Vattay (Niels Bohr Inst., Copenhagen, 2023).
- [3] R. Artuso and R. Strepparava, “Recycling diffusion in sawtooth and cat maps”, *Phys. Lett. A* **236**, 469–475 (1997).
- [4] P. Cvitanović, R. Artuso, R. Mainieri, G. Tanner, and G. Vattay, *Chaos: Classical and Quantum* (Niels Bohr Inst., Copenhagen, 2024).
- [5] J. Milnor and W. Thurston, “On iterated maps of the interval”, in *Dynamical Systems*, edited by J. C. Alexander (Springer, New York, 1988), pp. 465–563.
- [6] I. Percival and F. Vivaldi, “A linear code for the sawtooth and cat maps”, *Physica D* **27**, 373–386 (1987).

## Chapter 15

# Statistical mechanics applications

### 15.1 Cat map

HERE WE WILL DEAL WITH the prototype example of chaotic Hamiltonian maps, *hyperbolic toral automorphisms*, (subspecies of which, known as the as the ‘Arnol’d cat map’, you have most likely already encountered), acting on a cylinder or over  $\mathbb{R}^2$ . Their dynamics restricted to the elementary cell involves maps on  $\mathbf{T}^2$  (two-dimensional torus). On such torus an action of a matrix in  $SL(2, \mathbb{N})$  with unit determinant and absolute value of the trace bigger than 2 is known as the Anosov map. <sup>1</sup>

### 15.2 New example: Arnol’d cat map

the Arnol’d-Sinai cat is a practical cat

— Ian Percival and Franco Vivaldi [16]

The ‘standard’ generating partition code of Arnol’d and Avez [2] is rather simple - it is described in Devaney [9]. <sup>2</sup> It relies on a 3-rectangles complete partition of the torus. It is a subshift of finite type - it is well suited to the generation and counting of periodic orbits on the torus, see Isola [11] rational topological zeta function in sect. 2.3.7.

However, the Arnol’d–Avez alphabet has no easy translation to the integers shift on the unfolded torus (on the lattice, most of torus periodic orbits are relative periodic orbits). Furthermore, for  $N$  coupled cat maps the number of such

---

<sup>1</sup>Predrag 2018-02-11 rewrite appendix 15 *Statistical mechanics applications* in the style of ref. [13], or remove altogether. :

<sup>2</sup>Predrag 2016-08-03: I do not have either monograph at hand, but Creagh [7] summary in sect. 2.3.8 is pretty clear.



rectangles would grow exponentially [10].<sup>3</sup>

There is a general consensus in the cat map community [12] that the ‘linear code’ of Percival and Vivaldi [16] (here sect. 2.3.6) is deeper and more powerful. For deterministic diffusion developed in ChaosBook (chapter 15 here) that is the only choice, as one needs to convert symbolic dynamics of an relative periodic orbit to the integer shift (translation) on the lattice.<sup>4</sup> The downside is that the Markov/generating partition is infinite, meaning that for longer and longer orbits there are more and more new pruning (inadmissible blocks) rules, ad infinitum.

<sup>5</sup> Iterated area preserving maps of the form

$$p' = p + F(x) \tag{15.1}$$

$$x' = x + p' \pmod{1}, \tag{15.2}$$

where  $F(x)$  is periodic of period 1, are widely studied because of their importance in dynamics. They include the standard map of Taylor, Chirikov and Greene [5, 14], and also the sawtooth and cat maps that we describe here. Because values of  $x$  differing by integers are identified, whereas the corresponding values of  $p$  are not, the phase space for these equations is a cylinder.

These maps describe ‘kicked’ rotors that are subject to a sequence of angle-dependent impulses  $F(x)$ , with  $2\pi x$  as the configuration angle of the rotor, and  $p$  as the momentum conjugate to the configuration coordinate  $x$ . The time step has been set to  $\Delta t = 1$ . Eq. (15.1) says that the momentum  $p$  is accelerated to  $p'$  by the force pulse  $F(x)\Delta t$ , and eq. (15.2) says in that time the trajectory  $x$  reaches  $x' = x + p'\Delta t$ .

The phase space of the rotor is a cylinder, but it is often convenient to extend it to the plane or contract it to a torus. For the former case the “ $\pmod{1}$ ” is removed from (15.2) and for the latter it is included in (15.1).

Eqs. (15.1,15.2) are a discrete time form of Hamilton’s equations. But for many purposes we are only interested in the values of the configuration coordinate  $x$ , which satisfy the second-order difference equation (the discrete Laplacian in time)

$$\delta^2 x_t \equiv x_{t+1} - 2x_t + x_{t-1} = F(x_t) \pmod{1} \tag{15.3}$$

where  $t$  is a discrete time variable that takes only integer values. This equation may be considered as the Lagrangian or Newtonian equation corresponding to the Hamiltonian form (2.1), with  $p_t = x_t + x_{t-1}$ .

Rewrite (15.3) as

$$x_{t+1} = 2x_t + F(x_t) - x_{t-1} \pmod{1} \tag{15.4}$$

Call the 1-step configuration point forward in (15.2)  $x_t = y$ , and the next configuration point  $x_{t+1} = y'$ . This recasts the dynamical equation in the form of

<sup>3</sup>Predrag 2016-08-03: Have not checked that, or whether this is explained in ref. [10].

<sup>4</sup>Predrag 2016-08-03: I do not know why this symbolic dynamics is natural for extensions to  $N$  nearest-neighbor coupled maps.

<sup>5</sup>Predrag 2016-06-02: verbatim from Percival and Vivaldi [16]

an area preserving map in which only configurations at different times appear,

$$\begin{aligned} x' &= y \\ y' &= 2y + F(y) - x \quad \text{mod } 1. \end{aligned} \quad (15.5)$$

This they call the ‘two-configuration representation’.

The sawtooth map represents a rotor subject to an impulse  $F(x)$  that is linear in  $x$ , except for a single discontinuity. The impulse is standardised to have zero mean, the origin of  $x$  is chosen so that  $F(0)=0$ , so

$$F(x) = Kx \quad (-1/2 \leq x < 1/2) \quad (15.6)$$

With these conventions Hamilton’s equations for the sawtooth are

$$\begin{aligned} x' &= y \quad \text{mod } 1 \\ y' &= -x + sy \quad \text{mod } 1 \end{aligned} \quad (15.7)$$

in the two-configuration representation, where

$$s = K + 2. \quad (15.8)$$

For  $s > 2$  the map is unstable. In the two-configuration representation, Hamilton’s equations can be written in matrix form as

$$\begin{pmatrix} x' \\ y' \end{pmatrix} = M \begin{pmatrix} x \\ y \end{pmatrix} \quad \text{mod } 1 \quad (15.9)$$

with

$$M = \begin{pmatrix} 0 & 1 \\ -1 & s \end{pmatrix}, \quad (15.10)$$

characteristic polynomial

$$\Lambda^2 - s\Lambda + 1. \quad (15.11)$$

and eigenvalues

$$\Lambda = (s + \sqrt{D})/2, \quad \Lambda' = (s - \sqrt{D})/2, \quad (15.12)$$

where  $D = s^2 - 4$ . When  $s$  is an integer, then the map (15.9) is continuous on the torus, because the discontinuity of the sawtooth is an integer absorbed into the modulus. The map is then continuous; it is a toral automorphism, of a class called *cat maps*, of which the Arnol’d-Sinai cat map [2] with  $s = 3$  is a special case,

$$M = \begin{pmatrix} 0 & 1 \\ -1 & 3 \end{pmatrix}. \quad (15.13)$$

If instead of (15.4) dynamics on a torus, one considers motion on a line (no mod 1), one can land in any unit interval along the  $q$ -axis. Let then  $-b_t$  be the sequence of integer shifts that ensures that for all  $t$  the dynamics

$$x_{t+1} = 2x_t + F(x_t) - x_{t-1} - b_t \quad (15.14)$$

stays confined to the elementary cell  $x_t \in [-1/2, 1/2)$ . The Newton equation (15.3) then takes the form

$$(\delta^2 - K)x_t = -b_t \quad (15.15)$$

The linear operator or infinite tridiagonal matrix on the left of (15.15) has a Green's function or inverse matrix given by the unique bounded solution  $g_{ts}$  of the inhomogeneous equation<sup>6</sup>

$$g_{t+1,t'} - s g_{tt'} + g_{t-1,t'} = \delta_{tt'} , \quad (15.16)$$

which is given by

$$g_{tt'} = -\Lambda^{-|t-t'|} / \sqrt{D} . \quad (15.17)$$

This solution is obtained by a method that is directly analogous to the method used for second order linear differential equations [15] (click here). The solution of (15.15) for the orbit is therefore<sup>7</sup>

$$t_t = \sum_t^I g_{tt'}(-b_t) = \frac{1}{\sqrt{D}} \sum_t^I \Lambda^{-|t-t'|} b_{t'} = \delta_{tt'} , \quad (15.18)$$

defining the orbit uniquely in terms of the symbol sequence. That is to say that the code is complete. We shall refer to an integer code such as  $\{b_t\}$  for a linear system as a *linear code*: the orbit and the code are related to one another by a linear transformation. Clearly, a shift in the symbol sequence  $\{b_t\}$  corresponds to an equivalent time shift of the orbit.

The past and the future sums in (15.18) resembles the expression for a real number in terms of the digits  $b_t$ , using a representation of the reals in the non-integral base  $\Lambda$ , in contrast with the past and future coordinates for the baker's transformation, which have a similar form, to base 2. The 'present' symbol  $b_0$  is incorporated with the past in our convention.

## Commentary

**Remark 15.1.** Deterministic diffusion in Hamiltonian maps. (Continued from remark ??)

The quasilinear estimate (??) was given in ref. [4] and evaluated in refs. [3, 17]. Circulant matrices are discussed in Aitkenref. [1] (1939). The result (??) agrees with the saw-tooth result of ref. [4]; for the cat maps (??) is the exact value of the diffusion coefficient. This result was also obtained, by using periodic orbits, in ref. [8], where Gaussian nature of the diffusion process is explicitly assumed. Measure polytopes are discussed in ref. [6].

8

---

<sup>6</sup>Predrag 2016-05-29: still have to check this calculation

<sup>7</sup>Predrag 2018-03-11: Mestel and Percival [15] is very systematic, with Wronskians, etc., but I do not see this solution there. Percival and Vivaldi [16] state it, say it can be derived by the method of Mestel and Percival [15], and say "as may be verified by substitution."

<sup>8</sup>Predrag 2018-12-01: Had here Problems/exerAppStatM until 30dec2017, now only copy is the renamed ChaosBook exerAppDiff.tex.

REMEMBER: move the cat map exercises to exerCatMap.tex

## References

- [1] A. Aitken, *Determinants & Matrices* (Oliver & Boyd, Edinburgh, 1939).
- [2] V. I. Arnol'd and A. Avez, *Ergodic Problems of Classical Mechanics* (Addison-Wesley, Redwood City, 1989).
- [3] R. Artuso and R. Strepparava, "Recycling diffusion in sawtooth and cat maps", *Phys. Lett. A* **236**, 469–475 (1997).
- [4] J. R. Cary and J. D. Meiss, "Rigorously diffusive deterministic map", *Phys. Rev. A* **24**, 2664–2668 (1981).
- [5] B. V. Chirikov, "A universal instability of many-dimensional oscillator system", *Phys. Rep.* **52**, 263–379 (1979).
- [6] H. S. M. Coxeter, *Regular Polytopes* (Dover, New York, 1948).
- [7] S. C. Creagh, "Quantum zeta function for perturbed cat maps", *Chaos* **5**, 477–493 (1995).
- [8] Dana, "Hamiltonian transport on unstable periodic orbits", *Physica D* **39**, 205 (1989).
- [9] R. L. Devaney, *An Introduction to Chaotic Dynamical systems*, 2nd ed. (Westview Press, Cambridge, Mass, 2008).
- [10] B. Gutkin and V. Osipov, "Classical foundations of many-particle quantum chaos", *Nonlinearity* **29**, 325–356 (2016).
- [11] S. Isola, " $\zeta$ -functions and distribution of periodic orbits of toral automorphisms", *Europhys. Lett.* **11**, 517–522 (1990).
- [12] J. P. Keating, "Asymptotic properties of the periodic orbits of the cat maps", *Nonlinearity* **4**, 277 (1991).
- [13] H. Liang and P. Cvitanović, "A chaotic lattice field theory in one dimension", *J. Phys. A* **55**, 304002 (2022).
- [14] A. J. Lichtenberg and M. A. Leiberman, *Regular and Chaotic Dynamics*, 2nd ed. (Springer, New York, 2013).
- [15] B. D. Mestel and I. Percival, "Newton method for highly unstable orbits", *Physica D* **24**, 172 (1987).
- [16] I. Percival and F. Vivaldi, "A linear code for the sawtooth and cat maps", *Physica D* **27**, 373–386 (1987).
- [17] R. Strepparava, Laurea thesis, MA thesis (Università degli Studi di Milano, 1995).

## Chapter 16

# Ising model in 2D

**ChaosBook Exercise 17.1 Time reversibility.** Hamiltonian flows are time reversible. Does that mean that their transition graphs are symmetric in all node  $\rightarrow$  node links, their transition matrices are adjacency matrices, symmetric and diagonalizable, and that they have only real eigenvalues?

Solution 14.1, 2021-12-07 Read refsect s:latt1d and on for a group-theoretic solution.

— An open exercise from ChaosBook.org

2CB

**2016-02-19 Predrag** A wild idea, to keep in mind, if we get to the point where QFT is within reach. ‘Fundamental domain’ appears in an interesting stat mech context in Wipf *et al.* [158, 159] *Generalized Potts-models and their relevance for gauge theories*. They study the 3-state Potts model, a natural extension of the Ising model with 3 vectors at each site, whose global symmetries are point group  $C_3$ , and the 1d lattice of discrete translations. The domain of the traced Polyakov loop variable (?) for  $SU(3)$  is a triangle, with a  $C_3$  fundamental domain. Then they compute leading terms in the strong coupling limit using characters  $\chi_{pq}$  for the  $SU(3)$  representation  $(p, q)$ . These characters transform under  $C_3$ , so they restrict calculations to the fundamental domain inside the above triangle. Or perhaps  $D_3$ , could not tell in my first, very superficial reading. These articles were immediately followed up by a bunch of other articles - there are too many quantum field theorists out there:)

In other words, Potts model could provide a bridge from Boris’ cat maps to QFT on lattices.

There is also a continuation with  $G_2$  Yang-Mills by the same authors, but that’s for another, more ambitious time...

**2016-10-03 Predrag** Not quick or easy to explain, but I have a hunch that the spatiotemporal zeta function should be something like the 2D Ising model

zeta function described by Aizenman ([click here](#)). It should assign a weight for every spatiotemporal domain, described by its 2D symbolic dynamics.

**2016-10-08 Predrag** qmath16 Aizenman talk notes (mostly gibberish - my fault):

It is known (?) that QM is emergent from the *classical* stat mech of Ising models. Key tools: Pfaffians. Random current representation of Ising.

Groenevald-Boel-Kasteleyn'78: describe correlations in the planar Ising model, by boundary segments, ordered cyclically. Pfaffian refers to spin-spin correlations along the boundary. There is a parity sign that makes it a non-interacting fermion model.

Aizenman et al. extend it to nonplanar modles, where planarity *emerges* at the critical point. ADTW'16 proof utilizes the *random current representation*. Starts with high temperature expansion. Partition function is a sum over loops. In a correlation, sources are connected pairwise by lines, ie, Gaussian limit. Above critical dimension - four - the theory is free (sum of products over pairs). In 2D, fermionic case, you get Pfaffian. Leads to the integrability of the model. (Read Chelkak-Cimasoni-Kassel '15.)

"Almost planar"

Order-disorder variables.

Aizenman: Two implications of planarity

1) For any planar graph, and a symmetric edge function

$$\mathcal{F}(\{K_\theta\}) = \det(1 - KW)$$

is the *square of a multilinear function* of the parameters  $\{K_\theta\}_{\theta \in \epsilon_0}$ . This is proven through a reduction to an antisymmetric matrix  $A$ , and (Kasteleyn matrix '63):

$$\det(A) = \text{Pf}[A]^2.$$

For planar models, done by Kac-Ward. Works for any planar graph ("amorphous graphs"), not only on a regular lattice.

2) For any planar loop of oriented non-backtracking edges  $\{e_1, e_2, \dots\}$

$$\prod_{j=1}^n \mathcal{W}_{e_{j+1}, e_j} = (-1)^{w(\rho^*)} = (-1)^{n(\rho^*)}.$$


with  $w(\rho^*) =$  winding number, and  $n(\rho^*) = \#$  of self crossings [Whitney's Thm].

This is then combined with the *Ihara relation*, for matrices indexed by oriented edges:

$$\det(1 - KW)_{\epsilon_0 \times \epsilon_0} = \prod_{\ell} \left[ 1 + (-1)^{n(\ell)} \chi_{-K}(\ell) \right]^2.$$

the product being over unoriented loops on  $\mathbb{G}$  (hence the power 2).

2020-09-30 Predrag .

 Michael Aizenman biographical sketch

Aizenman Rutgers talk (unrecorded) was a model of clear exposition. It is an audience friendly explanation of the background to, and advance for  $d = 4$  explained in Michael Aizenman and Hugo Duminil-Copin *Marginal triviality of the scaling limits of critical 4D Ising and  $\phi_4^4$  models*, [arXiv:1912.07973](#). Duminil-Copin will give a tutorial on this work on October 9-10, 2020, in [42nd Midwest Probability Colloquium](#).

I especially liked the ‘reminder’ explaining how  $\phi^4$  goes to Ising in particular limit.

Related publications to check:

Michael Aizenman and Simone Warzel *Kac-Ward formula and its extension to order-disorder correlators through a graph zeta function*, [arXiv:1709.06052](#)

Is the *loop-soup expansion* related to my random walk interpretation of the hypercubic orbit Jacobian matrix traces and the determinant? References might be in Michael Aizenman, Hugo Duminil-Copin and Simone Warzel *Dimerization and Néel order in different quantum spin chains through a shared loop representation*, [arXiv:2002.02543](#).

**2016-10-05 Predrag** Aizenman, Laínz Valcázar and Warzel [2] *Pfaffian correlation functions of planar dimer covers* does not seem to be what we need (no word ‘zeta’ in this paper). They refer to 2016 preprint of

M. Aizenman H. Duminil-Copin, V. Tassion, S. Warzel, *Fermionic correlation functions and emergent planarity in 2D Ising models*. (that paper does not seem to be available anywhere, as yet)

The structure of the solution of Kac and Ward has been explained in unpublished lectures by Feynman (Aizenman referred to Feynman’s stat mech book).

Sherman [140] *Combinatorial aspects of the Ising model for ferromagnetism. I. A conjecture of Feynman on paths and graphs*

Hurst and Green [83] *New solution of the Ising problem for a rectangular lattice*

Burgoyne [29] *Remarks on the combinatorial approach to the Ising problem*

Vdovichenko [155] *A calculation of the partition function for a plane dipole lattice*. The steps: a) the sum over polygons is reduced to a sum over closed loops without intersections; b) the sum over closed loops without intersections is transformed into a sum over all loops; c) the sum over all loops is reduced to a random-walk problem and is calculated easily.

Cimasoni [36] *A generalized Kac-Ward formula*: “ As a consequence of our second proof, we also obtain the following fact: the Kac-Ward and the Fisher-Kasteleyn methods for solving the Ising model are one and the same. ”

Cimasoni [37] *The critical Ising model via Kac-Ward matrices*: The Kac-Ward formula [93] allows to compute the Ising partition function on any finite graph  $G$  from a determinant with quite remarkable properties. First of all, they satisfy some generalized Kramers-Wannier duality: there is an explicit equality relating the determinants associated to a graph and to its dual graph. Also, they are proportional to the determinants of the discrete critical Laplacians on the graph  $G$ .

Fisher [61] *On the dimer solution of planar Ising models*

Kasteleyn [96] *The statistics of dimers on a lattice: I. The number of dimer arrangements on a quadratic lattice*

Kasteleyn [97] *Dimer statistics and phase transitions*

H. Au-Yang, J. H. H. Perk. Ising correlations at the critical temperature. *Physics Letters A* 104, 131–134 (1984).

Kager, Lis and Meester [95] *The signed loop approach to the Ising model: Foundations and critical point*

Lis [112] *A short proof of the Kac-Ward formula*:

$$\det (Id - \Lambda) = \mathbb{Z}^2 \tag{16.1}$$

The original proof of Kac and Ward [93] famously contained an error. We refer the reader to ref. [95] for a longer discussion on the history of this theorem. The main improvement here, in comparison with ref. [95], is that there is no need for expanding the generating functions into generating functions of collections of loops. The combinatorial mechanism of the Kac-Ward formula is here as transparent as the one of the loop-erased walks.

Chertkov, Chernyak and Teodorescu [34] *Belief propagation and loop series on planar graphs*, write: “ We discuss a generic model of Bayesian inference with binary variables defined on edges of a planar graph. The Loop Calculus approach of Chertkov and Chernyak [33] is used to evaluate the resulting series expansion for the partition function. We show that, for planar graphs, truncating the series at single-connected loops reduces, via a map reminiscent of the Fisher transformation [60], to evaluating the partition function of the dimer-matching model on an auxiliary planar graph. Thus, the truncated series can be easily re-summed, using the Pfaffian formula of Kasteleyn [96]. This allows us to identify a big class of computationally tractable planar models reducible to a dimer model via the Belief Propagation (gauge) transformation. The Pfaffian representation can also be extended to the full Loop Series, in which case the expansion becomes a sum of Pfaffian contributions, each associated with dimer matchings on an extension to a subgraph of the original graph. Algorithmic consequences of the Pfaffian representation, as well as relations to quantum and non-planar models, are discussed. ”



“ As the seminal work of Onsager [124] on the two-dimensional Ising model and its combinatorial interpretation by Kac and Ward [93] have shown, the planarity constraint dramatically simplifies statistical calculations. ”

Onsager [124] computed the free energy, and Yang [161] obtained a formula for the magnetization. In particular, this formula implies that the magnetization is zero at criticality. These results have been reproved in a number of papers since then. See Werner [157] for a recent proof.

Onsager’s computation of the free energy is based on the study of the eigenvalues of the so-called transfer matrices. The original strategy used by Onsager is based on the fact that the transfer matrix is the product of two matrices whose commutation relations generate a finite dimensional Lie algebra. Later on, Kaufman [101] gave a simpler solution using Clifford algebra and anti-commuting spinor (free-fermion) operators (Predrag: I have looked at [Bruria Kaufman’s](#) article, do not recommend reading it - complicated).

The most famous expansions of the partition function are called the low and high temperature expansions. An expansion in terms of subgraphs of the original graph, called the random-cluster model, was found by Fortuin and Kasteleyn [62]. The strength of all these expansions is that they work for all graphs. They do not lead to an explicit computation of the partition function or the free energy, but they provide new insight and often highlight specific properties of the model.

**2023-09-16 Predrag** Shimizu [141] *Tensor renormalization group approach to a lattice boson model*, (2012),

Follow ups:

Akiyama, Kadoh, Kuramashi, Yamashita and Yoshimura *Tensor renormalization group approach to four-dimensional complex  $\phi^4$  theory at finite density* (2020) [arXiv:2005.04645](#)

Hirasawa, Matsumoto, Nishimura and Atis *Tensor renormalization group and the volume independence  $n$  2D  $U(N)$  and  $SU(N)$  gauge theories* (2021) [arXiv:2110.05800](#) has lots of SVD.

Akiyama, Kuramashi and Yoshimura *Quantum field theories with tensor renormalization group* (2021) [arXiv:2111.04240](#), on (3+1)-dimensional ((3+1)d) complex  $\phi^4$  and other theories.

**2017-09-18 Predrag** R J Baxter, *Some comments on developments in exact solutions in statistical mechanics since 1944* (2010)

We draw the square lattice diagonally, with  $M$  rows of sites and  $L$  sites per row. We are particularly interested in calculating the partition function per site:

$$\kappa = Z^{1/LM} ,$$

the dimensionless free energy  $f = -\ln \kappa$  and averages such as the magnetization. We expect  $\kappa$  to tend to limit when  $L, M \rightarrow \infty a$ .

[...] Later, combinatorial ways were found of writing the partition function of the Ising model on a finite lattice directly as a determinant or a pfaffian (the square root of an antisymmetric determinant).

**2017-09-11 Predrag** Bhat and Osting [23] *Diffraction on the two-dimensional square lattice* write: The lattice Green's function is quite well known [53, 99].

**2017-09-11 Predrag** The real part of the square lattice Green's function (8.43) is odd or even function of  $s$ , and the imaginary part is even or odd function of  $s$ , if the sum of  $n$  and  $t$  is even or odd, respectively.

**2017-09-11 Predrag** Morita and Horiguchi [121] *Calculation of the lattice Green's function for the bcc, fcc, and rectangular lattices*: see the appendix *The lattice Green's functions for the rectangular lattice* (includes the square lattice as a special case). They integrate (8.43) and express it as the complete elliptic integral of the first kind (8.170).

Katsura, Inawashiro and Abe [100] *Lattice Green's function for the simple cubic lattice in terms of a Mellin-Barnes type integral*

Horiguchi [78] *Lattice Green's function for the simple cubic lattice* - GaTech does not have online access to it.

Horiguchi and Morita [80] *Note on the lattice Green's function for the simple cubic lattice*: " A simple recurrence relation connecting the lattice Green's function at  $(l, m, n)$  and the first derivatives of the lattice Green's function at  $(l \pm 1, m, n)$ , is presented for the simple cubic lattice. By making use of that recurrence relation, the lattice Green's functions at  $(2, 0, 0)$  and  $(3, 0, 0)$  are obtained in closed forms, which contain a sum of products of the complete elliptic integrals of the first and the second kind, see (8.170). "

Asad [8] *Differential equation approach for one- and two-dimensional lattice Green's function* seems a continuation of ref. [80]: " A first-order differential equation of Green's function, at the origin  $G(0)$ , for the one-dimensional lattice is derived by simple recurrence relation. Green's function at site  $(m)$  is then calculated in terms of  $G(0)$ . A simple recurrence relation connecting the lattice Green's function at the site  $(m, n)$  and the first derivative of the lattice Green's function at the site  $(m \pm 1, n)$  is presented for the two-dimensional lattice, a differential equation of second order in  $G(0, 0)$  is obtained. By making use of the latter recurrence relation, lattice Green's function at an arbitrary site is obtained in closed form. "

**2023-05-18 Predrag** Besag [22] *On a system of two-dimensional recurrence equations* (1981).

[...] in principle, full solutions could be deduced in terms of the complete elliptic integrals K, E and  $\Pi$  of the first, second and third kinds, respectively.

Wortis [118] (1963) obtains simple formulae for the most important cases. Simple and highly efficient algorithms for evaluating  $K$ ,  $E$  and  $II$  are given by Bulirsch [27] (1965)

Bulirsch [27] *Numerical calculation of elliptic integrals and elliptic functions* (1965) very helpfully even provides ALGOL (!) code:)

Wortis [118] *Bound states of two spin waves in the Heisenberg ferromagnet* (1963). In a superficial scan, I do not see the "simple formulae" mentioned by Besag.

**2020-12-23 Predrag** Kaufman [101] *Crystal statistics. II. Partition function evaluated by spinor analysis* is an impressive paper. I have looked at **Bruria Kaufman's** article, do not recommend reading it - complicated.

**2020-06-16 Predrag** Shanker [139] *Exact solution of Ising model in 2d shortcut network*

Janke and Kenna [91] *Finite-size scaling and corrections in the Ising model with Brascamp-Kunz boundary conditions*

Izmailian, Oganessian and Hu [89] *Exact finite-size corrections for the square-lattice Ising model with Brascamp-Kunz boundary conditions*

Wu and Hu [160] *Exact partition functions of the Ising model on  $M \times N$  planar lattices with periodic-aperiodic boundary conditions*

Kastening [98] *Simplified transfer matrix approach in the two-dimensional Ising model with various boundary conditions*

Izmailian [87] *Finite-size effects for anisotropic 2D Ising model with various boundary conditions,*

Lyberg [113] *Free energy of the anisotropic Ising lattice with Brascamp-Kunz boundary conditions*

Poghosyan, Izmailian and Kenna [127] *Exact solution of the critical Ising model with special toroidal boundary conditions*

**2020-06-16 Predrag** Izmailian and Hu [88] *Finite-size effects for the Ising model on helical tori:* " We analyze the exact partition function of the Ising model on a square lattice under helical boundary conditions obtained by Liaw *et al.* [110]. We find that finite-size corrections for the free energy, the internal energy, and the specific heat of the model in a crucial way depend on the helicity factor of the lattice. "

**2019-11-04 Predrag** Hucht [82] *The square lattice Ising model on the rectangle I: finite systems*

**2019-11-04 Predrag** .

Hobrecht and Hucht [75] *Anisotropic scaling of the two-dimensional Ising model I: the torus:* They compute the partition function and the free energy of the finite two-dimensional square lattice Ising model with periodic boundary conditions.

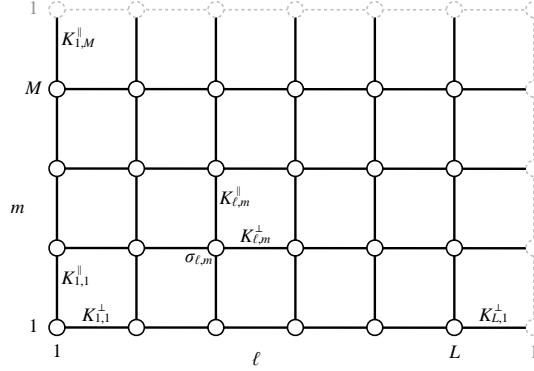


Figure 16.1: The square lattice with toroidal geometry for  $M = 4$  and  $L = 6$ .

[...] The two-dimensional Ising model on a finite  $L \times M$  square lattice with periodic boundary conditions (p) in both directions as depicted in figure 16.1, i. e., on the torus, is described by the reduced Hamiltonian

$$\mathcal{H}^{(p,p)} = - \sum_{\ell=1}^L \sum_{m=1}^M K_{\ell,m}^{\perp} \sigma_{\ell,m} \sigma_{\ell+1,m} + K_{\ell,m}^{\parallel} \sigma_{\ell,m} \sigma_{\ell,m+1}, \quad (16.2)$$

where  $K_{\ell,m}^{\perp}$  and  $K_{\ell,m}^{\parallel}$  are the reduced couplings between the nearest neighbours in perpendicular and parallel direction, respectively, and  $\sigma_{\ell,m}$  are spin variables with periodic indices, i. e.,  $\sigma_{\ell+L,m} \equiv \sigma_{\ell,m} \equiv \sigma_{\ell,m+M}$ . The partition function  $Z^{(p,p)} = \text{tr} e^{-\mathcal{H}^{(p,p)}}$  can be rewritten into a high-temperature expansion [93]

$$\frac{Z^{(p,p)}}{Z_0^{(p,p)}} = \frac{1}{2^{LM}} \sum_{\{\sigma\}} \prod_{\ell=1}^L \prod_{m=1}^M (1 + z_{\ell,m}^{\perp} \sigma_{\ell,m} \sigma_{\ell+1,m}) (1 + z_{\ell,m}^{\parallel} \sigma_{\ell,m} \sigma_{\ell,m+1}), \quad (16.3)$$

with  $z_{\ell,m}^{\delta} = \tanh K_{\ell,m}^{\delta}$  ( $\delta = \perp, \parallel$ ) and with the non-singular part

$$Z_0^{(p,p)} = \prod_{\ell=1}^L \prod_{m=1}^M 2 \cosh K_{\ell,m}^{\perp} \cosh K_{\ell,m}^{\parallel}. \quad (16.4)$$

[...]

The problem of finding the generating function of the closest-packed dimer configurations on an arbitrary planar graph was solved by Kasteleyn in terms of Pfaffians, as it gives the number of *perfect matchings* of a given directed planar graph with an even number of sites. This is especially powerful because of the connection between the Pfaffian and the determinant, namely

$$(\text{Pf} \mathcal{A})^2 = \det \mathcal{A}. \quad (16.5)$$

[...] The nearest-neighbour structure in a row and a column are both represented by the  $[n \times n]$  matrix

$$\mathbf{H}_{b,n} = \begin{pmatrix} 0 & 1 & 0 & \cdots & 0 \\ 0 & 0 & 1 & & 0 \\ \vdots & & & \ddots & \vdots \\ 0 & 0 & 0 & & 1 \\ -b & 0 & 0 & \cdots & 0 \end{pmatrix}, \quad (16.6)$$

with  $b \in \{+1, 0, -1\}$  accounting for  $b = 0$  open,  $b = +1$  periodic, and  $b = -1$  for anti-periodic boundary conditions.  $b = -1$  accounts for periodic boundaries on the directed graph, i. e., in the dimer system, in the sense that all edges are likewise aligned, while it accounts for antiperiodic BCs in the Ising model. However, the topology of the underlying directed graph is not representative for the Ising model, which is emphasised by the fact that the Ising partition function is a combination of four Pfaffians.

[...] the characteristic polynomials are

$$\mathcal{P}_\beta^\pm(N; \varphi) = \prod_{m=0}^{N-1} \left( e^{\pm i\varphi} - e^{i\varphi_m^{(\beta)}} \right) = e^{\pm iN\varphi} + \beta \quad (16.7)$$

with

$$\varphi_m^{(\beta)} = \begin{cases} 2m\pi/N & \text{if } \beta = -1 \\ (2m+1)\pi/N & \text{if } \beta = +1 \end{cases} \quad (16.8)$$

for  $m \in \{0, 1, 2, \dots, N-1\}$ , and thus we will call  $\beta = -1$  *even* and  $\beta = +1$  *odd*. Note that the eigenvalues lie equidistantly on the unit circle and thus we have a free shifting parameter for the spectrum. We have chosen it in such a way, that the eigenvalue  $\varphi_0^{(-)} = 0$  appears in the even spectrum; a shift by  $-\pi$  on the other hand would have given rise to a dependency on whether  $N$  is even or odd.

Characteristic polynomials (16.7) have a simple scaling form as one only have to replace  $\varphi = \Phi/N$  to obtain

$$\mathcal{P}_e^\pm(\Phi) = e^{\pm i\Phi} - 1, \quad (16.9a)$$

$$\mathcal{P}_o^\pm(\Phi) = e^{\pm i\Phi} + 1. \quad (16.9b)$$

They compute variety of determinants. Particularly suggestive is the product formula for translational invariance in both directions, their eq. (2.32), that looks like Han's determinant. This was previously computed by McCoy & Wu for the anisotropic torus [117]. There is an interesting matrix for the torus, their eq. (4.3). All in all, looks harder than what we need for the spatiotemporal cat.

**2019-11-04 Predrag** Hobrecht and Hucht [76] *Anisotropic scaling of the two-dimensional Ising model II: surfaces and boundary fields*

**2019-11-04 Predrag** Baxter [14] *The bulk, surface and corner free energies of the square lattice Ising model*

## 16.1 Ihara zeta functions

2020-05-12 Predrag .

- I think it should be little work to verify for temporal cat that the Boss determinant (16.16), (16.29), (16.36) for the Ihara zeta function (that counts undirected loops) is the Isola's Bowen-Ruelle zeta (16.43). This counts walks of the cat map directed Markov graph.
- Clair's square 2D lattice (16.14) presumably counts 1D loops (returning walks) on a 2D lattice. So does Kasteleyn [97] elliptic integral of the first kind (16.18) (see also (8.170)).
- For spatiotemporal cat we count 2D tori (Bravais lattices); expect a variable  $z_j$  for every translational symmetry direction, not a single  $z$  as in (16.18). In Ising models, one counts the 2D configurations - so how come Ihara functions can do that? Or can they?
- Explain the relation between a discrete torus and the Cayley graph. For example, given  $n \in \mathbb{N}^*$ , let  $G_n$  denote the Cayley graph  $(\mathbb{Z}/n\mathbb{Z}, \{\pm 1\})$ .

2020-06-04 Predrag Evgeny L. Korotyaev and Jacob Schach Møller [106], korotyaev@gmail.com, jacob@math.au.dk, arXiv:1701.03605: *Weighted estimates for the Laplacian on the cubic lattice*:

The starting point for their analysis is a representation of the summation kernel of the free resolvent (the propagator) in terms of a product of Bessel functions.

The momentum representation of the discrete Laplacian: one may diagonalize the discrete Laplacian, using the (unitary) Fourier transform  $\Phi: \ell^2(\mathbb{Z}^d) \rightarrow L^2(\mathbb{T}^d)$ , where  $\mathbb{T} = \mathcal{R}/(2\pi\mathbb{Z})$ . It is defined by

$$(\Phi f)(k) = \widehat{f}(k) = 1(2\pi)^{d/2} \sum_{n \in \mathbb{Z}^d} f_n e^{in \cdot k}, \quad \text{where } k = (k_j)_{j=1}^d \in \mathbb{T}^d.$$

Here  $k \cdot n = \sum_{j=1}^d k_j n_j$  is the scalar product in  $\mathcal{R}^d$ . In the resulting momentum representation of the discrete Laplacian  $\Delta$ , we write  $\widehat{\Delta} = \Phi \Delta \Phi^*$ . The Laplacian is transformed into a multiplication operator

$$(\widehat{\Delta} \widehat{f})(k) = \left( \sum_{j=1}^d \cos k_j \right) \widehat{f}.$$

The operator  $e^{it\Delta}$ ,  $t \in \mathcal{R}$  is unitary on  $L^2(\mathbb{T}^d)$  and has the kernel  $(e^{it\Delta})(n - n')$ , where for  $n \in \mathbb{Z}^d$ :

$$\begin{aligned} (e^{it\Delta})(n) &= 1(2\pi)^d \int_{\mathbb{T}^d} e^{-in \cdot k + it \sum_{j=1}^d \cos(k_j)} dk \\ &= \prod_{j=1}^d \left( \frac{1}{2\pi} \int_0^{2\pi} e^{-in_j k + it \cos(k)} dk \right) = i^{|n|} \prod_{j=1}^d J_{n_j}(t), \end{aligned}$$

where  $|n| = n_1 + \dots + n_d$ . Here  $J_n(z)$  denotes the Bessel function:

$$J_n(t) = (-i)^n 2\pi \int_0^{2\pi} e^{ink - it \cos(k)} dk \quad \forall (n, z) \in \mathbb{Z} \times \mathbb{R}.$$

The rest is all about bounds, we can safely ignore it.

**2020-05-14 Predrag** Lenz, Pogorzelski and Schmidt [109] *The Ihara zeta function for infinite graphs*, [arXiv:1408.3522](https://arxiv.org/abs/1408.3522), a very lengthy and ambitious paper, apparently gives yet another definition of an Ihara zeta function for infinite graphs. Dubout was unable to determine how it compares to his (18.15). I'm not frisky enough to read this paper, after having gone through Dubout already today...

### 16.1.1 Clair / Clair14

For the two dimensional integer lattice a zeta function has been defined and computed in Clair [40] *The Ihara zeta function of the infinite grid*

Bryan Clair is a great fan of [Ihara zeta functions](#).

Shahriar Mokhtari-Sharghi [41, 42] have shown that Ihara's construction can be extended to infinite graphs on which a discrete group acts isomorphically and with finite quotient. Their works seems to deal with trees, not lattices, though Clair [40] does discuss infinite square lattice, see (16.13).

The Ihara zeta function may be considered as a modification of the Selberg zeta function [13], and was originally written in terms of the variable  $s$ , where  $z = q^{-s}$ . One of main properties of the Ihara zeta function is the *determinant formula*, i.e., that its inverse is the determinant of a matrix-valued polynomial. A consequence of the determinant formula is that the Ihara zeta function meromorphically extends to the whole complex plane, and its completions satisfy a functional equation.

The main formula in all these papers gives a connection between the zeta function, originally defined as an infinite product, and the Laplacian of the graph.

Pollicott [129] explains in *Dynamical zeta functions* Sect. 3.3 what the Laplacian for a undirected graph is, relates it to the adjacency matrix in a somewhat obvious way, as we are used to on a lattice. He defines Ihara for undirected graph

1. the graph  $G$  has valency  $q+1$  with  $q \geq 2$  (i.e., every vertex has  $q+1$  edges attached)
2. there is at most one edge between any two vertices
3. there are no edges starting and finishing at the same vertex

He outlines a proof of the Bass determinant formula for the Bowen-Lanford zeta function.



**Loop:** A closed path in  $G$ , up to cyclic equivalence, without backtracking.

**Prime:** A loop  $p$  which is not a power (a repeat) of another loop.

**Back-track:** A path has a back-tracking if a subsequence of the form  $\dots, x, y, x, \dots$  appears.

The Ihara zeta function of a finite graph  $G$

$$\zeta(z) = \prod_p \frac{1}{1 - z^{n_p}} \quad (16.10)$$

It is instructive to have a look at the octahedral graph in Clair's talk above. There is no self-crossing condition, so  $\zeta(z)$  always has an infinity of prime cycles, of arbitrary length (as does any topological zeta function).

As a power series in  $z$ , the Ihara zeta has non-negative coefficients, and thus a finite radius of convergence. However, the inverse of the Ihara zeta is a polynomial.

Ihara considered the special case of regular graphs (those all of whose vertices have the same degree; i.e., the same number of oriented edges coming out of the vertex). A graph is  $k$ -regular if every vertex has degree  $k$ .

Terras [153] defines the  $m \times m$  adjacency matrix as,

$$A_{ij} = \begin{cases} k & \text{if a transition } \mathcal{M}_j \rightarrow \mathcal{M}_i \text{ is possible in } k \text{ ways} \\ 2\ell_j & \text{if } i = j \\ 0 & \text{otherwise,} \end{cases} \quad (16.11)$$

where  $\ell_j$  is the number of loops at vertex  $j$ . She then assigns to every of the  $e$  unoriented edges a pair of oriented edges. Her graphs are finite, connected and undirected, without "backtracks" and "tails". It will usually be assumed that they contain no degree 1 vertices (called "leaves" or "hair" or "danglers"). We will also usually assume the graphs are not cycles or cycles with hair. A cycle graph is obtained by arranging the vertices in a circle and connecting each vertex to the 2 vertices next to it on the circle. We will allow our graphs to have loops and multiple edges. For any closed loop, the equivalence class is the set of all its cyclic permutations. Two loops are equivalent if they differ only by the starting vertex.

Terras: We do not consider zeta functions of infinite graphs here. Nor do we consider directed graphs. Zeta functions for such graphs are discussed, for example, by Matthew Horton [81].

There is no unique factorization into primes. The only nonprimes are powers of primes. We distinguish prime  $p$  from  $p^{-1}$  which is the loop traversed in the opposite direction. All graphs have infinity of primes, with exception of the cycle graph that has only 2 primes  $p, p^{-1}$ , traversing the vertices in the opposite directions.

**Theorem [13, 84]:** Consider a finite connected graph  $G$  (without degree 1 vertices) with  $m$  vertices,  $e$  unoriented (or undirected) edges,  $\deg m_i$  the number of (undirected) edges going into vertex  $i$ . Let  $A$  be the adjacency matrix,  $Q$

be the  $m \times m$  diagonal matrix with  $Q_{ii} = \deg m_i - 1$ , and  $\Delta_z = I - zA + z^2Q$ . The (vertex) adjacency matrix  $A$  of  $G$  is a  $m \times m$  matrix whose  $ij$  entry is the number of directed edges from vertex  $i$  to vertex  $j$ . The matrix  $Q$  is a diagonal matrix whose  $j$ -th diagonal entry is 1 less than the degree of the  $j$ -th vertex. If there is a loop at a vertex, it contributes 2 to the degree.

$$1/\zeta(z) = (1 - z^2)^{e-m} \det \Delta_z \quad (16.12)$$

(then comes Riemann Hypothesis for the spectrum of a regular graph  $G$ , and Ramanujan graphs).

See **2020-05-11 Bharatram Rangarajan (16.35)** below for another derivation of the same.

Next, consider the ‘grid’ zeta function for  $G$  the infinite grid, i.e., a square 2D lattice. Let  $\pi = \mathbb{Z} \times \mathbb{Z}$  be a translation acting on  $G$ . The zeta function is still

$$\zeta(z) = \prod_{[p]} \frac{1}{1 - z^{n_p}} \quad (16.13)$$

where  $[p]$  is an equivalence class of loops under translation by  $\pi$ :

$$1/\zeta(z) = (1 - z^4)^2(1 - z^6)^4(1 - z^8)^{26}(1 - z^{10})^{152} \dots \quad (16.14)$$

(look at the 8-loops in Clair’s talk - there seems to be an extra factor 2 in loop counting. I only see two 6-loops, not four).

On infinite graphs, the adjacency matrix becomes an  $\ell^2(\mathbb{Z} \times \mathbb{Z}) \rightarrow \ell^2(\mathbb{Z} \times \mathbb{Z})$  adjacency operator. For the infinite grid,

$$\Delta_z = I - zA + z^3 \quad (16.15)$$

There is still a determinant formula for the zeta function:

$$1/\zeta_\pi(z) = (1 - z^2) \det_\pi \Delta_z. \quad (16.16)$$

With  $\pi = \mathbb{Z} \times \mathbb{Z}$ ,  $\det_\pi$  is an operator determinant:

$$\det_\pi \Delta_z = \exp \operatorname{Tr}_\pi \ln \Delta_z, \quad (16.17)$$

where  $\operatorname{Tr}_\pi$  is the trace on the group von Neumann algebra  $\mathcal{N}(\pi)$ .

The adjacency operator on a square lattice is essentially the 2D Laplacian. Clair throws in the 2D Ising, then Kasteleyn [97] and ends up with

$$1/\zeta_\pi(z) = (1 - z^2)(1 + 3z^2) \exp \mathbf{I}(k), \quad (16.18)$$

with a simple set of singularities, and  $\mathbf{I}(k)$  is related to an elliptic integral of the first kind (8.170), expressed in terms of theta functions (whose squares are modular forms of weight 1).

## 16.1.2 Ihara blog

**2016-10-03 Predrag** For further discussion, see [Wiki](#), and the notes for equation (16.22).

Ihara zeta function for undirected graphs satisfies a functional equation [153]. The formulation of the graph Riemann Hypothesis in terms of Ihara zeta function is based on the fact that the adjacency matrix of an undirected regular graph is symmetric. There is no analogue of Riemann Hypothesis for directed graphs.

A zeta function of a regular graph  $G$  associated to a unitary representation of the fundamental group of  $G$  was developed by Sunada [147].

**2016-10-03 Predrag** I cannot, at the moment, tell the difference between [Ihara](#) and what I call the topological zeta function in [ChaosBook.org](#) (section 18.4; the chapter alone is [here](#)). I find Aizenman's derivation of 2D Onsager solution beautiful - will have to chew on it.

**2018-03-22 Predrag** Trying to incorporate dynamics into a generalized, time-reversal invariant Laplacian by replacing a time forward cat map  $A$  by something like a time reversal invariant combination  $AA^T$ :

*Incidence matrix  $B$  entries are  $b_{ij} = \pm 1$ , depending on whether  $v_i$  is a target or a source.*

For literature and further discussion, see sect. 16.1 *Ihara zeta functions*.

For the finite transition graph figure 24.4 (d) and (2.82) the incidence matrix is **(2018-05-02 Predrag as they currently stand, the next two equation are wrong - they should be  $[\ell \times \ell]$  matrices, not 2-dimensional ones. Also, the literature discusses only 'simple' graphs, i.e., graphs without 1-loops)**

$$\begin{bmatrix} \phi'_A \\ \phi'_B \end{bmatrix} = B\phi = \begin{bmatrix} 2 & 1 \\ -1 & 1 \end{bmatrix} \begin{bmatrix} \phi_A \\ \phi_B \end{bmatrix} \quad (16.19)$$

and

$$BB^T = \begin{bmatrix} 2 & 1 \\ -1 & 1 \end{bmatrix} \begin{bmatrix} 2 & -1 \\ 1 & 1 \end{bmatrix} = \begin{bmatrix} 5 & -1 \\ -1 & 2 \end{bmatrix}. \quad (16.20)$$

Actually, we need something that acts on the whole chain, some Toeplitz matrix like

$$BB^T \text{ " = " } - \begin{bmatrix} -2 & 1 & & & 1 \\ 1 & -2 & 1 & & \\ & 1 & -2 & 1 & \\ & & 1 & \ddots & \\ 1 & & & 1 & -2 \end{bmatrix}, \quad (16.21)$$

but with 2 fields  $[\phi_{A,t}, \phi_{B,t}]^T$  at each site  $t$ .

**Proposition 17.2.** [Godsil and Royle [65]] Given any directed graph  $G$  if  $B$  is the incidence matrix of  $G$ ,  $A$  is the adjacency matrix of  $G$ , and  $D$  is the degree matrix such that  $D_{ii} = d(v_i)$ , then

$$BB^T = D - A. \quad (16.22)$$

The matrix  $L = D - A$  is called the (unnormalized) graph Laplacian of the graph  $G$ .  $BB^T$  is independent of the orientation of  $G$  and  $D-A$  is symmetric, positive, semidefinite; that is, the eigenvalues of  $D$ .

Each row of  $L$  sums to zero (because  $B^T \mathbf{1} = 0$ ). Consequently, the vector  $\mathbf{1}$  is in the nullspace of  $L$ .

The connection between the incidence matrix of a graph and its Laplacian is the well-known equation  $L = \partial\partial^T$ .

**2021-04-14 Predrag** Fan Chung [35] *Spectral Graph Theory* (revised and improved 2006) is the “bible” of spectral graph theory. Should read chapter *Eigenvalues and the Laplacian of a graph*.

See Gabriel Peyré [tweet](#).

Daniel A. Spielman *Spectral and Algebraic Graph Theory* deals with the combinatorial, normalized and random walk version of the Laplacian.

What -I think- is important for us is that any graph Laplacian can be written as

$$\mathcal{L} = SS^T, \quad (16.23)$$

where  $S$  is the matrix whose rows are indexed by the vertices and whose columns are indexed by the edges.

Let  $\mathbf{1}$  denote the constant function which assumes the value 1 on each vertex. This is an eigenfunction of  $\mathcal{L}$  with eigenvalue 0.

**2018-04-05 Predrag** There might be a related undirected network model, with a graph Laplacian (16.22). In that case a Lagrangian formulation (in terms of graph Laplacians) might be a more powerful formulation than their Hamiltonian one. “Arrow of time” is perhaps encoded by the orientations of the links in a directed complex network.

**2016-10-05 Predrag** Zeta functions of infinite graphs are discussed, for example, by

Bryan Clair and Shahriar Mokhtari-Sharghi [41],

Rostislav Grigorchuk and Andrzej Zuk [?46] (that one is about Cayley trees).

Guido, Isola, and Lapidus [69] *Ihara’s zeta function for periodic graphs and its approximation in the amenable case*.

Guido, Isola and Lapidus [70] *A trace on fractal graphs and the Ihara zeta function*

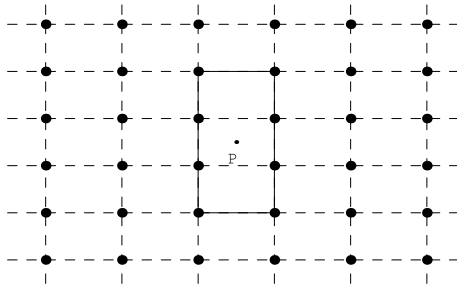


Figure 16.2: A cycle with  $|G_C| = 2$

2020-12-18 **Predrag** Daniele Guido, Tommaso Isola, and Michel Lapidus [68] *Ihara zeta functions for periodic simple graphs* [arXiv:math/0605753](https://arxiv.org/abs/math/0605753):

$$Z(G, u) = Z_G(u) = \prod_{[C]} \frac{1}{(1 - u^{[C]})^{1/|G_C|}}, \quad (16.24)$$

The standard lattice graph  $\mathcal{L} = \mathbb{Z}^2$  endowed with the action of the group  $G$  which is generated by the rotation by  $\frac{\pi}{2}$  around the point  $P$  and the translations by elements  $(m, n) \in \mathbb{Z}^2$  acting as  $(m, n)(v_1, v_2) := (v_1 + 2m, v_2 + 2n)$ , for  $v = (v_1, v_2) \in V\mathcal{L} = \mathbb{Z}^2$ .

Why face-centered point  $P$ ? why  $2m$ ? In their example, the length  $[C]$  in (16.24) is the number of group elements that map  $C$  into itself (the ‘stabilizer’), see figure 16.2, not what we need.

The main result in the theory of Ihara zeta functions (16.24) says that  $Z$  is the reciprocal of a holomorphic function, which, up to a factor, is the determinant of a deformed Laplacian on the graph.

2016-10-05 **Predrag** Unlike in dynamical systems, Ihara zeta functions are defined on graphs with unoriented (or undirected) edges.

Hashimoto [73] *Zeta functions of finite graphs and representations of  $p$ -adic groups*

2020-05-13 **Predrag** Bass [13] *The Ihara-Selberg zeta function of a tree lattice*. It seems that Ihara zeta function walks carry signs - investigate.

He also introduces the *edge zeta function* to give a determinant form of Ihara zeta function for undirected graph. This text is from Zhou, Xiao and He [163], [arXiv:1502.05771](https://arxiv.org/abs/1502.05771):

- The **edge matrix**  $W$  of size  $[2m \times 2m]$  for an undirected graph with  $m$  undirected edges has entries  $w_{ij}$ . The  $(i, j)$ -th entry of  $W$ ,  $w_{ij}$ , is a complex variable if the edge  $e_i$  is connected with edge  $e_j$  with  $e_j \neq e_i^{-1}$ , and the entry is 0 if otherwise.

- For a closed path  $C$  in an undirected graph  $X$  written as a sequence of edges  $C = e_1 e_2 \cdots e_s$ , the **edge norm** of  $C$  is

$$N_E(C) = w_{12} w_{23} \cdots w_{s1}.$$

The edge zeta function is defined as follows

$$\zeta_E(W, X) = \prod_{[P] \in \text{Prime Cycles}} (1 - N_E(C))^{-1}.$$

It is clear from this definition that if  $w_{ij}$  is set to  $z \in \mathbb{C}$ , we recover the original Ihara zeta function such that

$$\zeta_G(z) = \zeta_E(W_1, G),$$

where  $W_1$  is the edge matrix when all non-zero entries set to  $z$ .

Furthermore, we have the following formula (cf. Chapter 3 of Terras [153])

$$\zeta_E(W, G) = \text{Det}(I - W)^{-1}. \quad (16.25)$$

**2016-10-05 Predrag** In *A Window Into Zeta and Modular Physics* [102] (that should warm Li Han's heart) Audrey Terras discusses **Ihara zeta function**. She says: "the Ruelle zeta function of a dynamical system, will be shown to be a generalization of the Ihara zeta." Things are looking deep. "It turns out (using the Ihara determinant formula again) that the Riemann hypothesis means that the graph is Ramanujan", etc. She also discusses it in ref. [153] *Zeta Functions of Graphs: A Stroll through the Garden*.

To swoon over the multitude of zetas, read Bartholdi [12] *Zeta functions of graphs: a stroll through the garden, by Audrey Terras* [153]. *Book review*.

Teimoori Faal and M. Loeb [150] **Bass' identity and a coin arrangements lemma**

Like my topological zeta functions, **Loeb's** Ihara-Selberg function of  $G$  is the infinite product is over the set of the prime reduced cycles of  $G$ .

**2016-10-05 Predrag** da Costa [45] *The Feynman identity for planar graphs*: " The Feynman identity (FI) of a planar graph relates the Euler polynomial of the graph to an infinite product over the equivalence classes of closed nonperiodic signed cycles in the graph. The main objectives of this paper are to compute the number of equivalence classes of nonperiodic cycles of given length and sign in a planar graph and to interpret the data encoded by the FI in the context of free Lie superalgebras. This solves in the case of planar graphs a problem first raised by Sherman and sets the FI as the denominator identity of a free Lie superalgebra generated from a graph. Other results are obtained on the zeta functions of graphs. "

da Costa *Graphs and Generalized Witt identities* [arXiv:1409.5767](https://arxiv.org/abs/1409.5767)

**2016-10-05 Predrag Sato [136]** *Bartholdi zeta functions of group coverings of digraphs:*

The (Ihara) zeta function of a graph  $G$  is defined [84] to be a function of  $u$  with  $u$  sufficiently small, by

$$Z(G, u) = Z_G(u) = \prod_{[C]} \frac{1}{1 - u^{|C|}}, \quad (16.26)$$

where  $[C]$  runs over all equivalence classes of prime, reduced cycles of  $G$ .

Samuel Cooper and Stratos Prassidis (2010) *Zeta functions of infinite graph bundles*, DOI :

Originally, Ihara defined the zeta function on finite graphs imitating the classical definition of the zeta function, where the product is over all equivalence classes of primitive closed loops  $C$ , and  $|C|$  denotes the length of  $C$ .

**2016-10-05 Predrag Horton [81]** *Ihara zeta functions of digraphs* considers digraphs whose adjacency matrices are directed edge matrices.

Tarfulea and Perlis [149] An Ihara formula for partially directed graphs: " In 2001 Mizuno and Sato showed that the Ihara zeta function of a fully directed graph has a similar expression, and in 2005, Sato [136] generalized Ihara's formula to connected, simple, partially directed graphs. (Sato proved his formula for the more-general two-variable Bartholdi zeta function.) This paper provides a new proof of Ihara's formula for the Ihara zeta function of any finite graph, not necessarily connected or simple, no matter whether it is undirected, fully directed, or partially directed. "

**2016-10-30 Predrag** I worry a lot about what time-reversibility means - spatiotemporal cat is both time and space reversible, and then there are Ihara zeta functions for undirected graphs. So I find this interesting: Copper-smith, Kadanoff and Zhang [44] *Reversible Boolean networks I: distribution of cycle lengths*. They write: " We [...] consider time-reversible dynamics of  $N$  Boolean variables models, with the time evolution of each depending on  $K$  of the other variables, which necessarily have the property that every possible point in the state space is an element of one and only one cycle. The orbits can be classified by their behavior under time reversal. The orbits that transform into themselves under time reversal have properties quite different from those that do not; in particular, a significant fraction of latter-type orbits have lengths enormously longer than orbits that are time-reversal symmetric. For large  $K$  and moderate  $N$ , the vast majority of points in the state space are on one of the time-reversal singlet orbits. However, for any finite  $K$ , the random hopping approximation fails qualitatively when  $N$  is large enough ( $N > 22K$ ). When  $K$  is large, typical orbit lengths grow exponentially with  $N$ , whereas for small enough

K, typical orbit lengths grow much more slowly with N. The numerical data are consistent with the existence of a phase transition at which the average orbit length grows as a power of N at a value of K between 1.4 and 1.7. However, in the reversible models, the interplay between the discrete symmetry and quenched randomness can lead to enormous fluctuations of orbit lengths and other interesting features that are unique to the reversible case. ”

Need to check also

Toffoli and Margolus [154] *Invertible cellular automata: A review*

D’Souza and Margolus [48] *Thermodynamically reversible generalization of diffusion limited aggregation*

**2020-05-11 Predrag** Deitmar [52] *Ihara zeta functions of infinite weighted graphs:* “The theory of Ihara zeta functions is extended to infinite graphs which are weighted and of finite total weight. In this case one gets meromorphic instead of rational functions and the classical determinant formulas of Bass and Ihara hold true with Fredholm determinants.”

Tempesta [151] *A theorem on the existence of trace-form generalized entropies*

Tempesta [152] *Beyond the Shannon-Khinchin formulation: The composability axiom and the universal-group entropy*

**2020-05-11 Predrag** Supriyo Dutta and Partha Guha *Ihara Zeta Entropy*, [arXiv:1906.02514](#); *A System of Billiard and Its Application to Information-Theoretic Entropy*, [arXiv:2004.03444](#): they define Ihara entropy, an information-theoretic entropy based on the Ihara zeta function of a graph. A dynamical system consists of a billiard ball and a set of reflectors correspond to a combinatorial graph. The reflectors are represented by the vertices of the graph. Movement of the billiard ball between two reflectors is represented by the edges. The prime cycles of this graph generate the bi-infinite sequences of the corresponding symbolic dynamical system. The number of different prime cycles of a given length can be expressed in terms of the adjacency matrix of the oriented line graph. It also constructs the formal power series expansion of Ihara zeta function. Therefore, the Ihara entropy has a deep connection with the dynamical system of billiards.

**2017-03-08 Predrag** Reading Band, Harrison and Joyner [11] *Finite pseudo orbit expansions for spectral quantities of quantum graphs* one expects to run into another rediscovery of Ihara zeta functions, as the links are not directed:

“ The *quantum graphs* we consider are metric graphs equipped with a self-adjoint differential operator  $\mathcal{H}$ , the Hamiltonian. Here we are particularly interested in the negative Laplace operator,

$$\mathcal{H} : f(x) \mapsto -\frac{d^2 f}{dx^2}, \quad (16.27)$$



or the more general Schrödinger operator,

$$\mathcal{H} : f(x) \mapsto -\frac{d^2 f}{dx^2} + V(x)f(x), \quad (16.28)$$

where  $V(x)$  is a *potential*, which we assume to be bounded and piecewise continuous. Note that the value of a function or the second derivative of a function at a point on the bond is well-defined, thus it is not important which coordinate,  $x_b$  or  $x_{\bar{b}}$  is used. This is in contrast to the first derivative which changes sign according to the direction of the chosen coordinate.  
"

Indeed, they go through the usual steps of defining oriented graphs and then putting pairs of oriented bonds on each link, etc. This is explored further in

Ren, Aleksić, Emms, Wilson and Hancock [130] *Quantum walks, Ihara zeta functions and cospectrality in regular graphs*: review the literature on the discrete-time quantum walks and the Ihara zeta function.

Setyadi and Stor [137] *Enumeration of graphs with the same Ihara zeta function*

Higuchi, Konno, Sato and Segawa [74] *A remark on zeta functions of finite graphs via quantum walks*

Saito [134] *A proof of Terras' conjecture on the radius of convergence of the Ihara zeta function* has a nice explicit matrix example, and eigenvalues computation.

**2020-05-05 Predrag** Mizuno and Sato [119] *Zeta functions of digraphs* define a zeta function of a digraph and an L-function of a symmetric digraph. That is the usual Bowen-Ruelle (in ChaosBook topological) zeta function. Tarfulea and Perlis [149] do note: "The formula for the zeta function of a directed graph was proved in 1968, wearing a thin disguise, by Bowen and Lanford [25]. The elementary connection to directed graphs is made explicit in Th.6.4.6 of Lind Marcus [111]."

Various authors, such as Zhou, Xiao and He [163] *Seiberg duality, quiver gauge theories, and Ihara's zeta function*, nevertheless refer to it as "Ihara", see their Table 2 *Ihara zeta functions for various toric phases of del Pezzo and Hirzebruch quivers*. Apparently, "the toric phases are the most popular."

"The coefficients of the inverse of Ihara zeta function are related to simple cycles. In gauge theories, this translates to generic super-potentials that can be generated from certain quivers." This seems to be expansion of a topological zeta function in terms of fundamental cycles.

**2020-05-05 Predrag** Davey, Hanany and Pasukonis [49] *On the classification of brane tilings*, [arXiv:0909.2868](https://arxiv.org/abs/0909.2868). (See also [arXiv:hep-th/0503149](https://arxiv.org/abs/hep-th/0503149)) has an Appendix A *Tiling catalog*.

A brane tiling (or dimer model) is a periodic bipartite graph on the plane. Alternatively, we may draw it on the surface of a 2-torus by taking the smallest repeating structure (known as the fundamental domain) and identifying opposite edges [1]. The bipartite nature of the graph allows us to colour the nodes either white or black such that white nodes only connect to black nodes and vice versa.

**2020-05-05 Predrag** Sunada [148] *Topological Crystallography*. Have the book ([click here](#)), but do not know how to get useful info for spatiotemporal cat out of it.

“the Ihara zeta function [is] a graph-theoretic analogue of class field theory, discrete Laplacians, and harmonic maps.”

Again, “Abel–Jacobi maps” pop up, and again I have no idea what they are.

**2020-05-06 Predrag** Ren, Wilson and Hancock [131] *Graph characterization via Ihara coefficients*: For an unweighted graph, the Ihara zeta function is the reciprocal of a quasi characteristic polynomial of the adjacency matrix of the associated oriented line graph.

First, we demonstrate how to characterize unweighted graphs in a permutation-invariant manner using the polynomial coefficients from the Ihara zeta function, i.e., the Ihara coefficients.

Second, we generalize the definition of the Ihara coefficients to edge-weighted graphs, using the reduced Bartholdi zeta function.

Experimental results reveal that the Ihara coefficients are more effective than methods based on Laplacian spectra.

Bulò, Hancock, Aziz and Pelillo [28] *Efficient computation of Ihara coefficients using the Bell polynomial recursion*: They present a method for computing the Ihara coefficients in terms of complete Bell polynomials and show how the Ihara coefficients can be efficiently computed provided that the eigenvalues of the adjacency matrix are known.

**2020-05-05 Predrag** Arrigo, [Grindrod](#), Higham and Noferini [7] *On the exponential generating function for non-backtracking walks* do not mention “Ihara”, but seem to derive it anyway from a 3-term recurrence relation. They write:

We derive an explicit formula for the exponential generating function associated with non-backtracking walks around both undirected and directed graphs. Eliminating backtracking walks in this context does not significantly increase the computational expense. We show how the new measures may be interpreted in terms of standard exponential centrality computation on a certain multilayer network. Insights from this block matrix interpretation also allow us to characterize centrality measures arising from general matrix functions.

**2020-05-11 Predrag Bharatram Rangarajan** *A combinatorial proof of Bass's determinant formula for the zeta function of regular graphs*, [arXiv:1706.00851](https://arxiv.org/abs/1706.00851): The zeros and poles of the Selberg zeta function appear in the Selberg trace formula, which relates the distribution of primes with the spectrum of the Laplace-Beltrami operator of the surface. The idea of considering closed geodesics as primes inspired the work of Hashimoto [73], Bass [13], Kotani and Sunada [107] to come up with an analogous notion in the discrete setting.

Just like the Selberg zeta function is related to the spectrum of the Laplace-Beltrami operator of the surface, it is natural to ask if its discrete analogue, the Ihara zeta function of a graph, is related to the spectrum of the Laplacian matrix (or the adjacency matrix) of the graph. Bass [13] gives an expression for the Ihara zeta function of a graph  $G = (V, E)$  as

$$\zeta_G(t) = \frac{1}{(1-t^2)^{|E|-|V|} \det(I-tA+(D-I)t^2)}$$

where  $A$  is the adjacency matrix of  $G$  and  $D$  is the diagonal matrix of degrees of the vertices of  $G$ , or in other words,  $D = \text{diag}(A\vec{1})$ . In particular, if  $G$  is  $d$ -regular, then (see (16.15), derivation (16.36))

$$\zeta_G(t) = \frac{1}{(1-t^2)^{|E|-|V|} \det(I-tA+(d-1)t^2I)} \quad (16.29)$$

gives a way of obtaining the set of poles of  $\zeta_G(t)$ .

For a general, partially directed graph see Sato [136] and Tarfulea and R. Perlis [149].

Most proofs Bass's determinant formula start by expressing the zeta function in terms of not the adjacency matrix  $A$  of  $G$ , but the adjacency matrix  $H$  of the oriented line graph of  $G$  (called the Hashimoto edge-incidence matrix).

In this paper, we shall see a more elementary combinatorial proof of Bass's determinant formula in the case when  $G$  is regular. The proof goes as follows:

- The zeta function  $\zeta_G(z)$  has an expansion of the form

$$\zeta_G(z) = \exp\left(\sum_{k=1}^{\infty} N_k \frac{z^k}{k}\right)$$

where for  $k \in \mathbb{Z}$ ,  $N_k$  is the number of rooted, *non-backtracking* cycles in  $G$  of length  $k$ .

- An expression for  $N_k$  is not immediate, the starting point is the study of non-backtracking walks on  $G$ . We can construct the family  $\{A_k\}_{k \in \mathbb{Z}_{\geq 0}}$  of  $n \times n$  matrices such that for every  $k \in \mathbb{Z}_{\geq 0}$  and every  $v, w \in V$ ,  $(A_k)_{vw}$  is the number of non-backtracking walks on  $G$  of length  $k$  from  $v$  to  $w$ .

- $N_k$  is combinatorially computable from  $\text{Tr}(A_k)$ .
- $\text{Tr}(A_k)$  is well-understood in terms of the eigenvalues of  $A$  and a family of Chebyshev polynomials. These ingredients lead to a proof of Bass's determinant formula.

$(A^k)_{vw}$  counts the total number of walks (with backtrackings) on  $G$  from  $v$  to  $w$  of length  $k$ . Let

$$A_0, A_1, A_2, A_3, \dots$$

be  $[n \times n]$  matrices over  $\mathbb{C}$  such that the value  $(A_k)_{vw}$  is the number of *non-backtracking* walks on  $G$  from  $v$  to  $w$  of length  $k$ . This family  $\{A_k\}_{k \in \mathbb{Z}}$  can be recursively defined using powers of  $A$  as follows:

- $A_0 = I$
- $A_1 = A$
- $A_2 = A^2 - dI$
- For  $k \geq 3$ ,

$$A_k = A A_{k-1} - (d-1)A_{k-2}$$

This recurrence relation shows that the ordinary (matrix) generating function for the above sequence is

$$\sum_{k=0}^{\infty} z^k A_k = (1 - z^2)I \cdot (I - zA + (d-1)z^2I)^{-1}$$

i.e., generating function

$$\frac{1 - z^2}{1 - Az + (d-1)z^2}$$

Consider the family of Chebyshev polynomials of the second kind

$$U_0(x), U_1(x), U_2(x), \dots$$

defined by the recurrence

$$U_0(x) = 1$$

$$U_1(x) = 2x$$

and for  $k \geq 2$ ,

$$U_k(x) = U_{k-1}(x)U_1(x) - U_{k-2}(x)$$

and with generating function

$$\sum_{k=0}^{\infty} U_k(x)z^k = \frac{1}{1 - 2xz + z^2}$$

It is easy to see that

$$\sum_{0 \leq j \leq k/2} A_{k-2j} = (d-1)^{k/2} U_k \left( \frac{A}{2\sqrt{d-1}} \right)$$

implying that for  $k \geq 2$ ,

$$A_k = (d-1)^{k/2} U_k \left( \frac{A}{2\sqrt{d-1}} \right) - (d-1)^{k/2-1} U_{k-2} \left( \frac{A}{2\sqrt{d-1}} \right)$$

This holds for  $0 \leq k \leq 2$  as well, if

$$U_m(x) = 0$$

for every  $m < 0$ . This allows us to work with the above expression for  $A_k$  for *all* non-negative integers  $k$ .

Taking trace on both sides,

$$\text{Tr}(A_k) = (d-1)^{k/2} \sum_{j=0}^{n-1} U_k \left( \frac{\mu_j}{2\sqrt{d-1}} \right) - (d-1)^{k/2-1} \sum_{i=0}^{n-1} U_{k-2} \left( \frac{\mu_i}{2\sqrt{d-1}} \right)$$

where

$$d = \mu_0 \geq \mu_1 \geq \dots \geq \mu_{n-1} \geq d$$

are the  $n$  eigenvalues of the adjacency matrix  $A$ . Thus we have an expression for the trace of  $A_k$  as a polynomial in the eigenvalues of  $A$ . For a detailed and elementary exposition of Chebyshev polynomials and non-backtracking walks on regular graphs, the reader is referred to the monograph by Davidoff, Sarnak and Valette [50].

While  $(A_k)_{vw}$  counts the number of walks on  $G$  from vertex  $v$  to vertex  $w$  without backtracking, the diagonal element  $(A_k)_{vv}$  does *not* count the number of non-backtracking cycles of length  $k$  rooted at  $v$ . This is because  $(A_k)_{vv}$  also counts walks of the form

$$e_1 e_2 \dots e_k$$

where  $e_{i+1} \neq \bar{e}_i$  for any  $1 \leq i \leq k-1$  but  $e_k = \bar{e}_1$ . That is,  $e_1 e_2 \dots e_k$  is non-backtracking as a walk from  $v$  to  $v$ , but when considered as a closed walk (or a loop), the two end edges form a backtracking! Such an instance of a backtracking that gets overlooked in  $\text{Tr}(A_k)$  shall be referred to as a *tail*.

So  $\text{Tr}(A_k)$  counts the number of closed, rooted walks of length  $k$  that could have at most 1 tail, and hence does *not* count the rooted, non-backtracking cycles of length  $k$ . It is interesting to ask what the number of closed, rooted non-backtracking walks of length  $k$  is.

Relation between  $M_k = \text{Tr}(A_k)$  and  $N_k$ : For every  $k \geq 3$ ,

$$N_k = \begin{cases} M_k - (d-2)(M_{k-2} + M_{k-4} + \dots + M_1) & \text{odd } k \\ M_k - (d-2)(M_{k-2} + M_{k-4} + \dots + M_2) & \text{even } k \end{cases}$$

By linearity of trace,

$$N_k = \begin{cases} \text{Tr}(A_k - (d-2)(A_{k-2} + A_{k-4} + \dots + A_1)) & \text{if } k \text{ is odd} \\ \text{Tr}(A_k - (d-2)(A_{k-2} + A_{k-4} + \dots + A_2)) & \text{if } k \text{ is even} \end{cases}$$

[... after a few steps ... this is related to]

$$U_k(x) - U_{k-2}(x) = 2T_k(x)$$

where  $T_k(x)$  is the *Chebyshev polynomial of the first kind* defined by

$$\begin{aligned} T_0(x) &= 1, & T_1(x) &= x \\ T_k(x) &= 2xT_{k-1}(x) - T_{k-2}(x) & \text{for } k \geq 2, \end{aligned} \quad (16.30)$$

with the generating function

$$\sum_{k=0}^{\infty} T_k(x)z^k = \frac{1-xz}{1-2xz+z^2} \quad (16.31)$$

[... after a few probably unnecessary steps, ... taking a derivative ... this is related to]

$$N_1z + N_2\frac{z^2}{2} + N_3\frac{z^3}{3} + \dots \quad (16.32)$$

$$= -\frac{n(d-2)}{2} \ln(1-z^2) - \sum_{j=0}^{n-1} \ln(1 - \mu_j z + (d-1)z^2) \quad (16.33)$$

$$= -\left(\frac{nd}{2} - n\right) \ln(1-z^2) - \ln\left(\prod_{j=0}^{n-1} 1 - \mu_j z + (d-1)z^2\right) \quad (16.34)$$

$$= -(|E| - |V|) \ln(1-z^2) - \ln(\det(I - Az + (d-1)z^2I)) \quad (16.35)$$

resulting in (16.12):

**Bass's determinant formula** Let  $G = (V, E)$  be a  $d$ -regular graph with adjacency matrix  $A$ , and let  $N_k$  count the number of rooted, non-backtracking cycles of length  $k$  in  $G$ . Then

$$\zeta_G(z) = \frac{1}{(1-z^2)^{|E|-|V|} \det(I - zA + (d-1)z^2I)} \quad (16.36)$$

**2023-08-30 Predrag** Cris Moore, Santa Fe Institute, moore@santafe.edu, gave a [Rutgers seminar](#). My email to him:

I really liked the pedagogy and clarity of your talk - and I certainly did not understand the significance of these phase transitions and that mean field theory is trees (always think of trees as solutions of classical Euler-Lagrange equations, loops as perturbative non-linear corrections). Never connected Ihara to Hashimoto.

Except that now I see a ton of references to Hashimoto in my own blog on Ihara zeta functions:) What I want to say is I never thought of Hashimoto matrix as a linear operator whose (appropriate) determinant is Ihara zeta.

Anyway, the nitpicking: I disagree with your high-school teacher - the quadratic minimizer is not minimizing energy stored in springs - their spring constant is pure imaginary, ie, we are not finding extrema of a Helmholtz equation, but of its hyperbolic cousin, the damped Poisson (AKA Klein-Gordon or Yukawa or -please insert other names, I collect them-). Here Laplacian has to do with random walks, rather than with oscillations.

I obsess about this, because my world is not populated by vibrating spring mattress, but their [wild cousins](#), spatiotemporal cats (what in the 1980's, one-spacetime dimension was called "chaos"). If it's of interest, the details are [here](#). Embarrassingly, there is only one real paper, the rest we have been very slow to write in a digestible form.

### 16.1.3 Maillard

Another scary line of literature. Connecting Baxter to dynamical zeta functions. Maillardinians have a burst at the end of 20th century. Very easy to collect the literature, as only they cite their own articles, and nobody else cites them.

A cute cat map exercise - but I have to bike home, will continue later...

**2016-11-16 Predrag** Anglès d'Auriac, Boukraa and Maillard [6] *Functional relations in lattice statistical mechanics, enumerative combinatorics, and discrete dynamical systems* write " ... non-linear functional relations appearing in [...] lattice statistical mechanics [...] We then consider discrete dynamical systems corresponding to birational transformations. The rational expressions for dynamical zeta functions obtained for a particular two-dimensional birational mapping, depending on two parameters [...] compatible with a chaotic dynamical system.

They obsess about the Arnol'd complexity, which counts the number of intersections between a fixed line and its  $n$ th iterate. I do not see why we should care.

I like Bedford and Diller [15] *Real and complex dynamics of a family of birational maps of the plane: The golden mean subshift* better, so I follow their notation here. It's a rather impressive paper.

For reasons known to some people (symmetries of Baxter models?) they study a birational transformation and its inverse,

$$\begin{aligned} x_{n+1} &= y_n \frac{x_n + a}{x_n - 1} & x_{n-1} &= y_n + 1 - a \\ y_{n+1} &= x_n + a - 1 & y_{n-1} &= x_n \frac{y_n - aa}{y_n + 1}, \end{aligned} \quad a \in \mathbb{R} \quad (16.37)$$

The map is area-preserving in the sense that it preserves a meromorphic 2-form

$$\frac{dx \wedge dy}{y - x + 1}$$

and is reversible, which means that the map is conjugate to its inverse via involution  $(x, y) \rightarrow (-y, -x)$ . The inverse transformation amounts to  $y_n \leftrightarrow -z_n$ , i.e., the time reversal symmetry, and the  $x - y = 0$  line is the *time-reversal invariant line*. The topological zeta function for (16.37) is

$$1/\zeta_{AM}(z) = \frac{1 - z - z^2}{1 - z^2}. \quad (16.38)$$

It counts all periodic orbits, real and complex. Interestingly, this zeta satisfies an elegant functional relation relating  $\zeta(z)$  and  $\zeta(1/z)$ .

The zeta function for real roots is complicated and depends on the parameter  $a$ .

Bedford and Diller [15] construct a generating partition and the Markov diagram (they call that Graph of Filtration), including the transient nodes. The recurrent part of this graph is just the golden mean graph, with 11 repeats forbidden. They obsess much about their “rectangles.” Show that all periodic orbits are hyperbolic. Discuss pre-periodic orbits. Zeta functions are never mentioned, though topological entropy is computed.

Abarenkova *et al.* [1] *Rational dynamical zeta functions for birational transformations* is not worth reading - the material is better explained in their other papers.

If the dynamical zeta function can be interpreted as the ratio of two characteristic polynomials of two linear operators  $A$  and  $B$ , namely

$$\frac{1}{\zeta(z)} = \frac{\det(1 - zA)}{\det(1 - zB)}, \quad (16.39)$$

then the number of fixed points is given by

$$\text{Tr}(A^n) - \text{Tr}(B^n). \quad (16.40)$$

In this linear operators framework, the rationality of the  $\zeta$  function [67, 114], and therefore the algebraicity of the exponential of the topological entropy, amounts to having a finite dimensional representation of the linear operators  $A$  and  $B$ .



Their only explicit example of a rational zeta dynamical function is the case of the Arnol'd cat map on torus  $\mathbb{T}^2 = \mathbb{R}^2/\mathbb{Z}^2$ ,

$$A = \begin{pmatrix} 2 & 1 \\ 1 & 1 \end{pmatrix}, \quad B = \begin{pmatrix} 1 & 0 \\ 0 & 1 \end{pmatrix} \quad (16.41)$$

The topological zeta function [85] for Arnol'd cat map is

$$1/\zeta_{\text{AM}}(z) = \frac{\det(1 - zA)}{\det(1 - zB)} = \frac{1 - 3z + z^2}{(1 - z)^2}. \quad (16.42)$$

**2016-06-02, 2020-09-24 Predrag** From my notes on Isola [85]  $\zeta$ -functions and distribution of periodic orbits of toral automorphisms, see sect. 2.3.7: [...] The topological zeta function for cat-map class of models is (see (6.199))

$$1/\zeta_{\text{AM}}(z) = \frac{1 - sz + z^2}{(1 - z)^2}. \quad (16.43)$$

Define

$$d(s) = z^{-1} - s + z \quad (16.44)$$

then (compare with (16.39))

$$1/\zeta_{\text{AM}}(z) = \frac{d(s)}{d(2)} = 1 + \frac{d(s) - d(2)}{d(2)} = 1 - \mu^2 \frac{1}{d(2)} \quad (16.45)$$

I wonder whether the fact that this is quadratic in  $z$  has something to do with the time-reversibility, and the unsigned graph's Ihara zeta functions?

The "characteristic function" (8.167) for the 3-point recurrence centered on the  $s$  term,  $1/z - s + z$  suggests multiplying (16.43) by  $z^{-1}/z^{-1}$ . That leads to

$$1/\zeta_{\text{AM}}(z) = 1 + \frac{\mu^2}{(1 - z)(1 - 1/z)} = 1 + \left( \frac{z}{1 - z} + \frac{1/z}{1 - 1/z} \right) \mu^2. \quad (16.46)$$

Interpretation: the temporal cat zeta function denominator is the Laplacian, and  $\mu^2$  is measuring the deviation from the pure Laplacian case (marginal, no solutions other than the  $n = 1$  (line of) fixed point(s)).

Conversely, given the topological zeta function, the generating function for the number of temporal periodic states of period  $n$  is given by the

logarithmic derivative of the topological zeta function (2.13),

$$\begin{aligned}
 \sum_{n=0}^{\infty} N_n z^n &= \frac{2-sz}{1-sz+z^2} - \frac{2}{1-z} = \frac{2/z-s}{1/z-s+z} - \frac{2}{1-z} \\
 &= \frac{(2/z-s)(1-z) - 2(1/z-s+z)}{(1/z-s+z)(1-z)} \\
 &= \mu^2 \frac{1+z}{(1/z-s+z)(1-z)} \\
 &= \mu^2 [z + (s+2)z^2 + (s+1)^2 z^3 \\
 &\quad + (s+2)s^2 z^4 + (s^2+s-1)^2 z^5 + \dots] \quad (16.47)
 \end{aligned}$$

which is indeed the generating function for  $T_\ell(s/2)$ , the Chebyshev polynomial of the first kind.

To me it looks like we should include (time reflection symmetry!) also negative  $n$  in the  $z^n$  series (Laurent series?), with a negative sign, so I get

$$\begin{aligned}
 \sum_{n=-\infty}^{\infty} N_n z^n &= \frac{\mu^2}{z^{-1}-s+z} \left( \frac{1+z}{1-z} - \frac{1+z^{-1}}{1-z^{-1}} \right) \\
 &= \frac{\mu^2}{z^{-1}-s+z} \frac{(1+z)(1-z^{-1}) - (1-z)(1+z^{-1})}{(1-z)(1-z^{-1})} \\
 &= \frac{2\mu^2}{z^{-1}-\mu^2-2+z} \frac{z-z^{-1}}{(1-z)(1-z^{-1})} \\
 &= \frac{2\mu^2}{z^{-1}-\mu^2-2+z} \frac{z^{-1}-z}{z^{-1}-2+z}. \quad (16.48)
 \end{aligned}$$

**2020-09-24 Predrag** For 2-dimensional spatiotemporal cat the “characteristic function” (8.167) the above musings suggests a guess

$$\begin{aligned}
 1/\zeta_{AM}(z_1, z_2) &= \frac{z_1 + z_2 - 2s + z_1^{-1} + z_2^{-1}}{z_1 + z_2 - 4 + z_1^{-1} + z_2^{-1}} \\
 &= 1 - \frac{2\mu^2}{z_1 + z_2 - 4 + z_1^{-1} + z_2^{-1}} \quad (16.49) \\
 &= 1 + \frac{2\mu^2}{(1-z_1)(1-1/z_1) + (1-z_2)(1-1/z_2)}
 \end{aligned}$$

If we define

$$d(s) = z_1 + z_2 - 2s + z_1^{-1} + z_2^{-1} \quad (16.50)$$

then (compare with (16.39))

$$1/\zeta_{AM}(z_1, z_2) = \frac{d(s)}{d(2)} \quad (16.51)$$

suggest some derivatives, integrations with respect to the parameter  $s$ , resulting in  $\ln d(s) - \ln d(2)$  from the ends of the integration domain.

See also (16.42).

2020-05-05 **Predrag** Kotani and Sunada [107] *Zeta functions of finite graphs* seems cited a lot and perhaps belongs to *ChaosBook.org*.

2020-05-05 **Predrag** Stark and Terras [144] *Zeta functions of finite graphs and coverings* is cited a lot and perhaps belongs to *ChaosBook.org*.

Stark and Terras [145] *Zeta functions of finite graphs and coverings, Part II*

## 16.2 Gaussian model

2020-05-15 Predrag .

Kadanoff [94] ([click here](#)) 3.4 Lattice Green Function discussion of the “Gaussian model” coefficient matrix of his (3.12)

$$-\frac{1}{K}C_{nm} = \begin{cases} K^{-1} & \text{if } x_n = x_m \\ 1 & \text{if nearest neighbors} \end{cases} \quad (16.52)$$

is the same as our  $\mathcal{J}$  with  $d s = 1/K$ .

He writes “As we shall see this simple and exactly solvable problem is in fact closely related to several different situations involving phase transitions. The Gaussian problem itself undergoes a kind of phase transition at a point at which one of the eigenvalues of  $C$  approaches zero. When that happens, the correlation matrix  $G$  goes to infinity, and very large correlations tend to develop in the system. Some thermodynamic derivatives for the system become very large, and the system shows every sign of doing something interesting. We shall explore this interesting behavior in considerable detail below.”

He looks at the Fourier transformed  $\mathcal{J}$  and observes 0-Fourier mode is of form

$$C(0) = 1 - 2dK = 1 - 2/s, \quad (16.53)$$

so there is a phase transition as  $K$  approaches  $1/(2d)$  from below, or  $s$  approaches  $-2$  from above. He writes “We shall investigate this point in considerable detail in several of the chapters below.”

He returns to it in his eq. (4.38), where he notes (for 1-dimensional chain) that  $-1/2 < K < 1/2$ , i.e.,  $|s| > 2$ , so the Gaussian field theory operates in the same regime as the spatiotemporal cat. But I have not found a discussion in higher dimensions, or rather, while the Gaussian model is used throughout the book as the ‘opposite of’ the Ising model, I do not see what to make out of it from our perspective...

His lecture [is nice](#).

2019-11-04 Predrag Ivashkevich, Izmailian and Hu [86] *Kronecker’s double series and exact asymptotic expansions for free models of statistical mechanics on torus:*

*Gaussian model* is a boson analog of Ising model. Consider square lattice of size  $N \times M$  wrapped on a torus. To each site  $(m, n)$  of the lattice we assign a continuous variable  $\phi_{mn}$ . The Hamiltonian of the model is

$$H(\phi) = -J \sum_{n=0}^{N-1} \sum_{m=0}^{M-1} (\phi_{mn} \phi_{m+1,n} - 2\phi_{mn}^2 + \phi_{mn} \phi_{m,n+1}), \quad (16.54)$$

with the partition function

$$Z(J) = \int_{\mathbb{R}^{MN}} e^{-H(\phi)} d\sigma(\phi) \quad (16.55)$$

If the measure  $d\sigma(\phi)$  in the phase space  $\mathbb{R}^{MN}$  is Gaussian

$$d\sigma_{\text{Gauss}}(\phi) = \pi^{-MN/2} \prod_{n=0}^{N-1} \prod_{m=0}^{M-1} e^{-\phi_{mn}^2} d\phi_{mn}$$

the integration can be done explicitly and the partition function of the free boson model can be written in terms of the partition function with twisted boundary conditions (19.30)

$$Z_{\alpha,\beta}(\mu) = \prod_{n=0}^{N-1} 2 \left| \text{sh} \left[ M\omega_{\mu} \left( \frac{\pi(n+\alpha)}{N} \right) + i\pi\beta \right] \right| \quad (16.56)$$

and parameterization  $J^{-1} = 4 \text{ch}^2 \mu$  as

$$Z_{\text{Gauss}}(\mu) = \left( \sqrt{2} \text{ch} \mu \right)^{MN} \left[ Z_{0,0}(\mu) \right]^{-1} \quad (16.57)$$

where

$$Z_{0,0}^2(\mu) = \prod_{n=0}^{N-1} \prod_{m=0}^{M-1} 4 \left[ \sin^2 \left( \frac{\pi n}{N} \right) + \sin^2 \left( \frac{\pi m}{M} \right) + 2 \text{sh}^2 \mu \right]. \quad (16.58)$$

This model exhibit phase transition at the point  $\mu_c = 0$  where the partition function is divergent. This is due to the presence of so-called zero mode, i.e. due to the symmetry transformation  $\phi_{mn} \rightarrow \phi_{mn} + \text{const}$ , which leave the Hamiltonian (16.54) invariant. Correlation functions of disorder operator in this model have been studied by Sato, Miwa and Jimbo.

The reason why this model is often considered as boson analog of the Ising model is that one can choose another measure in the phase space, which makes this model equivalent to the Ising model considered above

$$d\sigma_{\text{Ising}}(\phi) = 2^{-MN} \prod_{n=0}^{N-1} \prod_{m=0}^{M-1} \left[ \delta(\phi_{mn} - 1) + \delta(\phi_{mn} + 1) \right] d\phi_{mn}$$

where  $\delta$ 's are Dirac  $\delta$ -functions. With such a definition the variables  $\phi_{mn}$  can actually take only two values:  $+1$  or  $-1$ , so that  $\phi_{mn}^2 = 1$ . In this case integration can be replaced by summation over discrete values of  $\phi_{mn} = \pm 1$  and the Hamiltonian (16.54) coincides with the Hamiltonian of the Ising model (19.25) up to a constant.

**2020-06-19 Predrag** Connect to (4.308)?

Recheck [2019-09-25 PC] Levit and Smilansky?

**2020-06-19 Predrag** P. A. P. Moran [120] *A Gaussian Markovian Process on a Square Lattice* is a very good paper that does all the right stuff with the Gaussian "model," and ends up with the complete elliptic integral of the first kind (8.170).

**2020-06-19 Predrag** Eduardo Fradkin [64] *Field Theories of Condensed Matter Physics*, discusses on p. 336 the quantum partition function of the dimer model which is given by the classical partition function of a discrete Gaussian model in three Euclidean dimensions on a cubic lattice. See also p. 332, 345 and 354. Not sure how to connect it to our work.

Shankar [138] *Quantum Field Theory and Condensed Matter* defines the Gaussian model in Eqs. (13.2), (6.219); sect 11.1 *The renormalization group: first pass*;

Marino [115] *Quantum Field Theory Approach to Condensed Matter Physics* (see 5.2 *Gaussian Functional Integrals*) does not seem to refer to the Gaussian model.

Chaikin and Lubensky [32] *Principles of Condensed Matter Physics* see 5.3 *Gaussian integrals*, 5.8.3 *Gaussian model*

*Lattice 89: Proceedings of the 1989 Symposium on Lattice Field Theory* edited by N. Cabbibo, E. Marinari, G. Parisi

**2020-09-06 Predrag** Kadanoff [94] on Gaussian model: sect. 3.4 *Lattice Green Function* and many more. The “coefficients matrix”  $C$  in Kadanoff eq. (3.9) is the inverse of our ‘propagator’  $\Delta$ .

A lattice with one field  $\phi_n$  for each site, then we can define a particularly simple and important problem by giving the coefficient matrix Kadanoff eq. (3.12)

$$C = \begin{pmatrix} 1 & -K & 0 & 0 & \dots & 0 & -K \\ -K & 1 & -K & 0 & \dots & 0 & 0 \\ 0 & -K & 1 & -K & \dots & 0 & 0 \\ \vdots & \vdots & \vdots & \vdots & \ddots & \vdots & \vdots \\ 0 & 0 & \dots & \dots & \dots & 1 & -K \\ -K & 0 & \dots & \dots & \dots & -K & 1 \end{pmatrix}. \quad (16.59)$$

The on-site interaction normalizes the Gaussian variables, for  $K = 0$  one gets the usual multi-dimensional Gaussian.  $-K$  is the nearest neighbor coupling strength, related to our case be  $-s \rightarrow 1$ , off-diagonal  $1 \rightarrow -K$ , so the conversion is  $s = -1/K$  (I believe).

Fourier transform of the  $d$ -dimensional Green’s function Kadanoff eq. (3.19)

$$G(q) = \frac{1}{1 - 2K \sum_{j=1}^d \cos(2\pi k_j/\ell_j)}, \quad q_j = \quad (16.60)$$

Compare with (8.53) and our Fourier-transformed field for  $k$ th discrete  $d$ -dimensional Fourier component on  $\ell_1, \ell_2, \dots, \ell_d$  torus, no tilt,

$$\hat{\phi}_k = \frac{1}{ds - 2 \sum_{j=1}^d \cos(2\pi k_j/\ell_j)} \hat{m}_k, \quad (16.61)$$

where  $k = (k_1, k_2, \dots, k_d)$ , so

$$K = \frac{1}{ds}, \quad (16.62)$$

Kadanoff eq. (4.38) shows that the  $d$ -dimensional Gaussian model only makes sense when  $K$  is in the interval  $[-1/2d, 1/2d]$ , i.e., if  $|s| > 2$ . If  $|K|$  exceeds this limit (Kadanoff says “dragons live here”), the Gaussian integrals diverge at infinite  $q$ -values, and the whole problem stops making sense. When there is any qualitative change in behavior of a many particle system we say that it undergoes a phase transition. The Gaussian model does so at the two points  $K = \pm 1/2d$ .

I still have some (conceptual) sign problems, as Kadanoff shows that his allowed values  $K$  correspond to harmonic oscillator states. I would like that to correspond to  $|s| < 2$ . I also need to explain why spatiotemporal cat has grammar, while Gaussian model has no restrictions... Inconclusive.

**2023-07-08 Predrag** Grad student **Jeffrey Chang**: The Gaussian Model is solvable, because it isn't exactly an interacting model: if we change coordinates into the Fourier modes, then we can write the Hamiltonian as a sum over modes without any cross-terms. That is, if we write the energy as a sum over sites, then we have cross-terms because the sites interact with each other, but if we take the Fourier Transform, we can instead write the energy as a sum over non-interacting modes. In terms of normal modes, the Gaussian model is just a bunch of uncoupled harmonic oscillators.

He evaluates the partition function explicitly in thermal bath (that's how it gets to be non-trivial, unlike our free-field Klein-Gordon theory with mass  $\mu^2$ ). He has spring constant multiplying the Laplacian, so this is imaginary mass  $\mu$  version of our free-field, with oscillatory solutions.

**2023-07-08 Predrag** Frank Nielsen has a useful list of lattice quantities for **lattice Gaussians**. In particular, he says: “lattice Gaussians are discrete distributions with lattice sample spaces used in differential privacy, cryptography, etc. Lattice Gaussians maximize Shannon entropy for exponential family with cumulant function related to Riemann theta function.”

Riemann theta function might be of use to us, if we use integer periodic state symbols instead of site fields  $\phi_z$ . **Mathworld** says: Let the imaginary part of a  $[g \times g]$  matrix  $F$  be positive definite, and  $m = (m_1, \dots, m_g)$  be a row vector with coefficients in  $\mathbb{Z}$ . Then the Riemann theta function is defined by

$$\theta(u|F) = \sum_{(m)} \exp[2\pi i(m^\top u + \frac{1}{2}m^\top Fm)]. \quad (16.63)$$

### 16.3 Tight-binding Hamiltonians

2017-09-11 Predrag Economou [53] *Green's Functions in Quantum Physics* ([click here](#)) contains a vast amount of useful information. Lattice shows up in chap. 5 *Green's Functions for tight-binding Hamiltonians*. Extracted text:

"[...] the Green's functions for the so-called tight-binding Hamiltonian (TBH) are calculated. The TBH is of central importance for solid-state physics because it is the simplest example of wave propagation in periodic structures. It is also important for quantum physics in general because it is rich in physical phenomena (e.g., negative effective mass, creation of a bound state by a repulsive perturbation) and, at the same time, simple in its mathematical treatment. Thus one can derive simple, exact expressions for scattering cross sections and for bound and resonance levels. The multiple scattering formalism is presented within the framework of the TBH and applied to questions related to the behavior of disordered systems (such as amorphous semiconductors)."

He studies the Green's functions associated with a class of periodic Hamiltonians, i.e., Hamiltonians remaining invariant under a translation by any vector on a regular  $d$ -dimensional lattice.

He also considers the more general case where the lattice can be divided into two interpenetrating sublattices such that each point of sublattice 1 is surrounded by points belonging to sublattice 2; the Hamiltonian remains invariant under translation by vectors of sublattice 1 or sublattice 2.

Periodic Hamiltonians are mathematically equivalent to a system of coupled 1-d harmonic oscillators and, as a result, they describe (by direct generalization to 3-d) the ionic motions in a crystalline solid.

In this approach one views the solids as being made up of atoms brought together from an infinite relative distance. It is then natural (following the usual practice for molecules) to try to express the unknown electronic wave functions as linear combinations of atomic orbitals (LCAO). The simplest version of this approach considers only one atom per primitive crystal cell, only one atomic orbital per atom, nearest-neighbor coupling only, and orthonormality of the atomic orbitals. This oversimplified version of the LCAO is known as the tight-binding model (TBM); the atomic orbital associated with the atom located at site  $\ell$  is symbolized by

$$w(r - \ell) = \langle r | \ell \rangle. \quad (16.64)$$

The matrix elements of the Hamiltonian within this subspace are

$$H = \sum_{\ell} |\ell\rangle \epsilon_{\ell} \langle \ell| + \sum_{\ell m} |\ell\rangle V_{\ell m} \langle m|. \quad (16.65)$$

The diagonal matrix elements are denoted by  $\epsilon_{\ell}$  and the off-diagonal matrix elements by  $V_{\ell m}$  ( $V_{\ell\ell} = 0$ ). The periodicity of the Hamiltonian, i.e., its invariance under translations by a lattice vector  $\ell$ , implies that

$$\epsilon_{\ell} = \epsilon_0 \quad (16.66)$$



$$V_{\ell m} = V_{\ell-m}. \quad (16.67)$$

For the sake of simplicity one assumes that

$$V_{\ell m} = \begin{cases} V & \text{if } \ell, m \text{ nearest neighbors} \\ 0 & \text{otherwise} \end{cases}. \quad (16.68)$$

There is only one quantity,  $V$ , which, following the usual practice in the literature, can be taken as negative (for s-like orbitals  $V$  is indeed negative).

$$H = \begin{pmatrix} \epsilon_0 & V & 0 & 0 & \dots & 0 & V \\ V & \epsilon_0 & V & 0 & \dots & 0 & 0 \\ 0 & V & \epsilon_0 & V & \dots & 0 & 0 \\ \vdots & \vdots & \vdots & \vdots & \ddots & \vdots & \vdots \\ 0 & 0 & \dots & \dots & \dots & \epsilon_0 & V \\ V & 0 & \dots & \dots & \dots & V & \epsilon_0 \end{pmatrix}. \quad (16.69)$$

A negative  $V$ , in contrast to a positive  $V$ , preserves the well-known property that as the energy of real eigenfunctions increases so does the number of their sign alternation.

The first term on the rhs of (16.65) describes a particle that can be trapped around any particular lattice site  $\ell$  with an eigenenergy  $\epsilon_\ell$ . The second term allows the particle to hop from site  $\ell$  to site  $m$  with a transfer matrix element  $V_{\ell m}$ . The quantum motion associated with the Hamiltonian (16.65) is equivalent to the wave motion of the coupled pendula, see figure 16.3.

$$\left( m_i \omega_i^2 + \sum_j \kappa_{ij} - m_i \omega^2 \right) u_i - \sum_j \kappa_{ij} u_j = 0. \quad (16.70)$$

where  $u_i$  is the 1-d displacement of the pendulum located at site  $i$ ,  $\omega_i$  is its eigenfrequency in the absence of coupling, and  $\sum_j \kappa_{ij}(u_i - u_j)$  is the force exercised on the pendulum at the  $i$  site as a result of the couplings with all the other pendula;  $m_i$  is the mass at  $i$ .

If we generalize to 3-d displacements, the problem of coupled pendula is reduced to that of the ionic (or atomic) motion in solids (by setting  $\omega_i = 0$ ) since each ion (or atom) is indeed performing small oscillations around its equilibrium position with the restoring force being equal to  $-\sum_j \kappa_{ij}(u_i - u_j)$ . This yields the electronic eigenfunctions and eigenenergies of the TBM. The eigenmodes are propagating waves such that the amplitude at each site is the same and the phase changes in a regular way. For a 2-d square lattice

$$E(\mathbf{k}) = \epsilon_0 + 2V[\cos(k_1 a) + \cos(k_2 a)], \quad (16.71)$$

where  $a$  is the lattice constant. In the 1d case, the function  $E(\mathbf{k})$  has an absolute maximum (which corresponds to the upper band edge) for  $k = \pi/a$  or  $-\pi/a$  with a value  $E_{max} = \epsilon_0 + 2|V|$ ; it has an absolute minimum (which corresponds

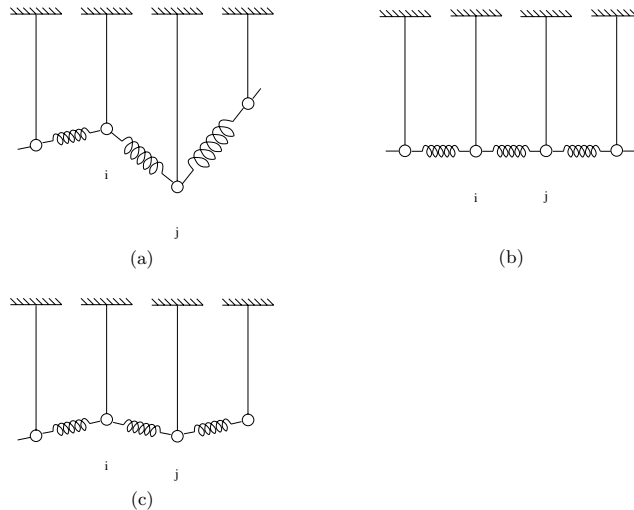


Figure 16.3: One-dimensional coupled pendulum analog of the tight-binding Hamiltonian, nearest-neighbor coupling (a). In the periodic case all pendula and all nearest-neighbor couplings are identical (b). The double spacing periodic case (c). (From Economou [53])

to a lower band edge) for  $k = 0$  with a value  $E_{min} = \epsilon_0 - 2|V|$ . Thus the spectrum is a continuum (a band) extending from  $\epsilon_0 - 2|V|$  to  $\epsilon_0 + 2|V|$ . The bandwidth is  $4|V|$ .

In his eq. (5.38) the diagonal matrix element of the square lattice Greens function is given by the complete elliptic integral of the first kind [79] (8.170).

**2020-10-04 Predrag** The reason I went above into detail with TBM is (1) it is spatiotemporal cat for  $s < 2$  and (2) has well known elliptic function solutions. According to (16.69), the precise formula relating  $\epsilon_0$  and  $V$  to spatiotemporal cat stretching factor  $s$  is

$$s = -\epsilon_0/V, \quad u_j \rightarrow u_j/\sqrt{-V}.$$

and the spectrum band extends from  $\epsilon_0/|V| - 2$  to  $\epsilon_0/|V| + 2$ , in other words, TBM assumes  $|s| < 2$ .

I assume the band structure for  $s < 2$  has no counterpart in the hyperbolic,  $s > 2$  case, but am not sure.

**2020-01-27 Predrag to Han** - For us there is no field  $\Phi(z)$  defined over continuum space  $z \in \mathbb{R}^d$ , only  $\phi_z$ . Our problems live on the integer lattices  $z \in \mathbb{Z}^d$ . This might be called 'tight-binding models'. Please verify whether that's what 'tight-binding models' are.

- 2020-01-13 Predrag** See Cserti [46] *Application of the lattice Green's function for calculating the resistance of an infinite network of resistors*, page 463, in particular the energy-dependent lattice Green's function of the tight-binding Hamiltonian for a square lattice, his eq. (30), with energy  $E$  playing the role of our stretching parameter  $s$ .
- 2020-01-13 Predrag** See also Cserti *et al.* [46, 47], in sect. 8.10 *Resistor networks*: The energy-dependent lattice Green's function of the tight-binding Hamiltonian for a square lattice, his eq. (30), has energy  $E$  playing the role of our stretching parameter  $s$ .
- 2019-07-13 Predrag** Kohler and Cubitt [105] *Translationally invariant universal classical Hamiltonians* give an explicit construction of a translationally invariant, 2D, nearest-neighbour, universal classical Hamiltonian with a single free parameter, drawing on techniques from theoretical computer science, in particular complexity-theoretic results on tiling problems. Seems too sophisticated for us.
- 2020-04-19 Predrag** See also chapter 13 *Chronotopic literature*, Politi, Torcini and Lepri [128] *Lyapunov exponents from node-counting arguments*: "That resembles the tight-binding approximation of the 1D Schrödinger equation (with imaginary time) in the presence of a random potential, i.e., the Anderson model."

## 16.4 Discrete Schrödinger equation

- 2020-12-06 Predrag** Marius Lemm, Arka Adhikari and Horng-Tzer Yau, *Global eigenvalue distribution of matrices defined by the skew-shift* [arXiv:1903.11514](https://arxiv.org/abs/1903.11514) study the following question:

*Suppose the entries of the large Hermitian matrices  $H_N$  are generated by sampling along the orbits of an ergodic dynamical system. Do their eigenvalues still exhibit random matrix statistics, like the Wigner semicircle law?*

We will answer this question in the affirmative for the model of  $H_N$  defined below, where the underlying dynamical system is generated from the skew-shift dynamics:

$$\begin{pmatrix} j \\ 2 \end{pmatrix} \omega + jy + x \pmod{1},$$

Here  $x, y \in \mathbb{T}$  (with  $\mathbb{T}$  being the torus) are the starting positions of the dynamical system and  $\omega \in \mathbb{T}$  is a (typically irrational) parameter called the frequency. The skew-shift dynamics possesses only weak ergodicity properties, e.g., it is not even weakly mixing. Nonetheless, it is believed

to behave in a quasi-random way (meaning like an i.i.d. sequence of random variables) in various ways reviewed at the end of the introduction. Moreover, the quasi-random behavior of the skew-shift should deviate from that of the more rigid standard shift  $j\omega + x \pmod 1$  (the circle rotation by an irrational angle  $\omega$ ). The key difference between the skew-shift and circle rotation is of course the appearance of a quadratic term  $j^2\omega$  for the skew-shift. This quadratic term has the effect of increasing the oscillations and thus improving the decay of the exponential sums over skew-shift orbits. This general fact is a central tenet of analytic number theory HL, Mont, W1, W2, and of our analysis here as well.

**The model.** Let  $\mathbb{T}$  be the one-dimensional torus, which we identify with  $[0, 1]$  in the usual way. For the skew-shift, the role of the “angle” is played by the frequency  $\omega \in [0, 1]$ . The skew-shift is then the transformation

$$T : \mathbb{T}^2 \rightarrow \mathbb{T}^2$$

$$(x, y) \mapsto (x + y, y + \omega).$$

We write  $T^j$  for the  $j$ -fold iteration of  $T$  and  $(T^j(x, y))_1$ , for the first component of the vector  $T^j(x, y) \in \mathbb{T}^2$ , i.e.,

$$(T^j(x, y))_1 = \binom{j}{2}\omega + jy + x. \tag{16.72}$$

We consider  $2N \times 2N$  Hermitian matrices of the form

$$H = \begin{pmatrix} 0 & X \\ X^* & 0 \end{pmatrix}$$

with  $X$  an  $[N \times N]$  matrix generated from the skew-shift via

$$X_{i,j} = \frac{1}{\sqrt{N}} e \left[ \left( \binom{j}{2} \omega_i + jy_i + x_i \right) \right], \quad e[t] := \exp(2\pi it) \tag{16.73}$$

Here the  $\omega_1, \dots, \omega_N$  are chosen deterministically (see the examples below), the  $y_1, \dots, y_N$  in (16.73) are sampled uniformly and independently from  $[0, 1]$ , and the  $x_1, \dots, x_N$  are arbitrary. (In particular, one can take  $x_1 = x_2 = \dots = x_N = 0$ .)

**Predrag: (16.73) is an  $[N \times N]$  matrix full of complex phases: it is unlike our 3-banded matrices, I think we can ignore these papers.**

Marius Lemm GaTech seminar 2020-04-09: “Global eigenvalue distribution of matrices defined by the skew-shift: A central question in ergodic theory is whether sequences obtained by sampling along the orbits of a given dynamical system behave similarly to sequences of i.i.d. random variables. Here we consider this question from a spectral-theoretic perspective. Specifically, we study large Hermitian matrices whose entries are defined by evaluating the exponential function along orbits of the skew-shift on the 2-torus with irrational frequency. We prove that their global

eigenvalue distribution converges to the Wigner semicircle law, a hallmark of random matrix statistics, which evidences the quasi-random nature of the skew-shift dynamics. ”

Kielstra and Lemm *On the finite-size Lyapunov exponent for the Schrödinger operator with skew-shift potential* [arXiv:1904.08871](https://arxiv.org/abs/1904.08871):

A one-dimensional quantum particle living on  $\mathbb{Z}$  with energy  $E \in \mathbb{R}$  is described by the discrete Schrödinger equation

$$\psi_{n+1} + \lambda v_n \psi_n + \psi_{n-1} = E\psi_n, \quad (16.74)$$

where  $\psi = (\psi_n)_{n \in \mathbb{Z}}$  is a sequence in  $\ell^2(\mathbb{Z}; \mathbb{C})$ . The real-valued potential sequence  $v = (v_n)_{n \in \mathbb{Z}}$  represents the environment that the particle is subjected to. (The “coupling constant”  $\lambda > 0$  is factored out for convenience.) Physically, one observes a sudden onset of insulating behavior in the presence of a random environment (“Anderson localization”). Mathematically, it is known that for arbitrarily small  $\lambda > 0$ , the one-dimensional Schrödinger operator

$$(H\psi)_n = \psi_{n+1} + \lambda v_n \psi_n + \psi_{n-1}. \quad (16.75)$$

has pure point spectrum with exponentially decaying eigenfunctions [31, 108].

A natural follow-up question is then: How random does the environment have to localize the quantum particle? Alternative “quasi-random” environments are generated by sampling a nice function along the orbit of an ergodic dynamical system. This question is interesting from a purely mathematical ergodic theory perspective, but it also has practical implications, since computer simulations are mostly based on appropriate pseudo-random number sequences.

A standing conjecture in this direction concerns the case when the potential is generated from the nonlinear skew-shift dynamics  $T : \mathbb{T}^2 \rightarrow \mathbb{T}^2$ ,  $T(x, y) = (x + y, y + \omega)$ , namely it is of the form

$$v_n = 2 \cos \left( \binom{n}{2} \omega + ny + x \right) \quad (16.76)$$

with  $\omega$  irrational (say Diophantine). The key difference between (16.76) compared to  $v_n = 2 \cos(n\alpha + \theta)$  is the appearance of the nonlinear quadratic term  $n^2\omega$ . The conjecture states that the associated Schrödinger operator  $H$  defined by (16.75) is Anderson localized for arbitrarily small  $\lambda > 0$  everywhere in the spectrum. Partial results in this vein are due to Bourgain and Bourgain-Goldstein-Schlag. Note that the conjecture says in particular that the skew-shift dynamics is appreciably more random-like than the circle rotation where  $v_n = 2 \cos(n\alpha + \theta)$ . (Recall that the latter is only localized for  $\lambda > 1$ , for us  $s > 2$ .) The observation that the skew-shift is more quasi-random than the shift has been made in another context by

Rudnick-Sarnak-Zaharescu RSZ and others DR,MY,RS (concerning the spacing distribution) and also recently in ALY (concerning eigenvalues of large Hermitian matrices).

**2020-12-06 Predrag** Possibly also of interest: Marius Lemm and David Sutter *Quantitative lower bounds on the Lyapunov exponent from multivariate matrix inequalities* [arXiv:2001.09115](https://arxiv.org/abs/2001.09115): The Lyapunov exponent characterizes the asymptotic behavior of long matrix products. Recognizing scenarios where the Lyapunov exponent is strictly positive is a fundamental challenge that is relevant in many applications. In this work we establish a novel tool for this task by deriving a quantitative lower bound on the Lyapunov exponent in terms of a matrix sum which is efficiently computable in ergodic situations. Our approach combines two deep results from matrix analysis — the  $n$ -matrix extension of the Golden-Thompson inequality and the Avalanche-Principle. We apply these bounds to the Lyapunov exponents of Schrödinger cocycles with certain ergodic potentials of polymer type and arbitrary correlation structure. We also derive related quantitative stability results for the Lyapunov exponent near aligned diagonal matrices and a bound for almost-commuting matrices.

**2020-12-06 Predrag** Carmona, Klein and Martinelli [31] *Anderson localization for Bernoulli and other singular potentials*:

Bernoulli potentials are potentials that take only two values

$$\mu = p\delta(v - a) + (1 - p)\delta(v - b), \quad 0 < p < 1.$$

Kunz and Souillard [108] *Sur le spectre des opérateurs aux différences finies aléatoires* is presumably similar - models for Anderson localization, we do not need them here.

**2022-04-17 Predrag** Oliver Knill and Folkert Tangerman [104] *Selfsimilarity and growth in Birkhoff sums for the golden rotation* [arXiv:1006.0285](https://arxiv.org/abs/1006.0285), and Oliver Knill *Birkhoff sum*. Check out their **3-term recurrences** in KAM (Kolmogorov-Arnold-Moser) problems, and Laplacian being degenerate.

"almost periodic discrete Schrödinger equations with cot potential which Barry Simon analyzed in the 80ties and called the **Maryland model**."

Predrag: The model is  $d$ -dimensional Laplacian  $(2d + 1)$ -term recurrence with almost periodic potential,  $V'(\phi_n) = \lambda \tan(\pi\alpha n + \theta)$ . What we call orbit Jacobian matrix Simon calls that the *Jacobi matrix* (= discrete Schrödinger operator)

A *Jacobi matrix* is a tridiagonal matrix with  $b_n$  on diagonal and  $a_n$  off

diagonal

$$\mathcal{J} = \begin{pmatrix} b_0 & a_0 & 0 & 0 & \dots & 0 & 0 \\ a_0 & b_1 & a_1 & 0 & \dots & 0 & 0 \\ 0 & a_1 & b_2 & a_2 & \dots & 0 & 0 \\ \vdots & \vdots & \vdots & \vdots & \ddots & \vdots & \vdots \\ 0 & 0 & \dots & \dots & \dots & b_{n-2} & a_{n-2} \\ 0 & 0 & \dots & \dots & \dots & a_{n-2} & b_{n-1} \end{pmatrix} \quad (16.77)$$

$\{a_j, b_j\}_{j=0}^{\infty}$  are Jacobi parameters, where each  $a_j$  is strictly positive and each  $b_j$  is real (Predrag 2022-07-05 so the opposite of our orbit Jacobian matrix (4.110)).

A 1948 theorem by Jacobi states that every symmetric matrix is congruent to a tridiagonal matrix. References about the spectral theory of Jacobi operators can be found in Rowan Killip and Barry Simon *Sum rules for Jacobi matrices and their applications to spectral theory*.

If  $b_j = b$ , can take  $b = 0$ , since this is an additive constant for each eigenvalue.

One-dimensional discrete Schrödinger operator on  $\ell_2$ :

$$(H\phi)_n = \phi_{n+1} + \phi_{n-1} + V'(\phi_n)\phi_n, \quad (16.78)$$

a special case  $a_n = 1$  of Jacobi matrices,

$$(\mathcal{J}\phi)_n = a_{n+1}\phi_{n+1} + a_{n-1}\phi_{n-1} + b_n\phi_n, \quad (16.79)$$

## 16.5 Harper's model

**2020-12-06 Predrag** Kielstra and Lemm *On the finite-size Lyapunov exponent for the Schrödinger operator with skew-shift potential* [arXiv:1904.08871](#) write: "For example, one can consider  $v_n = 2 \cos(n\alpha + \theta)$  generated from sampling cosine along an irrational circle rotation; this is the Harper [72] or almost-Mathieu [142] model. It turns out that these linear underlying dynamics only produce localization for sufficiently strong potentials, namely only for  $\lambda > 1$  (for us,  $s > 2$ ) [92]."

Jitomirskaya [92] *Metal-insulator transition for the almost Mathieu operator*.

Svetlana Jitomirskaya, Lyuben Konstantinov and Igor Krasovskiy  
*On the spectrum of critical almost Mathieu operators in the rational case*  
[arXiv:2007.01005](#):

The Harper operator, a.k.a. the discrete magnetic Laplacian a tight-binding model of an electron confined to a 2D square lattice in a uniform magnetic field orthogonal to the lattice plane and with flux  $2\pi\alpha$  through an elementary cell. It acts on  $\ell^2(\mathbb{Z}^2)$  and is usually given in the Landau gauge representation

$$(H(\alpha)\psi)_{m,n} = \psi_{m,n-1} + \psi_{m,n+1} + e^{-i2\pi\alpha n}\psi_{m-1,n} + e^{i2\pi\alpha n}\psi_{m+1,n}, \quad (16.80)$$

first considered by Peierls [125], who noticed that it makes the Hamiltonian separable and turns it into the direct integral in  $\theta$  of operators on  $\ell^2(\mathbb{Z})$  given by:

$$(H_{\alpha,\theta} \phi)_n = \phi_{n-1} + 2 \cos 2\pi(\alpha n + \theta) \phi_n + \phi_{n+1}, \quad \alpha, \theta \in [0, 1). \quad (16.81)$$

In physics literature, it also appears under the names Harper's or the Azbel-Hofstadter model, with both names used also for the discrete magnetic Laplacian  $H(\alpha)$ . In mathematics, it is universally called the critical almost Mathieu operator [142]. In addition to importance in physics, this model is of special interest, being at the boundary of two reasonably well understood regimes: (almost) localization and (almost) reducibility, and not being amenable to methods of either side.

Simon [142] *Almost periodic Schrödinger operators: A review*  
 [...] one-dimensional Schrödinger equation,  $H = -d^2/dx^2 + V(x)$  with  $V(x)$  almost periodic and the discrete (= tight binding) analog, i.e., the doubly infinite Jacobi matrix

$$h_{ij} = \delta_{i,j+1} + V_i \delta_{ij} + \delta_{i,j-1} \quad (16.82)$$

with  $V_n$  almost periodic on the integers.

The *Chambers' formula* presents the dependence of the determinant of the almost Mathieu operator with  $\alpha = p/n$  restricted to the period  $n$  with Floquet boundary conditions, on the phase  $\theta$  and quasimomentum  $k$ . In the critical case it is given by

$$\det(\mathcal{J}_{\theta,k,n} - E) = \Delta(E) - 2(-1)^n (\cos(2\pi n\theta) + \cos(kn)), \quad (16.83)$$

where  $\ell \in \mathbb{Z}/n$ , and in our notation (16.81) is written as (2.95)

$$\phi_{\ell+1} - d_\ell \phi_\ell + \phi_{\ell-1} = -s_\ell, \quad (16.84)$$

with site-dependent stretching  $d_\ell$  (so not a Toeplitz matrix, compare with (11.7), (12.49), (12.120), (21.241), (21.250), (12.46))

$$\mathcal{J}_{\theta,k,n} := \begin{pmatrix} -d_0 & 1 & 0 & 0 & \cdots & 0 & 0 & e^{-ikn} \\ 1 & -d_1 & 1 & 0 & \cdots & 0 & 0 & 0 \\ 0 & 1 & -d_2 & 1 & \cdots & 0 & 0 & 0 \\ \vdots & \vdots & \vdots & \vdots & \ddots & \vdots & \vdots & \vdots \\ 0 & 0 & 0 & 0 & \cdots & 1 & -d_{n-2} & 1 \\ e^{ikn} & 0 & 0 & 0 & \cdots & 0 & 1 & -d_{n-1} \end{pmatrix}, \quad (16.85)$$

compare with the orbit Jacobian matrix  $\mathcal{J}$  (8.79). For Harper model, stretching  $d_\ell$  is given by

$$d_\ell(\theta) = -2 \cos(2\pi \frac{p}{n} \ell + \theta), \quad s(x) = x, \quad (16.86)$$

and the discriminant  $\Delta$  is independent of  $\theta$  and  $k$ . They obtain a formula of this type for  $\det(B_{\theta,k,\ell} - E)$ .



**2021-08-11 Predrag** I have -an experiment- sat  $2\phi_j = -d_j$ , temporal cat style in (24.333) and (4.206), just to see how we like that. The signs might be wrong, please recheck.

This also connects to the Harper’s model (16.84), tight-binding model (16.65), and one-dimensional Schrödinger operator (16.82), (16.28) and (16.75), where  $\lambda v_n = -d_n$ . “The real-valued potential sequence  $v = (v_n)_{n \in \mathbb{Z}}$  represents the environment that the particle is subjected to, with the “coupling constant”  $\lambda > 0$  is factored out for convenience.”

**2023-09-16 Predrag** Movassagh *et al.* *The Green’s Function for the Hückel (tight binding) model* (2014), [arXiv:1407.4780](https://arxiv.org/abs/1407.4780)

The Hückel or tight binding model was originally introduced to describe electron hopping on a one-dimensional chain or ring. It has come to serve as a ubiquitous model in solid state chemistry and physics [9]. Two typical forms of the Hückel matrix, for a linear chain of  $N$  atoms, and for a cycle of  $N$  atoms, are given. The resulting banded matrix is isomorphic to the vertex adjacency matrix of a graph.

I find formulas for the determinant of the periodic primitive cell Hückel matrix, Lemma 2. on p. 5 interesting. Are they connected to my Laplacian eigenvalues calculation?

**2020-12-06 Predrag** For  $\alpha \in \mathbb{Z}$  this is a Helmholtz problem with stretching parameter  $s = 2 \cos 2\pi(\theta)$ .

For rational  $\alpha$  has periodic  $s$  [77], as in (16.86). Note the relative-periodic corner phases  $e^{\pm ikq}$  in (16.85)).

Hofstadter [77] *Energy levels and wave functions of Bloch electrons in rational and irrational magnetic fields* writes about rational case: “Algebra reveals the fact that this condition on  $\alpha$  is precisely that of rationality: We now proceed, making full use of this somewhat bizarre ansatz. ”

He, as everybody else, sooner or later, rewrites (16.84) in the “Percival-Vivaldi’ ‘two-configuration representation’ [126] matrix  $J$  (2.5),

$$\begin{pmatrix} \Delta\phi_t \\ \Delta\phi_{t+1} \end{pmatrix} = \begin{pmatrix} 0 & 1 \\ -1 & d_t \end{pmatrix} \begin{pmatrix} \Delta\phi_{t-1} \\ \Delta\phi_t \end{pmatrix}. \quad (16.87)$$

(note ‘upside-down’ 2D vector), and concerns himself with the rational, energy  $\text{tr } J^m < 2$ , oscillatory case.

Note, it’s only about the order of recurrence, nobody says the systems should be Hamiltonian / Lagrangian, works for dissipative systems as well.

The famed butterfly is a plot of the eigenvalues for all rational phases  $\alpha$ .

**2020-12-06 Predrag** I am looking at (16.81) because this is a different way to introduce a nonlinearity than the Hénon CML (13.4) because for irrational

$\alpha$  it has a quadratic dependence on the lattice site,

$$2 \cos(2\pi\alpha n) = 2 - (2\pi\alpha n)^2 + \dots$$

Nevertheless, this discrete Schrödinger is very different from temporal cat, so one more Sunday has been wasted (?) on learning other stuff.

**2021-06-25 Indubala Satija** *Geometry, Number Theory and the Butterfly Spectrum of Two-Dimensional Bloch Electrons* [arXiv:2106.1387](#):

We take a deeper dive into the geometry and the number theory that underlay the butterfly graphs of the Harper and the generalized Harper models of Bloch electrons in a magnetic field. Root of the number theoretical characteristics of the fractal spectrum is traced to a close relationship between the Farey tree – the hierarchical tree that generates all rationals and the Wannier diagram – a graph that labels all the gaps of the butterfly graph. The resulting Farey-Wannier hierarchical lattice of trapezoids provides geometrical representation of the nested pattern of butterflies in the butterfly graph. Some features of the energy spectrum such as absence of some of the Wannier trajectories in the butterfly graph fall outside the number theoretical framework, can be stated as a simple rule of "minimal violation of mirror symmetry". In a generalized Harper model, Farey-Wannier representation prevails as the lattice regroups to form some hexagonal unit cells creating new *species* of butterflies.

## 16.6 The sine-Gordon equation

Sine-Gordon, starting out as a cousin of the nonlinear pendulum, is much older than Klein-Gordon. It reappeared as the Frenkel-Kontorova model in 1939, and later as the Chirikov standard map.

The sine-Gordon equation might be of interest to us as a motivation for 'compact boson' theories. Here  $2\pi$  compactification of the field is built in from the start.

Most references [17], however, start with Villain action [156].

**2023-10-28 Predrag** The sine-Gordon Lagrangian [43] (see wiki)

$$\mathcal{L} = \frac{1}{2} \partial_\mu \phi \partial^\mu \phi - \frac{\mu^2}{\beta^2} (1 - \cos \beta \phi) \quad , \quad \phi \sim \phi + 2\pi/\beta. \quad (16.88)$$

is "the sophomore but unfortunately standard name for the theory of a single scalar field in one space and one time dimension. [...] We can gain some rough insight into the physical meaning of these parameters if, in the classical theory, we expand about the configuration of minimum energy ( $\phi = 0$ ).  $\mu^2$  is the "squared mass" (actually, since we are discussing a classical theory, squared inverse wavelength) associated with the spectrum of small oscillations about the minimum, and  $\beta$  is a parameter that measures the strength of the interactions between these small oscillations.

If  $\beta$  is less than  $8\pi$ , the theory is equivalent to the charge-zero sector of the massive Thirring model. This is a surprise, since the Thirring model is a canonical field theory whose Hamiltonian is expressed in terms of fundamental Fermi fields only.

In the special case  $\beta = 4\pi$ , the sine-Gordon equation describes the charge-zero sector of a free massive Dirac field theory. [...] The (massless) Thirring model is a theory of a single Dirac field in one space and one time dimension. [...]

I am indebted to [...] Konrad Osterwalder for reassuring me of my sanity. [...] Luther and I are in total agreement with Schroer on this point; we are also united in our embarrassment that we were incapable of reaching this conclusion unprompted. (Our offices are on the same corridor.) "

Noting  $1 - \cos \theta = 2 \sin^2(\theta/2)$ , and setting  $\beta = 2$  in (16.88), I get a suggestive -in terms of lattice momentum- form of sine-Gordon, for whatever that is worth:

$$\mathcal{L} = \frac{1}{2} \partial_\mu \phi \partial^\mu \phi - \frac{\mu^2}{2} \sin^2 \phi \quad , \quad \phi = \phi + \pi, \quad (16.89)$$

(see also free compact boson (16.120)).

**2023-10-28 Predrag Oliver Knill** (search for "Knill" in this blog) has a helpful overview over sine-Gordon, Frenkel-Kontorova, invertible Laplacians, coupled map lattices, discrete PDEs, Aubry anti-integrable limit (Bernoulli system in a Frenkel-Kontorova), almost Mathieu operators, mass gap, Dirac type solutions, Pesin positive entropy, in his [QuantumCalculus.org](https://www.quantumcalculus.org/). For Knill posts and videos, [see here](#).

## 16.7 Frenkel-Kontorova model

**2021-02-01 Predrag** The equilibria and relative equilibria of Frenkel-Kontorova models [10], widely studied in literature, might be closely related to temporal Hénon and  $\phi^4$  lattices.

It is difficult stuff, safely ignored, for now:)

Note the text below (12.17) and (16.90).

Search for **2019-12-12 Meisinger and Ogilvie** notes in this blog.

**2022-03-08 Predrag** It is difficult stuff, no more safely ignored :(

**2021-02-01 Anna Vainchtein** (U. Pittsburgh)

*Traveling waves in a driven Frenkel-Kontorova lattice:* Variants of Frenkel-Kontorova model, originally proposed to describe dislocations in crystal lattices, have been widely used to study a variety of physical phenomena, including dynamics of twin boundaries and domain walls, crystal

growth, charge-density waves, Josephson junctions and DNA denaturation. I discuss properties and stability of traveling waves in chains of Frenkel-Kontorova type driven by a constant external force. After reviewing some earlier studies for piecewise-smooth variants of the model, where exact and semi-analytical solutions can be constructed, I will describe numerical results for a fully nonlinear damped driven chain from a recent work with J. Cuevas-Maraver (U. of Sevilla), P. Kevrekidis (U. of Mass.) and H. Xu (Huazhong U.). In this setting, [traveling wave solutions are computed as fixed points of a nonlinear map](#). [...] Exploring the spectral stability of the obtained waveforms, we identify, at the level of numerical accuracy of our computations, a precise criterion for instability of the traveling wave solutions: monotonically decreasing portions of the kinetic curve always bear an unstable eigendirection.

The recorded talk will be available [here](#). It is a difficult subject, but our case - equilibria and relative equilibria is perhaps a trivial case described in this literature.

**2019-06-26 Predrag Mramor and Rink [122]** *Ghost circles in lattice Aubry-Mather theory*, [arXiv:1111.5963](#):

“Monotone lattice recurrence relations such as the Frenkel-Kontorova lattice, arise in Hamiltonian lattice mechanics as models for ferromagnetism and as discretization of elliptic PDEs. They are a multidimensional counterpart of monotone twist maps.”

The paper has an appendix of twist maps, refers to Mather and Forni [116] *Action minimizing orbits in Hamiltonian systems*. Example of exact symplectic twist maps are the Chirikov standard map and convex billiards. I think the focus in all this work is on *integrable*, not chaotic: “Under generic conditions, the Poincaré return map of a 2 degree of freedom Hamiltonian system near an elliptic equilibrium point is an exact symplectic twist map. In this case, the corresponding twist map is close to *integrable*, so that it allows for the application of various kinds of perturbation theory [116].” Lectures on *Equidistribution of periodic orbits: An overview of classical VS quantum results* by Degli Esposti, Graffi, and Isola in *Transition to Chaos in Classical and Quantum Mechanics* [16] are also of interest.

Twist maps often admit a variational structure, so that the solutions  $x : \mathbb{Z}^d \rightarrow \mathbb{R}$  are the stationary points of a formal action function  $W(x)$ . Given any rotation vector  $\omega \in \mathbb{R}^d$ , Aubry-Mather theory establishes the existence of a large collection of solutions of  $\nabla W(x) = 0$  of rotation vector  $\omega$ . For irrational  $\omega$ , this is the *Aubry-Mather set*. It consists of global minimizers and it may have gaps.

The part relevant to our spatiotemporal cat is the idea of studying globally stationary solutions by means of a formal gradient. We do not really know how to find all invariant 2-tori in 2 or more dimensions, even

though we know how to count them, right? They study the parabolic gradient flow  $\frac{dx}{dt} = -\nabla W(x)$  and prove that every Aubry-Mather set can be interpolated by a continuous gradient-flow invariant family, the so-called ‘ghost circle’. The existence of these ghost circles is known in dimension  $d = 1$ , for rational rotation vectors and Morse action functions.

**$d$ -dimensional Frenkel-Kontorova lattice:** Here, the goal is to find a  $d$ -dimensional “lattice configuration”  $x : \mathbb{Z}^d \rightarrow \mathbb{R}$  that satisfies

$$V'(x_i) - (\Delta x)_i = 0 \text{ for all } i \in \mathbb{Z}^d. \quad (16.90)$$

The smooth function  $V : \mathbb{R} \rightarrow \mathbb{R}$  satisfies  $V(\xi + 1) = V(\xi)$  for all  $\xi \in \mathbb{R}$ . It has the interpretation of a periodic onsite potential.

I like their definition of the discrete Laplace operator  $\Delta : \mathbb{R}^{\mathbb{Z}^d} \rightarrow \mathbb{R}^{\mathbb{Z}^d}$ , defined as

$$(\Delta x)_i := \frac{1}{2d} \sum_{\|j-i\|=1} (x_j - x_i) \text{ for all } i \in \mathbb{Z}^d. \quad (16.91)$$

where  $\|i\| := \sum_{k=1}^d |i_k|$ . Thus,  $(\Delta x)_i$  is the average of the quantity  $x_j - x_i$  computed over the lattice points that are nearest to that with index  $i$ , i.e., the graph Laplacian [37, 129] (16.22) for the case of hypercubic lattice, or the “central difference operator” [126].

One can think of (16.90) as a naive discretization of the nonlinear elliptic partial differential equation  $V'(u) - \Delta u = 0$  for a function  $u : \mathbb{R}^d \rightarrow \mathbb{R}$  and  $x_i = u(i)$ .

Eq. (16.90) is relevant for statistical mechanics, because it is related to the Frenkel-Kontorova Hamiltonian lattice differential equation

$$\frac{d^2 x_i}{dt^2} + V'(x_i) - (\Delta x)_i = 0 \text{ for all } i \in \mathbb{Z}^d. \quad (16.92)$$

This differential equation describes the motion of particles under the competing influence of an onsite periodic potential field and nearest neighbor attraction. Eq. (16.90) describes its stationary solutions.

In dimension  $d = 1$ , the solutions of equation (16.90) correspond to orbits of the Chirikov standard map  $T_V : \mathbb{A} \rightarrow \mathbb{A}$  of the annulus.

The Frenkel-Kontorova problem (16.90) is an example from a quite general class of lattice recurrence relations to which the results of this paper apply. These are recurrence relations for which there exists, for every  $j \in \mathbb{Z}^d$ , a real-valued “local potential” function  $S_j : \mathbb{R}^{\mathbb{Z}^d} \rightarrow \mathbb{R}$  so that the relation can be written in the form

$$\sum_{j \in \mathbb{Z}^d} \partial_i S_j(x) = 0 \text{ for all } i \in \mathbb{Z}^d. \quad (16.93)$$

It turns out that for the Frenkel-Kontorova problem (16.90), such local potentials exist and it is easy to check that they are given by

$$S_j(x) := V(x_j) + \frac{1}{8d} \sum_{\|k-j\|=1} (x_k - x_j)^2. \quad (16.94)$$

For the general problem (16.93), the functions  $S_j(x)$  will be required to satisfy some rather restrictive hypotheses. Physically, the most important of these hypotheses is the *monotonicity* condition. It is a discrete analogue of ellipticity for a PDE. Among the more technical hypotheses is one that guarantees that the sums in expression (16.93) are finite. For the purpose of this introduction, it probably suffices to say that the potentials (16.94) of Frenkel-Kontorova are prototypical for the  $S_j(x)$  that we have in mind. It is important to observe that the solutions of (16.93) are precisely the stationary points of the formal sum

$$W(x) := \sum_{j \in \mathbb{Z}^d} S_j(x). \quad (16.95)$$

This follows because differentiation of (16.95) with respect to  $x_i$  produces exactly equation (16.93) and it explains why solutions to (16.93) are sometimes called *stationary* configurations.

In the case that the periodic onsite potential  $V(\xi)$  vanishes, the Frenkel-Kontorova equation (16.90) reduces to the discrete Laplace equation  $\Delta x = 0$ , for which it is easy to point out solutions. For instance, when  $\xi \in \mathbb{R}$  is an arbitrary number and  $\omega \in \mathbb{R}^d$  is an arbitrary vector, then the linear functions  $x^{\omega, \xi} : \mathbb{Z}^d \rightarrow \mathbb{R}$  defined by

$$x_i^{\omega, \xi} := \xi + \langle \omega, i \rangle$$

obviously satisfy  $\Delta x = 0$ . It moreover turns out that the  $x^{\omega, \xi}$  are *action-minimizers*, in the sense that for every finite subset  $B \subset \mathbb{Z}^d$  and every  $y : \mathbb{Z}^d \rightarrow \mathbb{R}$  with support in  $B$ , it holds that

$$\sum_{j \in \mathbb{Z}^d} (S_j(x^{\omega, \xi} + y) - S_j(x^{\omega, \xi})) \geq 0.$$

Note that this sum is actually finite and can be interpreted as  $W(x^{\omega, \xi} + y) - W(x^{\omega, \xi})$ .

**Definition 16.1.** Let  $x : \mathbb{Z}^d \rightarrow \mathbb{R}$  be a  $d$ -dimensional configuration. We say that  $\omega \in \mathbb{R}^d$  is the *rotation vector* of  $x$  if for all  $i \in \mathbb{Z}^d$ , the limit

$$\lim_{n \rightarrow \infty} \frac{x_{ni}}{n} \text{ exists and is equal to } \langle \omega, i \rangle.$$

Clearly, the rotation vector of  $x^{\omega, \xi}$  is equal to  $\omega$ . On the other hand, in dimension  $d \neq 1$ , a solution to (16.90) does not necessarily have a rotation vector. An example is the hyperbolic configuration  $x^h$  defined by  $x_i^h = i_1 i_2 \cdots i_{d-1} i_d$  which solves  $\Delta x = 0$ .

**2022-04-17 Predrag** Oliver Knill and Folkert Tangerman [104] *Selfsimilarity and growth in Birkhoff sums for the golden rotation*, [arXiv:1006.0285](#), and Oliver Knill, *Birkhoff sum*. Check out their [3-term recurrences](#) in KAM (Kolmogorov-Arnold-Moser) problems, and Laplacian being degenerate.

His [Mathematica plots](#) might be useful templates for generating our figures.

**2022-04-17 Predrag** Sinai and Ulcigrai *A limit theorem for Birkhoff sums of non-integrable functions over rotations*, [arXiv:0710.1287](#) is a hard read.

**2022-04-17 Predrag** Oliver Knill and Folkert Tangerman [104] *Selfsimilarity and growth in Birkhoff sums for the golden rotation*, [arXiv:1006.0285](#): Critical KAM phenomena [103] lead us to the study of Birkhoff sums (4.121) for the function

$$a(x) = g(x) = \log(2 - 2 \cos(2\pi x)) = 2 \log |2 \sin(\pi x)| = 2 \log |1 - e^{2\pi i x}| \quad (16.96)$$

(see also (2.64)). with

$$a_j = g(j\alpha) = \log |2 - 2 \cos(2\pi j\alpha)|$$

at the golden mean rotation number  $\alpha = (\sqrt{5} - 1)/2$  with periodic approximants  $p_n/q_n$ .

We assume throughout this paper that  $\alpha$  is the golden mean  $\alpha = (\sqrt{5} - 1)/2$ . The dynamical system  $T(x) = x + \alpha \pmod{1}$  with this rotation number is the best understood and simplest aperiodic dynamical system.

Birkhoff's ergodic theorem  $A_k/k \rightarrow \int_0^1 g(x) dx$  relates Birkhoff averages  $A_k/k$  with the average of  $g$ . If  $g$  is continuous, this convergence is independent of the initial point if the dynamical system is an irrational rotation. If the mean  $\int g(x) dx = 0$ , one can ask how fast  $A_k$  grows. In the case of rigid rotation, the answer depends on the regularity of  $g$  and arithmetic properties of the rotation number. In the case of an irrational rotation we have  $A_k = O(1)$  for Diophantine  $\alpha$  and real analytic  $g$ . For functions  $g$  of bounded variation, Denjoy-Koksma theory allows estimates  $A_k = O(k^r)$  for  $0 \leq r < 1$  and of the form  $A_k = O(\log(k))$  for  $\alpha$  of constant type. There are also lower bounds on the growth rate: Herman, using it as a tool for higher dimensional considerations, gave example of Birkhoff sums, where  $\limsup A_k \geq \sqrt{k}$ . Bièvre and Forni have for any  $\epsilon > 0$  examples which achieve  $\limsup A_k \geq k^{1-\epsilon}$ . We look here at an  $L^1$ -integrable case of unbounded variation.

Hecke	$g(x) = [x] = x - [x]$	hecke1922 1921
Hardy-Littlewood	$g(x) = \sin(x)^{-1}$	HL 1928
Bryant-Reznick-Serbinowska	$g(x) = (-1)^{[x]}$	BS 2006
Sinai-Ulcigrai	$g(x) = 1/(1 - \exp(ix))$	[143] 2008
This paper	$g(x) = \log  1 - \exp(ix) $	2010

The authors were motivated by the study of

(1) determinants of truncated versions of the diagonalization of the linear operator,

$$h \rightarrow Lh = h(x + \alpha) + h(x - \alpha) - 2h \quad (16.97)$$

on  $L^2(\mathbb{T}^1)$ , where  $\mathbb{T}^1$  is the unit circle [103]. Perturbations of the operator  $L$  appear in the study of invariant circles in twist maps and the growth rate of determinants of truncated Fourier transformed matrices are used to estimate Green functions [24].

(2) the solution of the linear conjugacy relation:

$$m(\lambda z) + m(\lambda^{-1}z) - 2m(z) = zm(z) \quad (16.98)$$

where  $\lambda = e^{2\pi i\alpha}$  and  $m = \sum_{k=1}^{\infty} m_k z^k$  is a holomorphic function with  $m(0) = 0$ . (Perhaps related to formulations like Laurent monomials (8.119).) The coefficients  $m_k = e^{A_k}$  are positive. The logarithmic growth of the coefficients  $A_k$  shows that the power series for  $m$  is convergent in the interior of the unit disk. The distribution properties of the sequence  $A_k$  shows that this sequence does not converge at  $z = 1$ . It is not known if  $m$  has a meromorphic extension to the entire complex plane. Eq. (16.98) occurs in various KAM contexts, also as a first order solution occurring in the study of the boundary of KAM rings in conservative systems.

**4. Selfsimilarity in Hecke's example.** Birkhoff sums for bounded  $g$  have been studied first by number theorists like Hardy, Littlewood or Hecke. In the case of a golden rotation, there is a similar structure also but the story is different in that the limiting functions  $f$  and  $h$  are smooth. Their figure shows the Birkhoff sum in the situation studied by Hecke where  $g(x) = x - [x]$  is piecewise smooth. It is historically the first example studied for irrational rotation numbers. The functions  $f = \lim_n f_{2n}$  and  $h = \lim_n h_{2n}$  are explicitly known quadratic function in the case when the rotation number  $\alpha$  is the golden mean.

## 16.8 Mean field theory for the Ising model

According to E. Brézin and J. Zinn-Justin, finite-size mean field theory for the Ising model is described by the distribution

$$p_{\text{MFT}}(m) \propto \exp(-Nf(m)), \quad (16.99)$$

where  $N$  is the number of spins and the free energy (the large-deviation potential) at reduced temperature  $\tilde{t}$  is

$$f(m) = \frac{1}{2}\tilde{t}m^2 + \frac{1}{4!}m^4, \quad (16.100)$$

to leading order in  $N$ .



## 16.9 Clock model

The **free field solutions** of Potts models are most directly related to our dynamical considerations. If all states are allowed the underlying set of states is given by a full shift. If neighboring spins are only allowed in certain specific configurations, then the state space is given by a subshift of finite type. The partition function may then be written as a trace of the adjacency matrix, specifying which neighboring spin values are allowed.

The **wiki** says: The  $Z_N$  model, a generalization of the Ising model, sometimes known as the *clock model* or the *vector Potts model*, is defined by assigning a spin value at each node  $r$  on a graph, with the spins taking values  $S_r = \exp \frac{2\pi i q}{N}$ , where  $q \in \{0, 1, \dots, N-1\}$ . The spins therefore take values in the form of complex roots of unity. The spin assigned to each node of the  $Z_N$  model is pointing in any one of  $N$  directions. The Boltzmann weights for a general edge  $rr'$  are:

$$w(r, r') = \sum_{k=0}^{N-1} x_k^{(rr')} (S_r S_{r'}^*)^k$$

where  $*$  denotes complex conjugation and the  $x_k^{(rr')}$  are related to the interaction strength along the edge  $rr'$ . Note that  $x_k^{(rr')} = x_{N-k}^{(rr')}$  and  $x_0$  is often set to 1. The (real valued) Boltzmann weights are invariant under the transformations  $S_r \rightarrow \omega^k S_r$  and  $S_r \rightarrow S_r^*$ , the universal rotation and the reflection respectively.

The  $q$ -state clock model discretizes the rotor angle  $[0, 2\pi]$ , so that is not what we need; spatiotemporal cat has discrete winding numbers. It is  $X - Y$  model that has our  $s_n$  as vortex charges, and interactions between (mod 1) angles, except those are not the nearest neighbor, but logarithmic.

The local magnetic moment or “spin”, a 2D vector dimensionless vector of magnitude one,  $S_i = (\cos(2\pi qk), \sin(2\pi qk))$ , where  $k = 0, 1, \dots, q-1$ , at site  $i$  can point in any of the  $q$  directions in a given plane, with equal probability for all  $q$  values. The isotropic Hamiltonian for such a system can be written as:

$$H = -\frac{J}{2} \sum_{\langle ij \rangle} S_i \cdot S_j - B \cdot \sum_i S_i, \quad (16.101)$$

In the  $q$ -state clock model on each lattice point there is a vector spin pointing to  $q$  different directions, which differ by the angle  $2\pi/q$ . The 2D  $q$ -state clock model is defined by the Hamiltonian

$$H = -J \sum_{\langle ij \rangle} \cos(\theta_i - \theta_j) - h \sum_i \cos \theta_i, \quad (16.102)$$

where  $J$  is interaction strength, the summation is over the nearest neighbors,  $h$  is the applied weak magnetic field in units of  $J/\mu$ , where  $\mu$  is the magnetic moment of each spin usually set to 1, and  $\theta_i = 2\pi n_i/q$  with  $n_i = 0, \dots, q-1$ . Generalized Eq. (16.102) is of form

$$H = \sum_{\langle ij \rangle} V(\theta_i - \theta_j) - h \sum_i \cos \theta_i,$$

where the spin-interaction potential  $V$  has the  $Z_q$  symmetry. The Villain  $q$ -state clock model has

$$V(\phi) = -\frac{J}{\beta} \ln \left\{ \sum_{n=-\infty}^{\infty} \exp[-\beta(\phi - 2\pi n)^2/2] \right\},$$

where  $\beta \equiv 1/(k_B T)$  with the Boltzmann constant  $k_B$  and temperature  $T$ . This potential has been introduced to separate the vortex degrees of freedom from the spin-wave degrees of freedom as an approximate version of the  $XY$  model. The Villain clock model on the square lattice possesses self-duality.

The case  $q=2$  corresponds to the Ising model, the case  $q=3$  is a special case of the Potts model. Already for  $q=4$  the phase diagram is more complicated than for the Ising model: there are 3 phases, instead of 2.

Once the partition function is known, the thermodynamic observables, such as internal energy  $U$ , specific heat  $C$ , and entropy  $S$ , can be calculated by employing [123]:

$$U(T) = T^2 \frac{\partial}{\partial T} \ln Z(T, B). \quad (16.103)$$

$$C(T) = \frac{\partial U}{\partial T}, \quad (16.104)$$

$$S(T) = \frac{U}{T} + \ln Z(T, B). \quad (16.105)$$

The lattice average of the spin configuration, equivalent to the magnetization per site  $M$ , is given by

$$M = \frac{1}{N} \sum_j S_j. \quad (16.106)$$

They go on to compute the internal energy  $U$  and the specific heat  $C$ .

In all of the literature the focus is on Berezinskii-Kosterlitz-Thouless (BKT) transition, between a topological phase and the high-temperature paramagnetic (or disordered) phase, and phases possible for  $q > 5$ . If there is no continuous symmetry, existence of standard ferromagnetic order is allowed at low but finite temperature.

We are focused on the high-temperature paramagnetic (or disordered) phase.

**2019-12-12 Predrag** Jing Chen, Hai-Jun Liao, Hai-Dong Xie, Xing-Jie Han, Rui-Zhen Huang, Song Cheng, Zhong-Chao Wei, Zhi-Yuan Xie, and Tao Xiang, *Phase transition of the  $q$ -state clock model: duality and tensor renormalization*, [arXiv:1706.03455](https://arxiv.org/abs/1706.03455).

Now, memorize the authors:)

## 16.10 XY model

Restriction of the field  $\phi_t$  to the unit (or  $2\pi$ ) interval makes it a ‘compact boson’. There is a huge literature on temporal cat/spatiotemporal cat under the name ‘compact scalar’ or ‘compact boson’ (see also sect. 16.6).

The Villain [156]-type trick is to introduce a new field  $\varphi_z \in \mathbb{R}$  by inserting into the partition function an integrals over a periodic Dirac  $\delta$ -function (4.257) (a Poisson resummation?),

$$\delta(\varphi_z)_{circ} = \sum_{m_z \in \mathbb{Z}} e^{2\pi i m_z \varphi_z}.$$

**2023-10-28 Predrag Sulejmanpasic and Gatteringer [146] Abelian gauge theories on the lattice:  $\theta$ -terms and compact gauge theory with(out) monopoles, arXiv:1901.02637:**

The Villain-type discretization [156] of the XY model in  $d$ -dimensions is obtained by adding to the action

$$\sum_l \frac{\beta}{2} ((d\varphi)_l + 2\pi n_l)^2, \quad (16.107)$$

where the compact scalar field is represented by the pair  $\{\varphi_{\bar{s}} \in \mathbb{R}, n_{\bar{l}} \in \mathbb{Z}\}$

**2023-01-30 Predrag Tin Sulejmanpasic** has a bunch of potentially relevant ‘compact scalar’ papers. See also sect. 16.14.

Lucca Fazza and Tin Sulejmanpasic [59] *Lattice Quantum Villain Hamiltonians: Compact scalars, U(1) gauge theories, fracton models and Quantum Ising model dualities*, arXiv:2211.13047, have an operator (rather than mod 1 as in our temporal cat) that compactifies the field to a unit interval. Presumably one does not need quantum mechanics and commutators to implement such operator.

Consider a natural lattice discretization Hamiltonian of a free massless discrete scalar theory

$$H = \sum_x \left( \frac{1}{2Ja} \pi_x^2 + \frac{J}{2a} (\phi_{x+1} - \phi_x)^2 \right), \quad (16.108)$$

with  $[\phi_x, \pi_y] = i\delta_{xy}$ .  $J$  is dimensionless, while the lattice constant  $a$  is the only constant with dimension of length. We want  $\phi_x$  to be a *compact scalar*, i.e. that  $\phi_x \sim \phi_x + 2\pi$ . This is impossible with the Hamiltonian above, as shift of  $\phi_x$  by  $2\pi$  on distinct sites is not a symmetry. Instead we go to a Villain-type Hamiltonian

$$H = \sum_x \left( \frac{1}{2Ja} \pi_x^2 + \frac{J}{2a} (\phi_{x+1} - \phi_x + 2\pi n_x)^2 \right), \quad (16.109)$$

where  $n_x$  is an operator with only integer eigenvalues. To such an operator one naturally associates an angle-valued operator  $\tilde{\phi}_x$ , with canonical commutation relations

$$[\tilde{\phi}_x, n_y] = i\delta_{xy}. \quad (16.110)$$

Further we will assume that  $[n_x, \phi_y] = [n_x, \pi_y] = [\tilde{\phi}_x, \phi_y] = 0$ . The above implies that  $e^{i2\pi n_x} \tilde{\phi}_x e^{-i2\pi n_x} = \tilde{\phi}_x + 2\pi$ .

Predrag: there is an interesting self-duality (18.9) under  $J \leftrightarrow 1/J$ , read the paper.

**2020-08-06 Predrag** Sulejmanpasic [59] refers to it, I think we can ignore it: Yoneda [162] *Equivalence of the modified Villain formulation and the dual Hamiltonian method in the duality of the XY-plaquette model*, [arXiv:2211.01632](#).

**2025-01-16 Predrag** Have a look at Jacobson and Sulejmanpasic [90] *Modified Villain formulation of Abelian Chern-Simons theory* (2023). I have not read it.

**2019-12-22 Predrag** Peter N. Meisinger and Michael C. Ogilvie, *The Sign Problem, PT Symmetry and Abelian Lattice Duality*, [arXiv:1306.1495](#) (see also Meisinger and Ogilvie *The sign problem and Abelian lattice duality*, [arXiv:1311.5515](#)): The partition function of the two-dimensional XY model with an imaginary chemical potential term has the form

$$Z[K, \mu\delta_{\nu,2}] = \int_{S^1} [d\theta] \sum_{n_\nu} \exp \left[ -\frac{K}{2} \sum_{x,\nu} (\partial_\nu \theta(x) - i\mu\delta_{\nu,2} - 2\pi n_\nu(x))^2 \right].$$

Using the properties of the Villain action, we have

$$Z[K, \mu\delta_{\nu,2}] = \int_{S^1} [d\theta] \prod_{x,\nu} \sum_{p_\nu(x) \in Z} \frac{1}{\sqrt{2\pi K}} e^{-p_\nu^2(x)/2K} e^{ip_\nu(x)(\nabla_\nu \theta(x) - i\delta_{\nu,2}\mu)}.$$

[...] The partition function is now

$$Z = \sum_{\{m(X)\} \in Z} \frac{1}{\sqrt{2\pi K}} e^{-\sum_X [\sum_\nu (\nabla_\nu m(X))^2 / 2K + \mu \nabla_1 m(X)]}.$$

The final step is to introduce a new field  $\phi(x) \in R$  using a periodic  $\delta$ -function, effectively performing a Poisson resummation:

$$Z = \int_R [d\phi(X)] e^{-\sum_X [\sum_\nu (\nabla_\nu \phi(X))^2 / 2K + \mu \nabla_1 \phi(X)]} \sum_{\{m(X)\} \in Z} e^{2\pi i m(X) \phi(X)}.$$

If we keep only the  $m = 1$  contributions, we have a lattice sine-Gordon model

$$Z = \int_R [d\phi(X)] \exp \left[ -\sum_{X,\mu} \frac{1}{2K} (\nabla_\mu \phi(X))^2 - \sum_X \mu \nabla_1 \phi(X) + \sum_X 2y \cos(2\pi \phi(X)) \right]$$

with  $y = 1$ . This will be recognized as a two-dimensional lattice version of the Frenkel-Kontorova model, a sine-Gordon model with an additional

term proportional to  $\mu$ . For each fixed value of  $X_2$ , the term  $\sum_X \nabla_1 \phi(X)$  counts the number of kinks on that slice: The particles in the original representation manifest as lattice kinks in the dual representation.

The sign problem is explained clearly in Scott Lawrence, Yukari Yamauchi *Convex optimization of contour deformations* [arXiv:2311.13002](#).

**2020-06-15 Predrag** I do not even know what this is: Mazel, Stuhl and Suhov, *High-density hard-core model on  $\mathbb{Z}^2$  and norm equations in ring  $\mathbb{Z}[\sqrt{-1}]$* , [arXiv:1909.11648](#). They study the Gibbs statistics of high-density hard-core configurations on a unit square lattice  $\mathbb{Z}^2$ , for a general Euclidean exclusion distance  $D$ , with  $D^2 = a^2 + b^2$ ,  $a, b \in \mathbb{Z}$ . Pictorially, the problem is to study properties of configurations formed by non-overlapping ‘hard spheres’ of a given diameter (or exclusion distance)  $D$  with specified positions of the centers.

They say that a configuration  $\phi$  is periodic if there exist two linearly independent vectors  $e_1, e_2$  such that  $\phi(x) = \phi(x + e_1) = \phi(x + e_2)$ . If a periodic configuration  $\phi$  contains the origin, we say that  $\phi$  is a *sub-lattice*. The parallelogram with vertices  $0, e_1, e_2, e_1 + e_2$  is a *fundamental parallelogram* (FP) for  $\phi$ . We always assume that  $e_{1,2}$  are chosen so that the shorter diagonal of the FP divides it into two triangles with non-obtuse angles; one of these triangles, with a vertex at the origin, is referred to as a *fundamental triangle* (FT). They say that a sub-lattice is isosceles or non-isosceles if the FT is isosceles or not.

The term  $\mathbb{Z}^2$ -triangle means a triangle with vertices in  $\mathbb{Z}^2$ . Without loss of generality we will assume that one of the vertices is at the origin  $(0, 0)$ .

They say that a given value  $D$  exhibits *sliding* if exist two or more M-triangles  $T^{(1)}, T^{(2)}, \dots$ , with (i) a common side called a *sliding base*, with two common vertices, and (ii) distinct third vertices lying in the same half-plane relative to the shared side. Sliding leads to a multitude of periodic and non-periodic ground states characterized by layered or staggered patterns. The point is that under sliding there are countably many periodic and continuum of non-periodic ground states.

## 16.11 Rigid rotors model, dimer model

**2023-01-09 Predrag** Sushant Saryal and Deepak Dhar [[135](#)] *Exact results for interacting hard rigid rotors on a  $d$ -dimensional lattice*, [arXiv:2201.12866](#).

They study the entropy per site as a function of the dimensionless coupling parameter  $\ell/a$ , figure [16.4](#) (a).

Let the indicator function  $\eta(\mathbf{a}, \mathbf{b})$  be 1 if the rotors at sites  $\mathbf{a}$  and  $\mathbf{b}$ , with given orientations  $M(\mathbf{a})$  and  $M(\mathbf{b})$ , overlap, and zero otherwise. The

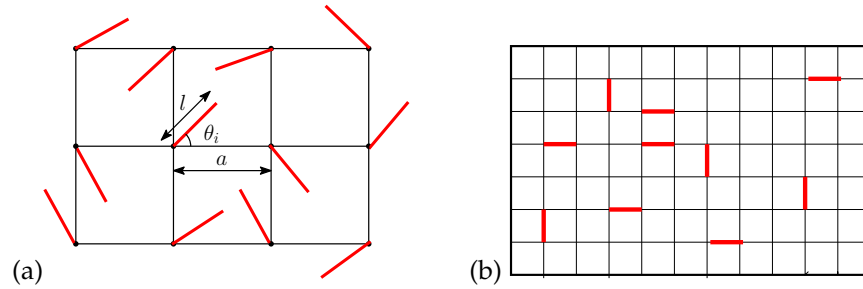


Figure 16.4: (a) Hard linear rods, pivoted at one end on a square lattice. Length of each rod is  $l$ , lattice spacing is  $a$ . The orientation of rotor at site  $i$  is given by the angle its long axis makes with the x-axis. (b) A typical term in the graphical expansion of the partition function (16.111) is a configuration of a set of dimers on the lattice.

partition function for this system is

$$\mathcal{Z}_N = \left[ \prod_{\mathbf{r}} \int dM(\mathbf{r}) \right] \prod_{\langle \mathbf{a}, \mathbf{b} \rangle} [1 - \eta(\mathbf{a}, \mathbf{b})], \quad (16.111)$$

where the second product is over all nearest neighbor pairs, and the integral over the matrix  $M(\mathbf{r})$  is the normalized Haar measure over the group  $SO(d)$ , so that  $\int dM(\mathbf{r}) 1 = 1$ . They only consider the case where rotors at sites farther than the nearest neighbors cannot overlap, so the second product is restricted to nearest neighbor pairs. The entropy per site  $s(\ell/a)$  is defined by

$$s(\ell/a) = \lim_{N \rightarrow \infty} [\log Z_N]/N, \quad (16.112)$$

where  $N$  is the number of sites in the lattice. If  $\ell/a < 1/2$ , then different rotors cannot overlap, and the entropy per rotor takes its maximum value, zero in this normalization. As the spacing  $a$  is decreased, keeping  $\ell$  constant, the entropy will also decrease. When  $a$  is decreased to the minimum allowed value, corresponding to closest packing, entropy per rotor will tend to  $-\infty$ .

Expand the product in (16.111), and make a graphical representation of the terms of the expansion, with a bond between vertices  $i$  and  $j$ , iff the term contains  $\eta(i, j)$ , see figure 16.4 (b). This is a lattice version of the Mayer cluster expansion. In the regime they study, only graphs with at most one bond coming to a site survive, so

$$\mathcal{Z}_N = \mathcal{Z}_{\text{dimers}}(z),$$

where  $\mathcal{Z}_{\text{dimers}}(z)$  is the grand partition function of partial covering of the vertices of the lattice by dimers (see figure 16.4 (b)),

$$\mathcal{Z}_{\text{dimers}}(z) = \sum_{\text{dimer-confgs}} z^{\text{number of dimers}},$$

with the fugacity of a dimer is the (negative ) real number, given by

$$z = - \int dM(\mathbf{i}) \int dM(\mathbf{j}) \eta(\mathbf{i}, \mathbf{j}). \quad (16.113)$$

This expression for  $z$  is the same as the second virial coefficient  $B_2$  of the virial expansion

$$P/(k_B T) = \rho + B_2 \rho^2 + B_3 \rho^3 + \dots$$

Let  $g(z)$  be the logarithm of the grand partition function per site,

$$g(z) = \lim_{N \rightarrow \infty} [\log \mathcal{Z}_{\text{dimers}}(z)]/N$$

Then, the entropy per site is  $s(\ell/a) = g(z)$ .

The equality of the dimer and rotor model partition functions holds also for finite lattices of size  $L_1 \times L_2 \times L_3 \dots$ . The dependence of these partition functions on one of the dimensions is of the form

$$\mathcal{Z} \sim \sum_{\alpha} c_{\alpha} \lambda_{\alpha}^{L_1},$$

where  $\lambda_{\alpha}$  are the eigenvalues of the transfer matrix in the direction 1, and  $c_{\alpha}$  are some constants. Since this is true for all  $L_1$ , we conclude that *all* the nonzero eigenvalues of the transfer matrix for the rotor model are the same as eigenvalues of the transfer matrix for the dimer model with activity  $z$ .

At this point my interest is dimming, but it might be revived by Dhar's Rutgers Seminar Wednesday, January 11, 2023.

**2023-01-31 Predrag** There is a huge literature on temporal cat/spatiotemporal cat relatives under the name 'compact scalar' or 'compact boson'. As far as I can tell, it starts with

De Angelis, De Martino and De Siena [51] *Reconstruction of Euclidean fields from plane rotator models* (1979)

but I still have to pinpoint where in the paper.

Possibly the story starts in 19th century, with sine-Gordon equation, see sect. 16.6.

I do not think we need the gauge theory as yet, only that the field is on a circle.

**2023-04-25 Predrag** Bricmont and Debacker-Mathot [26] *The Wegner approximation of the plane rotator model as a massless, free, lattice, Euclidean field*, (1977):

the classical plane rotator model is approximated by a lattice Gaussian spin model

Capitani [30] *Convergence of compact lattice scalar field theory to its continuum limit* (1991) is pretty clear; see the gaussian system generating functional of the correlation functions, the two-point Schwinger function in the first Brillouin zone (2.4) and the compactification of the field that follows. The theory of compact spins thus obtained is equivalent to a plane rotator model [26], and for small  $\beta$  is asymptotically equivalent to the usual lattice scalar theory

## 16.12 Many-body quantum chaos

**2016-01-12, 2023-04-04 PC** Engl, Dujardin, J. and Argüelles, A. and Schlagheck, P. and Richter Urbina [54] *Coherent backscattering in Fock space: A signature of quantum many-body interference in interacting bosonic systems*, (2014)

Engl, Plöss, Urbina, Richter [55] *The semiclassical propagator in fermionic Fock space* (2014)

Engl, Urbina, Hummel, Q. and Richter [56] *Complex scattering as canonical transformation: A semiclassical approach in Fock space* (2015)

Engl, Urbina, Richter [58] *The semiclassical propagator in Fock space: dynamical echo and many-body interference* (2016)

Engl, Urbina, Richter [57] *Periodic mean-field solutions and the spectra of discrete bosonic fields: Trace formula for Bose-Hubbard models* (2015)

Literature related to Klaus Richter - Engl et al. [54] *Coherent backscattering in Fock space: A signature of quantum many-body interference in interacting bosonic systems*; Engl et al. [56] *Boson sampling as canonical transformation: A semiclassical approach in Fock space*

Some of the stuff might already be in Richter [132] **book** *Semiclassical Theory of Mesoscopic Quantum Systems*.

Read Akila et al. [4] *Semiclassical identification of periodic orbits in a quantum many-body system*

**2022-05-09 Predrag** A new important paper for us to study: Klaus Richter, Juan Diego Urbina and Steven Tomsovic [133] *Semiclassical roots of universality in many-body quantum chaos* [arXiv:2205.02867](https://arxiv.org/abs/2205.02867).

**2022-05-09 Predrag** Akila, M. and Gutkin, B. and Braun, P. and Waltner, D. and Guhr [3] *Semiclassical prediction of large spectral fluctuations in interacting kicked spin chains* (2018)

Akila, Waltner, Gutkin and Guhr [5] *Particle-time duality in the kicked Ising spin chain* (2016)

Bertini, B. and Kos, P. and Prosen [18] *Exact spectral form factor in a minimal model of many-body quantum chaos* 2018

Bertini, B. and Kos, P. and Prosen [20] *Exact correlation functions for dual-unitary lattice models in 1+1 dimensions*, (2019)



Bertini, B. and Kos, P. and Prosen [19] *Entanglement spreading in a minimal model of maximal many-body quantum chaos* (2019)

Bertini, B. and Kos, P. and Prosen [21] *Operator entanglement in local quantum circuits i: Chaotic dual-unitary circuits*, (2020)

Fouxon, I. and Gutkin [63] *Local correlations in coupled cat maps with space-time duality* (2022)

Osipov, Krieger, Guhr and Gutkin *Local correlations in partially dual-unitary lattice models* (2024); [arXiv:2312.03445](https://arxiv.org/abs/2312.03445). Study sect. A. *Coupled cat maps*.

**2023-10-11 Predrag to Tomaž Prosen** Beautiful Rutgers seminar, both as the talk and as I happen to love these diagrams. I like going again over the old stuff –*repeticia est mater studiorum*– but alert me when you are going over the new stuff (or to online recording of such).

1. You mentioned that off the magic  $\pi/4$  you lose unitarity, as you get a projection operator, and that cannot be inverted. Attached work (the talk is presumably recorded) might be helpful, as the second best to unitarity. You can track the papers by having a look at [arXiv:2308.00747](https://arxiv.org/abs/2308.00747). As far as I can tell the defect and the  $1/2$  lattice arise from the Ising model being fermionic, but you'll know better.
2. Few comparisons to many-body folk (re Aizenman):  
We (GaTech group) always work ab initio on infinite spacetime, so there no thermodynamic limits to take. Your finite doubly periodic [LxT] rectangles (plus the relative- or screw-periodic primitive cells) are included in the partition function as contributions of multiply-periodic, infinite Bravais sublattices, what field theorists call 'sum over geometries'. We do not need noise. BTW, adding noise to evaluate things exactly reminds me of Cardy's recent Rutgers talk (it's on the seminar website).
3. Aizenman's transfer operators (your and Duisburg vertical and horizontal strips) are just one method of computing the rectangle primitive cell contribution to the partition sum. I believe that a better way is to evaluate it directly, globally, without transfer operators; that results seems to be a 2D lattice Green's function determinant as an elliptic integral, but I'm too uneducated to understand that - we have to compute the Brillouin zone bands integrals numerically anyway.
4. The 'sum over geometries' leads to the partition functions as sums over Euler 1741 pentagonal numbers, i.e. Dedekind eta function. If it rings any bells, alert me.

For more Dedekind, see sect. [19.2 Elliptic functions](#).

I have screen-shot some of Tomaž slides in [ChaosBook.org/library](https://ChaosBook.org/library), folder [Prosen23]. He credits [18] Akila, Waltner, Gutkin and Guhr [5] *Particle-time duality in the kicked Ising spin chain* (2016) with being first to note the

time-space self-duality of 2-dimensional square lattice partition sum, in unitary setting.

**2024-10-05 Predrag** Claeys and Lamacraft [38] *Maximum velocity quantum circuits* (2020); [arXiv:2003.01133](#).

Claeys and Lamacraft [39] *Operator dynamics and entanglement in space-time dual Hadamard lattices* (2024).

" Many-body quantum dynamics defined on a spatial lattice and in discrete time [...] evolving unitarily in space as well as in time, with space-time duality, has been shown to have a number of interesting features related to entanglement growth and correlations.

[...] operator dynamics in the case of Clifford cellular automata (Schlingemann et al 2008 J. Math. Phys. 49 112104) and in the  $q \rightarrow \infty$  limit to the classical spatiotemporal cat model of many body chaos (Gutkin et al. [71]). "

### 16.13 Lattice QED

Predrag would like to understand the 'compact boson' Villain trick. It's probably something simple that we already know: one introduces a new field by inserting into the partition function an integral over a periodic Dirac  $\delta$ -function. We are not using it in our spatiotemporal cat formulation, but much current lattice field theory literature does.

Lattice QED is currently not a part of Lan's PhD thesis, but might be a key to finally completing Predrag's [PhD thesis](#);)

**2023-10-28 Predrag** Berkowitz, Cherman and Jacobson [17] *Exact lattice chiral symmetry in 2d gauge theory*, [arXiv:2310.17539](#).

They integrate out a massless Dirac fermion in a Euclidean QFT

$$Z = \int \mathcal{D}\phi [\det \mathcal{D}(\phi)] e^{-S(\phi)} \tag{16.114}$$

where  $\mathcal{D}(\phi) = \gamma^\mu D_\mu(\phi)$  is the Dirac operator,  $\det \mathcal{D}(\phi)$  is given by (16.116), and  $\phi$  a set of bosonic fields with path integral measure  $\mathcal{D}\phi$ , and Euclidean action  $S(\phi)$ .

The det in (16.114) is upstairs and without a square root because the Grassmann-numbers integral is over fermions  $\bar{\psi} \cdots \psi$ , see [Field Theory eq. \(4.29\)](#).

[...] Domain-wall and overlap fermions satisfy the Ginsparg-Wilson relation  $\{\Gamma, \mathcal{D}\} = a\mathcal{D}\Gamma\mathcal{D}$ . They remove all of the undesired doubler modes at the cost of making both chiral symmetry transformations and the Dirac operator non-local at finite lattice spacing.

[...] Anomalies of locally-acting symmetries appear at finite lattice spacing [66, 146]. [...] lattice discretizations of Dirac fermions coupled to abelian gauge fields in  $d = 2$  which preserve the internal symmetries and anomalies *exactly*. [...] we discretize the resulting bosonic theory using a modified Villain action. [...] this works in 2d QED.

**The charge  $Q$  Schwinger model:** 2d QED with a massless Dirac fermion coupled to a  $U(1)$  gauge field  $a_\mu$  with electric charge  $Q \in \mathbb{Z}$ . [...] normalize  $a_\mu$  such that  $\frac{1}{4\pi} \int_M d^2x \epsilon^{\mu\nu} f_{\mu\nu} \in \mathbb{Z}$ , where  $f_{\mu\nu} = \partial_\mu a_\nu - \partial_\nu a_\mu$ , and write the action as

$$S = \int d^2x \left[ \frac{1}{4e^2} f_{\mu\nu} f^{\mu\nu} + \bar{\psi} \gamma^\mu (\partial_\mu - iQa_\mu) \psi \right]. \quad (16.115)$$

The Nielsen-Ninomiya theorem constrains discretizations of  $\mathcal{D}$ , but does not constrain  $\det \mathcal{D}$  [...] so they discretize  $\det \mathcal{D}$ . In  $d = 2$

$$\det \mathcal{D}(a_\mu) = \int \mathcal{D}\varphi \exp \left[ - \int d^2x \left( \frac{1}{8\pi} \partial_\mu \varphi \partial^\mu \varphi + \frac{iQ}{2\pi} \epsilon^{\mu\nu} a_\mu \partial_\nu \varphi \right) \right]. \quad (16.116)$$

[...]  $\varphi$  is a compact real scalar field (compact boson)

$$\varphi \equiv \varphi + 2\pi$$

and the mapping of the  $U(1)_V, U(1)_A$  currents is

$$\bar{\psi} \gamma^\mu \psi \leftrightarrow -\frac{1}{2\pi} \epsilon^{\mu\nu} \partial_\nu \varphi, \quad \bar{\psi} \gamma^\mu \gamma^5 \psi \leftrightarrow \frac{i}{4\pi} \partial_\mu \varphi.$$

[...] The spectrum in each degenerate discrete chiral vacuum consists of a single free massive scalar field, the Schwinger boson, with mass  $m_\gamma = eQ/\pi$ .

[...] Primitive cell  $[L \times L]$  Euclidean spacetime lattice with spacing  $a = 1$ , sites  $s$ , links  $\ell$ , and plaquettes  $p$ . [...] Following Villain [156], we represent the continuum  $U(1)$  gauge field  $a_\mu$  by a pair of lattice fields  $\{a_\ell \in \mathbb{R}, r_p \in \mathbb{Z}\}$  and the compact scalar field by the pair  $\{\varphi_{\bar{s}} \in \mathbb{R}, n_{\bar{\ell}} \in \mathbb{Z}\}$  on the dual lattice. [...] the modified [66, 146] Villain formulation (i.e., now applied also to gauge fields), and also introduce an auxiliary field  $\chi_s \in \mathbb{R}$  which can be viewed as the T-dual of  $\varphi_{\bar{s}}$ . [...] discretized  $N_f = 1$  QED action

$$S_{N_f=1} = \frac{\beta}{2} [(da)_p - 2\pi r_p]^2 + \frac{\kappa}{2} [(d\varphi)_{\bar{\ell}} - 2\pi n_{\bar{\ell}}]^2 - i\chi_s (dn)_{*s} + \frac{iQ}{2\pi} \varphi_{*p} [(da)_p - 2\pi r_p] - iQa_\ell n_{*\ell} \quad (16.117)$$

where  $d$  is the lattice exterior derivative  $(d\omega)_{c^{r+1}} = \sum_{c^r \in \partial c^{r+1}} \omega_{c^r}$  where  $c^r$  is an  $r$ -cell, so that, for example,  $(d\chi)_\ell = \chi_{s+\hat{\ell}} - \chi_s$ , and  $d^2 = 0$ . The

Hodge star  $\star$  maps an  $r$ -cell  $c^r$  on the lattice to the  $(d - r)$ -cell  $(\star c)^{d-r}$  on the dual lattice which pierces  $c^r$ .

The gauge redundancies of the lattice action (16.117) are

$$a_\ell \rightarrow a_\ell + (d\lambda)_\ell + 2\pi m_\ell, \quad r_p \rightarrow r_p + (dm)_p \quad (16.118a)$$

$$\varphi_{\bar{s}} \rightarrow \varphi_{\bar{s}} + 2\pi k_{\bar{s}}, \quad n_{\bar{\ell}} \rightarrow n_{\bar{\ell}} + (dk)_{\bar{\ell}} \quad (16.118b)$$

$$\chi_s \rightarrow \chi_s + Q\lambda_s + 2\pi h_s \quad (16.118c)$$

where  $\{\lambda_s \in \mathbb{R}, m_\ell, k_{\bar{s}}, h_s \in \mathbb{Z}\}$  are gauge parameters. They ensure that  $\{a, r\}$  and  $\{\chi, \varphi, n\}$  describe a  $U(1)$  gauge field and a  $2\pi$ -periodic boson with a conserved winding charge, with the topological properties one expects in the continuum.

[...] [...]

**2023-10-28 Predrag** The modified Villain formulation seems to have been introduced by Sulejmanpasic and Gattringer [146] *Abelian gauge theories on the lattice:  $\theta$ -terms and compact gauge theory with(out) monopoles*, [arXiv:1901.02637](#). For a Villain-type discretization of the  $XY$  model in  $d$ -dimensions, see (16.107).

Differential forms on the lattice are reviewed in Appendix A. Two useful facts are that  $\star^2 = (-1)^{r(d-r)}$  on an  $r$ -cell, and the identity  $\sum_{c^{r+1}} (dA)_{c^{r+1}} B_{\star c^{r+1}} = (-1)^{r+1} \sum_{c^r} A_{c^r} (dB)_{\star c^r}$ .

**2023-10-28 Predrag** Gorantla, Lam, Seiberg, and Shao [66] *A modified Villain formulation of fractons and other exotic theories*, [arXiv:2103.01257](#).

**2023-10-28 Predrag** Possibly more compact boson (?) papers of interest:

Christof Gattringer *Density of states techniques for fermion worldlines*, [arXiv:2211.15016](#).

Dominic Hirtler and Christof Gattringer *Massless Schwinger model with a 4-fermi interaction at topological angle  $\theta = \pi$* , [arXiv:2210.13787](#).

Mariia Anosova, Christof Gattringer, Nabil Iqbal, Tin Sulejmanpasic *Phase structure of self-dual lattice gauge theories in  $4d$* , [arXiv:2203.14774](#).

Mariia Anosova, Christof Gattringer, Tin Sulejmanpasic *Self-dual  $U(1)$  lattice field theory with a  $\theta$ -term*, [arXiv:2201.09468](#).

Christof Gattringer, Oliver Orasch *Density of states approach for lattice field theory with topological terms*, [arXiv:2111.09535](#): "A new density of states (DoS) approach to [...]  $U(1)$  lattice gauge theory in two dimensions [...] has an exact solution we may [...] establish the equivalence of the open boundary results with the periodic boundary conditions."

Tin Sulejmanpasic, Daniel Daniel Göschl, Christof Gattringer *First-principle simulations of  $1+1d$  quantum field theories at  $\theta = \pi$  and spin-chains*, [arXiv:2007.06323](#).

Christof Gattringer, Daniel Göschl, Pascal Törek *Exploring the worldline formulation of the Potts model*, [arXiv:1911.12728](#).

Gattringer and Törek *Topology and index theorem with a generalized Villain lattice action – a test in  $2d$* , [arXiv:1905.03963](#).

## 16.14 Seiberg lattice papers

**2020-06-11 Nathan Seiberg** Institute for Advanced Study talk: *Continuum Quantum Field Theories for Fractons*: “ Starting with a lattice system at short distances, its long-distance behavior is captured by a continuum Quantum Field Theory (QFT). This description is universal, i.e. it is independent of most of the details of the microscopic system. Surprisingly, certain recently discovered lattice systems, and in particular models of fractons, seem to violate this general dogma. We present exotic continuum QFTs that describe these systems. ”

I had a brief scan through

*Exotic Symmetries, Duality, and Fractons in 2+1-Dimensional Quantum Field Theory* [arXiv:2003.10466](https://arxiv.org/abs/2003.10466);

*Exotic U(1) Symmetries, Duality, and Fractons in 3+1-Dimensional Quantum Field Theory* [arXiv:2004.00015](https://arxiv.org/abs/2004.00015);

*Exotic  $Z_N$  Symmetries, Duality, and Fractons in 3+1-Dimensional Quantum Field Theory* [arXiv:2004.06115](https://arxiv.org/abs/2004.06115);

*More Exotic Field Theories in 3+1 Dimensions* [arXiv:2007.04904](https://arxiv.org/abs/2007.04904);

[www.scipost.org/SciPostPhys.9.5.073](https://www.scipost.org/SciPostPhys.9.5.073)

but I do not get them.

the 2 + 1-dimensional XY-plaquette model (winding dipole):

We study the system on a spatial lattice with  $L^x$  and  $L^y$  sites in the  $x$  and  $y$  directions and we use periodic boundary conditions. We label the sites by  $s = (\hat{x}, \hat{y})$ , with integer  $\hat{x} = 1, \dots, L^x$  and  $\hat{y} = 1, \dots, L^y$ . In the continuum limit, we use  $x = a\hat{x}$  and  $y = a\hat{y}$  to label the coordinates, and  $\ell^x = aL^x$  and  $\ell^y = aL^y$  to denote the physical size of the system.

The degrees of freedom are phase variable  $e^{i\phi_s}$ , so  $\phi_s \sim \phi_s + 2\pi$ . Their conjugate momenta  $\pi_s$  satisfy

$$[\phi_s, \pi_{s'}] = i\delta_{ss'}$$

The  $2\pi$ -periodicity of  $\phi_s$  implies that the eigenvalues of  $\pi_s$  are integers. The Hamiltonian is

$$H = \frac{u}{2} \sum_s (\pi_s)^2 - K \sum_s \cos(\Delta_{xy} \phi_s)$$

$$\Delta_{xy} \phi_{\hat{x}, \hat{y}} = \phi_{\hat{x}+1, \hat{y}+1} - \phi_{\hat{x}+1, \hat{y}} - \phi_{\hat{x}, \hat{y}+1} + \phi_{\hat{x}, \hat{y}}. \quad (16.119)$$

Predrag: too complicated. We are interested in  $(1+1)d$  compact scalar.

**2023-01-24 Nathan Seiberg** [Oxford Symmetry Seminar](#), with the video, no slides: *Symmetries and Anomalies in the Continuum and on the Lattice*, Seiberg and Cheng [arXiv:2211.12543](https://arxiv.org/abs/2211.12543).

It's all - almost all Hamiltonian and pretty ugly, wonder whether that's necessary, or just a habit. Seiberg is a field theorist, so Lagrangian formulation should feel natural? But it only enters in (16.120). This is an

80-page paper, and I've only grasped few things from it - currently we do not want to stray into QM, and 't Hooft anomalies.

The important contribuion here is the notion of an "emanant" global symmetry. It is not a symmetry of the UV theory, but unlike emergent (accidental) symmetries, it is not violated by any relevant or irrelevant operators in the IR theory. They discuss lattice models with anomalous lattice translation and relate them to an anomalous emanant symmetry in the IR theory. This connects to the Lieb-Schultz-Mattis theorem and to filling constraints like Luttinger theorem.

They discuss only anomalies in internal global symmetries. These anomalies involve coupling the system to classical background gauge fields for these symmetries, placing the system on a closed Euclidean spacetime, e.g., a torus, and studying the partition function. The anomaly is the statement that this partition function transforms with additional phase factors under gauge transformations of these background fields, and the phase factors cannot be removed by introducing local counterterms.

In quantum mechanics an anomaly means that the Hilbert space is in a projective representation of the internal symmetry group. A finite lattice system has a finite number of degrees of freedom and can be viewed as a particular quantum mechanical system.

$c = 1$  **free compact boson**

The theory is characterized by the free Lagrangian (see also (16.89))

$$\mathcal{L} = \frac{R^2}{4\pi} \partial_\mu \Phi \partial^\mu \Phi \quad , \quad \Phi \sim \Phi + 2\pi. \quad (16.120)$$

In the high-energy physics terminology, this means that the field is circle-valued, regardless of its action. This is to be contrasted with the notion of a compact field in the condensed-matter literature, which means that the lattice action does not preserve the winding symmetry.

### XY model

The Hamiltonian of the classical 2d XY model (sect. 16.10) can be thought of as an action for a 1+1d system in a discretized Euclidean time. Then, we can make time continuous and rotate to Lorentzian signature to find a Hamiltonian for a quantum 1+1d system. This Hamiltonian is known as the rotor model and it appears in various applications including a system of coupled Josephson junctions

$$H = \sum_{j=1}^L \left( \frac{U}{2} \pi_j^2 - J \cos(\Phi_{j+1} - \Phi_j) \right), \quad (16.121)$$

$$\Phi_j \sim \Phi_j + 2\pi,$$

$$[\Phi_j, \pi_{j'}] = i\delta_{j,j'}.$$

Yamada version [arXiv:2211.01632](https://arxiv.org/abs/2211.01632): the partition function of the lattice  $1 + 1d$  XY model:

$$Z(\beta_0, \beta_x) = \int \mathcal{D}\theta \exp \sum_{x, \tau} \left[ -\beta_0 (1 - \cos \nabla_\tau \theta) - \beta_x (1 - \cos \nabla_x \theta) \right],$$

$$\int \mathcal{D}\theta \equiv \prod_{\tau=0}^{N_\tau} \prod_{x=1}^{N_x} \int_{-\pi}^{\pi} \frac{d\theta(x, \tau)}{2\pi} \quad (16.122)$$

where  $\nabla_\tau \theta(x, \tau) \equiv \theta(x, \tau) - \theta(x, \tau - a)$  and  $\nabla_x \theta(x, \tau) \equiv \theta(x, \tau) - \theta(x - a, \tau)$  are the difference operators for the imaginary time and space components, respectively. The sums  $\sum_x \equiv \sum_{x=1}^{M_x}$  and  $\sum_\tau \equiv \sum_{\tau=1}^{M_\tau}$  are lattice summations of integral

$$\int_{-L/2}^{L/2} dx \text{ and } \int_0^\beta d\tau,$$

where  $\Delta\tau \equiv \tau_{\max}/M_\tau$ ,  $\tau_{\max}$ ,  $M_\tau$ ,  $M_x \equiv L/a$ ,  $L$ , and  $a$  are minimum imaginary time interval, the maximum imaginary time, the time division number, the space division number, the length of the  $x$ -space and the lattice spacing, respectively.  $\beta_0$  and  $\beta_x$  are the energies of the imaginary time  $\tau$  and the  $x$ -space component, respectively. In the  $\exp(\cos \theta)$  part of Eq. (16.122), Yamada introduces the ansatz as a periodic Gaussian approximation

$$e^{\alpha \cos \theta} \rightarrow R_v(\alpha) \sum_{n=-\infty}^{\infty} e^{-\frac{\beta_v(\alpha)}{2}(\theta - 2\pi n)^2}, \quad (16.123)$$

Predrag: For us, the crucial observation is that the coordinates  $\Phi_j$  are *circle valued*,  $\Phi_j \sim \Phi_j + 2\pi$  (a ‘compact scalar’? ‘compact boson’?), as in spatiotemporal cat, so their conjugate momenta  $\pi_j$  have integer eigenvalues.

The internal global symmetry of this system is  $O(2) = U(1) \times \mathbb{Z}_2^{\mathcal{R}}$ . Its  $U(1) \subset O(2)$  subgroup is generated by  $\sum_j \pi_j$  and the  $\mathbb{Z}_2^{\mathcal{R}}$  generator  $\mathcal{R}$  flips the signs of  $\Phi_j$  and  $\pi_j$ .

The rotor model with the Hamiltonian (16.121) is the standard lattice construction of the  $c = 1$  compact boson. The corresponding Euclidean spacetime lattice model is the famous XY model. The latter has a known Villain formulation, which uses a noncompact field  $\phi$  at the sites and a  $\mathbb{Z}$  gauge field  $n$  on the links. All these lattice models have only the  $U(1)_m \times \mathbb{Z}_2^{\mathcal{R}}$  symmetry.

They study a modified Villain model, with space one-dimensional lattice and time continuous. As in the Villain model, they start with a noncompact field at the sites  $\phi_j$ , and their conjugate momenta  $p_j$  at the sites. The

Hamiltonian is

$$H_{\text{matter}} = \sum_j \left( \frac{U_0}{2} p_j^2 + \frac{J_0}{2} (\phi_{j+1} - \phi_j)^2 \right) \quad (16.124)$$

$$[\phi_j, p_{j'}] = i\delta_{j,j'}.$$

This model is usually introduced in solid state physics as a simple model for phonons, where  $\phi_j$  is the displacement of an atom at site  $j$  from the lattice position.

The Hamiltonian is similar to that of the rotor model Hamiltonian (16.121), except that  $\phi_j$  is noncompact and the cosine potential is replaced by a harmonic potential. This model has an  $\mathbb{R}$  global shift symmetry:

$$\phi_j \rightarrow \phi_j + \xi, \quad \xi \in \mathbb{R}, \quad (16.125)$$

generated by  $\sum_j p_j$ . In addition there is a  $\mathbb{Z}_2^{\mathcal{R}}$  symmetry that flips the signs of all  $\phi_j$  and  $p_j$ .

They study a one-dimensional lattice with periodic boundary conditions. The sites are labeled by  $j = 1, 2, \dots, L$ . This system has a  $\mathbb{Z}_L$  translation symmetry generated by a shift by one lattice site  $T$  satisfying

$$T^L = 1. \quad (16.126)$$

We choose the convention that  $T$  acts on a local operator  $\mathcal{O}_j$  on a site  $j$  as

$$T\mathcal{O}_jT^{-1} = \mathcal{O}_{j+1}. \quad (16.127)$$

There can also be parity symmetry, extending it to  $\mathbb{D}_L$ . In addition, there is an internal symmetry group  $G$ . They assume that the full symmetry group  $\mathcal{G}$  factorizes as  $\mathcal{G} = G \times \mathbb{D}_L$ .

For a symmetry group to be on-site, we require that each symmetry transformation in the group is on-site, and they form a linear (rather than projective) representation for any system size.

They take the time direction to be Euclidean and compact (not discrete) and parameterize it by  $\tau \sim \tau + \beta$ . Then, the partition function is given in terms of the Hamiltonian  $H$  as

$$\mathcal{Z}(\beta, L) = \text{Tr} [e^{-\beta H}]. \quad (16.128)$$

**2024-11-09 Predrag** Understand what is "compact boson", possibly describe that in sect. 16.6? Is it mod 1 condition on the field?

I like referring to temporal systems like this:

"0+1d quantum mechanical systems"

Our spacetime is flat, either a plane  $\mathbb{R}^2$  or a two-torus  $\mathbb{T}^2$ . The signature can be either Lorentzian or Euclidean. We use  $x^i$  with  $i = 1, 2$  to denote the two spatial coordinates,  $x^0$  to denote Lorentzian time, and  $\tau$  for the Euclidean time.



## References

- [1] N. Abarenkova, J.-C. Anglès d’Auriac, S. Boukraa, S. Hassani, and J.-M. Maillard, “Rational dynamical zeta functions for birational transformations”, *Physica A* **264**, 264–293 (1999).
- [2] M. Aizenman, M. Laínz Valcázar, and S. Warzel, “Pfaffian correlation functions of planar dimer covers”, *J. Stat. Phys.* **166**, 1078–1091 (2017).
- [3] M. Akila, B. Gutkin, P. Braun, D. Waltner, and T. Guhr, “Semiclassical prediction of large spectral fluctuations in interacting kicked spin chains”, *Ann. Phys.* **389**, 250–282 (2018).
- [4] M. Akila, D. Waltner, B. Gutkin, P. Braun, and T. Guhr, “Semiclassical identification of periodic orbits in a quantum many-body system”, *Phys. Rev. Lett.* **118**, 164101 (2017).
- [5] M. Akila, D. Waltner, B. Gutkin, and T. Guhr, “Particle-time duality in the kicked Ising spin chain”, *J. Phys. A* **49**, 375101 (2016).
- [6] J.-C. Anglès d’Auriac, S. Boukraa, and J.-M. Maillard, “Functional relations in lattice statistical mechanics, enumerative combinatorics, and discrete dynamical systems”, *Ann. Comb.* **3**, 131–158 (1999).
- [7] F. Arrigo, P. Grindrod, D. J. Higham, and V. Noferini, “On the exponential generating function for non-backtracking walks”, *Linear Algebra Appl.* **556**, 381–399 (2018).
- [8] J. H. Asad, “Differential equation approach for one- and two-dimensional lattice green’s function”, *Mod. Phys. Lett. B* **21**, 139–154 (2007).
- [9] N. W. Ashcroft and N. D. Mermin, *Solid State Physics* (Holt, Rinehart and Winston, 1976).
- [10] S. Aubry and G. Abramovici, “Chaotic trajectories in the standard map. The concept of anti-integrability”, *Physica D* **43**, 199–219 (1990).
- [11] R. Band, J. M. Harrison, and C. H. Joyner, “Finite pseudo orbit expansions for spectral quantities of quantum graphs”, *J. Phys. A* **45**, 325204 (2012).
- [12] L. Bartholdi, “Zeta functions of graphs: a stroll through the garden, by Audrey Terras. book review”, *Bull. Amer. Math. Soc.* **51**, 177–185 (2014).
- [13] H. Bass, “The Ihara-Selberg zeta function of a tree lattice”, *Int. J. Math.* **3**, 717–797 (1992).
- [14] R. J. Baxter, “The bulk, surface and corner free energies of the square lattice Ising model”, *J. Phys. A* **50**, 014001 (2016).
- [15] E. Bedford and J. Diller, “Real and complex dynamics of a family of birational maps of the plane: The golden mean subshift”, *Amer. J. Math.* **127**, 595–646 (2005).
- [16] J. Bellissard, M. Degli Esposti, G. Forni, S. Graffi, S. Isola, and J. N. Mather, *Transition to Chaos in Classical and Quantum Mechanics* (Springer, Berlin, 1994).

- [17] E. Berkowitz, A. Cherman, and T. Jacobson, Exact lattice chiral symmetry in 2d gauge theory, 2023.
- [18] B. Bertini, P. Kos, and T. Prosen, “Exact spectral form factor in a minimal model of many-body quantum chaos”, *Phys. Rev. Lett.* **121**, 264101 (2018).
- [19] B. Bertini, P. Kos, and T. Prosen, “Entanglement spreading in a minimal model of maximal many-body quantum chaos”, *Phys. Rev. X* **9**, 021033 (2019).
- [20] B. Bertini, P. Kos, and T. Prosen, “Exact correlation functions for dual-unitary lattice models in 1+1 dimensions”, *Phys. Rev. Lett.* **123**, 210601 (2019).
- [21] B. Bertini, P. Kos, and T. Prosen, “Operator entanglement in local quantum circuits i: Chaotic dual-unitary circuits”, *SciPost Physics* **8**, 067 (2020).
- [22] J. Besag, “On a system of two-dimensional recurrence equations”, *J. R. Stat. Soc. B* **43**, 302–309 (1981).
- [23] H. S. Bhat and B. Osting, “Diffraction on the two-dimensional square lattice”, *SIAM J. Appl. Math.* **70**, 1389–1406 (2010).
- [24] J. Bourgain, *Green’s Function Estimates for Lattice Schrödinger Operators and Applications* (Princeton Univ. Press, Princeton NJ, 2005).
- [25] R. Bowen and O. Lanford, Zeta functions of restrictions of the shift transformation, in *Global Analysis (Proc. Sympos. Pure Math., Berkeley, CA, 1968)*, Vol. 1, edited by S.-S. Chern and S. Smale (1970), pp. 43–50.
- [26] J. Bricmont and F. Debacker-Mathot, “The Wegner approximation of the plane rotator model as a massless, free, lattice, Euclidean field”, *J. Math. Phys.* **18**, 37–40 (1977).
- [27] R. Bulirsch, “Numerical calculation of elliptic integrals and elliptic functions”, *Numer. Math.* **7**, 78–90 (1965).
- [28] S. R. Bulò, E. R. Hancock, F. Aziz, and M. Pelillo, “Efficient computation of Ihara coefficients using the Bell polynomial recursion”, *Linear Algebra Appl.* **436**, 1436–1441 (2012).
- [29] P. N. Burgoyne, “Remarks on the combinatorial approach to the Ising problem”, *J. Math. Phys.* **4**, 1320–1326 (1963).
- [30] S. Capitani, “Convergence of compact lattice scalar field theory to its continuum limit”, *J. Math. Phys.* **32**, 2880–2885 (1991).
- [31] R. Carmona, A. Klein, and F. Martinelli, “Anderson localization for Bernoulli and other singular potentials”, *Commun. Math. Phys.* **108**, 41–66 (1987).
- [32] P. M. Chaikin and T. C. Lubensky, *Principles of Condensed Matter Physics* (Cambridge Univ. Press, Cambridge UK, 1995).
- [33] M. Chertkov and V. Y. Chernyak, “Loop calculus in statistical physics and information science”, *Phys. Rev. E* **73**, 065102 (2006).

- [34] M. Chertkov, V. Y. Chernyak, and R. Teodorescu, “Belief propagation and loop series on planar graphs”, *J. Stat. Mech.* **2008**, P05003 (2008).
- [35] F. R. K. Chung, *Spectral Graph Theory* (American Math. Soc., 1996).
- [36] D. Cimasoni, “A generalized Kac-Ward formula”, *J. Stat. Mech.* **2010**, P07023 (2010).
- [37] D. Cimasoni, “The critical Ising model via Kac-Ward matrices”, *Commun. Math. Phys.* **316**, 99–126 (2012).
- [38] P. W. Claeys and A. Lamacraft, “Maximum velocity quantum circuits”, *Phys. Rev. Research* **2**, 033032 (2020).
- [39] P. W. Claeys and A. Lamacraft, “Operator dynamics and entanglement in space-time dual Hadamard lattices”, *J. Phys. A* **57**, 405301 (2024).
- [40] B. Clair, “The Ihara zeta function of the infinite grid”, *Electron. J. Combin.* **21**, P2–16 (2014).
- [41] B. Clair and S. Mokhtari-Sharghi, “Zeta functions of discrete groups acting on trees”, *J. Algebra* **237**, 591–620 (2001).
- [42] B. Clair and S. Mokhtari-Sharghi, “Convergence of zeta functions of graphs”, *Proc. Amer. Math. Soc.* **130**, 1881–1887 (2002).
- [43] S. Coleman, “Quantum sine-Gordon equation as the massive Thirring model”, *Phys. Rev. D* **11**, 2088–2097 (1975).
- [44] S. N. Coppersmith, L. P. Kadanoff, and Z. Zhang, “Reversible Boolean networks I: distribution of cycle lengths”, *Physica D* **149**, 11–29 (2001).
- [45] G. A. T. F. da Costa, “The Feynman identity for planar graphs”, *Lett. Math. Phys.* **106**, 1089–1107 (2016).
- [46] J. Cserti, “Application of the lattice Green’s function for calculating the resistance of an infinite network of resistors”, *Amer. J. Physics* **68**, 896–906 (2000).
- [47] J. Cserti, G. Széchenyi, and G. Dávid, “Uniform tiling with electrical resistors”, *J. Phys. A* **44**, 215201 (2011).
- [48] R. M. D’Souza and N. H. Margolus, “Thermodynamically reversible generalization of diffusion limited aggregation”, *Phys. Rev. E* **60**, 264–274 (1999).
- [49] J. Davey, A. Hanany, and J. Pasukonis, “On the classification of brane tilings”, *J. High Energy Phys.* **2010**, 078 (2010).
- [50] G. Davidoff, P. Sarnak, and A. Valette, *Elementary number theory, group theory and Ramanujan graphs* (Cambridge Univ. Press, Cambridge UK, 2001).
- [51] G. F. De Angelis, S. De Martino, and S. De Siena, “Reconstruction of Euclidean fields from plane rotator models”, *Phys. Rev. D* **20**, 451–455 (1979).

- [52] A. Deitmar, “Thara zeta functions of infinite weighted graphs”, *SIAM J. Discrete Math.* **29**, 2100–2116 (2015).
- [53] E. N. Economou, *Green’s Functions in Quantum Physics* (Springer, Berlin, 2006).
- [54] T. Engl, J. Dujardin, A. Argüelles, P. Schlagheck, K. Richter, and J. D. Urbina, “Coherent backscattering in Fock space: A signature of quantum many-body interference in interacting bosonic systems”, *Phys. Rev. Lett.* **112**, 140403 (2014).
- [55] T. Engl, P. Plöss, J. D. Urbina, and K. Richter, “The semiclassical propagator in fermionic Fock space”, *Theor. Chem. Acc.* **133**, 1563 (2014).
- [56] T. Engl, J. D. Urbina, Q. Hummel, and K. Richter, “Complex scattering as canonical transformation: A semiclassical approach in Fock space”, *Ann. Phys.* **527**, 737–747 (2015).
- [57] T. Engl, J. D. Urbina, and K. Richter, “Periodic mean-field solutions and the spectra of discrete bosonic fields: Trace formula for Bose-Hubbard models”, *Phys. Rev. E* **92**, 062907 (2015).
- [58] T. Engl, J. D. Urbina, and K. Richter, “The semiclassical propagator in Fock space: dynamical echo and many-body interference”, *Philos. Trans. Royal Soc. A* **374**, 20150159 (2016).
- [59] L. Fazza and T. Sulejmanpasic, “Lattice quantum Villain Hamiltonians: compact scalars, U(1) gauge theories, fracton models and quantum Ising model dualities”, *J. High Energy Phys.* **2023**, 17 (2023).
- [60] M. E. Fisher, “Statistical mechanics of dimers on a plane lattice”, *Phys. Rev.* **124**, 1664–1672 (1961).
- [61] M. E. Fisher, “On the dimer solution of planar Ising models”, *J. Math. Phys.* **7**, 1776–1781 (1966).
- [62] C. Fortuin and P. Kasteleyn, “On the random-cluster model: I. Introduction and relation to other models”, *Physica* **57**, 536–564 (1972).
- [63] I. Fouxon and B. Gutkin, “Local correlations in coupled cat maps with space-time duality”, *J. Phys. A* **55**, 504004 (2022).
- [64] E. Fradkin, *Field Theories of Condensed Matter Physics* (Cambridge Univ. Press, Cambridge UK, 2013).
- [65] C. Godsil and G. F. Royle, *Algebraic Graph Theory* (Springer, New York, 2013).
- [66] P. Gorantla, H. T. Lam, N. Seiberg, and S.-H. Shao, “A modified Villain formulation of fractons and other exotic theories”, *J. Math. Phys.* **62**, 102301 (2021).
- [67] J. Guckenheimer, “Axiom A + no cycles  $\Rightarrow \zeta_f(t)$  rational”, *Bull. Amer. Math. Soc.* **76**, 592–594 (1970).

- [68] D. Guido, T. Isola, and M. L. Lapidus, “Ihara zeta functions for periodic simple graphs”, in *C\*-algebras and Elliptic Theory II*, edited by D. Burghelea, R. Melrose, A. S. Mishchenko, and E. V. Troitsky (Birkhäuser, Basel, 2008), pp. 103–121.
- [69] D. Guido, T. Isola, and M. L. Lapidus, “Ihara’s zeta function for periodic graphs and its approximation in the amenable case”, *J. Funct. Analysis* **255**, 1339–1361 (2008).
- [70] D. Guido, T. Isola, and M. L. Lapidus, “A trace on fractal graphs and the Ihara zeta function”, *Trans. Amer. Math. Soc.* **361**, 3041–3041 (2009).
- [71] B. Gutkin, L. Han, R. Jafari, A. K. Saremi, and P. Cvitanović, “Linear encoding of the spatiotemporal cat map”, *Nonlinearity* **34**, 2800–2836 (2021).
- [72] P. G. Harper, “Single band motion of conduction electrons in a uniform magnetic field”, *Proc. Phys. Soc. London, Sect. A* **68**, 874–878 (1955).
- [73] K. Hashimoto, “Zeta functions of finite graphs and representations of p-adic groups”, *Adv. Stud. Pure Math.* **15**, 211–280 (1989).
- [74] Y. Higuchi, N. Konno, I. Sato, and E. Segawa, “A remark on zeta functions of finite graphs via quantum walks”, *Pacific J. Math. Industry* **6**, 1–8 (2014).
- [75] H. Hobrecht and F. Hucht, “Anisotropic scaling of the two-dimensional Ising model I: the torus”, *SciPost Phys.* **7**, 026 (2019).
- [76] H. Hobrecht and F. Hucht, “Anisotropic scaling of the two-dimensional Ising model II: surfaces and boundary fields”, *SciPost Phys.* **8**, 032 (2020).
- [77] D. R. Hofstadter, “Energy levels and wave functions of Bloch electrons in rational and irrational magnetic fields”, *Phys. Rev. B* **14**, 2239–2249 (1976).
- [78] T. Horiguchi, “Lattice Green’s function for the simple cubic lattice”, *J. Phys. Soc. Jpn.* **30**, 1261–1272 (1971).
- [79] T. Horiguchi, “Lattice Green’s functions for the triangular and honeycomb lattices”, *J. Math. Phys.* **13**, 1411–1419 (1972).
- [80] T. Horiguchi and T. Morita, “Note on the lattice Green’s function for the simple cubic lattice”, *J. Phys. C* **8**, L232 (1975).
- [81] M. D. Horton, “Ihara zeta functions of digraphs”, *Linear Algebra Appl.* **425**, 130–142 (2007).
- [82] A. Hucht, “The square lattice Ising model on the rectangle I: finite systems”, *J. Phys. A* **50**, 065201 (2017).
- [83] C. A. Hurst and H. S. Green, “New solution of the Ising problem for a rectangular lattice”, *J. Chem. Phys.* **33**, 1059–1062 (1960).
- [84] Y. Ihara, “On discrete subgroups of the two by two projective linear group over p-adic fields”, *J. Math. Soc. Japan* **18**, 219–235 (1966).

- [85] S. Isola, “ $\zeta$ -functions and distribution of periodic orbits of toral automorphisms”, *Europhys. Lett.* **11**, 517–522 (1990).
- [86] E. V. Ivashkevich, N. S. Izmailian, and C.-K. Hu, “Kronecker’s double series and exact asymptotic expansions for free models of statistical mechanics on torus”, *J. Phys. A* **35**, 5543–5561 (2002).
- [87] N. S. Izmailian, “Finite-size effects for anisotropic 2D Ising model with various boundary conditions”, *J. Phys. A* **45**, 494009 (2012).
- [88] N. S. Izmailian and C.-K. Hu, “Finite-size effects for the Ising model on helical tori”, *Phys. Rev. E* **76**, 041118 (2007).
- [89] N. S. Izmailian, K. B. Oganessian, and C.-K. Hu, “Exact finite-size corrections for the square-lattice Ising model with Brascamp-Kunz boundary conditions”, *Phys. Rev. E* **65**, 056132 (2002).
- [90] T. Jacobson and T. Sulejmanpasic, “Modified Villain formulation of Abelian Chern-Simons theory”, *Phys. Rev. D* **107**, 125017 (2023).
- [91] W. Janke and R. Kenna, “Finite-size scaling and corrections in the Ising model with Brascamp-Kunz boundary conditions”, *Phys. Rev. B* **65**, 064110 (2002).
- [92] S. Y. Jitomirskaya, “Metal-insulator transition for the almost Mathieu operator”, *Ann. of Math.* **150**, 1159–1175 (1999).
- [93] M. Kac and J. C. Ward, “A combinatorial solution of the two-dimensional Ising model”, *Phys. Rev.* **88**, 1332–1337 (1952).
- [94] L. P. Kadanoff, *Statistical Physics: Statics, Dynamics and Renormalization* (World Scientific, Singapore, 2000).
- [95] W. Kager, M. Lis, and R. Meester, “The signed loop approach to the Ising model: Foundations and critical point”, *J. Stat. Phys.* **152**, 353–387 (2013).
- [96] P. W. Kasteleyn, “The statistics of dimers on a lattice: I. The number of dimer arrangements on a quadratic lattice”, *Physica* **27**, 1209–1225 (1961).
- [97] P. W. Kasteleyn, “Dimer statistics and phase transitions”, *J. Math. Phys.* **4**, 287–293 (1963).
- [98] B. Kastening, “Simplified transfer matrix approach in the two-dimensional Ising model with various boundary conditions”, *Phys. Rev. E* **66**, 057103 (2002).
- [99] S. Katsura and S. Inawashiro, “Lattice Green’s functions for the rectangular and the square lattices at arbitrary points”, *J. Math. Phys.* **12**, 1622–1630 (1971).
- [100] S. Katsura, S. Inawashiro, and Y. Abe, “Lattice Green’s function for the simple cubic lattice in terms of a Mellin-Barnes type integral”, *J. Math. Phys.* **12**, 895–899 (1971).

- [101] B. Kaufman, “Crystal statistics. II. Partition function evaluated by spinor analysis”, *Phys. Rev.* **76**, 1232–1243 (1949).
- [102] K. Kirsten and F. L. Williams, *A Window Into Zeta and Modular Physics* (Cambridge Univ. Press, 2010).
- [103] O. Knill and J. Lesieutre, “Analytic continuation of Dirichlet series with almost periodic coefficients”, *Complex Anal. Oper. Th.* **6**, 237–255 (2010).
- [104] O. Knill and F. Tangerman, “Self-similarity and growth in Birkhoff sums for the golden rotation”, *Nonlinearity* **24**, 3115–3127 (2011).
- [105] T. Kohler and T. Cubitt, “Translationally invariant universal classical Hamiltonians”, *J. Stat. Phys.* **176**, 228–261 (2019).
- [106] E. L. Korotyaev and J. S. Møller, “Weighted estimates for the Laplacian on the cubic lattice”, *Ark. Matematik* **57**, 397–428 (2019).
- [107] M. Kotani and T. Sunada, “Zeta functions of finite graphs”, *J. Math. Sci. Univ. Tokyo* **7**, 7–25 (2000).
- [108] H. Kunz and B. Souillard, “Sur le spectre des opérateurs aux différences finies aléatoires”, *Commun. Math. Phys.* **78**, 201–246 (1980).
- [109] D. Lenz, F. Pogorzelski, and M. Schmidt, “The Ihara zeta function for infinite graphs”, *Trans. Amer. Math. Soc.* **371**, 5687–5729 (2018).
- [110] T. M. Liaw, M. C. Huang, Y. L. Chou, S. C. Lin, and F. Y. Li, “Partition functions and finite-size scalings of Ising model on helical tori”, *Phys. Rev. E* **73**, 041118 (2006).
- [111] D. A. Lind and B. Marcus, *An Introduction to Symbolic Dynamics and Coding* (Cambridge Univ. Press, Cambridge, 1995).
- [112] M. Lis, “A short proof of the Kac-Ward formula”, *Ann. Inst. H. Poincaré D* **3**, 45–53 (2016).
- [113] I. Lyberg, “Free energy of the anisotropic Ising lattice with Brascamp-Kunz boundary conditions”, *Phys. Rev. E* **87**, 062141 (2013).
- [114] A. Manning, “Axiom A diffeomorphisms have rational zeta function”, *Bull. London Math. Soc.* **3**, 215–220 (1971).
- [115] E. C. Marino, *Quantum Field Theory Approach to Condensed Matter Physics* (Cambridge Univ. Press, Cambridge UK, 2017).
- [116] J. N. Mather and G. Forni, “Action minimizing orbits in Hamiltonian systems”, in *Transition to Chaos in Classical and Quantum Mechanics*, edited by S. Graffi (Springer, Berlin, 1994), pp. 92–186.
- [117] B. M. McCoy and T. T. Wu, *The Two-Dimensional Ising Model*, 2nd ed. (Dover, 1973).
- [118] W. Michael, “Bound states of two spin waves in the Heisenberg ferromagnet”, *Phys. Rev.* **132**, 85–97 (1963).
- [119] H. Mizuno and I. Sato, “Zeta functions of digraphs”, *Linear Algebra Appl.* **336**, 181–190 (2001).

- [120] P. A. P. Moran, “A Gaussian Markovian process on a square lattice”, *J. Applied Prob.* **10**, 54–62 (1973).
- [121] T. Morita and T. Horiguchi, “Calculation of the lattice Green’s function for the bcc, fcc, and rectangular lattices”, *J. Math. Phys.* **12**, 986–992 (1971).
- [122] B. Mramor and B. Rink, “Ghost circles in lattice Aubry-Mather theory”, *J. Diff. Equ.* **252**, 3163–3208 (2012).
- [123] O. Negrete, P. Vargas, F. Peña, G. Saravia, and E. Vogel, “Entropy and mutability for the q-state clock model in small systems”, *Entropy* **20**, 933 (2018).
- [124] L. Onsager, “Crystal statistics. I. A Two-dimensional model with an order-disorder transition”, *Phys. Rev.* **65**, 117–149 (1944).
- [125] R. Peierls, “Zur Theorie des Diamagnetismus von Leitungselektronen”, *Z. Phys.* **80**, 763–791 (1933).
- [126] I. Percival and F. Vivaldi, “A linear code for the sawtooth and cat maps”, *Physica D* **27**, 373–386 (1987).
- [127] A. Poghosyan, N. Izmailian, and R. Kenna, “Exact solution of the critical Ising model with special toroidal boundary conditions”, *Phys. Rev. E* **96**, 062127 (2017).
- [128] A. Politi, A. Torcini, and S. Lepri, “Lyapunov exponents from node-counting arguments”, *J. Phys. IV* **8**, 263 (1998).
- [129] M. Pollicott, *Dynamical zeta functions*, in *Smooth Ergodic Theory and Its Applications*, Vol. 69, edited by A. Katok, R. de la Llave, Y. Pesin, and H. Weiss (2001), pp. 409–428.
- [130] P. Ren, T. Aleksić, D. Emms, R. C. Wilson, and E. R. Hancock, “Quantum walks, Ihara zeta functions and cospectrality in regular graphs”, *Quantum Inf. Process.* **10**, 405–417 (2010).
- [131] P. Ren, R. C. Wilson, and E. R. Hancock, “Graph characterization via Ihara coefficients”, *IEEE Trans. Neural Networks* **22**, 233–245 (2011).
- [132] K. Richter, *Semiclassical Theory of Mesoscopic Quantum Systems* (Springer, Berlin, 2000).
- [133] K. Richter, J. D. Urbina, and S. Tomsovic, “Semiclassical roots of universality in many-body quantum chaos”, *J. Phys. A* **55**, 453001 (2022).
- [134] S. Saito, “A proof of Terras’ conjecture on the radius of convergence of the Ihara zeta function”, *Discrete Math.* **341**, 990–996 (2018).
- [135] S. Saryal and D. Dhar, “Exact results for interacting hard rigid rotors on a  $d$ -dimensional lattice”, *J. Stat. Mech.* **2022**, 043204 (2022).
- [136] I. Sato, “Bartholdi zeta functions of group coverings of digraphs”, *Far East J. Math. Sci.* **18**, 321–339 (2005).
- [137] A. Setyadi and C. K. Storm, “Enumeration of graphs with the same Ihara zeta function”, *Linear Algebra Appl.* **438**, 564–572 (2013).



- [138] R. Shankar, *Quantum Field Theory and Condensed Matter* (Cambridge Univ. Press, Cambridge UK, 2017).
- [139] O. Shanker, “Exact solution of Ising model in 2d shortcut network”, *Mod. Phys. Lett. B* **23**, 567–573 (2009).
- [140] S. Sherman, “Combinatorial aspects of the Ising model for ferromagnetism. I. A conjecture of Feynman on paths and graphs”, *J. Math. Phys.* **1**, 202–217 (1960).
- [141] Y. Shimizu, “Tensor renormalization group approach to a lattice boson model”, *Mod. Phys. Lett. A* **27**, 1250035 (2012).
- [142] B. Simon, “Almost periodic Schrödinger operators: A review”, *Adv. Appl. Math.* **3**, 463–490 (1982).
- [143] Y. G. Sinai and C. Ulcigrai, “A limit theorem for Birkhoff sums of non-integrable functions over rotations”, in *Geometric and Probabilistic Structures in Dynamics*, Vol. 469, edited by K. Burns, D. Dolgopyat, and Y. Pesin (Amer. Math. Soc., 2008), pp. 317–340.
- [144] H. M. Stark and A. A. Terras, “Zeta functions of finite graphs and coverings”, *Adv. Math.* **121**, 124–165 (1996).
- [145] H. M. Stark and A. A. Terras, “Zeta functions of finite graphs and coverings, Part II”, *Adv. Math.* **154**, 132–195 (2000).
- [146] T. Sulejmanpasic and C. Gatteringer, “Abelian gauge theories on the lattice:  $\theta$ -terms and compact gauge theory with(out) monopoles”, *Nucl. Phys. B* **943**, 114616 (2019).
- [147] T. Sunada, “Unitary representations of fundamental groups and the spectrum of twisted Laplacians”, *Topology* **28**, 125–132 (1989).
- [148] T. Sunada, *Topological Crystallography* (Springer, Tokyo, 2013).
- [149] A. Tarfulea and R. Perlis, “An Ihara formula for partially directed graphs”, *Linear Algebra Appl.* **431**, 73–85 (2009).
- [150] H. Teimoori Faal and M. Loebl, “Bass’ identity and a coin arrangements lemma”, *Eur. J. Combinatorics* **33**, 736–742 (2012).
- [151] P. Tempesta, “A theorem on the existence of trace-form generalized entropies”, *Proc. Roy. Soc. Ser A* **471**, 20150165 (2015).
- [152] P. Tempesta, “Beyond the Shannon-Khinchin formulation: The composability axiom and the universal-group entropy”, *Ann. Phys.* **365**, 180–197 (2016).
- [153] A. Terras, *Zeta Functions of Graphs: A Stroll through the Garden* (Cambridge Univ. Press, 2010).
- [154] T. Toffoli and N. H. Margolus, “Invertible cellular automata: A review”, *Physica D* **45**, 229–253 (1990).
- [155] N. V. Vdovichenko, “A calculation of the partition function for a plane dipole lattice”, *Sov. Phys. JETP* **20**, 477–479 (1965).

- [156] J. Villain, "Theory of one- and two-dimensional magnets with an easy magnetization plane. II. The planar, classical, two-dimensional magnet", *J. Phys.* **36**, 581–590 (1975).
- [157] W. Werner, *Percolation et modèle d'Ising* (Société mathématique de France, 2009).
- [158] A. Wipf, T. Heinzl, T. Kaestner, and C. Wozar, "Generalized Potts-models and their relevance for gauge theories", *SIGMA* **3**, 6–14 (2007).
- [159] C. Wozar, T. Kaestner, A. Wipf, T. Heinzl, and B. Pozsgay, "Phase structure of  $\mathbb{Z}(3)$ -Polyakov-loop models", *Phys. Rev. D* **74**, 114501 (2006).
- [160] M.-C. Wu and C.-K. Hu, "Exact partition functions of the Ising model on  $M \times N$  planar lattices with periodic-aperiodic boundary conditions", *J. Phys. A* **35**, 5189–5206 (2002).
- [161] C. N. Yang, "The spontaneous magnetization of a two-dimensional Ising model", *Phys. Rev.* **85**, 808–816 (1952).
- [162] M. Yoneda, Equivalence of the modified Villain formulation and the dual Hamiltonian method in the duality of the XY-plaquette model, 2022.
- [163] D. Zhou, Y. Xiao, and Y.-H. He, "Seiberg duality, quiver gauge theories, and Ihara's zeta function", *Int. J. Mod. Phys. A* **30**, 1550118 (2015).

## Chapter 17

# Normalizing flows, machine learning, information

### 17.1 Normalizing flows

**Predrag:** What is here called

‘normalizing flow’  $f : \mathcal{X} \rightarrow \mathcal{X}$ , invertible and differentiable

Jacobian factor  $J(z) = |\det \partial f_i(z)/\partial z_j|$

is the main idea of our refs. [2, 3]); what they call their ‘latent’ space probability distribution being set to Gaussian is what we call ‘free field theory’. One pays a determinant of the Jacobian matrix of that field transformation, the same as for us. But Miranda Cheng (see **2021-11-01 Predrag** post below) says that this determinant “can be easily computed/approximated” which is news to me.

**2025-01-17 Predrag** to Ronnie, Yueheng, ... :

It looks to me that we have introduced ‘normalizing flow’ much earlier. Ronnie’s idea we implemented in Cvitanović, Dettmann, Mainieri and Vattay *Smooth conjugation method* [3] (1998) [arXiv:chao-dyn/9811003](https://arxiv.org/abs/chao-dyn/9811003). 20 total citations, some excerpts here in sect. 4.16 *Noise is your friend*, some posts in sect. 4.20 *em Field theory blog*, and a popularization in my *Chaotic Field Theory: A sketch* [2] (2000), but by now basically forgotten.

It also looks to me that we have introduced ‘normalizing flow’ in the context of

Cvitanović and Lan [4] *Turbulent fields and their recurrences* (2003); Lan and P. Cvitanović [10] *Variational method for finding periodic orbits in a general flow* (2004) and Y. Lan [9] *Dynamical Systems Approach to 1 – d Spatiotemporal Chaos – A Cyclist’s View* (2004), see also chapter 5 *Computing periodic states*.

but that is less clear.

I have started sketching that out in sect. [18.2.1](#) *Newton flows*, but maybe Yuehang can complete the argument? Or show that it is not relevant here?

Possible courses of action

1. Do nothing. At least in my case, everything I have ever done has somebody's (later work) name attached to it. Who wants to spell 'Cvitanović, when Penrose, Deligne, Feigenbaum, Gross, Tresser, ... are smooth to the tongue?
2. Complain. Write a very short, internal article, explaining our work, and where it shows up in current literature - send the complaint to every current coauthor of papers listed below, and more.
3. Write a very short article, as above, suitable to arXiv and some geezer friend's festschrift journal issue, then complain with the link to the publication.
4. Combine the recent ML wisdom with our specilaized chaos & turbulence wisdom, use this to compute numerically Hill determinants for fluid-dynamical invarinat solution. Thats the big outstanding problem for the spatiotemporal program, see [Turbulence in space-time](#) talks and papers. We could get Tobias Schneider's group, and Johanthan Halcrow at Google Research to do the heavy numerics, they understand why.

**2025-01-17 Predrag** Google Search Labs | AI Overview returns this:

**Concept** Normalizing Flows are a method for transforming a simple probability distribution into a more complex one by applying a series of invertible and differentiable transformations, allowing for better modeling of complex data distributions.

**Early work** Normalizing Flows in machine learning were popularized by Danilo Jimenez Rezende and Shakir Mohamed [arXiv:1505.05770](#) in the context of variational inference, with key contributions also coming from Laurent Dinh and Yoshua Bengio (2014) for their work on density estimation using this technique; however, the foundational framework was initially described in works by Tabak and Vanden-Eijnden (2010).

**Applications** Normalizing Flows are commonly used in generative modeling tasks like density estimation, where the goal is to learn the probability distribution of a dataset to generate new data points that resemble the original data.

**2025-01-17 Predrag** A selection of references related to Albergo *et al. Introduction to Normalizing Flows for lattice field theory* (2021); find the links in [arXiv:2101.08176](#); see also my **2025-01-17 Predrag** notes, around (17.5).

- **Normalizing flows:** Agnelli *et al.* (2010); Tabak and Vanden-Eijnden (2010); Dinh *et al.* (2014); Dinh *et al.* (2016); Papamakarios *et al.* *Normalizing flows for probabilistic modeling and inference* (2019), [arXiv:1912.02762](#);
- **Symmetries and equivariance:** Cohen and Welling (2016); Cohen *et al.* (2019); Rezende *et al.* (2019); Köhler *et al.* (2020); Luo *et al.* (2020); Favoni *et al.* (2020);
- **Flows on manifolds:** Gemici *et al.* (2016); Falorsi *et al.* (2019); Finzi *et al.* (2020); Mathieu and Nickel (2020); Falorsi and Forré (2020);
- **Applications of flows:** Müller *et al.* (2018) ; Noé *et al.* (2019); Wu *et al.* (2020); Dibak *et al.* (2020); Nicoli *et al.* (2021) [DOI](#)

**2023-12-06 Predrag** Yukari Yamauchi, Scott Lawrence *Normalizing flows for the real-time sign problem*, [arXiv:2112.15035](#).

A normalizing flow is a map  $\phi : \mathbb{R}^N \rightarrow \mathbb{R}^N$  obeying

$$\det \left( \frac{\partial \phi}{\partial x} \right) e^{-S(\phi(x))} = \mathcal{N} e^{-x \cdot x / 2}. \quad (17.1)$$

The normalization constant  $\mathcal{N}$  is given by the partition function of the physical model, and will drop out of all equations in this discussion.

Also: A normalizing flow (NF) is a map  $\mathbb{R}^N \rightarrow \mathbb{R}^N$  which induces a non-trivial distribution from a trivial distribution.

When the action is not complex-valued, and has no sign problem, a normalizing flow is guaranteed to exist, and for  $N > 1$ , is far from unique.

C. Villani, *Topics in optimal transportation*, 58 (American Mathematical Soc., 2003).

Consider *perturbative* normalizing flows of the  $\phi^4$  scalar theory, given by the action:

$$S = \sum_{ij} \phi_i M_{ij} \phi_j + \lambda \sum_i \Lambda_i \phi_i^4.$$

Here we fix  $\lambda$ , the magnitude of the strength of the coupling. We consider  $M$  and  $\Lambda$  as the action parameters, and will analytically continue a normalizing flow in the space of  $M, \Lambda$  to obtain a normalizing flow for a choice of these parameters [...].


At weak coupling, a normalizing flow is given by

$$\phi_i^{\text{weak}}(x) = x_i - \lambda \sum_j \left[ \frac{1}{2} M_{ij}^{-1} \Lambda_j x_j^3 + \frac{3}{4} M_{ij}^{-1} M_{jj}^{-1} \Lambda_j x_j \right]. \quad (17.2)$$

Thus the perturbative flow is the analytic function of the action parameter  $M, \Lambda$  except at vanishing  $\det M$ . [...] They also find the perturbative flow in the strong coupling limit [too complicate to detail here].

I see no calculation of the determinant of the Jacobian in the above discussion (??).

2021-11-01 **Predrag** Miranda Cheng

 *Machine learning and theoretical physics: some applications.*

Lattice field theory is the main tool for doing nonperturbative calculations in field theory. The idea of ML techniques, such as Normalizing Flows, is that if we can learn an invertible map that trivializes an interacting model to a free theory, we can easily sample the latter and push back the samples through the inverse map to obtain (proposed) samples from the original non-trivial distribution.

**Predrag:** this is the main idea of our ref. [2, 3]); what they call their ‘latent’ space probability distribution being set to Gaussian is what we call ‘free field theory’. One pays a determinant of the Jacobian matrix of that field transformation, the same as for us. But she says that this determinant “can be easily computed/approximated” which is news to me.

In the talk she defines the “observable” the way we would; I have not seen the definition yet in their papers.

The first part is based on

Pim de Haan, Corrado Rainone, Miranda Cheng and Roberto Bondesan *Scaling Up Machine Learning For Quantum Field Theory with Equivariant Continuous Flows*, [arXiv:2110.02673](https://arxiv.org/abs/2110.02673). Cheng has typos in her presentation (probability density ” + ”Det  $|J|$  rather than  $\times$ ).

the contributions of their paper:

- They extend and develop continuous normalizing flows for lattice field theories that are fully equivariant under lattice symmetries as well as the internal  $\phi \mapsto -\phi$  symmetry of the  $\phi^4$  model.
- They train their model for the  $\phi^4$  theory. For the  $32 \times 32$  lattice they improve the effective sample size from 1% to 66% w.r.t. a real NVP baseline of similar size.
- They study equivariance violations of real NVP models and contrast it with the exact equivariance of their flows.

If the vector field  $g$  is equivariant, the resulting distribution on  $\phi$  is invariant. They show how to construct a  $g$  equivariant to the square lattice symmetries.

**The  $\phi^4$  theory** possesses non-trivial symmetry properties and a phase transition. In the case of  $\phi^4$  theory in two dimensions, the *field configuration* is a real function on

the vertex set  $V_L$  of the square lattice

with periodic boundaries and size  $L \times L$ :  $\phi : V_L \rightarrow \mathbb{R}$ . The  $\phi^4$  theory is described by a probability density

$$p(\phi) = \exp(-S(\phi))/Z, \quad (17.3)$$

with action

$$S(\phi) = \sum_{x,y \in V_L} \phi(x) \Delta_{x,y} \phi(y) + \sum_{x \in V_L} m^2 \phi(x)^2 + \lambda \phi(x)^4 \quad (17.4)$$

Here  $\Delta$  is Laplacian matrix of the square lattice  $(\mathbb{Z}/L\mathbb{Z})^{\times 2}$ ,  $m$  and  $\lambda$  are numerical parameters. In the case of this and other non-trivial field theoretical densities,  $Z$  is the normalisation factor that is not known analytically for  $\lambda \neq 0$ .

Probability densities over those phase space manifolds:

- Prior density  $r(z)$
- Model density  $q(x)$
- Target density  $p(x)$

Note that, besides the space-time symmetries of the periodic lattice, the theory possesses a

discrete global symmetry  $\phi \mapsto -\phi$ .

We shall choose the couplings in such a way that only one minimum of the action, invariant under this symmetry, exists. See [??] for relevant work in the case of a symmetry-broken case.

(Was commented out:) We will work in the "unbroken" phase with  $m^2 > 0$ , where the minimum of the action is invariant under the global symmetry. See [arXiv:2107.00734](https://arxiv.org/abs/2107.00734) for relevant work in the broken phase.

The periodic lattice  $V_L$  has spatial symmetry group  $G = C_L^2 \rtimes D_4$ , the semi-direct product of two cyclic groups  $C_L$  of translations and dihedral group  $D_4$  of right angle rotations and mirrors. To ensure spatial equivariance of the vector field model, we should have that

$$\forall g \in G, x, y, a, f, W_{g(x)g(y)af} = W_{xyaf}.$$

Using the translation subgroup, we can map any point  $x$  to a fixed point  $x_0$ . This allows us to write  $W_{xyaf} = W_{x_0 t_x(y)af}$ ,  $t_x(y) = y - x + x_0$ .

(Predrag - they seem to be defining the point group here:)

Then let  $H \simeq D_4$  be the subgroup of  $G$  such that  $g(x_0) = x_0$  for all  $g \in H$ , and denote the orbit of  $y$  under  $H$  by  $[y] = \{y' \mid \exists g \in H, g(y) = y'\}$ .

For each such orbit  $[y]$  and dimension  $a$  and  $f$ , a free parameter  $W_{[y]af}$  exists, so that the other parameters are generated by  $W_{xyaf} = W_{[t_x(y)]af}$ .

(Was commented out; Predrag - they ignore symmetric lattice states here:) As most orbits are of size 8, the number of free parameters per  $a$  and  $f$  is approximately  $L^2/8$ .

The orbits of  $D_4$ , leaving point  $(0, 0)$  invariant, for  $L = 16$  are shown in Fig. 4. For each color in that figure, for each dimensions  $a$  and  $f$ , we have a free parameter.

(Predrag - that figure says the 1/8th fundamental domain tiles the square lattice, and ignores the symmetry boundaries. The “free parameter” is just the values of the field in the fundamental domain.)

**2021-12-05 Predrag** These papers seem to be more informative:

Rezende and Mohamed (2015) “normalizing flows” [arXiv:1505.05770](#)  
cites Jordan, Ghahramani, Jaakkola and Saul [6] *An introduction to variational methods for graphical models* (1999)

Del Debbio, Rossney and Wilson *Efficient Modelling of Trivializing Maps for Lattice  $\phi^4$  Theory Using Normalizing Flows: A First Look at Scalability*  
[arXiv:2105.12481](#)

**2025-01-17 Predrag** George Papamakarios, Eric Nalisnick, Danilo Jimenez Rezende, Shakir Mohamed, Balaji Lakshminarayanan *Normalizing Flows for Probabilistic Modeling and Inference*; [arXiv:1912.02762](#):

Normalizing flows provide a general mechanism for defining expressive probability distributions, only requiring the specification of a (usually simple) base distribution and a series of bijective transformations. We [...] by describing flows through the lens of probabilistic modeling and inference. We place special emphasis on the fundamental principles of flow design, and discuss foundational topics such as expressive power and computational trade-offs. We also broaden the conceptual framing of flows by relating them to more general probability transformations.

**2021-12-05 Predrag** Albergo, Boyda, Hackett, Kanwar, Cranmer, Racanière, Jimenez Rezende and Shanahan, *Introduction to Normalizing Flows for Lattice Field Theory* (2021), [arXiv:2101.08176](#):

This notebook tutorial demonstrates a method for sampling Boltzmann distributions of lattice field theories using a class of machine learning models known as normalizing flows. The ideas and approaches proposed in

Albergo, G. Kanwar, and P.E. Shanahan *Flow-based generative models for Markov chain Monte Carlo in lattice field theory*, [arXiv:1904.12072](#)

Nicoli, S. Nakajima, N. Strodthoff, W. Samek, K.-R. Müller, P. Kessel, *Asymptotically unbiased estimation of physical observables with neural samplers*, [arXiv:1910.13496](#)

[arXiv:2002.02428](#)

[arXiv:2003.06413](#)

are reviewed and a concrete implementation of the framework is presented. We apply this framework to a lattice scalar field theory and to U(1) gauge theory, explicitly encoding gauge symmetries in the flow-based approach to the latter.

I. Kobzyev, S. J. Prince, and M. A. Brubaker, *IEEE Transactions on Pattern Analysis and Machine Intelligence* 43, 3964 (2021).



The Box-Muller transform is an example of a ‘normalizing’ transformation: to produce Gaussian random variables, draw two variables  $U_1$  and  $U_2$  from  $\text{unif}(0, 1)$ , then change variables to

$$(Z_1, Z_2) = (r \cos(2\pi U_2), r \sin(2\pi U_2)), \quad r = \sqrt{-2 \ln U_1}. \quad (17.5)$$

The resulting variables  $Z_1, Z_2$  are then distributed according to an uncorrelated, unit-variance Gaussian distribution;  $U_1$  controls the radius, and  $U_2$  the angle of a  $2d$  Gaussian.

**Predrag:** This might relate Bernoulli and temporal cat to Gaussian field theories (see sect. 16.2), i.e., this maps fields in  $[0, 1)$  to fields in  $\mathbb{R}$ .

The density associated with output samples is computed by the *change-of-variables formula* relating the *prior density*  $\rho(U_1, U_2) = 1$  to the *output density*

$$\begin{aligned} q(Z_1, Z_2) &= \rho(U_1, U_2) \left| \det \frac{\partial Z_k(U_1, U_2)}{\partial U_l} \right|^{-1} \\ &= 1 \times \left| \det \begin{pmatrix} \frac{-1}{U_1 r} \cos(2\pi U_2) & -2\pi r \sin(2\pi U_2) \\ \frac{-1}{U_1 r} \sin(2\pi U_2) & 2\pi r \cos(2\pi U_2) \end{pmatrix} \right|^{-1} \\ &= \left| \frac{2\pi}{U_1} \right|^{-1}. \end{aligned} \quad (17.6)$$

$J(U_1, U_2) \equiv \det(\partial Z / \partial U)$  is the determinant of the Jacobian of the coordinates transformation  $(U_1, U_2) \rightarrow (Z_1, Z_2)$ . The Jacobian factor is a change in volume element, therefore the change-of-variables formula must contain the inverse of this factor (spreading out volume decreases density). As

$$U_1 = \exp(-(Z_1^2 + Z_2^2)/2)$$

and the initial density  $\rho(U_1, U_2)$  over the unit square was uniform, the transformed density is

$$q(Z_1, Z_2) = \frac{1}{2\pi} e^{-(Z_1^2 + Z_2^2)/2}. \quad (17.7)$$

This example has no free parameters because no extra parameters were needed to create a transform that exactly reproduced the desired target distribution, independent, unit-variance Gaussian. In general, we may not know a normalizing flow that exactly produces our desired distribution, and so instead construct parametrized models that we can variationally optimize to *approximate* that target distribution, and because we can compute the density these can be corrected to nevertheless guarantee exactness.

In some cases, it is easy to compute the Jacobian factor even when the whole Jacobian matrix is intractable; for example, only the diagonal elements are needed if the Jacobian matrix is known to be triangular.

The hypercubic lattice discretization of the derivatives of the continuum Euclidean action gives rise to a lattice Euclidean action,

$$\begin{aligned}
 S_{\text{cont}}^E[\phi] &= \int d^2\vec{x} (\partial_\mu\phi(\vec{x}))^2 + m^2\phi(\vec{x})^2 + \lambda\phi(\vec{x})^4 \\
 \rightarrow S(\phi) &= \sum_{\vec{n}} \phi(\vec{n}) \left[ \sum_{\mu \in \{1,2\}} -\phi(\vec{n} + \hat{\mu}) + 2\phi(\vec{n}) - \phi(\vec{n} - \hat{\mu}) \right] + m^2\phi(\vec{n})^2 + \lambda\phi(\vec{n})^4
 \end{aligned}
 \tag{17.8}$$

where now  $\phi(\vec{n})$  is only defined on the sites of the  $L_x \times L_y$  lattice,  $\vec{n} = (n_x, n_y)$ , with integer  $n_x, n_y$ . The discretized field  $\phi$  can be thought of as an  $(L_x \times L_y)$ -dimensional vector. We use periodic boundary conditions in all directions, i.e.  $\phi(L_x, y) \equiv \phi(0, y)$ , etc.

More details on  $\phi^4$  lattice scalar field theory can be found in Vierhaus's masters thesis [17] *Simulation of  $\phi^4$  theory in the strong coupling expansion beyond the Ising Limit* (DOI).

The lattice action then defines a probability distribution over configurations  $\phi$ ,

$$p(\phi) = \frac{1}{Z} e^{-S(\phi)}, \quad Z \equiv \int \prod_{\vec{n}} d\phi(\vec{n}) e^{-S(\phi)}, \tag{17.9}$$

where  $\prod_{\vec{n}}$  runs over all lattice sites  $\vec{n}$ . This is the distribution we are training the normalizing flows to reproduce. While  $Z$  is difficult to calculate, in practice we only need  $p(\phi)$  up to a constant. The action can be efficiently calculated on arbitrary configurations using Pytorch. Note that while the theory describes 2D spacetime, the dimensionality of distribution  $p(\phi)$  is the number of lattice sites, scaling with the volume of the lattice.

The theory has a symmetric phase and a broken symmetry phase, corresponding respectively to nearly one mode of the distribution or two widely separated modes (with intermediate configurations suppressed exponentially in volume). The broken symmetry phase can be accessed for  $m^2 < 0$  and  $\lambda$  less than a critical  $\lambda_c$ . For simplicity, we restrict focus to the **symmetric phase**, but remain close to this phase transition such that the system has a non-trivial correlation length.

**2022-05-11 Predrag** Liao and He [12] *Jacobian determinant of normalizing flows* [arXiv:2102.06539](https://arxiv.org/abs/2102.06539): [...] Jacobian determinant is a measure of local volume change and is maximized when MLE is used for optimization [...]. I do not understand the paper, but it has an introduction and lots of references that might be of some use.

**2024-07-22 Predrag** .

Surtej Kanwar *Flow-based sampling for lattice field theories* (2023); [talk slides](#).

Invariant prior + equivariant flow = symmetric model.


**2021-12-13 Predrag** Sara liked very much this morning's talk by [Max Welling](#) on ML for PDEs – the way he controls the PDE grid, incorporates symmetries into the NN part of the algorithm.

Garcia Satorras, Hoogeboom, Fuchs, Posner and Welling *E(n) Equivariant Normalizing Flows* Advances in Neural Information Processing Systems 34 (2021):

This paper introduces a generative model equivariant to Euclidean symmetries: E(n) Equivariant Normalizing Flows (E-NFs). To construct E-NFs, we take the discriminative E(n) graph neural networks and integrate them as a differential equation to obtain an invertible equivariant function: a continuous-time normalizing flow. We demonstrate that E-NFs considerably outperform baselines and existing methods from the literature on particle systems such as DW4 and LJ13, and on molecules from QM9 in terms of log-likelihood. To the best of our knowledge, this is the first flow that jointly generates molecule features and positions in 3D.

**2023-02-18 Predrag** Yubin Lu, Yang Li and Jinqiao Duan *Extracting stochastic governing laws by nonlocal Kramers-Moyal formulas* [arXiv:2108.12570](#) have a very simple, motivational introduction to [normalizing flows](#).

**2023-09-14 Predrag** .

 Tanaka *Towards physics of intelligence* (65 min)


in part about Kunin, Sagastuy-Brena, Ganguli, Yamins and Tanaka [8] *Neural mechanics: Symmetry and broken conservation laws in deep learning dynamics* (2020), [arXiv:2012.04728](#):

An important paper, uses 'batch normalization', not sure it fits under "normalizing":

Batch normalization leads to scale invariance during training.

geometric constraints on neural network gradients and Hessians (ie, our orbit Jacobians)

**2023-02-13 Predrag** (might belong more naturally to the Lippolis noise blog):

 Thierry Bodineau: *Stochastic dynamics and the Polchinski equation: an introduction*, presented a renormalisation group perspective on properties of stochastic dynamics associated with Ising type models and continuum systems. Uses the Polchinski equation which he explained, as well as the relationship of this approach to stochastic localisation and transport theory. Applies it to  $\phi^4$  model.

The trick is to use additivity of covariances to split a covariance  $Q$  into two, a sharp narrow one  $tQ$ , weighted by the broader reminder  $(1 - t)Q$ . That helps with establishing bounds.

Polchinski equation is an integral over  $t$ , so one uses all splittings on equal footing, I believe.

The paper is Bauerschmidt, Bodineau and Dagallier [arXiv:2307.07619](#): [...] a renormalisation group perspective on log-Sobolev inequalities and related properties of stochastic dynamics. We also explain the relationship of this approach to related recent and less recent developments such as Eldan’s stochastic localisation and the Föllmer process, the Boué–Dupuis variational formula and the Barashkov–Gubinelli approach, the transportation of measure perspective, and the classical analogues of these ideas for Hamilton–Jacobi equations which arise in mean-field limits.

**2024-11-18 Predrag** See also my notes on Cotler and Rezchikov *Renormalizing Diffusion Models*; [arXiv:2308.12355](#) after eq. (17.25).

**2025-01-17 Predrag** Might have a look at Andrea Perin, Stephane Deny *On the Ability of Deep Networks to Learn Symmetries from Data: A Neural Kernel Theory*; [arXiv:2412.11521](#).

[...] we aim to understand when and how deep networks can learn symmetries from data. We focus on a supervised classification paradigm where data symmetries are only partially observed during training: some classes include all transformations of a cyclic group, while others include only a subset. We ask: can deep networks generalize symmetry invariance to the partially sampled classes? [...] we derive a neural kernel theory of symmetry learning to address this question. The group-cyclic nature of the dataset allows us to analyze the spectrum of neural kernels in the Fourier domain; here we find a simple characterization of the generalization error as a function of the interaction between class separation (signal) and class-orbit density (noise). We observe that generalization can only be successful when the local structure of the data prevails over its non-local, symmetric, structure, in the kernel space defined by the architecture. This occurs when (1) classes are sufficiently distinct and (2) class orbits are sufficiently dense. [...] conventional networks trained with supervision lack a mechanism to learn symmetries that have not been explicitly embedded in their architecture a priori.

## 17.2 Information

See also sect. 4.2.1 *Laplacian notes 2012-2018*.

A proposal: use the smallest Kullback-Leibler divergence (relative information) [7]

$$D_{\text{KL}}[p[\Phi] \| p[\Phi']]_{\mathbb{A}} = p[\Phi] \ln \frac{p[\Phi]}{p[\Phi']} \quad (17.10)$$

as a measure of ‘distance’ between orbits of a pair of periodic states  $\Phi, \Phi'$  over primitive cell  $\mathbb{A}$ .

For a pair of Gaussians,

$$p(\Phi)_j = \frac{|\mathcal{J}_j|^{1/2}}{(2\pi)^{N/2}} \exp\left(-\frac{1}{2}(\Phi - \Phi_j)^T \mathcal{J}_j (\Phi - \Phi_j)\right).$$

we have the explicit formula (17.12),

$$\begin{aligned} D_{\text{KL}}[p[\Phi] \| p[\Phi']]_{\mathbb{A}} & \quad (17.11) \\ &= \frac{1}{2} \left( (\Phi - \Phi')^T \mathcal{J}_M (\Phi - \Phi') + \text{Tr}(\mathcal{J}_M \mathcal{J}_{M'}^{-1} - \mathbf{1}) - \ln \det \mathcal{J}_M \mathcal{J}_{M'}^{-1} \right). \end{aligned}$$

in terms of periodic states  $\Phi_p$  and  $\Phi_q$ , The  $D_{\text{KL}}[\dots \| \dots]$  square brackets indicate that in the continuum limit this is a field-theoretic functional.

Kullback-Leibler (hereafter: KL) divergence

$$\text{KL}(p\|q) = \frac{(\mu_q - \mu_p)^2}{2\sigma_p^2} - \frac{1}{2} \left( \log \frac{\sigma_q^2}{\sigma_p^2} + 1 - \frac{\sigma_q^2}{\sigma_p^2} \right).$$

between two univariate Gaussians. Note that

$$\log \left[ 1 - \left( 1 - \frac{\sigma_q^2}{\sigma_p^2} \right) \right] = - \left( 1 - \frac{\sigma_q^2}{\sigma_p^2} \right) - \frac{1}{2} \left( 1 - \frac{\sigma_q^2}{\sigma_p^2} \right)^2 + \dots,$$

so the leading covariances comparison term is of order  $\left( 1 - \frac{\sigma_q^2}{\sigma_p^2} \right)^2$ .

KL divergence between two multivariate Gaussians

$$\text{KL}(p\|q) = \frac{1}{2} (\mu_p - \mu_q)^T \Sigma_p^{-1} (\mu_p - \mu_q) + \frac{1}{2} \text{Tr} \left[ \ln \Sigma_p^{-1} \Sigma_q + \{ \Sigma_p^{-1} \Sigma_q - \mathbf{1} \} \right], \quad (17.12)$$

where we have used the  $\log \det = \text{tr} \log$  matrix identity, and

$$p(\mathbf{x}) = \frac{1}{(2\pi)^{d/2} |\Sigma|^{1/2}} \exp\left(-\frac{1}{2}(\mathbf{x} - \boldsymbol{\mu})^T \Sigma^{-1} (\mathbf{x} - \boldsymbol{\mu})\right).$$

The trace term is interesting. For  $p, q$  close, the ratio of covariances is close to  $\mathbf{1}$ , so expanding the log around  $\mathbf{1}$ ,

$$\ln(\mathbf{1} - (\mathbf{1} - \Sigma_p^{-1} \Sigma_q)) = -\frac{1}{\Sigma_p} (\Sigma_p - \Sigma_q) - \frac{1}{2} \left( \frac{1}{\Sigma_p} (\Sigma_p - \Sigma_q) \right)^2 + \dots.$$

The linear terms cancel, must be a consequence of some variational extremum. Where was it imposed? Everybody derives the above KL divergence, but nobody interprets the Tr terms.

This manipulation seems not to help.

$$\ln \Sigma_p^{-1} \Sigma_q + \ln e^{\Sigma_p^{-1} \Sigma_q - \mathbf{1}} = \ln \left( \frac{d}{d\epsilon} e^{\epsilon(\Sigma_p^{-1} \Sigma_q - \mathbf{1})} \right)_{\epsilon=1}.$$

The Kullback-Leibler divergence makes more sense to me than the *ad hoc*  $L2$  norm distance between periodic states:

$$|\Phi - \Phi'|^2 = \frac{1}{N_{\mathbb{A}}} \sum_{z \in \mathbb{A}} (\phi'_z - \phi_z)^2. \quad (17.13)$$

Instead, weigh the 'distances' by periodic state's weights

$$\frac{1}{|\text{Det } \mathcal{J}_{\mathbb{A},c}|} = e^{-N_{\mathbb{A}} \langle \lambda \rangle_{\mathbb{A},c}}. \quad (17.14)$$

I think we have to work in the reciprocal lattice, using  $\Phi_c$  in

$$\langle \lambda \rangle_{\mathbb{A}} = \frac{1}{Z_{\mathbb{A}}[0]} \sum_c \sum_{j=1}^{N_{\mathbb{A}}} \langle \lambda_j \rangle_c e^{-N_{\mathbb{A}} \langle \lambda_j \rangle_c}. \quad (17.15)$$

as the reference periodic state probability,

$$\rho[\Phi_c] = \frac{1}{Z_{\mathbb{A}}[0]} \sum_{j=1}^{N_{\mathbb{A}}} e^{-N_{\mathbb{A}} \langle \lambda_j \rangle_c}, \quad (17.16)$$

when measuring the  $\Phi_c, \Phi_d$  'distance'. Here  $j$  sum is over the orbit Jacobian matrix  $\mathcal{J}_{\mathbb{A},c}$  stability exponents. In that case, the information distance between the probabilities of periodic states  $\Phi_c$  and  $\Phi_d$  is something like (have to get rid of  $N_{\mathbb{A}}$ 's?)

$$\mathcal{S}(\rho_c || \rho_d) = \frac{1}{Z_{\mathbb{A}}[0]} \sum_{j=1}^{N_{\mathbb{A}}} (\langle \lambda_j \rangle_c - \langle \lambda_j \rangle_d) e^{-N_{\mathbb{A}} \langle \lambda_j \rangle_c}, \quad (17.17)$$

where the observable is the  $j$ th eigen-exponent  $\langle \lambda_j \rangle_c - \langle \lambda_j \rangle_d$ . Just like  $L2$  norm (17.13), this is an average over the *pointwise* 'distance' on the reciprocal lattice, zero when  $\Phi_c = \Phi_d$ , and weighted by  $\rho[\Phi_c]$  when  $\Phi_c \neq \Phi_d$ .

However, unlike field moments & correlations often computed in field theory and stat mech, relative information is very appealing to us, because it is invariant under general, smooth nonlinear field transformations, such as the 'normalizing flow' transformations from field  $\phi$  to field  $\psi(\phi)$ . The proof is elementary, see wiki [sect. Properties](#), essentially as in ChaosBook for the time evolution Jacobian/Floquet matrices, but now for the orbit Jacobian matrix  $\mathcal{J}_{\mathbb{A},c}$  stability exponents.

What Farshchian *et al.* [5] call multivariate Gaussian covariance matrix  $\Sigma$  is our orbit Jacobian matrix  $\mathcal{J}^{-1}$ . In our case the Kullback-Leibler divergence (17.24) is (17.11).

The divergence  $D_{\text{KL}}$  vanishes when  $\Phi_M = \Phi_{M'}$ . To insure that, we must minimize it by running through the translational and discrete reflections orbit of the reference periodic state  $\Phi_M$ , or section and slice the phase space before selecting the closest pair of periodic states.  $\Phi_M, \Phi_{M'}$ .

$(\Phi_M - \Phi_{M'})^T \mathcal{J}_M (\Phi_M - \Phi_{M'})$  is the ‘square’ of the distance between centers of  $\Phi_k, \Phi_M$ , asymmetrically weighted by the eigenvalues of  $\mathcal{J}_M$ . The phase space vector  $\Phi_M - \Phi_{M'}$  vanishes when  $\Phi_M = \Phi_{M'}$ , and the relative entropy  $\ln |\mathcal{J}_M \mathcal{J}_{M'}^{-1}|$  also vanishes when  $\Phi_M = \Phi_{M'}$ . Fourier-diagonalize everything.

Current  $D_{\text{KL}}$  is not correctly normalized for the  $N_{\mathbb{A}} \rightarrow$  large limit, clearly must divide by the lattice volume, so tentatively define KL divergence per lattice site as a ‘little’ divergence

$$d_{\text{KL}}[\cdots \|\cdots] = \frac{1}{N_{\mathbb{A}}} D_{\text{KL}}[\cdots \|\cdots]_{\mathbb{A}} \quad (17.18)$$

As  $\mathcal{J}$  is symmetric, its eigenvalues must be real, if unstable then strictly nonzero, but can be of either sign (see figure 22.2 (b)). We want to keep signs in (17.11). They cancel in the ratios of eigenvalues (if not, that signals something we would want to take a closer look at), and we do not want the solutions close in an eigenvalue magnitude, but of opposite sign to be misidentified as ‘close’.

**23-10-20 Predrag to Xuanqi** Please recover the eigenvalue signs from Q diagonal (?) of your QR calculation (23.40) for all periodic states of period 5. If the  $\phi^3$  calculation figure 22.2 (b) is correct, your  $\phi^3$  periodic states’ mosaics 0 symbol eigenvalues have one sign, the  $\pm 1$  the other sign, and self-dual periodic states (period 2 and onwards) might also have interesting signatures. This information might be important for the shadowing ‘distance’ quantification of this section.

The calculation is for the Gaussian field theory, so square roots of Hill determinants rather than Hill determinants as probabilities. Should be easily fixable? Or not, maybe for Dirac functions the center to center separation is infinite in standard deviation units?

Note that the divergence  $D_{\text{KL}}[p_{M'} \| p_0]_{\mathbb{A}}$  requires sitewise evaluation, cannot be simply a function of Hill determinants.  $\mathcal{J}_M, \mathcal{J}_{M'}$  can be simultaneously diagonalized by discrete Fourier transforms (ignoring the discrete point group for a while).

Dangling bits: define *pseudo-orbits*. The shadowing / curvature expansions need fleshing out.

**Punchline:**

Given a set of  $N$  periodic states over a primitive cell,  $d_{\text{KL}}[\Phi \|\Phi']$  is an asymmetric  $[N \times N]$  matrix of pairwise KL divergences. For each curvature expansion of orbits and pseudo-orbits there is the minimum one. When they fall below a given cutoff, we are done - further, larger volume periodic states give no additional information.

## 17.2.1 Information blog

### 2024-07-22 Predrag clippings

$$\begin{aligned} \text{KL}(p||q) &= \int p(x) \log \left( \frac{p(x)}{q(x)} \right) dx \\ &= \int p(x) \log \left( \frac{1}{q(x)} \right) dx - \int p(x) \log \left( \frac{1}{p(x)} \right) dx \\ &= H(P, Q) - H(P), \end{aligned} \tag{17.19}$$

where  $H(P, Q)$  is the cross-entropy of  $P$  and  $Q$ , and  $H(P)$  is the entropy of  $P$ , or the cross-entropy of  $P$  with itself.

I keep writing the wrong covariance in the quadratic separation, for example (17.11) and (17.12) were wrong. Farshchian *et al.* (17.24) is correct. For a derivation, see, for example, [Duchi notes, p. 13](#).

**2023-10-13 Predrag** The proof that relative information is invariant under general, smooth nonlinear field transformations answers, in a way, the question posed in the **2021-09-07 Sidney** post: we need the answer for Hill determinant, not the individual eigenvalue, anyway. I still do not know whether it applies to individual eigenvalue.

**2023-10-11 Predrag** Witten [arXiv:1803.04993](#) writes: “ [...] Our convention is to agree with quantum information theory, where it has become standard to define the relative entropy between density matrices  $\rho, \sigma$  as  $S(\rho||\sigma) = \text{Tr} \rho(\log \rho - \log \sigma)$ . ” He is concerned with quantum relative entropy (on modular domains!), has some cute inequalities, such as his eq. (3.39). The modular automorphism group shows up in -to me- unrecognizable form. I do not think we have to think about this now - classical Kullback-Leibler information theory should be good enough for us.

**2023-10-13 Predrag** The ‘Basic example’ in the [Kullback-Leibler wiki](#) is pretty clear.

We are almost doing something like that already, in our CL18 shadowing section:

$$\langle \lambda \rangle - \langle \lambda \rangle_{[L \times L]_0} = [\text{const}] \cdot e^{-1.05538 L}. \tag{17.20}$$

The [Fisher information metric](#) is the only Riemannian metric (up to rescaling) that is invariant under sufficient statistics. It is the infinitesimal form of the relative entropy (Kullback–Leibler divergence); it is the Hessian of the divergence.

**2023-10-13 Predrag** Why is this a [divergence](#)? Fedele says it is obvious - if you have information fluxes between modes, then the total relative information is an integral over divergences of these fluxes. That is the idea of Falkovich and Shavit *Singular measures and information capacity of turbulent cascades*, [arXiv:1911.12670](#), who also work in the Fourier space, just as in the above, in (17.17).



**2023-10-13 Predrag** Another notion of distance that seems related is **Wasserstein metric**. Wasserstein metric most commonly appears in optimal transport problems where the goal is to move things from a given configuration to a desired configuration in the minimum cost or minimum distance.

“Wasserstein metric main drawback: For instance, for homogeneous domains as simple as Poincaré upper half plane, Wasserstein metric is not invariant wrt the automorphism of this space. Only Fisher metric is valid, and its extension by Jean-Louis Koszul and Jean-Marie Souriau.”

**2023-10-20 Predrag** For the multivariate Gaussian distributions of dimension  $k$ , means  $\mu_i$ , and covariance matrices  $\Sigma_i$ ,  $i = 1, 2$  both Wasserstein distance and KL divergence have closed form expressions:

$$W_2(\mathcal{N}_0, \mathcal{N}_1)^2 = \|\mu_1 - \mu_2\|_2^2 + \text{tr}(\Sigma_1 + \Sigma_2 - 2(\Sigma_2^{1/2}\Sigma_1\Sigma_2^{1/2})^{1/2}).$$

This does not look invariant under coordinate transformations to me, so scratch Wasserstein.

**2023-10-13, 2024-07-17 Predrag** .

Dimitrios Bachtis, Gert Aarts, Biagio Lucini *Quantum field-theoretic machine learning*, [arXiv:2102.09449](https://arxiv.org/abs/2102.09449), published as **Phys. Rev. D**:

We derive machine learning algorithms from discretized Euclidean field theories [...] demonstrate that the  $\phi^4$  scalar field theory on a square lattice satisfies the Hammersley-Clifford theorem, therefore recasting it as a Markov random fields machine learning algorithm. We illustrate the concepts by minimizing an asymmetric distance between the probability distribution of the  $\phi^4$  theory and that of target distributions, by quantifying the overlap of statistical ensembles between probability distributions and through reweighting to complex-valued actions with longer-range interactions.

The local Markov property denotes that a variable  $\phi_k$  is conditionally independent of all other variables other than its neighbors. To understand intuitively the *local Markov property*, consider a Markov chain  $P(\phi_{k+1}|\phi_k, \dots, \phi_0) = P(\phi_{k+1}|\phi_k)$ : state  $\phi_k$  a future state  $\phi_{k+1}$  depends only on the current state  $\phi_k$ , and not on states that preceded it, such as  $\phi_{k-1}$ . The local Markov property extends this concept to higher dimensions by giving it a spatial representation via a Markov random field.

By searching for an optimal set of coupling constants they minimize the Kullback-Leibler divergence so that the probability distribution of the  $\phi^4$  scalar field theory converges to the target probability distribution.

**2023-10-13, 2024-07-17 Predrag** I see no difference (other than the addition of appendices) between the above and their next publication, Bachtis, Aarts and Lucini *Machine learning with quantum field theories*, [arXiv:2109.07730](https://arxiv.org/abs/2109.07730).

2023-10-13, 2024-07-17 Predrag .

Raymond Eveleth Fowler III PhD thesis *Information Theoretic Interpretations of Renormalization Group Flow* (2019):

we make use of the Kullback-Leibler (KL) divergence, which quantifies the information theoretic distance between two probability distributions. In order to use the KL divergence with quantum field theories, we study the probability distributions associated with Euclidean quantum field theories; the KL divergence thus computes the relative entropy between these Euclidean quantum field theories, as in statistical field theory.

Write probability density as a Boltzmann factor

$$p(\phi) = \frac{1}{Z_p} e^{-S_p(\phi)}, \quad (17.21)$$

then KL takes form

$$D(p||q) = \int d\phi p(\phi) \ln \frac{p(\phi)}{q(\phi)} = \ln \frac{Z_q}{Z_p} - \langle S_p - S_q \rangle_p, \quad (17.22)$$

To lowest order

$$\begin{aligned} Z_q &= \int d\phi e^{-S_q} = \int d\phi e^{-S_p} e^{S_p - S_q} \\ &= Z_p + \langle e^{S_p - S_q} - 1 \rangle_p \\ \ln \frac{Z_q}{Z_p} &= \ln \left( 1 - \frac{1}{Z_p} \langle 1 - e^{S_p - S_q} \rangle_p \right) \\ D(p||q) &= -\frac{1}{Z_p} \left( \langle 1 - e^{S_p - S_q} \rangle_p \right) - \\ D(p||q) &= \frac{1}{2} \left( \langle (S_p - S_q)^2 \rangle_p - \langle S_p - S_q \rangle_p^2 \right), \end{aligned} \quad (17.23)$$

2024-07-22 Predrag .

Vijay Balasubramanian, Jonathan J. Heckman, and Alexander Maloney *Relative Entropy and Proximity of Quantum Field Theories* (2015), [arXiv:1410.6809](https://arxiv.org/abs/1410.6809); DOI. They start with (17.22), then go to the Fisher information metric, etc. Did not finish reading it.

2023-10-13 Predrag We still to look at these:

Jacques Calmet and Xavier Calmet. Distance between physical theories based on information theory (2011). DOI; have not found it yet...

2023-10-18 Predrag Floerchinger has a very interesting information-theoretic reformulation of Euclidean field theory, but working through this would require some time.

Floerchinger *Information geometry of Euclidean quantum fields*, [arXiv:2303.04081](https://arxiv.org/abs/2303.04081):  
“ Information geometry provides differential geometric concepts like a

Riemannian metric, connections and covariant derivatives on spaces of probability distributions. We apply these to Euclidean quantum field theories / statistical field theories. The geometry has a dual affine structure corresponding to sources and field expectation values seen as coordinates. A key concept is a new generating functional, which is a functional generalization of the Kullback-Leibler divergence. From its functional derivatives one can obtain connected as well as one-particle irreducible correlation functions. It also encodes directly the geometric structure, i.e., the Fisher information metric and the two dual connections, and it determines asymptotic probabilities for field configurations. ”

Euclidean quantum field theories have a probability interpretation, or can be seen as classical statistical field theories with one more spatial dimension, from an information theoretic point of view. [...] concepts can be taken from classical information geometry, going from functions to functionals. [...] The Riemannian Fisher information metric corresponds to connected two-point correlation functions. [...] [...] [...]

**2023-10-18 Predrag** Stefan Floerchinger *Exact flow equation for the divergence functional*, [arXiv:2303.04082](https://arxiv.org/abs/2303.04082) is about renormalization flow, ignore for now: “ An exact functional renormalization group flow equation is derived for the divergence functional which is a generalization of the Kullback-Leibler divergence to quantum field theories in the Euclidean domain. It compares distributions with different sources and field expectation values. The renormalization group flow for a regularized version of this functional connects two limits: one where the functional is known in terms of the microscopic action or probability distribution, and the other where all fluctuations are taken into account. In the latter limit one can obtain full correlation functions from functional derivatives of the divergence functional. The flow equation provides a possibility to determine this functional non-perturbatively. ”

**2023-10-18 Sara to Predrag** Focus on eq (2) of Ali Farshchian, Juan A. Gallego, Joseph P. Cohen, Yoshua Bengio, Lee E. Miller and Sara A. Solla *Adversarial domain adaptation for stable brain-machine interfaces*, [arXiv:1810.00045](https://arxiv.org/abs/1810.00045) and [OpenReview](#), write:

**Kullback-Leibler divergence minimization (KLDM).** For the unsupervised approach, we seek to match the probability distribution of the latent variables of day- $k$  to that of day-0 [...] . We use the fixed AE trained on day-0 data to map the neural data of day-0 and day- $k$  onto two sets of  $l$ -dimensional latent variables,  $\{z_0\}$  and  $\{z_k\}$ , respectively. We then compute the mean and covariance matrices for each of these two empirical distributions, and capture their first and second order statistics by approximating these two distributions by multivariate Gaussians:  $p_0(z_0) \sim \mathcal{N}(z_0; \mu_0, \Sigma_0)$  and  $p_k(z_k) \sim \mathcal{N}(z_k; \mu_k, \Sigma_k)$ . We then minimize the KL

divergence between them,

$$D_{\text{KL}}(p_k(\mathbf{z}_k) \| p_0(\mathbf{z}_0)) \quad (17.24)$$

$$= \frac{1}{2} \left( \text{Tr}(\Sigma_0^{-1} \Sigma_k - \mathbf{1}) + (\boldsymbol{\mu}_0 - \boldsymbol{\mu}_k)^T \frac{1}{\Sigma_0} (\boldsymbol{\mu}_0 - \boldsymbol{\mu}_k) - \ln |\Sigma_0^{-1} \Sigma_k| \right).$$

To minimize the KL divergence, we implemented a map from neural activity to latent activity using a network with the same architecture as the encoder section of the BMI's AE. This network was initialized with the weights obtained after training the BMI's AE on the day-0 data. Subsequent training was driven by the gradient of the cost function of (??), evaluated on a training set provided by day- $k$  recordings of neural activity. This process aligns the day- $k$  latent PDF to that of day-0 through two global linear operations: a translation through the match of the means, and a rotation through the match of the eigenvectors of the covariance matrices; a nonuniform scaling follows from the match of the eigenvalues of the covariance matrices.

To improve on the Gaussian assumption for the distribution of latent variables, we have trained an alternative BMI in which the AE is replaced by a Variational AE. We train the VAE by adding to the interface loss function a regularizer term: the Kullback-Leibler (KL) divergence  $D_{\text{KL}}(p_0(\mathbf{z}_0) \| q(\mathbf{z}_0))$  between the probability distribution  $p_0(\mathbf{z}_0)$  of the latent activity on day-0 and  $q(\mathbf{z}_0) = \mathcal{N}(\mathbf{z}_0; 0, \mathbf{I})$ . The latent variables of the VAE are thus subject to the additional soft constraint of conforming to a normal distribution.


**2023-10-20 Predrag** The last sect. of John Duchy *Derivations for Linear Algebra and Optimization* [notes](#) gives the derivation of the KL divergence between two multivariate Gaussians (17.11). So does Rishabh Gupta's [website](#).

**2023-10-18 Predrag** Read:

J. Erdmenger, K. Grosvenor and R. Jefferson, *Information geometry in quantum field theory: Lessons from simple examples*, SciPost Physics 8 (2020) 073.

K. Grosvenor and R. Jefferson, *The edge of chaos: Quantum field theory and deep neural networks*, SciPost Physics 12 (2022) 081.

**2023-12-14 Ed Witten** .

 *A background independent algebra in quantum gravity*, see Chandrasekaran, Longo, Penington and Witten [1] *An algebra of observables for de Sitter space* (2023)

**2024-11-17 Predrag** Looking at [Jordan Cotler](#), publications on [Google Scholar](#) and [arXiv](#): some overlap with kinds of things we have been discussing and (should have been) writing up. I had only scanned over his publications, but in this seminar –two versions, the same slides– based on Cotler and Rezhikov [arXiv:2202.11737](#),

▶ [Renormalization group flow as optimal transport](#) (Apr 14, 2022)

▶ [Renormalization group flow as optimal transport](#) (Mar 30, 2022)

at about min 8:24, Cotler relates Euclidean scalar field theory (the same that we use) Polchinski [15] renormalization flow (see post **2023-02-13 Predrag**, we do not do that) to Kullback-Leibler divergence (17.10), see our sect. 17.2 *Information*: They show that Polchinski's equation can be written as

$$-\Lambda \frac{d}{d\Lambda} P_\Lambda[\phi] = -\nabla_{\mathcal{W}_2} S(P_\Lambda[\phi] \| Q_\Lambda[\phi]) \quad (17.25)$$

where  $\nabla_{\mathcal{W}_2}$  is a gradient with respect to a functional generalization of the Wasserstein-2 metric,  $S(P \| Q) = \int [d\phi] P[\phi] \log(P[\phi]/Q[\phi])$  is a functional version of the relative entropy (17.10), and  $Q_\Lambda[\phi]$  is a background probability functional that defines their RG scheme.

Polchinski's equation is a special case of the Wegner-Morris flow equation. The latter provides insights into the structure of RG flows which are obscured by Polchinski's formulation. The Wegner-Morris equation is

$$-\Lambda \frac{d}{d\Lambda} P_\Lambda[\phi] = \int d^d x \frac{\delta}{\delta\phi(x)} (\Psi_\Lambda[\phi, x] P_\Lambda[\phi]) \quad (17.26)$$

and implements ERG for a scheme determined by  $\Psi_\Lambda[\phi, x]$  where  $\Psi_\Lambda[\phi, x]$  will depend on  $P_\Lambda[\phi]$  in a non-trivial way. (Cotler likes most the exposition of Latorre and Morris [11] *Exact scheme independence* (2000); [arXiv:hep-th/0008123](#).)

Instead of relative entropy, they use

$$M_\Lambda(P_\Lambda) := S(P_\Lambda \| Q_\Lambda) - \log(Z_{Q,\Lambda}), \quad (17.27)$$

with  $Q_\Lambda[\phi] = e^{-S_{Q,\Lambda}[\phi]}/Z_{Q,\Lambda}$ , whose Wegner-Morris flow is monotone.

Polchinski equation is a type of a heat flow.

The heat flow is a gradient flow with respect to the  $L^2$  metric.

The heat flow is the gradient flow of the differential entropy with respect to the Wasserstein-2 metric.

Polchinski Wegner-Morris flow is the optimal transport gradient flow of relative entropy.

Intuitively, (17.25) says that the coarse-graining of their theory is generated by a decrease in a relative entropy.

Their sect. 6.1 *Variational discretization of the renormalization group flow* is interesting.

They use free field theory, and also do explicit perturbative computations for massive scalar  $\phi^4$  theory.

I believe Cotler's transport problem is related to our (Matt's) computation of periodic states by optimization, chapter 19.4 *Heat kernel, continuous space, fictitious time*. Our 'fictitious time' (in Newton iterations, for

example) is discrete, their renormalization flow is continuous in the cut-off scale  $\Lambda$ , so Cotler uses [Wasserstein metric](#), which I have not used, see post **2023-10-13 Predrag**.

Also of possible interest:

Cotler and Rezhikov *Renormalizing Diffusion Models*; [arXiv:2308.12355](#):

“ We explain how to use diffusion models to learn inverse renormalization group flows [...] These models achieve sample generation by learning the inverse process to a diffusion process which adds noise to the data until the distribution of the data is pure noise. Nonperturbative renormalization group schemes in physics can naturally be written as diffusion processes in the space of fields. [...] We also explain how to use diffusion models in a variational method to find ground states of quantum systems. We apply some of our methods to numerically find RG flows of interacting statistical field theories. ”

Bhattacharya, Cotler, Dersy and Schwartz *Renormalons as Saddle Points*; [arXiv:2410.07351](#)

Bhattacharya, Cotler, Dersy and Schwartz *The Collective Coordinate Fix*; [arXiv:2402.18633](#)

A popular blurb (unfortunately, I personally find *Quanta Magazine* ‘popularizations’ useless) [Physicists Rewrite a Quantum Rule That Clashes With Our Universe](#).

Busy beavers... Lots to unpack here.

**2024-11-17 Predrag** Read up on Lüscher’s ‘trivializing flows’, *Trivializing maps, the Wilson flow and the HMC algorithm*; [arXiv:0907.5491](#).

“ In lattice gauge theory, there exist field transformations that map the theory to the trivial one, where the basic field variables are completely decoupled from one another. Such maps can be constructed systematically by integrating certain flow equations in field space. [...] it is proposed to combine the Wilson flow [...] with the HMC simulation algorithm. ”

**2024-12-28 Predrag** I have a bunch of notes on Redfern, Lazer and Lucas [16] *Dynamically relevant recurrent flows obtained via a nonlinear recurrence function from two-dimensional turbulence* (2024); [arXiv:2408.05079](#)

in repo `pipes/blog/blog.tex` file `dailyBlog.tex`. Here I separate out the notes on their Kullback-Leibler.

For a given statistic  $\Gamma$  they seek a prediction based on an expansion in terms of  $N$  recurrent flows

$$\Gamma_{pred} = \sum_{j=1}^N w_j \Gamma_j \tag{17.28}$$

where the weights  $w_j$  are such that  $\sum_{j=1}^N w_j = 1$  and  $\Gamma_j$  is the statistic obtained for each individual solution.

Page *et al.* [14] shows evidence for the Markovian view of a turbulent trajectory “pinballing” between invariant sets by computing a transition matrix from shadowing events and using its invariant measure as the weights of the recurrent flow expansion. [...] we investigate some “optimal” expansions by obtaining the weights which minimize the Kullback-Leibler (KL) divergence, following Lucas and Kerswell [13];

$$\mathcal{L}(D) = \int \Gamma(D) \log \left( \frac{\Gamma_{pred}(D)}{\Gamma(D)} \right) + \Gamma(D) - \Gamma_{pred}(D) dD, \quad (17.29)$$

which is a loss function designed for minimizing the distance between probability distributions. We use the `scipy` minimiser with the L-BFGS-B algorithm. Here  $\Gamma(D)$  is the probability density function for the dissipation rate  $D$ . [...] here we use weights minimizing  $\mathcal{L}(D)$  and to reconstruct the other statistics [...] also very well approximated, [...] much better than the control weighting  $w_j = 1/N$ .

the weights  $w_j$  plotted against the sum of the real parts of the unstable Floquet exponents for each recurrent flow  $j$

$$\bar{\sigma} = \sum_i \sigma_i, \quad (17.30)$$

where  $\sigma_i$  are the real parts of individual unstable exponents. [...] the optimal set has many orbits with very small weights. [...] the minimization algorithm has returned a significant number of weights which are identically zero.

[...] to quantify the quality of the fit, independently of the KL-divergence, consider the mean squared error

$$\mathcal{E}(\Gamma) = \frac{1}{n} \sum_i^n (\Gamma - \Gamma_{pred})^2. \quad (17.31)$$

What is the minimal set of recurrent flows that represent well the turbulent state?

[...] a pruning strategy to find a minimal set of orbits [...] using  $\mathcal{L}(E)$  as loss function. [...] initialise a list with the pair of orbits which minimizes  $\mathcal{L}(E)$  and then iteratively append the orbit which reduces the loss the most [...] We find that 20 orbits are sufficient to provide an accurate representation of the energy PDF. [...]

[...] the cycle expansions of periodic orbit theory were trialed using this data set and showed less successful reconstructions than the ones shown here, severely underestimating the contributions from the extreme events.

**2024-12-28 Predrag** Compare our (17.11), (17.24) with their (17.29). We use KL to compare pairs of individual solutions

Their Fig. 6 plot of  $\bar{\sigma}$ , bottom right, makes no sense to me.

Why does KL in their Fig. 10 plateaus at  $N = 10$  orbits? Is there an orbit that should not be there? Is the real distribution bimodal, and this cannot fit it?

Regrettably, they again resurrect Zoldi & Greenside, Kazantsev nonsense.

**2024-12-28 Predrag** Redfern, Lazer and Lucas [16] "follow" Lucas and Kerswell [13] *Spatiotemporal dynamics in 2D Kolmogorov flow over large domains* (2014), but I see no Kullback-Leibler (?) there.

**2024-12-28 Predrag** However, a different Lucas, Simon M. Lucas and Vanessa Volz *Tile Pattern KL-Divergence for Analysing and Evolving Game Levels*; [arXiv:1905.05077](https://arxiv.org/abs/1905.05077) might be useful to us for measuring KL divergence between mosaics :)

[...] a detailed investigation of using the Kullback-Leibler (KL) divergence as a way to compare and analyse game-levels, and hence to use the measure as the objective function of an evolutionary algorithm to evolve new levels. We describe the benefits of its asymmetry for level analysis.

In order to apply the  $D_{KL}$ , we transform levels into probability distributions over tile pattern occurrences. Given a rectangular level of size  $(T_W \times T_H)$  and a rectangular filter window of size  $(F_W \times F_H)$ , the total number of tile patterns  $N$  is given by:

$$N = (1 + T_W - F_W)(1 + T_H - F_H) \quad (17.32)$$

Thus,  $X$  in (17.10) is the set of all tile patterns observed in either the set of training samples, or in the generated levels. For each experiment, we take the set of tile patterns that occur by sliding (convolving) a fixed-size window over a level, where a level is defined as a 2-d array of tiles.

## References

- [1] V. Chandrasekaran, R. Longo, G. Penington, and E. Witten, "An algebra of observables for de Sitter space", *J. High Energy Phys.* **2023**, 082 (2023).
- [2] P. Cvitanović, "Chaotic Field Theory: A sketch", *Physica A* **288**, 61–80 (2000).
- [3] P. Cvitanović, C. P. Dettmann, R. Mainieri, and G. Vattay, "Trace formulae for stochastic evolution operators: Smooth conjugation method", *Nonlinearity* **12**, 939 (1999).
- [4] P. Cvitanović and Y. Lan, Turbulent fields and their recurrences, in *Correlations and Fluctuations in QCD : Proceedings of 10. International Workshop on Multiparticle Production*, edited by N. Antoniou (2003), pp. 313–325.



- [5] A. Farshchian, J. A. Gallego, J. P. Cohen, Y. Bengio, L. E. Miller, and S. A. Solla, *Adversarial domain adaptation for stable brain-machine interface*, in *Internat. Con. Learning Representations* (2019), pp. 1–14.
- [6] M. I. Jordan, Z. Ghahramani, T. S. Jaakkola, and L. K. Saul, *“An introduction to variational methods for graphical models”*, *Machine Learning* **37**, 183–233 (1999).
- [7] S. Kullback and R. A. Leibler, *“On information and sufficiency”*, *Ann. Math. Statistics* **22**, 79–86 (1951).
- [8] D. Kunin, J. Sagastuy-Brena, S. Ganguli, D. L. K. Yamins, and H. Tanaka, *Neural mechanics: Symmetry and broken conservation laws in deep learning dynamics*, in *Intern. conf. learning representations* (2021).
- [9] Y. Lan, *Dynamical Systems Approach to 1 – d Spatiotemporal Chaos – A Cyclist’s View*, PhD thesis (School of Physics, Georgia Inst. of Technology, Atlanta, 2004).
- [10] Y. Lan and P. Cvitanović, *“Variational method for finding periodic orbits in a general flow”*, *Phys. Rev. E* **69**, 016217 (2004).
- [11] J. I. Latorre and T. R. Morris, *“Exact scheme independence”*, *J. High Energ. Phys.* **2000**, 004 (2000).
- [12] H. Liao and J. He, *Jacobian determinant of normalizing flows*, 2021.
- [13] D. Lucas and R. R. Kerswell, *“Spatiotemporal dynamics in 2D Kolmogorov flow over large domains”*, *J. Fluid Mech.* **750**, 518–554 (2014).
- [14] J. Page, P. Norgaard, M. P. Brenner, and R. R. Kerswell, *“Recurrent flow patterns as a basis for two-dimensional turbulence: Predicting statistics from structures”*, *Proc. Natl. Acad. Sci.* **121**, 23 (2024).
- [15] J. Polchinski, *“Renormalization and effective Lagrangians”*, *Nucl. Phys. B* **231**, 269–295 (1984).
- [16] E. M. Redfern, A. L. Lazer, and D. Lucas, *“Dynamically relevant recurrent flows obtained via a nonlinear recurrence function from two-dimensional turbulence”*, *Phys. Rev. Fluids* **9**, 124401 (2024).
- [17] I. Vierhaus, *Simulation of  $\phi^4$  Theory in the Strong Coupling Expansion beyond the Ising Limit*, MA thesis (Humboldt-Univ. Berlin, Math.-Naturwissen. Fakultät I, 2010).

# Chapter 18

## Heat kernel

This might go into Liang and Cvitanović [15] *A derivation of Hill's formulas* (2024): The general setting are Hill's formulas, relating zeta-regularized determinants of Jacobian operators with positive spectrum to Fredholm determinants of Hessians (forward-in-time determinants?).

**2024-12-01 Predrag** Starting this because I have a few hunches (not yet worked out)

1. Might maybe derive Xuanqi's  $2d$  Hill determinant as discrete random walks on square lattice, induced by Laplacian operator, see [QM lectures sect. 1.1 Wanderings of a drunken snail](#). It's OK for the free field theory, have not figured out yet how to insert nonlinear potentials.
2. Give us a discretized version of the *Gel'fand-Yaglom theorem's* 'Fredholm' operator, page 599. whose are stability is given by the orbit Jacobian operators. Can also think of this as infinitesimal fictitious time Newton methods steps stability matrix.
3. See also sect. 4.5 *Orbit stability*, sect. 4.16 *Noise is your friend*.

### 18.1 Heat kernel, continuous space, fictitious time

Let  $u(x, t)$  be a field at spatial position  $x \in \mathbb{R}^d$  at time  $t$ . The *heat equation* for  $u$  is <sup>1 2</sup>

$$\partial_t u = \frac{1}{2} \Delta u, \quad t > 0. \quad (18.1)$$

Laplacian  $\Delta$  is a negative operator, so  $e^{t\Delta/2}$  is the contraction time- $t$  *forward* heat operator. Given an initial density distribution  $\rho_0$  in  $L^2(\mathbb{R}^d, dx)$ ,

$$u(x, t) = (e^{t\Delta/2} \rho_0)(x), \quad (18.2)$$

---

<sup>1</sup>Predrag 2024-12-01: Should we use  $\square$  or  $\Delta$ , in all articles?

<sup>2</sup>Predrag 2024-12-01: Following Hall, see (18.23)

satisfies the heat equation (18.1) with the initial condition

$$\lim_{t \searrow 0} u(x, t) = \rho_0(x).$$

The *heat operator* is given by convolution

$$(e^{t\Delta/2}\rho_0)(x) = \int_{\mathbb{R}^d} \rho_t(x - x')\rho_0(x') dx' \quad (18.3)$$

with the Gaussian *heat kernel*

$$\rho_t(x) = (2\pi t)^{-d/2} e^{-x^2/2t}. \quad (18.4)$$

## 18.2 Wanderings of a drunken snail

Consider a lattice state is given by its phase space field values<sup>3</sup>  $i = (x_1, x_2, \dots, x_d)$ , and that the field is a scalar, with no further internal degrees of freedom.

TO BE CONTINUED

2020-05-05, 2024-11-29 **Predrag** See also:

Matthias Ludewig *Path Integrals on Manifolds with Boundary and their Asymptotic Expansions*, page 599.

2023-11-25 **Predrag** Dunne post.

Sect. 19.4 *Computing log det of Hill determinant*

One-dimensional discretized heat equation (2.99).

The elliptic  $\theta$ -functions heat equation (19.32).

2020-05-13 **Predrag** For general regular graphs with a transitive group action, in particular the discrete tori, a zeta function has been defined in an impressive paper by Chinta, Jorgenson and Karlsson [2] *Heat kernels on regular graphs and generalized Ihara zeta function formulas*: Let  $q$  be a positive integer and  $G$  be a  $(q + 1)$ -regular graph. There is an associated heat kernel  $K_G(t, x_0, x)$  corresponding to the Laplacian formed by considering the adjacency matrix on  $G$ . The building blocks of  $K_G$  are I-Bessel functions, and the number of geodesics from a fixed base point  $x_0$  to  $x$  of length  $m$ .

$N_m^0$  denotes the number of closed geodesics of length  $m$  in  $G$  with base point  $x_0$ .

They give a clear introduction into heat kernels on graphs, the origin of I-Bessel functions, and the relation to the number of paths. They also deduce the classical Ihara determinantal formula.

<sup>3</sup>Predrag 2024-11-21: It's not a field  $x_z$ , its a probability  $\rho_z$ , where we have set unit hypercube volume to unity.

There is a second expression for the heat kernel coming from spectral considerations. Equating the two expressions for the heat kernel, as in known approaches to the Poisson summation formula or the Selberg trace formula, one obtains an identity which is a type of theta inversion formula. To this identity they apply an integral transform, a Laplace transform with a change of variables, and obtain the logarithmic derivative of the Ihara zeta function.

For finite graphs, the classical Ihara zeta function is their Ihara zeta function raised to the power equaling the number of vertices (by fixing the base point  $x_0$ , they can work with infinite graphs). They give a formula, their Theorem 1.3, for  $1/\zeta$  as an integral over the spectral measure for the Laplacian.

They also count geodesics paths, not only closed geodesics paths. That corresponds to computing the Hurwitz zeta function instead of the Riemann zeta function, they say.

**2020-05-13 Predrag** Chinta, Jorgenson and Karlsson [1] *Zeta functions, heat kernels, and spectral asymptotics on degenerating families of discrete tori:*

By a discrete torus we mean the Cayley graph associated to a finite product of finite cycle groups with the generating set given by choosing a generator for each cyclic factor.

We examine the spectral theory of the combinatorial Laplacian for sequences of discrete tori when the orders of the cyclic factors tend to infinity at comparable rates. First, we show that the sequence of heat kernels corresponding to the degenerating family converges, after rescaling, to the heat kernel on an associated real torus.

We then establish an asymptotic expansion, in the degeneration parameter, of the determinant of the combinatorial Laplacian. The zeta-regularized determinant of the Laplacian of the limiting real torus appears as the constant term in this expansion.

By a classical theorem by Kirchhoff, the determinant of the combinatorial Laplacian of a finite graph divided by the number of vertices equals the number of spanning trees, called the complexity, of the graph. As a result, we establish a precise connection between the complexity of the Cayley graphs of finite abelian groups and heights of real tori.

It is also known that spectral determinants on discrete tori can be expressed using trigonometric functions and that spectral determinants on real tori can be expressed using modular forms on general linear groups. Another interpretation of our analysis is thus to establish a link between limiting values of certain products of trigonometric functions and modular forms. The heat kernel analysis which we employ uses I-Bessel functions. Our methods extend to prove the asymptotic behavior of other spectral invariants through degeneration, such as special values of spectral zeta functions and Epstein-Hurwitz-type zeta functions.

For any  $d \geq 1$ , let  $N = (n_1, \dots, n_d)$  denote a  $d$ -tuple of positive integers, and consider the product

$$D(N) = \prod_{K \neq 0} (2d - 2 \cos(2\pi k_1/n_1) - \dots - 2 \cos(2\pi k_d/n_d)); \quad (18.5)$$

where the product is over all  $d$ -tuples  $K = (k_1, \dots, k_d)$  of non-negative integers with  $k_j < n_j$ , omitting the zero vector in the product.

One can view  $D(N)$  as a determinant of a naturally defined matrix from graph theory. Quite generally, associated to any finite graph, there is a discrete Laplacian which acts on the finite dimensional space of complex valued functions whose domain of definition is the space of vertices of the graph.  $D(N)$  is equal to the product of the non-zero eigenvalues of the Laplacian associated to a graph which we call a discrete torus.

The  $d$ -dimensional discrete torus is defined as the product space

$$DT_N = \prod_{j=1}^d \ell_j \mathbb{Z} \backslash \mathbb{Z}, \quad (18.6)$$

See also

Yamasaki [19] *An explicit prime geodesic theorem for discrete tori and the hypergeometric functions*

Anders Karlsson *Spectral zeta functions*, [arXiv:1907.01832](https://arxiv.org/abs/1907.01832)

section 16.7

**2019-12-12 Predrag** Meisinger and Ogilvie *The Sign Problem, PT Symmetry and Abelian Lattice Duality* [arXiv:1306.1495](https://arxiv.org/abs/1306.1495): For Abelian models in the class of lattice field theories with the fundamental fields which are elements  $z = \exp(i\theta)$  of  $Z(N)$  or  $U(1)$ , with complex actions, lattice duality maps models with complex actions into dual models with real actions.

Explicit duality relations are given for models for spin and gauge models based on  $Z(N)$  and  $U(1)$  symmetry groups. The dual forms are generalizations of the  $Z(N)$  chiral clock model and the lattice Frenkel-Kontorova model, respectively.

We begin with duality for  $d = 2$   $Z(N)$  models with a chemical potential for the Villain, or heat kernel, action. Defining the site-based spin variables as  $\exp(2\pi i m(x)/N)$ , with  $m(x)$  an integer between 0 and  $N$ , the partition function is given by

$$Z[J, \mu\delta_{\nu,2}] = \sum_m \sum_{n_\nu} \exp \left[ -\frac{J}{2} \sum_{x,\nu} \left( \frac{2\pi}{N} \partial_\nu m(x) - i\mu\delta_{\nu,2} - 2\pi n_\nu(x) \right)^2 \right] \quad (18.7)$$

where  $\partial_\nu m(x) \equiv m(x+\hat{\nu}) - m(x)$  and the sum over link variables  $n_\nu(x) \in Z$  ensures periodicity. Using the properties of the Villain action, we can

write

$$Z[J, \mu\delta_{\nu,2}] = (2\pi J)^{-dV/2} \sum_m \sum_{p_\nu} \exp \left[ -\frac{1}{2J} \sum_{x,\nu} p_\nu^2(x) + i \sum_{x,\nu} p_\nu(x) \left( \frac{2\pi}{N} \partial_\nu m(x) - i\mu\delta_{\nu,2} \right) \right]$$

where  $V$  is the number of sites on the lattice such that  $dV$  is the number of links. Summation over the  $m(x)$ 's give a set of delta function constraints:

$$Z[J, \mu\delta_{\nu,2}] = (2\pi J)^{-dV/2} \sum_{p_\nu} \exp \left[ -\frac{1}{2J} \sum_{x,\nu} p_\nu^2(x) + \sum_{x,\nu} p_\nu(x) \mu \right] \prod_x \delta_{\partial \cdot p, 0(N)}$$

where the notation in the Kronecker delta function indicates  $\partial \cdot p = 0$  modulo  $N$ . We introduce a dual bond variable  $\tilde{p}_\rho(X)$  associated with the dual lattice via  $p_\nu(x) = \epsilon_{\nu\rho} \tilde{p}_\rho(X)$  and note that the constraint on  $p_\nu$  is solved by  $\tilde{p}_\rho(X) = \partial_\rho \tilde{q}(X) + N\tilde{r}_\nu(X)$ . We have

$$Z[J, \mu\delta_{\nu,2}] = (2\pi J)^{-dV/2} \sum_{\tilde{q}} \sum_{\tilde{r}_\nu} \exp \left[ -\frac{1}{2J} \sum_{x,\nu} (\partial_\rho \tilde{q}(X) + N\tilde{r}_\nu(X))^2 + \mu \sum_{x,\nu} (\partial_1 \tilde{q}(X) + N\tilde{r}_1(X)) \right]$$

which leads to

$$Z[J, \mu\delta_{\nu,2}] = (2\pi J)^{-dV/2} \exp \left[ +\frac{V}{2} J\mu^2 \right] Z \left[ \frac{N^2}{4\pi^2 J}, -i\frac{2\pi J\mu}{N} \delta_{\nu,1} \right]$$

The generalized duality here is

$$J \rightarrow \tilde{J} = \frac{N^2}{4\pi^2 J} \quad (18.8)$$

$$\mu\delta_{\nu,2} \rightarrow \tilde{\mu}\delta_{\nu,1} = -i\frac{2\pi J\mu}{N} \delta_{\nu,1}. \quad (18.9)$$

The dual of the original model, which has a complex action, is a chiral  $Z(N)$  model with a real action.

**2020-05-14 Predrag** I'm very impressed by Jérémy Dubout [5] *Zeta functions of graphs, their symmetries and extended Catalan numbers*, [arXiv:1909.01659](https://arxiv.org/abs/1909.01659):

It is natural to form symmetric functions of the eigenvalues of operators, in finite dimensions one has the trace and determinant. In infinite dimensions things become more complicated. For example, the determinant of

the Laplace operator on a manifold cannot be directly defined, but the following the heat kernel function can

$$\zeta_M(s) = \sum_{n \in \mathbb{N}} \lambda_n^{-s} = \frac{1}{\Gamma(s)} \int_0^\infty \text{tr} (e^{-t\Delta}) t^s \frac{dt}{t}, \quad (18.10)$$

for  $s$  in the half-plane  $\{s | \text{Re}(s) > 0\}$ . Since graphs have a natural Laplacian  $\Delta$ , Dubout considers sums over the eigenvalues as in (18.10), and introduces the *spectral zeta function* of a graph  $G$  as

$$\zeta_G(s) = \int_{\sigma(\Delta)} x^{-s} \mu_{\Delta}^{\delta_v, \delta_v}(dx),$$

where  $\mu_{\Delta}^{\delta_v, \delta_v}(dx)$  is a spectral measure of the Laplacian.  $\zeta_G$  provides an analogue of the right hand side of (18.10) for graphs. Dubout introduces a heat function  $H_t$  for infinite graphs [8] as an analogue of the heat kernel for manifolds:

$$\zeta_G(s) = \frac{1}{\Gamma(s)} \int_0^\infty H_t^G t^s \frac{dt}{t}.$$

This spectral zeta function recovers both previous definitions for finite graphs, the lattice  $\mathbb{Z}^d$  and the infinite  $d$ -regular tree. Dubout extends the  $\mathbb{Z}$  functional equation [8] to  $\mathbb{Z}^2$ . For more general  $s$  and  $d > 2$  the existence of such symmetries remains unknown. The formula acts can interpreted as a symmetry for Catalan numbers. Dubout is able to describe  $\zeta_G$  explicitly for  $G = \mathbb{Z}^d$  as well as for products for integers values.

Contrary to the compact manifold case, the heat kernel of an infinite graph is not always a trace-class operator. Instead of taking its trace, Dubout therefore evaluates it on the rooted graph, at some cost.

The resolvent

$$R(z, \Delta) = \frac{1}{z - \Delta}.$$

The heat kernel of  $\mathbb{Z}$  is given by

$$H_t^{\mathbb{Z}} = \int_0^4 \frac{e^{-tx}}{\pi \sqrt{x(4-x)}} dx = e^{-2t} I_0(2t),$$

where  $I_0$  a modified Bessel function of first kind, the same as ref. [13] (up to a factor 2, coming from their normalization of the Laplacian). Dubout extends this result to  $\mathbb{Z}^d$  with

$$H_t^{\mathbb{Z}^d} = e^{-2dt} I_0(2t)^d.$$

The spectral zeta function of  $\mathbb{Z}$  is given by

$$\begin{aligned} \zeta_{\mathbb{Z}}(s) &= \int_0^4 x^{-s} \frac{1}{\pi \sqrt{x(4-x)}} dx = \frac{1}{\pi} \int_0^1 4^{-s} x^{-s-\frac{1}{2}} (1-x)^{-\frac{1}{2}} dx \\ &= \frac{4^{-s}}{\pi} \mathbf{B} \left( \frac{1}{2} - s, \frac{1}{2} \right) = \frac{4^{-s}}{\sqrt{\pi}} \frac{\Gamma(\frac{1}{2} - s)}{\Gamma(1-s)}, \end{aligned} \quad (18.11)$$

where  $\mathbf{B}, \Gamma$  are the beta and gamma functions.

The function  $\zeta_{\mathbb{Z}}$  is meromorphic over  $\mathbb{C} \setminus \{\frac{1}{2}, \frac{3}{2}, \dots\}$  and satisfies

$$\zeta_{\mathbb{Z}}(s) = \begin{pmatrix} -2s \\ -s \end{pmatrix}$$

for any  $s$ .

For a finite transitive graph  $G$  with  $n$  vertices, the spectral zeta function  $\zeta_G$  can be written in explicit form, similar to the one in the first part of Equation 18.10, and analytically continued over  $\mathbb{C}$  with the formula

$$\zeta_G(s) = \frac{1}{n} \sum_{\lambda \neq 0} \lambda^{-s}, \quad (18.12)$$

where the sum is over the non-zero eigenvalues of  $\Delta_G$ . The Lebesgue's decomposition theorem allows us to split the spectral measure into an absolutely continuous part, a singular continuous part and a pure point part. The only issue with  $\zeta_G$ 's analyticity is the presence of 0 in the spectrum: A graph  $G$  is finite if and only if 0 belongs to the pure point part. Dubout then does some serious analysis.

Dubout introduces a *regularized determinant*. If  $G$  is finite and transitive, then  $\det^*(x + \Delta) = \det(x\mathbf{1} + \Delta)^{\frac{1}{|\mathbf{V}_G|}}$ . In the case of the regularized determinant for  $\mathbb{Z}$ , Dubout almost gets the generating function of the Catalan numbers:

$$\det^*(x + \Delta_{\mathbb{Z}}) = \frac{x}{2} + 1 + \frac{1}{2} \sqrt{x(4+x)} = x + 2 + \sum_{n \geq 1} C_n \frac{(-1)^n}{x^n}, \quad (18.13)$$

where  $C_n = \frac{1}{n+1} \binom{2n}{n}$  is the  $n$ -th Catalan number.

**Predrag:** Amusing, but I've also run into Catalan numbers while counting rooted trees, back in 1976: Cvitanović [4] *Group theory for Feynman diagrams in non-Abelian gauge theories*

Dubout computes the standard characteristic polynomial of the Laplacian of a cyclic graph, by a new, completely analytical way of obtaining the coefficients. Given  $n \in \mathbb{N}^*$ , let  $G_n$  denote the Cayley graph  $(\mathbb{Z}/n\mathbb{Z}, \{\pm 1\})$ . Then

$$\det(x + \Delta_{G_n}) = \sum_{l=0}^{n-1} \binom{2n-l}{l} \frac{2n}{2n-l} x^{n-l}. \quad (18.14)$$

The coefficients of  $\det(x + \Delta_{G_n})$  can be computed numerically using the eigenvalues of  $\Delta_{G_n}$ . Dubout gets the our usual discrete Fourier product formula

$$\det(x + \Delta_{G_n}) = \prod_{k=0}^{n-1} \left( x + 4 \sin^2 \left( \frac{k\pi}{n} \right) \right),$$



but he did not find a way to expand this product into a polynomial with integers coefficients.

**Predrag:** we should alert him to our integer-points counting formulas!

Dubout then relates the Ihara zeta function  $Z_G$  [18] of a  $d$ -regular finite graph  $G$

$$Z_G(u) = \left( (1 - u^2)^{\frac{(d-2)|V_G|}{2}} \det \left( 1 - (d - \Delta_G)u + (d - 1)u^2 \right) \right)^{-1}. \quad (18.15)$$

to his spectral zeta function. Given a  $d$ -regular finite graph  $G$  with  $n$  vertex, the Ihara zeta function of  $G$  can be computed as

$$Z_G(u) = (y_u \det^* (x_u + \Delta_G))^{-n}, \quad (18.16)$$

with  $y_u = u(1 - u^2)^{\frac{d}{2}-1}$  and  $x_u = (1 - \frac{1}{u})(u(d - 1) - 1)$ .

The appearance of  $|V_G|$  in (18.16) as only an exponent provides good motivation for defining a modified Ihara zeta function that extends to infinite graphs:

The *regularized Ihara zeta function* of a (possibly infinite)  $d$ -regular graph  $G$  is defined as

$$Z_G^*(u) = u^{-1}(1 - u^2)^{1-\frac{d}{2}} \det^* \left( \left( 1 - \frac{1}{u} \right) (u(d - 1) - 1) + \Delta_G \right)^{-1}. \quad (18.17)$$

This coincides with the known one for the Cayley graph of a finitely generated group.

It follows from (18.16) that if  $G$  is finite then  $Z_G^*(u)^{|V_G|} = Z_G(u)$ . This allows us to extend the functional equations to infinite regular graphs.

The regularized determinant of  $\mathbb{Z}$  was calculated in (18.13), and following (18.17) he obtains the regularized Ihara zeta function of  $\mathbb{Z}$ :

$$Z_{\mathbb{Z}}^*(u) = \begin{cases} 1 & \text{if } 0 < |u| < 1, \\ u^2 & \text{if } |u| > 1. \end{cases} \quad (18.18)$$

Note the functional equation

$$Z_{\mathbb{Z}}^* \left( \frac{1}{u} \right) = \frac{1}{u^2} Z_{\mathbb{Z}}^*(u).$$

That  $Z_{\mathbb{Z}}^*(u) = 1$  for  $0 < u < 1$  is a natural result, as the original definition of the Ihara zeta function is a generating function of weighted loops, and  $\mathbb{Z}$  does not have any, giving us only 1 as generating function. The same argument holds for any tree-like graph.

**2024-07-07 Predrag** To include into heat kernel references: [1, 5, 6, 12, 13, 16, 17, 19].

**2024-07-07 Predrag** Guido Caldarelli, Andrea Gabrielli, Tommaso Gili and Pablo Villegas *Laplacian Renormalization Group: An introduction to heterogeneous coarse-graining*, [arXiv:2406.02337](https://arxiv.org/abs/2406.02337).

We are not considering renormalization group here, so I have clipped only parts that interpret *the Laplacian as a generator of diffusion* (18.21) on networks (in our example, regular only).

The partition function  $Z$  determines all the thermodynamic properties of the system. Let us call  $\mathcal{F}_G[\phi(\mathbf{x}, t)]$  the quadratic part of  $\mathcal{F}[\phi(\mathbf{x}, t)]$ , giving rise to the Gaussian approximation of the theory, determined by the Laplacian  $\nabla^2$  operator of the embedding Euclidean space for the equilibrium models and by the heat equation operator  $\partial_t - D\nabla^2$  for out-of-equilibrium models (e.g., contact process) with local interactions and spatio-temporal homogeneity. It is convenient to use the Lagrangian as its exactly solvable Gaussian part takes a diagonal form. The plane waves  $\exp[i\mathbf{k} \cdot \mathbf{x}]$  are the eigenfunctions of the translation operator and, consequently, of the Laplacian  $\nabla^2$  with eigenvalues  $-k^2$ .

Facts on the effect of the introduction of quenched disorder in lattice models: in these out-of-equilibrium lattice models, ‘time’ and ‘space’ act differently on the process, it is customary to distinguish between spatial and temporal properties, denoting them respectively by the indices  $\perp$  and  $\parallel$ .

About the introduction of disorder in such lattice models: when dealing with dynamical models defined on strongly irregular networks, the topological disorder due to the embedding space can not be treated as a perturbation of the homogeneous lattice case.

Gaussian field theories can always be exactly solved, governed by the Laplace differential operator. So write the model on the basis that diagonalizes such Gaussian approximation, i.e., the basis of eigenstates of the Laplacian operator (in homogeneous spaces, these are the plane waves).

The Gaussian model on random graphs has the Hamiltonian

$$\mathcal{H} = \frac{1}{2} \sum_{ij} \phi_i (L_{ij} + m_i^2 \delta_{ij}) \phi_j, \quad (18.19)$$

where  $\phi_i$  is a real field, and  $m_i^2 = \alpha_i m^2$ , with  $1/K < \alpha_i < K$  for some positive  $K$  representing the square masses.

$\hat{L} = \hat{D} - \hat{A}$  is the analog of the continuous Laplace operator ( $-\nabla^2 \phi$ ) (in graph theory, the Laplacian operator is the network generalization of  $-\nabla^2$  instead of  $\nabla^2$ ), defined on a graph or a discrete grid, with  $\hat{A}$  the adjacency matrix of the network and  $\hat{D}$  the diagonal degree matrix of the network.

The symmetric graph Laplacian operator  $\hat{L} = \hat{D} - \hat{A}$  is the graph discrete representation of the continuous operator  $-\nabla^2$ .

The Laplacian matrix for general weighted but undirected networks is

$$L_{ij} = [(\delta_{ij} \sum_k A_{ik}) - A_{ij}], \quad (18.20)$$

where  $A_{ij}$  are the elements of the adjacency matrix  $A$ .

Using (18.20), we can now analyze how any scalar field evolves with time from a given initial specific state  $\phi(0)$ . This can be written as  $\phi(\tau) = e^{-\tau \hat{L}} \phi(0)$ , where the temporal evolution of  $\phi$  will depend on the *network propagator*,

$$\hat{K} = e^{-\tau \hat{L}}, \quad (18.21)$$

representing the discrete counterpart of the path-integral formulation of general diffusion processes, where now each matrix element  $\hat{K}_{ij}$  describes the sum of diffusion trajectories along all possible paths connecting nodes  $i$  and  $j$  at time  $\tau$ .

It grounds on two facts: (a) the Laplacian operator of a network describes the information diffusion dynamics on it so that it gives at each time the informationally equivalent neighborhood of each node of the network, proposing a natural extension to networks of the real space RG in homogeneous spaces à la Kadanoff; (b) the Laplacian RG can also be seen as a natural extension of the k-space RG à la Wilson in homogeneous spaces and practically all statistical dynamical models used to model physical processes on networks have a Gaussian approximation determined by the Laplacian operator.

Naoki Masuda, Mason A. Porter, Renaud Lambiotte *Random walks and diffusion on networks*; [arXiv:1612.03281](https://arxiv.org/abs/1612.03281). A review of possible interest...

**2024-11-14 Predrag** Ciaurri, Gillespie, Roncal, Torrea and Varona [3] *Harmonic analysis associated with a discrete Laplacian* (2017) ([click here](#)); [arXiv:1401.2091](https://arxiv.org/abs/1401.2091).

The fundamental solution of

$$u_t(n, t) = u(n + 1, t) - 2u(n, t) + u(n - 1, t), \quad n \in \mathbb{Z},$$

with  $u(n, 0) = \delta_{nm}$  for every fixed  $m \in \mathbb{Z}$ , is given by  $u(n, t) = e^{-2t} I_{n-m}(2t)$ , where  $I_k(t)$  is the Bessel function of imaginary argument. In other words, the heat semigroup of the discrete Laplacian the discrete Laplacian

$$\Delta f(n) = f(n + 1) - 2f(n) + f(n - 1), \quad n \in \mathbb{Z},$$

is described by the formal series

$$W_t f(n) = \sum_{m \in \mathbb{Z}} e^{-2t} I_{n-m}(2t) f(m).$$

The heat semigroup

$$W_t = e^{t\Delta}.$$

The fundamental solution of

$$u_t(n, t) = u(n + 1, t) - 2u(n, t) + u(n - 1, t), \quad n \in \mathbb{Z},$$

with  $u(n, 0) = \delta_{nm}$  for every fixed  $m \in \mathbb{Z}$ , is given by  $u(n, t) = e^{-2t} I_{n-m}(2t)$  (see [9] and [10]), where  $I_k(t)$  is the Bessel function of imaginary argument (for these functions, see [14, Chapter 5]). Consequently, the heat semigroup is given by the formal series

$$W_t f(n) = \sum_{m \in \mathbb{Z}} e^{-2t} I_{n-m}(2t) f(m). \quad (18.22)$$

**2024-11-14 Predrag** F. Alberto Grunbaum, Plamen Iliev *Heat kernel expansions on the integers*; [arXiv:math/0206089](#), [DOI](#).

Iliev [11] *Heat kernel expansions on the integers and the Toda lattice hierarchy*, (2008).

**2024-12-01 Predrag** Brian C. Hall *The range of the heat operator*; [arXiv:math/0409308](#), [DOI](#).

[...] Laplacian  $\Delta$  on  $\mathbb{R}^d$ ,

$$\Delta = \sum_{k=1}^d \frac{\partial^2}{\partial x_k^2}.$$

is a *negative* operator, which means that  $e^{t\Delta/2}$  is the *forward* heat operator. [...] The spectral theorem then allows us to define the heat operator  $e^{t\Delta/2}$  as a contraction operator on  $L^2(\mathbb{R}^d)$ . We will let “time- $t$  heat operator” denote  $e^{t\Delta/2}$  (with a factor of 2 in the exponent).

Given  $f$  in  $L^2(\mathbb{R}^d, dx)$ , if we define

$$u(x, s) = (e^{s\Delta/2} f)(x), \quad (18.23)$$

then  $u$  satisfies the heat equation

$$\frac{\partial u}{\partial s} = \frac{1}{2} \Delta u, \quad s > 0,$$

subject to the initial condition

$$\lim_{s \searrow 0} u(x, s) = f(x).$$

[...] the heat operator can be computed by convolution

$$(e^{t\Delta/2} f)(x) = \int_{\mathbb{R}^d} \rho_t(x - x') f(x') dx'. \quad (18.24)$$

against the *heat kernel*

$$\rho_t(x) = (2\pi t)^{-d/2} e^{-x^2/2t}, \quad (18.25)$$

where  $x^2 = x_1^2 + \dots + x_d^2$ . In this expression, we initially think of  $x$  as being in  $\mathbb{R}^d$ . However, it is easy to see that the heat kernel (18.25) has an entire analytic continuation to  $\mathbb{C}^d$ .

Then he works out Euclidean spaces, spheres, compact symmetric spaces, hyperbolic spaces, noncompact symmetric spaces, but I do not think we need to go there.

**2024-12-01 Predrag Jorgenson** and Lang [12] *The ubiquitous heat kernel* is a very advanced read for us. However, in their sect. *Variation formulas on moduli or fibered spaces*, they write:

[...] consider the simple example of a complex torus of real dimension 2. This is the example coming right after the circle. Such toruses are parametrized by a variable  $\tau$  in the upper half plane, giving rise to a lattice  $[1, \tau]$  generated over  $\mathbb{Z}$  by  $1, \tau$ . The *heat kernel*  $K_\tau$  is the periodization of the heat kernel on  $\mathbb{R}^2$ , and gives rise to the trace of the heat kernel  $(\text{tr } K_\tau)(t)$ . We let the zeta function  $\zeta_\tau$  be defined by

$$\Gamma(s)\zeta_\tau(s) = \int_0^\infty (\text{tr } K_\tau(t) - 1)t^s \frac{dt}{t} \quad (18.26)$$

So  $\xi_\tau(s) = \Gamma(s)\zeta_\tau(s)$  is the Mellin transform of the regularized heat trace (regularized because we subtracted 1 inside the integral, to make the integral converge for  $\text{Re}(s) > 0$ ).

[...] the variation formula ( **Kronecker Limit Formula** )

$$-\zeta'_\tau(0) = \ln \text{Im } \tau + \ln |\eta^2(\tau)| \quad (18.27)$$

Compare with (19.64), (19.37), (19.40), (19.79).

**2024-11-18 Predrag** See also my notes on Cotler and Rezhikov *Renormalizing Diffusion Models*; [arXiv:2308.12355](https://arxiv.org/abs/2308.12355) after eq. (17.25).

### 18.2.1 Newton flows

**2025-01-14 Predrag** Fornæss, Hu, Truong and Watanabe [7] *Backtracking new Q-Newton's method, Newton's flow, Voronoi's diagram and stochastic root finding*; [arXiv:2401.01393](https://arxiv.org/abs/2401.01393).

Newton's method

$$z_{n+1} = z_n - \frac{f(z_n)}{f'(z_n)}. \quad (18.28)$$

Relaxed Newton's method

$$z_{n+1} = z_n - \alpha \frac{f(z_n)}{f'(z_n)}, \quad \alpha \leq 1. \quad (18.29)$$

Newton flow in one real variable  $t$ :

$$\frac{dz}{dt} = -\frac{f(z)}{f'(z)} \quad (18.30)$$

with initial value  $z(0) = z_0$ . If a global solution  $z(t)$  exists, it satisfies

$$\frac{d}{dt}f(z(t)) = f'(z(t))\frac{dz}{dt} = -f(z).$$

Thus,  $f(z(t)) = f(z_0)e^{-t}$  and  $f(z(t)) \rightarrow 0$  as  $t \rightarrow \infty$ . The Euler discretization of the ODE (18.30)

$$\frac{z(t + \alpha) - z(t)}{\alpha} = -\frac{f(z(t))}{f'(z(t))}. \quad (18.31)$$

is the relaxed Newton's method,  $z(t + \alpha) = z(t) - \alpha f(z(t))/f'(z(t))$ .

The second Newton-type flow is the ordinary differential equation of complex-valued function  $z(t)$  of one real variable  $t$ :

$$\frac{dz}{dt} = -\frac{g(z)}{g'(z)}. \quad (18.32)$$

Here,  $g(z) = f(z)/f'(z)$  is a meromorphic function and  $f(z)$  is a holomorphic function. The roots of  $g$  are exactly the roots of  $f$ , with the advantage that their multiplicities are all 1. The ODE (18.32) is obtained by substituting  $g = f/f'$  for  $f$  in the ODE (18.30).

By a similar calculation, we can show that  $g(z(t)) = g(z_0)e^{-t} \rightarrow 0$  as  $t \rightarrow \infty$  if a global solution  $z(t)$  exists. Since the zeros of  $g$  is same as the zeros of  $f$ , we expect the flow  $z(t)$  will converge to a root of  $f$ .

The conceptual difference between two ODEs (18.30) and (18.32) is the singular sets. The singular set for (18.30) is  $\{f' = 0\} \setminus \{f = 0\}$ , while the singular set for (18.32) is contained in  $\{(f')^2 - ff'' = 0\}$ .

From now on, this version will be named Newton's flow vFraction.

Newton's method for systems of equations  $G(z) = 0$  is the iteration

$$z_{n+1} = z_n - J(z_n)^{-1} \cdot G(z_n), \quad (18.33)$$

where  $J$  is the Jacobian matrix of  $G$ .

Newton's method for optimization: Assume that one wants to find (local) minima of an objective function  $F : \mathbf{R}^m \rightarrow \mathbf{R}$ . Let  $\nabla F$  be the gradient of  $F$ , and  $\nabla^2 F$  be the Hessian of  $F$ . Choose  $z_0 \in \mathbf{R}^m$  an initial point, and define Newton's method for the function  $F$  is the iterative algorithm:

$$z_{n+1} = z_n - (\nabla^2 F(z_n))^{-1} \cdot \nabla F(z_n). \quad (18.34)$$

Newton's method is invariant under a linear change of coordinates.

The optimization version of Newton's flow is the ordinary differential equations related to the function  $z(t) = x(t) + iy(t)$  of one real variable  $t$ :

$$\frac{d}{dt} \begin{pmatrix} x \\ y \end{pmatrix} = -(\nabla^2 F(z))^{-1} \nabla F(z) \quad (18.35)$$

with initial value  $z(0) = z_0$ . Here,  $F(z) = \|f(z)\|^2/2$  and  $f(z)$  is a holomorphic function. Also, by identifying  $z = x + iy$ , we denote by

$$\nabla^2 F = \begin{pmatrix} F_{xx} & F_{xy} \\ F_{xy} & F_{yy} \end{pmatrix} \text{ and } \nabla F = \begin{pmatrix} F_x \\ F_y \end{pmatrix}$$

where  $F_x = \frac{\partial F}{\partial x}$ ,  $F_y = \frac{\partial F}{\partial y}$  and so on. The right-hand side of (18.35) is defined outside the singular set  $\{\det \nabla^2 F = 0\}$ .

If this ODE has a global solution  $z(t)$ , then we have

$$\frac{d}{dt} \nabla F(z(t)) = \nabla^2 F(z) \frac{dz}{dt} = -\nabla F(z(t)).$$

Therefore, the global solution satisfies  $\nabla F(z(t)) = e^{-t} \nabla F(z_0)$ , and hence we have  $\nabla F(z(t)) \rightarrow 0$  as  $t \rightarrow \infty$ . This shows that we can expect to obtain an approximation of points where  $\nabla F$  vanishes by solving the ODE. [...] This Newton's flow is named Newton's flow vOptimization.

[...] Newton's method for optimization has the tendency to converge to the nearest (non-degenerate) critical point of  $F$ . [...] a variant called New Q-Newton's method (NQN) [...] If one mimics Newton's method, in defining  $z_{n+1} = z_n - A(z_n)^{-1} \cdot \nabla F(z)$ , then the iteration still has the same tendency of convergence to the nearest critical point of  $F(z)$ . In NQN  $B(z)$  is the matrix with the same eigenvectors as  $A(z)$ , but whose eigenvalues are all absolute values of the corresponding eigenvalues of  $A(z)$ ,  $z_{n+1} = z_n - B(z_n)^{-1} \cdot \nabla F(z_n)$ .

### 18.2.2 Heat equation

<sup>4</sup> Let  $T_{nt}$  be temperature at spatial site  $n$  at time  $t$ . The heat equation for temperature field  $\mathbb{T} = \{T_{nt}\}$  is

$$\partial_t \mathbb{T} = D \Delta_x \mathbb{T}, \tag{18.36}$$

where  $D$  is the diffusion constant. Convert this into an integer lattice difference equation over a finite spacetime domain by the same rescaling as for (4.3). Then the heat difference equation for temperature field  $\mathbb{T} = \{T_{nt}\}$  over a finite tile  $[L \times T]_S$  is

$$\partial_t \mathbb{T} = \beta \Delta_x \mathbb{T}, \tag{18.37}$$

In the space and time continuum limits,  $\beta$  is related to the diffusion constant by

$$\beta = \frac{\Delta t}{(\Delta x)^2} D = \frac{L^2}{T} D.$$

---

<sup>4</sup>Predrag 2020-03-15: I like Elaydi [6]'s Sect. 3.5.5 *The heat equation*

## References

- [1] G. Chinta, J. Jorgenson, and A. Karlsson, “Zeta functions, heat kernels, and spectral asymptotics on degenerating families of discrete tori”, *Nagoya Math. J.* **198**, 121–172 (2010).
- [2] G. Chinta, J. Jorgenson, and A. Karlsson, “Heat kernels on regular graphs and generalized Ihara zeta function formulas”, *Monatsh. Math.* **178**, 171–190 (2014).
- [3] Ó. Ciaurri, A. T. Gillespie, L. Roncal, J. L. Torrea, and J. L. Varona, “Harmonic analysis associated with a discrete Laplacian”, *JAMA* **132**, 109–131 (2017).
- [4] P. Cvitanović, “Group theory for Feynman diagrams in non-Abelian gauge theories”, *Phys. Rev. D* **14**, 1536–1553 (1976).
- [5] J. Dubout, *Zeta functions of graphs, their symmetries and extended Catalan numbers*.
- [6] S. Elaydi, *An Introduction to Difference Equations*, 3rd ed. (Springer, Berlin, 2005).
- [7] J. E. Fornæss, M. Hu, T. T. Truong, and T. Watanabe, “Backtracking new Q-Newton’s method, Newton’s flow, Voronoi’s diagram and stochastic root finding”, *Complex Anal. Oper. Th.* **18**, 112 (2024).
- [8] F. Friedli and A. Karlsson, “Spectral zeta functions of graphs and the Riemann zeta function in the critical strip”, *Tohoku Math. J.* **69**, 585–610 (2017).
- [9] F. A. Grünbaum, “The bispectral problem: an overview”, *Special Functions 2000: Current Perspective and Future Directions*, 129–140 (2001).
- [10] F. A. Grünbaum and P. Iliev, “Heat kernel expansions on the integers”, *Math. Phys. Anal. Geom.* **5**, 183–200 (2002).
- [11] P. Iliev, “Heat kernel expansions on the integers and the Toda lattice hierarchy”, *Selecta Math. (N.S.)* **13**, 497–530 (2008).
- [12] J. Jorgenson and S. Lang, “The ubiquitous heat kernel”, in *Mathematics Unlimited - 2001 and Beyond* (Springer, Berlin, 2001), pp. 655–683.
- [13] A. Karlsson and M. Neuhauser, “Heat kernels, theta identities, and zeta functions on cyclic groups”, *Contemp. Math.* **394**, 177–190 (2006).
- [14] N. N. Lebedev, *Special Functions and Their Applications* (Dover, New York, NY, 1972).
- [15] H. Liang and P. Cvitanović, *A derivation of Hill’s formulas*, In preparation, 2024.
- [16] B. D. Mestel and I. Percival, “Newton method for highly unstable orbits”, *Physica D* **24**, 172 (1987).
- [17] I. Percival and F. Vivaldi, “A linear code for the sawtooth and cat maps”, *Physica D* **27**, 373–386 (1987).



- [18] A. Terras, *Zeta Functions of Graphs: A Stroll through the Garden* (Cambridge Univ. Press, 2010).
- [19] Y. Yamasaki, “An explicit prime geodesic theorem for discrete tori and the hypergeometric functions”, *Math. Z.* **289**, 361–376 (2017).

# Chapter 19

## Conformal field theory

### 19.1 Complex plane

#### 19.1.1 Integer lattice

**wiki:** *Gaussian integers* have many nice properties (factorization, primes, etc.).

**wiki:** A *fundamental pair of periods* is a pair of complex numbers  $\omega_1, \omega_2 \in \mathbb{C}$  such that, considered as vectors in  $\mathbb{R}^2$ , the two are not collinear. The lattice generated by  $\omega_1$  and  $\omega_2$  is

$$\mathcal{L} = \{m\omega_1 + n\omega_2 \mid m, n \in \mathbb{Z}\}$$

The two generators  $\omega_1$  and  $\omega_2$  are called the *lattice basis*. The parallelogram defined by the vertices  $0, \omega_1$  and  $\omega_2$  is called the *fundamental parallelogram*, see figure 19.1. The fundamental parallelogram contains no further lattice points in its interior or boundary. Conversely, any pair of lattice points with this property constitute a fundamental pair, and furthermore, they generate the same lattice.

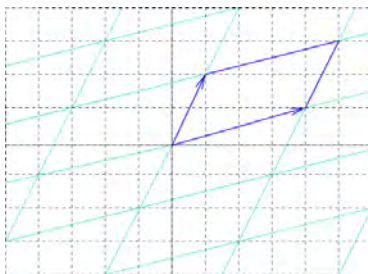


Figure 19.1: Integer lattice fundamental parallelogram spanned by  $(4,1)$  and  $(1,2)$  contains  $\text{Det } \mathcal{L} = 7$  points. Note that the far vertices  $(4,1)$ ,  $(1,2)$  and  $(5,3)$  are not counted, as they belong to other tiles.

A fundamental parallelogram spanned by (4,1) and (1,2) contains

$$\text{Det} \begin{pmatrix} 4 & 1 \\ 1 & 2 \end{pmatrix} = 7 \quad (19.1)$$

points, see figure 19.1.

There is no unique fundamental pair; an infinite number of fundamental pairs correspond to the same lattice. Any pair of fundamental parallelograms is related by a modular group matrix  $\in \text{SL}(2, \mathbb{Z})$ . This equivalence of lattices underlies many of the properties of elliptic functions (such as the Weierstrass elliptic function) and modular forms.

The abelian group  $\mathbb{Z}^2$  maps the complex plane into the fundamental parallelogram. That is, every point  $z \in \mathbb{C}$  can be written as  $z = p + m\omega_1 + n\omega_2$  for integers  $m, n$ , with a point  $p$  in the fundamental parallelogram.

## 19.2 Elliptic functions

If one identifies opposite sides of the parallelogram as being the same, the fundamental parallelogram has the topology of a torus; the quotient manifold  $\mathbb{C}/\mathcal{L}$  is a torus. We are interested in functions on  $\mathbb{C}/(\text{lattice})$ , functions on  $\mathbb{C}$  with a certain periodicity condition. These doubly periodic, meromorphic functions are called *elliptic*.

Define  $\tau$  as the ratio of Weierstrass half-periods,

$$\tau = \omega_2/\omega_1, \quad q = e^{2\pi i\tau}. \quad (19.2)$$

We can assume that  $\text{Im}(\tau) > 0$ , and also that the two periods are 1 and  $\tau$ . Next, we considered the lattice generated by 1 and  $\tau$ .

If the torus is thought of as a tube, the modular parameter is a complex number which parameterizes how the tube is stretched and twisted before its two ends are glued together. The shaded region  $\{\tau : |\tau| \geq 1, |\text{Re} \tau| \leq 1/2, \text{Im} \tau > 0\}$  shown in figure 19.3 is the *fundamental domain* of the modular parameter  $\tau$ . Each value of  $\tau$  in this region defines a triangle corresponding to a unique 2d lattice with periodic boundary conditions and the topology of a torus.

We are interested in meromorphic functions  $f$  on  $\mathbb{C}$  that have two periods; that is, there are two non-zero complex numbers  $\omega_1$  and  $\omega_2$  such that

$$f(z + \omega_1) = f(z) \text{ and } f(z + \omega_2) = f(z),$$

for all  $z \in \mathbb{C}$ . A function with two periods is said to be doubly periodic. The case when  $\omega_1$  and  $\omega_2$  are linearly dependent over  $\mathbb{R}$ , that is  $\omega_2/\omega_1 \in \mathbb{R}$ , is uninteresting.

A non-constant doubly periodic meromorphic function is called an *elliptic function*. Since a meromorphic function can have only finitely many zeros and poles in any large disc, we see that an elliptic function will have only finitely

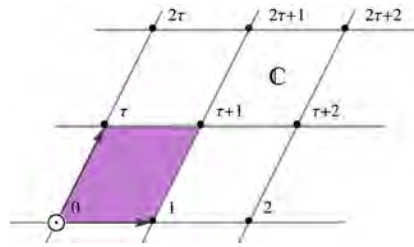


Figure 19.2: The two-dimensional lattice  $\mathcal{L}_\tau \subset \mathbb{C}$  is generated by the vectors  $(1, 0)$  and  $(0, \tau)$  spanning the fundamental lattice cell (shaded purple). Compare with figure 19.4.

many zeros and poles in any given period parallelogram.  $f$  can have a pole or zero on the boundary of fundamental parallelogram  $P_0$ . We count poles and zeros with multiplicities.

**Theorem** The number of poles of an elliptic function in  $P_0$  is always  $\geq 2$ .

The Weierstrass function is elliptic of order 2 with periods 1 and  $\tau$ . Its symmetries lead to the group of transformations of the upper halfplane  $\text{Im}(\tau) > 0$ , generated by the two transformations  $\tau \rightarrow \tau + 1$  and  $\tau \rightarrow -1/\tau$ . This group is called the *modular group*.

**2023-12-03 Predrag** Reading C. A. Lütken *A planar cubic derived from the logarithm of the Dedekind  $\eta$ -function* (2021), [click here](#).

To go from our definition of primitive cell to the Dedekind  $\eta$ -function primitive cell, scale out the lattice length (redefine lattice spacing unit of a square lattice). Then

$$L_p \rightarrow 1, \quad T_p \rightarrow \tau_2 = T_p/L_p, \quad S_p \rightarrow \tau_1 = S_p/L_p, \quad (19.3)$$

as in figure 19.2. See also Cardy (19.6). Dedekind lattice volume is  $V_{\mathcal{L}_\tau} = \tau_2$  (not 1!). Presumably that is the reason that  $\tau_2$  pops up in functional determinants, such as (19.64) and (19.65).

The group of substitutions generated by  $\tau \rightarrow \tau + 1$  and  $\tau \rightarrow -\frac{1}{\tau}$  is

$$\text{SL}(2, \mathbb{Z}) = \left\{ \begin{pmatrix} a & b \\ c & d \end{pmatrix}, \quad a, b, c, d \in \mathbb{Z} \text{ and } ad - bc = 1 \right\}. \quad (19.4)$$

See figure 19.3 and figure 19.5, and Brower and Owen [5] discussion on page 759.

**2023-03-15 Predrag** You might enjoy the modular flows part of Etienne Ghys and Jos Leys [21] *Lorenz and modular flows: a visual introduction* [Amer. Math. Soc. Feature Column](#) (2006). Starting with the famed (1801) paper of Gauss, one runs into it all the time (see figure 19.5, search here for ‘modular’). We slice all these orbits by picking the Hermite normal form representative for each.

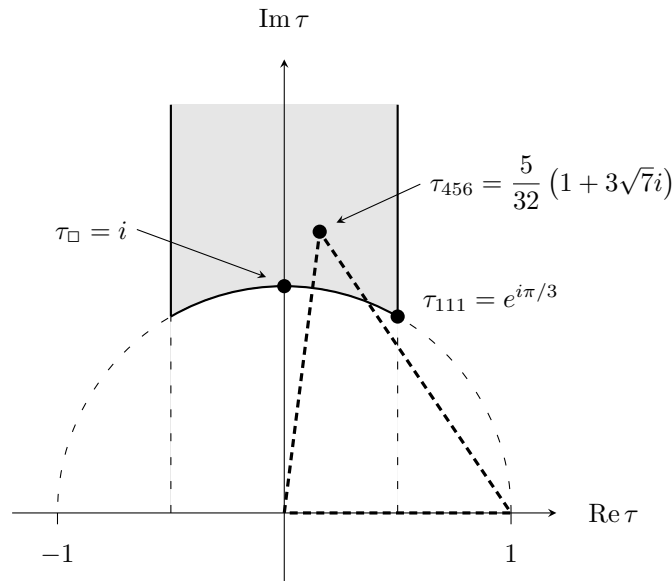


Figure 19.3: The fundamental domain of the modular parameter  $\tau$  (see also figure 19.5). A value of  $\tau$  defines a unique 2d lattice with periodic boundary conditions and the topology of a torus. Indicated: the equilateral triangle  $\tau_{111}$ , the square  $\tau_{\square}$ , and a skew triangle  $\tau_{456}$  primitive cells.

2023-12-06 **Predrag Alex Kontorovich** course *Complex Analysis, Rutgers Math 503*

▶ Lecture 29 *Elliptic integrals* 2023-12-01: Ellipse/lemniscate arclength calculations, elliptic integrals, elliptic functions, double periodicity, meromorphicity.

Kontorovich is wonderfully pedagogical. He motivates the subject by reviewing first the quadratic case, i.e. Apollonius 250 BC conic sections. Parametrized by  $\cos, \sin; \cosh, \sinh$ ; they are periodic over  $\mathbb{C}$ , either in the real or in the complex direction. Then he gives the story of why one wanted to look at double periodicity over  $\mathbb{C}$ , starting with 1650 Newton's gravity and ellipses.

Ellipse/lemniscate arclength calculations lead to elliptic integrals and their inverses, elliptic functions, elliptic curves. Jacobi discovers double periodicity in awkward form, three functions. Weierstrass combines them in one function. After that, the origin story is forgotten, and elliptic functions become synonymous with double periodicity, by  $\omega_1, \omega_2$  not collinear in  $\mathbb{C}$ .

He cites Stein and Shakarchi [42] *Complex Analysis* (2003), (click here); Chapter 9 *An Introduction to Elliptic Functions*.

▶ Lecture 30 *Weierstrass function* 2023-12-05

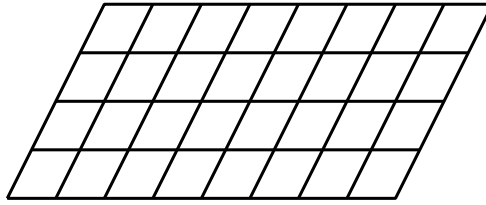


Figure 19.4:  $L \times T$  square lattice with tilt parameter  $c$ . Here,  $L = 8$ ,  $T = 4$  and  $c = 1/4$ , so  $S = L/4$ . The  $i$ -th site of the first row is identical with the  $\text{mod}(i + cL, L)$ -th site in the last row. The left-most site and the right-most site on the same horizontal line are identical.

Order of Elliptic functions, Weierstrass function, Parametrization of elliptic curves, universality of Weierstrass P

▶ Lecture 31 *Modular forms* 2023-12-08

Weierstrass P-function Taylor expansion, Eisenstein series, modular forms, space of lattices up to homothety, elliptic curves, Shimura-Taniyama-Weil, Frey curve, Fermat's Last Theorem, Wiles+Taylor/Wiles, Langlands, Birch+Swinnerton-Dyer

2024-03-06 **Mario Bonk** ▶ *Elliptic integrals, modular forms, and the Weierstrass zeta-function*. A very clear lecture, but actually, at the end, I did not get it. Why did Bonk do the thing he did?

The paper is pedagogical as well: Mario Bonk *The quasi-periods of the Weierstrass zeta-function*, [arXiv:2212.07012](https://arxiv.org/abs/2212.07012). It studies the ratio  $p = \eta_2/\eta_1$  of the pseudo-periods of the Weierstrass  $\zeta$ -function in dependence of the ratio  $\tau = \omega_2/\omega_1$ . What's the point I do not know.

2024-08-24 **Predrag Markus Schwagenscheidt** *Elliptic Functions and Elliptic Curves* (2022) look pedagogical, might be useful.

2023-05-05 **Predrag** Here is an enjoyable introduction into modular forms: **Dick Koch** *The pentagonal number theorem and modular forms* (2010).

2020-06-19 **Predrag** Okabe, Kaneda, Kikuchi and Hu [38] *Universal finite-size scaling functions for critical systems with tilted boundary conditions*, deal with the two-dimensional Ising model on  $L \times T$  square lattices with periodic boundary conditions in the horizontal  $L$  direction and tilted boundary conditions in the vertical  $T$  direction, such that the  $i$ -th site in the first row is connected with the  $\text{mod}(i + cL, L)$ -th site in the  $T$  row of the lattice, where  $1 \leq i \leq L$ ; see figure 19.4. They find that the finite-size scaling functions are universal for fixed sets of aspect ratio  $a = L/T$  and tilt parameter  $c = S/L$ .

It is interesting to discuss this problem in terms of the modular (conformal) transformation. According to Cardy [9], the shape of the 2D lattice

may be represented by the complex number

$$z = 1/a + i c. \quad (19.5)$$

This is usually called  $\tau$ , see (19.3). Then, Cardy asserted that the partition function becomes invariant under the transformations

$$z \rightarrow z + i \quad (19.6)$$

and

$$z \rightarrow 1/z, \quad (19.7)$$

in the limit that the system size becomes infinite. The first translates, the 2nd inverts: these are easiest to understand in the complex upper half-plane, see figure 19.5.

**2021-01-08 Predrag** Lecian [31] discusses this group in detail in [arXiv:1303.6343](#), see ‘big billiard’, ‘small billiard’, Sect. III.A. *The modular group*, Maass wavefunctions.

We have another invariant transformation

$$z \rightarrow z^*, \quad (19.8)$$

which corresponds to the fact that we can confine  $c$  to the interval of  $0 \leq c \leq 1/2$ . Starting from the recurrence relation

$$z_{n+1} = \frac{1}{z_n + i} + i, \quad (19.9)$$

we can easily show that (recheck!  $T, L$  rewrite wrong as it stands)

$$A = a/(c^2 a^2 + 1) = \frac{T}{L} \frac{1}{\frac{S^2 T^2}{L^2 L^2} + 1} \quad (19.10)$$

is an invariant, and can be regarded as the effective aspect ratio.

**2022-11-17, 2024-01-27 Predrag** Brower and Owen [5] *Ising model on the affine plane* (2022), [arXiv:2209.15546](#) is a pretty paper. Focus is on critical points and equivalence to CFT on  $\mathbb{R}^2$  at the second order phase point, but there is much lattice geometry -dual graphs, finite element framework, etc.- we might find inspirational.

**Richard C. Brower** does lattices for [living](#); graduate student Evan K. Owen [talks about them](#).

The discrete translations and the 4-fold and 6-fold discrete rotations (for the square and triangular lattice, respectively) are sufficient to guarantee the restoration of Poincaré invariance (1 rotation and 2 translations).

The star-triangle identity is interesting; presumably for a square lattice the dual is also a square lattice.

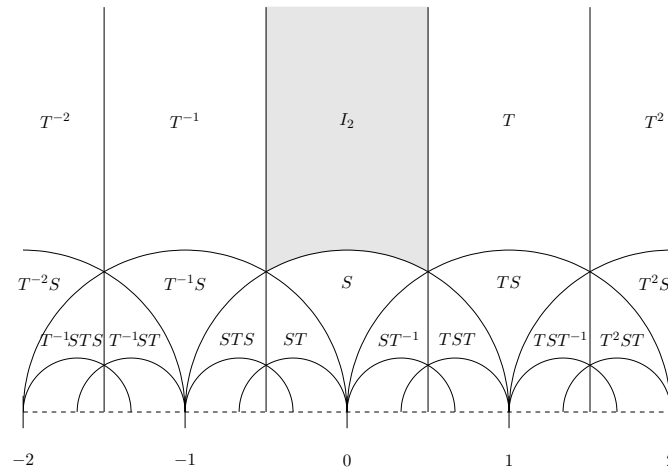


Figure 19.5: Action of  $SL(2, \mathbb{Z})$  on the complex upper half-plane by linear fractional transformations  $T$  and  $S$ . Taken from Keith Conrad. Ian Folkins caption for case where  $I_2$  is divided into domain  $D$  and its reflection: A division of the upper half complex plane into domains  $D$ . The domains become progressively smaller as you approach the real axis, so those closest to the axis are not shown. Each domain contains within it all possible two-dimensional Bravais lattices of a common value. The square and triangular structures are located at the vertices of the domains and are labeled accordingly. A particular domain has been shaded and labeled  $D$ . The boundary of  $D$  is made up of Bravais lattices having nontrivial point group symmetries, that is, a point group symmetry other than inversion. Structures on the imaginary axis are rectangular, those on the unit circle rhombohedral, and those with  $\text{Re } z = 1/2$  face centered rectangular. Structures with  $y \rightarrow \infty$  have  $\mathbf{a}_1 \rightarrow O$ . Hence, the physically relevant structures in  $D$  are those near the unit circle.



Traditionally the Ising model is studied only on square and rectangular lattices, but our formalism allows us to simulate the critical Ising model on a torus with arbitrary modular parameter  $\tau$ .

Each value of  $\tau$  in this region defines a triangle corresponding to a unique 2d lattice with periodic boundary conditions and the topology of a torus. For example, the heavy dashed lined is the triangle defined by  $\tau_{456}$ , where  $\tau_{ijk}$  indicates that the triangle side lengths are proportional to  $\{i, j, k\}$ .

The triangle condition:  $\vec{\ell}_1 + \vec{\ell}_2 + \vec{\ell}_3 = 0$ .

Without loss of generality, we can sort the triangular lattice lengths so that  $\ell_1 \leq \ell_2 \leq \ell_3$ . Then the modular parameter in the fundamental domain is

$$|\tau| = \frac{\ell_2}{\ell_1}, \quad \arg(\tau) = \cos^{-1}(-\hat{e}_1^* \cdot \hat{e}_2^*). \quad (19.11)$$

**2020-06-19 Predrag** Ziff, Lorentz and Kleban [45] *Shape-dependent universality in percolation*, [arXiv:cond-mat/9811122](https://arxiv.org/abs/cond-mat/9811122).

The torus with a twist has various topological symmetries that apply to any shape-dependent universal quantity  $u(r, t)$ . We consider a rectangular boundary with base 1 and height  $r$ , with a horizontal twist  $t$  in the periodic b. c. (Note that having twists in two directions leads to a non-uniform system, so we don't consider it.)  $u(r, t)$  satisfies the obvious symmetries of reflection

$$u(r, t) = u(r, -t) \quad (19.12)$$

and periodicity in the  $t$  direction

$$u(r, t) = u(r, 1 + t) \quad (19.13)$$

Another symmetry follows from the observation that the same rhombus can be made into a rectangle in two different ways, leading to:

$$u(r, t) = u\left(\frac{r}{r^2 + t^2}, \frac{t}{r^2 + t^2}\right) \quad (19.14)$$

Another construction shows that when  $t = 1/n$  where  $n$  is an integer,

$$u\left(r, \frac{1}{n}\right) = u\left(\frac{1}{n^2 r}, \frac{1}{n}\right) \quad (19.15)$$

which also follows from Eqs. (19.12-19.14). On the complex  $\tau = t + ir$  plane, (19.14) corresponds to  $\tau \rightarrow 1/\tau$  while (19.13) corresponds to  $\tau \rightarrow \tau + 1$ . These transformations generate the modular group, and functions invariant under them are called modular. Thus,  $b(r, t)$  must necessarily be a modular function.

Besides the excess number, another universal quantity on a torus is the cross-configuration probability  $\pi_+(r, t)$ , which can be expressed in a quite compact form. Things veer off to Dedekind eta function and such, and Predrag gives up.

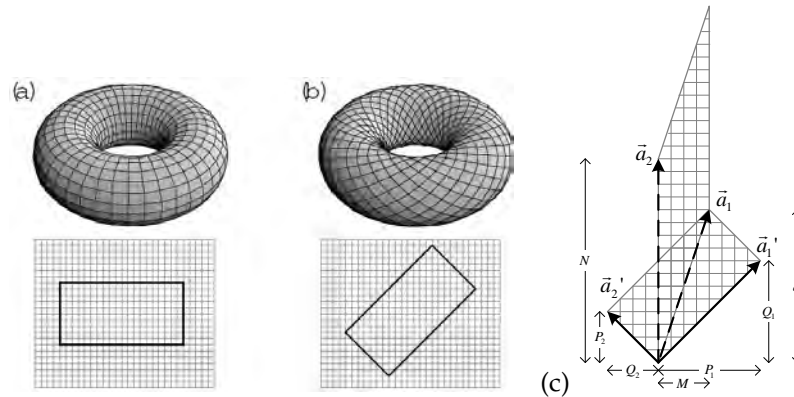


Figure 19.6: A helical tiling is formed by pairwise joining of the edges of the rectangle spanned by an orthogonal set of primitive vectors in the  $\mathbb{Z}^2$  lattice: (a) the direction of the primitive vectors coincides with the lattice orientations for the conventional toroidal bc's, and (b) a helical torus. (c) Equivalence between the bc's in helical and twisted schemes prescribed by  $\{\vec{a}_1, \vec{a}_2\}$  and  $\{\vec{a}'_1, \vec{a}'_2\}$  respectively, on a  $[M \times N]$  square lattice. For the helical bc's, the setting  $Q_1/P_1 = Q_2/P_2$  ensures that the two primitive vectors are orthogonal. On the other hand, twisting is generated by a  $d$ -unit traverse shift.

2020-06-19 Predrag Liaw *et al.* *Exact treatment of Ising model on the helical tori*, [arXiv:cond-mat/0512262](https://arxiv.org/abs/cond-mat/0512262), published as Liaw *et al.* [32] *Partition functions and finite-size scalings of Ising model on helical tori*: The exact closed forms of the partition functions of a two-dimensional Ising model on square lattices with twisted bc's are given.

A helical torus is related to the twisted boundary conditions tiling by an  $SL(2, \mathbb{Z})$  transformation. In  $d = 2$ , the equivalence transformations among the primitive cell vector-pairs preserve the area and are thus  $SL(2, \mathbb{Z})$ . This is the prototype of the modular symmetry of the conformal field theory.

In figure 19.6 they make a distinction between the 'helical', and the equivalent 'twisted' tiles.

Helical tori are tiled by pairwise joining the edges of the rectangle spanned by any orthogonal set of vectors on the lattice plane. This leads to distinct orientations of the underlying lattice, labelled by the chirality [sahito] as well as the chiral aspect ratio. The conventional periodic BC is referred as the helical primitive cell with trivial chirality, as depicted in figure 19.6 (a).

The twisted BC primitive cell is a modification to the conventional primitive cell by cutting the torus and then rejoining after twisting. Twisted tori are what we call Hermite normal form primitive cells. There are two types of twisting:  $Tw_I(M, N, d/M)$  primitive cell specified by  $\{\vec{a}_1 =$

$M\hat{x} + d\hat{y}$ ,  $\vec{a}_2 = N\hat{y}$ , and  $T_{w_{II}}(M, N, d/N)$  primitive cell specified by  $\{\vec{a}_1 = M\hat{x}, \vec{a}_2 = d\hat{x} + N\hat{y}\}$  used in ref. [12].

In CL18 [12] notation:  $T_{w_{II}}(L, T, S/T)$  primitive cell is specified by  $\{\vec{a}_1 = L\hat{x}, \vec{a}_2 = S\hat{x} + T\hat{y}\}$ .

It suffices to study the unique correspondence of a helical torus to the one of the above twistings, say  $T_{w_I}$ .

The helical tori primitive cell is given by the orthogonal primitive vector pair,

$$\begin{aligned}\vec{a}'_1 &= \hat{x} P_1 + \hat{y} Q_1, \\ \vec{a}'_2 &= -\hat{x} Q_2 + \hat{y} P_2,\end{aligned}\tag{19.16}$$

where the two radii for the torus are given as  $L_i = \sqrt{P_i^2 + Q_i^2}$  for  $i = 1, 2$ . They denoted the helical system by  $Hl(B, L_1, \chi)$ , where the chiral aspect ratio  $B = L_2/L_1$  and the chirality  $\chi = Q_1/P_1 \equiv Q_2/P_2$ . In order to furnish the equivalent structure  $Hl(B, L_1, \chi) \cong T_{w_I}(A, M, \alpha)$ ,  $\mathcal{M}_{11} = P_1/M$  and  $\mathcal{M}_{21} = -Q_2/M$  implies that

$$\mathcal{M}_{21} = -B\chi\mathcal{M}_{11}\tag{19.17}$$

$$1 = \mathcal{M}_{11}\mathcal{M}_{22} - \mathcal{M}_{21}\mathcal{M}_{12}.\tag{19.18}$$

$$A = \frac{(\mathcal{M}_{21})^2}{B} + B(\mathcal{M}_{11})^2,\tag{19.19}$$

$$\alpha = -\frac{\mathcal{M}_{21}\mathcal{M}_{22}}{B} - B\mathcal{M}_{11}\mathcal{M}_{12}.\tag{19.20}$$

The helical primitive cell is a subclass of twisted one by an  $SL(2, \mathbb{Z})$  equivalence relation, figure 19.6 (c) and (19.14).

They refer to  $\alpha = d/M$  (our notation:  $\alpha = S/T$ ) as a “twisting factor”.

$Q_{M,N}^\alpha = Q_{M,N}^{-\alpha}$  as twisting either clockwise or counterclockwise is not distinguished by the energy. Note that reversing the sign of a twist factor  $\alpha$  is not an  $SL(2, \mathbb{Z})$  transformation.

The  $[M \times N]$  square lattice with the helicity factor  $d = D/M$ , the system has periodic boundary conditions in the N direction and helical (tilted) boundary conditions in the M direction such that the  $i$ -site in the first column is connected with the  $\text{mod}(i + D, M)$ th site in the N column of the lattice.

R. Sahito, G. Dresselhaus and M. S. Dresselhaus, *Physical properties of Carbon Nanotubes*, (Imperial College Press, London, 1998).

Alexi Morin-Duchesne, Paul A. Pearce and Jorgen Rasmussen *Modular invariant partition function of critical dense polymers*, [arXiv:1303.4895](https://arxiv.org/abs/1303.4895): [...] The torus is formed by gluing the top and bottom of the cylinder. This gives rise to a variety of non-contractible loops winding around the torus.

[...] a parameter  $v$  that keeps track of the winding of defects on the cylinder. [...] The modified trace is constructed as a linear functional on planar connectivity diagrams in terms of matrix traces  $\text{Tr}_d$  (with a fixed number of defects  $d$ ) and Chebyshev polynomials of the first kind.

We assume helical boundary conditions in  $x$ -direction, i.e.,  $\phi_{L_{x+1},y} = \phi_{1,y+1}$ , and periodic boundaries in  $y$ -direction.

**2023-10-05 Predrag** Ian Folkins *Functions of two-dimensional Bravais lattices* (1991) ([click here](#)).

His basic reference is Audrey Terras [43] *Harmonic Analysis on Symmetric Spaces and Applications I* (1985). The Epstein zeta function and Mellin transform are discussed in Chap. 1, the two-dimensional fundamental domain and the Roelcke-Selberg decomposition in Chap. 3.

The physically meaningful Bravais lattices are those  $\mathbb{A} \in GL(n, \mathbb{R})$ , the group of real  $n \times n$  matrices with nonzero determinant.

Let  $f(\mathbb{A})$  be any real-valued function of  $\mathbb{A}$ , for example its energy, which is independent of the lattices' orientation. There are two symmetry constraints such a function must obey. The first arises from its invariance under rotations of the lattice, the second from the fact that there are an infinite number of sets of Bravais lattice vectors, and hence matrices  $\mathbb{A}$ , which generate the same Bravais lattice.

$$f\left(\begin{bmatrix} a & b \\ c & d \end{bmatrix}\right) = f\left(\begin{bmatrix} a & -b \\ -c & d \end{bmatrix}\right). \quad (19.21)$$

This symmetry comes from multiplying  $\mathbb{A}$  on both the right and left by  $\begin{pmatrix} 1 & 0 \\ 0 & -1 \end{pmatrix}$ , which corresponds physically to rotating the lattice by  $\pi$  and inverting  $\mathbf{a}_1$ .

Let  $H$  be the upper half complex plane. [...] A domain in figure 19.5 has the physical interpretation that it contains within it all inequivalent two-dimensional Bravais lattices (of a given cell volume). [...] Note the relation between primitive cell  $\mathbb{A}$  and the upper half complex plane

$$\begin{bmatrix} \sqrt{y} & \frac{\sqrt{x}}{\sqrt{y}} \\ 0 & \frac{1}{\sqrt{y}} \end{bmatrix} i \rightarrow x + iy. \quad (19.22)$$

[...] The function  $f(\mathbb{A})$  can be parametrized in terms of basis functions of  $H$ . This expansion has both a discrete sum and a continuous integral. [...] basis functions are eigenfunctions of the non-Euclidean Laplacian on  $H$ . [...]

[...] The  $2 \times 2$  symmetric matrix related to  $z = x + iy$  by

$$\begin{bmatrix} (x^2 + y^2)/y & x/y \\ x/y & 1/y \end{bmatrix} i = \mathbb{A}^\top \mathbb{A}. \quad (19.23)$$

Predrag: All this is supposed to enable us to compute free energy for a given atomic pair potential, but to me it is not clear how...

[...] Suppose that the Bravais lattice with the lowest free-energy of a crystal is square. A rectangular distortion of this structure corresponds to moving away from  $z = i$  up or down the imaginary axis, while moving to the left or right of  $i$  induces a rhombohedral distortion. The lowest order changes in the free-energy associated with these two displacements are given by the two respective elastic constants of the square lattice. These may be determined from  $f(z)$  by evaluating the second derivative of  $f(z)$  with respect to deviations in the real and imaginary parts of  $z$  from  $i$ , evaluated at  $i$ . In general, any crystal's elastic constants can be determined if  $f(z)$  is known.

[...] The central result of this paper is that the variation of any function of a two-dimensional Bravais lattice, under the constraint of constant volume, can be fully characterized in terms of a (presumably) finite number of coefficients, and a function defined on line in the upper half complex plane. One application of this characterization may be an attempt to find the energy of all Bravais lattice configurations of a crystal given knowledge of the energy at only a few of them. [...]

Predrag: I'm lost, give up.

**2020-10-16 Predrag** For me the problem is that I do not see any of the above formulas in Cardy [9], except for (19.5) that might correspond to his figure of a parallelepiped. I understand nothing in the paper. He writes though something intriguing: "the symmetry of the parallelogram, which corresponds to the invariance of  $Z(\delta)$  under the modular group, has recently been exploited to limit the possible gauge groups in heterotic string theories by D. Gross, J. Harvey, E. Martinec and R. Rohm, Phys. Rev. Lett. 54 (1985) 502." I would stay far away from such references.

**2023-06-26 Predrag** I see no modular group in the above Gross *et al. Heterotic String*

**2023-03-15 Predrag** Maybe too much math: Ghys [20] *Knots and dynamics* (2006), [click here](#).

**2023-03-15 Predrag** The reason why we might care: This associates to each unimodular matrix a periodic orbit with unique symbolic dynamics. Consider the two matrices [21]

$$\mathbb{U} = \begin{bmatrix} 1 & 1 \\ 0 & 1 \end{bmatrix}, \quad \mathbb{V} = \begin{bmatrix} 1 & 0 \\ 1 & 1 \end{bmatrix}. \quad (19.24)$$

Any integral matrix  $\mathbb{A}$  with determinant 1 (unimodular transformation) is conjugate, up to sign, to a product of  $\mathbb{U}$ 's and  $\mathbb{V}$ 's. The period-2  $UV$  example is given in (2.2). The word in  $\mathbb{U}$  and  $\mathbb{V}$  is uniquely defined up to a cyclic permutation. In other words, we should be able to enumerate,

construct and label all 2D Bravais lattice unimodular orbits using our usual full binary dynamics methods.

If we can see how to associate unimodular periodic orbits with different Bravais lattices, we might have a better way of enumerating Bravais lattices than the Hermite normal form, construction that breaks space-time symmetry.

**2019-11-04 Predrag** Ivashkevich, Izmailian and Hu [26] *Kronecker's double series and exact asymptotic expansions for free models of statistical mechanics on torus:*

Consider a planar square lattice of size  $M \times N$  with periodic boundary conditions, i.e. torus. To each site  $(m, n)$  of the torus a spin variable is ascribed,  $s_{mn}$ , with two possible values:  $+1$  or  $-1$ . Two nearest neighbor spins, say  $s_{mn}$  and  $s_{m,n+1}$  contribute a term  $-J s_{mn} s_{m,n+1}$  to the Hamiltonian, where  $J$  is some fixed energy. Therefore, the Ising model Hamiltonian is the sum of all such terms, one for each edge of the lattice

$$H(s) = -J \sum_{n=0}^{N-1} \sum_{m=0}^{M-1} (s_{mn} s_{m+1,n} + s_{mn} s_{m,n+1}) \quad (19.25)$$

(Predrag:) Note that this can be written in terms of a shift matrices  $\sigma_j$  as

$$H(s) = -J s^\top \cdot (\sigma_1 + \sigma_2) \cdot s,$$

which looks asymmetric - check whether this has a lattice Laplacian formulation?

The partition function of the Ising model is given by the sum over all spin configurations on the lattice

$$Z_{\text{Ising}}(J) = \sum_{\{s\}} e^{-H(s)}. \quad (19.26)$$

It is convenient to set up another parameterizations of the interaction constant  $J$  in terms of the mass variable  $\mu = \ln \sqrt{\text{sh } 2J}$ . Critical point corresponds to the massless case  $\mu = 0$ .

An explicit expression for the partition function of the Ising model on  $M \times N$  torus, which was given originally by Kaufman [29] (Predrag: I have looked at [Bruria Kaufman's](#) article, do not recommend reading it - complicated), can be written as

$$Z_{\text{Ising}}(\mu) = \frac{1}{2} \left( \sqrt{2} e^\mu \right)^{MN} \left\{ Z_{\frac{1}{2}, \frac{1}{2}}(\mu) + Z_{0, \frac{1}{2}}(\mu) + Z_{\frac{1}{2}, 0}(\mu) + Z_{0, 0}(\mu) \right\} \quad (19.27)$$

where we have introduced the partition function with twisted boundary conditions

$$Z_{\alpha, \beta}^2(\mu) = \prod_{n=0}^{N-1} \prod_{m=0}^{M-1} 4 \left[ \sin^2 \left( \frac{\pi(n+\alpha)}{N} \right) + \sin^2 \left( \frac{\pi(m+\beta)}{M} \right) + 2 \text{sh}^2 \mu \right] \quad (19.28)$$

Here  $\alpha = 0$  corresponds to the periodic boundary conditions for the underlying free fermion in the  $N$ -direction while  $\alpha = \frac{1}{2}$  stands for anti-periodic boundary conditions. Similarly  $\beta$  controls boundary conditions in  $M$ -direction. With the help of the identity [22]

$$4 |\operatorname{sh}(M\omega + i\pi\beta)|^2 = 4 [\operatorname{sh}^2 M\omega + \sin^2 \pi\beta] = \prod_{m=0}^{M-1} 4 \left[ \operatorname{sh}^2 \omega + \sin^2 \left( \frac{\pi(m+\beta)}{M} \right) \right] \quad (19.29)$$

partition function the partition function with twisted boundary conditions  $Z_{\alpha,\beta}$  can be transformed into simpler form

$$Z_{\alpha,\beta}(\mu) = \prod_{n=0}^{N-1} 2 \left| \operatorname{sh} \left[ M\omega_\mu \left( \frac{\pi(n+\alpha)}{N} \right) + i\pi\beta \right] \right| \quad (19.30)$$

where lattice dispersion relation has appeared

$$\omega_\mu(k) = \operatorname{arcsinh} \sqrt{\sin^2 k + 2 \operatorname{sh}^2 \mu} \quad (19.31)$$

This is nothing but the functional relation between energy  $\omega_\mu$  and momentum  $k$  of a free quasi-particle on the planar square lattice.

**2023-10-14 Predrag** Pavel Bleher, Brad Elwood and Dražen Petrović *Dimer Model: Full Asymptotic Expansion of the Partition Function*, [arXiv:1806.03742](https://arxiv.org/abs/1806.03742). “ We give a rigorous proof of the full asymptotic expansion of the partition function of the dimer model on a square lattice on a torus (rectangular primitive cell) of lattice periodicities  $m, n$ . We assume that  $m$  is even and we show that the asymptotic expansion depends on the parity of  $n$ . We review and extend the results of Ivashkevich, Izmailian and Hu [26], and we give a rigorous estimate of the error term in the asymptotic expansion of the partition function. ”

**2019-11-04 Predrag** Ivashkevich, Izmailian and Hu [26] **Elliptic Theta Functions**. We adopt the following definition of the elliptic  $\theta$ -functions:

$$\begin{aligned} \theta_{\alpha,\beta}(z, \tau) &= \sum_{n \in \mathbb{Z}} \exp \left\{ \pi i \tau \left( n + \frac{1}{2} - \alpha \right)^2 + 2\pi i \left( n + \frac{1}{2} - \alpha \right) \left( z + \frac{1}{2} - \beta \right) \right\} \\ &= \eta(\tau) \exp \left\{ \pi i \tau \left( \alpha^2 - \alpha + \frac{1}{6} \right) + 2\pi i \left( \frac{1}{2} - \alpha \right) \left( z + \frac{1}{2} - \beta \right) \right\} \\ &\times \prod_{n=0}^{\infty} \left[ 1 - e^{2\pi i \tau (n+\alpha) - 2\pi i (z-\beta)} \right] \left[ 1 - e^{2\pi i \tau (n+1-\alpha) + 2\pi i (z-\beta)} \right] \end{aligned}$$

These should be compared with the notations of Mumford.

The elliptic  $\theta$ -functions satisfies the heat equation

$$\frac{\partial}{\partial \tau} \theta_{\alpha,\beta}(z, \tau) = \frac{1}{4\pi i} \frac{\partial^2}{\partial z^2} \theta_{\alpha,\beta}(z, \tau) \quad (19.32)$$

**2023-09-16 Predrag** Campos, Sierra and López [8] *Tensor renormalization group in bosonic field theory* (2019), [arXiv:1902.02362](https://arxiv.org/abs/1902.02362): They compute the partition function of a massive free boson in a square lattice using a tensor network algorithm. They introduce a singular value decomposition (SVD) of continuous matrices that leads to accurate numerical results. The guiding principle is to preserve the Gaussian character of the statistical weights. This leads modifying the singular value decomposition to handle continuous degrees of freedom taking unbounded values.

They implement a tensor renormalization group protocol to reduce iteratively the number of degrees of freedom. The basic tool used in systems with a finite number of degrees of freedom is the *singular value decomposition* (SVD) of the network tensors. Any finite rank matrix can be decomposed as  $M = USV^\dagger$ , where  $U$  and  $V$  are unitary matrices and  $S$  is diagonal with non-negative entries.

This result has been used to implement the standard TRG approach to a  $\phi^4$ -boson field theory, see Shimizu [40] above.

The use of SVD looks very smart. They only need the free boson partition function, for a lattice of size  $L_1 \times L_2$  with periodic boundary conditions

$$Z_{L_1 L_2}^{\text{exact}} = \left(\frac{\pi}{2}\right)^{\frac{L_1 L_2}{2}} \prod_{n_1, n_2} \left( \sin^2 \frac{\pi n_1}{L_1} + \sin^2 \frac{\pi n_2}{L_2} + \frac{m^2}{4} \right)^{-\frac{1}{2}} \quad (19.33)$$

where  $n_i = 1, \dots, L_i$  ( $i = 1, 2$ ), to test the performance of their ‘gTRG method’. The square root is here because this is a Gaussian free boson theory, not our deterministic one.

In the massless limit, they reproduce the results of conformal field theory including a precise value of the central charge.

*Massless case:* We are avoiding this in CL18 manuscript, but it is very interesting, presumably easier than the massive case.

In the limit  $m \ll 1$  and  $L_1, L_2 \gg 1$ , with  $L_2/L_1$  constant, the exact partition function (19.33) can be approximated by

$$Z_{L_1 L_2}^{\text{exact}} \simeq \frac{e^{-f_\infty L_1 L_2}}{m(L_1 L_2)^{1/2}} Z_{\text{CFT}}(\tau), \quad (19.34)$$

where  $Z_{\text{CFT}}$  is the partition function of a massless boson [16] in a torus with moduli parameter  $\tau$ . In this case  $\tau = iL_2/L_1$ . A serious calculation (Appe. D on conformal field theory) follows, and the result is

$$Z(L_1, L_2) \simeq \frac{e^{-L_1 L_2 f_\infty}}{m\sqrt{L_1 L_2}} \times Z_{\text{CFT}}(\tau), \quad (19.35)$$

where  $f_\infty$  is the free energy per site

$$f_\infty = \frac{2G}{\pi} - \frac{\ln(2\pi)}{2}. \quad (19.36)$$



where  $G$  is the Catalan constant.  $Z_{\text{CFT}}(\tau)$  is the partition function of a massless boson on a torus with moduli parameter  $\tau$  [16]

$$Z_{\text{CFT}}(\tau) = \frac{1}{(\text{Im}\tau)^{1/2} |\eta(q)|^2}, \quad q = e^{2\pi i\tau}, \quad \tau = i \frac{L_2}{L_1}, \quad (19.37)$$

and

$$\eta(\tau) = q^{\frac{1}{24}} \prod_{n=1}^{\infty} (1 - q^n), \quad (19.38)$$

is the Dedekind eta function. Eq. (19.33) is symmetric under the exchange  $L_1 \leftrightarrow L_2$ , a condition that is guaranteed in (19.37) by the modular invariance of  $Z_{\text{CFT}}$ , see (19.7),

$$Z_{\text{CFT}}(\tau) = Z_{\text{CFT}}(-1/\tau). \quad (19.39)$$

Crucial for them, but we can ignore the renormalization flow part of the paper. Or maybe we should use it?! It might be a good way to compute large primitive cells: Their partition function of square lattices has  $L^2$  sites and periodic boundary conditions, with  $L = 2^S$ . After each gTRG step, the number of sites is reduced by 1/2. Therefore, after  $S-1$  RG steps their lattice only have 4 sites and there are only two tensors left. Then, performing another gTRG transformation the lattice becomes the tensor trace of just one tensor  $W_S^\pi$ .

**2024-10-05 Predrag** Di Francesco, Mathieu and Sénéchal [16] ([click here](#)) explain why the free-boson partition function (without zero-mode) (19.35), their eq. (10.13),

$$Z_{\text{bos}}(\tau) = \frac{1}{(\text{Im}\tau)^{1/2} |\eta(q)|^2}, \quad (19.40)$$

is modular invariant.

**2023-09-16 Predrag** Campos, López and Sierra [7] *Integrability and scattering of the boson field theory on a lattice* (2021), [arXiv:2009.03338](#): Free boson on a lattice is the simplest field theory one can think of. Its partition function can be easily computed in momentum space. They use the methods of exactly solvable models to a massless and massive free boson on a two dimensional square lattice.

The Boltzmann weights of the model are shown to satisfy the Yang-Baxter equation with a uniformization given by trigonometric functions in the massless case, and Jacobi elliptic functions in the massive case. [...] These results place the free boson model in 2D in the same position as the rest of the models that are exactly solvable à la Yang-Baxter.

In the Ising or XXZ models, fermions in the Hubbard model, etc., the local degrees of freedom are discrete. In the boson model we have to deal with continuous degrees of freedom given by the real values of the scalar field. Despite of this, the techniques mentioned above can be applied directly.

Consider a free scalar of mass  $m_0$  living on a 2D lattice with periodic boundary conditions. The Euclidean partition function of the model is

$$Z = \int \prod_{ij} d\phi_{ij} e^{-\frac{1}{2} \sum_{ij} a_x a_\tau \left[ \frac{(\phi_{ij} - \phi_{i+1j})^2}{a_x^2} + \frac{(\phi_{ij} - \phi_{ij+1})^2}{a_\tau^2} + \mu^2 \phi_{ij}^2 \right]}, \quad (19.41)$$

where  $a_x$  and  $a_\tau$  denote the lattice spacings in the spatial and euclidean time directions, and  $\phi_{ij} \in \mathbb{R}$ . The interactions described by (19.41) are pairwise between the variables at neighbour lattice sites.

Reformulate this partition function as a vertex model, where the fields live on the edges and the interactions take place at the lattice sites of a dual tilted lattice whose orientation is  $45^\circ$  degrees rotated with respect to the original one with statistical weights

$$W(\phi_i) = e^{-\frac{1}{2} \sum_{i=1}^4 \left[ (\phi_i - \phi_{i+1})^2 + \frac{\mu^2}{2} \phi_i^2 \right]}. \quad (19.42)$$

First they show that the massless case satisfies the Yang-Baxter equation. Massive case is harder. There is a two parameter family of solutions which generalizes those of the massless case by promoting trigonometric to elliptic functions. Define

$$c(u, \mu) = \sqrt{\mu_1} \frac{\text{sn}(u, \mu)}{\text{cn}(u, \mu) \text{dn}(u, \mu)}, \quad \tilde{m}(u, \mu) = \sqrt{\frac{4\mu}{\mu_1}} \text{cn}(u, \mu), \quad (19.43)$$

where  $\mu_1 = 1 - \mu$  and  $\text{sn}(u, \mu)$ ,  $\text{cn}(u, \mu)$ ,  $\text{dn}(u, \mu)$  are Jacobi elliptic functions of argument  $u$  and parameter  $\mu$  [1].

[...] A cyclic permutation

$$e^{i\mathbf{P}} |x_1, x_2, \dots, x_L\rangle = |x_L, x_1, \dots, x_{L-1}\rangle. \quad (19.44)$$

where  $a_x^{-1}\mathbf{P}$  is the lattice momentum, the first conserved charge derived from the transfer matrix expansion. They see a graphical derivation of the identification  $e^{i\mathbf{P}}$ , I don't.

They say: canonical commutations of the bosonic field  $\mathbf{x}$  and its conjugate momentum  $\boldsymbol{\pi}$  in the continuum, become in the discretized model

$$[\mathbf{x}(z), \boldsymbol{\pi}(z')] = i\delta(z - z') \longrightarrow [\mathbf{x}_i, \boldsymbol{\pi}_j] = ia_x^{-1} \delta_{ij}. \quad (19.45)$$

Therefore one can represent  $\boldsymbol{\pi}_i = -ia_x^{-1} \partial_{x_i}$ , where

$$\langle \vec{y} | \partial_{x_i} | \vec{x} \rangle = \delta'(x_i - y_i) \prod_{j \neq i} \delta(x_j - y_j). \quad (19.46)$$

Then they diagonalize the transfer matrix of the free boson lattice theory in a way that they find reminiscent to the coordinate Bethe ansatz for spin systems.

A natural ansatz for the eigenstates is

$$|\Psi\rangle = \int d\vec{x} f_n(\vec{x}) e^{-\frac{1}{2}\vec{x} K \vec{x}^T} |\vec{x}\rangle, \quad (19.47)$$

where  $K$  a symmetric matrix and  $f_n$  a polynomial of degree  $n$  in  $x_i$ . The eigenstate condition  $\mathbf{T}(u)|\Psi\rangle = \Lambda|\Psi\rangle$  implies [...] that

$$K^2 = (\tilde{m}_0^2 + 2) \mathbf{1} - S - S^T, \quad (19.48)$$

The eigenvalues of the shift matrix  $S$  are roots of unity of order  $L$ . Hence the eigenvalues of  $K$  are

$$\omega_k = \sqrt{\tilde{m}_0^2 + 4 \sin^2 \frac{p_k}{2}}, \quad k = 0, \dots, L - 1. \quad (19.49)$$

with  $p_k = \frac{2\pi k}{L}$ . [...] Note that, although  $K^2$  only has entries on the diagonal and one step above or below it, its square root is a non-local matrix.

OK,  $K^2$  is our orbit Jacobian matrix  $\mathcal{J}$ . But why is (19.48) one-dimensional? By this time, I'm totally lost...

**2017-09-18 Predrag** R J Baxter, *Some comments on developments in exact solutions in statistical mechanics since 1944* (2010)

We draw the square lattice diagonally, with  $M$  rows of sites and  $L$  sites per row. We are particularly interested in calculating the partition function per site:

$$\kappa = Z^{1/LM},$$

the dimensionless free energy  $f = -\ln \kappa$  and averages such as the magnetization. We expect  $\kappa$  to tend to limit when  $L, M \rightarrow \infty$ .

[...] Later, combinatorial ways were found of writing the partition function of the Ising model on a finite lattice directly as a determinant or a pfaffian (the square root of an antisymmetric determinant).

**2017-09-11 Predrag** Katsura and Inawashiro [27] *Lattice Green's functions for the rectangular and the square lattices at arbitrary points*. They start with product of two Bessel functions (8.47), then go hypergeometric, or  $K(u)$  complete elliptic. In the appendix they study lattice Green's function of the linear lattice (i.e.,  $d = 1$  lattice), and relate it to Chebyshev  $T_m(u)$  and in turn to the hypergeometric  ${}_2F_1$ .

**2017-09-11 Predrag** Bhat and Osting [4] *Diffraction on the two-dimensional square lattice* write: The lattice Green's function is quite well known [13, 27].

**2017-09-11 Predrag** The real part of the square lattice Green's function (8.43) is odd or even function of  $s$ , and the imaginary part is even or odd function of  $s$ , if the sum of  $n$  and  $t$  is even or odd, respectively.

**2017-09-11 Predrag** Morita and Horiguchi [37] *Calculation of the lattice Green's function for the bcc, fcc, and rectangular lattices*: see the appendix *The lattice Green's functions for the rectangular lattice* (includes the square lattice as a special case). They integrate (8.43) and express it as the complete elliptic integral of the first kind (8.170).

Katsura, Inawashiro and Abe [28] *Lattice Green's function for the simple cubic lattice in terms of a Mellin-Barnes type integral*

Horiguchi [24] *Lattice Green's function for the simple cubic lattice* - GaTech does not have online access to it.

Horiguchi and Morita [25] *Note on the lattice Green's function for the simple cubic lattice*: " A simple recurrence relation connecting the lattice Green's function at  $(l, m, n)$  and the first derivatives of the lattice Green's function at  $(l \pm 1, m, n)$ , is presented for the simple cubic lattice. By making use of that recurrence relation, the lattice Green's functions at  $(2, 0, 0)$  and  $(3, 0, 0)$  are obtained in closed forms, which contain a sum of products of the complete elliptic integrals of the first and the second kind, see (8.170). "

Asad [2] *Differential equation approach for one- and two-dimensional lattice Green's function* seems a continuation of ref. [25]: " A first-order differential equation of Green's function, at the origin  $G(0)$ , for the one-dimensional lattice is derived by simple recurrence relation. Green's function at site  $(m)$  is then calculated in terms of  $G(0)$ . A simple recurrence relation connecting the lattice Green's function at the site  $(m, n)$  and the first derivative of the lattice Green's function at the site  $(m \pm 1, n)$  is presented for the two-dimensional lattice, a differential equation of second order in  $G(0, 0)$  is obtained. By making use of the latter recurrence relation, lattice Green's function at an arbitrary site is obtained in closed form. "

**2023-05-18 Predrag** Besag [3] *On a system of two-dimensional recurrence equations* (1981).

[...] in principle, full solutions could be deduced in terms of the complete elliptic integrals  $K$ ,  $E$  and  $\Pi$  of the first, second and third kinds, respectively.

Wortis [36] (1963) obtains simple formulae for the most important cases.

Simple and highly efficient algorithms for evaluating  $K$ ,  $E$  and  $\Pi$  are given by Bulirsch [6] (1965)

Bulirsch [6] *Numerical calculation of elliptic integrals and elliptic functions* (1965) very helpfully even provides ALGOL (!) code:)

Wortis [36] *Bound states of two spin waves in the Heisenberg ferromagnet* (1963). In a superficial scan, I do not see the "simple formulae" mentioned by Besag.

**2020-06-16 Predrag** Machide [33] *An elliptic analogue of generalized Dedekind-Rademacher sums*: "We mention a relation between the generating func-

tion of Kronecker's double series [26] and that of the (Debye) elliptic polylogarithms studied by A. Levin."

Machide [34] *Sums of products of Kronecker's double series*

**2024-01-03 Predrag** Possibly of interest (have not checked):

S. D. Mathur, S. Mukhi, and A. Sen, *Reconstruction of Conformal Field Theories From Modular Geometry on the Torus*, Nucl. Phys. B318 (1989) 483

E. P. Verlinde, *Fusion Rules and Modular Transformations in 2D Conformal Field Theory*, Nucl. Phys. B300 (1988) 360

M. R. Gaberdiel and S. Lang, *Modular differential equations for torus one-point functions*, J. Phys. A42 (2009) 045405, [arXiv:0810.0106](#)

**2024-01-27 Predrag** Di Francesco, Saleur and Zuber [17] *Critical Ising correlation functions in the plane and on the torus* (1987). Do not have access to it.

Di Francesco, Saleur and Zuber [18] *Correlation functions of the critical Ising model on a torus* (1988). They consider critical correlation functions on a torus. Lots of elliptic functions, but no details that would be helpful to us. A detailed version of this work seems to be the above ref. [17].

They cite partition function evaluation of Itzykson C and Zuber J B 1986 Nucl. Phys. B 275 580.

**2024-03-25 Predrag** Eric Perlmutter papers are about calculations in the Poincaré upper half-plane figure 19.5.

Di Ubaldo and Perlmutter *AdS<sub>3</sub>/RMT<sub>2</sub> duality*, [arXiv:2307.03707](#), Sect. 2.1 *Lightning review of SL(2, Z) spectral theory in 2d CFT* might be helpful to us.

Paul, Perlmutter and Raj *Exact large charge in N = 4 SYM and semiclassical string theory*, [arXiv:2303.13207](#): [...] correlators are shown to be equivalent to a one-dimensional semi-infinite lattice of harmonic oscillators with nearest-neighbor interactions, evolving over the fundamental domain of SL(2, Z). [...]

**2024-08-24 Predrag** random clips from internet:

The logarithmic derivative of the  $\eta$ -function is the Eisenstein series  $G_2$ , up to elementary factors. The series for  $G_2$  does not quite converge when summed over a lattice, but can be regularized in various ways so that it does converge.

[Michael Somos](#) database of over 6300 of eta-product identities: [eta.math.georgetown.edu](#).

[The Somos Sequence Site](#).

**2024-08-24 Predrag** [Ryan Rueger](#) semester thesis *Eta Products* (2023).

Using the definition of Dedekind eta (19.38), he finds it convenient to define

$$e_{24}(\tau) = q^{\frac{1}{24}} = e^{\frac{\pi i \tau}{12}}$$

Then Rueger *Lemma 3.1* states a ‘ $q$ -expansion’ of the eta-function as sum of two integer  $n \geq 0$  sums over  $(-1)^n e_{24}((6n \pm 1)\tau)$ . As that is just Euler’s pentagonal numbers sum, not sure it is useful to us. The powers of  $q$  in the expansion grow quadratically. For a precision of  $q^k$  truncate the sums at  $n = \lceil \sqrt{24k} \rceil$  terms and then truncate  $q$  series at  $O(q^k)$ . “ The precision of eta products are trickier to manage since we allow negative exponents. That is to say, we must increase the precision when calculating the product, since negative powers may produce terms within our precision in a product. ”

Unfortunately, the actual Sect. 4 *Eta products* he considers is of a very specialized form, which is of no use to us. *Sagemath* includes an `EtaProduct` implementation, and might be useful as it

His adviser is [Markus Schwagenscheidt](#), now a high school teacher.

**2024-10-05 Predrag** Robin Chapman and William Har [Chapt. 6](#) *Evaluation of the Dedekind eta function* give a historical overview of methods for the evaluation of Dedekind functions. They evaluate it for specific values of  $\tau$  that we probably do not care about.

**2024-10-04 Sidney** (2002) Alan D. Sokal [\[41\]](#) *Numerical Computation of  $\prod_{n=1}^{\infty} (1 - tx^n)$* ; [arXiv:math/0212035](#).

“ The key lemma is a two-sided bound on the Dedekind eta function at pure imaginary argument,  $\eta(iy)$ , that is sharp at the two endpoints  $y = 0, \infty$  and is accurate to within 9.1% over the entire interval  $0 < y < \infty$ . ”

### 19.3 Zeta function regularization

Given operator  $\Delta$ , the spectral zeta function is the sum over its non-zero eigenvalues

$$\zeta(s) = \sum_{n=1}^{\infty} \lambda_n^{-s}. \tag{19.50}$$

Then the zeta-regularized determinant [\[39\]](#) is defined as

$$\text{Det}(\Delta) = \prod_{n=1}^{\infty} \lambda_n := e^{-\zeta'(0)}. \tag{19.51}$$

Zeta determinants only give the value of path integrals up to an arbitrary multiplicative constant. One can only calculate the quotient of two path integrals, which is then given by the quotient of the respective zeta determinants.

**2023-11-24 Predrag** Kirsten and Loya [\[30\]](#) *Calculation of determinants using contour integrals* (2008), [arXiv:0707.3755](#), is pedagogical, on undergraduate level.

Consider eigenvalues  $\{\lambda_k\}_{k=1}^n$  of a finite matrix  $L$ , assumed all non-zero,

$$\det L = \prod_{k=1}^n \lambda_k,$$

which implies

$$\ln \det L = \sum_{k=1}^n \ln \lambda_k = - \frac{d}{ds} \bigg|_{s=0} \sum_{k=1}^n \lambda_k^{-s}.$$

In the notation of (21.137) this shows

$$\ln \det L = -\zeta'(0) \quad \text{or} \quad \det L = e^{-\zeta'(0)}. \quad (19.52)$$

When the finite dimensional matrix is replaced by a differential operator  $L$  having infinitely many eigenvalues, in general  $\prod_{k=1}^{\infty} \lambda_k$  will not be defined. However, as it turns out for many situations of relevance, definition (21.138) makes perfect sense and has found important applications in mathematics and physics.

**2023-11-25 Predrag** Gerald V. Dunne *Functional Determinants in Quantum Field Theory*, [arXiv:0711.1178](https://arxiv.org/abs/0711.1178).

For Schrödinger operators with general potentials, or Dirac/Klein-Gordon operators with arbitrary gauge and/or gravitational backgrounds, we rely heavily on approximate methods. One such approximation is the heavy mass expansion. Define

$$\ln \det [m^2 + \mathcal{D}] = \text{tr} \ln [m^2 + \mathcal{D}] = - \int_0^\infty \frac{ds}{s} e^{-m^2 s} \text{tr} \{e^{-s \mathcal{D}}\}$$

Then an inverse mass expansion follows (after renormalization) from the small  $s$  asymptotic expansion of the heat kernel operator

$$\text{tr} \{e^{-s \mathcal{D}}\} \sim \frac{1}{(4\pi s)^{d/2}} \sum_{k=0}^{\infty} s^k a_k [\mathcal{D}] \quad .$$

Here the  $a_k [\mathcal{D}]$  are known functionals of the potentials appearing in  $\mathcal{D}$ . Similarly, a derivative expansion can be derived by expanding the heat kernel trace  $\text{tr} \{e^{-s \mathcal{D}}\}$  about the soluble constant background case, in powers of derivatives of the background. This corresponds to resumming all non-derivative terms in the inverse mass expansion. While very general, these expansions are asymptotic, with higher terms becoming rapidly unwieldy, and so have a somewhat limited range of application.

Another approach is to define the functional determinant via a zeta function

$$\zeta(s) \equiv \sum_{\lambda} \frac{1}{\lambda^s} \quad , \quad (19.53)$$

where the sum is over the spectrum of the relevant differential operator. Then, by the formal manipulations  $\zeta'(0) = -\sum_{\lambda} \ln \lambda = -\ln(\prod_{\lambda} \lambda)$ , one defines the determinant as

$$\det = e^{-\zeta'(0)} \quad . \quad (19.54)$$

The problem becomes one of analytically continuing  $\zeta(s)$  from the region in which it converges [typically  $\text{Re}(s) > d/2$ ] to the neighbourhood of  $s = 0$ . For example, in a radially separable problem, one might estimate the spectrum using WKB phase shifts [and the corresponding spectral function  $\rho(k) = \frac{1}{\pi} \frac{d\delta}{dk}$ ], thereby obtaining information about the zeta function. The zeta function approach is complementary to the so-called *replica method*, where one defines the logarithm of an operator by considering *positive* integer powers  $n$  of the operator, and then analytically continues to  $n = 0$ . There are also non-trivial interesting one-dimensional quantum mechanical problems for which the determinant can be computed from the zeta function [44].

**2023-11-21 Predrag** I like how Fadeev thinks about it, see [ChaosBook remark A22.1](#).

**2023-11-21 Predrag** Nicolas M. Robles [master's thesis Zeta Function Regularization](#) (2009) gives a nice overview.

**2024-07-19 Predrag** Chaumard [11] *Discrétisation de zeta-déterminants d'opérateurs de Schrödinger sur le tore* (2006), and references within, looks interesting, but I have not studied it.

**2023-11-21 Predrag** Emilio Elizalde, Klaus Kirsten, Nicolas Robles, Floyd Williams [15] *Zeta functions on tori using contour integration*, [arXiv:1306.4019](#).

Suppose we have a [...] Laplace-Beltrami operator  $\Delta$  with a discrete spectrum

$$0 = \lambda_0 < \lambda_1 < \lambda_2 < \dots, \quad \lim_{j \rightarrow \infty} \lambda_j = \infty. \quad (19.55)$$

Denote by  $n_j$  the finite multiplicity of the  $j$ -th eigenvalue  $\lambda_j$  of  $\Delta$ . Then the corresponding spectral zeta function is

$$\zeta_M(s) = \sum_{j=1}^{\infty} \frac{n_j}{\lambda_j^s}, \quad (19.56)$$

which is well-defined for  $\text{Re}(s) > \frac{1}{2} \dim M$ ,  $\dim M =$  manifold dimensions [...] Ray and Singer [39] define

$$\det(\Delta) = \prod_{k=1}^{\infty} \lambda_k^{n_k} := e^{-\zeta_M'(0)}, \quad (19.57)$$



(the zero eigenvalue of  $\Delta$  is not taken into the product). The motivation for this definition comes from the formal computation

$$\exp \left[ -\frac{d}{ds} \Big|_{s=0} \sum_{k=1}^{\infty} \frac{n_k}{\lambda_k^s} \right] = \exp \left[ \sum_{k=1}^{\infty} n_k \log \lambda_k \right] = \prod_{k=1}^{\infty} e^{n_k \log \lambda_k} = \prod_{k=1}^{\infty} \lambda_k^{n_k}. \quad (19.58)$$

[...] The group of substitutions generated by  $\tau \rightarrow \tau + 1$  and  $\tau \rightarrow -\frac{1}{\tau}$  is

$$\mathrm{SL}(2, \mathbb{Z}) = \left\{ \begin{pmatrix} a & b \\ c & d \end{pmatrix} \text{ such that } a, b, c, d \in \mathbb{Z} \text{ and } ad - bc = 1 \right\},$$

therefore modular forms of weight  $k$  satisfy

$$f \left( \frac{a\tau + b}{c\tau + d} \right) = (c\tau + d)^k f(\tau).$$

The Dedekind eta function is a modular form of weight  $k = \frac{1}{2}$  and we may assume without loss of generality that either  $c > 0$  or  $c = 0$  and  $d = 1$ . Moreover, if  $c = 0$  and  $d = 1$ , then it satisfies

$$\eta \left( \frac{a\tau + b}{c\tau + d} \right) = \varepsilon(a, b, c, d) (c\tau + d)^{1/2} \eta(\tau),$$

where  $\varepsilon(a, b, c, d) = e^{b\pi i/12}$ , and if  $c > 0$  then [...]

For fixed  $\tau = \tau_1 + i\tau_2 \in \mathbb{H}$  the  $\tau$ -Laplacian is

$$\Delta_\tau = -\frac{1}{\tau_2^2} \left[ \left( \frac{\partial}{\partial x} + \tau_1 \frac{\partial}{\partial y} \right)^2 + \left( \tau_2 \frac{\partial}{\partial y} \right)^2 \right] = -\frac{1}{\tau_2^2} \left[ \frac{\partial^2}{\partial x^2} + (\tau_1^2 + \tau_2^2) \frac{\partial^2}{\partial y^2} + 2\tau_1 \frac{\partial}{\partial x} \frac{\partial}{\partial y} \right]. \quad (19.59)$$

Let  $M = S^1 \times S^1$  be a complex torus and the corresponding integral lattice is

$$\mathcal{L}_\tau := \{a + b\tau \mid a, b \in \mathbb{Z}\}, \quad M := \mathbb{C} \setminus \mathcal{L}_\tau. \quad (19.60)$$

The eigenvalue problem is

$$\Delta_\tau \phi_\lambda(x, y) = \lambda^2 \phi_\lambda(x, y), \quad (19.61)$$

with periodic boundary conditions

$$\phi_\lambda(x, y) = \phi_\lambda(x + 1, y), \quad \frac{\partial}{\partial x} \phi_\lambda(x, y) = \frac{\partial}{\partial x} \phi_\lambda(x + 1, y), \quad (19.62)$$

on  $x$ , as well as

$$\phi_\lambda(x, y) = \phi_\lambda(x, y + 1), \quad \frac{\partial}{\partial y} \phi_\lambda(x, y) = \frac{\partial}{\partial y} \phi_\lambda(x, y + 1), \quad (19.63)$$

on  $y$ .

**The main result:** The functional determinant of the  $\tau$ -Laplacian on the complex torus is

$$\det(\Delta_\tau) = \tau_2^2 |\eta(\tau)|^4. \quad (19.64)$$

See (19.40).

**2023-11-26 Predrag** According to Bass and Todorov *Dedekind eta function for CY manifolds* (19.64) is a “well-known fact.” The rest is way above my pay grade.

nLab *Laplace operator on complex torus and Dedekind eta function* states it is well. It also helpfully gives this definition: “A differential or pseudodifferential operator is *elliptic* if its principal symbol is invertible.

A *principal symbol* is the highest homogeneous degree part of a symbol of a pseudodifferential operator. Some authors call a principal symbol a ‘symbol’, and symbol the ‘total symbol’.”

**2023-11-25 Predrag** The functional determinant for  $d$ -torus is computed in J. Angel-Ramelli, V. Giangreco M. Puletti, L. Thorlacius *Entanglement Entropy in Generalised Quantum Lifshitz Models*, [arXiv:1906.08252](https://arxiv.org/abs/1906.08252). For 2-torus, see eq. (C.20): it’s essentially a square root of (19.64).

They cite P. Di Francesco, P. Mathieu and D. Senechal *Conformal field theory*, Springer (1997), ([click here](#)), see sect. 10.2. *The free boson on the torus*.

[...] From Eqs. (10.5) and (7.16), we expect the partition to be of the form

$$Z \propto \frac{1}{|\eta(\tau)|^2}.$$

The proportionality constant is important, since the above expression is not modular invariant! With a suitable proportionality constant ensuring modular invariance, the free-boson partition function (without zero-mode) is (see (19.40)):

$$Z = \frac{1}{(\text{Im } \tau)^{1/2} |\eta(\tau)|^2}. \quad (19.65)$$

They (re)derive it using the  $\zeta$ -function regularization technique. The path-integral free-boson partition function without the zero-mode is written in their eq. (10.14).

Sect. 10.4.1. *Compactified boson* (see also sect. 6.3.5) leads to 2-winding numbers partition function eq. (10.56).

**2025-01-10 Predrag** Alexi Morin-Duchesne, Andreas Klümper, Paul A. Pearce *Critical site percolation on the triangular lattice: From integrability to conformal partition functions*; [arXiv:2211.12379](https://arxiv.org/abs/2211.12379).


Conformal partition functions of critical percolation from  $D_3$  Thermodynamic Bethe Ansatz equations; [arXiv:1701.08167](https://arxiv.org/abs/1701.08167)

Dedekind partition functions show up in Pearce's [slides](#), on p. 0.9. They are "well-known in the Coulomb gas formalism:

P. di Francesco, H. Saleur, J.-B. Zuber [17], *Relations between the Coulomb gas picture and conformal invariance of two-dimensional critical models*,

P. di Francesco, H. Saleur, J.-B. Zuber [19], *Generalized Coulomb-gas formalism for two-dimensional critical models based on  $SU(2)$  coset construction*,

2020-09-23 **Abhijit Gadde** [arXiv:2004.13490](https://arxiv.org/abs/2004.13490)

 Modularity of supersymmetric partition functions, a generalization of the modular invariance of two-dimensional supersymmetric theories on a torus i.e. of the elliptic genus.

The twisted partition function of the theory on a torus with periodic boundary conditions along both cycles, invariant under  $SL(2, \mathbb{Z})$  action on the parameters  $(z, \tau)$ ,

$$g_1 \cdot (z, \tau) = \left( \frac{z}{c\tau + d}, \frac{a\tau + b}{c\tau + d} \right), \quad g_1 = \begin{pmatrix} a & b \\ c & d \end{pmatrix} \in SL(2, \mathbb{Z}) \quad (19.66)$$

[...] Elements  $S$  and  $T$  are the generators of the modular group  $SL(2, \mathbb{Z})$ ,  $S : (z, \tau) \rightarrow (z/\tau, -1/\tau)$  and  $T : (z, \tau) \rightarrow (z, \tau + 1)$ . [...] Here  $\tau$  is the complex structure of the torus.

(Predrag: skipping the rest - this "review" of 2d case is above my head).

2024-10-05 **Predrag** Castro, Gaberdiel, Hartman, Maloney and Volpato [10] *Gravity dual of the Ising model* (2012):

" The torus partition function is given by a sum over geometries which is finite and computable. [...] in certain cases it agrees with the partition function of a known conformal field theory. For example, the partition function of pure Einstein gravity [...] equals that of the Ising model, providing evidence that these theories are dual.

In attempting to calculate the path integral for pure quantum gravity (1.3), we encounter two obstacles. [...] The second is that, at least in the semiclassical limit, the sum over geometries is badly divergent and needs to be regulated in some way.

[...] it is crucial that we are studying gravity in a strongly coupled regime where quantum effects are of order one. [...] the sum over geometries—i.e. the sum over distinct topologies in (1.3)—can be performed explicitly.

[...] In the semiclassical approximation, manifolds that contribute to the partition sum are the saddle point approximation, a sum over all solutions to the equations of motion,

In the semiclassical limit the only topologies which contribute to the path integral are those which admit a classical solution to the equations of motion.

[...] the geometries are labeled by the elements of the group  $SL(2, \mathbb{Z})$ .

So, is their geometry is trivial - it's the sum over all repeats??? Do, they seem to define what we call primitive cell partition sum  $Z_A$

[...] physically inequivalent saddles are labeled not by the group  $SL(2, \mathbb{Z})$  but by the coset  $\Gamma = T_\infty^2 \setminus SL(2, \mathbb{Z})$ , where  $T_\infty^2$  is the group of all translations, their eq. (2.11). "

Then the things get complicated, and I'm lost. Our path to Dedekind  $\eta$  is much shorter.

**2023-11-21 Predrag** A. A. Bytsenko, E. Elizalde *On Partition Functions of Hyperbolic Three-Geometry and Associated Hilbert Schemes*, [arXiv:1303.2265](#).

[...] Partition functions (elliptic genera) are conveniently transformed into product expressions, which may inherit the homology properties of appropriate (poly)graded Lie algebras. Specifically, the role of (Selberg-type) Ruelle spectral functions of hyperbolic geometry in the calculation of partition functions and associated q-series are discussed. [...] where one has Ruelle/Selberg spectral functions, whereas on the CFT side, partition functions and modular forms arise. These objects are here shown to have a common background, expressible in terms of Euler-Poincaré and Macdonald identities.

**2023-11-21 Predrag** Emilio Elizalde *Zeta function regularization in Casimir effect calculations and J.S. Dowker's contribution*, [arXiv:1205.7032](#). A summary of

contribution to the subject of operator zeta functions [...] contributions of Stephen Hawking and Stuart Dowker [...] recent results of the so called operator regularization procedure are presented.

Have the monograph Elizalde [14] *Ten Physical Applications of Spectral Zeta Functions* (2012), use as a reference.

**2023-11-21 Predrag** G. Cognola, E. Elizalde, S. Zerbini *Functional Determinant of the Massive Laplace Operator and the Multiplicative Anomaly*, [arXiv:1408.1766](#).

After a brief survey of zeta function regularization issues and of the related multiplicative anomaly, illustrated with a couple of basic examples, namely the harmonic oscillator and quantum field theory at finite temperature, an application of these methods to the computation of functional determinants corresponding to massive Laplacians on spheres in arbitrary dimensions is presented.

[...] regularized determinants do not satisfy the usual properties of  $\det$ 's, in particular, the multiplicative property.

**2023-11-24 Predrag** Holstein [23] *The harmonic oscillator propagator* (1998) is a pedagogical survey of Feynman propagator for the harmonic oscillator evaluated by a variety of path-integral-based means. Everything is done

for the Dirichlet boundary conditions, no periodic case. In particular, note the Euler product representation (3) for  $\sin(x)/x$ ; replacement of the functional determinant (19) by ratio of determinants (the other determinant being the Laplacian, zero mass propagator); replacing the logarithm of the operator by the integral (28); discretizing time and using our massive free field orbit Jacobian matrix (46), using the usual determinant recursion relation (49), our sect. 24.6.2;

**2023-12-06 Predrag** Reading C. A. Lütken *A planar cubic derived from the logarithm of the Dedekind  $\eta$ -function* (2021), [click here](#).

Periodic (circle) functions are called trigonometric functions. A product of two circles is a torus, which after a point of origin has been chosen is called an elliptic curve. If we do not impose any constraints, it is way too easy to make doubly periodic functions: the product  $P(x)Q(y)$  of any two periodic functions  $P$  and  $Q$  is doubly periodic, frequently finite, but never (by Liouville's theorem) holomorphic (complex analytic), except for constants; cf. Figure 2(a). The useful compromise is to consider meromorphic doubly periodic (toroidal) functions, which are called elliptic functions.

We can regard both periodic and doubly periodic functions as lattice functions, i.e., lattice sums that are manifestly periodic in one or two directions. Furthermore, we shall view a two-dimensional (2D) lattice as a stack of one-dimensional (1D) lattices, each of which is a string of lattice points parallel to the real line (cf. Figures 1 and 2) that we call a chain. We can dissect 2D sums by doing one chain at a time, and we therefore suspect that elliptic and trigonometric functions are close cousins. That this is indeed the case is most easily seen by constructing both as lattice sums.

This parsing of a 2D lattice as a stack of chains highlights the similarities between 1D and 2D lattice functions, and it is the main pedagogical device used here to explain that elliptic lattice functions (rather than Weierstrass functions) are the closest relatives of trigonometric functions.

Our convention is that the lattice is 1D with period  $\tau$  if  $\tau$  is a positive real number.

The lattice is 2D if  $\tau$  is not real, and we can without loss of generality parameterize all such lattices by the upper complex half-plane.

(He does 1D case very understandably, as intro to 2d case).

**2024-12-01 Predrag** See also (18.27).

## 19.4 Computing log det of Hill determinant

In [ChaosBook sect 4.7](#) *Neighborhood volume* I express the determinant of the linearized flow in terms of its average divergence in time, *without* computing

the detailed spectrum of the linearized flow.

We need something like that for Hill determinants. We do not have time to average over, but my hunch is that the fictitious heat kernel time of chapter 18 *Heat kernel* might do the job - compute periodic state's  $\ln \det$  of a Hill determinant, *without* computing first the spectrum of an orbit Jacobian matrix.

The idea is explained - for example - in Eduardo Fradkin's lectures (monograph?) [Sect. 8.8.2](#) *Functional determinants, heat kernels and  $\zeta$ -function regularization*.

The other option is a cop-out, but if it works, fine: use Hill-Gel'fand-Yaglom formula, compute  $\log \det$  Hill determinant as discretized divergence, time averaged.

## 19.5 Maloney-Witten partition functions, MalWit07

**2024-10-05 Predrag** H. Sun *Number Theory in 3d Gravity and from 4d Gauge Theory* [PhD thesis](#) (2020) has helpful introductory overview text in various chapters.

**2023-09-22 Predrag** notes:

Maloney and Witten [\[35\]](#) *Quantum Gravity Partition Functions in Three Dimensions* (2007), [arXiv:0712.0155](#), is a well written, pedagogical paper, with much wisdom. Basically, you understand that Witten has skills and insights well beyond an average theoretical physicist. Here I'm clipping only a few bits that lead to the partition function expressed as Dedekind eta function:

The automorphism group of  $AdS_3$  is  $SO(3, 1)$ , which is the same as  $SL(2, \mathbb{C})/\mathbb{Z}_2$ . If we combine the  $(z, u)$  coordinates into a single quaternion  $y = z + ju$ , the action of an element  $\begin{pmatrix} a & b \\ c & d \end{pmatrix} \in SL(2, \mathbb{C})$  can be written succinctly as

$$y \rightarrow (ay + b)(cy + d)^{-1}. \tag{19.67}$$

In this expression the element  $\begin{pmatrix} -1 & 0 \\ 0 & -1 \end{pmatrix} \in SL(2, \mathbb{C})$  acts trivially, so (19.67) actually describes the action of  $SL(2, \mathbb{C})/\mathbb{Z}^2$  on  $AdS_3$ . [...] The conformal boundary [...]  $SL(2, \mathbb{C})$  acts on this [...] in the familiar fashion

$$z \rightarrow \frac{az + b}{cz + d}.$$

The subgroup of  $SL(2, \mathbb{C})$  that leaves fixed the point at infinity consists of the triangular matrices

$$\begin{pmatrix} \lambda & w \\ 0 & \lambda^{-1} \end{pmatrix}. \tag{19.68}$$

The point  $z \in \mathbb{C}$  corresponds to  $\begin{pmatrix} z \\ 1 \end{pmatrix} \in CP^1$ , and a triangular matrix acts by  $z \rightarrow \lambda^2 z + \lambda w$ .

Since  $U$  is simply-connected,  $\Gamma$  must be isomorphic to  $\mathbb{Z} \oplus \mathbb{Z}$  [...] Any discrete group of triangular matrices that is isomorphic to  $\mathbb{Z} \oplus \mathbb{Z}$  is generated by two strictly triangular matrices

$$\begin{pmatrix} 1 & a \\ 0 & 1 \end{pmatrix}, \begin{pmatrix} 1 & b \\ 0 & 1 \end{pmatrix}, \quad (19.69)$$

where  $a$  and  $b$  are complex numbers that are linearly independent over  $\mathcal{R}$ . The subgroup of  $SL(2, \mathbb{C})$  that leaves fixed the point at infinity consists of the triangular matrices

$$\begin{pmatrix} \lambda & w \\ 0 & \lambda^{-1} \end{pmatrix}. \quad (19.70)$$

The point  $z \in \mathbb{C}$  corresponds to  $\begin{pmatrix} z \\ 1 \end{pmatrix} \in CP^1$ , and a triangular matrix acts by  $z \rightarrow \lambda^2 z + \lambda w$ .

Since  $U$  is simply-connected,  $\Gamma$  must be isomorphic to  $\mathbb{Z} \oplus \mathbb{Z}$  [...] Any discrete group of triangular matrices that is isomorphic to  $\mathbb{Z} \oplus \mathbb{Z}$  is generated by two strictly triangular matrices

$$\begin{pmatrix} 1 & a \\ 0 & 1 \end{pmatrix}, \begin{pmatrix} 1 & b \\ 0 & 1 \end{pmatrix}, \quad (19.71)$$

where  $a$  and  $b$  are complex numbers that are linearly independent over  $\mathcal{R}$ . Up to conjugacy by a diagonal matrix, the only invariant of such a group is the ratio  $b/a$ . Therefore, we can reduce to the case  $a = 1, b = \tau$ , and moreover by taking  $b \rightarrow -b$  (which does not affect the group generated by the two matrices) we can assume that  $\text{Im } \tau > 0$ .

We have therefore arrived precisely at the group of symmetries

$$z \rightarrow z + m + n\tau, \quad m, n \in \mathbb{Z} \quad (19.72)$$

of the complex  $z$ -plane. The quotient is a genus 1 surface  $\Sigma$  with an arbitrary  $\tau$ -parameter. [...] a Riemann surface of genus 1 [...] The complex modulus of this surface is  $\tau = \frac{\log q}{2\pi i}$ , i.e. it is given by  $q = e^{2\pi i \tau}$ . More generally, however, the modulus of this Riemann surface is defined only up to  $\tau \rightarrow (a\tau + b)/(c\tau + d)$  with integers  $a, b, c, d$  obeying  $ad - bc = 1$ . Therefore, we will get an equivalent Riemann surface if

$$q = \exp(2\pi i(a\tau + b)/(c\tau + d)) \quad (19.73)$$

for such  $a, b, c, d$ . [...] First, an overall sign change of  $a, b, c, d$  does not affect  $q$  or the associated three-manifold. Second, once  $c$  and  $d$  are given,  $a$  and  $b$  are uniquely determined by  $ad - bc = 1$  up to shifts of the form  $(a, b) \rightarrow (a, b) + t(c, d), t \in \mathbb{Z}$ . Under this transformation,  $q$  as defined in (19.73) is invariant. So the possible three-manifolds really only depend on the choice of the pair  $c, d$  of relatively prime integers, up to sign. For each such pair, we find integers  $a, b$  such that  $ad - bc = 1$ , and identify  $q$  via (19.73). This gives a manifold that we will call  $M_{c,d}$ . [...]

The path integral in this spacetime has a simple semiclassical meaning, since it may be interpreted in terms of Hamiltonian time evolution. A state is prepared at time zero and propagates a distance  $\beta = 2\pi \text{Im } \tau$  forward in Euclidean time. In this process, the state vector is multiplied by the time evolution operator  $\exp(-\beta H)$ , where  $H$  is the Hamiltonian. Then, after a spatial rotation by an angle  $\theta = 2\pi \text{Re } \tau$ , which acts on the state by  $\exp(-i\theta J)$ , we glue the top and bottom of the figure, which results in taking the inner product of the final state with the initial state. The whole operation gives the trace  $\text{Tr } \exp(-\beta H - i\theta J)$ . [...] We write  $Z_{c,d}(\tau)$  for the contribution to the partition function of the manifold  $M_{c,d}$ . Because the manifolds  $M_{c,d}$  are all diffeomorphic to each other, the functions  $Z_{c,d}(\tau)$  can all be expressed in terms of any one of them, say  $Z_{0,1}(\tau)$ , by a modular transformation. The formula is simply

$$Z_{c,d}(\tau) = Z_{0,1}((a\tau + b)/(c\tau + d)), \quad (19.74)$$

where  $a$  and  $b$  are any integers such that  $ad - bc = 1$ . The partition function, or rather the sum of known contributions to it, is

$$Z(\tau) = \sum_{c,d} Z_{c,d}(\tau) = \sum_{c,d} Z_{0,1}((a\tau + b)/(c\tau + d)). \quad (19.75)$$

The summation here is over all integers  $c$  and  $d$  which are relatively prime and have  $c \geq 0$ .

This formula shows that the key point is to evaluate  $Z_{0,1}(\tau)$ . We recall that this contribution is simply  $\text{Tr } \exp(-\beta H - i\theta J)$ , computed in the Hilbert space that describes small fluctuations about  $AdS_3$  (as opposed to black holes). If we know the eigenvalues of the commuting operators  $H$  and  $J$  in the Hilbert space of small fluctuations, then we can compute the trace.

This formula shows that the key point is to evaluate  $Z_{0,1}(\tau)$ . We recall that this contribution is simply  $\text{Tr } \exp(-\beta H - i\theta J)$  [...] If we know the eigenvalues of the commuting operators  $H$  and  $J$  in the Hilbert space of small fluctuations, then we can compute the trace.

In the most naive semiclassical approximation,  $Z_{0,1}(\tau)$  is just  $\exp(-I)$ , where  $I$  is the classical action. [...] in this approximation, we have

$$Z_{0,1}(\tau) \simeq |\bar{q}q|^{-k} \quad (19.76)$$

[...] (19.76) actually gives the exact result for the contribution of the ground state to the partition function. [...]

The contribution of these states to the partition function is then

$$Z_{0,1}(\tau) = |\bar{q}q|^{-k} \frac{1}{\prod_{n=2}^{\infty} |1 - q^n|^2} \quad (19.77)$$

It is convenient to introduce the Dedekind  $\eta$  function, defined by

$$\eta(\tau) = q^{1/24} \prod_{n=1}^{\infty} (1 - q^n). \quad (19.78)$$



(19.77) can then be rewritten

$$Z_{0,1}(\tau) = \frac{1}{|\eta(\tau)|^2} |\bar{q}q|^{-(k-1/24)} |1-q|^2. \quad (19.79)$$

[...]  $(\text{Im } \tau)^{1/2} |\eta(\tau)|^2$  is modular-invariant. [...]

As for why it is much simpler to compute the one-loop correction via the Hamiltonian route that we have followed, this should not really come as a surprise. In general, path integrals on a product  $S^1 \times Y$  are often most easily evaluated by constructing an appropriate Hilbert space in quantization on  $Y$  and then taking a trace. [...]

**Computing the sum over geometries.** [...] contributions to the partition function of pure gravity in a spacetime asymptotic to  $AdS_3$  come from smooth geometries  $M_{c,d}$ , where  $c$  and  $d$  are a pair of relatively prime integers (with a pair  $c, d$  identified with  $-c, -d$ ). Their contribution to the partition function [...] is

$$Z(\tau) = \sum_{c,d} Z_{0,1}(\gamma\tau), \quad (19.80)$$

where

$$\gamma\tau = \frac{a\tau + b}{c\tau + d}, \quad \gamma = \begin{pmatrix} a & b \\ c & d \end{pmatrix} \in \text{SL}(2, \mathbb{Z}) \quad (19.81)$$

and

$$Z_{0,1}(\tau) = \left| q^{-k} \prod_{n=2}^{\infty} (1-q^n)^{-1} \right|^2 = \frac{|\bar{q}q|^{-k+1/24} |1-q|^2}{|\eta(\tau)|^2}. \quad (19.82)$$

The summation in (19.80) is over all relatively prime  $c$  and  $d$  with  $c \geq 0$ . Since  $Z_{0,1}(\tau)$  is invariant under  $\tau \rightarrow \tau + 1$ , the summand in (19.80) is independent of the choice of  $a$  and  $b$  in (19.81). [...] Given any function of  $\tau$ , such as  $Z_{0,1}(\tau)$ , that is invariant under  $\tau \rightarrow \tau + 1$ , one may form a sum such as (19.80), known as a Poincaré series.

The function  $\sqrt{\text{Im } \tau} |\eta(\tau)|^2$  is modular-invariant. We can therefore write  $Z(\tau)$  as a much simpler-looking Poincaré series,

$$Z(\tau) = \frac{1}{\sqrt{\text{Im } \tau} |\eta(\tau)|^2} \sum_{c,d} \left( \sqrt{\text{Im } \tau} |\bar{q}q|^{-k+1/24} |1-q|^2 \right) \Big|_{\gamma}, \quad (19.83)$$

where  $(\dots)|_{\gamma}$  is the transform of an expression  $(\dots)$  by  $\gamma$ . [...]

If we set  $\kappa = n+m$ ,  $\mu = m-n$ , and use the fact that  $\text{Im } (\gamma\tau) = \text{Im } \tau / |c\tau + d|^2$ , then the basic Poincaré series can be written

$$E(\tau; \kappa, \mu) = \sqrt{\text{Im } \tau} \sum_{c,d} |c\tau + d|^{-1} \exp \{2\pi\kappa \text{Im } \gamma\tau + 2\pi i\mu \text{Re } \gamma\tau\}. \quad (19.84)$$

When  $\kappa = 0$  and  $\mu = 0$ , this sum is a non-holomorphic Eisenstein series of weight  $1/2$ . Sometimes we omit  $\tau$  and write just  $E(\kappa, \mu)$ . In terms of this function, the partition function is

$$Z(\tau) = \frac{1}{\sqrt{\text{Im } \tau} |\eta(\tau)|^2} \quad (E(2k-1/12, 0) + E(2k+2-1/12, 0))$$

$$-E(2k+1-1/12, 1) - E(2k+1-1/12, -1)). \quad (19.85)$$

[...] the first two terms in (19.85) diverge linearly as  $\sum_{c,d} |c\tau + d|^{-1}$  at large  $c$  and  $d$ . [...] this divergence has a natural regularization. On the upper half plane, which we call  $H$ , there is a natural  $\text{SL}(2, \mathbb{R})$ -invariant Laplacian:

$$\Delta = -y^2 \left( \frac{\partial^2}{\partial x^2} + \frac{\partial^2}{\partial y^2} \right). \quad (19.86)$$

A short calculation shows that the function  $y^{1/2}$  is an eigenfunction of  $\Delta$ :  $\Delta(y^{1/2}) = (1/4)y^{1/2}$ . Since  $\Delta$  is  $\text{SL}(2, \mathbb{R})$ -invariant, the same is true of  $(\text{Im } \gamma\tau)^{1/2}$  for any  $\gamma \in \text{SL}(2, \mathbb{Z})$  (or even  $\text{SL}(2, \mathbb{R})$ ):

$$\Delta \sqrt{\text{Im}(\gamma\tau)} = \frac{1}{4} \sqrt{\text{Im}(\gamma\tau)}. \quad (19.87)$$

[...] although the Poincaré series for  $E(\tau; \kappa, \mu)$  is divergent, the corresponding series for  $(\Delta - 1/4)E(\tau; \kappa, \mu)$  converges.

[...] the exact partition function  $Z_{0,1}$  associated with  $M_{0,1}$  [...]  $Z_{0,1} = F_k(q)F_k(\bar{q})$ , with

$$F_k(q) = q^{-k} \prod_{n=2}^{\infty} (1 - q^n)^{-1}. \quad (19.88)$$

To the extent that known formulations of three-dimensional gravity are valid, this sort of factorization holds for the contribution to the partition function of any classical geometry. [...] the theory is a product of two decoupled  $\text{SL}(2, \mathbb{R})$  theories, associated respectively with left- and right-moving modes in the boundary CFT, and this corresponds to holomorphic factorization in the Euclidean form of the theory.

Now let us discuss holomorphic factorization in view of the sum over geometries. Associated to an element

$$\gamma = \begin{pmatrix} a & b \\ c & d \end{pmatrix} \quad (19.89)$$

of  $\text{SL}(2, \mathbb{Z})$  is a classical spacetime  $M_{c,d}$ . Its action is obtained by applying a modular transformation:

$$I_\gamma(\tau) = 2\pi i k (\gamma\tau - \gamma\bar{\tau}). \quad (19.90)$$

As usual,  $\gamma\tau = (a\tau + b)/(c\tau + d)$ ,  $\gamma\bar{\tau} = (a\bar{\tau} + b)/(c\bar{\tau} + d)$ . The partition function of the manifold  $M_{c,d}$  is

$$Z_{c,d} = F_k(q)|_\gamma F_k(\bar{q})|_\gamma, \quad (19.91)$$

and is holomorphically factorized just like  $Z_{0,1}$ .

However, when we sum over geometries to evaluate the partition function

$$Z = \sum_{\gamma \in W} F_k(q)|_\gamma F_k(\bar{q})|_\gamma, \quad (19.92)$$

holomorphic factorization is lost [...] because the sum over topologies is a common sum for left- and right-movers. [...] If we formally introduce separate topological sums for holomorphic and antiholomorphic variables, defining an extended partition function

$$\hat{Z} = \sum_{\gamma, \gamma' \in W} F_k(q)|_{\gamma} F_k(\bar{q})|_{\gamma'}, \quad (19.93)$$

then holomorphic factorization is restored. [...]

**Black hole entropy and its corrections.** [...] formula for the microcanonical entropy:

$$\mathcal{N}(\Delta) = e^{\mathcal{S}(\Delta)} = 2\pi \sum_{\Delta' = -k}^{\infty} C_{\Delta} \sqrt{\frac{-\Delta'}{\Delta}} I_1(4\pi\sqrt{-\Delta\Delta'}). \quad (19.94)$$

In the semiclassical approximation, this formula will be dominated by the term with  $\Delta' = -k$ . We may then use the asymptotic formula for the Bessel function

$$I_1(z) = \frac{1}{\sqrt{2\pi z}} e^z \left( 1 - \frac{3}{8} z^{-1} + \dots \right), \quad \text{at } z \rightarrow \infty \quad (19.95)$$

to get

$$\mathcal{S}(\Delta) = \log \mathcal{N}(\Delta) = 4\pi\sqrt{k\Delta} + \frac{1}{4} \log k - \frac{3}{4} \log \Delta - \frac{1}{2} \log 2 + \dots \quad (19.96)$$

The first term is the usual Bekenstein-Hawking term, proportional to the area of the BTZ black hole. The other terms are logarithmic corrections that typically appear when the entropy is computed in microcanonical, as opposed to a canonical, ensemble. [...] The partition function factorizes as  $\hat{Z} = Z_k(q)Z_k(\bar{q})$ , where the function  $Z_k$  is a holomorphic and modular-invariant function.

## References

- [1] M. Abramowitz and I. A. Stegun, *Handbook of Mathematical Functions*, 3rd ed. (Dover, New York, 1965).
- [2] J. H. Asad, "Differential equation approach for one- and two-dimensional lattice green's function", *Mod. Phys. Lett. B* **21**, 139–154 (2007).
- [3] J. Besag, "On a system of two-dimensional recurrence equations", *J. R. Stat. Soc. B* **43**, 302–309 (1981).
- [4] H. S. Bhat and B. Osting, "Diffraction on the two-dimensional square lattice", *SIAM J. Appl. Math.* **70**, 1389–1406 (2010).
- [5] R. C. Brower and E. K. Owen, "Ising model on the affine plane", *Phys. Rev. D* **108**, 014511 (2023).
- [6] R. Bulirsch, "Numerical calculation of elliptic integrals and elliptic functions", *Numer. Math.* **7**, 78–90 (1965).

- [7] M. Campos, E. López, and G. Sierra, “Integrability and scattering of the boson field theory on a lattice”, *J. Phys. A* **54**, 055001 (2021).
- [8] M. Campos, G. Sierra, and E. López, “Tensor renormalization group in bosonic field theory”, *Phys. Rev. B* **100**, 195106 (2019).
- [9] J. L. Cardy, “Operator content of two-dimensional conformally invariant theories”, *Nucl. Phys. B* **270**, 186–204 (1986).
- [10] A. Castro, M. R. Gaberdiel, T. Hartman, A. Maloney, and R. Volpato, “Gravity dual of the Ising model”, *Phys. Rev. D* **85**, 024032 (2012).
- [11] L. Chaumard, “Discrétisation de zeta-déterminants d’opérateurs de Schrödinger sur le tore”, *Bull. Soc. Math. France* **134**, 327–355 (2006).
- [12] P. Cvitanović and H. Liang, *A chaotic lattice field theory in two dimensions*, In preparation, 2024.
- [13] E. N. Economou, *Green’s Functions in Quantum Physics* (Springer, Berlin, 2006).
- [14] E. Elizalde, *Ten Physical Applications of Spectral Zeta Functions*, 2nd ed. (Springer, Berlin, 2012).
- [15] E. Elizalde, K. Kirsten, N. Robles, and F. Williams, “Zeta functions on tori using contour integration”, *Int. J. Geom. Methods M.* **12**, 1550019 (2015).
- [16] P. di Francesco, P. Mathieu, and D. Sénéchal, “Quantum field theory”, in *Conformal Field Theory* (Springer, New York, 1997), pp. 15–59.
- [17] P. di Francesco, H. Saleur, and J. B. Zuber, “Relations between the Coulomb gas picture and conformal invariance of two-dimensional critical models”, *J. Stat. Phys.* **49**, 57–79 (1987).
- [18] P. di Francesco, H. Saleur, and J.-B. Zuber, “Correlation functions of the critical Ising model on a torus”, *Europhys. Lett.* **5**, 95–99 (1988).
- [19] P. di Francesco, H. Saleur, and J.-B. Zuber, “Generalized Coulomb-gas formalism for two dimensional critical models based on  $SU(2)$  coset construction”, *Nucl. Phys. B* **300**, 393–432 (1988).
- [20] É. Ghys, “Knots and dynamics”, in *Proc. intern. congress math., madrid* (European Mathematical Society Publishing House, 2006), pp. 247–277.
- [21] É. Ghys and J. Leys, “Lorenz and modular flows: a visual introduction”, *Amer. Math. Soc. Feature Column* (2006).
- [22] I. S. Gradshteyn and I. M. Ryzhik, *Tables of Integrals, Series and Products*, 8th ed. (Elsevier LTD, Oxford, New York, 2014).
- [23] B. R. Holstein, “The harmonic oscillator propagator”, *Am. J. Phys.* **66**, 583–589 (1998).
- [24] T. Horiguchi, “Lattice Green’s function for the simple cubic lattice”, *J. Phys. Soc. Jpn.* **30**, 1261–1272 (1971).

- [25] T. Horiguchi and T. Morita, “Note on the lattice Green’s function for the simple cubic lattice”, *J. Phys. C* **8**, L232 (1975).
- [26] E. V. Ivashkevich, N. S. Izmailian, and C.-K. Hu, “Kronecker’s double series and exact asymptotic expansions for free models of statistical mechanics on torus”, *J. Phys. A* **35**, 5543–5561 (2002).
- [27] S. Katsura and S. Inawashiro, “Lattice Green’s functions for the rectangular and the square lattices at arbitrary points”, *J. Math. Phys.* **12**, 1622–1630 (1971).
- [28] S. Katsura, S. Inawashiro, and Y. Abe, “Lattice Green’s function for the simple cubic lattice in terms of a Mellin-Barnes type integral”, *J. Math. Phys.* **12**, 895–899 (1971).
- [29] B. Kaufman, “Crystal statistics. II. Partition function evaluated by spinor analysis”, *Phys. Rev.* **76**, 1232–1243 (1949).
- [30] K. Kirsten and P. Loya, “Calculation of determinants using contour integrals”, *Am. J. Phys.* **76**, 60–64 (2008).
- [31] O. M. Lecian, “Reflections on the hyperbolic plane”, *Intern. J. Modern Phys. D* **22**, 1350085 (2013).
- [32] T. M. Liaw, M. C. Huang, Y. L. Chou, S. C. Lin, and F. Y. Li, “Partition functions and finite-size scalings of Ising model on helical tori”, *Phys. Rev. E* **73**, 041118 (2006).
- [33] T. Machide, “An elliptic analogue of generalized Dedekind-Rademacher sums”, *J. Number Theory* **128**, 1060–1073 (2008).
- [34] T. Machide, “Sums of products of Kronecker’s double series”, *J. Number Theory* **128**, 820–834 (2008).
- [35] A. Maloney and E. Witten, “Quantum gravity partition functions in three dimensions”, *J. High Energy Phys.* **2010**, 029 (2010).
- [36] W. Michael, “Bound states of two spin waves in the Heisenberg ferromagnet”, *Phys. Rev.* **132**, 85–97 (1963).
- [37] T. Morita and T. Horiguchi, “Calculation of the lattice Green’s function for the bcc, fcc, and rectangular lattices”, *J. Math. Phys.* **12**, 986–992 (1971).
- [38] Y. Okabe, K. Kaneda, M. Kikuchi, and C.-K. Hu, “Universal finite-size scaling functions for critical systems with tilted boundary conditions”, *Phys. Rev. E* **59**, 1585–1588 (1999).
- [39] D. B. Ray and I. M. Singer, “R-Torsion and the Laplacian on Riemannian manifolds”, *Adv. Math.* **7**, 145–210 (1971).
- [40] Y. Shimizu, “Tensor renormalization group approach to a lattice boson model”, *Mod. Phys. Lett. A* **27**, 1250035 (2012).
- [41] A. D. Sokal, Numerical computation of  $\prod_{n=1}^{\infty} (1 - tx^n)$ , 2002.
- [42] E. M. Stein and R. Shakarchi, *Complex Analysis* (Princeton Univ. Press, Princeton, 2003).

- [43] A. Terras, *Harmonic Analysis on Symmetric Spaces and Applications I* (Springer, Berlin, 1985).
- [44] A. Voros, "Spectral zeta functions", *Adv. Stud. Pure Math* **21**, 327–358 (1992).
- [45] R. M. Ziff, C. D. Lorenz, and P. Kleban, "Shape-dependent universality in percolation", *Physica A* **266**, 17–26 (1999).

## Chapter 20

# Metamaterials

### 20.1 Checkerboard model

2019-03-08 Zeb Rodrigues *et al.* [5] looks very interesting.

I'm interested in whether the nonlinearities of these flexible structures can lead to interesting chaotic behavior. The thing foremost on my mind is the structure (not dynamics) of a 1D chain of repeating mechanical elements. A rigid-body mechanism would lead to a nonlinear transfer function between the configuration of one element and its neighbors. That seems like it could lead to something like the logistic equation, and perhaps different structures depending on the shape of the unit cell and the "initial" (i.e., boundary) conditions.

I couldn't get that to work out, but Michael, see figure 20.1 (a), found something that suggests it could work. Specifically, he found a structure that is repeated every three unit cells.

Two-dimensional structures like the origami are also quite interesting, of course, but the 1D chain seems easier to us as a starting point.

2019-03-08 Michael D. Czajkowski <michael.czajkowski@physics.gatech.edu>

I have located a configuration of a chain of 1-d rotors which repeats in three cycles, see figure 20.1 (a).

It is not unlike the wheels on a classical steam engine, but with the rod lengths varied around to produce a mismatch. We are thinking, of course, of the sequence of rotors going from left to right (or vice versa) as like time going forward in the iterative cycles of the logistic map. Despite the simplicity it seems promising in identifying a deterministic geometric system, which will never repeat, by varying the intrinsic parameters (like the rotor radius, connector length, etc).

There is one caveat to this, which is that we are thinking of the (for instance) orientation of the leftmost rotor as the input which (together with

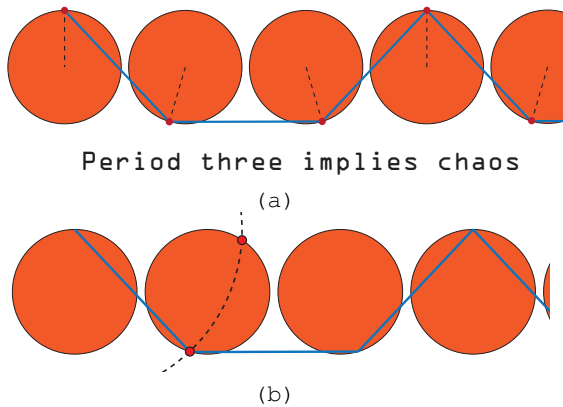


Figure 20.1: (a) The wheels on a steam engine, with the rod lengths varied around to produce a mismatch. (b) Forward-iteration almost always has two solutions, as there are two points at which the two circles intersect.

the intrinsic length of our blue rod, the radius of the orange circles and the spacing between them) determines the next orientation of the following rod to the right of it. However, this almost always has two solutions, as there are two points at which the two circles intersect, see figure 20.1 (b). So we are not entirely sure yet how to think of determinism in this system. Perhaps that is a bad thing, or perhaps it will be an interesting source of additional richness.

There is a separate perspective on this same mechanical system where there may be an analogue of chaos in a correspondence with topological mechanical polarization, but this is less developed and I will wait to share until I have gathered my thoughts a bit more.

### 20.1.1 Checkerboard literature

For the latest entry, go to the bottom of this section

2019-03-08 **Predrag** Rodrigues, Fonseca, Savi and Paiva [5] *Nonlinear dynamics of an adaptive origami-stent system*

## 20.2 Zero bulk modulus model

2019-03-08 **Adrian** James McInerney work is focused on origami.

2023-09-30 **Zeb** McInerney, Paulino and Rocklin *Discrete symmetries control mechanical response in parallelogram-based origami* [arXiv:2108.05825](https://arxiv.org/abs/2108.05825)



**2023-09-30 Zeb** Nan Cheng, Francesco Serafin, James McInerney, Zeb Rocklin, Kai Sun, Xiaoming Mao *Band theory and boundary modes of high-dimensional representations of infinite hyperbolic lattices*, [arXiv:2203.15208](https://arxiv.org/abs/2203.15208):

Euclidean lattices' wave eigenstates Bloch's theorem. Because the translation group  $T$  of Euclidean lattices is abelian and all elements of  $T$  commute with the Hamiltonian  $H$  (which has the same periodicity as the lattice), one can choose a set of waves that are eigenstates of  $H$  and all elements  $t_R$  in  $T$

$$t_R \psi(r) \equiv \psi(t_R^{-1} r) = \psi(r) e^{ikR}, \quad (20.1)$$

and these waves can be written as

$$\psi(r) = e^{-ikr} u(r), \quad (20.2)$$

where  $r$  is the position in space,  $k$  is the crystal momentum, and  $u(r)$  is a function with the same periodicity as that of the lattice. This theorem from Bloch has an equivalent description, using the Wannier basis, a complete orthogonal basis that characterizes localized molecular orbitals of crystalline systems

$$\psi(r) = \sum_R \phi_R(r) e^{-ikR} = \sum_{t_R \in T} [t_R \phi(r)] e^{-ikR}, \quad (20.3)$$

where the Wannier function  $\phi_R(r)$  obeys  $\phi_R(r) = t_R \phi(r) = \phi(t_R^{-1} r)$ . The sum here is over all lattice vectors, (or equivalently all elements of the lattice translation group). These three formula Eqs. (20.1)-(20.3) are equivalent to each other.

the lattice is guaranteed to have zero modes under open boundary conditions

[...] For tight-binding models (or models with a finite number of DOFs per cell) [...] we consider models defined in continuous space, with infinite DOFs in each unit cell, and we show a systematic approach of solving Wannier functions [...] although the procedure above involves a function  $\phi_0$ , which we choose arbitrarily, the final results (eigenvalues and Bloch waves) are independent of this choice: the functions  $u(r)$  depend on the choice of  $\phi_0(r)$ , but  $u(r)\phi_0(r)$  doesn't depends on it, and the same applies to the Bloch wave  $\psi(r)$ , which is proportional to  $u(r)\phi_0(r)$ .

[...] Interestingly, in the mechanical hyperbolic lattice we considered here,  $k = 0$  modes in 1D representation and  $\lambda = 0$  modes in 2D (reducible) representation all have finite frequencies  $\omega > 0$ , in contrast to acoustic phonon modes in Euclidean lattices, which are protected to have  $\omega = 0$  at  $k = 0$  by Goldstone's theorem. The reason is that uniform translations in hyperbolic lattices are isometries which can be described as boosts in the hyperboloid model, instead of  $k = 0$  modes. It would be very interesting to show the new form of Goldstone's theorem.

[...] [...] [...] [...] [...] [...]

**2023-09-28 Han Liang** We do not need to consider the L-shaped tessellations, see figure 24.85.

**2023-09-28 Predrag** So we do not need to worry about not-parallelogram primitive cells when enumerating 'geometries' (AKA Bravais lattices).

You will have to sum over all geometries when computing expectation values of material properties of bulk modulus  $B \rightarrow 0$  materials.

That will require work. I know of only one set of papers that describes that [1, 4, 7]. Prove me wrong:)

People quotient continuous dilatation symmetry, but to see it in a square lattice metamaterial is very interesting to us. Hope we can write a partition function that would return expectation values of material properties of interest to you.

To Zeb: Neel and I had a good conversation, but there are lots of details that will take a while to fill in. As to the papers, I believe the only ones are the ones Han and I are working on.

**2023-09-29 Neel Singh** I agree with Han that the parallelogram primitive cells can be found for any periodic lattice with two unique well-defined lattice vectors. For the rotating square, such a cell would include parts of neighbouring squares that add up to two complete squares.

I have many questions about this interesting statistical mechanics approach to dynamics of lattices. For starters, how are ensembles constructed, and how and what kind of properties can you get an expectation value for. I'm guessing there is a common action defined for all geometries.

**2023-10-06 Predrag 2 Zeb** I misunderstood what zero bulk modulus limit is in your 'rhombus' squishes dilatation, so all my short-wavelength modes partition function dreams for this metamaterial are wrong - only the nearly marginal modes matter. The discussion this morning was very good, I have no good suggestions how to think about conformally conserved quantities. Franco Fedele suggested looking at the 2-dimensional fluid dynamics in the complex functions formulation, there might be some wisdom there.

Neel proved me wrong. So no need to meet today:(

**2023-10-06 Franco Fedele** The condition for a mechanism can be derived as follows. The eigenfrequency  $\omega$  satisfies

$$\| -\omega^2 M + K \| = 0$$

where M and K are the mass and stiffness matrices of size (NxN). That yields a polynomial in  $\omega^2$  of order N

$$F(\omega) = a_0 + a_1\omega^2 + a_2(\omega^2)^2 \dots a_N(\omega^2)^N = 0$$

$a_0 = 0$  gives the condition for a zero-frequency mode, or mechanism

$$a_0 = F(\omega = 0) = \|\ -0 \cdot M + K \| = \|K\|$$

so the condition for a mechanisms is that the determinant of the stiffness matrix vanishes.

Depending on the structure of the matrix, the vanishing of the determinant could be due to the submatrix associated with the rhomboid.

Please check remark 3.1 at page 16 of my ref. [3].

**2023-10-06 Neel Singh** This work is a follow-up on Czajkowski, Coulais, van Hecke and Rocklin [2] *Conformal elasticity of mechanism-based metamaterials*, with actual calculations in [supplementary information](#).

Determinant of K in long wavelength limit:

$$-16 q_1^2 q_2^2 (k_l + k_s)^2 k_l k_s \cos^2 \theta_0 (4(k_l - 3k_s)k_t - k_l k_s \sin^2 \theta_0) = 0$$

$\theta_0$  is the reference angle - (related to the initial angle of rhomboid holes in reference configuration) - it can be anywhere between 0 (fully expanded) and  $\pi/4$  (fully contracted) but we don't want to look at the extreme points, since the lattice behaviour and symmetries are significantly different there.

$k_l, k_s, k_t$  are effective stiffnesses of the ligament (hinge) for stretching, shearing and bending respectively. Typically  $k_t < k_s \ll k_l$ .

The determinant does go to zero at  $q_1 = q_2 = 0$ , which implies at least two zero modes. But these zero modes exist irrespective of the stiffness parameters. Since, even with a hinge that is difficult to bend the periodic lattice has two zero modes, this can't be a mechanism. In fact, the eigenvalues and vectors of  $K(q_1 = 0, q_2 = 0)$  show that there are exactly two zero modes corresponding to translation in x and y.

Note that the dispersion comes from a linear Bloch analysis. One might hope to find a third mechanism zero-mode: uniform dilation when the relevant stiffness (kt) goes to zero. But a uniform dilation  $u(x, y) = x_i + y_j$  cannot be expressed as a Bloch wave and therefore it will never show up in this analysis.

**2023-10-06 Predrag** (misunderstanding everything, so this post is to be ignored) In the spatiotemporally chaotic lattice field theory, we have a scalar/boson field lattice propagator of the usual form,  $1/(p^2 + \mu^2)$ , and  $\text{Det} / (p^2 + \mu^2)$  always has  $k_1 = k_2 = 0$  eigenvalue  $\mu^2$ , so that vanishes in the  $\mu^2 \rightarrow 0$  limit, as the Laplacian  $p^2$  always has a zero eigenvalue, corresponding to the constant eigenstate.

But we definitely do not have two zero modes corresponding to translation in x and y, perhaps because our Bravais lattices are defined over  $Z^2$ , not over reals  $R^2$ . I would quotient  $q_1 q_2$  out. You probably want to replace  $1 - \cos 2t\theta$  by  $\sin^2 t\theta$ .

Also, time might be boring part of this, so maybe one can immediately go to time-independent formulation? Not sure about that...

The rest of the determinant looks unfamiliar to me, but that's because I have not used elasticity in this context. How can there be an eigenvalue that is not symmetric in  $k_l, k_s$  interchange? I have worked on related things [6, 8] (click [here](#) and [here](#)), but this does not ring any bells:)

Bloch or no Bloch, I think the dilatation eigenvalue (eigenvalues? One along each diagonal?) should show up in stability analysis of energy eigenstates.

## References

- [1] P. Cvitanović and H. Liang, [A chaotic lattice field theory in two dimensions](#), In preparation, 2024.
- [2] M. Czajkowski, C. Coulais, M. van Hecke, and D. Z. Rocklin, [“Conformal elasticity of mechanism-based metamaterials”](#), *Nat. Commun.* **13**, 211 (2022).
- [3] F. Fedele, P. Suryanarayana, and A. Yavari, [“On the effective dynamic mass of mechanical lattices with microstructure”](#), *J. Mech. Phys. Solids* **179**, 105393 (2023).
- [4] H. Liang and P. Cvitanović, [“A chaotic lattice field theory in one dimension”](#), *J. Phys. A* **55**, 304002 (2022).
- [5] G. V. Rodrigues, L. M. Fonseca, M. A. Savi, and A. Paiva, [“Nonlinear dynamics of an adaptive origami-stent system”](#), *Int. J. Mech. Sci.* **133**, 303–318 (2017).
- [6] N. Søndergaard, P. Cvitanović, and A. Wirzba, [“Periodic orbits in scattering from elastic voids”](#), *AIP Conference Proceedings* **834**, 175–183 (2006).
- [7] S. V. Williams, X. Wang, H. Liang, and P. Cvitanović, [Nonlinear chaotic lattice field theory](#), In preparation, 2024.
- [8] A. Wirzba, N. Søndergaard, and P. Cvitanović, [“Wave chaos in elastodynamic cavity scattering”](#), *Europhys. Lett.* **72**, 534–540 (2005).

# Chapter 21

## Article edits

### 21.1 Cats' GHJSC16blog

Internal discussions of ref. [52] edits: Move good text not used in ref. [52] to this file, for possible reuse later.

**2016-12-06 Boris** I prefer a precise title. E.g. :

*Linear encoding of cat map lattices*

Some earlier titles:

*Linear encoding of the spatiotemporal cat*

*A spatiotemporal cat encoded*

*A spatiotemporal code for a coupled maps lattice*

*A spatiotemporal symbolic dynamics for a coupled maps lattice*

*A spatiotemporal symbolic dynamics for a coupled cat maps lattice*

*A linear symbolic dynamics for coupled cat maps lattices*

*A spatiotemporal herding of coupled lattice cats*

*Herding five cats*

**2016-11-18 Predrag** A theory of turbulence that has done away with *dynamics*?

We rest our case.

**2016-10-05 Predrag** My approach is that this is written for field theorists, fluid dynamicists etc., who do not see any reason to look at cat maps, so I am trying to be pedagogical, motivate it as that chaotic counterpart of the harmonic oscillator, something that field theorists fell comfortable with (they should not, but they do).

**2016-11-13 Predrag** The claim "the cat map  $A = \begin{pmatrix} a & c \\ d & b \end{pmatrix}$  is assumed to be time-reversal invariant, i.e.  $c = d$ ." seems to be in conflict with Boris choice  $A = \begin{pmatrix} s-1 & 1 \\ s-2 & 1 \end{pmatrix}$

We write (4.178) as

$$(\square + 2 - s)x_t = s_t, \quad (21.1)$$

Percival and Vivaldi [79] write their Eq. (3.6)

$$(\square + 2 - s)x_t = -b_t \quad (21.2)$$

so their “stabilising impulses”  $b_t$  (defined on interval  $x \in [-1/2, 1/2)$ ) have the opposite sign to our “winding numbers”  $s_t$  (defined on  $x \in [0, 1)$ ).

Did not replace Arnol’d by PerViv choice.

$$A = \begin{pmatrix} 0 & 1 \\ -1 & s \end{pmatrix}, \quad (21.3)$$

$$\begin{aligned} x_{t+1} &= p_t \quad \text{mod } 1 \\ p_{t+1} &= -x_t + s p_t \quad \text{mod } 1 \end{aligned} \quad (21.4)$$

Predrag’s formula, removed by Boris 2017-01-15:

$$\begin{aligned} x_{t+1} &= (s - 1)x_t + p_t \\ p_{t+1} &= (s - 2)x_t + p_t \end{aligned} \quad \text{mod } 1, \quad (21.5)$$

Predrag’s formula, replaced by a more abstract form by Boris 2017-01-15: a  $d$ -dimensional spatiotemporal pattern  $\{x_z\} = \{x_{n_1 n_2 \dots n_d}\}$  requires  $d$ -dimensional spatiotemporal block  $\{m_z\} = \{m_{n_1 n_2 \dots n_d}\}$ ,

for definiteness written as

$$A = \begin{pmatrix} 2 & 1 \\ 1 & 1 \end{pmatrix}, \quad (21.6)$$

**2016-05-21 Predrag** Behrends [14, 15] *The ghosts of the cat* is fun - he uncovers various regular patterns in the iterates of the cat map.

**2016-09-27 Boris** **Cat maps and spatiotemporal cats**

In the spatiotemporal cat, “particles” (i.e., a cat map at each periodic lattice site) are coupled by the next-neighbor coupling rules:

$$q_{n,t+1} = p_{nt} + (s - 1)q_{nt} - q_{n+1,t} - q_{n-1,t} - m_{n,t+1}^q$$

$$p_{n,t+1} = p_{nt} + (s - 2)q_{nt} - q_{n+1,t} - q_{n-1,t} - m_{n,t+1}^p$$

The symbols of interest can be found by:

$$s_{nt} = q_{n,t+1} + q_{n,t-1} + q_{n+1,t} + q_{n-1,t} - s q_{nt}.$$

**2016-10-27 Boris** Gutkin and Osipov [53] write: “In general, calculating periodic orbits of a non-integrable system is a non-trivial task. To this end a number of methods have been developed,” and then, for a mysterious reasons, they refer to ref. [11].

**2016-11-17 Predrag** Adler and Weiss [1] discovered that certain mappings from the torus to itself, called hyperbolic toral automorphisms have Markov partitions, and in fact these partitions are parallelograms. One famous example is the Arnol’d Cat Map

(Axiom A; Anosov)

are a family of analytic hyperbolic automorphisms of the 2-dimensional torus which

The “linear code” was introduced and worked out in detail in influential papers of Percival and Vivaldi [16, 79, 80].

For  $d = 1$  lattice,  $s = 5$  the spatial period 1 fixed point is equivalent to the usual  $s = 3$  Arnol’d cat map.

The cat map partitions the phase space into  $|\mathcal{A}|$  regions, with borders defined by the condition that the two adjacent labels  $k, k + 1$  simultaneously satisfy (4.178),

$$x_1 - sx_0 + x_{-1} - \epsilon = k, \quad (21.7)$$

$$x_1 - sx_0 + x_{-1} + \epsilon = k + 1, \quad (21.8)$$

$$x_2 - sx_1 + x_0 = s_1, \quad (21.9)$$

$$x_1 - sx_0 + x_{-1} = s_0, \quad (21.10)$$

$$(x_0, x_1) = (0, 0) \rightarrow (0, 0), \quad (1, 0) \rightarrow (0, -1), \quad (0, 1) \rightarrow (1, s), \quad (1, 1) \rightarrow (1, s-1)$$

**2016-11-05 Predrag** Dropped this:

Note the two symmetries of the dynamics [60]: The calculations generalize directly to any cat map invariant under time reversal [62].

**2016-11-11 Boris** “Deeper insight” into  $d = 2$  symbolic dynamics Information comes locally (both in space and time). Allows to understand correlations between invariant 2-tori. Connection with field theories.

To Predrag: we have similar results on  $2 \times 1$  blocks, but I think  $1 \times 1, 2 \times 2$  is enough. Agree?

**2016-12-08 Predrag:** I agree

**2016-12-06 Boris** Predrag’s statement “Essentially, as the stretching is uniform, distinct admissible symbol patterns count all patterns of a given size, and that can be accomplished by construction the appropriate finite size transition matrices [31].” is true only for symbolic dynamics based on Markov partitions. Wrong e.g., for linear coding.

**2016-12-08 Predrag:** I rewrote that now, is it correct?

[the same plot as figure ??]

Figure 21.1: (Color online) Newtonian Arnol'd cat map  $(x_0, x_1)$  phase space partition into (a) 4 regions labeled by  $s_0$ , obtained from  $(x_{-1}, x_0)$  phase space by one iteration (the same as figure 2.2). (b) 14 regions labeled by past block  $s_{-1}s_0$ , obtained from  $(x_{-2}, x_{-1})$  phase space by two iterations. (c) 44 regions, past block  $s_{-2}s_{-1}s_0$ . (d) 4 regions labeled by  $.s_1$ , obtained from  $(x_2, x_1)$  phase space by one backward iteration. (e) 14 regions labeled by future block  $.s_1s_2$ , obtained from  $(x_3, x_2)$  phase space by two backward iterations. (f) 44 regions, future block  $s_3s_2s_1$ . Each color has the same total area ( $1/6$  for  $s_t = \underline{1}, 2$ , and  $1/3$  for  $s_t = 0, 1$ ). All boundaries are straight lines with rational slopes.

[the same plot as figure ??]

Figure 21.2: Newtonian Arnol'd cat map  $(x_0, x_1)$  phase space partition into (a) 14 regions labeled by block  $b = s_0.s_1$ , the intersection of one past (figure 21.1 (a)) and one future iteration (figure 21.1 (d)). (b) block  $b = s_{-1}s_0.s_1$ , the intersection of two past (figure 21.1 (b)) and one future iteration (figure 21.1 (d)). (c) block  $b = s_{-1}s_0.s_1s_2$ , the intersection of two past (figure 21.1 (b)) and two future iterations (figure 21.1 (e)). Note that while some regions involving external alphabet (such as  $_{-22}$  in (a)) are pruned, the interior alphabet labels a horseshoe, indicated by the shaded regions. Their total area is (a)  $4 \times 1/8$ , (b)  $8 \times 1/21$ , and (c)  $16 \times 1/55$ .

**2016-12-12 Predrag** My claim (in a conversation with Boris) that spatiotemporal cat symbolic dynamics is “ $d$ -dimensional” was nonsensical. I have now removed this from the draft: “ The key innovation of ref. [53] is the realization (an insight that applies to all coupled-map lattices, and all PDEs modeled by them, not only the system considered here) that  $d$ -dimensional spatiotemporal orbit  $\{x_z\}$  requires  $d$ -dimensional symbolic dynamics code  $\{m_z\} = \{(m_1, m_2, \dots, m_d)\}$ , rather than a *single* temporal symbol sequence (as one is tempted to do when describing a finite coupled  $N^{d-1}$ -“particle” system).”

Li Han text: “ To generate such phase space partitions, we start with length  $\ell = 1$ . Consider first the symbol  $s_0 = sx_0 - (x_1 + x_{-1}) = \lfloor sx_0 - x_1 \rfloor$ ,

[the same plot as figure ??]

Figure 21.3: (Color online)  $\ell = 1$  phase spaces on  $(x_0, x_1)$  phase space with respect to symbols  $s_t$ ,  $t = 0, -1, -2, 1, 2, 3$  for  $s = 3$ . In each block values of  $s_t = -1, 0, 1, 2$  are shaded with light red, green, blue, and yellow, respectively, and each color has the same total area ( $1/6$  for  $s_t = -1, 2$ ,  $1/3$  for  $s_t = 0, 1$ ) in all blocks. All boundary lines are straight lines with rational slopes, while the slopes tend to irrational values set by stable/unstable directions of the cat map exponentially fast in the limit  $t \rightarrow \pm\infty$ .



[the same plot as figure ??]

Figure 21.4:  $\ell = 2, 3, 4$  phase spaces on  $(x_0, x_1)$  phase space for  $s = 3$ , using blocks  $s_0s_1$ ,  $s_{-1}s_0s_1$ , and  $s_{-1}s_0s_1s_2$  from the  $\ell = 1$  diagrams. Shaded diamonds or rectangles correspond to sequences of all interior symbols  $(0, 1)^{\otimes \ell}$ , having a total area of  $4 \times 1/8$ ,  $8 \times 1/21$ ,  $16 \times 1/55$  respectively from left to right.

where  $\lfloor \dots \rfloor$  is the floor function.  $s_0$  has symbol boundaries which are equally spaced parallel lines of slope  $s$  and passing through  $(x_0, x_1) = (0, 0), (1, 1)$ . We then look at the time-evolved images of these symbol regions under forward map (2.75). The transformed region therefore means that at coordinate  $(x_{t+1}, Fx_{t+2})$  the point has symbol  $s_t$ , which in turn implies that when interpreted back to  $(x_0, x_1)$  phase space, a point is associated with symbol  $s_{-1}$ . As a result, we can generate all length-1 phase spaces corresponding to symbols  $s_t$ ,  $t = 0, \pm 1, \pm 2, \dots$  on the  $(x_0, x_1)$  phase space simply by applying the forward map (2.75) or its inverse. We plot such length-1 diagrams in figure ?? for symbols  $s_0, s_{-1}, s_{-2}$  (top), and  $s_1, s_2, s_3$  (bottom), and call them different blocks. Note that any of the blocks can be used to recover the 1-symbol measure  $f_1(m)$  by calculating the total of respective region areas, while with blocks  $s_0 = \lfloor sx_0 - x_1 \rfloor$  and  $s_1 = \lfloor sx_1 - x_0 \rfloor$  the computations are the easiest, which have symbol boundaries of slopes  $s$  and  $1/s$  respectively.

The fact that  $\mu(m \in \mathcal{A}_0)$  are all equal and twice of  $\mu(m \in \mathcal{A}_1)$  is also obvious from the  $s_0, s_1$  blocks of length-1 phase spaces.

A length- $\ell$  phase space is then the superposition of any  $\ell$  consecutive blocks of length-1 diagrams, while a choice that is symmetric about block  $s_0$  or  $s_0$  and  $s_1$  will make the amount of calculations minimal. We have evaluated  $\mu(m)$  up to  $\ell = 12$  from both (??) and symbolic diagrams for  $s = 3, 4, 5$ , and they are consistent. In figure ?? we plot the symbolic diagrams for 2, 3, and 4 consecutive symbols using blocks  $s_{0,1}$ ,  $s_{-1,0,1}$ , and  $s_{-1,0,1,2}$  of figure ?. Sequences of all interior symbols correspond to congruent parallelogram regions whose opposite sides are exactly parallel, and for even  $\ell$  the regions are diamonds whose sides are of equal length. Sequences of symbols from both  $\mathcal{A}_0$  and  $\mathcal{A}_1$  are not all admissible, which is the topic of next section. Here we note that the corresponding regions of such sequences have general polygon shapes and are not parallelograms, no matter which consecutive set of blocks we use.

All boundary lines are straight lines with rational slopes, while the slopes tend to irrational values set by stable/unstable directions of the cat map exponentially fast in the limit  $t \rightarrow \pm\infty$ .

From (??) the measure  $\mu(b)$  for a block  $b = s_1s_2 \dots s_\ell$  is proportional to the area of the polygon defined by inequalities (??).

The full list of measures  $\mu(s_1s_2 \dots s_\ell)$  has a tensor structure of tensor rank  $\ell$  with each index running over  $\mathcal{A}$  and can be interpreted as a joint prob-

ability function. ”

Boris results.tex text: “ whose lower left corner is the  $(n, t)$  lattice site

$$\mathcal{R}_{nt} = \{(n + i, t + j) | i = 0, \dots, \ell_1 - 1, j = 0, \dots, \ell_2 - 2\},$$

It is straightforward to see that when  $M$  is such that all symbols  $s_z$  belong to  $\mathcal{A}_0 = \{0, \dots, s - 4\}$  then  $M$  is always admissible. By positivity of Green’s function (see appendix ??) it follows immediately that  $0 < x_z$  while the condition  $\sum_{z' \in \mathbb{Z}} g_{zz'} = s - 2$  implies that  $x_z \leq 1$ .

”

Predrag text, recycle: “ Here the piecewise linearity of the spatiotemporal cat enables us to go far analytically. Essentially, as the cat map stretching is uniform, distinct admissible symbol blocks count all blocks of a given shape (they all have the same stability, and thus the same dynamical weight), and that can be accomplished by linear, Green’s function methods. ”

Predrag removed Boris poetry: “ The alphabet separation into interior and external parts nicely illustrates the transition of the model from the correlated regime to the uncorrelated Bernoulli process as parameter  $s$  in (24.43) tends to  $\infty$ . Indeed, the number of external symbols in  $\mathcal{A}_1$  is fixed within a given differential operator  $\square$  structure, while the number of interior symbols in  $\mathcal{A}_0$  grows linearly with the parameter  $s$  controlling the strength of chaos in a single map. For cat map this transition can be achieved by merely increasing the time step of time evolution. Increasing the time step from 1 to 2 leaves the form of equation (4.178) intact, but renormalizes the constant  $s \rightarrow s^2 - 1$ . This reflects the fact that  $\phi^2$  is more “chaotic” than  $\phi$ . With an increase of  $k$  the map  $\phi^k$  resembles more and more uncorrelated Bernoulli process. Similar transition can be observed in the coupled  $\mathbb{Z}$  map lattices, with a caveat that switch from  $\Phi$  to  $\Phi^k$  renormalizes not only the constant  $s$ , but  $\square$  itself. The resulting equation of motion will contain an elliptic operator  $\square^{(k)}$  of higher order. Still, it is straightforward to see that the number of external symbols is controlled by the order of the operator  $\square^{(k)}$  which grows linearly with  $k$ . On the other hand, the number of interior symbols grows in the same way as the constant  $s$  i.e., exponentially. ”

Replaced  $N$  (for  $N$  “particles”) by  $L$  (for spatial extent) throughout

**2019-09-10 Boris** Old version, now replaced in results.tex by a more compact paragraph:

To be specific, let  $\mathcal{R}$  be a rectangular  $[\ell_1 \times \ell_2]$  region, and let  $M_{\mathcal{R}}$  be the  $[\ell_1 \times \ell_2]$  block of  $M$  symbols from the alphabet  $\mathcal{A}$ . Let  $\mathcal{N}(M_{\mathcal{R}} | M_{[L \times T]})$  be the number of times a given symbol block  $M_{\mathcal{R}}$  appears anywhere within a much larger admissible symbol block  $M_{[L \times T]}$  cut out from a spatiotemporally infinite generic solution  $M$  of the spatiotemporal cat (24.43). The

$d = 1$  cat map is known to be fully hyperbolic and ergodic for  $s > 2$ , with a unique invariant natural measure  $\mu$  in the phase space (8.58) of the system. The  $d = 2$  spatiotemporal cat is fully hyperbolic and ergodic for  $s > 4$ , see (??). In the language of spatially extended systems, we assume that a steady state spatiotemporally chaotic solution is on average spatiotemporally invariant, so the number of times a *given* admissible block  $M_{\mathcal{R}}$  shows up over a region  $[L \times T]$  is expected to grow linearly with the area  $LT$ . Hence a *relative* frequency of the occurrence of the block  $M_{\mathcal{R}}$  can be defined as

$$f(M_{\mathcal{R}}|M_{[L \times T]}) = \frac{1}{LT} \mathcal{N}(M_{\mathcal{R}}|M_{[L \times T]}). \quad (21.11)$$

With  $L$  and  $T$  increasing at comparable rates (for example, take a square  $[L \times T]$ , with  $L = T$ ), the ergodic measure of finding the block  $M_{\mathcal{R}}$  across the infinite spatiotemporal domain is given by

$$\mu(M_{\mathcal{R}}) = \lim_{L, T \rightarrow \infty} f(M_{\mathcal{R}}|M_{[L \times T]}), \quad \sum_{M_{\mathcal{R}}} \mu(M_{\mathcal{R}}) = 1. \quad (21.12)$$

For an ergodic system with a unique invariant natural measure  $\mu$ , the limiting frequencies  $f(M_{\mathcal{R}})$  are equal to the measures  $\mu(\mathcal{M}_{\mathcal{R}})$  of the cylinder sets  $\mathcal{M}_{\mathcal{R}}$ , defined as sets of phase space points  $X_{\mathcal{R}}$  having  $M_{\mathcal{R}}$  symbolic representation over the region  $\mathcal{R}$ . For this reason, we sometimes refer, with a slight abuse of notation, to the frequencies  $f(M_{\mathcal{R}})$  defined by (21.11) as measures of  $M_{\mathcal{R}}$  in the limit  $L, T \rightarrow \infty$ , and denote them by  $\mu(M_{\mathcal{R}})$  in what follows.

**2016-11-20 Boris** The spatiotemporal symbols follow from the Newtonian equations in  $d$  spatiotemporal dimensions

$$\begin{aligned} s_{n,j} &= (q_{n,j+1} - 2q_{n,j} + q_{n,j-1}) + (q_{n+1,j} - 2q_{n,j} + q_{n-1,j}) - (s-4)q_{n,j} \\ m &= [\square + 2d1 - s1] q. \end{aligned} \quad (21.13)$$

**2017-08-02 Boris** Yes, and it is OK with our present convention - Green's functions must be positive.

**2017-08-02 Boris** Rule-of-thumb - internal symbols are non-negative, Green's functions are positive.

**2017-07-31 Boris** "As every Anosov automorphism is topologically conjugate to a linear cat map ..." Is it really true ?

**2017-08-11 Predrag** That's what I read in some of the articles cited. But no need to say it here, so now this is removed from our article.

**2016-11-13 Predrag** to all cats - where we write (4.178), Percival and Vivaldi [79] write their Eq. (3.6)  $(\square + 2 - s)x_t = -b_t$  so their "stabilising impulses"

$b_t$  have the opposite sign to our “winding numbers”  $s_t$  (defined on  $x \in [0, 1)$ ).

To all cats: keep checking that after your flip of signs of  $s_t$ 's Eqs. (24.43), (4.178), (??) and (21.13) are consistent.

**2017-07-31 Boris** Changed time ago. They should have the same sign as Percival and Vivaldi i.e., our  $m$  are positive!

**2017-08-11 Predrag** I now get it.  $LT$  is the area of  $\mathcal{R}$ . The total number of blocks grows exponentially with the size of  $\mathcal{R}$  and is bounded from above by  $(LT)^{|\mathcal{A}|}$ . You are saying that the number of times a *single* admissible block  $M_{\mathcal{R}}$  shows up over a region  $[L \times T]$  grows linearly with the area  $LT$ , and so does the sum over frequencies of all distinct admissible blocks  $M'_{\mathcal{R}}$ ? These “frequencies” are *relative*, in the sense that correct normalization is not (21.12), but

$$\mu(M_{\mathcal{R}}) = \frac{f(M_{\mathcal{R}})}{\sum_{M'_{\mathcal{R}}} f(M'_{\mathcal{R}})}. \quad (21.14)$$

**2017-08-05 Predrag** Cylinder sets are subtle: if we were counting only *admissible*  $X$ , the cylinder set would be much smaller. But we almost never know all inadmissible states.

**2017-07-31 Boris** Li subsection *Blocks of length  $\ell$* , was `siminos/cats/catGenerL.tex` 2017-02-17, mostly contained repetitions of the previous stuff. Did not think we needed it. Few usable things could be brought to other places. Agree?

**2017-08-23 Predrag** Done.

**2017-08-26 Predrag** Removed: “ The term  $\square + 2d1$  is the standard statistical mechanics diffusive inverse propagator that counts paths on a  $d$ -dimensional lattice [95], and  $-s1$  is the on-site cat map dynamics (for the Hamiltonian formulation, see appendix ??).

**2017-08-05 Boris** Something unclear here (at least for me). “The iteration of a map  $g(x_t)$  generates a group of *time translations*”. Why translations?  $g$  is a (time) map acting on all sites of lattice independently (no interaction). Note: I think the models in [81] and [22] are of the same type. Both can be thought of as products of two maps: “ Interactions” · “Single particle propagations” (i.e., product of  $g$ 's)

**2017-09-04 Predrag:** You are right, I have rewritten that text now.

**2017-08-28 Predrag** For the Dirichlet (as opposed to periodic) boundary condition, which breaks the translational symmetry, we take the very unphysical b.c.  $x_z = 0$  for  $z \in \mathcal{R}$ . Finite windows into turbulence that we describe by our symbol blocks never have such edges. Methinks...

2017-09-12 Boris This equation

$$\begin{aligned} x_{n,t+1} &= p_{nt} + (s-3)x_{nt} - (x_{n+1,t} - 2x_{nt} + x_{n-1,t}) - m_{n,t+1}^x \\ p_{n,t+1} &= p_{nt} + (s-4)x_{nt} - (x_{n+1,t} - 2x_{nt} + x_{n-1,t}) - m_{n,t+1}^p \end{aligned} \quad (21.15)$$

seems wrong. We use (??).

2017-09-14 Boris Recall that (the Dirichlet)  $g_{zz''}$  is a function of both  $z$  and  $z''$  and not just of the distance between them  $|z - z''|$ .

2017-09-04 Predrag "integer  $s > 4$ " is not the correct condition, for  $d = 2$   $s = 4$  is presumably already hyperbolic. To add to the confusion, in his report Adrien computes for  $s = 3$ , the case with no interior alphabet symbols. So  $s > 2$  is the correct hyperbolicity condition for all  $d$ ? Give the correct condition on  $s$ , explain it.

2017-09-12 Boris Here are the answers to this and co. questions over the paper.

1. The system is uniformly (fully) hyperbolic for  $s > 2d$ . This means all eigenvalues of linearized map (see (??) for  $d = 2$ ) are either  $|\Lambda| < 1$  (stable subspaces) or  $|\Lambda| > 1$  (unstable subspaces).
2. For  $s = 2d$  the system is partially hyperbolic. This means everything as above except two Lyapunovs for which  $\Lambda = 1$  (neutral subspaces).
3. For  $|s| < 2d$  system is non-hyperbolic. Apparently for everything in this paper 1 & 2 is OK. But
4. drastically changes everything (suspect a phase transition in physics jargon i.e., non-unique SRB measure). So whatever we consider in the paper should be for  $s \geq 2d$ .

2017-09-14 Boris A comment on  $s = 2d$  case (do not know how much of it we need for the paper). Our results in this paper require in principle  $s > 2d$  (all Lyapunovs are positive). However certain things still work (by whatever reason) for  $s = 2d$  as two figs in sect. ?? show. In this case the total momentum  $\sum_{n=1}^L p_{nt}$  is preserved. This can be seen from the invariance of (24.43) under translation  $x_{nt} \rightarrow x_{nt} + \alpha$ . So the system is not ergodic and linear encoding is not one to one (different trajectories might have the same symbolic representation). However, it is (probably) ergodic on the shell  $\sum_{n=1}^L p_{nt} = \text{const}$ . This is probably the reason why our formulas for frequencies of  $M_{\mathcal{R}}$  still work.

2017-09-26 Boris Dropped this: " with the corresponding probability of occurrence of a fixed symbol block  $M_{\mathcal{R}}$  given by

$$\mu(M_{\mathcal{R}}|M_{[L \times T]}) = \frac{f(M_{\mathcal{R}}|M_{[L \times T]})}{\sum_{M'_{\mathcal{R}}} f(M'_{\mathcal{R}}|M_{[L \times T]})}, \quad \sum_{M_{\mathcal{R}}} \mu(M_{\mathcal{R}}|M_{[L \times T]}) = 1,$$

where the sum goes over all distinct admissible blocks  $M'_{\mathcal{R}}$ ."

The point is that

$$\sum_{M_{\mathcal{R}}} \mathcal{N}(M_{\mathcal{R}} | M_{[L \times T]}) = LT - \text{"Terms linear in L and T"}$$

So no need in an artificial normalization - normalization in (21.12) would follow anyhow.

2017-09-14 **Boris** Replaced this eq.

$$M \cup \partial \mathcal{R} = \begin{bmatrix} x_{12} \\ x_{01} & s_{11} & x_{21} \\ x_{10} \end{bmatrix} = \begin{bmatrix} x_2 \\ x_1 & s_{11} & x_3 \\ x_4 \end{bmatrix} \quad (21.16)$$

by the first plot in figure ??.

2016-11-15, 2017-08-28 **Predrag** Note: When I look at the intersection of the diagonal with the partition strips in by inspecting figure ??, I find that the Fibonacci numbers 1,2,3,5, ... give the numbers of periodic points, in agreement with the Adler-Weiss Markov partition. So the linear code is not a generating partition, but periodic orbits do the right thing anyway.

2018-04-05 to **Adrien from Predrag** I think figure 21.8 is really hard to explain to a reader; why these axes, how did all points get mapped into the same unit square, why there are huge empty swaths - all stuff that distracts from the main point which is that  $x_z$ 's within the center of the shared symbol block are exponentially close.

2018-04-05 **Predrag** I think we can simplify this greatly, using the fact that the (damped) screened Poisson equation (??) is linear, so one can subtract patterns in order to visualize their distance.

In order to have a 2-dimensional visualization for each block, color the symbol  $M_j [L_1 \times L_2]$  block with discrete color alphabet  $\mathcal{A}_0$ , as in figure 21.6, and the corresponding state  $X_j [L_1 \times L_2]$  block with colors chosen from a continuum color strip.

As this is a linear problem, you can also represent closeness of two  $[L_1 \times L_2]$  blocks by using this coloring scheme for  $M_2 - M_1$  and  $X_2 - X_1$ .

For pairs of distinct 2-tori which share the same region of  $s_z$ 's, or a single 2-torus in which the same region of  $s_z$ 's appears twice, the states  $x_z$  in the center of the region should be exponentially close, in order to demonstrate that they shadow each other.

So, replace figure 21.8 by (a)  $M_2 - M_1$  from figure 21.6 (it will be all the same color in the shared region), and (b) plot  $X_2 - X_1$ . Mark the lattice point  $z$  with the minimal value of  $|x_z^{(2)} - x_z^{(1)}|$  on this graph, and in the

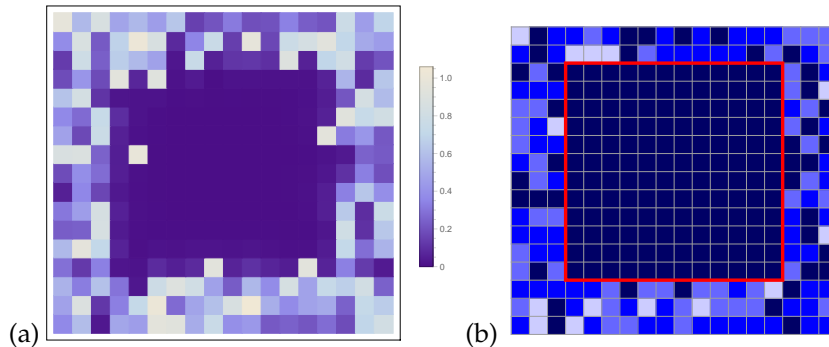


Figure 21.5: (Color online) (a)  $X_{2,z} - X_{1,z}$ , the site-wise distance between the invariant 2-tori fields corresponding to the two  $[18 \times 18]$  blocks  $M_1, M_2$  (colored tiles) of figure 21.6 (a,b). (b) The plot of the site-wise symbol difference  $|M_{2,z} - M_{1,z}|$  of figure 21.6 (b) and (b) (for a better visualization, see figure 21.9).

text state the minimal value of  $|x_z^{(2)} - x_z^{(1)}|$ . You can also state the mean Euclidean (or L2) distance between the two invariant 2-tori:

$$d_{x_2-x_1} = \left( \frac{1}{LT} \sum_z (x_z^{(2)} - x_z^{(1)})^2 \right)^{1/2}, \quad (21.17)$$

or distance averaged over the lattice points restricted a region  $\mathcal{R}$ .  
(taken care of by AKS)

**2018-04-13 Adrien** After reconstructing the orbits separately, I plotted the distance between the positions in  $(q, p)$  space for each lattice site  $z$ , see the new figure 21.5, meant to replace the current figure 21.8. Still have to use sensible color ranges, and compute figure 21.5 (b).  
(taken care of by AKS)

**2018-04-13 to Adrien from Predrag** Also of interest might be the color-coded plot of value of  $x_{q,p}$  for at least one of them. Would be nice to check -at least once- whether there is any relation to the corresponding  $m_{q,p}$  (probably there is no relation).

**2019-08-27 Predrag** If you mean “metric distances” of Gutkin-Osipov figures A3 and C2, that is quite different than our  $\log(\text{distance})$  plots. Problem is that Gutkin-Osipov measure Euclidean distance between symplectic phase-space points, not a meaningful distance. Would have to subtract actions, but this is not a thing for this paper..

**2019-08-26 Boris** Still not good enough. The coloring is too jumpy. It should range from white or light blue to dark blue. For a more reasonable coloring of this type see figure 14 from Our Paper [53] [arXiv:1503.02676](https://arxiv.org/abs/1503.02676).

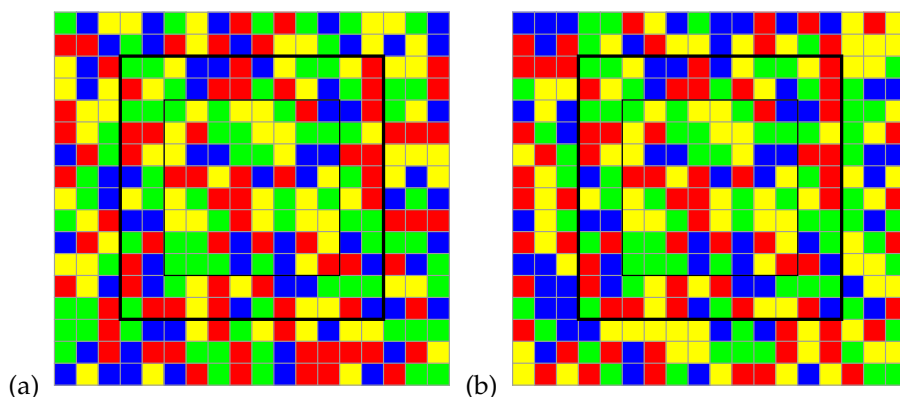


Figure 21.6: Figure nixed by Boris 2019-08-21, replaced by digits figure ??  
 Symbolic representation (colored tiles) of two  $[L \times T] = [18 \times 18]$  invariant 2-torus solutions of (??),  $s = 7$ , that shadow each other within the shared block  $M_{\mathcal{R}} = M_{\mathcal{R}_0} \cup M_{\mathcal{R}_1}$  (blue). The symbols within  $\mathcal{R}$ , drawn randomly from the interior alphabet  $\mathcal{A}_0$ , are the same for both solutions; the symbols outside  $\mathcal{R}$ , also drawn randomly from  $\mathcal{A}_0$ , differ. The shared block  $\mathcal{R} = \mathcal{R}_0 \cup \mathcal{R}_1$  is split into the interior region  $\mathcal{R}_0$  (bold blue) and the border strip  $\mathcal{R}_1$  (blue).

Maybe also the periods of tori L, T should be larger to make things smoother.  
 (taken care of by AKS)

2019-09-07 Boris redundant, removed:

**Answer to Q1.** *The spatiotemporal cat admits a natural 2-dimensional linear symbolic code with a finite alphabet. In principle, we can compute analytically the measure of a given finite spatiotemporal symbol block  $M_{\mathcal{R}}$  over a region  $\mathcal{R}$ .*

2017-09-04 Predrag Border notation in (??) conflicts with (??). Shouldn't it be  $+g_{t,0}x_0 + g_{t,\ell+1}x_{\ell+1}$  ?

2019-09-12 Boris No way :) I checked, (??) is correct.

2019-09-12 Boris I found the calculation following originally upon (??) redundant, so I removed it to here. Hope you understand everything without it.

The  $\mathcal{M}_b$  are partitions of the  $(x_0, x_1)$  phase space, in contrast to the polygons  $\mathcal{P}_b$ , plotted in the Lagrangian coordinates  $(x_0, x_{\ell+1})$ , see figure ??  
 Hence the interior alphabet measures  $\mu(b)$ ,  $s_i \in \mathcal{A}_0$ , are given by the Jacobian (??) of coordinate transformation from the Lagrangian coordinates  $(x_0, x_{\ell+1})$  to the phase space  $(x_0, x_1)$ ,  $\mu(b) = U_{|b|}(s/2)^{-1}$ . The value of  $U_{|b|}(s/2)$  is always an integer greater than 1, and thus the  $(x_0, x_1)$  phase space is "magnified" and wrapped around the  $(x_0, x_{\ell+1})$  phase space



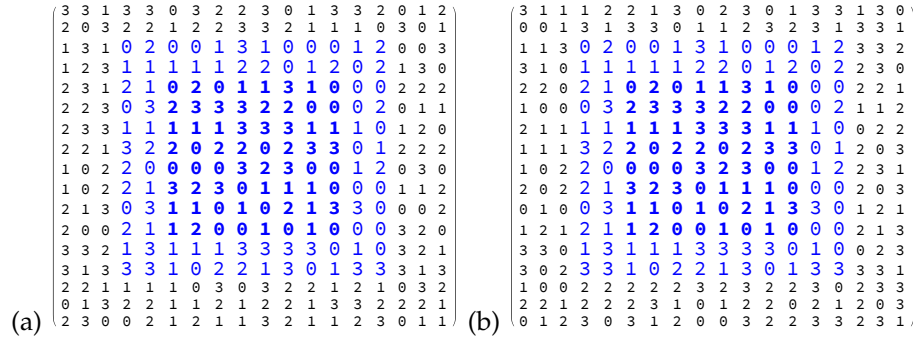


Figure 21.7: (Color online) Symbolic representation (numbered tiles) of two  $[L \times T] = [18 \times 18]$  invariant 2-torus solutions of (??),  $s = 7$ , that shadow each other within the shared block  $M_{\mathcal{R}} = M_{\mathcal{R}_0} \cup M_{\mathcal{R}_1}$  (blue). The symbols within  $\mathcal{R}$ , drawn randomly from the interior alphabet  $\mathcal{A}_0$ , are the same for both solutions; the symbols outside  $\mathcal{R}$ , also drawn randomly from  $\mathcal{A}_0$ , differ. The shared block  $\mathcal{R} = \mathcal{R}_0 \cup \mathcal{R}_1$  is split into the interior region  $\mathcal{R}_0$  (bold blue) and the border strip  $\mathcal{R}_1$  (blue).

$U_{|b|(s/2)}$  times through  $\ell$  iterations of the cat map. Lagrangian coordinates  $(x_0, x_{\ell+1})$  are related to phase space coordinates  $(x_k, p_k)$ ,  $p_t = (x_t - x_{t-1})/\Delta t$ , at time  $t \in (0, \ell + 1)$  by

$$\begin{aligned}
 x_t &= \bar{x}_t(b) + \frac{U_{\ell-t}(\frac{s}{2})}{U_{\ell}(\frac{s}{2})} x_0 + \frac{U_{t-1}(\frac{s}{2})}{U_{\ell}(\frac{s}{2})} x_{\ell+1} \\
 p_{t+1} &= \bar{x}_{t+1}(b) - \bar{x}_t(b) + \frac{U_{\ell-t-1}(\frac{s}{2}) - U_{\ell-t}(\frac{s}{2})}{U_{\ell}(\frac{s}{2})} x_0 + \frac{U_t(\frac{s}{2}) - U_{t-1}(\frac{s}{2})}{U_{\ell}(\frac{s}{2})} x_{\ell+1}.
 \end{aligned}$$

This is a linear map, so its Jacobian  $d_{\ell} = |\partial(x_0, x_1)/\partial(x_0, x_{\ell+1})|$  is simply

$$d_{\ell} = \frac{1}{U_{\ell}(\frac{s}{2})^2} \det \begin{pmatrix} U_{\ell}(\frac{s}{2}) & U_{-1}(\frac{s}{2}) \\ U_{\ell-1}(\frac{s}{2}) & U_0(\frac{s}{2}) \end{pmatrix} = \frac{1}{U_{\ell}(\frac{s}{2})}. \quad (21.18)$$

**2019-10-08 Predrag** Cannot beat the post-Soviet perfectionism :)

**2019-09-30 Boris** We need Hamiltonian formulation for two reasons. First, our measure  $dp dq$  comes from there. Second, for all numerics we actually use initial data problem i.e., Hamiltonian formulation. We need appendix ??, but should keep it compact.

**2019-10-03 Boris** A risky statement below. Did anybody checked this? "As  $X_z$  take rational values for any finite  $[L \times T]$  invariant 2-tori, for sites sufficiently close to the center of  $\mathcal{R}$  the cancelation  $x_{2,z} - x'_z$  can be exact."  
**Predrag:** dropped it.

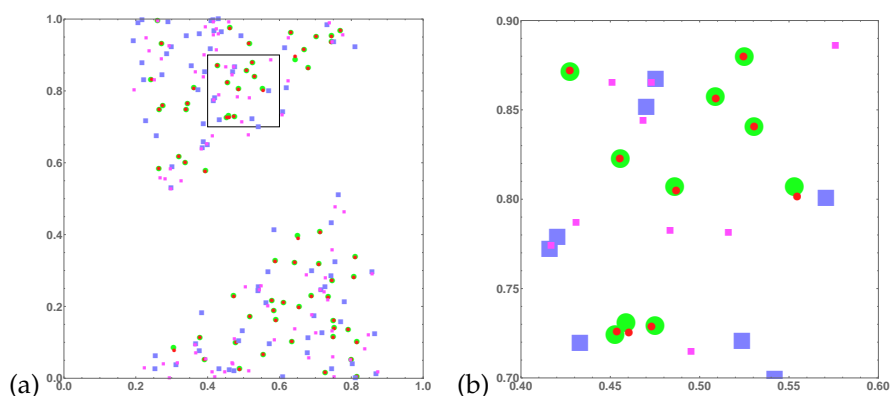


Figure 21.8: (Color online) (a) Phase space representation  $(q_z^{(i)}, p_z^{(i)})$ , where  $i = 1, 2$  refers to the two invariant 2-tori of figure 21.7. (b) A zoom into small rectangular area shown on the left. The phase space is covered only partially, as symbols in blocks  $M$  are restricted exclusively to the interior alphabet. Only data for  $z = (n, t) \in \mathcal{R}$  are shown in the figure. The centers of red (small) circles and green (large) circles are the points  $(q_z^{(i)}, p_z^{(i)})$  of the first ( $i = 1$ ) and the second ( $i = 2$ ) invariant 2-torus for  $z$ 's from the interior  $\mathcal{R}_0$ . The centers of violet (large) and magenta (small) squares show the respective points from the border  $\mathcal{R}_1$ , see figure 21.7. All  $(q_z^{(1)}, p_z^{(1)})$  and  $(q_z^{(2)}, p_z^{(2)})$  in the interior are well paired, while the separations are larger for  $z$ 's in the border region  $\mathcal{R}_1$ . This illustrates shadowing being exponentially stronger the closer the point is to the center of  $\mathcal{R}$ , see (??).

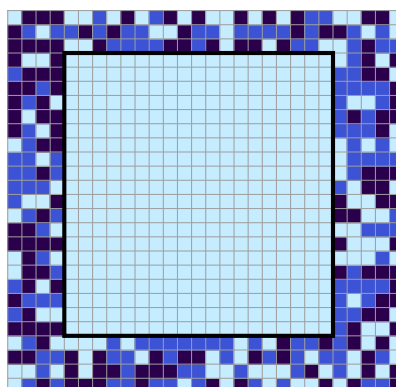


Figure 21.9: The site-wise distance  $M_{2,z} - M_{1,z}$  between the  $[28 \times 27]$  symbol blocks  $M_1, M_2$  of figure ?? . (For a worse visualization, see figure 21.5.)

**2017-01-25 Predrag** Gutkin and Osipov refer to the map generated by the action (21.20) as non-perturbed *coupled cat map*, and to an invariant 2-torus  $p$  as a “many-particle periodic orbit” (MPO) if  $x_{nt}$  is doubly-periodic, or “closed,” i.e.,

$$x_{nt} = x_{n+L, t+T}, \quad n = 0, 1, 2, \dots, L-1, \quad t = 0, 1, 2, \dots, T-1. \quad (21.19)$$

Action of an invariant 2-torus  $p$  is

$$S_p = -\frac{1}{2} \sum_{t=1}^T \sum_{n=1}^L s_{nt} x_{nt}. \quad (21.20)$$

**2019-10-08 Boris** Do you want formula for action in the paper?

**2017-01-25 Predrag** Not unless it is necessary to discuss it anywhere in the paper... Besides, to me (21.20) seems almost surely wrong.

**2017-09-05 Li Han** I’m looking at numerical data. The number of total admissible rules of cat map takes an exponential law:  $\sim 2.63^n$  for  $s=3$ ,  $\sim 3.74^n$  for  $s=4$  for example. i.e., effectively 2.63/3.74 symbols are needed for  $s=3/s=4$ . They agree with that from the topological entropy and Lyapunov exponent, which are  $(3 + \sqrt{5})/2, 2 + \sqrt{3}$ , respectively. Intuitively this should hold (that  $\log[\text{number of admissible rules}]/n = \text{topological entropy}$ ), but is it well-known/justified in symbolic dynamics?

**2017-08-02 Boris** figure ?? “Any  $4 \times 4$  block of symbols appears one and the same number of times in both representations.”

means the following: If we scroll/peep through the (upper) torus symbolic representation with  $4 \times 4$  window, there are exactly  $NT$  different  $4 \times 4$  blocks of symbols. Each of them appears the same number of times, as well, in the symbolic representation of the bottom tori (but for possibly different window positions).

**2017-09-14 Predrag** Spatiotemporal cat metric entropy (??) is presumably exact for spatiotemporal cat as long as  $T$  and  $L$  are going large at comparable rates. For systems without the space-time symmetry  $t \leftrightarrow x$ ,  $h_k$  should be different along the time and the space directions, so I do not think we can define one spacetime entropy? Enlightenment on this point would be very welcome.

**2019-10-20 Adrien** to Predrag and Boris: I can see why we would want to plot the logarithm of the site-wise distance  $\ln|x_z - x'_z|$  between the states  $X, X'$ . The idea would be to remain in the Lagrangian picture. To be clear, right now:

- figure ?? is actually plotting  $\ln\left(\sqrt{(q_z - q'_z)^2 + (p_z - p'_z)^2}\right)$  which is the site-wise distance in the Hamiltonian picture ( $q = x$  and  $p$  is

momentum). I already have generated the figure that corresponds to the Lagrangian site-wise distance, which is simply  $\ln |x_z - x'_z|$ . We want that one, correct?

(taken care of by AKS)

**2019-10-19 Predrag** Green's function notation is  $g_t$  is not helpful - it's a matrix, so easier to use  $g_{tt'}$  throughout. Green's function notation is  $g_{nt}$  is not helpful, and here even misleading - it's a tensorial matrix, so less confusing to use  $g_{zz'}$  notation throughout.

**2016-11-08 Predrag** Say: THE BIG DEAL is

for  $d$ -dimensional field theory, symbolic dynamics is not one temporal sequence with a huge alphabet, but  $d$ -dimensional spatiotemporal tiling by a finite alphabet

"Classical foundations of many-particle quantum chaos" I believe could become a game-changer. Corresponding dynamical zeta functions should be sums over invariant 2-tori (as is done in the kittens paper [35]), rather than 1-dimensional periodic orbits.

**2016-11-20 Boris** All papers that I know were dances around question of uniqueness SRB measure. Either show that measure is unique or opposite way around (phase transitions). We know from the start that system is in the high temperature regime, so the measure is unique.

**2019-09-12 Boris** Two remarks

1. In several cases you call  $\mathcal{A}_0$  as a "full shift". This looks wrong. As far as I understand (see [Scholarpedia](#)), one can call  $\mathcal{A}_0^{\mathbb{Z}}$  (together with the shift map  $T$ ) as a "full shift", but not  $\mathcal{A}_0$ . "Full shift" is a dynamical system = state space ( $\mathcal{A}_0^{\mathbb{Z}}$ ) + map (shift) not just alphabet.
2. Regarding notion of generating partition. "A partition  $Q$  is called a generator or generating partition if  $\mu$ -almost every point  $x$  has a unique symbolic name". So the partitions which we consider here are generating. I think what you mean by "generating" are rather called "Markov partitions".

**Predrag 2019-09-17** Thanks, for me these are very important remarks, to be fixed also in ChaosBook. Will chew on them... Until then, keep this remark here, as a reminder.

**2019-10-19 Predrag** I would like to use only one Green's function notation, i.e.,  $g_{zz'}^0$ , and not  $g(z, z')$ .

**2019-10-19 Boris** Do you mean  $g_{zz'}$  ( $g_{zz'}^0$  is reserved for periodic boundary conditions)? I have changed  $g(z, z')$  to  $g_{zz'}$ , everywhere except section A3.

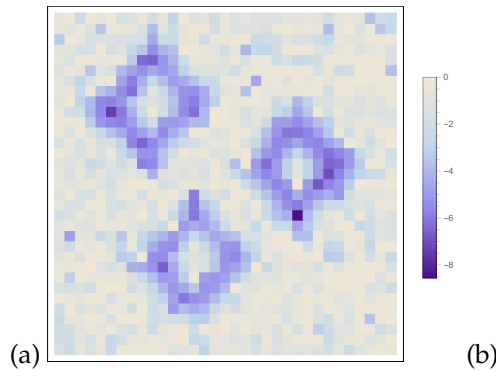


Figure 21.10: (Color online) The plots of the logarithm of the site-wise distance  $\ln |x_z - x'_z|$  (a) of the states  $X_1, X_2$  of figure ?? illustrate the exponential fall-off of the site-wise distances within the shared doughnut blocks  $M_{\mathcal{R}_1}, M_{\mathcal{R}_2}$ ; (b) of one of the three pairs of states  $X_i, X_j$  of figure ??; the other combinations have similar site-wise distance plots. Outside of the shared domains the distances are of the order 1. 2019-10-30 Boris: “completely wrong!”

2019-10-20 Predrag to Boris: A typical reader (if there will be any:)) of this opus magnum will not be encumbered by precisely your flavor of your quantum chaos baggage. To motivate this funky section full of peculiar doughnuts and their permuted holes, you need to explain why action differences (are the defined anywhere?) need to be small for close periodic orbit encounters in the quantum work that connects periodic orbits and quantum chaos spectral distributions.

2019-10-26 Boris It was done already in our paper with Vladimir. No need to repeat. Motivation here is somewhat different - By using internal symbols you can easily manufacture invariant 2-tori with whatever properties you wish/need (like in baker’s map).

2019-10-28 Boris Returned figure 21.10 back to Blogosiberia

2017-08-31 Boris On my current level of resolution (5 in the morning) the paper is completely ready for submission at any journal of this galaxy.

### 21.1.1 Cats/nonlin-v2/ GHJSC16 revisions

2020-10-16 Boris This paper builds explicit 2-dimensional spatiotemporal cat symbolic dynamics using winding numbers  $m_z$ . (An alternative construction, based on generating Adler-Weiss partition for the cat map, and a periodic orbit theory for spatiotemporal cat in higher dimensions are formulated in the parallel paper [35].)

2020-10-16 Boris added:

The following theorem allows for evaluation of symbol blocks measures.

**Theorem 21.1.** *Let  $b$  be a finite sequence of symbols. The corresponding measure is given by the product*

$$\mu(b) = d_\ell |\mathcal{P}_b|, \quad d_\ell = 1/U_\ell(s/2), \quad (21.21)$$

where  $|\mathcal{P}_b|$  is the area of the polygon  $\mathcal{P}_b$  defined by the inequalities

$$0 \leq \bar{x}_i(b) + \frac{U_{\ell-i}(s/2)}{U_\ell(s/2)} x_0 + \frac{U_{i-1}(s/2)}{U_\ell(s/2)} x_{\ell+1} < 1, \quad i = 1, \dots (21.22)$$

$$0 \leq x_0 < 1, \quad 0 \leq x_{\ell+1} < 1 \quad (21.23)$$

in the plane  $(x_0, x_{\ell+1})$ .

2020-10-16 Predrag Boris has now renamed refeq FreqDecomp to (?). While Boris-introduced (?) is cited many times, (?) is never cited.

Too many 'In general,'s

mark as EDITED:

Since all coefficients in (?) are given by rational numbers, the polygon areas  $|\mathcal{P}_b|$  are rational too. The same holds for the  $d_\ell$  factor. As a result, measures  $\mu(b)$  are always rational (see, for example, table ?). This allows for their exact evaluation by integer arithmetic. As the factor  $d_\ell$  in (?) is known explicitly, the

2020-10-16 Boris rewrote:

**Interior symbols.** For blocks composed of interior symbols only, the inequalities (?) are always satisfied, and  $\mathcal{P}_b$  are unit squares of area 1. The corresponding measure

$$\mu(b) = 1/U_{|b|}(s/2), \quad s_i \in \mathcal{A}_0, \quad i = 1, \dots |b|$$

depends only on the length of the block  $b$ .

**Rationality.** Since all coefficients in (?) are given by rational numbers, the polygon areas  $|\mathcal{P}_b|$  are rational too. The same holds for the  $d_\ell$  factor. As a result, measures  $\mu(b)$  are always rational (see, for example, table ?). This allows for their exact evaluation by integer arithmetic.

2020-10-31 Predrag Dropped: " The always trustworthy but so un-cited Soviet scientists (1781–1840) teach us that..."

**2020-10-17 Predrag** Edited everything down to  $d = 2$  dimensions. Was:

The temporal cat map (??), and the spatiotemporal cat (??) can be brought into uniform notation and generalized to  $d$  dimensions by converting the spatiotemporal differences to discrete derivatives. This yields the discrete screened Poisson equation [37, 55] for the  $d$ -dimensional *spatiotemporal cat*.

The key insight is that  $d$ -dimensional spatiotemporal lattice of integers  $\{m_z\} = \{m_z, z \in \mathbb{Z}^d\}$  is the natural encoding of a  $d$ -dimensional spatiotemporal state.

Eq. (24.43) was

$$(-\square + 2(s - 2))x_z = s_z, \quad s_z \in \mathcal{A},$$

$$\mathcal{A} = \{-2d + 1, -2d + 2, \dots, s - 2, s - 2\} \quad (24.43)$$

**2020-11-12 Boris** With the redefined stretching parameter  $s$  alphabet runs up to  $2s - 1$ .  $s$  can attain half-integer values.

**2020-11-15 Predrag** Thanks for noticing that  $\mathcal{A} = \{-3, -2, \dots, s - 2, s - 1\}$  in (24.43) was not updated to (??). Fixed now. Yes,  $s > 2$  can attain half-integer values, the lowest one is  $s = 5/2, \mu^2 = 1$ .

**2020-11-15 Predrag** I do not remember the unnumbered equation after (??) any longer. Do I know this identity? Does it follow from Green's function being the inverse of the linear operator in (??)? From appendix ?? *Lattice Green's identity*? I changed it to  $2(s - 2)$  rather than the old convention  $(s - 4)$ .

**2020-11-12 Boris** Text below (??) - "from which the above 'generic' state X is assumed to be drawn."

This part is very unclear. To obtain a generic solution X you need to draw generic (with respect to mu) initial conditions and then apply the map which is defined in the appendix. This how we check our results numerically.

**2020-11-15 Predrag** Ok. Go ahead with the rewrite.

**2020-11-12 Boris** Have we defined  $\mathcal{R}$  before the end of "Answer to Q1"?

**2020-11-15 Predrag** Yes, see 4 lines above Q1..

**2020-11-12 Boris**  $s = 2$  is the marginal case, with one zero Lyapunov exponent. Apparently the results are applicable to this case as well, as numerics shows.

**2020-10-17 Predrag** In figure ?? we are simulating the marginal,  $s = 2$  (Laplace operator) case. I do not trust student's simulations here -it's so easy to miss power laws- but it's too late to do anything about that. We will pass it over in silence, unhappily.

To Boris: This Dirichlet bc is lots of pain for a no gain. Again I do not know what even  $\mathcal{R} = [1]$  means. Or Figure 4. (a) A  $[5 \times 3]$  domain  $\mathcal{R}$  I would like to think of as a  $[4 \times 2]$  domain, centered on  $(\ell_j + 1)/2$ . Will rethink this tomorrow. For now, Good night.



## 21.2 Kittens' CL18blog

Internal discussions of ref. [35] edits: Move good text not used in ref. [35] to this file, for possible reuse later.

Tentative title: "Is there anything cats cannot do?"

**2016-11-18 Predrag** In this paper we have analyzed [...]. We now summarize our main findings.

**2023-08-01 Predrag** In the overview sect. 4.12.3 we start by introducing concepts such as the partition sum over a finite volume (finite number of lattice sites) primitive cell

Our periodic states are always periodic functions on infinite Bravais lattices

How is the deterministic chaotic field theory different from the

How is a deterministic chaotic field theory different from a conventional field theory?

In textbook descriptions of such systems one starts with a system confined to a large box, and then takes a 'thermodynamic' limit.

**2016-10-05 Predrag** My approach is that this is written for field theorists, fluid dynamicists etc., who do not see any reason to look at cat maps, so I am trying to be pedagogical, motivate it as that chaotic counterpart of the harmonic oscillator, something that field theorists felt comfortable with (they should not, but they do).

**2016-11-13 Predrag** We write

$$(-\square + (s - 2)\mathbb{1})X = M. \quad (21.25)$$

screened Poisson equation as

$$(\square + 2 - s)x_t = s_t, \quad (21.26)$$

Percival and Vivaldi [79] write their Eq. (3.6)

$$(\square + 2 - s)x_t = -b_t \quad (21.27)$$

so their "stabilising impulses"  $b_t$  (defined on interval  $x \in [-1/2, 1/2)$ ) have the opposite sign to our "winding numbers"  $s_t$  (defined on  $x \in [0, 1)$ ).

Did not replace Arnol'd by PerViv choice.

$$A = \begin{pmatrix} 0 & 1 \\ -1 & s \end{pmatrix}, \quad (21.28)$$

$$\begin{aligned} q_{t+1} &= p_t \pmod{1} \\ p_{t+1} &= -x_t + s p_t \pmod{1} \end{aligned} \quad (21.29)$$

Predrag's formula, removed by Boris 2017-01-15:

$$\begin{aligned} x_{t+1} &= (s-1)x_t + p_t \\ p_{t+1} &= (s-2)x_t + p_t \end{aligned} \pmod{1}, \quad (21.30)$$

Predrag's formula, removed by Boris 2017-01-15:

As the 3-term discretization of the second time derivative  $d^2/dt^2$  (central difference operator) is  $\square x_t \equiv x_{t+1} - 2x_t + x_{t-1}$  (with the time step set to  $\Delta t = 1$ ), the *temporal* cat map (21.37) can be rewritten as the discrete time Newton equation for inverted harmonic potential,

$$(\square + 2 - s)x_t = s_t. \quad (21.31)$$

a  $d$ -dimensional spatiotemporal pattern  $\{x_z\} = \{x_{n_1 n_2 \dots n_d}\}$  requires  $d$ -dimensional spatiotemporal mosaic  $\{m_z\} = \{m_{n_1 n_2 \dots n_d}\}$ ,

**2016-08-20 Predrag** “ The fact that even Dyson [42] counts cat map periods should give us pause - clearly, some nontrivial number theory is afoot. ”

Not sure whether this is related to cat map symbolic dynamics that we use, dropped for now: “ Problems with the discretization of Arnol'd cat map were pointed out in refs. [17, 18]. Ref. [17] discusses two partitions of the cat map unit square. ”

“ and resist the siren song of the Hecke operators [64, 75] ”

**2016-05-21 Predrag** Behrends [14, 15] *The ghosts of the cat* is fun - he uncovers various regular patterns in the iterates of the cat map.

**2016-09-27 Boris** **Cat maps and spatiotemporal cats**

In the spatiotemporal cat, “particles” (i.e., a cat map at each periodic lattice site) are coupled by the next-neighbor coupling rules:

$$q_{n,t+1} = p_{nt} + (s-1)q_{nt} - q_{n+1,t} - q_{n-1,t} - m_{n,t+1}^q$$

$$p_{n,t+1} = p_{nt} + (s-2)q_{nt} - q_{n+1,t} - q_{n-1,t} - m_{n,t+1}^p$$

The symbols of interest can be found by:

$$s_{nt} = q_{n,t+1} + q_{n,t-1} + q_{n+1,t} + q_{n-1,t} - s q_{nt}.$$

**2016-10-27 Boris** Gutkin and Osipov [53] write: “In general, calculating periodic orbits of a non-integrable system is a non-trivial task. To this end a number of methods have been developed,” and then, for a mysterious reasons, they refer to ref. [11].

**2023-11-07 Predrag** Periodic field configuration calculations are carried out either over a finite volume primitive cell  $\mathbb{A}$ , or over the infinite Bravais lattice. In what follows, suffix  $(\dots)_{\mathbb{A}}$  indicates that the calculation is carried out over the  $V_{\mathbb{A}}$  primitive cell lattice-site fields.

**2016-11-15 Predrag Homework for all cats:** Write the correct reseq cycleIgnorant for an  $n$ -cycle. For inspiration: check ChaosBook.org discussion of the kneading theory, where such formula is written down for unimodal maps. Might require thinking.

Hint: the answer is in the paper:)

**2016-11-17 Boris** Unlike the systems studied in ref. [22], spatiotemporal cat cannot be conjugated to a product of non-interacting cat maps; a way to see that is to compare the numbers of periodic orbits in the two cases – they differ.

As these equations are symmetric under interchange of the ‘space’ and the ‘time’ directions, their temporal and spatial dynamics are strongly coupled, corresponding to  $\epsilon \approx O(1)$  in reseq KanekoCML, in contrast to the traditional spatially weakly coupled CML [22].

**2016-11-17 Predrag** The cat map partitions the phase space into  $|\mathcal{A}|$  regions, with borders defined by the condition that the two adjacent labels  $k, k+1$  simultaneously satisfy (21.25),

$$x_1 - sx_0 + x_{-1} - \epsilon = k, \quad (21.32)$$

$$x_1 - sx_0 + x_{-1} + \epsilon = k + 1, \quad (21.33)$$

$$x_2 - sx_1 + x_0 = s_1, \quad (21.34)$$

$$x_1 - sx_0 + x_{-1} = s_0, \quad (21.35)$$

$$(x_0, x_1) = (0, 0) \rightarrow (0, 0), \quad (1, 0) \rightarrow (0, -1), \quad (0, 1) \rightarrow (1, s), \quad (1, 1) \rightarrow (1, s-1)$$

**2016-12-12 Predrag** Predrag text, recycle: “ Here the piecewise linearity of the spatiotemporal cat enables us to go far analytically. Essentially, as the cat map stretching is uniform, distinct admissible mosaics count all mosaics of a given shape (they all have the same stability, and thus the same dynamical weight), and that can be accomplished by linear, Green’s function methods. ”

**2017-08-28 Predrag** “Average state” depends on bc’s. Average state GHJSC16.tex eq. catMapAverCoord is computed for the very unphysical Dirichlet bc’s  $x_z = 0$  for  $z \in \mathcal{R}$  which breaks translation invariance. If one takes the much gentler, translationally invariant doubly periodic b.c., the “average state”  $\bar{x}_z$  is the periodic state periodic point, a more natural choice.

**2017-08-28 Predrag** Probably lots of repeats with existing text:

Consider a linear, area preserving map of a 2-torus onto itself <sup>1</sup>

$$\begin{pmatrix} x_{t+1} \\ p_{t+1} \end{pmatrix} = A \begin{pmatrix} x_t \\ p_t \end{pmatrix} \pmod{1}, \quad A = \begin{pmatrix} s-1 & 1 \\ s-2 & 1 \end{pmatrix}, \quad (21.37)$$

where both  $x_t$  and  $p_t$  belong to the unit interval. For integer  $s = \text{tr } A > 2$  the map is referred to as a cat map [4]. It is a fully chaotic Hamiltonian dynamical system, which, rewritten as a second-order difference equation in  $(x_t, x_{t-1})$  takes a particularly simple form (21.31) with a unique integer “winding number”  $s_t$  at every time step  $t$  ensuring that  $x_{t+1}$  lands in the unit interval [79]. While the dynamics is linear, the nonlinearity comes through the  $(\pmod{1})$  operation, encoded in  $s_t \in \mathcal{A}$ , where  $\mathcal{A}$  is finite alphabet of possible values for  $s_t$ .

A generalization to the *spatiotemporal* cat map is now immediate. Consider a one-dimensional spatial lattice, with field  $x_{n,t}$  (the angle of a kicked rotor “particle” at instant  $t$ ) at site  $n$ . If each site couples only to its nearest neighbors  $x_{n\pm 1,t}$ , and if we require (1) invariance under spatial translations, (2) invariance under spatial reflections, and (3) invariance under the space-time exchange, we arrive at the two-dimensional Euclidean cat map lattice (??). Note that both equations (21.31), (??) can be brought into uniform notation and generalized to  $d$  dimensions by converting the spatiotemporal differences to discrete derivatives. This yields the Newton (or Lagrange) equation for the  $d$ -dimensional *spatiotemporal cat* (21.79) where  $\square$  is the discrete  $d$ -dimensional Euclidean space-time Laplacian, given by  $\square x_t \equiv x_{t+1} - 2x_t + x_{t-1}$ ,  $\square x_{n,t+1} \equiv x_{n,t+1} + x_{n,t-1} - 4x_{n,t} + x_{n+1,t} + x_{n-1,t}$  in  $d = 1$  and  $d = 2$  dimensions, respectively.

the cat map in one dimension (temporal dynamics of a single “particle”) and for the spatiotemporal cat (21.79) in  $d$  dimensions (temporal dynamics of a  $(d-1)$ -dimensional spatial lattice of  $N^{d-1}$  interacting “particles,”  $N \rightarrow \infty$ ).

In this paper we focus on the  $d = 1$  case (introduced in ref. [79]), and the  $d = 2$  case (introduced in ref. [53]).

**2018-11-16 Predrag** We illustrate this by solving what is arguably the simplest deterministic field theory, the discretized screened Poisson equation, or the “spatiotemporal cat”, and describe its repertoire of admissible spatiotemporal patterns. We encode these by spatiotemporal symbol dynamics (rather than a single temporal string of symbols).

<sup>1</sup>Predrag 2019-10-31: compare with

$$\begin{pmatrix} q_{t+1} \\ p_{t+1} \end{pmatrix} = \mathbb{J} \begin{pmatrix} q_t \\ p_t \end{pmatrix} \pmod{1}, \quad \mathbb{J} = \begin{pmatrix} a & c \\ d & b \end{pmatrix}, \quad (21.36)$$

where  $a, b, c, d$  are integers whose precise values do not matter, as long as  $\det \mathbb{J} = 1$ , i.e., the map is area-preserving.

Herding cats

the theory is formulated in terms of prime orbits, minimal tilings of space-time.

In the spatiotemporal formulation of turbulence the zeta functions (Fredholm determinants) are presumably 2-d or (1+3)-d Laplace/Fourier transforms of trace formulas, one dimension for each continuous symmetry: one Laplace transform for time, and one Fourier transform for each infinite spatial direction.

We sketch how these are to be encoded by spatiotemporal symbol dynamics, in terms of minimal exact coherent structures. To determine these, radically different kinds of codes will have to be written, with space and time treated on equal footing.

- review cat map in damped Poisson formulation
- explain solution for temporal cat
- show few plots of 2D solutions
- future: computational literature that advocates for spatiotemporal computations

**2019-05-20 Han** My action of cat map is different from Keating's action [61] by two constant terms, which do not affect the computation.

**2018-02-16 Predrag** Dropped this: Adler-Weiss codes still have one fatal shortcoming, and are therefore not used in this paper: for  $L$  coupled cat maps the size of the alphabet  $|\mathcal{A}|$  (the number of partitions of the phase space, a  $2L$ -dimensional unit hypercube) grows exponentially with  $L$ .

**2019-08-10 Predrag** .

$$N_n = |\det(A^n - \mathbf{I})| = |\operatorname{tr}(A^n) - 2| = |\Lambda^n + \Lambda^{-n} - 2|, \quad (21.38)$$

if, or

$$N_n = |\operatorname{tr}(A^n)| = |\Lambda^n + \Lambda^{-n}|, \quad (21.39)$$

if  $\det(A^n) = -1$ .

**2018-12-01 Predrag** Give reference for (21.39). I see it nowhere in Isola [57] or Keating [61].

**2019-06-06 Han** I cannot find (21.39) either, but it can be proved by explicitly computing the determinant.

**2023-09-04 Predrag** Dropped this:

For our problem,  $-L_{12}[i, i + 1] = 1$ .

**2018-11-30 Han** In practice one can supply only symbol sequences of finite length, in which case the truncated (2.99) returns a finite trajectory  $x_t$ , with a finite accuracy. However, a periodic orbit  $p$  of period  $n$  (an  $n$ -cycle) is infinite in duration, but specified by a finite admissible mosaic  $p = [s_1 s_2 \cdots s_n]$ . To generate all admissible  $n$ -cycles for a given  $n$ , list all orbit symbol sequences  $[s_1 s_2, \cdots s_n]$ , (one string per its  $n$  cyclic permutations, not composed from repeats of a shorter cycle), apply (2.99) with cyclic  $[n \times n]$   $g_{tt'}$ , and then apply modulus one to all points in the cycle,

$$x_t = \sum_{t'=t}^{n+t-1} g_{tt'} s_{t'} \pmod{1}. \quad (21.40)$$

If the cycle is admissible,  $\pmod{1}$  does not affect it. If it is inadmissible, add the string to the list of pruned symbol strings. One can even start with any random sequence  $[s_1 s_2 \cdots s_n]$ , have  $\pmod{1}$  corral back the stray  $x_t$ 's into the unit interval, and in this way map any inadmissible symbol sequence into an admissible trajectory of the same duration.

**2016-11-15 Predrag Homework for all cats:** Write the correct (21.40) for an  $n$ -cycle. For inspiration: check ChaosBook.org discussion of the kneading theory, where such formula is written down for unimodal maps. Might require thinking.

Hint: the answer is *this* paper :)

**2019-08-04 Predrag** Note configuration part of the map (21.41) differs from Percival-Vivaldi [79] (2.1). However, it agrees with MacKay, Meiss and Percival [72] definition (3.4), and Meiss [74] (no discussion of cat maps) definition of the standard map (1.36).

**2019-08-04 Predrag** Percival-Vivaldi [79] get (21.31) immediately, their (2.2) for any force from their Hamiltonian (2.1), rather than our Hamiltonian of form

$$q_{t+1} - q_t = p_{t+1} \pmod{1}, \quad (21.41)$$

$$p_{t+1} - p_t = P(q_t), \quad (21.42)$$

**2019-08-05 Predrag** Rewrite refeq eq:HamEqMot as:

$$\begin{aligned} q_{t+1} &= q_t + p_t + (s-2)q_t - s_{t+1}^q \\ p_{t+1} &= p_t + (s-2)q_t - s_{t+1}^q - (s_{t+1}^p - s_{t+1}^q). \end{aligned} \quad (21.43)$$

Comparing this with the Hamiltonian mapping (21.41,21.42) we identify the impulse  $F(q_t)$

$$\begin{aligned} q_{t+1} &= q_t + p_{t+1} \\ p_{t+1} &= p_t + (s-2)q_t - s_{t+1}^p. \end{aligned} \quad (21.44)$$

<sup>2</sup>Predrag 2018-12-03: Mixing  $s_{t'}$  and  $\pmod{1}$  strikes me as profoundly wrong.

where the  $s_{t+1}^q$  seems happily absorbed into  $p_{t+1}$ . The generating function (1-step Lagrangian density) is

**2019-08-06 Predrag** We shall refer here to the least unstable of the cat maps (21.36), with  $s = 3$ , as the ‘Arnol’d’, or ‘Arnol’d-Sinai cat map’ [4, 36].

**2019-05-27 Predrag** I see no (21.38) in Percival and Vivaldi [79, 80] or Isola [57] - papers preceding Keating [61], though it is implicit in Isola [57] eq. (11).

**2019-06-06 Han** The method of using the determinant  $\det(A^n - \mathbf{I})$  to count periodic points is given by Keating [61] eq.(28) and the following paragraph.

**2021-07-28 Predrag** Jaidee, Moss and Ward [59], *Time-changes preserving zeta functions*, say that a Lehmer–Pierce sequence [65, 82], with  $n$ th term  $|\det(A^n - I)|$  for some integer matrix  $A$ , counts periodic points for an ergodic toral endomorphism if it is non-zero for all  $n \geq 1$ .

**2017-01-25 Predrag** Do not remember where it came from, but it sure looks wrong: Action of an periodic state  $p$  is

$$S_p = -\frac{1}{2} \sum_{t=1}^T \sum_{n=1}^L s_{nt} x_{nt} \quad (21.45)$$

Still, why the ‘-’ sign?

**2019-08-04 Predrag** By MacKay, Meiss and Percival [72, 74] convention (3.2), and Li and Tomsovic [66] convention (9) we should always have  $L(q_t, q_{t+1})$ . Unfortunately Keating [61] definition (3) corresponds to  $L(q_t, q_{t-1})$ , but we do not take that one.

**2019-05-16 Han** Will need to change the range of  $x_z$  to  $-1/2 \leq x_z < 1/2$  if we add the shadowing to this paper.

**2019-08-08 Han** In examples of sect. ?? and refsect s:catlattRel2x1 I used the symmetric  $x \in [-1/2, 1/2)$  field range of values. And the shadowing that we did before is also in the symmetric domain. I can change them back to the asymmetric  $x \in [0, 1)$  domain if needed, since in refsect s:catlatt the alphabet (21.79) is asymmetric.

**2019-08-08 Han** Periodic states (21.126) written out:

$$\begin{aligned} X_{33} &= \frac{1}{9} \begin{bmatrix} -3 & 3 \end{bmatrix}, & X_{22} &= \frac{1}{9} \begin{bmatrix} -2 & 2 \end{bmatrix}, & X_{11} &= \frac{1}{9} \begin{bmatrix} -1 & 1 \end{bmatrix}, \\ X_{00} &= \frac{1}{9} \begin{bmatrix} 0 & 0 \end{bmatrix}, & X_{11} &= \frac{1}{9} \begin{bmatrix} 1 & -1 \end{bmatrix}, & X_{22} &= \frac{1}{9} \begin{bmatrix} 2 & -2 \end{bmatrix}, \\ X_{33} &= \frac{1}{9} \begin{bmatrix} 3 & -3 \end{bmatrix}, & X_{44} &= \frac{1}{9} \begin{bmatrix} 4 & -4 \end{bmatrix}. \end{aligned} \quad (21.46)$$

Our notational convention, in the spirit of refeq 4-cyclePPs, (21.46):

$$X_{44} = \frac{1}{9} \begin{bmatrix} 4 & -4 \end{bmatrix}, \quad (21.47)$$

use M array as a subscript of the periodic state X, (the label for orbit  $p$ ).

**2019-08-12 Han** I have figures in the blog tried to visualize the orbit Jacobian matrix (??). The figures and the post are moved here. We can only visualize this for  $n \leq 3$ . A longer period can only be shown in higher dimensional space. The two figures in figure 21.20 are made with asymmetric admissible domain  $x \in [0, 1)$ . If these two figures are helpful I can redo these using the symmetric domain  $x \in [-1/2, 1/2)$ .

**2019-08-08 Predrag** Expand the determinant of  $\mathcal{J}_n$  by minors at the first row, use  $U_n(x)$  recurrence relations and a relation between  $U_n(x)$ 's and  $T_n(x)$ 's to derive (21.153).

**2019-01-08 Han** I made figure 21.20 to show how the volume (area) of the stretched torus counts the number of periodic points. Consider the cat map with  $s = 3$ . The periodic solutions satisfy:

$$\mathcal{J}X = -M, \quad (21.48)$$

where  $\mathcal{J}_n$  is the orbit Jacobian matrix of the periodic orbit with period  $n$ . If any  $x$  on the torus satisfies (24.151), this  $x$  is a periodic solution. So we can count the periodic points using  $\mathcal{J}_n$  to stretch the torus and counting the number of integer points enclosed in the stretched region. I plotted the stretched region of periodic solutions with  $n = 2$  and  $n = 3$ . The orbit Jacobian matrix for  $n = 2$  and  $n = 3$  are:

$$-\mathcal{J} = \begin{pmatrix} 3 & -2 \\ -2 & 3 \end{pmatrix} \quad (21.49)$$

$$-\mathcal{J} = \begin{pmatrix} 3 & -1 & -1 \\ -1 & 3 & -1 \\ -1 & -1 & 3 \end{pmatrix} \quad (21.50)$$

Let the range of the field value  $x$  be  $0 \leq x < 1$ . Figure 21.20 (a) shows the number of periodic points with length 2. The unit square enclosed by black lines is the available region of  $(x_n, x_{n+1})$ . The parallelogram with red borders are the region of the unit square stretched by the orbit Jacobian matrix  $\mathcal{J}$ . There are 4 blue dots which are the integer points in the fundamental parallelepiped. Each one of these blue dots corresponds to a periodic point. The 4 green dots are integer points on the vertices of the fundamental parallelepiped. These 4 points contribute to 1 periodic point. So there are 5 periodic points with period 2, corresponding to 3



periodic solutions (1 fixed point and 2 2-cycles). The area of this fundamental parallelepiped is 5.

Figure 21.20 (b) shows the periodic points with length 3. The square cube with black border is the available region of torus  $(x_n, x_{n+1}, x_{n+2})$ . After stretched by orbit Jacobian matrix  $\mathcal{J}$  it becomes the fundamental parallelepiped with red border. There are 6 blue dots which are the integer points completely enclosed in the fundamental parallelepiped. The 8 green dots are integer points on the vertices of the fundamental parallelepiped, which contribute to 1 periodic points. There are 18 pink points which are integer points on the surface of the fundamental parallelepiped. These 18 points contribute to 9 periodic points. So the number of periodic points is 16 which is also the volume of the fundamental parallelepiped

I have a Mathematica notebook with this 3d plot in [siminos/figSrc/han/Mathematica /HLCCountingFigures.nb](#) so you can rotate it.

**2019-08-13 Han** I get refeq POsChebyshev by calculating the determinant of the circulant orbit Jacobian matrix directly (basically a recurrence relation). I haven't figured out how to get the Chebyshev polynomial using the orthonormality of discrete Fourier eigenmodes...

**2019-08-13 Predrag** I remember this funky argument from your blog (right?), was never a fan. If you just copied that to here with on further edits, we can erase it again.

Try substituting (??) into topological zeta function refeq Isola90-13, see whether there are some doable sums over discrete Fourier eigenvalues  $\exp 2\pi jk/n$ ?

**2020-05-28 Predrag** Perhaps use

$$\cos(a - b) = \cos(a) \cos(b) + \sin(a) \sin(b) ?$$

$$\cos(2a) = \cos(a)^2 - \sin(a)^2 = 1 - 2 \sin(a)^2 ?$$

$$s - 2 \cos k_1 = (s - 2) + 4(\sin(k_1/2))^2$$

$$s - 2 \cos k_2 = (s - 2) + 4(\sin(k_1/2))^2$$

Set  $q_1 = 2\pi k_1/L$ ,  $q_2 = 2\pi k_2/T$ ,  $C = L/T$ ,

$$2 \cos(q_2 - Cq_1) = 2 \cos(q_2) \cos(Cq_1) + 2 \sin(q_2) \sin(Cq_1)$$

or

$$\lambda_m = 2 - 2 \cos \alpha_m = 4 \sin^2 (\alpha_m/2) , \quad \alpha_m = \pi m/n$$

we should state the  $\sin^2 (\alpha_m/2)$  version of the eigenvalues at least once.

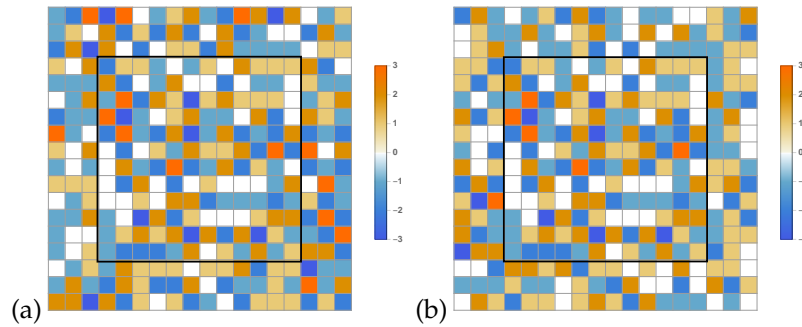


Figure 21.11: (a) and (b) are two admissible  $[18 \times 18]$  mosaics corresponding to the two distinct periodic states of figure 21.12. They coincide within the shared  $[12 \times 12]$  mosaic  $M_{\mathcal{R}}$ , region  $\mathcal{R}$  indicated by the black border.

**2019-08-21 Han** I redid the shadowing plot in a larger  $[18 \times 18]$  mosaic with  $s = 5$ . The algorithm is same as before:

- (1) Start with a random admissible state  $X^0$  with  $-1/2 \leq x_z < 1/2$ . Calculate the corresponding mosaic  $M^0$ . The  $s_z$ s in this mosaic are not integers. So we need to round these  $s_z$ s to the nearest integers and get mosaic  $M^1$
- (2) Use the Green's function and the integer mosaic  $M^1$  to calculate the state  $X^1$ . If the maximum  $x_{max}$  is larger or equal to  $1/2$ , calculate the distance  $\delta x_{max} = x_{max} - 1/2$ . Round up  $s \delta x_{max}$  (and call it  $\delta s_{max}$ ). Then change the corresponding symbol  $s_{max}$  to  $s_{max} - \delta s_{max}$ . If the minimum  $x_{min}$  is smaller than  $1/2$ , calculate the distance  $\delta x_{min} = -x_{min} - 1/2$ . Round up  $s \delta x_{min}$  (and call it  $\delta s_{min}$ ). Then change the corresponding symbol  $s_{min}$  to  $s_{min} + \delta s_{min}$ .
- (3) Now we get a new mosaic  $M^2$ . Repeat step (2) until all  $x_z$  in  $X$  are in the admissible range.

Using this method we get two periodic mosaics shown in figure 21.11. In these two mosaics the  $s_z$  within the  $[12 \times 12]$  square region with black borders are the same. The periodic state generated by these two mosaics are shown in figure 21.12. Figure 21.13 shows the pointwise distance and the logarithm of the absolute value of the pointwise distance between the two periodic states in figure 21.12.

**2019-08-21 Han** I also did the shadowing plot of  $[18 \times 18]$  mosaics with a smaller shared region of symbols. As shown in figures 21.14 and 21.15, the shared region is a  $[8 \times 8]$  sub-mosaic.

What I'm considering is: the symbols are on periodic states, so as we go further from the center of the shared region, we are getting closer to the shared region of the next tile. Using a smaller shared region we can probably reduce the effect of the next shared region. But compare figure 21.13

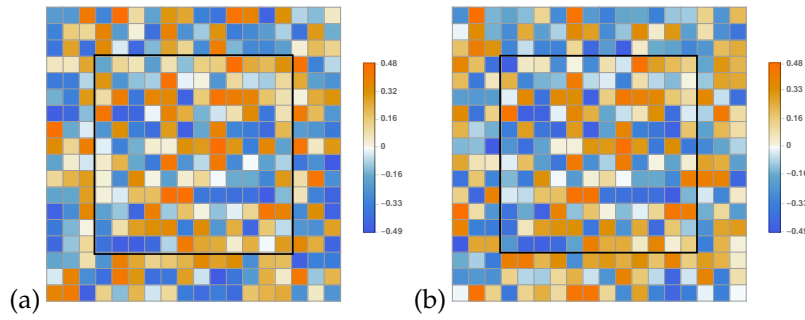


Figure 21.12: (a) and (b) are two periodic states whose symbol arrays are given by the  $[18 \times 18]$  mosaics of figure 21.11.

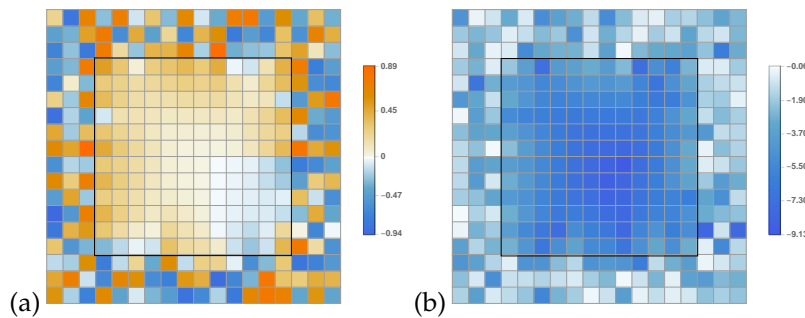


Figure 21.13: (a) The pointwise distance between the two periodic states of figure 21.12. (b) The logarithm of the absolute value of the distance between the two periodic states indicate exponential shadowing close to the center of the shared  $M_{\mathcal{R}}$ .

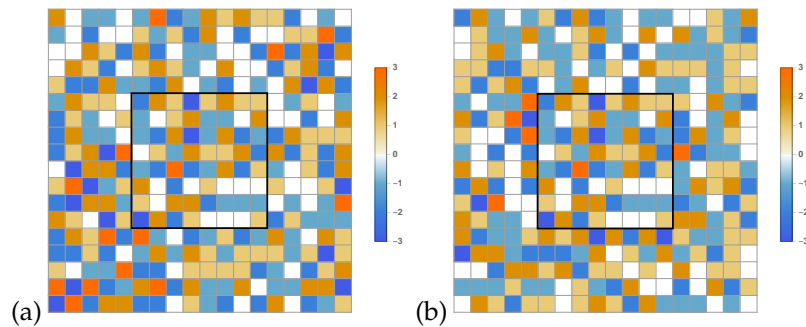


Figure 21.14: (a) and (b) are two admissible  $[18 \times 18]$  mosaics corresponding to the two distinct periodic states of figure 21.15. They coincide within the shared  $[8 \times 8]$  mosaic  $M_{\mathcal{R}}$ , region  $\mathcal{R}$  indicated by the black border.

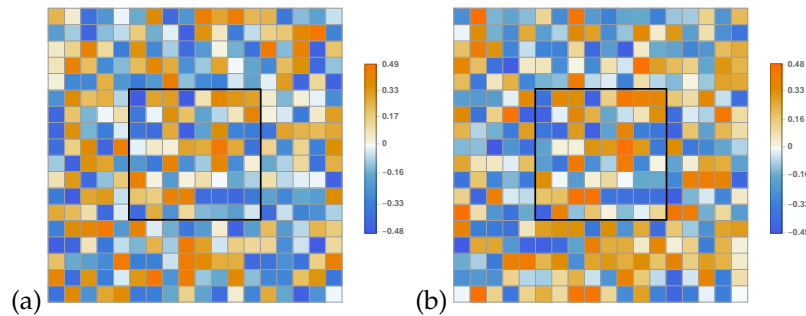


Figure 21.15: (a) and (b) are two periodic states whose symbol arrays are given by the  $[18 \times 18]$  mosaics of figure 21.14.

(b) and figure 21.16 (b), the logarithm of the distance is not too different. So I guess we don't need these figures with small shared region...

Also I think this exponential shadowing only exist in the region with shared symbols? In figure 21.13 (b) and figure 21.16 (b), the distance outside of the shared region looks random, while the distance within the shared region shrink exponentially as we go closer to the center.

**2019-08-21 Han** Another thing I tried is to generate 11 different  $[18 \times 18]$  periodic states shared a same  $[12 \times 12]$  sub-mosaic. Take one of these periodic states and compute the distance between this periodic state and other 10 periodic states, then compute the ensemble average. The result is shown in figure 21.17, which looks very similar to figure 21.13. Perhaps using a larger group of ensemble we can get a better result?

**2019-08-22 Han** I generated 500 different periodic states with a shared  $[12 \times 12]$  sub-mosaic at the center, labeled as  $X_1, X_2, \dots, X_{500}$ . Then I compute the distance between  $X_i$  and  $X_{i+250}$  where  $i$  goes from 1 to 250, and get 250

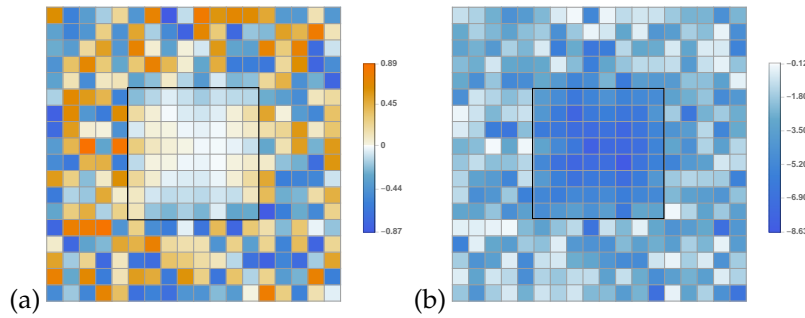


Figure 21.16: (a) The pointwise distance between the two periodic states of figure 21.15. (b) The logarithm of the absolute value of the distance between the two periodic states indicate exponential shadowing close to the center of the shared  $M_{\mathcal{R}}$ .

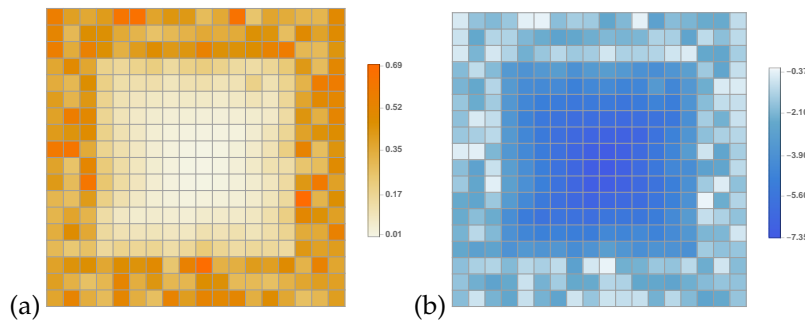


Figure 21.17: (a) The average of the absolute value of the pointwise distance between the one periodic state and other 10 different periodic states with shared  $[12 \times 12]$  sub-mosaic. (b) The logarithm of the average of the absolute value of the distance between the periodic states indicate exponential shadowing close to the center of the shared  $M_{\mathcal{R}}$ .

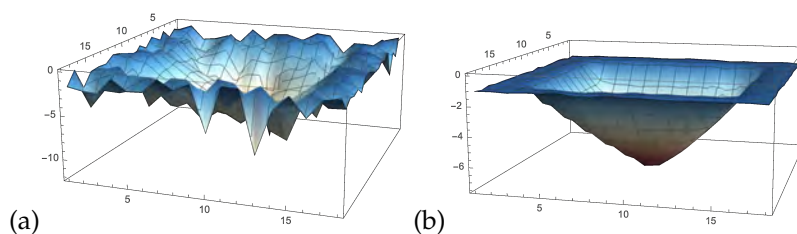


Figure 21.18: (a) The logarithm of the absolute value of the pointwise distance between the solutions  $X_1$  and  $X_{251}$  with shared  $[12 \times 12]$  sub-mosaic at the center. (b) The logarithm of the average of the absolute value of 250 different distance fields.

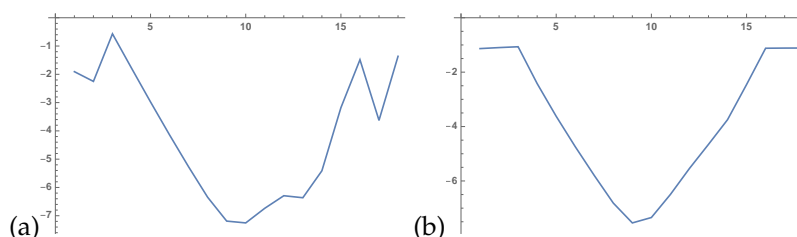


Figure 21.19: (a) The cross section through the center of the figure 21.18 (a). (b) The cross section through the center of the figure 21.18 (b). The logarithm of the distance decreases linearly as the coordinate of the field approaches the center of the shared sub-mosaic.

distance field. Figure 21.18 is the log plot of the absolute value of the distance field. Figure 21.18 (a) is the logarithm of the distance between field  $X_1$  and  $X_{251}$ , and (b) is the the logarithm of the average of the 250 distance field. By doing the average, the distance field becomes smooth. Figure 21.19 is the cross section of figure 21.18 through the center of the field. In figure 21.19 (b) the logarithm of the distance is straight line in the region with shared symbols, which shows that the distance shrink exponentially as getting closer to the center.

In figure 21.19 (b), the logarithm of the distance outside of the shared mosaic is approximately equal to  $\ln(1/3) = -1.0986$ , where  $1/3$  is the average distance between two random numbers within the range  $[-1/2, 1/2)$ .

I still need to add axis labels to these figures... (It seems like Mathematica doesn't allow me to use LaTeX for writing the labels.)

**2023-07-15 Predrag** To Han: Actually, figure ?? is maybe too complicated. It would be simpler to fix a band around the torus, have the complementary band with random symbols, or a single line around the torus with one (inner alphabet?) symbol in one periodic state, another in the shadowing periodic state. In continuum that would be related to a a Green's function

in half-plane. That is constructed by the method of images. For Laplace and Poisson this leads to logarithmic falloff, but I have not seen it for screened Poisson.

However, you are right: the closest distance from the "center" of fixed torus to the boundary decaying exponential might dominate the estimate.

**2023-09-24 Predrag** a numerical example of shadowing for two-dimensional spatiotemporal cat: dependence of the error in an observable (here the stability exponent  $\langle \lambda \rangle$ ) on the size of the approximating primitive cell

a plot of  $\ln(\langle \lambda \rangle - \langle \lambda \rangle_{\mathbb{A}})$  as a function of  $V_{\mathbb{A}}$ . If all errors are of order  $\propto \exp(-V_{\mathbb{A}} \langle \lambda \rangle)$ , you expect families with slopes  $-\langle \lambda \rangle$ .

Two families are of interest: the most space-time symmetric square primitive cells  $[L \times L]_0$ , and the most asymmetric spatially periodic, time-constant  $[L \times 1]_0$ , in particular  $[L^2 \times 1]_0$  which has the same lattice volume as  $[L \times L]_0$ , but has temporal cat stability exponent.

Not clear to me that the errors fall off like  $\propto \exp(-V_{\mathbb{A}} \langle \lambda \rangle)$  in the shadowing plot figure 21.19 (b): could be that the Green's function estimates lead to  $\propto \exp(-d(c - e)_{\mathbb{A}} \langle \lambda \rangle)$  where  $d(c - e)_{\mathbb{A}}$  is the linear distance from the center of primitive cell  $\mathbb{A}$  to its edge.

**2019-09-05 Predrag** dropped this:

Following eqs. PerViv2.1aB and PerViv2.1bB: Here  $2\pi q$  is the angle of the rotor,  $p$  is the momentum conjugate to the angular coordinate  $q$ , the angular pulse  $P(q) = P(q + 1)$  is periodic with period 1, and the time step has been set to  $\Delta t = 1$ . Eq. (21.41) says that in one time step  $\Delta t$  the configuration trajectory starting at  $q_t$  reaches  $q_{t+1} = q_t + p_{t+1} \Delta t$ , and (21.42) says that at each kick the angular momentum  $p_t$  is accelerated to  $p_{t+1}$  by the force  $P(q_t) \Delta t$ . As the values of  $q$  differing by integers are identified, and the momentum  $p$  is unbounded, the phase space is a cylinder. However, one can analyze the dynamics just as well on the compactified phase space, with the momentum wrapped around a circle, i.e., adding mod 1 to (21.42). Now the dynamics is a toral automorphism acting on a  $(0, 1] \times (0, 1]$  phase space square of unit area, with the opposite edges identified.

**2019-12-14 Predrag** restore this somewhere in cat map discussions:

The key property of hyperbolic flows is that nearby trajectories can *shadow* each other for finite times controlled by their stability exponents. One common way to quantify 'nearness' is to determine the minimal Euclidean distance between pairs of trajectories. That kind of distance is not invariant under symplectic transformations, and is thus meaningless in the Hamiltonian phase space. Here the notion of action comes to rescue: *the symplectic invariant distance between a pair of shadowing orbits is given by the difference of their actions* [66].

**2019-12-20 Predrag** dropped

Incorporate *spatiotemp/Examples/tempStab3cyc.tex*, eq. tempStab3cyc:inv

**2019-08-04 Predrag** to Han - Please make sure that all definitions and signs agree with the discrete lattice sections of ChaosBook [33].

**2019-12-18 Predrag** turn the final version into *spatiotemp/chapter/examSawtoothLin.tex* examples, then move to ChaosBook.

**2020-01-24 Predrag** I think (now commented out) reffigf:FundPar (b) was illegal - we are not allowed to define a primitive cell off the unit cell, on the 1/2 integer lattice. Removed, unless Han has a counterargument. It is kept for the record in *spatiotemp/chapter/catHamilton.tex*

**2020-01-21 Han** A possible problem with (4.126) is that  $\mathcal{J}$  could be negative. And here we have the one time step Jacobian matrix instead of a scalar  $s$  so I'm not sure if we can expand  $\ln(\mathbf{1} - \mathbb{J} \otimes r^{-1})$  as a series in  $\mathbb{J} \otimes r^{-1}$ ...

**2020-01-27 Predrag** Dropped: We are not aware of any useful visualizations of orbit Jacobian matrix fundamental parallelepiped for  $n > 3$  temporal cat and 2- and  $d$ -dimensional spatiotemporal cat of refsect s:catlatt.

$$\varphi_z(\mathbf{k}) = e^{i\mathbf{k}\cdot\mathbf{z}} = \exp\left[i\frac{2\pi}{V_{\mathbb{A}}}(m_1 T z_1 - m_1 S z_2 + m_2 L z_2)\right], \quad (21.51)$$

$$(-\square + s - 4)_{0,0,i_2,j_2} = (\mathcal{J}_{0,0})_{i_2,j_2} = \begin{bmatrix} -1 & -1 & 0 \\ 5 & -1 & -1 \end{bmatrix}_{i_2,j_2},$$

$$(-\square + s - 4)_{0,1,i_2,j_2} = (\mathcal{J}_{0,1})_{i_2,j_2} = \begin{bmatrix} 5 & -1 & -1 \\ -1 & 0 & -1 \end{bmatrix}_{i_2,j_2},$$

$$(-\square + s - 4)_{1,0,i_2,j_2} = (\mathcal{J}_{1,0})_{i_2,j_2} = \begin{bmatrix} 0 & -1 & -1 \\ -1 & 5 & -1 \end{bmatrix}_{i_2,j_2},$$

$$(-\square + s - 4)_{1,1,i_2,j_2} = (\mathcal{J}_{1,1})_{i_2,j_2} = \begin{bmatrix} -1 & 5 & -1 \\ -1 & -1 & 0 \end{bmatrix}_{i_2,j_2},$$

$$(-\square + s - 4)_{2,0,i_2,j_2} = (\mathcal{J}_{2,0})_{i_2,j_2} = \begin{bmatrix} -1 & 0 & -1 \\ -1 & -1 & 5 \end{bmatrix}_{i_2,j_2},$$

$$(-\square + s - 4)_{2,1,i_2,j_2} = (\mathcal{J}_{2,1})_{i_2,j_2} = \begin{bmatrix} -1 & -1 & 5 \\ 0 & -1 & -1 \end{bmatrix}_{i_2,j_2}.$$

To diagonalize this rank-4 orbit Jacobian matrix we need to use the eigenvectors refeq 2DEigenvector to form a rank-4 tensor:

$$U_{i_1,j_1,i_2,j_2} = \exp\left(i\frac{2\pi}{6}(2i_2i_1 - i_2j_1 + 3j_2j_1)\right).$$



The inverse of this tensor is the conjugate transpose  $U^\dagger$ :

$$(U^\dagger)_{i_1, j_1, i_2, j_2} = (U_{i_2, j_2, i_1, j_1})^* .$$

The diagonalized orbit Jacobian matrix is:

$$(\mathcal{J}_{\text{diagonalized}})_{i_1, j_1, i_2, j_2} = \sum_{i_3=0}^2 \sum_{j_3=0}^1 \sum_{i_4=0}^2 \sum_{j_4=0}^1 (U^\dagger)_{i_1, j_1, i_3, j_3} \mathcal{J}_{i_3, j_3, i_4, j_4} U_{i_4, j_4, i_2, j_2} .$$

The diagonalized orbit Jacobian matrix's element  $(\mathcal{J}_{\text{diagonalized}})_{i_1, j_1, i_2, j_2}$  is not 0 only when  $i_1 = i_2$  and  $j_1 = j_2$ . We can get the inverse of this diagonalized tensor,  $\mathcal{J}_{\text{diagonalized}}^{-1}$ , by changing the non-zero elements to their inverse. Then inverse of the orbit Jacobian matrix is:

$$(\mathcal{J}^{-1})_{i_1, j_1, i_2, j_2} = \sum_{i_3=0}^2 \sum_{j_3=0}^1 \sum_{i_4=0}^2 \sum_{j_4=0}^1 U_{i_1, j_1, i_3, j_3} (\mathcal{J}_{\text{diagonalized}}^{-1})_{i_3, j_3, i_4, j_4} (U^\dagger)_{i_4, j_4, i_2, j_2} .$$

The elements of the inverse orbit Jacobian matrix are:

$$(\mathcal{J}_{0,0}^{-1})_{i_2, j_2} = \frac{1}{35} \begin{bmatrix} 5 & 5 & 4 \\ 11 & 5 & 5 \end{bmatrix}_{i_2, j_2} ,$$

$$(\mathcal{J}_{0,1}^{-1})_{i_2, j_2} = \frac{1}{35} \begin{bmatrix} 11 & 5 & 5 \\ 5 & 4 & 5 \end{bmatrix}_{i_2, j_2} ,$$

$$(\mathcal{J}_{1,0}^{-1})_{i_2, j_2} = \frac{1}{35} \begin{bmatrix} 4 & 5 & 5 \\ 5 & 11 & 5 \end{bmatrix}_{i_2, j_2} ,$$

$$(\mathcal{J}_{1,1}^{-1})_{i_2, j_2} = \frac{1}{35} \begin{bmatrix} 5 & 11 & 5 \\ 5 & 5 & 4 \end{bmatrix}_{i_2, j_2} ,$$

$$(\mathcal{J}_{2,0}^{-1})_{i_2, j_2} = \frac{1}{35} \begin{bmatrix} 5 & 4 & 5 \\ 5 & 5 & 11 \end{bmatrix}_{i_2, j_2} ,$$

$$(\mathcal{J}_{2,1}^{-1})_{i_2, j_2} = \frac{1}{35} \begin{bmatrix} 5 & 5 & 11 \\ 4 & 5 & 5 \end{bmatrix}_{i_2, j_2} .$$

**2019-11-24 Predrag** Do you have a closed form formula for counting these? We will need to include it in the paper. My  $[2 \times 2]$  count  $36 = 9 + 8 + 7 + \dots + 1$  was wrong.

**2020-02-02 Predrag** It is hard to find spatiotemporal cat in Gutkin-Osipov [53]. The paper is mostly about the Hamiltonian formulation. Their (3.4) is the equation, once on sets  $c = d$  space-time isotropy, and drops their potential  $V$ . Their perturbed equation (7.1) comes close to it. Their action (3.9) is a bit mysterious as well.

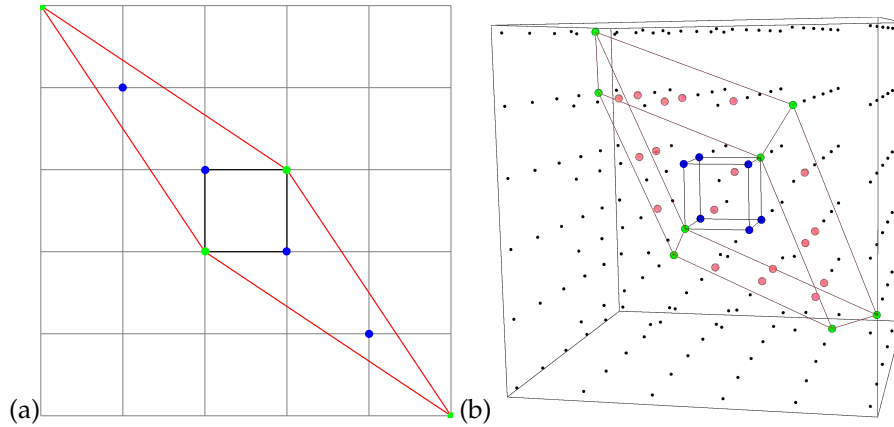


Figure 21.20: (a) A 2-dimensional torus (with black border) stretched by  $\mathcal{J}$ . The blue dots are internal integer points in the fundamental parallelepiped (with red border). The green dots are on the vertices of the fundamental parallelepiped. (b) A 3-dimensional torus (with black border) stretched by  $\mathcal{J}$ . The blue dots are internal integer points in the stretched fundamental parallelepiped (with red border). The green dots are on the vertices of the fundamental parallelepiped. The pink dots are on the surface of the fundamental parallelepiped.

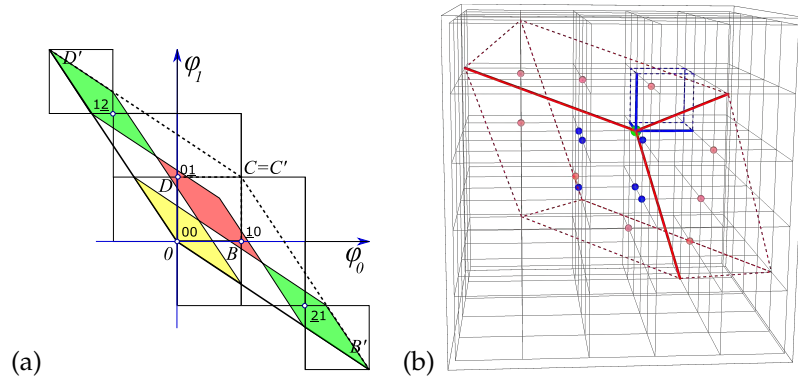


Figure 21.21: Was reffig:catCycJacob, now superannuated: (a)  $[2 \times 2]$  orbit Jacobian matrix  $\mathcal{J}$  refeqcatFundPar2 had a wrong sign, meaningless partition into 9 rectangles. (b) Han 2020-02-11: Intermediate attempt to draw reffig:catCycJacob.  $[3 \times 3]$  orbit Jacobian matrix  $\mathcal{J}$  had tons of irrelevant points plotted, is unintelligible.

Gutkin and Osipov [53] refer to an screened Poisson equation periodic state solution  $p$  as a ‘many-particle periodic orbit’, with  $x_{nt}$  ‘doubly-periodic’, or ‘closed,’

$$x_{nt} = x_{n+L_p, t+T_p}, \quad n = 0, 1, 2, \dots, L_p - 1; \quad t = 0, 1, 2, \dots, T_p - 1.$$

**2020-02-02 Predrag** Note that in (??) and throughout I have redefined the stretching parameter  $s$  to be stretching per dimension, i.e.,  $s$  in (??) is replaced by  $ds$ . This is consistent with how one defines a diffusion constant on an isotropic  $d$ -dimensional hypercubic lattice.

**2019-08-06 Predrag** Please strictly follow the nomenclature of a single reference -presumably Dresselhaus *et al.* [38], or Barvinok [12] or whatever - and state so clearly in your text.

integer lattices counting [12] enable us to count spatiotemporally finite mosaics, and give explicit formulas for the number of invariant  $d$ -torus solutions for mosaics of any size.

**2020-02-20 Han** Figure 21.22 is the fundamental parallelepiped of a  $[2 \times 1]_1$  periodic state. The pattern of this periodic state is shown in figure ?? (a). The orbit Jacobian matrix of this periodic state can be written as a  $[2 \times 2]$  matrix:

$$\mathcal{J} = \begin{pmatrix} -2s & 4 \\ 4 & -2s \end{pmatrix}.$$

The shape of the fundamental parallelepiped is very similar to reffig:catCycJacob (a).

**2018-12-13 Predrag** Must rethink the DIMENSION of  $F[X]$  and  $\mathcal{J}$ .  $F[X]_i$  is a  $n$ -dimensional vector function - is it dimensionally the same as  $x_j$ ? Otherwise orbit Jacobian matrix is not dimensionless, and cannot be referred to as a ‘Jacobian’. Relation (4.126) only makes sense for the dimensionless case. I think we are OK, but we have to be sure.

**2019-08-11 Predrag** to Han: this is wrong alphabet, for the symmetric unit interval  $x \in [-1/2, 1/2)$ . For all our examples we pick the ‘least stretching’ spatiotemporal cat with  $s = 5/2, \mu^2 = 1$ , with 9-letter alphabet

$$\mathcal{A} = \{\underline{4}, \underline{3}, \underline{2}, \underline{1}, 0, 1, 2, 3, 4\}. \quad (21.52)$$

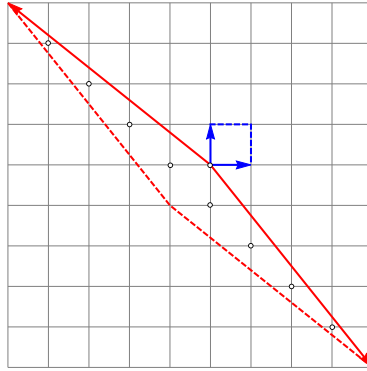


Figure 21.22: The fundamental parallelepiped of a  $[2 \times 1]_1$  periodic state with  $s = 5/2, \mu^2 = 1$ . Admissible field values lie within the unit square with blue boundaries. This unit square is stretched by the orbit Jacobian matrix  $\mathcal{J}$  into the fundamental parallelepiped with red boundaries. Integer points in the fundamental parallelepiped are marked by the circles. There are 9 integer points in the fundamental parallelepiped, in agreement with the counting formula.

2020-02-17 **Predrag** Now in reftab tab:LxTs:

$$\begin{aligned}
 N_{[1 \times 1]_0}(s) &= 2(s - 2) \\
 N_{[2 \times 1]}(s) &= 4(s - 2)s \\
 N_{[2 \times 1]_1}(s) &= 4(s - 2)(s + 2) \\
 N_{[2 \times 2]}(s) &= 16(s - 2)s^2(s + 2) \\
 N_{[3 \times 2]_0}(s) &= 4(s - 2)s(2s - 1)^2(2s + 3)^2 \\
 N_{[3 \times 2]_1}(s) &= 64(s - 2)s^3(s + 1)^2 \\
 N_{[3 \times 2]_2}(s) &= 64(s - 2)s^3(s + 1)^2 \\
 N_{[3 \times 3]}(s) &= -32(s - 2)(s + 1)^4(2s - 1)^4.
 \end{aligned} \tag{21.53}$$

2023-04-27 **Predrag** Superseded by the  $\mu^2$ -parametrized table 9.3.

2019-11-23 **Predrag** Dropped: For all our examples we pick the ‘least stretching’ hyperbolic spatiotemporal cat with  $s = 5$ , and restrict the admissible field values  $x_z$  at lattice site  $z = (n_1, n_2)$  to the symmetric unit interval  $x \in [-1/2, 1/2)$ , with 9-letter alphabet (21.52)

the code depends on the choice of the unit interval: the alphabet  $\mathcal{A}$  for  $x_t \in [-1/2, 1/2)$  differs from the alphabet for  $x_t \in [0, 1)$ .

Here  $s = 5/2, \mu^2 = 1$  and  $x_z \in [-1/2, 1/2)$ , so the interior alphabet is one letter alphabet  $\mathcal{A}_0 = \{0\}$ ...

2020-02-24 **Predrag** Not urgent, but can you complete the primitive counts  $M_{[L \times T]_s}$  and decompositions of  $N_{[L \times T]_s}$  into primitive periodic states in table 9.1 and perhaps also in table 9.3?

**2020-03-05 Predrag** Temporal cat counting (all messed up, fix using *CatMaptopZeta.nb* output):

$$\begin{aligned} \sum_{n=0}^{\infty} N_n z^n &= \frac{2 - sz}{1 - sz + z^2} - \frac{2}{1 - z} \\ \{N_n\} &= s - 2, s^2 - 4, s^3 - 3s - 2, s^4 - 4s^2, \\ &2(s^5 - 4s^3 + 3s) - s(s^4 - 3s^2 + 1) - 2, \\ &-2(s^3 - 2s) - s(s^4 - 3s^2 + 1) \\ &-2 - s(-1 + 6s^2 - 5s^4 + s^6) + 2(-4s + 10s^3 - 6s^5 + s^7), \\ &-2s(s^5 - 4s^3 + 3s) - 2(s^4 - 3s^2 + 1) - 2, \\ &-2(s^5 - 4s^3 + 3s) + s(s^6 - 5s^4 + 6s^2 - 1) - 2, \end{aligned} \quad (21.54)$$

**2020-03-23 Predrag** Lot's of headless Kuramoto–Sivashinsky equation floundering in preparing *BlogCats.tex* refsect s:KSe saved below. Hopefully the resulting discretized Kuramoto–Sivashinsky equation (21.61) is correct...

The discretized Kuramoto–Sivashinsky equation is of the form

$$\partial_t U + \frac{\alpha}{2} \partial_x U^2 - \beta \Delta_x U + \gamma \Delta_x^2 U = 0. \quad (21.55)$$

Rescale  $U \rightarrow U/\Delta t$

$$\frac{\partial_t}{\Delta t} U + \frac{(\Delta x)^2}{\Delta t} \frac{\alpha}{2} \frac{\partial_x}{\Delta x} U^2 - \frac{(\Delta x)^2}{\Delta t} \beta \frac{\Delta_x}{(\Delta x)^2} U + \frac{(\Delta x)^4}{\Delta t} \gamma \frac{\Delta_x^2}{(\Delta x)^4} U = 0. \quad (21.56)$$

Our canonical choice is setting these

$$\alpha = \frac{\Delta t}{(\Delta x)^2}, \quad \beta = -\frac{\Delta t}{(\Delta x)^2}, \quad \gamma = \frac{\Delta t}{(\Delta x)^4}, \quad (21.57)$$

equal to 1, parametrizing the problem with  $L = 1/\Delta x, T = 1/\Delta t$ ,

$$\frac{1}{T} \frac{\partial_t}{\Delta t} U + \frac{1}{L} \frac{\alpha}{2} \frac{\partial_x}{\Delta x} U^2 - \frac{1}{L^2} \beta \frac{\Delta_x}{(\Delta x)^2} U + \frac{1}{L^4} \gamma \frac{\Delta_x^2}{(\Delta x)^4} U = 0. \quad (21.58)$$

Rescale  $U \rightarrow UT$

$$\frac{\partial_t}{\Delta t} U + \frac{T^2}{L} \frac{\alpha}{2} \frac{\partial_x}{\Delta x} U^2 - \frac{T}{L^2} \beta \frac{\Delta_x}{(\Delta x)^2} U + \frac{T}{L^4} \gamma \frac{\Delta_x^2}{(\Delta x)^4} U = 0. \quad (21.59)$$

Our canonical choice is setting these

$$\alpha = L/T^2, \quad \beta = -L^2/T, \quad \gamma = L^4/T, \quad (21.60)$$

equal to 1,

$$\frac{\partial_t}{\Delta t} U + \frac{1}{2} \frac{\partial_x}{\Delta x} U^2 + \frac{\Delta_x}{(\Delta x)^2} U + \left( \frac{\Delta_x}{(\Delta x)^2} \right)^2 U = 0, \quad (21.61)$$

**2019-12-28 Predrag** My argument along the following lines was unnecessarily complicated:

$$\epsilon^0 \epsilon^1 \epsilon^2 \dots \epsilon^{n-1} = 1. \quad (21.62)$$

can be eliminated by going from products to sums over cyclic eigenvalues. For example, if a polynomial is of form  $G(x)/(x - \lambda_0)$ , with the zeroth root  $(x - \epsilon^0) = (x - 1)$  quotiented out from the characteristic polynomial,

$$\frac{x^N - 1}{x - 1} = (x - \epsilon)(x - \epsilon^2) \dots (x - \epsilon^{N-1}).$$

Consider a sum of the first  $N$  terms of a geometric series, multiplied by  $(x - 1)/(x - 1)$ :

$$1 + x + \dots + x^{N-1} = \sum_{m=0}^{N-1} x^m = \frac{1}{x - 1} \sum_{m=0}^{N-1} (x - 1) x^m = \frac{x^N - 1}{x - 1}. \quad (21.63)$$

So, the products can be written as sums

$$(x - \epsilon)(x - \epsilon^2) \dots (x - \epsilon^{N-1}) = 1 + x + \dots + x^{N-1}. \quad (21.64)$$

In  $C_N$   $P_n$  projection operators, the denominators are evaluated by substituting  $x \rightarrow 1$  into (21.64); that adds up to  $N$ . The numerator is evaluated by substituting  $x \rightarrow \epsilon^{-n} M$ . We obtain the projection operator as a discrete Fourier weighted sum of matrices  $M^m$ ,

$$P_n = \frac{1}{N} \sum_{m=0}^{N-1} e^{-i \frac{2\pi}{N} nm} M^m, \quad (21.65)$$

instead of the usual product form.

**2020-05-31 Predrag** Politi and Torcini [83] 1992 *Periodic orbits in coupled Hénon maps: Lyapunov and multifractal analysis* is quite close to our spatiotemporal cat. The problem is harder, as the Hénon map is nonlinear.

**2020-05-28 Predrag** Track this down: Vicky Weiskopf: "It is better to uncover a little than cover a lot"

**2019-08-11 Predrag** to Han - we need something like

For the  $s = 5/2, \mu^2 = 1$  example at hand, (??) yields the numbers of relative prime orbits  $[L \times 1]_1$

$$\{M_{[L \times 1]_0}\} = (M_{[1 \times 1]_0}, M_{2 \times 1}, M_{3 \times 1}, \dots) = (1, 9, ?, ?, ?, \dots), \quad (21.66)$$

to be contrasted with temporal cat counting  $\text{refeq noPrimeCycs}=3$ , this time for  $s = 3$ ,

$$\{M_L\} = (M_1, M_2, M_3, M_4, M_5, \dots) = (1, ?, ?, ?, ?, \dots). \quad (21.67)$$

**2019-11-24 Han** A brute way to determine the *admissible* mosaics, is to compute  $X_p$  for each prime mosaic  $M_p$ , and eliminate every  $X_p$  which contains a lattice site or sites on which the value of the field violates the admissibility condition  $x_z \in [0, 1]^2$ .

The interior alphabet depends on the value of  $s$  and the admissible range of  $x_z$ . For  $s = 5/2, \mu^2 = 1, x_z \in [0, 1)$ , the interior alphabet is  $\mathcal{A}_0 = \{0, 1\}$  (see eq. (38) in ref. [52]). For  $s = 7/2, x_z \in [0, 1)$ , the interior alphabet is  $\mathcal{A}_0 = \{0, 1, 2, 3\}$  (eq. (46) in ref. [52]).

**2020-09-06 Predrag** Removed the Mathematica expansion of (21.125)

$$\begin{aligned} \sum_{n=0}^{\infty} N_n z^n &= \frac{2 - sz}{1 - sz + z^2} - \frac{2}{1 - z} \\ &= (s - 2) [z + (s + 2)z^2 + (s + 1)^2 z^3 \\ &\quad + (s + 2) s^2 z^4 + (s^2 + s - 1)^2 z^5 + \dots] \end{aligned} \quad (21.68)$$

$$\begin{aligned} &s - 2, s^2 - 4, s^3 - 3s - 2, s^4 - 4s^2, -2(s^3 - 2s) + s(s^4 - 3s^2 + 1) - 2, \\ &s(s^5 - 4s^3 + 3s) - 2(s^4 - 3s^2 + 1) - 2, -2(s^5 - 4s^3 + 3s) + s(s^6 - 5s^4 + 6s^2 - 1) - 2, \end{aligned}$$

**2016-11-01 Boris** “Deeper insight” into  $d = 2$  symbolic dynamics: “Classical foundations of many-particle quantum chaos” I believe could become a game-changer

**2016-12-24 Predrag** “ Alternatively, one can consider the dynamics on the infinite line, and interpret  $s_t$  as a jump to  $s_t$ th interval. This leads to the phenomenon of “deterministic diffusion” [51, 87], and its periodic orbit theory [6, 34], with unit circle periodic orbits in one-to-one relation to the relative periodic (“running”) orbits on the line, and symbolic dynamics given by  $s_t$ ’s.

For single-parameter, one-dimensional sawtooth maps, it is possible to find infinitely many values of the parameter such that the grammar is finite (a finite subshift), and the exact diffusion constant is given by a finite-polynomial topological zeta function [7]. For cat maps, deterministic diffusion constants are not known exactly [8]. ”

**2020-07-15 Predrag** Perhaps refer to ChaosBook [ChaosBook 8.1 Hamiltonian flows](#), when discussing ‘two-configuration’ form (21.240).

**2020-09-19 Predrag** solution  $X$  of a global fixed-point condition  $F[X] = 0$  is uniquely encoded by a finite alphabet  $d$ -dimensional symbol periodic state  $M$

In particular, the following questions seem to be of fundamental importance:

- Can an effective  $d = 2$  symbolic dynamics with finite alphabet be constructed for an example of a PDE with spatiotemporal chaos, such that (a) Connection between periodic state solutions and their symbolic representation is unique; (b) The local symbolic content would define the values of the corresponding fields with the exponentially decreasing errors?

**2020-09-21 Predrag** As we shall here have to traverse territory unfamiliar to many, we follow Mephistopheles pedagogical dictum “You have to say it three times” [49], I hereby exorcise Liang-Gudorf-Williams heresy by singing my song thrice:

refsect s:bernIntLat *Coin is not the table off which it bounces*

refsect s:bernIntLat *Cat is not the floor on which it dances*

refsect s:catlatt *Cats are not the spacetime over which we herd them*

**2020-02-16 Predrag** Recheck - is there something called ‘characteristic function’ in integer lattice and other lattice literature?

**2023-01-19 Han** Removed from sect. ??:

**Relative  $[2 \times 2]_0$  periodic state.**

Consider  $[2 \times 2]_0$  Bravais lattices prime mosaic

$$M_p = \begin{bmatrix} s_{01} & s_{11} \\ s_{00} & s_{10} \end{bmatrix}, \quad (21.69)$$

**Relative  $[3 \times 2]_1$  periodic state.** Consider the Bravais lattice of figure ??, tiled by periodic state defined by the primitive cell with primitive vectors  $\mathbf{a}_1 = (3, 0)$  and  $\mathbf{a}_2 = (1, 2)$ , see figure ?? (b). There are 6 independent field values in the repeating cell, which can be written as an  $[3 \times 2]$  array:<sup>3</sup>

$$[3 \times 2]_1 = \begin{bmatrix} & x_{11} & x_{21} & x_{01} \\ x_{00} & x_{10} & x_{20} & \end{bmatrix}.$$

*Example:  $[3 \times 2]_0$  Bravais lattices prime mosaics.*

orbit Jacobian matrix (??) is the block-matrix (21.239), a block circulant matrix with circulant blocks [27],

$$\mathcal{J}_{[3 \times 2]_0} = \left( \begin{array}{cc|cc|cc} -2s & 2 & 1 & 0 & 1 & 0 \\ 2 & -2s & 0 & 1 & 0 & 1 \\ \hline 1 & 0 & -2s & 2 & 1 & 0 \\ 0 & 1 & 2 & -2s & 0 & 1 \\ \hline 1 & 0 & 1 & 0 & -2s & 2 \\ 0 & 1 & 0 & 1 & 2 & -2s \end{array} \right). \quad (21.70)$$

of  $[L \times L]$  block form,  $L = 3$ , with  $[T \times T]$  blocks,  $T = 2$ .

<sup>3</sup>Predrag 2020-02-23: Where is the source code for figure ???



The fundamental parallelepiped generated by the action of orbit Jacobian matrix  $\mathcal{J}_{[3 \times 2]_0}$  is spanned by  $LT = 6$  primitive vectors, the columns (??) of the orbit Jacobian matrix (21.70):

$$\mathcal{J}_{[3 \times 2]_0} = \begin{pmatrix} -2s & 2 & 1 & 0 & 1 & 0 \\ 2 & -2s & 0 & 1 & 0 & 1 \\ 1 & 0 & -2s & 2 & 1 & 0 \\ 0 & 1 & 2 & -2s & 0 & 1 \\ 1 & 0 & 1 & 0 & -2s & 2 \\ 0 & 1 & 0 & 1 & 2 & -2s \end{pmatrix}. \quad (21.71)$$

Consider the Bravais lattice

$$\mathbf{M} = \begin{bmatrix} s_{12} & s_{22} & s_{32} \\ s_{11} & s_{21} & s_{31} \end{bmatrix}. \quad (21.72)$$

A correct definition of a *prime* periodic state [32] is subtler than for the one-dimensional temporal lattice case. If a given periodic state over lattice  $\mathcal{L}$  is not periodic under translations  $R \in \mathcal{L}_p$  on any sublattice  $\mathcal{L}_p$  (except for  $\mathcal{L}$  itself), we shall refer to it here as a *prime periodic state*, a periodic orbit of the smallest periodicity in all spacetime directions.

### 21.2.1 Prime Bravais lattices

4

It might be possible to tile a given Bravais lattice  $\mathcal{L}_a$  by a finer lattice  $\mathcal{L}_p$ . Lattice  $\mathcal{L}_p$ , defined by a primitive cell

$$\mathbf{a}_1^p = \begin{pmatrix} L_p \\ 0 \end{pmatrix}, \quad \mathbf{a}_2^p = \begin{pmatrix} S_p \\ T_p \end{pmatrix}, \quad (21.73)$$

is a *prime* Bravais lattice, if there is no finer primitive cell, other than the unit volume  $[1 \times 1]_0$  primitive cell, that can tile it.

In order to determine all prime lattices  $\mathcal{L}_p$  (21.73) that tile a given Bravais lattice  $\mathcal{L}$  refeq Hermite2d,

$$\begin{aligned} \mathbf{a}_1 &= k \mathbf{a}_1^p + \ell \mathbf{a}_2^p \\ \mathbf{a}_2 &= m \mathbf{a}_1^p + n \mathbf{a}_2^p, \end{aligned}$$

observe that a prime tile  $(\mathbf{a}_1^p, \mathbf{a}_2^p)$  tiles the larger tile only if larger tile's width  $L$  is a multiple of  $L_p$ , the height  $T$  is a multiple of  $T_p$ , and the two tile 'tilts' satisfy

$$\mathbf{a}_2 = m \mathbf{a}_1^p + \frac{T}{T_p} \mathbf{a}_2^p \quad \rightarrow \quad S = mL_p + \frac{T}{T_p} S_p.$$

<sup>4</sup>Predrag 2024-02-08: Do not ever mention a "Prime Bravais lattice"

Hence a prime lattice  $\mathcal{L}_p$  tiles the given lattice  $\mathcal{L}$  only if the area spanned by the two ‘tilted’ primitive vectors

$$\mathbf{a}_2 \times \mathbf{a}_2^p = ST_p - TS_p \quad (21.74)$$

is a multiple of the prime tile area  $L_p T_p$ .

**2023-02-05 Predrag** Dropped this:

As the lattice fields we study here are defined on the sites of the integer lattice  $\mathbb{Z}^2$ , the periodicities are given by Bravais lattice with integer components, i.e.,  $\mathbf{A} \in \mathbb{Z}^{2 \times 2}$ .

For a periodic lattice field configuration, knowing the lattice fields in the primitive cell, the lattice field configuration in the infinite spacetime can be retrieved by tiling the spacetime with the primitive cell and the translation group. For simplicity, instead of the parallelogram spanned by the primitive vectors, we choose a rectangular primitive cell:

$$P_{[L \times T]_s} = \left\{ \left[ \begin{array}{cc} L & 0 \\ 0 & T \end{array} \right] \mathbf{x} \mid \mathbf{x} \in [0, 1)^2 \right\}. \quad (21.75)$$

The lattice field configuration with periodicity  $[2 \times 1]_1$  looks same as the field configuration with periodicity  $[2 \times 1]_0$ , but it has Figure ?? (a) is the field configuration  $[2 \times 1]_1$  in the infinite spatiotemporal domain.

**Lattice field configuration with periodicity  $[3 \times 2]_1$ :**

$$\mathbf{X} = \begin{bmatrix} x_{01} & x_{11} & x_{21} \\ x_{00} & x_{10} & x_{20} \end{bmatrix}.$$

The primitive cell we choose for this field configuration is a rectangular  $[3 \times 2]$  cell. This field configuration in the infinite spatiotemporal domain is shown in figure ?? (b).

**2023-02-14 Predrag** I would like to keep Birkhoff sum and Birkhoff average notation  $A[\mathbf{X}]$ ,  $a_z$ , as in ChaosBook. For that reason I’ve now introduced another letter, hopefully ‘standard’, for primitive cell:  $\mathbb{A}$ .

**2023-02-18 Predrag** Dropped this:

The semiclassical partition sum is the sum over all exact, deterministic solutions of system’s Euler–Lagrange equation:

$$\begin{aligned} Z &= \int [d\mathbf{X}] e^{\frac{i}{\hbar} S[\mathbf{X}]}, \\ &\approx \sum_c \frac{e^{\frac{i}{\hbar} S[\mathbf{X}] + im_c}}{|\text{Det}(\mathcal{J}_c/\hbar)|^{1/2}} \end{aligned} \quad (21.76)$$

We shall set  $\hbar = 1$ , and henceforth ignore the Maslov phases as they are of no concern for what follows.

**2023-02-19 Predrag** The raw text of sect. ?? *Semiclassical field theory* was taken from `siminos/presentations/kittens/semiClassic.tex` of 2023-01-29, click here: [overheads/traceSemicl/semiClassic.pdf](#).

**2023-02-10 Predrag** A small, irrelevant thing, but Eq. (??) would involve an ordinary matrix  $\{a_{ij}\}$

$$r = \mathbf{n} \mathbf{A}^\top = [n_1, n_1] \begin{bmatrix} \mathbf{a}_1 \\ \mathbf{a}_2 \end{bmatrix} = [n_1, n_1] \begin{bmatrix} (\mathbf{a}_1)_1 & (\mathbf{a}_1)_2 \\ (\mathbf{a}_2)_1 & (\mathbf{a}_2)_2 \end{bmatrix}, \quad (21.77)$$

if we used row vectors  $\mathbf{a}_j$ ,  $\mathbf{n}$  rather than column ones. That would correspond to the lower-triangular Hermite normal form.

**2023-04-20 Han** The term ‘**primitive rectangular lattice**’ is used in crystallography. But I’m not sure if we want to be so specific. Maybe ‘rectangular lattice’ is good enough.

The Hill determinant can be computed directly from the orbit Jacobian matrix, Euler–Lagrange equation linearized at the corresponding periodic state.

The most common application of the symmetry reduction is to compute the Hill determinant of a periodic state that is a repeat of a prime orbit.

So the asymptotic growth rate of stability of a periodic state at large spacetime limit is more important to us, compared to the stability of a periodic state in a finite spatiotemporal domain.

In this section we will use one-dimensional temporal systems examples to illustrate reciprocal lattice computation of orbit Jacobian matrices spectra.

For a  $d$ -dimensional deterministic field theory, the *orbit Jacobian matrices* are order  $2d$  tensors.

**2023-07-15 Predrag** Han’s thesis, but not CL18:

set all nearest neighbors at  $x_{z'} = 1 - \epsilon$ . That gives for the  $d$ -dimensional *spatiotemporal cat*

$$\mathcal{A} = \{-2d+1, -2d+2, \dots | 0, 1, \dots, \mu^2 | \mu^2+1 \dots, 2s-2, 2s-1\}, \quad (21.78)$$

where  $\square$  is the discrete  $d$ -dimensional Euclidean space-time Laplacian.

**2023-02-20 Predrag** Dropped from `refsect s:catlatt`:

Now that we have mastered the *temporal cat* (??), a generalization to the *spatiotemporal cat* (??) is immediate. Consider a one-dimensional spatial lattice, with field  $x_{nt}$  (the angle of a kicked rotor (21.265) at instant  $t$ ) at spatiotemporal site  $z = (n, t) \in \mathbb{Z}^2$ . If each site couples only to its nearest spatial neighbors  $x_{n\pm 1, t}$ , and if we require (1) invariance under spatial translations, (2) invariance under spatial reflections, and (3) invariance under the space-time exchange, we arrive at the two-dimensional Euclidean lattice difference equations (??).

In multi-index, or ‘tensorial’ notation, the spatiotemporal cat equation (??) can be written as

$$\begin{aligned}
 (\mathcal{J}x)_z &= \sum_{z'} \sum_{i=1}^d (r_i - s \mathbf{1} + r_i^{-1})_{zz'} x_{z'} = -s_z, \quad s_z \in \mathcal{A}, \\
 z &= (n_1, n_2, n_3, \dots, n_d) \in \mathbb{Z}^d \\
 \mathcal{A} &= \{-2d + 1, -2d + 2, \dots, 2s - 2, 2s - 1\}, \quad (21.79)
 \end{aligned}$$

with field  $x_z$  and source  $s_z$  labelled by the  $d$  indices of lattice site  $z$ . Sources  $s_z \in \mathcal{A}$  keep the field (‘rotor angle’  $x_z$ ) within the unit interval on every site. The orbit Jacobian matrix  $\mathcal{J}$ , labelled by  $d$  pairs of indices, acts on the periodic state  $X$  by usual matrix multiplication. We illustrate how that works by working out in detail an example in appendix ???. As yet another notational choice, in (21.239) we recast the orbit Jacobian matrix (??) as a  $[LT \times LT]$  Kronecker product block matrix.

The simplest dissipative spatiotemporal lattice field theory is the first order in time, second order in space difference equation, the ‘spatiotemporal Bernoulli’,

$$-\square x_{z,t} - x_{z,t} + s x_{z,t} - s_{z,t} = 0, \quad z \in \mathbb{Z}^{d-1}, \quad t \in \mathbb{Z}, \quad (21.80)$$

where the discrete Laplace operator only acts on the first  $(d - 1)$  indices.

The discretized Euler–Lagrange equation

$$F[X_c] = 0,$$

is a search for zeros of functions  $F[X_c]_z$ .

<sup>5</sup> The orbit Jacobian matrix of a two-dimensional lattice field theory can be written in a spatiotemporal block matrix form, as a temporal lattice

$$\mathcal{J} = \begin{pmatrix} s_0 & -\mathbf{1}_1 & & & -\tilde{\mathbf{r}}_1^\top \\ -\mathbf{1}_1 & s_1 & -\mathbf{1}_1 & & \\ & \ddots & \ddots & \ddots & \\ & & -\mathbf{1}_1 & s_{T-2} & -\mathbf{1}_1 \\ -\tilde{\mathbf{r}}_1 & & & -\mathbf{1}_1 & s_{T-1} \end{pmatrix}, \quad (21.81)$$

with the spatial dependence treated as a multicomponent field at each

<sup>5</sup>Predrag 2023-03-13: Not sure it is a good idea to introduce block matrix notation here, maybe an appendix, or not at all.

temporal lattice site, where  $[L \times L]$  matrix block  $\mathbf{s}_t$  is:

$$\mathbf{s}_t = \begin{pmatrix} d_{0,t} & -1 & & -1 \\ -1 & d_{1,t} & -1 & \\ & \ddots & \ddots & \ddots \\ & & -1 & d_{L-2,t} & -1 \\ -1 & & & -1 & d_{L-1,t} \end{pmatrix}, \quad (21.82)$$

the  $\mathbf{1}_1$  is a  $[L \times L]$  identity matrix, and  $\tilde{\mathbf{r}}_1$  is a  $[L \times L]$  shift matrix.  $L$  and  $T$  are the spatial and temporal periods of the periodic state, and the spatial shift  $\tilde{\mathbf{r}}_1$  depends on the relative-periodic shift on the boundary of the periodic state.

For uniform stretching systems such as the spatiotemporal cat, the orbit Jacobian matrix is a block Toeplitz, spatiotemporal translation invariant matrix. The spatial matrix block  $\mathbf{s}_t$  in (21.81) is:

$$\mathbf{s} = \begin{pmatrix} 2s & -1 & & -1 \\ -1 & 2s & -1 & \\ & \ddots & \ddots & \ddots \\ & & -1 & 2s & -1 \\ -1 & & & -1 & 2s \end{pmatrix}, \quad (21.83)$$

which does not depend on the lattice site of each periodic state. The spatiotemporal-translation invariance allows one to compute the eigenvalues of the orbit Jacobian matrix using the discrete Fourier transform.

As an example, consider the temporal Hénon period-2 periodic state  $X_p$  (??), with a two-dimensional repeating block `refeq henFundPar2` orbit Jacobian matrix. The orbit Jacobian matrix of an infinite periodic state tiled by repeats of  $X_p$  is the infinite-dimensional linear operator

$$\mathcal{J} = \begin{pmatrix} \ddots & \ddots & & & & \\ & \ddots & d_1 & -1 & & \\ & & -1 & d_0 & -1 & \\ & & & -1 & d_1 & \ddots \\ & & & & \ddots & \ddots \end{pmatrix}, \quad \begin{pmatrix} d_0 \\ d_1 \end{pmatrix} = \begin{pmatrix} -2 - 2\sqrt{a-3} \\ -2 + 2\sqrt{a-3} \end{pmatrix} \quad (21.84)$$

whose eigenstates are plane waves of form (??), where  $u_k(t)$  is periodic with period 2. Now there are two families of  $\mathcal{J}$  eigenvalues:

$$\Lambda_{LR,\pm}(k)\psi_k = \text{CORRECT THIS } \mathcal{J}\psi_k = -2(1 \pm \sqrt{a-3 + \cos^2 k})\psi_k, \quad (21.85)$$

plotted in the Brillouin zone  $k \in (-\pi/2, \pi/2]$  in figure ?? (b).

In companion paper III [94] notation:

$$\begin{bmatrix} x_0 \\ x_1 \end{bmatrix} = \begin{bmatrix} \frac{2}{\mu^2} - \frac{1}{2}\sqrt{1 - \frac{16}{\mu^4}} \\ \frac{2}{\mu^2} + \frac{1}{2}\sqrt{1 - \frac{16}{\mu^4}} \end{bmatrix}, \quad (21.86)$$

**2023-05-01 Predrag** Pure unfounded speculation: The requisite two-dimensional lattice integrals, one for each eigenvalue, might be hypergeometric functions, or  $K(u)$  complete elliptic functions.

Prime orbits  $p$  are themselves searched for and ordered by the hierarchy of primitive cells

$$\sum_p \cdots = \sum_{r_1=1}^{\infty} \sum_{r_2=1}^{\infty} \sum_{r_3=0}^{r_1-1} \cdots, \quad (21.87)$$

$$\sum_{r=1}^{\infty} \sum_{r'=1}^{\infty} z^{rr'} = \sum_{r=1}^{\infty} \frac{1}{1 - z^r}$$

Had here a wrong sum

$$Z[\beta]_p = e^{V_p W[\beta]_p} = V_p \sum_{r_1=1}^{\infty} \sum_{r_2=1}^{\infty} t_p^{r_1 r_2} = V_p \frac{t_p}{(1 - t_p)^2}. \quad (21.88)$$

**2023-03-15 Predrag** **This statement is wrong:** Repeated *prime orbit*  $p_{\mathbb{A}\mathbb{R}}$  over all slants  $s$  is the same prime orbit  $p$ , and should be counted *only once*. Ergo, always use only the  $s = 0$  primitive cell, there is no  $s$  sum in (21.87), and all is well.

A stronger argument why we should rescale the Bravais lattice by multiplying it by  $\mathbb{A}^{-1}$ , send it into the unit integer lattice.

a more 'pedagogical' attempt:

consider a prime orbit over  $P_{\mathbb{A}}$ . Now the tile  $\mathbb{A}$  Bravais lattice is the smallest possible tile. Rescale the Bravais lattice by multiplying it by  $\mathbb{A}^{-1}$  - that sends it into the usual unit integer lattice. Generate all multiple tilings in the usual way, and rescale them back to the prime Bravais lattice  $\mathcal{L}_{\mathbb{A}}$  by multiplying with  $\mathbb{A}$ .

Pure unfounded speculation: as the prime orbit *unit* primitive cell increases in volume, the interactions are becoming more local to it, as the number of Laplacian connections to its neighbors is proportional to its boundary.

For that one would think that one needs a cumulant expansion of the Helmholtz 'free energy'  $W[\beta] = \ln Z[\beta]$ . But no:

Note that, as a special case, for a one-dimensional lattice field theory, lattice  $G = \mathbb{Z}$  and  $H = n\mathbb{Z}$ , where  $n \geq 1$ . Then the zeta function (??) is the Artin-Mazur zeta function

This zeta function applies equally well to multi-dimensional lattice field theories as to the time evolution problem.

where  $p$  is the label of prime orbit, and  $z_p = z^{L_p T_p}$ .  $L_p$  and  $T_p$  are the spatial period and temporal period of the prime orbit  $p$  in the Hermite normal form.

(the symbolic dynamics definitions used throughout the paper are collected in `refappe s-SymbDynGloss`).

**2023-03-25 Predrag** In the spirit of the time-evolution periodic orbit, we approach the infinite spacetime (??) by a hierarchy of lattice field configurations over periodic lattices (discrete  $d$ -tori), ordered by increasing spatiotemporal periods.

**2023-03-25 Predrag** Re. *hyperbolicity assumption*: Sounds too simple. What about temporal evolution complex eigenvalues of magnitude 1? There we have to worry about  $1 - \exp(ir\theta)$  coming close to 0 for some repeat  $r$ ?

**2023-03-25 Predrag** A given Bravais lattice  $\mathcal{L}$  can be defined by any of an infinity of equivalent primitive cells.

with matrix  $\mathbb{A}$  defining one of the Bravais lattice's infinity of equivalent primitive cells) to label given Bravais lattice-specific quantities

The discretized lattice fields we study in this paper are defined on the integer lattice, so it is sufficient to consider only the discrete translations from a sublattice of the integer lattice.

In what follows, we shall deal only with deterministic field theory (4.53) and mostly omit the subscript 'c' in  $X_c$  when referring to periodic states.

**2023-05-06 Predrag** Adopted this convention throughout: "... the basis vectors that define the lattice geometry, commonly referred to as 'primitive vectors' [29]"

**2023-05-25 Predrag** Dropped this(looks wrong):

where  $u_k(z)$  is a  $\mathcal{L}_{\mathbb{A}}$ -periodic function, and the  $k$ -band can be confined to the Brillouin zone  $k_j = 2\pi/\ell_j$  of the reciprocal lattice  $\tilde{\mathcal{L}}_{\mathbb{A}}$ , with  $\ell_j$  the  $\mathcal{L}_{\mathbb{A}}$  period along  $j$ th lattice direction.

The eigenstates of the translation operator  $r$  which satisfy the periodicity of the Bravais lattice  $\mathcal{L}_{\mathbb{A}}$  are then of form (see sect. ?? for details)

$$\varphi_k(r) = e^{ik \cdot r}, \quad k \in \mathcal{L}_{\mathbb{A}}. \quad (21.89)$$

If a discrete field configuration  $X$  is invariant under Bravais lattice translations (??),

$$x_{z+r} = x_z \quad \text{for all } r \in \mathcal{L}, \quad (21.90)$$

we say that the field configuration is Bravais lattice  $\mathcal{L}$ -periodic.

$[L \times T]_S = [2 \times 2]_0$  in the primitive cell:

$$X = \begin{bmatrix} b & a \\ a & b \end{bmatrix}.$$

This is a repeat of the field configuration:

$$X_p = [ a \quad b ]$$

with periodicity  $[L \times T]_S = [2 \times 1]_1$  in its primitive cell.

repeats of the three 'bricks', on top, sideways, and on top and shifted:

$$[2 \times 1]_0 \simeq \begin{bmatrix} a & b \\ a & b \end{bmatrix}, \quad [1 \times 2]_0 \simeq \begin{bmatrix} b & b \\ a & a \end{bmatrix}, \quad [2 \times 1]_1 \simeq \begin{bmatrix} a & a & b \\ a & b & \end{bmatrix}.$$

**2023-06-01 Han** Dropped from refsect s:POT:

former subsection *Deterministic partition sum in terms of prime orbits*

The deterministic partition sum (21.98) is the sum over all periodic states  $X_c$  over all Bravais lattices  $\mathcal{L}$ ,

$$Z[\beta] = \sum_c t_c, \quad t_c = e^{V_c(\beta \cdot \langle a \rangle_c - \langle \lambda \rangle_c) z^{V_c}}, \quad (21.91)$$

where  $t_c/Z[0]$  is the observable-weighted probability of periodic state  $X_c$ ,  $\langle \lambda \rangle_c$  the stability exponent (??) evaluated on the Bravais lattice  $\mathcal{L}_c$ , and  $z$  a bookkeeping variable that we use to organize generating functions and normalize the probabilities.

A periodic state  $X_c$  is either prime, or a repeat (sect. ??) of a prime orbit  $X_p$ . A prime orbit over  $\mathcal{L}_\mathbb{A}$  has the same Hill determinant (refsect s:JacobianOrb) and Birkhoff sum (4.122) for the  $V_\mathbb{A}$  periodic states in its  $G = C_{L_\mathbb{A}} \otimes C_{T_\mathbb{A}}$  translational group orbit (for time being we assume only translational symmetries, ignore the discrete point group of sect. ??). Its contribution to the deterministic partition sum (21.91) is

$$V_p t_p = \frac{V_p}{|\text{Det}_\mathbb{A} \mathcal{J}_p|} e^{\beta V_p a_p}, \quad V_p = V_\mathbb{A} = L_\mathbb{A} T_\mathbb{A}. \quad (21.92)$$

A prime orbit  $X_p$  over primitive cell  $\mathbb{A}$  is the smallest tile that tiles Bravais lattice  $\mathcal{L}_\mathbb{A}$ . One can view it as the irreducible *unit cell*  $[1 \times 1]_0$  of  $\mathcal{L}_\mathbb{A}$ , a square lattice  $\mathbb{Z}^d$ , with lattice field on site  $z$  now an  $V_\mathbb{A}$ -dimensional multiplet of lattice site fields within primitive cell  $\mathbb{A}$ . The repeats matrix  $\mathbb{R}$  (sect. ??), acting on the unit cell  $\mathbb{A}$

$$\mathbb{R} = \begin{bmatrix} r_1 & s \\ 0 & r_2 \end{bmatrix}, \quad \mathbb{A} = \begin{bmatrix} 1 & 0 \\ 0 & 1 \end{bmatrix}, \quad \mathbb{A}\mathbb{R} = \begin{bmatrix} r_1 & s \\ 0 & r_2 \end{bmatrix}, \quad (21.93)$$

generates all distinct  $\mathcal{L}_{\mathbb{A}\mathbb{R}}$  Bravais sublattices of  $\mathcal{L}_\mathbb{A}$ .



The wonderful thing about Bravais lattice  $\mathcal{L}_{\mathbb{A}}$  Hill determinant (??) (as opposed to a *finite volume* primitive cell  $\mathbb{A}$  Hill determinant (??)) is that it is multiplicative for the prime orbit  $X_p$  repeated over a larger  $\mathbb{A}\mathbb{R}$  primitive cell (sect. ??): the contribution of a repeat to the partition sum is

$$\frac{V_p}{|\text{Det}_{\mathbb{A}\mathbb{R}}\mathcal{J}_p|} e^{\beta V_{\mathbb{A}\mathbb{R}} a_p} = V_p t_p^{r_1 r_2}, \quad t_p = \left( e^{\beta \cdot \langle a \rangle_p - \langle \lambda \rangle_p - s} \right)^{V_p}, \quad z = e^{-s}, \quad (21.94)$$

where  $\exp(\beta \cdot \langle a \rangle_c - \langle \lambda \rangle_c + s)$  is the observable weighted probability density per lattice site, The sum over all prime orbits  $X_p$  and their repeats ( $\mathbb{A}\mathbb{R}$  primitive cells) yields deterministic partition sum  $Z[\beta]$  (21.91) expressed in terms of prime orbits  $X_p$ . For a two-dimensional square lattice this is

$$Z[\beta] = \sum_p Z_p[\beta], \quad Z_p[\beta] = V_p \sum_{r_1=1}^{\infty} \sum_{r_2=1}^{\infty} \sum_{s=0}^{r_1-1} t_p^{r_1 r_2}.$$

The  $V_p$  prefactor arises because all periodic states in the group orbit of a prime orbit  $X_p$  have the same weight. For each width  $r_1$ , height  $r_2$ , the number of Hermite normal form (??) relative periodic primitive cells  $[r_1 \times r_2]_s$  is

$$\sum_{s=0}^{r_1-1} 1 = r_1, \quad \text{so } Z_p[\beta] = V_p \sum_{r_1=1}^{\infty} \sum_{r_2=1}^{\infty} r_1 (t_p^{r_1})^{r_2}.$$

As the  $r_2$  sum is a geometric series, the deterministic partition sum (21.91)

$$Z[\beta] = \sum_p V_p \sum_{n=1}^{\infty} \frac{n t_p^n}{1 - t_p^n} \quad (21.95)$$

is expressed as the sum of all prime orbits and their repeats, the two-dimensional spacetime generalization of the temporal deterministic partition sum (21.160). The prime repeats sum

$$\begin{aligned} \frac{1}{V_p} Z_p[\beta] &= \sum_{n=1}^{\infty} \sigma(n) t_p^n \\ &= t_p + 3t_p^2 + 4t_p^3 + 7t_p^4 + 6t_p^5 + 12t_p^6 + 8t_p^7 + \dots, \end{aligned} \quad (21.96)$$

where  $\sigma(n)$  is the Euler **sum-of-divisors function**.

Given the deterministic partition sum, we can compute the expectation value (4.122) of an observable  $a_z = a(x_z)$ ,  $t_p = e^{-V_c \langle \lambda \rangle_c z V_c}$ ,<sup>6</sup>

$$\langle a \rangle = \left. \frac{\partial}{\partial \beta} \ln Z[\beta] \right|_{\beta=0} = \frac{1}{Z[0]} \sum_p V_p A_p t_p \sum_{\ell=1}^{\infty} \frac{\ell + \ell(\ell-1)t_p^\ell}{(1-t_p^\ell)^2}. \quad (21.97)$$

<sup>6</sup>Predrag 2023-05-06: This is wrong, recompute:

Now, in the deterministic partition sum (21.91) everything contributes to periodic state weights with positive signs, there are *no shadowing cancellations*. The smart thing is to replace the partition sum by the appropriate zeta function.

**2024-02-03 Predrag** Now the deterministic partition sum (??) takes form

$$Z_{\mathbb{A}}[\beta] = \sum_c Z_c, \quad Z_c = e^{V_{\mathbb{A}}(\beta \cdot a_c - \lambda_c)}, \quad (21.98)$$

where the sum is over all periodic states  $c$  with primitive cell periodicity  $\mathbb{A}$ , and

$$p_{\mathbb{A}}[X_c] = e^{-V_{\mathbb{A}} \lambda_c} / Z_{\mathbb{A}}[0] \quad (21.99)$$

is the probability (4.95) of periodic state  $X_c$ . What is this partition sum good for? To paraphrase Baxter [13]: “We are particularly interested in calculating the partition sum (21.98) per site,

$$e^W = Z^{1/V_{\mathbb{A}}}, \quad V_{\mathbb{A}} = LT,$$

[...]. We expect  $W$  to tend to limit when  $L, T \rightarrow \infty$ ”.

**2023-04-20 Han**  $d_{lt} = \mu^2(\delta_{lt} - 3x_{lt}^2) + 4\delta_{lt}$ .

**2023-05-17 Predrag** The square brackets  $[\dots]$  in quantities such as  $Z_{\mathbb{A}}[J]$  is a convention inherited from [quantum field theory](#) [30], where coordinate label are continuous, and  $Z$ 's are functionals. Here we work only with functions, do not take continuous limit, but we already use a lots of  $(\dots)$  as is. However, [Scholarpedia](#) uses  $\mathcal{Z}(\beta)$ , maybe  $(\dots)$  would be more consistent. In any case, using both  $Z[\beta, z]$  and  $\zeta(\beta, z)$  in (4.127) is not a good look, we might prefer  $\zeta[\beta, z]$  to emphasize this is a spatiotemporal field theory zeta function, rather than the temporal chaotic dynamics of few degrees of freedom dynamical zeta function.

**2023-06-20 Predrag** Dropped: with reciprocal lattice volume

$$V_{\mathbb{A}} = (2\pi)^d / |\det \mathbb{A}|. \quad (21.100)$$

An example is the fundamental parallelepiped

$$P_{\mathbb{A}} = \{\mathbb{A}\mathbf{x} \mid \mathbf{x} \in [0, 1)^2\} \quad (21.101)$$

generated by the action of matrix  $\mathbb{A}$  on the unit square.

Let  $M_d$  denote the set of all  $d$ -mosaics.

An example of a  $\mathcal{L}$ -periodic field configuration (??) is the two-dimensional spatiotemporal array of  $V_{\mathcal{L}} = 70$  field values over a rectangular primitive cell of spatial period  $L = 10$ , temporal period  $T = 7$ , sketched in

figure ??, ‘Unrolled’ over the two-dimensional infinite lattice, a periodic field configuration (??) field values are

$$x_{l't'} = x_{lt}, \quad l' = l \pmod{L}, \quad t' = t \pmod{T}. \quad (21.102)$$

An example is determination of periodic states, solutions of system’s Euler–Lagrange equation (4.53) which shall need to determine for a given field.

**2023-06-26 Predrag** Question to Han: currently we have 3 primitive cell notations:  $\mathbb{A}$ ,  $[L \times T]_S$  and the Hermite normal form (??). Would replacement to 2 notations,  $\mathbb{A}$  and replacing  $[3 \times 2]_1$  by  $\begin{bmatrix} 3 & 1 \\ 0 & 2 \end{bmatrix}$  help?

**2023-07-14 Han** I think  $[L \times T]_S$  is easy to understand. The primitive cell of a periodic state is a  $[L \times T]$  rectangular region, and there is a relative shift  $S$  at the boundaries. It also emphasizes that the periodicities are only determined by 3 parameters instead of 4. And more importantly, 2 by 2 matrices look very awkward in the text.

Throughout the paper, we denote by  $\mathbb{A}$  both the primitive vectors matrix (??), and the corresponding primitive cell  $[L \times T]_S$ .

For a two-dimensional lattice, the translational symmetry is a cyclic group along each dimension (??), restricted to a two-dimensional primitive cell  $\mathbb{A}$  shift operators (22.100).

with relative-periodic bc’s.

**2023-07-21 Predrag** The wave vectors of the eigenvalues land on the reciprocal lattice of  $[8 \times 8]_0$ , where  $k_1$  and  $k_2$  are multiples of  $\pi/4$ .

**2023-07-20 Predrag** *Trying to always do calculations on reciprocal lattice, from the very start. If the unit hypercube (??) is taken as primitive cell, the only periodic state is  $x_0$ , and the Bloch eigenstates (??) are all the constant  $x_0$ , as the only lattice point is  $z = 0$ , and  $\exp ik \cdot z = 1$ .*

$$\mathbf{X}^\top = (x_0, x_1, x_2, x_3, \dots, x_{n-1}). \quad (21.103)$$

In solid state physics [9], a primitive cell can have any shape in the underlying continuous coordinates space that, translated in all possible ways, tiles all of the space without a gap or an overlap.

For the  $d$ -dimensional spatiotemporal cat the repertoire of periodic tilings is richer. In  $d = 2$  and 3 the basic facts are well known both from crystallography, and from the number theory of integer lattices.

determine  $N_{[L \times T]_S}$ , the number of *doubly-periodic state* solutions, by evaluating the associated Hill determinants.

**2023-07-06 Predrag** Thinking about group-theory formulation of (??)...

Goal: construct all distinct subgroups of the abelian translation group (??).

General primitive cell (??) as a subgroup generator:

$$\{(r_1^{a_{11}} r_2^{a_{12}})^{n_1} (r_1^{a_{21}} r_2^{a_{22}})^{n_2} \mid n_j \in \mathbb{Z}\}, \quad (21.104)$$

the abelian translation subgroup of the translation group (??),  $T = C_{\infty,1} \otimes C_{\infty,2}$ ,

$$H_{[L \times T]_S} = \{(r_1^L)^{n_1} (r_1^S r_2^T)^{n_2} \mid n_j \in \mathbb{Z}\}, \quad (21.105)$$

periodic state is a fixed point of the two primitive cell translations

$$[\mathbf{1} - (r_1^L)(r_2^T r_1^S)]X_c = 0$$

and satisfies the Euler–Lagrange equation, with the two-dimensional space-time Laplace operator (??)

$$\square = r_1 + r_2 - 4\mathbf{1} + r_2^{-1} + r_1^{-1}, \quad (21.106)$$

written out in terms of lattice site fields

$$x_{nt} = x_{n+L+S,t+T}, \quad n = 0, 1, 2, \dots, L-1; \quad t = 0, 1, 2, \dots, T-1.$$

$$n_1 = 0, n_2 = 1$$

$$x_{nt} = x_{n+S,t+T}.$$

Example

$$H_{[2 \times 1]_1} = \{(r_1^2)^{n_1} (r_2^1 r_1^1)^{n_2} \mid n_j \in \mathbb{Z}\}, \quad (21.107)$$

$$x_{nt} = x_{n+2+1,t+1}.$$

$$r_1^L \square = r_1 + r_2 - 4\mathbf{1} + r_2^{-1} + r_1^{L-1}$$

$$r_1^S r_2^T \square = r_1^{S+1} + r_1^S r_2 - 4r_1^S + r_1^S r_2^{T-1} + r_1^{S-1}$$

the diagonalized, reciprocal lattice orbit Jacobian matrix is

$$(\tilde{\mathcal{J}}_{\mathbb{A}})_{m_1 m_2} = [4 \sin^2(k_{m_1}/2) + 4 \sin^2(k_{m_2}/2 - k_{m_1} S/2T) + \mu^2].$$

**2024-02-08 Han** as the partition sum has a support on *all* Bravais lattices. In illustrating this, the calculation of steady state primitive cell stability of sects. ?? and ?? is particularly helpful. For both linear and nonlinear field theories, steady states  $x_z = x$ , whose primitive cell is the hypercubic unit cell (??), have orbit Jacobian matrices (4.107)–(4.109) with a single, constant stretching factor  $d_z = s$ .

2023-06-23 Predrag .

$$\tilde{X} = \begin{array}{cccccc} \cdots & \cdots & \cdots & \cdots & \cdots & \cdots & \cdots \\ \cdots & \tilde{\phi}_{-2,1} & \tilde{\phi}_{-1,1} & \tilde{\phi}_{0,1} & \tilde{\phi}_{1,1} & \tilde{\phi}_{2,1} & \cdots \\ \cdots & \tilde{\phi}_{-2,0} & \tilde{\phi}_{-1,0} & \tilde{\phi}_{0,0} & \tilde{\phi}_{1,0} & \tilde{\phi}_{2,0} & \cdots \\ \cdots & \tilde{\phi}_{-2,-1} & \tilde{\phi}_{-1,-1} & \tilde{\phi}_{0,-1} & \tilde{\phi}_{1,-1} & \tilde{\phi}_{2,-1} & \cdots \\ \cdots & \cdots & \cdots & \cdots & \cdots & \cdots & \cdots \end{array} \quad (21.108)$$

[5 × 3] torus field configuration

$$\tilde{X} = \begin{bmatrix} \tilde{\phi}_{-2,1} & \tilde{\phi}_{-1,1} & \tilde{\phi}_{0,1} & \tilde{\phi}_{1,1} & \tilde{\phi}_{2,1} \\ \tilde{\phi}_{-2,0} & \tilde{\phi}_{-1,0} & \tilde{\phi}_{0,0} & \tilde{\phi}_{1,0} & \tilde{\phi}_{2,0} \\ \tilde{\phi}_{-2,-1} & \tilde{\phi}_{-1,-1} & \tilde{\phi}_{0,-1} & \tilde{\phi}_{1,-1} & \tilde{\phi}_{2,-1} \end{bmatrix} \quad (21.109)$$

**2023-05-20 Predrag** The number of periodic states is then given by the Hill determinant of the orbit Jacobian matrix, which is the product of the eigenvalues:

$$N_{[L \times T]_S} = 2^{LT} \prod_{k_1=0}^{L-1} \prod_{k_2=0}^{T-1} \left[ s - \cos\left(\frac{2\pi k_1}{L}\right) - \cos\left(\frac{2\pi k_2}{T} - \frac{2\pi k_1 S}{L T}\right) \right] \quad (21.110)$$

As the field has support on the square lattice sites, it suffices to use the wave vectors  $k = n_1 \tilde{a}_1 + n_2 \tilde{a}_2$  with  $n_1$  from 0 to  $L - 1$  and  $n_2$  from 0 to  $T - 1$  to get all the reciprocal lattice eigenvectors.

**2023-07-23 Predrag** (1) Inverts the lattice, with all primitive cells  $\mathbb{A}$ , no matter how large...

(2) diagonalizes  $r$  operator.

**2023-06-19 Predrag** Move to ChaosBook: In refsect s:CCMs we review the traditional coupled map lattice model discretizations of dissipative PDEs, as well as many-body Hamiltonian models, refsect s:HCCMs.

**2023-07-23 Predrag** The cyclic group  $C_n$  elements are generated by the  $[n \times n]$  shift matrix (??) which translates a periodic state forward-in-time by one site,  $(rX)^\top = (x_1, x_2, \dots, x_{n-1}, x_0)$ . After  $n$  shifts, the periodic state returns to the initial state, yielding the characteristic equation for the matrix  $r_j$

$$r_1^L - \mathbf{1} = 0, \quad r_2^T - \mathbf{1} = 0, \quad (21.111)$$

and share its discrete Fourier eigenstates

$$\varphi_k(z) = e^{ik \cdot z}, \quad k \in (2\pi\mathbb{Z})^d. \quad (21.112)$$

$r_{\mathbb{A},j}$  shift operators with  $(r_{\mathbb{A},1})_{L+1,tL,t'} = (r_{\mathbb{A},1})_{1,tL,t'} = 1$  matrix element enforcing the spatial periodicity  $L$

$$(r_{\mathbb{A},1})_{nt\ n't'} = \begin{pmatrix} 0 & 1 & & & \\ & 0 & 1 & & \\ & & \ddots & \ddots & \\ & & & 0 & 1 \\ 1 & & & & 0 \end{pmatrix}_{nn'} \begin{pmatrix} 1 & & & & \\ & 1 & & & \\ & & \ddots & & \\ & & & 1 & \\ & & & & 1 \end{pmatrix}_{tt'} \quad (21.113)$$

and

$$(r_{\mathbb{A},2})_{nt\ n't'} = \begin{pmatrix} 1 & & & & \\ & 1 & & & \\ & & \ddots & & \\ & & & 1 & \\ & & & & 1 \end{pmatrix}_{nn'} \begin{pmatrix} 0 & 1 & & & \\ & 0 & 1 & & \\ & & \ddots & \ddots & \\ & & & 0 & 1 \\ \dots & \dots & \dots & \dots & \dots \end{pmatrix}_{tt'} \quad (21.114)$$

with  $(r_{\mathbb{A},2})_{n,T+1\ n'T} = (r_{\mathbb{A},2})_{n,t\ n',T} = 1$  matrix element enforcing the temporal periodicity  $T$  and tilt  $S$ .

Fundamental fact states that a torus mapped by an integer matrix  $\mathcal{J}$  will cover itself exactly  $|\text{Det } \mathcal{J}|$  times.

Consider temporal cat. The orbit Jacobian matrix  $\mathcal{J}$  stretches the phase space unit hypercube  $X \in [0, 1)^n$  into the  $n$ -dimensional *fundamental parallelepiped*, and maps each periodic state  $X_M$  into an integer lattice  $\mathbb{Z}^n$  site, which is then translated by the winding numbers  $M$  into the origin, in order to satisfy the Euler–Lagrange equation (??). Hence  $N_n$ , the total number of the solutions of the Euler–Lagrange equation equals the number of integer lattice points within the fundamental parallelepiped, a number given by what Baake *et al.* [10] call the ‘*fundamental fact*’,

$$N_n = |\text{Det } \mathcal{J}|, \quad (21.115)$$

i.e., fact that the number of integer points in the fundamental parallelepiped is equal to its volume, or, what we refer to as its Hill determinant.

**2023-08-16 Predrag** (see [ChaosBook 22.5 Spectral determinants vs. dynamical zeta functions](#)).

(see (??))

throughout, as in crystallography.

Experimentalist’s sample of a crystal is finite, but it has some  $10^{23}$  lattice sites, so it would never occur to anyone to first compute a small crystal of, let’s say, 4 lattice sites, than double that, redo the calculation, and so on. No, ...

Politi ..., with orbit weights depending exponentially both on the space and the time variables,  $\propto e^{-LT\lambda_p}$ .

The spatiotemporal symmetries of the lattice discretization play a crucial role in determining the form of the partition sum.

In the field-theoretic formulation, dynamical systems time-periodic orbits are replaced by  $d$ -dimensional periodic Bravais tilings of spacetime.

In refsect s:catlatt we generalize the temporal cat model to the  $d$ -dimensional *spatiotemporal* cat, and show that the system admits a  $d$ -dimensional symbolic code with a finite alphabet.

We return to the computation of the spectra of orbit Jacobian matrices in sect. ??.

We discuss stability in more detail in refsect s:JacobianOrb, and

The form of the partition sum is to a large extent determined by the symmetries of the theory, i.e., by the space group of its lattice discretization discussed in sect. ??

Sect. ?? illustrates our periodic state spatiotemporal cat solutions by several explicit examples.

**2019-08-06 Predrag** In appendix ?? we enumerate prime orbits of two-dimensional spatiotemporal cat and check the evaluation of the Hill determinant.

Appendix ?? tabulates our prime periodic orbits counts.

**2023-08-05 Predrag** The lattice site field is on a circle, so  $|x_z - x'_z| \leq 1/2$ . Are you possibly making errors when  $x_z$  is close to 1,  $x'_z$  close to 0, for example? Then  $|x_z - x'_z| \approx x'_z$ , not  $|x_z - x'_z| \approx 1$ .

**2023-07-23 Predrag** A circulant matrix is constant along each diagonal,

$$C = \begin{pmatrix} c_0 & c_{n-1} & \cdots & c_2 & c_1 \\ c_1 & c_0 & c_{n-1} & & c_2 \\ \vdots & c_1 & c_0 & \ddots & \vdots \\ c_{n-2} & & \ddots & \ddots & c_{n-1} \\ c_{n-1} & c_{n-2} & \cdots & c_1 & c_0 \end{pmatrix}, \quad C_{jk} = c_{j-k}, \quad (21.116)$$

diagonalizable by a discrete Fourier transform,

$$U^\dagger C U = \text{diag}(\lambda), \quad U_{jk} = \frac{1}{\sqrt{n}} \epsilon^{(j-1)(k-1)}, \quad (21.117)$$

with discrete Fourier mode eigenvectors

$$\tilde{e}_k = \frac{1}{\sqrt{n}} (1, \epsilon^k, \epsilon^{2k}, \dots, \epsilon^{k(n-1)})^T, \quad k = 0, 1, \dots, n-1, \quad (21.118)$$

and eigenvalues  $C \tilde{e}_k = \lambda_k \tilde{e}_k$ ,

$$\lambda_k = c_0 + c_{n-1} \epsilon^k + c_{n-2} \epsilon^{2k} + \dots + c_1 \epsilon^{k(n-1)}, \quad (21.119)$$

where

$$\epsilon = e^{2\pi i/n} \tag{21.120}$$

is an  $n$ th root of unity.

where the  $\tilde{X}_k$  and  $\tilde{M}_k$  are the  $k$ th Fourier modes of the periodic state  $X$  and symbol block  $M$ :

$$\tilde{X}_k = (\tilde{e}_k^\top X) \tilde{e}_k, \quad \tilde{M}_k = (\tilde{e}_k^\top M) \tilde{e}_k. \tag{21.121}$$

**2023-08-31 Predrag** Dropped this: The discrete Fourier transform reciprocal lattice state  $\tilde{X}$  is a *point* in system's *reciprocal* phase space

$$\mathcal{M}_{\tilde{A}} = \{ \tilde{X} \mid \tilde{\phi}_k \in \mathbb{C} \}. \tag{21.122}$$

**2023-07-23 Predrag** .

22 centuries might have passed, but we are in the same boat as Greek astronomers, as by discretizing compact lattices we are replacing circle arcs by cords.

It is conventional to visualize a Bravais lattice  $\mathcal{L}$  by tiling it with repeats of a primitive cell  $\mathbb{A} = [L \times T]_S$ , as in figure ?? . In calculations, however, we often find it convenient to use a *rectangular*  $[L \times T]$  primitive cell, and impose the relative-periodic shift as a boundary condition, translating the successive layers of field configuration ‘bricks’ by shift  $S$ , as in figure ?? .

In the lattice formulation, the two-dimensional spatiotemporal cat happens to involve two quite distinct lattices:

- (i) In the latticization of a spacetime continuum, one replaces a spacetime-dependent field  $x(x, t)$  at spacetime point  $(x, t) \in \mathbb{R}^2$  of *any* field theory by a discrete set of its values  $x_{nt} = x(n\Delta L, t\Delta T)$  on lattice sites, where the index  $(n, t) \in \mathbb{Z}^2$  is a discrete two-dimensional spacetime *coordinate* over which the field  $x$  lives. We describe the properties of this integer lattice  $\mathbb{Z}^2$  and its sublattices in sect. ?? .
- (ii) A peculiarity of the spatiotemporal cat is that the *field*  $x_{nt}$  (??) is confined to the unit interval  $[0, 1)$ , imparting a  $\mathbb{Z}^1$  lattice structure –in any spacetime dimension  $d$ – onto the computationally intermediate fundamental parallelepiped  $\mathcal{J}$  basis vectors (see, for example, (21.71)).

**2023-07-25 Predrag** In LC21.tex we called the eigenvectors ‘ $\psi$ ’ rather than ‘ $\varphi$ ’. Do that here for consistency?

**2023-09-03 Predrag** Gave up on making up a  $[3 \times 2]_0 \rightarrow \mu^2(\mu^2 + 3)^2(\mu^2 + 4)(\mu^2 + 7)^2$  example.



**2023-09-09 Predrag** Dropped:

but for the integer spatiotemporal lattice (4.46), the lattice spacing takes now a non-integer value  $2\pi/n$ .

This is a one-dimensional example of a reciprocal lattice, with the  $n$  distinct wave numbers (??) contained within the  $k \in [0, 2\pi)$  interval.

A period- $n$  field configuration  $X$  expressed in the  $\varphi(k)$  basis is its discrete Fourier transform  $\tilde{X} = \{\tilde{\phi}_k\}$ .

**2023-09-09 Predrag** (4.49) Dropped:

that define the  $d$ -dimensional primitive cell

with the wave number spacing along  $j$ th direction

$$2\pi/L_j, \quad j = 1, \dots, d, \quad (21.123)$$

where  $L_j$  is the extent of the primitive cell  $\mathbb{A}$  in  $j$ th direction.

The reciprocal primitive cell  $\tilde{\mathbb{A}}$  contains only a single lattice site.

Any parallelepiped of the reciprocal lattice volume  $(2\pi)^d$  –see the light grey lines in figure ?? (b)– can serve as the Brillouin zone.

**2023-08-10 Predrag** I find the angle  $\theta = k_2 - k_1 S/T$  hard to understand.

$$k_2 = \frac{2\pi}{LT}(-m_1 S + m_2 L)$$

**2017-09-18 Predrag**

$$p = \frac{1}{2i}(S - S^\dagger)$$

Does not work for us. It gives, for example, 1/5th of a circle eigenvalues  $0, \pm \sin(2\pi/5), \pm \sin(4\pi/5)$  (full angle) but we need 1/2 angle...

**2023-09-10 Predrag** Dropped:

By construction, each orbit is a fixed point of  $G$ . For one-dimensional temporal evolution dynamical systems this is a familiar fact: periodic points of a period- $n$  orbit are fixed points of the  $n$ th iterate of system's forward-in-time mapping. Here this is generalized to prime orbits of multi-periodic, higher-dimensional lattices' field configurations.

(or  $G$ -orbits)

Lattice  $\mathcal{L}_{\mathbb{A}}$  is relatively prime with respect to sublattice  $\mathcal{L}_{\mathbb{A}\mathbb{R}}$  in the sense that  $r_1 r_2$  translational copies of the primitive cell  $\mathbb{A}$  fully tile the sublattice primitive cell  $\mathbb{A}\mathbb{R}$ . Dudgeon and Mersereau [40] explain how to get the quotient  $\mathbb{A}$  when dividing  $\mathbb{A}\mathbb{R}$  by  $\mathbb{R}$ , but, as we shall show in sect. ??, there is no need to explore further the notion of 'prime' on the level of Bravais lattices.

10. The Bloch theorem: compute the Brillouin zone bands,

2. Find prime orbits for each, their Brillouin zone eigenvalues
4. Work with the corresponding sublattice  $\mathcal{L}_p$  on the reciprocal state - there is a 2-dimensional band surface for each eigenvalue of  $\mathcal{J}_p$ .

**2023-09-14 Predrag** Dropped: Now that we have derived the new, spatiotemporal zeta function, the paper is finished. However, there are still a couple of loose ends left to tie up that the reader is free to ignore.

**2023-10-11 Predrag** 2 Han: Please think this through. I might have forgotten the entropy (see Pesin's formula, connecting Kolmogorov entropy and the Lyapunov exponent, [ChaosBook eq. \(A33.16\)](#)). I think not. Due to probability conservation, the escape rate  $\gamma = 0$ .

**2023-09-26 Predrag** Rewrote this:

**Time-equilibria over  $[L \times 1]_0$ .** Consider the time-equilibrium  $x_{nt} = x_{n1}$  for all spatial sites  $n$ , and all times  $t$ . To see that this is the one-dimensional lattice temporal cat tiles of period  $L$  already counted in ref. [67], note that the 5-term recurrence relation (??) reduces to the 3-term recurrence

$$x_{n+1,1} - 2(s_2 - 1)x_{n1} + s_{n1} + x_{n-1,1} = 0, \quad (21.124)$$

where we have temporarily added index '2' to the stretching parameter  $s_2$  to indicate that it refers to the two-dimensional spatiotemporal cat. Comparing with the temporal cat (??),  $x_{t+1} - s_1 x_t + x_{t-1} = -s_t$ , we see that we have already counted all periodic states on primitive cells of form  $[L \times 1]_0$ , provided we replace  $s_1 \rightarrow 2(s_2 - 1)$  in

$$\begin{aligned} \sum_{n=0}^{\infty} N_n z^n &= \frac{2 - sz}{1 - sz + z^2} - \frac{2}{1 - z} \\ &= (s - 2) [z + (s + 2)z^2 + (s + 1)^2 z^3 \\ &\quad + (s + 2)s^2 z^4 + (s^2 + s - 1)^2 z^5 + \dots] \end{aligned} \quad (21.125)$$

For the values chosen in our numerical examples,  $s_1 = 3$  and  $s_2 = 5/2$ , the two counts happen to be the same and given by (21.125).

However, already the smallest *relative*-periodic  $[L \times 1]_S$  Bravais lattices are new, and perhaps surprising.

**Relative  $[2 \times 1]_1$  periodic state.**

Consider a  $[2 \times 1]_1$  periodic state with tilt periodic bc's, periodic state  $X_{s_1 s_2} = [x_1 \ x_2]$ , tiled by the Bravais lattice (??) with primitive vectors  $\mathbf{a}_1 = \{2, 0\}$  and  $\mathbf{a}_2 = \{1, 1\}$ , see figure ?? (a).<sup>7</sup>

$$X_{\underline{s}s} = \frac{1}{9} \begin{bmatrix} -s & s \end{bmatrix}, \quad s \in \mathcal{A}, \quad (21.126)$$

<sup>7</sup>Predrag 2020-02-23: This is wrong, it is written for the symmetric alphabet that we do not use. Fix.

for example

$$M = \begin{bmatrix} -4 & 4 \end{bmatrix} \Rightarrow X_{44} = \frac{1}{9} \begin{bmatrix} -4 & 4 \end{bmatrix}.$$

Note that these are ‘periodic state’ solutions: there is one *prime orbit* for each set of period-2 periodic states related by cyclic permutations,  $\overline{ss} = (X_{ss}, X_{ss})$ , and there are only 4 of those, as  $X_{00} = X_0$  is a repeat of the 1-block.

By (??) the number of  $[2 \times 1]_1$  relative periodic states with the given Bravais lattice bc’s is 9. Using the Green’s function method (??) one can verify that there are indeed 9 such periodic states, one periodic state solution for each letter of alphabet (??),

$[2 \times 1]_0$  **periodic state.**

To determine the *admissible* mosaics,

(7) compute  $X_p$  for each prime mosaic  $M_p$ , and eliminate every  $X_p$  which contains a lattice site or sites on which the value of the field violates the admissibility condition  $x_z \in [0, 1)$ .

$[3 \times 2]_0$  *periodic state.* For  $s = 5/2, \mu^2 = 1$  spatiotemporal cat only 850 prime  $[3 \times 2]_0$  mosaics are admissible. There are 5 admissible repeating prime  $[3 \times 1]_0$  mosaics, 2 admissible repeating prime  $[1 \times 2]_0$  mosaics, and 1 admissible mosaic which is a repeat of 0. The total number of admissible solutions obtained by all cyclic permutations of admissible prime mosaics is:

$$N_{[3 \times 2]_0} = 5120 = 850 [3 \times 2]_0 + 5 [3 \times 1]_0 + 2 [1 \times 2]_0 + 1 [1 \times 1]_0, \quad (21.127)$$

summarized in table 9.1. The count is in agreement with the Hill determinant formula (4.30) for the  $[3 \times 2]_0$  periodic states.

*Example: Relative  $[2 \times 2]_0$  periodic state.*

According to (9.1), the number of prime  $[2 \times 2]_0$  periodic states is

$$M_{[2 \times 2]_0} = \frac{1}{2 \cdot 2} (N_{[2 \times 2]_0} - 2M_{[2 \times 1]_0} - 2M_{[1 \times 2]_0} - 2M_{[2 \times 1]_1} - M_{[4 \times 1]_0}) \quad (21.128)$$

We can work this out explicitly as follows:

(3) The  $[2 \times 1]_1$  relative-periodic mosaic ??refeq eq:block2x1rp is counted as the  $[2 \times 2]_0$  periodic state.

(5) Throw away all mosaics which are repeats of smaller mosaics.

*Example:  $[3 \times 2]_0$  Bravais lattices prime mosaics.*

According to (9.1), the number of prime  $[3 \times 2]_0$  periodic states is

$$M_{[3 \times 2]_0} = \frac{1}{3 \cdot 2} (N_{[3 \times 2]_0} - 3M_{[3 \times 1]_0} - 2M_{[1 \times 2]_0} - M_{[1 \times 1]_0}) \quad (21.129)$$

Unlike the  $[2 \times 2]_0$  case, there are no sub-mosaics with relative-periodic boundary contributing to the  $[3 \times 2]_0$  mosaics count, since  $[3 \times 1]_0$  and  $[1 \times 2]_0$  sub-mosaics cannot fit into the  $[3 \times 2]_0$  doubly-periodic Bravais lattice without a shift.

**2020-10-03 Predrag** For periodic boundary conditions, the Laplacian  $\square$  in (??) and (??) has a translational zero mode,  $\lambda_0 = 0$ , corresponding to a constant eigenvector, so the matrix  $\square$  is singular. That is the reason why our counting formulas (21.125) and table 9.3 have a prefactor  $(s - 2)$ ; in the Laplacian limit the corresponding determinant has a zero eigenvalue, and therefore vanishes.

**2020-02-08 Predrag** Note:  $N_2 = \text{Det } \mathcal{J} = (s - 2)(s + 2)$ ,  $N_3 = (s - 2)(s + 1)^2$ ,  $N_4 = (s - 2)(s + 1)s^2$ ,  $N_5 = (s - 2)(s^2 + s - 1)^2$ . I think the factorization is true for all  $n$ , as the  $s = 2$  Laplacian has a zero mode (constant  $x_i$ , I think).

an sequence of non-negative integers counting the orbits of a map; the sequence of periodic points for that map.

**2023-09-14 Predrag** In other words: on the reciprocal lattice any infinite Bravais lattice is mapped into the same compact Brillouin zone, of width  $2\pi$  in each lattice direction. A fact familiar from the discrete Fourier transform of an infinite chain, generalized to multi-dimensional periodic lattices.

**2024-02-08 Predrag** As we shall now show, for higher-dimensional lattices the notion of 'prime' is subtler than for a one-dimensional lattice. We develop it in two stages, first for the integer lattice *coordinate* system, sect. ??, and then for the *field configurations* over these coordinates, sect. ??.

**2023-12-03 Predrag** is helpful in illuminating the relation between the Klein-Gordon mass  $\mu^2$  and the stability of a periodic state  $c$ .

$$a[X_c]_j = \ln |\Lambda_{c,j}|, \quad (21.130)$$

Using the partition sum our goal is to compute the expectation values of observables in large spatiotemporal domains.

$$[\varphi^{(\alpha)}(\mathbf{k})]_z = e^{i\mathbf{k} \cdot \mathbf{z}} [u^{(\alpha)}(\mathbf{k})]_z, \quad z \in \mathbb{A}, \mathbf{k} \in \mathbb{B},$$

Using these eigenstates one can compute the eigenvalues of orbit Jacobian matrices as functions of  $k$ .

The most important observation for what follows is that while each primitive cell  $\mathbb{A}$  repeat has its own complicated discrete orbit Jacobian matrix spectrum, for the Bravais lattice  $\mathcal{L}_{\mathbb{A}}$  there is *only one* continuous orbit Jacobian operator Bloch band. Why is that?

The primitive cell  $P_{\mathbb{A}\mathbb{R}}$  obtained by repeating this tile  $r_1$  times horizontally and  $r_2$  times along the ‘slanted’ primitive vector  $\mathbf{a}_2 = (S, T)$ ,

$$\mathbb{A}\mathbb{R} = \begin{bmatrix} r_1 L & sL + r_2 S \\ 0 & r_2 T \end{bmatrix}, \quad \mathbb{A} = \begin{bmatrix} L & S \\ 0 & T \end{bmatrix}, \quad \mathbb{R} = \begin{bmatrix} r_1 & s \\ 0 & r_2 \end{bmatrix}, \quad (21.131)$$

$0 \leq s < r_1$ , results in a larger rectangular tile / primitive cell that defines a sublattice  $\mathcal{L}_{\mathbb{A}\mathbb{R}}$ . The ‘slant’ component  $sL + r_2 S$  is taken  $\pmod{(r_1 L)}$ , and the repeat numbers are positive integers,  $r_j \geq 1$ .

The ‘slant’ component  $sL + r_2 S$  is taken  $\pmod{(r_1 L)}$ , and the repeat numbers are positive integers,  $r_j \geq 1$ .

The action of shift  $r_j$  in the Laplacian (??) is to cyclically permute lattice site fields, as in (??) and (??):

$$\tilde{\mathcal{J}} = (\mathbf{p}^2 + \mu^2) \mathbf{1}, \quad \mathbf{p}^2 = \sum_{j=1}^d p_j^2, \quad p_j = 2 \sin \frac{k_j}{2},$$

$$\begin{aligned} [\mathcal{J}_{\mathbb{A}}\varphi(k)]_z &= (4\mathbf{1} - r_1 - r_1^{-1} - r_2 - r_2^{-1} + \mu^2) e^{i[k_1 z_1 + (k_2 - k_1 \frac{S}{T}) z_2]} \\ &= (4 - 2 \cos k_1 - 2 \cos(k_2 - k_1 S/T) + \mu^2) [\varphi(k)]_z. \end{aligned}$$

Replacing ‘ $\cos(\dots)$ ’s with lattice momenta  $p$ , as in (??),

The ‘brick’ outlined in (9.18) is the rectangular primitive cell depicted in figure ?? (b), with momentum squared  $\mathbf{p}^2$  taking values on reciprocal lattice sites  $m_1 m_2$ .

$$(\tilde{\mathcal{J}}_{\mathbb{A}})_{m_1 m_2} = p(k_1)_{m_1 m_2}^2 + p(k_2)_{m_1 m_2}^2 + \mu^2. \quad (21.132)$$

**2024-03-26 Predrag** *Lorenz and modular flows: a visual introduction* Amer. Math. Soc. Feature Column (2006).

While we make no use of this parametrization here (reader might enjoy Ghys and Leys [48] visual introduction to the subject), the Dedekind eta function  $\eta(\tau)$  will come to play a key role in sect. ??.

**2024-03-26 Predrag** Dropped from sect. ??:

instead of a discrete set of points as (??).

**2024-02-06 Predrag** Use this?

$$\tilde{\mathbb{A}} = \frac{2\pi}{\tau_2} \begin{bmatrix} \tau_2 & 0 \\ -\tau_1 & 1 \end{bmatrix}. \quad (21.133)$$

2024-02-17 **Predrag** REUSE THIS:

An example, worked out in sect. ??, is given in figure ?? (b).

2024-04-05 **Han** Not used in this paper:

The reciprocity condition (??) maps a field configuration  $X$  (??) over the primitive cell  $\mathbb{A}$  into the reciprocal field configuration  $\tilde{X}$  over  $V_{\mathbb{A}}$  reciprocal lattice sites  $k$  within the interior of the reciprocal primitive cell  $\tilde{\mathbb{A}}$  (the shaded parallelogram in figure ?? (b)). The reciprocal phase space (the space of discrete Fourier coefficients),

$$\mathcal{M}_{\tilde{\mathbb{A}}} = \left\{ \tilde{X} \mid \tilde{\phi}_k \in \mathbb{C}, k \in \tilde{\mathbb{A}} \right\}, \quad (21.134)$$

is naturally foliated by orbits: on the reciprocal lattice all field configurations in an orbit such as (??) have the same magnitude  $|\tilde{\phi}_k|$  reciprocal lattice site fields, with a translation in  $j$ th direction  $X \rightarrow r_j X$  only affecting their phases (??).

2024-04-23 **Predrag** Dropped:

The shift  $r$  thus acts by rotating the eigenvector's overall phase.

The reciprocal lattice orbit Jacobian matrix evaluated above in (??) is the special, tilt  $S = 0$ , rectangular primitive cell case.

and the weight (??) is a functional determinant [44].

the Bravais lattice eigenvalue spectrum consists of  $n$  continuous Brillouin zone bands  $\Lambda(k)$  and Bloch eigenstates (??)

The key tool that a crystallographer uses next is

Its stability is the stability of a constant state, with any primitive cells  $\mathbb{A}$  tiled by repeats of the unit hypercube (??) primitive cell periodic state.

$$(\mathcal{J}_c)_{zz'} = \frac{\delta F[X_c]_z}{\delta x_{z'}}, \quad z \in \mathbb{Z}^d, \quad (21.135)$$

orbit Jacobian operator (4.103) does not depend on the field values at each lattice site, so the periodicity of the orbit Jacobian operator is given by the integer lattice  $\mathbb{Z}^2$ , with the corresponding reciprocal lattice  $(2\pi\mathbb{Z})^2$ . Any square of area  $(2\pi)^2$  can serve as the Brillouin zone, with Bloch eigenstates (??),

$$\tilde{\mathcal{J}}\varphi(k)_z = (p^2 + \mu^2)\varphi(k)_z. \quad (21.136)$$

The determinant of the infinite-dimensional orbit Jacobian operator is computed using the Bloch theorem, with the eigenstates of a linear operator acting on a Bravais lattice  $\mathcal{L}_{\mathbb{A}}$  of the form (??) where  $u_k(z)$  is a function with periodicity  $\mathcal{L}_{\mathbb{A}}$ , wave vector  $k$  within the Brillouin zone of  $\mathbb{B}$ . (see sect. ??).

For two-dimensional lattice field theories, the periodicities of the orbit Jacobian operators are given by two-dimensional Bravais lattice  $\mathcal{L}_{[L \times T]_S}$  (??) instead of only a temporal period. The Bloch eigenstate (??) is a continuous function of the wave vector  $\mathbf{k}$  over the reciprocal lattice Brillouin zone  $\mathbb{B}$  of the Bravais lattice  $\mathcal{L}_{[L \times T]_S}$ .

References Guttman. The answer might be expressible in terms of the [complete elliptic integral of the first kind](#).

**2023-12-03 Predrag** Associated with the Hill determinant (??) is the spectral zeta function, the sum over its non-zero eigenvalues

$$\zeta(\beta) = \sum_k |\Lambda_k|^{-\beta}. \quad (21.137)$$

The two are related by

$$\ln \text{Det } \mathcal{J} = \sum_k \ln |\Lambda_k| = - \left. \frac{d}{d\beta} \sum_k |\Lambda_k|^{-\beta} \right|_{\beta=0},$$

so

$$\text{Det } \mathcal{J} = e^{-\zeta'(0)}. \quad (21.138)$$

When the finite dimensional matrix is replaced by the operator  $\mathcal{J}$  having infinitely many eigenvalues, the eigenvalue product (??) is in general not defined. However, the definition (21.138) makes perfect sense: Ray and Singer [86] define the zeta-regularized determinant as

$$\text{Det } \mathcal{J} = \prod_{n=1}^{\infty} \Lambda_n := e^{-\zeta'(0)} \quad (21.139)$$

(the zero eigenvalue of  $\mathcal{J}$  is not taken into the product).

**2024-02-17 Predrag** The stability exponent  $\langle \lambda \rangle$  of an infinite periodic state is:

$$\langle \lambda \rangle = \frac{1}{4\pi^2} \int_{-\pi}^{\pi} dk_1 \int_{-\pi}^{\pi} dk_2 \ln (2s - 2 \cos k_1 - 2 \cos k_2). \quad (21.140)$$

**2024-02-08 Predrag** whose generating function is the analytically elegant topological zeta function [57].

**2020-01-28 Han** The simplest way to prove that the product of cosines gives a Chebyshev polynomial is to use Grashteyn and Ryzhik [50] identity 1.395.2:

$$\cosh nx - \cos ny = 2^{n-1} \prod_{k=0}^{n-1} \left\{ \cosh x - \cos \left( y + \frac{2k\pi}{n} \right) \right\}. \quad (21.141)$$

Let  $y = 0$ ,  $\cosh x = s/2$ , and multiply both side by 2, (21.141) becomes:

$$\prod_{k=0}^{n-1} \left\{ s - 2 \cos\left(\frac{2k\pi}{n}\right) \right\} = 2\{\cosh[n \operatorname{arcosh}(s/2)] - 1\}. \quad (21.142)$$

By the definition of the Chebyshev polynomials of the first kind,

$$T_n(x) = \cosh(n \operatorname{arcosh} x), \quad \text{if } x \geq 1,$$

the right hand side of (21.142) is  $2T_n(s/2) - 2$ , same as (21.153).

2018-12-01 Han Wu [96] proves that:

$$\prod_{m=0}^{n-1} \left( 2 \cosh \lambda - 2 \cos \frac{2\pi}{n} m \right) = 2^n \sinh^2(n\lambda/2).$$

$$2 \sinh(n\lambda/2) = \Lambda^{n/2} - \Lambda^{-n/2}$$

$$s = 2 \cosh \lambda = e^\lambda + e^{-\lambda} = \Lambda + \Lambda^{-1} = \mu^2 + 2$$

$$2 - 2 \cos \frac{2\pi}{n} m = 4 \sin^2 \frac{2\pi}{n} \frac{m}{2}$$

2023-07-23 Predrag The Chebyshev polynomials of the first kind [20] satisfy  $T_n(\cos(x)) = \cos(nx)$ , for  $x = 2\pi k/n$ ,  $k = 0, 1, \dots, n - 1$ .  $\cos(2\pi k/n)$  is the  $k$ th root of equation

$$T_n(x) - 1 = 0,$$

which, written as a product over the eigenvalues

$$2T_n(x) - 2 = 2^n \prod_{k=0}^{n-1} [x - \cos(2\pi k/n)]. \quad (21.143)$$

For  $x = s/2$ , this is the Hill determinant formula (21.153)

$$|\operatorname{Det} \mathcal{J}| = \prod_{k=0}^{n-1} [s - 2 \cos(2\pi k/n)] = 2T_n(s/2) - 2. \quad (21.144)$$

It is not immediately obvious that such products of trigonometric functions should be integer-valued [39], and establishing that might require some work [96].

2024-02-08 Predrag More generally, in lattice field theory every periodic state is a *fixed point* of a subgroup of the symmetry group of the theory.

2023-08-05 Predrag How does that play out for the continuum Bravais lattice? the massless theory, which always has a zero eigenvalue (??), is not discussed here.

As long as the ‘anti-integrability’ parameter (here the Klein-Gordon mass  $\mu^2$ ) is sufficiently large, the eigenvalues  $|\Lambda_{c,j}|$  in (??) are all strictly positive, and the system is fully spatiotemporally chaotic.



**2024-02-08 Predrag** The maximal subgroup  $G_p \subseteq G$  of actions which permute periodic states within the orbit set  $\mathcal{M}_p$ , but leave the set invariant, is the *symmetry* group of  $\mathcal{M}_p$ ,

$$G_p = \{g \in G_p \mid g\mathcal{M}_p = \mathcal{M}_p\}. \quad (21.145)$$

The orbit  $\mathcal{M}_p$  is then said to be  $G_p$ -symmetric (symmetric, set-wise symmetric). The *index* of orbit  $\mathcal{M}_p$

$$m_p = |G|/|G_p| \quad (21.146)$$

is the number of distinct periodic states in the orbit (see [Wikipedia \[93\]](#) and Dummit and Foote [41]).

**2024-04-29 Predrag** A Hill determinant of an orbit Jacobian matrix evaluated over a primitive cell  $\mathbb{A}$  is a determinant of a finite-dimensional matrix, for example matrix (??). In sect. ?? we show how the Hill determinant of periodic state  $c$ , given by the product of orbit Jacobian matrix's eigenvalues (??) is evaluated on the reciprocal lattice. In appendix 6.12 we show that one can also visualize and compute a Hill determinant geometrically, as the volume of the orbit Jacobian matrix fundamental parallelepiped.

**2024-04-29 Han** Dropped:

*Bravais lattice stability of one-dimensional lattice periodic state*

As explained in sect. ??, the orbit Jacobian *operator* acts on the *infinite* Bravais lattice  $\mathcal{L}_{\mathbb{A}}$  and has a continuum spectrum over its reciprocal lattice Brillouin zone. For a one-dimensional lattice field theory, a Bloch eigenstate (??) of the orbit Jacobian operator (??) is a discrete field configuration over integer lattice  $z \in \mathbb{Z}$ , with its phase  $e^{ikz}$  a continuous function of  $k$  over the reciprocal lattice Brillouin zone  $\mathbb{B}$ .

The one-dimensional steady state orbit Jacobian operator (4.103) has no lattice site dependence, so the periodicity of the orbit Jacobian operator is given by the integer lattice  $\mathbb{Z}$ , with the corresponding reciprocal lattice  $2\pi\mathbb{Z}$ . Conventionally we pick the interval  $(-\pi, \pi]$  as the first Brillouin zone, with Bloch eigenstates of the propagator (??),

$$\tilde{\mathcal{J}}\varphi(\mathbf{k})_z = (\mathbf{p}^2 + \mu^2)\varphi(\mathbf{k})_z. \quad (21.147)$$

As shown in sect. ??, the number of primitive cell orbit Jacobian matrix eigenvalues equals to the volume of the primitive cell. Naturally the determinant of the infinite Bravais lattice orbit Jacobian operator is not finite, but the finite mean eigenvalue of the orbit Jacobian operator is obtainable. Since the determinant of a finite-dimensional orbit Jacobian matrix can be computed as the product of its eigenvalues, instead of the mean eigenvalue, we compute the mean value of the logarithm of eigenvalues, the *stability exponent*, which is discussed in refsects:HillExpBlatt with more details.

*Stability exponent of a Bravais periodic state*

The field configurations we consider here are not the primitive cell  $\mathbb{A}$  periodic states  $X_c$  with only  $V_{\mathbb{A}}$  field values, but the infinite spatiotemporal Bravais lattice states, with each orbit Jacobian operator  $\mathcal{J}_c$  an  $\infty$ -dimensional linear operator.

Consider approximating the Bravais lattice  $\mathcal{L}_{\mathbb{A}}$  periodic state  $X_c$  (4.47) by  $r$  repeats (a finite ‘box’) of the primitive cell periodic state (??) in every spacetime direction (here just one), computing the eigenvalues of the  $[rV_{\mathbb{A}} \times rV_{\mathbb{A}}]$  orbit Jacobian matrix and taking the  $r \rightarrow \infty$  limit,

$$\langle \lambda \rangle_c = \lim_{r \rightarrow \infty} \langle \lambda \rangle_{r\mathbb{A},c} = \lim_{r \rightarrow \infty} \frac{1}{rV_{\mathbb{A}}} \sum_{j=1}^{rV_{\mathbb{A}}} \ln |\Lambda_{c,j}|. \quad (21.148)$$

But a better way of computing the stability exponent is to find the spectrum of the orbit Jacobian matrix on the reciprocal lattice. We show in sect. ?? that the Birkhoff average  $\langle \lambda \rangle_c$  is an average over the Brillouin zone.

For spatiotemporal systems, a  $\mathcal{L}_{\mathbb{A}_p}$ -periodic state is prime if there is no other  $\mathcal{L}_{\mathbb{A}}$ -periodic state that represents a same state in the infinite spacetime, where  $\mathcal{L}_{\mathbb{A}_p}$  is a sublattice of  $\mathcal{L}_{\mathbb{A}}$ . The totality of spatiotemporal translations of a prime periodic state is a *prime orbit*.

**2023-10-14 Predrag** Ponder, but seems too much work at this stage: instead of pointwise distance  $|x_z - x'_z|$  in figure ??, is there some version of pointwise *relative information* as a measure of distance? Presumably not, relative information refers to periodic states, not lattice sites...

**2023-10-11 Predrag** A proposal: instead of Green’s function (2.99), use *relative information* as a measure of distance, weigh the distance by periodic state’s probability (17.14). See blogCats.tex, sect. 5.2 *Information*.

**2024-04-25 Han** In dealing with a non-prime periodic state, the Bloch theorem simplifies the computation of the eigenvalues and determinant of its orbit Jacobian matrix. However, for pedagogical reasons we defer the discussion of its application to sect. ?? and appendix ??. In this section our focus is solely on observing the eigenvalues and determinants of orbit Jacobian matrices of non-prime periodic states.

**2024-04-25 Han** It is important to highlight that while Hill determinants of periodic states in nonlinear theories generally require numerically computation, for steady states they can be analytically computed for steady states via discrete Fourier diagonalization. The reason is that orbit Jacobian matrices have same symmetries as their corresponding periodic states. When the periodic states are steady states, their orbit Jacobian matrices are invariant under any spacetime translations (22.100). Thus these matrices share same set of plane wave (??) eigenstates and can be

diagonalized by Fourier transform. The orbit Jacobian matrix of a steady state, denoted as  $\bar{x}$ , in the primitive cell of lattice  $\mathcal{L}_A$ , takes the form of a Laplacian with a constant along the diagonal. As a result, their eigenvalues are summations of the local stretching factors and the square of the lattice momenta  $p$  (??), evaluated in the same way as the free-field theory and spatiotemporal cat (??-??):

$$(\tilde{\mathcal{J}}_A)_{m_1 m_2} = p_{m_1 m_2}^2 + \tilde{\mu}^2 \quad (21.149)$$

where the local stretching factor  $\tilde{\mu}^2$  is  $-2\mu^2 x$  for the spatiotemporal  $\phi^3$  (4.159) and  $\mu^2(1 - 3x^2)$  for the spatiotemporal  $\phi^4$  (4.105).

The orbit Jacobian operators (4.103) of the steady state do not depend on the periodic states and their periodicities. Thus every periodic state has a same orbit Jacobian operator and stability exponent.

The contrast between the discrete and the continuous spectra is illustrated by figure ?? (a) which shows the spectra of one-dimensional steady state orbit Jacobian matrices, and figure ?? (a) of the two-dimensional steady state as a function of the wave vector(s)  $k$ , or  $k = (k_1, k_2)$ , in the one-, or two-dimensional Brillouin zone  $\mathbb{B}$ , respectively.

However, using the Bloch theorem we can compute the spectrum of the infinite-dimensional orbit Jacobian operators of periodic states.

**2023-05-06 Predrag** An inspiration, but wrong in their execution: Credit Pughe-Sanford and Quinn [85] for the idea to sum  $p$  and all its repeats first.

**2023-09-09 Predrag Temporal cat: Difference equation.** Inserting a solution of form [43]  $x_t = \Lambda^t$  into the  $s_t = 0$  associated homogenous temporal cat 2nd-order difference equation (??)

$$x_{t+1} - s x_t + x_{t-1} = 0$$

yields the characteristic equation

$$\Lambda^2 - s\Lambda + 1 = 0, \quad (21.150)$$

which, for  $|s| > 2$ , has two real roots  $\{\Lambda, \Lambda^{-1}\}$ ,

$$\Lambda = \frac{1}{2}(s + \sqrt{(s-2)(s+2)}). \quad (21.151)$$

The result is that the Hill determinant of temporal periodic state of period  $n$  is

$$|\text{Det } \mathcal{J}_n| = \Lambda^n + \Lambda^{-n} - 2, \quad (21.152)$$

often written as

$$|\text{Det } \mathcal{J}_n| = 2 T_n(s/2) - 2, \quad (21.153)$$

where  $T_n(s/2)$  is the Chebyshev polynomial of the first kind.

2024-07-08 **Predrag** Stability (??) is checked in blogCats, search for Eq. 4.226 .

2023-03-06 **Predrag** The most important observation for what follows is that while each primitive cell  $\mathbb{A}$  has its own distinct orbit Jacobian matrix spectrum, for a steady  $x_z = x$  state there is *only one* orbit Jacobian operator spectrum. Why is that?

2023-03-06 **Predrag** Weave prime orbit as a ‘motif’ [38] into the narrative: “ If we add two-dimensional objects, e.g., a set of atoms, to each cell of a Bravais lattice, we can change the symmetry of the lattice. If the object, sometimes called a motif, lowers the symmetry to that of another group, then the resulting symmetry space group for the structure is identified with the lower symmetry space group. ”

2023-07-21 **Predrag** move: for orbit Jacobian operators only *prime orbits* matter. The observation that the spectra of orbit Jacobian *operators* depend only on *prime orbits*, and not on their repeats, is the key to the main result of this paper, the periodic orbit theory of spatiotemporal chaos to be formulated in sect. ??.

2023-08-05 **Predrag** Rethink seriously the ‘hyperbolicity assumption’: no imaginary eigenvalues? Check  $\phi^3$  for  $\mu^2$  or  $a$  values where it has an attractive 2-cycle?

2024-02-08 **Predrag** More generally, in lattice field theory every periodic state is a *fixed point* of a subgroup of the symmetry group of the theory.

2024-07-16 **Predrag**

$$\mathcal{M}_p = \{r_1^{m_1} r_2^{m_2} \mathcal{X}_p \mid r_1^{m_1} r_2^{m_2} \in T\} \quad (21.154)$$

The number of distinct periodic states in the orbit is  $V_{\mathbb{A}}$ , or a divisor of  $V_{\mathbb{A}}$ .

2023-09-03, 2024-07-28 **Predrag** Appendix s:jacobianOrbBlock was not referred to, so moved from appePrime.tex to blogCats.

2023-03-13 **Han** Global methods find periodic orbits of deterministic dynamical systems by solving the Euler–Lagrange equations  $F[\mathcal{X}_c] = 0$  on the spatiotemporal lattices. The stabilities of periodic orbits are given by the orbit Jacobian matrices evaluated for site field values of a given periodic state, for example (4.107)–(4.109).

2024-03-19 **Han** Prime orbits are the building blocks of the periodic orbits theory. To use the prime orbits, one needs to know the contribution of a prime orbit to periodic states with given periodicities, or in other words, how does a prime orbit tile a periodic state that is a repeat of the prime.

We have shown in sect. ?? how to determine if a Bravais lattice is a sublattice of another Bravais lattice. The repeats of a prime  $\mathcal{L}_{\mathbb{A}_p}$ -periodic state have periodicities given by  $\mathcal{L}_{\mathbb{A}}$ , the sublattice of  $\mathcal{L}_{\mathbb{A}_p}$ , where  $\mathbb{A} = \mathbb{A}_p \mathbb{R}$  (??).

$n$	1	2	3	4	5	6	7	8	9	10	11
$N_n$	1	5	16	45	121	320	841	2205	5776	15125	39601
$M_n$	1	2	5	10	24	50	120	270	640	1500	3600

Table 21.1:  $\mu^2 = 1$  temporal cat periodic state and prime orbit counts,  $N_n$  and  $M_n$  respectively.

View the primitive cell  $\mathbb{A}_p$  as the *unit* square of a new integer lattice, a unit square that supports a multiplet of  $V_{\mathbb{A}_p}$  fields belonging to a prime  $\mathcal{L}_{\mathbb{A}_p}$ -periodic state. Under lattice translations, this multiplet is an  $V_{\mathbb{A}}$ -dimensional steady state. The same procedure as finding the periodic states applies: a  $\mathcal{L}_{\mathbb{A}_p\mathbb{R}}$ -periodic state is a  $\mathcal{L}_{\mathbb{R}}$  periodic state in the new integer lattice.

To find all repeats of the prime periodic states one only needs to find all Bravais lattice  $\mathcal{L}_{\mathbb{R}}$ , which can be accomplished using the Hermite normal form of  $\mathbb{R}$  (??). Each  $\mathbb{R}$  gives a periodic state over a larger-periodicity Bravais sublattice  $\mathcal{L}_{\mathbb{A}_p\mathbb{R}}$ .

For example, one can repeat a  $\mathcal{L}_{\mathbb{A}_p} = [3 \times 2]_1$  prime periodic state to get a  $\mathcal{L}_{\mathbb{A}} = [6 \times 4]_2$  periodic state, as shown in figure ?? (a). In figure ?? (b) the primitive cell of the prime  $\mathcal{L}_{\mathbb{A}_p}$ -periodic state is transformed into the unit square of the new integer lattice, where each unit square supports a multiplet of 6 fields. In this new integer lattice, the primitive cell of the repeat  $\mathcal{L}_{\mathbb{A}}$ -periodic state is given by  $\mathcal{L}_{\mathbb{R}} = [2 \times 2]_0$ , where  $\mathbb{A} = \mathbb{A}_p\mathbb{R}$ .

**2019-06-10 Predrag** See table 21.1.

**2023-05-11 Predrag** Why do we care about the Hill determinant of repeats of primes, except for avoiding repeating computations?

**2023-05-11 Predrag** There are many different ways to skin this cat, some discussed in companion paper I [67], where we review the one-dimensional temporal lattice Isola [57] topological zeta function  $1/\zeta_{\text{AM}}(z)$  and its relation to  $T_n(s/2)$ , the Chebyshev polynomials of the first kind.

**2024-02-08 Predrag** This observation motivates Lind’s [69] census of invariant solutions of any system with discrete symmetries, based on enumeration of all fixed points of all subgroups of the symmetry group of a given theory (see sect. ??).

Then the set of all periodic states contributing to the partition sum (??) consists of the  $n$  cyclic rotations of  $X_p$  plus  $n_{p'}$  cyclic rotations of all shorter prime orbits  $X_{p'}$  whose  $r$ th repeat is of period  $n = rn_{p'}$ . So all we have to do is to determine the *prime orbits* of the translation equivalent periodic states.

**2024-02-08 Predrag** For example, if system's defining equations are of the same form for all times and everywhere in the space, they retain their form under action of one-lattice-spacing shift operator  $r_1, r_2, \dots, r_d$  (22.100) in  $j$ th lattice direction. A periodic state  $X_p$ , however, is transformed by 1-step translation into -in general- a distinct periodic state  $r_j X_p$ , with each translated periodic state  $X'_p$  having its own, periodic state dependent orbit Jacobian matrix  $\mathcal{J}'_p = \mathcal{J}[X'_p]$ , with the stretching factor (4.106) at the lattice site  $z$  a function of the periodic state.

**2023-04-20 Han** If the periodic state has symmetries, this computation can be obscured further.

**2023-10-11 Predrag** Gave up on including this proposal into CL18. (Maybe include in WWL AFC22?):  
should we use *relative information* as a measure of distance? KL divergence makes more sense to me than the *ad hoc*  $L2$  norm distance between periodic states (17.13): instead, weigh the distance by periodic state's probability refreq??.

See blogCats.tex, sect. 5.2 *Information*.

**2020-09-24 Predrag** spatiotemporal cat

$$\text{Det } \mathcal{J} = \text{Det} (-\square + \mu^2), \quad (21.155)$$

Trace is logarithmic derivative of the determinant, in any spacetime dimension

$$\text{Tr} \frac{1}{-\square + \mu^2} = \frac{d}{d\mu^2} \ln \text{Det} (-\square + \mu^2) \quad (21.156)$$

Specialising to temporal cat:

$$\begin{aligned} \text{Tr} \frac{1}{-\square + \mu^2} &= \text{Tr} \frac{1}{2 - 2 \cos(k) + \mu^2} = \text{Tr} \frac{1}{4 \sin^2(k/2) + \mu^2} \\ &= \frac{1}{2\pi} \int_{-\pi}^{\pi} dk \frac{1}{(\mu - i 2 \sin(k/2)) (\mu + i 2 \sin(k/2))} \end{aligned} \quad (21.157)$$

looking like an exercise in contour integration.

To recover  $\text{Det} (-\square + \mu^2)$  integrate both sides with respect to  $\mu^2$ ,

$$\int_{\mu_0^2}^{\mu^2} du \text{Tr} \frac{1}{-\square + u} = \ln \frac{\text{Det} (-\square + \mu^2)}{\text{Det} (-\square + \mu_0^2)},$$

and exponentiate. In this form, the determinant is regularized (not sure

this is needed on a lattice)

$$\begin{aligned}
 \frac{\text{Det}(-\square + \mu^2)}{\text{Det}(-\square + \mu_0^2)} &= \exp\left(\int_{\mu_0^2}^{\mu^2} du \text{Tr} \frac{1}{-\square + u}\right) \\
 &= \exp\left(\int_0^\infty dt \int_{\mu_0^2}^{\mu^2} du \text{Tr} e^{-t(-\square + u)}\right) \\
 &= \exp\left(-\int_0^\infty dt \frac{1}{t} \text{Tr} \left(e^{-t(-\square + \mu^2)} - e^{-t(-\square + \mu_0^2)}\right)\right) \\
 &= .
 \end{aligned}$$

**2023-05-16 Predrag** intro,tex has some **Bard's** "improvements". **GTPchat's** "improvements" were useless.

**2024-08-08 Han** Dropped from sect. ??:

For two-dimensional case (??), consider a steady state  $X_{2\mathbb{A}}$  over primitive cell of volume  $2V_{\mathbb{A}}$  obtained by joining a steady state  $X_{\mathbb{A}}$  and its repeat. The reciprocal primitive cell (7.5) is the same, but now there are  $2V_{\mathbb{A}}$  reciprocal lattice sites within it. Repeat this in all possible ways (sect. ??). The result is a tiling of the infinite Bravais lattice  $\mathcal{L}_{\mathbb{A}}$  by all repeats of steady state  $X_{\mathbb{A}}$ , with the infinity of reciprocal lattice sites all within the reciprocal primitive cell  $\tilde{\mathbb{A}}$  (the shaded region in figure ?? (b)).

**2018-08-06 Han** for spatiotemporal cat we have in the square lattice first Brillouin zone periodic orbit stability exponent

$$\lambda = \frac{1}{4\pi^2} \int_{-\pi}^{\pi} dk_1 \int_{-\pi}^{\pi} dk_2 \ln \left( 2s - 2 \cos(k_1) - 2 \cos(k_2) \right) \quad (21.158)$$

Evaluating this numerically for  $s = 5/2, \mu^2 = 1$  we get that the topological entropy density per unit spacetime volume is  $h \approx 1.508$ .

**2018-08-09 Predrag** Removed the above, as (24.97) is an earlier version of (24.506).

**2024-08-09 Han** We do not need this, so dropped:

It is noteworthy that the eigenvalues of finite-dimensional non-prime orbit Jacobian matrices can also be computed using the Bloch theorem. A  $\mathcal{L}_{\mathbb{A}}$ -prime periodic state can tile the primitive cell of lattice  $\mathcal{L}_{\mathbb{A}'}$  which is a sublattice of  $\mathcal{L}_{\mathbb{A}}$ . The orbit Jacobian matrix of the periodic state in the primitive cell  $\mathbb{A}'$  is  $\mathcal{L}_{\mathbb{A}}$ -periodic. According to the Bloch theorem, eigenstates of this  $V_{\mathbb{A}'}$ -dimensional orbit Jacobian matrix is a product of a plane wave and a  $\mathcal{L}_{\mathbb{A}}$ -periodic function. So the  $V_{\mathbb{A}'}$  eigenvalues of the orbit Jacobian matrices exist on the  $V_{\mathbb{A}}$  eigenvalue bands of the corresponding orbit Jacobian operator. However, for the eigenstates to be  $\mathcal{L}_{\mathbb{A}'}$ -periodic and fit within the primitive cell  $\mathbb{A}'$ , the wave numbers  $k$  can only take positions at the reciprocal lattice sites of  $\mathcal{L}_{\mathbb{A}'}$ .

**2023-09-08 Predrag** regrets writing this: “ I am no fan of shrinking ‘Brillouin zones’, I prefer always having reciprocal primitive cell  $\tilde{\mathbb{A}}$ , shaded in figure ?? (b), of Brillouin zone volume  $(2\pi)^2$ .”

**2024-02-17 Predrag** What’s the mosaic (symbol array) for this orbit? For one-dimensional  $\phi^4$  there is one symmetric period-2 periodic state  $\overline{LR}$  a pair of period-2 asymmetric periodic states  $\overline{LC}, \overline{CR}$  related by reflection symmetry (time reversal).

**2024-08-04 Predrag** A periodic state  $X_c$  is either prime, or a repeat (sect. ??) of a prime orbit  $X_p$  with periodicity  $\mathcal{L}_{\mathbb{A}}$ . A prime orbit  $X_p$  over its primitive cell of  $\mathcal{L}_{\mathbb{A}}$  has the same Hill determinant and Birkhoff sum (4.122) for the  $V_p$  periodic states in its translational group orbit, so its contribution to the deterministic partition sum (??) is  $V_p t_p$ , where

$$t_p = (e^{\beta \cdot a_p - \lambda_p z})^{V_p}, \quad V_p = V_{\mathbb{A}} = L_{\mathbb{A}} T_{\mathbb{A}}. \quad (21.159)$$

For any periodic state over the infinite spacetime, a prime orbit over its primitive cell  $\mathbb{A}$  is the smallest tile that tiles the infinite periodic state.

For a one-dimensional, temporal Bravais lattice, the generating function of the deterministic partition sum (21.98) is known as the deterministic trace formula (see ChaosBook eq. (21.24)),

$$Z[\beta, z] = \sum_p \sum_{r=1}^{\infty} V_p t_p^r = \sum_p \frac{T_p t_p}{1 - t_p}, \quad (21.160)$$

with the primitive cell volume  $V_p = T_p$  equal to the time period of a prime orbit (see sect. ??) of temporal evolution equation  $x_{t+1} - f(x_t) = 0$ .

The repeat matrix  $\mathbb{R}$  (sect. ??), acting on the unit cell  $\mathbb{A}$  generates all distinct  $\mathcal{L}_{\mathbb{A}\mathbb{R}}$  Bravais sublattices of  $\mathcal{L}_{\mathbb{A}}$ .

The sum over all prime orbits  $X_p$  and their repeats ( $\mathbb{A}\mathbb{R}$  primitive cells) yields the deterministic partition sum  $Z[\beta, z]$  (??) expressed in terms of prime orbits  $X_p$ . For the two-dimensional square lattice this is

$$Z[\beta, z] = \sum_p Z_p, \quad Z_p = V_p \sum_{r_1=1}^{\infty} \sum_{r_2=1}^{\infty} \sum_{s=0}^{r_1-1} t_p^{r_1 r_2}.$$

The  $V_p$  prefactor arises because all periodic states in the group orbit of a prime orbit  $X_p$  have the same weight. For each width  $r_1$ , height  $r_2$ , the number of Hermite normal form (??) relative periodic primitive cells  $[r_1 \times r_2]_s$  is

$$\sum_{s=0}^{r_1-1} 1 = r_1 \text{ so } Z_p = V_p \sum_{r_1=1}^{\infty} \sum_{r_2=1}^{\infty} r_1 (t_p^{r_1})^{r_2}.$$



As the  $r_2$  sum is a geometric series, the deterministic partition sum (??)

$$Z[\beta, z] = \sum_p V_p \sum_{n=1}^{\infty} \frac{nt_p^n}{1-t_p^n} \quad (21.161)$$

is expressed as the sum of all prime orbits and their repeats, the two-dimensional spacetime generalization of the temporal deterministic partition sum (21.160).

In the spirit of the Lind zeta function, we define the two-dimensional spatiotemporal zeta function, now not as a solution-counting generating function (??), but *probability weighted* by  $t_p$  (21.159),

$$\zeta[\beta, z] = \prod_p \zeta_p[\beta, z], \quad \ln \zeta_p[\beta, z] = \sum_{r_1=1}^{\infty} \sum_{r_2=1}^{\infty} \sum_{s=0}^{r_1-1} \frac{t_p^{r_1 r_2}}{r_1 r_2} = - \sum_{r_1=1}^{\infty} \ln(1 - t_p^{r_1}) \quad (21.162)$$

**2023-08-03 Han** Lind zeta function and spatiotemporal zeta function of the two-dimensional spatiotemporal cat

The Lind zeta function (??) of the two-dimensional spatiotemporal cat can be computed by substitute the number of the spatiotemporally periodic states (??):

$$1/\zeta_{Lind}(z) = \exp \left( - \sum_{L=1}^{\infty} \sum_{T=1}^{\infty} \sum_{S=0}^{L-1} \frac{V_{[L \times T]_S}}{LT} z^{LT} \right). \quad (21.163)$$

We do not know how to compute (21.163) for the two-dimensional spatiotemporal cat.

The spatiotemporal zeta function of spatiotemporal cat has a same form as the Lind zeta function up to a rescaling:

$$\begin{aligned} 1/\zeta[0, z] &= \exp \left[ - \sum_{L=1}^{\infty} \sum_{T=1}^{\infty} \sum_{S=0}^{L-1} \frac{V_{[L \times T]_S}}{LT} (ze^{-\langle \lambda \rangle})^{LT} \right] \\ &= 1/\zeta_{Lind}(t), \quad t = ze^{-\langle \lambda \rangle}. \end{aligned} \quad (21.164)$$

If we use the stability exponents of finite periodic states  $\lambda_c$  (??) instead of the stability exponents of infinite periodic states  $\langle \lambda \rangle$ , the spatiotemporal zeta function can be evaluated analytically, due to the fundamental fact:

$$\begin{aligned} 1/\zeta[0, z] &= \exp \left[ - \sum_{L=1}^{\infty} \sum_{T=1}^{\infty} \sum_{S=0}^{L-1} \frac{V_{[L \times T]_S}}{LT} \left( \frac{z}{e^{\lambda_c}} \right)^{LT} \right] \\ &= \exp \left( - \sum_{L=1}^{\infty} \sum_{T=1}^{\infty} \sum_{S=0}^{L-1} \frac{z^{LT}}{LT} \right) \\ &= \prod_{n=1}^{\infty} (1 - z^n) = \phi(z), \end{aligned} \quad (21.165)$$

where  $\phi(z)$  is the Euler function (??).

**2024-09-16 Han** To evaluate the expectation value of the stability exponent for the spatiotemporal cat, we use the Bravais lattice stability as the observable, and use the primitive cell stability as the weight of periodic orbits. The deterministic zeta function is:

$$\begin{aligned} 1/\zeta[\beta, z] &= \exp \left[ - \sum_{L=1}^{\infty} \sum_{T=1}^{\infty} \sum_{S=0}^{L-1} \frac{V_{[L \times T]_S}}{LT} \left( \frac{ze^{\beta\lambda}}{e^{\lambda e}} \right)^{LT} \right] \\ &= \exp \left( - \sum_{L=1}^{\infty} \sum_{T=1}^{\infty} \sum_{S=0}^{L-1} \frac{t^{LT}}{LT} \right), \quad t = ze^{\lambda\beta} \\ &= \prod_{n=1}^{\infty} (1 - t^n) = \phi(t). \end{aligned} \quad (21.166)$$

The leading root of the zeta function is  $t = 1$ ,  $z = e^{-\lambda\beta}$ . Using (??) we have  $\langle \lambda \rangle = \lambda$ .

**2023-08-03 Han** Every periodic state of spatiotemporal cat has a same stability exponent  $\langle \lambda \rangle$ :

$$\langle \lambda \rangle = \frac{1}{(2\pi)^2} \int_{-\pi}^{\pi} dk_1 \int_{-\pi}^{\pi} dk_2 \ln(2s - 2 \cos k_1 - 2 \cos k_2) \quad (21.167)$$

which can be evaluated numerically.

**2019-11-23 Predrag** We always reduce relative-shift symmetries, so I am not happy about the  $[2 \times 1]_1$  relative-periodic mosaic ??refeq eq:block2x1rp being counted as the  $[2 \times 2]_0$  periodic state. We'll have to revisit symmetry reduction...

**2024-08-22 Han** Fixed frame of figure 14. Predrag LaTeX labeled it.

Saved svg source files:

reffig f:BravLatt (a), reffig f:reciprLatt (a), reffig f:BlochBrillouin (a) figSrc/inkscape/HLBravaisCell  
reffig f:BravLatt (b) figSrc/inkscape/HLBravaisCell2.svg  
reffig f:2x1rpo (a) figSrc/inkscape/HL2by1shift1Lst.svg  
reffig f:2x1rpo (b) figSrc/inkscape/HL3by2shift1Lst.svg  
reffig f:pcellAsUnitSq (a) figSrc/inkscape/HLBravaisCellTiling3.svg  
reffig f:pcellTiling (a) figSrc/inkscape/HLBravaisCellTiling1.svg  
reffig f:pcellTiling (b) figSrc/inkscape/HLBravaisCellTiling2.svg  
reffig f:reciprLatt (b) figSrc/inkscape/HLBravaisCellTiling4.svg  
reffig f:reciprLatt (b) figSrc/inkscape/HLReciprocalLattice4.svg  
reffig f:recipCatCn (a) figSrc/inkscape/tempCatRecip.svg, figs/tempCatRecip.pdf  
reffig f:recipCatCn (b) figSrc/inkscape/tempHenRecip.svg  
reffig f:BlochBrillouin (b) figSrc/inkscape/HLReciprocalLattice3.svg  
reffig f:2dCatLattBand (a) figSrc/inkscape/HL2dCatBand.svg, figs/HL2dCatBand.pdf

reffig f:2dCatLattBand (b) figSrc/inkscape/HL2dPhi4Band.svg, figs/HL2dPhi4Band.pdf  
 reffig fig:stabExpLxL figSrc/inkscape/HLStbExpntNb.svg, figs/HLStbExpntNb.pdf  
 figSrc/han/Mathematica/CL18Figure/SptCatSpectra.nb  
 figSrc/han/Mathematica/CL18Figure/SptPhi4Spectra.nb  
 figSrc/han/Mathematica/CL18Figure/TemporalCatSpectra.nb

**2024-08-27 Han** Parameters used in figure ??: (a) Temporal cat with  $\mu^2 = 1$ .  
 (b) Temporal  $\phi^3$  with  $\mu^2 = 5$ . Figure ??: (a) Spatiotemporal cat with  
 $\mu^2 = 1$ . (b) Spatiotemporal  $\phi^4$  with  $\mu^2 = 5$ . Figures ??, ?? and ?? are  
 spatiotemporal cat with  $\mu^2 = 1$ .

**2024-08-15 Predrag**  $\beta$  is a parameter (set of parameters) that aids us in evalu-  
 ating expectation values and cumulants of observable(s),

**2024-08-08 Predrag** For temporal cat the stability multiplier  $\Lambda$  in (??) is known  
 analytically, so maybe one should seek for analytic spatiotemporal cat  
 ‘stability multiplier’

$$\Lambda = e^\lambda = 2.274013 \dots \quad (21.168)$$

Not clear, as this might be some kind of an average over 2 expanding  
 multipliers  $\Lambda_1 \Lambda_2$ , but they are the same by symmetry. The discrete sym-  
 metry  $D_4$  might relate this to something simple...

**2023-10-11 Predrag** Rewriting (??) as a multiplier:

$$\lambda - \lambda_{[L \times L]_0} = [const] \cdot e^{-1.05538 L} = [const] \cdot (1.113827 \dots)^L \quad (21.169)$$

**2023-09-25 Predrag** Always list only the significant digits that you trust. 6 dig-  
 its seems too much to me.

**2023-09-09 Predrag** I do not know why, but I never see (4.127) in field-theoretic  
 or solid state literature... Is this true re. (??)?  
 Variants of such partition sums had been derived, by various methods  
 and in different contexts, in refs. [24, 58, 73].

**2016-11-07 Predrag** The dynamical systems literature tends to focus on *local*  
 problems: bifurcations of a single time-invariant solution (equilibrium,  
 relative equilibrium, periodic orbit or relative periodic orbit) in low-dim-  
 ensional settings (3-5 coupled ODEs, one-dimensional PDE). The prob-  
 lem that we face is *global*: organizing and relating *simultaneously* infinities  
 of unstable relative periodic orbits in  $\infty$ -dimensional phase spaces, orbits  
 that are presumed to form the skeleton of turbulence and are typically  
 not solutions that possess the symmetries of the problem. In this quest  
 we found the standard equivariant bifurcation theory literature not very  
 helpful, as its general focus is on bifurcations of solutions, which admit  
 all or some of the symmetries of the problem at hand.

2023-07-24 Predrag The ‘compact boson’ references [28, 47] in refsect s:catlatt are very recent, track down the early, perhaps even original references...

By “spontaneous breaking of the symmetry” in a conventional theory one means that a solution does not satisfy a symmetry of the action, such as  $\phi \rightarrow -\phi$ ; we, however, always work in the “broken-symmetry” regime, as almost every ‘turbulent’, spatiotemporally chaotic deterministic solution breaks all symmetries.

This might be too obscure. Or even incorrect :)

In language of statistical mechanics, in this paper we focus on the description of the high-temperature paramagnetic (or disordered) phase.

A key advantage of the spatiotemporal code  $M$  is illustrated already by the  $d = 2$  case. While an Adler-Weiss type partition, forward-in time Hamiltonian evolution alphabet would grow exponentially with the “particle number”  $L$ , the number of letters (??) of the spatiotemporal code  $\mathcal{A}$  is finite and the same for any spatial extent  $L$ , including the infinite  $L, T \rightarrow \infty$  lattice.

For the spatiotemporal code, a field  $X$  over a periodic spatiotemporal domain is encoded by a doubly periodic two-dimensional mosaic  $M$  of symbols from a small alphabet, rather than by a 1-dimensional temporal string of symbols from the exponentially large (in  $L$ ) ‘ $L$ -particle’ alphabet  $\bar{\mathcal{A}}$ .

of fixed spatial width, large alphabet.

We are interested in averages of observables over arbitrarily large space-time domains.

Spatiotemporal dynamical systems are often described by partial differential equations in continuous spacetime, or by difference equations on the lattice. These defining equations of the dynamical systems are the Euler–Lagrange equations of the corresponding lattice field theories.

[Revolution] WHY? The primary claim that we make is that in hindsight, describing turbulence via an exponentially unstable dynamical equation never could have worked.

Only field theorists and general relativists are trained to think in space-time.

, we use the volume notation  $V_{\mathbb{A}} = |\text{Det } \mathbb{A}|$ , rather than the lattice sites count  $V_{\mathbb{A}}$

(indeed, any theory in which a neighborhood of a phase space point is approximated by a local  $d$ -dimensional piecewise linear chart)

Elizalde *et al.* [45] evaluate the Hill determinant using zeta function regularization.

this problem in terms of the modular (conformal) transformation, Cardy [25],

What we find appealing is that Witten arrives the form of their partition sum by symmetry reasoning, invariance under modular transformations (what we call unimodular transformations).

So not at all by counting different Bravais lattice (what they call the “sum over geometries”).

Our Hill determinant factorization is for them [58, 73] “holomorphic factorization”, arises because the theory is a product of two decoupled theories, associated respectively with “left- and right-moving modes”, which is how I think of our ‘metal means’, linear in lattice momentum Euler–Lagrange equations.

The massive boson partition sum for rectangular primitive cells is known, in terms of Jacobi elliptic functions, but I have not been able identify it in any simple form.

Witten’s black hole entropy has a Bessel function  $J_1$ . It might be related to our Green’s function modified Bessel function  $K_0$ , in the stability exponent shadowing calculations.

**2024-09-18 Han** Deterministic zeta function computation of temporal cat stability exponent. Dropped.

One can compute the expectation value of the stability exponent using the deterministic zeta function. Take the logarithm of periodic state’s stability as the Birkhoff sum  $A$  (4.122) and compute the corresponding deterministic zeta function:

$$1/\zeta[\beta, z] = \exp\left(-\sum_{n=1}^{\infty} \frac{N_n e^{n\lambda\beta} z^n}{\Lambda^n}\right) = 1/\zeta_{AM}(t), \quad t = \frac{ze^{\lambda\beta}}{\Lambda}, \quad (21.170)$$

where  $\lambda$  is the stability exponent for all periodic states of temporal cat, and  $\zeta_{AM}$  is the topological zeta function (??). Using (??) the expectation value of the stability exponent is:

$$\begin{aligned} \langle \lambda \rangle &= \frac{1}{z} \left( \frac{\partial \zeta_{AM}(t(\beta, z))}{\partial \beta} \bigg/ \frac{\partial \zeta_{AM}(t(\beta, z))}{\partial z} \right) \bigg|_{\beta=0, z=z(0)} \\ &= \frac{1}{z} \frac{\partial t}{\partial \beta} \bigg/ \frac{\partial t}{\partial z} \bigg|_{\beta=0, z=1} \\ &= \lambda, \end{aligned} \quad (21.171)$$

which is the obvious result as every periodic state has a same stability exponent  $\lambda$ . The same result can also be computed from solving  $1/\zeta[\beta, z(\beta)] = 0$  (21.170) for  $\zeta(\beta)$ , which gives us:

$$t = \Lambda^{-1} \rightarrow z(\beta) = e^{-\lambda\beta}. \quad (21.172)$$

Using (??) we have:

$$\gamma = 0, \quad \langle \lambda \rangle = \lambda. \quad (21.173)$$

2024-09-18 Han Derivation of (??):

The computation of (??) is the one I did for Josh and Sam. Compare (??) and (??) we see that the expectation value is computed over every periodic state with a weight given by  $1/\Lambda^n$ , then normalized by the sum of the weights. The sum of the weights do not converge to a finite value. So equation (??) is a  $\infty/\infty$  ratio. The **Stolz-Cesàro theorem** is a discrete version of **L'Hôpital's rule**. In the computation we used the last term of the sum, which is a discrete analogue of the derivative of the integral, to replace the infinite sum. To derive (??), let:

$$a_n = \sum_{m=1}^n \frac{(\Lambda^m + \Lambda^{-m} - 2) \ln(\Lambda^m + \Lambda^{-m} - 2)}{m\Lambda^m}, \quad (21.174)$$

and

$$b_n = \sum_{m=1}^n \frac{(\Lambda^m + \Lambda^{-m} - 2)}{\Lambda^m}. \quad (21.175)$$

Then the ratio of (??) is:

$$\langle \lambda \rangle = \lim_{n \rightarrow \infty} \frac{a_n}{b_n}. \quad (21.176)$$

Since both  $a_n$  and  $b_n$  are strictly increasing and approaching  $+\infty$ , according to the Stolz-Cesàro theorem, the ratio at the limit  $n \rightarrow \infty$  is the ratio of the  $n$ th terms in the sums:

$$\begin{aligned} \langle \lambda \rangle &= \lim_{n \rightarrow \infty} \frac{a_n}{b_n} = \lim_{n \rightarrow \infty} \frac{a_n - a_{n-1}}{b_n - b_{n-1}} \\ &= \lim_{n \rightarrow \infty} \frac{(\Lambda^n + \Lambda^{-n} - 2) \ln(\Lambda^n + \Lambda^{-n} - 2)}{n\Lambda^n} \bigg/ \frac{\Lambda^n + \Lambda^{-n} - 2}{\Lambda^n} \end{aligned} \quad (21.177)$$

2024-10-10 Predrag This claim is wrong, my bad:

Furthermore, while a primitive cell  $\mathbb{A} = [L \times T]_S$  Hill determinant depends on the tilt  $S$  relative periodic bc's (see, for example, Hill determinants listed in table 9.3), stability exponent (??) Brillouin zone integration domain (23.87) depends only on spacetime periodicities  $L_j$ .

2024-10-16 Han The deterministic partition sum  $Z[\beta, z]$  (??) is the generating function of  $Z_{\mathbb{A}}[\beta]$ , and it is only valid for systems with discrete spacetime.

2024-08-06 Predrag An inspiration for construction of the Ruelle dynamical zeta function (4.128) is the Artin-Mazur zeta function [5, 31, 67],

$$\zeta_{\text{AM}}(z) = \exp \left( \sum_{n=1}^{\infty} \frac{V_n}{n} z^n \right), \quad (21.178)$$

which counts the numbers of the periodic points  $V_n$  of a discrete-time dynamical system.

**2024-10-20 Predrag** The relation is one of the Hamiltonian mechanics to its imaginary time, Euclidean sister. Hamiltonian mechanics solutions are oscillatory,  $\propto \exp(-iE_n t/\hbar)$ , with eigenenergy  $E_n$  a dual variable to the lattice volume for a one-dimensional temporal lattice, time  $t$ . Here the solutions  $\propto \exp(-sV_c)$  are exponentially decaying, with the decay rate  $s$  a dual variable to the spacetime volume  $V_c$ .

**2018-11-16 Predrag** Witten has an interesting speculation about how “holomorphic factorization” is restored for the “sum over geometries” that they were unable to implement. But it works for us in the Isola zeta function factorization.

**2024-11-23, 2025-05-15 Predrag** Was "The section involves many computation which reader can safely skim over, as these are *not* the computations our theory requires."

Not true. One always has to compute  $\text{Det } \mathcal{J}_p = \text{Det } \mathcal{J}_p(0)$  value of  $\text{Det } \mathcal{J}_p(\mathbf{k})$ .

but now with stability exponent  $\lambda_c$  (??) in  $1/|\text{Det } \mathcal{J}_c| = \exp(-V_{\mathbb{A}}\lambda_c)$  evaluated over  $\mathcal{L}_{\mathbb{A}}$  Brillouin zone  $\mathbb{B}$ , as in sect. ??.

exponentially bound each primitive cell partition sum,

Note to Predrag - send this paper to Vladimir Rosenhaus <vrosenhaus@gc.cuny.edu>, Ivashkevich *et al.* [58], Xiangyu Cao <xiangyu.cao08@gmail.com>, George Savvidy, “Demokritos”, Athens, David Berenstein <dberens@physics.ucsb.edu> Manuel Campos, Esperanza López german.sierra@uam.es, Germán Sierra javi.molina@upct.es?, Madrid,

## 21.3 Reversal' LC21blog

The latest entry at the bottom of this section, page 899

Internal discussions of ref. [67] [arXiv:2201.11325](https://arxiv.org/abs/2201.11325) (uploaded 27 Jan 2022) edits: we had saved text not used in ref. [67] here, for possible reuse in ref. [35], or elsewhere.

Tentative title: "Is there anything cats cannot do?"

**2016-11-18 Predrag** A theory of turbulence that has done away with *dynamics*? We rest our case.

The deep insight here is the realization that the *Hill determinant*, i.e., the volume of the *orbit Jacobian matrix* (figure 1.3 and ??) partitions system's phase space.

**2016-11-18 Predrag** The dynamics is breathtakingly simple on the reciprocal lattice. Spatial period- $n$  primitive cell maps onto a regular  $n$ -gon in the reciprocal lattice. Time reversal fixes the symmetric solutions to sit on the symmetry axes, the boundaries of the fundamental domain. Lattice shift  $r_j$  maps out the  $G$ -orbit by running on circles, and orbits visit the  $1/2n$  wedge only once, so the points in the fundamental domain represent an orbit each.

with all reciprocal lattice Brillouin zone solutions orbits in an  $1/n$  sliver of a  $n$ -gon.

No self-respecting crystallographer would be drawing longer and longer periodic states (??)-(12.125) - they eventually run off the sheet of paper, no matter how wide. A professional crystallographer plots all periodic states snugly together in the first Brillouin zone, where the translational orbit of a periodic state is -literally- a circle, symmetric periodic states sit on boundaries of point group's fundamental domain, and everything is maximally diagonalized in term's of space group  $G$  irreps.

Consider

$$\rho_{\vec{G}}(\vec{x}) = e^{i\vec{G}\cdot\vec{r}(\vec{x})},$$

where  $\vec{G}$  is a reciprocal lattice vector. By definition,  $\vec{G} \cdot \vec{a}$  is an integer multiple of  $2\pi$ ,  $\rho_{\vec{G}} = 1$  for lattice vectors. For any other state, reciprocal periodic state is given by

$$e^{i\vec{G}\cdot\vec{a}(\vec{x})} \neq 1.$$

When a cube is a building block that tiles a 3D cubic lattice, it is referred to as the 'elementary' or 'Wigner-Seitz' cell, and its Fourier transform is called 'the first Brillouin zone' in 'the reciprocal space'.

the time-reversal pairs to be the complex-conjugate pairs in Fourier space, as  $C_\infty$  shift moves them in opposite directions.



The eigenvectors of the translation operator which satisfy the periodicity of the Bravais lattice are plane waves of form:

$$f_{\mathbf{k}}(\mathbf{z}) = e^{i\mathbf{k}\cdot\mathbf{z}}, \quad \mathbf{k} \in \bar{\mathcal{L}}, \quad (21.179)$$

where the wave vector  $\mathbf{k}$  is on the reciprocal lattice  $\bar{\mathcal{L}}$ .

A general plane wave does not satisfy the periodicity, unless

$$e^{i\mathbf{k}\cdot\mathbf{R}} = 1. \quad (21.180)$$

Since  $\mathbf{R}$  is a vector from the Bravais lattice  $\mathcal{L}$ , the wave vector  $\mathbf{k}$  must lie in the reciprocal lattice of  $\mathcal{L}$ :

$$\mathbf{k} \in \mathcal{L}^*, \quad \mathcal{L}^* = \{m\mathbf{b} \mid m \in \mathbb{Z}\}, \quad (21.181)$$

where the primitive reciprocal lattice vectors  $\mathbf{b}$  satisfies:

$$\mathbf{b} \cdot \mathbf{a} = 2\pi. \quad (21.182)$$

Barvinok [arXiv:/math/0504444](https://arxiv.org/abs/math/0504444):

Let  $V$  be a  $d$ -dimensional real vector space with the scalar product  $\langle \cdot, \cdot \rangle$  and the corresponding Euclidean norm  $\| \cdot \|$ . Let  $\mathcal{L} \subset V$  be a lattice and let  $\mathcal{L}^* \subset V$  be the *dual* or the *reciprocal* lattice

$$\mathcal{L}^* = \left\{ x \in V : \langle x, y \rangle \in \mathbb{Z} \quad \text{for all } y \in \mathcal{L} \right\}.$$

**2021-08-10 Han** When we write period- $n$  periodic states as  $n$ -dimensional vectors, and write the shift operator  $r$  as a  $[n \times n]$  matrix (??) which applies cyclic permutation to the periodic state, the matrix representation of shift operators forms a permutation representation of the cyclic translation group  $C_n$ . This permutation representation is a reducible representation, i.e., it can be block diagonalized by a similarity transformation. Each block on the diagonal is an irreducible representation (irrep).

The abelian group  $C_n$  only has 1-dimensional irreps. The permutation representation of  $C_n$  can be diagonalized by discrete Fourier transform. After the transform the representation of the shift operator becomes,

$$r^m = \begin{pmatrix} 1 & & & & \\ & \omega^m & & & \\ & & \omega^{2m} & & \\ & & & \ddots & \\ & & & & \omega^{(n-1)m} \end{pmatrix}, \quad \omega = e^{2\pi i/n}, \quad (21.183)$$

with periodic states projected onto 1-dimensional subspaces in which action of the shift operators is given by corresponding irrep. As we transform the permutation representation of the shift operator into the block

diagonal form, the periodic states  $(x_0, x_1, x_2, \dots, x_{n-1})$  are spanned by the Fourier modes basis, with components  $(\tilde{\phi}_0, \tilde{\phi}_1, \tilde{\phi}_2, \dots, \tilde{\phi}_{n-1})$ . When the shift operator acts on the periodic state:  $X \rightarrow rX$ , the irreducible representations act on the components in the corresponding subspace:  $\tilde{\phi}_k \rightarrow \omega^k \tilde{\phi}_k$ .

**Dihedral group**

In the  $n$ -dimensional space of the period- $n$  periodic states, the permutation representation of the Dihedral group  $D_n$  can be generated by the shift operator matrix representation (??) and the reflection operator matrix representation:

$$\sigma = \begin{pmatrix} 1 & & & & 0 \\ & & & & 0 \\ & & & & 1 \\ & & \cdot & \cdot & 1 \\ & & & & \\ & 0 & \cdot & \cdot & \\ 0 & 1 & & & \end{pmatrix}. \tag{21.184}$$

The Dihedral group  $D_n$  has: 2 1-dimensional irreps and  $[(n-1)/2]$  2-dimensional irreps if  $n$  is odd, or 4 1-dimensional irreps and  $(n/2 - 1)$  2-dimensional irreps if  $n$  is even. If  $n$  is odd, the permutation representation can be block diagonalized into irreps:  $A_0 \oplus E_1 \oplus \dots \oplus E_{(n-1)/2}$ . If  $n$  is even, the permutation representation can be block diagonalized into irreps:  $A_0 \oplus B_1 \oplus E_1 \oplus \dots \oplus E_{n/2-1}$ .

**2021-09-02 Predrag** Why do you mark 1/8 in figures ?? and ??, when the units are 1/7's? I see. You have  $1/\sqrt{3}$  and  $\pi$ 's floating around, unless you redefine units...

**2021-07-07 Predrag** Experimenting with (21.185) by: a flip across the  $k$ th axis,  $k = 0, 1, 2, \dots, n - 1$ ,

$$\text{dihedral } D_n : H_{n,k} = \langle r, \sigma_k = r^k \sigma \mid \sigma_k r \sigma_k = r^{-1}, r^n = \sigma_k^2 \rangle \tag{21.185}$$

that Han had replaced with (??) and  $n$  with  $|n|$  in (6.155).

**2021-07-07 Predrag** A presentation of the infinite dihedral group [63] is

$$D_\infty = \langle r_i, \sigma_j \mid r_i \sigma_j = \sigma_j r_{-i}; \sigma_j^2 = 1; i, j \in \mathbb{Z} \rangle. \tag{21.186}$$

**2021-08-10 Predrag** dropped:

Applying the projection operator  $P_{0-} = \frac{1}{2}(1 - \sigma_0)/2$  we obtain a periodic state

$$\dots y_4 y_3 y_2 y_1 \boxed{0} y_1 y_2 y_3 y_4 \dots, \tag{21.187}$$

antisymmetric under reflection, where the field  $\boxed{0} = (x_0 - x_0)/2 = 0$  at the reflection lattice site 0 vanishes by antisymmetry, while the rest,

$y_j = (x_j - x_{-j})/2$ , are pairwise antisymmetric under the reflection  $\sigma$ . The underline indicates the negative of, i.e.,  $\underline{y}_j = -y_j$ .

Applying the antisymmetric projection operator  $P_{1-} = \frac{1}{2}(\mathbf{1} - \sigma r)/2$  we obtain a periodic state

$$\cdots \underline{y}_4 \underline{y}_3 \underline{y}_2 \underline{y}_1 | y_1 y_2 y_3 y_4 \cdots, \quad (21.188)$$

antisymmetric under reflection, where  $y_j = (x_j - x_{1-j})/2$ , are pairwise antisymmetric under the reflection  $\sigma_1$ .

**2021-10-29 Predrag** Dropped: Cat maps are beloved by ergodicists and statistical mechanics because, even though the field  $(q_t, p_t)$  is 2-dimensional, for integer values of the stretching parameter  $s$ , a cat map has a finite alphabet linear code, just like the Bernoulli map, and its unit torus can be tiled by two rectangles, <sup>8</sup> in analogy with the forward-in-time Bernoulli map subinterval partitioning of figure 1.2.

**2021-10-29 Predrag** Dropped: The Lagrangian formulation requires only temporal periodic states and their actions, replacing the phase space ‘cat map’ (21.36) by a ‘temporal cat’ lattice (4.178). The temporal cat has no generating partition analogue of the Adler-Weiss partition for a Hamiltonian cat map (see <sup>9</sup>). As we have shown here, no funky Hamiltonian phase space partitioning magic (such as <sup>10</sup>) is needed to count the periodic states of a temporal cat. Not only are no such partitions needed to solve the system, but the Lagrangian,

**2021-08-12 Predrag** Sidney will chuckle at this comment: The usual  $ax_t^2$  form (3.23) might be preferable, as the ‘ $a$ ’ is a stretching parameter, just like in (4.180). See sect. 3.2 Temporal Hénon.

**2021-08-17 Predrag** See (24.339). We also MUST explain the relation to literature, as in the post including (24.338).

**2020-12-17 Predrag** Link to the ChaosBook? or drop?

In sect. ?? we review the traditional cat map in its Hamiltonian formulation. (but relegate to the explicit Adler-Weiss generating partition of the cat map phase space).

We evaluate and cross-check Hill determinants by two methods, either the ‘fundamental fact’ evaluation, or by the discrete Fourier transform diagonalization, sect. ??.

**2021-10-13 Predrag** Is there a - sign specific to Sidney’s definition of the Hénon orbit Jacobian matrix Han and Predrag have to redefine both temporal cat and temporal Hénon orbit Jacobian matrix throughout, so we do not pick

---

<sup>8</sup>Predrag 2020-12-17: Link to the ChaosBook.

<sup>9</sup>Predrag 2020-12-17: Link to the ChaosBook.

<sup>10</sup>Predrag 2020-12-17: Link to the ChaosBook.

up an extraneous ‘-’ sign for odd period periodic states. See also (8.203), and Pozrikidis [84] ([click here](#)) eq. (1.8.2). The main thing is to have a Laplacian with positive eigenvalues, right? Maybe not, the main thing is to have hyperbolic eigenvalues for  $s > 2$ . Rethink. determinants in periodic orbit formulas.

$Z[J]$  notation extracted from *lattFTnotat.tex*, called by *lattFT.tex*.

, in field theorist’s parlance,  $s_z$  are ‘sources’, and

The orbit Jacobian matrix  $\mathcal{J}[X]$  is best understood by starting with the period- $n$  primitive cell stability.

As in sect. ??, the fundamental parallelepiped given the stretching of the  $n$ -dimensional phase space unit hypercube  $X \in [0, 1]^n$  by the orbit Jacobian matrix counts periodic states, with the admissible periodic states of period  $T$  constrained to field values within  $0 \leq x_t < 1$ . The fundamental parallelepiped contains images of all periodic states  $X_M$ , which are then translated by integer winding numbers  $M$  into the origin, in order to satisfy the fixed point condition (??).

**2021-10-21 Predrag Han**, RECHECK all  $s_t$ , as well as formulas starting with (??)!!! Bernoulli  $s_t$  in (??) conflicted with the old definition (??), so I changed (??).

When the force is proportional to displacement, that is, when Hooke’s law is obeyed, the spring is said to be linear, the potential is quadratic.

A matrix  $\mathbb{J}$  with no eigenvalue on the unit circle is called hyperbolic.

Ignoring (mod 1) for a moment, we can use (??) to eliminate  $p_t$  from (??) and rewrite the kicked rotor equation as the

For the problem at hand, it pays to go from the Hamiltonian (configuration, momentum) phase space formulation to the discrete Lagrangian  $(x_{t-1}, x_t)$  formulation.

*temporal lattice* condition

‘Temporal’ again refers to the discretized time  $1d$  lattice

In atomic physics applications, the values of the angle  $q$  differing by integers are identified, but the momentum  $p$  is unbounded. In dynamical systems theory one compactifies the momentum as well, by adding (mod 1) to (??), as for the Bernoulli map (??). This reduces the phase space to a square  $[0, 1) \times [0, 1)$  of unit area, with the opposite edges identified, i.e., 2-torus.

Thom-Anosov diffeomorphism

Cat maps with the same  $s$  are equivalent up to a similarity transformation, so it suffices to work out a single convenient realization, as we shall do here for the Percival-Vivaldi [79] ‘two-configuration representation’ (??).

**2021-11-29 Predrag** **!!!WARNING!!!** Following Han (8.82), we are changing the sign of the action  $S[X]$  and the orbit Jacobian matrix, as in (3.9), **THROUGH-OUT!** (Totally Predrag's fault). This makes spatiotemporal cat and  $\phi^4$  theory action strictly positive for  $s > 2$ , as needed for the probability interpretation (4.95). Han, Sidney and Predrag have to redefine temporal cat, spatiotemporal cat and temporal Hénon orbit Jacobian matrices throughout, to avoid the extraneous '-' sign for odd period periodic states. See also (8.203), and Pozrikidis [84] ([click here](#)) eq. (1.8.2).

**2016-11-08 Predrag** Say: THE BIG DEAL is

for  $d$ -dimensional field theory, symbolic dynamics is not one temporal sequence with a huge alphabet, but  $d$ -dimensional spatiotemporal tiling by a finite alphabet

**2021-12-27 Predrag** removed:

**Hill determinant: time-evolution evaluation**

However, in classical and statistical mechanics, one often computes the Hill determinant using a Hamiltonian, or 'transfer matrix' formulation.

Define

$$\hat{\phi}_t = \begin{bmatrix} x_{t-1} \\ x_t \end{bmatrix}, \quad \hat{s}_t = \begin{bmatrix} 0 \\ s_t \end{bmatrix},$$

where the hat ^ indicates a 2-dimensional 'two-configuration' [79] lattice site  $t$  state.

The 1-dimensional field theory three-term recurrence (3.9) written in the Percival-Vivaldi [79] 'two-configuration representation' (??).

$\mathcal{J}_1$  is the spatial  $[L \times L]$  orbit Jacobian matrix of  $d = 1$  temporal cat form (??),

This proves that  $\det \hat{\mathcal{J}}$  of the 'Hamiltonian' or 'two-configuration'  $[2Ln \times 2Ln]$  'phase space' orbit Jacobian matrix  $\hat{\mathcal{J}}$  defined by (21.247) equals the 'Lagrangian' Hill determinant of the  $[Ln \times Ln]$  orbit Jacobian matrix  $\mathcal{J}$ .

**2021-12-26 Han** I think (??-??) should be written as:

$$q_{t+1} = q_t + p_{t+1} \pmod{1}, \quad (21.189)$$

$$p_{t+1} = p_t + P(q_t). \quad (21.190)$$

Otherwise the angle of the rotor  $q$  is not constrained to  $[0, 1)$ .

Predrag: you are right, corrected.

**2021-12-29 Predrag** The phase space  $\mathcal{M}$  of a  $D_\infty$  invariant dynamical is union of 4 subspaces of periodic states 4 distinct symmetries (see figure 6.1)

$$\mathcal{M} = \mathcal{M}_a \cup \mathcal{M}_o \cup \mathcal{M}_{ee} \cup \mathcal{M}_{ee}, \quad (21.191)$$

where

$X \in \mathcal{M}_a$  no reflection symmetry (12.123), see figure ??

orbit  $p = \{X, rX, \dots, r_{n-1}X, \sigma X, \sigma_1 X, \dots, \sigma_{n-1}X\}$

$X \in \mathcal{M}_o$  odd period, reflection-symmetric: (??) see figure 6.1

orbit  $p = \{X, rX, \dots, r_{n-1}X\}$

$X \in \mathcal{M}_{ee}$  even period, even reflection-symmetric: (12.124)

$X \in \mathcal{M}_{eo}$  even period, odd reflection-symmetric: (12.125).

Let  $\mathcal{M}_a$  be the set of pairs of asymmetric orbits (12.123), each element of the set a forward-in-time orbit and the time-reversed orbit. If prime cycle  $p \in \mathcal{M}_a$  exists, it and each of its repeats counts as 1:

$$1/\zeta_p(t) = \exp\left(-\sum_{r=1}^{\infty} \frac{1}{2n_p r} t^{2n_p r}\right) = \sqrt{1 - t^{2n_p}}. \quad (21.192)$$

prime periodic state  $p \in \mathcal{M}_o$  exists, periodic state invariant under the dihedral group  $H_{n,k}$ ,  $n_p$  values of  $k$

$$1/\zeta_p(t) = \exp\left(-\sum_{r=1}^{\infty} \frac{1}{r} t^{n_p r}\right) = \exp\left(-\sum_{r=1}^{\infty} \frac{t^{n_p}}{1 - t^{n_p}}\right). \quad (21.193)$$

prime cycle  $p \in \mathcal{M}_{ee}$  exists

$$1/\zeta_p(t) = \exp\left(-\sum_{m=1}^{\infty} \left\{ N_{2m-1,0} t^{2m-1} + (N_{2m,0} + N_{2m,1}) \frac{t^{2m}}{2} \right\}\right). \quad (21.194)$$

Let  $\mathcal{M}_s$  be the collection of finite orbits with time reversal (flip) symmetry, and  $\mathcal{M}_a$  be the collection of the pairs of orbits without time reversal symmetry, each an orbit and the flipped orbit. A finite orbit  $p$  is a periodic points set

$$p = \{x, f(x), \dots, f^{n_p-1}(x)\}$$

if  $p \in \mathcal{M}_s$ , and

$$p = \{x, f(x), \dots, f^{k-1}(x)\} \cup \{\sigma(x), f \circ \sigma(x), \dots, f^{k-1} \circ \sigma(x)\}$$

if  $p \in \mathcal{M}_a$ , where  $k = n_p/2$ .

If  $p \in \mathcal{M}_s$ ,

$$\zeta_p(t) = \sqrt{\frac{1}{1 - t^{2n_p}}} \exp\left(\frac{t^{n_p}}{1 - t^{n_p}}\right), \quad (21.195)$$

The product form of the zeta function is:

$$1/\zeta_{\text{KLP}}(t) = \prod_{p_1 \in \mathcal{O}_1} \sqrt{1 - t^{2n_{p_1}}} \exp\left(-\frac{t^{n_{p_1}}}{1 - t^{n_{p_1}}}\right) \prod_{p_2 \in \mathcal{M}_a} (1 - t^{n_{p_2}}). \quad (21.196)$$

How to count the number of periodic states for temporal cat?

No symmetry periodic states Hill determinant:

$$N_n = \prod_{j=0}^{n-1} \left( s - 2 \cos \frac{2\pi j}{n} \right).$$

The products of eigenvalues for the  $C_n$  discrete Fourier case follows from (21.142):

$$\prod_{j=0}^{n-1} \left( s - 2 \cos \frac{2\pi j}{n} \right) = (\Lambda^{n/2} - \Lambda^{-n/2})^2, \quad (21.197)$$

It's a square, because of the  $D_n$  symmetry. Consider even, odd cases, use  $\cos 0 = 1$ ,  $\cos \pi = -1$ ,  $\cos(-\theta) = \cos \theta$ . The product over non-trivial eigenvalues is:

$$n = 2m \quad M_{n,0} = \prod_{j=1}^{m-1} \left( s - 2 \cos \frac{\pi j}{m} \right) = \frac{|\Lambda^{n/2} - \Lambda^{-n/2}|}{\mu \sqrt{\mu^2 + 4}} \quad (21.198)$$

$$n = 2m - 1 \quad M_{n,1} = \prod_{j=1}^{m-1} \left( s - 2 \cos \frac{2j\pi}{2m-1} \right) = \frac{|\Lambda^{n/2} - \Lambda^{-n/2}|}{\mu} \quad (21.199)$$

Next, look at the *symmetric* periodic states Hill determinants:

For odd  $n = 2m - 1$ ,

$$N_{n,1} = \prod_{j=0}^{m-1} \left( s - 2 \cos \frac{2\pi j}{n} \right) = \mu M_{n,1}. \quad (21.200)$$

For  $n = 2m$ ,

$$\begin{aligned} N_{n,1} &= \prod_{j=0}^{m-1} \left( s - 2 \cos \frac{2\pi j}{n} \right) \\ N_{n,0} &= (s + 2) N_{n,1}, \end{aligned} \quad (21.201)$$

and

$$\frac{1}{2} (N_{n,0} + N_{n,1}) = \frac{\mu^2 + 5}{2} \prod_{j=0}^{m-1} \left( s - 2 \cos \frac{2\pi j}{n} \right) = \frac{\mu^2 + 5}{2\mu} \sqrt{\frac{(\Lambda^n + \Lambda^{-n} - 2)}{\mu^2 + 4}} \quad (21.202)$$

The number of periodic states can be written as polynomials: For  $n = 2m - 1$ :

$$\begin{aligned} N_{n,0} &= \mu \left( \Lambda^{n/2} - \Lambda^{-n/2} \right) \\ &= \mu^2 \Lambda^{-1/2} \left( \Lambda^m - \Lambda^{-m+1} \right). \end{aligned} \quad (21.203)$$

For  $n = 2m$ :

$$\begin{aligned} \frac{1}{2}(N_{n,0} + N_{n,1}) &= \frac{s+3}{2(\Lambda - \Lambda^{-1})} (\Lambda^{n/2} - \Lambda^{-n/2}) \\ &= \frac{\mu^2 + 5}{2\mu\sqrt{\mu^2 + 4}} |\Lambda^m - \Lambda^{-m}|. \end{aligned} \quad (21.204)$$

Now we can compute the  $h(t)$  from (21.233)

$$\begin{aligned} h(t) &= \sum_{m=1}^{\infty} \left[ N_{2m-1,0} t^{2m-1} + (N_{2m,0} + N_{2m,1}) \frac{t^{2m}}{2} \right] \\ &= \mu \frac{\Lambda^{1/2} t}{1 - \Lambda t^2} - \mu \frac{\Lambda^{-1/2} t}{1 - \Lambda^{-1} t^2} \\ &\quad + \frac{\mu^2 + 5}{2(\Lambda - \Lambda^{-1})} \frac{\Lambda t^2}{1 - \Lambda t^2} - \frac{\mu^2 + 5}{2(\Lambda - \Lambda^{-1})} \frac{\Lambda^{-1} t^2}{1 - \Lambda^{-1} t^2}. \end{aligned} \quad (21.205)$$

Using (21.232) we have the symmetric periodic states part of the Kim-Lee-Park zeta function. Expanding this zeta function using (21.215), we have:

$$\begin{aligned} -t \frac{\partial}{\partial t} (\ln e^{-h(t)}) &= t + 6t^2 + 12t^3 + 36t^4 + 55t^5 + 144t^6 \\ &\quad + 203t^7 + 504t^8 + 684t^9 + 1650t^{10} + \dots \end{aligned} \quad (21.206)$$

which is in agreement with (21.215) and table 24.3.

### 21.3.1 Counting periodic states

Given the topological zeta function (21.230) we can count the number of periodic states from the generating function: <sup>11</sup>

$$\frac{-t \frac{d}{dt} (1/\zeta_{\sigma}(t))}{1/\zeta_{\sigma}(t)} = \sum_{n=1}^{\infty} N_n t^{2n} + \sum_{n=1}^{\infty} \sum_{k=0}^{n-1} N_{n,k} t^n = \sum_{m=1}^{\infty} a_m t^m, \quad (21.207)$$

where the coefficients are:

$$a_m = \begin{cases} \sum_{k=0}^{m-1} N_{m,k}^{\sigma} = m N_{m,0}^{\sigma}, & m \text{ is odd,} \\ N_{m/2} + \sum_{k=0}^{m-1} N_{m,k}^{\sigma} = N_{m/2} + \frac{m}{2} (N_{m,0}^{\sigma} + N_{m,1}^{\sigma}), & m \text{ is even.} \end{cases} \quad (21.208)$$

<sup>11</sup>Predrag 2021-08-25: We have the counts of the periodic states  $N_n, N_{n,k}$  already, from (21.231), so why don't we reverse the logic, start here, and get the zeta function (21.232) by integration? Mention that this is an example of Lind zeta function [69] (??) without ever writing it down, so we do not have to explain it? It's a side issue for us, really.



Using the product formula of topological zeta function (21.196) and the numbers of orbits with length up to 5 from the table 24.3, we can write the topological zeta function:

$$\begin{aligned} 1/\zeta_\sigma(t) &= \sqrt{1-t^2} \exp\left(-\frac{t}{1-t}\right) (1-t^4) \exp\left(-\frac{2t^2}{1-t^2}\right) (\sqrt{1-t^6})^3 \\ &\quad \exp\left(-\frac{3t^3}{1-t^3}\right) (1-t^6)(1-t^8)^3 \exp\left(-\frac{6t^4}{1-t^4}\right) \\ &\quad (1-t^8)^2(1-t^{10})^5 \exp\left(-\frac{10t^5}{1-t^5}\right) (1-t^{10})^6 \dots \end{aligned} \quad (21.209)$$

The generating function is:

$$\frac{-t \frac{d}{dt}(1/\zeta_\sigma)}{1/\zeta_\sigma} = t + 7t^2 + 12t^3 + 41t^4 + 55t^5 + \dots, \quad (21.210)$$

which is in agreement with (21.208), where the  $N_n$  and  $N_n^\sigma$  are the  $C_n$  and  $SF_n$  in the table 24.3.

We are not able to retrieve the numbers of fixed points by their symmetry groups using this topological zeta function (21.230), unless we rewrite the topological zeta function with two variables:

$$\zeta_\sigma(t, u) = \exp\left(\sum_{n=1}^{\infty} \frac{N_n}{2n} t^{2n} + \sum_{n=1}^{\infty} \sum_{k=0}^{n-1} \frac{N_{n,k}}{n} u^n\right). \quad (21.211)$$

Using this topological zeta function  $\zeta_\sigma(t, u)$  we can write two generating functions:

$$\frac{-t \frac{\partial}{\partial t}(1/\zeta_\sigma(t, u))}{1/\zeta_\sigma(t, u)} = \sum_{n=1}^{\infty} N_n t^{2n}, \quad (21.212)$$

and

$$\frac{-u \frac{\partial}{\partial u}(1/\zeta_\sigma(t, u))}{1/\zeta_\sigma(t, u)} = \sum_{n=1}^{\infty} \sum_{k=0}^{n-1} N_{n,k} u^n. \quad (21.213)$$

Using the product formula of this topological zeta function and the numbers of orbits with length up to 5 from the table 24.3, the Kim-Lee-Park zeta function is:

$$\begin{aligned} 1/\zeta_\sigma(t, u) &= \sqrt{1-t^2} \exp\left(-\frac{u}{1-u}\right) (1-t^4) \exp\left(-\frac{2u^2}{1-u^2}\right) (\sqrt{1-t^6})^3 \\ &\quad \exp\left(-\frac{3u^3}{1-u^3}\right) (1-t^6)(1-t^8)^3 \exp\left(-\frac{6u^4}{1-u^4}\right) \\ &\quad (1-t^8)^2(1-t^{10})^5 \exp\left(-\frac{10u^5}{1-u^5}\right) (1-t^{10})^6 \dots \end{aligned} \quad (21.214)$$

And the generating function from this topological zeta function is:

$$\frac{-u \frac{\partial}{\partial u}(1/\zeta_\sigma(t, u))}{1/\zeta_\sigma(t, u)} = u + 6u^2 + 12u^3 + 36u^4 + 55u^5 + \dots, \quad (21.215)$$

which is in agreement with (21.213), where the  $N_n^\sigma$  is the  $SF_n$  in the table 24.3.

2021-12-10 Predrag

$$-\square x_t + a x_t^2 - 2 x_t - s_t = 0. \quad (21.216)$$

$$V(X, M) = \sum_{t \in \mathcal{L}} \left( \frac{g}{k} x_t^k - x_t^2 - s_t x_t \right), \quad s_t = -1. \quad (21.217)$$

Works also for temporal cat:

$$V(X, M) = \sum_{t \in \mathcal{L}} \left( \frac{s}{2} x_t^2 - x_t^2 - s_t x_t \right) = \sum_{t \in \mathcal{L}} \left( \frac{s-2}{2} x_t^2 - s_t x_t \right), \quad (21.218)$$

### 21.3.2 Hill determinant: fundamental parallelepiped evaluation

As a concrete example consider the Bravais lattice with basis vector

The orbit Jacobian matrix is the  $\delta/\delta x_k$  derivative of the temporal Hénon three-term recurrence relation (3.26)

$$\mathcal{J}_p = -r + 2 \mathbb{X}_p - r^{-1}, \quad (21.219)$$

where  $\mathbb{X}_p$  is a diagonal matrix with  $p$ -periodic state  $x_k$  in the  $k$ th row/column, and the '1's in the upper right and lower left corners enforce the periodic boundary conditions.

The action of the temporal Hénon orbit Jacobian matrix can be hard to visualize, as a period-2 periodic state is a 2-torus, period-3 periodic state a 3-torus, etc.. Still, the fundamental parallelepiped for the period-2 and period-3 periodic states, should suffice to convey the idea. The fundamental parallelepiped basis vectors (??) are the columns of  $\mathcal{J}$ . The  $[2 \times 2]$  orbit Jacobian matrix and its Hill determinant follow from (3.64)

$$\mathcal{J} = \begin{pmatrix} 2x_0 & -2 \\ -2 & 2x_1 \end{pmatrix}, \quad \text{Det } \mathcal{J} = 4(x_0 x_1 - 1) = -4(a - 3). \quad (21.220)$$

The resulting fundamental parallelepiped shown in figure ?? (a). Period-3 periodic states for  $s = 3$  are contained in the half-open fundamental parallelepiped of figure ?? (b), defined by the columns of  $[3 \times 3]$  orbit Jacobian matrix

$$\mathcal{J} = \begin{pmatrix} 2x_0 & -1 & -1 \\ -1 & 2x_1 & -1 \\ -1 & -1 & 2x_2 \end{pmatrix}, \quad \text{Det } \mathcal{J} = 8x_0 x_1 x_2 - 2(x_0 + x_2 + x_3) + 2, \quad (21.221)$$

**2021-12-31 Han** Note that in the temporal lattice reformulation, the Bernoulli system involves two distinct lattices:

- (i) Any lattice field theory: in the discretization (4.46) of the time continuum, one replaces *any* dynamical system's time-dependent field  $x(t) \in \mathbb{R}$  at time  $t \in \mathbb{R}$  by a discrete set of its values  $x_t = x(at)$  at time instants  $t \in \mathbb{Z}$ . Here  $t$  is a *coordinate* over which the field  $x$  is defined.
- (ii) Specific to the Bernoulli system: the site  $t$  field value  $x_t$  (??) is confined to the unit interval  $[0, 1)$ , imparting integer lattice structure onto the intermediate calculational steps in the extended phase space (??) on which the orbit Jacobian matrix  $\mathcal{J}$  (1.19) acts.

12

**2020-05-31 Predrag Simó** [89] *On the Hénon-Pomeau attractor* is a very fine early paper. Cite it in Hénon remark.

Miguel, Simó and Vieir [76] *From the Hénon conservative map to the Chirikov standard map for large parameter values* ([click here](#)):

Endler and Gallas [46]. method resembles the methods earlier employed for quadratic polynomials (and their Julia sets) by Brown [21] and Stephenson [90]. (PC 2022-01-03 now referred to.)

Brown gives cycles up to length 6 for the logistic map, employing symmetric functions of periodic points.

Hitzl and Zele [54] study the of the Hénon map for cycle lengths up to period 6.

**2021-10-29 Predrag** Dropped: , all five of form  $\{X_{s_0 s_1 s_2}, X_{s_1 s_2 s_0}, X_{s_2 s_0 s_1}\}$ .

**2020-12-17 Predrag** Gave up on linking temporal cat to ChaosBook, as Adler-Weiss partitions are not there yet. Maybe refer to Adler-Weiss in later version.

**2021-12-28 Han** Statement after reseq recipCircl is not correct. In the  $k = 1$  and  $k = n - 1$  subspaces, all reciprocal periodic states lie in complex plane on vertices of regular  $n$ -gons. Generally this is not true. See figures 24.57 and 24.58  $k = 2$  and  $k = 3$  (in blogCat), where the shift  $r$  rotate the reciprocal periodic state by  $2\pi/3$  and  $2\pi/2$ , instead of  $2\pi/6$ . I suggest we only mention  $k = 1$  here.

**2021-12-30 Predrag** It does not say in The Bible that vertices of an  $n$ -gon have to be visited in increments of one. Periodic states lie on the vertices of  $n$ -gons for any  $k$ , they are just visited in different order for different  $k$ .

---

<sup>12</sup>Predrag 2021-10-25: Combine the above with the temporal cat page ?? discussion into a remark that temporal Bernoulli and temporal cat aslo have a *dynamical*  $D_1$  symmetry, not utilized in this paper, as nonlinear field theories such as temporal Hénon do not have such symmetries. Here we study only the symmetries of the floor, not the dancer.

An if  $n$  is not prime, some visitation sequences do not visit all vertices. That's OK. Every vertex is occupied.

**2021-12-30 Predrag** (??) formulas do not make sense to me for  $n$  odd...

$$\begin{aligned} N_n &= \left( \Lambda^{n/2} - \Lambda^{-n/2} \right)^2, \\ N_{n,0} &= \Lambda^{n/2} - \Lambda^{-n/2} \end{aligned} \quad (21.222)$$

but I do remember all  $\Lambda^{1/2}$  eventually going away... Never mind.

**2021-12-30 Han** For general  $s$  we have:  $N_{n,0} = \sqrt{(s-2)N_n}$  (12.126). This is in agreement with table ??.

**2021-12-26 Han** Given the symmetry group of the periodic states, we can find a fundamental domain in the space of field configurations such that each orbit in this space visits the fundamental domain only once. Each periodic state in the fundamental domain is a representative periodic state of an orbit.

A natural way to choose the fundamental domain of  $C_n$  symmetry group is to divide the subspace of a component of the reciprocal lattice configuration. In the subspace of the  $k = 1$  Fourier mode, the fundamental domain is an  $1/n$  wedge. The lattice shift  $r$  maps the fundamental domain by rotation and tiles the whole complex plane. Orbits visit the  $1/n$  wedge only once, so the points in the fundamental domain represent an orbit each.

Repeats of the shorter periodic states sit on the 0 of the complex plane, which is on the boundary of the fundamental domain.

For example, one can choose the region in the complex plane of  $\tilde{\phi}_1$  with argument  $-\pi/2n \leq \theta_1 < \pi/2n$  to be the fundamental domain. Each orbit can visit the fundamental domain only once. For the period-3 periodic states of the temporal Bernoulli system with  $s = 2$  shown in figure ??, there are 3 points in this region, which are representative periodic states of two different period-3 orbits and the fixed point 0.

13

**2022-01-04 Han** Moved from the end of sect. ??

If, in addition, the law is time-reversal (or time-inversion) invariant, the symmetry includes time-reflection, ie, it is dihedral group  $D_n$  with  $2n$  elements, so the reciprocal lattice should be a half of the above  $1/n$  sliver of a  $n$ -gon, and irreps are now either 1 or 2 dimensional. Even  $n$  is different from odd  $n$ , and solutions either appear in pairs, or are self dual under reflection in 3 different ways.

Due to the time reversal, all  $k = 2\pi/5$  irrep states are the same as the  $k = 4\pi/5$  irrep states.

<sup>13</sup>Predrag 2021-08-20: Merge figure 6.1 (a) with 1dLatStatC\_5\_0x3.svg.

**2022-01-15 Han** where  $X$  and  $\hat{f}(X)$  are  $nd$ -dimensional column vectors with  $(id + j)$ th components  $(x_t)_j$  and  $[\hat{f}(x_t)]_j$ , where  $0 \leq i < n - 1, 0 \leq j < d - 1$ , and  $r$  is the cyclic  $[nd \times nd]$  time translation operator (compare with (??), (12.58)):

$$r = \begin{pmatrix} 0 & \mathbf{1}_d & & & \\ & 0 & \mathbf{1}_d & & \\ & & & \ddots & \\ & & & 0 & \mathbf{1}_d \\ \mathbf{1}_d & & & & 0 \end{pmatrix}, \quad (21.223)$$

where  $\mathbf{1}$  is the  $d$ -dimensional identity matrix.

Just as a scalar field satisfying a  $k$ th order differential equation can be replaced by a  $k$ -component field, each satisfying a first order equation, a  $k$ th order difference equation for a scalar field can be replaced by a  $k$ -component lattice site field, satisfying  $k$  1st order difference equations.

**2022-01-16 Predrag** Now I get it. To get from  $\prod d^2x_t$  in (??) to  $\prod dx_t$  in (??) we note that the first component of time-step (??) written in terms of 1-dimensional Dirac delta functions is trivial,

$$\begin{aligned} \int d\hat{x}_t \delta(\hat{x}_{t+1} - \hat{f}(\hat{x}_t)) &= \int d\hat{x}_{t,1} d\hat{x}_{t,2} \delta(\hat{x}_{t+1,1} - \hat{x}_{t,2}) \delta(\hat{x}_{t+1,2} - f(\hat{x}_{t,1}, \hat{x}_{t,2})) \\ &= \int d\hat{x}_{t,1} d\hat{x}_{t,2} \delta(\hat{x}_{t+1,1} - \hat{x}_{t,2}) \delta(\hat{x}_{t+2,1} - f(\hat{x}_{t,1}, \hat{x}_{t+1,1})) \\ &= \int d\hat{x}_{t,1} \delta(\hat{x}_{t+2,1} - f(\hat{x}_{t,1}, \hat{x}_{t+1,1})) \\ &= \int dx_{t-1} \delta(x_{t+1} - f(x_{t-1}, x_t)) \end{aligned} \quad (21.224)$$

where we have used periodicity and dropped the component subscript,  $\hat{x}_{t,1} \rightarrow x_{t-1}$  ? Looking back: we should get rid of field component indices by using two Greek letters,  $\hat{x}_t = (x_t, \varphi_t)$ , where  $\varphi_t = x_{t+1}$ .

**2020-02-08 Predrag** Gave up on this:

Complain about ref. [52] Dirichlet bc's stupidity clearly both in the intro and in conclusions.

**2022-01-17 Han** I changed (12.57) from

$$\Delta x_t - r^{-1} \mathbb{J}_t \Delta x_t = 0$$

which is incorrect. The shift matrix  $r$  cannot act on the  $d$ -dimensional vector.

PC: OK.

**2022-01-19 Predrag** Dropped:

For the 1-dimensional temporal lattice examples studied here, the reader

might not see much of an advantage in the global stability ('Lagrangian') formulation over the forward-in time stability ('Hamiltonian') formulation. The real payback is in the higher-dimensional spacetimes.

The fundamental fact does not apply to orbit counting for reversal-invariant nonlinear field theories, such as the temporal Hénon.

It is *prime* in the same sense that Leibnitz monad is indivisible.

Toeplitz, i.e., matrix constant along each diagonal,  $\mathcal{J}_{k\ell} = j_{k-\ell}$ .

For a finite set of neighbors, Allroth [2] has partial results in the context of Frenkel-Kontorova models.

we will spare the reader the group-theorist's cosets and group quotients.

**2021-12-24 Predrag** We have found MacKay [70] 1982 PhD thesis lists the periodic periodic states and orbits counts, together with the counts of time reversal invariant periodic states and orbits. Do cite in our paper(s). MacKay had these numbers already listed in Table 1.2.3.5.1 of his 1982 PhD thesis [70].

**2022-01-22 Predrag** Gave up on this confused insert on **Physical dimension**

Time evolution Jacobian matrices are nice, as to their multiplicative structure (??), the Floquet matrix for the  $r$ th repeat of a prime period- $n$  periodic state  $X_p$  (??) is known, once the prime periodic state  $X_p$  Floquet matrix (??) is known.

But that is actually quite meaningless, especially for infinite dimensional physical systems. What matters is the Hill determinant  $|\text{Det } \mathcal{J}_c| = |\det(\mathbf{1} - \mathbb{J}_c)|$ , which is a finite number as long as there is a finite number of expanding directions; the contracting ones are only small corrections to 1.

If  $\partial_i v_i < 0$  at a given phase space point  $x$ , the flow is *locally* contracting, and the trajectory might be falling into an attractor. If  $\partial_i v_i(x) < 0$  for all  $x \in \mathcal{M}$ , the flow is *globally* contracting, with the dimension of the attractor necessarily smaller than the dimension of phase space  $\mathcal{M}$ . For  $\infty$ -dimensional dissipative flows, such as Navier–Stokes, the  $\infty$  of stability multipliers  $\Lambda_i$  in can be arbitrarily small; as such exponents represent damping of arbitrarily kinky modes of a viscous fluid, they are of no interest for study of steady turbulence. So the product should be truncated to a finite number  $d_{phys}$  of leading stability exponents. We shall refer to this integer as a *physical* dimension of a *strange attractor*, in fluid dynamics often referred to as the *inertial manifold*. Every expanding or marginal direction contributes 1 to  $d_{phys}$ , and then to get a lower bound on  $d_{phys}$ , one has to keep at least as many contracting  $\Lambda_i$  as needed to ensure that the product is globally contracting. As nonlinear terms can mix various terms in such a way that expansion in some directions overwhelms the strongly contracting ones,  $d_{phys}$  is larger than this bound, but still a finite number.

This is an amazing result: a fluid's phase space is  $\infty$ -dimensional, but its long term dynamics is confined to a finite-dimensional(!) subspace, the reason why we can apply the few degrees of freedom technology developed here to  $\infty$ -dimensional field theories.

**2022-01-27 Predrag** Uploaded LC21 [67] as [arXiv:2201.11325](https://arxiv.org/abs/2201.11325).

For details, see `reversal/00ReadMe.txt`.

**2022-01-30 Predrag** Submitted LC21 [67] to

`mc04.manuscriptcentral.com/jphysa-iop`

For referees, see `reversal/jphysa-v1/referees.txt`

**2022-04-09 Predrag** At the moment I do not remember the logic of labels in figure 1.2(b) - good for desymmetrization? and why '6' rather than '0'?

**2022-04-29 Han** The subsection of  $D_\infty$  or Kim-Lee-Park zeta function needs to be rewritten.

If the assumed symmetry  $G$  is not the maximal symmetry group, let's say we assume only  $G = C_\infty$  whereas the full symmetry is  $D_\infty$ , Lind zeta function (??) reduces to the Artin-Mazur zeta (??) which counts reflection symmetry-related periodic states as belonging to separate 'prime orbits', a problem that repeatedly bedevils the [ChaosBook.org](https://chaosbook.org) exposition of periodic orbit theory.



So our next task is to evaluate Lind zeta function when the symmetry group  $G$  of temporal lattice of a given dynamical system is the infinite dihedral group  $D_\infty$ , the group of all translations and reflections, i.e., system's defining law is time and time-reversal invariant. For the infinite translation  $H_a$  subgroup (6.244) the index is (as illustrated by figure ??)

$$|D_\infty/H_n| = 2n. \quad (21.225)$$

As explained in sect. ??, the  $D_\infty$  orbits of reflection-symmetric periodic states contain only translations, so the index of each infinite dihedral subgroup  $H_{a,k}$  (??) is

$$|D_\infty/H_{n,k}| = n. \quad (21.226)$$

Thus the phase space  $\mathcal{M}$  of a  $D_\infty$  invariant dynamical system is the union

$$\mathcal{M} = \mathcal{M}_a \cup \mathcal{M}_s, \quad (21.227)$$

where  $\mathcal{M}_a$  is the set of pairs of asymmetric orbits (12.123), each element of the set a forward-in-time orbit and the time-reversed orbit, and  $\mathcal{M}_s$  is the set of time reversal symmetric orbits, invariant under reflections (??-12.125).

The Lind zeta function (??) now has contributions from asymmetric periodic states, whose index is (21.225), and symmetric periodic states, index

(21.226):

$$\zeta_{D_\infty}(t) = \exp\left(\sum_{n=1}^{\infty} \frac{N_n}{2} \frac{t^{2n}}{n} + \sum_{n=1}^{\infty} N_n^s \frac{t^n}{n}\right). \quad (21.228)$$

$N_n/2$  counts each asymmetric orbit pair of period  $n$  only once, so the first sum yields the Artin-Mazur zeta function  $\zeta_a(t^2)$  for the asymmetric periodic states:

$$\zeta_{D_\infty}(t) = \zeta_a(t^2) \zeta_s(t). \quad (21.229)$$

In order to count the symmetric periodic states, we have to take into account the fact that the three types of symmetric periodic states of sect. ?? have to be counted separately, as their orbit Jacobian matrices satisfy different boundary conditions,

$$\zeta_s(t) = \exp\left(\sum_{n=1}^{\infty} \sum_{k=0}^{n-1} \frac{N_{n,k}^s}{n} t^n\right). \quad (21.230)$$

The number of reflection-symmetric periodic states does not depend on the location of the reflection point  $k$ , only on the type of symmetry (see the class counts (??) and (??)), so

$$N_{n,k}^s = \begin{cases} N_{n,0}^s & \text{if } n \text{ odd} \\ N_{n,0}^s & \text{if } n \text{ and } k \text{ are even} \\ N_{n,1}^s & \text{if } n \text{ even and } k \text{ is odd,} \end{cases} \quad (21.231)$$

and the Lind zeta function takes the form that we refer to as the Kim-Lee-Park [63] zeta function

$$\zeta_{D_\infty}(t) = \zeta_a(t^2) e^{h(t)}, \quad (21.232)$$

where

$$h(t) = \sum_{m=1}^{\infty} \left\{ N_{2m-1,0}^s t^{2m-1} + (N_{2m,0}^s + N_{2m,1}^s) \frac{t^{2m}}{2} \right\}. \quad (21.233)$$

### Euler product form of Kim-Lee-Park zeta function.

Kim *et al.* [63] show that the contribution of a single prime orbit  $p$  to the Kim-Lee-Park zeta function is:

$$1/\zeta_{D_\infty}(t)|_p = \begin{cases} 1 - t^{n_p} & \text{if } p \in \mathcal{M}_a, \\ \sqrt{1 - t^{2n_p}} \exp\left(-\frac{t^{n_p}}{1 - t^{n_p}}\right) & \text{if } p \in \mathcal{M}_s, \end{cases} \quad (21.234)$$

with the zeta function written as a product over prime orbits:

$$1/\zeta_{D_\infty}(t) = \prod_{p_a \in \mathcal{M}_a} (1 - t^{n_{p_a}}) \prod_{p_s \in \mathcal{M}_s} \sqrt{1 - t^{2n_{p_s}}} \exp\left(-\frac{t^{n_{p_s}}}{1 - t^{n_{p_s}}}\right), \quad (21.235)$$



to be expanded as a power series in  $t$ .

The Euler product form of topological zeta functions makes it explicit that they count *prime orbits*, i.e., sets of equivalent periodic states related by symmetries of the problem. The remainder of this section the reader might prefer to skip: we verify by explicit temporal cat calculation that the Kim-Lee-Park zeta function indeed counts infinite dihedral group  $D_\infty$  orbits and the corresponding periodic states.

**2022-05-02 Predrag to Angelo Vulpiani**

Long silence because I have not YET (!) started reading *Il Libro* [26] ([click here](#)). Grazie for sharing it, and I'll get to it eventually, but... The usual physicist obsession – we had run into a wall exploring “exact coherent structures” in fluid dynamics, and my resolution is to take the revolutionary road: kill dynamical systems and retreat to field theory/stat mech. It has been very hard to write it up in a way that gets it across – here is part of it (with video clips) <https://chaosbook.org/overheads/spatiotemporal/LC21.pdf>  
And much talking about it over last few years:  
<https://chaosbook.org/overheads/spatiotemporal/>  
I think it might align with some of your work way back then, tell me if I should read/cite something in particular.

**Note to Han & Predrag send**

<https://chaosbook.org/overheads/spatiotemporal/LC21.pdf>  
link to

Michael Aizenman

(R. E. Amritkar and gade are not active)

S. Anastassiou

Ping Ao [aoping@sjtu.edu.cn](mailto:aoping@sjtu.edu.cn)

Roberto Artuso [artuso@fis.unico.it](mailto:artuso@fis.unico.it)

Serge Aubry

Erik Aurell [eaurell@kth.se](mailto:eaurell@kth.se)

Bountis

Dwight Barkley [d.barkley@warwick.ac.uk](mailto:d.barkley@warwick.ac.uk) University of Warwick

A. Bäcker

A. Barvinok

David Berenstein <[dberens@physics.ucsb.edu](mailto:dberens@physics.ucsb.edu)>

Ofer Biham

Erik M. Bollt [ebollt@clarkson.edu](mailto:ebollt@clarkson.edu) Clarkson University

S. V. Bolotin

A. Bountis

H. Chat'e

Xiangyu Cao <[xiangyu.cao08@gmail.com](mailto:xiangyu.cao08@gmail.com)>

B. Clair

A. M. Ozorio de Almeida

Carl Dettmann  
 H. R. Dullin  
 Marco Falconi marco.falconi@polimi.it  
 Farazmand  
 Jason Gallas  
 Gutkin  
 Jonathan Halcrow  
 Masanori Hanada <hanadamasanori@gmail.com>  
 J. H. Hannay  
 S. Isola  
 W. Just  
 Jon Keating j.p.keating@bristol.ac.uk University of Bristol  
 J. Li  
 Douglas Lind  
 R. S. MacKay  
 Ronnie Mainieri  
 James Meiss jdm@colorado.edu University of Colorado  
 Kevin Mitchell kmitchell@ucmerced.edu University of California Merced  
 I. Montvay  
 G. Münster  
 E. Ott  
 Kyewon Koh Park kkpark@kias.re.kr Korea Inst. Adv. Study  
 Antonio Politi a.politi@abdn.ac.uk U Aberdeen  
 M. Pollicott  
 C. Pozrikidis  
 Tomaz Prosen tomaz.prosen@fmf.uni-lj.si University of Ljubljana  
 Putkaradze  
 Klaus Richter klaus.richter@physik.uni-regensburg.de Universität Regensburg  
 Martin Richter <martin.richter@nottingham.ac.uk>  
 Ruelle  
 S. Saito  
 Marcos Saraceno saraceno@tandar.cnea.gov.ar CNEA-GIyA Laboratorio Tandar  
 George Savvidy, "Demokritos", Athens  
 (the other two not active? Young-One Kim, Jungseob Lee)  
 Tobias Schneider  
 Michele Schiavina (ETH Zürich)  
 Steve Shenker  
 David G. Sterling dsterling@somalogic.com (old?)  
 T. Sunada  
 G. Tanner  
 Jean-Luc Thiffeault jeanluc@gmail.com 2022-05-02  
 S. Tomsovic  
 Alessandro Torcini <alessandro.torcini@u-cergy.fr>  
 D. V. Treschev  
 Tuckermann

*CHAPTER 21. ARTICLE EDITS*

---

Gabor Vattay

Divakar Viswanath divakar@umich.edu University of Michigan

Franco Vivaldi f.vivaldi@qmul.ac.uk Queen Mary University of London

Angelo Vulpiani angelo.vulpiani@roma1.infn.it 2022-05-02

Wiegmann

Ashley Willis

**Contacted**

Vladimir Rosenhaus <vrosenhaus@gc.cuny.edu>

Baladi

Rafael De La Llave

## 21.4 Hill determinant: stability of an orbit vs. its time-evolution stability

The deep insight here is that the two formulations of mechanics, the forward-in-time Hamiltonian evolution, and the global, Lagrangian, temporal cat formulation are related by the *Hill's formula*.

The relation is so elementary that many practitioners routinely use it without ever having heard of any 'Hill's formula'.

One can compute the orbit Jacobian matrix of a scalar field periodic state of such system using the forward-in-time Hill's formula for the  $k$ -component lattice site field, with the corresponding  $[kn \times kn]$  orbit Jacobian matrix determinant (??).

The  $d = 2$  lattice spatiotemporal cat equations can be recast in a matrix form, by rewriting the defining equations in terms of *block matrices* [23, 27, 37, 56], constructed by the **Kronecker product**  $\mathbf{A} \otimes \mathbf{B}$ , an operation (introduced by Zehfuss in 1858) that replaces the  $a_{ij}$  element of an  $[n \times n]$  matrix  $\mathbf{A}$  by  $[m \times m]$  matrix block  $a_{ij}\mathbf{B}$ , resulting in an  $[mn \times mn]$  block matrix [3, 92]

$$\mathbf{A} \otimes \mathbf{B} = \begin{bmatrix} a_{11}\mathbf{B} & \cdots & a_{1n}\mathbf{B} \\ \vdots & \ddots & \vdots \\ a_{n1}\mathbf{B} & \cdots & a_{nn}\mathbf{B} \end{bmatrix}. \quad (21.236)$$

Consider  $\mathbf{A}, \mathbf{A}'$  square matrices of size  $[n \times n]$ , and  $\mathbf{B}, \mathbf{B}'$  square matrices of size  $[m \times m]$ . The matrix product of two block matrices is a block matrix [3, 91],

$$(\mathbf{A} \otimes \mathbf{B})(\mathbf{A}' \otimes \mathbf{B}') = (\mathbf{A}\mathbf{A}') \otimes (\mathbf{B}\mathbf{B}'). \quad (21.237)$$

The trace and the determinant of a block matrix are given by (12.20). The two  $[mn \times mn]$  block matrices  $\mathbf{A} \otimes \mathbf{B}$  and  $\mathbf{B} \otimes \mathbf{A}$  are equivalent by a similarity transformation

$$\mathbf{B} \otimes \mathbf{A} = \mathbf{P}^\top (\mathbf{A} \otimes \mathbf{B}) \mathbf{P}, \quad (21.238)$$

where  $\mathbf{P}$  is permutation matrix. As  $\det \mathbf{P} = 1$ , the block matrix determinant  $\det (\mathbf{A} \otimes \mathbf{B}) = \det (\mathbf{B} \otimes \mathbf{A})$  is independent of the order in which blocks are constructed.

Consider a rectangular  $d = 2$  lattice  $[L \times T]_0$  primitive cell. The orbit Jacobian matrix (??) written as a  $[LT \times LT]$  Kronecker product block matrix is

$$\mathcal{J} = \mathbf{1}_1 \otimes (r_2 + r_2^{-1}) - 2s \mathbf{1}_1 \otimes \mathbf{1}_2 + (r_1 + r_1^{-1}) \otimes \mathbf{1}_2, \quad (21.239)$$

where the (21.236) matrix  $\mathbf{A}$  and identity  $\mathbf{1}_1$  matrix are 'spatial'  $[L \times L]$  matrices, with blocks  $\mathbf{B}$  and identity  $\mathbf{1}_2$  'temporal'  $[T \times T]$  matrix blocks. Indices '1', '2' referring to 'spatial', 'temporal' lattice directions, respectively.

Our task is to compute the Hill determinant  $|\text{Det } \mathcal{J}|$ . We first show how to do that directly, by computing the volume of the fundamental parallelepiped.

### 21.4.1 Hill determinant: time-evolution evaluation

In practice, one often computes the Hill determinant using a Hamiltonian, or ‘transfer matrix’ formulation. An example is the temporal cat 3-term recurrence (??),

$$\begin{aligned} x_t &= x_t \\ x_{t+1} &= -x_{t-1} + s x_t - s_t, \end{aligned}$$

in the Percival-Vivaldi [79] ‘two-configuration’ cat map representation (21.265)

$$\hat{\phi}_{t+1} = \hat{\mathbb{J}}_1 \hat{\phi}_t - \hat{s}_t, \quad (21.240)$$

with the one-time step temporal evolution  $[2 \times 2]$  Jacobian matrix  $\hat{\mathbb{J}}_1$  generating a time orbit by acting on the two-dimensional ‘phase space’ of states on successive lattice sites

$$\hat{\mathbb{J}}_1 = \begin{bmatrix} 0 & 1 \\ -1 & s \end{bmatrix}, \quad \hat{\phi}_t = \begin{bmatrix} x_{t-1} \\ x_t \end{bmatrix}, \quad \hat{s}_t = \begin{bmatrix} 0 \\ s_t \end{bmatrix}, \quad (21.241)$$

Similarly, for the  $d = 2$  spatiotemporal cat lattice at hand, one can recast the 5-term recurrence (??)

$$\begin{aligned} x_{nt} &= x_{nt} \\ x_{n,t+1} &= -x_{n,t-1} + (-x_{n-1,t} + 2s x_{nt} - x_{n+1,t}) - s_{nt} \end{aligned} \quad (21.242)$$

in the ‘two-configuration’ matrix form (21.240) by picking the vertical direction (indexed ‘2’) as the ‘time’, with temporal 1-time step Jacobian  $[2L \times 2L]$  block matrix

$$\hat{\mathbb{J}}_1 = \left[ \begin{array}{c|c} \mathbf{0} & \mathbf{1}_1 \\ \hline -\mathbf{1}_1 & -\mathcal{J}_1 \end{array} \right], \quad (21.243)$$

(known as a transfer matrix in statistical mechanics [77, 78]) generating a ‘time’ orbit by acting on a  $2L$ -dimensional ‘phase space’ lattice strip  $\hat{\phi}_t$  along the ‘spatial’ direction (indexed ‘1’),

$$\hat{\phi}_t = \begin{bmatrix} \phi_{t-1} \\ \phi_t \end{bmatrix}, \quad \hat{s}_t = \begin{bmatrix} \mathbf{0} \\ s_t \end{bmatrix}, \quad \phi_t = \begin{bmatrix} x_{1t} \\ \vdots \\ x_{Lt} \end{bmatrix}, \quad s_t = \begin{bmatrix} s_{1t} \\ \vdots \\ s_{Lt} \end{bmatrix},$$

where the hat  $\hat{\phantom{x}}$  indicates a  $2L$ -dimensional ‘two-configuration’ state, and  $\mathcal{J}_1$  is the spatial  $[L \times L]$  orbit Jacobian matrix of  $d = 1$  temporal cat form (??),

$$\mathcal{J}_1 = r_1^{-1} - 2s \mathbf{1}_1 + r_1 \quad (21.244)$$

The first order in time difference equation (21.240) can be viewed as a periodic state fixed point condition, a zero of the function  $F[\hat{X}] = \hat{\mathcal{J}}\hat{X} + \hat{M} = 0$ , with the

entire periodic *periodic state*  $\hat{X}_M$  treated as a single fixed *point* in the  $2LT$ -dimensional phase-space unit hyper-cube, and the  $[2LT \times 2LT]$  block matrix orbit Jacobian matrix given either by

$$\hat{\mathcal{J}} = \hat{\mathbf{1}} - \hat{\mathbb{J}}_1 \otimes r_2^{-1}, \quad (21.245)$$

or by

$$\hat{\mathcal{J}}' = \hat{\mathbf{1}} - r_2^{-1} \otimes \hat{\mathbb{J}}_1. \quad (21.246)$$

Here the unity  $\hat{\mathbf{1}} = \hat{\mathbf{1}}_1 \otimes \mathbf{1}_2$  is a  $[2LT \times 2LT]$  block matrix, and the time-evolution Jacobian matrix  $\hat{\mathbb{J}}_1$  (21.243) is a  $[2L \times 2L]$  matrix.

The order in which the block matrix blocks are composed does not matter, yielding the same the Hill determinant  $\det \hat{\mathcal{J}} = \det \hat{\mathcal{J}}'$  by (21.238). However, written out explicitly, the two orbit Jacobian matrices (21.247) and (21.250) are of a very different form.

For example, for the  $[L \times T]_0$  rectangular primitive cell, the spatiotemporal cat orbit Jacobian matrix (21.245) involves the  $[T \times T]$  time shift operator block matrix  $r_2$  (??) with the one-time-step  $[2L \times 2L]$  time-evolution Jacobian matrix  $\hat{\mathbb{J}}_1$  (21.243)

$$\hat{\mathcal{J}} = \left[ \begin{array}{c|c} \mathbf{1}_1 \otimes \mathbf{1}_2 & -\mathbf{1}_1 \otimes r_2^{-1} \\ \hline \mathbf{1}_1 \otimes r_2^{-1} & \mathbf{1}_1 \otimes \mathbf{1}_2 + \mathcal{J}_1 \otimes r_2^{-1} \end{array} \right], \quad (21.247)$$

and for spatiotemporal cat (21.242) this is a time-periodic  $[T \times T]$  shift operator block matrix  $r_2$  (??), each block now a space-periodic  $[2L \times 2L]$  matrix  $\hat{\mathbb{J}}_1$  (21.243).

If a block matrix is composed of four blocks, its determinant can be evaluated using Schur's 1917 formula [88, 91]

$$\det \left[ \begin{array}{c|c} \mathbf{A} & \mathbf{B} \\ \hline \mathbf{C} & \mathbf{D} \end{array} \right] = \det(\mathbf{A}) \det(\mathbf{D} - \mathbf{C}\mathbf{A}^{-1}\mathbf{B}). \quad (21.248)$$

so, noting (21.237), (21.239) and (21.244), we find that

$$\begin{aligned} \det \hat{\mathcal{J}} &= \det \left[ \begin{array}{c|c} \mathbf{1}_1 \otimes \mathbf{1}_2 & -\mathbf{1}_1 \otimes r_2^{-1} \\ \hline \mathbf{1}_1 \otimes r_2^{-1} & \mathbf{1}_1 \otimes \mathbf{1}_2 + \mathcal{J}_1 \otimes r_2^{-1} \end{array} \right] \\ &= \det [\mathbf{1}_1 \otimes \mathbf{1}_2 + \mathcal{J}_1 \otimes r_2^{-1} + (\mathbf{1}_1 \otimes r_2^{-1})(\mathbf{1}_1 \otimes \mathbf{1}_2)(\mathbf{1}_1 \otimes r_2^{-1})] \\ &= \det [\mathbf{1}_1 \otimes \mathbf{1}_2 + \mathcal{J}_1 \otimes r_2^{-1} + \mathbf{1}_1 \otimes r_2^{-2}] \\ &= \det(\mathbf{1}_1 \otimes r_2^{-1}) \det [\mathbf{1}_1 \otimes r_2^{-1} + (r_1^{-1} - 2s \mathbf{1}_1 + r_1) \otimes \mathbf{1}_2 + \mathbf{1}_1 \otimes r_2] \\ &= \text{Det } \mathcal{J}, \end{aligned} \quad (21.249)$$

where we have used  $\det \mathbf{1}_1 = \det \mathbf{1}_2 = \det r_1 = \det r_2 = 1$ .

This proves that  $\det \hat{\mathcal{J}}$  of the 'Hamiltonian' or 'two-configuration'  $[2LT \times 2LT]$  'phase space' orbit Jacobian matrix  $\hat{\mathcal{J}}$  defined by (21.247) equals the 'Lagrangian' Hill determinant of the  $[LT \times LT]$  orbit Jacobian matrix  $\mathcal{J}$ .

### 21.4.2 Hill's formula: stability of an orbit vs. its time-evolution stability

2020-07-21 Han The orbit Jacobian matrix of the temporal cat has form:

$$\mathcal{J} = \begin{pmatrix} -s & 1 & 0 & 1 \\ 1 & -s & 1 & 0 \\ 0 & 1 & -s & 1 \\ 1 & 0 & 1 & -s \end{pmatrix},$$

while the orbit Jacobian matrix from refeqbernNotHill is

$$\mathcal{J}' = \mathbf{1} - r^{-1} \otimes \mathbb{J} = \left( \begin{array}{cc|cc|cc|cc} 1 & 0 & 0 & 0 & 0 & 0 & 0 & -1 \\ 0 & 1 & 0 & 0 & 0 & 0 & 1 & -s \\ \hline 0 & -1 & 1 & 0 & 0 & 0 & 0 & 0 \\ 1 & -s & 0 & 1 & 0 & 0 & 0 & 0 \\ \hline 0 & 0 & 0 & -1 & 1 & 0 & 0 & 0 \\ 0 & 0 & 1 & -s & 0 & 1 & 0 & 0 \\ \hline 0 & 0 & 0 & 0 & 0 & -1 & 1 & 0 \\ 0 & 0 & 0 & 0 & 1 & -s & 0 & 1 \end{array} \right).$$

We know that

$$\det(\mathbf{1} - r^{-1} \otimes \mathbb{J}) = \det(\mathbf{1} - \mathbb{J} \otimes r^{-1}) = \det[(\mathbf{1} - \mathbb{J} \otimes r^{-1})(\mathbf{1}_{[2 \times 2]} \otimes r)],$$

where

$$\mathbf{1} - \mathbb{J} \otimes r^{-1} = \left( \begin{array}{cccc|cccc} 1 & 0 & 0 & 0 & 0 & 0 & 0 & -1 \\ 0 & 1 & 0 & 0 & -1 & 0 & 0 & 0 \\ 0 & 0 & 1 & 0 & 0 & -1 & 0 & 0 \\ 0 & 0 & 0 & 1 & 0 & 0 & -1 & 0 \\ \hline 0 & 0 & 0 & 1 & 1 & 0 & 0 & -s \\ 1 & 0 & 0 & 0 & -s & 1 & 0 & 0 \\ 0 & 1 & 0 & 0 & 0 & -s & 1 & 0 \\ 0 & 0 & 1 & 0 & 0 & 0 & -s & 1 \end{array} \right),$$

and

$$(\mathbf{1} - \mathbb{J} \otimes r^{-1})(\mathbf{1}_{[2 \times 2]} \otimes r) = \left( \begin{array}{cccc|cccc} 0 & 1 & 0 & 0 & -1 & 0 & 0 & 0 \\ 0 & 0 & 1 & 0 & 0 & -1 & 0 & 0 \\ 0 & 0 & 0 & 1 & 0 & 0 & -1 & 0 \\ 1 & 0 & 0 & 0 & 0 & 0 & 0 & -1 \\ \hline 1 & 0 & 0 & 0 & -s & 1 & 0 & 0 \\ 0 & 1 & 0 & 0 & 0 & -s & 1 & 0 \\ 0 & 0 & 1 & 0 & 0 & 0 & -s & 1 \\ 0 & 0 & 0 & 1 & 1 & 0 & 0 & -s \end{array} \right).$$

The determinant of a block matrix is

$$\det \begin{pmatrix} A & B \\ C & D \end{pmatrix} = \det(A) \det(D - CA^{-1}B).$$

Then we have:

$$\det [(\mathbf{1} - \mathbb{J} \otimes r^{-1}) (\mathbf{1}_{[2 \times 2]} \otimes r)] = \det [-s \mathbf{1} + r - \mathbf{1}r^{-1}(-\mathbf{1})] = \text{Det } \mathcal{J}.$$

What happens if we change the order of how we block the matrix, and consider  $\mathbb{J}_1 \otimes r_2^{-1}$  instead of  $r_2^{-1} \otimes \mathbb{J}_1$  in (21.250)?

In particular, by similarity relation (21.238), (21.250) is equivalent to ...

### 21.4.3 Hill's formula

Consider next (21.246), the equivalent way of forming of the block matrix for the  $[L \times T]_0$  rectangular primitive cell, with temporal period taken for definitiveness  $T = 4$ . The spatiotemporal cat orbit Jacobian matrix (21.246) is now constructed as the  $[4 \times 4]$  time shift operator block matrix  $r_2$  (??), with the one-time-step  $[2L \times 2L]$  time-evolution Jacobian matrix  $\hat{\mathbb{J}}_1$  (21.243) and unit matrix  $\hat{\mathbf{1}}_1$  as blocks

$$\hat{\mathcal{J}}' = \mathbf{1}_2 \otimes \hat{\mathbf{1}}_1 - r_2^{-1} \otimes \hat{\mathbb{J}}_1 = \begin{bmatrix} \hat{\mathbf{1}}_1 & \mathbf{0} & \mathbf{0} & -\hat{\mathbb{J}}_1 \\ -\hat{\mathbb{J}}_1 & \hat{\mathbf{1}}_1 & \mathbf{0} & \mathbf{0} \\ \mathbf{0} & -\hat{\mathbb{J}}_1 & \hat{\mathbf{1}}_1 & \mathbf{0} \\ \mathbf{0} & \mathbf{0} & -\hat{\mathbb{J}}_1 & \hat{\mathbf{1}}_1 \end{bmatrix}. \quad (21.250)$$

From the block-matrix multiplication rule (21.237) and the determinant rule (12.20) it follows that

$$(r_2^{-1} \otimes \hat{\mathbb{J}}_1)(r_2^{-1} \otimes \hat{\mathbb{J}}_1) = r_2^{-2} \otimes \hat{\mathbb{J}}_1^2, \quad \text{so } (r_2^{-1} \otimes \hat{\mathbb{J}}_1)^k = r_2^{-k} \otimes \hat{\mathbb{J}}_1^k, \quad (21.251)$$

and

$$\det (r_2^{-1} \otimes \hat{\mathbb{J}}_1) = (\det r_2)^{-L} (\det \hat{\mathbb{J}}_1)^T = \det \hat{\mathbb{J}}_p, \quad \hat{\mathbb{J}}_p = \hat{\mathbb{J}}_1^T, \quad (21.252)$$

where  $\hat{\mathbb{J}}_p$  is the Jacobian matrix of a temporal periodic orbit  $p$ . Expand  $\ln \det \hat{\mathcal{J}}' = \text{tr } \ln \hat{\mathcal{J}}'$  as a series using (12.20) and (21.251),

$$\text{tr } \ln \hat{\mathcal{J}}' = \text{tr } \ln (\mathbf{1} - r_2^{-1} \otimes \hat{\mathbb{J}}_1) = - \sum_{k=1}^{\infty} \frac{1}{k} \text{tr } (r_2^{-k}) \text{tr } \hat{\mathbb{J}}_1^k, \quad (21.253)$$

and use  $\text{tr } r_2^k = T$  if  $k$  is a multiple of  $T$ , 0 otherwise (follows from  $r_2^T = \mathbf{1}$ ):

$$\ln \det (\mathbf{1} - r_2^{-1} \otimes \hat{\mathbb{J}}_1) = - \sum_{r=1}^{\infty} \frac{1}{r} \text{tr } \hat{\mathbb{J}}_p^r = \ln \det (\hat{\mathbf{1}}_1 - \hat{\mathbb{J}}_p).$$

So for the spatiotemporal cat the orbit Jacobian matrix and the temporal evolution (21.240) stability  $\hat{\mathbb{J}}_p$  are related by the remarkable (discrete time) Hill's formula [19, 71]

$$|\text{Det } \mathcal{J}| = |\det (\hat{\mathbf{1}}_1 - \hat{\mathbb{J}}_p)|. \quad (21.254)$$

which expresses the Hill determinant of the arbitrarily large orbit Jacobian matrix  $\mathcal{J}$  in terms of a determinant of a small  $[2L \times 2L]$  time-evolution Jacobian matrix  $\hat{\mathbb{J}}_p$ .



**2018-12-01 Predrag** Include here the song and dance from the remark.

What Hill's formula? Is it refeq MacMei83(17)? Not any longer sure that [71] contains the Hill's formula...

discrete Hill's formula [19]:

$$\det(\mathbb{J}_M - \mathbf{1}) = \frac{(-1)^n \text{Det } \mathcal{J}_M}{\prod_{i=1}^n \det B_i}, \quad (21.255)$$

where for the one dimensional cat map the  $B$  here is an  $[1 \times 1]_0$  matrix:

$$B = -\frac{\delta^2 L[x_{n+1}, x_n]}{\delta x_{n+1} \delta x_n} = 1, \quad (21.256)$$

subsection Hill's formula: stability of an orbit vs. its time-evolution stability

**2020-07-21 Han** The orbit Jacobian matrix of the temporal cat has form:

$$\mathcal{J} = \begin{pmatrix} -s & 1 & 0 & 1 \\ 1 & -s & 1 & 0 \\ 0 & 1 & -s & 1 \\ 1 & 0 & 1 & -s \end{pmatrix},$$

while the orbit Jacobian matrix from refeqbernNotHill is

$$\mathcal{J}' = \mathbf{1} - r^{-1} \otimes \mathbb{J} = \left( \begin{array}{cc|cc|cc|cc} 1 & 0 & 0 & 0 & 0 & 0 & 0 & -1 \\ 0 & 1 & 0 & 0 & 0 & 0 & 1 & -s \\ \hline 0 & -1 & 1 & 0 & 0 & 0 & 0 & 0 \\ 1 & -s & 0 & 1 & 0 & 0 & 0 & 0 \\ \hline 0 & 0 & 0 & -1 & 1 & 0 & 0 & 0 \\ 0 & 0 & 1 & -s & 0 & 1 & 0 & 0 \\ \hline 0 & 0 & 0 & 0 & 0 & -1 & 1 & 0 \\ 0 & 0 & 0 & 0 & 1 & -s & 0 & 1 \end{array} \right).$$

We know that

$$\det(\mathbf{1} - r^{-1} \otimes \mathbb{J}) = \det(\mathbf{1} - \mathbb{J} \otimes r^{-1}) = \det[(\mathbf{1} - \mathbb{J} \otimes r^{-1})(\mathbf{1}_{[2 \times 2]} \otimes r)],$$

where

$$\mathbf{1} - \mathbb{J} \otimes r^{-1} = \left( \begin{array}{cccc|cccc} 1 & 0 & 0 & 0 & 0 & 0 & 0 & -1 \\ 0 & 1 & 0 & 0 & -1 & 0 & 0 & 0 \\ 0 & 0 & 1 & 0 & 0 & -1 & 0 & 0 \\ 0 & 0 & 0 & 1 & 0 & 0 & -1 & 0 \\ \hline 0 & 0 & 0 & 1 & 1 & 0 & 0 & -s \\ 1 & 0 & 0 & 0 & -s & 1 & 0 & 0 \\ 0 & 1 & 0 & 0 & 0 & -s & 1 & 0 \\ 0 & 0 & 1 & 0 & 0 & 0 & -s & 1 \end{array} \right),$$

and

$$(\mathbf{1} - \mathbb{J} \otimes r^{-1}) (\mathbf{1}_{[2 \times 2]} \otimes r) = \left( \begin{array}{cccc|cccc} 0 & 1 & 0 & 0 & -1 & 0 & 0 & 0 \\ 0 & 0 & 1 & 0 & 0 & -1 & 0 & 0 \\ 0 & 0 & 0 & 1 & 0 & 0 & -1 & 0 \\ 1 & 0 & 0 & 0 & 0 & 0 & 0 & -1 \\ \hline 1 & 0 & 0 & 0 & -s & 1 & 0 & 0 \\ 0 & 1 & 0 & 0 & 0 & -s & 1 & 0 \\ 0 & 0 & 1 & 0 & 0 & 0 & -s & 1 \\ 0 & 0 & 0 & 1 & 1 & 0 & 0 & -s \end{array} \right).$$

The determinant of a block matrix is

$$\det \begin{pmatrix} A & B \\ C & D \end{pmatrix} = \det(A) \det(D - CA^{-1}B).$$

Then we have:

$$\det [(\mathbf{1} - \mathbb{J} \otimes r^{-1}) (\mathbf{1}_{[2 \times 2]} \otimes r)] = \det [-s \mathbf{1} + r - \mathbf{1}r^{-1}(-\mathbf{1})] = \text{Det } \mathcal{J}.$$

2020-07-25 Predrag using

$$\det \begin{pmatrix} A & B \\ C & D \end{pmatrix} = \det(D) \det(A - BD^{-1}C). \quad (21.257)$$

so (not rechecked),

$$\begin{aligned} \det(1 - \mathbb{J} \otimes r^{-1}) &= \det \begin{bmatrix} \mathbf{1}_1 & -\mathbf{1}_1 \\ \mathbf{1}_1 & \mathbf{1}_1 + \mathcal{J}_1 \end{bmatrix} = \det(2\mathbf{1}_1 + \mathcal{J}_1) \det(\mathbf{1}_1) \\ &= \det[r - 2(s-1)\mathbf{1} + r^{-1}] = |\text{Det } \mathcal{J}|. \end{aligned} \quad (21.258)$$

in time with a  $[2L \times 2L]$  block matrix  $\hat{\mathbb{J}}$ ,<sup>14</sup>

$$\hat{X}_{t+1} = \hat{\mathbb{J}}\hat{X}_t - \hat{s}_t, \quad \hat{\mathbb{J}} = \begin{bmatrix} \mathbf{0} & \mathbf{I} \\ -\mathbf{I} & -\mathcal{J}_t \end{bmatrix}. \quad (21.259)$$

The **Kronecker product**  $\mathbf{A} \otimes \mathbf{B}$  is an operation by  $[m \times n]$  matrix  $\mathbf{A}$  on  $[p \times q]$  matrix  $\mathbf{B}$ , resulting in an  $[pm \times qn]$  block matrix:

$$\mathbf{A} \otimes \mathbf{B} = \begin{pmatrix} a_{11}\mathbf{B} & \cdots & a_{1n}\mathbf{B} \\ \vdots & \ddots & \vdots \\ a_{m1}\mathbf{B} & \cdots & a_{mn}\mathbf{B} \end{pmatrix}, \quad (21.260)$$

$$\text{tr}(\mathbf{A} \otimes \mathbf{B}) = \text{tr } \mathbf{A} \text{tr } \mathbf{B} \quad \text{and} \quad \det(\mathbf{A} \otimes \mathbf{B}) = (\det \mathbf{A})^m (\det \mathbf{B})^n. \quad (21.261)$$

<sup>14</sup>Predrag 2020-07-15: Rewriting here refeq HLpartition2d, refeq HLpartition2d2 as (21.242); will use U for the variation of X.

$\mathcal{J}_1$  is the spatial  $[L \times L]$  orbit Jacobian matrix of form (XX),

$$\begin{aligned} \mathcal{J}_1 &= r_1^{-1} - 2s \mathbf{1}_1 + r_1 \\ &= \begin{pmatrix} -2s & 1 & 0 & \dots & 1 \\ 1 & -2s & 1 & \dots & 0 \\ \vdots & \vdots & \vdots & \ddots & \vdots \\ 1 & 0 & \dots & 1 & -2s \end{pmatrix}. \end{aligned} \quad (21.262)$$

If  $\mathbf{A}$ ,  $\mathbf{B}$ ,  $\mathbf{C}$  and  $\mathbf{D}$  are matrices of such size that one can form the matrix products  $\mathbf{AC}$  and  $\mathbf{BD}$ , then the product of two block matrices is a block matrix:

$$(\mathbf{A} \otimes \mathbf{B})(\mathbf{C} \otimes \mathbf{D}) = (\mathbf{AC}) \otimes (\mathbf{BD}). \quad (21.263)$$

If  $\lambda_1, \dots, \lambda_n$  are the eigenvalues of  $\mathbf{A}$ , and  $\mu_1, \dots, \mu_m$  the eigenvalues of  $\mathbf{B}$ , then the eigenvalues of  $\mathbf{A} \otimes \mathbf{B}$  are

$$\lambda_i \mu_j, \quad i = 1, \dots, n, j = 1, \dots, m, \quad (21.264)$$

temporal Jacobian matrix

$$\mathbb{J} = \begin{pmatrix} 0 & 1 \\ -1 & s \end{pmatrix} = \omega \left( \mathbf{1} - \omega \begin{pmatrix} 0 & 0 \\ 0 & s \end{pmatrix} \right). \quad (21.265)$$

$$\begin{aligned} \hat{\mathbf{X}}_{t+1} &= \mathbb{J}_{PV} \hat{\mathbf{X}}_t - \hat{\mathbf{s}}_t \\ \mathbb{J}_{PV} &= \begin{bmatrix} \mathbf{0} & \mathbf{I} \\ -\mathbf{I} & -\mathcal{J}_t \end{bmatrix} = \omega - \begin{bmatrix} \mathbf{0} & \mathbf{0} \\ \mathbf{0} & \mathcal{J}_t \end{bmatrix} \end{aligned} \quad (21.266)$$

as a generalization of the  $L = 1$  cat map (21.240), where

$$\omega = \begin{bmatrix} \mathbf{0} & \mathbf{I} \\ -\mathbf{I} & \mathbf{0} \end{bmatrix}, \quad (21.267)$$

is an antisymmetric  $[2L \times 2L]$  matrix,  $\omega^2 = -\mathbf{1}$ ,

## 21.5 Hill's formula LC22blog

Internal discussions of ref. [68] edits: Move good text not used in ref. [68] to this file, for possible reuse later.

Tentative title: "Is there anything cats cannot do?"

**2024-11-29 Predrag** Might want to include sect. 19.4 *Heat kernel* into this, Hill's formula paper.

**2021-10-25 Predrag** A succinct explanation of the Hill's formula:

If you evaluate stability of the three-term recurrence (3.9) on a periodic lattice you get the orbit Jacobian matrix  $\mathcal{J}$ ; if you evaluate it by multiplying the 'two-configuration representation' matrix  $J$ , you get the 'time evolution' side of the Hill's formula.

**2022-01-16 Predrag** The embarrassing fact is that I no longer get what is "succinct" about this statement...

**2019-06-26 Predrag** Currently the argument flow of ref. [68] (this paper) is:

1. Bernoulli map
  - (a) coin flip map
  - (b) temporal Bernoulli orbits, linear code, discrete Fourier transform
2. Hamiltonian cat map
  - (a) Percival-Vivaldi map
  - (b) Appendix: Adler-Weiss generating partition, transition graph
3. Temporal cat
  - (a) Hamiltonian  $\rightarrow$  Lagrangian
  - (b) screened Poisson equation
4. Periodic orbits theory of cat maps
  - (a) orbit counting
  - (b) Adler-Weiss zeta function of transition graph
  - (c) Hamiltonian volume formula
  - (d) Lagrangian orbit Jacobian matrix
  - (e) Hill's formula
5. Spatiotemporal cat (Predrag: spatiotemporal cat, as it is not a "map")
  - (a) time, space Laplacians  $\rightarrow$  screened Poisson equation
  - (b) Lagrangian
  - (c) orbit Jacobian matrix, reciprocal lattice, spectrum formula for volume

In language of statistical mechanics and  $q$  state clock models, in this paper we focus on the description of the high-temperature paramagnetic (or disordered) phase.

Then we can use the Hill's formula to show that the two counting methods are equivalent.

**2019-08-08 Han** We derived generating function because the orbit Jacobian matrix is defined by the second order partial derivatives of the generating function,  $-(\mathcal{J})_{ij} = \partial^2 L(\mathbf{x}) / \partial x_i \partial x_j$ . This concept is used in the Hill's formula (21.256) [19]. I think it's fine to keep that in the appendix.

2022-02-25 **Burak** Your shadow state method looks very much like the predictor-corrector method.

2022-02-28 **Predrag** I do not quite see it. Both methods are implicit, but predictor-corrector is forward in time, while shadow state is global. We should check whether there is a Hill's formula relation between the two - might help us transfer some of the predictor-corrector techniques into the global setting.

2023-10-?? **Predrag** Dropped:

## 21.6 Nonlinear deterministic field theory WWL AFC22blog

The latest entry at the bottom of this section, page 911

Internal discussions of ref. [94]: we saved text not used in ref. [94] here, for possible reuse in ref. [35], or elsewhere.

**2022-04-03 Predrag** the initial version of rescaling, from **2022-03-14**. Leads to a pesky parameter  $\mu^2/2$ , superseded by sect. 4.10 *Deterministic  $\phi^3$  lattice field theory*:

$$V_1(x) = -\frac{g}{3!}x^3 + \frac{\mu^2}{2}x^2 = -\frac{g}{3!}(x^3 - 3\lambda x^2), \quad \lambda = \mu^2/g, \quad (21.268)$$

$$f(x) = x^3 + px, \quad (21.269)$$

field translation  $x \rightarrow x + \epsilon$ :

$$-\frac{g}{3!}((x+\epsilon)^3 - 3\lambda(x+\epsilon)^2) = -\frac{g}{3!}(x^3 + 3(\epsilon-\lambda)x^2 + 3\epsilon(\epsilon-2\lambda)x) + (\text{const}).$$

field translation  $\epsilon = \lambda$ , such that the  $x^2$  term vanishes,

$$V_1(x) = -\frac{g}{3!}(x^3 - 3\lambda^2 x) + (\text{const}).$$

Rescale the field  $x \rightarrow \lambda x$ , and drop the (const) term:

$$V_1(x) = -\frac{g}{3!}x^3 + \frac{\mu^2}{2}x \rightarrow -\lambda^2 \frac{\mu^2}{3!}(x^3 - 3x).$$

$$S[\mathbb{X}] = \frac{\mu^4}{g^2} \sum_z \left\{ -\frac{1}{2}x_z \square x_z - \frac{\mu^2}{3!}(x_z^3 - 3x_z) \right\}. \quad (21.270)$$

$$-x_{t+1} + 2x_t - x_{t-1} - \frac{\mu^2}{2}x_t^2 + \frac{\mu^2}{2} = 0, \quad (21.271)$$

**Period-1 periodic states.**

$$F[\bar{x}] = \frac{\mu^2}{2}(1 - x_t^2), \quad (21.272)$$

with two real roots  $\bar{x}_s$

$$(\bar{x}_L, \bar{x}_R) = (-1, 1). \quad (21.273)$$

**Period-2 periodic states. (Never crosschecked)**

four period-2 periodic states  $\bar{X}_s = \overline{x_0 x_1}$ , set  $x = x_{2k}$ ,  $y = x_{2k+1}$  in the Euler–Lagrange equation (21.271), and seek the zeros of

$$F[x, y] = \begin{pmatrix} 2(x - y) - \frac{\mu^2}{2}(x^2 - 1) \\ 2(y - x) - \frac{\mu^2}{2}(y^2 - 1) \end{pmatrix}. \quad (21.274)$$

$$F_2[x, y(x)] = \frac{\mu^4}{16}(x - 1)(x + 1)\left(x^2 - \left(1 - \frac{8}{\mu^2}\right)\right) \quad (21.275)$$

symmetric period-2 periodic state  $\bar{12}$

$$x = -y = \pm\sqrt{1 - 8/\mu^2}, \quad (21.276)$$

prime period-2 periodic state exists for  $\mu > 8$ .

2024-03-06 Predrag

$$\mathcal{J}_H = \begin{pmatrix} 2a\gamma_0 & -1 & 0 & 0 & \cdots & 0 & -1 \\ -1 & 2a\gamma_1 & -1 & 0 & \cdots & 0 & 0 \\ 0 & -1 & 2a\gamma_2 & -1 & \cdots & 0 & 0 \\ \vdots & \vdots & \vdots & \vdots & \ddots & \vdots & \vdots \\ 0 & 0 & 0 & 0 & \cdots & 2a\gamma_{n-2} & -1 \\ -1 & 0 & 0 & 0 & \cdots & -1 & 2a\gamma_{n-1} \end{pmatrix} \quad (21.277)$$

## References

- [1] R. L. Adler and B. Weiss, “Entropy, a complete metric invariant for automorphisms of the torus”, *Proc. Natl. Acad. Sci. USA* **57**, 1573–1576 (1967).
- [2] E. Allroth, “Ground state of one-dimensional systems and fixed points of 2n-dimensional map”, *J. Phys. A* **16**, L497 (1983).
- [3] G. B. Arfken, H. J. Weber, and F. E. Harris, *Mathematical Methods for Physicists: A Comprehensive Guide*, 7th ed. (Academic, New York, 2013).
- [4] V. I. Arnol’d and A. Avez, *Ergodic Problems of Classical Mechanics* (Addison-Wesley, Redwood City, 1989).
- [5] M. Artin and B. Mazur, “On periodic points”, *Ann. Math.* **81**, 82–99 (1965).
- [6] R. Artuso, “Diffusive dynamics and periodic orbits of dynamic systems”, *Phys. Lett. A* **160**, 528–530 (1991).
- [7] R. Artuso and P. Cvitanović, “Deterministic diffusion”, in *Chaos: Classical and Quantum*, edited by P. Cvitanović, R. Artuso, R. Mainieri, G. Tanner, and G. Vattay (Niels Bohr Inst., Copenhagen, 2023).

- [8] R. Artuso and R. Strepparava, “Recycling diffusion in sawtooth and cat maps”, *Phys. Lett. A* **236**, 469–475 (1997).
- [9] N. W. Ashcroft and N. D. Mermin, *Solid State Physics* (Holt, Rinehart and Winston, 1976).
- [10] M. Baake, J. Hermisson, and A. B. Pleasants, “The torus parametrization of quasiperiodic LI-classes”, *J. Phys. A* **30**, 3029–3056 (1997).
- [11] M. Baranger, K. T. R. Davies, and J. H. Mahoney, “The calculation of periodic trajectories”, *Ann. Phys.* **186**, 95–110 (1988).
- [12] A. Barvinok, *Integer Points in Polyhedra* (European Math. Soc. Pub., Berlin, 2008).
- [13] R. J. Baxter, “Some comments on developments in exact solutions in statistical mechanics since 1944”, *J. Stat. Mech.* **2010**, P11037 (2010).
- [14] E. Behrends, “The ghosts of the cat”, *Ergod. Theor. Dynam. Syst.* **18**, 321–330 (1998).
- [15] E. Behrends and B. Fielder, “Periods of discretized linear Anosov maps”, *Ergod. Theor. Dynam. Syst.* **18**, 331–341 (1998).
- [16] N. Bird and F. Vivaldi, “Periodic orbits of the sawtooth maps”, *Physica D* **30**, 164–176 (1988).
- [17] M. Blank and G. Keller, “Random perturbations of chaotic dynamical systems: stability of the spectrum”, *Nonlinearity* **11**, 1351–1364 (1998).
- [18] M. L. Blank, *Discreteness and Continuity in Problems of Chaotic Dynamics* (Amer. Math. Soc., Providence RI, 1997).
- [19] S. V. Bolotin and D. V. Treschev, “Hill’s formula”, *Russ. Math. Surv.* **65**, 191 (2010).
- [20] J. P. Boyd, *Chebyshev and Fourier Spectral Methods*, 2nd ed. (Dover, New York, 2000).
- [21] A. Brown, “Equations for periodic solutions of a logistic difference equation”, *J. Austral. Math. Soc. Ser. B* **23**, 78–94 (1981).
- [22] L. A. Bunimovich and Y. G. Sinai, “Spacetime chaos in coupled map lattices”, *Nonlinearity* **1**, 491 (1988).
- [23] B. L. Buzbee, G. H. Golub, and C. W. Nielson, “On direct methods for solving Poisson’s equations”, *SIAM J. Numer. Anal.* **7**, 627–656 (1970).
- [24] M. Campos, G. Sierra, and E. López, “Tensor renormalization group in bosonic field theory”, *Phys. Rev. B* **100**, 195106 (2019).
- [25] J. L. Cardy, “Operator content of two-dimensional conformally invariant theories”, *Nucl. Phys. B* **270**, 186–204 (1986).
- [26] M. Cencini, A. Puglisi, D. Vergni, and A. Vulpiani, *A Random Walk in Physics* (Springer, 2021).
- [27] M. Chen, “On the solution of circulant linear systems”, *SIAM J. Numer. Anal.* **24**, 668–683 (1987).



- [28] M. Cheng and N. Seiberg, Lieb-Schultz-Mattis, Luttinger, and 't Hooft – anomaly matching in lattice systems, 2022.
- [29] M. M. P. Couchman, D. J. Evans, and J. W. M. Bush, “The stability of a hydrodynamic Bravais lattice”, *Symmetry* **14**, 1524 (2022).
- [30] P. Cvitanović, *Field Theory*, Notes prepared by E. Gyldenkerne (Nordita, Copenhagen, 1983).
- [31] P. Cvitanović, “Counting”, in *Chaos: Classical and Quantum* (Niels Bohr Inst., Copenhagen, 2023).
- [32] P. Cvitanović, “World in a mirror”, in *Chaos: Classical and Quantum* (Niels Bohr Inst., Copenhagen, 2023).
- [33] P. Cvitanović, R. Artuso, R. Mainieri, G. Tanner, and G. Vattay, *Chaos: Classical and Quantum* (Niels Bohr Inst., Copenhagen, 2024).
- [34] P. Cvitanović, P. Gaspard, and T. Schreiber, “Investigation of the Lorentz gas in terms of periodic orbits”, *Chaos* **2**, 85–90 (1992).
- [35] P. Cvitanović and H. Liang, A chaotic lattice field theory in two dimensions, In preparation, 2024.
- [36] R. L. Devaney, *An Introduction to Chaotic Dynamical systems*, 2nd ed. (Westview Press, Cambridge, Mass, 2008).
- [37] F. W. Dorr, “The direct solution of the discrete Poisson equation on a rectangle”, *SIAM Rev.* **12**, 248–263 (1970).
- [38] M. S. Dresselhaus, G. Dresselhaus, and A. Jorio, *Group Theory: Application to the Physics of Condensed Matter* (Springer, New York, 2007).
- [39] J. Dubout, *Zeta functions of graphs, their symmetries and extended Catalan numbers*.
- [40] D. Dudgeon and R. M. Mersereau, *Multidimensional Digital Signal Processing* (Prentice-Hall, Englewood Cliffs, NJ, 1984).
- [41] D. S. Dummit and R. M. Foote, *Abstract Algebra* (Wiley, 2003).
- [42] F. J. Dyson and H. Falk, “Period of a discrete cat mapping”, *Amer. Math. Monthly* **99**, 603–614 (1992).
- [43] S. Elaydi, *An Introduction to Difference Equations*, 3rd ed. (Springer, Berlin, 2005).
- [44] E. Elizalde, *Ten Physical Applications of Spectral Zeta Functions*, 2nd ed. (Springer, Berlin, 2012).
- [45] E. Elizalde, K. Kirsten, N. Robles, and F. Williams, “Zeta functions on tori using contour integration”, *Int. J. Geom. Methods M.* **12**, 1550019 (2015).
- [46] A. Endler and J. A. C. Gallas, “Reductions and simplifications of orbital sums in a Hamiltonian repeller”, *Phys. Lett. A* **352**, 124–128 (2006).

- [47] L. Fazza and T. Sulejmanpasic, “Lattice quantum Villain Hamiltonians: compact scalars,  $U(1)$  gauge theories, fracton models and quantum Ising model dualities”, *J. High Energy Phys.* **2023**, 17 (2023).
- [48] É. Ghys and J. Leys, “Lorenz and modular flows: a visual introduction”, *Amer. Math. Soc. Feature Column* (2006).
- [49] J. W. von Goethe, *Faust I, Studierzimmer 2*. M. Greenberg, transl. (Yale Univ. Press, 1806).
- [50] I. S. Gradshteyn and I. M. Ryzhik, *Tables of Integrals, Series and Products*, 8th ed. (Elsevier LTD, Oxford, New York, 2014).
- [51] S. Grossmann and H. Fujisaka, “Diffusion in discrete nonlinear dynamical systems”, *Phys. Rev. A* **26**, 1779–1782 (1982).
- [52] B. Gutkin, L. Han, R. Jafari, A. K. Saremi, and P. Cvitanović, “Linear encoding of the spatiotemporal cat map”, *Nonlinearity* **34**, 2800–2836 (2021).
- [53] B. Gutkin and V. Osipov, “Classical foundations of many-particle quantum chaos”, *Nonlinearity* **29**, 325–356 (2016).
- [54] D. L. Hitzl and F. Zele, “An exploration of the Hénon quadratic map”, *Physica D* **14**, 305–326 (1985).
- [55] G. Y. Hu and R. F. O’Connell, “Analytical inversion of symmetric tridiagonal matrices”, *J. Phys. A* **29**, 1511 (1996).
- [56] G. Y. Hu, J. Y. Ryu, and R. F. O’Connell, “Analytical solution of the generalized discrete Poisson equation”, *J. Phys. A* **31**, 9279 (1998).
- [57] S. Isola, “ $\zeta$ -functions and distribution of periodic orbits of toral automorphisms”, *Europhys. Lett.* **11**, 517–522 (1990).
- [58] E. V. Ivashkevich, N. S. Izmailian, and C.-K. Hu, “Kronecker’s double series and exact asymptotic expansions for free models of statistical mechanics on torus”, *J. Phys. A* **35**, 5543–5561 (2002).
- [59] S. Jaidee, P. Moss, and T. Ward, “Time-changes preserving zeta functions”, *Proc. Amer. Math. Soc.* **147**, 4425–4438 (2019).
- [60] J. P. Keating, “Asymptotic properties of the periodic orbits of the cat maps”, *Nonlinearity* **4**, 277 (1991).
- [61] J. P. Keating, “The cat maps: quantum mechanics and classical motion”, *Nonlinearity* **4**, 309–341 (1991).
- [62] J. P. Keating and F. Mezzadri, “Pseudo-symmetries of Anosov maps and spectral statistics”, *Nonlinearity* **13**, 747–775 (2000).
- [63] Y.-O. Kim, J. Lee, and K. K. Park, “A zeta function for flip systems”, *Pacific J. Math.* **209**, 289–301 (2003).
- [64] P. Kurlberg and Z. Rudnick, “Hecke theory and equidistribution for the quantization of linear maps of the torus”, *Duke Math. J.* **103**, 47–77 (2000).

- [65] D. H. Lehmer, “Factorization of certain cyclotomic functions”, *Ann. of Math. (2)* **34**, 461–479 (1933).
- [66] J. Li and S. Tomsovic, “Exact relations between homoclinic and periodic orbit actions in chaotic systems”, *Phys. Rev. E* **97**, 022216 (2017).
- [67] H. Liang and P. Cvitanović, “A chaotic lattice field theory in one dimension”, *J. Phys. A* **55**, 304002 (2022).
- [68] H. Liang and P. Cvitanović, “A derivation of Hill’s formulas”, In preparation, 2024.
- [69] D. A. Lind, “A zeta function for  $Z^d$ -actions”, in *Ergodic Theory of  $Z^d$  Actions*, edited by M. Pollicott and K. Schmidt (Cambridge Univ. Press, 1996), pp. 433–450.
- [70] R. S. MacKay, *Renormalisation in Area-preserving Maps* (World Scientific, Singapore, 1993).
- [71] R. S. MacKay and J. D. Meiss, “Linear stability of periodic orbits in Lagrangian systems”, *Phys. Lett. A* **98**, 92–94 (1983).
- [72] R. S. MacKay, J. D. Meiss, and I. C. Percival, “Transport in Hamiltonian systems”, *Physica D* **13**, 55–81 (1984).
- [73] A. Maloney and E. Witten, “Quantum gravity partition functions in three dimensions”, *J. High Energy Phys.* **2010**, 029 (2010).
- [74] J. D. Meiss, “Symplectic maps, variational principles, and transport”, *Rev. Mod. Phys.* **64**, 795–848 (1992).
- [75] F. Mezzadri, “On the multiplicativity of quantum cat maps”, *Nonlinearity* **15**, 905–922 (2002).
- [76] N. Miguel, C. Simó, and A. Vieiro, “From the Hénon conservative map to the Chirikov standard map for large parameter values”, *Regul. Chaotic Dyn.* **18**, 469–489 (2013).
- [77] I. Montvay and G. Münster, *Quantum Fields on a Lattice* (Cambridge Univ. Press, Cambridge, 1994).
- [78] L. Onsager, “Crystal statistics. I. A Two-dimensional model with an order-disorder transition”, *Phys. Rev.* **65**, 117–149 (1944).
- [79] I. Percival and F. Vivaldi, “A linear code for the sawtooth and cat maps”, *Physica D* **27**, 373–386 (1987).
- [80] I. Percival and F. Vivaldi, “Arithmetical properties of strongly chaotic motions”, *Physica D* **25**, 105–130 (1987).
- [81] Y. B. Pesin and Y. G. Sinai, “Space-time chaos in the system of weakly interacting hyperbolic systems”, *J. Geom. Phys.* **5**, 483–492 (1988).
- [82] T. A. Pierce, “The numerical factors of the arithmetic forms  $\prod (1 \pm \alpha_i^m)$ ”, *Ann. of Math. (2)* **18**, 53–64 (1916).
- [83] A. Politi and A. Torcini, “Periodic orbits in coupled Hénon maps: Lyapunov and multifractal analysis”, *Chaos* **2**, 293–300 (1992).

- 
- [84] C. Pozrikidis, *An Introduction to Grids, Graphs, and Networks* (Oxford Univ. Press, Oxford, UK, 2014).
- [85] J. L. Pughe-Sanford, S. Quinn, L. L. Balabanski, and R. O. Grigoriev, Learning the ergodic averages of non-linear systems from linear regression, 2023.
- [86] D. B. Ray and I. M. Singer, “R-Torsion and the Laplacian on Riemannian manifolds”, *Adv. Math.* **7**, 145–210 (1971).
- [87] M. Schell, S. Fraser, and R. Kapral, “Diffusive dynamics in systems with translational symmetry: A one-dimensional-map model”, *Phys. Rev. A* **26**, 504–521 (1982).
- [88] I. Schur, “Über Potenzreihen, die im Innern des Einheitskreises beschränkt sind”, *J. reine angewandte Math.* **147**, 205–232 (1917).
- [89] C. Simó, “On the Hénon-Pomeau attractor”, *J. Stat. Phys.* **21**, 465–494 (1979).
- [90] J. Stephenson and D. T. Ridgway, “Formulae for cycles in the Mandelbrot set II”, *Physica A* **190**, 104–116 (1992).
- [91] Wikipedia contributors, [Block matrix](#) — Wikipedia, The Free Encyclopedia, 2020.
- [92] Wikipedia contributors, [Kronecker product](#) — Wikipedia, The Free Encyclopedia, 2020.
- [93] Wikipedia contributors, [Index of a subgroup](#) — Wikipedia, The Free Encyclopedia, 2022.
- [94] S. V. Williams, X. Wang, H. Liang, and P. Cvitanović, *Nonlinear chaotic lattice field theory*, In preparation, 2024.
- [95] A. Wirzba and P. Cvitanović, “Appendix: Discrete symmetries of dynamics”, in *Chaos: Classical and Quantum* (Niels Bohr Inst., Copenhagen, 2023).
- [96] F. Y. Wu, “Theory of resistor networks: the two-point resistance”, *J. Phys. A* **37**, 6653–6673 (2004).

## Chapter 22

# Sidney's blog

Sidney V. Williams work blog  
swilliams425@gatech.edu  
sidneywilliams1231@gmail.com  
subversion siminos : swilliams425  
cell 208 310 3866

The latest entry at the bottom for this blog, page 1067

### 22.1 2020 blog

**2020-05-20 Predrag** to Sidney:

You can write up your narrative in this file. Can clip & paste anything from above sections you want to discuss, that saves you LaTeXing time.

**2021-09-09 Predrag** The 3rd line of *siminos/spatiotemp/blogCats.tex* says

```
\input{inputs/inclOnlyCats} %process only the files you are editing
```

you uncomment a single line in that file to "process only the files you are editing".

**2021-07-04 Predrag to Sidney** Pro tip: compile *blogCats.tex* often, as you write, and fix errors as you write. I had to go all the way back to May to find one of your unbalanced “{” and make the entire blog compile without errors...

**2020-08-22 Predrag** First task:

Start reading kittens/CL18.tex [6] sect. *Bernoulli map*. Everything up to CL18 sect. s:1D1dLatt *Temporal Bernoulli* you know from the ChaosBook course.

New stuff starts here. See how much you understand. Write your study notes up here, ask questions - this is your personal blog.

You refer to an equation like this: CL18 eq. (1.19);

to figure like this: CL18 figure fig:BernCyc2Jacob;

to table like this: table 9.1;

to a reference like this: Gutkin and Osipov [18] (*GutOsi15* refers to an article listed in *../bibtex/siminos.bib*).

and to external link like this: "For great wallpapers, see overheads in Engel's course [13]."

**2020-08-22 Predrag** An example of referring to the main text: Why do you write *orbit Jacobian matrix* CL18 eq. *jacobianOrb* as a partial derivative, when you already know  $\mathcal{J}$ , see CL18 eq. *tempFixPoint*?

**2020-08-24 Sidney** Started reading from the beginning as that only adds an additional 4 pages, and it would be beneficial to review.

General Notes: Showing what modern chaos calculations look like. The spatiotemporal cat is the arbitrary dimension generalization of the 1-D Bernoulli map.

(mod 1) subtracts the integer part of  $s\phi_t$ , this keeps  $\phi_{t+1}$  within the unit interval (group theoretic analogue?). Also partitions the state-space into  $s$  sub-intervals.

**2020-08-24 Predrag** The group theory here compatifies translations on the (infinite) line  $\phi \in (-\infty, \infty)$  to translations on the (compact) circle  $\phi \in [0, 2\pi)$ .

**2020-08-24 Sidney** Reminder to self: review the symbolic dynamics, and binary operations from chapter 14 of *ChaosBook*. **ChaosBook Chapter XXX**. The unit interval is partitioned into  $s^n$  subintervals, each with one unstable period-n point, except the rightmost fixed point is the same as the fixed point at the origin. So there are  $s^n - 1$  total period-n periodic points.  $r$  in (1.19) is a cyclic permutation that translates forward in time the periodic state by one site. Inverse  $r$  because the second term is always one step behind the first term and an inverse  $r$  moves the state back one.

Questions 1. I've pretty much never done modular arithmetic before, I understand CL18 eq. *BerStretch* in the idea that the circle map wraps in on itself and contributes the value of its slope after one go around, but I am unsure on how to use the modular arithmetic to do that, should I look into that?

**2020-08-24 Predrag** As I do not know what "modular arithmetic" is, don't worry about :)

2020-08-25 Sidney General Notes

CL18 eq. pathBern appears to be a vector of a periodic (or relative periodic orbit) through the Bernoulli map. Review Multishooting. Total number of periodic points of period  $n$  is  $N_n = s^n - 1$  but it also equals the magnitude of the determinant of the orbit Jacobian matrix. (got to page 7)

- Q1 Is CL18 eq. tempBernFix the evolution function  $f^t(y)$  that was referenced throughout ChaosBook?
- Q2 What exactly is meant by a "lattice"?

2020-08-24 Predrag .

- A1 The whole point of the paper is that ChaosBook is obsolete - in the new formulation, there is no 'time' evolution, no time trajectory  $f^t(y)$ , there are only sets of fields that live on lattice points that satisfy recurrence relations. CL18 eq. tempBernFix is *orbit Jacobian matrix*, the stability of a periodic state, to be related to stability forward in time in CL18 sect. s: Hill. This is a revolution: there is no more time, there is only spacetime.
- A2 Temporal lattice  $\mathbb{Z}$  is defined in CL18 eq. pathBern. Spacetime integer lattice  $\mathbb{Z}^2$ , (or more generally  $\mathbb{Z}^d$ ) in CL18 eq. KanekoCML, CL18 eq. CatMap2d. When you get to it, a 2-dimensional *Bravais lattice*  $\Lambda$  is defined in CL18 eq. 2DBravaisLattice.

If this is unclear, read up on integer lattices, give your own precise definition.

2020-08-26 Sidney Point Lattice (integer lattice is a special case of point lattice) notes from **Wolfram**: "A point lattice is a regularly spaced array of points." The integer lattice is where all of these points are integers. I will look at the Barvinok lecture tomorrow, I have to finish moving to a different house today. (Stayed on page 7)

- Q3 Please correct me if I am wrong, but a lattice seems to be a collection of points where all are regularly spaced, so does "regularly" mean that it is controlled by a deterministic law? If this is the case, the  $\phi_n$  states in a periodic orbit can be grouped as a lattice and ordered by location along the periodic orbit, then the associated "winding" number  $m_t$  can be grouped in its own lattice, which in this case is an integer lattice. What is the "regular" spacing for the winding numbers? Have missed the point?
- A3 Wolfram is right. When you have a discrete time map, time takes integer values  $t = \dots, -1, 0, 1, 2, \dots$ . That is called 1-dimensional integer lattice  $\mathbb{Z}$ . Once you are in  $d = 2$  or higher, the name makes

sense, as you can visualize  $\mathbb{Z}^2$  as a 'lattice'. It is regular, because all spacings between neighboring points are 1. There is nothing 'deterministic' about this, it just says that time takes its values on integers, rather than on a continuum.

There is only one lattice, but on each lattice site there is a real-valued field  $\phi_t$  and the integer valued 'source'  $m_t$ .

**2020-08-27 Sidney** Thank you for A1, that makes complete sense now. Calculated the orbit Jacobian matrix using equation CL18 eq. tempBernFix, matched with the paper, yay. Orbit Jacobian matrix maps the basis vectors of the unit hyper-cube into a fundamental parallelepiped basis vectors, each of which is given by a column in the orbit Jacobian matrix.  $|\text{Det}(s/r)| = s^n$  because  $r$  and its inverse are both unitary matrices, and if you multiply every row of an  $[n \times n]$  matrix, the determinant is multiplied by the constant raised to the power  $n$ . Periodicity  $r^n = 1$  accounts for  $\bar{0}$  and  $\overline{s-1}$  fixed points being a single periodic point. (got to page 9)

Q4 I was trying to calculate the orbit Jacobian matrix using the  $r$  matrix, but the delta function equation CL18 eq. hopMatrix for  $r$  doesn't seem to work for the Bernoulli map, I know that  $r_{2,1} = 1$  and  $r_{1,2} = 1$  which works with the delta function definition. However,  $r_{2,1} = \delta_{3,1}$  from CL18 eq. hopMatrix, which should equal zero. Other than just the idea of being cyclic, I don't know why it yields one instead of zero, what am I missing?

A4 Work it out  $r$  matrices for  $n = 1, 2, 3, \dots$ . It will start making sense.

Q5 So, does "periodic state" mean the set of all points (field of all points?) which running through the Bernoulli map requires the specific winding number at that lattice site?

A5 Interesting, grad students too seem to confuse coordinates (for example,  $(x, t) = (3.74, -0.02)$  in continuum,  $(n, t) = (7, -6)$  on a discretized space) and the fields  $\phi(n, t)$ . Physical "state" refers to value of field  $\phi$  over every  $(n, t)$  - is the grass high or low? rather than the coordinates of spacetime.

How would you state this precisely if you were trying to explain this paper to another student?

**2020-08-30 Sidney**

A5.1 Sidney: "  $\Phi_M$  is the set of all values the field  $\phi_z$  takes over the set of coordinates  $M$ . "

A5.2 Predrag: Please reread 2nd paragraph of CL18 sect. s:1D1dLatt and explain what is wrong with your answer A5.1

Notes: For an period- $n$  periodic state  $\Phi_M$  the Jacobian matrix is now a function of a  $[d \times d]$  matrix  $J$ , so the formula for the number of periodic



points of period  $n$  (number of periodic states of period  $n$ ) is now  $|\det(1 - J_M)|$  where  $J_M = \prod_{t=1}^n J_t$  where  $J_t$  is the one-step Jacobian matrix which is assumed to vary in time.

Note to self: look back over the topological zeta function, specifically try to understand derivation of:

$$\frac{1}{\zeta_{top}(z)} = \exp\left(-\sum_{n=1}^{\infty} \frac{z^n}{n} N_n\right)$$

(got to CL18 page s:bernODE)

Predrag: [ChaosBook \(click here\)](#)

- Q6 Is "there are  $s$  fundamental periodic states, and every other periodic state is built from their concatenations and repeats" is simply a restatement of the fact that the Bernoulli map is a full shift?
- A6 For Bernoulli, yes. But search for word 'fundamental' in [Chaos-Book Counting](#). For example, 'We refer to the set of all non-self-intersecting loops  $\{t_{p_1}, t_{p_2}, \dots, t_{p_f}\}$  as the *fundamental cycles*'. Write up here a more nuanced statement of 'fundamental' cycles might be (I do not have firm grip on this either...).
- Q7 Is CL18 eq. bernN\_n-s=2 a result of expanding in a Taylor the result of the derivative (and product of  $1/\zeta_{top}$  and  $z$ )? Because the topological zeta function of the Bernoulli map is a closed form function, not an infinite sum.

**2020-08-31 Sidney** Via a finite difference method, CL18 eq. (1.18) can be viewed as a first order ODE dynamical system. Back-substituted with (1.19) to show that with  $\Delta t = 1$  the velocity field does satisfy the diffeq (11.18). The Bernoulli system can be recast into a discretized ODE whose global linear stability is described by the orbit Jacobian matrix. (Stayed on CL18 page s:bernODE))

**2020-09-01 Sidney** Started reading CL18 sect. s:kickRot *A kicked rotor*.

(12.100) and (12.101) describe the motion of a rotor being subjected to periodic momentum pulses. The mod is present for the  $q$  equation to make sure that the angle varies from 0 to  $2\pi$ . As in the Bernoulli map case, here mod is also added to the momentum equation to keep it bounded to a unit square. Cat maps with the stretching parameter  $s$  are the same up to a similarity transformation. An automorphism is an isomorphism of a system of objects onto itself. An isomorphism is a map that preserves sets and relations among elements.

- Q8 Do the kicked rotor equations with Hooke's law force, and bounded momentum (mod 1 added to CL18 eq. PerViv2.1a) only take the form of CL18 eq. catMap if  $K$  is an integer?

A8 The text states: "The (mod 1) added to CL18 eq. PerViv2.1a makes the map a discontinuous 'sawtooth,' unless  $K$  is an integer." How would you make that clearer?

Q9 How does CL18 eq. catMap have a state space which is a 2-torus? I am having a hard time visualizing how this came about.

A9 Do you understand how (mod 1) operation turns unbounded stretch CL18 eq. BerStretch into a circle map CL18 eq. n-tuplingMap? Circle map is 1-torus. If both  $(q_t, p_t) \in (0, 1] \times (0, 1]$  are wrapped into unit circles, the phase space  $(q_t, p_t)$  is not an infinite 2-dimensional plane, but a compact, doubly periodic unit square with opposite edges glued together, i.e., 2-torus.

2020-09-03 **Sidney** I was typing my description into "summary" textbox above the commit to master button. Obviously I was incorrect, I'll try to type in the "description" for this commit.

2020-09-02 **Predrag** "Tripping Through Fields" showed up :)

2020-09-03 **Sidney**

A5.3 **Sidney:** I'm not actually quite sure what's wrong with my given definition. From your answer A5 it seems that  $M$  is a set of coordinates (the location of the blade of grass) and  $\Phi_M$  is the value at that coordinate (the height of the grass at that point). Perhaps I forgot that these periodic states are for periodic orbits, so I forgot the second coordinate (period of length  $n$ ).

A5.4 **Predrag:** The textbook inhomogeneous *Helmoltz equation* (8.10) is an elliptical equation of form

$$(\square + k^2) \phi(z) = -m(z), \quad z \in \mathbb{R}^d, \quad (22.1)$$

where the *field*  $\phi(z)$  is a  $C^2$  functions of *coordinates*  $z$ , and  $m(z)$  are *sources*. For example, charge density is a *source* of electrostatic *field*.

Suppose you are so poor, your computer lacks infinite memory, you only have miserly only 10 Tb, so you cannot store the infinitely many values that *coordinates*  $z \in \mathbb{R}^d$  take. So what do you do?

Perhaps a peak at ChaosBook [ChaosBook A24.1 Lattice derivatives](#) can serve as an inspiration. And once you have done what a person must do, your Helmloltz equation (hopefully) has the form of CL18 eq. OneCat. What is a *field*, a *source*, a *coordinate* then?

2020-09-03 **Sidney**

A8.1 The sawtooth statement made sense, what made it unclear for me was the second sentence which started with "in this case" it was (again for me, I might not have been paying enough attention) ambiguous, I didn't know if it was talking about the integer case or the sawtooth case.

A8.2 Predrag: thanks, I rephrased that sentence.

A9.1 I understand, your explanation makes sense, thank you :).

Notes: The discrete time Hamiltonian system induces forward in time evolution on the 2-torus phase space. The orbit Jacobian matrix can take many different forms depending on the map. Despite this the Hill determinant can still count the number of periodic states. (got to page CL18 page s:tempCatCountTEMP)

#### 2020-09-05 Sidney

A5.5 If I was so unlucky to only have 10Tb of memory, I would take a finite interval of points  $z$  that I was interested in, and discretize them (evenly, or unevenly) and then evaluate the field (that was probably the wrong wording) at a finite set of points, either of particular interest within the interval, or closely spaced enough so that the values were representative of the values the field took over a continuum. I think that a coordinate is a point in state space specified by specific values of state variables (position, time, momentum etc.). To try to answer source, and field, I'll be thinking of an electric charge, a source is what generates the medium by which other sources are effected, and the field is the medium which acts upon other sources.

A5.6 I did look at [ChaosBook A24.1 Lattice derivatives](#), but it didn't seem to address quite the fundamental confusion I seem to be facing. I'm relatively confident in my coordinate definition, but not at all in my source, and field definition.

#### 2020-09-05 Sidney

A5.8 I read the pink bits of CL18 sect. s:lattState *Periodic states* (as I assume that was the parts that you rewrote specially). From it I (think) I understand. We're looking at two coordinates for most of the Bernoulli and cat map stuff: a spatial one, and a temporal one, the maps only effect the temporal placement, but effect it differently depending on where the point was in space when the map acted on it, because the field takes a different value at every point in space (and time). So the coordinates are the field point placement in time and space. The field is the value that is assigned to every lattice point.  $M$  keeps getting referred to as an alphabet, so that makes me think that it is similar (perhaps the multidimensional generalization) to the "alphabet" which was used to partition state space in the 1D maps of Chaosbook, such as 0 for the left half of the interval and 1 for the right, and then further partitioning the more the map is applied. Is that close at least?

#### 2020-09-05 Predrag .

- A5.9 Getting hotter. Look at CL18 eq. circ-m and CL18 eq. catMapNewt;  $\phi_t$  and  $m_t$  are the same kind of a beast,  $m_t$  is just the integer part of the "stretched" field in CL18 eq. BerStretch. In this particular, linear map setting, this integer does double duty, as a letter of an "alphabet". It cannot possibly be a "coordinate", it like saying that a dancer's head is "floor."
- A5.10 In temporal lattice formulation no "map is applied." That is the brilliance of the global spatiotemporal reformulation: there is no stepping forward in time, so there is no map - the only thing that exists is the global fixed point condition that has to be satisfied by field values everywhere on the lattice, simultaneously.  
Time is dead.

2020-09-08 Sidney

- Q11 So the temporal cat / spatiotemporal cat equations are moving around points in the lattice instead of through time?
- Q12 Is something of the form of CL18 eq. tempFixPoint an example of the "global fixed point condition"?

2020-09-14 Predrag .

- A11 An equation does not have to be "moving around" anything: think of a quadratic equation  $x^2 + bx + c = 0$ . Does it "move" anything? No. It's a condition that a single "field"  $x$  has to satisfy, and the solution is a root of that equation. The temporal cat / spatiotemporal cat equations are "equations" in the same sense, [bunch of terms involving  $\phi_z$ ]=0.

A12 Yes.

2020-09-09 Sidney Notes: Equations such as CL18 eq. catMapNewt can be solved using similar methods to linear odes: guessing a solution of the form  $\Lambda^t$  and finding the characteristic equation. Then assuming all terms are site independent because the difference of any two solutions of CL18 eq. catMapNewt solve its homogeneous counterpart CL18 eq. diffEqs:CatCharEq. Got to CL18 page s:tempCatZeta.

Notes: Topological zeta functions count orbits, i.e. time invariant sets of equivalent periodic states related by cyclic permutations. The "search for zeros" CL18 eq. tempCatFixPoint is the "fixed point condition." Which is a global statement which enforces CL18 eq. catMapNewt at every point in the lattice. Got to CL18 page s:catlatt

2020-09-13 Sidney The temporal cat is a special case of the spatiotemporal cat, defined on a one-dimensional lattice  $\mathbb{Z}^1$ . In this case the associated topological zeta function is known in a closed, analytic form.

*Coupled map lattices:* Starts with a review of finite difference methods for PDEs. The d dimensions in the lattice are d-1 spatial lattice points and 1

temporal one. The PDE is reduced to dynamics of a coupled map lattice, with a set of continuous fields on each site.

A5.11 I have experience with finite difference methods for solving a discretized form of a PDE, but I'm having a hard time visualizing the idea of having a discrete coordinate system in  $d$  different directions, but with a continuous field on each site. This may be valuable as it is a specific statement of where I'm getting stuck.

Q13 My current understanding is that at each point in the  $d$ -dimensional integer lattice ("point" as in a lattice node with  $d$  specified coordinates), but at each point (site) there is a continuous field. What is this field continuous over? It's at one point in a discrete coordinate system. And why is there a continuum at each point? And finally, I assume that these continuous fields are the values of the function being solved for at that point, however, shouldn't that just be a single value? Not a field? I'm sorry if this is a rather silly question, but I'll keep thinking about it and I'll make a note if my understanding (or lack thereof) changes.

A13 Predrag: In CL18 figure 1.2 field  $x_t$  or  $\phi_t$  and  $f(\phi_t)$  on the discrete site  $t$  run over continuous values. For example, at temporal lattice site  $t = 7$  the field value is  $\phi_7 = 0.374569263952942 \dots$ . OK now?

Q13.1 Slight update, it seems that the field is the state of the system and at each discretized point there is a map acting on the state, although that conflicts with the notion that time is dead, so I'm probably still misunderstanding.

A13.1 Predrag: Yes.

Thinking of this as a spring mattress. Often starts out with chaotic on-site dynamics weakly coupled to neighboring sites. In this paper one sets the lattice spacing constant equal to one. Diffusive coupled map lattices introduced by Kaneko:

$$\phi_{n,t+1} = g(\phi_{n,t}) + \epsilon [g(\phi_{n-1,t}) - 2g(\phi_{n,t}) + g(\phi_{n+1,t})],$$

where each individual spatial site's dynamical system  $g(x)$  is a 1D map, coupled to the nearest neighbors by the discretized second order *spatial* derivative. The form of time-step map  $g(\phi_{n,t})$  is the same for all time i.e. invariant under the group of discrete time translations. Spatial stability analysis can be combined with temporal stability analysis, with orbit weights depending exponentially both on the space and the time variables:  $t_p \propto e^{-LT\lambda_p}$ .  $r_i$  translates the field by one lattice spacing in the  $i^{th}$  direction.

Q14 What is a lattice period?

A14 Predrag: Does the paragraph above CL18 eq. catlattFix answer you question? I would like to refer to the *set* of numbers  $\{\ell_1, \ell_2, \dots, \ell_a\}$  as the *period* of lattice  $\Lambda$ . Would that be confusing?

- Q15 Is  $z$  in the definition of a periodic state both a temporal and a spatial index? So equivalent to both  $n$  and  $t$ ?
- A15 Predrag: after CL18 eq. CatMap2d I write "a 1-dimensional spatial lattice, with field  $\phi_{nt}$  (the angle of a kicked rotor (12.100) at instant  $t$ ) at spatiotemporal site  $z = (n, t) \in \mathbb{Z}^2$ ." Should this " $z = (n, t) \in \mathbb{Z}^2$ " be repeated elsewhere. If so, where?
- Q16 Often a member of the alphabet can be a negative number, which I assume means that the state is taken out of unity in the negative direction.
- A16 Do you understand CL18 figure fig:BernCyc2Jacob and CL18 figure fig:catCycJacob?

The spatiotemporal cat has the point-group symmetries of the square lattice. A periodic state is a set of all field values  $\Phi = \{\phi_z\}$  over the  $d$ -dimensional lattice that satisfies the spatiotemporal cat equation, with all field values constrained between zero and one. A periodic state  $\Phi_\Lambda$  is a *invariant 2-torus* if it satisfies  $\Phi_\Lambda(z + R) = \Phi_\Lambda(z)$  for any discrete translation  $R = n_1 \mathbf{a}_1 + n_2 \mathbf{a}_2 \in \Lambda$ . Got to CL18 page s:catLatt1x1.

**2020-09-14 Sidney**

- A13.1 I think I'm OK now. I think what I was trying to visualize was a stack of an infinite number of values at each lattice point, which was confusing, but this makes sense.
- A14.1 Unfortunately I don't think I quite understand. I understand the idea of the different directions, I understand treating  $\Phi_M(\phi_z)$  as a singular fixed point, but I do not understand  $\ell_i$ .
- A15.1 I think that I lost that definition of  $z$  around CL18 eq. dDCatsT, but I think that may have been a factor of how long it takes me personally to digest this material.
- A16.1 After reading the descriptions and staring at it for awhile, I think that I do.
- Q17 I tried a couple days back (Thursday or Friday I think, they all blend together) to log in to your bluejeans office. But it must have been one of the times that it had logged you off due to inactivity. There was also another person their I didn't recognize, and I didn't want to step on their toes if they were waiting for you to get back, so I logged off. So, when in general would good times to try hopping into your office?

**2020-09-16 Sidney** A Bravais lattice can be denoted  $\Lambda = [L \times T]_S$  where  $L$  is the spatial lattice period,  $T$  is the temporal lattice period,  $S$  imposes the tilt to the cell. Basis vectors for the primitive cell can be written as:

$$\mathbf{a}_1 = \begin{pmatrix} L \\ 0 \end{pmatrix}, \quad \mathbf{a}_2 = \begin{pmatrix} S \\ T \end{pmatrix}$$

Q18 If something is written as  $850[3 \times 2]_0$  what is the numerical value? More importantly, how is it found? I know it has to do with the cyclic permutations of the prime blocks, but I'm not sure how to get a numerical value.

Got to page CL18 page s:catLattCount

**2020-09-17 Sidney** For the Bernoulli map its stretching uniformity allows the use of combinatorial methods for lattice points. For temporal (not spatiotemporal) the number of periodic states is the same as the volume of the fundamental parallelepiped, so the magnitude of the determinant of the orbit Jacobian matrix. The block M can be used as a 2D symbolic representation of the lattice system state. For a given admissible source block M, the periodic field can be computed by:

$$\phi_{i_1 j_1} = \sum_{i_2=0}^2 \sum_{j_2=0}^1 \mathbf{g}_{i_1 j_1, i_2 j_2} M_{i_2 j_2}$$

**2020-09-19 Predrag** Sorry, I've been a bit overwhelmed with lecture preparations, so I will not answer any of the questions quite yet. But I have rewritten the abstract, and the introduction to the paper, up to the start of CL18 sect. s:Bernoulli *Bernoulli map*. Can you have a critical look at the new text, report here if something does not make sense to you?

**2020-09-19 Sidney**

Update I read through, and aside from some very minor grammar issues (forgetting a "have" after "we") it all makes sense.

**2020-09-20 Predrag** .

A15.2 I now added the  $z$  definition to CL18 eq. dDCatsT, is that clearer?

**2020-09-20 Sidney**

A15.3 Yes, that makes it clearer.

$$-\sum_{r=1}^{\infty} \frac{1}{r} \text{tr} \hat{\mathbf{J}}_p^r = \text{tr} \left( -\sum_{r=1}^{\infty} \frac{1}{r} \hat{\mathbf{J}}_p^r \right) = \text{tr} \ln \left( \hat{\mathbf{1}}_1 - \hat{\mathbf{J}}_p \right) = \ln \det \left( \hat{\mathbf{1}}_1 - \hat{\mathbf{J}}_p \right)$$

I liked the text cut from the introduction on page 44, it made the idea of time's death more easily digestible. Finished main paper, will look at the appendices for math.

**2020-09-22 Sidney**

**Math Review Part 1**

**Updated 9/29/20**

**Bravais lattice** From [Wikipedia](#): A Bravais lattice is an infinite array of discrete points generated by a set of discrete translation operations described in two dimensional space by:

$$\mathbf{R} = n_1 \mathbf{a}_1 + n_2 \mathbf{a}_2$$

where  $n_i$  is any integer and  $\mathbf{a}_i$  is a primitive vector, each  $\mathbf{a}_i$  lie in different directions, but are not necessarily mutually perpendicular, but they do span the lattice. A fundamental aspect of a Bravais lattice is that no matter the direction of the primitive vectors, the lattice will look exactly the same from each of the discrete lattice points when looking in that direction. A Lattice is a periodic array of points where each point is indistinguishable from any other point and has identical surroundings. A unit cell expands the idea of the infinite array of discrete points to include the space inbetween the points, if we are looking at a physical system this includes the atoms in this space. There are two main types of unit cells: primitive unit cells and non-primitive unit cells. A unit cell is the smallest group of atoms of a substance that has the overall symmetry of a crystal of that substance, and from which the entire lattice can be built up by the repetition in three dimensions. A primitive cell must contain only one lattice point, generally, lattice points that are shared by  $n$  cells are counted as  $\frac{1}{n}$  of the lattice points contained in each of those cells. So traditional primitive cells only contain points at their corners. The most obvious way to form a primitive cell is to use the primitive vectors which the lattice is constructed from:

$$C(\mathbf{a}_1, \mathbf{a}_2) = \mathbf{r} = x_1 \mathbf{a}_1 + x_2 \mathbf{a}_2$$

$$0 \leq x_i \leq 1$$

The scaling factors are to ensure that lattice points are placed on the corners of the cell. In the current paper the primitive unit cell of a d-dimensional Bravais lattice tiles the spacetime.  $C(\mathbf{a}_1, \mathbf{a}_2)$  is the primitive cell of a Bravais lattice spanned by primitive vectors  $(\mathbf{a}_1, \mathbf{a}_2)$ . A given Bravais lattice  $\Lambda$  can be defined by an infinity of primitive cells. Hermite normal form: the analogue of reduced echelon form for matrices over  $\mathbb{Z}^n$ . Each family of primitive cells contains a unique cell of the Hermite normal form, this can be written in terms of L, T, and S, where L, and T are respectively the spatial, and temporal lattice periods, S is the "tilt" of the cell. Hence the lattice can be defined as  $[L \times T]_S$ .

**Prime Bravais lattices** It may be possible to tile a given Bravais lattice  $\Lambda$  by a finer lattice  $\Lambda_p$ . A Bravais lattice is prime if there is no finer primitive cell, other than the unit volume  $[1 \times 1]_0$  that can tile it. If  $\det \Lambda$  is a prime number, then  $\Lambda$  is a *prime matrix*. If  $\Lambda$  is neither prime nor unimodular (a square integer matrix having determinant



of  $\pm 1$ ), it is composite can be decomposed into a product of two non-unimodular matrices  $\Lambda = PQ$ . In order to determine all prime lattices  $\Lambda_p$  that tiles a given Bravais lattice  $\Lambda$ :

$$\mathbf{a}_1 = k\mathbf{a}_1^p + l\mathbf{a}_2^p$$

$$\mathbf{a}_2 = m\mathbf{a}_1^p + n\mathbf{a}_2^p$$

observe that a prime tile  $(\mathbf{a}_1^p, \mathbf{a}_2^p)$  tiles the large tile only if the larger tile's width  $L$  is a multiple of  $L_p$ , and the height  $T$  is a multiple of  $T_p$ , and the two tile "tilts" satisfy:

$$\mathbf{a}_2 = m\mathbf{a}_1^p + \frac{T}{T_p}\mathbf{a}_2^p \rightarrow S = mL_p + \frac{T}{T_p}S_p$$

A prime lattice only tiles the given lattice if the area spanned by the two tilted primitive vectors:

$$\mathbf{a}_2 \times \mathbf{a}_2^p = ST_p - TS_p$$

is a multiple of the prime tile area  $L_pT_p$ . A periodic state is a set of all field values  $\Phi = \{\phi_z\}$  over the  $d$ -dimensional lattice  $z \in \mathbb{Z}$  that satisfies the spatiotemporal cat equation. Periodic state  $\Phi$  is a periodic orbit if  $\Phi(z + R) = \Phi(z)$  for any discrete translation  $R = n_1\mathbf{a}_1 + n_2\mathbf{a}_2$ . If a given periodic orbit over lattice  $\Lambda$  is not periodic under translations  $R \in \Lambda_p$  for any sublattice  $\Lambda_p$  (except for  $\Lambda$  itself) we shall refer to it as an orbit: a periodic state of smallest periodicity in all spacetime directions.

**Shift Operator** Shift operator is a matrix:  $r_{ij} = \delta_{i+1,j}$ , this along with a periodic boundary condition assuming  $[n \times n]$  matrix  $r^n = I$  yields

$$\begin{pmatrix} 0 & 1 & 0 & 0 \\ 0 & 0 & 1 & 0 \\ 0 & 0 & 0 & 1 \\ 1 & 0 & 0 & 0 \end{pmatrix}$$

A periodic state is a vector with all the values that the field takes on at each point on the lattice. Shift operator is cyclic permutation of a periodic state, changes only the coordinates of the periodic state.

$$r\Phi = \begin{bmatrix} \phi_1 \\ \phi_2 \\ \vdots \\ \phi_0 \end{bmatrix}$$

$r^T = r^{-1}$  cyclic permutation in the opposite direction, does not destroy anything, only changes the coordinates.

**Lattice Derivatives** Hypercube in d-dimensions with unit sides. Each side is described by a unit vector in direction  $\mu \hat{n}_\mu \in \{\hat{n}_1, \hat{n}_2, \hat{n}_3, \dots, \hat{n}_d\}$  unit lattice cell, points along  $\mu'$ th direction.

Forward Lattice Derivative (a is lattice spacing):

$$(\partial_\mu \phi)_l = \frac{\phi(x + a\hat{n}_\mu) - \phi(x)}{a} = \frac{\phi_{l+\hat{n}_\mu} - \phi_l}{a}$$

Backward Lattice Derivative (transpose of forward lattice derivative):

$$(\partial_\mu \phi)^T = \frac{\phi(x - a\hat{n}_\mu) - \phi(x)}{a} = \frac{\phi_{l-\hat{n}_\mu} - \phi_l}{a}$$

**Lattice Discretization, Lattice State** Divide interval of separation  $a$  creating a discrete coordinate system. At each point read off the value of the continuous counterpart. Field has a constant value over the interval. Lattice is a coordinate, set of points, the values of the field at each lattice point is a periodic state.

field  $\phi = \phi(x) \quad x = al \quad l \in \mathbb{Z}$

Lattice State  $\phi = \{\phi_0, \phi_1, \phi_2, \dots, \phi_{n-1}\}$  "configuration".

**N-Site Periodic Lattice** After N steps, back

$$r^N = I$$

eigenvalues= $\omega = e^{\frac{i2\pi}{N}}$

$$r^N - I = \prod_{k=0}^{N-1} (r - \omega^k I)$$

N distinct eigenvectors, N-dim space (N irrep)

N projection operators

$$P_k = \prod_{j \neq k} \frac{r - \omega^j I}{\omega^k - \omega^j}$$

**Discrete Fourier Transforms** Have a periodic state  $\phi = \{\phi_0, \phi_1, \dots, \phi_{N-1}\}$

Kth Fourier Coeff=projection of  $\phi$  onto eigen vector  $\varphi$

$$\tilde{\phi}_k = \varphi_k^\dagger \cdot \phi = \frac{1}{\sqrt{N}} \sum_{l=0}^{N-1} e^{-\frac{i2\pi}{N} kl} \phi_l$$

**Q19** I think I may have gotten to the point where I can go beyond exclusively reading the paper, what should I do beyond? As well, what times would be good for me to drop in on your Bluejeans office during the week?

**Q20** I believe I've asked this before, or a form of it, but it seems that the periodic boundary condition is in direct conflict with the definition of the shift operator. Am I missing something?

**2020-10-15 Sidney** A reread.

The Bernoulli shift map is a circle map due to the mod 1 operation for  $[1/s, 1)$  where  $s$  is the "stretching parameter" of the general Bernoulli map:  $\phi_{t+1} = s\phi_t \pmod{1}$ . ( $\pmod{1}$  subtracts the integer part of  $s\phi_t$  yielding the "winding number"  $m_{t+1}$ . This keeps  $\phi_{t+1}$  in the unit interval, and divides this interval into  $s$  subintervals. The winding number is also the alphabet of the system, denoting at time  $t$ , it visits interval  $m$ . Brief note from Chaosbook: we can represent a state as a base  $s$  decimal of the resulting visitation sequence:  $\phi_0 = .m_1m_2m_3\cdots$ . The Bernoulli map operates on a state by shifting this itinerary over by one:  $\phi_0 = .m_1m_2m_3\cdots \rightarrow \phi_1 = .m_2m_3\cdots$ . The preimages of critical points (the point which when input into the map yield a maximum value on in the map) partition the map into  $s^n$  subintervals, where  $n$  is the orbit length. There is no pruning in the Bernoulli map, as its critical points are all unity, however, as it is a circle map the first and last fixed point (rightmost fixed point, and the fixed point at the origin) are the same, so they are counted as one fixed point, and thus the number of periodic orbits is  $N_n = s^n - 1$ . There can only be one periodic orbit per subinterval because each subinterval is treated as a single point where a certain orbit is possible, thus, there can only be one orbit. For the temporal Bernoulli, 'Temporal' here refers to the state (field)  $\phi_t$  and the winding number  $m_t$  (source) taking their values on the lattice sites of a 1-dimensional temporal lattice  $t \in \mathbb{Z}$ . Over a finite lattice segment they can be written as a state, and a symbol block. The Bernoulli equation can be written as a first order difference equation  $\phi_t - s\phi_{t-1} = -m_t$  where  $\phi_t$  is contained within the unit interval. This is the condition which each point on the lattice must fulfill. This can then be written in terms of the orbit Jacobian matrix, which is a sum of the identity and cyclic permutation matrix which has the condition  $r^n = I$ . This permutation permutes forward in time the periodic state by one site. The temporal Bernoulli condition can be viewed as a search for zeros of the function involving the orbit Jacobian matrix operating on the periodic state summed with the symbol block  $M$ . This allows the entire periodic state which solves for zero  $\Phi_M$  to be treated as a single fixed point. The orbit Jacobian matrix stretches the unit hyper cube such that every periodic point is mapped onto an integer lattice  $\mathbb{Z}^n$  site, which is then translated by the winding numbers into the origin to satisfy the fixed point condition. Therefore  $N_n$  the number of solutions to the fixed point condition is the number of lattice sites within the fundamental parallelepiped (fp), which is equivalent to the volume of the fp because each unit cell in the lattice only contains one lattice point. So  $N_n$  is the magnitude of the determinant of the orbit Jacobian matrix, this is called Hill's determinant, or the Fundamental Fact. The orbit Jacobian matrix maps the unit hyper

cube into the basis vectors of the fundamental parallelepiped which are given by columns of the orbit Jacobian matrix.

**2020-10-18 Sidney** My notes on Barvinok [2] *Lecture notes*

The theory discussed in these lectures are inspired by a few series formulas, the first being:

$$\sum_{m=1}^n x^m = \frac{1 - x^{n+1}}{1 - x}$$

We take the interval  $[0, n]$  and for every integer point in the interval we write the monomial  $x^m$  and then take the sum over each integer point on the interval. It gives a polynomial with  $n+1$  terms, but can be written in the form given, later we will cover doing the same over a 2D plane (evaluating at each integer point on the plane and summing over every integer point  $\mathbf{m} = (m_1, m_2)$  with bivariate monomials  $\mathbf{x}^{\mathbf{m}} = x^{m_1} x^{m_2}$ ). The second formula is the infinite geometric series:

$$\sum_m x^m = \frac{1}{1 - x}$$

This makes sense if  $|x| < 1$  similarly

$$\sum_{-\infty}^0 x^m = \frac{1}{1 - x^{-1}} = \frac{-x}{1 - x}$$

This converges if  $|x| > 1$

$$\sum_{m=-\infty}^{\infty} x^m$$

This converges for no values, so we will say that it equals zero, this can be reasoned through as every positive integer added to every negative integer is zero, we then subtract zero, as it was double counted:

$$\sum_{m=-\infty}^{\infty} x^m = \sum_{m=0}^{\infty} x^m + \sum_{m=-\infty}^0 x^m - x^0 = 0$$

This suggestively agrees with

$$\frac{-x}{1 - x} + \frac{1}{1 - x} - 1 = 0$$

Geometrically, the real line  $\mathbb{R}^1$  is divided into two unbounded rays intersecting in a point. For every region (the two rays, the line and the point), we construct a rational so that the sum of  $x^m$  over the lattice points in the region converges to that rational function, if it converges at all.

**2020-10-19 Sidney**

**Inclusion-exclusion principle**

$$|A \cup B| = |A| + |B| - |A \cap B| \quad (22.2)$$

where  $|A \cap B|$  is the number of elements which are in both A and B. This avoids double counting.

If we think of a plane of points, we can draw lines which subdivide the plane, each line makes the plane two half planes, and every two lines form four angles, this forms several regions. Among these regions there are regions  $\mathcal{R}$  where the sum:

$$\sum_{m \in \mathcal{R} \cap \mathbb{Z}^2} \mathbf{x}^m$$

converges for some  $\mathbf{x}$ , and some regions where the sum will never converge.

We shall show that it is possible to assign a rational function to every region simultaneously so that each series converges to the corresponding rational function, if it converges at all, it will also satisfy the inclusion-exclusion principle.

**Definition 1** The scalar product in  $\mathbb{R}^d$  is

$$\sum_{i=1}^d x_i y_i$$

for  $x = (x_1, \dots, x_d)$  and  $y = (y_1, \dots, y_d)$ , and the same for  $\mathbb{Z}^d \subset \mathbb{R}^d$ .

**Definition** Polyhedron P is the set of solutions to finitely many linear inequalities:

$$P = \left\{ \phi \in \mathbb{R}^d : \sum_{i=1}^d a_{ij} x_j \leq b_i \right\}$$

If all  $a_{ij}$  and  $b_j$  are integers the polyhedron is rational.

Barvinok notes concern themselves with the set  $P \cap \mathbb{Z}^d$  of integer points in a rational polyhedron P. He introduces the algebra of polyhedra to account for all relations among polyhedra.

**2020-11-29 Predrag** We only need to understand parallelepipeds, not polyhedra in general. Should be easier.

**2020-11-30 Sidney** I understand your comments. Thank you, I am pretty sure that the general polyhedra stuff can be put in terms of parallelepipeds, so at least it wasn't wasted knowledge, but I'm glad that I don't need to know all of it, it's on the edge of my proof abilities.

**2020-11-29 Predrag**

**Definition 2** For a set  $\mathcal{B} \in \mathbb{R}^d$ , the function

$$[\mathcal{B}](\phi) = \begin{cases} 1 & \text{if } \phi \in \mathcal{B} \\ 0 & \text{otherwise} \end{cases} \quad (22.3)$$

is called the *indicator* of  $\mathcal{B}$ .

**2020-10-24 Sidney**

The intersection of finitely many (rational) polyhedra is a (rational) polyhedron. The union doesn't have to be, but may be a polyhedron.

Union: The union of a collection of sets is the set of all elements in the collection.

Intersection:  $A \cap B$ , is the intersection of two sets A and B, i.e., the set containing all elements of A that also belong to B.

The algebra of rational polyhedra is the vector space  $\mathcal{P}(\mathbb{Q}^d)$  spanned by the indicators  $[P]$  for all rational polyhedra  $P \subset \mathbb{R}^d$

**2020-11-29 Predrag**  $\mathbb{Q}$  is the *field of rationals*.

**2020-10-24 Sidney**

**Valuations**

Let  $V$  be a vector space. A linear transformation  $\mathcal{P}(\mathbb{Q}^d) \rightarrow V$  is called a valuation. This course is on the particular valuation  $\mathcal{P}(\mathbb{Q}^d) \rightarrow \mathbb{C}(x_1, \dots, x_d)$ , where  $\mathbb{C}(x_1, \dots, x_d)$  is the space of d-variate rational functions.

**Theorem 1** There exists a unique valuation  $\chi : \mathcal{P}(\mathbb{R}^d) \rightarrow \mathbb{R}$  called the Euler characteristic, such that  $\chi([P]) = 1$  for any non-empty polyhedron  $P \subset \mathbb{R}^d$

**2020-11-30 Predrag** Klain and Rota [20] *Introduction to Geometric Probability*:

A *valuation* on a lattice  $L$  of sets is a function  $\mu$  defined on  $L$  that takes real values, and that satisfies the following conditions:

$$\mu(A \cup B) = \mu(A) + \mu(B) - \mu(A \cap B), \quad (22.4)$$

$$\mu(\emptyset) = 0, \quad (22.5)$$

where  $\emptyset$  is the empty set. By iterating the identity (24.251) we obtain the inclusion-exclusion principle for a valuation  $\mu$  on a lattice  $L$ , namely

$$\begin{aligned} \mu(A_1 \cup A_2 \cup \dots \cup A_n) &= \sum_i \mu(A_i) - \sum_{i < j} \mu(A_i \cap A_j) \\ &+ \sum_{i < j < k} \mu(A_i \cap A_j \cap A_k) + \dots \end{aligned} \quad (22.6)$$

for each positive integer  $n$ .

Barvinok [2] Lecture 1, Problem 1 statement of (24.253) is less intelligible: Take sets  $A_1, A_2, \dots, A_n \in \mathbb{R}^d$ . The inclusion-exclusion formula is

$$\cup A_i = \sum_I (-1)^{|I|-1} [\cap_{i \in I} A_i], \quad (22.7)$$

where the sum is taken over all non-empty subsets  $I \subset \{1, \dots, n\}$  and  $|I|$  is the cardinality of  $I$ .

2020-10-25 Sidney

### Identities in the Algebra of Polyhedra

The image of a polyhedron under a linear transformation is a polyhedron.

**Theorem 1** Let  $P \subset \mathbb{R}^d$  be a polyhedron and let  $T: \mathbb{R}^d \rightarrow \mathbb{R}^k$  be a linear transformation. Then  $T(P) \subset \mathbb{R}^k$  is a polyhedron. Furthermore, if  $P$  is a rational polyhedron and  $T$  is a rational linear transformation (that is, the matrix of  $T$  is rational), then  $T(P)$  is a rational polyhedron.

Linear transformations preserve linear relations among indicators of polyhedra.

**Theorem 2** Let  $T: \mathbb{R}^d \rightarrow \mathbb{R}^k$  be a linear transformation. Then there exists a linear transformation  $T: P(\mathbb{R}^d) \rightarrow P(\mathbb{R}^k)$  such that  $T(P) = [T(P)]$  for every polyhedron  $P \subset \mathbb{R}^d$ .

Most sensible polyhedra have vertices, but some don't.

**Definition 1** Let  $P \subset \mathbb{R}^d$  be a polyhedron. A point  $v \in P$  is called a vertex of  $P$  if whenever  $v = (x + y)/2$  for some  $x, y \in P$ , we must have  $x = y = v$ .

If  $v$  is a point in  $P$ , we define the tangent cone of  $P$  at  $v$  as:

$$co(P, v) = \{x \in \mathbb{R}^d : \epsilon x + (1 - \epsilon)v \in P \text{ for all sufficiently small } \epsilon > 0\}$$

Not all polyhedra have vertices. In fact, a non-empty polyhedron has a vertex if and only if it does not contain a line.

**Definition 2** We say that a polyhedron  $P$  contains a line if there are points  $x$  and  $y$  such that  $y \neq 0$  and  $x + ty \in P$  for all  $t \in \mathcal{R}$ .  $P_0(\mathbb{R}^d) \subset P(\mathbb{R}^d)$  is the subspace spanned by the indicators of rational polyhedra that contain lines.

*Theorem 3* Let  $P \subset \mathbb{R}^d$  be a polyhedron. Then there is a  $g \in P_0(\mathbb{R}^d)$  such that

$$[P] = g + \sum_v [co(P, v)],$$

where the sum is taken over all vertices  $v$  of  $P$ . If  $P$  is a rational polytope then we can choose  $g \in P_0(\mathbb{Q}^d)$

**Definition 3-0** A polytope is a high dimensional generalization of a polyhedron.

**Definition 3** Let  $A \subset \mathbb{R}^d$  be a non-empty set. the set

$$A^\circ = \{y \in \mathbb{R}^d : \langle x, y \rangle \leq 1 \text{ for all } x \in A\}$$

is called the polar of A, where  $\langle x, y \rangle$  is the inner product.

**2020-10-27 Sidney**

A set  $S$  in a vector space over  $\mathbb{R}^d$  is convex, if the line segment connecting any two points in  $S$  lies entirely within  $S$ . If  $P$  is a rational polyhedron then  $P^\circ$  is also a rational polyhedron.

**Theorem 4** There exists a linear transformation  $D : P(\mathbb{Q}^d) \rightarrow P(\mathbb{Q}^d)$  such that  $D[P] = [P^\circ]$  for every non-empty polyhedron  $P$ .

It follows from Theorem 4 that whenever we have a linear identity  $\sum_{i=1}^m \alpha_i [P_i] = 0$  among the indicator functions of polyhedra, we have the same identity  $\sum_{i=1}^m \alpha_i [P_i^\circ] = 0$  for the indicator functions of their polars.

Barvinok [2] Lecture 3.

For an integer point  $\mathbf{m} = (m_1, \dots, m_d)$  we introduce the monomial  $\mathbf{x}^{\mathbf{m}} = x_1^{m_1} \dots x_d^{m_d}$ . Given a set  $S \subset \mathbb{R}^d$ , we consider the sum

$$f(S, \mathbf{x}) = \sum_{\mathbf{m} \in S \cap \mathbb{Z}^d} \mathbf{x}^{\mathbf{m}} \tag{22.8}$$

Our goal is to find a reasonably short expression for this sum as a rational function in  $\mathbf{x}$ .

**Example 1** Let  $\mathcal{R}_+^d$  be the non-negative orthant, that is the set of all points with all coordinates non-negative. We have

$$\sum_{\mathbf{m} \in \mathcal{R}_+^d \cap \mathbb{Z}^d} \mathbf{x}^{\mathbf{m}} = \left( \sum_{m_1=0}^{\infty} x_1^{m_1} \right) \dots \left( \sum_{m_d=0}^{\infty} x_d^{m_d} \right) = \prod_{i=1}^d \frac{1}{1-x_i}$$

provided that  $|x_i| < 1$

**Definition** Let  $u_1, \dots, u_d \in \mathbb{Z}^d$  be linearly independent integer vectors. The simple rational cone generated by  $u_1, \dots, u_d$  is the set:

$$K = \left\{ \sum_{i=1}^d \alpha_i u_i : \alpha_i \geq 0 \text{ for } i = 1, \dots, d \right\}$$



The fundamental parallelepiped of  $u_1, \dots, u_d$  is the set

$$\Pi = \left\{ \sum_{i=1}^d \alpha u_i : 1 > \alpha_i \geq 0 \text{ for } i = 1, \dots, d \right\}$$

**Theorem** For a simple rational cone  $K = K(u_1, \dots, u_d)$  we have

$$f(K, \mathbf{x}) = \left( \sum_{m \in \Pi \cap \mathbb{Z}^d} \mathbf{x}^m \right) \prod_{i=1}^d \frac{1}{1 - \mathbf{x}^{u_i}}$$

**Theorem** The number of integer points in the fundamental parallelepiped is equal to its volume.

**Sketch of Proof** Let  $\Lambda$  be the set of all integer combinations of  $u_1, \dots, u_d$ :

$$\Lambda = \left\{ \sum_{i=1}^d \alpha_i u_i : \alpha_i \in \mathbb{Z} \text{ for } i = 1, \dots, d \right\}$$

Let us consider all translates  $\Pi + u$  with  $u \in \Lambda$ . We claim that  $\Pi + u$  can cover all  $\mathbb{R}^d$  without overlapping, this can be extracted from the proof of theorem 1. Let us take a sufficiently large region  $X \subset \mathbb{R}^d$  and let us count the number of integer point in  $X$ , the set is roughly covered by  $\text{vol} X / \text{Vol} \Pi$  translations of the parallelepiped, and each translation carries the same number of points hence we must have  $|\Pi \cap \mathbb{Z}^d| = \text{vol} \Pi$ .

**Barvinok [2] Lect. 3, Definition 2.** Let  $u_1, \dots, u_d \in \mathbb{Z}^d$  be linearly independent vectors and let  $K$  be the simple cone generated by  $u_1, \dots, u_d$ . We say that  $K$  is *unimodular* if the volume of the fundamental parallelepiped  $\Pi$  is 1. Equivalently,  $K$  is unimodular if the origin is the unique integer point in  $\Pi$ . Equivalently, (22.8) is of form

$$f(K, \mathbf{x}) = \prod_{i=1}^d \frac{1}{1 - x^{u_i}}. \quad (22.9)$$

**2021-01-01** I have been looking at the flow conservation sum rule for the Hénon map, as of today I had my suspicions confirmed that the Hénon map is not flow conserving so, the sum rule will not go to 1. However, I am still investigating the relation between the orbit Jacobian matrix (the Hill matrix) and the local Jacobian  $J_M$ . To do this, I have been looking over the proof that was done with the cat map to show that  $|\text{Det } \mathcal{J}| = |\det(I - J_M)|$ . I am hoping that I can find something similar to this identity for the Hénon map. I have been looking at section five of the cat paper to see if I can adapt anything. I am also going to look at the relaxation method for finding periodic orbits so I can start working within Orbithunter and finding periodic orbits.

Q21 Is XXX?

Q22 What exactly is meant by XXX?

2021-01-02 Sidney Here are my notes from section 5:

Kronecker product  $A \otimes B$   $A$  is  $[n \times n]$  and  $B$  is  $[m \times m]$

$$A \otimes B = \begin{pmatrix} a_{11}B & \cdots & a_{1n}B \\ \vdots & \ddots & \vdots \\ a_{n1}B & \cdots & a_{nn}B \end{pmatrix}$$

for  $A, A'$   $[n \times n]$  matrices and  $B, B'$   $[m \times m]$

$$(A \otimes B)(A' \otimes B') = AA' \otimes BB'$$

$$\text{tr}(A \otimes B) = \text{tr}(A)\text{tr}(B)$$

$$\det(A \otimes B) = \det(A)^m \det(B)^n$$

the two  $[mn \times mn]$  block matrices  $A \otimes B$  and  $B \otimes A$  are equivalent by a similarity transformation

$$B \otimes A = P^T(A \otimes B)P$$

where  $P$  is a permutation matrix, as  $\det(P) = 1$

$$\det(A \otimes B) = \det(B \otimes A)$$

Consider a rectangular  $d=2$  lattice  $[L \times T]_0$  primitive cell, for this cell, the spatiotemporal orbit Jacobian matrix is

$$\mathcal{J} = r_1 + r_2 - 2sI + r_2^{-1} + r_1^{-1}$$

The index 1 is the spacial direction, and the index 2 is the temporal direction. The  $[LT \times LT]$  orbit Jacobian matrix can be rewritten using Kronecker products:

$$\mathcal{J} = I_1 \otimes (r_2 + r_2^{-1}) - sI_1 \otimes I_2 + (r_1 + r_1^{-1}) \otimes I_2$$

$$I_1 = [L \times L] \text{ Identity}$$

$$I_2 = [T \times T] \text{ Identity}$$

Hill determinant: fundamental parallelepiped example Consider the Bravais lattice with primitive vectors  $\vec{a}_1 = \langle 3, 0 \rangle$  and  $\vec{a}_2 = \langle 0, 2 \rangle$  a periodic orbit over this primitive cell has 6 field values, one for each lattice site  $z = (n, t)$  on a  $[3 \times 2]_0$  rectangle:

$$\begin{bmatrix} \phi_{01} & \phi_{11} & \phi_{21} \\ \phi_{00} & \phi_{10} & \phi_{20} \end{bmatrix}$$

We can stack up the columns of this periodic state and the corresponding sources into 6-dimensional vectors

$$\begin{pmatrix} \phi_{01} \\ \phi_{00} \\ \phi_{11} \\ \phi_{10} \\ \phi_{21} \\ \phi_{20} \end{pmatrix}, \quad \begin{pmatrix} m_{01} \\ m_{00} \\ m_{11} \\ m_{10} \\ m_{21} \\ m_{20} \end{pmatrix}$$

The corresponding orbit Jacobian matrix block-matrix:

$$\mathcal{J}_{[3x2]_0} = \left[ \begin{array}{cc|cc|cc} -2s & 2 & 1 & 0 & 1 & 0 \\ 2 & -2s & 0 & 1 & 0 & 1 \\ \hline 1 & 0 & -2s & 2 & 1 & 0 \\ 0 & 1 & 2 & -2s & 0 & 1 \\ \hline 1 & 0 & 1 & 0 & -2s & 2 \\ 0 & 1 & 0 & 1 & 2 & -2s \end{array} \right]$$

The fundamental parallelepiped generated by the action of the orbit Jacobian matrix is spanned by  $LT = 6$  primitive vectors: the columns of the orbit Jacobian matrix. The fundamental fact now yields the Hill determinant as the number of periodic states

$$N_{[3x2]_0} = |\text{Det}(\mathcal{J}_{[3x2]_0})| = 4(s-2)s(2s-1)^2(2s+3)^2$$

In practice, one often computes the Hill determinant using a Hamiltonian or "transfer matrix" formulation. An example is the temporal cat 3-term recurrence

$$\begin{aligned} \phi_t &= \phi_t \\ \phi_{t+1} &= -\phi_{t-1} + s\phi_t - m_t \end{aligned}$$

In the Percival-Vivaldi "two-configuration" cat map representation

$$\begin{aligned} \hat{\phi}_{t+1} &= \hat{J}_1 \hat{\phi}_t - \hat{m}_t \\ \hat{J}_1 &= \begin{bmatrix} 0 & 1 \\ -1 & s \end{bmatrix}, \quad \hat{\phi}_t = \begin{bmatrix} \phi_{t-1} \\ \phi_t \end{bmatrix}, \quad m_t = \begin{bmatrix} 0 \\ m_t \end{bmatrix} \end{aligned}$$

Similarly for the d=2 spatiotemporal cat lattice at hand, one can recast into a 5-term recurrence relation:

$$\begin{aligned} \phi_{nt} &= \phi_{nt} \\ \phi_{n,t+1} &= \phi_{n,t-1} - \phi_{n-1,t} + 2s\phi_{nt} - \phi_{n+1,t} - m_{nt} \\ \hat{J}_1 &= \left[ \begin{array}{c|c} 0 & I_1 \\ \hline -I_1 & -\mathcal{J} \end{array} \right] \end{aligned}$$

This  $[2L \times 2L]$  block matrix generates a "time" orbit by acting on a 2L-dimensional "phase space" lattice strip  $\hat{\phi}_t$  along the "spatial" direction

**2021-01-04 Sidney** I am going to take a break from the sum rule proof. However, I do know that the Hénon map is not a closed system so the sum rule does not converge to 1. For this blog entry, I shall take notes on the relaxation method for finding cycles, I will also try to write some code today, if I do, I will post my initial python code here too.

**Notes** All methods for finding unstable cycles are based on the idea of constructing a new dynamical system such that (i) the position of the cycle is the same for the original system and the transformed one, and (ii) the unstable cycle in the original system is a stable cycle of the transformed system. For example, the Newton-Raphson method replaces iteration of  $f(x)$  by iteration of the Newton-Raphson map:

$$x'_i = g_i(x) = x_i - \left( \frac{1}{M(x) - I} \right)_{ij} (f(x) - x)_j$$

A fixed point  $x_*$  for a map  $f(x)$  is also a fixed point of  $g(x)$ , indeed a superstable fixed point since  $\frac{\partial g_i(x_*)}{\partial x_j} = 0$ . The relaxation methods start with a guess of not a few points along an orbit, but a guess of the entire orbit. The relaxation algorithm for finding cycles is based on the observation that a trajectory of a map such as the Hénon map (see the discussion leading up to (3.28)):

$$\begin{aligned} x_{i+1} &= 1 - ax_i^2 + by_i \\ y_{i+1} &= x_i \end{aligned}$$

Is a stationary solution of the relaxation dynamics defined by the flow

$$\frac{dx_i}{d\tau}$$

for any vector field  $v_i$  which vanishes on the trajectory. Here  $\tau$  is a "fictitious time" variable, unrelated to the dynamical time (in this example, the discrete time of map iteration). As the simplest example, take  $v_i$  to be the deviation of an approximate trajectory from the exact 2-step recurrence form of the Hénon map:

$$v_i = x_{i+1} - 1 + ax_i^2 - bx_{i-1}$$

For fixed  $x_{i-1}$  and  $x_{i+1}$  there are two values of  $x_i$  satisfying  $v_i = 0$ . These solutions are the two extremal points of a local "potential" function:

$$v_i = \frac{\partial}{\partial x_i} V_i(x)$$

$$V_i = x_i(x_{i+1} - bx_{i-1} - 1) + \frac{a}{3}x_i^3$$

Assuming that the two extremal points are real, one is a local minimum of  $V_i(x)$  and the other is a local maximum. We can modify our vector field differential equation with

$$\frac{dx_i}{d\tau} = r_i v_i$$
$$r_i = \pm 1$$

The modified flow will be in the direction of the extremal point given by the local maximum of  $V_i$  if  $r_i = 1$  is chosen, or in the direction of the one corresponding to the local minimum if we take  $r_i = -1$ . I think that this is because a negative slope seeks to minimize a value, whereas a positive slope seeks to maximize it, therefore, if we can somehow keep the flow from going off into positive or negative infinity, it will go to either a local maximum or local minimum. The goal of the relaxation method is that instead of searching for an unstable periodic orbit of a map, one searches for a stable attractor of a vector field. More generally, consider a  $d$ -dimensional map  $x' = f(x)$  with a hyperbolic fixed point  $x_*$ . Any fixed point  $x_*$  is by construction an equilibrium point of the fictitious time flow

$$\frac{dx}{d\tau} = f(x) - x$$

If all eigenvalues of the Jacobian matrix  $J(x_*) = Df(x_*)$  have real parts smaller than unity, then  $x_*$  is a stable equilibrium point of the flow. If some of the eigenvalues have real parts larger than unity, then one needs to modify the vector field so that the corresponding directions of the flow are turned into stable directions in a neighborhood of the fixed point. To do this, we can modify the flow by

$$\frac{dx}{d\tau} = \mathbf{C}(f(x) - x),$$

where  $\mathbf{C}$  is a  $[d \times d]$  invertible matrix. The aim is to turn  $x_*$  into a stable equilibrium point of the flow by an appropriate choice of  $\mathbf{C}$ . It can be shown that a set of permutation/reflection matrices with one and only one non-vanishing entry  $\pm 1$  per row or column (for  $d$ -dimensional systems, there are  $d!2^d$  such matrices) suffices to stabilize any fixed point. In practice, one chooses a particular matrix  $\mathbf{C}$ , and the flow is integrated. For each choice of  $\mathbf{C}$ , one or more hyperbolic fixed points of the map may turn into stable equilibria of the flow. We can change the algorithm to a discrete method which solves the issue of lengthy integrations of the fictitious time method. The idea is to construct a very simple map  $g$ , a linear transformation of the original  $f$ , for which the fixed point is stable. We take the Newton-Raphson map and replace the Jacobian prefactor in it with a constant matrix prefactor:

$$x' = g(x) = x + \Delta\tau \mathbf{C}(f(x) - x),$$

where  $\Delta\tau$  is a positive real number, and  $\mathbf{C}$  is a  $[d \times d]$  permutation and reflection matrix with one and only one non-vanishing entry  $\pm 1$  per row or column. A fixed point of  $f$  is also a fixed point of  $g$ . Since  $\mathbf{C}$  is invertible, the inverse is also true. This construction is motivated by the observation that for small  $\Delta\tau \rightarrow d\tau$  the map is the Euler method for integrating the modified flow with integration step  $\Delta\tau$ . The argument why a suitable choice of matrix  $\mathbf{C}$  can lead to the stabilization of an unstable periodic orbit is similar to the one used to motivate the construction of the modified vector field. In fact, for very small  $\Delta\tau$  this construction just becomes the flow. For a given fixed point of  $f(x)$  we again chose a  $\mathbf{C}$  such that the flow in the expanding directions of  $M(x_*)$  is turned into a contracting flow. The aim is to stabilize  $x_*$  by a suitable choice of  $\mathbf{C}$ . In the case where the map has multiple fixed points, the set of fixed points is obtained by changing the matrix  $\mathbf{C}$  (in general different for each unstable fixed point) and varying initial conditions for the map  $g$ . For example, for 2-dimensional dissipative maps it can be shown that the 3 matrices:

$$\begin{pmatrix} 1 & 0 \\ 0 & 1 \end{pmatrix}$$

$$\begin{pmatrix} -1 & 0 \\ 0 & 1 \end{pmatrix}$$

$$\begin{pmatrix} 1 & 0 \\ 0 & -1 \end{pmatrix}$$

suffice to stabilize all kinds of possible hyperbolic fixed points. If  $\Delta\tau$  is chosen sufficiently small, the magnitude of the eigenvalues of the fixed point  $x_*$  in the transformed system are smaller than one, one has a stable fixed point. However,  $\Delta\tau$  should not be chosen too small: since the convergence is geometrical with a ratio  $1 - \alpha\Delta\tau$  (where the value of the constant  $\alpha$  depends on the stability of the fixed point in the original system), small  $\delta\tau$  can slow down the speed of convergence. The critical value of  $\Delta\tau$ , which just suffices to make the fixed point stable can be read off from the quadratic equations relating the stability coefficients of the original system and those of the transformed system. In practice, one can find the optimal  $\Delta\tau$  by iterating the dynamical system stabilized with a given  $\mathbf{C}$  and  $\Delta\tau$ . In general, all starting points converge on the attractor provided  $\Delta\tau$  is small enough. If this is not the case, the trajectory either diverges (if  $\Delta\tau$  is far too large) or it oscillates in a small section of the state space (if  $\Delta\tau$  is close to its stabilizing value). A fixed point can now be found by choosing a starting point in the global neighborhood of the fixed point, and iterating the map  $g$  which now converges to the fixed point due to its stability. The basin of attraction is very large. The step size  $|g(x) - x|$  decreases exponentially when the trajectory approaches the fixed point. To get the coordinates of the fixed points with a high precision, one therefore needs a large number of iterations for the trajectory which is already in

the linear neighborhood of the fixed point. To speed up the convergence of the final part of the approach to a fixed point, it is recommended to do a combination of this approach and the Newton-Raphson method. The fixed points of the  $n$ th iterate  $f^n$  are periodic points of a cycle of period  $n$ . If we consider the map

$$x' = g(x) = x + \Delta\tau \mathbf{C}(f^n - x)$$

the iterates of  $g$  converge to a fixed point provided that  $\Delta\tau$  is sufficiently small and  $\mathbf{C}$  is a  $[dx/d]$  constant matrix chosen such that it stabilizes the flow. As  $n$  grows,  $\Delta\tau$  has to be chosen smaller and smaller.

**2021-01-05 Sidney .**

Q23 How does one choose what  $r$  or  $\mathbf{C}$  to use? I know that for sigma, I chose 1 if I want to drive it to converge to a local maximum in the potential, and -1 if I want a local minimum, but how do I know if the fixed point I am dealing with is a maximum or minimum?

**2021-01-05 Predrag .**

A23

**2021-01-05 Sidney** I have been hard at work trying to understand relaxation for cyclists. And I have gotten somewhere, not to a solution just yet, but somewhere. I decided that it would be best if I tried to understand the numerical methods employed by OrbitHunter [16] before I started using it, to this end, I have constructed a crude python code that can find the fixed points of the Hénon map, and the two cycle. My next step is to make the two cycle program more efficient and cleaner, and then to generalize it to  $n$ -length orbits. After this has been done I can start work on the exercise that I was set. The code is in

`siminos/williams/python/relax1.py`

**2021-01-14 Sidney** I have contacted Matt about OrbitHunter [16] and he says that he's working on fixing some things so it's easier for people that are not him to work with. He recommended that I try to work on my own code, so I have been doing that. I was able to get the Two\_Cycle working with the modification that it can now determine the sigma itself, but the four\_cycle code is still not working, I think I need to change the differential equation solver to a Runge-Kutta algorithm instead of the Euler one I've been using, I'll paste the code under here, please please help if you can.

**2021-02-01 Predrag .**

Do this Save and svn commit this code as `siminos/williams/python/XXX.py`, then remove the inset from here

```

\#def four_cycle(guesstrajjectory,dt):
\#  henon = Henon(1.4, 0.3)
\#  x0=guesstrajjectory
\#  vi=np.zeros(4)
\#  vi[0]=x0[0]-henon.oneIter(np.roll(x0,2))
\#  vi[1]=x0[1]-henon.oneIter(np.roll(x0,1))
\#  vi[2]=x0[2]-henon.oneIter(np.roll(x0,0))
\#  vi[3]=x0[3]-henon.oneIter(np.roll(x0,-1))
\#  ep=10**(-7)
\#  x=np.zeros(4)
\#  sigma=np.zeros(4)
\#  sigma[:]=1
\#  iglob=0
\#  while np.all(abs(vi))>ep:
\#      iglob+=1
\#      for i in range(0,4):
\#          x[i]=x0[i]-dt*vi[i]
\#          vi[i]=x[i]-henon.oneIter(np.roll(x,(2-i)))
\#          x0[i]=x[i]
\#          print(x[i])
\#          #print(i)
\#          #time.sleep(1)
\#          if abs(x[i])>5 or iglob>100000:
\#              print(x)
\#              return "Diverged"
\#              sigma[i]=-1
\#              x=np.zeros(4)
\#              x0=np.zeros(4)
\#              vi[0]=x0[0]-henon.oneIter(np.roll(x0,2))
\#              vi[1]=x0[1]-henon.oneIter(np.roll(x0,3))
\#              vi[2]=x0[2]-henon.oneIter(np.roll(x0,4))
\#              vi[3]=x0[3]-henon.oneIter(np.roll(x0,5))
\#              iglob=0
\#  return x

```

For the guess trajectory I put in "np.zeros(4)" and for dt I put in 0.1 to get: [ 1.11534978 -0.83649258 0.74365269 -0.33467244] close but no cigar. Also, this is not intended to be a "best practices" code, I shall work on that once I have made it work.

**2021-01-15** Matt to Sidney **Please comment your code so it is easier to read.** Comments are lines which start with '#' Pain is a part of the learning process for programming, at least in my experience. Especially for interpreted languages like Python; compiled languages like C, C++, C#, F# etc. are much more explicit and "logical", at the expense of flexibility. You'll be able to look back at old code and be able to write it in a much



clearer and nicer way in the future, that I can guarantee.

**For now, I'm going to refactor your code; I do not know if it will give the desired results, but hopefully it will get you back on track.** You can use this refactored code or simply use it as a guide, but you have to understand its incredibly hard to interpret someone else's code.

The way you have your cycle functions set up is not going to scale, as you'll have to write each component and index separately. Imagine doing this for a thirty two cycle.

Here are some signs that you need to vectorize or refactor your code. I'll explain what this means in the code itself.

1. you start labeling your variables with indices (point1, point2, etc.)
2. You have multiple functions that could be converted into a single function + parameter (two cycle and four cycle can be combined into a "cycle" function)
3. You have functions which are special cases of other functions. A single iteration oneIter should be produced by multiIter plus parameter that says iteration = 1.

One way of testing if you need a higher order integration scheme is to test large vs. small step sizes. I.e. the step size in Euler can control error, it simply requires a much smaller step size to do so. Also, you might look towards implicit integration schemes which are always stable, for example, backwards Euler would be the simplest.

**2021-01-15** Sidney to Matt Thank you very much for the help, I agree that pain seems to be a necessary ingredient in coding, and it is definitely extremely difficult to interpret another person's code. I can try to rewrite my code to make it more readable, along with references of where I am getting this method if that would be helpful, I shall wait for your response on that as I do not want to take more of your time. Also, I should definitely change the cycle functions, thank you, I will update that in the next iterate of the code. I have made my code all comments (I started each line with #).

**2021-01-15** Matt:

Sidney the refactored code is available on an old branch of orbithunter GitHub [16]:

[GitHub.com/mgudorf/orbithunter/blob/henon/notebooks/sidney\\_refactoring.ipynb](https://github.com/mgudorf/orbithunter/blob/henon/notebooks/sidney_refactoring.ipynb)

The issue was setting sigma to be a constant and not dependent on  $i$ . In other words, to need a sigma for each dimension of the cycle.

**2021-01-15 Sidney** I have been looking at the refactored code, and I see how it works, in fact, I understand it enough to work with it, and have generated a good number of orbits. Unfortunately, the generated periodic points are

not the same as they are in [ChaosBook Table 34.2](#) the last 1 to 2 digits are different. I am really unsure as to why this discrepancy exists. The values of the error function  $v_i$  get to values below the cutoff of  $10^{-7}$ , and my original `Two_Cycle` code gave me values equal to those of table 34.2, but with different values of sigma. I am tired, and I have a headache, so I will just take notes on the "Cartesian Product" that I had to use to construct a function to find all possible sigma matrices (C in Chaosbook), and paste in my current working code (the modified one that I took from Matt). My goal over the next few days is to better understand the code, and figure out why there is that small difference between my calculated values and table 34.2.

The Cartesian Product of two sets  $A$  and  $B$ , denoted by  $A \times B$ , is the set of all ordered pairs  $(a, b)$  where  $a$  is an element of set  $A$  and  $b$  is an element of set  $B$  or:

$$A \times B = \{(a, b) \mid a \in A \text{ and } b \in B\}$$

For two sets the Cartesian Product can be computed by constructing a table where one set is the row index and the other is the column index. or  $A \times B_{i,j} = (a_i, b_j)$ , due to the tabular nature of this product the number of ordered pairs is  $L_A L_B$  where  $L_A$  is the number of elements in set  $A$  and  $L_B$  is the number of elements in set  $B$  (from [Wikipedia](#)).

#### 2021-02-01 Predrag .

Do this Save and svn commit this code as `siminos/williams/python/XXX.py`, then remove the inset from here.

Update 2021-05-17: I removed the code here, and put the actual python file in `williams/relax`

**1-17-2021 Sidney** I was able to get the code to match the table in Chaosbook, I did this by changing the while loop condition to `# np.any(abs(cycle.deviation())) > ep`

Will discuss whether this is better or not at the next meeting

**1-28-2021 Sidney** Lots of coding issues later I finally have a working algorithm for calculating the periodic points and expanding eigenvalues for the Hamiltonian Hénon map ( $b = -1, a = 6$ ). It is messy, and I have not written the loop to calculate, and then write to an external document all cycles up to length  $n$ , but that should not be difficult, I also need to write this loop for my (still working) non-Hamiltonian code. Matt has been helping me clean up my code, I have been finding that my skills in matrix manipulation within Python are sorely lacking, and I hope that I can fix this. Once I have cleaned up the code, added the last few loops, and added comments and other such things to make it more readable, I shall upload it to the repository. After that point I hope to read at least some of Han's blog and take notes on it so that I can better understand what the rest of the group is doing.

## 22.2 2021 blog

**2021-02-01 Predrag** to Sidney - sorry about the Frenkel-Kontorova interruption, not worth your time right now, but Han and I might profit from being the first to read it. We'll keep it here until then.

**2021-02-07 Sidney** No issues with the interruption. I have been working towards understanding the next step, which is applying a Fourier transform on my states (cycles) to get them into Fourier space. From Han and other resources (Strang Linear Algebra), I know that all I have to do is apply a discrete Fourier transform on the periodic cycle vector, so it boils down to matrix vector multiplication where the elements are  $F_j k = w^{jk}$  where  $w$  is a complex root of unity. I think I could easily code this myself, however, I feel like I could use a prebuilt package to go much faster, so I will use the numpy fft package, and from there figure out how to create plots like Han did. I will hopefully soon have a full functional nice code to put into the repository.

**Q24 Sidney** I know that the Fourier modes make it a lot easier to see the symmetries, but is there a reason for that? Or is it just coincidence? Or, is it too far beyond my level of pure math to appreciate?

**2021-02-09 Sidney** I have modified my code and made it so I can generate the symbol sequences for all orbits (001101 etc.) up to a certain length  $n$  and store them in a list. I can then take this list and find the actual points of the cycle using my inverse iteration code, but for some reason the code diverges if I put the symbol sequence in the "wrong" order. For example, it gets the correct points if I put in 10 but not if I put in 01 which is weird. I still need to fix it. I have also used the fast Fourier transform from numpy to get the cycles into Fourier space. Now all I need to do is figure out why the code doesn't like some orders, and then figure out how to plot the points in Fourier space.

**2021-02-24 Sidney** I have officially completed my code, I will ask about how to upload my data and images here, I will also work on cleaning my code up a bit, and perhaps adding in the Fourier bit to the non-Hamiltonian Hénon map. Until that point though, it has become extremely obvious that I need to look at the theory about WHY I am doing Fourier transforms, so I am going to turn [Michael Engel's course \[13\]](#), based on Sands [\[29\] Introduction to crystallography \(1969\) \(click here\)](#). My notes:

Point Symmetry **Definition 1:** An Euclidean move  $\mathcal{T} = \{A, b\}$  is a linear transformation that leaves space invariant:

$$x \mapsto \mathcal{T}(x) = Ax + b$$

Here,  $x$  is a vector,  $A$  a  $[3 \times 3]$  orthogonal matrix and  $b$  a 3-vector.

**Definition 2:** The product of two transformations  $\mathcal{T}_1 = \{A_1, b_1\}$  and  $\mathcal{T}_2 = \{A_2, b_2\}$  is:  $\mathcal{T}_2 \circ \mathcal{T}_1 = \{A_2A_1, A_2b_1 + b_2\}$  ( $\mathcal{T}_1$  is applied first)

**Definition 3:** The order of a transformation  $\mathcal{T}$  is the smallest integer  $n$  such that  $\mathcal{T}^n(x) = \mathcal{T} \circ \mathcal{T} \circ \mathcal{T} \circ \dots \circ \mathcal{T} = x$  one can also say this transformation is  $n$ -fold.

**Observations:**

1. The inverse is:  $\mathcal{T}^{-1} = \{A^{-1}, -A^{-1}b\}$
2. Every transformation of finite order  $n$  (ie  $\mathcal{T}^n = 1$ ) leaves at least one point invariant.

2021-02-27 Sidney Notes from Engel's course [13].

A group  $G$ , together with an operation, that combines any two elements  $a$  and  $b$  to form another element  $a \cdot b$ . To qualify as a group, the set and the operation must satisfy the group axioms:

Closure For all  $a$  and  $b$  in  $G$ , the result of the operation  $a \cdot b$  is also in  $G$

Associativity For all  $a, b$ , and  $c$  in  $G$ ,  $(a \cdot b) \cdot c = a \cdot (b \cdot c)$

Identity Element There must exist an identity element in  $G$

Inverse Element For each  $a$  in  $G$  there must exist an inverse which yields the identity element when the group operation is applied between the two elements.

A symmetry of an object in space is an Euclidean move which leaves the object indistinguishable. The order of the group is equal to the number of elements in that group.

2021-02-27 Sidney Figure 22.1 shows all Hamiltonian Hénon (3.28),  $a = 6$  periodic states of period  $n = 6$ , in the  $C_6$  reciprocal lattice.

2021-02-27 Sidney Notes from Engel's course [13].

If  $G$  is a group and  $X$  is a set, then a left group action of  $G$  on  $X$  is a binary function:

$$GX \rightarrow X$$

denoted

$$(g, x) \mapsto g \cdot x$$

Which satisfies the following two axioms:

$$1. (gh)x = g(hx)$$

$$2. ex = x$$

The set  $X$  is called a left  $G$ -set. The group  $G$  is said to act on  $X$  on the left. When a group  $G$  acts on a set  $X$  the orbit of a point  $x$  in  $X$  is the set of elements of  $X$  to which  $x$  can be moved by the elements of  $G$ . The orbit of  $x$  is denoted as  $Gx$ :

$$Gx = \{g \cdot x | g \in G\}$$

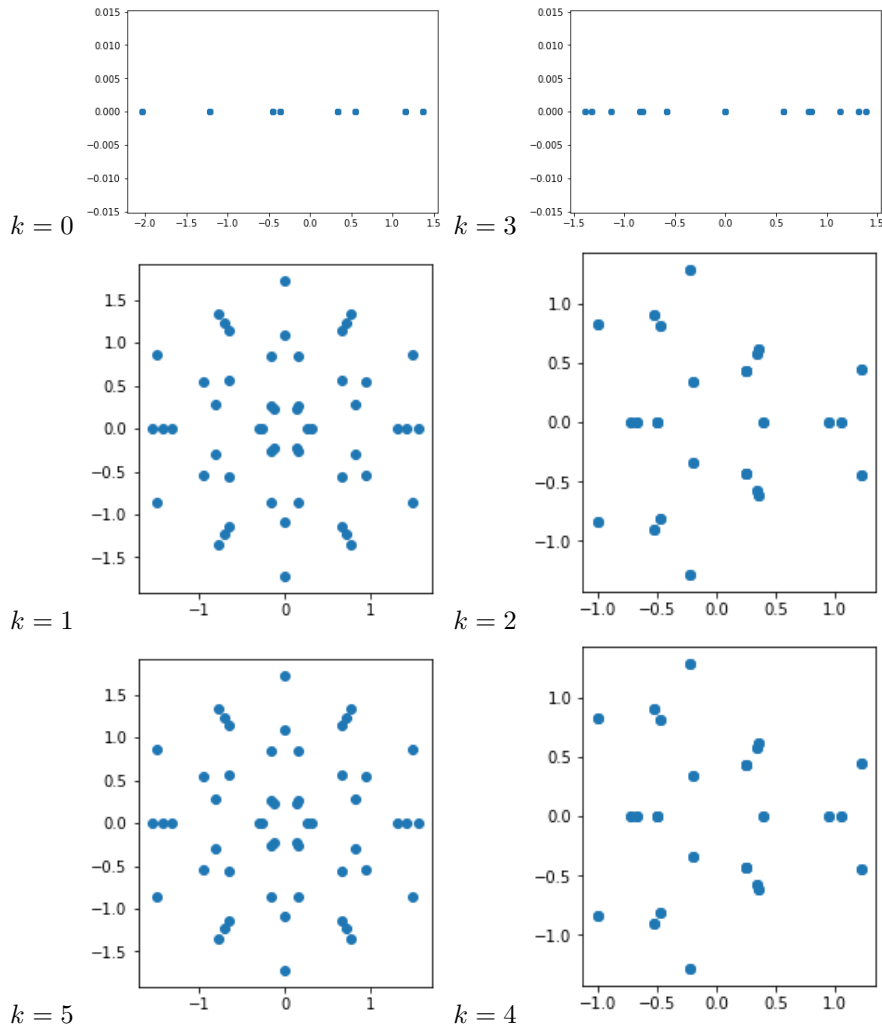


Figure 22.1: Hamiltonian Hénon (3.28),  $a = 6$  periodic states of period  $n = 6$ , in the  $C_6$  reciprocal lattice,  $k = 0, 1, 2, 3, 4, 5$ .  $k = 0, 3$  are purely real.  $k = 5, 4$  are the same as  $k = 1, 2$ , respectively, up to time reversal. Compare with Han's figure 24.59, for example.

The properties of a group guarantee that the set of orbits of  $X$  under the action of  $G$  form a partition of  $X$ . The associated equivalence relation is  $x \sim y$  if and only if there exists a  $g$  in  $G$  with  $gx = y$ . The orbits are then the equivalence classes under this relation, two elements  $x$  and  $y$  are equivalent if and only if their orbits are the same ie  $Gx = Gy$ . For every  $x$  in  $X$ , we define the stabilizer subgroup of  $x$  (also called the isotropy group or little group) as the set of all elements in  $G$  that fix  $x$ :

$$G_x = \{g \in G \mid g \cdot x = x\}$$

In short: the orbit consists of all points that are equivalent under symmetry. And the stabilizer consists of all symmetries that leave a point invariant.

**Definition 6:** A point symmetry is a symmetry which leaves a point  $x_0$  invariant:  $T(x_0) = x_0$

So, we can see that translations cannot be point symmetries, symmetries with finite order are point symmetries, symmetries with infinite order cannot be point symmetries.

**Definition 7:** A point group is a group of point symmetries which leave a common point  $x_0$  invariant.

So, we can see that a point group is a finite subgroup of  $O(3)$ , this space of three dimensional orthogonal matrices.

$$\text{Note: } O(3) = \{A \in \mathcal{R}^{3 \times 3} : A^T A = 1\}$$

$$SO(3) = \{A \in \mathcal{R}^{3 \times 3} : A^T A = 1, \det(A) = 1\}$$

**Definition 8:** Two subgroups  $H_1$  and  $H_2$  of a group  $G$  are conjugated if there exists a  $g \in G$ , such that:

$$H_2 = g^{-1}H_1g$$

**Example:**  $G = O(3)$ . Two point groups are conjugated, if there is a change of basis that maps them into each other.

**Cyclic groups:**  $C_1, C_2, C_3, \dots$  where  $C_n$  consists of all rotations about a fixed point by multiples of  $360/n$

**Dihedral groups:**  $D_1, D_2, D_3, D_4, \dots$  where  $D_n$  (of order  $2n$ ) consists of the rotations in  $C_n$  together with reflections in  $n$  axes that pass through the fixed point.

**2021-03-07 Predrag** For the current project, we need to understand  $D_n$  symmetry: see [Ding thesis example 2.9](#).

pdflatex *siminos/lyapunov/blog.tex*, read sect. 7.11.2 Factorization of  $C_n$  and  $D_n$ .

See also sect. [26.3 Pow wow 2021-01-08](#).

2021-03-07 **Sidney** I shall now attempt some of the exercises in Engel's [13] **Point Groups** lecture.

exercise 3.3

Exercise 1

Exercise 3

exercise 3.4

Determination of the point group of an object in space

1. Object linear:  $C_{\infty v}$  or  $D_{\infty h}$
2. High symmetry, non-axial:  $T, T_h, T_d, O, O_h, I, I_h$
3. No rotation axis:  $C_1, C_i, C_s$ .

Carolyn's packings of small spheres on a big sphere

The point groups are for the sphere on the left:  $C_{2v}$  because it has 3 axes that it can rotate  $180^{\text{deg}}$  around, and for each one it can then perform a flip and remain unchanged, I am unsure about the second sphere.

2021-03-07 **Predrag** For the current project, it will suffice to focus on 1-dimensional and 2-dimensional crystals (wallpaper groups). Engel is a chemist, so 3-dimensional symmetries are the most important thing, but we are good enough keeping to 2 dimensions.

2021-03-13 **Sidney** Here are my notes on Xiong Ding's example 2.9 and 2.8 in his thesis which is referenced above.

Example 2.8 Character table of dihedral group  $D_n = C_{nv}$   $n$  odd

$$D_n = \{e, C_n, C_n^2, \dots, C_n^{n-1}, r, C_n r, \dots, C_n^{n-1} r\}$$

$D_n$  has  $n$  rotation elements and  $n$  reflections. Group elements satisfy  $C_n^i C_n^j r = C_n^j r C_n^{n-i}$ , so  $C_n^i$  and  $C_n^{n-i}$  form a class. Also,  $C_n^{n-i} C_n^{2i+j} r = C_n^j r C_n^{n-i}$  implies that  $C_n^j r$  and  $C_n^{2i+j} r$  are in the same class. Therefore, there are only three different types of classes:

$\{e\}$ ,  $\{C_n^k, C_n^{n-k}\}$ ,  $\{r, C_n r, \dots, C_n^{n-1} r\}$ . The total number of classes is  $(n+3)/2$ . In this case, there are 2 one dimensional irreducible representations (symmetric  $A_1$  and antisymmetric  $A_2$ ) and  $(n-1)/2$  two-dimensional irreducible representations. In the  $j^{\text{th}}$  two-dimensional irreducible representation, class  $\{e\}$  has form  $\begin{pmatrix} 1 & 0 \\ 0 & 1 \end{pmatrix}$ , class  $\{C_n^k, C_n^{n-k}\}$

has form  $\begin{pmatrix} \exp(\frac{i2\pi ki}{n}) & 0 \\ 0 & \exp(-\frac{i2\pi ki}{n}) \end{pmatrix}$ , and class  $\{r, C_n r, \dots, C_n^{n-1} r\}$

has form  $\begin{pmatrix} 0 & 1 \\ 1 & 0 \end{pmatrix}$

Definition of Irreducible Representation (and Representation): Will be using the Dresselhaus lecture notes from 2002 downloaded from the [Chaosbook website](#):

Representation: A representation of an abstract group is a substitution group (matrix group with square matrices) such that the substitution group is homomorphic (or isomorphic) to the abstract group. We assign a matrix  $D(A)$  to each element  $A$  of the abstract group such that  $D(AB) = D(A)D(B)$ .

Homomorphic/Isomorphic: Two groups are isomorphic or homomorphic if there exists a correspondence between their elements such that each

$$\begin{aligned} A &\rightarrow \hat{A} \\ B &\rightarrow \hat{B} \\ AB &\rightarrow \hat{A}\hat{B} \end{aligned}$$

If the two groups have the same order, then they are isomorphic.

Irreducible Representation: If by one and the same equivalence transformation, all the matrices in the representation of a group can be made to acquire the same block form, then the representation is said to be reducible, otherwise it is irreducible. Thus, an irreducible representation cannot be expressed in terms of representations of lower dimensionality.

Aside: how to find a character table of a group. See [here](#) for the source, symbol  $A$  denotes symmetric with  $C_n$  so yields a 1 in the character table for all  $C$ . The subscripts 1, and 2 are symmetric (1) and antisymmetric (-1) respectively with respect to flips  $r$ . I am unsure about how the  $E_j$  column got its entries, it looks like it was a trace of the matrix representations, but I don't know the rule for that.

Q Sidney Conventionally, the irreps are the rows, and the symmetry operations are the columns, why are they transposed here?

2021-03-18 Sidney A review of the Group theory from Chaosbook, especially the irreps, and character tables. The goal of this is so that I can actually understand the character tables presented in the examples of Xiong Ding's thesis.

Q2 Sidney I am a little unsure about the statement in example 2.8 of Ding's thesis "in the  $j$ th two-dimensional irreducible representation class  $\{r, rC_n, \dots, rC_n^{n-1}\}$  has the form  $\begin{pmatrix} 0 & 1 \\ 1 & 0 \end{pmatrix}$ . Shouldn't there a contribution from the rotation group  $C_n$ ? This looks just like the inversion (reflection?) group  $r$ .

From Dresselhaus again.

The Unitary of Representations: This theorem which shows that in most physical cases, the elements of a group can be represented by unitary matrices.

Theorem: Every representation with matrices having non-vanishing determinants can be brought into unitary form by an equivalence



transformation. Skipping writing out the nitty gritty of the proof, we can first form a hermitian matrix using the representations of the group. We can then take advantage of the fact that any Hermitian matrix can be diagonalized by a suitable unitary transformation. We can construct this by doing a similarity transformation with some  $U$  from there we can redefine  $\hat{A}_x = d^{-1/2}U^{-1}A_xUd^{1/2}$  where  $d$  is the diagonal matrix. We can then show that  $\hat{A}_x$  is unitary by simple calculation, thus we have proved the theorem.

We can use this theorem to prove Schur's Lemma which is: A matrix which commutes with all matrices of an irreducible representation is a constant matrix (a constant times the unit matrix). Therefore, if a non-constant commuting matrix exists, the representation is reducible.

Proof: Let  $M$  be a matrix which commutes with all matrices of the representation  $A_1, A_2, \dots, A_h$ :

$$MA_x = A_xM$$

Take the adjoint of both sides:

$$A_x^\dagger M^\dagger = M^\dagger A_x^\dagger$$

From the Unitary Representations theorem, with no loss of generality we can assume that  $A_x$  is unitary, so we can multiply on the left and right to obtain:

$$M^\dagger A_x = A_x M^\dagger$$

So, if  $M$  commutes with  $A_x$  then so does  $M^\dagger$ .

2021-03-22 Sidney I read through the rest of the proof, and I will continue Dresselhaus notes later, but now, I will review some [Chaosbook](#) material. I also looked at the decomposition of the cat map done by Predrag, but I do not understand it enough to see if it works with the Hénon map, so I will discuss in tomorrow's meeting. Anyway, here are notes for Week 13.

Video 1: Hard Work Builds Character Elementary examples of discrete groups: the character table characterizes the finite group.  
 2-element group:  $\{e, g\}$   $g^2 = e$ .  $S_2, D_1, C_2, \dots$  used to tile our space. Imagine butterfly, symmetry axis across the middle. Can separate the space into two spaces  $\tilde{\mathcal{M}} \in \{\tilde{x}\}$  and  $\tilde{\mathcal{M}}_2 = \{-\tilde{x}\}$  (top view of butterfly space). On the side, it is just a line, half of the line can be the fundamental domain, everything else is a copy of the fundamental domain. (Order of the group is the number of elements in it). Think of scalar functions defined on this domain  $\rho(x)$ . Can divide it into two functions  $\rho_1(\tilde{x})$  (defined on fundamental domain) and  $\rho_2 = \rho(-\tilde{x})$ . Can decompose this function into a vector of functions evaluated on the

fundamental domain, the vector will have a length equal to the order of the group. Can write the original function on the fundamental domain as  $\rho(\tilde{x}) = \frac{1}{2}(\rho(\tilde{x}) + \rho(-\tilde{x})) + \frac{1}{2}(\rho(\tilde{x}) - \rho(-\tilde{x}))$  (decompose into symmetric, and antisymmetric components).  $\rho(\tilde{x}) = \rho_+(\tilde{x}) + \rho_-(\tilde{x})$ .  $\rho_\alpha = \frac{1}{|G|} \sum_g \chi_\alpha(g)\rho$ . Where  $\chi$  is the characters from the character table.

Video 2: The Symmetry Group of a Propeller 3 elements.  $G = \{e, g_2, g_3\}$   $g^3 = e$ , rotation by  $2\pi/3$   $C_3$  cyclic group with three elements. Can look at this as an abstract group (no physical, or geometrical realization):  $g_2 = \omega$   $g_3 = \omega^3$   $\omega^3 = e$ . Can write a multiplication table from these relationships with the inverses, there is the identity along the diagonal. Matrix representation: in 2D plane the identity is just the unit matrix, and the other elements are just the rotation matrices.

I shall end my notes here for today (it is getting late).

**2021-04-19 Sidney** I have been working through the chapter 10 [ChaosBook problems](#) and I'm pretty confident with all but problem 10.2, could I possibly have a hint on where to start?

**2021-03-07 Predrag** I put all solutions that I have [here](#). They are pretty incomplete. If you have solutions that I do not have, or better / comparable solutions to those that I do have, let me know.

**2021-04-24 Sidney** Here I will attempt to derive the orbit Jacobian matrix, so that I can later find the eigenvalues and eigenvectors. I will start with analytically finding periodic states, and eigen-things. We will see how well that goes. First, the temporal Hénon is  $x_{n+1} + ax_n^2 + x_{n-1} - 1 = 0$  this was drawn from the beginning of chapter 3 *Temporal Hénon*. Following the formalism of the CL18 paper, I can rewrite the map as  $r + 2a\mathbb{X} + r^{-1} - I = 0$  where the 2 has come from the fact that finding the orbit Jacobian matrix is in effect taking a derivative, now the orbit Jacobian matrix is **[2021-05-01 Sidney: this has wrong entries on the diagonal, (22.10), (21.219) is the correct formula.]**

$$\mathcal{J} = r + 2a\mathbb{X} + r^{-1} = \begin{bmatrix} 2ax_n & 1 & 0 & 0 & \dots & 0 & 1 \\ 1 & 2ax_n & 1 & 0 & \dots & 0 & 0 \\ 0 & 1 & 2ax_n & 1 & \dots & 0 & 0 \\ \vdots & \vdots & \vdots & \vdots & \ddots & \vdots & \vdots \\ 0 & 0 & \dots & \dots & \dots & 2ax_n & 1 \\ 1 & 0 & \dots & \dots & \dots & 1 & 2ax_n \end{bmatrix},$$

where the ones on the upper right and lower left corners, are a result of the periodic boundary conditions. The goal is to adapt this so that we can apply the time reversal boundary conditions, and thus construct time-symmetric periodic states.

**2021-05-01 Sidney** Here is the correct orbit Jacobian matrix (in the above I made a mistake):

$$\begin{aligned} \mathcal{J} &= r + 2a\mathbb{X} + r^{-1} \\ &= \begin{bmatrix} 2ax_0 & 1 & 0 & 0 & \dots & 0 & 1 \\ 1 & 2ax_1 & 1 & 0 & \dots & 0 & 0 \\ 0 & 1 & 2ax_2 & 1 & \dots & 0 & 0 \\ \vdots & \vdots & \vdots & \vdots & \ddots & \vdots & \vdots \\ 0 & 0 & \dots & \dots & \dots & 2ax_{n-2} & 1 \\ 1 & 0 & \dots & \dots & \dots & 1 & 2ax_{n-1} \end{bmatrix} \end{aligned} \quad (22.10)$$

I'll look at (and try to understand) the proof of the Hill's formula.

**2021-05-05 Predrag** Please modify your code so you are computing the (rescaled) temporal Hénon (3.62), orbit Jacobian matrix (21.219).

**2021-05-05 Sidney** I shall modify my code to do that, first, I will look at the rescaled temporal Hénon (3.62). Just for my own satisfaction, I shall re-derive (3.62) and (21.219). The Hamiltonian Hénon map is given by

$$x_{n+1} = 1 - ax_n^2 - x_{n-1}$$

We note that an n-step recurrence relation is the discrete analogue to an order-n differential equation. We can now introduce the change of variables  $\phi_n \equiv ax_n$  this turns our map into:

$$\frac{1}{a}\phi_{n+1} = 1 - \frac{1}{a}\phi_n^2 - \frac{1}{a}\phi_{n-1}$$

Rearranging, we get

$$a = \phi_{n+1} + \phi_n^2 + \phi_{n-1}. \quad (22.11)$$

The derivative of this map yields its orbit Jacobian matrix:

$$\mathcal{J}_p = r + 2\mathbb{X} + r^{-1}$$

Thus, we have rederived (3.62) and (21.219). I can now put it into my code. I am currently trying to understand the derivation of:

$$\hat{\mathcal{J}}_p = \begin{bmatrix} \mathbf{1} & & & & -J(\phi_0) \\ -J(\phi_1) & \mathbf{1} & & & \\ & \ddots & \ddots & & \\ & & -J(\phi_{n-2}) & & \\ & & & \mathbf{1} & \\ & & & -J(\phi_{n-1}) & \mathbf{1} \end{bmatrix},$$

Any hints would be much appreciated.

**2021-05-10 Predrag** It's all in the blog, and the *siminos* repo. But why don't you go back where you started, and reread CL18 [6]:

[sect. 1.5 Stability of an orbit vs. its time-evolution stability](#)

[appendix C Spatiotemporal stability](#)

**2021-05-10 Predrag** One thing you can maybe help Han and me with; we find the block matrix formulation of [sect. 12.5 Spatiotemporal cat Hill's formula](#) quite reader-unfriendly. I like the latest version, [sect. 12.11 Han's Hénon map Hill's formula](#) better. Any suggestions how to make this easier to read are welcome!

**2021-05-06 Matt to Sidney** It's not clear to me what you need help with, but the origin of the derivation of the aforementioned matrix is the Jacobian of a multipoint shooting method (see [ChaosBook sec. 16.2 Multipoint shooting method](#) and [ChaosBook example 16.2](#)) vector  $x_n - f(x_{n-1})$ ,  $n \in 0, \dots, N$  (indices may be off depending on how matrix is ordered), which finds cycles of length  $n$  by solving a system of single steps. If the vector equals 0 then this means that we have found a cycle/orbit as we have found a set of points which is closed under evolution (we can take  $N$  steps and return to our original position, starting from any of the  $N$  points defining the cycle). The actual matrix, as with all Jacobians, tells us how the tangent space evolves. In terms of the multipoint shooting, this is the combination of  $N$  single step Jacobians. If you are on the cycle (i.e. no deviations, or components in the tangent space) which evolve other than the velocity, which is mapped into the velocity at the new point. This is a quick and dirty explanation which is probably over simplifying, but the near-tautological explanation is: if you're on the cycle, then you don't get pushed away from the cycle due to your deviation from the cycle.

**tl;dr** It's the Jacobian of the multipoint shooting equation  $x_n - f^t(x_{n-1})$ .

**2021-05-10 Predrag** Talking about multishooting, the material around eq. (12.120) might be worth revisiting.

**2021-05-09 Sidney** Thank you Matt, it makes sense now, given the definition of the single step Jacobian it just sort of pops out. So, at this point I know how to get both the traditional orbit Jacobian matrix (which I am currently working on coding in) and the orbit Jacobian matrix in terms of the single step Jacobian (which I also know how to derive).

**2021-05-09 Sidney** At this point, I am trying to understand the block matrix form that can be generated by applying a permutation matrix defined by the circular Kronecker delta. What I do not understand, is:

What is the difference between the circular Kronecker delta, and the regular one?

**2021-05-10 Predrag** Regular one is defined on  $\mathbb{Z}$  (no restrictions), the circular one on  $C_n$  (periodic chain, so  $\text{mod } n$ ). (Re)read [ChaosBook appendix X.3](#) *Discrete Fourier transforms*.

**2021-05-09 Sidney** And I am also having difficulty deriving the appropriate permutation matrix. I want to try turning the two-cycle orbit Jacobian matrix (in terms of single-step Jacobians) into the block matrix form. The following is my (incorrect) derivation of the 4x4 permutation matrix. I have assumed that when the index for the circular Kronecker delta reads something like  $4, j$  it is equivalent to  $0, j$ , as that would be equivalent to going to the end of the columns (index  $j$ ) and then starting back at the beginning. By doing this I get:  $P$  is a  $[2n \times 2n]$  permutation matrix. Defined through the circular Kronecker delta:  $P_{k,j} = \delta_{2k-1,j}$ , for a periodic orbit of length  $n = 2$   $P$  is

$$P = \begin{bmatrix} 1 & 0 & 0 & 0 \\ 0 & 0 & 1 & 0 \\ 1 & 0 & 0 & 0 \\ 0 & 0 & 1 & 0 \end{bmatrix}$$

(This is wrong)

What did I do wrong?

**2021-05-10 Predrag** By 'permutation matrix' you mean the one-step cyclic permutation  $r$ , or the shift matrix (11.7)? The circular Kronecker delta is just the  $[n \times n]$  identity matrix. I leave it to Han and you to figure out what went wrong :)

**2021-05-13 Han** My Kronecker delta representation was wrong... (12.93) should be correct. I don't have a more compact way to write this permutation matrix. The permutation matrix for  $n = 2$  is:

$$\begin{bmatrix} 1 & 0 & 0 & 0 \\ 0 & 0 & 1 & 0 \\ 0 & 1 & 0 & 0 \\ 0 & 0 & 0 & 1 \end{bmatrix}.$$

**2021-05-10 Predrag** Regarding sect. 3.1 "Center of mass" puzzle:

Relevant Gallas papers are all in [ChaosBook.org/library](http://ChaosBook.org/library), for example ([click here](#)), with their names (always!) given by their BibTeX ID.

Predrag's unpublished 2004 drafts and calculations can be accessed by clicking on the link given there:

[ChaosBook.org/projects/revHenon](http://ChaosBook.org/projects/revHenon)

There is no need to look at old drafts of papers, as the most of the relevant stuff is already included in that section, but the link includes some data files, orbit plots and programs that might be useful to Sidney as cross-checks on his calculations.

**2021-05-12 Sidney** Here are some notes from the last meeting: Any matrix can be written as a sum of projections into the different eigendirections. An anti-diagonal matrix, as well as the anti-diagonal matrix multiplied by sigma and its powers give the reflection matrix, and the reflection matrix across all axes.

**Q** What are these axes? A reflection matrix has two eigenvalues  $\pm 1$  (corresponding to either the symmetric, or antisymmetric subspace), and a projection operator can be constructed by subtracting out the opposite of the subspace you want to project onto. This projection operator can be applied to the left of the orbit Jacobian matrix to project it onto either the symmetric, or antisymmetric space. In this way, the orbit Jacobian matrix can be written as  $\mathcal{J} = \mathcal{J}_- + \mathcal{J}_+$ , it is worth noting that  $\det(A + B) \neq \det(A) + \det(B)$ . In the case of a linear map (where the fundamental fact still applies) the determinant of  $\mathcal{J}_\pm$  counts the number of time symmetric/antisymmetric orbits. Note that we need to apply the time symmetric boundary conditions in order to enforce time symmetric orbits.

**Q2** Is this last statement correct? I have now updated my code to work with the scaled Hénon map. Actually, I just did the lazy thing of dividing all values in all orbits by  $a$ . I also added a function to generate the (scaled) orbit Jacobian matrix, and I tried calculating its eigenvalues and vectors, it all seems to work, but I'm really not sure what I should be seeing for eigenvalues and vectors, I will paste my code below (I will past all of it, but it's mostly the same as before, just with a little added on the end): There is probably some extra code in there that just isn't being used, but hey, it's a work in progress. Update 2021-05-17: I have added this code to the williams/relax folder in the subversion, so I have now deleted the code here.

**2021-05-13 Sidney** With Han's help I was able to see the permutation matrix, and I was able to reproduce the Hill's formula "proof" for the specific case of  $n=2$  (I use quotation marks because I only proved it for one case, and not all cases) I will probably keep thinking about how to generalize it, but I now feel better about applying Hill's formula to my orbit Jacobian matrix. I have been trying to work through the algebra with the reflection, and the corresponding projection matrices described in Han's most recent blog post. I understand qualitatively what's happening, effectively the projection operator is just the reflection operator with one of the eigenspaces subtracted out, with an additional weight that forces the identity  $\mathbb{K} = \sum_i P_{A_i}$ , this is a formula for a generic matrix. I cannot find anywhere in lectures, or textbooks where this is formalized, so I am not sure how the weights are constructed, but I'll keep looking at it.

**2021-05-15 Matt** I'll put a couple of responses here to hopefully help Sidney out. Response to questions in 2021-05-12 Sidney. It seems like the ques-

tions are with respect to the proceeding sentences but they are in different paragraphs so it is unclear to me if that is what you meant.

**Q What are these axes?** Is the question with respect to a specific system or just in general? If we're talking about reflection in  $D$  dimensional euclidean space then we can reflect over any  $D - 1$  dimensional hyperplane, so I'm assuming it's talking about reflection where the eigenvectors are the normal vectors to these planes, so the hyperplane which is normal to each eigenvector can define a reflection so maybe this is what you're referring to?

**Q2 Is this last statement correct?** What is "the last statement"? The last statement before the question, the last statement of the previous paragraph...? Is it the following?

Note that we need to apply the time symmetric boundary conditions in order to enforce time symmetric orbits

To ensure that you get a time symmetric orbit then yes you have to impose boundary conditions which constrain you to that subspace. The unconstrained method (if variational in formulation) could possibly find these orbits, but there would be no guarantee.

Response to 2021-05-13 Sidney.

I understand qualitatively what's happening, effectively the projection operator is just the reflection operator with one of the eigenspaces subtracted out, with an additional weight that forces the identity  $\mathbb{I} = \sum_i P_{A_i}$ , this is a formula for a generic matrix. I cannot find anywhere in lectures, or textbooks where this is formalized, so I am not sure how the weights are constructed, but I'll keep looking at it.

Where "this" is formalized: The "weights" are simply normalization coefficients. The sum of the projection operators equaling the identity essentially says that the "full" space can be decomposed into projection subspaces, each of which has its own projection operator. I.e. each subspace is a component of the full space. Predrag formalizes the projection operators *a lot*; especially in his group theory stuff which this is directly related to.

For a reflection operator we can decompose

$$\sum P_{\pm} = \frac{1}{2}(\mathbb{I} \pm R) = 1/2(\mathbb{I} + \mathbb{I} + R - R) = 1/2(2\mathbb{I}) = \mathbb{I}.$$

For a symmetry subspace that can be broken into 4 subspaces, the normalization would be 1/4, etc.

**2021-05-23 Sidney** Thank you to Matt for the explanation, I also have now attended the group theory lecture on projection operators (I've actually

been thinking about this a good bit, but taking the time to condense my thoughts onto my blog is not one of my strong suits). Anyway, the projection operator formalism for matrices can be derived from the Hamilton-Cayley theorem:

$$\prod_i (M - \lambda_i \mathbb{I}) = 0$$

In words, this is just the statement that a matrix satisfies its own characteristic equation. However, if we take one element out of the product, the RHS will no longer be zero:

$$\prod_{i \neq j} (M - \lambda_i \mathbb{I}) = \prod_{i \neq j} (\lambda_j - \lambda_i) \mathbf{e}_i$$

We can rearrange to get:

$$\mathbb{P}_j = \prod_{i \neq j} \frac{M - \lambda_i \mathbb{I}}{\lambda_j - \lambda_i}$$

Which is the definition of the projection operators that Han used, I was also able to reproduce his results. I also found out an issue with my code for finding time-reversal symmetric orbits. I was not taking into account permutations, but that is an easy fix, that I hope to fix quickly.

When I have, I can create a bank of orbits appropriate to use with the orbit Jacobian matrix projected into the symmetric subspace using projection operators, I know how to construct this both by hand, and by code, I just need to implement it. I also need to go through chapter 15 in Chaosbook, as it gives good visualization of what the Hamiltonian Hénon map does. I will add my notes here when I have a chance, hopefully tonight, or tomorrow. I also think that I should explore the volume of the parallelpiped represented by the orbit Jacobian matrix. I could probably use a package for that, but what I'll most likely do is just use the fact that the determinant of a matrix is just the product of its eigenvalues:

$$\det A = \prod_i \lambda_i$$

Then take the absolute value. I can then check the volumes generated by different orbits.

**2021-05-26 Sidney** I reviewed the spatiotemporal cat derivation to see if I could extend the idea to the Hénon map, I think I have.

If we enforce the following restrictions, we can qualitatively derive the spatiotemporal Hénon map:

- Each site couples to its nearest neighbors
- Spatial and temporal coupling is of the same strength



- Invariant under spatial translations
- Invariant under spatial reflections
- Invariant under space time exchange

With these conditions our temporal Hénon (3.62), (22.11)

$$a = \phi_{t+1} + \phi_t^2 + \phi_t$$

generalizes to my proposal for the spatiotemporal Hénon

$$\phi_{n,t+1} + \phi_{n,t-1} + 2\phi_{n,t}^2 + \phi_{n+1,t} + \phi_{n-1,t} = a. \quad (22.12)$$

The factor of two comes from adding together two Hénon maps (one spatial and one temporal), following the derivation of the spatiotemporal cat. I need to try to read Gutkin and Osipov [18] [arXiv:1503.02676](https://arxiv.org/abs/1503.02676) to get a better idea of the derivation.

**2021-05-28 Predrag** Your spatiotemporal Hénon (22.12) looks OK to me, except maybe adding the maps for each direction of a  $d$ -dimensional lattice results in  $da$  on the RHS? In the spirit of eq. (80) in CL18.pdf?

**2021-05-28 Predrag** I doubt you will find it in Gutkin and Osipov [18] - if you do, cite their words in detail here. The above argument is mine, from Gutkin *et al.* [17] and CL18 (kittens/ folder in this repository).

**2021-05-28 Predrag** How does your spatiotemporal Hénon compare to Politi and Torcini [26], sect. 13.3 Periodic orbits in coupled Hénon maps?

**2021-05-27 Sidney** Here is my attempt at looking at the eigenvalues, eigenvectors, and the determinants of the orbit Jacobian matrix. My orbit Jacobian matrix constructor only works with orbits of length 3 and above, this is because is row has three values in it that permute, and I'm not sure how to scale it down, will discuss this at the next meeting. I cannot tell anything about the eigen stuff so far, it seems almost random, however, the determinant values are each approaching an integer value, so maybe that is something.

Note: I removed the table here because it was wrong

I will hopefully rearrange some of these tables to group them by orbit in a later post, but for now, here is the "raw" data, let me know if anything appears.

**2021-05-31 Sidney** I'm not sure why, but the large table with all of the eigenvalues does not appear in the pdf version of the blog. I am not sure how to fix that, if anyone could let me know, that would be great. I still need to put it into a more readable format anyway. I also looked at eq. (80) in CL18.pdf, and it is the reason that I did not have  $d * a$  on the RHS, the form of the spatiotemporal cat eq. (79), has only  $\mathbf{M}$  not  $2\mathbf{M}$ , which

it would have if both sides were added (right?), I need to read up on the coupled maps, that will be something I do next (along with the better tables).

That would also say that '1100' is symmetric under time inversion.

**2021-06-03 Sidney** I want to try to take advantage of Hill's formula:

$$\text{Det}(\mathcal{J}_p) = \det(\mathbb{1} - \mathbb{J}_p) = (1 - \Lambda_p) \left(1 - \frac{1}{\Lambda_p}\right) = 2 - \Lambda_p - 1/\Lambda_p. \quad (22.13)$$

So, I need to calculate the eigenvalues for the scaled time-step Jacobian matrix, but first I need to find the form of the scaled time-step Hénon map (3.5)

$$\begin{aligned} x_{n+1} &= 1 - ax_n^2 + by_n \\ y_{n+1} &= x_n \end{aligned} \quad (22.14)$$

We scale  $x \rightarrow \frac{1}{a}\phi$ ,  $y \rightarrow \frac{1}{a}\varphi$ , and the Hénon map becomes:

$$\begin{aligned} \phi_{n+1} &= a - \phi_n^2 + b\varphi_n \\ \varphi_{n+1} &= \phi_n \end{aligned} \quad (22.15)$$

Temporal stability of the  $n$ th iterate of the Hamiltonian Hénon map is <sup>1</sup>

$$M^n(\phi_0) = \prod_{m=n}^1 \begin{bmatrix} -2\phi_m & -1 \\ 1 & 0 \end{bmatrix}, \quad \phi_m = f_1^m(\phi_0, \varphi_0). \quad (22.16)$$

It is very important to understand the Floquet multipliers are invariant under all smooth coordinate changes, see [ChaosBook sect. 5.4](#), so they are not affected by this rescaling.. When we find the eigenvalues of this matrix they give contracting and expanding, we are interested in the expanding stability multiplier. There are three period 4 orbits: 1110, 1100, 1000, they have the following expanding Floquet multipliers:

**2021-06-04 Predrag** I do not seem to have handy list of the Hamiltonian  $a = 6$  Hénon map Floquet multipliers. Floquet exponents for many  $a = 1.4, b = 0.3$  orbits are listed in [ChaosBook table 34.2](#). I believe that [sect. 12.11 Han's Hénon map Hill's formula](#) also applies to the dissipative case, might be worth by repeating the derivation with  $b \neq -1$ , or at least checking it for a few short periodic orbits.

**2021-06-11 Sidney** I have read some of Wen's 2014 project [ChaosBook.org/projects/Wen14.pdf](#), I should take some notes and put them here.

<sup>1</sup>Predrag 2021-06-04: Was

$$\begin{bmatrix} -2\phi_n & \frac{b}{a} \\ 1 & 0 \end{bmatrix}$$

The correct form is (3.45). Hence, with Sidney's "scaled Jacobian," the four cycle Floquet multipliers were all wrong.

**2021-06-11 Sidney** The Hill determinant should equal  $2 - \Lambda_p - 1/\Lambda_p$  by Hill's formula (22.13), where  $\Lambda_p$  is the expanding eigenvalue of the time-step Jacobian for that orbit, see table 22.1.

**2021-06-11, 2021-06-23 Sidney** Table 22.2 lists the Hill determinants computed from the orbit Jacobian matrices. Comparing with table 22.1 period-4 Hill determinants, we see that the Hill's formula (22.13) is satisfied to high precision.

**2021-06-12 Predrag** It looks like you now have the correct Hill determinants. Their numbers agree with ChaosBook Table 18.1; there are 6 period-5 orbits, and 9 period-6 orbits. The period-6 itineraries are not yet correctly assigned, fix that. The ones with even #'s of '1's are presumably the positive ones.

**2021-06-12 Sidney** I shall fix the itineraries for 6 cycles, and I'll add the itineraries of the other, shorter cycles later. Some were correct, and the negative determinants were in fact the odd number of 1s.

**2021-06-13 Predrag** Do include fixed points and the period 2 in table 22.2; might be helpful for understanding magnitudes of longer period Hill determinants.

**2021-06-13 Predrag to Han and Sidney** If you think of the Hénon map as a fattened parabola, then 0 fixed point has large positive slope (4 for the Ulam map), and 1 fixed point has small negative slope (-2 for the Ulam map). This explains the magnitudes, and should also determine the signs of Hill determinants in table 22.2.

However, either there is a - sign specific to Sidney's definition of the Hénon orbit Jacobian matrix, or Han and Predrag have to redefine both temporal cat and temporal Hénon orbit Jacobian matrix, so we do not pick up an extraneous '-' sign for odd period periodic states.

See also (8.203).

Fixing this is not essential, as we use only the absolute values of determinants in periodic orbit formulas.

**2021-06-13 Sidney** In the 2014 project paper by Haoran Wen, it is stated that for a range of a and b, the Hénon map is "structurally stable" and that means that the transport properties of the system have a smooth dependence on the parameters. And then it states that the lack of structural stability will result in the creation and destruction of infinitely many periodic orbits for any parameter change. Does that mean that a structurally stable system has relatively few bifurcations?

**2021-06-13 Predrag** It's a long story, starting with a wrong conjecture by Smale, but the answer is NO bifurcations for open intervals of system parameter

values. Tends to be possible only for repellers, that is why you are working with Hénon  $a > 6$  which has all possible binary symbolic dynamics cycles, and no bifurcations as you increase the parameter  $a$ .

Cat map has a finite grammar (is a "generating partition") for precisely  $s = \text{integer} > 2$ , but change  $s$  to an open interval of real values around -let's say-  $s = 3$ , and infinity of cycle get created and destroyed for any finite change in  $s$ .

**2021-06-13 Sidney** So, at  $a = 6$  we achieve all binary symbolic dynamics, and anything more than that we still have all binary symbols? No creation or destruction? Is there a proof for this in the blog or somewhere else easily linkable to, that wouldn't take me days to digest?

**2021-06-13 Predrag** No, not  $a = 6$  - that's just the closest integer value. [Chaos-Book sect. 15.2 Horseshoes](#) explains it, and -for example- Endler and Galas [12] say "This classification is independent of the control parameter  $a$ . Orbits are specially interesting for  $a > 5.69931\dots$ , since beyond this value there is a complete Smale horseshoe [34] and all orbits are real."

**2021-06-14 Sidney** blogCats is being weird for me, it is only showing the most recently added parts, plus the table of contents, so right now when I build it, it only gives the dihedral groups chapter, even though all the include commands are not commented out.

**2021-06-14 Predrag** In `inclOnlyCats.tex` the uncommented line was

```
\includeonly{chapter/groups}
```

so `blogCats.tex` was doing what it should.

**2021-06-14 Sidney to Predrag and Han** I am having trouble defining the orbit Jacobian matrix for orbit length 1 and 2, this is because my code is designed to have a minimum width of 3 for the matrix, because there needs to be the terms for  $\phi_{n+1}, \phi_{n-1}, \phi_n$ , and I am not sure how to do that for 1 and 2 orbit lengths, should I just have the orbit repeat?

**2021-06-14 Predrag** The fixed points and period-2 lattices you can evaluate by hand, I believe. CL18 [sect. 1.4 Fundamental fact](#) and [sect. 2.4 Fundamental fact](#) evaluate the period-2 lattice orbit Jacobian matrices. If you understand how (24.147), (24.148), and CL18 (103) were derived, you will understand all such special cases.

**2021-06-14 Sidney to Predrag and Han** Is 6 digits of accuracy good enough? Is there a different method I should use? I am using the one from [Chaos-Book chapter 7 Fixed points](#) (the link is right here, I'll use that style of referencing in the future).

**2021-06-18 Sidney to Predrag and Han** I am trying to reproduce the projection operator analysis for  $D_6$  symmetric periodic states and I am not really sure how to do that, which of Han's posts talks about the periodic states? As well, doesn't the projection analysis apply for  $D_n$  in general, not just specific periodic states?

**2021-06-19 Sidney to Predrag and Han** I tried to read Endler and Gallas [11] 2006 paper (not the Endler and Gallas paper [12] that Predrag mentioned) because Predrag said that it explained two period 3, one period 4, and two period 6 values in my table 22.2, but I am not quite sure how the authors are getting their P polynomials, or their S polynomials, specifically, I am not sure where the a value comes in, because when I just try to expand their eq. (3) and regroup it into eq. (6), I could not, so I am very confused. What obvious thing am I missing?

**2021-06-19 Predrag** To "expand their eq. (3) and regroup it into eq. (6)" you need to know analytically all period-4 periodic points, do you know them? They claim that "the solution of this problem is trivial because ref. [10] contains the solution for arbitrary  $a$  and  $b$ ."

However, I was referring to the Endler and Gallas [12] Table 1. The invariant quantity that they associate with a periodic orbit is the orbital sum (3.32), the sum over the periodic points, while the Hill determinant involves various sums over values of fields raised to various powers. You will immediately note that the cases that have integer orbit sums correspond to your integer-valued Hill determinants. They had no reason to think of Hill determinants, so that would be a major reworking of their paper(s); I do not think you want to do that.

**2021-06-20 Sidney to Predrag and Han** Oops

I agree that a major reworking is probably not in the cards, I will go back to trying to understand orbit Jacobian matrices for the fixed point, and period 2 orbits. Endler and Gallas [10, 11] look exceptionally cool, I'll give them a whirl.

**2021-06-23 Sidney** I worked through both Endler and Gallas papers [10, 11], as much as I could. Here is what I came up with: in ref. [11] the two important equations are  $P_k(x)$  and  $S_k(\sigma)$ , where  $S_k(\sigma)$  is found through manipulating the (scaled) Hénon map and  $\sigma$  is the sum of all points in the cycle,  $P_k(x)$  is defined as

$$P_k = \prod_{\ell=1}^k (x - x_\ell),$$

where  $x_\ell$  is the  $\ell$ th orbit point. The algorithm is simple: construct  $P_k(x)$  by expanding the product and putting each coefficient in terms of  $\sigma$ , then use  $S_k(\sigma) = 0$  to determine how many unique orbits of length  $k$  and 2.

what values  $\sigma$  can take, then combine with  $P_k(x)$  to solve for each orbit point. I will work two examples, first an orbit of length 1:

$$\begin{aligned}\sigma &= x_1 \\ P_1 &= x - \sigma \\ x_{t+1} &= a - x_t^2 - x_{t-1} = x_1 = a - x_1^2 - x_1\end{aligned}$$

Or

$$2\sigma + \sigma^2 - a = 0 = S_1(\sigma)$$

As this is a quadratic equation, we know that there are two different fixed points, and we can solve for them directly via  $S_1(\sigma) = 0$ , now for an orbit of length 2:

It is useful to first state that  $a = 2x_2 + x_1^2 = 2x_1 + x_2^2$  by the Hénon map, and  $\sigma = x_1 + x_2$

$$P_2(x) = (x - x_1)(x - x_2) = x^2 - \sigma x + x_1 x_2 = x^2 - \sigma x + \frac{1}{2}a - \frac{1}{2}\sigma^2 - \sigma$$

If we subtract the two  $a$  equations we get

$$0 = 2x_2 - 2x_1 + x_1^2 - x_2^2 = 2(x_2 - x_1) + (x_1 + x_2)(x_1 - x_2)$$

so

$$S_2(\sigma) = \sigma - 2 = 0$$

From this we know that there is one 2 cycle and this can be solved by solving for  $\sigma$  and solving for the roots of  $P_2(x)$ . There's a lot of algebra here, but I am sure there is some number theory trick that can be used that I am unaware of. I am also a little confused by the factorization (3.34)

$$S_k(\sigma) = C_k^2(\sigma)D_k(\sigma)N_k(\sigma),$$

I think that it is a statement that the polynomial  $S_k(\sigma)$  can be decomposed into polynomials that each give roots for the Chiral, Diagonal, and Non-diagonal orbits respectively. So it should be a way to count the number of each type of orbit. However, I am not sure how to tell the difference between any of them, I sort of understand that  $C_k$  has to be squared, and that could distinguish it, but I'm really not sure how to tell them apart.

Q16.1 Any suggestions for this?

A16.1 **Predrag 2021-07-04** Work through papers, they are clear and pedagogical

I have also figured out how to get the determinants of period 1 and period 2 cycles, I updated table 22.2 to include them. You'll notice that the determinant for  $\bar{0}$  and  $\bar{1}$  were negatives of each other up to six decimal places, neat. 10 was the integer  $-12$  up to six decimal places, again, neat.

Q16.2 How do I calculate eigenvalues for periods 1 and 2?

A16.2 Here is how:

**Period 1:** For the fixed points, I get

$$\phi_{0,1} = -1 \pm \sqrt{1+a} \rightarrow -1 \pm \sqrt{7} \quad (22.17)$$

$\mathcal{J}_{0,1}$  are  $[1 \times 1]$  matrices

$$\begin{aligned} \phi_{t+1} + \phi_t^2 + \phi_{t-1} &= a \\ F[\phi] &= 2\phi + \phi^2 - a = 0, \end{aligned}$$

Evaluating the Hill determinants (11.6) for both fixed points:

$$\mathcal{J}_{0,1} = 2(1 + \phi), \quad \text{Det } \mathcal{J}_{0,1} = \pm 2\sqrt{1+a} \rightarrow \pm 5.2915026, \quad (22.18)$$

in agreement with the numerical estimates of table 22.2. The Hill determinants of the two fixed points are negatives of each other.

**Period 2:** The periodic points in the 10 orbit are (I did it on paper, do not want to reproduce it here):

$$\phi_{1,2} = 1 \pm \sqrt{a-3} \rightarrow 1 \pm \sqrt{3} \quad (22.19)$$

$\mathcal{J}_{10}$  follows

$$\begin{aligned} F[\phi]_1 &= 2\phi_2 + \phi_1^2 - a = 0 \\ F[\phi]_2 &= 2\phi_1 + \phi_2^2 - a = 0, \\ \mathcal{J}_{10} &= \begin{bmatrix} 2\phi_{01} & 2 \\ 2 & 2\phi_{10} \end{bmatrix}. \end{aligned} \quad (22.20)$$

Hill determinants are *symmetric polynomials* in lattice fields  $\{\phi_1, \phi_2, \dots, \phi_n\}$ , which are, by construction, all *prime cycle  $p$  invariants*. The orbital sum (3.32) is one example. Another one is (22.21).

In case at hand,

$$\text{Det } \mathcal{J} = 4(\phi_{01}\phi_{10} - 1) = 4(3 - a) \rightarrow -12. \quad (22.21)$$

The Hill determinant is *exactly* 12, up to the annoying overall sign that **cries out** for a *redefinition* of orbit Jacobian matrices.

**2021-06-25 Sidney** With the above analytic calculations, I feel very confident in stating that my code is accurate up to 6 decimal places.

Q16.3 Is there a way to rigorously prove that the code is accurate up to 6 decimal places?

Q16.4 Is this worth doing if it exists?

A16.4 **Predrag 2021-07-04** No.

Q16.5 What do these values mean? An integer Hill determinant should mean something right?

Table 22.1: Hill determinants for the Hamiltonian  $a = 6$  Hénon map, period-4 periodic states, computed from time-evolution side of the Hill's formula (22.13). The pesky overall 'sign' presumably means we have to change the overall sign in the definition of orbit Jacobian matrix  $\mathcal{J}$  everywhere.

Orbit	Hill determinant
1110	105.697960425014
1100	-576.000010077746
1000	1046.301985671792

Table 22.2: Hill determinants for the Hamiltonian  $a = 6$  Hénon map, with correct symbolic dynamics. Indicated in red are values presumably explained by Endler and Gallas [12].

Period 1		
0	5.291502844	
1	-5.291502494	
Period 2		
10	-12.000000720	
Period 3		
110	-53.914854639	
100	133.914853323	
Period 4		
1110	-105.697960425	
1100	576.000010077	
1000	-1046.301985671	
Period 5		
11110	-388.996791481	
11100	591.500599893	
11010	712.689732105	
00101	-768.203977660	
00011	-4443.524089969	
00001	7608.534459743	
Period 6		
111110	-1045.3849327	
111100	3899.9387739	
111010	1092.9103354	
111000	-4786.6149478	
101000	5135.6190985	
110100	-6396.0000670	
001011	-6395.9999673	
110000	32220.0609406	
100000	-54576.5295457	



A16.4 **Predrag 2021-07-04** It is well explained in papers you have been reading. Integer Hill determinant is a historical accident, due to our (arbitrary) choice  $a = 6$ . But it gave Gallas and collaborators a clue that something is going on. As does (22.26). Be Gallas.

And finally, I was thinking about the multidimensional Hénon map. Since this is not a physical problem, there is no "physical" definition about what makes a map "Hénon map" like, so it would be good to stick to the mathematical requirement of the folding being linearly related to  $b$ , so I was thinking that for the multidimensional map, the Hénon-ness could be satisfied if the appropriate time Jacobian matrix determinant would be  $-b^d$ , unfortunately, I don't know how to define the correct time Jacobian.

**2021-07-03 Sidney** I have not had much time outside of my internship lately, so I haven't done much. However, I did make an attempt at showing that the eigenvalues of the orbit Jacobian matrix are coordinate-choice independent. It did not go well. First, I must remember that

$$\mathcal{J}_{ij} = \frac{\delta F[\phi]_i}{\delta \phi_j},$$

evaluated at a periodic state  $\phi_M$

$$F[\phi_M] = 0.$$

This gives a problem when I try to repeat the proof done for time-step Jacobians, because I get

$$\mathcal{J}'(\phi'_M)_{ij} = \Gamma(0)_{ik} \mathcal{J}_{kl} \Gamma^{-1}(\phi_M)_{lj}, \quad (22.22)$$

which means that I cannot cancel the  $\Gamma$ s in the determinant. So, I have failed to prove anything.

**2021-06-24 Predrag** Wow, I did not expect  $\text{Det } \mathcal{J}_0 = -\text{Det } \mathcal{J}_1!$  But Sidney's (22.17) nails it.

**2021-06-13 Predrag** Note the '.91485' decimal digits for period 3. Those are presumably explained by Endler and Gallas [12] analytic expressions, see their Table 1. For us they mean that Sidney's code is accurate to ca. 6 significant digits.

The 1100 Hill determinant is integer  $576 = (6 \times 4)(-6 \times -4)$ , (see (22.26)). Explain this factorization.

(22.20) explains 01 Hill determinant=12, but do you have an argument that this is the symmetry reduced Hill determinant= $2\sqrt{3}$  squared?

Show that 001011 and 001101 Hill determinants are (integer)<sup>2</sup> (are they?).

This is also a helpful check on the time-inversion factorization formulas Han and I are trying to establish.

**2021-07-06 Sidney** I have considered showing that the Hill determinant is coordinate invariant, but I think that's just a matter of mentioning that Jacobian matrix has coordinate invariant eigenvalues. I'll formalize that in a later post (most likely the next one).

I have also come up with a proof that the  $\mathcal{J}$  has the same set of eigenvalues evaluated at every point in the orbit, I suspect that there is a proof for the eigenvectors, but I don't know how to do it, again, will formalize on my next post.

**2021-07-07 Predrag** The orbit Jacobian matrix  $\mathcal{J}$  is global, a property of the entire periodic state, so I do not understand " $\mathcal{J}$  has the same set of eigenvalues evaluated at every point in the orbit."

**2021-07-06 Sidney** I am not sure what was meant by "do you have an argument that this is the symmetry reduced Hill determinant= $2\sqrt{3}$  squared?". I assume this is something either from the group theory course, or blog which I have not yet gone over, but does this mean that I should look for some symmetry reduction of a matrix whose Hill determinant has the value  $2\sqrt{3}$ ?

**2021-07-07 Predrag** Basically, yes. I'm referring to  $C_n^2$  term in (3.33),  $\sqrt{\zeta_{top}(t^2)}$  in (6.162), etc., throughout the time-reversal discussions in the blog.

Endler and Gallas [11] eq. (9) and Table 1 has

$$D_{0011} = \sigma, \quad P_{0011} = (x^2 - a)^2, \quad (22.23)$$

There are two period 6 diagonal orbits

$$D_6 = \sigma^2 + 4\sigma - 4a, \quad \text{orbits } 000111 \text{ and } ??, \quad (22.24)$$

but 000111 of figure 3.2(c) belongs to  $N_6$  messy polynomial eq. (14).

My reasoning is that due to the  $\{1, s\}$  time-reversal symmetry, any  $t < 0$  temporal lattice site can be mapped into  $t > 0$  by time reversal  $s$ , so the  $D_\infty$  'configuration' fundamental domain is the  $t \geq 0$  temporal half-lattice. Full lattice periodic states Hill determinants for orbits such as 01, 0011 in table 22.2 are then (that's not quite right) squares (twice the relative periodic orbit period) of the fundamental domain orbit Hill determinants, as in example 6.11  $D_1$  factorization.

But there no reason why you should know that, Han and I are still working it out, will have more concrete suggestions for the Hénon case once we understand it better.

**2021-06-13 Predrag** If you think of the Hénon map as a fattened parabola, then 0 fixed point has large positive slope (4 for the Ulam map), and 1 fixed point has small negative slope (-2 for the Ulam map). This explains the magnitudes, and should also determine the signs of Hill determinants in table 22.2.

**2021-07-07 Predrag** Endler and Gallas [11] eq. (13) presumably explains the integer valued pair of period-6 orbits in table 22.2:

$$C_6 = \sigma - 2, \quad \text{orbits } 110100, 001011, \quad (22.25)$$

**2021-06-25 Sidney** My numerical values for period 4 eigenvalues:

$$\begin{array}{ll} 1000 & 6.77624515, -7.4374406, -4.23778399, -\sigma, \\ 1110 & -2.39080489, 1.58070478, 5.70907942, \sigma, \\ 1100 & 6, 4, -6, -4 \end{array} \quad (22.26)$$

**2021-07-04 Predrag to Sidney and Han** What's up with two distinct orbits  $\overline{1000}$  and  $\overline{1110}$  in (22.26), with different Hill determinants in table 22.2, sharing the eigenvalue  $\sigma = 2\sqrt{6} = 4.89897947$  (see (22.27))? Well... when two numbers agree to 9 significant digits, it's usually a mere numerical coincidence. Happens 1/1 000 000 000 of time :)

**2021-07-25 Predrag** Endler and Gallas [10] have all period-4 periodic points:

$$S_4(\sigma) = \sigma(\sigma^2 - 4a) \quad (22.27)$$

The the 2-points on diagonal  $\overline{0011}$  of figure 3.2 (b) has  $\sigma = 0$ . For  $a = 6$  the  $\overline{1000}$  has  $\sigma = -2\sqrt{6} = -4.898979485566356$  and  $\overline{1110}$  has  $\sigma = 2\sqrt{6}$ , which happens to be their common eigenvalue in (22.26). Endler and Gallas [11] also define

$$\begin{aligned} \alpha &= \sqrt{6 + 2\sqrt{6}} = 3.3013602478 \\ \beta &= \sqrt{6 - 2\sqrt{6}} = 1.04929524655. \end{aligned} \quad (22.28)$$

and the corresponding orbital equations

$$\begin{aligned} P_{1000}(x) &= (x^2 - \alpha^2)(x + \sqrt{6})^2 \\ P_{0111}(x) &= (x^2 - \beta^2)(x - \sqrt{6})^2 \\ P_{0011}(x) &= (x^2 - 6)^2. \end{aligned} \quad (22.29)$$

**2021-07-25 Predrag** For a period-4  $p$ , the Hill determinant of the orbit Jacobian matrix (21.219) is the polynomial

$$\text{Det}(\mathcal{J}_p) = 2^2 [2^2 x_0 x_1 x_2 x_3 - x_0 x_3 - x_1 x_2 - x_2 x_3 - x_1 x_0], \quad (22.30)$$

not involving the orbit sum  $\sigma$ , not in the form currently written. Looks like one should rescale  $\phi_i$  (again?).

The quadratic part is a sum of sequential pairs. There are two kinds of ways in which it can be time-reversal invariant:

- 2 on diagonal  $x_0x_2$  fixed,  $x_1 = -x_3$

$$\text{Det}(\mathcal{J}_p) = 2^2 [-2^2 x_0 x_1^2 x_2], \quad (22.31)$$

- none on diagonal,  $x_0 = -x_1, x_2 = -x_3$

$$\begin{aligned} \text{Det}(\mathcal{J}_p) &= 2^2 [2^2 x_0^2 x_2^2 + 2x_0x_2 + x_2^2 + x_0^2] \\ &= 2^2 [(2x_0x_2)^2 + (x_0 + x_2)^2], \end{aligned} \quad (22.32)$$

At the first glance, Hill determinants do not seem to factorize, but the time reversal symmetry assumptions (and signs) have to be checked.

**2021-07-25 Predrag** Some while-falling-asleep reflections on orbits  $\overline{1000}$  and  $\overline{1110}$  in (22.26), sharing the eigenvalue  $\sigma = 2\sqrt{6}$ :

If an orbit has a symmetry  $H$ , all of its periodic states (periodic points) presumably live in an invariant subspace  $\mathcal{M}_H$ . An example is Kuramoto–Sivashinsky, where orbits that start in the antisymmetric subspace stay in this lower dimensional subspace.

Example 6.11 possibly explains this for binary symbolic dynamics (note: there our '0, 1' are denoted '-, +'). In table 6.5 the pair  $\{- + ++, + - --\} \rightarrow$  fundamental domain  $\overline{0011}$ , i.e., we are back to our perennial problem of mistaking internal symmetries for time reversal, not sure this symmetry reduction is the one we need.

My hunch is that *all* short orbits live in invariant subspace(s), with  $\overline{110100}$  and  $\overline{001011}$  being the first exceptions.

Orbit  $\overline{1000}$  is like figure 3.2 (c), placed in the upper right corner, with no points on the diagonal. Orbit  $\overline{1110}$  is in the lower left, also symmetric across the diagonal. Endler and Gallas [11] plot them in their fig. 2. According to J. Montaldi table 6.4, the  $D_4$  permutation representation irreps are  $A_0 + B_1 + E$ .

In the 2-dimensional invariant subspace  $E$  (?) orbits  $\overline{1000}$  and  $\overline{1110}$  are period-2 orbits (I'm guessing, have not checked) and their eigenvalues might be related, like, for example,  $\bar{0}$  and  $\bar{1}$  in table 22.1. Or there is shared eigenvalue in one of the 1-dimensional subspaces. Remember the  $z$ -axis dynamics for the Lorenz flow? Read [ChaosBook Desymmetrization of Lorenz flow](#) (here example 6.4) to understand that not every linearly independent space is invariant under time dynamics.

However, the orbit Jacobian matrix  $\mathcal{J}$  is always a perturbation in the full  $\mathcal{M}$ , thus 3 other eigenvalues, all different. I would be happier if there were only 2 distinct eigenvalues per each cycle, but you cannot have everything. At least, not if you don't try.



example 6.28  
p. 359



example 6.4  
p. 346

Basically, also for nonlinear systems orbit Jacobian matrix is linear, so irreps of the symmetry group do block-diagonalize it. A stronger claim; symmetry can restrict entire orbits to flow-invariant subspaces of the phase space  $\mathcal{M}$ , even for nonlinear flows. Then some of the orbit Jacobian matrix eigenvectors point into that subspace.

**2021-07-25 Predrag** Combination  $r + r^{-1}$  in (22.10) commutes with  $\sigma$ , and  $\sigma$  conjugacy reverses  $\mathbb{X}$

$$\begin{aligned} \sigma \mathcal{J} \sigma &= r + 2\sigma \mathbb{X} \sigma + r^{-1} \\ &= \begin{bmatrix} 2x_{n-1} & 1 & 0 & 0 & \dots & 0 & 1 \\ 1 & 2x_{n-2} & 1 & 0 & \dots & 0 & 0 \\ 0 & 1 & 2x_2 & 1 & \dots & 0 & 0 \\ \vdots & \vdots & \vdots & \vdots & \ddots & \vdots & \vdots \\ 0 & 0 & \dots & \dots & \dots & 2x_1 & 1 \\ 1 & 0 & \dots & \dots & \dots & 1 & 2x_0 \end{bmatrix} \end{aligned} \quad (22.33)$$

Next, evaluate Hill determinant with a projection operator inserted. Should factorize?

$$\begin{aligned} \text{Det } \mathcal{J} &= \text{Det } (r + 2\sigma \mathbb{X} \sigma + r^{-1}) \\ &= \text{Det } (r + 2\mathbb{X} + r^{-1})(P_+ + P_-) \\ &= \text{Det } (P_+ \mathcal{J}) \text{Det } (P_- \mathcal{J}) \end{aligned} \quad (22.34)$$

**2021-08-04 Han** Yes! Read the text starting about (24.331) to see how that works.

**2021-08-08 Sidney** I have been out of the loop for awhile, so what I'm going to try to do is read up on what I missed, and take notes on that, and write it up in my blog, and then continue on with the work here, hopefully that can all happen in a timely fashion.

**2021-08-20 Sidney** I have been reading LC21 [21] and Han's blog and taking notes as appropriate, as this already exists in this blog, I'll only talk about it when I can add something. Anyway, I've been thinking about the time reversal pairs in the temporal Hénon. In the case of 110100 and 001011, the determinants of the orbit Jacobian matrices were equal and they are a time reversal pair. I think that maybe we can try to make a global statement about the relative weights of time reversal pairs. So, here is the first step in trying to see that.

First, I will remind everyone of the definition of the orbit Jacobian matrix:

$$\mathcal{J}_{ij} = \frac{\partial F[\Phi]_i}{\partial \phi_j}$$

This is defined for any periodic state:  $\Phi = [\phi_1, \phi_2, \dots, \phi_n]$ ,  $i$  defines the lattice point which is considered the "current" location, ie. for the temporal Hénon,  $i = 1$  says that the first periodic state is what we should use

for  $n^{\text{th}}$  in time, instead of  $n + 1$  or  $n - 1$ .  $j$  defines the lattice point which the defining equation will be differentiated with respect to. By definition, any periodic orbit can be cyclically permuted and still be the same periodic orbit. When this happens the indices in the periodic state get shifted, say  $1 \rightarrow 3$ . In this case, the indices in the orbit Jacobian matrix must be redefined in accordance to the shift, if we want to know how the "original" orbit and the "permuted" Jacobians relate. As both indices in the definitions of the orbit Jacobian matrix depend on the same index definition for the periodic state, when the periodic state is permuted by some number of steps  $p$  the indices in the definition for orbit Jacobian matrix change as follows

$$i \rightarrow \alpha \equiv i + r, \quad j \rightarrow \gamma \equiv j + r. \quad (22.35)$$

In fact, if we ignore the rules for "sameness" of orbit and say that the order of the periodic state can be arranged arbitrarily, the indices in the orbit Jacobian matrix definition are mapped as follows:  $i \rightarrow \alpha \equiv f(i)$  and  $j \rightarrow \gamma \equiv f(j)$ , where  $f(x)$  is some one-to-one map appropriate for the rearrangement applied to the periodic state. If we define a "diagonal entry" of the orbit Jacobian matrix as when the difference between the indices is zero, we can construct two indicator functions:

$$\Delta_{ij} = i - j$$

$$\Delta'_{\alpha\gamma} = \alpha - \gamma = f(i) - f(j)$$

As can be seen, when  $i = j$  both indicator functions are zero, indicating that a diagonal entry in one index space, is a diagonal entry in the other index space. In fact, as  $f(x)$  is one-to-one by definition there are an equal number of diagonal entries in each index space. And finally, as the definitions of the orbit Jacobian matrix in either index space are isomorphic:

$$\frac{\partial F[\Phi]_i}{\partial \phi_j} \simeq \frac{\partial F[\Phi]_\alpha}{\partial \phi_\gamma}$$

and as the individual lattice values are unchanged by the rearranging, not only are there an equal number of diagonal entries in each index space, but the same values exist in each. Thus, the (unordered) set of diagonal orbit Jacobian matrix entries is invariant under one-to-one index mappings, ie. arbitrary rearrangements of periodic state order.

This shows that under time reversal, the diagonal entries of an orbit Jacobian matrix are preserved, even if the orbit is not time reversal symmetric. I may have made a mistake here, either in the math, or just basic notation, please let me know!

**2021-08-23 Predrag** I am not sure about this proof, discuss it with Matt and Han first.

Here how I think about (as always, I might be wrong): The beauty of our spatiotemporal, global approach is that every periodic state (ie, a solution of the defining equations of a particular problem) is a fixed point in its high-dimensional phase space. So, if you can show that the eigenvalues of a fixed point problem in 1, 2, 3,  $\dots$ , 63 873,  $\dots$ , dimensions do not change under a smooth nonlinear change of fields, you have proven what we need to prove.

If you understand it 1 or 2 dimensions, you probably understand it any number of dimensions.

Reflection symmetry (sometime known as time reversal) comes in (see [ChaosBook sect. 8.3](#)) as an additional set of relations between the stability eigenvalues.

**2021-08-23 Sidney** At this point, I have pretty much settled on wanting to work on the mathematical physics end of plasma physics. Specifically with turbulence, and nonlinear aspects of fusion and astrophysics. But I quite frequently worry that I will miss out a great deal by not working with quantum, especially path integrals and field theories. I know that you transitioned from high energy to nonlinear dynamics and turbulence. How did you find that? And how analogous is the math? I know that for awhile there was quite a bit of overlap between turbulence and QFT methods, but that seems to have fallen by the wayside.

**2021-08-23 Predrag** Mhm. My impression is that [much is going on](#), for example [here](#), and you just happen to be on the most fearless and inventive team in the field.

Don't be [Fritz Haake](#) (who accepted the invitation on 30 May 2011). He, who hesitates, is lost.

**2021-08-25 Predrag** I keep saying that the proof of the invariance of orbit Jacobian matrix  $\mathcal{J}$  eigenvalues for a nonlinear but nonsingular redefinition of fields  $\phi_i$  is a variant of [ChaosBook sect. 5.4 Floquet multipliers are metric invariants](#), but I'm not getting traction on that from anyone.

In today's group meeting, I interpreted Sidney's proof of the invariance of orbit Jacobian matrix  $\mathcal{J}$  eigenvalues ([22.35](#)) as a permutation matrix on site labels, made a claim that any other permutation than  $D_n$  cyclic ones or their reversals will change the value of temporal Hénon Hill determinant, and challenged Sidney to compute Hill determinant for other permutations, see that the resulting determinant is different.

But for temporal Hénon I am probably wrong, as Endler and Gallas [[11](#)] prove that all their polynomials depend only on the orbital sum ([3.32](#)).

I believe that will not be true for the  $\phi^4$  theory ([4.182](#)) on  $d$ -dimensional lattice ([23.22](#)), with the Hill determinant of the same form ([3.26](#)), see [sect. 4.12.5 Deterministic  \$\phi^4\$  lattice field theory](#), because in that case bilinear terms in lattice fields arising from ([24.331](#)) cannot be eliminated.

**2021-08-26 Sidney** I mostly tried to write the proof to see if I could show that the diagonal values were an invariant set for rearrangements of the orbits, because if I could, I could say something about the equal determinants of the length 6 time reversal pairs I calculated for the temporal Hénon. I need to look more at other cases.

As well, I tried again to look at varying the proof from [ChaosBook sect. 5.4](#) *Floquet multipliers are metric invariants*. But I run into the issue that the fixed point condition for the map which is having its derivative taken for the orbit Jacobian matrix, is different that the fixed point condition for the map having its derivative taken for the time-step Jacobian. Namely, from CL18 eqn 13, it is stated that  $F[\Phi] = 0$  is the fixed point condition, NOT  $F[\Phi] = \Phi$  which would be required for the proof from Chaosbook to be carried out in the same way. I also tried to take Predrag's suggestion of looking directly at permutation matrices, and then taking the determinant to show that everything is invariant around an orbit. I tried the shift, i.e., the permutation matrix (??)

$$r_{ij}^s = \delta_{i,j+s},$$

shifting each entry backwards by  $s$  steps. Shifting the  $n$ -dimensional vector  $F[\Phi]$

$$f[\varphi] = F[r^{-s}\Phi]$$

a function of the  $n$ -dimensional periodic state vector  $\Phi$ , such that the orbit Jacobian matrix

$$\mathcal{J} = \frac{\partial f[\varphi]}{\partial \varphi} = \frac{\partial r^s F[r^{-s}\Phi]}{\partial r^{-s}\Phi}.$$

And after this point I am stuck, mostly because I am not sure if this is right, and it's weird dividing by a matrix, although, I probably need to take the derivative of the change of coordinates that I defined.

**2021-08-26 Sidney** For the one-dimensional case (eqn 5.15 in Chaosbook) the final conclusion relies on the fixed point condition being  $f(x) = x$ . However,  $F[\Phi]$  is effectively defined as  $f(x) - x$ . This causes a problem whether we're looking at scalars or vectors.

I thought a little more about the permutation proof,  $r^s$  is not position dependent, so there is no weird Jacobian shenanigans, using the chain rule we should just get

$$\mathcal{J} = \frac{\partial f[\varphi]}{\partial \varphi} = r^s \frac{\partial F[\Phi]}{\partial \Phi} r^{-s}.$$

I think that this is right, then we can just move around the determinant by the permutation property. I should think more how to relate this to eigenvalues.

**2021-08-27 Sidney** What is this "square root" thereof thou speaketh?



**2021-08-05, 2021-08-28 Predrag** It's been fuzzy all along, but roughly speaking it is this: Stability (at least, temporal evolution stability) is multiplicative along an orbit, so if you go twice as many time steps (lattice sites in our perspective), the stability gets squared.

Conversely, in going from period  $n = 2m$  (24.324)  $D_8$  symmetric orbit  $\overline{\phi_1\phi_2\phi_3\phi_4|\phi_4\phi_3\phi_2\phi_1}$  to the orbit Jacobian matrices evaluated on the  $m$ -dimensional  $\phi_1\phi_2\phi_3\cdots\phi_m$  subspaces (24.326), the stability gets square-rooted. There are many little things that I do not understand about how this works in detail that you could easily work out

1. What type from the list (6.14)-(6.17) is each of the short temporal Hénon orbits that you have? Han tells me my guesses (22.36) to (22.38) are wrong.
2. What is its Hill determinant? Which block of orbit Jacobian matrices (24.326) goes with which orbit? What are its eigenvalues, the symmetries of eigenvectors?
3. What is the relation between our (6.14)-(6.17) and Endler and Gallas [11] symmetry classifications?

Inspecting Endler and Gallas [11] fig. 2: the Hénon period-4 orbits,  $n = 2m$ , are of form

$$\overline{1000} : \overline{\phi_0|\phi_1|\phi_0\phi_1}, \quad (22.36)$$

and

$$\overline{1110} : \overline{\phi_0|\phi_1|\phi_2\phi_1}, \quad (22.37)$$

with symmetric-antisymmetric subspace dimensions  $d_+ = 3, d_- = 1$ , and

$$\overline{1100} : \overline{\phi_2|\phi_1|\phi_1\phi_2}, \quad (22.38)$$

with symmetric-antisymmetric subspace dimensions  $d_+ = 2, d_- = 2$ .

I leave it to the gentlepersons of this blog to compute the  $[1 \times 1]$  Hill determinants  $\text{Det}(\mathcal{J}_-)$  for  $\overline{1000}$  and  $\overline{1110}$  in (22.26), show their sole eigenvalue is  $\pm\sigma = 2\sqrt{6}$ .

**8/29/2021 Sidney** I am very confused. First off, I found out that I don't know how to block-diagonalize matrices using symmetry operators, I tried to recreate the  $CO_2$  example in the group theory notes, but to no avail. So I turned to trying to show Hill determinants  $\text{Det}(\mathcal{J}_-)$  for  $\overline{1000}$  and  $\overline{1110}$  in (22.26) is,  $\pm\sigma = 2\sqrt{6}$ . But I am missing a factor of two, and I don't know why. I did the following:

The symmetry is an "even" reflection as defined in (6.32), so the symmetry matrix is

$$\sigma = \begin{bmatrix} 1 & 0 & 0 & 0 \\ 0 & 0 & 0 & 1 \\ 0 & 0 & 1 & 0 \\ 0 & 1 & 0 & 0 \end{bmatrix}$$

From here, I can construct projection operators for the symmetric and anti-symmetric subspaces of this operator:

$$P_+ = \frac{1}{2}(I + \sigma) \quad P_- = \frac{1}{2}(I - \sigma)$$

Taking the trace of each of these operators gives me the dimension of each of these subspaces:  $d_+ = 3, d_- = 1$ . Now, let's look at  $\mathbb{T}^4$   $\phi_0, \phi_1, -\phi_0, \phi_1$ . In this case the (incorrect! - see (22.40)) orbit Jacobian matrix is

$$\mathcal{J} = \begin{bmatrix} \phi_0 & 1 & 0 & 1 \\ 1 & \phi_1 & 1 & 0 \\ 0 & 1 & -\phi_0 & 1 \\ 1 & 0 & 1 & \phi_1 \end{bmatrix} \quad (22.39)$$

$$\sigma \mathcal{J} = \begin{bmatrix} \phi_0 & 1 & 0 & 1 \\ 1 & 0 & 1 & \phi_1 \\ 0 & 1 & -\phi_0 & 1 \\ 1 & \phi_1 & 1 & 0 \end{bmatrix}$$

The trace of  $P_- \mathcal{J} = \frac{1}{2}(\mathcal{J} - \sigma \mathcal{J})$  should give me the eigenvalue for the asymmetric subspace, this gives  $\phi_1$  which equals  $\sqrt{6}$  from Endler and Gallas [11], which is missing a factor of -2, I have no idea what's wrong (since corrected in(22.40)).

**2021-08-29 Predrag** Getting it up to factor of 2 is a triumph! The rest is work :) Have you tried cross-checking formulas? One cannot trust anyone, one always makes sure that the formulas are as you yourself have derived them. I would not be surprised if there should be  $2\phi_j$  along the diagonal...

In this context: (4.181) and the footnote next to it will amuse you.

A small aside - when you refer to an equation, like (6.32), refer to it, rather than having the reader try to figure out where it came from. It's much faster for everyone if you just do it.

A much less important thing at this stage: The macros such as  $\sigma$  [backslash Refl] are here for a reason - as the research progresses we often find that a better notation exists in literature. That can be fixed by editing a few characters in *siminos/inputs/defsSpatiotemp.tex*.

**2021-08-29 Predrag to Sidney** Here is a request that requires minimal work - you have it in your code or data sets: Plot the values of periodic state fields for the 6 periodic states of table 3.3 and figure 3.3 in the same format as figure 6.1 (b).

Note - temporal Hénon fields can be positive or negative. I'm particularly interested to see if any of your periodic states are antisymmetric under reflection across  $\phi_0$ .

**2021-09-01 Sidney** In my last post I used the incorrect definition (22.39) of  $\mathcal{J}$ , the correct definition is

$$\mathcal{J} = \begin{bmatrix} 2\phi_0 & 1 & 0 & 1 \\ 1 & 2\phi_1 & 1 & 0 \\ 0 & 1 & -2\phi_0 & 1 \\ 1 & 0 & 1 & 2\phi_1 \end{bmatrix} \quad (22.40)$$

This, along with remembering that  $\phi_1$  is negative for the 1000 orbit, fixes the factor of negative 2 I was missing. I have also figured out my block diagonalization issue from before. Now the question is, why would  $\overline{1000}$  and  $\overline{0111}$  have equal but opposite eigenvalues for the asymmetric subspace of the reflection operator (is this the correct vocab?). I also think I know what is wanted for the plots, I will do that.

Back to an earlier project: eigenvalues of  $\mathcal{J}$  in different coordinates.  $\mathcal{J}$  is not a derivative on space (like the one time step Jacobian is), it is instead a derivative on periodic lattice points (again, could be incorrect vocab, will work on this). So, maybe instead of using a regular coordinate transform, we should transform specifically on the periodic orbit? Maybe that would help with the issue of the fixed point condition being  $F[\Phi] = 0$  instead of  $F[\Phi] = \Phi$ .

**2021-09-01 Sidney to Predrag** What colors should I use for the bars when I do your plotting suggestion for temporal Hénon, the colors mattered in the other bar graphs.

**2021-09-01 Predrag** Quality of a plot does not matter much at the exploratory stage, I know by plotting by hand the shapes of the 6 periodic states - they follow from their symbolic dynamics. However, if you have accurate numbers for fields and eigenvalues, you could discover the symmetries that I am missing in hand-sketches. Or you can put intelligible data files in your computing folder *siminos/williams/* and make Predrag do your work, as in (22.26) :

Plot the values of periodic state fields for the 6 periodic states of table 3.3 and figure 3.3 in the same format as figure 6.1 (b), using the same color scheme. When I plot them, I place the yellow bar at 0, then two red bars to the left and two blue to the right. You can also superimpose symbolic dynamics code upon it - you will immediately understand '0's are negative and '1's are positive.

**2021-09-03 Predrag** To determine  $C_5$  period-5 states of table 3.3 you only need to determine the  $D_5$  length-3 block periodic state defined by boundary conditions of (??) - you might want to check whether the periodic states so obtained agree with the ones you already have.

Their Hill determinants are the determinants of the 3-dimensional orbit Jacobian matrix (??).

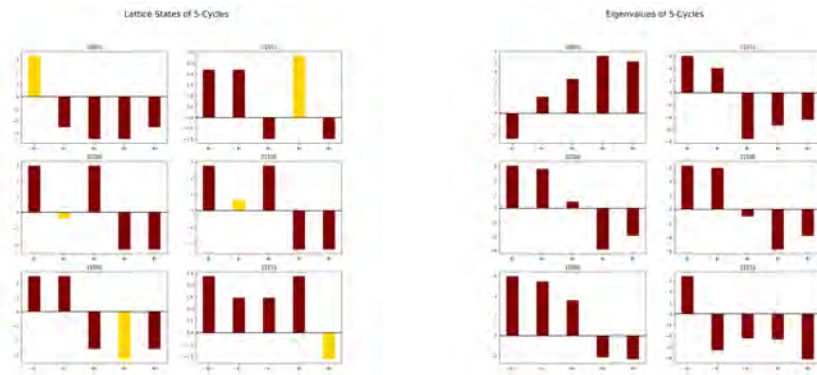


Figure 22.2: Temporal Hénon (3.62),  $a = 6$ : (left) The associated orbit Jacobian matrix eigenvalues (?). Currently we have no interpretation. Should't the corresponding eigenvectors be (anti)symmetric?

To determine  $C_6$  period-6 states of table 3.3 you only need to determine the corresponding  $D_6$  length-4 or -3 block periodic state defined by boundary conditions analogous to (?). Their Hill determinants are the determinants of 4- or 3-dimensional orbit Jacobian matrix (6.29) or (6.30).

2021-09-03 Predrag 2 Andrew afugett3 = fuggedaboutit

2021-09-06 Sidney 2 Everyone Sorry for the long silence, just settling back into everything. I will be working on the plots today, and will update as I go along, as well, I will show Andrew how to get the repository on his laptop.

Period  $n = 5$  periodic states of table 3.3 plotted as in figure 6.1. They are all reflection symmetric, with fixed lattice field  $\phi_0$  colored gold. Note that the symbolic dynamics is given by the signs of lattice site fields. This plot is now superseded by figure ??. (right)

2021-09-06 Sidney I completed the plots for both lattice field values, and the associated eigenvalues. The formatting is not finished yet, but I will change that later. Currently, I have the lattice state that remains fixed colored gold, and the ones that flip colored maroon.

2021-09-07 Predrag .

1. Figure 22.2 (a) agrees with my own sketch, but only examination of the actual  $\phi_j$  values can reveal further symmetries and factorizations.
2. Figure 22.2 (b) currently does not make much sense to me. 3 of the eigenvalues should belong to the symmetric subspace (22.41), (6.22), 2 to the antisymmetric subspace (6.24).

3. 2021-09-27: Figure 22.2 (a) is now superseded by figure ??.

**2021-09-06 Sidney** For a  $D_5$  lattice state, the following boundary conditions are respected:  $\phi_i = \phi_{i+5}$  and  $\phi_{-i} = \phi_i$ , if we follow (??), we find the temporal Hénon orbit Jacobian matrix in the symmetric subspace is

$$\mathcal{J}_+ = \begin{pmatrix} 2\phi_0 & 2 & 0 \\ 1 & 2\phi_1 & 1 \\ 0 & 1 & 2\phi_2 + 1 \end{pmatrix} \quad (22.41)$$

As well, from (??), I can find the 3 equations that define this sort of orbit for temporal Hénon

$$\begin{aligned} \phi_0^2 + 2\phi_1 &= a \\ \phi_0 + \phi_1^2 + \phi_2 &= a \\ \phi_1 + \phi_2^2 + \phi_2 &= a \end{aligned} \quad (22.42)$$

Is there a good way of solving this system analytically? Otherwise, should I just check it by numerically finding solutions?

**2021-09-07 Predrag** No, for us getting into the Endler-Gallas analytic solutions is getting too deep into the weeds. Use the same Biham-Wentzel program you have already written, with the boundary conditions added. The wonderful thing is that you are looking for the roots of an order  $2^3$  polynomial rather than  $2^5$ .

To compute the Hill determinant  $\text{Det } \mathcal{J}_+$ , Han would recommend doing the discrete Fourier transform first.

**2021-09-07 Predrag** Currently I prefer the (4.181) form of the temporal Hénon to (3.62), but that is not very important at this stage.

**2021-09-07 Sidney** The full orbit Jacobian matrix for the  $D_5$  cycles of the temporal Hénon commutes with reflection about the center lattice state (??). Therefore, we can block diagonalize to find the orbit Jacobian matrices of the symmetric and antisymmetric subspaces:

$$\mathcal{J}_{D_5} = \begin{pmatrix} 2\phi_2 - 1 & 1 & 0 & 0 & 0 \\ 1 & 2\phi_1 & 0 & 0 & 0 \\ 0 & 0 & 2\phi_0 & 2 & 0 \\ 0 & 0 & 1 & 2\phi_1 & 1 \\ 0 & 0 & 0 & 1 & 2\phi_2 + 1 \end{pmatrix} \quad (22.43)$$

Which gives the same matrix for the symmetric subspace as (22.41), therefore either boundary conditions or projection operators are effective for these sort of calculations.

I took a look at my code, and it seems that I wrote it with no ability to scale  $a$ , I will fix that, and add in the functionality of using the traditional field theory formulation and the rescaled "Gallas" notation that I have been using for awhile.

**2021-09-09 Predrag** You sure about (22.43)? It might be correct, but how did you derive it?

**2021-09-13 Sidney** I am quite sure of (22.43). I noticed that the orbit Jacobian matrix for a time reversal invariant orbit commutes with the  $[5 \times 5]$  reflection matrix

$$\sigma = \begin{pmatrix} 0 & 0 & 0 & 0 & 1 \\ 0 & 0 & 0 & 1 & 0 \\ 0 & 0 & 1 & 0 & 0 \\ 0 & 1 & 0 & 0 & 0 \\ 1 & 0 & 0 & 0 & 0 \end{pmatrix} \quad (22.44)$$

So, I found all the eigenvectors associated with (22.44) by an online calculator and arranged them so that the ones associated with  $-1$  (antisymmetric) and  $1$  (symmetric) were grouped together in a matrix  $S$ , I then used an online calculator to perform

$$S^{-1} \mathcal{J} S = \mathcal{J}_{BD}$$

And after shuffling around the columns of  $S$  (which is allowed for diagonalization), I got (22.43).

**2021-09-07 Sidney** This brings me to what Predrag has asked me to do:

#### Predrag check list

1. I will need to reformulate everything back into the unscaled field values so that  $a$  multiplies the quadratic term.
2. Find eigenvalues of  $D_5$  lattice states in the symmetric subspace to explain figure 22.2 (right).
3. Prove (or disprove) that the eigenvalues of the orbit Jacobian matrix are metric invariants. I am stuck here.
4. Implement Han's boundary conditions into my code so that I can directly find orbits with specific symmetries.

**2021-09-12 Sidney** I will start working on adding boundary conditions to find different symmetries (a task I have added to the list) after I clean up my code, and make it easy to switch between Gallas form, and Field Theory form.

**2021-09-13 Sidney** I have changed my code so that it can be easily switched between the Hénon [19] (3.21), and Endler and Gallas [12] rescaled (3.38), I have added this updated code *Relaxation Method Henon with orbit Jacobian matrix.py* to *siminos/williams/python/relax*.

**2021-09-14 Predrag 2 Sidney** Added exercise 3.5 *The matrix square root*.

**2021-09-14 Sidney 2 Predrag and Han** I looked at exercise 3.5 *The matrix square root*. I feel confident in being able to do that. However, I am not sure why I am looking at the square root here. From what I gathered during today's meeting, taking the square root of the time-step Jacobian at the boundary point did not give equality to the Hill determinant of the symmetry reduced orbit Jacobian matrix. My impression was that I would instead need to look for a "square root" of the temporal Hénon is that incorrect?

**2021-09-17 Sidney 2 Anyone** Just for clarification, I should be looking at (24.360) for time symmetric orbits of the temporal Hénon. I was thinking that since this is an identity for the forward in time  $2 \times 2$  Jacobian, for orbits symmetric with respect to time reversal, I would look at the Hill determinant  $\text{Det } \mathcal{J} = \det(\mathbf{1} - J)$  and check to see that the equality holds for when I take the half orbit of time-step  $J$ , compare to the symmetric part of (22.43). Is that a good strategy?

**2021-09-17 Sidney** I have completed exercise 3.5, the solution I got on pen and paper matches the solution that Predrag provided. I will take Andrew through it tomorrow.

**2021-09-17 Sidney** With respect to adding boundary conditions to my code: I do not know how to do it as I am not using the Biham-Wentzel method for the temporal Hénon, instead (a detail nowhere described in the blog) I invert it and feed the code a symbol sequence, see Vattay's *ChaosBook* exercise 7.2, copied to here as exercise 5.1.

**2021-09-17 Sidney** I do not know how to change the boundary conditions.

**2021-09-30 Sidney** The above statement is still true, although, around studying for tests, and other homework, I been working on testing the formula (24.360) numerically. I have also been review some of the group theory lectures from over the summer. What I did, was say that the "factored" time-step Jacobian for a time symmetric period-5 is

$$\tilde{J} = J_2 J_1 \sqrt{J_0} \tag{22.45}$$

Where  $\sqrt{J_0}$  can be calculated through the methods worked through in exercise 3.5. I then did the following calculation for every  $\sqrt{J_0}$

$$|\text{Det } \mathcal{J}_+| - |\det(I - \tilde{J})|(\text{should}) = 0, \tag{22.46}$$

where  $\mathcal{J}_+$  is the  $[3 \times 3]$  block in (22.43). This did not work. The closest I got to getting zero was 3.4, which isn't even an integer. So, I turned to Mathematica, and found that  $\text{Det } \mathcal{J}_+$  has a fundamentally different form from  $\det(I - \tilde{J})$  for the temporal Hénon with a time symmetric five cycle, so, I went back to the drawing board. In the meeting at the beginning of the week, it was mentioned that the time-step Jacobians had to satisfy the time symmetry boundary conditions, and my thought was to try to force

this by finding the Jacobian for each equation along a time symmetric period-5 which, with boundary conditions, yields a 3 equations:

$$2\phi_1 + \phi_0^2 = a \quad (22.47)$$

$$\phi_2 + \phi_1^2 + \phi_0 = a \quad (22.48)$$

$$\phi_2 + \phi_2^2 + \phi_1 = a \quad (22.49)$$

The time step Jacobian from (22.47) is  $J_0 = -\phi_0$ , and the time step Jacobian from (22.48) is just the normal one for the temporal Hénon. I am not sure how to get a Jacobian out of (22.49), perhaps the quadratic equation? If anyone has suggestions, that would be lovely.

I tried stating that (22.49) could be written as  $\phi_3 = a - \phi_2^2 - \phi_1$ , which would give just the normal temporal Hénon Jacobian, but it did not match with the determinant of the  $[3 \times 3]$  block in (22.43). So my hunch was wrong. Not quite sure where to go from here in that area.

2021-10-05 Sidney See sect. 5.1 *Vattay inverse iteration method* for how I compute temporal Hénon periodic states.

2021-10-12 Sidney I am currently trying to address "Find eigenvalues of  $D_5$  lattice states in the symmetric subspace to explain figure 22.2 (right)." from 22.2. I found a equation for the symmetric part of the orbit Jacobian matrix  $\mathcal{J}_+$  (22.43), it is of the form  $a\lambda^3 + b\lambda^2 + c\lambda + d$  where the coefficients are all inelegant sums of the lattice field values of a given orbit, it is not particularly helpful.

2021-10-15 Predrag You have to check that the "inelegant sums" are invariant under  $D_n$  symmetries. Han knows and explains how to compute the eigenvalues and eigenvectors (irreps of  $D_n$ ) on the reciprocal lattice.

I think you will eventually end up with evrything being expressible in terms of traces of powers of  $\text{Tr } \mathcal{J}_+^k$ .

I am curious how many orbit Jacobian matrix  $\mathcal{J}$  eigen-directions are expanding, what do they look like, stuff like that.

2021-10-12 Sidney I think that part of the confusion of the right hand side of figure 22.2 is that I tried to assign eigenvalues to individual lattice sites, which is just incorrect, right?

2021-10-15 Predrag Eigenvalues are properties of the whole matrix, not a single site. Only if the matrix is diagonalized are they associates with eigenstates ('lattice sites' of the reciprocal lattice).

2021-10-12 Sidney I am going to look at (22.28) again to see if I can see some pattern. But as of right now, I think the main conclusion is that the eigenvalues do not necessarily have the same symmetries as the orbit they belong to.



**2021-10-15 Predrag** Eigenvectors have symmetries, not the eigenvalues.

**2021-10-25 Sidney** I have generated some good data for the eigenstuff, see figure ???. I need to do further analysis to see which eigenstate(s) is most important. As well, I think I have some insight into why (24.360) does not work. The orbit Jacobian matrix can be block diagonalized into symmetric and antisymmetric blocks. As this is the case, Hill's formula can be written as

$$\text{Det}(\mathcal{J}_-)\text{Det}(\mathcal{J}_+) = \det |I - J|$$

If we assume we can write  $J$  as  $(J')^2$  (which is what (24.360) assumed), we can then write Hill's formula as

$$\text{Det}(\mathcal{J}_-)\text{Det}(\mathcal{J}_+) = \det |I - J'| \det |I + J'|$$

Which does not imply that  $\text{Det}(\mathcal{J}_+) = \det |I - J'|$  which I numerically showed to be incorrect a few weeks ago. This does not necessarily help find a correct factorization, but it at least shows us what is wrong.

**2021-11-11 Sidney** I added the plots of the eigenstates for every 5-cycle, as well as the decomposition for each period lattice state. Unfortunately, there seems to be no correlation between the important eigenstates and the size of the eigenvalues.

**2021-11-11 Predrag to Sidney** .

The figures currently in *siminos/williams/python/Figures/* are not \*.svg vector graphics - they are bit images. To see them, download [Inkscape](#) and try to edit them.

**2021-11-11 Sidney** I suppose that almost makes sense because treating the whole cycle as a fixed point removes iteration from our calculations, perhaps they will be useful for global stability analysis?

**2021-11-11 Predrag to Sidney** I think so too. Note that as the orbit Jacobian matrix is symmetric (at least for the full primitive cell - you have to show it also works for the symmetry-reduced case and  $b \neq -1$ ) all multipliers  $\Lambda_j$  are real. Their signs might mean something.

**2021-11-11 Predrag to Han** .

1. Before Sidney automatizes looking at eigenvectors, what output format do you prefer? Sidney's narrow bars as field values, as in figure 22.2, or Han's fat bars, as in figure ???
2. The problem with temporal Hénon is that due to all period-5 periodic states being symmetric, we are getting only 3-dimensional examples. For temporal cat you have asymmetric period-5 periodic states, there is more information in them.

3. Can you take your beloved temporal cat products of  $[s - 2 \cos(\frac{2\pi j}{n})]$  and do the corresponding eigenvector plots as [siminos/williams/python/Figures/](#) for (some of) illustrative temporal cat period-5 periodic states? Any striking similarities?

**2021-11-11 Predrag .**

I find the eigenvectors currently in [siminos/williams/python/Figures/](#) utterly fascinating.

The  $n$  multipliers  $\Lambda_j, j = 1, 2, \dots, n$  (ChaosBook reserves the lower case  $\lambda_j$  to exponents, but we might change that for the spatiotemporal theory) seem all to be of the same order of magnitude - that will be more apparent when we see their lists for examples of periodic states of periods  $n = 6, 7, 8, \dots$ .

**2021-12-06 Sidney** I am still a little unsure how to get the files saved as \*.svg vector graphics, the line which saves the pictures is given by

```
plt.savefig(name+'.svg',dpi=300)
```

where name is defined earlier in the code. I am not sure why that does not work. I am also quite close to automating the cycle finding process with nice looking, and useful figures, I will do that after finals.

I am still stuck on proving that the eigenvalues of the orbit Jacobian matrix are invariant under nonlinear coordinate transforms, the fixed point condition under the field theory just does not seem to allow for it.

I now understand how Han was able to find  $2\cos(k) - s$  for the eigenvalues, but I am currently having a hard time generalizing that to temporal Hénon I will keep working.

Finally, I have found a (probably useless) tensorial formulation of our theory which allows for the analysis of multiple equation systems (think the Lorenz equations discretized, or temporal Hénon before being compressed into a single equation). It is as follows

$$G^{kl}[\Phi] = \Gamma_{ij}^{kl} \Phi^{ij} + M^{kl} = 0^{kl}, \tag{22.50}$$

Where the index  $k$  is for the  $k^{th}$  equation, and index  $l$  is for the  $l^{th}$  lattice point. The index  $i$  ranges from 1 to  $n$  for a length  $n$  orbit, it is the field value on the  $l^{th}$  lattice point for the  $j^{th}$  variable (think  $x$  and  $y$  for Hénon).

$$\Gamma_{ij}^{kl} \equiv \frac{\delta G^{kl}[\Phi]}{\delta \Phi_{ij}}, \tag{22.51}$$

Several caveats here, I am sure that I could condense this, perhaps combining the  $i$  and  $l$  index, I am also pretty sure that I messed up the Einstein notation with the co and contravariant indicies. And finally, this is likely completely useless as I am pretty sure that given a system of  $k$  first order difference equations, it can be combined into a single higher order equation like what was done with temporal Hénon.

**2021-12-17 Sidney** I have been trying to get an equation which shows the bounds of the eigenvalues of the temporal Hénon but the method of just guessing  $e^{\omega^n z}$  doesn't work for the orbit Jacobian matrix for Hénon because it does not commute with the shift operator  $(\delta_{j+1,k})$ , so there is probably some other  $u(z)$  that I need to use, I am not sure though.

**2021-12-18 Sidney** I am trying to establish bounds for the temporal Hénon. I can do this numerically, with the minimum value being -0.607625218511 etc. and the maximum still to be calculated with the code provided for ChaosBook.org/course1 [homework 7](#). The stable and unstable manifolds trace out the region that is bounded  $(\Omega)$ , and the maxima and minima are determined by their intersections, and I know that these manifolds can be calculated numerically through forward and backward iteration, but I feel like I should be able to find these intersections analytically. Is there something else that I could do? Or do I have to resort to numerics?

**2021-12-20 Predrag** I do not believe I have ever seen an analytic expression for a non-trivial intersection of stable / unstable manifolds: for such calculation, see sect. [4.12.7](#). The lower left corner of [ChaosBook fig. 15.5](#) you know analytically: it is the stability of fixed point  $\bar{0}$ . The upper right corner of the Smale horseshoe non-wandering set is the heteroclinic point - lacking something more clever, one might approximate it by the longest nearby periodic orbit, of form  $\overline{100 \cdots 0}$ . You only need an lower bound on the magnitude of the multiplier, it's OK to be crude about such a bound.

An example of  $\overline{100 \cdots 0}$  sequence of periodic orbits is given in Artuso, Aurell and Cvitanović *Recycling of strange sets: II. Applications*, see their [fig. 2](#). That would correspond to the tangency stretching parameter  $a$  value (??); you are looking at a larger stretching so there is no funny  $\sqrt{\cdots}$  limit in your case, your limit is cleanly hyperbolic, see figure ??.

**2021-09-12 to 2021-09-14, 2021-12-22 Sidney, Predrag** It looked like a wild goose chase, so not to distract Sidney further I had moved the discussion of anti-integrable "perturbation theory" to sect. [3.2 Temporal Hénon](#). But it remains of interest: many new references there in sect. [3.2 Temporal Hénon in anti-integrable limit](#).

I have added my guess ([4.228](#)) for the infinite coupling  $g$  anti-integrable limit of  $\phi^4$  theory. That gives a 3-letter alphabet  $\mathcal{A} = \{-1, 0, 1\}$ . One can use it to find by continuation any periodic state, at  $g$  as low as possible. 'Generalized Hénon maps' AKA  $\phi^4$  field theory posts are in sect. [4.12.5 Deterministic  \$\phi^4\$  lattice field theory](#).

**2021-12-27 Sidney** I have figured out how to effectively bound the eigenvalues for any matrix whose rows have the form  $[0 \cdots 01V''(\phi)10 \cdots 0]$  using the Gershgorin circle theorem ([wiki](#)), I will talk about it in depth once the repository is back up and I can update my blog.

Additionally, if anyone knows anything about machine learning, I would appreciate some help with that so that I can try using it to more accurately find the bounds of the temporal Hénon orbit Jacobian matrix eigenvalue spectrum.

## 22.3 2022 blog

**2022-01-01 Sidney** Do you have any good recommendations for a look at the Smale horseshoe? There doesn't seem to be an introduction to it in Chaos-Book.

**2022-01-01 Predrag** .

[ChaosBook Horseshoes](#)

[ChaosBook 15.1 Remark](#)

[ChaosBook 1.1 Remark](#) "Strogatz [35] [...] is not strong on chaos. There the textbook of Alligood, Sauer and Yorke [1] is preferable: an elegant introduction to maps, chaos, period doubling, symbolic dynamics, fractals, dimensions—a good companion to Chaos-Book. Introduction more comfortable to physicists is the textbook by Ott [23], with the baker's map used to illustrate many key techniques in analysis of chaotic system."

**2022-01-02 Sidney** Why does drawing the line  $y = x$  and then drawing horizontal and vertical lines between the line and the map work to determine orbits visually? I understand why it works for fixed points, but not orbits.

**2022-01-02 Sidney** Here is the explanation for the Gershgorin circle theorem bounding of the eigenvalues for non-circulant orbit Jacobian matrices: The theorem is

$$|\lambda - \mathcal{J}_{tt}| \leq \sum_{t' \neq t} |\mathcal{J}_{tt'}|, \quad (22.52)$$

For the types of lattice equations we are working with the RHS is always 2, and so the eigenvalues are contained within circles of radius 2 in the complex plane centered according to the diagonal values of the orbit Jacobian matrix. Therefore, the minimum value which can be obtained for an eigenvalue is  $\mathcal{J}_{ii}^{min} - 2$  and the maximum is  $\mathcal{J}_{ii}^{max} + 2$ , the values  $\mathcal{J}_{ii}^{min}$  and  $\mathcal{J}_{ii}^{max}$  are determined by the lattice states of whichever orbit we are analyzing, which can be bounded in and of itself.

**2022-01-04 Predrag** Our orbit Jacobian matrices are circulant matrices.

Have you checked your bounds against your eigenvalues, for example figure 22.2?

I am fairly sure that if you redefine  $\phi_j$  coordinates you can change  $\mathcal{J}_{tt}$ , so these bounds move. That might be an argument for that the orbit Jacobian matrix eigenvalues have no invariant meaning.

2022-01-02 **Sidney** Although, how do we bound  $\phi^4$ ?

2022-01-12 **Sidney** I have been reading the periodic orbit theory notes linked [here](#),

2022-01-12 **Sidney** I'm about a third of the way through, as it is quite dense reading. I have two questions right now, first, the Perron-Frobenius operator is defined as the following in the notes:

$$\mathcal{L} = \int \delta(x - f(\xi)) d\xi$$

Why is the trace of this

$$\text{tr } \mathcal{L} = \int \delta(x - f(x)) dx ?$$

Is that just a definition of taking a trace over a continuous operator instead of a matrix?

2022-01-14 **Yes.**

2022-01-12 **Sidney** On a related note, why can we write the following

$$\text{tr} \left( \sum_{n=1}^{\infty} z^n \mathcal{L}^n \right) = \text{tr} \frac{z \mathcal{L}}{1 - z \mathcal{L}}$$

I understand the geometric series, but why is it the above instead of

$$\frac{z \text{tr } \mathcal{L}}{1 - z \text{tr } \mathcal{L}}$$

Why can we pull out the trace?

2022-01-12 **Sidney** I have a question about the binary symbolic dynamics. How do we know that a given binary sequence is unique to a single orbit?

2022-01-14 **Predrag to Ibrahim and Xuanqi** It is important that you be able to explain this to Sidney, at least on the [level of matrices](#). Write up the answer here by 2022-01-21, at the latest.

2022-01-18 **Ibrahim and Harrison to Sidney** So before we try to look at the trace of the geometric series, let us rewrite its final expression as

$$\frac{z \mathcal{L}}{1 - z \mathcal{L}} = (z \mathcal{L}) (1 - z \mathcal{L})^{-1}$$

So now if we think about this term as the product of two matrices, and we know that the trace of a product is not equal to the product of the traces.

$$\text{tr}(AB) \neq \text{tr}(A) \text{tr}(B)$$

In your previous note you phrase it as "why can we pull out the trace?" But rather it is not that we are pulling out the trace, but that we are not distributing the trace operation to each of the two matrices that make up the term on the right. You can see this by first just showing the equality of the sum to the geometric series solution and then applying the trace operation to both sides.

**2022-01-12 Sidney** Why is the escape rate  $e^{-\gamma}$  the leading eigenvalue of  $\mathcal{L}$ ? I understand why it is an eigenvalue, but I don't know why it's the LEADING one.

**2022-01-14 Predrag** [ChaosBook Index](#) has 23 entries under 'escape rate'. Check them out, come back with specific comments if that is not explained well enough.

**2022-01-12 Sidney** The new material: First a counting formula for the number of prime cycles of length  $n$  in complete binary symbolic dynamics. First, each entry in the length  $n$  string can either be 0 or 1 so we have a contribution of  $2^n$ . For each of  $n$ 's factors, we must subtract out the shorter orbits that can be built up to form the longer orbit ex:  $n = 3$  must subtract out  $2 \ n = 1$  orbits. Additionally, in our theory, each orbit is  $C_n$  invariant, so we must divide by  $n$  to remove orbits that are simple cyclic permutations of each other, since the shorter orbits cannot have  $n$  unique cyclic permutations, we have to multiply the number of shorter cycles by  $\frac{n_k}{n}$ . Where  $n_k$  is the length of the shorter cycle, we do this instead of just dividing by  $n$ . So, for a cycle of length  $n$ , the number of prime orbits is

$$\frac{1}{n} (2^n - \sum_k q_k n_k) , \tag{22.53}$$

where Einstein notation has been used, and where  $q_k$  is the number of prime orbits of length  $n_k$ . The  $k$  values of  $n_k$  are just all the divisors of  $n$  that are not equal to  $n$ .

**2022-01-12 Sidney** Now, I am claiming that I have found a proof that shows that the eigenvalues of the orbit Jacobian matrix are not invariant by the definition of the orbit Jacobian matrix. We can see this, by looking at the temporal Hénon if the eigenvalues were invariant under coordinate change, the bounds in (22.52) would also be invariant. We can see that it is now. First we note that to be invariant, the expression produced by the Gershgorin circle theorem must be able to be reverted to  $2a\phi_{max/min} \pm 2$ . Let us try to do this. First, we can introduce the mapping  $\phi = f(p)$ . Plugging this mapping into temporal Hénon and applying the orbit Jacobian matrix definition, and the Gershgorin circle theorem, we see that our condition is that the eigenvalues are contained in circles of radius

$f'(p_{n+1}) + f'(p_{n-1})$  centered at  $2af(p_n)f'(p_n)$ . Now, the minimum value achievable by the temporal Hénon is simply the fixed point  $\bar{0}$ , so we can write the minimum as  $f'(f^{-1}(\phi_{min}))(2a\phi_{min} - 2)$ . Therefore, unless  $f'(f^{-1}(\phi_{min})) = 1$  the minimum bound changes, and therefore, the achievable range of the eigenvalues change, and thus, the eigenvalues are not invariant under all smooth coordinate changes. And since the orbit Jacobian matrix for the temporal Hénon does not have invariant eigenvalues, we can state that invariant eigenvalues is not a general property of the orbit Jacobian matrix. Which begs the question, what are the eigenvalues?

**2021-12-27 Sidney** I have calculated the prime periodic orbits up to length 15 for the temporal Hénon, I'll be generating data for all 4,720 of them over the next few days. The length of the calculation makes me think that I need to be a bit more clever with my code writing.

**2022-01-16 Predrag** If you can compute the eigenvalues of the orbit Jacobian matrix for periodic states that you have, plot them all together in the first Brillouin zone as Han has done for temporal cat in figure 24.65, I think that would be very interesting. The plot should be symmetric under  $k \rightarrow -k$ , but asymmetric under reflection across the horizontal axis, possibly in a rather interesting way.

I have never been able to discern a pattern in what you have shared with us so far (figure 22.2, 2021-09-07 Predrag, 2021-09-07 Sidney posts). We do not expect an infinite lattice limit continuous curve (blue sinusoid in his plot), but I expect the eigenvalues to lie on a fractal set with nice binary symbolic dynamics interpretation.

**2022-01-19 Sidney** Here is the Cantor-Style plot of the eigenvalues for the Galas scaled temporal Hénon of orbits up to length 8. Yes, this file (which is located in the figs folder in siminos) is a .png. I am still dealing with getting everything moved onto my new laptop, and I will figure out the svg stuff soon, as it stands though, this file is only 44kb, which should hopefully not crash the repo.

I want to make an additional figure where I try to plot the fractilic sinusoids which Predrag is interested in. I am having a very difficult time thinking of how to do this. I know how to convert to reciprocal space, however, my eigenvectors are linear combinations of Fourier modes, which means that the calculated eigenvalues are associated with multiple scaled Fourier modes. So, I cannot think of a way to plot this on the  $k - \lambda$  plane, without plotting a scaled  $\lambda$  at multiple  $k$  values (the scaling would be the same as what is necessary in the linear combination which builds the calculated eigenvectors). I could also do as Han suggests and look at infinite orbit Jacobian matrices with varying periodicities and apply Bloch's theorem with the hope of making something analytic pop out. However, I

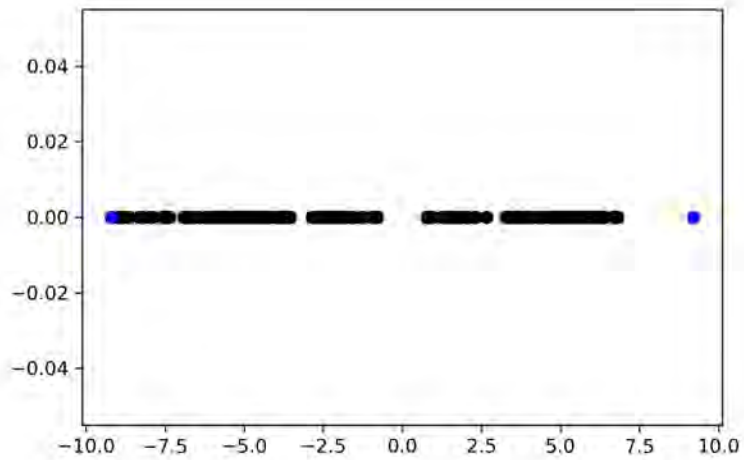


Figure 22.3: The eigenvalues plotted along the x-axis. The blue dots represent the bounds predicted by (22.52). The inaccuracy of the right bound is due to the fact that no orbit stays at the maximum achievable positive value, whereas  $\bar{0}$  is the minimum achievable value. Perhaps a better bound would be  $\approx 7.2$  which is what is achieved by (22.52) if we do not add the radius of two onto the central point ( $2 * \phi$  for Gallas). This could perhaps be justified by some averaging argument.



have no idea how to compare that with the numerically calculated eigenvalues...please help.

And now, a proof of the circle theorem, taken, basically verbatim, from [Wikipedia](#). First, we let  $A$  be a complex matrix, with entries  $a_{ij}$ . Now, we let  $R_i$  be the sum of absolute values of the off diagonal elements on the  $i$ th row:

$$R_i = \sum_{j \neq i} |a_{ij}|$$

We can then define a Gershgorin disc as a disk with radius  $R_i$  centered at  $a_{ii}$  in the complex plane:  $D(a_{ii}, R_i) \subset \mathbb{C}$ . Now, if we let  $\lambda^k$  be the eigenvalue associated with the  $k$ th eigenvector, we can write  $A\vec{x}^k = \lambda^k \vec{x}^k$ , we can always rescale  $\vec{x}^k$ , so we choose to scale it s.t. 1 is the largest value in the vector, allowing us to write

$$\sum_{j \neq i} a_{ij} x_j^k + a_{ii} = \lambda^k, \quad |x_j^k| \leq 1$$

By applying the triangle inequality ( $|\vec{x} + \vec{y}| \leq |\vec{x}| + |\vec{y}|$  note that this expression is valid in any metric space) we can write

$$|\lambda^k - a_{ii}| \leq \left| \sum_{j \neq i} a_{ij} x_j^k \right| \leq \sum_{j \neq i} |a_{ij}| |x_j^k| \leq \sum_{j \neq i} |a_{ij}| = R_i, \quad (22.54)$$

which is Gershgorin circle theorem!

Finally, I am working on improving my code a bit. It is not necessary, but the function which finds the symbol sequences for all prime orbits is painfully slow, so I am working on it. It may be helpful for future group members.

**2021-07-06, 2022-01-22 Predrag** Reposting this, as it is related to yesterday's discussion of how Bloch theorem works for Bravais lattices.

Regarding Sidney's attempt (22.22) to prove that the eigenvalues of the orbit Jacobian matrix  $\mathcal{J}$  are coordinate-choice independent:

The time-evolution Jacobian matrix in general has a different left  $\Gamma(\phi_t)_{ik}$  and right  $\Gamma^{-1}(\phi_0)_{lj}$  [ $d \times d$ ] matrices, they line up only for the period value  $t = n$ , so the periodic boundary condition will have to be a part of your proof.

How the time-periodicity is built into orbit Jacobian matrices is explained by (4.304). From that you can perhaps see how the periodicity is imposed on the coordinate-change Jacobian [ $nd \times nd$ ] matrices  $\Gamma(\Phi)_{lj}$ ...

See whether you can prove it first for the Hill determinant  $\det \mathcal{J}$ ?

To get it for individual eigenvalues, you'll have to write the eigenvalue, eigenvector equation for the orbit Jacobian matrix  $\mathcal{J}$ , then apply coordinate transformation  $\Gamma(\Phi)_{lj}$ .

2022-01-22 Sidney Predrag brings up an interesting method, that I will return to. However, my 2022 January 12th blog entry gives an informal proof showing that the lower eigenvalue bound is variable, thus implying that the eigenvalues themselves vary between coordinate transforms. Does that proof look incorrect?

It is at this point that I am trying to make an attempt at the Bloch theorem. Effectively, Han says that for every repeat of a prime orbit (say a length 3 orbit repeated once to give length 6) gives another Fourier mode. I do not understand why that is, and I'd really appreciate an explanation, but perhaps I can find it in the blog. So, I will make an attempt here, say that I have a length 3 orbit repeated 3 times, making a length 9 orbit in total. According to Bloch, we can write the eigenvector associated with  $\lambda^{(1)}$  as

$$v^{(1)} = \begin{bmatrix} v_1^{(1)} e_0 \\ v_2^{(1)} e_1 \\ v_3^{(1)} e_3 \\ v_0^{(1)} e_4 \\ \vdots \\ v_3^{(1)} e_8 \end{bmatrix}, \quad (22.55)$$

Where  $v_1^{(1)} \dots v_3^{(1)}$  are the elements of the original length 3 eigenvector, and  $e_j = e^{i*j*k}$ . Now, using the length 9, period 3 orbit with Gallas scaling, we see that matching either side of the eigenvalue equation (noting that we are using the new sign definition that was introduced) we get

$$\left( 2\phi_1 - \left( \frac{v_2^{(1)}}{v_1^{(1)}} e_1 + \frac{v_3^{(1)}}{v_1^{(1)}} e_{-1} \right) \right) e_0 v_1^{(1)} = \lambda^{(1)} v_1^{(1)} e_0$$

I need to work on this formula more, this is due to the fact that the fractions next to the remaining complex exponentials have varying indicies, and I need to think of what the pattern is. However, we can say that this is not as helpful as the cat map version, as the eigenvalues do not reduce down to a clean real-number only form... disappointing. How would I plot this? Is this right?

In addition, I think I have an idea as to why having repeats adds one to the available k, it is because the discrete Fourier transform is the generator of the  $C_n$  group, and a repeat adds periodicity, so now there is a first Fourier mode, and a second rotated one available. Is that close?

I am also not sure if in  $e_j$   $j$  should vary from 0 to 8 or from 0 to 2 and just be repeated. Because, the repeated "prime" orbit Jacobian matrix is only block diagonalized by the discrete Fourier, and there should only be 3 Fourier modes, instead of 9 for a prime orbit run through a total of 3 times...Will have to think.

**2022-01-23 Predrag** In the current version of *siminos/reversal/*, Han and I explain the orbit Jacobian matrix spectra of repeats of a prime periodic state  $\Phi_c$ . Each prime periodic state eigenvalue owns one blue sinusoid in figure 24.65, on which all of it repeats lie.

If you Google 'block-circulant matrix', there is a huge literature about their spectra - here is a random DOI. I have not studied it.

**2022-01-23 Sidney** Obviously, I have some reading to do. I found this paper, it seems to be pretty close to what I need to learn. I will read it, along with LC21 [21].

**2022-01-23 Predrag** Gade and Amritkar [14] do orbit stability of repeated blocks in detail: check sect. 11.2.2 *Repeats blog*. They have too complicated off-diagonal entries - rewrite everything for temporal Hénon case, and it will all make sense.

**2022-01-24 Sidney** I saw Han's post, it looks understandable, I will read it, and then extend it to arbitrary period.

Ok, so I think I understand how Han found his eq. (24.390). I can also solve for them using pen and paper via the following method. I can rearrange eq. (24.389) as the following

$$\begin{aligned} \left( -2 \cos(k) \frac{u_{k,1}}{u_{k,0}} + s_0 \right) u_{k,0} &= E_k u_{k,0} \\ \left( -2 \cos(k) \frac{u_{k,0}}{u_{k,1}} + s_1 \right) u_{k,1} &= E_k u_{k,1} \end{aligned}$$

Now, we can define  $\eta \equiv \frac{u_{k,1}}{u_{k,0}}$  and rearrange the above equations to get a quadratic equation in  $\eta$

$$0 = \eta^2 - \frac{s_0 - s_1}{2 \cos(k)} \eta - 1$$

Solving we get

$$E_{k,1,2} = \left( \frac{s_1 - s_0}{2} \pm \sqrt{\left( \frac{s_0 - s_1}{2} \right)^2 + 4 \cos^2(k)} \right) + s_0, \quad (22.56)$$

Inserting period-2 lattice sites field values (22.19) into  $s_0$  and  $s_1$ , this agrees with Han's (24.390).

**2022-01-24 Predrag** Cool!

**2022-01-24 Sidney** We can extend this a bit further by taking Han's equation, and assuming an arbitrary period  $n$

$$-u_{k,(j-1)} e^{i(j-1)k} + s_j e^{ijk} u_{k,j} - u_{k,(j+1)} e^{i(j+1)k} = E_k e^{ijk} u_{k,j}, \quad (22.57)$$

$$u_{k,t} = u_{k,t(\text{mod}(n))}$$

This gives us a set of  $n$  equations, so it is very unlikely that we can get analytic closed forms for these, but perhaps Mathematica, or python could do something?

**2022-01-25 Sidney** PROBLEM: Using eq. (22.57) makes it so we either have imaginary eigenvalues, imaginary eigenvectors, or the only allowed  $u_k$  being period-2. I may have to do more of the readings, but I don't know how to fix this.

**2022-01-28 Sidney** I am still looking at the results of Gade and Amritkar [14], I still need to try to get it to match up with the  $2 \times 2$  case that was worked out above, but it may solve all problems, we'll see.

Anyway, I have been thinking about an interpretation of the orbit Jacobian matrix eigenvalues. And I think I may have come up with one. In CL18 equation 10, we have

$$\mathcal{J}\phi = -M$$

Where  $M$  are the source terms. So, I think that perhaps the orbit Jacobian matrix eigenvalues represent how the field deforms in response to the source terms. Think how the strength and direction of an Electric field shifts in response to point charges being added. This needs to be refined, but I think it may be in the right direction.

**2022-01-30 Sidney** I have done a lot of algebra, and (of course) Han was right, there is no issue with Bloch, it just becomes difficult to evaluate eigenvalues. I will write out all the algebra later. I will now work on figuring out the nuts and bolts of Gade and Amritkar [14].

**2022-01-31 Predrag** I think it would be fastest to compute eigenvalues of all (prime, symmetry reduced) orbit Jacobian matrices up to some periodic state period, let's say 6 or 7, using *any code* that returns the eigenvalues to something like 3-4 significant digits, and plot them along the  $k = 0$  axis of figure 24.69. In contrast to figure 22.3, I would recommend thin line ticks or similar. One also has to keep track of symbolic dynamics of the corresponding periodic states. My draft of email to Bagrov around (4.318) explains why.

Later I would be curious to see whether there is any advantage of diagonalizing these matrices on the reciprocal lattice...

**2022-01-30 Sidney** Is there anything in particular in Predrag's quantum field theory notes that we should try to learn?

**2022-01-31 Predrag** Have look at the start of chapter 4 *Field theory*.

**2022-02-04 Sidney** I have been revisiting Smale horseshoes. I must understand the  $a = 6$  stretching parameter value, and that seems like the first step. I am starting to work with Andrew on this so that he can see if there is a similar limit he needs to work with for the spatiotemporal  $\phi^3$ .

**2022-02-04 Predrag**  $a = 6$  stretching parameter value is not a limit of anything. It's a convenient first integer above the stable/unstable manifold tangency value (4.246).

The full gang, one and all, *must* understand the  $2^n$  Smale horseshoe for  $\phi^3$  1-d forward-in time map, in the  $(\phi_t, \phi_{t+1})$  plane, see [ChaosBook fig. 15.5](#) for Hénon map (3.25), (13.2), and be able to explain to anyone the significance of the  $a$  tangency value (4.246).

**2022-02-04 Sidney** I have been trying to understand the LC21 [21] partition function, I think I'm nearly there. I shall also try to take some notes on the saddle point approximation stuff.

I have started working on producing plots of the repeated lattice state eigenvalues.

Questions:

1. Why is the action the negative inverse temperature multiplied by the system's Hamiltonian?
2. How would I determine which calculated eigenvalue is associated with which mode? I understand that there are  $n$   $r$  eigenvectors, and only  $r$  repeats Fourier modes. But how do I determine, given an eigenvector and its associated eigenvalue, what mode it is associated with? My only thought is that since the second element in the vector is  $v_1 \exp(ik)$ , I could take the ratio of imaginary component and real component, and then the inverse tangent to find  $k$ , but that seems a bit complicated, and inverse tan is a multivalued function.
3. Why are we looking at eigenvalues?
4. Why are we looking at eigenvalues as a function of the Fourier mode?

**2022-02-04 Predrag 2 Han** Sidney questions are all questions that anybody reading LC21 [21]. Can you answer them one by one today, we'll record the answers, and if appropriate, add these video snippets to *LC21.pdf*.

**2022-02-04 Predrag** Hereby resolved in today's meeting:

1. Sidney will, before doing *anything else* for this project, plot the orbit Jacobian matrices eigenvalues of all temporal Hénon prime periodic states up to period 5 or 6, clearly indicating the itinerary of each, as given in table 22.2 and [ChaosBook table 18.1](#), in a plot where one horizontal line of figure 22.3 contains eigenvalues of a single prime periodic state, with lines of shortest periodic state on top, and longer ones on subsequent lines.

2. Then and only then will Sidney attempt to check Han's figure 24.69 for repeats of the above prime primitive cells, i.e., non-zero wavenumbers  $k$ .

2022-02-05 **Sidney** Do you have a copy of Davis [7] *Circulant Matrices*? Gade and Amritkar [14] reference it for block-diagonalizing block circulant matrices.

2021-04-24, 2022-02-05 **Predrag** .

- (1) Please plot the orbit Jacobian matrices eigenvalues of all temporal Hénon prime periodic states up to period 5 or 6, one line per each entry in table 22.2, as we have agreed on Friday, see the above.  
You cannot diagonalize repeats of a period  $n$  primitive cell unless you *first* compute the  $n$  eigenvalues the  $m = 1$  single repeat, i.e., the  $[n \times n]$  orbit Jacobian matrix.
- (2) Yes, we have Davis [7] ([click here](#)) - it is a reference in sects. 2.5 and 11.2.2. It might be useful after you have computed (1).

2022-02-07 **Sidney** I looked at the [14] definition for the block matrices in the block diagonal form of the block circulant matrices:

$$A + \omega_r B + \omega_r^{k-1} C, \quad (22.58)$$

Where  $A$  is the tridiagonal part of the orbit Jacobian matrix, and  $B$  is the matrix with zeros everywhere but for a 1 in the upper right, and  $C$  is the same, except for a 1 in the lower left.

I tried using (22.58) to reproduce (24.390). I did this with the determinant of the matrix

$$\begin{bmatrix} s_0 - \lambda & 1 + e^{ik} \\ 1 + e^{-ik} & s_1 - \lambda \end{bmatrix}, \quad (22.59)$$

This yields the equation  $\lambda_{1,2} = -2 \pm \sqrt{14 + 2 \cos(k)}$  for the appropriate  $s_1$  and  $s_0$ . This does not match Han's equation, although, it gives the correct values for  $k = 0$ . So, this removes my idea of just evaluating the eigenvalues of a given block to place on the plot, any ideas why the discrepancy?

remark 3.2

I have also been looking at some material on deriving the  $a$  tangency value...it is hard. Here are the papers I've been looking at: [Chen](#) and [Devaney and Nitecki \[8\] Shift automorphisms in the Hénon mapping \(1979\)](#). I will also look at [ChaosBook horseshoes](#) and the associated videos.

2022-02-07, 2022-02-20 **Sidney** Predrag had requested a plot with a horizontal line with eigenvalues for each individual prime orbit, labeled by its itinerary. The current version of my plot is figure 22.4, with  $a = 6$  temporal Hénon orbit Jacobian matrix eigenvalues, marked black dots, lumped together by the orbit period  $n = 1, 2, \dots, 12$ , none of them labelled. The

eigenvalues have a remarkable fractal, Cantor set distribution, with a large gap around 0, two smaller gaps around  $\pm 3$ . Turned on the side, they are the values at which every continuous  $k$  family in figure 24.69 crosses the  $k = 0$  axis, implying that our chaotic field theories have fractal spectra, rather than the usual condensed matter bands.

I will understand the nature of these gaps, once I mark the eigenvalues with their itineraries, and identify the sequences that converge to the boundaries of Cantor set gaps, as is done, for example, in figs. 2 and 5 of this [recent publication](#).

I have included the Gershgorin circle theorem bound (22.54), plotted as  $\pm \bullet$ . As expected for  $a = 6$  Hénon, which is barely hyperbolic, and far away from the anti-integrable limit, the bound is not good: the left bound is far off from the most negative eigenvalue. However, the right bound seems surprisingly good. Whys is that? Gershgorin circle theorem is the crudest possible bound, one does not expect it to be a tight bound. The left bound it would be closer if we added 2 to it, perhaps an averaging argument is needed?

I have also verified that under  $\phi \mapsto -\phi$  field redefinition, all eigenvalues in figure 22.4 change sign. As far as I can see here, the most useful information from such plots is that they provide direct evidence that the eigenvalues of the orbit Jacobian matrix are not invariant under field redefinition, as under  $\phi \mapsto -\phi$  field redefinition, all eigenvalues in figure 22.4 change sign.

**2022-02-20 Sidney** Lots of updates. I have a plot of the spectrum of the homoclinic orbits  $\overline{011 \cdots 1}$  and  $\overline{100 \cdots 0}$ , compared to the spectrum of all possible orbits, see figure 22.4. I have gotten up to length 12, and I am working on my code to make longer calculations more feasible.

The eigenvalues are invariant under Gallas rescaling (3.62), or any positive constant scalings.

There is a lot of interesting structure here. Especially the "Christmas Trees" on the left and right, which seem to be contained within the Gershgorin bounds of the fixed points. The most confusing part is the left bound, which seems to be traced out by the spectrum of  $\overline{011 \cdots 1}$ , I am not sure why that is the case. My general theory of this whole thing, is that the location of the orbit Jacobian matrix eigenvalues are organized according the horseshoe structure of the temporal Hénon. I also think that the extremal values should be approaching Han's eigenvalue curves for the temporal cat, as the longer the orbit the closer the orbit Jacobian matrix is to a circulant matrix. Although, this may not be the case, as there is so much structure that is not explained with that idea. A final idea of explanation, is some cycle expansion argument...but I am not sure.

Figure 22.5 is a plot of the period-12 periodic states  $10^{n-1}$  and  $01^{n-1}$  in Fourier space. Questions:

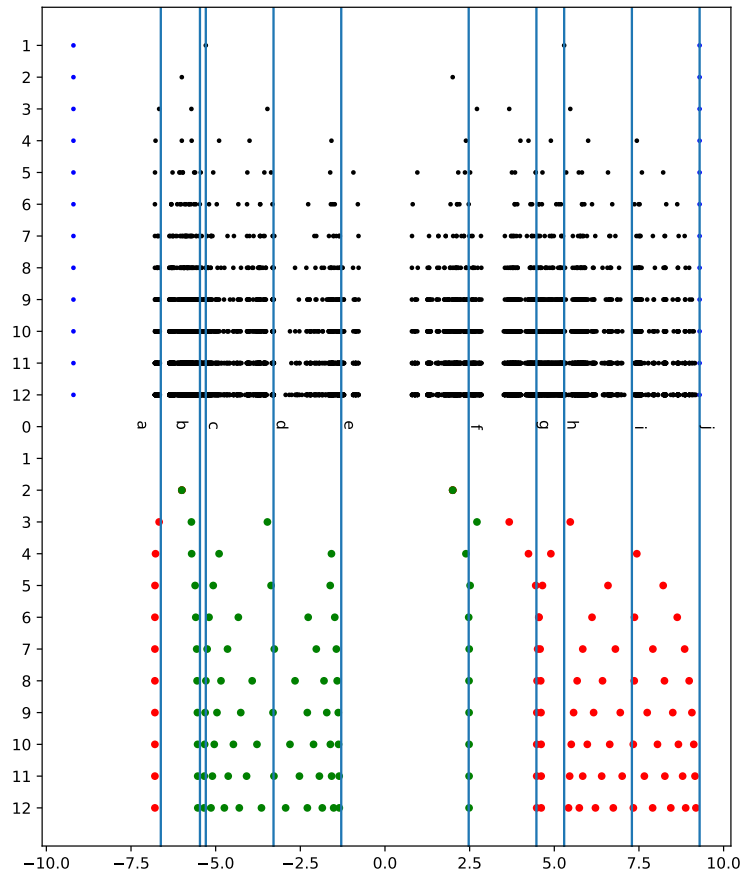
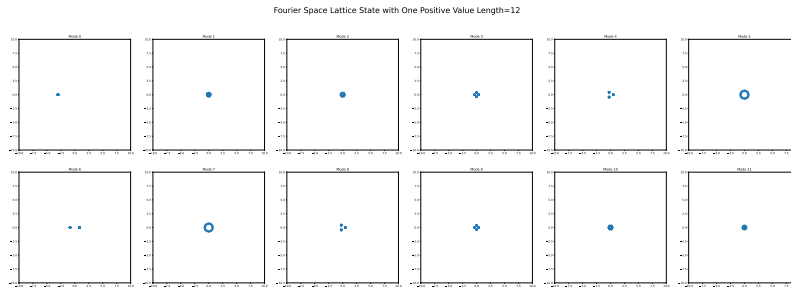
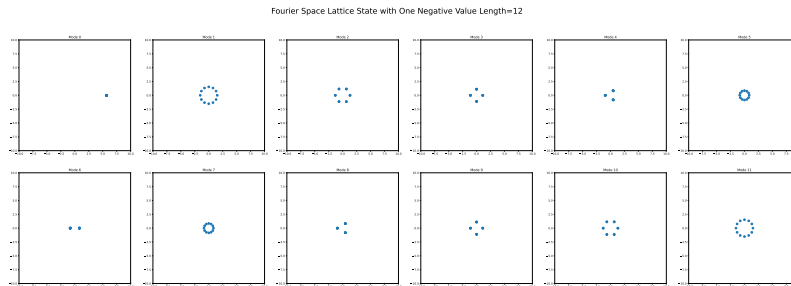


Figure 22.4:  $a = 6$  temporal Hénon (4.187) with Smale horseshoe indicated in figure 5.1. (top frame) orbit Jacobian matrix eigenvalues for all prime orbits of periods  $n = 1$  to 12, plotted on top of each other, with (•) Gershgorin bounds. (bottom frame) The eigenvalues of (red)  $10^{n-1}$  and (green)  $01^{n-1}$ . The vertical blue lines indicate various  $\lambda$  values. The fixed points (4.192) field values  $(\phi_0, \phi_1)$  appear to be the centers of the Christmas trees at  $d = 2a\phi_1$  and  $i = 2a\phi_0$ , bracketed by  $c = 2a\phi_1 - 2 =$  the minimum, and  $e = 2a\phi_1 + 2 =$  maximum Gershgorin bound for  $\phi_1$ ; and  $h = 2a\phi_0 - 2 =$  the minimum, and  $j = 2a\phi_0 + 2 =$  the maximum Gershgorin bound of  $\phi_0$ . Eigenvalue series are also converging to values that presumably have nothing to do with the  $10^{n-1}$  and  $01^{n-1}$  orbits. Period-2 orbit (4.193) field values are  $(\phi_{10}, \phi_{01})$ :  $b = 2a\phi_{10}$  seems close to a series, but not quite. I know numerically calculated period-3 orbit field values:  $f = \sqrt{6} = 2 \times$  the center value of  $\overline{101}$  seems pretty good (at least until I start plotting the differences),  $g = 4.47213 \dots$  which is twice either positive value in  $\overline{010}$  is off the mark, and so is  $a = -6.6204 \dots =$ , which  $2 \times$  the center value of  $\overline{11011}$ .





(a) Fourier transform of the 12 translated periodic states in the  $C_{12}$  orbit of period-12 periodic state  $01^{11}$ .



(b) The same for  $10^{11}$ .

Figure 22.5: We note that  $10^{11}$  modes have larger magnitudes than the corresponding  $01^{11}$  modes. The  $\tilde{\phi}_0$  mode is outside the box, for  $01^{11} \approx -18.0788$ , and for  $10^{11} \approx 34.08$ .

- What does the magnitude mean?  
**Predrag** LC21 sect. 10.1 *Reciprocal lattice states*; radius matters, the phase is just running on a circle.  
 Due to time reversal,  $(\tilde{\phi}_k)^* = \tilde{\phi}_{-k}$ , so the 2nd row of each panel in figure 22.5 is the repetition of the 1st row (for even  $n$ , the  $\tilde{\phi}_{n/2}$  mode is special).  
 $\tilde{\phi}_0$  = is the trace of orbit Jacobian matrix,  $\text{Tr } \mathcal{J} / \sqrt{n}$ , that grows like  $\sqrt{n}$ .
- In the meeting, Predrag kept mentioning that the number of dots related to the number of associated eigenvalues. What is the relation and why?  
**Predrag** phases are proportional to  $k/n$ . For  $n = 12$  you get fractions of form  $p/1, p/2, p/3, p/4, p/6$ , i.e., periods of your circles in figure 22.5 are 1, 2, 3, 4, 6 and 12.

That is all so far. I am going to try to improve my code a bit to find longer orbits (maybe about 20 I think is about what I can expect if I improve it some, and give a day or two for computation time), and I am going to plot the stable and unstable manifold intersections to see how that relates to figure 22.4.

2022-02-20 **Predrag** The  $\phi^3$  field theory is in LC21 defined as (4.187)

$$-\phi_{t+1} + a\phi_t^2 - \phi_{t-1} = 1.$$

2022-02-21 **Sidney** In previous calculations I was using the Gallas scaling (3.62),

$$-\phi_{t+1} + \phi_t^2 - \phi_{t-1} = a,$$

but have now switched to the LC21 convention (4.187).

2022-02-21 **Predrag** The Hénon map, as introduced by Hénon [19], is (4.186). Written as a 2nd-order inhomogeneous difference equation [9], (4.186) takes the *temporal Hénon* 3-term recurrence form (4.187). Its Smale horseshoe is generated by iterates of the region plotted in figure 5.1.

BTW, Xuanqi and I still do not see how our definition (4.216) relates to earlier  $\phi^4$  literature, see sect. 4.12.7, so maybe these definitions do have to be revisited.

2022-02-21 **Sidney** I have changed the symbol sequences and the Fourier plots to the LC21 convention (4.187). I will update the axis size the Fourier plots later this week when I have time.

2022-02-23 **Predrag** In sect. 5.2 *Shadow state method* I explain how to build in symbolic block translations into the defining equations of nonlinear field theories.

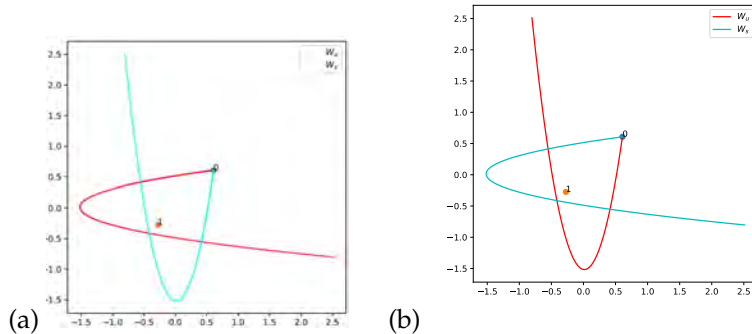


Figure 22.6: (a) Maybe instead I should just plot as was given in the homework 7 code (which is what this was based on) and then flip it over the  $y = -x$  line. Please help. (b) I have added the code which produced this in the same folder as the code for figure 22.6 (b). In this case, there is no issue with double values, so I don't have to plot everything with dots.

**2022-02-26 Sidney** After much fiddling, I was able to get a somewhat decent stable/unstable manifold plot for (4.187). It was strange as I had to use the negative of what python found as the eigenvectors to get something sensible. Of course, a negative eigenvector is still an eigenvector, so it shouldn't matter, but I still found it strange. Additionally, I had to plot everything as dots because the unstable manifold (the manifold which is produced through forward iteration) is double valued after applying the transformation  $x_t \rightarrow -\phi_t$ , and thus when python interpolated a line, it plotted extraneous line segments.

My code is in [williams/python/Misc/](#).

I cannot figure out how to get it to plot the stable manifold (the manifold produced by iteration backwards) first using the reverse iteration (I used equations  $x_{n-1} = y_n$  and  $y_{n-1} = ay_n^2 - x_n - 1$ ). I am thinking I may have to define the timestep Jacobian from these equation to do the backwards iteration manifold creation stuff. But we'll see. Anyway, figure 22.6 (a) is what I plotted.

In figure 22.6 (a) I assumed that the single valued manifold was  $W_s$ . Upon further inspection, this makes sense, as the stable manifold is that which is generated by iteration backwards, and that is what one has to do in order to generate the single-valued manifold. This means that I will need to change the labeling in figure 22.6 (b).

Ideally, I will add several more partitions, and then start explaining the eigenvalue structure of figure 22.4.

ADDITIONAL UPDATE: I tried creating a "y-Jacobian" using the back-

wards iteration equations:

$$\begin{bmatrix} 0 & 1 \\ -1 & 2ay_n \end{bmatrix} \quad (22.60)$$

And it worked! By implementing this Jacobian, I was able to produce figure 22.6 (b). The eigenvalues for this Jacobian evaluated at  $\bar{0}$  are the same as with the "x-Jacobian" which are  $-\sqrt{2\sqrt{7}+7}+1+\sqrt{7} \approx 0.13983$ , and  $1+\sqrt{7}+\sqrt{2\sqrt{7}+7} \approx 7.15168$ , I used this second eigenvalue and its associated eigenvector in the backwards iteration, as this would be the expanding eigenvalue over the course of iteration.

**2022-02-26 Predrag** Your figure 22.6 looks prefect to me - agrees with Chaos-Book.org  $x_t \rightarrow -\phi_t$  figure 5.1, in every detail.

Xuanqi has in his codes' folder the really pretty [xuanqi/matsuoka/](#) python code - you might enjoy it.

**2022-03-03 Sidney** So, I have a couple of new contributions. I have found that my original plan of plotting the stable/unstable manifolds for 10+ iterations is not practical. I am working with Matt to try to improve my code for the root finding, but as of now, I am just going to use an initial partition. Additionally, I have plotted the lattice states in the first partition in 22.7

We can also see where the general structure of figure 22.4 comes from by looking at the homoclinic lattice states plotted by orbit length.

Figure 22.8 shows that the lattice states organize themselves in approximately the same way as the eigenvalues in figure 22.4. Unfortunately, due to the nature of the homoclinic orbits, there are a lot of repeated lattice state values. This means that the exact structure is not replicated, but it seems that the non-diagonal form of the orbit Jacobian matrix spreads out the repeating lattice state values. I am not sure how, or why, but that will be the subject of further inquiry.

Additionally, I saw Harrison's new  $\phi^4$  definition. Should I start looking into the similar  $-\phi_{t+1} + (a\phi_t^2 + s\phi_t) - \phi_{t-1} = 1$ ? I would obviously prefer not to, as there is none of the pre-established nice results (such as Gallas, and the correct  $a$  value, but it may be necessary).

**2022-03-08 Sidney** As of yesterday, we started talking about writing a paper on nonlinear lattice field theory. Personally, I feel that we should at the very least, explain the field theory formulation, and how it applies to our theory (perhaps showing how our  $\phi^4$  theory relates to the one in say David Tong's notes), then presenting Hill's formula, and proving that it still applies in nonlinear theories. Then defining orbit Jacobian matrix  $\mathcal{J}$  with the following lemma:

**Lemma 22.1.** *The orbit Jacobian matrix  $\mathcal{J} \equiv \frac{\delta F[\phi]_i}{\phi_i}$  does not, in general, have eigenvalues which are invariant under smooth coordinate transformations.*

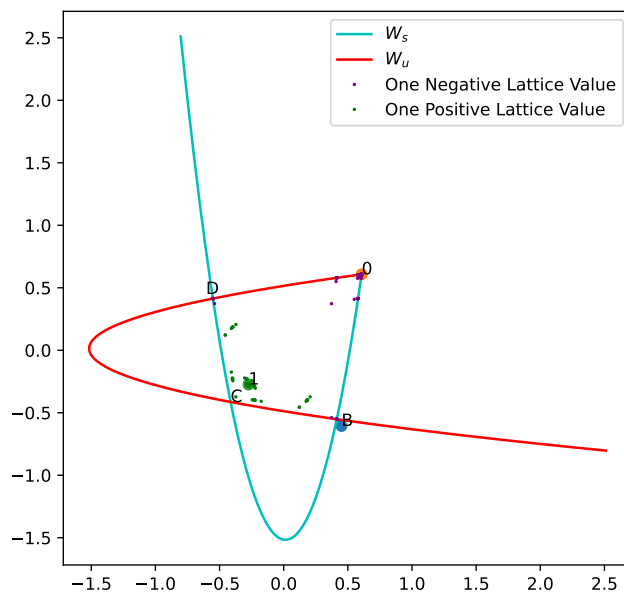


Figure 22.7: Using the LC21 definition of the temporal Hénon I generated the stable and unstable manifolds, and then plotted the homoclinic orbits in the form  $(\phi_t, \phi_{t+1})$ . As can be seen, there is a huge amount of symmetry. Additionally, we can see the 10000... (one negative lattice state) orbit contains all the extremal values achievable by the temporal Hénon which explains why in fig.22.4 all eigenvalues are bounded by the 1000... orbit eigenvalues.

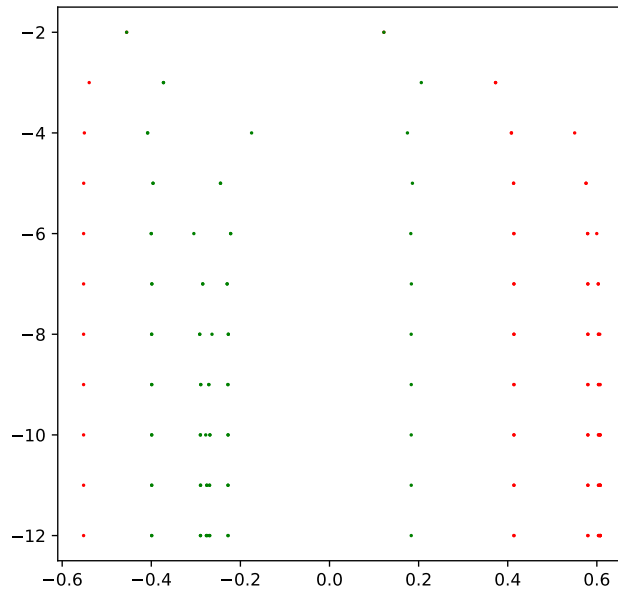


Figure 22.8: Plotting 1000... (Red one negative lattice state) and 01111... (Green one positive lattice state), by orbit length

*Proof.* One only needs to find one example to show this lemma holds. As such, we will consider the orbit Jacobian matrix for the temporal Hénon:  $-x_{t+1} + ax_t^2 - x_{t-1} = 1$ , whose rows are given by  $\text{circ}(2ax_n, -1, \dots, -1)$  with  $n$  entries for a period- $n$  orbit. By the Gershgorin circle theorem, the bounds of this orbit Jacobian matrix eigenvalues are given by  $2ax_{max/min} \pm 2$ . The horseshoe structure of the temporal Hénon gives that either  $x_{max}$  or  $x_{min}$  (depending on coordinate definition) is a fixed point of the map. We can define a smooth coordinate transformation as  $x_n = f(\phi_n)$ , changing the map to  $-f(\phi_{n+1}) + a(f(\phi_n))^2 - f(\phi_{n-1}) = 1$ . By the definition of the orbit Jacobian matrix the rows are given by  $\text{circ}(2af(\phi_n)f'(\phi_n), -f'(\phi_{n+1}), \dots, -f'(\phi_{n-1}))$ . So, the extremal Gershgorin bound associated with the fixed point is  $2af(\phi_{max/min})f'(\phi_{max/min}) \pm 2|f'(\phi_{max/min})|$ . By pulling out the absolute value of  $f'(\phi_{max/min})$ , we obtain

$$|f'(f^{-1}(x_{max/min}))|(\text{sign}(f'(f^{-1}(x_{max/min})))2ax_{max/min} \pm 2)$$

So, unless  $f'(f^{-1}(x_{max/min})) = \text{const}$  (at which point it would be divided out during the coordinate transformation), and  $\text{sign}(f'(f^{-1}(x_{max/min}))) = 1$ , the bound will not be invariant under  $f$ , and thus, the orbit Jacobian matrix cannot have eigenvalues which are invariant under all smooth coordinate transformations. An explicit example would be  $f(\phi) = -\phi$  as  $\text{sign}(f'(f^{-1}(x_{max/min}))) = -1$ .  $\square$

There are lots of other things I plan to do to try to put in the paper, here is a list

- Identify the symmetric and antisymmetric eigenvalues in figure 22.4, and remove the antisymmetric eigenvalues to see if the new structure is the same as figure 22.8.
- Use cycle expansions to calculate the temporal Hénon escape rate use both configuration space, and Fourier space. I honestly don't know how to use the Fourier space in this case, so I will need help with that.
- Fix the labeling in figure 22.7.

I also want to talk with Andrew, Harrison, Han and Ibrahim about what to include in the paper, but I feel like this is a good start.

**2022-03-11 Sidney** Here is a short commit to look at adding the extra linear term to the temporal Hénon through coordinate transform. If we define a mapping  $\phi \rightarrow \varphi + \epsilon$ , then the temporal Hénon becomes  $-\varphi_{t+1} + a(\varphi_t + \epsilon)^2 - \varphi_{t-1} - 2\epsilon = 1$ , rearranging we find  $-\varphi_{t+1} + a\varphi_t^2 + 2a\epsilon\varphi_t - \varphi_{t-1} + a\epsilon^2 - 2\epsilon = 1$ . We do not want extra constants floating around, and the potential of  $\phi^3$  theory is antisymmetric under the transform  $\phi \rightarrow -\phi$  so we want our lattice equation to reflect that, therefore, I am keeping the 1 on the right hand side of the equation. By remembering that we

set  $a = 6$  for full binary symbolic dynamics, we find the new temporal Hénon

$$\begin{aligned} -\varphi_{t+1} + \varphi_t^2 + s\varphi_t - \varphi_{t-1} &= 1 \\ a = 6 \quad s = 4 \end{aligned} \tag{22.61}$$

Note that those values of  $s$  and  $a$  correspond to a transformation  $\phi \rightarrow \varphi + \frac{1}{3}$ . If we look at the proof of lemma 22.1, we see that the transformation applied to obtain (22.61) does not change the distribution of the eigenvalues of the orbit Jacobian matrix. Note that we can have the RHS of (22.61) be  $= 0$  but that would make the map invariant under  $\varphi \rightarrow -\varphi$  instead of antisymmetric, and  $s$  would equal  $2 \pm 2\sqrt{7}$ . I will later explore to see what scaling arguments I can make to mirror Harrison's work on  $\phi^4$ .

**2022-03-12 Sidney** I looked at the eigenvalues and fixed points of this new definition of the temporal Hénon. For the definition with 1 on the RHS the fixed points are

$$\frac{-\mu^2 \pm \sqrt{\mu^4 + 4a}}{2a},$$

where  $\mu^2 = s - 2$  is the Klein-Gordon mass. The orbit Jacobian matrix eigenvalues are just the slope:

$$\frac{dF[\gamma]}{d\gamma} = 2a\gamma + \mu^2 = \pm\sqrt{\mu^4 + 4a}$$

If we use the definition with 0 on the RHS we get fixed points  $0, \frac{\mu^2}{a}$  and eigenvalues  $\pm\mu^2$ . So, it seems that the independence on coupling constant comes directly from the symmetry of the potential under the transformation  $\phi \rightarrow -\phi$ . Note that this analysis shows that should we choose to use the definition with RHS = 0 we would have to choose  $s = 2 + 2\sqrt{7}$  from the  $s = 2 \pm 2\sqrt{7}$  derived in my previous post.

**2022-03-12 Predrag** I believe we have the final formulation of  $\phi^4$  theory, see sect. 4.12.5 *Deterministic  $\phi^4$  lattice field theory*.

**2022-03-12 Sidney** I looked through sect. 4.12.5 *Deterministic  $\phi^4$  lattice field theory*, I still need to work through the algebra, but I think it looks good, however, I am not sure how the values of  $j_t$  were justified, I feel like that would be something good to mention. Anyway, I found a way to finalize the  $\phi^3$  theory. We have our temporal Hénon and multiply both sides by  $-1$  and we get  $\phi_{t+1} - a\phi_t + \phi_{t-1} = -1$ , and then we apply the transformation  $\phi \rightarrow -\gamma + \frac{1}{3}$ , and we get

$$-\gamma_{t+1} + \left(-\frac{g}{2}\gamma_t^2 + s\gamma_t\right) - \gamma_{t-1} = -1$$



Where  $g = 12$  and  $s = 4$ . From my other 2022-03-12 post, I don't think that the coupling coefficient is a mirage, due to the  $-1$  on the RHS which is unfortunate.

Additionally, could someone point me towards the literature where the discrete Euler–Lagrange equation is derived? It confuses me.

**2022-03-14 Sidney** Here is my derivation of what (I think) should be the  $\phi^3$  theory. We begin with the free energy

$$S[\phi] = \sum_z \left\{ \frac{1}{2} \sum_{\mu=1}^d (\Delta_\mu \phi_z)^2 + \frac{\mu^2}{2} \phi_z^2 - \frac{g}{k!} \phi_z^k \right\}$$

The non-Laplacian part, with the cubic Biham-Wenzel lattice site potential, is

$$\bullet -\frac{g}{3!} \phi^3 + \frac{\mu^2}{2} \phi^2 = -A\phi^3 + B\phi^2$$

I will begin by shifting the field by a constant  $\phi \rightarrow \phi + m$  then

$$\begin{aligned} -A(\phi+m)^3 + B(\phi+m)^2 &= -A\phi^3 - 3Am\phi^2 - 3Am^2\phi - Am^3 + B\phi^2 + 2Bm\phi + Bm^2 \\ &= -A\phi \left( \phi^2 + 3m\phi + 3m^2 - \frac{B}{A}\phi - 2\frac{B}{A}m \right) + const. \\ &= -A\phi \left( \phi^2 + \left( 3m - \frac{B}{A} \right) \phi + \left( 3m - 2\frac{B}{A} \right) m \right) + const. \end{aligned}$$

If we drop the constant term, and set  $m = \frac{B}{3A}$

$$\bullet = -A\phi \left( \phi^2 - \frac{B^2}{3A^2} \right) = -A\phi \left( \phi^2 - 3\frac{B^2}{9A^2} \right).$$

Now, defining  $\lambda = B/3A = \mu^2/g$ , noting that  $A\lambda = B/3 = \mu^2/6$ , and rescaling  $\phi \rightarrow \lambda\phi$

$$\bullet = -\lambda^2 \frac{\mu^2}{6} \phi(\phi^2 - 3).$$

**2022-03-14 Predrag** Thanks for fixing the algebra here! I get  $\mu^2/2$  in (??),  $1/2$  of what you have in (22.62).

**2022-03-14 Sidney** **2022-04-03 Predrag superseded by the scaling choice of sect. 4.10** continued: The  $\phi^3$  field theory action is the sum over Lagrangian density per lattice site,

$$S[\phi] = \lambda^2 \sum_z \left\{ \frac{1}{2} \phi_z \square \phi_z - \frac{\mu^2}{3!} \phi_z (\phi_z^2 - 3) \right\}. \quad (22.62)$$

Plugging this into the discrete Euler–Lagrange equation

$$-\square \phi_t + V'(\phi_t) = 0$$

We get

$$-\phi_{t+1} + 2\phi_t - \phi_{t-1} - \mu^2\phi_t^2 + \mu^2 = 0$$

Thus, the fixed points satisfy

$$-\mu^2\phi^2 + \mu^2 = 0$$

Which gives fixed points of  $\pm 1$ .

**2022-03-14 Sidney** **2022-04-03 Predrag** superseded by the scaling choice of sect. 4.10

We can transform this into the classic temporal Hénon by translating the field  $\phi = \varphi + \epsilon$  and rescaling:

$$-\varphi_{t+1} - \epsilon + 2\varphi_t + 2\epsilon - \varphi_{t-1} - \epsilon - \mu^2(\varphi_t + \epsilon)^2 + \mu^2 = 0$$

$$-\varphi_{t+1} + 2\varphi_t - \varphi_{t-1} - \mu^2(\varphi_t^2 + 2\epsilon\varphi_t + \epsilon^2) + \mu^2 = 0$$

$$-\varphi_{t+1} + 2\varphi_t - \varphi_{t-1} - \mu^2\varphi_t^2 - 2\mu^2\epsilon\varphi_t - \mu^2\epsilon^2 + \mu^2 = 0$$

If we define  $\epsilon = \frac{1}{\mu^2}$  we get

$$-\varphi_{t+1} - \varphi_{t-1} - \mu^2\varphi_t^2 - \frac{1}{\mu^2} + \mu^2 = 0$$

$$\varphi_{t+1} + \mu^2\varphi_t^2 + \varphi_{t-1} = \frac{\mu^4 - 1}{\mu^2}$$

Now, we rescale by  $\varphi \rightarrow -c\varphi$  giving us

$$-\varphi_{t+1} + \mu^2c\varphi_t^2 - \varphi_{t-1} = \frac{\mu^4 - 1}{c\mu^2}$$

We now have a system of equations to solve to find  $a$

$$c\mu^2 = a$$

$$\frac{\mu^4 - 1}{\mu^2} = c$$

So,

$$-1 + \mu^4 = a \rightarrow \mu^2 = \sqrt{a + 1} \quad (22.63)$$

**2022-04-03 Predrag** to be recomputed for the scaling choice of sect. 4.10. and we find our temporal Hénon

$$-\varphi_{t+1} + a\varphi_t^2 - \varphi_{t-1} = 1.$$

**2024-03-09 Predrag** Almost agrees with the convention used in ref. [37]. See Xaunqi's (23.54), and the Tiger's nonlinear paper appendix [37] for a concise derivation.

**2022-03-17 Sidney** I am currently working on finding the period 2 points. I will update you on it when I finish.

**2022-03-14 Predrag** I think you got it. Will redo the algebra, see the next edition of sect. [4.12.5](#) *Deterministic  $\phi^4$  lattice field theory*.

**2022-01-02 Predrag** Ultimately, a theorist needs to understand the theory, and for me that is trace formulas, zeta functions, and cycle expansions. Chaos-Book is long. For a quick tour, try taking [Omri Gat's 2015 \*Periodic orbit theory of chaos\*](#) (all of it in a [Mathematica notebook](#)) for a spin. Let me know if that works, maybe some of it can be used to improve DasBuch...

**2022-03-16 Sidney** I have a question. How can we show that the zeta function gives us the same leading eigenvalue as the spectral determinant? I understand heuristically, that for longer orbits we can ignore the corrections and just treat the weight as the product of the expanding eigenvalues, but I am not sure how to be more rigorous with that. The Omri Gat's lecture notes said on page 12 that the zeta function could be expressed as the ratio of two spectral determinants, so for nice enough systems, it would share the same zeros. How would I go about showing that?

**2022-03-16 Predrag** Good questions. I wrote a book that answers them. I recommend reading the relevant chapters, and if answers are not clear, point out here in the blog where the problem is in the text, and I'll try to make them clearer.

**2022-03-14 Predrag** I have redone the algebra, see sect. [4.10](#) *Deterministic  $\phi^3$  lattice field theory*. I get  $\mu^2/2$  instead of your  $\mu^2$ , not sure I'm right.

**2022-03-17 Sidney** You are not right, but it's an easy mistake to fix. In [\(4.149\)](#), you pulled the  $\frac{1}{2}$  out for the discrete Laplacian, but not for the potential term, pulling out for both would give the  $\mu^2$  present in my derivation.

**2022-03-14 Predrag** I must have a blind spot here... For me, the Euler–Lagrange equation functional derivative  $\delta S[\Phi]/\delta\phi_t$  of [\(4.149\)](#) yields

$$-\frac{1}{2}\phi_z\Box\phi_z \rightarrow -\phi_{t+1} + 2\phi_t - \phi_{t-1}. \quad (22.64)$$

and

$$-\frac{\mu^2}{3 \cdot 2}(\phi_z^3 - 3\phi_z) \rightarrow -\frac{\mu^2}{2}\phi_t^2 + \frac{\mu^2}{2}. \quad (22.65)$$

**2022-03-17 Sidney** From previous derivations, I thought that

$$-\phi_z\Box\phi_z \rightarrow -\phi_{t+1} + 2\phi_t - \phi_{t-1}. \quad (22.66)$$

This intuition (although possibly wrong) came from the original  $\phi^3$  derivation, and the current  $\phi^4$  derivation. However, if [\(22.64\)](#) is correct, so is the  $\frac{\mu^2}{2}$  actor.

**2022-03-17 Predrag** Mhm... It is not an intuition, it's a calculation. Please do the calculation, convince yourself. Never trust other people's calculations. Especially professors' :)

**2022-03-17 Sidney** My zeta function question: in [ChaosBook sect. 22.3 Dynamical zeta functions](#) there is only the statement that as  $rT_p \rightarrow \infty$  the dominant term from  $|\det(1 - M_p)|$  becomes  $|\Lambda_p|$ , the product of the expanding eigenvalues of the orbit. However, to me this seems only valid for long orbits, instead of every orbit (which the zeta function is built out of). Additionally, this would seem to imply that the zero is only an approximation to the leading zero of the determinant, which I do not believe it is.

**2022-03-17 Predrag** Every prime orbit repeated  $r$  times is a long orbit, dominated by  $|\Lambda_p^r|$ . The next eigenvalue is 1, or exponentially shrinking, so  $|\det(1 - M_p^r)| = |\Lambda_p^r| + O(1)$ .

You have studied [ChaosBook sect. 21.1.1 Hyperbolicity assumption](#) and understand that the hyperbolicity is the key to everything? Assuming that one has read this, what do you suggest I change in [ChaosBook sect. 22.5 Spectral determinants vs. dynamical zeta functions](#)?

**2022-03-17 Sidney** I would personally much appreciate a sketch of how to write the zeta function as a ratio of determinants as mentioned in the Omri Gat lecture, ideally with a sentence pointing out how writing it in such a fashion shows that the spectral determinant, and the dynamical zeta function share a leading zero.

**2022-03-17 Predrag** I assume you have studied [ChaosBook sect. 22.5 Spectral determinants vs. dynamical zeta functions](#) and all examples of this section. What should I elaborate? Maybe if you write up here what you feel would help other readers, I can include it into ChaosBook.org text?

**2022-03-17 Sidney** I have read both of those sections, though not closely enough to make comments, I will reread, and get back to you. Likely, this is all due to me not thinking hard enough!

**2022-03-19 Sidney** I have not yet finished figuring out the zeta function stuff... soon hopefully. Anyway, I was looking at [sect. 4.1 Lattice discretization of a field theory](#), and I think there may be a mistake in (4.7), I believe that the  $\partial_\mu$  should be  $\partial_\mu^2$  so as to accurately be kinetic energy, and to match with the box operator clearly being a second derivative. Additionally, I am really unsure how in (4.7)  $(\partial_\mu \phi(x))_z^2 = -\phi_z \square \phi_z$  please enlighten me.

**2022-03-20 Predrag** In continuum the sign comes from integration by parts. In discretized field theory it comes from the matrix transposition of the difference operator: [ChaosBook sect. A24.1.1 Lattice Laplacian](#).

**2022-03-21 Sidney** I am still looking at [ChaosBook sect. A24.1.1 Lattice Laplacian](#), but I think I have an argument for pulling out the  $\frac{1}{2}$  in our  $\phi^3$  theory. The variational extremization condition (4.53) is

$$\frac{\delta S[\Phi]}{\delta \phi_z} = 0$$

If we apply this to our  $\phi^3$  action, we find

$$\frac{\delta S[\Phi]}{\delta \phi_z} = \frac{\mu^4}{2g^2} \frac{\delta}{\delta \phi_{z'}} \sum_{z'} \{-\phi_{z'} \square \phi_{z'} - \frac{\mu^2}{3} (\phi_{z'}^3 - 3\phi_{z'})\} = 0 \quad (22.67)$$

Dividing through by the constants, and assuming that our action sum converges absolutely, and uniformly (par for the course in variational calculus), we obtain

$$\sum_z \{-\square \phi_z - \mu^2 (\phi_z^2 - 1)\} = 0$$

Which gives us our lattice Euler-Lagrange equation

$$-\square \phi - \mu^2 (\phi^2 - 1) = 0$$

$\frac{1}{2}$  free! Anyway, now it 3zis time to learn how to evaluate lattice states.

**2022-03-22 Predrag** I'm sorry, but

$$\frac{d}{dx} \frac{x^3}{3!} = \frac{x^2}{2},$$

there is no sum, and there is no term in (22.67) that is correct. For me (4.53) leads to (4.150).

**2022-03-22 Predrag** I have an offer to you that you cannot refuse:)

Read sect. 4.10 *Deterministic  $\phi^3$  lattice field theory*, in particular the main result (4.150). It removes the pesky  $1/2$ .

The reason I prefer temporal Hénon period-1 periodic states to be  $\pm 1/2$  is that now their separation is 1, giving a very pretty shadow state table 5.2. Please recompute this table for action (4.149).

**Period-2 periodic states. (PLEASE COMPUTE THIS)**

Please recompute conversion from  $a$ -parameter Hénon action to the current  $\mu^2$ -parameter action (4.149). Hill determinants should remain the same, but orbit Jacobian matrix spectra will change.

Once you are confident that you can convert all your already computed periodic states, can we decide that (4.150) is the final form of  $\phi^3$  theory for the contemplated publication?

**2020-03-22 Predrag** If you ever want to cross-check your temporal Hénon periodic states, check out the first two formulas in *Beyond the periodic orbit theory*.

**2022-03-22 Sidney** I corrected (22.67), by adding the derivative, there should be a sum as I am keeping with Munster's action which is a sum over all lattice states. Could you please enlighten me on how

$$\frac{\delta}{\delta\phi_z} \left( \sum_z \frac{1}{2} \phi_{z'} \square\phi_{z'} \right) = \square\phi_z$$

If I assume that  $\square\phi_z$  is a different variable from  $\phi_z$  (similar to how the Euler–Lagrange equations treat  $x$  and  $\dot{x}$  as different variables), taking the derivative would give  $\frac{1}{2}\square\phi$ . However, if we expand out the box operator for a temporal lattice, and apply the product rule, we find that taking the derivative gives  $\frac{1}{2}(\phi_{t-1} - 2\phi_t - \phi_{t+1} - 4\phi_t)$  (because  $\phi\square\phi = \phi(\phi_{t-1} - 2\phi_t + \phi_{t+1})$ ).

Additionally, there should be an extra  $\lambda$  in this:

$$V_1(\phi) = -\frac{g}{3!}\phi^3 + \frac{\mu^2}{2}\phi^2 \rightarrow -4\lambda^2\mu^2\left(\frac{\phi^3}{3} - \frac{\phi^2}{4}\right).$$

somewhere, as  $\phi \rightarrow 2\lambda\phi$  means  $\phi^3 \rightarrow 8\lambda^3\phi^3$  I will investigate later.

**2020-03-22 Predrag** Do you compile LaTeX before you committing it? It's

`\Box` , not `\box`

**2022-03-25 Predrag** Matt commits a breakthrough, see page 269. Should work equally well for  $\phi^3$  / temporal Hénon.

**2022-03-27 Matt** Regarding the functional derivative and factor of one half. I think there is nuance resulting from discretization which is causing the issue; in fact I think this is one of the points implicitly captured by professor Tao's statement

"The only difference is we first do the first variation of the action and then discretize the Euler–Lagrange equation, and you first discretize the action (for impeccable reasons) and then do the variation."

Anyway, looking at the statement

If I assume that  $\square\phi_z$  is a different variable from  $\phi_z$

This begs the question: *why do we even do this in the continuous case?* Any second order system requires two values to specify the state, the position and velocity. In the continuous case, we have to specify the velocity independently because at any *instant* in time there is no other way of doing

so. However, the discrete differentiation operator requires, *by definition*, two values; in this case are the field values at different times. In other words upon discretization, the first order derivative is uniquely defined by the "position". It is no longer an independent instantaneous tangent known as "velocity".

What does this look like in terms of the action functional? We need to rethink the Lagrangian; instead of being defined as  $\mathcal{L}(t, \phi, \dot{\phi})$ , the discretized functional (on a uniformly spaced lattice) can be defined by  $\mathcal{L}(\phi_z, \phi_{z+1})$ .

Formal definitions of "discretization" are how mathematicians keep the lights on; but I think Cuell and Patrick [4] *Geometric discrete analogues of tangent bundles and constrained Lagrangian systems*, [arXiv:0807.1511.pdf](#), does a good job of summarizing my point:

In the discrete context, the association of configurations to points of velocity phase space is artificial — like the invocation of a metric or connection where none is really natural. This, of course, is somewhat unintuitive after such concentration on the continuous systems. The reflex to associate a unique configuration to a velocity has to be unlearned.

All of this to explain a rational number; how do we then take the functional derivative? Well, first we need to explain the action functional more precisely. We are saying there isn't a difference between contravariant and covariant derivatives in this case; typically you need to write something like  $\partial_\mu \phi \partial^\mu \phi$  which are related by the metric  $\partial_\mu \phi = \eta_{\mu\nu} \partial^\nu \phi$ , which we are taking to be the identity, hence why rewriting  $(\partial_\mu \phi)^2$  into  $\phi \square \phi$  without any extras was possible in the first place. Additionally, the functional derivative commutes with these partial derivatives; this requires writing too many indices so I leave the proof to the internet. Applying the functional derivative to the action functional, written in a vector notation  $\phi^\top \square \phi$  we get  $\phi^\top \square + \square \phi$ . This looks like we're adding row and column vectors, but it's just another one of those things taken for granted; the box operator being self-adjoint results in  $\square^\top \phi + \square \phi = \square \phi + \square \phi = 2 \square \phi$ , hence the factor of one half yields  $(\frac{\partial}{\partial \phi} [-\frac{1}{2} \phi \square \phi]) = -\square \phi)_z = -\phi_{z+1} + 2\phi_z - \phi_{z-1}$  as desired.

**2022-03-30 Sidney urgent** to all Tigers (relating to the calculations to be included in our planned siminos/tigers/ paper):

How is eq. [ChaosBook \(20.17\)](#) derived? I can see how taking the spatial average over x and y of  $L^t$  would make the Dirac delta contribution in L an identity, which in turn would give something that looks very close to

$$\langle e^{\beta A} \rangle = \frac{1}{|M|} \int_M dx e^{\beta A}$$

however, since we would take two space integrals, there should be a  $\frac{1}{|M|^2}$  term instead of a  $\frac{1}{|M|}$  term, how do I resolve that so that I can reproduce eqn. (20.10) from eq. (20.17)?

I need to understand this **as soon as possible**, as I am going to present it tomorrow in **week 11, Thursday lecture**. We can meet any time at our usual Zoom link, if you want to discuss this. You are encouraged to join the presentation, as it is essential to our planned *Nonlinear deterministic field theory*.

**2022-03-31 Predrag** I cannot see your figures, as LaTeX does not like spaces in file names. Intriguing that your configuration of MS Windows does not mind, but do avoid spaces anyhow, because Linux does mind.

**2022-03-31 Predrag** Escape rate is defined many times, see for example **Chaos-Book eq. 1.7**.

**2022-04-03 Sidney** I am now going to write out my **ChaosBook.org/course1, ChaosBook Chap. 22 Spectral determinants discussion presentation**:

First, we expect the averaged value of the integrated observable

$$\langle e^{\beta A} \rangle$$

to decay or grow exponentially because we expect (with mixing) that the time average along all trajectories to approach the same value  $\bar{a}$ , and the integrated observable to approach  $\bar{a}t$ . So we can write

$$\langle e^{\beta A} \rangle \rightarrow (const)e^{ts(\beta)}$$

This fact means that we can write the integral

$$|\mathcal{M}(t)| = \int_{\mathcal{M}} dx dy \delta(y - f^t(x)) \sim |\mathcal{M}(0)| e^{-\gamma t}$$

Which is telling us that the state space volume is contracting exponentially at rate  $\gamma$ . Now, we can write the fraction of trapped trajectories as

$$\Gamma_{\mathcal{M}}(t) = \frac{\int_{\mathcal{M}} dx [\mathcal{L}^t \rho](x)}{\int_{\mathcal{M}} dx \rho(x)}$$

This effectively reads, "divide the number of trajectories contained in  $\mathcal{M}$  after time  $t$  by the initial number of trajectories". By expanding the density in the eigenfunction basis of  $\mathcal{L}$  we get  $\rho = \sum_{\alpha} a_{\alpha} \varphi_{\alpha}(x)$ . Plugging this expansion into our integrals we obtain

$$\Gamma_{\mathcal{M}}(t) = e^{s_0 t} \left( (const.) + O\left(e^{(s_1 - s_0)t}\right) \right)$$

where  $e^{s_0 t}$  is the leading eigenvalue of  $\mathcal{L}^t$ . This gives us the relation  $\gamma = -s_0$  from the volume contraction statement earlier. Now, if we move



onto the spectral determinant  $\det(1 - z\mathcal{L})$ , we note that the values of  $z$  at which this polynomial is zero are actually the inverse of the eigenvalues of  $\mathcal{L}$  due to the nature of the characteristic polynomial. I feel that it is not made particularly clear that this is the case in [ChaosBook eq. \(21.20\)](#), but I was rushed, and that could also be the answer.

So, we can write that the leading eigenvalue of  $\mathcal{L}$  is actually the inverse of the smallest (in magnitude) root of the spectral determinant, or the dynamical zeta function. Although, I am not completely sure what to do about signs. For example, the Hénon cycle expansion of the dynamical zeta function had two zeros  $\approx -10$  and  $\approx 2$ . My thought is that the escape rate should be  $\approx \ln(2)$  as  $\gamma = -s_0 \approx -\ln\left(\frac{1}{2}\right) = \ln(2)$ . Is this correct?

**2022-04-03 Predrag** No.

**2022-04-03 Sidney** Anyway, the next step is to finish calculating the length 3 points analytically, as [listed in](#) Endler and Gallas [12].

Then, I will look at a more exact cycle expansion of the dynamical zeta function. Additionally, I need to implement finding the symmetric and antisymmetric eigenvalues of the orbit Jacobian operator, should not be hard. And finally, I need to actually write out a good zeta function expansion in my, or Matt's (well a copy of) code.

I am well aware that my explanation here of escape rates was a little hand-wavey, any tips on tightening it up would be very much appreciated.

**2022-04-03 Predrag** Euler–Lagrange equation (21.271) is superseded by (4.150) of sect. 4.10 *Deterministic  $\phi^3$  lattice field theory*, please use that definition from now on.

**2022-04-04 Sidney** I will rederive (22.63).

**2022-04-04 Sidney** There seems to be a lot of errors in compiling the blog (even if I try to just do FTlatt blogSVW and blogAJF)

**2022-04-04 Predrag** You always have to

*svn up siminos*

update the entire repository, not just a subfolder or file.

*siminos/inputs/biblatex.tex* has changed as there is a conflict with *includeOnly* in the current release.

If that fails, uninstall *MikTeX*, and install the current version. That is safe, does not affect any edits in *siminos*. If that fails, ask Tigers for help again.

**2022-04-04 Sidney** Could anyone please explain how "So, we can write that the leading eigenvalue of  $\mathcal{L}$  is actually the inverse of the smallest (in magnitude) root of the spectral determinant, or the dynamical zeta function.

Although, I am not completely sure what to do about signs. For example, the Hénon cycle expansion of the dynamical zeta function had two zeros  $\approx -10$  and  $\approx 2$ . My thought is that the escape rate should be  $\approx \ln(2)$  as  $\gamma = -s_0 \approx -\ln(\frac{1}{2}) = \ln(2)$ ." Is this not correct?

**2022-04-04 Predrag** No. There is no substitute for elbow grease. Work through

1. [ChaosBook sect. 1.5 Chaos for cyclists](#)
2. [ChaosBook sect. 18.4 Topological zeta function](#)
3. [ChaosBook sect. 27.1 Escape rates](#)

I suspect you are mistaking the topological zeta function (counting only, complete Hénon horseshoe entropy  $h = \ln 2$ ) for the non-trivial, dynamical, instability weighted zeta function.

**2022-04-10 Sidney** Lots of work...not enough results, but I will report on what I did succeed in, and ask questions in what I am confused about. I now understand the dynamical zeta function zeros that I was having issues with. First, in (22.63) we note that the only change between that  $\phi^3$  definition and the current one is that the constant  $\mu^2$  term in the initial definition is now  $\frac{\mu^2}{4}$  so  $-\varphi_{t+1} - \varphi_{t-1} - \mu^2\varphi_t^2 - \frac{1}{\mu} + \frac{\mu^2}{4} = 0$ , so our system of equations (just following through the original derivation) becomes

$$c\mu^2 = a$$

$$\frac{\mu^4 - 4}{4\mu^2} = c$$

So  $\mu^4 - 4 = 4a$  or

$$-4 + \mu^4 = 4a \rightarrow \mu^2 = 2\sqrt{a+1} \quad (22.68)$$

**2024-03-09 Predrag** Agrees with the convention used in ref. [37]. See Xaunqi's (23.54), and the Tiger's nonlinear paper appendix [37] for a concise derivation.

**2022-04-10 Sidney** Using this, we can now establish a map from temporal Hénon to  $\phi^3$  and back

$$-\phi_{t+1} + a\phi_t^2 - \phi_{t-1} = 1 \rightarrow -\varphi_{t+1} + 2\varphi_t - \varphi_{t-1} - \mu^2\varphi_t^2 + \frac{\mu^2}{4} = 0 :$$

$$\phi = -\frac{2\sqrt{a+1}}{a}\varphi + \frac{1}{a}$$

$$-\varphi_{t+1} + 2\varphi_t - \varphi_{t-1} - \mu^2\varphi_t^2 + \frac{\mu^2}{4} = 0 \rightarrow -\phi_{t+1} + a\phi_t^2 - \phi_{t-1} = 1 :$$

$$\varphi = -\frac{a}{2\sqrt{a+1}} + \frac{1}{2\sqrt{a+1}} \quad (22.69)$$

Both of the maps given here are smooth, so we know that the Floquet multipliers are invariant, and so any cycle expansion work done for temporal Hénon or for  $\phi^3$  applies to either map. Speaking of cycle expansions, I have nearly completed my dynamical zeta function cycle expansion code. I am thinking I'll use my root from my quadratic approximation as my initial guess for the Newton solver. Additionally, if we look at (22.69) we see that the  $\phi^3$  theory period-2 periodic states (4.156) that Predrag calculated are incorrect, and should be

$$\frac{2 \pm \sqrt{3}}{2\sqrt{7}}. \quad (22.70)$$

**2022-04-10 Sidney** I have been trying to figure out how to extract the "symmetric" eigenvalues from a given orbit Jacobian operator. My initial thought was to apply the appropriate projection operator to the orbit Jacobian operator, and find those eigenvalues. However, that is wrong. I know that if I use the permutation matrix which leaves a given lattice state invariant to block diagonalize the orbit Jacobian operator, one of the submatrices will be associated to the symmetric subspace, and the other to anti-symmetric subspace, and then I can find the eigenvalues of that specific submatrix. However, I don't know how to automate this for python, or even how to tell which block is which if the two subspaces are of equal size. Can someone please help me with this? I feel like this is the key to understanding my earlier eigenvalue plots.

**2022-04-11 Predrag** Have you tried using (Newton's, I believe) expansion (24.331) of a determinant in terms of traces?

**2022-04-13 Sidney** I have not yet, hopefully this week. Anyway, I have been working on calculating the escape rate for my temporal Hénon or the  $\phi^3$ . Any advice would be great. I am getting imaginary roots for my zeta function expansion. Here is my code

```
def dyn_zetafunc_expansion(order, cycles):
    zeta=1
    z = sp.Symbol('z')

    for item in cycles:
        if len(item)>order:
            break

    timejacob=np.identity(2)

    for point in item[::-1]:
        timejacob=np.matmul(timejacob,timestep_jacobian(point)[0])

    vals,vecs=np.linalg.eig(timejacob)
```

```

expandval=np.prod(vals[(np.abs(vals)>1)])

zeta=zeta*(1-z**(len(item))/expandval)

zeta = ( zeta.expand() + sp.O(z**(order+1)) ).removeO()

print("zeta function at order: ", order)
print(zeta)

# for efficacy, we choose to use np.roots() instead sp.solve()
coe = sp.Poly(zeta, z).coeffs() # get the coefficients => a_n, a
zps = np.roots(coe) # find the zeros points of zeta function
minzero=zps[np.argmin(np.abs(zps))]
escape=np.log(minzero)

return escape

```

Is there anything here where I was doing something stupid? Here is the path to the code:

[/siminos/williams/python/relax](#)

I have labeled it with "cycle expansion" on the end.

**2022-04-13 Predrag** On reinventing the wheel: there is a bunch of codes around that generates cycle expansions for various situations, see page [510](#).

**2022-04-17 Sidney** I am aware that reinventing the wheel is not necessary, however, I wanted to take this as an exercise to try to fully understand cycle expansions. Unfortunately, I have run into a major problem: analytically calculating the escape rate up to order 2 gives me an imaginary root...which matches with my code. So, something is very wrong. I have used just the basic Hénon map [\(3.5\)](#) so as to not to confuse myself with our myriad of coordinate changes:

$$\begin{aligned}x_{n+1} &= 1 - ax_n^2 - y_n \\ y_{n+1} &= x_n\end{aligned}\tag{22.71}$$

This gives me the 1-time-step Jacobian matrix [\(3.45\)](#)

$$J = \begin{bmatrix} -2ax_n & -1 \\ 1 & 0 \end{bmatrix}\tag{22.72}$$

Now, the fixed points are  $\frac{-1 \pm \sqrt{7}}{6}$  and the period-2 points are  $\frac{1 \pm \sqrt{3}}{6}$ . We can calculate the eigenvalues for  $J_0$ ,  $J_1$  and  $J_{10}J_{01}$  to find

$$\Lambda_1 = \sqrt{2\sqrt{7} + 7} + \sqrt{7} + 1, \quad \Lambda_0 = 1 - \sqrt{7 - 2\sqrt{7}} - \sqrt{7},$$

and  $\Lambda_{10} = -5 - 2\sqrt{6}$ . Using the order 2 cycle expansion

$$1 - \left(\frac{1}{\Lambda_0} + \frac{1}{\Lambda_1}\right)z - \left(\frac{1}{\Lambda_{10}} - \frac{1}{\Lambda_0} \frac{1}{\Lambda_1}\right)z^2 = 0 \quad (22.73)$$

we ONLY get imaginary zeros. What is wrong? Additionally, we only get a negative zero for an order one approximation, which does not work with the logarithm.

**2022-04-18 Predrag** Use  $1/|\Lambda_p|$ , absolute value weights.

**2022-04-18 Predrag** Looking at [ChaosBook fig. 15.5](#), I expect  $\Lambda_1$  to be negative and smaller in magnitude than the positive  $\Lambda_0$ , due to its proximity to the near stable / unstable manifold tangency.  $\Lambda_p$  are tabulated in [ChaosBook exer. 7.2](#).

**2022-04-20 Sidney** I was able to get an escape rate of  $\gamma = 0.6421284201916422$  with an order 12 cycle expansion of the dynamical zeta function. From fixed points alone I get  $\gamma = 0.73713426$ , already OK to 10%. However, I am not sure how well this is converging as I tracked the differences between orders from order 1 to order 12 and got the following

$$|\gamma^{(i)} - \gamma^{(i-1)}| = \begin{bmatrix} 0.17897830012360127 \\ 0.14845337007623427 \\ 0.0742695173094986 \\ 0.0010576075438910593 \\ 0.007391408206467331 \\ 0.003993490989758652 \\ 0.0006028655480873057 \\ 0.0001069284762463818 \\ 4.289378461741489e - 05 \\ 2.0835294710641605e - 06 \end{bmatrix} \quad (22.74)$$

Note that I did not take any logarithms, could someone please explain why I should do that? I know that it should be converging exponentially, but I don't think the exponential factor is constant...

**2022-04-21 Predrag** See discussion around eq. [\(22.79\)](#).

**2022-04-20 Sidney** What is the point of developing all of this field theory formalism, if it is my belief that it falls apart when faced with a dissipative system? The nonlinear dynamics systems we are primarily interested in are all dissipative.

**2022-04-21 Predrag** Can you reread the discussion of humble parabola [Chaos-Book example. 3.7](#)? Our formulation of spatiotemporal field theory applies to both phase-space volume preserving as well as phase-space contracting (dissipative) systems. Han and I chose to illustrate 'dissipative' systems by the piece-wise linear temporal Bernoulli, rather than by the

nonlinear  $|b| \rightarrow 0$ , Hénon  $\rightarrow$  parabola, to keep the things as simple as possible, as well as for its relation to the temporal cat.

**2022-04-21 Predrag to all Tigers** If anyone wants to advance this discussion to a deeper level - it would be very welcome to write that up for our (forthcoming?) publications: while our 'Euler-Lagrange equations' work for all (discretized) systems, action formulation applies only to the Hamiltonian systems. Biham-Wenzel [3] ([click here](#)) discuss in detail how they get their 'Euler-Lagrange equations' for the dissipative case.

**2022-04-22 Sidney** I will look at the dissipative discussion, and related paper later, hopefully tomorrow. Anyway, I have figured out how to extract the symmetric eigenvalues. First, I take each orbit of interest and see what permutation matrix commutes with the associated orbit Jacobian operator, this is done through this code snippet here:

```
def permutation_mat(orbit):
    n=len(orbit)
    I=np.identity(len(orbit))
    m=1

    for i in range(len(orbit)):
        if(i != n):
            for j in range(i+1, len(orbit)):
                if(abs(orbit[i]-orbit[j]) <= 1e-7):
                    I[[i, j]]=I[[j, i]]
                    m += 1
                    n=j
                    break
            if((i+m)==(len(orbit)+1)):
                break
    return(I)
```

Then, I can use this permutation matrix to construct a projection operator into the symmetric subspace, by taking the trace of this operator, I can find the dimension of the subspace (I don't 100% understand that yet, will explore and learn). From there, I find the eigenvectors of the permutation matrix and use that to form an ordered matrix, where the order is columns symmetric under application of the permutation are placed furthest left, and those antisymmetric furthest right. I then use this matrix to block diagonalize my orbit Jacobian operator, and as the eigenvectors were ordered, I know that the upper-left block is the symmetric block of the orbit Jacobian operator, and thus contains the symmetric eigenvalues (in fact, if I do what I was talking about in my last post—write out the temporal Hénon while taking symmetries into account, and then find the orbit Jacobian operator for the reduced system of equations—I obtain this upper-left block). I then store the dimension of the symmetric subspace

and the block-diagonalized orbit Jacobian operator, and use the dimension of the subspace to extract the upper left block. This can then be used to find the desired eigenvalues. I do all this with the following code snippet:

```
def blockdiag_orbit_jacobian(orbit, orbitlength, k):
    J=orbit_jacobian(orbit, orbitlength, k)
    P=permutation_mat(orbit)
    Proj=0.5*(permutation_mat(orbit)+np.identity(len(orbit)))
    d=np.trace(Proj)

    D, Sn=np.linalg.eig(P)
    S=np.zeros(np.shape(Sn))
    Asym=np.zeros([len(Sn[:,0]),int(len(Sn[:,0])-d)])
    iglob=0
    jglob=0
    for i in range(0, len(Sn[:,0])):
        if (np.linalg.norm(np.matmul(P, Sn[:,i])-Sn[:,i])<1e-6):
            S[:,iglob]=Sn[:,i]
            iglob+=1
        else:
            Asym[:,jglob]=Sn[:,i]
            jglob+=1

    S[:,iglob:(iglob+jglob)]=Asym
    BJ=np.matmul(np.linalg.inv(S), J, casting='same_kind')
    BJ=np.matmul(BJ, S, casting='same_kind')
    BJ[np.abs(BJ) < 1e-6] = 0

    return BJ, d
```

Note that I have included the updated code in the repository, and the only reason I have full code snippets here is because I can give context to them, and a heuristic explanation. Additionally, if any tiger wants to give me suggestions on how to speed this up, please do, it's pretty fast already, but faster is always better.

Anyway, this works, but I still feel like there should be a more systematic way to just find the eigenvalues associated with a specific subspace. I know that there is a trace formula for a specific subspace, and a determinant (as derived by Han earlier) but those only give the sum, and product of the desired values, which is not helpful in actually finding anything, except in very fringe cases.

**2022-04-20 Sidney** I have continued to try to find a way to extract the symmetric eigenvalues from the orbit Jacobian operator. I have determined how to for symmetries of the form  $x_0x_1x_1x_0$  and  $x_0x_1x_1$ , but I cannot find a

way for  $x_0x_1x_2x_1$  as with longer strings I think I could have a string of the form  $x_0x_1x_2x_3x_4x_1x_5x_6$  and that would break my pattern... so again, I implore how do I systematically extract the symmetric/antisymmetric eigenvalues from a matrix which commutes with a permutation matrix?

**2022-04-20 Sidney** So far, I have written our the temporal Hénon equation over and over again applying the symmetry, and then thrown out the repeated equations, this can work for two of the symmetries, but not the third, unless I am misunderstanding. Please help.

**2022-04-21 Han** You should ...

**2022-04-22 Predrag** See figure 6.1 and (6.14–6.17). This is explained in detail in LC21 [21]. Your examples in the above post are:

(eo)  $\phi_0\phi_1|\phi_1\phi_0|$ , swap the 'reds' and 'blues' in figure 6.1 (eo)

(o)  $\boxed{\phi_0}\phi_1|\phi_1$

(ee)  $\boxed{\phi_0}\phi_1\boxed{\phi_2}\phi_1$ , two fixed 'yellow' sites, the rest in figure 6.1 (ee) swapped

(a)  $\phi_0\phi_1\phi_2\phi_3\phi_4\phi_1\phi_5\phi_6$  (why is this string different from all other strings?)

To generate all symmetric periodic states, proposal:

use as the 'atom'  $\tilde{\Phi}$  in (6.13) all symbol strings  $\tilde{M}$  of lengths  $m = 0, 1, 2, 3, \dots$ , then order them lexically to eliminate repeats, and next, remove the corresponding prime periodic states from the  $C_n$  list of primes; that yields the list of  $D_n$  primes divided into four sets, the asymmetric (a), and the 3 symmetric sets (o), (ee), (eo).

As you work this out, please write up the details step by step in the draft [37], here sect. 4.10, it does not help us if the mathematics is only in your code.

**2022-04-27 Sidney** Today is a research day, so hopefully there will be several commits. I am working on finally completely understanding the field theory derivation of  $\phi^3$ , and that involves not only explaining the  $\frac{1}{2}$ , but also explaining integration (or summation) by parts with respect to the  $(\partial_\mu\phi)^2$  term.

First, with the one half, Matt explained pretty well in his page 1014 March 27<sup>th</sup> post, but I feel like it is necessary to state that he wrote  $\phi^T\Box + \Box\phi = \Box^T\phi + \Box\phi = 2\Box\phi$  the last equality is obvious due to  $\Box$  being a self-adjoint operator, however, I am not so sure about  $\phi^T\Box = \Box^T\phi$  I am pretty sure that this can be explained via the definition of an inner product. But this is confusing because  $\Box$  is an operator, but is it a scalar operator? Please help me make this more rigorous.

Now, integration by parts, there is a direct derivation in ChaosBook sect. A24.1.1 Lattice Laplacian for this procedure on the lattice, but I would like to understand as well for the continuum. Since we are working with



the metric being the identity  $\partial_\mu \phi = \eta_{\mu\nu} \partial^\nu \phi$  gives  $\partial_\mu \phi = \partial^\mu \phi$  and we can write the kinetic energy contribution as

$$\int d^d x \partial_\mu \phi \partial_\mu \phi$$

Which under the application of integration by parts gives

$$\oint_{\partial} \phi \partial_\mu \phi - \int \phi \partial_\mu \partial_\mu \phi d^d x = \int \phi \square \phi d^d x$$

Where the last equality comes about because integrating along the **periodic** boundary gives zero. This is because the start and end points of a periodic boundary are the same.

**2022-04-27 Sidney** I looked at the figures suggested from the 1989 Predrag paper [here](#), I think I understand what is wanted of me, but I am not sure completely how to get the "best estimate" of  $\gamma^\infty$ . To extrapolate, I would need an idea of how the data is evolving. I know that it is asymptoting to some value, but I don't know how to estimate that value systematically... will keep looking, but input would also be nice. Additionally, where does equation (22.79) come from? I understand that the idea is that we want to see that the difference between the "current and the next" is less than the difference from the "last to the current" but is there some derivation that makes this more enlightening?

**2022-04-28 Predrag** Perhaps [convergence tests wiki](#) helps.

**2022-04-27 Sidney** I understand now how  $(\partial_\mu \phi)^2 \rightarrow -\phi \square \phi$  in the lattice formulation. First, we note that  $\square \equiv -\partial^T \partial$  because  $\square$  is the lattice Laplacian which, in finite difference notation, is given by  $\square = \frac{1}{a^2} (\sigma^{-1} - 2I - \sigma)$  and  $\partial^T \partial = \frac{1}{a^2} (\sigma^{-1} - I) (\sigma - I) = \frac{1}{a^2} (2I - \sigma - \sigma^{-1})$ . Now, if we take  $(\partial_\mu)^T \phi \partial_\mu \phi = \phi \partial_\mu^T \partial_\mu \phi = -\phi \square \phi$  which is what we were looking for, all just from carrying out a transposition!

Let's explore our Euler-Lagrange equations. We can write our action as

$$S[\phi] = \sum_{\mu} \frac{1}{2} (\partial_\mu \phi)^2 + V(\phi) = \sum_{\mu} -\frac{1}{2} \phi \square \phi + V(\phi) \quad (22.75)$$

This should encompass all our Hamiltonian field theories (those that are non-dissipative can be treated through an action formulation). Now, the functional derivative commutes with the partial derivatives present in  $\square$ , and  $\square$  is self-adjoint, so it works the same acting from the right as it does acting from the left. Therefore, we can write

$$\frac{\delta S[\phi]}{\delta \phi} = \sum_{\mu} -\frac{1}{2} \phi \square - \frac{1}{2} \square \phi + V'(\phi) = 0 \quad (22.76)$$

Summing over independent directions to get zero implies that each member of the sum is zero, so we get

$$-\square\phi + V'(\phi) = 0 \quad (22.77)$$

as our lattice Euler–Lagrange equations. Note that this includes any extra minus sign we choose to have in front of our  $V$ , it is just absorbed in to the potential energy term.

**2022-04-28 Predrag** Compare your action with Han's argument, starting with (24.432).

**2022-04-30 Predrag** Primes are important, so let's discuss them in a space of their own, chapter 9 *Counting*.

**2022-05-02 Sidney** I am not sure how to compute the action from Hamilton's equations. Could you point me somewhere? I am now looking at Han's algorithm.

**2022-05-19 Sidney** Ok...I have now compared the EL equations generated by Hamilton's equations, and by varying the action, and they are not compatible. We have our EL equation as

$$\square\phi + V'(\phi_z) = 0$$

Which can be derived from the discretized Hamilton's equations by stating  $p_t = \phi_t - \phi_{t-1}$ , however, this does not agree with our current  $\phi^3$  equation (4.150), this can instead be derived from my EL equations which I found by varying the action:

$$-\square\phi + V'(\phi_z) = 0 \quad (22.78)$$

This is worrying, as that means our two methods are incompatible somewhere. Will keep looking.

**2022-05-21 Sidney** I am trying to understand the usage of a Wick rotation to transform between Lorentzian space and Euclidean space. The Wick rotation is simply the transformation  $t = -i\tau$  which rotates time in a Minkowski metric to being purely on the imaginary axis. this gives us (in natural units)

$$\square \equiv -\frac{\partial^2}{\partial t^2} + \nabla^2 \rightarrow \square \equiv \frac{\partial^2}{\partial t^2} + \nabla^2$$

This allows us to convert between the Hamiltonian EL equations (4.144) for ONLY 1D time systems which seems to be how this was derived...maybe? Is this correct?

**2022-05-23 Sidney** After some thought, I have come to the conclusion that my above post is correct. Han's argument starting with (24.432) is only valid in the 1D time regime, so his EL equation is simply

$$\frac{d^2\phi}{dt^2} + \frac{dV}{d\phi} = 0$$

which through wick rotation yields

$$-\frac{d^2\phi}{d\tau^2} + \frac{dV}{d\phi} = 0$$

which is equivalent to my (22.78) for a 1D time system. I do not believe that Han's argument works so cleanly for n-dimension systems, so I can only assume that the action variation derivation is valid as the general equation.

**2022-04-21, 2022-06-17 Predrag** Successive differences (22.74) are not the best way to numerically demonstrate exponential convergence, but check

$$\epsilon_\ell = \frac{\gamma^{(\ell+1)} - \gamma^{(\ell)}}{\gamma^{(\ell)} - \gamma^{(\ell-1)}} \quad (22.79)$$

I prefer plots of  $\epsilon_\ell = \log_{10} |\gamma^{(\ell)} - \gamma^*|$  where  $\gamma^*$  is your best estimate of  $\gamma = \gamma^{(\infty)}$  obtained by extrapolating your data, see figs. 3 and 7 [here](#). See also figs. 10 and 11, and Han's figure 24.74.

Once you implement spectral determinant cycle expansion, [ChaosBook sec. 23.2.2](#), you will demonstrate *superexponential* convergence see fig. 1 [here](#), and [ChaosBook table 23.2](#).

Note also that eventually, inevitably, in the present formulation, the cycle-expansion coefficients get swamped by numerical errors, see my post on page [1327](#).

**2022-07-30 Sidney** I am currently trying to get my cycle expansion code for the spectral determinant to work. I am doing this by working through [Homework 12](#) using my own code. However, I am now running into a lack of mastery of spatial ordering and symbolic dynamics.

Specifically, I want to generate initial guesses for fsolve using formula 14.4 in Chaosbook:

$$w_{n+1} = \begin{cases} w_n & \text{if } s_n = 0 \\ 1 - w_n & \text{if } s_n = 1 \end{cases} \quad (22.80)$$

This gives a binary number of the form  $0.w_1w_2w_3\dots$  which can then be converted to a decimal number for the location of a periodic point of a unimodal map. However, doing so does not give the right values for the quadratic map  $x_{n+1} = 6x_n(1 - x_n)$  whose  $\bar{1}$  fixed point is calculated as  $\frac{5}{6}$ ,

whereas the binary number prediction gives asymptotically  $\frac{2}{3}$ . I realize that with  $A = 6$  as in Homework 12, there are pruned orbits, but I am unsure how to get better initial guesses using kneading theory, and I am also unsure why this unimodal map does not match up with the spatial ordering presented in chapter 14. I know that I can use a variational method to find the roots, but I feel like I should be able to do it without. Anyway, I am going to brute force as I only need to find about 6 orbits and that is doable by guessing and checking via Desmos, but I would really appreciate help if anyone can.

**2022-08-05 Sidney** Well, figured it out! Turns out that the spatial position stuff generated by (22.80) is so laughably inaccurate for the quadratic map that using it as guesses for even the multishooting method gives the incorrect orbits. The only way to take advantage of kneading theory, therefore, is to remember that the ordering of the symbol sequences is the same as for the tent map (also pruning, but I don't want to deal with that right now). Anyway, I found out that there is definitely some typo in my spectral determinant cycle expansion code, it does not match homework 12...I will fix that over the weekend. However, in my bumping around I had a very fruitful email chain with Matt that I will now transcribe:

**Sidney:** I am currently trying to get better at kneading theory...and I am very confused. How can I get better guesses for the quadratic map  $f(x) = 6x(1 - x)$ ? Its fixed point to the right of the critical point is at  $5/6$ , whereas the unimodal binary number stuff from chapter 14 of chaosbook predicts  $2/3$ . Why is that? Do I have to find some similarity transform to transform  $6x(1-x)$  to  $4x(1-x)$  which I believe has complete binary dynamics? (Granted...it I could do that  $6x(1-x)$  would have complete binary dynamics and that would not make sense).

**Matt:** I'm not really sure what you are asking; but the section mentions the difference in behavior depending on whether  $A > 4$  or  $A < 4$ . "If the parameter in the quadratic map (14.20) is  $A > 4$ , or the top of unimodal map in figure 14.9 exceeds 1, then the iterates of the critical point  $x_c$  diverge from 1, and any sequence  $S_+$  composed of letters  $s_i = \{0, 1\}$  is admissible" In regards to  $2/3$ ... I see a table with that value for fixed point 1; but I'm not sure that that table corresponds to the quadratic map at all; it may be the dike map. Sorry I can't help more than that.

**Sidney:** I'm more asking the question: how can I get good guesses for the roots of the quadratic map and its iterates with  $A=6$ . Also doesn't "and any sequence  $S_+$  composed of letters  $s_i = \{0, 1\}$  is admissible" mean any binary sequence is allowed? So, do I have to use like a variational method? Or is there some symbolic dynamics stuff I can do to get good guesses which can then be used in fsolve?

**Matt:** The last statement you made implies that  $6x(1-x)$  doesn't have complete dynamics; maybe you meant "would not"? I was just trying to help with what seemed like a contradiction.

"(Granted...it I could do that  $6x(1-x)$  would have complete binary dynamics and that would not make sense)."

In regards to your actual question about initial conditions; there are a couple of techniques, each of which depends on the method you are using to solve the equations, but it sounds like you're not trying to do a variational method.

method 1: Brute force. 1. Just select a very large number of points from the domain and see what converges.

method 2: Recurrence. For initial conditions for length  $N$  cycles, 1. generate a set of initial conditions; the most uninformed prior is to simply use a uniform sampling 2. iterate the map  $N$  times 3. Compute the norm (absolute or relative) with the initial condition and take the ones with the smallest values, or those which satisfy some tolerance.

$$|f^N(x_0) - x_0| < \epsilon$$

method 3: spatiotemporal approach If you are using a variational method, simply try to pick points which exist in the intervals corresponding to the admissible cycles; i.e. if I was trying to find the fixed point 1, you could uniformly sample the interval corresponding to symbol 1. In this case you're trying to exploit your domain expertise of the attractor as much as possible; in the continuous field case this can be done by trying to impose particular spatial and temporal scales on your initial condition, for example.

method 4: dark arts In all honesty it's a dark art which depends highly on both the problem and formulation being worked with.

In either case, you will likely end up finding the same solution many, many times, and so you need to get creative so that you are getting a representative sample of the solution space. I don't recall seeing a method like this in the literature, and so maybe we should bring it up with predrag, but presumably if you are sampling the space of  $N$ -cycles then the distribution of your sample points should be similar to the distribution of the  $N$ -th iterates, therefore maybe you could use an information theoretic function like Kullback-Leibler divergence (measures the similarity between distributions) between the distribution of your initial conditions and the distribution of the iterates.

I'm not really an expert in iterative maps where the symbolic grammar is 100% known, there might be something analytic I am not remembering.

**Sidney:** Ok... that gives some ideas, and I definitely need to reread that last bit. But I'm looking at example 14.10 I think it is, it gives a "systematic" way of finding things for unimodal maps... is there a bisector method that I could use to make use of that interval that I can set up? At the moment, I am simply iterating the map, and then trying to find roots

via fsolve as the 12th homework suggests. Technically, I could do it via desmos... but that seems really inelegant. Also, why doesn't the conversation from binary to decimal work for the quadratic map with  $A=6$ ? Is it just because there is not a similarity transform between it and the tent map?

**Matt:** It would help me out if I knew what the overall goal is; what are you trying to accomplish? What context are we working in? You have to remember I have no idea what you're working on and I haven't seen this stuff in this level of detail in years. Are we fixing  $A=6$  and trying to find all cycles? I don't know what this is supposed to mean: "why doesn't the conversation from binary to decimal work". I get that you probably meant to say conversion and conversation; I don't know what that means though. Again, I never really studied iterative maps that hard. Also if this is homework I'd prefer that you reach out to Predrag or your TA to talk about it; they have a much closer understanding about what the question is and what it's trying to accomplish.

**Sidney:** Well, strictly, my cycle expansion code for spectral determinants and the cycle expansion code for the dynamical zeta function that I have written for the Hénon map give two different answers for the escape rate. Therefore, I thought that if I could work through the homework which dealt with cycle expansions using my code, I could troubleshoot better. In doing this, I ran into the problem where I needed to find

0,1,01,001,011,0001,0011,0111  
cycles for The map  $f(x)=Ax(1-x)$  with  $A=6$ . I know how to do this in a very inelegant way which is effectively using desmos as a way to generate initial guesses for each periodic point. This is neither satisfying, nor particularly instructive. So, I am hoping to understand how to find these orbits in a more theoretically sound way. Also, the conversion (silly autocorrect before) from binary to decimal I was talking about was using equation 14.4 to get a spatial position from the temporal (binary) code.

**Matt:** Okay I think I'm understanding slightly better now. Is it possible to simply look for the intervals which could contain your potential cycles?  $f(x)$  exists in  $[0, 1]$  only if  $x$  is in  $[0, 1/2 - 1/\sqrt{12}]$  or  $[1/2 + 1/\sqrt{12}, 1]$ , so  $f^2(x)$  exists in  $[0, 1]$  only if  $f(x)$  is in  $[0, 1/2 - 1/\sqrt{12}]$  or  $[1/2 + 1/\sqrt{12}, 1]$ . Applying this iteratively derives a cantor set which removes the middle portion of the quadratic map where the image is  $> 1$ . I.e. If I was trying to find the 01 cycle, then I know that  $x$  has to be in  $[0, 1/2 - 1/\sqrt{12}]$  and  $f(x)$  has to be in  $[1/2 + 1/\sqrt{12}, 1]$  by definition. This implies that  $x$  has to be in the interval  $[0.15568308, 1/2 - 1/\sqrt{12}]$ , the first number found by solving  $6x(1-x) - (1/2 + 1/\sqrt{12}) = 0$ , constrained to one half of the parabola (because the first symbol is 0)  $x$  in  $[0, 1/2 - 1/\sqrt{12}]$ . I believe by solving this iteratively you should be able to find the boundaries of the interval that any specific cycle has to exist within; sampling from that interval for initial conditions is probably what I would do. What I would check is whether or not you can do that analytically; I'm so used to doing

everything numerically sometimes I lose the forest for the trees.

**Sidney:** If I could establish intervals, I could switch root finding method and I wouldn't have to rely on guesses. . . I believe. How did you find the  $1/\sqrt{12}$ ?

**Matt:** Solving  $6x(1-x) = 1$

**Sidney:** Why equal to 1?

**Matt:** To find the subsets which map to the unit interval; i.e. the subsets of the domain whose range is  $[0, 1]$ ; it was my understanding that anything that gets mapped outside of the unit interval is going to escape, and can't be a cycle.

**Sidney:** I need to reread that section of the book. . .

**Matt:** I didn't really get it from the book, I just looked at what happens to points uniformly sampled from  $[0,1]$  when mapped iteratively and tried to describe the points which do not diverge to infinity. I'm a hands on learner, you see.

**Sidney:** Is the "relaxation for cyclists" chapter in chaos book using about the same variational method as your code for phi-4 is using?

**Matt:** I hate to be "that guy" but in my experience "variational method" is just a fancy term for creating a scalar function and finding its extrema. It of course comes from lagrangian/hamiltonian mechanics, but at the end of the day the action is just a scalar functional whose extrema we find by marching in the direction of its gradient. What I do is the following: I define my equations in the following form  $F(x) = 0$ ,  $x$  is now a set of variables which represent the full spatiotemporal state. I.e. if I give you  $x$ , and  $F(x) = 0$ , then  $x$  is a periodic orbit. I then construct a cost function (functional technically) by simply taking the  $L_2$  norm of  $F(x)$ .

$$L(x) = 1/2F^2$$

Then I find the gradient, which in this case is the product of (orbit) jacobian transpose and F.

$$\nabla L(x) = J^T(x)F(x)$$

Then I pass the function and its gradient to whatever pre-programmed solver is the flavor of the day. If it helps, you can think of  $L(x)$  as a "formal" Lagrangian (a mathematical construction rather than a representation of a physical system) with a Lagrange multiplier.

$$L(x) = \lambda F(x)$$

Where the choice of lambda has been made to derive a lagrangian whose solutions to the euler-lagrange equations necessarily satisfy our equations. I would say the main distinguishing factor of what makes it "variational" is simply that we are keeping the entire spatiotemporal state in

memory; so we are optimizing the entire path rather than a single point. I should mention that in the world of iterative maps, there might be better things to do, but generally speaking if you can create a function  $F(x) = 0$  whose solutions  $x$  are orbits/cycles, you will be off to a good start, and lots of doors open from there.

**Sidney:** Thank you! I will add this to my blog tomorrow and then share these conversations with everybody. Realistically, I was thinking that it would be interesting to have the quadratic map  $4x(1-x)$  as the nonlinear equivalent of what the original spatiotemporal paper used the Bernoulli map for: a motivating example for the method and formalism we are using. And I would like to try to solve the map in the same way phi-4 (and eventually phi-3) is solved.

**Matt:** The variational methods work better with field like equations because of the smoothness implications. I'm not sure how well it would work in an iterative map. It would be an interesting problem to tackle to find a way to "smooth" the dynamics to be more befitting of a variational method; or at least that is my intuition.

**Sidney:** I was just thinking of rewriting the quadratic as a lattice field equation like we did with temporal Hénon . . . unless I am misinterpreting something

**Matt:** I will only know when I see the result :) There's some intuition about iterative maps that my brain is missing despite being "easier" than PDEs. The human brain is a perplexing thing

As mentioned above, I think it would be interesting to rewrite the quadratic map as a lattice field equation:

$$g(x_n, x_{n+1}) = 4x_n(1 - x_n) - x_{n+1} \quad (22.81)$$

And then use it like the Bernoulli map in CL18 to introduce our variational method, and motivate  $\phi^3$  and  $\phi^4$ . What do all of you think?

**2022-08-15 Predrag** Does [ChaosBook eq. \(31.2\)](#) help you understand the relation between Perron-Frobenius operators and Koopman operators? Yesterday's soliloquy on Budišić, M. and Mohr, R. M. and Mezić [22] *Applied Koopmanism* (2012):

 [Koopmanism, the idea.](#)

**2022-08-17 Sidney** I honestly don't understand [ChaosBook eq. \(31.2\)](#) yet. I will read chapter 31 until that point and see if I understand it better. Additionally, I have reworked my dynamical zeta function code to work on a recursion relation like the spectral determinant code. It is much much faster, and gives the same answer up to  $10^{16}$ . I will talk about it more, and do a convergence test later.



**2022-08-18 Predrag** A reminder: it's good to keep learning new stuff, but if we are to write the nonlinear field theory article [37], we need to understand the eigenvalue spectra of orbit Jacobian matrixs, the work you started 2022-02-20, see figure 22.4.

**2022-08-18 Sidney** I am still pretty unsure how to approach the eigenvalue problem. I have a couple ideas: 1. Try to understand the Hessian matrix spectrum for Lagrangian systems, 2. Use Han's Bloch theorem work from the cat map to look at the repeats of fixed point eigenvalues and compare to the Homoclinic eigenvalues in figure 22.4. The real issue is that I am not completely sure what the eigenvalues of the orbit Jacobian operator are, and what it means that they are not invariant under smooth coordinate transforms. Any input at all here would be much appreciated, and would greatly speed up this process.

After some thought, and looking at [this Hessian Document](#) I realized that the eigenvalues describe the curvature of the surface (our action) at a given point (our lattice state). I think that the eigenvalues are the slopes of the unstable manifold (or perhaps the map itself) at each point in the lattice state. That way, the spacing is governed by the spatial ordering of kneading theory. I need to explore this numerically. Thoughts?

**2022-08-21 Sidney** I think that I have figured out why the maximum Gershgorin bound in figure 22.4 appears to be a limit point, whereas the minimum Gershgorin bound is not. The fixed point eigenvalues are given by  $2a\phi_{0,1} - 2\cos k$ , where  $k = 2\pi i/n$  where  $i$  is an integer and  $n$  is the number of times the fixed point cycle is repeated. The maximum achievable value for  $\phi$  is a fixed point, whereas the minimum achievable value is not. So the maximum Gershgorin bound is  $2\pi\phi_0 + 2$  which is the value of  $\cos \pi$ , this is achievable by the fixed point. However, the minimum value, is not a fixed point and thus does not fill out the Gershgorin interval near the minimum bound. This needs to be made more rigorous I think. How much do we need to know about the eigenvalues? What are the eigenvalues?

**2023-07-09 Sidney** Weird to think that it's been almost a year since my last post...a PhD sure is time consuming. Anyway, I'm here to add in some more stuff for [37] that I think would be useful, it definitely brings up my work to the equivalent of what's written about  $\phi^4$ . First, I checked and

$$F[x, y] = \begin{pmatrix} -\mu^2(x^2 - 1/4) + 2x - 2y \\ -\mu^2(y^2 - 1/4) + 2y - 2x \end{pmatrix} \quad (22.82)$$

is correct. This gives me  $y = x - \mu^2/2(x^2 - \frac{1}{4})$  plugging this into the second equation of (22.82) we get

$$F_2[x, y(x)] = -\mu^2\left(\frac{\mu^4}{4}x^4 - \mu^2x^3 + \left(2 - \frac{\mu^4}{8}\right)x^2 + \frac{\mu^2}{4}x + \frac{\mu^4}{64} - \frac{1}{2}\right) \quad (22.83)$$

We can then do long division and divide out  $(x - \frac{1}{2})$  and  $(x + \frac{1}{2})$  from (22.83) to obtain

$$F_2[x, y(x)] = -\mu^2(x + 1/2)(x - 1/2)\left(\frac{\mu^4}{4}x^2 - \mu^2x + \left(2 - \frac{\mu^4}{16}\right)\right) \quad (22.84)$$

This gives me roots of

$$\frac{2 \pm 2\sqrt{\frac{\mu^4}{16} - 1}}{\mu^2} \quad (22.85)$$

So for  $\mu^2 > 4$  we have a valid period two orbit, note that to match temporal Hénon we have  $\mu^2 = 3\sqrt{3} > 4$ . For a period-1 start the orbit Jacobian operator is just a stretching factor, we can calculate it by enforcing the period-1 condition:  $\phi_{t-1} = \phi_t = \phi_{t+1} \quad \forall t$  so  $F[\phi] = \mu(\frac{1}{4} - \phi^2)$  so

$$\mathcal{J} = \mp \mu^2 \quad (22.86)$$

Doing similar to (22.82) we obtain

$$\mathcal{J} = \begin{pmatrix} 2 - 2\mu^2x & -2 \\ -2 & 2 - 2\mu^2y \end{pmatrix} \quad (22.87)$$

With the fringe cases out of the way, we can write the orbit Jacobian operator for a period-n orbit as an operator

$$\mathcal{J}_{zz'} = -\square_{zz'} - 2\mu^2\phi_z\delta_{zz'} \quad (22.88)$$

I also found the anti-integrable limit ( $\mu \rightarrow \infty$ ) of my period-2 polynomial

$$F_2[x, y(x)] \rightarrow \frac{\mu^6}{16}(x + 1/2)(x - 1/2)(1 - 4x^2) \quad (22.89)$$

This shows that the anti-integrable limit pushes the period-2 orbit towards the period-1 orbits. Something that is also useful (as I ended up using it in the code to solve for the orbits)  $\mu^2 = a(\frac{a}{4} - \frac{1}{a})^{-1/2}$ . I think it is worth mentioning that what I used to find solutions for  $\phi^3$  (and what Xuanqi used for  $\phi^4$  I think) is a Newton's method with the shadow state used as an initial guess, not the Vattay inversion method. As well, from (22.85) we can see that shifted from temporal Hénon to  $\phi^3$  actually changes the demarcation of the symbolic dynamics, eg. the symbol '0' does not necessarily mean "a negative number" it now means "anything smaller than  $1/(3\sqrt{3})$ " which is the constant shift which I wrote out in WWLAF21. This may have to have a deeper explanation, but we could always just say that the symbolic dynamics for  $\phi^3$  were defined through the connection to temporal Hénon. Finally, I plotted the shadow state versus an actual state, I have done minimal formatting, so I will fix it when I know what to base things off.

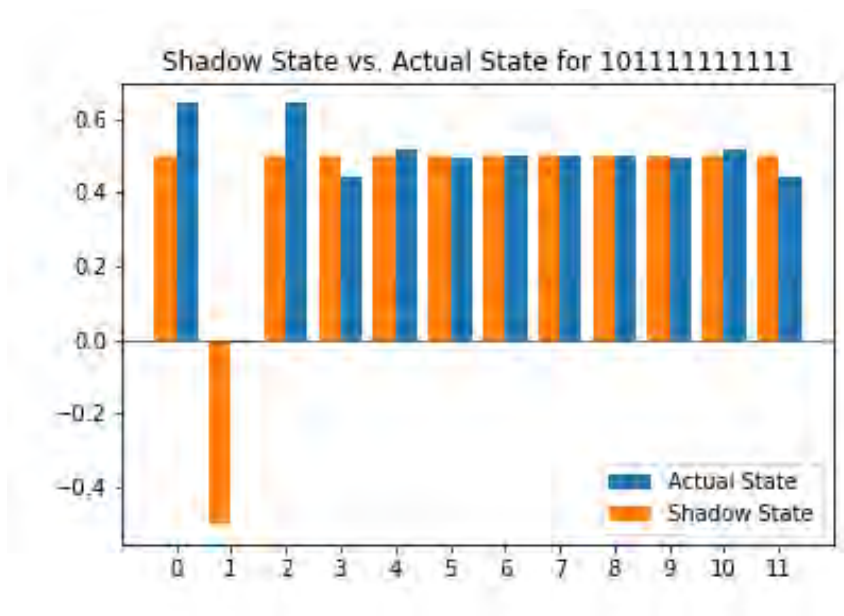


Figure 22.9: Showing the agreement between the most simple shadowing algorithm and an actual state. The lattice site  $z = 1$  field is happens to be small,  $\phi_1 \approx -0.006$ .

From here I want to try to organize my thoughts on my work on eigenvalues, was that ever resolved? Is there any symmetry, or cycle expansion stuff I need to address? A list of what else I need to accomplish given after this post would be much appreciated.

**2023-07-09 Sidney** Here's just a short update on my plan.

- Understand Xuanqi's horseshoe code and plot and make my own temporal Hénon /  $\phi^3$  one
- Finish Bloch analysis of Christmas Trees
- Smooth out proof of lack of invariance of orbit Jacobian operator eigenvalues
- Write eigenvalue and (small) Hill determinant section
- Construct example bloch integral and partition function for  $\phi^3$

I think this is decent progress, and relatively doable.

## 22.4 2024 blog

**2024-02-13 Sidney's secretary** Is there a "classical"  $\phi^4$  calculation that we could do using the nonlinear dynamics machinery that we've developed? Something that we could use to link our theory to regular lattice QFT?

**2024-02-13 Predrag** My reading of the literature is in sect. 4.13  $\phi^k$  field theory blog, and also spread out over that chapter. I believe Bloch bands are a tight-binding model calculation, you can search for that as well throughout the blogCats.pdf. See whether some of that is what you have in mind.

**2024-02-15 Sidney** I have reworked Temporal Hénon shadow states in terms of the current  $\phi^3$  parametrization by  $\mu^2$ .

I will post my reworked section in this blog so that the tigers paper is not besmirched.

**2024-02-15 Predrag** Made this into sect. 5.3 *Shadow state,  $\phi^3$* , so we can compare with the old Hénon map version sect. 5.2 *Shadow state, Temporal Hénon*, line by line.

**2024-02-15 Sidney** Should we also do the same for  $\phi^4$ ?

**2024-02-15 Predrag** Yes, you and Xuanqi decide who does the first pass.

**2024-05-20 Sidney** I am looking at calculating the stability integral for  $\phi^3$ , I think that all I really do is apply Bloch theorem, but have the coefficients be matrices, however, in trying to relearn Bloch I tried to reproduce the result in CL18 of the eigenvalues of our circulant Jacobian:  $2 \sin^2(k/2) + \mu^2$  how do we find this? When I work through it I get  $\mu^2 - (e^{ik} + e^{-ik}) = \mu^2 - 2 \cos(k) = \mu^2 + 4 \sin^2(k/2) - 2$ , Han, could you write out what you did, or point me to where this is written out?

**2024-05-26 Sidney** on the “block form of orbit Jacobian matrix”: I’m trying to reproduce equation (E.1) in [CL18](#). I’m not quite able to get it and I’m not quite sure what to do to fix it. Could you explain it to me? I get a block circulant matrix, but it is not of the form of (E.1).

**2024-05-28 Predrag** The orbit Jacobian matrix of a two-dimensional lattice field theory can be written in a spatiotemporal block matrix form, as a temporal lattice (21.81), with the spatial dependence treated as a multicomponent field at each temporal lattice site.

For an example, see  $\mathcal{J}_{[4 \times 2]} = (8.57)$ , of  $[L \times L]$  block form,  $L = 4$ , with  $[T \times T]$  blocks,  $T = 2$ .

There is a whole section [sect. 21.4 Hill determinant: stability of an orbit vs. its time-evolution stability](#) on this

**2024-05-21 Sidney** In regards to my post yesterday, I have now figured out what Han did, I had forgotten a factor in the box operator, including that fixes my issue.

**2024-05-26 Sidney** Han, I am very confused over eqs. (D.2) and (E.1) in [CL18](#). I spent a good chunk of today trying to reproduce them to absolutely no avail. First, for (E.1) where you claimed that we could rewrite our orbit Jacobian matrix as a large block matrix depending on the single  $L \times L$  matrix that would make up one repeat and  $L \times L$  identity matrices. That seems to be wrong. For example if I look at the  $9 \times 9$  (aka the  $[3 \times 3]_0$  mosaic) of three repeats of  $\phi^3$  (or really anything that has a variable diagonal)

$$\begin{bmatrix} s_0 & -1 & 0 & 0 & 0 & 0 & 0 & 0 & -1 \\ -1 & s_1 & -1 & 0 & 0 & 0 & 0 & 0 & 0 \\ 0 & -1 & s_2 & -1 & 0 & 0 & 0 & 0 & 0 \\ 0 & 0 & -1 & s_0 & -1 & 0 & 0 & 0 & 0 \\ 0 & 0 & 0 & -1 & s_1 & -1 & 0 & 0 & 0 \\ 0 & 0 & 0 & 0 & -1 & s_2 & -1 & 0 & 0 \\ 0 & 0 & 0 & 0 & 0 & -1 & s_0 & -1 & 0 \\ 0 & 0 & 0 & 0 & 0 & 0 & -1 & s_1 & -1 \\ -1 & 0 & 0 & 0 & 0 & 0 & 0 & -1 & s_2 \end{bmatrix} \quad (22.90)$$

This is indeed block circulant, but the blocks are not the identity or the single repeat matrix. I am sure I am missing something, but I do not see it. If I am not missing anything, this breaks Bloch for getting things in terms of nice trig functions. Now, for (D.2), I tried recalculating by using (E.1) as the base, this gives me something like

$$\begin{bmatrix} 2 - 2\mu^2\phi_0 - 2\cos(k) & -2 \\ -2 & 2 - 2\mu^2\phi_1 - 2\cos(k) \end{bmatrix}$$

Plugging in (D.2) from CL18 (which gives the period-2 points) and sim-

plifying  $2 - 2 \cos(k) = 4 \sin^2(k/2)$  this gives me

$$\begin{bmatrix} \sqrt{\mu^4 - 16 - 4 + p^2(2k)} & -2 \\ -2 & -\sqrt{\mu^4 - 16 - 4 + p^2(2k)} \end{bmatrix} \quad (22.91)$$

Which does not have the same eigenvalues that Han gave.

**2024-05-27 Sidney** Never mind, I figured it out, not the (E.1) equation, but I figured out the rest, and was able to match Han's (D.2), I'll write that up after I wake up in 8ish hours.

**2024-05-28 Predrag** :(

**2024-08-09 Sidney** That was a very long 8 hours...I'll write up what I said I would, and I'll include some bad news about  $\phi^3$ . First, the bad news, I calculated the convergence of the cycle expansion of the  $\phi^3$  escape rate, it has a weird periodic bouncing shape, my only idea is that since we aren't factoring out symmetries, when there is more than one symmetry in the orbits being included convergence patterns get disrupted. But that's all I have, I haven't tried the integral orbit Jacobian operator weighting yet, but I sort of doubt, that, that will fix anything. One hope is that the n=3 approximation giving really good values is observable when calculating up to n=7, n=7 can be found semi analytically using Endler and Gallas, so perhaps investigating that avenue would yield something.

Anyway, here's the Bloch derivation I promised in May: If we write out the large (infinite) orbit Jacobian operator we can pick out the repeating blocks, for a length n orbit yield  $n \times n$  repeating blocks. Consisting of the "prime" orbit Jacobian operator (sans the 1s in the upper right and lower left corners) and two matrices with ONLY a one in the upper right or lower left corner, these sparse matrices are then multiplied by  $\exp(\pm ik)$  and subtracted from the "prime" orbit Jacobian operator. The determinant of the resulting matrix is integrated over the appropriate Brillouin zone (width of  $2\pi/n$ ).

**2024-08-17 Sidney** I checked my transformation from  $\phi^3$  to Hénon, also my first thoughts about 2D  $\phi^3$ , I don't think its worth spending a bunch of time on it, but I am trying to figure out a good value for  $\mu^2$  in 2D, Xuanqi, Predrag, Han do you have any ideas on how to look at the 2D stable unstable manifold horseshoes?

**2024-08-18 Predrag** I have explained in a Zoom my shadow state proposal for determining low values of  $\mu^2$  for which one still has full-shift grammar, please blog your progress here.

And please, keep writing Tigers' draft [37]. I do not even see a phrase like "the first Brillouin zone" anywhere, but presumably that's what you are computing?

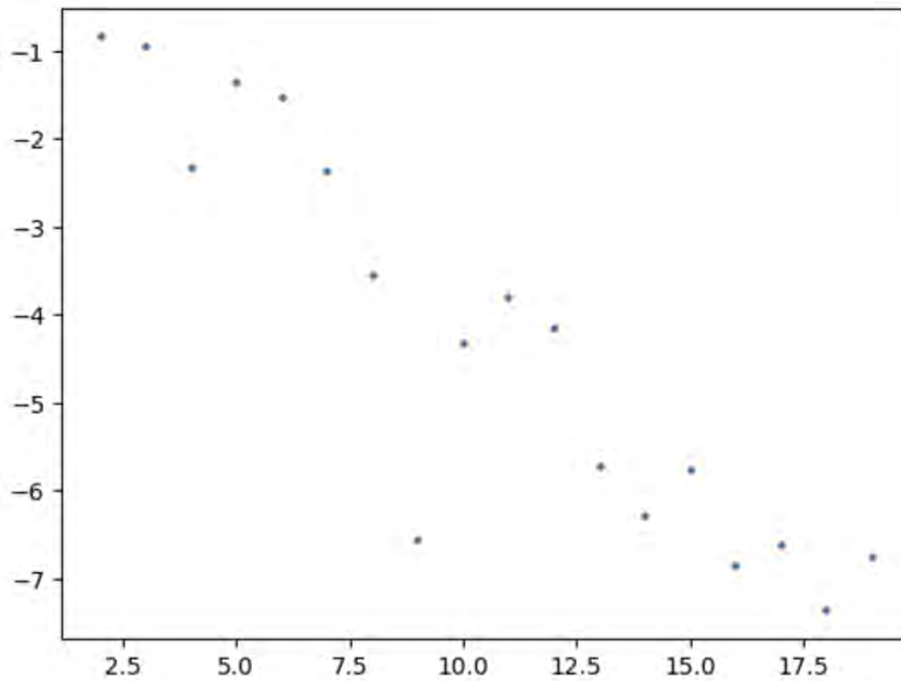


Figure 22.10: The weird convergence of  $\phi^3$  escape rate using the spectral determinant. The y axis is the logarithm of the difference between the current order of approximation of the escape rate, and the final (in this case order 20) order of approximation. This was calculated as a "double blind" test where I used Matt's cyclehunter along with Xuanqi's code.

It is possible that Sterling *et al.* [32–34] already have rigorous bounds and optimal numerical values for  $\mu^2$ , see Han's notes starting around eq. (24.512), also eq. (4.246); those you will have to convert into our  $\mu^2$  units.

**2024-08-17 Sidney** I have checked my derivation for mapping temporal Hénon to  $\phi^3$ , I was correct, but I committed an arithmetic error (no idea how) instead of  $3\sqrt{3}$  it should be  $2\sqrt{7}$  which is slightly larger at about 5.3. This still has weird behavior for the convergence of the spectral determinant at cycle length of 4, but it is much smoother. However, I think moving forward we will be using  $\mu^2 = 5.5$  my suggestion is that in the Tigers paper we state that we chose 5.5 in lieu of 5.3 as the point of the paper is to develop the simplest working case of a nonlinear field theory, so there serves little to no point in introducing additional complexities. However, I did print out the eigenvalues of the timestep Jacobian for length 4, nothing was very close to 1, so I am not quite sure what else I should be looking for, even in comparison to length 3 and length 5.

**2024-08-18 Predrag** I agree we should chose one  $\mu^2$  for all one-dimensional  $\phi^3$  numerical work, and another for all two-dimensional  $\phi^3$  numerical work. I thought we already had some blog entries about the choices? Before you and Xuanqi finalize that for both  $\phi^3$  and  $\phi^4$ , try having a look at Sterling, above. If they have a rigorously proven value, might just follow that, in the spirit of respecting people who were ahead of us.

**2024-08-17 Sidney** Next on the agenda, I've been looking at 2D  $\phi^3$ , specifically trying to determine the value needed for  $\mu^2$ . My initial thought is to repeat Xuanqi's analysis of stable/unstable manifolds, however, in 2D I would have to look at a 3D plot to determine when the horseshoe becomes complete. Any tips on this?

**2024-08-17 Sidney** A question about the following paragraph from sect. 13.3:

"A problem in reconstructing the statistical properties of an attractor from periodic orbits is ensuring that all orbits used belong to the natural invariant measure. For instance, in the single Hénon map, one of the two fixed points is isolated and it does not belong to the strange attractor. Something similar should occur in the CML."

How do we know that one of the fixed points is not in the strange attractor? Is it because we have the same sign for eigenvalues? Also, it seems that the coupled map lattices from ref. [27] are not super useful as they have quadratic terms for both backward and forward in time.

**2024-08-18 Sidney** I've worked a bit on the spatiotemporal  $\phi^3$ . I can now analytically work out the most basic shifted periodic states, specifically  $[2 \times 1]_1$ , this boundary condition forces  $\phi_{n,t+1} = \phi_{n-1,t} = \phi_{n+1,t}$  plugging



this into our map yields a set of nonlinear equations to be solved:

$$\begin{aligned} -4\phi_{10} + 4\phi_{00} - \mu^2(\phi_{00}^2 - 1/4) &= 0 \\ -4\phi_{00} + 4\phi_{10} - \mu^2(\phi_{10}^2 - 1/4) &= 0 \end{aligned} \quad (22.92)$$

This yields

$$\phi_{00}, \phi_{10} = \frac{4 \pm 4\sqrt{\mu^4/64 - 1}}{\mu^2} \quad (22.93)$$

This puts a requirement on the Klein-Gordon mass:  $\mu^2 > 8$  which is twice the 1D case, so I'll propose that we use  $\mu^2 = 11$  for Spatiotemporal  $\phi^3$  calculations.

**2024-08-18 Predrag** That's risky -  $\mu^2 > 8$  only ensures that relative periodic state of period 2 exist, says nothing about whether  $\mu^2 = 11$  is high enough for having the full grammar. You will get a better sense for it if you plot all larger  $V_{\mathbb{A}}$  lattice site field values  $\phi_{z,t}$  as we had discussed in the Zoom.

**2024-08-17 Sidney** I would still like to find a better estimate, but it seems that there's not a great way to write  $-\square\phi - \mu^2(\phi_{nt}^2 - 1/4) = 0$  as a forward in "time" map for  $d > 1$  and I'm not sure how else to define the Jacobian needed to find the stable/unstable manifolds.

**2024-08-17 Sidney to Han** Could you please explain to me the time reversal factorization? In [LC21 section 11.2 Kim-Lee-Park zeta function](#) the time factorized zeta function was only used to count admissible states. That seems underwhelming, what am I missing?

**2024-08-17 Sidney to Han and Predrag** In CL18 it seems that the spatiotemporal zeta function doesn't yield to the cycle expansion aspect of periodic orbit theory that I view as being the most impactful. However, in the shadowing section, it is numerically shown that there is exponential shadowing of longer orbits by shorter orbits. What gives? It seems that we have simultaneously found that shadowing is and isn't useful.

**2024-09-15 Sidney** For Bloch bands theory, I like

Singleton [30] *Band Theory and Electronic Properties of Solids* (2001), ([click here](#)).

**2024-10-20 Sidney** Finally got the first pruned orbits for  $\phi^3$  and  $\phi^4$ , I have plots, but I need to think a little harder on how to organize them. In order to find the orbits, I started at a large  $\mu^2$  and lowered it incrementally until the program was no longer able to converge every binary/ternary symbol sequence. After finding a coarse number, I went digit by digit until I found the accuracy needed to have only one orbit pruned. I then plotted this single orbit and saw what points moved the most before it ceased to converge, this allowed me to guess the orbit that annihilates with the one

I discovered. For  $\phi^3$  I went out to a maximum volume of 12, which allowed both spatial and temporal periods to reach a maximum of 12, this was so I could reproduce the temporal calculations. Similarly I went to volume 8 for  $\phi^4$  per the suggestion of Xuanqi.

$\phi^3$  : The orbits which seem to annihilate first for  $\phi^3$ ,  $\mu^2$  decreasing to  $\mu^2 = 10.279330575$ , are the 6 space, 2 time, i.e., Bravais lattice  $[6 \times 2]_0$  mosaics

$[0,1,0,0,1,0]$

$[0,0,0,1,0,1]$

with

$$\begin{array}{|c|c|c|c|c|c|} \hline 0 & 1 & 0 & 0 & 1 & 0 \\ \hline 0 & 0 & 0 & 1 & 1 & 1 \\ \hline \end{array} \quad (22.94)$$

I have a 3D plot showing these periodic states annihilating, will put it here.

$\phi^4$  : For  $\phi^4$  at  $\mu^2 = 7.50862409827$  they are periodicity  $[8 \times 1]_0$  pair of mosaics:

$[-1, 0, -1, 1, -1, 1, -1, 1]$

with

$[-1, -1, -1, 1, -1, 1, -1, 1]$ .

This is the 1D temporal lattice, so I will show where these points are on a blowup of figure 23.15, and on the periodic state of periodicity  $[8 \times 1]_0$  version of figure 23.16a.

With these results in mind, my suggestion is to use in all our calculations

$$\begin{array}{l} \phi^3 : \quad \mu^2 = 11 \\ \phi^4 : \quad \mu^2 = 8 \end{array} \quad (22.95)$$

**2024-10-22 Predrag** For 2D spatiotemporal periodic states, such as (22.94), the plot where one can study whether there is a gap between neighborhoods of (anti-integrable) shadow states is the plot together in one column all lattice site field values  $\phi_z$ , as we had discussed in the Zoom (see **2024-08-18 Predrag** above).

**2024-10-20 Sidney** Next step: I am pretty sure that if we calculate the Dedekind eta functions to high enough accuracy the convergence in terms of periodic orbits should clear up. I do not have Han's program for 2D spatiotemporal cat (I don't think), so if Han has the time to implement Sokal [31] paper I keep advertising, I think it will help with the main thing about this multiperiodic orbit theory that has been bothering me.

**2024-10-20 Sidney** I have been thinking about an orbit Jacobian operator for continuum systems. If we calculate the linear response of our continuum theory we should get something like

$$\hat{\mathcal{J}}\delta u = \delta F[\tilde{u}]$$

Where  $\tilde{u}$  is some multi-periodic orbit which satisfies our law at all points in space and time.

So, now we have an equation

$$\hat{\mathcal{J}} = \frac{\delta F}{\delta u}[\tilde{u}] \quad (22.96)$$

But this doesn't seem to be self consistent. For example, let's use Kuramoto–Sivashinsky. Linearization looks like

$$[\partial_t + \partial_x^2 + \partial_x^4 + \partial_x(u \cdot)]\delta u = \delta F[\tilde{u}]$$

Where it is important to note that the application of  $\partial_x(u \cdot)$  yields  $\partial_x(u\delta u)$ . In my mind, this should be factored as  $\partial_x(u) + \partial_x$  and this seems to be in conflict with the functional derivative formula (22.96) as applying that to Kuramoto–Sivashinsky would leave the nonlinear term as just  $\partial_x(u)$ , though, a similar conflict appears to occur when discretizing the nonlinear derivative:  $\frac{1}{2}\partial_x(u^2) \approx \frac{1}{4}((u_{n+1})^2 - (u_{n-1})^2)$  which would seem to be different from the discretization post chain-rule:  $u\partial_x(u) \approx \frac{1}{2}u_n(u_{n+1} - u_{n-1})$ . Anyway, once this discrepancy is solved, I believe we can simply discretize (22.96) and we'll have a perfectly good orbit Jacobian operator for continuum systems, with reasonable theoretical backing (see Peskin and Schroeder [24], for examples of taking the determinant of a differential operator).

**2024-10-21 Predrag to Sidney** `blog.tex` in this directory, as well as some of my talks have Burak's implementation of continuous spacetime Kuramoto–Sivashinsky equation. Run your attempt by Matt, see whether he has a discretization that makes sense to you (in his thesis, also in this repository).

**2024-10-21 Predrag** A very obscure use of Sokal's product [31]:

García-Etxebarria and Heidenreich [15] *New  $\mathcal{N} = 1$  dualities from orientifold transitions Part I: Field theory* (2013).

In Appe. G  $SO(N) \leftrightarrow Sp(-N)$  duality leads them to conjecture a new identity for elliptic hypergeometric integrals. Sokal's product [31] is here eq. (G.7).

**2024-10-22 Sidney** I will look at ref. [15] and try to figure out better the plotting suggestion that Predrag gave, as it seems I misinterpreted the suggestion somewhat.

2024-10-22 Sidney I think I've figured out a 2D version of Predrag's determinant calculation for square lattice states, sect. 6.4.2.

I'll start with my factored orbit Jacobian operator (the same idea as in 1D)

$$\mathcal{J}_{\pm} = \tilde{\mathcal{D}} \otimes \tilde{\mathcal{D}} - r_1 \otimes r_2 = -r_1 \otimes r_2 (\mathbf{1}_1 \otimes \mathbf{1}_2 - r_1^{-1} \tilde{\mathcal{D}}_p \otimes r_2^{-1} \tilde{\mathcal{D}}_p) \quad (22.97)$$

Notation  $\tilde{\mathcal{D}}_p \otimes \tilde{\mathcal{D}}_p$  might strike as odd, as there is only one, diagonal, (doubly) periodic 'stretching factors' matrix  $\tilde{\mathcal{D}}_A$ . Maybe index notation helps here: one means (no sum over repeated indices)

$$(\tilde{\mathcal{D}}_p \otimes \tilde{\mathcal{D}}_p)_{zz'} = \tilde{\mathcal{D}}_{nt,n't'} = \sigma_{nt} \delta_{nn'} \delta_{tt'}$$

Obvious, no? Just work out commutators  $[\tilde{\mathcal{D}}, r_j]$ , and you got it.

As a product of matrices (21.237) factors, pure shifts determinant (12.20) is nonzero (see wiki),

$$\text{Det} \left( r_1^{L_2} \right) \text{Det} \left( r_2^{L_1} \right) = 1$$

for multiples of primitive cell periodicities only. Use trace-log:

$$\ln \text{Det} (\mathbf{1}_1 \otimes \mathbf{1}_2 - r_1^{-1} \tilde{\mathcal{D}}_p \otimes r_2^{-1} \tilde{\mathcal{D}}_p) = \text{Tr} \ln (\mathbf{1}_1 \otimes \mathbf{1}_2 - r_1^{-1} \tilde{\mathcal{D}}_p \otimes r_2^{-1} \tilde{\mathcal{D}}_p)$$

Now, since the Kronecker product of two identity matrices is just another (larger) identity matrix we can directly use a Taylor series

$$\text{Tr} \ln (\mathbf{1}_1 \otimes \mathbf{1}_2 - r_1^{-1} \tilde{\mathcal{D}}_p \otimes r_2^{-1} \tilde{\mathcal{D}}_p) = - \sum_{l=1}^{\infty} \frac{1}{l} \text{Tr} (r_1^{-1} \tilde{\mathcal{D}}_p \otimes r_2^{-1} \tilde{\mathcal{D}}_p)^l$$

Since block matrices distribute in Kronecker traces (12.20),

$$\text{Tr} (A \otimes B) = \text{Tr} (A) \text{Tr} (B)$$

and since the shift matrices don't change behavior subspace to subspace, I guess my formula for  $\text{Det} \mathcal{J}_{\pm}$  in (6.54)

$$- \sum_{r=1}^{\infty} \frac{1}{r} \sigma_p^r = \ln(1 - \sigma_p), \quad \sigma_p = \sigma_{n,t} \sigma_{n-1,t} \sigma_{n,t-1} \dots \quad (22.98)$$

I need to double check this, but it all should be approximately right. As far as Bloch's theorem goes,  $\exp(ik)$  shouldn't effect traces, and so all of the wavenumber info should just be stored in the determinant that I pulled out at the very beginning of this calculation.

Finally, if I square  $\text{Det} \mathcal{J}_{\pm}$  I almost get

$$\tilde{\mathcal{D}}_p^2 \otimes \tilde{\mathcal{D}}_p^2 - r_1 \tilde{\mathcal{D}}_p \otimes r_2 \tilde{\mathcal{D}}_p - \tilde{\mathcal{D}}_p r_1^{-1} \otimes \tilde{\mathcal{D}}_p r_2^{-1} + \dots$$

which is symmetric to the 1D case, but would suggest that we would need to rescale something to isolate  $\tilde{\mathcal{D}}_p$ .

**2024-10-27 Predrag** In (22.100), double-index notation [6]  $z = nt$ , the two-dimensional square lattice orbit Jacobian operator

$$\begin{aligned} \mathcal{J} &= -r_1 - r_2 + 2\mathcal{D} - r_2^{-1} - r_1^{-1} \\ \mathcal{D}_{zz'} &= d_z \delta_{zz'}, \quad d_z = V''(\phi_z)/d + 2, \end{aligned} \quad (22.99)$$

site-stretching, diagonal operator  $\mathcal{D}_{zz'} = s_z \delta_{zz'}$  can be factorized as

$$\mathcal{D} = \tilde{\mathcal{D}}^\dagger \tilde{\mathcal{D}} \quad s_z = \sigma_z^* \sigma_z \quad \tilde{\mathcal{D}}_{nt,n't'} = \sigma_{nt} \delta_{nn'} \delta_{tt'}.$$

Shift operators  $r_1, r_2$

$$(r_1)_{nt,n't'} = \delta_{n+1,n'} \delta_{tt'}, \quad (r_2)_{nt,n't'} = \delta_{nn'} \delta_{t+1,t'} \quad (22.100)$$

translate a field configuration  $\Phi = \{\phi_z\}$ ,

$$(r_1 \phi)_{nt} = \phi_{n+1,t}, \quad (r_2 \phi)_{nt} = \phi_{n,t+1},$$

and the stretching operator

$$(r_1 \mathcal{D})_{nt} = d_{n+1,t} \delta_{nn'} \delta_{tt'}, \quad (r_2 \mathcal{D})_{nt} = d_{n,t+1} \delta_{nn'} \delta_{tt'} \quad (22.101)$$

by one lattice spacing in the spatial, temporal direction, respectively. Their products, commutators are

$$\begin{aligned} r_i r_j &= r_j r_i, \quad i \neq j, \\ r_j^n r_j^m &= r_j^{n+m}, \end{aligned}$$

**2024-10-30 Sidney** Unfortunately, it seems that trying to take the square root of our orbit Jacobian operator has again resulted in naught. I worked through Xuanqi's trace calculations, seems to makes sense. I've also looked through Peskin and Schroeder [24] and found that in my 2019 paperback reprint it walks through evaluation of functional determinants on pages 304 and 374. But both can be found in the index under "functional determinant methods of evaluation". However, the way the evaluation is conducted assumes a linear operator writing  $Tr(\partial^2 + m^2) = \sum_k (k^2 + m^2) \rightarrow \int d^4k \dots$  perhaps then Kuramoto-Sivashinsky would yield something like  $-i\omega - k^2 + k^4 + ik\hat{u}$  where  $u$  is evaluated on the orbit being considered? I think I also need to discuss more about the plots mentioned by Predrag in **2024-08-18 Predrag**

**2024-11-03 Sidney** I've been thinking about how we could extend our theory (painlessly) to maps with multiple fields. I've started with the "inverted potential" temporal Hénon

$$\begin{aligned} F_1 &= ax_n^2 - y_n - x_{n+1} + 1 \\ F_2 &= x_n - y_{n+1}. \end{aligned} \quad (22.102)$$

2024-11-03 **Sidney** In much the same way the timestep Jacobian is defined, I'll define the multi-field orbit Jacobian operator as

$$\mathcal{J} \equiv \frac{\delta \vec{F}}{\delta \vec{x}}[\vec{X}], \quad (22.103)$$

where I have used  $\vec{X}$  to show that the orbit Jacobian matrix is evaluated on a solution state for each field. For temporal Hénon, (22.103) becomes a  $2 \times 2$  block matrix, which I'll write out for a length 3 orbit as an example

$$\mathcal{J}_3 = \left( \begin{array}{ccc|ccc} 2ax_0 & -1 & 0 & -1 & 0 & 0 \\ 0 & 2ax_1 & -1 & 0 & -1 & 0 \\ -1 & 0 & 2ax_2 & 0 & 0 & -1 \\ \hline 1 & 0 & 0 & 0 & -1 & 0 \\ 0 & 1 & 0 & 0 & 0 & -1 \\ 0 & 0 & 1 & -1 & 0 & 0 \end{array} \right) \quad (22.104)$$

(Compare with (22.10) and (22.108).)

Note that the bottom-right block is just  $r$  from our regular field-theory orbit Jacobian operators. Now, using an identity proved [here](#) we can write the determinant of this block matrix as (using standard notation)

$$\text{Det}(\mathcal{J}_3) = \text{Det}(S - r - r^{-1})\text{Det}(r)$$

Which, up to a sign is EXACTLY what we see for a 1D  $\phi^3$  theory. This should also work for Bloch theorem, as now each field (and therefore each block in the multifield orbit Jacobian operator) repeats infinitely and picks up a Bloch phase. The only issue is that the Hill determinant would seem to pick up an extra phase from  $\text{Det}(r)$  however, maybe that drops out somehow.

I think that this could be a very nice section to add to the paper, it adds no additional work (since it seems to convert one-to-one into  $\phi^3$ ) and it shows that our theory is directly applicable (and easy to apply!) to multifield theories.

2024-11-08 **Sidney** I've fixed some typos from my last entry, I know that there was some gripes with my notation in (22.103), I tried to update it to be more similar to what was used in LC21, let me know if this is better

$$(\mathcal{J}_c)_{z'z}^i \equiv \frac{\delta F_{z'}^i}{\delta x_z} [X_c] \quad (22.105)$$

I have used the superscript  $i$  to denote which equation is being varied, it corresponds to rows of blocks in the orbit Jacobian operator.

2024-11-08 **Sidney** I reached out to [John McGreevy](#), the resident theoretical condensed matter/quantum field theorist at UCSD to ask about evaluating functional determinants. He told me that he viewed the periodic

boundary conditions as quantizing the momentum, so we'd be evaluating infinite sums in the "compact" domain. Here is the transcribed conversation:

**2024-11-08 Sidney** I have been working on a project that needs me to take determinants of operators (specifically differential operators of the form  $dt + d^2x + d^4x + \text{function of } x, t$ ) defined on infinite repeats of a periodic domain (think infinite lattice with a periodic wave on top).

I've seen examples in Peskin and Schroeder [24] of this sort of determinant but on operators without a function, and on a domain with no prescribed periodicity. The only thing I can think of is perhaps some "compact" integral similar to Peskin for the periodicity, and then Bloch theorem for the infinite lattice. This seems something similar to integrating over continuous bands in condensed matter physics... do you have any ideas or tips on how I may approach this?

**2024-11-08 John** I don't think you should expect an exact solution of such a problem, but you can probably make some progress.

Indeed if your differential operator is

$$\partial_t + \partial_x^2 + \partial_x^4 + V(x, t)$$

with  $V$  a \*constant\* then it is diagonal in momentum space, and the problem reduces to computing some infinite sums. If  $V$  actually depends on  $x$  and  $t$  only for very special cases can we solve it, just like only for special potentials can we find the spectrum of the Schrödinger operator  $-\partial_x^2 + V(x)$ .

An example where it can be done even when  $V$  is not constant is the SHO. For a good discussion see appendix A of volume 1 of Polchinski [25], ([click here](#)) (you don't need to know any string theory for this section).

I don't know a method for exactly computing the det that doesn't involve knowing the whole spectrum of the operator.

For the more general case, which I assume you are in, I think the way to proceed is perturbation theory in  $V$ , or in the deviation of  $V$  from a constant. That is, write your operator as  $L_0 + W$ , where  $L_0$  is a part you understand (e.g.  $\partial_t + \partial_x^2 + \partial_x^4$ , which is diagonal in momentum space), and  $W$  is regarded as "small". Then  $\det(L_0 + W) = \det(L_0) \exp \text{tr} \log(1 + L_0^{-1}W)$  where  $L_0^{-1}$  is the propagator, and you can use the expansion  $\log(1 - x) = -x - x^2/2 - x^3/3 - \dots$ . You can think about the  $n$ th order term in  $W$  as a Feynman diagram with a single loop and  $n$  insertions of the perturbation  $W$ .

Depending on what you want to know about the functional determinant, a few low orders in this expansion may be enough.

**2024-11-09 Predrag** At the moment, you two are too far apart. You should probably walk John through relevant parts CL18, up to Xuanqui's 1D Hill determinant (23.75), to focus him on *lattice* functional determinants.

I've had a superficial look at appendix A of volume 1 of Polchinski [25], (click here). Covers the same ground as my [5] (1983) *Field Theory*.

Most of it does not apply to lattice, as these determinants are evaluated over continuum and are rotationally invariant. We did use a rotationally invariant form, though, to approximate lattice Green's function for larger distance in the 'shadowing' section of CL18, eq. (150).

We tend to compute our determinants numerically exactly, not truncate the tr-log expansion as John proposes for his  $W^n$  log expansion. I keep suggesting, though, such truncations to Xuanqi, in order to settle the  $(k_1, k_2)$  dependence of 2D Hill determinants..

**2024-11-08 Sidney** That makes sense, eventually (by the nature of  $V(x,t)$ ) I'll need to turn to numerics, but I want to understand the theory first.

Does this apply to the periodic domain I was talking about? That is the second part that I find really difficult to put into math.

**2024-11-08 John** Right, from the point of view of the approach I was advocating, the periodic boundary conditions just mean that the momenta are quantized, so you have to do sums instead of integrals in the diagrams. It may be helpful to use the techniques people use for doing Matsubara sums, which use Sommerfeld-Watson transformation to rewrite the sum over integers as a contour integral against a function with poles at the integers.

See e.g. problem 3 in the attached problem set (added to the repo as `siminos/sidney/2022-215C-hw05-sol.pdf`) for a simple example. The [Matsubara frequency](#) wiki is also pretty good.

I recommend trying to understand the case with  $V=\text{constant}$  well first.

**2024-11-09 Predrag** Watson-Sommerfeld transform [36] might be something for every Tiger's toolbox (for example, [ChaosBook Chapter 41 Chaotic multiscattering](#)):

Michael G. Rozman lecture notes [Summation of series: Sommerfeld-Watson transformation](#) (2017)

William G. Melbourne, *Radio Occultations Using Earth Satellites: A Wave Theory Treatment*, Appendix G [Using the Sommerfeld-Watson Transformation](#) (2004)

Giuseppe Iurato *An historical prolegomenon to the occurrence of the resonance dual models: the Watson-Sommerfeld transform* [arXiv:1505.06638](#).

**2024-11-09 Sidney** I agree that what John and I were talking about doesn't really apply to our issues of evaluating lattice determinants. However,



I think it may apply to evaluating my weird operator determinants for PDEs.

**2024-11-09 Sidney** I know that we've talked a bit on zoom about rotationally invariant determinants, but I don't think I understood as well as I thought I did, could you explain why something like the Kuramoto-Sivashinsky operator that I was talking about yields a rotationally invariant determinant that then doesn't apply to lattices? (or is the nonapplicability to lattices just due to the continuum assumption?)

**2024-11-09 Predrag** I have not gone through your (22.96) and the Kuramoto-Sivashinsky operator example, but on a square lattice you can rotate only by multiples of  $90^\circ$ . In continuum by any continuous angle, so eigenfunctions of operators are totally different. Kuramoto-Sivashinsky has no rotational symmetries in 1+1 dimension, as time and space directions cannot be rotated into each other. In 2+1 dimension, there are rotations in the spatial plane.

**2024-11-09 Predrag** If we are going to use your example in the Tigers paper, what version of Hénon map is (22.102)? It is not (3.5), (3.59), (4.186), (22.14) or (22.71), is it?

**2024-11-09 Sidney** No, it is not quite, it is the "inverted potential" Hénon map where I've reflected the field values in everybody's Hénon map  $(x_n, y_n) \rightarrow (-x_n, -y_n)$  and then multiplied both sides of the equation by  $-1$ . However, it is worth pointing out that my conclusion that we can reproduce the one field  $\phi^3$  form of the orbit Jacobian matrix Hill determinant is not effected, as I kept everything in terms of the the diagonal  $S$  stretching matrix. No Heisenberg here:)

**2024-11-09 Predrag** It looks like we need to explain *internal* symmetries in some depth, so I sketched a possible sect. 4.9 for the Tiger's paper. The point is that if a group  $G$  is *not* a symmetry, it generates a whole orbit of Euler-Lagrange equations, each of different form. Therefore one sticks to one convention, and if referee sees that we have two forms of the same equation in the same paper, for no good reason, she will -rightly- kill us. Life is hard enough as is, without throwing in sneaky '-' signs. Stick to our (and Hénon's) convention.

**2024-11-10 Sidney** There was a long period of time where we were focussing on the inverted Hénon map so I did that so as to match the Tiger's paper section sect. 4.10 and sect. 4.10.1. The Hénon stretching parameter  $a$  in (3.31) and the Klein-Gordon mass  $\mu^2$  in (4.150) are related by

$$\mu^2 = 2\sqrt{a+1} \tag{22.106}$$

and now all we have (which I will correct in the field theory blog after discussion) is

$$\phi_t = \frac{6}{2\sqrt{7}}\varphi_t + \frac{1}{2\sqrt{7}} \tag{22.107}$$

This gives us back the map which is written in ChaosBook and other traditional references for  $a = 6$  and  $b = -1$ . With that in mind, the conventional block matrix (22.104) is

$$\mathcal{J}[\Phi]_3 = \left( \begin{array}{ccc|ccc} -2ax_0 & -1 & 0 & -1 & 0 & 0 \\ 0 & -2ax_1 & -1 & 0 & -1 & 0 \\ -1 & 0 & -2ax_2 & 0 & 0 & -1 \\ \hline 1 & 0 & 0 & 0 & -1 & 0 \\ 0 & 1 & 0 & 0 & 0 & -1 \\ 0 & 0 & 1 & -1 & 0 & 0 \end{array} \right) \quad (22.108)$$

and the Euler–Lagrange equations for the Hénon map are the 2-component field conditions that

$$\begin{aligned} F_1[\Phi]_n &= -ax_n^2 - y_n - x_{n+1} - 1 \\ F_2[\Phi]_n &= x_n - y_{n+1} \end{aligned} \quad (22.109)$$

simultaneously vanish on all lattice sites  $n$ .

Everything else is the same, and using (22.107) gives me our  $\phi^3$  orbit Jacobian operator.

I have not yet looked at the Watson-Sommerfeld transforms, this week project. I read through the internal symmetries section for the Tigers paper, I'd like to keep exploring that topic, so I'll try factoring the internal  $D_1$  symmetry for  $\phi^4$ .

I understand the group orbit of Euler–Lagrange equations.

**2024-11-10 Sidney** I was under the impression that we wanted an inverted potential to get the hyperbolic sines and cosines.

**2024-11-10 Predrag** We'll have to rewrite that, both in CL18 and the Tigers paper. To be in the anti-integrable regime we need  $|V'[\Phi]_n|$  evaluated on the non-wandering set of periodic states to be much larger than the contributions from the Laplacian terms. Then it works for both  $\phi^3$  and  $\phi^4$  theories.

**2024-11-10 Predrag** BTW, Polchinski [25] is all about partition functions which are Dedekind eta functions. In this context, Eudaemonist [Stany M. Schrans'](#) notes on [Polchinski book](#) might be helpful. Or not.

**2024-11-12 Sidney** Still working through some Polchinski, will write that up when I understand it. I also saw the comments in Xuanqi's blog about pub quality figures, I was planning on working on the figures that I used to determine appropriate  $\mu^2$ 's tomorrow, may as well do well with the figures. Additionally, I can do some writing to spare Predrag (some of the work).

Finally, in the meantime, I was doing some lit review and I'd like a clarification of something. In Predrag's 2013 paper on the clockwork of turbulence it says:

"once the periodic orbits form the skeleton (symbolic dynamics) underpinning the chaotic dynamics, their unstable manifolds trace out connections between neighborhoods of important recurrent flows (Markov graphs), the recurrent flows are organized hierarchically and the search for longer-period solutions is systematic[. It is only at this point that the exact cycle averaging formulas have a chance of converging."

This statement is equivalent to saying that we need to complete our library of short orbits correct? And by "completing our library" and "short orbits" I mean that we have amassed a collection of solutions that can connect any part of the chaotic attractor to any other, right? I think I need to reread chapter 14 of ChaosBook, but the picture I have right now, is that an "incomplete" Markov graph would be like having our three post billiard game, but not recognizing any angle of incidence, or location along the post where a ball could fly off and hit the third post. Is that about the idea?

**2024-11-13 Sidney** Figure 22.11, figure 22.12 and figure 22.13 are the plots I promised, see the captions for explanations

I realize that figure 22.13 is not quite what Predrag had in mind, this is what I visualized after our Boston Cafe zoom call, I would like to discuss. Also, it is worth noting that reducing the minimum  $\mu^2$  by one at the smallest decimal place would result in exactly one orbit being pruned. I do need to go through once more to double check about slants, and that it really is exactly one orbit, *but* I do know that all orbits converge at the  $\mu^2$  that I selected.

**2024-11-17 Sidney** Here is a much more thorough look at the annihilation of orbits. I made sure to check the slant, and label everything correctly. Additionally, I made sure that to within effectively machine precision what I report on are the first orbits to die. Next, since in both cases the orbits which annihilate are homoclinic (I took some notes on this, but tomorrow I'll ask for some clarification) they have the same shape and slant, and so I could just take a Frobenius norm and check to make sure that every point of the two orbits I'm considering are becoming close. I went until changing the last digit of  $\mu^2$  to be one smaller would cease to converge completely, and at that stage the Frobenius norm of the two considered orbits for both  $\phi^4$  and  $\phi^3$  were  $\sim 10^{-9}$  I plotted this convergence and got the behavior Predrag expected. There were some orbits that also seemed to converge to where the first eliminated orbits did, to repeat my analysis I would have to evolve each state forward in time and space to make sure they matched at each step as these other orbits were of different shapes. Additionally, there seems to be a huge amount of symmetry in the  $\phi^4$  orbits of interest. This probably means I need to actually factor something, I did not do that this weekend. Figure 22.14 to figure 22.14 are the plots.

They exhibit the same pattern as reported (only verbally) last week for the  $[8 \times 1]_3$  orbit.

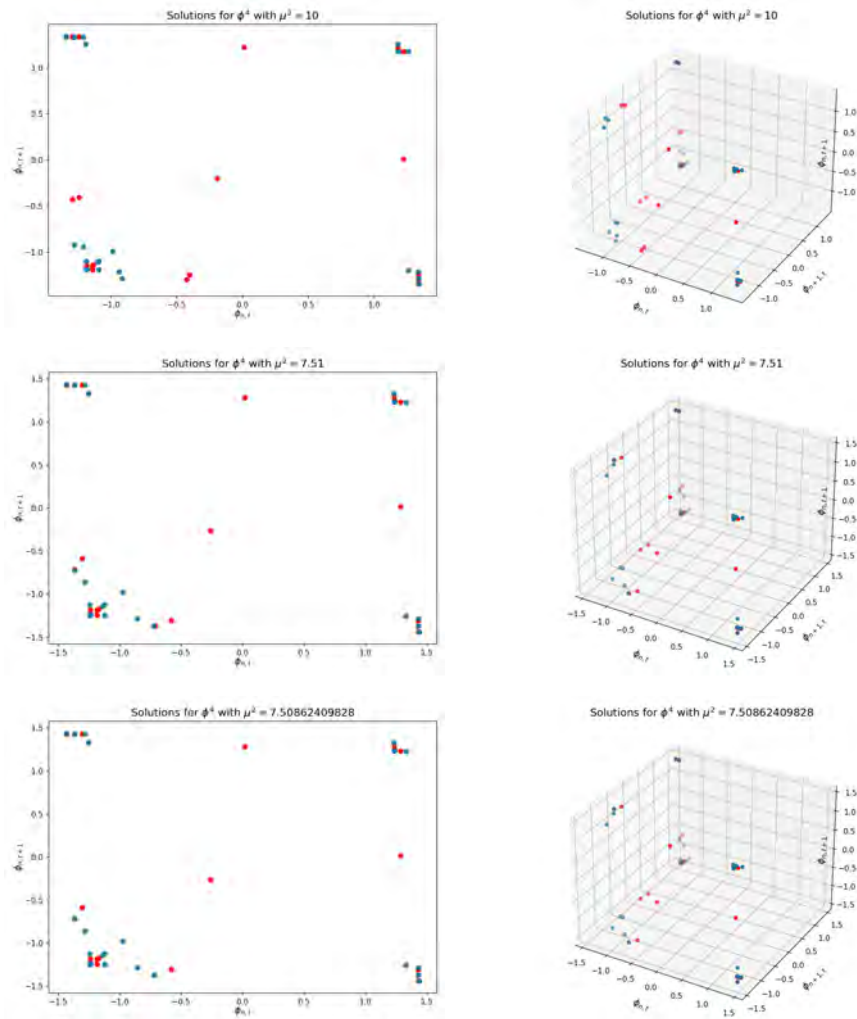
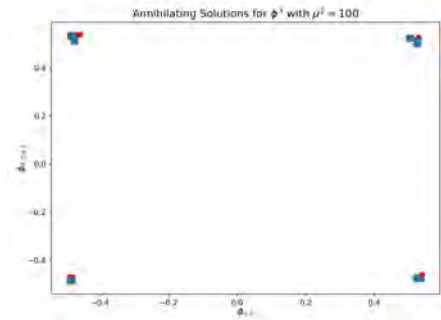


Figure 22.11: Annihilation of  $[7 \times 1]_0$  periodic states of  $\phi^4$  with mosaics  $[-1, 0, -1, 1, -1, 1, -1, 1]$  and  $[-1, -1, -1, 1, -1, 1, -1, 1]$ . Look at the lower left corner of the 2D plots and you'll see the points merge as  $\mu^2$  becomes smaller.



Missing: 100\_3D\_annihilation

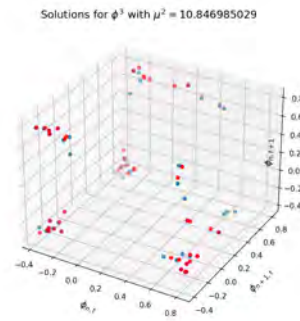
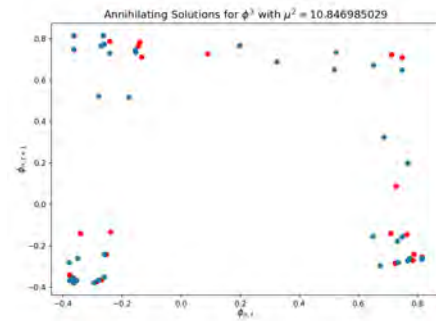
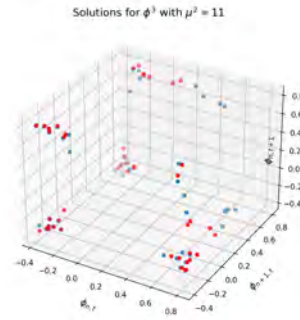
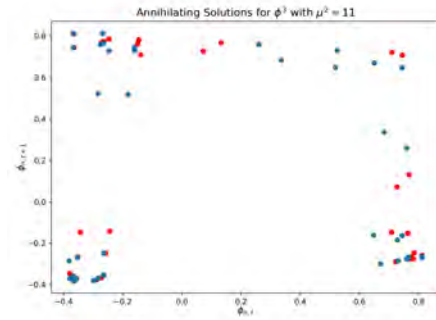


Figure 22.12: Annihilation of  $[6 \times 2]_0$  periodic states of  $\phi^3$  with mosaics  $\begin{bmatrix} 0 & 0 & 0 & 1 & 0 & 1 \\ 0 & 1 & 0 & 0 & 1 & 0 \end{bmatrix}$  and  $\begin{bmatrix} 0 & 0 & 0 & 1 & 1 & 1 \\ 0 & 1 & 0 & 0 & 1 & 0 \end{bmatrix}$ . Look at the middle right and you'll see the points merge as  $\mu^2$  becomes smaller.

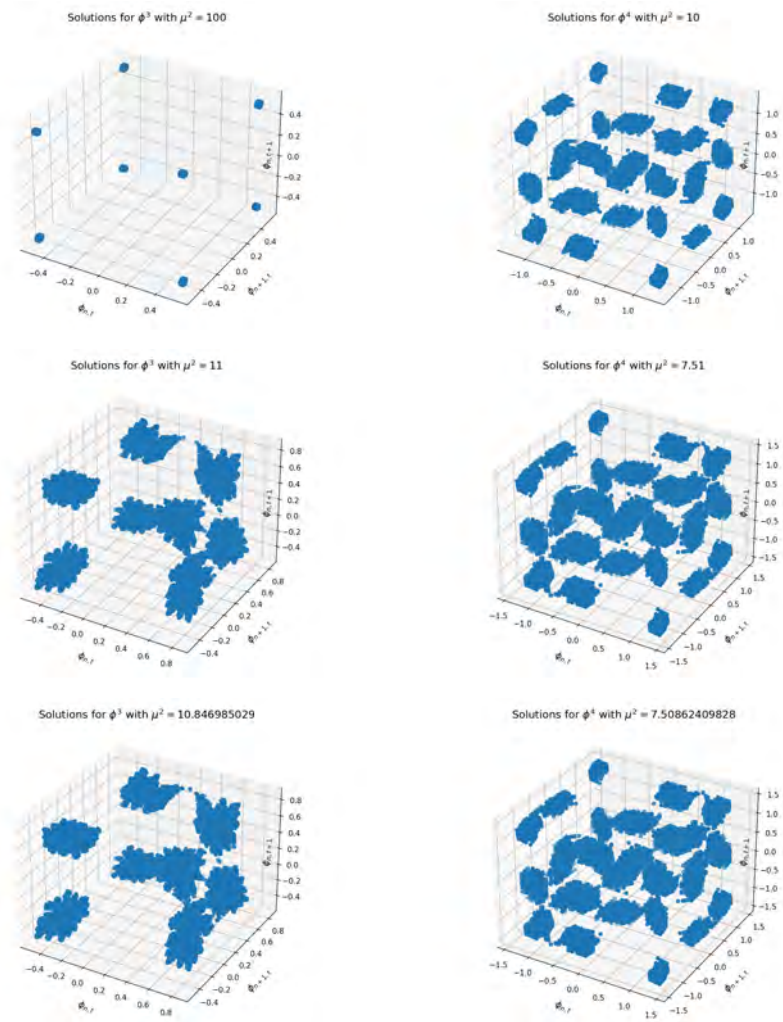


Figure 22.13: Plots of the periodic states for  $\phi^3$  and  $\phi^4$  up to periods 12 and 8 with max volumes 12 and 8, respectively.

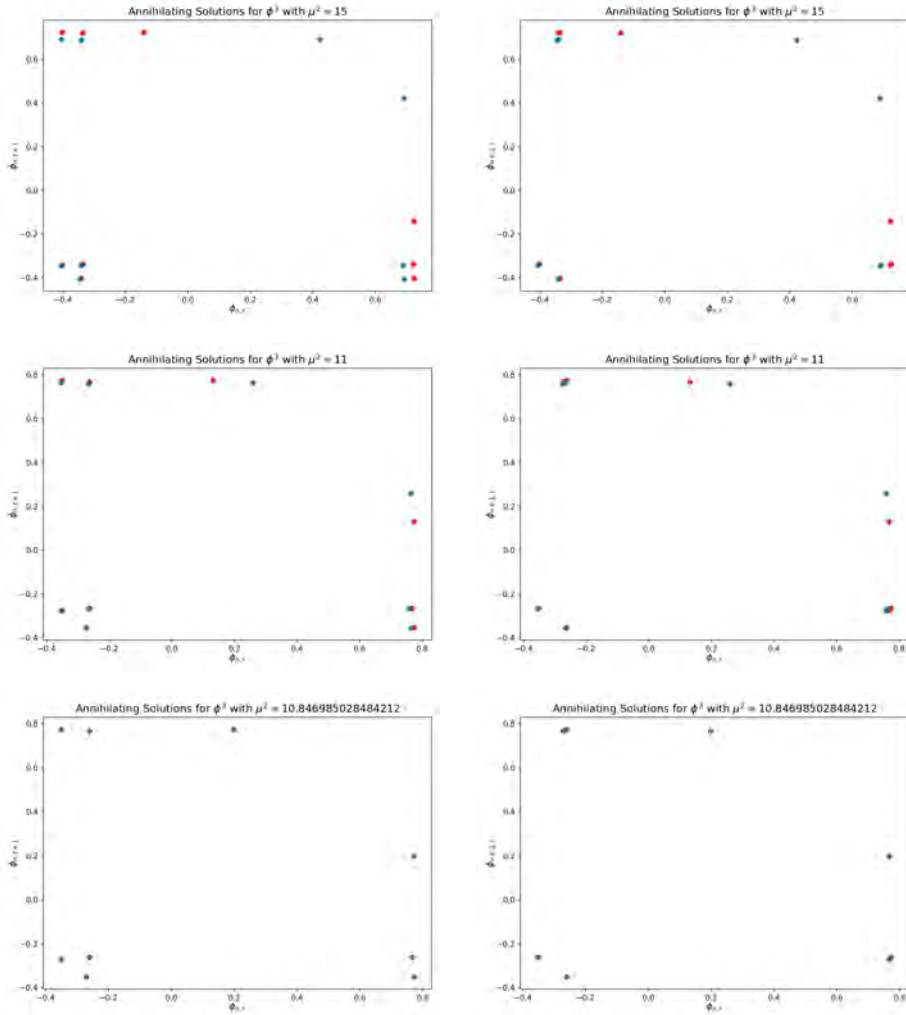


Figure 22.14: Annihilation plots for the  $[4 \times 3]_2$  periodic states  $\begin{bmatrix} 0 & 0 & 0 & 1 \\ 0 & 1 & 0 & 0 \\ 1 & 0 & 1 & 0 \end{bmatrix}$  and

$$\begin{bmatrix} 0 & 0 & 0 & 1 \\ 0 & 1 & 0 & 0 \\ 1 & 1 & 1 & 0 \end{bmatrix}.$$

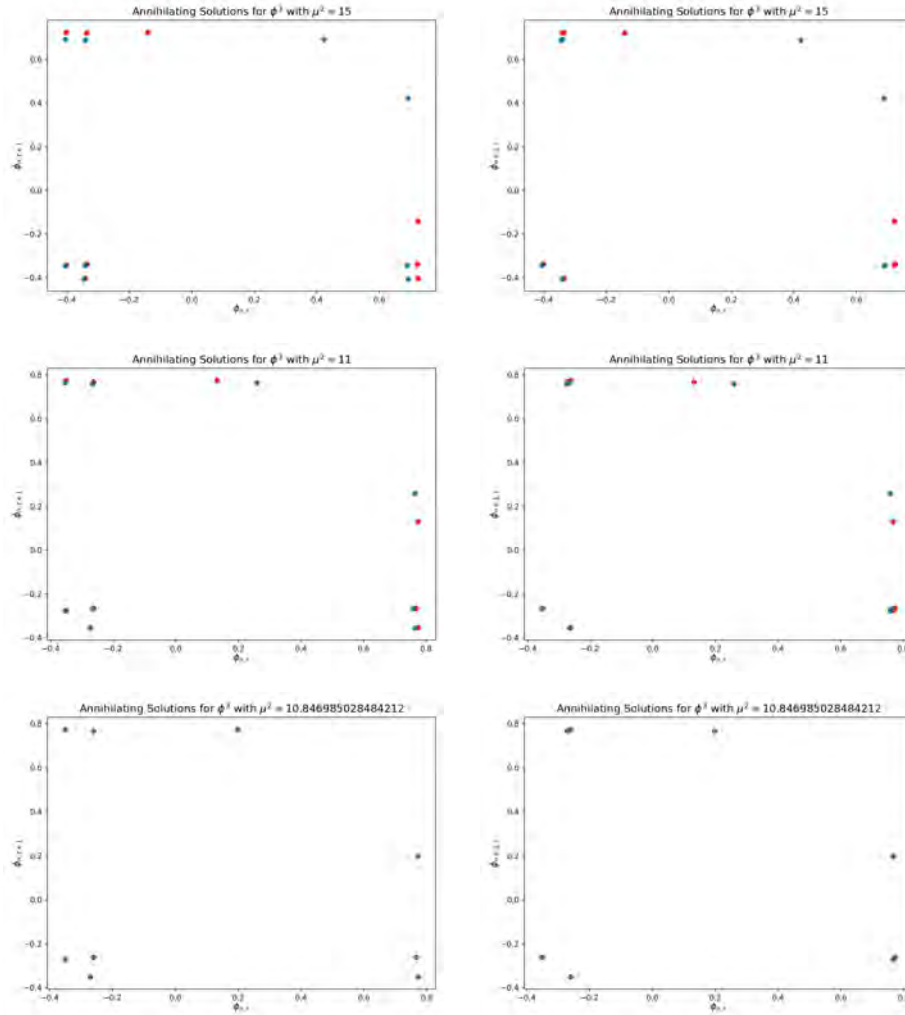


Figure 22.15: Annihilation plots for  $[4 \times 3]_2$  periodic states  $\begin{bmatrix} 0 & 0 & 0 & 1 \\ 0 & 1 & 0 & 0 \\ 1 & 0 & 1 & 0 \end{bmatrix}$  and  $\begin{bmatrix} 0 & 0 & 0 & 1 \\ 0 & 1 & 0 & 0 \\ 1 & 1 & 1 & 0 \end{bmatrix}$ .



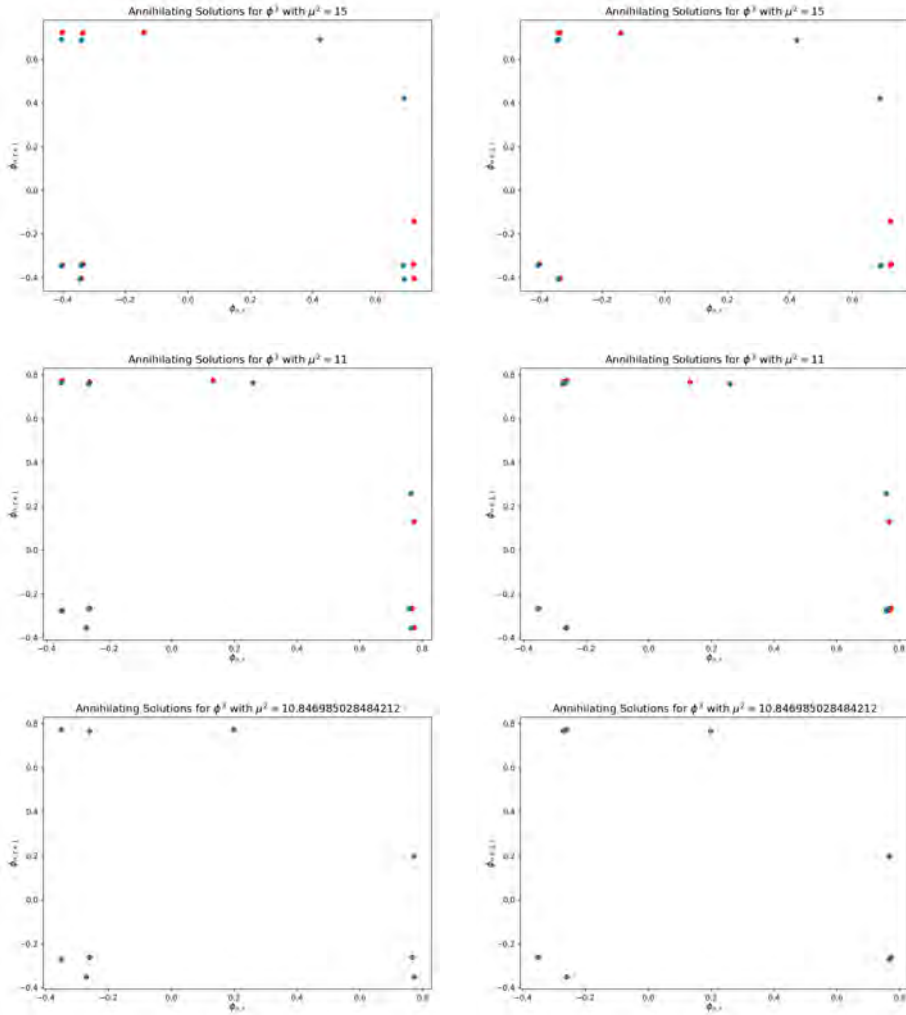


Figure 22.16: Annihilation plots for the  $[4 \times 3]_2$  periodic states  $\begin{bmatrix} 0 & 0 & 0 & 1 \\ 0 & 1 & 0 & 0 \\ 1 & 0 & 1 & 0 \end{bmatrix}$  (red) and  $\begin{bmatrix} 0 & 0 & 0 & 1 \\ 0 & 1 & 0 & 0 \\ 1 & 1 & 1 & 0 \end{bmatrix}$  (blue).

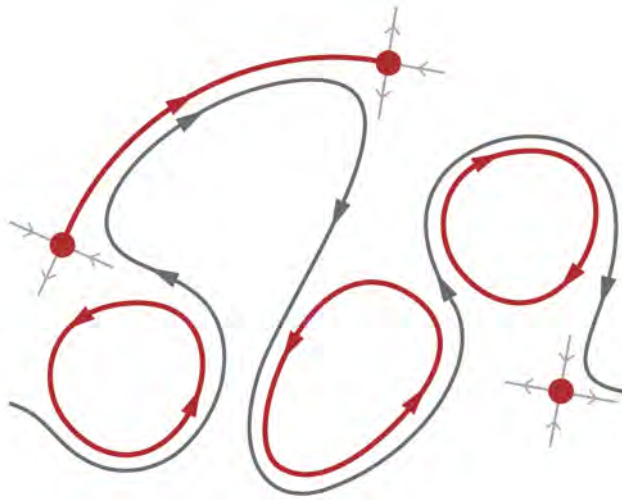


Figure 22.17: A cartoon of periodic (not multi-periodic) orbit theory as a skeleton for chaos, taken from uncited PhD thesis of a nameless student of Tobias Schneider. Any ideas how to modify this idea for us?

**2024-11-20 Sidney** Been thinking about the blobs, and I have no idea how to make them 2D, what would the y-axis be?! Otherwise we just have Cantor-ish plots. Also, I found this really neat figure 22.20 in a thesis from this year. It depicts in a cartoon how an arbitrary trajectory is sucked into the neighborhood of an equilibrium point via its stable manifold, and spat out along its unstable manifold. I was trying to think of a good way to redraw this to account for our multi-periodic orbits. Does anyone have ideas?

**2024-11-21 Sidney** Here is a short thought about trying to get the 2D zeta function to converge better. What if instead of trying to evaluate eta functions, we used the preexisting nice properties of the dynamical zeta function and then truncated the second product. I'll work through this thought a bit. First a couple of assumptions which may make my argument completely incorrect:

1. It is allowed to switch the order of our infinite products. I can't find a good requirement for this, so if someone could help, that would be awesome
2. The systems we are considering are hyperbolic enough that the coefficients of their dynamical zeta function as a polynomial are exponentially suppressed. eg.  $c_{m+1}/c_m \sim e^{-1}$  where I have used "m" to denote period length.
3. The coefficients of  $\prod_p (1 - t_p^n)$  are  $\sim e^{-mn}$ , I am working on showing that the coefficients are bounded by this, and I can do it for the

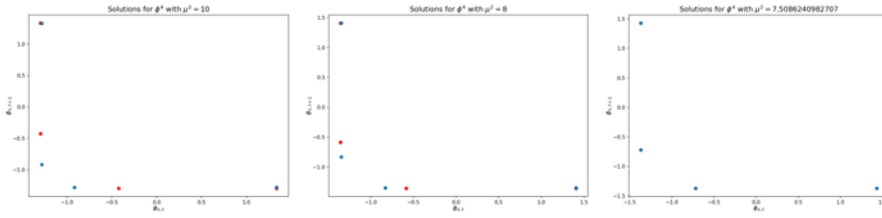


Figure 22.18: Decreasing  $\mu^2$  inverse bifurcation sequence for the merger of  $\phi^4$  theory  $[4 \times 2]_2$  periodic states with mosaics  $\begin{bmatrix} -1 & 0 & -1 & +1 \\ +1 & -1 & +1 & -1 \end{bmatrix}$  (red) and  $\begin{bmatrix} -1 & -1 & -1 & +1 \\ +1 & -1 & +1 & -1 \end{bmatrix}$  (blue). The forward temporal  $(\phi_{n,t}, \phi_{n,t+1})$  and right-side spatial projections  $(\phi_{n,t}, \phi_{n+1,t})$  are the same (still to be established by symmetry analysis), so the spatial projection plots are omitted.

second term  $t_{01}^n - t_0^n t_1^n$  but I haven't fleshed it out for the rest.

With my assumptions out of the way I can now write

$$\begin{aligned} \prod_n \prod_p (1 - t_p^n) &\sim \prod_n (1 - \sum_m e^{-mn} z^{mn}) \\ &= \prod_n \left( -\frac{e^{-n} z^n}{1 - e^{-n} z^n} \right) \sim \prod_n (1 - e^{-n} z^n - e^{-2n} z^{2n}) \end{aligned} \quad (22.110)$$

You can then show that if you truncate the outer product at  $N$  to obtain polynomial  $P_N$  the error is  $E_N \sim P_N \left( \frac{e^{-(N+1)}}{1 - e^{-1} z} + \frac{e^{-2(N+1)}}{1 - e^{-2} z^2} \right)$

I like thinking about it this way because by switching the products, we can still see the shadowing within the resulting equation.

**2024-11-22 Predrag** Have a look at Bountis and Helleman sect. III, our blog sect. 11.1.3. It is an interesting investigation of the "border of order" for the 1-dimensional standard map, starting with low "stretching" parameter  $K$  stable orbits. The estimates obtained from their eq. (3.23) are significantly lower than the actual values at which the corresponding orbit turns unstable. You might compare this to your decreasing  $\mu^2$  bifurcation value (I think it's a small modification of your  $\phi^3$  code). For period  $n = 3$ , I expect a big gap.

**2024-11-22 Predrag** For 2D spatiotemporal periodic states, such as (22.94), the plot where one can study whether there is a gap between neighborhoods of (anti-integrable) shadow states is the plot together in one column all lattice site field values  $\phi_z$ , as we had discussed in the Zoom (see 2024-10-22 Predrag above).

**2024-11-17 Sidney** In figure 22.18, the  $[4 \times 2]_2$  periodic states of  $\phi^4$  with mosaics

$$\begin{bmatrix} -1 & 0 & -1 & +1 \\ +1 & -1 & +1 & -1 \end{bmatrix}, \quad \begin{bmatrix} -1 & -1 & -1 & +1 \\ +1 & -1 & +1 & -1 \end{bmatrix}, \quad (22.111)$$

merge into the bifurcation periodic state

$$\begin{bmatrix} \phi_{-1} & \phi_c & \phi_{-1} & \phi_{+1} \\ \phi_{+1} & \phi_{-1} & \phi_{+1} & \phi_{-1} \end{bmatrix}, \quad (22.112)$$

where the  $\phi_{21}^0 = \phi_0$  and  $\phi_{21}^{-1} = \phi_{-1}$  have merged into their bifurcation value  $\phi_{21}^c = \phi_c$ ,

$$\begin{bmatrix} \phi_{-1} & = & -1.370951078751742 \\ \phi_c & = & -0.7188411823826567 \\ \phi_{+1} & = & 1.4295473539522372 \end{bmatrix}. \quad (22.113)$$

**2024-11-23 Predrag** You might want to explore what the  $[4 \times 2]_2$  not-prime periodic state of  $\phi^4$  with mosaic

$$\begin{bmatrix} -1 & +1 & -1 & +1 \\ +1 & -1 & +1 & -1 \end{bmatrix}, \quad \text{a repeat of } \begin{bmatrix} -1 & +1 \\ +1 & -1 \end{bmatrix}, \quad (22.114)$$

merges with. It might be the mother of the whole (22.111) family of periodic states.

In general, two periodic states should have twice  $4 \times 2 = 8$ , in all 16 distinct lattice sites field values  $\phi_{nt}$ . The internal  $Z_2$  symmetry under  $\phi_z \rightarrow -\phi_z$  ( $\phi_{n,t}, \phi_{n,t+1}$ ) maps at least the  $[2 \times 2]_?$  periodic state, (22.114), into itself, so that might have 2 or 3 distinct lattice site values, unless it is actually a repeat of  $[2 \times 1]_1$ , which make it have 2 distinct lattice site values. And so on: one should explain why in figure 22.18, before the merger, there are only 8 points (not 16!), and why at the merger, the 3 field values  $\phi_c = -0.7 \dots$ , and  $\phi_{+1} = 1.43 \dots$ ,  $\phi_{-1} = 1.37 \dots$  are all there is.

All this is clearly seen in the figure 22.18 temporal ( $\phi_{n,t}, \phi_{n,t+1}$ ) projection of the phase space.

**2024-11-23 Predrag** Note that in  $\phi^4$  mosaics, alphabet  $\mathcal{A} = \{-1, 0, +1\}$  consists of letters, *not* numbers. So do not omit "+" from "+1". At least, in my aesthetics.

That's why we usually write the  $\phi^4$  alphabet as in (2.9)

$$\mathcal{A} = \{\underline{1}, 0, 1\}. \quad (22.115)$$

If there is only one defect lattice site going through the bifurcation, I would the periodic state in the orbit where it is at the origin. For example, rotate (22.111) into

$$\begin{bmatrix} \underline{1} & 1 & \underline{1} & 1 \\ 0 & \underline{1} & 1 & \underline{1} \end{bmatrix}, \quad \begin{bmatrix} \underline{1} & 1 & \underline{1} & 1 \\ \underline{1} & \underline{1} & 1 & \underline{1} \end{bmatrix}, \quad (22.116)$$

and rotate (22.112) into

$$\begin{array}{|c|c|c|c|} \hline \phi_{\perp} & \phi_1 & \phi_{\perp} & \phi_1 \\ \hline \phi_c & \phi_{\perp} & \phi_1 & \phi_{\perp} \\ \hline \end{array} \tag{22.117}$$

preferably represented as its heat map. I find it easier to see symmetries in a colored pattern than in a heap of ternary symbols. But that's just me.

Not obvious, maybe one wants to keep the defect at the center of the primitive cell.

Now, we *know* that if you have a  $Z_2$  symmetry -any symmetry- you *must* quotient it. Its in [ChaosBook](#) . But ever since I have left QFT, I have not met a student who *gets* it. Professors of plumbing, fuggetit. So that's just my life now.

**2024-11-23 Predrag** If you stack  $[4 \times 2]_2$  periodic state colored bricks on top of each other, in the style of [CL18 fig. 7](#), you might see more clearly the symmetries of you periodic states.

**2024-12-03 Sidney** I have not yet done the heat maps, will tomorrow (hopefully)

What I have done though, is an attempt to extend Hill's formula to continuum. I'll look at the case which is first order in time, so

$$0 = \partial_t u - F[u] \tag{22.118}$$

Where  $F[u]$  could depend on derivatives of fields. According to (22.98) the orbit Jacobian operator is

$$\mathcal{J} = \partial_t - \frac{\delta F[u]}{\delta u} = \partial_t - A(u) \tag{22.119}$$

Where  $A$  is the stability matrix from Chaosbook. Note that this is valid because once you take the variational derivative, you can convert the spatial derivatives into Fourier space. Let's write this in terms of different operators

$$\mathcal{J} \approx \frac{\sigma_{\delta t} - \mathbf{1}}{\delta t} - A(u) = \frac{\sigma_{\delta t}}{\delta t} (\mathbf{1} - \sigma_{\delta t}^{-1} (\mathbf{1} + \delta t A(u))) \tag{22.120}$$

Here, I have defined the operator  $\sigma_{\delta t}$  which shifts the field forward in time by  $\delta t$ .  $\sigma_{\delta t}/\delta t$  is just our familiar  $r$  from our lattice model.  $\sigma_{\delta t}$  has a zero trace unless it is raised to an "infinite" power, ie the continuous analog of the nonzero trace for  $r$  on lattices

Now, here is where I make the largest leap: I will say that in the Eulerian definition of  $e$  the infinity that must be approached in  $\lim_{m \rightarrow \infty} (1 + \frac{1}{m})^m$

is contained within the infinity used in Taylor expansions. With that out of the way, I can write

$$\begin{aligned} \ln \text{Det}(\mathcal{J}) &= \text{Tr} \ln(\mathbf{1} - \sigma_{\delta t}^{-1}(\mathbf{1} + \delta t A(u))) = - \sum_{k=1}^{\infty} \frac{1}{k} \text{tr}(\sigma_{\delta t}^{-1}(\mathbf{1} + \delta t A(u)))^k \\ &= -\text{tr} \sum_{r=1}^{\infty} \frac{1}{r} e^{r \int^t d\tau A(u(\tau))} = \ln \det(\mathbf{1} - J) \end{aligned} \quad (22.121)$$

Where time ordering is assumed. I am honestly pretty uncomfortable with my "infinities contained in infinities" argument, is there anything I could do to tighten it up?

**2024-12-04 Sidney** I figured out how to tighten it up, and I did the blob plots. First, I'll work through the improved derivation. I'll rewrite (22.120) so that I use the definition of the derivative

$$\mathcal{J} = \lim_{\delta t \rightarrow 0} \frac{\sigma_{\delta t} - \mathbf{1}}{\delta t} - A(u) = \lim_{\delta t \rightarrow 0} \frac{\sigma_{\delta t}}{\delta t} (\mathbf{1} - \sigma_{\delta t}^{-1}(\mathbf{1} + \delta t A(u))), \quad \delta t = \frac{T}{m}, \quad m \in \mathbb{Q} \quad (22.122)$$

All definitions are the same as in the previous post, although, what I have defined is what is called a "restricted derivative" as  $\delta t$  is rational, not real. As we go on to assume that everything is well behaved, this shouldn't be a problem, but I'd need to relearn some real analysis if we wanted to be more rigorous.

From here, I'll go through the same motions, and go into the power series of the natural logarithm. As we are working with a power series, we have nice convergence properties and can switch the order of the sum and the limit, giving us

$$\ln \text{Det}(\mathcal{J}) = - \lim_{\delta t \rightarrow 0} \sum_{k=1}^{\infty} \frac{1}{k} \text{tr}(\sigma_{\delta t}^{-1}(\mathbf{1} + \delta t A(u)))^k \quad (22.123)$$

Now, before taking the limit,  $\sigma_{\delta t}^{-1}$  is just an  $m \times m$  matrix with the same properties as our lattice  $r^{-1}$  so allowing the trace to kill the appropriate terms in the sum, we obtain

$$\begin{aligned} - \lim_{\delta t \rightarrow 0} \sum_{k=1}^{\infty} \text{tr} \frac{1}{r} (\mathbf{1} + \delta t A(u))^{rm} &= - \lim_{m \rightarrow \infty} \text{tr} \sum_{k=1}^{\infty} \frac{1}{r} \left( \prod_{n=m}^1 e^{\delta t A(u_n)} \right)^r \\ &= -\text{tr} \sum_{r=1}^{\infty} \frac{1}{r} e^{r \int^t d\tau A(u(\tau))} = \ln \det(\mathbf{1} - J) \end{aligned} \quad (22.124)$$

Where again, time ordering is assumed. Great, now the long asked for "blob plots".

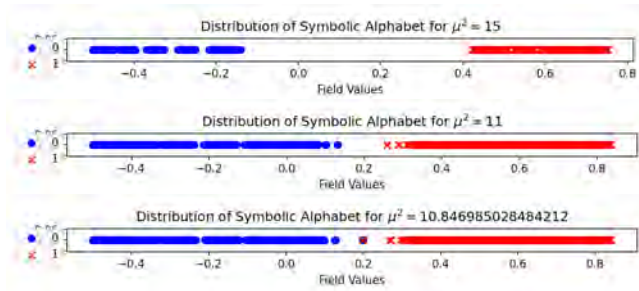


Figure 22.19:  $\phi^3$  theory: Decreasing  $\mu^2$  to see the first bifurcation on a global level for  $\phi^3$ , by plotting all lattice site field values  $\phi_{nt}$  up to volume  $V = 12$  (Predrag 2024-12-23: I have no idea why is this “Distribution of Symbolic Alphabet”? You mean, color-coded by the “binary alphabet”? See figure 22.22. I’m just guessing.)

I kept track of the field value for every 0 and 1 alphabet member regardless of shift, or Bravais cell shape and plotted them on the real number line, with 0 as blue dots, and 1 as red crosses. As you can see, at the value I’ve determined as my critical value  $\mu_c^2$ , the two symbols meet at a single lattice site. In the anti-integrable limit, as  $\mu^2$  grows larger, the distribution of field values clumps onto to me obvious Cantor-like set. For  $\phi^4$ , see figure 22.22.

These figures need to be visually adjusted, but this should do for discussion.

2024-12-23 Predrag Re. figure 22.19: I would plot as horizontal variable  $\sqrt{|\mu^2 - \mu_c^2|}$  of (22.127), values of  $\phi_{nt}$  vertically (make the rows of figure 22.19 columns of the new plot), replace blue dots by blue “+”s, plot a few more columns for  $\mu^2$  closer to  $\mu_c^2$ . eventually you need to track only bifurcating pairs, not all  $2^V$  lattice site field values.

2024-12-23 Predrag Re. temporal shadowing plot of figure 22.20: Gutkin *et al.* have replaced this by spatiotemporal shadowing, see figure 14 in ref. [6] and figure 10 in ref. [17]. In spacetime, homo-/hetero-clinic periodic states are not natural - they require very long primitive cells, of repeated fixed point symbols, with nothing much else happening.

2024-11-17 Sidney Frobenius norm

$$\|\Phi\|_F = \sqrt{\sum_n^L \sum_t^T |\phi_{ij}|^2} \quad (22.125)$$

distances between anonymous  $\phi^3$  and  $\phi^4$  bifurcations pairs of periodic states  $\Phi = \Phi^{(+)} - \Phi^{(-)}$  are plotted in figure 22.21.

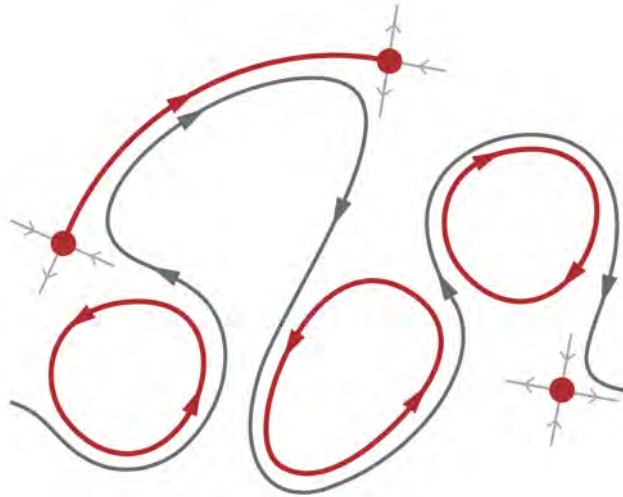


Figure 22.20: A cartoon of periodic (not multi-periodic) orbit theory as a skeleton for chaos, taken from uncited PhD thesis of a nameless student of Tobias Schneider. Any ideas how to modify this idea for us?

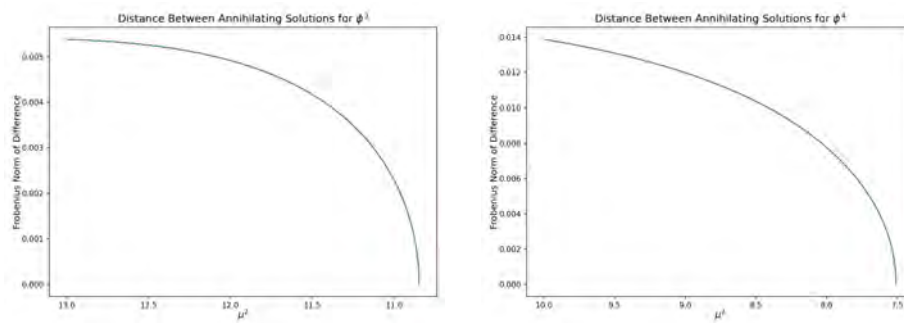


Figure 22.21: The Frobenius norm (22.125) of the difference between unnamed bifurcating pairs of periodic states for  $\phi^3$  and  $\phi^4$ . The  $\mu^2$  values were sampled logarithmically, with a higher concentration (smaller step size) near the bifurcation value. See (22.127) for a suggestion what to plot instead of the Frobenius distance.



**2024-12-23, 2025-01-15 Predrag** The most common bifurcation encountered in polynomial stretch-&-fold maps (parabola, Hénon map, Kuramoto–Sivashinsky, Navier–Stokes) is a **saddle-node** (fold, tangential, blue sky) bifurcation. In one dimension, the normal form has {unstable,stable} pair of fixed points

$$\begin{aligned} x_{t+1} &= \beta + x_t + \alpha x_t^2, \quad -\alpha\beta \geq 0 \\ \{x^{(-)}, x^{(+)}\} &= \{-\sqrt{-\alpha\beta}, \sqrt{-\alpha\beta}\}, \end{aligned} \quad (22.126)$$

bifurcating from the tangency fixed point  $x^{(0)} = 0$ , slope = 1, at  $\beta = 0$ .

In higher dimensions, generically one of the eigendirections at the fixed points goes through slope 1, dominating the neighborhood as the slow center manifold, with the rest hyperbolic, exponentially expanding or contracting, so 1d picture still applies, with fixed points separation dominated by the kissing site distance

$$|\phi_{nt}^{(+)} - \phi_{nt}^{(-)}| \propto \sqrt{|\mu^2 - \mu_c^2|}, \quad (22.127)$$

with  $\{\Phi^{(+)}, \Phi^{(-)}\}$  the pair of periodic states born/destroyed at the bifurcation value parameter= $\mu_c^2$ , and  $nt$  is the lattice site at which the two 'kiss'. If I were to plot this, I would set  $nt = 00$ , but placing the kissing site into the middle of the primitive cell might be easier on the eye.

You can tell that figure 22.21 is most likely a humble saddle-node bifurcation, as the slope is infinite at the bifurcation value, behaving the slope of  $\sqrt{\epsilon}$ ,  $\epsilon \rightarrow 0_+$ .

Instead of figure 22.21, I would plot

$$f(x) = (\phi_{nt}^{(+)} - \phi_{nt}^{(-)})^2, \quad x = \mu^2 - \mu_c^2, \quad (22.128)$$

where  $f(x)$  = the kissing distance, as a function of parameter distance to the bifurcation value. That should grow from the bifurcation value 0 as a straight line of slope 1. The Frobenius norm (22.125) averages over the whole primitive cell, and thus suppresses and obscures the role that the kissing lattice site plays.

Continued in **2025-01-15 Predrag**.

**2024-11-23 Predrag** Replace figure 22.18 by 5 heat maps of (22.112). Perhaps the first two plots with pointwise distances between the two periodic states, in the style of figure 21.16 (a). That would make bifurcation as a "defect" very dramatic.

**2024-12-24 Sidney** Trying to upload the codes

**2024-12-28 Predrag** I have a bunch of notes on Redfern, Lazer and Lucas [28] *Dynamically relevant recurrent flows obtained via a nonlinear recurrence function from two-dimensional turbulence* (2024); [arXiv:2408.05079](https://arxiv.org/abs/2408.05079) in repo

pipes/blog/blog.tex file dailyBlog.tex. My hunch is that Fourier space triads have something to do with the kissing lattice sites, but that's so vague that Tigers might prefer to ignore the remark.

**2025-01-05 Sidney, 2025-01-07 Predrag** No real work (as warned earlier) but an attempt at clarification regarding our discussion on applying Bloch theorem to finite sized systems such as Kuramoto Sivashinsky. In the most basic understanding of the physical picture of Bloch, we have an infinitely large crystal, and a field associated with each point along this massive crystal. Bloch comes in when we perturb the ENTIRE field configuration, not just a primitive cell which is then enumerated across the rest of the crystal (eg. there are different perturbations at different scales, and Bloch accounts for this).

For a finite system (say our flame front on top of a bunsen burner) there is an infrared cutoff of wave number, which, should we wish to continue with Bloch, should probably be approximated as 0. Now, the system which Kuramoto Sivashinsky models in plasma physics is the interaction between electrostatic "drift waves" and ions trapped in a nonhomogeneous magnetic field. Outside of the realm of marginal stability, the trapped ions resonate with many different "modes" of the drift waves, leading to turbulent fluctuations. Ignoring the infrared cutoff, would this multitude of resonances be equivalent to the "non-periodic perturbations on an infinite crystal" that we're applying to our lattice field theories?

Just to make absolutely sure:

Floquet-Bloch continuous Fourier spectra account for perturbations at all scales, whether this manifests as an infinite lattice where a periodic state is perturbed non-periodically, an infinite continuous space where a periodic state is perturbed non-periodically, or a continuous round flame front where there is an (ignorable) IR cutoff and a *discrete* but infinite spectrum of Fourier modes, wave numbers which include the arbitrarily small discrete UV wavelengths.

Take away: Floquet-Bloch theorem accounts for perturbations to periodic orbits on all scales. Yay?

**2025-01-07 Predrag** For lattices (where lattice constant is the ultraviolet (UV) cutoff, a 'Bunsen burner' has finite, discrete spatial  $k$  Fourier spectrum, with the number of eigenvalues (including repeats of degenerate ones) is  $V_A$ .

A PDE 'Bunsen burner' there is no UV cutoff, so infinite discrete spatial  $k$  Fourier spectrum, with the number of eigenvalues (including repeats of degenerate ones) infinite. Might need UV regularization, see [ChaosBook](#). In practice one truncates high  $k$  numerically.

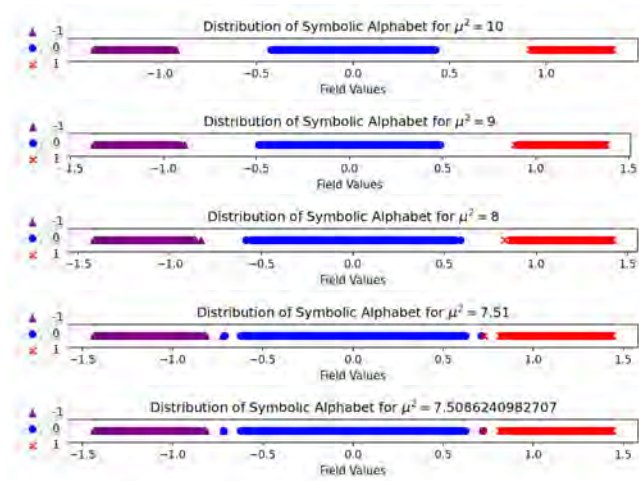


Figure 22.22:  $\phi^4$  theory. Lattice site field values  $\phi_z$ , up to volume 8, color-coded by the corresponding alphabet ternary letter of the lattice site  $z$  mosaic value  $m_z$ . For the  $\phi^3$  theory, see figure 22.19.

2025-01-07 **Predrag** Read today's pow wow on page 1416.

2025-01-15 **Sidney** Finally posting some figures, specifically the blobs of  $\phi^4$  and the kissing states...orbit Jacobian operator calculations still need some work

2025-01-15 **Predrag** There are two critical saddle-node bifurcation values of the parameter:  $\mu_{c1}^2$ , where elliptic equilibrium (a pair of imaginary eigenvalues) is born, so hyperbolicity is lost, and  $\mu_c^2$  where it annihilates the sister hyperbolic eigenvalues pair, and pruning sets in. My (22.127) probably does not work in  $d = 2$  spatiotemporal theory. To fix it, read January 9 pow wow, "Saddle-node bifurcations in Hamiltonian systems" discussion, start on page 1419.

## References

- [1] K. T. Alligood, T. D. Sauer, and J. A. Yorke, *Chaos, An Introduction to Dynamical Systems* (Springer, New York, 1996).
- [2] A. Barvinok, *Lattice Points, Polyhedra, and Complexity*, tech. rep. (Univ. of Michigan, Ann Arbor MI, 2004).
- [3] O. Biham and W. Wenzel, "Characterization of unstable periodic orbits in chaotic attractors and repellers", *Phys. Rev. Lett.* **63**, 819 (1989).

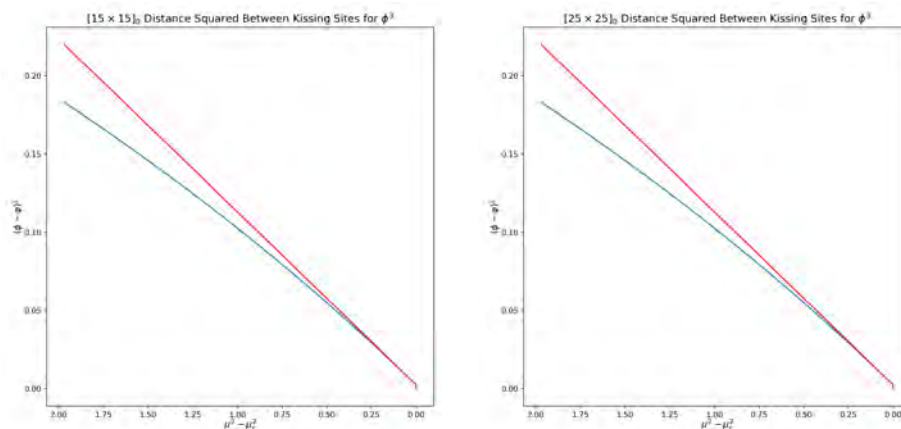


Figure 22.23:  $\phi^3$  theory: The kissing distance  $(\phi_{nt}^{(+)} - \phi_{nt}^{(-)})^2$  as a function of parameter distance to the bifurcation value,  $\mu^2 - \mu_c^2$ , see (22.128). Reference line with slope determined by the last  $10^{-6}$  difference,  $\mu_c^2 = 11.03079258$

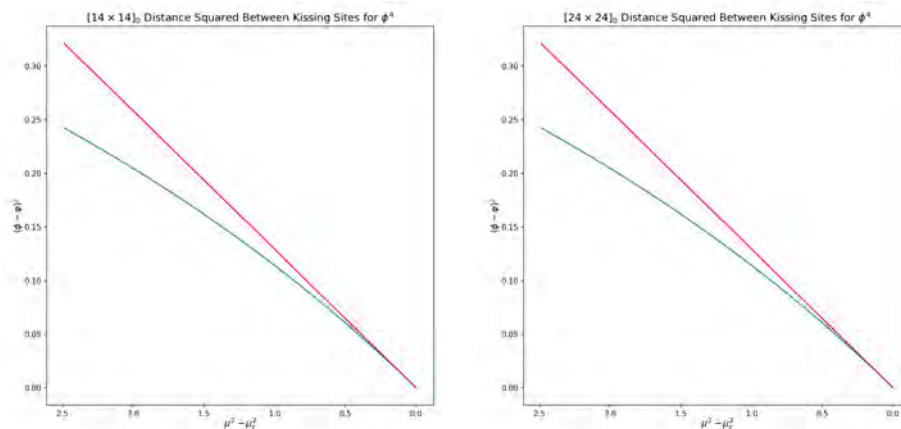


Figure 22.24: Kissing distance between annihilating field values for  $\phi^4$ , see (22.128). Reference line with slope determined by the last  $10^{-6}$  difference,  $\mu_c^2 = 7.51194731$ .

- [4] C. Cuell and G. W. Patrick, “Geometric discrete analogues of tangent bundles and constrained Lagrangian systems”, *J. Geom. Phys.* **59**, 976–997 (2009).
- [5] P. Cvitanović, *Field Theory*, Notes prepared by E. Gylstenkerne (Nordita, Copenhagen, 1983).
- [6] P. Cvitanović and H. Liang, *A chaotic lattice field theory in two dimensions*, In preparation, 2024.
- [7] P. J. Davis, *Circulant Matrices*, 2nd ed. (Amer. Math. Soc., Providence RI, 1979).
- [8] R. L. Devaney and Z. Nitecki, “Shift automorphisms in the Hénon mapping”, *Commun. Math. Phys.* **67**, 137–146 (1979).
- [9] H. R. Dullin and J. D. Meiss, “Generalized Hénon maps: the cubic diffeomorphisms of the plane”, *Physica D* **143**, 262–289 (2000).
- [10] A. Endler and J. A. C. Gallas, “Arithmetical signatures of the dynamics of the Hénon map”, *Phys. Rev. E* **65**, 036231 (2002).
- [11] A. Endler and J. A. C. Gallas, “Conjugacy classes and chiral doublets in the Hénon Hamiltonian repeller”, *Phys. Lett. A* **356**, 1–7 (2006).
- [12] A. Endler and J. A. C. Gallas, “Reductions and simplifications of orbital sums in a Hamiltonian repeller”, *Phys. Lett. A* **352**, 124–128 (2006).
- [13] M. J. Engel, *Short Course on Symmetry and Crystallography*, 2011.
- [14] P. M. Gade and R. E. Amritkar, “Spatially periodic orbits in coupled-map lattices”, *Phys. Rev. E* **47**, 143–154 (1993).
- [15] I. García-Etxebarria, B. Heidenreich, and T. Wrase, “New  $\mathcal{N} = 1$  dualities from orientifold transitions Part I: Field theory”, *J. High Energy Phys.* **2013**, 7 (2013).
- [16] M. N. Gudorf, *Orbithunter: Framework for Nonlinear Dynamics and Chaos*, tech. rep. (School of Physics, Georgia Inst. of Technology, 2021).
- [17] B. Gutkin, L. Han, R. Jafari, A. K. Saremi, and P. Cvitanović, “Linear encoding of the spatiotemporal cat map”, *Nonlinearity* **34**, 2800–2836 (2021).
- [18] B. Gutkin and V. Osipov, “Classical foundations of many-particle quantum chaos”, *Nonlinearity* **29**, 325–356 (2016).
- [19] M. Hénon, “A two-dimensional mapping with a strange attractor”, *Commun. Math. Phys.* **50**, 94–102 (1976).
- [20] D. A. Klain and G.-C. Rota, *Introduction to Geometric Probability* (Cambridge Univ. Press, 2006).
- [21] H. Liang and P. Cvitanović, “A chaotic lattice field theory in one dimension”, *J. Phys. A* **55**, 304002 (2022).
- [22] M. M. Budišić, R. M. Mohr, and I. Mezić, “Applied Koopmanism”, *Chaos* **22**, 047510 (2012).

- [23] E. Ott, *Chaos and Dynamical Systems* (Cambridge Univ. Press, Cambridge, 2002).
- [24] M. E. Peskin and D. V. Schroeder, *An Introduction to Quantum Field Theory* (Perseus Books, Cambridge, Massachusetts, 1995).
- [25] J. Polchinski, *String Theory. Vol 1: An Introduction to the Bosonic String* (Cambridge Univ. Press, 1998).
- [26] A. Politi and A. Torcini, "Periodic orbits in coupled Hénon maps: Lyapunov and multifractal analysis", *Chaos* **2**, 293–300 (1992).
- [27] A. Politi and A. Torcini, "Towards a statistical mechanics of spatiotemporal chaos", *Phys. Rev. Lett.* **69**, 3421–3424 (1992).
- [28] E. M. Redfern, A. L. Lazer, and D. Lucas, "Dynamically relevant recurrent flows obtained via a nonlinear recurrence function from two-dimensional turbulence", *Phys. Rev. Fluids* **9**, 124401 (2024).
- [29] D. E. Sands, *Introduction to Crystallography* (Dover, 1969).
- [30] J. Singleton, *Band Theory and Electronic Properties of Solids* (Oxford Univ. Press, Oxford, UK, 2001).
- [31] A. D. Sokal, Numerical computation of  $\prod_{n=1}^{\infty} (1 - tx^n)$ , 2002.
- [32] D. Sterling and J. D. Meiss, "Computing periodic orbits using the anti-integrable limit", *Phys. Lett. A* **241**, 46–52 (1998).
- [33] D. G. Sterling, *Anti-integrable Continuation and the Destruction of Chaos*, PhD thesis (Univ. Colorado, Boulder, CO, 1999).
- [34] D. G. Sterling, H. R. Dullin, and J. D. Meiss, "Homoclinic bifurcations for the Hénon map", *Physica D* **134**, 153–184 (1999).
- [35] S. H. Strogatz, *Nonlinear Dynamics and Chaos* (Westview Press, Boulder, CO, 2014).
- [36] G. N. Watson, "The diffraction of electric waves by the earth", *Proc. R. Soc. Lond. A* **95**, 83–99 (1918).
- [37] S. V. Williams, X. Wang, H. Liang, and P. Cvitanović, *Nonlinear chaotic lattice field theory*, In preparation, 2024.

## Chapter 23

# Xuanqi's blog

Xuanqi Wang  
xwang3021@gatech.edu  
subversion siminos : xwang3021  
cell +1 4047715611  
WeChat y2528742620

The latest entry at the bottom for this blog, page 1134

**2021-12-07 Predrag** to Xuanqi:

As you go along, write up your narrative in this file, ask questions - this is your personal blog, like an experimentalist's log - everything that you learn and want to share goes in here. Clip & paste anything from other sections you want to discuss, that saves you LaTeXing time.

**2021-12-07 Predrag** The deal is: If you have not entered one word into the blog in a week means that you have done nothing on this project in a week. The rule of thumb is not less than an entry twice a week.

**2021-09-09 Predrag** The 3rd line of *siminos/spatiotemp/blogCats.tex* says "process only the files you are editing",

```
\input{inputs/inclOnlyCats}
```

you uncomment a single line in that file to "process only the files you are editing".

**2021-12-07 Predrag to Xuanqi** .

You refer to a reference like this: Gutkin and Osipov [8] (*GutOsi15* refers to an article listed in *../bibtex/siminos.bib*).

and to external link like this: "For great wallpapers, see overheads in Engel's course [6]."

Pro tip: compile *blogCats.tex* often, as you write, and fix errors as you write. I had to go all the way back to May to find one of Sidney's unbalanced "{" and make the entire blog compile without errors...

## 23.1 2022 blog

**2021-12-08 Predrag** I believe that the  $\phi^4$  is not very different from the  $\phi^3$  theory for sufficiently strong stretching parameter. Here are proposed exercises for you to develop intuition about that:

1. Plot the  $3^n$  Smale horseshoe for  $\phi^4$  1-d forward-in time map, in the  $(\phi_t, \phi_{t+1})$  plane, paralleling [ChaosBook fig. 15.5](#) for  $\phi^3$ , i.e., Hénon map (3.25), (13.2).  
The intuition is topological; 1-d parabola repeller (with parabola height larger than 1) has the same kind of Cantor set as the complete Smale horseshoe repeller for the Hénon map. Similarly, I expect [ChaosBook fig. 11.4](#), here (6.225), to capture the topology of the  $\phi^4$  repeller.
2. For the  $b = -1$  Hénon map stretching parameter values  $a$  larger than (3.57), the 'critical' value  $a_h = 5.69931 \dots$  guarantee a complete horseshoe. What is (very roughly) a corresponding value for the  $\phi^4$  theory?
3. (harder, not essential as yet) Quotient the  $D_1$  symmetry for  $\phi^4$ , as in [ChaosBook fig. 11.5](#). It is an 'internal symmetry', see sect. 4.9.

Ibrahim and you should form a study group to understand this - it's absolutely essential.

**2021-12-08 Predrag** The above approaches should be safe for multimodal maps with complete repelling sets, and it should work for finite-grammar Smale horseshoe repellers. Smale's original horseshoe [13], his fig. 1 was unimodal, but he also explicitly gives our  $\phi^4$  bimodal repeller, his fig. 5.

**2021-12-07, 2022-01-16 Predrag** Parallel reading, while you work on the above:

Study [LC21 paper](#), in this repo `siminos/reversal/LC21.tex` *A chaotic lattice field theory in one dimension*, in particular sect. 4 *A  $\phi^3$  field theory*, and sect. 5 *A  $\phi^4$  field theory*.

Sorry about many broken equation links (??) - they are referring to equations in `LC21.tex`, now a separate article removed from this blog.

Write your study notes up here.

**2021-09-12 to 2021-12-22 Predrag** I have added my guess (4.228) for the infinite coupling  $g$  anti-integrable limit of  $\phi^4$  theory. That gives a 3-letter alphabet  $\mathcal{A} = \{-1, 0, 1\}$ . One can use it to find by continuation any periodic state, at  $g$  as low as possible. 'Generalized Hénon maps' AKA  $\phi^4$  field theory posts are in sect. 4.12.5 *Deterministic  $\phi^4$  lattice field theory*.



**2022-01-21 Xuanqi** I'm calculating eigenvalues for the Jacobian now of the  $\phi^4$  horseshoe map. The matrix seem very simple, but the coordinate for fixed point are is a cubic equation, whose analytic solution is too complicated to be included. So I think I should probably generate a list of parameters first and then calculate the fixed points separately. Now I have no sense what range of parameter should be chosen, just randomly decided that probably I should start as 1-10, because for Hénon it is 6.

**2022-01-21 Sidney 2 Xuanqi** I am going to copy this to both Harrison's and Ibrahim's blog. For an explanation of my method, look at my blog (entry for 2021-10-05), if you have question there, let me know. When I say "sign generated by symbol sequence" I mean either 1 or  $-1$ , depending if the symbol is a 1, or a 0 respectively. Note that  $\pm 1$  are the square roots of unity. I have to edit the loop to account for the change of sign, but that is ok. Anyway, for  $\phi^4$  we have to deal with a cubed root, and thus a cubed root of unity:  $\gamma$ . These are complex numbers, so I am not sure how useful that is, but it seems that unless  $g$  and  $m_t$  is set appropriately, some of the fixed points are complex, so maybe having complex numbers isn't too out of the ordinary. Anyway, the formula should be (I think)

$$\phi_t = \gamma \sqrt[3]{\frac{m_t + \phi_{t+1} + \phi_{t-1}}{g}}$$

Where  $\gamma$  is a different root of unity depending on the symbol sequence, I am not sure how that will work with the imaginary numbers. If this is a valid method for you, I would be interested in learning WHY it is. I am quite interested in numeric theory, but I have not yet bothered to see why this specific map inversion is valid. It could be interesting.

Additionally, the 6 in the Hénon map was determined via a sort of bifurcation analysis (that I need to actually nail down how it was done, but all the same). Effectively, 6 is larger than the 5.6... that is the minimum value of  $a$  which allows for all binary sequences, and it is an integer, thus 6 is convenient.

**2022-01-31 Xuanqi** I have figured out the recurrence relation, but the problem is that it cannot be symmetric around the origin, or we will be trapped by origin being a center.

**2022-01-31 Predrag** Can you be explicit, write down formulas down that led you to this 'center'?

Does (4.234) help you? I pointed out to the Gang that **2021-12-22 Predrag Anastassiou, Bountis and Bäcker [1] *Homoclinic points of 2D and 4D maps via the parametrization method* (2017)** plots the horseshoe you are trying to plot, see their fig. 1). Maybe just reproduce their results, for starters? See my notes following (4.229).

**2022-01-31 Xuanqi** I'm thinking about the deduction of recurrence. Is it just the second order difference equation of position equal to the gradient of potential function?

**2022-01-31 Predrag** Maybe. Hamiltonian is the sum of kinetic + potential, Lagrangian is their difference. I prefer not to think about "Hamiltonian vs. Lagrangian" but about spatiotemporal cat's Klein-Gordon mass squared  $\mu^2 = s - 2$ . Sufficiently strong stretching, the system is unstable. For weak stretching the "mass" is imaginary, you have to think about a spring constant again. Study LC21 [fig. 1](#)).

**2022-02-03 Xuanqi** I read the first few sections of Anastassiou *et al.* [1] *Homoclinic points of 2D and 4D maps via the parametrization method* (2017), see sect. [4.12.7](#), it helps. They took the potential function of form

$$V(\phi_t) = \frac{g}{4}\phi_t^4 + \frac{c}{2}\phi_t^2 + d. \quad (23.1)$$

I observe that it has a 'dynamical' reflection symmetry  $\phi_t \rightarrow -\phi_t$ , referred to in [2021-12-08 Predrag](#) post above as  $\dots$  harder, not essential as yet - quotient the  $D_1$  symmetry for  $\phi^4$ , as in [ChaosBook fig. 11.5](#)  $\dots$  .

This is not the temporal lattice reflection symmetry  $\phi_t \rightarrow \phi_{-t}$  .

**2022-02-06 Predrag** Can't distinguish a cat from a parquet floor? Read sect. [6.1](#).

**2022-02-03 Xuanqi** I calculated

(**2022-02-04 Predrag** Write down here the formulas of your calculation step by step. What you did by hand in the meeting today was very clear, it needs to be LaTeXed here for possible future use in a paper or a report.)

the eigenvalues of the 1-time step time evolution Jacobian matrix, and found that for  $c > 2$  ( $c$  is the coefficient for quadratic term in potential [\(23.1\)](#)), all fixed points are saddle points. This being Hamiltonian system, the determinant of time evolution Jacobian matrix always equals one, and the stability multipliers

$$(\Lambda^+, \Lambda^-) = (\Lambda, \Lambda^{-1}), \quad |\Lambda| > 0 \quad (23.2)$$

are real.

Now the thing is to chose a value  $c$ , as we surely don't want two free parameters in the equation. Should we choose some value close to 2 or far away from it? My guess is that for some value close to 2, the points in unstable manifold will be pushed away from origin.

As it so happens, Anastassiou *et al.* [1] have already made a choice, and once I understand what their choice was based on, I expect to follow it.

2022-02-03 Xuanqi Authors of ref. LC21 [9] claim that their action

$$V(\phi_t, m_t) = -\frac{g}{4}\phi_t^4 + \phi_t^2 + m_t \phi_t, \quad (23.3)$$

leads to the Euler–Lagrange equations for ‘ $\phi^4$  lattice field theory’ of form

$$-\phi_{t+1} + g\phi_t^3 - \phi_{t-1} = m_t. \quad (23.4)$$

Substituting  $\phi_t \rightarrow (\phi'_t + b); m_t \rightarrow 0 \dots$  I show that the two formulations disagree, as follows:

$$\phi'_{t+1} + g a^3 (\phi_t - b)^3 - \phi'_{t-1} = \phi'_{t+1} + g a^3 (\phi'_t)^3 - 3g a^3 b (\phi'_t)^2 + 3g a^3 b^2 (\phi'_t) - g a^3 b^3 - \phi'_{t-1}.$$

In order to agree with the form

$$\phi_{t+1} + \phi_{t-1} - 2\phi_t = g\phi_t^3 + c\phi_t + m_t. \quad (23.5)$$

we need  $b = 0$ , as there is no quadratic term here. However, this immediately result in a zero linear term, as we have  $b^2$  in the coefficient. Parameter  $a$  is only a rescaling of axis, but 0 is always invariant under rescaling, so I conclude that these formulae cannot agree.  $\dots$

2022-02-11 Xuanqi Anastassiou *et al.* [1] potential function is

$$V(\phi_t) = \frac{g}{4}\phi_t^4 + \frac{c}{2}\phi_t^2 + m_t \phi_t, \text{ with } g > 0. \quad (23.6)$$

In the discrete lattice site, we have the twice difference equals to the gradient of potential. That is

$$\phi_{t+1} - 2\phi_t + \phi_{t-1} = g\phi_t^3 + c\phi_t + m_t. \quad (23.7)$$

Rewrite this three terms recurrence relation as a two terms recurrence for a two-component field  $\varphi_t = (\phi_{t+1}, \phi_t)$ :<sup>1</sup>

$$\begin{aligned} \phi_{t+1} &= g\phi_t^3 + (c+2)\phi_t - \phi_{t-1} \\ \phi_t &= \phi_t. \end{aligned} \quad (23.8)$$

In matrix notation.

$$\varphi_t = \begin{pmatrix} g\phi_t^3 + (c+2)\phi_t & -1 \\ 1 & 0 \end{pmatrix} \varphi_{t-1} \quad (23.9)$$

Take  $\phi_t = \phi$  fixed point. It is a solution of the cubic equation  $g\phi^3 + c\phi + m_t = 0$ . The forward-in-time Jacobian matrix (12.66) evaluated at the fixed point at the origin (where  $m_t = 0$ ) is

$$\begin{pmatrix} 3g\phi_t^2 + (c+2) & -1 \\ 1 & 0 \end{pmatrix} = \begin{pmatrix} c+2 & -1 \\ 1 & 0 \end{pmatrix} \quad (23.10)$$

---

<sup>1</sup>Predrag 2022-02-11: I do not get (23.8) - it is a still a 3-point recurrence?

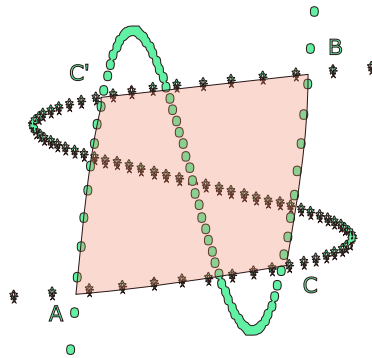


Figure 23.1:  $\phi^4$  theory (23.6) stable, unstable manifolds, for Anastassiou *et al.* [1] choice of coupling constant  $g = 10$ ,  $c = -4.5$ . (stars) Unstable manifold. (dots) Stable manifold. The primary cover ACBC'A. Its iterate forward and backward will yield 9 covers of the next level of the cubic Hénon map Smale horseshoe. Continued in figure 23.2.

Looking for the eigenvalues  $\Lambda$  of this matrix, we have  $\Lambda$ . By the Vieta's theorem that every school child knows,  $\Lambda_1\Lambda_2 = 1$ , and  $\Lambda_1 + \Lambda_2 = c$ . To ensure that both eigenvalues are real, we need  $(\Lambda_1 + \Lambda_2)^2 \geq 4\Lambda_1\Lambda_2 = 4$ . Now, looking at the origin, it's easy to see that if  $|c + 2| > 2$ , there should be one eigenvalue greater than 1 and the other smaller than 1. The remaining two fixed points are also saddle points, as we will always have  $\phi_t^2 > 0$ . Anastassiou *et al.* [1] chose  $c = -4.5$ , which satisfies  $c < 0$  needed for all 3 fixed points to be real.

I think the difference between the formula in LC21 and Anastassiou *et al.* [1] is merely a difference in the quadratic coefficient and the source term, which has no effect on the neighborhood of origin.

**2022-02-11 Xuanqi** I had a discussion with Ibrahim (see his post page ??), and he showed me a website that plots the horseshoe for Hénon map. That website started with a circular region, and then map the region and let image and pre-image intersect. However, it didn't show a full horseshoe in the first iteration, and we guess it's because the circular region is not a natural region to choose. For my replication, I will just start with a unit square, as in the paper, which is neither a natural set in the topological meaning but good enough to show the entire horseshoe.

**2022-02-11 Predrag** I found this top secret, very exclusive website, where every student plots the Hénon stable-unstable manifolds just as a humble homework 7. Student evaluation praise this course specifically for this problem set, because it taught them that stable-unstable manifolds are not a big deal.

**2022-02-17 Xuanqi** Figure 23.1 looks like what we expected. How do we de-

fine the non-wandering set  $\Omega$  here, as there are four regions bounded by  $W_u$  and  $W_s$  now.

**2022-02-18 Predrag** Wow, that looks great. Next, bring it to the publication level graphics.

**2022-02-18 Xuanqi** (Predrag acting as Xuanqi's blog ghost secretary) The next step is to replace dots by a "contour line", and use  $ABCC'A$  as the region for a backward and a forward iteration, as explained in the [ChaosBook fig. 11.5 Hénon map example](#).

I am using python with [Matplotlib](#).

**2022-02-11, 2022-02-18 Predrag** What I mean by the [...] following (23.15) is that you write down a *formula*, a parameter transformation formula like the one given in [ChaosBook example 14.6 Unimodal maps](#). You help Han and me finalize the convention for you, Sidney's and Ibrahim's work that way.

**2022-02-18 Predrag** For Anastassiou *et al.* [1] conventions, see sect. 4.12.7.

**2022-02-23 Xuanqi** My idea is that the definition in LC21 will not work, as it gives no linear term for  $\phi_t$ . Now my trouble is that this region  $\Omega$  that we start with is very hard to define. I tried the whole region with all the arms and legs, and it destroys the intersection in the middle, which is absolutely what we don't want. After that, I tried to work with two regions, i.e., iterate one region M forward and region N backward. Figure 23.2 (a) illustrates the region (shaded) I chose to map backward, denoted by  $\widehat{ACDEGHA}$  (I forgot to include that last "A" in my script with the figure). In the same fashion, the region I mapped forward is  $\widehat{ABCEFGA}$ .

Personally I think figure 23.2 (b) is not what we want. There are corners due to a very unnatural choice of boundary, as the stable and unstable manifolds are passing through our region. And also, as I discussed with Han today, we both think that it is somehow problematic to iterate two different regions forward and backward. Can we have a meeting, as I cannot understand how we should choose the region to iterate now. Han had a fascinating thought, but there is not enough space on the margin to stick it into this figure.

**2022-02-23 Predrag** Can you plot the stable-unstable manifolds for the fixed point  $\phi_R$  close to  $E$  in figure 23.2 (a)? In our discussion we concluded that it has positive stability multipliers, and that means that it might define the outer boundary of Smale horseshoe. The fixed point  $(0, 0)$  has negative multipliers, which means it gets buried within the horseshoe, cannot define a boundary.

**2022-02-23 Xuanqi** Works! See figure 23.3 :)

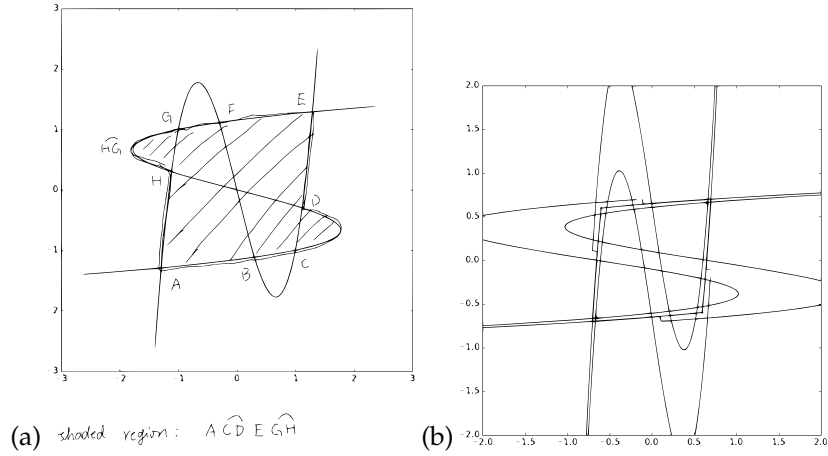


Figure 23.2: (a) Region  $N$  sent backward. (b) Somewhat strange horseshoe for  $g = 15, c = -8.5$ . The tilted square is the intersection of  $AB\widehat{C}E\widehat{F}G\widehat{A}$  and  $AC\widehat{D}E\widehat{G}\widehat{H}A$ , which is essentially  $\Omega$ . The Lo Fan [1] formulation of  $\phi^4$  theory (23.6),  $g = 15, c = -8.5$ . Continued in figure 23.3.

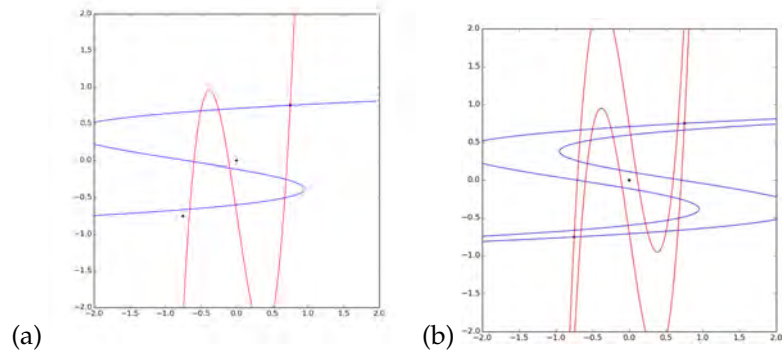


Figure 23.3: (a) Fixed point  $\phi_R$  stable-unstable manifold. (b) Fixed points  $\phi_L, \phi_R$  stable-unstable manifolds. The Lo Fan [1] formulation of  $\phi^4$  theory (23.6),  $g = 15, c = -8.5$ . Continued in figure 23.4.

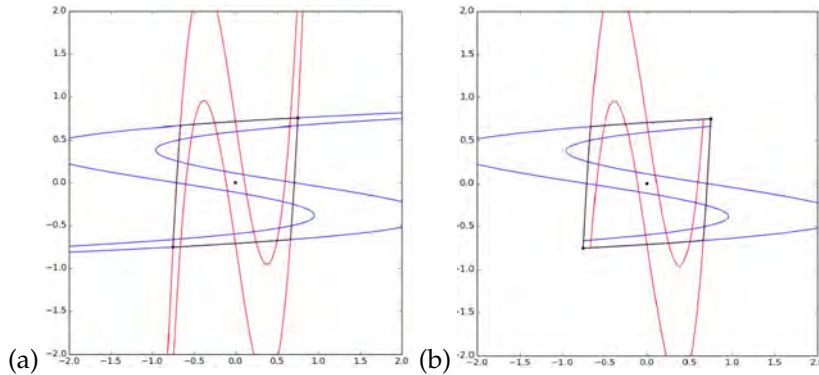


Figure 23.4: (Continued from figure 23.3.) (a) The intersections of fixed points'  $\phi_L, \phi_R$  stable-unstable manifolds form the level 0, single domain 'diamond' cover of the bimodal Smale horseshoe non-wandering set. (b) Iterating the 'diamond' forward and backward yield the level 2,  $3^2$  domains cover. As this is the Lo Fan [1] formulation of  $\phi^4$  theory (23.6),  $g = 15, c = -8.5; \phi_L = -0.7527, \phi_R = 0.7527$ , I will have to replot this for our group's formulation of  $\phi^4$  theory. (Continued in figure 23.6).

**2022-02-23 Xuanqi to Ibrahim** I just realized that the ellipse you figured out for the 2-cycle put the same condition on  $c < -4$  magically. I thought that it would be natural if my condition contains your, as if there is only one fixed point you won't expect the 2-cycle, but actually they are just the same set. Do you think that this double containment has some implication about saddle point?

I also updated the disagreement with LC21, proved that a coordinate transform won't compromise this disagreement. I think this region will work better, as it has two positive eigenvalues. Probably  $\phi^4$  is somehow trickier than we thought.

**2022-02-23 Predrag** Not tricky at all: do the same for the left fixed point  $L$  (or reflect figure 23.3 over the horizontal and vertical axes - would have done it for you, had you also committed the `figSrc/inksacape/XWwuWs1.svg` file) and you are done! That's the optimal cover, with 9 pretty intersections. Would be nicer if one could make it fatter...

**2022-02-24 Xuanqi** Several discoveries. (1) We now have a correct and beautiful horseshoe now. I calculated stable-unstable manifolds near both fixed points, see figure 23.4(a). And if we choose the region whose boundary contains these two fixed points, shown in black, and iterate this region forward and backward, we obtain the pretty bimodal Smale horseshoe of figure 23.4(b).

In fact, I thoroughly understand why this time it works. As explained in distant past, **2022-02-23 Predrag** post on page 1077.

1. Predrag's fixed point  $\phi_C$  stable-unstable manifolds 'diamond' figure 23.1 looks right, but it is **WRONG**. The fixed point  $\phi_C$  at  $(0, 0)$  has negative multipliers, with iterates of points close to the fixed points jumping across the unstable manifold, which means it gets buried within the horseshoe, and cannot define a boundary.
2. The reflection-symmetry related pair  $\phi_L = -\phi_R$  has positive stability multipliers, meaning that their unstable manifolds separate 'inside' from 'outside' iterating forward in time, their stable manifolds separate 'inside' from 'outside' iterating backward in time, precisely as they do for the  $\phi^3$  field theory in figure 5.1.

**2022-02-24 Xuanqi** Discovery (2): the  $\phi_L, \phi_R$  Jacobian (who I do not want to write it down - that's a secret) doesn't depend on the coupling constant  $g$ . Stability is solely determined by parameter  $c$ .

Also, I think it might be more convenient if we make a transformation  $c \rightarrow c - 2$  in our potential, as it always appears in my secret calculations as  $c + 2$  in any expression such as (23.8) and (23.10), except for fixed point condition.

**2022-02-24 Predrag** I do not see your (23.6) in Anastassiou *et al.* [1], where is it?

**2022-02-24 Xuanqi** Some thoughts on the non-wandering set: I think that for any periodic point  $p$  that is not on the stable-unstable manifold, it must have a neighborhood (with stable-unstable manifolds as its boundary) that is entirely in the non-wandering set, as a homeomorphism always maps boundary to boundary, and stable-unstable manifold is closed under map.

**2022-02-24 Xuanqi** Does every connected set in non-wandering set contains a periodic point?

**2022-02-24 Predrag** Yes. BTW, it's not "any" connected set. Also, every periodic point has its own stable-unstable manifolds pair, only one.

**2022-02-24 Predrag** You are learning this the hard way. It's inefficient for you not to follow [ChaosBook.org/course1](https://ChaosBook.org/course1), because that's what the course is for.

But OK. Once you convince yourself that there is only one periodic point per cover for the Bernoulli map figure 1.2, and you'll understand it for Smale horseshoes.

**2022-02-18 Predrag** Wow, figure 23.4 looks great. To bring your figures closer to the publication level graphics

- Always use 'tight' bounding box in your programs, leaving no huge white borders around figures, as for example in the original *XW-boundedRegion.pdf*, *XWphi4horseshoe.pdf*.



- Always use the same units vertically and horizontally, so square does not get printed as a squashed rectangle.
- Save the program that generated the final version of an important figure in the repo, with indication in the figure (commented out) where to find it.
- Save important figures' *figSrc/inkscape/\*.svg*, if possible.
- Draw stable and unstable manifolds as thin lines, not as collection of fat dots.
- Remove the gray frame around plots.
- Use symbolic dynamics of [ChaosBook fig. 11.4](#). Eventually Ibrahim or you will reduce the  $D_1$  symmetry, as in [ChaosBook fig. 11.5](#), but one step at a time.

**2022-02-23 Predrag** Curious: what happens if you start with the  $\phi^4$  field theory as defined in sect. [5.2 Shadow state method](#), with the 3-term recurrence like [\(5.9\)](#):

$$-\phi_{t+1} + g\phi_t^3 - \phi_{t-1} = j_t, \quad j_t = j = \text{const}. \quad (23.11)$$

That gives you two parameters,  $g$  and  $j$ . To me it looks like you can rescale  $g$  and  $\phi_t$  so  $j \rightarrow \pm 1$ , so only the sign of  $j$  matters (have not checked that). Can you make all 3 fixed points saddles?

**2022-02-28 Predrag** OK, the life is too short, so I wrote it down for you in sect. [4.12.5 Deterministic  \$\phi^4\$  lattice field theory](#).

Please construct the 1-time step  $[2 \times 2]$  Jacobian matrix, plot the unstable / stable manifolds, etc, etc, as in figure [23.4](#), for various  $g$ , and determine a small but sufficiently strong stretching  $g$  that yields a complete horse-shoe. To do that, it suffices to iterate once forward, get three region, each containing a shadow state  $\bar{\phi}_m$ .

Propose the smallest, simple to write (a fraction?)  $g$  value that we will use from now on for all  $\phi^4$  calculations.

**2022-02-23 Predrag** In sect. [5.2 Shadow state method](#) I explain how to build-in symbolic block translations into the defining equations of your problem. Can you implement it?

**2020-03-01 Predrag to Xuanqi** Would lattice 'scalar  $\phi^4$  field theory' ([23.22](#))

$$-\phi_{t+1} + (-g\phi_t^3 + s\phi_t) - \phi_{t-1} = j_t, \quad j_t = 0 \quad (23.12)$$

work for you? Needs  $s > 2$ , so that the Klein-Gordon mass  $\mu^2 > 0$ .

Now the problem is that we have to rethink the lattice 'scalar  $\phi^3$  field theory' ([4.187](#))

$$-\phi_{t+1} + (a\phi_t^2 + s\phi_t) - \phi_{t-1} = j_t, \quad j_t = -1. \quad (23.13)$$

**Deterministic  $\phi^4$  lattice field theory** quartic lattice site potential (4.137)

$$V(\phi_t, m_t) = -\frac{g}{4}\phi_t^4, \quad (23.14)$$

our example of the lattice 'scalar  $\phi^4$  field theory'

$$-\phi_{t+1} + (-g\phi_t^3 + s\phi_t) - \phi_{t-1} = j_t, \quad j_t = 0. \quad (23.15)$$

**2020-03-01 Xuanqi** The definition works, as long as we have  $g > 0$  here. I finished my calculation for what range of parameter will give a complete horseshoe (though with only two significant digits now). The result might be a bit surprising, as it doesn't depend on  $g$ , but only depends on  $s$ , the quadratic coefficient. My result yields  $s > 7.5$ , if I didn't mess up any calculation (which is highly likely!)

Now, another surprising thing is that the number of two-cycles is also independent of  $g$ . We will have all nine roots for  $s > 4$ , five roots for  $4 > s > 2$ . This leads me to think that we might want to abandon  $g$ , as it seems redundant here. So I did the follow transformation: Consider two different quartic coefficient  $g_1$  and  $g_2$  both negative, and the recurrence generated by the first potential:

$$-\phi_{t+1} + (g_1\phi_t^3 + s\phi_t) - \phi_{t-1} = 0 \quad (23.16)$$

We have  $\sqrt{\frac{g_2}{g_1}} > 0$ , so let's make a stretch  $\sqrt{\frac{g_2}{g_1}}\phi \rightarrow \xi$ , then we have

$$\sqrt{\frac{g_1}{g_2}}(-\xi_{t+1} + (g_2\xi_t^3 + s\xi_t) - \xi_{t-1}) = 0,$$

which is nothing but

$$-\xi_{t+1} + (g_2\xi_t^3 + s\xi_t) - \xi_{t-1} = 0$$

It is just the defining equation for  $g_2$ . So the quartic terms doesn't nothing but stretching the mesh. That why we didn't see any quartic coefficient in Anastassiou *et al.* [1], but a rescaling of  $x$  and  $y$ .

**2020-03-02 Predrag** Apologies again, I had a wrong sign :( in front of  $g$  in (23.22), fixed now, corrections marked in red, so we have converged. I would have preferred to vary coupling constant  $g$ , fix  $\mu^2$  to a constant value in (4.238), but you are right, we'll just have to ride with it, and explain to the reader that for  $\phi^4$  theory the coupling constant  $g$  can be scaled away for free.

**2020-03-10 Xuanqi** Now I'm reading some papers and books about field theory. I think I need to understand, at least a little bit, the Klein-Gordon equation. I also read Anastassiou *et al.* [1] again, and I found that they are not varying the quadratic coefficient for homoclinic intersection. Their determinant of the Jacobian doesn't equal to 1 anymore. I'm not sure I can understand what they are doing, so I am trying to enhance my background.

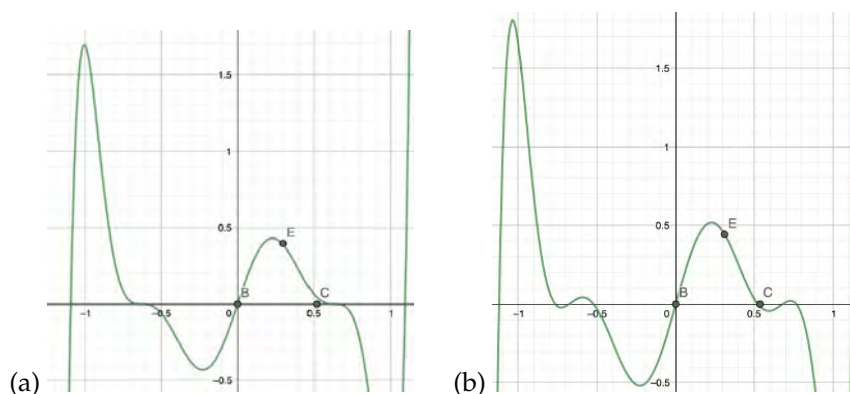


Figure 23.5:  $\phi^4$  theory (23.22) unwritten function  $g(\phi) = \phi(A\phi^8 + B\phi^6 + C\phi^4 + D\phi^2 + E)$ , whose zeros have something to do with period-2 periodic states. (a)  $s = 4$  is the bifurcation value, corresponding to  $\mu^2 = s - 2 = 0$  in (23.22). For higher  $s$  values all nine roots are real, for example for (b)  $s = 4.4$ .

2020-03-10 Predrag It would be helpful to refer to equation numbers in their paper, otherwise other people in the group have to reread the entire paper to understand your comment. Is my (4.216) wrong?

2020-03-10 Xuanqi I think it (what is it?) differs from the original figure in the axes scale, as we changed the definition of coupling constant  $g$  in (23.22), and I chose  $g = -1/2$  here. I will fix that in the next update.

2020-03-10 Predrag Shouldn't  $g > 0$ ? Or my steady states (4.169) for  $s = 4$ ,

$$(\bar{\phi}_L, \bar{\phi}_C, \bar{\phi}_R) = (-2\sqrt{2}, 0, 2\sqrt{2})$$

and the symmetric period-2 (4.174) are wrong? They do not fit figure 23.5 (a) roots.

2020-03-10 Xuanqi Plots from last week: In figure 23.5 (a) the quadratic coefficient  $s = 4$  is the bifurcation value, above which all nine roots are real, for example for  $s = 4.4$  in figure 23.5 (b).

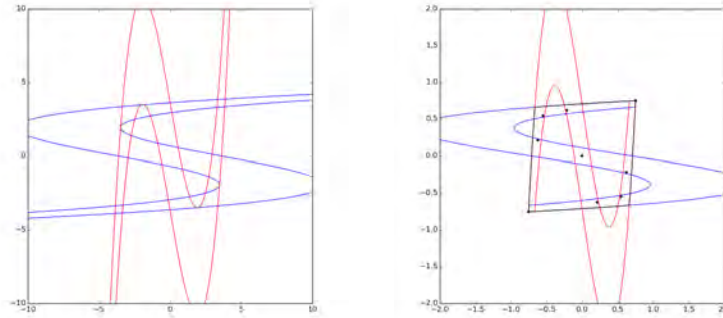
According to my program, the homoclinic tangency value is  $s \simeq 4.95 \dots$ , figure 23.6 (a). Above that, the horseshoe is complete, see for example figure 23.6 (b).

2020-03-10 Predrag What is (23.9)?

2020-03-10 Xuanqi And I think I should write a paragraph to explain our formula for  $\phi^4$  theory. Is it necessary?

2020-03-10 Predrag What do you think?

2020-03-02 Predrag It's possible that (4.224) is a better way to think about this.



(a) (b)

Figure 23.6: (Continued from figure 23.4 and figure 23.5)  $\phi^4$  theory (23.22). (a) The homoclinic tangency value is  $s \simeq 4.95 \dots$  (b) unknown value of parameter  $s$ . Iterating the 'diamond' forward and backward yield the level 2,  $3^2$  domains complete horseshoe cover. Can you spot the forming difference from figure 23.4? A hint is on page 1080.

2020-03-12 Predrag Indeed, (4.224) is a better way to think about this. Xuanqi's intuition agrees with what had been derived in the literature [10, 15, 17] 35-40 years ago. Yes, reading literature can be a real time saver, and it is really easy when somebody else does the literature search for you. Anyway:

I believe we have the final formulation of  $\phi^4$  theory. Please check carefully sect. 4.12.5 *Deterministic  $\phi^4$  lattice field theory*, and alert Han and me if there is something that should be corrected or improved. If everybody agrees, from now on all  $\phi^4$  calculation follow the conventions of that section.

2020-03-15 Xuanqi Start with our finalized version of action (4.166), we have the Euler-Lagrange equation

$$-\phi_{t+1} + [-\mu^2 \phi_t^3 + (\mu^2 + 2) \phi_t] - \phi_{t-1} = 0, \quad (23.17)$$

Set  $x_t = \phi_{t+1}, y_t = \phi_t$ , and rewrite the second-order recurrence as forward-in-time, 2-component field iteration:

$$\begin{aligned} x_t &= -\mu^2 x_{t-1}^3 + (\mu^2 + 2)x_{t-1} - y_{t-1} \\ y_t &= x_{t-1}, \end{aligned} \quad (23.18)$$

with the forward-in-time Jacobian matrix

$$J_t = \begin{pmatrix} -3\mu^2\phi_t^2 + \mu^2 + 2 & -1 \\ 1 & 0 \end{pmatrix} \quad (23.19)$$

At fixed points  $(-1, 0, 1)$ , this is

$$\begin{pmatrix} 2 - 2\mu^2 & -1 \\ 1 & 0 \end{pmatrix} \quad (23.20)$$

for left and right fixed points, and

$$\begin{pmatrix} \mu^2 + 2 & -1 \\ 1 & 0 \end{pmatrix} \quad (23.21)$$

for the center fixed point.

Take a real Klein-Gordon mass  $\mu^2 > 0$ , evaluate eigenvalues for these matrices. For the left and right fixed points, eigenvalue equation is

$$\Lambda(\Lambda + 2\mu^2 - 2) + 1 = 0.$$

Apply Vieda's theorem, we have  $\Lambda_1\Lambda_2 = 1 \rightarrow \Lambda_2 = \Lambda_1^{-1}$  corresponding to stable/unstable manifolds, and the discriminant is  $\Delta = b^2 - 4ac = 4(\mu^2 - 1)^2 - 4 \geq 0$ , when  $\mu^2 \geq 2$  which leads to two real eigenvectors. And for the center fixed point, the algebraic equation for eigenvalues is  $\Lambda(\Lambda - s) - 1 = 0$ . Similarly we will have  $\Lambda_1\Lambda_2 = 1$ , and the discriminant is now  $\Delta = b^2 - 4ac = s^2 - 4 = (\mu^2 + 2)^2 - 4 \geq 0$ , which also gives two real eigenvalues  $(\Lambda, \Lambda^{-1})$ .

The eigenvalues and eigenvectors ???.

**2020-03-17 Xuanqi** For  $\mu^2 = 3$  the period-1  $L, R$  periodic states eigenvalues are  $(\Lambda_L, \Lambda_R) = (-2 - \sqrt{3}, -2 + \sqrt{3})$ , both negative for the left and right fixed points for our choice of  $\mu^2 = 3$ . Thus, the the period-1  $L, R$  periodic states are buried within the horseshoe.

It's strange that the iterated regions protrude the original one. Is it because something went wrong? I thought the boundaries of iterated regions should smoothly slide on the original stable/unstable manifolds.

I'm still learning to compile equations and insert svg figures. This time the figures are not very big, only 49 kB each.

Figure 23.7 (b) looks like it is for  $\mu^2 < 2.95$ : It's not a complete horseshoe. But it is possible that the diamond iterates look like this, as they are not on the horseshoe boundary.

**2020-03-17 Predrag** The cubic potential (23.22) starts out large and positive for large negative values of  $\phi$ , so you are right about the eigenvalue signs. But I actually like  $C$  eigenvalue being positive. You might like it too

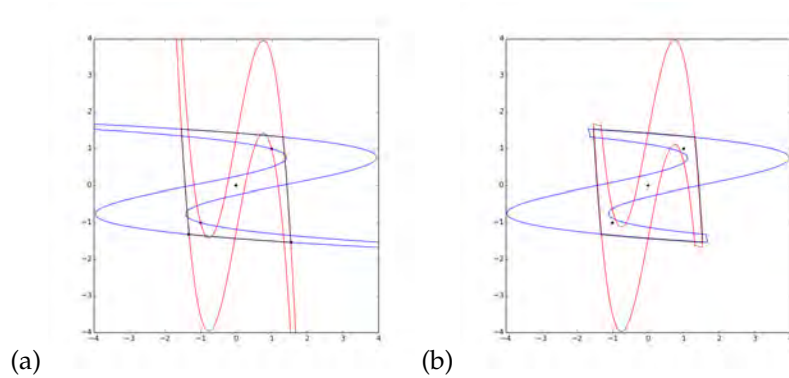


Figure 23.7: Continued from figure 23.6: note that the cubic has been flipped. Something seems not right. (a) The stable/unstable manifolds near left and right fixed points according to (23.22), with  $\mu^2 = 3$  for stable/unstable manifolds to intersect. (b) Result of iterating the black region in (a) forward and backward in time.

when you get to reducing the  $D_1$  symmetry, as in ChaosBook fig. 11.5. The point is, even the standard, unimodal Smale horseshoe has different space-orderings depending on the signs of eigenvalues, see ChaosBook exer. 15.3 and the next 2 exercises.

So, this time follow the  $\bar{\phi}_C = 0$  unstable manifold. I expect that the diamond you get this time will define 1/2 of the horseshoe -  $\bar{\phi}_C$  is in the middle of it, right? Then it's  $\bar{\phi}_t \rightarrow \bar{\phi}_t$  reflection will give you the other 1/2.

2022-02-18, 2022-02-23, 2020-03-17 Predrag I understand that it's wrong to try to put order in chaos, but cat herding is what it is. So reposting this:

Use symbolic dynamics of ChaosBook fig. 11.4. Eventually you will reduce the  $D_1$  symmetry, as in ChaosBook fig. 11.5, but one step at a time.

2022-03-21 Predrag I have a hunch (with a caveat that my hunches are almost always wrong) that if you reduce the symmetry, the unstable manifold of  $\bar{\phi}_C$  will be the *outer* boundary of the symmetry reduced horseshoe (also with  $3^k$  covers, but all periodic states symmetry reduced), and all will be well again.

This might not help you, but maybe - example 6.11  $D_1$ -reduced binary symbolic dynamics also has to do with  $\phi^4$ , in the limit where the slope of  $\bar{\phi}_C$  is so steep (vertical!) that it becomes the Bernoulli map discontinuity...

2022-03-25 Xuanqi & Predrag The  $\phi^4$  horseshoe diamond's boundary are the  $LR$  period-2 periodic state stable/unstable manifolds.

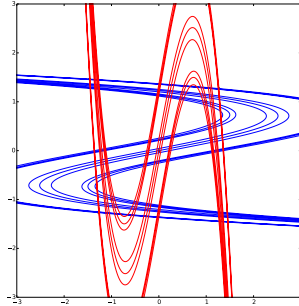


Figure 23.8: Result of mapping stable/unstable manifolds 3 times forward in time, with a choice of parameter  $s = 5.5$ . Two black dots on off-diagonal are two period-2 solutions. A fair guess would be that these two points lies on the limit of stable/unstable manifolds

**2022-03-25 Predrag** Matt commits a breakthrough, fills in the horseshoe Cantor set, see page [269](#).

**2020-03-31 Xuanqi** This is a record of my struggle with  $\phi^4$  horseshoe during the spring break.

03/21: As I said, this time I tried the larger diamond. The result is, as we expected, nine intersections. However, the two period-2 points on anti-diagonal are not covered by the non-wandering set. Therefore, we should push the boundaries further out. As I plotted below, the two period-2 points are always outside the stable/unstable manifolds, but as we iterate more, the boundaries gradually approach these two points. Therefore, a very natural way is to choose a limit (if it really exists). That is to say, after infinitely many times of iteration, the stable/unstable manifolds will go through these two period-2 points, and the region bounded by these stable/unstable manifolds should be our boundary. Now my question is whether this boundary really exists. According to my intuition, they must exist, because otherwise the neighborhood of period-2 points will not behave.

Also, the minimum value for  $s$  to generate a complete horseshoe is  $s=5.5$  at the center fixed point.

03/27: According to Predrag, we should consider the stable/unstable manifolds near the two period-2 points on the anti-diagonal, and we should use two-times forward in time map instead of one-time forward in time map. This perfectly agrees with my intuition, as I was just thinking about what stable/unstable manifolds can go through these period-2 solutions. Let's do it!

Now we finally have the complete horseshoe, and a brand new Xuanqi

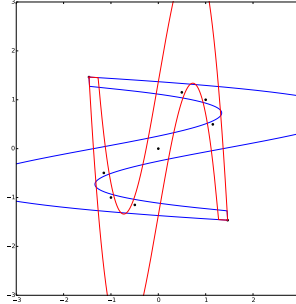


Figure 23.9: A complete horseshoe map with  $s = 5.5$  according to definition (4.166). 9 black dots are all period-2 solutions (including fixed points).

who knows how to add SVG files to the blog! But I still don't know how to control the position of figures. They just keep flying around the page.

I believe the next step is to look for periodic solutions with longer periods and shadowing method. Whatever the next step is, it should be time to wrap up this stage. I will make my program more readable and then upload it to the repository. Also, I'm trying to work out a concise proof for our choice of non-wandering set. Although it is much much much harder than just choosing a random square like Anastassiou *et al.* [1] did, the process of looking for the non-wandering set really teaches me a lot about maps and stable/unstable manifolds.

**2020-04-25 Xuanqi** Notes on Frasca [7] *Exact solutions of classical scalar field equations:*

This paper provides an exact solution of continuum scalar  $\phi^4$  theory, which involves a Jacobi elliptical function  $\text{sn}$ .

$$\phi(\vec{x}) = \sqrt{\frac{\mu^4}{\mu_0^2 + \sqrt{\mu_0^4 + 2\lambda\mu^4}}} \text{sn}(\vec{p} \cdot \vec{x} + \theta \sqrt{\frac{-\mu_0^2 + \sqrt{\mu_0^4 + 2\lambda\mu^4}}{-\mu_0^2 - \sqrt{\mu_0^4 + 2\lambda\mu^4}}}))$$

where  $p^2 = \mu_0^2 + \frac{\lambda\mu^4}{\mu_0 + \sqrt{\mu_0^4 + 2\lambda\mu^4}}$  Here  $\vec{x}, \vec{p}$  are both defined in 4-dimensional spacetime. Field is in Minkowski metric, which is different from our Euclidean field. We can divide this paper into two parts. In the first part, the author expands the exact solution in Fourier series, chose a rest frame in which there is no velocity (three of four components of  $(\vec{p})$  is zero), and found a mass spectrum from it (which I don't understand).

$$\epsilon_n = (2n + 1) \frac{\pi}{2K(k)} m \quad \text{where} \quad K'(k) = K(\sqrt{1 - k^2})$$



and

$$k = \sqrt{\frac{-\mu_0^2 + \sqrt{\mu_0^4 + 2\lambda\mu^4}}{-\mu_0^2 - \sqrt{\mu_0^4 + 2\lambda\mu^4}}}$$

and  $m = \sqrt{\mu_0^2 + \frac{\lambda\mu^4}{\mu_0 + \sqrt{\mu_0^4 + 2\lambda\mu^4}}}$ . Then he calculated the mass spectrum for  $\mu_0 = 0$ , which is a massless field, and found that there is a mass term arise from coupling constant.

$$\epsilon_n = (2n + 1) \frac{\pi}{2K(i)} \left(\frac{\lambda}{2}\right)^{1/4} \mu$$

In the second part, he wrote the action, then partition function, deduced Euler-Lagrange equation via path integral, and then solved for the Green function. By similar trick, he found that the mass spectrum of Green's function is the same as that from the exact solution, and he reached a conclusion that each exact solution correspond to a quantum field theory. As there are infinitely many exact solutions, there are also infinitely many equivalent quantum field theories. I guess this paper will not be very helpful for what we are doing now.

**2020-04-29 Predrag** LaTeX pro tip. Install [JabRef](#). It is the best app for \*.bib maintenance.

**2022-05-11 Xuanqi** If we start with our current definition of action (4.166), then our Euler Lagrange equation is simply (23.22). Here we can make no mistake. The finite difference equation is

$$-\phi_{t+1} + [-\mu^2 \phi_t^3 + (\mu^2 + 2) \phi_t] - \phi_{t-1} = 0, \quad (23.22)$$

Following Han, we define  $p_t = \phi_t - \phi_{t-1}$ , and we can rewrite our equation as

$$p_{t+1} - p_t = -\mu^2 \phi_t^3 + \mu^2 \phi_t \quad (23.23)$$

This equation indicates that we have  $V = \mu^2(\frac{\phi^4}{4} - \frac{\phi^2}{2})$ , which is a potential with a maximum and negative quadratic coefficient. I'm not sure this is what we want.

Actually, I'm more confused with the backward iteration. When I first derived it, I used the forward in time iteration, and the result is that change in momentum at time  $t$  depends on the gradient of potential at  $\phi_{t+1}$ , which is somehow inconsistent with Hamilton's equation. After all, if every step depends on the potential gradient at my destination, then I have to calculate some global equation before every local step, which seems absurd. Thus I checked Han's blog, and found that he used backward iteration. I understand why this definition is called backward, as the set of condition  $(q_t, p_t)$  and uniquely determine  $(q_{t-1}, p_{t-1})$ , instead of the usual  $(q_{t+1}, p_{t+1})$ , but I don't know why we are adopting this definition.

Also, I looked through the blog for negative potential but didn't find it, so I still don't understand why our definition of Lagrangian is  $L = T + V$

instead of  $L = T - V$ . And also, if we are really doing  $L = T + V$ , then I think we don't need to worry about Hamilton's equations, which presumed  $L = T - V$  for Hamiltonian action.

**2022-05-11 Xuanqi** For escape rate, we can start from Chaosbook (27.1)

$$\hat{\Gamma}_{\mathcal{M}}(t) = \frac{1}{|\mathcal{M}|} \iint_{\mathcal{M}} dx dy \delta(y - f^t(x)). \quad (23.24)$$

If we choose  $\mathcal{M}$  to be our diamond region for horseshoe, then this is exactly the area of the 'S' inside  $\mathcal{M}$ ?

**2022-05-11 Predrag** Yes. Probably (27.2) is closer to what you have in mind.

If by  $S$  you mean the sum over the  $3^t$ ,  $t \in \mathbb{Z}$ , Smale horseshoe intersection areas, then  $\hat{\Gamma}_{\mathcal{M}}(t)$  is the fraction of initial  $(\phi_t, \phi_{t+1})$  points that survive  $t$  iterations. The escape rate is the limit

$$\gamma = \lim_{t \rightarrow \infty} \frac{1}{t} \ln \hat{\Gamma}_{\mathcal{M}}(t),$$

i.e., average rate of loss of initial trajectories per iteration.

**2022-06-15 Xuanqi** I'm writing this note from my notes on stochastic process.

What I understand now is that we have a Perron-Frobenius operator, which is similar to Markov transition matrix, that represents the time evolution, but infinite dimensional (probably uncountable). Perron-Frobenius theorem states that there must be a unique leading eigenvalue, whose eigenvector could be chosen positive, which is the steady state that we are looking for. To guarantee that our time evolution operator is Perron-Frobenius, we have to first prune all the inadmissible regions, and thus making sure that the operator is irreducible, and then make sure that it is aperiodic, which is a necessary condition for the system to be ergodic (this part I'm not sure). After that we look for the leading eigenvalue through topological zeta function, which is essentially the characteristic polynomial for our time evolution operator (still reading this part, including escape rate).

Now, for us to have a symbolic dynamics, we have to do something similar to Markov chain: dividing the phase space and prune out inadmissible regions. This should be related to the horseshoe I drew, as it's a natural way to divide the phase space, and the discussion then goes to cycle expansions, because we are dividing it according to periodic solutions. Thus, if we can find the steady state solution, we know how often the ergodic solution would pass each region, so that we can multiply this probability with the expectation value for this periodic solution, sum over all regions, and thus obtain the expectation value of the ergodic solution. (I'm confused about many details, but I hope the general structure is correct).

**2022-05-20 Predrag** Bit of a fog of war here :) Will clear up when the sun comes up.

**2022-07-01 Xuanqi** Now I can calculate and truncate the dynamical zeta function properly using Python. I tested with period 2 cycles and the result is correct. My problem is that since I'm using MacBook with M1 chip, it seems that scipy (which Matt used in his program) is incompatible with my computer. I tried to run my vscode in Rosetta but it still doesn't work. Might need some help from people who can understand this error: (see the source file)

**2022-07-05 Xuanqi** Here are my results computing dynamical zeta function: first, most of the expanding eigenvalues of Jacobian matrix come in pairs, which is what we expected, as we haven't quotient time reversal now. So far as I observed, all the pairs have product one, but some are much larger than I expected (a two cycle yielded an eigenvalue with absolute value more than 100, which I didn't expect). As I truncated to 7, the roots are

$$\{x \rightarrow -4.54858\},$$

$$\{x \rightarrow -2.26341 - 6.29981i\},$$

$$\{x \rightarrow -2.26341 + 6.29981i\},$$

$$\{x \rightarrow 2.21287\},$$

$$\{x \rightarrow 3.77873\},$$

$$\{x \rightarrow 4.07239 - 4.71141i\},$$

$$\{x \rightarrow 4.07239 + 4.71141i\},$$

so the leading zero should be  $x=2.21287$ . Does it mean that the escape rate is  $\ln(2.21287) = 0.7943$  ?

**2022-08-08 Xuanqi** after a month Covid hiatus, as emailed to secretary Predrag:

The computation of multipliers takes longer than I imagined. It took me four hours to compute the dynamical zeta function truncated at period 11, though I will not reveal here the steps of my computation, or deposit my code anywhere. The distribution of roots in the complex plane is still not like what we expected (namely they are not in a circle), see figure 23.10. Probably we need more terms to see the circle, but it's out of my ability to compute more. I don't have a desktop computer that can run for a long time.

What is promising is that the leading root is  $s = 2.2088$ , the leading eigenvalue of the Perron-Frobenius operator, i.e., the escape rate  $s_0 = 2.20882$ , which is very close to 2.2128 that I computed for period 7. I check period 8,9,10, and the leading root is always about 2.21. Thus, if we are only looking for the leading zero, this result should be satisfactory enough, as illustrated by its convergence, see figure 23.11.

**2022-08-08 Predrag** Check Sidney's blog post **2022-04-21**, **2022-06-17 Predrag** for some pointers as how to plot the convergence results.

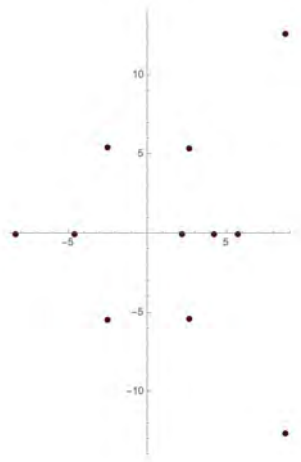


Figure 23.10: The [missing] plot of the  $\phi^4$  temporal field theory roots of dynamical zeta function  $1/\zeta(z)$  in the complex plane, Klein-Gordon mass  $\mu^2 = 3.5$ .

**2022-08-18 Xuanqi** Now I'm checking my results for convergence. The problem is how to find the best estimation of escape rate. For the former plot I just calculated it by least chi-square fitting, which is designed for a Poisson distribution, not our case. The result was  $s_0 = 2.20872$ , see figure 23.11 (a). However, if I observe the result by my eyes, the best fitting escape rate should be around 2.20882-2.20883. I tried 2.20882, and the figure looks like figure 23.11 (b). As we can see, the value of best estimation strongly affects our result, and  $s_0 = 2.20872$  is clearly not a good estimation. We can determine the slope and intercept of the log plot, but still we need a criterion to determine what does "the best fit" mean. In my opinion it we should look at the  $R^2$  for linear fitting, and I'm figuring out how to calculate that using Python.

**2022-08-21 Predrag** To me it looks like at the truncation cutoff  $N = 7$  things go south. You will need to look at the cycle weights, find whether a subset of them is numerically over- or under-flowing, in which case the coefficients of  $z^n$  are not meaningful for larger  $n$ .

**2022-08-21 Predrag** A random link for [R-squared, R2 in Linear Regression](#). Maybe it helps.

**2022-08-21 Xuanqi** Sorry for didn't explain clearly. (a) is the result of my eye-ball fitting, which I think is pretty linear. (b) is the result I showed last week, with the best estimation calculated by least-chi square. Personally I think that result ( $s_0 = 2.28072$ ) is somehow problematic. That's why I'm trying to find a better fitting method.

Also, by over- or under-flowing, do you mean that it is smaller than  $10^{-8}$

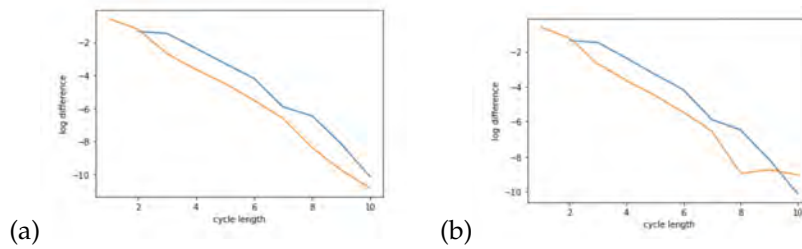


Figure 23.11: A plot of the convergence of  $|\ln z_n - \ln z_\infty|$ , where  $z_\infty = e^\gamma$ ,  $\gamma = -s_0$  the escape rate, is estimated by (a) eyeballing  $s_0$  to be  $s_0 = 2.20882$ , and the result looks pretty linear (b) least chi-square fitting  $s_0 = 2.20872$ , which is designed for a Poisson distribution, not our case;  $\phi^4$  temporal field theory dynamical zeta function  $1/\zeta(z)$ . Klein-Gordon mass  $\mu^2 = 3.5$ .

so that Python recognized this number as zero?

**2022-08-24 Xuanqi** Here I update my result for calculation of escape rate for  $\phi^4$  with  $\mu^2 = 3.5$ , as  $\mu^2 = 3.5$  is just enough for horseshoe to be complete.

To find the escape rate, first we will need the field values for all prime cycles up to a given period. For this part I used Matt's package cyclehunter to generate all prime cycles up to period 11. By prime cycles we didn't quotient out any symmetry except cyclic permutation.

Now we calculate the expanding Floquet multiplier for each prime cycle  $p$  we have. To do so, we calculate the forward-in-time Jacobian matrix at each point of orbit  $p$  and multiply them together. The forward-in-time Jacobian takes form

$$J_t = \begin{pmatrix} -3\mu^2\phi_t^2 + \mu^2 + 2 & -1 \\ 1 & 0 \end{pmatrix} \quad (23.25)$$

The expanding Floquet multiplier related to cycle  $p$  is the expanding eigenvalue of the product of matrices (remember that the product of two eigenvalues is always unity for forward-in-time Jacobian matrix). And then we put these multipliers into dynamical zeta function for maps  $1/\zeta(s) = \prod_p(1 - t_p)$  where  $t_p = \frac{1}{|\Lambda_p|} e^{\beta A_p} z^{n_p}$ . Here  $\Lambda_p$  is the multiplier related to prime orbit  $p$  and  $n_p$  is the period of orbit  $p$ . The result of escape rate with cycle period up to eleven is presented below. On the left is the period of longest cycle included and on the right is escape rate calculated.

- 1 → 1.65102,
- 2 → 1.91070,
- 3 → 2.41268,
- 4 → 2.14103,
- 5 → 2.23481,

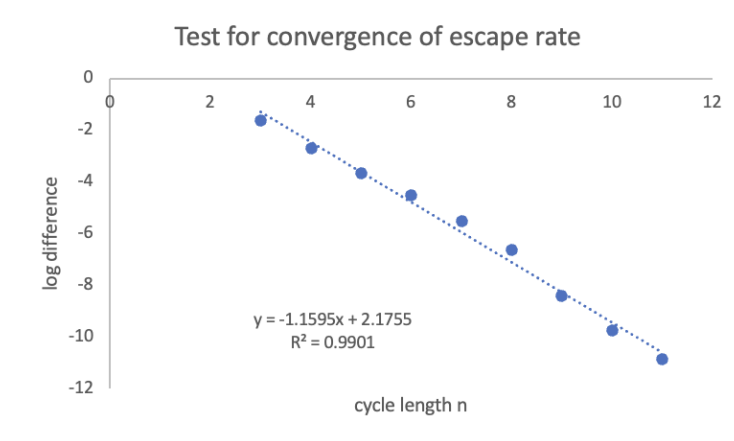


Figure 23.12: The plot of  $\ln(|s_\infty - s_n|)$  v.s.  $n$  where  $n$  is the period of longest prime cycle included for  $\phi^4$  temporal field theory with  $\mu^2 = 3.5$ . We take  $s_\infty = 2.20882$  as our best estimation. The best fit linear fit and its  $R^2$  are included in the figure.

6  $\rightarrow$  2.19772,  
 7  $\rightarrow$  2.21287,  
 8  $\rightarrow$  2.21017,  
 9  $\rightarrow$  2.20859,  
 10  $\rightarrow$  2.20888,  
 11  $\rightarrow$  2.20884,

To be confident with this result, we have to check convergence. For this, we will need an estimation of escape rate  $s_\infty$  based on what we have. For now this estimation is done by observation. I'm still figuring out a way to determine this quantitatively. In figure 23.12 we use  $s_\infty = 2.20882$ .

As we can see in figure 23.12, this relation is strongly linear (with  $R^2 = 0.9901$ ). Later we shall change it to a more professional version, but since Excel can display everything very clear I think it's not a bad idea to use an Excel figure here. Since we expect an exponential decay of error in escape rate, we are pretty confident now about the calculation.

Next we will want to verify that if we quotient out certain symmetry, the result would be the same. The first apparent symmetry is  $\phi \rightarrow -\phi$  internal symmetry (see sect. 4.9). Because of this symmetry, every prime cycle  $p$  has a mirrored prime cycle  $p'$  with no additional information. So in fact we only have to include one of them. The calculation is still on going. Result will be reported next week.

**2022-09-30 Xuanqi** The convergence test of the leading zero for dynamical zeta function showed a strange pattern. There seems to be some oscillation besides linearity that nobody understands. Han's calculation showed a

slower convergence for spectral determinant than dynamical zeta function. A bit confusing.

Now I'm looking at a generating function that can help us quotient discrete symmetries. Let's say that we have a prime orbit  $p = a_1, a_2, \dots, a_n$ , define its generating function  $g_p(z) = \sum_{i=1}^n a_i z^i$ . If we look at a new sequence  $q = g_p(\omega), g_p(\omega^2), \dots, g_p(\omega^{n-1})$  where  $\omega = e^{i2\pi/n}$ , it's nothing but a discrete Fourier transform. As we can write this  $p \rightarrow q$  relation as a Vandermonde matrix, this relation is apparently unique. But I want to push this result further. Uniqueness is not our ultimate goal. We look at prime cycles instead of arbitrary cycles, so we want those cycles that are equivalent under cyclic permutation to be the same point in k-space. Thus we need to find a proper quotient space of the original k-space.

Here generating function gives more space to operate than Fourier transform. As we are evaluating the generating function to create a sequence, we can also evaluate any function that composite with this generating function, such as the square of generating function.

As we argued that if  $p'$  is equivalent to  $p$  under cyclic permutation (say shift by 1), then we have  $g_{p'}(z) = z g_p(z)$ , so if we evaluate  $(g_p(\omega^k))^{n/k}$ , then  $p'$  and  $p$  gives exactly the same sequence  $q$ . But what we need is an "if and only if" statement. Now it's only " $p$  and  $p'$  are equivalent if they are equivalent under cyclic permutation", but we want to make sure that "only if" also holds so that we don't put different prime orbits into one element in the quotient space. As we don't have any uniqueness for this new operator, my idea is to use the pre-image to look for uniqueness under the original discrete Fourier transform operator. But this indeed requires hard work because this "inverse" is not strictly defined. There is a whole set that is mapped to a point, which means there are more than one pre-image. What we want is that exactly  $n$  points in that set is allowed under our symbolic dynamics, but I haven't proved this fake uniqueness.

**2022-10-28 Xuanqi** We still follow the same way that we define generating function, which is  $g_p(z) = \sum_{i=1}^n a_i z^i$ , and we look at a new  $n$ -dimensional vector

$$q = (g_p(\omega), [g_p(\omega^2)]^{1/2}, \dots, [g_p(\omega^k)]^{1/k}, \dots, [g_p(\omega^{n-1})]^{1/n-1})$$

where  $\omega = e^{i2\pi/n}$ . Now we notice that if  $p$  and  $p'$  are equivalent under cyclic permutation, then  $q$  and  $q'$  differs only by some power of  $\omega$ . Thus, if we write  $[\omega] = \{\omega, \omega^2, \dots, \omega^{n-1}\}$ , then we can define

$$P = q[\omega] = \{\omega q, \omega^2 q, \dots, \omega^{n-1} q\},$$

and a map  $\psi(p) = P$ . Note that for any prime orbit  $p$ , if  $\psi(p) = P$ , then  $P$ , as a set, contains all the vector  $q$ 's that are generated by the cyclic permutations of  $p$ . This the map from  $p$  to  $q$  is an injective, and the set

$P$ , if  $p$  is a prime orbit, contains exactly  $n$  elements. So  $\psi(p) = \psi(p')$  if and only if  $p$  and  $p'$  are related by a cyclic permutation. Also, for an orbit  $p$  with period  $n$ , if  $p$  is composed of shorter orbits, the group  $P$  has less than  $n$  elements, because  $P$  is essentially a cyclic group, and for repeat of shorter orbits the degree of generating element is less than  $n$ , which gives a group with less than  $n$  elements. So map  $\psi$  is a way to distinguish prime orbits.

Next we need to consider more symmetries. We have the (internal) reflection symmetry for  $D_1$ , composed of the identity and the reflection across  $y$  axis. This turns symbol  $1$ 's into  $-1$ 's, and  $-1$ 's into  $1$ 's, while zero doesn't change, so we just replace our  $g_p$  by  $-g_p$ . Another important symmetry is time reversal, which we can prove by a little trick that it turns vector  $q$  into its complex conjugate. I haven't looked deeply into these two symmetries, but I think this method is still promising, at least under  $D_1$  symmetry.

After this there are two things to do. The first one is to generalize this result to  $D_n$ , which is interesting but doesn't necessarily build up to what we do, and the other is to write this method of generating function into code and develop some more efficient algorithm, which is not very interesting but very useful. I will start to do both at the same time to make life busier and more interesting.

**2022-10-30 Xuanqi** Realized one more thing for the purpose of computation. As we defined above, the function  $\psi$  maps an orbit to a set of  $n$  vectors. This set is very special because it is  $P = q[\omega] = \{\omega q, \omega^2 q, \dots, \omega^{n-1} q\}$ , which means that if we look at the first component of the vectors, it must spread out evenly in complex plane. Thus, if we divide the complex space into  $n$  pizza slices, each slice must contain exactly one point (we take left boundary open and right boundary close). Therefore, we can reduce this set to one vector whose first component lies in a given slice, let's say the first one. This new vector is the new representation of the original symbol string. I will explain this in detail in Monday's meeting.

**2023-02-05 Xuanqi** My effort over the last few months are mainly on finding a new generating function for periodic orbits, but that didn't actually work very well. I think the reason is that I only considered cyclic permutation, so the result was quite unnatural. Thus, I decided to first replicate the discrete symmetry quotient in Chaosbook (the example is a two symbol string but also  $D_2$ ), and I believe this can help me understand more about what happens on these lattice. There are quite a lot of things to consider here, but I just cannot connect them and think about them as an entity.

Now let's consider the discrete symmetry for  $\phi_4$ . If we think about cyclic permutation, the picture is a circle, reflection symmetry comes with a natural interpretation, but time reversal is somehow harder to imagine, but in complex space it can be related with complex conjugate. There might be a better way to include all three symmetries.



For calculation, my understanding is that if we want to quotient reflection symmetry, we first merge left and right, then we count how many times an orbit cross the boundary. If this number is even, then it's a global periodic solution; if it's odd, then it's a relative periodic solution. I believe there will be more detailed problems when I write the actual program, but hopefully I can start now (after my midterm Wednesday).

**2023-02-05 Xuanqi** Here is my update for a systematic way to get symbolic dynamics in fundamental domain. First, we denote by  $A$  the set of all alphabets, and let  $S = (s_1, s_2, \dots, s_n)$  be a string with  $s_k \in A$  for all  $k$ . Let  $G$  be the symmetry group of our state space, and we reduce our alphabet to  $A'$  such that we only pick out one element from each orbit (orbit of  $x \in X$  is defined as  $O_x = \{y : y = gx, g \in G\}$ ). This way, the cosets of  $G$  in  $A'$  makes a partition of  $A$ , and we define whichever region that encompasses this set  $A'$  our fundamental domain (so that we can use the fundamental domain to reconstruct the full state space). Our goal here is to represent each string in reduced alphabet  $A'$  without losing any information about dynamics. To do so, the first step we do is to turn each symbol  $a$  in full alphabet into a tuple  $(a', g)$ ,  $a' \in A', g \in G$  such that  $ga' = a$ . Notice that this representation is not unique, but we can always modify it by quotient an equivalence relation later. Now our original string  $S$  is  $S = ((s'_1, g_1), (s'_2, g_2), \dots, (s'_n, g_n))$ , and by this we can easily see that the set of strings is a  $G$ -set, and  $gS = ((s'_1, gg_1), (s'_2, gg_2), \dots, (s'_n, gg_n))$ . With all these notations defined, let's fold our state space into the very fundamental domain. The orbit  $S'$  in fundamental domain is

$S' = ((s'_1, g_n^{-1}g_1), (s'_2, g_1^{-1}g_2), \dots, (s'_n, g_{n-1}^{-1}g_n))$ . As always, the group operation (second component) represents which region of partition it goes through, and the reduced symbol gives us the precise location in this region. What is different is that we do not automatically have a starting point. Instead, we visit the next neighborhood from where we are now, so there is no "special" region in the state space where we always root our solution. Conceptually it does make sense, because every copy generated from the symmetry group should be equivalent.

One notable feature of our symbolic dynamics is that it doesn't change under any group operation  $g \in G$ , because  $(gg_k)^{-1}(gg_{k+1}) = g_k^{-1}g^{-1}gg_{k+1} = g_k^{-1}g_{k+1}$ , so the new string is fully symmetrized by symmetric group of state space. Now there are two problems we need to address for our new symbolic dynamics: uniqueness and cyclic permutation. And also, our discussion is still on general orbits instead of prime orbits that we care, so at some point we need to bring it back, but the algebraic structure is the same as we discussed above.

**2023/05/28 Xuanqi** Using the new symbolic system, it's easy to prove that the symmetry group of  $p$  is not trivial if and only if  $\hat{p}$  in fundamental domain is shorter than  $p$ . The order of symmetry group of  $p$  is then the cardinality of stablizer of  $p$ . I laid out a sketch of the proof, but haven't written them

up yet. Now I'm trying to work out the group theory version of proof for 25.16. The main difficulty is that I don't quite understand the choice of  $h_{\hat{p}}$  now. Once I work this out, we can have a better way to view the fundamental domain, without referring to  $p$  and  $hat{p}$  all the time.

For computation part, I'm working on hashing map, which should take almost no computation time and thus make our algorithm more efficient. This part should be pretty easy once I found a suitable dictionary. I will try to wrap them all up before June.

The next thing to check is prune rules, which is actually the reason I suggested using this model. The example of three pinballs should be my start, and hopefully we can generalize to any case we like.

**2023/06/14 Xuanqi** A short summary on my work with symbolic dynamics.

For hyperbolic systems we consider (??), symbolic dynamics for a system with trivial symmetric group is straight forward. Thus, our discussion of symbolic dynamics will be closely related to the symmetry group which we denote by  $G$ .

The main idea is to divide  $G$  into two subgroups that we call state space symmetry  $G_s$  and lattice symmetry  $G_l$ . For one-dimensional case,  $G_l$  is just the infinite translation group, and the spatiotemporal case is just what we have in the previous draft. I'm considering to add time reversal to this group, because they are all symmetries on lattice, and together they form a normal subgroup of  $G$ . So here let's consider  $G_l$  as  $C \times e, \sigma$ , which is the product of infinite cyclic group with the subgroup generated by time reversal operator  $\sigma$ . Then we perform the standard quotient to form a quotient point group  $G/T$ . This subgroup is isomorphic to  $G_s$ , I claim, and all the elements in  $G_s$  commutes with elements in  $G_l$  as  $G_l$  is a normal subgroup (??). A non-trivial example of  $G_s$  is provided by temporal  $\phi^4$  theory, whose state space symmetry group is  $D_1$ .

Now, my claim is that the quotient point group  $G_s$  is not simply a byproduct of some boring mathematics. Instead,  $G_s$  is exactly the operations on state space that leaves the lattice field equation unchanged, like putting a negative sign on temporal  $\phi^4$  equation (??). (I will add more details to make this claim more persuasive, but still thinking about it).

Inspired by this, we will adopt a set of new notation system for symbolic dynamics for hyperbolic systems with non-trivial symmetry group (by which we mean  $G_s$  is not isomorphic to trivial group). In these systems, the symbolic dynamics is called reduced, because orbits that are related by symmetry operation have the same dynamical property. Denote by  $\mathbb{M}$  the whole state space, and as in Chaosbook  $\hat{\mathbb{M}}$  the fundamental domain. The whole state space is generated by fundamental domain and state space symmetry group  $G_s$ .

$$\mathbb{M} = \bigcup_{g \in G_s} g\hat{\mathbb{M}} \quad (23.26)$$

Inspired by this equation, we try to separate the state space symmetry operations with actual symbols in fundamental domain, which we can view as reduced state space. Thus, we introduce our new notation for symbolic dynamics.

First, denote by  $A$  the set of all alphabets, and let  $S = (s_1, s_2, \dots, s_n)$  be a string with  $s_k \in A$  for all  $k$ . Let  $G_s$  be the state space symmetry group, and we reduce our alphabet to  $A'$  such that we only pick out one element from each orbit in  $G$  (orbit of  $x \in X$  is defined as  $O_x = \{y : y = gx, g \in G_s\}$ ). This way, the cosets of  $G_s$  in  $A'$  makes a partition of  $A$ , and we define whichever region that encompasses this set  $A'$  our fundamental domain (so that we can use the fundamental domain to reconstruct the full state space). Our goal here is to represent each string in reduced alphabet  $A'$  without losing any information about dynamics. To do so, the first step we do is to turn each symbol  $a$  in full alphabet into a tuple  $(a', g)$ ,  $a' \in A', g \in G_s$  such that  $ga' = a$ . Notice that this representation is not unique, but we can always modify it by quotient an equivalence relation later. Now our original string  $S$  is

$$S = ((s'_1, g_1), (s'_2, g_2), \dots, (s'_n, g_n)) \quad (23.27)$$

and by this we can easily see that the set of strings is a  $G$ -set for point group  $G_s$ , and its action is naturally defined as

$$gS = ((s'_1, gg_1), (s'_2, gg_2), \dots, (s'_n, gg_n)) \quad (23.28)$$

With all these notations defined, let's fold our state space into the very fundamental domain. The orbit  $S'$  in fundamental domain is

$$S' = ((s'_1, g_n^{-1}g_1), (s'_2, g_n^{-1}g_2), \dots, (s'_n, g_n^{-1}g_n)) \quad (23.29)$$

As always, the group operation (second component) represents which region of partition it goes to (according to equation 21.26), and the reduced symbol gives us the precise location in this region. What is different is that we do not automatically have a starting point. Instead, we visit the next neighborhood from where we are now, so there is no "special" region in the state space where we always root our solution. Conceptually it does make sense, because every copy generated from the symmetry group should be equivalent.

One notable feature of our symbolic dynamics is that it does not change under any group operation  $g \in G_s$ , because  $(gg_k)^{-1}(gg_{k+1}) = g_k^{-1}g^{-1}gg_{k+1} = g_k^{-1}g_{k+1}$ , so the new string is fully symmetrized by symmetric group of

state space. Now there are two problems we need to address for our new symbolic dynamics: uniqueness and cyclic permutation. And also, our discussion is still on general orbits instead of prime orbits that we care, so at some point we need to bring it back, but the algebraic structure is the same as we discussed above.

From the new notation, it's easy to see how lattice symmetry is different from state space symmetry. Lattice symmetry action results in a permutation of symbols in a given string but does not change any symbol, while state space symmetry changes symbols without permutation any of them. Thus, without much difficulty we can argue that any actions from the two groups ( $G_l$  and  $G_s$ ) commutes. As we argued, this is because these two symmetry groups have different origins. The lattice symmetry group comes from the symmetry of lattice. For temporal case, our lattice is a one-dimensional infinite lattice, thus is unchanged under any finite shift, and the symmetry group is thus a infinite cyclic group. Therefore, any two orbits related by lattice symmetry are actually the SAME orbit if they are put on the whole infinite lattice. In contrast, two orbits that are related by state space symmetry are not the same orbits, but they have the same dynamical property. We shall see the merit of such division immediately.

TO BE CONTINUED

In fact, I think we can have a new perspective prime orbits. If we start from the set of infinite string, a periodic orbit is a string that has finite order, or in the words of group theory its orbit in  $G_l$  is finite. So if we look at this subset of periodic orbit, its quote space is the set of all prime orbits. Based on this, we further quotient state space symmetry in the same way to get reduced strings in fundamental domain. I'm still thinking about how to explain this idea better, so most likely I will write it up in the next version.

**2023-08-08 Predrag** Have a look at **2023-01-18 Predrag** post around (11.34), about evaluating Hill determinants by methods other than what Han and I have used so far: QR (used much by Xiong Ding), SVD, PCA, and others might offer more efficient numerical (maybe even analytical) evaluation methods, and hopefully new insights in Hill determinants. I think (but have not tried to do this myself) that it should be rather quick to recompute results we already have, for example table 9.2, or, preferably table 9.3, table 9.1 (always use  $\mu^2$  rather than  $s$ ), (24.390), table 22.1, table 22.2 (?), (always use  $\mu^2$  rather than Hénon  $a$ ).

Han will have a ton of results that you might want to recompute.

2023-08-30 Xuanqi Here is the calculation for Chebyshev polynomials.

By definition of the *Chebyshev polynomial of the first kind*,

$$\begin{aligned} T_0(x) &= 1 \\ T_1(x) &= x \\ T_{n+1}(x) &= 2xT_n(x) - T_{n-1}(x) \quad \text{for } n \geq 2 \end{aligned}, \quad (23.30)$$

(see, for example, eqs. (4.180), (16.30), (24.146), (21.125), (6.139), (24.211); example 2.5; search for "Weijie Chen"). The 3-term recurrence (23.30) has the same form as the homogenous ( $m_t = 0$ ) temporal cat Euler–Lagrange equation (2.95)

$$-\phi_{t+1} + (s\phi_t - m_t) - \phi_{t-1} = 0. \quad (23.31)$$

What's not obvious to Predrag is how do you show that you can substitute  $\phi_t \rightarrow T_t(s/2)$  and that computes Hill determinants?

To prove that

$$\Lambda^n + \Lambda^{-n} = 2T_n(s/2) \quad (23.32)$$

is a solution to the 3-term recurrence (23.30), note that<sup>2</sup>

$$\begin{aligned} s\Lambda - 1 &= \frac{1}{2}(s^2 + s\sqrt{(s-2)(s+2)}) - 1 \\ &= \frac{1}{4}(s^2 + 2s\sqrt{(s-2)(s+2)} + s^2 - 4) \\ &= \Lambda^2 \end{aligned} \quad (23.33)$$

and similarly

$$s\Lambda^{-1} - 1 = \Lambda^{-2}. \quad (23.34)$$

Then, take the Chebyshev polynomials 3-term recurrence (23.30) to prove by induction that

$$\begin{aligned} T_{n+1}(s/2) &= 2(s/2)(\Lambda^n + \Lambda^{-n}) - (\Lambda^{n-1} + \Lambda^{-(n-1)}) \\ &= (s\Lambda - 1)\Lambda^{n-1} + (s\Lambda^{-1} - 1)\Lambda^{-(n-1)} \\ &= \Lambda^{n+1} + \Lambda^{-(n+1)} \end{aligned} \quad (23.35)$$

Thus,  $\frac{1}{2}(\Lambda^n + \Lambda^{-n}) = T_n(s/2)$ , and  $N_n = \Lambda^n + \Lambda^{-n} - 2 = 2T_n(s/2) - 2$  is the desired analytical expression for the Hill determinant<sup>3</sup>. This gives an intuition that the number for states allowed almost grow exponentially as the size of primitive cell grows. Han might take a part of this proof into CL18 to relate the two different forms of Chebyshev polynomials.

---

<sup>2</sup>Predrag 2023-08-31: Where does this come from? I might have edited this incorrectly. This is useful in the proof of recurrence relation, and it is the characteristic equation if we assume  $\phi_t = \Lambda^t$

<sup>3</sup>Predrag 2023-08-31: Where does '-2' come from?

'-2' come from the spectrum of Hill determinant, and I cannot immediately figure out its physical meaning

**2023-08-31 Xuanqi** I investigated the algorithms previously mentioned by Predrag. QR decomposition seems to be the best way for our purpose of computing Hill's determinant. It basically is to decompose a real value matrix as a product of an orthogonal matrix and an upper triangular matrix. The orthogonal matrix has determinant 1 or -1, and the determinant of triangular matrices are the product of entries on the main diagonal. I will write the code tomorrow for realization, but this idea seems very reasonable.

PCA, principal component analysis, is basically a transformation of coordinates. It is usually used for a set of data represented as a matrix, say experiment results. Each of is one outcome of the results, and each column is a feature value. After this transformation, the rows are permuted according to their variance. So far I didn't see how it might be very useful in our computation, but I will check more.

**2023-09-06 Xuanqi** To Predrag: I have been thinking about the reason why we can relate Chebyshev Polynomials with Hill's determinant of Cat map, but it seems that there does not exist a straight-forward way to relate them. However, it came across me that if we assume the solution of Cat map has form

$$\phi_t = \Lambda^t \quad (23.36)$$

we can solve to have

$$\Lambda = \frac{1}{2}(s - \sqrt{(s-2)(s+2)}) \quad (23.37)$$

but at the same time, we can see that

$$\phi_t = \Lambda^{-t} \quad (23.38)$$

is also a solution to cat map without any winding number. Then, the interesting thing is that any linear combination of  $\Lambda^t$  and  $\Lambda^{-t}$  is a solution. Thus, we can somehow obtain a general solution of reduced Cat map. It should not be very hard to prove that this is in one-to-one correspondence with solutions of original cat map, so there is a way to write every solution of Cat map into

$$\phi_t = c_1 \Lambda^t + c_2 \Lambda^{-t} \pmod{1} \quad (23.39)$$

I don't know whether this would be helpful at all, but it just occurred to me on Monday when I tried to see more about Chebyshev Polynomials.

**2023-09-16 Predrag** Have a look at **2023-09-16 Predrag** posts around (19.41), about evaluating  $\phi^4$  theories by SVD methods. I have not studied them myself, and much of this (tensor renormalization groups) is good stuff, but you probably do not need it for the Tigers paper.

4

<sup>4</sup>Predrag 2023-09-18: This sure looks familiar. Have not checked why...

**2023-09-25 Xuanqi** Now the problem is with tigers is that we have some roughly equivalent definition of non-wandering set, and we want to get thing out correct so that the set indeed is the closed and invariant subset that on which the dynamics is ergodic. It seems that I have never understood the word ergodicity. However, the most robust version should come from **Poincaré recurrence theorem**, saying that any region consists of bounded orbits is infinitely recurrent. i.e. it intersects any open set in this region infinitely often, and then Birkhoff theorem suggests that we can have a well defined ergodic mean for the calculation of any expectation value but picking out a "representative point" and map that point forward in time. It does require some more careful thoughts and will take much longer than I expected, but the rough idea is there so maybe we can just make it like a correct version and add more details later.

**2023-10-05 Predrag** Our  $\phi^k$  and spatiotemporal cat systems happen to satisfy this: "Systems to which the Poincaré recurrence theorem applies are called conservative systems", but for us ergodicity works also for non-conserving systems, such as the temporal Hénon ( $\phi^3$  theory) for  $b \neq -1$ .

"The theorem: If a flow preserves volume and has only bounded orbits, then, for each open set, any orbit that intersects this open set intersects it infinitely often."

I think this definition makes it clear why Poincaré recurrence theorem does not apply to repelling sets: they have both bounded orbits (the non-wandering set) and unbounded orbits (the cats that manage to escape). In addition, existence of a non-wandering set do not require conserved phase space volume:

" The proof, hinges on two premises:

- (1) For a mechanical system, this bound can be provided by requiring that the system is contained in a bounded physical region of space (so that it cannot, for example, eject particles that never return).
- (2) The phase volume of a finite element under dynamics is conserved."

What you want to understand is Birkhoff's notion of '**wandering set**'.

**2023-10-06 Xuanqi** For non-wandering set, I perfectly understand that Poincaré recurrence doesn't apply to our system, However, if we restrict our state space to only the non-wandering set, which consists of only bounded orbit, then take the time-evolution operator to be the restriction of the original one on non-wandering set (which is a subset of the whole state space). As non-wandering set is invariant, the operator is still an automorphism on state space, and then we have a bounded system (in fact, I think topologically it should also be compact), as non-wandering set excludes all the orbits that gets repelled. The difficulty is to relate these two notions of boundedness and non-wandering, as opposed to wandering set introduced by Birkhoff.

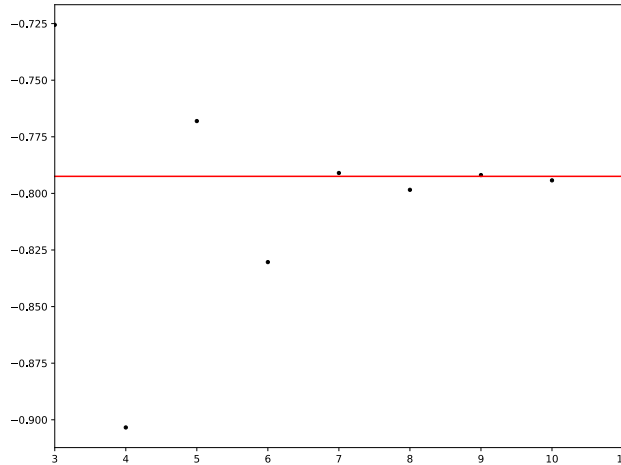


Figure 23.13: The plot of (23.40), where  $n$  (horizontal axis) is the period of periodic states  $c$  for  $\phi^4$  temporal field theory, with  $\mu^2 = 3.5$ . We take  $e^{s'_0} = e^{s(13)} = -0.79247$  (calculated from spectral determinant, see [ChaosBook eq. \(23.16\)](#), with periodic state period 13) as our best estimate of the infinite-time  $s_0$ , to check the convergence of our escape rate estimates.

**2023-10-05 Xuanqi** I calculated the Hill determinants for  $\phi^4$  periodic states up to period 9, one-dimensional temporal lattice using QR decomposition, and when I sum up  $1/|\text{Det } \mathcal{J}_c|$  for all periodic states  $c$  over a primitive cell of period  $n$  (the crudest version of the trace formula), using a secret value of Klein-Gordon mass  $\mu^2 = 3.5$ , the result is a nearly perfect exponential

$$\frac{\sum_c^{(n+1)} \frac{1}{|\text{Det } \mathcal{J}_c|}}{\sum_c^{(n)} \frac{1}{|\text{Det } \mathcal{J}_c|}} \approx e^{-0.79247}, \quad \mu^2 = 3.5, \quad (23.40)$$

see figure 23.13.

The problem is that it takes forever to calculate this, and I'm afraid that we cannot get to the period we need based on the algorithm we have now.

The code is essentially the same for  $\phi^3$  and  $\phi^4$ . The fits are surprisingly good.

**2023-10-06 Xuanqi** I haven't include a figure yet, because it only contains six points, and I want to calculated to a longer periods. So either we find a better way of this calculation, or I can just run it for a longer time or put it on some computational cluster of GaTech to produce more points.



**2023-10-10 Xuanqi** I computed the spectral determinant. The result is quite surprising: we don't have a good estimate of escape rate until cycle period 7. However, it does start to converge to a certain value with longer cycles added to it. Not surprisingly, it converged to approximately the same value as dynamical zeta function does, but very surprisingly, it converged any specific zero of zeta function, but the approximation I constructed for the test of convergence. This means that dynamical zeta function does have some error larger than we expected, but by assuming that it should converge exponentially, we should still have a good estimation.

Now it yields, with period 13, 7 significant digits (compare with (23.40))

$$e^\gamma = z_0 = 2.208846 \quad \text{for } \mu^2 = 7/2,$$

$z_0$  the leading zero of the spectral determinant, see [ChaosBook eq. \(1.7\)](#), and I'm now computing the period 15, which is done without referring to prime cycles. Convergence is not as fast as we imagined, but not bad, either.

**2023-10-10 Predrag** Think of your blog as you being a scientist, and recording your results as you go. Kepler did it, Gauss did it, Faraday did it, it's a necessity. Had you blogged the escape rate estimates using the trace sums that you had showed to me on-screen, one could track the relative merits of different approaches you have tried so far.

**2023-10-10 Xuanqi** Seems it is surely useful to update blog. I found that  $e^\gamma = 2.208846$  is not the value that yields the most linear relation, as what I wrote in figure [23.12](#) the value  $z_0^{(\infty)} = 2.20882$  yields a better linear relation with  $R^2 = 0.9901$ , but somehow the final version I saved was with  $z_0^{(\infty)} = 2.208847$ . It seems there is no more record about this in my blog, but if I did remember it correctly, it was some manual manipulation (or I just received some universe message that told me I should use this value).

I will try to clean up data and update before Friday with figures. Period 15 seems to be unattainable, as my computer crushed this evening for some unknown reasons. So I will try period 14 first. Also I think I can try to fit figure [23.13](#) with an exponentially decaying  $\cos$  function. It seems that it's not the first time we see some sinusoidal wave in convergence test for  $\phi^4$  theory.

**2023-10-11 Predrag** What you call  $z_0^{(\infty)}$  is the leading eigenvalue of the Perron-Frobenius operator (for  $\beta = 0$ ). I call it  $e^{s_0}$  in [ChaosBook sect. 20.2.3](#) and [ChaosBook eq. \(21.9\)](#). More precisely, as the dimension of  $s_\alpha$  is  $1/[t]$ , the leading eigenvalue for both discrete time maps and continuous time flows is  $e^{s_0 t}$  evaluated at  $t = 1$ . The result that you state is not  $s_\infty$  (your notation), but rather  $s_{13}$ . In ChaosBook notation I might write

$$e^{s_0, (13)} \quad \text{or simply} \quad e^{s(13)}.$$

However, from numerical data such as figure 23.13, you can gain a bit more accurate estimate of  $s_0 = s_{(\infty)}$  by fitting the known  $|s_{(n)}| - s'_{(\infty)}$  as initial terms in a geometric series, and then using that to sum up the infinite tail as the rest of a geometric series. If you do that, please write down the exact formula you have used, or point to it in a reference you have used. Always.

When you think of it a bit, you'll probably find better ways to estimate  $s_0$ . That's called 'accelerating convergence', numerics literature explains it. It is no substitute for thinking;) There is no mindless routine that outperforms a proof that a Fredholm determinant is an entire function.

**2023-10-15 Xuanqi** The leading zero of the spectral determinant is (from orbits of period 7 to period 13) :

$$\begin{aligned}
 z_7 &= 2.212 \\
 z_8 &= 2.210 \\
 z_9 &= 2.2086 \\
 z_{10} &= 2.20886 \\
 z_{11} &= 2.20884545 \\
 z_{12} &= 2.20884607 \\
 z_{13} &= 2.208848372 \\
 z_\infty &\approx z_{13} = 2.20884837. \tag{23.41}
 \end{aligned}$$

If we take the last one as our best approximation (i.e.  $z_0^{(\infty)}$ ), then we have a convergence shown in figure 23.14.

We can see that periods 8, 9, 10, 11 form a perfect straight line, but 12 somehow deviates. The reason might be that 12 is the first number that has 4 divisors and thus process a more complicated structure of periodic solutions, but it seems not quite a strong argument. And I want to check it by comparing that with 13, and that's why I desperately want to compute to longer periods.

**2023-10-10 Predrag** It's great to see that two honestly totally independent calculations figure 23.14 and figure 24.79 return the same plot (period  $n = 12$  seems to be where numerical double-precision is exhausted). I think if you quotient the internal  $D_2$  symmetry of  $\phi^4$ , as in [ChaosBook sect. 20.2.3](#) and [ChaosBook eq. \(21.9\)](#),

**2023-10-30 Xuanqi** My notes on the factorization of cumulant expansion. The ideal case is that if we can write trace as

$$\text{tr} \frac{z\mathcal{L}}{1 - z\mathcal{L}} = \sum_{\mu} G_{\mu}(z) \tag{23.42}$$

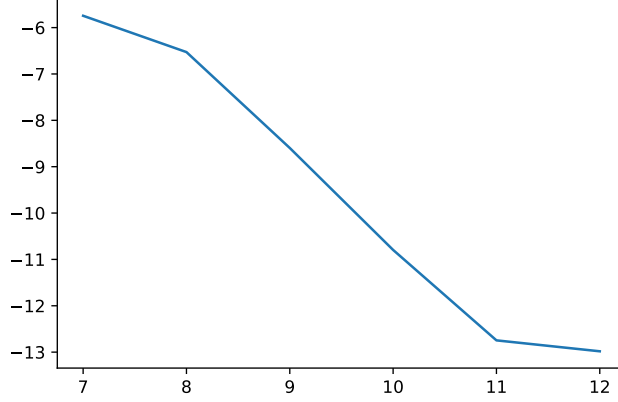


Figure 23.14: A plot somehow related to the undefined refeq XW\_Spectral\_D\_Convergence, where  $n$  is the period of periodic states  $c$  for  $\phi^4$  temporal field theory with  $\mu^2 = 3.5$ . We take  $s_\infty = 2.20884837$  (23.41) as the reference value (calculated from spectral determinant with cycle period  $n = 13$ ).

and use only the coefficients of  $G_\mu(z)$  to figure out the cumulant  $F_\mu(z)$  of spectral determinant, where

$$\det(1 - z\mathcal{L}) = \prod_{\mu} F_{\mu} \quad (23.43)$$

is the factorization of spectral determinant. This would provide a computational-feasible way for spectral determinant. To conform with formula

$$\text{tr} \frac{z\mathcal{L}}{1 - z\mathcal{L}} \det(1 - z\mathcal{L}) = -z \frac{d}{dz} \det(1 - z\mathcal{L}) \quad (23.44)$$

we must have

$$G_{\mu}(z)F_{\mu}(z) = -z \frac{d}{dz} F_{\mu}(z) \quad (23.45)$$

for every  $\mu$ . In fact, let's start with factorization into two components (i.e. two invariant subspaces)  $G_1 = \sum_{i=1} C_i^1 z^i$  and  $G_2 = \sum_{i=1} C_i^2 z^i$  for trace (similarly  $F_1 = \sum_{i=1} Q_i^1 z^i$  and  $F_2 = \sum_{i=1} Q_i^2 z^i$  for spectral determinant). Then it follows that

$$(G_1(z) + G_2(z))F_1(z)F_2(z) = -zF_1'(z)F_2(z) - zF_2'(z)F_1(z) \quad (23.46)$$

from chain rule. Notice that if such factorization of different invariant subspaces are indeed independent like (23.45) suggests, then

$$\begin{cases} G_1(z)F_1(z) = -zF_1'(z) \\ G_2(z)F_2(z) = -zF_2'(z) \end{cases} \quad (23.47)$$

we multiply the first equation by  $F_2(z)$  and second equation by  $F_1(z)$ , then add them together to get (23.46). However, it doesn't guarantee uniqueness, as we can only say that if (23.45) is correct, then (23.46) holds true, but not the reverse direction. But the case here is that (23.44) doesn't provide enough number of equation to uniquely determine every  $Q_n^\mu$ . Thus, I think it makes sense to conclude that

$$Q_n^\mu = \frac{1}{n}(C_n^\mu - C_{n-1}^\mu Q_1^\mu - \dots - C_1^\mu Q_{n-1}^\mu) \quad (23.48)$$

**2023-11-17 Xuanqi** Too many things clustered here. I will first make a list of it and finish them one by one.

1. Shadowing lemma and Anosov diffeomorphism for state space, want to show that non-wandering set is the closure of periodic solution.
2. Symmetry factorization of spectral determinant in cumulant sum format. The key idea here is how to define orbit Jacobian matrix for the half orbit.
3. Also have to summarize the discussion with Matheus about how to compute expectation using conditioning formula. I'm trying to use Riemann sphere for a better illustration for our case. Hopefully it will work. This conditioning is based on periodic orbits, and works for any choice of absorber set.
4. Need to generate one more figure for tigers paper for the illustration of optimal cover (which is also connected to the previous point). This should be fast.

**2024-01-08 Xuanqi** Turns out that our examples are not Anosov diffeomorphism, as hyperbolicity is limited in non-wandering set instead of the whole state space. I found out that Axiom A diffeomorphism such that

$$\begin{aligned} (i) \Omega(f) \text{ is compact} \\ (ii) \text{ The set of periodic point is dense in } \Omega(f) \end{aligned} \quad (23.49)$$

guarantees a Markov partition (shown by Bowen in 1970), density of periodic orbit, and non-wandering set as intersection of horseshoe (local maximality), and Axiom A in two-dimension is hyperbolicity. Now what I am still unclear is that how hyperbolicity is connected with homoclinic tangency of invariant manifolds, and for sake of generality the sufficient condition for Axiom A in higher dimensions.

**2024-01-19 Xuanqi** I am studying

Xu Zhang [18] *Hyperbolic invariant sets of the real generalized Hénon maps.*

generalized Hénon map  $F(x, y) = (y, ag(y - \delta x))$ , where  $g(y)$  is a monic real-coefficient polynomial of degree  $d \geq 2$ ,  $a$  and  $\delta$  are non-zero parameters

He gives a theorem with the lower bound on  $a$  (??), but no explicit numerical values or parameter plane graphs, so not clear how tight the bound is.

**2024-02-13 Xuanqi** I learnt from ref. [14] that dynamics in anti-integrable limit is what we call symbol mosaics, and there is a range of parameter where a continuation from anti-integrable limit exists. This notion, after reading [18] and [5], is widely used in the study of hyperbolic structure of invariant sets. A better phrase is that the dynamics is topologically conjugate to a  $m$ -symbol full shift ( $m=2$  for Henon and 3 for  $\phi^4$ ). Now the two things I don't understand is local maximality, which seems to be the case when horseshoe intersect at every possible point, and homoclinic tangle. The latter is related to Smale-Birkhoff theorem, and I think that is what I was looking for. I have found some materials on these topics, so I will take my time to read them.

While reading, I will continue to collect my findings and see how to write them into tigers' paper.

Also, for the reproduction of figures in CL18, I read through that chapter. I can understand the case of cat map, where stretching parameter is a constant. For the case of non-linear theories, I am having troubles with the fact that  $\phi_k$  is no longer eigenvectors as desired. Such calculation should be straight-forward numerically, but I don't have much idea of the analytical expression (seems like a trigonometric function from the figure).

**2024-02-13 Predrag** Have a look at day's version of CL18, sect. 5.3. *A doubly-periodic prime orbit, and its repeats*. The main thing to understand is that the prime orbit varies within the primitive cell, it is **not** translation invariant, so a discrete Fourier transform (the reciprocal lattice) does not diagonalize it. What remains is  $[N_{\mathbb{A}} \times N_{\mathbb{A}}]$  matrix.  $[2 \times 2]$  matrix you can diagonalize by hand (maybe do the  $k = 0$  case first). You can do that.

For any other primitive cell, condensed matter physicists always compute bands numerically.

We actually only need the Hill determinant, so I am hoping we compute that directly, rather than first computing the  $N_{\mathbb{A}}$  bands individually, than adding up their eigenexponents into a Birkhoff sum. That is why CL18 currently has Appendix C. *Spatiotemporal cat: Fundamental fact*. Look ma: Hill determinant, no cosines!

**2024-02-22 Xuanqi** This is about the calculation of spectrum of orbit Jacobian matrix for some  $n$  repeat of prime orbit of period 2. In other words, this is when we tile the space with a prime cell made up by a period  $2n$  orbit, which is  $n$  repeats of a period 2 prime orbit.

By the periodicity of orbit Jacobian matrix,

$$r^{-2} \mathcal{J} r^2 = \mathcal{J}, \tag{23.50}$$

and, since the shift operator  $r$  is reversible, we apply  $r^{-1}$  to both sides and get

$$[\mathcal{J}, r^2] = 0.$$

Assuming that both  $\mathcal{J}$  and  $r^2$  have a complete set of eigenvectors, basic linear algebra requires that these two operators have a common set of eigenvectors. The set of eigenvectors of  $r^2$ , as a basis of period  $2n$  orbits, is has very special form,

$$\begin{aligned}\varphi_{2t-1} &= e^{ik_1 t} \phi_1 \\ \varphi_{2t} &= e^{ik_2 t} \phi_2,\end{aligned}$$

where  $k_1, k_2 = \frac{2\pi k}{n}$  and  $t = 1, 2, \dots, n$ , and  $\phi_1, \phi_2$  are two independent field values. Looking globally, this equation also requires that  $k_1 = k_2$ , so just denote by  $k_1 = k_2 = k$ . To solve for the spectrum, assume that the eigenvalue corresponding to  $\varphi$  is  $\lambda$ ,

$$\begin{aligned}-e^{-ik} \phi_1 + s_1 \phi_2 - e^{ik} \phi_1 &= \lambda \phi_2 \\ -e^{-ik} \phi_2 + s_2 \phi_1 - e^{ik} \phi_2 &= \lambda \phi_1,\end{aligned}\tag{23.51}$$

where  $s_1 = s(\phi_1)$  and  $s_2 = s(\phi_2)$ . This reduces to the  $[2 \times 2]$  matrix eigenvalue problem

$$\mathbf{A} \varphi' = 0,$$

where

$$\begin{aligned}\mathbf{A} &= \begin{bmatrix} s_1 - \lambda & -2 \cos(k) \\ -2 \cos(k) & s_2 - \lambda \end{bmatrix}, \\ \varphi' &= \begin{bmatrix} \phi_1 \\ \phi_2 \end{bmatrix}.\end{aligned}$$

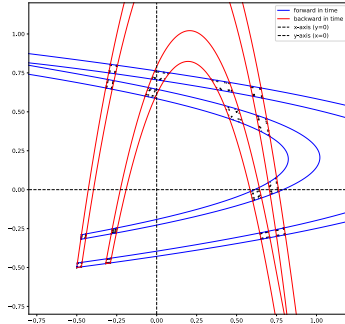
This results in a quadratic equation for  $\lambda$ , whose solution is given by

$$\lambda_{\pm} = \frac{(s_1 + s_2) \pm \sqrt{(s_1 + s_2)^2 - 4(4 \cos^2(k) + s_1 s_2)}}{2}.\tag{23.52}$$

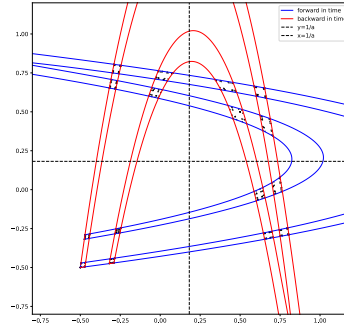
Note that this spectrum only depend on the trace  $(s_1 + s_2)$  and determinant  $s_1 s_2$  of the period-2 truncation of operator  $s$ , and this result can be generalized to prime cells consist of prime orbits with arbitrary period  $l$ , but all the other cases cannot be easily solved analytically because they would involve solving an eigenvalue problem with  $l \times l$  matrix. And this also doesn't depend on the specific form of field theory that we are considering. It applies equally well to all non-linear field theories that are not translationally-invariant.

**2024-03-07 Xuanqi** Last week I was working on the plots of  $\phi^3$  and fix up the package, as it seems that we chose a quite special presentation for  $\phi^3$ . The resulting transform is

$$\phi \rightarrow -\frac{2\sqrt{a+1}}{a} \phi + \frac{1}{a}\tag{23.53}$$



(a)  $\phi^3$  horseshoe before shift



(b)  $\phi^3$  horseshoe after shift

Figure 23.15:  $\phi^3(\phi_t, \phi_{t+1}, \dots)$  plot populated with periodic solutions up to period 7 to illustrate the fractal non-wandering set. Not that the time-reversal symmetry leads to the stable-unstable manifolds symmetry under the flip across the diagonal, but the  $\phi_t \leftrightarrow \phi_{t+1}$

$$\mu^2 = 2\sqrt{a+1} \tag{23.54}$$

So the result is not only a rescaling but also a shift. This makes division of symbolic mosaic a bit different, as we need to account for the shift. This is illustrated in figure 23.15, where the left one is when we use old tradition, dividing using x-axis, and the right one is after the adjustment. We can see that there is clearly a region in low branch (which symbol 0) above x-axis.

2024-03-09 Predrag Xuanqi's (23.54) agrees with Sidney's (22.68) and the convention used in ref. [16]. See the Tiger's nonlinear paper appendix [16] for a concise derivation.

2024-03-07 Xuanqi For the illustration of field values, I included both  $\phi^3$  and  $\phi^4$  in figure 23.16. There is not much to say about  $\phi^4$ , other than that its Euler-Lagrange equation is

$$-\square \phi_z + \mu^2(\phi_z - \phi_z^3) = 0, \tag{23.55}$$

and we can see that this time  $\phi^3$  agrees with the previous figure we see (view dashed line as original x-axis).

2024-03-07 Predrag Almost there. But, you don't mean that the relation (??) between  $a$  and  $\mu^2$  depends on a field value, do you?

2024-03-07 Predrag  $\phi^3$  in figure 23.16 (a) is interesting - does seem to align with reffig fig:PCchenlatt5cyc (vanished from blogCats.tex, but you know what

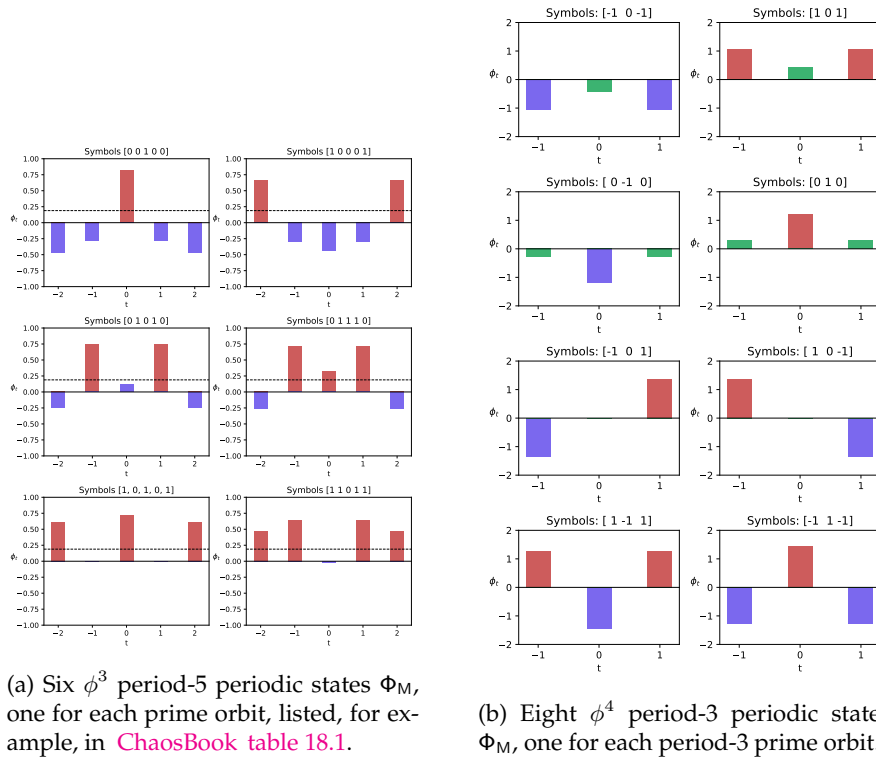


Figure 23.16: Examples of periodic states: (a)  $\phi^3$  Euler-Lagrange equation (4.150), with  $\mu^2 = 5.5$ , and (b)  $\phi^4$  Euler-Lagrange equation (23.55), with  $\mu^2 = 3.5$ .



I mean - it's in the Hénon appendix of the Tiger' paper). If  $\mu^2 = 20$ , does it approach  $\phi_t = \pm 1/2$ ? No need to put such figure here, just a sanity check.

## 23.2 Notes on zeta function

**2024-04-19 Xuanqi** We defined partition function on primitive cell  $\mathbb{A}$  to be

$$Z_{\mathbb{A}}[\beta] = \sum_c \int_{\mathcal{M}_c} d\Phi_{\mathbb{A}} \delta(F[\Phi]) e^{V_{\mathbb{A}} \beta \langle a \rangle_c} = \sum_c e^{V_{\mathbb{A}} (\beta \langle a \rangle_c - \lambda_c)} \quad (23.56)$$

Now, we used to write the generating function as

$$Z[\beta, z] = \sum_{\mathbb{A}} Z_{\mathbb{A}}[\beta] z^{V_{\mathbb{A}}} \quad (23.57)$$

The partial derivative  $\frac{\partial}{\partial \beta} \ln(Z)$  brings out a factor of  $V_{\mathbb{A}}$  for each term. If we write the generating function as

$$Z[\beta, z] = \sum_{\mathbb{A}} Z_{\mathbb{A}}[\beta] z^{V_{\mathbb{A}}/V_{\mathbb{A}}} \quad (23.58)$$

instead, without changing the partition function  $Z_{\mathbb{A}}$ , we can express  $Z_p[\beta, z]$  as

$$\begin{aligned} Z[\beta, z] &= \sum_{r_1=1}^{\infty} \sum_{r_2=1}^{\infty} \sum_{s=0}^{r_1-1} \frac{1}{r_1 r_2} t_p^{r_1 r_2} \\ &= \sum_{r_1=1}^{\infty} \sum_{r_2=1}^{\infty} \frac{1}{r_2} t_p^{r_1 r_2} \\ &= - \sum_{r_1=1}^{\infty} \ln(1 - t_p^{r_1}) \end{aligned} \quad (23.59)$$

as  $V_{\mathbb{A}} = r_1 r_2 V_p$  for repeats, and we use summation formula  $\sum_{n=1}^{\infty} \frac{a^n}{n} = -\ln(1-a)$  Per this definition, we have relation  $1/\zeta = \exp(Z[\beta, z])$ , which I think is simpler. Also, getting rid of the derivative  $\frac{\partial}{\partial z}$  will enable us to evaluate the Birkhoff average directly. I don't know whether this is desirable.

**2024-06-07 Xuanqi** This proof is inspired by the famous Cantor's intersection theorem. For hyperbolic dynamics, the locally maximal invariant set is constructed by

$$\Omega = \bigcap_{n=-\infty}^{\infty} f^n(U) \quad (23.60)$$

for some open set  $U \subset \mathcal{M}$  and  $f : \mathcal{M} \rightarrow \mathcal{M}$  invertible. We construct a sequence of nested compact (i.e. close and bounded in  $\mathbb{R}^2$ ) sets  $\{\Omega_k\}$  such that

$$\Omega_k = f^k(N) \cap N \cap f^{-k}(N) \quad (23.61)$$

where  $N \subset \mathcal{M}$  is the compact optimal cover that we choose, whose boundary is given by invariant manifolds. We will prove that  $\{\Omega_k\}$  is indeed a sequence of nested compact sets, and this sequence will be very useful in understanding  $\Omega$ . The key of this proof lies in the fact that

$$\Omega_k = \bigcap_{n=-k}^k f^n(N) \quad (23.62)$$

We begin by proving the following lemma.

Lemma 1:  $\Omega_m \subset \Omega_n$  for all  $m > n$ .

Proof: It suffices to prove that  $\Omega_{n+1} \subset \Omega_n$ . Assume there is  $x \in \mathcal{M}$  such that  $x \in \Omega_{n+1}$  and  $x \notin \Omega_n$ . Then, without loss of generality assume  $x \in f^{n+1}(N) \setminus f^n(N)$ . By invertibility of  $f$ , we can conclude that  $f^{-n}(x) \in f(N) \setminus N$ , which is the colored region shown in figure 23.17. However,  $f(N) \setminus N$  lies on the "wrong" side of stable manifolds  $W_1^s$  and  $W_2^s$ , which means that  $f(N) \setminus N$  never intersects  $N$  in any forward in time image of  $f$ . Therefore,  $f^n(f^{-n}(x)) = x \notin N$ , contradicts with the assumption  $x \in \Omega_{n+1}$ .

In fact, the reason that any forward in time image of  $f(N) \setminus N$  would never intersect  $N$  is clearer when looking at the direction of its boundary (which is piecewisely given by three invariant manifolds). This argument is more apparent when we look at all of the "smallest" regions in  $\Omega_0 \setminus \Omega_1$  whose boundaries are given by  $\partial f(N) \cup \partial f^{-1}(N)$ .

Intuitively, this lemma suggests that if a point  $x \in N$  runs out of  $N$  (i.e.  $f^k(x) \notin N \exists k \in \mathbb{Z}$ ), then it can never return to  $N$ . The important condition here is that  $x$  has to start out in  $N$ , because points that are outside  $N$  can enter, but such entrance is allow for only once.

Corollary:  $\Omega_k = \bigcap_{n=-k}^k f^n(N)$

Proof: It is the direct result by applying Lemma 1.

$$\bigcap_{n=-k}^k f^n(N) = \bigcap_{n=-k}^k f^n(N) \cap N = f^k(N) \cap N \cap f^{-k}(N) = \Omega_k \quad (23.63)$$

as  $f^k(N) \cap N \cap f^{-k}(N) \subset f^m(N) \cap N \cap f^{-m}(N)$  by Lemma 1.

The structure of invariant set  $\Omega = \lim_{n \rightarrow \infty} \bigcap \Omega_n$  is revealed by the sequence of  $\{\Omega_n\}$ . Write  $\Omega_n = (f^n(N) \cap N) \cap (f^{-n}(N) \cap N)$ , it is clear that  $f^n(N) \cap N$  resembles the construction of Smale's horseshoe map, where the existence of a transversally homoclinic point guarantees that

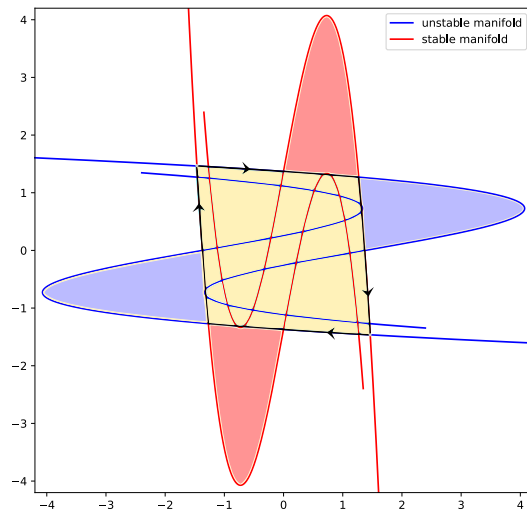


Figure 23.17: A visualization aid to understanding  $f(N) \setminus N$ , with example from  $\phi^4$  theory,  $\mu^2 = 3.5$ .

$f^n(N) \cap N$  is a disjoint union of  $m^n$  regions (where  $m$  is a positive integer), each being compact and connected. Therefore, we can label the  $2m^n$  disjoint connected regions in  $\Omega_n$  by a period  $2n$  string with  $m$  symbols.

$$\Omega_n = \bigsqcup_{s \in S} \Omega_n^s, \quad S = \mathcal{A}^{2n}, \quad |\mathcal{A}| = m. \quad (23.64)$$

We arrange the symbol strings in such a way that if  $s = s_{-n+1}s_{-n+2}\dots s_0s_1\dots s_n$  and  $s' = s'_{-m+1}s'_{-m+2}\dots s'_0s'_1\dots s'_m$  ( $n > m$ ) and  $s_k = s'_k$  ( $\forall |k| \leq m$ ), then  $\Omega_n^s \subset \Omega_m^{s'}$ . With this arrangement, for each bi-infinite string  $s = \dots s_{-1}s_0s_1s_2\dots \in \mathcal{A}^{\mathbb{Z}}$ , we can construct a sequence of nested compact sets  $\{\Omega_n^{s^n}\}$  where  $s^n = s_{-n+1}\dots s_0s_1\dots s_n$  denote the finitely truncated substring of  $s$  of period  $2n$ . Let  $\Omega^s = \lim_{n \rightarrow \infty} \bigcap \Omega_n^{s^n}$ , by Cantor's intersection theorem  $\Omega^s$  is non-empty. Since  $\Omega$  is the disjoint union of  $\Omega^s$

$$\Omega = \bigsqcup_{s \in \mathcal{A}^{\mathbb{Z}}} \Omega^s. \quad (23.65)$$

and  $\Omega$  is, by its nature, a totally disconnected, whose connected components are only singletons, we just need to prove that  $\Omega^s$  is connected to establish the one-to-one correspondence between  $\Omega$  and  $\mathcal{A}^{\mathbb{Z}}$  and prove that the dynamics is conjugated to a  $m$ -symbol full shift.

Lemma 2:  $\Omega^s$  is connect

Proof: We prove by contradiction. Assume that  $\Omega^s$  is disconnected, covered by  $U, V \subset \mathcal{M}$  open, then we construct a new sequence of nested sets  $\{\Omega_n^{s^n} \setminus (U \sqcup V)\}$ . Since  $U, V$  are open, all the sets in this sequence are still compact. And as  $\Omega_n^{s^n}$  are connected,  $\Omega_n^{s^n} \setminus (U \sqcup V)$  much be non-empty for each  $n$ . Then, there exists  $x \in \bigcap \Omega_n^{s^n} \setminus (U \sqcup V) = \Omega^s \setminus (U \sqcup V)$ , contradicts with the assumption that  $U \sqcup V$  covers  $\Omega^s$ .

Therefore, we conclude that the locally maximal invariant set  $\Omega$  has its points in one-to-one correspondence with  $\mathcal{A}^{\mathbb{Z}}$ . This construction naturally manifests the fact that dynamics in  $\Omega$  is conjugated to a  $m$ -symbol full shift, which is the important conclusion we will use in shadow state method.

**2024-07-10 Xuanqi** I'm reading Ruelle's paper on dynamical zeta function. Here are the links: [fea-ruelle](#) and "[what are they good for?](#)".

The first one is more technical and contains much richer details, while the second one should be the script of a talk based on content of the one (Fea-Ruelle paper).

**2024-07-10 Predrag** A math or theoretical physics research requires mastery of BibTex. When you are adding a reference, check first whether the entry is already in `siminos.bib`. We have them already:

D. Ruelle [12] *Dynamical zeta functions and transfer operators* (2002), briefly referred to on page 336.

D. Ruelle [11] *Dynamical zeta functions: Where do they come from and what are they good for?* (1992); [IHES preprint](#).

### 23.3 2024 blog, continued

**2024-07-23 Xuanqi** Some notes on the discussion yesterday. Predrag mentioned that we have always overlooked the case when some restriction is put on the system, like a fixed energy dissipation rate, and whenever such a condition is imposed, some periodic states are "killed". For me, I would rather think of this "imposing a condition" as driving the system in a certain way, pretty much like the masting effect when we study ODE (Lotka-Volterra system to be specific).

Specify this down to our case, it could be that we introduce a source term, just like cat map (and for cat map this term is designed so that all solutions are kept in the unit hypercube). In this way, the equation can be thought as

$$-\partial^2 \phi + V''(\phi) = j_t(\phi) \quad (23.66)$$

The subscript for source means that it can change with respect to time. If we consider the case that such change doesn't occur too often so that we can have enough time for the system to reach equilibrium at every stage, then we shall define some

$$V''_{new}(\phi) = V''(\phi) - j_t(\phi) \quad (23.67)$$

for each stage ( $T_i < t < T_{i+1}$ ). Then this reduces to a new system, whose Hamiltonian is perturbed by the source term. And if we drive the system periodically, it switch between this family of systems determined by this source, and whose expectation value is easy to compute as a weighted average.

I think a more delicate model can be made so that source term would simply give a new invariant measure based on the new time evolution operator, but the driving model should be more promising, I guess.

**2024-08-11 Predrag** There is a huge number of papers on necklaces, i.e., one-dimensional periodic lattices / primitive cells, once you have figured it out for yourself, might want to have a look to see whether your idea of ordering them by the largest number in  $n$ -ary orbit is already worked out, give proper credit to Euler or whoever.

I have added a few references of possible interest to the (current) end of sect. [9.2 Counting prime periodic states](#).

**2024-09-18 Xuanqi** Is it possible that the dependence of product of all  $\Lambda_c^\alpha(k)$  turns out to be just  $A = B \cos(nk)$  where  $n$  is the volume of primitive cell? I am working on the anti-symmetric trace formula, and it seems to suggest a quite simple dependence on  $k$ .

Let first focus on dimension one, where the period of a periodic state is  $n$ . Then the shifting operator gives  $r^n \phi^\alpha(k) = e^{ink} \phi^\alpha(k)$  for all  $\alpha$ . Then temporal cat  $\mathcal{J}_c = -r + s\mathbf{1} - r^{-1}$ , and

$$\text{Tr}(\mathcal{J}_c^m) = \text{Tr} \sum_{j=0}^{\lfloor m/2 \rfloor} \binom{2j}{j} s^{m-2j} \mathbf{1}, \quad (23.68)$$

where  $C_k^{2k}$  is the combinatoric coefficient of  $2k$  choose  $k$ , has only contributions from powers of  $s$ , expect for when  $m = n$  there is an additional  $2 \cos(nk)$  shows up from  $r^n + r^{-n}$ . (Because any non-zero shift of diagonal matrix  $s$  will result in a zero trace for simple reason). As since the determinant expressed in anti-symmetric trace formula only consists of combination of these traces and their powers, and this  $2 \cos(nk)$  only shows up in  $\text{tr}(\mathcal{J}_c^n)$ , which always has coefficient 1, it seems that this implies a rather simple dependence on  $k$  and we shall be able to work out the semi-analytical result of stability exponent.

**2024-09-24 Predrag** Whenever you commit LaTeX that does not compile, you make me or someone else spend 15 min debugging your commit to be able to read what you want us to read. That is inefficient use of our collective workhours, in many ways.

**2024-09-24 Predrag** sect. 12.7.1 Hill's formula for a first-order system, sect. 12.9.1 Hill's formula for a second-order system might remind you of calculations you sketched for us in the Tuesday's Tigers' Zoom.

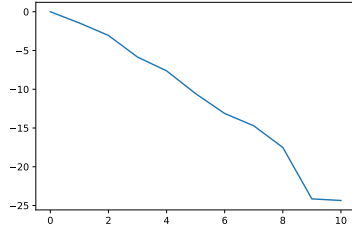
**2024-09-24 Predrag** Cannot find references that build upon my birdtrack determinant formulas, but there is no need for you to suffer through bird-tracking. There are perfectly fine online derivations of the formulas you are using in familiar notations. I've collected some for you [here](#). Ignore long-winded bloggery, go straight to the last entry before references.

**2024-09-26 Predrag** You also need to evaluate Hill determinant for  $\mathbb{A} = [L \times T]_S, S > 0$ .

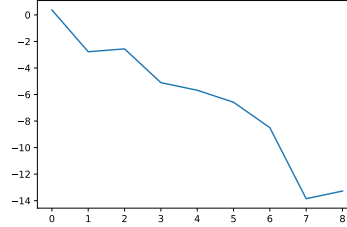
**2024-09-26 Predrag** The formulas for determinants are throughout the blog, and much of it has to do with symmetries. For example, see sect. 6.12 *Discrete factorization of the dynamical zeta function*: "the regular representation of a group element has nonzero trace if and only if this group element is  $e$ ."

Cyclic  $C_n$  symmetry (the only one we assume in CL18) is the easiest case. Our three model theories are time reversal symmetric, so they have the dihedral  $D_n$  symmetry, which requires a bit more work, see, for example, the above section, and LC21 [9].

**2024-09-26 Predrag** Some incomplete musings.... Expand  $\ln \text{Det}_{\mathbb{A}} \mathcal{J} = \text{Tr}_{\mathbb{A}} \ln \mathcal{J}$  as a series in momentum  $p/\mu$  in Klein-Gordon mass units, vanishing in



(a) Numerically generated exponentially decaying random coefficients (in log scale), positive or negative.



(b) Convergence of leading root found by the set of coefficients given above.

Figure 23.18: Checked the convergence pattern of algebraic equation (finitely truncated zeta function) with absolute value of coefficients exponentially decay.

the anti-integrable limit:

$$\text{Tr}_{\mathbb{A}} \ln(p^2 + \mu^2) - N_{\mathbb{A}} \ln \mu^2 = \text{Tr}_{\mathbb{A}} \ln \left( \mathbf{1} + \left( \frac{p}{\mu} \right)^2 \right) = - \sum_{m=1}^{\infty} \frac{1}{m} \text{Tr}_{\mathbb{A}} \left( i \frac{p}{\mu} \right)^{2m}.$$

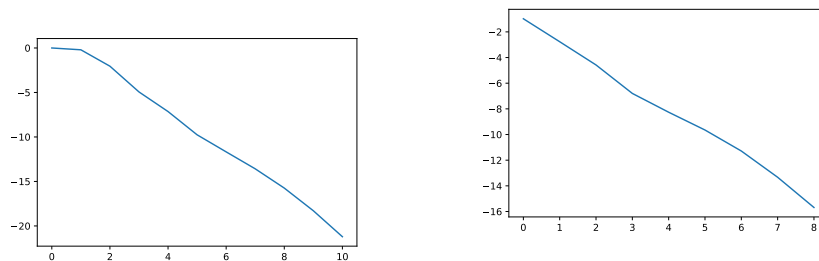
Note that  $\text{Tr}_{\mathbb{A}} r^m$  is non-zero only when  $m$  is a multiple of  $n$ , so Xuanqi's idea of using orbit Jacobian matrices in the diagonal stretching (4.107)–(4.109) form seems smarter.

**2024-09-29 Xuanqi** For higher dimensions, the result would be much more complicated. If I understood it correctly, then in 2-d we will have to calculate trace up to  $n_1 n_2$  where  $n_i$  is the period in each direction, so we will have non-zero terms from  $\text{Tr}(\mathcal{J}^{\ell_1 n_1 + \ell_2 n_2})$ , which would contribute  $4 \cos(\ell_1 n_1 k_1) \cos(\ell_2 n_2 k_2)$ , and for generality  $\ell_1$  can take value  $0, 1, \dots, n_2 - 1$  and similar for  $\ell_2$ . But since we can complete a cycle in both direction, we would also have terms like  $r_1^{n_1} s$ , which have non-zero trace, and the fact that  $\mathcal{J}$  does not commute with  $r_i$  makes the evaluation harder. However, it still provides with a structure of the spectrum, and my intuition is that most terms will be cancelled out. leaving with those that are highly "asymmetric".

When considering slanting, my argument is that, by replacing  $r_2'$  with  $r_2 r_1^s$ , what used to be  $4 \cos(\ell_1 n_1 k_1) \cos(\ell_2 n_2 k_2)$  becomes  $4 \cos(\ell_1 n_1 k_1) \cos(\ell_2 n_2 (k_2 + s k_1))$ .

**2024-10-13 Xuanqi** A few numerical results. First, I found that convergence of zeta function might not be what I expected. The results are figure 23.18a and figure 23.19b.

(Figure 23.19 itself not referred to.)



(a) Kept only the positive coefficients.

(b) Used the absolute value of all coefficients.

Figure 23.19: Exploring the convergence of the leading root of truncated cumulant sums, with numerically generated exponentially decaying *random coefficients* (in log scale).

We can see that cumulant sum, which contains only positive terms, has a better convergence pattern, but it does not mean that it converges faster. So I am not very sure that we would have perfect exponential convergence for zeta function calculation of escape rate. I did not include the actual result, as I think some more details has to be checked in my program.

The good news comes from the spectrum of spatiotemporal orbit Jacobian operator, which I showed in figure 23.20. We can see that there are exactly  $3 \times 5$  peaks in  $(-\pi, \pi)^2$  in k-space, and in primitive cell it is clear that this spectrum is an even function, which means that in power series there is no  $k_1$  or  $k_2$  terms, nor  $k_1 k_2$  terms, so the series starts with  $\det(0) + c_1 k_1^2 + c_2 k_2^2$  as we wished.

**2024-10-28 Xuanqi** The calculation for 1st order system yields no problem. It is particularly beautiful. However, when we try to generalize to second order systems, there seems to be a problem. First we define

$$p = i(r - 1) \quad p^\dagger = -i(r^T - 1) \quad (23.69)$$

Then  $p^\dagger p = -r + 2 - r^T$  has no problem, but if we include  $\mu$  into this, the fact that  $\mu$  does not commute with  $r$  and  $r \neq r^T$  yield some problems.

$$(p^\dagger + \mu)(p + \mu) = -r + (\mu^2 + 2) - r^T - ir^T \mu + i\mu r \neq \mathcal{J} \quad (23.70)$$

I guess, if physics does not prevent me from it, we should include the potential term into the definition of  $p$ , as this would reduce the problem for  $r \neq r^T$ , but still it does not solve this problem. If we define  $p$  to be

$$p = i(r - a) \quad (23.71)$$





(a) Orbit Jacobian operator spectrum for  $[3 \times 5]_0$  with constant stretching in k-space  $(-\pi, \pi)^2$ , i.e., 15 times the Brillouin zone.

(b) Orbit Jacobian operator spectrum for  $[3 \times 5]_0$  with constant stretching in primitive cell.

Figure 23.20: Checked the convergence pattern of algebraic equation (cumulant sum) with absolute value of coefficients exponentially decay.

then momentum square yields

$$p^\dagger p = (1 + a^2 - r^T a - ar) = a(1/a + a) - r - a^{-1} r^T a \quad (23.72)$$

What we need would be  $a + 1/a = S$ , but still we are left with a  $a^{-1} r^T a$  term unresolved.

2024-10-31 Xuanqi .

### Spectrum of orbit Jacobian operator

Here I summarize my work regarding the spectrum of orbit Jacobian operator. This result mainly uses the notion of anti-symmetrized trace in Predrag's group theory. For a temporal periodic state of length  $n$ , its orbit Jacobian operator is reduced to a  $n \times n$  matrix  $\mathcal{J}$ , and the determinant of this matrix can be given by

$$\text{Det}(\mathcal{J}) = \text{Tr}_p A \mathcal{J} = \frac{1}{n} \sum_{m=1}^n (-1)^{m-1} (\text{Tr}_{n-m} A \mathcal{J}) \text{Tr} \mathcal{J}^m \quad (23.73)$$

where  $A$  denote the anti-symmetrized tensor with  $\text{Tr}_0 A M = 1$ . Then, we can recursively decompose  $\text{Tr}_i A M$  into sum of products of  $\text{tr}(M^n)$  for  $n \leq i$ . If we request  $M = \text{diag}(x_1, x_2, \dots, x_n)$  is a diagonal matrix, then (??) exploits all possible terms in a homogenous polynomial  $p(x_1, x_2, \dots, x_n)$  of degree  $n$ . But we know that an extricate leaves only one last term. This expression of  $\text{Det} \mathcal{J}$  in a finite sum of traces is especially useful in the calculation of spectrum of  $\mathcal{J}$ .

### One-dimensional systems

For one-dimensional systems, we realize through Bloch theorem that since  $r^n \mathcal{J} = \mathcal{J}$ , we have  $\mathcal{J}(e^{ikr} \psi_k^\alpha(r)) = \Lambda(k)^\alpha e^{ikr} \psi_k^\alpha(r)$  and the wave function  $\psi_k^\alpha(r) = \psi_k^\alpha(r+n)$  has the same periodicity as underlying periodic state. In this case, one should aware that it is a wise choice to absorb all the phase into an operator  $\Psi: \mathbb{R}^n \rightarrow \mathbb{R}^Z$  such that  $\Psi(\psi_k^\alpha(r)) = e^{ikr} \psi_k^\alpha(r)$  is extended from the primitive cell to all space with proper phase factor.

Now, to work our the spectrum of orbit Jacobian operator, we still need to figure out how to put it into primitive cell so that it can be reduced to a matrix whose determinant is well-defined. To do so, we need to figure how to change order of  $\mathcal{J}$  and  $\Psi$  on lattice. Write  $\mathcal{J} = -r - r^{-1} + \mathbf{S}$ , where  $\mathbf{S}$  is a diagonal operator that commutes with  $\Psi$ , we get

$$\mathcal{J}\Psi = (-r - r^{-1} + \mathbf{S})\Psi = -\Psi r e^{ika} - \Psi r^{-1} e^{-ika} + \Phi \mathbf{S} = \Psi \mathcal{J}(k) \quad (23.74)$$

where  $a = 1$  should be the lattice constant and  $\mathcal{J}(k)$  is the orbit Jacobian operator in primitive cell (i.e. matrix), with the shift operator  $r$  replaced by  $r e^{ika}$ .

The spectrum of orbit Jacobian operator is  $\prod_\alpha \Lambda^\alpha(k) = \text{Det } \mathcal{J}(k)$  is reduced to the spectrum of a  $n \times n$  matrix that suits the setup of trace calculation. As we should find immediately that  $\text{tr}(r^m \mathbf{S}) \neq 0$  only for  $m|n$ , which means that diagonal matrix  $\mathbf{S}$  has to be put into its original position. Since we have all terms homogenous degree  $n$ , it is impossible to shift  $\mathbf{S}$  exactly  $n$  times, so we have to make sure that shift cancels in order to contribute anything in trace. This important observation then asserts that the only term in  $\text{Det } \mathcal{J}(k)$  that depends on  $k$  should come from  $\text{tr}(r e^{ika})^n = n e^{inka}$  and  $\text{tr}(r e^{-ika})^n = n e^{-inka}$ . Then trace calculation gives

$$\text{Det } \mathcal{J}(k) = \text{Det } \mathcal{J}(0) - 4 \sin^2(nk/2) \quad (23.75)$$

which is strikingly simple. (See Bountis and Helleman, sect. 11.1.3.) Here we have to aware that  $\text{Det } \mathcal{J}(0)$  can be negative, so upon taking absolute value moment  $\sin^2(nk/2)$  term can change sign according to the sign of  $\text{Det } \mathcal{J}(0)$ . In figure 23.21 I showed two spectra numerically calculated, and we can see that the prediction matches these calculations perfectly.

### Higher dimensional theories, still to be worked out better

The natural next step is to generalize this result to higher dimension, and we will first try 2-dimensional square lattice. Similar to the case in one dimension, we can absorb the phase into some operator  $\Phi$  and multiply  $\psi_k^\alpha(r)$  by  $\Phi$  to extend primitive cell to all space. I found it convenient to define  $\Phi_1$  and  $\Phi_2$  for two dimensions separately, and clearly  $r_i \Phi_j$  commutes when  $i \neq j$ . Thus, for a  $m \times n$  2-dimensional periodic state, the

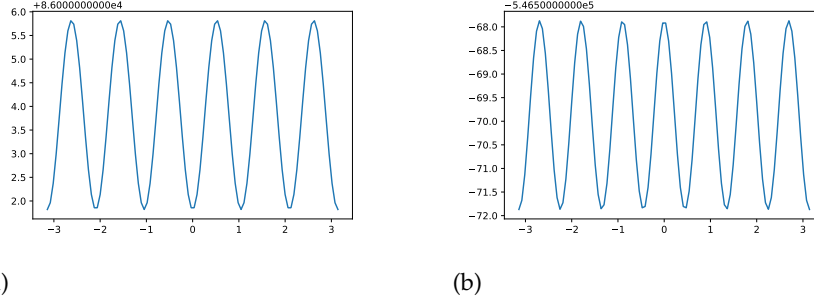


Figure 23.21: Spectrum of  $\text{Det } \mathcal{J}(k)$  plotted over  $(-\pi, \pi)$  for an random period-6 (left) and period-7 orbit (right) for  $\phi^4$  theory. We can see all expected features from these figures, includes the number of peaks equal to period, even function, oscillation with amplitude = 2

spectrum of orbit Jacobian operator can be found by push it into the flattened  $mn \times mn$  primitive cell orbit Jacobian operator, where  $r_1 = r \otimes \mathbf{1}$  and  $r_2 = \mathbf{1} \otimes r$ . We define the primitive cell orbit Jacobian operator to be

$$\mathcal{J}(k) = -(r_1 e^{ik_1 a_1} + r_1^{-1} e^{-ik_1 a_1} + r_2 e^{ik_2 a_2} + r_2^{-1} e^{-ik_2 a_2}) + S \quad (23.76)$$

We can still do the trace calculation, but this time it takes up power  $m \times n$ , and it is possible to complete multiple cycles in both direction. Then, the spectrum is now a trigonometric polynomial

$$\sum_{pm+nq \leq mn} [\sum_{\vec{\mu}=\vec{p}} \sum_{\vec{m} \cdot \vec{\nu}=q} C(\mu, \nu) \times \prod_{i=1}^n \cos^{\mu_i}(imk_1) \prod_{j=1}^m \cos^{\nu_j}(jnk_2)] \quad (23.77)$$

where we define  $\vec{m} = (1, 2, \dots, m)$  and similarly  $\vec{n} = (1, 2, \dots, n)$ , and we request all  $p, q, \mu_i, \nu_j$  to be non-negative. To reduce notation, it is more convenient to define  $\langle \mu \rangle = \vec{n} \cdot \vec{\mu}$  and  $\langle \nu \rangle = \vec{m} \cdot \vec{\nu}$ . We can decompose the cos's into momentum square and leave out the most important constant term

$$\text{Det } \mathcal{J}(k) = \text{Det } \mathcal{J}(0) + \sum_{p,q} [\sum_{\substack{\langle \mu \rangle = p \\ \langle \nu \rangle = q}} C_{\mu, \nu} \prod_{i=1}^n \sin^{2\mu_i}(\frac{imk_1}{2}) \prod_{j=1}^m \sin^{2\nu_j}(\frac{jnk_2}{2})] \quad (23.78)$$

We can even reduce this a little bit by coupling the periodicity with wave length to define  $k'_1 = \frac{mk_1}{2}$ ,  $k'_2 = \frac{nk_2}{2}$

$$\text{Det } \mathcal{J}(k) = \text{Det } \mathcal{J}(0) + \sum_{p,q} [ \sum_{\substack{\langle \mu \rangle = p \\ \langle \nu \rangle = q}} C_{\mu,\nu} \prod_{i=1}^n \sin^{2\mu_i}(ik'_1) \prod_{j=1}^m \sin^{2\nu_j}(jk'_2) ] \quad (23.79)$$

The coefficients  $C_{\mu,\nu}$  are exponentially suppressed as

$$|C_{\mu,\nu}| \sim C^{[1 - (\frac{\langle \mu \rangle}{n} + \frac{\langle \nu \rangle}{m})]} \quad (23.80)$$

and  $C = \text{Det } \mathcal{J}(0)$ . To understand this formula, we have to recall the explanation of trace formula as a homogenous polynomial. Here, the independent variables are  $e^{imk_1}$ ,  $e^{-imk_1}$ ,  $e^{ink_2}$ ,  $e^{-ink_2}$ , which form pairwise cancellations. Due to symmetry, all of the  $k$ -dependent terms appear as  $\cos(n_i k_i)$  for some direction  $i$ . And to summarize the condition for homogeneity in degrees, we separate the degree for each direction, as different directions can only possibly couple through multiplication, and their sum cannot exceed the volume of primitive cell  $m \times n$ . The degree of each term  $\cos(n_i k_i)$  is defined to be  $n_i$ , and in multiplication (either in the same direction or different directions), degrees add up. In ?? we label by  $mp = m\langle \mu \rangle$  the degree of  $k_1$  terms and  $nq = n\langle \nu \rangle$  the degree of  $k_2$  terms, and each is composed by product of different modes specified by vector  $\mu, \nu$ . This exponential decay in ?? is an exponential in total degree of each term, and clearly the constant term, with degree zero, is the most dominant. I took the product to be upper-bounded by  $n$  and  $m$  respectively because superposition of fundamental modes up to these numbers (which is essentially  $V/n_i$ ) would have reached the volume of primitive cell.

Although this spectrum is much more complicated than that for one dimension, it still gives us good intuition. First of all, we can see that this spectrum is dominated by the constant part. Then, if we look at the next level of contribution in  $k_1$  and  $k_2$ , we can see that the direction with shorter period dominates its longer counterpart. Finally, this spectrum is an even function for both wave numbers, and the crossing term of  $k_1$  and  $k_2$  comes first with  $k_1^2 k_2^2$ , the 4th order term. This means that in continuous limit, we should be able to decorelate perturbation in different directions. For even higher dimension, we only need to introduce more sets of vector subscripts, and clearly all of the observation made above generalize to arbitrarily high dimension.

To get the feeling of this 2D orbit Jacobian operator spectrum, it is better to work out an example. We first compare the  $[2 \times 2]_0$  state and  $[2 \times 3]_0$  states of cat map with stretching  $\mu^2 = 4$ . To better understand the figures we should, at this time, change from  $\sin^2$  to  $\cos$ . First, we list out the possible modes for each case, which is not very hard (7 terms for  $[2 \times 2]_0$  and 10 terms for  $[2 \times 3]_0$ )

To get the feeling of this 2D orbit Jacobian operator spectrum, it is better to work out an example. We first compare the  $[2 \times 2]_0$  state and  $[2 \times 3]_0$  states of cat map with stretching  $\mu^2 = 4$ . To better understand the figures we should, at this time, change from  $\sin^2$  to  $\cos$ . First, we list out the possible modes for each case, which is not very hard (7 terms for  $[2 \times 2]_0$  and 10 terms for  $[2 \times 3]_0$ )

$$\begin{aligned}
 [2 \times 2]_0 : \\
 & \cos(2k_1), \cos(2k_2), \\
 & \cos(2k_1)^2, \cos(2k_2)^2, \cos(4k_1), \cos(4k_2), \cos(2k_1)\cos(2k_2)
 \end{aligned} \tag{23.81}$$

$$\begin{aligned}
 [2 \times 3]_0 : \\
 & \cos(2k_1), \\
 & \cos(3k_2), \\
 & \cos(2k_1)^2, \cos(4k_1), \\
 & \cos(2k_1)\cos(3k_2), \\
 & \cos(6k_1), \cos(2k_1)\cos(4k_1), \cos(2k_1)^3, \cos(6k_2), \cos(3k_1)^2
 \end{aligned} \tag{23.82}$$

Then we check the dominant modes for both cases, which I showed in figure 23.22. We can see that for  $[2 \times 2]_0$  this spectrum is symmetric, while for  $[2 \times 3]_0$  there is oscillation in both directions, but the amplitude for x direction (with period 2) is much larger than that in y direction (with period 3). To further analyze this spectrum for  $[2 \times 3]_0$ , we take a slice in primitive cell, fixing  $k_2 = 0$  and plot over  $k_1 \in (-\pi/2, \pi/2)$ , and we see from figure 23.23 that the deviation from  $\cos(2k_1)$  by nearly  $\cos(4k_1)$ , and the amplitude is much smaller for this mode. If we look carefully enough we can see the  $\cos(6k_1)$  from how the dots deviates from the curve periodically.

**2024-11-01 Xuanqi** After discussion with Predrag yesterday, we decided to check the cross term by factoring the spectrum by irreducible representation of  $D_4$  for  $[2 \times 2]_0$  square lattice, first on spatiotemporal cat examples.

**2024-11-01 Predrag to Xuanqi** One of the reasons we use macros is that one can easily search for macros, like " $D_4$ " or " $[2 \times 3]_0$ ".

**2024-11-01 Predrag** I'm worried that this might be a wild goose chase, but here some links to our  $D_4$  notes:

Figure 6.2, eq. (6.32), figure 6.6, figure 24.68.

Eq. (6.204): for a two-dimensional square integer lattice, a possible symmetry of the theory can be the *space group*  $p4mm$  symmetry operations (23.83).

$$D_4 = \{e, r, r^2, r^3, \sigma, \sigma_1, \sigma_2, \sigma_3\}. \tag{23.83}$$

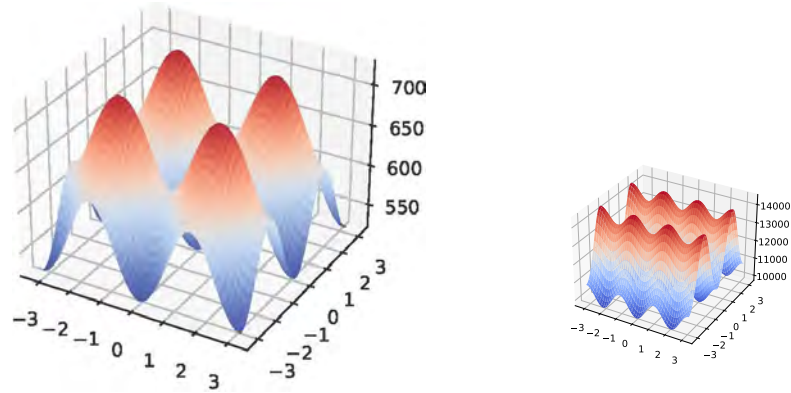


Figure 23.22: Spectra for spatiotemporal orbit Jacobian operator for cat map  $\mu^2 = 4$  for  $[2 \times 2]_0$  (left) and  $[2 \times 3]_0$  (right). We can see how amplitude in the major direction (with short period) can differ from that in minor direction (with longer period)

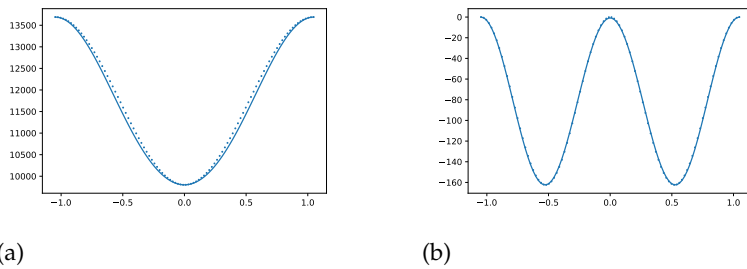


Figure 23.23: On the left is a snapshot taken at  $k_2 = 0$  in primitive cell  $k_1 \in (-\pi/2, \pi/2]$ , and the dots are results from fitting it to  $\cos(2k_1)$ . On the right is the residual of fitting in on left figure, and we fit it again with  $\cos(4k_1)$  (dots).

Blogpost **2021-07-08 Predrag** applies Burnside's method to  $D_4$ .  
table [6.4](#).

Blogpost **2019-01-28 Predrag** useful wikis.

Blogpost **2020-12-20 Predrag**

Blogpost **2020-12-20 Predrag** massless, Poisson equation value.

Example [6.27](#), example [6.28](#).

Blogpost **2021-07-07 Predrag** in `groups.tex`, and Cini and Stefanucci [[3](#)] *Antiferromagnetism of the two-dimensional Hubbard model at half-filling: The analytic ground state for weak coupling*, [arXiv:cond-mat/0009058](#), uses Dirac characters to diagonalize a square integer  $[N \times N]$  lattice with  $D_4$  symmetry. Might help us with the temporal cat desymmetrization.

**2023-03-06 Predrag** A way to explain it: rescale the Bravais lattice by multiplying it by  $\mathbb{A}^{-1}$ , send it into the unit integer lattice. A prime orbit usually has less symmetry than point group  $D_4$  of square lattice  $p4mm$  [[4](#)]. Mapped back into the unit square, its point group will be one of the square lattice point groups  $p4$  or  $p4gm$ , in the [wallpaper classification](#), see, for example, table 9.2 in Dresselhaus [[4](#)].

The same procedure as finding the periodic states applies: a  $\mathcal{L}_{\mathbb{A}_p\mathbb{R}}$ -periodic state is a  $\mathcal{L}_{\mathbb{R}}$  periodic state in the new integer lattice.

The repeats of a prime  $\mathcal{L}_{\mathbb{A}_p}$ -periodic state have periodicities given by  $\mathcal{L}_{\mathbb{A}}$ , the sublattice of  $\mathcal{L}_{\mathbb{A}_p}$ , where  $\mathbb{A} = \mathbb{A}_p\mathbb{R}$ .

**2024-11-10 Predrag** .

 Just do it! But not in 30 min :)

**2024-11-10 Xuanqi** I found out two things today about spectra of orbit Jacobian operators in higher dimensions. First, the formula is not very different from the one dimensional case, just a little bit more complicated, as more than one mode in each direction is introduced. Second, I found the way to solve for all coefficients, and show that the cross term does exist. I will briefly outline the result here, and write the derivation in a new section later this week.

The day's version of the Hill determinant has form

$$\begin{aligned} \text{Det } \mathcal{J}(k) &= \text{Det } \mathcal{J}(0) + \sum_{i=1}^L C_{1,i} \sin^2(iTk_1/2) + \sum_{j=1}^T C_{2,j} \sin^2(jLk_2/2) \\ &+ \sum_{Li+Tj \leq LT} C_{i,j} \sin^2(iTk_1/2) \sin^2(jLk_2/2), \end{aligned} \quad (23.84)$$

with a finite harmonic modes sum in each direction, and a finite cross terms sum. I evaluated the coefficients by undetermined coefficients, which is very simple and takes no time to compute. The result is shown in figure [23.24](#).

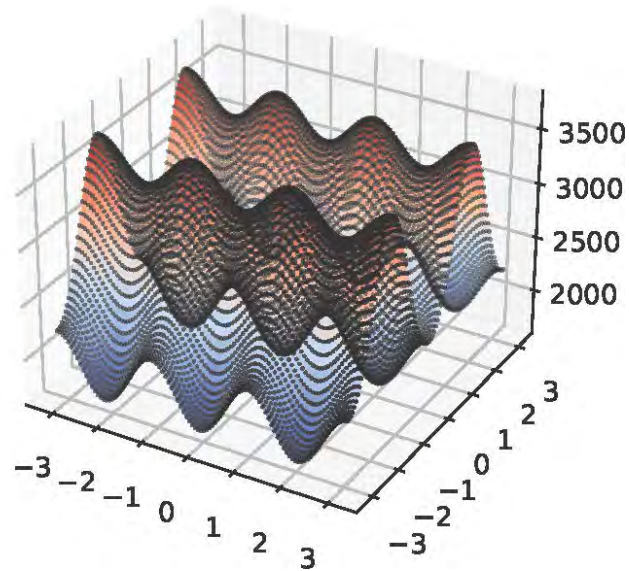


Figure 23.24: (black dots) The semi-analytic form of 2D orbit Jacobian operator (23.84) compared to with (colored surface) the numerical result. Spatiotemporal cat,  $\mu^2 = 4$  periodic state  $[2 \times 3]_0$ , repeated  $L = 2 \times T = 3$  times. I like to see 6 copies of the Brillouin zone.



**2024-11-11 Predrag** The Tiger's paper is getting so good that I might have to take the bullet and -student's professional training be damned- write the paper. For that, it's time to start writing figure-plotting that are asymptoting smoothly to the publication quality. This is not a criticism, just a time-saving proposal. Han has been plotting in this spirit for quite a while.

- Generate small figure sizes. I've been routinely converting figures in format 10'th of the initial size. Intelligent plotting routines (for example, Mathematica) should be generating LaTeX formatted figures for you already now.
- For example, labels sizes in figure 23.24 are suitable for publication, but scales have to be explained at least once in the article. What Fourier coefficient could be size 35,000? Maybe you are missing a  $N_p = L_p T_p$ ? Even then...
- It suffices to have one figure in the paper exhibiting reciprocal state reciprocity, like figure 23.24. The rest should only be plotted over the fundamental domain.
- Time reversal and space reflection invariance (will not be true for temporal Hénon) means you need to plot only  $(k_1, k_2)$  in the upper right quadrant of the Brillouin zone (23.87).
- For square-shaped primitive cell, the fundamental domain is given in figure 6.6.
- When comparing two almost equally precise calculations, it's easiest to understand a plot of differences of the two. For example, if you plot figure 6.6 this way, only over the upper right Brillouin zone wavenumber quadrant, you might find the plot much more informative.

**2024-11-11 Predrag** hoped that 2D Hill determinant for primitive cell  $[L \times T]_S$  is

$$\begin{aligned} \text{Det } \mathcal{J}(k) &= |\text{Det } \mathcal{J}| + p(L_1 k_1)^2 + p(L_2 k_2 - \frac{S}{L_1} k_1)^2 \\ \mathcal{J} &= \mathcal{J}(0), \quad p(k) = \frac{1}{2} \sin \frac{k}{2}, \end{aligned} \quad (23.85)$$

but Xuanqi found that it involves finite sums of (sub?)harmonics and cross terms,

$$\begin{aligned} \text{Det } \mathcal{J}(k) &= \text{Det } \mathcal{J} + \sum_{i=1}^{L_1-1} c_i^{(1)} p(ik_1)^2 + \sum_{j=1}^{L_2-1} c_j^{(2)} p(jk_2)^2 \\ &\quad + \sum_{L_2 q + L_1 r \leq L_2 L_1} c_{qr} p(qk_1)^2 p(rk_2)^2 \\ \mathcal{J} &= \mathcal{J}(0), \quad p(k) = \frac{1}{2} \sin \frac{k}{2}. \end{aligned} \quad (23.86)$$

Here the continuum wave numbers (what Pikovsky calls 'quasi-momenta')  $k \in \mathbb{B}$  are restricted to the 1st Brillouin zone,

$$k_j \in (-\pi/L_j, \pi/L_j] \quad j = 1, 2, \dots, d. \quad (23.87)$$

What bothers me: why don't we see a (sub?)harmonics sum already in the 1-dimensional case (23.75)?

$$\text{Det } \mathcal{J}(k) = \text{Det } \mathcal{J}(0) + p^2(L_k). \quad (23.88)$$

Isn't that just the  $L_2 = 1, [L \times 1]_0$  subcase?

**2024-11-14 Xuanqi** I found that instead of using the inverse of Chebyshev polynomials, we can directly use

$$T_n(\cos(\theta)) = \cos(n\theta),$$

and write the spectrum is powers of  $p_i = 2 \sin^2(T_i k_i / 2)$  as

$$\begin{aligned} \text{Det } \mathcal{J}(k) = & \text{Det } \mathcal{J}(0) + \sum_{i=1}^L C_{1,i} p_1^i + \sum_{j=1}^T C_{2,j} p_2^j \\ & + \sum_{Li+Tj \leq LT} C_{i,j} p_1^i p_2^j, \end{aligned} \quad (23.89)$$

This way it is easier for numerical calculation of coefficients, and I think this "momentum" form is more illustrative to compare to harmonics.

And we can even combine the three sums together to get

$$\text{Det } \mathcal{J}(k) = \text{Det } \mathcal{J}(0) + \sum_{Li+Tj \leq LT} C_{i,j} p_1^i p_2^j \quad (23.90)$$

One interesting thing is that in anti-integrable limit (23.90) looks like

$$\text{Det } \mathcal{J}(k) = \text{Det } \mathcal{J}(0) \left( 1 + \sum_{Li+Tj \leq LT} C^{-Li-Tj} p_1^i p_2^j \right) \quad (23.91)$$

where  $C = |\text{Det } \mathcal{J}(0)|^{1/LT}$ . In my opinion we can even collect it as  $\frac{p_1}{C^L}$  and then the second term is just a geometric series. And if we have the size of primitive cell goes to infinity we have

$$\text{Det } \mathcal{J}(k) = \text{Det } \mathcal{J}(0) \left( 1 + \frac{1}{1 + p_1/C^L} \frac{1}{1 + p_2/C^T} \right) \quad (23.92)$$

**2024-11-18 Predrag** (To be eventually moved to sect. 6.4.2 *Primitive cell Hill determinant for a 1-order system.*)

What academic feat made Professor Moriarty, arch enemy of Sherlock Holmes, *Professor Moriarty*?

In  $d$  dimensions, the orbit Jacobian operator takes the  $2d+1$  banded form (4.106)

$$\mathcal{J} = \sum_{j=1}^d \mathcal{J}_j, \quad \mathcal{J}_j = \mathcal{D}_p - (r_j + r_j^{-1}), \quad (23.93)$$

where  $r_j$  shift operators (22.100) translate the field configuration by one lattice spacing in the  $j$ th hypercubic lattice direction,  $d_z$  is the stretching factor evaluated at lattice site  $z$ . For the spatiotemporal cat (4.103), with the constant stretching factor  $d_z = s$  (4.107), the directional orbit Jacobian operators

$$\mathcal{J}_j = \frac{s}{2} \left( \mathbf{1} - \frac{2}{s} (r_j + r_j^{-1}) \right) \quad (23.94)$$

in (23.93) commute, and we can use the binomial formula

$$(x + y)^n = \sum_{k=0}^n \binom{n}{k} x^{n-k} y^k, \quad (23.95)$$

so

$$\text{Tr} (\mathcal{J}_1 + \mathcal{J}_2)^n = \sum_{k=0}^n \binom{n}{k} \text{Tr} \mathcal{J}_1^{n-k} \mathcal{J}_2^k. \quad (23.96)$$

In  $d = 2$  dimensions the trace (12.20) of a block matrix is given by

$$\text{tr} (\mathbf{A} \otimes \mathbf{B}) = \text{tr} \mathbf{A} \text{tr} \mathbf{B}, \quad (23.97)$$

so there are nonvanishing contributions only (?think about relative primes?) for a subset of repeats  $n = rN_p$ .

For the  $\phi^3$  (4.159),  $\phi^4$  (4.105) theories the stretching factor  $d_z$  in (4.109) is multi-periodic, and the orbit Jacobian operator in the orbit  $r_1^{m_1} r_2^{m_2} \mathcal{J}$  do not commute with each other. From  $r_j \mathcal{D} r_j^{-1} = \mathcal{D}$  it follows that (2024-11-23 Predrag obviously wrong, the correct form is (23.100))

$$\mathcal{D} r_j = r_j^{-1} \mathcal{D}, \quad (23.98)$$

so you can bring all products in the canonical form for the orbit of  $\mathcal{J}$ ,

$$\{r_1^{m_1} r_2^{m_2} \mathcal{D}\}, \quad 0 \leq m_1 < L_1, \quad 0 \leq m_2 < L_2. \quad (23.99)$$

— ignore what follows —

Expand  $\ln \text{Det}_{\mathbb{A}} \mathcal{J} = \text{Tr}_{\mathbb{A}} \ln \mathcal{J}$  as a series in momentum  $\mathbf{p}/\mu$  in Klein-Gordon mass units, vanishing in the anti-integrable limit:

$$\text{Tr}_{\mathbb{A}} \ln (\mathbf{p}^2 + \mu^2) - N_{\mathbb{A}} \ln \mu^2 = \text{Tr}_{\mathbb{A}} \ln \left( \mathbf{1} + \left( \frac{\mathbf{p}}{\mu} \right)^2 \right) = - \sum_{m=1}^{\infty} \frac{1}{m} \text{Tr}_{\mathbb{A}} \left( i \frac{\mathbf{p}}{\mu} \right)^{2m}.$$

Note that  $\text{Tr}_{\mathbb{A}} r^m$  is non-zero only when  $m$  is a multiple of  $n$ , so Xuanqi's idea of using orbit Jacobian matrices

Comments

1. Please complete this section, then we'll note them to a section shared with the Tigers paper.
2. Please work out the  $S > 1$  case.
3. Re. "Predrag's" birdtracks determinant (23.73): I think (not sure) this formula is useful when the matrix is 'full', meaning has nonzero entries (almost) everywhere. We probably will not need to refer to it in the Tigers paper.

We are computing determinants of sparse,  $2d + 1$  banded matrices. For them,  $\log \det = \text{tr} \log$  is particularly efficient, and for that reason frequently used in perturbation theory of QFT and solid state physics.

**2024-11-19 Xuanqi** Predrag's (23.98) is wrong. The shifts  $r_j$  cyclically permute diagonal elements, putting  $d_2$  in the place of  $d_1$ , and so on.

**2024-11-23 Predrag** (23.98) has a sign wrong :( . The correct statement is that the shift can be put on either side of the diagonal,

$$\mathcal{D}r_j = r_j\mathcal{D}. \quad (23.100)$$

In the index notation (22.101) we can stick the shift on either side of the diagonal matrix. I think :)

**2024-11-19 Xuanqi** There are two reasons that I see this idea as unpractical. First, the shifting operator does not commute with diagonal matrix, when diagonal is not a constant. The second reason is that the formula for tensor product of trace, (23.97), will not be very useful, as we cannot write the diagonal part in this tensor form. There are some other difficulties I encountered when I evaluated this spectrum, which I can write up in my next update, that made me think this might be nearly the best we can do. However I do have some other thoughts on this that I want to give a shot, but most likely it will turn out to be incorrect.

Now, the analytical expression of  $C_{i,j}$ , with primitive cell  $[2 \times 3]_0$ , is listed below, when we define  $p_i = 2 \sin(n_i k_i / 2)$

$$\begin{aligned}
 [2 \times 3]_0 : \\
 C_{0,0} &= s^6 - 9s^4 - 4s^3 + 12s^2, \\
 C_{1,0} &= \frac{3}{2}s^4 - 6s^2 + 6s - 2, \\
 C_{0,1} &= 2s^3 - 4, \\
 C_{2,0} &= \frac{3}{2}s^2, \\
 C_{1,1} &= -3s, \\
 C_{3,0} &= \frac{1}{2}, C_{0,2} = 1
 \end{aligned} \quad (23.101)$$

**2024-11-09 Predrag** Can you rederive your  $\text{Det } \mathcal{J}(k)$  (23.75) also for the general 1D temporal Hénon,  $|b| < 1$  case? For consistency, use the conventional Hénon's equation (3.5), (22.109), not Sidney's equivalent form (22.102).

1. Hénon map case, using Ofer-Biham potential, sect. 4.10.2.
2. Wash and repeat for our  $\phi^3$  theory, now with a dissipative term, by constructing the time-asymmetric potential that corresponds to our Euler-Lagrange equation (4.108). That would be for inclusion into the Tigers paper.
3. If you really get into the groove, you can try to see what happens for classical Hénon map parameter values  $a = 1.4, b = 0.3$ . My guess is that some eigenvalues of orbit Jacobian matrix would be complex.
4. Wash and repeat for our  $\phi^4$  theory (4.109).

**2024-11-10 Xuanqi** For dissipative temporal Hénon, I believe that we just need to play with the shift operator and the spectrum might have some imaginary component.

**2024-11-22 Predrag** Actually, it's already done by Bountis and Helleman [2], see sect. 11.1.3, and it is quite interesting. So what you have to do is write it up concisely in Tigers paper, harmonize with its spirit and notation.

**2024-12-02 Predrag** It's perfectly fine (recommended, indeed) to write your own reports in your language and style, before we incorporate (parts of) them into the Tigers's paper.

I suggest you make such reports / drafts subfolders of your own territory, in folder `siminos/xuanqi/`.

**2024-11-14 Xuanqi** Recently I contacted Jordan Cotler, assistant professor at Harvard, who works on quantum chaos and quantum gravity. I think his work is somehow related to our work in higher dimensions.

**2024-11-17 Predrag** He looks sharp, and has many interests, see my notes on his work around eq. (17.25).

**2024-11-14 Xuanqi** He invited me to give a talk to his group about our work next semester Should we have a discussion over this, or I just prepare it by myself?

**2024-11-17 Predrag** This is serious. "You come at the King, you best not miss." You get only one chance, if you do not leave a good impression, you will never be asked again. Or worse. Try your best to understand the relevant Cotler's publications.

Start preparing slides. Some source-code examples are in this repository, in `siminos/presentations/`, some examples of what these slides look like are in [ChaosBook.org/overheads/spatiotemporal](https://ChaosBook.org/overheads/spatiotemporal). 'Beamer' is what

math and theoretical physics people use. Some people (biology, business, ...) prefer PowerPoint or the Apple equivalent. Then you give a trial seminar in a group meeting, at least once, probably several times, before giving a presentation to external people. External audiences are not friendly, and can be aggressive. Competition among theoretical physicists is off-putting. The main reason so few women chose this as a profession.

**2024-11-14 Xuanqi** I am also interested in his work in QFT quantum scars, and I believe that you must be very familiar with this topic.

**2024-11-17 Predrag** I'm not a fan of Heller's original work - seems like expecting that a Fourier transform of a localized object is also localized. But I might be wrong.

**2024-12-29 Predrag** There should be (?) some well known (?) identity that says that  $\text{Tr} \ln$  is simpler than  $\ln \text{Det}$  for antisymmetrization operators

**2025-01-07 Predrag** Read today's pow wow on page [1416](#).

**2025-01-09 Predrag** Read today's pow wow on page [1419](#).

**2025-01-14 Predrag** Read today's pow wow suggestions for your presentation on page [1423](#).

## References

- [1] S. Anastassiou, A. Bountis, and A. Bäcker, "Homoclinic points of 2D and 4D maps via the parametrization method", *Nonlinearity* **30**, 3799–3820 (2017).
- [2] T. Bountis and R. H. G. Helleman, "On the stability of periodic orbits of two-dimensional mappings", *J. Math. Phys* **22**, 1867–1877 (1981).
- [3] M. Cini and G. Stefanucci, "Antiferromagnetism of the two-dimensional Hubbard model at half-filling: The analytic ground state for weak coupling", *J. Phys.: Condens. Matter* **13**, 1279–1294 (2001).
- [4] M. S. Dresselhaus, G. Dresselhaus, and A. Jorio, *Group Theory: Application to the Physics of Condensed Matter* (Springer, New York, 2007).
- [5] H. R. Dullin and J. D. Meiss, "Generalized Hénon maps: the cubic diffeomorphisms of the plane", *Physica D* **143**, 262–289 (2000).
- [6] M. J. Engel, *Short Course on Symmetry and Crystallography*, 2011.
- [7] M. Frasca, "Exact solutions of classical scalar field equations", *J. Nonlinear Math. Phys.* **18**, 291 (2021).
- [8] B. Gutkin and V. Osipov, "Classical foundations of many-particle quantum chaos", *Nonlinearity* **29**, 325–356 (2016).

- [9] H. Liang and P. Cvitanović, “A chaotic lattice field theory in one dimension”, *J. Phys. A* **55**, 304002 (2022).
- [10] M. Lüscher and P. Weisz, “Scaling laws and triviality bounds in the lattice  $\phi^4$  theory (I). One-component model in the symmetric phase”, *Nucl. Phys. B* **290**, 25–60 (1987).
- [11] D. Ruelle, Dynamical zeta functions: Where do they come from and what are they good for?, in *Mathematical Physics X*, edited by K. Schmüdgen (1992), pp. 43–51.
- [12] D. Ruelle, “Dynamical zeta functions and transfer operators”, *Notices Amer. Math. Soc.* **95**, 887–895 (2002).
- [13] S. Smale, “Differentiable dynamical systems”, *Bull. Amer. Math. Soc.* **73**, 747–817 (1967).
- [14] D. Sterling and J. D. Meiss, “Computing periodic orbits using the anti-integrable limit”, *Phys. Lett. A* **241**, 46–52 (1998).
- [15] I. Vierhaus, Simulation of  $\phi^4$  Theory in the Strong Coupling Expansion beyond the Ising Limit, MA thesis (Humboldt-Univ. Berlin, Math.-Naturwissen. Fakultät I, 2010).
- [16] S. V. Williams, X. Wang, H. Liang, and P. Cvitanović, *Nonlinear chaotic lattice field theory*, In preparation, 2024.
- [17] U. Wolff, “Triviality of four dimensional  $\phi^4$  theory on the lattice”, *Scholarpedia* **9**, 7367 (2014).
- [18] X. Zhang, “Hyperbolic invariant sets of the real generalized Hénon maps”, *Chaos Solit. Fract.* **43**, 31–41 (2010).

# Chapter 24

## Han's blog

Don't be [Fritz Haake](#). He, who hesitates, is lost.

Han Liang <[han\\_liang@gatech.edu](mailto:han_liang@gatech.edu)> work blog  
Orcid number [orcid.org/0000-0001-7181-8166](https://orcid.org/0000-0001-7181-8166)  
cell: +1 (401) 651-4482  
WeChat lhan118

[The latest entry at the bottom for this blog, page 1370](#)

### Contents

- [24.1 Rhomboid corner partition](#)
- [24.2 Rhomboid center partition](#)
- [24.3 Time reversal](#)
- [24.4 Reduction to the fundamental domain](#)
- [24.5 Spatiotemporal cat partition](#)
- [24.6.1 Stability of a periodic point vs. stability of the orbit](#)
- [24.6.2 Temporal cat counting by determinant recursion](#)

The latest post is on page [1370](#)

**2018-01-12, 2022-01-30 Predrag** to Han

On [zero.physics.gatech.edu](#), or Matt's [light.physics.gatech.edu](#), or your [hard.physics.gatech.edu](#), or visitor office [love.physics.gatech.edu](#), or any other CNS linux workstation your login is with your GaTech credentials.

Do not do calculations on the CNS servers: [zero.physics.gatech.edu](#) which is physically [one.physics.gatech.edu](#) or [two.physics.gatech.edu](#) - from any CNS machine.

```
ssh XXXX?@hard.physics.gatech.edu
```

save all data on the local hard disk `/usr/local/home/han/`. make a link in your CNS home directory:

```
cd homeHard
```



Help for CNS system, and all our documentation is on [www.cns.gatech.edu/CNS-only](http://www.cns.gatech.edu/CNS-only) cnsuser cnsweb

but current crop of grad students, as a matter of principle, never look at any info, or add to these homepages.

Good luck - Matt knows `linux` best, also Simon Berman, Xiong Ding and Burak Budanur (via Skype) know a lot.

**2018-01-19 Han** Here is an example of [text edit by me](#), and here one of a footnote by me<sup>1</sup>.

**2018-01-19 Han** (Discussion with Predrag, cat maps project Spring 2018:

- blog the project progress here
- blog whatever I'm reading and learning about dynamical systems here

**2018-06-05 to 06-11 Predrag** Read chapter ?, part of ?, and ? of Chaosbook. Do homework of online Course 1, Weeks ? and ?.

**2018-01-19 to 02-11 Han** Read Chapters ?, ?, part of ?, and ? of Chaosbook. Did homework of Weeks ? and ?.

**2018-01-11 Predrag** to Han: Caution - my posts can be erased your edits, if you omit to *svn up* before starting your edit.

Regarding new figures: always save *HL\*.png* (or *HL\*.pdf*) in *siminos/figs/*, then *svn add HL\*.png* (where \* is a name of the figure).

Remember, always, before starting your work session with *svn up* and colcluding it with

*svn ci-m"added entropy figures"* you have to go to the root directory, *cd [...]/siminos*. Otherwise you are not refreshing all bibtex, figures and other files in the repository.

## 24.1 Rhomboid corner partition

**Partitions, alphabets.** A division of phase space  $\mathcal{M}$  into a disjoint union of distinct regions  $\mathcal{M}_A, \mathcal{M}_B, \dots, \mathcal{M}_Z$  constitutes a *partition*. Label each region by a symbol  $m$  from an  $N$ -letter *alphabet*  $\mathcal{A} = \{A, B, C, \dots, Z\}$ , where  $N = n_{\mathcal{A}}$  is the number of such regions. Alternatively, one can distinguish different regions by coloring them, with colors serving as the "letters" of the alphabet. For notational convenience, in alphabets we sometimes denote negative integer  $m$  by underlining them, as in  $\mathcal{A} = \{-2, -1, 0, 1, 2\} = \{\underline{2}, \underline{1}, 0, 1, 2\}$ .

A generating partition must map borders onto borders under dynamics (Adler-Weiss).

---

<sup>1</sup>Han 2018-01-19: Han test footnote

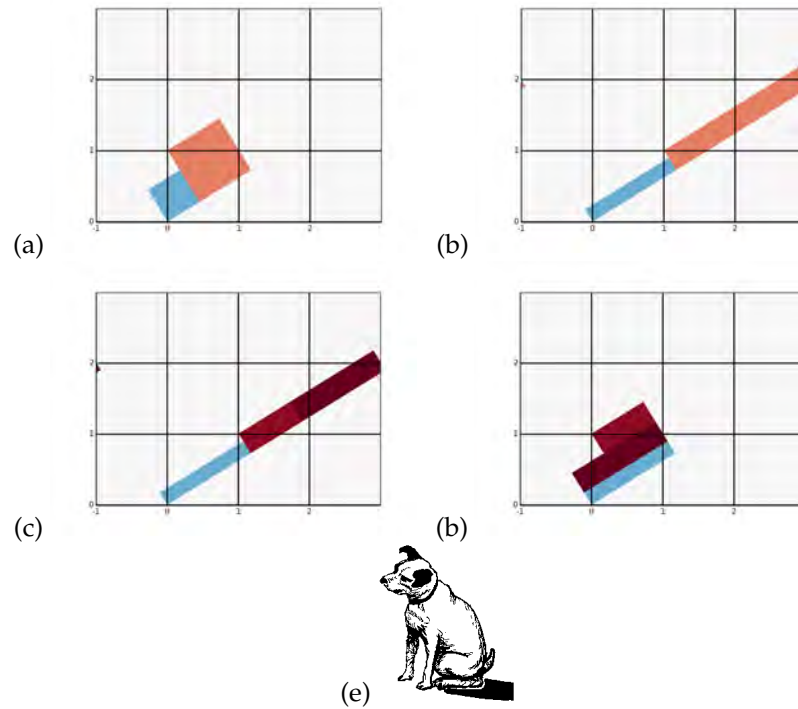


Figure 24.1: Figure 2.1 recomputed with my python code. (a) Two-squares Adler-Weiss generating partition for the canonical Thom-Arnol'd cat map (2.1), with borders given by stable-unstable manifolds of the unfolded cat map lattice points near to the origin. (b) The first iterate of the partition. (c) The first iterate of the partition intersections, (d) The iterate pulled back into the generating partition, and (e) the corresponding 5-letter transition graph. In (b) and (c) we still have to relabel Crutchfield's arbitrary partition labels with our shift code. This is a "linear code," in the sense that for each square one can count how many side-lengths are needed to pull the overhanging part of (c) back into the two defining squares.

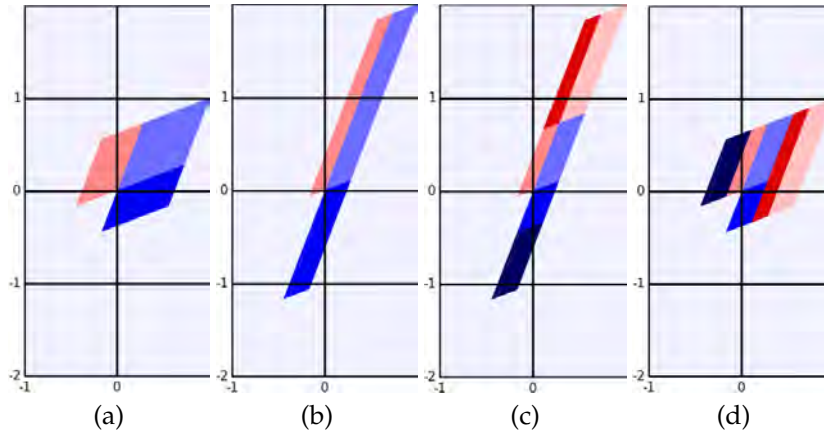


Figure 24.2: Figure 2.6 recomputed with my python code. (a) 3-rectangle, time-reversal symmetric Percival-Vivaldi cat map (2.5) partition. (b) The first forward iterate of the partition. (c) The first forward iterate of the partition, with the stable manifold intersections dividing it into 6 regions. (d) The 6 rhomboids (5 when the two blue regions are treated as one) are translated back into the generating partition, with the subscript label indicating the square-lattice vertical translation group elements:  $\{T_{AA} = g_0^{A \rightarrow A}, T_{BB} = g_0^{B \rightarrow B}, T_{BA} = g_{-1}^{A \rightarrow B}, T'_{AA} = g_1^{A \rightarrow A}, T_{AB} = g_1^{B \rightarrow A}\}$ . If the two blue regions are considered as a single partition, one obtains the standard Adler-Weiss 2-partition, with 5 distinct return maps one step forward in time, and the corresponding 5-letter transition graph of figure 24.1 (e). Together, these transitions make up the transition graph of figure 2.1 (c). The partition is generating, in the sense that the walks on this transition graph generate all admissible sequences.

**2018-01-18 Han** `figSrc/han/python/HLcatmapArnold.py` reproduces the standard Arnol'd map partition, figure 24.1. The plots are in `siminos/figs/figSrc/han/python/HLcatmapPV.py` reproduces Predrag's hand-sketch of the Percival-Vivaldi [62] "two-configuration representation" cat map partition, figure 24.2.

**2018-01-19 Predrag** In the Percival-Vivaldi partition, (2.5) there is only one partition, the  $[\phi_0, \phi_1]$  unit square. In the Adler-Weiss partition of figure 24.2 (a) there are two rhomboid partitions, each with its own coordinates, let's say the big rhomboid  $[\phi_0^A, \phi_1^A]$  and the small rhomboid  $[\phi_0^B, \phi_1^B]$  (and perhaps also its time-reversal partner  $[\phi_0^{B'}, \phi_1^{B'}]$ ), each bounded not by a unit square, but by the vectors  $(S^A, U^A), (S^B, U^B)$  of the stable/unstable manifold segments that border the rhomboids. As this is a symplectic mapping, the important property of these rhomboids is their (oriented) area, for 1D dof given by the wedge or skew-symmetric product

$$A^\alpha = U^\alpha \wedge S^\alpha = U_i^\alpha \epsilon^{ij} S_j^\alpha, \quad \alpha \in \{A, B\}. \quad (24.1)$$

The figure 24.1 and figure 24.2 partitions are related by canonical (in  $1D$  dof area-preserving) transformations, so for given stretching  $s$ , the small and the large rectangle/rhomboid areas are the same in any partition. Likewise, topologically the dynamics should be the same, i.e., have the same transition graph figure 2.1 (c).

That should naturally follow from the generator (Lagrangian) formulation sect. 12.2 in any choice of symplectically-paired coordinates.

Having several coordinate systems, one for each partition, is standard; a typical example are the three Poincaré sections of the 3-disk pinball, Fig. 15.15: *Poincaré section coordinates for the 3-disk game of pinball*, Chaos-Book chapter *Charting the state space* [23].

**2018-01-25 Predrag** Figure out Toeplitz matrix for the simplest cycle(s) of period two (for Toeplitz matrices, see the post of 2017-09-09 on page 415, and the posts in sect. 2.5).

Hopefully only a  $[2 \times 2]$  matrix. Understand its stability multipliers, eigenvectors.

**2018-01-19 Han** I've been working on reading the ChaosBook materials and doing the online Course 1.

**2018-01-26 Predrag** to Han: Can you compute analytically areas of partitions in figure 24.2, show that they are the same as those in figure 2.1 and figure 24.1? I expect them to be simple formulas in terms of stability multipliers (21.151).

**2018-01-27 Han** I have computed the area of the small partition  $B$  in figure 24.2 and figure 24.1. The areas of the small partitions are the same, for  $s = 3$  they are  $A_B = \frac{1}{2}(1 - \frac{1}{\sqrt{5}})$ . If the stability multipliers are  $(\Lambda, 1/\Lambda)$ , where  $\Lambda > 1$ , as in (21.151), the area of the small partition  $B$  in figure 24.1 is given by

$$A_B = \frac{1 - 1/\Lambda}{\sqrt{D}} = \frac{1}{\Lambda + 1}. \quad (24.2)$$

The area of figure 24.2 is  $A_B = \frac{(\Lambda-1)/\Lambda}{\sqrt{D}}$ , i.e., the same.

**2018-02-16 Predrag** Is  $|\mathcal{M}_B| = (\Lambda - 2)/\sqrt{D}$  in (2.86), for  $s = 3$ , the same as  $|\mathcal{M}_B| = \frac{1-1/\Lambda}{\sqrt{D}} = \frac{1}{\Lambda+1}$  of (24.2)? Indeed, that follows from (??) by inspection.

**2018-01-27 Predrag** Thanks! Did you use (24.1) to compute them? I think we need that formalism to harmonize the discussion with sect. 12.2 generating functions.

Did you also check that the area of the big partition is  $A_A = (1+1/\Lambda)/\sqrt{D}$ ?

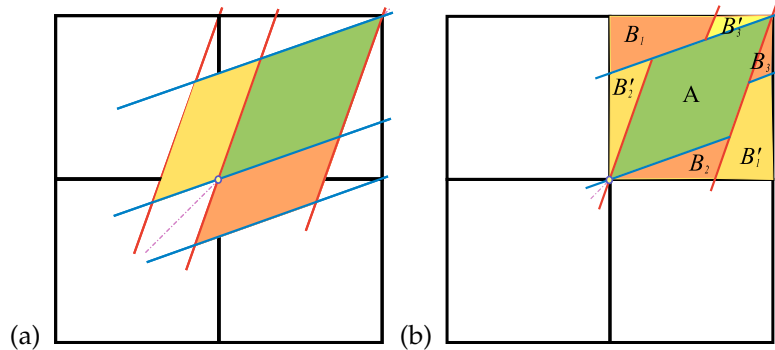


Figure 24.3: Abandoned attempt: (a) The three-rectangle, time reversal symmetric generating partition for the Percival-Vivaldi cat map (2.5), with borders given by cat map stable-unstable manifolds. (b) The three-rectangle partition of the unit square. In this partition  $A$ ,  $B_2$ ,  $B'_2$  already lie within the unit square, while  $B_1$  is shifted by  $(-1, 0)$ ,  $B_3$  is shifted by  $(-1, -1)$ , and  $B'_1$  is shifted by  $(0, -1)$ ,  $B'_3$  is shifted by  $(-1, -1)$ . It is more partitions than going forward in time, but I hope it will be the right thing for the Lagrangian formulation.

**2018-01-27 Predrag** Maybe you do not see what has happened in the blog - I always use `svn diff` (it works nicely in the Windows GUI) to see what has changed.

Anyway, I started the explicit construction of the Perron-Frobenius operator in example 2.4, so we also need the sub-partitions areas to check that.

**2018-01-31 Han** I have checked the area of the big partition. Adding the areas of each partition together we will get 1, so it should be correct. I didn't use (24.1) to compute the area. I found the coordinates of all the vertices on the edges of the parallelograms and got the vectors that border the partition then did the cross product (kind of tedious...). Using (24.1) to compute the areas should be very easy.

**2018-02-10 Predrag** computed them in (2.86).

**2018-01-19 Predrag** Read chapter *Walkabout: Transition graphs* [24]. Always try to work through examples. Eventually we want to try to solve Exercise 17.1 *Time reversibility*. The solution might be someplace here, in sect. 16.1 *Ihara zeta functions*.

**2018-01-31 Han** I have read chapter *Walkabout: Transition graphs*.

**2018-02-01 Predrag** I think a good partition is given in figure 24.3. The symbolic dynamics notation should probably be a 7-letter alphabet, some-

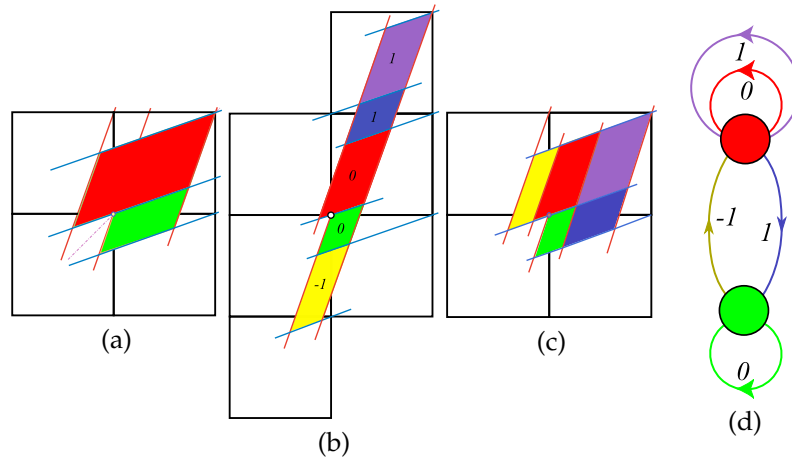


Figure 24.4: (Color online) (a) An Adler-Weiss generating partition of the unit torus into rectangles  $\mathcal{M}_A$  (red) and  $\mathcal{M}_B$  (green) for the Percival-Vivaldi cat map (2.5), with borders given by the cat map stable (blue) and unstable (red) manifolds. (b) Mapped one step forward in time, the rectangles are stretched along the unstable direction and shrunk along the stable direction. Sub-rectangles  $\mathcal{M}_j$  that have to be translated back into the partition are indicated by color and labeled by their lattice translation  $m_j \in \{\underline{1}, 0, 1\}$ . (c) The sub-rectangles  $\mathcal{M}_j$  translated back into the unit square yield a generating partition labelled by the 5-letter alphabet (24.10), with (d) the finite grammar given by the transition graph for this partition. The nodes refer to the rectangles  $A$  and  $B$ , and the five links correspond to the five sub-rectangles induced by one step forward-time dynamics. (Compare with figure 2.2. For details, see ChaosBook [25]).

thing like

$$\begin{aligned}
 A &\rightarrow A_{(0,0)}, & B_2 &\rightarrow B_{(0,0)}, & B'_2 &\rightarrow B'_{(0,0)} \\
 B_1 &\rightarrow B_{(-1,0)}, & B'_1 &\rightarrow B_{(0,-1)} \\
 B_3 &\rightarrow B_{(-1,-1)}, & B'_3 &\rightarrow B'_{(-1,-1)}.
 \end{aligned}
 \tag{24.3}$$

**2018-02-01 Predrag** [2018-02-11 accomplished for the two-rectangle partition]

Han points out that the unit square borders, have no physical meaning, and that the partition still has only three regions  $A, B, B'$ , as in figure 2.8. The time forward partition is given in figure 2.7 (b).

**2018-02-11 Han** I have verified some admissible and inadmissible orbits by the Green's function. The Percival-Vivaldi cat map matrix with  $s = 3$  is:

$$\mathbf{A} = \begin{bmatrix} 0 & 1 \\ -1 & 3 \end{bmatrix}
 \tag{24.4}$$

For the period  $T = 4$  we can represent the orbit Jacobian matrix  $\mathcal{J}$  with periodic boundary conditions by a  $[4 \times 4]$  circulant matrix

$$-\mathcal{J} = \begin{bmatrix} 3 & -1 & 0 & -1 \\ -1 & 3 & -1 & 0 \\ 0 & -1 & 3 & -1 \\ -1 & 0 & -1 & 3 \end{bmatrix} \quad (24.5)$$

The corresponding Green's function is the inverse of matrix of orbit Jacobian matrix  $-\mathcal{J}$

$$\mathbf{g} = \begin{bmatrix} \frac{7}{15} & \frac{1}{5} & \frac{2}{15} & \frac{1}{5} \\ \frac{1}{5} & \frac{7}{15} & \frac{1}{5} & \frac{2}{15} \\ \frac{2}{15} & \frac{1}{5} & \frac{7}{15} & \frac{1}{5} \\ \frac{1}{5} & \frac{2}{15} & \frac{1}{5} & \frac{7}{15} \end{bmatrix} \quad (24.6)$$

Then given symbol block  $M = m_0 m_1 m_2 m_3$ , we can calculate the corresponding orbit  $\Phi_M = (x_1, x_2, x_3, x_4)$ . For example, if

$$M = \begin{bmatrix} 0 \\ 2 \\ 2 \\ 0 \end{bmatrix} \Rightarrow \Phi = \frac{1}{3} \begin{bmatrix} 2 \\ 4 \\ 4 \\ 2 \end{bmatrix}. \quad (24.7)$$

This orbit should be inadmissible since it contains the pruned block 22, and indeed the corresponding periodic points fall outside the unit interval,  $\{x_1, x_2\} > 1$ . Examples of two admissible 4-cycles:

$$\begin{bmatrix} 0 \\ 2 \\ 0 \\ 0 \end{bmatrix} \Rightarrow \Phi = \frac{1}{15} \begin{bmatrix} 6 \\ 14 \\ 6 \\ 4 \end{bmatrix}; \quad \begin{bmatrix} 0 \\ 1 \\ 1 \\ 0 \end{bmatrix} \Rightarrow \Phi = \frac{1}{3} \begin{bmatrix} 1 \\ 2 \\ 2 \\ 1 \end{bmatrix}$$

We can verify that these are periodic orbits by iterating

$$\mathbf{A} \begin{bmatrix} x_{t-1} \\ x_t \end{bmatrix} = \begin{bmatrix} x_t \\ x_{t+1} \end{bmatrix} + \begin{bmatrix} 0 \\ m_t \end{bmatrix}. \quad (24.8)$$

**2018-02-11 Predrag** Very nice! Let's take your Green's function (24.6) for 4-cycles

$$\mathbf{g} = \frac{1}{15} \begin{bmatrix} 7 & 3 & 2 & 3 \\ 3 & 7 & 3 & 2 \\ 2 & 3 & 7 & 3 \\ 3 & 2 & 3 & 7 \end{bmatrix} \quad (24.9)$$

but now test whether all period 4 closed walks on the transition graph of figure 24.7 (d) yield admissible 4-cycles.

The partition figure 24.4 (c) is labeled / colored by a 5-symbol alphabet (2.9):

$$A = \{1, 2, 3, 4, 5\} = \{A^0 A, B^1 A, A^1 A, B^0 B, A^1 B\}, \quad (24.10)$$

that labels the five sub-rectangles  $\mathcal{M}_{m_j}$  of the cat map phase space,  $\mathcal{M} = \cup \mathcal{M}_{m_j}$ , by the links of the transition graph of figure 2.9 (d), with all admissible itineraries generated by all walks on the transition graph. Rational values correspond to periodic orbits, with the phase space periodic points uniquely labeled by the admissible itineraries of symbols from  $\mathcal{A}$ .

Bird and Vivaldi [14] tabulate the numbers of orbits (they call that  $N_T(\lambda)$  in their Table 1, with  $s = K = 3$  and 4),

$$\sum_{T=1}^{\infty} z^T N_T = z + 2z^2 + 5z^3 + 10z^4 + 24z^5 \dots \quad (24.11)$$

They say that there are  $N_4(\lambda) = 10$  admissible period 4 orbits. They can be read off as walks on figure 24.4 (d):

$$\begin{array}{ccccc} \overline{1113} & \overline{1125} & \overline{1245} & \overline{1253} & \overline{1325} \\ 0001 & 001\overline{1} & 010\overline{1} & 011\overline{1} & 011\overline{1} \\ \overline{1133} & \overline{3325} & \overline{3331} & \overline{3245} & \overline{4452} \\ 0011 & 111\overline{1} & 1110 & 110\overline{1} & 00\overline{11} \end{array} \quad (24.12)$$

with the corresponding translations read off the superscripts in (24.10). My sub-rectangles alphabet (24.10) is superfluous; the translations

$$m_t \in \{\underline{1}, 0, 1\} \quad (24.13)$$

from (24.10) alone label uniquely the admissible orbits, as they should, as the relation is linear. We have to figure out how to argue that reading  $\{m_t\}$  off the graph alone suffices to label the orbit. Not obvious, as links 0 and 1 occur twice. Green 0 has to be followed by  $\underline{1}$ , the red 0 has to be followed by 3 or 2, so they are distinct. The blue 1 must eventually be followed by  $\underline{1}$ , but how is that different from the purple 1?

Some clever recoding idea is called for.

**2018-02-11 Han** I have computed all ten 4-cycles using Green's function (24.9) and plotted all their periodic points in figures 24.5 and 24.6.

$$M = \begin{bmatrix} 0 \\ 0 \\ 0 \\ 1 \end{bmatrix} \Rightarrow \Phi_{0001} = \frac{1}{15} \begin{bmatrix} 3 \\ 2 \\ 3 \\ 7 \end{bmatrix}.$$



Likewise,

$$\begin{aligned}
 \Phi_{001\bar{1}} &= \frac{1}{15} \begin{bmatrix} -1 & 1 & 4 & -4 \end{bmatrix}, & \Phi_{010\bar{1}} &= \frac{1}{15} \begin{bmatrix} 0 & 5 & 0 & -5 \end{bmatrix} \\
 \Phi_{01\bar{1}\bar{1}} &= \frac{1}{15} \begin{bmatrix} 4 & 6 & -1 & 6 \end{bmatrix}, & \Phi_{01\bar{1}\bar{1}} &= \frac{1}{15} \begin{bmatrix} 2 & 8 & 7 & -2 \end{bmatrix} \\
 \Phi_{0011} &= \frac{1}{15} \begin{bmatrix} 5 & 5 & 10 & 10 \end{bmatrix}, & \Phi_{11\bar{1}\bar{1}} &= \frac{1}{15} \begin{bmatrix} 9 & 11 & 9 & 1 \end{bmatrix} \\
 \Phi_{11\bar{1}0} &= \frac{1}{15} \begin{bmatrix} 12 & 13 & 12 & 8 \end{bmatrix}, & \Phi_{110\bar{1}} &= \frac{1}{15} \begin{bmatrix} 7 & 8 & 2 & -2 \end{bmatrix} \\
 \Phi_{00\bar{1}\bar{1}} &= \frac{1}{15} \begin{bmatrix} 1 & -1 & -4 & 4 \end{bmatrix} & & (24.14)
 \end{aligned}$$

I verified these orbits by finding the position of each point  $(\phi_t, \phi_{t+1})$  on the partition  $\mathcal{M}_A$  or  $\mathcal{M}_B$ . They are all admissible. The count agrees with table 21.1.

**2018-02-11 Predrag** It feels like magic; we know that what the 2-rectangle partition is, and we have derived the transition graph of figure 24.4 (d), and that by similarity transformation this is the same for any  $s = 3$  cat map, but it is still not obvious that the 3-letter alphabet (24.13) does the job. I assume you have not checked any of the original literature, but I do not recall seeing such alphabet...

**2018-02-11 Predrag** Next: I have mostly solved and moved example 2.4 Perron-Frobenius operator for the Arnol'd cat map to section sect. 2.8 Examples. It would be good if you worked through it and understood the transfer matrix  $L$  (2.87), which I am reading off figure 24.7, in particular computed it eigenvalues (interpret the  $\lambda = 1$  eigenvalue) and eigenvectors (the leading one should be the natural measure). Here

$$s = 3, \text{ so } \Lambda = \frac{3 + \sqrt{5}}{2} = 2.6180, \text{ and } D = 5.$$

**2018-02-12 Predrag** Can you plot the stretched domains corresponding to figure 24.4 (b) for one step back in time (inverse map)? Should look something like figure 24.8.

**2018-03-01 Han** I have calculated the stretched domains corresponding to figure 24.4 (b) for one step back in time. The result is in figure 24.9 (c) which is not same as figure 24.8 (b). I guess this is because I start from partition in figure 24.9 (a). If I start from the partition flipped from figure 24.9 (a) across the  $\phi_1 = \phi_0$  I will get figure 24.8 (b). The overlap 2 partition is also different from figure 24.8 (c). I'm not sure...

**2018-03-01 Predrag** My figure 24.8 was just a quick sloppy sketch. I'm confident that your figure 24.9 is right.

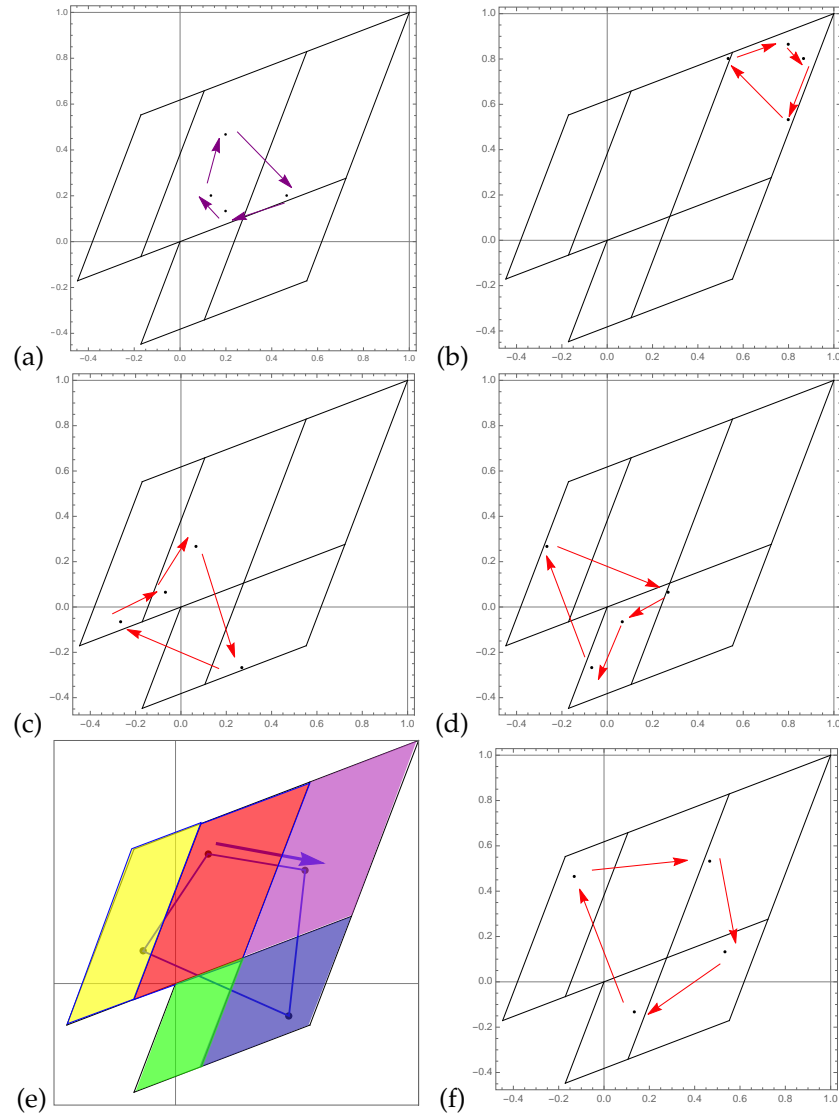


Figure 24.5: Abandoned attempt: All 4-cycles from (24.14): (a)  $\Phi_{0001} = \Phi_{1113}$ , (b)  $\Phi_{1110}$ , (c)  $\Phi_{001\bar{1}}$ , (d)  $\Phi_{00\bar{1}1}$ , (e)  $\Phi_{011\bar{1}}$ , (f)  $\Phi_{110\bar{1}}$ , (g) to (j) continued in figure 24.6.

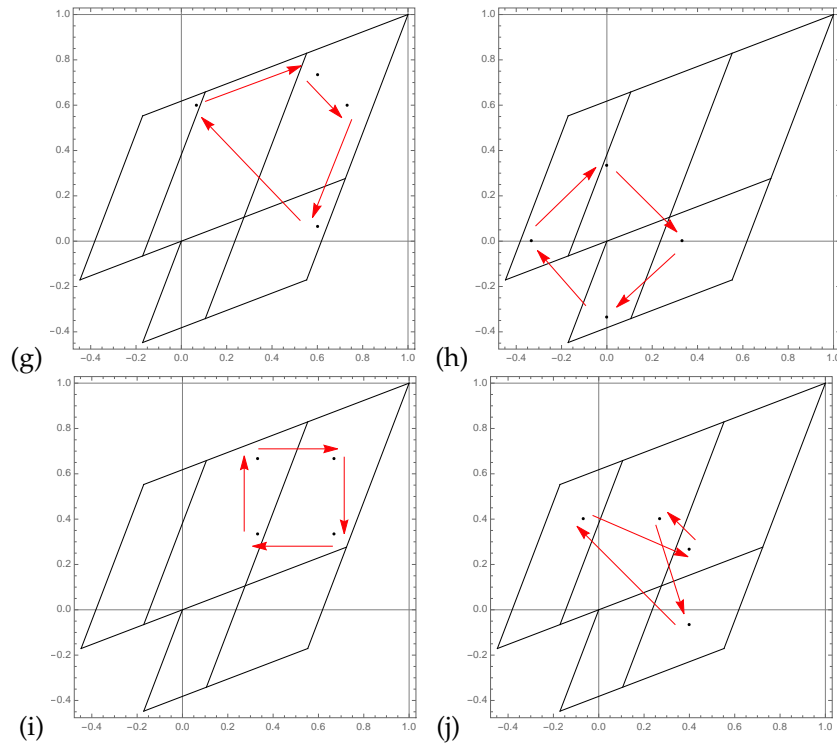


Figure 24.6: Continuation of figure 24.5: (g)  $\Phi_{1111}$ , (h)  $\Phi_{0011}$ , (i)  $\Phi_{0011}$ , and (j)  $\Phi_{0111}$ ,

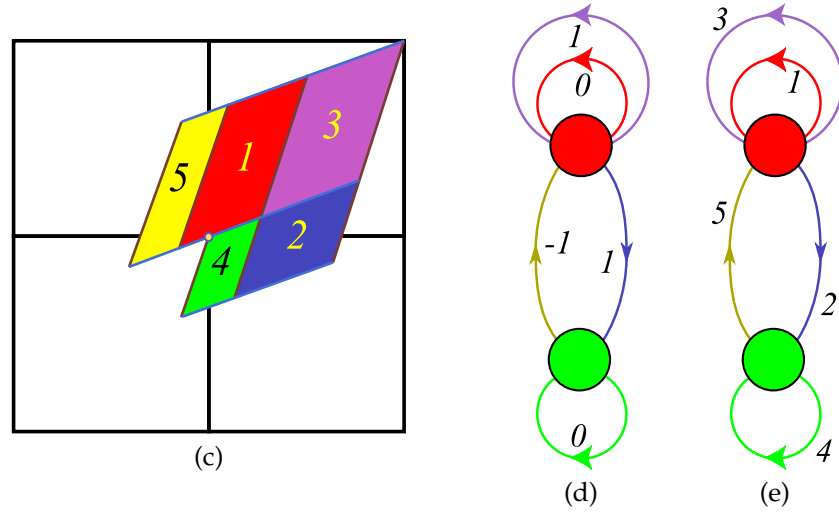


Figure 24.7: (Figure 24.4 continued) (c) The sub-rectangles  $\mathcal{M}_j$ , indicated by the compact 5-letter alphabet (24.10). (d) Admissible orbits correspond to walks on the transition graph for this partition. The nodes refer to the rectangles  $A$  and  $B$ , and the five colored links, labeled by their lattice translation  $m_j \in \{1, 0, -1\}$ , correspond to the five sub-rectangles reached in one step forward-time dynamics. (e) Compact labeling, see (24.10).

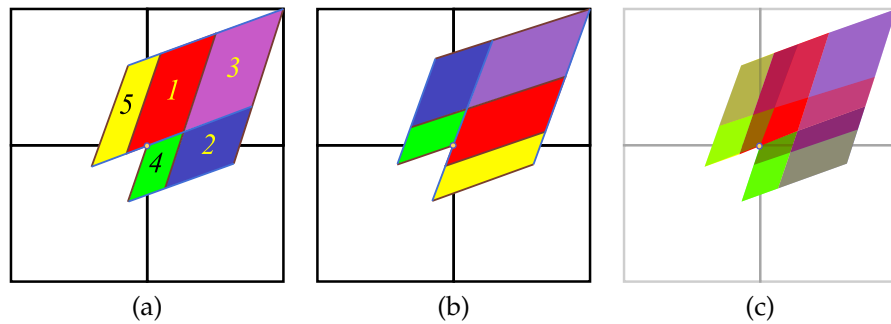


Figure 24.8: (From figure 24.4) (a) The forward in time sub-rectangles  $\mathcal{M}_j$ , indicated by color / 5-letter alphabet (24.10). (b) The corresponding partition defined for one step backward in time (not the partition (a) iterated back). (c) The overlap 2-step partition. Not sure this is right.

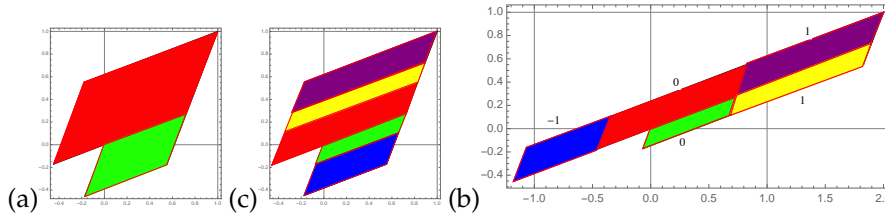


Figure 24.9: (a) The two rectangles partition of the Percival-Vivaldi cat map. (b) Mapped one step backward in time. (c) The stretched partition has been translated back to the original shape.

**2018-02-15 Han** I have read the section *Markov Partitions for Hyperbolic Toral Automorphisms* of Robinson's book. I'm currently working on example 2.4. The (2.87) seems not correct. I'm working on it.

**2018-02-16 Predrag** I'm complicating this unnecessarily - it would be nice to get the correct 5-rectangles transfer matrix (2.87), but it is unnecessary for our purposes: for the two-rectangle partition  $[2 \times 2]$  Markov matrix, see example 2.3.

**2018-02-16 Predrag** For  $s \geq 3$ , the 3-letter alphabet (2.9) generalizes to

$$\mathcal{A} = \{\underline{1}, 0, 1, \dots, s - 2\}. \quad (24.15)$$

What keeps the forward iterates of the small rectangle in check is the way this area shrinks with large  $\Lambda$  in (2.86).

**2018-02-18 Han** For  $s \geq 3$  the alphabet for the 2- (and 3-) rectangle partition is (24.15): see the 3-rectangle stable and unstable manifolds borders partition for  $s = 5$  in figure 24.10.

**2018-02-18 Predrag** Great. It should led to more sensible labelling of figure 24.7 (e) transition graph, for arbitrary  $s$ . You can see that, much like in the Percival-Vivaldi figure 2.2, there is an *interior*  $(s - 1)$ -letter alphabet  $\mathcal{A}_0$  which is a full shift  $((s - 1)$  loops attached to node  $A$ ), and some kind of 2-letter *exterior* alphabet  $\mathcal{A}_1$  that has to do with node  $B$ .

A well-understood alphabet can help us with solving the 2-dimensional spatiotemporal cat - there the interior alphabet  $\mathcal{A}_0$  is still a full shift, while the exterior alphabet  $\mathcal{A}_1$  is a bit bigger.

**2018-02-19 Predrag** The alphabet (24.13),  $m_t \in \{\underline{1}, 0, 1\}$  is not good, as it seems not to encode any of the symmetries of orbits in figures 24.5 and 24.6.

**2018-02-19 Predrag** I wonder why all cycles (except for a small kink in  $\Phi_{0111}$ ) turn clockwise? Reminds me of harmonic oscillator, that also has a unique rotation direction - might be a consequence of symplectic dynamics.

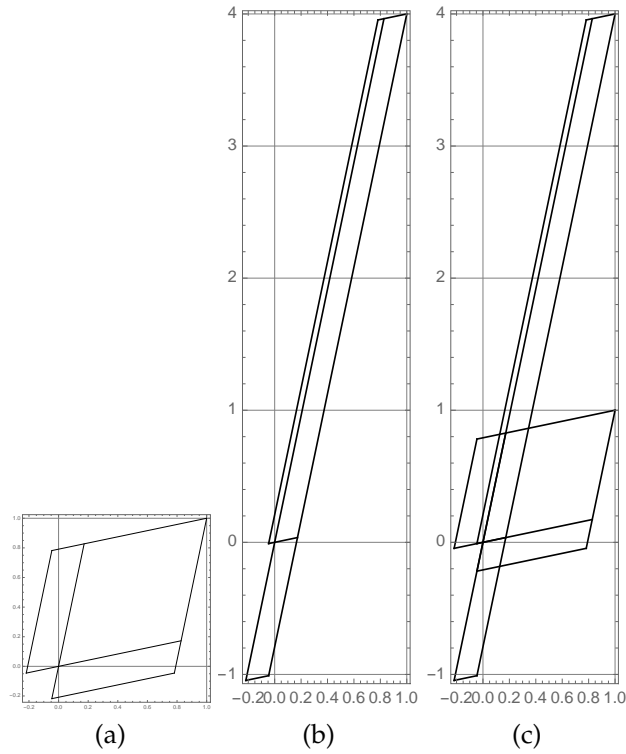


Figure 24.10: (a) The 3-rectangle partition for  $s = 5$ . (b) The first forward iterate of the partition. (c) I put (a) and (b) together so it obvious that the alphabet is from  $-1$  to  $4$ .

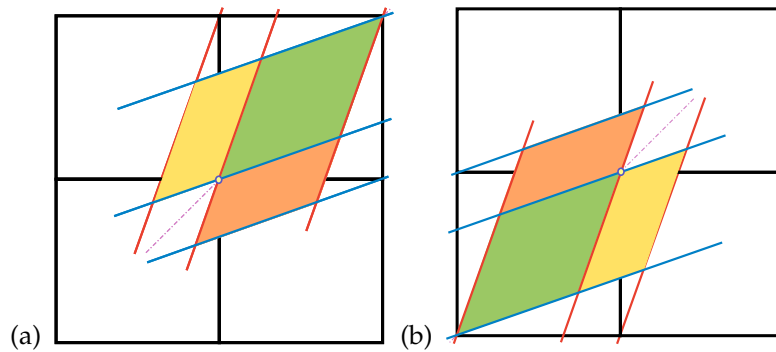


Figure 24.11: Abandoned attempt: (a) The three-rectangle, time reversal symmetric generating partition for the Percival-Vivaldi cat map (2.5), with borders given by cat map stable-unstable manifolds. (b) The three-rectangle partition obtained by space reversal (reflection across the anti-diagonal) is also a valid generating partition, but the distinct from (a). Thus this partition does not exhibit in a simple way the space reflection symmetry that is evident in figure 2.2.

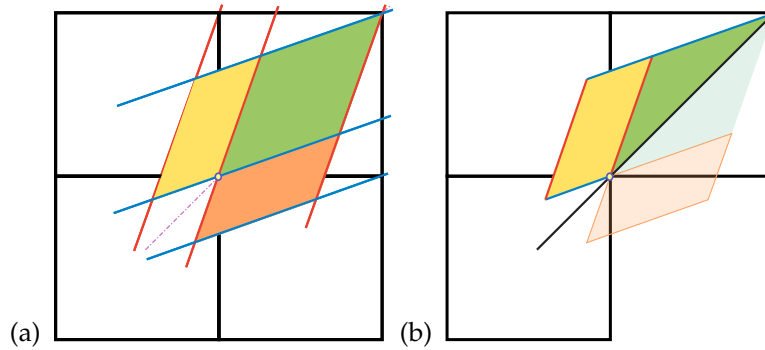


Figure 24.12: Abandoned attempt: (a) The three-rectangle, time reversal symmetric generating partition for the Percival-Vivaldi cat map (2.5), with borders given by cat map stable-unstable manifolds. Large rectangle is self-dual under time reversal (reflection across the diagonal), while the two small rectangles are mapped into each other. This implies that we should go to a fundamental domain (positive time only), and recode the dynamics according to example 6.11  $D_1$  factorization: (b) The three-rectangle partition time reversal fundamental domain (the half of the full partition, cut in two by the time reflection diagonal). Need to check whether we can handle the reflection of  $m_n$  as well.

2018-02-27 Han I have read the Chapter 15 *Counting* of Chaosbook. It's not easy. Finally have some general ideas about the topological zeta function.

2018-01-31 Han Matrices (2.8) can diagonalize (2.5) (I may be wrong).

2018-02-13 Predrag Your Green's function is symmetric. Diagonalize?

2018-02-13 Han The eigenvalues of this Green's function are  $1, 1/3, 1/3, 1/5$ . These are also the diagonal elements of the diagonalized matrix.

2018-02-13 Predrag Mhm - you sure? I was expecting  $\sqrt{5}$ 's. What about eigenvectors? Try period-5. 5 is a prime.

2018-02-13 Han When the circulant matrix and the Green's function are  $[5 \times 5]$  matrices, the eigenvalues of the Green's function are

$$1, (7 + \sqrt{5})/2, (7 + \sqrt{5})/2, (7 - \sqrt{5})/2, (7 - \sqrt{5})/2, \quad (24.16)$$

corresponding to eigenvectors:

$$\begin{aligned} &(1, 1, 1, 1, 1), \\ &((-1 + \sqrt{5})/2, (1 - \sqrt{5})/2, -1, 0, 1), \\ &(-1, (1 - \sqrt{5})/2, (-1 + \sqrt{5})/2, 1, 0), \\ &((-1 - \sqrt{5})/2, (1 + \sqrt{5})/2, -1, 0, 1), \\ &(-1, (1 + \sqrt{5})/2, (-1 - \sqrt{5})/2, 1, 0). \end{aligned}$$

**2018-02-13 Predrag** Mhm - surprised again. I was motivated by (2.36) and (2.72), and expected you to (re)discover sort of a **discrete Fourier transform**, but with hyperbolic functions. Back to drawing board.

**2018-04-22 Predrag** Fourier-transformed cycle points  $\hat{M}$  for the periodic points of figure 24.5:

$$\begin{aligned}
 \hat{M}_{0001} &= \frac{1}{2} [1, -i, -1, i] \Rightarrow \hat{\phi} = [0, , 0, ] \\
 \hat{M}_{1110} &= \frac{1}{2} [3, i, 1, -i] \Rightarrow \hat{\phi} = [0, , 0, ] \\
 \hat{M}_{0011} &= \frac{1}{2} [0, -1 + i, 2, -1 - i] \Rightarrow \hat{\phi} = [0, , , ] \\
 \hat{M}_{0011} &= \frac{1}{2} [0, 1 - i, -2, 1 + i] \Rightarrow \hat{\phi} = [0, , , ] \\
 \hat{M}_{0111} &= \frac{1}{2} [1, -1 + 2i, 1, -1 - 2i] \Rightarrow \hat{\phi} = [0, , , ] \\
 \hat{M}_{1101} &= \frac{1}{2} [1, 1 + 2i, 1, 1 - 2i] \Rightarrow \hat{\phi} = [0, , , ] \\
 \hat{M}_{1111} &= \frac{1}{2} [2, 2i, 2, -2i] \Rightarrow \hat{\phi} = [ , , , ] \\
 \hat{M}_{0011} &= \frac{1}{2} [0, -1 + i, 2, -1 - i] \Rightarrow \hat{\phi} = [ , , , ] \\
 \hat{M}_{0011} &= \frac{1}{2} [2, -1 - i, 0, -1 + i] \Rightarrow \hat{\phi} = [0, , , ] \\
 \hat{M}_{0111} &= \frac{1}{2} [1, 1, -3, 1] \Rightarrow \hat{\phi} = [0, , , ]
 \end{aligned}
 \tag{24.17}$$

Each cycle has 3 further cycle points, not computed here (but that should be plotted in the Brilluon zone). I did not compute  $\hat{\phi}_k$ , as that is a trivial multiplication by the diagonalized Green's function (24.30).

Take home messages; writing Fourier transforms of periodic points analytically is not useful. Only cycle-4 orbits are related to Gaussian integers, for other orbits there will be no nice analytic formulas. And already for 4-cycles, the phases are not rational fractions of  $2\pi$ . For example for  $1 + 2i$  the polar form phase in radians is  $\arctan 2 = 1.10715$ .

**2018-02-21 Predrag** The Green's function (24.9) and eigenvalues and eigenvectors (24.16) all have Toeplitz matrix structure. In case like this, when the problem has been around for centuries, reading literature is a great time saver, especially if someone has already done the dive into literature for you. You can understand your Mathematica results by the analytic solution for any cycle lengths and any  $s$ , for example (2.49) and (2.52). Here you learn, explicitly, that for  $s > 2$ , the lattice should not be expanded in Fourier modes, but in  $\sinh$  and  $\cosh$ 's. There are some other cute formulas in literatures, for example (2.72) and (2.73).



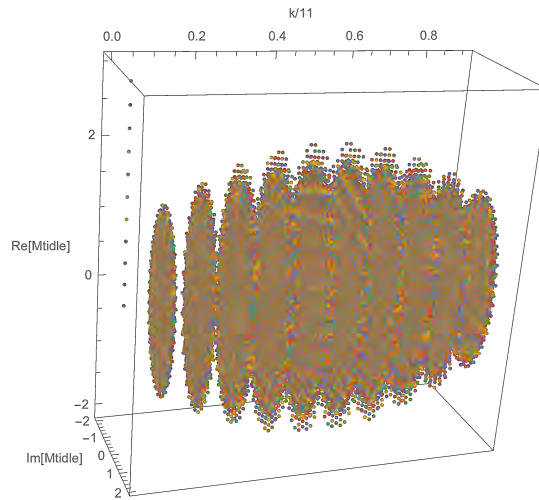


Figure 24.13: The Fourier transform of the 39601 period  $n = 11$  periodic states (see (2.14)) of the rhomboid corner partition in the complex plane.

**2018-04-25 Predrag** Reciprocal lattice is standard. I think you need to use stable / unstable eigenvectors in configuration space, compute reciprocal lattice with respect to them. Will continue writeup (unless you beat me to it:)

**2018-04-25 Predrag** Scratch stable / unstable eigenvectors - there is no integer-multiple tiling along those directions (I guess it is a antiperiodic tiling), the only configuration space vector is 1-dimensional, pointing for Percival-Vivaldi cat map along the vertical direction.

**2018-04-22 Predrag** Trying to get some feeling for the Fourier space representation, by computing the rhomboid corner partition 4-cycles (24.17), to see how they differ from the rhomboid center partition 4-cycles (24.29). The main take home message; analytic form of these Fourier transforms does not seem helpful, seems best to plot them numerically, in complex plane for the reciprocal lattice / Brilluion zone (not attempted yet).

**2018-04-25 Han** I plotted all of the admissible 11-cycles of the rhomboid corner partition in complex plane in figure 24.13. It looks like if I plot the figure with  $k$  from -5 to 5 instead of from 0 to 10 (which is to move the part with  $k > 5$  to the left side of the origin), this figure will be symmetric about  $k = 0$  plane. I tried to make some changes to the figure but the program keep getting frozen when I plot the figure. I will try again later on a desktop.

**2018-04-25 Predrag** Fascinating. Is it possible to generate a version that is 3D live (can be rotated)? Also, we need to plot these in the Brilluion zone,

not just raw Fourier...

## 24.2 Rhomboid center partition

A generating partition must map borders onto borders under dynamics (Adler-Weiss), but a really nice partition should also embody all symmetries of the dynamics; invariance under spatial reflections and the time reversal.

For the Percival-Vivaldi cat map the dynamics commutes with the spatial reflection  $\sigma$  (across anti-diagonal), while time reversal will require extra thinking.

For the Percival-Vivaldi cat map the flip across the  $\phi_1 = \phi_0$  diagonal together with the reversal of the direction of evolution is the  $D_1$  symmetry that corresponds to the invariance of cat map under time reversal.

**2018-04-20 Predrag** Currently figure 24.16 (b) does not map a border onto a border within region D of figure 24.17 (a); sadly, the partition studied in this section is not generating.

**2018-02-18 Predrag** Percival-Vivaldi alphabet can be made symmetric under spatial reflection by picking the origin in the middle of the unit interval, see sect. ?? . The tiling figure 2.4 (b) and the partition figure 24.3 (b) suggests that partition should be centered differently to fully exploit the symmetries of the tiling - perhaps with the fixed point in the center of the square, rather with the fixed point in the corner.

**2018-02-28 Predrag** A proposal for a space and time symmetric partition in figure 24.14. Do you see how to fix it?

**2018-02-28, 018-03-18 Han** Yes! A space reflection symmetric partition in figure 24.14 is obtained by cutting the yellow and orange rectangles into halves, as shown in figure 24.15. That is natural in the centered unit square tiling of the plane, i.e., the grid going through multiples of  $(1/2, 1/2)$ . Figure 24.15 (c) shows that this partition tiles the whole space. The forward image of the partition of figure 24.15 (b) figure 24.16. Figure 24.16 is the labeled 7-rectangle partition, together with the transition graph. The alphabet is

$$m_t \in \{\underline{2}, \underline{1}, 0, 1, 2\}. \quad (24.18)$$

**2018-03-18 Predrag** Staring at the partition of figure 24.16: no wonder I failed to draw it by hand. In figure 24.16 (b) there are little holes next to  $D$  and  $G$  and the weird overlaps  $\mathcal{M}_D \cap f(\mathcal{M}_E)$ ,  $\mathcal{M}_G \cap f(\mathcal{M}_F)$ , it's a miracle that the partition works. You might want to check it for longer period orbits in  $\mathcal{M}_D$ .

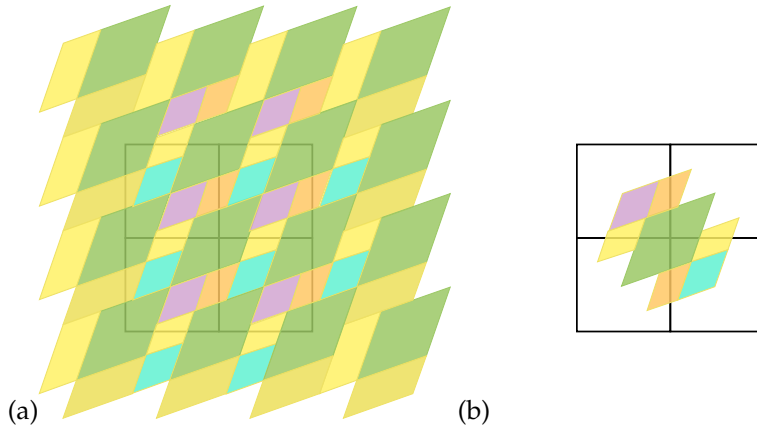


Figure 24.14: Abandoned attempt: (a) Tiling of the square lattice by a five-rectangle, time reversal and space reflection symmetric partition. Note that we have used the continuous translation invariance to place the center of the large tile  $A$  at the origin. (b) An almost a generating five-rectangle, time reversal and space reflection symmetric partition, except that the yellow / orange rectangles appear twice, so the area this covers exceeds the unit area.

2018-03-05 Han All period 4 orbits in the symmetric partition figure 24.15 (b) are

$$\begin{aligned}
 \Phi_{1111} &= \frac{1}{15} [ 5 \quad 5 \quad -5 \quad -5 ], & \Phi_{0202} &= \frac{1}{15} [ 0 \quad -10 \quad 0 \quad 10 ] \\
 \Phi_{0011} &= \frac{1}{15} [ -1 \quad 1 \quad 4 \quad -4 ], & \Phi_{0011} &= \frac{1}{15} [ 1 \quad -1 \quad -4 \quad 4 ] \\
 \Phi_{1221} &= \frac{1}{15} [ 2 \quad -7 \quad 7 \quad -2 ], & \Phi_{2211} &= \frac{1}{15} [ 7 \quad -7 \quad 2 \quad -2 ] \\
 \Phi_{0111} &= \frac{1}{15} [ 4 \quad 6 \quad -1 \quad 6 ], & \Phi_{1011} &= \frac{1}{15} [ -6 \quad -4 \quad -6 \quad 1 ] \\
 \Phi_{1012} &= \frac{1}{15} [ 3 \quad 2 \quad 3 \quad -8 ], & \Phi_{1012} &= \frac{1}{15} [ -3 \quad -2 \quad -3 \quad 8 ]
 \end{aligned}
 \tag{24.19}$$

The orbits are in figures 24.18 and 24.20. All orbits are symmetric about both  $\phi_1 = \phi_0$  and  $\phi_1 = -\phi_0$ , either self-dual or come in pairs.

2018-03-05 Predrag Beautiful! We have the doubly symmetric partition nailed. I do not think this is anywhere in the literature. Can you connect to symmetries to cycle itineraries?

2018-04-08 Han I have recomputed the 4-cycles of (24.19) in the face-centered Percival-Vivaldi unit square non-partition. That screws up the above

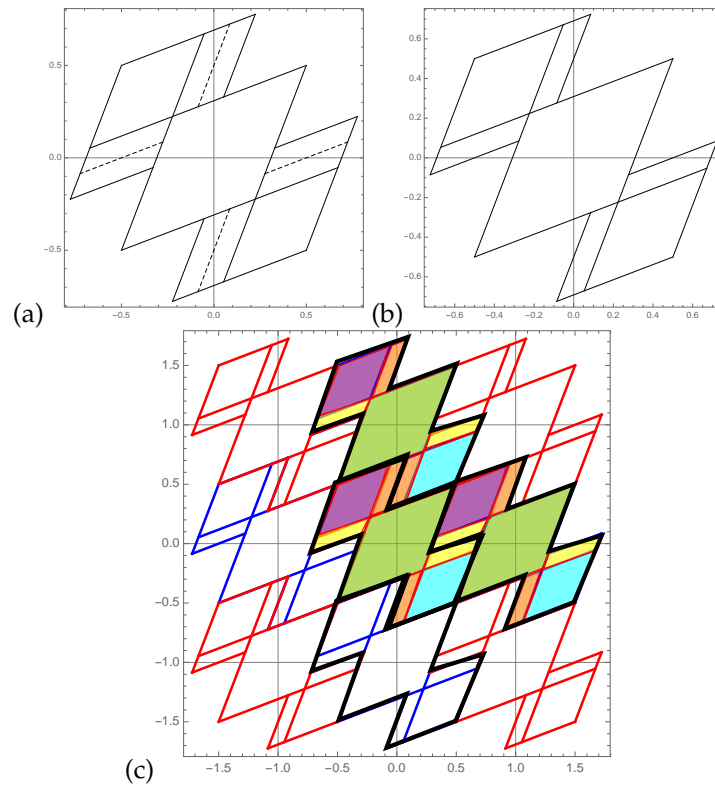


Figure 24.15: (a) Start with the partition of figure 24.14 (b). The dashed lines in the directions of stable and unstable manifolds cut the yellow and orange rectangles into halves. (b) The symmetric partition obtained by removing halves of yellow and orange rectangles has area 1. (c) The partition tiles the square lattice.

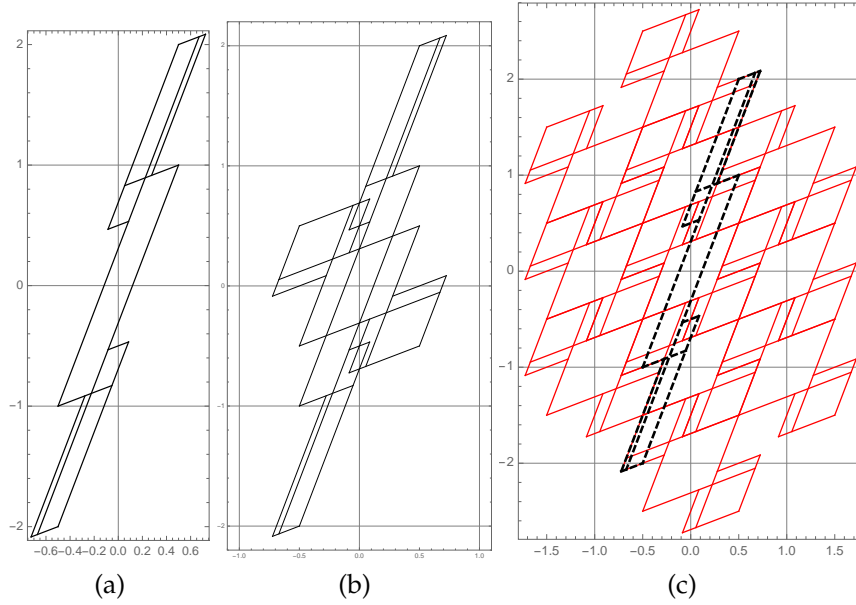


Figure 24.16: (a) The forward image of the 7-rectangle partition figure 24.15 (b). (b) The stretched partition overlaid over the original partition. (c) The stretched partition overlaid over the tiled lattice. The  $x$  and  $y$  axes are not plotted to the same scale.

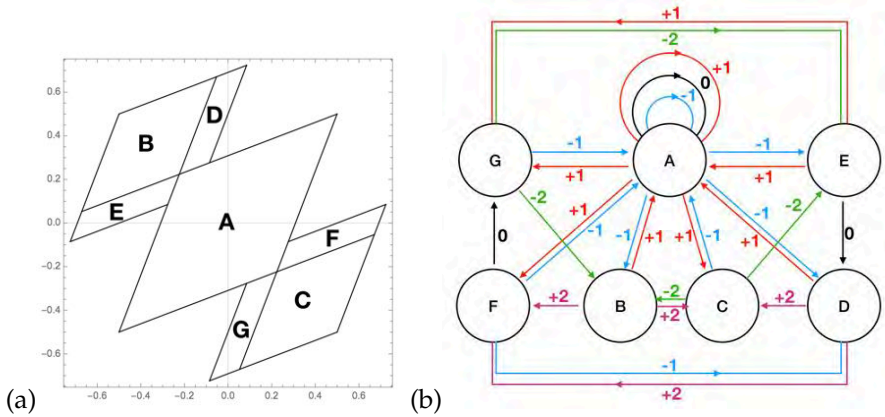


Figure 24.17: (a) The labeled 7-rectangle partition, and (b) the corresponding 7-node transition graph.

$\Phi_{1012}$ ,  $\Phi_{0202}$ , and  $\Phi_{1012}$ :

$$\begin{aligned}
 \Phi_{1111} &= \frac{1}{15} \begin{bmatrix} -5 & -5 & 5 & 5 \end{bmatrix}, & \Phi_{1010} &= \frac{1}{15} \begin{bmatrix} -5 & 0 & 5 & 0 \end{bmatrix} \\
 \Phi_{0011} &= \frac{1}{15} \begin{bmatrix} -1 & 1 & 4 & -4 \end{bmatrix}, & \Phi_{0011} &= \frac{1}{15} \begin{bmatrix} 1 & -1 & -4 & 4 \end{bmatrix} \\
 \Phi_{1221} &= \frac{1}{15} \begin{bmatrix} 2 & -7 & 7 & -2 \end{bmatrix}, & \Phi_{2211} &= \frac{1}{15} \begin{bmatrix} 7 & -7 & 2 & -2 \end{bmatrix} \\
 \Phi_{0111} &= \frac{1}{15} \begin{bmatrix} 4 & 6 & -1 & 6 \end{bmatrix}, & \Phi_{1011} &= \frac{1}{15} \begin{bmatrix} -6 & -4 & -6 & 1 \end{bmatrix} \\
 \Phi_{0001} &= \frac{1}{15} \begin{bmatrix} 3 & 2 & 3 & 7 \end{bmatrix}, & \Phi_{1000} &= \frac{1}{15} \begin{bmatrix} -7 & -3 & -2 & -3 \end{bmatrix}
 \end{aligned}
 \tag{24.20}$$

**2018-03-05 Predrag** I still think that if one day you plot all cycle *points* (no lines connecting them) on a single copy of the generating partition, you'll find the resulting picture very cute:)

A hint from literature: Percival and Vivaldi [62] write: "For the cat maps the periodic orbits lie on a rational lattice, so all surds cancel, as shown in the companion paper [63] on the number theory of the periodic orbits of the automorphisms of the torus."

Sect. ?? *Numbers of periodic orbits* and sect. ?? *Periodic orbits - first approach* might also help with developing some intuition about figure 24.22.

**2018-03-07 Predrag** The alphabet (24.18) seems to make sense. Space reflection acts as

$$j \leftrightarrow \bar{j}. \tag{24.21}$$

The total translation (the sum of symbols) is zero (the orbit is periodic, standing) for all, except for figure 24.20 (i) and (j) which translate by  $\pm 1$  (the orbit is relative periodic, running).

The time reversal should reverse the order of symbols, which it seems to do, at least for figures 24.18 and 24.20:

$$(c, d) 001\bar{1} \leftrightarrow 00\bar{1}1, \quad (e, f) \bar{1}1\bar{2}2 \leftrightarrow 2\bar{2}1\bar{1}, \tag{24.22}$$

rest self-dual.

**2018-03-15 Han** In figure 24.22 I plotted all the cycle points on a single copy of the partition for both partitions of figures 24.4 and 24.15.

**2018-03-22 Han** I have added the period 1, 2 and 3 orbits to figure 24.23. The period 1 and 2 orbits fill the holes of figure 24.22 (b). Each of the period 3 orbits has only one symmetry, and they have the other symmetry in pairs.

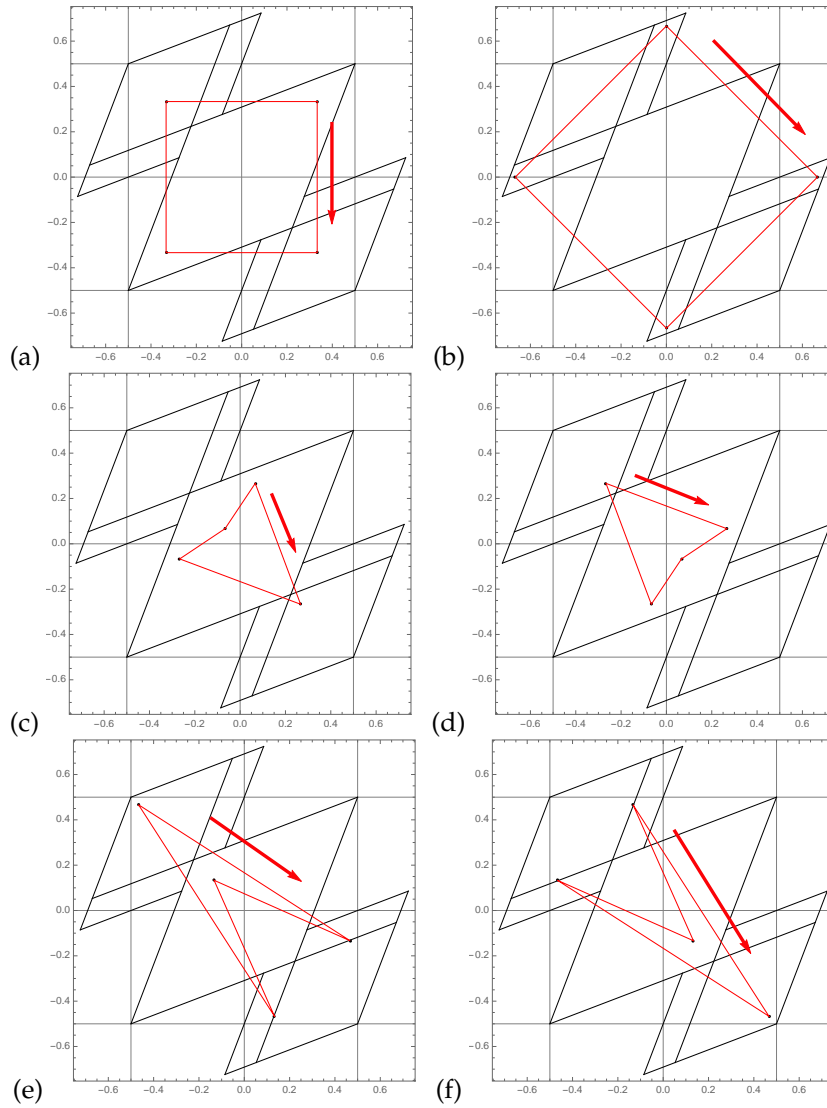


Figure 24.18: All 4-cycles from (24.19): (a)  $\Phi_{1111}$  (b)  $\Phi_{0202}$ , (c)  $\Phi_{0011}$ , (d)  $\Phi_{0011}$ , (e)  $\Phi_{1122}$ , (f)  $\Phi_{2211}$ , (g) to (j) continued in figure 24.20.

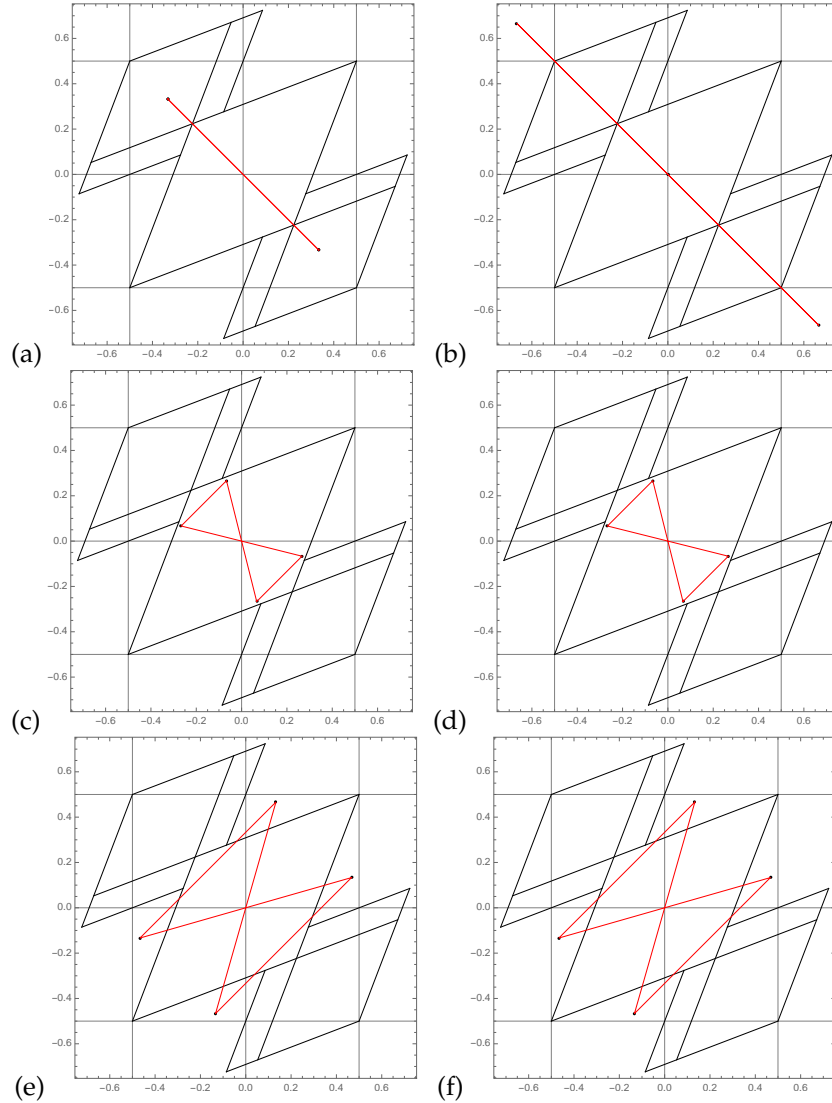


Figure 24.19: All 4-cycles from (24.19) plotted in “Lagrangian” coordinates  $\{\phi_{t-1}, \phi_{t+1}\}$ , in the order of figure 24.18. The 7-rectangle partition figure 24.15 (b), appropriate to  $\{\phi_t, \phi_{t+1}\}$  plots, is included only to guide the eye. (a)  $\Phi_{1111}$  is a “Laplacian” self-retracing 2-cycle (24.34). (b)  $\Phi_{0202}$  is a “Laplacian” self-retracing 2-cycle (24.35). (c)  $\Phi_{0011}$  and its time reversal (d)  $\Phi_{0011}$  map into one cycle; (e)  $\Phi_{1221}$  and its time reversal (f)  $\Phi_{2211}$  map into one cycle; (g) to (j) continued in figure 24.21.



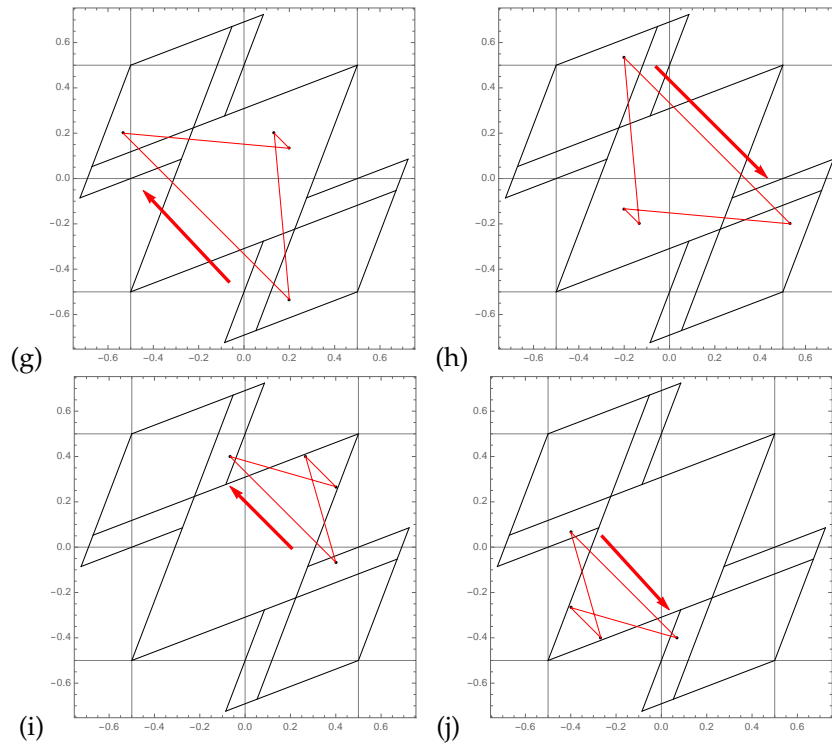


Figure 24.20: Continuation of figure 24.18: (g)  $\Phi_{1012}$ , (h)  $\Phi_{1012}$  (i)  $\Phi_{0111}$ , and (j)  $\Phi_{0111}$ ,

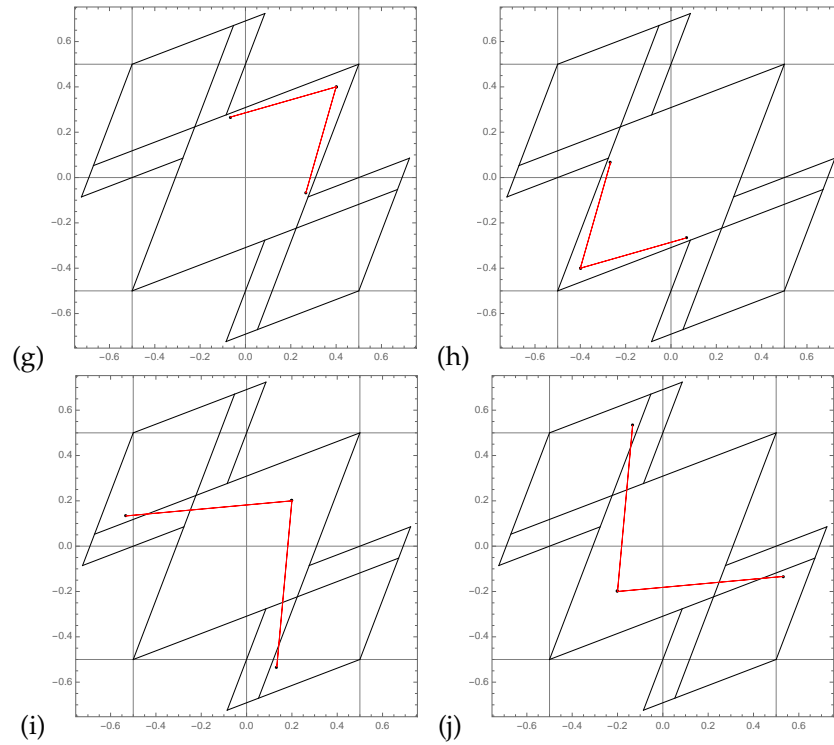


Figure 24.21: Continuation of figure 24.19 - the space reflection dual pairs: (g)  $\Phi_{0111}$  and its time reversal (h)  $\Phi_{1011}$  map into space-reflection dual 4-cycles; (i)  $\Phi_{1012}$  and (j)  $\Phi_{1012}$  map into space-reflection dual 4-cycles.

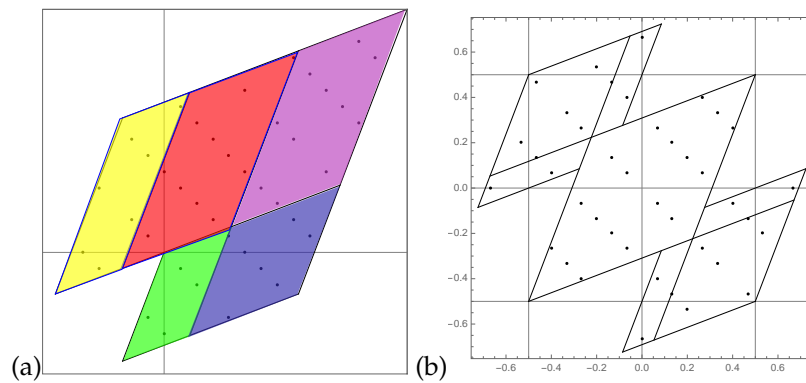


Figure 24.22: All period 4 orbits in the partition of (a) figure 24.4, and (b) figure 24.15. The holes correspond to missing cycle-1 and cycle-2 points.

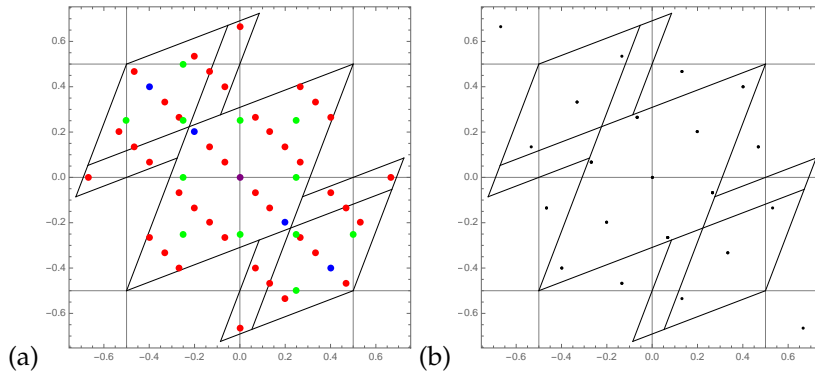


Figure 24.23: (a) All periodic points that belong to the 1 (purple), 2 (blue) and 4 (red) orbits, plotted in “Hamiltonian” coordinates  $\{\phi_t, \phi_{t+1}\}$ . The period 1- and 2-orbits fill the holes between period 4 orbits in the figure 24.22 (b). The 3 (green) orbits start a new grid, to be filled out by the period 6, 9, etc orbits. (b) All periodic points that belong to the period 4 orbits of figure 24.23 plotted in “Lagrangian” coordinates  $\{\phi_{t-1}, \phi_{t+1}\}$ . The 7-rectangle partition figure 24.15 (b), appropriate to  $\{\phi_t, \phi_{t+1}\}$  plots, is included only to guide the eye. The numbers of orbits are listed in (24.11).

**2018-03-13 Predrag** An aside, **not even right, a failed attempt kept here only for the record**: going from the partition of figure 24.4 to the partition of figure 24.15 we have translated the origin to  $\hat{\phi}_t = \phi_t - 1/2$ , so the map (2.5) is now

$$\begin{bmatrix} \hat{\phi}'_{t+1} \\ \hat{\phi}'_t \end{bmatrix} = \mathbf{A} \begin{bmatrix} \hat{\phi}_t \\ \hat{\phi}_{t-1} \end{bmatrix} - \frac{1}{2} \begin{bmatrix} 0 \\ s - 2 \end{bmatrix}. \quad (24.23)$$

I’m not sure why we would be allowed to drop such translational terms. A cute fact is that Percival and Vivaldi [62] actually define the map (2.5) on  $\phi_t \in [-1/2, 1/2]$  interval, i.e., without the translation term in (24.23). Such translations should not affect the map (it’s the same automorphism of the torus, just in different coordinates) but I do not have a clean argument that they do not matter.

**2018-03-15 Han** We didn’t change the origin when the partition changed from figure 24.4 to figure 24.15. The map is also not changed. What we did is changing the boundary of the partition. So the map is still:

$$\begin{bmatrix} \phi_{t+1} \\ \phi_t \end{bmatrix} = \mathbf{A} \begin{bmatrix} \phi_t \\ \phi_{t-1} \end{bmatrix}. \quad (24.24)$$

**2018-04-20 Predrag** Currently figure 24.16 (b) does not map a border onto a border within region D of figure 24.17 (a); it looks as though D would have to be cut horizontally into two halves, and even that does not complete the task. So, sadly, the partition studied in this section is not gen-

erating, and (for time being?) we have to give up on the whole section.

### 24.2.1 Reduction to the reciprocal lattice

**2018-03-18 Predrag** Check in  $d = 1$  whether (24.56) together with the inverse Fourier transform (24.60) recovers any of your periodic orbits?

Does the circulant eigenvalue formula (24.48) explain your (24.16)?

**2018-03-19 Predrag** Does the inverse Fourier transform of the propagator in (24.56) reproduce the usual  $d = 1$  configuration Green's function (2.105)?

**2018-03-22 Han** In  $d = 1$ , (24.56) can recover the periodic orbits. (24.56) can be written as:

$$\hat{\phi} = \text{diag}(\lambda)^{-1} \hat{m}, \quad (24.25)$$

where  $\lambda$  is the eigenvalue of the damped Poisson matrix (24.46). Then we have:

$$\phi = U^\dagger \text{diag}(\lambda)^{-1} U m, \quad (24.26)$$

When  $d = 1$ ,  $s = 3$  and  $n = 4$  (4-cycles),

$$\text{diag}(\lambda)^{-1} = \begin{pmatrix} 1 & 0 & 0 & 0 \\ 0 & 3 & 0 & 0 \\ 0 & 0 & 5 & 0 \\ 0 & 0 & 0 & 3 \end{pmatrix} \quad (24.27)$$

Then the Green's function for 4-cycle is:

$$\mathbf{g} = U^\dagger \text{diag}(\lambda)^{-1} U = \frac{1}{15} \begin{pmatrix} 7 & 3 & 2 & 3 \\ 3 & 7 & 3 & 2 \\ 2 & 3 & 7 & 3 \\ 3 & 2 & 3 & 7 \end{pmatrix} \quad (24.28)$$

which is same as (24.9).

Using (24.48) we can also get the result of (24.16).

**2018-04-18 Predrag** Can you plot the Fourier space (24.56) points  $\hat{\phi}_k, \hat{m}_k$  corresponding to your periodic orbits of figure 24.23 (a)? Interpret what you get?

2018-04-18 Han  $\hat{\phi}_k, \hat{m}_k$  for the periodic points of figure 24.23 (a):

$$\begin{aligned}
 \hat{M}_{1111} &= \begin{bmatrix} 0 & \sqrt{2} e^{i\pi/4} & 0 & \sqrt{2} e^{-i\pi/4} \end{bmatrix} \Rightarrow \hat{\Phi} = \begin{bmatrix} 0 & \frac{\sqrt{2} e^{i\pi/4}}{3} & 0 & \frac{\sqrt{2} e^{-i\pi/4}}{3} \end{bmatrix} \\
 \hat{M}_{0202} &= \begin{bmatrix} 0 & -2 e^{i\pi/2} & 0 & -2 e^{-i\pi/2} \end{bmatrix} \Rightarrow \hat{\Phi} = \begin{bmatrix} 0 & -\frac{2}{3} e^{i\pi/2} & 0 & -\frac{2}{3} e^{-i\pi/2} \end{bmatrix} \\
 \hat{M}_{0011} &= \begin{bmatrix} 0 & -\frac{e^{-i\pi/4}}{\sqrt{2}} & 1 & -\frac{e^{i\pi/4}}{\sqrt{2}} \end{bmatrix} \Rightarrow \hat{\Phi} = \begin{bmatrix} 0 & -\frac{e^{-i\pi/4}}{3\sqrt{2}} & \frac{1}{5} & -\frac{e^{i\pi/4}}{3\sqrt{2}} \end{bmatrix} \\
 \hat{M}_{0011} &= \begin{bmatrix} 0 & \frac{e^{-i\pi/4}}{\sqrt{2}} & -1 & \frac{e^{i\pi/4}}{\sqrt{2}} \end{bmatrix} \Rightarrow \hat{\Phi} = \begin{bmatrix} 0 & \frac{e^{-i\pi/4}}{3\sqrt{2}} & -\frac{1}{5} & \frac{e^{i\pi/4}}{3\sqrt{2}} \end{bmatrix} \\
 \hat{M}_{1221} &= \begin{bmatrix} 0 & -\frac{e^{i\pi/4}}{\sqrt{2}} & 3 & -\frac{e^{-i\pi/4}}{\sqrt{2}} \end{bmatrix} \Rightarrow \hat{\Phi} = \begin{bmatrix} 0 & -\frac{e^{i\pi/4}}{3\sqrt{2}} & \frac{3}{5} & -\frac{e^{-i\pi/4}}{3\sqrt{2}} \end{bmatrix} \\
 \hat{M}_{2211} &= \begin{bmatrix} 0 & \frac{e^{-i\pi/4}}{\sqrt{2}} & 3 & \frac{e^{i\pi/4}}{\sqrt{2}} \end{bmatrix} \Rightarrow \hat{\Phi} = \begin{bmatrix} 0 & \frac{e^{-i\pi/4}}{3\sqrt{2}} & \frac{3}{5} & \frac{e^{i\pi/4}}{3\sqrt{2}} \end{bmatrix} \\
 \hat{M}_{0111} &= \begin{bmatrix} 1/2 & 1/2 & -3/2 & 1/2 \end{bmatrix} \Rightarrow \hat{\Phi} = \begin{bmatrix} 1/2 & 1/6 & -3/10 & 1/6 \end{bmatrix} \\
 \hat{M}_{0111} &= \begin{bmatrix} -1/2 & -1/2 & 3/2 & -1/2 \end{bmatrix} \Rightarrow \hat{\Phi} = \begin{bmatrix} -1/2 & -1/6 & 3/10 & -1/6 \end{bmatrix} \\
 \hat{M}_{1012} &= \begin{bmatrix} 0 & e^{i\pi/2} & 2 & -e^{-i\pi/2} \end{bmatrix} \Rightarrow \hat{\Phi} = \begin{bmatrix} 0 & \frac{e^{i\pi/2}}{3} & 2/5 & -\frac{e^{-i\pi/2}}{3} \end{bmatrix} \\
 \hat{M}_{1012} &= \begin{bmatrix} 0 & -e^{i\pi/2} & -2 & e^{-i\pi/2} \end{bmatrix} \Rightarrow \hat{\Phi} = \begin{bmatrix} 0 & -\frac{e^{i\pi/2}}{3} & -2/5 & \frac{e^{-i\pi/2}}{3} \end{bmatrix}
 \end{aligned} \tag{24.29}$$

2018-04-18 Predrag The 0th Fourier component of  $M = 0111$  equals  $\hat{m}_0 = 1/2$ , as it should.

I would expect the time-reversal pairs to be the complex-conjugate pairs in Fourier space, as  $C_4$  shift moves them in opposite directions.

2018-04-18 Han The Green's function (24.56) that relates  $\hat{\phi}_k$  to  $\hat{m}_k$  is:

$$\hat{\phi} = \begin{pmatrix} 1 & 0 & 0 & 0 \\ 0 & \frac{1}{3} & 0 & 0 \\ 0 & 0 & \frac{1}{5} & 0 \\ 0 & 0 & 0 & \frac{1}{3} \end{pmatrix} \hat{m} \tag{24.30}$$

If we shift the orbit to the left by one time step, each component of the Fourier transform will be multiplied by the  $C_4$  cyclic group phase factor. For a 4-cycle the phase factors are

$$e^{-i2\pi k/4} = (1, e^{-i\pi/2}, -1, e^{-i3\pi/2}) = (1, i, -1, -i). \tag{24.31}$$

2018-04-18 Han The  $\hat{m}$  in (24.32) are transforming under the  $C_4$  shift by phase factors (24.31). For example, the  $1221$  and  $2211$  which correspond to successive periodic points in the same 4-cycle, have the correct Fourier transforms,

$$\begin{aligned}
 m &= \begin{bmatrix} 1 & -2 & 2 & -1 \end{bmatrix} \Rightarrow \hat{m} = \begin{bmatrix} 0 & -\frac{e^{i\pi/4}}{\sqrt{2}} & 3 & -\frac{e^{-i\pi/4}}{\sqrt{2}} \end{bmatrix} \\
 m &= \begin{bmatrix} -2 & 2 & -1 & 1 \end{bmatrix} \Rightarrow \hat{m} = \begin{bmatrix} 0 & -\frac{e^{-i\pi/4}}{\sqrt{2}} & -3 & -\frac{e^{i\pi/4}}{\sqrt{2}} \end{bmatrix}
 \end{aligned} \tag{24.32}$$

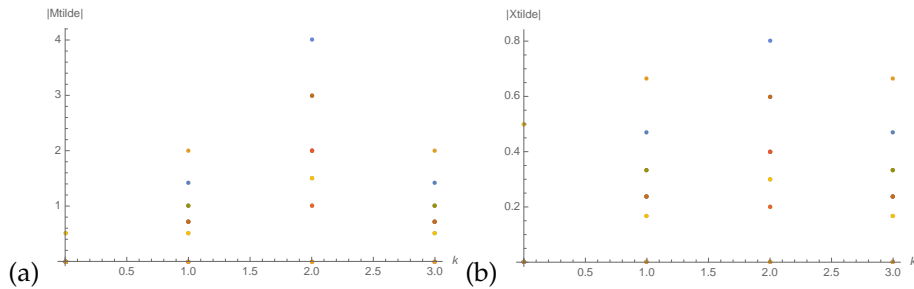


Figure 24.24: (a) The Fourier space points  $\hat{m}_k$  of all the periodic orbits with period 1, 2 and 4. The x-axis is  $k$  and y-axis is the absolute value of  $\hat{m}_k$ . (b) The Fourier space points  $\hat{\phi}_k$ .

**2018-04-18 Han** I plot the Fourier space points of all of the orbits of period 1, 2 and 4 in figure 24.24 using the absolute value of  $\hat{\phi}_k$  and  $\hat{m}_k$ .

**2018-04-18 Predrag** My hunch is that we do not want to plot the absolute values of  $\hat{\phi}_k$ . You might want to plot in the complex plane instead. We have to review what Brillouin zone means for 1D crystals. Mourigal, DeHeer and Berger students presumably understand that...

### 24.3 Time reversal

For our main thrust on understanding both the forward and backward in time, and the global temporal cat time-reversal symmetry, see sect. 6.4 *Temporal cat reversibility factorization*.

**2018-02-12 Predrag** Can you plot the stretched domains for one step back in time (inverse map)? The intersections of the past and future might help you intuition, in the way staring at the figure following figure 2.2 in Gutkin *et al.* [36] reveals the Smale-horseshoe structure.

Remember, our goal is to reformulate the problem in a global, Lagrangian way that is explicitly invariant under time reversal.

**2018-02-19 Predrag** The flip across the  $\phi_1 = \phi_0$  diagonal together with the reversal of the direction of evolution is the  $D_1$  symmetry that corresponds to the invariance of cat map under time reversal. There are at least two kinds of orbits:

1. self-dual, here figure 24.5 (a) and (b), figure 24.6 (g), (h), (i) and (j)
  - even period cycles have 0, 2, 4, ... points on the diagonal
  - odd period cycles have 1, 3, 5, ... points on the diagonal (need to plot odd period cycles to see that they always have at least one point on the diagonal)

2. orbits that come in pairs, here figure 24.5 (c) ↔ (d), (e) ↔ (f)
3. There is also invariance of the cat map dynamics (2.95) spatial reflection flip across the  $\phi_1 = -\phi_0$  anti-diagonal, together with  $m_n \rightarrow -m_n$  so the full symmetry is in some sense  $D_1 \times D_1$ .
  - 1 copy, self-dual under both symmetries: figure 24.6 (h)
  - Figure 24.5 (a) ↔ (b), self-dual under time reversal
  - Figure 24.5 (c) ↔ (d) is self-dual under the second reflection
  - 4 copies (need to get longer cycles to see examples)
4. However, as figure 24.11 illustrates, the partition is only in part invariant under the spatial reflection, resulting in some cycles missing their spatial-reflection sisters:
  - Figure 24.5 (e) and (f)
  - Figure 24.6 (g) and (j)

**2018-02-21 Predrag** The time reversal symmetry fundamental domain is given in figure 24.12 (b). One needs to describe the symmetry reduced dynamics on the fundamental domain, as in ChaosBook.org Figure 11.7: “The bimodal Ulam sawtooth map restricted to the fundamental domain.”

**2018-04-08 Han** I have plotted in figures 24.19 and 24.21. all 4-cycles in ‘Lagrangian’ coordinates  $\{\phi_{t-1}, \phi_{t+1}\}$ , in the unit-square face centered partition of figure 24.17. The periodic orbits in this partition are given by (24.20) (which seems to be (24.19) modulo some cyclic permutations). Note that sometimes different solutions appear to have the same orbit, and that sometimes points belonging to different solutions appear in the same position. The reason is that given the field values  $\phi_{t-1}$  and  $\phi_{t+1}$  we cannot decide  $\phi_t$  without knowing the  $m_t$ . For example, the points  $\{\phi_1, \phi_3\}$  for the first two solutions  $\Phi_{\underline{1111}}$  and  $\Phi_{\underline{1010}}$  are the same.

I also plotted all of the solutions in figure 24.23 (b). There are fewer points than figure 24.23 (a), because some of the points coincide. The 2-cycle and the fixed point solutions

$$\begin{aligned} \Phi_{\underline{11}} &= \frac{1}{15} \begin{bmatrix} -3 & 3 \\ 0 & 0 \end{bmatrix}, & \Phi_{\underline{22}} &= \frac{1}{15} \begin{bmatrix} -6 & 6 \\ 0 & 0 \end{bmatrix} \\ \Phi_0 &= \begin{bmatrix} 0 \\ 0 \end{bmatrix} \end{aligned} \tag{24.33}$$

also coincide with points of the 4-cycle solutions.

**2018-04-05 Predrag** In the “Lagrangian” coordinates  $\{\phi_{t-1}, \phi_{t+1}\}$  formulation the 2-cycles are self-dual, as in (24.34), and the fixed point is very special, as it sits in the maximally invariant subspace.

**2018-04-05 Predrag** Everything works like charm in the “Lagrangian” coordinates  $\{\phi_{t-1}, \phi_{t+1}\}$  formulation, except that you should fix a few cycles in figure 24.23 (b), figures 24.19 and 24.21: so far you are plotting periodic points in Percival-Vivaldi face centered unit square non-partition,

rather than our 7-region partition. Please replace all plots by plots with the 7-rectangle partition of figure 24.15 (b) indicated, as in figure 24.18.

If

$$\Phi_{1111} = \frac{1}{15} [ 5 \ 5 \ -5 \ -5 ]$$

then points on the orbit are (ignoring the 1/15 factor) a self-retracing 2-cycle

$$(\phi_{t-1}, \phi_{t+1}) = \{(-5, 5), (5, -5), (5, -5), (-5, 5)\} = \Phi_{11} + \Phi_{11}^\top. \quad (24.34)$$

If

$$\Phi_{0202} = \frac{1}{15} [ 0 \ -10 \ 0 \ 10 ]$$

then points on the orbit are (ignoring the 1/15 factor) a self-retracing 2-cycle

$$(\phi_{t-1}, \phi_{t+1}) = \{(10, -10), (0, 0), (-10, 10), (0, 0)\} = \Phi_{02} + \Phi_{02}^\top, \quad (24.35)$$

where '+' stands for string concatenation.

**2018-04-10 Predrag** My hunch is that we need a simpler transition graph than figure 24.17 (b), hopefully an undirected graph. Maybe we do not need a transition graph at all, or we need to formulate the graph is the 2-step "Lagrangian" coordinates  $\{\phi_{t-1}, \phi_{t+1}\}$ .

Can you list the pruned (inadmissible, forbidden) strings in the alphabet (24.18)? Presumably only blocks of period-2 and 3 are needed, and they are hopefully explicitly time-reversal invariant.

**2018-04-12 Han** I tried to get the pruned string from the transition graph figure 24.17. The pruned strings for blocks of period-2 are of two types:

$$12, 21, \underline{12}, \underline{21}, 22, \underline{22}, \quad (24.36)$$

but I'm not so sure...

Compare with (24.33); of the  $5 \times 4 - 6 = 14$  remaining non-repeating admissible 2-blocks, the period-2 periodic points  $\underline{11}, \underline{11}, \underline{22}, \underline{22}$ , are realized, but not the  $\underline{12}, \underline{21}, \underline{12}, \underline{21}, 01, 10, 0\underline{1}, \underline{1}0$  and  $02, 20, 0\underline{2}, \underline{2}0$  2-cycles.

**2018-04-18 Han** The three types of *new* period-3 pruned blocks from transition graph figure 24.17 are:

$$\begin{aligned} &002, 200, 00\underline{2}, \underline{2}00, \\ &102, 201, \underline{102}, \underline{201}, \\ &202, \underline{202}, \end{aligned} \quad (24.37)$$



*new* in the sense that the remaining blocks contain (24.36) blocks of period-2, which are pruned 2-blocks:

$$\begin{aligned}
 & \underline{122}, \underline{121}, \underline{120}, \underline{121}, \underline{122}, \underline{112}, \underline{112}, \underline{121}, \underline{122} \\
 & \underline{122}, \underline{121}, \underline{120}, \underline{121}, \underline{122}, \underline{112}, \underline{112}, \underline{121}, \underline{122} \\
 & \underline{212}, \underline{221}, \underline{222}, \underline{212}, \underline{211}, \underline{210}, \underline{211}, \underline{212}, \underline{222}, \underline{221}, \underline{220}, \underline{221}, \underline{222} \\
 & \underline{212}, \underline{221}, \underline{222}, \underline{222}, \underline{221}, \underline{220}, \underline{221}, \underline{222}, \underline{212}, \underline{211}, \underline{210}, \underline{211}, \underline{212} \\
 & 021, 022, \underline{021}, \underline{022}, 012, \underline{012}. \tag{24.38}
 \end{aligned}$$

Length-2 and -3 pruned blocks form space-reflection and time-reversal invariant sets. We expect that each such sets gets replaced by one pruning block in the fundamental domain of figure 24.25 (b).

**2018-04-12 Predrag** Lets hope that there are no *new* period-4 pruned block's.

**2018-04-11 Predrag** Maybe in the "Lagrangian" coordinates  $\{\phi_{t-1}, \phi_{t+1}\}$  we need to recode (24.19) 4-cycles, so I tried summing the pairs of successive shifts:

$$\begin{aligned}
 \Phi_{1111} &\Rightarrow 2020, & \Phi_{0202} &\Rightarrow 2222 \\
 \Phi_{0011} &\Rightarrow 0101 = \Phi_{0011} &\Rightarrow 0101 \\
 \Phi_{1221} &\Rightarrow 1010 = \Phi_{2211} &\Rightarrow 0101 \\
 \Phi_{0111} &\Rightarrow 1001, & \Phi_{1011} &\Rightarrow 1100 \\
 \Phi_{1012} &\Rightarrow 1111, & \Phi_{1012} &\Rightarrow 1111. \tag{24.39}
 \end{aligned}$$

What that does is to replace the shifts coded by alphabet (24.18) by averages (modulo factor 1/2) of pairs of successive shifts. Everybody is self-dual under time, and the last two pairs are related by space reflections, as it should be. However (c,d) should not be the same as (e,f), and (i,j) is already self-dual under both reflections, so this is recorded here just as **another failed attempt** to understand undirected graphs.

**2018-04-12 Han** I have replaced the plots in figure 24.23 (b), figures 24.19 and 24.21. The solutions I used are in (24.19). Note that for this partition, in order to decide whether a solution is admissible we only need to check whether  $\{\phi_{t-1}, \phi_t\}$  (**not** the Lagrangian coordinates  $\{\phi_{t-1}, \phi_{t+1}\}$ ) is in the partition. So we can see that some of the points are out of the partition. Actually, since we don't check if the Lagrangian coordinates are in the partition, I probably shouldn't put the partition in the figure. If we want to let the Lagrangian coordinates to be in the 7-region partition, we will be using another partition in which the solutions are different from (24.19).

**2018-03-22 Predrag** I think you have the spatial inversion fundamentally nailed. What about the transition graph?

**2018-04-27 Predrag** Continuing on the (16.20) theme, we also transform the identity (2.2), noted by string people, to Percival-Vivaldi coordinates:

$$\begin{aligned} \mathbf{L}' &= \begin{bmatrix} -1 & 2 \\ 1 & 0 \end{bmatrix} \begin{bmatrix} 1 & 1 \\ 0 & 1 \end{bmatrix} \begin{bmatrix} -1 & 2 \\ 1 & 0 \end{bmatrix} = \begin{bmatrix} 1 & -1 \\ 0 & 1 \end{bmatrix} \\ \mathbf{L}'^\top &= \begin{bmatrix} -1 & 2 \\ 1 & 0 \end{bmatrix} \begin{bmatrix} 1 & 0 \\ 1 & 1 \end{bmatrix} \begin{bmatrix} -1 & 2 \\ 1 & 0 \end{bmatrix} = \begin{bmatrix} -1 & 4 \\ -1 & 3 \end{bmatrix}, \end{aligned} \quad (24.40)$$

so

$$\mathbf{L}'\mathbf{L}'^\top = \begin{bmatrix} 1 & -1 \\ 0 & 1 \end{bmatrix} \begin{bmatrix} -1 & 4 \\ -1 & 3 \end{bmatrix} = \begin{bmatrix} 0 & 1 \\ -1 & 3 \end{bmatrix}.$$

Under the similarity transformation, the transpose (time reversal?) structure of (2.2) is lost, so this transpose structure (16.22) does not seem to play nice with symplectic transformations.

**2018-02-11 Predrag** In (the current draft of) Gutkin *et al.* [36] I wrote “The Adler-Weiss Markov partition for the Arnol’d cat map [1–3] utilizes the stable / unstable manifold of the fixed point at the origin to partition the torus into a 3-rectangles generating partition (see, for example, Devaney [21, 28]). It is a subshift of finite type (3 symbols alphabet  $\mathcal{A}$ , with a finite grammar), or a 5 symbols full shift.”

This is discussed in 2016-06-02 sect. 2.3.8 notes on Creagh [21], *Quantum zeta function for perturbed cat maps*. Creagh explains both the 3-letter and the 5-letter alphabet in ref. [21] Sect. III. A. *The classical map*. Robinson [66] goes through the construction clearly, step by step. The 3-rectangles generating partition is constructed for the antisymplectic map  $\mathbf{C}$  given in (8.111) and (6.185), whose double iteration is the Arnold cat map - orbits of the cat map are then coded by sequences whose period is even. I do not see how this would result in our pretty shifts 3-letter alphabet (24.13).

**2018-03-26 Predrag** I have a hunch that the partition can be related to the Lagrangian (the generating function).

Area-preserving maps that describe kicked rotors subject to a discrete time sequence of angle-dependent impulses  $P(x_n)$  of form (12.100), (12.101) have a *generating function* (8.80)

$$F(q_n, q_{n+1}) = \frac{1}{2}(q_n - q_{n+1})^2 - V(q_n)^2, \quad P(q) = -\frac{dV(q)}{dq}. \quad (24.41)$$

This generating function is the discrete time Lagrangian for a particle moving in potential  $V(x)$ . Eq. (12.100) says that in one time step  $\Delta t$  the configuration trajectory starting at  $\phi_n$  reaches  $\phi_{n+1} = \phi_n + p_{n+1}\Delta t$ , and (??) says that at each kick the angular momentum  $p_n$  is accelerated to  $p_{n+1}$  by the force pulse  $P(x_n)\Delta t$ .

**2018-04-12 Predrag** My hunch is that to go from the time evolution (Hamiltonian), initial point formulation to the Lagrangian, end points formulation, we will have to do it not by groping blindly, but by the standard

Hamiltonian  $\rightarrow$  Lagrangian transformation. The Legendre transforms between Hamiltonian and Lagrangian generating functions of sect. 12.2 are of form (this formula might be wrong in detail!)

$$H(q_k, p_k) = p_k q_{k+1} - L(q_k, q_{k+1}), \quad (24.42)$$

where  $q_{k+1}$  is implicitly defined by  $p_k = \partial_{q_k} L(q_k, q_{k+1})$ .

## 24.4 Reduction to the fundamental domain

**2018-03-07 Predrag** While the original cell has edges of length 1, the quarter cells with edges of length 1/2 are already set up for a reduction to 1/4 fundamental domain, whose sides are the diagonal and the anti-diagonal. That might be the justification for halving the side-strips as you have done: the cutting line goes through the length 1/2 lattice.

**2018-03-11 Predrag** Figure 24.25 (b) is cute. To me it suggests a 3-node ( $A, B, C$ ) transition graph, with alphabet to be figured out.

- (a)  $\overline{1111} \rightarrow \overline{A}$  ? (on both space and time symmetry lines) and
  - (b)  $\overline{0202} \rightarrow \overline{C}$  (space, time flip symmetric) are now fixed points.
  - (c)  $\overline{0011}$  and (d)  $\overline{0011}$  (2 points on space symmetry line) are now one 2-cycle  $\rightarrow \overline{AB}$ ,
  - (e)  $\overline{1122}$  and (f)  $\overline{2211}$  (on space symmetry line) are now one 2-cycle  $\rightarrow \overline{A?B?}$ ,
  - (g)  $\overline{1012}$  and (h)  $\overline{1012}$  (time flip symmetric) are now one 2-cycle  $\rightarrow \overline{A?B?}$ ,
  - (i)  $\overline{0111}$ , and (j)  $\overline{0111}$  (time flip symmetric) are now one 2-cycle  $\rightarrow \overline{AC}$ .
- This 3-partitions alphabet is not the right alphabet - still need to work out the the corresponding 5-letter transition graph links alphabet.

**2018-03-15 Han** The fundamental domain figure 24.25 (b) symbolic dynamics

- (a)  $\overline{1111} \rightarrow \overline{AB}$  (on both space and time symmetry lines, see figure 24.28 (a)) and
- (b)  $\overline{0202} \rightarrow \overline{C}$  (space, time flip symmetric) are now fixed points.
- (c)  $\overline{0011}$  and (d)  $\overline{0011} \rightarrow \overline{AAAB}$ ,
- (e)  $\overline{1122}$  and (f)  $\overline{2211} \rightarrow \overline{ABBB}$ ,
- (g)  $\overline{1012}$  and (h)  $\overline{1012}$  (time flip symmetric)  $\rightarrow \overline{AABB}$ ,
- (i)  $\overline{0111}$ , and (j)  $\overline{0111}$  (time flip symmetric)  $\rightarrow \overline{AACC}$ .

**2018-03-22 Han** If we reduce the partition by the spatial inversion symmetry, the fundamental domain is shown in figure 24.26 (a). Note that the boundary  $\{0, 0\} \rightarrow \{\infty, -\infty\}$  goes to  $\{0, 0\} \rightarrow \{-\infty, \infty\}$  after inversion. So for the boundary I only keep the points on  $(\{0, 0\}, \{-\infty, \infty\})$  half-diagonal (the thick black line in figure 24.26 (a)). For example, consider the orbit of  $\overline{1111}$ . This orbit is shown in figure 24.28 (a). The inversion will move the point  $\frac{1}{3}\{1, -1\}$  to  $\frac{1}{3}\{-1, 1\}$ , so I only keep the  $\frac{1}{3}\{1, -1\}$  and discard  $\frac{1}{3}\{-1, 1\}$  which is on the dashed line. Then this orbit become a 2-cycle  $\overline{AB}$ .

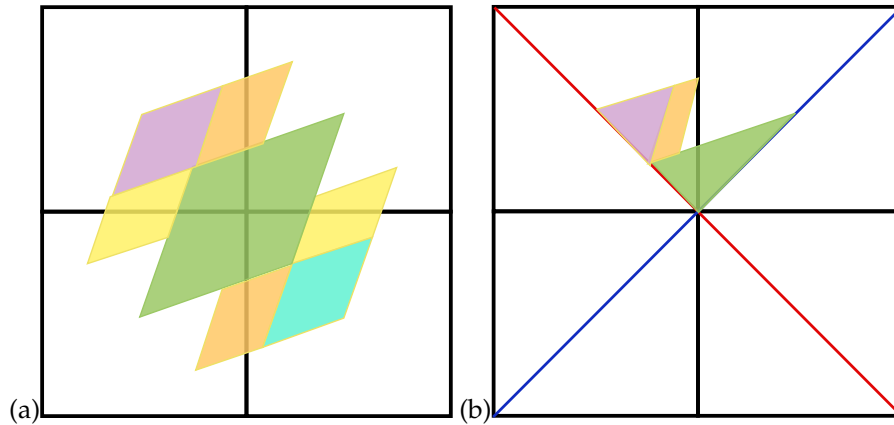


Figure 24.25: Figure 24.14 (b) continued. (a) Almost correct time reversal and space reflection symmetric partition - the correct one is figure 24.15 (b). (b) Three triangles/rectangles fundamental domain partition. Could it be cuter?

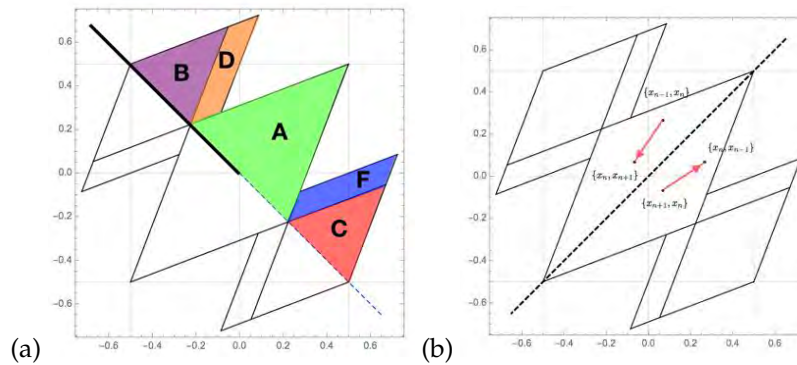


Figure 24.26: (a) The labeled space inversion fundamental domain partition. (b) The 1-step orbit after *time reversal*.

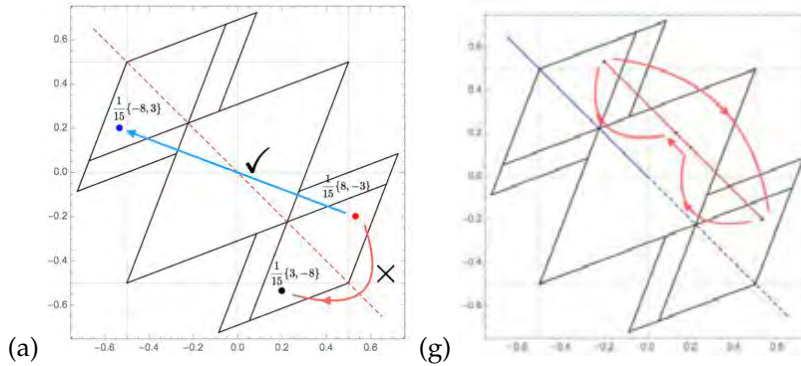


Figure 24.27: (a) The *space inversion* operation. Point  $(-8/15, 3/15)$  happens to be a periodic point of period 4, cycle  $\overline{1012} \rightarrow \overline{CAAB}$ , see (24.18) (g,h). Actually, any fractional coordinate belongs to a periodic orbit. The orange line is here just to confuse you; under inversion  $(3/15, -8/15)$  maps into  $(-3/15, 8/15)$  (not drawn). (g) The two corresponding 4-cycles reduced to a single 4-cycle in the space inversion fundamental domain,  $\overline{1012}$  and  $\overline{1012} \rightarrow \overline{CAAB}$ .

From figure 24.28 we can see that the rest of the cycles in figures 24.18 and 24.20 are:

- (a)  $\overline{1111} \rightarrow \overline{AB}$
- (b)  $\overline{0202} \rightarrow \overline{DF}$ ,
- (c)  $\overline{0011}$  and (d)  $\overline{0011} \rightarrow \overline{AAAB}$ ,
- (e)  $\overline{1122}$  and (f)  $\overline{2211} \rightarrow \overline{BBCA}$ ,
- (g)  $\overline{1012}$  and (h)  $\overline{1012} \rightarrow \overline{CAAB}$ ,
- (i)  $\overline{0111}$ , and (j)  $\overline{0111} \rightarrow \overline{AAFD}$ .

Now we have two 2-cycles but the rest of the 4-cycles are still 4-cycles. The two 2-cycles (blue points in figure 24.23) in the full domain are now fixed points.

**2018-03-22 Han** If we have an orbit  $\{\phi_{n-1}, \phi_n\} \rightarrow \{\phi_n, \phi_{n+1}\}$ , the time reversal will change this orbit to  $\{\phi_{n+1}, \phi_n\} \rightarrow \{\phi_n, \phi_{n-1}\}$ . Do a flip across the diagonal we will get the orbit after time reversal but the direction of the orbit also changed, as shown in figure 24.26 (b). I guess this is why the time reversal is more tricky...

**2020-01-10 Predrag** Stewart and Gökaydin [71] *Symmetries of quotient networks for doubly periodic patterns on the square lattice*, ([click here](#)).

## 24.5 Spatiotemporal cat partition

Consider a  $d$ -dimensional hypercubic lattice, infinite in extent, with each site labeled by  $d$  integers  $z \in \mathbb{Z}^d$ . The  $d$ -dimensional *spatiotemporal cat* is defined by

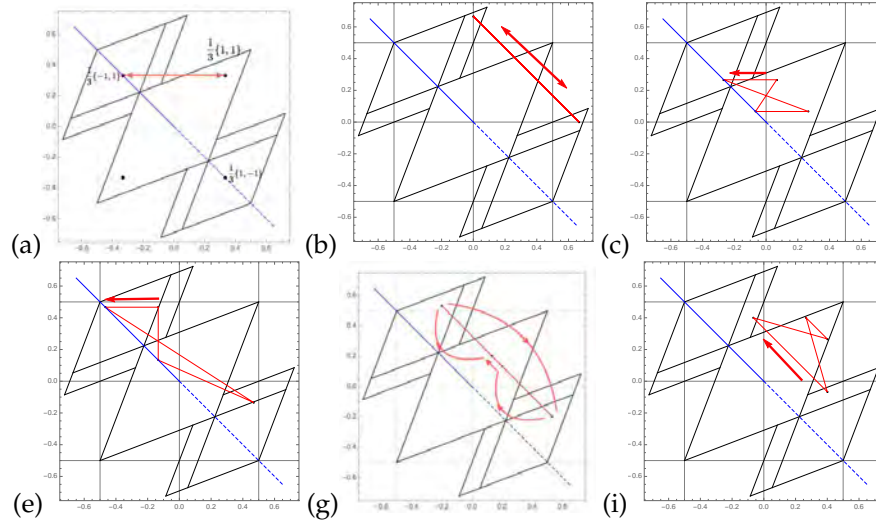


Figure 24.28: The orbits in the fundamental domain of 4-cycles (a)  $\overline{1111} \rightarrow \overline{AB}$  in the fundamental domain. (b)  $\overline{0202} \rightarrow \overline{DF}$ , (c)  $\overline{0011}$  and  $\overline{0011} \rightarrow \overline{AAAB}$ , (e)  $\overline{1122}$  and  $\overline{2211} \rightarrow \overline{BBCA}$ , (g)  $\overline{1012}$  and  $\overline{1012} \rightarrow \overline{CAAB}$ , (i)  $\overline{0111}$ , and  $\overline{0111} \rightarrow \overline{AAFD}$ . Compare with figures 24.18 and 24.20.

the discrete screened Poisson equation

$$(-\square + s - 2d)\phi_z = m_z, \quad m_z \in \mathcal{A}, \quad (24.43)$$

$$\mathcal{A} = \{-(s+1)/2, \dots, -1, 0, 1, 2, \dots, (s+1)/2\},$$

where  $\phi_z \in [-1/2, 1/2]^2$  (compare with (24.154)). It is a convention that we do not use, as that is not defined on the integer lattice). The map is smooth and fully hyperbolic for integer  $s > 2d$ .

For a discrete  $d$ -dimensional Euclidean spacetime the Laplacian is given by

$$\square \phi_n \equiv \phi_{n+1} - 2\phi_n + \phi_{n-1} \quad (24.44)$$

$$\square \phi_{n_1 n_2} \equiv (\square_1 + \square_2) \phi_{n_1 n_2} \quad (24.45)$$

$$\square_1 \phi_{n_1 n_2} = \phi_{n_1+1, n_2} - 2\phi_{n_1 n_2} + \phi_{n_1-1, n_2}$$

$$\square_2 \phi_{n_1 n_2} = \phi_{n_1, n_2+1} - 2\phi_{n_1 n_2} + \phi_{n_1, n_2-1}$$

in  $d = 1, 2, \dots$  dimensions.

What role do the spatiotemporal neighbors play? The local strength of “turbulence” at each site is parameterized by the stretching parameter  $s$ . The effect of neighbors is to “calm down” the local turbulence by distributing the stretching parameter  $s - 2$  along the  $d$  directions in (24.43), effectively decreasing it as  $s - 2 \rightarrow s/d - 2$ ,

$$\sum_{j=1}^d (-\square_j + s/d - 2)\phi_z = m_z. \quad (24.46)$$

An  $[L \times L]$  circulant matrix

$$C = \begin{bmatrix} c_0 & c_{L-1} & \cdots & c_2 & c_1 \\ c_1 & c_0 & c_{L-1} & & c_2 \\ \vdots & c_1 & c_0 & \ddots & \vdots \\ c_{L-2} & & \ddots & \ddots & c_{L-1} \\ c_{L-1} & c_{L-2} & \cdots & c_1 & c_0 \end{bmatrix}, \quad (24.47)$$

has eigenvectors (discrete Fourier modes) and eigenvalues  $Cv_k = \lambda_k v_k$

$$\begin{aligned} v_k &= \frac{1}{\sqrt{L}}(1, \epsilon^k, \epsilon^{2k}, \dots, \epsilon^{k(L-1)})^T, \quad k = 0, 1, \dots, L-1 \\ \lambda_k &= c_0 + c_{L-1}\epsilon^k + c_{L-2}\epsilon^{2k} + \dots + c_1\epsilon^{k(L-1)}, \end{aligned} \quad (24.48)$$

where

$$\epsilon = e^{2\pi i/L} \quad (24.49)$$

is a root of unity.

For the determinant of a circulant matrix, see [here](#). For the “definitive book on circulants,” see [Alun Wyn-jones](#). It is long - I have not checked whether it is good.

The unitary matrix  $U$  obtained by stacking eigenvectors (24.48) into a Vandermonde matrix is the discrete Fourier transform

$$U_{kj} = \frac{1}{\sqrt{L}}e^{2\pi i k j/L}, \quad (24.50)$$

which diagonalizes any circulant matrix  $C$ ,

$$U^\dagger C U = \text{diag}(\lambda).$$

The eigenvalues of the  $[L \times L]$  left-shift matrix

$$C = \begin{bmatrix} 0 & 1 & 0 & 0 & 0 \\ 0 & 0 & 1 & 0 & 0 \\ 0 & 0 & 0 & \ddots & 0 \\ 0 & 0 & 0 & 0 & 1 \\ 1 & 0 & 0 & 0 & 0 \end{bmatrix} \quad (24.51)$$

that shifts the orbit of an  $L$ -cycle to the left by one step and generates the cyclic group  $C_L$  are

$$(\lambda_k) = (e^{-i2\pi k/L}) = (1, e^{-i2\pi/L}, e^{-i3\pi/2}, \dots, e^{-i2\pi(L-1)/L}). \quad (24.52)$$

Thus, if the orbit is shifted to the left by one step, each component of its Fourier transform will be multiplied by the  $C_L$  cyclic group phase factor. That implies that for any cyclic-permutation invariant set, such as (14.10), the set of periodic

points  $\mathcal{M}_p$  that belong to a given  $p$ -cycle, one only needs to specify the magnitude of  $k$ th Fourier component, the rest is generated by cyclic transformations <sup>2</sup>

Take a cycle point block  $M = 1221$  and stack its cyclic permutations (the successive periodic points in its 4-cycle)  $M = 2211, \dots$ , into the circulant matrix (24.47),

$$[M]_{1221} = \begin{bmatrix} 1 & -2 & 2 & -1 \\ -2 & 2 & -1 & 1 \\ 2 & -1 & 1 & -2 \\ -1 & 1 & -2 & 2 \end{bmatrix}. \quad (24.53)$$

Its discrete Fourier transform is given by circulant matrix eigenvalues (24.48):

$$\hat{M}_{1221} = \frac{1}{2} \begin{bmatrix} 1 - 2 + 2 - 1 \\ 1 - 2\epsilon + 2\epsilon^2 - 1\epsilon^3 \\ 1 - 2\epsilon^2 + 2 - 1\epsilon^2 \\ 1 - 2\epsilon^3 + 2\epsilon^2 - 1\epsilon \end{bmatrix} = \frac{1}{2} \begin{bmatrix} 0 \\ -(1+i) \\ 6 \\ -(1-i) \end{bmatrix} = \begin{bmatrix} 0 \\ -\frac{1}{\sqrt{2}}\epsilon^{1/2} \\ 3 \\ -\frac{1}{\sqrt{2}}\epsilon^{-1/2} \end{bmatrix}.$$

It suffices to compute the Fourier transform of a single periodic point, as the rest, obtained by the  $C_L$  shifts, is generated by multiplication by phase factors (24.52).

For example, the Fourier transformed cycle points  $\hat{M}_{1221}$  and  $\hat{M}_{2211}$ ,

$$\hat{M}_{2211} = \frac{1}{2} \begin{bmatrix} -2 + 2 - 1 + 1 \\ -2 + 2\epsilon - 1\epsilon^2 + 1\epsilon^3 \\ -2 + 2\epsilon^2 - 1 + 1\epsilon^2 \\ -2 + 2\epsilon^3 - 1\epsilon^2 + 1\epsilon \end{bmatrix} = \frac{1}{2} \begin{bmatrix} 0 \\ -(1-i) \\ -6 \\ -(1+i) \end{bmatrix} = \begin{bmatrix} 0 \\ -\frac{1}{\sqrt{2}}\epsilon^{-1/2} \\ -3 \\ -\frac{1}{\sqrt{2}}\epsilon^{1/2} \end{bmatrix}.$$

which correspond to successive periodic points in a 4-cycle, have the correct Fourier transforms,

$$M_{1221} \Rightarrow \hat{M}_{1221} = \begin{bmatrix} 0 & -\frac{1}{\sqrt{2}}\epsilon^{1/2} & 3 & -\frac{1}{\sqrt{2}}\epsilon^{-1/2} \end{bmatrix} \\ CM_{1221} = M_{2211} \Rightarrow e^{-i2\pi k/4} \hat{M}_{1221,k} = \hat{M}_{2211} = \begin{bmatrix} 0 & -\frac{1}{\sqrt{2}}\epsilon^{-1/2} & -3 & -\frac{1}{\sqrt{2}}\epsilon^{1/2} \end{bmatrix}.$$

The eigenvalues of the damped Poisson matrix (24.46) in  $d = 1$  are

$$\lambda_k = s - \epsilon^k - \epsilon^{-k} = s - 2 \cos(2\pi k/L). \quad (24.54)$$

In  $d$  dimensions the discrete Fourier transform is no longer a 2-index matrix, but it acts tensorially,

$$U_{kz} = U_{k_1 k_2 \dots k_d, n_d \dots n_2 n_1} = \frac{1}{\sqrt{L_1 \dots L_d}} e^{2\pi i \sum_{j=1}^d k'_j n_j / L_j}. \quad (24.55)$$

<sup>2</sup>Predrag 2018-04-21: Not true - need to specify the relative phases between successive Fourier components, unless we can prove that each cycles has unique set of Fourier component magnitudes.



As the  $d$  translations commute,  $U$  diagonalizes the  $d$ -dimensional (damped) screened Poisson equation (24.46) yielding the Fourier-transformed field for each discrete  $d$ -dimensional Fourier component

$$\hat{\phi}_k = \frac{1}{2d - s + 2 \sum_{j=1}^d \cos(2\pi k_j / L_j)} \hat{m}_k, \quad (24.56)$$

where  $k = (k_1, k_2)$ ,  $\hat{\phi} = U\phi$ ,  $\hat{m} = Um$ , and  $U$  is the discrete Fourier transformation (24.55).

**2018-03-05 Predrag** Not sure you have ever worked through these formulas, so here they are as exercise 2.1 and exercise 2.2. Can you go through them, and fix both the formulation of the problems, and current sketches of the solutions?

**2018-03-08 Han** Wrote up solution 2.1 and solution 2.2. I have compared (2.119) with the Green's function of 4-cycles (24.9) for  $s = 3$ , but prefer to keep the actual calculations secret. Trust me: each cycle point matches.

Disposed of Predrag's wild guess (2.108) for the  $d = 2$  Green's function. Wrote up solution 2.3.

**2018-03-11 Predrag** In  $d = 2$  dimensions any solution  $\Phi$  uniquely recovered from its symbolic representation  $M$ ,

$$\phi_z = \sum_{z' \in \mathbb{Z}^2} g_{zz'} m_{z'}, \quad g_{zz'} = \left( \frac{1}{-\square + s - 4} \right)_{zz'}, \quad (24.57)$$

where  $g_{zz'} = g_{nt, n't'}$ ,  $z = (nt)$ ,  $z' = (n't') \in T_{[L_1 \times L_2]}^2$ , is the Green's function for the 2-dimensional (damped) screened Poisson equation. A periodic state  $M$  is admissible if and only if all  $\phi_z$  given by (24.57) fall into the generating partition.

Take  $\mathcal{R} = \mathcal{R}^{[L_1 \times L_2]}$  to be a rectangular region. Any  $L \times T$  block of interior symbols  $M = \{m_z \in \mathcal{A}_0 | z \in \mathbb{Z}_{LT}^2\}$ ,

$$\mathbb{Z}_{LT}^2 = \{z = (n, t) | n = 1, \dots, L, t = 1, \dots, T\},$$

is admissible and generates a invariant 2-torus solution. Its coordinate representation  $\Gamma = \{\phi_z, z \in \mathbb{Z}_{LT}^2\}$ , is obtained by taking inverse of (24.43):

$$\phi_z = \sum_{z' \in \mathbb{Z}_{LT}^2} g_{zz'}^0 m_{z'}, \quad m_{z'} \in \mathcal{A}_0, \quad (24.58)$$

where  $g_{zz'}^0$  is the corresponding Green's function with periodic boundary conditions. The block  $M = \{m_{nt} \in \mathcal{A}, (n, t) \in \mathbb{Z}^2\}$  can be used as a 2-dimensional symbolic representation of the lattice system state.

**2018-03-15 Han** I have found a solution of the Green's function in 2-dimensional lattice in Morita [61] *Useful procedure for computing the lattice Green's function - square, tetragonal, and bcc lattices*. Our Green's function should be:

$$g_{l't',lt} = \frac{1}{\pi^2} \int_0^\pi dy \int_0^\pi dz \frac{\cos[(l-l')y] \cos[(t-t')z]}{s - \cos y - \cos z}. \quad (24.59)$$

I threw this to Mathematica and it told me it's a hypergeometric function. Maybe it can be written in a easier form... I'm still trying.

**2018-03-15 Predrag** I had read Morita [61], and a number of similar papers, see sect. 8.5 Green's blog. We had used (24.59) in our paper [36], see (8.43). I would be very impressed if Mathematica fetched this bone you threw at it, and brought back anything intelligent. When you read this literature, be alert for what boundary conditions they use. We only need the periodic bc. Any other bc, such as Dirichlet, breaks translation invariance, and makes evaluation of Green's functions a very difficult problem.

I'm hoping we can simply verify a simple guess (the wrong guess (2.108) was not it), for any  $d$ , that would be so much simpler to write up.

**2018-03-16 Predrag** The bold and reckless proposal of **2018-03-05**, **2018-03-11 Predrag** continued: I believe we have the lattice Green's functions in  $d$  dimensions nailed.

- consider a  $d$ -dimensional discretized torus, with  $(n_1, n_2, \dots, n_d)$  points along each direction
- for each lattice site  $z$  pick admissible block  $\{m_z\}$  allowed by our generating partition for given  $s$
- Do the  $d$ -dimensional discrete Fourier transform of our (damped) screened Poisson equation. This yields the Fourier-transformed field for each discrete  $d$ -dimensional Fourier component, where  $\hat{\phi} = U\phi$ ,  $\hat{m} = Um$ , and  $U$  is the discrete Fourier transformation (a stack of Fourier eigenfunctions).
- Then get the field in the original configuration space by the inverse Fourier transform (relax - it is just a matrix multiplication)

$$\phi = U^\dagger \hat{\phi}. \quad (24.60)$$

I've been always asking myself what would a Fourier transform of a periodic orbit look like, and what it would mean. Well, now we can plot  $(\hat{\phi}_k, \hat{\phi}_{k+1})$  for each periodic orbit  $p$ , and ponder it.

(Han, continue at your leisure:)

**2018-03-05 Predrag** With period-5 I expect that you will find orbits that have only one or no symmetries.

**2018-03-18 Predrag** As illustrated in figure 24.16 (a), dynamics commutes with the spatial reflection  $\sigma$  (across anti-diagonal), while time reversal will require extra thinking. Why don't you first implement symmetry reduction for the spatial reflection  $\sigma$ , with the fundamental domain the partition being half above the anti-diagonal in figure 24.25 (a), and we postpone figure 24.25 (b) for later?

**2018-03-05, 2018-03-18 Predrag** I have flashed out in the above the bold and reckless proposal for symbolic dynamics in  $d$  dimensions. We probably do not need the  $d = 2$  Green's function in configurations space, as all periodic orbits can be computed directly in the momentum space, then Fourier transformed.

**2018-03-22 Han** I think the operation corresponding to the spatial reflection  $\{\phi_{n-1}, \phi_n\} \rightarrow \{-\phi_{n-1}, -\phi_n\}$  is not the reflection  $\sigma$  across the anti-diagonal but the rotation of  $\pi$  about the origin as shown in figure 24.27 (a).

**2018-03-22 Predrag** I might be wrong, but I would not go for a rotation interpretation - I think it is identical to the parity operation in case at hand.  $\phi_t \in T^1$  is the only phase space coordinate at lattice site  $t$ . Parity sends  $\phi_t \rightarrow -\phi_t, m_t \rightarrow -m_t$ . It is a symmetry of the equations of motion, see (24.8) for the time-forward 2D version, or (24.43) for the  $d = 1$  lattice formulation. To be able to rotate, you need to think of  $\phi_t \in (-\infty, \infty)$  as embedded in 2 or 3 dimensions. That is motivated by our 2D plots, but not necessary.

I replaced "rotation" by "inversion" in your notes - if I am wrong, we can easily revert the commented-out parts.

**2018-03-05 Predrag** In  $d = 2$  case compute the eigenvalues, eigenvectors for  $s = 5$  and the transition graph (I think you already have them). Then you can test it by generating a bunch of admissible  $[2 \times 2]$  or  $[3 \times 2]$  or  $[4 \times 2]$  blocks. The number of distinct ones can be reduced by reflection symmetries. It is not clear to me which ones are admissible, as yet, so you can generate all, solve by inverting corresponding the doubly-periodic 2-tori Toeplitz (tensor) matrix  $\rightarrow$  Green's function which gives you doubly-periodic periodic states. Then you can check which ones are within your Adler-Weiss partition.

**2018-03-29 Han** In  $d = 2$  dimensions the Green's function  $g_{zz'} = g_{\ell t, \ell' t'}, z = (\ell t), z' = (\ell' t') \in T_{(n_1, n_2)}^2$  is a  $[3 \times 3] \times [3 \times 3]$  tensor. Using the tensor Fourier transform (24.55), I calculated several periodic  $[3 \times 3]$  blocks, with  $z = (\ell t), z' = (\ell' t') \in T_{(3,3)}^2$ . For example, the symbol blocks and the corresponding 9 field values of two admissible 2-torus states are, in the

notation of (14.11),

$$M_1 = \begin{pmatrix} 1 & 0 & 0 \\ 0 & 1 & 0 \\ 0 & 0 & 1 \end{pmatrix} \Rightarrow \Phi_1 = \frac{1}{14} \begin{pmatrix} 6 & 4 & 4 \\ 4 & 6 & 4 \\ 4 & 4 & 6 \end{pmatrix} \quad (24.61)$$

$$M_2 = \begin{pmatrix} 1 & 0 & 0 \\ 0 & 1 & 2 \\ 0 & 0 & 1 \end{pmatrix} \Rightarrow \Phi_2 = \frac{1}{14} \begin{pmatrix} 8 & 6 & 7 \\ 7 & 9 & 12 \\ 6 & 6 & 9 \end{pmatrix} \quad (24.62)$$

In this calculation I used the Percival-Vivaldi partition of figure 2.2, with  $0 \leq x < 1$ , and  $s = 5$ .

As the blocks are doubly periodic, a single prime 2-torus  $p$  represents all vertical and horizontal cyclic permutations of the corresponding symbol block  $M_p$ . Furthermore, by lattice symmetries,  $M_p$  related by reflection and axes interchange symmetries are equivalent, (and -not sure of this- by the site symmetries, also internally space and time reversed) states are equivalent.

In  $d = 1$  dimension, the Percival-Vivaldi partition alphabet is an  $s = (s - 2) + 2$  letter alphabet (24.15). It has been shown in Gutkin *et al.* [36] that in  $d = 2$  dimensions the Percival-Vivaldi partition  $s + 3 = (s - 4) + 7$  letter alphabet  $\mathcal{A} = \mathcal{A}_0 \cup \mathcal{A}_1$  can be split into into the interior  $\mathcal{A}_0$  and exterior  $\mathcal{A}_1$  alphabets

$$\mathcal{A}_0 = \{0, \dots, s - 4\}, \quad \mathcal{A}_1 = \{\underline{3}, \underline{2}, \underline{1}\} \cup \{s - 3, s - 2, s - 1\}. \quad (24.63)$$

For example, for  $s = 5$  the interior, respectively exterior alphabets are

$$\mathcal{A}_0 = \{0, 1\}, \quad \mathcal{A}_1 = \{\underline{3}, \underline{2}, \underline{1}\} \cup \{2, 3, 4\}. \quad (24.64)$$

If all  $m_z$  belong to  $\mathcal{A}_0$  then  $M = \{m_z | z \in \mathbb{Z}^2\}$  is a full shift (14.6). In particular, the above  $M_1$  is admissible, while  $M_2$  could have been pruned (in this case the explicit calculation shows it is admissible).

**2018-03-29 Predrag** Make sure you understand the alphabet (24.183). My alphabet (24.43) might be wrong; for  $s$  large the number of letters does grow as  $s$ , but I do not quite see what corresponds to the  $\mathcal{A}_1$  letters. It has something to do with distributing  $s$  between  $d$  dimensions, as in (24.46).

**2018-03-29 Predrag** We'll have to think of how to visualize the states  $\Phi$ , something analogous to figure 24.18. There is no preferred time evolution direction, so it does not make sense to connect them by lines. But the states will align on lattices, as in figure 24.23.

**2018-03-29 Predrag** Keeping in mind where we want to go with this, might be better to use spatially-symmetric, unit-square face centered partition (24.43), rather than the unit-square corner (vertex?) partition of figure 2.2.

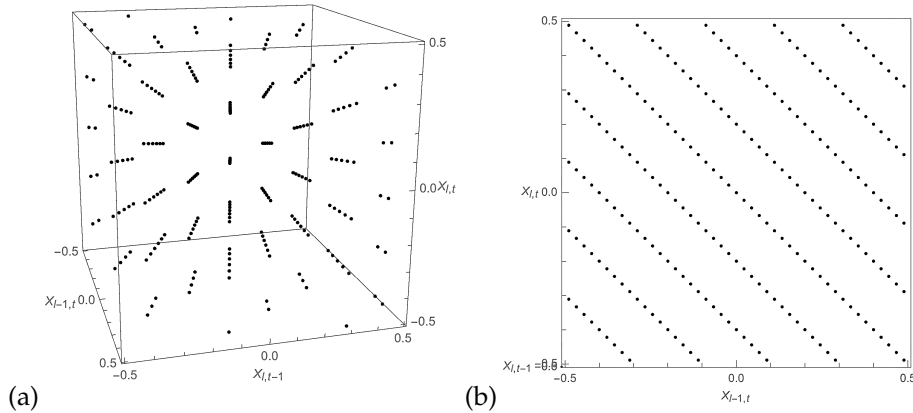


Figure 24.29: (a) All of the points in the periodic  $[2 \times 2]$  blocks. The coordinates of each points are  $\phi_{l-1,t}$ ,  $\phi_{l,t-1}$  and  $\phi_{l,t}$ . (b) The front view of (a). Clearly these points are arranged in lines.

**2018-03-30, 2023-03-10 Predrag** I have moved some of our space groups posts to sect. 7.1 Reduction to the reciprocal lattice.

**2018-04-05 Han** I have calculated all admissible  $[2 \times 2]$  periodic blocks in the unit-square face centered partition,  $-\frac{1}{2} \leq \phi_{n_1 n_2} < \frac{1}{2}$ , for  $s = 5$ . The alphabet is:

$$\mathcal{A} = \{-4, -3, -2, -1, 0, 1, 2, 3, 4\} \quad (24.65)$$

Using the coordinates  $\{\phi_{l-1,t}, \phi_{l,t-1}, \phi_{l,t}\}$  to represent a point in the block, I plot all periodic points of the admissible blocks in a 3-dimensional unit cube, as shown in figure 24.29.

**2018-04-05 Predrag** Were there any inadmissible blocks in the unit-square face centered partition? Or are you using the transition graph for  $s = 5$  to generate only admissible blocks?

**2018-04-05 Predrag** The visualization of figure 24.29 is quite interesting. All periodic points  $\phi_{n_1 n_2}$  have the same denominator?

**2018-04-05 Predrag** If you want to have a 2-dimensional visualisation for each block analogous to (24.61), color the symbol  $M_j [L_1 \times L_2]$  block with 9 discrete color alphabet  $\mathcal{A}$  from (24.65), and the corresponding state  $\Phi_j [L_1 \times L_2]$  block with colors chosen from a continuum color strip.

**2018-04-05 Predrag** As this is a linear problem, you can also represent closeness of two  $[L_1 \times L_2]$  blocks by using this coloring scheme for  $M_2 - M_1$  and  $\Phi_2 - \Phi_1$ . To find the closest “distance” between 2-tori, you will have to go through all cyclic permutations of the second one to align it optimally (or, if you understand ChaosBook course, you’ll have to ‘slice’).

For pairs of distinct 2-tori which share the same region of  $m_z$ 's, or a single 2-torus in which the same region of  $m_z$ 's appears twice, the states  $\phi_z$  in the center of the region should be exponentially close, in order to argue that they shadow each other.

This is illustrated in ref. [36], but there we do not use the linearity to actually subtract  $\Phi_2 - \Phi_1$ .

**2018-04-05 Predrag** Mark the lattice point  $z$  with the minimal value of  $|x_z^{(2)} - x_z^{(1)}|$  on above graphs, and in the text state the minimal value of  $|x_z^{(2)} - x_z^{(1)}|$ .

You can also state the mean Euclidean (or L2) distance between the two invariant 2-tori:

$$d_{\Phi_2 - \Phi_1} = \left( \frac{1}{LT} \sum_z (x_z^{(2)} - x_z^{(1)})^2 \right)^{1/2}, \quad (24.66)$$

or distance averaged over the lattice points restricted a region  $\mathcal{R}$ .

An aside: not sure that the Euclidean distance is the correct one. A better one might be the overlap, with the Green's function sandwiched something like

$$\frac{\Phi_2^\top \mathbf{g} \Phi_1}{\Phi_2^\top \Phi_1} \quad (24.67)$$

correctly normalized (as it stands, it is dimensionally wrong - is this "fidelity"?), and maximized by going through all cyclic permutations of  $\Phi_2$  (to align it optimally, or by 'slicing'). The overlap is maximal for  $\Phi_2 = \Phi_1$ , and falls off exponentially, depending on how much of the two invariant 2-tori differ.

The correct distance really should be the difference between two actions - that is symplectically invariant.

**2018-04-05 Han** This problem probably is not important. And I might be wrong. In the  $[2 \times 2]$  blocks if we use the unit-square corner partition, we have the symbol block and the corresponding 4 field values:

$$M = \begin{pmatrix} 1 & 1 \\ 1 & 1 \end{pmatrix} \Rightarrow \Phi = \begin{pmatrix} 1 & 1 \\ 1 & 1 \end{pmatrix} \quad (24.68)$$

which is not admissible, since for the unit-square corner partition the range of the field values is  $0 \leq \phi_{lt} < 1$ . But if all  $m_z$  belong to  $\mathcal{A}_0 = \{0, 1\}$  then  $M = \{m_z | z \in \mathbb{Z}^2\}$  should be a full shift (according to (24.183)).

**2018-04-05 Predrag** This, I think, is important (search for 'Manning' in this blog), and we have to understand it. I think you have to define *all* partition regions *including* the borders, in this example as  $0 \leq \phi_{lt} \leq 1$ , and then take care of over-counting the border points, such as (24.68) by quotienting the zeta function as in (??).

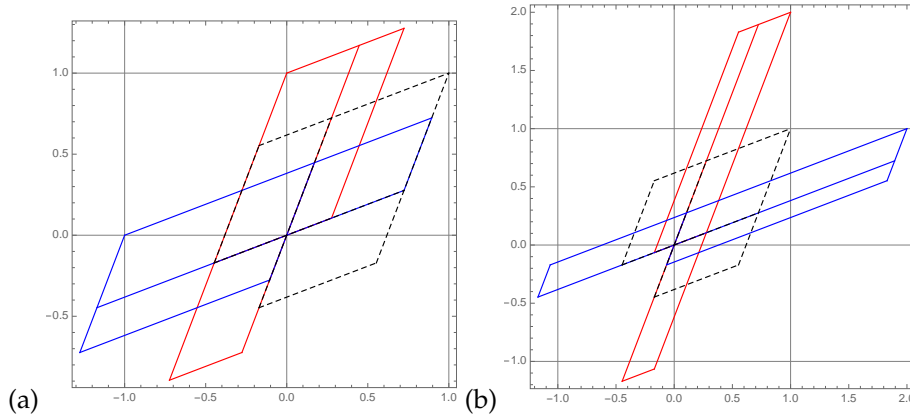


Figure 24.30: (a) The 3-rectangle rhomboid corner partition mapped half a step forward and half a step backward in time. (b) The partition mapped one step forward and one step backward in time. The black dashed lines are the 3-rectangle partition. The red lines are the partition mapped half a step or one step forward in time. The blue lines are the partition mapped half a step or one step backward in time.

## 24.6 Running blog

This section contains recent entries, before they are moved to the appropriate specific section above.

**2018-04-25 Predrag** Moved all our time-reversal invariant formulation musings into sect. [24.3 Time reversal](#).

**2018-05-10 Han** The Percival-Vivaldi cat map and the corresponding "square root" matrix are:

$$\mathbf{B} = \tilde{\mathbf{C}}^2 = \begin{bmatrix} 0 & 1 \\ -1 & 3 \end{bmatrix}, \quad \tilde{\mathbf{C}} = \mathbf{S}^{-1}\mathbf{C}\mathbf{S} = \begin{bmatrix} -1 & 1 \\ -1 & 2 \end{bmatrix}. \quad (24.69)$$

I plotted the 3-rectangle partition that mapped one step forward and one step backward using the matrix  $\tilde{\mathbf{C}}$  (which can be seen as half a step forward and backward with Percival-Vivaldi cat map). Figure [24.31](#) is the partition mapped half a step forward in time. And figure [24.32](#) is the partition for half a step backward in time. Figure [24.33](#) is the overlap of the two partitions.

**2018-05-10 Predrag** Is it interesting to see the explicit form of the unimodular transformation  $\mathbf{S}$  in [\(24.69\)](#)?

Figure [24.31](#), figure [24.32](#) and Figure [24.33](#) are presumably partitioned in too many subregions.

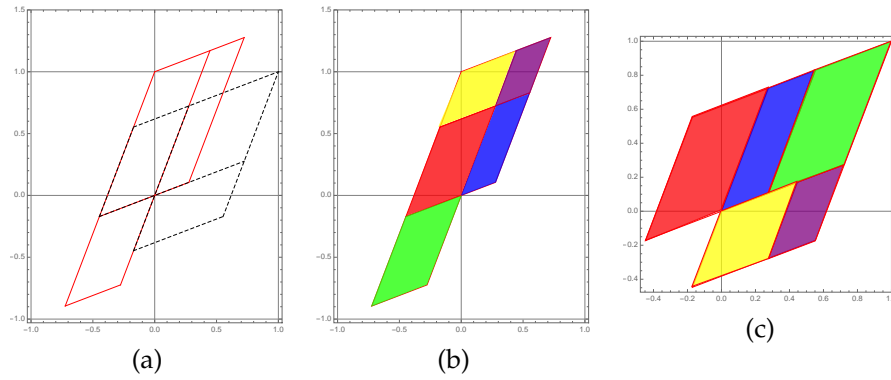


Figure 24.31: (a) and (b) are the partition that mapped half a step forward in time. (c) The mapped partition translated back to the original unit area.

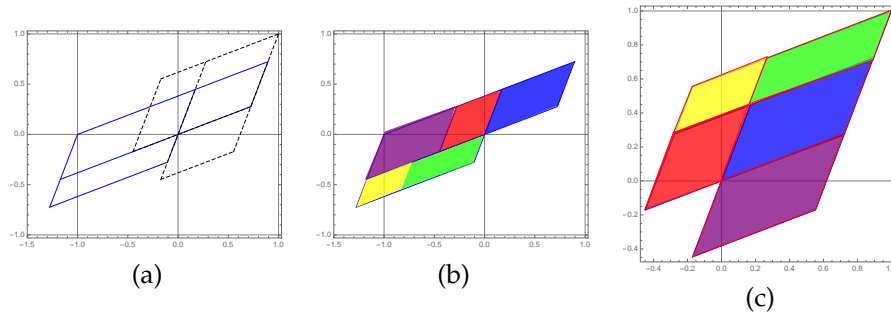


Figure 24.32: (a) and (b) are the partition that mapped half a step backward in time. (c) The mapped partition translated back to the original unit area.

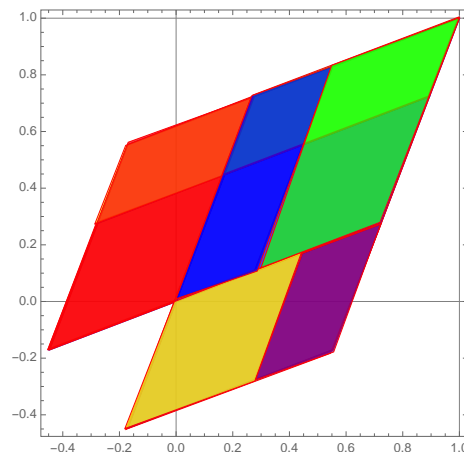


Figure 24.33: The overlap of figure 24.31 (c) and figure 24.32 (c).



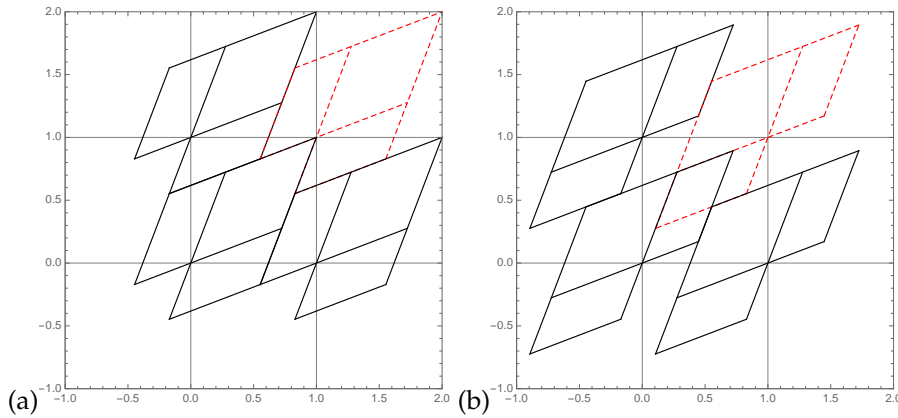


Figure 24.34: (a) The generating partition tiling the square lattice. (b) The flipped partition.

**2018-05-10 Han** From figure 24.33 we can see that the overlap of the figure that mapped half a step forward and backward is not symmetric about the diagonal  $x_1 = x_0$ . Actually in figure 24.30 we can see that the partition that mapped half a step forward and backward are symmetric about the antidiagonal  $x_1 = -x_0$  while the partition that mapped one step forward and backward in figure 24.30 (b) are symmetric about the diagonal  $x_1 = x_0$ . The reason is that the map  $\tilde{C}$  has a negative eigenvalue that flips the partition in the direction of stable manifold. If we use a partition that is symmetric about antidiagonal  $x_1 = -x_0$ , perhaps the overlap of the half a step forward and backward will be symmetric about antidiagonal  $x_1 = -x_0$ . But I'm not sure if this is what we want...

**2018-05-10 Predrag** You are starting from figure 24.32 (a) dotted lines partition (ie, figure 2.9 (a) that I had pulled out of a hat). But the literature suggests that for the golden cat map (8.111) Adler-Weiss partition might look something like Exercise 8.4 and Fig. 37. *Partition from the "behold" proof of the Pythagorean theorem.* That looks very space- and time-reflection symmetric, in contrast to figure 2.8 (b). Does it become something interesting for the Percival-Vivaldi golden cat map?

**2018-05-13 Han** Flipping the partition along the stable direction doesn't work. As shown in figure 24.34, the flipped partition cannot tile the square lattice.

**2018-05-22 Han** I plotted the Fourier transform of all the admissible period-5 of the rhomboid corner partition in the Brillouin zone in figure 24.35. For a 1-dimensional lattice with lattice spacing 1, the reciprocal lattice has spacing  $2\pi/1 = 2\pi$ , with the (first) Brillouin zone from  $k = -\pi$  to  $k = \pi$ . From figure 24.35 we can see that the Fourier transform in the Brillouin

zone is symmetric about the  $k = 0$ . And if we rotate this figure, we can see that some points lie on a straight line. Figure 24.35 (b) is all irreps overlaid. Due to the time reversal, all  $k = 2\pi/5$  irrep states are the same as the  $k = 4\pi/5$  irrep states.

I have put the Mathematica notebook in  
`siminos/figSrc/han/Mathematica/HLFourierTransform5Cycles.nb`  
 so one can rotate the figure.

**2021-01-27 Han** Figure 24.35 (c,d) is the  $C_5$  discrete Fourier transform of symbol blocks  $M$ . Note that on the reciprocal lattice symbol blocks  $\hat{M}$  lie on the straight lines.

**2018-06-11 Han** I have finished reading that introduction to group theory. I knew some basic concept of group theory before but never learned it systematically. It is interesting.

**2018-06-11 Han** This is one possible way to get the generating partition for a 2-dimensional lattice, but I'm not sure if this is useful.

I understand on each lattice site there is a two-torus. In our case the  $x$  and  $y$  coordinates are  $x_{\ell,t-1}$  and  $x_{\ell,t}$  separately (Is this right?). But I don't know how can we have the generating partition in this torus, since the evolution of the field value is affected by the neighboring sites.

**2018-06-21 Predrag** Your difficulty is that you keep on thinking in Hamiltonian way, where one steps in time, using the Hamilton's equations for  $(q_t, p_t)$ , where we had replaced the momentum  $p_t$  (at spatial position  $\ell$ ) by velocity  $p_t = (x_{\ell,t} - x_{\ell,t-1})/\Delta t$ , and thus initializing the Hamiltonian, a second-order difference equation for *evolution in time* by two horizontal rows  $(x_{\ell,t}, x_{\ell,t-1})$ ,  $\ell \in \mathbb{Z}$  in the spacetime plane.

You have to think in the spacetime, Lagrangian way instead. On each lattice site  $z = (\ell, t)$  there is a scalar field  $x_{\ell,t}$ , not a two-torus. The field  $x_{\ell,t-1}$  belongs to a neighboring site  $z = (\ell, t-1)$ . The two fields do not form a dynamical system on a two-torus, as the dynamics is also influenced by spatial neighbors  $x_{\ell\pm 1,t}$ .

**2018-06-11 Han** In order to integrate a 2nd order differential equation with only one variable, we need a 2-points initial condition. This the case in the time evolution 1-dimensional problem, where the equation (24.44) is a discrete "differential equation" in one-dimension. When we solve a 2-dimensional partial differential equation, we need the boundary condition. In the Dirichlet case, these are the field values on the boundary of the two-dimensional domain.

So if we use the similar way as one-dimension to treat the two-dimensional problem, we probably should start with not a single point, but the field values on all lattice sites at a certain time. In other words, the partition is defined by  $x_{t-1}$  and  $x_t$  in one-dimension, where in two-dimension it

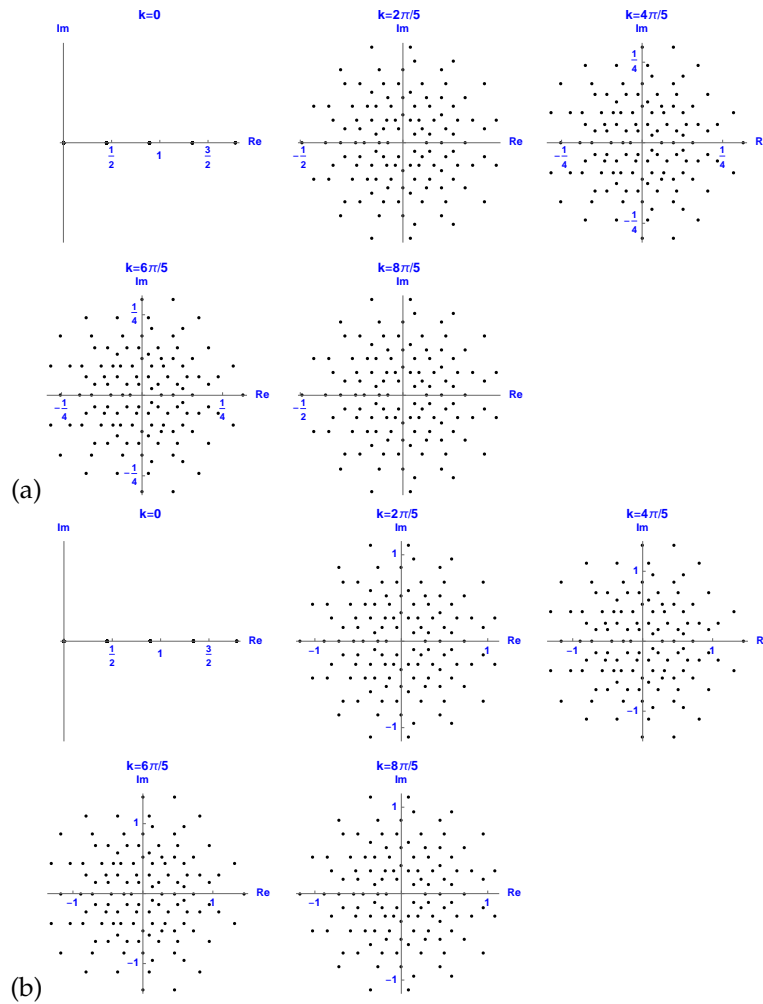


Figure 24.35: (a) The 121 period  $n = 5$  reciprocal periodic states  $\hat{\Phi}$  (see table 21.1) of the  $s = 3$  temporal cat, obtained by  $C_5$  discrete Fourier transform diagonalization, plotted in the Brillouin zone for the rhomboid corner partition. (b) The 121 period  $n = 5$  reciprocal lattice admissible symbol blocks  $\hat{M}$  of the  $s = 3$  temporal cat, obtained by  $C_5$  discrete Fourier transform diagonalization, plotted in the Brillouin zone for the rhomboid corner partition. (Continued in figure 24.51.)

is defined in a higher dimensional torus with coordinates  $x_{\ell,t-1}$  and  $x_{\ell,t}$ , and  $\ell$  is an integer from  $-\infty$  to  $\infty$ . When we have a periodic boundary in  $\ell$ , the number of coordinates will be reduced.

**2018-06-21 Predrag** You keep on thinking in Hamiltonian way. “The field values on all lattice sites at a certain time” is a horizontal line in the space-time plane. Yes, you need two successive lines to initiate Hamiltonian time evolution. Those equations are ugly (see this blog, for example (8.3), Gutkin and Osipov [37], and Gutkin *et al.* [36]) an we only know how to solve them for small “number of particles”  $L$ , not for  $\ell \in \mathbb{Z}$ .

**2018-06-21 Predrag** The problem you are solving is a Helmholtz equation. You do not do that by specifying initial conditions. With Dirichlet b.c.'s that is the equation for a drum, with a specified boundary, a hard problem to solve in general. However, with periodic b.c.'s, on a spatiotemporal 2-torus it is much easier, as it is an algebraic equation for the spatiotemporal discrete Fourier coefficients.

**2018-06-21 Predrag** Can we get “the generating partition” which is a 4-torus? Not obvious...

**2018-06-11 Han** If the spatial period is larger than 2, the dimension of the partition will be also larger.

**2018-06-21 Predrag** Can we get “the generating partition” which is a  $2L$ -torus? Not obvious, and it probably gets uglier and uglier...

**2018-06-11 Han** Using the method in Robinson's book, I think we will get the generating partition from these eigenvectors. But these are at least in 4-dimensions. It is not obvious what the partition looks like. And I think this is not Lagrangian... More important thing is, if we decide the period in space, can we still see the spatiotemporal symmetry?

**2018-06-21 Predrag** My experience from Kuramoto–Sivashinsky is that every small spatial length torus (really a cylinder, as the time is infinite) has its own grammar, and I expect the grammar for the  $t \in \mathbb{Z}$  be simpler than all these small spatial domains.

**2018-06-27 Predrag** Just that we are on the same page: In  $d$ -dimensional phase space, a partition is a  $d$ -dimensional volume, and its borders are co-dimension 1, i.e.,  $(d - 1)$ -dimensional. In case at hand, the partition borders are 3-dimensional hyper-planes, not 2-dimensional planes. By “the planes given by 3 of the eigenvectors” you mean a 3-dimensional hyper-plane, I assume.

**2018-06-26 Han** To find the planes given by 3 of the eigenvectors, we simply find the normal vector that is perpendicular to the 3 eigenvectors. The 4

normal vectors we have are:

$$\begin{aligned}L_{123} &= (-\Lambda_3, -\Lambda_3, 1, 1) \\L_{124} &= (1, 1, -\Lambda_3, -\Lambda_3) \\L_{134} &= (\Lambda_1, -\Lambda_1, -1, 1) \\L_{234} &= (-1, 1, \Lambda_1, -\Lambda_1)\end{aligned}\tag{24.70}$$

$L_{123}$  means this is the normal vector that is perpendicular to the eigenvectors  $e_1, e_2$  and  $e_3$ . Using these normal vectors we can easily get the expression of the planes. The 4 planes passing through the origin are:

$$\begin{aligned}-\Lambda_3x - \Lambda_3y + z + w &= 0 \\x + y - \Lambda_3z - \Lambda_3w &= 0 \\\Lambda_1x - \Lambda_1y - z + w &= 0 \\-x + y + \Lambda_1z - \Lambda_1w &= 0\end{aligned}\tag{24.71}$$

The first problem is: the last two planes in (24.71) pass through both the origin and the point  $(1, 1, 1, 1)$ .

**2018-06-27 Predrag** After you take mod 1? Otherwise the hyperplanes are distinct, right?

**2018-06-26 Han** So if we follow the same method we used in the one-dimensional case as I state above, the partition won't exist... But I guess my method is not correct anyway. To find the correct partition we will have to understand the structure of these vectors in this 4-dimensional space. And as you can see from (24.234-24.71), there are many symmetries. I expect the partition will still be very similar to the one-dimensional case of figure 24.3. I'm still working on this.

**2018-06-28 Han** The four hyperplanes in (24.71) are distinct. The last two hyperplanes pass through both the origin and the point  $(1,1,1,1)$ .

**2018-06-28 Han** I just realize that using the hyperplane passing through the origin and the point  $(1, 1, 1, 1)$ ,  $(1, 0, 0, 0)$ ,  $(0, 1, 0, 0)$ ,  $(0, 0, 1, 0)$  and  $(0, 0, 0, 1)$  won't give us the correct partition.

Now I'm thinking given 3 distinct planes in 3-dimensions, how to construct a region whose volume is 1 enclosed by planes that are parallel to these 3 planes. And the origin and the point  $(1, 1, 1)$  should be on the borders. And this region should "tile" the 3-dimensional space. Intuitively this region should be enclosed by the planes passing through the points with integer coordinates (like  $(1, 1, 0)$ ,  $(1, 0, 0)$ ). I have tried many ways to enclose the region but I can't get the correct volume. The most straightforward way should be cutting a unit cube with one of the planes and move the cut off part to the other end of the cube. But it is still hard to imagine. Currently I think there may be more subregions than just 1 large cube and 3 small cubes.

**2018-06-29 Han** I have solved the 3-dimensional tiling problem. It's not too complicated. The most important idea is: since the region will tile the whole 3-dimensional space, when we move the region along the direction of an axis by 1 unit of length, the borders of the new region must touch the borders of the old region. So if the planes passing through the origin and point  $(1, 1, 1)$  are the borders, the planes passing through the points  $(1, 0, 0)$ ,  $(0, 1, 0)$ ,  $(0, 0, 1)$ ,  $(1, 1, 0)$ ,  $(1, 0, 1)$ , and  $(0, 1, 1)$  must also be the borders (because these planes can be moved from the planes passing through the origin and  $(1, 1, 1)$  by 1 unit length).

Now I'm able to find the tiling region given 3 distinct planes and get the correct result. Hopefully this will help me to get the correct partition in 4-dimensions.

**2018-07-09 Han** I will start with the result: I already have the partition (which I think is a generating partition) of the two-dimensional problem with spatial length of two, and use this partition to calculate the solutions of all admissible  $2 \times 2$  blocks. From the solutions I find that the alphabet is reduced, but not in a perfect way. The left site and right site have different alphabet.

The partition is defined in a four-dimensional space  $\{x_{1,t-1}, x_{2,t-1}, x_{1,t}, x_{2,t}\}$ . It has the time reversal symmetry, i.e., if you swap  $x_{1,t-1}, x_{2,t-1}$  with  $x_{1,t}, x_{2,t}$ , the partition is unchanged. Because of the periodic spatial boundary, it should also have the space reflection symmetry (the partition should be invariant when we swap  $x_{1,t-1}, x_{1,t}$  with  $x_{2,t-1}, x_{2,t}$ ). But I can't find such a symmetric generating partition. So the result is if we have a solution  $\{x_{1,t-1}, x_{2,t-1}, x_{1,t}, x_{2,t}\}$ ,  $\{x_{2,t-1}, x_{1,t-1}, x_{2,t}, x_{1,t}\}$  is not necessarily an admissible solution. Another result is the alphabet of the left site (corresponding to  $x_{1,t}$ ) has different alphabet from the right site (corresponding to  $x_{2,t}$ ).

Remember that when we use the "square cube" partition for two-dimensional problem, the letters of the alphabet are from -4 to 4 if the field values are  $-\frac{1}{2} \leq x \leq \frac{1}{2}$ . And if the field values are  $0 \leq x \leq 1$ , the alphabet is from -3 to 4. Using my new partition to calculate all admissible  $2 \times 2$  blocks, the alphabet for the left site is from -1 to 5, and the alphabet for the right site is from -4 to 1. There is only one solution with left site  $m = -1$ . So I think if we use a longer block, the complete alphabet of the right site should be from -5 to 1 (because they should have same number of letters). Anyway, I think this shows that this new partition is very likely to be a generating partition.

**2018-07-13 Predrag** That's scary: "The left site and right site have different alphabet." But already had the unwelcome asymmetry in the forward / backward in time generating partition, that we could never resolve, so that might be a disease of the concept of generating partitions.

Mention that  $s = 5$ ?

**2018-07-09 Han** The next part is the tedious detailed method that find the partition in four-dimensions. In fact I should call it the method of finding the tiling region in four-dimensions enclosed by boundaries with given directions passing through the points with integer coordinates. Like I said one week ago, the boundaries must consist of hyperplanes that passing through all of the neighboring points, not just  $(1, 1, 1, 1)$ ,  $(1, 0, 0, 0)$ ,  $(0, 1, 0, 0)$ ,  $(0, 0, 1, 0)$  and  $(0, 0, 0, 1)$ , but also  $(0, 1, 1, 1)$ ,  $(1, 0, 1, 1)$ ,  $(1, 1, 0, 1)$ ,  $(1, 1, 1, 0)$ ,  $(1, 1, 0, 0)$ ,  $(1, 0, 1, 0)$ ,  $(1, 0, 0, 1)$ ,  $(0, 1, 1, 0)$ ,  $(0, 1, 0, 1)$  and  $(0, 0, 1, 1)$ . So the structure is actually very complex. I figured out a easy way to get the correct partition.

We know that these points listed above are fixed points if included in our partition. So we want some of these points to be on the boundary or on the cross section of several different boundaries, but not necessarily on the vertex of our partition. But to make the partition simpler and similar to the figure 24.2, I choose the point  $(1, 1, 1, 1)$  to be a vertex of our partition, which is a cross point of four hyperplanes. The expression of these four hyperplanes are:

$$\begin{aligned}
 -\Lambda_3x - \Lambda_3y + z + w &= 2 - 2\Lambda_3 \\
 x + y - \Lambda_3z - \Lambda_3w &= 2 - 2\Lambda_3 \\
 \Lambda_1x - \Lambda_1y - z + w &= 0 \\
 -x + y + \Lambda_1z - \Lambda_1w &= 0
 \end{aligned} \tag{24.72}$$

So these four hyperplanes will be the boundaries of our partition. The next step is to write down all of the hyperplanes passing through all of the neighboring points listed above. For each of these points, there will be four hyperplanes that are similar to the (24.71–24.72) but have different constants at the right hand side. Then we find four hyperplanes that are parallel to the four hyperplanes in (24.72) respectively that we can enclose the largest possible volume with these eight hyperplanes. For example, if we look at all of the hyperplanes that are parallel to the third hyperplane in (24.72), we find that the possible constants on the right hand side are  $\Lambda_1$ ,  $-\Lambda_1$ ,  $1$ ,  $-1$ ,  $0$ ,  $\Lambda_1 - 1$ ,  $\Lambda_1 + 1$ ,  $1 - \Lambda_1$  and  $-1 - \Lambda_1$ . So to enclose the largest possible volume we will pick the hyperplane with right hand side of  $\Lambda_1 + 1$  or  $-1 - \Lambda_1$ . We have two options, and I think this is why the rules for the left site and right site are different. I chose  $\Lambda_1 + 1$  when I get the partition. If I use  $-1 - \Lambda_1$  I think the rule of the left site and the right site will be swapped.

Now we have a very large and simple region in four-dimensions. And we know that the point  $(1, 1, 1, 1)$  will be on a vertex of our partition. And the four hyperplanes passing through it will be the boundaries, but only the parts that are close to the vertex is guaranteed. The next step is to move this large region by one unit length along the coordinate axes. Our original region has a vertex on  $(1, 1, 1, 1)$ . And now we have 15 new regions that have vertices on  $(1, 0, 0, 0)$ ,  $(0, 1, 0, 0)$ ,  $(0, 0, 1, 0)$ ,  $(0, 0, 0, 1)$ ,

$(0, 1, 1, 1), (1, 0, 1, 1), (1, 1, 0, 1), (1, 1, 1, 0), (1, 1, 0, 0), (1, 0, 1, 0), (1, 0, 0, 1), (0, 1, 1, 0), (0, 1, 0, 1), (0, 0, 1, 1)$  and  $(0, 0, 0, 0)$ . Our partition should be a region that has one unit volume, and tiles the whole space. So if we move the partition to these positions they should have no overlaps. But using this large region we will have overlaps for sure. So we just need to find the overlaps between these 15 new regions and our original region, and cut off these overlapped region from the original region. Then what we get is the correct partition. It has no overlap with the neighboring region, and I have calculate that the volume of this partition is one.

**2018-07-10 Han** I have the hyperplanes passing through the origin and the point  $(1, 1, 1, 1)$  in (24.71–24.72). Other hyperplanes are:

Hyperplanes passing through  $(1, 0, 0, 0)$ :

$$\begin{aligned} -\Lambda_3x - \Lambda_3y + z + w &= -\Lambda_3 \\ x + y - \Lambda_3z - \Lambda_3w &= 1 \\ \Lambda_1x - \Lambda_1y - z + w &= \Lambda_1 \\ -x + y + \Lambda_1z - \Lambda_1w &= -1 \end{aligned} \tag{24.73}$$

Hyperplanes passing through  $(0, 1, 0, 0)$ :

$$\begin{aligned} -\Lambda_3x - \Lambda_3y + z + w &= -\Lambda_3 \\ x + y - \Lambda_3z - \Lambda_3w &= 1 \\ \Lambda_1x - \Lambda_1y - z + w &= -\Lambda_1 \\ -x + y + \Lambda_1z - \Lambda_1w &= 1 \end{aligned} \tag{24.74}$$

Hyperplanes passing through  $(0, 0, 1, 0)$ :

$$\begin{aligned} -\Lambda_3x - \Lambda_3y + z + w &= 1 \\ x + y - \Lambda_3z - \Lambda_3w &= -\Lambda_3 \\ \Lambda_1x - \Lambda_1y - z + w &= -1 \\ -x + y + \Lambda_1z - \Lambda_1w &= \Lambda_1 \end{aligned} \tag{24.75}$$

Hyperplanes passing through  $(0, 0, 0, 1)$ :

$$\begin{aligned} -\Lambda_3x - \Lambda_3y + z + w &= 1 \\ x + y - \Lambda_3z - \Lambda_3w &= -\Lambda_3 \\ \Lambda_1x - \Lambda_1y - z + w &= 1 \\ -x + y + \Lambda_1z - \Lambda_1w &= -\Lambda_1 \end{aligned} \tag{24.76}$$

Hyperplanes passing through  $(0, 1, 1, 1)$ :

$$\begin{aligned} -\Lambda_3x - \Lambda_3y + z + w &= 2 - \Lambda_3 \\ x + y - \Lambda_3z - \Lambda_3w &= 1 - 2\Lambda_3 \\ \Lambda_1x - \Lambda_1y - z + w &= -\Lambda_1 \\ -x + y + \Lambda_1z - \Lambda_1w &= 1 \end{aligned} \tag{24.77}$$



Hyperplanes passing through  $(1, 0, 1, 1)$ :

$$\begin{aligned}
 -\Lambda_3x - \Lambda_3y + z + w &= 2 - \Lambda_3 \\
 x + y - \Lambda_3z - \Lambda_3w &= 1 - 2\Lambda_3 \\
 \Lambda_1x - \Lambda_1y - z + w &= \Lambda_1 \\
 -x + y + \Lambda_1z - \Lambda_1w &= -1
 \end{aligned} \tag{24.78}$$

Hyperplanes passing through  $(1, 1, 0, 1)$ :

$$\begin{aligned}
 -\Lambda_3x - \Lambda_3y + z + w &= 1 - 2\Lambda_3 \\
 x + y - \Lambda_3z - \Lambda_3w &= 2 - \Lambda_3 \\
 \Lambda_1x - \Lambda_1y - z + w &= 1 \\
 -x + y + \Lambda_1z - \Lambda_1w &= -\Lambda_1
 \end{aligned} \tag{24.79}$$

Hyperplanes passing through  $(1, 1, 1, 0)$ :

$$\begin{aligned}
 -\Lambda_3x - \Lambda_3y + z + w &= 1 - 2\Lambda_3 \\
 x + y - \Lambda_3z - \Lambda_3w &= 2 - \Lambda_3 \\
 \Lambda_1x - \Lambda_1y - z + w &= -1 \\
 -x + y + \Lambda_1z - \Lambda_1w &= \Lambda_1
 \end{aligned} \tag{24.80}$$

Hyperplanes passing through  $(1, 1, 0, 0)$ :

$$\begin{aligned}
 -\Lambda_3x - \Lambda_3y + z + w &= -2\Lambda_3 \\
 x + y - \Lambda_3z - \Lambda_3w &= 2 \\
 \Lambda_1x - \Lambda_1y - z + w &= 0 \\
 -x + y + \Lambda_1z - \Lambda_1w &= 0
 \end{aligned} \tag{24.81}$$

Hyperplanes passing through  $(1, 0, 1, 0)$ :

$$\begin{aligned}
 -\Lambda_3x - \Lambda_3y + z + w &= 1 - \Lambda_3 \\
 x + y - \Lambda_3z - \Lambda_3w &= 1 - \Lambda_3 \\
 \Lambda_1x - \Lambda_1y - z + w &= \Lambda_1 - 1 \\
 -x + y + \Lambda_1z - \Lambda_1w &= \Lambda_1 - 1
 \end{aligned} \tag{24.82}$$

Hyperplanes passing through  $(1, 0, 0, 1)$ :

$$\begin{aligned}
 -\Lambda_3x - \Lambda_3y + z + w &= 1 - \Lambda_3 \\
 x + y - \Lambda_3z - \Lambda_3w &= 1 - \Lambda_3 \\
 \Lambda_1x - \Lambda_1y - z + w &= \Lambda_1 + 1 \\
 -x + y + \Lambda_1z - \Lambda_1w &= -\Lambda_1 - 1
 \end{aligned} \tag{24.83}$$

Hyperplanes passing through  $(0, 1, 1, 0)$ :

$$\begin{aligned}
 -\Lambda_3 x - \Lambda_3 y + z + w &= 1 - \Lambda_3 \\
 x + y - \Lambda_3 z - \Lambda_3 w &= 1 - \Lambda_3 \\
 \Lambda_1 x - \Lambda_1 y - z + w &= -\Lambda_1 - 1 \\
 -x + y + \Lambda_1 z - \Lambda_1 w &= \Lambda_1 + 1
 \end{aligned} \tag{24.84}$$

Hyperplanes passing through  $(0, 1, 0, 1)$ :

$$\begin{aligned}
 -\Lambda_3 x - \Lambda_3 y + z + w &= 1 - \Lambda_3 \\
 x + y - \Lambda_3 z - \Lambda_3 w &= 1 - \Lambda_3 \\
 \Lambda_1 x - \Lambda_1 y - z + w &= 1 - \Lambda_1 \\
 -x + y + \Lambda_1 z - \Lambda_1 w &= 1 - \Lambda_1
 \end{aligned} \tag{24.85}$$

Hyperplanes passing through  $(0, 0, 1, 1)$ :

$$\begin{aligned}
 -\Lambda_3 x - \Lambda_3 y + z + w &= 2 \\
 x + y - \Lambda_3 z - \Lambda_3 w &= -2\Lambda_3 \\
 \Lambda_1 x - \Lambda_1 y - z + w &= 0 \\
 -x + y + \Lambda_1 z - \Lambda_1 w &= 0
 \end{aligned} \tag{24.86}$$

So all of these hyperplanes are perpendicular to one of the four vectors in (24.70). When I get the large original region, I use the boundaries:

$$\begin{aligned}
 \Lambda_1 x - \Lambda_1 y - z + w &= 0 \\
 -x + y + \Lambda_1 z - \Lambda_1 w &= 0 \\
 \Lambda_1 x - \Lambda_1 y - z + w &= \Lambda_1 + 1 \\
 -x + y + \Lambda_1 z - \Lambda_1 w &= \Lambda_1 + 1
 \end{aligned} \tag{24.87}$$

These are four of the eight boundaries that enclose the large region. These four hyperplanes are perpendicular to the last two vectors in (24.70). And you can see why we have different rules for the left site and right site. If I use :

$$\begin{aligned}
 \Lambda_1 x - \Lambda_1 y - z + w &= \frac{\Lambda_1 + 1}{2} \\
 -x + y + \Lambda_1 z - \Lambda_1 w &= \frac{\Lambda_1 + 1}{2} \\
 \Lambda_1 x - \Lambda_1 y - z + w &= \frac{\Lambda_1 + 1}{2} \\
 -x + y + \Lambda_1 z - \Lambda_1 w &= \frac{\Lambda_1 + 1}{2},
 \end{aligned} \tag{24.88}$$

instead of (24.87) I will have a partition that is invariant under the swap of  $x_{1,t-1}, x_{1,t}$  and  $x_{2,t-1}, x_{2,t}$  (in the equation of the planes it is a swap of

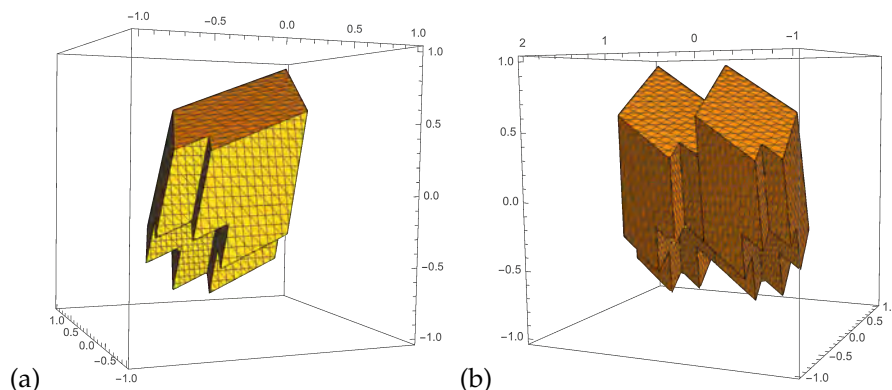


Figure 24.36: (a) A tiling region in three-dimensions. (b) The tiling region and one nearest neighboring region. You can see the boundaries exactly matched.

$x, z$  and  $y, w$ ). Then we will have the same rule for both the left site and right site. But unfortunately these hyperplanes don't pass through the fixed points (points with integer coordinates). From the experience of the one-dimensional problem I don't think this will give us the generating partition.

**2018-07-10 Han** This part is not important. The problem of finding a tiling region in three-dimensions is very instructive when we find the generating partition in four-dimensions. Assuming we are given 3 independent planes in three-dimensions. We want to find a region that can be used to tile the whole space by moving integer number of unit length along the coordinate axes. This region has unit volume. And we want to use the planes passing through the points with integer coordinates to enclose this region. Figure 24.36 is the tiling region that I get. It's not unique. From this figure you can imagine the structure of the four-dimensional partition. I have a Mathematica notebook in [siminos/figSrc/han/Mathematica/HL3-dimensional\\_tiling.nb](#) so you can rotate the figure.

**2018-07-13 Predrag** If you are very lucky, 1-step in space direction might suffice to understand all steps in space, just like for time evolution one step in time gave partition for times. However, you are not using the symplectic structure of the Hamiltonian formulation you are exploring. The Hamiltonian phase space for this problem are the four 4-vectors, something like

$$(\vec{x}_{1,t}, \vec{p}_{1,t}, \vec{x}_{2,t}, \vec{p}_{2,t}),$$

where the symplectic 2- and 4-volumes

$$\vec{x}_{1,t}^\top \omega \vec{p}_{1,t} + \vec{x}_{2,t}^\top \omega \vec{p}_{2,t},$$

and  $\det(\vec{x}_{1,t}, \vec{p}_{1,t}, \vec{x}_{2,t}, \vec{p}_{2,t}) = 4$ -volume. where you can chose  $\vec{x}_{1,t}^\top \cdot \vec{x}_{2,t} = 0$ .

**2018-08-02 Han** I have been trying to get a general formula of the number of periodic orbits. In fact given (24.237–24.239) we can write down the general formula explicitly:

$$N_{[L \times T]} = \prod_{i=1}^L \left[ \sum_{n=0}^{T/2} \sum_{m=0}^n \sum_{q=0}^{T-2m} \binom{T}{2n} \binom{n}{m} \binom{T-2m}{q} (-1)^{m+q} 2^{-T+2m+q+1} s^{T-2m-q} \cos^q\left(\frac{2\pi i}{L}\right) - 2 \right] \quad (24.89)$$

when  $T$  is an even number (if  $T$  is odd we only need to change the  $T/2$  to  $(T+1)/2$ ). But I cannot find a easier form where  $T$  and  $L$  are interchangeable. I'm trying to simplify (24.89) and thinking that using the [multiple-angle formulas](#) and some identities of the combinations we can cancel the cosine terms. Because generally they are irrational numbers but the results of (24.89) are always integers.

I was hoping that each term of the product in (24.89) is an integer but this is not true. One example is when  $L = 5$  and  $T = 1$ , one of the eigenvalues of the evolution matrix is  $\Lambda(L)_1 = 1/2(s - 2 \cos(2\pi/5) + \sqrt{(s - 2 \cos(2\pi/5))^2 - 4})$ . The corresponding term in the product is:

$$(\Lambda_1 + \Lambda_1^{-1} - 2) = s - 2 - 2 \cos\left(\frac{2\pi}{5}\right) = \frac{1}{2}(7 - \sqrt{5}) \quad (24.90)$$

which is not an integer. The term corresponding to the eigenvalue containing  $\cos(4\pi/5)$  is equal to  $\frac{1}{2}(7 + \sqrt{5})$ . Multiplying these two terms together gives us an integer. This means that each term in the product is not necessarily an integer and I will need to evaluate the product explicitly to cancel the trigonometric functions.

I also tried to evaluate (24.237) for several different  $L$  and  $T$ s, hoping to find the expression directly. But I didn't find any valid expression. I guess the general formula cannot be trivial. I observed something but they are not helpful... Rana already stated this in her report, see (??). When the spatial length is 1, the number of periodic orbits can be expressed with Fibonacci numbers. And when  $L = 2$  or  $L = 3$ , we can also express the number of periodic orbits by Fibonacci numbers but in very different forms.

**2018-08-03 Han** I think I remember everything in the online meeting, but not necessarily understand everything. Here is my best attempt at a summary:

- (1) Understand the eigenvalues of Toeplitz tensors. When we calculated the Green's function of the 2-dimensional spatiotemporal cat

we used the tensor Fourier transform (24.55) to diagonalize the circulant tensor (2.125). And the diagonal elements are the eigenvalues of the circulant tensor?

- (2) Go from the Hamiltonian formulation (24.232) to the Lagrangian formulation (8.4), as in sect. 12.2. Use symplectic transformations.
- (3) Use the symmetries of the system, see sect. ???. We have time reversal symmetry and space inversion symmetry, and more.
- (4) By Noether's theorem, sect. 11.4, for each symmetry there should exist a conserved quantity, such as energy, the discrete momentum, discrete rotations; it's a research active subject, here is a recent [conference](#). For field theory one expects infinitely many conserved quantities. Crazy idea, but very satisfying if true: could the conserved quantities be the numbers of periodic orbits?
- (5) I'm not sure about this last thing. By similarity transformation we can interchange change the  $L$  and  $T$ ?

**2018-08-03 Han** I just realized that I can also use the "determinant" of the circulant tensor to get the number of the periodic orbits directly... I believe you already know this and this is why you told me to look at the Toeplitz tensors... <sup>3</sup>

For the  $d = 1$  case, the number of the periodic orbits is the determinant of the circulant matrix (2.114). When the dimension is larger than 1, we have a circulant tensor instead of the circulant matrix. And the determinant can be given by the product of all the eigenvalues. (I guess I need to think more before we can call it determinant...) When we calculate the Green's function, we use the tensorial Fourier transform to diagonalize the tensor. For a tensor  $\mathcal{D}_{tt,l'l'}$  the diagonal elements are  $\mathcal{D}_{tt,tt}$ . Then the determinant is given by:

$$\det(\mathcal{D}) = \prod_{t=1}^T \prod_{l=1}^L \mathcal{D}'_{tt,tt} \quad (24.91)$$

where the  $\mathcal{D}'$  is the diagonalized  $\mathcal{D}$ . I have tried a few blocks and this gives me correct number of periodic orbits. Everything is clear now. I will get the general form as soon as possible.

---

<sup>3</sup>Predrag 2018-08-010: Is the "determinant" of the circulant tensor defined anywhere in the literature?

2018-08-06 Han The number of periodic points of the discrete 2-torus is: <sup>4</sup>

$$N_{[L \times T]} = \prod_{t=1}^T \prod_{l=1}^L \left( s - 2 \cos\left(\frac{2\pi l}{L}\right) - 2 \cos\left(\frac{2\pi t}{T}\right) \right) \quad (24.92)$$

In all  $d = 2$  examples we take  $s = 5$ . <sup>5</sup>

2018-08-06 Han I have calculated the topological entropy using (24.237). The topological entropy of spatially periodic discrete domain of period  $L$  is

$$h(L) = \lim_{T \rightarrow \infty} \frac{1}{T} \ln N_{LT} \quad (24.93)$$

Using (24.237) we have:

$$\begin{aligned} h(L) &= \lim_{T \rightarrow \infty} \frac{1}{T} \ln \prod_{i=1}^L (\Lambda_i^T + \Lambda_i^{-T} - 2) \\ &= \sum_{i=1}^L \ln \Lambda_i = \sum_{i=1}^L \ln \frac{\lambda_i + \sqrt{\lambda_i^2 - 4}}{2} \end{aligned} \quad (24.94)$$

where  $\lambda_i$  is given by (24.238).

Using (24.92) we can get the same result. Substituting (24.92) into (24.93) we have:

$$\begin{aligned} h(L) &= \lim_{T \rightarrow \infty} \frac{1}{T} \ln \prod_{t=1}^T \prod_{l=1}^L [5 - 2 \cos\left(\frac{2\pi l}{L}\right) - 2 \cos\left(\frac{2\pi t}{T}\right)] \\ &= \sum_{l=1}^L \lim_{T \rightarrow \infty} \frac{1}{T} \sum_{t=1}^T \ln [5 - 2 \cos\left(\frac{2\pi l}{L}\right) - 2 \cos\left(\frac{2\pi t}{T}\right)] \end{aligned} \quad (24.95)$$

When  $T$  goes to infinity, we can change the sum over  $t$  to an integral. Let  $a_l = 5 - 2 \cos(2\pi l/L)$ . Then (24.96) becomes:

$$\begin{aligned} h(L) &= \sum_{l=1}^L \int_0^1 \ln [5 - 2 \cos\left(\frac{2\pi l}{L}\right) - 2 \cos(2\pi t)] dt \\ &= \sum_{l=1}^L \int_0^1 \ln [a_l - 2 \cos(2\pi t)] dt \\ &= \sum_{l=1}^L \ln \frac{a_l + \sqrt{a_l^2 - 4}}{2}, \end{aligned} \quad (24.96)$$

<sup>4</sup>Predrag 2018-08-25: My conceptual problem is totally elementary, and I probably have seen the answer and forgotten it: how does this product of various cos's yield integers? It has to, as we started with integers and then went through Fourier transforms to get this diagonalized formula. Wonder whether there is a more direct way of seeing it... Also, why is everything cos's, whereas we know that for sufficiently large  $s$  everything is cosh's? For  $d = 1$  the eigenvalues, eigenvectors [60] are cos's for  $-2 < s < 2$ , but cosh's for  $s > 2$ , see (2.49). Note also that there is one trivial eigenvalue (rotational invariance?) and  $T - 1$  non-trivial ones.

<sup>5</sup>Predrag 2018-08-25: Notation  $N_{[L \times T]}$  is experimental.

which is same as (24.94).

**2018-08-06 Han** The rate of growth of the number of periodic orbits per unit spatial length is  $h(L)/L$ . As  $L$  goes to infinity, we have

$$\begin{aligned}
 h &= \lim_{L \rightarrow \infty} \frac{h(L)}{L} = \lim_{\substack{L \rightarrow \infty \\ T \rightarrow \infty}} \frac{1}{L} \frac{1}{T} \ln N_{[L \times T]} \\
 &= \lim_{L \rightarrow \infty} \frac{1}{L} \sum_{l=1}^L \lim_{T \rightarrow \infty} \frac{1}{T} \sum_{t=1}^T \ln \left( 5 - 2 \cos\left(\frac{2\pi l}{L}\right) - 2 \cos\left(\frac{2\pi t}{T}\right) \right) \\
 &= \int_0^1 \int_0^1 \ln[5 - 2 \cos(2\pi x) - 2 \cos(2\pi t)] dt dx \\
 &= \int_0^1 \ln \frac{[5 - 2 \cos(2\pi x)] + \sqrt{[5 - 2 \cos(2\pi x)]^2 - 4}}{2} dx \quad (24.97)
 \end{aligned}$$

Evaluating this numerically we get that the topological entropy density per unit length and unit time is  $h \approx 1.508$ .

**2018-08-010 Predrag** The number of periodic orbits (24.92) seems to be the product of Harshaw (8.53) eigenvalues for a doubly-periodic torus, just have to get the  $s$  dependence right. <sup>6</sup> The eigenvalues of the damped Poisson matrix (24.46) in  $d = 1$  are given by (24.54) or (24.238)

$$\lambda(L)_k = s - 2 \cos(2\pi k/L) . \quad (24.98)$$

**2018-08-010 Predrag** I'm optimistic about the drift of our argument. We are almost home. We should be able to relegate the Hamiltonian derivation to a tedious exercise in ChaosBook. Laplacian, or more precisely, the Green's function counts all paths. The trace of Green's function (i) counts all periodic points  $N_{[L \times T]}$ , and (ii) is given by the sum of eigenvalues (24.92). As explained in ChaosBook, the trace is a derivative of the determinant (topological zeta function), and thus we should be able to write down the spatiotemporal cat topological zeta function.

*The deterministic trace formula and zeta function follow from the Green's function evaluated on all doubly periodic invariant 2-tori.*

**2018-08-15 Han** By Green's function I guess you don't mean the inverse of the matrix at the left hand side of the (damped) screened Poisson equation (8.4) (We used to call it Green's function)? Because the trace of this matrix doesn't give us the number of the periodic orbits.

The trace of the Green's function is:

$$\text{Tr}(\Delta) = \sum_{T=1}^{\infty} \sum_{L=1}^{\infty} z^{L+T} \prod_{t=1}^T \prod_{l=1}^L \left( s - 2 \cos\left(\frac{2\pi l}{L}\right) - 2 \cos\left(\frac{2\pi t}{T}\right) \right) \quad (24.99)$$

---

<sup>6</sup>Predrag 2018-12-01: Do not remember where I got these Harshaw eigenvalues?

I'm not sure about the  $z^{L+T}$  (maybe it should be  $z^{LT}$ ?). The topological zeta function can be gotten from:

$$\text{Tr}(\Delta) = -z \frac{d}{dz} \ln \frac{1}{\zeta(z)} \quad (24.100)$$

So now the problems are how to evaluate the sum of the number of periodic orbits, and what is the correct form of  $z^{L+T}$ .

**2018-08-15 Han** From the definition of the topological zeta function:

$$1/\zeta_{\text{AM}}(z) = \exp\left(-\sum_{n=1}^{\infty} \frac{z^n}{n} N_n\right) \quad (24.101)$$

we can get the topological zeta function by substituting the number of periodic points to (24.101). But now we have number of points in the doubly periodic invariant 2-tori  $N_{[L \times T]}$  instead of 1-dimensional loops  $N_n$ . So I'm not sure what is the correct form of the topological zeta function of our problem.

**2018-08-23 Han** I haven't figured out how to evaluate the sum of the number of the periodic blocks. Assume the topological zeta function of the 2-torus is:

$$\zeta(z_1, z_2) = \exp\left(\sum_{T=1}^{\infty} \sum_{L=1}^{\infty} \frac{z_1^L z_2^T}{LT} N_{[L \times T]}\right) \quad (24.102)$$

We will need to evaluate the sum:

$$\sum_{T=1}^{\infty} \sum_{L=1}^{\infty} \frac{z_1^L z_2^T}{LT} N_{[L \times T]} = \sum_{L=1}^{\infty} \frac{z_1^L}{L} \sum_{T=1}^{\infty} \frac{z_2^T}{T} N_{[L \times T]} \quad (24.103)$$

The second sum can be evaluated using (24.237). (we don't like this formula because this expression is not compact and it's not symmetric about  $L$  and  $T$ , but it has the time period  $T$  in the exponent which makes it easier to calculate the sum) Expanding (24.237) each term is a constant times a combination of eigenvalues to the power of  $T$ , and the sum over all time period  $T$  will give us a logarithm of a product of eigenvalues, similar to (24.240). Then we evaluate the sum over  $L$ , which is a sum of logarithms. I haven't figured out how to evaluate this.

**2018-08-23 Han** I spent some time trying to understand the meaning of this experimental topological zeta function of 2-torus (24.102). If we write the local trace of a periodic block as  $t_p$ , then we have:

$$\begin{aligned} z_1^L z_2^T N_{[L \times T]} &= \sum_{\substack{L_p|L \\ T_p|T}} L_p T_p t_p^{\left(\frac{L}{L_p} \frac{T}{T_p}\right)} \\ &= \sum_p L_p T_p \sum_{r_1=1}^{\infty} \sum_{r_2=1}^{\infty} \delta_{L, L_p r_1} \delta_{T, T_p r_2} t_p^{r_1 r_2} \end{aligned} \quad (24.104)$$



Substitute (24.104) into (24.102):

$$\begin{aligned}
 1/\zeta_{\text{AM}}(z_1, z_2) &= \exp\left(-\sum_{T=1}^{\infty} \sum_{L=1}^{\infty} \frac{z_1^L z_2^T}{LT} N_{[L \times T]}\right) \\
 &= \exp\left(-\sum_p \sum_{\substack{r_1 \\ r_2}} \frac{t_p^{r_1 r_2}}{r_1 r_2}\right) \\
 &= \exp\left(\sum_p \sum_{r_1} \frac{1}{r_1} \sum_{r_2} -\frac{1}{r_2} (t_p^{r_1})^{r_2}\right) \\
 &= \exp\left(\sum_p \sum_{r_1} \frac{1}{r_1} \ln(1 - t_p^{r_1})\right) \quad (24.105)
 \end{aligned}$$

This sum over  $r_1$  is convergent for small  $t_p$  but I can't get a simpler formula. Let:

$$f(t_p) = \exp\left(\sum_{r_1} \frac{1}{r_1} \ln(1 - t_p^{r_1})\right) \quad (24.106)$$

Then the topological zeta function becomes:

$$1/\zeta_{\text{AM}}(z_1, z_2) = \prod_p f(t_p) \quad (24.107)$$

This is not a product of  $(1 - t_p)$  as I was hoping. But it is still a product of all the prime periodic blocks.

I also found Ban, Hu, Lin, and Lin [8], *Zeta functions for two-dimensional shifts of finite type*, see post **2016-05-04 Predrag** above. I'm not sure if that is applicable to our problem.

**2018-08-23 Han** Here I will explain why (24.92) gives us the number of periodic blocks.

Consider first a 1-dimensional discrete time lattice of period  $T$ . The admissible periodic orbits are the solutions of the (damped) screened Poisson equation

$$\mathcal{D}\phi = m, \quad (24.108)$$

where  $\phi$  is a vector in  $T$ -dimensional space, and  $\mathcal{D}$  is the circulant matrix given by (2.38). If we set each element of  $\phi$  to be larger or equal to 0 and smaller than 1 (the shape of the partition does not affect the number of solutions), all admissible  $\phi$  are in a  $T$ -dimensional hypercube of unit volume. The block  $m$  is also a  $T$ -dimensional vector but with integer coordinates. The matrix  $\mathcal{D}$  acting on a unit hypercube stretches it into a hyper-parallelepiped in  $T$ -dimensional space. Within each unit

volume of the stretched region there is a unique point with integer coordinates, corresponding to one periodic solution. Hence the volume of the stretched region, which is equal to the absolute value of the determinant of the matrix  $\mathcal{D}$ , is the number of periodic solutions of the given time period  $T$ .

For 2 or more spacetime dimensions the (damped) screened Poisson equation is always of the form (24.108). As the rank of tensors  $\phi$  and  $m$  is  $d$ , one can always relabel the  $d$  indices as one vector index. For a 2-dimensional lattice,  $\phi$  and  $m$  are 2-index tensors which can be relabelled as  $LT$ -dimensional vectors, and  $\mathcal{D}$  is a (tensor) matrix with its two pairs of indices ranging over  $(LT, LT)$ . The initial vector  $x$  is in a unit volume  $LT$ -dimensional hypercube, which is stretched by the (tensor) matrix  $\mathcal{D}$  into a hyper-parallelepiped whose volume is given by the determinant (24.91) of the (tensor) matrix  $\mathcal{D}$ .

The  $[L \times T \times L \times T]$  tensor  $\mathcal{D}$  can be viewed as a  $(LT, LT)$  matrix, with the same number of elements. This rank 4 tensor, written as matrix, is in general not a circulant matrix. But the eigenvalues are same as the eigenvalues of the tensor; it is a block matrix which has a similar pattern as a circulant matrix. The determinant of this matrix is given by (24.91), and it indeed gives us the volume of the stretched region, i.e., the number of invariant 2-tori.

The determinant of  $\mathcal{D}$  (24.92) is the product of all the eigenvalues calculated by the discrete Fourier transform diagonalization of  $\mathcal{D}$ .

**2018-08-30 Han** The above attempt at a definition of the topological zeta function of the two-torus (24.102) is wrong because I only count the periodic blocks that tile the space (and time) by moving in the direction of space or time. A more appropriate definition of the topological zeta function of two-dimensional torus is given in Lind [49] *A Zeta function for  $\mathbb{Z}^d$ -actions* (Predrag found the paper [here](#). If needed, his book [50] is in the CNS library.).

Lind [49] defines the topological zeta function as <sup>7</sup>

$$\zeta_\alpha(s) = \exp\left(\sum_{J \in \mathcal{J}_d} \frac{p_J(\alpha)}{[J]} s^{[J]}\right) \quad (24.109)$$

where  $\alpha : X \rightarrow X$  is a  $\mathbb{Z}^d$ -action.  $\mathcal{J}_d$  is the collection of finite-index subgroups in  $\mathbb{Z}^d$ . For  $J \in \mathcal{J}_d$  put  $[J] = |\mathbb{Z}^d/J|$ , and

$$p_J(\alpha) = |\{x \in X : \alpha^n x = x \text{ for all } \mathbf{n} \in J\}|. \quad (24.110)$$

For 2-dimensional lattice, a convenient general form of  $\mathcal{J}_2$  is:

$$\mathcal{J}_2 = \left\{ \begin{bmatrix} a & b \\ 0 & c \end{bmatrix} \in \mathbb{Z}^2 : a \geq 1, c \geq 1, 0 \leq b \leq a - 1 \right\} \quad (24.111)$$

<sup>7</sup>Han 2018-08-31: In Lind's article the subgroup of  $\mathbb{Z}^d$  is written as  $L$ . To avoid confusion with our spatial length  $L$ , I change it to  $J$  in this blog.

which gives us a complete collection of the tiling patterns, with each pattern only listed once. Each  $J$  is corresponding to one given tiling pattern, and

$$\mathbb{Z}^2/J = \begin{bmatrix} a & b \\ 0 & c \end{bmatrix}. \quad (24.112)$$

**2018-10-09 Predrag** Lind and Schmidt [48] *Symbolic and algebraic dynamical systems*, ([click here](#)) studies zeta functions for  $\mathbb{Z}^d$  actions.

**2018-08-31 Han** For each  $J$ , the corresponding periodic solutions satisfy:

$$x\left(\begin{bmatrix} l \\ t \end{bmatrix}\right) = x\left(\begin{bmatrix} l \\ t \end{bmatrix} + \begin{bmatrix} a & b \\ 0 & c \end{bmatrix} \begin{bmatrix} i \\ j \end{bmatrix}\right), \begin{bmatrix} i \\ j \end{bmatrix} \in \mathbb{Z}^2 \quad (24.113)$$

When  $b = 0$ , we are tiling the area by moving the block (the smallest repeating unit) along the time direction and along the space direction. The number of points in these solutions is given by (24.92).

To find the solution satisfies the relation (24.113), we need to modify the boundary of the tensor (2.38). I haven't figured out how to imagine the modified tensor. A easier way is to expand the tensor into a  $LT \times LT$  matrix then modify it. Using the inverse of this matrix (the Green's function) we can solve for the periodic block that satisfies (24.113). And the determinant of the modified matrix is the number of periodic points.

I already found the general formula counting the number of periodic points, though I don't know why this works. Define:

$$B = \mathbb{Z}^2/J = \begin{bmatrix} a & b \\ 0 & c \end{bmatrix} \quad (24.114)$$

which is uniquely corresponding to a tiling pattern. Then the number of periodic points is:

$$N_J = \prod_{t=1}^T \prod_{l=1}^L \left( s - 2 \cos\left(\frac{2\pi l'}{\det(B)}\right) - 2 \cos\left(\frac{2\pi t'}{\det(B)}\right) \right) \quad (24.115)$$

where  $l'$  and  $t'$  are given by:

$$\begin{bmatrix} t' \\ l' \end{bmatrix} = B \begin{bmatrix} t \\ l \end{bmatrix} = \begin{bmatrix} a & b \\ 0 & c \end{bmatrix} \begin{bmatrix} t \\ l \end{bmatrix} \quad (24.116)$$

The  $L$  and  $T$  in (24.115) are the spatial and the time periods, and from (24.113) we know that  $L = a$  and  $T = c$ .  $N_J$  is the determinant of the modified matrix, and each terms in (24.115) is an eigenvalue of the modified matrix.

I haven't understood why (24.115) works. And I'm sure (24.115) is not a good way to write the formula, because in (24.113)  $l$  is first component in

the column vector but in (24.115) it becomes the second component. We can't generalize this formula to three-dimensions. Perhaps a better way is to let:

$$\begin{bmatrix} l'' \\ t'' \end{bmatrix} = C \begin{bmatrix} l \\ t \end{bmatrix} = \frac{1}{ac} \begin{bmatrix} c & 0 \\ -b & a \end{bmatrix} \begin{bmatrix} l \\ t \end{bmatrix}, \quad (24.117)$$

where  $C$  is the cofactor matrix of  $B$ . The number of periodic points is:

$$N_J = \prod_{t=1}^T \prod_{l=1}^L (s - 2 \cos(2\pi l'') - 2 \cos(2\pi t'')) \quad (24.118)$$

(24.115) and (24.118) give the same result. The eigenvalues are also the same.

I don't understand these formulas. But good thing is these formulas are modified from (24.92) using the matrix  $B = \mathbb{Z}^2/J$ , so given a translation pattern we can count the number of periodic points directly.

**2018-02-16 Predrag** We need a simple explanation for why the 2-dimensional  $A^n$  and the linearization of the  $2n$ -dimensional matrix give the same multipliers, so I am re-reading Mackay and Meiss [53], *Linear stability of periodic orbits in Lagrangian systems* and incrementally editing the discussion of sect. 12.1.

**2018-09-25 Predrag** The 2018-09-27 math seminar by Igor Pak, UCLA, might be related to our invariant 2-tori counting: " Given a convex polytope  $P$ , what is the number of integer points in  $P$ ? This problem is of great interest in combinatorics and discrete geometry, with many important applications ranging from integer programming to statistics. From computational point of view it is hopeless in any dimensions, as the knapsack problem is a special case. Perhaps surprisingly, in bounded dimension the problem becomes tractable. How far can one go? Can one count points in projections of  $P$ , finite intersections of such projections, etc? We will survey both classical and recent results on the problem, emphasizing both algorithmic and complexity aspects. Some elegant hardness results will make an appearance in dimension as small as three. If time permits, we will discuss connections to Presburger Arithmetic and decidability problems for irrational polyhedra. Joint work with Danny Nguyen. "

We went, were dazzled and understood very little of it all.

**2018-10-02 Han** I tried to use (12.103) as the Lagrangian. It will give a result (12.107) different from (12.110). But I think this is not correct. The first reason is: using (12.99) we can eliminate all of the  $p$ 's, and get an equation of  $q_{n+1}$ ,  $q_n$ , and  $q_{n-1}$ . The equation we get is (12.110).

The second reason is: we should be able to use the Lagrangian to get the momentum by (8.69). But using Lagrangian (12.103) we can't get the

correct momentum. Using (12.108) we can get the correct momentum for both  $p_{n+1}$  and  $p_n$ .

I haven't read through Percival and Vivaldi [62]. But in their definition of Lagrangian they used  $X_t$  instead of  $x_t$ . It seems like this capital  $X$  is not constrained by modulo 1? I might be wrong. I'm still reading this article.

**2018-10-19 Han Note:** this entry is superseded by the derivation 2019-03-20 Han below, starting with eq. (24.157).

I have found a way to prove that (24.118) gives the determinant of the orbit Jacobian matrix for the two-dimensional lattice, for both the periodic boundary and relative periodic (twisted) boundary.

The orbit Jacobian matrix can always be written as:

$$\mathcal{J} = \sum_{j=1}^d (-s\mathbf{1} + r_j + r_j^\top). \quad (24.119)$$

But for blocks with different size or different boundary, the shift matrices  $r_j$  satisfy different conditions. For example, consider the periodic blocks satisfying (24.113). The shift matrices satisfy:

$$\begin{aligned} r_l^a r_t^0 &= \mathbf{1} \\ r_l^b r_t^c &= \mathbf{1}. \end{aligned} \quad (24.120)$$

If  $b = 0$ , this is a regular periodic block. From (24.120) we can see that:

$$\begin{aligned} r_l^a &= \mathbf{1} \\ r_l^{ab} r_t^{ac} = r_t^{ac} &= \mathbf{1}. \end{aligned} \quad (24.121)$$

So the eigenvectors of  $r_l$  and  $r_t$  are also the eigenvectors of the shift matrices in a  $a \times ac$  regular periodic block (The size of the eigenvector of the shift matrix with relative periodic (twisted) boundary is  $a \times c$ , but we can repeat this eigenvector to fill a  $a \times ac$  block). The eigenvector of this large block can be written as:

$$\mathbf{e}_{lt} = e^{2\pi i(\frac{ll'}{a} + \frac{tt'}{ac})}, \quad (24.122)$$

where  $l' = 1, 2, \dots, a$  and  $t' = 1, 2, \dots, ac$ . Here the subscripts  $l$  and  $t$  are the indices of the elements. For this large block, the number of eigenvectors is  $a \times ac$ . But only  $ac$  of these eigenvectors satisfy (24.120):

$$\begin{aligned} r_l^b r_t^c \mathbf{e} &= \mathbf{e} \\ \implies e^{2\pi i[\frac{(l+b)l'}{a} + \frac{(t+c)t'}{ac}]} &= e^{2\pi i(\frac{ll'}{a} + \frac{tt'}{ac})}. \end{aligned} \quad (24.123)$$

So to make the eigenvectors satisfy (24.120), we must have:

$$\begin{aligned} \frac{(l+b)l'}{a} + \frac{(t+c)t'}{ac} &= \frac{ll'}{a} + \frac{tt'}{ac} + n \\ t' &= -bl' + na, \quad n \in \mathbb{Z} \end{aligned} \quad (24.124)$$

Let  $l' = 1, 2, \dots, a$ , and let  $n = 1, 2, \dots, c$ , we will get  $ac$  sets of  $l'$  and  $t'$ s. Write the elements of the eigenvectors as:

$$\begin{aligned} \mathbf{e}_{lt} &= e^{2\pi i[\frac{lc'l'}{ac} + \frac{t(-bl'+na)}{ac}]} \\ &= e^{2\pi i[l'l^* + tt^*]} \end{aligned} \quad (24.125)$$

where:

$$\begin{bmatrix} l^* \\ t^* \end{bmatrix} = \frac{1}{ac} \begin{bmatrix} c & 0 \\ -b & a \end{bmatrix} \begin{bmatrix} l' \\ n \end{bmatrix} = C \begin{bmatrix} l' \\ n \end{bmatrix}, \quad (24.126)$$

The matrix  $C$  is the cofactor matrix of the matrix in (24.113) divided by the determinant of this matrix (which is also the transpose of the inverse matrix). So for a given set of  $l'$  and  $n$ , we have a specific eigenvector that has:

$$\begin{aligned} (\sigma_l + r_l^\top) \mathbf{e}_{l',n} &= 2 \cos(2\pi l^*) \mathbf{e}_{l',n} \\ (r_t + r_t^\top) \mathbf{e}_{l',n} &= 2 \cos(2\pi t^*) \mathbf{e}_{l',n}. \end{aligned} \quad (24.127)$$

The subscripts  $l'$  and  $n$  mean that this is the eigenvector that given by a certain set of  $l'$  and  $n$  (So  $\mathbf{e}_{l',n}$  here is a vector, not the  $l'$ th and  $n$ th component.).  $l^*$  and  $t^*$  are determined by  $l'$  and  $n$  using (24.126).

So the eigenvalues of the orbit Jacobian matrix are:

$$\sum_{j=1}^2 (-s\mathbf{1} + r_j + r_j^\top) \mathbf{e}_{l',n} = [-2s + 2 \cos(2\pi t^*) + 2 \cos(2\pi l^*)] \mathbf{e}_{l',n}, \quad (24.128)$$

and the determinant is the product of all eigenvalues is

$$\det \sum_{j=1}^2 (-s\mathbf{1} + r_j + r_j^\top) = \prod_{l'=1}^a \prod_{n=1}^c [-2s + 2 \cos(2\pi t^*) + 2 \cos(2\pi l^*)], \quad (24.129)$$

the same as (24.118).<sup>8</sup>

Now a problem is: I don't know why in (24.126) the matrix is a transpose of the inverse of the matrix in (24.113). I just calculate the eigenvectors explicitly and the result I get is a cofactor matrix. I don't know if this is correct for higher dimensional lattice.

Another possible problem is: in (24.124), choose  $l'$  from  $1, 2, \dots, a$  and  $n$  from  $1, 2, \dots, c$  will give us a set of eigenvectors. But are these eigenvectors always independent? If we choose  $l'$  and  $n$  in this way, the  $t'$  we get is not always in  $1, 2, \dots, ac$ . But as long as the  $t'$ s we get can form different eigenvectors we should be fine. I'm sure the eigenvectors are independent, but I'm still thinking how to prove it.

<sup>8</sup>Predrag 2019-07-11: to Han - correct the notation  $l', n, t^*, l^*$

**2018-10-26 Han** Using the reciprocal lattice I found that using the transpose of inverse matrix as (24.126) is correct for three-dimensional lattice. I tried to prove that this method is correct for any dimensions.

For  $d$ -dimensional lattice, the size and the way of tiling of a periodic block can be given by:

$$x \begin{pmatrix} l_1 \\ l_2 \\ \vdots \\ l_d \end{pmatrix} = x \begin{pmatrix} l_1 \\ l_2 \\ \vdots \\ l_d \end{pmatrix} + \mathbf{A} \begin{pmatrix} j_1 \\ j_2 \\ \vdots \\ j_d \end{pmatrix}, \begin{pmatrix} j_1 \\ j_2 \\ \vdots \\ j_d \end{pmatrix} \in \mathbb{Z}^d, \quad (24.130)$$

where:

$$\mathbf{A} = \begin{bmatrix} a_{11} & a_{12} & a_{13} & \dots & a_{1d} \\ 0 & a_{22} & a_{23} & \dots & a_{2d} \\ 0 & 0 & a_{33} & \dots & a_{3d} \\ \vdots & \vdots & \vdots & \ddots & \vdots \\ 0 & 0 & 0 & \dots & a_{dd} \end{bmatrix}, \quad (24.131)$$

where  $a_{ii} \geq 1$  and for  $j \neq i, 0 \leq a_{ij} \leq a_{ii} - 1$ . All elements are integers.

Follow the same procedure as above, we know that the eigenvectors of the shift matrices with the periodic boundary conditions defined in (24.130) have the form:

$$\vec{e}_{\vec{l}} = e^{2\pi i[l_1 l_1^* + l_2 l_2^* + \dots + l_d l_d^*]}. \quad (24.132)$$

This is an element of the eigenvector for a given set of  $\vec{l}^*$ .

The shift matrices need to satisfy the relations:

$$\begin{aligned} r_{l_1}^{a_{11}} &= \mathbf{1} \\ r_{l_1}^{a_{12}} r_{l_2}^{a_{22}} &= \mathbf{1} \\ r_{l_1}^{a_{13}} r_{l_2}^{a_{23}} r_{l_3}^{a_{33}} &= \mathbf{1} \\ &\vdots \\ &\dots \end{aligned} \quad (24.133)$$

Using these operators acting on the eigenvectors (24.132), we have:

$$\begin{bmatrix} a_{11} & 0 & 0 & \dots & 0 \\ a_{12} & a_{22} & 0 & \dots & 0 \\ a_{13} & a_{23} & a_{33} & \dots & 0 \\ \vdots & \vdots & \vdots & \ddots & \vdots \\ a_{1d} & a_{2d} & a_{3d} & \dots & a_{dd} \end{bmatrix} \begin{bmatrix} l_1^* \\ l_2^* \\ l_3^* \\ \vdots \\ l_d^* \end{bmatrix} = \mathbf{A}^\top \begin{bmatrix} l_1^* \\ l_2^* \\ l_3^* \\ \vdots \\ l_d^* \end{bmatrix} = \begin{bmatrix} q_1 \\ q_2 \\ q_3 \\ \vdots \\ q_d \end{bmatrix}, \begin{bmatrix} q_1 \\ q_2 \\ q_3 \\ \vdots \\ q_d \end{bmatrix} \in \mathbb{Z}^d. \quad (24.134)$$

So  $\vec{l}^*$  satisfies:

$$\begin{bmatrix} l_1^* \\ l_2^* \\ l_3^* \\ \vdots \\ l_d^* \end{bmatrix} = (\mathbf{A}^{-1})^\top \begin{bmatrix} q_1 \\ q_2 \\ q_3 \\ \vdots \\ q_d \end{bmatrix}, \quad (24.135)$$

which is the general form of (24.126).

Given these eigenvectors, the determinant of the orbit Jacobian matrix is:

$$\text{Det} \left[ \sum_{j=1}^d (-s\mathbf{1} + r_j + r_j^T) \right] = \prod_{q_1=1}^{a_{11}} \prod_{q_2=1}^{a_{22}} \cdots \prod_{q_d=1}^{a_{dd}} \left[ -ds + \sum_{j=1}^d 2 \cos(2\pi l_j^*) \right], \quad (24.136)$$

where the  $l_j^*$  is given by (24.135). This is the general form of the determinant of the orbit Jacobian matrix, for any given dimensions, for both regular and relative periodic (twisted) boundary.

But there is one last thing that I haven't figure out... How do I know the indexes of the product in (24.136) is  $q_d$  from 1 to  $a_{dd}$ ? It's obvious in low dimensions. But I don't know how to prove this in any dimensions. I'm still working on this.

**2018-11-29 Han** Here I will summarize how do we count the number of periodic solutions and what do we still need to prove.

For a  $d$ -dimensional hypercubic lattice with each site labeled by  $d$  integers  $z \in \mathbb{Z}^d$ , we already know that the field value on each lattice site can be solved from:

$$(-\square + s - 2d) \phi_z = m_z, \quad (24.137)$$

where  $m_z$  is a given integer. If we want to solve for the periodic solutions, we will need to use the Laplacian  $\square$  with periodic boundaries. Eq. (24.137) holds for all kinds of periodic solutions. All properties of the periodic blocks are embedded in the Laplacian, including the spatial length, time period and the way in which the block is twisted when it tiles the space.

$\phi_z$  is on a torus with length 1. The range of this torus can be simply as from 0 to 1, or a very complicated form as what we do in figure 24.2. But the range and partition of the torus will not affect the number of periodic solutions. The range of  $m_z$  depends on the range of the torus.

So the counting problem becomes solving:

$$(-\square + s - 2d) \phi = \mathbf{m}, \quad (24.138)$$



and count how many sets of integers  $\mathbf{m}$  can be given to (24.138) that have solutions  $\Phi$  enclosed in the unit volume torus. Here  $\Phi$  and  $\mathbf{m}$  have  $d$  indices. The range of these indices are from 1 to the length of the periodic block in the corresponding directions. Equation (24.138) is a set of linear equations. Even though  $\Phi$  and  $\mathbf{m}$  are rank  $d$  tensors and  $(-\square + s - 2d)$  is a rank  $2d$  tensor, they are calculated as vectors and matrix.

Since the range of the torus will not affect the number of solutions, here we will choose the simplest torus:  $0 \leq \phi_z < 1$ . Then the admissible region of the vector  $\mathbf{x}$  is a high dimensional hypercube with all coordinates larger or equal to 0 and smaller than 1. The dimension of vector  $\Phi$  and  $\mathbf{m}$  is  $\prod_{i=1}^d L_i$ , where  $L_i$  is the length of periodic block in the  $i$ th directions. To count the number of solutions, imagine the admissible unit volume hypercube is mapped by matrix  $(-\square + s - 2d)$  into a larger region. And each integer point enclosed in this region is corresponding to a periodic solution. (Unfinished)

**2018-12-06 Han** I checked that using the Chebyshev polynomial of the first kind we can calculate determinant of the circulant matrix (the orbit Jacobian matrix).

We already know that the determinant of the  $[n \times n]$  Toeplitz matrix:

$$\mathcal{D}_n = \begin{pmatrix} s & -1 & 0 & 0 & \dots & 0 & 0 \\ -1 & s & -1 & 0 & \dots & 0 & 0 \\ 0 & -1 & s & -1 & \dots & 0 & 0 \\ \vdots & \vdots & \vdots & \vdots & \ddots & \vdots & \vdots \\ 0 & 0 & \dots & \dots & \dots & s & -1 \\ 0 & 0 & \dots & \dots & \dots & -1 & s \end{pmatrix} \quad (24.139)$$

can be calculated using the Chebyshev polynomial of the second kind:

$$\det(\mathcal{D}_n) = U_n(s/2). \quad (24.140)$$

Now we want to calculate the determinant of the  $n \times n$  circulant matrix:

$$-\mathcal{J} = H_n = \begin{pmatrix} s & -1 & 0 & 0 & \dots & 0 & -1 \\ -1 & s & -1 & 0 & \dots & 0 & 0 \\ 0 & -1 & s & -1 & \dots & 0 & 0 \\ \vdots & \vdots & \vdots & \vdots & \ddots & \vdots & \vdots \\ 0 & 0 & \dots & \dots & \dots & s & -1 \\ -1 & 0 & \dots & \dots & \dots & -1 & s \end{pmatrix}. \quad (24.141)$$

Expand the determinant of  $H_n$  by minors at the first row:

$$\begin{aligned} \det(H_n) &= \sum_{j=1}^n (-1)^{j+1} (H_n)_{1,j} M_{1j}(H_n) \\ &= s M_{11}(H_n) + (-1)(-1) M_{12}(H_n) + (-1)^{n+1} (-1) M_{1n}(H_n). \end{aligned} \quad (24.142)$$

The  $M_{ij}(H_n)$  is a minor of matrix  $H_n$ , obtained by taking the determinant of  $H_n$  with row  $i$  and column  $j$  removed. The three minors in (24.142) are:

$$M_{11}(H_n) = \det(\mathcal{D}_{n-1}), \quad (24.143)$$

$$\begin{aligned} M_{12}(H_n) &= \det \begin{pmatrix} -1 & -1 & 0 & 0 & \dots & 0 & 0 \\ 0 & s & -1 & 0 & \dots & 0 & 0 \\ 0 & -1 & s & -1 & \dots & 0 & 0 \\ \vdots & \vdots & \vdots & \vdots & \ddots & \vdots & \vdots \\ 0 & 0 & \dots & \dots & \dots & s & -1 \\ -1 & 0 & \dots & \dots & \dots & -1 & s \end{pmatrix} \\ &= (-1)\det(\mathcal{D}_{n-2}) \\ &\quad + (-1)^n(-1)\det \begin{pmatrix} -1 & 0 & 0 & \dots & 0 & 0 \\ s & -1 & 0 & \dots & 0 & 0 \\ -1 & s & -1 & \dots & 0 & 0 \\ \vdots & \vdots & \vdots & \ddots & \vdots & \vdots \\ 0 & \dots & \dots & \dots & s & -1 \end{pmatrix} \\ &\quad \text{(expand by minor at the first column)} \\ &= (-1)\det(\mathcal{D}_{n-2}) + (-1)^n(-1)(-1)^{n-2} \\ &\quad \text{(the last matrix is a lower triangular matrix)} \\ &= -\det(\mathcal{D}_{n-2}) - 1, \quad (24.144) \end{aligned}$$

$$\begin{aligned} M_{1n}(H_n) &= \det \begin{pmatrix} -1 & s & -1 & 0 & \dots & 0 \\ 0 & -1 & s & -1 & \dots & 0 \\ \vdots & \vdots & \vdots & \vdots & \ddots & \vdots \\ 0 & 0 & \dots & \dots & \dots & s \\ -1 & 0 & \dots & \dots & \dots & -1 \end{pmatrix} \\ &= (-1)\det \begin{pmatrix} -1 & s & -1 & 0 & \dots & 0 \\ 0 & -1 & s & -1 & \dots & 0 \\ \vdots & \vdots & \vdots & \vdots & \ddots & \vdots \\ 0 & 0 & \dots & \dots & \dots & s \\ 0 & 0 & \dots & \dots & \dots & -1 \end{pmatrix} \\ &\quad + (-1)^{n-2}(-1)\det \begin{pmatrix} s & -1 & 0 & \dots & 0 & 0 \\ -1 & s & -1 & \dots & 0 & 0 \\ \vdots & \vdots & \vdots & \ddots & \vdots & \vdots \\ 0 & 0 & \dots & \dots & s & -1 \\ 0 & 0 & \dots & \dots & -1 & s \end{pmatrix} \\ &\quad \text{(expand by minor at the first column)} \\ &= (-1)(-1)^{n-2} + (-1)^{n-2}(-1)\det \mathcal{D}_{n-2}. \quad (24.145) \end{aligned}$$

So the determinant of the  $n \times n$  circulant orbit Jacobian matrix is:

$$\begin{aligned}
 \text{Det}(-\mathcal{J}) &= \det(H_n) \\
 &= s M_{11}(H_n) + (-1)(-1)M_{12}(H_n) + (-1)^{n+1}(-1)M_{1n}(H_n) \\
 &= s \det(\mathcal{D}_{n-1}) + (-1)(-1)(-\det(\mathcal{D}_{n-2}) - 1) \\
 &\quad + (-1)^{n+1}(-1)[(-1)(-1)^{n-2} + (-1)^{n-2}(-1)\det \mathcal{D}_{n-2}] \\
 &= s U_{n-1}(s/2) - 2U_{n-2}(s/2) - 2 \\
 &= U_n(s/2) - U_{n-2}(s/2) - 2 \\
 &\quad \text{(use recurrence relation } U_{n+1}(x) = 2xU_n(x) - U_{n-1}(x)) \\
 &= 2T_n(s/2) - 2 \\
 &\quad \text{(use relation } T_n(x) = \frac{1}{2}(U_n(x) - U_{n-2}(x))), \quad (24.146)
 \end{aligned}$$

In agreement with (??).

When the time period  $n$  is 1 and 2, the orbit Jacobian matrix will be special:

$$-\mathcal{J} = \begin{pmatrix} s - 2 \end{pmatrix}, \quad (24.147)$$

$$-\mathcal{J} = \begin{pmatrix} s & -2 \\ -2 & s \end{pmatrix}. \quad (24.148)$$

These determinants still satisfy (??).

**2018-12-06 Predrag** Wow - very impressive! I remember the proof of (24.140) being very quick, basically a 3-term recurrence relation (second-order difference equation [31]), in a reference cited someplace close to (2.41). Maybe you can show it by induction, assuming that if (??) is true for  $n - 1$ , then it is true for  $n$ . Then you start the recursion with (24.147) and (24.148).

**2018-12-11 Han** I have read Kook and Meiss [46] *Application of Newton's method to Lagrangian mappings*. The Newton's method here is a computational algorithm.

In this article the orbit Jacobian matrix is written as a block matrix and they invert the orbit Jacobian matrix via block-diagonalization. A block matrix is a matrix defined by smaller matrices, called blocks. I tried to write the orbit Jacobian matrix of 2-dimensional cat map (a rank 4 tensor) explicitly as a matrix (write the  $L \times T \times L \times T$  tensor as a  $LT \times LT$  matrix). The matrix can be written as a block matrix. For example, the orbit Jacobian matrix of a  $[3 \times 3]$  periodic block (not relative periodic) is:

$$-\mathcal{J}_{[3 \times 3]_0} = \begin{pmatrix} \mathbf{S} & -\mathbf{I} & -\mathbf{I} \\ -\mathbf{I} & \mathbf{S} & -\mathbf{I} \\ -\mathbf{I} & -\mathbf{I} & \mathbf{S} \end{pmatrix}, \quad (24.149)$$

which is a circulant block matrix. The  $\mathbf{S}$  and  $\mathbf{I}$  are  $3 \times 3$  matrices:

$$\mathbf{S} = \begin{pmatrix} s & -1 & -1 \\ -1 & s & -1 \\ -1 & -1 & s \end{pmatrix}, \quad \mathbf{I} = \begin{pmatrix} 1 & 0 & 0 \\ 0 & 1 & 0 \\ 0 & 0 & 1 \end{pmatrix}. \quad (24.150)$$

So perhaps using the Fourier transform to diagonalize the orbit Jacobian matrix tensor in each direction can be interpreted as doing the block-diagonalization to the block matrix and diagonalizing the block.

But for blocks with relative periodic (twisted) boundaries, the orbit Jacobian matrix will become more complicated...

**2019-01-08 Han** I made figure 24.37 to show how the volume (area) of the stretched torus counts the number of periodic points. Consider the cat map with  $s = 3$ . The periodic solutions satisfy:

$$\mathcal{J} \Phi = -M, \quad (24.151)$$

where  $\mathcal{J}$  is the orbit Jacobian matrix of the periodic orbit with period  $n$ . If any  $\phi$  on the torus satisfies (24.151), this  $\phi$  is a periodic solution. So we can count the periodic points using  $H_n$  to stretch the torus and counting the number of integer points enclosed in the stretched region. I plotted the stretched region of periodic solutions with  $n = 2$  and  $n = 3$ . The orbit Jacobian matrix for  $n = 2$  and  $n = 3$  are:

$$-\mathcal{J} = \begin{pmatrix} 3 & -2 \\ -2 & 3 \end{pmatrix} \quad (24.152)$$

$$-\mathcal{J} = \begin{pmatrix} 3 & -1 & -1 \\ -1 & 3 & -1 \\ -1 & -1 & 3 \end{pmatrix} \quad (24.153)$$

Let the range of the field value  $\phi$  be  $0 \leq \phi < 1$ . Figure 24.37 (a) shows the number of periodic points with length 2. The unit square enclosed by black lines is the available region of  $(\phi_n, \phi_{n+1})$ . The parallelogram with red borders are the region of the unit square stretched by the orbit Jacobian matrix  $\mathcal{J}$ . There are 4 blue dots which are the integer points in the parallelogram. Each one of these blue dots corresponds to a periodic point. The 4 green dots are integer points on the vertices of the parallelogram. These 4 points contribute to 1 periodic point. So there are 5 periodic points with period 2, corresponding to 3 periodic solutions (1 fixed point and 2 2-cycles). The area of this parallelogram is 5.

Figure 24.37 (b) shows the periodic points with length 3. The square cube with black border is the available region of torus  $(\phi_n, \phi_{n+1}, \phi_{n+2})$ . After stretched by orbit Jacobian matrix  $\mathcal{J}$  it becomes the parallelepiped with red border. There are 6 blue dots which are the integer points completely

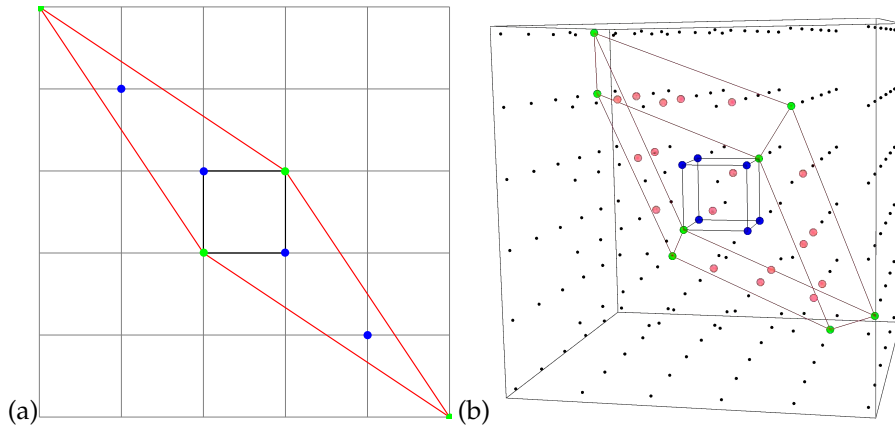


Figure 24.37: (a) A 2-dimensional torus (with black border) stretched by  $-\mathcal{J}$ . The blue dots are internal integer points in the stretched parallelogram (with red border). The green dots are on the vertices of the parallelogram. (b) A 3-dimensional torus (with black border) stretched by  $-\mathcal{J}$ . The blue dots are internal integer points in the stretched parallelepiped (with red border). The green dots are on the vertices of the parallelepiped. The pink dots are on the surface of the parallelepiped.

enclosed in the parallelepiped. The 8 green dots are integer points on the vertices of the parallelepiped, which contribute to 1 periodic points. There are 18 pink points which are integer points on the surface of the parallelepiped. These 18 points contribute to 9 periodic points. So the number of periodic points is 16 which is also the volume of the parallelepiped. I have a Mathematica notebook with this 3d plot in [siminos/figSrc/han/Mathematica/HLCCountingFigures.nb](#) so you can rotate it.

**2019-01-16 Han** According to (24.43), the covering alphabet for the  $s = 5$  spatiotemporal cat is

$$\mathcal{A} = \{\underline{3}, \underline{2}, \underline{1}, 0, 1, 2, 3\}.$$

I plotted two  $[12 \times 12]$  blocks of  $d = 2$ ,  $s = 5$  spatiotemporal cat. I choose the field to be in the range  $\phi_z \in [-1/2, 1/2)$ . Figure 24.38 are blocks corresponding to two admissible invariant 2-tori of figure 24.39. The  $m_z$  within the black borders are the same. Figure 24.40 shows the distance and the logarithm of the absolute value of the distance between these two invariant 2-tori.

The covering alphabet for this  $\phi_z \in [-1/2, 1/2)$  spatiotemporal cat is

$$m_z \in \{-4, -3, -2, -1, 0, 1, 2, 3, 4\}. \quad (24.154)$$

<sup>9</sup> To make it easier to find and admissible field here I only used  $m_z \in$

<sup>9</sup>Predrag 2019-01-16: Is (24.43) wrong?

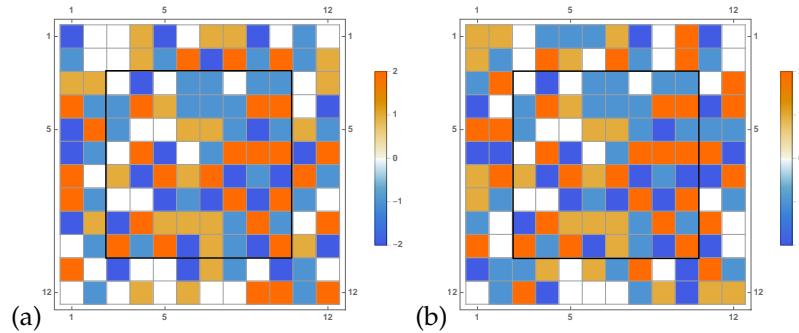


Figure 24.38: (a) and (b) are two admissible  $[12 \times 12]$  blocks corresponding to the two distinct invariant 2-tori of figure 24.39. They coincide within the shared  $[8 \times 8]$  block  $M_{\mathcal{R}}$ , region  $\mathcal{R}$  indicated by the black border.

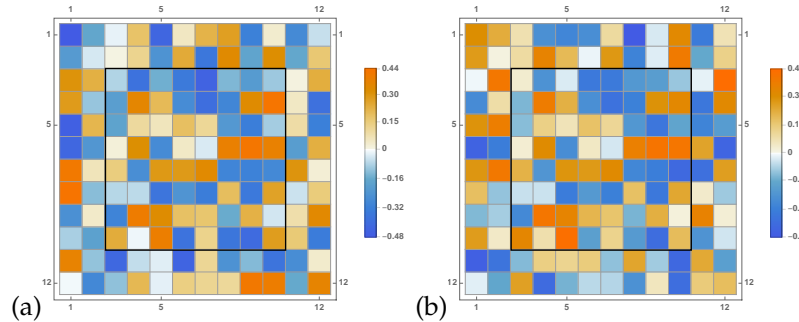


Figure 24.39: The two invariant 2-tori whose symbol arrays are given by the admissible  $[12 \times 12]$  blocks of figure 24.38.

$\{-2, -1, 0, 1, 2\}$ . But using  $m_z$  in this range does not guarantee that corresponding field is admissible. The starting random block of  $m_z$  usually yields some  $\phi_z$  outside  $[-1/2, 1/2)$ , so we keep changing the corresponding  $m_z$  until we find an admissible block. I can also redo this using (24.154).

The  $[12 \times 12]$  blocks might be too small. As this block is periodic we might need a larger block to observe fields that differ exponentially. Adrien used  $[18 \times 18]$  blocks.

**2019-01-16 Predrag** Shadowing looks promising. The Gutkin version has an argument about exponentially close shadowing using Green's functions.

You have to be very precise in explaining the algorithm that gets you from the initial random  $[L_1 \times L_2]$  block to an admissible block. You know the number of distinct invariant 2-tori from your orbit Jacobian matrix determinant counting formula. If you have a systematic way of generating blocks for all admissible invariant 2-tori, that would be satisfying, even if

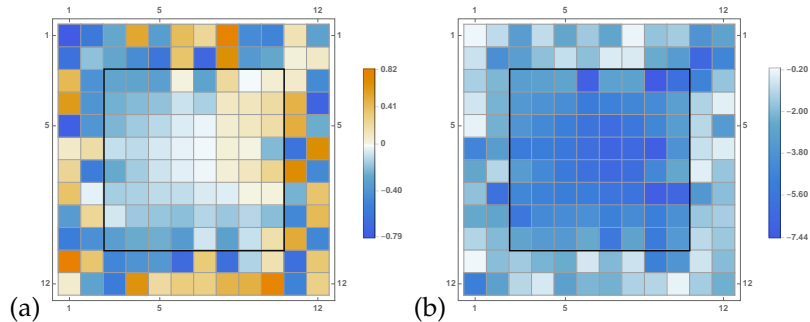


Figure 24.40: (a) The pointwise distance between the invariant 2-tori of figure 24.39. (b) The logarithm of the absolute value of the distance between the two invariant 2-tori indicate exponential shadowing close to the center of the shared  $M_{\mathcal{R}}$ .

we do not have a walks-on-Markov graph interpretation.

**2019-01-16 Predrag** As  $\phi_z$  are rational numbers (presumably with large denominators, you can have a look), some distances in figure 24.40 (a) could be exactly zero.

**2019-01-18 Han** Figure 24.41 is an example of admissible symbol block M and the corresponding state  $\Phi$  for a  $[12 \times 12]$  2-torus of the  $d = 2, s = 5$  spatiotemporal cat. Here I started with random symbol block M with  $m_z$  from -4 to 4. The algorithm:

Use the Green's function to calculate the state  $\Phi$  given the random symbol block M. If the maximum  $\phi_z$  is larger or equal to  $1/2$ , find the position  $z$  of this maximum and change the corresponding symbol  $m_{max}$  to  $m_{max} - 1$ . If the minimum of this field is smaller than  $-1/2$ , find the position of the minimum and change the corresponding symbol  $m_{min}$  by  $m_{min} + 1$ . Then use the new block M to calculate the state  $\Phi$ , and repeat this procedure until the state  $\phi_z$  at every site is larger or equal to  $-1/2$ , and smaller than  $1/2$ . Generally it takes 70 to 100 iterations to reach an admissible block M.

As we expected, the symbol 4 and -4 are not very likely to exist in the admissible field. Because the maximum (minimum) of the field are likely to have 4 (-4) on its site (but not always). Figure 24.41 is a very rare case which still has a symbol equal to 4. In most of my runs I end up with all symbol from -3 to 3.

**2019-01-19 Predrag** Why go in steps of one? Symbol  $m_z$  is the integer part of  $\phi_z$  that implements the translation to the desired unit interval (modulo 1 operation). So do not change  $m_z \rightarrow m_z \pm 1$ , but replace  $m_z$  by the integer translation that places  $\phi_z$  into the admissible range. Also, start at one point  $z$ , and do this along a rectangular "out-spiral" around it. That will

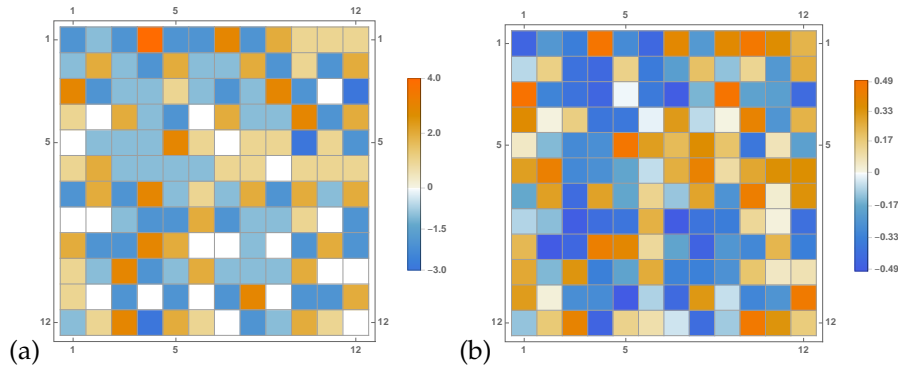


Figure 24.41: (a) An example of an admissible block  $M$ , initiated by a guess block with many  $m_z = 4$ . Row 1, column 3 site is the only one with  $m_{(3,12)} = 4$ . (b) The corresponding invariant 2-torus.

ensure that the center is exponentially well determined, and I expect that all inadmissible site values will sit outside the spiral.

**2019-01-19 Predrag** Matt, Han and I are using different words for the same things, so I keep editing everybody notes into the ‘standard’ notation. Probably best to read chapter 14 *Symbolic dynamics: a glossary*, and we discuss if something has to be changed.

**2019-01-19 Predrag** In our convention, the first lattice index is ‘space’, increasing from left to right, and the second index is ‘time’, increasing from bottom up, see for example (14.8), so the  $y$ -axis labels in figure 24.41 (a) and all other figures of symbol blocks  $M$  should be increasing as one goes up. For symbol blocks the alphabet / number of colors is a discrete set, so the color bar on the right should be a set of colored squares. The states  $\Phi$ , however, do need a continuous color bar.

**2019-01-24 Han** I redid the shadowing using symbol block  $M$  with  $m_z$  from  $-4$  to  $4$ . Figure 24.42 are blocks corresponding to two admissible invariant 2-tori of figure 24.43. The  $m_z$  within the black borders are the same. Figure 24.44 shows the distance and the logarithm of the absolute value of the distance between these two invariant 2-tori.

The algorithm I used is:

- (1) Start with a random admissible state  $\Phi^0$  with  $-1/2 \leq \phi_z < 1/2$ . Calculate the corresponding symbol block  $M^0$ . The  $m_z$ s in this symbol block are not integers. So we need to round these  $m_z$ s to the nearest integers and get symbol block  $M^1$
- (2) Use the Green’s function and the integer symbol block  $M^1$  to calculate the state  $\Phi^1$ . If the maximum  $\phi_{max}$  is larger or equal to  $1/2$ , calculate the distance  $\delta\phi_{max} = \phi_{max} - 1/2$ . Round up  $5\delta\phi_{max}$  (and call it



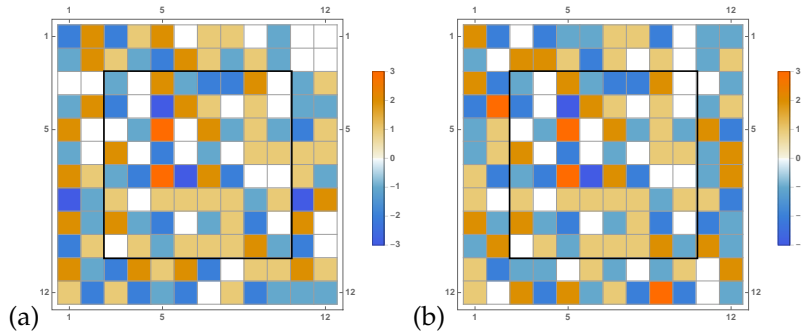


Figure 24.42: (a) and (b) are two admissible  $[12 \times 12]$  blocks corresponding to the two distinct invariant 2-tori of figure 24.43. They coincide within the shared  $[8 \times 8]$  block  $M_{\mathcal{R}}$ , region  $\mathcal{R}$  indicated by the black border.

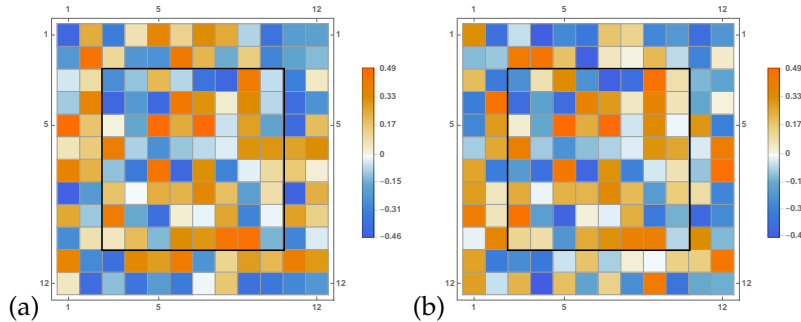


Figure 24.43: The two invariant 2-tori whose symbol arrays are given by the admissible  $[12 \times 12]$  blocks of figure 24.42.

$\delta m_{max}$ ). Then change the corresponding symbol  $m_{max}$  to  $m_{max} - \delta m_{max}$ . If the minimum  $\phi_{min}$  is smaller than  $1/2$ , calculate the distance  $\delta\phi_{min} = -\phi_{min} - 1/2$ . Round up  $5\delta\phi_{min}$  (and call it  $\delta m_{min}$ ). Then change the corresponding symbol  $m_{min}$  to  $m_{min} + \delta m_{min}$ .

(3) Now we get a new symbol block  $M^2$ . Repeat step (2) until all  $\phi_z$  in  $\Phi$  are in the admissible range.

Since we start with a state  $\Phi$  with only admissible  $\phi_z$ , now we only need no more than 10 iterations to reach an admissible block. Here we have to round up  $\delta m_{max}$  and  $\delta m_{min}$  so we always make a non-zero change. If we don't do this the program will very likely run into an endless loop.

The color bar of the symbol block should be colored squares. I haven't fixed this and the awkward axes due to "technical reasons"... Will fix that soon.

2019-03-01 Han To summarize why can we use the determinant of orbit Jacobian matrix to count the number of periodic solutions: For one-dimensional

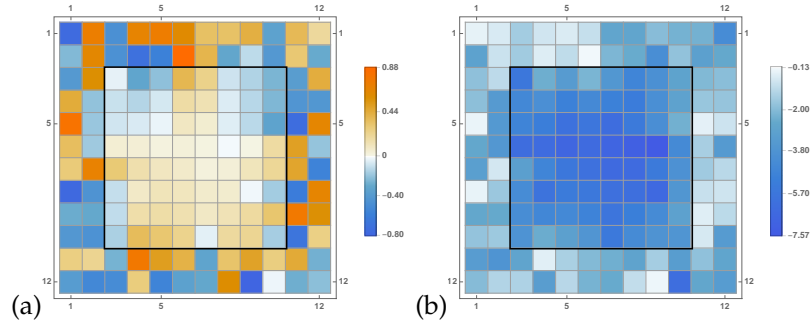


Figure 24.44: (a) The pointwise distance between the invariant 2-tori of figure 24.43. (b) The logarithm of the absolute value of the distance between the two invariant 2-tori indicate exponential shadowing close to the center of the shared  $M_{\mathcal{R}}$ .

cat map, the problem of solving for a periodic string eventually becomes solving the linear equations

$$\begin{bmatrix} s & -1 & 0 & \dots & -1 \\ -1 & s & -1 & \dots & 0 \\ 0 & -1 & s & \dots & 0 \\ \vdots & \vdots & \vdots & \ddots & \vdots \\ -1 & 0 & 0 & \dots & s \end{bmatrix} \begin{bmatrix} x_1 \\ x_2 \\ x_3 \\ \vdots \\ x_T \end{bmatrix} = \begin{bmatrix} m_1 \\ m_2 \\ m_3 \\ \vdots \\ m_T \end{bmatrix}, \begin{bmatrix} m_1 \\ m_2 \\ m_3 \\ \vdots \\ m_T \end{bmatrix} \in \mathbb{Z}^T. \quad (24.155)$$

for  $x$ 's.

For any set of integers  $m_z$ , there is a solution  $x_z$ . But the solution is admissible only when each one of the field values  $x_z$ 's is larger or equal to 0 and smaller than 1. So all admissible solutions of period  $T$  are constrained to a  $T$ -dimensional hypercube with unit volume (all the field values within  $0 \leq x_z < 1$ ). This hypercube will be stretched to a  $n$ -dependent parallelepiped by the orbit Jacobian matrix in (24.155). And each of the integer points inclosed within stretched parallelepiped will correspond to a periodic solution with period  $n$ . So the problem of counting the number of period solutions becomes counting the number of integer points enclosed in a parallelepiped.

Since all the field values can be equal to 0 but not equal to 1, when counting the integer points we must not count the points on the boundaries which correspond to field values 1. So counting the number of integer points in the parallelepiped is like counting the number of atoms in a unit cell. The parallelepiped can tile the space like the unit cell of a crystal lattice. And when the parallelepipeds tile the space, each of them is a cell of integer points, i.e., each of them is a repeating unit of integer points.

The number of points in a large space is equal to the number of parallelepipeds times the number of integer points within one parallelepiped. The density of integer points in the space is 1 per unit volume. So for an infinitely large space the number of integer points in it is equal to its volume. The number of the tiling parallelepipeds is equal to the space's volume divided by the volume of one parallelepiped. So the number of points in one parallelepiped is equal to the volume of the parallelepiped, which is given by the determinant of the orbit Jacobian matrix in (24.155).

To summarize, the reason that we can use the volume to count integer points is:

1. The region is a parallelepiped (so it can tile the space).
2. All vertices of the parallelepiped are integer points (so when tiling the space, each of these parallelepipeds is a repeating unit of integer points).
3. The density of integer points is one per unit volume.

**2019-03-02 Han** In order to count the cat map periodic solutions, and compute the field configuration given a symbol string, we diagonalize the orbit Jacobian matrix by a Fourier transform and compute its inverse, i.e., the Green's function. For the  $d$ -dimensional spatiotemporal cat, fields and symbol arrays are rank  $d$  tensors, related by the orbit Jacobian matrix in (24.155) which is a rank  $2d$  tensor. This is still a linear equation, so the above method of counting and computing  $d$ -periodic solutions still applies. For a  $d$ -periodic block we now use the  $d$ -dimensional Fourier transform to invert the orbit Jacobian matrix and compute the  $d$ -periodic field configuration.

For a relative periodic block, with relative periodic (twisted) boundary, we cannot use Fourier transform. I have explained everything clearly to Glen. He doesn't think there is any problem in these computations.

**2019-02-04 Predrag** What follows are some raggedly thoughts, you have already thought through all of them... My problem is I do not understand Lind [49] and your notes starting with **2018-08-30 Han** above.

We need to count all periodic and relative periodic orbits. In ChaosBook this is no harder than counting periodic orbits, but one has to quotient the symmetries first: for 2-dimensional spatiotemporal cat those are first the time and space translations, then the point group. The goal is to enumerate all distinct tilings of a square (hypercubic) lattice. I believe they have to be doubly (in general,  $d$ -)periodic, but we have not proven it. Is it obvious that a -let's say-  $L$ -shaped region is not a legal tile? A quick sketch shows that a 3-sites  $L$ -shaped tile is equivalent to both  $[1 \times 3]$  and  $[3 \times 1]$  relative-periodic tilings, but is such a thing true in general?

Consider a finite block of symbols  $M_{\mathcal{R}} \subset M$ , over a finite  $[L_1 \times L_2 \times \dots \times L_d]$  hyper-parallelepiped region  $\mathcal{R} \subset \mathbb{Z}^d$ . In particular, let  $M_p$  over a finite rectangular  $[L_1 \times L_2 \times \dots \times L_d]$  lattice region be the  $[L_1 \times L_2 \times \dots \times L_d]$   $d$ -periodic block of  $M$  whose repeats tile  $\mathbb{Z}^d$ .

Rectangles  $[L_1 \times L_2]$  are obviously tiles, however the shape of a general tile does not have to be rectangular, or even connected - one is allowed to shift  $j$ th column  $[1 \times L_2]$  by an arbitrary vertical shift  $r_2^{s_j}$ ,  $0 \leq s_j < L_2$ , and  $k$ th row  $[L_1 \times 1]$  by an arbitrary horizontal shift  $r_1^{s_k}$ , and any such raggedly 'tile' tiles the (hyper-)lattice.

Here I'm visualizing fields as residing on face-centered lattice, and translation shifts as acting across the vertical / horizontal boundary lines. Each solution finite block  $\Phi_{\mathcal{R}} \subset M$  breaks translational invariances, but the quotient (lattice)/ $\mathcal{R}$  is still translationally invariant for  $\mathcal{R}$  a rectangle. But what if  $\Phi$  is relative-periodic?

The reason I'm sketching such raggedly tiles is to try to visualize a 'natural' tile for a relative periodic tiling. In continuum dynamics one can go to a co-moving frame, where the trajectory on average looks stationary (no phase drift) but on a lattice there is no way of drawing a parallelepiped with straight sides - they must be raggedly...

Be it as it may, I define a relative (relative) periodic field by demanding that it satisfy

$$x_{jk} = r_1^{S_1} r_2^{S_2} x_{j+L_1, k+L_2} \text{ on every } z = (j, k) \text{ lattice site} \quad (24.156)$$

$0 \leq S_1 < L_1$ ,  $0 \leq S_2 < L_2$ . i.e., field value  $x_{jk}$  reappears spatiotemporally after periods  $(L_1, L_2)$  (in that case, we can draw a rectangle tile), and, in general, translated by shifts  $(r_1^{S_1}, r_2^{S_2})$  bounded by corresponding periods.

Field configuration (24.156) is a legal (though not yet necessarily admissible) field configuration. One first has to enumerate such configurations distinct under the  $d$ -translations. There are clearly many equivalent relative tilings, for example easy to sketch vertical  $[1 \times 3]$  and horizontal  $[3 \times 1]$  relative-periodic tilings...

Next one has to quotient the point-group, for example the  $D_4$  symmetry for the square lattice.

**2019-03-20 Han** Using the reciprocal lattice to determine the eigenvalues turns out to be much simpler than my previous method to find the eigenvectors for a relative periodic (twisted) boundary, leading to my formula (24.118) for the number of periodic points.

The idea is: a periodic tiling pattern is given by a Bravais lattice. All possible eigenmodes (eigenvalues, eigenvector pairs) are given by the reciprocal lattice wave vectors.

Imagine we have an infinite  $d$ -dimensional space with a field on it. There are translation operators in  $d$  independent directions. The eigenvectors (eigenstates) of these translation operators are plane waves:

$$f_{\mathbf{k}}(\Phi) = e^{i\mathbf{k} \cdot \Phi}, \quad (24.157)$$

where  $\mathbf{k}$  is any  $d$ -dimensional vector. Now we put a Bravais lattice in it, with lattice points given by

$$\mathbf{R} = \sum_{i=1}^d n_i \mathbf{a}_i, \quad (24.158)$$

with  $\mathbf{a}_i$  are the  $d$  independent primitive cell vectors, and  $n_i \in \mathbb{Z}$ . In order that wave vectors  $\mathbf{k}$  in (24.157) have the periodicity of the Bravais lattice, they must satisfy

$$f_{\mathbf{k}}(\Phi + \mathbf{R}) = e^{i\mathbf{k} \cdot \Phi} e^{i\mathbf{k} \cdot \mathbf{R}} = e^{i\mathbf{k} \cdot \Phi} = f_{\mathbf{k}}(\Phi), \quad (24.159)$$

so  $\mathbf{k} \cdot \mathbf{R}$  must equal to an integer times  $2\pi$ . The admissible  $\mathbf{k}$  lie on the reciprocal lattice if

$$\mathbf{K} = \sum_{i=1}^d k_i \mathbf{b}_i, \quad (24.160)$$

where the  $k_i$  are integers, and  $\mathbf{b}_i$  satisfy

$$\mathbf{b}_i \cdot \mathbf{a}_j = 2\pi \delta_{ij}. \quad (24.161)$$

Each lattice site in this reciprocal lattice corresponds to one eigenmode (eigenvalues, eigenvector pair), so there are still an infinity of them. But this is only true when we have a continuous periodic field in the space. For the cat map, the field has support only on the lattice sites. So the coordinates  $\Phi$  of this field are not continuous numbers but integer indices. In this case we only need wave vectors in a small region. This region is given by the **first** Brillouin zone of the reciprocal lattice.

For example, consider the  $2D$  spatiotemporal cat. We want to find solutions with periodicity given by Bravais lattice:

$$\mathcal{L} = \{n_1 \mathbf{a}_1 + n_2 \mathbf{a}_2 | n_i \in \mathbb{Z}\}. \quad (24.162)$$

If these two primitive vectors  $\mathbf{a}_1$  and  $\mathbf{a}_2$  are in the directions of the basis of the integer lattice, this is a regular periodic condition. A general periodic condition is  $\mathbf{a}_1 = (l_1, l_2)$  and  $\mathbf{a}_2 = (0, l_3)$ .<sup>10</sup> In Lind's paper this periodicity is written as a matrix, in the Hermite normal form (8.124).

$$[\mathbf{a}_1 \quad \mathbf{a}_2] = \begin{bmatrix} l_1 & l_2 \\ 0 & l_3 \end{bmatrix}. \quad (24.163)$$

The reciprocal lattice of this Bravais lattice is:

$$\bar{\mathcal{L}} = \{n_1 \mathbf{b}_1 + n_2 \mathbf{b}_2 | n_i \in \mathbb{Z}\}. \quad (24.164)$$

---

<sup>10</sup>Han 2019-06-25: (Should be  $\mathbf{a}_1 = (l_1, 0)$  and  $\mathbf{a}_2 = (l_2, l_3)$ ?)  
 Predrag 2019-06-26: Sorry, at the moment I'm not thinking about this, can you derive the correct  $\mathbf{a}_j$  for me?

These two primitive vectors satisfy (24.161). In this example they are

$$[ \mathbf{b}_1 \quad \mathbf{b}_2 ] = \frac{2\pi}{l_1 l_3} \begin{bmatrix} l_3 & 0 \\ -l_2 & l_1 \end{bmatrix}, \quad (24.165)$$

which is the transpose of the inverse matrix of (24.163) times  $2\pi$ . This is true in any dimension, as to satisfy (24.161), we must have

$$\begin{bmatrix} \mathbf{a}_1 \\ \mathbf{a}_2 \\ \vdots \\ \mathbf{a}_d \end{bmatrix} [ \mathbf{b}_1 \mathbf{b}_2 \cdots \mathbf{b}_d ] = 2\pi \mathbf{1}. \quad (24.166)$$

So for any wave vector on the reciprocal lattice  $\mathbf{k} = n_1 \mathbf{b}_1 + n_2 \mathbf{b}_2$ , there is an eigenvector that satisfies the periodicity of the Bravais lattice:

$$f_{\mathbf{k}}(\Phi) = e^{i\mathbf{k}\cdot\Phi} = e^{i(n_1 \mathbf{b}_1 \cdot \Phi + n_2 \mathbf{b}_2 \cdot \Phi)}, \quad (24.167)$$

where  $\Phi = \{x_1, x_2\}$  are a lattice site vector. This is the same as my relative periodic (twisted) boundary eigenvectors (24.125).

But I have concern for the range of  $n_1$  and  $n_2$  in (24.167).  $n_1$  and  $n_2$  give us the position of the wave vector. The range of these two should make sure the wave vector is in the Brillouin zone of the integer lattice. Consider a very specific example: let the primitive vectors of the Bravais lattice be:

$$[ \mathbf{a}_1 \quad \mathbf{a}_2 ] = \begin{bmatrix} l_1 & l_2 \\ 0 & l_3 \end{bmatrix} = \begin{bmatrix} 3 & 1 \\ 0 & 2 \end{bmatrix}. \quad (24.168)$$

We can find the reciprocal lattice by compute the inverse of matrix in (24.168). The Bravais lattice and the reciprocal lattice are shown in figure 24.45. Figure 24.45 (a) is the Bravais lattice which gives us the periodicity. Each parallelogram is a repeating unit of the field. The red and blue arrows are the two primitive vectors  $\mathbf{a}_1$  and  $\mathbf{a}_2$ . Figure 24.45 (b) is the reciprocal lattice. Each lattice site is a wave vector of the eigenvalue of the translation operator that satisfies the periodicity given by the Bravais lattice. The square enclosed by green dashed lines is the first Brillouin zone of the integer lattice. The field of spatiotemporal cat is a discrete field only defined on the integer points. Any field defined only on the discrete lattice can be transformed to a continuous field in the first Brillouin zone of the discrete lattice by Fourier transform. So all of the eigenvectors of this discrete field can be expressed with wave vectors in this Brillouin zone. This periodic block has 6 lattice sites in it, so each state is a 6-dimensional vector. There should be 6 eigenvectors. In figure 24.45 (b) we do have 6 points in the green square (the two points on the boundary should be counted as one).

The problem is: the reciprocal lattice is not a square lattice as the Brillouin zone of the integer lattice. We cannot give a range of  $n_1$  and  $n_2$  in (24.167)

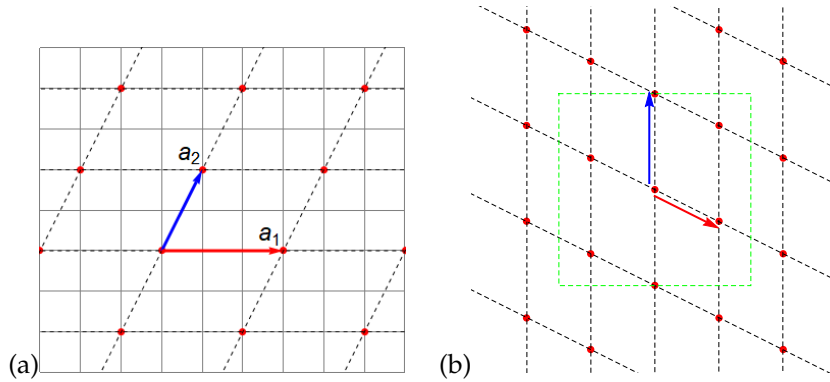


Figure 24.45: (a) The Bravais lattice defines the periodicity of the field. The red arrow is  $\mathbf{a}_1 = (3, 0)$  and the blue arrow is  $\mathbf{a}_2 = (1, 2)$ . (b) The reciprocal lattice of the Bravais lattice (a). Each reciprocal lattice point is a wave vector of the eigenvector of the translation operator with periodicity given by the Bravais lattice (a). The green dashed lines enclose the first Brillouin zone of the **integer lattice** (not the Bravais lattice (a)). The wave vectors in this first Brillouin zone give us all the eigenvectors of the translation operator. The wave vectors outside of this region (the first Brillouin zone enclosed by the green dashed lines) are equivalent to a wave vector in the region (2019-03-20 PC: what regions?).

separately. In my previous method I just used  $n_1 = 0, 1, 2$  and  $n_2 = 0, 1$ . These are corresponding to the wave vectors enclosed in the square with green dashed boundaries in figure 24.46. In figure 24.46 the blue gridlines are reciprocal lattice of the integer lattice. We don't really need to use the wave vectors in the first Brillouin zone to express the eigenvectors. Any two wave vectors that differ by a vector in the reciprocal lattice of the integer lattice (in figure 24.46 it's the lattice of blue lines) should give us equivalent eigenvectors. So can we use the green square in figure 24.46 to enclose the wave vectors instead of the green square in figure 24.45 (b), and have  $n_1$  and  $n_2$  go over a set of integers independently? I think the answer is yes. I just need to think a bit more about this...

**2019-04-12 Han** After we get the eigenvectors of the translation operator, we can compute the eigenvalues of the orbit Jacobian matrix. For a  $d$ -dimensional cat map, the orbit Jacobian matrix is:

$$H = \sum_{j=1}^d \frac{s}{d} - r_j - r_j^\top. \quad (24.169)$$

The eigenvectors of the translation operators are eigenvectors of this orbit Jacobian matrix. All the eigenvectors have the form  $f_{\mathbf{k}}(\Phi) = e^{i\mathbf{k}\cdot\Phi}$ , where the wave vector  $\mathbf{k}$  is a vector on the reciprocal lattice of the direct lattice

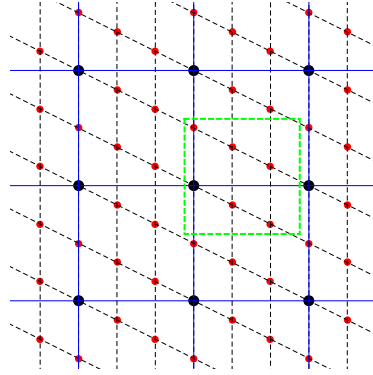


Figure 24.46: The reciprocal lattice of both the original direct lattice and the integer lattice. The red points are the reciprocal lattice of the Bravais lattice in figure 24.45 (a). The black points are the reciprocal lattice of the integer lattice. Each of these squares enclosed by the blue lines has edge length  $2\pi$ . And these squares are also repeating unit of the wave vectors (the red dots in this figure). Two wave vectors are equivalent if they are different by a vector on the reciprocal lattice of the integer lattice.

which gives the periodic tiling pattern. Let

$$\mathbf{k} = \begin{bmatrix} k_1 \\ k_2 \\ \vdots \\ k_d \end{bmatrix}, \quad \Phi = \begin{bmatrix} x_1 \\ x_2 \\ \vdots \\ x_d \end{bmatrix}. \quad (24.170)$$

Then we have:

$$(r_j + r_j^\top) f_{\mathbf{k}}(\Phi) = e^{i(\mathbf{k} \cdot \Phi - k_j)} + e^{i(\mathbf{k} \cdot \Phi + k_j)} = 2 \cos k_j e^{i\mathbf{k} \cdot \Phi} = 2 \cos k_j f_{\mathbf{k}}(\Phi). \quad (24.171)$$

The eigenvalue of the orbit Jacobian matrix corresponding to the eigenvector labeled by  $\mathbf{k}$  is:

$$\lambda_{\mathbf{k}} = \sum_{j=1}^d \frac{s}{d} - 2 \cos k_j. \quad (24.172)$$

Then the problem becomes finding  $k_j$ .  $\mathbf{k}$  can be written as:

$$\mathbf{k} = \begin{bmatrix} k_1 \\ k_2 \\ \vdots \\ k_d \end{bmatrix} = [\mathbf{b}_1 \quad \mathbf{b}_2 \quad \dots \quad \mathbf{b}_d] \begin{bmatrix} n_1 \\ n_2 \\ \vdots \\ n_d \end{bmatrix} = n_1 \mathbf{b}_1 + n_2 \mathbf{b}_2 + \dots + n_d \mathbf{b}_d. \quad (24.173)$$



$\mathbf{b}_i$ s are the vertical primitive vectors of the reciprocal lattice that satisfy (24.161).  $[\mathbf{b}_1 \ \mathbf{b}_2 \ \dots \ \mathbf{b}_d]$  is a  $d \times d$  matrix.  $n_i$ s are integers. Each wave vector  $\mathbf{k}$  is corresponding to a set of integers  $n_i$ .

A simple example is a two-dimensional cat map with the periodic pattern described by direct lattice with primitive vectors given in (24.163). The matrix of the primitive vectors of the reciprocal lattice is  $2\pi$  times the transpose of the inverse of matrix in (24.163), given by (24.165). Then wave vector is:

$$\mathbf{k} = \begin{bmatrix} k_1 \\ k_2 \end{bmatrix} = [\mathbf{b}_1 \ \mathbf{b}_2] \begin{bmatrix} n_1 \\ n_2 \end{bmatrix} = \begin{bmatrix} \frac{2\pi n_1}{l_1} \\ \frac{2\pi n_2}{l_3} - \frac{2\pi l_2 n_1}{l_1 l_3} \end{bmatrix}. \quad (24.174)$$

Substitute into (24.172):

$$\begin{aligned} \lambda_{\mathbf{k}} &= \sum_{j=1}^2 \frac{s}{2} - 2 \cos k_j \\ &= s - 2 \cos k_1 - 2 \cos k_2 \\ &= s - 2 \cos\left(\frac{2\pi n_1}{l_1}\right) - 2 \cos\left(\frac{2\pi n_2}{l_3} - \frac{2\pi l_2 n_1}{l_1 l_3}\right). \end{aligned} \quad (24.175)$$

And this is the eigenvalue of the orbit Jacobian matrix corresponding to the eigenvector with wave vector  $\mathbf{k} = n_1 \mathbf{b}_1 + n_2 \mathbf{b}_2$ .

The determinant of the orbit Jacobian matrix is the product of all the eigenvalues:

$$\det H = \prod_{\mathbf{k}} \lambda_{\mathbf{k}} = \prod_{n_1=0}^{l_1-1} \prod_{n_2=0}^{l_3-1} s - 2 \cos\left(\frac{2\pi n_1}{l_1}\right) - 2 \cos\left(\frac{2\pi n_2}{l_3} - \frac{2\pi l_2 n_1}{l_1 l_3}\right). \quad (24.176)$$

I haven't found an elegant way to prove the product after the second equals sign is correct, that  $n_1$  is from 0 to  $l_1 - 1$  and  $n_2$  is from 0 to  $l_3 - 1$ . One way to understand this is by looking at figure 24.46. The red points are the reciprocal lattice of the original direct lattice given by (24.168). The black points are the reciprocal lattice of the integer lattice. Since the field value only appears on the integer points, any two Fourier modes with wave vectors that are different by a vector on the reciprocal lattice of the integer lattice (in figure 24.46 they are different by a vector on the black points) are equivalent. So we only need wave vectors in a primitive cell of the reciprocal lattice of the integer lattice. When we choose  $n_1$  from 0 to  $l_1 - 1$  and  $n_2$  from 0 to  $l_3 - 1$  we find all the wave vectors in the primitive cell enclosed by the green dashed line in figure 24.46. The  $l_1$  and  $l_3$  here are two elements on the diagonal of the matrix (24.168). And choosing  $n_1$  and  $n_2$  using the numbers on the diagonal of the matrix of the primitive vectors is only correct when the matrix is an upper triangular matrix. For a more general matrix we are not able to let  $n_1$  and  $n_2$  go through a set of numbers independently. But if Lind is correct then all periodic patterns

on an integer lattice can be described by a set of primitive vectors which can form an upper triangular matrix.

The number of periodic solutions with periodic pattern given by (24.168) is equal to the determinant of the orbit Jacobian matrix given by (24.176).

**2019-11-11 Han** One possible way to evaluate determinant (24.92) is to compute the sum:

$$\sum_{n=0}^{N-1} \sum_{m=0}^{M-1} \frac{1}{s - 2 \cos(2\pi n/N) - 2 \cos(2\pi m/M)}. \quad (24.177)$$

Let  $s = \cosh \lambda$ , multiply (24.177) by  $\sinh \lambda$ , and integrate over  $\lambda$ , we have:

$$\begin{aligned} & \sum_{n=0}^{N-1} \sum_{m=0}^{M-1} \int d\lambda \frac{\sinh \lambda}{\cosh \lambda - 2 \cos(2\pi n/N) - 2 \cos(2\pi m/M)} \\ &= \sum_{n=0}^{N-1} \sum_{m=0}^{M-1} \ln[\cosh \lambda - 2 \cos(2\pi n/N) - 2 \cos(2\pi m/M)] \\ &= \ln \prod_{n=0}^{N-1} \prod_{m=0}^{M-1} [\cosh \lambda - 2 \cos(2\pi n/N) - 2 \cos(2\pi m/M)], \end{aligned} \quad (24.178)$$

which is logarithm of the determinant.

This method is used by Wu in *Theory of resistor networks: the two-point resistance* [75]. He defines

$$I_\alpha(\ell) = \frac{1}{N} \sum_{n=0}^{N-1} \frac{\cos(\alpha \ell \frac{n\pi}{N})}{\cosh \lambda - \cos(\alpha \frac{n\pi}{N})}, \quad \alpha = 1, 2,$$

and proves for  $\alpha = 2$ :

$$I_2(\ell) = \frac{\cosh(N/2 - \ell)\lambda}{(\sinh \lambda) \sinh(N\lambda/2)}, \quad 0 \leq \ell < N.$$

Setting  $\ell = 0$ , multiplying  $I_2(\ell)$  by  $\sinh \lambda$  and integrating over  $\lambda$ , he proves that:

$$\prod_{n=0}^{N-1} \left( \cosh \lambda - \cos \frac{2n\pi}{N} \right) = \sinh^2(N\lambda/2), \quad (24.179)$$

and this is also applicable to our counting formula of the cat map.

To evaluate the determinant one first evaluates the sum (24.177). Wu introduces  $S_\alpha(\ell)$  (8.179) and evaluates it by carrying out the summation:

$$\mathcal{R}e \frac{1}{N} \sum_{n=0}^{N-1} \frac{1}{1 - a e^{i2\theta_n}}, \quad a < 1$$

in different ways. This method works out because:

$$\mathcal{R}e \frac{1}{1 - a e^{i2\theta_n}} = \frac{1 - a \cos(2\theta_n)}{1 + a^2 - 2a \cos(2\theta_n)},$$

which gives the constant term minus  $\cos \theta_n$  in the denominator that one needs. But the method does not work for (24.177). The denominator one wants to evaluate is a constant term minus  $\cos \theta_n$  minus  $\cos \phi_m$ . Intuitively one wants to evaluate:

$$\mathcal{R}e \frac{1}{NM} \sum_{n=0}^{N-1} \sum_{m=0}^{M-1} \frac{1}{1 - a e^{i2\theta_n} - a e^{i2\phi_m}}.$$

But

$$\mathcal{R}e \frac{1}{1 - a e^{i2\theta_n} - a e^{i2\phi_m}} = \frac{1 - a \cos(2\theta_n) - a \cos(2\phi_m)}{1 + 2a^2 - 2a \cos(2\theta_n) - 2a \cos(2\phi_m) + 2a^2 \cos(2\theta_n - 2\phi_m)}.$$

There is a  $\cos(2\theta_n - 2\phi_m)$  in the denominator that we don't want. We will need use a different way to evaluate (24.177). I'm still trying other ways. I think this may work out.

**2019-11-11 Han** Ivashkevich, Izmailian and Hu [42] *Kronecker's double series and exact asymptotic expansions for free models of statistical mechanics on torus partition function with twisted boundary conditions*

$$Z_{\alpha,\beta}^2(\mu) = \prod_{n=0}^{N-1} \prod_{m=0}^{M-1} 4 \left[ \sin^2 \left( \frac{\pi(n+\alpha)}{N} \right) + \sin^2 \left( \frac{\pi(m+\beta)}{M} \right) + 2 \operatorname{sh}^2 \mu \right]$$

is exactly what is needed. Note that setting  $\alpha = \beta = 0$ :

$$\sin^2 \left( \frac{\pi(n+\alpha)}{N} \right) + \sin^2 \left( \frac{\pi(m+\beta)}{M} \right) + 2 \operatorname{sh}^2 \mu = 4 \cosh(2\mu) - 2 \cos \left( \frac{2\pi n}{N} \right) - 2 \cos \left( \frac{2\pi m}{M} \right).$$

They use the identity

$$4 |\sinh(M\omega + i\pi\beta)|^2 = \prod_{m=0}^{M-1} 4 \left[ \sinh^2 \omega + \sin^2 \left( \frac{\pi(m+\beta)}{M} \right) \right]$$

to get rid of one product, and obtain

$$Z_{\alpha,\beta}^2(\mu) = \prod_{n=0}^{N-1} 4 |\sinh [M\omega_\mu \left( \frac{\pi(n+\alpha)}{M} \right) + i\pi\beta]|^2 \quad (24.180)$$

where  $\omega_\mu(k) = \operatorname{arc} \sinh \sqrt{\sin^2 k + 2 \sinh^2 \mu}$ . Then they use a formula in the appendix that I haven't gone through yet.

To be continued...

**2019-11-23 Predrag** Moved to sect. ?? *Prime invariant 2-tori* / ref. [26].

Restrict the admissible field values  $\phi_z$  at lattice site  $z = (n_1, n_2)$  to the symmetric unit interval  $\phi \in [-1/2, 1/2)$ , with 9-letter alphabet now in CL

$$\mathcal{A} = \{\underline{4}, \underline{3}, \underline{2}, \underline{1}, 0, 1, 2, 3, 4\}. \quad (24.181)$$

**2019-11-23 Predrag** For uses of the lexical ordering, table **ChaosBook 18.1: Orbits for the binary symbolic dynamics up to length 9**, and appendix **Chaos-Book A18.2 Prime factorization for dynamical itineraries** might be of interest.

**Kai Hansen** and I found it very useful to plot periodic points as ‘Danish pastry’, see **ChaosBook Sect. 15.3 Symbol plane**, which gave us very clean illustration of pruning rules. For that, one has to recode symbolic dynamics, the symbols  $m_z$  shifted into nonnegative integers,

$$\gamma_z = m_z + 4.$$

A way to map the array such as (21.69) onto a ‘Danish pastry’ unit square is to write it as something like (wrong as it stands)

$$(\gamma_1, \gamma_2)_{(M_{\mathcal{R}})} = (0.\gamma_{11}\gamma_{21}\gamma_{31}\gamma_{41}\cdots\gamma_{L1}, 0.\gamma_{11}\gamma_{12}\gamma_{13}\gamma_{14}\cdots\gamma_{1T}) \quad (24.182)$$

in base  $s + 3$ , where  $\gamma_k \in \{0, 1, \dots, s + 3\}$

**2019-11-23 Predrag** For  $d = 2$ ,  $s = 5$  spatiotemporal cat with Dirichlet b.c.’s, ref. [36] splits the  $s + 3$  letter alphabet  $\mathcal{A} = \mathcal{A}_0 \cup \mathcal{A}_1$  into the interior  $\mathcal{A}_0$  and exterior  $\mathcal{A}_1$  alphabets

$$\mathcal{A}_0 = \{0, 1\}, \quad \mathcal{A}_1 = \{\underline{3}, \underline{2}, \underline{1}\} \cup \{2, 3, 4\}. \quad (24.183)$$

If all  $m_z \in M$  belong to  $\mathcal{A}_0$ ,  $M$  is admissible, i.e.,  $\mathcal{A}_0^{\mathbb{Z}^2}$  is a full shift.

If you look at your  $[2 \times 2]$  inadmissible blocks do you see any indication that invariant 2-tori alphabets also split into the interior  $\mathcal{A}_0$  and exterior  $\mathcal{A}_1$  alphabets?

**2019-11-23 Predrag** I forgot to mention the most important thing - when studying pruning, we focus on the inadmissible blocks; often they give us the grammar of the admissible blocks.

**2019-11-24 Predrag** Thanks for (9.9) and (9.10) counts! It is wonderful to have several independent confirmations of the invariant 2-tori count volume formula (8.214). Clearly my suggestion of constructing covering prime blocks wildly overcounts the candidates for admissible prime invariant 2-tori, so we should give up this avenue of constructing them - no need to count any larger Bravais lattices.

**2020-01-11 Predrag** Pondering figure 8.5; for both temporal cat and spatiotemporal cat, we should order the ‘spring mattress’ normal modes like we always do. For example, we have from **2018-02-13 Han (24.16)** (that should

have been written in terms of  $\Lambda = (3 + \sqrt{5})/2 = 2.6180$  for  $s = 3$ ) the eigenvalues of the  $[5 \times 5]$  Green's function,

$$(\lambda_0, \lambda_1 = \lambda_2, \lambda_3 = \lambda_4) = (1, 2.38, 2.38, 4.62, 4.62) \quad (24.184)$$

and the corresponding (normalized) eigenvectors:

$$\begin{aligned} \mathbf{e}^{(0)} &= \frac{1}{\sqrt{5}}(1, 1, 1, 1, 1) \\ \mathbf{e}^{(1)} &= \frac{1}{2.689}(-1.618, 1.618, -1, 0, 1) \\ \mathbf{e}^{(2)} &= \frac{1}{2.689}(-1, 1.618, -1.618, 1, 0) \\ \mathbf{e}^{(3)} &= \frac{1}{1.662}(0.618, -0.618, -1, 0, 1) \\ \mathbf{e}^{(4)} &= \frac{1}{1.662}(-1, -0.618, 0.618, 1, 0). \end{aligned} \quad (24.185)$$

By orthogonality to the ground state  $\mathbf{e}^{(0)}$ , the mean values of other eigenvectors are 0.  $\mathbf{e}^{(1)} \rightarrow \mathbf{e}^{(2)}$  and  $\mathbf{e}^{(3)} \rightarrow \mathbf{e}^{(4)}$  have the same energy by time-reversal invariance.

As the action has form

$$S[\Phi] = \frac{1}{2} \sum_{t=1}^n \left\{ (\partial \phi_t)^2 + \frac{1}{2}(2-s)\phi_t^2 \right\} + \sum_{t=1}^n m_t \phi_t. \quad (24.186)$$

For  $0 \leq s < 2$  this is the action for a 1-dimensional chain of nearest-neighbor coupled harmonic oscillators. Here we are, however, interested in the everywhere hyperbolic, unstable, anti-harmonic or inverted parabolic potential,  $s \geq 2$  case. The energy of a normalized eigenmode  $\mathbf{e}_{(j)} \cdot \mathbf{e}^{(j)} = 1$  is obtained by flipping the sign of the potential term.

$$E_j = \frac{1}{2} \sum_{t=1}^n \mathbf{e}_{(j)}^t \square \mathbf{e}^{(j)}_t + \frac{n}{2}(s-1) = \frac{n}{2} \left( \frac{\omega_j^2}{n} + (s-1) \right), \quad (24.187)$$

for temporal cat, and

$$E_j = \frac{LT}{2} \left( \frac{\omega_j^2}{LT} + (s-1) \right), \quad (24.188)$$

for spatiotemporal cat, where  $\omega_j^2$  are the Laplacian eigenvalues. This spatiotemporal cat energy is wrong, in the sense that I have not picked out a time direction - it's really an Euclidean, 'elasticity' mode.

Not sure whether we should be looking at normalized eigenmodes, but at least the energy density  $E_j/(LT)$  looks sensible in this definition, extensive with the system size. However, looking at the eigenvector signs, to me it looks like  $\mathbf{e}^{(1)}$  should have a higher energy than  $\mathbf{e}^{(3)}$  (more wiggles).

**2020-01-11 Predrag** So you are saved by the bell again: Have to compute and plot the lowest energies eigenmodes for large  $n$  temporal cat, and for as large  $[L \times T]$  spatiotemporal cat. So you can avoid actual paper writing while you do that.

The point is to demonstrate that even though the microscopic, site dynamics is chaotic, the most important lattice modes are 'hydrodynamic', i.e., long wavelength in units of the lattice spacing.

Once you see the eigenfunctions, it will be very hard to explain why would not one exploit the  $D_4$  and spacetime reflection symmetries.

**2020-01-16 Han** I computed the 5776 periodic states  $\Phi$  of period  $n = 9$  for the  $s = 3$  temporal cat (see (2.14)); corresponding to 960 prime periodic states, see (2.15)) with the with the 3-letter alphabet  $\mathcal{A}$  (2.9) defined in figure 2.9. The action, according to ref. [26], is

$$S[\Phi] = \frac{1}{2} \Phi^\top \mathcal{J} \Phi + \Phi^\top M = \frac{1}{2} \sum_{t,t'=1}^T \phi_{t'} \mathcal{J}_{t't} \phi_t + \sum_{t=1}^T m_t \phi_t. \quad (24.189)$$

I omitted the sources  $M$ , and computed  $2S[\Phi] = \Phi^\top \mathcal{J} \Phi$  for these solutions. The (twice the) action ranges between 0 and  $239/76 = 3.1447 = \pi + 0.0031$ . The lowest action 0 comes from the solution which has 0 field  $\Phi$  everywhere.

The second lowest action is  $17/76 = 0.224$ . This action comes from the single source periodic state

$$\begin{aligned} M_1 &= (\underline{1}, 0, 0, 0, 0, 0, 0, 0, 0) \\ \Phi_1 &= \frac{1}{76}(-34, -13, -5, -2, -1, -1, -2, -5, -13) \\ &\approx -\frac{1}{4}(1 + \cos 2\pi t/n), \end{aligned} \quad (24.190)$$

its  $m_t \rightarrow -m_t$  reflection

$$\begin{aligned} M_2 &= (1, 0, 0, 0, 0, 0, 0, 0, 0) \\ \Phi_2 &= \frac{1}{76}(34, 13, 5, 2, 1, 1, 2, 5, 13), \end{aligned} \quad (24.191)$$

and their translations. The state (and its reflection) with the third lowest action has source:

$$\begin{aligned} M_3 &= (\underline{1}, 1, 0, 0, 0, 0, 0, 0, 0) \\ M_4 &= (1, \underline{1}, 0, 0, 0, 0, 0, 0, 0). \end{aligned} \quad (24.192)$$

So the lowest actions correspond to the states disturbed by the smallest sources.

Then I computed the energy (24.187) of these solutions. If I neglect the sources, the energy is given by  $E = 1/2 \Phi^\top (-\square + 2 - s)\Phi$ . The energy of these solutions range from  $-3/8$  to  $5233/2888$ . The solution with lowest energy is the period-3 periodic state  $\Phi_{\perp 00}$

$$\begin{aligned} \Phi &= \frac{1}{4}(-2, -1, -1, -2, -1, -1, -2, -1, -1) \\ M &= (\underline{1}, 0, 0, \underline{1}, 0, 0, \underline{1}, 0, 0), \end{aligned} \quad (24.193)$$

its reflection, and its translations.

But if we compute the energy with source,  $E = 1/2 \Phi^\top (-\square + 2 - s)\Phi + M^\top \Phi$ , the energy of these solutions will range from 0 to  $23397/2888$ . The 0 energy again comes from the fixed point solution with 0 field. And the second lowest energy,  $1161/2888$ , comes from solutions with second lowest action, (24.191–24.192) and their translations.

**2020-01-17 Predrag** I have no idea how you count periodic states, so I included the official, ChaosBook style census in (2.14), and the prime periodic states (2.15), in sect. 2.3.2.

I think it is worth your time understanding that, as we hope to generalize it to spatiotemporal cat counting, see sect. ??.

**2020-01-21 Han** Moved the proof of not-Hill's formula using LU decomposition to here:

### 24.6.1 Stability of a periodic point vs. stability of the orbit

Consider a  $d$ -dimensional map  $\phi_{t+1} = f(\phi_t)$ , where  $\phi_t = \{\phi_{t,1}, \phi_{t,2}, \dots, \phi_{t,d}\}$  is the state of the system at time  $t$ . In case at hand, the one time step Jacobian matrix

$$J(\phi_t)_{ij} = \left. \frac{\partial f(\phi)_i}{\partial \phi_j} \right|_{\phi_i = \phi_{i,t}} \quad (24.194)$$

stretches uniformly, so the Jacobian matrix does not depend on the field value  $\phi_t$  or time  $t$ ,  $J(\phi_t) = J$ .

For a periodic state  $\Phi_p$  with period  $n_p$ , the orbit Jacobian matrix is a  $[n_p d \times n_p d]$  block matrix

$$\mathcal{J}_p = \begin{pmatrix} \mathbf{1} & & & -J \\ -J & \mathbf{1} & & \\ & \dots & \mathbf{1} & \\ & & \dots & \mathbf{1} \\ & & & -J & \mathbf{1} \end{pmatrix} = \mathbf{1} - Jr^{-1}, \quad (24.195)$$

where  $\mathbf{1}$  is a  $d$ -dimensional identity matrix, and  $J$  is the one time step  $[d \times d]$  Jacobian matrix (24.194).

To evaluate the determinant of the orbit Jacobian matrix, let  $L$  be a  $[n_p d \times n_p d]$  block lower-triangular matrix:

$$L = \begin{pmatrix} \mathbf{1} & & & & & \\ J & \mathbf{1} & & & & \\ \vdots & J & \mathbf{1} & & & \\ J^{n_p-2} & & \ddots & \mathbf{1} & & \\ J^{n_p-1} & J^{n_p-2} & \dots & J & \mathbf{1} & \end{pmatrix}, \quad (24.196)$$

and  $U$  be a  $[n_p d \times n_p d]$  block upper-triangular matrix:

$$U = \begin{pmatrix} \mathbf{1} & & & -J & & \\ & \mathbf{1} & & -J^2 & & \\ & & \mathbf{1} & -J^3 & & \\ & & & \dots & & \\ & & & & \mathbf{1} & -J^{n_p} \end{pmatrix}. \quad (24.197)$$

Note that:

$$L\mathcal{J}_p = U, \quad (24.198)$$

and the determinant of  $L$  is 1. The determinant of orbit Jacobian matrix is:

$$\det \mathcal{J}_p = \det (L\mathcal{J}_p) = \det U = \det (\mathbf{1} - J^{n_p}). \quad (24.199)$$

## 24.6.2 Temporal cat counting by determinant recursion

2020-06-12 Han From (2.90) to (2.96) we solved an inhomogeneous difference equation

$$\phi_{t+2} - s\phi_{t+1} + \phi_t = -2(s-2),$$

and the general solution is (2.96) with  $m = -2(s-2)$ . But then we use this general solution to find the number of solutions, which assumes that the number of solutions  $N_n$  satisfies the difference equation:

$$N_{t+2} - sN_{t+1} + N_t = -2(s-2).$$

And this is the recurrence relation that we need to prove.

I can only prove this recurrence relation by expanding the determinant of the orbit Jacobian matrix. Here is a method that is slightly simpler than the old one:



$$N_n = |\text{Det } \mathcal{J}_n| = \begin{vmatrix} s & -1 & 0 & 0 & \dots & 0 & -1 \\ -1 & s & -1 & 0 & \dots & 0 & 0 \\ 0 & -1 & s & -1 & \dots & 0 & 0 \\ \vdots & \vdots & \vdots & \vdots & \ddots & \vdots & \vdots \\ 0 & 0 & \dots & \dots & \dots & s & -1 \\ -1 & 0 & \dots & \dots & \dots & -1 & s \end{vmatrix}_{[n \times n]} \quad (24.200)$$

$$= \begin{vmatrix} s & -1 & 0 & 0 & \dots & 0 & 0 \\ -1 & s & -1 & 0 & \dots & 0 & 0 \\ 0 & -1 & s & -1 & \dots & 0 & 0 \\ \vdots & \vdots & \vdots & \vdots & \ddots & \vdots & \vdots \\ 0 & 0 & \dots & \dots & \dots & s & -1 \\ -1 & 0 & \dots & \dots & \dots & -1 & s \end{vmatrix}_{[n \times n]} \quad (24.201)$$

$$+(-1)^{n+1}(-1) \begin{vmatrix} -1 & s & -1 & 0 & \dots & 0 \\ 0 & -1 & s & -1 & \dots & 0 \\ \vdots & \vdots & \vdots & \ddots & \vdots & \vdots \\ 0 & 0 & \dots & \dots & -1 & s \\ -1 & 0 & \dots & \dots & \dots & -1 \end{vmatrix}_{[(n-1) \times (n-1)]} \quad (24.202)$$

$$= \begin{vmatrix} s & -1 & 0 & 0 & \dots & 0 & 0 \\ -1 & s & -1 & 0 & \dots & 0 & 0 \\ 0 & -1 & s & -1 & \dots & 0 & 0 \\ \vdots & \vdots & \vdots & \vdots & \ddots & \vdots & \vdots \\ 0 & 0 & \dots & \dots & \dots & s & -1 \\ 0 & 0 & \dots & \dots & \dots & -1 & s \end{vmatrix}_{[n \times n]} \quad (24.203)$$

$$+(-1)^{n+1}(-1) \begin{vmatrix} -1 & 0 & 0 & \dots & 0 & 0 \\ s & -1 & 0 & \dots & 0 & 0 \\ -1 & s & -1 & \dots & 0 & 0 \\ \vdots & \vdots & \vdots & \dots & \ddots & \vdots \\ 0 & \dots & \dots & -1 & s & -1 \end{vmatrix}_{[(n-1) \times (n-1)]} \quad (24.204)$$

$$+(-1)^{n+1}(-1)^n(-1) \begin{vmatrix} s & -1 & 0 & 0 & \dots & 0 \\ -1 & s & -1 & 0 & \dots & 0 \\ 0 & -1 & s & -1 & \dots & 0 \\ \vdots & \vdots & \vdots & \vdots & \ddots & \vdots \\ 0 & 0 & \dots & \dots & \dots & s \end{vmatrix}_{[(n-2) \times (n-2)]} \quad (24.205)$$

$$+(-1)^{n+1}(-1) \begin{vmatrix} -1 & s & -1 & 0 & \dots & 0 \\ 0 & -1 & s & -1 & \dots & 0 \\ \vdots & \vdots & \vdots & \ddots & \vdots & \vdots \\ 0 & 0 & \dots & \dots & -1 & s \\ 0 & 0 & \dots & \dots & \dots & -1 \end{vmatrix}_{[(n-1) \times (n-1)]} \quad (24.206)$$

$$9051 \text{ (predrag-7373)} \det(-\mathcal{J}_n) - 1 - \det(-\mathcal{J}_{n-2}) - 1, \quad 09/28/2023 \text{ blogHL} \quad (24.207)$$

where  $-\mathcal{J}_n$  is the  $[n \times n]$  tridiagonal matrix:

$$-\mathcal{J}_n = \begin{pmatrix} s & -1 & 0 & 0 & \dots & 0 & 0 \\ -1 & s & -1 & 0 & \dots & 0 & 0 \\ 0 & -1 & s & -1 & \dots & 0 & 0 \\ \vdots & \vdots & \vdots & \vdots & \ddots & \vdots & \vdots \\ 0 & 0 & \dots & \dots & \dots & s & -1 \\ 0 & 0 & \dots & \dots & \dots & -1 & s \end{pmatrix}. \quad (24.208)$$

The determinant of  $-\mathcal{J}_n$  satisfy the recurrence relation:

$$-\det(-\mathcal{J}_n) + s \det(-\mathcal{J}_{n-1}) - \det(-\mathcal{J}_{n-2}) = 0. \quad (24.209)$$

So the determinant of the orbit Jacobian matrix satisfies:

$$\begin{aligned} & N_{n+2} - sN_{n+1} + N_n \\ = & [-\det(-\mathcal{J}_{n+2}) + s \det(-\mathcal{J}_{n+1}) - \det(-\mathcal{J}_n)] \\ & + [-\det(-\mathcal{J}_n) + s \det(-\mathcal{J}_{n-1}) - \det(-\mathcal{J}_{n-2})] - 2(2-s) \\ = & 2(s-2), \end{aligned} \quad (24.210)$$

which is the difference equation that we use to solve for  $N_n$ .

**2020-01-28 Predrag** Is (6.139) or (2.44) the recursion we need for Chebyshevs?  
Or 2017-09-09 Predrag post?

**2020-01-31 Predrag** Here is a [stackexchange](#) recurrence relation for  $U_n(s/2)$  determinants of a circulant matrix. Can you do the same for  $T_n(s/2)$ . Then we are done with the spatiotemporal cat zeta function.

**2019-09-27, 2020-01-31 Predrag** Write this up here, then distill into a paragraph, insert into the *kittens/CL18.tex*:

Littlejohn [notes](#) are simple and clear on how one evaluates determinants of 3-diagonal matrices, via 3-term recurrence (second-order difference equation [31]), see his eq. (74). For temporal cat substitute  $-c_j \rightarrow s - 2 = \mu^2$ , specify the boundary condition, identify it as the recursive definition of the appropriate Chebyshev polynomials:

This is an  $[(n-1) \times (n-1)]$  tridiagonal matrix (see  $-\mathcal{J}_n = \mathcal{D}_n$  in (2.45)). To prove that  $\text{Det}(-\mathcal{J}_n) = 2T_n(s/2) - 2$ ,  $T_n(s/2)$  Chebyshev polynomial of the first kind, define  $\text{Det}(-\mathcal{J}_k)$  as the determinant of the upper  $[k \times k]$  diagonal block, and set  $\text{Det}(-\mathcal{J}_0) = 1$ . Then by Cramer's rule, we find the recursion relation (something like (24.146), but make it more compact),

$$T_{k+1}(s/2) - sT_k(s/2) + T_{k-1}(s/2) = 0. \quad (24.211)$$

Littlejohn then rescales the equation in the form appropriate to taking a continuum limit - we do not have to do that here.

**2019-09-27 PC Question:** Is there such recurrence relation for the 2-dimensional spatiotemporal cat? I suspect that at the worst it is two 3-term recurrences (second-order difference equations [31]), one for each index. Because of the space  $\Leftrightarrow$  time symmetry they might turn into something simple for square domains.

**2020-03-03 Predrag** For spatiotemporal cat the block circulant matrix with circulant blocks has for  $[3 \times 2]_0$  form

$$\mathcal{J}_{[3 \times 2]_0} = \left( \begin{array}{cc|cc|cc} -2s & 2 & 1 & 0 & 1 & 0 \\ 2 & -2s & 0 & 1 & 0 & 1 \\ \hline 1 & 0 & -2s & 2 & 1 & 0 \\ 0 & 1 & 2 & -2s & 0 & 1 \\ \hline 1 & 0 & 1 & 0 & -2s & 2 \\ 0 & 1 & 0 & 1 & 2 & -2s \end{array} \right). \quad (24.212)$$

of  $[L \times L]$  block form,  $L = 3$ , with  $[T \times T]$  blocks,  $T = 2$ .

**2020-03-03 Han** For  $\mathcal{J}_{[3 \times 3]_0}$  the block circulant matrix is:

$$\left( \begin{array}{ccc|ccc|ccc} -2s & 1 & 1 & 1 & 0 & 0 & 1 & 0 & 0 \\ 1 & -2s & 1 & 0 & 1 & 0 & 0 & 1 & 0 \\ 1 & 1 & -2s & 0 & 0 & 1 & 0 & 0 & 1 \\ \hline 1 & 0 & 0 & -2s & 1 & 1 & 1 & 0 & 0 \\ 0 & 1 & 0 & 1 & -2s & 1 & 0 & 1 & 0 \\ 0 & 0 & 1 & 1 & 1 & -2s & 0 & 0 & 1 \\ \hline 1 & 0 & 0 & 1 & 0 & 0 & -2s & 1 & 1 \\ 0 & 1 & 0 & 0 & 1 & 0 & 1 & -2s & 1 \\ 0 & 0 & 1 & 0 & 0 & 1 & 1 & 1 & -2s \end{array} \right), \quad (24.213)$$

in agreement with *Tensors.nb*.

**2020-03-03 Predrag** Can you compare  $[3 \times 1]_0$  with the temporal cat  $n = 3$  case,

$$\mathcal{J}_3 = \left( \begin{array}{c|c|c} -s & 1 & 1 \\ \hline 1 & -s & 1 \\ \hline 1 & 1 & -s \end{array} \right). \quad (24.214)$$

**2020-03-03 Han** The correct form is:

$$\mathcal{J}_{[3 \times 1]_0} = \left( \begin{array}{c|c|c} -2s+2 & 1 & 1 \\ \hline 1 & -2s+2 & 1 \\ \hline 1 & 1 & -2s+2 \end{array} \right). \quad (24.215)$$

The block on the diagonal has a form similar to the orbit Jacobian matrix of the temporal cat. For  $n = 2$  the orbit Jacobian matrix has the form (24.148), and for  $n = 1$  the orbit Jacobian matrix has the form (24.147), because for a fixed point (1-cycle) in temporal cat, the field value and source satisfy:

$$(-s+2)\phi_t = -m_t.$$

**2020-08-16 Predrag** to Han: Figure 8.3 is an example to rethink. It shows four parallelograms of area 10. The two blue parallelograms are claimed to be 'primitive'. The two red parallelograms can clearly be tiled by either 2 or 5 smaller tiles. I do not trust Holmin [40] on this. *Bravais lattices* clearly must be tiled by 1/2 or 1/5th prime Bravais lattices in all four cases.

1. Can you bring the first 3 parallelograms into the Hermite normal form primitive vectors (4.79)?
2. Are they distinct?
3. Are they  $[5 \times 2]_S$  or  $[10 \times 1]_S$ ?

Note,  $[10 \times 1]_S$  does not make 10 a 'prime', as that can be tiled by  $[5 \times 1]_{S_p}$  and  $[2 \times 1]_{S_p}$ .

**2020-08-18 Han** The the first 3 primitive cells in figure 8.3 are:

$$\Lambda'_1 = \begin{bmatrix} 3 & 1 \\ 2 & 4 \end{bmatrix}, \quad \Lambda'_2 = \begin{bmatrix} 3 & 1 \\ -1 & 3 \end{bmatrix}, \quad \Lambda'_3 = \begin{bmatrix} 3 & 2 \\ 1 & 4 \end{bmatrix}.$$

Unimodular matrices ( $U_j \in \text{SL}(2, \mathbb{Z})$ , special linear group over integers of degree 2) <sup>11</sup>

$$U_1 = \begin{bmatrix} 2 & 1 \\ -1 & 0 \end{bmatrix}, \quad U_2 = \begin{bmatrix} 3 & 2 \\ 1 & 1 \end{bmatrix}, \quad U_3 = \begin{bmatrix} 4 & 1 \\ -1 & 0 \end{bmatrix},$$

bring these to the Hermite normal form:

$$\begin{aligned} \Lambda_1 &= \Lambda'_1 U_1 = \begin{bmatrix} 5 & 3 \\ 0 & 2 \end{bmatrix}, & \Lambda_2 &= \Lambda'_2 U_2 = \begin{bmatrix} 10 & 7 \\ 0 & 1 \end{bmatrix} \\ \Lambda_3 &= \Lambda'_3 U_3 = \begin{bmatrix} 10 & 3 \\ 0 & 1 \end{bmatrix}. \end{aligned} \tag{24.216}$$

So these 3 bases span 3 different lattices. None of them is a prime lattice.  $[5 \times 2]_3$  is a sublattice of  $[5 \times 1]_4$  and  $[1 \times 2]_0$ ,  $[10 \times 1]_7$  is a sublattice of  $[5 \times 1]_2$  and  $[2 \times 1]_1$ , and  $[10 \times 1]_3$  is a sublattice of  $[5 \times 1]_3$  and  $[2 \times 1]_1$ .

**2020-08-21 Han** In this paper, we are able to systematically enumerate all possible solutions of the spatiotemporal cat in two steps. The first step is to generate the Bravais lattices which describe the periodicities of the solutions. The second step is to compute the solutions with the given periodicities and to count the number of the solutions, which can be done in two ways: using the Fourier transform to diagonalize the orbit Jacobian matrix, or computing the determinant of the orbit Jacobian matrix directly.

**2020-08-28 Han** Periodicity: The field is invariant under a discrete translation group, which is isomorphic to a Bravais lattice.

<sup>11</sup>Predrag 2020-08-18: where do your  $U_j$ 's come from?

**2020-09-08 Predrag** I do not know whether you have read any literature that defines precisely our lattices, but if you have, use that knowledge now. Clearly, we have to give up on “Bravais” lattices as all references say there are only 5 Bravais lattices in  $d = 2$ , so we are misusing the term - my bad. Keep on reading.

**2020-09-24 Predrag** While writing up tomorrow's talk, I came up with a simple guess (16.49) for spatiotemporal cat zeta function. The factor  $2(s - 2)$  the we see in every  $N_{[L \times T]_s}$  is automatic. Can you check whether it agrees with our periodic state counts? It has no tilt  $S$  anyplace, so if it works, it should generate the sums of all states whose tile has area  $[L \times T]$ . To recover periodic state counts  $N_{[L \times T]}$  you probably have to take derivatives of  $\ln \det$  in both  $z_1$  and  $z_2$ , something like

$$\sum_{L=1}^{\infty} \sum_{T=1}^{\infty} z_1^L z_2^T N_{[L \times T]} = -\frac{1}{1/\zeta_{AM}} z_1 z_2 \frac{d}{dz_1} \frac{d}{dz_2} (1/\zeta_{AM}). \quad (24.217)$$

Have not checked any of that. For once, the real time pressure is on - if true, I can announce it at 10am Friday. Who knows when I get to give another talk on spatiotemporal cat? :)

**2020-09-24 Han** It does not work. If zeta function we have is:

$$1/\zeta_{AM} = \exp \left( \sum_{L=1}^{\infty} \sum_{T=1}^{\infty} \frac{z_1^L z_2^T}{LT} N_{[L \times T]} \right), \quad (24.218)$$

then we have

$$f(z_1, z_2) = \sum_{L=1}^{\infty} \sum_{T=1}^{\infty} z_1^L z_2^T N_{[L \times T]} = z_1 z_2 \frac{\partial^2}{\partial z_1 \partial z_2} \ln(1/\zeta_{AM}). \quad (24.219)$$

From the guess “zeta” function (16.49)

$$1/\zeta_{AM}(z_1, z_2) = 1 - \frac{2(s - 2)}{z_1 + z_2 - 4 + z_1^{-1} + z_2^{-1}} \quad (24.220)$$

I get

$$f(z_1, z_2)/4(s - 2) = \frac{(z_1 - z_1^{-1})(z_2 - z_2^{-1})(z_1 + z_2 - s - 2 + z_1^{-1} + z_2^{-1})}{(z_1 + z_2 - 4 + z_1^{-1} + z_2^{-1})^2 (z_1 + z_2 - 2s + z_1^{-1} + z_2^{-1})^2}, \quad (24.221)$$

which changes sign separately under each spacetime reflection (reversal  $z_1 \rightarrow z_1^{-1}$ , and is invariant under the space  $\leftrightarrow$  time diagonal reflection  $z_1 \leftrightarrow z_2$ ). Doing the same for the 1-dimensional temporal cat, I rederive (21.125):

$$f(z) = (s - 2) \frac{1}{z^{-1} - s + z} \frac{1 + z}{1 - z} = \frac{2 - sz}{z^2 - sz + 1} - \frac{2}{1 - z}.$$

I rechecked that this, expanded as a power series, gives the correct periodic points count.

To count  $N_{[L \times T]}$ , we can either compute:

$$N_{[L \times T]} = \frac{1}{L!T!} \lim_{z_1, z_2 \rightarrow 0} \frac{\partial^L}{\partial z_1^L} \frac{\partial^T}{\partial z_2^T} f(z_1, z_2), \quad (24.222)$$

or:

$$N_{[L \times T]} = \frac{1}{(L-1)!(T-1)!} \lim_{z_1, z_2 \rightarrow 0} \frac{\partial^L}{\partial z_1^L} \frac{\partial^T}{\partial z_2^T} \ln(1/\zeta_{AM}). \quad (24.223)$$

I have tried both (24.222) and (24.223). The results for small  $L$  and  $T$  are either 0 or not converge. And this happens in most of the spatiotemporal cat zeta functions that we guessed.

**2020-09-24 Predrag**  $f$  (24.221) is pretty close in form to (16.48), but why are denominators squared? It's almost like our derivatives are not right, might be something like

$$\frac{1}{2} \left( z \frac{\partial}{\partial z} - z^{-1} \frac{\partial}{\partial (z^{-1})} \right)$$

would be better. In  $d = 2$  there might be some conformal, complex plane, Cauchy-Riemann magic going on, compare with use of 'time reversal' in (19.5), (19.7) and figure 19.5.

**2020-10-06 Han** Revisiting my attempt of 2 years ago, see (24.104): We need a definition of the topological zeta function of fields on the 2-dimensional lattice. (24.218) is incorrect. We want to find a topological zeta function that can be written into the product formula of prime orbits.

I tried to prove that (24.218) gives us a topological zeta function in (24.104–24.107). But there is a mistake in the beginning. If the  $N_{[L \times T]}$  means number of fixed points on  $[L \times T]_0$ , we will let each of the prime orbits  $[L_p \times T_p]_{S_p}$  with non-zero  $S_p$  that tiles  $[L \times T]_0$  contributes  $LT$  times in the  $N_{[L \times T]_0}$ , where they actually only contribute  $L_p T_p$  times.

If the  $N_{[L \times T]}$  is the sum of all states whose tile is  $[L \times T]$ , then this is intuitively wrong since we will overcount some solutions. For example, the trivial solution, fixed point on  $[1 \times 1]_0$ , is counted in all states whose tile is  $[L \times T]$  with different  $S$ .

Assume the weight assigned to a prime orbit  $p$  is:

$$t_p = t_{p1} t_{p2}, \quad \text{where } t_{p1} = z_1^{L_p}, t_{p2} = z_2^{T_p}. \quad (24.224)$$

Rewrite the number of periodic states as:

$$\begin{aligned}
 z_1^L z_2^T N_{[L \times T]_S} &= \sum_{L_p | L} L_p t_{p1}^{\frac{L}{L_p}} \sum_{T_p | T} T_p t_{p2}^{\frac{T}{T_p}} \sum_{L_p T_p | ST_p - TS_p} 1 \quad (24.225) \\
 &= \sum_p L_p T_p \sum_{r_1=1}^{\infty} \sum_{r_2=1}^{\infty} t_{p1}^{r_1} t_{p2}^{r_2} \delta_{r_1 L_p, L} \delta_{r_2 T_p, T} \\
 &\quad \sum_{r_S=-\infty}^{\infty} \delta_{r_S L_p, S - r_2 S_p},
 \end{aligned}$$

where

$$\begin{aligned}
 L &= r_1 L_p, \quad T = r_2 T_p \\
 ST_p - TS_p &= r_S L_p T_p \\
 \Rightarrow S &= r_S L_p + r_2 S_p \pmod{L}. \quad (24.226)
 \end{aligned}$$

The next step is to sum over  $L$ ,  $T$  and  $S$ . Taking sum of (24.225) over  $L$  and  $T$  from 1 to  $\infty$ , we will get rid of the Kronecker deltas, as in (24.105). The geometric series in powers of  $L_p$  sums up as in the  $d = 1$  case, but  $T$  and  $S$  sums are entangled through  $r_2$ . The generating function for the numbers of periodic states is

$$\begin{aligned}
 \Gamma(z_1, z_2) &= \sum_{L=1}^{\infty} \sum_{T=1}^{\infty} z_1^L z_2^T \sum_{S=0}^{L-1} N_{[L \times T]_S} \\
 &= \sum_p \frac{L_p t_{p1}}{1 - t_{p1}} T_p \sum_{r_2=1}^{\infty} t_{p2}^{r_2} \\
 &\quad \sum_{S=0}^{L-1} \sum_{r_S=-\infty}^{\infty} \delta_{r_S L_p + r_2 S_p, S} \quad (24.227)
 \end{aligned}$$

The sum over  $S$  is tricky. For  $S = 0$ ,

$$r_S L_p = -r_2 S_p$$

and as  $0 \leq S_p/L_p < 1$ , so  $-r_2 < r_S \leq 0$  is non-positive. For  $S = L - 1$ ,

$$r_S = r_1 - \frac{1 + r_2 S_p}{L_p}.$$

$r_S$  is strictly positive.

But if we take  $r_S$  from  $-\infty$  to  $\infty$ , for some of the  $r_S$  there will not be a  $S \in [0, L - 1]$  such that  $ST_p - TS_p = L_p T_p r_S$ . Maybe we need to find a range of  $r_S$  in the sum in (24.225) such that for any  $r_S$  there exists one  $S$  that have  $\delta_{r_S L_p + r_2 S_p, S} = 1$ .

The weight (24.224) is likely incorrect, and it will determine the factor in front of  $N_{[L \times T]_S}$  in the zeta function. But I think we need to first know how to write the zeta function into the product form, then we will be able to interpret and construct the zeta function.

**2020-10-09 Han** We need to reduce the range of the sum of  $r_S$  such that for any  $r_S$  in the range there is one  $S \in [0, L)$  that satisfy:

$$r_S = \frac{S - r_2 S_p}{L_p}.$$

Known the range of  $S$  and the relation between  $S$  and  $r_S$ , the reduced range of  $r_S$  is:

$$r_S \in \left[ -\frac{r_2 S_p}{L_p}, r_1 - \frac{r_2 S_p}{L_p} \right).$$

Sum the separated term with  $S$  in (24.225) over  $S$ :

$$\sum_{S=0}^{L-1} \sum_{r_S = \left\lceil -\frac{r_2 S_p}{L_p} \right\rceil}^{\left\lceil r_1 - \frac{r_2 S_p}{L_p} - 1 \right\rceil} \delta_{r_S L_p + r_2 S_p, S} = \sum_{r_S = \left\lceil -\frac{r_2 S_p}{L_p} \right\rceil}^{\left\lceil r_1 - \frac{r_2 S_p}{L_p} - 1 \right\rceil} 1 = r_1. \quad (24.228)$$

The  $\lceil x \rceil$  is the least integer greater than or equal to  $x$ .

The zeta function (24.218) can be written into product formula:

$$\begin{aligned} 1/\zeta_{AM} &= \exp \left( - \sum_{L=1} \sum_{T=1} \sum_{S=0}^{L-1} \frac{z_1^L z_2^T}{LT} N_{[L \times T]_S} \right) \\ &= \exp \left( - \sum_p \sum_{r_1=1}^{\infty} \sum_{r_2=1}^{\infty} \frac{t_p^{r_1 r_2} r_1}{r_1 r_2} \right) \\ &= \exp \left( \sum_p \sum_{r_1=1}^{\infty} \ln(1 - t_p^{r_1}) \right) \\ &= \prod_p \left[ \prod_{r_1=1}^{\infty} (1 - t_p^{r_1}) \right]. \end{aligned} \quad (24.229)$$

This result is very similar to the zeta functions in Lind [49]. In Lind [49], the function

$$\prod_{r_1=1}^{\infty} \frac{1}{1 - t_p^{r_1}}$$

is called the generating function for the partition function.

**2020-10-07 Predrag** The Kronecker (circular) delta function for a periodic lattice



$$\delta_{kj} = \frac{1}{L} \sum_{\ell=0}^{L-1} e^{i \frac{2\pi}{L} (k-j)\ell}. \quad (24.230)$$

takes care of  $\text{mod } L$  and  $\text{mod } T$  in (24.225), but what is Kronecker delta for  $S$ ? What is the periodicity there? I suspect one has to average over the unimodular group there, with a double sum over 2 generators, as in (19.6), (19.7) and figure 19.5. The eigenfunctions might be some fancy 19th century special functions.

**2020-10-07 Predrag** As far as I can see,  $S$  sum can be separated as in my rewritten version of (24.225). That looks strange.

**2020-10-07 Han** Counting formulas like (21.128), for the number of prime  $[2 \times 2]_0$  periodic states is

$$M_{[2 \times 2]_0} = \frac{1}{2 \cdot 2} (N_{[2 \times 2]_0} - 2M_{[2 \times 1]_0} - 2M_{[1 \times 2]_0} - 2M_{[2 \times 1]_1} - M_{[1 \times 1]_0}),$$

relate numbers  $N_{[L \times T]_S}$  and  $M_{[L \times T]_S}$ . Numbers such as the number of orbits  $M_p$  do not appear in formula (24.225) because when we compute the sum over all the prime orbits, labeled by  $p$ , each prime orbit will contribute once to the sum. If the number of prime  $[2 \times 2]_0$  periodic states is  $M_{[2 \times 2]_0}$ , there will be  $M_{[2 \times 2]_0}$  orbits with  $[L_p \times T_p]_{S_p} = [2 \times 2]_0$  that will be summed.

**2020-10-07 Predrag** Not getting a simpler formula than (24.106) is OK; looks like you are dealing with polylogs (wiki), and specifically with dilogs (wiki), and/or Spence's function (wiki).

Some random references, hopefully we do not need them:

Zagier (Predrag's MIT wunderkid) *The Dilogarithm Function*.

*Dilogarithm identities in conformal field theory and group homology*.

**2018-06-11 Han** For example, consider the simplest case in two-dimensions, with the period of  $\ell$  is  $L = 2$ . In this case, we will need to know  $x_{1,t-1}$ ,  $x_{2,t-1}$ ,  $x_{1,t}$  and  $x_{2,t}$  to solve for the field values on all of the lattice sites,  $t \in \mathbb{Z}$ . And we can also define the generating partition in the space spanned by these four values. If the field value satisfies (24.43) where  $d = 2$ , the state evolves with time as:

$$A \begin{bmatrix} \phi_{1,t-1} \\ \phi_{2,t-1} \\ \phi_{1,t} \\ \phi_{2,t} \end{bmatrix} = \begin{bmatrix} 0 & 0 & 1 & 0 \\ 0 & 0 & 0 & 1 \\ -1 & 0 & s & -2 \\ 0 & -1 & -2 & s \end{bmatrix} \begin{bmatrix} \phi_{1,t-1} \\ \phi_{2,t-1} \\ \phi_{1,t} \\ \phi_{2,t} \end{bmatrix} = \begin{bmatrix} \phi_{1,t} \\ \phi_{2,t} \\ \phi_{1,t+1} \\ \phi_{2,t+1} \end{bmatrix} + \begin{bmatrix} 0 \\ 0 \\ m_{1,t} \\ m_{2,t} \end{bmatrix} \quad (24.231)$$

The matrix  $A$  gives us the cat map for the lattice with spatial period of 2. If the spatial period is longer, the general matrix  $A$  will be:

$$A = \left[ \begin{array}{cccc|cccc} 0 & \dots & 0 & & 1 & 0 & \dots & 0 & 0 \\ \vdots & \ddots & \vdots & & \vdots & & \ddots & & \vdots \\ 0 & \dots & 0 & & 0 & 0 & \dots & 1 & 0 \\ - & - & - & - & - & - & - & - & - \\ -1 & 0 & \dots & 0 & 0 & s & -1 & \dots & 0 & -1 \\ 0 & -1 & \dots & 0 & 0 & -1 & s & -1 & & 0 \\ \vdots & \ddots & \vdots & & \vdots & \ddots & \ddots & \ddots & \vdots \\ 0 & 0 & \dots & -1 & 0 & 0 & & -1 & s & -1 \\ 0 & 0 & \dots & 0 & -1 & -1 & 0 & \dots & -1 & s \end{array} \right] \tag{24.232}$$

which is very similar to the cat map matrix in one-dimension.

**2020-07-12 Predrag** See (12.10) for a compact rewrite.

**2018-06-21 Predrag** This is nice. In principle it should be already in this blog, for example (8.3), and in Gutkin and Osipov [37], and Gutkin *et al.* [36], but I do not recognize the equations. My impression is that the spectrum of  $A$  for going forward in time is hard to interpret, but I have not tried.

**2018-06-11 Han** After we get the matrix  $A$ , we can get the eigenvalues and eigenvectors. There will be 4 eigenvectors for the case (24.231) where the spatial period is 2. With these four eigenvectors we can define the generating partition in the space spanned by  $x_{1,t-1}$ ,  $x_{2,t-1}$ ,  $x_{1,t}$  and  $x_{2,t}$  which is a 4-torus.

**2018-06-26 Han** I have tried to get the partition for spatiotemporal cat with spatial period  $L = 2$ . But this is more complex than I thought. I thought the partition will be same as the one-dimensional case. So using the 4 eigenvectors we will have 4 planes, and each of them is parallel to 3 of the eigenvectors. The 4 planes passing through the origin and the 4 planes passing through the point  $(1, 1, 1, 1)$  will enclose a four-dimensional "cube" which is corresponding to the large rectangle in the figure 24.3 (a). And using 4 planes passing through the points  $(1, 0, 0, 0)$ ,  $(0, 1, 0, 0)$ ,  $(0, 0, 1, 0)$  and  $(0, 0, 0, 1)$  separately we will have 4 small region corresponding to the 2 small rectangle in figure 24.3. This is the simplest case, but it doesn't work out.

The eigenvalues of the matrix in (24.231) where  $s = 5$  are:

$$\begin{aligned}
 \Lambda_1 &= \frac{1}{2}(7 + 3\sqrt{5}) \\
 \Lambda_2 &= \frac{1}{2}(7 - 3\sqrt{5}) = \Lambda_1^{-1} \\
 \Lambda_3 &= \frac{1}{2}(3 + \sqrt{5}) \\
 \Lambda_4 &= \frac{1}{2}(3 - \sqrt{5}) = \Lambda_3^{-1}
 \end{aligned} \tag{24.233}$$

The corresponding eigenvectors are:

$$\begin{aligned}
 e_1 &= (-1, 1, -\Lambda_1, \Lambda_1) \\
 e_2 &= (-\Lambda_1, \Lambda_1, -1, 1) \\
 e_3 &= (1, 1, \Lambda_3, \Lambda_3) \\
 e_4 &= (\Lambda_3, \Lambda_3, 1, 1)
 \end{aligned} \tag{24.234}$$

Note that  $\Lambda_3$  and  $\Lambda_4$  are the eigenvalues of the Percival-Vivaldi cat map with  $s = 3$ . These two eigenvectors are corresponding to the case when all of the sites are having a same value at a given time.

**2018-06-27 Predrag** Looks like the configuration eigenvectors,

$$e_{2i+1}^\top \cdot e_{2j+1} = 0, \quad i \neq j,$$

and the momentum eigenvectors,

$$e_{2i}^\top \cdot e_{2j} = 0, \quad i \neq j,$$

will be separately orthogonal for the  $L$ -“particles” lattice. If we are lucky, the  $j$ th phase-space area  $e_{2j}^\top \cdot e_{2j+1} = A_j$  is preserved by the (symplectic?) map (24.232); generically I think only the sum of areas is preserved.

**2018-07-13 Predrag** discussion with Han: think how to generalize the number of periodic orbits (??) to the  $L = 2$  case. Your arbitrary  $L$  evolution matrix (24.232) has a very nice form, which might lead to some nice generalization of eigenvalue formulas (24.233) to arbitrary  $L$ . We do not really need explicit alphabets; to get topological zeta functions for this problem, we only need formulas like (??) that only need eigenvalues (coordinate choice invariant properties of dynamics). For  $L = 1$  case the object of interest is the topological entropy  $\ln \Lambda$  (the rate of growth of the number of periodic orbits with  $T \rightarrow \infty$ ). For large  $L$  you need the rate of growth of the number of periodic orbits per unit length, i.e.,  $(\ln \Lambda_j)/L$ , where  $\Lambda_j$  is the leading eigenvalue in the generalized (24.233).

**2018-07-27 Predrag** That suggests computing analytic expressions for eigenvalues for invariant 2-tori  $\mathcal{R} = [2 \times 2]$ ,  $\mathcal{R} = [3 \times 3]$ ,  $\mathcal{R} = [4 \times 4]$ ,  $\dots$ , try to divine  $T \leftrightarrow L$  interchange symmetry from those...

**2018-08-02 Predrag** Have you had a look at sect. 8.4 *Toeplitz tensors*? References cited there might offer efficient ways of computing spectra of your doubly cyclic tensorial matrices.

**2018-07-24 Han** The number of periodic points for the  $L = 2$  case is easy to get. The number of periodic points with time period  $T$  is:

$$N_{[L \times T]} = |\det(\mathbf{A}(L)^T - \mathbf{I})| \quad (24.235)$$

In all examples we take  $s = 5$ . Since the matrices  $\mathbf{A}$  and  $\mathbf{I}$  can be diagonalized simultaneously, the number of periodic points for the  $L = 2$  case is:

$$\begin{aligned} N_{[2 \times T]} &= |(\Lambda_1^T - 1)(\Lambda_1^{-T} - 1)(\Lambda_3^T - 1)(\Lambda_3^{-T} - 1)| \\ &= |[2 - (\Lambda_1^T + \Lambda_1^{-T})][2 - (\Lambda_3^T + \Lambda_3^{-T})]| \end{aligned} \quad (24.236)$$

As the Hamiltonian evolution matrix (24.232) is symplectic, its eigenvalues come in pairs for any  $L$  (for any eigenvalue  $\Lambda_j$ ,  $\Lambda_j^{-1}$  is also an eigenvalue). So the number of periodic orbits with time period  $T$  and spatial period  $L$  is

$$\begin{aligned} N_{[L \times T]} &= \prod_{i=1}^L |(\Lambda_i^T - 1)(\Lambda_i^{-T} - 1)| \\ &= \prod_{i=1}^L (\Lambda_i^T + \Lambda_i^{-T} - 2) = N_{[T \times L]}. \end{aligned} \quad (24.237)$$

The problem is how to get a general form of the eigenvalues. We have the same number of orbits for the  $[T \times L]$  block and the  $[L \times T]$  block, so (24.237) must be a function of  $L$  and  $T$  invariant under the  $T \leftrightarrow L$  exchange.

**2018-07-24 Han** Perhaps there is a better way to get the general formulas of the eigenvalues of (24.232), I just haven't figured it out. It seems like the eigenvalues of (24.232) are completely determined by the eigenvalues of the small Toeplitz matrix at the bottom right corner of this matrix (The large evolution matrix itself is not a Toeplitz matrix). For example, when  $L = 2$  and  $s = 5$  the eigenvalues of the Toeplitz matrix are 7 and 3. The eigenvalues of the evolution matrix are  $\frac{1}{2}(7 + 3\sqrt{5})$ ,  $\frac{1}{2}(7 - 3\sqrt{5})$ ,  $\frac{1}{2}(3 + \sqrt{5})$  and  $\frac{1}{2}(3 - \sqrt{5})$ . When  $L = 3$ , the eigenvalues of the Toeplitz matrix are 6, 6 and 3, while the eigenvalues of the evolution matrix are  $\frac{1}{2}(6 + 4\sqrt{2})$ ,  $\frac{1}{2}(6 + 4\sqrt{2})$ ,  $\frac{1}{2}(6 - 4\sqrt{2})$ ,  $\frac{1}{2}(6 - 4\sqrt{2})$ ,  $\frac{1}{2}(3 + \sqrt{5})$  and  $\frac{1}{2}(3 - \sqrt{5})$ .

So generally, the eigenvalues of (24.232) can be expressed as  $\frac{1}{2}(a + b)$  and  $\frac{1}{2}(a - b)$ . And we know that  $\frac{1}{2}(a + b) \times \frac{1}{2}(a - b) = \frac{1}{4}(a^2 - b^2) = 1$ . And we know that  $a$  is an eigenvalue of the small Toeplitz matrix at the bottom right corner of (24.232). The general expression for the Toeplitz matrix is (from (24.48)):

$$\lambda(L)_i = s - 2 \cos\left(\frac{2\pi i}{L}\right), \quad i = 1, 2, \dots, L \quad (24.238)$$

where  $L$  is the spatial period of the lattice and the rank of the Toeplitz matrix. The eigenvalues of (24.232) are:

$$\Lambda(L)_i^\pm = \frac{1}{2}(\lambda_i \pm \sqrt{\lambda_i^2 - 4}), \quad i = 1, 2, \dots, L. \quad (24.239)$$

From (24.238) you can see that for any  $L$ , when  $i = L$  we will get the eigenvalue  $\lambda(L)_L = s - 2$ . That is why when  $s = 5$  the Toeplitz matrix will always have eigenvalue 3. And this will give us the eigenvalues of the large evolution matrix  $\frac{1}{2}(3 + \sqrt{5})$  and  $\frac{1}{2}(3 - \sqrt{5})$ , which are corresponding to the case when all of the sites have a same field value at a given time (same as the one-dimensional case).

Now we have the general formula of the matrix (24.232). In principle I can get a general expression of number of periodic orbits with a given length  $L$  and period  $T$ . The number of periodic orbits will be a function of  $s$ ,  $L$  and  $T$ . But as you can see my formula of eigenvalues of arbitrary  $L$  evolution matrix (24.232) is not pretty. When  $L < 5$ , (24.238) will be an integer but when  $L = 5$  the eigenvalue in (24.238) starts to become an irrational number and the eigenvalue of (24.232) also becomes uglier. So I'm still trying to find an elegant expression.

I haven't figured out how to prove that the eigenvalues of (24.232) are  $\frac{1}{2}(a + b)$  and  $\frac{1}{2}(a - b)$  where  $a$  is eigenvalue of the small Toeplitz matrix and  $b = \sqrt{a^2 - 4}$ . I just calculated all of the eigenvalues of the (24.232) and the small Toeplitz matrix from  $L = 1$  to  $L = 5$ . And they are all matched. I will think about how to prove this.

**2018-08-15 Han** This part is not important. It's just a practice for myself. Given a spatial length  $L$ , the topological zeta function can be calculated from (24.237). For example, if  $L = 2$ , we will have four eigenvalues from matrix (24.232). Let these four eigenvalues be  $\Lambda_1^+$ ,  $\Lambda_1^-$ ,  $\Lambda_2^+$  and  $\Lambda_2^-$ . Expand (24.237) we can see that each term is a constant times a combination of eigenvalues to the power of  $n$ . Substitute (24.237) into (24.101) we have the topological zeta function:

$$\zeta(z) = \frac{(1 - z\Lambda_1^+)^2(1 - z\Lambda_1^-)^2(1 - z\Lambda_2^+)^2(1 - z\Lambda_2^-)^2}{(1 - z\Lambda_1^+\Lambda_2^+)(1 - z\Lambda_1^-\Lambda_2^+)(1 - z\Lambda_1^+\Lambda_2^-)(1 - z\Lambda_1^-\Lambda_2^-)(1 - z)^4} \quad (24.240)$$

As  $L$  becomes larger, the topological zeta function becomes more complicated but it can still be written in a similar form.

**2020-10-20 Predrag** We have temporal cat relations (21.151), (2.7), (2.37), (2.40),  $s = 2 \cosh(\lambda)$ ,

$$2T_T(s/2) = \Lambda^T + \Lambda^{-T} = 2 \cosh(T\lambda),$$

and the Hill determinant formula

$$N_T = |\text{Det } \mathcal{J}| = \prod_{k=0}^{T-1} [s - 2 \cos(2\pi k/T)] = 2 \cosh(T\lambda) - 2. \quad (24.241)$$

Consider the Hermitian orbit Jacobian matrix:

$$\mathcal{J}_T(\theta) = \begin{pmatrix} s & -e^{i\theta} & 0 & 0 & \dots & 0 & -e^{-i\theta} \\ -e^{-i\theta} & s & -e^{i\theta} & 0 & \dots & 0 & 0 \\ 0 & -e^{-i\theta} & s & -e^{i\theta} & \dots & 0 & 0 \\ \vdots & \vdots & \vdots & \vdots & \ddots & \vdots & \vdots \\ 0 & 0 & \dots & \dots & \dots & s & -e^{i\theta} \\ -e^{i\theta} & 0 & \dots & \dots & \dots & -e^{-i\theta} & s \end{pmatrix} \quad (24.242)$$

The usual Toeplitz eigenvalues formula yields the right-hand side of the identity:

$$\det \mathcal{J}_T(\theta) = 2 \cosh(T\lambda) - 2 \cos(T\theta) = \prod_{t=0}^{T-1} \left[ s - 2 \cos \left( \theta + \frac{2\pi t}{T} \right) \right].$$

The left-hand side presumably comes from the Hill's formula - have not checked.

**2020-10-20 Predrag** Taking  $\theta = 2\pi S/T$  does not do anything -  $\det \mathcal{J}_T(\theta)$  is the same for all  $S$ .

**2020-10-20 Han** Using identity (21.141)

$$\cosh(nx) - \cos(ny) = 2^{n-1} \prod_{k=0}^{n-1} \left[ \cosh x - \cos \left( y + \frac{2k\pi}{n} \right) \right],$$

the counting formula (24.176) can be rewritten as:

$$\begin{aligned} N_{[L \times T]_S} &= \left| \prod_k \lambda_k \right| \\ &= \prod_{n_1=0}^{L-1} \prod_{n_2=0}^{T-1} \left[ 2s - 2 \cos \left( \frac{2\pi n_1}{L} \right) - 2 \cos \left( -\frac{2\pi n_1 S}{LT} + \frac{2\pi n_2}{T} \right) \right] \\ &= \prod_{n_1=0}^{L-1} \left[ \prod_{n_2=0}^{T-1} \left( 2s - 2 \cos \frac{2\pi n_1}{L} - 2 \cos \frac{2\pi n_2}{T} \right) - \left( 2 \cos \frac{2\pi n_1 S}{L} - 2 \right) \right]. \end{aligned} \quad (24.243)$$

Let

$$\tilde{N}_{[L \times T]}(n_1) = \prod_{n_2=0}^{T-1} \left( 2s - 2 \cos \frac{2\pi n_1}{L} - 2 \cos \frac{2\pi n_2}{T} \right).$$

Then

$$N_{[L \times T]_S} = \prod_{n_1=0}^{L-1} \left[ \tilde{N}_{[L \times T]}(n_1) - \left( 2 \cos \frac{2\pi n_1 S}{L} - 2 \right) \right].$$

For a  $L$  sites 1-dimensional chain involves with time, the number of fixed points that are invariant after  $T$  time steps with a tilt  $S$  is:

$$\begin{aligned} N_{[L \times T]_S} &= \prod_{n_1=0}^{L-1} \left( \Lambda_{n_1}^T + \Lambda_{n_1}^{-T} - 2 \cos \frac{2\pi n_1 S}{L} \right) \\ &= \prod_{n_1=0}^{L-1} \left[ 2 \cosh(T\lambda_{n_1}) - 2 \cos \frac{2\pi n_1 S}{L} \right], \end{aligned} \quad (24.244)$$

where

$$\lambda_{n_1} = \cosh^{-1} \left( s - \cos \frac{2\pi n_1}{L} \right).$$

When  $S = 0$ , (24.244) becomes (24.237).

**2020-12-23 Predrag** Looks like (19.28), where one allows tilts in both time and space directions, no? There one uses  $4 \sin^2 \theta/2$  instead of  $2 \cos \theta$ , as in (6.52).

**2020-10-30 Han** The determinant of the orbit Jacobian matrix (24.242) is:

$$\det \mathcal{J}_T(\theta) = \prod_{t=0}^{T-1} \left[ s - 2 \cos \left( \theta + \frac{2\pi t}{T} \right) \right] = 2 \cos(T\lambda) - 2 \cos(T\theta), \quad (24.245)$$

where  $\lambda = \arccos(s/2)$ , if the stretching parameter  $s < 2$ . Here I used the oscillatory counterpart (in the sense of (8.31) and (8.32)) of the identity (21.141)

$$2 \cos(nx) - 2 \cos(ny) = \prod_{k=0}^{n-1} \left[ 2 \cos x - 2 \cos \left( y + \frac{2k\pi}{n} \right) \right], \quad (24.246)$$

from [Gradshteyn and Ryzhik \[34\]](#) (1965) *Table of Integrals, Summations and Products* 1.395.2. It can also be proved by using the Chebyshev polynomial identity of [Wikipedia](#):

$$T_n(x) = \begin{cases} \cos(n \arccos x) & \text{if } |x| \leq 1 \\ \cosh(n \operatorname{arcosh} x) & \text{if } x \geq 1 \\ (-1)^n \cosh(n \operatorname{arcosh}(-x)) & \text{if } x \leq -1 \end{cases}.$$

In the continuous limit of the spatiotemporal cat equation becomes Helmholtz equation, whose solutions are also cosine and sines.

**2020-10-31 Predrag** Please read and correct/improve my attempt to consolidate this material in a single sect. [8.2 Helmholtz type equations](#).

**2020-10-31 Predrag** I think of Helmholtz  $\rightarrow$  screened Poisson equation relation as the Helmholtz wavenumber  $ik = m$  conversion, where  $m$  is the mass of the scalar Yukawa particle. The relations (2.49), (2.51), and (2.52) are then "trivial", in the sense that they are just examples of (8.31) and (8.32) conversion of oscillating solutions to exponentials.

**2020-10-31 Predrag** Perhaps of interest to Han: Wu [75] (8.177), (8.178).

**2020-10-31 Predrag** Please abandon the stretching parameter  $s$ , and rewrite everything in terms of the mass  $\mu^2 = d(s - 2) > 0$ ?

Chebyshev polynomials such as (24.241) are written in terms of  $s$ , but our Hill determinants / periodic orbit counts look more natural as polynomials in  $\mu^2$ .

**2020-11-13 Han** Using the counting formula (24.237) the topological zeta function of 2-dimensional spatiotemporal cat with  $L = 3$  I get:

$$\begin{aligned} \frac{1}{\zeta(z)} &= \exp\left(-\sum_{T=1}^{\infty} \frac{z^T}{T} N_{[3 \times T]}\right) \\ &= \frac{N(z)}{D(z)}, \end{aligned} \quad (24.247)$$

where the numerator and denominator of the zeta function are:

$$\begin{aligned} N(z) &= (1 - \Lambda_1^{-1}z)^4 (1 - \Lambda_1 z)^4 (1 - \Lambda_2^{-1}z)^4 \\ &\quad (1 - \Lambda_2 z)^4 (1 - \Lambda_3^{-1}z)^4 (1 - \Lambda_3 z)^4 \\ &\quad (1 - \Lambda_1 \Lambda_2 \Lambda_3^{-1}z) (1 - \Lambda_1^{-1} \Lambda_2^{-1} \Lambda_3 z) (1 - \Lambda_1^{-1} \Lambda_2 \Lambda_3^{-1}z) \\ &\quad (1 - \Lambda_1 \Lambda_2^{-1} \Lambda_3 z) (1 - \Lambda_1 \Lambda_2^{-1} \Lambda_3^{-1}z) (1 - \Lambda_1^{-1} \Lambda_2 \Lambda_3 z) \\ &\quad (1 - \Lambda_1^{-1} \Lambda_2^{-1} \Lambda_3^{-1}z) (1 - \Lambda_1 \Lambda_2 \Lambda_3 z), \end{aligned} \quad (24.248)$$

and

$$\begin{aligned} D(z) &= (1 - \Lambda_1 \Lambda_2^{-1}z)^2 (1 - \Lambda_1^{-1} \Lambda_2 z)^2 (1 - \Lambda_1^{-1} \Lambda_2^{-1}z)^2 (1 - \Lambda_1 \Lambda_2 z)^2 \\ &\quad (1 - \Lambda_1 \Lambda_3^{-1}z)^2 (1 - \Lambda_2 \Lambda_3^{-1}z)^2 (1 - \Lambda_1^{-1} \Lambda_3 z)^2 (1 - \Lambda_2^{-1} \Lambda_3 z)^2 \\ &\quad (1 - \Lambda_1^{-1} \Lambda_3^{-1}z)^2 (1 - \Lambda_1 \Lambda_3 z)^2 (1 - \Lambda_2^{-1} \Lambda_3^{-1}z)^2 (1 - \Lambda_2 \Lambda_3 z)^2 \\ &\quad (1 - z)^8 \end{aligned} \quad (24.249)$$

**2020-11-29 Predrag** For a set  $\mathcal{B} \in \mathbb{R}^d$ , the function

$$[\mathcal{B}](\phi) = \begin{cases} 1 & \text{if } \phi \in \mathcal{B} \\ 0 & \text{otherwise} \end{cases} \quad (24.250)$$

is called the *indicator* of  $\mathcal{B}$ .

**2020-11-30 Predrag** Klain and Rota [45] *Introduction to Geometric Probability*:

A *valuation* on a lattice  $L$  of sets is a function  $\mu$  defined on  $L$  that takes real values, and that satisfies the following conditions:

$$\mu(A \cup B) = \mu(A) + \mu(B) - \mu(A \cap B), \quad (24.251)$$



$$\mu(\emptyset) = 0, \tag{24.252}$$

where  $\emptyset$  is the empty set. By iterating the identity (24.251) we obtain the inclusion-exclusion principle for a valuation  $\mu$  on a lattice  $L$ , namely

$$\begin{aligned} \mu(A_1 \cup A_2 \cup \dots \cup A_n) &= \sum_i \mu(A_i) - \sum_{i < j} \mu(A_i \cap A_j) \\ &+ \sum_{i < j < k} \mu(A_i \cap A_j \cap A_k) + \dots \end{aligned} \tag{24.253}$$

for each positive integer  $n$ .

Barvinok [10] Lecture 1, Problem 1 statement of (24.253) is less intelligible: Take sets  $A_1, A_2, \dots, A_n \in \mathbb{R}^d$ . The inclusion-exclusion formula is

$$\mu(\cup A_i) = \sum_I (-1)^{|I|-1} [\cap_{i \in I} A_i], \tag{24.254}$$

where the sum is taken over all non-empty subsets  $I \subset \{1, \dots, n\}$  and  $|I|$  is the cardinality of  $I$ .

**2020-12-15 Han** Figure 24.47 is the fundamental parallelepiped of the symmetry reduced temporal Bernoulli system with  $s = 2$ . The fundamental domain hypercube  $\hat{\Phi} \in [0, 1/2]^n$  is divided into  $2^n$  smaller hypercubes by the symbolic dynamics  $\hat{A}$ . Each one of the smaller hypercubes is subject to different orbit Jacobian matrix, so the orbit Jacobian matrix maps these hypercubes into different positions.

Each integer point in the fundamental parallelepiped is corresponding to one periodic state of the symmetry reduced temporal Bernoulli system. But now the number of integer points is no longer equal to the volume of the fundamental parallelogram. So we need a smart way to count the number of periodic states. It's possible that the volume of the fundamental parallelogram mapped from the unit hypercube  $[0, 1]^n$  gives the correct number of fixed points. Still need to understand why can we count in this way...

**2020-12-16 Predrag** Figure 24.47 is cool, and you are right, now orbit Jacobian matrices differ because of  $\pm s$  on the diagonal, so different fundamental parallelepipeds go to different places.

Do prove that the |Hill determinant| is the same for all of them.

I expect  $\det(\mathcal{J}\mathcal{L})/\det \mathcal{L}$  from (8.103) to be the correct formula, so we have to divide the volumes you get by  $2^{-n}$ . Or maybe rescale fields  $\phi_t$  as we discussed, so you apply the fundamental fact to unit hypercube.

Sidney has gone through the lattice points enumeration [9, 11, 12, 27] proof, ask him to explain it to you.

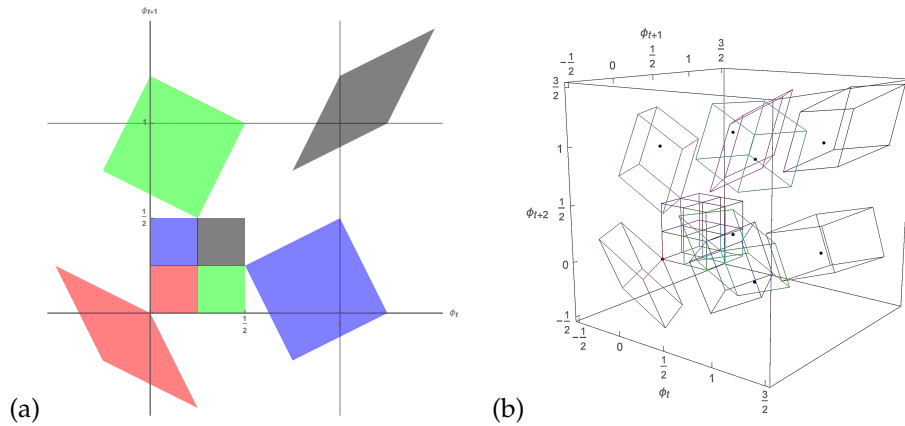


Figure 24.47: The fundamental parallelepiped of the symmetry reduced temporal Bernoulli system with  $s = 2$ . (a) The fundamental parallelogram of length 2 periodic state. The fundamental domain hypercube  $\hat{\Phi} \in [0, 1/2]^2$  is mapped into four fundamental parallelograms by the orbit Jacobian matrix. Each one of them contains one integer point, which is corresponding to a periodic state with length 2. The total area of the four fundamental parallelograms is  $4 \times 1/4$ . (b) The fundamental parallelepiped of length 3 periodic state. The fundamental domain hypercube  $\hat{\Phi} \in [0, 1/2]^3$  is divided into  $2^3$  hypercubes, and each one of them is mapped to a fundamental parallelepiped. The black dots are integer points. Each one of the fundamental parallelepipeds contains one integer point. So the number of the periodic states with length 3 is 8. The total volume of the 8 fundamental parallelepipeds is  $8 \times 1/8$ .

**2020-12-22 Han** Expand the antisymmetric contribution of an orbit into the trace form:

$$H_p = \{e\} : (1 - t_{\hat{p}}) = \exp[\ln(1 - t_{\hat{p}})] = \exp \left[ - \sum_{n=1}^{\infty} \frac{t_{\hat{p}}^n}{n} \right]$$

$$H_p = \{e, \sigma\} : (1 + t_{\hat{p}}) = \exp \left[ - \sum_{n=1}^{\infty} \frac{(-1)^n t_{\hat{p}}^n}{n} \right]$$

**2020-12-24 Han** The attempt described in this post [failed](#), as the fundamental domain is **not**  $\hat{\phi}_t \in [0, 1/2]$ :

Quotient the cat map

$$\phi_{t+1} - s\phi_t + \phi_{t-1} = -m_t \quad \phi_t \in [0, 1)$$

to the fundamental domain by the dynamical  $D_1 = \{e, \sigma\}$  symmetry. The fundamental domain is  $\hat{\phi}_t \in [0, 1/2]$ . The map in the fundamental domain is:

$$\begin{aligned} \hat{\phi}_{t+1} - s\hat{\phi}_t + \hat{\phi}_{t-1} &= -m_t, & -\hat{\phi}_{t-1} + s\hat{\phi}_t - m_t &\leq 1/2 \\ 1 - \hat{\phi}_{t+1} - s\hat{\phi}_t + \hat{\phi}_{t-1} &= -m_t, & -\hat{\phi}_{t-1} + s\hat{\phi}_t - m_t &> 1/2. \end{aligned} \tag{24.255}$$

Figure [24.48](#) (a) is the 3 points recurrence relation of the cat map with  $s = 3$ , and (b) is the recurrence relation in the fundamental domain.

**2020-12-24 Han** The cat map is a map:  $[0, 1)^2 \rightarrow [0, 1)^2$ . So using the reflection symmetry we can only reduce the state space to the fundamental domain which is a half of the full phase space, not a quarter. In the figure [24.48](#) (a) we can see that by using the symmetry  $\{\phi_{t+1}, \phi_t, \phi_{t-1}\} \rightarrow \{\sigma\phi_{t+1}, \sigma\phi_t, \sigma\phi_{t-1}\}$  we reduce the phase space volume by half.

Another way to see why the  $\hat{\phi}_t \in [0, 1/2]$  fundamental domain is incorrect: Assuming that  $\phi_t \in [0, 1/2]$  and  $\phi_{t-1} \in (1/2, 1)$ , we can compute

$$\phi_{t+1} = +s\phi_t - \phi_{t-1} \pmod{1}. \tag{24.256}$$

But in the fundamental domain we have  $\hat{\phi}_t = \phi_t$ ,  $\hat{\phi}_{t-1} = 1 - \phi_{t-1}$  and using the map [\(24.255\)](#)

$$\hat{\phi}_{t+1} = \begin{cases} -1 + \phi_{t-1} + s\phi_t \pmod{1}, & -\hat{\phi}_{t-1} + s\hat{\phi}_t - m_t \leq 1/2, \\ 2 - \phi_{t-1} - s\phi_t \pmod{1}, & -\hat{\phi}_{t-1} + s\hat{\phi}_t - m_t > 1/2. \end{cases}$$

And neither of them is equal to  $\phi_{t+1}$  or  $1 - \phi_{t+1}$ . So this periodic state in the full space  $\{\phi_{t-1}, \phi_t, \phi_{t+1}\}$  does not have a corresponding periodic state in the fundamental domain. The correct fundamental domain should be  $\{\hat{\phi}_{t-1}, \hat{\phi}_t\} \in [0, 1)^2/D_1$  which is not  $[0, 1/2]^2$ .

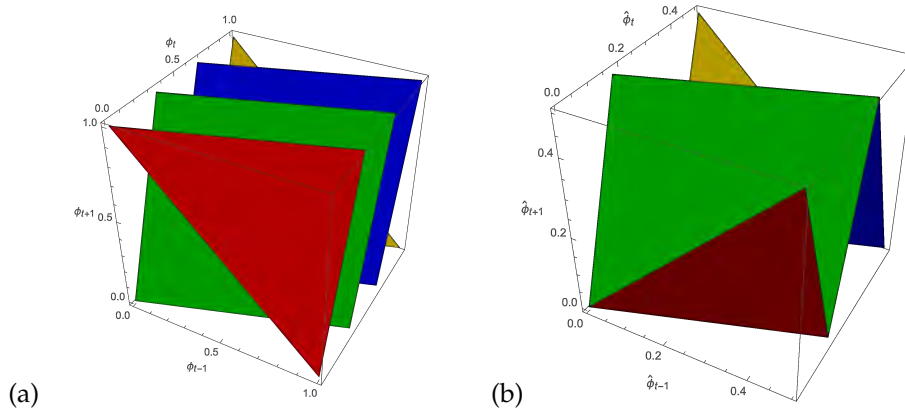


Figure 24.48: (a) A 3D visualization of the forward-in-time figure 2.2 cat map 3-term recurrence condition for the  $s = 3$  cat map (24.256) of,  $\{\phi_t\} \in [0, 1]$ . (b) **Incorrect:** The 3 points recurrence relation in the fundamental domain  $\{\hat{\phi}_{t-1}, \hat{\phi}_t, \hat{\phi}_{t+1}\} \in [0, 1/2]^3$ . To rotate the figures, use the notebook [siminos/figSrc/han/Mathematica/HLSymmReducedCat.nb](https://siminos.com/figSrc/han/Mathematica/HLSymmReducedCat.nb).

2020-12-24 Predrag I think you are right - the fundamental domain  $\hat{\mathcal{M}} = \mathcal{M}/D_L$ , should be  $1/2$  of  $\mathcal{M}$ , but my previous attempts (above in the blog) to quotient that have failed...

Thinking forward in time is a human condition, difficult to cure. Figure 24.48 (a) is a nice 3D visualization of the forward-in-time figure 2.2 cat map which leads to the total mess described in Gutkin *et al.* [36]. That is why I included figure 2 and table 2 in that paper – an impossible number-theoretic problem created by ignoring the well-known generating partition construction.

Try plotting instead the temporal cat condition

$$\phi_t = \frac{1}{s}(\phi_{t+1} + \phi_{t-1} + m_t) \pmod{1}. \quad (24.257)$$

As illustrated by figure 2.2, there are the two kinds of pieces within the state space partition: the rectangles  $\mathcal{M}_0, \dots, \mathcal{M}_{s-2}$ , and the two exterior half sized triangles  $\mathcal{M}_1, \mathcal{M}_{\mu^2}$ , labeled by the  $(\mu^2 + 1)$ -letter interior alphabet  $\mathcal{A}_0$ , and the two-letter exterior alphabet  $\mathcal{A}_1$ , respectively. For integer  $s \geq 2$  these alphabets are

$$\mathcal{A} = \mathcal{A}_0 \cup \mathcal{A}_1, \quad \mathcal{A}_0 = \{0, \dots, \mu^2\}, \quad \mathcal{A}_1 = \{-1, \mu^2 + 1\}. \quad (24.258)$$

For the interior alphabet  $\mathcal{A}_0$  there will be two complete rectangles in the plot corresponding to figure 24.48 (a); for the alphabet  $\mathcal{A}_1$  two triangles. You can plot the (exponentially many) admissible intermediate  $\{\phi_t\}$  planes; you'll see that  $1/s$  prefactor is  $1/|\text{Det } \mathcal{J}_T|$ . We still do not know

a simple grammar rule for spatiotemporal cat, so understanding these plots might help, but we had already gone that way [36], and failed. My hunch is that understanding  $D_1$  quotiented orbit Jacobian matrix  $\hat{\mathcal{J}}$  is our best chance.

**2020-12-29 Predrag** Temporal cat *dynamical*  $D_1 = \{e, \sigma\}$  symmetry is

$$\sigma\phi_t = 1 - \phi_t, \quad \sigma m_t = \mu^2 - m_t, \quad \text{for all } t \in \mathbb{Z}, \quad (24.259)$$

where  $m_t$  takes values in the  $s$ -letter alphabet (24.258).

Any codimension-1 hyperplane going through the center of mass point  $\phi_t^* = 1/2$  divides the unit hypercube phase space  $\mathcal{M} = \{\phi_t\} \in [0, 1]^n$  into two equal parts related by inversion through center (24.259) and can thus serve as a boundary  $\hat{\mathcal{M}} \cap (\sigma\hat{\mathcal{M}})$  of a fundamental domain  $\hat{\mathcal{M}}$ , and its copy  $\sigma\hat{\mathcal{M}}$ . By the inclusion-exclusion principle (24.251)

$$\mathcal{M} = \hat{\mathcal{M}} + \sigma\hat{\mathcal{M}} - \hat{\mathcal{M}} \cap (\sigma\hat{\mathcal{M}}). \quad (24.260)$$

The natural fundamental domain  $\hat{\mathcal{M}} = \{\hat{\phi}_t\} \in [0, 1]^n / D_1$  for an period-3 periodic state that satisfies the half-phase space condition and fits into the unit hypercube is given by the plane that goes through all the  $1/2$  edges, i.e., a hexagon. In 4 dimensions the intersection is 2-dimensional, an **octahedron**.

A hyperplane:

$$\sum_{k=1}^n \alpha_k \phi_k = 1, \quad \alpha_k \geq 0.$$

There are  $n2^n$  edges in a hypercube. The simplest choice would be vector  $\alpha$  connecting two opposite corners of a hypercube. The bisecting hyperplane has to cut  $2n$  edges (?) in a symmetric way under  $C_n$  rotations about the vector  $\alpha$ .

I'm starting to feel that construction explicit fundamental domain in this case is a bad idea...

(what follows is currently **incorrect**!)

$$\text{if } \sum_t \phi_t \begin{cases} < 1, & \hat{\phi}_t = \phi_t \text{ is in the fundamental domain} \\ = 1, & \hat{\phi}_t = \phi_t = \sigma\phi_t \text{ is in the border} \\ > 1, & \hat{\phi}_t = \sigma\phi_t = 1 - \phi_t. \end{cases} \quad (24.261)$$

The temporal cat condition in/out of the fundamental domain is:

$$\begin{aligned} \hat{\phi}_{t+1} - s\hat{\phi}_t + \hat{\phi}_{t-1} &= -m_t, \\ 1 - \hat{\phi}_{t+1} - s\hat{\phi}_t + \hat{\phi}_{t-1} &= -m_t, \end{aligned} \quad (24.262)$$

Can you figure out how does the  $\hat{m}_t$   $s$ -letter alphabet come out of the full alphabet (24.258)?

**2021-01-13 Han** The factorization of (6.199) can be interpreted as the product of the topological zeta function of a half time step cat map. The topological zeta function of the cat map has a rational form:

$$\frac{1}{\zeta(z)} = \frac{\det(1 - zA)}{\det(1 - zB)}, \quad A = \begin{pmatrix} 2 & 1 \\ 1 & 1 \end{pmatrix}, \quad B = \begin{pmatrix} 1 & 0 \\ 0 & 1 \end{pmatrix}. \quad (24.263)$$

where the matrix  $A$  and  $B$  are the transition matrices of the Markov diagrams in figure 6.5 (a) and (b). When the topological zeta function has a fractional form (24.263), the number of the periodic points with period  $n$  is given by

$$\text{Tr } A^n - \text{Tr } B^n.$$

Using the Markov diagram, the number of periodic points is given by the number of the closed walks in the graph of matrix  $A$ , with the closed walks in the graph of matrix  $B$  eliminated.

The topological zeta function of the half time step map is

$$\frac{1}{\tilde{\zeta}(t)} = \frac{\det(1 - tA')}{\det(1 - tB')}, \quad A' = \begin{pmatrix} 1 & 1 \\ 1 & 0 \end{pmatrix}, \quad B' = \begin{pmatrix} 0 & 1 \\ 1 & 0 \end{pmatrix}, \quad (24.264)$$

where

$$A'^2 = A, \quad B'^2 = B.$$

Let  $t^2 = z$ , we can factorize the topological zeta function of cat map:

$$\frac{1}{\zeta(z)} = \frac{1}{\tilde{\zeta}(t)} \frac{1}{\tilde{\zeta}(-t)}.$$

And the Markov diagram of the transition matrix  $A'$  and  $B'$  are shown in figure 6.5 (c) and (d). If we map the figure (c) and (d) two times forward in time we will get the figure (a) and (b).

So in (6.199) we factorized the topological zeta function using the "half map". To use the symmetries we probably need a different factorization...

**2018-02-11 Han** Bird and Vivaldi [14] say that for  $s = 3$  there are  $N_4(\lambda) = 10$  admissible period 4 orbits. They can be read off as walks on figure 24.4 (d), see (24.12). We have also computed them in sect. 24.2 *Rhomboid center partition*, see (24.19), as well as (24.20).

**2018-04-22 Predrag** The discrete Fourier-transformed cycle points  $\hat{M}$  for the periodic points of figure 24.5 are complex vectors (24.17). Similarly for (24.29). [...] Take-home messages is that writing Fourier transforms of periodic points analytically is not useful. Only cycle-4 orbits are related to Gaussian integers, for other orbits there will be no nice analytic formulas. And already for 4-cycles, the phases are not rational fractions of  $2\pi$ .

**2021-01-16 Han** The state space of the 1-dimensional periodic state can be divided into subspaces by the irreps of the dihedral group. For example, when the period of the periodic state is 4, the dihedral group has a  $[4 \times 4]$  matrix representation which act on the 4-dimensional state space of the periodic state. This representation can be generated by the reflection operator: <sup>12</sup>

$$\sigma = \begin{pmatrix} 0 & 0 & 0 & 1 \\ 0 & 0 & 1 & 0 \\ 0 & 1 & 0 & 0 \\ 1 & 0 & 0 & 0 \end{pmatrix},$$

and the shift operator:

$$r = \begin{pmatrix} 0 & 1 & 0 & 0 \\ 0 & 0 & 1 & 0 \\ 0 & 0 & 0 & 1 \\ 1 & 0 & 0 & 0 \end{pmatrix}.$$

They both commute with the orbit Jacobian matrix. Using the sine and cosine basis we can block diagonalize this representation such that each block on the diagonal is an irrep of the  $D_4$  group, using the orthogonal matrix:

$$T = \begin{pmatrix} \mathbf{e}_1 \\ \mathbf{e}_2 \\ \mathbf{e}_3 \\ \mathbf{e}_4 \end{pmatrix} = \begin{pmatrix} \frac{1}{2} & \frac{1}{2} & \frac{1}{2} & \frac{1}{2} \\ -\frac{1}{2} & \frac{1}{2} & -\frac{1}{2} & \frac{1}{2} \\ 0 & -\frac{1}{\sqrt{2}} & 0 & \frac{1}{\sqrt{2}} \\ \frac{1}{\sqrt{2}} & 0 & -\frac{1}{\sqrt{2}} & 0 \end{pmatrix},$$

each row of which is a primitive vector. The  $k$ th components of these primitive vectors are:

$$\mathbf{e}_{1k} = \frac{1}{2}e^{\frac{2\pi i 0k}{4}}, \mathbf{e}_{2k} = \frac{1}{2}e^{\frac{2\pi i 2k}{4}}, \mathbf{e}_{3k} = \frac{1}{\sqrt{2}}\cos\left(\frac{2\pi k}{4}\right), \mathbf{e}_{4k} = \frac{1}{\sqrt{2}}\sin\left(\frac{2\pi k}{4}\right).$$

Using this set of basis we can block diagonalize the reflection and shift operators:

$$T\sigma T^\top = \begin{pmatrix} 1 & 0 & 0 & 0 \\ 0 & -1 & 0 & 0 \\ 0 & 0 & 0 & 1 \\ 0 & 0 & 1 & 0 \end{pmatrix},$$

$$TrT^\top = \begin{pmatrix} 1 & 0 & 0 & 0 \\ 0 & -1 & 0 & 0 \\ 0 & 0 & 0 & 1 \\ 0 & 0 & -1 & 0 \end{pmatrix},$$

<sup>12</sup>Predrag 2021-06-13: You could not have chosen more devious notation: pretty much everywhere I (and some sophisticated wiki's) write  $r$  for the  $2\pi/n$  rotation (translation), and  $s_j$  for reflection across  $j$ th symmetry axis, see table ???. I'm experimenting with writing this up as in sect. 6.7.

which contain 3 irreps along the diagonal. The first one is the 1-dimensional symmetric irrep. The second one is antisymmetric under shift by one lattice site and one type of reflections, symmetric under other group operations. This representation is called  $B_1$  or  $B_2$ . The third one is the 2-dimensional irrep.

Using the orthogonal matrix  $T$  we can rewrite a periodic state into the space with sine and cosine basis. For example, a periodic state  $\{a, b, c, d\}$  becomes:

$$T \begin{pmatrix} a \\ b \\ c \\ d \end{pmatrix} = \begin{pmatrix} \frac{a}{2} + \frac{b}{2} + \frac{c}{2} + \frac{d}{2} \\ -\frac{a}{2} + \frac{b}{2} - \frac{c}{2} + \frac{d}{2} \\ \frac{d}{\sqrt{2}} - \frac{b}{\sqrt{2}} \\ \frac{a}{\sqrt{2}} - \frac{c}{\sqrt{2}} \end{pmatrix}.$$

The shifted and reversed periodic states  $\{d, a, b, c\}$  and  $\{d, c, b, a\}$  become:

$$T \begin{pmatrix} d \\ a \\ b \\ c \end{pmatrix} = \begin{pmatrix} \frac{a}{2} + \frac{b}{2} + \frac{c}{2} + \frac{d}{2} \\ \frac{a}{2} - \frac{b}{2} + \frac{c}{2} - \frac{d}{2} \\ \frac{c}{\sqrt{2}} - \frac{a}{\sqrt{2}} \\ \frac{d}{\sqrt{2}} - \frac{b}{\sqrt{2}} \end{pmatrix}, \quad T \begin{pmatrix} d \\ c \\ b \\ a \end{pmatrix} = \begin{pmatrix} \frac{a}{2} + \frac{b}{2} + \frac{c}{2} + \frac{d}{2} \\ \frac{a}{2} - \frac{b}{2} + \frac{c}{2} - \frac{d}{2} \\ \frac{a}{\sqrt{2}} - \frac{c}{\sqrt{2}} \\ \frac{d}{\sqrt{2}} - \frac{b}{\sqrt{2}} \end{pmatrix}.$$

So in the subspace of the last two components in the new basis, the shift and time reflection act as rotation and reflection in 2-dimensional space. The sign of the second component is changed because the second irrep contained in the reducible representation is  $-1$  for the reflection  $\sigma$  and shift  $r$ .

To find the fundamental domain of the cyclic permutation symmetry and time reversal symmetry in this new state space, we need to quotient the subspace of the last two components to  $1/8$  of the full subspace.

But I still need to think about how does the second 1-dimensional irrep affect the fundamental domain. Moreover, the boundary of the fundamental domain is a 3-dimensional space, which can have a complicated structure. I assume we will reach the boundary when some of the field values are equal. For example, the periodic states  $\{a, b, a, b\}$  and  $\{b, a, b, a\}$  are:

$$T \begin{pmatrix} a \\ b \\ a \\ b \end{pmatrix} = \begin{pmatrix} a+b \\ b-a \\ 0 \\ 0 \end{pmatrix}, \quad T \begin{pmatrix} b \\ a \\ b \\ a \end{pmatrix} = \begin{pmatrix} a+b \\ a-b \\ 0 \\ 0 \end{pmatrix}.$$

The last two components are on the origin, which is on the boundary of the fundamental domain. The periodic state  $\{a, b, a, b\}$  is a repeat of a shorter lattice, so perhaps the position in the subspace and the second component (subspace of the second 1-dimensional irrep) tell us information about whether the periodic state can be reduced to shorter prime state.



**2021-01-22 Han** It's easier to see the discrete Fourier transform (sine and cosine transform) of the periodic state space in 3-dimensional space. In the state space of the periodic state with period-3, the reflection and shift operators are:

$$\sigma = \begin{pmatrix} 0 & 0 & 1 \\ 0 & 1 & 0 \\ 1 & 0 & 0 \end{pmatrix}, \quad r = \begin{pmatrix} 0 & 1 & 0 \\ 0 & 0 & 1 \\ 1 & 0 & 0 \end{pmatrix}.$$

Using the sine and cosine basis:

$$T = \begin{pmatrix} \frac{1}{\sqrt{3}} & \frac{1}{\sqrt{3}} & \frac{1}{\sqrt{3}} \\ -\frac{1}{\sqrt{6}} & -\frac{1}{\sqrt{6}} & \sqrt{\frac{2}{3}} \\ \frac{1}{\sqrt{2}} & -\frac{1}{\sqrt{2}} & 0 \end{pmatrix},$$

the reflection and shift operators are block diagonalized:

$$T\sigma T^\top = \begin{pmatrix} 1 & 0 & 0 \\ 0 & -\frac{1}{2} & \frac{\sqrt{3}}{2} \\ 0 & \frac{\sqrt{3}}{2} & \frac{1}{2} \end{pmatrix}, \quad TrT^\top = \begin{pmatrix} 1 & 0 & 0 \\ 0 & -\frac{1}{2} & \frac{\sqrt{3}}{2} \\ 0 & -\frac{\sqrt{3}}{2} & -\frac{1}{2} \end{pmatrix},$$

which contain a symmetric 1-dimensional irrep and a 2-dimensional irrep. The orbit Jacobian matrix is diagonalized in this basis:

$$TJT^\top = \begin{pmatrix} -1 & 0 & 0 \\ 0 & -4 & 0 \\ 0 & 0 & -4 \end{pmatrix}.$$

Note that in the subspace of 2-dimensional irrep the orbit Jacobian matrix is  $-4 \times$  identity matrix.

Figure 24.49 shows the fundamental parallelepipeds of the period 3 periodic states in the configuration space and the "Fourier space". The shapes of the unit cube and the fundamental parallelepiped are not changed.

Figure 24.50 shows the fundamental parallelepipeds of the period 3 periodic states observed from the direction of the symmetric eigenvector of the reflection and shift operators. In the configuration space this eigenvector is  $\{1, 1, 1\}$  and in the "Fourier space" this eigenvector is  $\{1, 0, 0\}$ . These 2 figures are projections of the fundamental parallelepipeds in the subspace of the 2-dimensional irrep. The red and blue dots are the periodic points mapped by the orbit Jacobian matrix. In this figure we see that the periodic points exist on the same positions in the 2-dimensional subspace.

In the [wikipedia of the orthogonal transformation](#), the orthogonal transformation is a linear transformation that preserves length of vectors and the angles between them.

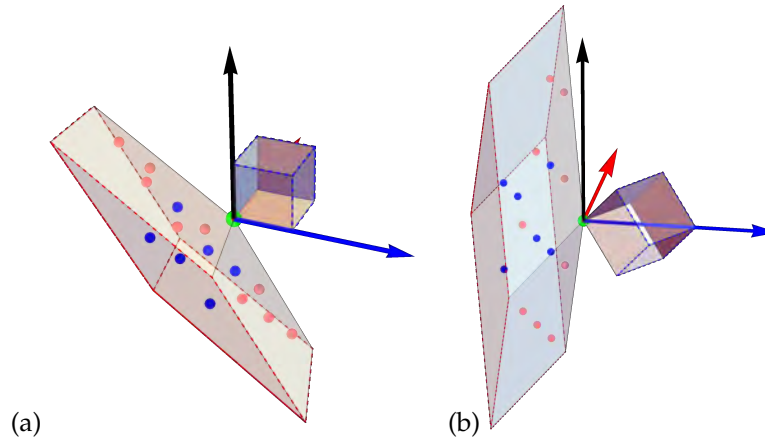


Figure 24.49: (a) The fundamental parallelepiped and the unit cube of the periodic state with period 3 in the configuration space. (b) The fundamental parallelepiped and the unit cube of the periodic state with period 3 in the "Fourier space". The 3 arrows are the axes of the space. The fundamental parallelepiped in the "Fourier space" is different from the fundamental parallelepiped in the configuration space by a rotation. To rotate the figures, use the notebook [siminos/figSrc/han/Mathematica/HLIrrepsBlockLength3.nb](https://www.math.ucdavis.edu/~siminos/figSrc/han/Mathematica/HLIrrepsBlockLength3.nb).

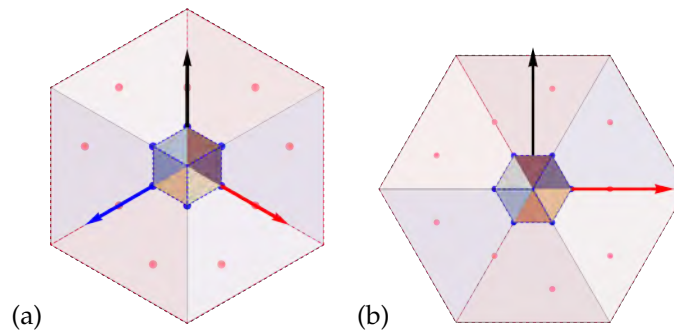


Figure 24.50: (a) The fundamental parallelepiped and the unit cube of the periodic state with period 3 in the configuration space observed from the direction of  $\{1, 1, 1\}$ . (b) The fundamental parallelepiped and the unit cube of the periodic state with period 3 in the "Fourier space" observed from the direction of  $\{1, 0, 0\}$ . In the figure (a) the blue and red dots are integer points enclosed by the fundamental parallelepiped. Each one of the integer points is related to one periodic point. In the "Fourier space", the blue and red dots are integer points transformed by the matrix  $T$ . They still form a cubic lattice, but the coordinates are no longer integers.

**2021-01-25 Predrag** Just so we do not forget: this eventually goes into our main thrust on understanding both the forward and backward in time, and the global temporal cat time-reversal symmetry, see sect. 6.4 *Temporal cat reversibility factorization*.

For our many (mostly failed) attempts to find an Adler-Weiss forward and backward in time symmetric partition, see sect. 24.3 *Time reversal*.

[Birdtracks.eu Sect. 8.2.3](#) *Time reversal symmetry* might be relevant to spatiotemporal cat: when the Hamiltonian is invariant under time reversal, the symmetry group is enlarged.

Not to reinvent the wheel: sect. 7.1 *Reduction to the reciprocal lattice* has various references to the standard space groups theory. It proceeds in two steps

1. Discrete Fourier transform diagonalizes the translational symmetry  $C_T$ ; that is the “reduction to the reciprocal lattice,” with complex eigenvectors.

My problem with figure 24.49 (b) and figure 24.50 (b) is that I expected to see the infinite lattice  $\mathbb{Z}$  eigenstates represented by a *unit interval* on the reciprocal lattice.

2. Point group  $D_1$  irreps ‘diagonalization’ reduces this to  $D_T$ , with real 1- and 2-dimensional irreps.

My problem with figure 24.49 (b) and figure 24.50 (b) is that I expected to see the infinite lattice  $\mathbb{Z}$  with reflection represented by a  $1/2$  *unit interval* fundamental domain on the reciprocal lattice.

For  $D_n$  symmetry: see [Ding thesis example 2.9](#).

Also, change to *siminos/lyapunov* subdirectory,

`pdflatex blog`

read sect. 7.11.2 *Factorization of  $C_n$  and  $D_n$* .

**2021-01-26 Han** Figure 24.51 (a) shows the the period-5 reciprocal periodic states the temporal cat for  $s = 3$ . The total number of the periodic states is given by  $N_5 = |\text{Det } \mathcal{J}| = 121$ .

See also the discussion in blog post **2018-05-22 Han** above, a few pages after (24.69).

Figure 24.51 (b) shows the periodic states in the fundamental domain. The fundamental domain contains periodic states with the argument of the second component of the Fourier transform of the periodic states greater or equal to  $-2\pi/10$ , less than  $2\pi/10$ .

The number of periodic states in the fundamental domain is 25. One of them is the constant  $\{0, 0, 0, 0, 0\}$  state. Each one of the other, prime solutions contributes 5 times to  $N_5$ , the total number of periodic states belong to the same time orbit. So we have the total number of solutions:  $N_5 = 121 = 1 + M_5 \times 5 = 1 + 24 \times 5$ , see table 21.1.

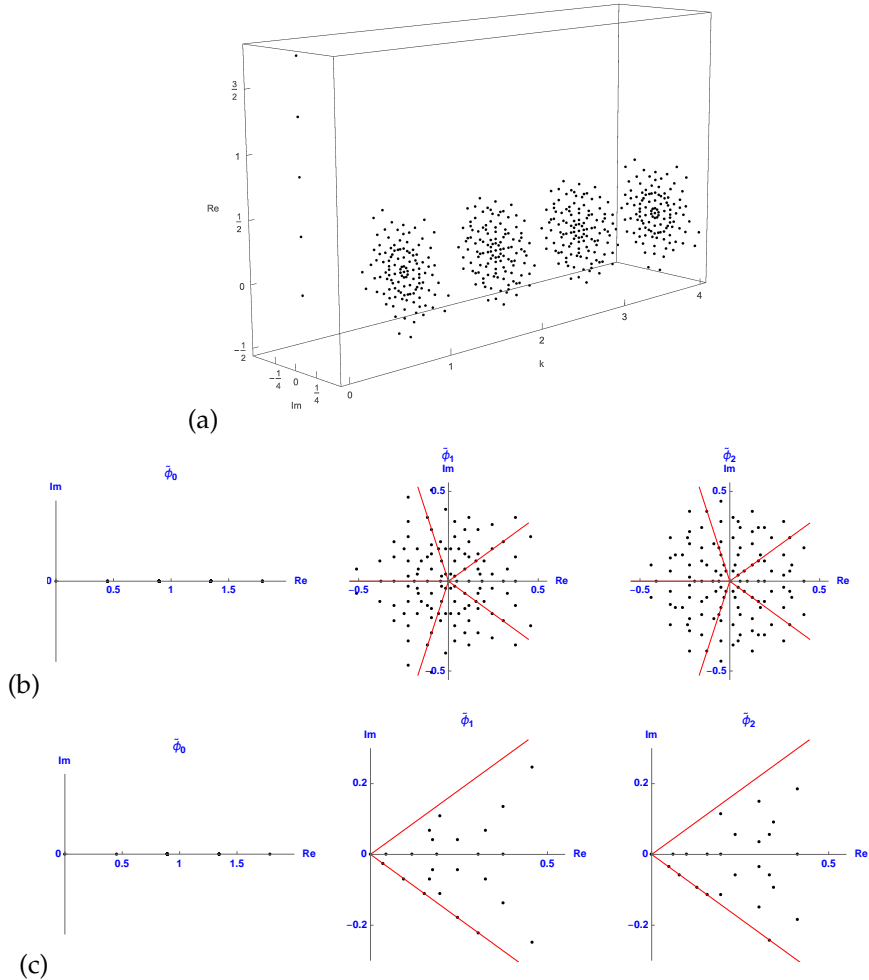


Figure 24.51: (Continuation of figure 24.35.) The 121 period  $n = 5$  reciprocal periodic states (see table 21.1) of the  $s = 3$  temporal cat, obtained by discrete  $C_5$  Fourier transform diagonalization. (a) A perspective view. (b)  $k = 0, 1, 2$  irreps of  $C_5$ . By time reversal  $k = 3$  has the same prime orbits as  $k = 2$ , and  $k = 4$  as  $k = 1$ . (c) The  $C_5$  symmetry reduced fundamental domain contains reciprocal periodic states whose phases lie in  $[-2\pi/10, 2\pi/10)$ , one reciprocal periodic state for each  $C_5$  group orbit. The constant periodic state  $\{0, 0, 0, 0, 0\}$  lives in a boundary, the intersection of the fundamental domain and all its images, with each reciprocal periodic state a  $k = 0$  average over corresponding periodic states, hence real. For  $C_{11}$  reciprocal periodic states, see figure 24.13. (Continued in figure 24.52.)

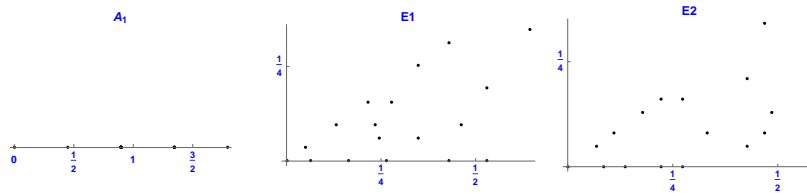


Figure 24.52: The  $C_5$   $k = 0, 1, 2$  fundamental domains  $[-2\pi/10, 2\pi/10]$  of figure 24.51 (c) are complex conjugation symmetric, so they can be tiled by a  $1/2$  domain  $[0, 2\pi/10]$  and its complex-conjugate image. In the  $[0, 2\pi/10]$  domain there are 18 reciprocal periodic states. One of them is the origin. Excluding origin, there are 10 points on the  $1/2$  domain boundaries, 5 points on the real axis (with phase 0), and 5 points with phase  $2\pi/10$  belonging to the same set of states in the time orbit, but with reverse rotation in time. The remaining 7 points lie inside the  $1/2$  domain. Their group orbits, generated by rotations and reflections include 10 periodic states. So the total number of the  $C_5$  periodic states is  $1 \times 1 + 10 \times 5 + 7 \times 10 = 121$ , where 121 is the coefficient of the  $z^5$  term in the number of states generating function  $F(z)$  of (2.14). This is *not* a  $D_5$  symmetry-reduction, as self-dual orbits are not represented as repeats of prime orbits of  $1/2$  period (coefficients of the  $D_5$  generating function  $F'(t)$ ,  $t^2 = z$ ) and time-reversal pairs are counted as distinct orbits, whereas under  $D_5$  each such pair is a single prime orbit, see the  $D_3$  example figure ?? (Continued in figure 24.53.)

**2021-01-26 Predrag** I think a very nice picture is emerging of fundamental domains and prime orbits for temporal cat, and hopefully eventually for spatiotemporal cat.

You need to explain what every periodic lattice concept becomes on reciprocal lattice, in particular how prime periodic states in the reciprocal lattice fundamental domain relate to the periodic states.

If one reduces only the  $C_n$  symmetry, the numbers of reciprocal periodic states in the fundamental domain are presumably given by  $M_n$  in table 21.1. Not that for non-prime  $n$  there will be more prime orbits, and more points in invariant subspaces (borders).

Once one also reduces the reflection symmetry, the numbers of reciprocal periodic states in the  $D_n$  fundamental domain are given by  $\tilde{M}_n$  in the golden (Fibonacci [5]) cat map table 6.2 and (6.198). This should be the same as counting walks on the "half time-step" Markov graph figure 6.5.

Is figure 24.51 (b) for  $k = 4\pi/5$  correct? I think you have to rotate by the appropriate  $2\pi\ell/5$  the points that are outside the fundamental domain.

**2021-01-27 Han** I believe figure 24.51 (b) for  $k = 4\pi/5$  and  $k = 6\pi/5$  is correct. To make this figure, I plotted all of the solutions then only kept the solutions with the  $k = 2\pi/5$  component in  $[-2\pi/10, 2\pi/10)$ . If you rotate the solutions to move the  $k = 4\pi/5$  component into the fundamental domain, the  $k = 2\pi/5$  component will come out of the fundamental domain.

Figure 24.35 shows the solutions in the generating partition (the rhomboid corner partition), while figure 24.51 are solutions with field values in  $[0, 1)$ .

For the Fourier transform of the field of figure 24.35, see figure 24.51 (a,b).

**2021-01-27 Han** Apparently I was wrong assuming the Fourier transforms of the symbol blocks appear on straight lines when the Fourier transforms of the fields are not... The figure 24.35 (a) and (b) are almost identical. The only difference is the scale. The reason is that in the Fourier space, orbit Jacobian matrix is diagonalized so the source terms are equal to the fields times the eigenvalues.

**2021-01-27 Predrag** I think this all is falling into place in a very nice way. This is all about the symmetry reduction of the space lattice (the "floor"), we still have to do the dynamical  $D_1$  temporal cat (the "cat") symmetry separately.

A system other than the temporal cat organized by  $D_{n_n}$  irreps is a convex regular polygon (a polygon that is equiangular and equilateral)  $n$ -disk scatterer. In ChaosBook we work out the  $n = 2, 3, 4$  cases. Unlike the temporal cat, if disks are sufficiently thin, all symbol blocks are admissible (full grammar, no pruning).

Temporal cat periodic states correspond to all  $n$  at one go.

(a)  
(b)

Figure 24.53: (Continuation of figure 24.51.) The 9 period  $n = 5$  reciprocal periodic states (hopefully given by (6.198)) of the  $s = 3$  temporal cat, obtained by discrete  $D_5$  irreps  $A_1 \otimes E_2 \otimes E_2$  diagonalization of the  $1/2$  time step or the temporal golden (Fibonacci [5]) cat lattice (generating functions in powers of  $t^n$ ). (a)  $A_1, E_2$  and  $E_2$  irreps of  $D_5$ . For  $D_5$  all reciprocal periodic states are real. (b) The  $D_5$  symmetry-reduced fundamental domain contains reciprocal periodic states whose phases lie in  $[0, 2\pi/10]$ , one reciprocal periodic state for each  $D_5$  group orbit. The constant periodic state  $\{0, 0, 0, 0, 0\}$  lives in the intersection of the fundamental domain and all its images. The time reversal symmetry corresponds to complex conjugation, with opposite direction orbits identified. The phase =0 states are self-dual, reciprocal periodic states on the real axis that is a fundamental domain boundary, and are correctly counted by the inclusion-exclusion principle (24.251). See 2021-01-27 Predrag above to see how this is done correctly for  $D_3$  and  $D_4$ .

**2021-01-27 Predrag** The brilliant thing about my fellow Dane Caspar Wessel's great invention is that in the complex plane the unit circle is a *circle*, not squashed into an ellipse :) Can you replot figure 24.35 and figure 24.51, so Re and Im axes have the same scale? Label them as Re and Im, instead of the awkward long labels you have now - you can explain axes in the figure caption. Also, in this  $C_5$  example, plot the 5 irreps (Fourier components in the  $C_5$  case) side by side, rather than a perspective drawing of 5 planes cutting across a parallelepiped. Use the same names for the figure files, just plot them Wessel's way.

I think you might want to repeat this for  $C_6$ , as there you get two extra sets of boundaries between 2-state and 3-state repeats, that's more like the case of general  $C_n$  reciprocal periodic state.

**2021-01-27 Predrag** The brilliant thing about  $D_n$  irreps is that they are all real, so you don't have to plot Wessel's 2D complex plane. However they all (except the two or 4 1-dimensional irreps) are 2-dimensional, so you still have to plot  $\cos 2\pi k/n, \sin 2\pi k/n$  planes. How do your reciprocal periodic states look in these 2-dimensional irreps for the  $C_5$  and  $C_6$  examples?

**2021-01-29 Predrag 2 Han** Can you plot the  $D_5$ -symmetry reduced figure 24.53? If the caption is not clear, call me, let's discuss.

**2021-02-01 Predrag 2 Han** About plotting the  $D_n$ -symmetry reduced figure 24.53: not sure what the good way is plotting the 2-dimensional representations.

Maybe complex regular irreps ChaosBook example 25.7 Basis for irreps of  $D_3$  suggest the way to plot?

I find Harter's Sect. 3.3 Second stage of non-Abelian symmetry analysis particularly illuminating. It shows how physically different (but mathemati-

cally isomorphic) higher-dimensional irreps are constructed corresponding to different subgroup embeddings. One chooses the irrep that corresponds to a particular sequence of physical symmetry breakings.

**2021-02-02 Han** In figure 24.52, there are 18 periodic states in the fundamental domain. The periodic state on the origin is  $\{0, 0, 0, 0\}$ .

The 5 periodic states  $\Phi$  on the boundary with phase 0 are:

$$\begin{aligned} & \frac{1}{11}\{2, 1, 1, 2, 5\}, \quad \frac{1}{11}\{4, 2, 2, 4, 10\}, \quad \frac{1}{11}\{6, 3, 3, 6, 4\}, \\ & \frac{1}{11}\{8, 4, 4, 8, 9\}, \quad \frac{1}{11}\{10, 5, 5, 10, 3\}. \end{aligned} \quad (24.265)$$

The 5 periodic orbits on the boundary with phase  $2\pi/10$  are:

$$\begin{aligned} & \frac{1}{11}\{6, 1, 8, 1, 6\}, \quad \frac{1}{11}\{7, 3, 2, 3, 7\}, \quad \frac{1}{11}\{8, 5, 7, 5, 8\}, \\ & \frac{1}{11}\{9, 7, 1, 7, 9\}, \quad \frac{1}{11}\{10, 9, 6, 9, 10\}. \end{aligned} \quad (24.266)$$

Orbits on the boundaries are invariant under reflection.

The 7 periodic orbits in the fundamental domain are:

$$\begin{aligned} & \frac{1}{11}\{4, 3, 5, 1, 9\}, \quad \frac{1}{11}\{4, 5, 0, 6, 7\}, \quad \frac{1}{11}\{7, 0, 4, 1, 10\}, \\ & \frac{1}{11}\{8, 7, 2, 10, 6\}, \quad \frac{1}{11}\{10, 0, 1, 3, 8\}, \quad \frac{1}{11}\{9, 0, 2, 6, 5\}, \\ & \frac{1}{11}\{9, 3, 0, 8, 2\}. \end{aligned} \quad (24.267)$$

**2021-02-09 Han** Also note that the orbits with time reversal symmetry (24.265–24.266) have phase  $2\pi/10$  in the subspace of  $E_1$  and  $4\pi/10$  in the subspace of  $E_2$ , or phase 0 in both  $E_1$  and  $E_2$  subspaces. So when a periodic state has time reversal symmetry, this periodic state exists in the 3-dimensional subspace. The dimension of the subspace is probably the period of the orbit after quotienting by the symmetry.

**2021-02-02 Han** The transition matrix of the half step map is given by the matrix  $A'$  in (24.264). The map

$$\begin{pmatrix} q_{t+1} \\ p_{t+1} \end{pmatrix} = A' \begin{pmatrix} q_t \\ p_t \end{pmatrix} \pmod{1} \quad (24.268)$$

can be rewritten as:

$$\begin{pmatrix} q_t \\ q_{t+1} \end{pmatrix} = \begin{pmatrix} 0 & 1 \\ 1 & 1 \end{pmatrix} \begin{pmatrix} q_{t-1} \\ q_t \end{pmatrix} \pmod{1}. \quad (24.269)$$

(Predrag: see (6.185), (6.188). This is not the Percival-Vivaldi two configuration representation.)



For  $s = 3$ ,  $\mathcal{J} = \tilde{\mathcal{J}}^\top \tilde{\mathcal{J}}$ , where the inversion-reduced orbit Jacobian matrix is:

$$\tilde{\mathcal{J}} = \begin{pmatrix} 1 & -1 & 0 & 0 & \dots & 0 & 1 \\ 1 & 1 & -1 & 0 & \dots & 0 & 0 \\ 0 & 1 & 1 & -1 & \dots & 0 & 0 \\ \vdots & \vdots & \vdots & \vdots & \ddots & \vdots & \vdots \\ 0 & 0 & \dots & \dots & \dots & 1 & -1 \\ -1 & 0 & \dots & \dots & \dots & 1 & 1 \end{pmatrix}, \quad (24.270)$$

as in (6.77).

This map has  $\tilde{N}_5 = 11$  period  $n = 5$  periodic states. One of them is the fixed point  $\{0, 0, 0, 0, 0\}$ . The other 10 periodic states are the  $\tilde{M}_5 = 2$  prime orbits:

$$\frac{1}{11}\{9, 3, 1, 4, 5\}, \quad \frac{1}{11}\{10, 7, 6, 2, 8\}, \quad (24.271)$$

and the cyclic permutations, in agreement the golden cat map counts table 6.2 and (6.198). The repeats of these two orbits are the orbits

$$\frac{1}{11}\{4, 3, 5, 1, 9\}, \quad \frac{1}{11}\{8, 7, 2, 10, 6\} \quad (24.272)$$

in the (24.267).

The half step lattice has 121 period  $n = 10$  periodic states. Some of the orbits are:

$$\begin{aligned} & \frac{1}{11}\{7, 8, 4, 1, 5, 6, 0, 6, 6, 1\}, \quad \frac{1}{11}\{7, 9, 5, 3, 8, 0, 8, 8, 5, 2\}, \\ & \frac{1}{11}\{7, 10, 6, 5, 0, 5, 5, 10, 4, 3\}, \quad \frac{1}{11}\{4, 2, 6, 8, 3, 0, 3, 3, 6, 9\}, \\ & \frac{1}{11}\{8, 2, 10, 1, 0, 1, 1, 2, 3, 5\}, \quad \frac{1}{11}\{5, 4, 9, 2, 0, 2, 2, 4, 6, 10\}, \\ & \frac{1}{11}\{7, 3, 10, 2, 1, 3, 4, 7, 0, 7\}, \quad \frac{1}{11}\{6, 4, 10, 3, 2, 5, 7, 1, 8, 9\}, \\ & \frac{1}{11}\{9, 7, 5, 1, 6, 7, 2, 9, 0, 0\}, \quad \frac{1}{11}\{9, 8, 6, 3, 9, 1, 10, 0, 10, 10\}, \\ & \frac{1}{11}\{10, 8, 7, 4, 0, 4, 4, 8, 1, 9\}. \end{aligned} \quad (24.273)$$

Each one of these orbits is corresponding to two orbits in (24.265–24.267)

**2021-02-04 Predrag** Sect. 6.5.2 contains my 2008 Baake, Roberts and Weiss [6] *Periodic orbits of linear endomorphisms on the 2-torus and its lattices* [arXiv:0808.3489](https://arxiv.org/abs/0808.3489) reading notes. Please improve them, if you read the paper. In any case, we must read 1997 sect. 6.5.3 Baake, Hermisson and Pleasants [4] *The torus parametrization of quasiperiodic LI-classes*, add your notes to the subsection there.

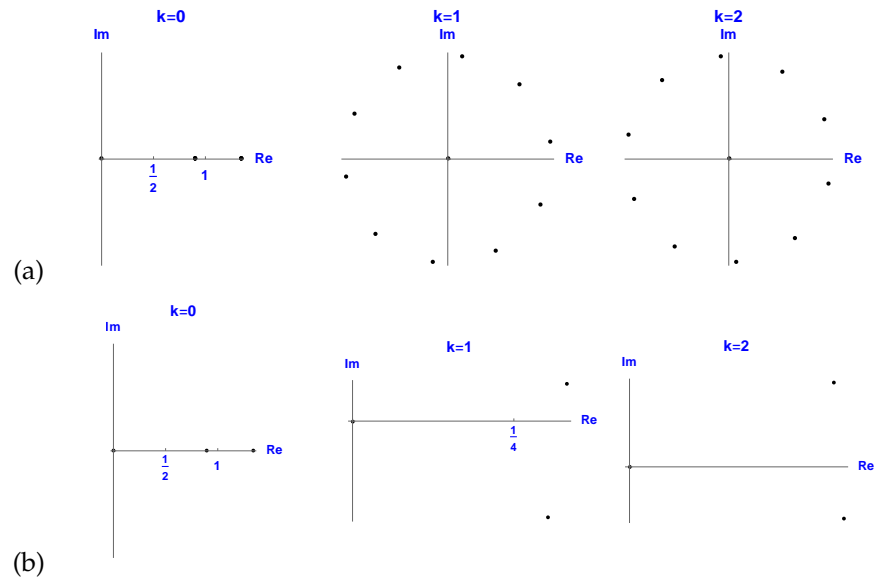


Figure 24.54: (a) The  $\tilde{N}_5 = 11$  period  $n = 5$  reciprocal periodic states of the  $1/2$  time step lattice (temporal golden cat) of the  $s = 3$  temporal cat, obtained by discrete  $C_5$  irreps diagonalization. (b) The  $C_5$  symmetry-reduced fundamental domain contains  $\tilde{M}_5 = 2$  prime reciprocal periodic states whose phases lie in  $[-2\pi/10, 2\pi/10)$ , one prime reciprocal periodic state for each  $C_5$  group orbit. The constant periodic state  $\{0, 0, 0, 0, 0\}$  lives in the intersection of the fundamental domain and its images.

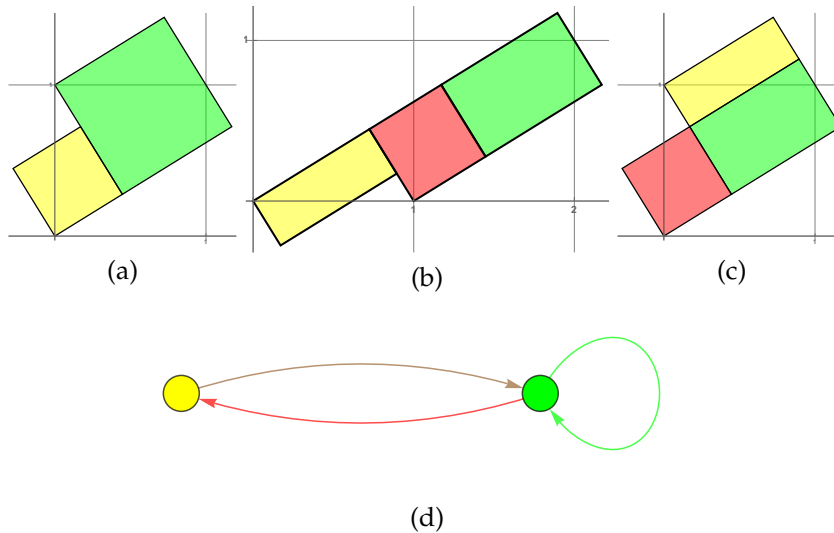


Figure 24.55: (a) An Adler-Weiss generating partition of the unit torus for the golden cat map (1/2 time step map) (6.185), (6.188), (24.269), the time-reversal reduction of the  $s = 3$  Thom-Arnol'd cat map (2.1) and figure 2.1, with rectangle  $\mathcal{M}_A$  (green) and  $\mathcal{M}_B$  (yellow) borders given by the stable and unstable manifolds, i.e., along the two eigenvectors corresponding to the eigenvalues of the matrix  $A'$  in (24.268). (b) Mapped one step forward in time, the rectangles are stretched along the unstable direction and shrunk along the stable direction. The eigenvectors are the same as for the Arnol'd cat map, but eigenvalue  $\tilde{\Lambda}$  (8.113) is a square root of the Arnol'd cat map eigenvalue (21.151),  $\Lambda = \tilde{\Lambda}^2$ , hence less stretching. As always, sub-rectangles have to be translated back into the initial partition. (c) The sub-rectangles translated back into the initial partition yield a generating partition, with the finite grammar given by the transition graph (d) of figure 6.5. The nodes refer to the rectangles  $A$  and  $B$ , and the three links correspond to the three sub-rectangles induced by one step forward-time dynamics. The generating partition of the half-step  $\mu = 1$  Percival-Vivaldi cat map is shown in figure 24.56.

**2021-02-06 Han** Added figure 24.55, the generating partition of the golden cat map (1/2 time step map) (6.185), (6.188), (24.269), the time-reversal reduction of the  $s = 3$  Thom-Arnol'd cat map (2.1) and figure 2.1.

**2021-02-06 Predrag** Note: this is *not* the time-reversal reduction (8.112) of the Percival-Vivaldi cat map figure 2.9 and (24.69), that is done in figure 24.56. I would prefer such Percival-Vivaldi golden cat map figure for inclusion into ChaosBook.

The colors in figure 24.55 (a) and (b) should be consistent, as in figure 2.9. But do not waste time on fixing that, draw the Percival-Vivaldi golden cat map instead.

In despair, I had drawn the original by hand, see *PVAdlerWeissB-a.svg*, *PVAdlerWeissB-b.svg*, *PVAdlerWeissB-c.svg* and *PVAWMkovCol.svg*. How do I know that? Every figure I draw has the source program indicated as a comment. You can edit \*.svg files using Inkscape, all you have to do is to replace  $\Lambda \rightarrow \tilde{\Lambda}$  in figure 2.9 (b), remove the extra sub-partitions. Almost done in figure 24.32 (c).

**2021-02-08 Han** Using (24.69), the generating partition of the half-step  $\mu = 1$  Percival-Vivaldi cat map is shown in figure 24.56.

**2021-02-06 Predrag** Very nice, thank you. Still, it would be nice to also have the  $\mu > 1$  generating partition, no necessarily as a drawing.

**2021-02-06 Predrag** OK, we are done. You know what to do next. We now have the golden cat orbit Jacobian matrix (6.77) on the half-time step lattice for any  $\mu$ . We had it all along, but I made a few trivial errors, and you did not check those calculations, so it took a bit too long...

1. You can now compute

$$\begin{aligned} \sum_{n=1} \tilde{N}_n(\mu)t^n &= -\tilde{\zeta}t \frac{d}{dt} \frac{1}{\tilde{\zeta}} \\ &= ??t+??t^2 + \mu(\mu^2 + 3)t^3+??t^4+??t^5+??t^6+??t^7 \\ &\quad +??t^8+??t^9 + \dots \end{aligned} \tag{24.274}$$

2. Does it agree with (6.198)?
3. Does your  $N(s)_n = \tilde{N}(\mu)_n^2$  agree with (6.88) for  $n = 3$ ?
4. Does it agree with our temporal cat  $N(s)_n$  series? For example, with (8.161).
5. Derive  $1/\tilde{\zeta}(t)$
6. Does it agree with (6.55)? with (6.197)?

You'll be glad to hear that have named "golden" cats for  $\mu > 1$  "metal cats" in a paper that was published, so that will be the official name for those zeta's :)

**2021-02-06 Predrag** Started drafting sect. 6.4 *Time reversal symmetry reduction* for CL18.

**2021-02-08 Han** We are not done yet... While in the above we here use Percival-Vivaldi [62] "two-configuration representation" cat map (2.5)

$$\mathbf{A} = \begin{bmatrix} 0 & 1 \\ -1 & s \end{bmatrix} \quad (24.275)$$

Gutkin *et al.* [36] cat map (derived as a niece of the standard map, see (3.84)) is of form:

$$A = \begin{pmatrix} s-1 & 1 \\ s-2 & 1 \end{pmatrix}. \quad (24.276)$$

The square root of this matrix is not an integer matrix if  $s \neq 3$ .

$\tilde{A}$  and  $A$  can be diagonalized simultaneously if  $\tilde{A}^2 = A$  (Predrag feels a bit unconformable taking a square root of an asymmetric matrix, even though you diagonalize it first...). We can always use matrix:

$$\mathbf{S} = ( e^{(+)} \quad e^{(-)} )$$

to diagonalize the matrix  $A$ , where  $e^{(+)}$  and  $e^{(-)}$  are the two eigenvectors of the matrix  $A$ :

$$\mathbf{S}^{-1} \mathbf{A} \mathbf{S} = \begin{pmatrix} \Lambda & 0 \\ 0 & \Lambda^{-1} \end{pmatrix}.$$

Then there are four possible  $\tilde{A}$ s:

$$\begin{aligned} & \mathbf{S} \begin{pmatrix} \sqrt{\Lambda} & 0 \\ 0 & \sqrt{\Lambda^{-1}} \end{pmatrix} \mathbf{S}^{-1}, \quad \mathbf{S} \begin{pmatrix} \sqrt{\Lambda} & 0 \\ 0 & -\sqrt{\Lambda^{-1}} \end{pmatrix} \mathbf{S}^{-1}, \quad (24.277) \\ & \mathbf{S} \begin{pmatrix} -\sqrt{\Lambda} & 0 \\ 0 & \sqrt{\Lambda^{-1}} \end{pmatrix} \mathbf{S}^{-1}, \quad \mathbf{S} \begin{pmatrix} -\sqrt{\Lambda} & 0 \\ 0 & -\sqrt{\Lambda^{-1}} \end{pmatrix} \mathbf{S}^{-1}. \end{aligned}$$

I found these four solutions for general  $s - 2 = \mu^2$ :

$$\begin{aligned} \tilde{A} &= \begin{pmatrix} a & b \\ c & d \end{pmatrix}, \quad \text{where} \\ &= \begin{pmatrix} -\mu & -\mu^{-1} \\ -\mu & 0 \end{pmatrix}, \quad \text{negative trace, usually not a solution} \\ &= \begin{pmatrix} \mu & \mu^{-1} \\ \mu & 0 \end{pmatrix}, \quad \text{and also solutions for which trace} \neq \mu: \\ & a = -\frac{\mu^2 + 2}{\sqrt{\mu^2 + 4}}, b = -\frac{1}{\sqrt{\mu^2 + 4}}, c = -\frac{\mu^2}{\sqrt{\mu^2 + 4}}, d = -\frac{2}{\mu^2 + 4} \\ & a = \frac{\mu^2 + 2}{\sqrt{\mu^2 + 4}}, b = \frac{1}{\sqrt{\mu^2 + 4}}, c = \frac{\mu^2}{\sqrt{\mu^2 + 4}}, d = \frac{2}{\mu^2 + 4} \quad (24.278) \end{aligned}$$

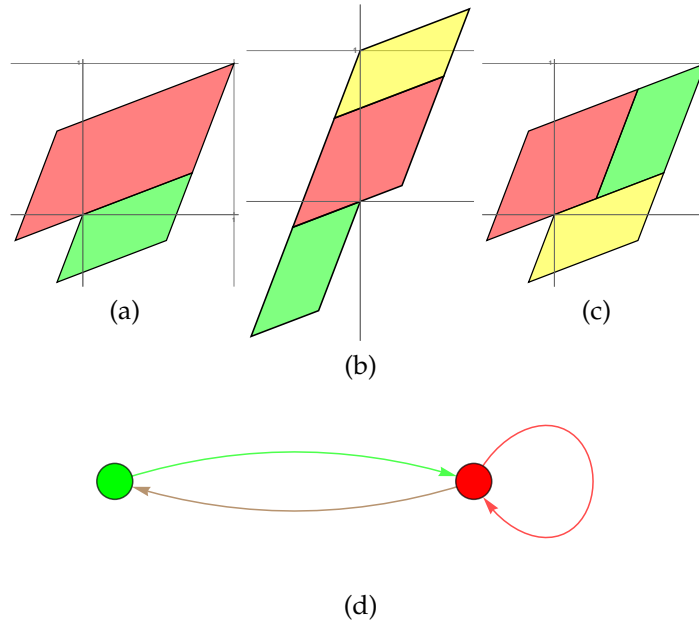


Figure 24.56: (a) An Adler-Weiss generating partition of the unit torus for the golden cat map (1/2 time step map) (8.112), (24.69), the time-reversal reduction of the  $s = 3$  or  $\mu = 1$  Percival-Vivaldi cat map (2.5) and figure 2.9, with rectangle  $\mathcal{M}_A$  (red) and  $\mathcal{M}_B$  (green) borders given by the stable and unstable manifolds, i.e., along the two eigenvectors corresponding to the eigenvalues of the matrix  $\tilde{C}$  in (24.69). (b) Mapped one half time-step forward in time, the rectangles are stretched along the unstable direction and shrunk along the stable direction. The eigenvectors are the same as for the Percival-Vivaldi cat map, but eigenvalue  $\tilde{\Lambda}$  (8.113) is a square root of the Percival-Vivaldi cat map eigenvalue (21.151),  $\Lambda = \tilde{\Lambda}^2$ , hence less stretching. (c) As always, the sub-rectangles translated back into the initial partition yield a generating partition, with the finite grammar given by the transition graph (d) of figure 6.5. The nodes refer to the green and red rectangles, and the three links correspond to the three sub-rectangles induced by one forward half time-step.

So only when  $s = 3$  or  $\mu = 1$  Thom-Arnol'd cat map we can find an integer matrix  $\tilde{A}$ .

And we cannot find square root of the Percival-Vivaldi cat map. Solving (24.69):

$$\mathbf{B} = \tilde{\mathbf{C}}^2 = \begin{pmatrix} 0 & 1 \\ -1 & s \end{pmatrix},$$

the four solutions are

$$\tilde{\mathbf{C}} = \begin{pmatrix} a & b \\ c & d \end{pmatrix}, \quad \text{where}$$

$$a = \mu^{-1}, b = -\mu^{-1}, c = \mu^{-1}, d = \frac{1-s}{\mu}, \quad \text{negative trace } \mu$$

$$a = -\mu^{-1}, b = \mu^{-1}, c = -\mu^{-1}, d = \frac{s-1}{\mu}$$

$$a = -\frac{1}{\sqrt{\mu^2+4}}, b = -\frac{1}{\sqrt{\mu^2+4}}, c = \frac{1}{\sqrt{\mu^2+4}}, d = \frac{-1-s}{\mu}$$

$$a = \frac{1}{\sqrt{\mu^2+4}}, b = \frac{1}{\sqrt{\mu^2+4}}, c = -\frac{1}{\sqrt{\mu^2+4}}, d = \frac{s+1}{\sqrt{\mu^2+4}} \quad (24.279)$$

2021-02-08 Han For me  $\mathcal{J} \neq \tilde{\mathcal{J}}^\top \tilde{\mathcal{J}}$ . Let

$$\tilde{\mathcal{J}} = \begin{pmatrix} \mu & -1 & 0 & 0 & \dots & 0 & 1 \\ 1 & \mu & -1 & 0 & \dots & 0 & 0 \\ 0 & 1 & \mu & -1 & \dots & 0 & 0 \\ \vdots & \vdots & \vdots & \vdots & \ddots & \vdots & \vdots \\ 0 & 0 & \dots & \dots & \dots & \mu & -1 \\ -1 & 0 & \dots & \dots & \dots & 1 & \mu \end{pmatrix}.$$

Then we have (6.49), and I believe that the determinant  $\det \mathcal{J}$  and  $\det (\tilde{\mathcal{J}}^\top \tilde{\mathcal{J}})$  are only equal when the period of the periodic state is an odd number.

2021-02-09 Predrag I expect the forward-in-time Jacobian  $\tilde{\mathcal{J}}$  to be related to the orbit Jacobian matrix  $\tilde{\mathcal{J}}$  as in sect. 12.5 *Spatiotemporal cat Hill's formula*. You have explicit orbit Jacobian matrix  $\tilde{\mathcal{J}}$  (6.77), so write down the corresponding  $\tilde{\mathcal{J}}$  acting on 1/2 time-step lattice.

2021-02-12 Han [2021-02-15 Predrag moved this post to the draft of *reversal.tex*, see (6.56).]

2021-02-13 Predrag I think it might be perhaps more informative and easier to survey the symmetries if one lists periodic states by their symbol blocks rather than lattice fields in listings such as (24.265), (24.266), (24.267) and (24.273), as you did for period-4 periodic states (24.14), (24.17) and (24.29).

Note that golden/metal cat number of alphabet letters  $\tilde{\mathcal{A}}$  is about  $\sqrt{\cdot}$  of the cat map alphabet  $\mathcal{A}$ .

**2021-02-24 Han** I computed the period-6 periodic states of the temporal cat with  $s = 3$ . Figures 24.57 and 24.58 are the reciprocal periodic states obtained by discrete  $C_6$  irreps diagonalization.

The  $C_6$  group has 4 subgroups, which are  $\mathbf{1}$ ,  $C_2$ ,  $C_3$  and  $C_6$ . In the space of the irreps of  $C_6$ , the subspace spanned by the  $k = 0$  Fourier mode is the subspace of the  $\mathbf{1}$  subgroup.  $k = 0$  and  $k = 3$  Fourier modes span the subspace of the  $C_2$  subgroup.  $k = 0, k = 2$  and  $k = 4$  Fourier modes span the subspace of the  $C_3$  subgroup. Using the subspaces of these subgroups, we can divide the periodic states into 4 categories.

The first category includes periodic states that are in the subspace of  $\mathbf{1}$ . We only have 1 periodic state in this category, which is the  $\{0, 0, 0, 0, 0, 0\}$ .

The second category includes periodic states that are in the subspace of  $C_2$  but not in the subspace of  $\mathbf{1}$ . These periodic states have non-zero components only in the subspace spanned by  $k = 0$  and  $k = 3$  Fourier modes, as shown in figure 24.57 (a). There are 4 periodic states in this subspace, which are the 2 period-2 orbits and their cyclic permutations.

The third category includes periodic states that are in the subspace of  $C_3$  but not in the subspace of  $\mathbf{1}$ . These periodic states have non-zero components only in the subspace spanned by  $k = 0, k = 2$  and  $k = 4$  Fourier modes, as shown in figure 24.57 (b). There are 15 periodic states in this category, which are the 5 period-3 orbits and their cyclic permutations.

The last category includes periodic states that are not in the subspace of  $\mathbf{1}$ ,  $C_2$  or  $C_3$ . These periodic states are the prime period-6 periodic states, which are not repeats of shorter periodic states. Note that some of these periodic states have 0 component in the  $k = 1$  subspace, but they have non-zero components in both the  $k = 2$  and  $k = 3$  subspaces, so they are not in the subspace of  $C_2$  or  $C_3$ . Figure 24.58 (a) shows the reciprocal periodic states with non-zero  $k = 1$  component. Figure 24.58 (b) shows the reciprocal periodic states with zero  $k = 1$  component but non-zero  $k = 2$  and  $k = 3$  components. There are 276 reciprocal periodic states in the Figure 24.58 (a) and 24 periodic states in the Figure 24.58 (b).

To get the number of orbits, we need to count the number of reciprocal periodic states in the fundamental domain. For the reciprocal periodic states with non-zero  $k = 1$  component, the fundamental domain contains reciprocal periodic states whose phase of the  $k = 1$  component lies in  $(-\pi/6, \pi/6]$ . For the reciprocal periodic states with zero  $k = 1$  component and non-zero  $k = 2$  and  $k = 3$  components, the fundamental domain contains reciprocal periodic states whose phase of the  $k = 2$  component lies in  $(-\pi/3, \pi/3]$  and  $k = 3$  component lies in  $(-\pi/2, \pi/2]$ . The reciprocal periodic states in the fundamental domain are shown in figure 24.59. There are 46 reciprocal periodic states in figure 24.59 (a) and 4 reciprocal periodic states in (b). Each one of the them is corresponding to a prime period-6 periodic orbit.



**2021-02-24 Han** Now we want to find the periodic states that are invariant under reflection. For  $D_6$  there are 6 group elements with reflection. Reflection operators will reflect the reciprocal periodic states over an axis in each one of the subspaces (except for the  $k = 0$  subspace, which is the symmetric irrep). Let  $\theta_n$  be the polar angle of the reflection axis in the subspace of  $k = n$ . The 6 reflection operators will reflect the subspaces over the axes:

- (1).  $\theta_1 = 0, \theta_2 = 0, \theta_3 = 0$ .
- (2).  $\theta_1 = \pi/6, \theta_2 = \pi/3, \theta_3 = \pi/2$ .
- (3).  $\theta_1 = \pi/3, \theta_2 = 2\pi/3, \theta_3 = 0$ .
- (4).  $\theta_1 = \pi/2, \theta_2 = 0, \theta_3 = \pi/2$ .
- (5).  $\theta_1 = 2\pi/3, \theta_2 = \pi/3, \theta_3 = 0$ .
- (6).  $\theta_1 = 5\pi/6, \theta_2 = 2\pi/3, \theta_3 = \pi/2$ .

If a reciprocal periodic state lies on one set of these axes, then the periodic state is invariant under one of the reflections.

Now check the figure 24.59 (a). The points in  $k = 1$  subspace are in the fundamental domain. So we can only have reciprocal periodic states on the first two sets of axes, which are plotted by the green and red lines in the figure.

Figure 24.60 (a) are the reciprocal periodic states that lie on the red axes,  $\theta_1 = \pi/6, \theta_2 = \pi/3, \theta_3 = \pi/2$ . There are only two orbits:

$$\frac{1}{8}\{5, 5, 2, 1, 1, 2\}, \quad \frac{1}{8}\{7, 7, 6, 3, 3, 6\}. \quad (24.280)$$

Figure 24.60 (b) are the reciprocal periodic states that lie on the green axes,  $\theta_1 = 0, \theta_2 = 0, \theta_3 = 0$ . There are 14 periodic states:

$$\begin{aligned} & \frac{1}{40}\{6, 29, 1, 14, 1, 29\}, \quad \frac{1}{40}\{10, 35, 15, 10, 15, 35\}, \\ & \frac{1}{40}\{14, 21, 9, 6, 9, 21\}, \quad \frac{1}{40}\{18, 27, 23, 2, 23, 27\}, \\ & \frac{1}{40}\{24, 36, 4, 16, 4, 36\}, \quad \frac{1}{40}\{26, 39, 11, 34, 11, 39\}, \\ & \frac{1}{40}\{18, 7, 3, 2, 3, 7\}, \quad \frac{1}{40}\{30, 25, 5, 30, 5, 25\}, \\ & \frac{1}{40}\{32, 28, 12, 8, 12, 28\}, \quad \frac{1}{40}\{34, 31, 19, 26, 19, 31\}, \\ & \frac{1}{40}\{36, 34, 26, 4, 26, 34\}, \quad \frac{1}{40}\{38, 37, 33, 22, 33, 37\}, \\ & \frac{1}{40}\{36, 14, 6, 4, 6, 14\}, \quad \frac{1}{40}\{38, 17, 13, 22, 13, 17\}. \end{aligned} \quad (24.281)$$

The rest 30 reciprocal periodic states are not invariant under time reflec-

tion. There are 15 periodic states:

$$\begin{aligned}
 & \frac{1}{40}\{18, 17, 33, 2, 13, 37\}, & \frac{1}{40}\{20, 25, 15, 20, 5, 35\}, \\
 & \frac{1}{40}\{21, 29, 26, 9, 1, 34\}, & \frac{1}{40}\{36, 9, 31, 4, 21, 19\}, \\
 & \frac{1}{40}\{21, 39, 16, 9, 11, 24\}, & \frac{1}{40}\{28, 7, 33, 12, 3, 37\}, \\
 & \frac{1}{40}\{32, 18, 22, 8, 2, 38\}, & \frac{1}{40}\{28, 17, 23, 12, 13, 27\}, \\
 & \frac{1}{40}\{32, 23, 37, 8, 27, 33\}, & \frac{1}{40}\{36, 29, 11, 4, 1, 39\}, \\
 & \frac{1}{40}\{31, 29, 16, 19, 1, 24\}, & \frac{1}{40}\{25, 35, 0, 5, 15, 0\}, \\
 & \frac{1}{40}\{31, 39, 6, 19, 11, 14\}, & \frac{1}{40}\{32, 3, 17, 8, 7, 13\}, \\
 & \frac{1}{40}\{38, 7, 23, 22, 3, 27\}, &
 \end{aligned} \tag{24.282}$$

and their reflections.

In the figure 24.59 (b) there are only 4 reciprocal periodic states. Two of them are on the red and green axes:

$$\frac{1}{20}\{14, 1, 9, 6, 9, 1\}, \quad \frac{1}{20}\{19, 11, 14, 11, 19, 6\}. \tag{24.283}$$

The rest two are:

$$\frac{1}{20}\{17, 3, 12, 13, 7, 8\}, \tag{24.284}$$

and its reflection.

Note that in the figure 24.59 (b), the red axes are  $\theta_1 = 2\pi/3$ ,  $\theta_2 = \pi/3$ ,  $\theta_3 = 0$ , which are different from the red axes in the figure 24.59 (a).

**2021-02-26 Matt** They are palindromes.

**2021-03-09 Han** When we found the periodic states of the golden cat (Fibonacci [5]) in (24.271–24.273), we did not use the time reflection symmetry. That is why periodic states in (24.271) are corresponding to the cat map's periodic states without reflection symmetry. The boundary of the periodic states of golden cat in (24.271) is periodic, not periodic with reflection.

**2021-03-10 Predrag** Correct. When you quotient a symmetry, the symmetry-reduced map does not have that symmetry. Golden cat is clearly not time-reversal invariant.

**2021-03-09 Han** We can find the periodic states with reflection symmetry by finding short periodic state with periodic reflection boundary conditions.

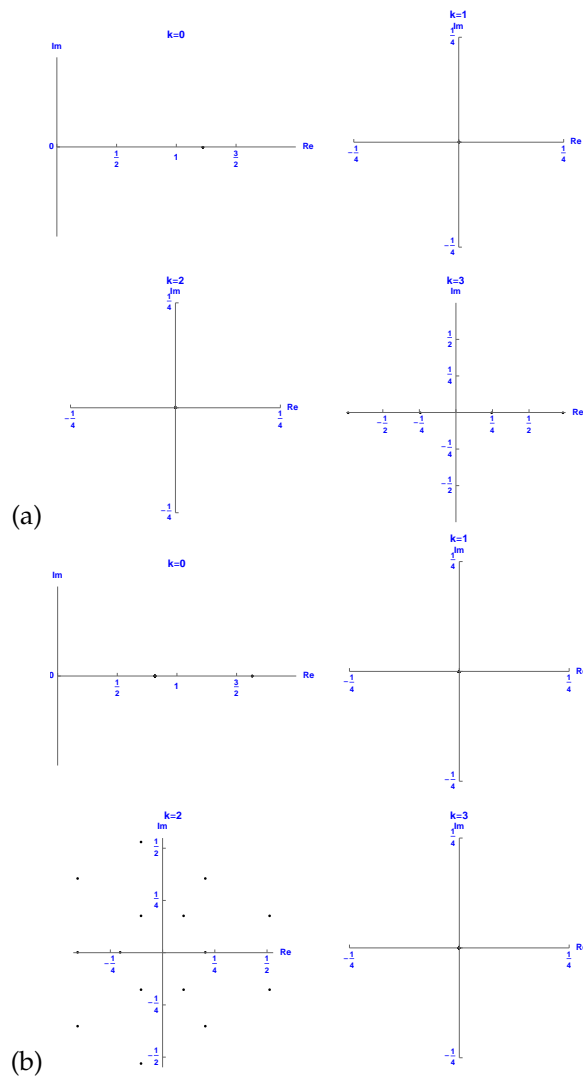


Figure 24.57: The period-6 reciprocal periodic states of the temporal cat with  $s = 3$ , obtained by discrete  $C_6$  irreps diagonalization. (a) The reciprocal periodic states in the subspace of  $C_2$ , whose components are non-zero only in the  $k = 0$  and  $k = 3$  subspace. These periodic states are repeats of period-2 periodic states. (b) The reciprocal periodic states in the subspace of  $C_3$ , whose components are non-zero only in the  $k = 0$ ,  $k = 2$  and  $k = 4$  subspace. These periodic states are repeats of period-3 periodic states.

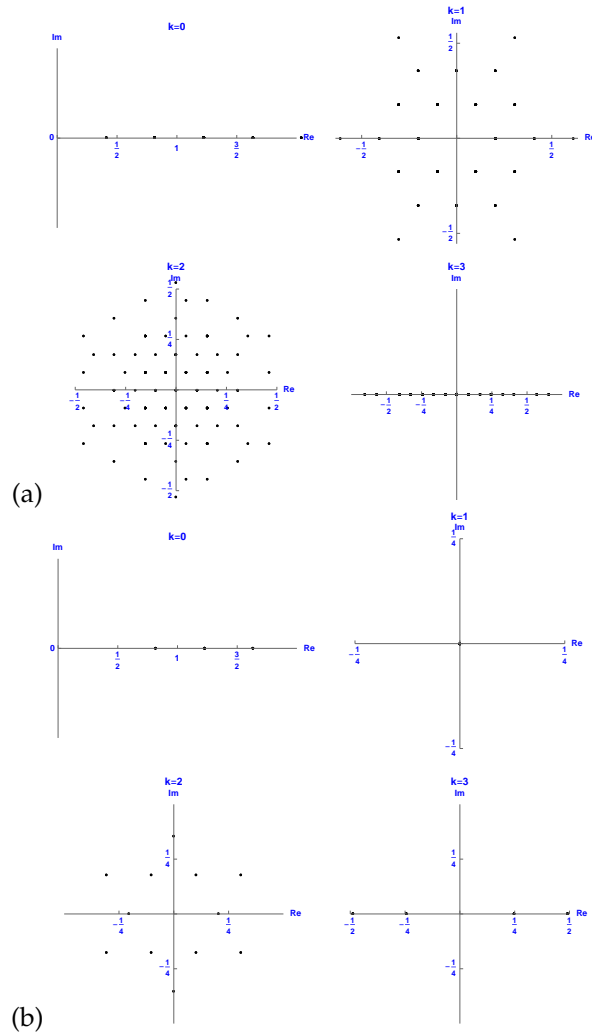


Figure 24.58: The period-6 reciprocal periodic states of the temporal cat with  $s = 3$ , obtained by discrete  $C_6$  irreps diagonalization. (a) The reciprocal periodic states that are not in the subspace of  $C_2$  or  $C_3$ , which have non-zero component in the  $k = 1$  subspace. (b) The reciprocal periodic states that are not in the subspace of  $C_2$  or  $C_3$ , which have zero component in the  $k = 1$  subspace and non-zero components in the  $k = 2$  and  $k = 3$  subspaces.

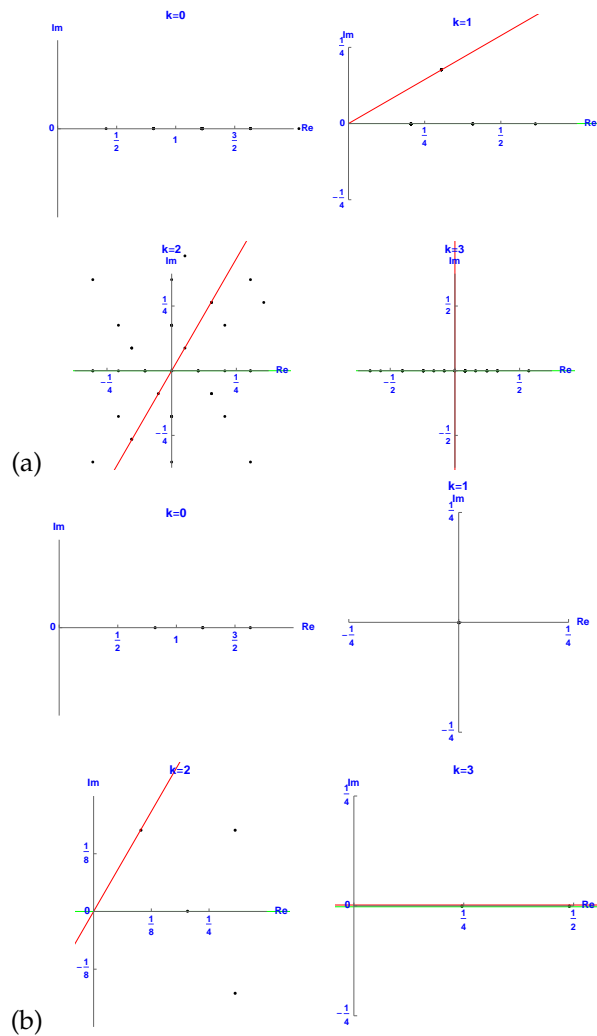


Figure 24.59: The period-6 reciprocal periodic states of the temporal cat with  $s = 3$ , obtained by discrete  $C_6$  irreps diagonalization. (a) The reciprocal periodic states that are not in the subspace of  $C_2$  or  $C_3$ , which have non-zero component in the  $k = 1$  subspace. The symmetry-reduced fundamental domain contain reciprocal periodic states whose phase of the  $k = 1$  component lies in  $(-\pi/6, \pi/6]$ . (b) The reciprocal periodic states that are not in the subspace of  $C_2$  or  $C_3$ , which have zero component in the  $k = 1$  subspace and non-zero components in the  $k = 2$  and  $k = 3$  subspaces. The symmetry-reduced fundamental domain contain reciprocal periodic states whose phase of the  $k = 2$  component lies in  $(-\pi/3, \pi/3]$ , and phase of the  $k = 3$  component lies in  $(-\pi/2, \pi/2]$ . The red and green lines are axes of reflections. For  $D_n$  irreps, see the  $D_3$  example figure ??.

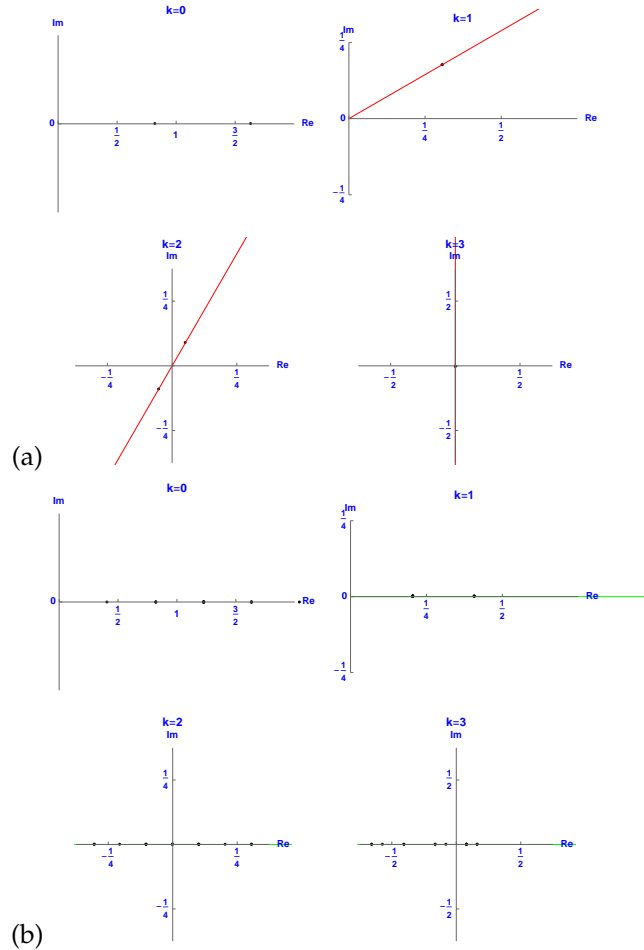


Figure 24.60: (a) The period-6 reciprocal periodic states with non-zero  $k = 1$  components, which are in the fundamental domain and on the axes of reflection  $\theta_1 = \pi/6, \theta_2 = \pi/3, \theta_3 = \pi/2$  (the red lines). (b) The reciprocal periodic states with non-zero  $k = 1$  components, which are in the fundamental domain and on the axes of reflection  $\theta_1 = 0, \theta_2 = 0, \theta_3 = 0$  (the green lines). These two sets of reciprocal periodic states are invariant under time reflection.

*Odd period* example: a period-5 reflection symmetric periodic states tiles the infinite lattice  $\mathcal{L}$  with a reflection-fixed  $\boxed{\phi_0}$ , and a length-2 block  $(\phi_1, \phi_2)$ ,

$$\cdots \phi_2 \phi_1 \boxed{\phi_0} \phi_1 \phi_2 \mid \phi_2 \phi_1 \boxed{\phi_0} \phi_1 \phi_2 \mid \cdots . \quad (24.285)$$

The boundary conditions are the index 5-periodicity mod 5, and the even reflection across  $\boxed{\phi_0}$ , or odd reflection after  $\phi_2$ :

$$\phi_i = \phi_{i+5}, \quad \phi_{-i} = \phi_i .$$

The temporal cat defining equation (??)

$$\phi_{t+1} - d_t \phi_t + \phi_{t-1} = -m_t , \quad (24.286)$$

is a length 3 block periodic state condition of form

$$\begin{aligned} -d_0 \phi_0 + 2\phi_1 &= -m_0 \\ \phi_0 - d_2 \phi_1 + \phi_2 &= -m_1 , \\ \phi_1 - (d_3 - 1)\phi_2 &= -m_2 \end{aligned} \quad (24.287)$$

Starting with  $\boxed{\phi_0}$ , followed by the block  $(\phi_1, \phi_2)$ , yields a 3-dimensional orbit Jacobian matrix  $\mathcal{J}_+$

$$\begin{pmatrix} -d_0 & 2 & 0 \\ 1 & -d_1 & 1 \\ 0 & 1 & -d_2 + 1 \end{pmatrix} = \begin{pmatrix} -d_0 & 1 & 1 \\ 1 & -d_1 & 1 \\ 1 & 1 & -d_2 \end{pmatrix} + \begin{pmatrix} 0 & 1 & -1 \\ 0 & 0 & 0 \\ -1 & 0 & 1 \end{pmatrix} \quad (24.288)$$

where the last matrix is displayed just to indicate the form of the even  $\boxed{\cdot}$  and odd  $\mid$  bc's, and that they only affect the top and the bottom rows. The translational symmetry is broken.

For  $d_j = 3$  the determinant of this orbit Jacobian matrix is 11, which counts the number of periodic states that satisfy the reflection symmetry (24.285). There are 10 period-5 periodic state with time reflection symmetry (24.265–24.266), and 1 period-1 periodic state, see table 24.3.

**2021-03-09 Han** *Even period, odd reflection* example: the period-6 periodic states with odd reflection symmetry, are tiled by length-3 blocks  $\{\phi_0, \phi_2, \phi_2\}$  that tile the infinite lattice as:

$$\cdots \phi_2 \phi_2 \phi_0 \mid \phi_0 \phi_2 \phi_2 \mid \phi_2 \phi_2 \phi_0 \mid \phi_0 \phi_2 \phi_2 \mid \cdots , \quad (24.289)$$

*Even period, even reflection* example: length-4 blocks  $\{\phi_0, \phi_2, \phi_3, \phi_4\}$  that tile the infinite lattice as:

$$\cdots \phi_3 \phi_2 \boxed{\phi_0} \phi_2 \phi_3 \boxed{\phi_4} \phi_3 \phi_2 \boxed{\phi_0} \phi_2 \phi_3 \boxed{\phi_4} \cdots . \quad (24.290)$$

The orbit Jacobian matrix of the period-3 periodic states is:

$$-\mathcal{J} = \begin{pmatrix} s-1 & -1 & 0 \\ -1 & s & -1 \\ 0 & -1 & s-1 \end{pmatrix} . \quad (24.291)$$

The determinant of this orbit Jacobian matrix is 8. The 8 orbits are:

$$\phi_{000} = \{0, 0, 0\},$$

$$\phi_{010} = \frac{1}{4}\{1, 2, 1\}, \phi_{111} = \frac{1}{2}\{1, 0, 1\}, \phi_{101} = \frac{1}{4}\{3, 2, 3\},$$

and

$$\phi_{001} = \frac{1}{8}\{1, 2, 5\}, \phi_{011} = \frac{1}{8}\{3, 6, 7\}, \phi_{100} = \frac{1}{8}\{5, 2, 1\}, \phi_{110} = \frac{1}{8}\{7, 6, 3\}.$$

The 8 periodic states consist of 1 period-1 orbit, 3 period-3 orbits and 4 period-6 periodic states from (24.280). Each invariant periodic state in (24.280) appears twice because we haven't quotiented the time translation symmetry.

The orbit Jacobian matrix of the period-4 periodic states is:

$$-\mathcal{J} = \begin{pmatrix} s & -2 & 0 & 0 \\ -1 & s & -1 & 0 \\ 0 & -1 & s & -1 \\ 0 & 0 & -2 & s \end{pmatrix}. \quad (24.292)$$

For  $s = 3$  the determinant of this orbit Jacobian matrix is 40. The 40 periodic states include: 1 period-1 orbit,

$$\phi_0 = \{0\},$$

2 period-2 orbits, corresponding to 4 periodic states:

$$\phi_{12} = \frac{1}{5}\{1, 4\}, \phi_{01} = \frac{1}{5}\{2, 3\},$$

3 period-3 orbits, 9 periodic states in all <sup>13</sup>

$$\phi_{111} = \frac{1}{2}\{0, 1, 1\}, \phi_{011} = \frac{1}{4}\{2, 3, 3\}, \phi_{100} = \frac{1}{4}\{2, 1, 1\},$$

and 16 period-6 orbits from (24.281) and (24.283), each one of which appears twice.

**2021-03-09 Han** Finding the periodic states with reflection symmetry by setting the boundary conditions with reflection is not efficient, because it becomes harder to separate shorter orbits from the long prime orbits.

Perhaps the smarter way is to still use the periodic boundary conditions and only use the Fourier modes with the reflection symmetries that we need.

<sup>13</sup>Predrag 2021-03-10: I shortened these to period 3



The eigenvectors of the orbit Jacobian matrix (24.292) are:

$$\begin{aligned} \mathbf{e}_0 &= (1, 1, 1, 1), \mathbf{e}_1 = (1, 1/2, -1/2, -1), \\ \mathbf{e}_2 &= (1, -1/2, -1/2, 1), \mathbf{e}_3 = (1, -1, 1, -1), \end{aligned} \quad (24.293)$$

with eigenvalues:

$$\lambda_0 = 1, \lambda_1 = 2, \lambda_2 = 4, \lambda_3 = 5.$$

The  $k$ th component of the  $j$ th eigenvector is:

$$\mathbf{e}_{jk} = \cos\left(\frac{\pi}{3}jk\right). \quad (24.294)$$

Compare with ChaosBook eq. (A24.25) notation; for period-6

$$\mathbf{e}_k^{(j)} = \cos\left(\frac{2\pi}{6}jk\right). \quad (24.295)$$

The eigenvalue of the  $j$ th eigenvector is:

$$\lambda_j = s - 2 \cos\left[\frac{2\pi}{6}(j-1)\right]. \quad (24.296)$$

Comparing the eigenvectors of the orbit Jacobian matrix of the period-6 cat map with periodic boundary condition, with the eigenvectors in (24.293), we can see that the eigenvectors in (24.293) are given by the first 4 components of the cosine basis vectors, which are the eigenvectors of the period-6 orbit Jacobian matrix with periodic boundary condition and reflection symmetry.

**2021-03-10 Predrag** This discussion reminds me of Baake *et al.* 1997 paper [4] *The torus parametrization of quasiperiodic LI-classes* (click here), sect. 2.3 *Symmetry*. Note the factorization of orbit Jacobian matrix, their eq. (11) (enter what you learn from that paper into sect. 6.5.3 - remember, it's the only one we found that introduces 1/2 unit length lattice). Have no feeling whether we are to worry about their 'inflation'.

**2021-03-10 Predrag** Boring remarks, but easiest to be consistent in the notation early on, so do not have to fix these later:

Remember, discrete Fourier modes are always counted starting with zero,  $k = 0, 1, \dots, n-1$ , see ChaosBook eq. (A24.32). The constant eigenvector in (24.293) is always  $\mathbf{e}^{(0)} = (1, 1, 1, 1)$  (why have you gone to curly vector =  $\{\dots\}$  notation?), and you avoid the awkward  $(j-1)(k-1)$  in (24.294), (24.296).

Please fix that throughout your blog, so I do not have to waste time on that.

**2021-03-10 Predrag** For  $D_n$  irreps, I think we should use the (6.52) form of eigenvalues, and Klein-Gordon mass  $\mu$

$$\begin{aligned}\lambda_m &= \mu^2 + 4 \sin^2(\alpha_m/2) \\ &= \left(\mu - i 2 \sin\left(\frac{\alpha_m}{2}\right)\right) \left(\mu + i 2 \sin\left(\frac{\alpha_m}{2}\right)\right) \\ \alpha_m &= 2\pi m/n,\end{aligned}\tag{24.297}$$

rather than (24.296) and stretching  $s$ , which is appropriate to  $C_n$  irreps. Identities like (19.29), (24.180), (16.58) and Gradshteyn and Ryzhik [34] Eq. 1.317.1 (click here)

$$2 \sin^2(\theta/2) = 1 - \cos(\theta)\tag{24.298}$$

are also suggestive in this context.

**2021-03-10 Predrag** In time evolution setting, it's important for me to distinguish Floquet multipliers  $\Lambda$ , see ChaosBook eq. (4.8) from Floquet exponents  $\lambda$ , see ChaosBook eq. (5.4). So I suspect for orbit Jacobian matrix we want to use  $\Lambda_j$  in formulas such as (24.296). But I'm not sure, have not thought that through yet...

**2021-03-10 Predrag to Han** Grava, Kriecherbauer, Mazzuca and McLaughlin [35] *Correlation functions for a chain of short range oscillators*, arXiv:2010.09612 (enter your notes into sect. 6.5.1) is interesting for us. The setting is  $N$ -body, coupled harmonically to neighbors up to a finite distance  $m$  away, i.e., period  $N$  1-dimensional discrete spatial lattice, continuous in time, see (6.115). Our problem corresponds essentially their spatial eigenstates (we still seem to be only ones that are thinking of this for a temporal lattice.

1. Like us in (6.49), they construct a 'localized square root' (6.118)
2. Trigonometric relations like (6.52) and functional factorizations are a result from 1915, known as Fejér and Riesz [65, pg. 117 f] lemma (6.125), (6.128).
3. Do you understand what to they gain by (6.121) going from half- $m$ -physical vector to  $m$ -physical vector?
4. They seem to separate the symmetric and antisymmetric subspaces in the Hamiltonian formulation (6.133).
5. Hénon system must be some version of their nonlinear system (6.134), with the cubic nonlinearity  $\chi \neq 0$ .
6. They only do the harmonic  $s = 2, \mu = 1$  case.
7. I have not yet seen any papers that do this for the discrete temporal lattice.

**2021-03-23 Han** Following the method used in Grava, Kriecherbauer, Mazzuca and McLaughlin [35], we first write the "Hamiltonian" form of the cat map:

$$\begin{bmatrix} q_{t+1} \\ p_{t+1} \end{bmatrix} = \begin{bmatrix} s-1 & 1 \\ s-2 & 1 \end{bmatrix} \begin{bmatrix} q_t \\ p_t \end{bmatrix} \pmod{1}.$$

Define  $\dot{q}_t \equiv q_t - q_{t-1}$  and  $\dot{p}_t \equiv p_{t+1} - p_t$ . We have:

$$\begin{cases} \dot{q}_t = p_t = \frac{\partial H}{\partial p_t}, \\ \dot{p}_t = (s-2)q_t = -\frac{\partial H}{\partial q_t}, \end{cases} \quad (24.299)$$

then the Hamiltonian of cat map is:

$$H_t = \frac{1}{2}p_t^2 - \frac{1}{2}(s-2)q_t^2. \quad (24.300)$$

The coefficient of the  $q_t^2$  term is negative because this is a kicked rotor. If the coefficient of the  $q_t^2$  term is positive then this will become a harmonic oscillator.

**2021-03-24 Han** Note that I defined  $\dot{p}_t \equiv p_{t+1} - p_t$  instead of  $p_t - p_{t-1}$ , because otherwise I cannot find a Hamiltonian that satisfies the Hamilton's equations (24.299).

**2021-03-24 Han** By factorizing the matrix generated by the  $m$ -physical vector (6.114) into the matrix generated by the half- $m$ -physical vector (6.118), they rewrote the Hamiltonian into a sum of a set of local Hamiltonian:

$$e_j = \frac{1}{2}p_j^2 + \frac{1}{2}r_j^2.$$

**2021-03-24 Han** To reverse time in the phase space  $\{q_t, p_t\}$ , we need to use the time-reversal operator:

$$T = \begin{bmatrix} 1 & 0 \\ 2-s & -1 \end{bmatrix}. \quad (24.301)$$

This operator satisfies:

$$TT = \begin{bmatrix} 1 & 0 \\ 0 & 1 \end{bmatrix},$$

and

$$TAT = A^{-1},$$

where

$$A = \begin{bmatrix} s-1 & 1 \\ s-2 & 1 \end{bmatrix}.$$

But if we write the Hamiltonian as:

$$H_t = \frac{1}{2} \mathbf{x}^\top H \mathbf{x},$$

where

$$\mathbf{x} = \begin{bmatrix} q_t \\ p_t \end{bmatrix}$$

and

$$H = \begin{bmatrix} -(s-2) & 0 \\ 0 & 1 \end{bmatrix},$$

we will find that  $[T, H] \neq 0$ ...

**2021-03-25 Predrag** This  $T$  is one of the two involutions but you are right, they do not commute.

**2021-03-25 Predrag** Re.  $\dot{p}_t \equiv p_{t+1} - p_t$  convention you mention above, I understand. One always has to be explicit about how you define lattice derivatives: forward/backward difference operators, see (4.3), (4.4) or centered, reflection (anti)symmetric difference operators (4.6), that we use in (6.46). Bolotin and Treschev [15] eq. (2.5) discuss this at length, see their symmetric generating function  $L(q_t, q_{t+1})$  defined in (8.80), and the discussion and references in that part of the blog. These just coordinate changes, should not effect any invariant quantities, like what solutions exist, of what stabilities they have.

**2021-03-26 Predrag** I'm frustrated not to see a clear connection between the discrete time-reflection symmetry and zeta function factorization (6.192), if there is any. <sup>14</sup> How about this: You have verified factorizations such as (6.54). You know  $|\det \mathcal{J}| = |\det(\hat{\mathbf{I}}_1 - \hat{\mathbf{J}}_p)|$  from (12.38).

Can you use  $|\det \mathcal{J}_\pm| = |\det(\hat{\mathbf{I}}_1 - \hat{\mathbf{J}}_{\pm,p})|$  to reverse engineer the Hamiltonian for each subspace, and explain how the time reversal relates the two (three) Hamiltonians?

**2021-03-26 Han** We can use the product formula (6.284) to check if the factorization (6.199) is given by the time-reversal symmetry.

An orbit  $p$  with length  $n_p$  will contribute to the zeta function as:

$$\begin{aligned} \mathcal{H}_p = \{e\} : & \quad (1 - z^{n_p})^2 = (1 - z^{n_p})^{A_1} (1 - z^{n_p})^{A_2} \\ \mathcal{H}_p = \{e, r\} : & \quad (1 - z^{n_p}) = (1 - z^{n_p/2})^{A_1} (1 + z^{n_p/2})^{A_2} \end{aligned} \quad (24.302)$$

We know the number of prime orbits of the cat map with  $s = 3$ , and the number of prime orbits that are invariant under time reflection up to length 6 (table 24.1).

<sup>14</sup>Predrag 2021-03-25: Have you ever checked whether my factorization (6.192) is correct?

$n$	1	2	3	4	5	6
$N_n$	1	5	16	45	121	320
$M_n$	1	2	5	10	24	50
$\tilde{M}_n$	1	2	3	6	10	18

Table 24.1: Periodic states and orbit counts for the  $s = 3$  cat map.  $\tilde{M}_n$  is the number of prime orbits with length  $n$  that are invariant under time reflection.

Let  $z = t^2$ . The zeta functions factorized by the time-reversal symmetry are:

$$\begin{aligned}
 1/\zeta_{A_1} &= (1-t)(1-t^2)^2(1-t^3)^3(1-t^6)(1-t^4)^6(1-t^8)^2 \\
 &\quad (1-t^5)^{10}(1-t^{10})^7(1-t^6)^{18}(1-t^{12})^{16} \dots \\
 &= 1-t-2t^2-t^3-2t^4+t^5+39t^7+34t^8+t^9-38t^{10}+O(t^{11}),
 \end{aligned} \tag{24.303}$$

$$\begin{aligned}
 1/\zeta_{A_2} &= (1+t)(1+t^2)^2(1+t^3)^3(1-t^6)(1+t^4)^6(1-t^8)^2 \\
 &\quad (1+t^5)^{10}(1-t^{10})^7(1+t^6)^{18}(1-t^{12})^{16} \dots \\
 &= 1+t+2t^2+5t^3+10t^4+23t^5+48t^6 \\
 &\quad +73t^7+130t^8+247t^9+422t^{10}+O(t^{11}).
 \end{aligned} \tag{24.304}$$

And the zeta functions from (6.199) are:

$$\begin{aligned}
 1/\zeta_- &= \frac{1-t-t^2}{1-t^2} \\
 &= 1-t-t^3-t^5-t^7-t^9+O(t^{11}),
 \end{aligned} \tag{24.305}$$

$$\begin{aligned}
 1/\zeta_+ &= \frac{1+t-t^2}{1-t^2} \\
 &= 1+t+t^3+t^5+t^7+t^9+O(t^{11}).
 \end{aligned} \tag{24.306}$$

These two factorizations are both correct if we expand their product:

$$\frac{1}{\zeta_{A_1}} \frac{1}{\zeta_{A_2}} = 1-t^2-2t^4-3t^6-4t^8-5t^{10}+O(t^{11}),$$

$$\frac{1}{\zeta_-} \frac{1}{\zeta_+} = 1-t^2-2t^4-3t^6-4t^8-5t^{10}+O(t^{11}).$$

So the factorization of (6.199) is correct but it is not factorized by the time reversal symmetry. But the factorization (24.302) may be wrong because I did not treat the boundary orbits correctly...

2021-04-09 Han (Continuation of (24.288), (24.291) and (24.292).)

The numbers of periodic states self-dual under time reversal are given by the Hill determinants of the orbit Jacobian matrix with the reflection-symmetric boundary conditions (24.309), (24.308), and (24.307), corresponding to (3.50), (3.51) and (3.54).

When the period  $n = 2m - 1$  of the orbit is odd, there is only one kind of reflection boundary condition:

$$\overline{|\phi_0| \phi_1 \phi_2 \cdots \phi_m | \phi_m \cdots \phi_2 \phi_1}. \quad (24.307)$$

This period  $2m - 1$  periodic state has the  $[n \times n]$  orbit Jacobian matrix:

$$\mathcal{J} = \begin{pmatrix} s & -2 & 0 & 0 & \cdots & 0 & 0 \\ -1 & s & -1 & 0 & \cdots & 0 & 0 \\ 0 & -1 & s & -1 & \cdots & 0 & 0 \\ \vdots & \vdots & \vdots & \vdots & \ddots & \vdots & \vdots \\ 0 & 0 & \cdots & \cdots & \cdots & s & -1 \\ 0 & 0 & \cdots & \cdots & \cdots & -1 & s-1 \end{pmatrix}.$$

The Hill determinant of this orbit Jacobian matrix is:

$$|\det \mathcal{J}| = \prod_{j=0}^{n-1} \left[ s - 2 \cos \left( \frac{2\pi j}{2n-1} \right) \right].$$

An example is period-5 orbit (24.288).

When the period of the orbit is even,  $n = 2m$  there are two kinds of boundary conditions with reflection symmetry.

The first kind of boundary condition is:

$$\overline{\phi_1 \phi_2 \phi_3 \cdots \phi_m | \phi_m \cdots \phi_2 \phi_1}. \quad (24.308)$$

The  $[n \times n]$  orbit Jacobian matrix is:

$$\mathcal{J} = \begin{pmatrix} s-1 & -1 & 0 & 0 & \cdots & 0 & 0 \\ -1 & s & -1 & 0 & \cdots & 0 & 0 \\ 0 & -1 & s & -1 & \cdots & 0 & 0 \\ \vdots & \vdots & \vdots & \vdots & \ddots & \vdots & \vdots \\ 0 & 0 & \cdots & \cdots & \cdots & s & -1 \\ 0 & 0 & \cdots & \cdots & \cdots & -1 & s-1 \end{pmatrix}.$$

The determinant of this orbit Jacobian matrix is:

$$|\det \mathcal{J}| = \prod_{j=0}^{n-1} \left[ s - 2 \cos \left( \frac{2\pi j}{2n} \right) \right].$$

The second kind of boundary condition is:

$$\overline{\phi_0 \phi_1 \phi_2 \cdots \phi_{m-1} \phi_m \phi_{m-1} \cdots \phi_2 \phi_1}. \quad (24.309)$$

Each  $\overline{\phi_1 \phi_2 \cdots \phi_{n-1} \phi_n \phi_{n+1}}$  corresponds to a period- $2n$  periodic state. The  $[(n+1) \times (n+1)]$  orbit Jacobian matrix is:

$$\mathcal{J} = \begin{pmatrix} s & -2 & 0 & 0 & \cdots & 0 & 0 \\ -1 & s & -1 & 0 & \cdots & 0 & 0 \\ 0 & -1 & s & -1 & \cdots & 0 & 0 \\ \vdots & \vdots & \vdots & \vdots & \ddots & \vdots & \vdots \\ 0 & 0 & \cdots & \cdots & \cdots & s & -1 \\ 0 & 0 & \cdots & \cdots & \cdots & -2 & s \end{pmatrix},$$

with Hill determinant

$$\begin{aligned} |\det \mathcal{J}| &= \prod_{j=0}^n [s - 2 \cos \alpha_j], \quad \alpha_j = 2\pi j/2n \\ &= \prod_{j=0}^n \left( \mu + e^{i\alpha_j/2} - e^{-i\alpha_j/2} \right) \left( \mu + e^{i\alpha_j/2} - e^{-i\alpha_j/2} \right)^* . \end{aligned} \quad (24.310)$$

where we have replaced  $(s - 2 \cos \alpha)$  by  $(\mu^2 + 4 \sin^2(\alpha/2))$ , in the (6.52) time-reversal spirit.

The above Hill determinants count the number of periodic states that have time reversal symmetry.

In order to compare with Gallas [33] (a step not needed for our calculations): his orbits with time reversal symmetry are categorized into two classes: diagonal class and non-diagonal class. For orbits with even period, the diagonal class orbits satisfy the boundary condition (24.308), and the non-diagonal class orbits satisfy the boundary condition (24.309).

Let  $A_n$  be the number of periodic states with period  $n$  that satisfy the boundary condition (24.307) if  $n$  is odd and the boundary condition (24.308) if  $n$  is even. And let  $Q_n$  be the number of periodic states with period  $n$  that satisfy the boundary condition (24.307) if  $n$  is odd and the boundary condition (24.309) if  $n$  is even.

$$A_n = \begin{cases} \prod_{j=0}^{\frac{n-1}{2}} \left[ s - 2 \cos \left( \frac{2\pi j}{n} \right) \right], & n \text{ is odd,} \\ \prod_{j=0}^{\frac{n}{2}-1} \left[ s - 2 \cos \left( \frac{2\pi j}{n} \right) \right], & n \text{ is even.} \end{cases}$$

$n$	1	2	3	4	5	6	7	8	9	10	11
$D_n$	1	0	3	1	10	2	28	9	72	22	198
$N_n$	0	2	0	5	0	16	0	45	0	130	0

Table 24.2: Time reversal symmetric prime orbit counts for the  $s = 3$  cat map.  $D_n$  is the number of symmetric orbits with points on the diagonal in the state space.  $N_n$  is the number of symmetric orbits without points on the diagonal.

$$Q_n = \begin{cases} \prod_{j=0}^{\frac{n-1}{2}} \left[ s - 2 \cos \left( \frac{2\pi j}{n} \right) \right], & n \text{ is odd,} \\ \prod_{j=0}^{\frac{n}{2}} \left[ s - 2 \cos \left( \frac{2\pi j}{n} \right) \right], & n \text{ is even.} \end{cases}$$

Now let  $D_n$  be the number of orbits with period  $n$  that satisfy the boundary condition (24.307) if  $n$  is odd and (24.308) if  $n$  is even. And  $N_n$  is the number of orbits with period  $n$  that satisfy the boundary condition (24.307) if  $n$  is odd and (24.309) if  $n$  is even. Then we have the relation:

$$A_n = \sum_{d|n} a_n D_n,$$

$$Q_n = \sum_{d|n} a_n N_n,$$

where

$$a_n = \begin{cases} 1, & n \text{ is odd,} \\ 2, & n \text{ is even.} \end{cases}$$

We can use the Möbius inversion formula to compute the number of the orbits with the time reversal symmetry:

$$D_n = \frac{1}{a_n} \sum_{d|n} \mu \left( \frac{n}{d} \right) A_n,$$

$$N_n = \frac{1}{a_n} \sum_{d|n} \mu \left( \frac{n}{d} \right) Q_n,$$

where  $\mu(n)$  is the Möbius function. Note that using these formulas we will have  $D_n = N_n$  if  $n$  is odd. In Gallas [33], by definition  $N_n = 0$  if  $n$  is odd. Set  $N_n = 0$  for odd  $n$ . The number of orbits with time reversal symmetry is shown in table 24.2.

**2021-04-13 Han** Let  $A : (x, y) \rightarrow (x', y')$  be the cat map with  $s = 3$ :

$$A \begin{bmatrix} x \\ y \end{bmatrix} = \begin{bmatrix} 0 & 1 \\ -1 & 3 \end{bmatrix} \begin{bmatrix} x \\ y \end{bmatrix} \pmod{1}.$$



And  $T$  is the time reflection:

$$T \begin{bmatrix} x \\ y \end{bmatrix} = \begin{bmatrix} 0 & 1 \\ 1 & 0 \end{bmatrix} \begin{bmatrix} x \\ y \end{bmatrix}.$$

Fixed points of  $T$  satisfy:

$$x = y.$$

Fixed points of  $A \circ T$  satisfy:

$$A \circ T \begin{bmatrix} x \\ y \end{bmatrix} = \begin{bmatrix} 1 & 0 \\ 3 & -1 \end{bmatrix} \begin{bmatrix} x \\ y \end{bmatrix} \pmod{1} = \begin{bmatrix} x \\ y \end{bmatrix},$$

which can be written as:

$$3x - 2y \pmod{1} = 0.$$

For time reversal symmetric periodic orbits with odd period, each orbit has one point on the  $\text{Fix}(AT)$  and one point on the  $\text{Fix}(T)$ . If the period is  $2n + 1$  and  $(\phi_0, \phi_1)$  is on  $\text{Fix}(AT)$ , then  $(\phi_n, \phi_{n+1})$  is on  $\text{Fix}(T)$ . So we have:

$$3\phi_0 - 2\phi_1 \pmod{1} = 0,$$

and

$$A^n \begin{bmatrix} \phi_0 \\ \phi_1 \end{bmatrix} = \begin{bmatrix} \phi_n \\ \phi_n \end{bmatrix}.$$

$A^n$  is:

$$A^n \begin{bmatrix} x \\ y \end{bmatrix} = \begin{bmatrix} \frac{2^{-n+1}[(3-\sqrt{5})^{n-1} - (3+\sqrt{5})^{n-1}]}{\sqrt{5}} & \frac{2^{-n}[-(3-\sqrt{5})^n + (3+\sqrt{5})^n]}{\sqrt{5}} \\ \frac{2^{-n}[(3-\sqrt{5})^n - (3+\sqrt{5})^n]}{\sqrt{5}} & \frac{2^{-n-1}[-(3-\sqrt{5})^{n+1} + (3+\sqrt{5})^{n+1}]}{\sqrt{5}} \end{bmatrix} \begin{bmatrix} x \\ y \end{bmatrix} \pmod{1}.$$

For example, if  $n = 4$  and the period of the orbit is  $2n + 1 = 9$ , we have:

$$A^4 \begin{bmatrix} \phi_0 \\ \phi_1 \end{bmatrix} = \begin{bmatrix} -8 & 21 \\ -21 & 55 \end{bmatrix} \begin{bmatrix} \phi_0 \\ \phi_1 \end{bmatrix} \pmod{1} = \begin{bmatrix} \phi_n \\ \phi_n \end{bmatrix},$$

which can be written as:

$$-13\phi_0 + 34\phi_1 \pmod{1} = 0.$$

So we have:

$$\begin{bmatrix} 3 & -2 \\ -13 & 34 \end{bmatrix} \begin{bmatrix} \phi_0 \\ \phi_1 \end{bmatrix} \pmod{1} = 0.$$

Then the number of periodic points on the  $\text{Fix}(AT)$  is given by the determinant:

$$\left| \det \begin{bmatrix} 3 & -2 \\ -13 & 34 \end{bmatrix} \right| = 76.$$

When the period of the orbit is even, each orbit has two points on  $\text{Fix}(AT)$  and none on  $\text{Fix}(T)$ , or two points on  $\text{Fix}(T)$  and none on  $\text{Fix}(AT)$ . For example, if the period is 10, when the orbits have no point on  $\text{Fix}(AT)$ , we have:

$$\phi_0 = \phi_1,$$

and

$$A^5 \begin{bmatrix} \phi_0 \\ \phi_1 \end{bmatrix} \pmod{1} = \begin{bmatrix} -21 & 55 \\ -55 & 144 \end{bmatrix} \begin{bmatrix} \phi_0 \\ \phi_1 \end{bmatrix} \pmod{1} = \begin{bmatrix} \phi_n \\ \phi_n \end{bmatrix}.$$

Then the periodic point  $(\phi_0, \phi_1)$  satisfies:

$$\begin{bmatrix} 1 & -1 \\ -34 & 89 \end{bmatrix} \begin{bmatrix} \phi_0 \\ \phi_1 \end{bmatrix} \pmod{1} = 0.$$

So the number of points on the  $\text{Fix}(T)$  is:

$$\left| \det \begin{bmatrix} 1 & -1 \\ -34 & 89 \end{bmatrix} \right| = 55.$$

When the orbits have no periodic point on  $\text{Fix}(T)$ , we have:

$$3\phi_0 - 2\phi_1 \pmod{1} = 0,$$

and

$$A^5 \begin{bmatrix} \phi_0 \\ \phi_1 \end{bmatrix} \pmod{1} = \begin{bmatrix} -21 & 55 \\ -55 & 144 \end{bmatrix} \begin{bmatrix} \phi_0 \\ \phi_1 \end{bmatrix} \pmod{1} = \begin{bmatrix} \phi_n \\ \phi_{n+1} \end{bmatrix},$$

where

$$3\phi_n - 2\phi_{n+1} \pmod{1} = 0.$$

So we have:

$$\begin{bmatrix} 3 & -2 \\ 47 & -123 \end{bmatrix} \begin{bmatrix} \phi_0 \\ \phi_1 \end{bmatrix} \pmod{1} = 0.$$

$$\left| \det \begin{bmatrix} 3 & -2 \\ 47 & -123 \end{bmatrix} \right| = 275.$$

Using the number of periodic points on  $\text{Fix}(T)$  and  $\text{Fix}(AT)$  we can count the number of orbits. The result is shown in table [24.3](#).

**2021-04-13 Predrag** Pozrikidis [64] *An introduction to grids, graphs, and networks*, ([click here](#)) has a clear discussion of various boundary conditions, (see some of my clippings around [\(8.205\)](#), but it is better to check out the book). For an example of *Dirchlet boundary conditions* orbit Jacobian matrix  $-\mathcal{J}$  [\(2.38\)](#). See also antiperiodic sum [\(2.48\)](#).

**2021-04-13 Predrag** My problems with bc's approaches is they are a natural starting point, but they do not scale up. At all. Even for the 3-disk pinball you start by thinking of symmetry axes as mirrors, but then what do you do with the 2-dimensional irreps? Hill's formula  $\det H = \det(1 - J_p)$  for the periodic case.

$n$	$F_n$	$C_n$	$SF_n$		$SC_n$	
1	1	1	1		1	
2	5	2	1	5	0	2
3	16	5	4		3	
4	45	10	3	15	1	5
5	121	24	11		10	
6	320	50	8	40	2	16
7	841	120	29		28	
8	2205	270	21	105	9	45
9	5776	640	76		72	
10	15125	1500	55	275	22	130

Table 24.3:  $F_n$  is the number of periodic states with period  $n$ .  $C_n$  is the number of periodic orbits with period  $n$ .  $SF_n$  is the number of symmetric fixed points of  $A^n$  on  $\text{Fix}(T)$  for odd  $n$ , and on  $\text{Fix}(T), \text{Fix}(AT)$  for even  $n$ .  $SC_n$  is the number of symmetric orbits with periodic points on  $\text{Fix}(T)$  for odd  $n$ , and on  $\text{Fix}(T), \text{Fix}(AT)$  for even  $n$ . The notations are same as the notations used in Table 1.2.3.5.1 of MacKay's thesis [52].

**2021-05-11 Han** The product of eigenvalues of the antisymmetric eigenvectors of the orbit Jacobian matrix does count the number of antisymmetric periodic states.

For example, if the period of the periodic states is 6, we have two kinds of reflections. If the periodic state is antisymmetric under reflection over half lattice sites, the antisymmetric subspace is 3-dimensional. And the periodic state tiles the infinite lattice as:

$$\overline{\phi_1 \phi_2 \phi_3 | \phi_3 \phi_2 \phi_1} = \dots \phi_3 \phi_2 \phi_1 | \phi_1 \phi_2 \phi_3 | \phi_3 \phi_2 \phi_1 | \phi_1 \phi_2 \phi_3 \dots, \quad (24.311)$$

where the underline means negative.

The orbit Jacobian matrix in the 3-dimensional antisymmetric subspace is:

$$\mathcal{J} = \begin{bmatrix} s+1 & -1 & 0 \\ -1 & s & -1 \\ 0 & -1 & s+1 \end{bmatrix}.$$

The eigenvalues of this orbit Jacobian matrix in the 3-dimensional antisymmetric subspace are  $s - 1, s + 1$  and  $s + 2$ , which are the eigenvalues of the antisymmetric eigenvectors of the orbit Jacobian matrix in the full space.

If the periodic state is antisymmetric under reflection over integer lattice sites, the antisymmetric subspace is 2-dimensional. The periodic state tiles the infinite lattice as:

$$\overline{\overline{0} \phi_1 \phi_2 | \phi_3 \phi_2 \overline{0}} = \dots \phi_2 \phi_1 \overline{0} | \phi_1 \phi_2 \overline{0} | \phi_2 \phi_1 \overline{0} | \phi_1 \phi_2 \dots, \quad (24.312)$$

The orbit Jacobian matrix in the 2-dimensional antisymmetric subspace is:

$$\mathcal{J} = \begin{bmatrix} s & -1 \\ -1 & s \end{bmatrix}.$$

The eigenvalues of this orbit Jacobian matrix in the 2-dimensional antisymmetric subspace are  $s - 1, s + 1$ , which are the eigenvalues of the antisymmetric eigenvectors of the orbit Jacobian matrix in the full space.

**2021-06-13 Predrag** I think I'm starting to understand *Máo Zhǔxí Yǔlù*. The 3 types of  $D_\infty$  symmetric states  $\Phi$  are -well- symmetric, and that means that the number  $\sim m$  of distinct fields that describe the corresponding period- $n$  primitive cell is  $\sim n/2$ . They satisfy non-periodic bc's equations such as (??).

**2021-06-13 Predrag** That block-diagonalizes into eigenvectors that *point within* the symmetry subspace of the same symmetry as the periodic state, and the (antisymmetric) rest, that *point out* of it. That's all as it should be for a fixed point with a symmetry.

**2021-05-11 Han** To write the orbit Jacobian matrix in the reflection symmetric or antisymmetric subspace, we can use the projection operators.



example 6.29  
p. 360

To get the orbit Jacobian matrix in the antisymmetric subspace, we can project the orbit Jacobian matrix of the full space into the antisymmetric subspace:

$$\mathcal{J}P_{R^-} = \frac{1}{2} \begin{bmatrix} s+1 & -1 & 0 & 0 & 1 & -s-1 \\ -1 & s & -1 & 1 & -s & 1 \\ 0 & -1 & s+1 & -s-1 & 1 & 0 \\ 0 & 1 & -s-1 & s+1 & -1 & 0 \\ 1 & -s & 1 & -1 & s & -1 \\ -s-1 & 1 & 0 & 0 & -1 & s+1 \end{bmatrix},$$

$$\mathcal{J}P_{T R^-} = \frac{1}{2} \begin{bmatrix} 0 & 0 & 0 & 0 & 0 & 0 \\ 0 & s & -1 & 0 & 1 & -s \\ 0 & -1 & s & 0 & -s & 1 \\ 0 & 0 & 0 & 0 & 0 & 0 \\ 0 & 1 & -s & 0 & s & -1 \\ 0 & -s & 1 & 0 & -1 & s \end{bmatrix}.$$

And the orbit Jacobian matrix of the antisymmetric subspace can be found in the top left blocks of  $\mathcal{J}P_{R^-}$  and  $\mathcal{J}P_{T R^-}$ .

**2021-06-01 Han** I'm still not able to use the number of symmetric periodic states from table 24.3 to compute the factor of the topological zeta function which is corresponding to the symmetric orbits.

Remember that for the number of the periodic points  $N_n$ , we have:

$$z^n N_n = \sum_{n_p | n} n_p t_p^{\frac{n}{n_p}} = \sum_p n_p \sum_{r=1}^{\infty} \delta_{n, r n_p} t_p^r.$$

Then the topological zeta function is:

$$\begin{aligned} \frac{1}{\zeta(z)} &= \exp\left(-\sum_{n=1}^{\infty} \frac{z^n N_n}{n}\right) \\ &= \exp\left(-\sum_{n=1}^{\infty} \frac{1}{n} \sum_p n_p \sum_{r=1}^{\infty} \delta_{n, r n_p} t_p^r\right) \\ &= \exp\left(-\sum_p \sum_{r=1}^{\infty} \frac{1}{r} t_p^r\right) \\ &= \prod_p (1 - t_p). \end{aligned} \tag{24.313}$$

Now let  $D_n$  be the number of symmetric periodic states with points on the diagonal. we have

$$z^n D_n = \sum_{n_p | n} a_p t_p^{\frac{n}{n_p}} = \sum_p a_p \sum_{r=1}^{\infty} \delta_{n, r n_p} t_p^r,$$

where

$$a_p = \begin{cases} 1, & n_p \text{ is odd,} \\ 2, & n_p \text{ is even.} \end{cases}$$

And

$$\sum_{n=1}^{\infty} z^n D_n = \sum_p a_p \sum_{r=1}^{\infty} t_p^r.$$

To find the topological zeta function that count the number of orbits with symmetry, I need to find a function  $f(n)$  such that:

$$f(r n_p) = r a_p.$$

So

$$\sum_{n=1}^{\infty} \frac{1}{f(n)} z^n D_n = \sum_p \sum_{r=1}^{\infty} \frac{a_p}{r a_p} t_p^r.$$

**2021-06-25 Han** I realized why figure 6.14 (b) is unnatural to me. If the time is continuous, we cannot have an orbit with reflection symmetry like figure 6.14 (b), because if the system has reflection symmetry, then the reflection axis (the boundary) is an invariant set, and orbit cannot cross it. So orbit with reflection symmetry can only exist on the boundary.

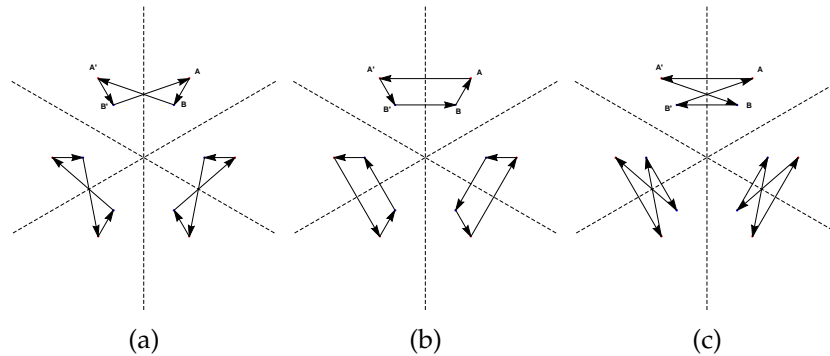


Figure 24.61: (a): Reflection invariant orbits of system with  $D_3$  symmetry. The orbit  $ABA'B'$  will be changed to  $A'B'AB$  after reflection. (b) and (c): Orbits that cannot exist for system with  $D_3$  symmetry. Although the sets of periodic points in these orbits are invariant under reflection, the order of the periodic points in these orbits will be changed to the opposite direction.  $AA'B'B$  will be changed to  $A'ABB'$  and  $AA'BB'$  will be changed to  $A'AB'B$ .

If the time is discrete then orbit with reflection symmetry can exist as shown in figure 24.61 (a). Note that figure 24.61 (b) and (c) cannot exist because these two orbits will change direction after reflection, i.e., the orbit will go opposite direction in the flipped fundamental domain. Even though these two kinds of orbits will not exist for system with reflection symmetry, these are the orbits that will exist for system with time reversal symmetry.

**2021-07-04 Predrag to Han** I think I have finally found the ‘dihedral’ zeta function in the literature. The much desired -see (3.34)- square root and dependence on  $t^2$  makes an appearance in the Lind zeta function (6.162)!

Please drop everything, and check and correct my draft sect. 6.6 *A Lind zeta function for flip systems*. I hope this finally leads to a paper on zeta-function factorization in time-reversal invariant temporal lattices.

**2021-07-09 Han** Figure ?? shows period-3 periodic states of  $s = 3$  temporal cat, plotted in the subspace of the irreps (6.180) of the permutation representation. Using these 16 periodic states as a set on which the  $D_3$  group acts, we can apply the Burnside theorem (24.316), using the  $D_3$  table of marks table 6.3 to compute the number of periodic states that are invariant under the action of each subgroup.

Since irrep  $A_1$  is a symmetric irrep, we only need to study the orbits in the subspace of irrep  $E_1$ . Periodic states related by cyclic permutations are connected by blue lines in the figure ?? (a). The two biggest triangles are two orbits without time reflection symmetry. There are three smaller

triangles which are orbits with time reflection symmetry. And the point on the center is invariant under all group actions. This set of periodic states is corresponding to an element of the *Burnside ring*  $\Omega(D_3)$ :

$$a_{[D_3/1]} \begin{bmatrix} D_3 \\ \mathbf{1} \end{bmatrix} + a_{[D_3/D_1]} \begin{bmatrix} D_3 \\ D_1 \end{bmatrix} + a_{[D_3/C_3]} \begin{bmatrix} D_3 \\ C_3 \end{bmatrix} + a_{[D_3/D_3]} \begin{bmatrix} D_3 \\ D_3 \end{bmatrix}. \quad (24.314)$$

In this expression,  $[D_3/H]$  is a kind of group orbits that are generate by factor group  $D_3$  on a point  $x$  in the orbit, and  $x$  is invariant under the action of subgroup  $H$ . And  $a_{[D_3/H]}$  is the number of this kind of group orbits.

For the period 3 periodic states of cat map,  $a_{[D_3/1]}$  is the number of group orbits that is only invariant under the identity subgroup  $\mathbf{1}$ , which is 1. Note that the two biggest triangles are one group orbit.  $a_{[D_3/D_1]}$  is 3, since there are 3 smaller triangles that are invariant under reflection subgroup  $D_1$ .  $a_{[D_3/C_3]}$  is 0. Although there is one point on the center that is invariant under  $C_3$ , the stabilizer (isotropy) subgroup is  $D_3$  itself. So this point will contribute to  $a_{[D_3/D_3]}$  instead of  $a_{[D_3/C_3]}$ .

The expression of the ring element of this set of orbits is

$$1 \begin{bmatrix} D_3 \\ \mathbf{1} \end{bmatrix} + 3 \begin{bmatrix} D_3 \\ D_1 \end{bmatrix} + 0 \begin{bmatrix} D_3 \\ C_3 \end{bmatrix} + 1 \begin{bmatrix} D_3 \\ D_3 \end{bmatrix}.$$

Let

$$\mathbf{a} = (a_{[D_3/1]}, a_{[D_3/D_1]}, a_{[D_3/C_3]}, a_{[D_3/D_3]}) = (1, 3, 0, 1), \quad (24.315)$$

we can use the Burnside theorem (6.179)

$$\mathbf{a}M = \mathbf{u}, \quad (24.316)$$

to compute the  $\mathbf{u}$  which are the numbers of states fixed by the subgroups.  $M$  is the matrix of the table of marks of  $D_3$  table 6.3. The result is:

$$\mathbf{u} = (16, 4, 1, 1).$$

16 is the number of states that are invariant under the identity group  $\mathbf{1}$ , which is the total number of states. 4 is the number of states that are invariant under a reflection subgroup  $D_1$ . As shown in figure ?? (b), there are 4 points on each one of the reflection axis (red dashed lines). The number of states that are invariant under  $D_3$  and  $C_3$  subgroups is 1, which is the fixed point state, or the center.

It is easy for me to find the number of states invariant under the action of a group. So to make a good use of (24.316) we should find the number of periodic states that are invariant under subgroup actions, then use the inverse of the table of marks to find the numbers of each kind of orbit.

Table 24.4:  $D_6$  table of marks, taken from [GAP sect. 70.12-2 Table of marks dihedral](#). For  $D_3$ , see table [6.3](#).

$D_6$	$\mathbf{1}$	$C_2$	$D_{1,0}$	$D_{1,1}$	$C_3$	$D_2$	$C_6$	$D_{3,0}$	$D_{3,1}$	$D_6$
$D_6/\mathbf{1}$	12									
$D_6/C_2$	6	6								
$D_6/D_{1,0}$	6	0	2							
$D_6/D_{1,1}$	6	0	0	2						
$D_6/C_3$	4	0	0	0	4					
$D_6/D_2$	3	3	1	1	0	1				
$D_6/C_6$	2	2	0	0	2	0	2			
$D_6/D_{3,0}$	2	0	2	0	2	0	0	2		
$D_6/D_{3,1}$	2	0	0	2	2	0	0	0	2	
$D_6/D_6$	1	1	1	1	1	1	1	1	1	1

2021-07-10 Han The dihedral group

$$D_6 = \langle r, s \mid srs = r^5, r^6 = s^2 = 1 \rangle.$$

has 10 subgroup conjugacy classes (see [\(6.154\)](#) for notation):

- The identity subgroup  $\mathbf{1} = \{1\}$ .
- Dihedral subgroup  $D_{1,0} = \{1, s\} = \langle s \rangle$  and its conjugate subgroups.
- Dihedral subgroup  $D_{1,1} = \{1, rs\} = \langle rs \rangle$  and its conjugate subgroups.
- Cyclic subgroup  $C_2 = \{1, r^3\} = \langle r^3 \rangle$ .
- Dihedral subgroup  $D_2 = \{1, r^3, s, r^3s\} = \langle r^3, s \rangle$  and its conjugate subgroups.
- Cyclic subgroup  $C_3 = \{1, r^2, r^4\} = \langle r^2 \rangle$ .
- Dihedral subgroup  $D_{3,0} = \{1, r^2, r^4, s, r^2s, r^4s\} = \langle r^2, s \rangle$ .
- Dihedral subgroup  $D_{3,1} = \{1, r^2, r^4, rs, r^3s, r^5s\} = \langle r^2, rs \rangle$ .
- Cyclic subgroup  $C_6 = \{1, r, r^2, r^3, r^4, r^5\} = \langle r^5 \rangle$ .
- $D_6$  group.

The table of marks of these subgroups is give in table [24.4](#).

2021-07-10 Han For the temporal cat with  $s = 3$ , we have 320 periodic states with period 6. Let  $u_H$  be the number of states that are invariant under the action of the subgroup  $H$ . Then

$$\begin{aligned} \mathbf{u} &= (u_{\mathbf{1}}, u_{C_2}, u_{D_{1,0}}, u_{D_{1,1}}, u_{C_3}, u_{D_2}, u_{C_6}, u_{D_{3,0}}, u_{D_{3,1}}, u_{D_6}) \\ &= (320, 16, 8, 40, 5, 4, 1, 1, 5, 1). \end{aligned} \tag{24.317}$$



Using the Burnside theorem (6.179) we have the corresponding Burnside ring:

$$\begin{aligned} \mathbf{a} &= \mathbf{u}M^{-1} \\ &= (16, 1, 2, 16, 0, 3, 0, 0, 2, 1). \end{aligned} \quad (24.318)$$

The interpretation of these numbers (see also (24.315)):

- $a_{[D_6/\mathbf{1}]} = 16$ : there are 16 pairs of  $C_6$  orbits without any symmetry.
- $a_{[D_6/C_2]} = 1$ : there is 1 pair of  $C_3$  period 3 orbits without any symmetry, see figure ??.
- $a_{[D_6/D_{1,0}]} = 2$  and  $a_{[D_6/D_{1,1}]} = 16$  are the numbers of  $C_6$  period 6 orbits that are invariant under two types of reflections, in agreement with table 24.3  $SC_6$ .
- $a_{[D_6/C_3]} = 0$ : there is no orbit of  $C_2$  period 2 without reflection symmetry.
- $a_{[D_6/D_2]} = 3$ : there are 3  $C_3$  period 3 orbits with reflection symmetry, in agreement with table 24.3  $SC_3$ .
- $a_{[D_6/C_6]} = 0$ : there is no fixed point periodic state without reflection symmetry.
- $a_{[D_6/D_{3,0}]} = 0$  and  $a_{[D_6/D_{3,1}]} = 2$  are the numbers of  $C_2$  period 2 orbits invariant under both types of reflections, in agreement with table 24.3  $SC_2$ .
- $a_{[D_6/D_6]} = 1$ : there is one fixed point periodic state with reflection symmetry.

**2021-07-11 Predrag** To me indicating  $D_6$  in  $a_{[D_6/D_{1,0}]}$ , etc, in (24.315) and (24.318) seems redundant. Is that a notation literature uses? Otherwise indicating just the subgroup, as in  $a_{D_{1,0}}$ , should suffice?

**2021-07-11 Predrag** A remark on the level of ChaosBook generality: Looks like one should abandon the notion of 'prime', 'relative prime' orbit. The notion of 'orbit' covers all that, so the distinction is only between 'periodic state' and 'orbit', there is no 'non-prime' orbit.

**2021-07-11 Predrag** Very nice - I have changed the notation following (6.154), and tentatively reordered the list (but not in the table, there we follow GAP) by grouping  $C_n$ 's,  $D_n$ 's together, and putting  $D_1$ 's ahead of  $C_2$ 's, though ordering by the order of the group might be more logical.

A beautiful thing is that the Lind zeta function (6.162), (6.166) does not seem to depend on all these subgroup lattice details. That might be the genius of zeta functions; the 'prime' orbits are only defined in terms of  $C_n$ 's,  $D_n$ 's, and all these subgroup complications arise only when one insists on counting the periodic states. Which is what is fundamentally not needed, that should be emphasized in the putative paper.

**2021-07-17 Predrag to Han** Before we can hope that sect. 6.6 *A Lind zeta function for flip systems* is publishable, we have to explain clearly that the quotient taken is a lattice/sublattice quotient, isomorphic to a point group. I've used the *CL18.tex* spatiotemporal cat text as a starting point for sect. ?? *1-dimensional lattices and sublattices* - please shorten it to a few paragraphs? To make that understandable, I believe we need to draw some 1-dimensional lattice, line group figures, illustrating

1. the unit tile has no symmetry (and arrow? a fish? drawn in it, pointing to the right?) for a generic dynamical system, such as the usual Hénon map.
2. Reversible dynamical system's unit tile has a midpoint and edge-flip reflection symmetry (draw left-right arrow? moustache?)
3. Draw a figure illustrating that  $rH(n, k)r^{-1} = H(n, k + 2)$ .
4. draw (for example?) a 1-dimensional, period 4 primitive cell, and draw the (6.154)  $k = 0, 1, 2, 3$  flips of it.

**2021-07-21 Han** In the Lind zeta function (6.150), each subgroup  $H$  is a symmetric group of a set of periodic states. For the flip system (dynamical system with time reversal symmetry), there are two kinds of subgroups of  $D_\infty$  (6.7):  $H(n)$  and  $H(n, k)$  (6.154). These two subgroups act on infinite periodic states.  $N_n$  and  $N_{n,k}^\sigma$  are the numbers of periodic states that are invariant under the  $H(n)$  and  $H(n, k)$ .

We need to define the action of the  $D_\infty$  on the periodic state. Let the generator  $r$  shift the periodic state one step to the left, and the generator  $\sigma$  reflect the periodic state over the 0th lattice point. Then figure 24.62 shows periodic states that are invariant under subgroups of  $D_\infty$ .

**2021-07-22 Predrag** I was wrong: color-coded figure 24.62 is useless, while the field figure 6.1 is much easier to understand.

**2021-07-27 Han** The two small triangles in figure ?? are related by the  $D_1$  :  $S\phi_i = 1 - \phi_i$  symmetry. Let  $T$  be the irreps transformation,  $\phi_1$  and  $\phi_2$  be two periodic states related by  $\phi_1 = 1 - \phi_2$ . Then we have :

$$T\phi_1 = T\mathbf{1} - T\phi_2 = (1, 0, 0, \dots) - T\phi_2, \quad (24.319)$$

where  $(1, 0, 0, \dots)$  is a vector with the first component 1 and other components 0. The first component in the space of irreps is the component in the subspace of the 1-dimensional symmetric irrep, which is the average value of the periodic state. The effect of the action of  $S$  is to inverse the sign of the periodic state in the space of irreps except for the subspace of the 1-dimensional symmetric irrep.

But why the two big triangles and the one medium size triangle do not have inversions? The orbit of these triangles are  $1/4(0, 1, 3)$  and  $1/2(1, 1, 0)$ . When we apply the inversion  $S$ , 0 is mapped to 0 instead of 1. So these

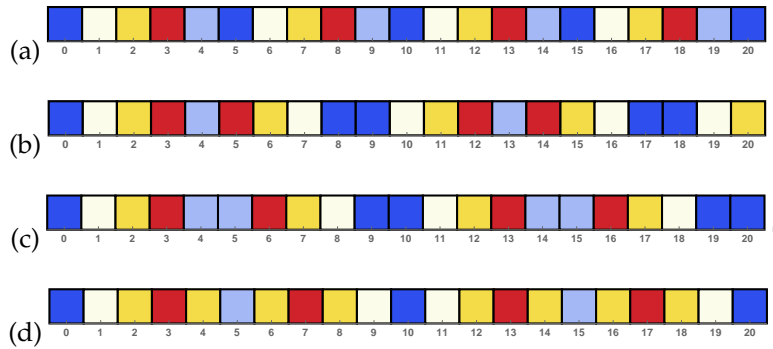


Figure 24.62: Periodic states same as figure 6.1 but the field values are color coded (we have since abandoned this approach), rather than plotted as  $\phi_t \in [0, 1)$ . Horizontal: lattice sites labelled by  $t \in \mathbb{Z}$ . Vertical: value of field  $\phi_t$ , plotted as a bar centred at lattice site  $t$ . A period  $n$  periodic state  $\Phi$  has one of the 4 possible symmetries, illustrated by: (a) A period-5 periodic state  $\Phi$  invariant under the translation group  $H(5)$ , with no reflection symmetry. Its  $D_5$  orbit are  $2n = 10$  distinct periodic states,  $5 C_\infty$  translations and  $5 D_\infty$  translate-reflections. (b) A period 9, odd-period periodic state (??), invariant under the space group  $H(9, 8)$ . This periodic state has reflection symmetry over the 4th lattice point (as in figure ?? (a)), and the midpoint between 8th and 9th lattice points (as in figure ?? (b)). (c) A period 10, even-period periodic state (12.124), invariant under the space group  $H(10, 9)$ . This periodic state has reflection symmetry over the midpoint between the 4th and 5th lattice points and the midpoint between 9th and 10th lattice points. (d) A period 10, even-period periodic state (12.125), invariant under the space group  $H(10, 0)$ . This periodic state has reflection symmetry over the 0th lattice point and the 5th lattice point. Note that  $H(10, 9)$  and  $H(10, 0)$  are not conjugate subgroups, so we cannot use translations or reflections to make the periodic state (c) satisfy the symmetry of periodic state (d). The  $D_n$  orbits of reflection-symmetric periodic states (b-c) contain only  $n$  periodic state  $C_n$  translations, as any reflection results in a translation of the initial periodic state.

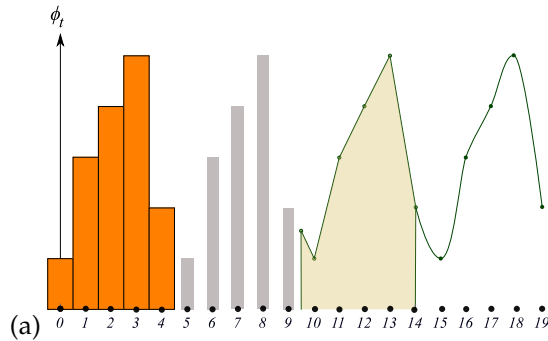


Figure 24.63: For a time-reversal invariant system, a period  $n$  periodic state  $\Phi$ , plotted here as the field values  $\phi_t$ , each bar centred at lattice site  $t$ , has one of the 4 possible symmetries, illustrated by: (a) A period-5 periodic state  $\Phi$  invariant under the translation group  $H(5)$ , with no time reversal symmetry.

two orbits are mapped to  $1/4(0, 3, 1)$  and  $1/2(1, 1, 0)$ , which are themselves.

2021-07-28 Predrag Moved the two “ $H(n, k)$  is not a normal subgroup” posts to example 6.18. I agree with both.

2021-07-28 Predrag I feel that the coset count is easiest to understand looking at the 3-disk billiard, ChaosBook example 11.6. I find the notion of “isotropy” group too restrictive, and prefer “symmetry of a solution”, see ChaosBook eq. (11.2). Let me know if you agree, and if not, suggest rewrites for the ChaosBook text.

2021-08-04 Han To block diagonalize the orbit Jacobian matrix by the symmetric and antisymmetric subspace of the reflection operator as in (22.34), we need to use the eigenvectors of the reflection operator. For example, generally the orbit Jacobian matrix of the Hénon map (21.219) is not invariant under reflection and translation. But if the orbit has the reflection symmetry, we can use the reflection operator, under the action of which the orbit is invariant, to project the orbit Jacobian matrix into symmetric and antisymmetric subspace, or block diagonalize the orbit Jacobian matrix.

If the period of the orbit is odd, there is only one kind of reflections. For example, if the period is 9, the orbit can be written as a vector in the 9 dimensional space of periodic state:

$$\overline{\phi_1\phi_2\phi_3\phi_4\phi_5\phi_4\phi_3\phi_2\phi_1}. \tag{24.320}$$

This orbit is invariant under the reflection operator:

$$\sigma = \begin{bmatrix} 0 & 0 & 0 & 0 & 0 & 0 & 0 & 0 & 1 \\ 0 & 0 & 0 & 0 & 0 & 0 & 0 & 1 & 0 \\ 0 & 0 & 0 & 0 & 0 & 0 & 1 & 0 & 0 \\ 0 & 0 & 0 & 0 & 0 & 1 & 0 & 0 & 0 \\ 0 & 0 & 0 & 0 & 1 & 0 & 0 & 0 & 0 \\ 0 & 0 & 0 & 1 & 0 & 0 & 0 & 0 & 0 \\ 0 & 0 & 1 & 0 & 0 & 0 & 0 & 0 & 0 \\ 0 & 1 & 0 & 0 & 0 & 0 & 0 & 0 & 0 \\ 1 & 0 & 0 & 0 & 0 & 0 & 0 & 0 & 0 \end{bmatrix}. \quad (24.321)$$

Let the diagonalizing matrix  $V$  be:

$$V = \begin{bmatrix} 1 & 0 & 0 & 0 & 0 & -1 & 0 & 0 & 0 \\ 0 & 1 & 0 & 0 & 0 & 0 & -1 & 0 & 0 \\ 0 & 0 & 1 & 0 & 0 & 0 & 0 & -1 & 0 \\ 0 & 0 & 0 & 1 & 0 & 0 & 0 & 0 & -1 \\ 0 & 0 & 0 & 0 & 1 & 0 & 0 & 0 & 0 \\ 0 & 0 & 0 & 1 & 0 & 0 & 0 & 0 & 1 \\ 0 & 0 & 1 & 0 & 0 & 0 & 0 & 1 & 0 \\ 0 & 1 & 0 & 0 & 0 & 0 & 1 & 0 & 0 \\ 1 & 0 & 0 & 0 & 0 & 1 & 0 & 0 & 0 \end{bmatrix}, \quad (24.322)$$

each column of which is an eigenvector of the reflection operator. The first 5 vectors span the symmetric subspace of reflection and the last 4 vectors span the antisymmetric subspace. Using the eigenvectors the orbit Jacobian matrix can be block diagonalized as:

$$V^{-1}\mathcal{J}V = \left[ \begin{array}{ccccc|cccc} 2\phi_1 + 1 & 1 & 0 & 0 & 0 & 0 & 0 & 0 & 0 \\ 1 & 2\phi_2 & 1 & 0 & 0 & 0 & 0 & 0 & 0 \\ 0 & 1 & 2\phi_3 & 1 & 0 & 0 & 0 & 0 & 0 \\ 0 & 0 & 1 & 2\phi_4 & 1 & 0 & 0 & 0 & 0 \\ 0 & 0 & 0 & 2 & 2\phi_5 & 0 & 0 & 0 & 0 \\ \hline 0 & 0 & 0 & 0 & 0 & 2\phi_1 - 1 & 1 & 0 & 0 \\ 0 & 0 & 0 & 0 & 0 & 1 & 2\phi_2 & 1 & 0 \\ 0 & 0 & 0 & 0 & 0 & 0 & 1 & 2\phi_3 & 1 \\ 0 & 0 & 0 & 0 & 0 & 0 & 0 & 1 & 2\phi_4 \end{array} \right] \quad (24.323)$$

If the period of the orbit is even, there are two kinds of reflections. For example, the orbit

$$\overline{\phi_1\phi_2\phi_3\phi_4|\phi_4\phi_3\phi_2\phi_1} \quad (24.324)$$

is invariant under the 1/2 lattice spacing reflection:

$$\sigma = V = \begin{bmatrix} 1 & 0 & 0 & 0 & -1 & 0 & 0 & 0 \\ 0 & 1 & 0 & 0 & 0 & -1 & 0 & 0 \\ 0 & 0 & 1 & 0 & 0 & 0 & -1 & 0 \\ 0 & 0 & 0 & 1 & 0 & 0 & 0 & -1 \\ 0 & 0 & 0 & 1 & 0 & 0 & 0 & 1 \\ 0 & 0 & 1 & 0 & 0 & 0 & 1 & 0 \\ 0 & 1 & 0 & 0 & 0 & 1 & 0 & 0 \\ 1 & 0 & 0 & 0 & 1 & 0 & 0 & 0 \end{bmatrix}, \quad (24.325)$$

we can block diagonalize the orbit Jacobian matrix as:

$$V^{-1} \mathcal{J} V = \left[ \begin{array}{cccc|cccc} 2\phi_1 + 1 & 1 & 0 & 0 & 0 & 0 & 0 & 0 \\ 1 & 2\phi_2 & 1 & 0 & 0 & 0 & 0 & 0 \\ 0 & 1 & 2\phi_3 & 1 & 0 & 0 & 0 & 0 \\ 0 & 0 & 1 & 2\phi_4 + 1 & 0 & 0 & 0 & 0 \\ \hline 0 & 0 & 0 & 0 & 2\phi_1 - 1 & 1 & 0 & 0 \\ 0 & 0 & 0 & 0 & 1 & 2\phi_2 & 1 & 0 \\ 0 & 0 & 0 & 0 & 0 & 1 & 2\phi_3 & 1 \\ 0 & 0 & 0 & 0 & 0 & 0 & 1 & 2\phi_4 - 1 \end{array} \right] \quad (24.326)$$

If the orbit is

$$\overline{\phi_1 \phi_2 \phi_3 \phi_4 \phi_5 \phi_4 \phi_3 \phi_2}, \quad (24.327)$$

the corresponding reflection operator leaves sites 1 and 4 invariant:

$$\sigma_1 = \begin{bmatrix} 1 & 0 & 0 & 0 & 0 & 0 & 0 & 0 \\ 0 & 0 & 0 & 0 & 0 & 0 & 0 & 1 \\ 0 & 0 & 0 & 0 & 0 & 0 & 1 & 0 \\ 0 & 0 & 0 & 0 & 0 & 1 & 0 & 0 \\ 0 & 0 & 0 & 0 & 1 & 0 & 0 & 0 \\ 0 & 0 & 0 & 1 & 0 & 0 & 0 & 0 \\ 0 & 0 & 1 & 0 & 0 & 0 & 0 & 0 \\ 0 & 1 & 0 & 0 & 0 & 0 & 0 & 0 \end{bmatrix}. \quad (24.328)$$

Using the eigenvector matrix:

$$V = \begin{bmatrix} 1 & 0 & 0 & 0 & 0 & 0 & 0 & 0 \\ 0 & 1 & 0 & 0 & 0 & -1 & 0 & 0 \\ 0 & 0 & 1 & 0 & 0 & 0 & -1 & 0 \\ 0 & 0 & 0 & 1 & 0 & 0 & 0 & -1 \\ 0 & 0 & 0 & 0 & 1 & 0 & 0 & 0 \\ 0 & 0 & 0 & 1 & 0 & 0 & 0 & 1 \\ 0 & 0 & 1 & 0 & 0 & 0 & 1 & 0 \\ 0 & 1 & 0 & 0 & 0 & 1 & 0 & 0 \end{bmatrix}, \quad (24.329)$$

the orbit Jacobian matrix can be block diagonalized as:

$$V^{-1} \mathcal{J} V = \left[ \begin{array}{ccccc|ccc} 2\phi_1 & 2 & 0 & 0 & 0 & 0 & 0 & 0 \\ 1 & 2\phi_2 & 1 & 0 & 0 & 0 & 0 & 0 \\ 0 & 1 & 2\phi_3 & 1 & 0 & 0 & 0 & 0 \\ 0 & 0 & 1 & 2\phi_4 & 1 & 0 & 0 & 0 \\ 0 & 0 & 0 & 2 & 2\phi_5 & 0 & 0 & 0 \\ \hline 0 & 0 & 0 & 0 & 0 & 2\phi_2 & 1 & 0 \\ 0 & 0 & 0 & 0 & 0 & 1 & 2\phi_3 & 1 \\ 0 & 0 & 0 & 0 & 0 & 0 & 1 & 2\phi_4 \end{array} \right]. \quad (24.330)$$

**2021-08-04 Han** The choice of eigenvectors in the symmetric and antisymmetric subspaces is not unique, and it will not affect the determinant of the orbit Jacobian matrix in the subspaces. So we can compute the determinant of the orbit Jacobian matrix in the subspaces without using any eigenvector.

The determinant of a matrix can be written as the antisymmetrized trace of the matrix [22]:

$$\text{Det } M = \text{Tr}_p AM = \frac{1}{p} \sum_{k=1}^p (-1)^{k-1} (\text{Tr}_{p-k} AM) \text{Tr } M^k, \quad (24.331)$$

where  $A$  is the antisymmetrization projection operator,  $p$  is the dimension of the matrix  $M$ . To compute the determinant of the orbit Jacobian matrix in the subspace, we need to first project the matrix into the subspace, then compute the antisymmetrized trace with the dimension of the subspace.

For example, consider (24.324) symmetric orbit  $\overline{\phi_1 \phi_2 \phi_3 \phi_4 | \phi_4 \phi_3 \phi_2 \phi_1}$ . The determinant of the orbit Jacobian matrix  $\mathcal{J}_+$  in the symmetric subspace is:

$$\begin{aligned} \text{Det}(P_+ \mathcal{J}) &= \left\| \begin{array}{cccc} -d_1 + 1 & 1 & \cdot & \cdot \\ 1 & -d_2 & 1 & \cdot \\ \cdot & 1 & -d_3 & 1 \\ \cdot & \cdot & 1 & -d_4 + 1 \end{array} \right\| \\ &= d_1 d_2 d_3 d_4 + d_1 d_2 d_3 + d_2 d_3 d_4 \\ &\quad + d_1 d_2 + d_2 d_3 + d_1 d_4 + d_3 d_4 + d_1 + d_2 + d_3 + d_4. \end{aligned} \quad (24.332)$$

Alternatively, using the projection operator to project the orbit Jacobian matrix into the symmetric subspace  $P_+ \mathcal{J} = \mathcal{J}_+$ :

$$\mathcal{J}_+ = \frac{1}{2} \left[ \begin{array}{ccccccccc} 2\phi_1 + 1 & 1 & 0 & 0 & 0 & 0 & 1 & 2\phi_1 + 1 \\ 1 & 2\phi_2 & 1 & 0 & 0 & 1 & 2\phi_2 & 1 \\ 0 & 1 & 2\phi_3 & 1 & 1 & 2\phi_3 & 1 & 0 \\ 0 & 0 & 1 & 2\phi_4 + 1 & 2\phi_4 + 1 & 1 & 0 & 0 \\ 0 & 0 & 1 & 2\phi_4 + 1 & 2\phi_4 + 1 & 1 & 0 & 0 \\ 0 & 1 & 2\phi_3 & 1 & 1 & 2\phi_3 & 1 & 0 \\ 1 & 2\phi_2 & 1 & 0 & 0 & 1 & 2\phi_2 & 1 \\ 2\phi_1 + 1 & 1 & 0 & 0 & 0 & 0 & 1 & 2\phi_1 + 1 \end{array} \right] \quad (24.333)$$

and using (24.331) we have:

$$\begin{aligned}
 \text{Det}(\mathcal{J}_+) &= \text{Tr}_4(A\mathcal{J}_+) \\
 &= \frac{1}{4!} \{ (\text{Tr } \mathcal{J}_+)^4 - 6(\text{Tr } \mathcal{J}_+)^2 \text{Tr } \mathcal{J}_+^2 + 3(\text{Tr } \mathcal{J}_+^2)^2 \\
 &\quad + 8\text{Tr } \mathcal{J}_+^3 \text{Tr } \mathcal{J}_+ - 6\text{Tr } \mathcal{J}_+^4 \} \\
 &= 16\phi_1\phi_2\phi_3\phi_4 + 8\phi_1\phi_2\phi_3 + 8\phi_2\phi_3\phi_4 - 4\phi_1\phi_2 + 4\phi_2\phi_3 \\
 &\quad - 4\phi_1\phi_4 - 4\phi_3\phi_4 - 2\phi_1 - 2\phi_2 - 2\phi_3 - 2\phi_4, \quad (24.334)
 \end{aligned}$$

the same result as computing the determinant of the  $[4 \times 4]$  matrix.

If the orbit is  $\overline{[\phi_1\phi_2\phi_3\phi_4\phi_5]\phi_4\phi_3\phi_2}$ , see (24.327), the determinant of the orbit Jacobian matrix in the symmetric subspace is:

$$\begin{aligned}
 \text{Det}(\mathcal{J}_+) &= \text{Det} \begin{bmatrix} 2\phi_1 & 2 & 0 & 0 & 0 \\ 1 & 2\phi_2 & 1 & 0 & 0 \\ 0 & 1 & 2\phi_3 & 1 & 0 \\ 0 & 0 & 1 & 2\phi_4 & 1 \\ 0 & 0 & 0 & 2 & 2\phi_5 \end{bmatrix} \\
 &= 32\phi_1\phi_2\phi_3\phi_4\phi_5 - 16\phi_1\phi_2\phi_3 - 8\phi_1\phi_2\phi_5 \\
 &\quad - 8\phi_1\phi_4\phi_5 - 16\phi_3\phi_4\phi_5 + 4\phi_1 + 8\phi_3 + 4\phi_5. \quad (24.335)
 \end{aligned}$$

We can get the same result from the orbit Jacobian matrix projected into the symmetric subspace:

$$P_+\mathcal{J} = \frac{1}{2} \begin{bmatrix} 4\phi_1 & 2 & 0 & 0 & 0 & 0 & 0 & 2 \\ 2 & 2\phi_2 & 1 & 0 & 0 & 0 & 1 & 2\phi_2 \\ 0 & 1 & 2\phi_3 & 1 & 0 & 1 & 2\phi_3 & 1 \\ 0 & 0 & 1 & 2\phi_4 & 2 & 2\phi_4 & 1 & 0 \\ 0 & 0 & 0 & 2 & 4\phi_5 & 2 & 0 & 0 \\ 0 & 0 & 1 & 2\phi_4 & 2 & 2\phi_4 & 1 & 0 \\ 0 & 1 & 2\phi_3 & 1 & 0 & 1 & 2\phi_3 & 1 \\ 2 & 2\phi_2 & 1 & 0 & 0 & 0 & 1 & 2\phi_2 \end{bmatrix}. \quad (24.336)$$

The determinant is:

$$\begin{aligned}
 \text{Det}(\mathcal{J}_+) &= \text{Tr}_5(A\mathcal{J}_+) \\
 &= \frac{1}{5!} \{ (\text{Tr } \mathcal{J}_+)^5 - 10(\text{Tr } \mathcal{J}_+)^3 \text{Tr } \mathcal{J}_+^2 + 15(\text{Tr } \mathcal{J}_+)(\text{Tr } \mathcal{J}_+^2)^2 \\
 &\quad + 20\text{Tr } \mathcal{J}_+^3 (\text{Tr } \mathcal{J}_+)^2 - 20\text{Tr } \mathcal{J}_+^2 \text{Tr } \mathcal{J}_+^3 \\
 &\quad - 30\text{Tr } \mathcal{J}_+^4 \text{Tr } \mathcal{J}_+ + 24\text{Tr } \mathcal{J}_+^5 \} \\
 &= 32\phi_1\phi_2\phi_3\phi_4\phi_5 - 16\phi_1\phi_2\phi_3 \\
 &\quad - 8\phi_1\phi_2\phi_5 - 8\phi_1\phi_4\phi_5 - 16\phi_3\phi_4\phi_5 \\
 &\quad + 4\phi_1 + 8\phi_3 + 4\phi_5. \quad (24.337)
 \end{aligned}$$



**2021-08-04 Han** Using the antisymmetrized trace formula (24.331) we can compute the determinant of a matrix in the subspace. The reason is simple: when the matrix is diagonalized, some elements on the diagonal will be zero. These zeros will not contribute to the trace of the matrix. So if we use the antisymmetrized trace formula with the correct dimension, the determinant we get is the determinant of the matrix in the subspace with non-zero eigenvalues.

**2021-08-04 Predrag** Very nice!

**2021-08-04 Predrag** It might that the above symmetric polynomials in  $\phi_i$  are all reducible to powers of the orbital sum  $r_p$  defined in (3.32), a orbit  $p$  invariant. For an example, see (3.42). But probably specific to Hénon only...

**2021-08-05 Predrag** Added

`\newcommand{\sitebox}[1]`

that enables you to control the margin around  $\overline{\phi_{n-1}}$ . Gave up on playing with  $\overline{\phi_n}$  and  $\phi_n$ .

**2021-08-04 Predrag** You are using the wrong definition of Hénon orbit Jacobian matrix, there are no factors of  $a$  in (21.219). Please fix throughout. We prefer Gallas *et al.* convention (21.219).

**2021-08-04, 2021-08-11 Predrag** I have -an experiment- sat  $2\phi_j = -d_j$ , temporal cat style in (24.333) and (4.206), just to see how we like that. The signs might be wrong, please recheck.

This also connects to the one-dimensional Schrödinger operator (16.75), where  $\lambda v_n = -d_j$ . "The real-valued potential sequence  $v = (v_n)_{n \in \mathbb{Z}}$  represents the environment that the particle is subjected to, with the "coupling constant"  $\lambda > 0$  is factored out for convenience."

**2021-08-04 Predrag** It seems better to number lattice sites as  $\phi_0 \phi_1 \phi_2 \cdots \phi_{n-1}$ , at least when one or two lattice sites are invariant under the reflection, see (24.339) and (24.340).

**2021-08-04 Predrag** Let us try to explicitly connect and generalize Kim *et al.* [44] orbit-counting "generating function" (6.163) counts

$$N_{2m-1,0}, N_{2m,0}, N_{2m,1} \tag{24.338}$$

as well as MacKay's thesis [52] table 24.3, and Gallas *et al.* (3.33), to the Hill determinant-weighted, symmetry reduced and factorized periodic orbit weights  $t_{\bar{p}}$ , by connecting

period  $n = 2m - 1$  odd ( $N_{2m-1,k}, SC_n$ )  $n$  cyclicly related periodic states

$$\overline{\phi_0 \phi_1 \phi_2 \cdots \phi_m | \phi_m \cdots \phi_2 \phi_1}. \tag{24.339}$$

to 1 boundary point 'diagonal' class **D** (3.54), (24.285), (24.307), (24.320);  $m$ -dimensional symmetric,  $(m - 1)$ -dimensional antisymmetric subspace (24.323).

period  $n = 2m$  even,  $k = \text{even}$  ( $N_{2m,k}$ ,  $SF_n$  (?))  $m = n/2$  cyclicly related periodic states

$$\overline{\phi_0 \phi_1 \phi_2 \cdots \phi_{m-1} \phi_m \phi_{m-1} \cdots \phi_2 \phi_1}. \quad (24.340)$$

to no boundary point 'non-diagonal' class **N** (3.49), (24.290), (24.309), antisymmetric (24.312), (24.327);  $(m + 1)$ -dimensional symmetric,  $(m - 1)$ -dimensional antisymmetric subspace (24.330).

period  $n = 2m$  even,  $k = \text{odd}$  ( $N_{2m,k}$ ,  $SF_n$  (?))  $m = n/2$  cyclicly related periodic states

$$\overline{\phi_1 \phi_2 \phi_3 \cdots \phi_m \phi_m \cdots \phi_2 \phi_1}. \quad (24.341)$$

to 2 boundary points 'diagonal' class **D** (3.53), (24.289), (24.308), antisymmetric (24.311), (24.324), (24.333);  $m$ -dimensional symmetric,  $m$ -dimensional antisymmetric subspace (24.326). Also and (4.206).

I have almost certainly mixed up the two even-period classes, please correct.

**2021-08-05 Predrag** We have to distinguish the symmetric (24.308) from the antisymmetric (24.311), (24.312) throughout.

I started writing this up in sect. 6.3.3 *Reflection-symmetric periodic states*.

Orbit Jacobian matrix  $\mathcal{J}$  is linear, so the antisymmetric-symmetric factorization will always apply to it. However, I expect the antisymmetric subspace to be flow-invariant for nonlinear systems (such as temporal Hénon; but also temporal cat should have an interesting space of antisymmetric solutions), with periodic states within that lower-dimensional subspace. That would explain shared eigenvalues such as (22.26): do the two distinct Hénon orbits  $\overline{1000}$  and  $\overline{1110}$  both live in the lower-dimensional antisymmetric subspace, and because of that share the eigenvalue  $r$ ?

See my post that includes (22.36).

My hunch based on the experience with Kuramoto–Sivashinsky antisymmetric subspace being flow-invariant, see example 6.4 *Desymmetrization of Lorenz flow*, [ChaosBook example 30.1 Kuramoto–Sivashinsky antisymmetric subspace](#) and [ChaosBook example 30.2 Cyclic subgroups of  \$SO\(2\)\$](#) .

**2021-08-11 Predrag** Let's get Hamiltonian Hénon system (3.28) even closer to the temporal cat, by multiplying both sides by  $-2a$  and taking  $\phi_j = -2ax_j$ . The rescaled temporal Hénon is (3.22). Now the orbit Jacobian matrix is of the desired temporal cat form (3.26), with  $d_j = \phi_j$ , and once you have an expression for Hill determinant  $\|\mathcal{J}[\Phi]\|$  in terms of traces  $\text{Tr } \mathcal{J}^k$ , i.e., the  $D_n$  invariant orbital sums for products of fields on consecutive lattice sites, they will be the same for the temporal cat and the temporal Hénon.

Not only that, but we should be able to write (4.224) action  $S[\Phi]$  such that the derivative of the quartic term yields classical  $\phi^4$  theory (4.221) on  $d$ -dimensional lattice (23.22), with the Hill determinant of the same form (3.26).

**2021-08-11 Predrag** It would be good to evaluate small Hill determinants both in terms of traces (24.331), and on the  $C_n$  and  $D_n$  reciprocal lattices. Reciprocal lattice is diagonalized, and eigenvectors are presumably explicit.

**2021-08-11 Predrag** If you use birdtracks, determinant is the full antisymmetrizer, and time reversal is a permutation with all lines crossed. The contraction with antisymmetrizer might simplify some calculations.

**2021-08-11 Predrag** I have a hunch why for Hénon only the orbital sum  $\text{Tr } \mathcal{J}$  matters. For  $\text{Tr } \mathcal{J}^2$  you can use the temporal Hénon recurrence (3.22) to eliminate  $\phi_t^2$  in terms of terms linear in  $\phi_{t\pm 1}$ . The same, but for  $\text{Tr } \mathcal{J}^3$ , might apply to the  $\phi^4$  theory  $\phi_t^3$  terms in (23.22).

**2021-08-14 Predrag** About 'right' and 'left'. We have to distinguish the action of the translation operator  $r$  on coordinates (lattice site label  $i$  in discretizing  $x \rightarrow x_i$ ):

$r_j$  is a counterclockwise rotation of a polygon by  $j$  vertices, or right translation of a  $\mathbb{Z}$  lattice by  $j$  sites (we follow [Dihedral group wiki](#)).

vs. its action on *fields*, i.e., functions  $\phi_i = \phi(x_i)$ , given by the Wigner definition of the effect of transformations on functions, [ChaosBook eq. \(25.2\)](#). I hope our introduction of translations (??) is in agreement for the convention for fields.

Time evolution clearly increases the field's site index,  $\phi_t \rightarrow \phi_{t+1}, \dots$ , and thus shift the periodic state to the left; if I sit at the origin, lattice site '0', I should be seeing  $\phi_0$ , then the one time-step  $r$  'later'  $\phi_1$ , and so on.

We also have to make sure that the direction of shift [ChaosBook eq. \(14.12\)](#) is consistent with our usage here.

Am I correct?

**2021-08-14 Predrag** Experimenting with periodic state plots of figure 6.1 see figure 24.63 and figure 24.64. I still find bar graph figure 6.1 the best.

If a Mathematica figure

siminos/figs/\*.pdf

is getting into almost publishable shape, please save it also as a

siminos/figSrc/inkscape/\*.svg.

Makes easier for me to fine-tune it for the publication.

**2021-08-14 Predrag** I hope figure 24.64 settles for once and all the 'odd' and 'even' reflections.

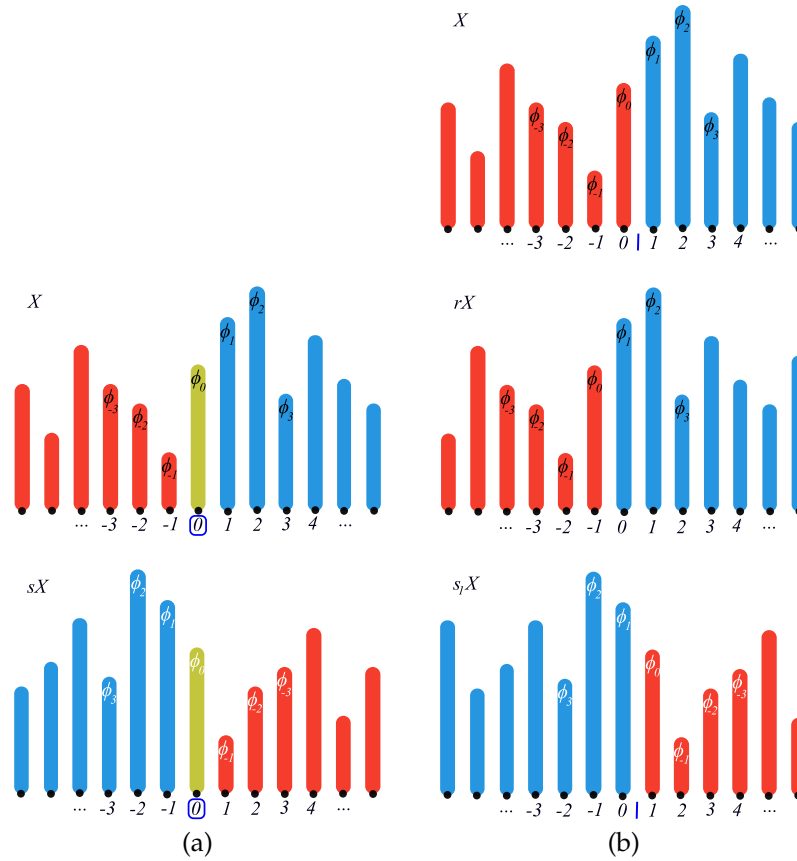


Figure 24.64: There are two classes (??) of periodic state reflections: even, across a lattice site, and odd, across the mid-point between a pair of adjacent lattice sites. (a) In example (??) even reflection  $\sigma$  exchanges (blue  $\phi_j$ )  $\leftrightarrow$  (red  $\phi_{-j}$ ) while leaving the field  $\phi_0$  at lattice site  $\bar{0}$  fixed. (b) In example (??) odd  $\sigma_1 = \sigma r$  swaps the ‘blues’ and the ‘reds’ by a lattice translation  $\Phi \rightarrow r\Phi$ , followed by a reflection  $\sigma$ . The result is a reflection across the midpoint of the  $[01]$  interval, marked ‘|’. Horizontal: lattice sites  $j \in \mathbb{Z}$ . Vertical: lattice site fields  $\phi_j$ , labeled by their values before the reflection.

**2021-08-17 Han** I redid figure 24.64 in figure ?? using Mathematica, so the style of the figure is similar to figure 6.1. The periodic states in figure ?? and figure 6.1 are actual solutions of temporal cat with  $s = 3$ .

**2021-08-17 Predrag** Experimenting with colors in figure ?? (a) and figure 6.1 (b). There is no need to change your Mathematica code, this is best done for the publication version in Inkscape LaTeX labeled svg.

**2021-05-11, 2021-08-05, 2021-08-22 Predrag zu Sam** Spielen Sie es noch einmal, bitte:

What I do not understand is the relation between the symmetry of a periodic state (6.14) - (6.17), and the Hill determinant factorization of it. Am I supposed to extend this list to include the antisymmetric periodic states (6.20), (6.39)? Does each carry only the Hill determinant of the orbit Jacobian matrix  $\text{Det}(\mathcal{J}_{\pm})$  with the same symmetry as the corresponding periodic state? If so, how do we get rid of the other  $\text{Det}(\mathcal{J}_{\pm})$  in the factorized  $\text{Det}(\mathcal{J})$ ?

Can you plot the appropriate periodic states, for temporal cat, but preferably for temporal Hénon, with analytic formulas for  $\text{Det}(\mathcal{J}_{\pm})$ ?

**2021-08-26 Han** We already know how to count the number of periodic lattice states for temporal cat:

$$N_n = \prod_{j=0}^{n-1} \left( s - 2 \cos \frac{2\pi j}{n} \right) = 2T_n(s/2) - 2 = \Lambda^n + \Lambda^{-n} - 2, \quad (24.342)$$

where  $\Lambda = \frac{1}{2}(s + \sqrt{(s-2)(s+2)})$ . For  $n = 2m - 1$ ,

$$N_{n,0} = \prod_{j=0}^{m-1} \left( s - 2 \cos \frac{2\pi j}{n} \right) = \sqrt{(\Lambda^n + \Lambda^{-n} - 2)(s-2)}. \quad (24.343)$$

For  $n = 2m$ ,

$$\begin{aligned} N_{n,0} &= \prod_{j=0}^m \left( s - 2 \cos \frac{2\pi j}{n} \right) \\ N_{n,1} &= \prod_{j=0}^{m-1} \left( s - 2 \cos \frac{2\pi j}{n} \right), \end{aligned} \quad (24.344)$$

and

$$\frac{1}{2}(N_{n,0} + N_{n,1}) = \frac{s+3}{2} \prod_{j=0}^{m-1} \left( s - 2 \cos \frac{2\pi j}{n} \right) = \frac{s+3}{2} \sqrt{\frac{(\Lambda^n + \Lambda^{-n} - 2)(s-2)}{(s+2)}} \quad (24.345)$$

Note that:

$$\sqrt{\Lambda^n + \Lambda^{-n} - 2} = \sqrt{\Lambda^n (1 - \Lambda^{-n})^2} = |\Lambda^{n/2} - \Lambda^{-n/2}|. \quad (24.346)$$

Using this identity, the number of lattice states can be written as polynomials: For  $n = 2m - 1$ :

$$\begin{aligned} N_{n,0} &= \sqrt{s-2} \left| \Lambda^{n/2} - \Lambda^{-n/2} \right| \\ &= \sqrt{\frac{s-2}{\Lambda}} \left| \Lambda^m - \Lambda^{-m+1} \right|. \end{aligned} \quad (24.347)$$

For  $n = 2m$ :

$$\begin{aligned} \frac{1}{2} (N_{n,0} + N_{n,1}) &= \frac{s+3}{2} \sqrt{\frac{s-2}{s+2}} \left| \Lambda^{n/2} - \Lambda^{-n/2} \right| \\ &= \frac{s+3}{2} \sqrt{\frac{s-2}{s+2}} \left| \Lambda^m - \Lambda^{-m} \right|. \end{aligned} \quad (24.348)$$

Now we can compute the  $h(t)$  from (??)

$$\begin{aligned} h(t) &= \sum_{m=1}^{\infty} \left[ N_{2m-1,0} t^{2m-1} + (N_{2m,0} + N_{2m,1}) \frac{t^{2m}}{2} \right] \\ &= \sqrt{s-2} \frac{\Lambda^{1/2} t}{1 - \Lambda t^2} - \sqrt{s-2} \frac{\Lambda^{-1/2} t}{1 - \Lambda^{-1} t^2} \\ &\quad + \frac{s+3}{2} \sqrt{\frac{s-2}{s+2}} \frac{\Lambda t^2}{1 - \Lambda t^2} - \frac{s+3}{2} \sqrt{\frac{s-2}{s+2}} \frac{\Lambda^{-1} t^2}{1 - \Lambda^{-1} t^2}. \end{aligned} \quad (24.349)$$

Using (??) we have the "flip" part of the zeta function. Testing this zeta function using (21.215), we have:

$$\begin{aligned} -t \frac{\partial}{\partial t} (\ln e^{-h(t)}) &= t + 6t^2 + 12t^3 + 36t^4 + 55t^5 + 144t^6 \\ &\quad + 203t^7 + 504t^8 + 684t^9 + 1650t^{10} + \dots \end{aligned} \quad (24.350)$$

which is in agreement with (21.215) and table 24.3.

**2021-08-29, 2021-08-30 Predrag** I have been struggling with antisymmetric periodic states - see around eq. (6.40) - the Hill determinant that I got is wrong, will remove it from your blog.

Antisymmetric periodic states do not exist. I sketched - by hand, not posted here - the values of periodic state fields for the 6 temporal Hénon periodic states of table 3.3 and figure 3.3 in the same format as figure 6.1 (b). They are all nicely symmetric.

**2021-08-30 Predrag** I think I'm starting to understand *Máo Zhǔxí Yǔlù*. The 3 types of  $D_{\infty}$  symmetric states  $\Phi$  are -well- symmetric, and that means that the number  $\sim m$  of distinct fields that describe the corresponding period- $n$  primitive cell is  $\sim n/2$ . They satisfy non-periodic bc's equations such as (24.287).

The orbit Jacobian matrix  $\mathcal{J}[\Phi]$  is best understood by starting with the period- $n$  primitive cell stability. That block-diagonalizes into eigenvectors that *point within* the symmetry subspace of the same symmetry as the periodic state, and the (antisymmetric) rest, that *point out* of it. That's all as it should be for a fixed point with a symmetry.

It is all breathtakingly simple on the reciprocal lattice. Period- $n$  primitive cell maps onto a regular  $n$ -gon in the reciprocal lattice, with the usual  $D_n$  symmetry axes. Time reversal amounts to complex conjugation, and the symmetric solutions sit on the symmetry axes, which are also the boundaries of the fundamental domain. Lattice shift  $r_j$  maps out the  $G$ -orbit by running on circles, and orbits visit the  $1/2n$  wedge only once, so the points in the fundamental domain represent an orbit each.

**2021-08-30 Predrag** Back to fuzzy thinking...

Q. can one construct invariant, lower dimensional subspace like (24.287), such that all 'dynamics' is restricted to it? In reciprocal space, only the orbits that sit on symmetry axes? What I call a 'flow-invariant subspace.'

That would be the famed 'square root' or 'golden' temporal Hénon.

**2021-09-03 Predrag** *Slicing the reciprocal lattice; stretching out the pizza slice into a full pizza per each Fourier mode.*

Inspect figure ??, 24.35, 24.51, 24.52, 24.57, 24.58, 24.59, ...: for  $C_n$ , wavenumbers  $k > 1$  they have  $k$ -fold symmetry; for  $D_n$ , the  $2k$ -fold symmetry. Why? If you plot all period- $n$  periodic states at one go, you plot all their group orbits at one go. In  $k$ th mode, they rotate  $k$  times faster than the  $k = 1$  irrep. It will amount to a Bernoulli map with slope  $k$  per each Fourier mode, with phase written as an integer (integer part of the phase  $k\theta_k$  in units of  $2\pi$ ) + remainder representing angle across the fundamental pizza slice, scaled to  $2\pi$  for  $C_n$ , and to  $\pi$  for  $D_n$ . There each orbit is represented by a single reciprocal periodic state.

That is illustrated by the  $C_5$  figure 24.51 (c) and  $D_5$  figure 24.52 (c)  $k = 0, 1, 2$  fundamental domains  $[-2\pi/(2nk), 2\pi/(2nk))$ . Multiplied by  $n k$  they fill out the whole (semi)circle for all  $n$ .

**2021-09-06 Han** Bloch theorem is not very useful to us. Let the (??) be the orbit Jacobian matrix that acts on the infinite lattice. The orbit Jacobian matrix  $\mathcal{J}$  commute with the translation operator  $r$  and the reflection operator  $\sigma$ , so it has the  $D_\infty$  symmetry. The translation group of  $D_\infty$  is described by a Bravais lattice, which is the integer lattice. So the reciprocal lattice of this Bravais lattice is spanned by the primitive vector  $b = 2\pi$ . The eigenstates of the orbit Jacobian matrix have the form:

$$\psi_k(z) = e^{ikz} u(z),$$

where  $z$  is the coordinate on the 1-dimensional direct temporal space,  $u(z)$  is a periodic function with period 1 (the periodicity of  $u(z)$  is given

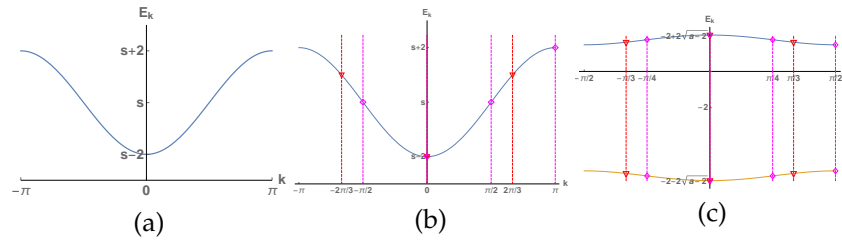


Figure 24.65: (a) The eigenvalue  $E_k$  of the orbit Jacobian matrix on the infinite lattice as a function of the wave vector  $k$  in the first Brillouin zone. The orbit Jacobian matrix has the reflection symmetry so the eigenvalue is also invariant under the reflection  $k \rightarrow -k$ . (b) For period 3 lattice states, the wave vectors of the eigenstates exist on the reciprocal lattice spanned by  $2\pi/3$ . These lattice sites are labeled by the red dashed lines. There are only 3 period 3 eigenstates, with eigenvalues  $-1 - s$ ,  $2 - s$  and  $-1 - s$ . (c) For period 4 lattice states, the wave vectors of the eigenstates exist on the reciprocal lattice spanned by  $\pi/2$ . These lattice sites are labeled by the red dashed lines. There are only 4 period 4 eigenstates, with eigenvalues  $-s$ ,  $2 - s$ ,  $-s$  and  $-2 - s$ .  $k = \pi$  and  $k = -\pi$  are different by a reciprocal lattice translation, so they are a same wave vector and should be only counted once.

by the integer lattice), and  $k$  is a wave vector in the first Brillouin zone  $k \in (-\pi, \pi]$ . For our problem the value of the function only exist on the integer lattice site, so function  $u(z)$  with period 1 can be seen as a constant. The eigenstates of the orbit Jacobian matrix can always be written as:

$$\psi_k(z) = e^{ikz}$$

with eigenvalue  $E_k = 2 \cos k - s$ , which does not depend on the period of the eigenstate. Known that the wave vector  $k$  is in the first Brillouin zone, we can plot the 'eigenvalue band' of the orbit Jacobian matrix, as shown in figure 24.65.

After we have the 'eigenvalue band', we can find eigenstates that satisfy periodic boundary condition. If the period of the lattice state is  $n$ , the wave vector can only exist on a finer lattice in the reciprocal space, the lattice spanned by  $2\pi/n$ . Then only finite amount of wave vectors can be used as wave vectors of these periodic eigenstates. For example, in figure 24.65 (b) the reciprocal lattice sites of the period 3 lattice states are labeled by red dashed lines. There are only 3 reciprocal lattice sites in the first Brillouin zone. So we find 3 eigenstates, with wave vectors  $k = -2\pi/3$ ,  $0$  and  $2\pi/3$ , and eigenvalues  $-1 - s$ ,  $2 - s$  and  $-1 - s$ . In figure 24.65 (c) the reciprocal lattice sites of the period 4 lattice states are labeled by red dashed lines. There are only 4 reciprocal lattice sites in the first Brillouin zone. We find 4 eigenstates, with wave vectors  $k = -\pi/2$ ,



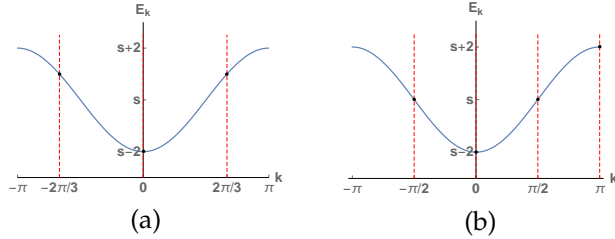


Figure 24.66: (Removed from LC21) The temporal cat infinite lattice orbit Jacobian matrix spectrum (??) plotted in blue in the first Brillouin zone, as a function of the wavenumber  $k$ . As the system is time-reflection invariant, the spectrum is invariant under the  $k \rightarrow -k$  reflection. A period- $n$  Bravais lattice spectrum consist of  $n$  discrete points on this spectrum. (a) Period-3 reciprocal lattice points  $k = (-2\pi/3, 0, 2\pi/3)$  eigenvalues are  $\lambda_k = (s + 1, s - 2, s + 1)$ . (b) Period-4 reciprocal lattice points  $k = (-\pi/2, 0, \pi/2, \pi)$  eigenvalues are  $\lambda_k = (s, s - 2, s, s + 2)$ . There are only 4 reciprocal periodic states, as  $k = \pi$  and  $k = -\pi$  differ by a reciprocal lattice translation, and should be counted only once.

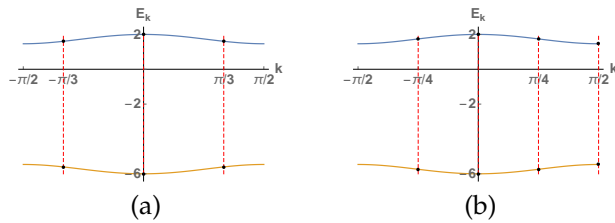


Figure 24.67: (Removed from LC21) The orbit Jacobian matrix spectrum (??) of the  $a = 6$  temporal Hénon infinite lattice tiled by period-2 prime periodic state plotted in blue in the first Brillouin zone, as a function of the wavenumber  $k$ . As the system is time-reflection invariant, the spectrum is invariant under the  $k \rightarrow -k$  reflection. A  $m$ -th repeat Bravais lattice spectrum consist of  $m$  discrete points on this spectrum. (a) 3rd repeat Bravais reciprocal lattice points  $k = (-\pi/3, 0, \pi/3)$  eigenvalues are  $\lambda_k = (-2 \pm \sqrt{13}, -2 \pm 4, -2 \pm \sqrt{13})$ . (b) 4th repeat Bravais reciprocal lattice points  $k = (-\pi/4, 0, \pi/4, \pi/2)$  eigenvalues are  $\lambda_k = (-2 \pm \sqrt{14}, -2 \pm 4, -2 \pm \sqrt{14}, -2 \pm 2\sqrt{3})$ . There are only 4 reciprocal periodic states, as  $k = \pi$  and  $k = -\pi$  differ by a reciprocal lattice translation, and should be counted only once.

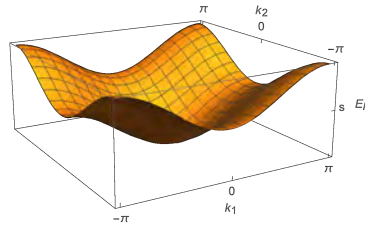


Figure 24.68: The eigenvalue  $E_k$  of the orbit Jacobian matrix on the infinite spatiotemporal lattice as a function of the wave vector  $k$ . The point group symmetry of the orbit Jacobian matrix is  $D_4$  so the eigenvalue function also has the  $D_4$  symmetry.

$0, \pi/2$  and  $\pi$ , and eigenvalues  $-s, 2-s, -s$  and  $-2-s$ . Note that  $k = -\pi$  and  $k = \pi$  are a same wave vector as they are different by a reciprocal lattice translation.

The point group symmetry of the orbit Jacobian matrix is also the symmetry of the 'eigenvalue band' in the reciprocal space. For the temporal cat lattice, we only need to know the eigenstates with wave vectors  $k \geq 0$  as other eigenstates can be found by a reflection, and the eigenvalues are invariant under the reflection. For the 2-dimensional spatiotemporal cat lattice, as shown in figure 24.68, we only need eigenstates with wave vectors in  $1/8$  of the first Brillouin zone, the rest of the eigenstates can be found by reflections and rotations from the  $D_4$  group.

**2021-09-06 Han** The function  $E_k$  in the figure 24.65 is  $E_k = 2 \cos(k) - s$ . We can compute:

$$\exp \int_{-\pi}^{\pi} \ln |E_k| dk = \exp(2\pi \ln \Lambda) = \Lambda^{2\pi}, \quad (24.351)$$

where  $\Lambda$  is the expanding eigenvalue of the cat map. This result is not surprising, because by computing the exponential of trace of the logarithm I'm hoping to find the determinant of the orbit Jacobian matrix on the infinite lattice. And the determinant of this orbit Jacobian matrix is probably the weight of a infinitely long lattice state which should converge to  $\Lambda^n$  as  $n \rightarrow \infty$ . The  $2\pi$  is probably introduced by the integral which can be fixed. But I'm hoping to find a formula that I can compute the determinant or trace of the orbit Jacobian matrix on infinite lattice times variable  $z$  plus some other operators and then retrieve, hopefully, the contribution to the dynamical zeta function from a single prime orbit.

**2021-09-10 Han** I do not have the Hamiltonian, forward-in-time Jacobian matrix  $J_t$  for an orbit with time reflection symmetry.

Let  $f(\phi_{n-1}, \phi_n) = (\phi_n, \phi_{n+1})$  be the map forward in time. For cat map we have:

$$f(\phi_{n-1}, \phi_n) = (\phi_n, -\phi_{n-1} + s\phi_n) \pmod{1}. \quad (24.352)$$

And let map  $t(\phi_{n-1}, \phi_n) = (\phi_n, \phi_{n-1})$  be the time reflection in the state space.

The Hamiltonian forward in time orbit Jacobian matrix is the Jacobian matrix of  $(\phi_0, \phi_1) - f^n(\phi_0, \phi_1)$ , if the time reversal symmetry is not taken into account. With the time reversal symmetry, a periodic point needs to satisfy a different set of conditions. Consider period-7 periodic state

$$\phi_0 | \overline{\phi_1 \phi_2 \phi_3 \phi_4 \phi_3 \phi_2 \phi_1} |. \quad (24.353)$$

**2021-09-11 Predrag** I do not like the interloper  $\phi_0$  in (24.353); notation  $\overline{\phantom{x}}$  means infinite repeat of "block". At  $-\infty$  you stick in  $\phi_0$ ; cannot do that. Also, please follow our convention (??) for odd period orbits:

$$\overline{\phi_0 \phi_1 \phi_2 \phi_3 \phi_3 \phi_2 \phi_1}. \quad (24.354)$$

**2021-09-10 Han** If the period-7 periodic state is  $\overline{\phi_0 \phi_1 \phi_2 \phi_3 \phi_4 \phi_3 \phi_2 \phi_1}$ , the two boundaries need to satisfy

$$t(\phi_0, \phi_1) = (\phi_0, \phi_1), \quad (24.355)$$

and

$$t \circ f(\phi_3, \phi_4) = (\phi_3, \phi_4). \quad (24.356)$$

So now we have 3 conditions that need to be satisfied:

$$\begin{aligned} (\phi_0, \phi_1) - t(\phi_0, \phi_1) &= 0, \\ (\phi_3, \phi_4) - t \circ f(\phi_3, \phi_4) &= 0, \\ (\phi_3, \phi_4) - f^3(\phi_0, \phi_1) &= 0. \end{aligned} \quad (24.357)$$

If we compute the determinant of the Jacobian matrix of the first and second conditions, the results are 0, which means that there are a continuous set of points in the state space that satisfy these two conditions. I have tried to use the first two conditions to write  $\phi_1$  is a function of  $\phi_0$ , and  $\phi_4$  and a function of  $\phi_3$ , then compute the determinant of the Jacobian matrix:

$$\tilde{\mathcal{J}} = \frac{\partial[(\phi_3, \phi_4(\phi_3)) - f^3(\phi_0, \phi_1(\phi_0))]}{\partial(\phi_0, \phi_3)}, \quad (24.358)$$

but the result is apparently wrong (not an integer for cat map). So we cannot perturb any two field values and get the correct Hill determinant.

Let  $F(\phi_0, \phi_1, \phi_3, \phi_4)$  be a function with 4 components. The first two components are given by  $(\phi_3, \phi_4) - f^3(\phi_0, \phi_1)$ . The third and fourth components are  $\phi_0 - \phi_1$  and  $2\phi_3 - s\phi_4$  (for cat map), which are equal to 0 if the first two conditions in (24.357) are satisfied. Then the Hill determinant is:

$$\begin{aligned} \text{Det}(\tilde{\mathcal{J}}) &= -s^4 + s^3 + 4s^2 - 3s - 2 \\ &= -\mu^2 (\mu^6 + 7\mu^4 + 14\mu^2 + 7), \end{aligned} \quad (24.359)$$

which is equal to -76 if  $s = 3, \mu = 1$ , in agreement with table 24.3. I wonder if the coefficients 7 and 14 have something to do with the periodic state period being 7.

**2021-09-11 Predrag** I get  $\text{Det}(\tilde{\mathcal{J}}) = -29$ , which is -up to the sign- in agreement with table 24.3.

**2021-09-11 Predrag** We really have to rethink the definition of orbit Jacobian matrices to avoid this pesky minus signs for odd period Hill determinants.

**2021-09-11 Predrag** I was expecting vaguely something like

$$\begin{aligned} J^7(\phi_0) &= \overline{\phi_0 \phi_1 \phi_2 \phi_3 | \phi_3 \phi_2 \phi_1} \\ &= \sqrt{J_0} J_1^\top J_2^\top J_3^\top J_3 J_2 J_1 \sqrt{J_0} \\ &= \sigma_{\tilde{J}_p} \sigma_1 \tilde{J}_p \\ \text{Det}(\tilde{\mathcal{J}}_p) &= \det(\mathbf{1} - \tilde{J}_p), \end{aligned} \quad (24.360)$$

where  $J_t = J(\phi_t)$  is the 1-time-step Jacobian matrix evaluated on lattice site  $\phi_t$ ; see example 3.4 for what these 2-dimensional Jacobian matrices products look like.

The square roots are in the spirit of the boundary orbit treatment in [Chaos-Book Example 25.9. Reflection symmetric 1-d maps](#).

**2021-09-12 Predrag** The above square roots are suspect, they come from my insistence on the reflection border being "shared" by the adjacent tiles. The correct formulation is probably the inclusion-exclusion principle (24.251), (1.33).

**2021-09-14 Predrag** Some matrix square roots around eq. (3.93). See also the discussion around eq. (24.278).

**2021-09-14 Predrag** Checked that the orbit Jacobian matrix factorization (6.49), metal temporal lattice condition (6.50) works also for the orbit  $\Phi$  dependent case (3.26).

That presumably takes care of the no reflection symmetry case figure 12.123. Symmetric cases (??)-(12.125) still require boundary conditions treatment.

As to the time-step case (24.360), I would prefer 1/2 time step  $J = \tilde{J}^\top \tilde{J}$ -type factorization to taking a square. It's the right form for time-reversal symmetry, I think.

**2021-09-24 Predrag to Han** Looking at sect. ?? *Cyclic groups*, I think there is more to get out of the  $s = 2$  Bernoulli example.

On the reciprocal lattice only symmetry subspace is the origin (I think); you can define the fundamental domain as any wedge of angular width  $2\pi/n$  (I think) but thinking ahead to the  $D_n$  case, it's natural to take real axis as the border included in the fundamental domain, and its  $2\pi/n$  rotation as the other, open set border, not a part of the fundamental domain.

For a generic dynamical system there is no time reversal symmetry, so no lattice state lies on the real axis. For Bernoulli you can probably show it, as you have all lattice states in the analytic form (1.25).

Here is my question:

We know all [ChaosBook binary-labelled](#) Bernoulli orbits and their [Chaos-Book numbers](#) for  $s = 2, 3, 4$ . My current understanding that each orbit visits the fundamental domain only once, with all irrep points rotated into the fundamental domain, different rotation for each wavenumber  $k$ . Is that correct?

**2021-10-18 Predrag** This one, also available online, has "Burnside" in their index: Tom Judson's online [Abstract Algebra: Theory and Applications](#).

Obviously, I've fallen into a major rabbit hole, better stop now:)

**2021-10-31 Predrag to Han** I have mentioned that you have to derive trace formula / spectral determinant only for a single unstable periodic state. Once you have that, you simply put the infinity of them together. That is explained in [ChaosBook Appendix A39 Semiclassical quantization, with corrections](#), see [ChaosBook eq. \(39.11\)](#).

You would do Vattay a favor if you drew [ChaosBook Figure A39.1](#), he was too excited with the implications of this chapter to actually do himself such a lowly thing.

**2021-11-18 Predrag to Han** Have a look at [ChaosBook Append. A33 Statistical mechanics recycled](#). Might be not useful for what you are thinking about now, but the original intention was along the lines we are exploring now: connecting dynamics approaches to the traditional statistical mechanics. Ronnie also wrote a series of articles on this approach [54–59], and there might be more.

**2021-11-16 Han** In Lind [49] and Kim *et al.* [44] the maps of a dynamical system are related to group operations. For a system with time reversal symmetry, there are two maps.  $f : \mathcal{M} \rightarrow \mathcal{M}$  is the map forward in time and  $t : \mathcal{M} \rightarrow \mathcal{M}$  is the flip in the state space. These two maps satisfy:

$$t \circ t = 1, \quad t \circ f \circ t = f^{-1}. \quad (24.361)$$

The kernels of the Perron-Frobenius operators of these two maps are

$$\mathcal{L}_f(x, y) = \delta(x - f(y)), \quad \mathcal{L}_t(x, y) = \delta(x - t(y)). \quad (24.362)$$

The Perron-Frobenius operators satisfy the same relation as the group operation:

$$\begin{aligned}
 (\mathcal{L}_t \circ \mathcal{L}_f \circ \mathcal{L}_t \rho)(x) &= \int_{\mathcal{M}} dy dz dw \delta(x - t(y)) \delta(y - f(z)) \delta(z - t(w)) \rho(w) \\
 &= \int_{\mathcal{M}} dz dw \delta(x - t \circ f(z)) \delta(z - t(w)) \rho(w) \\
 &= \int_{\mathcal{M}} dw \delta(x - t \circ f \circ t(w)) \rho(w) \\
 &= \int_{\mathcal{M}} dw \delta(x - f^{-1}(w)) \rho(w) \\
 &= (\mathcal{L}_{f^{-1}} \rho)(x)
 \end{aligned} \tag{24.363}$$

$$\begin{aligned}
 (\mathcal{L}_t \circ \mathcal{L}_t \rho)(x) &= \int_{\mathcal{M}} dy dz \delta(x - t(y)) \delta(y - t(z)) \rho(z) \\
 &= \int_{\mathcal{M}} dz \delta(x - z) \rho(z) \\
 &= \rho(x).
 \end{aligned} \tag{24.364}$$

So we have:

$$\mathcal{L}_t \circ \mathcal{L}_f \circ \mathcal{L}_t = \mathcal{L}_{f^{-1}}, \quad \mathcal{L}_t \circ \mathcal{L}_t = 1. \tag{24.365}$$

So the Perron-Frobenius operators are linear representations of the  $D_\infty$  group. Then the leading eigenvalue of  $\mathcal{L}_f$  is 1, which is incorrect because it implies that the system is bounded.

**2021-10-29 Han** A lattice state is a set of lattice site field values  $\Phi = \{\phi_z\}$  that satisfies the defining equation at every lattice site. The defining equation can be rewritten as a fixed point condition  $F[\Phi] = 0$ . The fixed point condition satisfied by a periodic lattice state with period  $n$  is  $F_n[\Phi_n] = 0$ , where  $F_n[\Phi_n]$  and  $\Phi_n$  are  $n$ -dimensional vectors.

The weight of lattice states are computed from:

$$\int \delta(F_n[\Phi_n]) e^{\beta A(\Phi)} d\Phi_n = \sum_{\{\Phi_i: F_n[\Phi_i]=0\}} \frac{e^{\beta A(\Phi_i)}}{|\det \mathcal{J}_i|} \tag{24.366}$$

where

$$\mathcal{J}_i = \frac{\partial F_n[\Phi_i]}{\partial \Phi_i}$$

is the orbit Jacobian matrix. From the Hill's formula we know that this is equal to the trace of the time evolution operator:

$$\text{tr } \mathcal{L}^n = \int \delta(\phi - f^n(\phi)) e^{\beta A(\phi)} d\phi = \sum_{\phi_i \in \text{Fix } f^n} \frac{e^{\beta A_i}}{|\det(\mathbf{1} - M^n(\phi_i))|} \tag{24.367}$$

**2021-10-29 Han** The expectation value of an observable can be computed from the expectation value of the time evolution operator:

$$\langle e^{\beta A} \rangle = \frac{1}{|\mathcal{M}|} \int_{\mathcal{M}} dx \int_{\mathcal{M}} dy \delta(y - f^t(x)) e^{\beta A} = \frac{1}{|\mathcal{M}|} \langle \mathcal{L}^t \rangle. \quad (24.368)$$

Set  $\beta = 0$ . The time evolution operator acts on a density distribution function as:

$$\begin{aligned} [\mathcal{L}^n \psi](\phi_n)|_{\psi(\phi_0)=1} &= \int_{\mathcal{M}} d\phi_0 \delta(\phi_n - f^n(\phi_0)) \\ &= \int_{\mathcal{M}} d\phi_{n-1} d\phi_{n-2} \dots d\phi_2 d\phi_1 d\phi_0 \\ &\quad \delta(\phi_n - f(\phi_{n-1})) \delta(\phi_{n-1} - f(\phi_{n-2})) \\ &\quad \dots \delta(\phi_2 - f(\phi_1)) \delta(\phi_1 - f(\phi_0)). \end{aligned} \quad (24.369)$$

Let  $\Phi$  be the lattice state:

$$\Phi = \begin{pmatrix} \phi_0 \\ \phi_1 \\ \phi_2 \\ \vdots \\ \phi_{n-2} \\ \phi_{n-1} \end{pmatrix}. \quad (24.370)$$

And function  $F$  be:

$$F(\Phi, \phi_n) = \begin{pmatrix} \phi_1 \\ \phi_2 \\ \phi_3 \\ \vdots \\ \phi_{n-1} \\ \phi_n \end{pmatrix} - \begin{pmatrix} f(\phi_0) \\ f(\phi_1) \\ f(\phi_2) \\ \vdots \\ f(\phi_{n-2}) \\ f(\phi_{n-1}) \end{pmatrix}. \quad (24.371)$$

The product of delta function is a delta function of function  $F$ :

$$\prod_{i=0}^{n-1} \delta(\phi_{i+1} - f(\phi_i)) = \delta(F(\Phi, \phi_n)). \quad (24.372)$$

And the time evolution operator can be rewritten as:

$$[\mathcal{L}^n \psi](\phi_n)|_{\psi(\phi_0)=1} = \int d\Phi \delta(F(\Phi, \phi_n)). \quad (24.373)$$

The trace of the time evolution operator is:

$$\begin{aligned} \text{tr } \mathcal{L}^n &= \int d\phi_n d\phi_0 \delta(\phi_n - \phi_0) \mathcal{L}^n(\phi_n, \phi_0) \\ &= \int d\Phi \delta(F(\Phi, \phi_0)). \end{aligned} \quad (24.374)$$

Let

$$F(\phi_0, \phi_1, \dots, \phi_{n-1}, \phi_0) = F_p(\phi_0, \phi_1, \dots, \phi_{n-1}) = F_p(\Phi). \quad (24.375)$$

$F_p(\Phi) = 0$  is the fixed point condition of the lattice state. Compute the trace in a small neighborhood around a fix point  $\phi_j$ :

$$\begin{aligned} \int_{\mathcal{M}_j} d\phi \delta(\phi - f^n(\phi)) &= \int_{\mathcal{M}_{\Phi_j}} d\Phi \delta(F(\Phi)) \\ \frac{1}{|\det(\mathbf{1} - \mathbb{J}(\phi_j))|} &= \frac{1}{|\text{Det } \mathcal{J}_j|}. \end{aligned} \quad (24.376)$$

$$\mathcal{J}_j = \frac{\partial F(\Phi_j)}{\partial \Phi_j}, \quad (24.377)$$

is the Jacobian matrix of function  $F(\Phi)$  at  $\Phi_j$ , which is a periodic lattice state that starts with  $\phi_j$ .

In the previous example, the state  $\phi$  generally is a vector. So this relation (Hill's formula) applies to maps with any dimension. If there exists a multiple points recurrence relation, the orbit Jacobian matrix can be written in a more compact way.

Consider a map with a 3-point recurrence relation. Let  $\hat{\phi}_i = (\phi_i, \phi_{i+1})$ . The map in the 2-dimensional state space has the form:

$$\begin{aligned} \hat{\phi}_i &= \hat{f}(\hat{\phi}_{i-1}) \\ (\phi_i, \phi_{i+1}) &= (\phi_i, f(\phi_{i-1}, \phi_i)). \end{aligned} \quad (24.378)$$

The the time evolution operator satisfies:

$$\begin{aligned} [\mathcal{L}^n \psi](\hat{\phi}_n) \Big|_{\psi(\hat{\phi}_0)=1} &= \int_{\mathcal{M}} d\hat{\phi}_0 \delta(\hat{\phi}_n - \hat{f}^n(\hat{\phi}_0)) \\ &= \int_{\mathcal{M}} d\phi_0 d\phi_1 \delta(\hat{\phi}_n - \hat{f}^n(\hat{\phi}_0)) \\ &= \int_{\mathcal{M}} d\phi'_n d\phi'_{n-1} d\phi_{n-1} d\phi'_{n-2} \dots d\phi_2 d\phi'_1 d\phi_1 d\phi_0 \\ &\quad \delta(\phi_n - \phi'_n) \delta(\phi_{n+1} - f(\phi'_n, \phi'_{n-1})) \\ &\quad \delta(\phi'_{n-1} - \phi_{n-1}) \delta(\phi'_n - f(\phi'_{n-2}, \phi_{n-1})) \\ &\quad \dots \\ &\quad \delta(\phi'_2 - \phi_2) \delta(\phi_3 - f(\phi_1, \phi_2)) \\ &\quad \delta(\phi'_1 - \phi_1) \delta(\phi_2 - f(\phi_0, \phi_1)) \\ &= \left( \prod_{i=0}^{n-1} \int_{\mathcal{M}} d\phi_i \right) \left( \prod_{i=0}^{n-1} \delta(\phi_{i+2} - f(\phi_i, \phi_{i+1})) \right). \end{aligned} \quad (24.379)$$



Let  $\Phi$  be the lattice state:

$$\Phi = \begin{pmatrix} \phi_0 \\ \phi_1 \\ \phi_2 \\ \vdots \\ \phi_{n-2} \\ \phi_{n-1} \end{pmatrix}. \quad (24.380)$$

And function  $F$  be:

$$F(\Phi, \phi_n, \phi_{n+1}) = \begin{pmatrix} \phi_2 \\ \phi_3 \\ \phi_4 \\ \vdots \\ \phi_n \\ \phi_{n+1} \end{pmatrix} - \begin{pmatrix} f(\phi_0, \phi_1) \\ f(\phi_1, \phi_2) \\ f(\phi_2, \phi_3) \\ \vdots \\ f(\phi_{n-2}, \phi_{n-1}) \\ f(\phi_{n-1}, \phi_n) \end{pmatrix}. \quad (24.381)$$

$$[\mathcal{L}^n \psi](\hat{\phi}_n) \Big|_{\psi(\hat{\phi}_0)=1} = \int d\Phi \delta(F(\Phi, \phi_n, \phi_{n+1})). \quad (24.382)$$

The trace of the time evolution operator is:

$$\begin{aligned} \text{tr } \mathcal{L}^n &= \int d\hat{\phi}_n d\hat{\phi}_0 \delta(\hat{\phi}_n - \hat{\phi}_0) \mathcal{L}^n(\hat{\phi}_n, \hat{\phi}_0) \\ &= \int d\phi_{n+1} d\phi_n \dots d\phi_1 d\phi_0 \delta(F(\phi_0, \phi_1, \dots, \phi_n, \phi_{n+1})) \delta(\phi_0 - \phi_n) \delta(\phi_1 - \phi_{n+1}) \\ &= \int d\Phi \delta(F(\Phi, \phi_0, \phi_1)). \end{aligned} \quad (24.383)$$

Let

$$F_p(\Phi) = F(\phi_0, \phi_1, \dots, \phi_{n-2}, \phi_{n-1}, \phi_0, \phi_1). \quad (24.384)$$

$F_p(\Phi) = 0$  is the fixed point condition. Compute the trace in a small neighborhood around a fix point  $\hat{\phi}_j$ :

$$\begin{aligned} \int_{\mathcal{M}_j} d\hat{\phi} \delta(\hat{\phi} - \hat{f}^n(\hat{\phi})) &= \int_{\mathcal{M}_{\Phi_j}} d\Phi \delta(F(\Phi)) \\ \frac{1}{|\det(\mathbf{1} - \mathbb{J}(\hat{\phi}_j))|} &= \frac{1}{|\text{Det } \mathcal{J}_j|}, \end{aligned} \quad (24.385)$$

where

$$\mathcal{J}_j = \frac{\partial F(\Phi_j)}{\partial \Phi_j}, \quad (24.386)$$

is jacobian matrix of  $F(\Phi)$  at  $\Phi_j$ , a periodic lattice state that starts with  $\hat{\phi}_j$ . The  $\mathcal{J}_j$  is a  $[n \times n]$  orbit Jacobian matrix.

**2022-01-02 Han** Lind zeta function was introduced for actions on high-dimensional lattices ( $\mathbb{Z}^d$ -actions). I think what we do not have is a dynamical zeta function that relates the expectation values of observables to lattice states with point group symmetry, or higher-dimensional lattice states.

**2022-01-24 Han** Eigenvalue spectrum of the orbit Jacobian matrix of  $a = 6$  Henon period-2 prime periodic state  $(\frac{-1-\sqrt{3}}{6}, \frac{-1+\sqrt{3}}{6})$ .

The orbit Jacobian matrix on the period-2 lattice is:

$$\mathcal{J} = \begin{pmatrix} s_0 & -2 \\ -2 & s_1 \end{pmatrix}. \quad (24.387)$$

The two eigenvalues of this matrix are  $-6$  and  $2$ . The eigenvectors of the linear operator  $\mathcal{J}$  on infinite lattice are:

$$\psi_{k,t} = e^{ikt} u_{k,t}. \quad (24.388)$$

$u_{k,t}$  is periodic with period-2, so

$$u_{k,t} = u_{k,t \bmod 2}.$$

The periodic function  $u_{k,t}$  is not the eigenvector of the  $[2 \times 2]$  orbit Jacobian matrix, unless  $k = 0$ . To find the eigenvalues  $E_k$ , solve the equations:

$$\begin{aligned} (\mathcal{J}\psi_k)_0 &= -e^{-ik}u_{k,1} + s_0u_{k,0} - e^{ik}u_{k,1} \\ &= -2\cos(k)u_{k,1} + s_0u_{k,0} = E_k u_{k,0} \\ (\mathcal{J}\psi_k)_1 &= -u_{k,0} + s_1e^{ik}u_{k,1} - e^{2ik}u_{k,0} \\ &= e^{ik}(-2\cos(k)u_{k,0} + s_1u_{k,1}) = E_k e^{ik}u_{k,1}. \end{aligned} \quad (24.389)$$

Solve for the eigenvector  $u_{k,0}$  and  $u_{k,1}$ , and the eigenvalue  $E_k$ , we find two eigenvalues from two bands:

$$\begin{aligned} E_{k,1} &= -2 + 2\sqrt{3 + \cos^2(k)} \\ E_{k,2} &= -2 - 2\sqrt{3 + \cos^2(k)}, \end{aligned} \quad (24.390)$$

where, for whatever that is worth,

$$3 + \cos^2(k) = 2^2 - (1 - \cos^2(k)) = 2^2 - \sin^2(k) = (2 - \sin(k))(2 + \sin(k)).$$

See figure [24.69](#).

**2022-01-24 Predrag 2 Han** This is great, but you can do even better.

In this case, probably equally easy to solve it for  $a$  stretching parameter, without setting it to 6. You probably want to use orbital sum (3.32) as the parameter, rather than  $a$ .

Now, you have a great opportunity to illustrate in LC21 what happens for a symmetric periodic state. In any case, you should combine the two figures 12(a) and 12(b) into one, by marking the period-3 and period-4

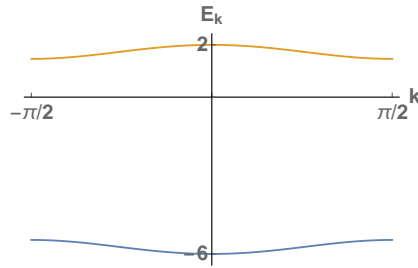


Figure 24.69: The eigenvalue  $E_k$  of the period-2  $a = 6$  Hénon's orbit Jacobian matrix on the infinite lattice as a function of the wave vector  $k$ .

reciprocal lattice eigenvalues by circles and diamonds, and make your current figure 24.69 the new 12 (b).

Period-2 periodic state (22.19) is  $D_1$  symmetric (remember table 3.3, (22.21), etc.). Like (22.38), if the 2-cycle would be of type (eo)

$$\overline{10} : \overline{\phi_1 | \phi_1}, \quad (24.391)$$

it would reduce to the  $[1 \times 1]$  prime orbit Jacobian matrix  $\mathcal{J}$ .

But, as you had mentioned earlier, the symmetry type is (ee) -two unequal heights  $\overline{\phi_0 | \phi_1}$  yellow bars in our figures (where in permutation representation the even reflection  $\sigma = 1?$ )- then the prime  $\mathcal{J}$  is  $[2 \times 2]$ , as you and Sidney get by explicit calculation. You are surely right, as the Hill determinant (21.220) is not a square of a 1-dimensional Hill determinant.

2022-01-24 Predrag 2 The Gang Is figure 6.2 easier to grasp than LC21 figure 8?

2022-03-08 Predrag Have a quick look (again?) at (19.29), (19.30), (19.16), and (16.5), just in case it is useful in writing up the Hill's formula for the relative-periodic  $[L \times T]_S$  case, or in case we should refer to them.

For possible use:

A definition of a  $d$ -dimensional discrete torus (18.6).

In sect. 16.2 the definition (16.54) of the *Gaussian model* action is identical in form to the  $\mu^2 = 0$ , Laplacian part of our (4.138). Temporal cat, however, is *nonlinear* because of the restriction of  $\phi_z$  to the unit interval.

2020-03-02 Predrag It's possible that (4.224) is a better way to think about  $\phi^4$  theory.

2020-03-12 Predrag Indeed, (4.224) is a better way to think about this. Xuanqi's intuition agrees with what had been *derived* in the literature [51, 72, 74] 35-40 years ago. Yes, reading literature can be a real time saver, and it is

really easy when somebody else does the literature search for you. Anyway:

I believe we have the final formulation of  $\phi^4$  theory. Please check carefully sect. 4.12.5 *Deterministic  $\phi^4$  lattice field theory*, and alert us if there is something that should be corrected or improved. If everybody agrees, from now on all  $\phi^4$  calculation follow the conventions of that section.

2020-03-20 **Predrag** Beware of

[ChaosBook sect. 22.4 False zeros](#)

 *Moral tale: Perils of infinite products*

2022-03-20 **Han** I computed the Lind's topological zeta function (24.109) of  $s = 5/2$  2-dimensional spatiotemporal cat numerically, truncated the cycle expansion at  $z^{100}$ .

I first compute the number of periodic states  $N_{[L \times T]_S}$  with the area of the periodic block  $LT \leq 100$ . Substitute the number of the periodic states into the formula (24.109):

$$\exp\left(-\sum_{[L \times T]_S: LT \leq 100, 0 \leq S < L} \frac{N_{[L \times T]_S}}{LT} z^{LT}\right), \quad (24.392)$$

then truncate the expansion at  $z^{100}$ :

$$\begin{aligned} 1/\zeta^{(100)} = & 1 - z - 9z^2 - 34z^3 - 230z^4 - 291z^5 - 4759z^6 + 4452z^7 \\ & - 33313z^8 + 71765z^9 + 618748z^{10} + \dots \\ & + 2.09371 \times 10^{64} z^{98} + 1.05257 \times 10^{65} z^{99} \\ & + 6.09136 \times 10^{65} z^{100}. \end{aligned} \quad (24.393)$$

The roots of (24.393) are plotted in figure 24.70 (c). Let  $\mathcal{L}$  be the Bravais lattice  $[L \times T]_S$ , and  $[\mathcal{L}]$  be the index:

$$[\mathcal{L}] = |\mathbb{Z}^2 / \mathcal{L}| = LT.$$

Then the growth rate of periodic points is defined as:

$$g = \limsup_{[\mathcal{L}] \rightarrow \infty} \frac{1}{[\mathcal{L}]} \ln N_{[L \times T]_S}. \quad (24.394)$$

For  $s = 5/2, \mu^2 = 1$  the growth rate of periodic points  $g = 1.508$  is computed numerically in (24.97). In (24.97) Bravais lattices with  $S \neq 0$  are not considered. Including the non-zero  $S$  the growth rate becomes:

$$g = \int_0^1 \int_0^1 dl dt \ln [2s - 2 \cos(2\pi l) - 2 \cos(2\pi t - 2\pi pl)], \quad (24.395)$$

where  $p$  is a constant which depends on  $S/T$ . But the value of  $p$  will not affect the result. The growth rate is still  $g = 1.508$ . The radius of convergence of the Lind zeta function is  $e^{-g} = 0.2213$ .

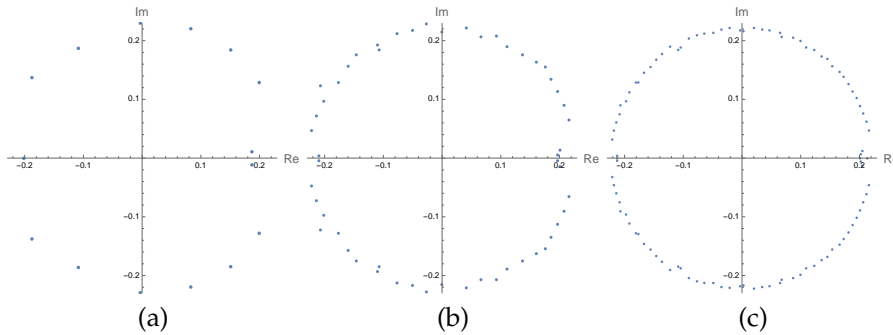


Figure 24.70: Roots of the topological zeta function  $1/\zeta$  (24.112) truncated at  $z^{20}$ ,  $z^{60}$  and  $z^{100}$ . (a) Roots of the zeta function  $1/\zeta$  truncated at  $z^{20}$ . The truncated zeta function has two real roots  $-0.201607$  and  $1.34409$  (much greater than the radius of convergence). (b) Roots of the zeta function  $1/\zeta$  truncated at  $z^{60}$ . Two real roots are  $-0.245602$  and  $0.702541$  (greater than the radius of convergence, not shown in the figure). (c) Roots of the zeta function truncated at  $z^{100}$ . This polynomial has four real roots:  $-0.234093$ ,  $-0.212601$ ,  $0.200788$  and  $0.213615$ .  $0.200788$  is the smallest positive root.

As shown in the figure 24.70(c), the smallest root of the zeta function  $1/\zeta^{(100)}$  (24.393) is not near  $0.2213$ . Most of the roots roughly appear on a circle with radius given by the radius of convergence  $0.2213$ .

Figure 24.70(a) and (b) are the topological zeta functions truncated at  $z^{20}$  and  $z^{60}$ . The radius of convergence is approximately  $0.22$ . There are some roots near the real axis that is close to  $0.2$ , smaller than the radius of convergence.

So the smallest root of the truncated Lind zeta function does not approach to the prediction from the growth rate of the periodic points  $e^{-g}$ . However, I tried to compute a zeta function without including the periodic state with  $S \neq 0$ , which is obviously wrong, and the smallest root of the truncated zeta function approaches to a value near  $e^{-g}$ .

Let the zeta function be:

$$1/\zeta(z) = \exp \left( - \sum_{L=1, T=1}^{\infty} \frac{N_{[L \times T]_0}}{LT} z^{LT} \right). \quad (24.396)$$

To truncate this topological zeta function, again substitute the number of periodic states with  $LT \leq 100$  into the equation, then truncate the expansion at  $z^{100}$ :

$$\begin{aligned} 1/\zeta^{(100)} = & 1 - z - 4.5z^2 - 5.833z^3 - 58.0417z^4 + \dots \\ & -6.24692 \times 10^{61} z^{98} - 3.38178 \times 10^{62} z^{99} \\ & -7.79114 \times 10^{62} z^{100}. \end{aligned} \quad (24.397)$$

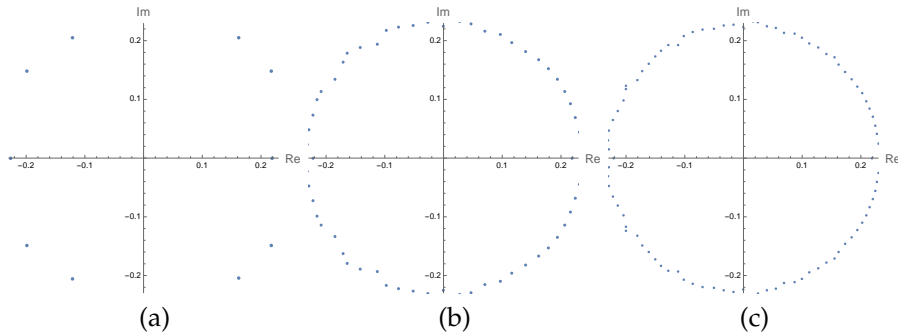


Figure 24.71: Roots of the truncated topological zeta function (24.396). (a) Roots of the topological zeta function (24.396) truncated at  $z^{20}$ . The truncated function has two real roots: -0.226954 and 0.21926. (b) Roots of the zeta function truncated at  $z^{60}$ . The two real roots are -0.221874 and 0.218601. (c) Roots of the zeta function truncated at  $z^{100}$ . The two real roots are -0.221433 and 0.21947.

Then coefficients of this polynomial are not even integers. But the smallest positive root of this polynomial is 0.21947 (it also has a negative root at -0.221433), very close to  $e^{-g} = 0.2213$ .

Roots of the zeta function (24.396) truncated at  $z^{20}$ ,  $z^{60}$  and  $z^{100}$  are plotted in figure 24.71. The smallest root of the truncated zeta function is close to  $e^{-g}$  and other roots appear on a circle with radius greater than the radius of convergence  $e^{-g}$  of the topological zeta function (24.396).

**2020-03-21 Predrag** Wow! Very impressive! The sobering news is that if you are right, the 2-dimensional spatiotemporal cat has no finite graph, with a finite pruning grammar.

**2020-03-21 Predrag** These are weird sequences, but sometimes one can identify a sequence by checking it in the [On-Line Encyclopedia of Integer Sequences](#).

**2020-03-21 Predrag** I believe that the topological zeta function (24.392) is Artin-Mazur. Lind would be quotiented by  $D_4$ , with different indices for different sequences of subgroups; that seems like a lot of work, still to be done for (hopefully for CL18).

**2020-03-21 Predrag** As a sanity check, do you mind running the temporal cat through the same program, see whether one can use numerics to get back to the cat map topological entropy (21.151)  $h = \lambda = \ln \Lambda$ ?

In particular, your program should ‘discover’ the finite Artin-Mazur-Isola *rational* topological polynomial (2.28), and, with some luck, the golden Lind-Y.K. Hu topological polynomial (6.199), (6.197), (6.192), for any  $\mu^2$ , not only  $\mu^2 = 1$ .

The point is that if you do not realize you have a rational polynomial, the cycle expansion might look infinite and generate poles that are actually not a big deal, can be removed by multiplying with a polynomial.

**2020-03-21 Predrag** I might be not remembering right how Fredholm determinants work, but for a finite grammar, 2-dimensional Hamiltonian, forward in time  $\zeta$  should be a ratio of two *entire* (no poles or cuts, i.e., not rational) Fredholm determinants, see ChaosBook, boyscout edition extract sect. 6.4.4 *Poles of dynamical zeta functions*. For uniform, constant piecewise linear expansion systems, various poles and zeros exactly cancel, leading to simple rational-polynomial  $\zeta$  functions. In particular, the moment there is such a cancelation, the radius of convergence expands to the next (uncancelled) pole.

My guess is that overcounting due to neglecting the time-reversal, Chaos-Book style, does not affect the leading eigenvalue. Anyway, you have that already in LC21, should be a quick check?

**2022-03-21 Han** I computed the truncated topological zeta function of  $\mu^2 = 1$  temporal cat. The polynomial truncated at  $z^{20}$  is:

$$1/\zeta^{(20)} = 1 - z - 2z^2 - 3z^3 - 4z^4 - \dots - 19z^{19} - 20z^{20}. \quad (24.398)$$

The roots of the zeta function truncated at  $z^{10}$  and  $z^{20}$  are plotted in figure 24.72(a) and (b). Smallest of roots of  $1/\zeta^{(10)}$  and  $1/\zeta^{(20)}$  are 0.382047 and 0.381966, while the radius of convergence of the zeta function computed from the topological entropy is  $e^{-\lambda} = 1/\Lambda = 0.381966$ .

I also computed the roots of the zeta function truncated at  $z^{100}$ , and found a problem. The truncated polynomial is:

$$\begin{aligned} 1/\zeta^{(100)} = & 1 - z - 2z^2 - 3z^3 - 4z^4 - \dots - 29z^{29} - 30z^{30} \\ & - 31.0003z^{31} - 31.9999z^{32} - \dots - 41.3659z^{41} \\ & - 42.6667z^{42} - 23.814z^{43} - 58.1818z^{44} \dots \end{aligned} \quad (24.399)$$

The coefficients of higher order terms are incorrect, compare to the expansion from the known zeta function (2.12):

$$1/\zeta = 1 - \sum_n n z^n. \quad (24.400)$$

Figure 24.72 (c) shows the roots of the incorrect truncated topological zeta function  $1/\zeta^{(100)}$ . The radius of convergence is significantly less than the radius of convergence of  $1/\zeta^{(10)}$  and  $1/\zeta^{(20)}$ . But the smallest root is still 0.381966.

2CB

**2020-03-22 Predrag** If you really wanted to push these calculation further, for counting problems integer arithmetic (forget Fourier) would help. But I am afraid I might have '*forgotten*' (that I have to fix) to mention the

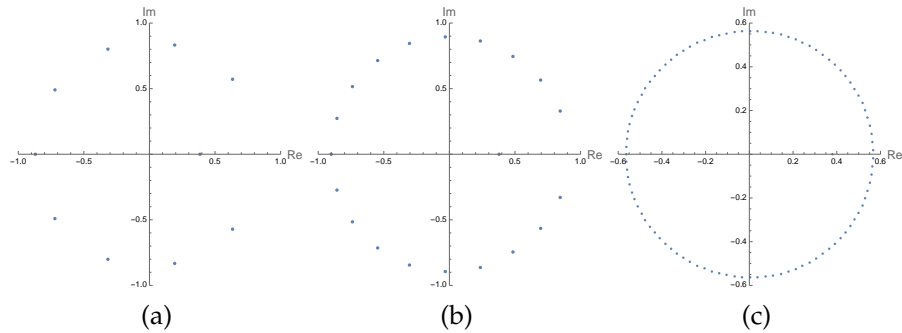


Figure 24.72: Roots of the truncated topological zeta function of the  $s = 3$  cat map. (a) Roots of the topological zeta function truncated at  $z^{10}$ . The smallest root is 0.382047. (b) Roots of the zeta function truncated at  $z^{20}$ . The smallest root is 0.381966. (c) Roots of the zeta function truncated at  $z^{100}$ . The smallest root is 0.381966.

main problem of long-period terms in cycle expansions: we are evaluating pseudo-cycle cancellation between exponentially many exponentially flow terms. If I remember correctly, the resulting errors eat up 1/2 of the significant digits of accuracy. That is why I had tried hard to kill periodic orbit theory, replace it with some integral representation (a ‘sum rule’) that directly computes the pseudocycles *sum*, rather than breaking it up first into individual periodic orbits and then summing them, see (but do not use much time on them right now):

*ChaosBook Thermodynamics of Farey tree: Farey model*  
*Kill periodic orbit theory*

2023-05-02 Predrag Lind [49] example 3.1 ... trivial  $\mathbb{Z}^2$ -action on a single point

$$\begin{aligned} 1/\zeta(t) &= \exp\left(-\sum_{n=1}^{\infty} \sum_{m=1}^{\infty} \sum_{s=0}^{n-1} \frac{1}{nm} t^{nm}\right) = \exp\left(-\sum_{n=1}^{\infty} \sum_{m=1}^{\infty} \frac{(t^n)^m}{m}\right) \\ &= \exp\left(\sum_{n=1}^{\infty} \ln(1-t^n)\right) = \prod_n (1-t^n), \end{aligned} \quad (24.401)$$

Seams to use the Hermite normal form, breaks the spacetime symmetry.

2022-03-26 Han I computed the Lind topological zeta function using the product formula [49]:

$$\zeta(z) = \prod_p \pi_d(z^{|p|}), \quad (24.402)$$

where  $d$  is dimension of the lattice,  $|p|$  is the volume of the primitive cell of the prime orbit labeled by  $p$ , and  $\pi_d(z)$  is the zeta function of the trivial



$\mathbb{Z}^d$ -action. For 1-dimensional lattice


$$\pi_1(z) = \frac{1}{1-z}, \quad (24.403)$$

and for 2-dimensional lattice

$$\pi_2(z) = \prod_{n=1}^{\infty} \frac{1}{1-z^n}. \quad (24.404)$$

The  $\pi_2(z)$  is the classical generating function for the partition function  $p(n)$  of the number of ways integer  $n$  can be partitioned into sum of integers:

$$\pi_2(z) = \sum_{n=1}^{\infty} p(n)z^n. \quad (24.405)$$

**2023-05-01 Predrag** See  Kidambi 2 hour lecture. He says Hardy and Ramanujan worked on this, mentions complex norm of a torus, relates this generating function to the Dedekind eta function  $\eta(\tau)$ , see [wiki](#), or the Euler function, see [wiki](#). The eta function is easy to compute numerically from its power series. Much is known about it (A collection of over 6300 product identities for the Dedekind eta function in a canonical, standardized form is available:). So our prime sum could be the "modular discriminant of Weierstrass".

I do not see how or why are we partitioning  $n = LT$  into sums of integers, but given that, for the classical generating function for the partition function  $p(n)$  see [wiki](#). In [strict partition function](#) no part occurs more than once, reminiscent of a prime orbit contributing to the zeta function only once. Do not know whether this has implications for us.

Check out post **2020-06-16 Predrag** and the text below (19.15). Search also for "pentagonal numbers" in this blog.

**2023-05-04 Predrag** No need for these power series, [Mathematica](#) yields Dedekind eta function  $\eta(\tau)$  to high accuracy. My guess is that  $\tau$  is a better variable than our (multiplicative) weight  $t_p$  which is decreasing exponentially with the primitive cell volume, but that will not matter much for small tiles.

**2023-05-11 Han** There was a mistake in CL18.tex eq. partFprime:2d, now fixed:

$$Z_p[\beta] = V_p \sum_{r_1=1}^{\infty} \sum_{r_2=1}^{\infty} r_1 (t_p^{r_1})^{r_2} = V_p \sum_{l=1}^{\infty} \frac{\ell t_p^\ell}{1-t_p^\ell} \neq V_p t_p \sum_{l=1}^{\infty} \frac{\ell}{1-t_p^\ell}. \quad (24.406)$$

Alternatively, computing the sum over  $r_1$  first we have:

$$Z_p[\beta] = V_p \sum_{r_1=1}^{\infty} \sum_{r_2=1}^{\infty} r_1 (t_p^{r_1})^{r_2} = V_p \sum_{l=1}^{\infty} \frac{t_p^\ell}{(1-t_p^\ell)^2}. \quad (24.407)$$

It is not obvious that

$$V_p \sum_{\ell=1}^{\infty} \frac{\ell t_p^\ell}{1-t_p^\ell} = V_p \sum_{\ell=1}^{\infty} \frac{t_p^\ell}{(1-t_p^\ell)^2}. \quad (24.408)$$

But expand these two functions we get same polynomial:

$$\begin{aligned} \frac{1}{V_p} Z_p[\beta] &= \sum_{\ell=1}^{\infty} \sigma(\ell) t_p^\ell \\ &= t_p + 3t_p^2 + 4t_p^3 + 7t_p^4 + 6t_p^5 + 12t_p^6 + 8t_p^7 + 15t_p^8 + 13t_p^9 + 18t_p^{10} + O(t_p^{11}), \end{aligned} \quad (24.409)$$

where  $\sigma(\ell)$  is the Euler [sum-of-divisors function](#).

**2023-05-11 Predrag** The wiki remarks "Euler proved this by logarithmic differentiation of the identity in his [pentagonal number theorem](#)". If you read about polylogs, I think you will find the relation (24.408), as a derivative of a polylogarithm is itself a polylogarithm.

**2023-05-07 ChatGTP** Some formulas not to trust until we have rederived them

$$\sum_{n=1}^{\infty} \frac{n}{1-x^n} = PolyLog[2, x] / \log[x] \quad (24.410)$$

This one is OK: it is the definition

$$\ln_2(z) = \sum_{n=1}^{\infty} \frac{z^n}{n^2} \quad (24.411)$$

$$\frac{d}{dx} \log(2, x) = \frac{1}{x \log(2)} \quad (24.412)$$

**2023-05-12 ChatGTP** Formulas not to trust until we have rederived them :)

The connection between the sum and the dilogarithm function can be seen by first expressing the general term of the sum as a geometric series:

$$\frac{z^n}{(1-z^n)^2} = \frac{z^n}{1-z^n} \frac{1}{1-z^n} = \sum_{k=1}^{\infty} k z^{nk}.$$

Summing over  $n$  yields:

$$\sum_{n=1}^{\infty} \sum_{k=1}^{\infty} k z^{nk} = \sum_{k=1}^{\infty} k \sum_{n=1}^{\infty} z^{nk} = \sum_{k=1}^{\infty} \frac{k z^k}{1-z^k}$$

This sum can then be expressed in terms of the dilogarithm function as:

$$\sum_{k=1}^{\infty} \frac{k z^k}{1-z^k} = -\frac{1}{2} (\text{Li}_2(z) + \text{Li}_2(1/z))$$

Therefore, the original sum can be written as (compare with (24.414)):

$$\sum_{n=1}^{\infty} \frac{z^n}{(1-z^n)^2} = -\frac{1}{2}(\text{Li}_2(z) + \text{Li}_2(1/z)) \quad (24.413)$$

**2023-05-12 Bard** Some formulas not to trust until we have rederived them :)

The polylogarithm is a special function of the form

$$\text{Li}_s(z) = \sum_{n=1}^{\infty} \frac{z^n}{n^s},$$

where  $s$  is a complex number. The polylogarithm with  $s = 2$  is called the dilogarithm  $\text{Li}_2(z)$ .

The dilogarithm can be expressed in terms of the sum (compare with (24.413)):

$$\sum_{n=1}^{\infty} \frac{z^n}{(1-z^n)^2} = \text{Li}_2(z) + \frac{1}{2} \log^2(1-z) \quad (24.414)$$

Also, claims Bard:

$$\sum_{n=1}^{\infty} \frac{nz^n}{1-z^n} = \frac{1}{(1-z)^2}$$

$$\sum_{n=1}^{\infty} \frac{z^n}{(1-z^n)^2} = \frac{1}{(1-z)^3}$$

**2023-05-11 Predrag** A proposal for a new, 2-dimensional lattice cycle expansion.  $\zeta_p(z) = \phi(t_p)$  is the **Euler function**. Absorb the higher order  $t_p^n$  dependence into a function  $\gamma_p$  (or some other, perhaps more appropriate symbol) which you can evaluate numerically (using Mathematica)

$$\begin{aligned} \zeta_p(z) &= 1 - \gamma_p \\ \gamma_p &= 1 - \phi(t_p) = t_p + O(t_p^2). \end{aligned} \quad (24.415)$$

$-\gamma_p$  is the pentagonal numbers series (24.425), with the term '1' omitted, but idea is not use a truncation of the series, but evaluate it numerically to a desired accuracy, using Mathematica.

Denote by  $\gamma_\pi = (-1)^{k+1} \gamma_{p_1} \gamma_{p_2} \dots \gamma_{p_k}$  an element of the set of all distinct products of the prime cycle weights  $\gamma_{p_i}$ , and label each such *pseudo-cycle* by

$$\pi = p_1 + p_2 + \dots + p_k \quad (24.416)$$

The formal power series expansion is now compactly written as

$$1/\zeta = 1 - \sum'_{\pi} \gamma_{\pi}. \quad (24.417)$$

Expand this as a the usual *cycle expansion*. For example, in the full-binary case, we have

$$\begin{aligned} 1/\zeta &= (1 - \gamma_0)(1 - \gamma_1)(1 - \gamma_{01})(1 - \gamma_{001})(1 - \gamma_{011}) & (24.418) \\ &\times (1 - \gamma_{0001})(1 - \gamma_{0011})(1 - \gamma_{0111})(1 - \gamma_{00001})(1 - \gamma_{00011}) \\ &\times (1 - \gamma_{00101})(1 - \gamma_{00111})(1 - \gamma_{01011})(1 - \gamma_{01111}) \dots \end{aligned}$$

The first few terms of the expansion ordered by increasing total pseudo-cycle length are:

$$\begin{aligned} 1/\zeta &= 1 - \gamma_0 - \gamma_1 - [(\gamma_{01} - \gamma_{0+1})] - [(\gamma_{001} - \gamma_{0+01}) + (\gamma_{011} - \gamma_{01+1})] \\ &- [(\gamma_{0001} - \gamma_{0+001}) + (\gamma_{0111} - \gamma_{011+1}) \\ &+ (\gamma_{0011} - \gamma_{001+1} - \gamma_{0+011} + \gamma_{0+01+1})] - \dots & (24.419) \end{aligned}$$

The new cycle expansion agrees with the usual one in the leading term  $t_p$  in (24.415), the product of primes accounts for the entropy, so I expect this expansion to converge as well as the traditional one.

Han, can you take this cycle expansion out for a spin? Find  $1/\zeta(z) = 0$  for our  $\phi^3$  theory?

**2023-05-11 Han** Let consider the cycle expansion for topological zeta function first,  $t_p = z^{n_p}$ . for  $\phi^3$  theory with sufficiently large stretching parameter the number of periodic states is same as a 2-letter full shift on a 2-dimensional lattice. The first few terms of the zeta function are:

$$\begin{aligned} 1/\zeta &= 1 - \gamma[0] - \gamma[1] - \gamma \begin{bmatrix} 0 & 1 \\ 0 & 1 \end{bmatrix}_0 - \gamma \begin{bmatrix} 0 & 1 \\ 1 & 1 \end{bmatrix}_1 - \gamma \begin{bmatrix} 0 & 1 \\ 1 & 1 \end{bmatrix}_0 \\ &+ \gamma[0]\gamma[1] - \dots \\ &= 1 - 2\gamma(z) - [3\gamma(z^2) - \gamma^2(z)] - \dots & (24.420) \end{aligned}$$

where  $\begin{bmatrix} 0 & 1 \\ 0 & 1 \end{bmatrix}_0$  means a  $[2 \times 1]_0$  block with two symbols 0 and 1. And we already know that the zeta function is

$$1/\zeta = 1 - \gamma(2z). \tag{24.421}$$

Compare these two formulae we see that the cancellation of orbits and pseudo-orbits does not happen. And it should not happen, as unlike the temporal systems,  $\gamma(2z) \neq 2\gamma(z)$ .

**2022-03-26 Han** I counted the number of prime solutions of the  $s = 5/2, \mu^2 = 1$  spatiotemporal cat with the area of the primitive cell less than 100, computed the zeta function  $1/\zeta$  using the product formula (24.402) and truncated the formula to  $z^{100}$ . The result is same as (24.393), as it should be. The coefficients of the expanded polynomial grow exponentially, which implies that the pseudo-cycles do not cancel with the short periodic orbits.

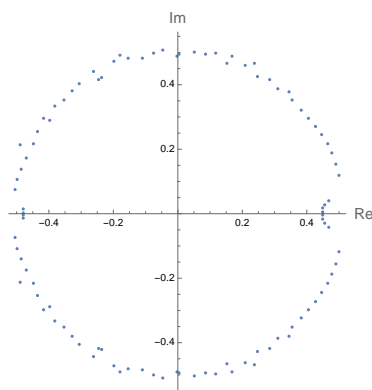


Figure 24.73: Roots of the topological zeta function of the 2-letter full shift on a 2-dimensional lattice truncated to  $z^{100}$ . The growth rate of periodic points is  $\ln 2$  and the radius of convergence is  $1/2$ .

However, I also computed the truncated Lind zeta function of a 2-letter full shift on a 2-dimensional lattice, and the result is surprising: coefficients of many terms cancel out exactly, although the terms not cancelled out still grow exponentially.

I used both the product formula (24.402) and the exponential sum (24.392) to compute and truncate the zeta function at  $z^{100}$ , and got a same result:

$$\begin{aligned}
 1/\zeta^{(100)} = & 1 - 2z - 4z^2 + 32z^5 + 128z^7 - 4096z^{12} - 32768z^{15} \\
 & + 4.1943 \times 10^6 z^{22} + 6.71089 \times 10^7 z^{26} - 3.43597 \times 10^{10} z^{35} \\
 & - 1.09951 \times 10^{12} z^{40} + 2.2518 \times 10^{15} z^{51} + 1.44115 \times 10^{17} z^{57} \\
 & - 1.18059 \times 10^{21} z^{70} - 1.51116 \times 10^{23} z^{77} + 4.95176 \times 10^{27} z^{92} \\
 & + 1.26765 \times 10^{30} z^{100}. \quad (24.422)
 \end{aligned}$$

The coefficients of a lot of terms are 0, but the non-zero terms still grow very fast. I also tried to use the product formula but not including the relative periodic orbits, and the result is much worse: none of the coefficients is cancelled out. So the Lind product formula is still better than others.

The roots of the truncated zeta function are plotted in figure 24.73. The growth rate of periodic points is  $\ln 2$ , and the radius of convergence is  $1/2$ . The radius of the ring in figure 24.73 is approximately  $1/2$ , and it also has the small half circle near the real axis, the same as figure 24.70.

**2022-03-26 Predrag** You forgot to blog the important thing that you had already checked - that if you write  $\mu^2 = 1$  temporal cat (24.398) in the correct, rational polynomial Isola form (24.422) it stops at  $z^2$ , all other roots in figure 24.72 are spurious.

That 2D lattice full 2-shift (24.422) blows up exponentially is a puzzling, but it is possible that 2D  $\zeta$  is rational polynomial.

Is it too much to identify the symbolic dynamics of uncanceled terms? If they have long sequences of 0's or 1's it means that you have to divide them by polynomials whose Taylor series causes these noncancellations.

That there were no cancellations in the product formula that excluded the relative periodic orbits means that my suggestion to first count periodic states for square and rectangular primitive cells was a bad suggestion. Quite possible, as we know that looking at time evolution of cells of fixed spatial width is complicated.

The problem with the Lind zeta (6.150) for me is that it is not clear how it would lead to rational polynomials. Are you able to derive Isola zeta (24.422) starting with the temporal cat Lind zeta? What about the metal cat map zeta (6.55)?

We might want to revisit (8.121) and (10.9). Also, give chapter 10 *Zeta functions in 2D* a quick scan. There might be something there related to this...

**2022-03-30 Han** The Lind zeta function of the 2-letter full shift on a 2-dimensional lattice has a simpler form:

$$1/\zeta(z) = 1/\pi_2(2z) = \prod_{n=1}^{\infty} [1 - (2z)^n]. \quad (24.423)$$

In fact Lind has showed that the  $k$ -letter full shift on a 2-dimensional lattice has zeta function:

$$1/\zeta(z) = 1/\pi_2(kz) = \prod_{n=1}^{\infty} [1 - (kz)^n]. \quad (24.424)$$

If the zeta function of the 2-dimensional spatiotemporal cat has a rational polynomial form, it probably is an infinite product of polynomials.

**2022-11-28 Han** (24.422) is the expansion of the Lind zeta function of a full  $\mathbb{Z}^2$  2-shift (24.423). The expansion of the Lind zeta function of a trivial  $\mathbb{Z}^2$  1-shift is

$$\begin{aligned} 1/\zeta^{(100)} = & 1 - z - z^2 + z^5 + z^7 - z^{12} - z^{15} \\ & + z^{22} + z^{26} - z^{35} - z^{40} + z^{51} + z^{57} \\ & - z^{70} - z^{77} + z^{92} + z^{100} + \dots \end{aligned} \quad (24.425)$$

which is also the contribution from one prime orbit (24.404). This expansion has same terms as the 2-shift (24.422), except that the coefficients are  $\pm 1$ . According to [On-Line Encyclopedia of Integer Sequences](#), the sequence

$$0, 1, 2, 5, 7, 12, 15, 22, 26, 35, 40, \dots$$

is known as the [generalized pentagonal numbers](#):

$$\frac{m(3m-1)}{2}, \quad m = 0, \pm 1, \pm 2, \pm 3, \dots \quad (24.426)$$

"Generalized pentagonal numbers are important to Euler's theory of partitions, as expressed in his [Pentagonal number theorem](#)".

The contribution from one prime orbit (24.404), (24.425) is called the [Euler function](#).

**2022-11-28 Han** Uploaded Mathematica notebook of computing orbits of one and two-dimensional  $\phi^4$ .

figSrc/han/Mathematica/HLPhi4.nb

figSrc/han/Mathematica/HL2dPhi4.nb

**2022-11-28 Predrag** Wiki says The  $n$ th pentagonal number is the sum of  $n$  integers from  $n$  to  $2n - 1$ . The following recursions hold:

$$p_n = p_{n-1} + 3n - 2 = 2p_{n-1} - p_{n-2} + 3 \quad (24.427)$$

Pentagonal numbers are closely related to triangular numbers. The  $n$ th pentagonal number is one third of the  $(3n - 1)$ th triangular number. Each  $n$ th triangular number is the sum of the first  $n$  positive integers:

$$1, 1 + 2 = 3, 1 + 2 + 3 = 6, 1 + 2 + 3 + 4 = 10, \dots$$

The recursive process of producing this number can be visualized as adding a row of  $n$  dots to the top of the previous triangular number to obtain the next one in the pattern. For pentagonal numbers put together from rectangular and triangular numbers, see [Michael Shaughnessy](#): reminiscent of slant sums.

In addition, where

$$T_n = \sum_{k=1}^n k = 1 + 2 + 3 + \dots + n = \frac{n(n+1)}{2} = \binom{n+1}{2} \quad (24.428)$$

is the  $n$ th triangular number.

$$p_n = T_{n-1} + n^2 = T_n + 2T_{n-1} = T_{2n-1} - T_{n-1} \quad (24.429)$$

[Generating function for pentagonal numbers](#):

The  $k$ th pentagonal number is

$$a_k = (3k^2 - k)/2 \quad (24.430)$$

**2022-11-28 Predrag** To get this, keep differentiating the geometric series

$$\begin{aligned} \sum_{i=0}^{\infty} x^{i+1} &= \frac{x}{(1-x)} \\ \sum_{i=0}^{\infty} ix^i &= \frac{x}{(1-x)^2} \\ \sum_{i=0}^{\infty} i^2 x^i &= \frac{x(1+x)}{(1-x)^3} \\ \sum_{i=0}^{\infty} \frac{(3i^2 - i)}{2} x^i &= \frac{3}{2} \sum_{i=0}^{\infty} i^2 x^i - \frac{1}{2} \sum_{i=0}^{\infty} ix^i = \frac{2x^2 + x}{(1-x)^3} \quad (24.431) \end{aligned}$$

**2022-03-30 Predrag** Could be. Someplace in ChaosBook I have such infinite products of ratios of Fredholm determinants; they have to do with skew-product formulas for determinants.

Still, I'm hopeful :) If you can bring spatiotemporal cat  $\zeta$  into rational polynomial form, be it infinite product, would be nice.

**2022-03-30 Predrag** Our expression for deterministic **periodic state probability** is obvious: it simply states what we always say in words, that Euler-Lagrange equation is satisfied at ever site.

One of the methods for evaluating path integrals is called 'decimation'. A random reference that I happen to have read: Feigenbaum and Hasslacher [32] *Irrational decimations and path-integrals for external noise*.

For future work: decimation in the sense of -for example- reducing ten invading soldiers to one is the essence of Kadanoff-Migdal discrete lattice renormalization theory.

Your derivation of Hill's formula in terms of 'time-stepping' transfer operator is another example. We should really write it down for  $C_\infty$  symmetry unit cell Bravais lattice, then reduce to finite primitive cell sublattices.

The 2nd order difference equation (special case  $D_\infty$  reversal invariant field theory) might have other decimation schemes than the one you used to prove Hill's formula.

For example, the 2-dimensional square lattice does not count neighbors along diagonals as the nearest neighbors - they are nearest neighbors in the 1-step shifted lattice, so a square lattice is really two intercalated lattices. Maybe there is a decimation scheme that takes advantage of that.

I'm sure that has already been done or tried by many people in statistical mechanics. It might be even cited in this blog, but I am not a person that could remember 3 000 references :)

**2022-04-01 Han** The Bernoulli map:

$$f(\phi) = s\phi \pmod{1}$$



is equivariant under the  $D_1$  inversion:

$$\sigma\phi_t = 1 - \phi_t \pmod{1},$$

as

$$f(\sigma\phi) = \sigma f(\phi).$$

But the map is invariant under the  $C_s$  cyclic shift:

$$r_n\phi_t = \phi_t + \frac{n}{s} \pmod{s}, \quad n \in \mathbb{Z},$$

because:

$$f(r_n\phi) = f(\phi).$$

Consider a period-2 periodic state of  $s = 6$  temporal Bernoulli:  $\Phi = \overline{\phi_1\phi_2}$ , where

$$\phi_1 = \frac{2}{35}, \quad \phi_2 = \frac{12}{35}.$$

The  $\overline{(\sigma\phi_1)(\sigma\phi_2)}$  with

$$\sigma\phi_1 = \frac{33}{35}, \quad \sigma\phi_2 = \frac{23}{35},$$

is also a periodic state. But  $\overline{(r_1\phi_1)(r_1\phi_2)}$  where

$$r_1\phi_1 = \frac{2}{35} + \frac{1}{6} \pmod{s} = \frac{47}{210}, \quad r_1\phi_2 = \frac{12}{35} + \frac{1}{6} \pmod{s} = \frac{107}{210},$$

is not a periodic state.

**2022-03-31 Han** [This post is wrong.](#)

The temporal Bernoulli has an internal symmetry. The Euler–Lagrange equation of the temporal Bernoulli is invariant under the inversion of the field thought the center of the  $0 \leq \phi_t < 1$  unit interval  $\sigma$ ,

$$\sigma\phi_t = 1 - \phi_t \pmod{1},$$

and the cyclic translation  $r_n$ ,

$$r_n\phi_t = \phi_t + \frac{n}{s} \pmod{s}, \quad n \in \mathbb{Z}.$$

So the temporal Bernoulli has a  $D_s$  internal symmetry. If  $\Phi = \{\phi_t\}$  is a periodic state of the temporal Bernoulli, then the inversion and translations of this periodic state  $g\Phi = \{g\phi_t\}$ , where  $g$  is a group element of the  $D_s$  internal symmetry group, are also admissible periodic states. Periodic states of the system can satisfy all of system's symmetries, a subgroup of them, or have no symmetry at all.

**2022-04-17 Predrag** sect. 4.7.3 *Birkhoff sums* connection of  $\ln(\text{Hill determinant})$  to deterministic random walks might be of interest: the logs in (16.96) correspond to factors of Hill determinant, exponentiated sum corresponds to  $|\text{Hill determinant}|$ . Of course, there is a ton of literature that comes along.

**2022-04-18 Han** To derive the Hamiltonian form of the  $\phi^4$  field theory, let

$$\begin{aligned}\phi_{t+1} &= \phi_t + p_{t+1}, \\ p_{t+1} &= p_t - V'(\phi_t).\end{aligned}\tag{24.432}$$

Using the Euler–Lagrange equation:

$$\phi_{t+1} = -\mu^2 \phi_t^3 + (\mu^2 + 2)\phi_t - \phi_{t-1},\tag{24.433}$$

we get:

$$p_{t+1} = -\mu^2 \phi_t^3 + (\mu^2 + 1)\phi_t - \phi_{t-1}.\tag{24.434}$$

To get rid of the  $\phi_{t-1}$ , note that:

$$p_t = \phi_t - \phi_{t-1}.\tag{24.435}$$

Substitute  $p_t$  into  $p_{t+1}$ :

$$p_{t+1} = p_t - \mu^2 \phi_t^3 + \mu^2 \phi_t.\tag{24.436}$$

So the potential is:

$$V(\phi) = \frac{\mu^2}{4} \phi^4 - \frac{\mu^2}{2} \phi^2.\tag{24.437}$$

**2022-04-21 Predrag** we use backward (24.435), not forward partial difference operator (4.4),

$$p_t = \phi_t - \phi_{t-1},\tag{24.438}$$

so (24.432) is OK.

**2022-04-28 Han** There is a simple way to understand the integral of the "eigenvalue band" of the orbit Jacobian matrix of repeats of prime orbits.

The continuous eigenvalue band is the eigenvalue spectrum of the orbit Jacobian matrix of an infinite repeat of a prime orbit. As shown in (24.351), the integral of  $\ln |E_k|$  in the first Brillouin zone gives us the logarithm of the product of the eigenvalues, which is the logarithm of the determinant. The determinant of the orbit Jacobian matrix of an infinite repeat of a prime orbit should be infinite, so the  $\Lambda^{2\pi}$  we computed here should be a weight per unit length of the orbit (?). The  $2\pi$  is introduced by the integral over the first Brillouin zone.

This result is not surprising. As the orbit gets longer, the Hill determinant is dominated by the expanding eigenvalues of the Floquet matrix. To test this result, I computed the integral of the band of  $a = 6$  length 2 temporal Hénon. The prime period-2 periodic state of the temporal Hénon is  $(\phi_0, \phi_1) = \left(\frac{-1-\sqrt{3}}{6}, \frac{-1+\sqrt{3}}{6}\right)$ . The forward-in-time Jacobian matrices at  $\left(\frac{-1-\sqrt{3}}{6}, \frac{-1+\sqrt{3}}{6}\right)$  and  $\left(\frac{-1+\sqrt{3}}{6}, \frac{-1-\sqrt{3}}{6}\right)$  are:

$$\mathbb{J}_0 = \begin{pmatrix} 0 & 1 \\ -1 & 2(-1 + \sqrt{3}) \end{pmatrix}$$

and

$$\mathbb{J}_1 = \begin{pmatrix} 0 & 1 \\ -1 & 2(-1 - \sqrt{3}) \end{pmatrix}.$$

The Floquet matrix at  $\left(\frac{-1-\sqrt{3}}{6}, \frac{-1+\sqrt{3}}{6}\right)$  is

$$\mathbb{J}_c = \mathbb{J}_1 \mathbb{J}_0 = \begin{pmatrix} -1 & 2(\sqrt{3} - 1) \\ 2(1 + \sqrt{3}) & -9 \end{pmatrix},$$

whose eigenvalues are  $\Lambda = (-5 - 2\sqrt{6})$  and  $\Lambda^{-1} = (-5 + 2\sqrt{6})$ . Analytical formulas of two bands in (24.69) are (24.390). Compute the determinant by the integral:

$$\begin{aligned} & \exp\left(\int_{-\frac{\pi}{2}}^{\frac{\pi}{2}} \ln |E_{k,1}| dk + \int_{-\frac{\pi}{2}}^{\frac{\pi}{2}} \ln |E_{k,2}| dk\right) \\ &= \exp\int_{-\frac{\pi}{2}}^{\frac{\pi}{2}} \ln[4(3 + \cos^2(k)) - 4] dk \\ &= (5 + 2\sqrt{6})^\pi = |\Lambda|^\pi. \end{aligned} \tag{24.439}$$

The result is the expanding eigenvalue to the power of  $\pi$ . In this computation we have  $\pi$  instead of  $2\pi$ , because the size of the first Brillouin zone for a length-2 prime orbit is  $\pi$ , while for temporal cat the size is always  $2\pi$ .

**2022-05-10 Han** I computed several  $s = 3$  temporal cat examples of 2-lattice sites correlation function, defined as an average of the  $M_p$  translation or cyclic group  $C_\infty$  prime orbits over a primitive cell of period  $n$ ,

$$\langle \phi_t \phi_0 \rangle_n = \frac{1}{nM_p} \sum_p \sum_{\Phi \in p} \phi_t \phi_0. \tag{24.440}$$

For  $s \in \mathbb{Z}$  temporal cat primitive cell lattice sites fields  $\phi_t$  take rational values, so all correlation functions are rational numbers.

When the primitive cell period  $n$  is odd, the correlation function has two values, the (auto) correlation value with zero distance  $\langle \phi_0 \phi_0 \rangle$ , and correlation value with nonzero distance,  $\langle \phi_t \phi_0 \rangle$ ,  $t \neq 0$ .

For example, the correlation functions on period-9 and period-11 prime orbits are:

$$\begin{aligned} \{\langle \phi_t \phi_0 \rangle\}_9 &= \{0.32708333, 0.24375, 0.24375, 0.24375, 0.24375, \\ &\quad 0.24375, 0.24375, 0.24375, 0.24375\}, \\ \{\langle \phi_t \phi_0 \rangle\}_{11} &= \{0.330833, 0.2475, 0.2475, 0.2475, 0.2475, 0.2475, \\ &\quad 0.2475, 0.2475, 0.2475, 0.2475\}. \end{aligned} \quad (24.441)$$

If the primitive cell period  $n$  is even, the correlation function has three different values,  $\langle \phi_0 \phi_0 \rangle$ ,  $\langle \phi_{n/2} \phi_0 \rangle$  and the correlation at other distances. This arises because the sum is over the  $C_\infty$  prime orbits, but the symmetry of temporal cat is  $D_\infty$ , with two kinds of prime orbits (6.16), (6.17).

For example, the 'prime' correlation functions on period-4 (see (24.14)), period-6, and period-10 primitive cells are, respectively,

$$\begin{aligned} \{\langle \phi_t \phi_0 \rangle\}_4 &= \frac{1}{120} \{37, 27, 26, 27\} \\ &= \{0.30833333, 0.225, 0.21666667, 0.225\} \\ \{\langle \phi_t \phi_0 \rangle\}_6 &= \frac{1}{300} \{98, 73, 73, 72, 73, 73\} \\ &= \{0.32667, 0.24333, 0.24333, 0.24, 0.24333, 0.24333\} \\ \{\langle \phi_t \phi_0 \rangle\}_{10} &= \frac{1}{7500} \{2489, 1864, \dots, 1860, \dots, 1864\} \\ &= \{0.33186667, 0.24853333, \dots, 0.248, \dots, 0.24853333\}. \end{aligned} \quad (24.442)$$

For period-2 see (24.33), for period-3 see (24.38).

**2022-05-11 Predrag** This is a very pedagogical exercise.

The field  $\phi_t$  is not even translation invariant, depends on where does one center the unit interval. That is presumably fixed by redefining the 'average' (24.440) as the fluctuation from the mean

$$\langle (\phi_t - \langle \phi \rangle)(\phi_0 - \langle \phi \rangle) \rangle = \langle \phi_t \phi_0 \rangle - \langle \phi \rangle^2 \quad (24.443)$$

The 'average' (24.440) is not the correct cycle averaging formula. That one -still to be made explicit- follows from example 2.4 and/or sect. 2.3.2, with extra observable weight  $\exp(\beta \phi_t)$  included. We know the answer in the Ulam piecewise constant approximation. For 2 areas, the two probabilities are the green-red areas given in (2.86), and for 5 areas approximation I hope one gets the same answer - your  $\langle \phi_0 \phi_0 \rangle$ , and  $\langle \phi_t \phi_0 \rangle$ ,  $t \neq 0$  are presumably converging to that.

Lattice sites correlation functions are not invariant under field  $\phi_t$  translations, etc., so they have no invariant meaning in themselves. That's why we are getting different estimates for each primitive cell period.

An invariant observable is, for example, the reciprocal lattice observable  $\ln |\text{Det } \mathcal{J}_c|$ .

**2022-05-12 Predrag** Probably want to use the connected correlation function (24.443), see, for example, eq. (6) in ref. [67] (click [here](#)).

## 24.7 Cycle expansion

**2022-06-14 Han** I compute the expectation values and correlation functions of temporal Bernoulli and temporal cat using cycle expansions of the dynamical zeta function.

To approximate the dynamical zeta function using the cycle expansion, all prime orbits with short periods are generated. The dynamical zeta function is computed using the product formula:

$$1/\zeta = \prod_p (1 - t_p), \quad t_p = \frac{z^{n_p} e^{\beta A_p}}{|\Lambda_p|}, \quad (24.444)$$

where  $\Lambda_p$  is the product of expanding eigenvalues of the Floquet matrix of the orbit  $p$ . To evaluate the cycle expansion of the dynamical zeta function, first compute

$$1/\zeta_{(N)} = \prod_{n_p \leq N} (1 - t_p), \quad (24.445)$$

using all prime orbits with periods  $n_p \leq N$ . Then truncate the function to a polynomial of order  $N$ :

$$1/\zeta_N = 1 - \sum_{n=1}^N c_n z^n. \quad (24.446)$$

### 24.7.1 Temporal Bernoulli escape rate and field expectation value

To evaluate the escape rate and the expectation value of the field of the  $s = 2$  temporal Bernoulli (see chapter 1), all prime orbits with periods less or equal to 12 and their Birkhoff sums

$$A_p = \sum_{i=1}^{n_p} \phi_i \quad (24.447)$$

are used to compute the cycle expansion approximation of the dynamical zeta function. The 12th order polynomial approximation of the zeta function is:

$$\begin{aligned} 1/\zeta_{12} = & 1 - \frac{1}{2}z - \frac{1}{4}e^\beta z^2 - \frac{1}{8}e^{2\beta} z^3 - \frac{1}{16}e^{3\beta} z^4 \\ & - \dots - \frac{1}{2048}e^{10\beta} z^{11} - \frac{1}{4096}e^{11\beta} z^{12}. \end{aligned} \quad (24.448)$$

The leading zero of (24.448) is an approximation to the inverse of the leading eigenvalue of the evolution operator  $e^{s(\beta)}$ , which satisfies:

$$s(\beta) = \lim_{t \rightarrow \infty} \frac{1}{t} \ln \langle e^{\beta A} \rangle. \quad (24.449)$$

When  $\beta$  is set to 0, the leading zero of the dynamical zeta function is  $e^\gamma$ , where  $\gamma$  is the escape rate. The leading zero computed from (24.448) is

$$e^\gamma = 1.00012. \quad (24.450)$$

So the escape rate is close to 0. The expectation value of the field is computed by:

$$\left. \frac{\partial s(\beta)}{\partial \beta} \right|_{\beta=0} = \lim_{t \rightarrow 0} \frac{1}{t} \langle A \rangle = \langle \phi \rangle = 0.499327 \quad (24.451)$$

which is close to the correct expectation value  $1/2$ .

We already know that the dynamical zeta function of the temporal Bernoulli is a rational polynomial, whose denominator is contributed by the fixed point  $\bar{1}$ , which is not admissible. The accuracy of the computation can be significantly improved by removing the denominator of the dynamical zeta function. To remove the denominator, one can multiply the product of prime orbits (24.445) by the contribution from the not admissible prime orbit:

$$1/\zeta_{(N)} = (1 - t_1) \prod_{n_p \leq N} (1 - t_p), \quad t_1 = \frac{ze^\beta}{s}. \quad (24.452)$$

Then truncate the product to a polynomial of order  $N$ . The dynamical zeta function of the temporal Bernoulli becomes very simple after we remove the denominator:

$$1/\zeta_{12} = 1 - \frac{1 + e^\beta}{2} z. \quad (24.453)$$

The leading zero of this zeta function is

$$e^{-s(\beta)} = \frac{2}{1 + e^\beta}. \quad (24.454)$$

The escape rate  $\gamma$  is 0:

$$\gamma = \ln e^{-s(0)} = 0. \quad (24.455)$$

$t$	0	1	2	3	4	5	6
$\langle \phi_0 \phi_t \rangle$	0.33333	0.29167	0.27083	0.26042	0.25520	0.25260	0.25130
$\langle \phi_0 \phi_t \rangle_{12}$	0.33337	0.29172	0.27092	0.26058	0.25554	0.25326	0.25261
$t$	7	8	9	10	11	12	13
$\langle \phi_0 \phi_t \rangle$	0.25065	0.25032	0.25016	0.25008	0.25004	0.25002	0.25001
$\langle \phi_0 \phi_t \rangle_{12}$	0.25326	0.25554	0.26058	0.27092	0.29172	0.33337	0.29172

Table 24.5:  $\langle \phi_0 \phi_t \rangle$  and  $\langle \phi_0 \phi_t \rangle_{12}$  are the exact two-point correlation function and the correlation function computed from the cycle expansion using prime orbits with periods up to 12, respectively, for the  $s = 2$  temporal Bernoulli.

And the expectation value of the field is:

$$\langle \phi \rangle = \left. \frac{\partial s(\beta)}{\partial \beta} \right|_{\beta=0} = \left. \frac{\partial}{\partial \beta} \ln \left( \frac{1 + e^\beta}{2} \right) \right|_{\beta=0} = \frac{1}{2}. \quad (24.456)$$

Note that the expanded dynamical zeta function (24.453) is a polynomial of order 1. To get the accurate escape rate and expectation value we only need to use prime orbits of period 1.

### 24.7.2 Correlation function of temporal Bernoulli

The numerator of the rational polynomial zeta function is used to compute the two-point correlation function of the  $s = 2$  temporal Bernoulli. To compute the correlation function  $\langle \phi_0 \phi_t \rangle$ , the Birkhoff sum

$$A_p = \sum_{i=1}^{n_p} \phi_i \phi_{(i+t) \bmod n_p} \quad (24.457)$$

is computed for every prime orbit with period less or equal to 12. The exact correlation:

$$\langle \phi_0 \phi_t \rangle = \frac{1}{4} + \frac{1}{12 \times 2^{|t|}} \quad (24.458)$$

and the correlation computed from the cycle expansion are listed in the table 24.5. The correlation function computed from the cycle expansion is accurate when the time separation is small. But as the time separation increases, the accuracy becomes worse. The correlation  $\langle \phi_0 \phi_t \rangle_{12}$  starts to increase when the time separation is greater than 6, which is half of the period of the longest prime orbit used in this computation.

The correlation function computed using the cycle expansion converges to the exact correlation function exponentially with increasing cycle lengths. Figure 24.74 is the log plot of errors of correlation functions,  $|\langle \phi_0^2 \rangle_N - \langle \phi_0^2 \rangle|$  and

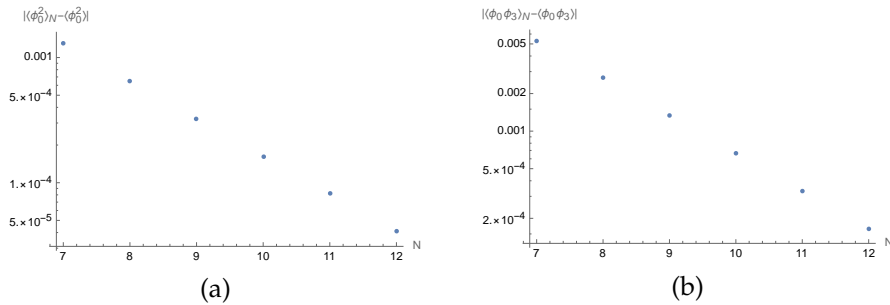


Figure 24.74: Log plots of errors of correlation functions, (a)  $\langle \phi_0^2 \rangle_N$  and (b)  $\langle \phi_0 \phi_3 \rangle_N$ , computed from the cycle expansion, as functions of the length of the longest prime orbit  $N$ .

$|\langle \phi_0 \phi_3 \rangle_N - \langle \phi_0 \phi_3 \rangle|$ , as functions of the length of the longest prime orbit  $N$ . The relationship between logarithmic errors and the cycle length are approximated by linear fits:

$$\begin{aligned} \ln |\langle \phi_0^2 \rangle_N - \langle \phi_0^2 \rangle| &= -1.77582 - 0.694554N, \\ \ln |\langle \phi_0 \phi_3 \rangle_N - \langle \phi_0 \phi_3 \rangle| &= -0.374023 - 0.694554N, \end{aligned} \quad (24.459)$$

where the slope is close to negative  $\ln 2 = 0.693147$ .

### 24.7.3 Correlation function of the 'golden mean' map

As a warmup for temporal cat (two-dimensional Hamiltonian system), work through the 'golden mean' map, the simplest example of a one-dimensional tent map with pruning.

[ChaosBook exercise 14.6](#) 'Golden mean' pruned map

[ChaosBook example 17.5](#) 'Golden mean' pruning

[ChaosBook example 17.8](#) 'Golden mean' pruning (a link-to-link version of example 17.5)

[ChaosBook example 18.4](#) 'Golden mean' pruning. (continued from example 17.5?)

[ChaosBook exercise 18.5](#) Transition matrix and cycle counting

[ChaosBook exercise 18.6](#) Alphabet  $\{0, 1\}$ , prune \_00\_

[ChaosBook exercise 18.7](#) 'Golden mean' pruned map

[ChaosBook exercise 18.8](#) A unimodal map with 'golden mean' pruning

[ChaosBook exercise 22.1](#) Spectrum of the 'golden mean' pruned map (medium - exercise 18.7 continued)

[ChaosBook example 1](#) the 'golden mean' pruning  $x_p = .11$



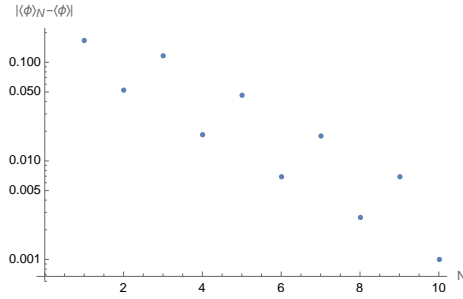


Figure 24.75: Log plot of errors of field expectation values,  $\langle \phi \rangle_N$ , computed from the cycle expansion, as functions of the longest cycle length  $N$ .

### 24.7.4 Temporal cat escape rate and field expectation value

Repeat the same procedure to compute the escape rate and the field expectation value for the  $s = 3$  temporal cat. To perform the cycle expansion, all prime cycles with period less or equal to 10 and their Birkhoff sums (24.447) are computed. Known that the topological zeta function is a rational polynomial, and the denominator is contributed by two nonexistent fixed points, one can remove the denominator by multiplying the zeta function with the contribution from the two fixed points,  $\bar{0}$  and  $\bar{1}$  (possibly wrong).

Set  $\beta$  to 0 the cycle expansion of the dynamical zeta function is a finite polynomial:

$$\frac{1}{\zeta_{10}(z, \beta)} \Big|_{\beta=0} = 1 - \frac{6z}{3 + \sqrt{5}} + \frac{4z^2}{(3 + \sqrt{5})}. \quad (24.460)$$

The leading zero of the dynamical zeta function is  $e^{-s(\beta)}$ , and  $e^{-s(0)} = e^\gamma = 1$  is the leading zero of (24.460). So the escape rate  $\gamma$  is 0. The field expectation value is computed from

$$\langle \phi \rangle = \frac{\partial s(\beta)}{\partial \beta} \Big|_{\beta=0}. \quad (24.461)$$

The exact expectation value of the field is  $1/2$ . The errors of the expectation value computed from the cycle expansion are plotted in figure 24.75. The expectation value computed from the cycle expansion converges with increasing cycle lengths, and it belongs to one of the two branches, depending on whether the longest cycle length is odd or even.

### 24.7.5 Correlation function of temporal cat

The final version is in sect. 4.12.3 *Deterministic lattice field theory*

To compute the correlation function  $\langle \phi_0 \phi_t \rangle$ , the Birkhoff sum (24.457) is computed for all prime cycles with period up to 10. The exact correlation function

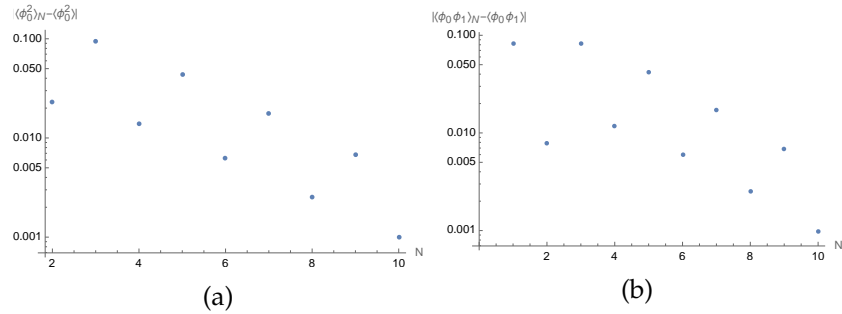


Figure 24.76: Log plots of errors of correlation functions, (a)  $\langle \phi_0^2 \rangle_N$  and (b)  $\langle \phi_0 \phi_1 \rangle_N$ , computed from the cycle expansion, as functions of the longest cycle length  $N$ .

for  $s = 3$  is:

$$\langle \phi_0 \phi_t \rangle = \begin{cases} \frac{1}{3}, & t = 0, \\ \frac{1}{4}, & t \neq 0. \end{cases} \quad (24.462)$$

The errors of the correlation function with  $t = 0$  and  $t = 1$  computed from the cycle expansion are plotted in figure 24.76.

The correlation function computed from the cycle expansion converges to the exact correlation function exponentially with increasing cycle lengths. But correlation functions computed from cycle expansions with odd and even longest cycle lengths belong to two different branches. The slope of each branch is approximately -0.4, while  $\ln \Lambda = 0.962424$ .

**2022-06-17 Predrag** The current version of Han's Sect. 24.7 stops here.

Then the Han's blog restarts here.

**2022-06-29 Han** One possible problem of computing the cycle expansion of cat map is that the two nonexistent fixed points are not necessarily  $\bar{0}$  and  $\bar{1}$ . We got the fixed points  $\bar{0}$  and  $\bar{1}$  only from the generating partition figure 24.4. I'm hoping that by multiplying the zeta function with correct fixed points we can fix the problem caused by periodic points on the boundary, like in temporal Bernoulli. Replacing 0 by 1/2 in the prime orbits is a very rough approximation. I hope we don't need to do that.

**2022-08-23 Han** The cycle expansion approximations of the dynamical zeta function and the spectral determinant of the  $\phi^4$  field theory with  $\mu^2 = 3.5$  are computed, using periodic orbits with cycle lengths up to 10.

To find the expectation value of the observable  $\phi^2$ , compute the Birkhoff sum:

$$A_p = \sum_{i=1}^{n_p} \phi_i^2 \quad (24.463)$$

$N$	1	2	3	4
$\gamma_N$	0.501392566025	0.64746721655	0.88073776270	0.76123260117
$N$	5	6	7	8
$\gamma_N$	0.80418397752	0.787425111103	0.794287322781	0.793070367149
$N$	9	10	11	12
$\gamma_N$	0.792352913555	0.79248721925	0.792468936955	0.792470271806

Table 24.6:  $\gamma_N$  is the escape rate of the  $\phi^4$  field theory with  $\mu^2 = 3.5$  computed from the cycle expansion approximation of the dynamical zeta function truncated at cycle length  $N$ .

on each prime orbit. But to compute the escape rate, we will first set  $\beta = 0$  and compute the first 10 terms of the dynamical zeta function:

$$\begin{aligned}
 1/\zeta(z) = & 1 - 0.605687z + 0.0430822z^2 + 0.0149915z^3 - 0.00227791z^4 \\
 & + 0.000501066z^5 - 0.0000766518z^6 + 0.0000151082z^7 \\
 & - 1.16159 \times 10^{-6}z^8 - 3.15225 \times 10^{-7}z^9 \\
 & + 2.68629 \times 10^{-8}z^{10} + \dots
 \end{aligned} \tag{24.464}$$

and the first 10 terms of the spectral determinant:

$$\begin{aligned}
 \det(1 - z\mathcal{L}) = & 1 - 0.571429z + 0.0229144z^2 + 0.016139z^3 - 0.00175346z^4 \\
 & + 0.000432593z^5 - 0.0000604386z^6 + 0.000012724z^7 \\
 & - 6.77323 \times 10^{-7}z^8 - 3.47905 \times 10^{-7}z^9 \\
 & + 1.57257 \times 10^{-8}z^{10} + \dots
 \end{aligned} \tag{24.465}$$

The escape rate  $\gamma$  computed from the dynamical zeta function truncated at different cycle length are listed in tables 24.6 and 24.7.

Figure 24.77 (a) and (b) are the log plots of the differences between the escape rate  $\gamma_N$  computed at cycle lengths  $N$  and the estimate computed at cycle length 10, using the cycle expansion approximation of the dynamical zeta function and the spectral determinant, respectively. The slope of the linear fit of figure 24.77 (a) is -0.947979. There is no obvious super exponential convergence appeared in the cycle expansion approximation of the spectral determinant figure 24.77 (b).

After we find the escape rate,  $\gamma = \ln e^{-s(0)}$ , use the derivative of  $s(\beta)$  with respect to  $\beta$  to compute the expectation value of the observable,  $\phi^2$ . Figure 24.78 (a) and (b) are the log plots of the differences between the expectation value  $\langle \phi^2 \rangle$  computed at cycle lengths  $N$  and the estimate computed at cycle length 10, using the cycle expansion approximation of the dynamical zeta function and the spectral determinant, respectively.

$N$	1	2	3	4
$\gamma_N$	0.559615787935	0.638597025400	0.839780478985	0.765874710451
$N$	5	6	7	8
$\gamma_N$	0.800465998104	0.788419720702	0.793797091291	0.793141668813
$N$	9	10	11	12
$\gamma_N$	0.792406782127	0.792479699371	0.792470069283	0.792470198802

Table 24.7:  $\gamma_N$  is the escape rate of the  $\phi^4$  field theory with  $\mu^2 = 3.5$  computed from the cycle expansion approximation of the spectral determinant truncated at cycle length  $N$ .

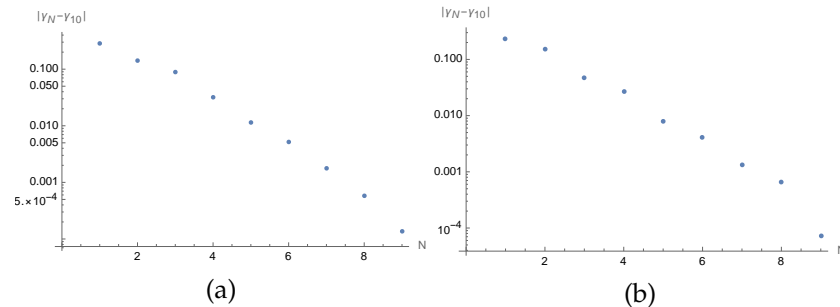


Figure 24.77: Log plots of the difference between the escape rate  $\gamma_N$  of the  $\mu^2 = 3.5 \phi^4$  theory computed at cycle length  $N$  and the estimate computed at cycle length 10, using the cycle expansion approximation of (a) the dynamical zeta function and (b) the spectral determinant.

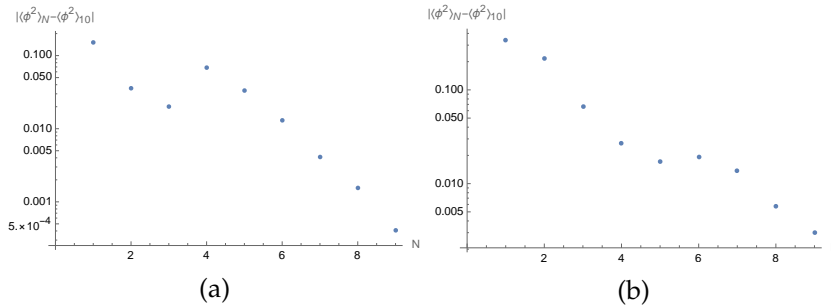


Figure 24.78: Log plots of the difference between expectation value  $\langle \phi^2 \rangle$  of the  $\mu^2 = 3.5 \phi^4$  theory computed at cycle length  $N$  and the estimate computed at cycle length 10, using the cycle expansion approximation of (a) the dynamical zeta function and (b) the spectral determinant.

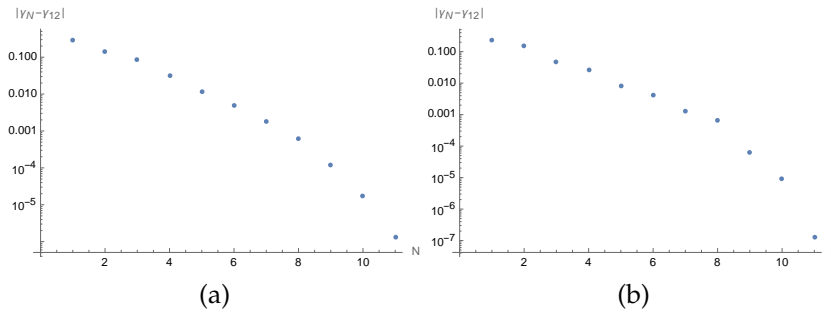


Figure 24.79: Log plots of the difference between the escape rate  $\gamma_N$  of the  $\mu^2 = 3.5 \phi^4$  theory computed at cycle length  $N$  and the estimate computed at cycle length 12, using the cycle expansion approximation of (a) the dynamical zeta function and (b) the spectral determinant.

The cycle expansion approximation is converging, but not exponentially or super exponentially from the beginning.

**2022-08-29 Han** With the cycle expansion truncation of the  $\mu^2 = 3.5 \phi^4$  field theory extended to  $N = 12$ , the escape rate computed from the cycle expansion truncation starts to converge faster, as shown in figure 24.79. The cycle expansion approximation of escape rates computed at cycle length 11 and 12 are now included in tables 24.6 and 24.7.

**2022-09-06 Han** For a 1-dimensional map, the weight of the  $r$ th repeat of a prime orbit  $p$  is:

$$\frac{1}{|\det(\mathbf{1} - M_p^r)|} = \frac{1}{|\Lambda_p|^r (1 - 1/\Lambda_p^r)} = \frac{1}{|\Lambda_p|^r} \sum_{k=0}^{\infty} \frac{1}{\Lambda_p^{kr}}. \quad (24.466)$$

The spectral determinant is

$$\begin{aligned}
 \det(\mathbf{1} - z\mathcal{L}) &= \exp\left(-\sum_p \sum_{r=1}^{\infty} \frac{1}{r} \frac{z^{rn_p} e^{\beta A_p r}}{|\det(\mathbf{1} - M_p^r)|}\right) \\
 &= \exp\left(-\sum_p \sum_{k=1}^{\infty} \sum_{r=1}^{\infty} \frac{1}{r} \frac{(z^{n_p} e^{\beta A_p})^r}{(|\Lambda_p| \Lambda_p^k)^r}\right) \\
 &= \exp\left(-\sum_p \sum_{k=1}^{\infty} \ln\left(1 - \frac{z^{n_p} e^{\beta A_p}}{|\Lambda_p| \Lambda_p^k}\right)\right) \\
 &= \prod_p \prod_{k=0}^{\infty} \left(1 - \frac{t_p}{\Lambda_p^k}\right) \\
 &= \prod_{k=0}^{\infty} 1/\zeta_k
 \end{aligned} \tag{24.467}$$

where

$$t_p = \frac{z^{n_p} e^{\beta A_p}}{|\Lambda_p|}, \tag{24.468}$$

and

$$1/\zeta_k = \prod_p \left(1 - \frac{t_p}{\Lambda_p^k}\right). \tag{24.469}$$

Using the identity

$$\frac{1}{|\Lambda|} = \frac{1}{|\Lambda|(1 - 1/\Lambda)} - \frac{1}{|\Lambda|\Lambda(1 - 1/\Lambda)} \tag{24.470}$$

the dynamical zeta function can be rewritten as:

$$\begin{aligned}
 \frac{1}{\zeta} &= \exp\left(-\sum_p \sum_{r=1}^{\infty} \frac{1}{r} \frac{z^{rn_p} e^{\beta A_p r}}{|\Lambda_p|^r}\right) \\
 &= \exp\left[-\sum_p \sum_{r=1}^{\infty} \left(\frac{1}{r} \frac{z^{rn_p} e^{\beta A_p r}}{|\Lambda_p|^r (1 - 1/\Lambda_p^r)} - \frac{1}{r} \frac{z^{rn_p} e^{\beta A_p r}}{|\Lambda_p|^r \Lambda_p^r (1 - 1/\Lambda_p^r)}\right)\right].
 \end{aligned} \tag{24.471}$$

Note that

$$\frac{1}{|\Lambda_p|^r (1 - 1/\Lambda_p^r)} = \frac{1}{|\det(\mathbf{1} - M_p^r)|}. \tag{24.472}$$

(24.471) becomes

$$\frac{1}{\zeta} = \frac{\det(\mathbf{1} - z\mathcal{L})}{\det(\mathbf{1} - z\mathcal{L}_{(1)})} \tag{24.473}$$

where the cycle weight in  $\mathcal{L}_{(1)}$  is given by replacement  $t_p \rightarrow t_p/\Lambda_p$ . Alternatively, using (24.467) the spectral determinant  $\det(1 - z\mathcal{L}_{(1)})$  is:

$$\begin{aligned} \det(1 - z\mathcal{L}_{(1)}) &= \prod_p \prod_{k=0}^{\infty} \left(1 - \frac{t_p}{\Lambda_p^{k+1}}\right) \\ &= \prod_p \prod_{k'=1}^{\infty} \left(1 - \frac{t_p}{\Lambda_p^{k'}}\right) \\ &= \frac{\det(1 - z\mathcal{L})}{1/\zeta}. \end{aligned} \quad (24.474)$$

Next, retyping example 2.7, example 2.8 and example 2.9:

To write the dynamical zeta function in terms of the spectral determinant for 2-dimensional Hamiltonian maps, write the weight of orbits as

$$\frac{1}{|\det(\mathbf{1} - M_p^r)|} = \frac{1}{|\Lambda_p|^r (1 - 1/\Lambda_p^r)^2} = \frac{1}{|\Lambda_p|^r} \sum_{k=0}^{\infty} \frac{k+1}{\Lambda_p^{kr}}. \quad (24.475)$$

Then substitute the identity:

$$\frac{1}{|\Lambda|} = \frac{1}{|\Lambda|(1 - 1/\Lambda)^2} (1 - 2/\Lambda + 1/\Lambda^2) \quad (24.476)$$

into the dynamical zeta function and get

$$1/\zeta = \frac{\det(1 - z\mathcal{L}) \det(1 - z\mathcal{L}_{(2)})}{\det(1 - z\mathcal{L}_{(1)})^2}. \quad (24.477)$$

The identity (24.476) can be substituted into the dynamical zeta function  $1/\zeta_k$  (24.469), and factorize it into:

$$1/\zeta_k = \frac{\det(1 - z\mathcal{L}_{(k)}) \det(1 - z\mathcal{L}_{(k+2)})}{\det(1 - z\mathcal{L}_{(k+1)})^2}. \quad (24.478)$$

**2022-09-30 Han** The partition function of a temporal lattice deterministic field theory is:

$$Z(\beta) = \sum_c \frac{e^{A_c \beta}}{|\mathcal{J}_c|}, \quad (24.479)$$

where the sum is over all periodic states  $c$  and  $A_c$  is the Birkhoff sum of the observable over the **periodic state**. To evaluate expectation values of observables using periodic states with finite period, first set the period of the temporal domain to  $n$  and find all period- $n$  periodic states. Then use the partition function with sum over the finite period- $n$  periodic states to approximate the exact zeta function and expectation values.

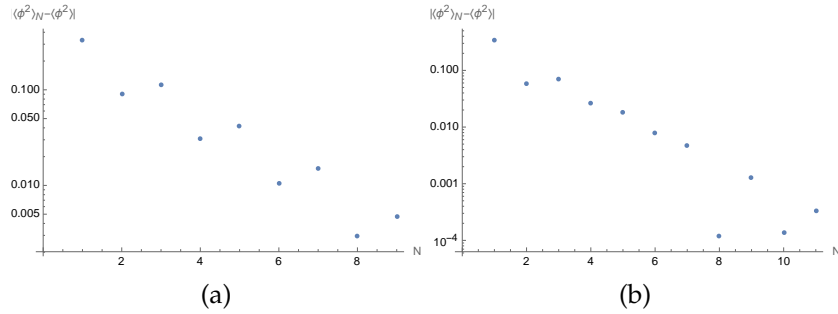


Figure 24.80: Log plots of the difference between the expectation value  $\langle \phi^2 \rangle_n$  computed using the partition function (24.480–24.481) and the best estimation of (a) the  $s = 3$  temporal cat, and (b) the  $\mu^2 = 3.5$   $\phi^4$  field theory.

I have computed the approximation of expectation values of observables for the temporal cat and the  $\phi^4$  field theory. The observable I choose is  $\phi^2$ . This is the simplest non-trivial observable for the  $\phi^4$  field theory. To simplify the computation I computed the prime orbits instead of the periodic states. And the partition function I used for period- $n$  periodic states is:

$$Z_n(\beta) = \sum_{n_p|n} \frac{e^{A_p \beta}}{|\mathcal{J}_p^{n/n_p}|}. \quad (24.480)$$

Note that this partition function is different from the partition function (24.479). The sum of (24.480) is over **prime orbits** whose period  $n_p$  is a divisor of  $n$ , and  $\mathcal{J}_p^{n/n_p}$  is the Jacobian matrix of the  $(n/n_p)$ th repeat of the prime orbit  $p$ . Since each prime orbit only contribute once in (24.480), this partition function can be written as

$$Z_n(\beta) = e^{W_n(\beta)} \quad (24.481)$$

instead of  $e^{nW_n(\beta)}$ . And the expectation value of the observable is:

$$\langle a \rangle_n = \left. \frac{d}{d\beta} W_n(\beta) \right|_{\beta=0}. \quad (24.482)$$

The log plot of errors between the expectation value of  $\phi^2$  computed using periodic states with period  $n$  and the best estimation is shown in figure 24.80. The best estimation of  $\langle \phi^2 \rangle$  is  $\langle \phi^2 \rangle_{10} = 0.3315173553719008$  for  $s = 3$  temporal cat and  $\langle \phi^2 \rangle_{12} = 0.8431130603441963$  for  $\mu^2 = 3.5$   $\phi^4$  theory.

2022-10-03 Han Let the generating function of the zeta function be:

$$G(z) = \sum_{n=1}^{\infty} Z_n z^n \quad (24.483)$$



where  $Z_n$  is the partition function computed on the primitive cell with size  $n$ . Then the contribution from one **prime** orbit  $p$  to the generating function is

$$G_p(z) = \frac{Z_p z^{n_p}}{1 - Z_p z^{n_p}}, \quad (24.484)$$

where  $n_p$  is the period of the prime orbit  $p$  and  $Z_p$  is the contribution from the prime orbit  $p$  to the partition function computed on the period- $n_p$  primitive cell  $Z_{n_p}$ .

The generating function of partition function can be written as a sum over all prime primitive cells, each getting contributions only from prime orbits:

$$G(z) = e^W(z) = \sum_p \frac{Z_p z^{n_p}}{1 - Z_p z^{n_p}}. \quad (24.485)$$

If we compute the generating function using all prime orbits with period less than  $n$ , after the expansion (24.483) the coefficients of the terms up to  $z^n$  are correct. The problem is that to compute the expectation value, we will only use the coefficient of  $z^n$ , instead of the entire generating function truncated at  $z^n$ . The coefficient of  $z^n$  is not computed using all prime orbits with period less than  $n$ .

**2022-10-08 Predrag** What do you think of the repeats of 2-dimensional prime primitive cell summed up as in (4.99)? The crucial thing is that the 'path integral' over  $d\Phi_{\mathbf{a}} = \prod_z^{\mathbf{a}} d\phi_z$  is performed after the resummation. That will probably lead to the correct reciprocal lattice 'Bloch theorem' weights, and the correct, nontrivial cumulant expansions for observables.

**2022-10-11 Han** The probability of the occurrence of a periodic state  $\Phi_{\mathbf{a}}$  is proportional to the inverse of the Hill determinant:

$$1/|\text{Det } \mathcal{J}_{\mathbf{a}}| = \int_{\mathcal{M}_{\mathbf{a}}} d\Phi_{\mathbf{a}} \delta(F[\Phi_{\mathbf{a}}]), \quad d\Phi_{\mathbf{a}} = \prod_z^{\mathbf{a}} d\phi_z. \quad (24.486)$$

The contribution from a prime periodic state  $p$  to the generating function of the partition function (24.483) is:

$$G_p(z) = \sum_{r=1}^{\infty} \frac{e^{r\beta A_p} z^{rn_p}}{|\text{Det } \mathcal{J}_{rp}|}, \quad (24.487)$$

where  $\mathcal{J}_{rp}$  is the orbit Jacobian matrix computed at the  $r$ th repeat of the periodic state  $p$ . Let  $\mathcal{M}_{rp}$  be the neighborhood of the periodic state  $\Phi_{rp}$  in the  $rn_p$ -dimensional field configuration state space.

$$1/|\text{Det } \mathcal{J}_{rp}| = \int_{\mathcal{M}_{rp}} d\Phi_{rp} \delta(F[\Phi_{rp}]), \quad d\Phi_{rp} = \prod_z^{rn_p} d\phi_z. \quad (24.488)$$

To compute the generating function of partition functions (24.483), sum (24.487) over all prime periodic states:

$$G(z) = \sum_p \sum_{r=1}^{\infty} \frac{e^{r\beta A_p} z^{rn_p}}{|\text{Det } \mathcal{J}_{rp}|}. \quad (24.489)$$

**2022-10-14 Han** The generating function on a 2-dimensional spatiotemporal lattice is more complicated. Let the generating function of the partition function be:

$$G(z_1, z_2, z_3) = \sum_{L=1}^{\infty} \sum_{T=1}^{\infty} \sum_{S=0}^{L-1} Z_{[L \times T]_S} z_1^L z_2^T z_3^S, \quad (24.490)$$

where  $Z_{[L \times T]_S}$  is the partition function computed on the  $[L \times T]_S$  primitive cell. The contribution from a prime periodic state  $p$  to the partition function on the  $[L_p \times T_p]_{S_p}$  primitive cell is:

$$Z_{[L_p \times T_p]_{S_p}}^p = \frac{e^{\beta A_p}}{|\text{Det } \mathcal{J}_{[L_p \times T_p]_{S_p}}|}. \quad (24.491)$$

Then the contribution from the prime periodic state  $p$  to the generating function is:

$$G_p(z_1, z_2, z_3) = \sum_{r_1=1}^{\infty} \sum_{r_2=1}^{\infty} \sum_{r_3=0}^{r_1-1} \frac{e^{r_1 r_2 \beta A_p} z_1^{r_1 L_p} z_2^{r_2 T_p} z_3^{r_2 S_p + r_3 L_p}}{|\text{Det } \mathcal{J}_{[r_1 L_p \times r_2 T_p]_{r_2 S_p + r_3 L_p}}|}, \quad (24.492)$$

where  $\mathcal{J}_{[r_1 L_p \times r_2 T_p]_{r_2 S_p + r_3 L_p}}$  is the orbit Jacobian matrix computed at the repeat of the periodic state  $p$  on the  $[r_1 L_p \times r_2 T_p]_{r_2 S_p + r_3 L_p}$  primitive cell. The generating function (24.490) can be computed by sum (24.492) over all prime periodic states:

$$G(z_1, z_2, z_3) = \sum_p \sum_{r_1=1}^{\infty} \sum_{r_2=1}^{\infty} \sum_{r_3=0}^{r_1-1} \frac{e^{r_1 r_2 \beta A_p} z_1^{r_1 L_p} z_2^{r_2 T_p} z_3^{r_2 S_p + r_3 L_p}}{|\text{Det } \mathcal{J}_{[r_1 L_p \times r_2 T_p]_{r_2 S_p + r_3 L_p}}|}. \quad (24.493)$$

**2022-11-01 Predrag 2 all felines** Yet another attempt to entice Tigers to take Helmholtz free energy seriously: see links to ChaosBook at the start of the sect. 4.7.

**2022-11-06 Predrag 2 all felines** Now that we are thinking of spatiotemporal field theory as thermodynamics, is our "free energy" (related to) Ruelle's 'pressure', see [ChaosBook Remark 20.2. 'Pressure'](#)? That would be a very nice outcome, get Ruelle to pay attention to our deterministic field theory.

**2022-11-17 Predrag** Continuing on the last tiger's meeting, a brand new start proposal: maybe we should forget translations, and tile the 2D square lattice by reflections only? The corresponding group is the 'triangular group'  $D(2, 4, 4)$ . Can you figure out the Lind zeta function for the triangular group?

A possible starting point - the Brower, Cogburn, Fitzpatrick, Howarth and Tan *Lattice Setup for Quantum Field Theory in  $AdS_2$*  [arXiv:1912.07606](https://arxiv.org/abs/1912.07606):

On two-dimensional manifolds of constant curvature, the triangle group provides an elegant approach to maintaining a maximal discrete subgroup of the  $AdS_2$  isometries. The approach is essentially to choose a fundamental triangle and generate the lattice by reflection on the edges. For example a familiar case in flat space is that starting with an equilateral triangle, one generates the infinite triangulated lattice.

The full **triangle group**  $\Delta(p, r, q)$  is a group that can be realized geometrically as a sequence of reflections along the sides of a triangle with angles  $(\pi/p, \pi/r, \pi/q)$  [20].

$D(3, 3, 3)$  generates the triangular flat space lattice.  $D(2, 4, 4)$  utilizes the right triangle for the standard square lattice.

**2022-11-28 Han** Spatiotemporal  $\phi^4$  field theory has good symbolic dynamics on the two-dimensional lattice. Using the initial guess constructed by the symbol blocks, the corresponding periodic states can be easily computed using Newton's method.

**2022-12-07 Han** Two different choices of basis of the Bravais lattice  $[3 \times 2]_1$  are shown in figure 24.81. The primitive vectors in figure 24.81 (a) are in the Hermite normal form:

$$A = [\mathbf{a}_1, \mathbf{a}_2] = \begin{bmatrix} 3 & 1 \\ 0 & 2 \end{bmatrix}. \quad (24.494)$$

And the primitive vectors in figure 24.81 (b) are:

$$A = [\mathbf{a}_1, \mathbf{a}_2] = \begin{bmatrix} 2 & -1 \\ -2 & 4 \end{bmatrix}. \quad (24.495)$$

While the primitive cells spanned by these two sets of primitive vector are different, the corresponding Bravais lattices are the same.

A periodic state with the periodicity given by a Bravais lattice is prime if it is not a repeat of a periodic state whose periodicity is given by a finer Bravais lattice. If a periodic state is not prime then corresponding primitive cell can be tiled by a smaller primitive cell, and the Bravais lattice is a subset of a finer Bravais lattice. Each Bravais lattice is contained by a finite set of Bravais lattices, if all lattices are subsets of the integer lattice  $\mathbb{Z}^2$ . If we choose to span the primitive cells with the primitive vectors in the Hermite normal form, the tiling of primitive cells is often not

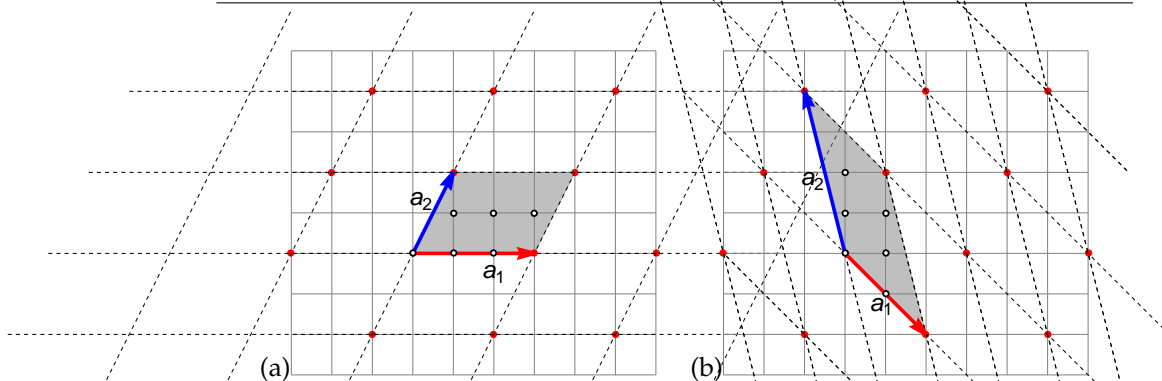


Figure 24.81: The Bravais lattice (red dots) defines the periodicity of the field. Intersections of the solid lines are the integer lattice, on which the discrete field is defined. The choice of primitive vectors is not unique. (a) The primitive cell (green parallelogram) is spanned by the primitive vectors  $\mathbf{a}_1 = (3, 0)$  and  $\mathbf{a}_2 = (1, 2)$ , which are in the Hermite normal form. (b) Alternatively, the same Bravais lattice can be spanned by the primitive vectors  $\mathbf{a}_1 = (2, -2)$  and  $\mathbf{a}_2 = (-1, 4)$ . The primitive cell (green parallelogram) spanned by these primitive vectors is different from (a).

obvious. But by changing the primitive vectors we can make the tiling understandable. Figure 24.82 is an example of tiling the primitive cell of  $[3 \times 2]_1$  using the primitive cell of  $[3 \times 1]_2$ .

2022-12-07 Predrag Nice examples!

I think you want to combine them with prior text explaining primitive cell orbits under *unimodular* matrix  $U \in \mathbb{Z}^{2 \times 2}$  transformations, see mentions of 'unimodular' and/or 'Hermite' around eqs. (8.104), (8.106), (8.115), (8.116), (10.4), (4.93); the text following (8.124); (12.46), (19.16), (4.81), (19.1), (19.5), (24.216), and figure 19.5; Brower and Owen [18] discussion on page 759; and explain and display unimodular matrices that relate these primitive cells.

2022-12-07 Predrag Can one say that *given* the Bravais lattice  $\mathcal{L}$  one can pick as  $\mathbf{a}'_1$  any point on the lattice, and the corresponding *primitive cell*  $\mathbf{a}'_2$  is uniquely fixed by the equal (signed) area condition  $\mathbf{a}'_1 \times \mathbf{a}'_2 = \mathbf{a}_1 \times \mathbf{a}_2$ ? Not sure, as this is one condition, but one needs to determine two components  $\mathbf{a}'_2 = (a'_{2,1}, a'_{2,2})$ . Use Hermite normal form for that? That yields the  $\mathbb{Z} \times \mathbb{Z}$  equivalent primitive cells in each orbit, one of them illustrated by figure 24.81 (b). There is only one Hermite normal form per orbit, with  $a_{1,1} > 0 \in \mathbb{Z}$ ,  $a_{1,2} = 0$ , here figure 24.81 (a).

2023-02-14 Predrag To construct the mother of all partition functions

1. Enumerate all Hermite normal form primitive cells in increasing order by area.

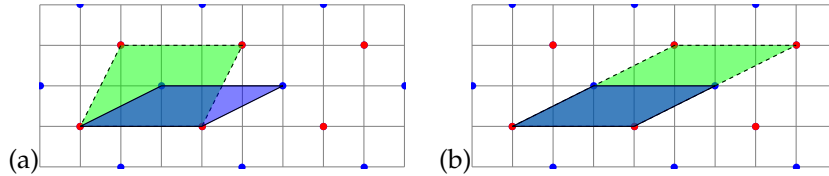


Figure 24.82: A periodic state with the periodicity given by a Bravais lattice is prime if it is not a repeat of a periodic state whose periodicity is given by a finer Bravais lattice. If a periodic state is not prime then the corresponding primitive cell can be tiled by a smaller primitive cell, and the Bravais lattice is a subset of a finer Bravais lattice. Each Bravais lattice is contained by a finite set of Bravais lattices, if all lattices are subsets of the integer lattice  $\mathbb{Z}^2$ . (a) The lattice  $[3 \times 2]_1$  is contained by the lattice  $[3 \times 1]_2$ . But the primitive cell of  $[3 \times 2]_1$  (green parallelogram spanned by primitive vectors  $(3,0)$  and  $(1,2)$ ) is not obviously tiled by the primitive cell of  $[3 \times 1]_2$  (blue parallelogram spanned by primitive vectors  $(3,0)$  and  $(2,1)$ ). (b) If we choose different primitive vectors  $(3,0)$  and  $(4,2)$  for  $[3 \times 2]_1$ , and span the primitive cell using these two vectors, the tiling becomes obvious.

2. Find prime periodic states for each, their first Brillouin zone eigenvalues
3. NOW: For each prime periodic state, use its primitive cell as the *unit* cell, enumerate all of its Hermite normal form primitive cells in increasing order by area: this yields all contributions prime orbit  $p$  to the probability  $w_p$ . Work with the corresponding sublattice  $\mathcal{L}_p$  on the reciprocal state - there might be a 2-dimensional band surface for each eigenvalue.

2023-02-14 Predrag .

4. Pure unfounded speculation: The requisite 2-dimensional lattice integrals, one for each eigenvalue, might be hypergeometric functions, like (24.59), (8.170), or like (8.56), (8.53),  $K(u)$  complete elliptic [38, 43, 76]. We have lots of notes on such in this blog.
5. Pure unfounded speculation: as the prime periodic state *unit* primitive cell increases in volume, the interactions are becoming more local to it, as the number of Laplacian connections to its neighbors is proportional to its boundary.
6. Perhaps a more natural definition of primitive cells would be to draw them face-centered; no need to indicate outer edges as being open-ended. Then the center on the integer lattice unit primitive cell indicates the activity local to the cell, and a prime periodic state over a primitive cell  $\mathbb{A}$  is the activity local to  $P_{\mathbb{A}}$ , with  $\mathbb{A}$  taken to be the unit cell of the corresponding Bravais lattice.

7. As long as we study translations only. Once there are discrete symmetries, having boundaries go through the lattice sites might be demanded by the discrete symmetry.

2023-02-16, 2023-03-05 Predrag .

8. Probably unnecessary, but here is a more 'pedagogical' attempt: consider a prime periodic state over  $P_{\mathbb{A}}$ . Now the tile  $\mathbb{A}$  Bravais lattice is the smallest possible tile. Rescale the Bravais lattice by multiplying it by  $\mathbb{A}^{-1}$  - that sends it into the usual unit integer lattice. Generate all multiple tilings in the usual way, and rescale them back to the prime Bravais lattice  $\mathcal{L}_{\mathbb{A}}$  by multiplying with  $\mathbb{A}$ .  
It makes sense: every prime periodic state over  $P_{\mathbb{A}}$  is the smallest possible tile, so one has to treat it as the irreducible unit cell.  
There might be some subtleties concerning relative-periodic states translations in units of the underlying integer lattice space - they might help us understand the Kuramoto–Sivashinsky case better.
9. A stronger argument why we should rescale the Bravais lattice by multiplying it by  $\mathbb{A}^{-1}$ , send it into the unit integer lattice. A prime periodic state usually has less symmetry than  $D_4 / p4mm$  [30]. Mapped back into the unit square, its point group will be one of the square lattice point groups in the [wallpaper classification](#).
10. This finite tilings approach feels wrong. We should really start with the infinite Bravais lattice, go directly for Bloch theorem and compute the band, without constructing the set of all finite 2-tori first.

2023-02-16 Predrag If we lump slanted families in the same  $z_1^L z_2^T$  term, and sum over all prime orbit  $p$  repeats (all  $\mathbb{A}\mathbb{R} + \dots$  primitive cells), we have the  $p$  contribution to the partition sum written as a double sum

$$\begin{aligned} e^{N_p W[\beta]_p} &= \sum_{r_1=1}^{\infty} \sum_{r_2=1}^{\infty} \sum_{r_3=0}^{r_1-1} \frac{N_p}{|\text{Det}_{\mathbb{A}\mathbb{R}} \mathcal{J}_p|} (e^{\beta N_p a_p})^{r_1 r_2} (z_1^L)^{r_1} (z_2^T)^{r_2} \\ &= N_p \sum_{r_1=1}^{\infty} \sum_{r_2=1}^{\infty} (e^{\beta N_p a_p})^{r_1 r_2} (z_1^L)^{r_1} (z_2^T)^{r_2} \sum_{r_3=0}^{r_1-1} \frac{1}{|\text{Det}_{\mathbb{A}\mathbb{R}} \mathcal{J}_p|} . \end{aligned} \tag{24.496}$$

Then  $W[\beta]_p$  is given by a corresponding double-sum version of the *cumulant-generating function*

$$\ln \langle e^{\beta a} \rangle = \sum_{k=1}^{\infty} \frac{\beta^k}{k!} \langle a^k \rangle_c , \tag{24.497}$$

where the subscript  $c$  indicates a *cumulant*, or, in statistical mechanics and quantum field theory contexts, the 'connected Green's function'. See

[ChaosBook Appendix: Averaging](#) and  
[ChaosBook Remark A20.1. Cumulants](#)

**2023-03-15 Predrag** Current text in CL18:

Consider a primitive cell  $\mathbb{A}$  rectangular *tile* defined by Hermite normal form matrix  $\mathbb{A}$ . The primitive cell  $P_{\mathbb{A}\mathbb{R}}$  obtained by repeating this tile  $r_1$  times horizontally and  $r_2$  times along the 'slanted' primitive vector  $\mathbf{a}_2 = (S, T)$ ,

$$\mathbb{A}\mathbb{R} = \begin{bmatrix} r_1 L & sL + r_2 S \\ 0 & r_2 T \end{bmatrix}, \quad \mathbb{A} = \begin{bmatrix} L & S \\ 0 & T \end{bmatrix}, \quad \mathbb{R} = \begin{bmatrix} r_1 & s \\ 0 & r_2 \end{bmatrix}, \quad (24.498)$$

$0 \leq s < r_1$ , results in a larger rectangular tile / primitive cell that defines a sublattice  $\mathcal{L}_{\mathbb{A}\mathbb{R}}$ . By the Hermite normal form condition (??), the upper right 'slant' component  $s_1 L + r_2 S$  is taken  $\text{mod } r_1 L$ , and the repeat numbers are positive integers,  $r_j \geq 1$ .

A  $[3 \times 1]_2$  example is given in figure 24.82. Consider its  $r_1 = 2$  repeat:

$$\mathbb{A}\mathbb{R} = \begin{bmatrix} 6 & 2 \\ 0 & 1 \end{bmatrix}, \quad \mathbb{A} = \begin{bmatrix} 3 & 2 \\ 0 & 1 \end{bmatrix}, \quad \mathbb{R} = \begin{bmatrix} 2 & 0 \\ 0 & 1 \end{bmatrix}. \quad (24.499)$$

(Could draw this as well.)

Consider now its  $r_1 = 2$  repeat, but with slant  $s = 1$ :

$$\mathbb{A}\mathbb{R} = \begin{bmatrix} 6 & 5 \\ 0 & 1 \end{bmatrix}, \quad \mathbb{A} = \begin{bmatrix} 3 & 2 \\ 0 & 1 \end{bmatrix}, \quad \mathbb{R} = \begin{bmatrix} 2 & 1 \\ 0 & 1 \end{bmatrix}. \quad (24.500)$$

$[6 \times 1]_2$  and  $[6 \times 1]_5$  are indeed distinct primitive cells on the  $[3 \times 1]_2$  sublattice. But look at them: the once-repeated *prime* periodic state  $p_{\mathbb{A}\mathbb{R}}$  over either is the *same* prime periodic state repeat of  $p$ , and should be counted *only once*. Ergo, always use only the  $s = 0$  primitive cell, there is no  $s$  sum in (9.20), and all is well.

**2020-10-20 Predrag** What are these  $\theta = 2\pi S/T$  phases? Remember that  $[L \times 1]_0$  can be thought of 1-dimensional lattice, but with  $s$  appropriately redefined, as in (24.504). When one considers  $[L \times 1]_S$ , the tilt  $S$  can be distributed uniformly over the lattice by picking  $\theta = 2\pi S/L$ .

**2023-04-18 Predrag** Copying from the current version of CL18:

**Time-equilibria over  $[L \times 1]_0$ .**

Consider the time-equilibrium  $\phi_{nt} = \phi_{n1}$  for all spatial sites  $n$ , and all times  $t$ . To see that this is the 1-dimensional lattice temporal cat tiles of period  $L$  already counted in ref. [47], note that the 5-term recurrence relation for the 2-dimensional spatiotemporal cat [26, 36]

$$\phi_{n,t+1} + \phi_{n,t-1} - 2s \phi_{nt} + \phi_{n+1,t} + \phi_{n-1,t} = -m_{nt}, \quad m_{nt} \in \mathcal{A}, \quad (24.501)$$

with alphabet

$$\mathcal{A} = \{-3, -2, -1, 0, \dots, \mu^2 + 1, \mu^2 + 2, \mu^2 + 3\}, \quad (24.502)$$

$[L \times T]_S$	$[1 \times 1]_0$	$[2 \times 2]_0$	$[2 \times 5]_0$	$[5 \times 5]_0$	$[5 \times 10]_0$	$[10 \times 10]_0$	$[\infty \times \infty]_0$
$\langle \lambda_c \rangle$	0	1.354025	1.441989	1.506464	1.507260	1.507979	1.507983

Table 24.8: Stability exponents  $\langle \lambda_c \rangle$  of finite periodic states of  $s = 5/2$  spatiotemporal cat, compare to the stability exponent of infinite periodic states  $\langle \lambda \rangle$ . As the size of the primitive cells increase, the stability exponents of finite periodic states approach  $\langle \lambda \rangle$  rapidly.

reduces to the 3-term recurrence

$$\phi_{n+1,1} - 2(s_2 - 1)\phi_{n1} + \phi_{n-1,1} = -m_{n1}, \quad (24.503)$$

where we have temporarily added index '2' to the stretching parameter  $s_2$  to indicate that it refers to the 2-dimensional spatiotemporal cat. Comparing with the temporal cat (??),  $\phi_{t+1} - s_1\phi_t + \phi_{t-1} = -m_t$ , we see that we have already counted all periodic states on primitive cells of form  $[L \times 1]_0$ , provided we replace in (21.125)

$$s_1 \rightarrow 2(s_2 - 1), \quad \mu_1^2 \rightarrow \mu_2^2 \quad (24.504)$$

(in agreement with (4.245), seems to show again that  $\mu^2$  is the parameter to use, not the "stretching"  $s_z$ , always) then

$$\begin{aligned} \sum_{n=0}^{\infty} N_n z^n &= \frac{2 - sz}{1 - sz + z^2} - \frac{2}{1 - z} \\ &= (s - 2) [z + (s + 2)z^2 + (s + 1)^2 z^3 \\ &\quad + (s + 2)s^2 z^4 + (s^2 + s - 1)^2 z^5 + \dots] \end{aligned} \quad (24.505)$$

For the values chosen in our numerical examples,  $s_1 = 3$  and  $s_2 = 5/2$ ,  $\mu_2^2 = 1$  the two counts happen to be the same and given by (24.505).

Might want to revisit (24.218), (10.1).

**2023-05-18 Predrag 2 Han** Check out Besag [13] and other square lattice references, after (19.32). I have not found the particular elliptic function that is your spatiotemporal cat 2D band integral, so what you have done so far in (24.97) is still the best we have.

**2023-06-22 Predrag** Table 24.8 looks better if replaced by the figure 24.83 plot of  $\ln(\langle \lambda \rangle - \langle \lambda \rangle_{\mathbb{A}})$  as a function of  $V_{\mathbb{A}}$ . If all errors are of order  $\propto \exp(-V_{\mathbb{A}} \langle \lambda \rangle)$ , you expect families with slopes  $-\langle \lambda \rangle$ . Two families are of interest: the most space-time symmetric square primitive cells  $[L \times L]_0$ , and the most asymmetric spatially periodic, time-constant  $[n \times 1]_0$ , in particular  $[n^2 \times 1]_0$ .

Not clear to me that the errors fall off like  $\propto \exp(-V_{\mathbb{A}} \langle \lambda \rangle)$  in the shadowing plot figure 21.19 (b): could be that the Green's function estimates



lead to  $\propto \exp(-d(c - e)_{\mathbb{A}} \langle \lambda \rangle)$  where  $d(c - e)_{\mathbb{A}}$  is the linear distance from the center of primitive cell  $\mathbb{A}$  to its edge. Or the square root of it, if the dominant effect are Brownian walks (one of the ways of understanding Laplacians).

The stability exponents of finite periodic states  $\langle \lambda_c \rangle$  approach the stability exponents of their infinite repeats  $\langle \lambda \rangle$  rapidly as the size of the spatiotemporal primitive cells increase. Table 24.8 shows the stability exponents  $\langle \lambda_c \rangle$  of finite primitive cell periodic states of  $\mu^2 = 1$  spatiotemporal cat, compared to the stability exponent of infinite Bravais lattice periodic states  $\langle \lambda \rangle'$

$$\langle \lambda \rangle = 1.507983 \dots \approx 1.005322 \frac{3\mu}{2}. \quad (24.506)$$

I did not expect  $\langle \lambda \rangle_{[1 \times 1]_0} = 0$  in table 24.8. Nobody expects Spanish Inquisition.

**2023-09-20 Predrag** Where is (24.395), (24.506), evaluated for  $\mu = 1$ ? Could it be that  $\langle \lambda \rangle = 3\mu/2$ , exactly? If it is anything similar to the massless case (19.36), that's very unlikely.

**2023-08-31 Han** Stability exponents  $\langle \lambda \rangle_{\mathbb{A}}$  computed using the finite-dimensional orbit Jacobian matrix converge to the one computed on the infinite spatiotemporal lattice  $\langle \lambda \rangle$  as the size of the primitive cells increase. To find the rate of the convergence, stability exponents of  $\mu^2 = 1$  spatiotemporal cat are computed using both the finite and infinite-dimensional orbit Jacobian matrices. The logarithm of their differences are plotted in figure 24.83.

Stability exponents  $\langle \lambda \rangle_{\mathbb{A}}$  of the orbit Jacobian matrices on square primitive cells  $\mathbb{A} = [n \times n]_0$  are computed for  $n$  from 1 to 25. As the size of the primitive cell increases, the stability exponent of the finite primitive cell  $\langle \lambda \rangle_{\mathbb{A}}$  converges to the infinite spacetime stability exponent  $\langle \lambda \rangle$ . The logarithm of the differences  $|\langle \lambda \rangle_{\mathbb{A}} - \langle \lambda \rangle|$  is plotted in figure 24.83 (a) as a function of the volume of the primitive cells  $V_{\mathbb{A}} = n^2$ . From the figure 24.83 (b) we can see that  $\langle \lambda \rangle_{\mathbb{A}}$  is not converging to  $\langle \lambda \rangle$  exponentially as a function of  $V_{\mathbb{A}}$ .

However,  $\langle \lambda \rangle_{\mathbb{A}}$  is converging to  $\langle \lambda \rangle$  as a function of the side length  $n$ , as shown in figure 24.83 (c) and (d). The logarithm of the difference between  $\langle \lambda \rangle_{\mathbb{A}}$  and  $\langle \lambda \rangle$  decreases linearly as the side length  $n$  increases. The straight line in figure 24.83 (b) is the linear fit of the logarithm of the distance as function of  $n$ :

$$y = -1.05538x - 2.04611.$$

The slope of the linear fit is close to the stretching parameter  $\mu$ .

For primitive cells with different shapes, the stability exponents of primitive cell  $\mathbb{A} = [rL \times rT]_0$  converge to  $\langle \lambda \rangle$  exponentially as a function of the scale factor  $r$ , with a same converging rate of -1.0553.

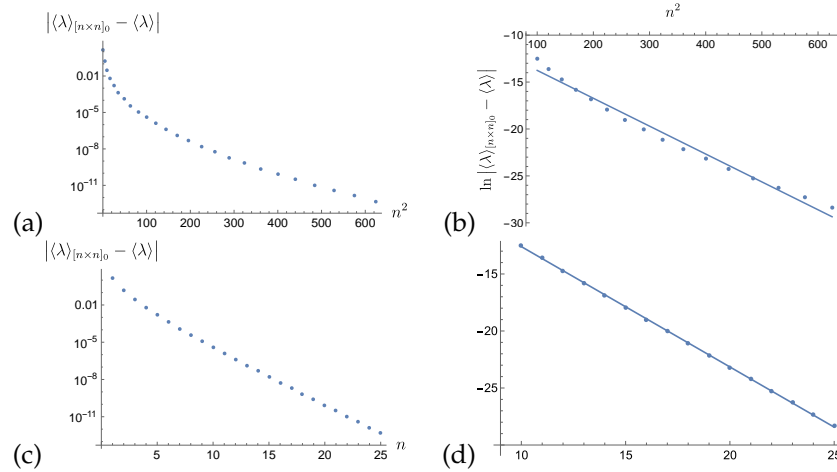


Figure 24.83: (a) Log plot of the distance between the stability exponents of the finite primitive cells and the infinite spacetime, as a function of the volume of the primitive cells  $V_{\mathbb{A}}$ . (b) The straight line is a linear fit of the logarithm of the distance between  $\langle \lambda \rangle_{\mathbb{A}}$  and  $\langle \lambda \rangle$  as a function of  $n^2$ . (c) Log plot of the distance between the stability exponents of the finite primitive cells and the infinite spacetime, as a function of the side length of the primitive cells  $n$ . (d) The straight line is a linear fit of the logarithm of the distance between  $\langle \lambda \rangle_{\mathbb{A}}$  and  $\langle \lambda \rangle$  as a function of  $n$ .

**2023-09-16 Predrag 2 Han** A few facts (rather recent!) that you will find interesting:

The free boson partition function for  $\mu^2$  evaluation is a conformal field theory calculation, known analytically (19.37) and is the Dedekind eta function. For the massless,  $\mu^2 = 0$ , theory, the free energy per site (19.36) -I believe that is our stability exponent- is also known analytically.

The massive boson partition function for rectangular primitive cells is known, in terms of Jacobi elliptic functions (19.43), but I have not been able identify it in any simple form.

**2023-09-22 Predrag** I spent the morning reading the Maloney-Witten paper on (what I believe are conformal) partition functions, sect. 19.5. What I find appealing is that Witten arrives the form of his partition function (19.77) by symmetry reasoning, invariance under modular transformations (19.74) (what we call unimodular transformations). So not at all by counting different Bravais lattice (what they call the "sum over geometries").

Our Hill determinant factorization is for them "holomorphic factorization" (19.91), arises because the theory is a product of two decoupled theories, associated respectively with "left- and right-moving modes", which is how I think of our 'metal means', linear in lattice momentum Euler-Lagrange equations. Witten has an interesting speculation about how "holomorphic factorization" is restored "sum over geometries" that they were unable to implement. But it works for us in the Isola zeta function factorization (6.55) and (6.192).

Witten's black hole entropy (19.94) has a Bessel function  $J_1$ . It might be related to our Green's function figure 24.83 modified Bessel function  $K_0$ , in the stability exponent shadowing calculations. I think our calculation is also entropy calculation (via fundamental fact: log of counting = log of stability; that is called Pesin's formula, connecting Kolmogorov entropy and the Lyapunov exponent, see [ChaosBook eq. \(A33.16\)](#)).

**2016-05-04, 2023-09-22 Predrag** Hu and Lin [41] ([click here](#)), *On spatial entropy of multi-dimensional symbolic dynamical systems*, (see the [blogCats](#) post preceding (10.1)) Of immediate relevance to you: They discuss multi-dimensional shift space for a rectangular spatial entropy which is the limit of growth rate of admissible local patterns on finite rectangular sublattices. In their eq. (3) they define 'the rectangular entropy' which is a topological, mosaics-counting entropy, and for the spatiotemporal cat (which I do not see in their paper, and their literature) this might be your figure 24.83 stability exponent. If so, we might have to cite them, and whoever is cited by them for doing it before them. Potentially (uuurgh!)

Chow, Mallet-Paret and Van Vleck [19], *Pattern formation and spatial chaos in spatially discrete evolution equations* (1996). See

2023-05-20 Predrag post. Remeber to include into tigers paper III [73].

P. Ballister, B. Bollobas and A. Quas [7], *Entropy Along Convex Shapes, Random Tilings and Shifts of Finite Type* (2002).

M. Boyle, R. Pavlov and M. Schraudner [17], *Multidimensional sofic shifts without separation and their factors* (2010), 4617–4653.

M. Hochman and T. Meyerovitch [39], *A characterization of the entropies of multidimensional shifts of finite type* (2010).

Other the papers on “mosaics” do not seem relevant to our project:

Abell, Humphries and Van Vleck, *Mosaic solutions and entropy for spatially discrete Cahn–Hilliard equations* IMA Journal of Applied Mathematics, 65, 219-255(2000).

There is just too much literature out there...

2023-09-28 Han I computed the convergence rate of the stability exponent of the temporal cat. The temporal cat stability exponent for the infinite Bravais lattice is:

$$\langle \lambda \rangle = \ln \Lambda = \lim_{n \rightarrow \infty} \frac{1}{n} \ln (\Lambda^n + \Lambda^{-n} - 2), \quad \Lambda = \frac{1}{2} \left( \mu^2 + 2 + \mu \sqrt{\mu^2 + 4} \right). \quad (24.507)$$

The stability exponent of a period- $n$  periodic state in its primitive cell is

$$\begin{aligned} \langle \lambda \rangle_n &= \frac{1}{n} \ln (\Lambda^n + \Lambda^{-n} - 2) \\ &= \frac{1}{n} \left[ \ln \Lambda^n + \frac{\Lambda^{-n} - 2}{\Lambda^n} - \frac{(\Lambda^{-n} - 2)^2}{\Lambda^{2n}} + \dots \right]. \end{aligned} \quad (24.508)$$

The difference between  $\langle \lambda \rangle_n$  and  $\langle \lambda \rangle$  decreases exponentially as the size of the primitive cell  $n$  increases:

$$\begin{aligned} |\langle \lambda \rangle - \langle \lambda \rangle_n| &= \frac{1}{n} \left[ \frac{2 - \Lambda^{-n}}{\Lambda^n} - \frac{(2 - \Lambda^{-n})^2}{\Lambda^{2n}} + \dots \right] \\ &\approx \frac{2}{n\Lambda^n}. \end{aligned} \quad (24.509)$$

The stability exponents of  $\mu^2 = 1$  temporal cat are computed numerically and the difference between  $\langle \lambda \rangle_n$  and  $\langle \lambda \rangle$  are plotted in figure 24.84. The stability multiplier  $\Lambda$  and stability exponent  $\langle \lambda \rangle$  for the infinite Bravais lattice are (accurate up to 12 digits):

$$\Lambda = 2.61803398875, \quad \langle \lambda \rangle = \ln \Lambda = 0.962423650119.$$

Figure 24.84 is the logarithm of the difference between the stability exponents of the infinite lattice  $\langle \lambda \rangle$  and the finite size- $n$  primitive cell  $\langle \lambda \rangle_n$ . The

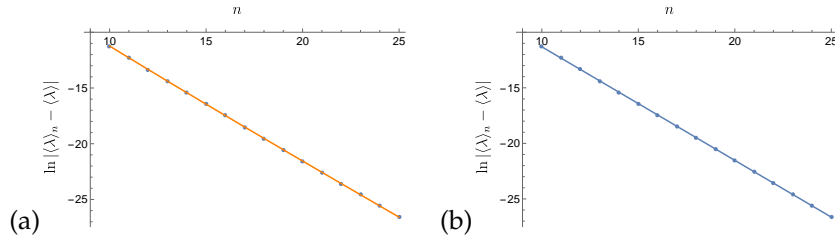


Figure 24.84: (a) Logarithm of the distance between the stability exponents of the finite primitive cells and the infinite lattice, as a function of the volume of the primitive cells  $n$ . The dots are the logarithm of the distance computed numerically. The line is analytical result computed from (24.509). (b) The straight line is a linear fit of the logarithm of the distance between  $\langle \lambda \rangle_n$  and  $\langle \lambda \rangle$  as a function of  $n$  (24.510).

logarithm of the difference decreases linearly as the size of the primitive cell  $n$  increases. A linear fit of the relation is plotted in figure 24.84 (b):

$$\ln |\langle \lambda \rangle - \langle \lambda \rangle_n| = -1.08639130893 - 1.02217046593n. \quad (24.510)$$

The analytical result (24.509) suggests linear decreasing at large  $n$ :

$$\ln |\langle \lambda \rangle - \langle \lambda \rangle_n| = \ln 2 - \ln n - (\ln \Lambda)n + \dots, \quad (24.511)$$

where the slope equals to the negative stability exponent  $-\langle \lambda \rangle = -0.9624$ . The slope from the linear fit is not close enough to the stability exponent because the size of primitive cells are not large enough. But compare figure 24.84 (a) and (b) we can see that they both fit the numerical result very well.

**2016-05-04, 2023-09-22 Predrag** Hu and Lin [41] (click here), *On spatial entropy of multi-dimensional symbolic dynamical systems*, (see the blogCats post preceding (10.1))

They write: “A finite subset is called a *tessellation* of  $\mathbb{Z}^2$  if there exists a sequence [...] such that [...] is a partition of  $\mathbb{Z}^2$ .” Tessellations subsume our primitive cells. In their Fig. 2.2 they draw two Hermite normal form primitive cells that we use, but also consider L-shaped tessellations that we *do not* use. Looks like we should, but have overlooked them - they are translations of each other, they can support perfectly fine periodic state extrema of our partition functions, and thus contribute. I do not see how they would be a subset of Bravais lattices that we do include in our sums over geometries, so I see no reason to exclude them into our partition functions:(

Maybe you can quickly compute the spectrum of spatiotemporal cat orbit Jacobian matrix  $\mathcal{J}_\mathbb{A}$  for the smallest, 3-sites L-shape, check that is not one of the  $V_\mathbb{A} = 3$  that we already have?

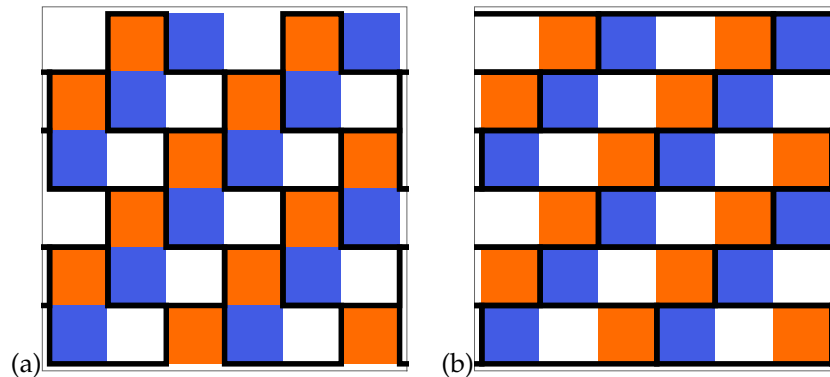


Figure 24.85: A field configuration over Bravais lattice  $[3 \times 1]_1$ . (a) The 2-dimensional  $\mathbb{Z}^2$  spacetime lattice can be tiled by L-shape, volume  $V_{\mathbb{A}}$  primitive cells  $\mathbb{A}$ . (b) But one can also use the  $[3 \times 1]$  rectangular primitive cells to tile the Bravais lattice  $[3 \times 1]_1$ .

**2023-09-28 Han** I don't think we need to consider the L-shaped tessellations. If the periodicity of a field is given by a Bravais lattice, there always exist rectangular primitive cells with at least one edge along a primitive vector. The simplest example of the L-shape tessellation has a primitive cell with volume 3. The only way to tile the spacetime with this L-shape (using only the translations) is plotted in figure 24.85 (a). But observing the field, one immediately realizes that this is a field configuration with periodicity  $[3 \times 1]_1$ . So L-shaped primitive cell tiles the same Bravais lattice as the Hermite normal form, volume 3 rectangular primitive cell, plotted in figure 24.85 (b).

**2023-10-18 Predrag** Sect. 17.2 *Information*: A proposal (17.11) for a site-wise evaluation of the Kullback-Leibler divergence.

**2023-10-25 Predrag** We could maybe use your thesis + the papers + drafts of papers to put together a short-book length *Elements in Dynamical Systems* monograph. If we do a good job, my colleagues would happy to publish it.

**2023-10-25 Predrag** I like the grayed-out convention of figure 16.1 for the open-boundary edges of a primitive cell. Makes it very clear why those lattice sites do not belong to it. Maybe we should adopt it?

**2024-01-08 Han** Sterling *et al.* [68–70] assign the global symbolic representation to periodic states by continuation from the anti-integrable limit. At the anti-integrable limit the dynamical systems (single and coupled Hénon map) are no longer deterministic maps, and periodic states are arbitrary arrays of points from a set of anti-integrable states  $\{-1, 1\}$ . The anti-integrable states are used as the symbols of the mosaics. The Euler–Lagrange

equation of their Hénon map is

$$-x_{t+1} - bx_{t-1} - k + x_t^2 = 0 \quad (24.512)$$

and the Euler–Lagrange equation of the (2-dimensional) coupled Hénon map is:

$$-x(m)_{t+1} - bx(m)_{t-1} - k + x^2(m)_t + c(WX_t)(m) = 0 \quad 1 \leq m \leq N, \quad (24.513)$$

where the  $W$  is a linear spatial coupling function and  $N$  is the number of the spatial lattice sites.

At the anti-integrable limit where  $k \rightarrow \infty$ , they use the scaled variable  $z = \epsilon x$ , where  $\epsilon = 1/\sqrt{k}$ . The Euler–Lagrange equation of the Hénon map is converted to:

$$\epsilon(z_{t+1} - bz_{t-1}) + 1 - z_t^2 = 0. \quad (24.514)$$

At  $\epsilon = 0$ , the orbits of this map are sequences  $\{z_t\} \in \{\pm 1\}^{\mathbb{Z}}$ . Denote the set of bi-infinite sequences with two symbols by:

$$\mathbb{S} = \{s : s_t \in \{1, -1\}, t \in \mathbb{Z}\}. \quad (24.515)$$

The Euler–Lagrange equation (24.514) can be rewritten as

$$z_t = \pm \sqrt{1 + \epsilon(z_{t+1} + bz_{t-1})}, \quad (24.516)$$

so that  $z(\epsilon)$  is a fixed point of the operator  $T : l_\infty \rightarrow l_\infty$  whose  $t$ -th component is

$$T_t(v) \equiv s_t \sqrt{1 + \epsilon(v_{t+1} + bv_{t-1})} \quad (24.517)$$

and the sign of the square root is determined by the sequence  $s \in \mathbb{S}$ . Note that the map  $T$  is Vattay's inverse iteration.

They proved the theorem that for every  $s \in \mathbb{S}$ , there exist a corresponding unique orbit,  $z(\epsilon)$ , of the Hénon map (24.514) such that  $z(0) = s$ , providing

$$\gamma < \gamma_\infty \equiv 2\sqrt{1 - 2/\sqrt{5}} \approx 0.649839, \quad (24.518)$$

where  $\gamma = |\epsilon|(1 + |b|)$ . They showed that the orbit  $z(\epsilon)$  is contained in the closed ball of radius  $M_\infty$  around the point  $s$ :

$$B_{M_\infty}(s) = \{z : \|z - s\|_\infty \leq M_\infty\}, \quad (24.519)$$

where

$$M_\infty = 1 - \sqrt{1 - \gamma_\infty \frac{\gamma_\infty + \sqrt{\gamma_\infty^2 + 4}}{2}} \approx 0.675078. \quad (24.520)$$

The conclusion of this theorem follows from finding the maximum value of  $\epsilon$  for which there is an  $n$  such that  $T^n$  is a contraction mapping (i.e.,

$T^n : B_M \rightarrow B_M$  and  $\|DT^n\| < 1$ ). The fact that  $T$  is a contraction implies that there are no bifurcations in the range of (24.518).

For the coupled Hénon map, the Euler–Lagrange equation can be scaled as:

$$\epsilon[z(m)_{t+1} + bz(m)_{t-1}] - \epsilon^2 k + z^2(m)_t + \epsilon c(WZ_t)(m) = 0 \quad (24.521)$$

where  $z = \epsilon x$ . The anti-integrable limit is reached when  $k \rightarrow \infty$ ,  $\epsilon^2 k \rightarrow 1$  and  $\epsilon c \rightarrow 0$ . With an  $N$  site lattice a mosaic is given by  $s \in \mathbb{S}^N$ :

$$\mathbb{S}^N = \{s : s(j)_t \in \{1, -1\}, 1 \leq j \leq N \text{ and } t \in \mathbb{Z}\}. \quad (24.522)$$

As in the uncoupled case they rewrite the Euler–Lagrange equation in terms of the component at time  $t$ :

$$z(m)_t = \pm \sqrt{1 + \epsilon(z(m)_{t+1} + bz(m)_{t-1} + cW[Z_t](m))}. \quad (24.523)$$

The orbit  $z(\epsilon)$  is a fixed point of the operator  $T : (l_\infty)^N \rightarrow (l_\infty)^N$  whose  $t$ -th component at index  $m$  is:

$$T(m)_t(z) \equiv s(m)_t \sqrt{1 + \epsilon(z(m)_{t+1} + bz(m)_{t-1} + cW[Z_t](m))}, \quad (24.524)$$

where the sign of the square root is determined by the symbol mosaic  $s \in \mathbb{S}^N$ . When  $\epsilon = 0$ , the operator becomes  $T(z) = s$ . Again using the contraction mapping theorem, they showed that for small enough  $\epsilon$  the fixed point persists. They proved that for every symbol tensor  $s \in \mathbb{S}^N$  there exists a corresponding unique periodic state,  $z(\epsilon)$ , of the coupled Hénon map lattice such that  $z(0) = s$  providing

$$\gamma \equiv \epsilon(1 + |b| + |c|\|W\|_\infty) < \gamma_\infty \equiv 2\sqrt{1 - 2/\sqrt{5}} \approx 0.649839. \quad (24.525)$$

The orbit  $z(\epsilon)$  is contained in the ball  $B_{M_\infty}(s)$  where

$$M_\infty = 1 - \sqrt{1 - \gamma_\infty \frac{\gamma_\infty + \sqrt{\gamma_\infty^2 + 4}}{2}} \approx 0.675078. \quad (24.526)$$

$\|W\|_\infty$  in (24.525) is the norm of the coupling function. For one dimensional diffusive coupling, where the coupling function  $W$  is the 1-dimensional Laplacian in the spatial direction, this theorem gives

$$\epsilon < \frac{2}{1 + |b| + 4|c|} \sqrt{1 - 2/\sqrt{5}}. \quad (24.527)$$

Note that this bound does not depend on the spatial period of systems, as the norm of the coupling  $\|W\|_\infty$  is the leading eigenvalue of  $W$ , which is (4d) for the  $d$ -dimensional Laplacian.



**2023-01-10 Han** The bound of  $\epsilon$  provided by (24.518) is not a tight bound. For the Hamiltonian Hénon map (3.61) the range of  $a$  that guarantees a hyperbolic horseshoe given by (24.518) is

$$a > \frac{1}{1 - 2/\sqrt{5}} \approx 9.47214. \quad (24.528)$$

This is in agreement with the range of  $a$  given by Devaney and Nitecki [29], in which the non-wandering set has a hyperbolic structure and is conjugate to the 2-shift. But this is different from the tight bound (4.246)

$$a > 5.699310786700 \dots \quad (24.529)$$

Sterling *et al.* [70] numerically computed the bound of  $\epsilon$  from the continuation of all symbol sequences for orbits of periods up to 24. For the Hamiltonian Hénon the first bifurcation occurs for

$$\epsilon \approx 0.41888,$$

corresponding to  $a \approx 5.69929$ , which is still different from (4.246). Then they showed that in the area preserving Hénon map, the first homoclinic bifurcation of the invariant manifolds of the fixed point  $(+)^{\infty}$  is

$$\text{sn} \{ +^{\infty} - (+) - +^{\infty}, +^{\infty} - (-) - +^{\infty} \} \quad (24.530)$$

and "there is a saddle-node bifurcation of the type 1 homoclinic orbits,

$$\text{sn} \{ +^{\infty} - (+) - +^{\infty}, +^{\infty} - (-) - +^{\infty} \} \quad (24.531)$$

at

$$\epsilon_{sn}(1) \approx 0.418879233367 \quad \text{or} \quad k_{sn}(1) \approx 5.699310786700. \quad (24.532)$$

This also corresponds to the parameter value at which the topological horseshoe for the Hénon map is destroyed." The  $k_{sn}(1)$  is critical value of the stretching parameter  $a$  (4.246).

**2024-11-22 Predrag** Joined Han's reading of Bountis and Helleman [16] to previous and subsequent notes on the paper, sect. 11.1.3.

**2024-12-11 Han** Reread Mackay and Meiss (1983) [53]. In this paper they compute the multipliers of a discrete-time one-degree-of-freedom system using second variations of the action in the space of periodic paths (orbit Jacobian matrices).

To compute the multipliers, they consider variations along a periodic orbit over infinite time (referred to as a tangent orbit in their paper). For a periodic orbit of period  $q$ , they define the multipliers  $\lambda$  by the existence of a tangent orbit satisfying:

$$\delta x_{i+q} = \lambda \delta x_i. \quad (24.533)$$

Combining this with the second derivative of action, the equations they need to solve are:

$$M(\lambda)\delta x = 0 \quad (24.534)$$

where  $M(\lambda)$  is a  $[q \times q]$  matrix which is same as the orbit Jacobian matrix, but has  $M_{1,q} = \lambda^{-1}L_{21}[0, 1]$  and  $M_{q,1} = \lambda L_{12}[q, q + 1]$  at the top right and bottom left corners. Note that they essentially applied Floquet theorem, even though they did not explicitly mention it in their paper. The multiplier  $\lambda$  is  $e^{iqk}$  in our formula.

They define  $D(\lambda) = \det M(\lambda)$ . There is a non-trivial solution for  $\delta x$  iff  $D(\lambda) = 0$ . By collecting terms appropriately in the expansion of the determinant, they find:

$$D(\lambda) = D(1) + 4R \prod_{i=0}^{q-1} (-L_{12}[i, i + 1]) \quad (24.535)$$

where  $R$  is the residue  $R = (2 - \lambda - \lambda^{-1})/4$ . Setting  $D(\lambda) = 0$  they get the Hill's formula (12.17).

In this derivation, it seems that the Floquet multiplier  $\lambda$  is the Floquet-Bloch theorem phase factor  $e^{iqk}$  at which the Hill determinant reaches 0. Hill determinant  $\text{Det } \mathcal{J}(k)$  goes to 0 when

$$k = \frac{-i}{q} \ln \lambda. \quad (24.536)$$

For a hyperbolic orbit this critical value of  $k$  is not a real number.

No one ever promised us [A Rose Garden](#) :)

## References

- [1] R. L. Adler and B. Weiss, "Entropy, a complete metric invariant for automorphisms of the torus", *Proc. Natl. Acad. Sci. USA* **57**, 1573–1576 (1967).
- [2] R. L. Adler and B. Weiss, *Similarity of Automorphisms of the Torus* (Amer. Math. Soc., Providence RI, 1970).
- [3] V. I. Arnol'd and A. Avez, *Ergodic Problems of Classical Mechanics* (Addison-Wesley, Redwood City, 1989).
- [4] M. Baake, J. Hermisson, and A. B. Pleasants, "The torus parametrization of quasiperiodic LI-classes", *J. Phys. A* **30**, 3029–3056 (1997).
- [5] M. Baake, N. Neumärker, and J. A. G. Roberts, "Orbit structure and (reversing) symmetries of toral endomorphisms on rational lattices", *Discrete Continuous Dyn. Syst.* **33**, 527–553 (2013).

- [6] M. Baake, J. A. G. Roberts, and A. Weiss, “Periodic orbits of linear endomorphisms on the 2-torus and its lattices”, *Nonlinearity* **21**, 2427 (2008).
- [7] P. Balister, B. Bollobás, and A. Quas, “Entropy along convex shapes, random tilings and shifts of finite type”, *Illinois J. Math.* **46**, 781–795 (2002).
- [8] J.-C. Ban, W.-G. Hu, S.-S. Lin, and Y.-H. Lin, *Zeta Functions for Two-dimensional Shifts of Finite Type*, Vol. 221, *Memoirs Amer. Math. Soc.* (Amer. Math. Soc., Providence RI, 2013).
- [9] A. Barvinok, *A Course in Convexity* (Amer. Math. Soc., New York, 2002).
- [10] A. Barvinok, *Lattice Points, Polyhedra, and Complexity*, tech. rep. (Univ. of Michigan, Ann Arbor MI, 2004).
- [11] A. Barvinok, *Integer Points in Polyhedra* (European Math. Soc. Pub., Berlin, 2008).
- [12] M. Beck and S. Robins, *Computing the Continuous Discretely* (Springer, New York, 2007).
- [13] J. Besag, “On a system of two-dimensional recurrence equations”, *J. R. Stat. Soc. B* **43**, 302–309 (1981).
- [14] N. Bird and F. Vivaldi, “Periodic orbits of the sawtooth maps”, *Physica D* **30**, 164–176 (1988).
- [15] S. V. Bolotin and D. V. Treschev, “Hill’s formula”, *Russ. Math. Surv.* **65**, 191 (2010).
- [16] T. Bountis and R. H. G. Helleman, “On the stability of periodic orbits of two-dimensional mappings”, *J. Math. Phys* **22**, 1867–1877 (1981).
- [17] M. Boyle, R. Pavlov, and M. Schraudner, “Multidimensional sofic shifts without separation and their factors”, *Trans. Amer. Math. Soc.* **362**, 4617–4653 (2010).
- [18] R. C. Brower and E. K. Owen, “Ising model on the affine plane”, *Phys. Rev. D* **108**, 014511 (2023).
- [19] S.-N. Chow, J. Mallet-Paret, and E. S. Van Vleck, “Pattern formation and spatial chaos in spatially discrete evolution equations”, *Random Comput. Dynam.* **4**, 109–178 (1996).
- [20] H. S. M. Coxeter and W. O. J. Moser, *Generators and Relations for Discrete Groups* (Springer, Berlin, 1957).
- [21] S. C. Creagh, “Quantum zeta function for perturbed cat maps”, *Chaos* **5**, 477–493 (1995).
- [22] P. Cvitanović, *Group Theory: Birdtracks, Lie’s and Exceptional Groups* (Princeton Univ. Press, Princeton NJ, 2008).
- [23] P. Cvitanović, “Charting the state space”, in *Chaos: Classical and Quantum*, edited by P. Cvitanović, R. Artuso, R. Mainieri, G. Tanner, and G. Vattay (Niels Bohr Inst., Copenhagen, 2023).

- [24] P. Cvitanović, “Walkabout: Transition graphs”, in *Chaos: Classical and Quantum*, edited by P. Cvitanović, R. Artuso, R. Mainieri, G. Tanner, and G. Vattay (Niels Bohr Inst., Copenhagen, 2023).
- [25] P. Cvitanović, R. Artuso, R. Mainieri, G. Tanner, and G. Vattay, *Chaos: Classical and Quantum* (Niels Bohr Inst., Copenhagen, 2024).
- [26] P. Cvitanović and H. Liang, *A chaotic lattice field theory in two dimensions*, In preparation, 2024.
- [27] J. A. De Loera, R. Hemmecke, J. Tauzer, and R. Yoshida, “Effective lattice point counting in rational convex polytopes”, *J. Symbolic Comp.* **38**, 1273–1302 (2004).
- [28] R. L. Devaney, *An Introduction to Chaotic Dynamical systems*, 2nd ed. (Westview Press, Cambridge, Mass, 2008).
- [29] R. L. Devaney and Z. Nitecki, “Shift automorphisms in the Hénon mapping”, *Commun. Math. Phys.* **67**, 137–146 (1979).
- [30] M. S. Dresselhaus, G. Dresselhaus, and A. Jorio, *Group Theory: Application to the Physics of Condensed Matter* (Springer, New York, 2007).
- [31] S. Elaydi, *An Introduction to Difference Equations*, 3rd ed. (Springer, Berlin, 2005).
- [32] M. J. Feigenbaum and B. Hasslacher, “Irrational decimations and path-integrals for external noise”, *Phys. Rev. Lett.* **49**, 605–609 (1982).
- [33] J. A. C. Gallas, “Counting orbits in conjugacy classes of the Hénon Hamiltonian repeller”, *Phys. Lett. A* **360**, 512–514 (2007).
- [34] I. S. Gradshteyn and I. M. Ryzhik, *Tables of Integrals, Series and Products*, 8th ed. (Elsevier LTD, Oxford, New York, 2014).
- [35] T. Grava, T. Kriecherbauer, G. Mazzuca, and K. D. T.-R. McLaughlin, “Correlation functions for a chain of short range oscillators”, *J. Stat. Phys.* **183**, 1 (2021).
- [36] B. Gutkin, L. Han, R. Jafari, A. K. Saremi, and P. Cvitanović, “Linear encoding of the spatiotemporal cat map”, *Nonlinearity* **34**, 2800–2836 (2021).
- [37] B. Gutkin and V. Osipov, “Classical foundations of many-particle quantum chaos”, *Nonlinearity* **29**, 325–356 (2016).
- [38] A. J. Guttmann, “Lattice Green’s functions in all dimensions”, *J. Phys. A* **43**, 305205 (2010).
- [39] M. Hochman and T. Meyerovitch, “A characterization of the entropies of multidimensional shifts of finite type”, *Ann. Math.* **171**, 2011–2038 (2010).
- [40] S. Holmin, *Geometry of Numbers, Class Group Statistics and Free Path Lengths*, PhD thesis (KTH Royal Inst. Technology, Stockholm, 2015).

- [41] W.-G. Hu and S.-S. Lin, "On spatial entropy of multi-dimensional symbolic dynamical systems", *Discrete Continuous Dyn. Syst. Ser. A* **36**, 3705–3717 (2016).
- [42] E. V. Ivashkevich, N. S. Izmailian, and C.-K. Hu, "Kronecker's double series and exact asymptotic expansions for free models of statistical mechanics on torus", *J. Phys. A* **35**, 5543–5561 (2002).
- [43] S. Katsura and S. Inawashiro, "Lattice Green's functions for the rectangular and the square lattices at arbitrary points", *J. Math. Phys.* **12**, 1622–1630 (1971).
- [44] Y.-O. Kim, J. Lee, and K. K. Park, "A zeta function for flip systems", *Pacific J. Math.* **209**, 289–301 (2003).
- [45] D. A. Klain and G.-C. Rota, *Introduction to Geometric Probability* (Cambridge Univ. Press, 2006).
- [46] H.-T. Kook and J. D. Meiss, "Application of Newton's method to Lagrangian mappings", *Physica D* **36**, 317–326 (1989).
- [47] H. Liang and P. Cvitanović, "A chaotic lattice field theory in one dimension", *J. Phys. A* **55**, 304002 (2022).
- [48] D. Lind and K. Schmidt, "Symbolic and algebraic dynamical systems", in *Handbook of Dynamical Systems*, Vol. 1, edited by B. Hasselblatt and A. Katok (Elsevier, New York, 2002), pp. 765–812.
- [49] D. A. Lind, "A zeta function for  $Z^d$ -actions", in *Ergodic Theory of  $Z^d$  Actions*, edited by M. Pollicott and K. Schmidt (Cambridge Univ. Press, 1996), pp. 433–450.
- [50] D. A. Lind and B. Marcus, *An Introduction to Symbolic Dynamics and Coding* (Cambridge Univ. Press, Cambridge, 1995).
- [51] M. Lüscher and P. Weisz, "Scaling laws and triviality bounds in the lattice  $\phi^4$  theory (I). One-component model in the symmetric phase", *Nucl. Phys. B* **290**, 25–60 (1987).
- [52] R. S. MacKay, *Renormalisation in Area-preserving Maps* (World Scientific, Singapore, 1993).
- [53] R. S. MacKay and J. D. Meiss, "Linear stability of periodic orbits in Lagrangian systems", *Phys. Lett. A* **98**, 92–94 (1983).
- [54] R. Mainieri, Thermodynamic Zeta Functions for Ising Models with Long-Range Interactions, PhD thesis (Physics Dept., New York Univ., 1990).
- [55] R. Mainieri, "Thermodynamic zeta functions for Ising models with long-range interactions", *Phys. Rev. A* **45**, 3580–3591 (1992).
- [56] R. Mainieri, "Zeta-function for the Lyapunov exponent of a product of random matrices", *Phys. Rev. Lett.* **68**, 1965–1968 (1992).
- [57] R. Mainieri, Can averaged orbits be used to extract scaling functions?, 1993.

- [58] R. Mainieri, "Cycle expansions with pruned orbits have branch points", *Physica D* **83**, 206–215 (1995).
- [59] R. Mainieri, *Geometrization of spin systems using cycle expansions*, 1995.
- [60] C. Meyer, *Matrix Analysis and Applied Linear Algebra* (SIAM, Philadelphia, 2000).
- [61] T. Morita, "Useful procedure for computing the lattice Green's function - square, tetragonal, and bcc lattices", *J. Math. Phys.* **12**, 1744–1747 (1971).
- [62] I. Percival and F. Vivaldi, "A linear code for the sawtooth and cat maps", *Physica D* **27**, 373–386 (1987).
- [63] I. Percival and F. Vivaldi, "Arithmetical properties of strongly chaotic motions", *Physica D* **25**, 105–130 (1987).
- [64] C. Pozrikidis, *An Introduction to Grids, Graphs, and Networks* (Oxford Univ. Press, Oxford, UK, 2014).
- [65] F. Riesz and B. Sz.-Nagy, *Functional Analysis* (Dover Publ., Mineola, NY, 1955).
- [66] R. C. Robinson, *An Introduction to Dynamical Systems: Continuous and Discrete* (Amer. Math. Soc., New York, 2012).
- [67] J. Slipantschuk, O. F. Bandtlow, and W. Just, "Complete spectral data for analytic Anosov maps of the torus", *Nonlinearity* **30**, 2667 (2017).
- [68] D. Sterling and J. D. Meiss, "Computing periodic orbits using the anti-integrable limit", *Phys. Lett. A* **241**, 46–52 (1998).
- [69] D. G. Sterling, *Anti-integrable Continuation and the Destruction of Chaos*, PhD thesis (Univ. Colorado, Boulder, CO, 1999).
- [70] D. G. Sterling, H. R. Dullin, and J. D. Meiss, "Homoclinic bifurcations for the Hénon map", *Physica D* **134**, 153–184 (1999).
- [71] I. Stewart and D. Gökaydin, "Symmetries of quotient networks for doubly periodic patterns on the square lattice", *Int. J. Bifur. Chaos* **29**, 1930026 (2019).
- [72] I. Vierhaus, *Simulation of  $\phi^4$  Theory in the Strong Coupling Expansion beyond the Ising Limit*, MA thesis (Humboldt-Univ. Berlin, Math.-Naturwissen. Fakultät I, 2010).
- [73] S. V. Williams, X. Wang, H. Liang, and P. Cvitanović, *Nonlinear chaotic lattice field theory*, In preparation, 2024.
- [74] U. Wolff, "Triviality of four dimensional  $\phi^4$  theory on the lattice", *Scholarpedia* **9**, 7367 (2014).
- [75] F. Y. Wu, "Theory of resistor networks: the two-point resistance", *J. Phys. A* **37**, 6653–6673 (2004).
- [76] Y. Yamasaki, "An explicit prime geodesic theorem for discrete tori and the hypergeometric functions", *Math. Z.* **289**, 361–376 (2017).

## Chapter 25

# Spatiotemporal cat, blogged

I'm a space and time continuum  
— Red Wanting Blue

The latest entry at the bottom for this blog, page 1398

2016-01-12 PC

2016-05-16 **Predrag** I am putting all stuff about cat maps known to us into sect. 15.1.

2016-05-17 **Predrag** I have added for the time being chapter 15 *Statistical mechanics applications* from ChaosBook to this blog. Note that there are yet more references to read in the Commentary to the chapter 15.

2016-05-17 **Boris** There has been some progress in the cat maps direction. Li did a simple simulation for single cat map which has confirmed my guesses so far. General question is about 2D symbolic dynamics which we used in our paper with Vladimir [25]. We encoded trajectories by winding numbers so the alphabet is small. This radically differs from standard symbolic dynamics - Markov partitions, etc. which you normally find in the literature.

Question: Given rectangular domain of symbols - what is the probability to find it within a generic N-particle spatiotemporal cat trajectory of duration T (N and T are large)? To my surprise an answer for this question might be within reach (at least for most of the sequences, small rectangles, etc.) This symbolic dynamics is much nicer than what I thought it would be. If true, this will be a nice project for students. I am writing some notes, will send this crude stuff at night today - hopefully it will be digestible.

**2016-05-18 Boris** To speed up everything I send my notes ([click here](#)) on recent progress on cat map symbolic dynamics. Very crude, limited edition (probably barely digestible :). This what I managed to put in latex tonight. More stuff and explanations will come on Friday . So far only few things (and only for single cat) were checked numerically.

**2016-05-21 Boris** The current version of my notes: ([click here](#)), with more stuff, more or less the same level of disorder. The main news - this symbolic dynamics (for single cat) was investigated a time ago by Percival and Vivaldi [41]. At least some of their results are of relevance for us and maybe overlap with my results. Need some time to digest their paper.

**2016-05-21 Predrag** For simple linear maps with integer coefficient it might be possible to write explicitly all period points in terms of rational numbers. See [ChaosBook](#) example 14.10 *Periodic points of the full tent map*.

**2016-06-01 Predrag** The downside the Percival-Vivaldi [41] 'linear code' is that the Markov/generating partition is infinite, meaning that for longer and longer orbits there are more and more new pruning (inadmissible blocks) rules, ad infinitum.

As far as I can tell, for  $N$  coupled maps this gets harder to describe, as in general there is an coupling strength parameter. Perhaps for rational values of it some miracles might happen.

**2016-07-10 Boris** The current ver. 5020 of my notes: ([click here](#)),

Main attractions:

1. Single cat: Frequencies of sequences which are composed of internal symbols eq. (2.23) - analytic answer.
2. Infinity of cats, pp. 9-11: Results for single symbol frequency. Some results for  $[2 \times 2]$  squares - Rana eqs, internal symbols, forbidden sequences. Looks like extendable to general rectangles (Future looks bright [gotta wear shades](#)).

To Rana, Adrien and Li - we Skype Wednesday 5pm.

**2016-08-15 Predrag** : Before I start sounding critical: Rana, Adrien and Li are all good students / postdoc, and the work and what people learned this summer is very good. Now, to my first impressions (Boris still has to chime in, and we should all meet soon to discuss).

Boris was the primary advisor for Adrien and Rana, and he did not push them to write; European style, more hands off than is the American custom. Rana has written too little, not covering all the work that she did (which was good, but only Boris knows what it was). Adrien also has some work to do before the report can be read by anyone other than the members of this team.



For me, what lacks in Rana, Adrien and Li's work is that they did not (on their own initiative) read the literature, or if they did, they never summarized what they learned in their blogs, or cited the original sources in their reports (if it is not recorded, I assume it did not happen). I did an exhaustive literature search for them (for coupled maps, see above in this blog, chapter 25; for cat maps see sect. ?? and sect. 15), but they did not pick it up, so I'll have to do that work myself.

**2016-10-03 Predrag** Not quick or easy to explain, but I have a hunch that the spatiotemporal zeta function should be something like the 2D Ising model zeta function described by Aizenman, see chapter 16.

**2016-11-06 Predrag** Early references on the spatiotemporal invariants and invariant measures:

Grassberger [22] *Information content and predictability of lumped and distributed dynamical systems* " ... we point out the difference between difficulty and possibility of forecasting, illustrating it with quadratic maps. Next, we ask ourselves how this should be generalized to distributed, spatially extended and homogeneous systems. We point out that even the basic concepts of how information is processed by such systems are unknown. Finally, we discuss some intermittency-like effects in coupled maps and cellular automata.

Most interesting systems are spatially extended ("distributed") and have thus, in the infinite-volume limit, an infinite number of degrees of freedom. Nevertheless, concepts developed for dynamical system with few degrees of freedom can be applied.

Let us first consider a system located in a finite space volume  $V$  with fixed boundary conditions. For the moment we assume that the field variables (local observables) are continuous, while space and time are discrete.

It is very plausible that the number of excited degrees of freedom in such a system is proportional to the volume, at least in typical situations. More precisely, we expect that both the metric entropy  $h$  and the dimension  $D$  are extensive quantities. This is supported by overwhelming theoretical [19, 39, 48] and numerical evidence that the Lyapunov exponents (ordered such that  $\lambda_2$  decreases with  $i$ ) scale as

$$\lambda_i \approx f(i/V) \tag{25.1}$$

[...] The limit  $\eta = \lim_{V \rightarrow \infty} (h/V)$  is called density of metric entropy. [...] more interesting is the information needed to describe a finite part of an infinite system than that needed to describe the system as a whole. "

**2016-11-06 Boris** Papers to read:

Bardet and Keller [6] *Phase transitions in a piecewise expanding coupled map lattice with linear nearest neighbour coupling* write: " We construct a mixing continuous piecewise linear map on  $[-1,1]$  with the property that a

two-dimensional lattice made of these maps with a linear north and east nearest neighbour coupling admits a phase transition. We also provide a modification of this construction where the local map is an expanding analytic circle map. The basic strategy is borrowed from Gielis and MacKay (2000 *Nonlinearity* 13 867-88 ); namely, we compare the dynamics of the CML with those of a probabilistic cellular automaton of Toom's type; see MacKay (2005) *Dynamics of coupled map lattices and of related spatially extended systems* (Lecture Notes in Physics vol 671) ed J-R Chazottes and B Fernandez (Berlin: Springer) pp 65–94) for a detailed discussion. "

de Maere [34] *Phase transition and correlation decay in coupled map lattices* writes: " For a Coupled Map Lattice with a specific strong coupling emulating Stavskaya's probabilistic cellular automata, we prove the existence of a phase transition using a Peierls argument, and exponential convergence to the invariant measures for a wide class of initial states using a technique of decoupling originally developed for weak coupling. This implies the exponential decay, in space and in time, of the correlation functions of the invariant measures. "

Schmitt [52] *Spectral theory for nonanalytic coupled map lattices* write: " We consider weakly coupled strong mixing interval maps on the infinite lattice with finite range couplings. We construct Banach spaces defined by bounded variation conditions such that the transfer operator associated with the full infinite system has a simple eigenvalue 1 (corresponding to a unique natural invariant probability measure) and a spectral gap. "

**2017-02-13 Predrag** Consider admissible Lagrangian trajectories in the  $[x_0, x_{\ell+1}]$  plane. The 1-step Lagrangian map is

$$x_2 = (s x_1 - m_1) - x_0. \quad (25.2)$$

For  $s = 3$  have  $m_j \in \{-1, 0, 1, 2\}$ , and the partition borders are slope -1 lines defined by  $x_1 = 0$  or 1.

$$-m_1 - x_0 \leq x_2 \leq s - m_1 - x_0. \quad (25.3)$$

Anything outside  $0 \leq x_2 \leq 1$  is not a constraint.

$$1 - x_0 \leq x_2^{(-1)} \leq 4 - x_0. \quad (25.4)$$

$$-x_0 \leq x_2^{(0)} \leq 3 - x_0. \quad (25.5)$$

$$-1 - x_0 \leq x_2^{(1)} \leq 2 - x_0. \quad (25.6)$$

$$-2 - x_0 \leq x_2^{(2)} \leq 1 - x_0. \quad (25.7)$$

So, there is no pruning for  $x_2^{(0)}$  and  $x_2^{(1)}$ ; the only pruning constraints are

$$1 - x_0 \leq x_2^{(-1)}, \quad (25.8)$$

$$x_2^{(2)} \leq 1 - x_0. \quad (25.9)$$

2-step Lagrangian map

$$x_3 = (s - 1)(x_2 + x_1) - x_0 - m_2 - m_1, \quad (25.10)$$

Eliminate  $x_2$  by (25.2)

$$x_2 + x_1 = ((s + 1)x_1 - m_1) - x_0. \quad (25.11)$$

$$x_3 = (s^2 - 1)x_1 - s x_0 - m_2 - s m_1, \quad (25.12)$$

**2016-09-28 Predrag** Learned much more from [Rafael de la Llave](#) that I can possibly remember.

He says that fancy Smaliens, like Pugh and Shub, who studied dynamical systems with ‘multiple times’. The results are expressed in terms of ‘Weyl chambers’. They are particularly simple if symmetries commute. They call that the ‘Abelian case’.

**2016-09-28 Predrag** Volevich [55] *Kinetics of coupled map lattices* writes: “ A simple example of coupled map lattices generated by expanding maps of the unit interval with some kind of diffusion coupling is considered. The author proves that probability measures from some natural class weakly converge to the unique invariant mixing measure under the actions of dynamics. The main idea of the proof is the symbolic representation of his system by two-dimensional lattice model of statistical mechanics. ”

**2016-09-28 Predrag** Giberti and Vernia [11, 20] *Normally attracting manifolds and periodic behavior in one-dimensional and two-dimensional coupled map lattices* study weakly coupled logistic maps in one- and two-dimensional lattices. They show numerically for some classes of coupled map lattices that the stability of a spatial structure is determined by the stability of its pattern with the minimal (spatial) scale, i.e. by the tiniest detail of this structure.

Continued in Livi, Martínez-Mekler and Ruffo [5, 12, 30] *Periodic orbits and long transients in coupled map lattices*.

Hopefully something we can ignore as long as we are interested into the “high-temperature” phase.

**2016-10-03 Predrag** In 1986 Zimmer outlined a general program directed at understanding smooth actions of lattices in semisimple Lie groups on compact manifolds. So hopefully this has nothing to do with CLMs.

de la Llave and Mireles James [31] *Connecting orbits for compact infinite dimensional maps: Computer assisted proofs of existence* is indigestible from get go.

**2016-11-11 Predrag** Boris A. Khesin [course notes](#) might be helpful if we ever get to Hamiltonian PDEs :)

**2016-11-11 Predrag** Belykh and Mosekilde [7] *One-dimensional map lattices: Synchronization, bifurcations, and chaotic structures study*

$$\begin{aligned} x_{n,t+1} &= f(x_{n,t}) + \epsilon[x_{n+1,t} - (1 + \gamma)x_{n,t} + \gamma x_{n-1,t}] \\ &= f(x_{n,t}) + (1 - \gamma)\epsilon(x_{n,t} - x_{n-1,t}) + 2\epsilon \square x_{n,t}, \end{aligned} \quad (25.13)$$

asymmetrically drifting due to coupling by  $(1 - \gamma)$ . With  $g(x) = f(x) - x$ , and rescaling the nonlinearity, this is a discretization of a dynamics of extended, non-equilibrium media PDE

$$\frac{\partial x}{\partial t} = g(x) + (1 - \gamma) \frac{\partial x}{\partial s} + \frac{\partial^2 x}{\partial s^2}. \quad (25.14)$$

Consider the diffusively coupled maps (25.13) for  $\gamma = 1$  and  $N = 2m$  and assume periodic boundary conditions ( $m \rightarrow \infty$  when the array is unbounded). As this has a spatial Laplacian (the dynamics is now reflection-symmetry invariant) they construct a pair of new variables  $x_{n,t}, y_{n,t}$  from  $x_n$  with odd or even  $n$ , and obtain a 2D lattice symmetric under  $(x, y) \leftrightarrow (y, x)$ . Then the symmetric and asymmetric spaces behave differently. In particular, the second period-doubling bifurcation for can be changed into a torus bifurcation [46].

**2016-11-11 Predrag** Belykh and Mosekilde [7] is a descendent of the system previously studied by Reick and Mosekilde [46] in *Emergence of quasiperiodicity in symmetrically coupled, identical period-doubling systems*: “ When two identical period-doubling systems are coupled symmetrically, the period-doubling transition to chaos may be replaced by a quasiperiodic transition. The reason for this is that at an early stage of the period-doubling cascade, a Hopf bifurcation instead of a period-doubling bifurcation occurs. Our main result is that the emergence of this Hopf bifurcation is a generic phenomenon in symmetrically coupled, identical period-doubling systems. The whole phenomenon is stable against small nonsymmetric perturbations. Our results cover maps and differential equations of arbitrary dimension. As a consequence the Feigenbaum transition to chaos in these coupled systems - which exists, but tends to be unstable - is accompanied by an infinity of Hopf bifurcations.”

The seemingly first remark on this splitting is due to Ruelle [47]. He noted that the symmetry of the coupling results in a splitting into a symmetric solution and a nonsymmetric solution, where for the latter the two subsystems are 180° out of phase. Later Neu [37, 38] specialized the problem to linear coupling and analyzed the stability of the symmetric and nonsymmetric solutions by singular perturbation methods.

All of these might be of importance for Burak’s torus birth and destruction [9].

As for the cats crowd, these seem to suggest that spacetime interchange symmetry  $t \leftrightarrow n$  of the spatiotemporal cat [24] should lead to different

dynamics (and symbolic dynamics! only positive  $(n, t)$  are needed after the decomposition) in symmetrized and anti-symmetrized lattices, with a possible flow-invariant subspace currently invisible. In Gibson, Halcrow and Cvitanović [21] *Visualizing the geometry of state-space in plane Couette flow* we also had a  $D_1 \times D_1$  symmetry, with important consequences on types of solutions, and invariant subspaces.

**2016-11-23 Predrag** Symmetries of the action are more powerful than symmetries of the Euler–Lagrange equations for theories without Lagrangian formulation because of Noether’s theorem.

Having a variational principle (action (11.37) in case at hand) and a continuous symmetry means that the **Noether’s theorem** applies

“To every one-parameter, continuous group of symmetries of a Lagrangian dynamical system there corresponds a scalar, real-valued conserved quantity.”

Is there is a version of it for discrete translations? What is the conserved quantity for a single cat map? What is it for the lattice? Internet says many contradictory things:

“The fact that a Lagrangian is unchanged by a discrete transformation is of no significance. There is no conserved quantity associated with the transformation.”

“For infinite symmetries like lattice translations the conserved quantity is continuous, albeit a periodic one. So in such case momentum is conserved modulo vectors in the reciprocal lattice. The conservation is local just as in the case of continuous symmetries.”

Read about it [here](#).

Mansfield [35] in [proceedings](#) and in her [talk](#) defines *total difference* and says “Just as an integral of a total divergence depends only on the boundary data, so does the sum over lattice domain of a total difference.”

She states the discrete Noether’s Theorem, and in Example 1.3.7 she shows that for a discretization of a standard mechanical Lagrangian, time invariance yields “energy” as a the conserved quantity.

Hydon and Mansfield [26].

Capobianco and Toffoli [14] Can anything from Noether’s Theorem be salvaged for discrete dynamical systems? is fun to read (but ultimately unsatisfactory):

“ we take the Ising spin model with both ferromagnetic and antiferromagnetic bonds. We show that-and why- energy not only acts as a generator of the dynamics for this family of systems, but is also conserved when the dynamics is time-invariant.”

The *microcanonical Ising model* is strictly deterministic and invertible: on a given step, a spin will flip (that is, reverse its orientation) if and only if

doing so will leave the sum of the potential energies of the four surrounding bonds unchanged. The Ising dynamics is a second-order recurrence relation. They define “energy” as the length of the boundary between ‘up’ and ‘down’ domains. While the magnetization-number of spins up minus number of spins down-may change with time, that length, and thus the energy, remains constant. The total energy of a system may be defined as

1. A real-valued function of the system’s state,
2. that is additive,
3. and is a generator of the dynamics.

In a discrete Hamiltonian dynamics, a state is no longer a “position/momentum” pair  $\langle q, p \rangle$  as in the continuous case, but an ordered pair of configurations  $\langle q_0, q_1 \rangle$ .

A second-order dynamical system has an evolution rule of the form

$$x_{t+1} = g(x_t, x_{t-1}).$$

**2016-12-12 Predrag Spatiotemporal cat claim retracted:**

On the second thought, spatiotemporal cat is not radically different from the previous examples of  $(D+1)$ -dimensional spatiotemporal symbolic dynamics cited by Boris (Pesin and Sinai [42], Bunimovich and Sinai [13], Pethel, Corron and Bollt [43, 44]). In all coupled maps literature, the starting point is time evolution of a non-interacting particle at each site, with its 1-dimensional temporal symbolic dynamics, with spatial coupling to  $D$  spatial neighbors subsequently tacked on. While the *coordinate* of site is  $(D+1)$ -dimensional, its symbolic dynamics is 1-dimensional. In all models the I am aware of, with the exception of zeta functions in  $d = 2$ , the field being discretized (“particles” at sites) is *scalar*, and so is the spatiotemporal cat field (I was wrong when I claimed in a conversation with Boris that is a *vector* field). In  $d$  spatiotemporal dimensions it is  $d$ -dimensional, but its symbolic dynamics alphabet at each site is 1-dimensional set.

The zeta functions in  $d = 2$ , reviewed in chapter 10, are not based on any dynamics, and have problems of their own. In nutshell, for such zeta functions grammars are awkward, while in the spatiotemporal cat the grammar rules are automatically obeyed by any simulation, and can be explicitly computed as a finite set of rules for any given invariant 2-torus.

**2018-12-05 Predrag Liverani’s** paper Keller and Liverani [29] *Uniqueness of the SRB measure for piecewise expanding weakly coupled map lattices in any dimension* is an example of rigorous work on ergodicity of weakly couple chaotic maps. Cite, emphasize weak-coupling is NOT what we do. Also, our Euclidian metric leads to hyperbolicity, no attracting subsets and phase transitions in the evolution.

**2016-12-17 Predrag** Read Qin [45] *Bifurcations of steady states in a class of lattices of nonlinear discrete Klein-Gordon type with double-quadratic on-site potential*

**2017-02-17 Predrag** For a single cat map linear code is simply awkward

1. depends on choice of  $x_t$  origin: 4 letters for Boris, 5 for (symmetric) Vivaldi
2. linear code partition areas have no relation to periodic orbit weights
3. linear code pruning rules undercount periodic orbit pruning rules
4. periodic orbits are intrinsic to the flow, so makes more sense to use AW Markov partition

**Boris 2017-02-17** Mostly agree, but linear code has its own charm: internal part of the code has trivial grammar rules, it is very homogeneous, i.e., admissible sequences of finite length have volumes either close to zero or close to max (volumes of internal sequences).

**Boris 2017-02-17** For  $p$  iterations of the map situation rapidly improves - number of internal symbols grows exponentially with  $p$ , number of external symbols is fixed (kind of renormalization).

**Predrag 2017-03-04** That's just a cheat. For a piecewise linear expanding map of mod 1 variety, it is always the orbit of the outermost critical point (in your language, exterior alphabet) that defines the grammar, in the spirit of the kneading theory, with no grammar rules for the interior alphabet, see ChaosBook chapter *Deterministic diffusion*. If one looks at iterates of the map, of course the number of interior alphabet sequences grows exponentially, but that does not mean that they dominate the topological entropy - that one is what it is, an irrational number larger than  $\ln N_{\mathcal{A}_0}$ , the same number for the original map or any of its iterates.

**2017-04-29 Predrag** Tourigny [54] *Networks of planar Hamiltonian systems* writes things we probably disagree with:

“Hamiltonian systems famously do not admit attractors, but rather families of periodic orbits parameterised by level sets of the Hamiltonian. There have been surprisingly few attempts to study complex networks consisting of coupled Hamiltonian systems. Consequently, in this paper we initiate the study of complex networks whose autonomous units are planar Hamiltonian systems. We choose to focus on planar Hamiltonian systems because already there exists a rich theory that may be identified with the geometry of planar algebraic curves.

Define a weighted graph  $\mathcal{G}$  by assigning a vertex to each  $i \in V$  and an edge with “weight”  $W_{ij} = W(i, j)$  joining vertex  $i$  to  $j$ . We assume this graph  $\mathcal{G}$  is *undirected* (i.e.,  $W_{ij} = W_{ji}$ ) and *connected* meaning that there always exists a path from any vertex  $i$  to any other vertex  $j$ . The network is then defined to be the dynamical system on  $\mathbb{R}^{m \times n}$  whose time

evolution is governed by the equations

$$\dot{z}_i = F_i(z_i) + \sum_{j=1}^n W_{ij} U(z_i, z_j).$$

We will actually only be concerned with networks where the autonomous units are planar ( $m = 2$ ) and the coupling function is *diffusive*, implying  $U(z_i, z_j) = U(z_i - z_j)$ . We say that a network is an *oscillator network* if each of the underlying systems  $\dot{z}_i = F_i(z_i)$  admits at least one periodic solution. "

This work is inspired by Winfree, Kuramoto and Turing (rather than coupled maps lattices). If the dynamics on a node is the same everywhere, the network (graph) is "homogenous", otherwise it is "heterogenous." The diffusive coupling  $W_{ij} = W_{ji}$  couples all nodes, in his model with the same strength, but the nodes are assumed heterogenous. After further reading it seems that the networks are not Hamiltonian (coupling destroys that, and that we can safely avoid this literature.

Rest in pacem.

**2017-10-10 Boris** Our recent [1] *Semiclassical prediction of large spectral fluctuations in interacting kicked spin chains*, [arXiv:1709.03601](https://arxiv.org/abs/1709.03601), hides a feline creature in the form of (25.15):

"**Integrable Case:** For  $b^x = 0$  all rotations are around the  $z$ -axis and therefore commute with the Hamiltonian making the system integrable. As a result the dynamics of the kicked system for arbitrary times is equivalent to one at fixed time, e.g.  $T = 1$  with rescaled system parameters  $J \rightarrow JT$  and  $b^z \rightarrow b^z T$ . Moreover, the flow induced by the Hamiltonian  $\hat{H}_I + \hat{H}_K$  for time  $T$  is identical to the evolution of the kicked system for  $T$  time steps with the same parameters.

For the classical trajectories  $p_n = \text{const.}$  holds for each  $n$  and periodic orbits form  $L$  dimensional manifolds. To close a trajectory in phase-space after  $T$  iterations it is sufficient that the total change in angles  $\Delta q_n$  is a multiple of  $2\pi$ ,

$$\Delta q_n = 4T (J(p_{n-1} + p_{n+1}) + 2V p_n) + 2b^z T = 2\pi \hat{m}_n. \quad (25.15)$$

The  $\hat{m}_n \in \mathbb{Z}$  is a local winding number for spin  $n$ . Since the momenta are bounded,  $|p_n| \leq 1$ ,  $\chi_n = p_{n-1} + p_{n+1}$  resides within the interval  $[-2, +2]$ . Therefore, this equation has no solution if, for instance,  $b^z > 4(J + V)$  and  $4(J + V) + b^z < \pi/T$ . In such cases the system does not possess any classical periodic orbits of period  $T$  or shorter. If all parameters (times  $T$ ) are sufficiently small, the first accessible winding number is necessarily zero. With increasing time  $T$  the number of possible  $\hat{m}_n$  grows linearly, and with it the number of possible distinct periodic orbits grows algebraically. With respect to  $L$  the number of periodic orbits is determined



by all admissible combinations of the winding numbers. If there is more than one allowed  $m_n$  the growth is thus exponential in  $L$ . This exponential growth also holds for non-integrable parameter choices. "

Boris continues: This is the (dual) equation for "spatially" periodic orbits of an integrable spin chain. For  $4JT = 2\pi$  it is the cat map

$$p_{n+1} - s p_n + p_{n-1} = -m_n, \quad (25.16)$$

with the cat map "stretching" parameter  $s = -2TV/\pi$ , and the winding number  $m_n = b^z T/\pi - \hat{m}_n \in \mathbb{Z}$ . For other times  $T$ , the map is non-symplectic but still linear. The equation says, loudly, that temporally integrable system can be "spatially" chaotic (e.g., number of spatial periodic orbits grows exponentially with the spatial period  $L$  (in case at hand, the number of "particles").

On the quantum side the corresponding "dual" evolution is exactly the quantum cat map.

**2017-10-10 Predrag** Thanks for pointing it out, I would have never noticed that the very feline (25.16) is hiding within (25.15). So, whenever one has the nearest neighbor couplings, spatially, spatial translation invariance, a spatial reflection symmetry, and a linear dynamics on the site, one gets a spatial cat map. Your  $T = 1$  example is the discrete time analog of the Michelson [36]  $T = 0$  study of equilibria on the kneading sequence spatial  $L \rightarrow \pm\infty$  (described in the parallel `blog.tex`, in this subversion repo directory). This system is not integrable, but, needless to say, the number of equilibria does not grow with increasing  $T$  (it is constant).

This continues with **2020-01-11 Predrag** post below.

**2017-10-10 Predrag** Currently open ends:

1. Finish the Pythagorean tiling of figure ?? in terms of two rectangles. In these coordinates the cat map should again have a linear encoding, but with no pruning rules (the two rectangles are a generating partition).
2. Do the same for  $d > 1$ .
3. Redo everything with doubly-periodic boundary conditions, where all Green's functions trivial.
4. I have started writing up the spatiotemporal Jacobian and the  $\det(1-J)$  for  $d$ -tori in what is currently called Sect. 1.3.2 *Spatiotemporal stability* in the parallel `blog.tex`. In the discrete spacetime case, that should agree with the determinants that Boris has computed.

**2018-01-20 Predrag** Akila, Waltner, Gutkin, Braun and Guhr [2] *Collectivity and periodic orbits in a chain of interacting, kicked spins* is presumably closely related to ref. [1] *Semiclassical prediction of large spectral fluctuations in interacting kicked spin chains*, see **2017-10-10 Boris** post above.

**2018-01-20 Predrag** Catnipping is taking a delirious turn. Axenides, Floratos and Nicolis [3] *The quantum cat map on the modular discretization of extremal black hole horizons* write: “ We present a toy model for the chaotic unitary evolution of infalling black hole horizon single particle wave packets. We construct explicitly the eigenstates and eigenvalues for the single particle dynamics for an observer falling into the BH horizon, with time evolution operator the quantum Arnol’d cat map (QACM). Using these results we investigate the validity of the eigenstate thermalization hypothesis (ETH), as well as that of the fast scrambling time bound (STB). We find that the QACM, while possessing a linear spectrum, has eigenstates which are random and satisfy the assumptions of the ETH. We also find that the thermalization of infalling wave packets in this particular model is exponentially fast, thereby saturating the STB, under the constraint that the finite dimension of the single-particle Hilbert space takes values in the set of Fibonacci integers. ”

**2018-03-28 Predrag** Plasma physicists Xiao *et al.* [56] *A lattice Maxwell system with discrete space-time symmetry and local energy-momentum conservation*, [arXiv:1709.09593](https://arxiv.org/abs/1709.09593) might of interest to us. By ‘Maxwell’ they mean EM on a discrete spacetime lattice. Their system has gauge symmetry, symplectic structure and discrete space-time symmetry. They generalized Noether’s theorem to discrete symmetries for the lattice Maxwell system, and the system is shown to admit a discrete local energy-momentum conservation law corresponding to the discrete space-time symmetry. These conservation laws make the discrete system an effective algorithm for numerically solving the governing differential equations on continuous space-time.

There is also Stern *et al.* [53] *Geometric computational electrodynamics with variational integrators and discrete differential forms*, They write: “ We develop a structure-preserving discretization of the Lagrangian framework for electrodynamics, combining the techniques of variational integrators and discrete differential forms. This leads to a general family of variational, multisymplectic numerical methods for solving Maxwell’s equations that automatically preserve key symmetries and invariants. We generalize the Yee scheme to unstructured meshes in 4-dimensional spacetime, which relaxes the need to take uniform time steps or even to have a preferred time coordinate. We introduce a new asynchronous variational integrator (AVI) for solving Maxwell’s equations. These results are illustrated with some prototype simulations that show excellent numerical behavior and absence of spurious modes. ”

**2018-04-05 Boris** You show that your Adler-Weiss (Markov) partition can be used to get position of the points in the phase space by linear transformation. So your partition is good on both fronts = simple grammar rules + easy walk from phase space to symbolic representation and back (as opposed to the linear code of Percival-Vivaldi, where only the second

part is true).

Q: Was it known already (I mean simple connection between phase space and symbolic dynamics for Adler-Weiss partitions)?

**2018-04-08 Predrag** The generating partition of figure 24.4 is new.

Newer still is the generating partition of figure 24.17 (a) which incorporates the invariance of the cat map dynamics (2.95) under spatial reflection flip across the  $x_1 = -x_0$  anti-diagonal, together with  $s_n \rightarrow -s_n$  time reversal symmetry, so the full symmetry is  $D_1 \times D_1$ . This should lead to very simple symbolic dynamics, but sect. 24.4 *Reduction to the fundamental domain* has still to be completed.

**2018-04-05 Boris** Start from e.g., 5 letter alphabet, then translate admissible sequences (from the transition graph) into tree letter (-1,0,1) LINEAR alphabet (2.9), and use Green's function to get to the phase space points. Right?

**2018-04-08 Predrag** As explained in ChaosBook.org, in symmetry reduction the *links* of such graphs are not labelled arbitrarily, they have a precise group-theoretic meaning.

Figure 24.4 (d) indeed has 5 links (I prefer not use an arbitrary 'alphabet' to label them), but the important thing is that the links correspond to the symmetry group elements; they enable you to reconstruct from a walk on the torus. In the symmetry reduction of dynamical systems we call that "reconstruction equations". It is these group elements (24.15), (24.18), etc., that are the *alphabet*, as explained in [ChaosBook.org/paper.shtml#diffusion](http://ChaosBook.org/paper.shtml#diffusion) chapter, and the preceding chapters that deal with discrete symmetry reduction (like the 3-disk billiard).

To repeat: we are reducing translational symmetry. Hence the alphabet are the group elements that reduce global motions to the elementary cell, in this case our 2-rectangle partition.

**2018-04-05 Boris** If linear refers to linear connection between symbol sequences and phase space points (my definition) then your three letter code is indeed linear, but (probably) not the original 5-letter one.

**2018-04-08 Predrag** What code? There is no "original 5-letter" code... Maybe you mean link labels in the (2.84) calculation? That just looks like clumsy notation to me. Writing down a transition graph with 5 nodes corresponding to such 'alphabet' would be a mess, I did not do it.

**2018-04-05 Boris** I would say that under any Adler-Weiss looms a linear code

**2018-04-08 Predrag** I think so too. While the canonical Thom-Arnol'd cat map (2.1) and the Percival-Vivaldi [41] two-configuration representation (2.5) are related by the anti-symplectic transformation (8.110), the Thom-Arnol'd

cat map seems clumsier, as it seems to require 2D translations in figure 2.1 to return subpartitions back into the 2-rectangle partition (have not bothered to work that out). Still a linear code.

**2018-04-05 Boris** Adler-Weiss code is not linear on its own. Agree?

**2018-04-08 Predrag** I agree - I have never seen it recast in the group-theoretic symbolic dynamics. Percival-Vivaldi [41] do discuss Adler-Weiss, and do write down the 1D (damped) screened Poisson equation and 1D Green's functions, but they never saw that Adler-Weiss could be combined with their linear code. Would sure have saved a ton of needless work in the subsequent literature.

**2018-04-05 Boris** The biggest question to me what are you doing/going to do in  $d = 2$  case. For me, Adler-Weiss partitions can be (probably) turned to 1D linear code (with a huge alphabet), but not to the 2D linear code. Right, Wrong?

**2018-04-08 Predrag** Wrong. Why would one turn  $d = 2$  Adler-Weiss into 1D linear code? For finite spatial periodicity  $L$  that would not be smart, and for  $L \rightarrow \infty$  (the subject of these papers) impossible. No, for  $d = 2$  one has to partition the 4D invariant 2-torus partition hypercube. I'm optimistic about us being able to accomplish that. Symmetries should help. Percival-Vivaldi [41] hypercube is already working (see Han's examples (24.62), etc.), now we have to find a generating partition.

Just get cracking :)

**2017-12-18 Predrag** More seriously, what is wrong with the argument so far?

I used the Hamiltonian, evolution-in-time thinking to generate the  $d = 1$  generating partition. That will not work in higher dimensions, so the above argument has to be recast in the Lagrangian form.

In principle, it is just a discrete Legendre transform, see sect. 12.2 *Generating functions; action*, but I do not see it yet...

**2018-04-12 Boris** By the "original 5-letter" code I mean the one which appears in (24.10). You can use it to label paths on the transition graph = all admissible sequences/trajectories. The grammar rules for this encoding/labeling (call it whatever) are local - you just say which pairs of symbols are admissible. In other words if I give you an arbitrary sequence of symbols (from this five letter alphabet) you can easily say me whether it admissible or not. Right?

**2018-04-19 Predrag** If by "local" you mean "full shift", i.e., transition graph of memory 1, wrong. They are walks on the transition graph (24.8) (e), so 2 cannot be followed by 1 or 3, 5 cannot be followed by 4, etc. But any transition graph of *finite* memory encodes a finite grammar (subshift of finite type)- no need to recode it as a memory 1 code.

**2018-04-12 Boris** But what about your 3 letter code (24.13)? Given a sequence of symbols from this 3-letter alphabet, can you say easily whether it admissible or not (without going to the phase space)? In other words, whether the grammar rules are local here?

**2018-04-19 Predrag** Don't you see how brilliant our solution is?

1. Any walk  $M$  on the transition graph figure 24.4 (d) is admissible
2. By linearity of the (damped) screened Poisson equation, to each admissible block  $M$  corresponds a unique admissible state  $\Phi$ .

Done.

**2018-05-14 Predrag** There is some excitement about new regularities of Bragg peaks in diffraction patterns of 1-dimensional aperiodic crystal composed of primes. I find the limit periodic structures, such as the spatial period-doubling [4] particularly intriguing (see Fig. 6.1 in Torquato, Zhang and De Courcy-Ireland, arXiv:1804.06279).

**2018-10-06 Predrag** Ruelle [49] *Zeros of graph-counting polynomials*, and Ruelle [50] *Graph-counting polynomials for oriented graphs* deal with things like counting subgraphs, motivated by studies of zeros of the grand partition function, such the circle theorem of Lee and Yang. I truly do not understand why this is done... I am not alone, as very few people cite these articles.

**2018-11-05 Predrag Mark Paul** and Jonathan Barbish are testing their covariant vector codes on the diffusive coupled map lattices (CML) (8.2) of Kaneko [27, 28] type on finite spatial periodic lattice of period  $L$ ,

$$u_{j+1}^n = f(u_j^n) + [f(u_j^{n-1}) - 2f(u_j^n) + f(u_j^{n+1})] = (1 + \epsilon \square) f(u_j^n), \quad (25.17)$$

where the individual site dynamical system  $f(x)$  is the 1D quadratic map

$$f(x) = ax + bz(1 - z), z = x \bmod 1, \quad (25.18)$$

studied in Grigoriev and Cross [23] *Dynamics of coupled maps with a conservation law*.

A differential or discrete equation of this form represents the competition between: generation of chaotic perturbations by  $f(x)$  and their dissipation the diffusive coupling induced by the spatial Laplacian.

For map (25.17) the space average of the 'velocity field'  $u$

$$\langle u \rangle = \frac{1}{L} \sum_j u_j^n \quad (25.19)$$

is conserved (Galilean invariance), so the system has, in addition to the two parameters  $a$  and  $b$  of the local map  $f$ , as the additional control parameter the conserved quantity  $\langle u \rangle$ , which can be defined by the initial

condition. They give plots of possible phases in the  $[a, u]$  and  $[b, u]$  parameter planes.

Their objective is to determine the effect of this conservation law on the dynamics of the extended chaotic system; it leads to the singularity in Lyapunov spectrum at  $\lambda_j = 0$ , shown in their fig. 10(b). They break the conservation law in their eq. (70). In Kuramoto–Sivashinsky we do not seem to get anything much out of it, as far as I remember, but they comment on that in their eq. (18).

In their eqs. (10) and (13) they give analytically the two 2-cycles. As is the case for parabola, it might be possible to give 3-cycles analytically, but nothing beyond.

They state that there are non-linear waves (we call these relative equilibria or travelling waves), propagating through the laminar background with unit velocity, their fig. (3): “All defects move with a constant velocity, but while the majority of defects is moving with the maximal speed  $v = \pm 1$ , the rest have a smaller speed.” They neither derive nor prove existence of relative equilibria (travelling defects) with  $|v| \leq 1$ , nor do they study their stability.

If I were Jonathan, I would first look for equilibria  $u^n = u^{n+1}$  for small  $L$ , then for relative equilibria  $u^n = u^{n+q} + p$ . Show that phase velocity is maximal for  $v = 1$ , ( $q = p$ ). Determine their linear stability – perhaps  $v = 1$  is the least unstable, that’s why you see it all the time. The go on finding unstable periodic and relative equilibria for small  $(L, T)$  tori (periodic tilings).

**2019-09-28 Predrag Boris** gets a [prestigious grant](#).

**2019-11-18 Boris** There are some exciting developments during the last two years regarding quantum dual models, mostly by the group of Tomaž Prosen, see Bertini, Kos, and Prosen [8] *Exact correlation functions for dual-unitary lattice models in 1+1 dimensions*, [arXiv:1904.02140](#).

Although they go by some funny names - dual-unitary spin chains, dual local quantum circuits etc., behind each of these models sits a (quantized) spatiotemporal cat. Amazingly, we know how to calculate correlations between local operators in such models resp. in quantum spatiotemporal cat (even in perturbed one).

This generates some funny questions regarding classical cats as well. One should be able to do it also for the classical model as well. In short, if you look for an interesting problem – calculating classical correlators in spatiotemporal cats might be the hit.

In a week I will be able to send you a Duisburg preprint (with setting closer to cats).

**2020-01-11 Predrag** This continues the conversation that includes (25.15) above,

but I do not understand the details - some of the quantum notation obscures them for me.

No further peep from Boris, but this is presumably the Duisburg preprint: Boris Gutkin, Petr Braun, Maram Akila, Daniel Waltner and Thomas Guhr, *Local correlations in dual-unitary kicked chains*, [arXiv:2001.01298](#).

Turns out Boris knows how to upload to arXiv, but was too busy to do it with our preprint :)

**2023-03-02 Predrag** Moved notes on free cumulants discussed below to [GitHub](#) `reducesymm/QFT/planar.tex`

Laura Foini and Jorge Kurchan *The Eigenstate Thermalization Hypothesis and Out of Time Order Correlators*, [arXiv:1803.10658](#) (2019), and Silvia Pappalardi, Felix Fritzsche and Tomaž Prosen *General Eigenstate Thermalization via Free Cumulants in Quantum Lattice Systems*, [arXiv:2303.00713](#) (2023).

2CB

**2020-01-13 Predrag** MacKay, Johnson and Sansom [32] *How directed is a directed network?*, ([click here](#)):

We consider directed networks (also known as directed graphs or di-graphs) with set  $N$  of nodes (also known as vertices) and set  $E$  of directed edges (also known as links). We suppose that there is at most one edge from a node  $m$  to a node  $n$ , and denote the edge by  $mn$ . There can also be an edge from  $n$  to  $m$ . Each edge carries a weight  $w_{mn} > 0$ . This can represent the strength of the edge. We write  $w_{mn} = 0$  if there is no edge from  $m$  to  $n$  and we assemble the  $w_{mn}$  into a matrix  $W$ . The edge weights could be set to 1, as is common in the literature, and the array  $W$  is then called the adjacency matrix  $A$  of the network, but the ability to represent the strength of the edge is a useful extension. If there were multiple edges from  $m$  to  $n$  then we would amalgamate them into a single edge by adding the weights. Self-edges  $mm$  (also called loops) are permitted.

The *weight* of the node  $n$  is

$$u_n = w_n^{in} + w_n^{out}$$

and the *imbalance* for node  $n$  by

$$v_n = w_n^{in} - w_n^{out}$$

In matrix form the (weighted) graph-Laplacian operator  $\Lambda$  on functions  $h : N \rightarrow \mathbb{R}$  is defined by

$$\Lambda = \text{diag}(u) - W - W^T$$

They seek the solution  $h$  of the linear system of equations

$$\Lambda h = v$$

This always has a solution but it is non-unique, because one can add an arbitrary constant in each connected component of the network. Etc.

They seek levels to minimise the *trophic confusion* :)

A directed network is said to be normal if its weight matrix  $W$  commutes with its transpose  $W^\top$  :

$$WW^\top = W^\top W$$

Note that  $W^\top$  represents the same weighted network but with all the edges reversed. The term “normal” came from people who spent their lives with self-adjoint operators and unitary operators, both of which are normal, but people working in stability of ordinary differential equations are fully cognizant that most matrices are not normal.

For the unweighted case of an adjacency matrix  $A$ , normality implies the imbalance vector  $v = 0$ . This is because  $(A^\top A)_{mn}$  is the number of sources in common to nodes  $m$  and  $n$ , and  $(AA^\top)_{mn}$  is the number of sinks in common. In particular,  $(A^\top A)_{nn} = w_n^{in}$  and  $(AA^\top)_{nn} = w_n^{out}$ , so  $A^\top A = AA^\top$  implies that  $w^{in} = w^{out}$  and  $v = 0$ . When  $v = 0$  we say a network is balanced.

Another special case of normality is symmetric networks  $W^\top = W$ .

Normality of  $W$  is equivalent to existence of a unitary matrix  $U$  such that  $U^\dagger W U$  is diagonal.

A cycle in a directed network is a closed walk in it. We allow repeated edges and repeated nodes. In particular, we allow a cycle to be a periodic repetition of a shorter cycle. The weight  $w$  of a cycle is the product of the weights along its edges. The total weight of cycles of length  $p$  is given by the trace of the  $p$ th power of  $W$ :  $\text{tr } W^p$ .

The orbits are those which are not repetitions of a shorter cycle. We consider two orbits to be the same if they differ only by a cyclic permutation. We denote by  $\mathcal{P}$  the set of orbits,

$$1/\zeta_{AM}(z) = \prod_p (1 - z^{n_p} w_p)$$

This can be reduced to one in terms of “**elementary cycles**”, those which do not repeat a node before closing. They are prime and for a finite network there are only finitely many of them. The formula is

$$1/\zeta_{AM}(z) = 1 + \sum_C \prod_{p \in C} (-z^{n_p} w_p)$$

where the sum is over non-empty collections  $C$  of disjoint elementary cycles. Might want to study MacKay’s proof to see if it is better than what is in ChaosBook.

**2020-11-22 Predrag** Scher, Smith and Baranger [51] *Numerical calculations in elementary quantum mechanics using Feynman path integrals* (1980): “ We show that it is possible to do numerical calculations in elementary quantum



mechanics using Feynman path integrals. Our method involves discretizing both time and space, and summing paths through matrix multiplication. We give numerical results for various one-dimensional potentials. The calculations of energy levels and wave functions take approximately 100 times longer than with standard methods, but there are other problems for which such an approach should be more efficient. ”

**2020-11-23 Predrag** Could it be that in the large  $[L \times T]$  limit we should be looking at Floquet of ‘Brillouin’ bands?

**2020-11-23 Predrag** Temporal cat satisfies 1-d Klein-Gordon equation. Does it mean there is a Gaussian solution on it? Probably not, as the usual situation has a Gaussian spreading in time, but here time is taken to  $\infty$ ...

**2020-12-16 Predrag** Not exactly ‘Gaussian’, but maybe the outgoing Klein–Gordon Green’s function (8.12) or the ‘Yukawa potential’ (8.17) maybe answer the above random thought.

**2017-09-16 Predrag** We know the exact, Adler-Weiss answer, in terms of a golden mean - state it. The half-baked linear encoding is an arbitrary, infinite sequence of approximations to the exact answer.

**2021-02-01 Predrag** **Gabriel Peyré**: The Fiedler vector of a graph is the second eigenvector of the Laplacian. It is the lowest Fourier mode and is useful to order the nodes (clustering, dimensionality reduction, etc).

[Wiki](#).

**2021-09-23 Martin Richter** <martin.richter@nottingham.ac.uk>

Can you give a presentation here in Nottingham? The subject of Fritz Haake talk would be great. However, I would like to hear the second half in only 1/2-Tomaž-Prosen speed :-)

**2021-10-11 Predrag** A half? That would kill you, my talk was at 1.0 deciProsen. You are pleading for milliProsens, I assume. I make no promises in that spatiotemporal direction.

I would like to give a technical talk, because you guys have a lot of experience with Laplacians, and I’m puzzled.

**My schedule** is pretty flexible, and I do not mind getting up at 1:30am (for the pleasure of being slapped around by Tomaž Prosen, to give a random example. Or Bogomolny).

For the people who would rather just be entertained, I would suggest listening to one of the talks on [overheads/Spatiotemporal](#). Thanks to my graduate students (yet another level of paper-writing reluctant) there are no papers to read :-)

**2022-01-30 Predrag** The **Fourier approximation of a cat** we must weave into our **narrative**.

2022-03-25 **Predrag** We have competition: **TI:GER**

2022-04-08 **Predrag to Chris DuPre** U r on strike?

2022-04-08 **Chris** I don't know if I would say strike. I would just say I felt like my anxieties were not really relevant to the discussions and so it was best to stay away. Still reading the book and love the material!

2022-04-08 **Predrag** We MISS you! And you and I have to clean up "measures" vs. "probabilities" in ChaosBook.

**Chris DuPre** I still think it is best for me to stay away. I don't want to bog people down like that if people just want to learn the techniques. Happy to help write that out!

2022-05-09 **Predrag** We still have Gutzwiller trace formula / determinant to rederive spatiotemporally.

2022-10-28 **Predrag** Strictly speaking, applies only to the dissipative PDEs with continuous 'rubbery tile' families of solutions, but anyway: A major conceptual breakthrough - the day 'rubbery tiles' died!

For the Kuramoto–Sivashinsky system at hand, we impose the constant mean dissipation rate (computed as along-time average over any ergodic trajectory) to be satisfied by every compact solution, resulting in a single (or no) solution contribution for each continuous family, see *siminos/spatiotemporal/blog* sect. 1.9.4, or online [sect. 1.9.4 "Rubbery" tiles in far-from equilibrium dynamics](#).

Please either agree, or shoot me down. Important step in our program.

2023-02-17 **Predrag** **Varsha Subramanyan** *Non-linear dynamics of bosons and fermions in effective classical phase space*

Varsha told us about the T.H. Hansson, S.B. Isakov, J.M. Leinaas and U. Lindstrom *Classical phase space and statistical mechanics of identical particles* method, [arXiv:quant-ph/0003121](#), to obtain an effective classical phase space describing a system of  $N$  identical quantum particles, focusing on systems consisting of two bosons or two fermions in the presence of an elliptical trap potential. The resulting equations of motion yield non-trivial trajectories over the classical phase space, with possible chaotic motion. This presentation is an attempt to understand this problem better in the light of broader connections with non-linear systems.

**Smitha Vishveshwara**: We are looking at semiclassical orbits of lowest Landau level quasiparticles (where  $x$  and  $y$  don't commute) in the presence of quadratic potentials. While these orbits are closed for elliptical potentials, it no longer is the case when there's more than one particle. In the lovely formalism of Hans Hansson et al, one particle feels the presence of the other in a term in the equations of motion. And it seems to need only two particles, not three (like in classical chaos). Perhaps one

particle causes a deformation for the effective potential for the other, and so the orbit is no longer closed.


**2023-02-18 Hans Hansson** By the way, what is your problem with standard QM? Nothing wrong with semiclassics (I even say the name “Maslow” when I teach it and refer students to Gutzwiller as I say “Wiener measure” and refer to Glimm & Jaffe when I do path integrals — in both cases with very shallow mathematical understanding), but how do you deal with simple systems like spin 1/2? And even in systems where semiclassics work well like transport in Fermi liquids, the connection to the original electrons is either mysterious (Landau) or quite abstruse (Shankar). Not to speak about Luttinger liquids and stuff with quantum entanglement. Do you think that there is a “classical backbone” even in these cases?

**2023-02-19 Predrag** I’ve tried to distill semiclassical/Gutzwiller/ WKB approximation to QFT [here](#). Gutzwiller had only done it for QM; QFT formulation has been my problem since 1986, see [here](#).

So far, it only works for bosonic QM/QFT. My approach to fermions has been a bit funky, see [my lectures](#). In essence that “Archimedes principle” necessitates anticommuting variables.

That’s why I would love if your calculation was a simple (semi)classical example of antisymmetry -> fermions. That would be a long-sought “classical backbone” to fermions!

Don’t know about Luttinger liquids and quantum entanglement...

**2023-05-08 Predrag** Potentially interesting, should be here  .

**May 11, 2023 Shailesh Chandrasekharan** *Learning more about the magic of Wilson’s Renormalization Group* (have not found a recent paper on arXiv on this): Continuum quantum field theories can emerge from lattice field theories when the latter are tuned to critical points. However, this understanding has taken a somewhat magical twist: we are able to show that free Gaussian field theories with marginally relevant couplings seem to emerge at long distances from just a few discrete lattice degrees of freedom. After quickly reviewing an older result in the O(3) nonlinear sigma model which showed us this phenomenon, I will demonstrate that something similar occurs in the well-known BKT transition. Apparently, a simple loop-gas model on a square lattice with three degrees of freedom per lattice site can reproduce the massive phase of the transition.

**2023-05-20 Predrag Couchman, Evans and Bush [16]** *The stability of a hydrodynamic Bravais lattice* (2022):

[...] an investigation of the stability and collective vibrations of a two-dimensional hydrodynamic lattice [...] of a vibrating liquid bath. [...] the linearized equations of motion of a generic Bravais lattice, all possible tilings of parallelograms in an infinite plane-filling array. Focusing on square and triangular lattice geometries, we demonstrate that for relatively low driving accelerations of the bath, only a subset of inter-drop spacings exist for which stable lattices may be achieved. As the driving acceleration is increased progressively, the stationary lattices destabilize into coherent oscillatory motion.

[...] we consider the Bravais lattice, a theoretical construct used in solid-state physics to describe regular crystalline structures. [...] the Bravais lattice appears to be identical from each constituent lattice point. derive the dispersion relation governing the stability of a generic Bravais lattice.

If a wavevector  $k$  exists such that any root [...] has a positive real part, then the associated mode will grow and the lattice will destabilize, otherwise the lattice remains stable.

It suffices to consider only wavevectors  $k$  in the lattice's Brillouin zone, defined as the smallest set of  $k$  required to describe all distinguishable vibrations of the discrete lattice.

[...] the primitive vectors that define the lattice geometry, commonly referred to as 'primitive vectors'

Figure 7 is of interest to us: it shows rectangular lattice stable regions as function of the two lattice spacings; there should be something similar fixing periodicities of rubber tiles for Kuramoto-Sivashinsky rectangular primitive cells.

Eddi, Boudaoud and Couder [18] *Oscillating instability in bouncing droplet crystals* (2011) are the experimental observations.

[...] quasi-one-dimensional aggregates, with  $N$  droplets along one direction and only three droplets transversally. [...] instability corresponds to a spatial modulation of the periodic pattern. This mode is coherent all over the aggregate structure. They observe spatial period doubling: the second neighbours of a droplet have in-phase motions, the selected mode has a spatial wave number  $k_V = \pi/L$ . Their model eq. (9) has discrete Laplacians in discretized space and velocity. [...] Each sublattice has a spatial periodicity which is twice the original network periodicity. [...] Depending on the symmetry breaking involved, there are ten generic types of instabilities.

[...] 2-dimensional square and hexagonal lattices: the same period doubling as in the one-dimensional case occurs along the principal directions of the lattice. [...] They do not have a model in 2-dimensional, and they do not consider periodic state periodicities larger than 2.

2018-03-21 Predrag Hangout notes I:

**Burak on walking droplets:** returning to a 3-year old project, Burak is writing up a paper [10] on a droplet walking on a Faraday oscillating surface in a harmonic potential; he is able to reduce it to something that qualitatively looks like a Lorentz attractor. As a function of a parameter (driving amplitude?), the stability multipliers / exponents of relative equilibria and relative periodic orbit motions of the droplet go through interesting bifurcations. In particular, the first non-leading complex Floquet multiplier pair (and other sub-leading pairs?) seem to move on a circle in complex plane, with a constant (negative?) real part.

That is reminiscent of eigenvalue pairing for Gaussian thermostats, see Dettmann and Morriss [17] *Proof of Lyapunov exponent pairing for systems at constant kinetic energy*. In such models the dissipation does not fully destroy the symplectic structure. While for Hamiltonian systems stable/unstable exponents cancel pairwise, for thermostats they add up to a negative real number, the dissipation rate.

Burak shared a link to a review by John W. M. Bush. To best of my recollection, I had pointed Bush to Madelung [33], used in ChaosBook.org to derive semiclassical quantum mechanics, and discussed in this review at length. This leads to pilot wave theory, Nelson stochastic interpretation of quantum mechanics, and much else. To quote Michael Berry: “Bohmian quantum mechanics is Madelung plus hot air.” As to the source of this quote, it might be me - it is something I remember Berry telling me in my semiclassical days.

2024-09-20 Predrag for Dan Harris.

Dear President Harris, here are my notes following up on today’s discussion:

**Slicing.** In Budanur and Fleury [10] *State space geometry of the chaotic pilot-wave hydrodynamics* (2019) Burak slices the rotational symmetry of a pilot-wave model with central harmonic force [40]. Why slicing is helpful and, in my opinion necessary is illustrated by comparing the (full state space) trajectories and the reduced (i.e., ‘sliced’) trajectories in their Table I, and Fig. 10. Slicing is explained in our online course lecture 10. *Got a continuous symmetry? Freedom and its challenges*, and in ChaosBook Chapter 13. *Slice & dice*.

In Choueiri, Suri, Merrin, Serbyn, Hof and Budanur [15] *Crises and chaotic scattering in hydrodynamic pilot-wave experiments*, (2022) there are further examples of slicing (scan through the figures).

**Spatiotemporal stability exponent.** A good definition of what we believe to be the correct *spatiotemporal* stability exponent is harder to explain, and its evaluation even harder.

All our talks, papers, drafts, blogs are here. I keep trying to explain what the stability exponent is - here is an attempt for plumbers:

 *Herding cats: turbulence in spacetime*

and brain scientists:

 *Are we there yet?*

but they hate it. I can do it online for your group; talking to you today gave me an idea how to explain it better.

**2024-11-21 Predrag** read Vrahatis and Bountis, T.C. (1994). An Efficient Method for Computing Periodic Orbits of Conservative Dynamical Systems. In: Seimenis, J. (eds) Hamiltonian Mechanics. NATO ASI Series, vol 331. Springer, Boston, MA. DOI.

**2020-02-02 Predrag** *Cata at work*. Can we weave this into our presentations?

**2017-09-30 Predrag** *Cats rule*.

## References

- [1] M. Akila, B. Gutkin, P. Braun, D. Waltner, and T. Guhr, “Semiclassical prediction of large spectral fluctuations in interacting kicked spin chains”, *Ann. Phys.* **389**, 250–282 (2018).
- [2] M. Akila, D. Waltner, B. Gutkin, P. Braun, and T. Guhr, “Collectivity and periodic orbits in a chain of interacting, kicked spins”, *Acta Phys. Pol. A* **132**, 1661–1665 (2017).
- [3] M. Axenides, E. Floratos, and S. Nicolis, *The quantum cat map on the modular discretization of extremal black hole horizons*, 2017.
- [4] M. Baake and U. Grimm, “Diffraction of limit periodic point sets”, *Philos. Mag.* **91**, 2661–2670 (2011).
- [5] F. Bagnoli, S. Isola, R. Livi, G. Martínez-Mekler, and S. Ruffo, “Periodic orbits in a coupled map lattice model”, in *Cellular Automata and Modeling of Complex Physical Systems: Proceedings of the Winter School, Les Houches 1989*, edited by P. Manneville, N. Boccara, G. Y. Vichniac, and R. Bidaux (Springer, Berlin, 1989), pp. 282–290.
- [6] J.-B. Bardet and G. Keller, “Phase transitions in a piecewise expanding coupled map lattice with linear nearest neighbour coupling”, *Nonlinearity* **19**, 2193 (2006).
- [7] V. N. Belykh and E. Mosekilde, “One-dimensional map lattices: Synchronization, bifurcations, and chaotic structures”, *Phys. Rev. E* **54**, 3196–3203 (1996).
- [8] B. Bertini, P. Kos, and T. Prosen, “Exact correlation functions for dual-unitary lattice models in 1+1 dimensions”, *Phys. Rev. Lett.* **123**, 210601 (2019).

- [9] N. B. Budanur and P. Cvitanović, “Unstable manifolds of relative periodic orbits in the symmetry-reduced state space of the Kuramoto-Sivashinsky system”, *J. Stat. Phys.* **167**, 636–655 (2015).
- [10] N. B. Budanur and M. Fleury, “State space geometry of the chaotic pilot-wave hydrodynamics”, *Chaos* **29**, 013122 (2019).
- [11] L. A. Bunimovich, V. Franceschini, C. Giberti, and C. Vernia, “On stability of structures and patterns in extended systems”, *Physica D* **103**, 412–418 (1997).
- [12] L. A. Bunimovich, R. Livi, G. Martínez-Mekler, and S. Ruffo, “Coupled trivial maps”, *Chaos* **2**, 283–291 (1992).
- [13] L. A. Bunimovich and Y. G. Sinai, “Spacetime chaos in coupled map lattices”, *Nonlinearity* **1**, 491 (1988).
- [14] S. Capobianco and T. Toffoli, “Can anything from Noether’s theorem be salvaged for discrete dynamical systems?”, in *Unconventional Computation: 10th Intern. Conf., UC 2011, Turku, Finland*, edited by C. S. Calude, J. Kari, I. Petre, and G. Rozenberg (Springer, Berlin, Heidelberg, 2011), pp. 77–88.
- [15] G. Choueiri, B. Suri, J. Merrin, M. Serbyn, B. Hof, and N. B. Budanur, “Crises and chaotic scattering in hydrodynamic pilot-wave experiments”, *Chaos* **32**, 093138 (2022).
- [16] M. M. P. Couchman, D. J. Evans, and J. W. M. Bush, “The stability of a hydrodynamic Bravais lattice”, *Symmetry* **14**, 1524 (2022).
- [17] C. P. Dettmann and G. P. Morriss, “Proof of Lyapunov exponent pairing for systems at constant kinetic energy”, *Phys. Rev. E* **53**, R5545–R5548 (1996).
- [18] A. Eddi, A. Boudaoud, and Y. Couder, “Oscillating instability in bouncing droplet crystals”, *EPL* **94**, 20004 (2011).
- [19] C. Foias, O. Manley, R. Témam, and Y. Treve, “Asymptotic analysis of the Navier-Stokes equations”, *Physica D* **9**, 157–188 (1983).
- [20] C. Giberti and C. Vernia, “Normally attracting manifolds and periodic behavior in one-dimensional and two-dimensional coupled map lattices”, *Chaos* **4**, 651–663 (1994).
- [21] J. F. Gibson, J. Halcrow, and P. Cvitanović, “Visualizing the geometry of state-space in plane Couette flow”, *J. Fluid Mech.* **611**, 107–130 (2008).
- [22] P. Grassberger, “Information content and predictability of lumped and distributed dynamical systems”, *Phys. Scr.* **40**, 346 (1989).
- [23] R. O. Grigoriev and M. C. Cross, “Dynamics of coupled maps with a conservation law”, *Chaos* **7**, 311–330 (1997).
- [24] B. Gutkin, L. Han, R. Jafari, A. K. Saremi, and P. Cvitanović, “Linear encoding of the spatiotemporal cat map”, *Nonlinearity* **34**, 2800–2836 (2021).

- [25] B. Gutkin and V. Osipov, “Classical foundations of many-particle quantum chaos”, *Nonlinearity* **29**, 325–356 (2016).
- [26] P. E. Hydon and E. L. Mansfield, “Extensions of Noether’s Second Theorem: from continuous to discrete systems”, *Proc. R. Soc. London A* **467**, 3206–3221 (2011).
- [27] K. Kaneko, “Transition from torus to chaos accompanied by frequency lockings with symmetry breaking: In connection with the coupled-logistic map”, *Prog. Theor. Phys.* **69**, 1427–1442 (1983).
- [28] K. Kaneko, “Period-doubling of kink-antikink patterns, quasiperiodicity in antiferro-like structures and spatial intermittency in coupled logistic lattice: Towards a prelude of a “field theory of chaos””, *Prog. Theor. Phys.* **72**, 480–486 (1984).
- [29] G. Keller and C. Liverani, “Uniqueness of the SRB measure for piecewise expanding weakly coupled map lattices in any dimension”, *Commun. Math. Phys.* **262**, 33–50 (2006).
- [30] R. Livi, G. Martínez-Mekler, and S. Ruffo, “Periodic orbits and long transients in coupled map lattices”, *Physica D* **45**, 452–460 (1990).
- [31] R. de la Llave and J. D. Mireles James, “Connecting orbits for compact infinite dimensional maps: Computer assisted proofs of existence”, *SIAM J. Appl. Dyn. Sys.* **15**, 1268–1323 (2016).
- [32] R. S. MacKay, S. Johnson, and B. Sansom, “How directed is a directed network?”, *Proc. Natl. Acad. Sci. USA* **117** (2020).
- [33] E. Madelung, “Quantentheorie in hydrodynamischer Form”, *Z. f. Physik* **40**, 322–326 (1927).
- [34] A. de Maere, “Phase transition and correlation decay in coupled map lattices”, *Commun. Math. Phys.* **297**, 229–264 (2010).
- [35] E. L. Mansfield, Noether’s theorem for smooth, difference and finite element schemes, in *Foundations of Computational Mathematics, Santander 2005*, Vol. 331, London Math. Soc. Lect. Notes (2006), pp. 230–254.
- [36] D. Michelson, “Steady solutions of the Kuramoto-Sivashinsky equation”, *Physica D* **19**, 89–111 (1986).
- [37] J. C. Neu, “Coupled chemical oscillators”, *SIAM J. Appl. Math.* **37**, 307–315 (1979).
- [38] J. C. Neu, “Chemical waves and the diffusive coupling of limit cycle oscillators”, *SIAM J. Appl. Math.* **36**, 509–515 (1979).
- [39] B. Nicolaenko, “Some mathematical aspects of flame chaos and flame multiplicity”, *Physica D* **20**, 109–121 (1986).
- [40] A. U. Oza, R. R. Rosales, and J. W. M. Bush, “A trajectory equation for walking droplets: hydrodynamic pilot-wave theory”, *J. Fluid Mech.* **737**, 552–570 (2013).



- [41] I. Percival and F. Vivaldi, “A linear code for the sawtooth and cat maps”, *Physica D* **27**, 373–386 (1987).
- [42] Y. B. Pesin and Y. G. Sinai, “Space-time chaos in the system of weakly interacting hyperbolic systems”, *J. Geom. Phys.* **5**, 483–492 (1988).
- [43] S. D. Pethel, N. J. Corron, and E. Bollt, “Symbolic dynamics of coupled map lattices”, *Phys. Rev. Lett.* **96**, 034105 (2006).
- [44] S. D. Pethel, N. J. Corron, and E. Bollt, “Deconstructing spatiotemporal chaos using local symbolic dynamics”, *Phys. Rev. Lett.* **99**, 214101 (2007).
- [45] W.-X. Qin, “Bifurcations of steady states in a class of lattices of nonlinear discrete Klein-Gordon type with double-quadratic on-site potential”, *J. Phys. A* **36**, 9865–9873 (2003).
- [46] C. Reick and E. Mosekilde, “Emergence of quasiperiodicity in symmetrically coupled, identical period-doubling systems”, *Phys. Rev. E* **52**, 1418–1435 (1995).
- [47] D. Ruelle, “Some comments on chemical oscillations”, *Trans. N. Y. Acad. Sci.* **35**, 66–71 (1973).
- [48] D. Ruelle, “Large volume limit of the distribution of characteristic exponents in turbulence”, *Commun. Math. Phys.* **87**, 287–302 (1982).
- [49] D. Ruelle, “Zeros of graph-counting polynomials”, *Commun. Math. Phys.* **200**, 43–56 (1999).
- [50] D. Ruelle, “Graph-counting polynomials for oriented graphs”, *J. Stat. Phys.* **173**, 243–248 (2018).
- [51] G. Scher, M. Smith, and M. Baranger, “Numerical calculations in elementary quantum mechanics using Feynman path integrals”, *Ann. Phys.* **130**, 290–306 (1980).
- [52] M. Schmitt, “Spectral theory for nonanalytic coupled map lattices”, *Nonlinearity* **17**, 671 (2004).
- [53] A. Stern, Y. Tong, M. Desbrun, and J. E. Marsden, “Geometric computational electrodynamics with variational integrators and discrete differential forms”, in *Geometry, Mechanics, and Dynamics: The Legacy of Jerry Marsden*, edited by D. E. Chang, D. D. Holm, G. Patrick, and T. Ratiu (Springer, New York, 2015), pp. 437–475.
- [54] D. S. Tourigny, “Networks of planar Hamiltonian systems”, *Commun. Nonlinear Sci. Numer. Simul.* **53**, 263–277 (2017).
- [55] V. L. Volevich, “Kinetics of coupled map lattices”, *Nonlinearity* **4**, 37–48 (1991).
- [56] J. Xiao, H. Qin, Y. Shi, J. Liu, and R. Zhang, “A lattice Maxwell system with discrete space-time symmetry and local energy-momentum conservation”, *Phys. Lett. A* **383**, 808–812 (2019).

# Chapter 26

## Pow Wows

Scribes Sidney, Han and Matt.

The latest entry at the bottom for this chapter

### 26.1 Pow wow 2020-12-08

Scribe Predrag

One must distinguish *coordinate system* symmetries (the floor cat dances on) from *dynamical* symmetries (the cat reflected through its bisection plane).

**Hereby resolved:**

**Task 1** Define temporal cat phase space fundamental domain for the *dynamical*  $D_1 = \{e, \sigma\}$  symmetry  
Predrag 2020-12-XX: Done! See XXX

**Task 2** Define temporal cat phase space fundamental domain symbolic dynamics.  
XXX 2020-12-XX: Done! See XXX

**Task 3** Factorize temporal cat zeta using the *dynamical*  $D_1 = \{e, \sigma\}$  symmetry on the traces (periodic states count), then exponentiating.  
XXX 2020-12-XX: Done! See XXX

**Suggestion** Check the above guess factorization for the Bernoulli first. It is more instructive to assume that the  $s$  branch map is not piecewise linear, and work out weights  $t_p$  factorization, write down cycle expansions in terms of orbits.  
XXX 2020-12-XX: Done! See XXX

## 26.2 Pow wow 2020-12-28

Scribe Predrag

**2020-12-28 Han** (See the post above including (24.256).) The fundamental domain should be  $\{\hat{\phi}_{t-1}, \hat{\phi}_t\} \in [0, 1]^2/D_1$ , i.e.,  $1/2$  of the phase space unit square area, not the quarter of the area  $[0, 1/2]^2$ . Any codimension-1 hyperplane going through the center of mass  $\phi_t = 1/2$ , all  $t \in \mathbb{Z}$  point can serve as a boundary of the fundamental domain.

**2020-12-XX Predrag done!:** The natural fundamental domain is given by XXX

**Hereby resolved:**

**Task 1 Sidney** Define Hénon [ChaosBook \(15.20\)](#) phase space fundamental domain for the *coordinate* time reversal  $D_1 = \{e, \sigma\}$  symmetry. To Predrag, the [ChaosBook fig. 15.5](#) and Gutkin *et al.* [8] cat map [figure 2](#) suggest that the fundamental domain border is the diagonal, but Predrag is usually wrong.

**Sidney 2021-01-XX:** Done! See refeqXXX.

**Task 2 Sidney** Define Hénon phase space fundamental domain symbolic dynamics. Predrag expects it to be like what is described in [ChaosBook sect. 25.5  \$D\_1\$  factorization](#).

**Sidney 2021-01-XX:** Done! See XXX

**Task 3 Sidney** Factorize Hénon zeta using the *dynamical*  $D_1 = \{e, \sigma\}$  symmetry. Predrag expects it to be like what is described in [ChaosBook sect. 25.5  \$D\_{n1}\$  factorization](#).

**Sidney 2021-01-XX:** Done! See XXX

## 26.3 Pow wow 2021-01-08

Scribe Predrag

**2021-01-08 Predrag** Try to understand irreps of  $D_n$ : For worked out  $D_2$ ,  $D_4$  and  $D_n$  examples, see the text following (6.204).

**Hereby resolved:**

**Task 1 Han** Derive temporal cat factorization (6.199) and (6.197) into  $1/\zeta'(t)$ 's, either from the dynamical  $D_1$  symmetry, or from the lattice coordinate time-reversal  $D_1$  symmetry.

**Han 2021-01-XX:** Done! The  $D_1$  irrep decomposition of the temporal cat orbit Jacobian matrix  $\mathcal{J}$  is given by XXX

**Task 1 Predrag** Incorporate into ChaosBook the  $D_2$ ,  $D_4$  and  $D_n$  examples from the text following (6.204).

**Predrag 2021-01-XX:** Done!

## 26.4 Pow wow 2021-03-22

Scribe Predrag

Homework: verify whether

1. Hamiltonian (6.91) equations lead to the golden (Fibonacci [2]) cat map (6.194)?
2. is this consistent with the Yukawa massive field mass  $\mu$  relation (8.27) to the spatiotemporal cat stretching parameter  $s$  by  $\mu^2 = d(s - 2)$ . Note that Grava *et al.* [7] sect. 6.5.1 is full of such square roots relations for parameters, such as  $\tau_0 = -\sqrt{\kappa_1}$ .
3. is what they call “ $m$ -physical vector and half- $m$ -physical vector” the same as our  $\sqrt{\dots}$  or half-unit spacing lattice?
4. this leads to factorization (6.199), (6.192)?
5. this works (or not) for nonlinear systems? I believe we have to verify it for the orbit Jacobian matrix  $\mathcal{J}_{\pm}$ , for each solution, not on the periodic states themselves. Sidney’s Hénon (3.29) first, than
6. this works any nonlinear map?

The above is a failed attempt again, it seems...

## 26.5 Pow wow 2021-04-02

Scribe Predrag

1. Predrag believes that Han’s approach - for example (24.301) and thereabouts is the right way to go about it.
2. Sidney and Predrag should understand Gallas [6] *Counting orbits in conjugacy classes of the Hénon Hamiltonian repeller*, see (3.36)
3. Han should derive temporal cat formulas corresponding to Gallas Hénon  $C_n, D_n, N_n$ .
4. Han will presumably do it only for  $s = 3$ , but Predrag would be happier to see this done for arbitrary integer  $\mu$ ...
5. Then figure out what this has to do with  $D_n$
6. Added
  - (a) example 3.5 *Hamiltonian Hénon map, reversibility*
  - (b) example 3.6 *Symmetry lines of the standard map*
  - (c) remark 2.3 *Symmetries of the symbol square*
  - (d) sect. 3.5 *Symmetries of the symbol square*
  - (e) See eq. (3.34)

## 26.6 Pow wow 2021-04-09

Scribe Predrag

- (a) Han knows how to count the three types of time-reversal self-dual orbits, and has explicit trigonometric products expressions for their Hill determinants.
- (b) **2021-03-10 Predrag** The discussion reminds me of Baake *et al.* 1997 paper [1] *The torus parametrization of quasiperiodic LI-classes* ([click here](#)) (enter what you learn from that paper into sect. 6.5.3: is the only paper we found that associates a 1/2-shift unit length lattice with time reversal). But under my reading the paper does not seem to be applicable to our 1D lattice with time-inversion problem. Here is what we can adopt:
- (c) An infinite periodic state can be self-dual under time-inversion about an integer lattice point (with a single field  $\phi_0$  invariant under inversion), or about 1/2 midway point between two integer lattice sites, with all lattice fields paired as  $\phi_i = \phi_{-i}$ , with no invariant field. For a finite period  $n$  periodic state, there are four pairs of time-inversion points for self-dual periodic states

$$(0, 0) \quad (1/2, 0) \quad (0, 1/2) \quad (1/2, 1/2) \quad , \quad (26.1)$$

that form  $D_1 \times D_1$  the discrete subgroup of 'two-reflection points' of  $\mathbb{Z}/n$ . A periodic state starts at a reflection points, marches to the other reflection point, and then it marches back, so any self-dual periodic state has two reflections points, no more and no less. As reflection destroys cyclic invariance, all self-dual periodic states are prime, they cannot be tiled by repeats of a shorter segment (???)

(1/2, 0) and (0, 1/2) are the same by a half-period rotation, so there are three kinds of self-dual cycles illustrated in figure 3.2 (a,b,c). (compare with (3.34): Han has two diagonal classes instead of Gallas one)

- i. Both time-inversion invariant fields on the integer lattice (24.309) (Gallas [6] class ? $D_1$ ?)
  - ii. One time-inversion point on the integer lattice, the other on the 1/2-integer lattice (24.308) (class ? $D_2$ ?)
  - iii. Both time-inversion points on the 1/2-integer lattice (24.307) (class ? $N$ ?)
- (d) MacKay had the logistic map counts listed already in Table 1.2.3.5.1 of his 1982 PhD thesis [9] ([click here](#)). Should be the same as Gallas Table. 1, but I do not see the correspondence for all columns - you might want to check MacKay's construction, it is very clearly explained.

- (e) MacKay says that for self-dual cycles of odd period there is precisely one periodic point on the symmetry line; or two or none for even period cycles, so he correctly separates the two kinds of 'diagonal' cycles that Gallas lumps into one.
- (f) MacKay might be the first to note (p. 46) that period-6 is the smallest period for which there are non-symmetric periodic orbits.
- (g) The (3.34) hunch for time-reversal quotiented zeta function: in the numerator all cycles appear in pairs, but that overcounts the boundary cycles, which thus contribute  $(D_1 D_2 N)$  to the denominator???

## 26.7 Pow wow 2021-04-27

Scribe, for some inscrutable reason, always Predrag

2021-04-27 Predrag in progress:

example 3.2 *Temporal Hénon*

example 3.4 *Temporal Hénon stability*

Note the rescaled definition of the field  $\phi = a \phi$

**Hereby resolved:**

**Task 1 Sidney** compute the orbit Jacobian matrix  $\mathcal{J}_p$  for a set of shortest periods periodic states  $p$

**Task 2 Sidney** compute the periodic states  $p$  orbit Jacobian matrix eigen-values, -vectors.

**Task 3 Sidney** Interpret these eigen-values, -vectors.

**Task 1 Sidney & Han** compute analytically the orbit Jacobian matrix  $\det \mathcal{J}_p$  for fixed points, period-2 and periods-3.

**Task 2 Sidney & Han** verify Hill's formula for each

**Task 1 Han** time-symmetry reduce the orbit Jacobian matrix  $\det \mathcal{J}_p$  for fixed points, period-2 and periods-3.

**Task 1 Sidney & Han** verify the time-symmetry factorization of the Hill's formula for each

## 26.8 Pow wow 2021-05-04

Scribe, for some inscrutable reason, always Predrag

2021-05-04 Predrag in progress:

example 3.4 *Temporal Hénon stability*

Hereby resolved:

**Task 1 Han** Figure out how to piece together period  $rn$  repeats of period- $n$  orbit Jacobian matrix  $\mathcal{J}_p$ . (11.29) and (11.30) are failed attempts.

**Task 2 Han** Figure out how to piece together period  $\tilde{n}$   $\tilde{\mathcal{J}}_p$  with its time-reversed copy  $\tilde{\mathcal{J}}_p^\top$  by pulling out a matrix representation of the group element (in this case, a pair of the two types of reflections).

**Dream 1 Han** Replace the forward-in-time Perron-Frobenius operator by including the time-reversal into the operator definition. Perhaps by complexifying it, as in [ChaosBook \(28.10\)](#) and [ChaosBook \(29.17\)](#)? By replacing the monomial  $x^k$  eigenvectors [ChaosBook \(28.18\)](#), with exponential multipliers, with a time-reversal invariant combination of eigenvalues, something like  $\tanh$ ?

## 26.9 Pow wow 2021-05-07

Scribes Han, Predrag

1. Using the reflection operator in the space of periodic state, the orbit Jacobian matrix can be projected into symmetric and antisymmetric subspace of time reflection. Han used the symmetric eigenvectors of the orbit Jacobian matrix to project the orbit Jacobian matrix into symmetric subspace. A better way is to use the time reflection operator to find the projection operators as in (6.82–6.83).
2. There are two kinds of reflection points, corresponding to two kinds of reflection operators, denoted by a bar or a box, as in (24.307), and 3 (or 4) kinds of time-reversal self-dual orbits (3.50), (3.51) and (3.54), or (24.309), (24.308), and (24.307).
3. The eigenvalues of the antisymmetric eigenvectors *probably* count the number of antisymmetric periodic states:  $\{\Phi \in \mathbb{T}^{\mathbb{Z}} | R\Phi \pmod{1}\}$ .
4. However,  $\pmod{1}$  does not allow for  $\phi_t < 1$ . Perhaps we should replace the  $\pmod{1}$  condition by the  $\phi_t \in [-1/2, 1/2)$  condition. In that case, the antisymmetric eigenspace might be taking care of what we call the ‘dynamical’, site-wise symmetry under  $\phi_t \leftrightarrow -\phi_t$   $D_1$ , specific to temporal cat.
5. We still don’t know how to piece together orbit Jacobian matrices, other than by doing the multiplication along temporal evolution, and then using the Hill’s formula. The orbit Jacobian matrices for repeats of orbits do not multiply, as their determinants do not multiply.

6. The  $\sum 1/|\text{Det } \mathcal{J}_j|$  always satisfies the flow conservation sum rule [Chaos-Book \(23.18\)](#). Except that for Hénon we are working with [ChaosBook sect. 20.3 Open systems](#), so the sum is related to the escape rate.

## 26.10 Pow wow 2021-05-14

Scribe Predrag

**2021-05-14 Han** There is no proposal for time-reversal quotiented topological zeta function, dynamical zeta function or spectral determinant.

**2021-05-14 Predrag** We have: the topological zeta function for metal cat maps [\(6.55\)](#); the  $\mu = 1$  golden (Fibonacci [\[2\]](#)) cat zeta function [\(6.197\)](#); the time-reflection factorized (?)  $1/\tilde{\zeta}(t)$  [\(6.192\)](#); the Hamiltonian factorized [\(6.103\)](#), [\(6.111\)](#), [\(2.102\)](#), [\(2.103\)](#); the unique Euler product [\(6.141\)](#); the  $D_1$  dynamical zeta function factorization [\(6.284\)](#); something like [\(3.34\)](#) computed on the fundamental domain; spatiotemporal cat Z-transform (discrete Laplace transform)  $\zeta$  function [\(10.9\)](#); Ihara zeta functions [\(16.24\)](#), [\(16.29\)](#). The last I looked.

**2021-05-14 Han** I'm 99% sure that the metal [\(6.55\)](#); tand the golden cat [\(6.197\)](#) factorization have nothing to do with time-reversal.

**2021-05-14 Predrag** NOTHING to do with time-reversal? You are willing to bet \$100 to \$1 that they have NOTHING to do with time-reversal?

**2024-10-21 Predrag** As always, Han was right, see the next pow wow.

**Hereby resolved:**

**Task 1 Han** *Think* some more.

## 26.11 Pow wow 2024-10-21

Scribes: Zoom AI Companion, Predrag

**2024-10-19 Predrag** Challenge to all Tigers:

If sect. [6.4.2](#) and remarks at the end of section are correct, formulas for Hill determinants and stability exponents are insanely simple. Please verify, complete the calculations outlined in the remarks.

**2024-10-21 Predrag Zoom AI Companion Quick recap**

The team discussed the generalization of a formula from one dimension to higher dimensions, focusing on the properties of a square lattice and its implications for the orbit Jacobian matrix. They also explored simplifications of the problem, focusing on the determinant of a specific operator



and its relationship to the Laplacian and momentum in higher dimensions.

Lastly, AI Companion hallucinated pablum about the need for a focus on understanding the customer's needs and pain points, and effective communication and collaboration to ensure the project's success.

**Generalizing Formula to Higher Dimensions** Predrag and Xuanqi discuss the generalization of a formula from one dimension to higher dimensions. Xuanqi points out that in two dimensions, there can be non-zero trace contributions before reaching the full volume of the primitive cell, which is not the case in one dimension. Predrag argues that these contributions can be handled separately, but Xuanqi demonstrates that the sum of the periods in different dimensions can be much smaller than their product, leading to many non-zero trace terms. They do not reach a clear resolution on how to handle the higher-dimensional case.

**Square lattice and orbit Jacobian operator** Xuanqi and Predrag discussed the properties of a square lattice and its implications for the orbit Jacobian matrix. Xuanqi explained that even for a square lattice, the orbit Jacobian matrix would have many  $k$ -dependent terms, which would be problematic for intuition. Predrag suggested that if the square lattice was the simplest case, then it would be true for all lattices. Xuanqi agreed to show the  $[2 \times 2]_0$  Bravais lattice Hill determinant has  $k_1^2 k_2^2$  cross terms. Han proposed a method to compute the Laplacian as the product of two inner products of two vectors, which could simplify the computation. However, Xuanqi pointed out that this method would not work for the square root of the orbit Jacobian matrix. The team agreed to focus on the Laplacian for now and to compute the determinant of the vector of operators.

**Eigenvalues and Diagonalization in Lattices** Predrag explains that the eigenvalues of the operators can be written as a sum of two diagonal terms - one from the anti-integrable limit and one that depends on the momentum. He argues that this diagonalization should work in any dimension, and that the anti-integrable limit corresponds to the product of stretching factors for each lattice site. The momentum-dependent term is the square root of the sum of squares of the momentum components. Predrag shows how this can be computed explicitly on a reciprocal lattice for a specific example. He expresses optimism that this approach will work out for periodic solutions as well.

$$\mathcal{J}_p = p^2 + \tilde{\mu}^2 \mathbf{1} \quad (26.2)$$

where the local stretching factor  $\tilde{\mu}^2$  is  $-2\mu^2\phi$  for the spatiotemporal  $\phi^3$  (4.159) and  $\mu^2(1 - 3\phi^2)$  for the spatiotemporal  $\phi^4$  (4.105).

**$\phi^3$  field theory period-1 periodic states.** (Preliminary, correct!) From the Euler-Lagrange equation it follows that the period-1, constant periodic states,

$\phi_t = \bar{\phi}$ , for the  $d = 1$  lattice are the zeros of function

$$F[\bar{\phi}] = \mu^2 \left( \bar{\phi}^2 - \frac{1}{4} \right), \quad (26.3)$$

with two real roots  $\bar{\phi}_m$

$$(\bar{\phi}_L, \bar{\phi}_R) = \left( -\frac{1}{2}, \frac{1}{2} \right). \quad (26.4)$$

The stretching factor for the 2 steady periodic states is **in 2d**

$$d_z = -2\mu^2 \phi_z / d + 2 \rightarrow \pm(-\mu^2)/2 + 2, \quad (26.5)$$

**$\phi^4$  field theory period-1 periodic states.** (Preliminary, correct!) From the Euler–Lagrange equation (23.22) it follows that the period-1 periodic states,  $\phi_t = \bar{\phi}$ , for the  $d = 1$  lattice are the zeros of function

$$F[\bar{\phi}] = \mu^2 (1 + \bar{\phi}) \bar{\phi} (1 - \bar{\phi}). \quad (26.6)$$

As long as the Klein-Gordon mass is positive, there are 3 real roots  $\bar{\phi}_m$

$$(\bar{\phi}_L, \bar{\phi}_C, \bar{\phi}_R) = (-1, 0, 1). \quad (26.7)$$

The period-1 primitive cell orbit Jacobian matrix  $\mathcal{J}$  is a  $[1 \times 1]$  matrix

$$\mathcal{J} = d_m = \frac{dF[\bar{\phi}]}{d\bar{\phi}} = \mu^2 (1 - 3\bar{\phi}_m^2) = \mu^2 \text{ or } -2\mu^2, \quad (26.8)$$

so the stretching factor for the 3 steady periodic states is **(harmonize with (26.4))**

$$(d_L, d_C, d_R) = (-2\mu^2, \mu^2, -2\mu^2). \quad (26.9)$$

**Determinants and Smooth Transformations** Predrag discussed the properties of determinants in relation to smooth transformations of coordinates and fields. He emphasized that the determinant is invariant under these transformations and is not affected by the choice of coordinates. He also explained how to compute the determinant in one and two dimensions, and how to generalize this to higher dimensions. Sidney confirmed his understanding of these concepts. The conversation ended with Predrag explaining how to compute the logarithm of the determinant, which involves taking the trace of the logarithm and considering only contributions when the periods are multiples of the primitive cell periodicities.

**Simplifying Complex Mathematical Problem** Predrag discussed the simplification of a complex mathematical problem, focusing on the determinant of a specific operator. He explained that the problem could be simplified by considering the product of stretching factors and the volume, which would lead to a convergent series. He also discussed the relationship between the Laplacian and the momentum in higher dimensions, and how this could be used to simplify the problem further. Xuanqi asked about the decomposition of the

two-dimensional case into a product, and Predrag explained that the problem could be simplified by transforming into the reciprocal lattice and taking the square root of the diagonal elements. He also mentioned that the determinant function could be expressed as a square of another function, but with the variable being the square root of the stretching factor or mu square. Predrag concluded by stating that the problem agrees with what Xuanqi has done and that he couldn't see anything wrong with the current approach.

**Hereby resolved:**

1. Xuanqi and Sidney to verify the determinant calculation for the one-dimensional case as presented by Predrag.

**Sidney 2024-10-21:** Done! Everything looks correct for the 1D case, also checked that we could use this result to regain a general 1D lattice field theory Hill Determinant.

2. Han to further develop the approach of treating P as a vector and computing the determinants separately for  $p_1$  and  $p_2$  in the two-dimensional case.

**Han 2024-10-XX:** Done!

Xuanqi investigate how to generalize eq (7.45) to two dimensions, considering the cross-terms.

**Predrag 2024-10-24:** Done! Following Xuanqi documentation practices, which I find very efficient: I've done it all in my head, while taking a walk. All you need to know is that translation in different directions generators commute, and -voila!- no cross terms in  $d$  dimensions. The anti-integrable part -product over site values- is  $d$ -periodic, with all  $k$  phase and the tilt in the corner translations.

3. Team to examine the  $k_j$ -dependence in the two-dimensional case and its impact on the determinant calculations.

**Predrag 2024-10-24:** Xuanqi filling in the dotted lines here :)

4. Team to consider the implications of using direct sum versus direct product in the matrix calculations.

5. Team to analyze the validity of taking square roots of operators in the context of the Laplacian calculations.

6. Team to clarify the correct definition of the determinant in relation to the orbit Jacobian matrix and the shifting of the delta function integral.

7. Team to explore how to handle the zero eigenvalue of the Laplacian in the calculations.

8. Team to investigate the anti-integrable limit and its role in the stability matrix calculations for arbitrary perturbations.

9. Team to consider how to properly handle cases where ' $\mu^2$ ' might be negative, particularly for  $\phi^3$  and  $\phi^3$  theories.

**Sidney 2024-10-21:** Done! Empirically, there should be almost no cases where the large values of  $\mu^2$  allow for a positive determinant, but regardless, in the case that it does, Predrag's initial calculation is 100% correct, in the cases it is negative, we can verbatim repeat Han's calculation on page 17 and page 22, except replacing  $s^n$  with  $\text{Det}(S_p)$  and  $s^{-1}$  with  $S_p^{-1}$ , this works because  $S_p$  is diagonal, so it gives nice properties for both the inverse, and the eigenvalues.

## 26.12 Pow wow 2024-10-24

Scribes: Zoom AI Companion, Predrag

### 2024-10-24 Predrag Zoom AI Companion Quick recap

Predrag and Sidney discussed the challenges and potential solutions for understanding and applying operators in high dimensions, particularly in 2D space. They also explored the interpretation of determinants, the concept of trace, and the application of periodic orbit theory to fluid dynamics problems. Additionally, they discussed the discretization of the Kuramoto–Sivashinsky equation on a spacetime lattice and the potential for optimization algorithms to improve solution accuracy in fluid dynamics problems.

**Operator Factorization in High Dimensions** Predrag and Sidney discussed the challenges of understanding and applying the operator in high dimensions, particularly in 2D space. Predrag proposed a method to factorize the operator into a symmetric and anti-symmetric translation operator, which would simplify the problem. He explained that this method would result in two linear operators that are orthogonal and commute with each other. Sidney found the idea clear but needed to visualize it further. They also discussed the potential of this method to simplify the problem of determining the contribution of the operator to the traces.

**Derivatives in Discretized Wave Equation** Sidney and Predrag discuss a derivation related to a discretized wave equation involving derivatives in both time and space directions. Predrag initially expresses skepticism that a simple first-order derivative formula could apply to this case, but Sidney explains that it is still a first-order derivative in each direction. They explore the connection to continuous wave equations and the factorization into right and left-moving waves. Predrag becomes convinced that Sidney's approach could be valid for this type of problem.

**Determinants, Mixed Terms, and Operators** Predrag and Sidney discussed the interpretation of a determinant as a square of the terminal of a site field. They considered the possibility of missing terms and the issue of mixed terms. Sidney proposed that cross terms might show up when multiplying determinants together. They also discussed the definition of the square root of an op-

erator and how it could be used to derive equations. The conversation ended with Sidney acknowledging that there might be some errors in the equations they were discussing.

**Trace and Periodicity in Work** Sidney and Predrag discussed the concept of trace and its application in their work. They agreed on the importance of understanding the trace of a matrix and its relation to the determinant. They also discussed the concept of periodicity and its role in their work. Sidney suggested that the trace could be treated as the number of repeats multiplied together, which Predrag agreed with. They also discussed the possibility of having different multiples in two directions and how this could affect their calculations. The conversation ended with an agreement that their work was almost there, but they needed to clarify some details.

**Deriving Product of Kronecker Deltas** Sidney and Predrag discussed the derivation of a product of Kronecker deltas, which has to be a multiple of both  $r$ ,  $1$ , and  $n$ , which represents repeats in the spatial direction. They also discussed the relationship between this product and the Laplacian operator, with Predrag suggesting that Sidney should establish this relationship more explicitly. Sidney expressed uncertainty about how to proceed with this, but Predrag encouraged him to continue and to consider the boundary conditions. They also discussed the possibility of extending this work to all dimensions.

**Determinants and Generating Functions Formula** Sidney and Predrag discuss a mathematical formula related to determinants and generating functions. Predrag points out an issue with the formula and suggests that Sidney needs to prove it works for determinants. Sidney agrees and proposes expanding the formula, which should give cross terms matching numerical results. They plan to further refine the formula and proof.

**Double Index Notation and Operators** Predrag and Sidney discussed the concept of double-index notation (22.100) from ref. [3] and its application to the project.

Predrag prefers index notation to the outer-product notation, and explained how operators work in any dimension. They also discussed the commutation relation between the operator and the diagonal matrix, the concept of shifting elements in the diagonal matrix and how it is invariant under  $L$  and  $T$  shifts. They agreed to further explore the continuous orbit Jacobian in their next discussion.

**Indices and Operators in 3D Space** Predrag and Sidney discussed the concept of indices and operators in a three-dimensional space. Predrag explained that the concept is not new and is commonly used in physics. He also mentioned that the idea of multiple indices is standard and that it's not necessary to use the outer product notation. Sidney expressed his willingness to try using index notation. They also discussed the idea of a diagonal matrix that is not constant but periodic, and how it is invariant under two shifts to the periods. Predrag guided Sidney through the process of understanding this concept, emphasizing that it's not difficult once you work it out. They also touched on the idea of a slanted unit vector and how it adds a second matrix to the calculation. Predrag assured Sidney that once he works through the calculations, he

will understand the concept. They ended the conversation with plans to continue discussing other topics.

**Kuramoto Shivashinsky and Euler Lagrange Equations** Predrag discussed the concept of Kuramoto Shivashinsky, a spatiotemporal block, and its relation to the Euler Lagrange equations. He mentioned that it requires 4 initial conditions and is a dissipative system. Sidney asked about the possibility of a proper Lagrangian or action, to which Predrag responded that their theory doesn't require a variational principle and can be derived from equations alone. Predrag also mentioned that the Bernoulli map is not defined from an action principle and works well on a lattice. He suggested that the details might be found in his thesis or in some of his talks.

**Discretizing Kuramoto–Sivashinsky Equation on Lattice** Predrag explains how to discretize the Kuramoto–Sivashinsky equation on a spacetime lattice by introducing a tower of equations and replacing the field with its derivatives. This results in an algebraic equation for the Fourier coefficients on the discrete lattice sites. The nonlinearity comes from the convective term, which couples different lattice sites. Predrag mentions that some codes on GitHub solve these discretized equations for finite resolutions. He also discusses the sparsity of the Jacobian matrix for simpler models like the  $\phi^4$  theory, contrasting it with the more complex case where the solution depends on the entire lattice.

#### **Periodic Orbit Theory in Fluid Dynamics**

Predrag and Sidney discussed the application of periodic orbit theory to various fluid dynamics problems. They explored the use of Fourier and Chebyshev polynomials as bases for computations, particularly in the context of doubly periodic solutions and multiperiodic orbits. They also discussed the challenges of applying these methods to pipe flow and the potential for a spatiotemporal field theory reformulation to overcome computational limitations. The conversation concluded with a discussion on the potential for optimization algorithms to improve solution accuracy in fluid dynamics problems.

#### **Hereby resolved:**

1. Sidney to derive and write out the formulas for the determinant calculation in index notation, ensuring it works for rectangles first before adding slants.  
**Sidney 2024-10-22:** Done! I have a too-good-to-be-true Hill determinant (22.98).
2. Sidney to verify the relationship between the determinant of the Laplacian and the left and right waves expression.  
**Sidney 2024-10-XX:** Done! XX
3. Sidney to review Matt's thesis for potential Lagrangian formulations of the Kuramoto–Sivashinsky equation.  
**Han 2024-10-XX:** Done!

4. Sidney to apply the spatiotemporal field theory reformulation to the plasma equation, discretizing all derivatives.
5. Sidney to explore the application of periodic orbit theory to systems with mixed boundary conditions, such as plain Couette flow or pipe flow.
6. Predrag to compile and share the updated continuum block of the spatiotemporal blog with Sidney.  
**Predrag 2024-10-XX: Done! XX**
7. Sidney to investigate the use of Chebyshev polynomials and Bessel functions for expanding fields in non-periodic directions of fluid flow problems.  
**Predrag 2024-10-XX: Xuanqi filling in the dotted lines here :)**
8. Team to XX

## 26.13 Pow wow 2024-11-08

Scribes: Zoom AI Companion, Predrag

### 2024-10-24 Predrag Zoom AI Companion Quick recap

Predrag and Sidney discussed the differences between their work and others in condensed matter physics, focusing on the importance of enumerating solutions and considering hyperbolic solutions. They also explored the concept of symmetry in chaos theory and condensed matter physics, and how it relates to the counting of solutions and the stability of solutions. Lastly, they discussed the generalization of counting periodic orbits to calculate dynamical zeta functions and observables, and Sidney's ongoing work on block matrices and determinants.

**Condensed matter physics solution enumeration** They discussed the differences between their work and that of others in the field of condensed matter physics. We enumerate solutions on small Bravais lattices and consider hyperbolic solutions, while they focus on oscillatory solutions and countably many Eigenstates. They discussed enumerating solutions and giving them importance, and the need to find topologically possible solutions. Predrag mentioned that in ChaosBook the counting of Hamiltonian short period solutions was wrong, as it didn't account for time reversal.

**Symmetry in chaos theory and condensed matter physics** Predrag explained that the temporal lattice is a translation in time. He also mentioned that the Lind zeta function accounts for symmetries beyond just translation. Sidney understood the relevance of wanting to factor out all symmetries to get better convergence. Predrag further explained that in solid-state physics, the presence of discrete extra symmetry is crucial, as it leads to degenerate energy levels and higher-dimensional subspaces. He also mentioned that the inclusion of

time-reversal symmetry in calculations can significantly improve the accuracy of results.

**Generalizing counting of periodic orbits** They discuss how to generalize the counting of periodic orbits to calculate dynamical zeta functions and observables. The topological zeta function counts periodic orbits with weight 1, while the dynamical zeta function counts them with a weight related to their stability. To go from counting to dynamics, an extra sum over prime cycles is introduced, where each cycle is weighted by its stability instead of weight 1. This allows calculating observables like escape rates by averaging over the weighted periodic orbits. The discussion relates the formalism to concepts like graphs, incidence matrices, and averaging over probability densities.

**Symmetry Groups and Subgroups Theory** They discussed the concept of symmetry groups and their subgroups in the context of a theory. Predrag explained that the number of operations required to return to the original configuration,  $|G/H|$ , and the number of invariant sets are important factors. They also discussed the concept of fixed points and the role of prime cycles in the theory. Predrag mentioned that the weights of the repeats are multiplicative, leading to a structure similar to the zeta function.

**Block Matrices and Determinants Discussion** Sidney discussed his ongoing work on block matrices and determinants, mentioning a theorem he found that could be applied to more than 2 equations. He expressed a need to learn more about the mathematical structure of a ring to further his work. Sidney had given a talk on periodic orbits, which was well-received.

#### Hereby resolved:

- Sidney to study and understand the mathematical structure of rings to apply the theorem for block matrices with more than 4 blocks.
- Sidney to attempt implementing and calculating Lind zeta functions for the Hamiltonian Hénon map.
- Sidney to continue research on functional determinants and potentially reach out to colleagues for additional insights.

## 26.14 Pow wow 2025-01-07

Scribes: Zoom AI Companion, Predrag

### 2025-01-07 Predrag Quick recap

Xuanqi and Predrag discussed the setup for the deterministic lattice field theory, including the terminology, structure, and use of symbols and equations, and what to include in the presentation for Jordan Cotler's group



They explored the concept of a "Dance Marathon" and its application to the structure of non-wandering sets in dynamical systems, and the challenges of finding initial conditions for ergodic solutions in open systems.

The conversation ended with a discussion on the application of the Floquet-Bloch theorem in their work, the findings on celestial mechanics and chaos theory.

**Dynamical Systems and Poincaré Recurrences** According to the transcript, Xuanqi presents slides describing a dynamical system with a repelling region and a bounded region. Predrag advises not to use the term "Poincaré recurrence" since it has a specific meaning in statistical mechanics, and instead suggests referring to the concept as a "non-wandering set." Xuanqi plans to explain the concepts further in later slides, including clarifying the color-coded regions representing stable and unstable orbits.

**Exploring Dance Marathon and Plot Structure** The team discussed the concept of a "Dance Marathon" (Henri Siret held the world record for the marathon from October 10, 1908 until May 31, 1913, with a time of 2:37:23.). The plot should be explained in detail, with the yellow region representing dancers who can exit but never re-enter. They agreed to use this example to illustrate symbolic dynamics.

**Non-Wandering Sets and Ergodicity** Xuanqi and Predrag discussed the structure of non-wandering sets in dynamical systems. Xuanqi explained that these sets have a structure similar to  $n$ -symbol full shifts and can be used to define ergodic solutions and ergodicity. They also discussed the concept of normal numbers, which are numbers that have a uniform distribution of digits in their decimal representation. Xuanqi expressed interest in the computational complexity of spatial and temporal systems, an important topic.

**Ergodic Solutions and Global Shadow State** Xuanqi and Predrag discussed the challenges of finding conditions for ergodic solutions in open systems. Xuanqi explained that it's difficult to specify actual ergodic solutions due to the fractal nature of the solutions, which requires infinitely many digits to specify. They also discussed the concept of the global shadow state method and its application to higher dimensions. Xuanqi would focus on the spatiotemporal deterministic field theory and on finance 'state machines' in his upcoming presentation. Sidney and Predrag provided feedback, suggesting he avoid using the term "difficulty" twice and emphasize the importance of spatial temporal solutions. They suggested organizing the presentation into two topics: spatiotemporal deterministic field theory and finance (?) state machines.

**Floquet-Bloch Theorem and Resonances in Lattices** Sidney and Predrag discussed the application of the Floquet-Bloch theorem in their work, particularly in the context of an infinite lattice with periodic solutions. Predrag explained that the Floquet theorem is necessary when dealing with time, as the time is always infinite. He also mentioned the concept of regularization, which involves computing a ratio of two Hill determinants to handle divergent products of eigenvalues, see *ChaosBook Infinite dimensional operators*. They also touched on the idea of resonances in oscillatory systems and how they can be

avoided by having frequencies in the complex plane, see the Fenichel [4] post below. The discussion concluded with Predrag emphasizing the importance of considering multiperiodic solutions in nonlinear systems.

**Reevaluating Celestial Mechanics and Chaos** Predrag celestial mechanics and chaos theory. Xuanqi shared that their initial criteria for determining the existence of certain orbits might be incorrect, as he had found (in his private plots) that the orbit Jacobian matrix spectrum dropping to 0 is not a reliable indicator. Sidney expressed his satisfaction that the code he had put together worked well, despite the disappointing results. Xuanqi and Sidney discussed the possibility of postponing their work on two-dimensional systems due to the lack of conclusive results in one dimension. The conversation ended with Xuanqi mentioning that they would continue to explore other aspects of the Jacobian spectrum for insights.

**Hereby resolved:**

**Xuanqi** rethink and reorganize the content of his presentation for Jordan Cotler's group, focusing on spatiotemporal deterministic field theory and separating the topic of finite state machines.

**Xuanqi** review and potentially revise the slide about "actual ergodic solutions" based on Predrag's feedback.

**Xuanqi** write up the stability exponent section of the presentation.

**Sidney** continue investigating the spectrum behavior near bifurcation points in the one-dimensional case before moving on to two-dimensional analysis.

**Sidney** look for an analytical criterion for determining orbit existence, beyond just non-convergence.

**2015-09-15 Predrag** (reposted here from `elton/blog/AdamBlog.tex`)

Reading about robustness of invariant tori. Farazmand likes to refer to Fenichel [4] (to read it, [click here](#)). My understanding is that if a stability exponent is purely imaginary, it can destroy a torus at a rational resonance; but if it has a real part (hyperbolic case), there is no way for the Floquet exponent to approach the purely imaginary winding number of the torus, there can be no resonance, and the torus remains smooth and robust for an open interval of the system parameter values.

Figueras and Haro [5] write: "it has been known for a long time that persistence of invariant manifolds is closely related to the concept of normal hyperbolicity [4, 10]. We consider the analogous concept, tailored for skew products over rotations. Roughly speaking, an invariant torus is fiberwise hyperbolic if the linearized dynamics on the normal bundle is exponentially dichotomous, that is, the normal bundle splits into stable and unstable bundles on which the dynamics is uniformly contracting

and expanding, respectively. Notice that the tangent dynamics is dominated by the normal dynamics, since the former presents zero Lyapunov exponents. This implies that fiberwise hyperbolic invariant tori are robust and are as smooth as the system [28]. ”

Figueras’ thesis might be an easier read: [click here](#).

**Sidney** to explore creative and unconventional ideas for testing the hypothesis about ergodic orbits and spectrum.

## 26.15 Pow wow 2025-01-09

Scribes: Zoom AI Companion, Predrag

**2025-01-09 Zoom AI Companion Quick recap** The team discussed the development of a two-dimensional model from a one-dimensional model, focusing on the challenges of transitioning from one to two dimensions and the use of symbolic dynamics and the global shadow state method. They also analyzed the behavior of a spectrum as the period increases, the results of a logarithmically spaced set of  $\mu^2$  values, and the convergence of a numerical experiment. Lastly, they discussed issues with their data analysis, and explored the concept of bifurcation in a Hamiltonian system.

**Transitioning From One to Two Dimensions** Xuanqi and Han discussed the challenges of transitioning from one to two dimensions, including the loss of contact points (?) and the need for a modified gradient descent. They also discussed the use of symbolic dynamics and the global shadow state method, which they believe can help find all periodic states. Han expressed some uncertainty about the meaning of the global shadow state method, but Xuanqi clarified that he understood it as a method using fixed points to construct the model. They also discussed the need for more detailed explanations and visual aids for certain parts of the presentation.

**Spectrum Behavior and Determinant Discussion** Xuanqi and Han discussed the behavior of a spectrum as the period increases. Xuanqi presented a graph showing the spectrum’s behavior, noting that it doesn’t decrease to zero as the period increases. Han suggested that the graph might be a log plot, and Xuanqi agreed. They also discussed the possibility of the spectrum not decreasing to zero but (what?) still disappearing. Xuanqi mentioned that the spectrum’s behavior is not predictable, and Han suggested that the determinant might not be the best measure.

**Logarithmic  $\mu^2$  Analysis** Sidney discussed the results of a logarithmically spaced set of  $\mu^2$  values, noting a dip in the data at a specific point. He also shared that the data followed a linear relation until the end, as predicted by Predrag. Sidney further explained that the blue line in the plot represented the squared distance between two lattice states, while the red line was a straight

line with a slope of 0, as suggested by Predrag. Xuanqi asked about the periodic orbits used in the plot, to which Sidney clarified that he had tested two specific periodic orbits and another where he removed certain points. Xuanqi also inquired about the  $\mu^2$  values used, and Sidney explained that he had taken two  $\mu^2$  values, one of which was at the point where the data dips down. Xuanqi suggested that the plot could be improved by using two colors for the two orbits.

**Numerical Experiment Convergence Issues Discussed** Sidney shared that the experiment stops converging when the  $\mu$  value goes beyond a critical value, and it doesn't give any solution. Xuanqi suggested adding more values in between to understand the trend better. Sidney also mentioned that he had issues with numerical precision and tried coarse graining to fix it.

**Data Plot Critical Value Discussion** The team discussed issues with their data plot, particularly with the critical value and numerical methods. Xuanqi suggested that the critical value might be the actual value, and Han agreed, noting that going beyond this value could lead to different solutions. Sidney acknowledged the potential issue and decided to redo the plot based on the new critical value. The team also discussed the utility of the regime where all orbits exist to define their work.

**Saddle Node Bifurcation and System Application** Sidney and Xuanqi discussed the saddle node bifurcation and its application to their system. Xuanqi clarified that the bifurcation they proposed was not suitable for their system as it required a system with more than one co-dimension. Sidney then presented a plot showing a drop in values, which Xuanqi suggested might be due to large step sizes. Sidney agreed to fine-tune the plot and planned to verify the asymptotic nature of the dips. Xuanqi pointed out that the dips might not be exactly the same due to different sampling methods.

**Refining Mathematical Model With Precision** Sidney and Xuanqi discussed focusing on the (currently non-existent) Pruning Theory of spatiotemporal lattice field theories. Sidney suggested using  $T = 12$  instead of 11, which Xuanqi agreed with. They also discussed the importance of numerical precision and the need to adjust certain values to achieve a closer fit. Sidney made several adjustments, including adding more points to the start and end of the model, and adjusting the critical value. Xuanqi suggested adding more to the start and end to get a better approximation of the point where they touch.

**Eigenvalues and Convergence** Sidney and Xuanqi are discussing the results of a simulation or calculation related to some eigenvalues or lattice sites. They notice a value around 0.00005 where two quantities become infinitesimally close but do not fully converge. Predrag joins the discussion and they determine that there is a range around 0.01 where these two quantities coexist before fully converging. They debate whether the point of interest is when the quantities first get close or when they fully converge, and decide the range of coexistence spans about 4 orders of magnitude larger than their numerical precision.

**Numerical Experiments and PDE Formula** Sidney and Xuanqi discussed the critical value for their numerical experiments, with Xuanqi suggesting a

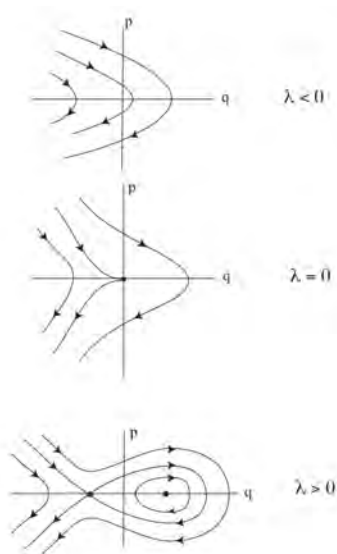


Figure 26.1: A set of portraits of one degree-of-freedom normal-form Hamiltonian saddle-node bifurcation of an equilibrium, illustrated by a forward-in-time phase-space plot.

larger size 25x25. They also discussed the behavior of lattice site fields, with Sidney explaining that the fields come close but do not reach a bifurcation or annihilation point.

**Exploring Bifurcation in Hamiltonian Systems** Sidney and Predrag discussed the concept of bifurcation in a Hamiltonian system. They explored the idea of islands of stability and the possibility of a pair of eigenvalues bifurcation to purely imaginary. They also discussed the potential for oscillatory behavior in the system and the importance of looking at the eigenvalue spectrum to understand the bifurcation. Predrag suggested that the bifurcation might show up in the orbit Jacobian matrix eigenvalues and that it could have a wavelength associated with it. They agreed to further investigate the spectrum to see if any eigenvalues become complex.

**Predrag: Saddle-node Bifurcation in Hamiltonian Systems** has not read up on this yet, but do have a look at (and blog whatever is of interest to us):

Check online-book by many authors, *Chemical Reactions : A Journey into Phase Space* (DOI); Chapter *Two Degree-of-Freedom Saddle-Node Hamiltonian*. Actually, already *One Degree-of-Freedom (DoF) Hamiltonian Bifurcation of Equilibria* figure 26.1 explains how the complex-stability equilibrium point (one to the two periodic states that will soon kill each other) shows up.

Víctor J. García-Garrido, Shibabrat Naik, Stephen Wiggins *Tilting and Squeezing: Phase space geometry of Hamiltonian saddle-node bifurcation and its influence on chemical reaction dynamics*; [arXiv:1907.03322](https://arxiv.org/abs/1907.03322).

'Glue' Figure 1 in L. M. Lerman *Hamiltonian Systems with Loops of a Separatrix of a Saddle-Center*, *Selecta Mathematica Sovietica* Vol. 10, No. 3 (1991); (click [here](#)) looks suggestive.

Saddle-node bifurcations in Figure 3, R. Barrio, F. Blesa and S. Serrano *Bifurcations and chaos in Hamiltonian systems* *Internat. J. Bif. Chaos*, Vol. 20, No. 5 (2010) 293–1319; [DOI](#); (click [here](#)) looks suggestive.

**Hereby resolved:**

**Sidney** refine the numerical analysis of the critical value for the bifurcation point in the spatiotemporal lattice field theory model.

**Sidney** check the orbit Jacobian matrix eigenvalues spectrum for complex/imaginary pairs near the critical value.

**Sidney** redo the pruning analysis for the 5,4 orbit using the new critical value method.

**Sidney** investigate the smooth transition of the distance between orbits near the critical value.

**Sidney** verify the asymptotic behavior of the critical value for different orbit lengths.

**Sidney** generate and send an updated plot for the 5,3 orbit to Xuanqi with a more accurate critical value.

**Sidney** investigate if the behavior observed at very small  $\mu$  step sizes is related to the complex eigenvalue phenomenon or is only numerical error.

**Sidney** create a new plot for the 15x15 orbit calculation, extending the range up to  $\mu^2 = 13$  and including a reference red line.

**Sidney** create a new plot with a larger range, up to  $10^{13}$ , including a reference red line.

**Sidney** continue working on the spatiotemporal Hill's formula for PDEs.

**Xuanqi** incorporate Sidney's updated plots into the presentation on the generalization from one-dimensional to two-dimensional systems.

**Xuanqi** review and revise the explanation of the global shadow state method, both in his MIT presentation and in Tigers' paper..

**Xuanqi** consider the implications of the new findings on the proposed bifurcation type for the presentation.

**Xuanqi** explain the new 15x15 orbit calculation results and discuss the possible type of bifurcation.

**Xuanqi** explain the purpose of the original blob plot and the new plot in the presentation or report.

**Xuanqi** discuss the possible kind of bifurcation that differs from common expectations.

**Han** provide input on the interpretation of the spectrum and determinant calculations near the critical value.

**Team** analyze the implications of potential complex eigenvalue pairs for both  $\phi^3$  and  $\phi^4$ . **Predrag 2025-0X-XX: Done!**

## 26.16 Pow wow 2025-01-14

Scribes: Zoom AI Companion, Predrag

**2025-01-14 Zoom AI Companion Quick recap** The team explored the challenges of working with infinite dimensional phase spaces in spatiotemporal theory, the concept of temporal shadowing in fluid turbulence, and the development of a new theory that treats space and time democratically. Lastly, they delved into the implications of breaking translational symmetry in one direction on periodic orbit theory and its applications, and discussed the key concepts of partition functions and zeta functions in deterministic classical field theory.

**Eigenvalues and Determinant Stability** Xuanqi and Sidney discussed the eigenvalues of the orbit Jacobian matrix and their implications for the determinant. Xuanqi asserted that a determinant cannot be considered zero if it has infinitely many entries, even if a single entry is zero. Sidney shared his findings on the  $\phi^4$  and  $\phi^3$ , 1 calculations, noting that the  $\phi^4$  calculation was more monotonic. Sidney mentioned that the orbit Jacobian spectrum had no pure imaginary values, only very small imaginary eigenvalues. Xuanqi is almost finished with his PowerPoint and has a question for **Pure Jack**.

**Deterministic Lattice Field Theory Discussed** Predrag and Xuanqi discussed the importance of deterministic lattice field theory in understanding chaos and turbulence. They explained that this theory is based on exact field equations and is particularly useful in situations where classical equations are dominant, such as in fluid dynamics and celestial mechanics, in contexts where weak noise or quantum effects can be neglected.

**Temporal Lattice Field Theory Challenges** Predrag suggested using the term 'coupling' instead of 'stretching' to avoid confusion. Xuanqi also discussed the challenges of moving to higher dimensions in temporal lattice field theory, particularly the issue of infinite dimensionality in the phase space. Sidney and Predrag attempted to clarify the concept of phase space, emphasizing that it refers to the space of all possible field configurations, not a particular method (Hamiltonian formulation, for example) of solving the equations.

**Infinite Dimensional State Spaces Challenges** Sidney, Xuanqi, and Predrag discussed the infinite dimensional phase spaces of spatiotemporal theory. Xuanqi emphasized the importance of following the anti-integrable limit, the periodic states, and the global shadow state method. Predrag emphasized the elegance and simplicity of treating space and time in the same way, as done in field theory.

**Shadowing in Fluid Turbulence** The team discussed the concept of temporal shadowing in the context of fluid turbulence, the close proximity of two surfaces in a high-dimensional space. Sidney uploaded

`figs/Closepass-ezgif.com-optimize.gif`,

a gif he made from [ChaosBook.org/tutorials](https://ChaosBook.org/tutorials) to help explain the concept of temporal shadowing. Predrag emphasized the importance of shadowing in chaos theory, explaining that it allows for the description of long orbits using shorter ones. They agreed to use the GIF in their presentations and to give credit to the creator, John Gibson.

**Bifurcations in Spacetime** Predrag and Xuanqi discussed the concept of shadowing in spacetime, its role in the bifurcation of periodic solutions in a spatiotemporal context.

**New Theory for Space and Time** Predrag discussed the development of our new theory that treats space and time democratically, focusing on doubly periodic solutions in space and time. He explained that this theory, which did not exist before, is being developed here and now, and is particularly useful for understanding the behavior of turbulent systems like chemical processes, flame fronts, fluids. The theory is still under development, they have not yet figured out how to compute with it. Predrag emphasized that the theory is new and has not been seen in the literature before.

**Translational Symmetry and Periodic Orbits** Sidney and Predrag discussed the implications of breaking translational symmetry in one direction on periodic orbit theory and its applications. They agreed that the theory heavily relies on time invariance, which is essential for the existence of useful periodic orbits. They also discussed the concept of shadowing, which might not hold in non-autonomous systems without time invariance. Predrag emphasized that the law governing the system should remain invariant in time and space for the theory to hold. They concluded that the rigid structure provided by periodic orbits in autonomous systems would be lost in non-autonomous systems.

**Partition Functions and Zeta Functions** Predrag explains the key concepts of partition functions and zeta functions in the context of deterministic classical field theory: the partition function is defined as a sum over all classical solutions, with each solution weighted by its stability computed from the Hill determinant. The zeta function arises by counting only prime *orbits*, rather than all distinct periodic states. One expresses the zeta function as a product over prime orbits, with connections to elliptic functions like the Dedekind eta function for doubly periodic solutions. While the formalism is elegant, he notes challenges in numerical evaluation. Xuanqi plans to include an overview of



these concepts in an upcoming talk, focusing on the main results without excessive technical details.

**Hereby resolved:**

**Xuanqi** to update presentation slides replacing "stretching parameter" by "coupling parameter" for clarity

**Xuanqi** add a slide explaining the concept of shadowing in both temporal, Sidney gif,

`figs/Closepass-ezgif.com-optimize.gif`,

and spatiotemporal cases

**Xuanqi** revise the slide on "critical" value to use the term "bifurcation value" instead

**Xuanqi** add a slide repeating the explanation of orbit Jacobian matrix before discussing stability of individual solutions

**Xuanqi** mention Hill's functional determinants and their relevance in field theory

**Xuanqi** add a slide on spatiotemporal zeta function and partition function, mentioning the Dedekind eta functions

**Xuanqi** remove the slide with the truncated series expansion plots of zeros of Euler function

**Xuanqi** incorporate Sidney's updated plots into the presentation on the generalization from one-dimensional to two-dimensional systems.

## 26.17 Pow wow 2025-01-16

Scribes: Zoom AI Companion, Predrag

**2025-01-16 Zoom AI Companion Quick recap** The team discussed the results of Sidney's calculations on the determinant of a [15x15] matrix and the concept of bifurcation in Hamiltonian systems.

**Improving Paper on Partition Sums** Predrag and Han focused on the CL18 section about partition sums, and the CL18 (non?) introduction of uniform hyperbolicity. The current section on partition sums was too long and needed improvement. They also discussed the need to define uniform hyperbolicity earlier in the paper, particularly in relation to the Hill determinant.

**Determinant and Eigenvalue Calculation Discussion** Sidney and Predrag discussed the results of Sidney's calculations on the determinant of a 15x15 matrix. Sidney shared a plot showing the determinant's behavior near the critical

value, noting that it doesn't go negative but becomes extremely large. Sidney also shared the difference in imaginary components of eigenvalues between the critical value and the value right before the change. Sidney found that a large number of these eigenvalues have positive imaginary components, with positive-negative pairs. Sidney also mentioned that the largest change in imaginary eigenvalue is of the order of  $10^{-14}$ , a number that might be within numerical accuracy and not meaningful.

**Bifurcation in Hamiltonian Systems** Predrag explained the concept of bifurcation in Hamiltonian systems, as illustrated by figure 26.1 set of portraits of one degree-of-freedom normal-form Hamiltonian saddle-node bifurcation of an equilibrium, a forward-in-time phase-space plot. He described how a pair of eigenvalues changes from hyperbolic to elliptic as the parameter  $\mu^2$  decreases, leading to a loss of hyperbolicity and the disappearance of a pair of solutions. Sidney, on the other hand, discussed his observations of the orbit Jacobian eigenvalues, noting that they barely change in magnitude before the bifurcation point. The team agreed to continue their exploration of the bifurcation process, with Sidney planning to analyze the imaginary parts of the eigenvalues.

**Tracking Eigenvalues and Bifurcation Points** The team discussed the tracking of eigenvalues in relation to bifurcation points. Han suggested that the smallest eigenvalue should be tracked, as it is likely to be the one that touches the critical value. Xuanqi presented a plot showing the smallest eigenvalue of the orbit Jacobian matrix for different primitive cell sites, but noted that there was no clear evidence of a quantitative change at the bifurcation point. Sidney confirmed that the minimum values before and at the critical  $\mu$  value did not change significantly.

The team discussed the possibility of computing eigenvalues directly over the infinite lattice, rather than imposing periodic boundary conditions. The conversation ended with Xuanqi planning to add more detail to the plot by adding the  $k$  dependence.

**Determinant of Infinite Operator Conditions** Xuanqi and others discuss the conditions for the determinant of an infinite operator to be zero. Xuanqi argues that for the determinant to be zero, it is not enough for one eigenvalue to be zero; rather, there must be an infinite subsequence of eigenvalues that is strictly bounded above by a value less than one. Predrag suggests that if the operator is in the trace class, the determinant can be defined as the integral of the logarithm over the Brillouin zone. They discussed whether a singular point in the integrand could make the integral undefined, depending on the type of singularity.

**Numerical Experiment Results and Integrals** Xuanqi and Predrag discussed the numerical experiment results and the implications of the integral of the logarithm of the spectrum. Xuanqi pointed out that the integral is undefined when the logarithm of the spectrum goes to negative infinity, which happens when the integrand is not continuous. However, they agreed that this issue does not arise when dealing with finite primitive cells, as the spectrum remains continuous. They also discussed the possibility of singularities in the integrand, but

concluded that these do not affect the integral's value. The discussion ended with the understanding that the integral is well-defined for finite primitive cells, but may become undefined when dealing with infinite primitive cells.

**Complex Eigenvalues and Singularities** Sidney and Xuanqi discussed the behavior of their numerical method, particularly focusing on the  $\phi^3$  figures. Sidney explained that the drop in the figures was intentional to signify a critical value. Xuanqi questioned the inclusion of a point with a huge drop, but Sidney clarified that it was included to visually represent the critical value. They also discussed the behavior of the  $\phi^4$  and  $\phi^3$  figures, with Sidney noting that  $\phi^4$  seemed to be better behaved. Xuanqi then discussed the issue of the orbit Jacobian not going to 0, and the implications of this for the stability exponent. Han and Xuanqi also discussed the concept of hyperbolicity and its relation to the eigenvalues of the orbit Jacobian matrix.

Predrag mentioned the "small denominator problem" in dynamical systems, which could potentially explain the critical  $\mu^2$  behavior observed for  $\phi^3$  by Xuanqi. If forward-in-time  $\det(1 - J^n)$  has  $J$  with eigenvalues on the unit circle, irrational phase angle, there might be repeats  $r$  for which the phase is arbitrarily close to 0, with the corresponding  $1/(1 - \Lambda_j)$  and arbitrarily small denominator.

Though for symplectic flows, eigenvalues come in complex-conjugate pairs,  $(1 - \Lambda_j)(1 - \Lambda_j^*) = 1 - \Lambda_j^2 = 0$ , exactly, for an interval of  $\mu^2$  values, no matter what the phase is. So seems a red herring.

Predrag mentioned that the Hessian matrix, which is a product of such matrices, can be problematic due to its symmetric nature. Han added that the determinant of the orbit Jacobian matrix equal to zero guarantees that the forward time Jacobian matrix will not have an eigenvalue of magnitude one. Xuanqi and Han discussed the stability exponent of a system, with Xuanqi plotting the logarithm of the determinant divided by the volume. They observed oscillations in the plot for certain values, but the trend generally looked credible. Predrag suggested dividing the logarithm also by the shadow state value ( $\mu^2$ ?) to collapse all plots on the same vertical scale.

**Determinant of Forward Jacobian** Xuanqi and Han discussed the determinant of the forward in time Jacobian in the context of the orbit Jacobian matrix. Xuanqi expressed confusion about the determinant approaching zero as the exponent goes to infinity. Han clarified that the determinant does not necessarily approach zero, but rather rotates around the unit circle. They also discussed the implications of the determinant approaching zero for the convergence of the orbit Jacobian.

**Hill Determinant and Newton Method** Predrag then introduced another interpretation of the orbit Jacobian, relating it to sect. 18.2.1 Newton's method for finding zeros of a function, in particular, Newton's method for optimization (18.34) that he assumes is included in the repertoire of the orbitHunter optimization routines. He explained that the determinant of the orbit Jacobian matrix is related to the convergence of the algorithm, and that a singular determinant could lead to divergence, i.e., no periodic state with the prescribed mosaic.

Predrag also mentioned the concept of Newton flow, which he hopes (but has not shown) can be interpreted as a heat equation (or machine learning ‘diffusion flows’, ‘normalizing flows’ (17.1))?. The conversation ended without a clear resolution to Xuanqi’s confusion (in AI Companion’s opinion) about the determinant of the forward-in-time Jacobian.

**Hyperbolicity and Bifurcations** Xuanqi and Predrag discussed the concept of hyperbolicity in dynamical systems and its relation to bifurcation. Xuanqi expressed interest in understanding the conditions under which a system loses hyperbolicity, particularly in the context of time evolution. Predrag suggested that bifurcation could be considered in the context of fictitious time, where the system’s ability to converge or diverge could be seen as a bifurcation point. Xuanqi, however, insisted on avoiding the criterion of non-convergence, seeking instead a more reliable indicator of hyperbolicity loss. The discussion also touched on the limitations of their current approach, which is limited to finite primitive cell volume and periodic states. Han suggested the possibility of extending the analysis to infinite space and time, potentially allowing for a more accurate calculation of the system’s stability.

**Localized Solutions and State Space** Predrag discussed the concept of localized solutions in a system, likening them to a ‘soliton’ or a ‘kink’ or a ‘breather’. Xuanqi questioned the nature of these solutions, suggesting they might not be ergodic. In Predrag’s opinion they are not ergodic, they are homo/heteroclinic. They also discussed the representation of these solutions in a time-evolution phase space, with Xuanqi noting that the points did not fill out the horseshoe as he would have expected. Predrag suggested that these solutions could be visualized by excluding the homoclinic points in the lower left corner: surviving points should reveal intermittent bursts.

The conversation ended with an unclear statement, in AI Companion’s opinion, from Predrag.

**Hereby resolved:**

**Han and Predrag** review and revise the explanation of uniform hyperbolicity in CL18. Decide where to best introduce the concept of uniform hyperbolicity.

**Han** investigate the possibility of computing the eigenvalues of the orbit Jacobian operator directly over the infinite lattice.

**Sidney** continue analyzing the eigenvalues of the orbit Jacobian matrix near the critical  $\mu^2$  value for different lattice sizes.

**Xuanqi** continue investigating the behavior of the orbit Jacobian matrix spectrum near the bifurcation point for the spatiotemporal  $\phi^4$  theory.

**Xuanqi** write up the section on semi-analytical spectrum of 2D spatiotemporal theory for the paper.

**Xuanqi** explore alternative criteria for determining the bifurcation point, beyond just non-convergence of numerical methods.

**Xuanqi** (perhaps?) incorporate sect. 18.2.1 Newton method interpretation of orbit Jacobian matrix determinants into his presentation.

**Xuanqi** consider analyzing localized solutions near the bifurcation point.

**Xuanqi** further examine the non-ergodic orbit behavior observed in the  $\phi^3$ .

**Xuanqi** analyze phase-space plot points that are not in the lower left corner of the graph to better visualize the system's behavior.

## References

- [1] M. Baake, J. Hermisson, and A. B. Pleasants, "The torus parametrization of quasiperiodic LI-classes", *J. Phys. A* **30**, 3029–3056 (1997).
- [2] M. Baake, N. Neumärker, and J. A. G. Roberts, "Orbit structure and (reversing) symmetries of toral endomorphisms on rational lattices", *Discrete Continuous Dyn. Syst.* **33**, 527–553 (2013).
- [3] P. Cvitanović and H. Liang, *A chaotic lattice field theory in two dimensions*, In preparation, 2024.
- [4] N. Fenichel, "Persistence and smoothness of invariant manifolds for flows", *Indiana Univ. Math. J.* **21**, 193–226 (1971).
- [5] J.-L. Figueras and À. Haro, "Reliable computation of robust response tori on the verge of breakdown", *SIAM J. Appl. Dyn. Syst.* **11**, 597–628 (2012).
- [6] J. A. C. Gallas, "Counting orbits in conjugacy classes of the Hénon Hamiltonian repeller", *Phys. Lett. A* **360**, 512–514 (2007).
- [7] T. Grava, T. Kriecherbauer, G. Mazzuca, and K. D. T.-R. McLaughlin, "Correlation functions for a chain of short range oscillators", *J. Stat. Phys.* **183**, 1 (2021).
- [8] B. Gutkin, L. Han, R. Jafari, A. K. Saremi, and P. Cvitanović, "Linear encoding of the spatiotemporal cat map", *Nonlinearity* **34**, 2800–2836 (2021).
- [9] R. S. MacKay, *Renormalisation in Area-preserving Maps* (World Scientific, Singapore, 1993).
- [10] R. J. Sacker, "A new approach to the perturbation theory of invariant surfaces", *Commun. Pure Appl. Math.* **18**, 717–732 (1965).